Canadian Journal of Chemistry

Issued by THE NATIONAL RESEARCH COUNCIL OF CANADA

VOLUME 33 JANUARY 1955 NUMBER 1

PHENOXYMETHYL 2-CHLOROETHYL ETHERS[1]

BY MARSHALL KULKA

ABSTRACT

A series of phenoxymethyl 2-chloroethyl ethers has been prepared for testing as possible insecticides.

In this investigation a series of phenoxymethyl 2-chloroethyl ethers, $ArOCH_2OCHXCH_2Cl$ (I, X = H or CH_3), was prepared for testing as possible insecticides by alkylating various phenols with 2-chloroethyl (1, 2) and 1-chloro-2-propyl (5) chloromethyl ether. The toxic effects of these ethers (I) on insects is described by Musgrave and Kukovica (3).

It is well known that the halogen atom linked α to the oxygen atom of chloroethers is more reactive than the β-halogen (2). This considerable difference in the halogen reactivities was also noted in the reactions between chloromethyl chloroethyl ether (II) and sodium phenoxides.

When chloromethyl 2-chloroethyl ether (II) was treated with aqueous or alcoholic solutions of a sodium phenoxide at room temperature, only a monophenoxy derivative was formed and a higher reaction temperature was necessary in order to form the diphenoxy derivative, $ArOCH_2OCH_2CH_2OAr$. In order to establish that the α-chlorine and not the β-chlorine reacted under the milder conditions, the reaction product (III) of sodium *p*-chlorophenoxide and II was heated with sodium 2,4-dichlorophenoxide. The resulting product (IV) on mild acid hydrolysis yielded *p*-chlorophenol and 2,4-dichlorophen-

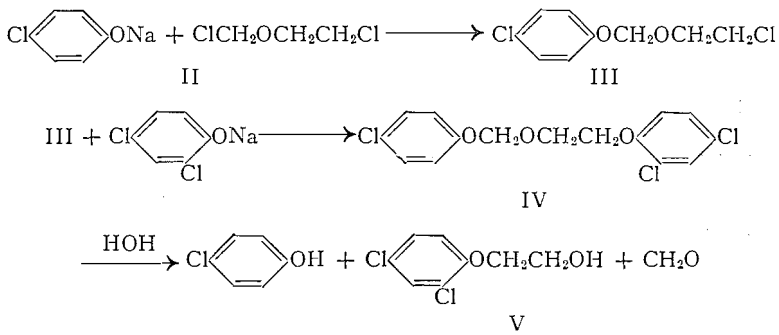

[1]*Manuscript received August 13, 1954.*
Contribution from the Dominion Rubber Company Limited Research Laboratories, Guelph, Ont.

oxyethanol (V) (4) and not 2,4-dichlorophenol and *p*-chlorophenoxyethanol, the products expected had the β-chlorine of II reacted before the α-chlorine. The wide difference in the degree of reactivity between the two chlorine atoms of II is further emphasized by the fact that III remains unaltered after boiling with diethylamine in benzene solution for several hours and requires prolonged boiling with alcoholic potassium thiocyanate in order to form 2-thiocyanatoethyl *p*-chlorophenoxymethyl ether. Phenoxymethyl 2-chloroethyl ether (I, Ar = C_6H_5, X = H) is stable in aqueous alkali but resinifies explosively when warmed with a drop of concentrated hydrochloric acid.

EXPERIMENTAL

Preparation of 2-Chloroethyl Phenoxymethyl Ethers

Method A

To a stirred solution of sodium (1 mole) in absolute ethanol (1 liter) was added the phenol (1 mole) and then dropwise chloromethyl 2-chloroethyl ether (1 mole) (1, 2) over about one-half hour, the temperature being kept at 20–25° by cooling. The reaction mixture was stirred for an additional two hours, the ethanol was distilled off *in vacuo*, and the residue treated with water. The product was extracted with benzene, washed with sodium hydroxide and with water. The solvent was then removed and the residue distilled.

Method B

To a stirred solution (or suspension) of sodium phenoxide (1 mole) in water (200 ml.) was added dropwise chloromethyl 2-chloroethyl ether (1 mole) in benzene (400 ml.) over about one-half hour, the temperature being kept at 10° by cooling. After the solution had been stirred for an additional two hours the benzene layer was separated from the reaction mixture, washed with sodium hydroxide and with water. The solvent was removed and the residue distilled.

TABLE I

PHENOXYMETHYL 2-CHLOROETHYL ETHERS ($ROCH_2OCH_2CH_2Cl$) FROM CHLOROMETHYL 2-CHLOROETHYL ETHER AND THE APPROPRIATE PHENOL

$ROCH_2OCH_2CH_2Cl$ R =	Method of prep.	% Yield	M.p. or b.p.	n_D^{20}	Formula	Analyses Calc. C	Calc. H	Found C	Found H
Phenyl	A	68	b_{12}=123	1.5170	$C_9H_{11}O_2Cl$	57.91	5.94	58.05	6.01
α-Naphthyl	A	88	b_{12}=200	1.5912	$C_{13}H_{13}O_2Cl$	65.97	5.50	66.12	5.51
p-t-Butylphenyl	A	64	b_{12}=163	1.5072	$C_{13}H_{19}O_2Cl$	64.33	7.84	64.41	7.87
p-Chlorophenyl	A	76	b_{12}=150	1.5300	$C_9H_{10}O_2Cl$	48.87	4.52	49.22	4.65
	B	64							
2,4-Dichlorophenyl	A	50	b_{12}=167	1.5465	$C_9H_9O_2Cl_3$	42.27	3.52	42.62	3.58
2,3,4,5,6-Pentachlorophenyl	A	60	m.p.=90		$C_9H_6O_2Cl_6$	30.08	1.67	30.30	2.11
p-Nitrophenyl	A	28	m.p.=70		$C_9H_{10}NO_4Cl$	46.65	4.32	46.89	4.50
	B	4							
	C	90							
2-Methoxy-4-formylphenyl	A	30	m.p.=59		$C_{11}H_{13}O_4Cl$	53.99	5.32	53.99	5.52
2,4-Dinitrophenyl	C	6	m.p.=80		$C_9H_9N_2O_6Cl$	39.06	3.26	39.32	3.08

Method C

A reaction mixture of chloromethyl 2-chloroethyl ether (1 mole), dry benzene (350 ml.), and the dry sodium phenoxide (1 mole) was heated under reflux for four hours. Water was added to the cooled reaction mixture, the benzene layer was separated, washed with sodium hydroxide and with water. The solvent was removed and the residue distilled.

p-Chlorophenoxymethyl 2-(2,4-Dichlorophenoxy)ethyl Ether (IV)

To a solution of sodium (5 gm.) in absolute ethanol (250 ml.) was added 2,4-dichlorophenol (34 gm.) and 2-chloroethyl *p*-chlorophenoxymethyl ether (45 gm.) and the resulting solution heated under reflux for 40 hr. About half of the ethanol was distilled off from the reaction mixture and the residue was treated with water and extracted with benzene.

The benzene extract was washed with water and the solvent was removed. Fractional distillation of the residue yielded unchanged *p*-chlorophenoxymethyl 2-chloroethyl ether (21 gm.) and a higher-boiling fraction, b.p. (0.2 mm.) = 170–172° (27 gm.). The latter was a viscous colorless liquid, n_D^{20} = 1.5752. Anal. calc. for $C_{15}H_{13}O_3Cl_3$: C, 51.81; H, 3.74. Found: C, 52.11; H, 3.60.

p-t-Butylphenoxymethyl 2-p-t-Butylphenoxyethyl Ether

This was prepared in 70% yield as above from *p-t*-butylphenoxymethyl 2-chloroethyl ether. It is a colorless viscous liquid, b.p. (12 mm.) = 245–250°, n_D^{20} = 1.5270. Anal. calc. for $C_{23}H_{32}O_3$: C, 77.54; H, 8.98. Found: C, 77.43; H, 9.06.

Hydrolysis of p-Chlorophenoxymethyl 2-(2,4-Dichlorophenoxy)ethyl Ether (IV)

A solution of *p*-chlorophenoxymethyl 2-(2,4-dichlorophenoxy)ethyl ether (15 gm.), water (150 ml.), ethanol (150 ml.), and concentrated hydrochloric acid (25 ml.) was heated under reflux for eight hours. Most of the ethanol was distilled and the cooled residue was extracted with ether. The ether was removed from the extract and the residue was fractionally distilled. Two main fractions were collected, fraction 1 boiling at 98–105° (12 mm.) (4 gm.) and fraction 2 boiling at 160–165° (12 mm.) (7 gm.). Fraction 1 solidified on cooling and melted at 35° alone or in admixture with *p*-chlorophenol. It depressed the melting point of 2,4-dichlorophenol. Fraction 2 after crystallization from benzene melted at 58–59° alone or in admixture with authentic 2,4-dichlorophenoxyethanol (4).

1,3-bis(2-Chloroethoxymethoxy)benzene

This was prepared in 20% yield by method A using two moles of sodium and two moles of chloromethyl 2-chloroethyl ether (II) per mole of resorcinol. It is a colorless liquid boiling at 150–154° (0.3 mm.), n_D^{20} = 1.5212. Anal. calc. for $C_{12}H_{16}O_4Cl_2$: C, 48.83; H, 5.41. Found: C, 48.80; H, 5.39.

1,4-bis(2-Chloroethoxymethoxy)benzene

This was prepared in 52% yield by method A as above from II and hydroquinone, b.p. (0.3 mm.) = 149–150°, n_D^{20} = 1.5197. Anal. calc. for $C_{12}H_{16}O_4Cl_2$: C, 48.83; H, 5.41. Found: C, 48.67; H, 5.31.

1,4-bis(2-Chloroethoxymethoxy)-2,3,5,6-tetrachlorobenzene

This was prepared in 12% yield by method A from tetrachlorohydroquinone and II. The white needles melted at 117–118° after crystallization from ethanol. Anal. calc. for $C_{12}H_{12}O_4Cl_6$: C, 33.26; H, 2.77. Found: C, 33.24; H, 2.82.

1,2-bis(2-Chloroethoxymethoxy)benzene

This was prepared in 41% yield by method A from II and catechol, b.p. (0.2 mm.) = 146–148°, n_D^{20} = 1.5222. Anal. calc. for $C_{12}H_{16}O_4Cl_2$: C, 48.83; H, 5.41. Found: C, 48.72; H, 5.18.

1,2,3-tris(2-Chloroethoxymethoxy)benzene

This was prepared in 15% yield by method A from II and pyrogallol, b.p. (0.2 mm.) = 212–215°. Anal. calc. for $C_{15}H_{21}O_6Cl_3$: C, 44.62; H, 5.25. Found: C, 44.91; H, 5.24.

p-Chlorophenoxymethyl 2,N-Morpholinoethyl Ether

A solution of *p*-chlorophenoxymethyl 2-chloroethyl ether (III) (16 gm.), morpholine (16 gm.), and toluene (100 ml.) was heated under reflux for 24 hr. The morpholine hydrochloride was filtered and the filtrate was extracted with dilute hydrochloric acid. The acid solution was basified with sodium hydroxide and extracted with benzene. Removal of the benzene and distillation of the residue yielded 14 gm. (or 68%) of a colorless liquid b.p. (12 mm.) = 196–198°, n_D^{20} = 1.5278. Anal. calc. for $C_{13}H_{18}NO_3Cl$: C, 57.45; H, 6.63. Found: C, 57.27; H, 6.54.

p-Chlorophenoxymethyl 2-Dimethylaminoethyl Ether

This was prepared as above from dimethylamine and *p*-chlorophenoxymethyl 2-chloroethyl ether (III), the reaction being carried out in a sealed bomb at 120–130°. It distilled as a colorless liquid boiling at 149–150° (12 mm.), n_D^{20} = 1.5100. Anal. calc. for $C_{11}H_{16}NO_2Cl$: C, 57.51; H, 6.97. Found: C, 57.24; H, 6.93. The *ethiodide* melted at 106–107° after crystallization from ethyl acetate. Anal. calc. for $C_{13}H_{21}NO_2ClI$: C, 40.46; H, 5.45. Found: C, 40.41; H, 5.59. The *butiodide* melted at 86–87° after crystallization from methanol. Anal. calc. for $C_{15}H_{25}NO_2ClI$: C, 43.53; H, 6.04. Found: C, 43.55; H, 6.13.

p-Chlorophenoxymethyl 2-Diethylaminoethyl Ether

This was prepared as above from diethylamine and III. It distilled as a colorless liquid boiling at 165–167° (12 mm.), n_D^{20} = 1.5032. Anal. calc. for $C_{13}H_{20}NO_2Cl$: C, 60.57; H, 7.77. Found: C, 60.68; H, 7.82.

p-Chlorophenoxymethyl 1-Chloro-2-propyl Ether

This was prepared in 63% yield by method A from chloromethyl 1-chloro-2-propyl ether (5) ($ClCH_2OCH(CH_3)CH_2Cl$) and *p*-chlorophenol. It distilled as a colorless liquid boiling at 155–157° (13 mm.), n_D^{20} = 1.5210. Anal. calc. for $C_{10}H_{12}O_2Cl_2$: Cl, 30.2. Found: Cl, 30.5.

p-Nitrophenoxymethyl 1-Chloro-2-propyl Ether

This was prepared in 63% yield by method C from chloromethyl 1-chloro-2-propyl ether and *p*-nitrophenol. It crystallized from methanol as white

prisms melting at 43–44°. Anal. calc. for $C_{10}H_{12}NO_4Cl$: C, 48.88; H, 4.89. Found: C, 49.00; H, 4.84.

p-Nitrophenoxymethyl 2-Thiocyanatoethyl Ether

A solution of *p*-nitrophenoxymethyl 2-chloroethyl ether (12 gm.) and potassium thiocyanate (6 gm.) in 95% ethanol (100 ml.) was heated under reflux for 24 hr. Most of the ethanol was distilled off and the residue treated with cold water. The white solid was filtered, washed, dried, and crystallized from benzene – petroleum ether. The white prisms melted at 58–59°. Anal. calc. for $C_{10}H_{10}N_2O_4S$: C, 47.26; H, 3.94. Found: C, 46.88; H, 4.05.

p-Nitrophenoxymethyl 1-Thiocyanato-2-propyl Ether

This was prepared as above from *p*-nitrophenoxymethyl 1-chloro-2-propyl ether. The white prisms melted at 42–43°. Anal. calc. for $C_{11}H_{12}O_4N_2S$: C, 49.25; H, 4.48. Found: C, 49.30; H, 4.78.

ACKNOWLEDGMENT

The author is indebted to Miss Gisela Rotermann for the microanalyses.

REFERENCES

1. FARREN, J. W., FIFE, H. R., CLARK, F. E., and GARLAND, C. E. J. Am. Chem. Soc. 47: 2419. 1925.
2. LINGO, S. P. and HENZE, H. R. J. Am. Chem. Soc. 61: 1574. 1939.
3. MUSGRAVE, A. J. and KUKOVICA, I. 85th Ann. Rept. Entomol. Soc. Ontario. 1954.
4. NEWMAN, M., FONES, W., and RENOLL, M. J. Am. Chem. Soc. 69: 718. 1947.
5. STAPPER, M. L. Rec. trav. chim. 24: 256. 1905.

SOME CHLORINATION PRODUCTS OF BUTYNE-1, BUTYNE-2, AND PENTYNE-1[1]

By A. T. Morse and L. C. Leitch

ABSTRACT

The following new compounds were isolated from the vapor phase chlorination of butyne-1, butyne-2, and pentyne-1: 1,1,2,2-tetrachlorobutane, 2,2,3,3-tetrachlorobutane, 1,1,2,2-tetrachloropentane, *trans*-1,2-dichloro-1-butene, *trans*-2,3-dichloro-2-butene, and *trans*-1,2-dichloro-1-pentene. Dehydrochlorination of 1,1,2,2-tetrachlorobutane and 1,1,2,2-tetrachloropentane gave 1,1,2-trichloro-1-butene and 1,1,2-trichloro-1-pentene respectively. Partial dechlorination of 1,1,2,2-tetrachlorobutane and 1,1,2,2-tetrachloropentane gave *cis* and *trans* isomers of 1,2-dichloro-1-butene and 1,2-dichloro-1-pentene respectively. 2,2,3,3-Tetrachlorobutane gave chiefly *trans*-2,3-dichloro-2-butene. 1,1,1,2,2-Pentachlorobutane and 1,1,1,2,2-pentachloropentane were prepared by chlorination of 1-chloro-1-butyne and 1-chloro-1-pentyne respectively.

In a previous communication (2) one of us reported the preparation of 1,1,2,2-tetrachloropropane and *trans*-1,2-dichloro-1-propene in 65 and 20% yields respectively by the vapor phase chlorination of propyne at 50° to 60°C. These compounds were in turn later used to synthesize others of the C_3 series (3). The successful outcome of this investigation led us to attempt the chlorination of other acetylenic hydrocarbons by the same method in the hope of obtaining some hitherto unknown polychlorinated hydrocarbons. Such studies might also enable us to correlate chemical behavior with structure. This paper deals with the chlorination products of butyne-1, butyne-2, and pentyne-1 and some of their reactions.

Chlorination of butyne-1 in the vapor phase at 40°C. gave a 36.5% yield of 1,1,2,2-tetrachlorobutane and 11% of *trans*-1,2-dichloro-1-butene. Between these compounds an intermediate fraction was collected over a wide range of temperature. A second careful fractionation of this mixture gave a product, b.p. 64–65°C. at 25 mm., which was first thought to be a trichlorobutane. However, dehalogenation in ethanol with zinc dust gave a mixture of compounds. The original material therefore appears to be a mixture of trichlorobutanes and/or trichlorobutenes. In addition to these fractions a considerable amount of distillate was obtained boiling above the tetrachlorobutane from which no pure compound could be separated. The presence of penta- and hexachlorobutanes was indicated by the index of refraction of the distillate.

Dehalogenation of 1,1,2,2-tetrachlorobutane with zinc dust in ethanol gave *trans*- and *cis*-1,2-dichloro-1-butene, b.p. 99.5° to 100°C. and 118° to 119°C. respectively. The yield of *cis* isomer was nearly twice that of the *trans*. Dehydrohalogenation of the tetrachlorobutane gave 1,1,2-trichloro-1-butene, b.p. 137°C. The latter compound was also obtained from butyne-1 by the sequence of reactions:

[1]*Manuscript received August 20, 1954.*
Contribution from the Division of Pure Chemistry, National Research Laboratories, Ottawa, Canada. Issued as N.R.C. No. 3439.
Presented at the 37th Canadian Chemical Conference, Toronto, Ontario, June, 1954.

$$C_2H_5C{\equiv}CH \xrightarrow{NaOCl} C_2H_5C{\equiv}CCl \xrightarrow{2Cl_2} C_2H_5CCl_2CCl_3 \xrightarrow{-Cl_2} C_2H_5CCl{=}CCl_2.$$

The physical constants of the two compounds were identical.

The chlorination of butyne-2 proceeded smoothly at room temperature. From the first fraction of chlorinated product *trans*-2,3-dichloro-2-butene, b.p. 99.5° to 100°C., was recovered in 23.6% yield. At this point the distillation had to be discontinued on account of the separation of solid from the residue which was removed by filtration. This product analyzed correctly for a tetrachlorobutane and was in fact 2,2,3,3-tetrachlorobutane, m.p. 174°C. The filtrate from the solid boiled over a wide range of temperature; its index of refraction indicated that it was a mixture of penta- and hexachlorobutanes.

2,2,3,3-Tetrachlorobutane was dehalogenated with zinc dust in ethanol. The chief product isolated was a substance b.p. 100°C., apparently *trans*-2,3-dichloro-2-butene. Very little of the *cis*-isomer was present. These compounds had been previously prepared by Tishchenko and Churbakov (4) by removal of hydrogen chloride from 2,2,3-trichlorobutane.

The chlorination of pentyne-1 gave a 19.3% yield of *trans*-1,2-dichloro-1-pentene and 15% of 1,1,2,2-tetrachloropentane. A large amount of by-products was obtained from which no pure compounds could be isolated.

Dechlorination of 1,1,2,2-tetrachloropentane gave *cis*- and *trans*-1,2-dichloro-1-pentene, b.p. 62° to 62.5°C. at 47 mm. and 49 to 50°C. at 47 mm. respectively. The proportion of *cis*- to *trans*- isomer was in the ratio 2:1. Removal of hydrogen chloride from the tetrachloro compound gave 1,1,2-trichloro-1-pentene, b.p. 74–75°C. at 45 mm. The same compound was prepared by the following sequence of reactions from pentyne-1:

$$C_3H_7C{\equiv}CH \xrightarrow{NaOCl} C_3H_7C{\equiv}CCl \xrightarrow{2Cl_2} C_3H_7CCl_2CCl_3 \xrightarrow{-Cl_2} C_3H_7CCl{=}CCl_2.$$

DISCUSSION

The chlorination of the acetylenic hydrocarbons described in the present work was much less specific than that of propyne. In all three instances chlorination by substitution took place to a certain extent as well as by addition. The formation of substitution products in the case of butyne-1 and pentyne-1 is consistent with Haas' rule (1) relating to the ease of substitution of chlorine for hydrogen in hydrocarbons, viz., that hydrogen is more readily replaced by chlorine in a methylene than in a methyl group. However, this does not account for the presence of appreciable amounts of products formed by substitutive chlorination in butyne-2, and none in propyne. It may well be that electron mobility in butynes and pentyne is greater than in propyne, and chlorination by substitution is thus facilitated.

Another curious observation made in the present work is the predominance of *cis*-isomer formed in the dechlorination of 1,1,2,2-tetrachlorobutane and pentane and the almost exclusive formation of *trans*-isomer in the dechlorination of 2,2,3,3-tetrachlorobutane. No obvious explanation can be offered for these results at this time.

EXPERIMENTAL

Chlorination of Butyne-1

This chlorination was carried out in an apparatus similar to that described in an earlier paper (2).

Dry chlorine gas and butyne-1 were introduced into the evacuated reaction flask in the ratio 2: 1. After they were heated to 40°C. with an infrared lamp, reaction began and proceeded smoothly at 55° to 60°C. without further external heating provided that the correct ratio of the gases was maintained. The liquid product collected in the trap at the bottom of the reactor. Under these conditions, 32.5 liters of butyne-1 were chlorinated in 12 hr. The crude product was shaken twice with 100 ml. of dilute sodium bicarbonate solution and finally washed with water. After drying over potassium carbonate, the dry product, weighing 227 gm., was fractionally distilled under reduced pressure.

Fraction I was collected over the range 23° to 28°C. at 27 mm. When refractionated through a Stedman column (12 in. × 3/8 in.) at atmospheric pressure, 15.8 gm. of *trans*-1,2-dichloro-1-butene were obtained. Yield 11.3%, b.p. 99.5° to 100.5°C., n_D^{20} 1.4522. Fraction II (35.0 ml.) distilled over the range 31° to 85°C. at 25 mm. When carefully refractionated, a sample of 12.0 ml. with constant boiling point (64 to 64.5°C. at 25 mm.) was collected. This material is probably a mixture of trichlorobutanes and/or trichlorobutenes.

Fraction III consisted of 80.0 gm. of 1,1,2,2-tetrachlorobutane. Yield 36.5%, b.p. 85° to 85.5°C. at 25 mm., n_D^{20} 1.4908; calc. for Cl, 72.39%, found, 72.17%. Fraction IV consisting of 8.0 ml. distilled over the range 88° to 105°C. at 25 mm., n_D^{20} 1.5000. Fraction V (13.5 ml.) was collected at 105° to 106.5°C. at 23 mm., n_D^{20} 1.5074. Fraction VI (4.0 ml.) distilled at 108° to 117°C. at 25 mm., n_D^{20} 1.5102. Fraction VII (10.0 ml.) distilled at 119° to 121°C. at 24 mm., n_D^{20} 1.5162.

cis- and trans-1,2-Dichloro-1-butene

1,1,2,2-Tetrachlorobutane (69.0 gm.) in 25 ml. of ethanol was added dropwise to a refluxing mixture of 30.0 gm. of zinc dust in 200 ml. of ethanol. After refluxing for 30 min. the reaction products were distilled off as azeotropes through a Stedman column. The distillate was washed with water and dried by distilling on the vacuum line through a U-tube filled with P_2O_5. The isomers were separated by fractional distillation through a Stedman column. The total yield was 80.0%. The *trans*-isomer weighed 12.6 gm. (37% of the total), distilled at 100° to 101.0°C., n_D^{20} 1.4526; calc. for Cl, 56.73%, found, 55.80%. The *cis*-isomer weighed 21.5 gm. (63% of the total) and distilled at 118.5° to 119.0°C., n_D^{20} 1.4598.

1,1,2-Trichloro-1-butene

1,1,2,2-Tetrachlorobutane (20.0 gm.) and calcium oxide (6.0 gm.) in 100 ml. of water were refluxed for eight hours. The yield of 1,1,2-trichloro-1-butene which distilled off as an azeotrope was nearly quantitative. After drying over calcium chloride, the halide was distilled through a Stedman column. It boiled at 137.0°C. at atmospheric pressure (58° to 58.5°C. at 46.0 mm.), n_D^{20} 1.4816; calc. for Cl, 66.71%, found, 66.06%.

1,1,1,2,2-Pentachlorobutane

1-Chlorobutyne-1 (15 gm.; prepared as in Ref. 3) was dissolved in 25 ml. of methylene chloride in a 100 ml. flask. The latter was fitted with a cold finger condenser filled with dry ice. Chlorine gas (28.4 gm.) was slowly distilled into this solution which was allowed to stand in the dark for four hours. The colorless solution was fractionally distilled at reduced pressure through a Stedman column. 1,1,1,2,2-Pentachlorobutane distilled at 102–103.5°C. at 25 mm. Yield 25.6%, n_D^{20} 1.5096; calc. for Cl, 76.95%, found, 71.03%. A sample of this compound added to zinc dust in ethanol gave a product identical with 1,1,2-trichloro-1-butene reported above.

Chlorination of Pentyne-1

Pentyne-1 (122 gm.) was placed in a 200 ml. flask, which was connected to the same apparatus as was used in the chlorination of butyne-1. The pentyne and vacuum line leading to the reaction flask were heated to 45°C. in order to keep the vapor pressure of the compound slightly above one atmosphere. By this means it was possible to feed it into the reaction flask as a vapor, in which form it reacted with the chlorine. As soon as the gases mixed chlorination began without external heating. Reaction temperature fluctuated between 45° and 50°C. On several occasions flashes occurred during the chlorination but these were neither dangerous nor did they retard reaction; they merely deposited carbon on the walls of the flask. After eight hours the pentyne was all reacted. The crude product (236 gm.) was treated in the same manner as described for the lower homologue. After drying it was fractionally distilled through a Stedman column.

Fraction I consisted of 51 gm. of unreacted pentyne-1.

Fraction II was collected over the range 31° to 51°C. at 24 mm. When refractionated at atmospheric pressure, 28.0 gm. of *trans*-1,2-dichloro-1-pentene were collected. Yield 19.3%, b.p. 124.5–125°C. (48° to 49°C. at 47 mm.), n_D^{20}1.4556.

Fraction III was a mixture of chloro compounds from which no single compound was isolated.

Fraction IV was 1,1,2,2-tetrachloropentane. It distilled at 95–97°C. at 23 mm. Yield 33.0 gm. (15.3%), n_D^{20} 1.4887; calc. for Cl, 67.61%, found, 66.61%.

A high boiling residue of 30 ml. remained but no pure compound was isolated from it.

cis- and trans-Dichloro-1-pentene

1,1,2,2-Tetrachloropentane (20.6 gm.) in 10 ml. of ethanol was added to a suspension of 10 gm. of zinc dust in 60 ml. of ethanol. The reaction products were distilled off as azeotropes and dried over calcium chloride. The yield of dry product was 13.0 gm. (95%). The two isomers were separated by careful distillation. *trans*-1,2-Dichloro-1-pentene distilled at 49–50°C. at 47 mm. Yield 4.0 gm. (34.8% of total), n_D^{20} 1.4552; calc. for Cl, 51.00%, found, 50.98%. The *cis*-isomer, 7.5 gm. (65.2% of total), distilled at 62–62.5°C. at 47 mm., n_D^{20} 1.4614; calc. for Cl, 51.00%, found, 51.04%.

1,1,2-Trichloro-1-pentene

This compound was prepared by adding 7.2 gm. of 1,1,2,2-tetrachloropentane to a mixture of 3.0 gm. of calcium oxide in 50 ml. of water. The dry 1,1,2-trichloro-1-pentene distilled at 74–75°C. at 45 mm. Yield 4.1 gm. (70%), n_D^{20} 1.4798; calc. for Cl, 61.31%, found 61.23%.

1,1,1,2,2-Pentachloropentane

Dry chlorine gas (0.80 mole) was slowly distilled into a solution of 40.0 gm. (0.39 mole) of 1-chloro-1-pentyne in 40 ml. of methylene chloride in the dark. The 1,1,1,2,2-pentachloropentane, fractionated through a Stedman column, distilled at 83–84°C. at 7.00 mm. Yield 44.8 gm. (47.2%), n_D^{20} 1.5062; calc. for Cl, 72.53%, found, 70.53%.

A sample of this compound treated with zinc dust in ethanol gave a product identical with 1,1,2-dichloro-1-pentene described above.

Chlorination of Butyne-2

Butyne-2 (45 gm.) was placed in a 100 ml. flask, and the flask connected to the chlorination apparatus. The hydrocarbon was heated to 32°C. at which it had a vapor pressure slightly above one atmosphere. Chlorine and butyne-2 were fed into the evacuated reaction flask in the ratio 2: 1. Reaction began at once and proceeded smoothly at 36–38°C. The liquid product collected in the receiver at the bottom of the apparatus. There was also evidence of solid product forming on the walls of the reaction flask.

After 10 hr. all the butyne-2 had been added and the product was fractionated without further treatment through a glass helices packed column.

Fraction I consisted of 4.0 gm. of unreacted butyne-2.

Fraction II was composed of 21 gm. of *trans*-2,3-dichloro-2-butene. Yield 22.0%, b.p. 98° to 100°C., n_D^{20} 1.4570.

A solid began to separate in the fractionating column and distilling flask shortly after the apparatus had been evacuated. The flask was cooled to −20°C. and the solid filtered off. A sample recrystallized from pentane gave pure 2,2,3,3-tetrachlorobutane. Yield 25 gm. (16.8%), m.p. 171.5–174°C.; calc. for Cl, 72.38%, found, 71.94%.

A high boiling residue of 34 gm. remained from which no pure compound could be isolated. It appeared to be a mixture of penta- and hexachlorobutanes.

cis- and trans-2,3-Dichloro-2-butene

2,2,3,3-Tetrachlorobutane (28 gm.) in 200 ml. of ethanol was added to a refluxing mixture of 15 gm. of zinc dust in ethanol. After reaction was complete the products were distilled as azeotropes with ethanol. About 200 ml. had to be distilled before all the halide had distilled. The distillate was worked up in the usual manner. The total yield was 60%. The *trans*-isomer weighing 9.1 gm. (90% of the total) distilled at 99–101°C., n_D^{20} 1.4582. The *cis*-isomer weighed 1.2 gm. (10% of the total), distilled at 124–126°C., n_D^{20} 1.4672.

REFERENCES

1. Haas, H. B., McBee, E. T., and Weber, P. Ind. Eng. Chem. 28: 333. 1936.
2. Leitch, L. C. Can. J. Chem. 31: 385. 1953.
3. Morse, A. T. and Leitch, L. C. Can. J. Chem. 32: 500. 1954.
4. Tishchenko, D. V. and Churbakov, A. J. Gen. Chem. (U.S.S.R.) 6: 1553. 1936. Chem. Abstr. 31: 2165. 1937.

ANTITUBERCULOUS ISONICOTINYLHYDRAZONES OF LOW TOXICITY[1]

By A. Zubrys and C. O. Siebenmann

ABSTRACT

In a search for antituberculous compounds of low toxicity, the isonicotinylhydrazones of monohydroxybenzaldehydes and of the corresponding aldehydophenoxyacetic acids were prepared. When tested *in vivo*, the isonicotinylhydrazones of 2-formyl-phenoxyacetic acid and of 6-methoxy-2-formyl-phenoxyacetic acid showed the most marked antituberculous activity combined with low toxicity. The preparation of 6-methoxy-2-formyl-phenoxyacetic acid and of the isonicotinylhydrazone of 2-formyl-phenoxyacetic acid are described as representative examples. The results of microanalysis include data which define the antituberculous isonicotinylhydrazones of 2-hydroxybenzaldehyde, 4-hydroxybenzaldehyde, and 2-hydroxy-3-methoxybenzaldehyde (*o*-vanillin).

INTRODUCTION

Following the discovery of the antituberculous activity of isonicotinic acid hydrazide (isoniazid) by Grunberg and Schnitzer (5) and by Bernstein *et al.* (1) we recorded the marked therapeutic action in the experimental tuberculous infection in mice of isonicotinylhydrazones of hydroxy substituted benzaldehydes (8). As a representative example of this group of compounds the isonicotinylhydrazone of 4-hydroxybenzaldehyde (I) was studied more closely (7).

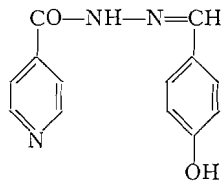

I

The low toxicity in mice shown by (I), as well as by isonicotinylhydrazones of other monohydroxybenzaldehydes, encouraged us to extend our research in this field.

As the *in vitro* antituberculous activity of (I) approaches that of isoniazid, it was considered likely that the limited *in vivo* activity of this compound, as compared to that of isoniazid, may in part be due to its low solubility. It appeared desirable, therefore, to introduce suitable modifications in the molecular structure to render this type of compound more soluble. On the basis of this idea we have prepared, as starting materials for isonicotinylhydrazones, a series of aldehydo-phenoxyacetic acids, namely:
4-formyl-phenoxyacetic acid (3) from 4-hydroxybenzaldehyde,
2-formyl-phenoxyacetic acid (2, 6) from salicylaldehyde,
6-methoxy-2-formyl-phenoxyacetic acid from *o*-vanillin (2-hydroxy-3-methoxybenzaldehyde), and

[1]*Manuscript received August 16, 1954.*
Contribution from the Connaught Medical Research Laboratories, University of Toronto, Toronto, Ont.

2-methoxy-4-formyl-phenoxyacetic acid (4) from vanillin (4-hydroxy-3-methoxybenzaldehyde).

One of these acids, namely, 6-methoxy-2-formyl-phenoxyacetic acid (II) was unknown.

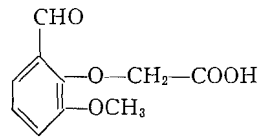

II

The isonicotinylhydrazones of all four above-mentioned aldehydophenoxyacetic acids, when tested in mice, showed a consistently higher antituberculous activity than the isonicotinylhydrazones of the corresponding unsubstituted hydroxybenzaldehydes. The best results were obtained with the isonicotinylhydrazones of 6-methoxy-2-formyl-phenoxyacetic acid (III) and of 2-formyl-phenoxyacetic acid (IV).

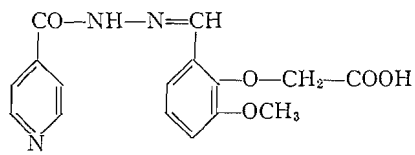

III

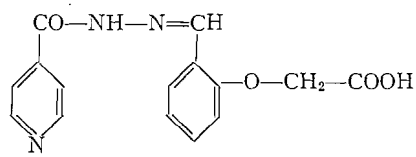

IV

The marked antituberculous activity of these two compounds, mentioned in an earlier communication (9), is of the order of 35–50% of that of isoniazid,

TABLE I

Compound	M.p., ° C. uncorrected	Empirical formula	Analysis, % Calc. C	Calc. H	Calc. N	Found C	Found H	Found N
6-Methoxy-2-formyl-phenoxyacetic acid (II)	118–121	$C_{10}H_{10}O_5$	57.14	4.79		57.02 56.89	4.83 4.68	
Isonicotinylhydrazones of:								
4-Hydroxybenzaldehyde* (I)	287–287.5	$C_{13}H_{11}N_3O_2 \cdot H_2O$	60.22	5.05	16.21	60.18	5.00	16.09
2-Hydroxybenzaldehyde	238–240	$C_{13}H_{11}N_3O_2$	64.72	4.59	17.42	64.52	4.43	17.29
4-Hydroxy-3-methoxy-benzaldehyde*	223–224	$C_{14}H_{13}N_3O_3 \cdot H_2O$	58.12	5.23	14.53	58.04	4.86	14.50
2-Hydroxy-3-methoxy-benzaldehyde	227–228	$C_{14}H_{13}N_3O_3$	61.98	4.84	15.49	62.00	5.00	15.09
6-Methoxy-2-formyl-phenoxyacetic acid (III)	233–234	$C_{15}H_{15}N_3O_5 \cdot H_2O$	55.32	4.93	12.1	55.00 55.19	4.88 4.98	12.30 12.16
2-Formyl-phenoxyacetic acid (IV)	247–248	$C_{15}H_{13}N_3O_4$	60.19	4.38	14.03	59.98 60.10	4.20 4.39	14.32 14.14

**Dried in vacuo (14 mm.) at 75°.*

and deserves special attention on account of the low toxicity which both compounds exhibit in laboratory animals. The acute oral toxicity of (III), when tested in mice, is less than $\frac{1}{40}$, and that of (IV) less than $\frac{1}{25}$, of that of isoniazid.

In the experimental part the synthesis of 6-methoxy-2-formyl-phenoxyacetic acid, 2-formyl-phenoxyacetic acid and its isonicotinylhydrazone are described as representative examples. The results of microanalysis (Table I) include data defining the antituberculous isonicotinylhydrazones, prepared by us in 1952, from 4-hydroxybenzaldehyde, 2-hydroxybenzaldehyde, 2-hydroxy-3-methoxybenzaldehyde, and vanillin. These hydrazones were prepared using essentially the same procedure as for the isonicotinylhydrazone of 2-formyl-phenoxyacetic acid. The biological properties of all above-mentioned compounds are the subject of a separate communication (10).

EXPERIMENTAL PART

6-Methoxy-2-formyl-phenoxyacetic Acid (II)

To a solution of 45.6 gm. (0.3 M.) of 2-hydroxy-3-methoxybenzaldehyde in 100 ml. of ether, 25 gm. of sodium hydroxide dissolved in 50 ml. of water were added slowly while the solution was cooled and stirred. To this mixture a solution of 28.35 gm. (0.3 M.) of chloracetic acid in 30 ml. of water was added in the same way. The ether was removed and the mixture heated under reflux for two hours at 120–125° C. (oil bath temp.). The resulting solution was cooled, diluted with water, acidified with hydrochloric acid to Congo red, and allowed to stand for three hours at room temperature. The precipitate which formed was filtered, dissolved in sodium bicarbonate solution, and extracted with ether. The aqueous layer was acidified to Congo red and left in the cold-room for two hours. The precipitated impure 6-methoxy-2-formyl-phenoxyacetic acid was crystallized from boiling water. Yield: 20 gm., m.p. 111–114.5° C. After two recrystallizations from benzene the m.p. rose to 118–121° C.

The 6-methoxy-2-formyl-phenoxyacetic acid crystallizes from benzene in white needles and has the characteristic properties of an aldehydo-carbonic acid. It reduces ammoniacal silver nitrate solution, gives a violet coloration with Schiff's reagent, forms a hydrazone with isonicotinic acid hydrazide, and a thiosemicarbazone with thiosemicarbazide. It dissolves slowly in sodium bicarbonate solution with elimination of carbon dioxide. The acid is easily soluble in ethanol, methanol, acetone, ethylacetate, amylacetate, ether, acetic acid, dimethylformamide, hot benzene, and hot water.

2-Formyl-phenoxyacetic Acid

This acid was prepared in a similar way as 6-methoxy-2-formyl-phenoxyacetic acid. The final product was crystallized from water. From 36.6 gm. of salicylaldehyde the yield was 25 gm., m.p. 130–132° C.

Isonicotinylhydrazone of 2-formyl-phenoxyacetic Acid (IV)

A hot solution of 13.7 gm. (0.1 M.) of isonicotinic acid hydrazide* in 100 ml.

**For the synthesis of isonicotinic acid hydrazide a generous initial supply of isonicotinic acid was obtained through the courtesy of Fine Chemicals of Canada, Ltd.*

of water was mixed with a hot solution of 18 gm. (0.1 M.) of 2-formyl-phenoxy-acetic acid in 120 ml. of ethanol, heated for 15 min. under reflux, and allowed to stand in the cold-room over night. The slightly yellowish precipitate which formed was filtered, washed with water, ethanol, acetone, and dried. Yield: 29 gm., m.p. 246–248° C. An analytical sample, recrystallized from 75% ethanol, had m.p. 247–248° C.

The hydrazone is soluble in dilute sodium bicarbonate solution; it reduces ammoniacal silver nitrate solution.

ACKNOWLEDGMENTS

The authors wish to thank the National Research Council for financial assistance which made this investigation possible. We are indebted to Dr. R. D. Defries, Director of the Connaught Medical Research Laboratories, for his encouragement and valuable support. Grateful acknowledgment is made to Prof. G. F Wright, University of Toronto, for the X-ray diffraction pattern and to Dr. R. N. Jones, Division of Pure Chemistry, National Research Council, for the infrared spectra taken of some of the compounds recorded in this report.

REFERENCES

1. BERNSTEIN, J., LOTT, W. A., STEINBERG, B. A., and YALE, H. L. Am. Rev. Tuberc. 65: 357. 1952.
2. CAJAR, H. Ber. 31: 2809. 1898.
3. ELKAN, T. Ber. 19: 3041. 1886.
4. ELKAN, T. Ber. 19: 3054. 1886.
5. GRUNBERG, E. and SCHNITZER, R. J. Quart. Bull. Sea View Hosp. 13: 3. 1952.
6. RÖSSING, A. Ber. 17: 2990. 1884.
7. SIEBENMANN, C. O. Am. Rev. Tuberc. 68: 411. 1953.
8. SIEBENMANN, C. O. and ZUBRYS, A. Can. J. Public Health (Abstr.), 44: 23. 1953.
9. SIEBENMANN, C. O. and ZUBRYS, A. Can. J. Public Health (Abstr.), 45: 34. 1954.
10. SIEBENMANN, C. O. and ZUBRYS, A. Antibiotics Annual, 1954–55. Medical Encyclopedia, Inc. In press. 1954.

A NEW MATERIAL AND TECHNIQUES FOR THE FABRICATION AND MEASUREMENT OF VERY THIN FILMS FOR USE IN 4π-COUNTING[1]

By B. D. Pate[2] and L. Yaffe

ABSTRACT

A new method for preparing thin films for use in beta-spectrometry and 4π-counting is described. These films, made of polyvinylchloride-acetate copolymer are readily prepared with superficial densities as low as 1 μgm. per cm.^{2} The films have good tensile strength and show excellent resistance to acids, alkalies, and many organic reagents. The thickness of the films may be determined (*a*) gravimetrically, (*b*) radiometrically, and (*c*) optically either by transmission or reflection. The films can be made conducting by distilling a thin gold layer on to them. The thickness of the gold layer can be determined spectrophotometrically.

INTRODUCTION

In the course of work in this laboratory (to be published shortly) on the improvement of the accuracy of disintegration-rate determinations by 4π gas-ion counting, it became necessary to develop methods for producing films of synthetic resin of superficial density much lower than hitherto reported. This paper reports the successful fabrication of films of good chemical and mechanical stability, of superficial densities down to below 1 μgm./cm.^{2} (thickness < 7 mμ) and of area up to 100 cm.^{2}

Materials used for the production of source-mounts for the purposes of 4π-counting or beta-spectrometry must satisfy a number of criteria. They must be of:

(*a*) minimal superficial density and low average atomic number, in order to reduce absorption and scattering of radiation;

(*b*) adequate mechanical strength to withstand shocks received during normal, careful handling and the pipetting out of radioactive solutions;

(*c*) adequate chemical resistance to reagents present during the rapid evaporation of these solutions, e.g. under infrared irradiation;

(*d*) adequate thermal resistance to withstand infrared irradiation during this evaporation procedure and during metallizing procedures if these are required (see later).

The use of a number of materials has been reported in the literature. Aluminum foil has been used (3, 4, 5, 6, 20, 21) in superficial densities as low as 260 μgm./cm.^{2} (19). Such foils will however be very weak mechanically, and in addition aluminum does not exhibit very good chemical resistance to acids or alkalies. Certain synthetic resins have been found to lend themselves to the fabrication of thin films suitable for source mounts and have been used extensively with conventional low-geometry counters and in beta-spectrometry where back-scattering effects were to be minimized (7, 15). Formvar (7, 9, 22),

[1]*Manuscript received August 13, 1954.*
Contribution from the Radiochemistry Laboratory, Department of Chemistry, McGill University, Montreal, Quebec, with financial assistance from the National Research Council of Canada.
[2]*Holder of a National Research Council Studentship.*

a polyvinylformal, has excellent mechanical properties, being strong and resistant to abrasion (8, 16, 17). A method (2) to produce films of less than 10 μgm./cm.^{2} superficial density by means of very specialized handling techniques has recently been described. Unfortunately Formvar is readily attacked by acids, concentrated alkalies, and organic solvents. It has however found application in laminates with films of polystyrene or Zapon (8, 10, 13) which possess better chemical properties, but are alone too fragile.

Cellulose nitrate (1, 11, 14) and acetate (19) are probably the most successful of the materials used up to this time. They are resistant to hydrochloric acid in all concentrations, oxidizing acids in concentrations up to 12 N, and dilute alkalies. They are attacked however by concentrated alkalies, and other substances, e.g. an aqueous slurry of a metallic sulphide. Films of these materials with a superficial density of as low as 3 μgm./cm.^{2} have been reported. However these are of small area, and it is found that films of less than 40 μgm./cm.^{2} do not make satisfactory mounts owing to increasing fragility which impedes their manufacture, handling, and use during pipetting operations.

When it is desired to work with source-mounting films of 5–10 μgm./cm.^{2}, therefore, it is clear that a material with much better characteristics is required. We propose the use of VYNS resin* (a polyvinylchloride-acetate copolymer). Films of this material can be made with superficial densities below 1 μgm./cm.^{2} These show remarkable tensile strength, and excellent chemical resistance to acids and alkalies in all concentrations and to most organic solvents. The only common chemicals found to attack the films are ketonic compounds and esters which act as solvents for the resin. These properties, together with resistance to all but the severest of shocks, make VYNS resin an ideal material for source mounts.

PROCEDURES

(1) *Film Production*

VYNS resin as supplied by the manufacturers is a finely ground white powder. The most convenient solvent is found to be cyclohexanone, one volume of resin requiring about two volumes of solvent for complete dissolution. First addition of solvent to the resin produces a gel, which dissolves in further solvent only slowly in the course of several days. The process can however be accelerated somewhat by maintaining the mixture at 50–60°C. for several hours. The saturated solution thus obtained forms a convenient stock solution. This is diluted with further cyclohexanone before use to give a one-third saturated solution.

VYNS in cyclohexanone does not spread satisfactorily on a water surface, and dilution with a second solvent produces on evaporation very weak and uneven films. The conventional techniques for film formation are therefore not applicable, and a new method has had to be developed. This is found to

**This material is a product of the Bakelite Co. N.Y., available in Canada through Canadian Resins and Chemicals Ltd., Montreal. We are indebted to Mr. I. Maclaine of Dominion Oilcloth and Linoleum Ltd. for introduction to this material, and to Mr. F. M. King of Canadian Resins and Chemicals Ltd. for a supply of the resin for experimental purposes.*

produce films whose constancy of thickness is better than previously obtainable, and possesses the additional merit of improving the tensile strength of the thinner films, possibly by orientation of polymer molecules.

The procedure used is as follows. A trough or sink is filled with water at room temperature and a floating wooden barrier placed in contact with one end. One to two milliliters of resin solution are pipetted between the barrier and the trough, so as to wet both the side of the trough and the barrier; the latter is released and the resin solution allowed to expand into a band about 2–3 cm. wide, the outer edge (nearest the barrier) of which immediately begins to solidify. The barrier is lifted from the water, lowered lightly on to the solidified film, and then moved away along the water surface at a speed of about 30–40 cm. per second. During this process a film of resin is observed to feed out of the solution band, and continues to do so covering the water surface, until either the barrier reaches the far end of the trough, or the band of solution is exhausted. The thickness of film produced is governed by the speed at which the barrier is pulled out, the thinnest films being obtained with the highest speeds. The evenness of the film in one direction is conditioned by the evenness of the original pipetting operation, and in the other by the constancy of barrier velocity. Success in operation of this procedure is largely a matter of manual dexterity, which can easily be obtained.

The film produced is quite dry and may be lifted from the water surface for use immediately. The lifting may be accomplished by the use of wire frames (coated with VYNS to give better film adhesion) which allow larger areas of film to be obtained, e.g. up to 40 cm. × 20 cm. of 10–20 μgm./cm.^{2} film. The film may then be transferred to other supports which have previously been wetted with water. Alternatively the supports, in our apparatus aluminum annuli of area 40 cm.^{2}, may be used to pick up the film directly, 30 or 40 rings being covered in one operation. In either case the support or frame is lowered to contact the upper surface of the film, the latter torn away at the edges, and the film lifted with a rolling motion, one edge separating first. This procedure often gives a film completely free of water droplets. Any that may be left can be cautiously pulled to the edge of the film with a wisp of absorbent material. An alternative procedure useful for the thinnest films is to sink the film and support carefully and to bring them out through the water surface at right angles, reducing the effect of surface tension forces. Marks remaining after evaporation of water droplets left by this procedure may be avoided by dipping the film on edge below the surface of some distilled water. VYNS is hydrophobic, and films produced by this method, once any adhering water is removed, are quite dry and ready for use. No appreciable change in weight is observed over long periods of time, either with plain films or after metallizing (see later).

This simple technique as described is suitable for the production of uniform films of up to 20 μgm./cm.^{2} superficial density. Films of greater thicknesses are conveniently produced by lamination, two films placed in contact adhering readily; laminates of greater than 100 μgm./cm.^{2} and quite even in thickness have been made in this way. Alternatively one can use a mechanical means of

ensuring constant barrier speed to produce the thicker films. The manual method does not operate too satisfactorily in this region.

It is standard procedure in this laboratory to store films on edge. This arrangement renders the stock of films less liable to damage by vibration, and further allows a large number of films to be stored in a small space.

(2) *Measurement of Film Superficial Density*

For the purposes of 4π-counting and beta-spectroscopy it is desirable to know the superficial density of the material used as a source mount. Four methods have been found useful in this connection.

(*a*) *Optical Reflection Method*

As is well known, thin films are often observed to be brilliantly colored by reflected light, owing to the occurrence of interference and reinforcement between the light reflected from the top and bottom surfaces of the film. The conditions for reinforcement and destructive interference for light of wave length λ are given by:

$$\text{reinforcement:} (n+\tfrac{1}{2})\lambda = 2\mu d \cos\theta,$$
$$\text{destruction:} \quad n\lambda = 2\mu d \cos\theta$$

where μ is the film refractive index (for VYNS = 1.5), d is the film thickness, θ is the angle of reflection, and n is an integer. The wave lengths for which interference is expected for various VYNS film thicknesses with normally incident light, together with the color actually observed, are listed in Table I. The effects observed below 10 μgm./cm.^{2} are due to a falling off in reflectivity of the film.

TABLE I

Superficial density of film (μgm./cm.^{2})	Film thickness (mμ)	Wave length for reinforcement calculated (mμ)	Wave length for destructive interference calculated (mμ)	Color observed
1	7	(14)	(21)	Dark gray
5	36	(72)	(108)	Light gray
10	70	(140)	(210)	White
20	140	280	420	Light yellow
25	180	360	540	Yellow-brown
30	210	420	630	Purple (First
35	250	500	750	Blue order
40	290	580	870	Yellow spectrum
45	320	640	960	Red ($n = 1$)
50 and above	360 and above	—	—	Second order and above ($n \geq 2$). Colors of diminishing intensity

We have used these color differences, as observed visually, for the rough sorting of films of differing thicknesses, and especially for the selection of areas of film of the desired thickness and evenness for lifting from the water surface. It is clear that this could be made into a precision method, if desired, by use of a spectrophotometer with a reflection attachment.

(*b*) *Gravimetric Method*

A five decimal place analytical balance is capable of measuring the superficial density of 40 cm.^{2} (for our apparatus) of 5 μgm./cm.^{2} film with an accuracy of 5%. This gives a very useful, absolute means of superficial density standardization. We have used films specially selected for their uniformity and calibrated gravimetrically to standardize other methods of determination. As a routine method, however, weighing has certain disadvantages:

(i) Measurements to the required accuracy are very tedious and time-consuming.

(ii) The superficial density measured is an average for the whole film, not for the region of interest (the center). This method is not therefore applicable to films with peripheral irregularities which are nevertheless quite suitable for source mounts.

(iii) Finally the mounting of a film on a weighed support is not easily accomplished without a concomitant change in support weight, and measurements are subject to random errors far in excess of those imposed by the sensitivity limit of the balance used.

(*c*) *Beta Radiation Absorption Method*

Figs. 1 and 2 show as a function of their superficial density the transmission of VYNS films for the beta radiation of Ni^{63} (which has a maximum energy of

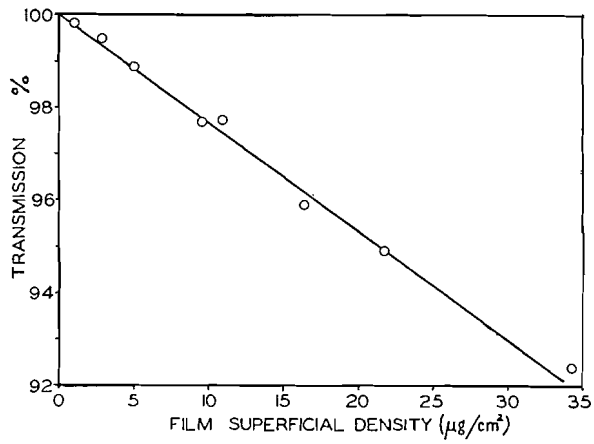

FIG. 1. Transmission of VYNS film to Ni^{63} beta radiation. Film superficial density range 0–35 μgm./cm.^{2}

67 kev.). Providing the radiation measurements can be made to the necessary precision, the method is limited by the accuracy of the superficial density values of the films used for calibration. We estimate that measurements can be made to 2 μgm./cm.^{2} in the range 0–30 μgm./cm.^{2}, and with a somewhat larger error at greater thicknesses. The actual form of the curves obtained depends a great deal on the radiation scattering and other characteristics of the apparatus used, but the details of procedure as used by us are as follows.

A Ni^{63} source of about 2×10^3 dis./sec. is deposited in a depression at the

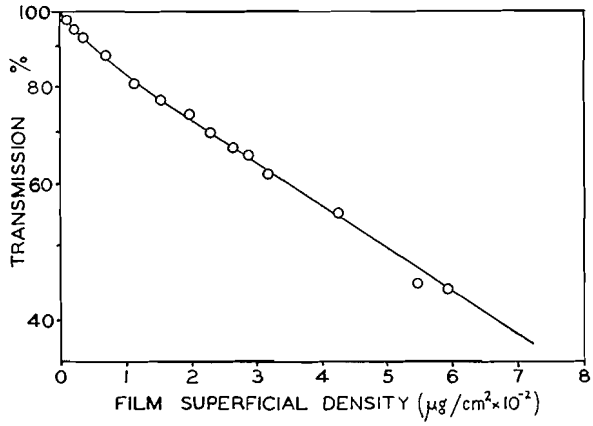

FIG. 2. Transmission of VYNS film to Ni^{63} beta radiation. Film superficial density range 0–600 μgm./cm.²

center of an aluminum plate, and the whole is covered with a VYNS film of about 50 μgm./cm.² to give a completely planar surface. This is then mounted in a conventional hemispherical 2π-proportional counter, and the counting rate measured to the required accuracy. Curves of transmission versus superficial density are then obtained, using specially selected gravimetrically calibrated films which are placed in contact with the plate. Advantages of the method include insensitivity to peripheral film irregularities—the superficial density measured is that observed by a source centrally located on the film used for a source mount—and a rapidity of operation much greater than for the gravimetric method. Disadvantages include the tendency for films of less than 10 μgm./cm.² to adhere to the plate and subsequently to rupture (which can to some extent be ameliorated by a light dusting of talc away from the central part of the film), the need for ensuring close contact between the film and plate (since a layer of methane counting-gas entrapped between them can cause considerable error in the apparent film thickness), and the need for electronic counting apparatus, etc.

(d) Optical Absorption Method

This method is now in routine use in this laboratory, and proves quite satisfactory for the measurement of superficial densities in the range 0–30 μgm./cm.² We employ a Beckman Model DU Spectrophotometer, which is first balanced against air, and then used to measure the optical transmission at a wave length of 360, 600, or 1300 mμ according to the thickness range and accuracy required. Calibration with selected weighed films produces curves as shown in Fig. 3, the features of which will be further discussed in a forthcoming publication. The potential precision of the method is about 0.05 μgm./cm.², but calibration difficulties impose at the moment a limit of ±0.5 μgm./cm.², which is nevertheless adequate for the present purposes. The method is found to be very rapid and facile in operation, and is applicable to the thinnest films since they need not be placed in contact with anything. It also meas-

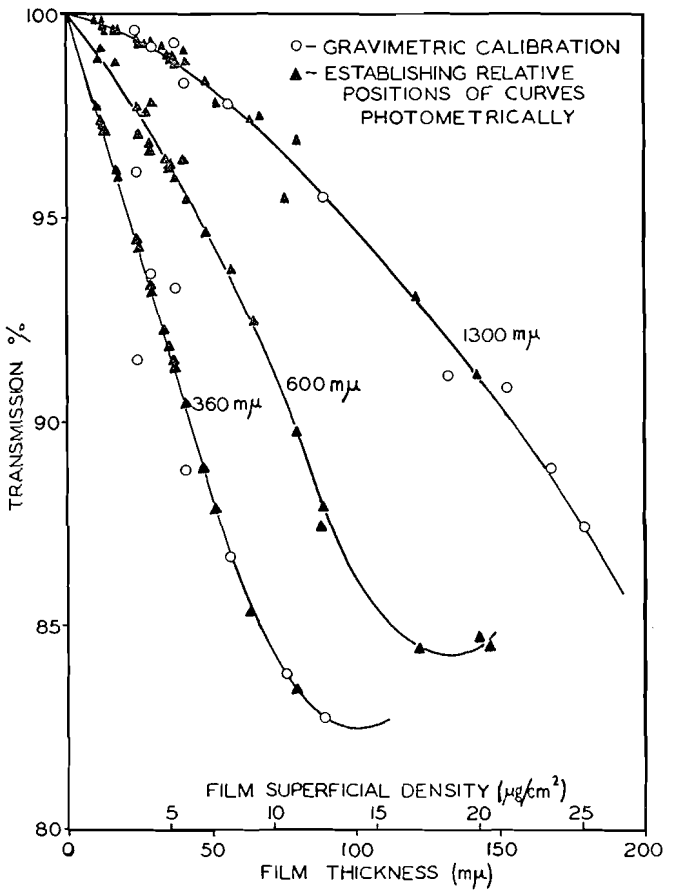

FIG. 3. Optical transmission of VYNS film.

ures the thickness of the center of the film, and is useful in measuring small irregularities of superficial density in this area.

(3) *Gold Coating*

The plastic film used for mounting a source within a counting chamber (or for beta-spectrometry) must be essentially at cathode potential in order that the counter shall function correctly. It has been reported (18) that a small area of plastic film can be satisfactorily used as a source mount, but most authors agree that films must be rendered conducting by a suitable coating, either of Aqua-dag (12, 15) or of metal applied by sputtering or distillation *in vacuo*. The use of aluminum (19), copper (11, 14), silver (1), and gold (7, 10) has been reported. We find gold coating of one side of the film by distillation from a tungsten ribbon filament at about 1200°C. and under <1 μ Hg to be satisfactory.

Low distillation rates of gold give approximately isotropic distribution of metal, and several films may be coated simultaneously if arranged spherically around the filament.

The progress of distillation may be followed by observing the color of the film by reflected light from the reverse face to that being coated. With an initially uncolored film of 5–10 μgm./cm.^{2} for example, a faint purple coloration is first noticed at a superficial density of 0.4 μgm./cm.^{2} gold, and this progressively deepens in shade until at 5 μgm./cm.^{2} a rich red-purple coloration is obtained. By transmitted light gold layers appear as increasing intensity of blue, and this color, due to absorption or reflection of light at about 600 mμ, has been made the basis of a satisfactory precision method of measuring the thickness of a gold layer applied. The Beckman Spectrophotometer is again used, balanced against air, and the transmission at 600 mμ of a series of films of known gold superficial density is measured, the film being arranged so that the light beam is incident on it from the uncoated side. A satisfactory method of preparing the calibration films is to employ increasing distillation times from a filament of constant distillation rate, which is known from gravimetric measurements. The optical transmission of the film plus gold as measured is the product of the transmission of the film and that of the gold. The former may be read from the 600 mμ curve in Fig. 3, and the curve of the gold transmission thus calculated versus gold superficial density is given in Fig. 4. The

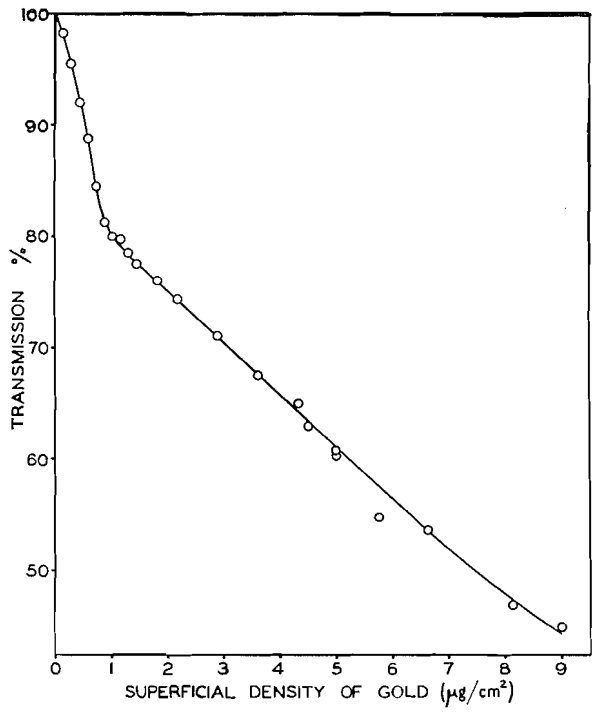

FIG. 4. Optical transmission of gold on VYNS film at 600 mμ wave length.

form of the curve, which has several unusual features, will be discussed in the forthcoming publication mentioned earlier. Spectrophotometer readings can be taken with an accuracy which gives a precision for the method of 0.05

μgm./cm.^{2} of gold, and in this case the calibration is probably of comparable accuracy.

ACKNOWLEDGMENTS

We wish to thank Mr. W. L. Elsdon of Dr. C. A. Winkler's laboratory for discussions on the spectrophotometric measurement of thin films. We would like to express our appreciation to the National Research Council for a grant-in-aid and to Atomic Energy of Canada Ltd. for loan of equipment. One of us (B. D. P.) wishes to thank the National Research Council for assistance received in the form of a studentship.

REFERENCES

1. BACKUS, J. Phys. Rev. 68: 59. 1945.
2. BARREAU, P., LÉGER, P., MOREAU, J., and PRUGNE, P. J. phys. radium, 15: Suppl. to No. 1, 4 A. 1954.
3. CHARPAK, G. and SUZOR, F. Compt. rend. 231: 1471. 1950.
4. CHARPAK, G. and SUZOR, F. Compt. rend. 232: 322. 1951.
5. COHEN, R. Compt. rend. 229: 356. 1949.
6. COHEN, R. Ann. phys. 7: 185. 1952.
7. Conference on absolute β counting. Prelim. Rept. No. 8. Nuclear Sci. Ser., N.R.C. Washington, D.C. Oct. 1950.
8. FRY, L. M. and OVERMAN, R.T. U.S. Atomic Energy Comm. Document 1800. 1948.
9. GERMER, L. H. Phys. Rev. 56: 58. 1939.
10. HAWKINGS, R. C., MERRITT, W. F., and CRAVEN, J. H. Proceedings of Symposium, Maintenance of Standards, Natl. Phys. Lab. May, 1951. H.M. Stationery Office, London. 1952.
11. HOUTERMANS, F. G., MEYER-SCHÜTZMEISTER, L., and VINCENT, D. H. Z. Physik, 134: 1 1952.
12. LANGER, L. M. Rev. Sci. Instr. 20: 216. 1949.
13. MANN, W. B. and SELIGER, H. H. J. Research Natl. Bur. Standards, 50: 197. 1953.
14. MEYER-SCHÜTZMEISTER, L. and VINCENT, D. H. Z. Physik, 134: 9. 1952.
15. NOVEY, T. B. Rev. Sci. Instr. 21: 280. 1950.
16. SCHAEFER, V. J. J. Phys. Chem. 45: 681. 1941.
17. SCHAEFER, V. J. and HARKER, D. J. Appl. Phys. 13: 427. 1942.
18. SELIGER, H. H. and CAVALLO, L. J. Research Natl. Bur. Standards, 47: 41. 1951.
19. SMITH, D. B. A.E.R.E. I/R 1210. 1953.
20. SUZOR, F. and CHARPAK, G. Compt. rend. 232: 720. 1951.
21. SUZOR, F. and CHARPAK, G. J. phys. radium, 13: 1. 1952.
22. YAFFE, L. and JUSTUS, K. M. J. Chem. Soc. Suppl. S. 341. 1949.

THE ALKALINE NITROBENZENE OXIDATION OF ASPEN WOOD AND LIGNIN MODEL SUBSTANCES[1]

By K. R. Kavanagh and J. M. Pepper

ABSTRACT

The yields of vanillin and syringaldehyde obtained by the alkaline nitrobenzene oxidation of aspen wood meal have been determined at various temperatures for various times. The maximum yield of each of these aldehydes, *ca.* 15 and 36% respectively, was obtained under the same conditions. Similar maximum yields result at 130±5°C. as at 170±5°C. if the reaction time is markedly increased. Treatment of the wood meal with sodium hydroxide at 160°C. for two and one half hours prior to the addition of nitrobenzene and subsequent heating under the same conditions decreases, by over 30%, the yields of aldehydes. Samples of 3,4,5-trimethoxybenzaldehyde, β-D-glucovanillin, and β-D-glucosyringaldehyde were oxidized by alkaline nitrobenzene at 160°C. for two and one half hours and yields of the corresponding phenolic aldehydes of 10.7, 69.6, and 71.9% respectively were obtained. These results are discussed with respect to the chemistry of aspen lignin.

Little has been reported regarding the establishment of the optimum conditions for obtaining the maximum yields for each of vanillin and syringaldehyde by the alkaline nitrobenzene oxidation of hardwood lignins. Brauns (2) has summarized the value of this technique in lignin chemistry. The major part of this work was concerned with softwood lignins and various reaction temperatures, ranging from that of boiling alkaline sulphite spent liquor to 200°C., and various reaction times from 10 min. to three hours. Since this book was published Leopold (9) has determined the vanillin yields obtainable from synthetic model lignin substances as a function of temperature and time and found that at 180°C. for two hours the best yields were obtained. Subsequently Leopold and co-workers (10, 11, 12) used these conditions to study the oxidation products of a wide variety of both hardwoods and softwoods. It is significant that almost all the conifers studied gave small amounts of *p*-hydroxybenzaldehyde while several (*Pinaceae* family) gave small amounts of syringaldehyde, this latter observation representing the first isolation of syringaldehyde from softwoods. Stone and Blundell (14) used a temperature of 160°C. for two and one half hours in their analytical micromethod for the alkaline nitrobenzene oxidation of plant materials.

A detailed study of these conditions of oxidation as applied to hardwoods was undertaken, therefore, with the belief that some useful information would be obtained with respect to the following problem. If vanillin and syringaldehyde arise by the hydrolysis and/or oxidative cleavage of different type linkages in the protolignin, then maximum yields of each might be obtained under different conditions. In this way a greater combined yield of aldehydes could result than that now obtained under conditions whereby both yields are deter-

[1]*Manuscript received September 1, 1954.*
Contribution from the Department of Chemistry, University of Saskatchewan, Saskatoon, Sask. This paper constitutes part of a thesis submitted by K. R. Kavanagh in partial fulfillment of the requirements for the degree of Master of Arts in Chemistry, November, 1953. Presented before the second Western Regional Conference, The Chemical Institute of Canada, Vancouver, September, 1954.

mined from the same reaction mixture. On the other hand, should the release of the two compounds be equally dependent on the conditions, some evidence would be presented for the existence of similar type linkages in the lignin. Other information, from such studies, such as the variance of the vanillin to syringaldehyde ratio with changing reaction conditions and the effect, on the aldehyde yield, of a prior treatment of the wood meal with alkali, could be interpreted with respect to the hardwood lignin structure. Little is known concerning the relative amount and the mode of linkage of the guaiacyl- and syringyl-containing nuclei in the protolignin of angiosperms.

For these experiments small (*ca.* 40 mgm.) samples of solvent extracted aspen wood meal were oxidized and the reaction mixture analyzed according to the procedure of Stone and Blundell (14). The results are given in Table I.

TABLE I

VARIATION OF ALDEHYDE YIELDS WITH TEMPERATURE[a]

	Temp., °C. ±5°								
	100	130	150	160	170	180	195	200[d]	215[d]
Syringaldehyde %[b]	0.77	11.9	32.2	33.8	35.8	36.2	30.2	23.1	17.3
	0.91	11.9	32.5	31.8	36.8	34.2	33.6	20.8	20.8
			32.1	35.8	{35.2[c]	{35.6	34.0	26.5	
			33.4	35.6	{35.2	{36.6			
			32.7	35.6					
				35.4					
Mean %	0.85	11.9	32.7	34.6	35.9	35.5	32.6	23.4	18.9
Vanillin %[b]	0.95	3.82	11.4	13.3	14.3	14.0	15.0	8.45	9.1
	1.51	3.96	11.5	12.2	17.5	13.9	13.0	8.25	10.3
			11.5	13.2	{15.4	{15.1	14.3	9.45	
			11.8	13.5	{14.6	{16.3			
			11.5	13.5					
				13.7					
Mean %	1.22	3.84	11.5	13.3	15.6	14.5	14.1	8.66	9.64
Total mean %	2.07	15.7	44.2	47.9	51.5	50.0	46.7	32.1	28.5
Ratio S/V	0.70	3.1	2.84	2.60	2.30	2.45	2.31	2.70	1.96

[a]*Each experiment was maintained at the stated temperature for two and one half hours but required from one half to one and a half hours to reach this temperature.*
[b]*Reported as percentage by weight of the Klason lignin.*
[c]*Bracketed results refer to duplicate chromatograms from the same oxidation product.*
[d]*Less significance should be given to these values; see text.*

It is significant that, at a temperature of 170–180°, the maximum yield of each of the individual aldehydes is obtained. This observation suggests that similar linkages are being cleaved to release each type of aldehyde. The decreasing ratio of syringaldehyde to vanillin with increasing temperature suggests that the 4-hydroxy grouping of the former is released more readily than that of the latter. Some support for this idea is found in the known ready selective demethylation of 3,4,5-trimethoxyphenyl compounds to the 3,5-dimethoxy-4-hydroxyphenyl derivatives. A similar decreasing ratio of syringaldehyde to vanillin was noted by Chisholm (5) in experiments wherein condi-

tions of progressively stronger severity of the alkaline nitrobenzene oxidation of aspen wood were made. These included experiments with no added nitrobenzene, with nitrobenzene at reflux temperatures, and with nitrobenzene at 160°C.

At the higher temperatures (200° and 215°) an increasing number of unknown interfering compounds began to appear on the developed chromatograms and therefore the absorption recorded may not have been due to the aldehydes only. Up to 195° however, this presented no problem since a comparison of the ultraviolet spectra of individual spots with those of authentic aldehyde samples showed excellent agreement.

On the basis that lignin may be represented as a polymer of phenylpropane units and that the major part of the wood methoxyl is associated with this lignin, then the total yield of aldehydes obtained represents only about a 60% recovery of the lignin both on a weight and on a methoxyl basis.* This consistent maximum total aldehyde yield was found even in experiments carried out at a lower temperature of 130°±5° but for an extended time and in those at 170° for periods longer than the normal two and one half hours. These data are given in Table II.

TABLE II

VARIATION OF ALDEHYDE YIELDS WITH TIME[a]

	At 130±5°C.					At 170±5°C.	
	2.5 hr.	4 hr.	8 hr.	13 hr.	19 hr.[c]	2.5 hr.	5 hr.
Syringaldehyde %[b]	11.9	25.8	32.7	33.4	31.8	35.8	34.6
	11.9	24.5	32.2	33.5	30.9	36.8	35.9
					26.2	35.2	35.2
					27.7	35.2	
Mean %	11.9	25.2	32.5	33.5	29.2	35.9	35.2
Vanillin %[b]	3.82	7.94	11.0	11.9	12.0	14.3	13.1
	3.86	8.18	11.0	12.4	11.8	17.5	14.1
					11.4	15.4	13.8
					11.2	14.6	
Mean %	3.84	8.06	11.0	12.2	11.6	15.6	13.7
Mean total aldehydes %	15.7	33.3	43.5	45.7	40.8	51.5	48.9
Ratio S/V	3.10	3.13	2.95	2.74	2.50	2.30	2.57

[a]*Time does not include that required to reach the reported temperature.*
[b]*Reported as percentages by weight of the Klason lignin.*
[c]*This chromatogram showed presence of additional products; see Table I*[d].

From these results it would appear that only part of the lignin has linkages amenable to cleavage to the simple aldehyde by this treatment. This may be interpreted to suggest that protolignin is a polymer of a repeating unit comprising a part from which the phenolic aldehydes arise and another part of

**It has been shown by A. J. McNamara in these laboratories that no change in total alkoxyl occurs during the alkaline nitrobenzene oxidation treatment of aspen wood at 160° for two hours.*

which little is known, rather than a simple polymer of a single phenylpropane structure.

The liberation of phenolic aldehydes by this oxidative process means that two processes at least are occurring, namely, that whereby the free phenolic group is released and that whereby the carbonyl group is established. It seems likely that these two reactions occur for the most part independently of each other. Therefore it would be of interest to arrive at the same final result but by means of two separate reaction stages. Experiments were conducted to determine the aldehyde yields as a result of an alkaline treatment alone at 160° and others to determine the effect of a similar alkaline treatment of the wood meal prior to the addition of nitrobenzene with subsequent heating under standard conditions. The results are compared in Table III.

TABLE III

VARIATION OF ALDEHYDE YIELDS WITH MODE OF ALKALINE TREATMENT

	With sodium hydroxide only		With sodium hydroxide only, prior to nitrobenzene addition		Sodium hydroxide and nitrobenzene
	2.5 hr.	5 hr.	2.5 hr.	5 hr.	2.5 hr.
Syringaldehyde %	2.71 2.94 2.20 1.97	1.77 1.95	23.5 23.6 24.5 21.7 19.5 21.9	21.4 21.4 22.2	
Mean %	2.46	1.86	22.6	21.7	34.6
Vanillin %	1.41 1.76 1.46 1.13	0.59 0.98	10.2 10.6 10.5 9.42 8.35 8.55	8.12 8.99 8.10	
Mean %	1.44	0.79	9.65	8.74	13.3
Mean total aldehydes %	3.90	2.65	32.3	30.4	47.9
Ratio S/V	1.69	2.36	2.34	2.48	2.60

The small yields of aldehyde obtained using alkali without nitrobenzene suggest the existence of a small percentage of much more readily cleaved units, e.g. those that are terminal. Or such yields may be the result of an hydrolysis and/or an alkaline oxidation reaction aided by the fact that no attempt was made to exclude the air in sealing the microbombs or that dissolved in the reagents. Of greater interest is the marked decrease in the yields of aldehydes that result if a prior alkali treatment at 160° is given the wood meal. This may mean that, by this treatment, part of the linkages have been modified so that it is no longer possible for them to be cleaved to yield the phenolic aldehydes. Whether this interference is concerned with the liberation of the phenolic or

aldehydic groups or whether it involves secondary reactions (see below) remains to be shown. Experiments are in progress to determine, by analysis, the extent of the individual liberation of the phenolic and carbonyl functional groups under varying conditions. Such information would assist in determining the mechanism by which the aldehydes are released.

Such a secondary reaction as mentioned above is that pointed out recently by Brickman and Purves (3) and Hlava and Brauns (7). These authors showed that under conditions of alkaline nitrobenzene oxidation similar to those used in this work, namely, 160° for three hours and 180° for two hours respectively, veratraldehyde is converted to vanillin in approximately 30% yield. Since vanillin itself is essentially unchanged by such a procedure (14) a major portion of the veratraldehyde has undergone other reactions, likely the Cannizzaro oxidation–reduction change (6). If a similar reaction for both the guaiacyl and syringyl nuclei were occurring during the oxidation of wood lignin, it would account for the low total aldehyde yields and also suggest that the carbonyl-releasing reaction is more rapid than that whereby the phenol hydroxyl is liberated. If the reverse were true very little of the liberated vanillin would undergo further reaction and higher yields might be expected. In order to gain some experimental evidence for or against these ideas, other model substances were similarly oxidized at 160° for two and one half hours and the yields of the corresponding phenolic aldehydes determined. These results are given in Table IV.

TABLE IV

OXIDATION OF MODEL LIGNIN SUBSTANCES

Model substance	Molar recovery, %			Remarks
	Vanillin	Syringaldehyde	Mean	
Vanillin	99.3 96.4 97.8		97.8	According to Stone and Blundell (14) corrected for chromatographic losses
Veratraldehyde	31.3 30.6 31.9		31.3	No unchanged veratraldehyde Reported by Brickman and Purves, 29.7 and 34.2%
β-D-Glucovanillin*	68.4 72.7 67.8		69.6	
Syringaldehyde		93.0 86.0	89.5	Uncorrected for chromatographic losses
3,4,5-Trimethoxy-benzaldehyde		12.5 9.5 11.2 11.2 9.1	10.7	No unchanged 3,4,5-trimethoxybenzaldehyde
β-D-Glucosyringaldehyde		69.2 74.6	71.9	

Sample donated by Dr. A. C. Neish, National Research Council, Saskatoon.

The chromatogram of the product of oxidation of the β-D-glucovanillin showed one other spot only which had the same R_f value as the starting material. This may mean that no other serious side reaction is occurring as was the case with the two methylated derivatives.

In the light of both the small recovery of phenolic aldehydes, especially syringaldehyde, from their fully methylated derivatives and of the amounts obtained from the wood, it seems likely that these nuclei are not joined by means of phenolic alkyl ether linkages if the liberation of the carbonyl grouping is the major primary reaction. On the other hand, should these nuclei be involved in phenolic glycosidic linkages, nothing can be said about the relative rates of release of the two functional groupings. It would seem that under these circumstances, whereby both aldehydes are released at the same rate, evidence is presented that suggests that in the aspen protolignin, a larger number of syringyl than guaiacyl nuclei exist.

EXPERIMENTAL

Aspen Wood Meal

Native Saskatchewan aspen sapwood (*Populus tremuloides*) was ground in a Wiley mill (20 mesh), extracted* with ethanol–benzene (4:1) for 48 hr., then with ethanol for 36 hr., thoroughly washed with hot water for eight hours, and air-dried. Anal.: Klason lignin, 16.5; moisture, 7.65; ash, 3.77%.**

Oxidation and Chromatographic Procedures

The general methods of microoxidations of plant material, the chromatographic separation of the oxidation products, and the spectrophotometric determination of the concentration of aldehydes were those described in detail by Stone and Blundell (14). All oxidations were made using 35–50 mgm. samples of wood meal and around 10 mgm. samples of pure compounds. The chromatograms were developed for two to two and one half hours using a solvent of *n*-butyl ether saturated with water. The presence of the aldehyde spots were revealed by spraying with the ferric chloride – potassium ferricyanide reagent (1). The standard concentration vs. optical density curves were those described previously (13). All results of the wood oxidations are expressed as percentage yields by weight based on the amount of Klason lignin in the ash-free oven-dried sample. No corrections were made for chromatographic loss so the results represent minimum values.

For those experiments involving a prior alkaline treatment, only the wood meal and the sodium hydroxide solution were heated initially. After the mixture was cooled, the microbombs were opened, the nitrobenzene added, and the bombs again sealed and heated under standard conditions.

Synthesis of Model Substances

3,4,5-Trimethoxybenzaldehyde.—Syringaldehyde was methylated with dimethyl sulphate in alkaline solution according to the standard procedure (4).

**The extractions and washings were carried out by Mr. A. J. McNamara in these laboratories.*
***The high ash content is believed due to the use of a copper condenser during the extensive extractions.*

3,4,5-Trimethoxybenzaldehyde was recovered in 44.5% yield, m.p. 73–74°C., reported, 74–75°C. The oxime was prepared in high yield, m.p. 81–84°C., reported, 82–84°C.

β-D-Glucosyringaldehyde

Tetraacetyl-β-D-glucosyringaldehyde.—The method used was similar to that reported by Kratzl and Billek (8). Acetobromo-D-glucose (1.5 gm.), potassium carbonate (0.6 gm.), and syringaldehyde (0.67 gm.) were dissolved in a mixture of acetone (13 ml.) and water (7.7 ml.). After six hours at room temperature, the acetone was removed under reduced pressure and the residue extracted with benzene. After washing with dilute potassium hydroxide and drying over sodium sulphate, the benzene solution was concentrated under reduced pressure and the resulting tetraacetyl-β-D-glucosyringaldehyde recrystallized from benzene, yield, 1.3 gm.

Deacetylation of Tetraacetyl-β-D-glucosyringaldehyde

The method of Zemplén and Pacsu (15) was followed. The crude product (1.3 gm.) obtained in the preceding step was warmed on a water bath with methanol (3.3 ml.) and $N/10$ sodium hydroxide (0.33 ml.). From the resulting solution, an orange-yellow colored precipitate resulted after one to two minutes, yield, 0.7 gm. After recrystallization twice from ethanol–water (4:1), m.p. 201–204°C., reported, 210–211°C.

ACKNOWLEDGMENT

The authors wish to thank the Saskatchewan Research Council for both the award of a Graduate Research Fellowship to one of them (K. R. K.) and for a research grant which supported this investigation.

REFERENCES

1. Barton, G., Evans, R. S., and Gardner, J. A. F. Nature, 170: 4319. 1952.
2. Brauns, F. E. Chemistry of lignin. Academic Press, Inc., New York. 1952.
3. Brickman, W. J. and Purves, C. B. J. Am. Chem. Soc. 75: 4336. 1953.
4. Buck, J. S. Organic syntheses. Collective Vol. 2. John Wiley & Sons, Inc., New York. 1944. p. 619.
5. Chisholm, A. M.A. Thesis, University of Saskatchewan, Saskatoon. 1950.
6. Decker, H. and Pschorr, R. Ber. 37: 3403. 1904.
7. Hlava, J. B. von and Brauns, F. E. Holzforschung, 7 (Nos. 2 and 3): 62. 1953.
8. Kratzl, K. and Billek, G. Holzforschung, 7: 66. 1953.
9. Leopold, B. Acta Chem. Scand. 4: 1523. 1950.
10. Leopold, B. Svensk Kem. Tidskr. 63: 260. 1951.
11. Leopold, B. Acta Chem. Scand. 6: 39. 1952.
12. Leopold, B. and Malmstrom, I. L. Acta Chem. Scand. 6: 49. 1952.
13. Pepper, J. M. and MacDonald, J. A. Can. J. Chem. 31: 476. 1953.
14. Stone, J. E. and Blundell, N. J. Anal. Chem. 23: 771. 1951.
15. Zemplén, G. and Pacsu, E. Ber. 62: 1613. 1929.

THE REACTION OF METHYL RADICALS WITH CH_3CHO AND CH_3CDO[1]

By P. Ausloos[2] and E. W. R. Steacie

ABSTRACT

Azomethane has been photolyzed in the presence of CH_3CHO and CH_3CDO, and the results compared with the direct photolysis of the aldehydes. The activation energies found were 6.8 and 7.8 kcal./mole, respectively, for the reactions

$$CH_3+CH_3CHO \rightarrow CH_4+CH_3CO \quad [1]$$
$$CH_3+CH_3CDO \rightarrow CH_3D+CH_3CO. \quad [2]$$

The results furnish evidence that only an acyl hydrogen is captured. Evidence has also been found for the occurrence of wall reactions and the disproportionation reaction

$$CH_3+CH_3CO \rightarrow CH_4+CH_2CO.$$

INTRODUCTION

By decomposing di-*t*-butyl peroxide in the presence of CH_3CHO, Volman and Brinton (6) obtained a value of 7.5 ± 0.3 kcal. for the activation energy for hydrogen abstraction by methyl from CH_3CHO. This value lies well below most previous estimates. Its acceptance has explained a number of anomalies in the acetaldehyde photolysis, and the value is therefore of considerable importance.

Up to the present no value has been obtained for the activation energy of the companion reaction

$$CH_3+CH_3CDO \rightarrow CH_3D+CH_3CO.$$

Also, there has been no definite proof whether it is an acyl or a methyl hydrogen which is captured in the reaction (4), although the acyl hydrogen is far more probable on general grounds.

The purpose of the present work was to compare the rates of abstraction from CH_3CHO and CH_3CDO, to obtain a check on the activation energy of the abstraction reaction using a different source of methyl radicals, and to determine whether an acyl or a methyl hydrogen is captured in the abstraction reaction. Azomethane has been used as a source of methyl radicals, since it can be photolyzed at wave lengths greater than 3400 Å where acetaldehyde is transparent. It can thus be photolyzed without complications due to the simultaneous photolysis of the aldehyde. The photolysis of CH_3CHO and CH_3CDO has also been investigated very briefly at 3130 Å in order to compare the results with those obtained with azomethane–acetaldehyde mixtures at longer wave lengths. By using relatively low pressures of acetaldehyde and higher intensities ($1–5 \times 10^{13}$ quanta per cc. per sec.) than have usually been used in the past, it is possible to obtain measurable amounts of ethane and thus to determine values of $R_{CH_4}/R_{C_2H_6}^{\frac{1}{2}}$ in the photolysis of acetaldehyde itself.

[1]*Manuscript received September 17, 1954.*
Contribution from the Division of Pure Chemistry, National Research Council, Ottawa, Canada. Issued as N.R.C. No. 3448.
[2]*National Research Council of Canada Postdoctorate Fellow, 1952–54. Present address: Departement de Chimie Physique, Université Laval, Québec.*

EXPERIMENTAL

Acetaldehyde-*d* was prepared by Dr. L. C. Leitch (5) of this laboratory by the reaction sequence

$$CH_3CH_2NO_2 \overset{D_2O}{\rightleftarrows} CH_3CD_2NO_2$$

$$CH_3CD_2NO_2 \xrightarrow[0°C.]{H_2SO_4(6M)} CH_3CDO + HDO + N_2O.$$

Mass-spectrometer analysis indicated that the CH_3CDO contained about one per cent CH_2DCDO and less than five per cent CH_3CHO.

The light source was a Hanovia S-500 medium pressure mercury arc. The cylindrical quartz reaction cell, 10 cm. long, 5 cm. diameter, was completely filled by a nearly parallel light beam. Four types of filter were used to limit the incident radiation to longer wave lengths:

Corning clear chemical glass 774 (0–53),
Corning 586 (7–37),
Corning 738 (0–52), and
Corning 970 (9–53).

The apparatus was essentially similar to that used in previous investigations. The methane, N_2, CO fractions were taken off at liquid nitrogen temperature and CO determined by passing over hot CuO. Further analysis was done with a mass spectrometer. The ethane fraction was separated at −170°C., and occasionally checked by mass-spectrometer analysis.

RESULTS AND DISCUSSION

(*A*) *The Reaction of CH_3 with CH_3CHO*

When azomethane is photolyzed in the presence of CH_3CHO the following reactions may be considered:

$$CH_3NNCH_3 + h\nu \rightarrow 2CH_3 + N_2 \quad [3]$$
$$CH_3 + CH_3 \rightarrow C_2H_6 \quad [4]$$
$$CH_3 + CH_3NNCH_3 \rightarrow CH_4 + CH_2NNCH_3 \quad [5]$$
$$CH_3 + CH_3CHO \rightarrow CH_4 + CH_3CO \quad [1]$$
$$CH_3CO \rightarrow CH_3 + CO \quad [6]$$
$$CH_3 + CH_3CO \rightarrow CH_3COCH_3 \quad [7]$$
$$2CH_3CO \rightarrow CH_3COCOCH_3 \quad [8]$$
$$CH_3 + CH_3CO \rightarrow CH_4 + CH_2CO \quad [9]$$
$$2CH_3CO \rightarrow CH_2CO + CH_3CHO \quad [10]$$

If reaction [9] is neglected for the moment, then

$$\frac{k_1}{k_4^{\frac{1}{2}}} = \left(\frac{R_{CH_4}}{R_{C_2H_6}^{\frac{1}{2}}} - \frac{k_5}{k_4^{\frac{1}{2}}} [CH_3NNCH_3] \right) \Big/ [CH_3CHO].$$

The values of $k_5/k_4^{\frac{1}{2}}$ which are required in the calculations have been taken from an experimental Arrhenius plot for azomethane alone (1).

The results of runs at different temperatures, intensities, and concentrations are given in Table I. As can be seen from Fig. 1 (Curve *B*), a plot of $\log R_{CH_4}/R_{C_2H_6}^{\frac{1}{2}}$ [Ald] against $1/T$ gives a straight line, except at temperatures below

TABLE I

THE PHOTOLYSIS OF AZOMETHANE IN THE PRESENCE OF CH_3CHO

Temp., °C.	Time, min.	Pressure, cm. CH_3NNCH_3	Pressure, cm. CH_3CHO	Rate, cc./min. × 10^4 N_2	CH_4	C_2H_6	CO	$\frac{k_1}{k_1^{\frac{1}{2}}} \times 10^{13}$
27	713	5.50	0.80	1.16	0.435	0.57	—	8.5
27	73	6.48	0.82	10.5	1.77	7.68	—	9.1
27	33	4.39	0.80	17.7	2.3	14.4	—	9.7
27	20	5.20	0.72	54.0	4.25	43.5	—	11.0
27	28	2.60	4.10	18.7	8.40	10.7	1.52	9.7
51	20	5.29	1.23	39	8.95	28.25	0.855	19.4
51	35	1.8	4.4	14.3	12.4	5.80	2.10	19.6
73	61	6.10	0.90	8.6	3.9	3.11	0.73	30.7
72	35	5.12	0.75	17.6	5.4	9.30	1.35	29.5
72	75	3.89	1.29	22.3	8.80	12.1	2.10	29.3
91	62	5.28	1.52	27.8	17.4	9.45	5.35	52.0
93	25	3.56	2.62	25.1	23.7	8.40	9.70	55.0
110	30	5.33	0.80	27.0	8.90	4.66	3.60	81.0
115	60	4.88	1.83	26.7	22.5	5.60	12.20	90.0
132	60	5.41	1.37	28.5	22.7	4.17	11.40	135.0
146	22	4.92	1.08	36.4	26.8	5.45	14.6	175.0
146	20	4.45	2.50	33.8	45.7	4.35	29.0	172.0
165	20	5.50	0.98	40.2	29.0	3.6	12.8	250.0
165	25	4.07	2.70	30.6	53.0	3.20	35.5	230.0

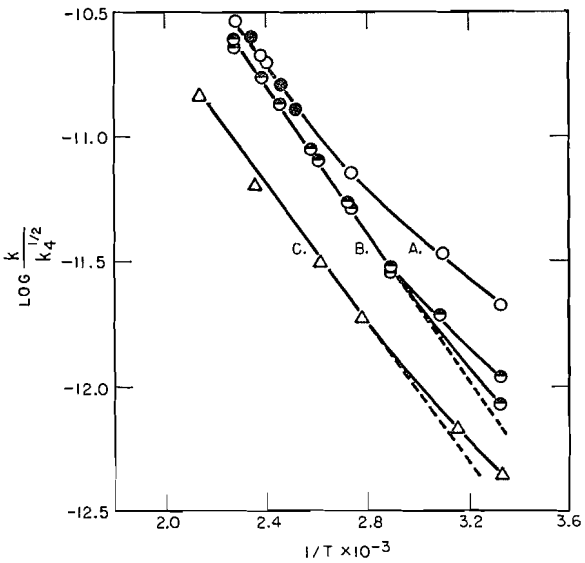

FIG. 1. Arrhenius plot of $R_{CH_4}/R_{C_2H_6}^{\frac{1}{2}}$[Aldehyde].
Curve *A*—CH_3CHO photolysis.
Curve *B*—Photolysis of azomethane in the presence of CH_3CHO.
Curve *C*—Photolysis of azomethane in the presence of CH_3CDO, containing 5% CH_3CHO.

75°C. where curvature is evident. (The units of k throughout are cm.^{3}, molecules, sec.)

From the first four runs at 27°C., it may be concluded that $R_{CH_4}/R_{C_2H_6}^{\frac{1}{2}}$[Ald] decreases with decreasing intensity as shown by Fig. 2. This can be explained by the occurrence of the disproportionation reaction [9]. Evidence for the

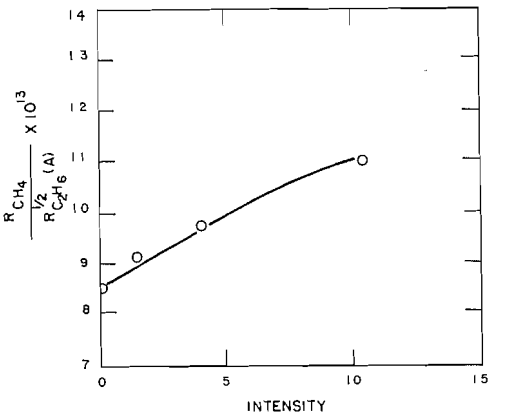

FIG. 2. The effect of intensity at 27°C. on the photolysis of azomethane in the presence of CH_3CHO.

occurrence of this reaction has been found in the photolysis of acetone (2) and biacetyl (3) as well. When the curve in Fig. 2 is extrapolated to zero intensity, a value of 8.4×10^{-13} is obtained for $k_1/k_4^{\frac{1}{2}}$. This is still higher than the value obtained by extrapolation of the linear portion of curve B in Fig. 1. This is therefore not due to reaction [9], and it is suggested that wall effects occur as well at low temperatures, as is the case with acetone and biacetyl.

From the slope of curve B in Fig. 1 at temperatures above 75°C. an activation energy difference $E_1 - \frac{1}{2}E_4$ of 6.8 kcal. is obtained. Since $E_4 = 0$, $E_1 = 6.8$ kcal. This is in excellent agreement with the value found by Volman and Brinton, whose results are also given in Fig. 1. The lower value for E_1 may therefore be considered to be established.

(B) The Photolysis of CH_3CHO

A few experiments were also made on the direct photolysis of CH_3CHO. A Corning Filter No. 970 (opaque at wave lengths below 2900 Å) was used, so that the light absorbed by acetaldehyde consisted mainly of the 3130 Å group of lines. The results are given in Table II. The rate of hydrogen formation has not been included since it was always too small to measure with any great accuracy. An Arrhenius plot of $R_{CH_4}/R_{C_2H_6}^{\frac{1}{2}}[CH_3CHO]$ is given in Fig. 1 (Curve

TABLE II

PHOTOLYSIS OF CH_3CHO

Temp., °C.	Time, min.	Pressure, cm.	Rate in cc./min. × 10^4 CH_4	C_2H_6	CO	$\frac{R_{CH_4}}{R_{C_2H_6}^{\frac{1}{2}}[CH_3CHO]} \times 10^{13}$
27	30	3.78	11.0	4.65	17.0	21.6
50	20	3.75	19.8	6.20	24.5	34.5
92	15	3.45	33.0	6.42	38.0	73.2
143	20	3.13	79.5	7.75	90.0	202.0
146	13	3.45	101.0	8.85	120.0	217.0
165	6	3.53	148.0	10.8	160.0	297.0

A). A curved line is obtained which at higher temperatures appears to become parallel to the line obtained by photolyzing azomethane in the presence of CH_3CHO. The curvature may largely be explained by the direct formation of some methane in the primary step. However, in the light of the azomethane results it is probable that the curvature also results in part from reaction [9] and from wall reactions. In spite of these complications the results indicate that at higher temperatures methane mainly results from reaction [1].

(*C*) *The Reaction of CH_3 with CH_3CDO*

When azomethane is photolyzed in the presence of CH_3CDO the same reaction scheme holds as for CH_3CHO, except that in place of [1] we have

$$CH_3+CH_3CDO \rightarrow CH_3D+CH_3CO. \qquad [2]$$

Also we may consider the possible reaction

$$CH_3+CH_3CDO \rightarrow CH_4+CH_2CDO. \qquad [11]$$

If it is assumed that only an acyl hydrogen is captured, then

$$\frac{R_{CH_3D}}{R_{C_2H_6}^{\frac{1}{2}}[CH_3CDO]} = \frac{k_2}{k_4^{\frac{1}{2}}},$$

and

$$\frac{R_{CH_4}}{R_{C_2H_6}^{\frac{1}{2}}[CH_3NNCH_3]} = \frac{k_5}{k_4^{\frac{1}{2}}}$$

The values of $k_2/k_4^{\frac{1}{2}}$ and $k_5/k_4^{\frac{1}{2}}$ given in columns 9 and 10 of Table III have been calculated in this way. In Fig. 3 curve *F*, the triangles represent the values of $\log k_5/k_4^{\frac{1}{2}}$, while the line drawn through them represents the results from the photolysis of azomethane alone. It is evident, therefore, that reaction [11] does not occur to an appreciable extent (i.e. not over five per cent of [2]) since all the CH_4 found can be accounted for by abstraction from azomethane. The small amount of CH_3CHO present in the CH_3CDO is not sufficient to alter the results appreciably.

The fact that no C_2H_5D or $C_2H_4D_2$ could be detected in the ethane fraction is further proof that no hydrogen atoms are captured from the methyl group of CH_3CDO. Also no CH_2D_2 was found in the methane fraction, which, as Blacet and Brinton point out (4) excludes a mixed mechanism.

An Arrhenius plot of $k_2/k_4^{\frac{1}{2}}$ (curve *E*) gives an activation energy of 7.9 kcal. for reaction [2], as compared with 6.8 kcal. for [1].

A very small amount of curvature is present in the $\log k_2/k_4^{\frac{1}{2}}$ plot at low temperatures. Since this plot involves CH_3D, the curvature cannot result from the disproportionation of methyl with acetyl, since all the acetyl radicals are CH_3CO. It is therefore probably to be explained by wall reactions.

No curvature was found in the $k_5/k_4^{\frac{1}{2}}$ plot (curve *F*). In this case the reaction

$$CH_3+CH_3CO \rightarrow CH_4+CH_2CO \qquad [9]$$

would cause such curvature. Its absence is presumably due to the much smaller rate of abstraction from CH_3CDO as compared with CH_3CHO (a factor of 20). This results in a much smaller concentration of acetyl, and the effect of reaction [9] is apparently negligible.

TABLE III

THE PHOTOLYSIS OF AZOMETHANE IN THE PRESENCE OF CH_3CDO

Temp., °C.	Time, min.	Pressure, cm. CH_3CDO	Pressure, cm. CH_3NNCH_3	Rate, cc./min. × 10^4 CH_3D	CH_4	C_2H_6	CO	$\frac{k_5}{k_4^{\frac{1}{2}}} \times 10^{13}$	$\frac{k_2}{k_4^{\frac{1}{2}}} \times 10^{13}$
27	125	1.08	5.26	0.115	0.465	10.2	0.02	0.435	0.530
27	125	0.74	5.38	0.08	0.495	10.0	0.02	0.463	0.54
61	60	1.20	4.88	0.460	1.55	16.3	0.15	1.40	1.70
62	126	1.00	5.14	0.385	1.17	6.9	0.16	1.50	1.80
85	60	0.72	5.70	0.52	3.36	12.9	0.40	3.12	3.90
86	100	1.06	4.29	0.49	1.52	4.4	0.34	3.24	4.20
126	50	0.84	5.30	1.14	5.50	5.4	1.24	9.00	12.30
127	100	1.65	5.50	1.29	2.90	1.62	1.27	9.40	13.00
158	55	0.83	5.58	1.52	6.82	2.60	—	17.30	26.00

TABLE IV

PHOTOLYSIS OF CH_3CDO

Temp., °C.	Time, min.	Pressure, cm.	Rate, cc./min. × 10^4 CH_3D	CH_4	Ethane	CO	$\frac{R_{CH_3D}}{R_{Ethane}^{\frac{1}{2}}[CH_3CDO]} \times 10^{13}$	$\frac{R_{CH_4}}{R_{Ethane}^{\frac{1}{2}}[CH_3CDO]} \times 10^{13}$
26	62	4.90	0.77	0.175	1.48	2.85	2.05	0.46
43	45	3.95	0.95	0.215	1.68	3.00	3.05	0.70
86	90	3.75	1.90	0.495	1.56	4.92	7.45	1.94
108	85	3.72	2.47	0.652	1.68	5.30	10.4	3.25
151	90	3.83	6.08	1.70	2.22	10.6	23.5	6.65
196	60	3.24	9.95	2.85	1.92	16.4	52.2	15.0

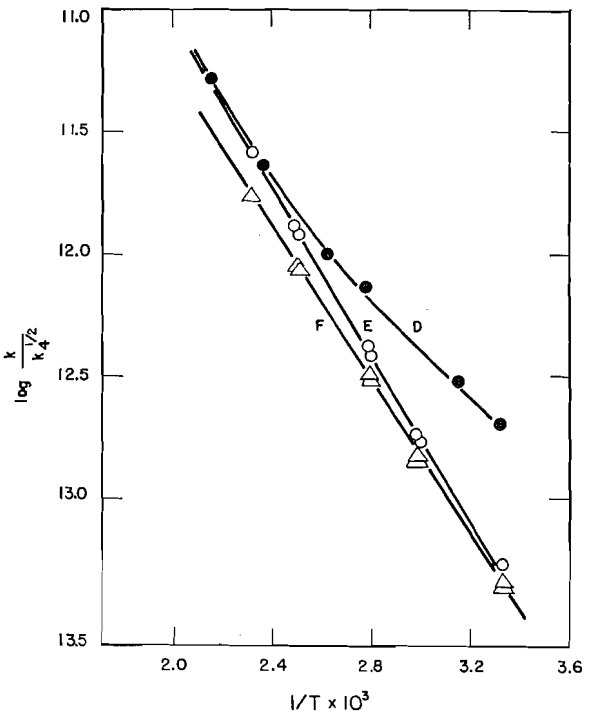

FIG. 3. The photolysis of CH_3CDO.

Curve *D*—Arrhenius plot of $R_{CH_3D}/R^{\frac{1}{2}}_{Ethane}$[Aldehyde] for the direct photolysis of CH_3CDO.

Curve *E*—Arrhenius plot of $R_{CH_3D}/R^{\frac{1}{2}}_{Ethane}$[Aldehyde] for the photolysis of azomethane in the presence of CH_3CDO.

Curve *F*—Arrhenius plot of $R_{CH_4}/R^{\frac{1}{2}}_{C_2H_6}$[Azomethane] for the photolysis of azomethane in the presence of CH_3CDO.

(*D*) *The Photolysis of CH_3CDO*

The photolysis of CH_3CDO was briefly investigated. A Corning 970 filter was used so that absorption was mainly of the 3130 Å group of lines. The results are given in Table IV. The fraction coming off at −195°C. consisted of CO, CH_4, and CH_3D. No CH_2D_2, D_2, or H_2 was found by mass-spectrometer analysis, so that they amounted to less than one per cent of the products. The ethane fraction consisted mainly of C_2H_6 (~60%); considerable amounts of deuterated ethanes were also present. Only the total ethane has been given in Table IV.

In Fig. 3 (curve *D*) an Arrhenius plot of $R_{CH_3D}/R^{\frac{1}{2}}_{Ethane}$[$CH_3CDO$] is given. A large curvature is present at low temperatures, while at higher temperatures the plot becomes parallel to the one found when azomethane is photolyzed in the presence of CH_3CDO. This appears to indicate that at high temperatures CH_3D is mainly formed by reaction [2], while at low temperatures the occurrence of the primary step

$$CH_3CDO + h\nu \rightarrow CH_3D + CO \qquad [12]$$

explains largely the excess of CH_3D responsible for the curvature in the Arrhenius plot.

Considerable CH_4 is formed in addition to CH_3D. This may be accounted for by the presence of about five per cent CH_3CHO in the CH_3CDO sample. Since abstraction by methyl is about 20 times faster from CH_3CHO than from CH_3CDO, even five per cent of CH_3CHO has a large effect. In Fig. 1 (curve *C*) an Arrhenius plot is given for this methane, i.e. a plot of $R_{CH_4}/R_{Ethane}^{\frac{1}{2}}$[Aldehyde]. Since the exact amount of CH_3CHO present is somewhat uncertain, but its percentage is constant, we have used the total aldehyde concentration. The actual value of the ratio $R_{CH_4}/R_{Ethane}^{\frac{1}{2}}[CH_3CHO]$ will therefore be approximately 20 to 25 times higher than the figures plotted in Fig. 1, and the results will therefore coincide approximately with the linear portion of curve *A* as they should. From the slope of curve *C* a value of 6.4 kcal. is obtained for E_1, in excellent agreement with the value of 6.8 kcal. obtained by photolyzing azomethane in the presence of CH_3CHO.

It may be noted that the deviation from linearity is much less for curve *C* than for curve *A*. This is to be expected since the relatively fast abstraction by methyl from CH_3CHO as compared with CH_3CDO, causes a small amount of CH_3CHO to have an important effect on the abstraction reaction. There is, however, no reason to suppose that reaction [11] will be more important for CH_3CHO than for CH_3CDO.

If CH_4 was also produced by abstraction from the methyl group

$$CH_3+CH_3CDO \rightarrow CH_4+CH_2CDO, \qquad [13]$$

a higher activation energy than 6.8 kcal. would be expected, and CH_2D_2 should also be produced. It may therefore be concluded that reaction [13] does not occur to an appreciable extent. However, no explanation can be given for the production of a considerable amount of C_2H_5D and $C_2H_4D_2$.

Since there is no appreciable abstraction from the methyl group in CH_3CDO, in spite of the higher acyl C—D bond strength, it is evident that no appreciable abstraction from the methyl group in CH_3CHO will occur.

ACKNOWLEDGMENT

The authors are indebted to Dr. R. E. Dodd for valuable advice, to Dr. L. C. Leitch for the preparation of the acetaldehyde-*d* sample, and to Miss F. Gauthier and Miss G. Fuller for the mass-spectrometer analysis.

REFERENCES

1. Ausloos, P. and Steacie, E. W. R. Can. J. Chem. 32: 593. 1954.
2. Ausloos, P. and Steacie, E. W. R. Can. J. Chem. 33: 47. 1955.
3. Ausloos, P. and Steacie, E. W. R. Can. J. Chem. 33: 39. 1955.
4. Blacet, F. E. and Brinton, R. K. J. Am. Chem. Soc. 72: 4715. 1950.
5. Leitch, L. C. To be published.
6. Volman, D. H. and Brinton, R. K. J. Chem. Phys. 20: 1764. 1952.

THE PHOTOLYSIS OF BIACETYL[1]

By P. Ausloos[2] and E. W. R. Steacie

ABSTRACT

The photolysis of biacetyl has been reinvestigated. The results are, in general, in excellent agreement with those of Blacet and Bell. Curvature occurs at low temperatures in the Arrhenius plot of $R_{CH_4}/R^{\frac{1}{2}}_{C_2H_6}$[Biacetyl], and this is attributed to wall reactions, and to the disproportionation reaction

$$CH_3+CH_3CO \rightarrow CH_4+CH_2CO.$$

Azomethane–biacetyl mixtures have been photolyzed to give further information on these points. An activation energy of 8.5 kcal. has been found for the reaction of methyl radicals with biacetyl.

INTRODUCTION

The photolysis of biacetyl has been thoroughly investigated by Blacet and Bell (4, 3). It has, however, been thought to be worth reinvestigating the reaction, especially in the low temperature region, to see if there were anomalies similar to those which occur with acetone. In particular we were interested in the possibility of complications due to wall effects and to the possible occurrence of the disproportionation reactions

$$CH_3+CH_3CO \rightarrow CH_4+CH_2CO$$

and

$$CH_3CO+CH_3CO \rightarrow CH_3CHO+CH_2CO.$$

In addition azomethane was photolyzed in the presence of biacetyl to obtain a further check on the activation energy of the reaction of methyl radicals with biacetyl.

EXPERIMENTAL

The reaction cell was a quartz cylinder 10 cm. long and 5 cm. diameter, with a volume of about 170 cc. A Hanovia S-500 medium pressure mercury arc was used for most of the experiments. For a few runs a B.T.H. ME/D 250 w. compact source lamp was used to obtain higher intensities. The reaction cell was completely filled by a nearly parallel light beam. The intensity was varied by means of neutral density filters of chromel deposited on quartz. No other filters were used, except where mentioned. The remainder of the apparatus was essentially similar to that described in previous papers from this laboratory.

Reagent grade biacetyl (Eastman white label) was used, and was distilled in vacuum with the rejection of a large head and tail fraction.

The analysis of the products was done in the usual way by taking off the CO, CH_4 or CO, CH_4, N_2 fraction at liquid nitrogen temperature. In CO, CH_4 samples the CO was determined by hot copper oxide. The samples containing nitrogen were analyzed with a mass spectrometer. The C_2H_6 fraction was

[1]*Manuscript received September 17, 1954.*
Contribution from the Division of Pure Chemistry, National Research Council, Ottawa, Canada. Issued as N.R.C. No. 3447.
[2]*National Research Council of Canada Postdoctorate Fellow, 1952–54. Present address: Departement de Chimie Physique, Université Laval, Québec.*

TABLE I

PHOTOLYSIS OF BIACETYL

Relative intensity	Temp., °C.	Pressure, cm.	R_{CO}	R_{CH_4}	$R_{C_2H_6}$	R_{CH_2CO}	$\frac{R_{CH_2CO}}{R_{CH_4}}$	$\frac{R_{CH_4}}{R_{C_2H_6}^{\frac{1}{2}}[CH_3COCOCH_3]} \times 10^{13}$
				cc. per min. $\times 10^4$				
20	27	2.6	17.5	0.34	4.50	—	—	0.985
20	27	2.1	16.5	0.27	4.0	—	—	1.04
20	27	2.3	17.3	0.31	4.20	—	—	1.06
1	27	2.45	0.37	0.029	0.08	—	—	0.67
1	27	2.4	0.36	0.03	0.087	—	—	0.67
20	28	2.55	17.78	0.34	4.40	0.39	1.15	1.01
50	28	2.3	56.1	0.78	14.3	1.2	1.54	1.45
50	27	2.6	59.5	0.95	15.0	1.3	1.4	1.51
20	81	2.2	28.0	1.22	8.3	0.432	0.34	3.67
1	81	2.3	1.05	0.20	0.25	0.013	0.06	3.35
20	119	2.15	48.5	3.80	15.6	—	—	9.3
1	119	2.3	2.22	0.58	0.36	—	—	8.80
20	137	2.32	58.0	6.60	18.8	0.47	0.07	15.0
1	137	2.28	3.0	1.04	0.43	0.05	0.05	15.0
20	196	2.35	109.0	26.4	25.0	15.6	0.59	56.0
1	196	2.35	8.85	4.15	0.7	1.7	0.41	53.0
20	204	2.2	125.0	29.2	27.5	—	—	64.0
1	204	2.16	9.0	3.8	0.53	2.55	0.67	61.0
20	162	2.2	79.2	11.8	21.3	—	—	27.2
1	162	2.5	5.3	1.95	0.54	—	—	25.0

TABLE II

PHOTOLYSIS OF AZOMETHANE–BIACETYL MIXTURES

Temp., °C.	Time, min.	Pressure, cm.		Products, cc./min. × 10^4				$\frac{R_{CH_4}}{R_{C_2H_6}^{\frac{1}{2}}[CH_3COCOCH_3]} \times 10^{13}$
		Azomethane	Biacetyl	N_2	CH_4	C_2H_6	CO	
27	32	2.09	2.26	27.7	0.995	24.0	<0.20	1.00
27	30	2.15	1.90	27.2	0.98	24.5	<0.20	1.15
77	30	2.07	1.6	29.5	2.85	23.3	1.71	3.68
78	60	1.65	2.15	7.8	1.41	5.15	—	3.50
140	30	2.25	1.90	39.5	12.0	18.2	9.80	18.5
198	15	2.21	1.81	44.7	28.5	12.1	31.7	70.0

TABLE III

EFFECT OF VARIATION OF INTENSITY

Relative intensity	Pressure, cm.	Time, min.	Products, cc./min. × 10^4				$\frac{R_{CH_4}}{R_{C_2H_6}^{\frac{1}{2}}[CH_3COCOCH_3]} \times 10^{13}$	Rate of formation of excess CH_4	$\frac{k_{11}}{k_{12}^{\frac{1}{2}} k_3^{\frac{1}{2}}}$
			CO	CH_4	C_2H_6	CH_2CO			
1	2.4	1050	0.36	0.03	0.087	—	0.67	—	—
4	2.3	1150	1.96	0.065	0.368	0.015	0.75	0.006	0.103
10	2.3	200	7.70	0.145	1.58	0.075	0.81	0.028	0.104
28	2.25	55	23.5	0.337	0.74	0.500	1.10	0.138	0.105
72	2.25	19	106.0	1.29	25.8	3.25	1.72	0.75	0.094
79	2.3	13	128.0	1.32	27.0	4.05	1.78	0.84	0.091
200	2.3	14	—	3.92	86.0	12.2	2.9	3.05	0.106
200	2.3	4	445.0	4.27	102.0	13.0	2.9	3.30	0.108

taken off at −175°C., and the ketene fraction at −135°C. Both fractions were occasionally checked with a mass spectrometer.

RESULTS

Table I gives the results of runs at temperatures between 27 and 200°C., and relative intensities varying by a factor of 20, where a relative intensity of 1 corresponds to an absorbed intensity of about 2×10^{14} quanta/sec. The amount of ketene formed was measured in only a few experiments. Velocity constants throughout are expressed in units of cm.^{3}, molecules, sec.

Table II gives the results obtained by photolyzing azomethane in the presence of biacetyl. For these runs a Corning 738 filter was used, which cut off wave lengths below 3400 Å.

The results in the last columns of Tables I and II, together with the results of Blacet and Bell, are plotted in Fig. 1. Table III and Fig. 2 show the effect of varying the intensity by a factor of 200 at 27°C. and constant biacetyl concentration.

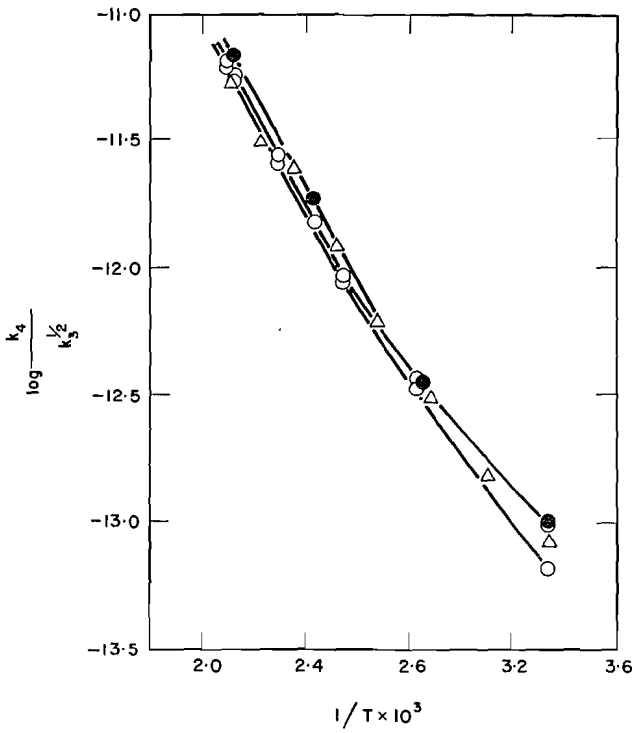

FIG. 1. Arrhenius plot of $k_4/k_3^{\frac{1}{2}}$ for the biacetyl photolysis.
○ Photolysis—relative intensities—lower curve, 1.
—upper curve, 20.
△ Photolysis—results of Blacet and Bell.
● Photolysis of azomethane in presence of biacetyl.

DISCUSSION

To explain their results Blacet and Bell proposed the following secondary reactions:

$$CH_3CO \rightarrow CH_3+CO \quad [1]$$
$$CH_3+CH_3CO \rightarrow CH_3COCH_3 \quad [2]$$
$$2CH_3 \rightarrow C_2H_6 \quad [3]$$
$$CH_3+CH_3COCOCH_3 \rightarrow CH_4+CH_2COCOCH_3 \quad [4]$$
$$CH_2COCOCH_3 \rightarrow CH_2CO+CH_3CO \quad [5]$$
$$CH_3+CH_3COCOCH_3 \rightarrow CH_3COCH_3+CH_3CO \quad [6]$$
$$CH_3+CH_2COCOCH_3 \rightarrow C_2H_5COCOCH_3 \quad [7]$$
$$2CH_3CO \rightarrow CH_3COCOCH_3 \quad [8]$$

Activation Energy of the Abstraction Reaction

If ethane and methane are formed only by reactions [3] and [4], then

$$\frac{R_{CH_4}}{R_{C_2H_6}^{\frac{1}{2}}[\text{Biacetyl}]} = \frac{k_4}{k_3^{\frac{1}{2}}},$$

so that a straight line may be expected on plotting the L.H.S. against $1/T$. The results given in Table I and Fig. 1 confirm this for the high-temperature region. However, at low temperatures a curvature becomes apparent in the Arrhenius plot. We have also shown Blacet and Bell's results in Fig. 1. Although their original plot was not drawn so as to show curvature, it is evident that if the two highest temperature points are ignored it is possible to draw a line through their remaining points which is strikingly similar to ours. The two plots thus drawn have the same slope and lead to an activation energy difference $E_4-\frac{1}{2}E_3$ of 8.5 kcal., or assuming $E_3 = 0$, $E_4 = 8.5$ kcal.

Wall Reactions

Fig. 1 also shows the results of experiments in which azomethane was photolyzed in the presence of biacetyl. The effective wave length was 3660 Å. Biacetyl also absorbs slightly under our conditions, but the amount decomposed was negligible compared with azomethane decomposed. This is shown by the very small amount of CO formed at room temperature. At this temperature CO is a measure of the amount of biacetyl photolyzed because of the unimportance of reactions [5] and [6]. At higher temperatures CO is formed by [5] and [6] from radicals resulting from the photolysis of azomethane.

When azomethane is photolyzed in the presence of biacetyl, the following reactions have to be taken into account to explain the formation of methane and ethane.

$$CH_3NNCH_3+h\nu \rightarrow 2CH_3+N_2 \quad [9]$$
$$2CH_3 \rightarrow C_2H_6 \quad [3]$$
$$CH_3+CH_3NNCH_3 \rightarrow CH_4+CH_2NNCH_3 \quad [10]$$
$$CH_3+CH_3COCOCH_3 \rightarrow CH_4+CH_2COCOCH_3 \quad [4]$$

whence

$$\frac{k_4}{k_3^{\frac{1}{2}}} = \left(\frac{R_{CH_4}}{R_{C_2H_6}^{\frac{1}{2}}} - \frac{k_{10}}{k_3^{\frac{1}{2}}}[CH_3NNCH_3]\right) \Big/ [CH_3COCOCH_3].$$

The values of $k_{10}/k_3^{\frac{1}{2}}$ have been taken from an experimental plot for the photolysis of azomethane alone (1). From Fig. 1 it is evident that the results agree

excellently with those from the photolysis of biacetyl itself. It is also apparent that curvature is still present in the Arrhenius plot, although there is none in the plot for azomethane itself. It is suggested that the curvature results from wall effects at lower temperatures where the diffusion of radicals to the wall is of more importance. More conclusive evidence for this will be discussed in a forthcoming paper (2).

Disproportionation of Acetyl

It is suggested that the reactions

$$CH_3+CH_3CO \rightarrow CH_4+CH_2CO \qquad [11]$$

and

$$2CH_3CO \rightarrow CH_2CO+CH_3CHO \qquad [12]$$

also occur. If this is so, the ratio $R_{CH_4}/R^{\frac{1}{2}}_{C_2H_6}[CH_3COCOCH_3]$ will become intensity dependent, i.e.

$$\frac{R_{CH_4}}{R^{\frac{1}{2}}_{C_2H_6}} = \frac{k_4}{k_3^{\frac{1}{2}}}[CH_3COCOCH_3] + \frac{k_{11}}{k_3^{\frac{1}{2}}}[CH_3CO].$$

To check this two series of runs were carried out at relative intensities which differed by a factor of 20. Fig. 1 shows that variation in intensity has little effect at temperatures above 100°C. At 27° however $R_{CH_4}/R^{\frac{1}{2}}_{C_2H_6}[CH_3COCOCH_3]$ decreases appreciably with intensity as may be expected if reaction [11] occurs, since CH_3CO radicals will be more stable at room temperature.

The amount of ketene formed was also measured at a few temperatures. From 200° to 137°C. a sharp decrease in ketene was observed (Table I) in agreement with the results of Blacet and Bell who measured the ketene formed at 200°, 150°, and 100°C. They explain the formation of ketene by reaction [5]. If this has an appreciable activation energy the drop in ketene with decreasing temperature is to be expected. If reactions [11] and [12] are neglected, the ratio takes the form

$$\frac{[CH_2CO]}{[CH_4]} = 1/\left(1+\frac{k_7}{k_5}[CH_3]\right).$$

Since $E_5 \gg E_7$, this predicts a drop in the ratio of ketene to methane with decreasing temperature, as is observed from 200° to 137°C. There are, however, three anomalies all of which point to the occurrence of [11] or [12]. (*a*) There is always an increase in the ratio CH_2CO/CH_4 with increasing intensity. (*b*) At temperatures below 137°C., the rate of ketene formation begins to increase again. At room temperature the ratio CH_2CO/CH_4 is larger than unity. (*c*) Mass-spectrometer analyses indicated the presence of acetaldehyde as a reaction product.

In order to obtain more definite information on these points, a series of runs were made in which the intensity was varied over a wider range (by a factor of 200). For these runs the temperature was 27 ± 1°C., and the biacetyl pressure was 2.3 cm. The results are given in Table III and Fig. 2. Fig. 2 indicates a considerable increase in the ratio $R_{CH_4}/R^{\frac{1}{2}}_{C_2H_6}[CH_3COCOCH_3]$ with increasing

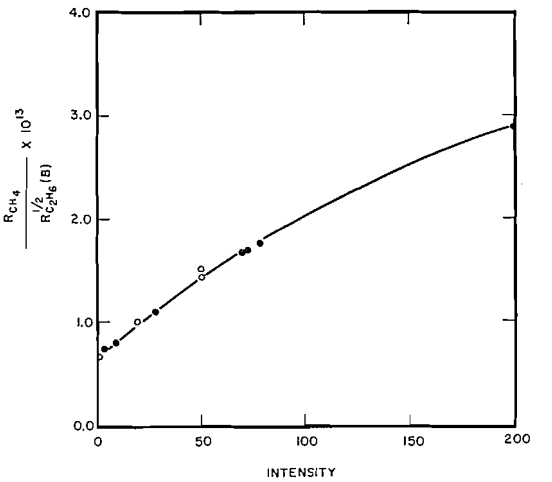

FIG. 2. Effect of intensity.
● B.T.H. lamp. Pressure 2.3 cm.
○ Hanovia lamp. Temperature 27°C.

intensity. If the curve in Fig. 2 is extrapolated to zero intensity a value of 0.65×10^{-13} is obtained for the ratio. This is higher than the value which would be expected from an extrapolation of the straight-line portion of the Arrhenius plot in Fig. 1. The curvature in Fig. 1 is thus in part but not solely due to disproportionation of acetyl radicals. The residual curvature is probably due to diffusion effects accompanying wall reactions.

The fact that the ratio CH_2CO/CH_4 becomes considerably higher than 1 at high intensities indicates that there is a further source of ketene in addition to reaction [11]. As pointed out previously the presence of acetaldehyde suggests reaction [12]. The direct production of acetaldehyde in the primary step

$$CH_3COCOCH_3 + h\nu \rightarrow CH_3CHO + CH_2CO$$

is unlikely on the basis of Blacet and Bell's results in the presence of iodine. Also, the fact that acetaldehyde has been observed in the acetone photolysis as well (2) suggests a common origin such as reaction [12].

A rough quantitative check on the validity of assuming reactions [11] and [12] can be made as follows. From reactions [11], [12], and [3] the relationship can be deduced

$$\frac{R^*_{CH_4}}{R^{\frac{1}{2}}_{CH_3CHO} R^{\frac{1}{2}}_{C_2H_6}} = \frac{k_{11}}{k_{12}^{\frac{1}{2}} k_3^{\frac{1}{2}}}$$

where $R^*_{CH_4}$ represents the amount of excess methane necessary to account for the increase in the ratio $R_{CH_4}/R^{\frac{1}{2}}_{C_2H_6}[CH_3COCOCH_3]$ above the limiting value 0.65×10^{-13}. Although the acetaldehyde concentration could not be quantitatively determined, it is evident that

$$R_{CH_3CHO} = R_{CH_2CO} - R^*_{CH_4}.$$

The values of $k_{11}/k_{12}^{\frac{1}{2}} k_3^{\frac{1}{2}}$ calculated in this way are given in the last column of Table III, and are independent of intensity.

In conclusion, it may be pointed out that the results given here indicate complications at low temperatures in all systems in which acetyl radicals are present, and in particular that such complicating processes will be intensity dependent. The analogous case of acetone is discussed in a forthcoming paper (2).

REFERENCES

1. AUSLOOS, P. and STEACIE, E. W. R. Can. J. Chem. 32: 593. 1954.
2. AUSLOOS, P. and STEACIE, E. W. R. Can. J. Chem. 33: 47. 1955.
3. BELL, W. E. and BLACET, F. E. J. Am. Chem. Soc. In press.
4. BLACET, F. E. and BELL, W. E. Discussions Faraday Soc. 14: 70. 1953.

SOME COMPLICATING FACTORS IN THE PHOTOLYSIS OF ACETONE[1]

By P. Ausloos[2] and E. W. R. Steacie

ABSTRACT

The photolysis of acetone has been investigated at room temperature using low pressures and high intensities. In addition an investigation was made of the photolysis of azomethane–acetone mixtures. The results indicate that the curvature at low temperatures of Arrhenius plots of $R_{CH_4}/R_{C_2H_6}^{\frac{1}{2}}$[Acetone] is due to two causes (*a*) a reaction between methyl radicals and adsorbed acetone and (*b*) to the occurrence of the disproportionation reaction

$$CH_3+CH_3CO \rightarrow CH_4+CH_2CO.$$

Confirmatory evidence for wall effects was obtained from experiments at low pressures and higher temperatures.

INTRODUCTION

The photochemical decomposition of acetone has been thoroughly investigated, especially by Noyes and his co-workers. In the temperature region from 120° to 200°C. it has been established that all the methane and ethane formed can be accounted for by the reactions:

$$CH_3+CH_3COCH_3 \rightarrow CH_4+CH_2COCH_3 \quad [1]$$

$$CH_3+CH_3 \rightarrow C_2H_6 \quad [2]$$

It has, however, been shown (6, 8, 9) that at lower pressures reaction [2] becomes dependent on a third-body. Whence at higher pressures

$$\frac{R_{CH_4}}{R_{C_2H_6}^{\frac{1}{2}}[\text{Acetone}]} = \text{Constant} = \frac{k_1}{k_2^{\frac{1}{2}}}$$

and at low pressures

$$\frac{R_{CH_4}}{R_{C_2H_6}^{\frac{1}{2}}[\text{Acetone}]^{\frac{1}{2}}} = \text{Constant}.$$

For the activation energy difference, $E_1-\frac{1}{2}E_2$, a value of 9.7 ± 0.1 kcal. has been generally accepted (12). This value has been deduced from experiments at temperatures above 100°C., and at pressures between 25 and 200 mm.

In the lower temperature region there are complications in the kinetics. Curvature has been observed in the Arrhenius plot between room temperature and 125°C. (7, 12). Several suggestions have been made as to the cause of the discrepancy (11). In the first place the presence of an appreciable amount of acetyl radicals constitutes the most striking difference between the low- and the high-temperature photolysis. The diffusion of radicals out of the light-beam and possible wall effects have also to be considered. As far as diffusion is concerned, Nicholson (10) has shown that although it is important in some

[1]*Manuscript received September 17, 1954.*
Contribution from the Division of Pure Chemistry, National Research Council, Ottawa, Canada. Issued as N.R.C. No. 3450.
[2]*National Research Council of Canada Postdoctorate Fellow, 1952–54. Present address: Departement de Chimie Physique, Université Laval, Québec.*

cases, the effect is still too small to account for the curvature in the Arrhenius plot at low temperatures.

The purpose of the present work was in the first place to study the reaction of methyl radicals with acetone in the absence of complications due to acetyl radicals. For this purpose azomethane was used as a source of methyl radicals. It has the advantage of absorbing at longer wave lengths where acetone is transparent. The second object of the work was to investigate the photolysis of acetone under special conditions (high intensities and low pressures), to obtain information regarding wall reactions and reactions of acetyl radicals.

EXPERIMENTAL

Azomethane was prepared by Dr. L. C. Leitch as described in previous papers from this laboratory. Acetone was obtained from the Eastman Kodak Co. Both compounds were thoroughly degassed and stored behind mercury cutoffs.

Two different types of apparatus were used. Apparatus I was of the conventional type which has been described elsewhere (1). A Hanovia S-500 medium pressure mercury arc was used as a light source. The cylindrical quartz reaction cell (5 cm. diameter, 10 cm. long) was completely filled with a nearly parallel light beam.

Apparatus II which was used for low pressure experiments was essentially the same as that described by Dodd and Steacie (6). The lamp was a B.T.H. ME/D 250 w. compact source. In some experiments a "packed" reaction vessel was used. For these the cell which was 70 cm. long contained two inner quartz tubes concentrically mounted. The surface/volume ratio of the packed cell was 7.1 cm^{-1}. The cell was completely filled by a parallel beam of light. An empty cell was also used, which was 100 cm. long.

In experiments with azomethane–acetone mixtures a Corning filter No. 7380 was used to limit radiation to wave lengths greater than 3400 Å. For other experiments a Corning No. 986 filter was used.

The N_2–CH_4 fractions of the products were removed at liquid nitrogen temperature and analyzed by the mass spectrometer. On a few occasions checks were made for CO in the N_2–CH_4 fraction from the photolysis of azomethane–acetone mixtures by passing the gas over hot copper oxide. The quantity of CO was invariably negligible. The CO–CH_4 fractions from the acetone photolysis were analyzed by combustion over hot copper oxide. The ethane fraction was separated at −175°C. and occasionally checked with the mass spectrometer.

RESULTS FROM RUNS AT NORMAL PRESSURES USING APPARATUS I

The results for the photolysis of azomethane and of azomethane–acetone mixtures are given in Tables I and II. In Fig. 1 Arrhenius plots are given for $k_1/k_2^{\frac{1}{2}}$ and $k_3/k_2^{\frac{1}{2}}$, where reaction [3] is

$$CH_3+CH_3NNCH_3 \rightarrow CH_4+CH_2NNCH_3. \qquad [3]$$

The units of k throughout are $cm.^3$, molecules, and sec.

Some experiments were also carried out in which acetone was photolyzed at room temperature and various intensities. The results are given in Table III.

TABLE I

THE PHOTOLYSIS OF AZOMETHANE

Temp., °C.	Pressure, cm.	Time, min.	R_{N_2}	R_{CH_4}	$R_{C_2H_6}$	$k_3/k_2^{\frac{1}{2}} \times 10^{13}$
			cc./min. $\times 10^4$			
28	5.85	47	17.0	0.64	14.8	0.455
28	4.14	85	23.5	0.56	22.5	0.458
49	5.2	80	30.2	1.42	24.75	0.95
53	4.88	85	28.3	1.69	22.3	1.225
68	3.4	95	19.7	1.33	14.75	1.86
91	4.95	80	28.4	3.59	14.0	3.72
112	4.1	100	24.0	3.65	8.60	6.20
133	4.48	70	24.0	5.62	5.78	11.4

TABLE II

PHOTOLYSIS OF AZOMETHANE–ACETONE MIXTURES

Temp., °C.	Pressure, cm.		Time, min.	R_{N_2}	R_{CH_4}	$R_{C_2H_6}$	$k_1/k_2^{\frac{1}{2}} \times 10^{14}$
	Azomethane	Acetone		cc./min. $\times 10^4$			
26	1.74	5.10	40	14.6	0.337	13.5	1.35
27	2.95	3.15	1030	0.41	0.059	0.267	1.64
27	1.18	3.42	36	10.4	0.20	9.85	1.47
27	1.73	3.72	65	6.92	0.205	6.08	1.55
27	1.32	5.20	40	12.3	0.305	11.6	1.66
57	2.28	4.62	41	17.5	1.08	14.6	4.2
58	1.57	5.05	40	11.21	0.77	9.7	4.2
109	3.01	4.64	60	6.00	1.64	1.92	26.6
109	2.18	5.70	28	16.2	3.79	8.2	24.2
140	3.03	4.27	35	22.9	6.88	5.2	69.0

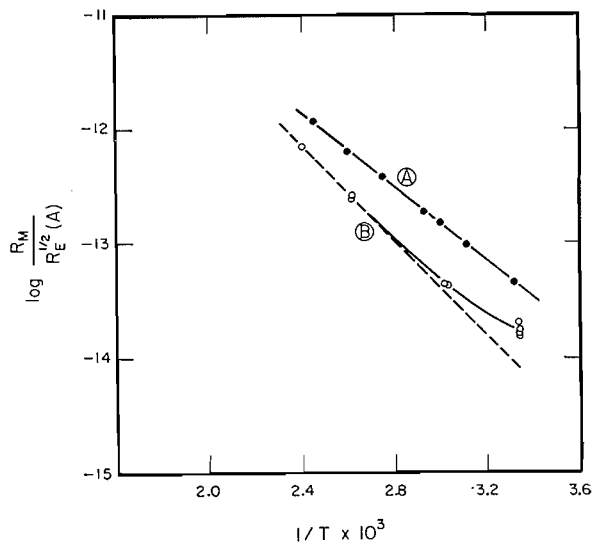

FIG. 1. Plot of $\log R_{CH_4}/R_{C_2H_6}^{\frac{1}{2}}[A]$ against $1/T$ for the photolysis of azomethane–acetone mixtures.

Curve *A*—photolysis of azomethane alone. Curve *B*—azomethane–acetone mixtures. The dotted line is an extrapolation to low temperatures of the results of Trotman-Dickenson and Steacie.

TABLE III

PHOTOLYSIS OF ACETONE AT ROOM TEMPERATURE AND VARYING INTENSITY
Temperature 27°C.

Relative intensity	Pressure, cm.	Time, min.	R_{CO} cc./min. $\times 10^4$	R_{CH_4} cc./min. $\times 10^4$	$R_{C_2H_6}$ cc./min. $\times 10^4$	$\frac{\frac{1}{2}CH_4+C_2H_6}{CO}$	$\frac{R_{CH_4}}{R^{\frac{1}{2}}_{C_2H_6}[\text{Acetone}]} \times 10^{14}$
1	5.85	4050	0.065	0.0194	0.067	1.18	2.02
1	5.6	1105	0.133	0.0275	0.166	1.36	1.95
3	5.45	1311	0.177	0.0334	0.236	1.43	2.02
3	5.6	1017	0.200	0.038	0.272	1.46	2.05
6.6	5.7	866	0.344	0.055	0.583	1.78	2.00
33	5.45	76	1.60	0.165	4.00	2.55	2.40
66	5.83	151	3.30	0.322	8.45	2.60	3.0
165	5.78	40	8.80	0.805	24.5	2.82	4.45
165	5.9	80	8.90	0.790	23.0	2.62	4.45

The relative intensity was varied by a factor of 165, where an intensity of 1 corresponds to approximately 5×10^{11} quanta per cc. per sec. The light intensity was varied by means of neutral density filters of chromel on quartz. The higher intensities are much higher than those used in most previous investigations at low temperatures. The values of $R_{CH_4}/R^{\frac{1}{2}}_{C_2H_6}[\text{Acetone}]$ have been plotted in Fig. 2.

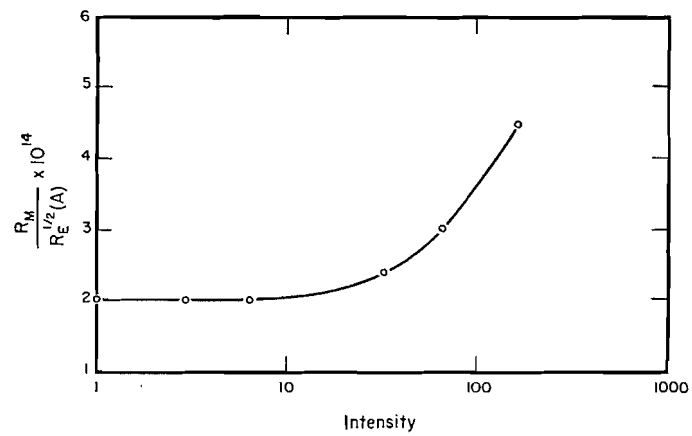

FIG. 2. The photolysis of acetone at 27°C. and 57 mm. with varying intensity.

In addition to the products listed, the highest intensity runs produced a very small amount of a material of intermediate volatility, which could be separated at −125°C. In order to obtain a larger amount of this fraction a run was made at the highest possible incident intensity using a cylindrical cell of 1 liter volume. Mass-spectrometer analysis of the −125°C. cut from this run showed that it consisted mainly of ketene and acetaldehyde.

DISCUSSION

The methane and ethane formed by photolyzing azomethane in the presence of acetone may be accounted for by the following reactions:

$$CH_3NNCH_3 + h\nu \rightarrow 2CH_3 + N_2$$
$$2CH_3 \rightarrow C_2H_6 \quad [2]$$
$$CH_3 + CH_3NNCH_3 \rightarrow CH_4 + CH_2NNCH_3 \quad [3]$$
$$CH_3 + CH_3COCH_3 \rightarrow CH_4 + CH_2COCH_3 \quad [1]$$

From this scheme

$$\frac{k_1}{k_2^{\frac{1}{2}}} = \frac{R_{CH_4}}{R_{C_2H_6}^{\frac{1}{2}}[\text{Acetone}]} - \frac{k_3[\text{Azomethane}]}{k_2^{\frac{1}{2}}[\text{Acetone}]}.$$

The values of $k_3/k_2^{\frac{1}{2}}$ required in the calculations have been taken from an experimental Arrhenius plot for azomethane (2). A few runs were repeated in the low-temperature region to check again the absence of curvature at low temperatures in the Arrhenius plot for azomethane. Fig. 1 shows the complete absence of curvature and the results coincide exactly with those previously obtained (2).

Fig. 1 also gives an Arrhenius plot for $k_1/k_2^{\frac{1}{2}}$, calculated from results with azomethane–acetone mixtures. The dotted line in the figure was obtained by extrapolation of the high-temperature results of Trotman-Dickenson and Steacie on the photolysis of acetone itself. It is evident that the results agree exactly at high temperatures, but that there is appreciable curvature at low temperatures in the results obtained with azomethane–acetone mixtures. At 27°C. a mean value of about 1.6×10^{-14} was found for $k_1/k_2^{\frac{1}{2}}$. This is in excellent agreement with the value of 1.55×10^{-14} found by Nicholson (10) in the direct photolysis of acetone at similar intensities. Since no acetyl radicals are present in the photolysis of azomethane–acetone mixtures, the curvature in the plot at low temperatures and low intensities cannot be due to reactions involving acetyl. Diffusion of radicals out of the light beam is not a possible explanation in the present case, since the cell was filled with light and the cell volume was used in the calculations. It is therefore suggested that wall reactions are involved, and specifically that methyl radicals react with adsorbed acetone to form methane. It may be mentioned that analogous curvature in Arrhenius plots has been found when azomethane was photolyzed in the presence of biacetyl (3) and methyl ethyl ketone (5).

Fig. 2 shows that in experiments on the photolysis of acetone alone the ratio $R_{CH_4}/R_{C_2H_6}^{\frac{1}{2}}[\text{Acetone}]$ does not vary with intensity in the low intensity region. Most previous work was done at still lower intensities. The constant low-intensity value (2×10^{-14}) lies well above the value obtained by extrapolating Trotman-Dickenson and Steacie's Arrhenius plot (12) to lower temperatures. The extrapolated value is in good agreement, however, with the value of 1.6×10^{-14} found by photolyzing azomethane–acetone mixtures. Interference by reactions of acetyl is excluded in this intensity range as the cause of the curvature in the Arrhenius plot. The evidence again strongly favors wall reactions as the cause of the discrepancy.

At higher intensities, however, a sharp increase of $R_{CH_4}/R_{C_2H_6}^{\frac{1}{2}}[\text{Acetone}]$ becomes apparent. This suggests the formation of methane in a radical–radical reaction. Further, since the effect only occurs at low temperatures, the

participation of acetyl is strongly indicated. It is therefore suggested that the additional methane arises by the disproportionation reaction,

$$CH_3+CH_3CO \rightarrow CH_4+CH_2CO. \quad [4]$$

The intensity dependence of methane formation can be explained on this basis, as well as the ketene formation at high intensities. The small amounts of acetaldehyde found by mass-spectrometer analysis may be accounted for by the similar reaction

$$2CH_3CO \rightarrow CH_2CO+CH_3CHO. \quad [5]$$

Evidence for both these reactions has been found also in the photolysis of biacetyl (3). Reaction [5] has also been suggested in the photolysis of acetaldehyde (4).

RESULTS FROM EXPERIMENTS AT LOW PRESSURES USING APPARATUS II

The results of a few experiments at low pressures using a "packed" reaction vessel are given in Table IV, and are plotted in Fig. 3 and compared with the

TABLE IV

PHOTOLYSIS OF ACETONE AT LOW PRESSURES
"Packed" cell

Pressure, mm.	Time, min.	Rate, molecules/cc./sec. $\times 10^{-10}$ CO	CH_4	C_2H_6	$\frac{R_{CH_4}}{R^{\frac{1}{2}}_{C_2H_6}[\text{Acetone}]^{\frac{1}{2}}} \times 10^5$	$\frac{\frac{1}{2}CH_4+C_2H_6}{CO}$	ϕ_{CO}
Temperature 235°C.							
0.105	875	1.14	0.75	0.395	2.65	0.68	0.76
0.22	720	3.17	2.04	1.29	2.80	0.73	1.0
0.53	313	7.6	3.90	3.6	2.06	0.73	
0.71	310	9.8	4.90	5.01	1.91	0.76	
0.90	190	12.8	5.77	6.71	1.72	0.74	$\sim$
2.1	76	28.5	13.0	17.0	1.59	0.82	1.0
4.5	76	67.7	30.6	42.6	1.60	0.85	
10.6	46	120	72.0	68	1.96	0.86	
21.0	20	260	157	135	2.17	0.82	
26.0	35	267	194	134	2.40	0.86	
Temperature 255°C.							
0.06	1485	0.93	0.73	0.278	4.26	0.68	0.79
0.08	1260	1.30	1.06	0.340	4.80	0.685	0.83
0.16	960	3.15	2.50	0.88	5.00	0.67	
0.40	273	7.8	5.21	3.08	3.50	0.72	$\sim$
0.82	180	16.8	9.88	8.28	2.80	0.79	1.0
1.5	60	31.5	16.7	16.8	2.50	0.80	
2.5	60	52	27.8	31.2	2.35	0.87	
7.6	30	146	90.0	86.0	2.63	0.90	

results of Dodd and Steacie (6). For these experiments the *incident* intensity was kept constant and the pressure was varied from 25 to 0.05 mm. The values of ϕ_{CO} in the last column of Table IV were determined in the usual way at higher pressures. The absorbed intensity at lower pressures was obtained by a Beer's law extrapolation.

Table V gives the results of experiments at 27°C. and varying intensities at four different pressures (from 0.6 to 4.7 mm.). The results are given in Fig. 4 in the form of a plot of $\log R_{CH_4}/R^{\frac{1}{2}}_{C_2H_6}$ against the logarithm of the *incident*

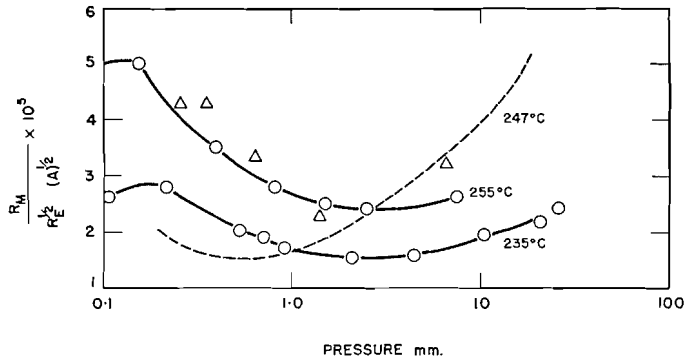

FIG. 3. The photolysis of acetone at higher temperatures and low pressures.
Dotted curve—results of Dodd and Steacie in an "unpacked" cell.
Triangles—Dodd and Steacie "packed" cell.
Circles—present work in "packed" cell.

TABLE V

EFFECT OF INTENSITY AT 27°C. AND LOW PRESSURES
Unpacked cell

Incident intensity	Pressure, mm.	Time, min.	Rate, molecules/cc./sec. $\times 10^{-10}$ CO	CH_4	C_2H_6	$\frac{R_{CH_4}}{R^{\frac{1}{2}}_{C_2H_6}} \times 10^{-3}$
8	0.6	8190	0.125	0.0168	0.285	3.14
50	0.56	1260	0.51	0.0685	1.62	5.4
100	0.6	1100	1.32	0.148	3.60	7.8
400	0.6	150	6.85	0.74	19.8	16.2
1000	0.6	63	20.9	2.0	59.0	26.0
8	1.25	4250	0.24	0.0235	0.56	3.15
20	1.25	2800	0.31	0.039	1.02	3.85
50	1.25	1370	0.81	0.111	3.35	6.1
1000	1.25	70	29.5	2.8	90.0	29.5
8	3.25	2675	0.41	0.0476	1.025	4.7
20	3.3	1120	0.95	0.1022	3.20	5.72
50	3.2	1095	1.90	0.235	7.60	8.5
400	3.0	75	10.6	1.80	58.5	23.5
1000	3.1	35	54.8	5.55	217	37.8
8	4.7	2715	0.760	0.075	1.55	6.0
20	4.75	1430	0.965	0.138	3.57	7.3
50	4.65	1122	2.68	0.354	11.2	10.6
250	4.8	133	22.8	2.4	93.0	25.0
1000	4.7	30	111	9.5	380	49.0

intensity. The lowest incident intensity is about eight times the lowest intensity used for the runs at usual pressures (Table III).

Since we were interested in possible wall reactions, the experiments given in Table IV were done. It is evident from Fig. 3 that the results agree excellently with those of Dodd. They confirm the fact that while the ratio $R_{CH_4}/R^{\frac{1}{2}}_{C_2H_6}$ [Acetone]$^{\frac{1}{2}}$ falls with decreasing pressure in agreement with the assumption that the recombination of methyl radicals is becoming pressure-dependent,

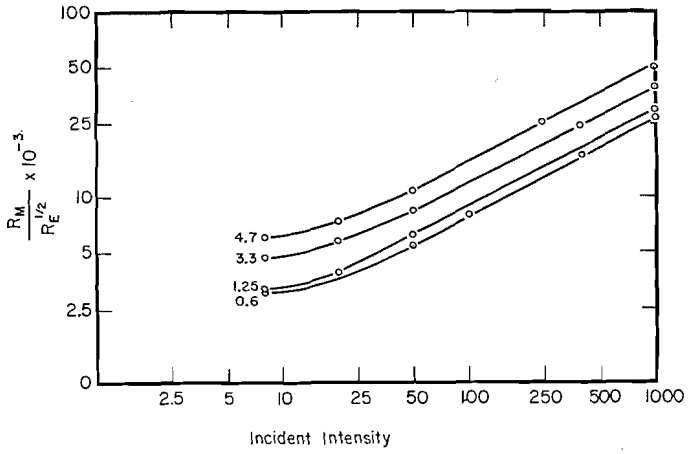

FIG. 4. Photolysis of acetone at 27°C. and low pressures, with varying intensity. The figures on the curves refer to the pressure in mm.

nevertheless at low pressures the ratio rises again instead of becoming constant. This increase commences at higher pressures in the packed cell, and there is no doubt that it is due to a wall reaction which produces methane. The only reasonable possibility seems to be a reaction between methyl radicals and adsorbed acetone. The results appear to indicate that the ratio decreases again at the lowest pressures, but it is difficult to be sure that this effect is real.

It may be mentioned that there is a gradual drop in the ratio $(\frac{1}{2}CH_4+C_2H_6)/CO$ with decrease in pressure in the packed vessel. No such effect was observed in the unpacked cell. We are unable to offer any convincing explanation of this.

The experiments at high intensities and room temperature, given in Table V, were done to obtain more information about the occurrence of reaction [4].

In this temperature region we are primarily concerned with the reactions:

$$CH_3+CH_3COCH_3 \rightarrow CH_4+CH_2COCH_3 \quad [1]$$

$$2CH_3 \rightarrow C_2H_6 \quad [2]$$

$$CH_3+CH_3CO \rightarrow CH_4+CH_2CO \quad [4]$$

$$2CH_3CO \rightarrow CH_3CHO+CH_2CO \quad [5]$$

$$CH_3+CH_3CO \rightarrow CH_3COCH_3 \quad [6]$$

$$2CH_3CO \rightarrow CH_3COCOCH_3 \quad [7]$$

As a *very rough approximation*, at constant temperature and pressure but varying intensity, we may put $[CH_3CO] \propto [CH_3]$, and thus $[CH_3CO] \propto I_{abs}^{\frac{1}{2}}$. Whence, if all methane is formed by [1] and [4], we have *at low pressures*

$$\frac{R_{CH_4}}{R_{C_2H_6}^{\frac{1}{2}}} = \frac{k_4}{k_2^{\frac{1}{2}}}[\text{Acetone}] + \frac{k_4}{k_2^{\frac{1}{2}}}[CH_3CO]$$

so that at constant low pressure and varying intensity

$$\frac{R_{CH_4}}{R_{C_2H_6}^{\frac{1}{2}}} = k'+k''I_{abs}^{\frac{1}{2}}$$

Since for constant acetone pressure $I_{\text{incident}} \propto I_{\text{abs}}$, $R_{CH_4}/R_{C_2H_6}^{\frac{1}{2}}$ will become constant at low incident intensities and proportional to $I^{\frac{1}{2}}$ at high intensities. Fig. 4 gives a plot of $\log R_{CH_4}/R_{C_2H_6}^{\frac{1}{2}}$ against log intensity for four different low pressures. At high intensities a series of straight lines is obtained with a slope of $\frac{1}{2}$, while at low intensities the ratio approaches a constant value. This furnishes further strong support for the postulation of reaction [4].

REFERENCES

1. AUSLOOS, P. and STEACIE, E. W. R. Bull. soc. chim. Belges, 63: 87. 1954.
2. AUSLOOS, P. and STEACIE, E. W. R. Can. J. Chem. 32: 593. 1954.
3. AUSLOOS, P. and STEACIE, E. W. R. Can. J. Chem. 33: 39. 1955.
4. AUSLOOS, P. and STEACIE, E. W. R. Can. J. Chem. 33: 31. 1955.
5. AUSLOOS, P. and STEACIE, E. W. R. Can. J. Chem. In press. 1955.
6. DODD, R. E. and STEACIE, E. W. R. Proc. Roy. Soc. (London), A, 223: 283. 1954.
7. DORFMAN, L. M. and NOYES, W. A., Jr. J. Chem. Phys. 16: 557. 1948.
8. KISTIAKOWSKY, G. B. and ROBERTS, E. K. J. Chem. Phys. 21: 1637. 1953.
9. LINNEL, R. H. and NOYES, W. A., JR. J. Am. Chem. Soc. 73: 3986. 1951.
10. NICHOLSON, A. J. C. J. Am. Chem. Soc. 73: 3981. 1951.
11. NOYES, W. A., JR. J. Phys. & Colloid Chem. 55: 925. 1951.
12. TROTMAN-DICKENSON, A. F. and STEACIE, E. W. R. J. Chem. Phys. 18: 1097. 1950.

CONSTITUTION OF A HEMICELLULOSE FROM WHEAT BRAN[1]

By G. A. Adams[2]

ABSTRACT

The hemicellulose prepared from wheat bran by alkaline extraction was an acidic polysaccharide containing arabinose (50.0%), xylose (38.5%), and uronic acid (9.0%). Graded hydrolysis with 0.02 *N* oxalic acid preferentially released 65% of the arabinose with only a small simultaneous production of xylose. Hydrolysis of the full methylated hemicellulose yielded 2,3,4-tri-*O*-methyl-, 2,3-di-*O*-methyl-, 2-*O*-methyl-, and free D-xylose; 2,3,5-tri-*O*-methyl-, 2,5-di-*O*-methyl-, and probably 3- and 5-*O*-methyl-L-arabinose. These data, together with those from periodate oxidation, strongly suggested that the molecule was a highly branched araboxylan. Viscosity measurements and reducing power determinations indicated a degree of polymerization of 300.

Investigations in this laboratory of the polysaccharides of the wheat plant have included those of patent white flour (10), straw (1), and leaf (2). The present paper concerns the hemicelluloses of wheat bran. Early studies on bran by Schulze (12) established xylose and arabinose as major constituents, and more recently, Norris and Preece (9) have demonstrated that glucuronic acid is a minor component. It was now of interest to examine the constitution of this hemicellulosic material in greater detail.

A suitable starting material appeared to be "bee-wing" bran which has an unusually high pentosan content (3) and consists mainly of the outer coatings of the wheat grain with very little starch.

The bran, after extraction with alcohol:benzene (2:1) and ammonium oxalate, contained 46% pentosan and 5.6% lignin. Extraction with dilute alkali gave a crude water-soluble hemicellulose in 37% yield having a pentosan content of 68% and a lignin content of 3%. Acid hydrolysis showed that arabinose and xylose were the main sugars present along with minor amounts of glucose, galactose, and uronic acid. To test the possibility that these sugars represented separate pentosans and hexosans, fractionation methods designed to separate polysaccharides were applied. The copper complexing method which is more or less specific for segregating xylans (5) gave no precipitate with the crude bran hemicellulose. Extraction with 70% ethanol, as used by Aspinall *et al.* (4) for separating an arabinose-rich pentosan from esparto grass, removed only a small portion of bran hemicellulose which varied insignificantly in composition from the original material. When the crude hemicellulose was acetylated and the acetate fractionated from chloroform solution with petroleum ether, most of the product was recovered within a narrow solvent mixture range. Deacetylation and hydrolysis showed that the main fractions contained arabinose and xylose in a ratio of 1.0:0.78; glucose and galactose were present only in the more soluble fractions. Hence it appeared that the hexosans were not a part of the hemicellulose molecule. The same finding was reported pre-

[1]*Manuscript received September 24, 1954.*
Contribution from the Division of Applied Biology, National Research Laboratories, Ottawa. Issued as Paper No. 174. of Uses of Plant Products and as N.R.C. No. 3451.
[2]*With the technical assistance of A. E. Castagne.*

viously for wheat straw (1) and wheat leaf hemicellulose (2). Lack of separation of araban from xylan by the methods just described strongly suggested that the sugars were combined chemically within the same molecule.

Hydrolysis of the hemicellulose with 0.02 *N* oxalic acid preferentially removed L-arabinose units. The stability of the xylose residues to the acid treatment showed that they were in the usual pyranoside form, while the ready removal of 65% of the arabinose units indicated that they were predominantly in the furanoside configuration and also were located towards the outside of the molecule. Slow release of arabinose units after hydrolysis for two and one-half hours in 0.02 *N* oxalic acid indicated that about 35% of the total amount of this sugar was part of the central core of the hemicellulose molecule and was doubly attached to other sugar units.

The main purified hemicellulose fraction was methylated initially with dimethyl sulphate and sodium hydroxide and finally with methyl iodide and silver oxide to a methoxyl value of 38.4% (calculated for $C_7H_{14}O_4$: (OCH_3, 38.8%); $[\alpha]_D^{25}$ −80.4° (*c*, 1.1% in chloroform). Fractionation using chloroform – petroleum ether yielded 10 fractions; of these, a fully methylated product (OCH_3, 38.8%), comprising 32% of the total, was selected for further study. Methanolysis followed by acid hydrolysis yielded the following products: (I) methylated uronic acid (not studied further in this investigation); (II) D-xylose (three parts); (III) 2-*O*-methyl-D-xylose (four parts); (IV) 3- and 5-*O*-methyl-L arabinose (three parts) (?); (V) 2,3-di-*O*-methyl-D-xylose (four parts); (VI) 2,5-di-*O*-methyl-L-arabinose (seven parts); (VII) 2,3,4-tri-*O*-methyl-D-xylose (five parts); (VIII) 2,3,5-tri-*O*-methyl-L-arabinose (six parts).

The methylation data indicated a highly branched structure. Almost 40% of the arabinose appeared on hydrolysis as 2,3,5-tri-*O*-methyl-L-arabinose and therefore existed as end groups in the original hemicellulose. Although the monomethyl arabinose units were not positively identified, their presence indicated branch points in the molecule where other groups were attached. Arabinose linked 1,3- in the original hemicellulose appeared as 2,5-dimethyl arabinose to the extent of about 45% of the total. It was not possible to determine whether these units indicated a structure in which several arabinose units were joined or one in which both arabinose and xylose units occurred. However, the graded hydrolysis data supported the view that about 70% of the arabinose units were joined together in short branches or side chains which were removable with only a slight release of xylose. The decreased rate of acid hydrolysis, which yielded a resistant portion containing about 35% of the arabinose, was not considered due to the pyranose form of arabinose since no direct evidence for this type of structure was found among the methylated sugars. The branching character of the bran hemicellulose involved also the xylose component. The 2-*O*-methyl-D-xylose and unmethylated D-xylose represented single and double branch points respectively. However the number of xylose end groups accounted for only half of these branch points (Table IV) and the assumption must be made that the remainder were linked to arabinose units. The presence of a high proportion of the methylated xylose as 2,3-dimethyl xylose proved that the xylose units were linked 1,4- and were in the pyranose form. The

change in rotation of the methylated polysaccharide on hydrolysis, from highly negative (−82°) to positive (+69.2°), indicated that the sugar units were primarily in the β configuration.

Although a specific structure for this hemicellulose cannot be formulated, methylation data showed that the following sugar residues were present:

D-xyl. $p1\ldots$; $\ldots$ 4-D-xyl. $p1\ldots$; $\begin{matrix}\ldots 3-\\ \ldots 4-\end{matrix}$D-xyl. $p1\ldots$; $\ldots$ L-arab. $f1\ldots$; $\ldots$ 3-L-arab. $f1\ldots$; and in addition $\begin{matrix}\ldots 2-\\ \ldots 5-\end{matrix}$ L-arab. $f1\ldots$; and $\begin{matrix}\ldots 2-\\ \ldots 3-\end{matrix}$ L-arab. $f1\ldots$ are indicated.

Periodate oxidation results supported the methylation data as further evidence for a highly branched structure. The consumption of approximately 0.59 mole of periodate per mole of sugar showed that about half of the sugar residues did not consume periodate and hence had a high proportion of branch attachments. The original sugar residues which yielded 2,3-di-*O*-methyl-D-xylose, 2,3,4-tri-*O*-methyl-D-xylose, and 2,3,5-tri-*O*-methyl-L-arabinose would consume periodate and, based on the proportion present as shown by the methylation data, should consume 0.62 mole of periodate per sugar unit. The yield of formic acid (0.18 mole) calculated from the amount of trimethyl xylose present was in reasonable agreement with the measured yield (0.22 mole per sugar unit). The relatively large amounts of formic acid produced indicated a high proportion of end groups. Mild acid degradation of the hemicellulose, which initially released a large proportion of the arabinose, caused a 10% increase in periodate consumption and a 40% increase in formic acid production. Such effects could be caused by simple degradation of a xylan chain or by removal of arabinose end groups linked to xylose units which in turn became new end groups. Hydrolysis of the unoxidized portion of the hemicellulose released xylose and arabinose in about equal amounts; all the xylose and that portion of arabinose which yielded monomethyl arabinose (see Table IV) represented branched units in the original hemicellulose.

Estimations of the molecular weight of the bran hemicellulose were obtained by viscosity measurements and reducing power determinations. With the exception of the viscosity measurements in water, the results agreed reasonably well and suggested that the molecule contained about 300 sugar residues. This is the same order of magnitude as was suggested for the soluble pentosan of wheat flour (10).

Although wheat bran hemicellulose resembles that of straw (1) and leaf (2) in having the same component sugars, some marked differences are apparent. The wheat bran molecule is much larger, more highly branched, and contains more arabinose than xylose, with the arabinose unit being branched. Although positive proof has not been obtained that a mixture of araban and xylan is not present, the available data indicate that wheat bran hemicellulose is a highly branched araboxylan. The purified cellulase enzyme of *Myrothecium verrucaria* which readily hydrolyzed wheat straw xylan did not attack bran hemicellulose; this observation supported the view that no free xylan was present. Removal

of 70% of the arabinose units by mild acid hydrolysis of the hemicellulose did not initiate enzyme action, thus indicating that the predominantly xylan residue was sufficiently different in structure from wheat straw xylan to resist enzymatic attack.

EXPERIMENTAL

The following solvents (v/v) were used to separate the sugars and their derivatives: (*A*) ethyl acetate – pyridine – water (2:1:2); (*B*) methyl ethyl ketone – water (2:1); (*C*) ethanol–benzene–water (47:200:15); and (*D*) N-butanol–ethanol–water (40:11:19). The R_g values refer to 2,3,4,6-tetra-*O*-methyl-D-glucose.

Preparation of Hemicellulose from Wheat Bran

The bran* was extracted exhaustively with benzene–alcohol (2:1) followed by ethanol to remove pigments, lipids, and waxy substances. Water-soluble materials were removed by two four-hour extractions at 85°C. Pectic substances were extracted by ammonium oxalate (0.5%) at 85°C. in two three-hour extraction periods. The residue was thoroughly washed with warm water and dried with ethanol and ether.

Air-dry extracted bran (160 gm.) was extracted with stirring for 20 hr. at room temperature with 8 liters of 4% potassium hydroxide in an atmosphere of nitrogen. After recovery by filtration on cloth, the residue was subjected to a further extraction for 48 hr. The combined alkaline filtrates were brought to pH 7.0 with acetic acid and then concentrated under reduced pressure at 30°C. to one-tenth their original volume. Only a faint trace of precipitate appeared in the neutral solution. The thick brown solution was dialyzed in cellophane tubes against running water for 48 hr. The dialyzed solution was again concentrated under reduced pressure to one-half its original volume. The hemicellulose was recovered by adding 1 volume of the solution to 4 volumes of ethanol which was rapidly stirred and by allowing the mixture to stand. The precipitated hemicellulose was centrifuged off and dried with ethanol and ether to yield a fluffy gray powder (60 gm.). Acid hydrolysis of the crude hemicellulose followed by chromatographic separation of the sugars (solvent *A*) showed the presence of xylose, arabinose, and glucose, with small amounts of galactose and uronic acids.

Purification Treatments on Crude Hemicellulose

Ethanol (70%) extraction.—Crude hemicellulose (25 gm.) was extracted under reflux with 1000 ml. of 70% ethanol for 24 hr. A fine precipitate which appeared on cooling the alcoholic solution was removed by centrifuging. Concentration of the solution at 30°C. to small volume yielded a light brown precipitate (wt. 0.7 gm.). After hydrolysis with 1% sulphuric acid and chromatographic separation of the sugars, the ratio of xylose to arabinose was 1.0:0.78, which was the same as that of the original hemicellulose. Hence no segregation of araban-rich material was achieved.

**The "bee-wing" bran was donated by Flour Mills of America Inc., Rosedale Mill, 914 Division St., Kansas City, Kansas, U.S.A.*

Copper complexing.—Crude hemicellulose (20 gm.) was dissolved with shaking in 4% sodium hydroxide (1250 ml.) and, to this solution, Fehling's solution (1250 ml.) was added with stirring. Even on prolonged standing no insoluble copper hemicellulose complex formed. Variation in ratio between the alkaline hemicellulose solution and Fehling's solution from 1:1 to 4:1 failed to yield an insoluble compound. By acidification, dialysis, and precipitation with ethanol, the original hemicellulose sample was recovered with its xylose to arabinose ratio unchanged.

Acetylation of crude hemicellulose.—Crude hemicellulose (50 gm.) was dispersed in 1000 ml. of formamide, stirred for two hours at 65°C., cooled to room temperature (20°C.), and 1000 ml. of dry pyridine added. After one hour's stirring, acetic anhydride (400 ml.) was added in 100 ml. quantities over a period of four hours. The acetylated product was recovered by pouring into ice water. After recovery and thorough drying, the partly acetylated hemicellulose was dissolved in pyridine and reacetylated with acetic anhydride. The acetylated product was recovered as before, yield 67.4 gm., acetyl content 38.3%.

Fractionation of hemicellulose acetates.—Acetylated hemicellulose (65 gm.) was dissolved in 3000 ml. of chloroform and filtered through sintered glass (porosity M). To the chloroform solution of the acetates, petroleum ether (b.p. 65–110°C.) was added with vigorous stirring. After the formation of a distinct cloudiness, the material was allowed to settle, removed by centrifuging, and dried *in vacuo*. A total of nine fractions were recovered with the bulk of the material precipitating in a fairly narrow solvent range. Fractions 3–5 inclusive comprised 80% of the acetates with fraction 4 being approximately 60%.

Analysis of the acetylated fractions.—The nine fractions were deacetylated with sodium hydroxide in acetone, precipitated with ethanol, and dried. Acid hydrolysis followed by quantitative chromatography (solvent *A*) showed that all fractions contained arabinose and xylose in an approximate ratio of 1.0:0.78. In addition, fractions 7, 8, and 9 contained small amounts of glucose and galactose. Fractions 2–6 inclusive contained approximately 9% uronic acid while fractions 7–9 contained about 3.5%. Since fraction 4 comprised 60% of the original hemicellulose and contained no hexose sugars, it was selected for the main constitutional studies. Its composition was as follows: ash, nil; nitrogen, nil; lignin, 0.9%; methoxyl, 1.06%; uronic acid anhydride, 9.00%; D-xylose, 38.5%; L-arabinose 50.0%; and $[\alpha]_D^{25}$ −83° (*c*, 1% in potassium hydroxide (2%)).

Graded Acid Hydrolysis

A concentration of 0.02 *N* oxalic acid was found to give preferential release of arabinose and was therefore selected as the most satisfactory concentration for graded hydrolysis of the hemicellulose. Three separate lots of hemicellulose (50 mgm.) were hydrolyzed with 0.02 *N* oxalic acid (5 ml.) at 98°C. with heating periods of two and one-half, four, and six hours respectively. After hydrolysis each solution was analyzed chromatographically for arabinose and xylose content (Table I). The unhydrolyzed portions (acid degraded hemi-

TABLE I

GRADED HYDROLYSIS OF BRAN HEMICELLULOSE WITH 0.02 *N* OXALIC ACID

Hydrolysis time, hr.	Percentage individual sugars released	
	Arabinose	Xylose
2.5	67.5	14.2
4.0	70.0	21.9
6.0	75.6	28.6

TABLE II

YIELD AND COMPOSITION OF ACID DEGRADED HEMICELLULOSES FROM GRADED HYDROLYSIS OF BRAN HEMICELLULOSE

Sample No.	Hydrolysis time, hr.	Yield, %	Composition	
			Arabinose, %	Xylose, %
I	2.5	60.0	33.8	56.9
II	4.0	51.3	30.7	60.1
III	6.0	44.6	28.8	64.4

celluloses I, II, and III) were recovered by complete precipitation with ethanol without any attempted fractionations, dried *in vacuo*, and weighed. These materials were completely hydrolyzed with 1% sulphuric acid and the proportion of arabinose and xylose determined by chromatographic analysis (Table II).

Enzyme Hydrolysis

The original bran hemicellulose and acid degraded hemicelluloses I and II were made up to 1% concentration in 1/25 *M* sodium chloride and the pH adjusted to 5.0 with hydrochloric acid. The purified cellulase enzyme of *Myrothecium verrucaria* in 1/25 *M* sodium chloride solution was added to the extent of 100 μgm. protein per ml. of substrate and incubated for 12 hr. at 30°C. with agitation. At the end of the incubation period, 2 volumes of hot ethanol were added to the substrate, the solution filtered, and the filtrate concentrated to a small volume at 40°C. Chromatographic examination of the solution showed only a trace of arabinose and xylose.

Methylation

Hemicellulose (20 gm.) was methylated with dimethyl sulphate and sodium hydroxide (40%) by a method previously described in detail (1). After each of two successive methylation treatments, the partly methylated crude product was recovered by neutralization, dialysis, and evaporation. After the material had been sufficiently methylated (nine treatments) to become soluble in methyl iodide, it was subjected to further methylation by Purdie's reagent. After four methylations with this reagent the methoxyl content was 38.3%. Further methylations increased the methoxyl content only slightly. The final

product was a friable yellow solid, yield 21.2 gm.; OCH_3, 38.4% (theoretical value for dimethyl xylan, 38.7%); $[\alpha]_D^{25}$ −80.4° (*c*, 1.1% in chloroform).

Fractionation.—The methylated hemicellulose (20.2 gm.) was extracted under reflux for a period of two hours with solvent mixtures of chloroform – petroleum ether (b.p. 30–60°C.). After filtration and removal of the solvent, the recovered product was dried *in vacuo* at 40°C. The results of the fractionation are given in Table III. Since fraction 8 comprised a large proportion of the product and was fully methylated, it was used in the subsequent studies of the methanolysis products.

TABLE III

FRACTIONATION OF METHYLATED BRAN HEMICELLULOSE

Fraction	Chloroform: petroleum ether solvent mixture	Yield, %	OCH_3, %	$[\alpha]_D^{25}$
1	0 : 100	0.52	22.6	− 5.48
2	20 : 180	0.41	23.3	−11.05
3	25 : 175	1.03	30.6	−11.30
4	30 : 170	1.85	37.1	−32.4
5	35 : 165	6.24	38.6	−81.0
6	40 : 160	25.79	38.7	−87.1
7	45 : 155	22.9	38.7	−80.0
8	50 : 150	32.50	38.8	−82.1
9	55 : 145	5.67	37.7	−80.0
10	100 : 0	1.23	35.0	−79.5

Methanolysis.—Fraction 8 (100 mgm.) was heated with methanolic hydrogen chloride (10 ml.; 8%) in a sealed tube in a boiling water bath for 16 hr. After removal of the solvent, the methyl glycosides were hydrolyzed with hydrochloric acid (10 ml.; 0.5 *N*) for eight hours at 100°C. The free methylated sugars ($[\alpha]_D^{25}$ +69°) were recovered and separated chromatographically on filter paper using solvent *B*. The sugar spots were developed with aniline phthalate spray. Authentic specimens of 2-*O*-methyl-D-xylose, 2,3-di-*O*-methyl-D-xylose, 2,3,5-tri-*O*-methyl-L-arabinose, and 2,3,4-tri-*O*-methyl-D-xylose were used as reference compounds. A total of eight sugar derivatives were located on the chromatogram and the following tentative identifications were made based on color reactions and positions relative to the reference compounds: methylated uronic acid (I); D-xylose (II); a monomethyl pentose corresponding to 2-*O*-methyl-D-xylose (III); monomethyl pentose (IV);

TABLE IV

COMPOSITION OF HYDROLYZATE FROM METHYLATED HEMICELLULOSE

Component sugar	Molar composition, %	Simple molar ratio
D-Xylose (II)	9.5	3
Monomethyl pentose (III)	12.0	4
Monomethyl pentose (IV)	9.0	3
Dimethyl pentose (V)	12.5	4
Dimethyl pentose (VI)	22.0	7
Trimethyl pentose (VII)	15.0	5
Trimethyl pentose (VIII)	18.0	6

dimethyl pentose corresponding to 2,3-di-*O*-methyl-D-xylose (V); dimethyl pentose (VI); a trimethyl pentose corresponding to 2,3,4-tri-*O*-methyl-D-xylose (VII); a trimethyl pentose corresponding to 2,3,5-tri-*O*-methyl-L-arabinose (VIII). The free methylated sugars were extracted from quantitative chromatograms with water and analyzed by the alkaline hypoiodite method (5). The results are given in Table IV.

Separation of the Methylated Sugars

To provide sufficient material for separation and identification of the products of methanolysis, a large quantity was prepared as follows: Fraction 8 (6.4 gm.) was refluxed with 285 ml. of methanolic hydrogen chloride (8%) until the rotation became constant ($[\alpha]_{25}^{D}$ +9.2°). After neutralization with silver carbonate, the methyl glycosides and uronosides were recovered as a brown sirup (6.7 gm.). Saturated barium hydroxide (75 ml.) was added to the sirup and the mixture heated for three hours at 60°C. on a steam bath. Excess barium hydroxide was removed with carbon dioxide and the solution heated for 15 min. at 85°C. Because of the volatility of the trimethyl pentosides, the solution was evaporated at room temperature in a current of air.

Recovery and Separation of Trimethyl Pentoses

Extraction of the methanolysis mixture with *n*-pentane removed the trimethyl pentosides almost quantitatively. They were hydrolyzed with 0.5 *N* hydrochloric acid and the free methylated sugars (1.86 gm.) were recovered in the usual way. Chromatography on filter paper showed that the two trimethyl pentoses contained a trace of a dimethyl pentose. A portion of the trimethyl pentose sirup (0.65 gm.) was separated chromatographically on large sheets of filter paper using solvent *C*. The individual sugars were recovered by elution with water and each solution concentrated to a small volume. Addition of methanol and clarification with charcoal yielded clear yellowish sirups VII and VIII.

Separation of Remaining Sugars

Although solvent *B* separated methylated uronic acids (barium salt form) and methylated sugars satisfactorily in small amounts, the uronic acid streaked into the xylose and two monomethyl pentose spots when the sirup was chromatographed in preparative quantities (conversion of the barium salt to the free acid did not improve the separation). The free xylose and monomethyl pentose areas on the paper which were overrun with uronic acid were cut out, eluted with water, and chromatographed again using solvent *A*. This procedure gave satisfactory separation of the methylated uronic acid (I), free xylose (II), and the two monomethyl pentoses (III) and (IV). The dimethyl pentoses were separated from each other satisfactorily in the first chromatogram using solvent *B*.

Examination of the Methylated Sugar Fractions

Fraction I.—This material was a methylated uronic acid complex which gave a cherry red spot on the paper chromatogram. It was not examined further in the present study.

Fraction II.—The sirup, on standing, crystallized almost completely. Recrystallization from glacial acetic acid yielded a crop of D-xylose crystals, m.p. 145–146°C. unchanged on admixture with an authentic sample, and $[\alpha]_D^{25}$ +19° (*c*, 1.0% in water). Chromatographic examination (solvent *A*) showed only xylose present. This fraction was therefore established as D-xylopyranose.

Fraction III.—On clarification with charcoal in methanol, a clear yellow sirup was obtained which partially crystallized on standing. Chromatography showed only one component with the same R_g value as 2-*O*-methyl-D-xylose (R_g 0.22–0.24, solvent *B*). On demethylation with hydrobromic acid (48%) (9), D-xylose was the only sugar produced. Recrystallization from methanol solution yielded 2-*O*-methyl-D-xylopyranose, m.p. 133°C., $[\alpha]_D^{25}$ + 34.8° (*c*, 1% in water). Analysis: calculated for $C_6H_{12}O_5 : OCH_3$, 18.9%; found: OCH_3, 18.8%. Treatment of this sugar with aniline in ethanol gave crystalline 2-*O*-methyl-N-phenyl-xylosylamine, m.p. 123°. The X-ray diffraction pattern of the crystals was identical with that of an authentic sample of 2-*O*-methyl-N-phenyl-xylosylamine.

Fraction IV.—This sirup was re-chromatographed on filter paper (solvent *B*) until only one spot was present. (R_g 0.37–0.38, solvent *B*; 0.68–0.69, solvent *D*). On spraying with aniline oxalate reagent a reddish color characteristic of pentose sugars was obtained. Demethylation with hydrobromic acid (48%) yielded only arabinose. The sirup (104 mgm.) was distilled (b.p. 140–150°C. at 0.05 mm.) to yield a product (74 mgm.) having methoxyl content 19.3% (calculated for $C_6H_{12}O_5 : OCH_3$, 18.9%) and $[\alpha]_D^{25}$ −4° (*c*, 1.75% in water). Hence the sirup was a monomethyl arabinose. Oxidation with lead tetraacetate (11) yielded 2 moles of formic acid and no formaldehyde. These results are most readily interpreted as indicating the presence of a mixture of 3- and 5-methyl arabinose.

Fraction V.—After repeated chromatographic separations, a sirup was recovered which had $[\alpha]_D^{25}$ +24° (*c*, 1.0% in water); η_D^{25} 1.4733; OCH_3, 34.8% (calculated for $C_7H_{14}O_5 : OCH_3$, 34.8%). With solvent *B* the R_g value was 0.67–0.68 and only a single pink spot was found with aniline phthalate spray on the paper chromatogram. Demethylation of the sirup (12 mgm.) with hydrobromic acid yielded only xylose. Oxidation of the sirup (80 mgm.) with bromine yielded a lactone which was converted into the corresponding crystalline amide with methanolic ammonia. On recrystallization from ethyl acetate 2,3-di-*O*-methyl xylonamide was recovered, m.p. and mixed m.p. 134°. The X-ray diffraction pattern was identical with that of authentic 2,3-di-*O*-methyl xylonamide. A crystalline anilide was prepared having m.p. 123–124°C. and an X-ray diffraction pattern identical with that of 2,3-di-*O*-methyl-N-phenyl-xylosylamine. Fraction V was, therefore, 2,3-di-*O*-methyl-D-xylose.

Fraction VI.—This sirup gave only one spot on chromatographic examination (R_g 0.80–0.81 solvent *B*; 0.88–0.89, solvent *D*); $[\alpha]_D^{25}$ −26° (reported value −18° (6)); OCH_3, 34.4% (calculated for $C_7H_{14}O_5 : OCH_3$, 34.8%). Demethylation yielded only one sugar which was identified as arabinose on paper chromatogram. Oxidation of the free sugar (173 mgm.) with bromine for 48 hr. at

room temperature yielded a lactone (126 mgm.). Distillation of the sirupy lactone (b.p. (bath) 130°–135°C. at 0.05 mm.) yielded a product which crystallized on seeding with a crystal of 2,5-di-*O*-methyl-L-arabonolactone, m.p. and mixed m.p. 60°C. The X-ray diffraction pattern was the same as that of 2,5-di-*O*-methyl-L-arabonolactone. Treatment of the lactone (33 mgm.) with methanolic ammonia gave the corresponding amide which on recrystallization from absolute ethanol yielded 2,5-di-*O*-methyl-L-arabonamide (24 mgm.), m.p. 130–131°. To another portion of the lactone (48 mgm.) phenylhydrazine (18 mgm.) in methanol (5 ml.) was added and the mixture refluxed two and one-half hours. After removal of the solvent, the sirup crystallized and recrystallization from alcohol–ether yielded a pure product (34 mgm.), m.p. 165–167° undepressed on admixture with an authentic sample of 2,5-di-*O*-methyl-L-arabinose phenylhydrazide. The X-ray diffraction pattern was identical with that of the authentic sample. Fraction VI, therefore, was 2,5-di-*O*-methyl-L-arabinose.

Fraction VII.—Purification of this sirup by paper chromatography using solvent *C* yielded a single sugar which gave a pink spot on spraying with aniline phthalate (R_g value was 0.86–0.88 solvent *C*). Demethylation showed xylose to be the only component sugar. On standing the sirup partially crystallized. Recrystallization from ethyl ether containing a small amount of petroleum ether yielded 2,3,4-tri-*O*-methyl-D-xylopyranose, m.p. 89–90°C. undepressed on admixture with an authentic sample, and $[\alpha]_D^{25}$ +20° (*c*, 1.0% in water); OCH_3, 48.2% (calculated for $C_8H_{16}O_5$: OCH_3, 48.4%).

Fraction VIII.—The sirup had an R_g 1.10–1.12 (solvent *B*) identical with that of 2,3,5-trimethyl arabinose; $[\alpha]_D^{25}$ −36°; OCH_3, 48.7% (calculated for $C_8H_{16}O_5$: OCH_3, 48.4%). Oxidation of the sugar with bromine yielded the corresponding lactone which on refluxing with methanolic ammonia was converted into the corresponding amide. Recrystallization of the amide yielded 2,3,5-tri-*O*-methyl-L-arabonamide, m.p. and mixed m.p. 137–138°C. and $[\alpha]_D^{25}$ +18 (*c*, 1.0% in water); OCH_3 44.7% (calculated for $C_8H_{17}O_5N$: OCH_3, 44.9%). The X-ray diffraction pattern showed that the product was 2,3,5-tri-*O*-methyl-L-arabonamide.

Periodate Oxidation

Bran hemicellulose (fraction 4) and acid degraded hemicelluloses I and II (100 mgm. each) were oxidized with 100 ml. of sodium metaperiodate (1%). All oxidations were done in the dark at 16°C. with shaking. Analyses for periodate consumption and formic acid production were made at various time intervals (5). The results are given in Table V.

In a separate experiment 50 mgm. of the original hemicellulose was oxidized to completion with periodate. On freezing and thawing of the solution, the unoxidized portion of the hemicellulose precipitated out and, when washed with ice water and dried with ethanol and ether, yielded a white product (wt. 40 mgm.). Hydrolysis of this polysaccharide with 1% sulphuric acid and separation of the sugars by chromatography yielded arabinose (38%), xylose (52%).

TABLE V

PERIODATE OXIDATION OF BRAN HEMICELLULOSE

	Time, hr.						
	48	72	96	120	144	168	192
Original hemicellulose Periodate consumed,* moles per $C_5H_8O_4$	—	0.58	—	0.58	0.58	0.58	0.59
Formic acid produced, moles per $C_5H_8O_4$	—	0.20	—	0.21	0.22	0.24	0.24
Acid degraded hemicellulose I Periodate consumed, moles per $C_5H_8O_4$	0.65	—	0.65	—	0.65	—	0.65
Formic acid produced, moles per $C_5H_8O_4$	0.29	—	0.32	—	0.33	—	0.34
Acid degraded hemicellulose II Periodate consumed, moles per $C_5H_8O_4$	—	0.62	0.65	—	0.64	0.65	0.66
Formic acid produced, moles per $C_5H_8O_4$	—	0.33	0.34	—	0.36	0.36	0.37

**Corrected for periodate consumed in formic acid production.*

Estimation of Degree of Polymerization

Viscosity measurements.—Viscosity measurements were made on three preparations, bran hemicellulose in water solution and in cupriethylenediamine solution, and bran hemicellulose acetate in acetone solution. The solutions used contained 0.50, 0.25, 0.125, 0.0625, and 0.0317% of the component. The measurements were made in Oswald-Cannon-Fenske viscometers in a water bath at 25°C.±0.02°C. Intrinsic viscosity $[\eta]$ was obtained by plotting η_{sp}/c against c (gm./liter). The results were calculated from Staudinger's equation using a K_m factor of 5.0×10^{-4} as proposed for xylans by Husemann (8). The degree of polymerization (P) for the hemicellulose in cupriethylenediamine solution and for the acetate in acetone solution was approximately 300. On the other hand, the value of P for hemicellulose in water was approximately 1000; this value suggested probable association of the molecules.

Reducing power.—The copper reduction method of Somogyi (13) was used for determination of reducing power of three samples of bran hemicellulose (29.6, 39.0, and 45 mgm. respectively). Increasing the reaction period from 30 min. to one hour did not affect the results. Based on the reducing power estimation, the hemicellulose contained one reducing group per 300±10 sugar units. A similar measurement based on estimation of reducing power by alkaline hypoiodite oxidation (5) gave a result of one reducing group for each 250 units.

ACKNOWLEDGMENTS

The author wishes to thank Dr. J. K. N. Jones, Queen's University, for samples of 2,5-di-*O*-methyl-L-arabonolactone, 2,5-di-*O*-methyl-L-arabonamide,

and 2,5-di-*O*-methyl-L-arabinose phenylhydrazide. Dr. D. R. Whitaker of this Division kindly supplied the purified cellulase enzyme.

REFERENCES

1. ADAMS, G. A. Can. J. Chem. 30: 698. 1952.
2. ADAMS, G. A. Can. J. Chem. 32: 186. 1954.
3. ADAMS, G. A. and CASTAGNE, A. E. Can. J. Research, B, 26: 314. 1948.
4. ASPINALL, G. O. and MAHOMED, R. S. J. Chem. Soc. 1731. 1954.
5. CHANDA, S. K., HIRST, E. L., JONES, J. K. N., and PERCIVAL, E. G. V. J. Chem. Soc. 1289. 1950.
6. HIRST, E. L., PERCIVAL, E. G. V., and WYLAM, C. B. J. Chem. Soc. 189. 1954.
7. HOUGH, L., JONES, J. K. N., and WADMAN, W. H. J. Chem. Soc. 1702. 1950.
8. HUSEMANN, E. J. prakt. Chem. 155: 13. 1940.
9. NORRIS, F. W. and PREECE, I. A. Biochem. J. (London), 24: 59. 1930.
10. PERLIN, A. S. Cereal Chem. 28: 382. 1951.
11. PERLIN, A. S. J. Am. Chem. Soc. 76: 5505. 1954.
12. SCHULZE, E. Z. physiol. Chem. (Hoppe-Seyler's), 16: 387. 1892.
13. SOMOGYI, M. J. Biol. Chem. 160: 61. 1945.

STUDIES IN THE POLYOXYPHENOL SERIES

VII. THE OXIDATION OF VANILLIN WITH SODIUM CHLORITE AND CHLORINE DIOXIDE[1]

By R. M. Husband,[2] C. D. Logan,[3] and C. B. Purves

ABSTRACT

Vanillin almost instantly reduced 1.2 to 1.5 moles of aqueous chlorine dioxide at 20°C. or 5°C. and any pH between 1.2 and 6.5, and a white crystalline substance with the composition of a dihydroxyvanillin, $C_7H_5O_4(OCH_3)$, was isolated in roughly 25% yield independently of the pH. When oxidized with aqueous sodium chlorite at 20°C. and pH 0.5, these crystals gave another crystalline substance with the composition of a dihydroxyvanillic acid, $C_7H_5O_5(OCH_3)$. Although both these substances decomposed readily to red oils and then to brown powders free of methoxyl groups, seven well characterized derivatives were prepared. The results showed that the substances were unsaturated, monohydroxy, diketone tautomers of a dihydroxyvanillin and the corresponding dihydroxyvanillic acid, but precise structures could not be assigned. Parallel oxidations of vanillin with aqueous sodium chlorite at 20°C. and pH 6 proceeded at a negligible rate, but near pH 5 a reaction that often seemed autocatalytic produced about 19% of 5-chlorovanillin. At pH 4 the aldehyde $C_7H_5O_4(OCH_3)$ was isolated in 19% yield; at pH 1 this aldehyde (15%) was mixed with 7.7% of the corresponding acid $C_7H_6O_5(OCH_3)$, but at pH 0.5 the latter alone was produced (28%). Chlorine dioxide and sodium chlorite therefore differed markedly in their oxidizing action and in the effect of pH upon it. When acting on vanillin, both oxidants also produced deep red, unstable oils with quinone-like properties and often containing chlorine.

INTRODUCTION

The earliest study of the action of chlorine dioxide on an organic substance was published in 1881 by Fürst (4), who noticed that the gas reacted rapidly with ethylene exposed to bright sunlight. Schmidt and his collaborators (17, 18, 19) used aqueous chlorine dioxide to remove lignin (a condensed phenolic ether) from wood, and extended Fürst's observation to many unsaturated aliphatic compounds and to phenols. Catalytic amounts of vanadium trichloride were sometimes used in these oxidations (19). The work of Fuchs and Honsig (3), later extended by Sarkar (15), showed that phenolic ethers and esters were oxidized by aqueous chlorine dioxide at a much slower rate than the phenols themselves, and that the oxidation products included carbon dioxide, oxalic acid, maleic acid, and small amounts of undefined, chlorinated compounds. With the exception of thio compounds and those containing reactive methylene groups, all saturated aliphatic substances examined, including polysaccharides and reducing sugars, were stable to aqueous chlorine dioxide. All of the above research was of a qualitative nature, and the hydrogen ion concentration was in no case controlled.

Since an acidified solution of sodium chlorite displayed the same selectivity as an oxidant, and spontaneously decomposed to chlorine dioxide, the assump-

[1]*Manuscript received September 21, 1954.*
Contribution from the Division of Industrial and Cellulose Chemistry, McGill University, and from the Wood Chemistry Division, Pulp and Paper Research Institute of Canada, Montreal, Que. Abstracted from Ph.D. theses submitted to the University in September 1947 by R. M. H., and in May 1949 by C. D. L.
[2]*Present address: State University of New York, College of Forestry, Syracuse 10, New York.*
[3]*Present address: The Ontario Paper Company, Limited, Thorold, Ontario.*

tion was often made that chlorine dioxide was the active agent in this case also. Jeanes and Isbell (7), however, observed that sodium chlorite oxidized aldose sugars quantitatively to the aldonic acids at a rate which increased as the pH decreased from 8, but that aqueous chlorine dioxide did so only with very great difficulty at any pH in the above range. Although chlorites and chlorine dioxide are now used to bleach cellulose pulps free from residual lignin, the above résumé shows that detailed knowledge concerning their oxidizing action on phenols and phenolic ethers is still exceedingly scanty. Information concerning vanillin, for example, is restricted to the remark that it is oxidized by chlorine dioxide (3, 15), and to the fact that a small yield of 2,4-furane dicarboxylic acid is formed in oxidations carried out with aqueous sodium chlorite near pH 3 (13). The present research had the object of extending these observations.

RESULTS AND DISCUSSION

The concentration of dilute aqueous solutions of sodium chlorite, buffered within 0.1 unit at various pH values and kept at 20°C., was determined from time to time by an iodometric method responsive to chlorite, chlorine dioxide, and hypochlorite, but not to chlorate. These solutions were stable for many hours except at pH 1, when loss by the volatilization of chlorine dioxide might sometimes have been appreciable. As the plots A in Fig. 1 show, aqueous

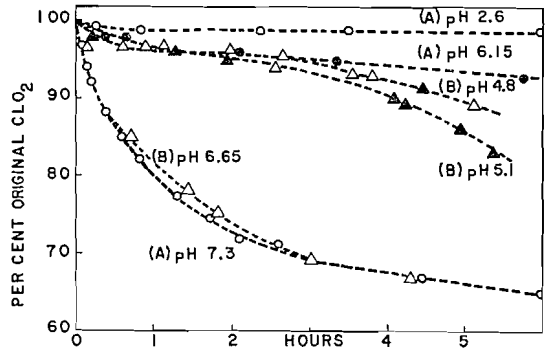

FIG. 1. Rate of decomposition of chlorine dioxide at 20°C. in aqueous 10% sodium acetate – acetic acid buffers. Plots A, 13.5 mM. of chlorine dioxide; plots B, 20 mM. to 25 mM., per liter.

solutions containing about 13.5 mM. of chlorine dioxide per liter were fairly stable on the acid side of pH 6, but at pH 7.3 decreased rapidly in strength owing to the formation of equimolecular amounts of chlorite and chlorate ion. The change was complete within 12 hr. More concentrated, 0.02 to 0.025 *M*, solutions of chlorine dioxide decomposed rather slowly when kept on the acid side of pH 4.5, but near pH 5 the decomposition assumed an autocatalytic form before becoming very rapid at pH 6.65 (plots B). This decomposition was among those reviewed by Taylor, White, Vincent, and Cunningham (22, 23) in their study of the inorganic chemistry of chlorine dioxide and chlorites. Taube and Dodgen (21) used radioactive chlorine to reveal the mechanisms involved when the oxidation state of the halogen changed.

A selection from more than thirty plots of the rate of reduction of the oxidant by vanillin is presented in Figs. 2 and 3, in which full lines refer to reductions of excess sodium chlorite, and broken lines to those of chlorine dioxide. Although the plots were corrected for the spontaneous decomposition of the oxidant, the rate of this decomposition might not be the same in the blank and in the presence of vanillin, since the residual concentrations at any time would be different. Moreover, most of the reductions were strongly exothermic, and it was difficult to keep the temperature at 20°C. during the initial period; the inorganic system was complex, and any quinone formed from the vanillin would interfere with the iodometric method used to determine the residual oxidant. Figs. 2 and 3, although reproducible, thus indicate merely the net change in the redox systems present, and details of the relevant estimations are omitted from this article.

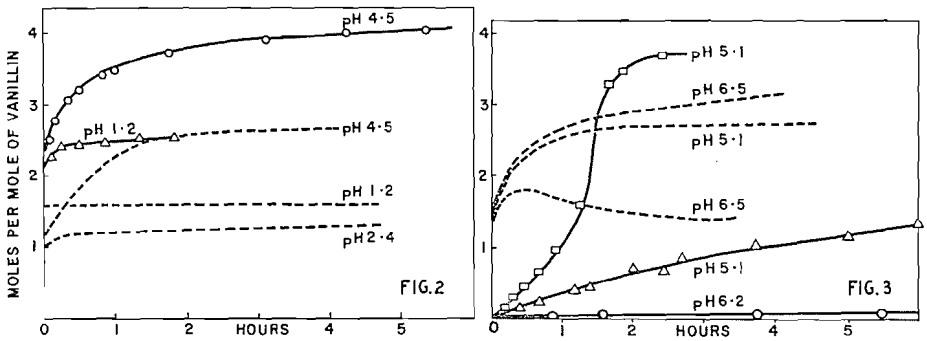

FIG. 2. Apparent rate of reduction of oxidant at 20°C. Solid lines: vanillin, 15 mM., and sodium chlorite, 60 mM. per liter. Broken lines: vanillin, 4 mM. and chlorine dioxide, 21 mM. to 29 mM. per liter.

FIG. 3. See legend for Fig. 2. Upper broken line at pH 6.5 uncorrected for chlorine dioxide blank. Upper solid line at pH 5.1, 65 mM. of sodium chlorite per liter; lower solid line at pH 5.1. 60 mM. per liter.

At pH 1.2, 1 mole of vanillin apparently reduced about 2.5 moles of sodium chlorite within a few minutes, and the reaction then became extremely slow. Although the initial rapid reduction was preserved at pH 4.5, a secondary reaction was now marked. When this experiment was repeated at 4°C., the initial reduction was almost unaffected, but the secondary one took more than two hours, instead of less than 20 min., to increase the total consumption of chlorite to 3.0 mole (not shown). The lower plot at pH 5.1 in Fig. 3 was obtained with the same concentration (60 mM. per liter) of sodium chlorite, but a slight increase in concentration to 65 mM. per liter produced the upper plot, whose form suggested an autocatalytic reaction. A reaction at pH 4.6 and 3°C. became apparently autocatalytic within two minutes, but this behavior was never observed on the alkaline side of pH 5.4, even when the concentration of chlorite was increased (not shown). In experiments carried out at pH 5.1 and 6°C., the initial, nearly linear portion corresponding to the consumption of about 1 mole of chlorite required 2.5 hr., instead of 1 hr.; and 4 hr., instead of about 1.5 hr., elapsed before the total consumption was 3.0 mole per mole of

vanillin. At 20°C. and on the alkaline side of pH 5.1, the linear portion of the plot decreased in slope very rapidly, until the consumption of 0.2 moles of chlorite required 14.25 hr. at pH 6.2. No odor of chlorine dioxide was ever noticed at any acidity in these oxidations until more than 2 moles of sodium chlorite per mole of vanillin had been utilized.

Figs. 2 and 3 (broken lines) also show that vanillin almost instantaneously reduced about 1.5 moles of chlorine dioxide at all pH values between 1.2 and 6.5. A slower secondary reduction was evident on the alkaline side of pH 4.5, but could not be even approximately assessed at pH 6.5 because the observed data (upper plot) gave an absurd result (lower plot) when corrected for the large and uncertain blank. The proper correction would probably have placed this plot close to that for the reduction at pH 5.1. This experiment differed from those carried out at pH values less than 6 in that a little by-product chlorate was formed, but aqueous potassium chlorate was found to have no action on vanillin at pH 6.9, 5.7, or even 2.6. When the plots in Figs. 2 and 3 were compared, it became evident that vanillin reduced approximately 1 mole more of sodium chlorite than of chlorine dioxide between pH 1 and pH 4.5 and at all times; between pH 5 and 6.5, however, the relationship was reversed. The course of the initial oxidation with sodium chlorite was highly sensitive to pH, whereas that with chlorine dioxide was apparently independent of this factor. The two oxidants were therefore by no means equivalent.

Much time was spent in attempts to isolate a crystalline product from the clear, bright red solutions that resulted when vanillin was oxidized with aqueous chlorine dioxide at pH 1 or pH 2.3. Such solutions, and also the unstable red oils isolated from them by evaporation or by extraction with ether, assumed a pale yellow color when reduced by sulphurous acid or by hydrogenation under mild conditions, and the red color was regenerated by the addition of benzoquinone or by the access of air. Condensations with aniline, *p*-anisidine, hydroxylamine, *o*-phenylenediamine, and diazotized anilines provided small yields of brown or black powders. The whole mass of observations suggested that the initial product of the oxidations was an unstable, methoxylated quinone that readily changed to brown, amorphous substances of lower methoxyl content. Eventually small yields of a white substance, melting at 101°C. and crystallizing as tufts of very fine needles or as prisms, were isolated. Success in isolating these crystals depended upon extracting the solution of the oxidized vanillin at the proper time with ether, upon maintaining a low temperature, and upon speed in freeing the extract from water and any traces of acid. Buffers employing sulphuric, phosphoric, or citric acid had to be used, because acetic acid was readily extracted from the aqueous solution by the ether and accelerated the decomposition of the product. The final procedure made it possible to isolate the purified crystals from oxidations at pH 1, pH 4, and pH 5.8 in a uniform yield of 25% to 30% by weight. In addition to these crystals, the ether extract contained considerable amounts of an unstable, chlorinated oil whose orange color quickly darkened on standing. Neither this oil nor the aqueous residue, which turned black when warmed to expel the ether, were examined further.

The crystalline product possessed the formula $C_7H_5O_4(OCH_3)$ and was extracted less readily by ether from solution in aqueous sodium bisulphite than from a more concentrated solution in water. Ammoniacal silver nitrate (Tollen's solution) was quickly reduced by the crystals, which also yielded a crystalline mono-2,4-dinitrophenyl hydrazone and a crystalline monosemicarbazone. This evidence for the presence of an aldehyde group was confirmed by oxidizing the substance at pH 0.5 with chlorous acid to a crystalline acidic substance, $C_7H_5O_5(OCH_3)$, decomposing at 143° to 144°C., and giving a nearly quantitative yield of a crystalline monoester when boiled with methanol containing a trace of sulphuric acid. Although two acidic groups were revealed in the acid by a potentiometric titration against standard sodium hydroxide, a marked buffering effect between pH 9 and pH 11 suggested that one of these groups was phenolic or enolic. When added to saturated sodium bicarbonate solution, the aldehyde displayed a slight acidity that was also attributed to a phenolic unit. Since both substances were derived from vanillin, $C_7H_5O_2(OCH_3)$, the aldehyde was at first regarded as a dihydroxy vanillin, and the acid as the corresponding dihydroxyvanillic acid.

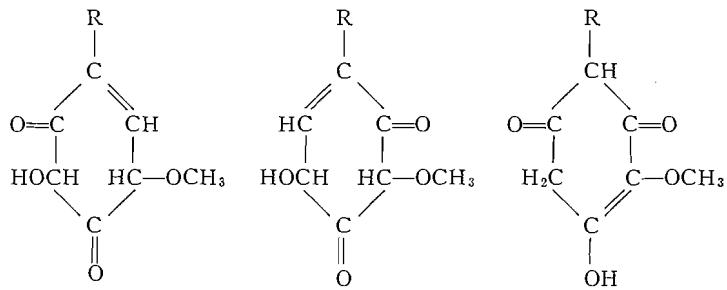

R = CHO or COOH

I II III

Both the aldehyde and acid, however, failed to give a distinctive color in the ferric chloride test for phenol. When examined by the Zerewitinoff method with methyl magnesium iodide, the aldehyde was found to contain only one atom, instead of the expected three atoms, of active hydrogen, and to add 3 moles, instead of the expected 1 mole, of the Grignard reagent. In similar fashion, the acid contained only 2 moles of active hydrogen and added 3 moles of the reagent. These observations suggested that the aldehyde and acid existed as ketonic tautomers analogous to the keto forms in which metapolyhydric phenols like resorcinol and phloroglucinol tended to react. Structures I, II, and III, which were metadiketones derived from 5,6-, 2,5-, and 2,6-dihydroxyvanillin, thus came into consideration.

Although the acid (R = COOH) slowly added two atoms of bromine per mole, an attempt to hydrogenate it over a palladium catalyst and with two atmospheres pressure of hydrogen ended with no absorption of the gas. Since double bonds conjugated with ketone or carboxyl groups tended to be hydrogenated less readily than isolated double bonds (5), the observation gave

support to Structures I and II rather than to Structure III. Hydrogenation of the aldehyde (R = CHO) under the same conditions required 2 moles per mole and yielded a distillable oil with the formula $C_7H_9O_4(OCH_3)$ which might have been a mixture of *cis–trans* isomers. Since this oil failed to form a phenylhydrazone and contained two atoms of active hydrogen, it appeared that the aldehyde had been reduced to a benzyl alcohol group, and that the double bond was then reactive enough to absorb the second mole of hydrogen. The replacement of the palladium by a platinum catalyst caused the consumption of a third mole of hydrogen, possibly by the reduction of the aldehyde to a methyl unit, as was shown to occur when vanillin was hydrogenated under the same conditions. An attempt to demonstrate the presence of ketone groups in the acid (R = COOH) by preparing a 2,4-dinitrophenyl hydrazone failed.

Methylation of the acid with silver oxide and methyl iodide gave a practically quantitative yield of a colorless, distillable oil with the composition, $C_7H_3O_3(OCH_3)_3$, expected for the monomethyl ether-monomethyl ester. An attempt to saponify this ester with hot 5% aqueous sodium hydroxide, however, produced a crystalline substance which contained no methoxyl groups and had the composition of a tetrahydroxybenzoic acid, $C_7H_2O_2(OH)_4$. When titrated potentiometrically with alkali, this substance gave a plot similar to that obtained in the titration of the original acid (R = COOH) and the presence of one carboxyl and one acidic hydroxyl group was inferred. The substance probably existed in a ketone form analogous to one or other of the Structures I, II, or III, because it contained only three atoms of active hydrogen per mole, instead of the five expected for a tetrahydroxybenzoic acid. This substance was also obtained in good yield when an attempt was made to methylate the original acid (R = COOH) with sodium hydroxide and dimethyl sulphate. Such easy demethylations of the acid and its monoether-monoester seemed consistent with the alternative structures advanced, since both the methyl ether and the phenolic hydroxyl positions would probably be highly activated by neighboring functional groups. The methylation of the acid (R = COOH) with diazomethane in ether yielded, not the expected monomethyl methyl ester, but unstable colorless needles melting with decomposition at 116° to 118°C. and having the formula $C_7H_3O_3(OCH_3)_3(CH_2N_2)_2$. Since treatment of the monomethyl methyl ester with diazomethane gave the same substance, it was thought probable that two molecules of diazomethane had added to the two ketone groups. The usual result of such addition is ring expansion with loss of nitrogen; but in this case the adduct was stable enough to be isolated. One mole of the diazomethane, of course, might have added to the double bond. An attempt to methylate the aldehyde (R = CHO) with diazomethane yielded 46% by weight of an unstable orange glass with the methoxyl content required for the adduct $C_7H_4O_3(OCH_3)_2(CH_2N_2)_2$, but the substance decomposed before further data could be secured.

Dr. D. A. Ramsay, of the National Research Council of Canada, kindly determined the infrared absorption of the acid (R = COOH) in the form of a mull in Nujol. He attributed a broad band from wavelength 3400 $cm.^{-1}$ to 3000 $cm.^{-1}$ to hydroxyl groups in a state of hydrogen bonding; the absence of a

sharp band in the region 3600 cm.$^{-1}$ to 3700 cm.$^{-1}$ indicated that no unbonded hydroxyl groups were present. Three bands at 1724 cm.$^{-1}$, 1704 cm.$^{-1}$, and 1689 cm.$^{-1}$ were consistent with a structure containing one carboxyl group and one unconjugated and one conjugated ketone group. Two bands at 1651 cm.$^{-1}$ and 1612 cm.$^{-1}$ suggested the presence of two, rather than only one, ethylenic linkages, and the bands at 1450 cm.$^{-1}$ and 1379 cm.$^{-1}$ might be correlated with the methoxy group. Although the remaining bands in the spectrum were difficult to interpret, the absorption at 835 cm.$^{-1}$ was consistent with triple substitution around a double bond ($R_1R_2C{=}CHR_3$) because such substitution was usually accompanied by absorption in the region 810 cm.$^{-1}$ to 840 cm.$^{-1}$. Thus the absorption in the infrared supported structures I, II, and III, but failed to discriminate sharply between them; the authors' preference for Structure I therefore rested on nothing more than the observation that vanillin was substituted as a rule in the fifth or sixth, rather than in the second, position. Baker and Brown (2), for example, obtained 5-hydroxyvanillin (3,4-dihydroxy-5-methoxy-benzaldehyde) in 3.6% yield by an Elbs oxidation of vanillin by potassium persulphate in alkaline solution.

Attempts to elucidate the nature of the aldehyde (R = CHO) were greatly hampered by its instability. Although the pure white crystals could be preserved for some time in a desiccator containing a dehydrating agent, a cold aqueous solution assumed a deep red color within a few hours. The same change occurred very quickly in cold, aqueous sodium bicarbonate. When a trace of pyridine or piperidine was added to a solution of the crystals in ether, a red oil quickly separated. This oil initially had a methoxyl content approaching that of the original aldehyde (16.9%), but when kept either *in vacuo* or in aqueous solution quickly changed to a brown, amorphous substance almost free of methoxyl groups and insoluble in ether, although still soluble in water. Attempts to acetylate the aldehyde with acetic anhydride and pyridine under various conditions gave red solutions from which no well-defined acetate could be recovered. A freshly prepared aqueous solution of the aldehyde had a marked tanning action on the skin, and much of the solute was absorbed by hide powder in the standard test for tannins. Aqueous solutions of the acid (R = COOH) were considerably more stable than those of the aldehyde, but nevertheless soon decomposed to red substances.

As already mentioned, the initial oxidation of vanillin by aqueous sodium chlorite, unlike that by chlorine dioxide, was greatly dependent upon the pH of the system (Figs. 2 and 3). At pH 0.5, the sodium chlorite oxidation yielded 40% by weight (28% of theory) of the acid (R = COOH), at pH 1.0 a mixture of the aldehyde (R = CHO) and acid resulted, and at pH 4.0 25% (19% of theory) of the aldehyde was the only product identified. Sodium chlorite therefore differed from chlorine dioxide in oxidizing the aldehyde group of vanillin when the pH was sufficiently low, as Jeanes and Isbell (7) had previously observed in their oxidations of glucose. The other product isolated when vanillin was oxidized with sodium chlorite was 5-chlorovanillin, which was carefully differentiated from the 6-chloro isomer. Experiments carried out at pH 4.7 and pH 5.05 near 5°C., and at pH 6.0 and higher at room temperature,

produced 4%, 17% to 19%, a trace, and 0%, respectively, of 5-chlorovanillin. A sharp maximum in yield therefore occurred near pH 5, or in the region where the rate of oxidation plot (Fig. 3) often suggested an autocatalytic reaction. The yield was negligible at pH 6 or more because the whole reaction was negligible, and trial showed that 5-chlorovanillin itself was rapidly oxidized to a dark colored oil in media more acidic than pH 5. The production of the 5-chloro derivative was attributed to a side-reaction peculiar to sodium chlorite; none was observed in the experiments with chlorine dioxide, but this oxidant was too active, even at pH 5, to permit any 5-chlorovanillin formed to survive unchanged.

EXPERIMENTAL

The vanillin used was recrystallized from aqueous alcohol until it melted correctly at 82° to 83°C. Sodium chlorite, of analytical grade, was kindly presented by the Mathieson Alkali Company of New York. The Coleman pH Electrometer was frequently standardized against 0.05 *M* potassium acid phthalate, whose pH at 25°C. was accepted as 4.0 (6, 11).

Reduction of Sodium Chlorite by Vanillin (Figs. 2 and 3)

The buffers used consisted of dilute sulphuric acid for pH 1, 10% acetic acid for pH 2.2, and 5.2% sodium acetate plus the appropriate amount of acetic acid for the higher pH range. Frequent tests during each experiment showed that these buffers maintained the original pH to within one-tenth of a unit. Vanillin, 0.913 gm. (6 mM.), was dissolved in 200 cc. of the buffer contained in a glass-stoppered, amber bottle maintained at 20°±0.1°C. in a thermostat. An equal volume of 0.12 *M* sodium chlorite, also at 20°C., was added at zero time with thorough mixing. A blank containing no vanillin was simultaneously prepared. At intervals a 10 cc. aliquot was removed and was mixed with about 90 cc. of water containing 10 cc. of aqueous 10% potassium iodide and 20 cc. of 20% sulphuric acid. The liberated iodine was titrated with 0.025 *N* sodium thiosulphate with a starch solution as indicator, and the result when corrected for the corresponding blank was expressed as moles of sodium chlorite reduced. One mole was considered equivalent to 4 liters of *N* iodine (22, 23). Concordant results were obtained by treating the 10 cc. aliquot with 15 cc. of the potassium iodide solution and 15 cc. of 30% acetic acid according to Jeanes and Isbell (7), but acidification with only 10 cc. of 20% sulphuric acid was insufficient.

5-Chlorovanillin

Three grams (19.7 mM.) of vanillin, dissolved in 200 cc. of an adequate sodium acetate buffer at pH 5.05, was mixed near 5°C. with 77.5 cc. of 1.04 *M* aqueous sodium chlorite (80.5 mM.). The separation of a buff-colored solid from the cold solution was essentially complete after 42 hr. and the clear, dark red color of the filtrate could be discharged to orange-yellow by sulphur dioxide. A 1.03 gm. sample of the solid was extracted with ether in a Soxhlet apparatus and, when concentrated, the red ether extract slowly deposited cubical crystals. The remainder of the product consisted of dark red, viscous oils which were soluble in benzene, and of amorphous, insoluble solids.

After several recrystallizations from benzene, the above crystals, now shining white leaflets, had the elementary analysis and the Rast molecular weight of a chlorovanillin. Their melting point, 164° to 165.4°C., was correct for 5-chlorovanillin, and was not depressed by admixture with an authentic sample: admixture with authentic 6-chlorovanillin (m.p. 170°C.) depressed the value below 143°C. Acetylation of 0.14 gm. of the crystals with 2 cc. of acetic anhydride and one drop of concentrated sulphuric acid gave a 90% yield of pure 3-methoxy-4-acetoxy-5-chlorobenzal diacetate melting correctly at 118°C. (corrected). Authentic samples of the above diacetate, and also of the 6-chloro isomer (m.p. 144°C.) were prepared according to the method of Raiford and Lichty (14) for comparison. The yield of pure 5- chlorovanillin was 0.62 gm. or 17% of theory, and was 19% in a duplicate experiment.

Preparation and Analysis of Aqueous Chlorine Dioxide

To avoid the risk of explosions, chlorine dioxide gas was always prepared in dilution with an equimolecular amount of carbon dioxide by Schacherl's method (16), as described in detail by Sarkar (15). This method involved heating a mixture of potassium chlorate, 25 gm., oxalic acid dihydrate, 20 gm., and 80 cc. of cold 33% (by volume) sulphuric acid to 30° to 60°C. The evolution of gases from larger-scale preparations occasionally became too violent to be easily controlled. An all-glass apparatus coated with black paint was used, and the effluent mixture of gases was scrubbed with a saturated solution of sodium chlorite to replace any chlorine with chlorine dioxide. The effluent chlorine dioxide was absorbed in ice-cold, distilled water contained in a glass-stoppered, amber bottle until a concentration of 0.2 *M* to 0.3 *M* was attained.

These solutions were tested for their content of chlorine or hypochlorous acid by titrating aliquots iodometrically in a phosphate buffer at pH 7, and then by continuing the titration to the end point in dilute sulphuric acid. The first titration measured only one of the five oxidizing equivalents of the chlorine dioxide, *plus* those of any chlorine or hypochlorous acid, while the second or "acid" titration determined only the remaining four oxidizing equivalents of the chlorine dioxide. Five-fourths of the "acid" titration therefore gave the molar equivalent of the chlorine dioxide, and the difference between one-fourth and the first titration corresponded to the content of chlorine and hypochlorous acid. In practice, this content never exceeded 2 mM. per liter, or was almost within the experimental error. Since the solutions were usually diluted to 0.03 *M* to 0.07 *M* in chlorine dioxide before use, they were considered to be free of chlorine. Routine estimations could then be performed in acid solution as described for sodium chlorite solutions, 1 mole of chlorine dioxide being assumed to liberate five atoms of iodine.

The rapid deterioration of 0.0134 *M* chlorine dioxide in a buffer at pH 7.3 (Fig. 1, plot A) was followed by titrating 10 cc. aliquots iodometrically in acid solution. After 12 hr. at 20°C., 16.57 cc. of 0.0246 *N* sodium thiosulphate was required, corresponding to 0.0082 *M* chlorine dioxide. Another 10 cc. aliquot was analyzed by the method of Kolthoff and Furman (9) to include chlorate by being boiled for one minute with 1.3 gm. of ferrous sulphate. Excess potas-

sium iodide was then added to reduce the ferric iron formed, and the liberated iodine was titrated with 35.5 cc. of the standard sodium thiosulphate. After correction for the ferrous sulphate blank (1.55 cc.) and for the chlorine dioxide (16.57 cc.), the chlorate corresponded to 17.4 cc. or was 0.0071 *M*. This value was in fair agreement with the figure of 0.0067 *M* calculated for the complete decomposition of chlorine dioxide into equimolecular amounts of chlorite and chlorate.

Reduction of Chlorine Dioxide by Vanillin (Figs. 2 and 3)

The buffers were those used in the parallel reductions of sodium chlorite. In a typical experiment, 100 cc. of 0.008 *M* vanillin in the desired buffer, contained in a glass-stoppered, amber bottle, was brought to 20°±0.05°C. in a constant temperature bath. A blank containing no vanillin was prepared. At zero time, cold, approximately 0.03 *M* aqueous chlorine dioxide, 100 cc., was added to the solution and the blank, and the stoppered bottles were quickly shaken. The heat of the initial reaction raised the temperature of the vanillin solution close to that of the bath almost immediately. From time to time, the residual oxidant in 10 cc. aliquots was determined iodometrically as chlorine dioxide. The apparent chlorine dioxide content of the blanks was plotted against time (cf. Fig. 1), and the difference between these plots and the corresponding values for the solution was accepted as the chlorine dioxide reduced by the vanillin.

Preparation of Aldehyde $C_7H_5O_4(OCH_3)$

(*a*) With chlorine dioxide. Thirty grams (0.2 mole) of vanillin was dissolved in 1400 cc. of a 0.4 *M* citric acid – 0.8 *M* disodium hydrogen phosphate buffer for pH 4.0 made up according to McIlvaine's proportions (10) but with four times the recommended concentrations. After this solution had been chilled, 820 cc. of 0.41 *M* aqueous chlorine dioxide (0.4 mole) was added near 0°C., and the flask was cooled efficiently to dissipate the considerable heat of the reaction. The solution immediately became dark red but this color changed in about two hours to a golden yellow. At this stage the excess chlorine dioxide was removed by passing nitrogen gas through the solution, which was then extracted with 2 liters of ether. Toward the end of the extraction the solution gradually became opaque and dark red-brown in color. The yellow ether extract was dried over anhydrous sodium sulphate and was concentrated to about 150 cc. on a steam bath. When this concentrate was further evaporated *in vacuo* without warming or access of moisture, it became very cold and deposited white crystals, which were recovered on a filter and were freed from traces of an orange-brown oil by washing with a small amount of cold, anhydrous ether. Concentration and "freezing out" were repeated three or four times to give a total yield of 9.0 gm. (25%) of the crystals, and the final mother liquor contained 7.1 gm. of a chlorine-containing, orange oil which darkened on standing. Benzene was the best solvent found for recrystallization, and the pure prisms melted at 104° to 105°C. Found: C, 52.1, 52.4; H, 4.4, 4.4; OCH_3, 16.7, 16.7%; mol. wt. (Rast) 182. Calc. for $C_7H_5O_4(OCH_3)$: C, 52.1; H, 4.4; OCH_3, 16.9%; mol. wt. 184.

The substance evolved 1.06, 1.01 atoms of active hydrogen in the Zerewitinoff (12) estimation, and 3.83, 3.90 moles of the Grignard reagent was consumed per gram mol. wt. Pyridine was the solvent for the sample and butyl ether for the methyl magnesium iodide.

(*b*) With sodium chlorite at pH 4. Two grams of vanillin was dissolved in 100 cc. of the McIlvaine standard buffer, pH 4.0, but used in four times the usual strength. When 5 gm. of sodium chlorite in 25 cc. of distilled water was added, the solution turned orange, green, and then yellow, and the presence of chlorine dioxide became apparent for the first time at the yellow stage. The aldehyde was isolated as already described in a yield of 0.5 gm. or 19%, m.p. 104° to 105°C., not depressed by admixture with a sample prepared with chlorine dioxide. None of the acid $C_7H_5O_5(OCH_3)$ (see below) could be isolated.

2,4-Dinitrophenylhydrazone of Aldehyde $C_7H_5O_4(OCH_3)$

A 0.20 gm. sample, dissolved in a few cc. of alcohol, was stirred with 60 cc. of filtered Brady's solution containing 4 gm. of the dinitrophenylhydrazine per liter. After about 20 sec. the solution became opalescent, and after one hour the bright yellow deposit was collected and thoroughly washed with water. Yield 0.37 gm. or 97% of theory, and m.p., 192° to 193° (uncorrected). Found: N, 15.7, 15.8%. Calc. for $C_{14}H_{12}N_4O_8$: N, 15.4%.

Semicarbazone of Aldehyde $C_7H_5O_4(OCH_3)$

The sample (0.05 gm.) was mixed in a small centrifuge tube with 0.05 gm. of semicarbazide hydrochloride and 0.75 gm. of anhydrous sodium acetate. A few cubic centimeters of water was added with stirring, and the semicarbazone separated as the original substance dissolved. The white precipitate, after being washed in water and dried at 50°C. *in vacuo*, was recovered in quantitative yield. Found: N, 16.9; 17.1%. Calc. for $C_9H_{11}N_3O_5$: N, 17.4%. The semicarbazone melted at 163° (uncorrected) with decomposition.

Hydrogenation of Aldehyde $C_7H_5O_4(OCH_3)$

(*a*) The sample, 1.84 gm. (0.01 mole) was dissolved in 30 cc. of anhydrous dioxane, and 20 mgm. of a palladium catalyst (20) was added. The mixture when shaken in an Adkins hydrogenator at room temperature and about 35 p.s.i. hydrogen pressure absorbed 2 moles per mole in two hours, and no more was consumed in an additional hour.

After filtration, the colorless solution was evaporated in a vacuum to a slightly discolored, viscous oil weighing 1.85 gm. This oil when distilled at 120°C. and 125μ pressure yielded a colorless product with refractive index η_D^{20} 1.4670. Found: C, 51.5, 51.4; H, 6.4, 6.3; OCH_3, 16.6, 16.7%. Calc. for $C_7H_9O_4(OCH_3)$: C, 51.1; H, 6.4; OCH_3, 16.5%. A Zerewitinoff estimation (12) showed the presence of 2.03, 1.97 atoms of active hydrogen per mole.

(*b*) A microscale hydrogenation was carried out in apparatus described by Johns and Seiferle (8). When the apparatus was tested with pure vanillin and a platinum oxide catalyst, 1.98 moles of hydrogen per mole was used. The aldehyde group in vanillin had therefore been reduced to a methyl group.

Samples of the aldehyde, $C_7H_5O_4(OCH_3)$, 6.04 mgm. and 6.13 mgm., required 2.23 cc. and 2.27 cc. of hydrogen at S.T.P., corresponding to consump-

tions of 3.03, 3.04 moles, respectively, per calculated mol. wt. of 184. A repetition of the hydrogenation on a larger scale gave a colorless glass unaffected by aqueous sodium bicarbonate and by 2,4-dinitrophenylhydrazine, and giving no distinct color with ferric chloride solution.

Methylation of Aldehyde $C_7H_5O_4(OCH_3)$ with Diazomethane

A solution of 1 gm. of the aldehyde in anhydrous ether was mixed with excess of an ether solution of diazomethane prepared from 10 gm. of nitrosomethylurea (1). A pale yellow precipitate, 0.46 gm., settled, which after recovery became dark orange in color. The substance decomposed when heated to 80°C., was insoluble in petroleum ether and benzene, but dissolved in methanol, ethanol, and acetone. All attempts at recrystallization yielded an orange glass. Found: OCH_3, 22.1, 22.2%. Calc. for $C_7H_4O_3(OCH_3)_2(CH_2N_2)_2$: OCH_3, 22.0%. The residue from the ether was also a yellow glass that became dark on exposure to air.

Preparation of the Acid $C_7H_5O_5(OCH_3)$

(*a*) At pH 0.5. Thirty grams (0.2 mole) of vanillin, dissolved in 1500 cc. of aqueous sulphuric acid (pH 0.5), was mixed with 72 gm. (0.8 mole) of sodium chlorite dissolved in 150 cc. of water. The solution became dark red, but this color gradually faded to orange and then to golden yellow. After 45 min. the chlorine dioxide formed in the reaction was removed by bubbling nitrogen through the solution, which was then saturated with sodium chloride and extracted with ether. The ether extract was dried over anhydrous sodium sulphate and concentrated to about 150 cc. When the remaining ether was evaporated *in vacuo* at room temperature, a total of 12 gm. (28% of theory) of white crystals was recovered from 17 gm. of a residual yellow oil. Qualitative tests revealed a high chlorine content in this oil, but when exposed to the air it quickly changed to a dark, viscous tar.

The crystals were washed with cold, anhydrous ether, and when recrystallized from a mixture of ether and low-boiling petroleum ether formed large, colorless, glistening plates melting with decomposition at 143° to 144°C. (uncorrected). Found: C, 48.0, 48.1; H, 4.1, 4.1; OCH_3, 15.6, 15.5%. Calc. for $C_7H_5O_5(OCH_3)$: C, 48.0; H, 4.0; OCH_3, 15.5%. The total Grignard reagent consumed in a Zerewitinoff (12) estimation was 4.80, 4.87 moles, and 2.01, 1.97 atoms of hydrogen were evolved, per calculated mol. wt. of 200. A 50 mgm. sample was neutralized to a potentiometric end point near pH 8 by 5.60 cc. of 0.0914 *N* caustic soda, corresponding to a neutralization equivalent of 98.

The acid was insoluble in petroleum ether and benzene, but dissolved in alcohol, water, chloroform, and ether.

(*b*) At pH 1.0. A solution of 10 gm. of vanillin in 500 cc. of distilled water adjusted to pH 1 with sulphuric acid was mixed with another made from 19 gm. of sodium chlorite and 50 cc. of water. After 2.5 hr., during which time the color changes already described occurred, the mixture was saturated with salt and extracted with ether. The crystalline product, 2.8 gm., recovered from the ether was separated by extraction with benzene into the benzene-soluble aldehyde $C_7H_5O_4(OCH_3)$ (1.8 gm. or 15% of theory) melting at 104° to 105°C.

and the benzene-insoluble acid $C_7H_5O_5(OCH_3)$ (1.0 gm. or 7.7%), melting at 143° to 144°C. Neither melting point was depressed when samples of each product were mixed with the appropriate authentic specimen.

(*c*) From the aldehyde $C_7H_5O_4(OCH_3)$. The oxidation (*a*) was repeated at pH 0.5 with 2 gm. (0.013 mole) of the aldehyde dissolved in 100 cc. of aqueous sulphuric acid, 4.5 gm. (0.05 mole) of sodium chlorite being used. After removing the by product chlorine dioxide, the colorless aqueous solution was extracted with ether. A quantitative yield of the acid remained, and the melting point of this product was not depressed by admixture with an authentic sample. Found: OCH_3, 15.4, 15.5%. Calc. for $C_7H_5O_5(OCH_3)$: OCH_3, 15.5%.

Methylation of the Acid $C_7H_5O_5(OCH_3)$

(*a*) With diazomethane. An excess of an ethereal solution of diazomethane was added to a solution of 1 gm. of the acid dissolved in ether. Large, colorless needles, melting at 116° to 118°C. with decomposition, separated from the solution after a short time. No solvent was found from which the product could be recrystallized without decomposition. Found: C, 46.5, 46.2; H, 5.0, 5.1; OCH_3, 29.9, 29.9; N, 17.8, 17.8%. Calc. for $C_7H_3O_3(OCH_3)_3 \cdot 2CH_2N_2$: C, 46.5; H, 5.2; OCH_3, 30.0; N, 18.1%.

(*b*) With methanol. One gram of the acid was heated under reflux for 10 hr. with 10 cc. of dry methanol containing two drops of concentrated sulphuric acid. Concentration of the solution under vacuum brought about the separation of a crystalline mass melting at 115° to 118°C. with previous softening. Recrystallization from a low-boiling petroleum ether – ether mixture yielded a product which melted at 125° to 126°C. after being washed with water and dried. Found: OCH_3, 29.2, 29.1%. Calc. for $C_7H_4O_4(OCH_3)_2$: OCH_3, 29.0%.

This ester, when re-methylated with diazomethane, yielded the substance $C_7H_3O_3(OCH_3)_3 \cdot 2CH_2N_2$ with the proper melting point of 115° to 117°C., undepressed by admixture with the specimen prepared directly from the acid $C_7H_5O_5(OCH_3)$.

(*c*) With dimethyl sulphate. A solution of the acid, 1.4 gm., and sodium hydrosulphite, 0.2 gm., in a small amount of water was methylated by the alternate addition, with continuous stirring, of 2 cc. volumes of dimethyl sulphate and 5 cc. volumes of 30% sodium hydroxide. The total volumes added were 10 cc. and 20 cc., respectively. After the mixture had been kept near 100°C. for an additional two hours, acidification and continuous extraction with ether yielded 1.2 gm. of a red oil. This oil partly crystallized one day later, and after recovery the crystals were recrystallized from a very small volume of ethyl acetate. The product, still slightly pink in color, decomposed at 172° to 175°C. with discoloration and the evolution of gas. Found: C, 45.4, 45.0; H, 3.27, 3.23; OCH_3, 0.0%. Calc. for $C_7H_6O_6$: C, 45.2; H, 3.2%. The substance evolved 2.95 atoms of hydrogen per mol. wt. 186 in a Zerewitinoff estimation (12). A 15.15 mgm. sample, when titrated to a potentiometric end point near pH 8, consumed 6.80 cc. of 0.0239 *N* sodium hydroxide. The neutralization equivalent was therefore 93.

(*d*) With silver oxide and methyl iodide. A mixture of the following substances was heated under reflux for four hours on a steam bath: 4.0 gm. of the

acid $C_7H_5O_5(OCH_3)$, 50 cc. of anhydrous acetone, 50 cc. of methyl iodide freshly distilled over phosphorous pentoxide, 12 gm. of dry silver oxide, and 8 gm. of regenerated Drierite. The acetone was included because the acid was insoluble in methyl iodide. The product, recovered by filtration of the reaction mixture and evaporation of the filtrate, consisted of a viscous, slightly yellow oil weighing 4.40 gm. One gram of this oil when distilled boiled at 92°C. and 120μ pressure, and the colorless product had the refractive index, η_D^{20}, 1.4940. Found: C, 52.4, 52.5; H, 5.3, 5.2; OCH_3, 40.7, 40.7%. Calc. for $C_7H_3O_3(OCH_3)_3$: C, 52.6; H, 5.3; OCH_3, 40.8%.

This oil, when re-methylated with diazomethane, yielded the crystals $C_7H_3O_3(OCH_3)_3 \cdot 2CH_2N_2$. Although the substance melted with decomposition at 110° to 112°C. instead of 116° to 118°C., and could not be recrystallized, a mixed melting point with a sample prepared directly from the acid $C_7H_5O_5(OCH_3)$ was not depressed.

Another portion of the above oil was heated on a steam bath with 5% aqueous sodium hydroxide; the solution was acidified and extracted with ether. The extract yielded a crystalline product whose melting point of 172° to 174°C. was not depressed by admixture with the crystals, $C_7H_6O_6$, obtained in the attempt to methylate the acid $C_7H_5O_5(OCH_3)$ with dimethyl sulphate and sodium hydroxide.

ACKNOWLEDGMENT

Two of us (R. M. H. and C. D. L.) wish to thank the Brown Company for the two Fellowships, and the Canadian Pulp and Paper Association for the total of two summer stipends, awarded to them during the research.

REFERENCES

1. ARNDT, F. *In* Organic syntheses. Collective Vol. II. John Wiley & Sons, Inc., New York. 1943. p. 165.
2. BAKER, W. and BROWN, N. C. J. Chem. Soc. 2303. 1948.
3. FUCHS, W. and HONSIG, E. Ber. 59: 2850. 1926.
4. FÜRST, E. Ann. 206: 78. 1881.
5. GILMAN, H. (*Editor*). Organic chemistry. Vol. I. John Wiley & Sons, Inc., New York. 1943. p. 802.
6. HITCHCOCK, D. I. and TAYLOR, A. C. J. Am. Chem. Soc. 60: 2710. 1938.
7. JEANES, A. and ISBELL, H. S. J. Research Natl. Bur. Standards, 27: 125. 1941.
8. JOHNS, I. B. and SEIFERLE, E. J. Ind. Eng. Chem., Anal. Ed. 13: 841. 1941.
9. KOLTHOFF, I. M. and FURMAN, N. H. (*Editors*). Volumetric analysis. Vol. II. John Wiley & Sons, Inc., New York. 1929. p. 388.
10. MCILVAINE, T. C. J. Biol. Chem. 49: 183. 1921.
11. MACINNES, D. A., BELCHER, D., and SHEDLOVSKY, T. J. Am. Chem. Soc. 60: 1094. 1938.
12. NIEDERL, J. B. and NIEDERL, V. (*Editors*). Organic quantitative microanalysis. 2nd ed. John Wiley & Sons, Inc., New York. 1942. p. 263.
13. PEARL, I. A. and BARTON, J. S. J. Am. Chem. Soc. 74: 1357. 1952.
14. RAIFORD, L. C. and LICHTY, J. G. J. Am. Chem. Soc. 52: 4576. 1930.
15. SARKAR, P. B. J. Indian Chem. Soc. 12: 470. 1935.
16. SCHACHERL, G. Ann. 206: 68. 1881.
17. SCHMIDT, E. and BRAUNSDORF, K. Ber. 55: 1529. 1922.
18. SCHMIDT, E. and GRAUMANN, E. Ber. 54: 1860. 1921.
19. SCHMIDT, E., HAAG, W., and SPERLING, L. Ber. 58: 1394. 1925.
20. SHRINER, R. L. and ADAMS, R. J. Am. Chem. Soc. 46: 1683. 1924.
21. TAUBE, H. and DODGEN, H. J. Am. Chem. Soc. 71: 3330. 1949.
22. TAYLOR, M. C., WHITE, J. F., VINCENT, G. P., and CUNNINGHAM, G. L. Ind. Eng. Chem. 32: 899. 1940.
23. WHITE, J. F., TAYLOR, M. C., and VINCENT, G. P. Ind. Eng. Chem. 34: 782. 1942.

STUDIES IN THE POLYOXYPHENOL SERIES

VIII. THE OXIDATION OF SUBSTANCES RELATED TO VANILLIN WITH SODIUM CHLORITE AND CHLORINE DIOXIDE[1]

By C. D. Logan,[2] R. M. Husband,[3] and C. B. Purves

ABSTRACT

The research confirmed the fact that chlorine dioxide and sodium chlorite were not equivalent in their oxidizing properties. At 22° C. or less, the oxidation of pyrogallol by aqueous sodium chlorite at pH 6 was very slow, but became very rapid on the acid side of pH 3.5. The amorphous, colored products probably did not include purpurogallin. Under similar circumstances *p*-hydroxybenzaldehyde was unaffected at pH 6; 22% was oxidized to *p*-benzoquinone (Dakin's reaction) at pH 5, and this amount increased to 39% at pH 1. The yield of benzoquinone was about 24% regardless of pH within the above range when aqueous chlorine dioxide was the oxidant. Sodium chlorite at pH 0.9 produced a 91% yield of methoxy-*p*-quinone from methoxy-*p*-hydroquinone; at pH 4 this product was mixed with 56% of 4,4′-dimethoxydiquinone, but near pH 6 a slower oxidation did not proceed beyond 4,4′-dimethoxyquinhydrone. Aqueous chlorine dioxide yielded at least 92% of monomeric methoxyquinone at all pH values between 1 and 6, probably in accord with the equation,

$$3\ \text{hydroquinone} + 3\ ClO_2 \longrightarrow 3\ \text{quinone} + 2\ HCl + HClO_3\ (+3\ O + 3\ H).$$

The simultaneous formation of hydrogen peroxide was suspected, but not proved. In sharp distinction to the behavior of free phenols, veratraldehyde was not oxidized by aqueous chlorine dioxide between pH 6 and pH 3, but at pH 1 a slow reaction yielded up to 15% of veratric acid. Sodium chlorite produced about 92% of the same acid at pH 1 and pH 4, but its action was negligible at pH 5. Since by-product chlorine dioxide was ineffective at pH 4, it was possible to confirm the validity of the Jeanes–Isbell equation for the reduction of chlorous acid:

$$C_6H_3(OCH_3)_2CHO + 3\ HClO_2 \longrightarrow C_6H_3(OCH_3)_2COOH + 2\ ClO_2 + HCl + H_2O.$$

The oxidation of acetylated vanillin was complicated by the occurrence of deacetylation. Red, chlorinated oils with quinoidal properties were also formed in most of the above oxidations.

INTRODUCTION

Although aqueous solutions of sodium chlorite and of chlorine dioxide have often been considered to be equivalent in their bleaching action, a recent research (11) showed that they oxidized vanillin in somewhat different ways. Oxidations with chlorine dioxide at 20° C. seemed to be independent of the hydrogen ion concentration between pH 1 and pH 6 and did not alter the aldehyde group in vanillin. Sodium chlorite, however, had no effect at pH 6, produced about 19% of 5-chlorovanillin at pH 5, appeared to duplicate the behavior of chlorine dioxide at pH 4, and produced derivatives of vanillic acid at pH 3 or less. In order to determine the characteristics of the two oxidants more fully, their action on several other phenolic substances has now been studied.

Schmidt, Hagg, and Sperlin (27) observed that an excess of chlorine dioxide in presence of a vanadium chloride catalyst produced about 25% yields of

[1]*Manuscript received September 21, 1954.*
Contribution from the Division of Industrial and Cellulose Chemistry, McGill University, and from the Wood Chemistry Division, Pulp and Paper Research Institute of Canada, Montreal, Que. Abstracted from Ph.D. theses submitted to the University in September 1947 by R.M.H., and in May 1949 by C.D.L.
[2]*Present address: The Ontario Paper Company, Limited, Thorold, Ontario.*
[3]*Present address: State University of New York, College of Forestry, Syracuse 10, New York.*

both oxalic acid and maleic acid from pyrogallol, one of the most readily oxidizable phenols. The present research employed a sixfold to sevenfold molar proportion of sodium chlorite buffered to within one-tenth of a pH unit, and the consumption of chlorite (Fig. 1) was followed by determining the amount remaining after various times. Iodometric methods of estimating chlorite in presence of pyrogallol proved unsuitable, and the method eventually used depended upon the quantitative oxidation of sodium bisulphite by chlorous acid to sodium sulphate (12), which was determined gravimetrically as the barium salt. This tedious method gave reproducible results (plot for pH 2), although complications introduced by the chlorine dioxide also formed made their absolute value uncertain.

When the solutions of pyrogallol and sodium chlorite were mixed at pH 3.5 or less, about 2.5 moles of oxidant per mole was rapidly consumed (plots for pH 2); the mixture slowly developed an orange color, an orange precipitate appeared but then quickly redissolved to leave a clear yellow solution. The production of chlorine dioxide became apparent only at this stage, which corresponded to the consumption of more than two molar equivalents of chlorite. Between pH 3 and pH 6, the solutions of pyrogallol and of sodium chlorite turned orange to orange-red when mixed, and dark-brown, amorphous solids separated within a few minutes. The rate at which the chlorite was consumed, however, decreased rapidly as the pH increased (plots at pH 4.5 and 5). Other experiments, not reproduced in Fig. 1, showed that a decrease in temperature to 5° C. or less had the same general effect on the shape of the rate-plots as an increase in pH; at pH 3 and 5° C. amorphous solids were still present after 200 hr., and at pH 6 and 5° C. 10 hr. were required for the reduction of 0.1 mole of chlorite per mole of pyrogallol.

The literature concerned with condensations of pyrogallol caused by other oxidants was reviewed by Erdtman (4) who concluded that vicinal, asymmetrical and symmetrical dipyrogallol (the 2,3,4,2′,3′,4′, the 2,3,4,3′,4′,5′, and the 3,4,5,3′,4′,5′-hexahydroxy derivatives of biphenyl) were among the first products formed by oxidation in alkaline, neutral, and acidic media, respectively. Henrich (10), who also suggested a mechanism for such condensations, apparently confused the vicinal with the symmetrical dipyrogallol. Purpurogallin (8), a well defined, crystalline product in certain oxidations, was probably derived from the asymmetrical derivative. The further oxidation and condensation of pyrogallol gave rise to amorphous, ill-defined "humic acids" not dissimilar in character to the colored solids that separated during the present experiments. All attempts to isolate a single chemical individual from these solids failed. Purpurogallin in particular was probably not present, because a pure, crystalline sample was very readily oxidized to soluble substances by sodium chlorite at pH 2 and 10° C. (Fig. 1). Even at pH 4.6, almost seven molar equivalents of the oxidant were consumed within 32 hr. (not shown).

The next experiments employed buffered solutions kept at 20° C. and containing 5 mM. of *p*-hydroxybenzaldehyde and about 20 mM. of chlorine dioxide per liter. Plots of the rate of reaction have not been reproduced,

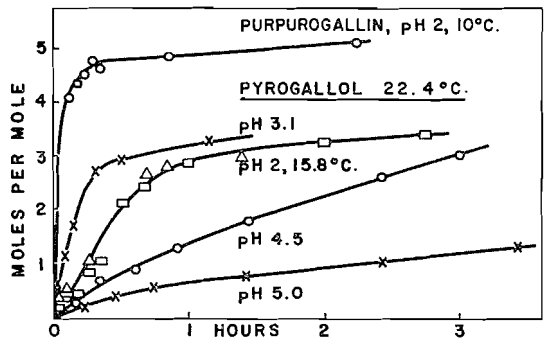

FIG. 1. Rate of oxidation of 0.015 *M* aqueous solutions of purpurogallin and pyrogallol with 0.097 *M* to 0.101 *M* sodium chlorite. Temperature 22.4° C. unless specially noted.

because quinones were formed that interfered with the iodometric method used to determine the remaining chlorine dioxide. The plots suggested that between 1 and 1.3 moles of oxidant per mole was reduced almost instantaneously at pH 5.4 or pH 6, but that the reduction decreased in rate and increased in extent as the pH was lowered, until two hours at pH 1.1 were required for the consumption of about 2.5 moles. No secondary consumption of oxidant was evident at any pH. As expected, one of the products of these oxidations was *p*-benzoquinone, but extraction of the liquors with ether yielded nothing but red tars when sodium acetate – acetic acid buffers had been employed. The substitution of citric acid and sulphuric acid buffers obviated this difficulty.

Although the quinone in the ether extract could be determined fairly accurately by iodometry (33) when the oxidation had been carried out near pH 5 or pH 6, oxidations in more acidic media contained interfering substances, and the method was discarded. Estimations based upon the reduction of the quinone to the hydroquinone by zinc and acid, and on the isolation of the crystalline dibenzoate of the hydroquinone, also failed to give quantitative results. Kimijima and Kishino (17), who encountered similar analytical

TABLE I

YIELD OF *p*-BENZOQUINONE FROM *p*-HYDROXYBENZALDEHYDE

pH†	With chlorine dioxide*		With sodium chlorite*	
	% after 30 min.	% after 60 min.	% after 30 min.	% after 60 min.
6.0	—	21.1	No reaction	
5.0	20.6	24.7	22.0	22.0
4.0	25.7	26.6	22.7	24.0
3.0	24.8	25.2	25.7	25.9
2.2	22.5	24.8	27.6	29.6
1.0‡	21.1	21.1	37.3	38.8

**The aldehyde, 0.01 mole, dissolved in the buffer, was mixed with aqueous solutions containing 0.031 mole of chlorine dioxide or 0.04 mole of sodium chlorite.*

†*Citric acid – sodium hydroxide buffers.*

‡*Sulphuric acid buffer.*

difficulties, finally added an excess of aqueous hydroquinone to the residue obtained by evaporating the ether extract, and weighed the crystalline quinhydrone that separated. This simple method gave good checks in the present work. Comparison of the data in columns 2 and 3 of Table I shows that the production of benzoquinone was practically complete in 30 min., and that the yield was almost independent of the pH of the oxidation. The slight decrease in yield observed at pH 2.2 and pH 1 was probably connected with the increase in other oxidations evidenced by the increase in the consumption of chlorine dioxide and in the depth of color of the reaction mixture.

In contrast to the almost instantaneous oxidation of *p*-hydroxybenzaldehyde by chlorine dioxide at pH 6 and 20° C., duplicate experiments with an excess of aqueous sodium chlorite showed that no appreciable reaction occurred. From pH 5 to pH 3, the two oxidants gave similar yields of benzoquinone (Table I, columns 4 and 5), but at pH 1 the yield with sodium chlorite was almost twice as great. No chlorine dioxide was evolved during the early part of the oxidation with sodium chlorite, and no red oil was isolated as a by-product. Red oils were obtained in addition to the quinone when chlorine dioxide was the oxidant, and were probably of a quinoidal nature since their color was completely discharged by reduction with sodium hydrosulphite, or with zinc and acid. The oils, which darkened quickly and became tars, were probably nuclear condensation products of a quinone, or of a hydroxylated quinone. Analogous products were described by Erdtman (4, 6).

The last two oxidations were examples of a general reaction discovered by Dakin (2) for free *o*- or *p*-phenols whose side chains contained an unsaturated carbon atom in the alpha position. In the case of *p*-hydroxybenzaldehyde, oxidation with an alkaline solution of hydrogen peroxide produced a nearly quantitative yield of hydroquinone, together with formic acid from the aldehydic group. Wacek and his collaborators (30, 31) discussed the probable mechanism of such oxidations, and isolated the monoformyl ester of hydroquinone as an intermediate when the oxidation was carried out with peracetic acid in acetic anhydride. The same type of oxidation could be effected by a few other peroxides (2), and also by ozonides decomposing in alkali (30) but not by the other common oxidants tried. In order to avoid the possibility of a Dakin reaction, methoxy-*p*-hydroquinone was chosen for study.

The oxidation of methoxyhydroquinone with twice the molar amount of aqueous chlorine dioxide at room temperature proved to be less complicated, for within 20 min. a heavy, yellow precipitate of methoxyquinone separated from solution. By extraction of the mother liquor with ether, the yield was increased to about 92% of theory from oxidations carried out at pH 1, pH 2.2, and pH 7.5, and iodometric titrations of the aqueous residues suggested that they retained another 7% of quinone-like substances. When the assumption was made that the yield of methoxyquinone was actually quantitative, it became possible to investigate the inorganic reactions involved in the reduction of the chlorine dioxide. To do this, 20 mM. samples of methoxyhydroquinone were oxidized in buffered solutions with 34 mM. to 38 mM. of chlorine dioxide, and after reaction was complete the excess of the gas was expelled

from solution by a stream of nitrogen into bubblers containing aqueous potassium hydroxide. All of the methoxyquinone formed was removed from the original liquor, whose content of "total chlorine" was determined by reducing an aliquot with ferrous sulphate and precipitating chloride as the silver salt. In all cases save run 7 (Table II, column 4) the "total chlorine"

TABLE II

REDUCTION OF CHLORINE DIOXIDE BY METHOXYHYDROQUINONE*

			Found in reaction mixture			Found in bubblers			
				Chloride			Chlorite		
Run	ClO_2 added, mM.	pH	Total chlorine, mM.	mM.	%†	Total chlorine, mM.	mM.	%‡	Halogen recovery, %§
(1)	(2)	(3)	(4)	(5)	(6)	(7)	(8)	(9)	(10)
1	—	2.2	19.7	16.9‖	86	—	—	—	—
2	—	2.2	19.4	12.7‖	65	—	—	—	—
3	38	2.2	20.5	18.9‖	92	14.0	7.0	50	91
4	36	1.0	19.4	9.3#	48	13.7	6.9	50	92
5	—	2.2	19.9	11.1#	56	—	—	—	—
6	34	2.2	20.8	13.1#	63	11.2	5.5	50	94
7	37	5.8	23.0	10.6#	46	10.7	5.3	50	91
8	—	1.0	20.1	12.5**	63	—	—	—	—
				12.7††					
9	37	2.2	20.5	13.3**	65	13.0	6.4	49	91
				13.4††					
10	—	2.2	20.3	12.7**	63	—	—	—	—
11	—	2.2	19.7	12.5**	64	—	—	—	—
				12.6††					

*Every experiment used 20 mM.
†Column 5 as per cent of column 4.
‡Column 8 as per cent of column 7.
§"Total chlorine" (columns 4 and 7) as per cent of chlorine dioxide added (column 2).
‖Determined with silver nitrate plus nitric acid.
#Determined with silver acetate plus water.
**Determined with silver acetate plus acetic acid.
††Determined by Mohr's titration with standard silver nitrate.

corresponding to 20mM. of the hydroquinone amounted to 20.1 ± 0.7 mM., or 1 mole of chlorine dioxide had supplied only two oxidizing equivalents, instead of the five equivalents found in an iodometric determination. The value of 23 mM. of "total chlorine" found in run 7 probably included chloride originating as chlorite, since the spontaneous decomposition of chlorine dioxide to chloride and chlorite was appreciable at pH 5.8 (11).

With the possible exception of run 7, no significant amount of chlorite was found in the oxidation liquors, and the "total chlorine" therefore originated exclusively in chloride and chlorate. A direct determination of chloride ion by precipitation as silver chloride in presence of nitric acid gave results (columns 5 and 6, runs 1, 2, 3) whose irreproducibility was traced to the action of the acid on the chlorate. The chloride ion was then precipitated with aqueous silver acetate, and any silver carbonate was removed from the precipitate by a subsequent extraction with dilute nitric acid. This method also was unsatisfactory (runs 4 to 7). The estimation of chloride in presence of chlorate was reproducible when silver acetate in 10% acetic acid was the precipitating agent, and these values agreed with those obtained by titrating the chloride ion in neutral solution with standard silver nitrate according to Mohr (18).

Experiments 8 to 11, which were considered reliable, showed that 63% to 65% or substantially two-thirds, of the "total chlorine" was present as chloride. Since chlorite was absent, the remaining one-third could be attributed to chlorate, and the equation for the oxidation of methoxyhydroquinone by chlorine dioxide could be written:

$$3\,C_6H_3(OCH_3)(OH)_2+3\,ClO_2\rightarrow 3\,C_6H_3(OCH_3)O_2+2\,HCl+HClO_3(+3\,O+3\,H).$$

Although this equation strongly suggested that hydrogen peroxide was formed, no reliable method could be found for detecting and estimating this substance in the reaction mixture. Hydrogen peroxide, however, is known to be a frequent by-product of the oxidation of hydroquinones to quinones, especially in alkaline solutions (13, 14).

The unsatisfactory oxygen and hydrogen balance in this equation made it desirable to complete the over-all chlorine balance by determining the excess halogen absorbed by the sodium hydroxide in the bubblers. Hypochlorite was absent, and therefore no free chlorine or chlorine monoxide gas had been transferred with the excess chlorine dioxide. Estimations for chloride gave a positive result of 2 mM. to 3 mM. in each case, but control experiments with pure sodium chlorite and sodium chlorate solutions of the relevant concentration, either alone or mixed, showed that the chlorite yielded 3 mM. of apparent chloride. The small chloride content of the bubblers was accordingly considered to be spurious. If this conclusion was correct, the traces of chloride found by Taylor and his collaborators (28) among the decomposition products of sodium chlorite in acid solution could perhaps be explained in the same way. Columns 7, 8, and 9 of Table II show that 50% of the chlorine was present as chlorite, and the remaining 50% was therefore chlorate. Since the above workers (28) demonstrated that no appreciable interaction occurred among the salts of the chlorine oxy-acids in alkaline solution, the fact that the chlorite and chlorate were in equimolecular amount was proof that the only form in which the halogen had entered the bubblers was as chlorine dioxide.

The total amount of halogen in the bubblers (column 7), plus that recovered in the reaction (column 4), amounted to 91% to 94% (column 10) of the chlorine dioxide originally used (column 2). Since the recovery of methoxyquinone was also about 92%, it seemed likely that up to 8% of chlorinated quinones had been formed during the oxidation. Such by-products would have remained in the reaction vessel, and their content of halogen might have escaped estimation as "total chlorine" (column 4).

A 91% yield of methoxyquinone was also obtained by oxidizing the hydroquinone at pH 0.9 with a fourfold molar amount of aqueous sodium chlorite, the initial red color of the liquor swiftly changing through green to yellow. The speed of this oxidation suggested that chlorous acid was the active agent, because the spontaneous decomposition of chlorous acid to chlorine dioxide in a control experiment was relatively slow. When this oxidation was repeated at pH 2.2, the initial red solution rapidly became opaque and after a few minutes deposited a 30.4% yield of the crystalline, purple 4,4′-dimethoxy diquinhydrone (Structure I*a* or I*b*) previously investigated by Erdtman (5). If the oxidation was allowed to proceed for about 10 min., the purple precipi-

tate of the diquinhydrone suddenly changed into a heavy, brown-yellow curd, and simultaneously the production of chlorine dioxide became apparent. A recrystallization of this precipitate gave a 30% yield of brilliant yellow needles which proved to be Erdtman's 4,4′-dimethoxydiquinone (II), and which when heated to about 210° C. underwent an intramolecular condensation to the red, crystalline isomer (III). Erdtman obtained the coupled products (I), (II), and (III) by oxidizing methoxyhydroquinone with ferric chloride or chromic acid, and suggested appropriate reaction mechanisms (3, 5).

In addition to the 30% yield of the diquinone (II) from the oxidation at pH 2.2, some monomeric methoxyquinone was extracted from the mother liquors. There were therefore two competing oxidations. At pH 4.0, the yield of the diquinone was 56% of theory; at pH 5.2, about 25%, and no methoxyquinone could be recovered. Near pH 6, the oxidations yielded precipitates of the purple diquinhydrone (I*a* or I*b*) but the transformation to the yellow diquinone (II) did not occur, presumably because the oxidation potential of aqueous sodium chlorite at pH 6 was insufficient.

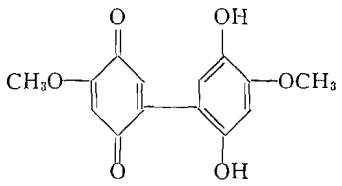

I*a* Purple. Decomp. 220° C.

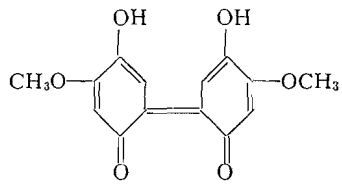

I*b*

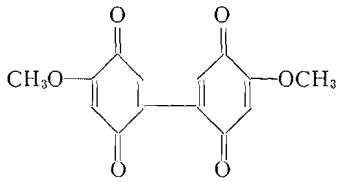

II. Yellow

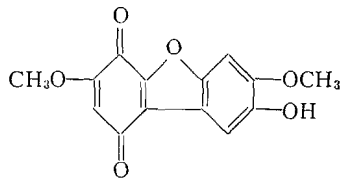

III. Red. Decomp. 250° C.

The experimental portion of this article does not record oxidations of salicylaldehyde, protocatechualdehyde, protocatechuic acid, and syringaldehyde with chlorine dioxide because no definite products were isolated. In each case the oxidation instantly produced a solution whose deep red color could be partially or completely discharged by zinc dust and acid, and which presumably contained unstable quinones. Syringaldehyde immediately reduced 1.1 to 1.5 molar equivalents of chlorine dioxide at 20° C.; at pH 2 or less the slow secondary reduction was minor, but at pH 4.5 a total of about 3 molar equivalents was consumed within two hours. When 1.5 moles per mole was used at pH 1 and near 5° C., the liquor, initially red, soon turned yellow, and then yielded a yellow oil when extracted with ether. This oil, like the aqueous residue, became deep red when kept.

In sharp contrast to the behavior of the free phenols hitherto discussed, the reduction of chlorine dioxide by a phenolic ether, veratric aldehyde, was

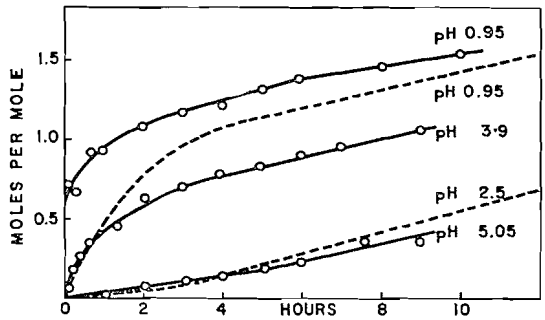

FIG. 2. Rate of oxidation of 0.001 *M* or 0.002 *M* solutions of veratraldehyde in 20% aqueous ethanol at 20° C. with approximately fourfold molar concentrations of oxidant. Solid lines, sodium chlorite; dotted lines, chlorine dioxide oxidations.

negligible at 20° C. and pH 6 to pH 3, was very slow at pH 2.5 (Fig. 2, broken lines), and even at pH 0.95 was not rapid. The liquors from oxidations carried out at pH 1, when extracted with ether, yielded yellow oils that were separated into acidic, aldehydic, and neutral fractions. The last two fractions were yellow-red oils whose color could be readily reduced by zinc and acid. They were not examined further. The acid fraction never exceeded 15% in yield, and contained veratric acid together with a chloro acid with the melting point, 185° to 187° C., of 5,6-dichloroveratric acid (24). Unfortunately, the amount of this acid was too minute to be definitely identified.

Fig. 2 (solid lines) also shows that the initial action of aqueous sodium chlorite on veratraldehyde at pH 0.95 was very rapid but, as in all other cases, became negligible on the alkaline side of pH 5. Yields of 91% and 92% of pure, crystalline veratric acid were isolated from experiments carried out at pH 1 and pH 4, respectively, and even more of the acid was produced, because some remained dissolved in the buffer. This method of preparing veratric acid was probably as convenient as any reported in the literature. Furthermore, since the yield at pH 4 could be assumed to be nearly quantitative, and since chlorine dioxide at this pH and 20° C. had no appreciable action on veratraldehyde for many hours, the reaction afforded a sound basis for studying the inorganic chemistry involved in the reduction of sodium chlorite without interference from the by-product chlorine dioxide.

Veratraldehyde, 10 mM., was oxidized with 29.4 mM. to 60.3 mM. of aqueous sodium chlorite in the apparatus previously used for the quantitative study of the reduction of chlorine dioxide by methoxyhydroquinone. The passage of nitrogen through the reaction liquor in experiments 1 and 2 (Table III) was slow, and eight or nine hours were required to transfer all of the chlorine dioxide into the traps containing aqueous potassium hydroxide. Subtraction of the "total chlorine" remaining in the reaction liquor (column 4) from the millimoles of sodium chlorite used (column 2) gave the amount of halogen expected in the traps. This amount was almost exactly recovered as "total chlorine" from the traps, and almost exactly 50% was present as chlorite, the remainder being assumed to be chlorate. The over-all chlorine

TABLE III

REDUCTION OF SODIUM CHLORITE BY VERATRALDEHYDE*

Run (1)	Chlorite added, mM. (2)	Hours (3)	Total chlorine, mM. (4)	Chloride, mM. (5)	Chlorite, mM. (6)	Chlorate,† mM. (7)	Chlorite‡ consumed, mM. (8)	Chlorine dioxide,§ mM. (9)
Chlorine dioxide slowly removed								
1	40.2	8	21.5	12.0	7.8	1.8	32.4	18.7‖
2	40.2	9	21.6	12.0	7.8	1.8	32.4	18.6#
Chlorine dioxide rapidly removed								
3	29.4	1.25	12.9	8.8	4.2	0.0	25.2	16.5
4	40.2	1.5	21.5	10.1	11.5	0.1	28.8	18.7
5	40.2	2	21.6	9.9	11.0	0.7	29.2	18.6
6	60.3	9	41.5	10.0	31.3	0.2	29.0	18.8

**Veratraldehyde, 10 mM., in 30 cc. of a sodium acetate – acetic acid buffer at pH 4.0, mixed near 20° C. with 50 cc. of aqueous sodium chlorite.*
†Column 4 minus columns 5 and 6.
‡Column 2 minus column 6.
§Column 2 minus column 4.
‖Chlorite, 9.2 mM. and "total chlorine", 18.3 mM, recovered in bubbler.
#Chlorite, 9.0 mM., and "total chlorine", 18.4 mM., recovered in bubbler.

balance was therefore satisfactory, and no volatile chlorine compound except chlorine dioxide had reacted with the alkali.

Of the "total chlorine" (column 4) found in experiments 1 and 2, 1.8 mM. was not accounted for as chloride and chlorite and was attributed to chlorate (column 7). On this assumption, a small amount of chlorine dioxide had decomposed during its long sojourn in the reaction mixture, and in consequence the amounts reported for chlorite consumed (column 8), chlorine dioxide (column 9), and for chloride (column 5), were not accurate. The observed molar ratios of 3.24: 1.87: 1.20 (with 1.0 for veratraldehyde) were nevertheless similar to those determined by Jeanes and Isbell (15) when they oxidized glucose with aqueous sodium chlorite in a sealed tube; that is, in contact with the by-product chlorine dioxide.

In order to confirm this interpretation of the data, in experiments 3 to 6 the chlorine dioxide was removed by a brisk current of nitrogen gas as soon as it was formed. Almost no chlorate was found in the reaction mixture and the content of chlorite plus chloride accounted satisfactorily for the "total chlorine" (columns 4 to 7). The mole ratios of chlorite: chlorine dioxide: chloride: veratraldehyde in experiments 4, 5, and 6 were 2.9 ± 0.02: 1.87 $\pm$ 0.01: 1.0 ± 0.01: 1.0, or were close to those required by the equation

$$RCHO + 3\ HClO_2 \rightarrow RCOOH + 2\ ClO_2 + HCl + H_2O.$$

Experiment 3, in which slightly less than 3 moles of sodium chlorite per mole of veratraldehyde was used, gave chlorite consumed: chlorine dioxide: chloride in the similar mole ratio of 2.86: 1.88: 1.0. The above equation was suggested by Jeanes and Isbell (15), and its validity for the oxidation of glucose was supported by the kinetic studies of Launer and Tominatsu (19, 20). Since 3 moles of sodium chlorite, corresponding to 12 oxidizing equivalents when determined iodometrically, were replaced by 2 moles of chlorine dioxide with

10 equivalents, the net response was only 2 equivalents, or one-sixth of the expected amount. The values in Fig. 2 giving the moles of sodium chlorite reduced at any time had therefore to be increased sixfold. Extrapolation to zero time of the later, nearly linear portion of the plot for the oxidation at pH 3.9 (solid line) pointed to an apparent consumption of about 0.5 mole of sodium chlorite per mole of veratraldehyde, in agreement with the very rapid initial oxidation at pH 0.95. The true consumption was therefore close to the proper value of 3 moles, and the later portions of the plots probably represented an iodometric response to the gradual decomposition of acidified sodium chlorite to chlorine dioxide and chlorate (28). This correction was not applied to the apparent consumption of chlorite by phenolic substances (e.g. Fig. 1) because in these cases the by-product chlorine dioxide was reduced to an unknown extent.

As expected, the rate plot for the oxidation of acetyl vanillin by aqueous sodium chlorite at 20° C. and pH 4.2 was similar to that of veratraldehyde at pH 3.9 (Fig. 2), although somewhat more of the oxidant was consumed and the yield of acetyl vanillic acid was only 78%. Small amounts of an unidentified, chlorinated product were also recovered. The above results were duplicated in an oxidation at pH 1. Acetyl vanillin failed to reduce aqueous chlorine dioxide at all at pH 2.3, pH 3.75, and pH 4.5, but at pH 1.1 an apparent consumption of 1.4 mole per mole occurred within one minute and did not increase thereafter. A 4% yield of 6-chlorovanillic acid was isolated; also a yellow oil with quinoidal properties, and 17% of an unresolved mixture that probably consisted of vanillic and chlorovanillic acid. Small amounts of vanillin and acetyl vanillic acid were recovered in some experiments. It appeared that at pH 1.1 most of the acetyl vanillin had first been hydrolyzed to vanillin, which had then been oxidized as described in the previous article (11). A portion, however, had probably been chlorinated and oxidized prior to deacetylation, because vanillin itself tends to become substituted in the 5-, rather than in the 6-position (25).

It was interesting to note that chlorine dioxide regained the capacity to oxidize acetyl vanillin at pH 5.65, the apparent consumption of 0.5 mole of oxidant being complete within one hour. At pH 6.0 about 1 mole per mole was reduced within 25 min. Yields of 35% and 25%, respectively, of acetyl vanillic acid were isolated, and the other product was unchanged acetyl vanillin. The oxidation of the aldehyde group therefore competed with the decomposition of the chlorine dioxide to chlorite and chlorate, which was rather rapid near pH 6 (15). The by-product chlorite, however, could hardly be responsible for the oxidation, because chlorite at pH 6 and 20° C. was incapable of oxidizing vanillin (15).

EXPERIMENTAL

Materials and Methods

Commercial *p*-hydroxybenzaldehyde, vanillin, and resublimed pyrogallol, also synthetic syringaldehyde kindly given by Dr. P. A. Pearl, of the Institute of Paper Chemistry, Appleton, Wis., were recrystallized to constant melting

point. Purpurogallin was prepared by oxidizing pyrogallol with a neutral solution of sodium iodate (7, 8), and the bright orange crystals were definitely identified by their decomposition point of 272° C., and by the correct melting points of their tetraacetate (9, 22) and trimethyl ether (8, 22), 187° C. and 177° C., respectively. Pure veratraldehyde was prepared by methylating vanillin (1), and the oxidation of vanillin with alkaline hydrogen peroxide as described by Dakin (2) yielded 70% of recrystallized methoxy-*p*-hydroquinone (3). This substance melted at 88° to 89° C., and not at 84° C., as found by Will (32). The acetylation of vanillin (23) yielded acetyl vanillin with the correct melting point of 77° C.

The sodium chlorite of Analytical Grade was the gift of the Mathieson Alkali Company of New York, and aqueous solutions of chlorine dioxide were prepared and standardized as described previously (11). All oxidations were carried out in the dark or in amber colored bottles in order to minimize the photochemical decomposition of chlorine dioxide. The previous iodometric methods were used to follow most of the oxidations.

Reduction of Sodium Chlorite by Pyrogallol (Fig. 1)

In a typical experiment, sodium chlorite, 4.61 gm. (0.05 mole, corrected for a purity of 98.1%) and pyrogallol, 0.945 gm. (0.0075 mole) were separately dissolved in 250 cc. volumes of 0.4 *M* phosphate buffer of the desired pH and were brought to 22.3° ± 0.1° C., or 15.8° ± 0.2° C. in a constant temperature bath. The solutions were then mixed, and kept at the desired temperature; small aliquots were removed at intervals and checked for constancy in pH.

In order to follow the reduction of the sodium chlorite, 25 cc. aliquots, which could not be more than 0.05 *M* in chlorite or pyrogallol, were discharged into 10 cc. of 4% aqueous sodium bisulphite. Concentrated hydrochloric acid, 1 cc., was added, and the mixture was boiled for 15 min. to expel all sulphur dioxide that had not been oxidized to sulphate (12). A few drops of concentrated nitric acid were then added to destroy the amorphous organic material that usually separated at some stage of the oxidation of pyrogallol, and after being boiled for some time longer, the mixture was diluted to 200 cc. with distilled water. The sulphate was estimated according to the standard procedure as the barium salt. After correction for the blank (about 0.1 gm.), 1 mole of sodium chlorite was assumed to be equal to 2 moles of barium sulphate. The experiments with purpurogallin were conducted in the same way.

Oxidation of p-Hydroxybenzaldehyde to Benzoquinone (Table I)

Samples of the aldehyde, 1.22 gm. or 0.01 mole, were dissolved in 50 cc. volumes of water adequately buffered with citric acid – sodium hydroxide to pH 6.0, 5.0, 3.0, and 2.2; sulphuric acid was used as the buffer for pH 1. After being mixed with 65 cc. of 0.48 *M* aqueous chlorine dioxide (0.031 mole), the mixtures were cooled to keep their temperature below 30° C. One hour or one-half hour later, the mixtures were flushed with nitrogen to expel chlorine dioxide, were saturated with sodium chloride, and were extracted with 250 cc. volumes of ether. Each extract was cautiously evaporated and the residue was dissolved in 25 cc. of distilled water; an equal volume of water containing

1.2 gm. of hydroquinone was added, and some time later the precipitate of the green, crystalline quinhydrone was recovered, dried, and weighed (17).

The experiments were repeated with the substitution of 50 cc. of water containing 0.04 mole of sodium chlorite for the aqueous chlorine dioxide. When desired, the above ether extract was dried, evaporated, and extracted with petroleum ether to recover the yellow needles of quinone. These crystals were readily reduced with sodium hydrosulphite and were identified as hydroquinone with the correct melting point of 171° C. (16).

Oxidation of Methoxyhydroquinone with Chlorine Dioxide (Table II)

(*a*) A solution of 2.8 gm. of methoxyhydroquinone (0.02 mole) in 28 cc. of 10% acetic acid (pH 2.2) was mixed with 80 cc. of 0.464 *M* aqueous chlorine dioxide (0.037 mole) at room temperature. After about 20 min. the green-yellow flocculent precipitate was recovered and dried; yield, 1.8 gm., m.p. 143° to 144° C. More of the product, 0.7 gm., was obtained by extracting the filtrate with ether, and the total yield was 92% of theory. After recrystallization from petroleum ether, the bright yellow substance had the melting point, 144° to 145° C., reported by Erdtman (3) for methoxyquinone.

The aqueous residues, now free of chlorine dioxide, required 27.8 cc. of 0.1 *N* sodium thiosulphate in an iodometric titration, an amount which suggested the presence of 1.39 millimoles (7%) of quinone-like substances.

(*b*) The all-glass apparatus used for studying the inorganic chemistry of the oxidation consisted of a 500 cc. round-bottom flask with an inlet for nitrogen reaching nearly to the bottom and an exit for chlorine dioxide. This exit conveyed the gas through two absorption vessels containing 20% aqueous potassium hydroxide. The best results were obtained when the inlet to the test tube which served as the second vessel was drawn out to a fine capillary.

The apparatus was immediately assembled after the mixture of 0.02 mole of methoxyhydroquinone and sodium chlorite described in (*a*) had been prepared in the 500 cc. flask. After 20 min., when the oxidation was known to be complete, the flask was covered with a dark cloth and nitrogen was passed through the apparatus at a rate slow enough for the chlorine dioxide to be completely absorbed in the alkali. This operation took up to eight hours. The two alkaline solutions were then combined and made up to 500 cc. with water. Methoxyquinone was removed from the reaction liquor, and the filtrate was also made up to 500 cc.

The method described by Treadwell (29) was used to determine total chlorine. A 100 cc. aliquot was boiled for 15 min. with 50 cc. of 10% aqueous ferrous sulphate in order to reduce any chlorite and chlorate to chloride. It was necessary to neutralize the alkaline aliquots before carrying out this reduction. After the mixture had been cooled, the brown precipitate was redissolved by adding nitric acid, and the chloride was determined gravimetrically as silver chloride. As previously noted, the chloride present as such in the reaction vessel could be determined most satisfactorily by the Mohr (18) method, a 100 cc. aliquot being carefully neutralized with sodium carbonate and then titrated with standard 0.1 *N* silver nitrate, with potassium chromate as the indicator.

To estimate chlorite, a 10 cc. aliquot of the alkaline solution was treated with excess potassium iodide and sulphuric acid, and the liberated iodine was titrated with 0.04 *N* sodium thiosulphate. One mole of chlorite was equivalent to four atoms of iodine. The chlorate was found by subtracting the chlorite content from the total chlorine present. Since the chlorine dioxide reacted with the potassium hydroxide to form 1 mole of chlorite and 1 mole of chlorate,

$$2\ ClO_2 + 2\ KOH \rightarrow KClO_2 + KClO_3 + H_2O,$$

the chlorine dioxide absorbed was twice the amount of chlorite formed (28).

Oxidation of Methoxyhydroquinone with Sodium Chlorite

(*a*) A solution of the hydroquinone (0.01 mole) in 10 cc. of 10% acetic acid (pH 2.2) was mixed with another containing 0.04 mole of sodium chlorite. A few minutes later, the purple precipitate (0.41 gm. or 30.4%) could be recovered on a filter and recrystallized from pyridine. The powder decomposed at 220° C. If the filtration was delayed for about 11 min., the product was a yellow powder isolated in 30% yield and insoluble in ether, alcohol, and other organic liquids tried with the exception of boiling acetic anhydride. Recrystallization from this solvent gave brilliant golden needles which turned red on heating to about 210° C. and melted at 250° C. The melting point and other properties agreed with those recorded by Erdtman (5) for 4,4′-dimethoxydiquinone.

(*b*) The experiment was repeated with the same quantities, but the 10% acetic acid was replaced by dilute sulphuric acid to adjust the pH to 0.9. In this case the mixture quickly turned red, and then a green precipitate settled which rapidly became yellow. The product (1.01 gm.) was recovered, and also a further 0.24 gm. by extracting the mother liquor with ether. This substance, isolated in a total yield of 91%, had the melting point, 146° C., of methoxyquinone, and a mixed melting point with an authentic sample was not depressed.

Oxidation of Veratraldehyde with Chlorine Dioxide (*Fig. 2*)

(*a*) Experiments on the rate of oxidation were carried out as described for those with *p*-hydroxybenzaldehyde, but the buffer solutions were made up in 20% aqueous ethanol because veratraldehyde was insoluble in water.

(*b*) Veratraldehyde, 4.98 gm. (0.03 mole), dissolved in 400 cc. of 20% alcohol buffered to pH 1.0 with sulphuric acid, was mixed with 0.06 mole of 0.38 *M* chlorine dioxide. No immediate change occurred and no obvious amount of heat was generated, but on standing an amber and finally a red color appeared. The solution was extracted with ether after 10 hr. and the extract in turn extracted, first with saturated sodium bisulphite solution to remove aldehydes, and then with saturated sodium bicarbonate to remove acids.

After recovery from the bicarbonate liquor, the crude acidic fraction, 0.90 gm., was extracted with petroleum ether to remove 0.40 gm. of a mixture of chlorinated acids that could not be thoroughly resolved. One small fraction of colorless needles melted sharply at 185° to 186° C. and might have been 5,6-dichloroveratric acid (24). The remaining 0.5 gm. when repeatedly re-

crystallized from benzene gave crystals whose melting point of 180° to 181° C. was not depressed by admixture with an authentic sample of veratric acid.

Oxidation of Veratraldehyde with Sodium Chlorite (Fig. 2, Table III)

(*a*) The rate of oxidation was determined in 20% aqueous ethanol buffered to the desired pH, and the consumption of chlorite was followed by iodometry. In larger scale experiments, 25 cc. of an aqueous solution contained 10.9 gm. of sodium chlorite (0.12 mole) was mixed with 125 cc. of water plus 18 cc. of ethanol buffered to pH 1.0 with sulphuric acid and containing 5 gm. (0.03 mole) of veratraldehyde. A pale pink precipitate, 5.1 gm., settled out of the solution almost immediately. A single recrystallization from dilute acetic acid yielded 4.9 gm. (91%) of colorless plates whose melting point of 180° to 181° C. was undepressed by admixture with pure veratric acid.

(*b*) The apparatus, the technique, and the analytical methods were the same as those employed in studying the oxidation of methoxyhydroquinone with chlorine dioxide. Veratraldehyde, 1.662 gm. (0.01 mole), dissolved in 30 cc. of an adequate sodium acetate – acetic acid buffer at pH 4.0, was mixed with 50 cc. of water containing 0.04 mole of sodium chlorite. The reaction vessel was aerated with nitrogen, either at a slow or fast rate, but never rapidly enough to bring about an incomplete absorption of by-product chlorine dioxide in the potassium hydroxide bubblers. Crystalline veratric acid separated almost immediately in 92% yield. This product was removed as soon as the absorption of chlorine dioxide was complete, the filtrate and the alkaline absorption liquors were separately diluted to volumes of 500 cc., and aliquots were analyzed.

Oxidation of Acetylvanillin with Chlorine Dioxide

A solution of acetylvanillin, 0.04 mole, buffered to pH 1.0 with 4% sulphuric acid, was mixed with 0.08 mole of aqueous chlorine dioxide. Eight hours later, when its color had turned orange-yellow, the solution was extracted with ether, the extract was shaken with barium carbonate to remove any entrained sulphuric acid, and was then dried over anhydrous sodium sulphate. The residue from the ether was extracted with petroleum ether, which removed a small quantity of a yellow oil, and then with boiling benzene. The latter extract on cooling deposited 0.31 gm. (4%) of colorless needles melting at 207° C. Found: OCH_3, 15.3, 15.1%. Calc. for $C_8H_7O_4Cl$: OCH_3, 15.3%. A mixed melting point with 6-chlorovanillic acid prepared according to Raiford and Potter (26) was not depressed.

When extracted with bisulphite, the benzene mother liquor yielded a small amount of vanillin, and, when re-extracted with sodium bicarbonate, the sodium salts of some acids. The free acids, amounting to 1.45 gm. after several recrystallizations from ether, melted from 185° C. to 187° C. with decomposition, and contained chlorine. Found: OCH_3, 17.1, 17.3%. Calc. for $C_8H_7O_4Cl$: OCH_3, 15.3%; for $C_8H_8O_4$: OCH_3, 18.5%. Vanillic acid melts at 208° to 210° C. (21) and the 6-chloro derivative at 207° C. In other runs small amounts of acetylvanillic acid were identified.

Oxidation of Acetylvanillin with Sodium Chlorite

Acetylvanillin, 4.0 gm. (0.021 mole), dissolved in 50 cc. of alcohol and 50 cc. of 4% sulphuric acid (pH 1), was oxidized with a solution of 7.3 gm. (0.08 mole) of sodium chlorite in 25 cc. of water. After 3.5 hr. the mixture was chilled to 5° C. and was diluted with water. The crystals which deposited melted at 147° to 147.5° C. and a mixed melting point with authentic acetylvanillic acid was not depressed. Yield, 3.4 gm. or 78.5% of theory. An oxidation carried out in a sodium acetate – acetic acid buffer at pH 4.2 gave the same yield.

ACKNOWLEDGMENT

Two of us (R.M.H. and C.D.L.) wish to thank the Brown Company for the two Fellowships, and the Canadian Pulp and Paper Association for the three summer stipends, awarded to them during the research.

REFERENCES

1. Buck, J. R. Organic syntheses. Collective Vol. II. John Wiley & Sons, Inc., New York. 1944. p. 619.
2. Dakin, H. D. Am. Chem. J. 42: 477. 1909.
3. Erdtman, H. G. H. Proc. Roy. Soc. (London), A, 143: 177. 1934.
4. Erdtman, H. G. H. Proc. Roy. Soc. (London), A, 143: 191. 1934.
5. Erdtman, H. G. H. Proc. Roy. Soc. (London), A, 143: 223. 1934.
6. Erdtman, H. G. H. Proc. Roy. Soc. (London), A, 143: 228. 1934.
7. Evans, T. W. and Dehn, W. M. J. Am. Chem. Soc. 52: 3647. 1930.
8. Haworth, R. D., Moore, B. P., and Pauson, P. L. J. Chem. Soc. 1045. 1948.
9. Haworth, R. D., Moore, B. P., and Pauson, P. L. J. Chem. Soc. 3271. 1949.
10. Henrich, F. Sitzber. physik.-med. Sozietät Erlangen, 71: 199. 1939. Chem. Abstr. 35: 3997. 1941.
11. Husband, R. M., Logan, C. D., and Purves, C. B. Can. J. Chem. 33: 81. 1955.
12. Jackson, D. T. and Parsons, J. L. Ind. Eng. Chem., Anal. Ed. 9: 14. 1937.
13. James, T. H., Snell, J. M., and Weissberger, A. J. Am. Chem. Soc. 60: 2087. 1938.
14. James, T. H. and Weissberger, A. J. Am. Chem. Soc. 60: 98. 1938.
15. Jeanes, A. and Isbell, H. S. J. Research Natl. Bur. Standards, 26: 205. 1941.
16. Kempf, R. J. prakt. Chem. 78 (2): 256. 1908.
17. Kimijima, T. and Kishino, N. J. Soc. Chem. Ind. Japan, 47: 273. 1944. Chem. Abstr. 42: 6769. 1948.
18. Kolthoff, I. M. and Sandell, E. B. Textbook of quantitative inorganic analysis. 3rd ed. The MacMillan Co., New York. 1952. p. 451.
19. Launer, H. F. and Tominatsu, Y. Anal Chem. 26: 382. 1954.
20. Launer, H. F. and Tominatsu, Y. J. Am. Chem. Soc. 76: 2591. 1954.
21. Misani, F. and Bogert, M. T. J. Org. Chem. 10: 347. 1945.
22. Perkin, A. G. and Steven, A. B. J. Chem. Soc. 83: 192. 1903.
23. Pschorr, R. and Sumuleanu, C. Ber. 32: 3405. 1899.
24. Raiford, L. C. and Floyd, D. E. J. Org. Chem. 8: 358. 1943.
25. Raiford, L. C. and Lichty, J. G. J. Am. Chem. Soc. 52: 4576. 1930.
26. Raiford, L. C. and Potter, D. J. J. Am. Chem. Soc. 55: 1682. 1933.
27. Schmidt, E., Hagg, W., and Sperlin, L. Ber. 58: 1394. 1925.
28. Taylor, M. C., White, J. F., Vincent, G. P., and Cunningham, G. L. Ind. Eng. Chem. 32: 899. 1940.
29. Treadwell, F. P. Analytical chemistry. Vol. II. 4th ed. *Translated by* W. T. Hall. John Wiley & Sons, Inc., New York. 1915. p. 461.
30. Wacek, A. v. and Bézard, A. Ber. 74, B: 845. 1941.
31. Wacek, A. v. and Eppinger, H. O. Ber. 73, B: 644. 1940.
32. Will, W. Ber. 21: 602. 1888.
33. Willstätter, R. and Majima, R. Ber. 43: 1171. 1910.

PRÉPARATION DE DÉRIVÉS DU PAPAVÉRINOL ET DES HYDROXYLAUDANOSINES[1]

PAR JEAN-LOUIS FERRON ET PHILIBERT L'ECUYER

SOMMAIRE

La préparation du papavérinol et des hydroxylaudanosines a été améliorée en apportant diverses modifications au mode opératoire déjà suivi. Par la méthode de Williamson, les éthers *n*-propylique, *n*-hexylique, *n*-décylique, et benzylique du papavérinol ont été obtenus avec d'excellents rendements. Par l'action des chlorures d'acide appropriés sur les hydroxylaudanosines en présence de pyridine, l'acétyl-salicylate, le benzoate, le butyrate, l'isovalérate, et le caproate de l'α-hydroxylaudanosine et le butyrate et le benzoate de la β-hydroxylaudanosine ont été synthétisés.

INTRODUCTION

Plusieurs travaux ont éte publiés concernant la préparation de dérivés ou d'homologues de la papavérine (1); un seul a été consacré à la synthèse de bases quaternaires et d'esters du papavérinol (II, R = H) (3), aucun à celle de dérivés des hydroxylaudanosines (III, R = H). Le présent travail avait pour but la synthèse d'éthers du papavérinol et d'esters de l'α- et de la β-hydroxylaudanosine.

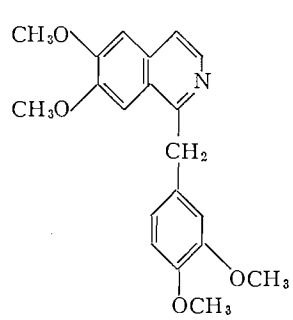

(I)

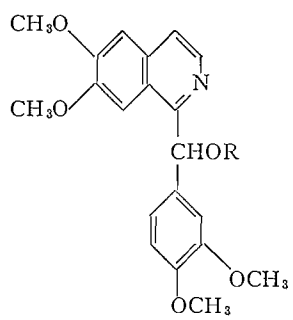

(II)

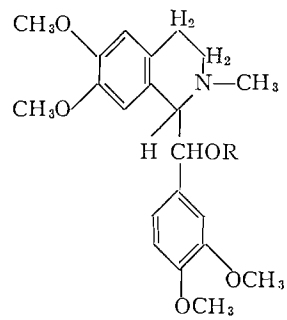

(III)

Nous avons préparé le papavérinol en oxydant la papavérine en solution acétique à l'aide de l'acétate mercurique selon la méthode de Gadamer (1), mais nous l'avons isolé et purifié par l'intermédiaire du perchlorate ce qui permet pratiquement de doubler le rendement.

Les hydroxylaudanosines sont facilement synthétisées par la réduction catalytique du méthochlorure de papavérinol (2), obtenu par la transformation du méthiodure à l'aide du chlorure d'argent. Nous avons préparé ce méthiodure avec un rendement de 86% en faisant réagir le papavérinol et l'iodure de méthyle sous pression et en purifiant le produit par l'intermédiaire du perchlorate.

En appliquant la méthode de Williamson (4) pour la préparation des éthers nous avons réussi avec d'excellents rendements la synthèse de quelques éthers du papavérinol en faisant bouillir à reflux une solution benzénique d'un

[1]*Manuscrit reçu le 29 septembre 1954.*
Contribution du Département de Chimie de l'Université Laval, Québec, Qué.

halogènure d'alkyle ou d'aryle en présence du sel de sodium du papavérinol. Nous avons ainsi obtenu les éthers *n*-propylique, *n*-hexylique, et *n*-décylique (II, R = C_3H_7, C_6H_{13}, et $C_{10}H_{21}$) identifiés sous forme de perchlorate, et l'éther benzylique (II, R = $CH_2C_6H_5$) caractérisé sous forme de picrate. Les rendements varient de 85 à 100%.

D'autre part, par l'action de chlorures d'acide sur les hydroxylaudanosines en présence de pyridine comme agent de condensation nous avons synthétisé quelques esters. L'acétyl-salicylate de l'α- et les benzoates de l'α- et de la β-hydroxylaudanosine (III, R = $C_6H_4(OCOCH_3)CO$ et C_6H_5CO) ont été obtenus à l'état solide. Les autres esters, le butyrate de la β- et l'isovalérate et le caproate de l'α-hydroxylaudanosine (III, R = C_3H_7CO, Me_2CHCH_2CO, $CH_3(CH_2)_4CO$), qui se séparent à l'état liquide, ont été purifiés sous forme de picrates. Les rendements varient de 25 à 50%.

PARTIE EXPÉRIMENTALE

Papavérinol

A de la papavérine (25.0 g., 0.073 mole) dissoute dans l'eau (125 ml.) et l'acide acétique (25 ml.) est ajoutée une solution d'acétate mercurique (50 g., 0.156 mole) dans l'acide acétique dilué (150 ml. d'acide 1 : 5). Après être laissé à la température ambiante pendant 24 h. le mélange est maintenu dans un bain d'eau à 70°C. pendant deux heures, refroidi, débarrassé par filtration de l'acétate mercureux et additionné d'acide chlorhydrique dilué (250 ml. d'acide 1 : 4). On porte la suspension sur bain-marie et on sature à chaud par un courant lent d'hydrogène sulfuré. Le précipité de sulfure de mercure est filtré et lavé à l'acide acétique dilué (50 ml. d'acide 1 : 4) et le filtrat alcalisé à la soude et extrait au chloroforme. Le résidu de papavérinol brut obtenu après l'évaporation à sec de la solution chloroformique sur bain-marie est dissous dans l'alcool éthylique (150 ml.) et la solution acidulée (pH2) à l'acide perchlorique à 70%. La perchlorate de papavérinol précipite sous forme de sel jaune pur de p.f. 201–202°C. Rendement: 96.7% (32.5 g.). Calculé pour $C_{20}H_{22}O_9NCl$: C, 52.7%; H, 4.9. Trouvé: C, 52.5%; H, 4.83%.

Le papavérinol est libéré en alcalisant à la soude la suspension du perchlorate dans l'eau chaude. Il est ensuite extrait au chloroforme et la solution chloroformique est séchée et évaporée à sec. Le résidu fournit après une cristallisation dans l'alcool éthylique le papavérinol pur de p.f. 138°C. Rendement: 86% (22.5 g.).

Méthiodure de papavérinol

Du papavérinol (10.0 g., 0.028 mole) et de l'iodure de méthyle (30 ml., 0.48 mole) sont chauffés pendant quatre heures dans une bouteille à pression dans un bain d'eau à 80°C. Le mélange est refroidi, l'excès d'iodure de méthyle est récupéré par distillation, et le résidu broyé dans l'acétone (environ 50 ml.). La suspension est filtrée et le méthiodure lavé avec une quantité additionnelle d'acétone (50 ml.). Rendement: 89.5% (12.6 g.).

Hydroxylaudanosines

Du méthiodure de papavérinol (78 g., 0.153 mole) dans l'alcool à 50% (250 ml.) est transformé en méthochlorure par réaction sur bain-marie avec du

chlorure d'argent fraîchement précipité (30 g., 0.2 mole). Le méthochlorure est cristallisé dans l'alcool éthylique, p.f. 205–206°C. Rendement: 97% (60.0 g.). Ce méthochlorure (0.168 mole) en solution dans l'alcool méthylique aqueux (400 ml., 5 : 3) est réduit catalytiquement à 55°C. sous pression (2–3 atmosphères) en présence de 3.0 g. d'un mélange hydroxyde de palladium – carbonate de calcium à 20% de $Pd(OH)_2$. Le catalyseur est filtré, le filtrat concentré sous pression réduite, dilué à environ 100 ml., et rendu alcalin par la soude à 30%. Les hydroxylaudanosines précipitées sont filtrées, séchées, et cristallisées dans l'alcool absolu (200 ml.). L'α-hydroxylaudanosine pure de p.f. 138°C. est obtenue après une seule cristallisation. Rendement: 41.7% (23.0 g.). Les eaux-mères saturées par un courant de gaz chlorhydrique sec donnent le chlorhydrate de la β-hydroxylaudanosine de p.f. 235°C. dont la base elle-même de p.f. 109°C. est libérée. Rendement du chlorhydrate: 24.5% (15.0 g.).

Ethers du papavérinol

On fait réagir à reflux, pendant 10 h., du papavérinol (1.0 g., 0.003 mole) avec un morceau de sodium (environ un gramme) dans du benzène anhydre (25 ml.). On retire l'excès de sodium, on ajoute le bromure d'alkyle ou d'aryle (1 ml.), et on chauffe de nouveau à reflux pendant cinq heures additionnelles. On chasse ensuite sous vide partiel le benzène et l'excès de bromure et on dissout dans l'éther (10–15 ml.). L'extrait éthéré est filtré, évaporé à sec sur bain-marie, et le résidu dissous dans l'alcool éthylique (10 ml.). On précipite ensuite, suivant le cas, soit sous forme de perchlorate en acidulant à pH 2 avec de l'acide perchlorique à 70% ou sous forme de picrate en ajoutant une solution saturée d'acide picrique dans l'alcool (10 ml.). On filtre, lave le précipité avec quelques millilitres d'alcool, et on cristallise le perchlorate dans un mélange alcool–dioxane (4 : 1) et le picrate dans l'alcool. Les rendements varient de 85 à 100%.

Les résultats de ces synthèses sont donnés dans le tableau I.

TABLEAU I

ETHERS DU PAPAVÉRINOL

Ethers	Rend., %	P.f., °C.	Solvant	Formule brute	Analyses			
					Carbone, %		Hydrogène, %	
					Calculé	Trouvé	Calculé	Trouvé
n-Propyle*	90	145–150 (déc.)	Alcool–dioxane 4 : 1	$C_{23}H_{28}O_9NCl$	55.5	55.3	5.7	6.1
n-Hexyle*	85	137	Alcool–dioxane 4 : 1	$C_{26}H_{34}O_9NCl$	57.8	57.3	6.3	6.5
n-Décyle*	95	180	Alcool–dioxane 4 : 1	$C_{30}H_{42}O_9NCl$	60.4	60.0	7.1	7.0
Benzyle†	100	126–127	Alcool	$C_{33}H_{30}O_2N_4$	58.7	58.9	4.5	4.9

**Les données sont celles du perchlorate.*
†*Les données sont celles du picrate.*
Les rendements ont été calculés d'après la quantité de sel brut précipité.

TABLEAU II

ESTERS DES HYDROXYLAUDANOSINES

Alcool	Ester	Rend., %		P.f., °C.		Solvant		Formule brute	Analyses					
									Carbone, %		Hydrogène, %		Azote, %	
		Ester	Picrate	Ester	Picrate	Ester	Picrate		Calculé	Trouvé	Calculé	Trouvé	Calculé	Trouvé
α-Hydroxyl-audanosine	Butyrate	—	24	—	139	—	Benzène	$C_{31}H_{36}O_{13}N_4$	55.3	55.3	5.4	5.2	8.0	8.1
	Isovalérate	—	27	—	151	—	Dioxane – éther de pétrole	$C_{32}H_{38}O_{13}N_4$	56.0	55.8	5.6	5.4	8.2	7.8
	Caproate	—	36	—	158	—	Benzène	$C_{33}H_{40}O_{13}N_4$	56.6	56.2	5.8	5.9	8.0	7.8
	Benzoate	45	—	120	182	Alcool – éther de pétrole	Propanol – dioxane	$C_{38}H_{31}O_6N$ (ester) $C_{34}H_{34}O_{13}N_4$	70.4	70.7	6.5	6.6	7.9	7.9
	Acétyl-salicylate	51	—	125	163	Alcool – éther de pétrole	Propanol–dioxane	$C_{30}H_{32}O_8N$ (ester) $C_{36}H_{36}O_{15}N_4$	67.3	67.3	6.2	5.8	7.4	7.3
β-Hydroxyl-audanosine	Butyrate	—	35	—	137	—	Benzène	$C_{31}H_{36}O_{13}N_4$	55.3	55.2	5.4	5.4	8.0	8.2
	Benzoate	49	—	130	187	Alcool – éther de pétrole	Dioxane	$C_{28}H_{31}O_6N$ (ester) $C_{34}H_{34}O_{13}N_4$	70.4	70.8	6.5	6.6	7.9	8.0

Tous les pourcentages sont ceux qui ont été déterminés à l'analyse des picrates sauf pour les benzoates et l'acétyl-salicylate dont les pourcentages de carbone et d'hydrogène ont été obtenus à l'analyse des esters libres.

Esters des hydroxylaudanosines

De l'hydroxylaudanosine (0.5 g.), de la pyridine (0.5 ml.), et du chlorure d'acide (0.5 ml.) sont chauffés sur bain-marie pendant quelques minutes et laissés à la température ambiante pendant 12 h. La gomme formée est triturée dans l'eau (5 ml.) et agitée avec l'éther (trois fois avec 10 ml.) jusqu'à l'obtention d'une solution limpide. Les extraits éthérés sont rejetés et la partie aqueuse est diluée à environ 15 ml. et filtrée. Le filtrat est neutralisé par un excès de bicarbonate de sodium. Le benzoate et l'acétyl-salicylate précipitent à l'état solide et sont purifiés directement par cristallisation dans un solvant approprié. Les autres esters se séparent sous forme d'huile et sont identifiés par la formation d'un picrate. L'ester est dissous dans l'alcool éthylique (5 ml.). Cette solution alcoolique est séchée sur du sulfate de sodium anhydre, filtrée, et le picrate de l'ester est précipité par l'addition d'une solution alcoolique saturée d'acide picrique (5 ml.). Le picrate est filtré, lavé avec quelques millilitres d'alcool, et recristallisé dans un solvant approprié. Les rendements varient de 25 à 50%.

Les résultats des synthèses de ces esters sont donnés dans le tableau II.

REMERCIEMENTS

Les auteurs remercient le Conseil National des Recherches et l'Office des Recherches de la Province de Québec pour l'aide financière accordée à l'un d'eux (J.-L. F.) sous forme de bourse ou d'octroi de recherches.

BIBLIOGRAPHIE

1. GADAMER, J. and SCHULEMANN. Arch. Pharm. 253: 284. 1915.
2. KING, F. E., L'ECUYER, P., and PYMAN, E. L. J. Chem. Soc. 731. 1936.
3 STUCHLIK, L. Monatsh. 21: 822. 1900.
4. WILLIAMSON. Phil. Mag. 337: 350. 1850.

ESSAI DE SYNTHÈSES PSEUDOPHYSIOLOGIQUES DE 6,7-DIMÉTHOXYISOQUINOLÉINES[1]

PAR JEAN-LOUIS FERRON ET PHILIBERT L'ECUYER

SOMMAIRE

L'acide diméthyl dihydrocaféique, l'eugénol glycol, le méthyleugénol glycol, et l'aldéhyde homovératrique ont été synthétisés par une nouvelle série de réactions. En aucun cas, il a été possible d'isoler une autre base que l'amine de départ lors des essais de condensation, dans des conditions pseudophysiologiques, de l'homovératrylamine et de la N-méthylhomovératrylamine avec divers aldéhydes et cétones bien que la récupération de la base ne dépasse jamais 84%. En dépit de certaines prétentions il semble donc que pour toute fin pratique ce mode de condensation soit irréalisable avec ces amines et d'autres du même genre à moins que les groupements hydroxyles de l'amine ne soient à l'état libre.

INTRODUCTION

A la suite de la synthèse de la tropinone par Robinson (12) plusieurs préparations d'alcaloides ont été effectuées *in vitro* à partir de substances supposées être des produits de dégradation des acides animés. Ces synthèses pseudophysiologiques s'effectuent simplement en laissant séjourner à la température ambiante les substances de départ dans des solutions tampons.

Parmi les substances synthétisées de cette façon il convient de mentionner la lobelamine (16), la pseudopelletiérine (16), la rutécarpine (18), la téloidinone (13), et le tétrahydroharmane (5). Dans le groupe de la quinoléine Schöpf et Lehmann (15) ont réussi la préparation de quinoléines mono- et bi-substituées en position 2 et 3 à partir de l'*o*-aminobenzaldéhyde (I) et de cétones (II, R_1 = H ou groupe alkyle; R_2 = CH_3 ou groupe aryle) ou d'acides β-cétoniques (II, R_1 = CO_2H; R_2 = groupe alkyle ou aryle). Dans la série de l'isoquinoléine

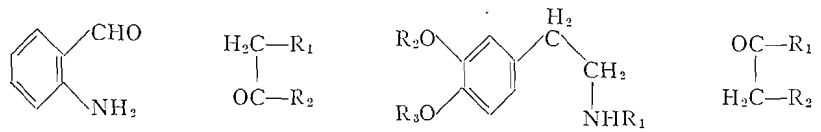

(I) (II) (III) (IV)

Schöpf et Bayerle (14) ont réalisé la condensation de l'acide acétique avec deux amines: la β-(3,4-dihydroxyphényl)-éthylamine (III, R_1 = R_2 = R_3 = H) et la N-méthyl-β-(3,4-dihydroxyphényl)-éthylamine (III, R_1 = CH_3; R_2 = R_3 = H) tandis que Schöpf et Salzer (17) ont réussi la synthèse de la 1-(3′4′-méthylènedioxybenzyl)-6,7-dihydroxytétrahydroisoquinoléine (V, R_1 = R_2 = OH; R_3R_4 = CH_2O_2) à partir du pipéronal (II, R_2 = H; R_1 = 3,4-méthylènedioxyphényl) et de la β-(3,4-dihydroxyphényl)-éthylamine (III, R_1 = R_2 = R_3 = H).

A la suite de ces travaux Schöpf (14) a émis l'hypothèse que la réussite des synthèses physiologiques de dérivés de la tétrahydroisoquinoléine à partir des

[1]*Manuscrit reçu le 29 septembre 1954.*
Contribution du Département de Chimie de l'Université Laval, Québec, Qué.

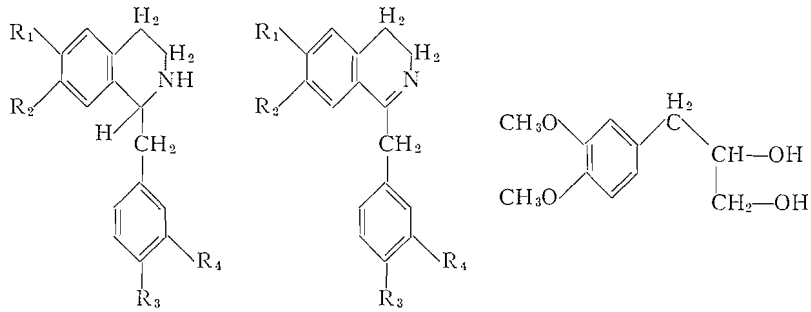

(V) (VI) (VII)

β-phényléthylamines exige la présence de groupements hydroxyles libres en position "*para*". Par contre, Hahn et Schales (6), alléguant que la présence dans la nature d'un grand nombre d'alcaloides méthylés contredisait la prétention de Schöpf, ont entrepris la condensation de l'homopipéronal avec l'homopipéronylamine et ont affirmé avoir isolé la 1-(3,4-méthylènedioxybenzyl)-6,7-méthylènedioxytétrahydroisoquinoléine (V, $R_1R_2 = R_3R_4 = CH_2O_2$).

Späth et ses collaborateurs (20) par ailleurs rapportent qu'ils ont tenté de répéter les travaux de Hahn et Schales (6) et qu'ils n'ont pas réussi à isoler le produit de condensation. Ils concluent que les prétentions de Hahn et Schales sont fausses. Späth, de plus, attribue à l'instabilité en milieu acide de l'homovératraldéhyde et de la base de Schiff intermédiaire (VI) la faillite de ces essais de condensation dans ces conditions aussi bien que le faible rendement obtenu en effectuant la synthèse de la tétrahydropapavérine à chaud en présence d'acide chlorhydrique concentré (19).

En face de l'hypothèse de Schöpf, des prétentions de Hahn, et des avancés de Späth, il convenait d'étudier et de tenter d'éclaircir ce problème. Nous avons essayé quatre séries de synthèses physiologiques avec l'homovératrylamine (III, $R_1 = H$; $R_2 = R_3 = CH_3$) et la N-méthylhomovératrylamine (III, $R_1 = R_2 = R_3 = CH_3$) comme amines de départ:

(1) condensation de l'homovératrylamine avec l'homovératraldéhyde;
(2) condensation de la N-méthylhomovératrylamine avec l'homovératraldéhyde;
(3) condensation de la N-méthylhomovératrylamine avec la benzaldéhyde;
(4) condensation de la N-méthylhomovératrylamine avec la formaldéhyde, l'acétone, et l'acétaldéhyde.

Nous avons préparé l'homovératrylamine en suivant la méthode de Fries et Bestian (4) qui consiste à décomposer l'azide de l'acide diméthyldihydrocaféique. Celui-ci avait déjà été préparé (11) par la réduction de l'acide non saturé par l'amalgame de sodium. Nous l'avons facilement obtenu en rendements quantitatifs par la réduction catalytique de l'acide caféique en présence de chlorure de palladium dispersé sur du noir animal.

La N-méthylhomovératrylamine a été synthétisée en suivant la méthode de Buck (1). Son picrate a un p.f. de 175°C. et non de 162–163°C. comme le donne l'auteur.

L'aldéhyde homovératrique a déjà été synthétisé par ozonisation du méthyleugénol suivie de la réduction de l'ozonide correspondant (7). Nous l'avons préparé par l'oxydation du méthyleugénol glycol au tétraacétate de plomb. Quant à ce glycol, il peut s'obtenir par l'oxydation du méthyleugénol au permanganate de potassium (9). Nous avons préféré le préparer par la méthylation du groupement phénolique de l'eugénolglycol à l'aide de l'iodure de méthyle.

Enfin, nous avons synthétisé avec un rendement de 90% l'eugénolglycol par l'oxydation de l'acétate d'eugénol à l'acide performique, suivie de la saponification des groupements acétyle et formyle. Freudenberg (3) avait préparé ce glycol à partir de l'eugénol par une série de quatre réactions difficiles avec un rendement final de seulement 43%.

PARTIE EXPÉRIMENTALE

Acide diméthyldihydrocaféique

De l'acide diméthylcaféique (41.6 g., 0.2 mole) est dissous dans la soude (100 ml. de solution à 10%) et la solution est réduite catalytiquement sous pression (2–3 atmosphères) à la température ambiante en présence d'un mélange chlorure de palladium – noir animal (5.0 g. à 8% de chlorure de palladium). Le catalyseur est récupéré par filtration et le filtrat acidulé. L'acide qui précipite est filtré, bien lavé à l'eau, et séché. Rendement: 99% (41.8 g.) d'acide pur de p.f. 97°C.

N-Méthylhomovératrylamine

Cette amine est préparée à partir de l'homovératrylamine (9.82 g., 0.055 mole) et de l'aldéhyde benzoique (5.75 g., 0.055 mole) selon le mode opératoire décrit par Buck (1). Rendement: 69% (11.95 g. d'iodhydrate). La N-méthylhomovératrylamine forme un picrate de p.f. de 175°C.; Buck (1) donne 162–163°C. Calculé pour $C_{17}H_{20}O_9N$: C, 48.1%; H, 4.7%.

Eugénolglycol

De l'acétate d'eugénol (31.7 g., 0.15 mole), de l'acide formique à 90% (320 ml.), et du peroxyde d'hydrogène à 30% (32 ml.) sont introduits dans un ballon. Une réaction exothermique s'amorce immédiatement et la température monte lentement à 40°C. On maintient le mélange réactionnel à cette température (±1°C.) d'abord par immersion intermittente dans un bain d'eau froide et ensuite, lorsque la vitesse de la réaction a diminué, par introduction dans un bain d'eau à 40°C. On laisse à cette température pendant deux heures et ensuite à la température ambiante pendant 12 h. On distille les acides formique et performique sous vide partiel, on dissout le résidu dans l'alcool méthylique (100 ml.), et on saponifie en faisant bouillir à reflux pendant 30 min. avec de l'hydroxyde de potassium (40 g. en solution dans 50 ml. d'eau et 100 ml. de méthanol). L'alcool et l'eau sont ensuite évaporés sous vide partiel et le résidu dissous dans l'acide chlorhydrique dilué (75 ml. d'acide 2 : 1). La solution acide est extraite à l'acétate d'éthyle (cinq portions de 100 ml.), les extraits combinés sont séchés sur du sulfate de sodium anhydre, filtrés, et concentrés. Le glycol brut est distillé sous pression réduite. Rendement: 90% (27.9 g.) de glycol pur de p.é. 146°C./0.0003 mm. Le glycol a été identifié

par la formation du tribenzoate de p.f. 100°C. Calculé pour $C_{31}H_{25}O_7$: C, 73.1%; H, 4.9%. Trouvé: C, 72.9%; H, 5.2%.

Méthyleugénolglycol

On dissout du sodium (3.3 g.) dans l'alcool méthylique anhydre (25 ml.) et à la solution de méthylate de sodium, on ajoute une solution d'eugénol glycol (27.9 g., 0.14 mole) dans du méthanol anhydre (100 ml.) et de l'iodure de méthyle (46 g., 0.32 mole). On fait bouillir la solution à reflux jusqu'à ce qu'elle devienne acide au tournesol. L'alcool est alors distillé sur bain-marie et le résidu dissous dans l'eau (environ 50 ml.). La solution aqueuse est rendue alcaline par addition de quelques millilitres de soude concentrée et extraite à l'alcool amylique (trois portions de 100 ml.). L'extrait est séché, l'alcool amylique chassé sous vide partiel, et le méthyleugénol glycol distillé sous pression réduite. Rendement: 74.5% (22.3 g.) de p.é. 134°C./0.0003 mm.

Aldéhyde homovératrique

Du méthyleugénol glycol (19.97 g., 0.094 mole) est dissous dans le benzène (250 ml.) et introduit dans un ballon à trois tubulures muni d'un agitateur mécanique et d'un condensateur à reflux. A cette solution bien agitée on ajoute à l'ébullition du tétracétate de plomb (41.5 g., 0.094 mole) en portions de 2 à 3 g. Lorsque l'oxydation est terminée (15–20 min.) la suspension est refroidie, l'acétate de plomb filtré, le filtrat lavé à l'eau, séché sur du sulfate de sodium anhydre, et concentré. Le résidu d'aldéhyde homovératrique est distillé sous pression réduite. Rendement: 67.5% (11.34 g.); p.é. 125°C./1.5 mm.

L'aldéhyde a été identifié par la préparation de la *p*-nitrophénylhydrazone de p.f. 158–159°C. (8) et de la 2,4-dinitrophénylhydrazone de p.f. 172°C. Calculé pour $C_{16}H_{16}O_6N_4$: C, 53.3%; H, 4.5%. Trouvé: C, 53.6%; H, 4.3%.

Essais de synthèses physiologiques

Les expériences ont été faites en mélangeant les réactifs de départ dans des solutions tampons. Trois séries de solutions tampons ont été préparées. Les pH ont été vérifiés par mesure électrométrique et les valeurs ont été trouvées exactes à ±0.05. Voici ces mélanges tampons:

SÉRIE A: Phosphate disodique et acide citrique (10)

No	pH	Na_2HPO_4 0.2 *M*	$C_6H_8O_7$ 0.1 *M*
1	4.2	8.28 ml.	11.72 ml.
2	5.2	10.72 ml.	9.28 ml.
3	6.2	12.63 ml.	7.37 ml.

SÉRIE B: Phthalate acide de potassium et hydroxyde de sodium (2)

No	pH	NaOH 0.2 *M*	$KHC_8H_4O_4$ 0.2 *M*
1	4.2	3.65 ml.	50.0 ml.
2	5.2	29.75 ml.	50.0 ml.
3	6.6	47.00 ml.	50.0 ml.

SÉRIE C: Acide acétique et acétate de sodium (21)

No	pH	CH_3CO_2H 0.2 *N*	CH_3CO_2Na 0.2 *N*
1	5.2	4.0 ml.	16.0 ml.

Dans le tableau I où sont compilés les résultats observés, ces mélanges tampons sont identifiés par la lettre de la série suivie du numéro de la solution.

A chacune des solutions tampons mentionnées dans le tableau sont ajoutés de l'amine pesée exactement (environ 0.5 g.) et, suivant le cas, de la cétone

TABLEAU I

RÉSULTATS DES ESSAIS DE CONDENSATION

No.	Réactifs: Aldéhyde ou cétone	Réactifs: Amine	Sol. tampon	pH	Poids en grammes: Aldéhyde ou cétone	Poids en grammes: Amine	Poids en grammes: Extrait en milalcalin	Poids en grammes: Picrate	P.f.,°C. picrate	Amine récupérée, %
1	Homovératraldéhyde	Homovératrylamine	A1	4.2	0.463	0.447	0.246	0.382	165–166	55
2	Homovératraldéhyde	Homovératrylamine	A2	5.2	0.446	0.441	0.245	0.424	165–166	55
3	Homovératraldéhyde	Homovératrylamine	A3	6.2	0.459	0.407	0.172	0.257	165–167	42
4	Homovératraldéhyde	Homovératrylamine	B1	4.2	0.453	0.433	0.272	0.474	165–167	63
5	Homovératraldéhyde	Homovératrylamine	B2	5.2	0.455	0.424	0.165	0.248	165–166	39
6	Homovératraldéhyde	Homovératrylamine	B3	6.2	0.445	0.432	0.048	0	——	11
7	Homovératraldéhyde	Homovératrylamine	C1	5.2	0.459	0.427	0.136	0.110	164–166	32
8	Homovératraldéhyde	N-Méthylhomovératrylamine	A1	4.2	0.505	0.499	0.249	0.449	175	84
9	Homovératraldéhyde	N-Méthylhomovératrylamine	A2	5.2	0.462	0.498	0.242	0.430	175	82
10	Homovératraldéhyde	N-Méthylhomovératrylamine	B1	4.2	0.600	0.499	0.262	0.454	175	88
11	Homovératraldéhyde	N-Méthylhomovératrylamine	B2	5.2	0.522	0.501	0.239	0.445	175	80
12	Homovératraldéhyde	N-Méthylhomovératrylamine	C1	5.2	0.507	0.497	0.243	0.436	175	82
13	Benzaldéhyde*	N-Méthylhomovératrylamine	B1	4.2	0.50	0.500	0.225	0.496	175	74
14	Benzaldéhyde*	N-Méthylhomovératrylamine	B3	6.2	0.50	0.500	0.219	0.498	174–175	73
15	Benzaldéhyde*	N-Méthylhomovératrylamine	C1	5.2	0.50	0.500	0.206	0.490	175	68
16	Formaldéhyde	N-Méthylhomovératrylamine	B2	5.2	1.5 ml.	0.500	0.152	——	175	51
17	Acétaldéhyde	N-Méthylhomovératrylamine	B2	5.2	0.5 ml.	0.500	0.203	——	175	68
18	Acétone	N-Méthylhomovératrylamine	B2	5.2	1.0 ml.	0.500	0.216	——	175	73

**Dans ces trois essais l'extraction en milieu acide a été faite à l'éther.*

ou de l'aldéhyde pesé exactement (environ 0.5 g.). Les mélanges sont d'abord agités vigoureusement et ensuite laissés au repos à la température ambiante pendant sept à huit jours, tout en agitant quotidiennement durant environ une heure. On extrait alors les solutions acides au chloroforme ou à l'éther selon le cas (trois fois avec 5 ml.). Les extraits chloroformiques ou éthérés sont décantés, séchés sur du sulfate de sodium anhydre, filtrés, et évaporés à sec sur bain-marie. Les résidus laissés par l'évaporation du solvant sont pesés et dissous dans de l'alcool absolu (5–10 ml.) et on ajoute une solution saturée d'acide picrique (9–12 ml.).

Les portions aqueuses sont alcalisées à la soude 30% et extraites au chloroforme (trois fois avec 5 ml.). Les extraits chloroformiques sont décantés, séchés sur du sulfate de sodium anhydre, et filtrés, puis le chloroforme est évaporé sur bain-marie. Le résidu considéré comme étant uniquement de l'amine de départ est pesé. Ce résidu est dissous dans l'alcool absolu (5–10 ml.). L'addition d'une solution alcoolique saturée d'acide picrique (5–10 ml.) fait précipiter un picrate qu'on filtre et recristallise dans un mélange dioxane–éthanol (1 : 4) jusqu'à constance du point de fusion.

Les résultats de ces expériences apparaissent au tableau I. On y trouve: (1) la nature des réactifs; (2) celle de la solution tampon; (3) le pH des solutions; (4) les poids de l'aldéhyde ou de la cétone et ceux de l'amine de départ; (5) le poids de l'extrait obtenu après alcalinisation à la soude; (6) le poids du picrate pur obtenu de l'extrait fait en milieu alcalin; (7) le point de fusion du picrate; (8) le pourcentage de récupération de l'amine. Ces pourcentages sont calculés en faisant le rapport du poids de l'amine brute récupérée sur le poids de l'amine de départ. Il n'est pas tenu compte des extraits faits en milieu acide, parce qu'ils n'ont jamais fourni de picrate lorsque traités par l'acide picrique.

CONCLUSIONS

Bien que la récupération de l'amine de départ ne soit jamais de 100% (une quantité variable d'amine disparaît au cours de l'essai de condensation), dans aucun cas il nous a été possible de déceler la présence d'une autre base que celle de départ dans les produits de la réaction. L'identité du picrate isolé et de celui de l'amine de départ a été vérifiée par la détermination de points de fusion mixtes et par l'analyse des picrates provenant des essais 3, 7, et 11. Il nous semble évident que, s'il y a condensation entre le composé carbonyle et l'amine, elle doit être négligeable et, en tous cas, insuffisante pour être décelée.

Voici donc les conclusions qui découlent de ces expériences:

(1) La condensation de la N-méthylhomovératrylamine avec les aldéhydes exclue la possibilité de la formation d'une base de Schiff instable comme produit intermédiaire, ce qui ne permet pas d'invoquer l'instabilité d'une telle base comme raison de la faillite des condensations pseudophysiologiques avec les N-méthyl-3,4-dihydroxyphényléthylamines éthérifiées.

(2) Comme certains essais de condensation ont été tentés avec des aldéhydes stables (formique, acétique, et benzoique), l'instabilité de l'aldéhyde ne peut pas non plus, dans ces cas, être le véritable facteur d'insuccès.

(3) Ces résultats négatifs confirment le point de vue de Schöpf qui veut que les groupements oxydriles dans l'homovératrylamine doivent être libres pour que la condensation avec les aldéhydes ou les cétones puisse se faire dans des conditions pseudophysiologiques.

REMERCIEMENTS

Les auteurs remercient le Conseil National des Recherches et l'Office des Recherches de la Province de Québec pour l'aide financière accordée à l'un d'eux (J.-L. F.) sous forme de bourse ou d'octroi de recherches.

BIBLIOGRAPHIE

1. Buck, J. S. J. Am. Chem. Soc. 52: 4119. 1930.
2. Clark, W. M. and Lubs, H. A. J. Biol. Chem. 25: 479. 1916.
3. Freudenberg, K. and Hemberger, W. Ber. 83: 529. 1950.
4. Fries, K. and Bestian, H. Ann. 533: 72. 1938.
5. Hahn, G. and Ludewig, H. Ber. 67B: 2031. 1934.
6. Hahn, G. and Schales, O. Ber. 68B: 24. 1935.
7. Harries, C. and Adam, H. Ber. 49: 1029. 1916.
8. Harries, C. and Haarmann, R. Ber. 48: 41. 1915.
9. Haufmann, E., Eliel, E., and Rosenkranz, H. Ciencia (Mex.), 7: 1936. 1946.
10. McIlvaine, T. C. J. Biol. Chem. 49: 193. 1921.
11. Perkin, W. E. and Robinson, R. J. Chem. Soc. 91: 1079. 1907.
12. Robinson, R. J. Chem. Soc. 111: 762. 1917.
13. Schöpf, C. and Arnold, W. Ann. 558: 109. 1947.
14. Schöpf, C. and Bayerle, H. Ann. 513: 190. 1934.
15. Schöpf, C. and Lehmann, G. Ann. 497: 7. 1932.
16. Schöpf, C. and Lehmann, G. Ann. 518: 1. 1935.
17. Schöpf, C. and Salzer, W. Ann. 544: 1. 1940.
18. Schöpf, C. and Steuer, H. Ann. 558: 1261. 1947.
19. Späth, E. and Berger, F. Ber. 63: 2098. 1930.
20. Späth, E., Haffner, F., and Kergler, F. Ber. 69B: 378. 1936.
21. Walpole, G. S. J. Chem. Soc. 105: 2501. 1914.

A COMPARISON OF THE PROPERTIES OF PENTAACETATES AND METHYL 1,2-ORTHOACETATES OF GLUCOSE AND MANNOSE[1]

By R. U. Lemieux[2] and Carol Brice

ABSTRACT

The rates of exchange of acetate—concurrent with anomerization—between the C1-acetoxy groups of the pentaacetates (0.05 *M*) of D-glucose and D-mannose and stannic trichloride acetate (0.05 *M*) in chloroform containing stannic chloride (0.05 *M*) were determined at 40°C. using isotopically labelled acetate. 1,2-*trans*-α-D-Mannose pentaacetate underwent exchange seven times more rapidly than the β-1,2-*cis*-anomer but eight times less rapidly than 1,2-*trans*-β-D-glucose pentaacetate. The latter compound was 450 times more reactive than the α-1,2-*cis*-anomer. In accordance with these results, the D-mannose pentaacetate underwent mercaptolysis in ethyl mercaptan containing zinc chloride at rates intermediate to those found for the D-glucose pentaacetates. The main product from the mannose pentaacetates was in each case ethyl 1,2-*trans*-α-D-1-thiomannopyranoside tetraacetate (60–70% yield). Tetra-*O*-acetyl-β-D-glucopyranosyl chloride with silver acetate gave β-D-glucose pentaacetate when the reaction was carried out in dry acetic acid but gave 2,3,4,6-tetra-*O*-acetyl-α-D-glucose in 90% aqueous acetic acid. Tetra-*O*-acetyl-β-D-glucopyranosyl chloride with methanol and silver carbonate gave a sirupy product with the properties expected for methyl 1,2-ortho-*O*-acetyl-α-D-glucopyranose triacetate. The substance was hydrolyzed by 0.005 *N* hydrochloric acid in 95% dioxane 18 times more rapidly than the corresponding derivative of β-D-mannose. The significance of these observations toward an understanding of the effect of configuration on reactivity is discussed.

INTRODUCTION

The technique developed by the authors (11), in which the exchange—concurrent with anomerization (13)—of acetate between the C1-acetoxy group of a sugar acetate and $SnCl_3OAc^*$ (labelled in the carboxyl group with carbon-14), was applied to the pentaacetates of D-mannose and D-glucose. In these experiments the non-radioactive sugar acetate (I) is treated in chloroform solution with equimolar amounts of stannic chloride and the radioactive

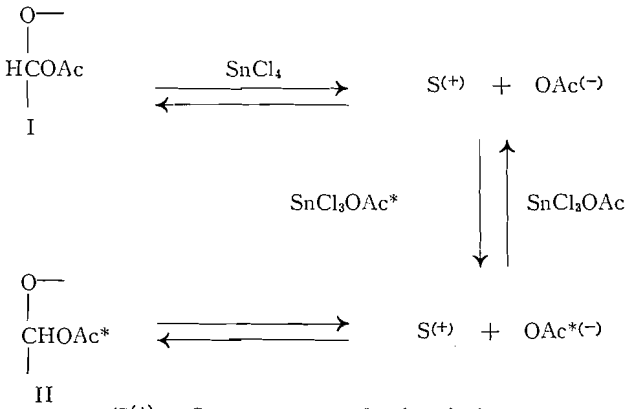

($S^{(+)}$ = Sugar acetate carbonium ion)

[1]*Manuscript received September 7, 1954.*
Contribution from the National Research Council of Canada, Prairie Regional Laboratory, Saskatoon, Saskatchewan. Issued as Paper No. 180 on the Uses of Plant Products and as N.R.C. No. 3463.
[2]*Present address: Department of Chemistry, University of Ottawa, Ottawa, Ontario.*

stannic trichloride acetate. At various times thereafter, the prevailing sugar derivatives (II) are isolated and their radioactivity is determined. It was shown (11) for the D-glucose pentaacetates that the exchange is specific for the C1-acetoxy group. The same situation is assumed for the D-mannose pentaacetates. The reaction rates obtained obviously are a measure of relative ease of bringing about dissociation of the C1 to acetoxy group bonds of the various sugar acetates whether or not anomerization takes place prior to the dissociation.

The exchange data obtained for the pentaacetates of D-mannose and D-glucose at 40°C. are plotted in Fig. 1. It is seen that, at least for the initial

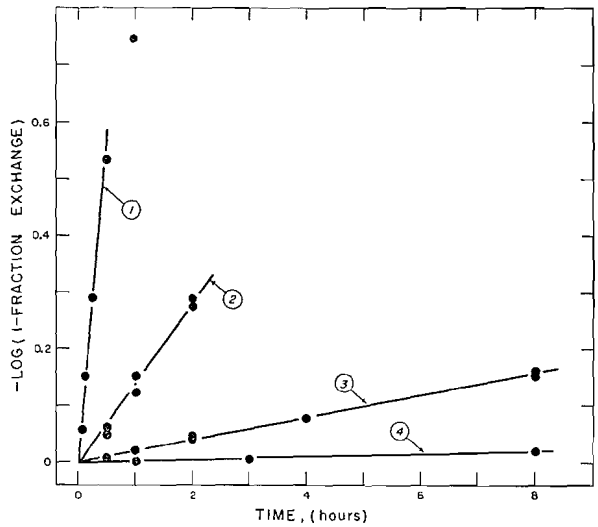

FIG. 1. Rates of exchange of sugar acetates (0.05 *M*) with labelled stannic trichloride acetate (0.05 *M*) in the presence of stannic chloride (0.05 *M*) in chloroform solution.
Plot 1—β-D-glucopyranose pentaacetate
2—α-D-mannopyranose pentaacetate
3—β-D-mannopyranose pentaacetate
4—α-D-glucopyranose pentaacetate

stages, the exchange reactions follow the simple exponential law expected for simple isotopic exchange reactions (2). The data from duplicate runs starting with the mannose pentaacetates are plotted in order to illustrate the reproducibility of these experiments. The relative rates of exchange at 40°C. obtained by comparing the slopes of the curves in Fig. 1 are listed in Table I.

TABLE I

RELATIVE RATES OF EXCHANGE OF THE C1-ACETOXY GROUP OF SUGAR ACETATES (0.05 *M*) WITH $SnCl_3OAc^*$ (0.05 *M*) IN THE PRESENCE OF $SnCl_4$ (0.05 *M*) IN CHLOROFORM AT 40°C.

Pentaacetate of	Relative rates of reaction
1,2-*cis*-α-D-glucose	1
1,2-*cis*-β-D-mannose	8
1,2-*trans*-α-D-mannose	56
1,2-*trans*-β-D-glucose	450

Thus, as found in other similar investigations (7), the rate of C1 to acetoxy group dissociation of sugar acetates is strongly affected by the relative configurations of all the asymmetric centers in the molecule.

The stereochemical route of the reaction of a sugar acetate with ethyl mercaptan catalyzed by zinc chloride (9) is readily established since the acetylated ethyl 1-thioglycosides which are formed are highly resistant to anomerization. Thus, the mercaptolysis of a sugar acetate can yield information on neighboring group participation in replacements of the C1-acetoxy group. Mercaptolysis of either α- or β-D-mannose pentaacetate for 50 hr. at 0°C. gave ethyl α-D-1-thiomannopyranoside tetraacetate. The yield was 70% from the β-D-pentaacetate and 60% from the α-D-anomer. Inspection of the residual sirups, after deacetylation, by preparative paper chromatography led in each case to the isolation of ethyl β-D-1-thiomannopyranoside in approximately 0.15% yield. Therefore, as was previously found (9) for the D-glucose pentaacetates, both the D-mannose pentaacetates yield essentially only the 1,2-*trans*-1-thioglycoside. Fried and Walz (3) have established the pyranoside structure for ethyl β-D-1-thiomannopyranoside tetraacetate. We have established the pyranoside structure of the α-D-anomer (III) by reductive desulphurization to form styracitol tetraacetate (IV). The latter compound was also obtained by reductive desulphurization of ethyl β-D-2-thiofructopyranoside tetraacetate (V). The retention of configuration obtained on mercaptolysis of

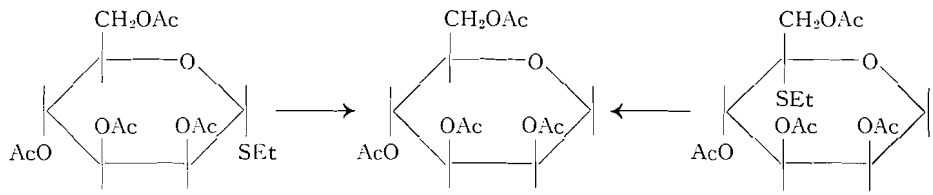

the α-D-mannose pentaacetate indicates the participation of a neighboring group in the first stage of the reaction. The fact that 1,2-*trans*-tetra-*O*-acetyl-α-D-mannopyranosyl halides yield 1,2-orthoacetates under the conditions of the Koenigs–Knorr reaction (1, 15 p. 83) supports this contention. The simple Walden inversion obtained on mercaptolysis of β-D-mannose pentaacetate may be the result of an S_N2 type replacement. However, other possible mechanisms, such as anomerization prior to mercaptolysis or the formation of intermediate carbonium ions which have a tendency to form the α-D-thiomannoside cannot at present be excluded.

Lemieux (9) found that β-D-glucose pentaacetate undergoes mercaptolysis much more rapidly than does the α-D-anomer. It was seen above with reference to Table I that a similar wide difference in reactivity exists for these compounds in undergoing exchange of the C1-acetoxy group with stannic chloride acetate. It was therefore of interest to compare the relative rates at which the D-mannose pentaacetates undergo mercaptolysis with those found for the exchange reactions. The rates of mercaptolysis were measured as described

previously (9) and the data are plotted in Fig. 2 where the data for the D-glucose pentaacetates are also included. It is important to note at this point

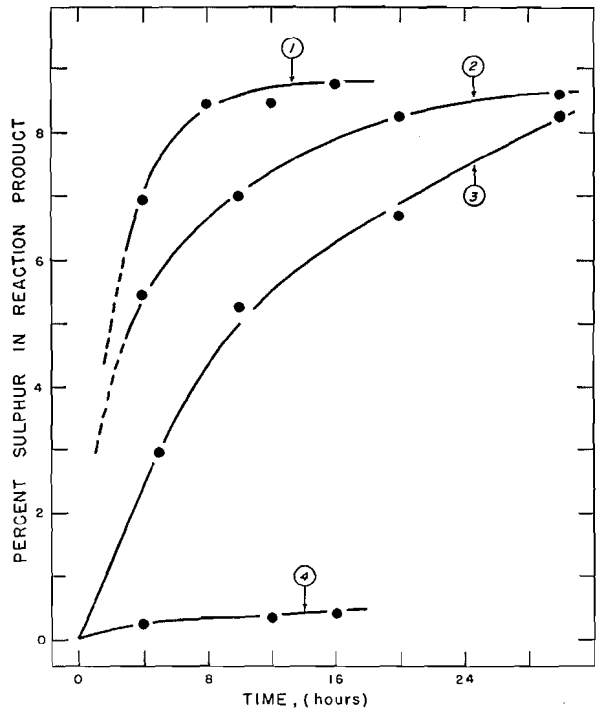

FIG. 2. A comparison of the rates of mercaptolysis (9) of sugar acetates at 0°C.
Plot 1—β-D-glucopyranose pentaacetate (9)
2—β-D-mannopyranose pentaacetate
3—α-D-mannopyranose pentaacetate
4—α-D-glucopyranose pentaacetate (9)

that these rates of mercaptolysis are only a very rough measure of the rates of ethyl 1-thioglycoside tetraacetate formation because of the presence of side reactions which yield materials with higher sulphur contents. It will be seen below that this is particularly true for the D-mannose pentaacetates. The plots in Fig. 2 show that, unlike the D-glucose pentaacetates, the D-mannose pentaacetates undergo mercaptolysis at not widely different rates. These results are roughly in agreement with those expected on the basis of the relative rates of exchange listed in Table I and show that the rates of exchange can be used as an indication of the ease of replacing the C1-acetoxy group of sugar acetates.

The data plotted in Fig. 3 show that an increase in temperature from 0°C. to 20°C. for the mercaptolysis of the D-mannose pentaacetates is accompanied by a large increase in the extent of side reactions. One of the by-products possessed, after deacetylation, the formula $C_{12}H_{26}O_4S_3$. The material may be epimeric to the 2-deoxy-2-ethylthio derivative of D-glucose diethyl thioacetal which was obtained in small yield on the mercaptolysis of the D-glucose pentaacetates (9).

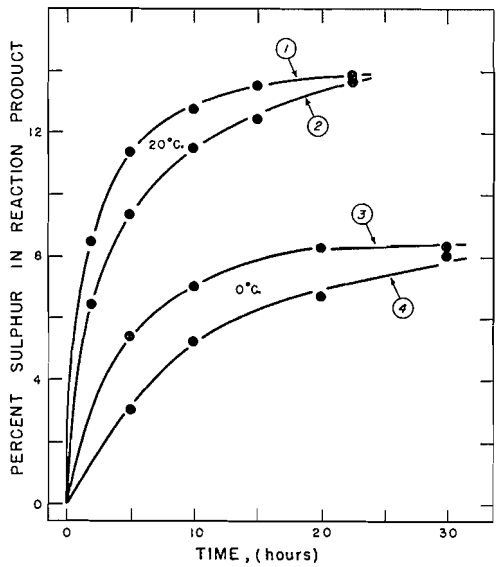

FIG. 3. The effect of temperature on the mercaptolysis of β-mannose pentaacetate (plots 1 and 3) and of α-mannose pentaacetate (plots 2 and 4).

The high reactivity of β-D-glucose pentaacetate as compared to the α-anomer in undergoing dissociation of the C1 to acetoxy group bond catalyzed by acids

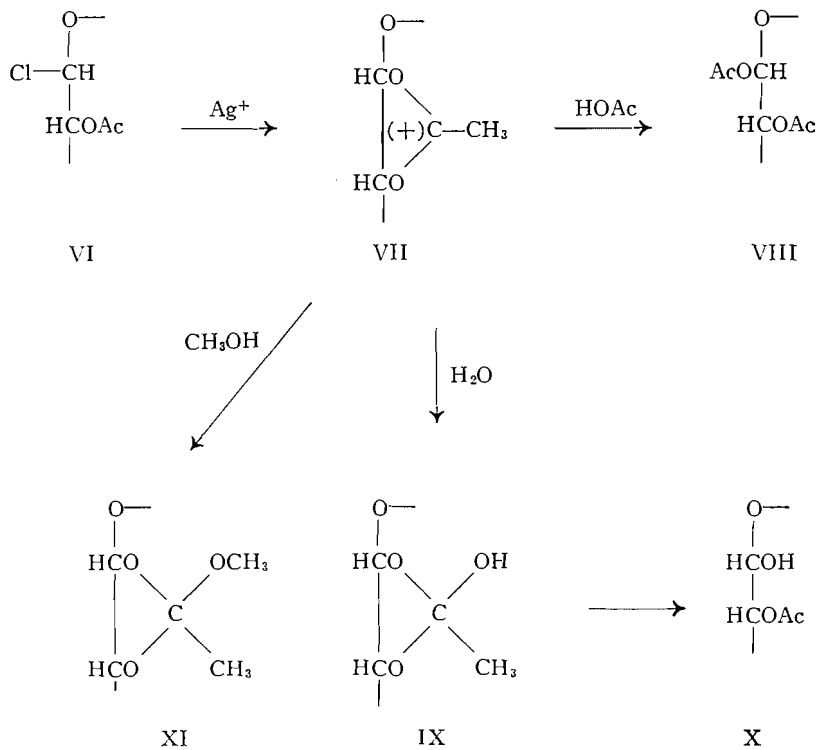

has been attributed to participation of the C2-acetoxy group in the case of the 1,2-*trans*-β-D-anomer (9, 11). We now wish to present further evidence for the participation based on the behavior of tetra-*O*-acetyl-β-D-glucopyranosyl chloride (VI) under conditions for solvolysis. This substance is readily obtained in high yield by reacting β-D-glucose pentaacetate with an equivalent amount of titanium tetrachloride in benzene for only five minutes at 40°C. The authors have described the nature of this reaction in a previous publication (11). The chloride (VI) reacted extremely rapidly with silver acetate in dry acetic acid to form β-D-glucose pentaacetate (VIII). However, when water was present in the reaction mixture, the product was strongly dextrorotatory, soluble in water, and readily yielded crystalline 2,3,4,6-tetra-*O*-acetyl-α-D-glucose (X). This was to be expected on the basis of the conclusions reached by Isbell and Frush (8). Winstein and Roberts (19) have recommended the procedure as a general test for carbonium ions derived through neighboring acetoxy group participation. Thus, the orthoacid (IX) was an intermediate in the reaction. It is of interest to note that the fact that this substance rearranged at least in part to the tetraacetate (X) indicates that 1,3,4,6-tetraacetyl-α-D-glucose (12) should possess a tendency to rearrange to the 2,3,4,6-tetraacetate (X). Schlubach and Wolf (17) have prepared the tetraacetate (X) by reaction of tetra-*O*-acetyl-β-D-glucopyranosyl chloride with silver carbonate in moist acetone.

When tetra-*O*-acetyl-β-D-glucopyranosyl chloride (VI) was reacted with silver carbonate in dry methanol, a highly acid-labile sirupy product was obtained which possessed the properties expected for methyl 1,2-ortho-*O*-

TABLE II

RATES OF HYDROLYSIS OF SUGAR ORTHOACETATES

The orthoester, 50 mgm., was dissolved at zero time in 3.16 ml. of 0.005 *N* hydrochloric acid in 95% dioxane and the solution was observed at room temperature, 23.5°C., in a 2 dm. tube.

t, min.	Observed rotation	*k*, min.$^{-1}$
Methyl 1,2-ortho-O-acetyl-α-D-glucopyranose triacetate		
0	+2.06° (Calc.)	—
4	3.25	0.28
5	3.37	0.28
6	3.48	0.29
7	3.56	0.29
8	3.62	0.29
9	3.66	0.29
10	3.69	0.28
25	3.79	—
30 (∞)	3.79	Average 0.29
1,2-Ortho-O-acetyl-β-D-mannopyranose triacetate (1)		
0	−1.012° (Calc.)	—
10	−0.860	0.016
20	−0.765	0.014
40	−0.560	0.015
60	−0.430	0.014
90	−0.270	0.015
120	−0.164	0.015
480 (∞))	0.000	Average 0.015

acetyl-α-D-glucopyranose triacetate (XI). That is, although acid hydrolysis gave four acetyl groups per methoxyl group, only three of the acetyl groups could be detected by saponification. Furthermore, the substance was extremely sensitive to acid hydrolysis—a fact which is characteristic of sugar orthoesters (15). Thus, there can be no doubt that the substance was methyl 1,2-ortho-*O*-acetyl-α-D-glucopyranose triacetate (XI). Unfortunately, the substance has not crystallized.

The rates of hydrolysis of both the D-glucose orthoacetate (XI) and the well-known methyl 1,2-ortho-*O*-acetyl-β-D-mannopyranose triacetate (1) in 95% dioxane 0.005 *N* with respect to hydrochloric acid were determined polarimetrically. The data, given in Table II, show that the D-glucose derivative is hydrolyzed 18 times faster than the D-mannose compound. This is reminiscent of the relative reactivities noted above for the 1,2-*trans*-pentaacetates of D-glucose and D-mannose. Winstein and co-workers (18) have established the inherent stability of 1,2-cyclic carbonium ions of structure XII. Consequently, it seems likely that the hydrolysis of 1,2-cyclic orthoacetates proceeds by way

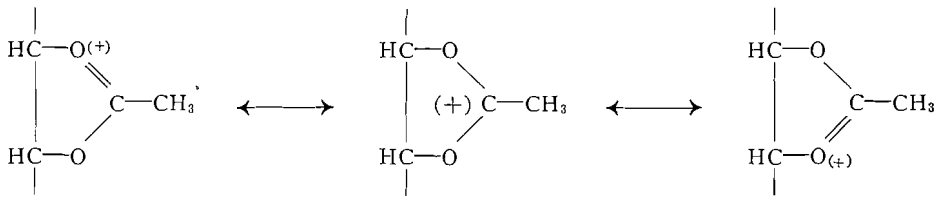

XII

of such ions and that the higher reactivity of both β-D-glucose pentaacetate and the D-glucose orthoacetate (XI) as compared to the corresponding derivatives of D-mannose is due in each case mainly to a greater stability of the 1,2-cyclic ion (VII) from D-glucose than for the corresponding ion (XIII) from D-mannose. This could be the result of a steric inhibition to resonance in the D-mannose carbonium ion (XIII) which is not present in the D-glucose carbonium ion. It is of interest to note that the presently described methyl 1,2-

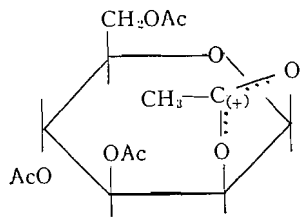

XIII

ortho-*O*-acetyl-α-D-glucopyranose triacetate (XI) appears to be about five times more sensitive to acid hydrolysis than the corresponding derivative of D-glucuronic acid methyl ester (5).

The greater reactivity of β-D-mannose pentaacetate over α-D-glucose pentaacetate both toward exchange (see Fig. 1) and mercaptolysis (see Fig. 2) may well be due to a weakening of the C1 to acetoxy group bond in the mannose derivative through the steric strain which should arise from the presence in this compound of four large substituents on one side of the ring. It has been suggested (6, 14) that the anomalous A-values which are obtained when Hudson's rules of isorotation are applied to anomeric mannose derivatives may be due to the occurrence in these compounds of internal strains which force the molecules into unusual conformations.

EXPERIMENTAL

Rates of Exchange

Stannic chloride, freshly distilled in a dry atmosphere, 3.30 gm. (12.6 mM.), was dissolved in 50 ml. of pure dry chloroform. Dry radioactive silver acetate, 1.045 gm. (6.25 mM.), 163,000 counts per min., was added and the mixture was refluxed in a dry apparatus for 20 min. The silver chloride was removed by filtration and was washed twice with 20 ml. volumes of the dry chloroform. The combined filtrates were diluted to 100 ml. The sugar acetate, 0.489 gm. (1.25 mM.), was dissolved in about 3 ml. of dry chloroform in 25 ml. volumetric flask. At zero time, exactly 20 ml. of the $SnCl_3OAc^* - SnCl_4$ solution was added at 40°C. and the solution was diluted to 25 ml. After the various reaction times, a 4 ml. sample was removed and plunged into 50 ml. of cold water. The mixture was extracted three times with chloroform. The chloroform extracts were washed in succession with sodium bicarbonate solution then with water, combined, and dried over sodium sulphate. The chloroform was removed *in vacuo* to yield a sirup which was dried at 60°C. in a high vacuum. The sample was converted to barium carbonate for counting at infinite thickness (11). Evidence was obtained (11) that stannic chloride reacts quantitatively with silver acetate. Therefore, complete exchange of the C1-acetoxy group of the sugar acetate with the stannic trichloride acetate thus formed would be expected to yield sugar acetate with a radioactivity of $163{,}000 \times 167/2 \times 16 \times 197 = 4300$ counts per min. when counted as barium carbonate. The results plotted in Fig. 1 were calculated on this basis.

Rates of Mercaptolysis

The rates of mercaptolysis were determined as previously described (9).

Mercaptolysis of β-D-Mannose Pentaacetate

Pure, dry β-D-mannose pentaacetate, 2.00 gm., was dissolved at 0°C. in 10 ml. of dry ethyl mercaptan which contained 1.00 gm. of anhydrous zinc chloride. The solution was left at 0°C. for 48 hr. and the product was isolated as previously described (9). Crystallization from ethanol gave 1.36 gm. (68% yield) of crude ethyl α-D-1-thiomannopyranoside tetraacetate, m.p. 98–106°C. The substance was pure, m.p. 107–108°C., $[\alpha]_D + 101°$ (*c*, 0.6 in chloroform), after two recrystallizations. These constants are in close agreement with those reported by Fried and Walz (3), m.p. 107–108°C., $[\alpha]_D^{25} + 104°$ (*c*, 0.88 in chloroform).

The mother liquors from the crystallizations were combined and evaporated to sirup, 0.75 gm., which was deacetylated with sodium methylate in dry methanol. Inspection of the product by partition chromatography on paper using butanol–ethanol–water (5 : 1 : 4) showed the presence of seven zones. The approximate R_f values were: I, 0.04; II, 0.12; III, 0.17; IV, 0.51; V, 0.64; VI, 0.75; VII, 0.87. The zones were detected on the paper by the periodate–permanganate spray reagent developed in this laboratory (10). Substance III appeared to be mannose and, as is shown below, substances IV and V were the β- and α-ethyl 1-thiomannopyranosides, respectively.

The deacetylated product was dissolved in water and the solution was extracted three times with ether. A very small amount of material, m.p. 108–110°C., was deposited on evaporation of the ether. The melting point was not depressed by the substance described below which was obtained in the same manner from α-D-mannose pentaacetate. The substances responsible for zones IV and V in the above chromatograms were isolated by preparative paper chromatography of the material which remained in the aqueous phase. The compounds were acetylated with sodium acetate and acetic anhydride for crystallization. Zone IV gave 2.7 mgm. of a substance, m.p. 159–160°C., which must be (see below) ethyl β-D-1-thiomannopyranoside tetraacetate, m.p. 161–162°C. Zone V gave 49 mgm. of pure ethyl α-D-1-thiomannopyranoside tetraacetate, m.p. 106–107°C.

When the mercaptolysis was carried out at room temperature for 23 hr., the yield of crude ethyl α-D-1-thiomannopyranoside tetraacetate was 60%.

Mercaptolysis of α-D-*Mannose Pentaacetate*

Mercaptolysis of 2.00 gm. of α-D-mannose pentaacetate under the above conditions led to the direct isolation of 1.18 gm. (59% yield) of crude ethyl α-D-1-thiomannoside tetraacetate, m.p. 98–104°C. The residual sirups were treated as described above. The same pattern was obtained on paper chromatography. The ether extraction gave enough of the by-product for purification and analysis. After recrystallization from water, the material melted at 110.5–111°C. Calc. for $C_{12}H_{26}O_4S_3$: C, 43.61; H, 7.93; S, 29.1%. Found: C, 43.61; H, 7.88; S, 28.1%. Zone IV gave, after acetylation, 3.0 mgm. of a substance, m.p. 157–160°C. This material was combined with the same material described above for a measurement of the specific rotation. The value, −65° (*c*, 0.05 in chloroform), is in good agreement with that, $[\alpha]_D$ −67° (*c*, 0.67 in chloroform), reported for ethyl β-D-1-thiomannopyranoside tetraacetate, m.p. 161–162°C. (3).

1,5-Anhydro-D-*mannitol* (*Styracitol*)

The ethyl α-D-1-thiomannopyranoside tetraacetate, 300 mgm., was treated with 6 ml. of settled Raney nickel in 30 ml. of 70% aqueous ethanol and the mixture was refluxed for 4.5 hr. The catalyst was removed by filtration and washed with hot ethanol. The combined filtrates were evaporated *in vacuo* to sirup which was deacetylated in methanol solution with dry ammonia. Solvent removal gave a sirup which soon crystallized. Recrystallization from methanol

gave 100 mgm. of material, m.p. 154.5–155°C., $[\alpha]_D - 50°$ (*c*, 0.9 in water). The constants for styracitol are, m.p. 155–156°C., $[\alpha]_D - 50°$ (*c*, 1 in water) (3).

Reductive desulphurization of ethyl β-D-2-thiofructopyranoside (20), 1.00 gm., under the above conditions and deacetylation of the product gave a sirup which crystallized after repeated extractions with ether. Recrystallization from methanol gave 91 mgm. of pure styracitol, m.p. 154–155°C., $[\alpha]_D - 50.5°$ (*c*, 0.4 in water). The melting point was unaffected by the styracitol from the α-D-thiomannoside.

Tetra-O-acetyl-β-D-glucopyranosyl Chloride (VI) (11, 16)

A solution of pure dry β-D-glucose pentaacetate, 10 gm., in 50 ml. of dry benzene was mixed at 40°C. with 50 ml. of benzene which contained 5 gm. (3 ml.) of titanium tetrachloride. After five minutes, when some yellow precipitate still remained, the mixture was poured into 150 ml. of ice water. After the mixture was vigorously shaken, the benzene layer was isolated and washed first with aqueous sodium bicarbonate solution and then with water. The benzene solution was dried for a few minutes over sodium sulphate and then evaporated *in vacuo* to a sirup. The sirup was dissolved in ether and Skellysolve F was added to turbidity. On standing at 0°C., 6.5 gm., 68% yield of essentially pure tetra-*O*-acetyl-β-D-glucopyranosyl chloride, m.p. 90–95°C., $[\alpha]_D - 20.3°$ (benzene), was deposited. Recrystallization from the same solvents yielded pure material, m.p. 95–97°C., $[\alpha]_D - 22°$ (*c*, 1 in chloroform). Schlubach (16) has reported tetra-*O*-acetyl-β-D-glucopyranosyl chloride to melt at 99–100°C. with $[\alpha]_D^{17} - 13.0°$ (*c*, 1 in chloroform).

2,3,4,6-Tetra-O-acetyl-α-D-glucopyranose (X) (4, 17)

Tetra-*O*-acetyl-β-D-glucopyranosyl chloride, 0.5 gm., was added to 10 ml. of dry acetic acid which contained 0.5 gm. silver acetate and the mixture was shaken at room temperature. Judging from the rate at which silver chloride was formed, the reaction was complete within one or two minutes. After 10 min., the silver salts were removed by filtration and the filtrate was evaporated to sirup, 0.539 gm., which crystallized completely. The material was pure β-D-glucopyranose pentaacetate (VIII) after one recrystallization from ethanol.

The reaction was repeated with the exception that 90% aqueous acetic acid was substituted for the glacial acetic acid. The product was strongly dextrorotatory, $[\alpha]_D + 110°$ (90% aqueous acetic acid), and crystallized readily from ether–Skellysolve F. The material, m.p. 89–96°C., $[\alpha]_D + 138°$ (*c*, 0.44 in chloroform), melted at 96–98°C. after one recrystallization from the same solvents. Calc. for $C_{14}H_{20}O_{10}$: acetyl, 49.5%. Found: acetyl, 51.1%. Georg (4) has reported 2,3,4,6-tetra-*O*-acetyl-α-D-glucose to melt at 99–100°C. with $[\alpha]_D + 135°$ (*c*, 4 in chloroform). When the reaction was carried out in ordinary glacial acetic acid, the product, $[\alpha]_D + 59°$ (acetic acid) was found to contain about equal amounts of 2,3,4,6-tetra-*O*-acetyl-D-glucose and β-D-glucose pentaacetate.

Methyl 1,2-Ortho-O-acetyl-α-D-glucopyranose Triacetate (XI)

Tetra-*O*-acetyl-β-D-glucopyranosyl chloride, 1 gm., was shaken with 50 ml. of dry methanol which contained 1.5 gm. of freshly prepared dry silver carbonate for 50 min. at room temperature. The solids were removed by filtration and washed with benzene. The combined filtrates were evaporated below 12°C. to a sirup which was dissolved in benzene. The solution was clarified by filtration and evaporated to a sirup, $[\alpha]_D+65°$ (*c*, 0.9 in chloroform) which was dried in a high vacuum at room temperature. Calc. for methyl 1,2-ortho-*O*-acetyl-α-D-glucopyranose triacetate, $C_{15}H_{22}O_{10}$: methoxyl, 8.56%; acetyl by saponification, 35.64%; acetyl by acid hydrolysis, 47.51%. Found: methoxyl, 8.30%; acetyl by saponification, 37.3, 37.3%; acetyl by acid hydrolysis, 47.6, 46.3%.

ACKNOWLEDGMENT

The microanalyses were performed by J. A. Baignee of this laboratory.

REFERENCES

1. Dale, J. K. J. Am. Chem. Soc. 46: 1046. 1924.
2. Duffield, R. B. and Calvin, M. J. Am. Chem. Soc. 68: 557. 1946.
3. Fried, J. and Walz, D. E. J. Am. Chem. Soc. 71: 140. 1949.
4. Georg, A. Helv. Chim. Acta, 15: 924. 1932.
5. Goebel, W. F. and Babers, F. H. J. Biol. Chem. 110: 707. 1935.
6. Hudson, C. S. J. Am. Chem. Soc. 61: 2972. 1939.
7. Isbell, H. S. and Frush, H. L. J. Research Natl. Bur. Standards, 24: 125. 1940.
8. Isbell, H. S. and Frush, H. L. J. Research Natl. Bur. Standards, 43: 161. 1949.
9. Lemieux, R. U. Can. J. Chem. 29: 1079. 1951.
10. Lemieux, R. U. and Bauer, H. F. Anal. Chem. 26: 920. 1954.
11. Lemieux, R. U. and Brice, C. Can. J. Chem. 30: 295. 1952.
12. Lemieux, R. U. and Huber, G. Can. J. Chem. 31: 1040. 1953.
13. Pacsu, E. Ber. 61: 137. 1928.
14. Pacsu, E. J. Am. Chem. Soc. 61: 2669. 1939.
15. Pacsu, E. *In* Advances in carbohydrate chemistry. Vol. 1. *Edited by* W. W. Pigman and M. L. Wolfrom. Academic Press Inc., New York. 1945. p. 77.
16. Schlubach, H. H. Ber. 59: 840. 1926.
17. Schlubach, H. H. and Wolf, I. Ber. 62: 1507. 1929.
18. Winstein, S., Grunwald, E., and Ingraham, L. L. J. Am. Chem. Soc. 70: 821. 1948.
19. Winstein, S. and Roberts, R. M. J. Am. Chem. Soc. 75: 2297. 1953.
20. Wolfrom, M. L. and Thompson, A. J. Am. Chem. Soc. 56: 880. 1934.

A MECHANISM FOR THE ANOMERIZATION OF ACETYLATED ALKYL GLYCOPYRANOSIDES[1]

By R. U. Lemieux[2] and W. P. Shyluk

ABSTRACT

Unequivocal evidence that the anomerization of acetylated alkyl glycopyranosides can proceed by way of an intramolecular mechanism was obtained through the observation that a racemic mixture of methyl β-glucopyranoside tetraacetate with the D-isomer labelled in the methoxyl group with carbon-14 is anomerized both by titanium tetrachloride and boron trifluoride without transfer of radioactive methoxyl groups to the L-isomer. It is submitted that these intramolecular anomerizations are best rationalized as the result of an unsuccessful attempt by the environment to bring about glycosidic cleavage and proceed by way of an ion-pair intermediate in which the anion is derived from the aglycon group.

INTRODUCTION

In 1928, Pacsu reported that methyl β-D-glucopyranoside tetraacetate was transformed to the α-anomer by refluxing a solution of the substance in chloroform containing either stannic chloride (20) or titanium tetrachloride (21). Titanium tetrachloride was the more effective catalyst and the method has found wide application for the preparation of alkyl glycosides anomeric to the form obtained by the Koenigs–Knorr reaction with stable 1,2-*cis*-*O*-acetylglycosyl halides (11, 14, 21, 22, 24). In 1944, Lindberg (10) showed that the *O*-acetylated ethyl β-glycopyranosides of D-glucose and cellobiose are rearranged to the α-anomer by heating a solution in benzene with hydrogen bromide and mercuric bromide. In 1948, Lindberg (11) reported the anomerization of a number of *O*-acetylated alkyl β-D-glucopyranosides in chloroform solution with boron trifluoride as catalyst. Recently, Reeves and Mazzeno (25) have used titanium tetrachloride to anomerize a variety of β-D-glucopyranoside tetrabenzoates.

In 1944, Montgomery *et al.* (17) found that a solution of methyl α-D-arabinopyranoside triacetate in a mixture of 4% sulphuric acid in 7 : 3 acetic anhydride – acetic acid changed in rotation from −19° to −114° in one minute and declined to an equilibrium value of −25° at the end of 20 min. When the experiment was interrupted at the rotation peak of −114°, a 14% yield of methyl β-D-arabinopyranoside triacetate was obtained. In more recent years, Lindberg has studied the polarimetric rates for the reactions of a variety of β-D-glucosides (12, 13, 14), β-D-galactosides (1), and β-D-xylosides (2) in 10 : 3 mixtures of acetic anhydride – acetic acid with sulphuric acid as catalyst. In most cases there was a rapid increase in rotation followed by a decrease to a constant value. The reaction products at maximum rotation gave ethyl, isopropyl, and tertiary butyl α-D-glucopyranoside tetraacetates in 60, 70, and

[1]*Manuscript received September 7, 1954.*
Contribution from the National Research Council of Canada, Prairie Regional Laboratory, Saskatoon, Saskatchewan, Issued as Paper No. 179 on the Uses of Plant Products and as N.R.C. No. 3462.
[2]*Present address: Department of Chemistry, University of Ottawa, Ottawa, Ontario.*

30% yields, respectively (12), and ethyl α-D-galactopyranoside tetraacetate in 55% yield (1). Thus, it was apparent that the initial rapid rise in rotation was related to the formation of the α-anomer. It is to be noted that Lemieux *et al.* (9) have shown that these polarimetric rates are complex expressions which are not susceptible to simple interpretation. For example, it was found (9) that although the change in rotation on the acetolysis of methyl β-D-glucopyranoside tetraacetate did not clearly pass through a maximum, the α-glucoside content did pass through a maximum in 60% yield. Montgomery *et al.* (18) have observed that methyl α-D-glucopyranoside tetraacetate was formed when the β-anomer was treated with an excess of phenol which contained either zinc chloride or *p*-toluenesulphonic acid.

It was apparent that the anomerization of acetylated alkyl glycosides proceeds by way of an intramolecular mechanism since the only attractive alternative mode of reaction was by way of intermediate carbonium ions and this was unlikely because of the presence in the environment of a large excess of nucleophilic substances when the reaction takes place under conditions for acetolysis or phenolysis. Lindberg (12) concluded that the reactions are intramolecular on the basis that he was able to isolate isopropyl α-D-glucopyranoside tetraacetate and ethyl α-D-cellobioside heptaacetate in 66 and 75% yields, respectively, on isomerizing a mixture of isopropyl β-D-glucopyranoside tetraacetate and ethyl β-D-cellobioside heptaacetate using titanium tetrachloride in chloroform. However, considering the rather low yields obtained, this evidence was not compelling in the absence of information on the relative rates for the anomerization of the two β-glycosides since it was possible that one of the anomerizations was substantially finished before the other was well under way. Unequivocal evidence appeared desirable since Lemieux and Brice (6) have found that stannic chloride rapidly dissociates β-D-glucopyranose pentaacetate to acetate and carbonium ions during the process of bringing about anomerization. Obviously, a similar situation could be anticipated for the interaction of the related acetylated glycosides and titanium tetrachloride. We have now obtained unequivocal evidence that acetylated methyl glucopyranosides are not dissociated under conditions for anomerization and that the anomerization must therefore proceed by way of an intramolecular mechanism. This was accomplished by anomerizing a racemic mixture of methyl β-glucopyranoside tetraacetate with the methoxyl group of the D-isomer labelled with carbon-14. Both boron trifluoride and titanium tetrachloride were used as catalysts. Analysis of the products by the method of isotopic dilution showed in both cases that all the radioactivity was in the methyl α-D-glucopyranoside tetraacetate portion.

Lindberg (12) has proposed that the anomerizations proceed by way of a ring-opening–ring-closing mechanism. The ring-opening stage was considered to lead either to a carbonium ion or a dipolar ion depending on whether or not the acid catalyst was positively charged. As was indicated above, such a mechanism is unlikely in view of the ability of the anomerization to proceed under conditions for acetolysis or phenolysis. The present authors believe that a more plausible mechanism can be postulated based on the recent discovery

by Winstein and associates (27, 28) of ion-pair intermediates in a wide variety of rearrangements.

The great ease with which an electronegative substituent (X) can be replaced from the α-carbon of an ether has long been recognized and has been attributed to the participation of the ether oxygen in the dissociation of the carbon to X bond which results in the formation of a resonance stabilized carbonium ion (I). Several investigators (4, 6, 12, 19, 23) have suggested the

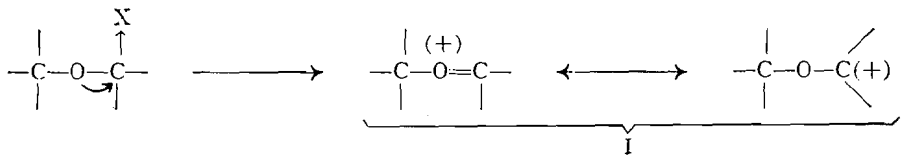

occurrence of an intermediate carbonium ion of this type in replacements at the anomeric center of sugar derivatives. On this basis and the fact that, as pointed out by Winstein and Schreiber (28), the ion-pair phenomenon can in principle be present in all processes which involve neighboring group participation, the anomerization of glycosides can be envisaged to proceed by way of either one of the two possible ion-pair intermediates represented by the formulas II and III. The postulation of the ion-pair (II) would be a refinement of the mechanism proposed by Lindberg (12). However, the present authors submit that the available evidence favors the ion-pair III. First of all, it is noteworthy that Hickinbottom (5) has shown 3,4,6-tri-*O*-acetyl-β-D-glucopyranosyl chloride to undergo anomerization as well as glucoside formation when dissolved in methanol. There can be no doubt that in this case the C1 to chlorine bond was the bond to be disrupted and the occurrence of anomerization in the presence of methanol precludes the presence of a solvated carbonium ion intermediate. Therefore, an ion-pair of the type depicted by structure III was most probably an intermediate for the reaction. Secondly, evidence for an intermediate of type III is provided by the effect of changes in the aglycon on the behavior of the compound under conditions for anomerization. The isotopic dilution analysis for methyl α-D-glucopyranoside tetraacetate in the product from the anomerization of the β-anomer which is described in the experimental portion of this paper shows that when titanium tetrachloride was used as catalyst, the yield of α-anomer was 76%. Reynolds (26) found that carboethoxymethyl β-D-glucopyranoside tetraacetate is not anomerized when treated with titanium tetrachloride in chloroform but instead is converted to tetra-*O*-acetyl-α-D-glucopyranosyl chloride in high yield (75%). Pacsu (21) has shown that β-D-glucopyranose pentaacetate is converted to the latter compound by titanium tetrachloride. Lemieux and Brice (6) have shown that the first reaction product is tetra-*O*-acetyl-β-D-glucopyranosyl chloride. Unsuccessful attempts to anomerize phenyl β-D-glucopyranoside tetraacetate are mentioned in the literature (15, 18). However, no experimental details were reported. We have found that phenyl β-D-glucopyranoside tetraacetate is

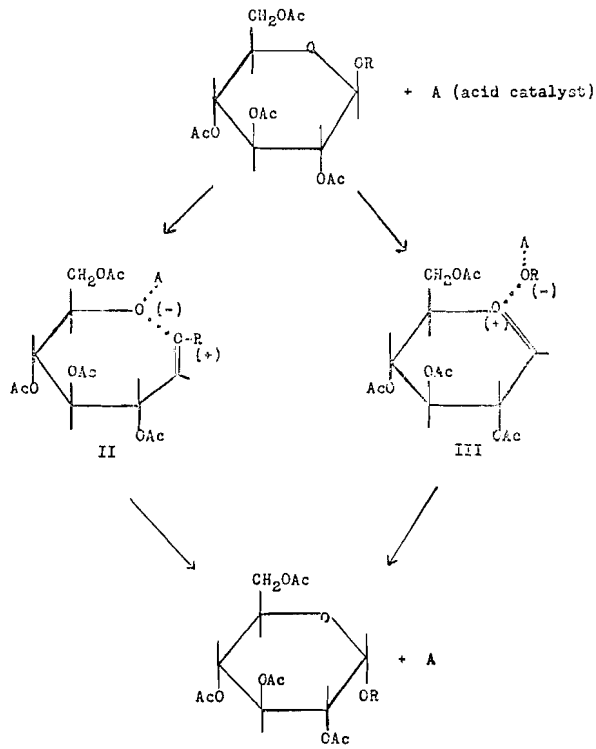

much more resistant to change by titanium tetrachloride than is methyl β-D-glucopyranoside tetraacetate and has little, if any, tendency for anomerization. Thus, while the conversion of methyl β-D-glucopyranoside tetraacetate to the α-anomer using an equimolar amount of titanium tetrachloride in boiling chloroform was complete within one hour, the much more drastic conditions of a threefold greater amount of titanium tetrachloride and six hour reaction time did not change more than 52% of phenyl β-D-glucopyranoside tetraacetate. When the product from the latter reaction was treated with silver acetate in acetic acid, little silver chloride was formed. This product, 60% yield by weight, specific rotation −5.9° in chloroform, was found by chromatography to comprise at least 81% starting material and 8% α-D-glucopyranose pentaacetate. Therefore, little, if any, phenyl α-D-glucopyranoside tetraacetate was formed. This result was not due to an unexpectedly high reactivity of the latter compound since under the same conditions for anomerization this substance was recovered in 95% yield. Reeves and Mazzeno (25) have recently shown that *O*-nitrophenyl β-D-glucopyranoside tetrabenzoate is more prone to glycosidic cleavage than to anomerization by titanium tetrachloride by finding that the substance was converted to tetra-*O*-benzoyl-α-D-glucopyranosyl chloride in 44% yield. Lemieux *et al.* (7) have recently shown that the anomerization of β-D-glucopyranose pentaacetate in a 0.5 *M* solution of sulphuric acid in 1 : 1 acetic acid – acetic anhydride mixture at 25°C. proceeds only to a very small extent by way of an intramolecular mechanism. On the other hand,

Lemieux *et al.* (9) have shown that under the same conditions methyl β-D-glucopyranoside tetraacetate passes into the α-form approximately four times

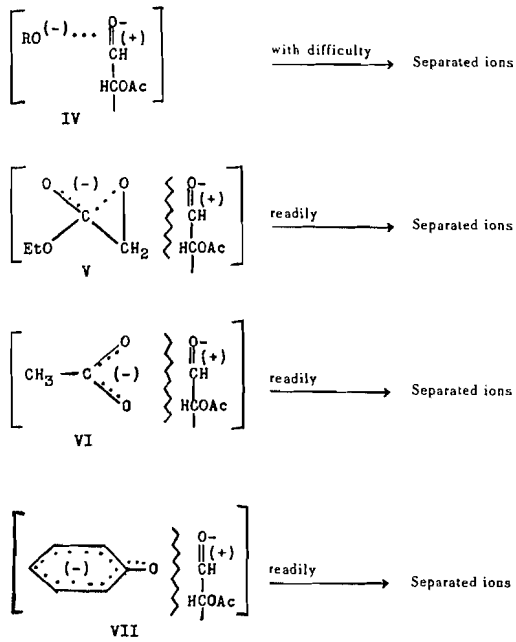

more rapidly than it is cleaved to form β-D-glucopyranose pentaacetate. These experimental facts appear to be best rationalized by assuming that both anomerization and glycosidic cleavage result from an attack by the acid catalyst at the aglycon group. When the aglycon group is derived from an anion such as alkylate ion (IV) where charge localization is high, a large proportion of the interactions can reasonably be expected to lead to a fairly stable ion-pair of structure III which can collapse to the α-glycoside instead of leading to separated ions. On the other hand, it is reasonable that ion separation leading to glycosidic cleavage should be extensive when the anion of the ion-pair can dissipate the negative charge through resonance as in the case for the carboethoxymethylate (V), acetate (VI), and phenolate (VII) ions.

EXPERIMENTAL

Methyl β-D-Glucopyranoside Tetraacetate

The substance was prepared labelled with carbon-14 in the methoxyl group by the procedure of Lemieux and Shyluk (8). β-D-Glucopyranose pentaacetate (1.77 mM.) was added to 9 ml. of dry benzene which contained 1.8 mM. of stannic chloride and 1.77 mM. of radioactive methanol. The solution was kept at 40°C. for one hour and the reaction product was isolated in the usual way (8). The substance was pure, m.p. 104.5–105°C., after three crystallizations from methanol and when counted as barium carbonate at infinite thickness possessed a radioactivity of 98,000 counts per minute.

Methyl β-L-Glucopyranoside Tetraacetate

L-Glucose, 1 gm., was converted to sirupy tetra-*O*-acetyl-L-glucopyranosyl bromide by the procedure of Bárczai-Martos and Kőrösy (3). The sirup was reacted with dry methanol, 30 ml., in presence of silver carbonate, 2 gm., at room temperature for 10 hr. The product was isolated in the usual manner and crystallized from 3 ml. of methanol to yield 1.06 gm. of crude methyl β-L-glucopyranoside tetraacetate, m.p. 103–104.5°C. The substance was pure after three recrystallizations from methanol, m.p. 104.8–105.2°C., $[\alpha]_D^{25}+19.3$ (*c*, 1 in chloroform).

Methyl α-L-Glucopyranoside Tetraacetate

Methyl β-L-glucopyranoside tetraacetate, 700 gm., was dissolved in 45 ml. of pure chloroform and the solution was saturated with dry boron trifluoride (11). The reaction mixture was allowed to stand at room temperature for 24 hr. and was then poured into saturated aqueous sodium bicarbonate solution and the product was isolated in the usual way. The substance, 350 mgm., was pure after three recrystallizations from ethanol, m.p. 102–102.5°C., $[\alpha]_D^{25}-130.5$ (*c*, 1 in chloroform).

Anomerization Catalyzed by Boron Trifluoride

Methyl β-D-glucopyranoside tetraacetate labelled in the methoxyl group with carbon-14, 11.04 mgm., 98,000 c.p.m., and non-radioactive methyl β-L-glucopyranoside tetraacetate, 9.98 mgm., were dissolved in 2 ml. of pure chloroform and the solution was saturated with boron trifluoride. After 24 hr. at room temperature, the reaction product was isolated in the usual manner (11). A sample of the sirupy product, 8.3 mgm., was mixed with 101 mgm. of pure methyl α-D-glucopyranoside tetraacetate for crystallization from ethanol. After six recrystallizations from ethanol, the substance melted at 101.5–102.5°C. and possessed a radioactivity of 3560 c.p.m. when counted as barium carbonate at infinite thickness. The radioactivity was unchanged, within experimental error, by further recrystallization. The radioactivity expected on the basis of an intramolecular mechanism and quantitative yield was 3860 c.p.m. The product of the anomerization, 7.8 mgm., was mixed with 99.5 mgm. of pure methyl α-L-glucopyranoside tetraacetate for crystallization from ethanol. After seven recrystallizations the melting point was 102–102.5°C. and the radioactivity was insignificant, 6 c.p.m.

Anomerization Catalyzed by Titanium Tetrachloride

Methyl β-D-glucopyranoside tetraacetate labelled in the methoxyl group with carbon-14, 10.9 mgm., 98,000 c.p.m., was dissolved in 0.3 ml. of pure chloroform which contained an equal amount of non-radioactive L-isomer. The solution was mixed with 0.3 mgm. of 0.2 *M* titanium tetrachloride in chloroform and the container was sealed for heating at 61°C. for five hours. The product was isolated in the usual way (21) and dissolved in 50 ml. of chloroform. The resulting solution was divided into two equal portions which were evaporated to yield two samples of dry sirupy product each weighing 11 mgm. One sample was diluted with 86.8 mgm. of non-radioactive methyl α-D-glucopyrano-

side tetraacetate for crystallization as described above in the anomerization using boron trifluoride. After seven recrystallizations, the material, m.p. 102–103°C., possessed a radioactivity of 4420 c.p.m. The radioactivity expected on the basis of an intramolecular mechanism and quantitative yield was 5840 c.p.m. The other sample of reaction product was mixed with 85.9 mgm. of methyl α-L-glucopyranoside tetraacetate and the mixture was recrystallized six times from ethanol to yield material, m.p. 101.5–102.5°C., which possessed insignificant radioactivity, 16 c.p.m.

Rate of Anomerization Catalyzed by Titanium Tetrachloride

At zero time, equal amounts, 0.6 ml., of 0.2 *M* solutions of methyl β-D-glucopyranoside tetraacetate and titanium tetrachloride in pure chloroform were mixed in glass tubes which were immediately sealed and placed in a water bath controlled at 61°C. After each of the various reaction times, a tube was placed in about 50 ml. of saturated aqueous bicarbonate solution contained in a stainless steel beaker and smashed with a heavy steel rod. The product was isolated by extraction with chloroform in the usual manner. The rotations of the product, measured in chloroform, were as follows: after 30 min. reaction time, +90°; 60 min., 112°; 90 min., 111°; 120 min., 113°.

Attempt to Anomerize Phenyl β-D-Glucopyranoside Tetraacetate

Dry phenyl β-D-glucopyranoside (8) tetraacetate, 424 mgm. (1 mM.) was added to a solution of 3 mM. of titanium tetrachloride in 10 ml. of pure chloroform and the mixture was refluxed for three hours. The brown colored solution was added to ice-water mixture and the resulting mixture was extracted four times with chloroform. The chloroform extracts were washed once with sodium bicarbonate solution, then with water, dried, and evaporated to a sirup which possessed a strong odor of phenol. The product was dissolved in 10 ml. of dry acetic acid which contained silver acetate (1 mM.) and the mixture was shaken at 60°C. for one hour. There appeared to be little reaction. The silver salts were removed by filtration and the filtrate was added to water before extraction with chloroform. The washed and dried chloroform extract was evaporated to a crystalline residue, 252 mgm. yield (60% by weight), $[\alpha]_D$ −5.9° in chloroform. Chromatography on Magnesol–Celite (5 : 1) according to the procedure of McNeely *et al.* (16) afforded 204 mgm. of essentially pure starting material, m.p. 123–125°C. and 20 mgm. of α-D-glucopyranose pentaacetate which was identified by mixed melting point, infrared spectra, and rotation.

When phenyl α-D-glucopyranoside tetraacetate (18), 424 mgm., was treated under the above conditions, the material was recovered in essentially pure condition, m.p. 110–112°C., $[\alpha]_D$ +161° in chloroform in 95% yield.

ACKNOWLEDGMENT

The authors are grateful to Carol Brice for valuable technical assistance and to A. C. Neish for kindly donating the L-glucose used in this work.

REFERENCES

1. ASP, L. and LINDBERG, B. Acta Chem. Scand. 4: 1386. 1950.
2. ASP, L. and LINDBERG, B. Acta Chem. Scand. 4: 1446. 1950.

3. BÁRCZAI-MARTOS, M. and KŐRÖSY, F. Nature, 165: 369. 1950.
4. BONNER, W. A. J. Am. Chem. Soc. 73: 2659. 1951.
5. HICKINBOTTOM, W. J. J. Chem. Soc. 1676. 1929.
6. LEMIEUX, R. U. and BRICE, C. Can. J. Chem. 30: 295. 1952.
7. LEMIEUX, R. U., BRICE, C., and HUBER, G. Can. J. Chem. 33: 134. 1955.
8. LEMIEUX, R. U. and SHYLUK, W. P. Can. J. Chem. 31: 528. 1953.
9. LEMIEUX, R. U., SHYLUK, W. P., and HUBER, G. Can. J. Chem. 33: 148. 1955.
10. LINDBERG, B. Arkiv. Kemi, Mineral. Geol., Ser. B, 18 (No. 9): 1. 1944.
11. LINDBERG, B. Acta Chem. Scand. 2: 426, 534. 1948.
12. LINDBERG, B. Acta Chem. Scand. 3: 1153. 1949.
13. LINDBERG, B. Acta Chem. Scand. 3: 1350. 1949.
14. LINDBERG, B. Acta Chem. Scand. 3: 1355. 1949.
15. LINDBERG, B. Acta Chem. Scand. 4: 49. 1950.
16. MCNEELY, W. H., BINKLEY, W. W., and WOLFROM, M. L. J. Am. Chem. Soc. 67: 527. 1945.
17. MONTGOMERY, E. M., HANN, R. M., and HUDSON, C. S. J. Am. Chem. Soc. 59: 1124. 1937.
18. MONTGOMERY, E., M. RICHTMYER, N. K., and HUDSON, C. S. J. Am. Chem. Soc. 64: 690. 1942.
19. NEWTH, F. H. and PHILLIPS, G. O. J. Chem. Soc. 2900. 1953.
20. PACSU, E. Ber. 61: 137. 1928.
21. PACSU, E. Ber. 61: 1508. 1928.
22. PACSU, E. J. Am. Chem. Soc. 52: 2563, 2568. 1930.
23. PAINTER, E. P. J. Am. Chem. Soc. 75: 1137. 1953.
24. PIEL, E. V. and PURVES, C. B. J. Am. Chem. Soc. 61: 2978. 1939.
25. REEVES, R. E. and MAZZENO, L. W., JR. J. Am. Chem. Soc. 76: 2219. 1954.
26. REYNOLDS, T. M. J. Proc. Roy. Soc. N.S. Wales, 66: 167. 1932.
27. WINSTEIN, S. and HECK, R. J. Am. Chem. Soc. 74: 5584. 1952.
28. WINSTEIN, S. and SCHREIBER, K. C. J. Am. Chem. Soc. 74: 2165. 1952.

THE SOLVOLYSIS OF THE *ALPHA*- AND *BETA*-3,4,6-TRI-*O*-ACETYL-D-GLUCOPYRANOSYL CHLORIDES[1]

By R. U. Lemieux[2] and G. Huber[3]

ABSTRACT

3,4,6-Tri-*O*-acetyl-β-D-glucopyranosyl chloride was found to undergo solvolysis in acetic acid to form 1,3,4,6-tetra-*O*-acetyl-α-D-glucopyranose as the main reaction product. The much less reactive anomeric α-chloride also appeared to undergo solvolysis with extensive inversion of the anomeric center. It is submitted that the tendencies for inversion obtained in these ionic reactions are due to the conformations imposed on the intermediate ions through distribution of the positive charge to the ring oxygen and the consequent introduction of double-bond character to the carbon-1 to ring-oxygen bond.

INTRODUCTION

It is now clear that the retention of configuration which is obtained in the replacement of the halogen atom of 1,2-*trans*-acetohalogenosugars (fully *O*-acetylated 1,2-*trans*-glycopyranosyl halides) by acetate is due to the participation of the C2-acetoxy group in the dissociation of the C1 to halogen bond (9, 10, 11). The high degree of inversion which usually is obtained in reactions of 1,2-*cis*-acetohalogenosugars could of course be the result of an S_N2 displacement-type mechanism. Isbell and Frush (8) have rationalized the formation of methyl β-D-glucopyranoside tetraacetate from α-acetobromoglucose in about 94% yield on this basis. This view has recently been challenged by Newth and Phillips (15) who suggested instead that these reactions proceed by way of carbonium ions with the positive charge distributed to the ring oxygen. Lindberg (14) had earlier produced kinetic evidence that the reaction of α-acetobromoglucose with water in acetone catalyzed by mercuric acetate was ionic in type. Chapman and Laird (5) have pointed out that some of the arguments used by Newth and Phillips are not acceptable and reported evidence that the reaction of 1,2-*cis*-acetohalogenosugars with amines usually is bimolecular in poorly solvating media. The present authors have recently shown (13) that the reactions of both the α- and β-3,4,6-tri-*O*-acetyl-D-glucosyl chlorides with acetic acid containing silver acetate proceed with inversion of the anomeric centers to a high degree. It was pointed out (13) that these results were in accordance with the idea that these reactions are of the S_N2 type. According to Hassel and Ottar (7) the β-chloride would be much less reactive than the α-anomer should these reactions in fact be of the S_N2 type. This investigation was undertaken to test this speculation made by Hassel and Ottar (7). However, the data obtained show that in all probability the reactions of the 3,4,6-tri-*O*-acetyl-D-glucosyl chlorides with acetic acid are of the S_N1 solvolytic type and that the β-chloride is far more reactive than the α-anomer.

[1]*Manuscript received September 7, 1954.*
Contribution from the National Research Council of Canada, Prairie Regional Laboratory, Saskatoon, Saskatchewan. Issued as Paper No. 176 on the Uses of Plant Products and as N.R.C. No. 3459.
[2]*Present address: Department of Chemistry, University of of Ottawa, Ottawa, Ontario.*
[3]*National Research Council of Canada Postdoctorate Fellow.*

TABLE I

POLARIMETRIC RATES FOR THE SOLVOLYSIS OF 3,4,6-TRI-*O*-ACETYL-β-D-GLUCOSYL CHLORIDE AT 20°C.

Expt.	Solvent	Initial concentration of the β-chloride	Observed rotation* Initial†	Observed rotation* Final	$k \times 10^4$, min.$^{-1}$‡
1	Acetic acid	0.025 *M*	0.486	2.263	65 ± 5
2	Acetic acid	0.05 *M*	1.024	4.460	63 ± 1
3	0.05 *M* potassium acetate in acetic acid	0.025 *M*	0.455	2.225	68 ± 5
4	0.05 *M* potassium acetate in acetic acid	0.05 *M*	0.995	4.560	69 ± 3
5	7:1 acetic acid – benzene (v/v)	0.025 *M*	0.486	2.285	49 ± 3
6	3:1 acetic acid – benzene (v/v)	0.025 *M*	0.547	2.265	36 ± 1
7	0.05 *M* mercuric acetate in acetic acid	0.025 *M*	—	2.260	Too fast to measure

*2 dm. tube.
†*Determined by extrapolation.*
‡*Calculated using the expression* $k = (2.303/t)\log[(\alpha_0 - \alpha_\infty)/(\alpha_t - \alpha_\infty)]$.

Table I summarizes the results of kinetic studies with 3,4,6-tri-*O*-acetyl-β-D-glucopyranosyl chloride (I). Experiments 1 and 2 show that the substance reacts rapidly when dissolved in acetic acid. The facts that the reaction product was strongly dextrorotatory, contained only a trace of chlorine, and afforded 1,3,4,6-tetra-*O*-acetyl-α-D-glucose in 72% crude yield show that the reaction proceeded to a large extent with inversion of the anomeric center. The results of experiments 3 and 4 show that the rate and stereochemical route of the reaction were unaffected by the presence of potassium acetate in the reaction mixture. Thus, it is clear that the rate of reaction is dependent only on the ionizing power of the solvent and therefore the reaction must be of the S_N1 solvolytic type. This conclusion is supported by the observation (experiments 5 and 6) that rendering the solvent less polar by dilution with benzene resulted in a substantial decrease in rate of reaction. Therefore, when 3,4,6-tri-*O*-acetyl-β-D-glucosyl chloride is dissolved in acetic acid the chlorine atom is replaced by acetate *by way of an intermediate carbonium ion with a strong tendency for inversion of the anomeric center.*

In contrast to the β-anomer, 3,4,6-tri-*O*-acetyl-α-D-glucosyl chloride (II) was too unreactive to allow the measurement of its rate of reaction in acetic acid. A comparison of the result of experiment 1 of Table II with that of experiment 2 of Table I shows that the α-chloride (II) is about 100 times less reactive than the β-anomer (I). In order to obtain convenient reaction rates in homogeneous solution, the Lewis acid mercuric acetate was used to catalyze the reaction. A comparison of the results of experiments 3 and 4 of Table II shows that the addition of benzene to the reaction mixture lowered the reaction rate by an extent comparable to that observed for the β-chloride. This observation cannot be taken as compelling evidence for an S_N1 mechanism. Never-

TABLE II

POLARIMETRIC RATES FOR THE SOLVOLYSIS OF 3,4,6-TRI-*O*-ACETYL-α-D-GLUCOSYL CHLORIDE AT 20°C.

Expt.	Solvent	Initial concentration of α-chloride	Observed rotation* Initial†	Final	$k \times 10^4$, min.$^{-1}$‡
1	0.05 *M* potassium acetate in acetic acid	0.05 *M*	3.813	1.600¶	0.69 ± 0.11
2	0.05 *M* mercuric acetate in acetic acid	0.05 *M*	3.999	1.600	2020 ± 50
3	0.05 *M* mercuric acetate in acetic acid	0.025 *M*	2.119	0.800	3310 ± 180
4	0.05 *M* mercuric acetate in 3:1 acetic acid – benzene (v/v)	0.025 *M*	2.095	0.806	2490 ± 180

*,†,‡*See footnote for Table I.*
¶*The final rotation observed in experiment 2.*

theless, the fact that it leads to the same conclusion as was reached by Lindberg (14) and Newth and Phillips (15) in kinetic studies with α-acetobromoglucose in solvating media leaves little doubt that the reaction proceeds by way of an intermediate carbonium ion. The polarimetric data listed in Table II and the fact that 1,3,4,6-tetra-*O*-acetyl-β-D-glucose could be isolated from the product in 72% crude yield show clearly that the reaction proceeds with a high degree of inversion at the anomeric center. Therefore, it can be concluded that *like its β-anomer* 3,4,6-tri-*O*-acetyl-α-D-glucosyl chloride *undergoes solvolysis with extensive inversion* at the anomeric center.

The fact that the reactions of the chlorides (I and II) proceed mainly with inversion shows the reactions to be essentially free of neighbor group participation. The ability of the reactions to proceed readily by way of ionic mechanisms must therefore be related to stabilization of the carbonium ion by interaction with the ring-oxygen atom (5, 15). The fact that this interaction must introduce double-bond character to the lactol carbon to ring-oxygen bond renders possible an interesting rationalization of the results which in turn gains support from a stereodynamic standpoint. The ability of an S_N1 reaction to proceed with a high degree of inversion must be related to the conformation of the carbonium ion. The introduction of double-bond character to the C1 to ring-oxygen bond renders possible two fairly rigid carbonium ions (III and IV) which differ only in conformation as has been suggested for cyclohexene (1). The orientations of the substituents in these ions are such that it can be reasonably expected that ion III prefers to accept an anion on the α-side of the ring and that ion IV is more open to attack on the β-side of the ring. Thus, the stereochemical routes followed in the solvolyses of the chlorides can be rationalized on the assumption that the β-anomer (I) dissociates to the ion III while the α-anomer yields the ion IV. This assumption is supported by the fact that these reaction routes are those to be expected on the basis of the stereochemical

requirements for elimination established by Barton and Miller (3). Thus, the preferred conformation for dissociation of the β-chloride (I) would be as shown where the ring-oxygen atom has a *p*-orbital in the same plane as the chlorine atom. This postulation appears particularly attractive when it is considered that it allows rationalization of the higher reactivity of the β-chloride (I) over the α-anomer (II) on the basis that the presence of the C3-acetoxy group, CH_2OAc group, and chlorine atom in axial orientation (2) can be expected to result in steric assistance to dissociation. That is, it appears likely that the achievement of the conformation I by the β-chloride through kinetic disturbance should result in considerable steric pressure by the C3-acetoxy and CH_2OAc groups on the chlorine atom and thus aid in its dissociation. Hassel and Ottar (7) have discussed the steric interaction which can be expected (4) between opposing groups in axial orientation in the sugar molecules. The postulate also appears attractive for the reason that the dissociation of I to ion III involves much less reorientation of the pyranose ring than the conversion of I to ion IV and as seen above ion III appears necessary to explain the stereochemical route of the reaction. The α-chloride (II) can be expected for similar reasons to react in the conformation shown to form the ion IV. The implication of these ideas on the mechanism of the anomerization of derivatives of glucose is dealt with in another communication (12).

Lemieux (9) has suggested that the high difference in reactivity which exists for the anomeric D-glucopyranose pentaacetates (which can be as great as 450 (10)) and the acetochloroglucoses (9, 10) is due mainly to anchimeric assistance to dissociation by the C2-acetoxy group in the case of the more reactive 1,2-*trans*-β-anomer. The facts that the β-chloride (I) is about 100

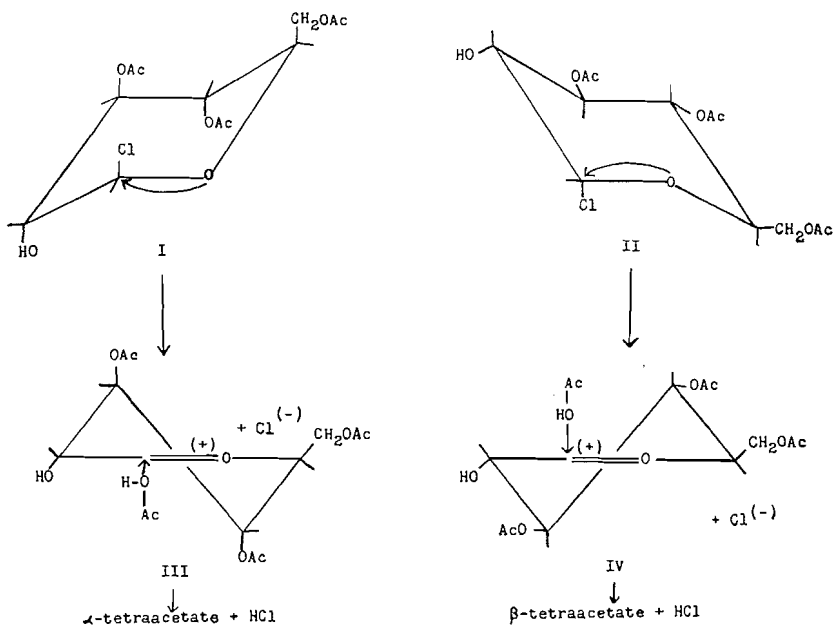

times more reactive than the α-chloride (II) and that the reaction was clearly free of neighboring group participation require that this idea be qualified. Nevertheless, the facts that inversion can be expected in the absence of participation of the C2-substituent and that the reactions of β-glucopyranose pentaacetate and β-acetochloroglucose proceed with very high degree of retention of configuration show clearly that C2-acetoxy group participation is extensive and must therefore provide an important driving force for the dissociation (16). This conclusion is strongly supported by the fact that 1,2-*cis*-β-mannopyranose pentaacetate is less reactive than the 1,2-*trans*-α-anomer in spite of the fact that the latter compound is the more stable substance (11). It is of definite interest to note that the higher reactivity of the β-chloride (I) over the α-chloride (II) is probably due to steric considerations which resemble those responsible for the higher reactivity of β-mannopyranose pentaacetate over α-glucopyranose pentaacetate (11). Winstein and Roberts (17) have pointed out that dissociation with participation of a neighboring acetoxy group probably requires an axial–axial orientation as shown in formula V for β-D-acetochloroglucose. This consideration lends considerable weight to the idea that the β-chloride (I) undergoes dissociation in the conformation shown.

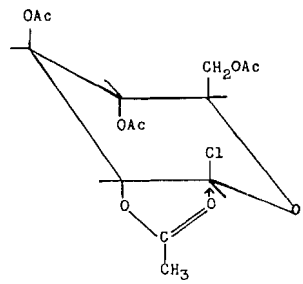

V

In contrast to reactions in acetic acid, the reactions of the glucosyl chlorides I and II with silver acetate in dry ether led to extensive racemization of the anomeric center. Gakhokidze (6) has reported the preparation of 1,3,4,6-tetra-*O*-acetyl-β-D-glucose by reaction of the β-chloride (I) under these conditions. We have now shown by isotopic dilution analysis that the product contains 43.3% of the 1,3,4,6-tetra-*O*-acetyl-α-D-glucose. Reaction of the α-chloride II gave only a 44.6% yield of the Walden inversion product. These results are in accordance with expectation for an ionic reaction under these reaction conditions since solvation of the carbonium ion by ether (8) would lead to an equilibrium mixture of the various possible conformations for the carbonium ion.

EXPERIMENTAL

Methods

The kinetic studies and the determinations of radioactivity were carried out as previously described (10, 11). Each experiment was done in duplicate.

Isolation and Analysis of Reaction Products

Table I, experiment 2—the solvent was removed *in vacuo* and the residue was crystallized from ether to give a 72% yield of crude 1,3,4,6-tetra-*O*-acetyl-α-D-glucose, m.p. 88–92°C. The melting point after one recrystallization, 96–98°C., was not depressed by the pure α-tetraacetate, m.p. 97–98°C. (13).

Table I, experiment 7—hydrogen sulphide was passed into the reaction mixture to precipitate mercuric sulphide and the filtrate was evaporated *in vacuo* to a sirup which was monochloroacetylated as previously described (13). The product was crystallized from ethanol to give a 90% yield of crude 2-*O*-monochloroacetyl-α-D-glucopyranose tetraacetate (13), m.p. 130–136°C., $[\alpha]_D$ +96° (chloroform). The substance was characterized by mixed melting point determination after purification.

The products from experiments 5 and 6 of Table I contained about 0.4% chlorine. Therefore, the reactions were essentially free of anomerization of the β-chloride (13).

Table II, experiment 2—hydrogen sulphide was used to precipitate mercuric sulphide and concentration of the filtrate *in vacuo* gave a sirup which was crystallized from ethanol. The yield was 72% of a substance, m.p. 132–135°C., whose melting point was not depressed by 1,3,4,6-tetra-*O*-acetyl-β-D-glucopyranose (13), m.p. 137–138°C.

The 3,4,6-tri-*O*-acetyl-D-glucosyl chloride, 1 mM., was shaken with 2 mM. silver acetate in 10 ml. dry ether for 16 hr. The product, isolated in the usual manner, was diluted with a known amount of radioactive 1,3,4,6-tetra-*O*-acetyl-D-glucose (13) of known radioactivity for isotopic dilution analysis. Starting with the β-chloride (I), the α-tetraacetate was isolated by crystallization and from the radioactivity it could be calculated that it comprised 43.3% of the reaction product. The reaction product from the α-chloride (II), was shown to contain 44.6% β-tetraacetate using this procedure.

REFERENCES

1. Barton, D. H. R., Cookson, R. C., Klyne, W., and Shoppee, C. W. Chemistry & Industry, 21. 1954.
2. Barton, D. H. R., Hassel, O., Pitzer, K. S., and Prelog, V. Nature, 172: 1096. 1953.
3. Barton, D. H. R. and Miller, E. J. Am. Chem. Soc. 72: 1066. 1950.
4. Beckett, C. W., Pitzer, K. S., and Spitzer, R. J. Am. Chem. Soc. 69: 2488. 1947.
5. Chapman, N. B. and Laird, W. E. Chemistry & Industry, 20. 1954.
6. Gakhokidze, A. M. J. Gen. Chem. (U.S.S.R.), 11: 117. 1941.
7. Hassel, O. and Ottar, B. Acta Chem. Scand. 1: 929. 1947.
8. Isbell, H. S. and Frush, H. L. J. Research Natl. Bur. Standards, 43: 161. 1949.
9. Lemieux, R. U. Can. J. Chem. 29: 1079. 1951.
10. Lemieux, R. U. and Brice, C. Can. J. Chem. 30: 295. 1952.
11. Lemieux, R. U. and Brice, C. Can. J. Chem. 33: 109. 1955.
12. Lemieux, R. U., Brice, C., and Huber, G. Can. J. Chem. 33: 134. 1955.
13. Lemieux, R. U. and Huber, G. Can. J. Chem. 31: 1040. 1953.
14. Lindberg, B. Acta Chem. Scand. 1: 710. 1947.
15. Newth, F. H. and Phillips, G. D. J. Chem. Soc. 2896, 2900, 2904. 1953.
16. Winstein, S., Grunwald, E., and Ingraham, L. L. J. Am. Chem. Soc. 70: 821. 1948.
17. Winstein, S. and Roberts, R. M. J. Am. Chem. Soc. 75: 2297. 1953.

THE EFFECT OF CHLORINE SUBSTITUTIONS AT THE C_2-ACETOXY GROUP ON SOME PROPERTIES OF THE GLUCOSE PENTAACETATES[1]

By R. U. Lemieux,[2] Carol Brice, and G. Huber[3]

ABSTRACT

The effects were studied of substituting one, two, and three chlorine atoms at the C2-acetoxy group of the α- and β-D-glucopyranose pentaacetates on the rates both of anomerization and of dissociation of the C1 to acetoxy group bond in 1 : 1 acetic acid – acetic anhydride 0.5 *M* with respect to sulphuric acid at 25°C. In the case of the α-anomers, the rates of anomerization appeared about equal to the rates of dissociation as measured by isotopic exchange. The β-anomers dissociated more rapidly than they underwent anomerization. The difference in rate decreased rapidly, however, with the introduction of chlorine atoms indicating that the tendency for C2-acyl group participation in the dissociation is reduced by the chlorine substitutions. Evidence was obtained that only a very small fraction, if any, of the C1-acetoxy group of β-glucose pentaacetate passes into the α-anomer without becoming completely dissociated. It is pointed out that the data for the anomerizations can be rationalized on the basis of ionic mechanisms, if specific conformations are allocated to the intermediate carbonium ions.

INTRODUCTION

The high reactivity of β-D-glucopyranose pentaacetate as compared to the α-anomer in undergoing dissociation of the C1 to acetoxy group bond through the agency of acid catalysts has been demonstrated under the following conditions: mercaptolysis using zinc chloride in ethyl mercaptan (4), exchange of acetate with stannic trichloride acetate in chloroform (5), replacement by chlorine using titanium tetrachloride in chloroform (5), methanolysis using stannic chloride as catalyst in either benzene or chloroform (9), and phenolysis using toluene sulphonic acid as catalyst (14, 18). Lemieux (4) has pointed out that the high reactivity of the 1,2-*trans*-β-anomer is in all probability related to participation of the C2-acetoxy group in the dissociation. Direct evidence for the participation was recently obtained through the preparation of methyl 1,2-ortho-*O*-acetyl-α-D-glucopyranose triacetate by reacting tetra-*O*-acetyl-β-D-glucopyranosyl chloride with methanol in the presence of silver carbonate (6).

It was now of interest to study the effect of varying substituents at the C2-position on the dissociation of the C1 to acetoxy group bond. The anomeric monochloroacetyl, dichloroacetyl, and trichloroacetyl derivatives of the 1,3,4,6-tetra-*O*-acetyl-D-glucopyranoses (7) were chosen for this purpose since the C2-substituents in these compounds vary widely in electronegativity. A study was made of the behavior of these substances under the conditions for anomerization using 0.5 *M* sulphuric acid in 1 : 1 acetic acid – acetic anhydride

[1]*Manuscript received September 7, 1954.*
Contribution from the National Research Council of Canada, Prairie Regional Laboratory, Saskatoon, Saskatchewan. Issued as Paper No. 175 on the Uses of Plant Products and as N.R.C. No. 3461. Presented in part before the Division of Carbohydrate Chemistry at the 125th Meeting of the American Chemical Society, Kansas City, Missouri, March 24, 1954.
[2]*Present address: Department of Chemistry, University of Ottawa, Ottawa, Ontario.*
[3]*National Research Council of Canada Postdoctorate Fellow.*

since Bonner (1) has shown these conditions to affect only the anomeric center and to be particularly well-suited for kinetic measurements. Painter (17) has also very recently made an extensive kinetic study of the behavior of the glucose pentaacetates in acetic acid – acetic anhydride mixtures which contained sulphuric acid.

The evidence, based mainly on qualitative infrared spectra (1), that anomerization of the glucose pentaacetates under these conditions leads to a product which contains only the α- and β-pentaacetates was substantiated by isotopic dilution analysis. The analytical results, listed in Table I, showed a composition for the equilibrium mixture which was in good agreement with the composition expected from its rotation. Bonner (1) has reported the equilibrium mixture to contain about 83% α- and 17% β-anomer. This conclusion was based on the rotation of the equilibrium product measured in chloroform. On the other hand, Painter (17) calculated the point of equilibrium from the kinetic data and concluded that the equilibrium mixture contains 87% α- and 13% β-anomer. We have substantiated both of these conclusions (see Table I)

TABLE I

ANALYSIS OF THE REACTION MIXTURE AT VARIOUS TIMES DURING THE ANOMERIZATION OF PENTA-*O*-ACETYL-β-D-GLUCOPYRANOSE

The anomerizations were carried out in 1 : 1 acetic acid – acetic anhydride 0.5*M* with respect to sulphuric acid at 25°C.

	Reaction mixture		Reaction product		
		% β-anomer		% β-anomer	
t (min.)	α*	Calc. from rotation	$[\alpha_D^{25}]$†	Calc. from rotation	Isotopic‡ dilution analysis
2	—	—	9.12	94.6	94
10	2.61	74.3	27.6	75.6	72
20	4.00	57.5	44.3	58.6	56
210	7.65	14.3	84.8	17.1	17§

**The rotation for the β-anomer (at zero time) was estimated to be +0.49°. In a separate experiment, the rotation of the α-anomer was estimated to be +8.76°.*

†Measured in chloroform under the conditions where the specific rotation of the β-anomer is +3.8° and that of the α-anomer is +101.6°.

‡Average of two analyses.

§By difference from the content of α-anomer.

but cannot explain the discrepancy. Since it is possible that the composition of the equilibrium product is altered during the isolation, Painter's method for obtaining the point of equilibrium was used in the present work.

Table I lists the results of isotopic dilution analyses performed on reaction products isolated at a variety of times during the course of reaction before equilibrium was achieved. These results establish that the anomerizations do not proceed by way of isolable intermediates.

Lemieux and Brice (5) have shown that β-glucose pentaacetate is dissociated by stannic chloride in chloroform solution much more rapidly than it is converted to the α-anomer. The same situation was to be expected under the

present conditions of acetolysis. In order to measure the rates of dissociation under the present conditions, all but one of the compounds used in these studies (i.e., compounds I*a*, I*b*, I*c*, I*d*, II*a*, II*b*, II*d*) were prepared labelled with carbon-14 in the carbonyl group of the C1-acetoxy group and the rates at which the substances lost radioactivity by exchange of the C1-acetoxy group with

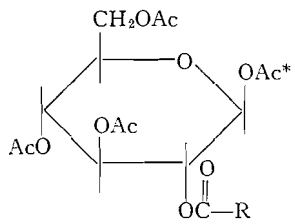

I*a*, R = CH_3
I*b*, R = CH_2Cl
I*c*, R = $CHCl_2$
I*d*, R = CCl_3

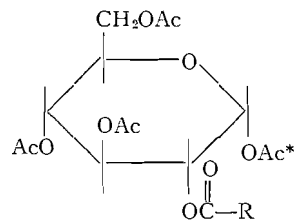

II*a*, R = CH_3
II*b*, R = CH_2Cl
II*c*, R = $CHCl_2$
II*d*, R = CCl_3

acetoxy groups from the environment were determined. The loss of radioactivity may of course have been brought about in two ways:

(*a*) by exchange of acetyl groups as acetyl carbonium ion,

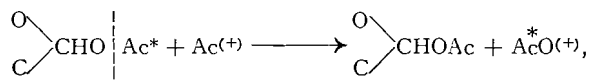

and,

(*b*) by exchange of acetoxy groups as acetate ion,

There can be no doubt that the environment can serve as a source of either acetyl carbonium ions or acetate ions. Although direct evidence for the relative importance of the two routes is at present not available, the behavior of the glucose pentaacetates under the variety of reaction conditions listed above clearly demonstrates the C1 to acetoxy group bond to be the most acid-labile linkage in these compounds. Furthermore, the results obtained in the present study can be clearly rationalized only on the assumption of exchange by way of C1 to acetoxy group bond cleavage. Therefore, it is considered completely safe to conclude that the only important route for exchange was that which involved acetoxy groups.

The C1-acetoxy group-labelled β-D-glucose pentaacetate was subjected to anomerization at 25°C. in 1 : 1 acetic acid – acetic anhydride 0.5 *M* with respect to sulphuric acid. The reaction was stopped after 3, 5, and 10 min., the D-glucose pentaacetates were separated by chromatography on Magnesol–Celite (5 : 1) (12) and their radioactivities were determined. The results are listed in Table II. It is seen that as expected (5) the β-pentaacetate underwent exchange much more rapidly than it underwent anomerization. The radioactivity found in the α-anomer will be considered later on.

TABLE II

RATE OF DISSOCIATION OF THE C1 TO ACETOXY GROUP BOND OF β-D-GLUCOSE PENTAACETATE AS MEASURED BY EXCHANGE
The reaction conditions were those reported in Table I

Time, (min.)	Reaction mixture: Composition, %		Reaction mixture: Radioactivity, c.p.m.		k, min.$^{-1}$ for β-anomer
	β-anomer	α-anomer	β-anomer	α-anomer	
0	100	0	11,800	—	
3	92.3	7.7	3500	280	0.41
5	87.6	12.4	1440	146	0.43
10	77.2	22.8	276	75	0.40
20 hr. (∞)				68	0.41 (average)

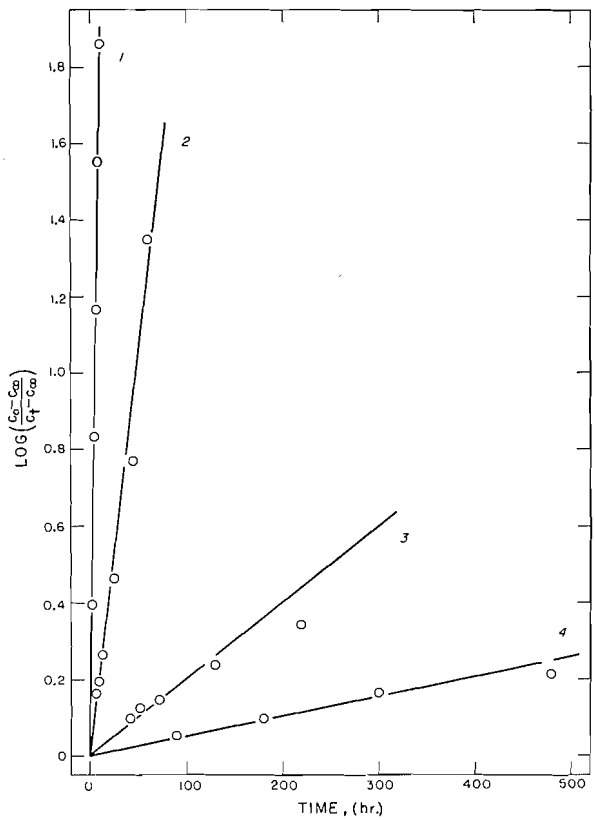

FIG. 1. Rate of exchange of the C1-acetoxy group of β-D-glucose derivatives in 1 : 1 acetic acid – acetic anhydride 0.5 *M* with respect to sulphuric acid at 25°C.
Curve 1—β-D-Glucopyranose pentaacetate.
Curve 2—2-*O*-Monochloroacetyl-β-D-glucopyranose tetraacetate.
Curve 3—2-*O*-Dichloroacetyl-β-D-glucopyranose tetraacetate.
Curve 4—2-*O*-Trichloroacetyl-β-D-glucopyranose tetraacetate.

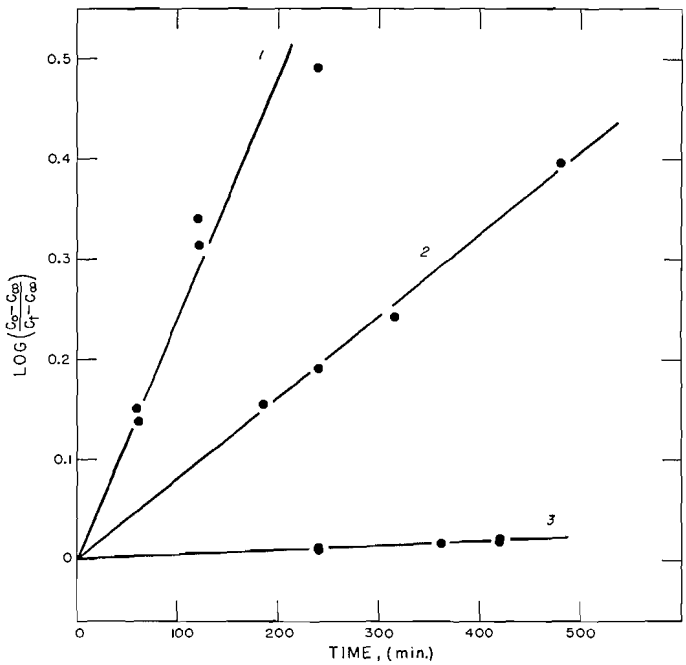

FIG. 2. Rate of exchange of the C1-acetoxy group of α-D-glucose derivatives in 1 : 1 acetic acid – acetic anhydride 0.5 *M* with respect to sulphuric acid at 25°C.
Curve 1—α-D-Glucopyranose pentaacetate.
Curve 2—2-*O*-Monochloroacetyl-α-D-glucopyranose tetraacetate.
Curve 3—2-*O*-Trichloroacetyl-α-D-glucopyranose tetraacetate.

The fact that a sufficiently accurate value for the velocity constant for the exchange of the β-anomer can be obtained simply by determining the radioactivity of the reaction product after various periods of time is shown by the data listed in Table III. It is seen that this procedure yields a value of 0.46 min.$^{-1}$ for the velocity constant instead of the value of 0.41 min.$^{-1}$ given in Table II. The velocity constants given in Table III are all based on the radioactivity of the isolated reaction products. The plots in Figs. 1 and 2 illustrate the reproducibility of the experimental data from which these constants were calculated.

The data in Table III show that β-D-glucose pentaacetate undergoes exchange about 80 times more rapidly than the α-anomer. This result is consistent with the conclusions previously reached (4, 5) regarding the relative reactivities of these substances. Electronic theory would predict that the introduction of chlorine atoms at the C2-acetoxy groups of the glucose pentaacetates would affect strongly the ease for dissociation of the C1 to acetoxy group bond. Lemieux (4) has pointed out that there should be a strong direct effect in the case of the β-anomer due to reduction in the nucleophilic properties of the carbonyl oxygen of the C2-acetoxy group which would be brought about by each successive substitution of chlorine atoms. Thus, the chlorine substitutions should result in a decreasing tendency for participation in the dissociation and,

TABLE III

RATES OF DISSOCIATION OF C1 TO ACETOXY GROUP BOND OF D-GLUCOSE DERIVATIVES AS MEASURED BY EXCHANGE
The reaction conditions were those reported in Table I

2-*O*-Acyl derivative of 1,3,4,6-tetraacetylglucose	$k \times 10^4$,* min.$^{-1}$	
I*a*, β-acetyl	4600	±160
II*a*, α-acetyl	55.7	±6.1
I*b*, β-monochloroacetyl	498	±72
II*b*, α-monochloroacetyl	18.8	±1.4
I*c*, β-dichloroacetyl	46.0	±6.3
I*d*, β-trichloroacetyl	12.0	±1.1
II*d*, α-trichloroacetyl	1.10	±0.04

**The standard deviations are from the average of five determinations.*

since the participation is the source of strong activation, a strong decrease in reactivity. That this is in fact the case is clear from the fact that the introduction of three chlorine atoms brought about a 390-fold reduction in reactivity. This should be compared to the case for the α-anomer where the introduction of three chlorine atoms brought about only a 50-fold reduction in reactivity. Here, the effect of the chlorine substituents on the dissociation must be exerted indirectly by induction transmitted *via* the C2-carbon atom. The introduction

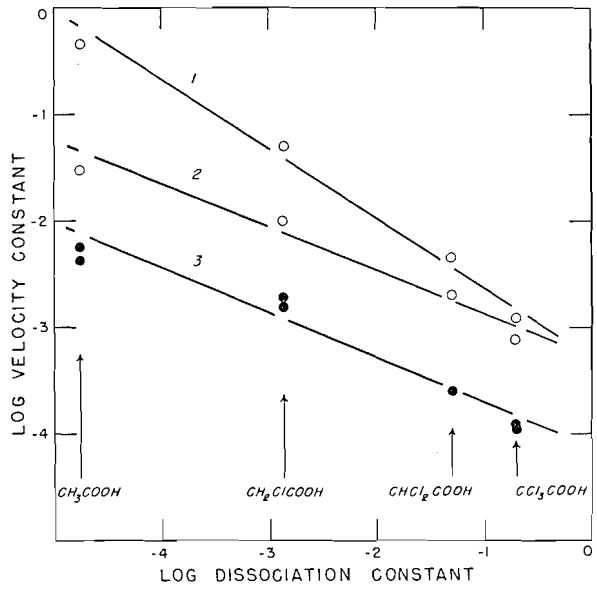

FIG. 3. Plots of log velocity constants (see Tables III and IV) against log dissociation constant for the acid derived from the C2-substituent of an acylated 1,3,4,6-tetra-*O*-acetyl-D-glucose. The dissociation constants are those published by Mason and Kilpatrick (13).
Curve 1—Dissociation of the C1-acetoxy group of β-D-glucose derivatives.
Curve 2—Anomerization of the β-D-glucose derivatives.
Curve 3—Dissociation and anomerization of α-D-glucose derivatives.

of chlorine atoms at the C2-acetoxy groups of the glucose pentaacetates of course adds greatly to the bulk of these groups. Consequently, it might be expected that these alterations would greatly affect the steric picture. The logarithms of the velocity constants for the exchange reactions are plotted in Fig. 3 against the logarithms of the dissociation constants for the acids present as esters at the C2-position. It is seen that the deviation from Hammett's linear free energy relationship (2) is not great. Consequently, it is apparent that in both series of compounds the steric requirements for reaction were not seriously affected by the introduction of chlorine atoms. Further support for this conclusion is given later on.

The results of polarimetric rate studies on the anomerization of the glucose derivatives (I*a*–I*d* and II*a*–II*d*) are listed in Table IV. The plots in Fig. 4 are

TABLE IV

RATES OF ANOMERIZATION

POLARIMETRIC DATA FOR THE ANOMERIZATION OF GLUCOSE DERIVATIVES IN 1 : 1 ACETIC ACID – ACETIC ANHYDRIDE 0.5 *M* WITH RESPECT TO SULPHURIC ACID AT 25°C.

2-*O*-Acyl derivative of 1,3,4,6-tetra-*O*-acetyl-D-glucose*	Initial rotation†	Equilibrium rotation	Equilibrium constant‡	$k_{\alpha\to\beta}+k_{\beta\to\alpha}$ $\times 10^4$, min.$^{-1}$§	$k_{\alpha\to\beta}\times 10^4$, min.$^{-1}$	$k_{\beta\to\alpha}\times 10^4$, min.$^{-1}$
I*a*, β-acetyl	0.295°	3.83°	0.140	349 ±8	43	306
II*a*, α-acetyl	4.325	3.83		327 ±15	40	287
I*b*, β-monochloroacetyl	0.575	3.96	0.151	114 ±4	15	99
II*b*, α-monochloroacetyl	4.475	3.96		121 ±5	16	105
I*c*, β-dichloroacetyl	0.824	4.06	0.122	23.2 ±1.5	2.5	20.7
II*c*, α-dichloroacetyl	4.454	4.06		22.6 ±1.5	2.5	20.1
I*d*, β-trichloroacetyl	0.811	4.10	0.154	8.7 ±0.2	1.2	7.5
II*d*, α-trichloroacetyl	4.605	—		8.7 ±0.8	1.2	7.5

**The starting material used for the measurements.*
†*The value obtained by graphical extrapolation.*
‡*The value calculated from the initial and equilibrium rotations.*
§*These values are the average of the values obtained in two separate runs.*

illustrative of the data from which the content of Table III was calculated. A consideration of the results shows that the point of equilibrium was affected only slightly by introducing chlorine atoms in the C2-acetoxy group of the glucose pentaacetates. Consequently, the velocity constants for the forward and reverse reactions were affected about equally by each successive substitution. This comprises strong evidence that the substitutional changes affected the rates of anomerization mainly through electronic phenomena and that the increase in the size of the group through substitution of chlorine for hydrogen had a relatively small effect. This conclusion should be compared with the views recently expressed by Newth and Phillips (15) who contended that the trichloroacetyl group in 2-*O*-trichloroacetyl-β-D-glucopyranosyl chloride exerts a strong shielding effect on the C1-chlorine atom.

It seems clear (10, 11) that acetylated alkyl glycopyranosides undergo anomerization under conditions for acetolysis by way of an intramolecular mechanism. Lemieux *et al.* (10) have studied the anomerization of methyl

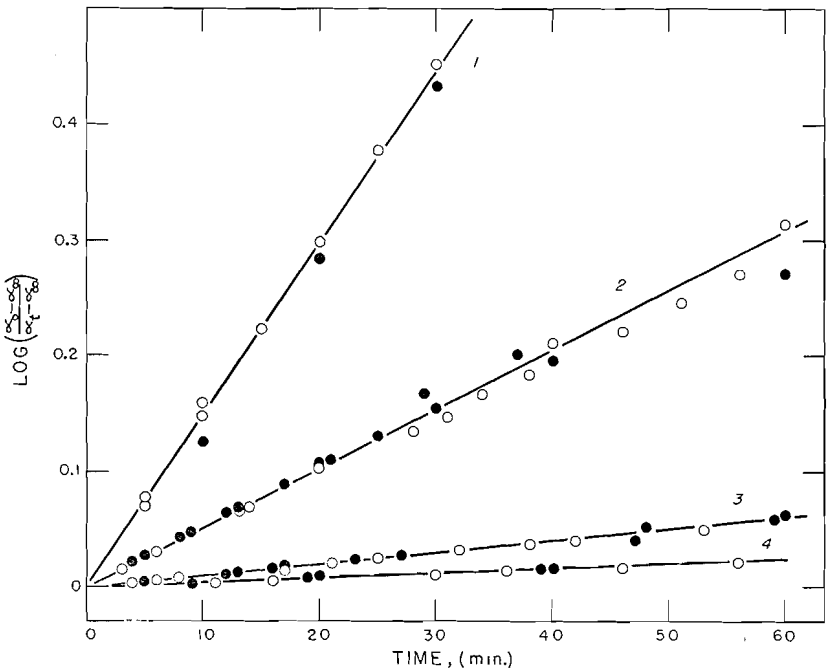

FIG. 4. Rates of anomerization of glucose derivatives determined polarimetrically in 1 : 1 acetic acid – acetic anhydride 0.5 *M* with respect to sulphuric acid at 25°C.
(○ and ● signify that the points of equilibrium were approached from the β- and α-anomers, respectively)
Curve 1—D-Glucopyranose pentaacetates.
Curve 2—2-*O*-Monochloroacetyl-D-glucopyranose tetraacetates.
Curve 3—2-*O*-Dichloroacetyl-D-glucopyranose tetraacetates.
Curve 4—2-*O*-Trichloroacetyl-D-glucopyranose tetraacetates.

β-D-glucopyranoside tetraacetate under the conditions used herein for the anomerization of the glucopyranose pentaacetates. Since it must be expected that the anomerization of β-D-glucopyranose pentaacetate would have a tendency to follow the same path as the anomerization of methyl β-D-glucopyranoside tetraacetate, any consideration of the mechanism of the latter reaction must first deal with the possibility that the reaction proceeds by way of an intramolecular mechanism.

C1-Acetoxy-group-labelled β-D-glucopyranose pentaacetate was subjected to anomerization and the α-anomer which had formed after various intervals of time was isolated by chromatography and its radioactivity was determined. The data which were obtained are listed in Table II. It is seen that the α-anomer appeared to gain radioactivity directly from the β-anomer since the initially formed α-anomer was more radioactive than samples isolated later on. It is possible that this result was due to the presence of a small amount (about 0.2%) of radioactive α-compound in the starting material. However, it is considered more probable that the result indicates the occurrence of intramolecular anomerization. It was found that the extent of the intramolecular route, if in fact present, was very small by comparing the experimental values

shown in Table II with those expected from calculations based on the assumption that anomerization occurred entirely by way of an intramolecular mechanism. The calculations were based on the following scheme where k_1 is the velocity constant for dissociation of the β-anomer (k_β of Table III), $k_2 = k_{\beta\to\alpha}$, and $k_3 = k_{\alpha\to\beta}$. The reconversion of radioactive α-form to radioactive β-form

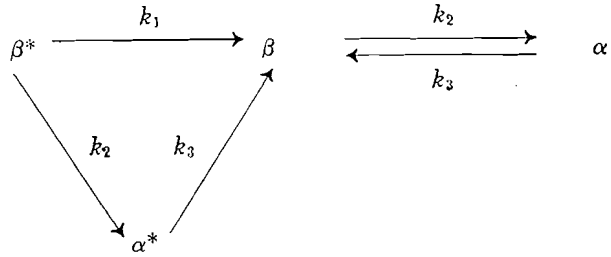

need not be considered since this would merely raise our calculated values for the radioactivity of the α-form at any given time by a negligible amount. The rate of formation of α^* can be expressed as,

$$d[\alpha^*]/dt = -d[\beta^*]/dt - d[\beta]/dt.$$

Since the rate of disappearance of β^* is expressed by

[1] $$-d[\beta^*]/dt = (k_1+k_2)\,[\beta^*]$$

and the rate of formation of β is given by

$$d[\beta]/dt = k_1[\beta^*]+k_3[\alpha^*],$$

then

$$d[\alpha^*]/dt = k_2[\beta^*]-k_3[\alpha^*].$$

Integration of equation [1] yields

$$[\beta^*] = [\beta^*]_0\, e^{-(k_1+k_2)\,t}.$$

Therefore,

$$d[\alpha^*]/dt = [\beta^*]_0\, k_2 e^{-(k_1+k_2)\,t} - k_3[\alpha^*].$$

Integration of this linear differential equation using the integrating factor $R = \exp \int k_3\, dt$ yields the expression,

$$[\alpha^*]_t = [\beta^*]_0 \frac{k_2}{k_3 - k_1 - k_2} (e^{-(k_1+k_2)\,t} - e^{-k_3 t}),$$

from which the concentration of α-anomer, $[\alpha^*]_t$, which was formed from radioactive β-anomer after any given time t can be calculated. The concentration of α-anomer, $[\alpha^*]+[\alpha]$, at any given time can be calculated from the integrated expression for reversible first-order reactions,

$$[\alpha^*] + [\alpha] = [\beta^*]_0 \frac{k_2}{k_2 + k_3} (1 - e^{-(k_2+k_3)\,t}).$$

Therefore, the radioactivity of α-anomer, C_t, isolated at time t would be,

$$c_t = c_0[\alpha^*]_t/([\alpha^*]+[\alpha]),$$

where c_0 is the original radioactivity of the β-anomer. The calculated values

for c_t after 3, 5, and 10 min. are given in Table V. A comparison of these results with the values actually obtained which are listed in Table II shows clearly that intramolecular anomerization is an unimportant reaction route.

TABLE V

DATA EXPECTED ON THE BASIS OF AN INTRAMOLECULAR MECHANISM FOR THE ANOMERIZATION OF β-D-GLUCOSE PENTAACETATE
Compare these data with the experimental values given in Table II

Time, (min.)	Calculated radioactivity, c.p.m.	
	β-Anomer	α-Anomer
0	11,800	
3	2985	6490
5	1180	4720
10	118	2714
∞	66	66

Bonner (1) has proposed a mechanism for the anomerization under the present reaction conditions which would involve a cyclic six-membered intermediate formed between the sugar acetate and a carbonium ion derived from acetic anhydride. Examination of the data in Tables III and IV shows that within experimental error* the velocity constants for anomerization of an α-anomer (compounds II*a*, II*b*, and II*d*) are equal in value to the velocity constants for exchange. This situation is required by Bonner's mechanism or any other S_N2 type mechanism which can be formulated. However, Painter (17) has recently published the results of an extensive kinetic study of the anomerization of the D-glucopyranose pentaacetates in mixtures of acetic acid – acetic anhydride catalyzed both by sulphuric acid and by perchloric acid and concluded from a consideration of the results that the anomerizations proceed by way of sugar acetate carbonium ions. Our present evidence that the rate of anomerization for the α-form was essentially equal to that of dissociation of the C1 to acetoxy group bond might appear to contradict this conclusion. However, Lemieux and Huber (8) have obtained evidence that other similar reactions of derivatives of D-glucopyranose proceed by way of carbonium ions with extensive inversion of the anomeric center. This result was rationalized on the basis of the assumption that the double-bond character introduced at the C1 to ring-oxygen bond imposed a conformation on the ion which rendered the ion more likely to form the inverted product.

We submit that the following mechanisms for the anomerization of the D-glucopyranose pentaacetates is an attractive rationalization of the experimental data thus far obtained. First of all, as was seen above, intramolecular anomerization is undoubtedly unimportant for the *beta* to *alpha* transformation. As it was indicated above, the data for the *alpha* to *beta* anomerization can be rationalized by assuming that the α-pentaacetate (V) dissociates to the

**The experimental error is rather large. For example, if Bonner's value for the equilibrium constant for the anomerization of the glucose pentaacetates is used to calculate the velocity constants, the value of $k_{\alpha\rightarrow\beta}$ becomes 0.0056 min.$^{-1}$ instead of 0.0042 min.$^{-1}$ as listed in Table III.*

carbonium ion (VI) which by virtue of its conformation tends to form the β-pentaacetate (III) on interaction with the environment. The *beta* to *alpha* transformation can be assumed to proceed by way of the carbonium ion (IV) which because of its conformation can be expected (8) to preferentially form the α-pentaacetate. However, as it was seen above the present data show clearly that the β-anomer (III) is rapidly dissociated to the 1,2-α-cyclic carbonium ion (VII). Since direct replacements with retention of configuration are not known, the α-pentaacetate cannot be expected to be formed by direct interaction of this ion with the environment. However, the discovery by Hurd and Holysz (3) that the 1,2-cyclic ketals are formed in the reaction of tetra-*O*-acetyl-α-D-glucopyranosyl bromide with dialkyl cadmium shows that the 1,2-α-cyclic carbonium ion (VII) can be formed from other carbonium ions. Since the reverse must be expected, the anomerization must follow to some extent the route III → VII → IV → V. The relative importance of these

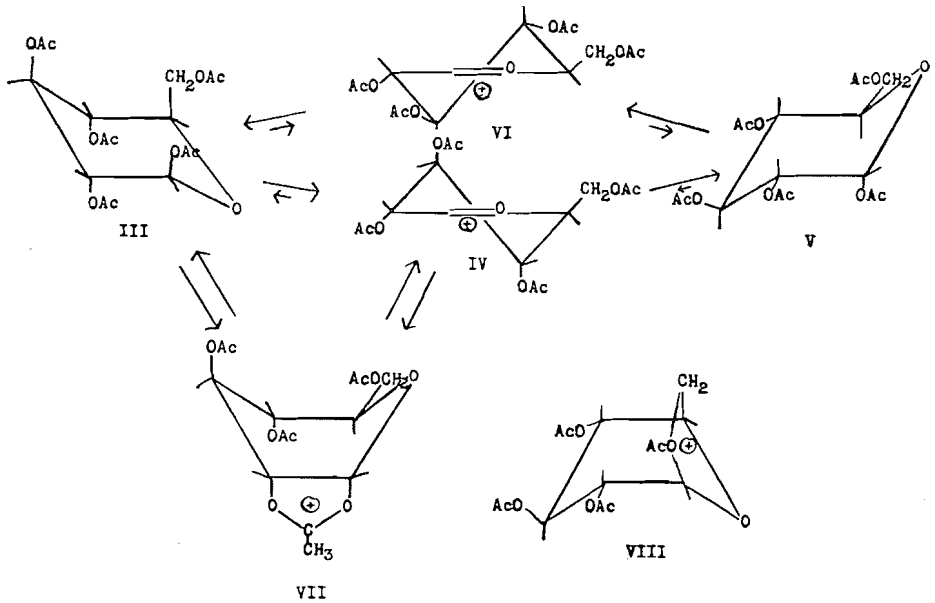

theoretically plausible routes for the *beta* to *alpha* conversion cannot be assessed. Lemieux and Brice (5) have proposed similar reaction routes for the anomerization of β-glucopyranose pentaacetate in chloroform catalyzed by stannic chloride. It was pointed out that the rearrangement of the 1,2-α-cyclic ion (VII) to the 1,6-β-cyclic ion (VIII) is a further stereochemically possible step for the reaction.

In summary, evidence was obtained to show that the substitution of chlorine atoms at the C2-acetoxy group of β-D-glucopyranose pentaacetate greatly reduces the tendency for this group to participate in dissociation of the C1 to acetoxy group bond. Thus, the fact that the velocity constants for dissociation were 15, 5, and 1.5 times that for β → α anomerization when the C2-substituent was acetoxy, monochloroacetoxy, and trichloroacetoxy, respectively,

renders clear the reason why β-D-acetochloroglucose and 2-*O*-trichloroacetyl-β-D-glucosyl chloride triacetate yield mainly β-D-glucose pentaacetate (6) and 2-*O*-trichloroacetyl-α-D-glucose tetraacetate (7) respectively, on reaction with silver acetate in acetic acid. The results comprise direct evidence in support of the contention (4) that participation of the C2-acetoxy group provides an important driving force for dissociation of a β-C1-substituent. The fact that 2-*O*-trichloroacetyl-β-D-glucopyranose tetraacetate underwent dissociation six times more rapidly than the α-anomer together with the previous observation (8) that 3,4,6-tri-*O*-acetyl-β-D-glucosyl chloride is more reactive than the α-anomer shows that the high reactivity of β-D-glucopyranose pentaacetate (4, 5) and β-D-acetochloroglucopyranose (6) as compared to their α-anomers is not entirely due to C2-acetoxy group participation. Lemieux and Huber (8) have suggested that the higher reactivity of a β-compound may be related to the presence of *cis* C3- and C5-substituents.

EXPERIMENTAL

Methods

The samples were converted to barium carbonate for measurement of the radioactivities at "infinite thickness" in a windowless counter operating with helium–isobutane. Appropriate resolving-time and background corrections were made. Duplicate determinations did not differ by more than 3%.

The polarimetric measurements were made using a 2 dm. polarimeter tube and precision polarimeter. The temperature was controlled within ±0.1°C.

The rates of reaction were measured as follows. The glucose derivative, 2 mM., was dissolved in 8 ml. of 50 : 50 acetic acid – acetic anhydride in a 20 ml. volumetric flask. Sulphuric acid, 1.026 gm. of 95.5% acid, 10 mM., was added to 8 ml. of the solvent mixture and the solution was cooled. The solutions, brought to 25°C., were mixed at zero time and the volume was adjusted to 20 ml. with solvent mixture. This could be done very rapidly by using syringes. The polarimetric rates were determined in the usual way (1). In order to follow the rate of disappearance of radioactivity, 2 ml. samples were removed at various time intervals and plunged into 50 ml. of water. The product was isolated by extraction with chloroform. The chloroform extract was washed with bicarbonate solution, then with water and dried over sodium sulphate. The chloroform was removed *in vacuo* and the sample was dried over phosphorus pentoxide in high vacuum before analysis.

In order to determine the radioactivities of both the β- and α-forms in a reaction mixture to yield the data listed in Table II, the major component was isolated by crystallization and the minor component was isolated by chromatography of the combined mother liquors on Magnesol–Celite (5 : 1) according to the procedure of McNeely *et al.* (12). The materials were recrystallized several times to achieve a very high degree of purity.

The isotopic dilution analyses listed in Table I were carried out by adding a sufficiently large radioactive sample of the anomer to be estimated to a sample of reaction product to allow the substance to be isolated from the resultant mixture by fractional crystallization. The amount of the anomer in the

reaction mixture was calculated from the expression,

$$\% \text{ anomer} = (100x/y)\,[(c_i - c_f)/c_f],$$

when x gm. of radioactive anomer of c_i c.p.m. was added to y gm. of reaction product to be analyzed and c_f was the radioactivity in counts per minute of the pure anomer isolated from the mixture.

The specific reaction rates listed in Tables II and III were calculated from the polarimetric data using the integrated rate expression,

$$k_\alpha + k_\beta = (2.303/t) \log [(\alpha_0 - \alpha_e)/(\alpha_t - \alpha_e)].$$

The rate of exchange, R, for a simple exchange reaction can be calculated from the relationship,

$$R = -\frac{[A][B]}{[A]+[B]} \cdot \frac{1}{t} \ln(1-F),$$

where $[A]$ is the concentration of the exchangeable group in one reactant (in the present case sugar acetate), $[B]$ is the concentration of the exchangeable group in the other reactant (in the present case the acetic acid and acetic anhydride), and the fraction exchange at time t is,

$$F = (c_t - c_0)/[(c_\infty - c_0)].$$

c_0, c_∞, and c_t are the radioactivities of the sugar acetate at zero time, infinite time, and time t, respectively. In the present case, the dissociation of the sugar acetate undoubtedly controlled the rate of exchange. Therefore, the specific rate of exchange, k, can be calculated from the relationship,

$$k = \frac{R}{[A]} = -\frac{[B]}{[A]+[B]} \cdot \frac{1}{t} \ln(1-F).$$

Since $[B]$ was great as compared to $[A]$, the specific reaction rates listed in Table II were calculated from the expression,

$$k = (2.303/t) \log(c_0 - c_\infty)/[(c_t - c_\infty)],$$

which is sufficiently accurate for the present purposes. Analysis showed the presence of 180 acetoxy groups in the environment per mole of glucose derivative. Thus, the radioactivity at infinite time would be expected to be 1/181 of the original radioactivity. In practice, the agreement with this value was very good (compare Tables II and V).

Materials

The radioactive acetate was labelled in the carboxyl group with carbon-14.

C1-Acetoxy-labelled penta-*O*-acetyl-β-D-glucopyranose was prepared by treating acetobromoglucose with radioactive silver acetate in dry acetonitrile (5). The product was recrystallized from ethanol until pure. Radioactive penta-*O*-acetyl-α-D-glucopyranose was prepared by anomerization of the β-anomer using stannic chloride in chloroform solution (5, 16). Purification was by recrystallization from ethanol.

The C1-acetoxy-labelled chloro-compounds were prepared by acylating the C1-acetoxy-labelled α- and β-1,3,4,6-tetra-*O*-acetyl-D-glucoses under the conditions described in a previous publication (7). The compounds were recrystallized from ethanol until pure. The C1-acetoxy-labelled glucose tetraacetates were prepared as follows. A mixture of radioactive silver acetate, 1.7 gm., 3,4,6-tri-*O*-acetyl-α-D-glucosyl chloride, 3.24 gm., and 75 ml. of dry ether which contained one drop of acetic acid was shaken for 12 hr. at room temperature. The silver salts were removed by filtration. Evaporation gave 3.1 gm. of product, m.p. 131–135°C. Pure 1,3,4,6-tetra-*O*-acetyl-β-D-glucopyranose, m.p. 137–138°, was obtained after two recrystallizations from ethanol. The 1,3,4,6-tetra-*O*-acetyl-α-D-glucose was prepared in the same manner starting from 3,4,6-tri-*O*-acetyl-β-D-glucosyl chloride except that the reaction time was extended to 24 hr. and purification was achieved by crystallization from ether – petroleum ether.

REFERENCES

1. BONNER, W. A. J. Am. Chem. Soc. 73: 2659. 1951.
2. HAMMETT, L. P. Physical organic chemistry. McGraw-Hill Book Company, Inc., New York. 1940.
3. HURD, C. D. and HOLYSZ, R. P. J. Am. Chem. Soc. 72: 2005. 1950.
4. LEMIEUX, R. U. Can. J. Chem. 29: 1079. 1951.
5. LEMIEUX, R. U. and BRICE, C. Can. J. Chem. 30: 295. 1952.
6. LEMIEUX, R. U. and BRICE, C. Can. J. Chem. 33: 109. 1955.
7. LEMIEUX, R. U. and HUBER, G. Can. J. Chem. 31: 1040. 1953.
8. LEMIEUX, R. U. and HUBER, G. Can. J. Chem. 33: 128. 1955.
9. LEMIEUX, R. U. and SHYLUK, W. P. Can. J. Chem. 31: 528. 1953.
10. LEMIEUX, R. U., SHYLUK, W. P., and HUBER, G. Can. J. Chem. 33: 148. 1955.
11. LINDBERG, B. Acta Chem. Scand. 3: 1153. 1949.
12. MCNEELY, W. H., BINKLEY, W. W., and WOLFROM, M. L. J. Am. Chem. Soc. 67: 527. 1945.
13. MASON, R. B. and KILPATRICK, M. J. Am. Chem. Soc. 59: 572. 1937.
14. MONTGOMERY, E. M., RICHTMYER, N. K., and HUDSON, C. S. J. Am. Chem. Soc. 64: 690. 1942.
15. NEWTH, F. H. and PHILLIPS, G. D. J. Chem. Soc. 2904. 1953.
16. PACSU, E. Ber. 61: 137. 1928.
17. PAINTER, E. P. J. Am. Chem. Soc. 75: 1137. 1953.
18. TSOU, K. C. and SELIGMAN, A. M. J. Am. Chem. Soc. 75: 1042. 1953.

THE ACETOLYSES OF THE *ALPHA* AND *BETA* METHYL D-GLUCOPYRANOSIDE TETRAACETATES[1]

By R. U. Lemieux,[2] W. P. Shyluk, and G. Huber[3]

ABSTRACT

The acetolyses of the *alpha* and *beta* methyl D-glucopyranoside tetraacetates in 1 : 1 acetic acid – acetic anhydride 0.5 *M* with respect to sulphuric acid were followed at 25°C. by isotopic dilution analysis of products isolated after various intervals of time. The reaction of the α-glucoside was found to proceed mainly with inversion of the anomeric center. On the other hand, the β-glucoside was found to undergo acetolysis with retention of configuration concurrent with anomerization. It was shown that the polarimetric changes observed in the course of the reactions could be satisfactorily accounted for on the basis of these reaction routes. Reaction mechanisms are suggested.

Montgomery *et al.* (15) investigated the use of either sulphuric acid or zinc chloride in acetic acid – acetic anhydride as a reagent for the acetolysis of glycosides. It was shown that in many cases the glycoside was converted to a mixture of the anomeric sugar acetates in high yield and the procedure has been widely used for the cleavage of acetal bonds in carbohydrate chemistry. Studies on the acetolysis of the anomeric methyl D-arabinopyranoside triacetates showed these reactions to be highly complex (15). A solution at 20°C. of methyl α-D-arabinopyranoside triacetate in a mixture of 4% sulphuric acid in 7 : 3 acetic anhydride – acetic acid changed sharply in specific rotation from −19° to −114° in one minute and declined to an equilibrium value of −25° at the end of 20 min. The hexaacetate of *aldehydo*-D-arabinose and β-D-arabinopyranose tetraacetate were isolated in yields of 50% and 12%, respectively, from the product. However, when the experiment was interrupted at the rotation peak of −114°, a 14% yield of methyl β-D-arabinopyranoside triacetate was obtained. Thus, it was apparent that the rapid initial rise in rotation was due to the anomerization of the α-anomer to the more stable β-form. This possibility was strengthened by the observation that methyl β-D-arabinopyranoside triacetate under the same conditions gave a solution which changed in specific rotation from −184° to a constant equilibrium value of −17° in three minutes. The hexaacetate and the β-tetraacetate could be isolated in 56% and 11% yields, respectively, after 24 hr. The occurrence of the hexaacetate in the reaction products suggested that the C1 to ring-oxygen bond may cleave in preference to the C1 to methoxyl group bond. This idea was substantiated by the acetolysis of the β-arabinoside under the milder conditions of 0.16% sulphuric acid in 7 : 3 acetic anhydride – acetic acid mixture. Both the anomeric forms of methyl hemiacetal pentaacetates (I) were isolated in good and approximately equal yields. It is to be noted that

[1]*Manuscript received September 7, 1954.*
Contribution from the National Research Council of Canada, Prairie Regional Laboratory, Saskatoon, Saskatchewan. Issued as Paper No. 177 on the Uses of Plant Products and as N.R.C. No. 3460.
[2]*Present address: Chemistry Department, University of Ottawa, Ottawa, Ontario.*
[3]*National Research Council of Canada Postdoctorate Fellow.*

the high levorotation which was achieved in the

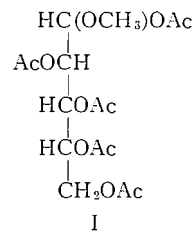

I

case of the α-D-arabinoside indicates that the susceptibility to ring cleavage is a property of the β-D-anomer.

More recently, Lindberg (1, 2, 13) has obtained further evidence that the acetolysis of an unstable *O*-acetylated alkyl glycopyranoside is accompanied by anomerization. This was shown to be so for a variety of glucosides (13), galactosides (1), and a xyloside (2) when treated in 10 : 3 acetic anhydride mixture containing sulphuric acid. Lindberg (13) obtained evidence for the presence of peracetylated *aldehydo*-sugar in the product of these reactions. A theory for the mechanism of the anomerization was formulated (13) on the basis of the presence of these open-chain compounds in the products and the polarimetric rates observed.

The present authors undertook to elaborate in detail the course of the acetolysis of both the α- and β-methyl D-glucopyranoside tetraacetates with the hope that the results would provide a firmer basis for work in this complex field. The glucosides were subjected to acetolysis at 25°C. in 1 : 1 acetic acid – acetic anhydride mixture 0.5 *M* with sulphuric acid since these conditions were chosen by Bonner (3) in a thorough kinetic study of the anomerization of the glucopyranose pentaacetates. Furthermore, Bonner's results were closely reproduced in this laboratory (9) in a study of the behavior of the glucopyranose pentaacetates and related compounds under conditions of acetolysis and it was desirable that the results of this study be of use in the present work.

First of all, it is of interest to note the polarimetric changes which occurred when the acetylated glucosides were subjected to the conditions for acetolysis. The results of typical runs are plotted in Fig. 1. Superficially, these results would appear to indicate that the two glucosides reacted at about equal rates, a result in complete disagreement with what could be expected on the basis of the rather great difference in reactivity noted for the glucopyranose pentaacetates under these conditions where β-anomer was found to dissociate 80 times more rapidly than the α-form (9). Thus, it was clear from the beginning that in all likelihood these polarimetric rates were complex expressions which were not susceptible to simple interpretation.

Methyl α-D-glucopyranoside tetraacetate was subjected to the acetolysis and reaction products were isolated after a variety of intervals of time. The methoxyl contents of these samples were determined by the procedure of Hoffman and Wolfrom (5). Care had to be taken in the interpretation of these values since in view of the above described experiences of Montgomery *et al.*

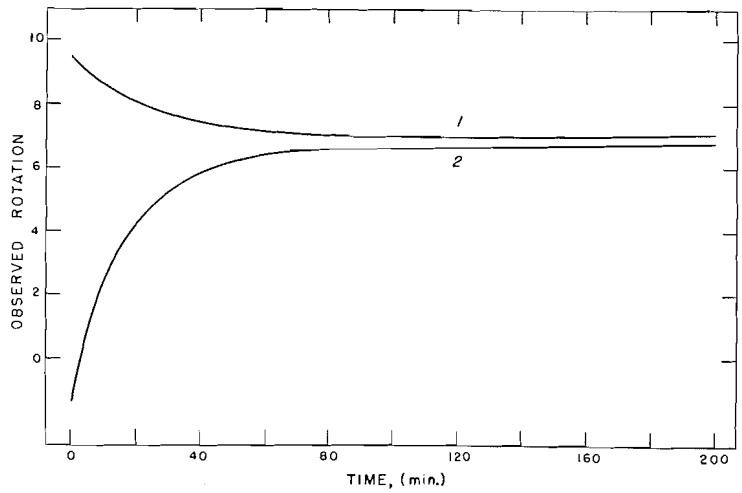

FIG. 1. Polarimetric rates for the acetolysis of the *alpha* (curve 1) and *beta* (curve 2) methyl D-glucopyranoside tetraacetates in 1 : 1 acetic acid – acetic anhydride 0.5 *M* with respect to sulphuric acid at 25°C.

(15) it was possible that these samples contained *aldehydo*-glucose methyl hemiacetal hexaacetate as well as methyl α-D-glucopyranoside tetraacetate. The following analytical method was designed to test for this possibility. The reaction products were saponified to liberate methanol from the acetylated hemiacetal group, and the methanol was removed from the reaction mixture by distillation for estimation by conversion to formaldehyde with potassium permanganate and determination of the formaldehyde by the chromotropic acid colorimetric method (4). The results are listed in Table I. The differences

TABLE I

ANALYSES OF REACTION PRODUCTS AND VELOCITY CONSTANTS FOR THE ACETOLYSIS OF METHYL α-D-GLUCOPYRANOSIDE TETRAACETATE
0.5 *M* H_2SO_4, 1 : 1 Ac_2O – AcOH, 25°C.

Time, min.	% methoxyl, total	% methoxyl, alk. labile	C_B*	C_E†	k_3+k_6, min.$^{-1}$	k_6, min.$^{-1}$
0	8.56	0	1	0	—	—
10	7.94	0.04	0.921	0.006	0.0080	0.00062
20	7.32	0.08	0.845	0.012	0.0074	0.00064
30	6.85	0.14	0.782 0.751‡	0.021	0.0076	0.00078
90	4.23	0.24	0.465 0.467‡	0.036	0.0084	0.00056
120	3.17	0.40	0.323	0.060	0.0094	0.00079
300	0.98	0.69	—	—	—	—
1440	0.56	—	—	—	—	—
				Average	0.0082 ±0.0007	0.0007 ±0.00008
				k_3 = 0.0075 min.$^{-1}$		

**Amount of methyl α-D-glucopyranoside tetraacetate in the product.*
†Amount of D-glucose methyl hemiacetal hexaacetate in the product.
‡Determined by isotopic dilution analysis.

between these methoxyl values and the total methoxyl content could be attributed to the starting material methyl α-D-glucopyranoside tetraacetate since, even though the anomerization of the glucosides is probably reversible, the amount of methyl β-D-glucopyranoside tetraacetate present at any time was undoubtedly negligible for the present purposes. This conclusion was substantiated by isotopic dilution analysis of the products isolated after 30 and 90 min. reaction times for their methyl α-D-glucopyranoside tetraacetate contents. The results, listed in Table I, show a good agreement between the methyl α-D-glucopyranoside tetraacetate contents when determined in both ways.

The reaction of methyl α-D-glucopyranoside tetraacetate (B) under the conditions for acetolysis could therefore be represented by the scheme

$$E \xleftarrow{k_6} B \xrightarrow{k_3} C$$

wherein glucosidic cleavage yields a glucopyranose pentaacetate (C) with the velocity constant k_3 and ring cleavage yields the *aldehydo*-glucose methyl hemiacetal hexaacetate (E) with the velocity constant k_6. On this basis, the fraction of B (C_B) in the product at any given time was

$$[1] \qquad C_B = e^{-(k_3+k_6)t}.$$

The rate of the appearance of E is expressed by

$$dC_E/dt = C_B k_6 = k_6 e^{-(k_3+k_6)t},$$

and integration of this expression yields

$$[2] \qquad C_E = \frac{k_6}{k_3+k_6}(1-e^{-(k_3+k_6)t}).$$

Using expression [1], the value for k_3+k_6 could be calculated from the data in Table I and found to be 0.0082 min.$^{-1}$ (average value). Knowing k_3+k_6 and values for C_E at a variety of times (see Table I), the value of k_6 could be calculated using expression [2]. Thus, as shown in Table I, the average values $k_3 = 0.0075$ min.$^{-1}$ and $k_6 = 0.0007$ min.$^{-1}$ were obtained for the acetolysis of methyl α-D-glucopyranoside tetraacetate in 1 : 1 acetic acid – acetic anhydride mixture 0.5 *M* with respect to sulphuric acid at 25°C.

It was now of interest to determine which of the anomeric D-glucopyranose pentaacetates was the first product of the main reaction path. A decision was reached by accounting for the polarimetric change which took place in the course of the reaction. For the reaction sequence

$$E \xleftarrow{k_6} B \xrightarrow{k_3} C \underset{k_5}{\overset{k_4}{\rightleftharpoons}} D,$$

where C and D are the two D-glucopyranose pentaacetates, the change in the

fraction of C (C_C) in the product with time is expressed by

$$dC_C/dt = C_B(k_3+k_6) - C_Bk_6 - C_Ck_4 + C_Dk_5.$$

Since $C_Dk_5 = k_5(1-C_B-C_C-C_E)$, this expression can be converted to

$$dC_C/dt = C_Bk_3 - C_Ck_4 + k_5 - C_Bk_5 - C_Ck_5 - C_Ek_5.$$

Substitution of expressions [1] and [2] for C_B and C_E yields the following equation,

$$dC_C/dt = (k_3-k_5)e^{-(k_3+k_6)t} - C_C(k_4+k_5) + k_5 - [k_5k_6/(k_3+k_6)](1-e^{-(k_3+k_6)t}).$$

Integration using the integrating factor $\exp \int (k_4+k_5)\,dt$ and solving for the integration constant yields the following expression for the fraction of C at any given time:

$$[3] \qquad C_C = \frac{k_3-k_5}{(k_4+k_5)-(k_3+k_6)}\left[e^{-(k_3+k_6)t} - e^{-(k_4+k_5)t}\right] + \frac{k_5}{k_4+k_5}\left[1-e^{-(k_4+k_5)t}\right] + \frac{k_5k_6}{(k_3+k_6)(k_4+k_5)}\left[e^{-(k_4+k_5)t}-1\right] + \frac{k_5k_6}{(k_3+k_6)(k_4+k_5-k_3-k_6)}\left[e^{-(k_3+k_6)t} - e^{-(k_4+k_5)t}\right].$$

The value of C_C at any given time could be calculated using this expression since the four velocity constants were known. As was mentioned above, Bonner (3) has published velocity constants for the anomerization of the D-glucopyranose pentaacetates under the present conditions for acetolysis and the values were reproduced by Lemieux *et al.* (9). The average values obtained by the latter workers, $k_{\beta\to\alpha} = 0.0306$ min.$^{-1}$ and $k_{\alpha\to\beta} = 0.0043$ min.$^{-1}$, were used in the present calculations. The amount of the other D-glucopyranose pentaacetate (C_D) was calculated by difference,

$$C_D = 1-(C_B+C_C+C_E).$$

Thus, the change in the composition of the reaction mixture could be calculated on the basis that β-D-glucopyranose pentaacetate was the first product (C) of the reaction in which case $k_4 = k_{\beta\to\alpha}$ and $k_5 = k_{\alpha\to\beta}$ or, on the other hand, on the basis that the α-pentaacetate was formed first and $k_4 = k_{\alpha\to\beta}$ and $k_5 = k_{\beta\to\alpha}$. The results of these calculations are plotted in Fig. 2.

The contribution to the rotation of the reaction mixture at any given time made by the small amount of by-product E must have been small and, therefore, the rotation of the reaction mixture (α_t) was essentially completely due to the presence of the three other components (B, C, and E). Since at unit concentration (0.1 *M*) methyl α-D-glucopyranoside tetraacetate, β-D-glucopyranose pentaacetate, and α-D-glucopyranose pentaacetate were found by extrapolation to possess rotations of +9.45°, +0.49°, and +8.76°, respectively, it could be expected that the rotation of the reaction mixture at any given time would be closely approximated by the expression

α_t = 9.45 × fraction of α-glucoside + 0.49 × fraction of β-pentaacetate + 8.76 × fraction of α-pentaacetate.

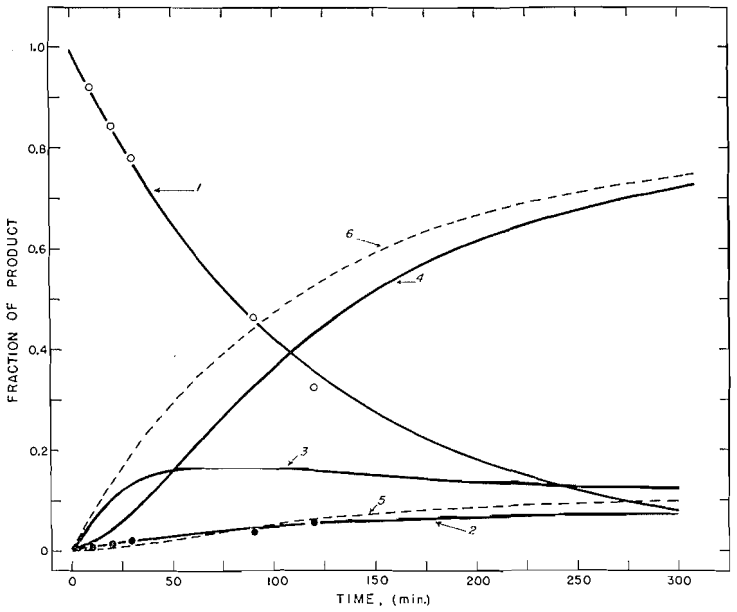

FIG. 2. Calculated curves (using equations [1], [2], and [3], and data listed in Table I) and experimental points for the acetolysis of methyl α-D-glucopyranoside tetraacetate in 1 : 1 acetic acid – acetic anhydride 0.5 *M* with respect to sulphuric acid at 25°C. Curves 3 and 4 are the result of calculations based on the assumption that β-D-glucopyranose pentaacetate is the first product of the reaction and curves 5 and 6 are the result of calculations based on the assumption that α-D-glucopyranose pentaacetate is the first product.

Curve 1—Methyl α-D-glucopyranoside tetraacetate content.
Curve 2—D-Glucose methyl hemiacetal hexaacetate content.
Curves 3 and 5—β-D-Glucopyranose pentaacetate content.
Curves 4 and 6—α-D-Glucopyranose pentaacetate content.

TABLE II

COMPARISON OF OBSERVED POLARIMETRIC RATE WITH CALCULATED VALUES FOR THE ACETOLYSIS OF METHYL α-D-GLUCOPYRANOSIDE TETRAACETATE
0.5 *M* sulphuric acid in 1 : 1 acetic acid – acetic anhydride at 25°C.

t, min.	Observed		Calculated*		Calculated†	
	α	*k*, min.$^{-1}$‡	α§	*k*, min.$^{-1}$‡	α§	*k*, min.$^{-1}$‡
0	9.45	—				
3.5	9.100	0.044				
4.5	9.025	0.048	9.45		9.45	—
10	8.580	0.043	8.84	0.034	9.31	0.0081
20	8.025	0.044	8.36	0.034	9.19	0.0079
30	7.660	0.044	8.05	0.032	9.04	0.0077
50	—	—	7.64	0.031	8.77	0.0077
80	—	—	7.34	0.030	8.42	0.0078
100			7.29	0.028	8.15	0.0085
∞	7.02	—	7.11	—	7.11	—

**Calculated on the basis that β-D-glucopyranose pentaacetate is the first reaction product.*
†Calculated on the basis that α-D-glucopyranose pentaacetate is the first reaction product.
‡Calculated using the expression $k = (2.303/t) \log [(\alpha_0 - \alpha_\infty)/(\alpha_0 - \alpha_t)]$.
§The rotation of the D-glucose methyl hemiacetal hexaacetate was neglected.

The results of calculations made on this basis are given in Table II. Furthermore, Table II contains the polarimetric velocity constants which can be calculated from these results. A comparison of the calculated polarimetric velocity constants with that observed shows that, while the results obtained on the basis that the β-pentaacetate was the first product agree fairly well with those observed, the results of calculations based on the assumption that the α-anomer was formed first are in strong disagreement. Thus, it was clear that the acetolysis of methyl α-D-glucopyranoside tetraacetate proceeds mainly with inversion of the anomeric center to yield β-D-glucopyranose pentaacetate. It is noteworthy in this respect that α-D-glucopyranose pentaacetate undergoes mercaptolysis (7) and acetolysis (9) with inversion of the anomeric center—a stereochemical route which has long been recognized for the reaction of acetylated α-D-glucopyranosyl halides under conditions for the Koenigs–Knorr type of reaction (6, 10, 16).

The above information on the acetolysis of methyl α-D-glucopyranoside tetraacetate allowed the consideration of the more complex reaction of the β-anomer under the same reaction conditions. The reaction was followed by isolating samples of the reaction product after various intervals of time and determining the amounts of unreacted methyl β-D-glucopyranoside tetraacetate, methyl α-D-glucopyranoside tetraacetate, β-D-glucopyranose pentaacetate, and α-D-glucopyranose pentaacetate in the material by isotopic dilution analysis. This was accomplished by adding weighed amounts of radioactive samples of these materials to a weighed sample of a reaction product, separating the four components by chromatography on Magnesol–Celite (14), determining the radioactivity of the pure compounds thus isolated, and calculating the fraction of each substance in the reaction product using the expression

$$\text{fraction in reaction product} = (x/y)[c_i - c_f)/c_f]$$

where x gm. of radioactive sample of c_i c.p.m. was added to y gm. of reaction product and c_f was the radioactivity in counts per minute of substance isolated. The results from these analyses are listed in Table III where the methoxyl

TABLE III

ANALYSES OF REACTION PRODUCTS FROM THE ACETOLYSIS OF METHYL β-D-GLUCOPYRANOSIDE TETRAACETATE
0.5 M H_2SO_4, 1 : 1 Ac_2O–AcOH, 25°C.

Time, min.	% methoxyl (total)	Content of β-glucoside* C_A	Content of α-glucoside* C_B	Glucoside content by methoxyl analysis	Glucoside content by isotopic dilution analysis	Content of β-penta-acetate*	Content of α-penta-acetate*	Amount of product accounted for*
0	8.56	1.0	0.0	—	—	—	—	—
4	8.30	0.828	0.151	0.969	0.979	0.040	0.010	1.029
8	7.78	0.672	0.243	0.908	0.915	0.068	0.014	0.997
12	7.27	0.523	0.343	0.849	0.866	0.088	0.027	0.981
24	—	0.238	—	—	—	0.126	0.050	
36	—	0.130	—	—	—	0.129	0.129	
48	—	0.077	—	—	—	0.121	0.243	
50.5	5.82	—	0.592	0.680	—			
102.5	4.44	—	—	0.515	—			
200	2.36	—	—	0.276	—			
300	1.46	—	—	0.170	—			
420	—	—	—	—	—	0.116	0.819	0.935

By isotopic dilution analysis.

contents found for each of the reaction products are also given. First of all, it is to be noted that for the first part of the reaction the methyl D-glucopyranoside tetraacetate contents expected from the methoxyl values were in good agreement with those found by isotopic dilution analysis. Secondly, it is to be noted that the analyses for the four components accounted very well for all of the reaction products. Therefore, it could be concluded that the α-glucoside and the two glucose pentaacetates were the only isolable reaction products formed in appreciable amounts and that the reaction could be represented by the following scheme wherein A, B, and C are the methyl β-D-glucopyranoside tetraacetate, methyl

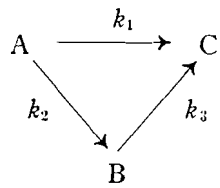

α-D-glucopyranoside tetraacetate, and D-glucopyranose pentaacetate, respectively. For this reaction scheme,

[4] $$-dC_A/dt = (k_1+k_2)C_A$$

and therefore,

[5] $$C_A = e^{-(k_1+k_2)t}.$$

Knowing C_A at a variety of times (Table II) and using equation [4], an average value for k_1+k_2 could be calculated (see Table III). The rate of change in the amount of B at any given time is expressed by

$$dC_B/dt = -(dC_A/dt)-(dC_C/dt)-(dC_D/dt).$$

Since $$dC_C/dt = C_Bk_3+C_Dk_5-C_Ck_4$$

and $$dC_D/dt = C_Ak_1+C_Ck_4-C_Dk_5,$$

then $$dC_B/dt = k_2C_A-k_3C_B$$

$$= k_2e^{-(k_1+k_2)t}-C_Bk_3.$$

Integration using the integrating factor $\exp \int k_3\,dt$ and solving for the integration constant yields

[6] $$C_B = \frac{k_2}{k_3-(k_1+k_2)}\,[e^{-(k_1+k_2)t}-e^{-k_3t}].$$

The value for k_3 under the present reaction conditions was determined in the above described study of the acetolysis of methyl α-D-glucopyranoside tetraacetate. Thus, k_3 and k_1+k_2 being known, using equation [6] and the values for C_B given in Table III, values for k_2 could be calculated. The results of these calculations are given in Table IV.

TABLE IV

VELOCITY CONSTANTS FOR THE ACETOLYSIS AND ANOMERIZATION OF METHYL β-D-GLUCOPYRANOSIDE TETRAACETATE
0.5 *M* H_2SO_4, 1 : 1 Ac_2O – AcOH, 25°C.

Time, min.	k_1+k_2, min.$^{-1}$*	k_2, min.$^{-1}$†
4	0.047	0.040
8	0.050	0.038
12	0.054	0.039
24	0.058	—
36	0.057	—
48	0.053	—
50.5	—	0.045
Average	0.053±0.004 k_1 = 0.012 min.$^{-1}$	0.041±0.003

*Calculated from the data in Table II and equation [5].
†Calculated from the data in Table II and equation [6].

Scheme 1

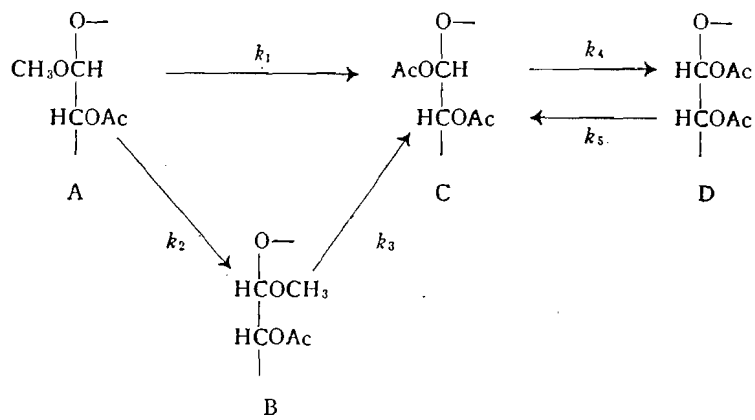

Scheme 2

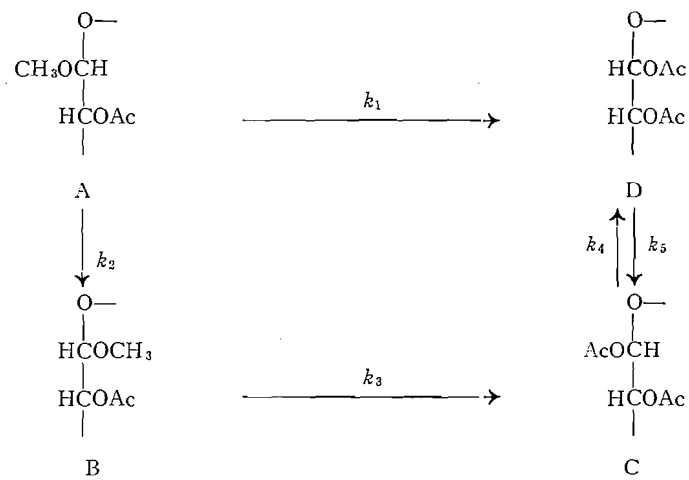

It was now of interest to attempt a decision on whether or not one of the anomeric D-glucopyranose pentaacetates was formed preferentially on the acetolysis of methyl β-D-glucopyranoside tetraacetate. A decision was reached by showing that the reaction (scheme 1) which possesses β-D-glucopyranose pentaacetate (C) as the first product of the reaction can account for the experimental data listed in Table III much more satisfactorily than that (scheme 2) which has α-D-glucopyranose pentaacetate as the initial product.

Equations [5] and [6] which relate the amounts of the substances A and B, respectively, in the reaction product after a given reaction time apply to both the schemes 1 and 2. The rate of change of the fraction of compound C (C_C) in the reaction product for scheme 1 is given by the expression,

$$dC_C/dt = C_A k_1 + C_B k_3 + C_D k_5 - C_C k_4.$$

Since

[7] $$C_D = 1-(C_A+C_B+C_C),$$

$$\frac{dC_C}{dt} = (k_1-k_5)\, e^{-(k_1+k_2)t} + k_5 + \frac{k_2(k_3-k_5)}{k_3-(k_1+k_2)}\,[e^{-(k_1+k_2)t} - e^{-k_3 t}] - (k_4+k_5)\, C_C.$$

Integration using the integrating factor $\exp \int (k_4+k_5)dt$ and solving for the integration constant yields

[8] $$C_C = \frac{k_1-k_5}{k_4+k_5-(k_1+k_2)}\,[e^{-(k_1+k_2)t} - e^{-(k_4+k_5)t}] + \frac{k_5}{k_4+k_5}\,[1-e^{-(k_4+k_5)t}] + \frac{k_2(k_3-k_5)}{k_3-(k_1+k_2)}\left[\frac{e^{-(k_1+k_2)t} - e^{-(k_4+k_5)t}}{k_4+k_5-(k_1+k_2)} - \frac{e^{-k_3 t} - e^{-(k_4+k_5)t}}{k_4+k_5-k_3}\right].$$

For scheme 2, the rate of change of the fraction of compound C (C_C) in the reaction product with time is expressed by

$$dC_C/dt = C_B k_3 + C_D k_5 - C_C k_4.$$

Integration of this expression after the appropriate substitutions have been made in the general manner outlined above for scheme 1 yields the following equation:

[9] $$C_C = \frac{k_2(k_3-k_5)}{k_3-(k_1+k_2)}\left[\frac{e^{-(k_1+k_2)t} - e^{-(k_4+k_5)t}}{k_4+k_5-(k_1+k_2)} - \frac{e^{-k_3 t} - e^{-(k_4+k_5)t}}{k_4+k_5-k_3}\right] + \frac{k_5}{k_4+k_5}\,[1-e^{-(k_4+k_5)t}] - \frac{k_5}{k_4+k_5-(k_1+k_2)}\,[e^{-(k_1+k_2)t} - e^{-(k_4+k_5)t}].$$

Thus, for scheme 1, the composition of the reaction product after any given time could be calculated using equations [5], [6], [7], and [8] and the same could be done for scheme 2 by employing equations [5], [6], [7], and [9]. The results of these calculations are plotted in Fig. 3 as are the experimental values given in Table III. It is seen that scheme 1 closely describes the reaction while scheme 2 does not. Therefore, it is clear that under the conditions for acetolysis, methyl β-D-glucopyranoside undergoes glycosidic cleavage to a large extent with retention of configuration to yield β-D-glucopyranose pentaacetate simultaneously with anomerization. The data listed in Table V show that the polari-

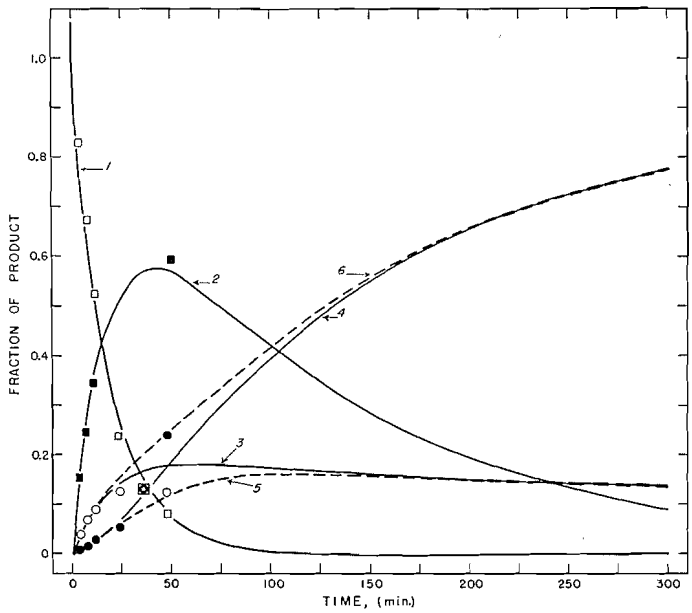

FIG. 3. Calculated curves (using equations [5], [6], [8], and [9], and data listed in Table IV) and experimental points for the acetolysis of methyl β-D-glucopyranoside tetraacetate in 1 : 1 acetic acid – acetic anhydride 0.5 *M* with respect to sulphuric acid at 25°C.
□—Methyl β-D-glucopyranoside tetraacetate content (curve 1—calculated).
■—Methyl α-D-glucopyranoside tetraacetate content (curve 2—calculated).
○—β-D-Glucopyranose pentaacetate content (curve 3—calculated on basis of scheme 1; curve 5—calculated on basis of scheme 2).
●—α-D-Glucopyranose pentaacetate content (curve 4—calculated on basis of scheme 1; curve 6—calculated on basis of scheme 2).

TABLE V

COMPARISON OF OBSERVED POLARIMETRIC RATE WITH CALCULATED VALUES FOR THE ACETOLYSIS OF METHYL β-D-GLUCOPYRANOSIDE TETRAACETATE
0.5 *M* sulphuric acid in 1 : 1 acetic acid – acetic anhydride at 25°C.

t, min.	Observed		Calc. for scheme 1		Calc. for scheme 2	
	α	*k*, min.$^{-1}$*	α	*k*, min.$^{-1}$*	α	*k*, min.$^{-1}$*
0	−1.30°	—	−1.30°	—	−1.30°	—
1	—	—	−0.831	0.053	−0.749	0.063
2	—	—	−0.394	0.053	−0.231	0.063
5	+0.82	0.060	+0.782	0.053	+1.125	0.063
10	2.35	0.059	2.366	0.052	2.921	0.063
20	4.31	0.058	4.610	0.053	5.329	0.066
30	5.34	0.056	5.773	0.051	6.469	0.065
∞	6.86	—	7.743†	—	7.743†	—

**Calculated using the expression* $k = (2.303/t) \log [(\alpha_0 - \alpha_\infty)/(\alpha_t - \alpha_\infty)]$.
†*The rotation for the equilibrium mixture of the α- and β-D-glucopyranose pentaacetates.*

metric change expected on the basis of scheme 1 is in good agreement with that observed. It is also seen, however, that the polarimetric rate based on scheme 2 is not greatly different from that based on scheme 1 and that therefore a definite decision on the reaction route would be achieved through polarimetric studies only with great difficulty.

In accordance with the mechanism proposed by Lemieux and Shyluk (12) for the anomerization of acetylated alkyl glycopyranosides, the behavior of methyl β-D-glucopyranoside tetraacetate (II) would be accounted for as follows. Under the influence of the acid catalyst (A), the transition state III is achieved. It is deemed necessary to postulate the participation of the C2-acetoxy group in the loosening of the C1 to methoxyl group bond in view of the strong activation this participation appears to provide to the reaction (7, 8). Also, it would otherwise be difficult to rationalize the apparent high degree of anomerization which occurs when methyl α-D-arabinopyranoside triacetate

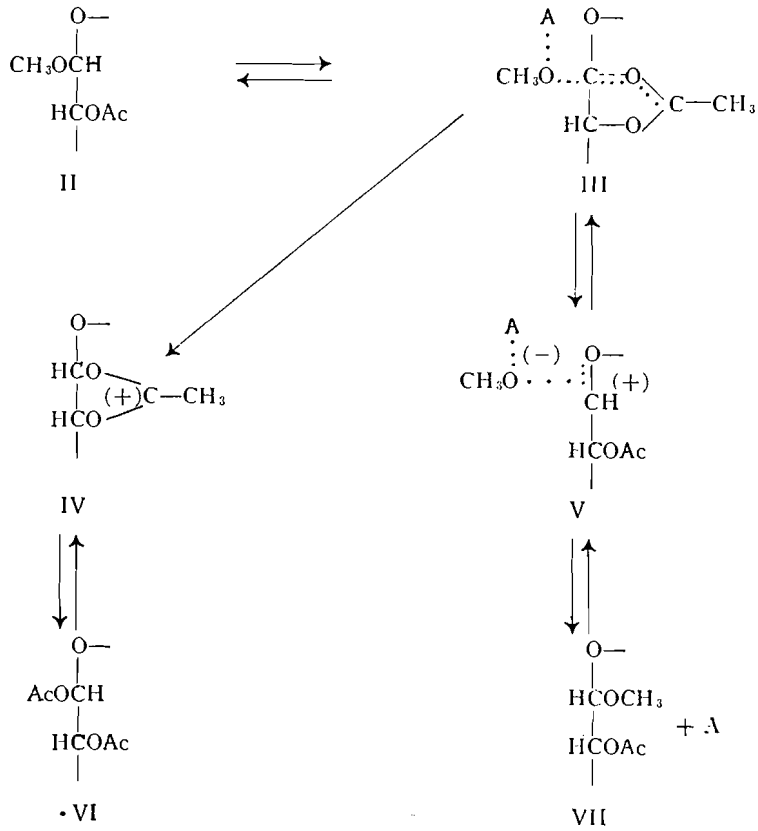

is subjected to acetolysis with the high lability of the ring structure as displayed by the β-anomer (15). Winstein and Heck (17) have shown that the 1,2-cyclic carbonium ion derived from participation of an acetoxy group shows little tendency for participation in an ion-pair. Consequently, it is conceivable that the transition state III can readily lead to the ion-pair V (12). The collapse of the ion-pair could then result in the formation of the α-glucoside (VII). In the event that the collision leading to the transition state III brought about separation of the ions, the 1,2-cyclic ion (IV) would result—an ion which is known to lead to β-D-glucopyranose pentaacetate as is required by the experimental data.

The acetolysis of methyl α-D-glucopyranoside tetraacetate with inversion of the anomeric center could, of course, be rationalized as a reversal of the above process. That is, the reaction would take place by VII ⟶ V ⟶ III ⟶ IV ⟶ VI. However, in view of the fact that evidence exists that 3,4,6-tri-*O*-acetyl-α-D-glucopyranosyl chloride appears to undergo solvolysis in acetic acid with a preponderance of inversion at the anomeric center (11) it is conceivable that the acetolysis of methyl α-D-glucopyranoside tetraacetate proceeds mainly by dissociation to a carbonium ion which possesses a strong tendency to form β-D-glucopyranose pentaacetate on interaction with the environment.

In conclusion, it is of interest to consider the implication of these results on the procedure used by Lindberg in his studies on the mechanism of the anomerization of acetylated alkyl glycopyranosides (1, 2, 13). First of all, the significance attached by Lindberg to the velocity constants which were calculated from polarimetric data only is questionable. The fact that the polarimetric change which accompanies a complex reaction is not readily amenable to interpretation is well illustrated by the data obtained for the acetolysis of methyl α-D-glucopyranoside tetraacetate. Inspection of Fig. 1 might lead one to believe that the reaction was essentially over in 90 min. The fact was, however, that the reaction was only 53.5% complete at this time. Thus, the common practice of following a carbohydrate reaction polarimetrically to the first point of inflection would in this case have led to nearly the worst possible mixture of starting material and reaction products. The course of the polarimetric change in the acetolysis of acetylated alkyl β-glucopyranosides is obviously determined by a wide variety of factors such as the relative rates of acetolysis and anomerization of the β-glucoside, the relative rates of glycosidic cleavage and ring cleavage for the α-glucoside, the relative rates of glycosidic cleavage, the stereochemical routes of the glucosidic cleavages which need not be the same for all glucosides and the relative rotatory powers of all the reaction products formed. Secondly, Lindberg attached considerable importance to presence of peracetylated *aldehydo*-sugars in the reaction products. It is to be noted in this respect that the present data indicate the formation of these products to be the result of a property of the more stable 1,2-*cis*-glycoside, a conclusion which is in accordance with the above mentioned experimental results obtained by Montgomery *et al.* (15) on the acetolysis of the methyl D-arabinopyranoside triacetates. This is reasonable since the acetolysis of the ring must be expected to be more important in the case of the acetylated 1,2-*cis*-glucosides where anchimeric assistance for glucosidic cleavage through participation of the C2-acetoxy group is not possible. The following deductions are of interest in this respect. The cleavage of the C1 to methoxyl group bond of a methyl D-glucopyranoside tetraacetate may occur either before or after the pyranose ring has undergone acetolysis. If the fission occurred before the ring was opened the product should be a D-glucopyranose pentaacetate; if afterward, the product can be expected to be *aldehydo*-D-glucose heptaacetate. Bonner (3) has shown the pyranose ring of the glucose pentaacetates to be stable under conditions for acetolysis and Lindberg's

experiments (13) indicate the same stability for the heptaacetate. Therefore, the identification by Lindberg (13) of only about 8% heptaacetate in the product from the acetolysis of methyl α-D-glucopyranoside tetraacetate suggests that for this compound the preferred reaction route was direct acetolysis of the C1 to methoxyl group bond. The C1 to acetoxy group bond of β-D-glucopyranose pentaacetate has been shown to be highly susceptible to dissociation as compared to the corresponding bond in the α-anomer (7, 8). It would therefore be surprising indeed if conditions which readily cleave the C1 to methoxyl group bond of methyl α-D-glucopyranoside tetraacetate would not dissociate much more readily the corresponding bond in the β-anomer as is suggested by Lindberg's arguments in support of his theory for the mechanism of the anomerization of acetylated glycopyranosides.

EXPERIMENTAL

The techniques used in carrying out the reaction and isolating samples after the various reaction times were the same as previously reported (9). In order to remove the chloroform, the material was twice dried *in vacuo* from solution in benzene before drying in a high vacuum first for several days at room temperature and then for several hours at 60°C.

The methods used to prepare the radioactive compounds have already been described (8, 12). The isotopic dilution analyses were carried out by adding weighed amounts, about 10 mgm., of the radioactive compounds to a weighed sample of the reaction product before chromatographic separation, purifying the compounds from the chromatogram by several recrystallizations, and then determining the radioactivities of the pure compound as was described in a previous communication (9). The amount of the reaction product used depended on the amount of the material to be analyzed which was present in the sample. Usually, about one gram of reaction product was used. The mixture was applied to the top of a column of Magnesol–Celite (5 : 1) 120 gm., 50 mm. in diameter, and the chromatogram was developed with 1500 ml. of benzene–ethanol (250 : 1) (14). The methyl β-D-glucopyranoside tetraacetate was found about one third of the way down the column and the remainder of the compounds were in the bottom quarter of the column. The α-D-glucopyranose pentaacetate occurred first and was well separated from the methyl α-D-glucopyranose tetraacetate which occurred next. The latter compound was not, however, well separated from the β-D-glucopyranose pentaacetate and was usually obtained by crystallization from the mother liquors from the isolation of the β-pentaacetate.

The contents of alkali-labile methoxyl groups listed in Table I were determined as follows. The sample, about 100 mgm., was dissolved in 1 ml. of diethylene glycol. Two milliliters of *N* sodium hydroxide solution was added and the solution was left at room temperature for one hour. The solution was then washed into a standard micro-Kjeldahl distillation apparatus for distillation in the usual manner. The distillate was collected in a 10 ml. volumetric flask kept in ice water. After about 9 ml. of distillate was collected, the solution was diluted to 10 ml. and the methanol in 1-ml. aliquots was determined by the

procedure described by Boos (4). A standard curve was set up by treating solutions which contained known amounts of methanol in the same manner. The results were reproducible within ± 5%.

ACKNOWLEDGMENT

The authors are indebted to Mr. J. A. Baignee of this laboratory for the microanalyses.

REFERENCES

1. Asp, L. and Lindberg, B. Acta Chem. Scand. 4: 1386. 1950.
2. Asp, L. and Lindberg, B. Acta Chem. Scand. 4: 1446. 1950.
3. Bonner, W. A. J. Am. Chem. Soc. 73: 2659. 1951.
4. Boos, R. N. Anal. Chem. 20: 964. 1948.
5. Hoffman, D. O. and Wolfrom, M. L. Anal. Chem. 19: 225. 1947.
6. Isbell, H. S. and Frush, H. L. J. Research Natl. Bur. Standards, 43: 161. 1949.
7. Lemieux, R. U. Can. J. Chem. 29: 1079. 1951.
8. Lemieux, R. U. and Brice, C. Can. J. Chem. 30: 295. 1952.
9. Lemieux, R. U., Brice, C., and Huber, G. Can. J. Chem. 33: 134. 1955.
10. Lemieux, R. U. and Huber, G. Can. J. Chem. 31: 1040. 1953.
11. Lemieux, R. U. and Huber, G. Can. J. Chem. 33: 128. 1955.
12. Lemieux, R. U. and Shyluk, W. P. Can. J. Chem. 33: 120. 1955.
13. Lindberg, B. Acta Chem. Scand. 3: 1153. 1949.
14 McNeely, W. H., Binkley, W. W., and Wolfrom, M. L. J. Am. Chem. Soc. 67: 527. 1945.
15. Montgomery, E. M., Hann, R. M., and Hudson, C. S. J. Am. Chem. Soc. 59: 1124. 1937.
16. Tipson, R. S. J. Biol. Chem. 130: 55. 1939.
17. Winstein, S. and Heck, R. J. Am. Chem. Soc. 74: 5584. 1952.

NOTE

SUBUNITS IN THE MOLECULE OF BOVINE PLASMA ALBUMIN[1]

By Manfred E. Reichmann[2] and J. Ross Colvin

Oxidation of intramolecular disulphide bridges in proteins, followed by determination of the molecular weight of the products, has been shown to be a valid method of investigating subunit structure in these substances. Sanger has shown (8) that such oxidation, if carried out at room temperature and for a short period only, irreversibly separates the molecule of insulin into component chains by oxidizing the cystine residues to cysteic acid, without attacking the primary polypeptide backbone. Anfinsen and co-workers (1) have confirmed the applicability of the method by their studies on ribonuclease. We wish to give a preliminary report of the results of an application of the same technique to bovine plasma albumin (B.P.A.).

After 20 min. oxidation of crystalline B.P.A. (Armour and Co.) by performic acid at room temperature, followed by hydrolysis, the cystine and cysteine spots disappeared from the chromatogram of the hydrolyzate (9). Repeated determinations of free α amino groups with Sanger's reagent (5, 7) showed that no α amino groups in other than aspartic acid residues could be detected in either native or oxidized B.P.A. These observations confirm those of Van Vunakis and Brand (10) and indicate that no significant hydrolysis of a peptide bond occurred during oxidation.

The weight average molecular weight of three preparations of oxidized B.P.A. at pH 7.4 in 0.2 *M* sodium chloride and 0.08 *M* borate buffer was determined by previously described light-scattering techniques (6) as $32{,}000 \pm 2000$. Under the same conditions, native B.P.A. gave a molecular weight of 77,000 in good agreement with previous results reported by Edsall *et al.* (3). Osmotic pressure measurements in the same buffer gave a number average molecular weight of 30,000 for oxidized B.P.A. and 66,000 for native B.P.A., the latter estimate being the same as that recently published by Gutfreund (4).

The difference between the molecular weights obtained by light-scattering and osmotic pressure data has usually been attributed to the presence of a small fraction of high molecular weight material in the samples (3). We have detected this fraction in our samples of native B.P.A. by sedimentation in the ultracentrifuge but have been unable to find evidence for it in the oxidized material. During our preparations of oxidized B.P.A., this small fraction of high molecular weight therefore seems to have been lost, and its disappearance accounts adequately for the otherwise surprising agreement between the light-scattering molecular weight of oxidized B.P.A. and that obtained by osmotic pressure.

[1]*Issued as N.R.C. No. 3449.*
[2]*National Research Council of Canada Postdoctorate Fellow, 1953–54.*

In contrast to previous suggestions of a single polypeptide chain for B.P.A. (2) these results demonstrate that the molecule is made up of at least two subunits (chains) which seem to be held together by —S—S— cross-links. The component parts are not dissociable, however, by variation of the pH of the solution (6). Full details of this work will be reported later in this journal.

1. ANFINSEN, C. B., REDFIELD, R. R., CHOATE, W. L., PAGE, J., and CARROL, W. R. J. Biol. Chem. 207: 201. 1954.
2. EDSALL, J. T. In Chap. 7. The proteins. Vol. 1, Pt. B. *Edited by* H. Neurath and K. Bailey. Academic Press, Inc., New York. 1953. p. 549–726.
3. EDSALL, J. T., EDELHOCH, H., LONTIE, R., and MORRISON, P. R. J. Am. Chem. Soc. 72: 4641. 1950.
4. GUTFREUND, H. Trans. Faraday Soc. 50: 628. 1954.
5. PORTER, R. R. and SANGER, F. Biochem. J.(London), 42: 287. 1948.
6. REICHMANN, M. E. and CHARLWOOD, P. A. Can. J. Chem. 32. 1092. 1954.
7. SANGER, F. Biochem. J.(London), 39: 507. 1945.
8. SANGER, F. Biochem. J.(London), 44: 126. 1949.
9. TOENNIES, G. and KOLB, J. J. Anal. Chem. 23: 823. 1951.
10. VAN VUNAKIS, H. Ph.D. Thesis, Columbia University, New York. 1951.
11. VAN VUNAKIS, H. and BRAND, E. Abstr. 119th Meeting Am. Chem. Soc. p. 28. c. April, 1951.

RECEIVED SEPTEMBER 29, 1954.
DIVISION OF APPLIED BIOLOGY,
NATIONAL RESEARCH LABORATORIES,
OTTAWA, CANADA.

Canadian Journal of Chemistry

Issued by THE NATIONAL RESEARCH COUNCIL OF CANADA

VOLUME 33 FEBRUARY 1955 NUMBER 2

Symposium on Physical Adsorption of Gases by Solids

FOREWORD

The papers that follow were presented at a symposium on "Problems Relating to the Physical Adsorption of Gases by Solids", held at the Royal Military College, Kingston, Ontario, September 10 and 11, 1954, under the auspices of the Physical Chemistry Subject Division of the Chemical Institute of Canada. A few of the papers presented are not being published here, owing either to prior commitments or to the authors' choice. The conveners of the symposium were of the opinion that it would be useful at this time to bring together various points of view on experimental methods and theoretical interpretations currently being applied to the study of physical adsorption of gases by solids. To this end they arranged a program of contributions concerned with the state of physically adsorbed films, the structure and energetics of solid surfaces, and theoretical aspects of adsorption phenomena. No record of discussion was kept as the attendant editing would have significantly delayed publication of these proceedings.

On behalf of the conveners of the symposium I should like to acknowledge the generous co-operation of the National Research Council, of the authorities of the Royal Military College, and of the Editor of the Canadian Journal of Chemistry.

R. MCINTOSH,
CHEMISTRY DEPARTMENT,
UNIVERSITY OF TORONTO.

SOME PROBLEMS IN SURFACE CHEMISTRY

An Invited Address by PROFESSOR SIR ERIC RIDEAL, F.R.S.

In 1917, Langmuir advanced the view that in heterogeneous catalytic reactions, chemisorbed reactants were involved. Work since that time has fully substantiated that view and at the present time enquiry is centering around the problem of distinguishing between two possible modes of reaction for the catalytic formation of a product by the interaction of two reactants, A and B, at the surface of a catalyst. These may be depicted as

$$\begin{matrix} A & B \\ | & | \\ M & M \end{matrix} \rightarrow C \qquad \text{or} \qquad \begin{matrix} A & B \\ | & \vdots \\ M & M \end{matrix} \rightarrow C$$

where — denotes a chemisorbed species and ---- a molecule in the gas phase or in the van der Waals field.

During the last quarter of a century we have been interested in the process of chemisorption and have attempted to examine it by a variety of methods.

Three of these have been successful in throwing a great deal of light on the process. These are very briefly (*a*) the use of a single wire on which the accommodation coefficient of a rare gas in the absence and presence of a chemisorbed layer is measured; a field explored in great detail by Dr. J. K. Roberts, (*b*) the contact potential method in which two crossed wires are employed, one as an electron emittor and the other as an acceptor, the acceptor being coated at will by a chemisorbed layer; a method taken up by Dr. R. C. L. Bosworth and more recently (*c*) Mr. M. McD. Baker has had some success in utilising the photoelectric threshold and its change on the adsorption of gases to investigate chemisorption. I might deal briefly with the main features of the results of these investigations.

In the first place, it was found that chemisorption took place readily on clean wires frequently with no detectable energies of activation and that many cases of apparently slow adsorption could be attributed either to a displacement of a previously adsorbed gas or to a slow diffusion into the interior. This does not preclude the fact that there are well established cases of activated adsorption e.g. hydrogen and oxygen on diamond, oxygen on silver and hydrogen on copper, but it does serve to emphasise the danger of attributing all slow processes to an activation energy for adsorption especially where clean metals are involved. It is only natural that activation energies are involved when adsorption on and reaction with oxides and the like are under consideration.

The second important point which emerged was that the molar heat of adsorption was not constant but varied as a function of the surface coverage from $\theta = 0$ to $\theta = 1$. These molar heats of adsorption can be determined directly, calorimetrically, even on a wire or preferably on a metallic mirror following Beeck's method, or calculated from the adsorption isotherms taken over a suitable temperature range. The form of the ΔH, θ curve was of some interest in that ΔH was found to be neither independent of nor a linear function of θ as might be at first sight anticipated but consisted in those cases which were carefully examined of three distinct portions, a high ΔH for a small region of $\theta = 0$ to *ca.* $\theta = 0.1$, a linear portion ΔH gradually falling from $\theta = 0.1$ to *ca.* $\theta = 0.6$, and a more rapid fall after this point sinking to quite low values as θ approaches unity. It is evident that this fact can be interpreted by two entirely different concepts, firstly that the adsorbing surface is heterogeneous in character or that there exist both repulsive fields between the ad-atoms or ad-radicals and that the bonding energy falls with increasing surface coverage.

The first view, viz. the assumption of heterogeneity of the surface, gained a good deal of support in the United States; we, however, were inclined to the alternative view, namely, that the phenomenon of chemisorption of gases at metallic surfaces bore a closer similarity to those phenomena dealing with the modification of the thermionic and photoelectric properties of metallic surfaces in the presence of adsorbed monolayers. It was also easy to show that if the ad-atoms or ad-radicals did indeed resemble dipoles and as a result repulsive fields existed between them, then the general form of the ΔH, θ curve for a dissociating gas such as hydrogen could be accounted for; if, in addition to this

hypothesis, the ad-atoms or ad-radicals could undergo surface diffusion and thus space themselves uniformly over the surface at a speed at least commensurate with the rate at which the experiment of gas admission was being conducted. Dr. Roberts' work is widely known on both sides of the Atlantic and for that reason I have given only the briefest summary of the more important conclusions derived from his investigations. It is interesting to note that recently the accommodation coefficient method of attack has been queried as to its accuracy but I am glad to see that recent work of Dr. Tompkins at Imperial College has fully substantiated Roberts' work.

Dr. Bosworth's work does not appear to be so well known so I am taking the liberty of giving this in slightly more detail.

Langmuir and Kingdon studied the impact of caesium atoms onto a tungsten surface and noted that when the surface was relatively bare every caesium atom evaporated as an ion. The electron work function of tungsten, ϕ, is 4.53 volts whilst the ionisation potential of caesium, I, is 3.88 volts, thus the passage of the electron from the donor caesium atom to the acceptor tungsten is facilitated. When, however, the caesium layer begins to populate the surface more thickly, this layer continues to lower the work function of the surface until, when ϕ has sunk to 3.88 volts, any further incident caesium atom will evaporate as an atom and not as an ion. We might regard the surface phase as consisting of a mixture of ad-atoms and ad-ions, their proportion being given by

$$\frac{n_{ions}}{n_{atoms}} = \frac{f_1}{f_2} e^{-(I-\phi)e/kT}$$

where f_1 and f_2 are the statistical weights of the ion and atom respectively in their ground states; or, we may regard the surface as consisting entirely of ad-atoms, the polarisation or dipole moment of which varies for a bare surface from that equivalent to an adsorbed ion to much smaller values as the surface becomes more crowded, evaporation from the surface taking place in the two stable states viz. atom and ion in a ratio defined by the energetics of the system. Langmuir obtained the following values for the dipole moment of caesium on tungsten:

θ	μ(Debyes)
0.0	14.6
0.5	6.1

Bosworth investigated potassium on tungsten in a similar manner and obtained:

θ	μ(Debyes)
0.012	23
0.025	21
0.10	13
0.50	6.0
1.0	2.8

We can note that the lattice constant of potassium is 5.25Å and if we regard it as a sphere with unit positive charge placed on an ideal plane conductor, the external field produced by an ion and its mirror image would be equivalent to

that of a dipole of electric moment

$$5.25 \times 4.77 = 25 \text{ Debyes},$$

a value very close to that obtained experimentally for extremely dilute films. Bosworth extended this investigation to oxygen on tungsten and computed the following tentative values:

θ	μ(Debyes)
0.05	3.4
0.10	3.0
0.20	2.1
0.40	1.0
0.60	0.8
0.80	0.8

Here again we note that there is a fall in the apparent polarisation as the surface becomes more densely populated. It is interesting to compare the work functions of stable close packed monolayers of electronegative gases on tungsten as determined by this method. ϕ for W = 4.56 volts at 300°A. Then at the same temperature we find ϕ for WO 6.34, WN 5.92, WH 5.82, WD 5.80. For a thick oxide film WO_x ϕ = 6.24 volts.

Bosworth also measured the rate of surface diffusion as a function of the surface concentration of potassium on tungsten. The energies of activation for the surface diffusion were found as expected to be relatively large for dilute films falling to smaller values for more concentrated films. I cite the following values:

θ	E (electron volts)	θ	E (electron volts)
0	0.72	0.1	0.59
0.015	0.69	0.25	0.52
0.025	0.67	0.5	0.35
0.05	0.63	1.0	0.29

From these data it is possible to calculate the spreading forces and these can be compared with say the spreading forces of formic acid adsorbed on mercury.

Potassium on tungsten		Formic acid on mercury	
Ad-atoms per sq. cm. ($\times 10^{-14}$)	F (dynes/cm.)	Molecules per sq. cm. ($\times 10^{-14}$)	F (dynes/cm.)
0.06	0.23	0.8	14
0.12	0.96	1.5	22
0.24	3.5	3.0	38
0.48	10	4.6	52
0.60	14.3		
1.20	38		
1.50	60		
2.40	142		
3.0	187		
4.8	322		

The spreading forces for the strong dipolar system potassium on tungsten are far greater than those for formic acid on mercury. For very dilute monolayers where the distances are too great for appreciable dipolar interaction we note

that the spreading forces which are kinetic thermal in origin for the two systems are of the same order of magnitude. As the surface concentration rises the increased spreading forces for the potassium can be shown to be due to the electrostatic dipole repulsion but for concentrated films the values obtained fall below those calculated, another confirmation that the magnitude of the dipole is falling with concentration.

It is difficult to attain such a high accuracy when wires or thin ribbons of metal are employed as can be attained with metallic mirrors. It also militates against the accuracy of the method when other extraneous metal has to be present or when local high temperatures as in thermionic emittors are employed. For this reason Mr. M. McD. Baker has been engaged in exploring the possibilities of using photoelectric thresholds in conjunction with freshly formed metallic mirrors derived by vaporisation from suitable filaments. So far we have confined our attention to the 1800 line of mercury and have used a silica window to our vessel. We hope to extend the method further into the ultraviolet so that we can examine chemisorption on such metals as copper. Mr. Baker has examined the chemisorption of hydrogen and of carbon monoxide on a variety of metals. It is interesting to note that the $\Delta\phi, \theta$ curve pursues a curve similar to the $\Delta H, \theta$ curve, namely on several metals there is an initial relatively large rise in $\Delta\phi$ indicating a large dipole, this is followed by a steady linear rise and then the curve bends over indicating that the magnitude of the dipole in the closely packed film is very small.

Finally by means of the method of contact potentials it is possible to measure the latent heats of evaporation. The experimental evidence suggests that on tungsten oxygen evaporates as molecules formed by the combination of two chemisorbed atoms i.e. a bi-molecular surface action whilst nitrogen evaporates in a unimolecular manner i.e. either as N_2 or WN. The values obtained for these two chemisorbed gases on tungsten were as follows:

ΔV (volts)	Nitrogen, E (kcal./mole)	Oxygen, E (kcal./mole)
−0.10	—	150
−0.20	28	147
−0.40	26	130
−0.60	23	113
−0.80	20	90
−1.00	19	83
−1.20	18	76
−1.70	—	67

It is from these experiments difficult to avoid the conclusions that monolayers chemisorbed on uniform metallic surfaces vary markedly in properties as their surface concentration is varied. Dilute monolayers are relatively firmly held and have large dipoles and large energies of activation for migration. As the packing density increases the polarisation of the dipoles decreases, the lateral mobility increases, the spreading force increasing and the energy of activation for migrations decreasing and, at the same time, the forces holding the ad-atom or ad-radical to the surface suffer a considerable diminution.

It is interesting to determine the energy changes associated with the ionisation of sodium, i.e. the reaction

$$Na^+ \rightarrow Na + \epsilon,$$

from Bosworth's data. For gaseous sodium vapour $E = 5.1$ electron volts; in a closely packed monolayer on tungsten it is $E = 1.7$ electron volts, whilst in a very dilute monolayer it is $E = -0.4$ electron volts.

It does not seem to be unreasonable to apply similar considerations to, say, hydrogen on nickel. We may regard a nickel surface when sparsely populated as capable of dissociating hydrogen. The resulting surface hydride is relatively polar and the reaction is strongly exothermic. The repulsive forces between the ad-atoms ensure an even distribution over the surface. For these, the rate of recombination and re-evaporation as molecules is extremely slow and the equilibrium pressure of hydrogen above a nickel surface for small values of θ is vanishingly small. As θ increases the interaction energy decreases and the reaction becomes increasingly less exothermic whilst the repulsive forces and the energy of activation for lateral migration become reduced, with the result that evaporation proceeds more readily and, as we have found with Trapnell, relatively large equilibrium pressures of hydrogen are necessary for θ to attain unity. We might also assume that there may be substrates with which the interaction energy for hydrogen sinks to such low values that surface dissociation ceases *before* θ reaches unity resulting in a mixed atomic and molecular film.

We have not succeeded in attempts to discover the mechanism of the surface migratory process. We could imagine it to take place by three different methods. If we regard each metallic atom as though it were a crater with the ad-atom in it then a migration might consist of a process of hopping from one crater to the next. Again there may be preferred directions, e.g. at an angle of 45° on the surface of a cubic crystal or a direction in which the lips of the crater are lower giving rise to directional migration.

Finally, we may conceive the existence of migratory levels involving the supply of energy to raise the ad-atom into the migratory level and then the supply of a much smaller energy of activation in the travel over the migratory level. The energies for migration in the migratory levels being naturally smaller the greater distance the level is from the metal atom surface and the greater the original energy of activation necessary to raise the ad-atom to that level.

This concept of chemisorption involves, as we have seen, electron transfer, either the ad-atom or ad-radical being the electron donor or acceptor, and I need only at this point draw your attention to the ever increasing amount of work now being devoted to the electronic structure of metals and to the production of p and n lattice defects to modify the electronic structure of catalysts.

Finally, I would like to express my gratitude for the kindness which the National Research Council is always extending to me especially in so far that they have made my attendance at this meeting possible. I would also like to congratulate all those who have taken part in getting this meeting together.

The meetings of the Faraday Society, deservedly some of us think, hold a high reputation in the world of science. The reason for the success of those meetings can be summed up in two words—hard work. I think those of us present here who have attended meetings of that society would consider this meeting as good as the best.

INVESTIGATION OF THE PHYSICALLY ADSORBED STATE BY MEANS OF DIELECTRIC MEASUREMENTS[1]

By E. W. Channen[2] and R. McIntosh[3]

ABSTRACT

Dielectric data obtained for a variety of adsorbates on porous silica gel and on nonporous rutile are summarized. Four methods of computing the polarizabilities or dielectric constants of the adsorbed matter are outlined and applied using the primary experimental data of capacitance change and volume adsorbed. All four methods contain somewhat arbitrary assumptions and at best are semi-empirical. None predicts values of the electrical constants of the adsorbed species which appear reasonable in all cases. It is concluded that an interpretation of the phenomena revealed by the primary data is not possible until improved methods of computing the polarizability of adsorbed material are developed.

INTRODUCTION

Attempts to elucidate the state of physically adsorbed films of vapors on solids have been reported particularly by Higuti (7), Kurbatov (12), and by McIntosh and his associates (13, 14, 17, 18, 20). These investigators have discovered the very interesting fact that when the change of capacity of the test cell is plotted against the volume of gas adsorbed, a sudden change of the slope of this plot is observed at some particular quantity of adsorbed matter. Typical observations for a variety of adsorbates on a porous adsorbent, silica gel, and on nonporous rutile are given below. The interpretation of this kind of data and of the variation of the slopes of such plots with temperature is, however, a very difficult matter.

In order to attempt an interpretation it appears necessary to evaluate the polarizability of the adsorbed species. The dielectric which is being examined is, of course, a heterogeneous one, and it is necessary to account correctly for such factors as the arrangement of the particles in the bed, the spaces between particles occupied by gaseous matter, and the contribution of the adsorbed matter. Up to the present the simpler situation of powdered solid and intervening space between particles has not been satisfactorily treated, although both Böttcher (1) and Kamiyoshi (9) have succeeded in developing formulae which yield reasonable values of the dielectric constant of the solid provided its dielectric constant is not above about 20.

In the present paper the general nature of the experimental findings is reviewed and information from further studies recorded. A comparison is then made of the values of the polarizability of the adsorbed matter or of the apparent dipole moments of polar adsorbates deduced by a number of procedures. It is thus shown that the values obtained are markedly dependent upon the method of computation. As each procedure involves an empirical step and usually also an arbitrary assumption in the method by which the

[1]*Manuscript received September 16, 1954.*
Contribution from the Department of Chemistry, University of Toronto, Toronto, Ont. This paper was presented at the Symposium on Problems Relating to the Adsorption of Gases by Solids, held at Kingston, Ontario, September 10–11, 1954.
[2]*Graduate Student.*
[3]*Professor of Chemistry.*

polarizability of the adsorbed matter is separated from that of the whole system, it has not been possible generally to assess the advantages of one method over the others. An obvious test is to rely upon the answer obtained for a nonpolar adsorbate, such as butane. In this case, however, owing probably to the low dielectric constant of the adsorbate, discrimination among the methods is not readily achieved. The contribution of the paper, therefore, is to point out the nature of the problem and to emphasize that the methods outlined are far from satisfactory. As these methods include that used by Kamiyoshi (10), it must be concluded that all values of the polarizability or of the permanent moment so far published are unlikely to be reasonable approximations to the effective molecular constants of adsorbed molecules.

SUMMARY OF EXPERIMENTAL OBSERVATIONS

The experimental observations made in this laboratory are briefly summarized below. As Higuti (7) and Kurbatov (12) have also reported the type of result to be found using porous adsorbents, the validity of the findings appears established.

I. *Porous Silica Gel*

(*a*) All adsorbates studied reveal two well-defined linear sections of the plots of capacitance change versus volume of gas adsorbed. (*b*) These linear sections are separated by a short transition region, so that extrapolation of the two lines defines a critical value of the volume adsorbed at which a change of the apparent polarizability of the adsorbed phase occurs. (*c*) The second linear section always has a lower slope than the first. (*d*) Depending upon the adsorbate, the critical value of the volume adsorbed may or may not change with temperature over the range of temperature which has been studied. (*e*) The critical value of the volume adsorbed does not agree with the value of V_m computed by the B.E.T. method. (*f*) Addition of water to the gel before admission of the second adsorbate may influence both the values of the slopes and the critical quantity of adsorbate. (*g*) The variation of the slopes of the linear sections with temperature depends upon the particular adsorbate. Nonpolar butane shows a negligible temperature dependence of the slopes. Polar adsorbates, such as ethyl chloride and water, show a negligible dependence on temperature of the slope of one section, while the slope of the other section may vary either as is normal for a polar substance or anomalously.

Details may be found in earlier publications, but typical plots for several adsorbates are shown in Fig. 1 as illustrations of the usual findings.

II. *Nonporous Rutile*

The measurements are more difficult to make using this adsorbent because of its low adsorptive capacity (specific surface to N_2 80 square meters) and the lower quantity which packs into the beds. The relative precision with which capacities are measured and the essentially similar results obtained with a different assembly (19) indicate that the results reported here are valid. It should be emphasized that linear sections of the usual type of plot are excellent, and in our opinion, it is justifiable only to draw straight lines through

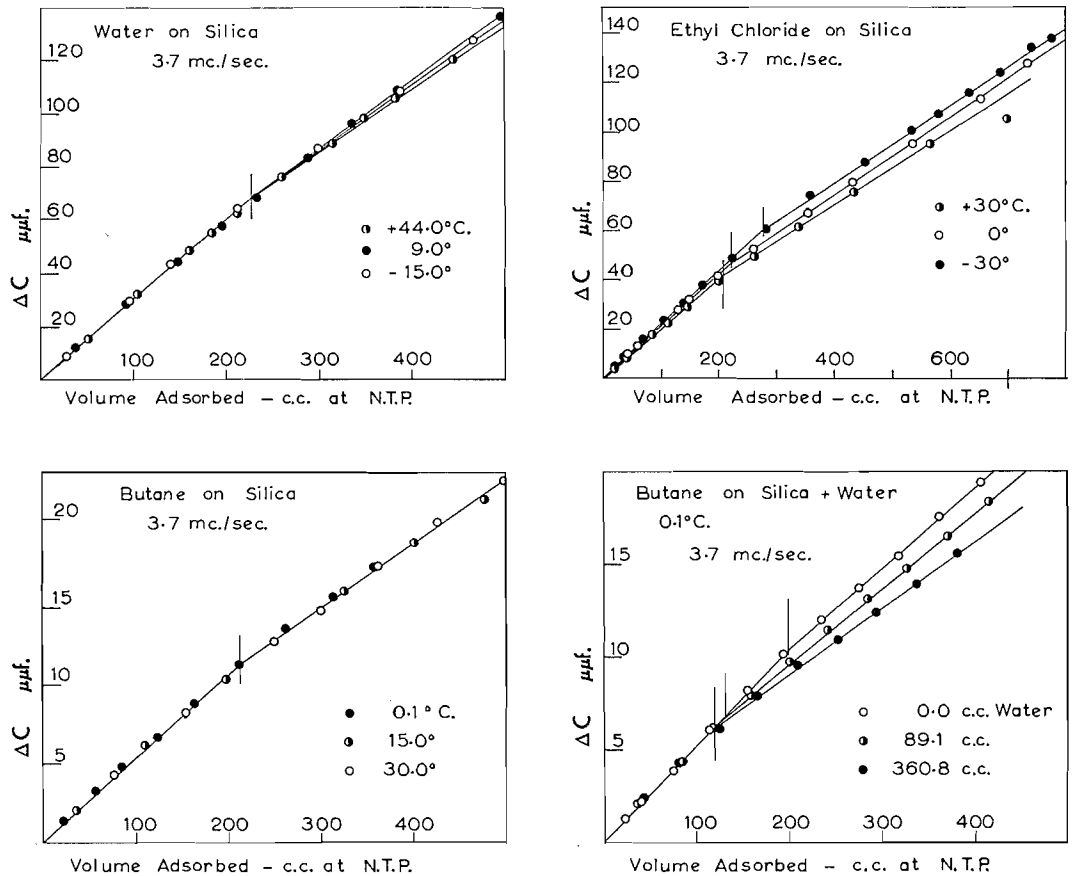

FIG. 1. Plots of capacitance change versus volume adsorbed for various adsorbates on silica.

the experimental points of the several sections of the graphically represented data.

The experimental observations may again be briefly summarized. (*a*) Nonpolar butane shows no discontinuity of the slope of the usual capacitance change versus volume adsorbed plot. (*b*) Three polar adsorbates, namely, ethyl chloride, sulphur dioxide, and ammonia, reveal two linear sections in the plots. (*c*) In these cases the second linear section possesses a higher slope than does the first, a fact which is in striking contrast with the behavior of polar adsorbates on porous silica. (*d*) The temperature coefficients of the slopes are negligible over the narrow temperature range of some thirty degrees which was feasible for the adsorbates other than dichlorofluoromethane. (*e*) The critical value of the quantity adsorbed at which the apparent polarization of the adsorbate changes is in good agreement with the value of V_m computed by use of the B.E.T. (4) or Hüttig equations (8). (*f*) Critical examination of these primary data shows that the sudden change cannot be accounted for by the gaseous matter between particles. (*g*) Dichlorofluoromethane[4] does not

[4]*The data for dichlorofluoromethane were obtained by Mrs. E. Petrie in this laboratory.*

exhibit the sudden change of apparent polarization at 20.2°C., but does so at −19.6°C., owing to a negligible temperature coefficient along the first section and a negative coefficient along the second. Representation of typical data is made in Fig. 2.

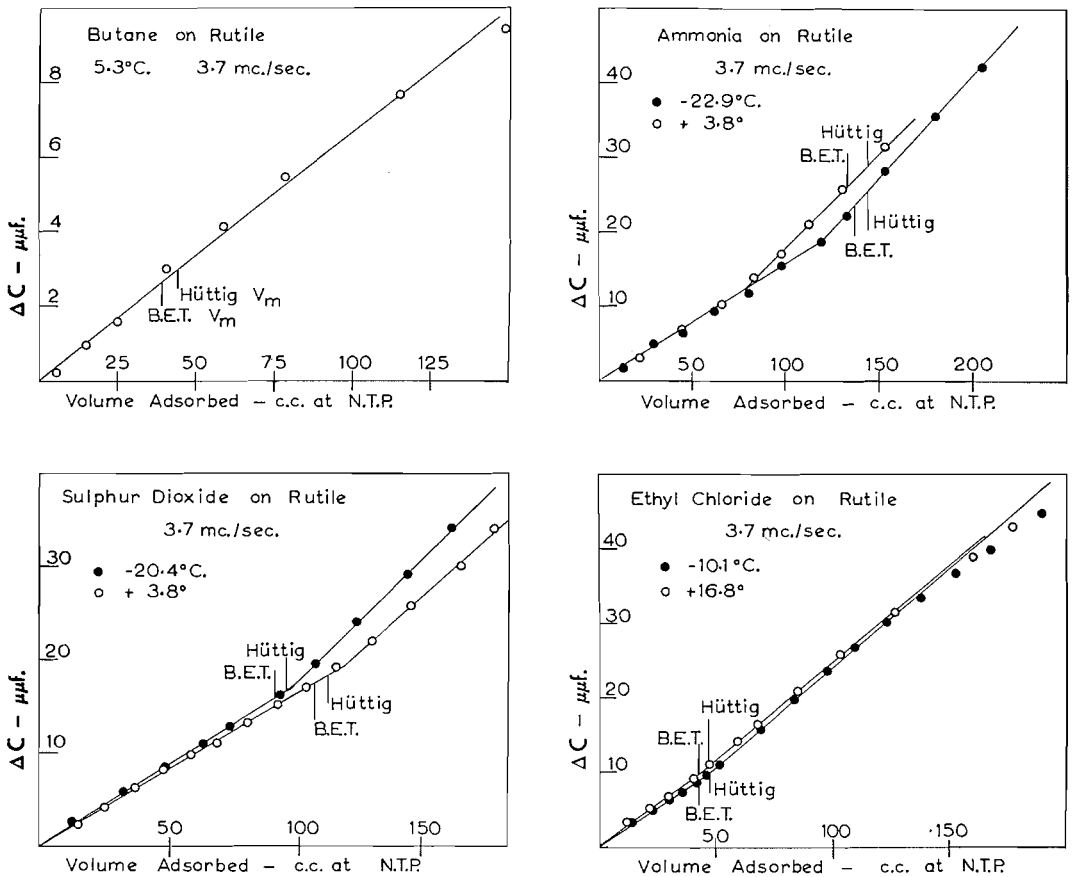

FIG. 2. Plots of capacitance change versus volume adsorbed for various adsorbates on rutile.

A comparison of these results with those obtained using silica suggests that porous structure has a bearing upon the results found. Moreover, the agreement between the values of V_m deduced from theories of adsorption and the critical values found from the electrical measurements using the nonporous adsorbent suggests that the change of apparent polarization occurs on the completion of the first molecular layer in the case of that adsorbent. It should be noted from the C values of the B.E.T. or Hüttig plots that the heat of adsorption in the first layer is quite large for these adsorbates.

General Theoretical Considerations

If the value of the directing field at the site of an adsorbed molecule were known, some theoretical knowledge is available to aid in the interpretation of the behavior of the adsorbed matter. McIntosh, Rideal, and Snelgrove (14)

showed that the orientational contribution to the total polarization of an adsorbed dipole constrained to rotate in the plane of the adsorbing surface is $\mathbf{E}_r(\mu^2/3kT)$, where $\mathbf{E}_r$ is the directing field. Kurbatov (12) treated the case of a dipolar molecule which can undergo rotational oscillations in three dimensions, and also the case of a rotating molecule constrained to rotate within a given cone angle. For the first case he established the important result that although the orientation of the oscillator may make an important contribution to the measured polarization, the temperature coefficient of the orientational effect will be negligible if there is a reasonable restoring force to the equilibrium position of the oscillator with no field applied. In the second case the usual inverse temperature relation should be observed. Snelgrove and McIntosh (18) applied this type of treatment to molecules constrained to move in the plane of the adsorbing surface with similar results. Although we have now shown (5) that equation [e] of their paper should be modified to the form

$$[a] \qquad \overline{\mathbf{m}} = \frac{\mu^2 \mathbf{E}_r}{3kT}\,(1-e^{-1/2\beta^2}) \qquad [a]$$

the important result is still valid, namely, that a higher polarizability than is to be expected for a nonpolar adsorbate and a negligible temperature variation of the orientational part of the polarization may be found. It is therefore not surprising that values of the polarizability of adsorbed molecules in excess of that predicted on the basis of refractive index data (or more properly, high frequency dielectric data) should be deduced from any method of computation which may be employed, even when the primary data appear independent of temperature. On the other hand, in our opinion, one should not expect to find an apparent permanent moment for an adsorbed nonpolar species. This statement is based upon the view that although a dipole may be induced in a nonpolar adsorbate by the field of the solid, the random orientation of the adsorbing surfaces should cause the net effect of these induced dipoles to be zero. Moreover, since the direction of the induced dipole depends upon the direction of the field from the surface, there is no tendency for the induced dipole to orientate with the applied field. When, therefore, a nonpolar adsorbate is found to possess a polarizability markedly in excess of α_0, the distortion polarizability, when the primary data have been treated by some procedure such as those to be discussed below, we believe that this result merely demonstrates the inadequacy of the treatment. A discussion of four procedures which we have employed with the type of data recorded above will now be given. These four procedures are (1) extension of Böttcher's powder method, (2) Böttcher's solution formulae applied to the adsorbate–adsorbent system, (3) a cluster model of the powder in conjunction with Böttcher's several methods, (4) the procedure due to Kamiyoshi.

METHODS OF OBTAINING DIELECTRIC QUANTITIES

I. *Extension of Böttcher's Powder Method*

The extension of Böttcher's powder method has been described earlier (14). It is useful, however, to review the assumptions which are made in it.

It is assumed (*a*) that the average field within the composite dielectric is given by the Clausius–Mosotti field $\frac{1}{3}(\epsilon+2)\mathbf{E}$, where ϵ is the average dielectric constant of the system and $\mathbf{E}$ is the applied field, (*b*) that the field in the interstices is given by the Onsager cavity field, namely, $[3\,\epsilon/(2\,\epsilon+\epsilon_g,)]\,\mathbf{E}$, where ϵ is the dielectric constant of the composite dielectric and ϵ_g is the dielectric constant of the gas at the equilibrium pressure over the solid, (*c*) that the average field in the composite system is given by adding the average internal fields in each constituent on a volume fraction basis, (*d*) that the total polarization of the composite dielectric is given by adding the polarization of each constituent on a volume fraction basis. It should be noted that an assumption concerning the density of the adsorbate is required, and there is thus an adjustable parameter in the final equation

$$[b]\qquad \frac{\epsilon+2}{3}-\frac{\epsilon}{2\epsilon+\epsilon_g}(\epsilon_g+2)\,\delta_3=\frac{\epsilon_i-1}{4\pi C_1}+\frac{\epsilon-\epsilon_i-(\epsilon_g-1)\frac{\epsilon}{2\epsilon+\epsilon_g}(\epsilon_g+2)\,\delta_3}{4\pi C_2}$$

TABLE I

DIELECTRIC CONSTANTS OR POLARIZATIONS PER CM.^{3} FOR ADSORBATES ON SILICA BY THE EXTENSION OF BÖTTCHER'S POWDER METHOD

Temp., °C.	First linear section	Second linear section	Refractive index squared	Dielectric constant from Onsager equation
Butane—dielectric constant				
0.1	1.80	1.61	1.81	—
15.0	1.78	1.58	1.79	—
30.0	1.74	1.55	1.77	—
Ethyl chloride—dielectric constant				
0.1	8.66	4.36	1.90	10.9
15.0	7.89	4.14	1.87	10.0
30.0	7.50	3.99	1.84	9.4
Methyl chloride—dielectric constant				
0.1	9.40	5.05	1.86	12.0
Water—polarization per cm.^{3}				Polarization from Onsager equation
−15.0	1.069	0.947		0.915
9.0	1.052	0.944		0.908
44.0	1.052	0.937		0.896

where δ_3 is the volume fraction occupied by gaseous matter, ϵ_i is the dielectric constant of the powder before addition of adsorbate, and C_1 and C_2 are respectively the volume average polarizabilities of the solid and of the adsorbate. The correction terms for gaseous matter given here are of some significance in dealing with rutile systems. McIntosh, Rideal, and Snelgrove (14) have pointed out how dielectric measurements might be employed to establish the value of the density of the adsorbed phase for nonpolar adsorbates, or for polar adsorbates at very high measuring frequencies. Without such knowledge the arbitrary assumption that the adsorbate has the density of liquid at the particular temperature has been made.

TABLE II

DIELECTRIC CONSTANTS* FOR ADSORBATES ON RUTILE BY THE EXTENSION OF BÖTTCHER'S POWDER METHOD

Temp., °C.	First linear section	Second linear section	Refractive index squared	Dielectric constant from Onsager equation
Butane				
5.3	2.05	—	1.80	—
Ethyl chloride				
0.6	6.2	7.2	1.90	10.9
−10.1	6.1	7.8	1.92	11.7
−19.2	6.2	9.2	1.94	12.3
Ammonia				
3.8	16.1	49	1.79	14.0
−22.9	15.6	69	1.84	16.7
Sulphur dioxide				
3.8	7.8	10	2.03	11.6
−20.6	8.2	16	2.09	13.4

**The number of significant figures stated is to show any variation with temperature. Absolute values of the dielectric constant of the adsorbate are not known.*

In conjunction with equation [*b*] the relation

$$[c] \qquad \frac{\epsilon_2-1}{\epsilon_2+2} = \frac{4\pi}{3} C_2$$

has been employed to give the dielectric constant of the adsorbate. The use of this formula follows from the definition of C_2 based upon assumption (*d*).

The application of this method to systems consisting of porous silica and various adsorbates seems reasonable, in view of the fact that the result obtained for the dielectric constant of the silica from the measured ϵ_i is about 6. On the other hand, as may be seen from Table I the value obtained for water is too high, and cannot reasonably be accounted for on the basis of experimental error. Application to systems of rutile and adsorbate is questionable, because the measured value of ϵ_i yields a wrong value for the dielectric constant of rutile (negative) while the known value is about 114 (11). It is not surprising, therefore, that the value of the dielectric constant of ammonia is found to be greater than that of bulk liquid. The use of the field in a spherical cavity is one source of error, since this approximation is poor when the dielectric constant of the powder particles is large (2). Values for several adsorbates are given in Table II.

II. *Solution Method*

Böttcher (3) has also treated the case of solutions. The requisite equations are:

$$[d] \qquad \frac{\epsilon+2}{3}\mathbf{E} = \sum_k \frac{4}{3}\pi a_k{}^3 N_k \mathbf{E}_{i_k} + \left(1 - \sum_k \frac{4}{3}\pi a_k{}^3 N_k\right)\frac{3\epsilon}{2\epsilon+1}\mathbf{E},$$

$$[e] \qquad \frac{\epsilon-1}{4\pi}\mathbf{E} = \sum_k \left(N_k \alpha_k \mathbf{E}_{i_k} + N_k \frac{\mu_k{}^2}{3kT}\mathbf{E}_{r_k}\right),$$

[f] $$\mathbf{E}_{i_k} = \left\{1+\frac{\mu_k^2}{3kT}\left(\frac{f_k}{1-f_k\alpha_k}\right)\right\}\mathbf{E}_{r_k}.$$

Here, a_k, α_k, and N_k are respectively the radius, the distortion polarizability, and the number of molecules per unit volume of the kth type of molecule. $\mathbf{E}_{i_k}$ and $\mathbf{E}_{r_k}$ are respectively the internal field and the directing field at the kth type molecule. If these equations for solution systems are combined with the equations of the Böttcher powder method, it follows that a constant C_2' for the adsorbed matter is now defined by the relation

[g] $$\left(\frac{4}{3}a_2^3C_2'N_2\right)\mathbf{E}_{i_2} = \alpha_2N_2\mathbf{E}_{i_2}+\frac{\mu_2^2}{3kT}N_2\mathbf{E}_{r_2}.$$

It can then be shown that

[h] $$\frac{\epsilon-\epsilon_i}{4\pi C_2'} = \frac{\epsilon+2}{3}-\frac{3}{2\epsilon+1}\left[\delta_4+\frac{4}{3}\pi a_3^3N_3\left\{\left(1+\frac{f_3}{1-f_3\alpha_3}\frac{\mu_3^2}{3kT}\right)\frac{1}{1-f_3\alpha_3}\right\}\right]$$
$$-\frac{\epsilon_i-1}{4\pi C_1'}+4\pi N_3\frac{1}{1-f_3\alpha_3}\frac{3\epsilon}{2\epsilon+1}\left\{\alpha_3\left(1+\frac{f_3}{1-f_3\alpha_3}\frac{\mu_3^2}{3kT}\right)+\frac{\mu_3^2}{3kT}\right\}\frac{1}{4\pi C_2'}$$

where δ_4 designates the volume fraction of free space and the subscript 3 designates the gaseous molecules. The symbols C_1' and C_2' refer to the solid and the adsorbed matter, respectively.

[i] $$\text{Also } f_k = \frac{1}{a_k^3}\left(\frac{2\epsilon-2}{2\epsilon+1}\right).$$

By this combination of equations the field within the solid is regarded as independent of the volume fraction of adsorbate and of gas, as in the extension of the powder method. Since the value of ϵ changes only slightly with increasing quantity of adsorbate, this approximation is not very serious.

Thus a plot of

$$\frac{\epsilon+2}{3}-\frac{3\epsilon}{2\epsilon+1}\left[\delta_4+\frac{4}{3}\pi a_3^3N_3\left\{\left(1+\frac{f_3}{1-f_3\alpha_3^3}\frac{\mu_3^2}{3kT}\right)\frac{1}{1-f_3\alpha_3}\right\}\right]$$

versus

$$\epsilon-\epsilon_i-4\pi N_3\frac{1}{1-f_3\alpha_3}\frac{3\epsilon}{2\epsilon+1}\left\{\alpha_3\left(1+\frac{f_3}{1-f_3\alpha_3}\frac{\mu_3^2}{3kT}\right)+\frac{\mu_3^2}{3kT}\right\}$$

should yield a straight line of slope $1/4\pi C_2'$. The values of α were taken from refractive index data, while the values of a were assigned from the van der Waals' constants of the adsorbate (6, 16). The value of C_2' obtained from the data is independent of the value assigned the volume fraction of the solid, δ_1, for changes of the order of 30%. Thus the apparent electrical characteristics of the adsorbate are not dependent upon whether or not a "free space" term should be included for the solid constituent.

Finally, the relation between dipole moment of the adsorbate and C_2' is given by

[j] $$\frac{\mu_2^2}{3kT} = \left\{1-\frac{\alpha_2}{a_2^3}\left(\frac{2\epsilon-2}{2\epsilon+1}\right)\right\}\left\{C_2'\frac{4\pi a_2^3}{3}-\alpha_2\right\}\Big/\left(1-C_2'\frac{4\pi}{3}\frac{2\epsilon-2}{2\epsilon+1}\right).$$

Some justification for using a solution model may be derived from the fact that the adsorbent has a large specific surface, so that its subdivision is great, and the system approximates to a mechanical mixture on the molecular scale. Further, the term $(\mu_2^2/3kT)\mathbf{E}_{r_2}$ is valid for a dipole constrained to rotate in the plane of the adsorbing surface (14), but would not be valid for a rotational oscillator. A likely source of failure is the spherical form of the model implicit in the equations, a criticism already mentioned in the preceding section. It should also be noted that the treatment implies a field within the solid independent of the numbers N_2 and N_3 of adsorbed and gaseous molecules.

It can be seen from equations [*d*], [*e*], and [*f*] that the selected values of α and a will influence the number obtained. In the case of a nonpolar adsorbate, the relation

$$[k] \qquad C_2'\frac{4\pi}{3}a_2^3 = \alpha_2$$

should apply, and may be used to test the measure of agreement between experiment and theory when the value of a_2 is taken from the van der Waals' equation of state. For butane the value of α_2 from refractive index data is 8.2×10^{-24} cc. per molecule. The experimental values of C_2' for butane on silica and rutile gave values of 5.7×10^{-24} and 7.1×10^{-24} cc. per molecule, respectively. It may be remarked that adjustment of the parameter a_2 may be made in a similar fashion to that mentioned in the preceding section. Examples of the numerical values of μ for various adsorbates on silica and rutile are recorded in Table III. The value of ϵ required in the calculations was taken about midway along the appropriate linear section of the plots.

TABLE III

APPARENT DIPOLE MOMENTS FOR ADSORBATES ON SILICA AND RUTILE BY THE "SOLUTION" METHOD OF COMPUTATION

Substance	Temp. (°C.)	Adsorbent	Molar volume	α per molecule from refractive index data $\times 10^{24}$	Apparent dipole moment $\times 10^{18}$	Gaseous dipole moment $\times 10^{18}$
NH_3	−22.9	TiO_2	8.80	2.02	0.53	1.47
NH_3	+ 3.8	TiO_2	8.80	2.02	0.56	1.47
SO_2	+ 3.8	TiO_2	14.0	5.56	0.0	1.61
C_2H_5Cl	+ 0.6	TiO_2	22.0	6.47	0.57	2.02
C_2H_5Cl	0.0	SiO_2	22.0	6.47	0.52	2.02
C_4H_{10}	0.1	SiO_2	30.4	8.20	α_2 from $C_2' = 5.7 \times 10^{-24}$	
C_4H_{10}	5.3	TiO_2	30.4	8.20	α_2 from $C_2' = 7.1 \times 10^{-24}$	

The most noteworthy feature of this method of computation is the terms arising from the presence of gaseous matter in the composite dielectric. This remark applies only to the rutile systems, where the relative quantities of adsorbate and gaseous material are such as to make the contribution from the

gas important. In the cases of ethyl chloride and sulphur dioxide the discontinuities evident in the slopes of the plots of the primary data disappear, or a lower polarizability is deduced for the second linear region. This suggests that an overcorrection is being made. As the correction terms are negligible for the first linear sections, the values of μ for these sections are given in the table.

III. *The "Cluster" Method*

It was pointed out that the application of Böttcher's formula to powdered rutile did not yield the correct value of the dielectric constant of crystalline rutile, namely, 114. As the specific surface of the sample is 80 square meters, the ultimate particles would be invisible and the particles seen are aggregates or clusters of these. Further, in packing the cell it was found that the volume fraction of solid always lay in the range 0.16–0.18. For powders of particle size of the order 0.005 cm. the volume fraction of solid is ordinarily in the range 0.4 to 0.6. The existence of clusters could explain this difference in the volume fraction of solid in the beds of rutile. By assigning a value for the volume fraction of the ultimate particles within the clusters, the volume fraction of the clusters themselves, considered as a homogeneous phase, can be calculated. By an application of Böttcher's powder method, the mean dielectric constant of the clusters can then be calculated. From this number, in conjunction with the previously assigned value of the volume fraction of solid within clusters, a second application of Böttcher's procedure yields the dielectric constant of the ultimate particles of solid.

This procedure was applied for two different values of the volume fraction within the clusters. The one corresponded with hexagonal close-packing of spheres, and gave a dielectric constant of 180 for the solid rutile. The other corresponded with cubical close-packing of spheres, and gave a dielectric constant of 50. If both the cluster model and Böttcher's equation are correct, the arrangement within the clusters must be something between the hexagonal and cubical close-packing arrangements. The volume fraction within the clusters can then be empirically adjusted to yield the correct value of the dielectric constant of the rutile.

Having established the distribution of the powder alone in this way, the dielectric data for the adsorbed gases may be treated in either of two ways on making the further assumption that the adsorbed matter is contained within clusters. These are: (*a*) Calculate the mean dielectric constant of the clusters as a function of the volume of adsorbed gas and then, using those results, calculate the dielectric constant by the extension of the powder method described earlier. (*b*) Calculate the mean dielectric constant of the clusters as in (*a*) above and then apply the solution method to the clusters to obtain the property of the adsorbed phase.

Method (*a*) yielded values of ϵ_2 approaching infinity. Method (*b*), led, in the case of butane, to a value of $\alpha_2 = 11.6 \times 10^{-24}$cc. per molecule, compared with 8.2×10^{-24} from refractive index measurements. This corresponds with a prediction of a permanent moment of 0.5×10^{-18} e.s.u. for a nonpolar

adsorbate. As already argued, such a prediction illustrates some inadequacy of the treatment. The apparent permanent moments of ethyl chloride and ammonia, as shown in Table IV, are in fair agreement with the known moments. On the other hand, a virtually infinite moment was deduced for sulphur dioxide. Furthermore, although both procedures (*a*) and (*b*) gave excellent straight lines over the entire range of quantity adsorbed they obscured the discontinuity of the slope of the primary data. On these grounds the method must be considered invalid.

Kamiyoshi's Method

Kamiyoshi (9, 10) starting with Rayleigh's formula for a cubical array of spheres (15) obtained expressions for the apparent dielectric constants of two types of region regarded as making up the composite dielectric. These regions were considered to consist of spheres of dielectric constant ϵ_0 in space and of spheres of dielectric constant 1 in a medium of dielectric constant ϵ_0. Then, on the assumption that the over-all dielectric constant may be obtained by combining these two types of region as a system of condensers in series and in parallel, a formula was deduced which would yield the value of the dielectric constant of the solid. Similar treatment would yield a value of the dielectric constant of solid plus adsorbed phase. If a porous adsorbent was employed an empirical correction factor had to be introduced to obtain the correct value of the dielectric constant of the solid, much as the packing factor was selected in the "cluster" treatment outlined earlier. Such an empirical factor had to be introduced in the case of rutile.

When the dielectric constant of adsorbent plus adsorbate is deduced by this method, some further means of separating the contributions of the two constituents must be employed. Kamiyoshi (10) used a solution model and the Debye equations for dilute solutions. Theoretically, this general procedure is hardly preferable to any of those with which we have already dealt. However, as each is semiempirical, Kamiyoshi's method was employed using ethyl chloride and butane on rutile. With ethyl chloride the value of μ_2 was found to be 1.41×10^{-18} e.s.u. In the case of butane, however, a permanent moment of about 1.6×10^{-18} e.s.u. was deduced, and on the arguments put forward earlier this demonstrates the inapplicability of the method. This is not an isolated example, since Kamiyoshi himself has reported apparent permanent moments of 0.57 and 0.47×10^{-18} e.s.u. for carbon tetrachloride and for benzene, respectively, adsorbed on silica gel (10). Owing to the tediousness of the computations by this method other data were not tested in view of these unsatisfactory results. An application of our modified solution treatment was not attempted because in this case the value of ϵ for the solid plus adsorbate varies appreciably over the range of quantity adsorbed.

GENERAL CONCLUSIONS

The interesting phenomena which may be observed on measuring capacity increments with increasing quantity of adsorbate on a solid have been shown to be of fairly general occurrence and to be specific to the adsorbent as well

as the adsorbate. Up to the present however, no satisfactory way of obtaining the apparent electrical properties of adsorbed matter has been developed, and until this is achieved no great clarification of the observations appears likely.

TABLE IV

APPARENT DIPOLE MOMENTS FOR ADSORBATES ON RUTILE BY THE "CLUSTER" METHOD OF COMPUTATION

Substance	Temp., °C.	Apparent dipole moment $\times 10^{18}$	Gaseous dipole moment $\times 10^{18}$
NH_3	−22.9	1.67	1.47
C_2H_5Cl	+ 0.6	1.65	2.02
SO_2	−22.9	∞	1.61
C_4H_{10}	+ 5.3		α_2 from $C_2' = 11.6 \times 10^{-24}$ apparent moment 0.5×10^{-18}

ACKNOWLEDGMENT

It is a pleasure to acknowledge the financial support of this work by the National Resaarch Council and by the Advisory Committee on Research, University of Toronto.

REFERENCES

1. BÖTTCHER, C. J. F. Rec. trav. chim. 64: 47. 1945.
2. BÖTTCHER, C. J. F. The theory of electric polarisation. Elsevier Publishing Co., Inc., Amsterdam. 1952, p. 418.
3. BÖTTCHER, C. J. F. The theory of electric polarisation. Elsevier Publishing Co., Inc., Amsterdam. 1952. Chap. VI.
4. BRUNAUER, S., EMMETT, P. H., and TELLER, E. J. Am. Chem. Soc. 60: 309. 1938.
5. CHANNEN, E. Unpublished.
6. DEBYE, P. J. Polar molecules. The Chemical Catalog Co., Inc., New York. 1929. p. 17.
7. HIGUTI, I. Bull. Inst. Phys. Chem. Research, (Tokyo), 20: 489. 1941.
8. HÜTTIG, G. F. Monatsh. 78: 770. 1948.
9. KAMIYOSHI, K. Science Repts. Research Insts. Tôhoku Univ. Ser. A, 2: 180. 1950.
10. KAMIYOSHI, K. Science Repts. Research Insts. Tôhoku Univ. Ser. A, 3: 513. 1951.
11. KLEBER, W. Chem. Abstr. 46: 10728$_d$. 1952.
12. KURBATOV, L. N. J. Phys. Chem. (U.S.S.R.), 24: 899. 1950.
13. McINTOSH, R., JOHNSON, H. S., HOLLIES, N., and McLEOD, L. Can. J. Research, B, 25: 566. 1947.
14. McINTOSH, R., RIDEAL, E. K., and SNELGROVE, J. A. Proc. Roy. Soc. (London), A, 208: 292. 1951.
15. RAYLEIGH, LORD. Phil. Mag. 34: 481. 1892.
16. SLATER, J. C. Introduction to chemical physics. McGraw-Hill Book Company, Inc., New York. 1939. p. 408.
17. SNELGROVE, J. A., GREENSPAN, H., and McINTOSH, R. Can. J. Chem. 31: 72. 1953.
18. SNELGROVE, J. A. and McINTOSH, R. Can. J. Chem. 31: 84. 1953.
19. WALDMAN, M. H. and McINTOSH, R. Can. J. Chem. 33: 268. 1955. Paper presented at the Symposium on Problems Relating to Physical Adsorption of Gases by Solids.
20. WALDMAN, M. H., SNELGROVE, J. A., and McINTOSH, R. Can. J. Chem. 31: 998. 1953.

THE GROWTH OF CRYSTALLINE LAYERS ON FOREIGN SURFACES[1]

By J. H. Singleton and G. D. Halsey, Jr.

ABSTRACT

When the bulk phase of an adsorbent is solid, it has been shown that adsorption often proceeds only to a finite limit as the pressure reaches saturation. A theory is developed for this finite limit, in terms of the excess forces at the surface and the incompatibility of the crystal lattices of the adsorbent and adsorbate. It is applied to the stepwise adsorption of krypton on graphitized carbon black. An extrapolation formula applicable to smooth isotherms at high coverages is developed and shown to be analogous to the Harkins–Jura equation. It is applied to argon adsorbed on carbon black, on xenon preadsorbed on carbon black, on silver iodide, and on anatase. The energies obtained are compared with a theoretical estimate based on the Kirkwood–Müller equation. A theory for calculating isotherms on preadsorbed layers is developed and compared with the data for argon on xenon.

In the temperature range of ordinary physical adsorption measurements, the adsorbate is usually a liquid in the bulk phase. It appears that, at least in the typical case, adsorption proceeds without limit as the pressure approaches saturation. At lower temperatures we have shown (8, 9) that there is a definite upper limit to the thickness of the adsorbed layer in a number of cases. The technique used involved following the change in the argon isotherm as the preadsorbed layer of the adsorbate was thickened. For the adsorption of xenon on anatase or silver iodide, only one or two atomic layers of the rare gas on the surface produced the saturation pressure of the bulk crystal. In the case of krypton on a graphitized carbon black, a definite upper limit was established between five and six layers.

It is clear that for growth to continue, a supersaturated atmosphere of xenon would be required, and that the degree of supersaturation would be related to the ability of the foreign surface to act as a nucleating agent for, in this case, xenon. Difficulties inherent in working with supersaturated vapors make it desirable to develop a theoretical method of calculating the degree of supersaturation from equilibrium data below saturation.

A Theory Predicting a Finite Adsorption Limit

The adsorption of argon on graphitized carbon black has been interpreted as evidence of surface homogeneity, because of the quasi-stepwise character of the isotherm. Our measurements with krypton at 77°K. on the same adsorbent show much more pronounced steps. Champion and Halsey (1) have modified the treatment of Hill (5) for adsorption on a uniform surface. His theory is essentially a generalization to n layers of the crude treatment of adsorption with lateral interaction given by Fowler and Guggenheim (2). He took into account the condensation energy of the adsorbate but neglected

[1]*Manuscript received September 16, 1954.*
Contribution from the Department of Chemistry, University of Washington, Seattle, Wash., U.S.A. This paper was presented at the Symposium on Problems Relating to the Adsorption of Gases by Solids, held at Kingston, Ontario, September 10–11, 1954.

the van der Waals forces transmitted from the surface to each succeeding layer. When these forces are included the isotherm that results is composed of a series of steps.

In an attempt to suppress these steps, and thus produce an ordinary smooth isotherm on a uniform surface, Champion and Halsey introduced the idea of an incompatibility between the crystal lattices of the adsorbent and the adsorbate. It was possible to make the steps disappear, but in order to have adsorption continue out to several layers it was necessary to increase the van der Waals forces and to change their decay law unreasonably. Thus, the theory developed was found not to apply to ordinary adsorption in the liquid range; however, it will now be applied to the problem of finite adsorption limits.

Hill's equations were modified to read

$$[1] \quad p/p_0 = [(\theta_n - \theta_{n+1})/(\theta_{n-1} - \theta_n)] \times \exp\{(-E_n/kT) + (w/kT)(-2g_n\theta_n - 1)\}.$$

Here, p/p_0 is the partial pressure in equilibrium with the adsorbed layers, θ_n the coverage in the nth layer, E_n the excess energy of adsorption transmitted to the nth layer, and w the lateral interaction energy. The last two are taken positive in sign for attractive interaction, which is the opposite of the usual thermodynamic convention. The compatibility factor, g_n, can vary from zero to unity. If it has the value zero, the lateral interactions are completely suppressed. If the factor is unity, it is implied that the lattices are completely compatible, and so the full energy of lateral interaction is operative. It will appear that the degree of incompatibility necessary to suppress growth beyond a few layers is not large. Since w is approximately equal to one half the energy of sublimation of the bulk crystal, and since g_n will always be near unity, calculations using equation [1] will lead to a completely stepwise isotherm (1). In order to find the positions of the risers of the steps in terms of p/p_0, the value one half is given to θ_n, unity to θ_{n-1}, and zero to θ_{n+1}. This yields a simple expression for the pressure at the nth step:

$$[2] \quad \ln(p/p_0)_n = -E_n/kT + (w/kT)(1 - g_n).$$

This equation can be put into usable form by making two assumptions; first that the energy E_n is given by the cube law (1, 6)

$$[3] \quad E_n = E_1/n^3,$$

and second that g_n has the constant value g in all layers. Thus

$$[4] \quad \ln(p/p_0)_n = -E_1/n^3kT + (w/kT)(1 - g).$$

We shall now use the positions of the steps for the second and third layers in the isotherm for krypton on graphitized carbon black to evaluate the parameters. The data so fitted are shown in Fig. 1. The values used to achieve this fit are $E_1/kT = 7.9$ and $(w/kT)(1-g) = 0.09$. The heat of sublimation of solid krypton is about 2.5 kcal. and T is 70°K. Thus g is 0.99 or almost unity. This value of g causes the isotherm to cross the axis $p/p_0 = 1$ at between four and five layers, whereas the actual crossing was one layer higher.

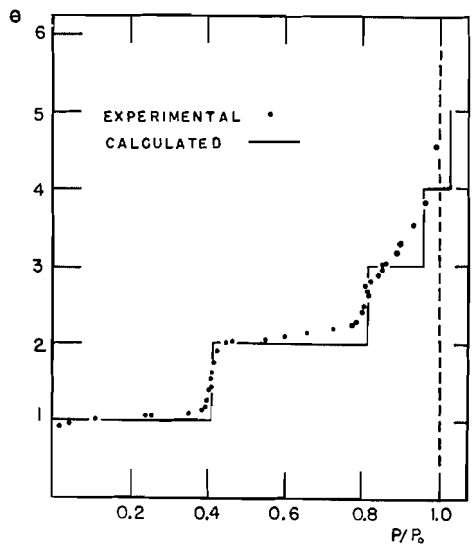

FIG. 1. Comparison of steps calculated from equation [4] with experimental isotherm points of krypton on graphitized carbon black at 77.1°K.

It appears that a very slight disturbance of the structure of the bulk crystal, at least as is reflected in its energy, is enough to halt the growth of the adsorbed phase at a definite limit. Note that this disturbance is nowhere nearly equal to the heat of fusion (which is about 12% of the heat of sublimation) so that the surmise that the adsorbed phase is "liquid" is definitely wrong.

An Extrapolation Formula

If the coverage on the surface is many layers thick, the integral layer number n in equation [4] can be replaced by the continuous variable, θ, the total coverage. An isotherm equation results:

$$\ln(p/p_0) = -E_1/\theta^3 kT - (w/kT)(1-g). \quad [5]$$

With $g = 1$, this equation reduces to a special case of an equation successfully applied to adsorption from the liquid phase:

$$\ln(p/p_0) = -E_1/kT\theta^r. \quad [6]$$

As we observed above, for the liquid, compatibility does not seem to present a problem. The present equation is analogous to the equation used by Harkins and Jura (4) in connection with their relative method of evaluating surface area:

$$\ln(p/p_0) = A - B/v^2. \quad [7]$$

Here A and B are constants and v is the volume adsorbed and is thus proportional to θ. The change in power of θ from the Harkins value of two to three in equation [5] attaches a definite meaning to the constants. The analogue of A in equation [5] is a measure of incompatibility. The interpretation of E_1 will be discussed in the next section.

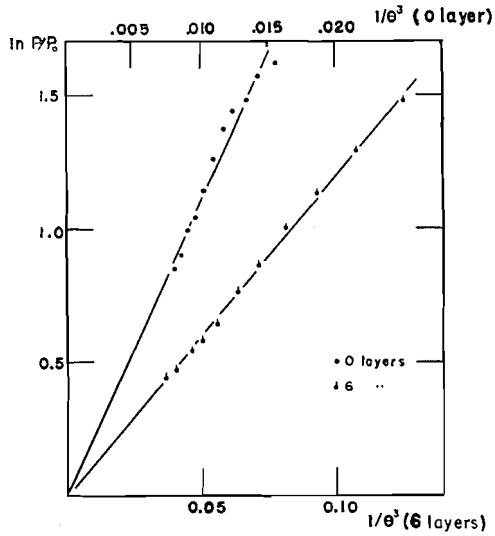

FIG. 2. Extrapolation from data for argon adsorption on graphitized carbon black using equation [5] (0 and 6 layers of preadsorbed xenon: 77.1°K.).

The data for the adsorption of argon on the graphitized carbon black, and for the adsorption of argon on six layers of xenon preadsorbed on the black are plotted according to equation 5 in Fig. 2. Note that the points for the six layers of xenon extrapolate to the origin, which shows that the solid argon is fully compatible with the preadsorbed xenon. It appears that the points for the bare carbon surface also extrapolate at least very near to the origin,

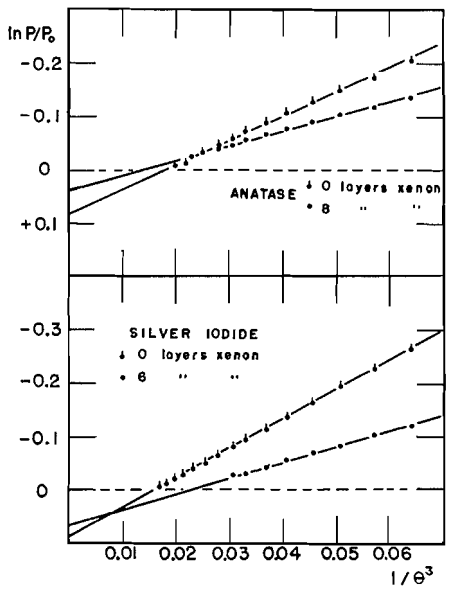

FIG. 3. Extrapolation from data for argon adsorption on anatase and silver iodide, using equation [5] (0 and 8, 0 and 6 layers of preadsorbed xenon, respectively: 77.1°K.).

although, because of the bumpiness in the isotherm, the straight line plot is not perfect.

In Fig. 3, some data that do not intercept the origin are presented. Argon is thus not compatible with either anatase or silver iodide. On both surfaces the intercept on the $\ln(p/p_0)$ axis is at about 0.09, which corresponds to a supersaturation ratio of 1.1. Note that when the surfaces are coated with as much xenon as they will support, the intercept is reduced, and the supersaturation ratio decreases to 1.05 for silver iodide and 1.08 on anatase. Thus the xenon forms sort of a "graded seal". In harmony with the greater thickness of xenon layer on silver iodide, the decrease in the supersaturation ratio is greater.

Comparison of E_1 with the Kirkwood–Müller Formula

When the extrapolation formula (5) is used to evaluate E_1 it is clear that the value found is unlikely to agree with E_1 values found experimentally using data over the first-layer range. Short-range forces, heterogeneity, crystal lattice periodicity, and incompatibility all operate to affect the real value of E_1. The E_1 evaluated using data at high coverages represents only the long-range surface forces, with local disturbances more or less averaged out. It is thus more nearly the ideal quantity to compare with theoretical estimates of the London force than calorimetric data are. Steele and Halsey (10) have calculated the energy of interaction of a single rare gas atom at a distance D from the surface using the following expression, which is based on a treatment due to Kirkwood and Müller (7):

$$[8] \qquad \epsilon^* = (N_2 mc^2 \pi/D^3)\{\alpha_1\alpha_2/[(\alpha_1/\chi_1)+(\alpha_2/\chi_2)]\}$$

N_2 is the number of atoms per cm.^{3} in the solid, mc^2 is the mass of the electron multiplied by the velocity of light squared, and α and χ are the atomic polarizability and atomic susceptibility respectively. The subscript one refers to the adsorbed atom and two refers to the adsorbent atoms.

Following Hill (6), we must now modify this expression so that it applies to an adsorbed atom surrounded by the other atoms of the adsorbed phase. E_n is defined as the excess energy available to the adsorbed atom in the nth layer because of the presence of the adsorbent n layers away. Because the absolute pressure, p, is divided by the reference-state pressure p_0, the energy must be corrected by the extent to which the adsorbed layers deviate from the bulk structure. Part of this deviation has been taken care of by the g factor of equation [5]. However, in introducing a semi-infinite slab of adsorbent n layers away, a similar slab of adsorbate has been removed. Therefore one must subtract this energy of self interaction from equation [8] to obtain the expression for E_n.

$$[9] \qquad E_n = \epsilon^* - (N_1 mc^2 \pi/D^3)(\alpha_1\chi_1/2)$$

N_1 is the number of atoms per cm.^{3} in the solid adsorbate. The distance D must now be evaluated in order to calculate E_1. Since the E_1 determined

using the extrapolation formula equation [5] refers to large distances from the surface, the appropriate distance is that between adjacent parallel planes of atoms in the bulk adsorbate. For the close-packed rare gas crystals, this is equal to $\sqrt{\frac{2}{3}}$ times the lattice parameter.

Comparison of the Calculated and Experimental Values of E_1

The constants used to calculate E_1/kT are presented in Table I. The temperature was 77°K. The density given was used to calculate the lattice parameter. It will appear in the analysis of the argon isotherms on xenon which follows below, that the argon isotherm on six atomic layers of xenon is sufficiently close to the calculated isotherm for an infinitely thick layer of xenon to calculate E_1/kT on this basis. The calculated value is 2.55 compared to the measured value 1.20. For argon on the bare carbon surface the calculated value is 13.8 compared to 11 measured. For the case of krypton on carbon, which was analyzed using the formula, equation [4], the calculated value is 15.3, compared to the measured value 7.9.

The calculated value for argon on silver iodide is 9.7; the experimental value is 11. No estimate of the diamagnetic susceptibility of anatase could be found. Since the theory is admittedly quite crude, the agreement, although not perfect, is satisfactory.

TABLE I

	Density (gm./ml.)	Atomic susceptibility $\times 10^{29}$	Atomic polarizability $\times 10^{24}$
Argon	1.65[a]	3.24[c]	1.623[e]
Krypton	2.994[a]	4.65[c]	2.46[e]
Xenon	3.56[a]	7.04[c]	4.00[e]
Silver iodide	5.67[b]	13.6[d]	9.28[f]
Carbon black	2.25[b]	3.79[d]	1.02[f]

[a] *Partington, J. R. An advanced treatise in physical chemistry. Vol. III. Longmans, Green & Company, Inc., New York. 1952. p. 149.*
[b] *International Critical Tables. Vol. I. McGraw-Hill Book Company, Inc., New York. 1926. pp. 102–174.*
[c] *Mann, K. E. Z. Physik, 98: 548. 1936.*
[d] *International Critical Tables. Vol. VI. McGraw-Hill Book Company, Inc., New York. 1928. pp. 354–364.*
[e] *Margenau, H. J. Chem. Phys. 6: 896. 1938.*
[f] *Calculated from refractive indices in International Critical Tables. Vol. I. McGraw-Hill Book Company, Inc., New York. 1926. pp. 102–174.*

A Theory for Adsorption on Top of Preadsorbed Layers

The two different preadsorbates that we have studied exhibited layer formation in the case of xenon and solution in the case of krypton when argon was subsequently adsorbed. It was possible to develop a crude theory for solution in preadsorbed layers (9) by modification of the regular solution theory of Fowler and Guggenheim (3) to include the free energy of adsorption. The essential assumption added to those of the bulk solution theory was that the presence of component B did not affect the molar contribution of component A to the adsorption energy, and vice versa. This amounted to assuming that

the two species were the same size; an equivalent assumption will be required here for a given total coverage $\theta_A+\theta_B$; the adsorption free energy was calculated from a weighted average of the energy for the pure components. It was then possible to calculate the mixed isotherms from the isotherms for the single components and the bulk solution data.

We shall now develop an analogous theory for the case (that of argon on xenon) where the essentially non-volatile component B forms an insoluble and distinct layer under the volatile A. The problem is to calculate intermediate isotherms for A from the isotherm for the surface bare of B, and the isotherm for the surface covered with an infinite number of layers of B. We shall see that this latter isotherm can be calculated although it may not be possible to measure it directly. Suppose that there are N_A molecules of A and N_B molecules of B adsorbed on the surface. (These numbers can be related to θ by dividing by the number of molecules in a monolayer.) We shall denote the isotherm for A on b layers of B by $(p/p_0)_b$ and the isotherm for pure B on the otherwise bare surface by $(p/p_0)_B$. The free energy of the adsorbent and its surface is a constant, F_s. (Note that since the reference state is a solid there is essentially no volume change associated with the adsorption process and that therefore F, the Helmholtz free energy, equals G, the Gibbs free energy, and so no distinction need be made.) Then, the total free energy of the surface plus N_A molecules of A and N_B molecules of B is

$$[10] \qquad F = F_s+kT\int_0^{N_B}\ln(p/p_0)_B dN+kT\int_0^{N_A}\ln(p/p_0)_b dN.$$

Then the chemical potential of A

$$[11] \qquad \mu_b^A = \partial G/\partial N_A = \partial F/\partial N_A = kT\ln(p/p_0)_b,$$

independent of F_s and the isotherm for component B.

We shall now divide the contributions to μ_b^A into two terms; one from the underlying solid and one from a slab b layers thick of component B. If we assume that these b layers are exactly equivalent to the same number of layers of A in reducing the contribution of the surface forces, then the first term in μ_b^A is the chemical potential of argon on the bare surface μ_0^A evaluated at $b+\theta_A$ layers. To this term must be added the term for the slab of B of thickness b layers. This is equal to the contribution from a slab of infinite thickness $\mu_\infty^A(\theta_A)$ minus the contribution from beyond $b+\theta_A$ layers, $\mu_\infty^A(\theta_A+b)$:

$$[12] \qquad \mu_b^A = \mu_0^A\,(b+\theta_A)+\mu_\infty^A(\theta_A)-\mu_\infty^A(b+\theta_A)$$

This relationship can be put in terms of the isotherm data by using equation [11], but actually it is more convenient to carry out the calculations in terms of the μ's. Note that for the relationship equation [12] to hold, the monolayer thickness of B must equal that of A, or else it will have a different effect in reducing the surface forces. This restriction corresponds to the restriction of regular solution theory that the molecules must be of the same size.

Calculation of the Limiting Isotherm $(p/p_0)_\infty$

If the known isotherm for argon on six layers of xenon, and thus μ_6^A is substituted into equation [12] a difference equation in the unknown μ_∞^A results. As a first approximation, the value of μ_6^A at $6+\theta_A$ can be used in place of $\mu_\infty^A(6+\theta_A)$ to calculate $\mu_\infty^A(\theta_A)$. This better value can then be used in the equation for a second approximation, etc. Throughout, the extrapolation formula equation [5] is used to obtain values beyond the experimental range. The result of this calculation is shown as an isotherm in Fig. 4. It is compared with

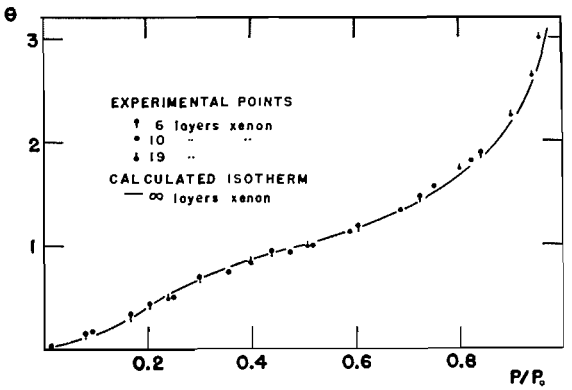

FIG. 4. Comparison of the limiting isotherm for argon on preadsorbed xenon, calculated according to equation [12], with experimental points taken at 77.1°K. (graphitized carbon black).

experimental points taken in the presence of enough xenon to make 6, 9.7, and 19.4 atomic layers. One can calculate from the extrapolation formula that going from 6 to 10 layers should change the upper part of the isotherm noticeably, and that the isotherm for 20 layers should be indistinguishable from the limiting curve. It would appear, then, that growth does stop between 6 and 10 layers. However, the continued change in the isotherm near a monolayer of argon, upon going from 6 to 10 layers of xenon, suggests that the surface arrangement of the xenon is different in the last few layers.

Calculation of the Intermediate Isotherms

In Fig. 5 isotherms calculated from the limiting isotherms are presented. They are compared with some of the experimental data. Although agreement is not quantitative, the general features of the data are well reproduced. Note that the calculated pressures are above the observed values, in keeping with the fact that the atomic layers of xenon are presumably thicker than the argon layers.

Previously (8), we had adjusted the monolayer volume of xenon by a 20% increase from the "point B" value, because when this volume was preadsorbed, a small "point B" appeared in the argon isotherm. No similar adjustment was made in the argon v_m, and therefore the isotherms here are presented in terms of the estimated "point B" volume. However, the calculated isotherm on one layer of xenon shows a "point B" of 0.1 monolayer. This at least suggests

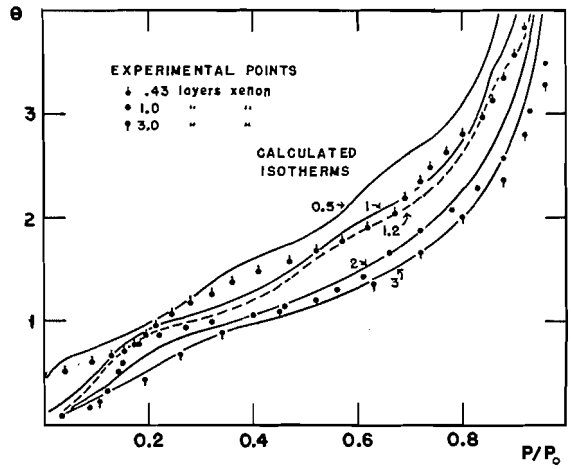

FIG. 5. Calculated isotherms for argon on preadsorbed xenon, using equation [12], compared with experimental points taken at 77.1°K. (graphitized carbon black).

that the true argon v_m should be larger also. This is in keeping with other independent estimates we have made of the area of this carbon black, all of which are larger than the B. E. T. area.

ACKNOWLEDGMENTS

We are indebted to Prof. J. R. Arnold for first mentioning this problem. The work was supported by contract AF19(604)–247 with the Air Force Cambridge Research Center.

REFERENCES

1. CHAMPION, W. M. and HALSEY, G. D., JR. J. Phys. Chem. 57: 646. 1953.
2. FOWLER, R. H. and GUGGENHEIM, E. A. Statistical thermodynamics. Cambridge University Press, London. 1939. Chap. X.
3. FOWLER, R. H. and GUGGENHEIM, E. A. Statistical thermodynamics. Cambridge University Press, London. 1939. Chap. XIII.
4. HARKINS, W. D. and JURA, G. J. Am. Chem. Soc. 66: 1366. 1944.
5. HILL, T. L. J. Chem. Phys. 15: 767. 1947.
6. HILL, T. L. J. Chem. Phys. 17: 590. 1949.
7. MÜLLER, A. Proc. Roy. Soc. (London), A, 154: 624. 1936.
8. SINGLETON, J. H. and HALSEY, G. D., JR. J. Phys. Chem. 58: 330. 1954.
9. SINGLETON, J. H. and HALSEY, G. D., JR. J. Phys. Chem. 58: 1011. 1954.
10. STEELE, W. A. and HALSEY, G. D., JR. J. Chem. Phys. 22: 979. 1954.

USE OF INTERPOLATION THEORY IN THE ANALYSIS OF GAS ADSORPTION ISOTHERMS

I. THEORY[1]

By J. M. Honig and P. C. Rosenbloom

ABSTRACT

The theory presented in this paper permits the determination of extremal bounds for a given adsorbate–adsorbent system within which the adsorption isotherms must fall if certain assumptions pertaining to the nature of the adsorption process are applicable. The use of interpolation theory in estimating lower and upper bounds on physical quantities of interest in adsorption theory is also discussed.

INTRODUCTION

The object of this paper is to present a new mathematical approach to the problem of surface heterogeneity and its effect on the physical sorption of gases by solids. In previous work of this type (1–5, 9, 13–16, 18) it has been customary to interpret a given isotherm in terms of a particular distribution of adsorption energies among the surface sites of the adsorbent. Several difficulties associated with this correlation procedure have by now emerged (6, 10, 11): First of all, the isotherm equation is quite insensitive to the choice of distribution function which characterizes the energy heterogeneity. Secondly, it is necessary to introduce a large number of simplifying assumptions in order to make the correlations mathematically feasible. It is often difficult to ascertain to what extent the simplifications are really applicable, the more so because the adsorption theories in themselves furnish no pertinent criteria. In view of these difficulties it would be instructive to estimate the maximum variation in the adsorption isotherm as the energy distribution is allowed to vary over all conceivable mathematical functions consistent with the physical requirements. Further, it is desirable to have at hand some method of checking the validity of the restrictive assumptions.

The present paper is devoted to a study of these subjects. It will be shown that by random selection of one or more points from a set of isotherm data one can construct lower and upper bounds which define the maximum possible variation in the isotherm data consistent with the simplifying restrictions. Failure of the remaining points to remain within these bounds is a clear indication that the restrictive postulates and the data are incompatible, at least over certain ranges of surface coverage. Lastly, the theory lends itself to a determination, without resorting to curve fitting procedures, of lower and upper bounds on quantities of interest in adsorption theory.

The mathematical theory is based on a publication by Rosenbloom (12) to which the reader is referred for verification of the theorems cited in the next

[1]*Manuscript received September 16, 1954.*
Contribution from the Department of Chemistry, Purdue University, Lafayette, Indiana, and the Department of Mathematics, University of Minnesota, Minneapolis 14, Minnesota. This paper was presented at the Symposium on Problems Relating to the Adsorption of Gases by Solids, held at Kingston, Ontario, September 10–11, 1954.

sections. The relevant parts of this theory are also summarized and made plausible in an appendix. Examples illustrating the application of this theory to experimental data will be presented elsewhere.

FUNDAMENTAL CONCEPTS

A. The following assumptions are used as a basis for further discussions (see also (7)): (*a*) Adsorption occurs on a fixed number of surface sites; (*b*) adsorption is limited to a monolayer; (*c*) each site is associated with a fixed adsorption energy; (*d*) no lateral interactions occur between adsorbed molecules; (*e*) each adsorbed particle is held rigidly to its site of adsorption; (*f*) the distribution of adsorption energies remains unaltered in the adsorption process. Using these assumptions it can be shown (1, 2, 4, 5, 9, 13–16, 18) that the fraction of surface sites covered, θ, is related to the gas pressure, p, and to the temperature T by the expression

$$[1] \qquad \theta(p, T) \equiv \frac{n}{n_m} = \int_0^\infty \frac{dF(\epsilon)}{1+[\beta(\epsilon, T)/p]\, e^{-\epsilon/kT}}.$$

Here ϵ is the adsorption energy associated with a given site and $dF(\epsilon) = f(\epsilon)\, d\epsilon$ is the fraction of all sites associated with adsorption energies in the range ϵ to $\epsilon+d\epsilon$. The quantity $\beta(\epsilon, T)$ is related (5) to the ratio of internal partition functions of molecules in the gas phase and on the surface; n and n_m are the quantities of adsorbate present on the surface at equilibrium and when the surface is covered by a monolayer.

It is shown (7) that by use of the substitutions

$$[2] \qquad \begin{aligned} &\eta = \epsilon-\epsilon_0 \geqslant 0, \\ &\alpha_0 = \alpha(0, \epsilon_0, T), \\ &\alpha(\eta, \epsilon_0, T) = \beta(\eta+\epsilon_0, T)\, e^{-\epsilon_0/kT}, \\ &y = \alpha_0/p+1, \\ &\lambda = (\alpha_0/\alpha)\, e^{\eta/kT}-1, \end{aligned}$$

the integral [1] can be converted into the simple form

$$[3] \qquad L(y, T) = \int_0^\infty \frac{dG(\lambda, T)}{\lambda+y}.$$

In equation [3], $L(y, T) \equiv \theta_1(\alpha_0/(y-1), T)$ and

$$[4] \qquad \begin{aligned} G(T) &= \int_0^\infty dG(\lambda, T) \equiv \int_0^\infty g(\lambda, T)\, d\lambda \\ &= \int_0^\infty (\alpha_0/\alpha)\, e^{\eta/kT} f(\eta+\epsilon_0)\, d\eta \\ &= \int_0^\infty (\lambda+1) dF(\epsilon). \end{aligned}$$

Note that the above substitutions were introduced in order to take into account

the possible dependence of β on ϵ, and the possibility that the lowest adsorption energy on the surface may have the value $\epsilon_0 > 0$.

B. According to theory (12), if L is a function of the form [3] and if $F(\epsilon)$ is a nonnegative, nondecreasing function such that $G(0) = 0$ then the function L must satisfy certain restrictive inequalities. Let us consider the class of all functions of the form [3] which are subject to $k+1$ restrictions

$$[5] \qquad L(y_i, T) = C_i, \qquad i = 0, 1, 2, \ldots k,$$

where $y_0 < y_1 < \ldots < y_k$ and where the C_i are given constants. Then there exist two uniquely determined functions L_a and L_b in this class such that for any other functions in this class the following inequalities hold:

$$[6] \qquad \begin{aligned} &L_a(y, T) \leqslant L(y, T) \leqslant L_b(y, T) \text{ for } y_k < y,\ y_{k-2} < y < y_{k-1},\ y_{k-4} < y < y_{k-3}, \text{ etc.;} \\ &L_a(y, T) \geqslant L(y, T) \geqslant L_b(y, T) \text{ for } y_{k-1} < y < y_k,\ y_{k-3} < y < y_{k-2}, \text{ etc.} \end{aligned}$$

Thus, in alternate intervals between the selected reference values y_i of equation [5], L_a and L_b represent extremal functions, each forming lower and upper bounds alternately in the consecutive intervals marked off by the y_i. L_a and L_b thus represent an interlacing structure on an L vs. y diagram.

Of the $k+1$ restrictions used in equation [5], k are obtained by arbitrary selection of k reference points $\theta(p_i, T)$ from the experimental isotherm data. An additional restriction arises from the normalization requirement

$$[7] \qquad 1 = \int_0^\infty dF(\epsilon) = \lim_{p\to\infty} \theta(p, T) \equiv \theta(\infty, T) = L(1, T).$$

C. Having examined the existence of extremal bounds, we now turn to a discussion of the conditions under which $L(y, T)$ assumes the limiting form L_a or L_b. It can be shown (see (12) and appendix) that the extremal functions L_a and L_b are obtained from equation [3] if $G(\lambda, T)$ is chosen to be a step function

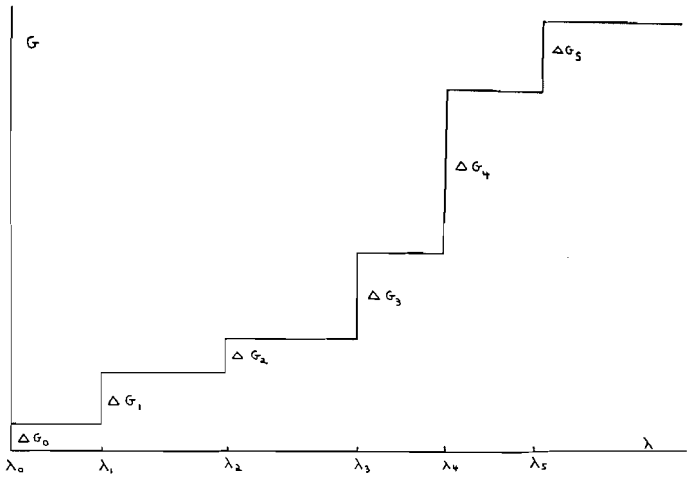

FIG. 1. The step function G.

with at most $k+1$ jumps at the points $\lambda_0, \lambda_1, \ldots, \lambda_k$. (See Fig. 1). In the open intervals $\lambda_i < \lambda < \lambda_{i+1}$ $(i = 0, 1, \ldots, k)$, $dG(\lambda, T) \equiv 0$; hence in these regions the integral vanishes identically. At each of the points of discontinuity, λ_i, however, the function G increases by an amount ΔG_i as shown in the figure, and the denominator in the integral [3] assumes the value λ_i+y. Thus, an increment $\Delta G_i/(\Delta_i+y)$ is associated with every stepwise increase in G; equation [3] is accordingly reduced to a summation of the form

$$[8] \qquad L_{a,b}(y, T) = \sum_{i=0}^{k} \frac{\Delta G_i}{\lambda_i+y}.$$

It is evident from equation [8] that the use of Stieltjes integrals lends itself particularly well to the type of interpolation theory described here. For a rigorous discussion of the theory and properties of such integrals the reader is referred to standard texts (17). In this connection it might be noted that the distribution density function $g(\lambda, T) = \partial G(\lambda, T)/\partial\lambda$, which corresponds to the step function G described above, is a linear combination of $k+1$ Dirac delta functions located at $\lambda = \lambda_i$.

D. To determine L_a or L_b uniquely it is now necessary to fix (*a*) the number of terms in the summation [8], (*b*) the size of the jumps ΔG_i, and (*c*) their location on the λ scale. (*a*) The theory of Reference 12 requires that we count each step in the function G that occurs in the open interval $0 < \lambda < \lambda_k$ with weight 2 and that we assign weight 1 to a jump by G at either end point 0 or λ_k. Let us define the *order* of a function of the form [8] as the total weight of all the steps. The theory of extremals (12) then demands that the order of L_a or L_b be at most $k+1$. This requirement determines the number of properly weighted terms to be included in the summation. (*b*, *c*) The values of λ_i and of ΔG_i may be determined from the conditions of constraint [5] imposed on the system. Detailed computational procedures for this step will be provided in the next two sections for the cases $k = 1$ (order two) and $k = 2$ (order three). The extension to larger k values is straightforward, but the mathematical complications become excessive in the higher order calculations.

It may be noted that L_a and L_b are continuous functions of the variable y. Since these extremals are also affected by the choice of reference values y_i, it is clear that any experimental errors in the reference points $\theta(p_i, T)$ will displace the calculated limiting curves from their correct positions. The magnitude of this effect can be computed by the standard calculational procedures.

E. To sum up: It is possible to specify two limiting isotherms L_a and L_b which delineate the greatest possible variations in θ as $F(\epsilon)$ assumes all functional relationships which leave the integral [1] convergent. The specification of L_a and L_b requires that $G(\lambda, T)$, related by equation [4] to the distribution $F(\epsilon)$ of energies over the surface sites, be a step function. This choice converts the Stieltjes integral [3] into a summation. The number of terms in that sum, the size of the jumps in G, and their location in the λ spectrum are all determined by the imposition of conditions of constraint. The latter are obtained from the normalization condition for $F(\epsilon)$ and by selection of a limited number of reference points from the experimental data, through which the limiting isotherms

are required to pass. If the remaining experimental points fall outside the prescribed bounds, the observed isotherm data are not compatible with assumptions (*a*)–(*f*).

SECOND ORDER THEORY

In the second order theory the two constraints on L are given by $L(1, T) = 1$ and $L(y_1, T) = C_1$. (See equations [7] and [5].) There are two extremal distribution functions G which can be specified to be of order two. One of these, G_a, is constant everywhere except for a jump ΔG_1 at some point λ_1 in the range $0 < \lambda < \lambda_m$. The second distribution, G_b, is likewise constant everywhere except for a jump ΔG_0 at $\lambda = 0$ and another jump ΔG_m at $\lambda = \lambda_m$. In these relations λ_m represents the maximum value of λ encountered for the adsorption system under study.

Using the first of these distributions functions in equation [8] one obtains

$$L_a(y, T) = \Delta G_1/(y+\lambda_1) \tag{9}$$

while use of the second distribution function in equation [8] yields

$$L_b(y, T) = \Delta G_0/y+\Delta G_m/(y+\lambda_m). \tag{10}$$

The constants ΔG_0, ΔG_1, ΔG_m, and λ_1 can be determined by application of the two conditions of constraint which the extremal functions must satisfy. Thus from [9] one finds

$$\begin{aligned} L_a(1, T) &= 1 = \Delta G_1/(1+\lambda_1), \\ L_a(y_1, T) &= C_1 = \Delta G_1/(y_1+\lambda_1). \end{aligned} \tag{11}$$

Similarly, from equation [10]

$$\begin{aligned} L_b(1, T) &= 1 = \Delta G_0+\Delta G_m/(1+\lambda_m), \\ L_b(y_1, T) &= C_1 = \Delta G_0/y_1+\Delta G_m/(y_1+\lambda_m). \end{aligned} \tag{12}$$

Solution of the two sets of simultaneous equations leads to

$$\begin{aligned} \lambda_1 &= (C_1y_1-1)/(1-C_1), \\ \Delta G_1 &= (C_1y_1-C_1)/(1-C_1), \end{aligned} \tag{13}$$

and

$$\begin{aligned} \Delta G_0 &= [1+\lambda_m-C_1(y_1+\lambda_m)]\, y_1/\lambda_m(y_1-1), \\ \Delta G_m &= (C_1y_1-1)(y_1+\lambda_m)(1+\lambda_m)/\lambda_m(y_1-1). \end{aligned} \tag{14}$$

Substitution of equations [13] into [9] results in the extremal isotherm

$$L_a(y, T) = [1+(y-1)(1-C_1)/C_1(y_1-1)]^{-1}. \tag{15}$$

Similarly, use of equations [14] in [10] yields the second extremal isotherm

$$\begin{aligned} L_b(y, T) = \lambda_m^{-1}(y_1-1)^{-1}\{&(y_1/y)[1-C_1y_1+\lambda_m(1-C_1)] \\ &+[(y_1+\lambda_m)/(y+\lambda_m)]\,[C_1y_1-1+\lambda_m(C_1y_1-1)]\} \end{aligned} \tag{16}$$

As a final step, it is only necessary to introduce the relations for y, L, and C_1 from equations [2], [3], and [5]. This gives us the explicit relations

$$\theta_a = p\theta_1/[p_1(1-\theta_1)+p\theta_1], \tag{17}$$

$$\theta_b = \frac{p_1/\alpha_0}{\lambda_m}\left\{\left(\frac{\alpha_0/p_1+1}{\alpha_0/p+1}\right)[(1+\lambda_m)(1-\theta_1)-\theta_1(\alpha_0/p_1)] + \left(\frac{\alpha_0/p_1+1+\lambda_m}{\alpha_0/p+1+\lambda_m}\right)(\lambda_m+1)[\theta_1(\alpha_0/p_1+1)-1]\right\}. \tag{18}$$

In the above relations $\theta_1 \equiv \theta(p_1, T)$ where θ_1, p_1 is the reference point, arbitrarily selected from the isotherm data, through which the limiting curves θ_a and θ_b are required to pass; $\lambda_m = [\alpha_0/\alpha(\eta_m, \epsilon_L, T)] \exp(\epsilon_m-\epsilon_0)/kT-1$.

The labor of evaluating θ_b can be considerably reduced by selecting a reference pressure p_1 such that $\alpha_0/p_1+1 << \lambda_m$. Then in the pressure range for which $\alpha_0/p+1 << \lambda_m$, equation [18] reduces to

$$\theta_b(p, T) = [p-p_1+(\alpha_0+p_1)\theta_1]/(\alpha_0+p). \tag{19}$$

It is readily verified that the exact functions [17] and [18] interlace at the common points $(0, 0)$, (θ_1, p_1), and $(1, \infty)$, as required. Equation [19] fails to meet the first requirement, which merely means that this limiting function, together with [17] bounds a wider region than equations [17] and [18] and thus furnishes less precise information.

It is instructive to determine which of the two limiting isotherms represents the lower and the upper bounds in the two regions $p < p_1$ and $p > p_1$. A mathematical analysis of this problem will be deferred to a later paper. One can, however, arrive at a decision by use of a qualitative argument. It is seen that θ_a represents the Langmuir adsorption isotherm; this is consistent with the assumption that the associated function $g(\lambda, T)$ vanishes everywhere except for a Dirac delta peak at $\lambda = \lambda_1$. The energy density distribution function $f(\epsilon)$ has a corresponding peak at $\epsilon = \epsilon_1$. In most experimental work, however, one encounters a much wider distribution in ϵ. In particular, at very low pressures the sites associated with adsorption energies near ϵ_m will be filled much more extensively than those associated with energies $\epsilon_1 < \epsilon_m$. It is thus to be expected that at these low pressures the experimental isotherm will be greater than the calculated Langmuir isotherm associated with the energy ϵ_1. By selecting a p_1 from the higher pressure range and by noting the interlacing properties discussed earlier it follows that

$$\theta_a < \theta < \theta_b \quad \text{for} \quad 0 < p < p_1,$$
$$\theta_a > \theta > \theta_b \quad \text{for} \quad p_1 < p < \infty. \tag{20}$$

THIRD ORDER THEORY

In this section we deal briefly with the problem of finding upper and lower bounds on $L(y, T)$ when three conditions of constraint are placed on $L(y, T)$. These are: $L(1, T) = 1$, $L(y_1, T) = C_1$, and $L(y_2, T) = C_2$. There exist two extremal distribution functions $G(\lambda, T)$ which can be specified to be of order

three. The first, G_a, is everywhere constant except for two jumps ΔG_m and ΔG_1 located at $\lambda = \lambda_m$ and at a point $0 < \lambda_1 < \lambda_m$. The second, G_b, is everywhere constant except for two jumps ΔG_0 and ΔG_2 located respectively at $\lambda = 0$ and at a point $0 < \lambda_2 < \lambda_m$. Use of the two distribution functions in equation [8] yields

[21] $$L_a = \Delta G_1/(y+\lambda_1)+\Delta G_m/(y+\lambda_m),$$

[22] $$L_b = \Delta G_0/y+\Delta G_2/(y+\lambda_2).$$

Application of the conditions of constraint to equation [21] results in the set of equations

$$\Delta G_1 = (y_1+\lambda_1)(y_2+\lambda_1)[C_1(y_1+\lambda_m)-C_2(y_2+\lambda_m)]/(\lambda_m-\lambda_1)(y_2-y_1),$$

$$\Delta G_m = (y_1+\lambda_m)(y_2+\lambda_m)[C_2(y_2+\lambda_1)-C_1(y_1+\lambda_1)]/(\lambda_m-\lambda_1)(y_2-y_1),$$

[23] $$\lambda_1 = \frac{C_2y_2(y_1-1)(y_2+\lambda_m)-C_1y_1(y_2-1)(y_1+\lambda_m)+(y_2-y_1)(1+\lambda_m)}{C_1(y_2-1)(y_1+\lambda_m)-C_2(y_1-1)(y_2+\lambda_m)+(y_1-y_2)(1+\lambda_m)}.$$

Similarly, the use of the conditions of constraint in [22] yields the unknowns:

$$\Delta G_0 = y_1y_2[C_1(y_1+\lambda_2)-C_2(y_2+\lambda_2)]/\lambda_2(y_2-y_1),$$

[24] $$\Delta G_2 = (y_1+\lambda_2)(y_2+\lambda_2)(C_2y_2-C_1y_1)/\lambda_2(y_2-y_1),$$

$$\lambda_2 = \frac{(y_1-1)(C_2y_2^2-1)-(y_2-1)(C_1y_1^2-1)}{(y_2-1)(C_1y_1-1)-(y_1-1)(C_2y_2-1)}.$$

The extremal isotherms θ_a and θ_b can now be found by setting $L = \theta$, $C_1 = \theta_1$, $C_2 = \theta_2$, $y = \alpha_0/p+1$ in equations [23] and [24] and substituting these quantities into [21] and [22]. It is evident that the limiting isotherms are very unwieldy.

Fortunately one obtains a much simpler formulation whenever it is possible to select two reference pressures p_1 and p_2 which satisfy the inequality

[25] $$1 << \alpha_0/p_i << \lambda_m.$$

If one now restricts the range of pressures to values $\alpha_0/p \ll \lambda_m$ then θ_a reduces to

[26] $$\theta_a = \frac{(\theta_2-\theta_1)\,p+[\theta_1p_2(1-\theta_2)-\theta_2p_1(1-\theta_1)]}{(\theta_2-\theta_1)\,p+[p_2(1-\theta_2)-p_1(1-\theta_1)]}.$$

Likewise, using assumption [25], but imposing no restriction on p, it can be shown that θ_b reduces to

[27] $$\theta_b = \frac{\theta_1\theta_2(p_1-p_2)}{[(\alpha_0+p)/\alpha_0p]\,p_1p_2(\theta_1-\theta_2)+(\theta_2p_1-\theta_1p_2)}.$$

At sufficiently low pressures this limiting expression reads

[28] $$\theta_b = \frac{\theta_1\theta_2(p_1-p_2)}{p_1p_2(\theta_1-\theta_2)/p+(\theta_2p_1-\theta_1p_2)}.$$

It can be shown that the exact relations [21] and [22] interlace at $(0, 0)$, (θ_1, p_1), (θ_2, p_2), $(1, \infty)$ as required. The approximate functions [26] and [27] or

[28] do not meet at (0, 0) or (1, ∞) and thus bound a wider region on the θ vs. p diagram than the exact functions. In fact, it follows from [26] and [28] that

$$[29] \qquad \lim_{p\to 0} \theta_b = 0, \qquad \lim_{p\to 0} \theta_a = \frac{\theta_1 p_2(1-\theta_2) - \theta_2 p_1(1-\theta_1)}{p_2(1-\theta_2) - p_1(1-\theta_1)}.$$

Equation [29] shows that $\lim_{p\to 0} \theta_a$ may be either positive or negative depending on the magnitudes of the terms involved in the fraction. One cannot decide as to which isotherm represents the upper and the lower bound in the various intervals until after numerical values have been substituted for the parameters.

In comparing the results of the second and third order theories, it is seen that use of the equations [26] and [28] does not require specification of numerical values for α_0 or λ_m. Moreover, equation [28] is independent of the choice of n_m, as may be verified by substitution of $\theta = n/n_m$ on both sides. For these reasons equations [26] and [28] are quite useful in the actual computation of limiting isotherms. On the other hand, these relations are only approximate and should be applied only to cases where it is known that the restrictive assumption [25] is applicable and where for all experimental pressures, $p \ll \alpha_0$.

APPENDIX

In this appendix we shall try to expound the relevant ideas of the article of reference 12, which is written primarily for mathematicians, in a less technical and more intuitive language. For this purpose let us consider an analogous problem with finite sums instead of integrals. Suppose we consider all sets of numbers $g_1 \ldots g_n$ which satisfy the inequalities

$$[30] \qquad g_j \geqslant 0, \qquad 1 \leqslant j \leqslant n,$$

and the set of equations

$$[31] \qquad \sum_{j=1}^{m} a_{ij} g_j = C_i, \quad i = 1, \ldots, k$$

where the a_{ij} and the C_i are given constants. Here the sequence $g_1 \ldots g_n$ corresponds to the nonnegative function $g(\lambda, T)$ of equation [4], while the constraints [31] correspond to the conditions $L(y_i, T) = C_i$ of equation [5]. In fact, $L(y_i, T)$ of equation [3] is the result of a linear operation (integrating $(y_i+\lambda)^{-1} g(\lambda, T)$) applied to g; the form of a linear operation applied to a finite sequence g_i is given by the left-hand side of [31]. The function $G(\lambda, T)$ corresponds to the sequence of the sums g_1; g_1+g_2; . . . ; $g_1+\ldots+g_n$. Let us now interpret conditions [30] and [31] geometrically.

If we think of $(g_1 \ldots g_n)$ as a point in n-dimensional space, then the linear equations [31] represent hyperplanes while the linear inequalities [30] represent half-spaces. Thus [30] and [31] together represent the intersection of a finite number of hyperplanes and half-spaces, i.e., a convex polyhedron. As an example, we may consider the three-dimensional space defined by three mutually perpendicular axes g_1, g_2, g_3. The inequalities $g_1 \geqslant 0$, $g_2 \geqslant 0$, $g_3 \geqslant 0$ represent

three mutually intersecting half-spaces which define a semi-infinite volume in space: this is our polyhedron P. The polyhedral volume may be made finite by the specification of another half-space, such as $g_1+g_2+g_3 \leqslant 1$; the resulting polyhedron now has vertices at (0, 0, 0), (1, 0, 0), (0, 1, 0), and (0, 0, 1), each vertex being formed by the intersection of three triangularly shaped bounding planes. Note that the bounding faces are described by replacing the inequality signs with equalities. If we now intersect the polyhedron with the plane $z = \frac{1}{2}$ the polyhedron will be projected onto this plane and form a triangle with vertices at $(0, 0, \frac{1}{2})$, $(\frac{1}{2}, 0, \frac{1}{2})$, $(0, \frac{1}{2}, \frac{1}{2})$. This example illustrates the general principle that the intersection of an n-dimensional polyhedron with a hyperplane results in a polyhedron of $n-1$ dimensions.

Suppose now we wish to find the maximum of a linear function

$$F(g) = \sum_{j=1}^{n} a_j g_j \text{ on } P.$$

If M is the maximum, then $F(g) \leqslant M$ for all points in P, while $F(g) = M$ for at least one point. In other words, the whole polyhedron lies on one side of the hyperplane, $F(g) = M$, and has at least one point in common with this hyperplane. Such a hyperplane is called a *supporting hyperplane.* It is intuitively obvious in ordinary three-dimensional space, and is easy to prove in any n-dimensional space, that a supporting hyperplane must contain at least one vertex of the polyhedron.

In three-dimensional space at least three of the bounding faces (planes) meet at a vertex. Similarly, in n-dimensional space at least n of the bounding faces meet at a vertex; algebraically, in the defining equations and inequalities of the polyhedron, at least n of the equality signs must hold. If we apply this to the polyhedron P defined by the half-spaces and hyperplanes [30] and [31], we see that since we already have k equality signs in [31], then at least $n-k$ of the equality signs in [30] must hold at a vertex, i.e., at most k of the g_i's can be different from 0 at a vertex. Therefore, the maximum of a linear function on P is attained at some point with at most k nonvanishing co-ordinates, where k is the number of linear constraints in the definition of P. Note that in the sequence corresponding to $G(\lambda, T)$, a nonvanishing g_j corresponds to a jump from $g_1+ \ldots +g_{j-1}$ to $g_1+\ldots+g_j$, so that this sequence has at most k jumps at a vertex. The same reasoning applies to the problem of minimizing $F(g)$ on P.

The maximizing vertex will be unique if no edge of the polyhedron is parallel to the supporting hyperplane. This geometrical condition can be expressed algebraically in terms of the nonvanishing of certain determinants formed from the numbers a_{ij} and g_j.

The above reasoning can be extended to certain infinite dimensional spaces. Physicists are already familiar with one infinite dimensional space, Hilbert space, as representing the state of a mechanical system in quantum mechanics. In the present problem under consideration, the space involved has as its "points" the functions $G(\lambda, T)$ of bounded variation (17) on the interval $[0, \lambda_m]$. The "polyhedron" P is now defined by the conditions

[32] $G(\lambda, T)$ is nondecreasing in $[0, \lambda_m]$

and

[33] $$L(y_i,T) = \int_0^{\lambda_m} K(y_i, \lambda)\, dG(\lambda, T) = C_i, \quad i = 0, 1, \ldots, k.$$

Here [32] corresponds to [30] and [33] to [31], with the kernel $K(y_i, \lambda)$ playing the role of the matrix (a_{ij}). We have replaced k by $k+1$ constraints in order to make the conditions agree with [5]. In our physical problem $K(y, \lambda) = 1/(y+\lambda)$. The set of functions $G(\lambda, T)$ satisfying [32] and [33] form a convex polyhedron P in the infinite dimensional space. The "vertices" of P are represented by G's which have at most $k+1$ jumps. The generalization of the "edge" criterion for uniqueness is as follows:

If $K(y, \lambda)$ is Cartesian, i.e., if the number of zeros of any linear combination $\sum_{i=1}^{r} a_i K(y_i, \lambda)$ in the interval $[0, \lambda_m]$, where $y_1 < y_2 \ldots < y_r$ is at most equal to the number of sign changes in the coefficients, then the G which makes a given integral of the form $\int_0^{\lambda_m} K(y, \lambda)\, dG(\lambda, T)$ a maximum or a minimum under the conditions [32] and [33] is a *uniquely determined* step function. Furthermore, if the kernel is Cartesian, then we can narrow down the positions of the jumps of the extremal G. This is expressed in the condition that its *order* must be at most $k+1$. The details of the proofs are beyond the scope of this brief summary. The kernel $K(y, \lambda) = 1/(y+\lambda)$ can easily be proved to be Cartesian by the use of problem 87 (8), and the standard formula for a Vandermonde determinant. (See also problem 48 (8).)

It is quite likely that this method can be applied to other problems of inference from empirical data.

ACKNOWLEDGMENT

The authors are pleased to acknowledge the assistance of Mr. Chi Chang in verifying some of the derivations.

REFERENCES

1. Cremer, E. and Schwab, G. M. Z. physik. Chem. A, 144: 243. 1929; B, 5: 406. 1929. Cremer, E. and Flügge, S. Z. physik. Chem. B, 41: 453. 1938.
2. Halsey, G. D., Jr. J. Chem. Phys. 16: 931. 1948.
3. Halsey, G. D., Jr. J. Am. Chem. Soc. 73: 2693. 1951.
4. Halsey, G. D., Jr. and Taylor, H. S. J. Chem. Phys. 15: 624. 1947.
5. Hill, T. L. J. Chem. Phys. 17: 762. 1949.
6. Honig, J. M. J. Phys. Chem. 57: 349. 1953.
7. Honig, J. M. and Hill, E. L. J. Chem. Phys. 22: 851. 1954.
8. Pólya, G. and Szegö, G. Aufgaben and Lehrsätze aus der Analysis. J. Springer, Berlin. 1925.
9. Roginsky, S. Doklady Akad. Nauk S.S.S.R. 45: 61, 194. 1944.
10. Roginskii, C. Z. Doklady Akad. Nauk S.S.S.R. 47: 412, 478, 558. 1945.
11. Roginskii, C. Z. and Todes, O. Acta Physicochim. U.R.S.S. 21: 519. 1946.
12. Rosenbloom, P. C. Bull. Soc. Math. France. In press.
13. Sips, R. J. Chem. Phys. 16: 490. 1948; 18: 1024. 1950.
14. Temkin, M. and Levich, V. Zhur. Fiz. Khim. 20: 1441. 1946.
15. Todes, O. M. and Bondareva, A. K. Zhur. Priklad. Khim. 21: 693. 1948.
16. Tompkins, F. C. Trans. Faraday Soc. 46: 569. 1950.
17. Widder, D. V. The Laplace transform. Princeton Univ. Press, Princeton, N.J. 1946.
18. Zeldowitsh, J. Acta Physicochim. U.R.S.S. 1: 961. 1934.

THERMODYNAMIC CONSIDERATIONS OF SURFACE REGIONS
ADSORBATE PRESSURES, ADSORBATE MOBILITY, AND SURFACE TENSION[1]

By E. A. Flood and Max Huber[2]

ABSTRACT

The flow of water through the micropore system of activated carbon has been described in previous papers as a hydrodynamic flow of liquid water under high pressure gradients due to surface forces. It is shown below that these high pressures are probably real and that the temperature coefficient of the flow rate is closely related to the temperature coefficient of the viscosity of liquid water. Surface tension is discussed.

If two volumes consisting of a single fluid substance have the same total Gibbs free energy[3] per unit mass and the same temperature, but have different positions in a scalar potential field, they will, in general, have different intrinsic thermodynamic potentials, different pressures and densities. They will, of course, be in a state of neutral equilibrium with respect to transformations into one another, the pressures and positions in the field remaining constant during the transformations.

The condition that these two systems remain in reversible equilibrium with one another as the pressures are varied is that $v_1 dp_1 = v_2 dp_2$, the positional coordinates x_1 and x_2 and the other variables remaining constant. This condition is necessary and sufficient regardless of whether the potential field is a function of pressure p_1 or not.

If a path of variation of the equilibrium pressure $p_1(n)$ is known as a function of the mass of material constituting the second system, as this mass varies from zero to n and the systems are in reversible equilibrium throughout this path, then the change in Gibbs free energy ΔF_1 at x_1 can be determined and must be equal to ΔF_2 at x_2 along this path of variation of the equilibrium pressure. Thus we can write for the process of filling the two volumes

$$\Delta F = \int_{x_1, p=0, n=0}^{x_1, p=p_1, n=n} v_1(n) dp_1(n) = \int_{x_2, p=0, n=0}^{x_2, p=p_2, n=n} v_2(n) dp_2(n)$$

and hence also

$$p_2 = \int_0^{p_1} \frac{\rho_2}{\rho_1} dp_1 \equiv \left| \frac{\rho_2}{\rho_1} \right| \cdot p_1.$$

The positional 'potential difference' between the two volumes $\Omega(x_2 - x_1)$ may be obtained from the following:

$$\Delta F = \int_{0, n=0, x_1}^{p_1, n, x_1} v_1(n) dp_1 + \int_{n, p_1, x_1}^{n, p_2, x_1} \left(\frac{\partial F}{\partial p} \right)_{x,n} dp + \int_{n, p_2, x_1}^{n, p_2, x_2} \left(\frac{\partial F}{\partial x} \right)_{p,n} dx$$

[1]*Manuscript received September 16, 1954.*
Contribution from the Division of Pure Chemistry, National Research Council, Ottawa, Canada. Issued as N.R.C. No. 3485. This paper was presented at the Symposium on Problems Relating to the Adsorption of Gases by Solids, held at Kingston, Ontario, September 10–11, 1954.

[2]*National Research Council of Canada Postdoctorate Fellow.*

[3]*The total Gibbs free energy, F, may be defined by* $F = F_0 + \omega = n\mu_0 + n\Omega$ *where* F_0 *is the Gibbs intrinsic free energy,* ω *the potential of position, n the mass,* μ_0 *the intrinsic thermodynamic potential, and* Ω *the potential of position of unit mass.*

and

$$\int_{n,p_1,x_1}^{n,p_2,x_1} v_1 dp_1 + \int_{n,p_2,x_1}^{n,p_2,x_2} f(x)dx = 0$$

where v_1 is written for $(\partial F/\partial p)_{x,n}$ and $f(x)$ for $(\partial F/\partial x)_{p,n}$. Accordingly,

$$\Omega(x_2-x_1, p_2) = -\frac{1}{n}\int_{n,p_1,x_1}^{n,p_2,x_1} v_1 dp_1 = \int_{n,p_2,x_1}^{n,p_2,x_2} f(x)dx$$

and

$$\Omega(x_2-x_1, p_1) = -\frac{1}{n}\int_{n,p_1,x_2}^{n,p_2,x_2} v_2 dp_2 = \int_{n,p_1,x_1}^{n,p_1,x_2} f(x)dx.$$

If the last two expressions for Ω are the same, Ω is independent of p, and v is independent of x or of the field.

In the case of equilibrium between a uniform reference volume and an assembly of elementary volumes of the same substance where the elementary volumes of the assembly have varying values of the x co-ordinate, i.e., varying values of the force function of the field, the conditions for reversibility are essentially similar and if $p_1(n)$ is known as a function of the mass of material in the whole assembly, then we may write

$$[1] \qquad \bar{p}_a = \int_0^{p_1} \frac{\bar{\rho}_a}{\rho_1} dp_1 \equiv \left|\frac{\bar{\rho}_a}{\rho_1}\right| . p_1$$

where $\bar{p}_a$ and $\bar{\rho}_a$ represent respectively the volumetric mean pressure and density of the assembly of volumes, $\Sigma v_{a_i} = v_a$.

In adsorption reactions $p_1(n)$ is given by the isotherm, where n is the mass adsorbed and p_1 the equilibrium pressure. If v_a, the adsorbate volume, is known, $\bar{\rho}_a$ and $|\bar{\rho}_a/\rho_1| . p_1$ and hence $\bar{p}_a$ can be calculated.

If the adsorbate can be regarded as an assembly of volumes of a single component and if $p_1(n)$ represents a path of thermodynamic reversibility, $\bar{p}_a$ as calculated from [1] will give the mean volumetric hydrostatic pressure of the adsorbate.

Under the usual methods of measuring adsorption isotherms, $p_1(n)$ cannot represent a path of thermodynamic reversibility if it is anywhere a decreasing function of n.

It is to be emphasized that Equation [1] is independent of the mechanism of adsorption and is equally applicable to adsorbate systems with or without menisci of various kinds, provided only that $p_1(n)$ represents a reversible path and that the adsorbate behaves as a single component substance in a scalar potential field.

From the above relations it is easily shown (4) that the change in volumetric average state of stress of the adsorbent as a result of adsorption of n moles of gas may be expressed as follows:

$$\delta\bar{p}_c{}^v = \left(1+\frac{v_a}{v_c}-\frac{v_a}{v_c}\cdot\alpha\right)\delta p_1$$

where $\bar{p}_c{}^v$ is the volumetric mean state of stress of the adsorbent; v_a and v_c are

the void volume and solid volume of the adsorbent respectively; and α is defined by $\bar{p}_a{}^v = \int (\bar{p}_a/\rho_1)\, dp_1 = \alpha \,.\, p_1$.

From Hooke's Law for isotropic bodies

$$\frac{\delta l}{l} = -\frac{1}{3}\beta\delta\bar{p}^l$$

where $\delta l/l$ is the length change per unit length, β is the bulk compressibility, and $\delta\bar{p}^l$ is the change in linear average state of stress along the length l. If the change in solid stress were due wholly to a change in hydrostatic pressure, $\delta\bar{p}^l$ would be equal to $\delta\bar{p}^v$. This would be the case if no surface field existed and the interaction of gas and solid were confined to an increase in hydrostatic pressure δp_1. Thus the change in state of stress of the solid may be thought of as consisting of two parts, one a change in hydrostatic stress, δp_1, and a second, $\delta(\bar{p}_c{}^v)'$, due to interaction. Accordingly, we may write

$$\delta\bar{p}_c{}^v = \delta p_1 + \delta(\bar{p}_c{}^v)' \quad \text{and} \quad \delta\bar{p}^l = \delta p_1 + \delta(\bar{p}^l)'$$

where, in general, $\delta(\bar{p}_c{}^v)'$ and $\delta(\bar{p}^l)'$ are not equal. Let

$$\delta(\bar{p}^l)' = K\,\delta(\bar{p}_c{}^v)',$$

then

$$\delta\bar{p}^l = \left(1 + K\frac{v_a}{v_c} - K\frac{v_a}{v_c}\cdot\alpha\right)\delta p_1;$$

and putting $v_a/v_c = \phi$, the adsorption extension is given by

$$\frac{\partial l}{l} = -\frac{1}{3}\beta(1 + K\phi - K\phi\alpha)\,\delta p_1. \qquad [2]$$

It is found that $\delta l/l$ as calculated by Equation [2] describes the data very well in the cases examined, as shown in Figs. 1 to 5.

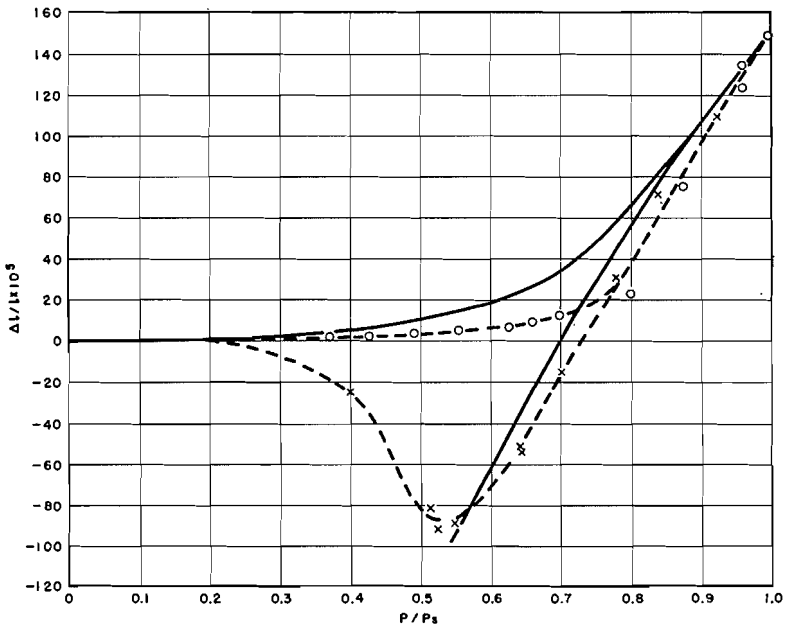

FIG. 1. Adsorption extension: Water vapor on carbon, data of Haines and McIntosh (7). Broken line drawn through experimental points. O, adsorption; ×, desorption. Solid line calculated from $\delta l/l = \frac{1}{3}\beta\phi K\alpha p_1 = 3.43 \cdot 10^{-7} \cdot \alpha p_1$. ($\beta K = 4.76 \cdot 10^{-7}$ p.s.i.; $\phi = 2.16$.)

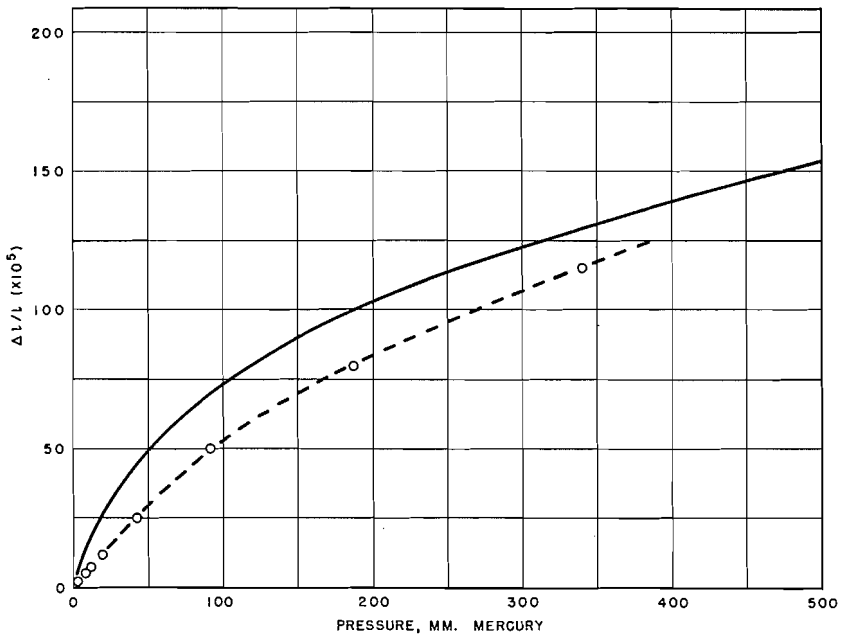

FIG. 2. Adsorption extension: Dimethyl ether on carbon, data of Haines and McIntosh (7). Broken line drawn through experimental points. Solid line calculated from $\delta l/l = 3.43 \cdot 10^{-7} \cdot \alpha p_1$.

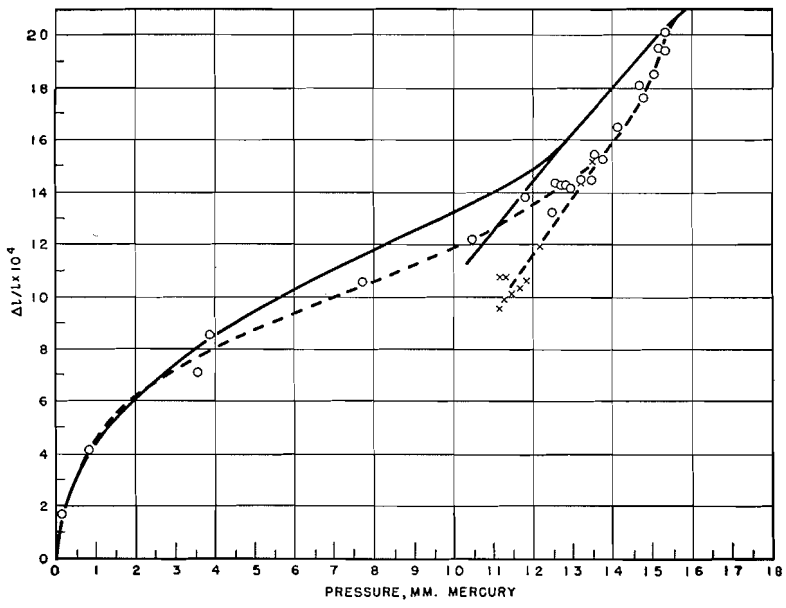

FIG. 3. Adsorption extension: Water vapor on porous glass, data of Amberg and McIntosh (1). Broken line drawn through experimental points. ○, adsorption; ×, desorption. Solid line calculated from $\delta l/l = \frac{1}{3}\beta\phi\, X\alpha p_1 = 3.69 \cdot 10^{-7} \cdot \alpha p_1$. ($\beta K = 5.76 \cdot 10^{-7}$ p.s.i.; $\phi = 1.92$.)

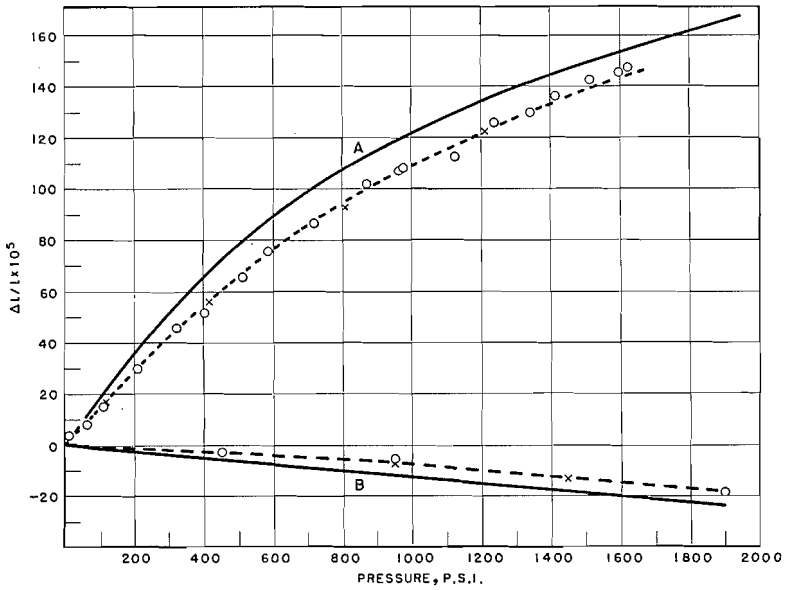

FIG. 4. Adsorption extension: Carbon rod No. 1 (25°C.) (cf. (4)). *A*, nitrogen; *B*, liquid water. Broken line drawn through experimental points. ○, adsorption; ×, desorption. Solid line calculated from $\delta l/l = \frac{1}{3}\beta(1+\phi K-\phi K\alpha)p_1$. ($\beta = 3.3\cdot 10^{-7}$ p.s.i.; $K = 2.91$; $\phi = 1.65$.)

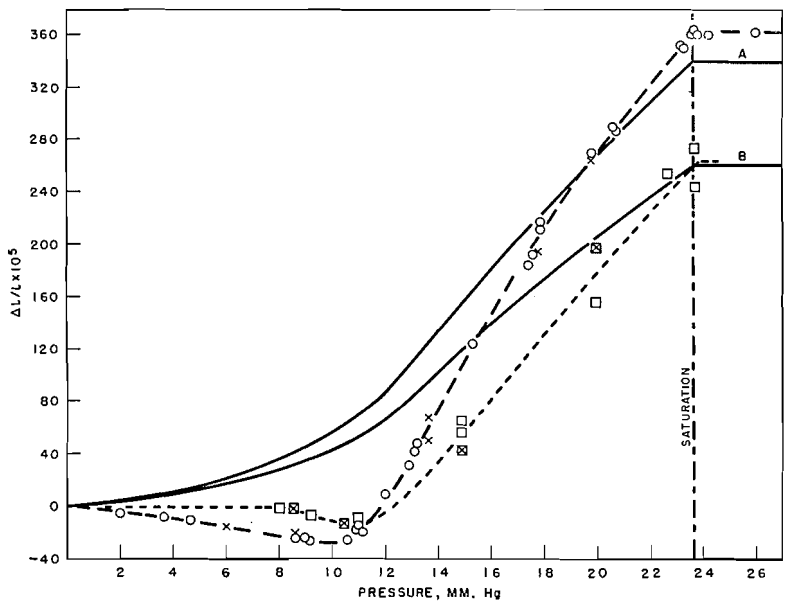

FIG. 5. Adsorption extension: Water vapor on Carbon rod No. 1 (25°C.) (cf. (4)). *A*, axial extensions; *B*, radial. Broken line drawn through experimental points. Solid line calculated. Axial, *A*, as for Fig. 8. Radial, *B*, as for Fig. 8, but $K = 2.23$.

The above relations may also be applied to permeability problems. It can be shown that if surface forces within a small capillary condense a dilute vapor to densities exceeding the saturation value and so cause a dense liquid film to form on the surface, and if the liquid film is greater than a few molecules deep, the flow rate can be written

$$Q_m = \frac{-A}{\eta_l}\rho_a \cdot \frac{dp_a}{dx} = \frac{-A}{\eta_l}\frac{\rho_a^2}{\rho_1}\frac{dp_1}{dx} = \frac{A}{\eta_l}\left|\frac{\rho_a^2}{\rho_1}\right|\frac{\Delta p_1}{L},$$

where p_1, p_a = pressures of gas and adsorbate, respectively; ρ_1, ρ_a = densities of gas and adsorbate, respectively; Q_m = flow in gm./min.; η_l = liquid viscosity.

It has been shown that this formula represents the flow rate of water through the micropore system of some carbons fairly well (5).

This formula indicates that at equal values of the pressure and concentration gradients, the relative flow rates at two temperatures (25° and 35°C.) can be expressed by

$$\frac{Q_{m25}}{Q_{m35}} = \frac{\eta^{35}}{\eta^{25}}\frac{T^{25}}{T^{35}} \text{ or } \frac{K_{25}}{K_{35}} = \frac{p_s^{35}}{p_s^{25}}\left(\frac{T^{25}}{T^{35}}\right)^2\frac{\eta^{35}}{\eta^{25}}$$

where $K = \frac{\text{cc.}}{\text{min.}}\frac{p_1}{\Delta p}$ and p_s^{35} = saturation pressure at 35°C.

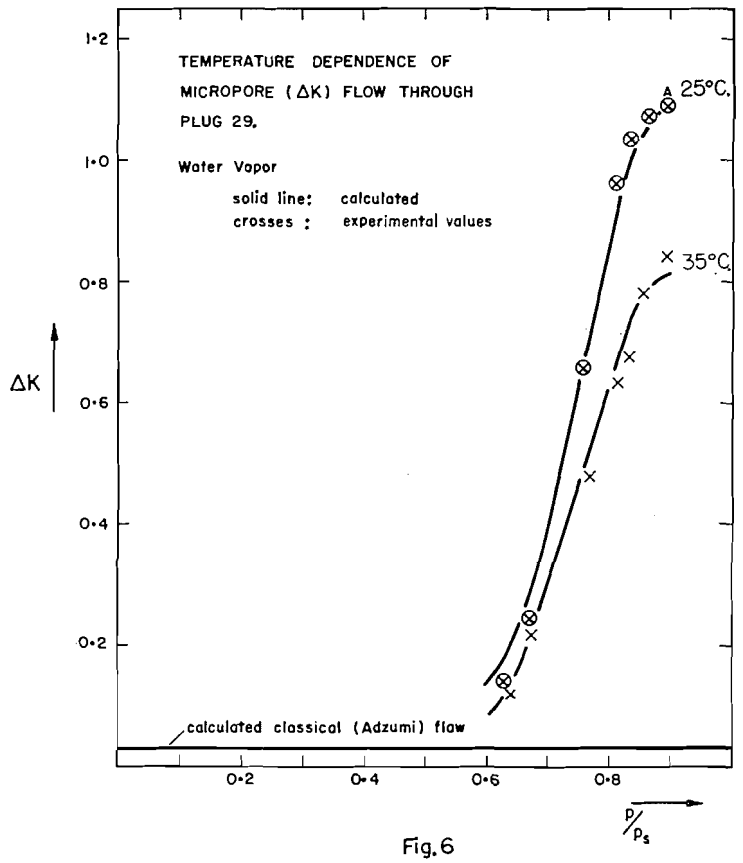

Fig. 6

Fig. 6 shows calculated and observed water flow rates for an active carbon where the macropores have been filled with a lead alloy, thus largely removing macropore flow. The constant A is calculated from the flow at 25°C. at the point $p/p_s = 0.89$. The curves at 25°C. and 35°C. are calculated using this value of A. Incidentally, A is almost identical with the calculated value based on pore size distributions reported by Emmet for similar carbons, and is nearly the same as the constant for unfilled carbon rods, when allowance is made for increased path lengths.

Between the region of classical hydrodynamic and/or effusive flow through large pores ($>10^{-5}$ cm.) and the region of slow diffusive flow through pores of molecular dimensions ($<10^{-7}$ cm.) where diffusion coefficients involve large activation energies and are often highly specific (cf. Barrer (2)), we should expect a pore size region (10^{-7} to 10^{-5} cm.) where the flow mechanisms are essentially classical but where fluid densities and pressure gradients within the pores are considerably increased by the surface forces. Our results strongly suggest that this is indeed the case.

Surface Tension of Fluid Interfaces

There appear to be some differences of opinion as to whether the Helmholtz free energy per unit surface and 'surface tension' are the same thing or not (cf. Shuttleworth (10)). Some authors treat the surface film as a separate thermodynamic system distinct from the material lying on either side of it, while other authors consider that the 'surface free energy' is the change in Helmholtz free energy of the whole system when it is changed in such a way that the surface increases while the volume of the whole system remains constant.

In a fluid interface, the pressure in every elementary volume must be the same in all directions. Following Tolman (11) we may think of the interface as made up of laminae parallel with the surface and we must suppose a pressure gradient along the normal to this surface. If the gradient extends a distance h along x, the normal to the interface, and if $\bar{p}(x)$ is the mean value of the stress intensities of the various laminae parallel with the surface, the stress intensities being averaged over the interval h, then $\bar{p}(x) \cdot h$ is the surface force exerted by unit length of the surface region. If $\bar{p}(x)$ is negative, $-\bar{p}(x) \cdot h$ is literally a positive 'surface tension'. In this case, if h is constant and $\bar{p}(x)$ is a function of T only, then $(\partial A/\partial\sigma)_T = -\bar{p}(x) \cdot h = \gamma$, and γ is unambiguously the Helmholtz free energy, A, per unit of surface area σ.

If we consider a spherical or cubical shell of thickness h where the mean parallel stress intensity in the surface shell is $\bar{p}(x)$, and p_0 is the uniform pressure outside of the body while p is that inside, then balancing forces, the pressure difference across the surface is given by

$$p - p_0 = (2[p_0 - \bar{p}(x)]h)/r \quad \text{or} \quad \Delta p \approx 2\gamma/r,$$

where r is either the radius of the sphere or one half the side length of the cube.

The reversible work of forming a drop of liquid within a large constant volume of gas is $\frac{1}{3}\gamma\sigma$ as shown by Gibbs (6). An assembly of drops (or cubes)

of various sizes contained within a constant volume does work w (not reversible in this case) when small drops are converted to larger drops, the work being very nearly equal to $\frac{1}{3}\gamma\sigma$. If we had defined the surface tension as $(\partial w/\partial\sigma)_{T_v}$ for this process, this 'surface tension' would be only one third of the actual surface tension. In this case, as in the case considered by Gibbs, the work consists of two parts, the work done by the surface, $\gamma\Delta\sigma$, less the work done on the interior mass, $v\Delta p$. In some cases we cannot measure surface tension directly and cannot distinguish between the work done by the surface and the work done simultaneously on or by the interior mass. 'Surface free energies' in such cases are 'surface differential free energies' of whole systems wherein surface tension proper may play only a very small part. It is only when the system consists wholly of a single kind of surface layer that $(\partial A/\partial\sigma)_T$ is reasonably unambiguous and that γ, the tension of the surface, measures the Helmholtz free energy of that surface. Evidently, in the case of liquids the 'surface tension' rather than the 'surface free energy' is the more directly observable quantity; and if there be any meaning to such distinctions, then as pointed out by Brown (3), the surface free energy is to be regarded as the 'useful fiction' and the surface tension the 'reality' rather than the other way about.

When a liquid is separated from its vapor by a flat fluid surface of tension the following conditions prevail. The Gibbs free energy of every lamina is the same and independent of their positions along x, the normal through the surface. The hydrostatic pressures are the same in the bulk liquid and in the gas, and densities of bulk liquid and vapor are constant. But within the interface density and pressure gradients exist. Thus, specific volumes, $v(x)$, and pressures, $p(x)$, of laminae are variable functions of x within the interfacial region. If we take x_0 as the end of the liquid region whose pressure is p_0, and $x = x_0$ to $x = h$ as the interfacial region, and if $\Omega(x)$ is the potential of field and $f(x)$ the force function of the field, we have the following necessary relations:

$$\Omega(x) = \int_{x_0}^{x} \frac{d\Omega(x)}{dx}\,dx = \int_{x_0}^{x} f(x)\,dx = \int_{x_0 p_0}^{x p_0} \left(\frac{\partial F}{\partial x}\right)_p dx$$

and

$$p(x) = p_0 + \int_{x_0}^{x} \frac{dp(x)}{dx}\,dx \quad x_0 \leqslant x \leqslant h.$$

The functions $v(x)$, $p(x)$, $\Omega(x)$, $f(x)$ etc. must conform to the following equations:

$$dF = \left(\frac{\partial F}{\partial x}\right)_p dx + \left(\frac{\partial F}{\partial p}\right)_x dp = f(x)\,dx + v(x)\,dp(x) = 0$$

and

$$\int_{x_0}^{h} \frac{d\Omega}{dx}\,dx = \int_{x_0}^{h} f(x)\,dx = -\int_{x_0}^{h} v(x)\frac{dp(x)}{dx}\,dx = 0,$$

$$\int_{x_0}^{h} \frac{dp(x)}{dx}\,dx = 0; \quad \int_{x_0}^{h} p(x)\,dx = \bar{p}(x).h = -\gamma.$$

These equations impose considerable restrictions on possible forms of the

various functions. Thus if $\Omega(x)$ have a single extreme, say a maximum at x_m, the minimum pressure must occur at x_m, and since the mean value of the magnitude of $dp(x)/dx$ in the interval x_0 to x_m must equal that in the interval x_m to h, and since from physical considerations the mean value of $v(x)$ must be greater in the later interval, $v(x)$ must have a maximum in the interval $0-x_m$,

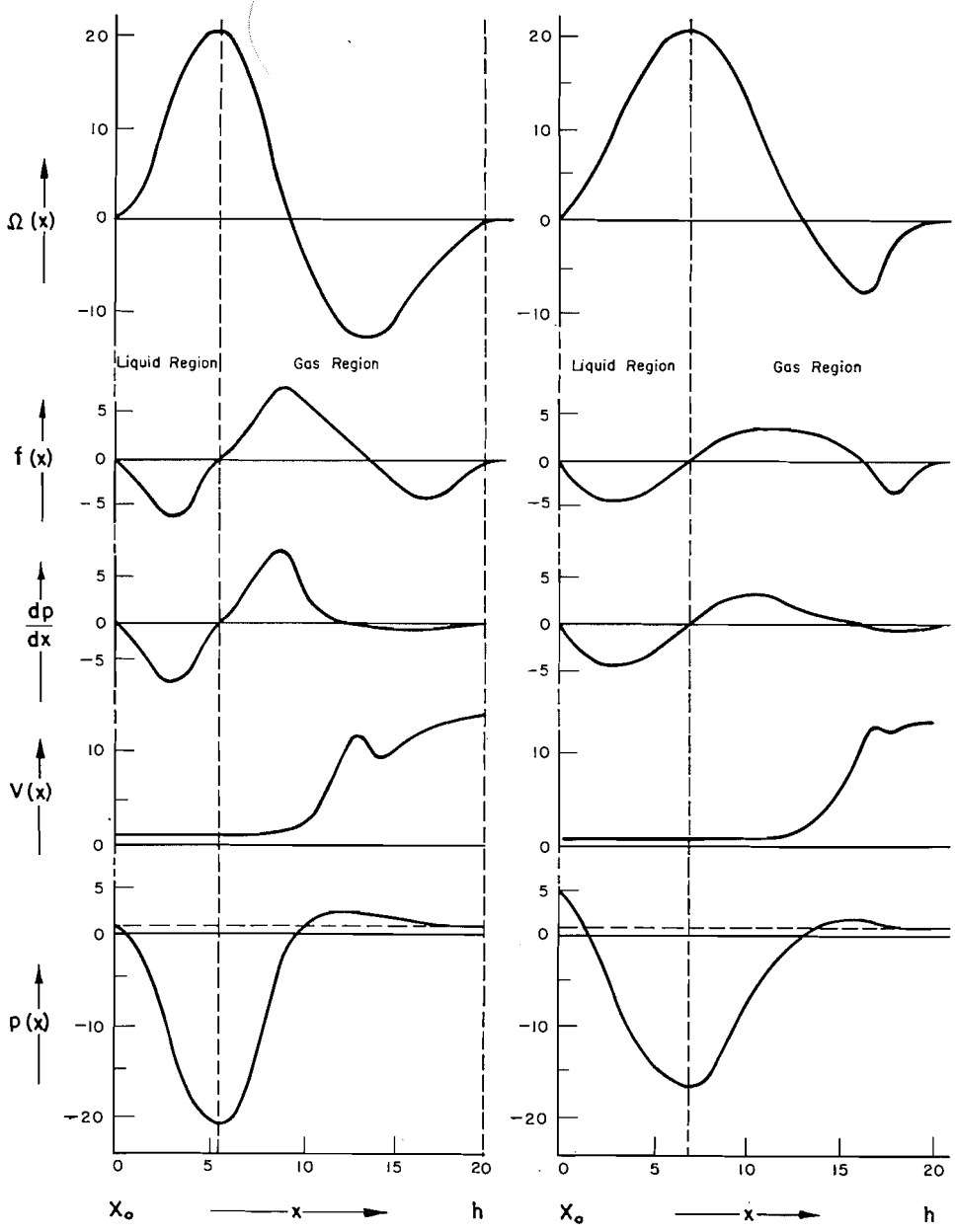

Fig. 7

i.e., in the region of lowest pressures. Accordingly $\Omega(x)$ cannot have a single extreme[4] when surface tensions have appreciable positive values and when vapor densities are low. Assuming a simple form for $\Omega(x)$ having a maximum and a minimum, and choosing a physically plausible form $v(x)$, the relations which must subsist between the various functions can be illustrated approximately (see Fig. 7*a*). Evidently, this surface adsorbs its own vapor (cf. Wyllie (12)). For convenience of illustration the difference between the specific volumes of liquid and vapor has been taken much less than is the case with liquid–vapor systems such as water. The magnitudes of the negative pressures are also much smaller with respect to vapor pressures than is the case in ordinary systems of appreciable surface tension. In the case of the water interface $-\bar{p}(x) \cdot h \approx 70$ dynes cm.$^{-1}$ at room temperature. If the thickness of the interface, h, lies between 10 and 1 Å, the mean negative pressure or mean stress intensity must lie between 700 and 7000 atm. Evidently such large tensile stresses cannot be sustained in the more dilute regions of the fluid interface and hence, practically the whole contribution to $p(x)$ must come from the region where the fluid has high tensile strengths, high densities, and low compressibilities, i.e., from the liquid region of the interface. The maximum tensile stress in this region will exceed the mean tensile stress by factors depending on the relative thicknesses of these regions, the factor being the greater, the smaller the ratio of the thickness of the dense region to the thickness of the whole interface. In the case illustrated in Fig. 7*a* the factor is about five and correspondingly, the maximum tensile stress is between 35,000 and 3500 atm. for total film thicknesses between 1 and 10 Å. The film thickness as measured by the Rayleigh method will be the region of rapid change of refractive index and thus will be the region of rapid increase in specific volume. The thickness of the water interface as measured by Raman and Ramdas (8) using the Rayleigh method is about 1 Å. If the relative thicknesses of the various regions are as illustrated, the total film thickness is somewhat less than 10 Å and the maximum tensile stress of the order of 4×10^3 atm. It seems very improbable that this figure can be much too low since it is comparable with the measured tensile strength of some metals.

Capillary Rise and Depression

As a variation of the 'flat' interface illustrated by Fig. 7*a* we may suppose the whole system raised or lowered in a potential field independent of surface potential fields. If we impose the condition $dF = 0$ for this variation the conditions are analogous to capillary rise or depression.

In order that $dF = 0$, the relative changes in liquid and gas pressures will be more or less proportional to densities. Accordingly the $p(x)$ curve must be distorted so that

$$\int_{x_0}^{h} \frac{dp(x)}{dx} \cdot dx \neq 0 .$$

However, for small rises or depressions $\bar{p}(x)$ and $\Omega(x)$ will not be changed appreciably, since the magnitudes of $\bar{p}(x)$, $p(x_m)$ etc. are large compared with

[4]*That is,* $\frac{d\Omega(x)}{dx} = 0$ *at more than one value of* x *between* x_0 *and* h.

the pressure changes introduced by the rise or depression. For large depressions, analogous to the effect of curvature on very small droplets, the pressure changes may be comparable with $\bar{p}(x)$. In such cases to retain constancy of surface tension either $\Omega(x)$ must change or the surface thickness or both must change. A natural assumption is that the tendency of the surface to adsorb its own vapor becomes less on surfaces concave toward the dense phase and hence that $\Omega(x)$ is changed. Fig. 7*b* illustrates a 'capillary depression' of the hypothetical system illustrated by Fig. 7*a*, the values of $\bar{p}(x)$ and h being unchanged, but $v(x)$, $p(x)$, and $\Omega(x)$ distorted so that there is a net pressure difference between liquid and vapor.

The energy of a vapor is in general much greater than the energy of the corresponding liquid. The heat energy or TS energy change from liquid to gas is somewhat greater than the corresponding internal energy change (i.e., by $p_0\Delta v$). In order that a positive potential of position exist in the interface $[\Delta(E+p_0v)/\Delta x]\ \Delta x$ must exceed $(T\Delta S/\Delta x).\ \Delta x$. Since $p_0\Delta v$ is small, especially in the dense region of the interface, we may ascribe the positive potential of position to an increase in energy without a compensating increase in entropy. In the more dilute region the negative potential of position may be ascribed to the large increase in entropy associated with the large volume change, the entropy in this region becoming too large with respect to the energy. The energy of a single phase (lamina in this case) of one component cannot vary continuously at constant μ, T, and P; consequently, strictly continuous density (energy) gradients must be associated with pressure gradients, i.e., potential gradients. Evidently surface potentials are in the main due to the very sharp density gradients in the neighborhood of the surface. Accordingly changes in surface conditions which tend to reduce density differences and which tend to equalize compressibilities will tend to reduce surface potentials. Thus, it would appear that the 'surface tension' of the flat surface is near the maximum and that either increasing or decreasing the equilibrium pressures by very large values will in the limit result in a vanishing surface tension. In the case illustrated in Fig. 7*b*, the mean potential of the matter in the surface region is increased by the distortion (cf. Rice (9)).

A primary objective of the inquiry outlined above is to obtain some notion of the physical factors controlling rates of flow of fluids through porous adsorbents. Evidence has been obtained that in the case of pores which are fairly large compared with molecular dimensions (10^{-7} to 10^{-5} cm.), flow mechanisms are essentially those of classical laminar flow, but are controlled by density and pressure gradients (both parallel and normal to the direction of flow) that are functions of the surface forces. Generally, these gradients are not directly observable and accordingly must be measured indirectly or inferred from measurements of adsorbate pressures, surface tensions, surface potentials, or other average properties. Where we can determine density gradients we can calculate corresponding pressure gradients and can make considerable progress in relating net flow rates to the physical structures of ultra fine grained porous adsorbents.

REFERENCES

1. AMBERG, C. H. and MCINTOSH, R. Can. J. Chem. 80: 1012. 1952.
2. BARRER, R. M. Diffusion in and through solids. Cambridge University Press, London. 1951. (Also numerous papers.)
3. BROWN, R. C. Proc. Phys. Soc. (London), 59: 429. 1947.
4. FLOOD, E. A. and HEYDING, R. D. Can. J. Chem. 32: 660. 1952.
5. FLOOD, E. A., TOMLINSON, R. H., and LEGER, A. E. Can. J. Chem. 30: 348, 389. 1952.
6. GIBBS, J. W. Collected works. Yale University Press, New Haven, Conn. 1948. p. 257.
7. HAINES, R. S. and MCINTOSH, R. Can. J. Phys. 25: 28. 1947.
8. RAMAN, C. V. and RAMDAS, L. A. Phil. Mag. 3: 220. 1927.
9. RICE, O. K. J. Chem. Phys. 15: 333. 1947.
10. SHUTTLEWORTH, R. Proc. Phys. Soc. (London), A, 62: 167. 1949.
11. TOLMAN, R. C. J. Chem. Phys. 16: 758. 1948.
12. WYLLIE, G. Proc. Roy. Soc. (London), A, 197: 383. 1949.

THE DETERMINATION OF PORE SIZE DISTRIBUTION AND SURFACE AREA FROM ADSORPTION ISOTHERMS[1]

By E. M. Voigt[2] and R. H. Tomlinson

ABSTRACT

Theoretical isotherms have been developed which when compared to experimental isotherms showing hysteresis, allow the calculation of pore size, pore size distribution, and surface area of the sorbent. Interpretation of some experimental isotherms obtained with porous vycor glass shows that this system can best be represented by the "ink bottle" pore model with a Gaussian distribution of pore sizes. The mean pore radius of the porous glass is about two thirds of the Kelvin radius, and the surface area greater than that obtained from the B.E.T. theory. The Kelvin radius is interpreted as a weighted average, but the B.E.T. surface area appears more fundamentally different.

INTRODUCTION

The B.E.T. (4) theory which has been widely used for interpretation of adsorption phenomena fails to account for the types IV and V isotherms of the Brunauer classification (3). The more complete B.D.D.T. theory (3), which takes capillary condensation into account, applies only to those systems where there is no distribution in pore size or where the variation from an average pore size is not too great.

Several attempts have been made to interpret adsorption, particularly at high relative pressures where hysteresis is encountered, in terms of pore distribution and capillary condensation. The radii of cylindrical capillaries which fill at a given partial pressure may be evaluated by means of the Kelvin equation:

$$\ln (P/P_0) = -2\gamma V_1/R R_0 T$$

where P = pressure,
P_0 = vapor pressure at the temperature T,
γ = surface tension,
V_1 = molal volume of the adsorbed liquid at the temperature T,
R = capillary radius,
R_0 = the gas constant,
T = absolute temperature.

The particular radius corresponding to the point of inflection on the hysteresis loop is known as the Kelvin radius. This radius may be interpreted as the radius of that pore having the most probable volume. If, however, there is a distribution of pore radii, the pore which has the most probable volume will have a greater than average radius. Whether the adsorption or desorption branch of the isotherm should be used for the determination of the Kelvin radius will be considered below. A more basic capillary condensation equation has recently been derived by Kistler (8):

$$[1] \qquad dA/dV = -\ln(P/P_0)R_0T/M\gamma,$$

[1]*Manuscript received June 11, 1954.*
Contribution from the Department of Chemistry, McMaster University, Hamilton, Ontario. This paper was presented at the Symposium on Problems Relating to the Adsorption of Gases by Solids, held at Kingston, Ontario, September 10–11, 1954.
[2]*Holder of Research Council of Ontario Scholarship.*

where A = pore area,
V = pore volume.

It may be seen that this relation reduces to the Kelvin equation for cylindrical capillaries or spherical pores.

From the experimental isotherm it is possible to obtain directly a plot of the pore volume distribution curve. Kubelka (10) has used a plot of

$$d(V_a/V_t)/d \log D \text{ vs. } \log D,$$

where V_a is the total volume adsorbed at a given relative pressure,
V_t is the total volume adsorbed at the saturation pressure,
D is the pore diameter as calculated from the Kelvin equation for the relative pressure corresponding to V_a.

The curves obtained resemble typical probability curves and Kubelka interpreted their maxima as corresponding to the capillary diameter that occurs most frequently in the adsorbent. Schuchowitski (13) has criticized Kubelka's plot on the basis that it did not differentiate between adsorption and capillary condensation. Foster (7) overcame this objection by plotting a function similar to that of Kubelka, but using only the hysteresis region of the isotherm. In either case, however, the peak of the distribution curve merely corresponds to the point of inflection on the original isotherm, and hence the "average" pore radius calculated from these methods is the Kelvin radius discussed above.

Wheeler (15) has suggested an integrated theory combining multilayer adsorption and capillary condensation. Following the suggestion of Wheeler, Shull (14) has assumed that multilayer adsorption reduces the pore size by an amount t at any given pressure. Thus one must use a modified Kelvin equation which relates the maximum pore that will be filled owing to capillary condensation at any given relative pressure:

$$\ln (P/P_0) = -2\gamma V_a/(R-t)R_0T,$$

where t = thickness of the adsorbed film. It was concluded that a plot of $V_c - V$ against $R-t$, where $R-t$ was evaluated by means of the above equation, should correspond to the integral:

$$V_c - V = \pi \int_R^\infty (R-t)^2 L(R)dR,$$

where $L(R)dR$ is the total length of pores whose radii fall between R and $R+dR$.

By assuming various forms of the distribution function $L(R)dR$, families of curves were obtained. Each member of a given family corresponded to a value of the most probable pore size. These theoretical curves could then be compared with experimental isotherms plotted in the same manner. That member of a given family of the theoretical curves which most closely represented the experimental curve would allow one to choose the type of distribution and mean pore radius of the pores in the experimental system. Whereas the method of Wheeler and Shull is adequate for many systems, it makes no allowance for the influence of pore shape. In any system having a distribution of pores, most of the total void volume will arise from those pores which are

greater than average in radius. It follows that volumes of sorbed material as obtained from capillary condensation measurements might well be more adequately represented by a $f(R^3)$ ('ink bottle') type of pore volume function than a $f(LR^2)$ (cylindrical type) volume function. The present work evaluates the theoretical form of capillary condensation isotherms for various pore shapes, sizes, and distributions. Further, it has been possible to obtain information about the thickness of the adsorbed film, and the surface area of the sorbent. The theory is discussed with reference to some experimental isotherms obtained by Barrer (2) and Emmett (6) for porous vycor brand glass.

THEORETICAL

Distribution of Capillary Condensation Radii

The Kistler equation [1] in the appropriate form indicates the relative pressure at which condensation will occur on a meniscus in a capillary of a given shape. Such condensation would also occur on an adsorbed layer covering the concave surfaces of a porous system. If such condensation leads to a reduction in the radius of curvature of the surface, condensation will continue on this surface at constant pressure as long as the radius of curvature continues to reduce. In this discussion a pore will be considered as any void region in a porous material which by virtue of this process completely fills at constant relative pressure. Also the pore radius will be considered as the radius of curvature of that surface on which the above pore filling process started to occur.

If a given porous system has a distribution of pore radii, one may expect that at a given partial pressure, pores of radius equal to or less than the value determined by the appropriate form of the Kistler equation [1] will be completely filled. That is, if the volume of a pore in the porous system is expressed by the function

$$V = f_1(R),$$

and if the number of pores having radii falling between R and $R+dR$ is given by

$$dn = f_2(R)dR,$$

then the volume of all pores with radii between R and $R+dR$ is

$$dV = Vdn = f_1(R) \times f_2(R)dR,$$

and the ratio of the sum of the volumes of all pores whose radii are equal to or less than R to the total volume of all the pores is given by

$$[2] \qquad V/V_c = \int_{\infty}^{R} (f_1(R) \times f_2(R)dR) / \int_{0}^{\infty} (f_1(R) \times f_2(R)dR).$$

In order to solve equation [2] it is necessary to obtain explicit functions for $f_1(R)$ and $f_2(R)$. Various pore models may be assumed.

(*a*) The cylindrical type pore model for which

$$f_1(R) = K_1LR^2,$$

where K_1 = shape factor ($K_1 = \pi$ for cylinders),

and L = length of pore.

(*b*) The 'ink bottle' type pore model for which

$$f_1(R) = K_2R^3,$$

where K_2 = shape factor ($K_2 = \frac{4}{3}\pi$ for spheres).

It is most reasonable to assume that the distribution in pore size is either Maxwellian or Gaussian, although in some porous systems other types of distribution may occur.

(*a*) For a typical Maxwellian distribution

$$f_2(R) = \frac{4N}{\sqrt{\pi}}\frac{R^2}{\alpha^3}\exp\left(-\frac{R^2}{\alpha^2}\right),$$

where N = number of pores per unit mass,
and α = a constant.

(*b*) For a typical Gaussian distribution

$$f_2(R) = NA\exp\left[-\frac{\beta^2}{\alpha^2}(R-\alpha)^2\right],$$

where A = normalization constant

$$= \int_0^\infty \exp\left[-\frac{\beta^2}{\alpha^2}(R-\alpha)^2\right]dR,$$

β = constant.

With both of these distributions α may be interpreted as the most probable radius, and β which occurs in the Gaussian function is a measure of the distribution width.

Four solutions to equation [2] may be obtained using the four possible combinations of the above pore models and distributions.

(*a*) Cylindrical type pore model with Maxwellian distribution of pore radii

$$[3] \qquad \frac{V}{V_c} = \frac{2}{\sqrt{\pi}}\int_0^x e^{-x^2}dx - \frac{4}{3\sqrt{\pi}}x^3e^{-x^2} - \frac{2}{\sqrt{\pi}}xe^{-x^2},$$

where $x = R/\alpha$.

(*b*) Cylindrical type pore model with Gaussian distribution of pore radii

$$[4] \qquad \frac{V}{V_c} = \frac{(\frac{1}{2}+\beta^2)\int_{-\beta}^{z} e^{-z^2}dz + e^{-\beta^2}(\beta-\frac{1}{2}\beta) - e^{-z^2}(\beta+\frac{1}{2}z)}{(\frac{1}{2}+\beta^2)\int_{-\beta}^{\infty} e^{-x^2}dz + (\beta-\frac{1}{2}\beta)\,e^{-\beta^2}},$$

where $z = \beta(R-\alpha)/\alpha$.

(*c*) 'Ink bottle' type pore model with Maxwellian distribution of pore radii

$$[5] \qquad \frac{V}{V_c} = 1-\left[\frac{x^4}{2}e^{-x^2}+x^2e^{-x^2}+e^{-x^2}\right],$$

where $x = R/\alpha$.

(*d*) 'Ink bottle' type pore model with Gaussian distribution of pore radii

$$[6]\quad \frac{V}{V_c} = \frac{-\frac{1}{2\beta^3}e^{-z^2}(1+3\beta^2+3\beta z+z^2)+\frac{1}{2\beta^3}e^{-\beta^2}(1+\beta^2)+\left(1+\frac{3}{2\beta^2}\right)\int_{-\beta}^{z}e^{-z^2}dz}{\frac{1}{2\beta^3}e^{-\beta^2}(1+\beta^2)+\left(1+\frac{3}{2\beta^2}\right)\int_{-\beta}^{\infty}e^{-z^2}dz},$$

where $z = \beta(R-\alpha)/\alpha$.

Values of the functions V/V_c versus R have been plotted in Figs. 1–6 corresponding to each of the various systems represented by equations [3, 4, 5, 6]. Each curve in a given figure is representative of a different value of the parameter α (the most probable pore size). Two families of curves have been plotted for each pore model with a Gaussian distribution, since these systems have a further parameter β. As β may have any positive value these are merely representative of a large number of families which may be plotted for these systems. The plot of V/V_c versus R for a particular value of α (and β for Gaussian distribution) will be known as a theoretical or normalized capillary condensation isotherm for the given pore model and distribution.

Distribution of Pore Radii Including the Thickness of the Adsorbed Layer

In addition to capillary condensation true adsorption contributes to the total amount of the sorbed material in a porous system. Since all adsorption in any pore must precede capillary condensation, the capillary condensation radii distributions evaluated in the previous section must be representative of pores which are reduced in radius by an amount equal to the thickness of the

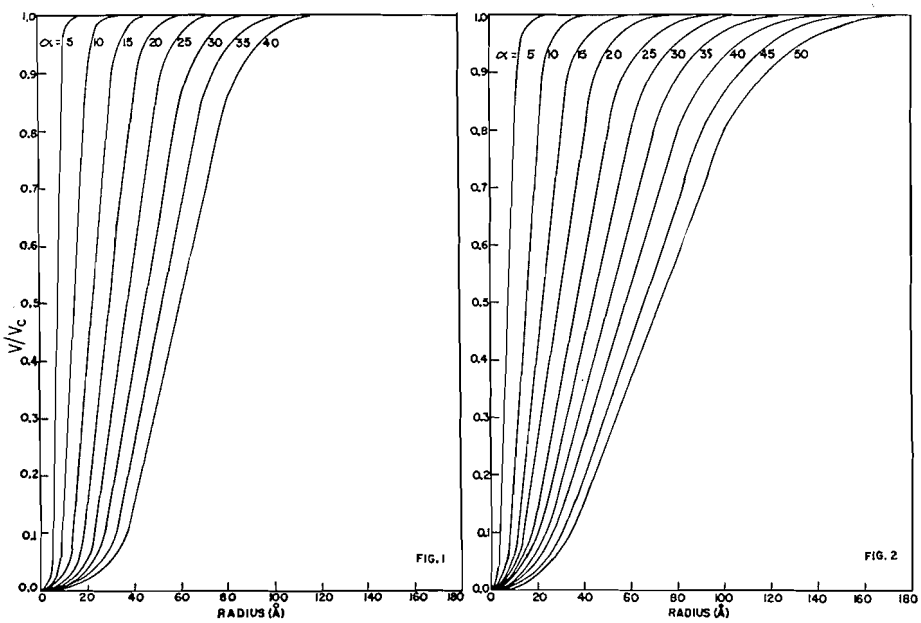

FIG. 1. Normalized isotherms—calculated for a Maxwellian distribution of pore sizes and cylindrical volume function as given by equation [3].

FIG. 2. Normalized isotherms—calculated for a Gaussian distribution of pore sizes and cylindrical volume function as given by equation [4] with $\beta = 2$.

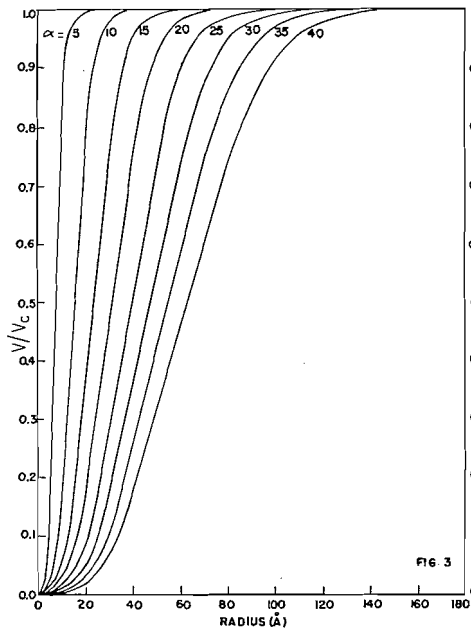

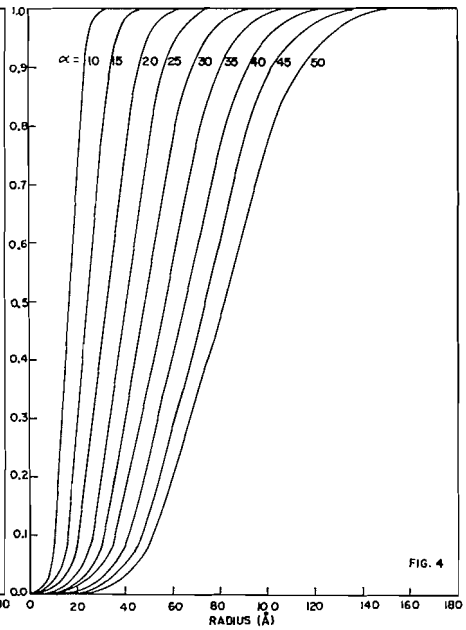

FIG. 3. Normalized isotherms—calculated for a Gaussian distribution of pore sizes and cylindrical volume function by equation [4] with $\beta = 1$.

FIG. 4. Normalized isotherms—calculated for a Maxwellian distribution of pore sizes and cubic volume function as given by equation [5].

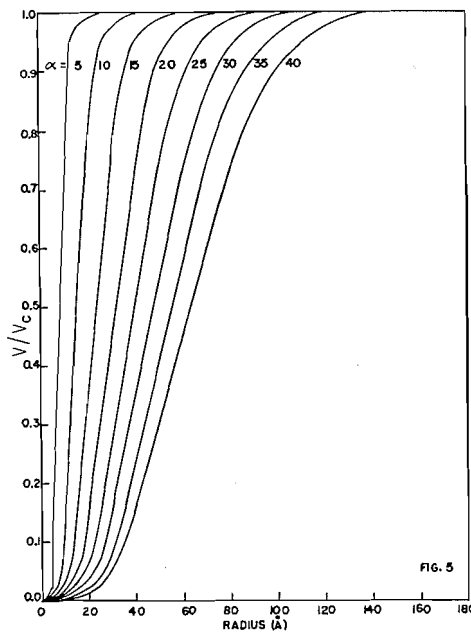

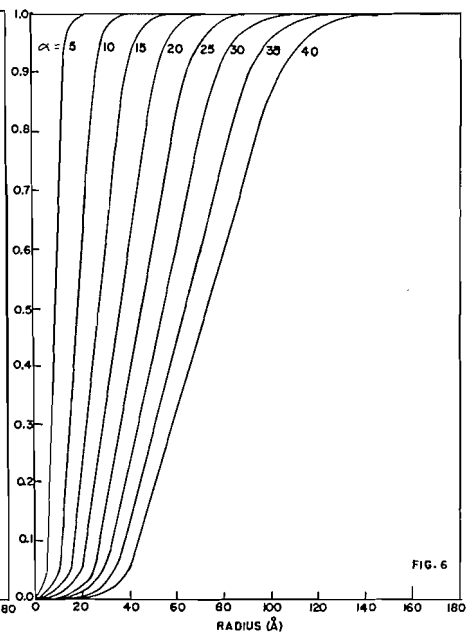

FIG. 5. Normalized isotherms—calculated for a Gaussian distribution of pore sizes and cubic volume function by equation [6] with $\beta = 2$.

FIG. 6. Normalized isotherms—calculated for a Gaussian distribution of pore sizes and cubic volume function by equation [6] with $\beta = 1$.

adsorbed layer. If it is assumed that at saturation the adsorbed material is equally distributed on all surfaces, the ratio of the volume filled by capillary condensation to the total volume of the system is given by

$$V_c/V_t = \int_0^\infty f_1(R)f_2(R)dR \Big/ \int_0^\infty f_1(R)f_2'(R)dR,$$

where $f_2'(R) = f_2(R)$ with $R-\alpha$ replaced by $R-(\alpha+t)$,
and t = thickness of adsorbed layer at saturation if equally distributed on all surfaces.

Thus for the Gaussian distributions

$$[7] \qquad \frac{V_c}{V_t} = \frac{\int_0^\infty R^n \exp\left[-\frac{\beta^2}{\alpha^2}(R-\alpha)^2\right]dR}{\int_0^\infty R^n \exp\left[-\frac{\beta^2}{\alpha^2}\{R-(\alpha+t)\}^2\right]dR},$$

where $n = 2$ for the cylindrical type pore model,
and $n = 3$ for the 'ink bottle' type pore model.

Solving equation [7] we obtain:

(*a*) cylindrical pore model

$$[8] \qquad \frac{V_c}{V_t} = \frac{\beta e^{-\beta^2} + (1+2\beta^2)I}{\beta\omega e^{-\beta^2\omega^2} + (1+2\beta^2\omega^2)I(t)};$$

where $\omega = \frac{a+t}{a}$, $I = \int_{-\beta}^{\infty} e^{-x^2}\,dx$ with $x = \frac{\beta}{a}(R-a)$, and $I(t) = \int_{-\beta\omega}^{\infty} e^{-x^2}\,dx$.

(*b*) 'Ink bottle' pore model

$$[9] \qquad \frac{V_c}{V_t} = \frac{(\beta^2+1)\,e^{-\beta^2} + (3\beta+\beta^3)I}{(\beta^2\omega^2+1)\,e^{-\beta^2\omega^2} + (3\beta\omega+\beta^3\omega^3)I(t)}.$$

Determination of Surface Area

The surface area of a given porous system may be represented by:

$$S_w = \int_0^\infty f_3(R)f_2(R)dR;$$

S_w = surface area per unit weight of porous material,
$f_3(R)$ = the surface area of a pore whose volume is $f_1(R)$,
$f_2(R)$ = the particular distribution function determined above in which α is set equal to $\alpha+t$.

Thus the surface area per unit mass of sorbent for the 'ink bottle' model with Gaussian distribution of pore radii is given by

$$[10] \qquad S_w = \int_0^\infty K_3R^2AN \exp\left[-\frac{\beta^2}{\alpha^2}(R-R_0)^2\right]dR,$$

where $R_0 = a+t$ (when assumption of equal distribution of adsorbed material is justified),
K_3 = shape factor ($K_3 = 4\pi$ for spherical pores).

To solve equations of type [10] requires a knowledge of the shape factor K_3 and the number of pores per unit mass N. Since these quantities can not be

evaluated from sorption data alone without further assumptions, it is considered simpler to evaluate the surface area of the porous material from V_m, the volume of adsorbed material required to form a monolayer on the surface of the sorbent. This calculation allows the use of more generally recognized assumptions.

It is apparent that the evaluation of V_m is analogous to the determination of the thickness of the adsorbed layer, except that in this case the value of the thickness may be assumed to be one molecular diameter. Thus

$$[11] \qquad \frac{V_t - V_m}{V_t} = \frac{\int_0^\infty R^n \exp\left[-\frac{\beta^2}{\alpha^2}\{R-(R_0-m)\}^2\right] dR}{\int_0^\infty R^n \exp\left[-\frac{\beta^2}{\alpha^2}\{R-R_0\}^2\right] dR},$$

where m = thickness of monolayer = 1 molecular diameter of adsorbate. Solving equation [11] for:

(*a*) Cylindrical pore model ($n = 2$)

$$[12] \qquad \frac{V_t - V_m}{V_t} = \frac{\eta\, e^{-\eta^2} + (1+2\eta^2)\, I(\eta)}{\tau\, e^{-\tau^2} + (1+2\tau^2)\, I(\tau)};$$

where $\eta = \frac{\beta}{\alpha}(R_0 - m)$, and $\tau = \frac{\beta}{\alpha}R_0$, $I(\eta) = \int_{-\eta}^{\infty} e^{-x^2} dx$ and $I(\tau) = \int_{-\tau}^{\infty} e^{-x^2} dx$.

(*b*) 'Ink bottle' pore model ($n = 3$)

$$[13] \qquad \frac{V_t - V_m}{V_t} = \frac{(\eta^2+1)\, e^{-\eta^2} + (3\eta+\eta^3)\, I(\eta)}{(\tau^2+1)\, e^{-\tau^2} + (3\tau+\tau^3)\, I(\tau)};$$

where $I(\eta)$ and $I(\tau)$ have the same meaning as in [12].

Surface area may then be evaluated in the usual manner from the relation

$$[14] \qquad S_w = \frac{V_m}{22400}\, x\, N_a\, x\, A_m,$$

where S_w = surface area per gram of adsorbent,
N_a = Avogadro's number,
A_m = surface area covered by a molecule as obtained from the equation

$$A_m = 4 \times 0.866\left[\frac{M}{4\,\gamma\, 2 \times N_a\, x\, \rho_l}\right]^{2/3},$$

where M = molecular weight of adsorbate,
ρ_l = density of the liquefied adsorbate at temperature of the isotherm.

EXPERIMENTAL INTERPRETATION

In order to find the distribution of capillary condensation radii in an experimental system, it is necessary to obtain the experimental values of V/V_c and plot these against R, where R is calculated from the Kistler equation [1] in the appropriate form for the relative pressure corresponding to V. That is, for the

Cylindrical pore model: adsorption—Cohan equation,
desorption—Kelvin equation;
KR^3 pore model: adsorption—Kelvin equation.

(For discussion see below.) The pore model and distribution parameters may then be obtained from the theoretical isotherm that gives the best fit to the experimental curve. Before it is possible to obtain these quantities from the experimental isotherm it is necessary to understand the mechanism of adsorption hysteresis. In some cases hysteresis is not reproducible. Zsigmondy (16) has suggested that this type of hysteresis probably results from the effects of surface impurities. Where the branches of the hysteresis loop are entirely reproducible, two main theories have been proposed. The 'ink bottle' theory of Kraemer (9) which has been adopted by McBain (11) suggests that during adsorption, capillary condensation occurs on a relatively large meniscus in the 'bottle' part of the pore, and that desorption must occur from the smaller meniscus of the 'neck' of the ink bottle pore. Although this theory has not yet been proved Rao (12) has shown that in a qualitative way it will explain his experimental data. Proponents of this theory have considered the adsorption branch of the isotherm as most significant in determining pore radius. The 'ink bottle' hypothesis does not necessarily imply that each 'bottle' has only a single neck, for the arguments would be equally valid for any porous network having larger pores connected by smaller ones.

Cohan (5) has suggested a theory of hysteresis which turns out to be very similar to the 'ink bottle' theory, except that it is subject to a more quantitative treatment because of a simpler pore model. Cohan considers the pores to be cylindrical in shape and that adsorption capillary condensation occurs as an annular ring on the wall of the pore rather than on a normal meniscus as required by the Kelvin equation. For these conditions the Kelvin equation must be modified, and Cohan has shown that this modified equation is identical in form to the Kelvin equation except for the disappearance of the numerical factor 2. This modification of the Kelvin equation can also be obtained directly from the Kistler equation [1]. Therefore radii calculated with Cohan's equation, using the adsorption branch of the isotherm, are one half those obtained when the normal Kelvin equation is used.

Desorption, on the other hand, occurs from the surface of a normal meniscus in a completely filled capillary, and the vapor pressure over the meniscus could therefore be represented by a normal Kelvin expression. Whereas Cohan has been able to obtain quantitative relations between adsorption and desorption for the cylindrical pore model, it is to be expected that in most systems the pore radii will vary from point to point along their lengths and the 'ink bottle' model will more nearly represent most porous systems. No quantitative expressions, however, have yet been developed to relate the adsorption and desorption pressures in the more complicated but realistic 'ink bottle' system.

There is, however, a good visual test which allows one to choose between the Cohan and the 'ink bottle' models. The difference may be seen when the weight adsorbed, after the contribution of reversible adsorption is subtracted, is plotted against the log of the relative pressure.[3] For the Cohan mechanism,

[3]*The reversible adsorption in the pressure region where hysteresis occurs may be approximately estimated from the slope of the top of the hysteresis loop which Amberg and McIntosh (1) have shown to be reversible.*

adsorption and desorption branches of the isotherm should then be entirely symmetrical since the form of the adsorption, as well as the desorption branch, is determined by the *same* pore radii distribution. Their relative positions, however, are determined by differences in the shapes of the menisci. In the case of the 'ink bottle' model the shapes of the menisci are the same and it is the largest pore neck which determines the relative pressure at which desorption occurs in a given pore. The amount desorbed, however, depends more on the volume of the pore than on the volume of the necks leading into it. The position and shape of the adsorption branch is then fixed by the distribution of pore sizes whereas the position and shape of the desorption branch is related to the radii distribution of the largest necks connecting the pores. Since there may be several necks to a given pore, the probability that all of these are much smaller than the mean radius of the necks is greatly reduced, and hence one would expect the desorption branch of the isotherm to represent an apparent distribution of pore necks with greatly reduced numbers of small necks. This difference will manifest itself in a much steeper desorption isotherm, particularly in the lowest relative pressure region where hysteresis is observed.

Whereas this test may allow one to establish the Cohan mechanism, it can only show in a qualitative way the possible validity of the 'ink bottle' model. A quantitative test of the 'ink bottle' model may be obtained by comparison of experimental and theoretical isotherms, but as yet this comparison applies to only the adsorption branch.

Further, it is necessary to interpret the form of the experimental isotherm in terms of the physical processes which give rise to it. If the partial pressure of a sorbable gas over a sorbent is increased, this pressure increase may lead to one, two, or three types of physical sorption:

(*a*) Complete filling of pores whose radii are equal to or less than the value required by the Kistler equation [1] in a form corresponding to the model.

(*b*) Adsorption on the surfaces of pores whose radii are larger than the value required for Kelvin condensation.

(*c*) Capillary condensation into the corners of pores which are too large to completely fill at the given partial pressure.

Types (*a*) and (*b*) are self-explanatory, but type (*c*) is best illustrated with reference to a specific model. For a boxlike pore capillary condensation may occur into the corners, but the addition of each layer of sorbate increases the radius of curvature of the menisci so that further condensation requires an increase in pressure. Gas condensed in this manner would show no hysteresis, and would be difficult to distinguish from multilayer adsorption. When, however, the corners of the boxlike pore are completely filled and only a single spherical hole remains, further condensation reduces the radius of curvature of the meniscus and the slightest increase in pressure will result in complete filling of the pore. This pore filling process is the type (*a*) condensation which results in the 'ink bottle' type hysteresis.

The value of V used in the theoretical isotherms corresponds to type (*a*) sorption only, while V_c is the value of V at saturation pressure. Since type (*a*) sorption always leads to hysteresis, the maximum value that V may have at any

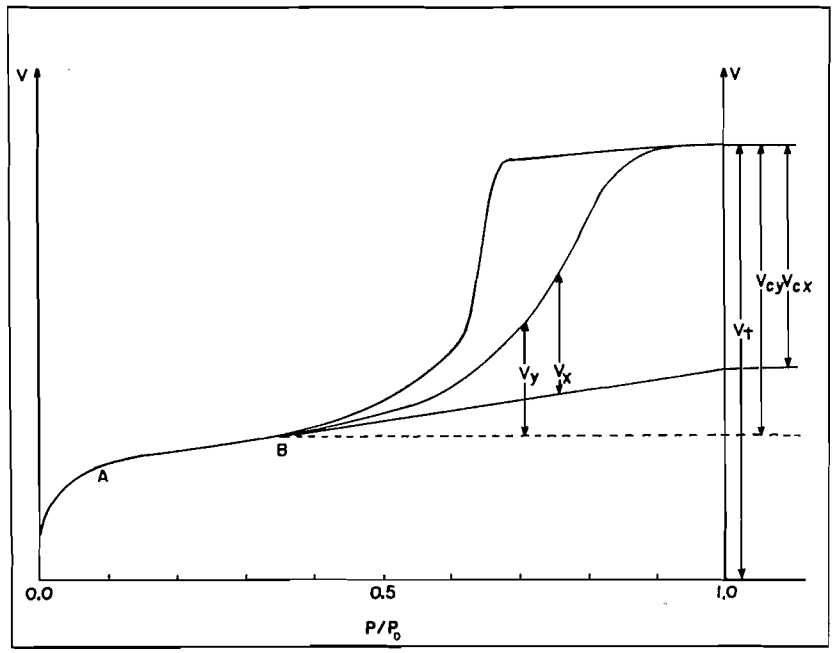

FIG. 7. Typical adsorption–desorption isotherm showing hysteresis.

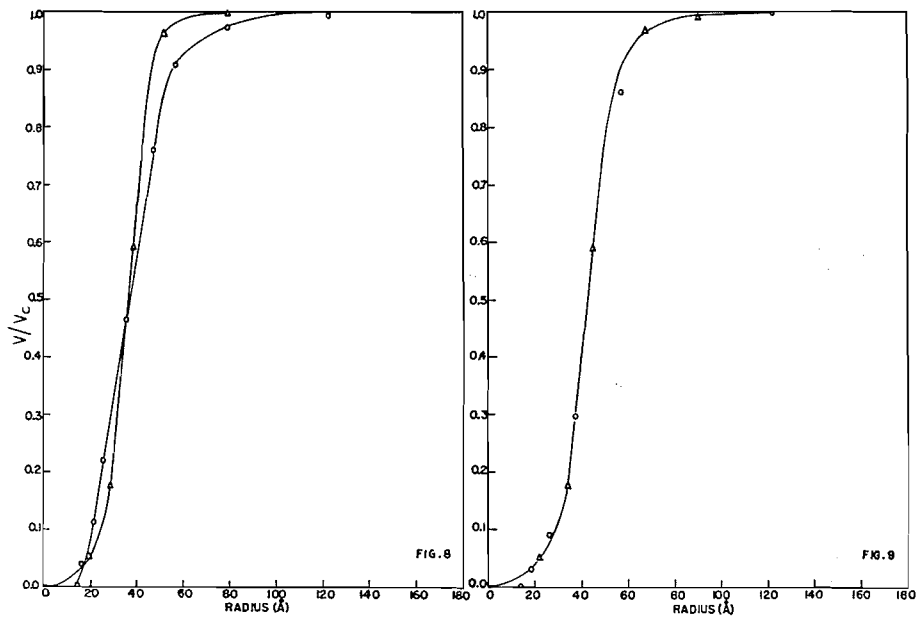

FIG. 8. Comparison of theoretical and experimental isotherms: experimental values from Emmett (6) using ratio of V_c/V_{cy} (FIG. 7).
Δ Selected Gaussian isotherm of cubic type with $\beta = 1$ and $\alpha = 10$Å (equation 6).
FIG. 9. Comparison of theoretical and experimental isotherms: experimental values from Emmett (6) using ratio of V_x/V_{cx} (Fig. 7).
Δ Selected Gaussian isotherm of cubic type with $\beta = 1$ and $\alpha = 22.5$Å (equation 6).

given relative pressure is equal to the total amount sorbed less the amount sorbed at the relative pressure where hysteresis becomes significant. Thus if only type (*a*) sorption occurs in pressure regions where hysteresis is observed then a plot of V/V_{cy} (see Fig. 7) should correspond to the theoretical isotherm. This ratio taken from Emmett's experimental isotherm for nitrogen on porous glass (6) has been found to fit best the theoretical isotherm (equation 6) for $\beta = 1$ and $\alpha = 13$ Å (see Fig. 8). If, however, sorption other than type (*a*) is contributing to the total sorption in the pressure region where hysteresis occurs, it is necessary to know what shape the adsorption isotherm would have had if capillary condensation had not contributed. Test extrapolations of the region A–B (see Fig. 7) of the experimental isotherm for porous glass show that the actual form of this extrapolation makes relatively small differences in the fit of the 'experimental' V/V_c and the theoretical isotherms. Thus the ratio V_x/V_{cx} (see Fig. 7) taken for the same nitrogen isotherm as above still fits the theoretical isotherm (equation 6) with $\beta = 1$ and $\alpha = 15$ Å (Fig. 9). Comparison of Figs. 8 and 9 shows that the fit of the 'experimental' isotherm to the theoretical isotherm is better in the case of Fig. 9 although the actual distributions and mean pore radii are not significantly different. Since this choice is not critical for the porous glass system the ratio V_x/V_{cx} (Fig. 7) has been used in this work as the experimental value comparable to the ratio V/V_c of the theoretical isotherm. In Table I the types of distribution, pore model, mean capillary condensation radius, and distribution width β are summarized for the experimental isotherms obtained by Barrer (2) and Emmett (6) for porous vycor glass.

TABLE I

MEAN PORE SIZE AND PORE SIZE DISTRIBUTION IN POROUS GLASS CALCULATED FROM VARIOUS ISOTHERMS

Substance adsorbed	Type of distribution	Character of volume function	Distribution width, β	Mean capillary condensation radius, α(Å)	Adsorbed layer thickness, t, (Å)	Mean radius after addition of adsorbed layer thickness, R_0, (Å)
Argon (Ref. 6)	Gaussian	Cubic	1	17.5	6.4	23.9
Nitrogen (Ref. 6)	Gaussian	Cubic	1	15.0	4.5	19.5
Butane (Ref. 6)	Gaussian	Cubic	2	15.0	(2.2)	19.9*
Oxygen (Ref. 2)	Gaussian	Cubic	1	18.0	6.18	24.2
Ammonia (Ref. 2)	Gaussian	Cubic	½	15.0	10.7	25.7

**Layer thickness assumed to be one molecular diameter (4.9 Å).*

DISCUSSION

The typical comparison between an experimental isotherm and a theoretical isotherm shown in Figs. 8 and 9 indicates that the adsorption isotherm in the

region where hysteresis is observed can for the porous system investigated be very closely represented by equation [6]. This tends to justify the assumptions which lead to this equation, i.e.

(*a*) There is a Gaussian distribution of pore radii;

(*b*) The pore volumes can be represented by an R^3 (ink bottle) function;

(c) All pores of radius equal to or less than that which is evaluated from the appropriate form of the Kistler equation [1] will be completely filled at a given partial pressure, i.e., the assumption that capillary condensation is the predominant factor in the region of hysteresis is valid.

From Table I it is apparent that the type of distribution, as well as the character of the volume function found for each gas, is very self-consistent. However, slight differences are found with respect to the values obtained for the parameters β and α. This can possibly be ascribed to the fact that the system has a most probable pore size comparable to the molecular dimensions. Thus, the size and shape of the adsorbed molecule may be expected to become influencing factors.

The fit of the 'experimental' and theoretical isotherm, as might be expected, is slightly better in the case of Fig. 9 than Fig. 8, although the actual distribution and mean radius obtained are not significantly different. It is apparent that with the relatively large contributions of capillary condensation found with porous glass it is the pressure and shape of the hysteresis region of the isotherm rather than the contribution of reversible sorption which are most significant in determining the fit of the 'experimental' and theoretical isotherms.

There are several differences between the theory introduced above and that described by Shull (14). Shull has only considered the cylindrical pore model whereas a better correlation between theoretical and experimental isotherms has been found with the 'ink bottle' model for the porous glass system. The present approach can, however, be used in cases where the cylindrical pore model might be desirable. Furthermore, it has been found convenient in this work to evaluate a normalized isotherm (V/V_c) rather than the inverted isotherm ($V_c - V$) used by Shull. The normalized isotherm not only allows the cancellation of arbitrary constants from the theoretical relations but also simplifies the necessary curve fitting. Shull has also used his method to determine pore sizes from isotherms where *hysteresis does not occur*. The theoretical curves evaluated either by Shull or in this work may well represent some part of any experimental isotherm—as a matter of fact, they may in their strictly mathematical form be used for the evaluation of any physical phenomenon showing such functional correlation. But, in the interpretation of such results, it must not be forgotten that any parameters, dependent or independent, appearing in the equations are now mathematical symbols only and therefore have no relation to the physical functions with which they were associated in the original theory. Thus, the evaluation of a mean or average pore size for a system that does not show hysteresis is inadvisable.

In the theoretical section, only the families of curves corresponding to $\beta = 1$ and $\beta = 2$ have been plotted for the Gaussian distribution. Since there is

no limitation on the possible values of β, there is an infinite number of such families that can be drawn. Presumably an experimental isotherm which will not fit one of the theoretical isotherms which have been plotted in the theoretical section may fit a member of a family of isotherms for a different value of β. It must be pointed out here, however, that Maxwellian distributions have the disadvantage of not by themselves allowing a decision regarding pore shape. For example, if the volume adsorbed can be represented by the integral of an expression $R^4e^{-\alpha^2R^2}dR$, one cannot interpret whether this expression is either (*a*) $K_1LR^2 \times R^2e^{-\alpha^2R^2}dR$ or (*b*) $K_2R^3 \times R\,e^{-\alpha^2R^2}\,dR$. The former case (*a*) would indicate a cylindrical pore volume whereas (*b*) would correspond to the 'ink bottle' pore. To distinguish between these two possibilities it is necessary to use further criteria such as the visual test described above.

In order to obtain the total pore radius, it is necessary to find the thickness of the adsorbed layer which must be added to the capillary condensation radius. This may be calculated from equation [9] which is the applicable relation for the previously established pore model and distribution. If, for the nitrogen isotherm of Emmett, all the gas sorbed at the relative pressure where hysteresis becomes significant were equally distributed on the surfaces of the pores, the thickness of the resultant adsorbed layer could be evaluated from the ratio V_{cv}/V_t (Fig. 7). Using the previously obtained value of α (i.e. 15 Å) a value of 4.5 Å is obtained for the layer thickness. That is, if the layer is equally distributed, the amount adsorbed at the partial pressure where hysteresis becomes significant is approximately the amount required to form a monolayer (i.e. 4 Å) on all surfaces. The values of t obtained for different sorbates together with the mean pore radius including the thickness of the adsorbed layer are listed in Table I. In the case of ammonia it is seen that t is approximately equal to three molecular diameters. Barrer (2) has pointed out that the high affinity of the ammonia molecule for the sorbent causes considerable swelling and hence the mean capillary radius obtained from the ammonia isotherm does not appear excessively large. For butane the calculated layer thickness is less than one molecular diameter and therefore the surface cannot be completely covered at the pressure where hysteresis occurs. Since condensation begins only after monolayer formation it has been assumed that the distribution of butane is not equal on all surfaces, and that the thickness of the adsorbed layer is equal to one molecular diameter at the pressure at which a pore fills by condensation. All above radii are seen to have values considerably less than the Kelvin values of 30–40 Å given by Emmett (6), which do not yet include the thickness of the adsorbed layer. This difference was to be expected, however, since it was realized at the outset that the Kelvin radius calculated from the relative pressure at the inflection point on the isotherm corresponded to the radius of the pore which has the most probable volume. That is, the Kelvin radius is the radius such that

$$d(dV/dR)/dr = 0.$$

If, therefore, the volume distribution function is known, the Kelvin radius may be calculated directly. For the model found applicable to the porous glass

system, the Kelvin radius is such that

$$\frac{R}{dR}\left[R^3\exp\left\{-\frac{\beta^2}{\alpha^2}(R-\alpha)^2\right\}\right] = 0,$$

whence the Kelvin radius = 1.82 α when $\beta = 1$.

Barrer (2) and Cohan (6) arrived at values similar to those obtained in this work by using the desorption branch of the isotherm. Barrer has corrected for the thickness of the adsorbed layer by the addition of two molecular diameters of the adsorbate. The highly polar molecules, however, give inconsistent values. Since these radii are calculated from the partial pressure corresponding to the point of inflection on the isotherm they must correspond to weighted values in the same sense as the Kelvin radii discussed above. The weighted radius obtained from the desorption isotherm happens to almost correspond to the mean radius obtained from the adsorption isotherm after allowance is made for the distribution in pore size. However, the pore model corresponding to the desorption isotherm has not been found applicable so that the apparent similarity seems largely fortuitous.

The model which most closely resembled the actual system was the 'ink bottle' model. This conclusion appears in direct opposition to that arrived at by Amberg and McIntosh (1), who decided that the cylindrical pore model was applicable to this same system. This difference is partly one of definition in so far as they have shown the pores to have a length to diameter ratio of about two, which these authors would consider 'ink bottle' rather than cylindrical type pores. Although this seems to be only a minor point of disagreement the relative forms of the expected adsorption and desorption isotherms are quite different for the two systems. The test described above which compares the relative shapes of the adsorption and desorption isotherms of the two models seems to eliminate the Cohan mechanism and is also qualitatively in agreement with the 'ink bottle' mechanism. The excellent correspondence between the theoretical cubic type isotherms and experimental adsorption isotherms over the complete applicable pressure range strongly indicates a basic equivalence between the 'ink bottle' model and the porous glass system.

When the smaller pore radii evaluated from the above methods are accepted, it is apparent that for a given pore volume a greater pore surface area should be expected. This may be calculated from V_m, the quantity of sorbate required to complete a surface monolayer. The value of V_m may be obtained from equation [11], which is the appropriate equation for the pore model established for the porous glass. Numerically, these values of V_m are greater than those obtained from the B.E.T. isotherm with the exception of ammonia (see Table II). In order to reconcile the differences, it is necessary to re-examine the postulates leading to the different V_m's. The V_m evaluated in this work corresponds to one of the several definite models used, rather than the V_m of the real system.

In order to evaluate the mean pore radius of the distribution it was necessary to assume the appropriate form of the Kistler equation [1]. In porous glass, where the pores have been formed in a solid non-crystalline mass by a preferential leaching process, it would appear that after the smoothing out of surfaces

by adsorption, condensation would occur on nearly spherical surfaces. This, as pointed out in the introduction, leads to the Kelvin relation. For capillary condensation causing hysteresis in the 'ink bottle' model this factor appears to be a maximum. Whereas altering this factor may change our conclusions with respect to the mean radius, it does not affect the conclusions with respect to the pore model and distribution. Any smaller value of the constant of the applicable form of the Kistler equation [1] would lead to a smaller mean pore radius and larger values of V_m and surface area.

For the V_m of the B.E.T. theory to be valid, it is necessary that the surface of the porous glass be homogeneous. Barrer (2) has already shown that the heats of sorption on the porous glass do not confirm this assumption and furthermore, the B.E.T. isotherm only fits the experimental data for the porous glass at low relative pressures. Kistler (8) has presented further arguments against the acceptance of the B.E.T. V_m.

TABLE II

COMPARISON OF CALCULATED V_m'S AND SURFACE AREAS WITH THOSE OBTAINED BY B.E.T. METHOD FOR POROUS GLASS

Substance adsorbed	V_m as determined from equation [13] (cc. at S.T.P. per gram material)	Total surface area of system as calculated from V_m ($m.^2$ $gm.^{-1}$ material)	B.E.T. V_m (cc. at S.T.P. per gram material)	B.E.T. surface area ($m.^2$ $gm.^{-1}$ material)
Argon (at 90°K.) (Ref. 6)	37.5	157	26.5	111.5
Nitrogen (Ref. 6)	34.1	143	29.0	121
Butane (Ref. 6)	24.6	212	8.6	74.5
Oxygen (at 79°K.) (Ref. 2)	46.7	178	36.5	139
Ammonia (Ref. 2)	40.6	138	59.9	204

In view of these factors the surface areas shown in Table II which are calculated from the V_m obtained in this work by means of equation [14] are considered more representative of the porous glass than those obtained using the B.E.T. V_m. The variations in the surface areas obtained for the different gases may well result from variations in the pore structure of the sorbent which were neglected in the present theory. This approach, then, appears to be generally applicable to other porous systems except where appreciable amounts of reversible capillary condensations might occur (type *c* physical adsorption defined above). Even with fibrous networks or compacted solids, however, one would expect hysteresis to result from the filling of nearly spherical type pores. In such systems the 'pore radius' would require a different interpretation with respect to the pore structure. Furthermore, the reversibly sorbed material would not be equally distributed on all surfaces and the evaluation of the surface area by the method described above would lead to inaccurate results.

ACKNOWLEDGMENTS

The authors are indebted to Dr. J. D. Bankier for helpful discussion and to the National Research Council of Canada for the financial assistance which made this investigation possible.

REFERENCES

1. AMBERG, C. H. and MCINTOSH, R. Can. J. Chem. 30: 1012. 1952.
2. BARRER, R. M. and BARRIE, J. A. Proc. Roy. Soc. (London), A, 213: 250. 1952.
3. BRUNAUER, S., DEMING, L. S., DEMING, W. E., and TELLER, E. J. Am. Chem. Soc. 62: 1723. 1940.
4. BRUNAUER, S., EMMETT, P. H., and TELLER, E. J. Am. Chem. Soc. 60: 309. 1938.
5. COHAN, L. H. J. Am. Chem. Soc. 60: 433. 1938.
6. EMMETT, P. H. and DEWITT, T. W. J. Am. Chem. Soc. 65: 1253. 1943.
7. FOSTER, A. G. Trans. Faraday Soc. 28: 645. 1932.
8. KISTLER, S. S., FISCHER, E. A., and FREEMAN, I. R. J. Am. Chem. Soc. 65: 1909. 1943.
9. KRAEMER, E. O. *In* A treatise on physical chemistry. *Edited by* H. S. Taylor. D. Van Nostrand Company, New York. 1931. Chap. 20. p. 1661.
10. KUBELKA, P. and MULLER, M. Kolloid-Z. 58: 189. 1932.
11. MCBAIN, J. W. J. Am. Chem. Soc. 57: 699. 1935.
12. RAO, K. S. J. Phys. Chem. 45: 506. 1941.
13. SCHUCHOWITSKI, A. A. Kolloid-Z. 66: 139. 1934.
14. SHULL, C. G. J. Am. Chem. Soc. 70: 1405. 1948.
15. WHEELER, A. Presentations at catalysis symposia, Gibson Island. Am. Assoc. Advance. Sci. Conf. June, 1945 and June, 1946.
16. ZSIGMONDY, R. Z. anorg. u. allgem. Chem. 71: 356. 1911.

SURFACE ENERGIES OF THE ALKALI HALIDES[1]

By G. C. Benson and G. W. Benson[2]

ABSTRACT

Previous theoretical calculations and experimental measurements of the surface energies or enthalpies of the alkali halides are reviewed briefly. A new attempt to determine the surface enthalpy associated with the {100} face of sodium chloride from a calorimetric study of the effect of particle size on the heat of solution is described. The result (305 ergs/cm.^{2} at 25°C.) appears to be larger than might be predicted on the basis of the classical Born-Mayer theory.

1. INTRODUCTION

The surface energies of ionic crystals have been considered theoretically a number of times during the past thirty years but very little work has been done on their experimental determination. A satisfactory comparison of experimental data with various theoretical models has not yet been achieved. Such a comparison is highly desirable since it would yield information concerning the force fields and distortion of the lattice near the surface of the crystal. Furthermore, at moderate pressures the surface energy differs only negligibly from the surface enthalpy and Jura and Garland (6) have shown that, in simple cases, a knowledge of this quantity at one temperature, together with the contribution of the surface to the specific heat of the crystal as a function of temperature, makes possible a calculation of all the surface thermodynamic properties.

In our laboratory a study of the surface energies of the alkali halides is in progress and the present paper is a report on the current status of this project. A brief review of some theoretical aspects of the problem is given in Section II. This is followed by a summary of the attempts of previous authors to determine the surface energies of the alkali halides calorimetrically. A description of our experimental work is given in Section IV and the preliminary results for sodium chloride are discussed in the last section.

II. SURFACE THERMODYNAMIC QUANTITIES AND THEORETICAL CALCULATIONS OF THE SURFACE ENERGIES OF THE ALKALI HALIDES

The variables, entropy, volume, and composition, are no longer sufficient to specify the thermodynamic state of a solid body having a significant extent of surface, and introduction of other variables becomes necessary. In the simplest case one new variable, the area A, is required and a term γdA is added to the usual expression for the differential of the energy of the system. In terms of more convenient variables, differential surface properties may be defined as derivatives with respect to A at constant temperature T, pressure p, and composition n. On this basis γ is identical with the surface Gibbs free energy $(\partial G/\partial A)_{T,p,n}$.

[1]*Manuscript received September 16, 1954.*
Contribution from the Division of Pure Chemistry, National Research Council, Ottawa, Canada. This paper was presented at the Symposium on Problems Relating to the Adsorption of Gases by Solids, held at Kingston, Ontario, September 10–11, 1954. Issued as N.R.C. No. 3487.
[2]*National Research Council of Canada Postdoctorate Fellow 1952–54. Present address: Division of Mechanical Engineering, National Research Council, Ottawa, Canada.*

Experimentally, surface properties are generally determined by comparing measurements on systems having different specific areas. The quantities obtained are really integral surface properties but when stated per unit area are identified with the differential properties. This involves the added assumption that γ is independent of A.

Theoretical calculations of the surface energy are usually based on atomistic models at zero pressure and temperature. In this case the surface energy, enthalpy, and various free energies become identical and are separately equal to the increase in potential energy of interaction between the ions when a new surface is formed by division of an infinite crystal as illustrated in Fig. 1.

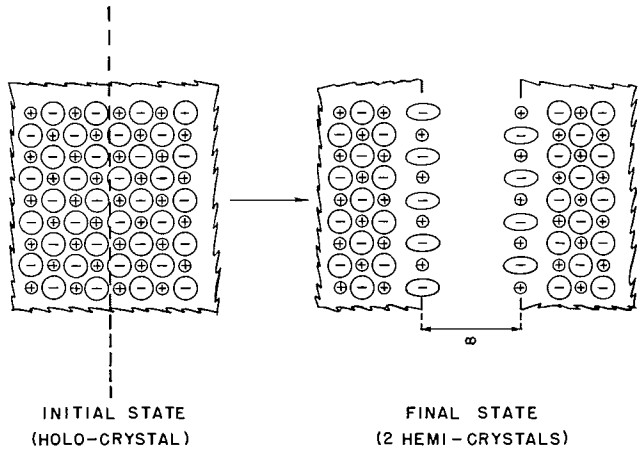

FIG. 1. Formation of two new surfaces by division of a holocrystal into two hemicrystals.

Thus the surface energy per unit area is given by

$$[1] \qquad E_s = (2\,U_{\text{hemi}} - U_{\text{holo}})/2A$$

where U_{holo} and U_{hemi} are the total energies of interaction for the initial crystal and for one of the hemicrystals respectively. A is the area of one of the newly created surfaces.

In classical calculations these energies are evaluated by adding up interactions between pairs of ions, assuming that these interactions can be represented as a sum of coulombic, dipole–dipole, dipole–quadrupole, and repulsive terms. Various types of distortion in the region of the surface such as changes in lattice spacing and polarization of the ions have been considered, and it is generally concluded that significant distortion is limited to one or two layers at the surface and makes a contribution of 10 to 20% to the surface energy.

The dependence of the calculated surface energies on the various types of interactions and distortion assumed in the model is shown in the cycle of values given in Table I. It will be noted that the recent calculation of Shuttleworth gives almost the same value as that of Born and Stern, though a number of refinements have been made in the model. One feature which appears in Shuttleworth's calculations is the relative importance of the van der Waals' attractive terms. Although these forces contribute only a few per cent to the

cohesive energy of the crystal, their contribution to the surface energy is 50% of the net value.

TABLE I

THEORETICAL VALUES OF THE SURFACE ENERGY OF A {100} FACE OF SODIUM CHLORIDE

Author	Description of model	E_s, erg/cm.^{2}	Ref.
Born and Stern 1919	Coulombic and inverse 10th power repulsive forces	150	1
Lennard-Jones and Taylor 1925	Coulombic and inverse 9th (Na—Na), 10th (Na—Cl), and 11th (Cl—Cl) power repulsive forces	96	7
Dent 1929	Same as L.-J. and T. but included polarization and a 5% contraction at the surface	77	3
Shuttleworth 1949	Coulombic, attractive van der Waals' and exponential repulsive forces; also included a correction for surface distortion	155	11

Recently a quantum mechanical calculation of the surface energy of LiF has been described by van der Hoff and Benson (5). In this an attempt is made to consider the electronic density distributions of the ions in more detail and to avoid the introduction of semiempirical force laws. The value of the cohesive energy of the crystal calculated by this model is in good agreement with that calculated in a classical fashion, but the surface energy is about two to three times larger than the classical value.

III. PREVIOUS EXPERIMENTAL MEASUREMENTS OF THE SURFACE ENERGIES OF THE ALKALI HALIDES

Sutherland (12) has given an excellent review of previous attempts to determine the surface energy, enthalpy, or free energy of a solid. A method which seems very likely to yield useful results in this field is the determination of the surface enthalpy from the effect of particle size on the heat of solution. Lipsett, Johnson, and Maass (8) measured this effect for sodium chloride in water. Their original result was 400 ergs/cm.^{2} at 25°C., but the salt in this experiment was exposed to water vapor for a period of time before the solution process. In a second paper (9) by the same authors, a new technique to avoid this exposure is described and a revised value of 386 ergs/cm.^{2} reported. Boyd and Harkins (2) performed similar experiments and obtained a value of 395 ergs/cm.^{2} The areas in both these sets of experiments were obtained from photomicrographs and are generally considered to be too small. Hence the values of the surface enthalpy are probably high. Wertz (13) working in Harkins' laboratory used a gas adsorption technique for measuring the area of the salt and obtained a value of 130 ergs/cm.^{2} for the surface enthalpy. Unfortunately this work was discontinued after a single determintion and the value cannot be considered as well established. In all these measurements the surface area of the salt used was in the range 1–5 square meters per gram

and no attempt was made to establish that the heat effect per unit weight was proportional to the specific surface area.

IV. EXPERIMENTAL DETERMINATION OF THE SURFACE ENTHALPY OF SODIUM CHLORIDE

It is apparent from the brief survey of theoretical and experimental work given in the two preceding sections that further investigation of the calorimetric method of determining the surface enthalpy would be of value. With this purpose in view, we have constructed an adiabatic calorimeter suitable for measuring heats of solution at 25°C.

The calorimeter vessel (190 cc. capacity) is constructed from a corrosion resistant stainless steel. It is hung by nylon loops inside an evacuated space surrounded by a water jacket. The temperature of the latter can be varied to maintain adiabatic conditions. The sample of salt sealed in a thin-walled glass bulb is held in a guillotine arrangement. Breaking the bulb and stirring the contents of the calorimeter is accomplished by an intermittent rotation of the whole assembly through 180°. Further details of the design and operation of the calorimeter will be given in another publication.

Emersleben (4) has deplored the failure of most workers to give information regarding particle size when reporting heats of solution and has criticized Wüst and Lange (14) in connection with their results for sodium chloride. It thus seemed desirable to carry out some measurements on "coarse" salt. At the same time this served to establish the accuracy of the calorimetric procedure.

The coarse salt was Merck reagent recrystallized three times from conductivity water. It was given a final drying in the sample bulb under vacuum at 300°C. for 12 hr. before being sealed off under a few millimeters pressure of helium. Attempts to measure the area of this salt by the usual B.E.T. nitrogen adsorption method at 78°K. indicated that the area was negligibly small (i.e. less than 0.1 square meter per gram, which corresponds to an average particle size exceeding 30μ). Equilibrium conductivity water was used in all solution experiments and no attempt was made to remove dissolved gases. Measurements were made in the concentration range 0.05 to 1.4 molal. The results appear to be more consistent internally than those of previous workers and fall between the values reported by Wüst and Lange (14) and by Lipsett, Johnson, and Maass (8, 9). The reproducibility of the present results is estimated to be about 0.1% down to 0.2 molal. Below this concentration the errors increase and are of the order of 0.5% at the lowest concentration studied. The solid curve in Fig. 2 was plotted from a table of our smoothed data. The calorie used in stating these values is defined as 4.1840 absolute joules. A more detailed analysis of the coarse salt results will be given in the paper on the operation of the calorimeter.

The fine salt was prepared in an apparatus similar to that described by Young and Morrison (15) but some changes were made in the method of heating the salt. Also contact between the salt and brass parts of the apparatus was eliminated. Some signs of non-stoichiometry have been observed for salt prepared

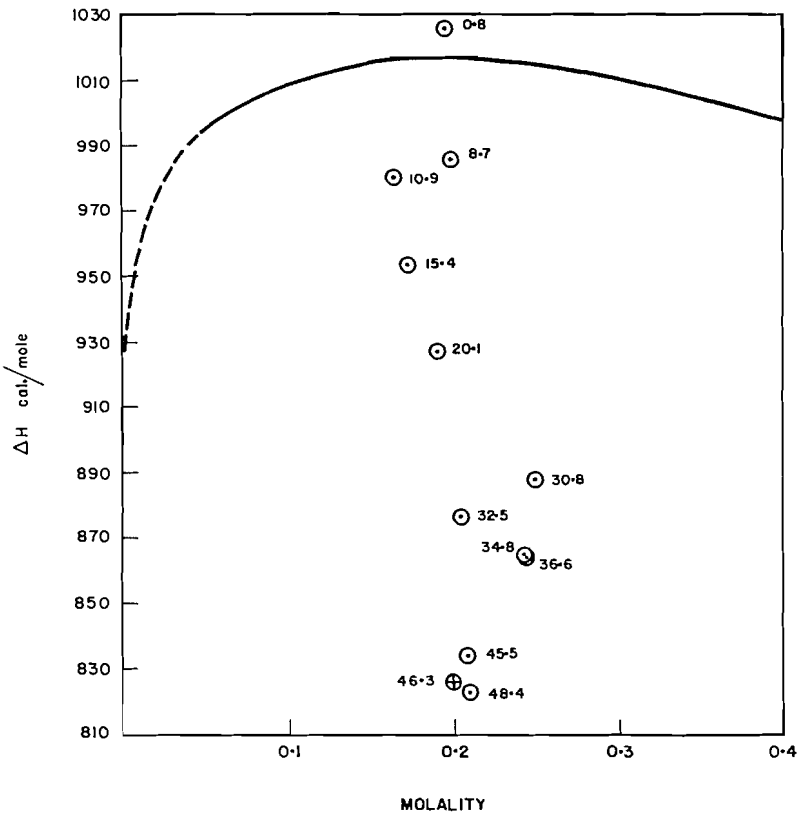

FIG. 2. The curve represents the $\triangle H$ for solution of coarse sodium chloride in water at 25°C. plotted as a function of molality. The results obtained for fine salt are indicated by the points labelled with the areas in square meters per gram. The point marked with a cross is for unsintered salt; all other points are for sintered samples.

by this method. Samples collected at high precipitator voltages sometimes have a slight blue color and give alkaline solutions when dissolved in water. This blue color probably indicates the presence of colloidal sodium produced by electrolysis or bombardment in the electrostatic precipitator. A careful check was kept on the pH of solutions of the fine salt and none of the material used in the present work showed this effect.

Care was taken to minimize any exposure of the fine material to water vapor. B.E.T. areas were measured on the actual samples to be dissolved in the calorimeter. The original preparation yielded material with a surface area of about 48 square meters per gram. It was found that controlled sintering offered a convenient method of producing samples with lower specific surfaces. Thus samples of fine salt were heated under vacuum for 14 hr. at temperatures from 70 to 200°C. before the area was measured. Below 100°C. the sintering was negligible, while at 200°C. nearly the whole area could be destroyed in the 14-hr. period.

Heats of solution measured with the fine salt are indicated by the points in Fig. 2 labelled with the specific areas of the samples. The point marked with a

cross was obtained with the original unsintered material; all other samples were sintered. The fact that one area is higher than the unsintered material is due to a slight non-uniformity of the original preparation.

V. DISCUSSION OF THE RESULTS

Excluding the smallest area sample, the points for fine salt fall below the curve for coarse salt, indicating a positive particle size effect. A plot of the deviation $(\Delta H)_s$ against surface area, given in Fig. 3, shows a definite linear

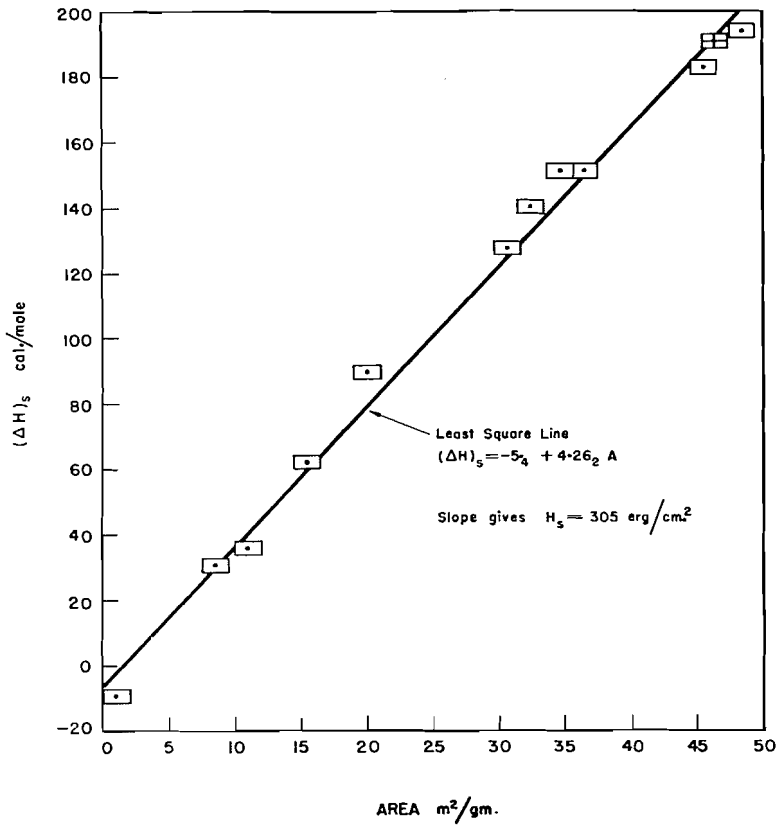

FIG. 3. Plot of the variation of the $\triangle H$ for solution of sodium chloride in water at 25°C. as a function of the surface area of the sample. The point marked with a cross is for unsintered salt; all other points are for sintered samples. The length and breadth of the rectangles correspond to ±1 square meter per gram and ±2 cal./mole respectively.

trend but does not go through the origin. The slope of the least square line corresponds to a surface enthalpy $H_s = 305$ ergs/cm.^{2} at 25°C. Electron micrographs of the salt prepared by Young and Morrison show that the crystals are predominantly cubic; hence the above value of H_s should be associated with the {100} face of sodium chloride.

It is difficult at present to place limits on the accuracy of this result. The B.E.T. method applied to materials like sodium chloride is generally considered to give the surface area to about 5 to 10% though the reproducibility of the

measurement is much better than this. The accuracy of the individual calorimetric determinations of $(\Delta H)_s$ is of the order of 2 or 3 cal./mole but variations from sample to sample are higher than this. The most disturbing feature is the negative value of $(\Delta H)_s$ obtained for the smallest area sample. This is further confirmed by the negative intercept of the least square line. Unfortunately the measurements were made in the order of decreasing area and the sign and magnitude of the intercept was not apparent for sime time. Since then spot tests done on the fine salt have indicated the presence of nitrate and nitrite impurities. Presumably these were formed in the Cottrell precipitator. Since all the data reported came from one preparation of fine salt, it is quite possible that a reasonable correction could be made by moving the line with fixed slope until it passes through the origin. This assumes the impurities are fairly homogeneously distributed in the original preparation. In this case the surface enthalpy is unchanged but it is for impure sodium chloride. The influence of these impurities on the surface enthalpy will depend to a large extent on their nature and on whether they are preferentially concentrated in the surface region.

The electron micrographs mentioned above also showed a broad distribution of particle size. Extremely small crystals may be expected to show deviations arising from the effects of edges and corners. Even for larger crystals surface structure such as steps and kinks may lead to irregularities in the apparent surface energy. In addition there is the further possibility of effects arising from strain energy in the small crystals. The present results with sintered samples indicate that if these effects are present and make significant contributions to the heat of solution they are proportional to the extent of surface and for practical purposes could be lumped with the ideal surface contribution. However, comparison of the result with a theoretical model requires a more detailed knowledge of these various factors.

Until the uncertainties outlined in the preceding two paragraphs are investigated further, the value 305 ergs/cm.^{2} must be considered as provisional. Nevertheless, a comparison of this value with the theoretical and previous experimental results summarized in Sections II and III is of interest. Our value is roughly 85 ergs/cm.^{2} lower than the values reported by Lipsett, Johnson, and Maass and by Boyd and Harkins. This is in line with the criticism of their area determination. Wertz's result is considerably lower but is based on an isolated measurement. The value of H_s at 0°K. is related to that at 298°K. by the equation

$$[2] \qquad H_s(0°) = H_s(298°) - \int_0^{298} C_s dT$$

where C_s is the surface contribution to the heat capacity. Patterson and Morrison (10) are studying this last term in detail but their results are incomplete as yet. At present all that can be deduced from [2] is that $H_s(0°)$ should be smaller than 305 ergs/cm.^{2} It seems rather doubtful that the temperature correction will reduce this to the classically calculated value of 155 ergs/cm.^{2}

An equivalent way of stating the present result is

$$[3] \qquad (\Delta H)_s = 11.8/l \text{ cal./mole}$$

where l is the length in microns of the edge of an average sized cubic particle. Emersleben (4) has given a theoretical value of 13.0 for the numerical coefficient. Although the derivation is based on a model assuming an ideal lattice and only coulombic forces, the expression does provide a useful approximation in the present case.

ACKNOWLEDGMENTS

The authors are indebted to Dr. H. P. Schreiber and Dr. F. W. Thompson for preparing the samples of fine salt and to Mr. P. D'Arcy for assistance with the calorimetric measurements. They also wish to thank Dr. J. A. Morrison and Dr. D. Patterson for many stimulating discussions of surface problems.

REFERENCES

1. Born, M. and Stern, O. Sitzber. preuss. Akad. Wiss. Physik.-math. Kl. 48: 901. 1919.
2. Boyd, G. E. and Harkins, W. D. J. Am. Chem. Soc. 64: 1190. 1942.
3. Dent, B. M. Phil. Mag. 8: 530. 1929.
4. Emersleben, O. Z. physik. Chem. 200: 1. 1952.
5. van der Hoff, B. M. E. and Benson, G. C. J. Chem. Phys. 22: 475. 1954.
6. Jura, G. and Garland, C. W. J. Am. Chem. Soc. 74: 6033. 1952.
7. Lennard-Jones, J. E. and Taylor, P. A. Proc. Roy. Soc. (London), A, 109: 476. 1925.
8. Lipsett, S. G., Johnson, F. M. G., and Maass, O. J. Am. Chem. Soc. 49: 925. 1927.
9. Lipsett, S. G., Johnson, F. M. G., and Maass, O. J. Am. Chem. Soc. 49: 1940. 1927.
10. Patterson, D., Morrison, J. A., and Thompson, F. W. Can. J. Chem. 33: 240. 1955.
11. Shuttleworth, R. Proc. Phys. Soc. (London), 62, A: 167. 1949.
12. Sutherland, K. L. Australian Chem. Inst. J. & Proc. 14: 268. 1947.
13. Wertz, J. E. Private communication.
14. Wüst, J. and Lange, E. Z. physik. Chem. 116: 161. 1925.
15. Young, D. M. and Morrison, J. A. J. Sci. Instr. 31: 90. 1954.

A LOW TEMPERATURE PARTICLE SIZE EFFECT ON THE HEAT CAPACITY OF SODIUM CHLORIDE[1]

By D. Patterson,[2] J. A. Morrison, and F. W. Thompson[2]

ABSTRACT

An effect of particle size upon the heat capacity of sodium chloride has been found in the temperature range 9° to 21°K. The experiments were done with three NaCl samples of specific surfaces between 38 and 59 sq. meters per gm. The observed effect has the temperature dependence predicted by theory but its magnitude is three to four times larger than expected. It is unlikely that adsorbed gases have made any significant contribution in the experiments. The accuracy with which the specific heat and surface area differences have been determined is not high enough to show definitely whether or not the surface specific heat is an extensive property of the surface.

INTRODUCTION

The existence of an effect of particle size on the thermodynamic properties of a solid is evident from the Einstein model which considers the solid as an assembly of oscillators identified with the atoms. Atoms on the free surface are less strongly bound than those in the interior so that their frequency is lowered, producing a change in thermodynamic properties which is proportional to the surface area. With the Debye or Born – von Karman models, however, the oscillators are identified with the normal modes of vibration of the whole solid. The effect of free boundaries is then not localized in the frequencies of oscillators associated with the surface but is spread throughout the frequency spectrum. Nevertheless, it may be shown that in particular cases the effect of finite particle size reduces to a contribution to the thermodynamic quantities which is extensive in the surface area, plus other contributions (e.g. edge contribution) which can ordinarily be neglected.

Brager and Schuchowitsky (2, 3), Montroll (8), and Stratton (11) give the following relation (low temperature form) for the heat capacity of small particles of rectangular cross-section and with perfect faces,

$$C_v = 464.5\ (T/\theta_D)^3 + B(T/\theta_D)^2 + \ldots \text{ cal./gm. atom deg.} \qquad [1]$$

where θ_D is the Debye characteristic temperature and B is a constant proportional to the specific surface area. According to [1] the surface contribution becomes more important at low temperatures since it is decreasing as T^2 while the volume contribution does so as T^3. If the density of modes in the frequency spectrum is too low, equation [1] breaks down and the specific heat is no longer an extensive property of the surface. This may occur if the particles are too small or if the temperature is too low, i.e. if $(h\nu_0/2kT) > (2N/\pi)$ (ν_0 is the maximum frequency of the solid lattice and N^3 is the number of atoms in the particle).

[1]*Manuscript received September 16, 1954.*
Contribution from the Division of Pure Chemistry, National Research Laboratories, Ottawa. Issued as N.R.C. No. 3478. This paper was presented at the Symposium on Problems Relating to the Adsorption of Gases by Solids, held at Kingston, Ontario, September 10–11, 1954.
[2]*National Research Laboratories Postdoctorate Research Fellow.*

Specific heat measurements on several samples of TiO_2 between 12° and 270°K. showed an effect of particle size above 50°K. (4) which could be explained to an order of magnitude as an effect on the optical modes of vibration of TiO_2 (10). However, the low temperature increase predicted by equation [1], which has to do with the acoustical modes, was not found. Since there were no grounds for doubting the theory, it was decided that the low temperature effect must have been masked by other effects. Therefore, it seemed worthwhile to try further experiments using the simpler solid, NaCl, about which more is known theoretically, and also to carry the experiments to as low a temperature as possible. With the NaCl, an increase of the specific heat with decreasing particle size has now been found at low temperatures. The temperature dependence of the effect is that required by theory but the magnitude is three to four times greater than anticipated.

Apart from the intrinsic interest in the effect itself, two other considerations exist. Recently there has been some discussion (1, 5, 6, 7) as to whether or not thermodynamic properties associated with solid surfaces are extensive properties of the surface in a real case, as has been predicted by [1]. An answer to this should be found in experiments such as the present ones, but unfortunately the accuracy achieved so far is not high enough to permit definite conclusions to be drawn. A further interest lies in the possibility of obtaining information about surface structure from measurements of particle size effects, but for this purpose the experiments must extend over a wide temperature range.

EXPERIMENTAL

Materials

The small particles of NaCl (mean specific surfaces between 38 and 59 sq. meters per gm.) were prepared by the method described by Young and Morrison (12) and by a recent modification of this method. The methods involve volatilizing NaCl in a platinum crucible and sweeping the crystals formed from the vapor into an electrostatic precipitator with a stream of dry nitrogen. The samples were handled in an inert gas atmosphere in either a dry box or a desiccator. Each sample was about 30 gm.

The specific surfaces of the samples were determined by nitrogen adsorption at liquid nitrogen temperatures. Determinations on the whole calorimetric samples and on aliquots (0.5 to 2 gm.) agreed to 10% or better.

Calorimetric Measurements

The details of the calorimetric method are given fully in a preceding paper (9) so that here it is only necessary to discuss special effects associated with the experiments on the small particles.

In the experiments with bulk NaCl (9) it was found that thermal equilibrium within the calorimeter vessel could be readily attained over the temperature range 2.5° to 20°K. with 10^{-6} moles of helium in the vessel. Further, this amount of helium did not make a significant contribution to the specific heat of the system. On the other hand, with the small particles of NaCl in the

calorimeter vessel, 10^{-6} moles of helium did not allow thermal equilibrium to be established in a reasonable time below about 9°K. Apparently the helium was being adsorbed on the large surface presented by the small particles. One set of experiments was done with 10^{-4} moles of helium in the calorimeter vessel but here also equilibrium times became much too long below 9°K. The heat capacity of this additional helium was very much less than it would have been if the helium had been present as a gas. This suggests that the helium was being strongly adsorbed in a localized array on the surface.

In principle, specific heat measurements such as these can be pursued to temperatures below 9°K. simply by increasing the amount of helium until some is left in the gas phase at the lowest temperature desired. Practically, however, correcting for the effect of helium on the specific heat would prove difficult. The additional results which might be obtained would hardly justify the labor involved in determining the heat capacity of the adsorbed helium, the heat of adsorption, etc., over a range of temperature and of concentration.

RESULTS AND DISCUSSION

Since the heat capacity of NaCl changes by about a factor of 20 in the range 9° to 20°K., the small observed dependence of the heat capacity upon particle size cannot be shown conveniently in a graph of the primary data.

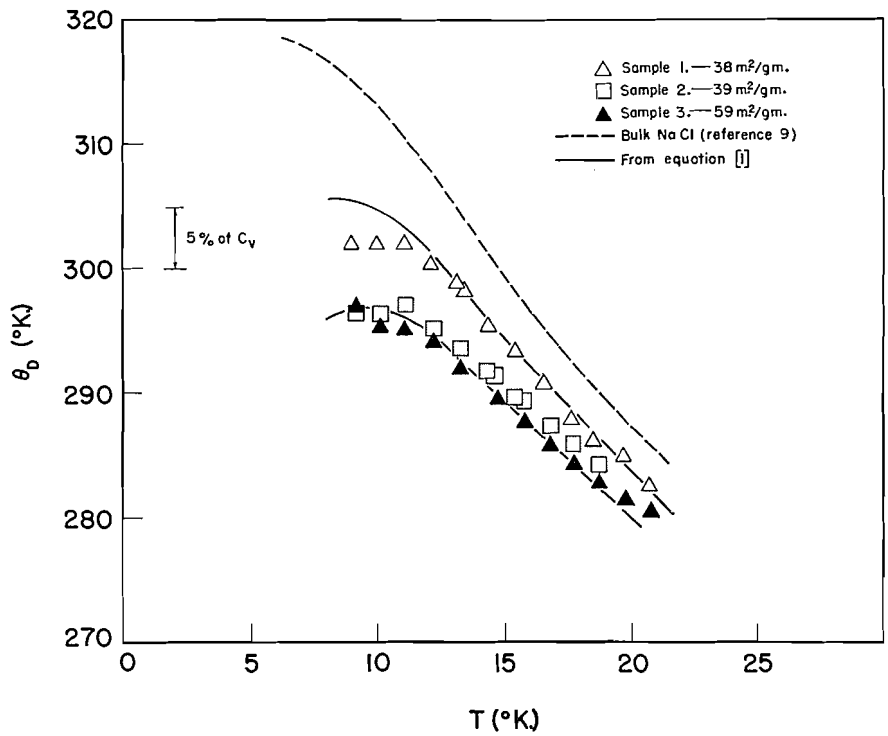

FIG. 1. The Debye characteristic temperature (Θ_D) for small particles of NaCl as a function of temperature.

Rather, recourse is had to a plot of the 'apparent' Debye characteristic temperature corresponding to each measured specific heat versus the absolute temperature. All of the results shown in this form in Fig. 1 were obtained with about 10^{-6} moles of helium in the calorimeter vessel. The significant point is that each of the three samples of small particles of NaCl has a larger specific heat (lower θ_D) than that of the bulk over the temperature range 9° to 21°K. As will now be shown, the temperature dependence of the specific heat is of the expected form.

The theoretical predictions are based on the Debye model, although it is recognized that it does not hold exactly for bulk NaCl, i.e. θ_D is a function of temperature. The consequences of the model are given by equation [1]. The two full curves of Fig. 1 have been calculated using the equation with the constant B fitted from the experimental points for samples 1 and 3 at 15°K. There is a certain arbitrariness involved in this fitting but it seemed most reasonable to select fixed points abut the middle of the temperature region. Although there appears to be a small systematic deviation at the higher temperatures for sample 3 and at the lower temperatures for sample 1, the curves reproduce the experimental results quite well. The deviation at the lower temperatures is probably due to the difficulty of attaining thermal equilibrium.

The actual values of B for samples 1 and 3 deduced from the experiments are 1.28 and 2.60 cal./mole deg. respectively whereas Montroll's theory (8) gives 0.42 and 0.64. The magnitude of the particle size effect is, therefore, three to four times larger than predicted. While no quantitative explanation for this difference can be offered as yet, the observed values might be increased by several things, e.g. by the presence of adsorbed gases or by surface roughness and non-stoichiometry. The effect of adsorbed gases must, however, be insignificant in these experiments. The excess of the specific heat of sample 1 over that of bulk NaCl is approximately 0.0055 cal./deg. at 20°K. Were this amount to be contributed by adsorbed atoms or molecules behaving as fully excited oscillators, nearly 10% of the surface would need to be covered. Such a surface concentration would seem unlikely because the weakly bound oscillators would readily desorb at room temperature. Any gases not removed by pumping at this temperature would be held to the surface so tightly as to have high frequencies of oscillation, at least of the order of 10^{13} sec.$^{-1}$. Oscillators of frequency higher than about 10^{12} sec.$^{-1}$ would make no significant specific heat contribution below 20°K.

Surface roughness and non-stoichiometry may well explain the difference in results between samples 1 and 3 and sample 2. The former two were made in the same apparatus, the only difference in their preparations being the temperature of volatilization of the NaCl. Sample 2 was prepared in another apparatus with a somewhat higher potential in the electrostatic precipitator, and it shows a particle size effect which is much too large compared with that for samples 1 and 3. Sample 2 must have contained an excess of sodium as the pH of its solution in water was about 9 compared with pH's of 6 to 6.5 for the solutions of the other two samples. Since the specific heat for this sample has the same temperature dependence as that for the other two, one might specu-

late that the excess sodium was in the surface. However, no attempt has been made yet to deduce quantitatively the effect of such a surface excess.

The ratio of the B's for samples 1 and 3 is 2.03, while the ratio of their surface areas is 1.55. The difference, approximately 25%, is just within the probable combined experimental error in determining the differences in specific heat and in surface area. The experiments, therefore, do not allow a definite decision as to whether or not the surface specific heat is an extensive property of the surface.

ACKNOWLEDGMENT

We are indebted to Dr. D. M. Young for assistance in the early stages of the work.

REFERENCES

1. BAUER, S. H. J. Am. Chem. Soc. 75: 1004. 1953.
2. BRAGER, A. and SCHUCHOWITSKY, A. Acta Physicochim. U.R.S.S. 21: 1001. 1946.
3. BRAGER, A. and SCHUCHOWITSKY, A. J. Chem. Phys. 14: 569. 1946.
4. DUGDALE, J. S., MORRISON, J. A., and PATTERSON, D. Proc. Roy. Soc. (London), A, 224: 228. 1954.
5. JURA, G. J. Chem. Phys. 17: 1335. 1949.
6. JURA, G. and GARLAND, C. W. J. Am. Chem. Soc. 74: 6033. 1952.
7. JURA, G. and GARLAND, C. W. J. Am. Chem. Soc.75: 1006. 1953.
8. MONTROLL, E. W. J. Chem. Phys. 18: 183. 1950.
9. MORRISON, J. A., PATTERSON, D., and DUGDALE, J. S. Can. J. Chem. 33: 375. 1955.
10. PATTERSON, D. To be published.
11. STRATTON, R. Phil. Mag. 44: 519. 1953.
12. YOUNG, D. M. and MORRISON, J. A. J. Sci. Instr. 31: 90. 1954.

REVERSIBILITY IN PHYSICAL ADSORPTION[1]

By E. L. Pace, K. S. Dennis, S. A. Greene, and E. L. Heric

ABSTRACT

The question of reversibility and equilibrium is considered in relation to the physical adsorption of gases on finely divided solid surfaces. Conclusions are drawn from calorimetric measurements of (1) adsorption isotherms, (2) integral, differential, and isosteric heats of adsorption, and (3) heat capacity of the adsorbed phase for surface coverages of the order of a monolayer or less. In line with the preceding, results are presented and discussed for calorimetric studies involving (1) heats of adsorption and heat capacities of methane adsorbed on rutile between 80 and 140°K., (2) heats of adsorption of argon on rutile between 60 and 90°K., and (3) the zero point entropy of krypton adsorbed on rutile at a coverage of about 0.57 of the monolayer capacity.

INTRODUCTION

The following paper will be directed towards the question of reversibility and equilibrium as related to the physical adsorption of gases on finely divided solid surfaces. Surface coverages under consideration will, in general, be of the order of a monolayer or less. The conclusions will be drawn from calorimetric measurements of (1) adsorption isotherms, (2) integral, differential, and isosteric heats of adsorption, and (3) heat capacity of the adsorbed phase.

Some methods used in establishing the reversibility of the adsorption process are essentially empirical in character. Those deserving mention here are (1) the reproducibility of the adsorption isotherm and its invariance with time and (2) comparison of the heat of adsorption with the heat of desorption at the same surface coverage and temperature. In the case of the adsorption isotherms, difficulties arise because of the slowness of the equilibrium process and the necessary measurement of very low pressures with precision. These difficulties have been emphasized in the recent work of Young *et al.* (10) with *n*-heptane on various solid surfaces and Crowell and Young (1) with the argon–graphite system. If heats of adsorption and desorption agree within the experimental error, this agreement is an indication that the adsorption and desorption paths are the same. The method, however, is not generally feasible at low equilibrium pressures because of the slow rate of the desorption process of the adsorbate. This second method has been used under suitable conditions by Pace *et al.* (8) in a study of the methane–rutile system and by Morrison and co-workers (5) in studies of argon adsorbed on rutile.

Some methods of establishing reversibility are fundamentally thermodynamic in character. It is possible by these methods to derive the same thermodynamic quantity from independent measurements of adsorption isotherms, heats of adsorption, and heat capacity at several coverages and temperatures.

[1]*Manuscript received September 16, 1954.*
Contribution from Morley Chemical Laboratory, Western Reserve University, Cleveland, Ohio. This paper was presented at the Symposium on Problems Relating to the Adsorption of Gases by Solids, held at Kingston, Ontario, September 10–11, 1954.

From the adsorption isotherm, we can obtain the isosteric heat (q_{st}) from the expression

[1] $$q_{st} = RT^2(d \ln P/dT)_{N_s}$$

in which P is the equilibrium pressure of the adsorbate, N_s is the number of adsorbed moles, and T is the absolute temperature. The isosteric heat q_{st} is related to the molar heat content of the gas (H_G) and differential molar heat content (considering adsorbed gas as one component system) of the adsorbed gas ($\bar{H}_s$) by the expression

[2] $$q_{st} = H_G - \bar{H}_s.$$

The experimental integral heat of adsorption (Q_{N_s}) is also related to q_{st} since

[3] $$Q_{N_s} = \int_0^{N_s} q_{st} dN_s.$$

A differential heat of adsorption can be defined in terms of the integral heat as $(dQ_{N_s}/dN_s)_T$. It can be evaluated either as the slope of the integral heat curve or by direct experimental measurement. If the increment of added gas is small enough, $(\Delta Q_{N_s}/\Delta N_s)_T$ is essentially the same as $(dQ_{N_s}/dN_s)_T$. It is also obvious that the differential heat of adsorption is identified thermodynamically with the isosteric heat. Kington and Aston (4) have pointed out that calorimetrically measured quantities can be interpreted without ambiguity in terms of the reversible thermodynamic properties of the system.

The heat capacity of the adsorbed phase can be measured directly and also can be derived from the temperature coefficient of the various heats of adsorption from the expressions

[4] $$(dQ_{N_s}/dT)_{N_s} = N_s(C_{PG} - C_{N_s})$$

and

[5] $$(dq_{st}/dT)_{N_s} = C_{PG} - \bar{C}_{N_s}.$$

In the preceding expressions, C_{PG} is the molar heat capacity of the gas, C_{N_s} is the molar heat capacity of the adsorbed gas, and $\bar{C}_{N_s}$ is the differential molar heat capacity.

Finally, the zero point entropy evaluated from heat capacity, heat of adsorption, and heat capacity measurements provides the most complete criterion for the reversibility of the adsorption process. The zero point entropy S_0 is calculated from

[6] $$S_0 = S_G(T, P_0) - \int_0^T (C_{N_s}/T)\, dT - Q_{N_s}(T)/T - R/N_s \int_0^{N_s} \ln P/P_0 dN_s$$

in which $S_G(T,P_0)$ is the molar entropy of the gas at temperature T and reference pressure P_0 and P is the equilibrium pressure of the adsorbate. A value of zero for S_0 would be a strong indication that the adsorption process was an equilibrium one. A non-zero value would have ramifications in terms of the configuration of the adsorbed phase, surface barriers, etc. Morrison and

co-workers (2, 5) have used this particular method very effectively in their study of the argon–rutile system.

In line with the preceding observations we are presenting the results of some calorimetric studies on (1) heats of adsorption and heat capacities of methane adsorbed on rutile between 80 and 140°K., (2) heats of adsorption of argon on rutile between 60 and 90°K., and (3) the entropy of krypton adsorbed on rutile at a coverage of about 0.57 of the monolayer capacity.

EXPERIMENTAL

The methane–rutile system was studied with a low temperature adiabatic calorimeter, the general features of which have been previously described (9). The adsorbate was Research Grade methane of 99.5% minimum purity obtained from the Phillips Petroleum Company. It was purified further by a one-step fractional distillation. The rutile was obtained from the National Lead Company. The monolayer capacity was 0.0311 moles of methane by the B.E.T. method.

The argon–rutile system was studied with a Nernst-Giauque type calorimeter. Some of the details concerning this calorimeter are to be found in the literature (7). The rutile sample, obtained from the National Lead Company, was from a different batch than for the preceding study. It was 94.3% titanium dioxide, the remainder being adsorbed or coordinately bound water. The monolayer capacity was 0.0541 moles of argon.

The entropy of the krypton–rutile system was determined with an adiabatic calorimeter which was almost identical with the one used for the methane–rutile study. The krypton was obtained from Matheson Company. The analysis supplied with the gas indicated a total impurity of 0.08 mole per cent. The rutile sample was taken from the same batch as that used in the argon–rutile system. Its monolayer capacity was 0.0283 moles of krypton.

The details involved in obtaining the calorimetric data on isotherms, heats of adsorption, and heat capacity, have been described adequately elsewhere (2, 5, 8, 9).

DISCUSSION

It has been pointed out that a certain internal consistency should exist between the heat capacity derived from the temperature coefficient of the integral heat of adsorption and the directly measured quantity if the adsorption is reversible. The heat capacity of methane adsorbed on rutile was measured at coverages of 0.00887, 0.01763, 0.02641, and 0.03463 moles of methane corresponding to the fractions 0.28, 0.56, 0.84, and 1.11 of the monolayer. Integral heats of adsorption were measured at 110, 120, 130, and 140°K. and the temperature coefficient used to evaluate values of c_{N_s}($c_{N_s} = N_s C_{N_s}$). The results are presented in Table I. The direct measurement of the heat capacity at some coverages was not extended to temperatures as high as those used for the integral heats. In these cases, the heat capacity curve was extrapolated for the purpose of comparing results. The heat capacities from the two sources agree well within the experimental error. Therefore, the adsorption

TABLE I

HEAT CAPACITY OF METHANE ADSORBED ON RUTILE*

Moles adsorbed	Temperature (°K.)	c_{N_s} from $(dQ_{N_s}/dT)_{N_s}$ (cal. deg.$^{-1}$)	c_{N_s} from direct measurement (cal. deg.$^{-1}$)
0.00887	135	0.133	0.127
0.01763	125	0.214	0.234
0.01763	135	0.219	0.240
0.02614	115	0.327	0.346†
0.02614	125	0.324	0.350†
0.02614	135	0.358	0.354†
0.03463	115	0.471	0.477†

A sample (48.5 gm.) with monolayer capacity of 0.0311 moles.
†Extrapolated from heat capacity curve.*

appears to be reversible for the methane–rutile system above 110°K. at all coverages.

The results of a study of the differential heats of adsorption of argon adsorbed on a rutile surface for coverages to a maximum of the order of a monolayer are summarized in Fig. 1. The measurements were carried out at temperatures of 63.5, 69.5, 73.0, 78.5, and 86.5°K. A warm thermal drift was encountered at 69.5°K. at low coverages which made the evaluation of the differential heat very uncertain. Therefore, the data at this temperature are not shown. The data at 73, 78.5, and 86.5°K. were used with directly measured heat capacities to reduce the results to a single curve at 63.5°K. The differential heats measured experimentally at 63.5°K. did not fall on the preceding curve, even though, unlike the measurements at 69.5°K., no prolonged thermal drift was observed within the limits of the sensitivity of the calorimeter (0.001 calorie per minute). The values which were obtained gave the two lower curves in Fig. 1. The path of adsorption in this case appears to depend on the size and the order of the increments of gas which are added. When the values of the differential heat at 63.5°K. are used with those at higher temperatures to determine an average value for the heat capacity of the adsorbed phase, the results are entirely unreasonable. Consequently, we conclude that the adsorption has taken place reversibly for the argon–rutile system only at temperatures above 73°K.

The results of a zero point entropy determination for a system consisting of 0.01627 moles ($\theta = 0.57$) of krypton adsorbed on rutile with a monolayer capacity of 0.0283 moles are presented in Table II. The value is 0.4 ± 1.0 cal. deg.$^{-1}$ mole^{-1}.

The precision in the value of the zero point entropy would allow one to draw two conclusions without a clear decision as to which is correct.

One conclusion is that the zero point entropy is zero at absolute zero for the adsorbed gas (assuming no surface perturbation) and hence, the adsorption process is reversible. This conclusion has been reached by Morrison and co-workers (2, 5) in their study of the argon–rutile system. The other conclusion is that the zero point entropy is a small, positive value. The appearance

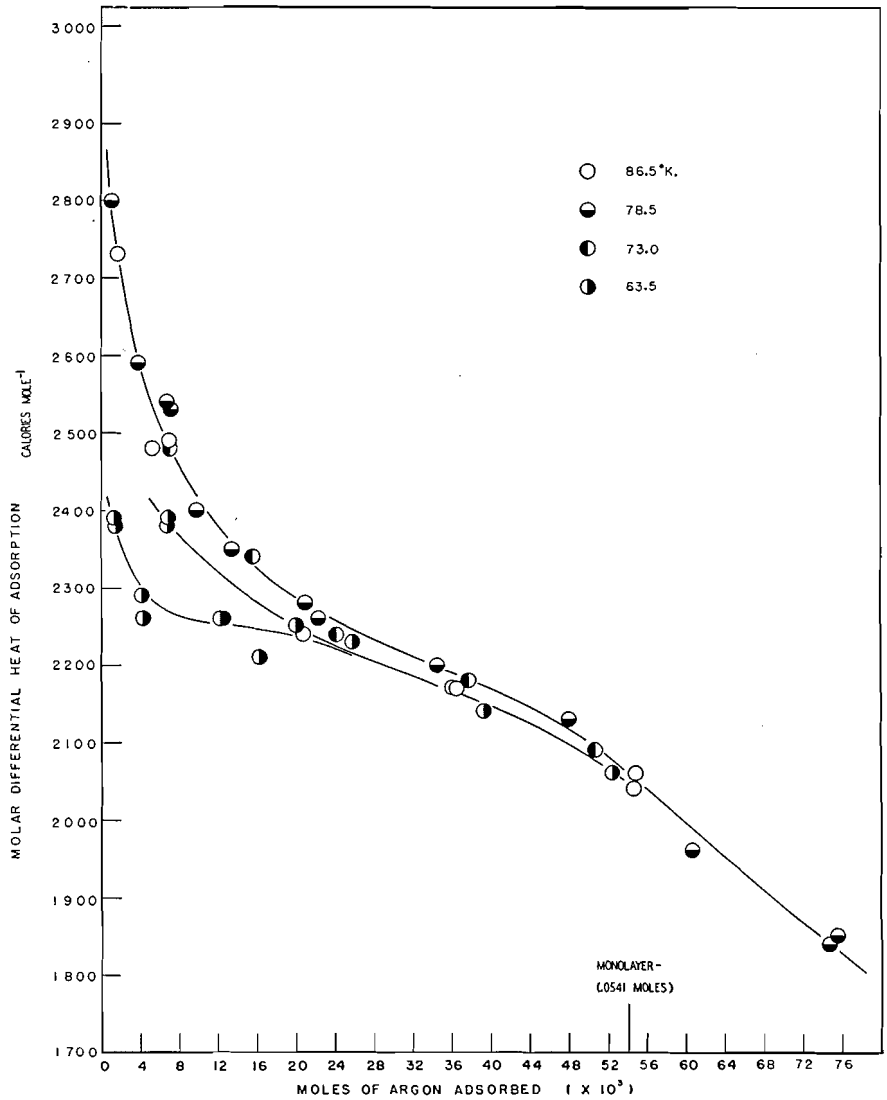

FIG. 1. Differential heat of adsorption of the argon–rutile system.

of such an entropy could arise from an appreciable number of molecules being present in a reasonably homogeneous but not completely filled group of sites at very low temperatures. The coverage which has been studied experimentally is a favorable one from this standpoint. At the lowest temperature of the heat capacity measurements, the group of sites at the peak of the distribution function, comprising about 10% of the total sites, is incompletely filled. Calculations of the type described by Hill (3) based on a unimolecular localized model show that this group of sites contributes a small configurational entropy (about 0.3 cal. deg.$^{-1}$ mole^{-1}) which is essentially temperature independent

TABLE II

ZERO POINT ENTROPY OF KRYPTON ADSORBED ON RUTILE
0.01627 moles adsorbed krypton; monolayer capacity 0.0283 moles; $\theta = 0.57$

$S_0^{18}(C_{osc}/T)\,dT$	2.39 cal. deg.$^{-1}$ mole^{-1}
$S_{18}^{126}(C_{N_s}/T)\,dT$	14.47
$Q_{N_s}/126$	28.07
$R/N_S\int_0^{N_s} \ln P/P_0\,dN_S$	−3.34
$S_G(126, P_0) - S_0$	41.59
$S_G(126, P_0)$ by Sackur-Tetrode equation	42.01
S_0	0.4*
S_0 for homogeneous surface	2.4

*Estimated uncertainty ±1.0 cal. deg.$^{-1}$ mole^{-1}.

between 10 and 125°K. The details concerning this calculation will be presented in a forthcoming publication (6) and so will not be discussed further here. Consequently, a zero point entropy of the order of that observed would result with a continuous energy distribution provided that the energy barriers in the surface are not surmounted by the adsorbed molecules within the experimental time of approximately 15 min. required for a heat capacity measurement. A rough calculation shows that, for energy barriers in the surface of the order of several hundred calories at the lowest experimental temperature, the time of passage over the barriers is of the same order as the time of the experiment. Without the "freezing in" of the adsorbed molecules, the observed zero point entropy could be accounted for by the existence of the distribution of energy among the sites, such that 10% of the sites is contained in a peak of width smaller than RT at the lowest experimental temperature. This possibility must also be considered in view of the fact that the rutile consists of acicular crystals in which 100 and 110 planes predominate.

ACKNOWLEDGMENT

We are pleased to acknowledge the support of portions of the work by (1) the Atomic Energy Commission under Contract No. AT (30-1)-824, (2) the Office of Naval Research under Contract No. 182(00), and (3) a Frederick Gardner Cottrell Grant from the Research Corporation.

REFERENCES

1. CROWELL, A. D. and YOUNG, D. M. Trans. Faraday Soc. 49: 1080. 1953.
2. DRAIN, L. E. and MORRISON, J. A. Trans. Faraday Soc. 48: 316. 1953.
3. HILL, T. L. J. Chem. Phys. 17: 762. 1949.
4. KINGTON, G. L. and ASTON, J. G. J. Am. Chem. Soc. 73: 1929. 1951.
5. MORRISON, J. A., LOS, J. M., and DRAIN, L. E. Trans. Faraday Soc. 47: 1023. 1951.
6. PACE, E. L., DENNIS, K. S., and BERG, W. T. To be published.
7. PACE, E. L. and GREENE, S. A. J. Am. Chem. Soc. 76: 3286. 1954.
8. PACE, E. L., HERIC, E. L., and DENNIS, K. S. J. Chem. Phys. 21: 1225. 1953.
9. PACE, E. L., SASMOR, D. J., and HERIC, E. L. J. Am. Chem. Soc. 74: 4413. 1952.
10. YOUNG, D. M., BEEBE, R. A., and BIENES, H. Trans. Faraday Soc. 49: 1080. 1953.

INTERACTION ENERGIES OF ORGANIC MOLECULES WITH RUTILE AND GRAPHON SURFACES FROM HEATS OF IMMERSION[1]

By J. J. Chessick, A. C. Zettlemoyer, F. H. Healey, and G. J. Young

ABSTRACT

The heats of immersion of rutile in a series of short chain organic liquids are found experimentally to be an approximate linear function of the dipole moment of the wetting liquid. The significance of the relation is discussed in terms of the polar van der Waals force contribution which is primarily dependent on dipole moment. The average distance of approach of a dipole to the rutile surface and the effective surface force field extending from the rutile surface are calculated.

The net adsorption energy, which is calculated directly from heat of immersion data, is related to the energy contributions resulting from the various polar and nonpolar van der Waals forces active in the adsorption process: These energy contributions which make up the total adsorption energy are calculated for the interaction of an alcohol and a hydrocarbon with both a heteropolar (rutile) and a homopolar (Graphon) surface. On the basis of the results obtained, the effects of chain length and functionality of the liquids on the heat of immersion are discussed.

INTRODUCTION

The heats of immersion of rutile and Graphon in a variety of organic liquids were reported in a previous paper (3). In particular the heats of immersion found with rutile for a series of *n*-butyl derivatives were shown to be a linear function of the dipole moments of the wetting liquid. From the slope of the line the average electrostatic field strength of the rutile surface at the position of the dipole was calculated. From this value, the distance from the rutile surface to the dipole center could be estimated.

In the present paper the heat of immersion measurements are extended to include organic liquids with a wider range of dipole moment. From the estimated field strength the approximate contributions of the various van der Waals forces to the total interaction energy are calculated. In addition, the similarities in the heats of wetting of several heteropolar solids in a variety of liquids relative to their respective heats of wetting in water are considered.

EXPERIMENTAL

Apparatus

The calorimeter, associated equipment, and general techniques were the same as those previously reported (3, 9). Special attention was given to the drying of the liquids and the interior of the calorimeter as well as to maintaining anhydrous conditions during the course of each run.

Solids

The titanium dioxide (rutile), du Pont Ti-pure R-300, Lot 5550, was activated at 400°C. and 1×10^{-5} mm. pressure for two hours before the samples

[1]*Manuscript received September 16, 1954.*
Contribution from Chemistry Department, Lehigh University, Bethlehem, Pa. This paper was presented at the Symposium on Problems Relating to the Adsorption of Gases by Solids, held at Kingston, Ontario, September 10–11, 1954.

were sealed off for heat of immersion determinations. The surface area as measured by the conventional B.E.T. method from nitrogen adsorption data was 7.3 square meters per gram.

The Graphon, Lot No. L-2808, supplied by the Godfrey L. Cabot Company, had a surface area of 95 square meters per gram. The activation of the Graphon samples was carried out at 25° and 1×10^{-5} mm. pressure for 24 hr. More rigorous activation conditions for the Graphon did not influence the heat of immersion values appreciably (8).

Liquids

The properties and purification of most of the wetting liquids have been reported (3). The three new wetting liquids, *n*-butyl iodide (b.p. 129–131°), *n*-butyraldehyde (b.p. 73–75°), and 1-nitropropane (pract.) were stored and fractionally distilled over anhydrous magnesium sulphate before use.

RESULTS AND DISCUSSION

Heats of immersion of rutile and Graphon in a variety of organic liquids are given in Table I. Many of these values have been reported in a previous paper (3) where it was pointed out that the heat of immersion of rutile in a series of straight chain compounds was a linear function of the dipole moment of the wetting liquid. Heat data for the additional liquids shown in Table I fall close to the same line presented previously (3).

TABLE I

HEATS OF IMMERSIONAL WETTING OF RUTILE AND GRAPHON AT 25°C. (Ergs/cm.^{2})

Liquid	Rutile	Graphon
Water	−550±18	− 32.2±0.1
Methyl alcohol	−426±11	−102±2
Ethyl alcohol	−397±3	−110±4
n-Butyl alcohol	−410±1	−114±5
n-Amyl alcohol	−413±8	−120±0
n-Butyl iodide	−395±16	——
n-Butyl aldehyde	−556±10	——
n-Nitropropane	−664±6	——
n-Butyl amine	−330±40	−106±6
n-Butyl chloride	−502±8	−106±2
Butyric acid	−506±11	−115±1
Hexane	−135±1	−103±3
Heptane	−144±9	−112±2
Octane	−140±5	−127±0

In systems which wet spontaneously (no contact angle) nearly the entire heat effect on immersion of the clean solid surface is due to the adsorption of

molecules in the first layer. Experimental proof comes from the fact that the heat of immersion per unit area of solid having a preadsorbed monolayer of the wetting liquid is usually very close to the value obtained on immersing a unit area of the liquid surface, h_L. A good approximation of the heat effect due to the adsorption of a monolayer is therefore given by $(h_{I(SL)}-h_L)$, where $h_{I(SL)}$ is the heat of immersion of the clean solid surface. This heat effect is directly related (5) to the net energy of adsorption, (E_A-E_L), by the equation

$$h_{I(SL)}-h_L = +N_A(E_A-E_L). \quad [1]$$

In this case (E_A-E_L) is the net integral energy of adsorption for a molecule in the monolayer and N_A is the number of molecules adsorbed per cm.^{2} in the monolayer. The net energy of adsorption thus represents the energy involved in removing a molecule from the bulk liquid and adsorbing it onto the surface. If it is assumed that interactions between molecules in the liquid are the same as in the adsorbed state, it follows that (E_A-E_L) represents only the interaction between the surface and an adsorbed molecule and does not include interactions between adsorbed molecules and themselves.

The total interaction energy between adsorbed polar molecules and a heteropolar surface consists of four principal parts: E_W, the nonpolar van der Waals contribution; E_α, the contribution due to the polarization of the adsorbate by the surface; E_μ, the contribution arising from the interaction between a permanent peripheral dipole in the adsorbate and the electrostatic field of the dielectric surface; and $E_{\text{int.}}$, the contribution arising from interaction between adsorbed molecules, thus:

$$E_A-E_G = E_w+E_\mu+E_\alpha+E_{\text{int.}}. \quad [2]$$

With the assumption that the interactions in the adsorbed state are the same as in the liquid state, then

$$E_{\text{int.}} = E_L-E_G \quad [3]$$

and

$$E_A-E_L = E_w+E_\mu+E_\alpha. \quad [4]$$

The various expressions developed for these energies are summarized by de Boer (1). The most useful forms of these equations for the purpose of this paper are

$$E_\alpha = \frac{-F^2\alpha_1}{2} \quad [5]$$

$$E_w = \frac{N_v}{4r^3}\alpha_1\alpha_2\frac{I_1I_2}{I_1+I_2} \quad [6]$$

$$E_\mu = -F\mu. \quad [7]$$

In these equations α_1 and α_2 are the polarizabilities of the adsorbate and adsorbent respectively, I_1 and I_2 the corresponding ionization energies, N_v the number of atoms of the dielectric per cm.^{3}, r_0 the nearest surface ion, μ the dipole moment, d the distance of charge separation in the dipole, and F is the average electrostatic force field of the surface.

The net energy of adsorption for a monolayer, $N_A(E_A - E_L)$ is plotted in Fig. 1 as a function of the dipole moment for a number of straight chain compounds on rutile. The $N_A(E_A - E_L)$ values were calculated from the heat of

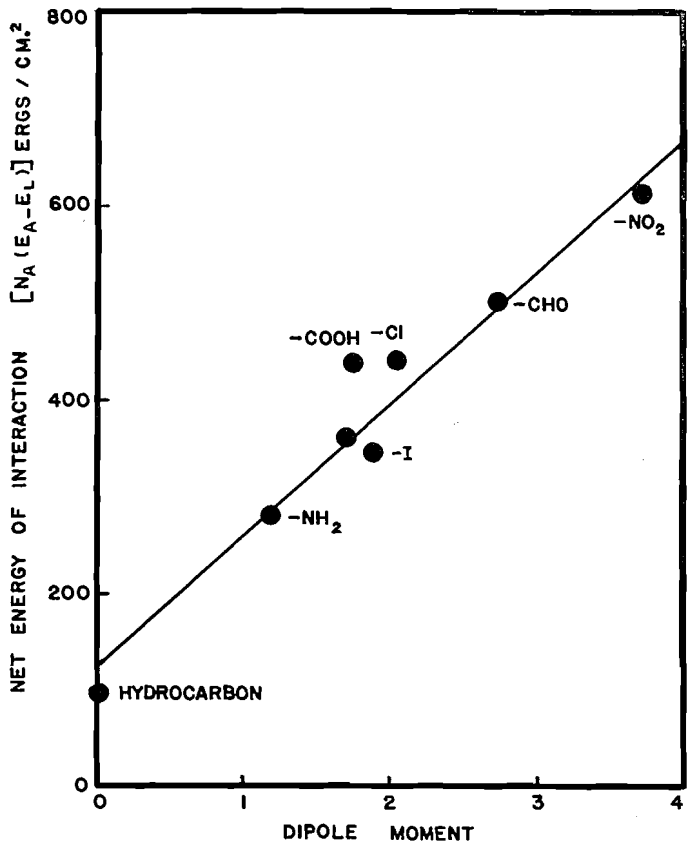

FIG. 1. Net interaction energy as a function of dipole moment of various polar molecules on rutile.

immersion data in Table I and a knowledge of h_L using equation [1]. The dipole moments are those of Smyth (7). If it is assumed that the differences in the total adsorption energy arise primarily from E_μ, then, according to equation [7], the slope of the line in Fig. 1 is a measure of the average electrostatic field strength of the rutile surface immersed in the liquids. Exact agreement of the heat data for all the liquids studied would be expected if the polarizabilities, cross-sectional areas, and distance from dipole to surface were the same. Since polar molecules at monolayer coverage no doubt have the polar end directed toward the rutile surface, these properties of the molecules probably do not differ markedly. The average effective field strength of the rutile surface was calculated to be 2.72×10^5 e.s.u.

The contributions of the various interaction energies to the net adsorption energies for hexane and *n*-butyl alcohol on the heteropolar surface, rutile, and the homopolar surface, Graphon, are given in Table II. Since Graphon has no

electrostatic surface field, E_μ and E_α are both zero and the total adsorption energy is due primarily to dispersion forces alone. Any "image" force between the alcohol and Graphon must be negligible since the heats of wetting of Graphon were found to be independent of the dipole moment of the liquid. The values of E_w for the Graphon systems were taken to be equal to the net adsorption energy $N_A(E_A - E_L)$ and were not calculated because of both the approximate nature of the equation and the lack of reliable values for the physical constants of the surface atoms.

TABLE II

CONTRIBUTION OF VARIOUS VAN DER WAALS' FORCES TO THE ADSORPTION ENERGY

System	Interaction energies (ergs/cm.^{2})		
	E_w	E_α	E_μ
Hydrocarbon on rutile	62	30	0
Hydrocarbon on Graphon	67	0	0
Alcohol on rutile	94	21	246
Alcohol on Graphon	66	0	0

The values of E_α and E_μ for alcohol on rutile were directly calculable from equations [5] and [7] respectively from the knowledge of the field strength. The polarizabilities of the OH and CH_2 groups were calculated from molar refraction data. The alcohol was assumed to be oriented perpendicularly to the surface at monolayer coverage. Calculation of the contribution to E_α due to the polarizability of the nearest CH_2 group showed this contribution to be negligible ($\sim$0.01 ergs/cm.^{2}) since the distance of approach of this group from the surface is prohibitively large (*ca.* 3.5 Å). The value of E_w was obtained here and in the case of the hydrocarbon on rutile by subtracting $E_\mu + E_\alpha$ from the net adsorption energy. The value of E_w calculated for alcohol on rutile by equation [6] agrees in magnitude with the value already obtained, but the approximate nature of the equation and the lack of knowledge of the physical constants of the surface atoms permit only an order of magnitude to be calculated.

For the hydrocarbon on rutile, an average distance of approach of 2.3 Å was estimated from considerations of bond distances and the geometry of the hydrocarbon molecule assuming a horizontal orientation. To calculate E_α from equation [5] the field strength corresponding to this distance was estimated from the exponential function of Hückel discussed in a later section. The calculation was made for the contribution for each CH_2 or CH_3 group since the number of carbon atoms in a monolayer is approximately the same for each of the hydrocarbons irrespective of the orientation of these molecules. For this reason also, E_α will be about the same for any of the hydrocarbons regardless of chain length.

For all the systems listed in Table II with the exception of alcohol–rutile, the contribution of the dispersion force is very nearly the same. Apparently the OH groups of the alcohol interact more strongly than the CH_2 or CH_3 groups of the hydrocarbon owing, primarily, to the closer average distance of approach of the OH group to the surface. It is important to note that the *direct* influence

of the surface is negligible for the second layer in these calculations because of the large distance of second layer molecules from the surface, and thus the use of the term $(h_{I(SL)}-h_L)$ to approximate the heat of adsorption in the first layer appears to be justified.

Variation of Field Strength with Distance of Approach

An equation for the field strength above an ion in a solid composed of singly charged ions has been given by Hückel (4) as

$$F = \frac{8\pi\epsilon}{r_c^2} \exp\left(-\pi\sqrt{2}\frac{r_0}{r_c}\right)$$

where ϵ is the electronic charge, r_c is the closest interionic spacing in the crystal, and r_0 is the distance from the center of a surface ion. The slope of Fig. 1 gave an independent measure of the field strength which was substituted in Hückel's equation to determine whether a reasonable value of r_0 would result even though adsorption did not necessarily occur above an ion site and the crystal was made up of doubly charged ions. Using a value of 1.96 Å for the r_c distance in rutile (6) the value of r_0 was calculated to be 2.08 Å. Estimates of the distance from the center of the alcohol dipole to the center of the surface oxide ions range from 2.06 to 2.37 Å depending on the assumed orientation.

If the exponential term in Hückel's equation is used to obtain the variation of the field with distance from the surface, it is found the field strength is negligible at the distance (*ca.* 3.5 Å) of the first CH_2 group of an alcohol molecule oriented perpendicular to the surface. Thus there is essentially no contribution to E_α from the carbon chain.

A consideration of the factors in the equation for the various contributing energies emphasizes the dominant role of the OH group for adsorption of an alcohol on rutile. The hydrocarbon portion of the molecule is too far from the surface to have any significant influence on the interaction energy. Thus, it would be reasonable to expect that chain length would have a negligible effect on the heat of immersion or net adsorption energy. This is indeed the case; the lower alcohols have essentially the same heat of immersion values as *n*-amyl alcohol. The same result, of course, would be expected with other relatively short-chain polar homologues. Similarly, for hydrocarbons on a polar or nonpolar surface, the CH_2 and CH_3 groups contribute in an approximately equal manner to the total adsorption energy. Regardless of orientation, the number of these groups is very nearly the same and here too, as was found experimentally, the heats of immersion would be expected to be independent of chain length.

Relative Heats of Immersion

It was pointed out in the previous paper (3) that rutile and barium sulphate had identical relative heats of immersion in water and in alcohol even though the actual values for the two solids were widely different. Harkins (2) had also

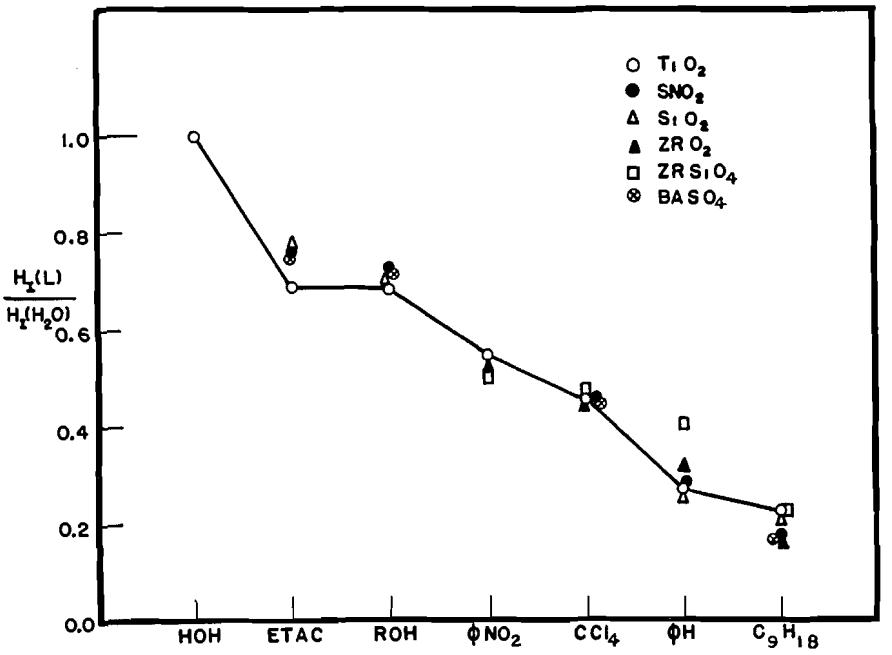

FIG. 2. Relative heats of immersion of several hydrophilic solids in various organic liquids.

noted this similarity in the relative heat of immersion values for a number of different solids and liquids. Fig. 2 shows a plot of the heats of immersion of various solids in liquids relative to their heats of immersion in water. The line was drawn through the values for titanium oxide, and the close agreement for the group of solids indicates that their relative interactions with the different liquids is the same. All of the solids are heteropolar and hydrophilic, and probably all present primarily an outer surface of oxygen ions. The similar behavior is, however, still surprising since such properties as polarizability, characteristic energies, and field strength all vary. A further study of the influence of crystal parameters on the various interaction forces is being undertaken to attempt to explain the differences in the absolute heats of wetting of the different solids.

The relative heats of wetting given in Fig. 2 show only a general correlation with dipole moment since the cross-sectional areas of the molecules are not the same and therefore the surface concentration of dipoles per square centimeter varies; also the polarizabilities are different. Thus nitrobenzene, with a very high dipole moment, has a relatively low heat of wetting indicating that the benzene ring is blocking off a considerable portion of the surface.

Because of the similarity in relative heats of wetting the results obtained with one solid should be applicable to all solids of the same type. Therefore, once heats of immersion of a reference solid in a series of liquids have been measured only one heat of immersion value for a new solid of the same type need be obtained in order to predict the values in the other liquids.

ACKNOWLEDGMENT

The authors wish to express their appreciation for the financial support provided by the Office of Ordnance Research, Ordnance Project No. TB2-0001 (457), Contract No. DA-36-034-ORD-935.

REFERENCES

1. DEBOER, J. H. Advances in colloid science. Vol. III. Interscience Publishers, Inc., New York. 1950.
2. HARKINS, W. D. The physical chemistry of surface films. Reinhold Publishing Corporation, New York. 1952.
3. HEALEY, F. H., CHESSICK, J. J., ZETTLEMOYER, A. C., and YOUNG, G. J. J. Phys. Chem. 58: 887. 1954.
4. HÜCKEL, E. Adsorption and Kapillarkondensation. Akad. Verlagsgesellschaft, Leipzig. 1928. p. 129.
5. JURA, G. and HILL, T. L. J. Am. Chem. Soc. 74: 1498. 1952.
6. PAULING, L. The nature of the chemical bond. 2nd ed. Cornell Univ. Press, Ithaca, N.Y. 1948.
7. WEISSBERGER, A. Physical methods of organic chemistry. Pt. II. Interscience Publishers, Inc., New York. 1949.
8. YOUNG, G. J., CHESSICK, J. J., HEALEY, F. H., and ZETTLEMOYER, A. C. J. Phys. Chem. 58: 313. 1954.
9. ZETTLEMOYER, A. C., YOUNG, G. J., CHESSICK, J. J., and HEALEY, F. H. J. Phys. Chem. 57: 649. 1953.

THERMODYNAMIC PROPERTIES OF HYDROCARBONS ADSORBED ON RUTILE II[1]

By H. P. Schreiber[2] and R. McIntosh[3]

ABSTRACT

Integral molar heats and entropies of adsorbed methane and propane on rutile have been computed from data of isotherms at 103.2° and 110.2°K. for methane and 166.3° and 224.6°K. for propane. Some resemblance has been found between these functions and those for argon, nitrogen, and oxygen adsorbed on rutile, reported by Drain and Morrison. The integral molar entropy of adsorption made possible a test of the model of a localized film without interactions on a heterogeneous substrate. The model was found to be a reasonable representation of the state of adsorbed methane up to about 0.5 of the monolayer and of propane up to about 0.3 of the monolayer. A unique heat of adsorption curve for the adsorption of methane, ethane, propane, and *n*-butane has been derived and its significance is briefly discussed. The curve has been employed to derive functions for the distribution of energies among the adsorption sites of the substrate.

INTRODUCTION

In a recent publication, hereafter referred to as I (8), the differential molar thermodynamic functions of methane, ethane, propane, and *n*-butane adsorbed on rutile were presented. These functions were computed from adsorption isotherms determined in a manner especially developed to provide accurate thermodynamic data. The results were of comparable accuracy with similar data obtained by calorimetry (7). It was therefore decided to attempt a calculation of the integral thermodynamic functions of the adsorbates, and to utilize them in combination with a simple model of a localized film in the manner developed by Drain and Morrison (1). Only the data for methane and propane were sufficiently detailed to make the additional calculations feasible, and the discussion is largely limited to these two systems.

The value of the integral thermodynamic functions has been amply stressed by Hill (4). A more significant description of the state of the adsorbed phase may be obtained from them, and the values of the integral molar entropy permit comparison with assumed models, the properties of which are computed by statistical methods. In this paper the integral heats and entropies of adsorption of methane and propane are presented and discussed.

RESULTS AND DISCUSSION

Thermodynamic Analysis

The integral molar thermodynamic functions of the adsorption process are obtained when the spreading force, ϕ, of the film is chosen as one of the independent variables describing the adsorbed phase. In order to evaluate these functions, ϕ must be known accurately over wide ranges of surface concentra-

[1]*Manuscript received September 16, 1954.*
Contribution from the Department of Chemistry, University of Toronto, Toronto, Ontario. This paper was presented at the Symposium on Problems Relating to the Adsorption of Gases by Solids, held at Kingston, Ontario, September 10–11, 1954.
[2]*Present address: Division of Pure Chemistry, National Research Council, Ottawa, Canada.*
[3]*Professor of Chemistry.*

tion. The values of ϕA were obtained according to the methods described by Hill, Emmett, and Joyner (6). The required equation is

$$[1] \qquad \phi A = R\,T \int \frac{V}{p}\,d\,p$$

where V is the volume of gas adsorbed per gm.,
p is the equilibrium pressure,
A is the surface area per gm. considered independent of T, and R and T have their usual significance.

In regions of higher equilibrium pressures the integration was performed graphically. In the low pressure region the isotherms could be represented analytically by the equation

$$[2] \qquad V = a\,p + b\,p^{\frac{1}{2}}$$

where a and b are constants, and the integration was performed using this relation. Values of ϕA were obtained at 103.2, 118.2, and 133.2°K. for methane, and at 166.3, 183.4, 197.6, and 224.6°K. for propane. The integral molar heats of adsorption were obtained from

$$[3] \qquad (H_g - H_s)_\phi = \frac{R \ln(p_2 - p_1)_\phi}{1/T_1 - 1/T_2}$$

and the integral molar entropies of adsorption from

$$[4] \qquad H_g - H_s + R\,T \ln p/p^\circ = T(S_g - S_s).$$

The subscripts g and s refer to the gas and the adsorbed phase, respectively. In several instances the integral heat of adsorption was evaluated from

$$[5] \qquad H_s - H_g = q_{st} - \frac{T}{\Gamma}\left(\frac{\partial \phi}{\partial \Gamma}\right)_T$$

where q_{st} is the isosteric heat of adsorption and Γ equals V/A. This serves as a check upon the correctness of the ϕ values (6). In all cases the value of $H_s - H_g$ so obtained agreed to within 150 cal. mole^{-1} with the values obtained from equation [4]. The rather large uncertainty is due to the fact that the errors in determining q_{st} and ϕ are combined here. It can be concluded, however, that the ϕ values are free from gross errors. In general, the integral thermodynamic functions are less well defined than their differential counterparts. This is because the correlation of the correct equilibrium pressure with some particular value of ϕ is less certain than the correlation of the equilibrium pressure at some particular value of the volume adsorbed. This is especially true at low equilibrium pressures. Thus the error in the integral heats of adsorption is $\pm$ 100 cal. mole^{-1} and in the integral molar entropies 1.0 cal. mole^{-1} degree^{-1}.

In order to make the entropy relationships easier to interpret, the integral and differential molar entropies of the adsorbed molecules themselves were evaluated and recorded herein. The entropy of the gas phase, necessary for this evaluation, was obtained by making appropriate corrections for the

pressure to the entropy in the standard state, taken as 1 atmosphere pressure and the temperature in question. The entropy in the standard state was taken from the literature (9).

Methane

The integral heat of adsorption of methane at 110.2°K. is shown in Fig. 1A as a function of θ. For comparison, the corresponding isosteric heat curve is also represented. The two curves show an expected similarity. The integral heat values did not vary with temperature in the range 103.2 to 133.2°K. The shape of the heat curves is that generally considered to be characteristic of physical adsorption on a heterogeneous substrate.

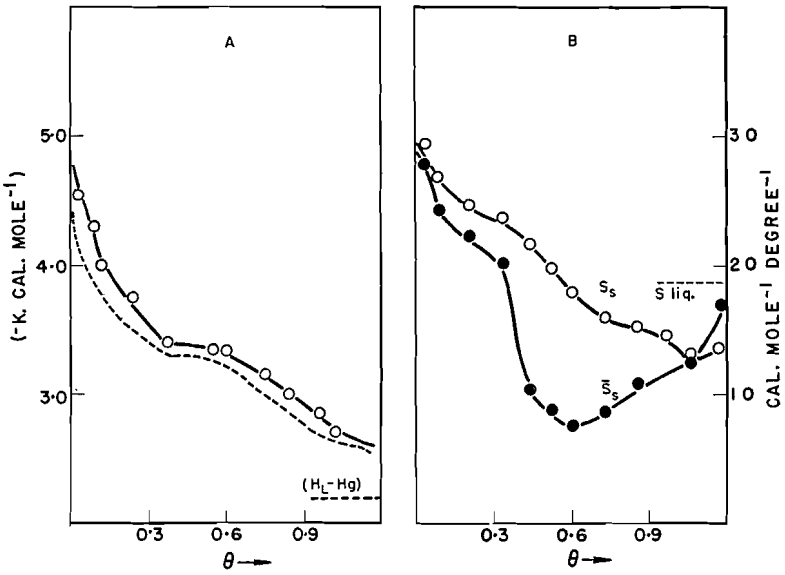

FIG. 1. A. Integral (—) and isosteric (— — —) heat of adsorption of methane on rutile at 110.2°K.

B. Integral molar (S_s) and differential molar ($\bar{S}_s$) entropy of methane adsorbed on rutile at 103.2°K.

The integral and differential molar entropies of methane adsorbed at 103.2°K. are shown in Fig. 1B. At first, both S_s and $\bar{S}_s$ decrease continuously with surface coverage, but the curve of the integral entropy exhibits a shallow minimum in the vicinity of $\theta = 1.0$. A deeper minimum occurs in the plot of $\bar{S}_s$ near $\theta = 0.6$. Both S_s and $\bar{S}_s$ are initially greater than the entropy of bulk liquid, but approach that value at high surface concentrations. The general shape of the curves is that which has been derived by Hill, Emmett, and Joyner(6) on the basis of the B.E.T. model for high values of the constant C. In this case the value of C was approximately 85. The results are similar to those reported by Drain and Morrison (1) for argon on rutile. Thus the initial decrease in the entropy may be interpreted as being caused by restrictions in the configuration of the adsorbate as the number of sites available for adsorption decreases. The increasing values of S_s beyond $\theta = 1$ is then due to the formation of multilayers.

Propane

The integral molar heats of adsorption for propane at average temperatures 174.8 and 210.3°K. are shown in Fig. 2, along with the corresponding isosteric heats of adsorption. It was pointed out in I that the shape of the isosteric heat curve might suggest a phase change in the adsorbed film at 185°K. This is again suggested by the integral heat of adsorption curve.

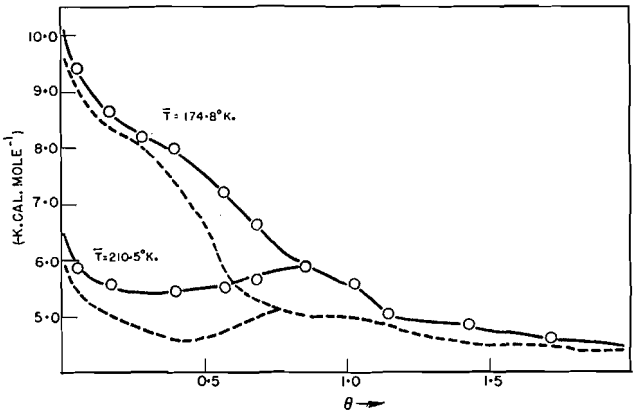

FIG. 2. Integral (—) and isosteric (— — —) heat of adsorption of propane on rutile.

Below 185°K. the integral heat of adsorption curve is of similar shape to that for methane, but at higher temperatures the plots are distinctly different. The junction of the two branches of the plot occurs near 0.8 θ instead of 0.6 θ as indicated by the plot of the isosteric heat of adsorption.

It was suggested in I, on the basis of the plots of $\bar{S}_s - S_g$ at 183.9 and 197.6°K., that the adsorption of propane differed from the adsorption of

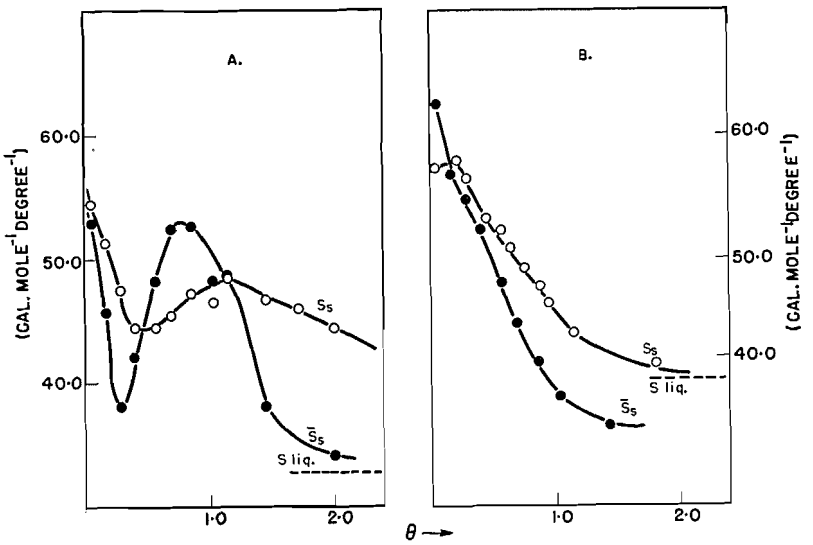

FIG. 3. A. Integral molar (S_s) and differential molar ($\bar{S}_s$) entropy of propane adsorbed on rutile at 166.3°K.
B. At 224.6°K.

methane and ethane. This view may be more closely examined with the aid of Figs. 3A and 3B, in which both S_s and $\bar{S}_s$ for propane are plotted at 166.3 and 224.6°K., respectively. It is evident from Fig. 3A that the curves of S_s and $\bar{S}_s$ for propane at the lower temperature are similar to the curves for methane. On the other hand, both S_s and $\bar{S}_s$ at 224.6°K. vary with θ in an entirely different manner. This fact again suggests a change in the physical state of adsorbed propane near 185°K. Unfortunately, the entropy values are dependent upon the heats of adsorption, and so cannot provide independent evidence of the validity of the postulated phase change.

While the entropy curves for propane at 166.3°K. are of the same general shape as those shown in Fig. 1B, some differences should be noted. The minimum value of S_s occurs near 0.4 θ, rather than near the monolayer. A comparable finding has been reported by Drain and Morrison (2) in the cases of oxygen and nitrogen adsorbed on rutile. It is difficult to interpret these differences in the entropy relationships. Contributions to the entropy from internal degrees of freedom of the adsorbed molecules as well as molecular interactions no doubt influence the shape of the curve.

Test of Localized Film Model

The values of the integral molar entropy permit a more detailed examination of the systems along lines developed by Drain and Morrison (1, 2). These authors showed that the assumption of a localized film upon a heterogeneous substrate led to theoretical values of S_s which agreed well with the experimentally measured values up to a surface coverage of 0.6 θ in the case of argon. The model was also successful in accounting for the behavior of oxygen and nitrogen, although the diatomic molecules offered a much more complex problem for treatment.

In the present case no detailed statistical treatment has been carried through. In the first place, the accuracy of the S_s values suffices only for semi-quantitative interpretation. Secondly, the increased complexity of the molecules makes the statistical problem virtually intractable. Finally, the problem of surface heterogeneity can only be satisfactorily resolved if isosteric heat of adsorption data can be derived for 0°K. Therefore heat capacity data are necessary, which will permit reduction of the q_{st} to 0°K. These data were not available.

In view of these limitations, it has been assumed that methane, adsorbed at 103.2°K., and propane, adsorbed at 166.3°K., form localized films. To reduce difficulties in interpretation, discussion is essentially limited to surface coverages well below the monolayer, where molecular interactions can be neglected. The postulate of the existence of a heterogeneous substrate may be supported by the usual arguments (1, 11). The assumed presence of localized films may also be justified. If the temperature region in which some degree of localization is considered to persist is taken as

$$\frac{\Delta U}{10R} < T < \frac{\Delta U}{R} \quad (3,11)$$

where ΔU is the energy barrier between neighboring sites, and if ΔU is

considered to be considerably less than 50% of the net heat of adsorption, the films of methane and propane may be considered as localized films. At 0.3 θ, for example, the net heat of adsorption of methane is 1300 cal. mole^{-1} and 3600 cal. mole^{-1} for propane. Hence, taking values of ΔU between 200 and 500 cal. mole^{-1} for methane, and between 500 and 1000 cal. mole^{-1} for propane, the assumption of localized films at the designated temperatures appears justified.

On the basis of the assumed model it becomes meaningful to split the molar entropy of the adsorbate into configurational and non-configurational parts according to the equation

[6] $$S_s = S_c + S_{nc}.$$

Both S_c and S_{nc} may be calculated from theory and Hill (5) has given the necessary formulae. The computations involve a knowledge of a distribution function for the energies of the sites of the heterogeneous surface, of the temperature dependence of the partition function of the adsorbate, and of the dependence of the partition function on the energy ϵ, of the adsorption site. Owing to the complexity of the methane and propane systems, S_c has been calculated by the use of the approximate equation due to Drain andMorrison (1)

[7] $$S_c = (\pi^2/3)\, R\, (d \ln V/d \ln p)$$

which is valid for energy distributions that are wide compared with RT. S_{nc} was then evaluated by means of equation [6]. The behavior of the quantities so calculated is the sole criterion of the applicability of the chosen model. On the basis of the findings of Drain and Morrison (1, 2) it would seem that for simple molecules, the variation of S_s with θ should initially be determined largely by configurational effects. Furthermore, at a given temperature and over the initial range of surface coverage, the dependence of S_{nc} on surface coverage should be determined largely by the variation of the vibrational frequency ν of the adsorbed molecules with the site energy ϵ. If $\nu \alpha \epsilon^n$ where n

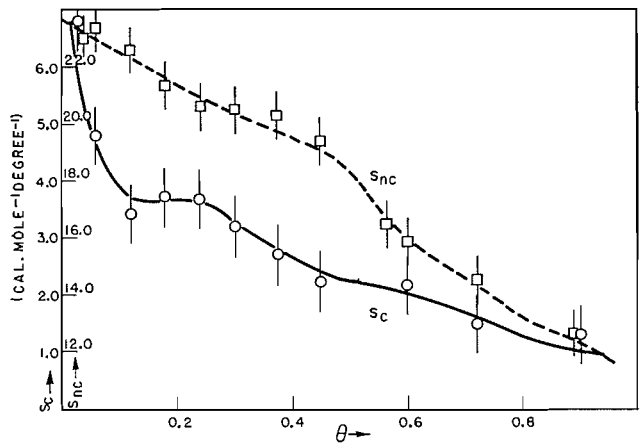

FIG. 4. Configurational molar (S_c) and non-configurational molar (S_{nc}) entropy of methane adsorbed on rutile at 103.2°K.

is of the order of unity, as suggested by Drain and Morrison, S_{nc} may be expected to vary only slightly with θ.

Methane

The configurational and non-configurational entropies of adsorbed methane are shown as functions of θ in Fig. 4. Comparison of Fig. 4 with Fig. 1B shows that the S_c curve for methane resembles the curve for S_s up to 0.5 θ. Moreover, the greater part of the variation of S_s with θ is accounted for by the change of S_c in this range of surface coverage. Beyond 0.5 θ the S_s and S_c plots begin to diverge and S_{nc} varies rapidly with θ. In this region, molecular interactions should become significant and the postulated model no longer is suitable. Therefore the model of a localized film without interaction on a heterogeneous surface seems an acceptable representation of the state of the adsorbed methane up to 0.5 θ.

Propane

The values of S_c and S_{nc} for adsorbed propane are represented in Fig. 5. Comparison with Fig. 3A again reveals that there is some resemblance in the

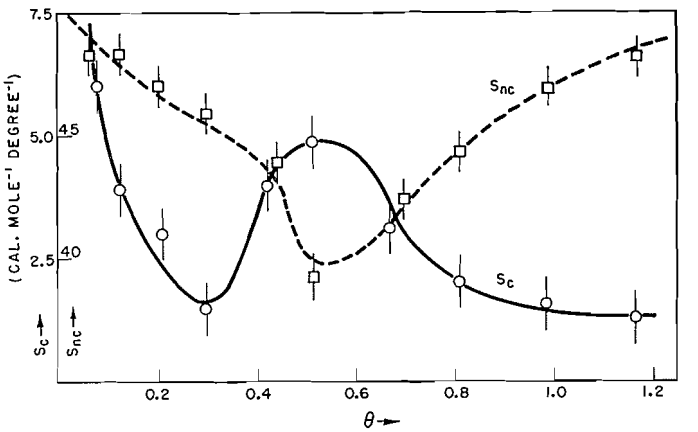

FIG. 5. Configurational molar (S_c) and non-configurational molar (S_{nc}) entropy of propane adsorbed on rutile at 166.3°K.

behavior of S_s and S_c up to about 0.3 θ. However, the variation of S_{nc} is greater than in the case of methane. This is not surprising, in view of the fact that Drain and Morrison found that even for nitrogen and oxygen the complications caused by added rotational and vibrational degrees of freedom were of importance. It should also be noted that S_{nc} for propane, unlike that for methane, has a minimum value near 0.5 θ and then increases rapidly. Thus, up to 0.5 of the monolayer the variations of the S_{nc} functions of the two adsorbates are similar, and the increasing rate of change between 0.4 and 0.5 θ may be due, as has been suggested in the case of methane, to interactions. The rapid increase of S_{nc} in the case of propane beyond this region indicates failure of the model from other causes.

The Surface Heterogeneity of the Rutile Adsorbent

The effects of surface heterogeneity can be taken into account quantitatively in a model describing physical adsorption. Specifically, Sips has shown (10) that a function giving the distribution of energies among adsorption sites can always be obtained from a given isotherm. Drain and Morrison have evaluated such distribution functions (2) and, using them, have carried out successful statistical analyses for nitrogen, oxygen, and argon adsorbed on rutile. They found that up to monolayer capacity, the various isosteric heats of adsorption were linear functions of each other, so that a unique heat of adsorption function could be reduced to 0°K. Since the distribution function of the energies

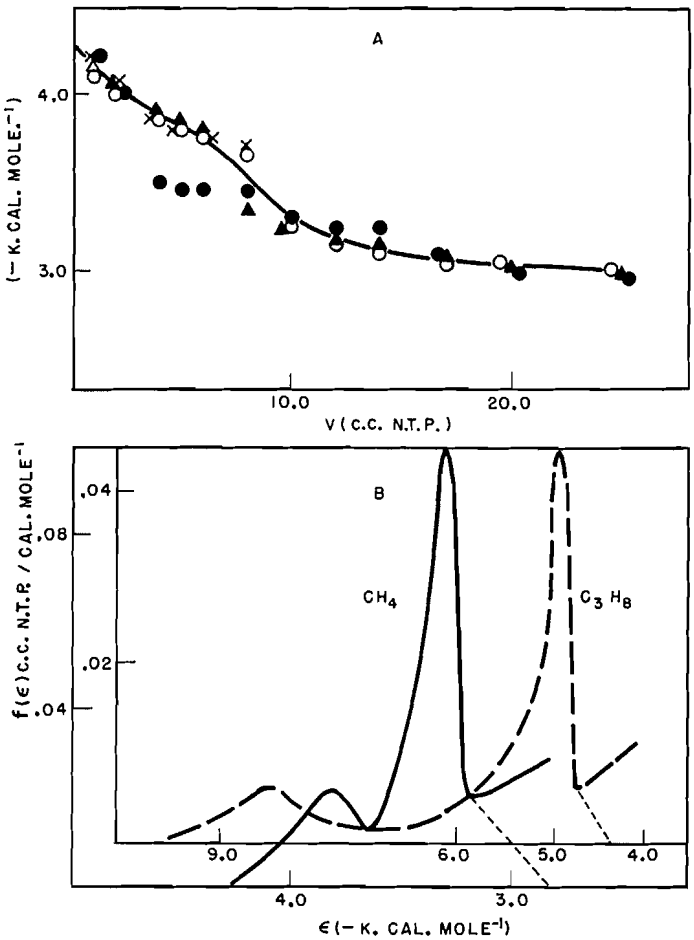

FIG. 6. A. Common isosteric heat of adsorption for hydrocarbons on rutile at the reduced temperature $T_r = 0.53$.
○—$q_{st.}$ (CH_4)
●—0.395 $q_{st.}$ (C_2H_6) + 1350
▲—0.250 $q_{st.}$ (C_3H_8) + 1900
×—0.065 $q_{st.}$ (C_4H_{10}) + 3320
B. Distribution of energies among the adsorption sites for methane and propane adsorbed on rutile. Broken line extrapolations are normalizing factors giving areas under the curves equal to the respective monolayer capacities.

of the adsorption sites is derived from the isosteric heat of adsorption curve, it also followed that the distribution functions had the same shape, although the range of energies varied with each adsorbate. They interpreted these findings as meaning that the same sites were involved in the adsorption of all three gases, but that the forces of interaction varied.

The same treatment has been followed in this study involving the four saturated hydrocarbons. Owing to the lack of heat capacity data, it was not possible to correct the isosteric heat of adsorption curves to the absolute zero as Drain and Morrison were able to do. The data for each vapor were compared at the common reduced temperature $T/T_c = 0.53$. This temperature corresponded to the temperature of the lowest isotherm in each case and also the temperature at which the relative value of ΔU and $R\,T$ was about equal. Again it was found possible to construct a unique isosteric heat of adsorption curve for the four hydrocarbons up to nearly the monolayer capacity. The curve is represented in Fig. 6A. Only certain values for ethane between 0.3 θ and 0.6 θ depart appreciably from the curve.

The unique heat of adsorption curve leads to a family of distribution curves of the same shape but of widths in the ratios 1:2.5: 4:15.4, if the width of the methane curve is taken as unity. Two of these curves, those for methane and propane, are shown in Fig. 6B.

An interpretation of the existence of a unique heat of adsorption curve along the lines given in the case of the simpler molecules by Drain and Morrison is not ruled out. However, in the present case this interpretation tends to lose its simplicity because, for example, it is difficult to imagine that a "site" for the adsorption of methane should also serve as a "site" for the adsorption of butane. If the existence of common isosteric heat curves is established for other series of complex molecules, the significance of curves such as that in Fig. 6A should be reconsidered.

ACKNOWLEDGMENTS

The authors are pleased to acknowledge financial assistance given by the National Research Council of Canada and by the Advisory Committee on Research, University of Toronto, Toronto, Canada, and the award of a N.R.C. Studentship to H. P. Schreiber.

REFERENCES

1. DRAIN, L. E. and MORRISON, J. A. Trans. Faraday Soc. 48: 316. 1952.
2. DRAIN, L. E. and MORRISON, J. A. Trans. Faraday Soc. 49: 654. 1953.
3. EVERETT, D. H. Trans. Faraday Soc. 46: 942. 1950.
4. HILL, T. L. J. Chem. Phys. 17: 520. 1949.
5. HILL, T. L. J. Chem. Phys. 17: 762. 1949.
6. HILL, T. L., EMMETT, P. H., and JOYNER, L. G. J. Am. Chem. Soc. 73: 5102. 1951.
7. PACE, E. L., HERIC, E. L., and DENNIS, K. S. J. Chem. Phys. 21: 1225. 1953.
8. SCHREIBER, H. P. and McINTOSH, R. Can. J. Chem. 32: 842. 1954.
9. Select values of properties of hydrocarbons. National Bureau of Standards, Washington, D.C. 1949.
10. SIPS, R. J. Chem. Phys. 18: 1024. 1950.
11. TOMPKINS, F. C. Trans. Faraday Soc. 46: 569. 1950.

AN APPARATUS FOR THE MEASUREMENT OF DIELECTRIC CONSTANTS OF ADSORBED GASES AT FREQUENCIES UP TO 100 Mc./sec.[1]

By M. H. Waldman[2] and R. McIntosh[3]

ABSTRACT

The design of an apparatus suitable for the measurement of dielectric constants at frequencies up to 106 Mc./sec. is shown. The apparatus was used to measure changes in capacitance with volume adsorbed for the system sulphur dioxide – rutile at about 3.5°C. and for frequencies of 13, 36, and 106 Mc./sec. The results failed to reveal any dispersion due to the adsorbed matter in this frequency range. The dielectric behavior observed is the same, within experimental error of a few per cent, as that found by Channen and McIntosh for the same system at 3.7 Mc./sec.

INTRODUCTION

From the work of Snelgrove, Greenspan, and McIntosh (6) and Waldman, Snelgrove, and McIntosh (7), who measured dielectric constants of gases on silica gel and rutile at radio frequencies, it became evident that it would be desirable to investigate these dielectric constants at much higher frequencies. The reasons for making high frequency measurements were:

(1) The method of calculating the dielectric constants from the primary data involved the knowledge of the density of the adsorbed matter. If the frequency of the applied field were made so high that the adsorbed dipole could no longer follow the changes in the field, then the adsorbate would act as nonpolar material and the densities could be determined by applications of laws for nonpolar dielectrics. The determined density could then be used in the low frequency calculations.

(2) It would be of interest to see whether the Debye dispersion range (2) of the adsorbed matter would correspond to the dispersion range, in magnitude and position in the frequency spectrum, of the bulk liquid, or whether the dispersion phenomena characteristic of a rotational oscillator would be observed.

Although the frequency at which dispersion would be found was unknown, the design and construction of a cell that would allow reliable measurement of dielectric constants at high frequencies up to about 100 Mc./sec. was attempted. Previous to this, cells were used which consisted of three co-axial cylinders with the center cylinder at high potential while the other two were grounded. The space between the cylinders was packed with the solid dielectric. The change in capacity in this test cell due to adsorption of gas on the solid was

[1]*Manuscript received September 16, 1954.*
Contribution from the Chemistry Department, University of Toronto, Toronto, Ontario. This paper was presented at the Symposium on Problems Relating to the Adsorption of Gases by Solids, held at Kingston, Ontario, September 10–11, 1954.
[2]*Graduate Student and Demonstrator in Chemistry.*
[3]*Professor of Chemistry.*

measured by adjusting a precision condenser connected in parallel with the test cell.

This method was quite suitable for the radio frequencies used, but the corrections to be applied for the lead connections between the two condensers became excessive for frequencies higher than about four megacycles/second.

It became clear, then, that the main requirement was to construct a cell with the shortest possible leads between the test cell and the measuring condenser so that lead corrections would be negligible. A modification of an apparatus due to Hartshorn and Ward (4) was used. In principle, these authors made the measuring condenser part of the test cell. In the present case, a very slight modification of the original test cell accomplished the same result. The innermost cylinder was made movable so that by raising or lowering this cylinder the capacity of the whole condenser was increased or decreased. The powder, of course, was packed only in the space between the two outermost cylinders. The changes in capacitance due to the movement of the innermost cylinder merely had to be calibrated against a standard condenser at low frequencies. Since the dielectric in the space between this cylinder and the next larger one was Teflon, its capacity would not alter with frequency.

The Principle of the Hartshorn and Ward Method

To grasp the principle of operation, consider an ideal circuit as envisaged by Hartshorn and Ward (4). Schematically, this may be shown as in Fig. 1.

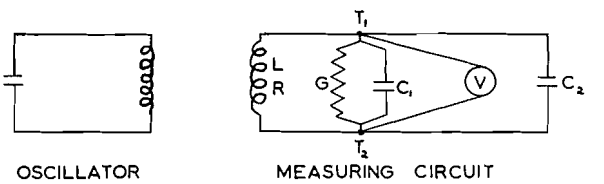

FIG. 1.

The only voltages considered are those between T_1 and T_2 which are common to all the components of the measuring circuit. C_1 is the test condenser containing the sample, and C_2 is the measuring condenser which is used to compensate for changes in capacity in C_1 and also to obtain the resonance curves.

Current considerations in the above circuit lead to an expression for C in terms of C_r, the resonance capacity, G, the conductance across the cell, and q, the square of the ratio of the voltage at resonance to the voltage at the particular capacity measured, as follows

$$[a] \qquad C = C_r \pm \frac{G\sqrt{(q-1)}}{\omega}$$

where ω is the frequency, in radians per second, of the circulating current Assuming G does not change, this expression shows that the resonance curve should be symmetrical about C_r as shown below.

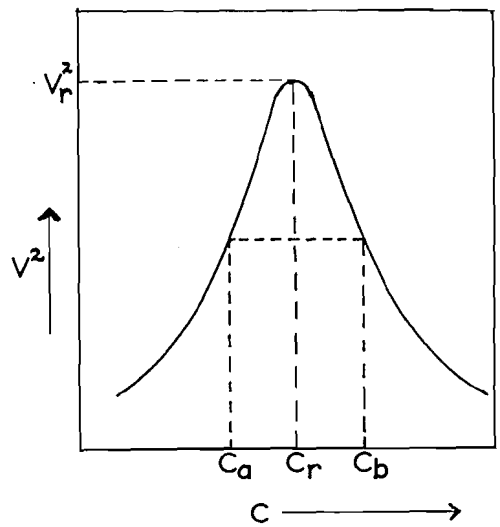

FIG. 2.

Thus, if one measures two values of C, C_a and C_b, for the same value of V^2 (or q) the resonance capacity may be calculated by

[b] $$C_r = \tfrac{1}{2}(C_a + C_b),$$

while the conductance of the system is given by

[c] $$G = \frac{(C_a - C_b)}{2\sqrt{(q-1)}}.$$

The above considerations are for an ideal circuit where the leads have zero impedance. In practice, the leads to the various components never have zero impedance. As Hartshorn and Ward have pointed out, the only quantities which require further consideration are the resistance and inductance in the leads to C_1 and C_2. The residual resistance and inductance are designated as R' and L'.

Taking R' and L' into consideration, it may be shown that the combination is equivalent to a capacitance C_p in parallel with a conductance G_p where C_p and G_p are given, after certain reasonable approximations, by

[d] $$C_p = C_t\,(1 + L'C_t\omega^2 - R'^2C_t^2\omega^2)$$

and

[e] $$G_p = G_t\,(1 - 2L'C_t\omega^2 - R'^2C_t^2\omega^2) + R'C_t^2\omega^2.$$

If both L' and R' are not very small [d] should be written

[f] $$C_p = \frac{C_t(1 - L'C_t\omega^2)}{(1 - L'C_t\omega^2)^2 + R'^2C_t^2\omega^2}.$$

If R' is found to be negligibly small but L' quite large, then [f] may be written

[g] $$C_p = \frac{C_t}{1 - L'C_t\omega^2};$$

[f] is, of course, the most rigorous expression for C_p.

The equations [*d*], [*f*], or [*g*] are used to correct for asymmetry in the resonance curve. Once the curve is made symmetrical, G_p may be calculated by use of [*c*].

In fact, in cases where R' is negligible, L' may be accurately found by determining the value of L' necessary to make an asymmetric curve symmetrical by use of [*g*]. With reasonable care in construction R' should be negligibly small at all frequencies so that [*g*] may indeed be used to correct for asymmetry.

If, on trial, it is found that the resonance curve is completely symmetrical without correction, then it may reasonably be assumed that the L' and R' are both negligibly small.

Further, even if there were appreciable lead corrections in this system the manner of operation would cause them to be cancelled out.

Consider equation [*d*]. Any L and R in the leads could be lumped with the L' and R' of the cell. We have for the first condition, before gas is adsorbed

$$C_{p_1} = \epsilon C_{t_1}(1+\omega^2 L'\epsilon C_{t_1} - R'^2\omega^2\epsilon^2 C_{t_1}^2)$$

where ϵ is the dielectric constant of the bare powder in the cell and C_{t_1} is the low frequency capacity of the empty cell determined from low frequency measurements and the reading of the calibrated micrometer.

After gas is adsorbed we have

$$C_{p_2} = \epsilon' C_{t_2}(1+\omega^2 L'\epsilon' C_{t_2} - R'^2\omega^2\epsilon'^2 C_{t_2}^2)$$

where ϵ' is the composite dielectric constant of the system and C_{t_2} would be the capacity of the empty cell at this setting.

By the method of operation $C_{p_1} = C_{p_2}$, since resonance is re-established at the same frequency and for the same coil. Since the correction term is thus the same in both cases, $\epsilon C_{t_1} = \epsilon' C_{t_2}$. C_{t_1} and C_{t_2} are determined directly from the positions of the piston as measured by the micrometer and ϵ is separately determined at low frequency by bridge methods. Thus, correct values of ϵ' may be measured by this method. This assumes that ϵ, the dielectric constant of the powder does not change with frequency in this frequency range. The evidence at hand indicates that this assumption is correct.

In order to show that the operation of the cell is such that lead corrections vanish, it is best to consider a diagram of the cell. This is shown in Fig. 3.

Design and Operation of the Cell

As may be seen, the cell consists of a cylinder with a thick flange, on top of which a lid may be bolted. The cylinder and its flange were machined out of a single block of brass. Inside this cylinder and resting on a block of Teflon on the bottom is a smaller cylinder with a short lug at the top to which a high potential lead may be soldered. Since the wall of the outer cylinder is well grounded, we thus have a condenser of two coaxial cylinders.

Fitting snugly inside the second cylinder is a cylinder of Teflon. Since the fit is quite snug, the second cylinder must be rigidly fixed if the Teflon cylinder is rigidly fixed. This is accomplished in two ways. (1) The Teflon disc

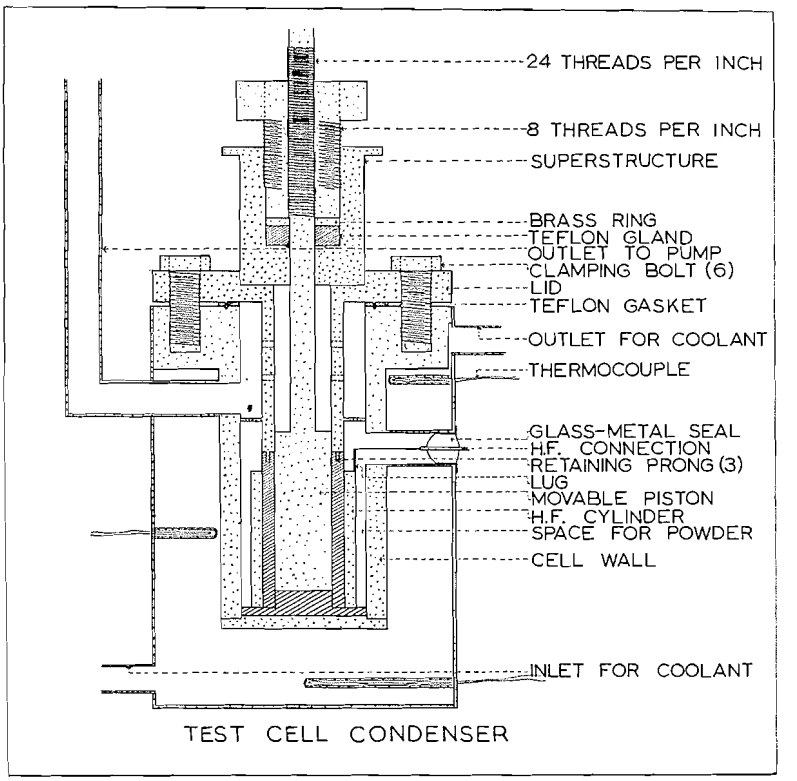

FIG. 3. Test cell for high frequency measurements.

at the bottom of the large cylinder has a raised circular portion over which the Teflon cylinder fits tightly. (2) The cell lid has a long sleeve extending down with three prongs cut out of the end of the sleeve. These prongs fit into three matching slots cut into the Teflon cylinder so that when the lid is tightly clamped the Teflon cylinder is held fixed.

Passing down through the sleeve and the Teflon cylinder is a brass piston on a long rod. The rod and the piston were machined out of a single piece of brass to ensure that they rotated about a common axis without a trace of wobble. Further, the piston was made to maintain good contact with the sleeve at all times as it was moved up or down. It will be noticed that the sleeve itself has a collar near the lower end that makes good contact with the walls of the outer cylinder. Thus, the piston is always grounded to the walls of the outer cylinder by a ground connection, the length of which does not change as the piston is moved. It will now be clear that this movable piston makes a variable condenser system with the second high potential cylinder. Small holes were drilled through the sleeve and collar to allow free passage of gas.

To ensure that no leakage would occur while the piston was moved, a superstructure was built on top of the lid. This superstructure consisted of a brass cup solidly soldered to the lid, and of a large heavily threaded brass bolt

pressing down on a brass ring resting on top of a Teflon gland at the bottom of the cup. The piston rod passed through the bottom of the cup, the Teflon gland, the brass ring, and the bolt. When the large bolt was screwed down tightly, the Teflon gland was squeezed out and made a very effective seal. If the operating temperature was lowered appreciably below room temperature, the large bolt had to be tightened further to prevent leaks. To accomplish the movement of the rod the inside of the bolt and the top part of the rod were threaded and the piston could be screwed up and down by the use of a small rachet wrench. The movement of the piston was measured by a micrometer (not shown) which could be read to 0.0001 in. also fastened to the top of the lid.

Taken as a whole, the cell is really a single variable condenser consisting of two parts, one of which is fixed, and one variable. The two parts have a common high potential plate so that, in effect, there is no high potential lead between them. Their respective grounds go to a common point and are very nearly the same short length.

The height of the fixed condenser part was 3.5 cm. The inside radius of the outer cylinder was 1.58 cm. with a gap of 0.27 cm. Thus, the volume of the space in which the powder was packed was 8.46 $cm.^3$ and the capacity when empty was 10.53 $\mu\mu f$. When filled with powder the capacity of the space increased to about 33.5 $\mu\mu f$. which value varied depending on the density of packing. When completely assembled the cell had a total capacity of about 50 $\mu\mu f$. with the piston resting on the bottom. The cell was operated at about 47 to 48 $\mu\mu f$. capacity to allow resonance curves to be taken at all points of operation. The total movement of the piston was 1 in. which could be measured accurately to 0.0002 in. The total change in capacity brought about by this 1 in. movement of the piston was 7.5 $\mu\mu f$.

With 48 $\mu\mu f$. total capacity, resonance could be obtained at 106 Mc./sec. with an inductance consisting of a straight piece of copper wire 2.5 cm. long connected across the cell from the high potential lead to ground. The lowest frequencies at which resonance could be made to occur would presumably be limited by the ability to wind a coil with enough turns of wire. In practice the cell was used at a frequency of 13 Mc./sec. by use of 10 turns of copper wire on a form 3.15 cm. in diameter.

To maintain a constant temperature, an outer jacket, through which coolant could be circulated, was built around the entire cell as shown in the diagram. In this case, it was felt to be more convenient to cause a low boiling liquid to boil in this outer jacket and condense in a coil immersed in a dry ice – acetone bath above the cell, and thus to maintain the temperature of the cell at that of the refluxing liquid. The temperature could be varied quite easily by altering the pressure at which boiling occurred. The temperature was checked by means of three thermocouples set into the boiling chamber. By this means the temperature could be kept constant to 0.1°C. with a temperature gradient of less than 0.2°C. from the bottom to the top of the cell.

It is worthwhile, now, to consider a certain aspect of the voltmeter used. This was a vacuum tube voltmeter employing two balanced tubes, as described

by Greenspan (3). The circuit diagram is given by Hartshorn and Ward (4). From this diagram it can be seen that the operation of the voltmeter is that of a Wheatstone bridge of which the plate resistances of the two tubes form two equal arms and the two tubes form the other two arms. The internal resistance of tube I is altered by the input voltage from the test cell to the grid of this tube. This will cause an unbalanced condition with respect to tube II and current will flow through the galvanometer. In most cases the swing of the galvanometer in response to this current is very large, and the galvanometer spot travels far off the scale. For determining resonance capacities alone, this causes no trouble, since the capacity of the test cell is changed till the galvanometer spot has swung through its farthest limit and has returned to the same position on the scale. When it is desired to determine an entire resonance curve, for the purpose of measuring the G of the circuit, however, the actual number of scale divisions traversed by the spot must be known. To accomplish this, just before the spot moves off the scale it is returned to the low point of the scale by altering the bias on tube II. Since the internal resistance of the tube is a function of the bias (viz. operation of tube I), changing the bias of tube II would also change its internal resistance. This would change an arm of the Wheatstone bridge that was supposed to have remained constant. Therefore, depending on the number of times the spot had to be returned to scale during a measurement, the top part of the resonance curve would have been determined at a different bias than the bottom part. Furthermore, owing to the change in the tube resistance, the top part of the curve would have been determined at a different amplification factor of the tube. This disadvantage could, of course, be overcome by operating the apparatus at such a low sensitivity that the whole curve could be taken on one scale length,

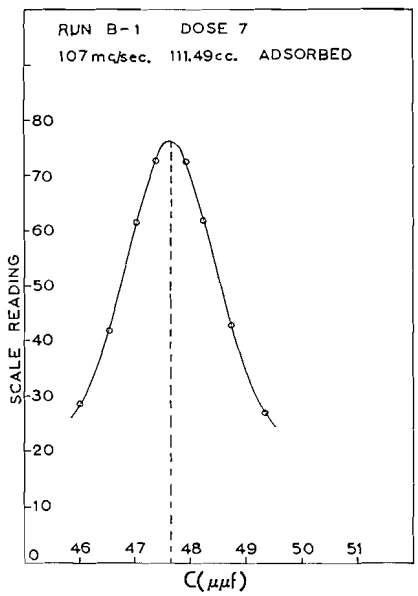

FIG. 4. Resonance curve for run B-1 addition 7.

or by using a scale of great length. Both alternatives were impractical. It was possible to show, from considerations of the galvanometer circuit, that the required change in bias on the grid of tube II did not change the tube constants to an appreciable extent.

It now was shown that the residual inductance and resistance of the cell were negligible. Plots of V^2 versus C_t were obtained for a variety of frequencies and these curves were found to be perfectly symmetrical, even at the highest frequency used. These symmetrical curves were obtained for the empty cell and for the cell packed with powder and with gas adsorbed. A typical curve taken from one of the runs is shown in Fig. 4.

Table I demonstrates the symmetry of the curve. As was pointed out earlier, such symmetry in the resonance curve can only mean no corrections need be made because of residual resistance and inductance.

TABLE I

$C_a(\mu\mu f.)$	$C_b(\mu\mu f.)$	$C_r(\mu\mu f.)$
47.41	47.97	47.69
47.32	48.07	47.70
47.03	48.37	47.70
46.77	48.61	47.69
46.43	48.93	47.68

It had next to be confirmed that true values of the dielectric constant could be obtained at all frequencies. For this test, glass was used as the dielectric, since its dielectric constant remained unchanged in the frequency range. The following procedure was used.

First, with the empty cell the resonance capacity was measured using a coil giving resonance at 73 Mc./sec. The top was removed and a piece of glass, cut into a half cylinder that partly filled the space to be occupied by the powder, was inserted into that space. The top was carefully replaced and the plunger moved until resonance was again obtained. Now the coil was changed to one that would allow resonance at 13 Mc./sec. Resonance was obtained with the glass in and the plunger nearly in the same position as it was at 73 Mc./sec. The top was removed, the glass taken out, the top replaced, and the plunger moved until resonance was again obtained. Thus the capacity change due to insertion of the glass could be compared for the frequencies of 13 Mc./sec. and 73 Mc./sec. since the position of the glass semicylinder was the same for both frequencies.

As an added assurance, this value was checked against the value obtained at 10.2 kc./sec. using a bridge method of measuring the capacity. The glass semicylinder was not an exact fit so that it was not possible to insert it in exactly the same way as for the high frequency trial. To compensate for this error, 10 trials were made by the bridge method and an average taken. Table II shows the remarkably close agreement in the result of all three tests and adequately shows that the cell will give true readings.

TABLE II

Frequency (Mc./sec.)	$\Delta C(\mu\mu f.)$
73.0	4.98
13.5	4.97
0.010	4.89 ± 0.06

RESULTS

The cell was used to measure the change in capacity when sulphur dioxide was adsorbed on nonporous rutile at frequencies of 13, 36, 106 Mc./sec. and the single temperature of 3.5°C.

From the primary data at these frequencies (a typical set is represented in Fig. 5), no appreciable frequency dependence could be detected. The plot is seen to have the same general characteristics as those shown by a similar

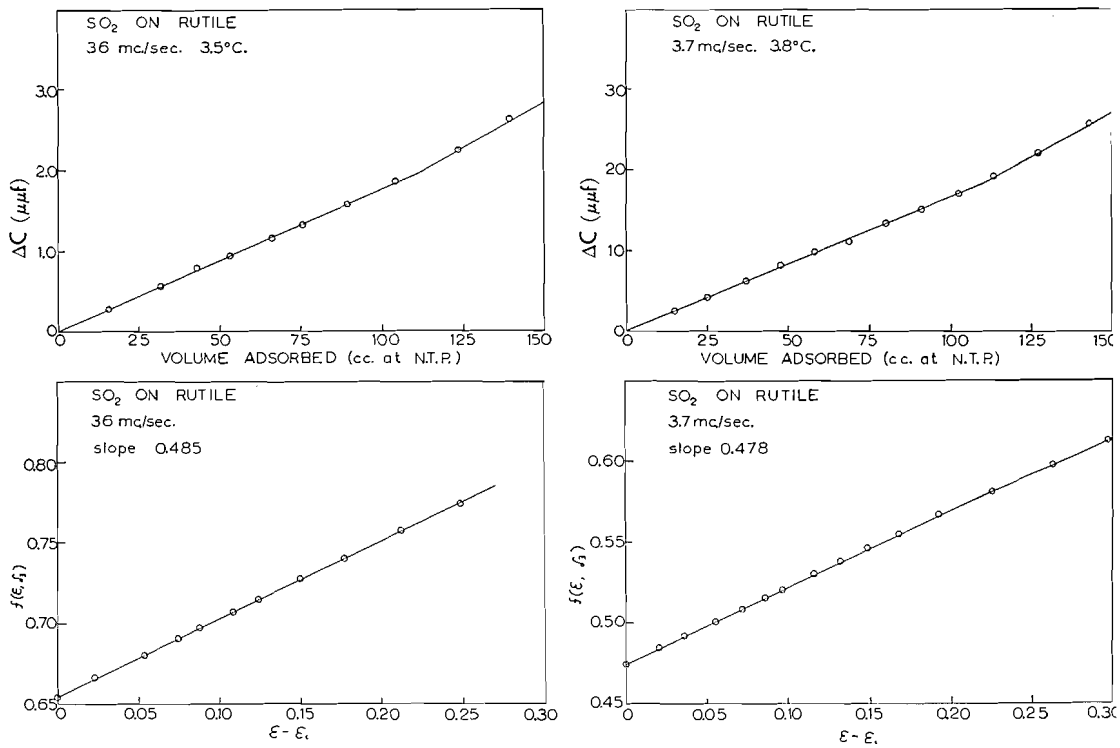

FIG. 5. Plots of ΔC versus volume adsorbed and functional plots for sulphur dioxide adsorbed on rutile.

plot given by Channen (1) at 3.7 Mc./sec. with the apparatus described by Snelgrove, Greenspan, and McIntosh (6). The characteristic change in the slope of the plot was also found here as observed by Channen and McIntosh for sulphur dioxide.

It is desirable to compare results obtained in this assembly with those obtained by Channen. Unfortunately, this comparison can not be made using

the primary data, owing to the difference in cell geometry and packing densities of the powder. A comparison using some functional plot must be made. The various functional plots that it is possible to use are discussed elsewhere in a paper by Channen and McIntosh (1). The one used here is the original function derived by McIntosh, Rideal, and Snelgrove (5) with a small correction for the material in the gas phase which was not necessary for silica systems. Using this method, the results obtained in this investigation agree very well with those of Channen, as a comparison of the slopes of the first linear sections of the functional plots given in Table III reveals.

TABLE III

Frequency (Mc./sec.)	Temp., °C.	Slope
13.0	3.2	0.471
36.0	3.5	0.485
106.0	3.7	0.469
3.7	3.8	0.478

From equation [*c*] one may obtain an expression for the power factor (or the loss tangent) of the adsorbed vapor in the form

$$[h] \qquad \tan \delta = \frac{(\Delta C_i - \Delta C_0)}{2\, C_{r_i} \sqrt{(q-1)}}$$

where $\tan \delta$ is the loss tangent.

ΔC_i is the change in capacity needed to go from one side of the resonance curve to the other at any chosen q after the ith addition of gas.

ΔC_0 is the change in capacity under the same conditions but for the bare powder.

C_{r_i} is the resonance capacity at the ith addition of gas.

There was no detectable loss tangent at any of the frequencies used. This result is not, in itself, conclusive, since the adsorbed phase is such a small fraction of the total system that, though the adsorbed phase itself may have an appreciable loss tangent, its contribution to the loss tangent of the system as a whole may be undetectable.

CONCLUSIONS

The above results show that the apparatus, as designed, works well at frequencies up to 106 Mc./sec. However, measurements at these frequencies have not shown any marked change in behavior of the adsorbed molecules from their behavior at low frequencies. Nevertheless, the conviction remains that some anomalous behavior, particularly the phenomenon of dispersion, must exist in some higher frequency range.

Since neither the cell capacitance nor the inductance used to obtain resonance can be greatly reduced, the principle employed in the construction of this apparatus has probably been pushed to near its upper frequency limit. If it is desired to investigate a higher frequency range, some other method, such as transmission lines or wave guides, will have to be tried.

ACKNOWLEDGMENT

It is a pleasure to acknowledge financial support of this work by the National Research Council and by the Advisory Committee on Research of the University of Toronto.

REFERENCES

1. CHANNEN, E. and MCINTOSH, R. L. Can. J. Chem. 33: 172. 1955.
2. DEBYE, P. Polar molecules. The Chemical Catalog Company, Inc., New York. 1929.
3. GREENSPAN, H. M. Sc. Thesis, University of Toronto, Toronto, Ont. 1951.
4. HARTSHORN, L. and WARD, W. H. J. Inst. Elec. Engrs. (London), 79: 597. 1936.
5. MCINTOSH, R. L., RIDEAL, E. K., and SNELGROVE, J. A. Proc. Roy. Soc. (London), A, 208: 292. 1951.
6. SNELGROVE, J. A., GREENSPAN, H., and MCINTOSH, R. L. Can. J. Chem. 31: 72. 1953.
7. WALDMAN, M. H., SNELGROVE, J. A., and MCINTOSH, R. L. Can. J. Chem. 31: 998. 1953.

ON THE CALCULATION OF THERMAL TRANSPIRATION[1]

By S. Chu Liang

ABSTRACT

The equation proposed earlier has been derived from a new kinetic concept. It is shown to be a reasonable approximation of this new consideration. The equation is also shown to be mathematically consistent with the general fact that when the thermomolecular pressure difference is plotted against the normally measured pressure, a single maximum is obtained. The curves calculated from this equation are shown to agree closely with those from the Weber equation using van Itterbeek and de Grande's data. The practical use of the equation is discussed.

INTRODUCTION

The problem of the effect of thermal transpiration on pressure, or the thermomolecular pressure difference, was observed and investigated by a number of workers both experimentally and mathematically (1, 4, 9). Although a practical solution was not obtained, the problem was neglected for many years. It was not even mentioned in most publications where it was obviously important.

Recently, Weber and his co-workers reinvestigated this problem and showed the extent to which a pressure measurement may be affected (11, 12). More recently, the problem was again brought to the general attention of this continent. Its practical importance was demonstrated by Liang (6) in the the case of vapor pressure measurement, and by Crowell and Young (2) in the case of physical adsorption.

Until very recently, the only available equation by which the thermal transpiration effect may be calculated was a semiempirical one obtained by Weber and his co-workers. The equation was derived along the line given by Maxwell with modifications suggested by Weber, and took the general form

$$[1] \qquad \ln \frac{p_1}{p_2} = \frac{1}{2} \ln \frac{T_1}{T_2} - \frac{1+2n}{2(1+n)} \left[B \ln \frac{y_1+m}{y_2+m} + C \ln \frac{y_1+m'}{y_2+m'} + D \ln \frac{y_1+m''}{y_2+m''} \right]$$

in which $y = R/\lambda$, R being the tube radius and λ the mean free path of the gas; n was related to the viscosity η by the equation

$$[2] \qquad \eta/\eta_0 = (T/T_0)^{\frac{1}{2}+n};$$

B, C, D, m, m', and m'' were constants calculated from another three semiempirical constants, k_1, k_2, and μ, which in turn were evaluated from the experimental data. Weber and Schmidt (13) calculated the constants for helium. van Itterbeek and de Grande (10) found that the values of k_1, k_2, and μ were functions of the nature of the gas and that separate determinations for different gases must be made. They extended the equation accordingly to cover the cases of hydrogen, deuterium, and neon.

[1]*Manuscript received September 16, 1954.*
Contribution from Research Laboratory, Dominion Tar & Chemical Co., Ltd., 3547 Allard Street, Ville LaSalle, Quebec. This paper was presented at the Symposium on Problems Relating to the Adsorption of Gases by Solids, held at Kingston, Ontario, September 10–11, 1954.

Los and Fergusson (8), in attempting to extend the Weber equation to the cases of nitrogen and argon, discovered that equation [1] was not applicable to argon. They also showed that by following the same general argument as Weber, mathematically, another equation of the general form

$$[3] \quad \ln\frac{p_1}{p_2} = \frac{1}{2}\ln\frac{T_1}{T_2} - \frac{1+2n}{2(1+n)}\left[B\ln\frac{y_1+m}{y_2+m} + \frac{C}{2}\ln\frac{y_1^2+m'y_1+m''}{y_2^2+m'y_2+m''} - \frac{D-\frac{1}{2}Cm''}{d}\left(\tan^{-1}\frac{y_1+\frac{1}{2}m'}{d} - \tan^{-1}\frac{y_2+\frac{1}{2}m'}{d}\right)\right]$$

is possible, where $d = (m''-\frac{1}{4}m'^2)^{\frac{1}{2}}$. The constants, while differing from those of equation [1], may be calculated in a similar fashion to that employed by Weber. This, of course, raises the intrinsic problem whether equation [1] or equation [3] should be employed when a new gas is being considered.

In the meantime, a different empirical formula was suggested by the present writer (5) in the form

$$[4] \quad R = p_1/p_2 = [\alpha(X/f)^2+\beta(X/f)+R_m]/[\alpha(X/f)^2+\beta(X/f)+1]$$

for the purpose of calculating the thermal transpiration effect R. Equation [4] was obtained by plotting R vs. p_2, the normally measured pressure. $X = p_2.d$, d being the tube diameter. $R_m = (T_1/T_2)^{\frac{1}{2}}$ and f is the "pressure shifting factor" which was used to correlate the different gases and was arbitrarily defined as $f_{N_2} \equiv 1$. The constants α and β were obtained by fitting the curve to the experimental data. Equation [3] was later modified slightly (7) to take a more readily usable form

$$[5] \quad p_1/p_2 = [\alpha_{He}(\phi_g X)^2+\beta_{He}\phi_g X+R_m]/[\alpha_{He}(\phi_g X)^2+\beta_{He}\phi_g X+1]$$

by referring to helium as the standard, and defining $\phi_{He} \equiv 1$. Equation [5] has been found to be applicable to at least eight gases, namely, helium, neon, hydrogen, argon, nitrogen, krypton, xenon, and ethylene; and it is expected to be equally applicable to others.

Equation [5] can be reduced readily to

$$[6] \quad \frac{p_2-p_1}{p_2} = \frac{\Delta p}{p_2} = \frac{1-R_m}{\alpha_{He}(\phi_g X)^2+\beta_{He}\phi_g X+1}.$$

The practical advantage of equation [6] over the Weber equation and its variation (equations [1] and [3]) is immediately obvious. It is therefore desirable to investigate whether there is any reasonable basis for its existence; and to examine whether, mathematically, it conforms to all the known facts. Such is the primary purpose of this communication.

DERIVATION OF EQUATION [5]

The purely mathematical approach to the problem has been exhausted by Chapman and Cowling (1). The final solution includes a cluster integral which is too complicated to solve for practical purposes. The recent thermodynamic approach made by de Groot (3) following the Onsager theory of reciprocal relations is deceptively simple. The many terms included in the final solution

are so far from the conventional thermodynamics that its usefulness for practical purposes is rather doubtful. The physical approach outlined by Maxwell has been followed up by Weber and his associates (11, 12) to reach useful but cumbersome results. It is thus decided that an entirely independent approach, a new kinetic approach, however empirical it may be, should be adopted.

We shall now consider the system composed of two regions at T_1 and T_2, connected by a tube of diameter d, and filled with *one* gas. After infinite time of waiting, the pressures are p_1 and p_2. We shall proceed to solve the relation between p_1 and p_2. At the offset, it should be pointed out that the system under consideration is not, and will never be, in thermodynamic equilibrium. Consequently, the conventional thermodynamics is of no great help. When the pressures between two regions of different temperatures reach "equilibrium", a stationary state, not an equilibrium, is established. The boundary conditions are that, at high pressures, i.e. $\lambda \ll d$, $p_1 = p_2$, and at low pressures, i.e. $\lambda \gg d$, $p_1/p_2 = (T_1/T_2)^{\frac{1}{2}}$. Furthermore, at high pressures the collisions for the transfer of energy take place predominantly in the gaseous phase while at low pressures the collisions take place predominantly via the wall. In the intermediate pressure region, the two types of collisions are both important, to varying degree as a function of the pressures. We assume that the collisions may be divided into the two types, each exerts its influence independently on the pressures, and the resultant effects are additive. Thus,

$$[7] \qquad p_1 = [N_G p_2 + N_W p_2 (T_1/T_2)^{\frac{1}{2}}]/(N_G + N_W),$$

where N_G and N_W are the number of collisions via the gaseous phase and wall respectively. It must be emphasized that N_G and N_W are not necessarily the physical numbers, but that they may be the equivalent numbers. The assumption of additivity may therefore be justified.

It follows readily that $N_G = k_1 p_1 p_2$ as N_G depends on the concentrations of molecules in both regions, where k_1 is a proportional constant; and $N_W = k_2 p_2$ (or $k_2' p_1$) where k_2 (or k_2') is *pressure dependent.*

Further, we will assume that p_1 may be represented by a polynomial of p_2, or

$$[8] \qquad p_1 = a p_2 + b p_2^2 + \ldots$$

Solving equation [7] by substituting the functions for N_G and N_W we have

$$[9] \qquad \frac{p_1}{p_2} = \frac{k_1 p_1 + k_2 (T_1/T_2)^{\frac{1}{2}}}{k_1 p_1 + k_2}.$$

Substituting equation [8] into equation [9], bearing in mind k_2 as a function of p's, we obtain

$$[10] \qquad \frac{p_1}{p_2} = \frac{k(p_2)(a p_2 + b p_2^2 + \ldots) + (T_1/T_2)^{\frac{1}{2}}}{k(p_2)(a p_2 + b p_2^2 + \ldots) + 1},$$

in which $k(p_2) = k_1/k_2$. Equation [10] may be rewritten in the form

$$[11] \qquad \frac{p_1}{p_2} = \frac{A p_2^2 + B p_2 + (T_1/T_2)^{\frac{1}{2}}}{A p_2^2 + B p_2 + 1},$$

when taking only the first two terms of equation [8]. By following the argument put forward earlier (5, pp. 150–151), equation [11] is transformed into equation [5].

DISCUSSION

Comparison with Weber Equation

The merit of the Weber equation cannot be denied. It has served well as far as accuracy is concerned. The starting point of Weber's treatment is very sound in principle. The approach of considering a stationary state established by the balance of an axial flow and a tangential flow is quite rigorous. That the original Maxwell treatment is inadequate to solve this problem has been adequately discussed in textbooks on the kinetic theory of gases and needs no further amplification. Weber, therefore, has to modify some of the Maxwellian terms, and an approximation is made. When the equation for the hydrodynamical region is applied to the molecular region, Weber is forced to make a further modification. Much of the original rigorousness is lost after the successive approximations, although the mathematical expression does not become any simpler. The complete solution (equations [1] and [3])is cumbersome yet still empirical. Actually, equations [1] and [3] are simple in appearance but unwieldy in use. For y_1 and y_2 are functions of λ's which are in turn functions of p_1 and p_2. Thus to calculate p_1 for a given value of p_2, the operation becomes extremely complicated. The alternative solution found by Los and Fergusson makes it even less attractive.

The present treatment gives a very simple formula and thus eliminates all the difficulties involved in the Weber equation. Besides, it leaves no ambiguity when a new gas is to be considered. The agreement between equation [6] and the experimental values is to be shown in the discussion to follow.

It might be questioned whether or not the rigorous starting mathematical treatment of Weber is a strong point in its favor. Actually, if the theoretical treatment is of interest, then those treatments given by Chapman (1) and de Groot (3) should be followed but not that of Weber.

Comparison with Experiments

For all the published cases known to the writer, T_2 and p_2 represent the conditions at room temperature, and T_1 and p_1 those at lower temperatures; the discussion will therefore be confined to this understanding.

Generally, when Δp is plotted against p_2,* the curve exhibits a single maximum. Equation [6] will be examined for this point. At Δp = maximum or $d(\Delta p)/dp_2 = 0$,

[12] $$\alpha_{\mathrm{He}}(\phi_g X)^2_{\max} = 1,$$

$$X_{\max} = (p_2 \,.\, d)_{\max} = (1/\alpha_{\mathrm{He}}\,\phi_g{}^2)^{\frac{1}{2}},$$

or

[13] $$(p_2)_{\max} = \frac{1}{\alpha^{\frac{1}{2}}_{\mathrm{He}}.d} \cdot \frac{1}{\phi_g}.$$

**In Weber's type treatment, the customary way is to plot Δp against $\bar{p}$, where $\bar{p} = \frac{1}{2}(p_1+p_2)$. The net result is the same.*

Equation [12] is of considerable practical importance. It not only indicates that equation [6] gives a single maximum, but also gives the pressure at which the maximum exists. Furthermore, for a given tube, $\alpha_{He}^{\frac{1}{2}}.d$ is constant, for various gases; the value of $(p_2)_{max}$ is therefore a function of ϕ_g *only*. Experimentally, the value of $(p_2)_{max}$ can be determined more accurately for a larger difference between T_1 and T_2. Once it is determined, it may be used for the cases of small temperature difference when direct determination often involves high uncertainty. The accuracy in the determination of $(p_2)_{max}$ may also be increased by using tubes of small diameter, which correspond to high values of $(p_2)_{max}$, and the $(p_2)_{max}$ so obtained may then be used for the cases of tubes of large diameters.

Since $\phi_{He} \equiv 1$, by measuring $(p_2)_{max}$ for helium accurately, α_{He} may be obtained with good accuracy. This makes it possible for ϕ_g for other gases to be obtained with low experimental uncertainty.

Equation [6] also makes it possible for the experimental results obtained with the same gas, same T_1 and T_2, but different tube diameter, to be cross-checked. Thus, if

$$Y = (\Delta p) \,.\, d,$$

the equation [6] gives

$$[14] \qquad \frac{Y}{X} = \frac{(\Delta p) \,.\, d}{p_2 \,.\, d} = \frac{1-R_m}{\alpha_{He}(\phi_g X)^2+\beta_{He}(\phi_g X)+1}.$$

Or, if Y is plotted versus X, measurements of different tube diameters will fall in a single curve.

The foregoing considerations are examined with the published experimental results. The equation is known to be applicable to the conditions for $T_1 = 78°$ and 195°K. (5, 6, 7). In order to test its applicability over wide temperature variations, the data of van Itterbeek and de Grande (10), which cover the temperature range of $T_1 = 20$–90°K. in a reasonably systematic way, are used. The constants for equation [5] at various temperatures are determined, and the curves so calculated are compared with the experimental data and also with the curves obtained according to the Weber equation by the original authors. The agreement is in general very close. One such comparison, the 69°K. results, is shown in Fig. 1. The open and closed points are the two sets of published data for $d = 1.236$ and 0.860 mm. respectively. The full lines are the curves calculated from equation [5]. In the case of helium, the dotted curve represents that calculated from the Weber equation. In the cases of neon and hydrogen, the difference between the Weber equation and equation [5] is too small to be shown. Thus, for all practical purposes, the two solutions, both empirical, are equal.

Substituting equation [12] into equation [14] gives

$$[15] \qquad \frac{Y_{max}}{X_{max}} = \frac{1-R_m}{2+\beta_{He}\phi_g X_{max}} = \frac{1-R_m}{2+\beta_{He}/\alpha_{He}^{\frac{1}{2}}}.$$

Equation [15] gives the value of Y_{max}/X_{max} for all gases. Thus, once the constants α_{He} and β_{He} are determined, the value of Y_{max}/X_{max} in all gases for all

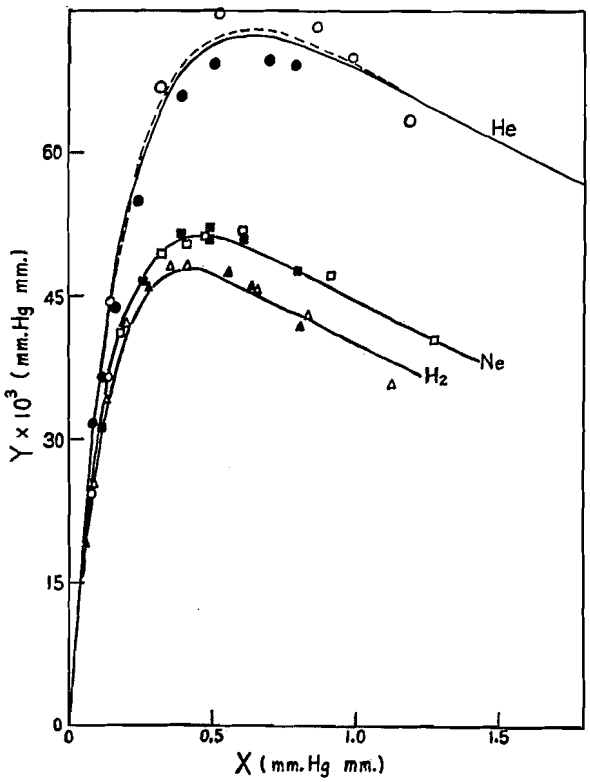

FIG. 1. Comparison of the curves calculated from the present equation and the Weber equation with experimental data (van Itterbeek and de Grande) for helium, neon, and hydrogen, at $T_1 = 69°K$. Tube diameter: open points, $d = 1.236$ mm.; closed points, $d = 0.860$ mm. Full lines, equation [5]; dotted line, the Weber equation.

tube sizes and at all temperature differentials may be evaluated readily. Table I gives one set of values of Y_{max}/X_{max} for helium, neon, and hydrogen at $T_1 = 69°K$. as an example.

TABLE I

Y_{max}/X_{max}— FOR HELIUM, NEON, AND HYDROGEN AT 69°K.

Gas	Y_{max} (mm. Hg mm.)	X_{max} (mm. Hg mm.)	Y_{max}/X_{max}
Helium	0.0730	0.63	0.116
Neon	0.0513	0.445	0.115
Hydrogen	0.0480	0.41	0.117

From equation [15], one may also obtain

$$[16] \qquad B = \beta_{He}\phi_0 = \frac{1-R_m}{Y_{max}} - \frac{2}{X_{max}}.$$

Thus, the B value for each gas may be calculated from experimental data for

each individual gas through the use of equation [16]. The ratio B_g/B_{He} gives ϕ_g which may thus be determined experimentally.

It should be emphasized that the thermal transpiration effect is a function of the nature of the tube. This has been pointed out previously (5) and has since been verified experimentally (8). The accommodation coefficient undoubtedly plays an important role. Thus Los and Fergusson have found that the effect produced in a metal tube differs from that in a glass tube.

The question of what role the length of the tube plays has been raised on many occasions. It is sufficient to say that as long as the length of the tube is such as to permit the establishment of the two regions at T_1 and T_2, the length is immaterial. If the tube is too short, then the two distinct regions cannot be established. In that case, of course, the basic conditions are not met, and it becomes a different problem altogether.

ACKNOWLEDGMENT

The author wishes to acknowledge his indebtedness to Dr. J. A. Morrison of the National Research Council of Canada who first interested him in this problem.

REFERENCES

1. CHAPMAN, S. and COWLING, T. G. The mathematical theory of non-uniform gases. The University Press, Cambridge. 1939. Chap. 7.
2. CROWELL, A. D. and YOUNG, D. M. Trans. Faraday Soc. 49: 1083. 1953.
3. DE GROOT, S. R. Thermodynamics of irreversible processes. Interscience Publishers, Inc., New York. 1952. p. 20ff.
4. KNUDSEN, M. H. C. The kinetic theory of gases. Methuen & Co., Ltd., London. 1934. pp. 33–39.
5. LIANG, S. C. J. Appl. Phys. 22: 148. 1951.
6. LIANG, S. C. J. Phys. Chem. 56: 660. 1952.
7. LIANG, S. C. J. Phys. Chem. 57: 910. 1953.
8. LOS, J. M. and FERGUSSON, R. R. Trans. Faraday Soc. 48: 730. 1952.
9. REYNOLDS, O. *See* The scientific papers of James Clark Maxwell, Vol. 2. *Edited by* W. D. Niven. 1890. p. 708.
10. VAN ITTERBEEK, A. and DE GRANDE, E. Physica, 13: 289. 1947.
11. WEBER, S. and KEESOM, W. H. Communs. Kamerlingh Onnes Lab. Univ. Leiden, No. 223, b. 1932.
12. WEBER, S. *et al.* Communs. Kamerlingh Onnes Lab. Univ. Leiden, Nos. 246, a–d. 1936.
13. WEBER, S. and SCHMIDT, G. Communs. Kamerlingh Onnes Lab. Univ. Leiden, No. 246, c. 1936. Rapp. et Communs. 7e Congr. intern. Froid. p. 72. 1936.

THE ADSORPTION OF ARGON ON SOME VACUUM DEHYDRATED SALTS[1]

By H. W. Quinn,[2] R. W. Missen,[3] and G. B. Frost

ABSTRACT

Isotherms for the adsorption of argon on amorphous products formed by the vacuum dehydration of several hydrated salts have been determined. These have shown that the adsorption is physical and that dehydration results in the formation of products of large capillary volume. The probable distribution of capillary diameters has been estimated and correlated with the effect of water vapor at low pressures in catalyzing the crystallization of the amorphous intermediates. Consideration of these findings, in the light of data for the heats of transition from the amorphous to the crystalline state, suggests that the X-ray amorphous character is not entirely due to the capillary structure but that other changes occur. The possible nature of these is discussed.

INTRODUCTION

When certain hydrated salts are dehydrated under vacuum or at very low pressures of water vapor, products are obtained which do not diffract X-rays. These products crystallize into the lattice of one of the crystalline lower hydrates in the presence of water vapor above certain limiting pressures which are specific for each salt but which depend on temperature. Crystallization also occurs when the amorphous material is heated at moderate temperatures for various periods. Hydrated salts known to behave in this manner are copper sulphate pentahydrate, zinc sulphate heptahydrate, manganous sulphate tetrahydrate, nickel sulphate hexahydrate, magnesium sulphate heptahydrate, and manganous oxalate dihydrate. There are probably others.

Discussion of the possible mechanism of formation of amorphous material under vacuum dehydration and its subsequent crystallization in the presence of water vapor has been given elsewhere (5, 9). It appears that as the parent lattice loses co-ordinated water molecules at the reaction interface, a skeleton lattice is formed which probably collapses at once into either a microcrystalline state (the microcrystals being below the limit in dimensions required for X-ray diffraction), or into some state of ionic randomness resulting in a disordered lattice of higher energy than its normal crystalline counterpart. The effect of water in inducing crystallization may be due to a catalytic effect whereby macrocrystals are formed from microcrystals (8), or to the effect of adsorbed water dipoles in lowering interionic attractive forces and diffusing into the strained lattice, thus increasing the mobility of the disordered ions and enabling them to orient themselves into an energetically stable arrangement.

[1]*Manuscript received September 16, 1954.*
Contribution from the Department of Chemistry, Queen's University, Kingston, Ontario. This paper was presented at the Symposium on Problems Relating to the Adsorption of Gases by Solids, held at Kingston, Ontario, September 10–11, 1954.
[2]*Present address: Holder of a National Research Council of Canada Studentship, University of Toronto, Toronto, Ontario.*
[3]*Present address: Athlone Fellow in Chemistry, Cambridge University, Cambridge, England.*

The limiting pressures of water vapor above which the formation of an amorphous intermediate is not observed vary from small fractions of a millimeter to a few millimeters. Observed values are given in Table I.

TABLE I

Salt	t, °C.	Approximate limiting pressure (mm.)
$MnC_2O_4.2H_2O$	60	0.2
$CuSO_4.5H_2O$	40	0.25
$MnSO_4.4H_2O$	50	1.2
$ZnSO_4.7H_2O$	40	1.5
$NiSO_4.6H_2O$	60	2.0
$MgSO_4.7H_2O$	40	4.5
$MgSO_4.7H_2O$	50	8.0
$MgSO_4.7H_2O$	60	12.5

The rate of dehydration of manganous oxalate dihydrate at a series of low pressures of water vapor has been determined by Volmer and Seydel (11) and by Topley and Smith (10). Similar rate determinations for the dehydration of copper sulphate pentahydrate have been made by Frost and Campbell (4), who interpreted these rates in terms of the formation of amorphous material and its subsequent crystallization. Wheeler (12) and Ford (3) have studied the rates of dehydration of the other salts mentioned and found that all were qualitatively similar in the dependence of rate on the water vapor pressure in the vicinity of the reaction interface.

Certain salts do not yield amorphous products on vacuum or low pressure dehydration. Nickel nitrate hexahydrate and magnesium nitrate hexahydrate undergo a series of crystalline phase changes. The rate of dehydration of chrome alum has been determined by Cooper and Garner (1) who made measurements of the rate of growth of nuclei on crystal surfaces. The product obtained on vacuum dehydration shows a definite pattern of X-ray diffraction lines, and the dependence of dehydration rate on water vapor pressure is quite different from that observed for hydrated salts which yield X-ray amorphous products. On vacuum dehydration, this salt appears to form a crystalline lower hydrate of large internal surface due to capillary formation, whereas dehydration in the presence of water vapor at low pressure yields normal crystal aggregates.

Ford (3) has shown that the dependence of rate of dehydration on water vapor pressure of cobalt chloride hexahydrate is very similar to that of chrome alum, and that the mechanism of dehydration is probably the same for the two salts.

Frost, Moon, and Tompkins (5) have calculated values for the heat of transition from the amorphous to crystalline forms of copper sulphate monohydrate and zinc sulphate monohydrate from measurements of the heat of solution of the amorphous and crystalline forms. Jamieson (7) has made similar determinations for magnesium sulphate monohydrate and nickel sulphate monohydrate. He also found that the heat of solution of vacuum dehydrated cobalt chloride differed from that of the normal crystalline monohydrate. Since all these salts

when dehydrated under vacuum have higher heats of solution than their macrocrystalline counterparts, regardless of whether or not X-ray diffraction lines are shown, it will be more convenient in what follows to use the term "active" rather than "amorphous" to describe them. Values of the heats of transition are as follows:

$$ZnSO_4 \cdot H_2O \text{ (active)} \rightarrow ZnSO_4 \cdot H_2O \text{ (cryst.)}; \quad \Delta H = -7600 \text{ cal. mole}^{-1},$$
$$CuSO_4 \cdot H_2O \text{ (active)} \rightarrow CuSO_4 \cdot H_2O \text{ (cryst.)}; \quad \Delta H = -7170 \text{ cal. mole}^{-1},$$
$$MgSO_4 \cdot H_2O \text{ (active)} \rightarrow MgSO_4 \cdot H_2O \text{ (cryst.)}; \quad \Delta H = -6550 \text{ cal. mole}^{-1},$$
$$NiSO_4 \cdot H_2O \text{ (active)} \rightarrow NiSO_4 \cdot H_2O \text{ (cryst.)}; \quad \Delta H = -4720 \text{ cal. mole}^{-1},$$
$$CoCl_2 \cdot H_2O \text{ (active)} \rightarrow CoCl_2 \cdot H_2O \text{ (cryst.)}; \quad \Delta H = -1390 \text{ cal. mole}^{-1}.$$

In view of the fact that the formation of these energy active products is a reaction step in the dehydration mechanism, and since the conversion of these products into crystalline forms depends in a very marked way on the action of water molecules adsorbed at very low pressures, it appeared desirable to study the adsorption of other gases on these intermediates. It was thought that a knowledge of such factors as the types of isotherms, the adsorptive capacity, the capillary structure, and the heats of adsorption might throw light on the nature of these products and on their role in the reaction mechanism. Preliminary experimental work has indicated a small but definite adsorption of hydrogen, carbon monoxide, and carbon dioxide. This paper, however, deals entirely with the adsorption of argon on various vacuum dehydrated salts.

EXPERIMENTAL METHOD

Recrystallized samples of hydrated salts were placed in a container which consisted essentially of two concentric cylinders of 100-mesh copper gauze, the sample being contained in the annular space between the inner and outer cylinders. The thickness of the sample so contained was about four millimeters. Dehydrations under vacuum were then carried out for several hours, usually at 40°C., preliminary experiments having indicated the time required to reach the stoichiometric monohydrate composition. Adsorption and desorption measurements were made following dehydration without disturbing the sample, the usual volumetric technique being used. Following these measurements, requisite weighings were made to determine the weight loss on dehydration and small samples removed for the making of X-ray powder photographs.

Crystalline copper sulphate monohydrate was prepared by placing pentahydrate crystals in the adsorbent container and allowing them to stand in an oven at 110°C. and atmospheric pressure for 60 hr. The final weight corresponded to the monohydrate composition and X-ray lines characteristic of the crystalline monohydrate were obtained.

Cobalt chloride hexahydrate, when dehydrated under vacuum as described above, yielded a crystalline product corresponding to the monohydrate composition. It is known, however, that under such conditions a sequence of changes occurs which involves the co-ordination of chloride ion and the

ultimate loss of hydrogen chloride. In order to determine the extent of this reaction, a 5-gm. sample was dehydrated, the water being trapped, and the hydrogen ion and chloride ion concentrations determined. It was found that approximately 0.025% of the weight loss was due to the formation of hydrogen chloride. Some slight heterogeneity in composition may therefore have been introduced from this source.

Isotherms were obtained at liquid air temperatures and at the boiling points of liquid oxygen and liquid nitrogen. The temperatures of these refrigerants were determined during the course of the adsorption measurements by means of a resistance thermometer.

RESULTS

Argon adsorption isotherms were obtained for several dehydrated salts. These are shown in Fig. 1. These isotherms were obtained at liquid air temperature (approximately 85°K.) with the exception of that for copper sulphate

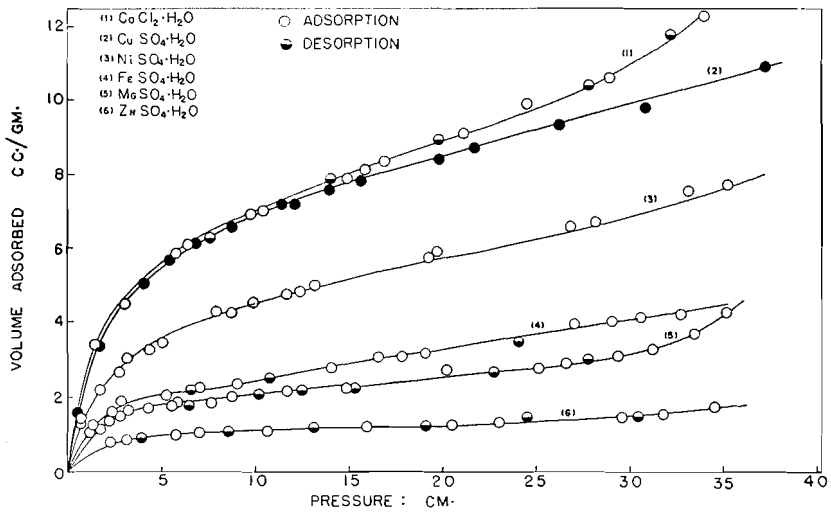

FIG. 1. Adsorption isotherms for argon on several vacuum dehydrated salts at approximately 85°K.

which was obtained at 90°K. All samples were of approximately the same weight and were all dehydrated at 40°C. to the monohydrate composition with the exception of nickel sulphate which retained about 1.5 mole of water. The final products showed no X-ray diffraction lines except in the case of cobalt chloride, where weak diffraction lines were observed.

It will be observed that the isotherms are similar in type. There is very little difference in adsorptive capacity between the active crystalline form of cobalt chloride and the X-ray amorphous copper sulphate. However, the adsorptive capacity of the other salts, which are also X-ray amorphous, varies widely.

In Figs. 2 and 3 are shown isotherms for active and macrocrystalline copper sulphate monohydrate at 78°K. and 90°K. respectively, both adsorption and desorption points being shown. The adsorptive capacity is much greater for the active form and there is a pronounced hysteresis loop in the isotherm at

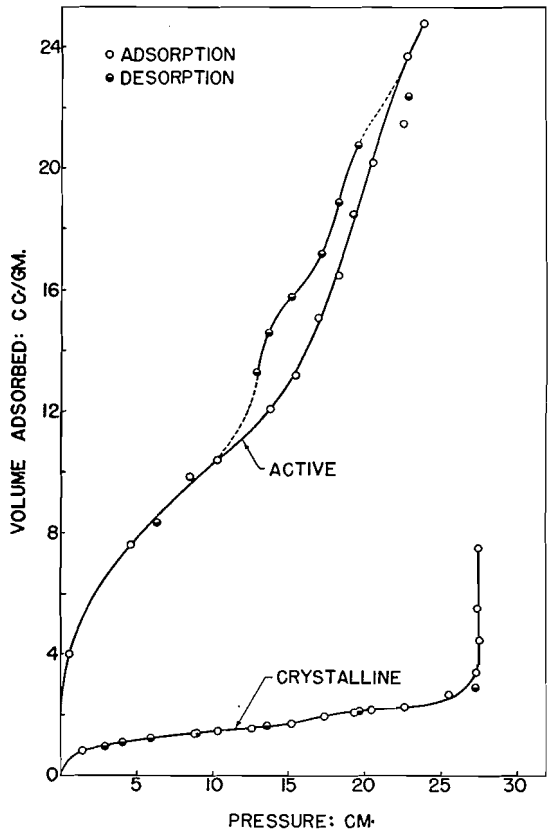

FIG. 2. Adsorption and desorption of argon on active and crystalline copper sulphate monohydrate at 78°K.

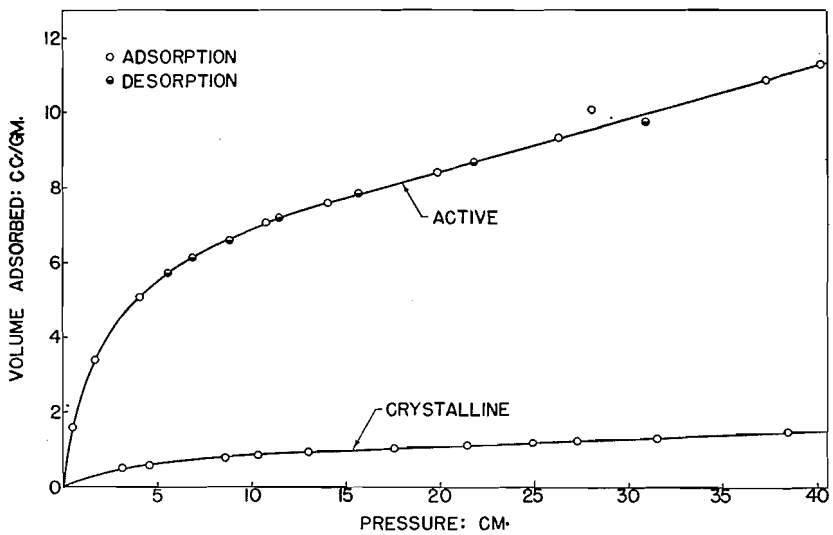

FIG. 3. Adsorption and desorption of argon on active and crystalline copper sulphate monohydrate at 90°K.

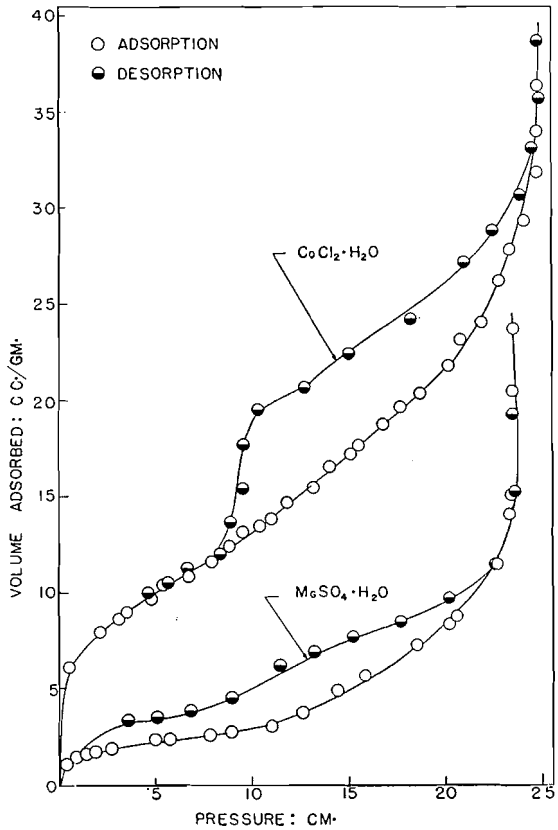

FIG. 4. Comparison of adsorption and desorption isotherms for active cobalt chloride and active magnesium sulphate at 78°K.

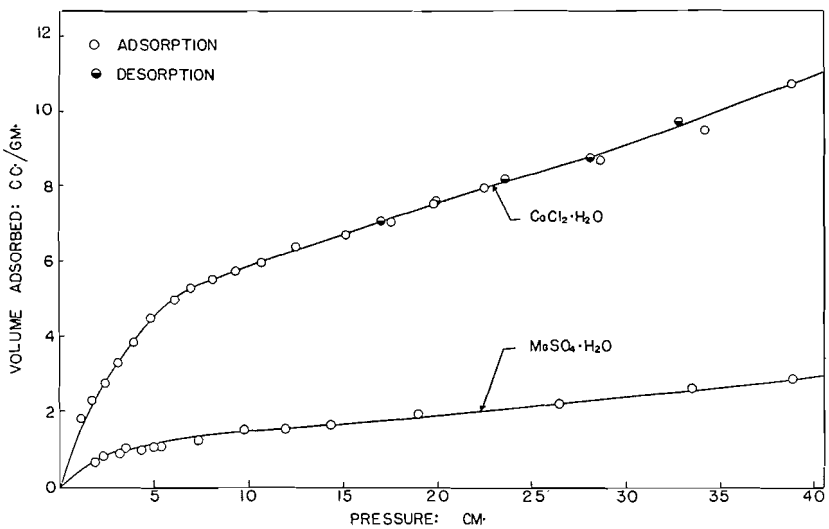

FIG. 5. Comparison of adsorption and desorption isotherms for active cobalt chloride and active magnesium sulphate at 90°K.

78°K. The sharp rise of the isotherm for the crystalline monohydrate at 78°K. is to be attributed to the condensation of argon at its saturation pressure.

The isotherms obtained for active cobalt chloride and for active magnesium sulphate at 78°K. are shown in Fig. 4. Those obtained at 90°K. are shown in Fig. 5. Pronounced hysteresis loops were obtained in the 78°K. isotherms, that for magnesium sulphate extending over a greater range of pressure.

Surface area values were calculated from the foregoing isotherms using both the B.E.T. method and the Hüttig method (2). These values are given in Table II.

TABLE II

SURFACE AREAS

Adsorbent	Method	T, °K.	V_m (cc. per gm.)	Area (sq. m. per gm.)
$CuSO_4.H_2O$ (C)	B.E.T.	78	1.04	3.94
$CuSO_4.H_2O$ (C)	B.E.T.	90	0.99	3.82
$CuSO_4.H_2O$ (A)	B.E.T.	78	7.04	26.7
$CuSO_4.H_2O$ (A)	B.E.T.	90	7.25	28.1
$CuSO_4.H_2O$ (A)	Hüttig	90	7.71	29.8
$CoCl_2.H_2O$ (A)	Hüttig	78	9.48	35.9
$CoCl_2.H_2O$ (A)	Hüttig	90	7.44	28.8
$MgSO_4.H_2O$ (A)	B.E.T.	78	1.97	7.50
$MgSO_4.H_2O$ (A)	Hüttig	78	2.20	8.30
$MgSO_4.H_2O$ (A)	Hüttig	90	1.74	6.74
$ZnSO_4.H_2O$ (A)	Hüttig	85	1.03	3.9
$NiSO_4.H_2O$ (A)	Hüttig	85	4.61	17.6
$FeSO_4.H_2O$ (A)	Hüttig	85	2.47	9.4

The adsorption data obtained from the isotherms at 78°K. for active copper sulphate, crystalline copper sulphate monohydrate, active cobalt chloride, and active magnesium sulphate were tested for specificity in the usual manner, by plotting the relative volume adsorbed (v/v_m) against the relative pressure (p/p_0). The results obtained are shown in Fig. 6. There is a marked absence of any specific effect for values of v/v_m up to and somewhat greater than unity;

TABLE III

DISTRIBUTION OF CAPILLARY DIAMETERS

Salt	Pressure, cm.	P/P_0	V/V_m	Diameter, Å	Position on hysteresis loop
$CoCl_2.H_2O$	8.5	0.31	1.29	18	Lower limit
	10.4	0.38	2.05	22	Sharp break in desorption curve
	18.3	0.67	2.54	53	
	24.5	0.89	3.49	190	Upper limit
$CuSO_4.H_2O$	11.2	0.41	1.56	25	Lower limit
	12.8	0.47	1.85	28	First break in curve
	18.4	0.67	2.70	53	Second break in curve
	19.8	0.72	2.98	66	
	22.2	0.81	3.27	100	Upper limit
$MgSO_4.H_2O$	1.5	0.05	0.77	7	Lower limit
	3.6	0.13	1.55	11	First break in curve
	11.5	0.42	2.82	25	Second break in curve
	17.7	0.65	3.86	49	
	22.6	0.82	5.18	112	Upper limit

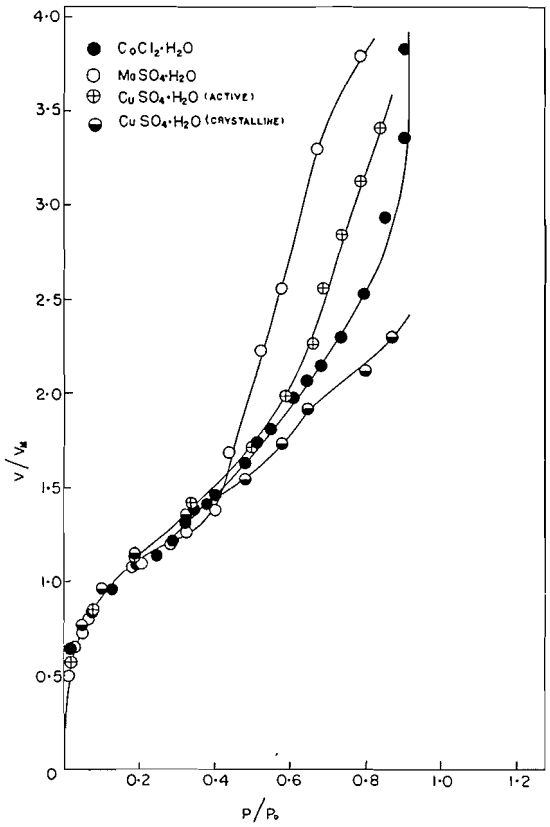

FIG. 6. Comparative specificity curves for three active and one macrocrystalline salt.

in other words, in this region, all the adsorbents differ in adsorptive capacity only by reason of differences in surface area. At higher values there is a marked divergence indicating a distinct difference in the distribution of capillary sizes.

Capillary diameters have been calculated assuming the validity of the Kelvin equation. Some values obtained are given in Table III.

From Table III, it will be observed that active magnesium sulphate contains capillaries which are much smaller in diameter than the smallest calculated for either active copper sulphate or active cobalt chloride, although it does have at its upper limit capillaries which are equal in diameter to the maximum size shown by copper sulphate. Active cobalt chloride, on the other hand, has capillaries which are nearly twice as large as the maximum size exhibited by the other two salts.

Differentiated structure curves, obtained by plotting dv/dr against r, are shown in Fig. 7. For cobalt chloride, the greatest contribution to the total capillary volume is made by capillaries of diameter of approximately 20 Å. For copper sulphate, these curves show two peaks at capillary diameters of approximately 28 Å and 53 Å. For magnesium sulphate there are also two peaks at 11 Å and 26 Å.

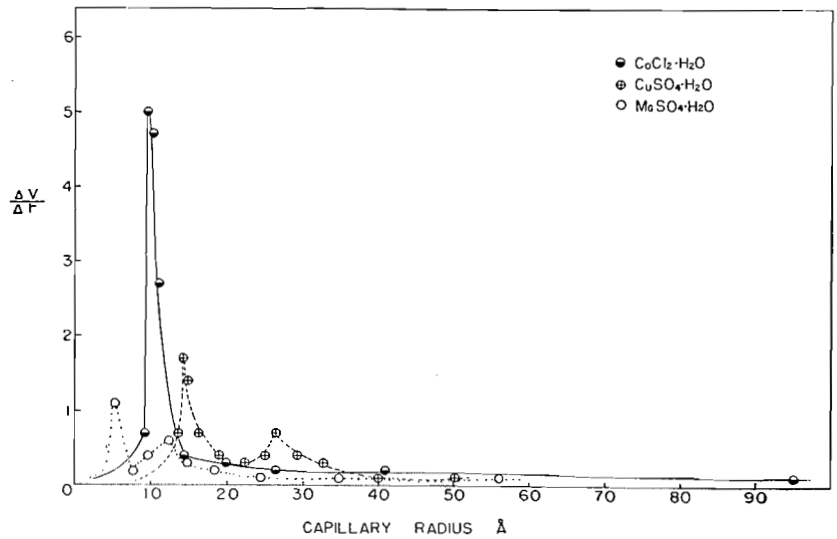

FIG. 7. Differentiated structure curves.

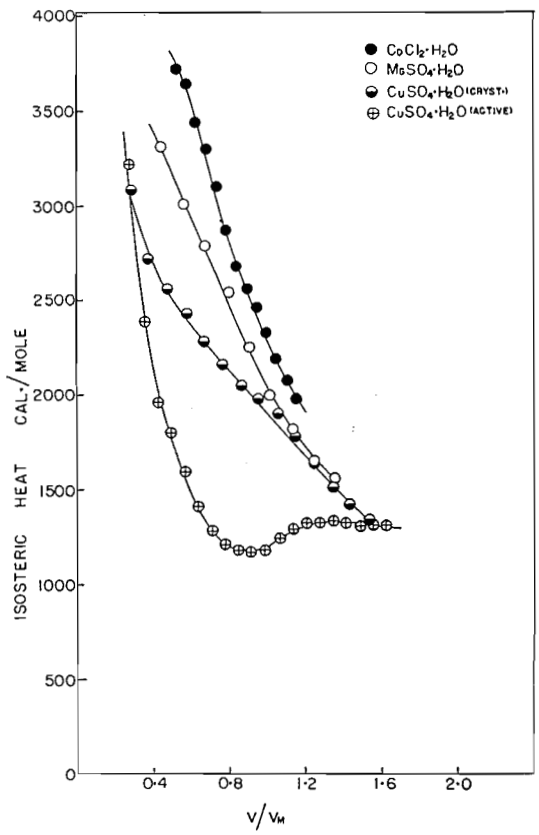

FIG. 8. Change in isosteric heat of adsorption with relative surface coverage.

Although the most frequently occurring capillary diameter for cobalt chloride is smaller than the diameters calculated for copper sulphate, the differentiated structure curve shows that the total number of these is approximately three times greater than that of the 28 Å diameter capillaries and somewhat over five times the number of the 53 Å capillaries of copper sulphate. For magnesium sulphate, the number of capillaries of either diameter which occurs most frequently is comparable with that of either diameter for copper sulphate. However, with magnesium sulphate, these diameters are very much smaller. It follows that the total capillary volume of magnesium sulphate is much smaller than that of either copper sulphate or cobalt chloride. Since there is a significant number of capillaries of wide diameter in copper sulphate, it is a little difficult, from the differentiated structure curves alone, to correlate its total capillary volume with that of cobalt chloride. However, the surface areas of these two active salts are nearly the same and, therefore, their capillary volumes must be comparable.

Isosteric heats were calculated from the isotherms at 78°K. and 90°K. The values obtained, plotted against v/v_m, are shown in Fig. 8. In all cases, there is a rapid decrease in isosteric heat with the extent of adsorption. The values calculated for active copper sulphate decrease much more rapidly than those for the other salts and at lower values of v/v_m. In the vicinity of the value of v/v_m corresponding to the formation of a monolayer, these values pass through a minimum. It was not possible to carry the adsorption measurements into a range of pressure from which the existence of minima for the other salts could be ascertained.

DISCUSSION

The adsorption of argon on these vacuum dehydrated salts follows, in the main, the pattern of the adsorption of non-polar gases on gel-like structures, the over-all heats of adsorption being of the order of magnitude which has been observed for such systems. However, there are some points of interest which it appears desirable to bring out in discussion.

It has been shown that, for the three salts most carefully studied, vacuum dehydration yields products of large capillary volume. The capillary volumes of active copper sulphate and of active cobalt chloride have been shown to be comparable, although the former is an X-ray amorphous product and the latter is a crystalline product of large internal surface. Active magnesium sulphate is X-ray amorphous but has a smaller internal surface.

The over-all spread in capillary diameter for the three active salts is from about 11 Å to nearly 200 Å. The diameters most likely to occur are much greater than those observed for dehydrations of the zeolitic type where the capillary diameters are less than 5 Å. It follows, therefore, that the loss in water is accompanied by a considerable contraction in volume in the reaction zone and that this contraction in volume continues as the reaction interface moves into the dehydrating lattice. Garner and Pike (6) have observed the shapes of the dehydration nuclei formed on the faces of copper sulphate pentahydrate crystals and have shown that dehydration occurs most rapidly along certain

crystal planes. Cooper and Garner (1) photographed, at various stages of growth, the nuclei formed on the dehydration of crystals of chrome alum. It was shown that, as the nuclei grow, radial cracks develop around a star-shaped hole at the center of the nucleus. In the absence of direct observation, it may be reasonably assumed that some like process occurs in the cases under consideration. The observed differences in most probable capillary diameter are likely due to differences in crystallographic character. If the parent lattice and the crystalline end product of dehydration differ in crystal parameters and in specific volume, the capillaries are likely to be large. Relative rates of dehydration along preferred planes may be a contributory factor in the distribution of capillary sizes.

The relative adsorptive capacity of the various adsorbents studied is clearly related to the capillary structure. Active magnesium sulphate with a surface area of approximately seven square meters per gram and probable distributions of capillary diameter about the values of 11 Å and 25 Å presents a much smaller total capillary volume than active copper sulphate or active cobalt chloride. The adsorptive capacities of the latter two salts are about the same, whereas that of magnesium sulphate is very much smaller.

This immediately suggests a correlation between the internal surface and the characteristic limiting pressures of water vapor above which amorphous intermediates do not occur. Cobalt chloride hexahydrate dehydrates at zero pressure of water vapor into a crystalline product of large internal surface. Active copper sulphate with nearly the same adsorptive capacity adsorbs a sufficient quantity of water at approximately 0.25 mm. pressure to induce crystallization; active magnesium sulphate of much lower adsorptive capacity shows a much greater stability in the amorphous state and does not crystallize below pressures of 4.5 mm. Of the salts for which isotherms are shown in Fig. 1, active nickel sulphate fits well into this correlation; active zinc sulphate does not. However, this salt behaves in a more complex fashion on dehydration and requires closer study. Although an isotherm has been reported for the dehydration product of ferrous sulphate heptahydrate, it is probable that this salt undergoes a series of crystalline changes on low pressure dehydration and consequently does not fit into the sequence under discussion. The behavior of manganous oxalate dihydrate with respect to this correlation should be of interest.

It has been pointed out that the heat of solution of vacuum dehydrated cobalt chloride hexahydrate is greater by 1390 cal. per mole than that of the normal crystalline monohydrate. This difference may be ascribed in part to the large internal surface. Since however, both active cobalt chloride and active copper sulphate have about the same capillary volume, it might be expected that the heat of solution relative to the crystalline form (or, therefore, the energy liberated on the amorphous to crystalline transition) of active copper sulphate should be of the same order as that observed for cobalt chloride. This is far from being the case, the value being over 7000 cal. per formula weight. All of the values for the X-ray amorphous to crystalline transitions, given earlier in this paper, are higher than those which might be expected from the

surface area or capillary data found, unless it is assumed that large differences in surface energy exist.

This suggests that some change, other than increased surface or capillary volume, occurs during vacuum dehydration. If there is a lack of conformity at the reaction interface between the dehydrating lattice and its crystal end product, it is possible that the ions of the lattice will collapse into whatever energy levels happen to be available, ordered arrangement being realized (as was suggested at the outset) as mobility is given to the ions by the adsorption and inward diffusion of water dipoles. A state of internal strain would therefore result which would manifest itself by a relatively high energy release on crystallization.

If such a state of internal strain were also a source of surface inhomogeneity, it might be expected that some specificity in adsorption would be observed for the active salts with reference to their crystalline counterparts. From Fig. 6, it is clear that no marked specific effects occur with active copper sulphate in reference to the crystalline monohydrate, at least up to the formation of the monolayer. However, the isosteric heat of adsorption falls off much more rapidly with increased adsorption for active copper sulphate than for the crystalline monohydrate and a minimum is observed at approximately the completion of the monolayer. The existence of such minima has, of course, been predicted theoretically and observed experimentally for certain ionic crystals. In the present work, no minimum has been observed for crystalline copper sulphate monohydrate, although a slight extrapolation of the adsorption isotherms suggests that one occurs just beyond the range of calculated values. It is possible that the more rapid drop in isosteric heat values and the location of the minimum in a lower range of adsorption for active copper sulphate has significance in terms of the possible ionic disorder of the surface and the effect of this on the induced dipoles of the adsorbed atoms. However, this possibility must remain in the region of speculation until more comprehensive experiments have been made.

ACKNOWLEDGMENTS

The award of a National Research Council bursary (R. W. M.) and of a Research Council of Ontario scholarship (H. W. Q.) during the period of this work is gratefully acknowledged.

REFERENCES

1. Cooper, J. A. and Garner, W. E. Proc. Roy. Soc. (London), A, 174: 487. 1940.
2. Fergusson, R. R. and Barrer, R. M. Trans. Faraday Soc. 46: 400. 1950.
3. Ford, R. M.A. Thesis, Queen's University, Kingston, Ont. 1954.
4. Frost, G. B. and Campbell, R. A. Can. J. Chem. 31: 107. 1953.
5. Frost, G. B., Moon, K. A., and Tompkins, E. H. Can. J. Chem. 29: 604. 1951.
6. Garner, W. E. and Pike, H. V. J. Chem. Soc. 1565. 1937.
7. Jamieson, J. W. S. M.Sc. Thesis, Queen's University, Kingston, Ont. 1953.
8. Lipsett, S. G., Johnson, F. M. G., and Maass, O. J. Am. Chem. Soc. 49: 925. 1927.
9. Symposium Discussion. Trans. Faraday Soc. 34: 976. 1938.
10. Topley, B. and Smith, M. L. J. Chem. Soc. 321. 1933.
11. Volmer, M. and Seydel, G. Z. physik. Chem. A, 179: 153. 1937.
12. Wheeler, R. C. M.Sc. Thesis, Queen's University, Kingston, Ont. 1951.

THE FORMATION OF THIN FILMS OF IRON OXIDE[1]

By E. J. Caule and M. Cohen

ABSTRACT

It is assumed that the free energy of a thin film of iron oxide is a function of its thickness. The effect on the dissociation pressure is calculated and the condition for stability of thickness is stated. A possible method for measuring the free energy change involved in oxide film formation on metal surfaces is presented which is based on measurements of the e.m.f. of the dry cell metal|oxide|oxygen.

INTRODUCTION

At ordinary temperatures and pressures the system iron+oxygen is unstable and will go spontaneously to one or more of the various iron oxides. For example, the equilibrium dissociation pressure of α Fe_2O_3 is about 10^{-80}mm. pressure of oxygen. Hence, when the process of oxidation halts it is natural to assume that kinetic conditions have imposed a very slow speed on the process, slow enough to give the appearance of a halt.

The influence of resistance to change can be seen very clearly in the formation of iron oxide films on massive iron at pressures of around, say, 3 cm. oxygen and at temperatures around 370°C. In this region the clear-cut result is obtained, by a variety of methods, that the rate of increase of the film thickness is inversely proportional to the thickness. The most reasonable interpretation of this result is that the rate is controlled by the diffusion of the reagents through the film. Subsidiary experiments on transport processes, such as conduction, in oxides have checked this conclusion directly.

This simple diffusion mechanism holds over a very wide range of film thicknesses—under the conditions mentioned above, from 800 Å up to thicknesses of the order of fractions of a millimeter where the film begins to lift from the metal and to scale off the surface. The range from 0 to 800 Å behaves anomalously, not following the diffusion law. Fig. 1 shows an oxidation for which the diffusion law is valid; the weight increase varies linearly with the square root of the time which follows from the varying of the rate of increase with the thickness. Fig. 2 can be regarded as a "blown-up" view of the anomalous region in Fig. 1; the data were obtained from observation of interference colors and the ordinate is plotted directly as Angstrom units since the interference colors can be correlated with film thickness. It is seen that the anomalous region has been divided into two stages. At any rate, from Fig. 1 it is clear that given a certain thickness iron oxide will limit the rate of its own further growth.

It is tempting to apply this conclusion to the data on iron oxidation at room temperature. At room temperature and below, iron will take up oxygen to form a film in the manner shown in Fig. 3. It is seen that the rate slows

[1]*Manuscript received September 16, 1954.*
Contribution from Division of Applied Chemistry, National Research Council, Ottawa, Canada. Issued as N.R.C. No. 3493. This paper was presented at the Symposium on Problems Relating to the Adsorption of Gases by Solids, held at Kingston, Ontario, September 10–11, 1954.

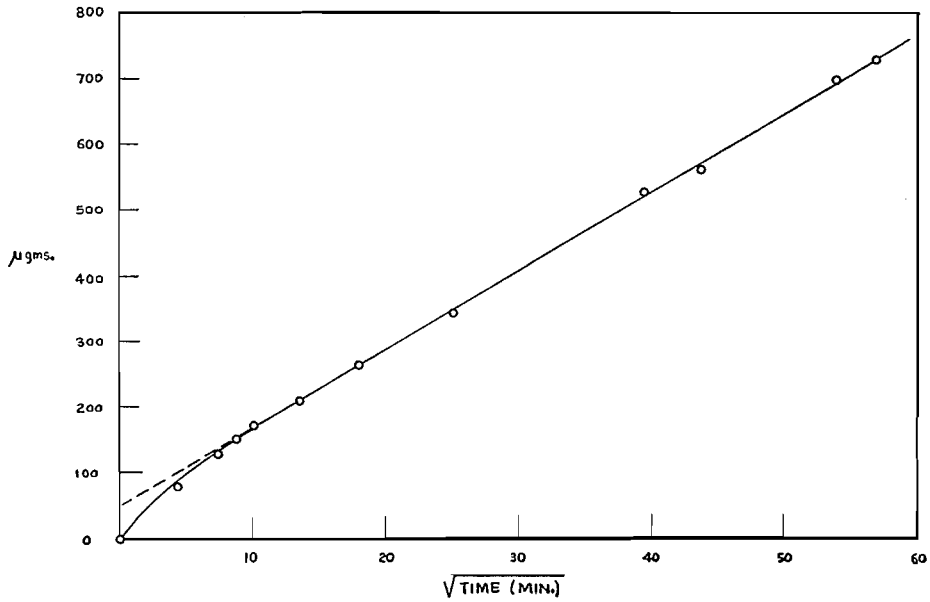

FIG. 1. Measurements of weight gain as a function of square root of time. Total area of specimen 15 cm.²

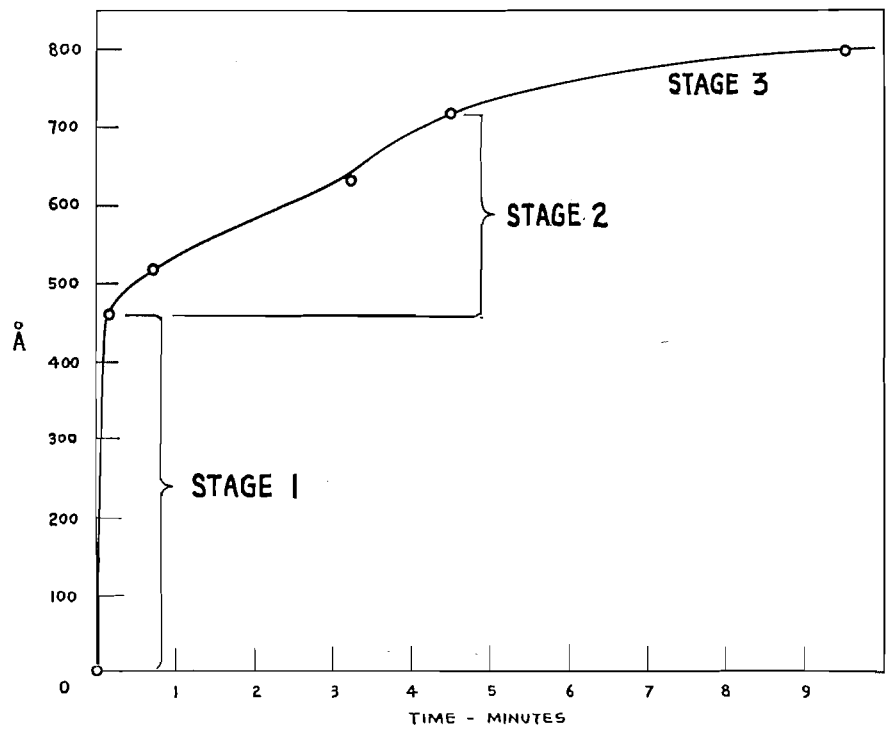

FIG. 2. Curve of oxide thickness as function of time; thickness derived from color observations.

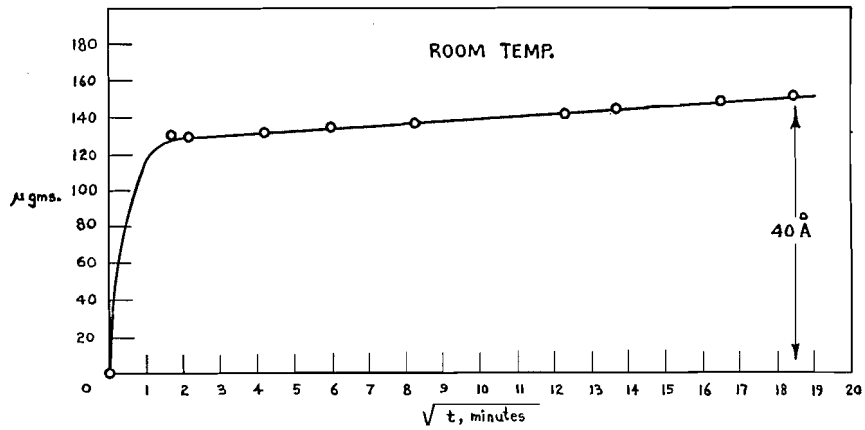

FIG. 3. Curve of weight gain as function of square root of time. Total area of specimen 15 cm.^{2} Specimen oxidized and reduced once previously.

practically to zero in the time shown. It is natural to assume that the process here is exactly the same as the high-temperature diffusion process, modified and reduced in scale by the drop in temperature, since the diffusion process has been found to have an activation energy of about 40 kcal. This paper will present an alternative explanation of the low-temperature phenomena, which can be extended to explain the initial section of the high-temperature curve. It will be claimed (*a*) that the film initially formed on iron at any temperature attains an equilibrium thickness, whose magnitude is a function of temperature and pressure, and (*b*) that a process of recrystallization transforms the initial oxide to a second variety not possessing an equilibrium thickness and that in this second form the diffusion process of the type shown in Fig. 1 takes place. Unless, then, process (*b*) occurs, growth of the film will cease entirely at a certain thickness which is truly stable in the absence of the second phase.

The most striking fact to consider is that all of the iron oxide phase is concentrated at an interface, where it is subject to peculiarly unbalanced forces. From this consideration comes the first assumption, that the free energy of the iron oxide per unit of weight or volume is a function of the thickness.

Let the free energy of the oxide phase, F_{ox}, be divided into two parts, one the free energy of the equivalent amount of iron oxide in the bulk phase, F_b, and the other the amount of free energy attributable to the existence of the oxide at an interface, F_s.

[1] Then $F_{ox} = F_b + F_s$.

[2] Similarly, $\mu_{ox} = \mu_b + \mu_s$.

The number of moles, N, of oxide can be related to the thickness, r, by the following equation:

[3] $$N = r.A.\rho/M$$

where A is the area considered, ρ is the density, and M the molecular weight. From [3] there is obtained:

$$dN = (A\rho/M).dr.$$

Consequently μ_s in [2] above can be expressed as a function of r:

$$[4] \qquad \mu_s = \frac{\partial F_s}{\partial N} = \frac{M}{A\rho} \cdot \frac{\partial F_s}{\partial r}.$$

At a fixed pressure of oxygen, p_{O_2}, the condition for equilibrium is

$$[5] \qquad 4\mu_{Fe} + 3\mu_{O_2} = 2\mu_{ox}.$$

This assumes that the oxide formed is Fe_2O_3, which below 550°C. is very probable.
Hence

$$4\mu_{Fe} + 3\mu^0_{O_2} + 3RT \ln p = 2\mu_{ox} = 2\mu_b + 2\mu_s,$$

from which

$$[6] \qquad 4\mu^0_{Fe} + 3\mu^0_{O_2} - 2\mu^0_b = 2\mu_s - 3RT \ln p.$$

But the left-hand side of this equation is then $-\Delta F^0$, which is equal to $RT \ln K$.
Hence

$$[7] \qquad RT \ln K = 2\mu_s - 3RT \ln p.$$

For bulk oxide equation [7] reduces to $K = p^{-3}$ which gives the equilibrium pressure when the free energy is not dependent on the thickness of film. Here, because of the introduction of $2\mu_s$, p will not have the value it would have for bulk oxide. If μ_s has a positive value, p will have to have a more positive value—and correspondingly for a negative value of μ_s.

There is a second important factor to be considered, namely, the slope of the μ_s vs. r curve. (*a*) If $\partial\mu/\partial r$ is negative in a range, no equilibrium can be established in the range at a given value of applied oxygen pressure, since an increase in r will result in a lower value of μ and thus a lower value of equilibrium pressure. (*b*) On the other hand, a positive value of $\partial\mu/\partial r$ in a certain range does permit the system to come to equilibrium at definite values of p which then define values of r. From the above considerations there are seen

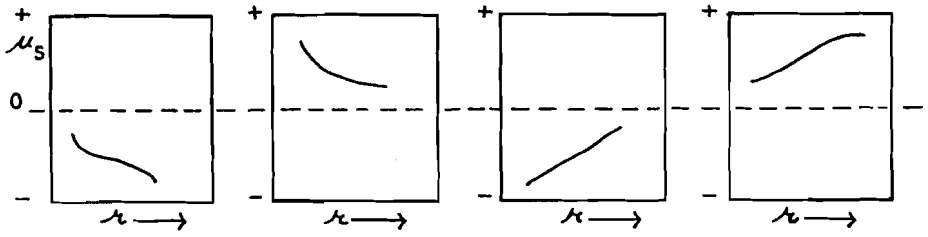

FIG. 4.

(i) $\mu_s < 0$, $\frac{\partial\mu}{\partial r} < 0$ — No equilibrium $p < p_b$

(ii) $\mu_s > 0$, $\frac{\partial\mu}{\partial r} < 0$ — No equilibrium $p > p_b$

(iii) $\mu_s < 0$, $\frac{\partial\mu}{\partial r} > 0$ — Equilibrium possible $p < p_b$

(iv) $\mu_s > 0$, $\frac{\partial\mu}{\partial r} > 0$ — Equilibrium possible $p > p_b$

to be four possibilities which are shown in Fig. 4. In the caption to this figure, p_b represents the dissociation pressure of the bulk oxide. It will be seen that the most probable situation is represented by (iv).

In the discussion so far the definition of μ_s has been by means of the differential equation [4]. It is important that it be emphasized that μ_s includes not only the free energy connected with the formation of the top layer of oxide but also the "reorganization" energy of the inner layers and of the metal–oxide interface.

Another major assumption must now be made in order to account for the experimental facts; the primary stable film is considered to be not a normal oxide, but one of higher total free energy content, perhaps amorphous in character. There are several reasons for this condition, one of which is that it is extremely difficult to obtain a definite and recognizable electron diffraction pattern from such thin films. Another is to be found in the results of high-temperature oxidation; a striking graph from a series of experiments is shown in Fig. 5, where there is clearly an induction period between stages 1 and 2.

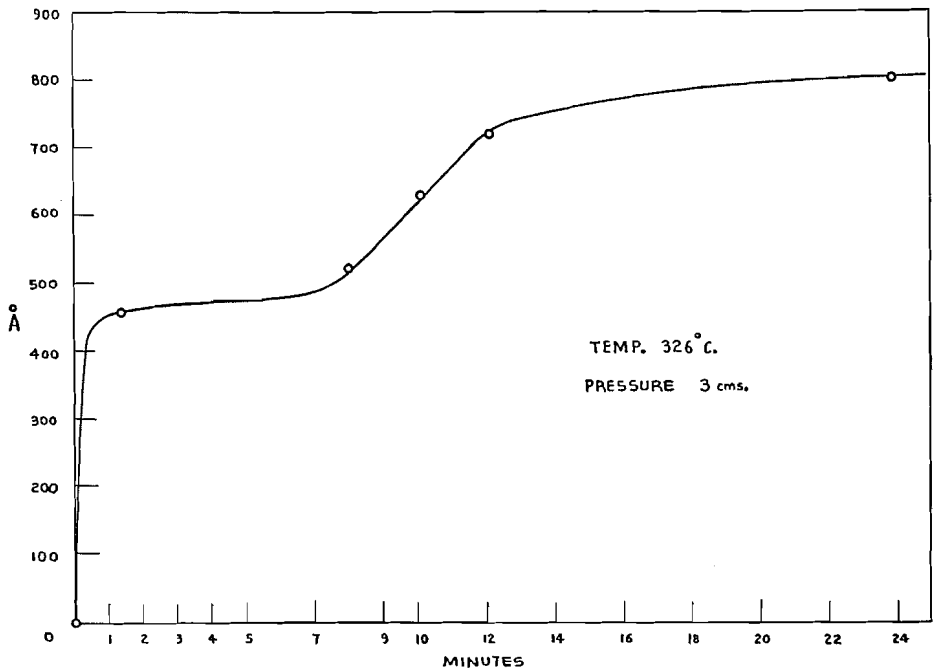

FIG. 5. Color measurement of thickness as function of time.

Mott (2) has obtained the same result for copper, by a method of direct weighing of oxygen uptake. In general, our results indicate that stage 2 can be explained on the basis of a nucleation and recrystallization process occurring to the oxide, assumed amorphous, formed in stage 1. The induction period demonstrates that the oxide in stage 1 is stable in the absence of the type of oxide formed in stage 3, which is the normal bulk crystalline α-ferric oxide.

At low temperatures the transformation does not occur readily and stable films are left on the metal.

The assumptions brought into the discussion so far could be tested if there were a direct method of measuring free energy as a function of thickness. Normally one of the most direct measurements is that of e.m.f., which is, of course, related to free energy by: $\Delta F = -n\mathcal{F}E$. There is a possibility of such a measurement here since the oxidation of iron is electrical in character and a current normally does flow in the oxide (3). An over-all equation showing the transfer of electrons can be written: $4(Fe-3e)+3(O_2+4e) \rightarrow 2Fe_2O_3$. In Mott's theory of oxidation (2) electrons are emitted from the metal through the oxide to combine with adsorbed oxygen on the oxide surface; the negative ions then set up a field across the oxide which pulls iron ions through the oxide. Unfortunately the electron current, which normally is in the external circuit, is here in the cell itself together with the ion current. This rules out direct measurement of the cell e.m.f. and destroys any simple analogy to cells containing liquid solutions.

There have been many measurements made, notably by Hackerman (1), of the contact potential difference between a noble reference electrode and an electrode of iron or other metal undergoing oxidation. The resultant readings, while showing that changes are taking place, have not been able to be interpreted. It is possible to set up a circuit which in most respects simulates the oxidizing system and produces an e.m.f. analogous to contact potential. Fig. 6 shows the proposed analogue.

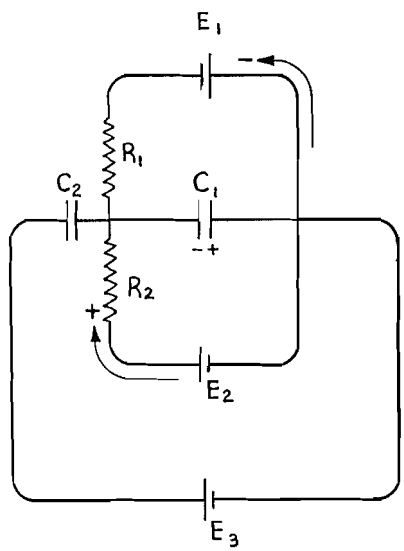

FIG. 6. Electrical analogue to pair of contacting metals, one of which is oxidizing in oxygen.

In this circuit the contact potential would appear across C_2, which is a condenser of very low capacity similar to the electrodes ordinarily used in contact potential measurements. Condenser C_1 represents the capacity of

the oxide film. R_1 is the resistance to electron flow of the oxide film, and R_2 is the resistance to positive ion flow of the same film. E_1 is the e.m.f. responsible for electron flow and according to Mott (2) is to be equated to $W+E^0-\phi$ where W is the binding energy of an adsorbed oxygen ion, E^0 is the electron affinity of oxygen, and ϕ is the work function of the metal against vacuum. E_2 is the e.m.f. equivalent to the free energy change of removing an iron ion from the metal and bringing it to the outer layer of the oxide. It is equal to $L-W_{Fe}$, where L is the sublimation energy of an iron ion and W_{Fe} is the binding energy in the external layer. E_3 is the contact potential difference between iron and the reference metal.

Before the system comes to equilibrium, growth occurs by the passage of a current around the circuit including E_1 and E_2. Growth will stop when this current drops to zero. The condenser C_1 allows simulation of the building-up of the charge on the surface of the oxide which is a feature of Mott's theory. The potential actually measured across C_2, the "contact potential", is the algebraic sum of e.m.f.'s around the circuit—it is the negative of the voltage which must be inserted to cause no current to flow when the capacity of C_2 is altered (which is the common method of measurement of contact potentials by the vibrating plate method). At equilibrium, then, the measured contact potential will be E_3-E_1 or E_3-E_2 since E_2 and E_1 must be equal and opposed. At other non-equilibrium stages, the measured contact potential will be E_3-E_2+potential drop across R_1.

The free energy change involved in the oxide growth is proportional to the algebraic sum of E_1+E_2. At equilibrium this sum is zero; consequently the relative magnitudes must change as the thickness increases.

The analogue is not too useful as yet but further study may prove its validity and increase its usefulness. The assumptions involved in the early part of this paper may be extreme and based on faulty experimental data, since accurate oxidation experiments are difficult to do. They too await further trial and proof.

REFERENCES

1. ANTES, L. and HACKERMAN, N. J. Appl. Phys. 22: 1395. 1951.
2. CABRERA, N. and MOTT, N. F. Repts. Progr. in Phys. 12: 163. 1948–49.
3. WAGNER, C. Corrosion and Material Protect. 5 (5): 9. 1948.

HEATS OF ADSORPTION OF KRYPTON ON HIGHLY GRAPHITIZED CARBON BLACK[1,2]

By C. H. Amberg, W. B. Spencer, and R. A. Beebe

ABSTRACT

Calorimetric heats have been determined at −183°C. for the adsorption of krypton on a highly graphitized sample of carbon black. This adsorption system is of particular interest because of the extreme step-wise nature of the isotherm. Both the heat-coverage curve and the isotherm appear to be indicative of a high degree of homogeneity of the adsorbing surface.

INTRODUCTION

Graphitized carbon blacks are among the very few known solid adsorbents which appear to exhibit energetically homogeneous adsorbing surfaces. Schaeffer, Smith, and Polley (21) have described the preparation of a number of these blacks. These authors (19) found a development of steps in the argon isotherms at −195°C. on carbon blacks heat treated at successively higher temperatures up to 3000°C. (notably the 'Spheron 6' and 'P-33' series), which they interpreted as indicative of increasing homogeneity of the surface. Steps were also observed with oxygen and to a lesser extent with nitrogen as the adsorbate. Champion and Halsey (8) have predicted step-wise isotherms on homogeneous surfaces on theoretical grounds. They made use of Hill's isotherm equations (14) modified so as to include the influence of the surface force field of the adsorbent up to the nth layer. Conversely, they have shown that the smoothing out of such steps on a homogeneous surface requires untenable assumptions, and they have therefore concluded that the more common smooth type of isotherm must be due to surface heterogeneity.

A number of publications from this laboratory concerning chiefly the adsorption of nitrogen and argon on carbon surfaces show evidence of a maximum value in the heat-coverage curve at the monolayer (3, 6, 7). The evolution of what is thought to be a homogeneous surface is particularly well demonstrated by the adsorption of argon on a series of Spheron blacks (7). With heat treatment to increasingly higher temperatures causing both the removal of oxygen and also increasing graphitization, the initial high section of the heat-coverage curve is gradually both lowered and flattened out, whilst the rise due to lateral interaction between the adsorbed molecules thus becomes more clearly delineated and the maximum value at the monolayer shows a slight increase. This behavior is reflected in the second layer, but to a lesser extent, probably because adsorption into separate layers is less pronounced at that stage.

[1]*Manuscript received September 16, 1954.*

Contribution from the Chemistry Department, Amherst College, Amherst, Mass. This work was supported by the U.S. Office of Naval Research. This paper was presented at the Symposium on Problems Relating to the Adsorption of Gases by Solids, held at Kingston, Ontario, September 10–11, 1954.

[2]*Work on the adsorption of sulphur dioxide and ammonia on carbon surfaces, presented together with this material at the Kingston meeting, is described in O.N.R. Reports Nos. 4 and 5 from this laboratory and will be submitted for journal publication in the near future.*

Further indication that there may be an increase in surface homogeneity with heat treatment is given by the growth of crystallites as determined by X-ray diffraction (19). Furthermore, taking the black P-33 (2700°) as an example, the particles appear to have a structure approaching that of graphite judging from their interplanar distance, which is 3.42 Å (19) as compared to 3.35 Å for graphite (17). Planar regions, probably exposed basal planes of the graphite type, may be distinguished on the surface of the carbon black particles in the electron microscope and these may well be a decisive factor in producing those phenomena which we attribute to a homogeneous surface.

In this connection, Crowell and Young (10) have shown that the potential energy calculated for an argon atom adsorbed on the basal plane of graphite is quite insensitive to position at a given distance from the surface. The experimental evidence from adsorption work also points towards surface homogeneity in the case of graphite. Thus, for instance, Gulbransen and Andrew (12) found a distinct step for the initial part (up to $P/P_0 = 0.4$) of a krypton isotherm on graphite.

Undoubtedly, the removal of oxygen from the carbon particle at the earlier stages of the heat treatment plays its part in removing more 'active' sites and thus rendering the surface more homogeneous, an effect particularly noticeable with polar adsorbates. A number of adsorption and heat of wetting studies have dealt with this subject (4, 24).

Along with plausible indications mentioned above, there is as yet little *direct* experimental evidence available to link the 'operationally defined' degree of homogeneity of a surface to its fine structure. The well known work of Rhodin (20) on the adsorption of nitrogen on single crystal copper surfaces, also discussed by Halsey (13), presents one of the most telling demonstrations of the difference between homogeneous and heterogeneous surfaces. On single crystal faces, which were demonstrably flat on the atomic scale, clean and undistorted, the isosteric heat of adsorption curves started with nearly constant values at lower coverage up to about $\theta = 0.5$. On polycrystalline copper Rhodin found disproportionately high initial heats along with the masking of lateral interaction effects in the adsorbate. This must have been caused largely by the presence of intercrystalline boundaries.

We are indebted to Dr. G. D. Halsey for calling our attention to the extreme step-wise type of isotherm for the system krypton – P-33 (2700°) first obtained in his laboratory (23). As Dr. Halsey suggested, it would obviously be interesting to obtain calorimetric heats of adsorption for this system. Because we had been building up a considerable backlog of adsorption data for a number of adsorbates on graphitized carbon blacks, it seemed to us worthwhile to add the krypton – P-33 (2700°) system to the list for the purpose of comparison and contrast.

EXPERIMENTAL

Materials

The adsorbent used was the highly graphitized P-33 carbon black, heat treated to 2700°C. It was kindly supplied by Dr. W. R. Smith of Godfrey L.

Cabot Inc., Boston. Its characteristics have been previously described in detail by Polley, Schaeffer, and Smith (19). It has a B.E.T. nitrogen surface area of 12.5 square meters per gram. The calorimeter was loaded with 10.18 gm. of this material.

Spectroscopically pure krypton furnished by the Air Reduction Sales Company was used as the adsorbate.

All runs were done at liquid nitrogen or liquid oxygen temperatures. The former were read with an argon vapor pressure thermometer and the latter with an open-ended oxygen vapor pressure thermometer.

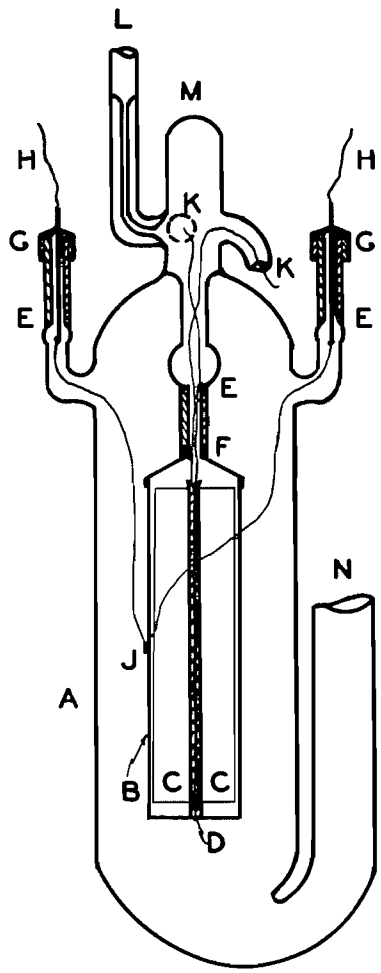

FIG. 1. Calorimeter.
A, Glass jacket; *B*, platinum cylinder; *C*, platinum fins; *D*, heater; *E*, Kovar-pyrex seals; *F*, Kovar-platinum seal; *G*, brass caps; *H*, thermocouple leads; *J*, copper–constantan thermal junction; *K*, heater leads (side arms not fully shown); *L*, inlet tube; *M*, top seal; *N*, connecting tube to pump and helium reservoir.

Apparatus and Procedure

The apparatus used for the determination of isotherms was of the conven-

tional type which has been described in previous publications from this laboratory (6).

Equilibrium pressures were read on a calibrated McLeod gauge up to 19 mm. mercury and above that on the constant volume mercury manometer using a Gaertner travelling microscope. Agreement between the two in overlapping regions was within 1%.

The calorimeter used in the present work is shown in Fig. 1. It consists of a platinum cylinder *B*, 7 cm. long, 2 cm. in diameter and of 0.25 mm. wall thickness. Into this was close-fitted a set of six platinum fins, *C*, symmetrically spaced about a central platinum tube of 3 mm. diameter which serves as the housing for heater, *D*. A clearance of 2 mm. is provided between the fins and the bottom of the cylinder to facilitate gas distribution. A platinum lid was silver soldered onto the cylinder after having been joined, at *F*, to a Kovar-pyrex seal, *E*. The Kovar inlet tube is 19 mm. long and has an inside diameter of 5.5 mm. Surrounding the platinum cylinder is a glass jacket, *A*, the spacing between the two being about one centimeter. One copper–constantan thermal junction, *J*, is silver soldered onto the outside of the platinum cylinder. The thermocouple wires (B&S No. 30 and No. 31 for copper and constantan respectively) are connected to short sections of heavier wire (B&S No. 18) and these in turn are sealed through side arms in the jacket as shown on the diagram at *G*. The heater leads are similarly sealed through side arms at *K* (not fully shown in the diagram).

Gas inlet *L* consists of a short section of 3 mm. capillary tubing, which was completely immersed in the constant temperature bath during runs; it is joined onto regular 8 mm. tubing. Thermal transpiration was thus minimized because of the relatively large diameter of the inlet tube in the region of the temperature gradient. The top of the instrument, *M*, was open for the purpose of inserting the adsorbent and installing the heater and was subsequently sealed off. The 15 mm. tube, *L*, is connected through stopcocks to the vacuum manifold as well as to a helium reservoir. Thus the calorimeter jacket may be pumped out during measurements or else helium may be admitted to it, if rapid heat exchange is desired, as it is between separate admissions of adsorbate.

The 160 ohm heater was wound from B&S No. 34 enamel covered 'Advance' wire. The coil was covered with a thin layer of aluminum foil which was held in place by four narrow strips of platinum shaped so as to provide a sliding fit with the heater housing.

The reference thermal junction was housed in an 8 mm. glass tube which, in turn, was held in a copper cylinder of 2 cm. inside diameter by a rubber stopper. The whole unit, not shown in the diagram, was wired to the calorimeter jacket. For runs at −195° the inner glass tube was filled with pump oil. This, however, was discarded for runs at liquid oxygen temperature with no apparent change in performance of the thermocouple.

Before each run the whole calorimeter was outgassed overnight at 200°. Next, the Dewar vessel containing liquid nitrogen or oxygen was raised around the apparatus and the system allowed to establish temperature equilibrium over a period of two to three hours. To accelerate this process, helium was

admitted to the jacket to a pressure of about one centimeter or higher. Finally, the jacket was pumped out and the instrument was then ready for measurements.

The methods used for the measurement of electrical energy input during calibrations and for amplification and recording of the thermal e.m.f. have been described in previous publications from this laboratory. A Perkin–Elmer d-c. breaker–amplifier was used in conjunction with an Esterline–Angus automatic recorder. The procedure outlined by Beebe and Dell (4) was followed.

RESULTS AND DISCUSSION

The results of two separate runs are shown in Figs. 2 and 3. Fig. 2 represents the isotherm of krypton on P-33 (2700°) at −183° plotted as volume adsorbed versus relative vapor pressure. Values for the saturation vapor pressures of solid krypton were taken from the data of Keesom, Mazur, and Meihuizen (16).

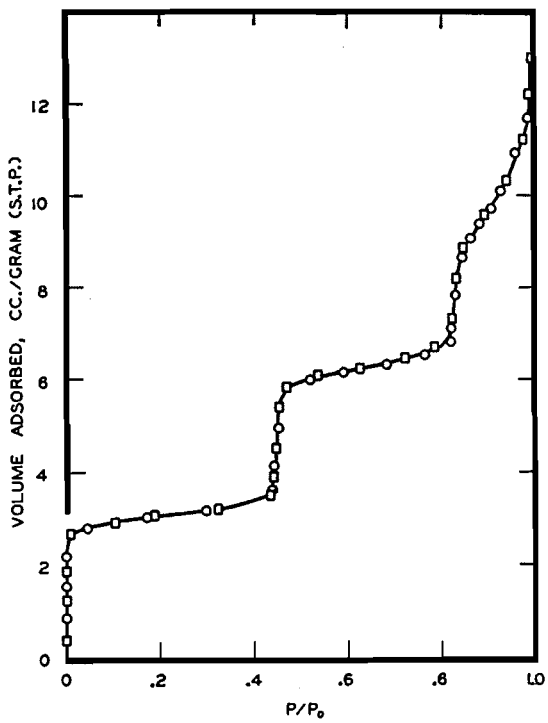

FIG. 2. Isotherm, adsorption of krypton on P-33 (2700°) carbon at −183°C.: ○, run 1; □, run 2.

The highly pronounced step-wise character of this isotherm had already been demonstrated by Singleton and Halsey at the boiling temperature of liquid nitrogen (23). There is no appreciable difference in the sharpness of comparable steps at the two temperatures. We have also determined a krypton isotherm on Spheron (2700°) which is known to be less highly graphitized than

the P-33 (2700°) sample. As expected the isotherm on Spheron (2700°) had a somewhat less step-wise character.

Singleton and Halsey argued that the adsorption of krypton in their case reached a definite limiting value at the saturation pressure of bulk solid krypton somewhere between the fifth and sixth layers. This was supported by a model (22) which predicts a limiting value between the fourth and fifth layers at saturation. We have repeated their calculation for the −183° isotherm with the same result. Unfortunately, our data near saturation are not sufficiently definitive to decide between an isotherm which crosses the $P/P_0=1$ ordinate or one which proceeds to a very large value at saturation. The latter was assumed to be the case with the systems studied by Beebe, Beckwith, and Honig (2) who employed vapor pressures of liquid krypton extrapolated to below the triple point.

In Fig. 3 the calorimetric heats for krypton on P-33 (2700°) at −183° are plotted as a function of the volume adsorbed. As corrections for the heats of compression are negligible, the calorimetric heats may be said to represent the true isosteric heats of adsorption.

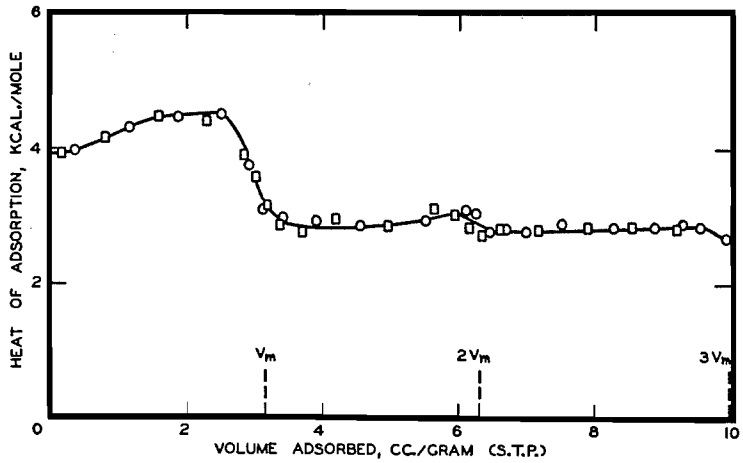

FIG. 3. Heats of adsorption, krypton on P-33 (2700°) carbon at −183°C.: ○, run 1; □, run 2.

The curve shows the expected rise due to lateral interaction between adsorbate molecules in the first layer, amounting to about 600 cal./mole adsorbed. A steep drop of about 1600 cal./mole occurs at the completion of the monolayer and the curve levels off at 200 cal. above the heat of sublimation of krypton. The latter was calculated by means of the Clapeyron equation from vapor pressures given by Mathias, Crommelin, and Meihuizen (18). (The analogous figures for argon on Spheron (2700°C.) (7) are about 400 cal./mole for the rise in the first layer and 800 cal./mole for the steep drop. These figures, of course, are not strictly comparable, since the two carbon surfaces represent a different degree of homogeneity.) The same pattern is reflected in the second adsorbed layer of krypton, although to a much smaller extent. The maximum

rises only 200 cal. above the minimum value in the second layer and the well defined drop into the third layer amounts to some 250 cal. A small rise in the second layer for argon was observed, but the descending part following it is more gradual than with krypton; this conforms well to the picture of less sharp separation into adsorbed layers in the case of argon. There is an indication of a third step into the fourth layer in our case. Since, however, heat values at coverages higher than those reported show an unreasonably large scatter (undoubtedly owing to condensation effects in the calorimeter) not too much reliability can be claimed for the third drop at the end of the curve.

The heats of adsorption and the isotherm of krypton on P-33 (2700°) were also measured at −195°. Our isotherm agreed well with that given by Singleton and Halsey (23) except in the first low pressure region, where our pressure values were somewhat higher. This was due to our not having waited longer than two hours for the attainment of equilibrium. Our attention was focused on the measurement of the heat evolved during the first few minutes following the admission of a gas increment to the system and the exact equilibrium pressure was not a critical quantity in our heat determination. The observed heats in the first layer at −195° are more or less constant with coverage, which leads one to suspect initial non-selective adsorption on the most readily accessible part of the carbon black, followed by a subsequent redistribution of the krypton too slow to be detected by our calorimeter (5). Beginning with the first steep drop in the heat curve, agreement between the heats of adsorption at the two temperatures was excellent. This is plausible, as one would not expect a very large temperature coefficient of the heat of adsorption; thus, for instance, the heats of vaporization of liquid krypton differ by only 0.14% over the 13° range, as calculated from the equation given by Mathias, Crommelin, and Meihuizen (18).

For the same reason it appears valid to employ the integrated form of the Clausius–Clapeyron equation over this temperature range in order to calculate the isosteric heats for an intermediate temperature from the two isotherms. It is worthy of note that the agreement was quite good beyond a coverage of 3.0 cc./gm., if we compared the heats obtained by calorimetry with those calculated from the isotherms. However, the calculated heats in the region 0–3.0 cc./gm. are far from being in agreement with the calorimetric values; this was to be expected because of the known errors in the pressure measurements in the region of low coverage.

Differential and integral molar entropies were calculated from the calorimetric heats and the isotherm at −183° (1) using the equations given by Drain and Morrison (11). The entropy-coverage curves follow the characteristic pattern found, for instance, by Hill, Emmett, and Joyner for the system nitrogen–Graphon (15). Crossing of the two curves takes place at the monolayer, where there is a minimum in the integral entropy curve. Although the curves as calculated do not actually cross at the completion of the second layer, a second minimum in the differential entropy approaches the integral curve very closely and the curves could be said to cross within the limit of error of these calculations.

In conclusion it may be said that both the isotherm and heat data point again to a highly homogeneous surface in the case of P-33 (2700°).

In view of the X-ray and electron micrograph data cited in the Introduction one might argue that the surface of these carbon particles consists chiefly of crystallites whose basal planes are arranged in directions parallel to the plane faces of the irregular polyhedra of the kind detectable by means of the electron microscope. This still leaves unanswered the question of why a surface, where lattice defects, crystallites in the surface oriented in directions other than parallel to it, and edge effects are bound to be significant factors in its topography, shows practically none of the experimental signs of heterogeneity such as smoothed out isotherms (such as type II of the B.E.T. classification) and monotonically decreasing heat of adsorption curves in the first and higher layers. One must remember, that the original P-33 particle before heat treatment consisted of a random arrangement of crystallites. It is not likely that these have arranged themselves to form a perfect surface of basal planes. Even if that were so, one might still expect boundaries between adjacent planes to be the seats of higher energy sites. Possibly the explanation is to be sought in terms of favorable packing of the crystallites even within the imperfectly ordered particle. It should be pointed out in this connection that although the distance between nearest neighbours in the hexagonal structure of the basal plane of graphite is 1.42 Å, or slightly less than half the distance between basal planes, the distance across the hexagon is of the same order of magnitude as that between planes. Thus a non-polar adsorbate atom or molecule placed over the center of a carbon hexagon may well be subjected to forces similar to those operative over the edges of a 'bundle' of planes oriented in a direction normal to a geometric plane which is tangential to the surface. In other words, if the distance between carbon neighbors on the surface nowhere exceeds the interplanar distance of 3.35 Å by a significant amount, the model of Crowell and Young (10) (or in a simpler form by Crowell (9)) may still be applicable for argon and other adsorbates which approach the surface less closely. Adsorbates with a closer approach may well be more sensitive to irregularities in the surface. It is therefore not surprising to find that a graphitized carbon black shows the symptoms of homogeneity to a more marked degree for krypton than it does for argon. It would be interesting to have data available for adsorbates of smaller atomic or molecular cross-section, such as neon or helium, on a highly graphitized carbon surface.

ACKNOWLEDGMENTS

The authors are indebted to Dr. G. D. Halsey for making available, prior to its publication, his manuscript containing krypton adsorption data (23). Our thanks are also due to Dr. J. M. Holmes for his helpful suggestions in working out some of the experimental details of this investigation.

REFERENCES

1. BEEBE, R. A., AMBERG, C. H., and SPENCER, W. B. U.S. Office of Naval Research Technical Report No. 6. To be issued. Contract N8—onr—66902.
2. BEEBE, R. A., BECKWITH, J. B., and HONIG, J. M. J. Am. Chem. Soc. 67: 1554. 1945.

3. BEEBE, R. A., BISCOE, J., SMITH, W. R., and WENDELL, C. B. J. Am. Chem. Soc. 69: 95. 1947.
4. BEEBE, R. A. and DELL, R. M. U.S. Office of Naval Research Technical Reports Nos. 4, 1953, and 5, 1954. Contract N8—onr—66902.
5. BEEBE, R. A. and DOWDEN, D. A. J. Am. Chem. Soc. 60: 2912. 1938.
6. BEEBE, R. A., MILLARD, B., and CYNARSKI, J. J. Am. Chem. Soc. 75: 839. 1953.
7. BEEBE, R. A. and YOUNG, D. M. J. Phys. Chem. 58: 93. 1954.
8. CHAMPION, W. M. and HALSEY, G. D. J. Phys. Chem. 57: 646. 1953.
9. CROWELL, A. D. J. Chem. Phys. 22: 1397. 1954.
10. CROWELL, A. D. and YOUNG, D. M. Trans. Faraday Soc. 49: 1080. 1953.
11. DRAIN, L. E. and MORRISON, J. A. Trans. Faraday Soc. 48: 840. 1952.
12. GULBRANSEN, E. A. and ANDREW, K. F. Ind. Eng. Chem. 44: 1039. 1952.
13. HALSEY, G. D. *In* Advances in Catalysis. Vol. IV. Academic Press, Inc., New York. 1952. p. 259.
14. HILL, T. L. J. Chem. Phys. 15: 767. 1947.
15. HILL, T. L., EMMETT, P. H., and JOYNER, L. G. J. Am. Chem. Soc. 73: 5102. 1951.
16. KEESOM, W. H., MAZUR, J., and MEIHUIZEN, J. J. Physica, 2: 669. 1935.
17. LIPSON, H. and STOKES, A. R. Proc. Roy. Soc. (London), A, 181: 101. 1942.
18. MATHIAS, E., CROMMELIN, C. A., and MEIHUIZEN, J. J. Physica, 4: 1200. 1937.
19. POLLEY, M. H., SCHAEFFER, W. D., and SMITH, W. R. J. Phys. Chem. 57: 469. 1953.
20. RHODIN, T. N. J. Am. Chem. Soc. 72: 5691. 1950.
21. SCHAEFFER, W. D., SMITH, W. R., and POLLEY, M. H. Ind. Eng. Chem. 45: 172. 1953.
22. SINGLETON, J. H. and HALSEY, G. D. Paper presented at the Symposium on Problems Relating to the Physical Adsorption of Gases on Solids. Kingston, 1954.
23. SINGLETON, J. H. and HALSEY, G. D. J. Phys. Chem. 58: 1011. 1954.
24. ZETTLEMOYER, A. C., CHESSICK, J. J., HEALEY, F. H., and YU, Y. U.S. Office of Naval Research Technical Reports Nos. 5, 1953, and 6, 1954. Contract N8—onr—74300.

PHYSICAL ADSORPTION STUDIES IN CARBON BLACK TECHNOLOGY[1]

By M. H. Polley, W. D. Schaeffer, and W. R. Smith

ABSTRACT

The adsorption isotherms of *n*-butane and butene-1 on typical furnace and channel carbon blacks were determined over a range of temperatures, 55°–250°C. The adsorption of *n*-butane on carbon black surfaces is attributed to physical adsorption; however, the extent of surface covered per unit area of carbon black is considerably greater at a given temperature than for a silica. Butene-1 is also physically adsorbed on the furnace blacks. The presence of approximately 3% chemisorbed oxygen on the surface of the channel blacks induces an isomerization of butene-1 to *cis*-butene-2. When oxygen is first chemisorbed on a furnace black surface, then that surface also interacts with butene-1. Those blacks which participate in the isomerization of butene-1 respond or "interact" in a cyclic heat treated Butyl rubber – carbon black masterbatch.

INTRODUCTION

In the field of carbon black technology, the properties that carbon black imparts to inks, lacquers, and rubber compounds are largely dependent upon the extent of surface and the nature of the carbon black employed. Of course, the extent of carbon surface is easily measured by low temperature nitrogen adsorption or by evaluation of electron micrographs. The former estimates the total surface area, while the electron micrograph pictures the external surface area. The nature of the carbon black surface, on the other hand, is not as easily defined but may be characterized by the concentration and type of chemisorbed complexes that reside on the carbon black surface. It is often the nature of the carbon black surface that is responsible for the marked effects some carbon blacks produce in application. The presence of chemisorbed complexes accounts for such effects as slowing the rate of cure in rubber compounds or developing flow in lithographic inks.

One industrial development in which the nature of the carbon black surface plays an important role is in the cyclic heat treatment of Butyl rubber. This process was developed by the Esso Laboratories and is described by Gessler and co-workers (2, 3, 5, 8). The cyclic heat treatment of Butyl rubber produces increased modulus, increased tensile, increased elasticity, and increased abrasion resistance. The processing involved is simply the heat treatment of a carbon black – Butyl rubber masterbatch at 160°C. followed by milling for five minutes. This is repeated for the desired number of cycles. The improvement in reinforcement properties is associated with the chemisorbed oxygen present on the channel black surface. Furnace blacks or "devolatilized" channel blacks did not show corresponding improvement. However, if a furnace black was first oxidized before it was compounded in Butyl rubber, it then responded to the cyclic heat treatment process. It was postu-

[1]*Manuscript received September 16, 1954.*
Contribution from the Research and Development Laboratories, Godfrey L. Cabot, Inc., Cambridge, Mass. This paper was presented at the Symposium on Problems Relating to Adsorption of Gases by Solids, held at Kingston, Ontario, September 10–11, 1954.

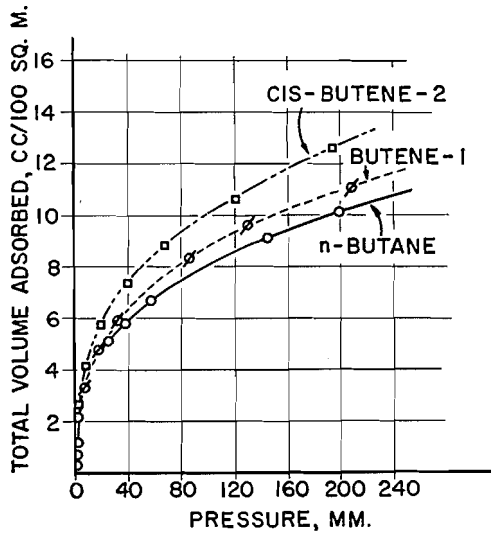

FIG. 1. The effect of unsaturation at 0°C., Spheron 6.

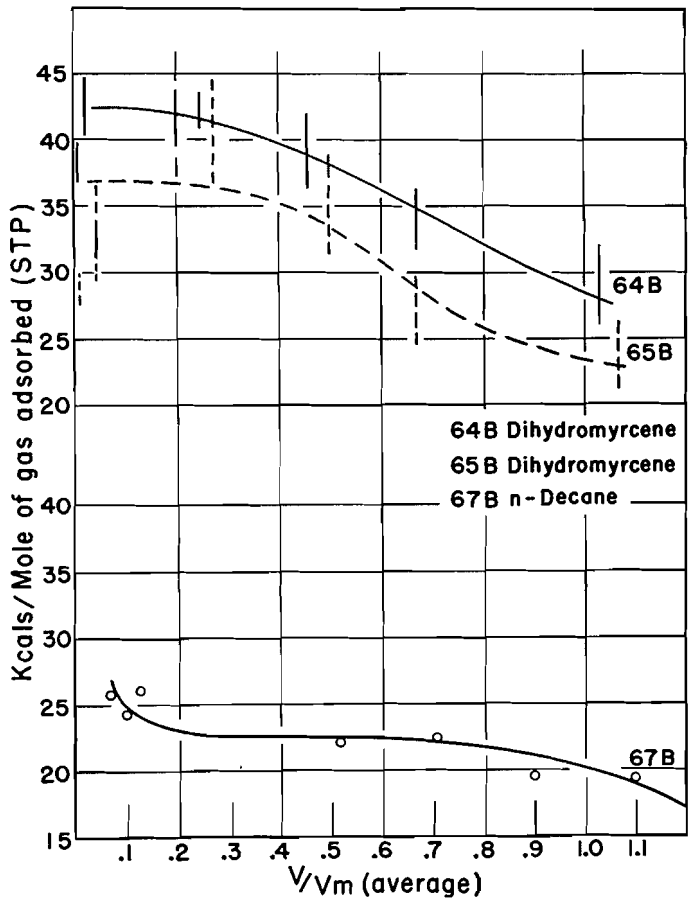

FIG. 2. Differential heats of adsorption at 100°C., Spheron 6.

lated that this cyclic heat treatment produces: (1) enhanced anchorage of polymer-to-carbon clusters or particles, and (2) subsequent milling disaggregates these carbon clusters by virtue of the enhanced anchorage, making new surface available for further polymer–carbon linkage.

If the reinforcement developed was due to this polymer–black interaction as suggested, then could this interaction be studied more simply by gas phase adsorption of hydrocarbons analogous to the Butyl polymer? Earlier studies (1) on the heats of adsorption of the four- and five-carbon hydrocarbons on carbon blacks at 0°C. were typical examples of *physical* adsorption. No interaction was apparent between any of the adsorbed molecules and the carbon blacks studied. In Fig. 1, the isotherms for *cis*-butene-2, butene-1, and *n*-butane on Spheron 6 carbon black are shown. Spheron 6 is a channel black having about 3% chemisorbed oxygen on the surface. If these isotherms were plotted against relative pressure, they would be nearly superimposed. Later work (4) with *n*-decane and dihydromyrcene at 100°C. did show evidence of some sort of interaction of the dihydromyrcene with Spheron 6 that was absent with the "devolatilized" Spheron 6, absent with the "ion-exchanged" Spheron 6, and absent with furnace black. The heats of adsorption in Fig. 2 illustrate the presence of this interaction, possibly a cyclization of the dihydromyrcene. Unfortunately, the reaction product was not identified.

The present work describes adsorption research continued with the four-carbon hydrocarbons, *n*-butane and butene-1, at higher temperatures than those used earlier. The temperatures were chosen to coincide with those employed in the Butyl heat cycling process.

EXPERIMENTAL

The carbon blacks chosen for study were similar types to those used by the Esso Laboratories and could be separated into two main groups, i.e., those that do not respond to the heat cycling process and those that do. With the first group of blacks no interaction would be expected between the butene-1 and the carbon black surface. With the second group, if the response to heat cycling is due to polymer–carbon linkage, then there may be evidence of interaction between the butene-1 and the chemisorbed oxygen on the carbon black surface.

The apparatus and procedures were similar to those used in earlier experiments (1). A constant temperature bath containing various refluxing liquids provided temperatures of 55°, 109°, and 179°C.

RESULTS

Fig. 3 illustrates the type of adsorption isotherm that is obtained for butene-1 on a variety of adsorbents at 109°C. or roughly 115° above the boiling point of the butene-1. The "devolatilized" Spheron 6 is simply a standard channel black which has been heated to 957°C. for one hour in a vacuum to remove most of the chemisorbed oxygen. The surface area was 109.7 sq. meters per gram. The Vulcan 3 and Vulcan 9 are oil furnace blacks containing less than 1% chemisorbed oxygen. They differ principally in surface area—the Vulcan

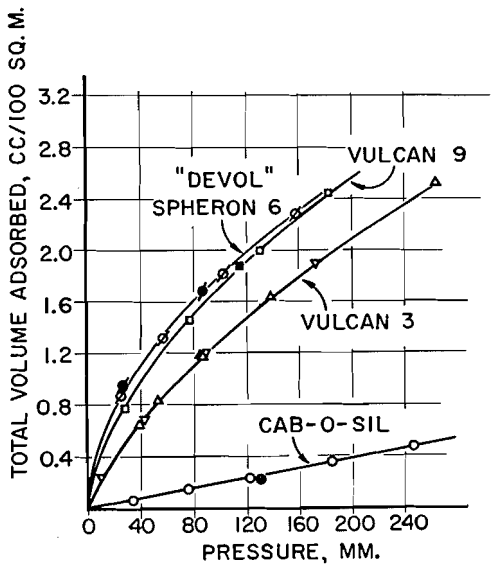

FIG. 3. The adsorption of butene-1 at 109°C., open points—adsorption; solid points—desorption.

3 having an area of 77 sq. meters per gram and the Vulcan 9 having an area of 134 sq. meters per gram. The Cab-O-Sil is a 99% pure silica formed in a high temperature flame process. Its surface area is 152 sq. meters per gram. To eliminate these surface area differences, the volume adsorbed has been expressed as cc. (S.T.P.) per 100 sq. meters. Surprisingly enough, the volume of gas adsorbed at 109°C. is as much as one sixth that of the volume adsorbed at 0°C. for the carbon blacks. Like the 0°C. data, these isotherms were completely reversible and reproducible. Pressure equilibration was fairly rapid—generally in about 10–15 min. Although not illustrated on this graph, the *n*-butane isotherm on the Vulcan 3 sample lies very close to the butene-1 curve for the same black. The most interesting feature in this set of isotherms is the large difference in the magnitude of adsorption of butene-1 on a non-polar carbon black surface as opposed to a polar silica surface. Our earlier work (6) with butene-1 on silica gel at 0°C. revealed heats of adsorption nearly identical with that of carbon black, and the silica gel isotherms when plotted per unit area were only about 10% lower than that of the carbon black. However, Emmett (7) found for *n*-butane on a silica alumina catalyst an adsorption of 0.04 cc. per 100 sq. meters at 100°C. and one atmosphere pressure. This is even a lower order of magnitude than the data for the Cab-O-Sil.

In the second group of pigments, i.e., those that do show a response to the Butyl heat cycling process, standard Spheron 6 is the most familiar. Fig. 4 shows that the adsorption per unit area has just about doubled in volume from the values of the blacks in the previous graph. The solid desorption points on the upper curve give evidence of hysteresis. The lower isotherm, which was a repeat run on the same Spheron 6 sample, shows the poisoning effect of the first experiment. In addition, the pressure equilibration time is now greater

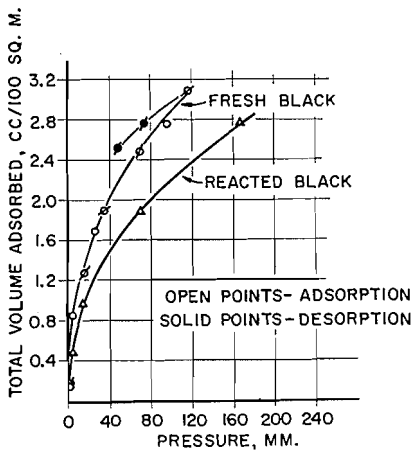

FIG. 4. The adsorption of butene-1 on Spheron 6 at 109°C.

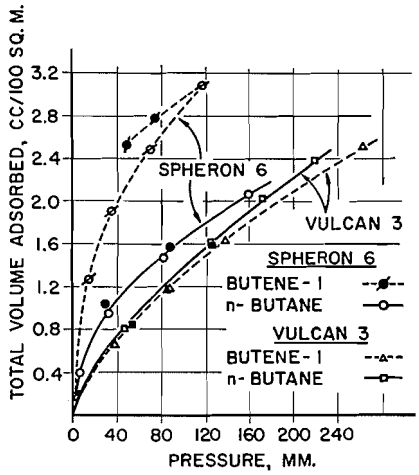

FIG. 5. The effect of unsaturation at 109°C., open points—adsorption; solid points—desorption.

than one hour. These isotherms do not represent true equilibrium points, as the final pressure reading was generally taken at some 95% of equilibrium. Considering this fact, the agreement of the two runs on fresh black in the upper curve is quite good. Thus, with hysteresis, poisoning, and slow pressure equilibration, it appears that there is evidence of some type of interaction occurring between the butene-1 and the chemisorbed oxides present on the Spheron 6 surface. This interaction is not evident when *n*-butane is adsorbed on Spheron 6. The effect of unsaturation on the adsorption isotherms for the Spheron 6 channel black as compared to the Vulcan 3 furnace black is shown in Fig. 5. The non-polar Vulcan 3 surface scarcely can differentiate between the two adsorbates, butene-1 and *n*-butane.

If this interaction was not seen at 0°C. either in the isotherms or in the heats of adsorption measurements, then at what point does it become evident? Fig. 6 illustrates the effect of temperature on the adsorption of butene-1 on Spheron 6. The desorption points are not plotted on the 0°C. isotherm, but at the high pressures they were coincident with the adsorption curve. Hysteresis is seen at 55°C. though the reaction is very slow at this temperature. Desorption points were not obtained on the 179° and 250°C. runs, but in these experiments the reaction rate had increased markedly.

Two other carbon blacks, in addition to Spheron 6, have been tested in Butyl rubber and did respond to the heat cycling process. They are oxidized Vulcan 3 and an experimental channel black. These two carbon blacks shown in Fig. 7 have about 3% chemisorbed oxygen on the surface, while the oxidized Printex U has about 9%. Volatile analysis experiments now in progress have shown differences in the type of volatile matter that is contained on these various surfaces.

Mass-spectrometer analysis has confirmed the purity of the original butene-1 and also has identified the desorbed gas from the butene-1-standard Vulcan 3

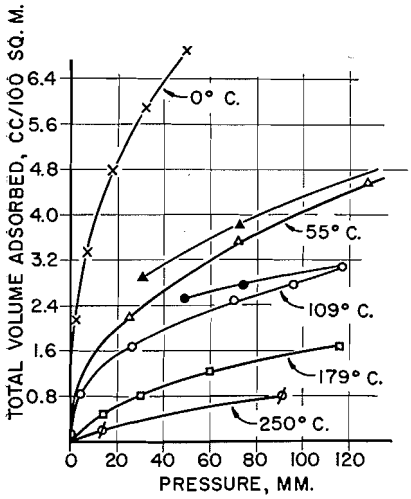

FIG. 6. The effect of temperature on the adsorption of butene-1 on Spheron 6.

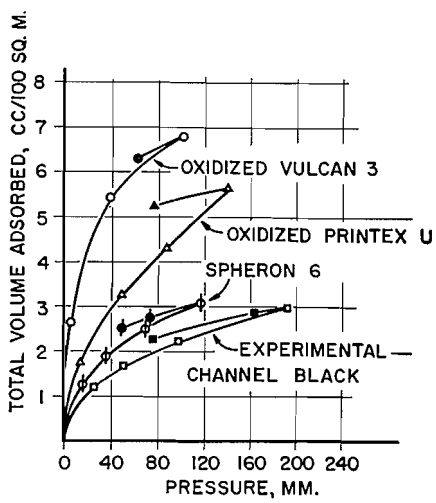

FIG. 7. The adsorption of butene-1 at 109°C.

isotherm as pure butene-1. The reaction product of the butene-1-Spheron 6 isotherm contained a mixture of butene-1 and *cis*-butene-2. Thus, the interaction is an isomerization reaction.

The nature of the carbon black – polymer association in the heat-cycled Butyl rubber is still undefined, yet, here, by a relatively simple adsorption experiment, it has been possible to predict the performance of a carbon black in a heat-cycled Butyl rubber compound.

ACKNOWLEDGMENT

The authors wish to thank Mr. Murray Bazinet of the National Research Corporation, Cambridge, Mass., for the mass-spectrometer analyses.

REFERENCES

1. BEEBE, R. A., POLLEY, M. H., SMITH, W. R., and WENDELL, C. B. J. Am. Chem. Soc. 69: 2294. 1947.
2. GESSLER, A. M. Rubber Age, (N.Y.), 74: 59. 1953.
3. GESSLER, A. M. and FORD, F. P. Rubber Age, (N.Y.), 74: 397. 1953.
4. POLLEY, M. H., SCHAEFFER, W. D., and SMITH, W. R. J. Am. Chem. Soc. 73: 2161. 1951.
5. REHNER, J. and GESSLER, A. M. Rubber Age, (N.Y.), 74: 561. 1954.
6. SMITH, W. R. and BEEBE, R. A. Ind. Eng. Chem. 41: 1431. 1949.
7. ZABOR, R. C. and EMMETT, P. H. J. Am. Chem. Soc. 73: 5639. 1951.
8. ZAPP, R. L. and GESSLER, A. M. Rubber Age, (N.Y.), 74: 243. 1953.

CHARCOAL SORPTION STUDIES

III. THE ADSORPTION OF ETHYLENE AND PERFLUOROETHYLENE BY AN ACTIVATED CHARCOAL[1]

By H. L. McDermot, J. C. Arnell, and B. E. Lawton

ABSTRACT

The adsorption of ethylene and perfluoroethylene by an activated charcoal has been measured over a range of temperatures. Integral and differential heats have been calculated and compared for the two gases. The heats of adsorption of perfluoroethylene are consistently higher than those of ethylene, but only by an amount to be expected from the difference in molecular weights. The absolute entropy of adsorbed ethylene has been calculated and found to be in agreement with a model in which the adsorbed molecules are mobile and possess at least two degrees of rotational freedom.

INTRODUCTION

The factors influencing the adsorption of hydrocarbons on carbon surfaces have been exhaustively studied by Beebe and his co-workers (1, 2). Beebe *et al.* (2) measured the heats of adsorption calorimetrically for the adsorption of a series of hydrocarbons on a non-porous carbon black. The hydrocarbons chosen were paraffins and olefins containing four or five carbon atoms, and included geometrical isomers and one positional isomer. It was found that for any given coverage the differential heat of adsorption was directly proportional to the number of carbon atoms in the hydrocarbon, but was independent of the presence of unsaturation in the compound or of the arrangement of the carbon atoms in the molecule. In a subsequent paper, Beebe *et al.* (1) showed that the heat of adsorption per carbon atom of the adsorbate was diminished with respect to the value found for the linear isomers, if the molecular arrangement of the adsorbate was such that one of the carbon atoms projected into space when the others were in the plane of the surface. For example at a coverage of $\theta = 0.2$, the differential heat of adsorption of neopentane was reported by these workers to be 1.6 kcal. per carbon atom compared with a value of 2.5 kcal. per carbon atom for *n*-pentane. The work of Beebe's group has demonstrated that with the exception of neopentane and cyclohexane the differential heat of adsorption per carbon atom of hydrocarbon at a coverage of $\theta = 0.2$ lies between 2.5 and 2.65 kcal. per carbon atom.

The present work was undertaken to make a careful study of the adsorption of a simple hydrocarbon on a carbon surface and to investigate the effect of replacing all the hydrogen atoms of the hydrocarbon by fluorine atoms. To this end adsorption isotherms are presented for the adsorption of ethylene and perfluoroethylene by an activated charcoal. Thermodynamic quantities for the adsorbed phase have been calculated by the methods outlined by Hill (6).

[1]*Manuscript received September 16, 1954.*
Contribution from the Defence Research Chemical Laboratories, Ottawa, Canada. Also issued as DRCL Report No. 178. This paper was presented at the Symposium on Problems Relating to the Adsorption of Gases by Solids, held at Kingston, Ontario, September 10–11, 1954.

PROCEDURE

The charcoal employed in this study was a zinc chloride activated maple charcoal of extremely low ash content whose properties have been reported elsewhere (10).

The ethylene was procured from the Ohio Chemical Co. It was reported to be 99.5% pure and was used without any further purification. The perfluoroethylene was made by the pyrolysis of polytetrafluoroethylene and purified by low temperature fractional distillation.

The charcoal was prepared for adsorption measurements by evacuation at 200°C. for at least 12 hr. The perfluoroethylene isotherms were measured by a gravimetric method. A sample of charcoal weighing approximately half a gram was placed in a bulb fitted with a stopcock and a tapered joint so that the sample could be removed from the system and weighed. The adsorption isotherm was measured by admitting gas to the charcoal, allowing the system to equilibrate, and then removing the sample from the system and weighing it. The weight of gas adsorbed was simply the difference between this weight and that of the evacuated sample. With the exception of the isotherm at 273.2°K. for which an ice bath was used, simple water thermostats were used for the measurements at all the other temperatures. Isotherms were measured at 273.2°, 290.5°, 295.8°, 302.0°, and 308.5°K. The isotherms are plotted in Fig. 1 and are reversible within the experimental error of the measurements.

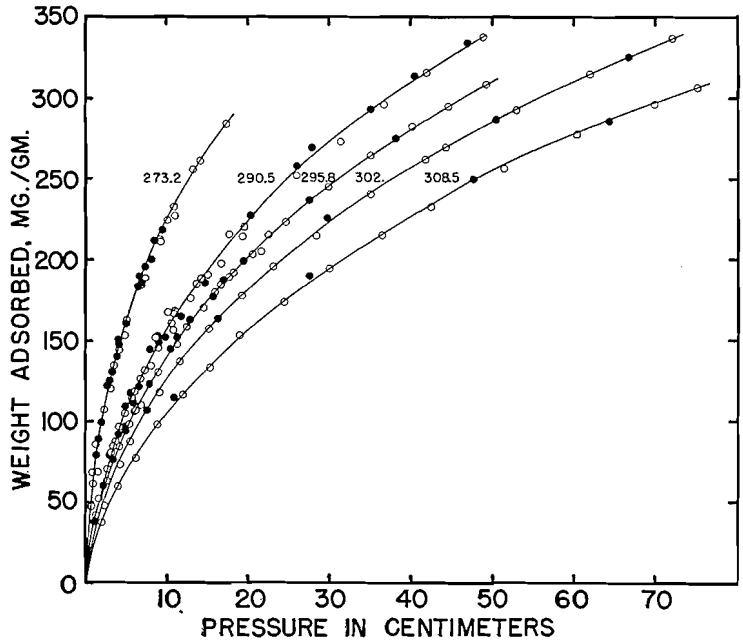

FIG. 1. Adsorption isotherms for perfluoroethylene on charcoal. Open symbols denote adsorption. Closed symbols denote desorption.

To achieve greater precision than was attained in the perfluoroethylene isotherms, the ethylene isotherms were measured volumetrically in a standard

volumetric adsorption system. A slightly larger sample of charcoal was used than that employed in the perfluoroethylene measurements, but its treatment prior to adsorption measurements was the same. An ice bath was used for measurement of the isotherm at 273.2°K. To attain the lower temperatures an ethylene glycol – water bath was used which was cooled by a copper coil through which liquid air was circulated at a rate controlled by a vapor pressure regulator. Sulphur dioxide was used in the regulator at 260.8°K. and methyl chloride at 245.4°K. The ethylene isotherms displayed a small amount of hysteresis over the pressure range studied. The adsorption points were somewhat scattered and slightly displaced in the direction of higher pressures with reference to the desorption points. It was also observed that on adsorption the system required extremely long periods of the order of eight hours to equilibrate compared with short periods of about 15 min. on desorption. The short equilibration times on desorption and the exact reproducibility of the desorption points taken over many separate runs are believed to be convincing proof that the adsorption points are not at true equilibrium, but represent metastable states due perhaps to slow diffusion of gas into the granules of the charcoal. Accordingly the adsorption points have not been plotted in Fig. 2, which

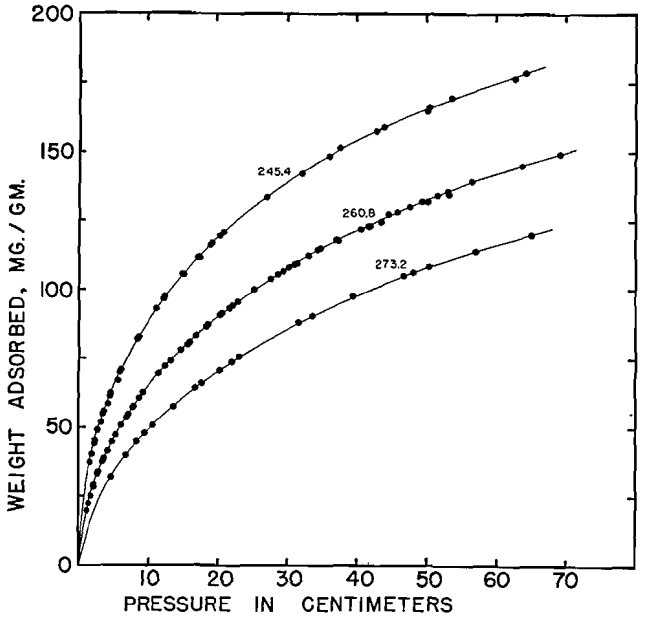

FIG. 2. Adsorption isotherms for ethylene on charcoal.

shows the desorption points for the isotherms at 273.2°, 260.8°, and 245.4°K. The absence of corresponding hysteresis effects in the perfluoroethylene–charcoal system can possibly be accounted for by the following: (1) the gravimetric method is not as sensitive as the volumetric, and (2) removal of the adsorption cell from the thermostat for weighing tends to obscure hysteresis effects if the bath temperature is lower than room temperature.

Thermodynamic quantities were calculated by the methods outlined by Hill (6). Isosteric heats and integral heats were calculated by means of the equations

$$Q_{ST} = \left(\frac{\partial \ln p}{\partial T}\right)_v RT^2,$$

$$H_G - H_S = \left(\frac{\partial \ln p}{\partial T}\right)_\phi RT^2,$$

$$\phi = RT \int_0^p \frac{V}{p}\, dp,$$

where Q_{ST} is the isosteric heat, $H_G - H_S$ is the integral heat, and the other symbols have their usual meaning. The fraction of the surface covered, θ, was estimated from the area of the charcoal as measured by the low temperature adsorption of nitrogen and from the areas of the adsorbate molecules as calculated from their liquid densities. The isosteric and integral heats are plotted as a function of θ in Figs. 3 and 4 respectively. As a check on the internal consistency of the calculations, the isosteric heat was computed also by means of the equation

$$Q_{ST} = H_G - H_S + \frac{T}{V}\left(\frac{\partial \phi}{\partial T}\right)_v$$

and compared with the isosteric heat calculated in the usual manner. The measure of agreement reached in the case of ethylene is shown in Fig. 5. The difference between the integral molar entropy of the adsorbed phase and that

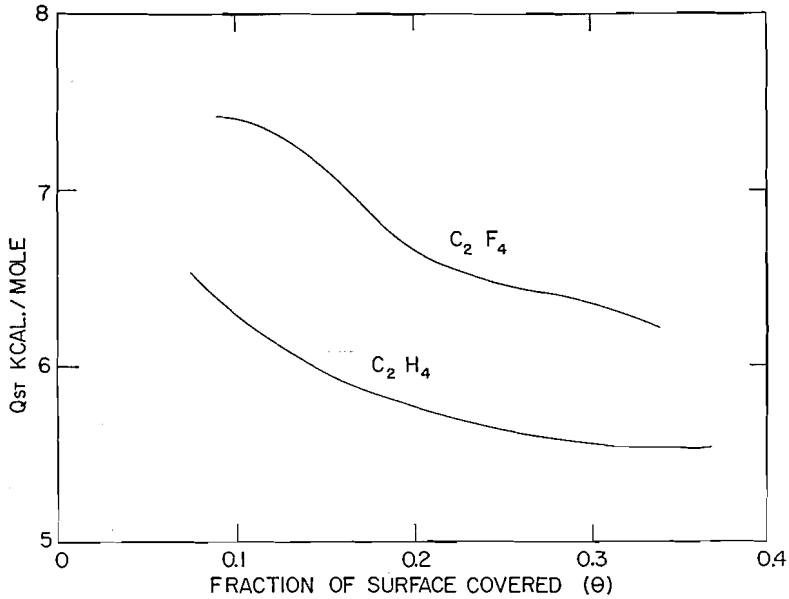

FIG. 3. Isosteric heats for the adsorption of ethylene and perfluoroethylene by charcoal.

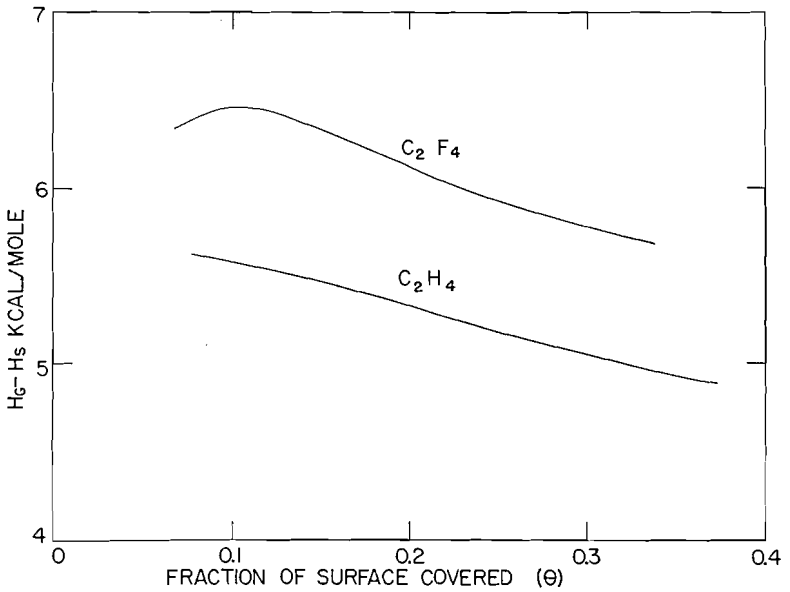

FIG. 4. Integral heats for the adsorption of ethylene and perfluoroethylene by charcoal.

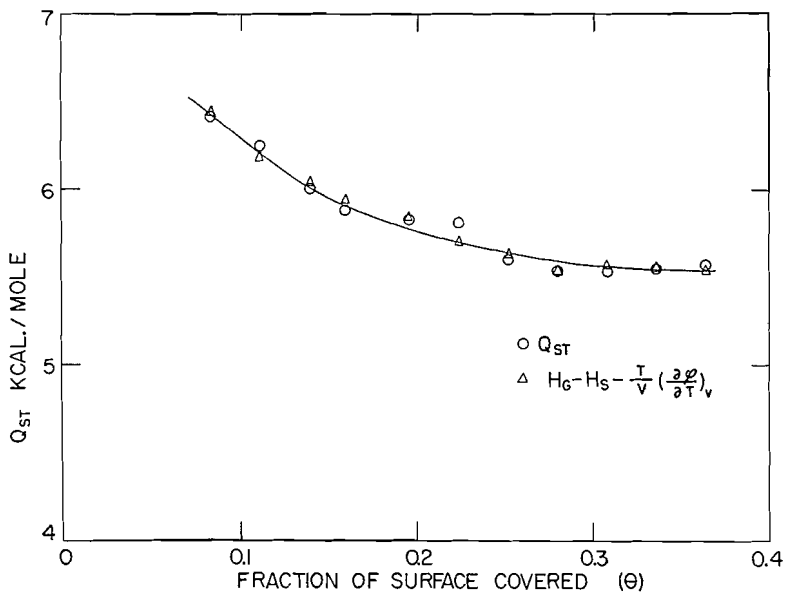

FIG. 5. Isosteric heats calculated in two different ways for the adsorption of ethylene by charcoal.

of the gas at the equilibrium pressure was computed from the equation

$$S_G - S_S = (H_G - H_S)/\bar{T},$$

where $\bar{T}$ is the mean temperature of the isotherms. The quantity $S_G - S_S$ is plotted as a function of θ for both gases in Fig. 6.

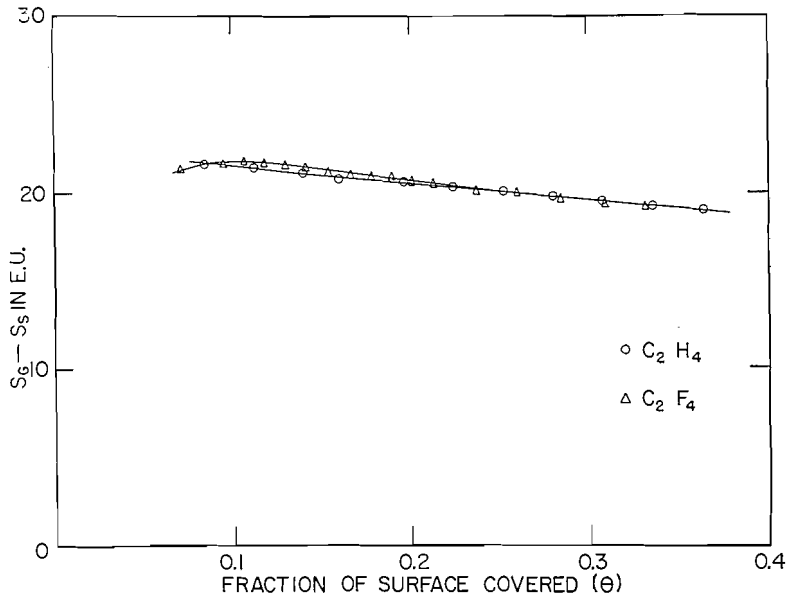

FIG. 6. Integral molar entropy changes accompanying the adsorption of ethylene and perfluoroethylene by charcoal.

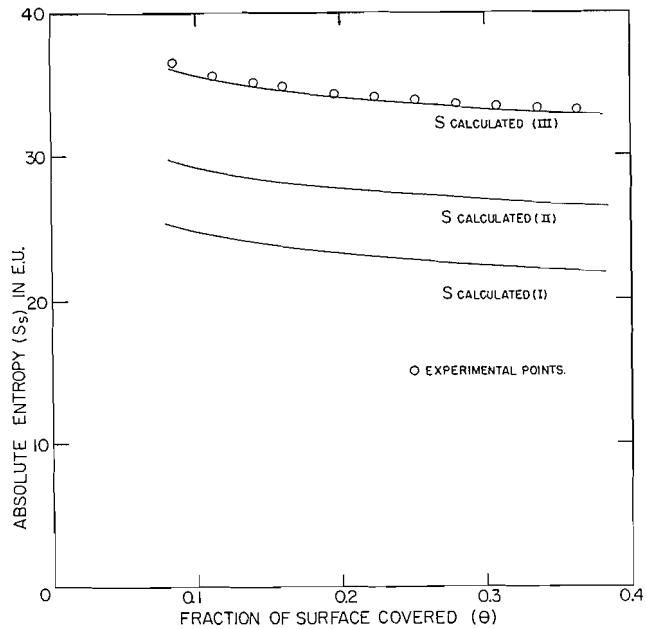

FIG. 7. Absolute entropy of ethylene adsorbed by charcoal. Circles denote experimental points. Solid lines are calculated values.

The absolute entropy, S_S, of the adsorbed ethylene was calculated from the quantity $S_G - S_S$ using the value of 51.1 e.u. (4) for the entropy of the gas at a pressure of 1 atm. and at the temperature $\bar{T}$. Experimental values of S_S are

presented in Fig. 7 along with theoretical curves based on three adsorption models.

DISCUSSION

Experimental values of the entropy of adsorbed ethylene are presented in Fig. 7 along with theoretical curves based on three adsorption models. The theoretical curves were calculated by means of the following equations derived from simple statistical thermodynamics

$$S_{\text{trans}} = R \ln \frac{2\pi mkTeA}{h^2} + 2,$$

$$S_{\text{rot}} = R\left[\ln \frac{1}{\pi\sigma}\left\{\frac{8\pi^3 (I_A^a\, I_B^b\, I_C^c)^{1/n} kT}{h^2}\right\}^{\frac{1}{2}n} + \frac{n}{2}\right]$$

where S_{trans} is the translational entropy, A is the area available per molecule, S_{rot} is the rotational entropy, $a+b+c = n$ is the number of degrees of rotational freedom possessed by the molecule, I_A, I_B, and I_C are the moments of inertia, and σ is the symmetry number. The area available per molecule, A, was calculated from the relationship $A = \Sigma/N$, where Σ is the area of the adsorbent. The first curve, labelled $S_{\text{calculated}}$(I), represents the case where the adsorbed molecules possess two degrees of translational freedom and one degree of rotational freedom in the plane of the surface. In the second model, $S_{\text{calculated}}$(II), the molecules are endowed with two degrees of translational freedom and two degrees of rotational freedom in the plane of the surface. The third curve, $S_{\text{calculated}}$(III), is calculated by assigning the molecules two degrees of translational freedom and all three degrees of rotational freedom.

Kemball (9) has suggested that a molecule that has lost one degree of translational freedom may acquire in its place a vibrational degree of freedom which may result in an entropy contribution of from 0 to 5 e.u. The following equations given by Kemball (9) have been used to estimate the entropy contribution due to vibration of the ethylene molecule:

$$\nu = L\, V_m^{-\frac{1}{3}}\, T_m^{\frac{1}{2}}\, M^{-\frac{1}{2}}$$

$$\text{and } S_{\text{vib}} = R[(h\nu/kT)(e^{+h\nu/kT}-1)^{-1} - \ln(1-e^{-h\nu/kT})],$$

where ν is the frequency, L is a constant having the value 2.8×10^{12}, V_m is the molecular volume, and T_m is the melting point. At 259°K., S_{vib} was calculated to be 4.1 e.u.

If interaction exists between the adsorbed molecules, an entropy contribution may be expected from this source. However in the present experiments, it is hoped that the coverage is sparse enough to lead to negligible interaction between adsorbed molecules. Some evidence exists to show that this is indeed the case. Graham (5) has suggested that adsorption systems may be characterized by the form of the curve obtained by plotting the quantity $\theta/(1-\theta)p$, which he calls the equilibrium function, against θ, the fraction of the surface covered. If this is done for ethylene and perfluoroethylene it is found that the equilibrium function decreases steadily with increasing θ. According to Graham, this type of behavior is characteristic of adsorption on a non-uniform surface with no interaction between adsorbed molecules. Consequently, it is believed that the contributions arising from molecular

interaction may be neglected up to the highest coverage attained in these experiments, although they would undoubtedly become important at higher coverages. If Kemball's suggestion is accepted, then the theoretical values presented in Fig. 7 must all be increased by 4.1 e.u. It is at once apparent that $S_{\text{calculated}}$(III) will be appreciably above the experimental values over the whole range of coverage investigated and that $S_{\text{calculated}}$(I) will still be considerably below the experimental values. Thus on this basis Model III may be ruled out and it may be inferred that insufficient degrees of freedom were assigned to the molecule in the case of Model I. Model II with the addition of a weak vibration remains as the final choice, and indeed the values so calculated account for 93% of the experimentally measured entropy. The difference between $S_{\text{calculated}}$(II) plus 4.1 e.u. and the experimental values is 2.4 e.u. over the coverage studied. The experimental values are accurate to approximately 1 e.u. and the method of calculating the vibrational entropy is an approximate one. Therefore, the agreement noted above is satisfactory. de Boer (3) has also calculated entropies of hydrocarbons adsorbed on charcoal and concluded that the adsorbed films are mobile. Although the authors of this paper believe this is true on the basis of their own findings, they do not feel that de Boer was justified in reaching this conclusion. In the first place his calculations were based for the greater part on work done by Ray and Box (11), which although adequate for the purpose intended is not accurate enough for making thermodynamic calculations. Secondly, de Boer calculated differential entropies, which Hill (7) has pointed out are unsuitable for comparison with those calculated from statistical–mechanical models.

The heats of adsorption and the entropies of adsorption for ethylene and perfluoroethylene have been compared in Figs. 3, 4, and 6. Over the range of coverage studied the heat of adsorption of perfluoroethylene is consistently higher than that of ethylene, although the entropies are almost identical at the temperatures chosen. For example, at $\theta = 0.2$ the differential heat of adsorption of ethylene was found to be 2.65 kcal. per carbon atom compared with 3.10 kcal. per carbon atom for perfluoroethylene. These values are in approximate agreement with values found by Beebe *et al.* (1, 2) for the adsorption of a number of hydrocarbons by carbon surfaces. In the discussion which follows, it will be shown that the mode of adsorption is the same for the two gases and that the differences in the heat of adsorption may be accounted for solely in terms of the difference in molecular weight between the two compounds. The physical properties of ethylene (8) and perfluoroethylene (12, 13) are listed below.

	Critical temp., °K.	Mean temp. of adsorp., °K.	Ads. temp. / Critical temp.	Heat of vaporization, kcal./mole	B.P., °K.	Entropy of vaporization, e.u.
Ethylene	283	259	0.92	3.33	169	19.7
Perfluoro-ethylene	307	297	0.97	4.10	197	20.8

It is seen that the mean temperatures of adsorption are close to 95% of the critical temperatures of the two gases. Since the forces which determine the critical temperature of the gas are similar to those active in physical adsorption, the agreement between the entropy curves of Fig. 6 at roughly the same fraction of the critical temperature is interpreted as meaning that the mechanisms of adsorption are identical for the two gases. This is believed to be exactly analogous to the agreement of the entropies of vaporization at the boiling points, which occur at approximately 60% of the critical temperatures.

The quantity $H_G - H_S - H_L$ is plotted in Fig. 8 as a function of θ. The curves fall close to each other indicating that the forces responsible for the

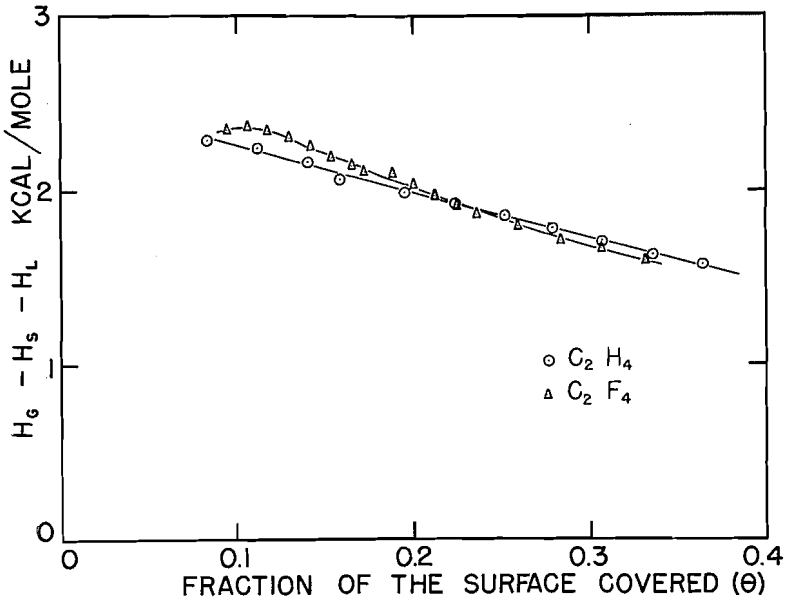

FIG. 8. The difference between the integral heat of adsorption and the heat of vaporization for ethylene and perfluoroethylene.

increase in the heat of vaporization of perfluoroethylene over that of ethylene are also responsible for the observed increase in the heat of adsorption. Since these two substances obey Trouton's rule quite closely, it may be assumed that the liquids are monomeric and that the increase in the heat of vaporization of perfluoroethylene over that of ethylene is simply a result of its higher molecular weight. Consequently, the heat of adsorption of perfluoroethylene is larger than that of ethylene by an amount that would be expected from its higher molecular weight. It is concluded therefore that there is no specific interaction between the fluorine atoms of the fluorocarbon and the carbon surface.

REFERENCES

1. BEEBE, R. A., KINGTON, G. L., POLLEY, M. H., and SMITH, W. R. J. Am. Chem. Soc. 72: 40. 1950.
2. BEEBE, R. A., POLLEY, M. H., SMITH, W. R., and WENDELL, C. B. J. Am. Chem. Soc. 69: 2294. 1947.

3. DE BOER, J. H. and KRUYER, S. Proc. Koninkl. Ned. Akad. Wetenschap. 56, B: 415. 1953.
4. GLASSTONE, S. Thermodynamics for chemists. D. Van Nostrand Company, Inc., New York. 1947.
5. GRAHAM, D. J. Phys. Chem. 57: 665. 1953.
6. HILL, T. L. J. Chem. Phys. 17: 520. 1949.
7. HILL, T. L. Trans. Faraday Soc. 47: 376. 1951.
8. International Critical Tables. Vol. III. McGraw-Hill Book Company, Inc., New York. 1928. p. 230.
9. KEMBALL, C. Proc. Roy Soc. (London), A, 190: 117. 1947.
10. McDERMOT, H. L. and ARNELL, J. C. Can. J. Chem. 30: 177. 1952.
11. RAY, G. C. and BOX, E. O. Ind. Eng. Chem. 42: 1315. 1950.
12. RENFREW, M. M. and LEWIS, E. E. Ind. Eng. Chem. 38: 870. 1946.
13. RUFF, O. and BRETSCHNIEDER, O. Z. anorg. u. allgem. Chem. 210: 173. 1933.

THE ADSORPTION OF ALIPHATIC ACIDS FROM AQUEOUS SOLUTIONS BY POROUS CARBONS[1]

By John L. Morrison[2] and David M. Miller[3]

ABSTRACT

The maximum adsorptions of the lower members of the mono- and di-carboxylic acids from aqueous solutions were determined for coconut charcoals of different degrees of activation. Based on these results, a method for estimating pore size was applied to the more finely porous charcoals. To corroborate the pore sizes estimated from acid adsorption, pore size – area distributions were calculated from measurements of the water vapor sorption isotherms of the charcoals. An alternation in the maximum amounts of adsorbed acids was observed with the more active charcoals. Acids with an even number of carbon atoms had larger adsorptions than acids with an odd number. The alternation was much more marked for the di- than for the mono-carboxylic acids. A remarkable correlation between the alternation of adsorptions and of melting points of both acid series was observed. An explanation for the general phenomenon of alternation based on rotational motion of molecules in the solid state is given as an alternative to the widely held one based on tilting of molecular chains.

A determination of the nature of the adsorbed layer is one of the principle objectives of adsorption studies. In the selective adsorption by a porous adsorbent of one component from a binary liquid mixture, two alternatives have been considered possible, either molecular layer adsorption (6, 10, 11) or capillary condensation (4, 5, 8). The present work concerning the adsorption of aliphatic acids from aqueous solutions by porous carbons appears to be an example of the first alternative.

Linner and Gortner (11) measured the adsorption isotherms of 31 organic acids from water solutions by one sample of Norite charcoal, and by applying the Langmuir equation, they calculated the maximum amounts adsorbed at higher concentrations. In the case of acid adsorption, the present work exclusively involves the direct measurement of the maximum amounts adsorbed. As Linner and Gortner suggest, this is "a more valid method of comparing the effect of molecular structure on adsorption".

EXPERIMENTAL

The coconut shell charcoal samples were obtained from the Standard Chemical Co. Ltd., Montreal. They consisted of two series of seven samples, each sample removed from the steam activator at approximate intervals of 24 hr. Some data on the series Charcoals 1 to 7 have already been given (10) and data for the series charcoals 1B to 7B are given in Table I.

[1]*Manuscript received September 16, 1954.*
Contribution from the Department of Chemistry, University of Alberta, Edmonton, Alberta. Part of this paper is taken from a thesis submitted to the University of Alberta in partial fulfillment of the requirements for the M.Sc. degree. This paper was presented at the Symposium on Problems Relating to the Adsorption of Gases by Solids, held at Kingston, Ontario, September 10–11, 1954.
[2]*Associate Professor of Chemistry.*
[3]*Graduate student, 1945–46. Present address: Science Service Laboratory, Canada Department of Agriculture, University Post Office, London, Ontario.*

TABLE I

DATA ON THE B SERIES OF COCONUT CHARCOALS[1]

Sample No.	Volume activity	Mercury density,[2] gm./cc.	Nitrogen adsorbed,[2] V_m mM./gm.
1 B	1.0	1.177	5.17
2 B	4.1	1.099	6.71
3 B	8.7	1.080	8.04
4 B	13.0	1.045	9.18
5 B	16.6	0.988	10.48
6 B	19.9	0.944	11.78
7 B	22.1	0.917	12.72

[1]*For the methods of obtaining these data, see Lemieux and Morrison (10).*
[2]*Determined by J. L. Morrison.*

Acid Adsorption

The data of Lemieux and Morrison for the adsorption of the aliphatic acids from acetic to valeric by Charcoals 1 to 7 are used here. The measurements on caproic acid and the dicarboxylic acids oxalic to adipic on the same charcoal series are new, as are all the measurements on Charcoals 1B to 7B.

Caproic acid was C. P., Fisher Scientific Co.; the other monocarboxylic acids and malonic, succinic, and adipic acids were chemically pure grade from Eastman Kodak Co.; oxalic acid was recrystallized from technical grade, Central Scientific Co.; glutaric acid was prepared from trimethylene bromide (14).

The procedure already described (10) was followed with slight modifications for the dicarboxylic acids. The adsorptions were carried out in 250-ml. ground glass stoppered flasks which were sealed by paraffin wax. At least two days were allowed for equilibration. The measurements on the B series were made at 25.0 ± 0.1°C., and the dicarboxylic acids were equilibrated at room temperature.

Owing to the large solubilities of malonic and glutaric acids, smaller amounts of solution and larger charcoal samples than above were used. Here 25 ml. portions of acid solution were added to 4 gm. of Charcoals 1 to 4 and to 3 gm. of Charcoals 5 to 7. They were allowed to stand until gas evolution ceased (seven to eight days). Then two 10-ml. samples were titrated. The two procedures checked for succinic acid within the experimental error.

The adsorptions at four or five concentrations were determined and averaged for each charcoal. The average deviation for the monocarboxylic acids adsorbed on the B series was ±2.0%, and for the dicarboxylic acids, excluding glutaric, ±3.6%. Glutaric acid had a deviation of ±9.2%. In all cases, the deviations decreased with increasing charcoal activity; for example, with Charcoal 7, glutaric acid deviated by ±4.7% and the average of the other dicarboxylic acids was ±2.6%.

Water Adsorption

To obtain an independent measure of the charcoal pore sizes, the water vapor adsorption isotherms were measured by the method of Wiig and Juhola

(23). As in their case, dibutyl phthalate manometers were used. Because they exhibited a very small vapor pressure (approx. 5×10^{-4} cm. Hg) on the McLeod gauge, they were replaced by Apiezon Oil B manometers for repeat determinations on two charcoals. No difference was found in the isotherms.

At least two hour and often overnight periods were used in the measurement of each point of an isotherm. Six to nine points were determined on each of the adsorption and desorption branches for each charcoal. The isotherms were measured at 22.9 ± 0.1°C.

RESULTS AND DISCUSSION

Acid Adsorption

All the data fitted Langmuir isotherms, as is generally observed for this type of system (6, 10, 11). Hansen, Fu, and Bartell (6) have shown that porous sugar charcoal in constrast with nonporous carbons exhibits a Langmuir isotherm with a value of 1 for the maximum number of adsorbed layers. The maximum amounts of the various acids adsorbed by the two charcoal series are given in Table II. Included for convenience are the corresponding results obtained by Lemieux and Morrison (10).

TABLE II

MAXIMUM NUMBER OF MILLIMOLES ACID ADSORBED PER GRAM CHARCOAL

Acid adsorbate	Charcoal number (first series)						
	1	2	3	4	5	6	7
Acetic	2.15	2.55	2.85	3.22	3.25	3.70	4.00
Propionic	1.63	2.04	2.47	2.91	2.93	3.46	3.75
Butyric	1.24	1.66	2.06	2.63	2.74	3.43	3.84
Valeric	0.88	1.31	1.75	2.40	2.41	3.18	3.66
Caproic	0.75	1.10	1.32	1.96	2.04	2.63	3.00
Oxalic	1.27	1.56	1.74	2.00	2.15	2.40	2.54
Malonic	0.60	0.78	1.09	1.40	1.52	1.62	1.87
Succinic	0.61	0.91	1.22	1.70	1.78	2.18	2.29
Glutaric	0.23	0.42	0.82	1.10	1.15	1.49	1.69
Adipic	0.43	0.68	0.99	1.48	1.44	1.88	2.08

	Charcoal number (second series)						
	1B	2B	3B	4B	5B	6B	7B
Acetic	1.90	2.14	2.59	2.74	2.89	3.15	3.36
Propionic	1.39	1.89	2.34	2.50	2.78	3.11	3.27
Butyric	1.01	1.71	2.24	2.45	2.82	3.19	3.39
Valeric	0.74	1.58	2.04	2.31	2.68	3.13	3.33
Caproic	0.44	0.98	1.46	1.73	2.15	2.54	2.70

Maximum adsorption occurs at about the following concentrations for the various acids: caproic—0.03 *M*, oxalic—0.09 *M*, malonic—4.8 *M*, succinic—0.5 *M*, glutaric—3.0 *M*, and adipic—0.05 *M*.

Pore Size from Acid Adsorption

The *less activated* members of the two charcoal series exhibit an inversion of Traube's rule when it is applied to the maximum number of moles of mono-

carboxylic acid adsorbed. Although some workers (5, 8) interpret this by a capillary condensation mechanism, we interpret it on the basis of oriented unimolecular adsorption and a sieving of the molecules according to chain length. Moreover, the fact as seen in Figs. 2 and 3 that for the less activated charcoals the *change* in the amount adsorbed for successive acids is comparable to the absolute adsorptions suggests that most pores are comparable in size to the length of the acid molecules. This suggestion led to a method for estimating the pore size of very finely porous carbon.

Qualitatively, the results indicate that Charcoals 1, 2, and 1B have "an even distribution of pore sizes" (10). On this basis, assume that the pores are like a set of open-ended regular cones; also assume vertical orientation of the monocarboxylic acids at the water–charcoal interface. The model is given in Fig. 1. The amount adsorbed will be proportional to the number of cones n,

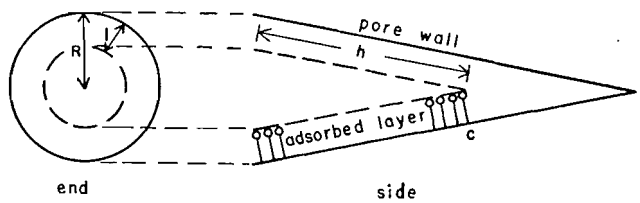

FIG. 1. Cone model of a charcoal pore. R—pore radius, l—acid chain length, h—slant height of cone radius $(R-l)$, c—"cutoff" radius.

and the lateral area of the cones of radius $(R-l)$ and slant height h, where R = pore radius and l = acid chain length. Thus

$$x_m = knh\ \pi(R-l), \qquad [1]$$

where x_m is the maximum number of millimoles adsorbed per gm. charcoal, and k is a proportionality constant.

For different acid chain lengths, the change in x_m for the same charcoal will be

$$dx_m/dl = -knh\pi. \qquad [2]$$

Here, the product nh is assumed constant as a first approximation. By substituting for nh in Equation [1] we obtain

$$R = 1-x_m/(dx_m/dl). \qquad [3]$$

In Figs. 2 and 3, the x_m values have been plotted against acid chain length, the latter having been estimated from the liquid molar volume by assuming a common cross-sectional area of 24.3 Å^2 for the acid molecules (19, 22). The pore radii given in Table III were obtained from plots similar to Figs. 2 and 3 after a correction varying from 1.2 to 3.1% was made for the alternation effect (to be discussed later). This correction placed the first three acids, acetic to butyric, on the same straight lines respectively for Charcoals 1,2, and 1B, with valeric lying somewhat above in each case.

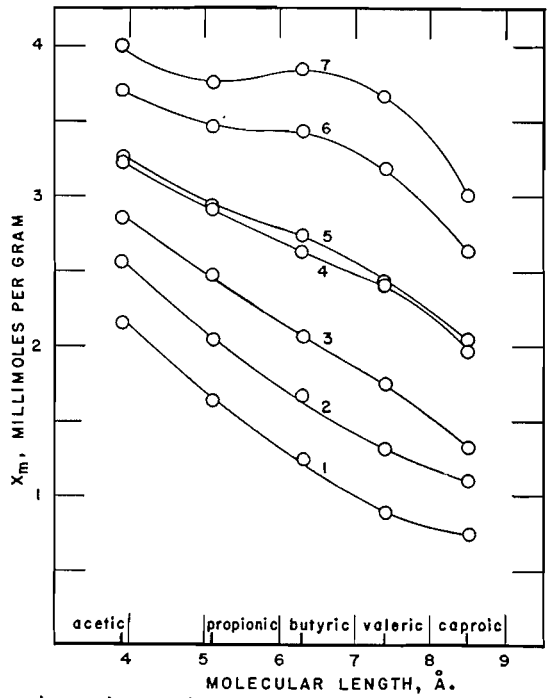

FIG. 2. The change in maximum adsorption of monocarboxylic acids with chain length for the first charcoal series.

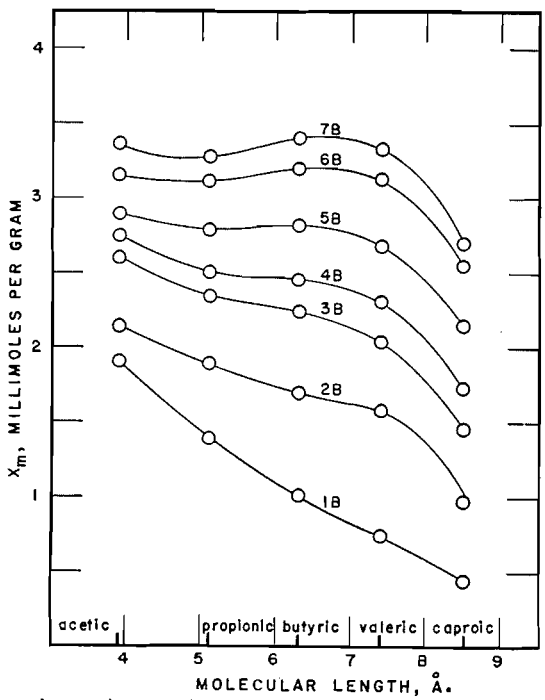

FIG. 3. The change in maximum adsorption of monocarboxylic acids with chain length for the B charcoal series.

The radii in Table III are the largest radii of the cones in the model, and depend on the molecular chain lengths chosen for the acids. In a later section it will be shown that these radii may be low by about 2Å.

TABLE III

PORE RADII (Å) OF CHARCOALS BY ACID ADSORPTION

Acid	Charcoal number			
	1	2	3	1B
Acetic	9.7	10.9	13.9	9.1
Propionic	9.7	10.9	14.2	9.1
Butyric	9.7	10.9	13.6	9.1
Valeric	9.9	11.2	13.9	9.5

The approximation assumption that the product '*nh*' in Equation [1] is constant apparently has some validity because of the constancy of the radii of particular charcoals for the first three acids. If the product '*nh*' is approximately constant, then, on the cone model, either or both of two possibilities are suggested. The number of pores, n, may be the same to all acids, in which case the apical angle would have to increase with increasing pore radius at such a rate as to keep h approximately constant, *or*, the apical angle may remain constant, in which case the number of pores would have to decrease with increasing pore radius.

Pore Radii from Water Adsorption

The water vapor adsorption isotherms are most conveniently reported in Table IV. These data are taken from smoothed curves drawn through the experimental points when the amount adsorbed was plotted against the relative water vapor pressure.

The area of charcoal occupied by water rather than the weight adsorbed, at various relative pressures, was considered the more valid parameter by which to compare the water adsorption radii with the acid adsorption radii. The distribution of pore areas for various pore radii was found in the following way.

The equation of Kistler, Fischer, and Freeman (9),

$$[4] \qquad \frac{dA}{dW} = \frac{2.303\,RT}{M\sigma\cos\theta}\log\frac{P_0}{P}$$

was applied to the desorption branch of the water isotherms (2). Here, A is the area occupied by W grams of water of molecular weight M, and surface tension σ, at a relative pressure of P/P_0. R is the gas constant and the $\cos\theta$ term was added by us to take account of the partial wettability of charcoal by water. The distribution of area with the weight of water was obtained by graphical integration.

Following Fineman, Guest, and McIntosh (2) and Wiig and Juhola (23), the Kelvin equation was used to calculate the pore radius R at various relative

TABLE IV

GRAMS WATER VAPOR SORBED PER GRAM CHARCOAL

Relative pressure	Charcoal number 1		2		3		4		5		6		7	
	A	D	A	D	A	D	A	D	A	D	A	D	A	D
0.10	.0050	.0050	.0050	.0050	.0050	.0050	.0055	.0055	.0040	.0045	.0035	.0035	.0050	.0050
0.20	.0115	.0115	.0110	.0110	.0110	.0120	.0115	.0115	.0100	.0100	.0090	.0090	.0120	.0120
0.30	.0200	.0205	.0190	.0190	.0180	.0220	.0185	.0195	.0170	.0185	.0175	.0185	.0195	.0200
0.40	.0335	.0395	.0335	.0355	.0350	.0400	.0315	.0390	.0330	.0425	.0305	.0340	.0305	.0355
0.45	.0490	.0720	.0570	.0645	.0590	.0620	.0520	.0640	.0525	.0665	.0440	.0540	.0470	.0560
0.50	.0845	.1135	.0920	.1160	.1000	.1180	.0950	.1090	.0930	.1135	.0740	.1060	.0810	.1300
0.55	.1165	.1450	.1410	.1680	.1535	.1990	.1635	.2340	.1580	.2260	.1430	.2530	.1540	.2620
0.60	.1395	.1585	.1704	.1820	.1860	.2120	.2040	.2445	.2025	.2345	.2165	.2790	.2465	.3220
0.70	.1585	.1640	.1845	.1915	.2105	.2185	.2415	.2540	.2330	.2435	.2690	.2880	.3090	.3355
0.80	.1655	.1680	.1920	.1965	.2205	.2245	.2570	.2605	.2440	.2510	.2855	.2930	.3285	.3425
0.90	.1715	.1720	.1980	.2005	.2280	.2295	.2650	.2660	.2535	.2570	.2930	.2960	.3430	.3495
1.00	.1755	.1755	.2030	.2030	.2340	.2340	.2705	.2705	.2620	.2620	.2965	.2965	.3560	.3560

Relative pressure	Charcoal number 1B		2B		3B		4B		5B		6B		7B	
	A	D	A	D	A	D	A	D	A	D	A	D	A	D
0.10	.0075	.0075	.0065	.0065	.0055	.0055	.0050	.0050	.0060	.0060	.0040	.0040	.0025	.0025
0.20	.0170	.0175	.0140	.0140	.0130	.0130	.0110	.0110	.0130	.0130	.0095	.0095	.0085	.0085
0.30	.0275	.0325	.0230	.0265	.0230	.0260	.0190	.0225	.0220	.0235	.0170	.0195	.0190	.0190
0.40	.0410	.0560	.0435	.0510	.0465	.0530	.0410	.0485	.0405	.0485	.0335	.0400	.0370	.0405
0.45	.0630	.0840	.0670	.0815	.0695	.0840	.0660	.0750	.0610	.0770	.0535	.0610	.0590	.0725
0.50	.1040	.1245	.1025	.1360	.1145	.1560	.1050	.1600	.1080	.1600	.0890	.1380	.1015	.1650
0.55	.1280	.1485	.1405	.1800	.1560	.2025	.1720	.2200	.1745	.2495	.1610	.2710	.1780	.2960
0.60	.1410	.1540	.1645	.1885	.1815	.2115	.2025	.2325	.2200	.2665	.2225	.2930	.2505	.3255
0.70	.1530	.1625	.1835	.1985	.2040	.2205	.2215	.2425	.2535	.2775	.2735	.3070	.3045	.3440
0.80	.1625	.1690	.1955	.2055	.2170	.2275	.2370	.2500	.2745	.2865	.2995	.3190	.3330	.3570
0.90	.1710	.1740	.2065	.2115	.2280	.2330	.2500	.2565	.2895	.2940	.3190	.3280	.3560	.3670
1.00	.1785	.1785	.2170	.2170	.2380	.2380	.2620	.2620	.3010	.3010	.3350	.3350	.3740	.3740

Note: A = adsorption; D = desorption.

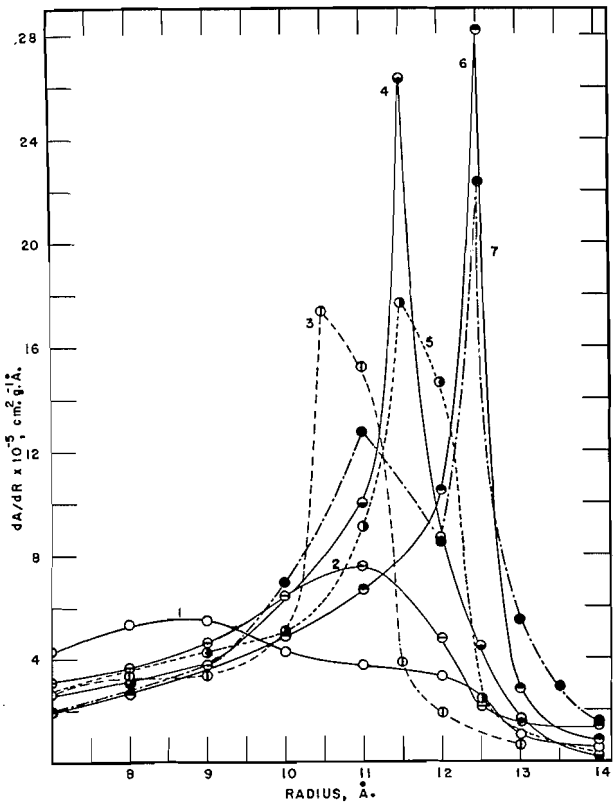

FIG. 4. The distribution of pore area with radius for the first charcoal series.

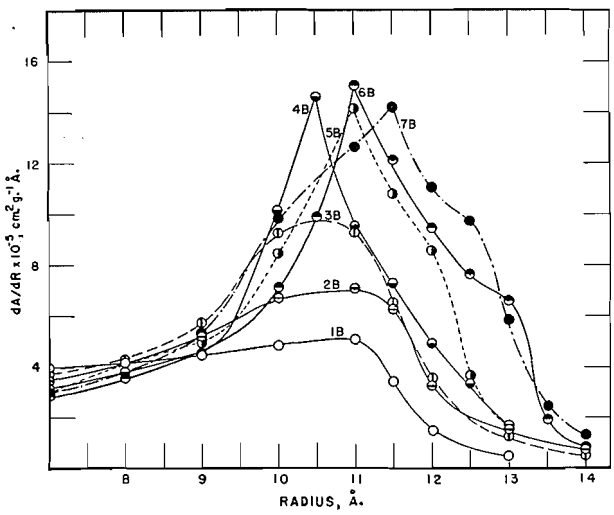

FIG. 5. The distribution of pore area with radius for the B charcoal series.

pressures, and thus at various adsorbed weights. In both expressions, the $\cos\theta$ term for partial wettability was given the value of 0.65 following the work of McDermot and Arnell (12). Areas were connected to radii by their relations to the adsorbed weights. Then, by graphical differentiation of the plots of the cumulative areas at various pore radii (Milligan and Adams (15) did the same for weights), the area – pore radius distribution curves were obtained for each charcoal. These are given in Figs. 4 and 5.

Two observations may be made. Confirming the qualitative picture of the pores of Charcoal 1 and 1B given by the acid adsorption results, it is seen that these charcoals have a fairly even pore size distribution. Also, the values of the radii from water adsorption compare reasonably well with those from acid adsorption.

Water–Acid "Cutoff" Areas

The combined water and acid adsorption data give another confirmation of the proposed model. Contrary to the suggestion (4, 5) that the acids are leaving the water solution to fill the charcoal pores, density measurements (16) indicate that water from the binary mixture can penetrate further into the charcoal than any of the acids.[4]

The areas reached by water were compared with those reached by the various acids. The latter were calculated by assuming vertical orientation and a cross-sectional adsorption area of 24.3 Å^2 (10, 19, 22) for the acid molecules. The excess area penetrated by water compared with that penetrated by a particular acid was approximately the same for the first four charcoals of each charcoal series. The "cutoff" radii (at *c* in Fig. 1) corresponding to the excess water penetration areas were determined from the composite Kistler–Kelvin data and are given in Table V. The radii are the average of Charcoals 1 to 4 and 1B to 4B.

TABLE V

"CUTOFF" RADII FOR WATER PENETRATION

Acid	Cutoff radius, Å	Acid chain length, Å
Acetic	6.5 ± 0.5	3.9
Propionic	7.7 ± 0.5	5.1
Butyric	8.7 ± 0.3	6.3
Valeric	9.5 ± 0.5	7.4
Caproic	10.3 ± 0.4	8.5

The differences between successive "cutoff" radii are consistent with the differences in acid chain lengths. However, the "cutoff" radii are about 2Å greater than the acid lengths. This is not unreasonable in such a dynamic system. If these radii are approximately correct, they increase the estimated acid pore radii given in Table III by about 2Å. The revised values are more

[4]*Such penetration would reduce the apparent selective acid adsorption but a calculation for the most extreme case, valeric acid solution on Charcoal 1, showed that the effect was about 8% which is within the experimental error.*

compatible with the water radii results, considering that the acids give *external* pore radii.

Alternation in Acid Adsorption

Alternation in the maximum adsorption of the successive members of the monocarboxylic series to valeric acid was observed for Charcoals 5 to 7 (Fig. 2) and Charcoals 3B to 7B (Fig. 3). The dicarboxylic acids exhibited a much more marked alternation in adsorption, as shown in Fig. 6. These

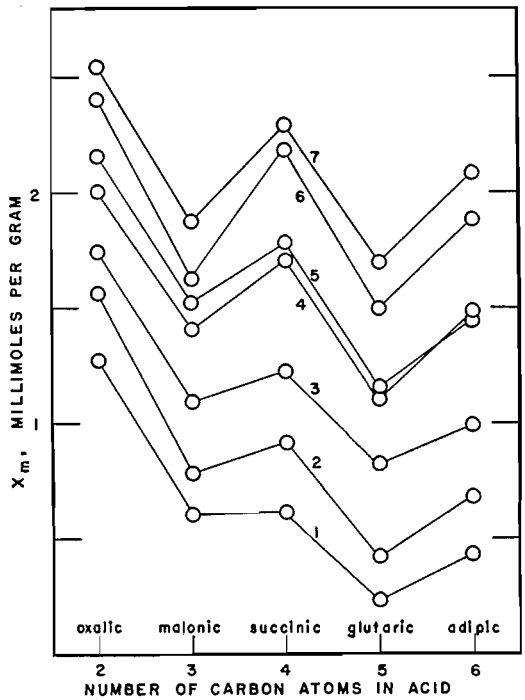

FIG. 6. The change in maximum adsorption of dicarboxylic acids with number of carbons in the chain for the first charcoal series.

observations greatly extend earlier ones made by Linner and Gortner (11) for the same acids on a single Norite charcoal. In their case, the monocarboxylic acids showed a slight alternation, without alternately larger and smaller values, while the dicarboxylic acids gave sufficient alternation to exhibit such a fluctuation. However, the authors remarked that "the results in themselves are not particularly striking".

The alternation increases with increasing charcoal activity. In the lesser activated charcoals, the alternation is markedly reduced, being practically non-existent for the monocarboxylic acids, but still quite definite for the dicarboxylic acids. Apparently for these charcoals progressive sieving of the longer molecules masks the alternation effect, and where the alternation is less marked as in the case of the monocarboxylic acids, the effect becomes negligible. However, alternation is not really absent even for Charcoals 1 and 1B

and corrections were made for the effect when the pore radii were estimated from the acid adsorption data.

Alternation in many of the physical properties of a number of long chain homologous series of compounds is well known and appears to be a characteristic of the solid state (18). In Fig. 7, the adsorptions of the two acid series on

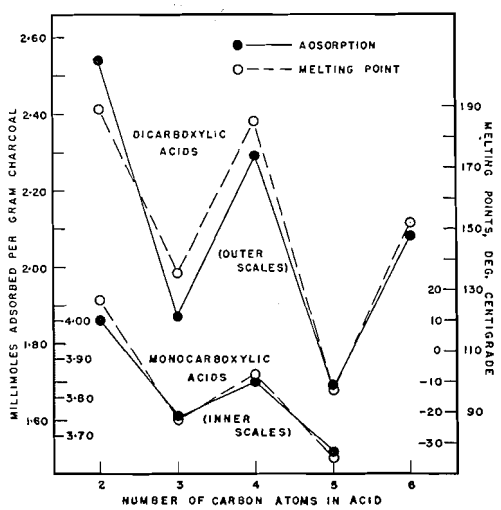

FIG. 7. A comparison of the alternation in melting points of mono- and di-carboxylic acids with their maximum adsorptions by Charcoal 7.

Charcoal 7 are compared with their melting points (3, 18). The scales of the two acid series were displaced so that each series would appear separately. The arbitrary elements in the figure are the adsorption and temperature scales which were adjusted so that a successive pair of acids approximately overlapped. However, the scale *intervals* are respectively the *same* for each acid series pointing to a remarkable correlation between the *alternations* in adsorption and in melting point.

On the basis of X-ray evidence, Malkin (13) suggests that alternation is a property of crystals with tilted molecular chains, "alternate planes of odd chains being less closely packed" than those of even chains. In support of his explanation is the fact that the dicarboxylic acid chains have an unusually large tilt in their crystals (1). Malkin's hypothesis requires association of the molecules along the long axis of the chain. However, the present adsorption results do not point to such association on the carbon surface. The internal consistency of the results appears to rule out that any *mixture* of associated and unassociated molecules is adsorbed. Dimers or higher associations may be ruled out by the calculations which, by assuming monomers, gave pore radii from the acid adsorptions that were consistent with those obtained from water vapor adsorption. Also, the monocarboxylic acids in water solutions give normal freezing point depressions (7). The molal freezing point of oxalic acid is 3.40°C. at 0.02 molal concentration and that of succinic 1.99° at 0.01

molal. So that although the aliphatic acids are known to associate in nonpolar solvents (18), they do not do so in water. Thus, it is difficult to reconcile the present observations with Malkin's explanation, and we must seek an alternative one. In fact, Malkin's hypothesis has been "vehemently criticized" as Smith has pointed out in his review (21).

Referring to Charcoal 7 in Fig. 6, the straight line drawn through oxalic, succinic, and adipic acids is nearly parallel to that drawn through malonic and glutaric acids. The same holds approximately for Charcoals 4 to 6. Since Charcoal 7 probably is equally open to all the acids with the possible exception of caproic, it appears that the addition of *two* methylene groups to the acid chain increases the molecular adsorption area (or section area) by a constant amount. However, the addition of *one* methylene group either decreases or increases the section areas by a much larger but also approximately constant amount.

Quantitatively, the addition of one methylene group as such (calculated for Charcoal 7 and with a cross sectional area of 24.3 $Å^2$ per molecule) increases the section area by about 2.4 $Å^2$. On the other hand, the fluctuations cause changes in the section areas of 12.3 $Å^2$ per fluctuation. It would appear that alternation is a reflection of the amount of space occupied by the carboxyl groups on the carbon surface, which in turn may be determined by their relative orientation in the chain.

In other words, the even acids in which the terminal carboxyl groups are *trans* to each other fit together closer than the odd acids in which the carboxyls are *cis*. The basic reason for this may have very little to do with tilt, but rather may be due to rotation of the chains along their long axis. It seems reasonable that the *cis* arrangement would sweep out larger areas than the *trans* arrangement. A similar explanation may apply to melting point alternation.

In the case of the monocarboxylic acids the similar but smaller effect would be explained by the fact that one of the terminal groups is smaller—a methyl replacing a carboxyl group.

Rotation of molecules in the solid state is not an uncommon phenomenon. Pauling says that "in general it is to be expected that rotational motion of molecules and complex ions of sufficiently low moment of inertia will set in below the melting point of the crystals" (17). Moreover, he points out that "the moment of inertia along a staggered chain about an axis along the chain would be very small". Further, Rideal and Tadayon (20) have shown the ease of motion of aliphatic acids in the solid state.

The rotational hypothesis is better able to account for the much greater alternation of the acids of shorter chain length (18) than is Malkin's hypothesis. The longer the chain, the more readily it will be able to accommodate *cis* rotations, and the less the carboxyl groups will dominate the rotational motion. Over a certain range of chain lengths we might expect a transition from one dominant type to the other. Such a transition is very apparent in the case of the monocarboxylic acids, both from melting point and adsorption evidence.

Caproic Acid

Caproic acid behaves anomalously compared with the lower monocarboxylic acids. At higher charcoal activities, its adsorption falls off sharply, as shown in Figs. 2 and 3. Linner and Gortner (11) observed a similar falloff in the adsorption of caproic acid on Norite charcoal. A possible explanation may be that its molecular chain length is sufficient to be sieved appreciably even by the highly activated charcoals.

An alternative explanation is suggested by the adsorption of caproic acid on Charcoals 1 and 2. In Fig. 2, the falloff in adsorption is not as great as would be expected from caproic acids behaviour with the other charcoals. This may mean that caproic acids' is partially curled up, thus reducing its effective chain length and permitting it to penetrate finer pores. At the same time, the concomitantly higher molecular adsorption area would reduce the number of moles adsorbed.

The anomalous adsorption behavior of caproic acid is paralleled by its melting point behavior. In a plot of the melting points of the monocarboxylic acids (3) against the number of carbons, a straight line drawn through valeric acid parallel to the melting point axis divides the plot into two parts which are approximately mirror images. Thus, while valeric acid is the last member of one group, caproic acid is the first member of the other group of acids. Considering the close parallel already observed between the alternations in adsorption and melting point, it is not surprising to find caproic acid behaving anomalously. On the basis of the rotational hypothesis given above, it is suggested that over the interval valeric to caproic acids, molecular rotation in the crystal changes from carboxyl dominance to hydrocarbon chain dominance.

ACKNOWLEDGMENTS

The authors thank Dr. J. C. Arnell for supplying and making certain measurements on some of the charcoals. They also acknowledge financial assistance from the National Research Council.

REFERENCES

1. Caspari, W. A. J. Chem. Soc. 3235. 1928.
2. Fineman, M. N., Guest, R. M., and McIntosh, R. Can. J. Research, B, 24: 109. 1946.
3. Handbook of physics and chemistry. Chemical Rubber Publishing Co., Cleveland, Ohio. 1953.
4. Hansen, R. D. and Hansen, R. S. J. Colloid Sci. 9: 1. 1954.
5. Hansen, R. S. and Craig, R. P. J. Phys. Chem. 58: 211. 1954.
6. Hansen, R. S., Fu, Y., and Bartell, F. E. J. Phys. & Colloid Chem. 53: 769. 1949.
7. International Critical Tables. McGraw-Hill Book Company, Inc., New York. Vol. 4. 1928.
8. Kisselev, A. and Shcherbakova, K. Acta Physicochim. U.R.S.S. 21: 539. 1946.
9. Kistler, S. S., Fischer, E. A., and Freeman, I. R. J. Am. Chem. Soc. 65: 1909. 1943.
10. Lemieux, R. U. and Morrison, J. L. Can. J. Research, B, 25: 440. 1947.
11. Linner, E. R. and Gortner, R. A. J. Phys. Chem. 39: 35. 1935.
12. McDermot, H. L. and Arnell, J. C. Can. J .Chem. 30: 177. 1952.
13. Malkin, T. Nature, 127: 126. 1931.
14. Marvel, C. S., Tuley, W. F., and McColm, E. M. Organic syntheses, collective volume. Vol. I. John Wiley & Sons, Inc., New York. 1941. pp. 289, 536.
15. Milligan, W. O. and Adams, C. R. J. Phys. Chem. 57: 885. 1953.
16. Morrison, J. L. Unpublished results.
17. Pauling, L. Phys. Rev. 36: 430. 1930.

18. RALSTON, A. W. Fatty acids and their derivatives. John Wiley & Sons, Inc., New York. 1948.
19. RIDEAL, E. K. An introduction to surface chemistry. Cambridge University Press, London. 1926. p. 50.
20. RIDEAL, E. K. and TADAYON, J. Proc. Roy. Soc. (London), A, 225: 346. 1954.
21. SMITH, J. C. Annual reports on the progress of chemistry. Vol. 35. Chemical Society, London. 1939.
22. VOLD, M. J. J. Colloid Sci. 7: 196. 1952.
23. WIIG, E. O. and JUHOLA, A. J. J. Am. Chem. Soc. 71: 561. 1949.

THE RATE OF ADSORPTION OF SOME LOW BOILING GASES ON A MODIFIED SARAN CHARCOAL[1]

By J. R. Dacey and D. G. Thomas[2]

ABSTRACT

The pyrolysis at 300°C. of vinylidene chloride monomer adsorbed on Saran charcoal alters the pore structure of the charcoal so that low boiling gases such as nitrogen are adsorbed slowly. The rates of adsorption of nitrogen, argon, and methane have been measured. They were found to vary with pressure and temperature, and from the temperature variation an activation energy may be calculated. A new method of determining this energy is described which involves changing the temperature during only one adsorption experiment.

INTRODUCTION

Previous work had shown that pressed Saran (polymerized vinylidene chloride) gave, when pyrolyzed *in vacuo*, a porous charcoal in which the pores were comparable in size with the size of simple hydrocarbon molecules (3). The pores were not cylindrical for although large bulky molecules such as neopentane were only adsorbed slowly, flat molecules such as benzene were adsorbed very rapidly as were thin molecules such as *n*-pentane. It seemed therefore as though there were slot-like constrictions in the charcoal, perhaps arising from the presence of graphitic platelets. The molecules which were adsorbed slowly diffused into the charcoal by an activated process, and the energy of activation, E, could be measured. It was suggested that E corresponded to the energy required to move a molecule from one position to another over the carbon surface, though for larger molecules, the energy required to squeeze through a small constriction may also play a part. Unfortunately the kinetic experiments, which were performed at temperatures ranging from about -50°C. upwards, were not always precisely reproducible even with consecutive runs on the same piece of charcoal. After each run it was necessary to heat the charcoal in order that the desorption should occur in a reasonable time, and it was thought that changes in the charcoal might take place during this heating, accounting for the irreproducibility. To offset these difficulties an attempt was made to block the interstices of the charcoal to a controlled extent, so that smaller and lighter molecules would be adsorbed slowly at low temperatures, desorption occurring at room temperature. The charcoal was successfully blocked, but the behavior was still not reproducible. At the same time a modified method of determining E during one adsorption run was devised.

EXPERIMENTAL

Materials

Charcoal

Saran charcoal was prepared in the manner previously described (3). Oxygen was used initially in an attempt to block the charcoal, which was

[1]*Manuscript received September 16, 1954.*
Contribution from the Department of Chemistry, Royal Military College of Canada, Kingston, Ontario. This paper was presented at the Symposium on Problems Relating to the Adsorption of Gases by Solids, held at Kingston, Ontario, September 10–11, 1954.
[2]*Present address: Bell Telephone Laboratories, Murray-Hill, New Jersey, U.S.A.*

hung from a quartz spiral and heated at 300°C. in an atmosphere of oxygen. There was, however, no change of weight and the sorption of benzene was still very rapid, so the method was abandoned.

Monomeric vinylidene chloride was adsorbed rapidly at room temperature. By pumping at 300°C. all the monomer was desorbed. But if the charcoal was heated at 300°C. in the presence of excess monomer vapor for an hour or so, some reaction took place, for pumping did not then remove all the monomer. Further heating and pumping caused further weight loss. One such sample with a 10% weight increase adsorbed benzene at a measurable rate (10% of the weight of the sample adsorbed in 25 min.) and gave a saturation value of 0.29 cc./gm. assuming the adsorbate to have the normal liquid density. Heating to redness essentially restored the charcoal to its original condition. Another piece, treated so that the weight increase was only 7%, adsorbed *n*-hexane more slowly (5% in one hour) than benzene (5% in 22 min.) at 20°C., and 2-methyl-pentane not at all.

Sample No. 3, on which most of the work was done, was heated at 300° in the presence of monomer for four and one-half hours and after pumping at 500°C. for 20 min. there was a weight increase of 16%. In this condition even nitrogen was not adsorbed at liquid air temperature and so the sample was pumped at red heat for five minutes, reducing the weight increment to 11%. Nitrogen was now slowly adsorbed at 90°K. (3% in one hour), but although desorption took place within a few minutes at room temperature the rate of adsorption steadily decreased from run to run. One per cent was adsorbed in 11 min. in the first run, but the third run required 19 min. to adsorb the same amount.

A further pumping at red heat for 10 min. reduced the weight increment to 9.0% and speeded the adsorption of nitrogen. Except for occasional heatings at 300°C., which increased the rate of adsorption without affecting the weight of the charcoal, the sample was examined in this condition.

Nitrogen — was commercially obtained 99.99% pure.
Methane — was commercially obtained 99.7% pure.
Argon — was commercially obtained 99.99% pure.
Benzene — was Analar grade dried with phosphorus pentoxide.

Apparatus and Procedure

The techniques used were similar to those described in a previous paper (3). About 0.07 gm. of charcoal was suspended from a quartz spiral, and the adsorption was followed by measuring the increase in length of the spiral. The extension of the spiral was 15 cm. for the original 0.07 gm. of charcoal. Pressures were measured with a mercury manometer. For pressures above one atmosphere a large manometer was used and taps were held in with special clamps. As the quantity of gas adsorbed during a run was small compared with the amount in the apparatus, the pressure remained virtually constant.

Temperatures were measured with a platinum resistance thermometer calibrated at the National Bureau of Standards. Commercial oxygen and nitrogen were liquefied, and when the liquefied gases were mechanically stirred in a Dewar Flask, they were found to remain at a constant temperature, to

within $\pm 0.01°$, over the period necessary to measure the rate of adsorption (about one hour). For temperatures slightly above the boiling point of liquid oxygen a Dewar Flask of Freon 12 was manually thermostatted by dropping liquid air into a copper tube immersed in the stirred Freon. Solid carbon dioxide and a bath of acetone cooled by occasionally adding solid carbon dioxide was also used as a thermostat. With the manually controlled thermostats the temperature control was only good to $\pm 0.1°$ but was adequate for our purpose.

The rate of adsorption increased rapidly with temperature and as before it was concluded that an activated diffusion process was the rate controlling factor. The activation energy, E, could be obtained by plotting the logarithms of the slopes of the initial straight part of the plot of amount adsorbed versus the square root of the time against the reciprocal of the absolute temperature. However, since the desorption process which was carried out at room temperature seemed to cause some change in the charcoal it was thought desirable to obtain the E value by changing the temperature during a run. This method of determining E was developed and tested for validity using neopentane on ordinary Saran charcoal as is described below.

The Determination of E by Changing the Temperature During One Run

For the initial stages of adsorption, that is before an appreciable quantity of the diffusing material has arrived at the center of the adsorbate, it can be shown that,

$$Q = kC_0 D^{\frac{1}{2}} t^{\frac{1}{2}} \qquad [1]$$

where Q is the total quantity of material adsorbed, k is a constant, C_0 is the surface concentration, D is the diffusion constant, and t is the time of adsorption (1, 2).

Consider now two runs performed at temperatures T_A and T_B. In Fig. 1 we see using equation [1],

$$Q_y = kC_{0_A} D_A^{\frac{1}{2}} t_{A_1}^{\frac{1}{2}} = kC_{0_B} D_B^{\frac{1}{2}} t_{B_1}^{\frac{1}{2}}$$

or

$$Q_y^2 = k^2 C_{0_A}^2 D_A t_{A_1} = k^2 C_{0_B}^2 D_B t_{B_1}.$$

Similarly

$$Q_x^2 = k^2 C_{0_A}^2 D_A t_{A_2} = k^2 C_{0_B} D_B t_{B_2}.$$

We thus have two values for $Q_x^2 - Q_y^2$ at temperatures T_A and T_B and we may equate these:

$$k^2 C_{0_A} D_A (t_{A_2} - t_{A_1}) = k^2 C_{0_B} D_B (t_{B_2} - t_{B_1})$$

or if

$$C_{0_A} = C_{0_B}$$

$$\frac{D_A}{D_B} = \frac{t_{B_2} - t_{B_1}}{t_{A_2} - t_{A_1}} = \frac{1/\tau_A}{1/\tau_B}, \qquad [2]$$

where τ_A and τ_B are the times required to adsorb between the limits Q_x and Q_y at the temperatures T_A and T_B respectively.

Suppose now that we begin the adsorption at T_B until Q is reached (Fig. 1), and at Q abruptly change the temperature to T_A. We may then observe the

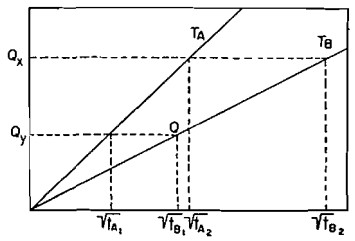

FIG. 1.

time τ_A required for adsorption from Q_y to Q_x at T_A, and we may safely predict the time τ_B by extrapolating the initial straight line plot at temperature T_B.

The energy of activation for the diffusion process may now be obtained from:

$$\log_{10}\frac{\tau_A}{\tau_B} = \frac{E}{2.3R}\left(\frac{1}{T_A}-\frac{1}{T_B}\right).$$

It is apparent that so long as we remain in the region for which equation [1] is valid, several temperature changes may be made and the same analysis applied.

It was observed that for neopentane the rate of adsorption changed 4% on changing the relative pressure at constant temperature from 0.1 to 0.2. When the relative pressure was increased from 0.2 to 0.9 the rate increased by only 2%. We therefore conclude that above a relative pressure of about 0.2 when adsorbing hydrocarbons the surface approaches saturation and C_0 remains almost constant. With neopentane our measurements were made with a relative pressure above 0.2. With nitrogen the saturation concentration is not closely approached until higher relative pressures are reached. This is discussed further below.

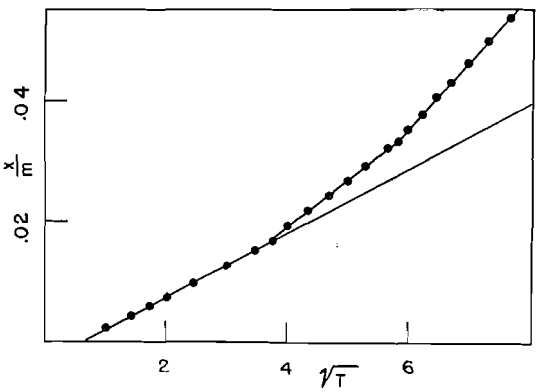

FIG. 2. The rate of adsorption of neopentane. The temperature was changed twice during the run.

This method was tested for the adsorption of neopentane on Saran charcoal. The results are plotted in Fig. 2. The first portion of the curve was obtained at 0°C. and this straight line was extrapolated to higher values of x/m, the ratio of the weight of the adsorbent to adsorbate. After 12 min. the temperature was increased to 9.9°C. $\tau_0°$ and $\tau_{9.9}°$ were taken between the values of x/m of 0.025 and 0.035. A third portion of the curve was obtained by increasing the temperature to 19.9°C. after 32 min. $\tau_0°$ and $\tau_{19.9}°$ were now obtained between $x/m = 0.045$ and $x/m = 0.055$. The E calculated from the first and second parts of the curve was 7700 cal./mole, and that calculated from the first and third was 7600 cal./mole. In most such cases the E values agreed to within 5%. For satisfactory results it was necessary to have fairly slow adsorption so that the x/m values used were less than 0.3 of the saturation value. Best results were obtained if the temperature changes did not exceed 10°C.

RESULTS

We have already indicated that by suitable treatment with monomeric vinylidene chloride the charcoal could be blocked to different degrees and that the adsorption in these different states was controlled by the shape and size of the adsorbed molecules.

Sample No. 3, after treatment with the monomer as described above, was saturated with nitrogen at 90.4°K. and gave 0.29 cc./gm. as the available pore volume assuming the nitrogen to have the normal liquid density. In the untreated charcoal the corresponding figure is 0.46 cc./gm. Since during its treatment with monomer the original charcoal had increased its weight by about 0.1 gm./gm., and as one may assume that the density of the material remaining in the charcoal is of the order of unity, we conclude that the adsorbed monomer does not block off large volumes but rather only blocks off that volume which it occupies, this being consistent with the picture of slot-like pores offered in the previous paper (3). This is supported by the behavior of benzene on another piece of charcoal which had also adsorbed about 0.1 gm./gm. The volume available to benzene was 0.28 cc./gm., whereas the original charcoal had 0.40 cc./gm. available to benzene.

The experiments described below were carried out on sample No. 3 which adsorbed nitrogen slowly and benzene and larger molecules not at all.

Nitrogen

For nitrogen the variation of C_0 with relative pressure was investigated in some detail. The pressure was changed in the middle of the run but the temperature was not altered; the time of passage between two values of x/m was determined in a manner similar to that described above. From the relation $\tau_A/\tau_B = C_{0_A}^2 D_A / C_{0_B}^2 D_B$ assuming that the coefficient of diffusion is independent of pressure, we can arrive at a relative value of C_0 at the two pressures. A typical run is shown in Fig. 3. By several such experiments at a series of overlapping pressures it is possible to build up a relative isotherm. Such an isotherm is shown in Fig. 4 which was calculated from data obtained at −183°C. except for one run at −196°C. where the relative pressure was changed from 0.29 to 0.99. It is seen to be of the Langmuir type without a large uprising as

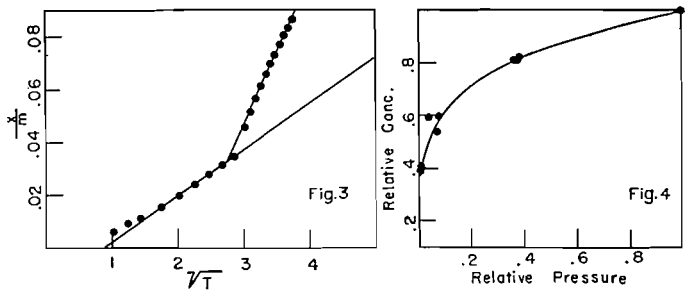

FIG. 3. The rate of adsorption of nitrogen. The pressure was changed during the run.
FIG. 4. The relative isotherm for nitrogen on the outer surfaces.

$p/p°$ approaches unity. At $p/p° = 0.2$ the surface was found to be only 75% saturated so it seemed best for the determination of E to make runs at different temperatures with $p/p°$ close to unity where the surface concentration should remain reasonably constant if the differences in temperature were not too great. The results of several such runs together with other runs in which $p/p°$ did not equal unity are presented in Table I. A typical experimental run is shown in Fig. 5.

TABLE I

ADSORPTION OF NITROGEN, ARGON, AND METHANE ON SAMPLE 3

Run No.	Temperatures, °K. T_1	T_2	Relative pressure at T_1	at T_2	E, cal./mole	Slope of x/m against $t^{\frac{1}{2}}$ at T_1
*Heat of liquefaction of nitrogen at its b.p. = 1330 cal./mole**						
5	76.98	87.43	0.035	0.038	1340	.00800
12	77.03	90.09	0.043	0.031	1410	.0053
15	77.05	90.30	0.035	0.032	1630	.0101
18	76.96	90.31	0.106	0.030	1610	.00724
22	77.19	90.42	0.282	0.278	2050	.00645
23	77.02	90.13	0.281	0.287	2060	.00890
24	77.06	90.18	0.289	0.083	1460	.00550
25	76.89	90.09	1.00	0.997	2920	.00755
26	76.89	90.05	1.00	0.997	1980	.00855
27	76.97	90.12	1.00	1.00	1910	.00639
Heat of liquefaction of argon at its b.p. = 1500 cal./mole						
33	76.87	90.09	0.96	0.97	2050	.00967
38	76.91	90.22	0.96	0.97	3160	.00184
Heat of liquefaction of methane at its b.p. = 2210 cal./mole						
34	194.75	215.17	16.2 cm.	74.5 cm.	7160	.00343
35	194.71	215.27	44.0 cm.	74.0 cm.	2880	.00619
37	116.20	129.20	$p/p° = .90$	$p/p° = .89$	4350	.0014

**Heat of adsorption on Saran charcoal at saturation pressure = 3200 cal./mole (3).*

Argon

Argon at liquid nitrogen and oxygen temperatures was adsorbed at a rate comparable with the rate at which nitrogen was adsorbed. In Table I are given

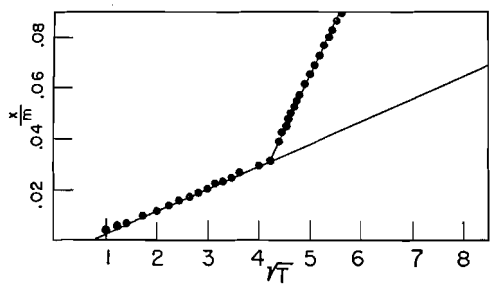

FIG. 5. The rate of adsorption of nitrogen. The temperature was changed during the run while the surface concentration remained constant.

the results of two runs on Sample 3. Between these runs methane had been adsorbed and the charcoal had been heated to 400°C. which had caused a loss in weight of 0.3%. A saturation value at 90.09°K. gave a pore volume of 0.26 cc./gm., assuming the normal liquid density for the adsorbed argon. This is in fair agreement with the nitrogen value.

Methane

Methane was adsorbed slowly. At first adsorption was studied above the critical temperature of methane (190.7°K.), then near its boiling point (111.7°K.). The results are given in Table I.

DISCUSSION

When vinylidene chloride is adsorbed on Saran charcoal it may be removed readily by pumping at room temperature and therefore does not polymerize. However, if the system is heated to 300°C. it cannot be removed. The adsorbed vinylidene chloride therefore polymerizes inside the capillaries of the charcoal. This polymer on further heating undoubtedly loses hydrogen chloride and would no doubt all eventually decompose leaving only carbon.

The additional carbon–polymer complex does not block off large voids in the original carbon because as was shown above the total pore volume was reduced by an amount roughly equivalent to the space required for the weight increase observed.

The carbon–polymer complex probably blocks off many of the entrances into the porous structure of the original carbon. At the same time the many entrances which must remain unblocked are reduced in size. This is clear from the fact that on the original charcoal both nitrogen and benzene were rapidly taken up while on the modified sample nitrogen was taken up slowly but benzene not at all. We therefore conclude the modification carried out as described above alters the slot-like constrictions which existed in the original sample, probably closing some of them completely while reducing the size of the others so that a benzene molecule cannot enter while a methane molecule can.

Unfortunately, a carbon with pores so small that small molecules could be adsorbed slowly at low temperatures and desorbed at room temperature did not overcome the difficulty of subtle changes occurring which altered the rates of adsorption from run to run. This phenomenon was attributed, in the case of

ordinary Saran charcoal, to the heating necessary for desorption but it appears now that the act of adsorption and desorption without heating above room temperature is sufficient to bring about small structural changes in the adsorbent.

However, despite this difficulty, methods were devised as described above, which make it possible to estimate the value of the energy of activation. The E values for nitrogen cannot be said to be entirely consistent though except for run 25 it appears that when the relative pressure is high, so that the changes in surface concentration brought about by the temperature changes are not great, E has a value of approximately 2000 cal./mole. For those runs in which the relative pressure has been kept nearly constant, at the two temperatures, at a comparatively low value, the E values are below 2000 cal. Presumably this is because the increase in temperature at the low coverage produces a large decrease in surface concentration which is not fully compensated for by the increase in pressure. This is to be expected if the heat of adsorption at low surface coverage is greater than the heat of vaporization of the liquid.

In considering the data on argon it must be noted that between runs 33 and 38 methane had been adsorbed and the charcoal had been heated to 400° which had caused a 0.3% loss of weight. This treatment seems to have substantially altered the adsorption kinetics. E has increased and the rate decreased, however, if E alone had changed, the slope of the x/m vs. $\sqrt{t}$ plot should have decreased by a factor of 1300 where in fact it has only decreased by a factor of 5.3. It seems that although in run 38 the diffusion process requires a higher activation energy the steric limitations have become much less stringent.

Considering Table I, the data on methane, the first two runs show that at low coverage the surface concentration is very sensitive to temperature changes, which is to be expected since at low coverage the heat of adsorption will be high. Thus the E values for these runs are of little significance, but for run 37, in which the pressures were kept near the saturation pressure, the E value should be more meaningful.

REFERENCES

1. BARRER, R. M. Diffusion in and through solids. Cambridge University Press, London. 1951.
2. BARRER, R. M. and IBBITSON, D. A. Trans. Faraday Soc. 40: 206. 1944.
3. DACEY, J. R. and THOMAS, D. G. Trans. Faraday Soc. 50: 740. 1954.

DÉDOUBLEMENT DES α- ET β-HYDROXYLAUDANOSINES[1]

PAR JEAN-LOUIS FERRON ET PHILIBERT L'ECUYER

SOMMAIRE

Les hydroxylaudanosines, α- et β-, ont été dédoublées en leurs énantiomorphes et les constantes physiques de ces derniers déterminées. Dans des conditions identiques le papavérinol ne s'est pas dédoublé en ses antipodes optiques; au contraire, il a donné de la papavéraldine lors des essais de dédoublement avec les acides *d*-tartrique, *l*-malique, et *d*-camphresulfonique.

INTRODUCTION

Le papavérinol (II) et les hydroxylaudanosines (III) sont obtenus, le premier par l'oxydation de la papavérine (I) et les dernières par la réduction

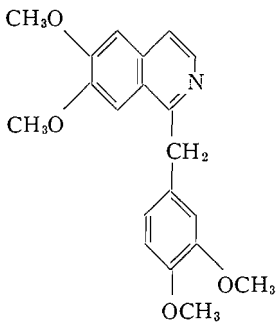

(I)

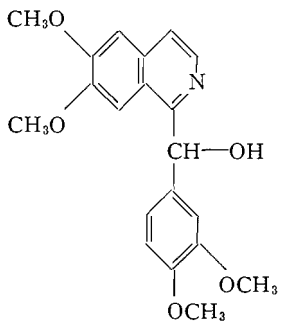

(II)

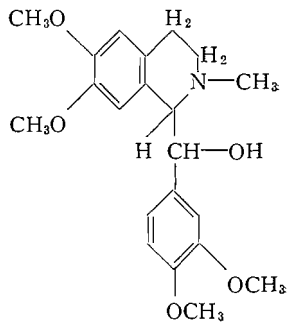

(III)

du méthochlorure de papavérinol (4). Ils possèdent respectivement un et deux carbones asymétriques laissant ainsi prévoir l'existence de deux et de quatre isomères optiques. Les quatres énantiomorphes des hydroxylaudanosines réunis deux à deux donnent deux formes racémiques connues sous le nom d'α- et de β-hydroxylaudanosines. D'autre part le papavérinol se présente également à l'état racémique. Le but du présent travail était de dédoubler ces diverses formes racémiques.

Parmi les multiples procédés utilisés pour le dédoublement des substances racémiques nous avons choisi la méthode de Ingersoll (2) qui se prête le mieux au dédoublement de l'une ou l'autre des trois catégories de formes racémiques possibles. Par cette méthode nous avons dédoublé l'α- et la β-hydroxylaudanosine en utilisant les acides *d*- et *dl*-tartriques comme agents de dédoublement. Ce même procédé appliqué au papavérinol avec les acides *d*-tartrique, *l*-malique, et *d*-camphresulfonique n'a permis l'isolement d'aucun sel. Le dédoublement ne s'est pas effectué. Une base de p.f. 210°C. a cependant été obtenue lors des essais de dédoublement avec les deux premiers acides et c'est la même qui précipite dans les deux cas; car il n'y a aucun abaissement du point de fusion si on mélange les deux échantillons en proportions égales. Cette substance possède une fonction cétonique comme le montre la formation d'une

[1]*Manuscrit reçu le 29 septembre, 1954.*
Contribution du Département de Chimie de l'Université Laval, Québec, Qué.

2,4-dinitrophénylhydrazone. Elle a été définitivement identifiée comme étant la papavéraldine. Comme le point de fusion du méthiodure du composé isolé (148–150°C.) différait considérablement de celui qui est donné par Menon (5), nous avons synthétisé la papavéraldine selon la méthode de Taylor (6) et préparé son méthiodure. Son p.f. est bien 148–150°C. et il ne varie pas lorsqu'on mélange le méthiodure avec celui qu'on obtient à partir de la base isolée au cours des essais de dédoublement du papavérinol.

Cette transformation du papavérinol en papavéraldine est sans doute due à une oxydation atmosphérique du genre de celle que subit la dihydroyobyrine pour donner la yobyrone (3).

Les pouvoirs rotatoires ont été déterminés sur des solutions à 1% pour le *d*-tartrate de la *d*-α-hydroxylaudanosine, le *l*-tartrate de la *l*-α-hydroxylaudanosine, le *d*-tartrate de la *d*-β-hydroxylaudanosine, et le *l*-tartrate de la *l*-β-hydroxylaudanosine ainsi que pour les bases optiquement actives obtenues par la neutralisation de chacun de ces sels et les pouvoirs rotatoires spécifiques ont été calculés.

PARTIE EXPÉRIMENTALE

Dédoublement de l'α-hydroxylaudanosine

De l'α-hydroxylaudanosine (4.00 g., 0.011 mole) et de l'acide *d*-tartrique (1.605 g., 0.011 mole) sont dissous dans l'alcool éthylique absolu (40 ml.) à l'ébullition. Par refroidissement à la température ambiante on obtient une gomme dont la cristallisation s'amorce lentement et se continue pendant une semaine. Le *d*-tartrate bien cristallisé est alors filtré, lavé avec quelques millilitres d'alcool absolu, et le filtrat (*a*) mis de côté pour l'isolement de l'autre isomère. Le sel (4.965 g.) est cristallisé une première fois dans l'alcool à 85% (50 ml.) contenant un peu d'acide *d*-tartrique pour empêcher la dissociation du sel et laissé pendant une semaine à la température ordinaire en contact avec les eaux-mères. Les cristaux sont alors filtrés et le filtrat (*b*) est ajouté au filtrat (*a*). Le *d*-tartrate de la *d*-α-hydroxylaudanosine (2.145 g.) est lavé avec quelques millilitres d'alcool éthylique à 85% et recristallisé dans le même solvant (30 ml.). Cette deuxième cristallisation fournit le sel pur de p.f. 208–209°C. Rendement: 60% (1.68 g.). Calculé pour $C_{21}H_{27}O_5N.C_4H_6O_6$: C, 57.4%; H, 6.4%. Trouvé: C, 57.5%; H, 6.3%. $[\alpha]_D = +76.2°$ (*c*, 1.004 dans l'eau). Le sel est ensuite dissous dans l'eau (35 ml.) et la solution rendue alcaline par addition d'un excès de soude 3*N*. La base précipite et fournit après une cristallisation dans l'alcool absolu (6–7 ml.) la *d*-α-hydroxylaudanosine pure de p.f. 151°C. Rendement: 60% (1.19 g.). $[\alpha]_D = +84.2°$ (*c*, 1.057 dans le chloroforme).

Les filtrats réunis (*a* et *b*) sont évaporés à sec sur bain-marie, le résidu est dissous dans l'eau (30–35 ml.), et la solution alcalisée par un excès de soude 3*N*. La base précipitée est extraite au chloroforme. La solution chloroformique est séchée, filtrée, puis évaporée à sec sur bain-marie. Le résidu (2.84 g., 0.007 mole) est traité à l'ébullition par de l'acide *dl*-tartrique (2.28 g., 0.014 mole) dans l'alcool absolu (20 ml.). Par refroidissement, un sel cristallise. On le laisse séjourner une semaine à la température ambiante. Le *l*-tartrate (3.32 g.) est

ensuite filtré, lavé avec quelques millilitres d'alcool à 85% (35 ml.) contenant un peu d'acide *dl*-tartrique. Recristallisé dans l'alcool à 85%, le *l*-tartrate de la *l*-α-hydroxylaudanosine est obtenu à l'état pur, p.f. 207°C. Rendement: 52% (1.49 g.). $[\alpha]_D = -75.9°$ (*c*, 1.001 dans l'eau). Le sel est ensuite dissous dans l'eau (35 ml.) et la solution neutralisée à la soude *N*. La base qui précipite est filtrée et lavée à l'eau. Une cristallisation dans l'alcool (4–5 ml.) donne la *l*-α-hydroxylaudanosine pure de p.f. 151°C. Rendement: 47% (0.95 g.). Calculé pour $C_{21}H_{27}O_5N$: C, 67.5%; H, 7.3%. Trouvé: C, 67.6%; H, 7.1%. $[\alpha]_D = -86.4°$ (*c*, 1.209 dans le chloroforme).

Un mélange à parties égales des deux inverses optiques, la *d*- et la *l*-α-hydroxylaudanosine, a un p.f. de 138°C. qui est le p.f. de la base racémique, l'α-hydroxylaudanosine.

Dédoublement de la β-hydroxylaudanosine

On procède avec les mêmes quantités de substances exactement comme précédemment lors du dédoublement de l'α-hydroxylaudanosine. Le *d*-tartrate de la *d*-β-hydroxylaudanosine (3.32 g.) précipite d'abord. Une première cristallisation dans l'alcool absolu (35 ml.) et une deuxième dans l'alcool éthylique à 95% (30 ml.) fournit le sel pur de p.f. 190–191°C. Rendement: 61.5% (1.76 g.). $[\alpha]_D = -19.5°$ (*c*, 1.000 dans l'eau).

La base obtenue par neutralisation du sel est cristallisée une fois dans l'alcool à 50% (10 ml.) et donne la *d*-β-hydroxylaudanosine pure de p.f. 104°C. Rendement: 47% (0.94 g.). Calculé pour $C_{21}H_{27}O_5N$: C, 67.5%; H, 7.3%. Trouvé: C, 67.2%; H, 7.3%. $[\alpha]_D = +11.2°$ (*c*, 1.030 dans le chloroforme).

Le *l*-tartrate est obtenu par l'action de l'acide *dl*-tartrique (1.74 g., 0.012 mole) sur la base *l*-impure (2.16 g., 0.006 mole) dans l'alcool absolu (15 ml.). Le sel qui se dépose par refroidissement est laissé au contact des eaux-mères pendant une semaine à la température ambiante. Le sel (1.82 g.) est ensuite filtré et lavé avec quelques millilitres d'alcool absolu. Après une cristallisation dans l'alcool à 90% (25 ml.) il donne le *l*-tartrate de la *l*-β-hydroxylaudanosine pur de p.f. 189–190°C. Rendement: 50.5% (1.44 g.). Calculé pour $C_{21}H_{27}O_5N.C_4H_6O_6$: C, 57.4%; H, 6.4%. Trouvé: C, 57.1%; H, 6.4%. $[\alpha]_D = +20.0°$ (*c*, 1.000 dans l'eau).

L'alcalisation de la solution aqueuse du sel par la soude 3*N* donne la *l*-β-hydroxylaudanosine. Celle-ci après une cristallisation dans l'alcool à 50% (8–10 ml.) est pure et a un p.f. de 103°C. Rendement: 34% (0.68 g.). $[\alpha]_D = -12.3°$ (*c*, 1.056 dans le chloroforme).

La détermination du point de fusion d'un mélange à parties égales des deux antipodes, la *d*- et la *l*-β-hydroxylaudanosine, donne 109°C. qui est le p.f. de la β-hydroxylaudanosine racémique.

Essais de dédoublement du papavérinol

Du papavérinol (1.121 g., 0.003 mole) et de l'acide *d*-tartrique (1.00 g., 0.006 mole) sont dissous dans l'alcool éthylique absolu (10 ml.) à l'ébullition et laissés à la température ambiante durant quatre mois. Le produit cristallin qui s'est alors déposé est filtré, lavé avec quelques millilitres d'alcool absolu, et séché. Cette substance (0.46 g.) insoluble dans l'eau et soluble dans le chloro-

forme donne par cristallisation dans le dioxane (5 ml.) un produit (0.28 g.) de p.f. 210°C. Un autre essai à partir de 2.0 g. de papavérinol et de 0.946 g. d'acide *d*-tartrique a donné après 22 jours 0.463 g. de produit brut. Si cependant l'acide *l*-malique (0.38 g. pour 1.0 g. de papavérinol) est employé, la quantité du produit de p.f. 209°C. obtenu n'est que de 0.10 g. La même substance a été isolée au cours de ces trois essais. C'est ce qu'ont montré les déterminations de points de fusion mixtes. Cette substance basique forme une 2,4-dinitrophénylhydrazone de p.f. 250–251°C. Calculé pour $C_{26}H_{25}O_8N_5$: C, 58.3%; H, 4.7%. Trouvé: C, 58.3%; H, 4.4%. C'est donc une cétone. Un méthiodure de p.f. 148–150°C. (déc.) a également été préparé. Il cristallise dans l'alcool éthylique. Calculé pour $C_{21}H_{25}O_5NI$: C, 50.7%; H, 4.8%. Trouvé: C, 50.1%; H, 4.6%.

Comme le point de fusion (148–150°C.) du méthiodure ne correspondait pas à celui (133–135°C.) qui est donné par Menon (5), de la papavéraldine a été préparée par la méthode de Taylor (6). Cette papavéraldine synthétique a également un p.f. de 210°C. seule ou mélangée au composé isolé. Le point de fusion de son méthiodure est aussi le même que celui du méthiodure de la base isolée, soit 148–150° (déc.), et il n'est pas affecté par le mélange des deux sels. Calculé pour la papavéraldine $C_{20}H_{19}O_5N$: C, 68.0%; H, 5.4%. Trouvé pour le composé isolé: C, 67.7%; H, 5.9%. Il s'ensuit donc que la base isolée est la papavéraldine.

REMERCIEMENTS

Les auteurs remercient le Conseil National des Recherches et l'Office des Recherches Scientifiques de la Province de Québec pour avoir accordé à l'un d'eux (J.-L. F.) un octroi et une bourse de recherches.

BIBLIOGRAPHIE

1. GADAMER, J. and SHULEMANN. Arch. Pharm. 253: 284. 1915.
2. INGERSOLL, A. W. J. Am. Chem. Soc. 64: 611. 1942.
3. JULIAN, P. L., KARPEL, W. J., MAGNANI, A. and MEYER, E. W. J. Am. Chem. Soc. 70: 180. 1948.
4. KING, F. E., L'ECUYER, P., and PYMAN, F. L. J. Chem. Soc. 731. 1936.
5. MENON, K. N. Proc. Indian Acad. Sci. A, 19: 21. 1944.
6. TAYLOR, E. P. J. Pharm. Pharmacol. 2: 325. 1950.

KINETICS OF THE CUPRIC ACETATE CATALYZED HYDROGENATION OF DICHROMATE IN AQUEOUS SOLUTION[1]

By E. Peters and J. Halpern

ABSTRACT

In aqueous solution, cupric acetate was found to act as a homogeneous catalyst for the reduction of dichromate by hydrogen, i.e.

$$Cr_2O_7^{--} + 3\,H_2 + 8\,H^+ \xrightarrow{[Cu(OAc)_2]} 2\,Cr^{+++} + 7\,H_2O.$$

The paper describes a kinetic study of this reaction. Rates were determined at temperatures between 80° and 140°C. and hydrogen partial pressures up to 27 atmospheres. The rate is independent of the dichromate concentration but varies directly with the partial pressure of hydrogen and is nearly proportional to the concentration of cupric acetate. The activation energy is 24,600 calories per mole. Cupric acetate, apparently acting as a true catalyst, activates the hydrogen through formation of a complex with it. An extension of the mechanism proposed earlier for the reaction of cupric acetate itself with hydrogen also accounts for the kinetics of the dichromate reaction.

INTRODUCTION

Dakers and Halpern (3) have recently shown that cupric acetate reacts homogeneously in aqueous solution with molecular hydrogen as follows:

$$2Cu(OAc)_2 + H_2 + H_2O \rightarrow Cu_2O + 4HOAc. \qquad [1]$$

The kinetics of this reaction are described in an earlier paper (3). The rate can be expressed by the equations:

$$-d[Cu(OAc)_2]/dt = k_2'[Cu(OAc)_2]\,P_{H_2} = k_2[Cu(OAc)_2]\,[H_2] \qquad [2]$$

where P_{H_2} is the partial pressure of hydrogen above the solution.

k_2', apparently independent of the hydrogen pressure and solution composition, was given by:

$$k_2' = 6.15 \times 10^{10} \exp[-24{,}200/RT]\ \text{atm.}^{-1}\ \text{min}^{-1}. \qquad [3]$$

To account for this kinetic behavior the reaction was postulated (3) to proceed through the following sequence of steps, the first step being rate determining:

$$Cu(OAc)_2 + H_2 \xrightarrow[\text{slow}]{k} Cu(OAc)_2 \cdot H_2 \qquad [4]$$

followed by:

$$Cu(OAc)_2 \cdot H_2 + Cu(OAc)_2 + H_2O \xrightarrow[\text{fast}]{} Cu_2O + 4HOAc. \qquad [5]$$

Cupric acetate thus appears to have the property of being able to activate molecular hydrogen homogeneously, through the formation of a complex with

[1]*Manuscript received September 17, 1954.*
Contribution from the Department of Mining and Metallurgy, University of British Columbia, Vancouver, B.C. This work was supported by a grant from the National Research Council of Canada and a Fellowship award to one of the authors (E. P.) from the Consolidated Mining and Smelting Company of Canada Ltd.

it, as represented in equation [4]. Only two other instances of comparable homogeneous activation of hydrogen, one involving cuprous acetate (1, 2, 8) and the other dicobalt octacarbonyl (5, 9) as the activating species, have previously been reported. This appears to be the first time that this type of activation has been observed in aqueous solution. The detailed mechanism of the process and its relation to the more common phenomenon of heterogeneous catalytic activation of hydrogen have not been resolved.

The reaction sequence represented in equations [4] and [5] above implies that cupric acetate should also be capable of functioning as a homogeneous catalyst for the reactions with hydrogen of other compounds which are thermodynamically reduced more readily than cupric acetate itself, but which do not react with hydrogen in the absence of a catalyst for kinetic reasons.

In accord with this it was found that the homogeneous reduction of dichromate salts by molecular hydrogen in aqueous solution, represented by the equation:

$$Cr_2O_7^{--} + 3H_2 + 8H^+ \rightarrow 2Cr^{+++} + 7H_2O, \qquad [6]$$

would proceed only in the presence of dissolved cupric acetate, the latter apparently acting as a true catalyst. The present paper describes a kinetic study of this reaction, undertaken with a view to obtaining further information about the mechanism of the hydrogen activation process.

EXPERIMENTAL

Sodium dichromate, cupric acetate, sodium acetate, and acetic acid, all of Reagent Grade, were supplied by Nichols Chemical Company. The solutions were prepared by dissolving weighed quantities of these chemicals in distilled water. Commercial hydrogen gas, supplied in cylinders by Canadian Liquid Air Company, was used without further purification.

The experiments were conducted in the stainless steel autoclave described in an earlier paper (3). Three liters of solution of desired composition were placed in the autoclave which was then sealed, flushed with nitrogen, and heated to the reaction temperature, maintained to within ±0.3°C. Hydrogen was introduced and maintained at a desired partial pressure with a standard gas pressure regulator. The solution was stirred with an impeller of 2.5 in. diameter which rotated at 900 r.p.m. Samples of the solution were withdrawn periodically for analysis. The concentration of unreacted dichromate was measured with a Beckman DU Spectrophotometer using the 3500 Å absorption peak. Cupric acetate concentrations were determined electrolytically.

RESULTS

In the absence of cupric acetate, no reaction between dichromate and hydrogen could be detected up to temperatures of 160°C. and hydrogen partial pressures of 30 atm. When cupric acetate was present, the reduction of dichromate proceeded measurably at temperatures as low as 80°C. Spectrophotometric identification of the product, chromic acetate, confirmed that the stoichiometry of the reaction is represented by equation [6].

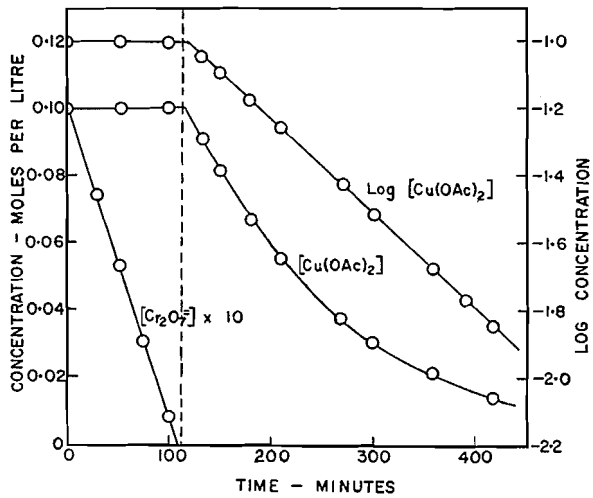

FIG. 1. Typical rate curves for the reactions of dichromate and cupric acetate with hydrogen. Temperature, 100°C. H_2 partial pressure, 13.6 atm.

The course of a typical experiment is depicted in Fig. 1. At constant temperature and hydrogen partial pressure, the concentration of $Cr_2O_7^{--}$ always

TABLE I

RATE OF REACTION BETWEEN HYDROGEN AND DICHROMATE IN SOLUTIONS OF DIFFERENT COMPOSITION

$[Cu(OAc)_2]$ = 0.1 M./liter, Temp. = 100°C., H_2 partial pressure = 13.6 atm.

Expt. No.	Solution composition			Rate of $Cr_2O_7^{--}$ reduction		
	$[Na_2Cr_2O_7]$, M./liter	[NaOAc], M./liter	[HOAc], M./liter	$k_0 \times 10^4$, mole liter^{-1} min.$^{-1}$	$k_3 \times 10^4$, min.$^{-1}$	$k_4' \times 10^4$, atm.$^{-1}$min.$^{-1}$
A–4	0.010	0.25	0.50	0.964	9.64	0.709
B–4	0.010	0.25	0.50	1.008	10.08	0.741
C–3	0.010	0.25	0.50	0.983	9.83	0.722
D–3	0.010	0.25	0.50	0.952	9.52	0.700
E–3	0.010	0.25	0.50	0.956	9.56	0.703
F–2	0.010	0.25	0.50	0.941	9.41	0.692
G–3	0.010	0.25	0.50	0.931	9.31	0.684
H–1*	0.010	0.25	0.50	0.932	9.32	0.685
C–4	0.005	0.25	0.50	1.026	10.26	0.754
C–3	0.010	0.25	0.50	0.983	9.83	0.722
C–2	0.015	0.25	0.50	0.923	9.23	0.679
C–5	0.020	0.25	0.50	0.952	9.52	0.700
F–5	0.010	0.00	0.50	0.923	9.23	0.680
F–4	0.010	0.05	0.50	0.941	9.41	0.692
F–3	0.010	0.15	0.50	0.947	9.47	0.698
F–2	0.010	0.25	0.50	0.941	9.41	0.692
F–1	0.010	0.50	0.50	0.957	9.57	0.704
G–2	0.010	0.25	0.50	0.931	9.31	0.684
G–3	0.010	0.25	0.75	0.950	9.50	0.698
G–4	0.010	0.25	1.00	0.925	9.25	0.680

**Stirring velocity reduced to 600 r.p.m. In all other experiments stirring velocity was 900 r.p.m.*

decreased linearly with time, corresponding to zero order kinetic behavior, i.e.

$$-d[Cr_2O_7^{--}]/dt = k_0. \quad [7]$$

Values of the zero order rate constant, k_0, determined from the slopes of the rate plots were reproducible to within $\pm 5\%$ (see Table I).

Further evidence for zero order kinetic behavior is provided by the results in Fig. 2 and Table I, which show k_0 to be independent of the initial $Cr_2O_7^{--}$ concentration. The fact that the rate was unchanged when the stirring velocity was varied from 600 to 900 r.p.m. indicates that the reaction was not limited by solution of hydrogen.

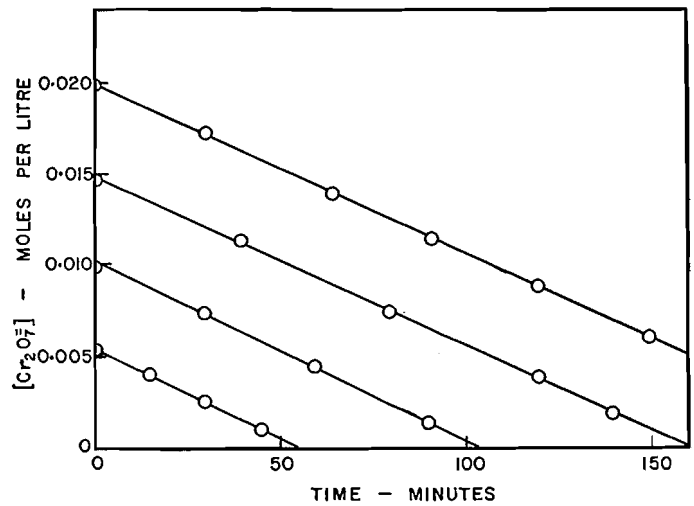

FIG. 2. Rate curves for the reduction of dichromate by hydrogen. $[Cu(OAc)_2]$, 0.10 M./liter. Temperature, 100°C. H_2 partial pressure, 13.6 atm.

Fig. 1 shows that the concentration of cupric acetate remained constant as long as dichromate was undergoing reaction. This was always found to be the case and is in accord with the view that cupric acetate is a true catalyst for the dichromate reaction. Only when the reduction of dichromate was complete, did the cupric acetate react with hydrogen to form cuprous oxide according to equation [1]. The first order kinetic behavior of this reaction, shown in Fig. 1, is in quantitative agreement with that reported earlier (3). Apparently the reduction of cupric acetate is not affected by the previous dichromate reaction or by the presence of small amounts of chromic salts in the solution.

The dependence of the rate of the dichromate reaction on the concentration of cupric acetate provides further support for the catalytic role of the latter. The results in Figs. 3 and 4 show that the rate increases in a nearly linear manner with increasing cupric acetate concentration, i.e.

$$k_0 = k_3 [Cu(OAc)_2]. \quad [8]$$

Actually the relation is seen to be not quite linear, k_3 showing a tendency to fall off slightly with increasing $[Cu(OAc)_2]$. Thus at 100°C. and 13.6 atm. of

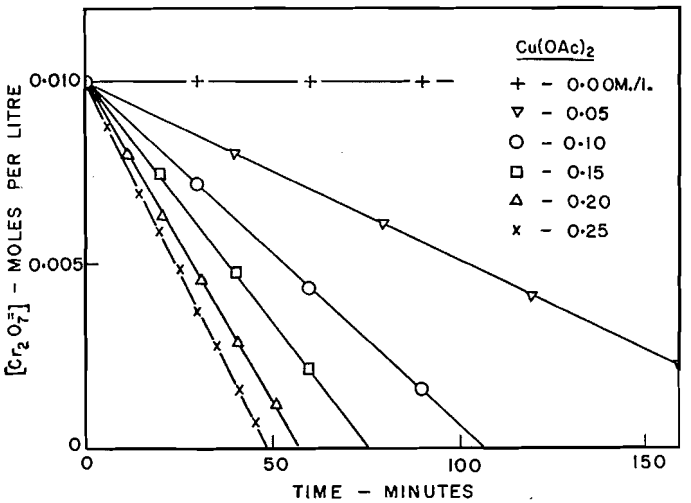

FIG. 3. Rate curves for the reduction of dichromate at different concentrations of cupric acetate. Temperature, 100°C. H_2 partial pressure, 13.6 atm.

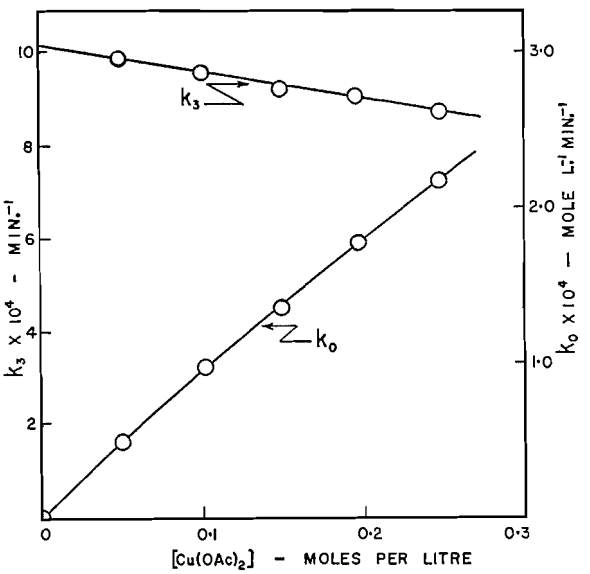

FIG. 4. Dependence of the rate of reaction of dichromate on the concentration of cupric acetate. Temperature, 100°C. H_2 partial pressure, 13.6 atm.

hydrogen, the value of k_3, extrapolated to zero [$Cu(OAc)_2$] (see Fig. 4), is given by:

$$k_3^0 = 0.00101 \text{ mole } Cr_2O_7^{=}/\text{mole } Cu(OAc)_2/\text{min.} \qquad [9]$$

At the highest cupric acetate concentration investigated, i.e. 0.25 M./liter, the value of k_3 was found to be 0.00087 or about 14% lower. The significance of this decrease will be discussed later.

The reduction of dichromate was studied at hydrogen partial pressures ranging from zero to 27.2 atm. The results, plotted in Fig. 5, show the rate to be directly proportional to the partial pressure of hydrogen throughout this

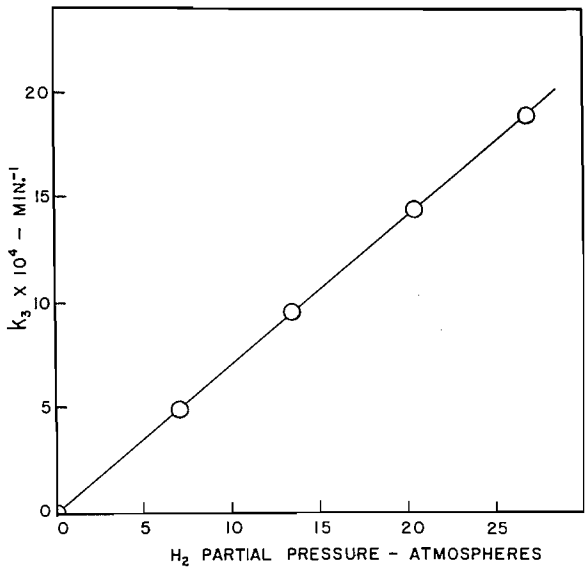

FIG. 5. Dependence of the rate on the hydrogen partial pressure. Temperature, 100°C.

range. Assuming that the solubility of hydrogen follows Henry's Law (3, 7), this relation also implies that the rate is proportional to the concentration of molecular hydrogen in solution.

The kinetics of the reaction are thus seen to conform to the bimolecular rate equation:

$$-d[Cr_2O_7^{--}]/dt = k_4'[Cu(OAc)_2]P_{H_2} = k_4[Cu(OAc)_2]\,[H_2]. \qquad [10]$$

The following relations are also seen to hold:

$$k_3 = k_4'\,P_{H_2} = k_4[H_2] \qquad [11]$$

and

$$k_4' = \alpha k_4 \qquad [12]$$

where α is Henry's constant denoting the solubility of hydrogen.

There is evident a formal similarity between equation [10] and equation [2], which expresses the rate of reaction of cupric acetate with hydrogen. Relations similar to equations [11] and [12] also apply in the case of the cupric acetate reaction (3).

The rate of the dichromate reaction was measured at temperatures ranging from 80° to 140°C. The results were found to give a good Arrhenius plot shown in Fig. 6. The activation energy, calculated from the slope of this plot, is 24,600±600 cal. per mole, in good agreement with the value of 24,200±800 cal. per mole reported earlier for the reaction of cupric acetate itself with hydrogen (3). It should be noted that in the series of experiments where the temperature was varied, the partial pressure of hydrogen, and not its con-

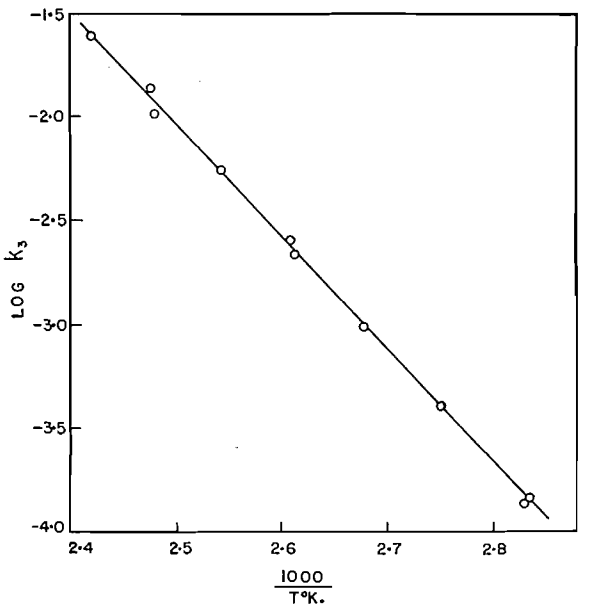

FIG. 6. Arrhenius plot for the cupric acetate catalyzed reaction of dichromate with hydrogen.

centration in solution, was held constant. The apparent activation should therefore be corrected for the change in solubility of hydrogen with temperature. This correction is probably small.

In most of these experiments the solutions contained, in addition to sodium dichromate and cupric acetate, 0.25 M./liter of sodium acetate and 0.5 M./liter of acetic acid. The pH was thus buffered at a value of about 4.5 and changed very little during the course of reaction. That these values are not critical is indicated by the results in Table I which show that wide variations in the acetate and acetic acid concentrations were substantially without effect on the rate.

DISCUSSION

The kinetic similarity of the dichromate and cupric acetate reactions supports the view that both have the same rate controlling step. In each case the pattern of kinetic behavior suggests that the rate is determined by a bimolecular process involving one molecule of cupric acetate and one molecule of hydrogen. The hydrogen must become activated in this step so that its subsequent reaction with either reducible substrate to give the observed reaction products is rapid.

A reaction mechanism incorporating such a rate controlling step has already been proposed for the reduction of cupric acetate (see equations [4] and [5]). An analogous mechanism can be written for the dichromate reaction, i.e.

$$3Cu(OAc)_2 + 3H_2 \xrightarrow[\text{slow}]{k} 3Cu(OAc)_2 \cdot H_2 \qquad [13]$$

followed by:

$$3Cu(OAc)_2 \cdot H_2 + Cr_2O_7^{--} + 8H^+ \xrightarrow[\text{fast}]{} 2Cr^{+++} + 7H_2O + 3Cu(OAc)_2. \quad [14]$$

The role of cupric acetate is seen to be that of a true catalyst, since it is regenerated as long as dichromate is undergoing reduction.

At 100°C., the rate constant for the cupric acetate reaction, k_2', was found to be 4.45×10^{-4} atm.$^{-1}$ min.$^{-1}$ (3). From equation [9], the value of the corresponding rate constant for the dichromate reaction, k_4', extrapolated to zero cupric acetate concentration, is seen to be 7.45×10^{-5} atm.$^{-1}$ min^{-1}. The ratio $k_2' : k_4'$ is thus found experimentally to be 5.95, in agreement with the theoretical value of 6.0, corresponding to the fact that the reduction of $Cr_2O_7^{--}$ involves six electrons as compared with one for $Cu(OAc)_2$.

Thus measurements of the dichromate reaction rate and of the cupric acetate reaction rate both yield the same value of k. It has previously been shown (3) that this value corresponds to a frequency factor of 4.8×10^{13} liter mole^{-1} min.$^{-1}$, or an equivalent activation entropy, $\Delta S_c^{\ddagger}$, of -6.5 e.u. These values are normal (3, 4, 6) for a simple bimolecular process such as that represented by equation [13].

The reaction mechanisms which have been proposed for both the dichromate and cupric acetate reactions thus appear to be in quantitative agreement with the kinetic results. In particular, this agreement may be taken as supporting the conclusion that cupric acetate rather than one of its reduction products (i.e. cuprous acetate or cuprous oxide) is the species responsible for activating molecular hydrogen. Other evidence for the same view has previously been presented (3). In the present case the evidence appears fairly conclusive, since no cupric acetate is reduced until all the dichromate has reacted. This is of special interest in view of Calvin's earlier work (1, 2), showing that cuprous acetate activates hydrogen homogeneously in quinoline solutions. It appears that the mechanism of activation in the two systems is not the same.

It is probable that the observed slight decrease in k_4' (and hence in the apparent value of the ratio $k_4' : k_2'$) with increasing cupric acetate concentration arises from a secondary effect of cupric acetate, the most likely one being a lowering of the solubility of hydrogen (i.e. of α). The mechanism which has been proposed above suggests that k_4 is independent of the concentration of hydrogen. At constant partial pressure, any change in α would therefore be reflected in k_4'. A lowering of the solubility of hydrogen in water is a well-known effect of many salts (7).

k_2', which is also proportional to α, should vary in a similar manner with the cupric acetate concentration. That the earlier work (3) did not reveal this variation is not surprising, since the values of k_2' were determined by measuring the rate of disappearance of cupric acetate, usually down to very low concentrations. The first order kinetics of this reaction would tend to mask a small change in the rate, apparent only in the first stages (i.e. when most of the cupric acetate was still unreacted). Recently more accurate determinations have been made of the initial rate of the cupric acetate reaction. The results

confirm that k_2' varies, in a similar manner to k_4', with the cupric acetate concentration, and thus that the ratio $k_2' : k_4'$ retains a constant value close to 6.

CONCLUSIONS

Further evidence has been provided that cupric acetate activates molecular hydrogen homogeneously in aqueous solution. One consequence of this is its ability to function as a true homogeneous catalyst for the hydrogenation of other compounds. An extension of the mechanism, proposed earlier (3) for the reaction of cupric acetate itself with hydrogen, also appears to explain the kinetics of the catalytic hydrogenation of dichromate.

REFERENCES

1. CALVIN, M. Trans. Faraday Soc. 34: 1181. 1938.
2. CALVIN, M. J. Am. Chem. Soc. 61: 2230. 1939.
3. DAKERS, R. G. and HALPERN, J. Can. J. Chem. 32: 969. 1954.
4. MOELWYN HUGHES, E. A. The kinetics of reactions in solution. 2nd ed. Oxford at the Clarendon Press. 1947. pp. 68–77.
5. ORCHIN, M. *In* Advances in catalysis. Vol. 5. Academic Press, Inc., New York. 1953. p. 385.
6. ROLLEFSON, G. K. J. Phys. Chem. 56: 976. 1952.
7. SEIDELL, A. Solubilities of inorganic and metal organic compounds. 3rd ed. Vol. 1. D. Van Nostrand Company, Inc., New York. 1940. pp. 553–601.
8. WELLER, S. and MILLS, G. A. J. Am. Chem. Soc. 75: 769. 1953.
9. WENDER, I., ORCHIN, M., and STORCH, H. H. J. Am. Chem. Soc. 72: 4842. 1950.

THE OXIDATION OF 3-(N-BENZYLACETAMIDO)-1,2-PROPANEDIOL TO N-BENZYLACETAMIDOACETALDEHYDE AND RING CLOSURE OF THE LATTER TO ISOQUINOLINE[1]

By Arlen W. Frank[2] and C. B. Purves

ABSTRACT

Fischer's synthesis of isoquinoline by the oxidative cyclization of benzylaminoacetaldehyde diethyl acetal with 20% oleum was found to give a yield of 8.5%, but his isolation of the intermediate aldehyde could not be repeated. The N-acetyl derivative, N-benzylacetamidoacetaldehyde, however, was synthesized as a somewhat unstable oil, b.p. 129–131° (0.12 mm.), and was cyclized in 7.5% yield to isoquinoline. This synthesis involved the hydrogenation of 3-benzylideneamino-1,2-propanediol to 3-benzylamino-1,2-propanediol, b.p. 152–155° (0.5 mm.); hydrochloride, m.p. 92–94.5°. The N-acetyl derivative, 3-(N-benzylacetamido)-1,2-propanediol, b.p. 188° (0.12 mm.), was then oxidized with sodium metaperiodate; the behavior of other intermediates in the synthesis toward periodate, and also lead tetraacetate, was studied. The following additional compounds were thought to be new: 3-veratrylideneamino-1,2-propanediol, m.p. 123–125°; 3-veratrylamino-1,2-propanediol, b.p. 207–214° (0.4 mm.); the hydrochloride, m.p. 151–152°; 3-(N-benzylacetamido)-1,2-diacetoxypropane, b.p. 196–199° (0.7 mm.), and N-benzylacetamidoacetaldehyde 2,4-dinitrophenylhydrazone, m.p. 315–316°.

INTRODUCTION

The synthesis of isoquinolines from substituted benzylideneaminoacetals (I) or benzylaminoacetals (II) suffers from the fact that the azomethine link is unstable in the sulphuric acid or polyphosphoric acid required for cyclization. While this difficulty is not great when simple aldimine Schiff bases are cyclized, it becomes serious with the more complex ketimine Schiff bases (12). In order to eliminate this difficulty, the azomethine group has been reduced to the more stable secondary amine (III), which has then been cyclized with sulphuric acid in the presence of an oxidizing agent.

In 1893 Fischer (10) reported that the oxidative cyclization of benzylaminoacetaldehyde with fuming sulphuric acid gave isoquinoline, isolated in low but unstated yield as the platinichloride. Since sulphur dioxide was evolved

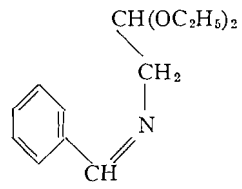

I

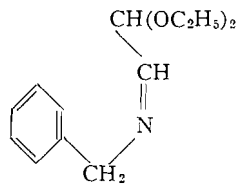

II

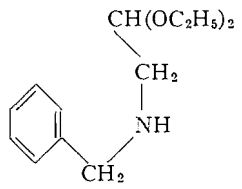

III

and no isoquinoline was obtained when cyclization was attempted with concentrated instead of fuming sulphuric acid, it appeared that one of the inter-

[1]*Manuscript received October 7, 1954.*
Contribution from the Division of Industrial and Cellulose Chemistry, McGill University, and from the Wood Chemistry Division, Pulp and Paper Research Institute of Canada, Montreal, Que. Abstracted from a Ph.D. thesis submitted to the University in August, 1954 by A. W. F.
[2]*Present address: Division of Pure Chemistry, National Research Council, Ottawa, Canada.*

mediates, probably 1,2-dihydroisoquinoline, was oxidized by the sulphur trioxide. Fischer's method, however, was obviously inapplicable to many compounds substituted in the benzene ring because of the ease with which such compounds were sulphonated. An alternative method, developed by Rügheimer and Schön (28) consisted of cyclization in concentrated sulphuric acid containing arsenic pentoxide as an oxidizing agent. Although veratrylaminoacetal yielded 21% of 6,7-dimethoxyisoquinoline (11), the method failed when applied to myristicinylaminoacetal (26) and to N-(α-veratrylveratryl)-aminoacetal (2). Attempts to isolate the intermediate 1,2-dihydroisoquinolines in the cyclization of benzyl- (10), myristicinyl- (29), piperonyl- (20), and N-methylpiperonylaminoacetal (31) were uniformly unproductive. In addition to sulphuric acid in various concentrations, other cyclizing agents such as concentrated hydrochloric acid and phosphorus oxychloride were tried without success.

Despite these disappointing results, the synthesis seemed to merit further study, because it offered a simple and direct way of preparing isoquinoline derivatives such as the alkaloid papaverine from readily available substances (2). In all save one of the cases cited, cyclization had to await the hydrolysis of the acetal to a free aldehyde (or to a vinyl derivative), and if the delay happened to be lengthy there would be opportunity for undesired side-reactions. The exception was Fischer's claim (9) that benzylaminoacetaldehyde could be isolated as a pale yellow, crystalline hydrochloride by evaporating to dryness a solution of the corresponding acetal (III) in concentrated hydrochloric acid. The free base was reported to be a colorless, ether soluble oil which strongly reduced Fehling's solution and which gave the low but unstated yield of isoquinoline when cyclized (10). Neither the base nor its hydrochloride was analyzed or assigned any physical characteristics other than those just stated, and the synthesis has apparently never been repeated nor applied successfully to any other compound in the benzylaminoacetal class. A reinvestigation of the original work was therefore undertaken.

Despite many attempts, Fischer's hydrochloride was invariably isolated as a black, gummy solid which could not be purified by recrystallization. Neutralization of these hydrochlorides gave no recognizable benzylaminoacetaldehyde, and Fischer's claim to have obtained it was finally considered to be in error. On the other hand, cyclization of the black, solid hydrochloride with 20% oleum at room temperature for 24 hr. did give isoquinoline, which was isolated as the picrate in 8.5% yield based on the original benzylaminoacetal. Stronger acid (30–35% SO_3) probably resulted in sulphonation, since the yield of isoquinoline decreased to only 0.07% of theory. The experiment with 20% oleum was then repeated with the acetal itself, and the yield of isoquinoline was 3.5%. When a solution of the acetal (III) in concentrated sulphuric acid was heated for 30 min. at 160–170° and the basic portion of the product was distilled in steam, a copious amount of oil was recovered but no isoquinoline picrate could be isolated from it. Under these conditions, benzylideneaminoacetal (I) was cyclized to isoquinoline in 50% yield (24). An experiment was also carried out using arsenic pentoxide instead of sulphur trioxide as the

oxidizing agent, but only an impure picrate was recovered in small yield. A condensation with concentrated sulphuric acid at 100° for four hours yielded an amorphous yellow solid softening at 185° to 190°, and containing 9.7% of nitrogen (calc. for isoquinoline: N, 10.9%); another condensation with 72% sulphuric acid for four days at room temperature gave a viscous yellow liquid with 8.3% of nitrogen. Neither of these substances was the 1,2-dihydroisoquinoline postulated by Fischer as an intermediate in the cyclization. A base, prepared by cyclizing benzylaminoacetal in cold concentrated sulphuric acid, according to Fischer's directions, was probably impure isoquinoline. The details of these negative experiments have been omitted from this article.

The failure to confirm Fischer's preparation of benzylaminoacetaldehyde made it desirable to develop a new synthesis for this class of compounds, and advantage was taken of the fact that the structure IV (and from this, V) could be readily obtained by condensing benzaldehyde with 3-amino-1,2-propanediol. The analogous veratryl derivatives were also prepared. Oxidation

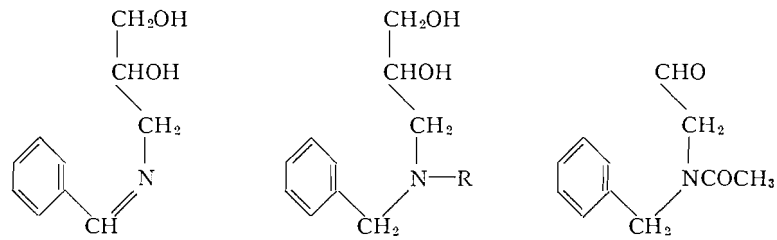

IV V (R = H or $COCH_3$) VI

of IV or V (R = H) with sodium periodate or lead tetraacetate would then be expected to cleave the 1,2-glycol units giving the aldehydes corresponding to the acetals I and III. No previous reference was found to the oxidation of a Schiff base like IV by periodate, other than the oxidation of mannose phenylhydrazone and of glucose phenylosazone (15), the latter giving a pyrazolone in which, of course, the C=N bonds were stabilized by resonance. Benzylidenimine was known to be dehydrogenated with lead tetraacetate in acetic acid to benzonitrile (8), and the imines produced by the oxidation of 2-aminoalcohols were considered to be further oxidized to nitriles (8, 18). McCasland and Smith (18) recently reviewed the rather extensive literature dealing with the action of both oxidants on the aminoalcohols themselves.

It was expected that the azomethine bond in 3-benzylideneamino-1,2-propanediol (IV) would be untouched by periodate in neutral or basic solution, but might be readily hydrolyzed in an acidic medium. An aqueous solution of IV, however, was reported as strongly basic (5), a property not characteristic of a Schiff base, and also at once developed the odor of benzaldehyde. The compound, therefore, appeared to exist in aqueous solution as a mixture of the Schiff base (and its cyclic oxazolidine form (4)), benzaldehyde, and 3-amino-1,2-propanediol in equilibrium. In keeping with this view, the compound IV, like 3-amino-1,2-propanediol (21), reduced 2 moles of periodate per mole both at

pH 8 and pH 4, and 1 mole of ammonia was liberated. It was interesting to note that when 1 mole of periodate per mole of Schiff base was used, no less than 0.55 mole of ammonia was formed; the N—C—C—O link in 3-amino-1,2-propanediol was therefore somewhat more sensitive than the glycol unit to cleavage by the periodate. Although Mead and Bartron (21) found that ammonia could not be reliably determined by the direct titration of solutions in which formaldehyde was present, accurate results were obtained in the present experiments by distilling the ammonia as in the standard Kjeldahl method.

In order to avoid hydrolysis, 3-benzylideneamino-1,2-propanediol was then oxidized with lead tetraacetate dissolved in benzene or in glacial acetic acid. Two moles per mole of diol was rapidly consumed in the former solvent, but in the latter the rate of consumption was slow enough to be followed by iodometry (13). The rate plot (Fig. 1) showed that 1 mole of the tetraacetate was

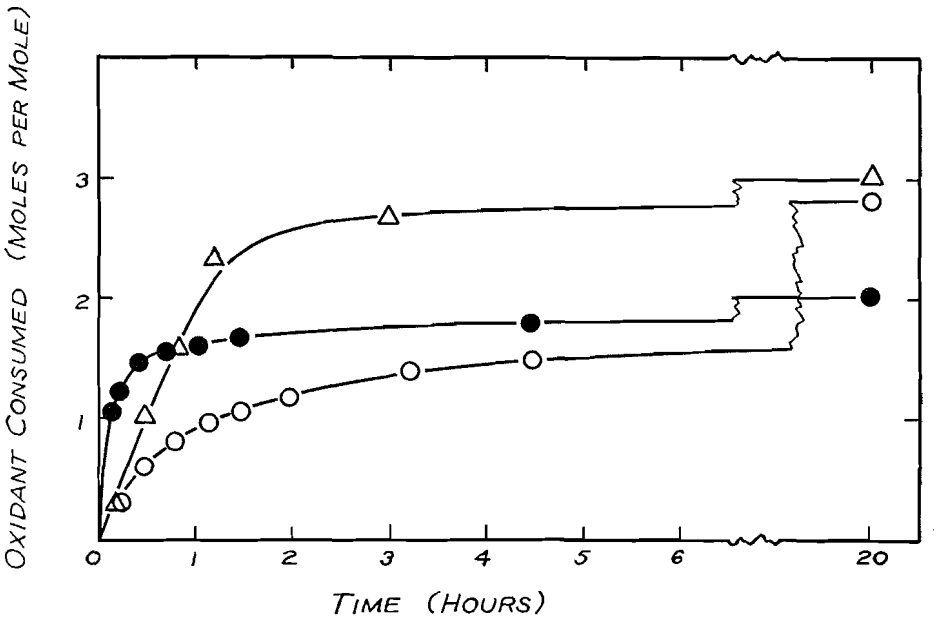

FIG. 1. Oxidation of the aminediols with excess 0.05 *M* lead tetraacetate in acetic acid at 26°.
△3-Amino-1,2-propanediol
●3-Benzylideneamino-1,2-propanediol
○3-(N-Benzylacetamido)-1,2-propanediol (3.04 moles tetraacetate consumed after 47 hr.)

consumed fairly quickly, while the second mole required about 20 hr. Fig. 1 also shows that under the same conditions 3-amino-1,2-propanediol required 3 moles of the tetraacetate, of which 1 mole was expended in slowly oxidizing one of the products, formic acid, to carbon dioxide (8, 23). Although it was plain that the consumption of 2 moles, instead of 1 mole, by IV was not caused by the solvolysis of the Schiff base group, no good explanation was found for

the anomaly. The fact that exactly 2 moles of lead tetraacetate were utilized, instead of a fractional amount, suggested that a specific, ionic reaction was occurring, rather than a non-specific, free-radical process such as addition or dehydrogenation (3, 8). These oxidations were not pursued because they were not likely to yield the desired product, benzylaminoacetaldehyde.

An easy hydrogenation of the Schiff base (IV) yielded 3-benzylamino-1,2-propanediol (V, R = H), which was found to reduce 2 moles of periodate per mole at pH 4, but only 1 mole when the solvent was 5% sulphuric acid. This behavior was not unexpected, because Tompsett and Smith (30) observed that periodate produced formaldehyde from aminoalcohols like ethanolamine and serine in neutral, but not in acid solution. The consumption of periodate by 2-aminocyclohexanol also decreased with decrease in pH (18). It seemed likely that the conversion of the amine to the ammonium salt in acid media prevented the formation of a cylic ester with the periodate ion, which was probably an essential intermediate in the oxidation (6). Attempts were made to use the above results on a preparative scale by destroying any excess periodate in the acidic reaction mixture with ethylene glycol, and then extracting the neutralized liquor with ether. No N-benzylaminoacetaldehyde could be recovered from the black gums produced. Attempts to prepare this compound by deacetylating its N-acetyl derivative (see below) also ended in failure.

3-(N-benzylacetamido)-1,2-propanediol (V, R = $COCH_3$) was then prepared, either directly from 3-benzylamino-1,2-propanediol (V, R = H) by acetylation in aqueous solution, or indirectly by the partial deacetylation of the O,O,N-triacetyl derivative. The consumption of periodate by the product (V, R = $COCH_3$) was 1.3 mole per mole after 30 min., and did not increase during 24 hr. One mole of lead tetraacetate was consumed rapidly, but a slow utilization of a further 2 moles during 47 hr. also occurred (Fig. 1). In other aminoglycols the introduction of an N-acyl group such as acetyl, benzoyl, or carbobenzyloxy prevented the oxidation from exceeding 1 mole (7, 14, 22). The oxidation of 3-(N-benzylacetamido)-1,2-propanediol with periodate, however, led to a successful preparation of N-benzylacetamidoacetaldehyde (VI), which was a colorless oil soluble in chloroform but not in ether, and which darkened quite rapidly. The crystalline 2,4-dinitrophenylhydrazone of the aldehyde was prepared and characterized.

When a solution of N-benzylacetamidoacetaldehyde (VI) in concentrated sulphuric acid was heated for 30 min. at 160–170°, the product included 7.5% of isoquinoline, but this yield decreased to 3% when the heating was only for five minutes. Cyclization in 20% oleum for 24 hr. at room temperature also gave isoquinoline picrate, but in extremely low yield. The odor of benzaldehyde was absent in these experiments, whereas in the Pomeranz (24) cyclization of benzylideneaminoacetal (I) a considerable amount of benzaldehyde was produced in a hydrolytic side-reaction. This difference suggested that the present reaction involved cyclization to 1,2-dihydroisoquinoline, or its N-acetyl derivative, followed by dehydrogenation or deacetylation. All attempts to isolate these supposed intermediates, or N-benzylaminoacetaldehyde, however, were in vain.

EXPERIMENTAL[3]

Materials and Analytical Methods

Glycidol (2,3-epoxy-1-propanol), prepared from 3-chloro-1,2-propanediol with alcoholic potassium hydroxide (25), was dissolved in aqueous ammonia (16) and the solution distilled 24 hr. later to give an 88.5% yield of 3-amino-1,2-propanediol as a colorless oil boiling at 154–156° (14 mm.). On redistillation the product boiled sharply at 153° (13 mm.). The picrolonate melted with charring at 216–218°.

Lead tetraacetate was prepared by adding red lead (Pb_3O_4) to a hot mixture of acetic acid and acetic anhydride, as described by McClenahan and Hockett (19). The consumption of the tetraacetate was followed iodometrically (13), and that of the periodate either iodometrically in acid solution, or by the arsenite–iodine titration near pH 9 (14). In order to determine the ammonia liberated in the oxidation of 3-benzylideneamino-1,2-propanediol (IV), samples, 0.03675 and 0.04360 gm., were dissolved in 20 ml. of 0.05 *M* sodium metaperiodate. After one hour at room temperature, the solutions were transferred to a semimicro Kjeldahl distilling apparatus, diluted with 10 ml. of 45% aqueous sodium hydroxide and steam distilled for 10 min., the distillates being collected in 25 ml. volumes of 0.8% aqueous boric acid containing five drops of methyl purple indicator. The distillates when titrated required 7.52 and 8.94 ml. of 0.02660 *N* hydrochloric acid, respectively, or 98, 98% of the theoretical amount. These results were corrected from blanks containing only sodium metaperiodate.

Benzylaminoacetaldehyde Diethyl Acetal (III)

The details, lacking in Rügheimer and Schön's (27) description, were as follows. A mixture of 53.5 gm. (0.35 mole) of chloroacetaldehyde diethyl acetal and 77.0 gm. (0.72 mole) of benzylamine was heated for 1.5 hr. at 145–150° with mechanical stirring. During this time the solution became deep red in color, gases were evolved, and benzylamine hydrochloride separated in a mass of white crystals. After cooling, water was added to dissolve the salt, the solution was made alkaline with 500 ml. of 10% sodium carbonate and extracted with ether. The extract was washed with water, dried over anhydrous sodium sulphate, and evaporated. The residual oil when distilled at 15 mm. pressure yielded 45.8 gm. (59%) of benzylaminoacetal boiling at 150–160°; redistillation of this fraction furnished a pure sample boiling correctly (9, 27) and sharply at 156° (15 mm.). Found: N, 6.22, 6.20%. Calc. for $C_{13}H_{21}O_2N$: N, 6.27%.

In attempts to prepare Fischer's benzylaminoacetaldehyde hydrochloride (9), 4.5 gm. of the above acetal was dissolved cautiously in 20 ml. of ice-cold, concentrated hydrochloric acid. After being heated for one hour at 50–60°, the solution was evaporated to dryness under reduced pressure. No crystalline material could be recovered from the black residue.

In a typical cyclization to isoquinoline the black hydrochloride from 4.5 gm. of the acetal was gradually added to 20 ml. of ice-cold oleum (20% SO_3),

[3]*Melting points were not corrected.*

solution being immediate and with the evolution of hydrogen chloride. After 24 hr. at room temperature, the wine-red solution was poured onto 50 gm. of crushed ice, diluted with 50 ml. of water, and extracted with ether. The aqueous layer was made strongly alkaline by adding 40 gm. of sodium hydroxide dissolved in 200 ml. of water, and was distilled in steam until 300 ml. of distillate was collected. Extraction of the distillate with ether removed an oil which was diluted with a little ethanol and added to a hot solution of picric acid, 2.5 gm., in 75 ml. of water. The picrate which separated, when recovered, washed with ethanol, and dried, weighed 0.61 gm. (8.5%) and melted at 225–227.5°. A mixed melting point with authentic isoquinoline picrate prepared from commercial isoquinoline was not depressed. When the mother liquors were concentrated to small volume 0.53 gm. of crude picric acid was all that separated.

3-Benzylideamino-1,2-propanediol (IV)

Condensation of 77.7 gm. of 3-amino-1,2-propanediol with 98.0 gm. of benzaldehyde in 40 ml. of ethyl acetate (5) gave a 70% yield of the above substance as white needles, m.p. 80–82°, from ethyl acetate. The reported melting point was 75–79° (17), but the almost quantitative yield, m.p. 72–78°, found by Bergmann *et al.* (5) was never attained. Found: N, 7.80, 7.80%; neutralization equivalent, 177, 178. Calc. for $C_{10}H_{13}O_2N$: N, 7.82%; neut. equiv., 179. This equivalent probably referred to the 3-amino-1,2-propanediol formed by hydrolysis during the titration.

The oxidations with aqueous sodium metaperiodate were carried out with a 0.05 *M* solution and 10 to 30 mgm. samples of the Schiff base. One mole of the Schiff base yielded 0.98, 0.98 mole of ammonia when excess periodate was used; 0.56, 0.55 mole with 1.0 mole of periodate, and 0.49, 0.49 mole with 0.9 mole. The oxidations with lead tetraacetate (Fig. 1) employed a 0.05 *M* solution in glacial acetic acid or benzene and 10 to 30 mgm. samples of the Schiff base.

3-Veratrylideneamino-1,2-propanediol

The preparation was adapted from that of the benzylidene derivative. A mixture of 66.4 gm. (0.40 mole) of veratraldehyde, 31.9 gm. (0.35 mole) of 3-amino-1,2-propanediol and 20 ml. of ethyl acetate was stirred until all the veratraldehyde dissolved. Within a few minutes, the solution suddenly became quite hot and solidified to a white, crystalline mass. After being washed thoroughly with ethyl acetate and dried *in vacuo*, the product weighed 78.8 gm. (94.5%) and melted at 121–124°. Two recrystallizations from ethyl acetate left the melting point almost unchanged (123–125°). Found: C, 60.2, 60.3; H, 7.2, 7.0; N, 5.71, 5.78; OCH_3, 25.6, 25.6%. Calc. for $C_{12}H_{17}O_4N$: C, 60.2; H, 7.2; N, 5.86; OCH_3, 25.9%.

3-Benzylamino-1,2-propanediol (V, R = H)

A mixture of 17.9 gm. (0.1 mole) of 3-benzylideamino-1,2-propanediol, 200 mgm. of Adams' platinum oxide catalyst (1), and 100 ml. of ethanol was shaken under 2–3 atm. pressure of hydrogen until the consumption of the gas

ceased (three to five hours). The liquor was decanted and the recovered catalyst used in two or three similar hydrogenations until it became inactive. The combined ethanolic solutions obtained from 104.2 gm. of the Schiff base were filtered and then evaporated to an oil which was distilled at 0.5 mm. pressure, the yield being 93.1 gm. boiling at 130–160°. Redistillation furnished 80.7 gm. (76.5%) of a viscous, colorless oil boiling at 152–155° (0.5 mm.). Found: C, 65.7, 65.7; H, 8.1, 8.1; N, 7.44, 7.48%; neut. equiv., 181, 182, 181. Calc. for $C_{10}H_{15}O_2N$: C, 66.3; H, 8.3; N, 7.73%; neut. equiv., 181.

A solution of the amine in an excess of hydrochloric acid was extracted with ether to remove any non-basic impurities, and was then evaporated to dryness under diminished pressure. The residue of 3-benzylamino-1,2-propanediol hydrochloride melted at 92–94.5° after two recrystallizations from isoamyl alcohol. Found: N, 6.28, 6.29%. Calc. for $C_{10}H_{16}O_2NCl$: N, 6.43%.

A 50 mgm. sample of the amine was dissolved in 15 ml. of 0.05 *M* sodium metaperiodate and at intervals 2-ml. aliquots were analyzed iodometrically. The consumption of periodate, 2.11 moles per mole after 30 min., was practically unchanged at 2.06 mole after one hour. In a second oxidation, a 50 mgm. sample was dissolved in 10 ml. of 10% sulphuric acid and 10 ml. of the 0.05 *M* periodate. After 15 min., 1 hr., 3 hr., and 17 hr. the consumption of periodate was 0.74, 1.10, 1.12, and 1.24 mole per mole, respectively.

3-Veratrylamino-1,2-propanediol Hydrochloride

3-Veratrylideneamino-1,2-propanediol, 23.9 gm. (0.1 mole) was dissolved in 100 ml. of ethanol and hydrogenated over 200 mgm. of platinum oxide catalyst as already described for the corresponding benzylidene Schiff base. The product from three such hydrogenations was dissolved in 100 ml. of water, 50 ml. of concentrated hydrochloric acid was added, and the solution extracted with ether to remove any non-basic impurities. Evaporation of the aqueous residue to dryness under reduced pressure left the white, crystalline hydrochloride. After one recrystallization from ethanol the yield was 64.7 gm. (89.5%) and the m.p., 151–152°. Found: N, 5.02, 5.01; OCH_3, 22.1, 22.3%. Calc. for $C_{12}H_{20}O_4NCl$: N, 5.04; OCH_3, 22.3%.

The free base, 3-veratrylamino-1,2-propanediol, distilled with some decomposition at 207–214° (0.4 mm.) as a pale yellow, viscous oil.

3-(N-Benzylacetamido)-1,2-diacetoxypropane

A mixture of 79.7 gm. (0.44 mole) of 3-benzylamino-1,2-propanediol (V, R = H), 400 ml. of acetic anhydride, and 40 gm. of fused sodium acetate was heated for several hours under reflux near 100°, and the solution was then decanted into 1300 ml. of water. After standing overnight to decompose the acetic anhydride, the clear solution was extracted with ether and the extract washed, twice with dilute hydrochloric acid and thrice with water. The residual oil remaining after evaporation of the dried extract was distilled, giving 81.8 gm. (61.5%) of product boiling at 196–199° (0.7 mm.). Found: C, 62.4, 62.5; H, 6.8, 6.9; N, 4.49, 4.47%. Calc. for $C_{16}H_{21}O_5N$: C, 62.5; H, 6.9; N, 4.56%. The compound was soluble in ether and water.

3-(N-Benzylacetamido)-1,2-propanediol (V, R = $COCH_3$)

(*a*) *From 3-(N-Benzylacetamido)-1,2-diacetoxypropane*

The above O,O,N-triacetyl derivative was selectively deacetylated by a procedure adapted from that used by Carter *et al.* (7) to de-O-acetylate hexa-acetyl inosamine to N-acetyl inosamine.

A 9.2 gm. (0.03 mole) sample, dissolved in 100 ml. of anhydrous methanol, was mixed with 150 ml. of methanol which had been saturated with ammonia gas at 26°. After being kept for 40 hr. at room temperature, the solution was evaporated to dryness under reduced pressure, and the residue was held at 150° and 0.4 mm. pressure until the acetamide was removed by distillation. The still residue when fractionated yielded 5.1 gm. (76%) of product boiling at 190–193° (0.3 mm.). Found: N, 5.78, 5.79%. Calc. for $C_{12}H_{17}O_3N$: N, 6.28%.

(*b*) *From 3-Benzylamino-1,2-propanediol Hydrochloride*

The hydrochloride from 49.5 gm. of the base was dissolved in 500 ml. of water, mixed with 83 ml. of acetic anhydride, and 39.0 gm. of sodium acetate trihydrate dissolved in 100 ml. of water was added at once. This solution was shaken for six hours at room temperature, then extracted with ether to remove any triacetyl derivative, and evaporated to dryness. The residue was mixed with chloroform and filtered to remove the inorganic salts. The chloroform filtrate was shaken thoroughly with water, both phases were transferred to a liquid–liquid extractor, and the aqueous layer was extracted with chloroform for 24 hr. The residual oil remaining after evaporation of the chloroform amounted to 35.5 gm. (58%). A small sample distilled as an extremely viscous yellow oil at 182–188° (0.12 mm.), for the most part at 188°. Found: C, 64.2, 64.3, 64.2; H, 7.6, 7.7, 7.7; N, 6.15, 6.11%. Calc. for $C_{12}H_{17}O_3N$: C, 64.5; H, 7.7; N, 6.28%. This compound was soluble both in water and in chloroform. One mole reduced 1.30 mole of sodium metaperiodate in neutral solution within 30 min., and this amount did not increase after 24 hr.

N-Benzylacetamidoacetaldehyde (VI)

A mixture of 11.3 gm. (0.05 mole) of 3-(N-benzylacetamido)-1,2-propanediol, 16.3 gm. (0.076 mole) of sodium metaperiodate, and 280 ml. of water was shaken vigorously for six hours and then extracted with chloroform. The residual oil from the evaporation of the extract was distilled at 0.4 mm. pressure, the fraction boiling at 136–139° weighing 5.6 gm. (58%). The sample redistilled for analysis had the boiling point 129–131° (0.12 mm.). Found: C, 69.1, 68.8; H, 6.9, 6.8; N, 7.29, 7.31, 7.33%. Calc. for $C_{11}H_{13}O_2N$: C, 69.1; H, 6.9; N, 7.33%. The aldehyde was a colorless oil after distillation, but darkened rapidly even when stored in a desiccator over potassium hydroxide or calcium chloride. The substance was soluble in chloroform, but was insoluble in ether and only slightly soluble in water.

The 2,4-dinitrophenylhydrazone of VI was prepared by adding the aldehyde in slight excess to an acid solution of 2,4-dinitrophenylhydrazine in ethanol. Brick red crystals, which separated slowly, were recovered after 24 hr. and were recrystallized from phenol containing a little ethanol. After being dried overnight *in vacuo* at 78° to remove any traces of phenol, the crystals melted

with effervescence at 315–316°, becoming black above 305°. Found: N, 18.5, 18.9%. Calc. for $C_{17}H_{17}O_5N_5$: N, 18.9%. The derivative was quite insoluble in ethanol, ethyl acetate, and other organic liquids tried, but dissolved in nitrobenzene and in hot phenol.

In a typical cyclization to isoquinoline, 1.21 gm. of N-benzylacetamidoacetaldehyde (VI) was dissolved cautiously in 10 ml. of ice-cold concentrated sulphuric acid and the solution heated for 30 min. at 160–170°. After cooling, the solution was poured onto 50 gm. of crushed ice, and the isoquinoline was recovered as in the cyclization of benzylaminoacetal. The picrate weighed 0.141 gm. (7.5%) and melted at 226–228°. A mixed melting point with an authentic sample of isoquinoline picrate, m.p. 226–227.5°, was not depressed.

ACKNOWLEDGMENT

One of us (A. W. F.) wishes to thank the National Research Council of Canada for the Studentship he was privileged to hold in 1953–54.

REFERENCES

1. Adams, R., Voorhees, V., and Shriner, R. L. Organic syntheses. Coll. Vol. 1. 2nd ed. John Wiley & Sons, Inc., New York. 1944. p. 463.
2. Allen, I. and Buck, J. S. J. Am. Chem. Soc. 52: 310. 1930.
3. Barron, H. E., Cavill, G. W. K., Cole, E. R., Gilham, P. T., and Solomon, D. H. Chemistry & Industry, 76. 1954.
4. Bergmann, E. D. Chem. Revs. 53: 309. 1953.
5. Bergmann, M., Brand, E., and Dreyer, F. Ber. 54: 936. 1921.
6. Buist, G. J. and Bunton, C. A. J. Chem. Soc. 1406. 1954.
7. Carter, H. E., Clark, R. K., Jr., Lytle, B., and McCasland, G. E. J. Biol. Chem. 175: 683. 1948.
8. Criegee, R. Angew. Chem. 53: 321. 1940.
9. Fischer, E. Ber. 26: 464. 1893.
10. Fischer, E. Ber. 26: 764. 1893; 27: 165. 1894.
11. Forsyth, R., Kelly, C. I., and Pyman, F. L. J. Chem. Soc. 127: 1659. 1925.
12. Gensler, W. J. Organic reactions. Vol. 6. John Wiley & Sons, Inc., New York. 1951. p. 191.
13. Hockett, R. C., Dienes, M. T., and Ramsden, H. E. J. Am. Chem. Soc. 65: 1474. 1943.
14. Jackson, E. L. Organic reactions. Vol. 2. John Wiley & Sons, Inc., New York. 1944. p. 341.
15. Karrer, P. and Pfaehler, K. Helv. Chim. Acta, 17: 766. 1934.
16. Knorr, L. and Knorr, E. Ber. 32: 750. 1899.
17. McCasland, G. E. and Horswill, E. C. J. Am. Chem. Soc. 73: 3923. 1951.
18. McCasland, G. E. and Smith, D. A. J. Am. Chem. Soc. 73: 5164. 1951.
19. McClenahan, W. S. and Hockett, R. C. J. Am. Chem. Soc. 60: 2061. 1938.
20. Mannich, C. and Kuphal, R. Arch. Pharm. 250: 539. 1912.
21. Mead, J. F. and Bartron, E. A. J. Am. Chem. Soc. 70: 1286. 1948.
22. Niemann, C., Benson, A. A., and Mead, J. F. J. Org. Chem. 8: 397. 1943.
23. Perlin, A. S. Anal. Chem. 26: 1053. 1954.
24. Pomeranz, C. Monatsh. 14: 116. 1893; 15: 299. 1894.
25. Rider, T. H. and Hill, A. J. J. Am. Chem. Soc. 52: 1521. 1930.
26. Rügheimer, L. and Ritter, G. Ber. 45: 1340. 1912.
27. Rügheimer, L. and Schön, P. Ber. 41: 17. 1908.
28. Rügheimer, L. and Schön, P. Ber. 42: 2374. 1909.
29. Salway, A. H. J. Chem. Soc. 95: 1204. 1909.
30. Tompsett, S. L. and Smith, D. C. Analyst, 78: 209. 1953.
31. Young, P. C. and Robinson, R. J. Chem. Soc. 275. 1933.

AN ADIABATIC CALORIMETER FOR THE TEMPERATURE REGION BELOW 20°K.—THE SPECIFIC HEAT OF SODIUM CHLORIDE[1]

By J. A. Morrison, D. Patterson,[2] and J. S. Dugdale[2,3]

ABSTRACT

A simple adiabatic calorimeter for specific heat measurements at very low temperatures is described. Liquid helium is made in the cryostat by the Simon expansion method. The calorimeter and adiabatic shield are cooled below 13°K. by conduction of heat along the lead wires rather than by conduction with exchange gas. The working thermometer is a carbon resistor which has been calibrated against a helium gas thermometer. The assembly has been used to determine the specific heat of rock salt between 2.5° and 20°K. The results are compared with the theoretically derived values of the specific heat and Debye characteristic temperature for sodium chloride.

INTRODUCTION

In recent years there has been an increasing interest in the specific heat of substances at very low temperatures to try to determine, for example, the electronic contribution to the specific heat or the effect of superconductivity on the heat capacity of metals (8). In many cases the substances used have been of such a form—blocks or large single crystals—as to permit use of very simple calorimeter assemblies (11) in which the calorimeter vessel exchanges heat continuously with its surroundings. Such assemblies work satisfactorily where thermal equilibrium times are short, i.e. of the order of seconds. The present apparatus was designed especially for experiments with samples of small particles where it was anticipated that equilibrium times of the order of minutes would be encountered. Hence, it seemed obligatory to make the assembly of the adiabatic type. This had the further advantage of achieving uniform and continuous operation throughout the temperature region 2.5° to 20°K. Although designed primarily for samples of small particles, the assembly may be used equally well for experiments on bulk solids as will be shown by the results for bulk sodium chloride.

Accurate values of the specific heat of bulk NaCl were needed for comparison with the specific heat of small particles of NaCl. Existing measurements by Clusius *et al.* (5) were not adequate as they went no lower than 11°K. At the same time, however, the results which have been obtained are of interest for comparison with theoretical values of the specific heat deduced from a Born–von Karman treatment of NaCl crystal (7), and with quantities deduced from elastic constants. As will be seen, the agreement between the experimental and theoretical results is gratifying.

[1]*Manuscript received October 14, 1954.*
Contribution from the Division of Pure Chemistry, National Research Laboratories, Ottawa, Canada. Issued as N.R.C. No. 3472.
[2]*National Research Laboratories Postdoctorate Research Fellow.*
[3]*Present address: Division of Physics, National Research Laboratories.*

APPARATUS AND EXPERIMENTAL TECHNIQUE

The Cryostat

The essentials of the calorimeter assembly are shown diagrammatically in Fig. 1. The outer part of the cryostat (the liquid nitrogen and liquid hydrogen stages) was patterned after a cryostat used for adsorption experiments which

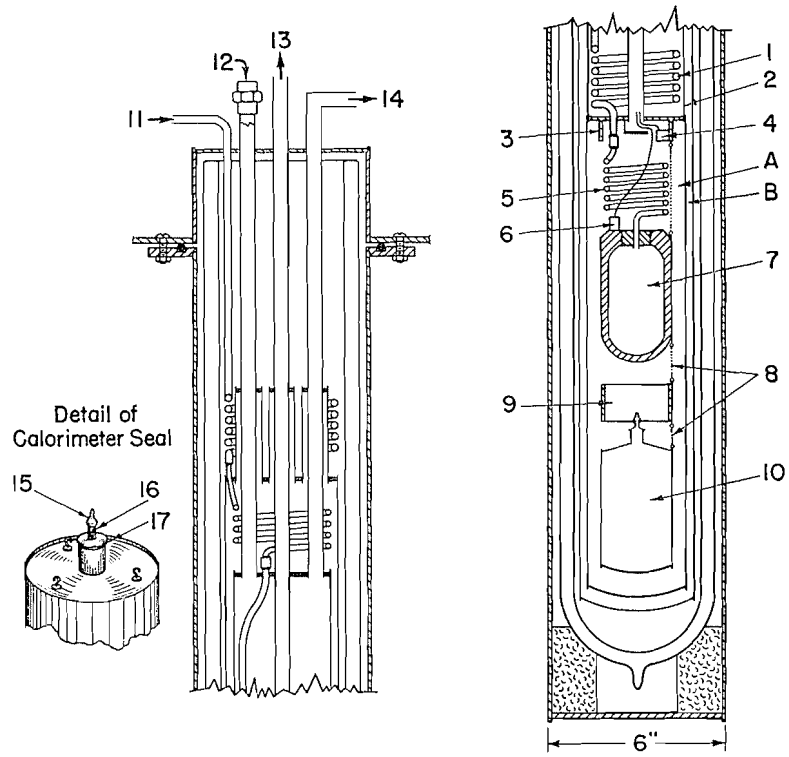

FIG. 1. The calorimeter assembly. A and B: vacuum spaces; 1: coil of copper tubing, 1 meter long, $\frac{3}{16}$ in. O.D., 0.035 in. wall thickness; 2: liquid hydrogen container; 3: anchoring ring for lead wires; 4: hydrogen vapor pressure thermometer; 5: coil of copper nickel tubing, 1 meter long, $\frac{1}{8}$ in. O.D., 0.018 in. wall thickness; 6: helium vapor pressure thermometer; 7: helium bomb (copper); 8: Nylon suspension cords; 9: adiabatic shield ($\frac{1}{16}$ in. thick copper), 10: calorimeter vessel; 11: high pressure helium line; 12: liquid hydrogen filling tube; 13: vacuum line; 14: gaseous hydrogen vent line; 15: soft glass seal; 16: platinum tube; 17: Wood's metal seal.

has been adequately described elsewhere (9). In order to reach temperatures below 10°K. a liquid helium stage has been added, the liquid helium being made by the Simon expansion method (12). The helium bomb, 7, of about 150 cm.^{3} internal volume, is hung by Nylon cords from the liquid hydrogen container, 2. An expansion of helium from a pressure of 130 atm. to 1 atm. with a starting temperature of 13°K. attained by pumping on the liquid hydrogen in 2 produces about 50 cm.^{3} of liquid helium which has proved to be adequate for 12 or more hours of experiments.

Previous experience showed that the use of exchange gas at liquid helium temperatures caused certain experimental difficulties. On the one hand, it

proved difficult to secure a satisfactory vacuum and on the other hand desorption of helium from the surface of the calorimeter vessel caused a perceptible fall in its temperature. Consequently, in these experiments no exchange gas was used below about 13°K. Temperatures below this were reached by conduction of heat from the calorimeter along the lead wires. This was, of course, a slow process and required three to five hours for liquid helium temperatures to be reached, but the advantages of the method greatly outweigh this disadvantage.

The Calorimeter and Shield

The adiabatic shield, 9, and the calorimeter vessel, 10, are hung below the helium bomb by Nylon cords, 8. Since the major heat exchange between the calorimeter vessel and shield was along lead wires, an elementary form of shield was permissible. However, experience showed that radiation exchange with the jacket was significant when extremes of temperature were reached, e.g. calorimeter at 4° and surrounding can at 20°. Therefore, a detachable cylindrical radiation shield (not shown in the diagram) of 0.001 in. thick copper foil which surrounded the calorimeter vessel was attached to the shield.

The lead wires from outside (No. 36 B. and S.D.S.C. copper) are brought in through the central tube and first make thermal contact with the anchoring ring, 3. Similar copper leads go between the bomb and the shield and make good thermal contact with each. Between the anchoring ring and the bomb, and between the shield and the calorimeter constantan leads (No. 30 B. and S.D.S.C. 15 cm. long) are used in order to reduce thermal conduction. The copper to constantan junctions were put close together at isothermal points in order to minimize thermal e.m.f.'s. Residual e.m.f.'s in the circuits were of the order of 0.1 μv. and were quite steady.

Adiabatic control was accomplished by manual regulation of the current passed through a heater wound on the shield. Temperature differences between the shield and calorimeter vessel were detected by a difference thermocouple made from two alloy wires—Ag – 0.37% Au/Au – 2.4% Co.* This thermocouple has adequate sensitivity even at the lowest temperature ~2.5°K. (e.g. 5 μv./deg. at 4°).

Since it was desired to do experiments with samples of particles of bulk density as low as 0.1, it was necessary to use a large calorimeter vessel (approximately 300 cm.^{3}). At the same time the mass of the vessel had to be kept small and this was accomplished by making the vessel of thin copper (0.007 in.) with light reinforcing rings on the cylindrical side. The bottom and top were made slightly conical for added strength. Light vertical vanes (0.001 in. copper) were attached to the inside wall of the vessel in order to enhance gross conduction of heat from the outer wall to the center of the sample.

Filling the Calorimeter

The method of putting samples into the calorimeter requires comment because of the possible significance of adsorbed gases in the specific heat

Cf. Keesom, W. H. and Matthijs, C. J. Physica, 2: 623. 1935.

measurements. It was important to be able to evacuate the filled calorimeter vessel and to seal it securely with a small amount of helium gas inside to assist in heat exchange. As may be seen from the diagram, the vessel is provided with a port approximately one-quarter inch in diameter through which the sample is admitted under an inert gas atmosphere. Connection to a vacuum line is made through a platinum-soft glass seal, 15,16, the platinum tube being fastened to the calorimeter vessel with Wood's metal, 17. Finally the glass tube is sealed off close to the platinum seal. In practice, the amount of glass in the seal averaged 100 mgm. with variations from experiment to experiment not exceeding 10 mgm. These variations were of no significance in the specific heat measurements.

Thermometer and its Calibration

The most important aspect of the calorimetry is the matter of a working thermometer and the temperature scale. It turns out that the accuracy of the specific heat measurements is determined by the accuracy with which the temperature scale can be fixed. No completely satisfactory thermometer exists for this temperature region, but recently carbon resistors have been tried. One of these (Ohmite, nominal value 10 ohms, $\frac{1}{2}$ watt) was used for the present assembly. The resistor was attached to the bottom of the calorimeter vessel with a light copper clip. Thermal contact between the thermometer and the calorimeter was established through the thermometer leads (No. 28 B. and S.D.C.C. copper) wrapped twice around and lacquered to the cylindrical side of the vessel. Experiment showed that the time lag between the heater (200 ohms of No. 40B. and S.D.G.C. manganin, wrapped on the side) and the thermometer was less than two seconds. Resistances of the thermometer were determined with a Mueller bridge in which the current was varied from 10 μa. to 65 μa., depending upon the temperature.

The attractive feature of using carbon resistance thermometers is the possibility of having to calibrate them only at the two ends of the temperature region, intermediate temperatures being obtained by a suitable interpolation formula. Two interpolation formulas have been suggested and as will be seen, one is much preferable to the other for the thermometer used in these experiments. Clement and Quinnell (4) have proposed the formula

$$\log R+(K/\log R) = A+(B/T) \qquad [1]$$

while Brown, Zemansky, and Boorse (3) have suggested a four-constant formula

$$\log R = A+(B/T)+(C/T^2)-KT^2. \qquad [2]$$

The constants of the formulas were determined in the following way. First, the indications of the carbon thermometer were compared with temperatures deduced from the hydrogen vapor pressure thermometer, 4, at several points in the range 14° to 20°. For the comparisons, exchange gas was admitted to space A and at least half an hour was allowed for equilibrium at each point. The vapor pressure thermometer was filled with normal hydrogen and tem-

peratures were deduced from the appropriate vapor pressure equation given by Woolley *et al.* (14). At the lower end of the temperature region the carbon thermometer was compared with the helium vapor pressure thermometer, 6. These comparisons had to be made with space A evacuated and therefore temperature differences between the bomb and shield and between the shield and calorimeter had to be taken into account. The latter was determined each time by means of the difference thermocouple but the former had to be deduced from a separate experiment in which a vapor pressure thermometer was attached to the calorimeter vessel. Small temperature differences (a few hundredths of a degree) were found which were due to small amounts of energy appearing in the calorimeter vessel as a result of vibration. It was not possible in practice to eliminate vibration completely. The observed vapor pressures of helium were converted to temperatures on the 'agreed' scale (13). The constants of the interpolation formulas were computed using comparison data at about 4°, 14°, and 20°K. for formula [1] and at about 4°, 14°, 17°, and 20°K. for formula [2]. The constants shifted each time that the thermometer was cooled from liquid nitrogen or higher temperatures. At 20°K. or below no shift in the constants could be detected over a period of two days.

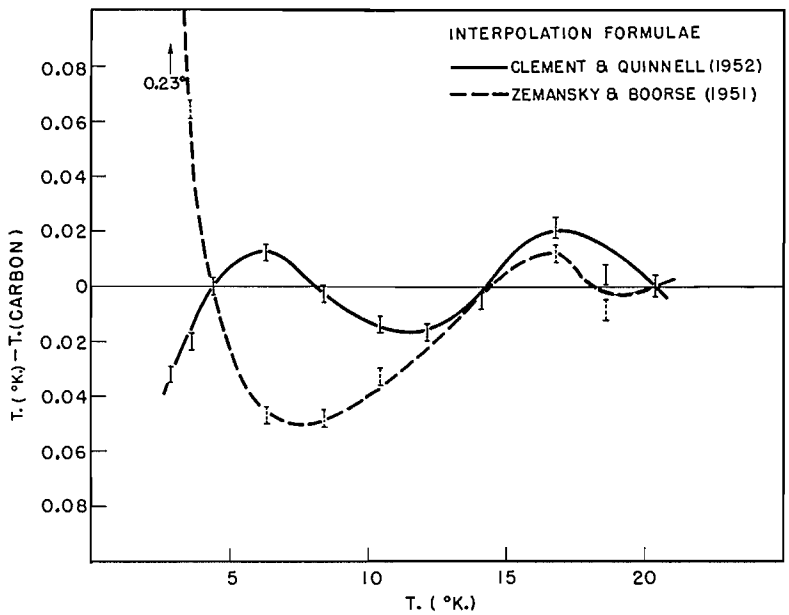

FIG. 2. Deviation of the carbon thermometer scale from the thermodynamic scale.

Finally in a separate experiment the carbon thermometer was compared with a helium gas thermometer (2 cm.^{3} bulb, 0.4 cm.^{3} external volume, ice point pressure approximately eight meters) attached to the calorimeter vessel. The results of the comparison are shown in Fig. 2 as a deviation plot. The deviations of formula [1] are relatively modest over the whole temperature

range but formula [2] becomes seriously off at the low temperature end. The difficulty would appear to be that the constant C in formula [2] turns out to be negative, which leads to a maximum in the R–T relation at low temperatures (at about 1.7° K. in this case). It was found most convenient to work out the experimental results on the scale given by formula [1] and as a last step to convert them to the thermodynamic scale using Fig. 2.

The matters of the precision and accuracy of the method are best discussed in connection with the specific heat results for NaCl.

THE SPECIFIC HEAT OF SODIUM CHLORIDE

Experimental Details

For these experiments two samples were used—pieces broken from a single crystal made by the Harshaw Chemical Company and fused lumps (Merck reagent grade). The Merck NaCl was fused in a platinum crucible and then poured onto a sheet of platinum in an inert gas atmosphere. Each sample was placed in the calorimeter under a helium atmosphere. The calorimeter vessel was evacuated to a pressure of 10^{-6} mm. Hg at room temperature and finally sealed off with 10^{-6} moles of helium inside as exchange gas. This amount of helium was so small as to not contribute to the specific heat even if it were all desorbed during one temperature increment. The samples were each about one-half mole and on the average contributed about one-third of the total specific heat. Temperature increments between 0.5° and 1° were used throughout. The equilibrium times following admission of energy to the calorimeter vessel varied from about 30 sec. at the lowest temperatures to about five minutes at 20°K.

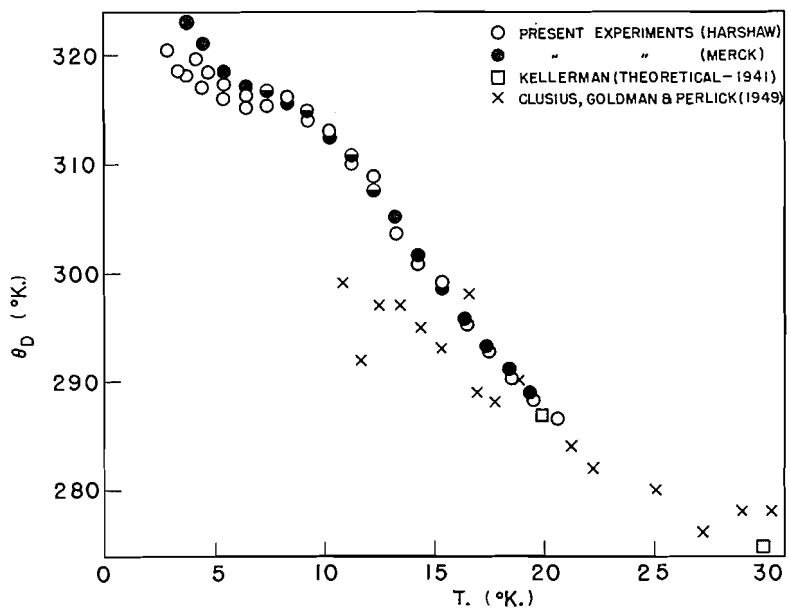

Fig. 3. The Debye characteristic temperature (θ_D) for NaCl as a function of temperature.

Results and Discussion

The results of the experiments are summarized in Fig. 3 in the form of a plot of the apparent Debye characteristic temperature, θ_D, versus the absolute temperature. θ_D was computed for each experimental value of the specific heat by means of the equation

[3] $$C_V = 464.5\ (T/\theta_D)^3 \text{ cal./gm. atom deg.}$$

The difference between C_p and C_V could reasonably be neglected in this temperature region. One notes that as T is reduced below 20°K. θ_D increases at first fairly rapidly but below about 8°K. much more slowly. This behavior is in agreement with the work of Blackman (2) who showed that an exact fit of the Debye model (θ_D practically a constant) was only to be expected at temperatures of the order of $\theta_D/50$ or less. The measured specific heat at 20°K. agrees almost exactly with the theoretical value deduced by Kellerman (7).

A limiting value of θ_D at 0°K. can be deduced from the elastic constants of the crystal. Kellerman (7) gives the value of 313° which he computed by the Hopf–Lechner method (6) using theoretically derived elastic constants. Recently Overton and Swim (10) have determined the elastic constants of NaCl down to 60°K. and have estimated the values at 0°K. by extrapolation. Using their values of the elastic constants and a simpler method of calculation due to Bhatia and Tauber (1), one derives the value of 321° for θ_D at 0°K., which agrees with θ_D deduced from the experiments at the lowest temperatures within the experimental uncertainty.

The agreement between the results for the two samples of NaCl is of interest as one might expect that imperfections in the fused sample could have a measurable effect on the low temperature specific heat.

Using the criterion that the specific heat should be a smooth function of the temperature, it was established that the precision of measurement of the total heat capacity was 0.3% at worst. That is, for any one set of experiments the results were consistent with a smoothed function to this extent. The accuracy, however, depends on the fixing of the temperature scale in an absolute sense. The possible errors involved in this can be estimated. Under the unfavorable condition of the NaCl contributing only one third to the total specific heat, it would appear that the accuracy of the results for NaCl is 1% or better from 20° down to about 7°K. Below the latter temperature the accuracy decreases to about 5% at the lowest temperature reached. Furthermore, the experimental and theoretical results for NaCl agree within these limits.

REFERENCES

1. Bhatia, A. B. and Tauber, G. E. Phil. Mag. 45: 1211. 1954.
2. Blackman, M. Proc. Roy. Soc. (London), A, 159: 416. 1937.
3. Brown, A., Zemansky, M. W., and Boorse, H. A. Phys. Rev. 84: 1050. 1951.
4. Clement, J. R. and Quinnell, E. H. Rev. Sci. Instr. 23: 213. 1952.
5. Clusius, K., Goldman, J., and Perlick, A. Z. Naturforsch. 4*a*: 424. 1949.
6. Hopf, J. and Lechner, G. Verhandl. deut. physik. Ges. 16: 643. 1914.
7. Kellerman, E. W. Proc. Roy. Soc. (London), A, 178: 17. 1941.
8. MacDonald, D. K. C. *In* Progress in metal physics. Vol. 3. Pergamon Press Ltd., London. 1952. Chap. 2.

9. MORRISON, J. A. and LOS, J. M. Discussions Faraday Soc., 8: 321. 1950.
10. OVERTON, W. C. and SWIM, R. T. Phys. Rev. 84: 758. 1951.
11. PEARLMAN, N. and KEESOM, P. H. Phys. Rev. 88: 398. 1952.
12. PICKARD, G. L. and SIMON, F. E. Proc. Phys. Soc. (London), 60: 405. 1948.
13. VAN DIJK, H. and SHOENBERG, D. Nature, 164: 151. 1949.
14. WOOLLEY, H. W., SCOTT, R. B., and BRICKWEDDE, F. G. J. Research Natl. Bur. Standards, 41: 379. 1948.

THE PHOTOLYSIS OF ACETONE IN THE PRESENCE OF HYDROGEN BROMIDE[1]

By M. J. Ridge[2] and E. W. R. Steacie

ABSTRACT

The presence of hydrogen bromide during the photolysis of acetone sharply inhibits the yields of carbon monoxide, ethane, and volatile methyl radical derivatives as measured by the function ($CH_4+2C_2H_6$). The observed effects can be explained on the assumption that both acetyl and methyl radicals react rapidly with HBr.

INTRODUCTION

The photolysis of acetone has been extensively used as a source of methyl radicals. The subsequent reactions of these with other substances are accessible to study when mixtures of acetone and a substrate are photolyzed. These methods have recently been applied by Raal and Steacie (6) to halogen-substituted hydrocarbons. It has, however, been discovered that the photolysis of acetone in the presence of certain chlorine-substituted hydrocarbons is accompanied by complicating side reactions leading to the formation of hydrogen chloride (2, 7). Cvetanovic and Steacie (3) have studied the photolysis of acetone in the presence of hydrogen chloride and have shown that methyl radicals react rapidly with hydrogen chloride which is largely regenerated by the abstraction of hydrogen atoms from acetone by chlorine atoms.

The work of Anderson and Kistiakowsky (1) indicates that methyl radicals react rapidly with hydrogen bromide also. However, there are reasons for believing that the photolysis of acetone in the presence of hydrogen bromide may not proceed entirely analogously with the hydrogen chloride case. In the oxidation of hydrocarbons the presence of hydrogen bromide profoundly modifies the reaction, the effect being attributed to the abstraction of a hydrogen atom from hydrogen bromide by peroxy radicals. Hydrogen chloride does not exert the same effect.

EXPERIMENTAL

Apparatus

The optical system was as previously described and included a G.E. 935 phototube so that the intensity of the incident light could be controlled (7). The light source was a Hanovia S-500, medium pressure lamp. The experiments were carried out using a Corning 0.53 filter (Pyrex) with a "cut-off" below 2800 Å. The analysis system was of the type usually used in this laboratory and included a Le Roy-Ward still, McLeod gauge, Toepler pump, and a gas burette. Since hydrogen bromide reacts slowly with mercury, a reaction

[1]*Manuscript received August 3, 1954.*
Contribution from the Division of Pure Chemistry, National Research Council, Ottawa, Canada. Issued as N.R.C. No. 3473.
[2]*On leave of absence 1952–53 from the Division of Tribophysics, Commonwealth Scientific and Industrial Research Organization, Melbourne, Australia.*

system was adopted in which taps greased with silicone grease were employed and contamination by mercury vapor was reduced to a minimum.

The acetone was prepared as previously described (7). Hydrogen bromide was prepared by adding bromine to tetralin. The crude hydrogen bromide was passed through a red phosphorus column to eliminate excess free bromine, and through a bubbler filled with a concentrated aqueous solution of hydrogen bromide in order to remove bromides of phosphorus. The gas was then subjected to three bulb to bulb distillations from acetone dry ice to liquid air temperatures, first and last thirds being rejected. The fraction retained was kept frozen in liquid nitrogen and samples were taken by warming to dry ice temperature. The frozen solid was quite white.

Preliminary Experiments

In view of the "tail-off" towards longer wave length in the absorption spectrum of hydrogen bromide, some preliminary experiments were carried out to determine the effect on hydrogen bromide of light of the wave lengths passed by the filter.

Hydrogen bromide, 635 mm., was admitted to the reaction vessel at 150°C. Within the experimental error the intensity of the emergent beam as determined by the phototube was unaffected by the admission of the reagent. In the pressure region of the photolysis experiments absorption could therefore be safely neglected.

Hydrogen bromide, 101 mm., was illuminated for four hours at 150°C. The fraction uncondensable at −196°C. was found to be negligibly small. In general, preliminary experiments indicated that decomposition of hydrogen bromide could be neglected. This conclusion is borne out in the experiments by the virtual absence of hydrogen among the products.

RESULTS

Products of the Photolysis of Acetone in the Presence of Hydrogen Bromide

The major products (Table I) were methane and carbon monoxide. A trace of hydrogen was detected in the run with 50 mm. hydrogen bromide, but none at all in the run with 20 mm. hydrogen bromide. In none of the remaining experiments (in which the analyses were carried out by conventional gas analysis methods) was there any indication of the presence of hydrogen, and

TABLE I

PRODUCTS OF THE PHOTOLYSIS OF ACETONE IN THE PRESENCE OF HYDROGEN BROMIDE

Run	Temp., °C.	Time, hr.	Concentration, micromoles/cc.		Products, micromoles			
			Acetone	Hydrogen bromide	Methane	Carbon monoxide	Hydrogen	Ethane
100	150	4	1.854	1.987	4.99	1.24	0.07	0.05
112	201	4	1.888	0.748	10.75	4.85	None detected	0.04

it may therefore be disregarded as a significant product. With the quantities of hydrogen bromide employed here, ethane has been reduced to almost negligible proportions.

Effect of Concentration of Hydrogen Bromide

The effect of hydrogen bromide over a range of concentrations is shown in Table II. The experiments were carried out with 50 mm. acetone at 150°. Throughout the series the light intensity was maintained constant.

TABLE II

THE EFFECT OF CONCENTRATION OF HYDROGEN BROMIDE ON THE PHOTOLYSIS OF ACETONE
Time of irradiation 4 hr.; Temp. 150°C.

Run	Concentration, micromoles/cc.		Products, micromoles			
	Acetone	Hydrogen bromide	Methane	Carbon monoxide	Ethane	$\frac{CH_4+2C_2H_6}{CO}$
105	1.900	—	4.29	7.76	4.29	1.66
110	1.889	0.068	9.99	3.88	0.07	2.61
106	1.901	0.190	7.41	1.95	0.02	3.82
107	1.891	0.372	5.80	1.34	0.02	4.36
109	1.889	0.778	4.83	0.76	0.02	6.4
108	1.904	1.934	4.32	0.82	0.02	5.3
104	1.900	3.870	4.47	0.90	0.02	5.0
111	1.892	—	4.23	7.45	4.01	1.65

Table II shows that the addition of hydrogen bromide to acetone has resulted in a striking reduction of the carbon monoxide, volatile methyl radical ($CH_4+2C_2H_6$) and ethane yields, the ethane yield being in most cases too small for accurate measurement. For small concentrations of hydrogen bromide the effect is strongly dependent upon hydrogen bromide concentration but becomes independent of hydrogen bromide at higher concentrations.

Another striking effect of hydrogen bromide is the inhibition of the carbon monoxide yield. The addition of only 20 mm. of hydrogen bromide (run 109) reduced the carbon monoxide yield to 10% of its value in the absence of hydrogen bromide. This behavior is contrary to that of hydrogen chloride, which produces no effect upon the carbon monoxide yield (3).

The Effect of Temperature on the Inhibition by Hydrogen Bromide

This is shown in Table III. At each temperature two photolyses were carried out at the same light intensity. One of these was a blank with acetone alone.

Throughout the series the time of irradiation and concentration of reagents were maintained constant, except with runs 194 and 195 where longer exposures were used so as to increase the amount of products. An attempt to maintain the illumination constant over the whole series had to be abandoned owing to difficulties arising from the fogging of the cell windows, which became more pronounced as the temperature was raised. Experiment pairs with the same number outside the bracket were carried out at the same light intensity.

TABLE III

THE EFFECT OF TEMPERATURE ON HBr INHIBITION OF ACETONE PHOTOLYSIS
Time 4 hr.

Run	Temp.	Concentration, micromoles/cc.		Products, micromoles			
		Acetone	Hydrogen bromide	CH_4	CO	C_2H_6	$\frac{CH_4+2C_2H_6}{CO}$
1 {113	51.1	1.895	—	0.64	1.18	1.26	2.68
{114	51.7	1.890	0.770	1.73	0.04	0.07	46.8
3 {123	99.8	1.900	—	0.97	5.16	4.62	1.99
{124	100.7	1.895	0.755	2.46	0.09	0.10	29.5
4 {125	119.7	1.891	—	1.68	5.57	4.46	1.90
{126	119.8	1.900	0.759	2.95	0.23	0.08	13.5
1 {105	149.6	1.900	—	4.29	7.76	4.29	1.66
{109	149.8	1.889	0.778	4.83	0.76	0.02	6.38
1 {119	199.4	1.898	—	11.82	11.04	2.54	1.53
{120	199.5	1.898	0.757	12.79	5.84	—	2.19
5 {127	219.6	1.881	—	10.84	8.00	0.80	1.56
{128	218.8	1.898	0.752	10.80	5.69	0.09	1.93
2 {121	249.7	1.893	—	17.42	11.59	0.63	1.61
{122	249.8	1.890	0.758	13.33	7.02	0.11	1.94
6 {168	299.8	1.850	—	13.60	8.26	0.02	1.65
{169	299.2	1.873	0.760	12.80	7.07	0.02	1.82
*7 {194	47.0	1.953	—	0.18	0.77	0.94	2.08
{195	48.0	1.947	0.791	1.09	0.07	0.02	16.1

**Time six hours.*

Table IV shows for each temperature the *carbon monoxide deficiency*, $-\Delta CO$, obtained by subtracting the carbon monoxide yield for the run with hydrogen bromide from the value for the run at the same temperature and light intensity with acetone alone, and the volatile *methyl radical deficiency*, $-\Delta CH_3$, obtained

TABLE IV

CARBON MONOXIDE AND VOLATILE METHYL RADICAL DEFICIENCIES RESULTING FROM THE ADDITION OF HYDROGEN BROMIDE TO ACETONE

Temp., °C.	$-\Delta CO$, micromoles	$-\Delta CH_3$, micromoles	CO yield for acetone, micromoles	$\frac{-\Delta CO}{CO}$	$\frac{-\Delta CH_3}{-\Delta CO}$
51	1.14	1.29	1.18	0.97	1.13
100	5.07	7.55	5.16	0.98	1.49
120	5.34	7.49	5.57	0.96	1.40
150	7.00	8.02	7.76	0.90	1.15
200	5.20	4.11	11.04	0.47	0.79
219	2.31	1.46	8.00	0.29	0.63
250	4.57	5.13	11.59	0.39	1.12
300	1.19	0.80	8.25	0.14	0.67
48	0.70	0.92	0.77	0.91	1.31

in the same way from the function ($CH_4+2C_2H_6$). The ratio of the carbon monoxide deficiency to the yield of carbon monoxide for the acetone photolysis is nearly unity up to 120°C. and then falls off as the temperature increases, but even at 300°C. it is still 0.14. Over the whole range the value of $-\Delta CH_3/\Delta CO$ is of the order of magnitude of unity.

The absolute values of the carbon monoxide deficiency and the volatile methyl radical deficiency are significant only as showing a general tendency, since illumination was maintained constant only over the pairs 113, 114; 105, 109; and 119, 120. It is seen that they rise to maximum at 150° and then fall away again.

The Effect of Time of Irradiation in the Presence of a Small Amount of Hydrogen Bromide

Table V shows the effect of increasing times of irradiation on 100 mm. of acetone at 150° in the presence of 0.3 mm. of hydrogen bromide. The results of an experiment with the same pressure of acetone in the absence of hydrogen

TABLE V

EFFECT OF TIME OF IRRADIATION ON THE PHOTOLYSIS OF ACETONE IN THE PRESENCE OF A SMALL AMOUNT OF HYDROGEN BROMIDE

Acetone 100 mm.; hydrogen bromide 0.30 mm.; Temp. 150°C.

Run	Concentration, micromoles/cc.		Time of run, hr.	Products, micromoles			$\frac{CH_4+2C_2H_6}{CO}$	$\frac{CO}{\text{Time, micromoles/hr.}}$	$\frac{R_{CH_4}}{R_{C_2H_6}}$
	Acetone	Hydrogen bromide		Methane	Carbon monoxide	Ethane			
130	3.779	—	3	5.89	7.73	3.34	1.63	2.58	1.76
132	3.774	0.0113	3	9.89	7.18	1.03	1.66	2.39	9.60
133	3.774	0.0113	6	18.11	15.12	3.18	1.62	2.52	5.70
131	3.779	0.0113	9	24.73	21.28	4.93	1.63	2.37	5.02

bromide are included for comparison. Although the carbon monoxide yields show more scatter than usual, it appears that even this amount of hydrogen bromide has inhibited the carbon monoxide yield to some extent.

The effect of the addition of 0.3 mm. of hydrogen bromide has been to increase the methane yield at the expense of the ethane yield, the ratio $CH_4+2C_2H_6/CO$ remaining constant. The ratio $R_{CH_4}/R_{C_2H_6}$ (R_{CH_4} = rate of methane formation etc.) shows a drop as the time of irradiation is increased, presumably indicating that hydrogen bromide is slowly spent as the photolysis proceeds. However, the magnitude of the effect produced is such that a large part of the HBr reacting must be regenerated.

DISCUSSION

The effect of hydrogen bromide on the photolysis of acetone is particularly striking. As little as 1.5 mm. in 50 mm. of acetone at 150° practically eliminates the ethane yield (run 110, Table II), reduces the carbon monoxide yield to almost half its value in the absence of hydrogen bromide, brings about a considerable increase in the yield of methane and an increase in the ratio

$(CH_4+2C_2H_6)/CO$ to a value well over 2. The last effect is a plain indication that the reaction is not a simple case of photodecomposition of acetone to give methyl radicals and carbon monoxide, followed by the abstraction of hydrogen from the hydrogen halide by the methyl radicals, as appears to be the case in the photolysis of acetone – hydrogen chloride mixtures (3).

That hydrogen abstraction (2) is, however, involved

$$CH_3+HBr = CH_4+Br \qquad [2]$$

is fairly clear from the results of the photolyses for various lengths of time, with very small additions of hydrogen bromide (see Table V). In this case the carbon monoxide yield was only slightly affected and the ratio $(CH_4+2C_2H_6)/CO$ remained the same as for acetone alone, the drop in the ethane yield on addition of hydrogen bromide being accounted for by a corresponding increase in the methane yield. From the same series of experiments it is likewise clear that the reaction

$$Br+CH_3.CO.CH_3 = HBr+CH_2.CO.CH_3 \qquad [4]$$

occurs sufficiently rapidly compared with other reactions of bromine atoms for the hydrogen bromide to be partly regenerated, as has already been discussed. This result is of significance for the photolysis of acetone in the presence of bromine substituted hydrocarbons, as it indicates that the formation of even small quantities of hydrogen bromide will result in serious complications as far as interpretation of the results and derivation of activation energies concerned.

Hydrogen bromide in greater concentration brings about a marked reduction in the volatile methyl radical yield $(CH_4+2C_2H_6)$; for example, at 150° the addition of 9.8 mm. hydrogen bromide to 50 mm. acetone reduces the volatile methyl radical yield to less than half its value in the absence of hydrogen bromide (run 107, Table II). This indicates that methyl radicals are either undergoing reactions not leading to methane or ethane production, or that the photolysis of acetone is so interfered with by the presence of hydrogen bromide, that there is a reduction in the number of methyl radicals produced.

A striking feature of the effect of hydrogen bromide is the sharp suppression of the carbon monoxide yield. This is almost certainly due to a rapid reaction of acetyl radicals with HBr to form acetaldehyde.

Table IV shows that the ratio $-\Delta CH_3/-\Delta CO$ is approximately unity over the range of temperature studied. If the values most likely to be in error are omitted, viz. for 300° where the degree of inhibition is small, and for 50° where the amount of products is small, the average value is 1.1. However, this ratio, as calculated from the figures of Table III, alone is of limited significance. It is, however, consistent within the experimental error with a mechanism in which the loss of CH_3 and of CO is due to loss of acetyl radicals.

Attempts were made to detect acetaldehyde among the products of photolysis of acetone – hydrogen bromide mixtures, but these were not successful. It is felt, however, that this is not a serious objection as there was a considerable amount of tarry products and acetaldehyde may well have been lost in these.

The Reaction Mechanism

The observed effects are therefore accounted for by the following reaction scheme:

$$\begin{aligned} CH_3.CO.CH_3+h\nu &= CH_3.CO+CH_3 && [I\phi] \\ CH_3.CO &= CH_3+CO && [1] \\ CH_3+HBr &= CH_4+Br && [2] \\ CH_3.CO+HBr &= CH_3.CHO+Br && [3] \\ Br+CH_3.CO.CH_3 &= HBr+CH_2.CO.CH_3 && [4] \\ CH_3+Br &= CH_3Br && [5] \end{aligned}$$

Since the light used in these experiments was largely 3130 Å, we assume that the initial decomposition of acetone proceeds predominantly to a methyl and an acetyl radical (5). The acetonyl radical will presumably disappear by association to form bromoacetone or methyl ethyl ketone.

From the above scheme

$$d[CH_3.CO]/dt = I\phi - k_1[CH_3.CO] - k_3[CH_3.CO]\,[HBr] = 0. \qquad I$$

Also $$d[CO]/dt = k_1[CH_3.CO],$$

$\therefore$ $$[CH_3.CO] = d[CO]/dt./k_1. \qquad II$$

Substituting II in I and rearranging

$$I\phi = d[CO]/dt + k_3/k_1.[HBr].d[CO]/dt.$$

Identifying $I\phi$ with R_{CO}, the rate of carbon monoxide formation for acetone alone, and setting R^*_{CO} equal to $d[CO]/dt$, the rate of carbon monoxide formation in the presence of hydrogen bromide, we obtain on rearranging:

$$R_{CO}/R^*_{CO} - 1 = k_3[HBr]/k_1$$

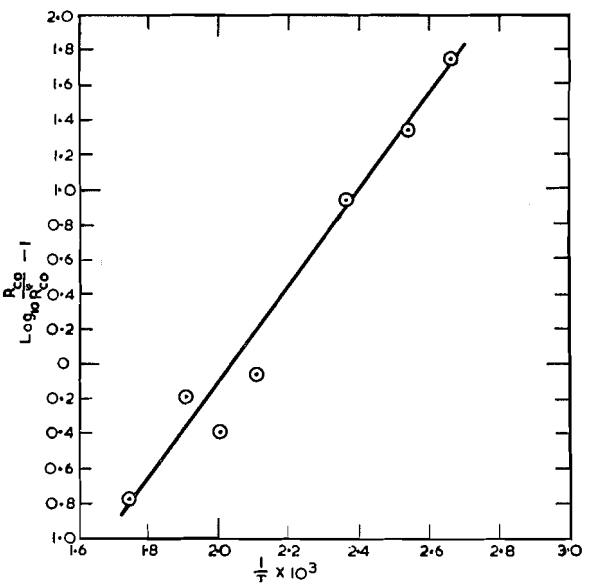

FIG. 1. $\text{Log}_{10} R_{CO}/R^*_{CO} - 1$ vs. $1/T \times 10^3$.

Fig. 1 shows log $R_{CO}/R^{*}_{CO}-1$ plotted against $1/T$. The points lie about a straight line with a slope corresponding to about -13 kcal./mole for the difference E_3-E_1. The activation energy of reaction (1) is not known precisely but has been estimated at from 10 to 18 kcal./mole (4). E_3 is unlikely to be more than 5 kcal./mole. Thus, in view of the drastic approximations made in the above derivation the value of -13 kcal./mole for E_3-E_1 is a reasonable one, and to this extent supports the mechanism suggested.

If the inhibition of the acetone photolysis by hydrogen bromide is due entirely to the reaction of acetyl radicals the yield of $(CH_4+2C_2H_6)$ for the inhibited reaction cannot be less than the carbon monoxide yield of the corresponding uninhibited reaction. However, reference to Table II shows that the volatile methyl radical yield of the inhibited reaction falls appreciably below the carbon monoxide yield for acetone alone. This may be attributed to reaction (5). As noted previously with the experiments with 0.3 mm. hydrogen bromide, hydrogen bromide is gradually spent despite the regenerative reaction. With the higher concentrations of hydrogen bromide used in the experiments over a range of temperatures, the production of bromine atoms must become appreciable.

ACKNOWLEDGMENT

We wish to thank Miss F. Gauthier and Dr. F. P. Lossing of this laboratory for the mass spectrometric analyses, and Drs. R. J. Cvetanovic and R. M. Heggie for many interesting discussions.

REFERENCES

1. Anderson, H. C. and Kistiakowsky, G. B. J. Chem. Phys. 11: 6. 1943.
2. Cvetanovic, R., Raal, F. A., and Steacie, E. W. R. Can. J. Chem. 31: 171. 1953.
3. Cvetanovic, R. and Steacie, E. W. R. Can. J. Chem. 31: 158. 1953.
4. Davis, W. Chem. Revs. 40: 201. 1947.
5. Noyes, W. A., Jr. and Dorfman, L. M. J. Chem. Phys. 16: 788. 1948.
6. Raal, F. A. and Steacie, E. W. R. J. Chem. Phys. 20: 578. 1952.
7. Ridge, M. J. and Steacie, E. W. R. Can. J. Chem. In press. 1955.

THE EFFECT OF PRECIPITATION CONDITIONS ON THE FLOW PROPERTIES OF SILICA DISPERSIONS[1]

By A. F. Sirianni and I. E. Puddington

ABSTRACT

The pH of the solutions in which silica is precipitated from sodium silicate has a marked effect on the flow properties of pastes prepared by subsequently dispersing the silica in liquid hydrocarbons. The yield value of this non-Newtonian suspension exhibits a pronounced maximum when silica precipitated at about pH 5 is used. An explanation based on the properties of the solid–liquid interface is proposed.

INTRODUCTION

When a dilute solution of sodium silicate is treated with acid, a sol of silicic acid is formed. On standing, this sol sets to a firm, transparent gel. Although the mechanism of this change is still a subject of investigation, it appears to be due to the formation of polymers from the liberated silicic acid and the cross-linking of these aggregates to form a three-dimensional structure. The time required for the sol–gel transformation to occur is termed the time of set and it is a function of the hydrogen ion concentration in the system when silica concentration and temperature are kept constant. The time of set and certain mechanical properties of the gel can also be altered by the use of chemical additives (12, 13). A number of substances show this effect, including alcohols, aldehydes, ketones, and sugars.

Since the time of set is an indication of particle–particle interaction, it might be expected that factors that change the time of set materially may also influence the other properties of the gel that depend on interaction between particles. A recent and interesting use to which silica has been put is its addition to liquid hydrocarbons to produce highly thixotropic pastelike dispersions. Since thixotropy is caused by the interaction of solid phase particles, it seemed probable that the conditions of preparation of the original silica gel would influence the properties of the paste. The present communication describes part of the work undertaken in this connection, viz., the effect, on the flow-properties of the hydrocarbon–silica dispersions, of altering the pH at which gels of constant concentration are prepared.

EXPERIMENTAL

The silica aqua gels were prepared by adding sulphuric acid to an appropriate concentration of *N* grade sodium silicate produced by the Philadelphia Quartz Company. The following procedure was typical: 100 gm. of 41° Baumé silicate were diluted to 450 cc. with distilled water in a 2 liter beaker. The silicic acid was precipitated during vigorous agitation by the addition of about 550 cc. of dilute sulphuric acid. The pH of the sol was taken with a Beckman pH meter before gelation occurred, the quantity of acid being adjusted to give

[1]*Manuscript received in original form August 11, 1952, and as revised, October 25, 1954.*
Contribution from the Division of Applied Chemistry, National Research Council, Ottawa, Canada. Issued as N.R.C. No. 3481.

gels that varied in pH from 1.0 to 8.6. Variations in the time of set of these sols were similar to those observed by other investigators. The concentration of SiO_2 in all the gels was approximately 2.8%.

The gels were allowed to age for 24 hr. at 25°C., after they had set. They were then washed until substantially free from soluble salts. This was normally accomplished with four 1-liter portions of distilled water, the gel and wash water being mixed in a Waring Blendor before filtering. In a few experiments the gel was extracted until no sulphate could be detected in the wash water. As subsequent experiments indicated no significant difference between these gels and those washed by the first procedure, the simpler method was used. Changes in pH of the gel during the setting period were small and in the expected direction (7).

Silica may be dispersed in non-aqueous media and still retain much of the structure developed during the sol–gel transformation by either of the following methods. In the first, the water in the aqua gel is exchanged with a solvent miscible both with water and with the liquid medium in which the silica is to be dispersed. This may be done conveniently by a process of exhaustive extraction. In the present work acetone was used as the solvent. The exchange was carried out in a continuous liquid extractor fitted with a fractionating column to deliver substantially dry acetone to the sample. Solvent replacement was considered complete when a test sample of silica did not shrink when placed in high boiling liquid hydrocarbon and the solvent flashed off. Silica–hydrocarbon dispersions could now be prepared by adding an appropriate quantity of silica–acetone gel to the hydrocarbon, flashing off the acetone, and subjecting the system to mild homogenization.

The second method consists in first producing a silica aerogel by the method of Kistler (8) followed by dispersing a known amount of the aerogel in the hydrocarbon using a shearing device.

The flow properties of the pastes produced by these methods could be examined using conventional apparatus.

The pastes from solvent exchanged silica were made up to contain 5.76% of silica by weight in a highly paraffinic oil having a viscosity of about 0.65 poise at 38°C. Pastes prepared from aerogels contained 5.0% of silica by weight. Owing to the similarity of refractive index of the two phases, the dispersions were quite transparent. Viscometric measurements were made using an extrusion plastometer that was equipped with a capillary having an orifice 0.089 cm. in diameter and 2.45 cm. in length. Compressed nitrogen provided a source of variable pressure. The samples were degassed by being placed in a vacuum desiccator for about 20 min. and were charged into the viscometer under reduced pressure to lessen the danger of entrapping air bubbles.

From the outflow time, weight of material extruded, and pressure used, the rates of shear and apparent viscosity were calculated for the various samples using Poiseuille's equation. The results were examined by plotting the apparent viscosities against the reciprocal of the rate of shear and by calculating the residual viscosity and coefficient of thixotropy or yield value from the intercept at infinite shear and the limiting slope of the graph at high shear rates.

RESULTS AND DISCUSSION

Typical data showing the changes in the yield value of the silica–oil dispersions with the variation of the pH at which the silica was precipitated are shown in Fig. 1. During a period of several years, more than 60 individual

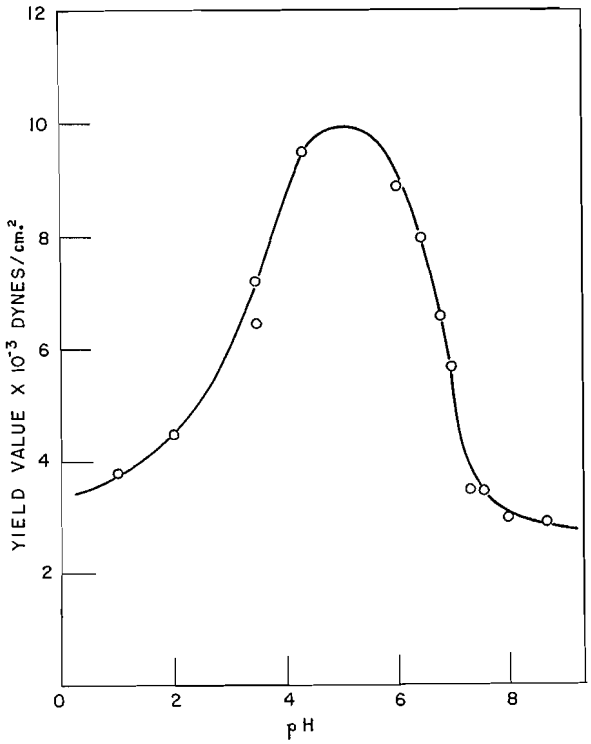

FIG. 1. Dependence of the yield value of silica–hydrocarbon pastes on the conditions under which the silica is precipitated.

experiments have been conducted using the silica obtained from several samples of sodium silicate and using both the solvent exchange and aerogel techniques in the preparation of the silica–oil pastes. With minor variations the flow properties of the dispersions follow the pattern indicated in Fig. 1. The maximum in the curve obtained with pastes prepared via the aerogel technique is usually displaced slightly to the left. However, by redispersing samples of the silicas in water, it was found that the pH of the dispersions prepared from the aerogels was higher than comparable samples prepared from solvent exchanged silica. The change in acidity apparently occurs during the preparation of the aerogel and compensates for the apparent displacement of the maximum.

Comparison of the residual viscosities of these systems (1, 5, 15) indicates an apparent increase in the axial ratio of individual particles of silica in the vicinity of pH 5. This, however, may actually be an increased porosity in particles of cross-linked gel at this pH. No differences could be detected in the

various samples of silica when the pastes prepared from them were examined with the electron microscope. To determine whether or not this apparent change in shape factor could account for the maximum found in the yield value, three silica aqua sols, adjusted to pH 5.0, 6.6, and 2.5 respectively, were prepared and allowed to gel. After the gels had aged for 24 hr., each was divided into three portions, extra water was added, and each portion agitated until a smooth slurry was produced. One of the portions from each batch was retained as a control and to each of the others acid or alkali was added to adjust the pH of the slurries to 2.9 and 7.1 for the first batch, 5.0 and 4.0 for the second, and 5.0 and 7.0 for the third. After a further 24 hr. period of aging, the silica samples were washed, solvent exchanged with acetone, and dispersed in oil as previously described. When the flow properties of these nine dispersions were examined and the yield values plotted as a function of conditioning pH it was found that a reasonably smooth curve very similar in shape to Fig. 1 could be drawn through the points. The apparent viscosity at infinite shear was virtually independent of the conditioning pH values in each of the three batches. These results would seem to indicate that the phenomenon is due predominantly to the surface properties of the silica rather than to the shape of the particles.

The maximum in yield value apparently bears no relation to the minimum time of set of silica gels since this occurs at about pH 8 (13), nor is it related to the rigidity of the aqua gels (11). It does appear to occur in a region where elastic recovery of the aqua gel is high and very near the isoelectric point determined by Batchelor (2).

Schneiderwirth (14) has noted that aqueous dispersions of insoluble alkaline earth salts show a maximum in thixotropy at pH 5 and the apparent viscosity of aqueous suspensions of TiC and TiN have been observed to pass through a maximum at pH 6 (16). Mukherjee and Mitra (10) have reported a very pronounced maximum in the viscosity of suspensions of bentonitic clay at about pH 6.5 and Hauth (6) has noted a similar phenomenon with aqueous alumina. Thus maxima in apparent viscosity with changes in pH do not appear to be uncommon with aqueous inorganic suspensions. No record of a similar occurrence with non-aqueous media was found, however.

Since the maximum in yield value must be associated with a high degree of flocculation and instability of the system, this is to be expected at or near an isoelectric point. Although it has been pointed out recently (9) that while the usual double layer considerations may apply in a number of non-aqueous systems they would not be expected in such apolar liquid media as hydrocarbons. Garner, Nutt, and Mohtadi have been able to demonstrate electrokinetic phenomena with carbon dispersed in highly non-polar systems (4). Electrokinetic effects could not be observed with these dispersions of silica after suitable dilution. However, it is perhaps not unreasonable that a partial layer of acid or alkali sorbed on the silica surface on either side of the isoelectric point would confer a degree of stability to the system in proportion to the percentage of surface covered, with a consequent reduction in the yield value. This effect may be enhanced by the presence of oil soluble polar compounds in the liquid phase.

Chaudhury (3) has suggested the possible influence of the free energy at the solid–liquid interface on the stability of colloidal systems. The effect of screening ions on the surface energy of quartz and its relation to the rheological properties of aqueous clay and sand suspensions has been emphasized recently in a review by Weyl (17). That the effect may be even more pronounced in non-aqueous media is also indicated. Certainly the initiation of flow in a thixotropic paste involves the creation of fresh solid–liquid interfaces, since electrical properties of pastes indicate solid–solid contact in the unsheared condition. High interfacial surface energies might be expected to contribute to the high yield values of the less stable systems, while the possible reduction of surface energies due to the adsorption of ions is in keeping with the greater stability found with the systems where the silica was precipitated above and below pH 5. Many examples can be cited where spontaneous adsorption of molecules dissolved in the liquid phase has increased the stability of suspensions in hydrocarbon media. This process presumably takes place with a substantial reduction of the free energy of the solid–liquid interface.

ACKNOWLEDGMENT

Preliminary experimental data contained in this paper were obtained when work was in progress under an industrial agreement between Imperial Oil Limited and the National Research Council. Our thanks are due Imperial Oil for permission to publish the results.

REFERENCES

1. ASBECK, W. K. and VAN LOO, M. Ind. Eng. Chem. 46: 1291. 1954.
2. BATCHELOR, H. W. J. Phys. Chem. 42: 575. 1938.
3. CHAUDHURY, S. G. J. Phys. Chem. 32: 148. 1928.
4. GARNER, F. H., NUTT, C. W., and MOHTADI, M. F. J. Inst. Petroleum, 38: 986. 1952.
5. GOODEVE, C. F. and WHITFIELD, G. W. Trans. Faraday Soc. 34: 511. 1938.
6. HAUTH, W. E., JR. J. Phys. & Colloid Chem. 54: 142. 1950.
7. HURD, C. B., FREDERICK, K. J., and HAYNES, C. R. J. Phys. Chem. 42: 85. 1938.
8. KISTLER, S. S. J. Phys. Chem. 36: 52. 1932.
9. KRUYT, H. R. and OVERBEEK, J. TH. G. In Colloid science. Vol. 1. *Edited by* H. R. Kruyt. Elsevier Publishing Co., Inc., New York. 1952. pp. 57 and 62.
10. MUKHERJEE, J. N. and MITRA, R. P. J. Colloid Sci. 1: 141. 1946.
11. MUNRO, L. A., MCNAB, J. G., and OTT, W. L. Can. J. Research, B, 27: 781. 1949.
12. MUNRO, L. A. and PEARCE, J. A. Can. J. Research, B, 16: 390. 1938.
13. MUNRO, L. A. and PEARCE, J. A. Can. J. Research, B, 17: 266. 1939.
14. SCHNEIDERWIRTH, H. J. U.S. Patent 2,487,600. 1950.
15. SIRIANNI, A. F., MOSES, G. B., and PUDDINGTON, I. E. Can. J. Chem. 29: 166. 1951.
16. VASILOS, T. and KINGERY, W. D. J. Phys. Chem. 58: 486. 1954.
17. WEYL, W. A. In Structure and properties of solid surfaces. *Edited by* R. Gomer and C. S. Smith. The University of Chicago Press, Chicago. 1953. p. 147ff.

THE PHOTOLYSIS OF MIXTURES OF ACETONE AND SOME HALOGENATED HYDROCARBONS[1]

By M. J. Ridge[2] and E. W. R. Steacie

ABSTRACT

The composition of the products of photolysis of acetone in the presence of methyl chloride, methyl bromide, methylene chloride, and methylene bromide has been determined. These reactions are attended by complications not found with the photolysis of acetone–hydrocarbon mixtures. Failure to take into account reactions resulting from the formation of halogen hydrides and to allow for the presence of ethylene invalidates the values obtained by Raal and Steacie for the activation energy for hydrogen abstraction by methyl radicals from some halogenated hydrocarbons.

INTRODUCTION

The photolysis of mixtures of acetone and some halogenated hydrocarbons has been investigated by Raal and Steacie (4), who found ethane, methane, and carbon monoxide as volatile products. Assuming that all methane arose from hydrogen abstraction by methyl radicals from acetone and the particular halogenated hydrocarbon, and that all ethane arose from the combination of methyl radicals, Raal and Steacie obtained values for the activation energy of a number of reactions of the type

$$CH_3+CH_3X = CH_4+CH_2X$$

where X = Cl, Br, or F.

However, the photolysis of acetone in the presence of carbon tetrachloride and chloroform has been studied by Cvetanovic *et al.* (1) and with both substrates hydrogen chloride was found among the reaction products. In view of the rapid hydrogen abstraction from hydrogen chloride by methyl radicals (2), the formation of hydrogen chloride during the course of the reaction invalidates the kinetic treatment applied by Raal and Steacie to the photolysis of acetone in the presence of chloroform.

The present paper describes the results of an investigation into the composition of the products of the photolysis of acetone in the presence of methyl chloride, methylene chloride, methyl bromide, and methylene bromide.

EXPERIMENTAL

The apparatus was of the same general design as that used by Cvetanovic and Steacie (2), with provision for the exclusion of mercury vapor from the reaction cell. Silicone grease was used as a stopcock lubricant. When constant illumination over a series of runs was required, the current through the lamp was adjusted to give constant intensity of the emergent light as measured by a phototube reading. In fact, the current through the lamp required to be con-

[1]*Manuscript received August 12, 1954.*
Contribution from the Division of Pure Chemistry, National Research Council, Ottawa, Canada. Issued as N.R.C. No. 3490.
[2]*On leave of absence 1952–53 from the Division of Tribophysics, Commonwealth Scientific and Industrial Research Organization, Melbourne, Australia.*

stantly increased as the exposure continued, owing to the deposition of opaque matter on the windows of the reaction cell (chiefly on the front window).

Two filters were used alternatively, viz.:

(*a*) A Corning 7.54, with a "cutoff" below 2300 Å.

(*b*) A Corning 0.53, with a "cutoff" below 2800 Å (Pyrex Filter).

Analysis of products was carried out by means of a modified Ward still (3) in conjunction with standard gas analysis methods. Analyses of fractions from the Ward still were also carried out by means of the mass spectrometer.

RESULTS

Acetone – Methyl Chloride Mixtures

The results of a number of experiments with acetone – methyl chloride mixtures are given in Table I. The products are those to be expected from the photolysis of acetone or from hydrogen abstraction by methyl radicals from

TABLE I

PHOTOLYSIS OF ACETONE – METHYL CHLORIDE MIXTURES AT 150°C.

Run	Concentration, μM./cc.		Time, sec.	Products, μM.				Remarks
	Acetone	CH_3Cl		CH_4	CO	C_2H_6	C_2H_4	
38	3.890	3.685	7200	17.23	11.19	3.0	2.36	
46	3.838	3.771	18,000	—	—	2.30	1.27	
52	3.785	—	3600	3.39	5.92	2.98	0.04	
53	3.816	—	7200	7.07	11.93	4.98	0.07	
58*	1.889	1.889	7200	36.51	25.60	1.88	1.45	Filter "A".
59*	1.889	1.919	7200	35.15	25.72	2.04	1.37	Mercury absent
56	1.911	—	7200	—	28.54	—	—	
57	1.885	23.76	7200	—	28.36	—	—	
157	—	14.84	57,600	0	0	(0.04)		
60*	1.965	1.889	7200	37.34	25.49	1.82	1.28	
61*	1.878	1.879	7200	36.14	24.58	1.89	1.43	
93	1.899	1.899	5400	31.16	21.90	1.72	1.32	
94	1.900	—	5400	6.02	22.19	16.37	0	Filter "A".
95	—	1.923	5400	0	0	0	0	Mercury present
96†	1.904	1.902	5400	0	0	0	0	
75	—	7.695	21,600	(0.04)		(0.04)		
64	1.891	1.903	7200	28.34	24.08	1.33	0.85	Filter "A".
65	1.897	1.927	7200	27.61	23.34	1.21	1.03	Mercury absent. Run No. 64 was carried out in the presence of 11.54μM. /cc. of CO_2

**Successive runs at same intensity.*
†No illumination.
—Product not determined.

methyl chloride. However, ethylene is also an important product. Tests for the presence of hydrogen chloride among the reaction products were made by the method previously described (1). A series of experiments was made at 150°C. When methyl chloride was irradiated alone, or when mixtures of acetone and methyl chloride were maintained at 150°C. for 15 hr. without irradiation, no

hydrogen chloride was detectable. Hydrogen chloride was, however, always found in irradiated mixtures of acetone and methyl chloride.

The following conclusions may be drawn:

(*a*) The formation of ethylene and HCl shows that the reaction is complex and invalidates the kinetic treatment of Raal and Steacie (4).

(*b*) The presence of mercury vapor has no effect.

(*c*) Runs 56 and 57 show that the quantum yield of CO is not affected by the presence of a large amount of methyl chloride.

(*d*) No appreciable quantity of gaseous products is formed on irradiating methyl chloride alone.

(*e*) The presence of a large excess of CO_2 (runs 64 and 65) does not affect the results. Surface effects or effects due to excited molecules are therefore unimportant.

A few experiments were also made with deutero-acetone and methyl chloride. The C_1 fraction consisted of CO, CD_3H, and CD_4. The absence of CH_4 and CH_3D is further evidence that no direct decomposition of CH_3Cl is occurring. The ethylene fraction was mainly $C_2D_2H_2$. This rules out the possibility of ethylene resulting from disproportionation of CH_2Cl or dimerization followed by decomposition. Ethylene presumably results from the decomposition of complex products perhaps formed from CH_2Cl and CH_3COCH_2.

Acetone – Methylene Chloride Mixtures

Similar experiments were carried out with methylene chloride. Appreciable amounts of hydrogen chloride were found among the reaction products. Traces of HCl were found, however, when methylene chloride alone was irradiated.

Acetone – Methyl Bromide Mixtures

Similar experiments were carried out with acetone – methyl bromide mixtures. The results for a typical run were:

Temperature:	150°C.
Filter:	"*b*"
Acetone:	100 mm.
Methyl bromide:	100 mm.
Time:	nine hours

Products	μM.
CH_4	24.37
CO	16.48
C_2H_6	1.11
C_2H_4	0.19

Ethylene was thus again formed, but in much smaller amount than with methyl chloride. Hydrogen bromide was not positively identified, since the unilluminated mixture gave a slight positive reaction.

The complications are thus not as pronounced as with methyl chloride, but the results of Raal and Steacie (4) should be regarded with some suspicion.

Similar results were obtained with methylene bromide.

REFERENCES

1. CVETANOVIC, R. J., RAAL, F. A., and STEACIE, E. W. R. Can. J. Chem. 31: 171. 1953.
2. CVETANOVIC, R. J. and STEACIE, E. W. R. Can. J. Chem. 31: 158. 1953.
3. LEROY, D. J. Can. J. Research, B, 28: 492. 1950.
4. RAAL, F. A. and STEACIE, E. W. R. J. Chem. Phys. 20: 578. 1952.

ORGANIC DEUTERIUM COMPOUNDS
XIII. THE MECHANISM OF THE NEF REACTION SYNTHESIS OF ETHANAL-1-*d*[1]

By Leonard C. Leitch

ABSTRACT

The mechanism of the Nef reaction was investigated with nitroethane-1,1-d_2. The isolation of 95 mole % ethanal-1-*d* in 70% yield renders a mechanism proposed by Mahler untenable, but supports others submitted by van Tamelen and Thiede and by Nametkin.

INTRODUCTION

The conversion of a primary nitroparaffin into an aldehyde or of a secondary nitroparaffin into a ketone is known, after its discoverer, as the Nef reaction (9). Its scope was later investigated by Johnson and Degering (4) when nitroparaffins became readily accessible from the nitration of aliphatic hydrocarbons. Mahler (7) defined the optimum conditions for the preparation of propionaldehyde from 1-nitropropane and suggested "the highly tentative mechanism" shown below.

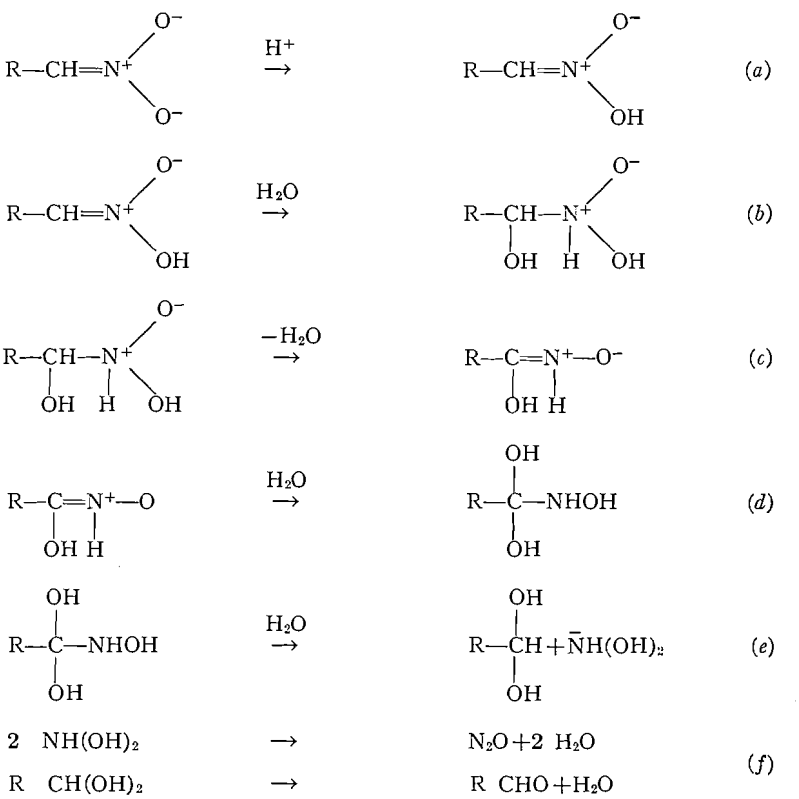

[1]*Manuscript received October 25, 1954.*
Contribution from the Division of Pure Chemistry, National Research Laboratories, Ottawa, Canada. Issued as N.R.C. No. 3489. Presented at the 126th meeting of the American Chemical Society, New York City, September, 1954.

This mechanism hinges on the addition of a mole of water in one direction, its elimination in another, then addition of a second mole of water, followed by hydrolysis. The addition of water in the manner indicated is improbable on account of the charge distribution between carbon and nitrogen. Also, this mechanism cannot account for the formation of ketones from secondary nitroparaffins.

An alternative mechanism which is shown below was recently advanced by van Tamelen and Thiede (11).

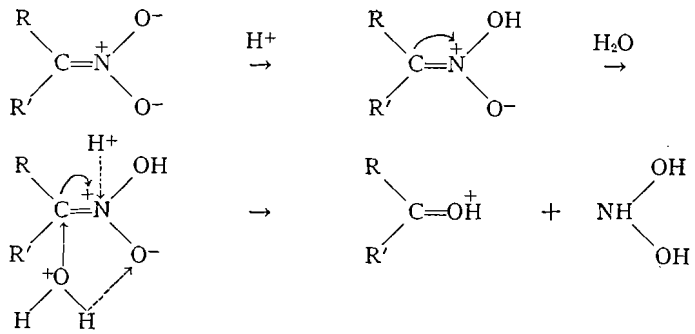

These authors point out a parallel between the Nef reaction and the hydrolysis of oximes and present evidence strongly in favor of this scheme.

The correctness or otherwise of these mechanisms may be readily tested using deuterated nitroethane as a tracer; for, if the reaction proceeds as proposed by Mahler, nitroethane-1,1-d_2 ($CH_3CD_2NO_2$) should give normal acetaldehyde because the hydrogen at C-1 is lost as water in step (*c*) and acetaldehyde is formed by hydrolysis in step (*e*). On the other hand acetaldehyde deuterated in the functional group should result if the reaction follows the course suggested by van Tamelen and Thiede (11).

Nitroethane-1,1-d_2 was prepared by exchanging nitroethane with deuterium oxide as described for nitromethane in a previous paper (5) but in the presence of a weak base. After two exchanges the bands at 1330, 1255, 1132, 994, and 811 cm.$^{-1}$ in the infrared spectrum of $CH_3CH_2NO_2$ were reduced in intensity while new bands corresponding to $CH_3CD_2NO_2$ appeared at 1305, 1289, and 1025 cm^{-1}. The mass spectrum of nitroethane shows no parent peak, but measurement of the peak intensity due to $CH_3\overset{+}{C}D_2$ indicated that the compound contained about 45 mole % $CH_3CD_2NO_2$ and unknown amounts of CH_3CHDNO_2 and $CH_3CH_2NO_2$. There was no peak corresponding to three deuterium atoms in the molecule so deuteration therefore does not extend to the H in the methyl group. The deuterated nitroethane was subjected to the Nef reaction essentially as described by Johnson and Degering (4) except that the acetaldehyde itself was isolated instead of its semicarbazone. The mass spectrum of the acetaldehyde indicated it was largely CH_3CDO. The mechanism of the Nef reaction as proposed by Mahler (7) is therefore incorrect. On the other hand, the present work supports the alternative and simpler mechanism of van Tamelen and Thiede (11).

A minor shortcoming of their interpretation of the Nef reaction is its failure to account for the appearance of a transient blue color in the reaction mixture prior to the evolution of nitrous oxide. Nametkin (8) attributed this color to the formation of a nitroso intermediate.* It is possible to modify the mechanism of van Tamelen and Thiede (11) to include a nitroso intermediate as shown below.

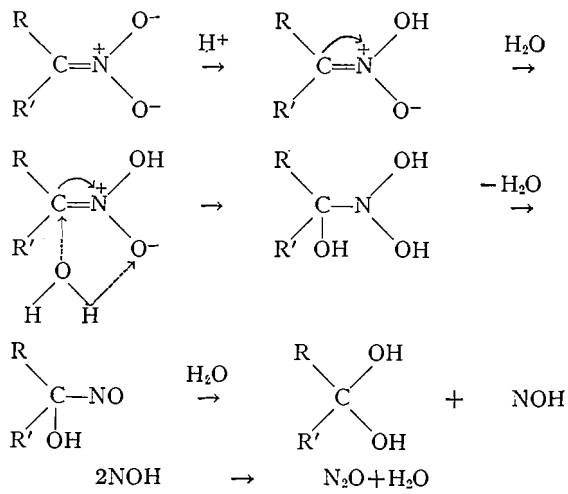

The Nef reaction is well adapted to the synthesis of ethanal-1-*d* and other aldehydes deuterated only in the formyl group on account of its simplicity and the high isotopic purity of the product, which is over 95% if we base our results on the theoretical calculation of Brinton and Blacet (3) for the mass ratio CDO/CHO obtained by mass spectrometry.

The apparent discrepancy between the deuterium content of the nitroethane and that of the acetaldehyde prepared from it may be readily reconciled by reference to data in a paper by Wynne-Jones (12). According to this author the relative rates of ionization of the hydrogen and deuterium atoms in nitroethane are in the ratio 10:1. Therefore, assuming the deuterated nitroethane contained 50% of the isotopic species, CH_3CHDNO_2, its ion, $CH_3CD{=}NO_2^-$ will be present to the extent of 45%; this, added to the 45% from $CH_3CD_2NO_2$, would lead to acetaldehyde containing 90% CH_3CDO.

Ethanal-1-*d* has been synthesized by Blacet and Brinton (2) in five steps starting from butyne-2. Another synthesis from diacetyl was reported recently by Loewus *et al.* (6). The first is tedious and leads to a product of low isotopic purity, while the second requires lithium aluminum deuteride which is both difficult to obtain and very expensive. Moreover, these methods are not suitable for the synthesis of other aldehydes deuterated in the functional group because the starting materials are not readily accessible.

**This information was kindly supplied by Dr. W. E. Noland, Department of Chemistry, University of Minnesota, Minneapolis, Minn.*

The ethanal-1-*d* reported in this work has since been used by others in these laboratories in spectroscopic and photochemical studies (1, 10).

EXPERIMENTAL

Nitroethane-1,1-d_2, $CH_3CD_2NO_2$

A mixture of nitroethane (25 ml.) and deuterium oxide (25 ml.) containing 10 mgm. of dissolved anhydrous sodium acetate was heated overnight in a sealed tube in a rocking furnace at 90°C. The tube containing the deep-yellow reaction mixture was opened, attached to a vacuum line, frozen, and evacuated. The supernatant layer of deuterated nitroethane was distilled off through a U-tube containing Drierite and condensed in a trap at −78°C. The yield of colorless liquid was 19.0 ml. The loss is due to the formation of a water-soluble product by a side reaction which was not further investigated.

The exchange was repeated with an equal volume of fresh deuterium oxide and sodium acetate. The yield of nitroethane-1,1-d_2 analyzing 45 mole % $CH_3CD_2NO_2$ was 11.0 ml.

Ethanal-1-d, CH_3CDO

Nitroethane-1,1-d_2 (3.0 ml.) was dissolved in 20 ml. of ice-cold 10% sodium hydroxide in a small separatory funnel. The solution was added slowly dropwise to one of 6 ml. sulphuric acid dissolved in 40 ml. of water, which was kept at 0 to 5°C. and stirred continuously. The addition of the sodium nitroethane solution produces a characteristic blue color in the sulphuric acid which fades as nitrous oxide is evolved. Any acetaldehyde entrained in the nitrous oxide was condensed in a U-tube cooled to −40°C. with dry ice and acetone. Stirring was continued for 15 min. after all the sodium salt solution had been added. When the reaction mixture was heated the acetaldehyde distilled and condensed in the U-tube. The product was then distilled from the U-tube into a graduated trap on the vacuum line. Yield: 0.8 ml. The mass spectrum gave the following principal peaks:

46	($CH_2D.CDO$)	3.82
45	(CH_3CDO)	136.0
30	($\overset{+}{C}DO$)	200.8
29	($\overset{+}{C}HO$)	24.83

Evidently, ethanal-1-*d* is largely produced in this reaction rather than normal acetaldehyde.

There is no advantage in dissolving the deuterated nitroethane in sodium deuteroxide. In fact, this leads to a higher peak at 46 due to CH_2DCDO produced by the exchange:

$$CH_3CDO + D^+ \rightleftarrows CH_2DCDO + H^+.$$

ACKNOWLEDGMENTS

The author is grateful to Dr. D. A. Ramsay for the interpretation of the infrared absorption spectra and to Miss F. Gauthier for the mass analyses.

REFERENCES

1. AUSLOOS, P. and STEACIE, E. W. R. Unpublished work.
2. BLACET, F. E. and BRINTON, R. K. J. Am. Chem. Soc. 22: 4715. 1950.
3. BRINTON, R. K. and BLACET, F. E. J. Chem. Phys. 17: 797. 1949.
4. JOHNSON, K. and DEGERING, E. F. J. Org. Chem. 8: 10. 1943.
5. LEITCH, L. C., GAGNON, P. E., and CAMBRON, A. Can. J. Research, B, 28: 256. 1950.
6. LOEWUS, F. A., WESTHEIMER, F. H., and VENNESLAUD, B. J. Am. Chem. Soc. 75: 5018. 1953.
7. MAHLER, H. R. U.S. Atomic Energy Comm. Document No. 2400. 1948. p. 40.
8. NAMETKIN, S. S. J. Russ. Phys. Chem. Soc. 45: 1414. 1913. Chem. Abstr. 8: 324. 1914.
9. NEF, J. U. Ann. 280: 263. 1894.
10. RAMSAY, D. A. Unpublished work.
11. VAN TAMELEN, E. E. and THIEDE, R. J. J. Am. Chem. Soc. 74: 2615. 1952.
12. WYNNE-JONES, W. F. K. J. Chem. Phys. 2: 381. 1934.

THE BIOGENESIS OF ALKALOIDS

XIV. A STUDY OF THE BIOSYNTHESIS OF DAMASCENINE AND TRIGONELLINE

By Edward Leete,[2] Léo Marion, and Ian D. Spenser[2]

ABSTRACT

Tryptophan-3-C^{14} was prepared from methyl labelled sodium acetate and fed to mature *Nigella damascena* L. plants. Radioactivity was translocated throughout the plant, but no activity was detected in the damascenine isolated from it. Similarly the radioactive tryptophan was fed to pea seedlings and trigonelline detected in the plant extracts. This was also inactive, and these results are discussed.

It has been suggested (25) that trigonelline (the methyl betaine of nicotinic acid) arises from proline by ring opening to δ-aminovaleric acid and thence to nicotinic acid by reaction with a one carbon fragment such as formic acid. Klein and Linser (18, 19) injected various amino acids into the hollow stems of *Dahlia variabilis* and other plants which produce trigonelline and they claimed that the amount of trigonelline increased, relative to that in control plants, after the feeding of ornithine, proline, glutamic acid, or δ-aminovaleric acid. No increase was observed after feeding arginine, tyrosine, aspartic acid, or other amino acids. Hexamethylene tetramine produced increases in the amount of alkaloid, possibly by acting as a source of formic acid. These results have been critically examined by James (15) who raised doubts about the supposed increases in the amount of alkaloid.

Barger (3) was the first to place damascenine (the methyl ester of 2-methylamino-3-methoxybenzoic acid) amongst the alkaloids derived from tryptophan by the oxidation of indole to anthranilic acid followed by hydroxylation and methylation. In animals and molds it has been conclusively proved that 3-hydroxyanthranilic acid and nicotinic acid arise in the course of tryptophan metabolism (4, 6, 14, 20). Many biological reactions which occur in plants have been shown to be similar to if not identical with those occurring in animals and molds. It was thus conceivable that tryptophan might be the source not only of damascenine, but also of trigonelline. It was therefore decided to feed tryptophan labelled with C^{14} in the 3-position of the indole nucleus to plants producing damascenine and trigonelline. If tryptophan were the precursor of these alkaloids radioactivity would be expected in the carboxyl group of both trigonelline and damascenine.

The preparation of tryptophan-3-C^{14} in 5% yield from carboxyl labelled benzoic acid in 11 steps has been reported (14). In the present work methyl labelled sodium acetate was converted to pyruvamide-3-C^{14} by the method described in the literature (2, 24) for the preparation of pyruvamide-2-C^{14} from carboxyl labelled sodium acetate. This was converted to the phenylhydrazone and quantitatively hydrolyzed to pyruvic acid phenylhydrazone

[1]*Manuscript received November 4, 1954.*
Contribution from the Division of Pure Chemistry, National Research Council, Ottawa, Canada. Issued as N.R.C. No. 3496.
[2]*National Research Council of Canada Postdoctorate Fellow.*

which was esterified with diazomethane and cyclized to methyl indole-2-carboxylate (7). The ester was hydrolyzed and the indole-2-carboxylic acid decarboxylated in quinoline in the presence of cupric oxide. The indole-3-C^{14} was converted via gramine to tryptophan-3-C^{14} (1, 13, 23). The over-all radiochemical yield from pyruvamide to tryptophan was 6%. Direct ring closure of pyruvic acid phenylhydrazone to indole-2-carboxylic acid failed completely (11) while cyclization of pyruvamide phenylhydrazone to indole-3-carboxamide was accomplished in 12% yield only. Attempts to synthesize pyruvic acid phenylhydrazone according to Japp and Klingemann (16) in two steps from methyl iodide and ethyl methylmalonate (10) or from methyl iodide and ethylacetoacetate (9) led to the desired product in poor yields only.

The labelled tryptophan was fed to mature five-month-old *Nigella damascena* plants via the roots and after eight days the damascenine isolated from the whole plant by ether extraction. The amino acid was also fed to five-week-old pea seedlings and after seven days trigonelline was detected in the extracts of the aerial parts of the plant. No trigonelline was found in the roots. Neither alkaloid, however, was radioactive.

EXPERIMENTAL[3]

Synthesis of Tryptophan-3-C^{14}

Pyruvamide-3-C^{14}.—This was prepared from methyl labelled sodium acetate by the same method as that described for the synthesis of pyruvamide-2-C^{14} (2, 24).

Pyruvic acid-3-C^{14} phenylhydrazone.—Pyruvamide-3-C^{14} (0.834 gm., 0.0096 mole) of activity 2.78×10^8 disintegrations per minute was dissolved in water (30 ml.) and a solution of freshly distilled phenylhydrazine (0.95 ml., 0.0096 mole) in 2 *N* hydrochloric acid (5 ml.) was added. The mixture was kept at 0° for one hour and the product filtered off and washed with water (100 ml.). It was wetted with a little methanol, dissolved in boiling water (100 ml.), 2 *N* hydrochloric acid (150 ml.) added, and the solution kept on the steam bath for two hours. The solution was cooled and the crystalline pyruvic acid-3-C^{14} phenylhydrazone filtered, m.p. 173–174°, wt. 1.382 gm., yield 81%.

Indole-3-C^{14}-2-carboxylic acid.—The pyruvic acid phenylhydrazone was suspended in ether and treated with excess diazomethane. The solvent and excess reagent were removed by distillation, the residual ester dissolved in glacial acetic acid (6 ml.), and after cooling concentrated sulphuric acid (0.7 ml.) was added. The resulting solution was kept at 80° for one hour when crystallization of ammonium acetate was complete. It was filtered, the filtrate cooled, water (250 ml.) and 2 *N* ammonium hydroxide (50 ml.) added, and the mixture kept at 0° for 48 hr. The supernatant liquor was sucked off and the crude methyl indole-2-carboxylate transferred to a sublimation tube and distilled at 120–140° at 0.001 mm. The white sublimate together with a small amount of yellow oil was washed out with methanol, taken to dryness, and hydrolyzed with hot *N* sodium hydroxide (10 ml.). 2 *N*-Hydrochloric acid (12 ml.) was added, the mixture cooled for 36 hr., and the acid filtered. After

[3]*All melting points are corrected.*

drying over concentrated sulphuric acid the crude indole-2-carboxylic acid, m.p. 176–179°, wt. 0.371 gm., was obtained in 29.7% yield based on pyruvic acid phenylhydrazone.

Indole-3-C^{14}.—The active indole-2-carboxylic acid was refluxed with cupric oxide (20 mgm.) in quinoline (6 ml.) in an atmosphere of nitrogen for 16 hr. The mixture was cooled, diluted with ether (200 ml.), filtered, and the filtrate washed with aqueous sodium hydroxide and then with dilute hydrochloric acid. The ether solution was dried over sodium sulphate and evaporated *in vacuo* at room temperature. It left a residue consisting of crude indole-3-C^{14} (0.290 gm.).

DL-Tryptophan-3-C^{14}.—The crude active indole was converted to gramine by reaction with formaldehyde and dimethylamine. The gramine (0.214 gm.) was diluted with inactive gramine to give a weight of 1.59 gm. which in a Mannich reaction yielded tryptophan-3-C^{14} acetate (with 1 mole of acetic acid of crystallization), wt. 1.342 gm., with a specific activity of 1.24×10^4 disintegrations per min. per mgm., or 4.02×10^6 disintegrations per min. per millimole, representing an over-all radiochemical yield of 6% from pyruvamide.

Pyruwamide Phenylhydrazone

In the course of the radioactive synthesis this compound was not isolated. Pyruvamide (1.09 gm., 0.0125 mole) in water (10 ml.) was added to a warm solution of phenylhydrazine (1.35 gm., 0.0125 mole) in 2 *N* hydrochloric acid (6.3 ml.). A bulky crop of crystals separated almost immediately. After being allowed to stand for 10 min. the product was filtered off and recrystallized from hot water containing a little sodium hydroxide. Pyruvamide phenylhydrazone separated as shiny plates (1.95 gm., 88% yield), m.p. 143–144°. The literature reports m.p. 144° for this compound prepared by another method (12). Calc. for $C_9H_{11}ON_3$: C, 61.00; H, 6.26; N, 23.72. Found: C, 61.21; H, 6.33; N, 23.34%. The substance is only very slowly hydrolyzed by 2 *N* aqueous sodium hydroxide, but is readily converted to pyruvic acid phenylhydrazone by dilute aqueous hydrochloric acid.

Indole-2-carboxamide.—Ring closure of pyruvamide phenylhydrazone could not be effected by means of a mixture of acetic and sulphuric acids, nor by dry ethanolic hydrogen chloride. Boron trifluoride gave the product in poor yield. Pyruvamide phenylhydrazone (0.89 gm., 0.005 mole) in glacial acetic acid (3 ml.) was treated with boron trifluoride dietherate (1 ml.). The mixture was heated for 20 min. on the water bath, cooled, poured into water and the suspension extracted with ether. The dried ether extract was distilled at 0.01 mm., yielding two products. The first fraction was an oil (0.31 gm.) which on standing for two months set to a glass and was not further investigated. The second fraction, a crystalline sublimate (0.10 gm., 12% yield), m.p. 234.5–235.5°, was the desired product. Calc. for $C_9H_8ON_2$: C, 67.48; H, 5.03. Found: C, 67.53; H, 5.09%.

Administration of the Tryptophan-3-C^{14} *to Nigella damascena L.*

Nigella damascena L. seeds were germinated in soil and allowed to grow for five months. Eighteen mature plants were transferred to a hydroponics set up

with the roots dipping into the nutrient solution. The nutrient solution contained, per liter, potassium nitrate (505 mgm.), calcium nitrate tetrahydrate (1180 mgm.), magnesium sulphate heptahydrate (495 mgm.), potassium dihydrogen phosphate (272 mgm.), ferrous sulphate heptahydrate (2 mgm.), plus traces of micronutrients (B, Mn, Zn, Mo, Cu). After two weeks in the nutrient solution new roots were being produced and some of the plants were flowering. At this stage the tryptophan-3-C^{14} acetate (580.1 mgm., with a specific activity of 4.02×10^6 disintegrations per min. per millimole, and a total activity of 7.21×10^6 disintegrations per min.) was equally divided between the plants. The tryptophan was taken up by the plant as shown by the day to day decreasing activity in the nutrient solution. The first day after feeding the total activity remaining in the nutrient solution was 5.9×10^6, second day 4.4×10^6, third day 2.9×10^6, fourth day 2.0×10^6, fifth day 0.8×10^6, sixth day 0.2×10^6, seventh day 0.1×10^6 disintegrations per min.

Isolation of Damascenine

On the eighth day the plants were harvested, dried at 50–60°, and ground in a Wiley mill. The ground material (18.8 gm.) was extracted with ether for three days in a Soxhlet extractor. This ether extract had a total activity of 1.07×10^4 disintegrations per min. The green solution was evaporated to dryness and a small sample of the residue chromatographed on Whatman No. 1 paper (buffered to pH 8 with phosphate – citric acid), with a mixture of *n*-butanol (80 ml.) and water (15 ml.) as the developing solvent. Authentic specimens of 3-hydroxyanthranilic acid, damascenine (obtained from *Nigella damascena* seeds according to the procedure of Ewins (8)), and damasceninic acid were run on the same chromatogram and had R_F values of 0.15, 0.88, and 0.76 respectively. The hydroxyanthranilic acid was detected by its pronounced fluorescence in ultraviolet light and the other two compounds with Dragendorff's reagent (21). Only damascenine was found in the plant extract. The residue from the ether extract of the plant was dissolved in *N* hydrochloric acid (100 ml.) and the solution extracted with ether. The aqueous layer was made alkaline with ammonia and the alkaloid extracted with ether. The fluorescent extract was dried and the ether removed by distillation under diminished pressure leaving a residue which was distilled *in vacuo*. Damascenine distilled as a colorless oil, b.p. 120° at 0.001 mm., wt. 5.6 mgm. This was completely non-radioactive.

The ground plant was further extracted with methanol, but no more alkaloid was obtained. The methanol extract was radioactive (1.6×10^5 disintegrations per min.) presumably owing to the extraction of uncombined radioactive tryptophan from the plant. After extraction with ether and methanol the plant had a total activity of 2.1×10^5 disintegrations per min.

Administration of Tryptophan-3-C^{14} to Garden Peas

Garden peas (Laxton's Progress) treated with fungicide (Semesan) were allowed to germinate in soil. After two weeks 48 plants were transferred to a hydroponic solution of the same composition as that used for the *Nigella*

damascena and the labelled tryptophan acetate (573.7 mgm. with a specific activity of 4.02×10^6 disintegrations per min. per millimole) was administered as in that case. The rate at which the amino acid was taken up by the plant was followed by determining the total activity of the nutrient solution every day. The plants were harvested on the seventh day and the roots and the aerial parts worked up separately. No trace of trigonelline was found in the roots. The aerial parts of the plant (64.9 gm. fresh weight) were extracted with water. The extract, having a total activity of 1.4×10^5 disintegrations per min., was treated with 20% lead acetate solution to precipitate the protein and then with hydrogen sulphide to remove the excess lead. The filtrate (having a total activity of 0.5×10^5 disintegrations per min.) was concentrated to 250 ml., made alkaline with ammonia, and treated with an excess of ammonium reineckate (3 gm. in 10 ml. of methanol) to precipitate the choline. The precipitate was centrifuged off after cooling overnight and the solution acidified with 1.0 *N* hydrochloric acid and kept cold for 24 hr. The precipitated reineckate was filtered off, washed with *n*-propanol, and dissolved in acetone. This acetone solution contained negligible radioactivity; it was chromatographed on Whatman No. 1 paper using the one phase system 95% ethanol–5% ammonia of d. 0.880 (5) which separates choline (R_F 0.45) from trigonelline (R_F 0.22), and the chromatogram developed with Dragendorff's reagent (21). The trigonelline spot on the chromatogram was not radioactive. Trigonelline reineckate was decomposed with silver sulphate and barium hydroxide (17), but only a trace of free base was obtained.

DISCUSSION

If the synthesis of damascenine and of trigonelline occurred in the plants while they were in contact with the radioactive tryptophan, the results would indicate that tryptophan was not utilized for the production of the bases. Since damascenine and trigonelline are methylated derivatives of 3-hydroxyanthranilic acid and of nicotinic acid respectively, both well established tryptophan metabolites in animals and in molds (4, 6, 14), and since methylation in plants has been shown to be a general and facile process, the present results would lead to the conclusion that tryptophan metabolism in the plants studied differs radically from that prevailing in animals and molds.

In feeding experiments with mature plants, there is the danger that alkaloids are no longer being actively produced at the time of the experiment. In our experiments, however, the labelled amino acid was fed while the plants were flowering and producing seeds. In both *Nigella damascena* (8) and peas (22) the alkaloid is present in the seeds, and while it is conceivable that it may be translocated there from other parts of the plant and that actual synthesis no longer takes place at the time, this seems unlikely.

ACKNOWLEDGMENT

The authors are indebted to Professor H. K. Mitchell of the California Institute of Technology for a sample of 3-hydroxyanthranilic acid and wish to acknowledge his courtesy.

REFERENCES

1. ALBERTSON, N. F., ARCHER, S., and SUTER, C. M. J. Am. Chem. Soc. 67: 36. 1945.
2. ANKER, H. S. J. Biol. Chem. 176: 1337. 1948.
3. BARGER, G. Bull. soc. chim. biol. 20: 685. 1938.
4. BONNER, D. Proc. Natl. Acad. Sci. U.S. 34: 5. 1948.
5. BREGOFF, H. M., ROBERTS, E., and DELWICHE, C. C. J. Biol. Chem. 205: 565. 1953.
6. DALGLEISH, C. E. Quart. Revs. (London), 5: 227. 1951.
7. ELKS, J., ELLIOTT, D. F., and HEMS, B. A. J. Chem. Soc. 629. 1944.
8. EWINS, A. J. J. Chem. Soc. 101: 544. 1912.
9. FAVREL, G. Bull. soc. chim. (3), 27: 324. 1902.
10. FEOFILAKTOV, V. V. Compt. rend. acad. sci. U.R.S.S. 24: 755. 1939.
11. FISCHER, E. Ann. 236: 126. 1886.
12. GASTALDI, C. Gazzetta, 54: 212. 1924.
13. HEIDELBERGER, C. J. Biol. Chem. 179: 139. 1949.
14. HEIDELBERGER, C., ABRAHAM, E. P., and LEPKOVSKY, S. J. Biol. Chem. 179: 151. 1949.
15. JAMES, W. O. The alkaloids. Vol. I. *Edited by* R. H. F. Manske and H. L. Holmes. Academic Press, Inc., New York. 1950. p. 58.
16. JAPP, F. R. and KLINGEMANN, F. Ann. 247: 190. 1888.
17. KAPFHAMMER, J. and BISCHOFF, C. Z. physiol. Chem. (Hoppe-Seyler's), 191: 179. 1930.
18. KLEIN, G. and LINSER, H. Z. physiol. Chem. (Hoppe-Seyler's), 209: 75. 1932.
19. KLEIN, G. and LINSER, H. Planta, 19: 366. 1933.
20. MITCHELL, H. K. and NYC, J. F. Proc. Natl. Acad. Sci. U.S. 34: 1. 1948.
21. MUNIER, R. and MACHEBOEUF, M. Bull. soc. chim. biol. 33: 846. 1951.
22. SCHULZE, E. and TRIER, G. Z. physiol. Chem. (Hoppe-Seyler's), 76: 258. 1911.
23. SNYDER, H. R. and SMITH, C. W. J. Am. Chem. Soc. 66: 350. 1944.
24. THOMAS, R. C., WANG, C. H., and CHRISTENSEN, B. E. J. Am. Chem. Soc. 73: 5914. 1951. Document 3354, American Documentation Inst. Washington, D.C.
25. WINTERSTEIN, E. and TRIER, G. Die Alkaloide. 2nd ed. Verlag von Gebrüder Borntraeger, Berlin. 1931. p. 346.

ABSORPTION SPECTRA OF METALS IN SOLUTION[1]

By H. Blades[2] and J. W. Hodgins[3]

ABSTRACT

Measurements of the absorption spectra were made on solutions of alkali and alkaline earth metals in ammonia, methylamine, ethylamine, and mixed solvents. In ammonia, a single absorption band was measured which is common to all the metals examined. In the amines and in mixtures of ammonia with methylamine, however, bands were found which were characteristic of the metal employed. A hypothesis has been advanced to explain the existence of the different types of energy traps responsible for the variations in spectra.

INTRODUCTION

The alkali metals and some of the alkaline earth metals dissolve in liquid ammonia without reaction; it is thought that simple dissolution occurs, yielding metal ions and electrons which are trapped or solvated in the liquid (5). Various physical properties have been examined which are consistent with this postulate, although a concise model has not yet been formulated for the electron traps. For example, the expansion exhibited on dissolving the metal has been attributed to the formation of holes in the liquid which represent energy barriers for the escape of electrons (8). The electrical conductivity in dilute solution is greater than can be explained by simple ionic transport, but less than would be expected by electronic conduction (5). Magnetic susceptibility measurements indicate that the metal is ionized, but some difficulty is experienced in explaining the variation of the susceptibility with temperature (3). The measurements of paramagnetic resonance absorption are consistent with the existence of trapped electrons (4). Finally, the absorption spectra of a number of the solutions have been measured, and the observation made that in ammonia there is a single absorption maximum whose position is independent of the particular metal in solution (1, 9). This maximum is in a region where none appears in the spectrum of bulk sodium metal; and in the spectrum of atomic sodium, very strong absorption occurs at 5889 Å (*D* line), which does not appear in the solution spectrum. Since the maximum observed is also absent from the spectrum of sodium ion and of liquid ammonia, it has been ascribed to the trapped electrons.

Primary amines will also dissolve some of the metals; sodium, cesium, potassium, lithium, and calcium are soluble in methylamine, while ethylamine dissolves at least lithium and potassium. Although these solutions have been examined less exhaustively than the ammonia solutions, their behavior is similar. Thus the variation of electrical conductivity with concentration in metal solutions in methylamine is similar to that in anhydrous ammonia (2), and the absorption spectra, although exhibiting maxima at a different wave

[1]*Manuscript received October 18, 1954.*
Contribution from Department of Chemistry and Chemical Engineering, Royal Military College of Canada, Kingston, Ontario. Issued as D.R.B. Report No. SW-2.
[2]*Present address: DuPont de Nemours Company, Wilmington, Delaware.*
[3]*Present address: Royal Military College of Canada, Kingston, Ontario.*

length, were shown to be independent of the metal for a limited number of solutions (1).

The experimental observations of the absorption spectra are limited to quite early work done with a visual spectrophotometer (1) and to some work by Vogt (9). Because the solutions in methylamine had maxima in the absorption spectrum at visible wave lengths, these were observed by the early workers, but the peaks for ammonia solutions were missed as they occur in the near infrared. Vogt describes the spectra of lithium and sodium in ammonia solutions of unspecified concentration. The dearth of spectrophotometric data is probably explained by the difficulty of manipulating the solutions, their very high absorbance, and the awkward spectral region in which the absorption maximum for ammonia is located.

In the present paper, absorption spectra are presented for solutions of lithium, sodium, potassium, and calcium in ammonia and in methylamine, lithium and potassium in ethylamine, sodium and potassium in mixed ammonia and methylamine, and sodium in mixed ammonia and ethylamine.

EXPERIMENTAL PROCEDURE

The main experimental problems associated with the measurement of liquid ammonia and amine spectra arise from the instability of the solutions, their low boiling points (which necessitate constant refrigeration), and the very high molar absorbancy index which make dilute solutions and very thin cells necessary.

The spectra were determined in two parts, the region from 0.3 to 1.0μ on a Beckman D.U. ultraviolet spectrophotometer and from 1.0 to 2.5μ on a Beckman IR-2 infrared spectrophotometer. Quartz cells of thickness 10, 1.0, and 0.1 mm. as supplied by the American Instrument Company were used. In both instruments the effective band width is considerably smaller than the half-height width of the maxima being investigated so that the shape of any spectrum was not affected by the dispersion of the instruments.

The cell was contained within a thick-walled Lucite box with quartz windows on either side for the passage of the light beam. The absorption cell was removed from the light path by moving it upwards. It was kept at the desired temperature by a stream of cold dry air, which entered the box by the ducts shown in Fig. 1 (at *G*). The air was dried with silica gel and cooled by liquid air. The outside windows of the box were kept clear of frost by jets of warm dry air.

The cold box made a light-tight fit into either spectrophotometer, and fogging of the instrument optics was prevented by the warm dry air which continually swept the volume outside the box. Temperature was controlled manually both by regulating the flow of air through the box and by regulating the temperature of the air entering it. A thermocouple cemented on the cell wall near the face showed fluctuations of two to three degrees.

The apparatus for manipulating the solvents and preparing the solutions is shown schematically in Fig. 1. Solvents were stored in a detachable trap *A*. Solutions were prepared in trap *B* by various methods and were transferred to

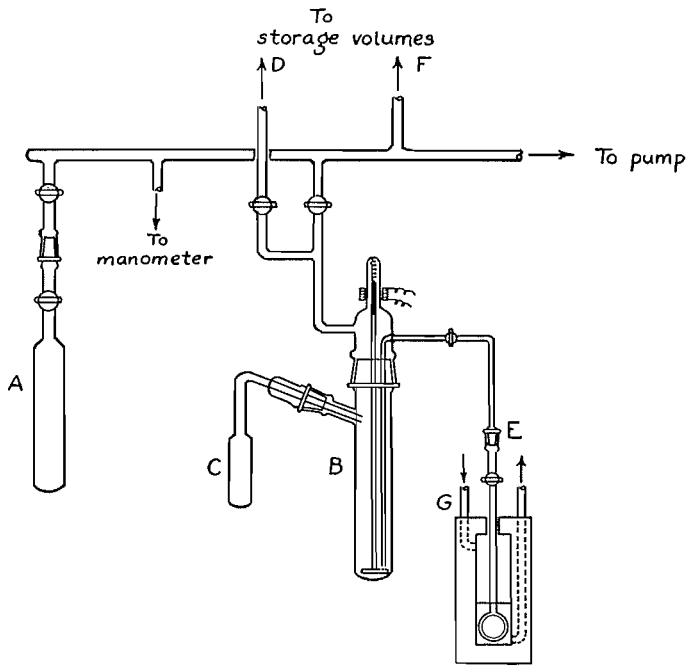

FIG. 1. Apparatus for preparing solutions and filling absorption cell.

the cell by admitting nitrogen from *D* thus forcing the liquid through the siphon into the cell. Excess liquid in the neck of the cell was removed by pumping off the nitrogen and distilling the solvent back into *B*.

The cell was disconnected at the ground glass joint *E* for measurements in the spectrophotometer. At the completion of these measurements the cell could be reconnected at *E* and the solvent distilled off. Another solvent could then be distilled into the cell thus avoiding the necessity of forcing over-all combinations of metals and solvents.

A saturated solution of potassium in methylamine was found to be quite stable, could be successfully forced over, and was just the correct concentration for spectral measurements in the 0.1 mm. cell. Solutions were thus prepared simply by placing a piece of potassium in trap *B* and distilling in a suitable quantity of methylamine. It thus became possible by the procedure described above to obtain spectra for any solvent in which potassium was more soluble than in methylamine.

A similar procedure could be used for sodium solutions although for this metal the combination of a saturated solution in methylamine and the 1.0 mm. cell was most convenient.

For more soluble metals it was necessary to resort to a dilution technique where a piece of the metal was placed in trap *C* and solvent added by distillation. Trap *C* could then be rotated on its ground glass joint until drops of solution poured from *C* into *B* where a relatively large volume of solvent diluted the drop to a suitable concentration.

Since lithium and calcium metal are relatively stable in the air, solutions of these metals were prepared either by the above dilution procedure or by placing a small piece of the metal in trap *B*. However, solutions of these metals are much less stable than those of sodium and potassium and hence greater difficulty was experienced in forcing them over.

When a solvent was distilled into the thin cells containing metal residue the first few drops of solution were sufficient to cover the whole cell face since the liquid rose by capillary action. Thus the concentrations of solutions prepared in this manner were not reproducible. Mixed solvents were condensed from a large gas storage bulb *F* in order to prevent preferential condensation. Table I

TABLE I

METHODS OF PREPARATION OF THE SOLUTION

Metal	Solvent	Method of preparation
Li	Methylamine	Small piece of metal placed in trap, or by diluton
Li	Ammonia	Residue from methylamine
Li	Ethylamine	Dilution
Na	Methylamine	Saturated solution
Na	Ammonia	Residue from methylamine
Na	Mixed solvent	Residue from methylamine
K	Methylamine	Saturated solution and dilution of saturated solution
K	Ammonia	Residue from methylamine
K	Ethylamine	Saturated solution
Ca	Ammonia	Small piece of metal placed in cell
Ca	Methylamine	Saturated solution

shows the specific fashion in which the various solutions were prepared. Solvents were distilled, before use, in a Podbielniak type of column and at a pressure of 300 to 400 mm. Hg. All the amines as received had ammonia fractions in them but the separation of this fraction was quite sharp on the still used. Only a middle fraction was used for the experiment. The solvents were dried over one of the alkali metals but ultimately it was found that lithium was the best drying agent probably because it is the most soluble.

No attempt was made to purify the metals used. It was observed, however, in the case of sodium and calcium that these metals did contain something which made it difficult to produce a solution in methylamine. This material could be removed in one of two ways. The metal could be fused in trap *B* under vacuum (feasible only for sodium) or a solution could be first made in ammonia and the ammonia subsequently evaporated. The latter method was

used for calcium, but either method left the metal in a finely divided state which caused some trouble because metal particles tended to remain suspended in the liquid.

The absorption spectra of liquid ammonia and methylamine are shown in Fig. 2. From these spectra it can be seen that little difficulty will be encountered from solvent contribution to solution spectra, down to about 7000 cm^{-1}. At frequencies above this almost any cell thickness is acceptable while below this a cell 0.1 mm. in thickness is desirable. Spectra of sodium solutions in the mixed solvent and in ammonia have a band at about 7350 $cm.^{-1}$ which for ease of preparation were measured in the 1.0 mm. cell. Consequently, measurements of this band are more uncertain than most of the spectra reported.

Considerable variation of absorbance was observed from solution to solution even in the case of those which were originally saturated. This was probably due to change in concentration which occurred when the liquid was forced over. It is possible that sufficient water and oxygen remained adsorbed on the surface of the vessels to affect the dilute solutions slightly, particularly in the region between the windows.

Variations in absorbance were also observed when the temperature of a specific solution was changed, particularly in the case of the saturated solutions. This variation followed no regular pattern and if the solubility changed with temperature and some suspended particles of metal were present such behavior would be predicted. However, when the temperature was held steady, absorbance measurements on solutions in pure solvents were reproducible throughout the time required for determination of the spectrum.

No detectable fading was observed in sodium or potassium solutions in methylamine up to −20°C. Lithium and calcium solutions in methylamine tended to fade at temperatures as low as −40°C. Solutions in ammonia were stable without exception but in this case the temperature was not allowed to rise above −40°C.

MATERIALS USED

Ammonia	Matheson	Anhydrous
Methylamine	Matheson	Anhydrous
Ethylamine	Matheson	Anhydrous
Sodium	Merck	Reagent grade
Potassium	Baker and Adamson	Reagent grade
Lithium	Metalloy	Low sodium, reagent grade
Calcium	Purest grade	Dominion Magnesium Limited

EXPERIMENTAL RESULTS

The spectra of lithium, sodium, potassium, and calcium in ammonia are identical, having a single broad band with a maximum at 6650 $cm.^{-1}$ (−60°C.)* and a half-height width of 2950 cm^{-1}. The specific observations are shown in

When a band was not determined at −60°C. a value has been estimated using the temperature coefficients given below.

TABLE II

SPECTRA OF LI, NA, K, AND CA IN AMMONIA, METHYLAMINE, ETHYLAMINE, AND MIXED SOLVENT

Solution	Temp., °C.	Position of maximum, cm.$^{-1}$	Half-height width, cm.$^{-1}$	Density at maximum	Cell thickness, mm.
Li in ammonia	−70	6700	3200	2.43	0.1
Na in ammonia	−62	6800	3370	2.57	1.0
K in ammonia	−42	6500	3250	2.36	0.1
	−52	6550	3150	2.47	0.1
	−60	6700	3100	2.58	0.1
	−61	6600	3150	2.91	0.1
	−63	6650	3050	2.60	0.1
	−71	6850	2900	2.70	0.1
	−78	6750	2900	2.82	0.1
Li in methylamine	−55	7350	4350	0.76	0.1
	−55	7600	4350	0.73	0.1
	−75	8000	4350	0.71	0.1
Na in methylamine	−14	14,700	3450	1.83	1.0
	−23	15,550	3000	0.42	1.0
	−25	15,000	3300	1.61	1.0
	−30	15,300	2950	0.45	1.0
	−48	15,450	3250	1.20	1.0
	−50	15,550	3000	0.57	1.0
	−66	15,750	2750	0.53	1.0
K in methylamine	−62	12,200 15,300 12,100			0.1
	−67	15,100 12,500			1.0
	−73	15,900			10
Ca in methylamine	−60	7800	4550	0.815	0.1
K in ethylamine	−64	15,500	3600	1.66	10.0
Li in ethylamine	−40	7050	5900	2.14	0.1
Na in 1:1 ammonia–methylamine	−81	7500*	3150	0.54	1.0
Same	−63	7500*	3750	0.61	1.0
Same	−79	7500*	3350	0.51	1.0
K in 1:1 ammonia–methylamine	−72	7500	3350	1.11	0.1
	−81	7600	3200	1.08	0.1
Same	−52	7000	3550	0.88	0.1
Same	−43	7200	3600	0.75	0.1

**Low frequency maximum only.*

Table II. Calcium does not appear there because the solution used was too concentrated, so that it was possible only to show that no additional bands appeared and that the maximum was located similarly to the other three metals.

In methylamine different bands were observed for the various metals. This is illustrated in Fig. 4. Lithium and calcium have a single band each, which is the same for both metals and appears at 7680 cm.$^{-1}$ (−60°C.). Sodium has a single band at 15,300 cm^{-1}. Potassium has two bands close together with the

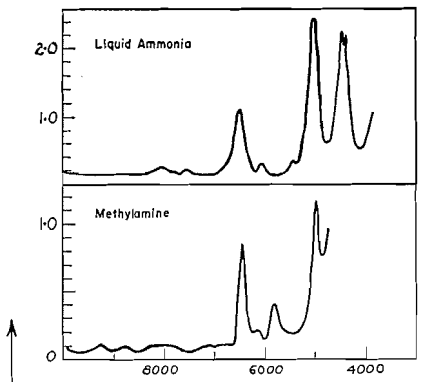

Fig. 2. Absorption spectra of pure solvents.

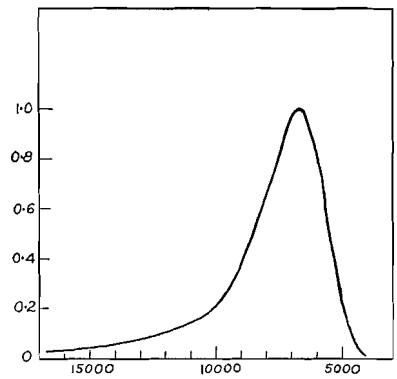

Fig. 3. Potassium in ammonia.

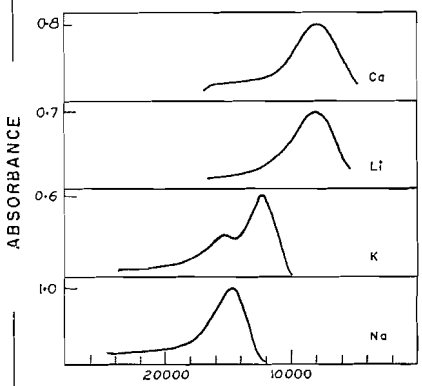

Fig. 4. Metals in methylamine.

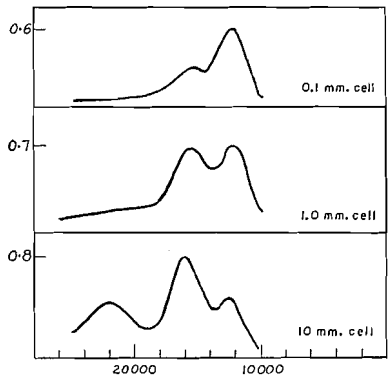

Fig. 5. Potassium in methylamine — concentration effect.

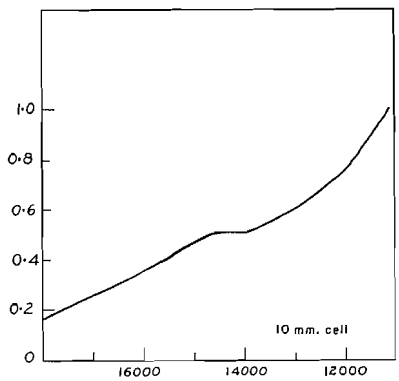

Fig. 6. Lithium in methylamine — dilute solution.

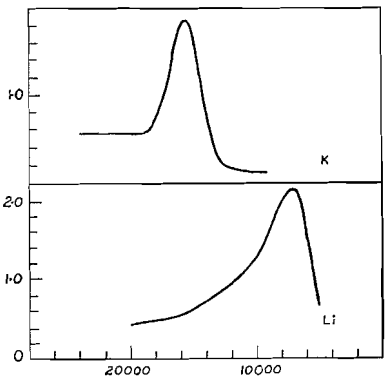

Fig. 7. Metals in ethylamine.

WAVE NUMBER, ($cm.^{-1}$)

result that the observed position of either band is somewhat affected by the other. It seems likely, however, that the high frequency band is identical with that found for sodium.

The effect of concentration on the potassium spectrum was investigated by adjusting the concentration, in three separate cells of 10, 1.0, and 0.1 mm. thickness, to give nearly constant absorbance. This will produce a change in concentration of about 100-fold. The resulting spectra are shown in Fig. 5. It will be noted here that the relative height of the two maxima varies with concentration and this indicates that absorption occurs by two independent processes.

In ethylamine only lithium and potassium were successfully dissolved. Their spectra are shown in Fig. 7. Two different bands are observed, the high frequency band being very similar to the high frequency band produced in methylamine. The low frequency band as observed for lithium, however, has a much greater half-height width than the comparable bands observed in methylamine.

The spectrum of sodium in a mixed solvent of methylamine and ammonia (molar ratio 1 : 1), shown in Fig. 8, exhibits two main absorption bands. The position of the high frequency band was established at 14,700 cm.$^{-1}$; its

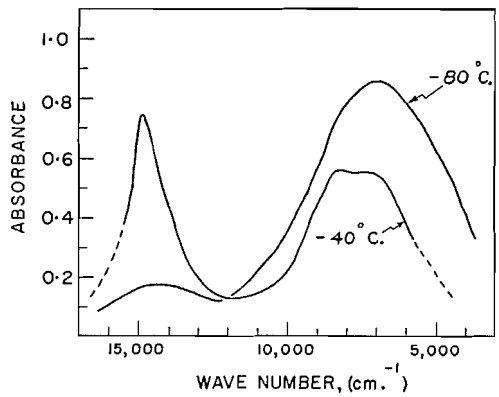

FIG. 8. Sodium in mixed ammonia–methylamine.

precise location was made difficult by the large variation of absorbance with temperature. The position and half-height width of the low frequency band are shown in Table II. From these it can be seen that this band is essentially the same as that observed for pure ammonia. Although its position is slightly shifted, its half-height width indicates that it does not contain a new hidden band. The temperature dependence of the absorbance at the maximum is shown for both bands in Table III.

The absorption spectrum of potassium in mixed methylamine and ammonia (molar ratio 1 : 1) reveals one band. The location and half-height width of this band serves to identify it with the low frequency band observed for sodium in the mixed solvent. This spectrum was obtained in the 0.1 mm. cell so that the concentration of potassium is probably about 10 times that of the corresponding sodium solution.

A solution of sodium in a mixture of ethylamine and ammonia (molar ratio 1 : 1) was examined for its absorption spectrum. This showed two bands, one at 7500 cm.$^{-1}$ and one at 14,800 cm^{-1}. The high frequency maximum can

TABLE III

EFFECT OF TEMPERATURE ON THE ABSORBANCE AT THE MAXIMA FOR THE MIXED SOLVENT

Temperature, °C.	Absorbance of the low frequency maximum	Absorbance of the high frequency maximum
−38	0.72	0.11
−49		0.13
−57		0.13
−59	0.68	0.16
−62		0.18
−63	0.61	
−68	0.62	0.21
−68	0.60	
−69		0.24
−71		0.25
−74	0.58	
−76		0.29
−78	0.51	
−79	0.52	
−80		0.33
−80		0.38
−81	0.44	
−82	0.43	0.44
−83	0.44	
−83	0.47	

probably be ascribed to sodium effectively dissolved in ethylamine although no solution is formed in the pure solvent.

From the data in Table II it might be expected that the position of the band in the spectrum of sodium in methylamine would be affected by both temperature and concentration. The effect of temperature on a specific solution for which the absorbance remained fairly constant is shown in Table IV. A plot of these data gives a temperature coefficient of −13 cm.$^{-1}$/degree. If the data in Table II for sodium in methylamine are now adjusted to a single temperature, using the above temperature coefficient it can be demonstrated that a change in position of the maximum is produced as the absorbance (i.e. concentration) is changed. The variation is 330 cm.$^{-1}$/unit of absorbance.

TABLE IV

THE EFFECT OF TEMPERATURE ON THE POSITION OF THE MAXIMUM FOR A SOLUTION OF SODIUM IN METHYLAMINE

Temperature, °C.	Position of maximum	Absorbance at maximum
−14	14,710	1.89
−25	14,810	1.80
−28	14,930	1.73
−50	15,150	1.53
−50	15,250	1.55
−58	15,270	1.45
−73	15,490	1.39
−73	15,380	1.65
−74	15,490	1.48

The position of the maximum for potassium in ammonia varies with temperature in a similar fashion, and the temperature coefficient for this system is -9 cm.$^{-1}$/degree.

The temperature coefficients for the half-height widths are 12 cm.$^{-1}$/°C. for potassium in ammonia and 14 cm.$^{-1}$/°C. for sodium in methylamine. As would be expected these coefficients are positive but the data are not precise enough to test the fit of a plot of $\sqrt{T}$ against band width.

The spectra of sodium and potassium in methylamine were observed for saturated solutions in a 1.0 mm. and a 0.1 mm. cell respectively. An attempt was made to determine the solubility of these two metals in methylamine. This was done by preparing saturated solutions at -80°C. and filling a small bulb with the solution in a manner similar to that used for filling the absorption cells. The solvent was then evaporated and the residual metal determined by measuring the hydrogen evolved on reacting it with water. The method of preparation of sodium solutions was such that the production of small particles of suspended metal was very likely. While this is not important in the measurement of spectra it does make analysis for the metal in solution difficult. Solutions were allowed to stand for some time before a sample was drawn off for analysis but this does not preclude the possibility of particles being swept off the delivery tube. With potassium the problem was not so severe because the metal was not in a finely divided state and particles were much less likely to be formed. Thus figures obtained for potassium are more likely to be accurate. The best estimates of concentration were 8×10^{-4} moles/liter and 1.9×10^{-3} moles/liter for saturated solutions of sodium and potassium respectively. It is suspected that the figure for sodium is somewhat high. A value of about 10^4 is thus observed for the molar absorbancy index of sodium in methylamine. The molar ratio of potassium to methylamine as used in the 0.1 mm. cell was thus about 5×10^{-5}; that for sodium to methylamine as used in the 1.0 mm. cell was probably 10^{-5} or less.

DISCUSSION

Originally it was hoped that information about the electron traps in liquid ammonia and amines could be obtained by observing spectra in mixtures of ammonia and an amine. It had been established that the spectrum in ammonia had a band at about 6000 cm.$^{-1}$ (9) and that a corresponding band occurred for methylamine at about 15,000 cm.$^{-1}$ (1). If traps exist in the structure of the liquid rather than in the form of a molecular orbital about a given molecule of solvent then it was reasoned that, in mixtures, intermediate bands between the two parent bands would appear. Indeed there was the possibility of only the intermediate band appearing.

The present observations confirm previous conclusions regarding the spectra in ammonia but the spectra for potassium, lithium, and calcium in methylamine are new and unexpected. At first glance it would appear that it is necessary to postulate a trap which will involve the metal ion as well as the solvent. But since identical bands appear for more than one metal (i.e. 7680 cm.$^{-1}$ band for lithium and calcium and the 15,500 cm.$^{-1}$ band for sodium and potassium) it is

evident that a given metal ion does not produce a unique trap. This is adequate evidence for rejecting a metal ammoniate or solvent metal complex as the location of the trap. It will be shown below that it is possible to fit all the observed facts into the presently held theory that the electron trap is formed by a hole in the liquid which has a more or less regular structure.

It is suggested by Lipscomb (6) that the density of metal ammonia solutions is consistent with the hypothesis of a hole in the liquid of 3 Å radius. The solvent molecules at the edge of such a hole will have their more positive ends, in this case the three hydrogen atoms, directed inwards thus forming a region of low potential in which the electron is trapped. By analogy with *F* centers and impurity phenomena in solids such a trap might be expected to have an excited state with an attendant energy transition which is manifested by the absorption spectrum.

The positive end of the ammonia molecule is made up of three hydrogen atoms and is symmetrical so that the array of molecules at the edge of any hole will be identical. This will make the configurational co-ordinates and consequently the transition levels for each hole identical, with the result that a single maximum is observed for all the solutions in liquid ammonia. As the temperature is changed the intermolecular association will be disturbed with the result that the configuration of the hole is slightly altered. This leads to a slight change in the transition levels in the trap and is manifested by a shift in the position of the absorption maximum.

The methylamine molecule is not symmetrical about the nitrogen atom and hence it is possible that two different aspects of the molecule may be presented at the boundary of a trap. These two orientations may or may not be mixed depending on how readily they fit around the hole, the size of the hole, and on what other forces are at work in the rest of the liquid. On the basis of this model the methylamine spectra can be broken into two groups, called for convenience, amine bands and aliphatic bands. The former represents the condition where the methylamine molecules are oriented so that an ammonia-like trap is produced. This case is probably represented by the spectra of calcium and lithium where a band is observed at about 7680 cm^{-1}. The small difference in position of the maximum from that observed in ammonia is accounted for by the effect of the methyl group on the intermolecular forces and hence on the configurational co-ordinates. Aliphatic bands arise from traps in which the methyl group takes part in the formation of the trap boundary. Such a trap would be expected to have quite different configurational co-ordinates and a different set of transition levels. Such a situation is in fact observed for the sodium and potassium spectra in methylamine where a band appears at about 15,500 cm^{-1}.

In potassium solutions in methylamine an intermediate band is produced which must arise from a third trap because the relative height of the two bands observed varies with concentration and temperature. Such behavior would not be observed if two transition levels in a single oscillator were being represented. The fact that there is a discrete additional band and not a diffuse broadening of the original implies that a fixed combination of the two possible orientations exists.

Aliphatic bands in ethylamine are represented by the spectrum of potassium in solution. A mixture of the orientations producing aliphatic and amine traps is probably represented by the lithium spectrum in ethylamine. The single band is very much broadened and close inspection shows that the broadening is largely on the high frequency side which is what would be expected for mixed traps where the amine orientation predominated.

The particular trap which is formed in the amines depends on the metal ion which is present in the solution. This implies that the metal ions have a relatively long range effect on the orientation of solvent molecules so that one trap or the other is formed depending on the strength of this influence. Thus as the potassium solutions were made more dilute the number of pure aliphatic traps tended to increase at the expense of the other mixed trap. In very dilute lithium solutions in methylamine (Fig. 6) there is definite evidence that a weaker band at about 15,000 cm.$^{-1}$ exists which was not observed in the more concentrated solutions. In even more dilute solutions this band presumably would become relatively stronger and in fact Gibson and Argo (1) report a definite band in that position. It would appear that aliphatic traps would normally form in methylamine but the influence of certain metal ions favors the amine type trap to a degree depending on their concentration.

Further evidence for the long range effect of the metal ions is presented by the concentration effect on the position of the maximum in sodium solutions in methylamine. Here it was observed that even in very dilute solutions a variation in concentration shifted the position of the maximum to a significant degree.

It will be shown below that the difference in depth of traps of the two kinds is only about 0.1 ev., so that even a very weak influence from the metal ion may be sufficient to favor the orientation producing one trap or the other.

In mixed ammonia and methylamine, the following six types of trap may be expected:

Amine type	Mixed type	Aliphatic type
1. Pure ammonia	3. Ammonia+methylamine (amine oriented)	6. Pure methylamine
2. Pure methylamine	4. Ammonia+methylamine (aliphatic oriented)	
	5. Methylamine (amine oriented) +methylamine (aliphatic oriented)	

In pure methylamine, a trap of type 5 above is represented only in the potassium spectrum; from this it can be predicted that traps of type 4 and 5 will be rare in the mixed solvents. In fact no corresponding bands have been observed.

Traps of types 1 and 2 have maxima which lie quite close together (Table V). In the mixed solvent an intermediate band is observed, probably due to traps of type 3. A similar band could of course be produced from the sum of two

TABLE V

AVERAGE VALUES, INDEPENDENT OF METAL, FOR BAND POSITION AND HALF-HEIGHT WIDTH FOR THE LOW FREQUENCY BANDS

Measurement	Solvent		
	Ammonia	1:1 Ammonia methylamine	Methylamine
Band maximum	6650	7310	7680
Half-height width, $cm.^{-1}$	3080	3460	4420

separate bands each representing the spectrum observed in the pure solvents, but such a band would be wider than either of the two parent bands. This, however, is not observed since the band width also is intermediate as shown in Table V. It is therefore concluded that the intermediate band observed results from the formation of combination traps involving both solvents.

The band of the pure aliphatic type is observed only for sodium in the mixed solvents. A corresponding band does not appear in the potassium solution. This is consistent with the pattern in pure methylamine where it is observed that potassium has a stronger directing influence towards the formation of amine type bands than does sodium.

The relative depths of traps of the two kinds, i.e. those involving the amine group only and those involving only the aliphatic group, can be estimated from the effect of temperature on the height of the two maxima appearing in the sodium solution in mixed methylamine and ammonia. Heights of these two maxima as a function of temperature are given in Table III. By plotting the absorbance of the two maxima against temperature it can be shown that the one maximum gains at the expense of the other when the temperature is changed.

If it is assumed that the activation energy for the formation of traps is zero, we may write:

[1] $$B/A = a\, e^{-(E_b - E_a)/RT}$$

where A = concentration of traps of the amine type,
B = concentration of traps of the aliphatic type,
a = constant,
E_a = energy of formation of Trap A,
E_b = energy of formation of Trap B.

If it is further assumed that Beer's Law holds for the maxima, it follows that

$$B^1/A^1 \propto B/A$$

where B^1 = absorbance at maximum of high frequency band when the concentration of aliphatic traps is B,
A^1 = absorbance at maximum of low frequency band when the concentration of amine traps is A.

Thus the plot of $\log B^1/A^1$ against $1/T$ should permit an estimation of $E_b - E_a$.

Such a plot is shown in Fig. 10 and from this a value of -0.17 ev. is obtained for $E_b - E_a$. Traps of mixed amine and ammonia types are thus slightly deeper than the aliphatic type. Because of the great similarity of these bands it is suggested that ammonia traps, methylamine traps of the amine type, and mixtures of the two will have approximately the same depth. The difference in depth between traps in ammonia and methylamine for a metal such as sodium then is about 0.2 ev.

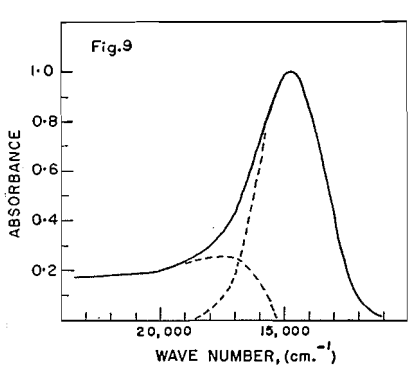

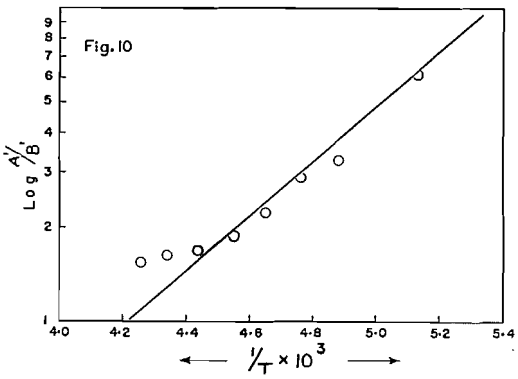

FIG. 9. Sodium in methylamine.
FIG. 10. Effect of temperature on peak height in spectrum of sodium in mixed ammonia–methylamine.

The separation of the two bands for spectra in methylamine and ammonia is about 1 ev. This value is much larger than the difference between the potential energies of the two traps so that it must be concluded at least for the low frequency bands that the absorption process involved in producing the bands is not one resulting in dissociation of the traps but rather is a transition between two energy levels of the trap.

Fig. 9 shows a more detailed representation of the absorption spectrum of sodium in methylamine. If this spectrum be compared with that found for potassium in ammonia (Fig. 3) it will be noted that for the high frequency band in methylamine there is a rather high level of continuous absorption on the high frequency side. In ammonia the level of absorption falls off much more quickly in the corresponding region.

By analogy with F centers in alkali halide crystals (7) it is suggested that the continuous absorption in the solution spectrum in methylamine represents a dissociation continuum which begins in the neighborhood of the main band. This implies a dissociation energy of about 2 ev. for the high frequency trap.

SUMMARY

1. A single band in the absorption spectra at 6650 cm.$^{-1}$ was found for all the solutions of metals in liquid ammonia which were studied.

2. The absorption spectra of solutions of metals in methylamine have a single band with the exception of potassium which has two. The position of the single band may be at one of two points, 15,300 cm.$^{-1}$ or 7680 cm.$^{-1}$ (-60°C.) depending on the metal.

3. The absorption spectrum of potassium in ethylamine has a single maximum in the 15,300 cm.$^{-1}$ region.

4. A solution of sodium in mixed methylamine–ammonia solvent has an absorption spectrum with two bands, one in the 15,300 cm.$^{-1}$ and one in the 7300 cm.$^{-1}$ region.

5. From the sodium in methylamine absorption spectrum it is argued that a dissociation continuum begins in the neighborhood of the band, which permits the estimation of 2 ev. for the depth of traps represented by bands in the 15,300 cm.$^{-1}$ region. From temperature effects in the mixed solvent it was shown that the trap represented by the band in the 7300 cm.$^{-1}$ region is about 0.2 ev. deeper.

6. Since the separation in trap depth is much less than the separation of the two bands it is argued that the absorption bands result from energy transitions and not from dissociation of the trap.

ACKNOWLEDGMENT

The foregoing investigation was part of the work performed at the Royal Military College under D.R.B. Research Grant No. 357. This opportunity is welcomed for thanking the Defence Research Board for its fine cooperation and financial assistance.

REFERENCES

1. GIBSON, G. E. and ARGO, W. L. J. Am. Chem. Soc. 40: 1327. 1918.
2. GIBSON, G. E. and PHIPPS, T. E. J. Am. Chem. Soc. 48: 312. 1926.
3. HUSTEN, E. Ann. Physik, 33: 477. 1938.
4. HUTCHISON, C. A., JR. and PASTOR, R. C. J. Chem. Phys. 21: 1959. 1953.
5. KRAUS, C. A. J. Am. Chem. Soc. 43: 749. 1921.
6. LIPSCOMB, W. N. J. Chem. Phys. 21: 52. 1953.
7. MOTT, N. F. and GURNEY, R. W. Electronic processes in ionic crystals. The Clarendon Press, Oxford. 1940. p. 114.
8. OGG, R. A., JR. J. Am. Chem. Soc. 68: 155. 1946.
9. VOGT, E. VON. Naturwissenschaften, 35: 298. 1948.

SOME OBSERVATIONS ON CYANIC ACID AND CYANATES[1]

By M. W. Lister

ABSTRACT

Various reactions of cyanic acid and the cyanate ion have been examined. Cyanic acid, in the presence of added hydrochloric or nitric acid, decomposes quantitatively according to the equation: $HNCO+H_3O^+ \rightarrow CO_2+NH_4^+$. The rate constant for this reaction was measured over a range of temperature and ionic strength, and was found to be 0.86 mole liter^{-1} min.$^{-1}$ at unit ionic strength and 1.5°C. The activation energy is 14½ kcal. The effect of ionic strength on the reaction with hydrochloric acid closely parallels that on the activity coefficients of the acid itself. Without added acid cyanic acid decomposes by a first order reaction: $HNCO+2H_2O \rightarrow NH_4HCO_3$, followed by a rapid second stage: $NH_4HCO_3+HNCO \rightarrow NH_4NCO+H_2CO_3$. This reaction has a rate constant of 0.011 min.$^{-1}$ at 0°C., and an activation energy of 16 kcal. There is also a few per cent of some side reaction. Cyanate ions in alkaline solution decompose thus: $OCN^-+2H_2O \rightarrow NH_4^++CO_3^{--}$. This reaction was examined over a range of temperature and ionic strength: it is first order with $k = 3.0 \times 10^{-3}$ min.$^{-1}$ at 100°C. (0.3 ionic strength) and 23½ kcal. activation energy. The rate is somewhat dependent on hydroxide concentration, when this is fairly low. The reaction is catalyzed by carbonate, but not by a number of other anions that were examined. The rate of the catalyzed reaction is proportional to the carbonate concentration, but independent of cyanate, at least over a considerable range. The ionization constant of cyanic acid has been measured by a method that avoids errors from hydrolysis; the value obtained was 2.0×10^{-4}. The oxidation of cyanate by hypochlorite and by chlorine was examined more briefly.

Past workers have established with reasonable certainty the qualitative aspects of the decomposition reactions of cyanic acid and the cyanate ion. However, quantitative measurements have not been too systematic, and it is hoped that the present work will give a more complete picture. Besides the decomposition reactions in aqueous solution, which are really hydrolyses, some observations are included on the oxidation of the cyanate ion.

1. DECOMPOSITION OF CYANIC ACID IN ACID SOLUTION

This acid decomposes fairly rapidly in dilute aqueous acid according to the equation:

$$HNCO+H_3O^+ \rightarrow CO_2+NH_4^+.$$

Cyanuric acid only results to any great extent in concentrated solution. The ammonium ions could react with cyanate ions to give urea; but this reaction is much slower, so that in acid solution it is negligible. Quantitative measurements on this reaction are rather limited. Taufel, Wagner, and Dunwald (8) report a reaction first order with respect to cyanic acid, and with a rate constant of 2.4×10^{-3} min.$^{-1}$ at 25°C. We have studied this reaction over a range of conditions with the following results.

Experimental Method

A good grade of potassium cyanate was recrystallized from a mixture of 10% water, 50% ethyl alcohol, and 10% methyl alcohol. A solution of this salt in water was made up; a sample was pipetted into a flask immersed in a

[1]*Manuscript received October 26, 1954.*
Contribution from the Department of Chemistry, University of Toronto, Toronto, Ont.

bath at the temperature being investigated. A sample of hydrochloric acid of known concentration was similarly pipetted out and to this was added sodium chloride solution to give the desired ionic strength. This also was brought to the correct temperature. The solutions were mixed and after a given time the reaction was stopped by adding excess sodium hydroxide. The actual reaction temperature was read from a thermometer graduated in 0.1°C. immersed in the reaction mixture.

The ammonia formed was estimated by distilling it into a known amount of standard acid, and titration. The distillation was brief enough so that only a very small amount of ammonia was formed by decomposition of cyanate during this operation; however as this reaction was also measured (see Part 3), this error could be allowed for. The solution was always distilled for the same length of time. Traces of ammonium ion initially present in the cyanate (or elsewhere) were estimated in a reagent blank run. The cyanate initially present was calculated from the strengths of the stock solutions, which were determined by silver nitrate titration (see Part 3 for details). At subsequent times it was assumed that the cyanate concentration was given by the initial concentration minus the ammonium ion formed. It was checked that if the reaction was allowed to go to virtual completion the ammonium ion formed was equal to the initial cyanate; i.e. side reactions are negligible. The same point was checked in another way. A potassium cyanate solution, containing some carbonate from its decomposition, was titrated with hydrochloric acid, and the pH followed. An inflection point was found at a pH of about 7.8. At this point the carbonate is just converted to bicarbonate. After this the pH meter was removed, and bromcresol green added. The solution was warmed and acid run in to maintain the color of the indicator at yellowish-green. Eventually the color did not change even on boiling, and at this point the reaction is just complete.

$$KOCN + 2HCl + H_2O \rightarrow KCl + NH_4Cl + CO_2$$

This is a method of estimating cyanate in the absence of interfering substances, and the results agreed with those of silver nitrate titration. Hence side reactions during the titration with acid are negligible.

Results

This reaction was examined at various temperatures and ionic strengths. Table I gives results all at an ionic strength of 1.0. This ionic strength is derived on the assumption that no cyanic acid is ionized; the value for the ionization constant obtained later shows that the fraction ionized would be less than 0.001. The reaction itself will not change the ionic strength.

Table I also gives values of the rate constant assuming that the reaction is first order with respect to cyanic acid and hydrogen ions; i.e. that

$$-dx/dt = kxy$$

where x = (HNCO), y = (H^+), and k is the rate constant. The most convenient integrated form of this equation is

$$k = \frac{1}{ct} \ln \frac{x_0(x-c)}{x(x_0-c)}$$

where x_0 and y_0 are the initial values of x and y, and $c = y_0 - x_0$. k was calculated from this equation. The values of k so obtained are reasonably constant, though at 25°C. the rate is too great for very accurate measurements. It can readily be checked that no other rate equation fits the results anything like as well. Run 12 differs from the others in being done with nitric acid; it gives

TABLE I

Run No.	Temp., °C.	Initial (H^+), M	Time, sec.	(HNCO), M	k, moles $l.^{-1}$ $min.^{-1}$
1	1.5	0.939	0	0.0859	—
			30	0.0540	1.00
			60	0.0382	0.889
			120	0.0177	0.882
			240	0.0059	(0.76)
2	1.5	0.783	0	0.0716	—
			15	0.0602	0.889
			30	0.0493	0.966
			60	0.0369	0.870
			120	0.0213	0.805
			240	0.0067	0.803
3	1.5	0.348	0	0.0763	—
			30	0.0661	0.838
			60	0.0562	0.907
			120	0.0433	0.860
			240	0.0274	0.801
4	13.1	0.290	0	0.1004	—
			15	0.0839	2.55
			30	0.0735	2.27
			60	0.0541	2.35
			120	0.0285	2.57
			240	0.0120	2.33
5	13.1	0.884	0	0.1004	—
			15	0.0575	2.59
			30	0.0369	2.31
			60	0.0124	2.54
			90	0.0040	2.64
			120	0.0027	2.23
6	25.5	0.275	0	0.1120	—
			15	0.0724	6.89
			30	0.0491	6.92
			45	0.0296	7.98
			60	0.0198	8.11
			90	0.0166	6.06
7	25.5	0.869	0	0.1120	—
			5	0.0635	8.08
			10	0.0376	7.69
			20	0.0132	7.99
			30	0.00612	7.33
12	13.4	0.150	0	0.0981	—
			60	0.0685	2.68
			120	0.0528	2.50
			240	0.0335	2.46
			480	0.0229	2.44

the same rate as with hydrochloric acid, showing that chloride has no catalytic effect.

Table II shows the effect of altering the ionic strength. These runs are all at 1.5°C. The constants were calculated as before, except for Run 8 where cyanic acid was in slight excess. Here if $b = x_0 - y_0$, then

$$k = \frac{1}{bt} \ln \frac{x(x_0-b)}{x_0(x-b)},$$

but as b is small this can be expanded as a series:

$$k = \frac{1}{t}\left[\frac{x_0-x}{x_0(x-b)} - \frac{b}{2}\frac{(x_0-x)^2}{x_0^2(x-b)^2} + \ldots\right].$$

For Run 8, k was calculated from this formula.

The results of these runs give the following average values for the constants. Firstly at an ionic strength of 1.0 we get:

T	1.5	13.1	25.5	°C.
k	0.86	2.44	7.45	moles liter^{-1} min.$^{-1}$

These give an activation energy of 14.5 kcal./gm-mol.

At 1.5°C. the dependence of k on the ionic strength, μ, is as follows:

μ	0.2	0.5	1.0	2.0	3.0
k	0.73	0.73	0.86	1.07	1.25 moles liter^{-1} min.$^{-1}$

TABLE II

Run No.	Ionic strength	Initial (H^+), M	Time, sec.	(HNCO), M	k, moles l.$^{-1}$ min.$^{-1}$
8	0.2	0.0944	0	0.0986	—
			15	0.0969	0.740
			60	0.0923	0.759
			120	0.0866	0.738
			240	0.0781	0.700
			480	0.0642	0.713
9	0.5	0.293	0	0.0986	—
			15	0.0934	0.764
			30	0.0889	0.726
			120	0.0667	0.713
			240	0.0470	0.704
10	2.0	0.285	0	0.0988	—
			30	0.0857	1.024
			60	0.0726	1.140
			120	0.0564	1.074
			240	0.0351	1.057
11	3.0	0.285	0	0.0987	—
			15	0.0903	1.260
			30	0.0839	1.173
			60	0.0695	1.302
			120	0.0515	1.261

It is interesting to note that this change closely parallels that of the activity

coefficient (f) of hydrochloric acid at similar ionic strengths (7):

μ	0.2	0.5	1.0	2.0	3.0
$\log f$	−0.116	−0.121	−0.091	0.008	0.120
$\log k$	−0.137	−0.137	−0.066	0.029	0.097

The next question is whether this is the same reaction as that examined by Taufel *et al.* (8). Cyanic acid itself could provide hydrogen ions; from the rate constants given above and that obtained by these authors, the observed rates would be the same if the pH were 3.5, which is a reasonable value for partially hydrolyzed cyanic acid. However if cyanic acid provided the hydrogen ions the rate would not appear to be first order, as reported by Taufel *et al.* In fact the reaction should follow the equation:

$$x_0/x - \ln(x_0/x) = 1 - 2k.k_a t$$

where x is the cyanic acid concentration, initially x_0, k is the rate constant, and k_a the ionization constant. It was therefore decided to investigate the decomposition of cyanic acid in the absence of added acid.

2. DECOMPOSITION OF CYANIC ACID WITHOUT ADDED ACID

The reaction here goes in two stages:

$$HNCO + H_2O \rightarrow NH_3 + CO_2,$$
$$NH_3 + HNCO \rightarrow NH_4^+ + NCO^-.$$

The first stage is, of course, the slower.

Experimental Method

Cyanic acid solution was prepared in the usual way by passing the gases formed by heating cyanuric acid through a red-hot tube and thence into ice-cold water (e.g. 1, 10). A slow stream of nitrogen was used to carry over the gas. The resulting solution of cyanic acid was used as soon as possible. It was contained in a flask immersed in a water bath of the desired temperature, and samples for analysis were taken at intervals.

The chief difficulty in following this reaction is to find an analytical method that distinguishes between cyanic acid and cyanate ions. As it is necessary to stop the reaction by the addition of alkali, only an acid–base titration seemed to offer much hope of a successful method. It was found that if a sample of partially decomposed cyanic acid were run into excess sodium hydroxide solution, and the mixture titrated with standard acid, then the pH of the mixture showed two inflection points, at 7.8 and at 5.1. The first inflection comes when carbonate ions have just been converted into bicarbonate; in effect this is the pH of ammonium bicarbonate solution. The second is due to the fact that at pH 5.1 most of the carbonate is now carbonic acid while the buffering action of cyanate is only just beginning. This is not a very well marked inflection, but it is quite distinguishable.

The procedure was therefore as follows. The sample was run into a known volume of standard sodium hydroxide solution, and this mixture was titrated with hydrochloric acid with the help of a pH meter. The volumes required to give pH 7.8 and 5.1 were noted. After this the pH meter was removed, brom-

cresol green was added, and the solution was heated. Hydrochloric acid was run in until the bromcresol green maintained a green color even on boiling; the volume of acid required was noted. It will be seen that the difference between the gram molecules of the sodium hydroxide and hydrochloric acid gives the number of gram molecules of the following constituents: (1) pH 7.8: HNCO+CO_2; (2) pH 5.1: HNCO; (3) bromcresol green end point: HNCO+2(NCO^-). From this the concentrations of cyanic acid, cyanate ion, and carbon dioxide can be found separately. There is a small correction to apply at pH 5.1, since about 4% of cyanate is already cyanic acid, and about 4% of the carbon dioxide is still present as bicarbonate. If any cyanuric acid (pK_a = 6.75(2)) is present it will appear as carbon dioxide in this scheme of analysis, but will not interfere with the analyses for cyanic acid or cyanate.

TABLE III

Run No.	Temp., °C.	Time, min.	(HNCO), *M*	(NCO^-), *M*
1*x*	5.0	0	0.0796	0.0305
		27	0.0298	0.0555
		62	0.0080	0.0646
		95	0.0025	0.0655
2*x*	5.0	0	0.1085	0.0059
		30.5	0.0390	0.0406
		65	0.0135	0.0516
		95	0.0040	0.0550
		125	0.0016	0.0540
3*x*	0.0	0	0.1784	—
		20	0.1232	0.0265
		43	0.0726	0.0390
		62.5	0.0440	0.0418
		81.5	0.0278	0.0494
5*x*	0.0	0	0.1692	—
		20	0.1157	0.0243
		40	0.0686	0.0448
		61	0.0423	0.0576
		80.5	0.0302	0.0609
6*x*	12.0	0	0.1191	0.0182
		11	0.0532	0.0496
		21	0.0246	0.0580
		31	0.0120	0.0632
		41.5	0.0049	0.0601

The results are given in Table III. A plot of log(HNCO) against time shows that the reaction is first order. The equation, $x_0/x - \ln(x_0/x) = 1+2k.k_a t$, derived above, is definitely not followed. These runs give the following first order rate constants:

Run	1*x*	2*x*	3*x*	5*x*	6*x*	
T	5.0	5.0	0.0	0.0	12.0	°C.
k	1.82	1.73	1.12	1.07	3.71	$\times 10^{-2}$ min.$^{-1}$

These constants make the activation energy about 16 kcal./gm-mol. Owing to the fact that the pH changes in the titration are not very sharp, these

constants are only moderately accurate. These results show that the $HNCO + H_3O^+$ reaction will be faster at pH less than about two; above pH 2 the $HNCO + H_2O$ reaction will be faster. The pH's of these reaction mixtures were followed during the runs, but are not worth reporting in detail, except to say that they ran from about 2.5 to 4.5, and agreed reasonably well with the analytical results.

It was found that the bromcresol green titer fell slowly during a run. If the reaction is solely

$$2HNCO + H_2O \rightarrow NH_4NCO + CO_2$$

this titer should not change. These experiments indicate that there is a few per cent of some other, or perhaps subsequent, reaction involving cyanate. The formation of urea is too slow (see, for example, Ref. 9) to account for the change; possibly some cyanuric acid is formed. However on the present evidence all that can be said is that such reactions, if present, would decrease the bromcresol green titer. This matter deserves further study.

3. DECOMPOSITION OF CYANATE IONS

This reaction has been investigated at 80°C. by Masson and Masson (4), who examined the decomposition of salts such as barium cyanate which give insoluble carbonates, and sodium cyanate which give soluble carbonates. The first salt reacts thus:

$$Ba(NCO)_2 + 2H_2O \rightarrow BaCO_3 + CO(NH_2)_2.$$

Ammonium ions are no doubt an intermediate. With sodium cyanate they find that the reaction approximates to

$$4NaOCN + 6H_2O \rightarrow 2Na_2CO_3 + (NH_4)_2CO_3 + CO(NH_2)_2.$$

They believe that the relative proportion of ammonium carbonate and urea is not essential from the reaction mechanism, but the chance result of the relative reaction rates. They found that the reaction was catalyzed by sodium ammonium carbonate ($NaNH_4CO_3$), and less so by sodium carbonate. They attribute the catalysis to the $NH_4CO_3^-$ ion, though it seems dubious to postulate this as a unit.

Taufel *et al.* (8) made a few measurements on the decomposition at 100°C. in the presence of excess alkali, which prevents urea formation by removing ammonium ions. They found a first order reaction with $k = 2.7 \times 10^{-3}$ min^{-1}.

The present work deals with the decomposition in the presence of excess sodium hydroxide (in most cases), over a variety of conditions, and in some runs with added carbonate or other ions to discover if they catalyze the reaction.

Method and Apparatus

The reaction was carried out in a flask fitted with a thermometer and a side tube for sampling. The flask was deeply immersed either in boiling water or, for lower temperatures, in a water thermostat of conventional design.

The reaction mixture was made up from stock solutions of potassium cyanate, sodium hydroxide, and sodium nitrate to bring the ionic strength to a known value. In some runs sodium carbonate or other salt was added to investigate the catalytic effect, and the amount of sodium nitrate was adjusted to maintain the ionic strength. Since the over-all reaction is

$$OCN^- + OH^- + 2H_2O \rightarrow NH_4OH + CO_3^{--},$$

it is, of course, impossible to keep constant ionic strength throughout the reaction, but the reactions were started at known values.

TABLE IV

Run No.	Temp., °C.	Initial (NaOH), *M*	Initial ionic strength	Time, min.	(OCN^-), *M*	*k*
1	100.0	0.143	0.28	0	0.1310	
				15	0.1247	
				60	0.1097	3.07×10^{-3}
				90	0.0994	
2	100.0	0.111	0.33	0	0.0968	
				21	0.0911	
				30	0.0902	
				45	0.0847	3.03×10^{-3}
				60	0.0797	
				120	0.0673	
3	100.0	0.036	0.28	0	0.1190	
				16	0.1131	
				30	0.1059	3.75×10^{-3}
				60	0.0950	
				90	0.0665	
				120	0.0414	
				150	0.0224	
				182	0.0026	
3a	100.0	0.589	1.02	0	0.427	
				16½	0.404	
				30	0.384	3.00×10^{-3}
				75	0.339	
				100	0.315	
				120	0.298	
4	100.0	0.321	0.39	0	0.0723	
				30	0.0667	
				60	0.0612	2.89×10^{-3}
				240	0.0371	
				345	0.0267	
5	65.0	0.143	0.30	0	0.1527	
				185	0.1492	
				1288	0.1339	1.081×10^{-4}
				1600	0.1285	
6	80.9	0.148	0.29	0	0.1384	
				240	0.1223	
				537	0.1033	5.41×10^{-4}
				603	0.0999	

Temp.	65.0	80.9	100.0 °C.
Mean *k*	1.08	5.4	30.0×10^{-4} min.$^{-1}$

The reaction was followed by pipetting out a sample, which was rapidly cooled and to which then a few drops of phenolphthalein were added and dilute acetic acid run in until the color was just discharged. Litmus paper was put in, and acetic acid was added drop by drop until the litmus was pink. This brings the pH to 5–6, and cyanate can now be titrated with silver nitrate without interference from carbonate or ammonia. Sodium chromate was used as indicator.

The results are given in Table IV. Within experimental error the results all conform to a first order reaction, and accordingly the first order constants are also given in Table IV. There seems to be a slight dependence on hydroxide concentration when this is small, but not at higher concentrations. Run 3 illustrates this point very well. In this run the hydroxide was completely used up when the cyanate concentration fell to 0.09 *M*. At about this point the rate increased rapidly, showing that other reactions are important once ammonium ions are present; but the point at 0.095 *M* cyanate (0.005 *M* hydroxide) is in line with the earlier points, showing that even at this low hydroxide concentration the rate had not increased very much. It was checked that when excess hydroxide was present all the carbon from cyanate appeared as carbonate. Hence side reactions only occur when ammonium ions are present.

Runs 1, 5, and 6 give a value of $23\frac{1}{2}$ kcal./gm-mol. for the activation energy. This is doubtless for the first stage of the reaction

$$OCN^- + 2H_2O \rightarrow NH_4^+ + CO_3^{--}$$

after which the ammonium ion reacts with hydroxide.

The next matter to be investigated was the catalytic effect of carbonate found by Masson and Masson for the reaction without added alkali. It was suspected at first that this might simply arise from the higher ionic strength

TABLE V

Run No.	Temp., °C.	Initial (NaOH), *M*	Initial ionic strength	Time, min.	(OCN^-), *M*	*k*
7	100.0	0.150	0.55 (Na_2SO_4)	0	0.1436	
				30	0.1333	
				60	0.1217	3.00×10^{-3}
				90	0.1117	
				120	0.1015	
				183	0.0839	
				221	0.0739	
8	100.0	0.141	2.68 (Na_2SO_4)	0	0.1389	
				30	0.1251	
				60	0.1170	3.04×10^{-3}
				92	0.1069	
				122	0.0959	
9	100.0	0.141	1.07 ($NaNO_3$)	0	0.1316	
				30	0.1207	
				66	0.1079	3.02×10^{-3}
				97.5	0.0984	
				127.5	0.0895	

of the solutions containing carbonate. Accordingly sodium sulphate was added to two runs; it was chosen as a 2:1 salt like sodium carbonate. A run was also carried out at high sodium nitrate concentration. The results are given in Table V. It will be seen that no very great change in k results; and there is no difference between nitrate and sulphate, so the small change probably is due to changing ionic strength.

Table VI gives the effect firstly of added carbonate, and secondly of adding some other ions derived from weak acids. The results show that acetate and borate do not catalyze the reaction, so that the catalytic effect of carbonate is not reproduced by the anion of any weak acid. This is perhaps only to be expected, since hydroxide ions were present in every run, and are also anions of a weak acid.

TABLE VI

Run No.	Temp., °C.	Added salt, M	Initial ionic strength	Initial (NaOH), M	Time, min.	(OCN^-), M
10	100.0	Na_2CO_3	0.52	0.141	0	0.1433
					30	0.1261
		0.076			60½	0.1158
					91	0.1066
					122	0.0925
					151	0.0842
11	100.0	Na_2CO_3	0.80	0.141	0	0.1275
					31	0.1158
		0.177			63½	0.0998
					109	0.0793
					142	0.0639
12	100.0	Na_2CO_3	1.60	0.141	0	0.1261
					32	0.1112
		0.445			62	0.0921
					115	0.0590
					154	0.0406
					185	0.0268
13	100.0	Na_2CO_3	2.41	0.141	0	0.1290
					30½	0.1068
		0.714			60	0.0875
					94	0.0620
					123	0.0409
					150	0.0277
14	100.0	Na acetate	1.12	0.141	0	0.1754
					32	0.1628
		0.80			64	0.1507
					93	0.1363
					155	0.1160
15	100.0	Na borate	1.11	0.141	0	0.1227
					30	0.1139
		0.79			69	0.1039
					96½	0.0961
					126	0.0883

In the runs with carbonate there is a marked catalytic effect and in addition the rate of the reaction no longer fits a first order equation. In fact in runs 11,

12, and 13, (HNCO) gives a linear plot against time. Run 10 is more or less intermediate, but on the whole fits a logarithmic plot best. In Runs 12 and 13 there is some sign that the rate falls off at low concentrations, but over most of the range the rate is constant. If we calculate the rate at various carbonate concentrations, the results are as follows:

Run	—	10	11	12	13	
(CO_3^{--})	low	0.105	0.21	0.49	0.76	M
Rate	3.0	3.9	4.4	5.6	7.15	$\times 10^{-4}$ moles liter^{-1} min.$^{-1}$

The first rate given above is that calculated from runs without added carbonate for a cyanate concentration about the average of those used in these runs. It roughly indicates what part of the rate is to be ascribed to the uncatalyzed reaction. In the other runs the carbonate concentrations are the averages during the run. These rates give a reasonably linear plot against (CO_3^{--}); that is, the catalyzed reaction conforms to the equation

$$-d(OCN^-)/dt = K_1(OCN^-)+K_2(CO_3^{--}).$$

The results make $K_2 = 6.2 \times 10^{-4}$ min^{-1}. This value of K_2 is obtained by calculating the rate due to the uncatalyzed reaction for all successive pairs of points in Runs 10–13, subtracting this from the observed rate, and dividing the difference by the carbonate concentration. The average result is that given above. Masson and Masson (4) propose an equation for the reaction without excess sodium hydroxide, which is in effect:

$$-d(OCN^-)/dt = \{K_1+K_2(CO_3^{--})\}(OCN^-),$$

but it does not seem possible to fit the present results to this equation. While the catalysis of this reaction by carbonate seems well established, it is not easy to propose a detailed mechanism; that is, to explain the nature of the interaction between cyanate and carbonate.

These results mean that the reaction

$$OCN^-+OH^-+2H_2O \rightarrow NH_4OH+CO_3^{--}$$

must be autocatalytic to a certain extent. The reason that this is not apparent from the results of Table IV (without added carbonate) is that the catalytic contribution is small in these runs: K_1 is about five times as large as K_2, and the runs were terminated after usually about 40% of the cyanate had decomposed.

4. IONIZATION CONSTANT OF CYANIC ACID

This quantity has been previously measured by Taufel *et al.* (8) using the color of bromphenol blue to give the pH of a cyanic acid solution; and by Naumann (5) from the conductivity of a solution containing equimolar amounts of potassium cyanate and hydrochloric acid. The values reported are (i) 2.2×10^{-4}, probably at 0°C.; and (ii) 1.2×10^{-4} at 0°C. Since the decomposition of cyanic acid is relatively rapid even at 0°C., it seemed desirable

to repeat this measurement by a method that avoids as far as possible the risk of error from hydrolysis. Accordingly a roughly 0.1 *M* solution of potassium cyanate was titrated with 0.1004 *M* hydrochloric acid, the pH being followed on a pH meter. The total concentration of cyanate was found by continuing the titration to the bromcresol green end point as described above. A value of the ionization constant, K_a, can be calculated from each pH reading. In this method any carbonate present in the cyanate can be measured and allowed for; the results given in Table VII are calculated on the

TABLE VII

Run 1, Temp. 27°C.											
Vol. HCl	0.72	1.09	1.47	1.99	2.50	3.03	4.03	4.96	6.00	7.07	7.91
pH	7.85	6.42	5.99	5.55	5.27	5.10	4.90	4.80	4.69	4.55	4.51
pK_a(calc.)	—	(3.52)	(3.80)	3.76	3.71	3.70	3.71	3.75	3.76	3.72	3.75
Vol. HCl to bromcresol green end point = 89.97 ml. Mean pK_a = 3.73.											
Run 2, Temp. 10°C.											
Vol. HCl	0.74	1.26	1.51	2.01	2.50	3.00	3.51	3.98	5.00	6.00	
pH	7.85	6.35	6.08	5.64	5.37	5.17	5.01	4.90	4.70	4.59	
pK_a(calc.)	—	3.68	3.79	3.75	3.72	3.68	3.65	3.64	3.59	3.60	
Vol. HCl to bromcresol green end point = 81.60 ml. Mean pK_a = 3.68.											

assumption that pK_a for carbonic acid is 6.46. Any hydrolysis of cyanic acid would show up as an upward drift in the calculated K_a values. As before it was assumed that the ammonium bicarbonate stage was just reached at a pH of 7.85. The best average for pK_a is 3.70, so K_a is 2.0×10^{-4}. It was checked by a rough calorimetric measurement that cyanic acid absorbs heat on ionization though the amount is small. This means that pK_a must fall as the temperature rises, so the difference between the two runs in Table VII must be due to experimental error.

5. OXIDATION OF CYANATE

This section briefly reports some observations on the oxidation of cyanate by the hypochlorite ion and by chlorine and on the similar oxidation of cyanide to cyanate.

The oxidation of cyanide by hypochlorite is known, though it does not seem to have been much investigated. It does however form the basis of a German patent for producing cyanate by passing chlorine into an alkaline cyanide solution, though this could go through cyanogen chloride. It was observed in the present work that potassium cyanide containing sodium hydroxide was oxidized quantitatively to cyanate by sodium hypochlorite. In the presence of hydroxide concentrations down to about 0.1 *M*, equal amounts (within experimental error) of cyanide and hypochlorite were used up in this reaction; that is, side reactions to the main reaction

$$CN^- + ClO^- \rightarrow OCN^- + Cl^-$$

are not present to more than 1% at the most. Attempts to measure the speed of the reaction were unsuccessful: the reaction was stopped by adding hydrogen

peroxide to destroy hypochlorite, but even when this was done only five seconds after the start of the reaction at 3°C., the reaction was already virtually complete. This perhaps merely proves that hypochlorite ions react with cyanide faster than with hydrogen peroxide, but the latter is certainly a rapid reaction.

With low concentrations of sodium hydroxide, cyanate is oxidized by hypochlorite. Under these conditions 1 gm-mol. of cyanide reacts with about 2.5 gm-mol. of hypochlorite; a typical example is the following experiment:

	Concentration, *M*			
Ion	Initial	Final	Difference	
CN^-	0.128	0	0.128	
ClO^-	0.577	0.231	0.346	
OH^-	0.019	0		
CO_3^{--}	0.015	0.034	0.128	carbonate
HCO_3^-	0	0.109		

The concentrations under 'initial' are those immediately on mixing, calculated on the assumption of no reaction. Under 'final' are the results of analyses after the reaction. Hence the reaction is, at least mainly:

$$2KCN+5NaOCl+H_2O \rightarrow 2KHCO_3+5NaCl+N_2$$

or, if we assume that cyanate is formed first, this is then oxidized:

$$2KOCN+3NaOCl+H_2O \rightarrow 2KHCO_3+3NaCl+N_2.$$

This last reaction occurred when cyanate and hypochlorite were mixed directly, as shown by the following experiment:

	Concentration, *M*		
Ion	Initial	Final	Difference
OCN^-	0.316	0	0.316
ClO^-	0.547	0.029	0.518

This gives a hypochlorite to cyanate ratio of 1.64. This is somewhat greater than 1.5, probably because at the end of the reaction the remaining hypochlorite was in a hot solution, containing bicarbonate, from which nitrogen was being evolved. Probably some hypochlorous acid was decomposed, or also evolved.

With fairly low concentrations of sodium hydroxide, the oxidation of cyanate appeared to have an induction period. In the following experiment cyanide (initial concentration 0.130 *M*) was mixed with hypochlorite and samples were taken at intervals and analyzed for hypochlorite. The concentration of sodium hydroxide was initially 0.038 *M*.

Time	0	0.75	2	3.67	5	32	min.
(NaOCl)	0.562	0.414	0.412	0.223	0.217	0.222	*M*
Temp.	22	33	34	40	43	—	°C.

The temperature was read from a thermometer immersed in the liquid, and it is probably because of lag in the thermometer that the temperature appears to rise between 3.67 and 5 min. though the reaction is already virtually complete. Note that here 2.61 hypochlorite ions vanished for each cyanide ion. The length of the induction period, as measured by the time for rapid nitrogen evolution to develop, was as follows (other conditions as in the last experiment):

Induction time	10 sec.	3–3.5 min.	long
(NaOH)	0.019	0.038	0.065 *M*

Similar experiments were made on mixtures of cyanate and hypochlorite. In Run 1 below, the hypochlorite concentration was followed by samples taken at intervals; initially the cyanate concentration was 0.316 *M*, and the sodium hydroxide concentration was 0.0735 *M*. The initial time is the time of mixing:

Run 1	Time	0	0.4	1.5	4.2	7.0	12.0	13.1	min.
	(NaOCl)	0.547	0.543	0.542	0.540	0.538	0.530	0.029	*M*

The temperature in this and similar runs was followed with the results in Table VIII.

TABLE VIII

Run	(NaOH) initial, *M*	Time, min.	Temp., °C.	Run	(NaOH) initial, *M*	Time, min.	Temp., °C.
1	0.0735	0.5	19.8	3	0.057	0.2	19.7
		8.0	19.9			1.0	19.9
		9.5	20.0			2.0	20.0
		11.0	20.2			2.3	22.0
		12.0	20.2			2.6	53.5
		12.7	54.5			2.8	54.8
		13.5	53.5			3.25	54.3
		15.0	51.0			4.0	53.5
2	0.0695	0.2	19.2	4	0.042	0.2	19.5
		2.0	19.8			0.5	41
		4.0	19.9			0.7	53
		6.0	20.0			0.8	54.5
		6.2	35			1.0	54.3
		6.5	45			2.0	53.0
		6.75	54.5				
		7.0	54.2				
		8.0	52.0				

There is evidently an induction period in all these runs, as was also apparent from the sudden evolution of gas after a certain time. The time required for rapid gas evolution to develop was:

Run	1	2	3	4	
(NaOH) initial	0.0735	0.0695	0.057	0.042	*M*
Induction time	12.3	6.2	2.4	0.3	min.

The explanation of this would seem to be that the oxidation of cyanate by hypochlorite ions is slow, but that hypochlorous acid oxidizes it rapidly.

As soon as the hydroxide is used up, the potassium bicarbonate formed is acid enough to liberate hypochlorous acid; cyanic acid is too strong an acid to be formed.

Similar experiments were made on the reaction between chlorine and cyanate. The reaction is fairly rapid in solution at room temperature. The results are not very clear-cut, probably because more than one reaction can occur. The products were found to be chloride, carbon dioxide, nitrogen, and ammonium chloride or hydrochloric acid depending on the relative amounts of chlorine and cyanate. No urea was detected by the xanthydrol test (3). With smaller amounts of chlorine the reaction approximated to

$$4KOCN+3Cl_2+4H_2O \rightarrow 4KCl+4CO_2+N_2+2NH_4Cl.$$

In one experiment 4.69 millimoles of potassium cyanate and 3.44 of chlorine disappeared (a ratio of 1.36 to 1); no acid and 1.74 millimoles of ammonium ion were formed: the above equation would lead one to expect 2.34 of ammonium ion, so about three quarters of the expected amount was formed. In another experiment 3.29 millimoles of potassium cyanate disappeared, and 0.86 of ammonium ion and 3.86 of acid appeared. If we assume the above equation, followed by attack of chlorine on ammonium chloride, to give nitrogen and hydrochloric acid, this reaction would have used up 4.01 millimoles of chlorine; actually 4.47 disappeared. Several other similar experiments were made, but the results were all about the same: the analyses for the products and reagents did not agree to better than 10% with the predictions of the equation above, allowing for subsequent reaction of chlorine and ammonium ions. It is not difficult to suggest side reactions, and the most that can be said is that this equation probably represents the main reaction. Normand and Cumming (6) report that bromine gives a reaction precisely analogous to the one suggested for chlorine. Here presumably the attack of bromine on ammonium ions, or other side reactions, is slower so that the reaction is more clear-cut.

REFERENCES

1. Eyster, E. H., Gillette, R. H., and Brockway, L. O. J. Am. Chem. Soc. 62: 3236. 1940.
2. Hantzsh, A. Ber. 39: 139. 1906.
3. Kny-Jones, F. G. and Ward, A. M. Analyst, 54: 574. 1929.
4. Masson, O. and Masson, I. Z. physik. Chem. 70: 290. 1910.
5. Naumann, R. Z. Elektrochem. 16: 773. 1910.
6. Normand, C. W. B. and Cumming, A. C. J. Chem. Soc. 1852. 1912.
7. Randall, M. and Young, L. E. J. Am. Chem. Soc. 50: 989. 1928.
8. Taufel, K., Wagner, C., and Dunwald, H. Z. Elektrochem. 34: 115. 1928.
9. Walker, J. and Hambly, F. J. J. Chem. Soc. 746. 1895.
10. Woo, S. C. and Liu, T. K. J. Chem. Phys. 3: 544. 1935.

NOTES

UNIT CELL, SPACE GROUP, AND INDEXED X-RAY DIFFRACTION POWDER DATA FOR THE C_{15} LUPINE ALKALOIDS, *l*-THERMOPSINE ($C_{15}H_{20}N_2O$), *dl*-LUPANINE ($C_{15}H_{24}N_2O$), AND *d*-HYDROXYLUPANINE ($C_{15}H_{24}N_2O_2$)[1]

By W. H. Barnes, D. M. Donaldson,* and D. C. Phillips

Thermopsine, $C_{15}H_{20}N_2O$, is the "blank-*cis*" (1) precursor of α-isosparteine, $C_{15}H_{26}N_2$, the structure of which (in the form of the monohydrate) has been studied in this laboratory (2). Lupanine, $C_{15}H_{24}N_2O$, is the first "*cis–trans*" hydrogenation product of the "blank-*trans*" isomer of thermopsine, namely anagyrine. As a preliminary step in possible structure investigations, the unit cell constants of *l*-thermopsine, *dl*-lupanine, and *d*-hydroxylupanine have been determined from precession photographs obtained with Mo K_α radiation (λ = 0.7107 Å), and the space group of each has been established. The density (at ~22°C.) of *l*-thermopsine and of *dl*-lupanine was measured by flotation in aqueous solutions of potassium iodide, while solutions of carbon tetrachloride and benzene were employed as the flotation liquid for *d*-hydroxylupanine.

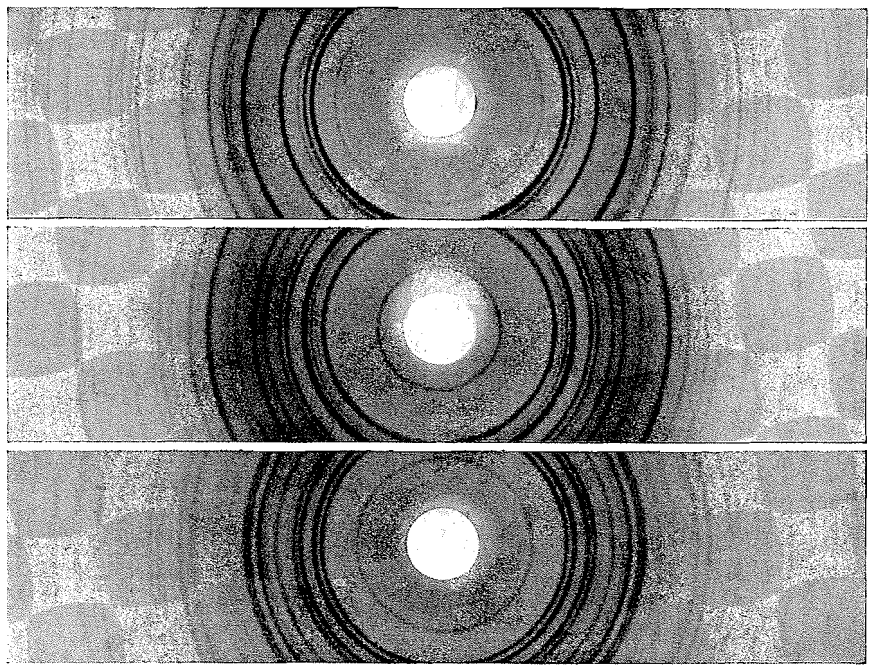

FIG. 1. X-ray diffraction powder photographs of A, *l*-thermopsine; B, *dl*-lupanine; C, *d*-hydroxylupanine. (Camera diameter: 114.6 mm.; radiation: Co K_α, λ = 1.790 Å)

[1]*Issued as N.R.C. No. 3495.*

**National Research Laboratories Postdoctorate Fellow, now I.C.I. Fellow, The University, Edinburgh, Scotland.*

TABLE I

SINGLE-CRYSTAL DATA FOR *l*-THERMOPSINE, *dl*-LUPANINE, AND *d*-HYDROXYLUPANINE

	l-Thermopsine	*dl*-Lupanine	*d*-Hydroxylupanine
Crystal system	Tetragonal	Monoclinic	Orthorhombic
Space group	$P4_1(C_4^2)$ or $P4_3(C_4^4)$	$P2_1/a(C_{2h}^5)$	$P2_12_12_1(D_2^4)$
a	8.26±0.03 Å	13.82±0.03 Å	12.84±0.04 Å
b		7.75±0.03 Å	17.98±0.05 Å
c	18.68±0.05 Å	12.82±0.04 Å	6.08±0.02 Å
β		96.5 ±0.2°	
Z	4 molecules per cell	4 molecules per cell	4 molecules per cell
ρ(Obs.)	1.257 gm./ml.	1.203 gm./ml.	1.261 gm./ml.
ρ(Calc.)	1.273 gm./ml.	1.208 gm./ml.	1.250 gm./ml.

TABLE II

X-RAY DIFFRACTION POWDER DATA FOR *l*-THERMOPSINE

I/I_1	d(Å) Obs.	d(Å) Calc.	*hkl*	I/I_1	d(Å) Obs.	d(Å) Calc.	*hkl*
10	8.23	8.26	010	—	—	2.28	134
20	7.49	7.55	011	—	—	2.27	231
90	6.19	6.19	012	2	2.24	2.25	018
50	5.83	5.84	110			2.24	027
20	5.57	5.57	111	—	—	2.22	035,232
70	4.98	4.97	013	20	2.17	2.17	118
		4.95	112	—	—	2.15	233
—	—	4.67	004	1	2.13	2.14	135
—	—	4.26	113			2.13	226
	*	4.13	020	25	2.07	2.07	040
100	4.03	4.07	014	—	—	2.06	036,234
		4.03	021	—	—	2.05	041
25	3.78	3.78	022	—	—	2.03	028
35	3.69	3.69	120			2.02	042
—	—	3.65	114	10BB	2.00	2.01	019
15	3.63	3.62	121			2.00	140
40	3.43	3.44	023,122			1.99	141
—	—	3.40	015	—	—	1.97	227
—	—	3.18	123	20	1.96	1.96	043,119
15	3.15	3.15	115				142
20	3.09	3.09	024	—	—	1.95	235,330
—	—	2.92	220		*	1.94	331
		2.91	016	—	—	1.92	037
1	2.89	2.90	124	1	1.91	1.91	143,332
		2.89	221	—	—	1.89	044
—	—	2.79	222	—	—	1.86	333
10B	2.74	2.77	025	5	1.85	1.85	029,236
		2.75	030,116				240
		2.72	031	—	—	1.84	144,241
25	2.64	2.64	032,223	1	1.82	1.82	0.1.10,228
		2.63	125	5	1.81	1.81	045,242
10	2.59	2.61	130	—	—	1.80	334
		2.59	131	1	1.78	1.78	1.1.10,038
	*	2.54	017	1	1.77	1.77	145,243
15	2.52	2.52	033,132	10	1.74	1.74	237
1	2.49	2.49	026	—	—	1.73	335
		2.48	224	1	1.72	1.72	046,244
15	2.43	2.43	117	1BB	1.63		
—	—	2.41	133	1B	1.59		
	*	2.37	034	1	1.56		
	*	2.34	008	1	1.28		
10	2.30	2.30	225	1	1.23		
	*	2.29	230	1	1.22		

X-ray diffraction powder patterns were obtained with a camera of 114.6 mm. diameter, Straumanis film mounting. Co K_α radiation ($\lambda = 1.790$ Å); the apparatus "cutoff" was 20 Å. Film shrinkage corrections were applied in the case of the precession photographs, but were too small to be significant for the powder films.

The single-crystal data are shown in Table I, and the powder data in Tables II, III, and IV, where B and BB designate lines that were broader and much broader, respectively, than the general average for the pattern examined and an asterisk (under d(Obs.)) indicates a line, the presence of which is probable, but which was too faint ($I/I_1 < 1$) for accurate measurement. The small-2θ end of each film is reproduced in Fig. 1, where, incidentally, the advantage of a capillary-tube container for the specimen (*l*-thermopsine, *dl*-lupanine) over a glass-fiber and adhesive (Household Cement) mount (*d*-hydroxylupanine) is apparent in the generally improved sharpness of the lines in the first and second patterns compared to the third.

TABLE III

X-RAY DIFFRACTION POWDER DATA FOR *dl*-LUPANINE

I/I_1	d(Å) Obs.	d(Å) Calc.	*hkl*	I/I_1	d(Å) Obs.	d(Å) Calc.	*hkl*
30	12.8	12.7	001	—	—	3.37	220
		6.87	200	—	—	3.31	022,22$\bar{1}$
70	6.79	6.75	110	2	3.26	3.26	12$\bar{2}$
		6.62	011	—	—	3.22	221,401
15	6.39	6.37	002			3.21	312
		6.35	20$\bar{1}$			3.18	004,122
30	6.11	6.11	11$\bar{1}$	25	3.16		40$\bar{2}$
100B	5.81	5.83	111			3.14	213,410
		5.78	201	—	—	3.12	41$\bar{1}$
65	5.13	5.14	210	5	3.04	3.05	22$\bar{2}$
		4.96	20$\bar{2}$			3.04	31$\bar{3}$
45	4.95	4.92	012	—	—	3.02	20$\bar{4}$
		4.91	21$\bar{1}$	15	2.95		
10	4.76	4.77	11$\bar{2}$	15	2.83		
	*	4.63	211	2	2.77		
45	4.52	4.51	112	10B	2.58		
	*	4.43	202	8	2.48		
65	4.24	4.25	003	1	2.42		
—	—	4.18	21$\bar{2}$	8	2.36		
—	—	3.94	310	15	2.29		
30	3.87	3.87	020,31$\bar{1}$	5	2.24		
		3.84	212	20	2.21		
—	—	3.81	20$\bar{3}$	2	2.12		
		3.73	120	5	2.09		
20	3.73	3.72	013	1B	2.05		
		3.71	021	5	2.01		
		3.69	11$\bar{3}$	2	1.96		
—	—	3.67	311	5	1.93		
8	3.61	3.61	12$\bar{1}$	1	1.85		
—	—	3.55	121	2	1.81		
1	3.52	3.51	113,31$\bar{2}$	3B	1.73		
		3.44	203	1	1.69		
		3.43	400				
60B	3.42	3.42	21$\bar{3}$				
		3.41	40$\bar{1}$				

TABLE IV

X-RAY DIFFRACTION POWDER DATA FOR *d*-HYDROXYLUPANINE

I/I_1	*d*(Å) Obs.	*d*(Å) Calc.	*hkl*	I/I_1	*d*(Å) Obs.	*d*(Å) Calc.	*hkl*
1	10.5	10.5	110	5	3.21	3.21	400
30	8.99	8.99	020			3.16	410
	*	7.36	120	25	3.14	3.15	241
70	6.42	6.42	200			3.14	250
100	6.03	6.05	210		*	3.10	051,340
5	5.74	5.76	011			3.04	002
80	5.48	5.50	101			3.02	331,420
		5.43	130	25B	3.00	3.01	151
65	5.22	5.26	111			3.00	012
		5.22	220	5	2.91		
5	5.02	5.04	021	15B	2.78		
35	4.66	4.69	121	15	2.70		
—	—	4.50	040	2	2.62		
10	4.40	4.41	201	2	2.54		
		4.38	230	10B	2.45		
		4.29	211	1	2.40		
70	4.25	4.27	031	25	2.32		
		4.24	140	2B	2.27		
—	—	4.16	310	10	2.20		
55	4.04	4.05	131	10	2.18		
55	3.95	3.96	221	1	2.13		
	*	3.86	320	20	2.07		
15	3.66	3.68	240	1	2.02		
—	—	3.61	041	10B	1.96		
—	—	3.55	231	10B	1.91		
—	—	3.50	301	1B	1.87		
		3.48	141,330	1	1.81		
15B	3.45	3.46	150	1	1.79		
		3.44	311	1	1.75		
—	—	3.26	321				

Dr. L. Marion kindly supplied authenticated specimens of the three alkaloids. Mrs. H. M. Sheppard and Mr. B. J. Cowick assisted with the powder investigations.

1. MARION, L. and LEONARD, N. J. Can. J. Chem. 29: 355. 1951.
2. PRZYBYLSKA, M. and BARNES, W. H. Acta Cryst. 6: 377. 1953.

RECEIVED OCTOBER 22, 1954.
DIVISION OF PHYSICS,
NATIONAL RESEARCH COUNCIL,
OTTAWA, CANADA.

UNIT CELL, SPACE GROUP, AND INDEXED X-RAY DIFFRACTION POWDER DATA FOR CERTAIN NARCOTICS
VI. NARCOTINE[1]

BY W. H. BARNES

X-ray diffraction powder photographs of narcotine ($C_{22}H_{27}O_7N$) were taken some time ago in connection with the collection of data for the identification of a number of narcotics (1, 3). The free base, unlike its hydrochloride salt, gave a satisfactory and reproducible pattern. Owing to the pressure of special

[1]*Issued as N.R.C. No. 3488.*

TABLE IV

X-RAY DIFFRACTION POWDER DATA FOR *d*-HYDROXYLUPANINE

I/I_1	*d*(Å) Obs.	*d*(Å) Calc.	*hkl*	I/I_1	*d*(Å) Obs.	*d*(Å) Calc.	*hkl*
1	10.5	10.5	110	5	3.21	3.21	400
30	8.99	8.99	020			3.16	410
	*	7.36	120	25	3.14	3.15	241
70	6.42	6.42	200			3.14	250
100	6.03	6.05	210		*	3.10	051,340
5	5.74	5.76	011			3.04	002
80	5.48	5.50	101			3.02	331,420
		5.43	130	25B	3.00	3.01	151
65	5.22	5.26	111			3.00	012
		5.22	220	5	2.91		
5	5.02	5.04	021	15B	2.78		
35	4.66	4.69	121	15	2.70		
—	—	4.50	040	2	2.62		
10	4.40	4.41	201	2	2.54		
		4.38	230	10B	2.45		
		4.29	211	1	2.40		
70	4.25	4.27	031	25	2.32		
		4.24	140	2B	2.27		
—	—	4.16	310	10	2.20		
55	4.04	4.05	131	10	2.18		
55	3.95	3.96	221	1	2.13		
	*	3.86	320	20	2.07		
15	3.66	3.68	240	1	2.02		
—	—	3.61	041	10B	1.96		
—	—	3.55	231	10B	1.91		
—	—	3.50	301	1B	1.87		
		3.48	141,330	1	1.81		
15B	3.45	3.46	150	1	1.79		
		3.44	311	1	1.75		
—	—	3.26	321				

Dr. L. Marion kindly supplied authenticated specimens of the three alkaloids. Mrs. H. M. Sheppard and Mr. B. J. Cowick assisted with the powder investigations.

1. MARION, L. and LEONARD, N. J. Can. J. Chem. 29: 355. 1951.
2. PRZYBYLSKA, M. and BARNES, W. H. Acta Cryst. 6: 377. 1953.

RECEIVED OCTOBER 22, 1954.
DIVISION OF PHYSICS,
NATIONAL RESEARCH COUNCIL,
OTTAWA, CANADA.

UNIT CELL, SPACE GROUP, AND INDEXED X-RAY DIFFRACTION POWDER DATA FOR CERTAIN NARCOTICS
VI. NARCOTINE[1]

BY W. H. BARNES

X-ray diffraction powder photographs of narcotine ($C_{22}H_{27}O_7N$) were taken some time ago in connection with the collection of data for the identification of a number of narcotics (1, 3). The free base, unlike its hydrochloride salt, gave a satisfactory and reproducible pattern. Owing to the pressure of special

[1]*Issued as N.R.C. No. 3488.*

problems that developed with certain narcotics during the survey (2, 3), it was impractical to obtain single-crystal data for the authentication of the powder patterns of the majority of the compounds which, like narcotine, presented no difficulties. Since that time, however, unit cell and space group data for narcotine have become available (4) and it has, therefore, become desirable to index the powder pattern. According to Lovell (4), narcotine is orthorhombic,

TABLE I

INDEXED X-RAY DIFFRACTION POWDER DATA ($d > 3.00$ Å) FOR NARCOTINE

I/I_1	d(Å) Obs.	d(Å) Calc.	hkl	I/I_1	d(Å) Obs.	d(Å) Calc.	hkl
25	16.2	16.3	002			3.88	117
3	14.0	13.9	011		*	3.87	126
20	11.2	11.2	012			3.85	040
10	8.85	8.88	013			3.84	202
1	8.15	8.15	004			3.83	210
75	7.64	7.70	020	50	3.81	3.82	041
		7.68	101			3.81	134
—	—	7.49	021			3.80	211
		7.20	014			3.75	042
30B	7.10	7.11	102			3.73	036
		7.03	110	30	3.75	3.72	212
	*	6.96	022			3.71	203
		6.87	111			3.63	043
35	6.48	6.45	112			3.62	108
	*	6.39	103			3.61	213
50	6.22	6.28	023	10B	3.58	3.60	028
35	5.91	6.00	015			3.59	135
		5.90	113			3.56	127
25	5.70	5.67	104			3.55	204
—	—	5.60	024	—	—	3.53	019,118
15	5.50	5.51	120			3.51	220
	*	5.44	121	100	3.49	3.49	221
		5.43	006			3.48	044
40	5.33	5.32	114			3.46	140,214
—	—	5.22	122	—	—	3.45	037
—	—	5.12	016			3.44	141,222
		5.07	031			3.39	142
20	5.06	5.03	105	1	3.38	3.38	205
		4.98	025			3.37	136
20	4.93	4.92	123	—	—	3.34	223
—	—	4.90	032			3.32	045
25	4.79	4.78	115	20	3.32	3.30	143,215
		4.64	033			3.29	109
		4.57	124	—	—	3.28	029,128
3B	4.53	4.48	106			3.26	0.0.10
		4.46	017		*	3.23	224
		4.44	026			3.22	119
		4.34	034			3.19	0.1.10,038
25	4.30	4.30	116,130	—	—		144,206
	*	4.27	131			3.16	137
	*	4.21	125			3.14	046
—	—	4.16	132	5	3.13	3.13	216,230
20	4.07	4.07	008			3.12	231
		4.03	035			3.09	225
—	—	4.01	107	—	—	3.07	051,232
		4.00	133			3.06	145
		3.98	027			3.03	052,129
15	3.96	3.95	200	2	3.02	3.01	1.0.10
		3.94	018				207,233
—	—	3.92	201			3.00	0.2.10

space group $P2_12_12_1$, with $a = 7.90$ Å, $b = 15.4$ Å, $c = 32.6$ Å. Retaining this orientation, the powder pattern, indexed on the basis of these data for all reflections corresponding to $d > 3.00$ Å, is given in Table I, where B identifies an unusually broad line and an asterisk (under d(Obs.)) indicates the probable presence of a line which was too faint ($I/I_1 < 1$) or diffuse for accurate measurement. The agreement between d(Obs.) and d(Calc.) is very satisfactory, particularly in view of the large number of possible reflections with the consequent difficulty of deciding precisely which contribute most probably to a given line on the film, and because the maximum error in the single-crystal numerical data is estimated as of the order of 1% (4).

1. BARNES, W. H. Bull. Narcotics U.N. Dept. Social Affairs, 6 (1): 20. 1954.
2. BARNES, W. H. and FORSYTH, W. J. Can. J. Chem. 32: 984, 988, 991, 993. 1954.
3. BARNES, W. H. and SHEPPARD, H. M. Bull. Narcotics U.N. Dept. Social Affairs. 6 (2): 27. 1954.
4. LOVELL, F. M. Acta Cryst. 6: 869. 1953.

RECEIVED OCTOBER 22, 1954.
DIVISION OF PHYSICS,
NATIONAL RESEARCH COUNCIL,
OTTAWA, CANADA.

NOTE ON THE VOLATILITY OF LITHIUM OXIDE

BY A. E. VAN ARKEL, U. SPITSBERGEN, AND R. D. HEYDING

Preliminary experiments in this laboratory on the reactions of lithium oxide with various metals in the presence of oxygen at 1000°C. were complicated by the apparent volatilization of Li_2O. Although there is considerable disagreement in the earlier literature in respect of the vapor pressure of Li_2O, recent reports by Brewer and Margrave (2) indicate that the vapor or decomposition pressure would probably be too low at 1000°C. to result in any significant losses. Moreover, during experiments on molten Li_2O at 1570°C. there was no indication that the vapor pressure was appreciable (1).

To confirm these observations, small magnesia boats containing powdered Li_2O were heated *in vacuo* at 1000°C. for extended periods of time. A small initial decrease in weight was observed and was found to be a function only of the quantity of oxide employed in the experiment. Such losses can be attributed to the decomposition of impurities which in these experiments amounted to some four per cent of the oxide and were in all probability hydroxide and carbonate. Following this initial decomposition no appreciable decrease in weight could be detected.

Similar small losses occurred when the same experiments were repeated using dry oxygen rather than a high vacuum. On the other hand the oxide disappeared rapidly in the presence of oxygen containing small amounts of water vapor. Brewer and Margrave also observed erratic losses when wet gases were passed over Li_2O at 1200°C. and have suggested the formation of a volatile 'hydenide'.

space group $P2_12_12_1$, with $a = 7.90$ Å, $b = 15.4$ Å, $c = 32.6$ Å. Retaining this orientation, the powder pattern, indexed on the basis of these data for all reflections corresponding to $d > 3.00$ Å, is given in Table I, where B identifies an unusually broad line and an asterisk (under d(Obs.)) indicates the probable presence of a line which was too faint ($I/I_1 < 1$) or diffuse for accurate measurement. The agreement between d(Obs.) and d(Calc.) is very satisfactory, particularly in view of the large number of possible reflections with the consequent difficulty of deciding precisely which contribute most probably to a given line on the film, and because the maximum error in the single-crystal numerical data is estimated as of the order of 1% (4).

1. BARNES, W. H. Bull. Narcotics U.N. Dept. Social Affairs, 6 (1): 20. 1954.
2. BARNES, W. H. and FORSYTH, W. J. Can. J. Chem. 32: 984, 988, 991, 993. 1954.
3. BARNES, W. H. and SHEPPARD, H. M. Bull. Narcotics U.N. Dept. Social Affairs. 6 (2): 27. 1954.
4. LOVELL, F. M. Acta Cryst. 6: 869. 1953.

RECEIVED OCTOBER 22, 1954.
DIVISION OF PHYSICS,
NATIONAL RESEARCH COUNCIL,
OTTAWA, CANADA.

NOTE ON THE VOLATILITY OF LITHIUM OXIDE

BY A. E. VAN ARKEL, U. SPITSBERGEN, AND R. D. HEYDING

Preliminary experiments in this laboratory on the reactions of lithium oxide with various metals in the presence of oxygen at 1000°C. were complicated by the apparent volatilization of Li_2O. Although there is considerable disagreement in the earlier literature in respect of the vapor pressure of Li_2O, recent reports by Brewer and Margrave (2) indicate that the vapor or decomposition pressure would probably be too low at 1000°C. to result in any significant losses. Moreover, during experiments on molten Li_2O at 1570°C. there was no indication that the vapor pressure was appreciable (1).

To confirm these observations, small magnesia boats containing powdered Li_2O were heated *in vacuo* at 1000°C. for extended periods of time. A small initial decrease in weight was observed and was found to be a function only of the quantity of oxide employed in the experiment. Such losses can be attributed to the decomposition of impurities which in these experiments amounted to some four per cent of the oxide and were in all probability hydroxide and carbonate. Following this initial decomposition no appreciable decrease in weight could be detected.

Similar small losses occurred when the same experiments were repeated using dry oxygen rather than a high vacuum. On the other hand the oxide disappeared rapidly in the presence of oxygen containing small amounts of water vapor. Brewer and Margrave also observed erratic losses when wet gases were passed over Li_2O at 1200°C. and have suggested the formation of a volatile 'hydenide'.

A series of very simple experiments to indicate the dependence of the volatility of Li_2O on the presence of water vapor has now been completed. A small platinum crucible containing the oxide was heated inductively in a system designed to permit the introduction of water vapor at relatively low pressures. A water cooled platinum disk was placed a few centimeters from the crucible to allow recovery of some of the condensable volatile material. The results may be indicated briefly as follows:

Time, hr.	Temp., °C.	v.p. H_2O, mm. Hg	Total loss in weight (%)
1.0	1000	Pumps on	5.7
2.5	1040	Pumps on	3.3
12.0	1000	Pumps on	4.4
16.0	1000	Pumps on	5.8
2.0	1040	10^{-8}	3.2
2.5	1040	10^{-4}	6.4
2.0	1040	10^{-3}	12.2
0.5	1020	10^{-2}	18.1

The rates of evaporation are necessarily qualitative since surface areas of the oxide samples were observed to alter considerably during the course of the experiments, and water vapor pressures are accurate only in order of magnitude.

Debye–Scherrer diagrams of the material collected on the target corresponded to the pattern of anhydrous lithium hydroxide. We cannot exclude the possibility that the powder initially deposited was not LiOH, but was subsequently converted to hydroxide during handling in spite of the precautions imposed. Nor do these experiments prove the nature of the volatile species. Nevertheless, since Smith and Sugden have shown that gaseous LiOH is stable at 2000°C. (3), there is reason to believe that the hydroxide was the primary product in these reactions. If such is the case, the apparent volatility of Li_2O at high temperatures in systems in which traces of water vapor are present can be ascribed to the simple reaction $Li_2O_{(s)}+H_2O_{(g)} \rightarrow 2LiOH_{(g)}$ in which the favorable change in free energy is mainly due to the large change in entropy associated with the formation of a second mole of gas.

The factors affecting the stability of gaseous LiOH are analogous to those affecting the stability of gaseous VCl_4 and $CrCl_4$. Provided the conditions of the system are such that the vapor pressure of the lower chloride (VCl_3 or $CrCl_3$) is negligible, the gaseous tetrachloride will not dissociate because the dissociation can proceed only with a decrease in entropy.

1. VAN ARKEL, A. E., FLOOD, E. A., and BRIGHT, N. F. H. Can. J. Chem. 31: 1009. 1953.
2. BREWER, L. and MARGRAVE, J. Vapor of alkali metal oxides, Univ. of Calif. Radiation Lab. U.C.R.L. 1864. 20 pp. 1952.
3. SMITH, H. and SUGDEN, T. M. Proc. Roy. Soc. (London), A, 219: 204. 1953.

RECEIVED OCTOBER 5, 1954.
LABORATORY FOR PHYSICAL AND INORGANIC CHEMISTRY,
UNIVERSITY OF LEIDEN,
THE NETHERLANDS.

ATISINE: THE FUNCTIONAL GROUPS[1]

By O. E. Edwards and Tara Singh[2]

The suggestion is implicit in the structure recently suggested for dihydroatisine (9) that atisine and isoatisine are oxazolidines rather than vinylamines. This possibility was ignored in our earlier consideration of the environment of the nitrogen in these alkaloids (2) because both bases gave methane equivalent to two active hydrogens when heated with methyl Grignard reagent at 100° in anisole. Since the value of this evidence has been questioned by Dr. Wiesner (private communication) it was decided to accumulate further evidence bearing on the question.

Infrared spectra of atisine, isoatisine, and dihydroatisine were compared at identical concentrations in chloroform. The intensity of the C=C stretching band in all three was identical, while an extra OH stretching band appeared in the latter. This indicates oxazolidine rather than vinylamine structures for the bases.

Pelletier and Jacobs (7) have very recently reached the same conclusion after examining the properties of several oxidation products of atisine and isoatisine.

On the basis of the oxazolidine structures, the bases should give monoacetate with no free hydroxyl, or diacetates with one free hydroxyl. Jacobs and Craig (5) obtained a diacetate hydrochloride from atisine hydrochloride. However, we have obtained instead a triacetate hydrochloride by the action of acetic anhydride or acetic anhydride – pyridine mixture on atisine or isoatisine hydrochlorides. The amorphous sensitive base liberated from this hydrochloride showed no hydroxyl absorption in the infrared. On hydrolysis with potassium hydroxide in aqueous methanol it gave isoatisine nearly quantitatively. However, on hydrolysis with sodium carbonate solution at room temperature atisine was obtained. Thus the triacetate is a derivative of atisine, probably containing the following partial structures:

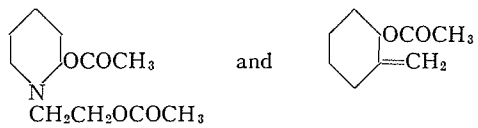

The formation of the triacetate from isoatisine involves the first example of the isomerization of isoatisine to atisine. So far, attempts to obtain crystalline mono- or di-acetates from atisine or isoatisine have failed.

Wiesner's structures do not readily account for the extra active hydrogen found in isoatisine and distilled atisine (2). These results seem to demand the presence of hydrogen on the carbons α to the masked aldehyde or ketone carbons.

[1]*Issued as N.R.C. No. 3491.*

[2]*National Research Council Postdoctorate Fellow. Present address: Government College, Ludhiana, East Punjab, India.*

Jacobs and Craig (5) showed that atisine gave 0.71 mole fraction of acetic acid in the Kuhn–Roth determination. There is some possibility that the exocyclic methylene might isomerize to give a C-methyl prior to oxidation by the chromic acid, although the experience of other workers with gelsemine (3) and bakankosine (1) makes this seem unlikely. Thus it proved desirable to investigate further the source of the acetic acid.

It has now been found that isoatisine, the $C_{20}H_{29}ON$ base (2), and the lactam tricarboxylic acid from isoatisine (4) give 0.52, 1.13, and 0.57 mole fraction of acetic acid in the Kuhn–Roth determination indicating one, two, and one C-methyl respectively.

The infrared spectrum of a film of atisine has a band at 1375 cm.$^{-1}$, which is also present in the spectra of chloroform solutions of isoatisine and the $C_{20}H_{29}ON$ base. These bands can be ascribed with certainty to a methyl group (6). A comparison of the apparent integrated absorption intensities (8) of this band in the last two bases indicated that two methyl groups are present in the C_{20} base if isoatisine has one, in agreement with the suggested mode of formation of this base (2) and with the results of the Kuhn–Roth determination. The infrared spectrum of a perfluorohydrocarbon mull of the lactam tricarboxylic acid from isoatisine contained a methyl band at 1380 cm^{-1}.

Thus all the evidence is consistent with the conclusion that atisine has one methyl group.

It is most probable that it is this C-methyl group which becomes the 1-methyl substituent on the phenanthrene derivatives obtained by selenium dehydrogenation of atisine derivatives. In this respect the structure suggested by Wiesner is satisfactory.

EXPERIMENTAL

Infrared spectra were determined on a Perkin–Elmer model 21 double beam spectrophotometer with a sodium chloride prism. In order to obtain a more reliable value for the integrated absorption intensity, a trace was made with two cells containing chloroform. The chloroform in one cell was then replaced by a chloroform solution of the compound and the spectrum recorded. The background trace was taken as the 0% absorption line for the calculations. Method 1 of Ramsay (8) was used and the value 1.57 was taken for K. Percentage absorption values are cited in brackets after the position of peaks in wave numbers.

Atisine

Obtained as a resin from ether solution. Infrared spectrum (65.8 mgm. per ml., 0.1 mm. cell): 3590 (20), 1655 (13).

Isoatisine

M.p. 152°. Found: C-methyl, 2.27. Calc. for $C_{22}H_{33}O_2N$: one C-methyl, 4.38. Infrared spectrum (30.6 mgm. per ml. in chloroform, 0.1 mm. cell): at 1375 cm.$^{-1}$ $\log_{10}(I_0/I) = 0.049$, $\Delta\nu_{\frac{1}{2}}^{c} = 10.5$ cm^{-1}. $A = 1800$. At a concentration of 63.2 mgm. per ml., 0.1 mm. cell: 3600 (19), 1652 (11).

Dihydroatisine

Infrared spectrum (64.8 mgm. per ml., 0.1 mm. cell): 3600 (21), 3470 (19), 1655 (12).

The $C_{20}H_{29}ON$ Base

M.p. 82–84°. Found: C-methyl 5.65. Calc. for $C_{20}H_{29}ON$: two C-methyls, 10.04. Infrared spectrum (30.0 per ml. in chloroform, 0.1 mm. cell): at 1376 cm.$^{-1}$ $\log_{10}(I_0/I) = 0.054$, $\Delta\nu_{\frac{1}{2}}^{a} = 17$ cm^{-1}. $A = 3300$. At 1710 cm.$^{-1}$ (62) and 1649 cm.$^{-1}$ (24).

Lactam Tricarboxylic Acid from Isoatisine

This was prepared by the method of Huebner and Jacobs (4). After two recrystallizations from aqueous methanol the tiny plates melted at 253–255° (dec.) when immersed at 230°. Found: C-methyl, 2.10. Calc. for $C_{21}H_{29}O_7N$: one C-methyl, 3.69. Infrared spectrum (perfluorohydrocarbon mull): a broad band centered about 1700 cm.$^{-1}$ (COOH); 1610 (lactam); 1515, 1465, 1450, 1405 (CH_2's); 1380 (CH_3).

Triacetylatisine Hydrochloride

(*a*) A suspension of atisine hydrochloride (0.15 gm.) in 3 cc. of acetic anhydride was boiled for 10 min. The crystals dissolved to give a light orange solution. The reagent was removed under reduced pressure, and the residue crystallized from methanol–ether. The 104 mgm. of crystals melted at 230° dec. After two recyrstallizations the melting point was 235°. The infrared spectrum was identical with that of the products from (*b*) and (*c*).

Atisine was left overnight in solution in acetic anhydride. The reagent was removed under reduced pressure, methanol added, and the solution again taken to dryness. The residue was converted to its hydrochloride. The crystalline product melted at 233°. After one recrystallization it melted at 242° dec., and did not depress the melting point of the triacetate hydrochloride.

(*b*) From 145 mgm. of isoatisine, treated as in (*a*), was obtained 96 mgm. of acetate hydrochloride. After one recrystallization from very concentrated methanol solution on addition of ethyl acetate, it melted at 241° dec. It showed no mixed melting point depression with product from (*c*) and had the same infrared spectrum.

(*c*) A suspension of 918 mgm. of finely divided atisine hydrochloride in 20 cc. of 50% pyridine – acetic anhydride was refluxed for five minutes. The solution was cooled to 0°, giving 984 mgm. of fine needles, m.p. 230° dec. After two recrystallizations from methanol – ethyl acetate the melting point was 241° when immersed at 210°. $[\alpha]_D^{22} -18 \pm 1°$ ($c = 2.0$ in ethanol). Found: C, 63.67, 63.76, 64.16; H, 8.49, 8.50, 8.11; Cl, 7.11, 7.17. Calc. for $C_{28}H_{42}O_6$ NCl: C, 64.16; H, 8.08; Cl, 6.77. I.R. spectrum: 3580 (40), 3440 (39), 3350 (40), 1740 (90), 1679 (40), 1650 (51), 1333 (29), 1320 (25), 1309 (29), 1250 (92), 1210 (46), 1128 (29), 1111 (23), 1094 (25), 1071 (45), 1060 (51), 1039 (53), 1020 (57), 985 (34), 973 (35), 955 (25), 948 (55), 902 (38), 843 (16), 831 (16). Isoatisine hydrochloride treated in the same way gave a good yield of the same triacetate hydrochloride.

Triacetyl Atisine

Cold potassium hydroxide solution was added to a cold solution of the triacetyl hydrochloride in water. The precipitate was extracted quickly into petroleum ether (30–60°), the solution dried, and the solvent removed under reduced pressure. The clear gum would not crystallize from ether or petroleum ether. Infrared spectrum (film): 3080 (18), 2945 (85), 2890 (75), 1740 (92), 1652 (35), 1582 (45), 1450 (57), 1415 (44), 1375 (76), 1329 (31), 1310 (31), 1240 (97), 1182 (32), 1155 (27), 1113 (31), 1070 (45), 1028 (78), 985 (57), 947 (33), 901 (49), 827 (25).

Saponification of the Triacetate

(*a*) A sample of the amorphous triacetate prepared as described above was hydrolyzed for four hours at room temperature followed by 0.5 hr. reflux in aqueous methanol containing potassium hydroxide. The solvent was largely removed under reduced pressure, the residue taken up in water and extracted with ether. The base crystallized readily and completely from concentrated ether solution. M.p. 149°; mixed m.p. with isoatisine 151°.

(*b*) A solution of 69 mgm. of triacetate hydrochloride and 100 mgm. of sodium carbonate in 2 cc. of water soon became milky. It was clarified by addition of methanol and left for 24 hr. at room temperature. The mixture was worked up as in (*a*) giving 39 mgm. of base. This would not crystallize. Its infrared spectrum (film) had every peak coincident with that of atisine except for a very small extra peak at 1727 cm^{-1}. It gave a hydrochloride, m.p. 300° dec., which when mixed with atisine hydrochloride melted at 302° dec.

ACKNOWLEDGMENT

The authors wish to thank Dr. R. N. Jones and Mr. R. Lauzon for taking the infrared spectra.

1. Balenovic, K., Daniker, H. U., Goutarel, R., Janot, M.-M., and Prelog, V. Helv. Chim. Acta, 35: 2519. 1952.
2. Edwards, O. E. and Singh, T. Can. J. Chem. 32: 465. 1954.
3. Goutarel, R., Janot, M.-M., Prelog, V., Sneedon, R. P. A., and Taylor, W. I. Helv. Chim. Acta, 34: 1139. 1951.
4. Huebner, C. F. and Jacobs, W. A. J. Biol. Chem. 174: 1001. 1948.
5. Jacobs, W. A. and Craig, L. C. J. Biol. Chem. 143: 589. 1942.
6. Jones, R. N. and Cole, A. R. H. J. Am. Chem. Soc. 74: 5648. 1952.
7. Pelletier, S. W. and Jacobs, W. A. J. Am. Chem. Soc. 76: 4496. 1954.
8. Ramsay, D. A. J. Am. Chem. Soc. 74: 72. 1952.
9. Wiesner, K., Armstrong, R., Bartlett, M. F., and Edwards, J. A. Chemistry & Industry, 132. 1954.

Received September 27, 1954.
Division of Pure Chemistry,
National Research Council,
Ottawa, Canada.

Canadian Journal of Chemistry

Issued by THE NATIONAL RESEARCH COUNCIL OF CANADA

VOLUME 33 MARCH 1955 NUMBER 3

ORGANIC FLUORINE COMPOUNDS

I. AN IMPROVED SYNTHESIS OF HEXAFLUOROACETONE[1]

BY A. T. MORSE, P. B. AYSCOUGH, AND L. C. LEITCH

ABSTRACT

The synthesis of hexafluoroacetone reported recently by Brice, Lazerte, Hals, and Pearlson has been improved in several particulars. Teflon was depolymerized to tetrafluoroethylene which was then dimerized to give a 50% yield of perfluoroisobutene in one step. Oxidation of the latter at 35–40°C. with aqueous potassium permanganate gave a 75% yield of hexafluoroacetone hydrate. The vapor pressure of hexafluoroacetone was measured between −60° and −28°C.

Hexafluoroacetone was first obtained by Fukuhara and Bigelow (2) among the products of the direct fluorination of acetone. It was subsequently prepared by Henne, Shepherd, and Young (3) by the oxidation of the chlorofluoroolefin $(CF_3)_2C=CCl_2$. While the yield of ketone is satisfactory, the preparation of the olefin is tedious and involves hydrofluorination at one stage. Brice, Lazerte, Hals, and Pearlson (1) recently obtained a 26% yield of hexafluoroacetone by the oxidation of perfluoroisobutene prepared by the thermal isomerization of perfluorocyclobutane. The latter was presumably prepared by polymerization of tetrafluoroethylene at 500°C. as reported by Miller (5).

It occurred to us that perfluoroisobutene might be obtained in one step from tetrafluoroethylene. The use of teflon was later suggested to us in a letter from Dr. W. H. Pearlson of the Minnesota Mining and Manufacturing Company, St. Paul, Minn. A furnace, described by one of us in an earlier paper (4), having three independent elements which permit the temperature to be controlled at different points appeared to be suitable for the preparation of perfluoroisobutene. Teflon was depolymerized at 450°C. to tetrafluoroethylene in the first section of the furnace and then dimerized to a mixture of perfluorobutenes by heating the monomer to 700°C. in the second and third sections. A 62% yield of fluorobutenes consisting of 85% perfluoroisobutene was thus obtained; the 2-isomer was formed to the extent of only 15%. These figures were arrived at by comparing the infrared spectrum of our product with the spectra of the pure compounds reported in the paper by Pearlson and co-workers (1).

The perfluorobutenes were oxidized with alkaline permanganate in the apparatus illustrated in the experimental part at 35 to 40°C. instead of in an auto-

[1]*Manuscript received November 16, 1954.*
Contribution from the Division of Pure Chemistry, National Research Council, Ottawa, Ontario, Canada. Issued as N.R.C. No. 3512.

clave at 100°C. as reported by Pearlson and co-workers. The yield of hexafluoroacetone hydrate was 70 to 80% of the theoretical amount. The dehydration to hexafluoroacetone was carried out according to the directions of Henne and co-workers (3). These authors reported the formation of a white solid during the dehydration of hexafluoroacetone hydrate which gave a semicarbazone melting very near hexafluoroacetone semicarbazone prepared from the hydrate. In the present work this substance was also detected when the hexafluoroacetone was fractionated on the vacuum line. It gives a mass spectrum identical with that of hexafluoroacetone. When sealed in a glass tube it can be sublimed by merely applying the heat of the hand. The sub-

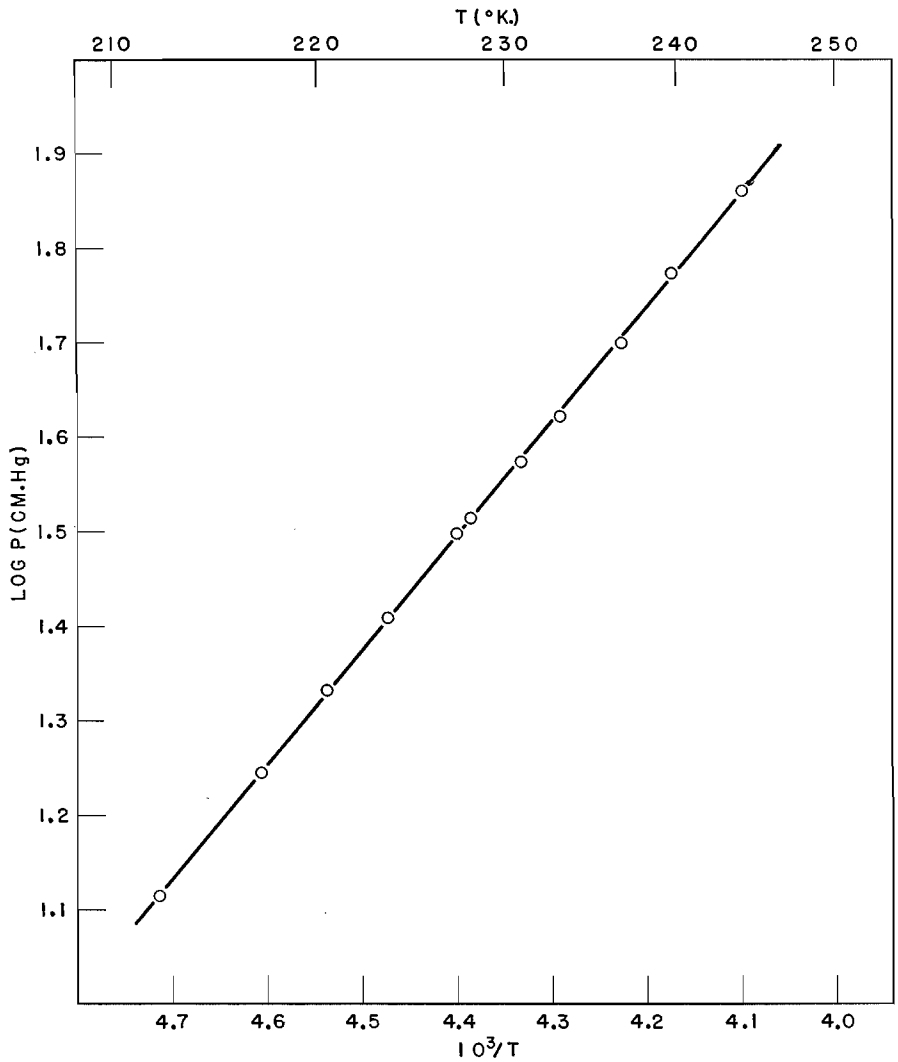

FIG. 1. Vapor pressure of hexafluoroacetone.

stance is considered to be a polymeric form of hexafluoroacetone and is provisionally assigned the structure I.

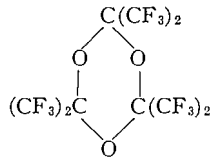

I

The vapor pressure of a sample of hexafluoroacetone purified by fractionation on the vacuum line was measured by the static method described in an earlier paper (4). The line shown in Fig. 1 gives the expression

$$\log p \text{ (mm.)} = 6.8060 - [(1.2074 \times 10^3)/T]$$

for the vapor pressure of hexafluoroacetone between −60°C. and −28°C.

EXPERIMENTAL

Perfluoroisobutene

The furnace used in this experiment was referred to in the Introduction. Teflon (200 gm.) cut into small pieces was placed at one end of the reactor while the other end was connected to a 150 ml. spiral trap cooled to −78°C. The section of the furnace containing the teflon was slowly heated to 450°C. while the temperature of the other two units was kept at 700–725°C. After two hours the temperature of the first section was raised to 550°C. to complete the depolymerization of the teflon. At the end of the experiment the trap contained 110 ml. of yellow liquid which was fractionated on the vacuum line. Forty milliliters of material with a very high vapor pressure, consisting chiefly of perfluoropropene, were distilled off. The remainder (70 ml.), which had a vapor pressure of 40 mm. at −78°C., was collected in another trap. Yield: 125 gm. By infrared analysis this product was found to contain 85% perfluoroisobutene, i.e. 106 gm., and 15% perfluorobutene-2.

Hexafluoroacetone Hydrate

The apparatus used in the oxidation is shown in Fig. 2. Potassium permanganate (300 gm.) and 1200 ml. of water were placed in the 3-liter reaction flask *B*. The fluoro-olefin (95 ml., 165 gm.) was condensed into the trap *A* which was then connected to the bubbler immersed in the permanganate solution. The contents of the flask were agitated by means of a magnetic stirrer. The temperature of the fluoro-olefin was raised to about 10°C. and maintained there while the vapor bubbled slowly into the permanganate solution. The rate of flow could be readily controlled by varying the temperature of the bath surrounding the olefin. Hexafluoroacetone hydrate produced by the oxidation remained in solution while unchanged perfluoroisobutene was returned to the flask by the cold finger *C* which was kept at −80°C. The carbon dioxide which was produced simultaneously passed into the atmosphere, any fluoro-olefin which it carried over being condensed in a second trap (*D*)

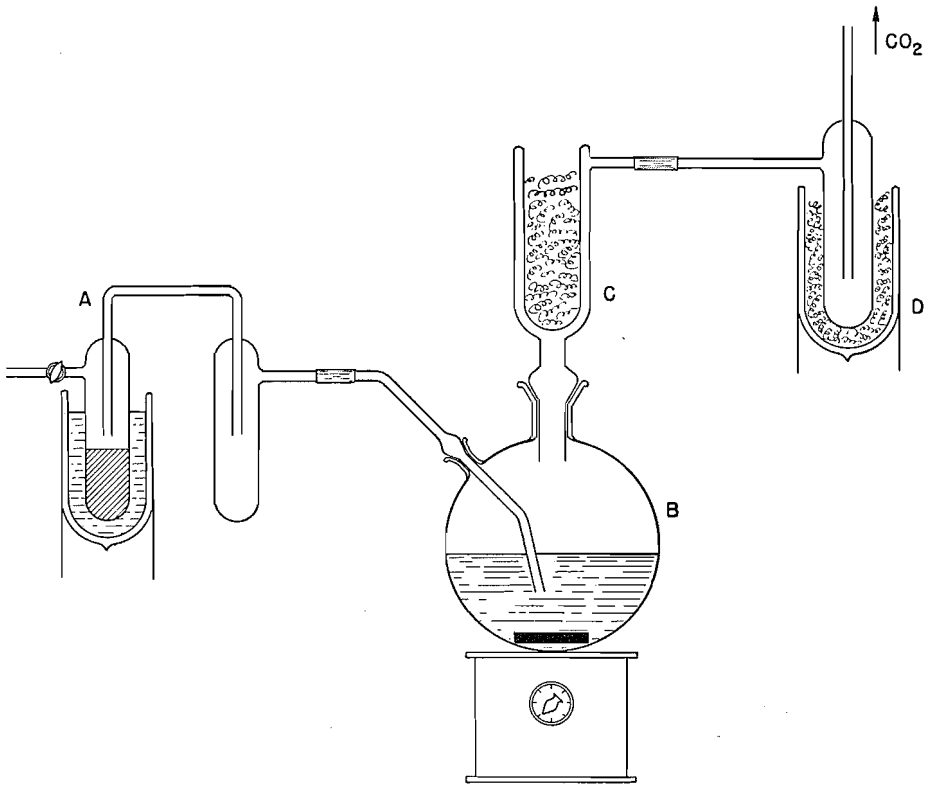

FIG. 2. Apparatus for the oxidation of perfluoroisobutene to hexafluoroacetone.

maintained at −80°C. Reaction was slow at first but became more rapid as the temperature increased to 35–40°C. The fluoro-olefin was absorbed at the rate of 20–25 gm. per hour.

The reaction mixture was then treated with sulphur dioxide to remove excess permanganate and the mixture filtered with suction. The precipitate on the filter was washed with 500 ml. of water and discarded. The combined filtrates were extracted with ether in a continuous extraction apparatus for 24 hr. The ether extract was separated, dried over sodium sulphate, and freed of solvent. The residue was fractionated under reduced pressure. The yield of hexafluoroacetone hydrate, b.p. 55–6°C. at 80 mm., n_D^{20} 1.3179 was 108 gm. (72% of the theoretical amount).

Hexafluoroacetone

The hydrate was treated with phosphorus pentoxide as directed by Henne, Shepherd, and Young (3). A middle fraction of 5.0 ml. from a total of 7.5 ml. of hexafluoroacetone was collected separately on the vacuum line. It distilled at a constant pressure of 32.6 mm. at −78°C. The vapor pressure of this fraction was measured at several temperatures, between −60°C. and −28°C. by the static method (4), and the values plotted logarithmically in

Fig. 2. The mass spectrum of the product was identical with that of Pearlson and co-workers (1).

ACKNOWLEDGMENT

The authors are extremely grateful to Dr. W. H. Pearlson of the Minnesota Mining and Manufacturing Company for a generous sample of hexafluoroacetone and suggestions.

REFERENCES

1. BRICE, T. J., LAZERTE, J. D., HALS, L. J., and PEARLSON, W. H. J. Am. Chem. Soc. 75: 2698. 1953. U.S. Patent No. 2,617,836. November, 1952.
2. FUKUHARA, N. and BIGELOW, L. A. J. Am. Chem. Soc. 63: 788. 1941.
3. HENNE, A. L., SHEPHERD, J. W., and YOUNG, E. J. J. Am. Chem. Soc. 72: 3577. 1950.
4. LEITCH, L. C. and RENAUD, R. Can. J. Chem. 30: 79. 1952.
5. MILLER, W. T. Chap. 32, p. 592. SLESSER, C. and SCHRAM, S. R. *In* Preparation, properties and technology of fluorine and organic fluoro compounds. Natl. Nuclear Energy Ser. Div. VII, Vol. I. McGraw-Hill Book Company, Inc., New York. 1951.

THE SYNTHESIS OF HEMOPYRROLE-DICARBOXYLIC ACID AND OF SOME DIPYRROMETHENES[1]

By S. F. MacDonald and R. J. Stedman[2]

ABSTRACT

The pyrrole II*e* was obtained through the known II*c* and hydrolyzed to III*b*. This last could be partially decarboxylated to hemopyrrole-dicarboxylic acid III*c* or, with formic acid, converted into the dipyrromethene VII*b*. The isomeric dipyrromethene VII*a* was obtained analogously.

Of the two key pyrroles related to the uroporphyrins, cryptopyrrole-dicarboxylic acid I*a* has already been synthesized (10). The synthesis of the second of these, hemopyrrole-dicarboxylic acid III*c*, is now reported.

With ethyl cyanoformate and hydrogen chloride, the pyrrole II*c* (10), for which an improved preparation is given, gave the glyoxylic ester II*d*. Consistently high yields were obtained only when the usual conditions (cf. (6)) were modified to ensure that the intermediate ketimine hydrochloride crystallized. The glyoxylic ester was catalytically reduced in acetic–sulphuric acid over palladium black (cf. (9)) to II*e*, which Treibs and Ott have obtained from II*c* by a different route (13). When this reduction was attempted with W-6 Raney nickel in refluxing ethanol (cf. (12)), with hydrogen (cf. (15)) at 130–150° and 3000 to 4000 lb. per sq. in. in ethanol over copper chromite (1), or with zinc dust in boiling acetic acid, the only product isolated was II*c* identified by melting point and mixed melting point, the positive Ehrlich's reaction in the cold, and, in the first case, by analysis for C, H, and N. The loss of an acyl group on catalytic reduction was unexpected but is not without analogy (cf. (8)).

Alkaline hydrolysis of II*e* resulted in III*a* or in III*b*, differing in their Ehrlich's reactions. These structures were confirmed by decarboxylating the latter to the known hemopyrrole-carboxylic acid IV*a*. With water at 100°, III*b* gave a dicarboxylic acid which could not be directly shown to be III*c* rather than IV*b*, for the latter is known only as a half-ester (7*b*). Under these conditions I*a* had been obtained from I*b* (10) and IV*b* would be expected to lose its α-carboxy group. Further, the dimethyl ester of the dicarboxylic acid gave a strongly positive Ehrlich's reaction in the cold, behavior consistent with III*c* but not with IV*b*. However, the dicarboxylic acid was shown definitely to be hemopyrrole-dicarboxylic acid III*c* by conversion of its dimethyl ester into V*e* (see below) with phosgene and methanol (cf. (7*c*)).

As the preparation of the intermediates might have proved more convenient using the higher-melting methyl esters, methyl α-oximino-β-ketoadipate and benzyl acetoacetate were combined in the Knorr synthesis to give V*a*, which

[1]*Manuscript received November 8, 1954.*
Contribution from the Division of Pure Chemistry, National Research Council, Ottawa, Canada. Issued as N.R.C. No. 3513. Reported in part at the Seminar in the Chemistry of Natural Products, University of New Brunswick, August, 1953, and in a preliminary communication (11).
[2]*National Research Council of Canada Postdoctorate Fellow.*

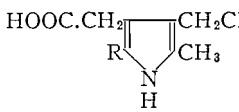

I*a*, R = H
b, R = COOH

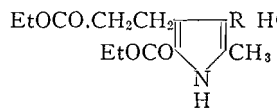

II*a*, R = $COOCH_2.C_6H_5$
b, R = COOH
c, R = H
d, R = CO.COOEt
e, R = CH_2.COOEt

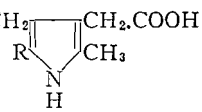

III*a*, R = COOEt
b, R = COOH
c, R = H

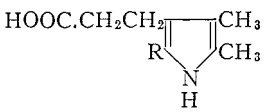

IV*a*, R = H
b, R = COOH

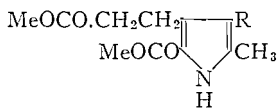

V*a*, R = $COOCH_2.C_6H_5$
b, R = COOH
c, R = H
d, R = CO.COOMe
e, R = CH_2.COOMe

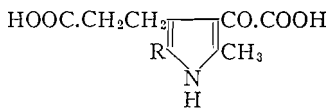

VI*a*, R = COOEt
b, R = COOH

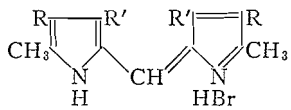

VII*a*, R = CH_2CH_2.COOH; R′ = CH_2.COOH
b, R = CH_2.COOH; R′ = CH_2CH_2.COOH

was converted into V*b*, V*c*, V*d*, and V*e*. The structures of these were confirmed by relating V*d* and V*e* to the ethyl esters for which there was independent analytical proof. Thus II*d* could be hydrolyzed either to VI*a* or VI*b*, and the latter gave V*d* with diazomethane; similarly II*e* was hydrolyzed to III*b*, which was converted into V*e* with diazomethane.

Two better methods were found for converting ethyl β-keto-α-carbethoxy-adipate into ethyl β-ketoadipate (cf. (5, 14)), an intermediate in the preparation of II*a*: the triester was allowed to stand with sulphuric acid, and alcohol added to the mixture, or the triester was boiled with water (cf. (4, 2)). To obtain the methyl β-ketoadipate of Bardhan (3) required in the synthesis of V*a*, β-carbomethoxy-propionyl chloride and the ethoxymagnesium derivative of ethyl malonate gave methyl δ,δ-dicarbethoxylevulinate, which was converted into β-ketoadipic acid with hydrochloric acid (cf. (5)), and the acid esterified.

Both the pyrroles I*b* and III*b* reacted normally with formic acid and hydrogen bromide at 100° (cf. (7*d*)) to give the dipyrromethenes VII*a* and VII*b* respectively. At lower temperatures, the hydrobromides of I*a* and III*c* were the predominant products (16).

EXPERIMENTAL

2-Methyl-5-carboxypyrrole-4-(propionic acid) Diethyl Ester, IIc

Up to 500 gm. of the benzyl ester II*a* have been hydrogenated in 1 liter of ethanol in a 3 liter autoclave as previously described (10). The mixture of crude acid II*b* and catalyst (277 gm.) from 378 gm. of the benzyl ester II*a* was dry distilled in two lots at 230° rising to 260° (air bath temperatures) under the water-pump vacuum (initially and finally 15 mm.). The pyrrole II*c* rapidly

solidified in the air condenser. It was recrystallized from pentane by extraction (Soxhlet) giving 155 gm. (63% from the benzyl ester), m.p. 67-67.5° (cf. (10)).

2-Methyl-5-carboxypyrrole-3-(glyoxylic acid)-4-(propionic acid) Triethyl Ester, IId

The pyrrole II*c* (45 gm.) in ethyl cyanoformate (45 ml.), dry ether (150 ml.), and chloroform (50 ml., dry and alcohol free) was stirred in an ice–salt bath and protected from moisture while dry hydrogen chloride was passed in for three hours. Dry air was then passed through without cooling until the mixture was largely crystalline. Ether (100 ml.) was added, the mixture kept at 0° overnight, the ketimine hydrochloride filtered off, washed with ether, dried *in vacuo*, and dissolved in ice-water (3 liters). After several hours, the glyoxylic ester was filtered off and washed with water. It was dissolved in alcohol, filtered with charcoal, and the charcoal washed with alcohol. After the filtrate and washings (110 ml.) were diluted with 85 ml. of water and allowed to stand at 25° then at 0°, 53 gm., m.p. 78–79°, were collected. The mother liquors diluted with 100 ml. of water and allowed to stand as above gave 4.8 gm., m.p. 77–78° (total, 92% as used for reduction). For analysis, the ester was recrystallized twice and dried *in vacuo*, forming colorless needles, m.p. 78.5°–79°. Ehrlich's reaction slowly positive hot. Found: C, 57.64; H, 6.72; N, 4.01%. Calc. for $C_{17}H_{23}O_7N$: C, 57.78; H, 6.56; N, 3.96%.

2-Methyl-5-carboxypyrrole-3-(acetic acid)-4-(propionic acid) Triethyl Ester (Ethyl α-Carbethoxyhemopyrrole-dicarboxylate), IIe

The glyoxylic ester II*d* (24 gm.) in acetic acid (100 ml.) and sulphuric acid (3.75 ml.) was shaken for six hours with palladium black (1.2 gm., freshly prepared (17)) under hydrogen (60 lb. per sq. in.) at 27°. After the theoretical uptake in two hours, absorption nearly ceased. The filtrate and washings from the catalyst were added to ice-water (3 liters) containing sodium bicarbonate (70 gm.), seeded, and left at 0° overnight. The solid was filtered off, washed, and dried. The acidified filtrate was extracted once with ether, and the ether evaporated from the extract.

Three reductions, using 57.8 gm. glyoxylic ester, were worked up together. When the solid was extracted with pentane (Soxhlet) most of the product crystallized from the pentane. More was obtained by combining the partially hydrolyzed pentane-insoluble material with the residue from the ether extract, esterifying it with 5% ethanolic hydrogen chloride at 25° overnight, pouring it into ice water, and extracting the dried solid with pentane (Soxhlet). Yield 44 gm. (79%), long colorless needles, m.p. 63–64°, or prisms, m.p. 64–65°. Ehrlich's reaction negative cold but positive hot. For analysis, it was recrystallized three times from aqueous ethanol and dried *in vacuo*, needles m.p. 63–64°. Found: C, 59.98; H, 7.26; N, 4.26%; mol. wt. (Rast) 333. Calc. for $C_{17}H_{25}O_6N$: C, 60.16; H, 7.43; N, 4.13%; mol. wt. 339.

When less active palladium black was used, the yield fell to about 50%.

This pyrrole and the isomeric ethyl α-carbethoxycryptopyrrole-dicarboxylate (10) were not clearly distinguished by their melting points or by their infrared

spectra in carbon disulphide. However, their mixed melting point showed a depression.

α-Carboxyhemopyrrole-dicarboxylic Acid, IIIb

The triethyl ester II*e* (2 gm.) in ethanol (25 ml.) and 10% sodium hydroxide (25 ml.) was heated for two and a half hours on the steam bath in an open flask. The solvent was removed *in vacuo*, the residual gum dissolved in water (25 ml.), warmed, and filtered with charcoal, and the product (1.27 gm., 84%), a yellow powder m.p. 144–145° (decomp.), precipitated with sulphur dioxide at 0° and washed with ice-water. After three recrystallizations from acetone (dried over potassium carbonate) (thimble) it formed small very pale violet needles, m.p. 155–156° (decomp.), Ehrlich's reaction strongly positive cold. Found in material dried *in vacuo*: C, 51.29; H, 5.36; N, 5.54%. Calc. for $C_{11}H_{13}O_6N$: C, 51.76; H, 5.13; N, 5.49%. It is stable when kept under nitrogen, or *in vacuo* over phosphorus pentoxide.

Hemopyrrole-dicarboxylic Acid, IIIc

The crude tricarboxylic acid III*b* (0.802 gm., m.p. 148°) in water (3 ml.) was heated under nitrogen on the steam bath to solution and cessation of effervescence (*ca.* 15 min.). After the solution was cooled to 0°, the product (0.544 gm., 84%) was collected and washed with a little ice-water, as very pale pink prisms, m.p. 150–150.5° (decomp.), Ehrlich's reaction positive cold, no insoluble picrate was formed in wet ether. After three recrystallizations from water (4 ml.) the melting point was unchanged. Found in material dried *in vacuo* and stored over nitrogen: C, 56.78; H, 6.26; N, 6.82%. Calc. for $C_{10}H_{13}O_4N$: C, 56.86; H, 6.20; N, 6.63%.

Dimethyl Hemopyrrole-dicarboxylate[3]

Hemopyrrole-dicarboxylic acid III*c* (3.05 gm.) was allowed to stand overnight with a cooled ethereal solution of diazomethane. After removing the ether *in vacuo*, the crystalline residue was distilled (135°, 5×10^{-5} mm.). The ester (3.33 gm., 96%) formed yellow crystals, m.p. 50–51°, raised to 51°–52.5° by resublimation, Ehrlich's reaction strongly positive cold. Found: C, 60.39; H, 7.35; N, 6.03%. Calc. for $C_{12}H_{17}O_4N$: C, 60.23; H, 7.16; N, 5.86%.

Unless protected from light and stored *in vacuo* or under nitrogen, the product turns red.

Conversion of Dimethyl Hemopyrrole-dicarboxylate to 2-Methyl-5-carboxypyrrole-3-(acetic acid)-4-(propionic acid) Trimethyl Ester, Ve

Dimethyl hemopyrrole-dicarboxylate (2.11 gm., distilled in high vacuum at 110–115°) was dissolved in dry ether (70 ml.), cooled in ice-water, and treated with a rapid stream of phosgene for 15 min. The solution initially became cloudy, but rapidly cleared and darkened. After one and a quarter hours at room temperature the ether and excess phosgene were removed by a stream of dry air, and the crystalline residue was briefly dried *in vacuo* and dissolved in dry methanol (50 ml.). Evaporation under reduced pressure after 60 hr. gave a

[3]*This preparation is due to Dr. K. H. Michl.*

dark gum which rapidly crystallized and was freed from hydrogen chloride by drying *in vacuo* over potassium hydroxide. Recrystallization from 15 ml. of methanol and 30 ml. of water (charcoal) gave the trimethyl ester (2.30 gm., 87%) as light brown crystals, m.p. 91°–91.5°.

A further crystallization from methanol–water gave light yellow plates, melting point unchanged, undepressed by authentic Ve (see below), and indistinguishable from it by its infrared spectrum in carbon disulphide. The Ehrlich's reaction was positive hot. Found, in material recrystallized from pentane (thimble) and dried at 60° *in vacuo*: C, 56.77; H, 6.55; N, 4.83%. Calc. for $C_{14}H_{19}O_6N$: C, 56.56; H, 6.44; N, 4.71%.

Hemopyrrole-carboxylic Acid, IVa, from α-Carboxyhemopyrrole-dicarboxylic Acid, IIIb

The tricarboxylic acid III*b* (0.583 gm., m.p. 155°) in glycerol was heated under nitrogen at 200° for 15 min. After the mixture was poured into water (100 ml.) and extracted with ether (4 × 25 ml.), the extract was washed with water (25 ml.), dried over sodium sulphate, and the ether evaporated. The crystalline residue on sublimation (100°, 5×10^{-4} mm.) gave cream colored crystals (0.224 gm., 58%), m.p. 120–125°. After three crystallizations from water it formed cream colored rectangular plates, m.p. 127–128° (lit. 130–131° (7*a*)), Ehrlich's reaction positive cold. Found in material stored under nitrogen: C, 64.60; H, 8.06; N, 8.65%. Calc. for $C_9H_{13}O_2N$: C, 64.65; H, 7.83; N, 8.38%.

Methyl Hemopyrrole-carboxylate

Hemopyrrole-carboxylic acid (77 mgm., m.p. 128–129°, from III*b*) was added to ethereal diazomethane (from 2 gm. nitrosomethylurea) under nitrogen. After one hour the ether solution was washed with dilute hydrochloric acid, the acid neutralized with sodium bicarbonate and washed with ether, the ether washed twice with water and dried over sodium sulphate. The dark crystalline residue left after evaporation of the ether was sublimed (50–60°, 10^{-3} mm.) giving methyl hemopyrrole-carboxylate as colorless prisms (31.5 mgm., 38%), m.p. 48–51°; after recrystallization from aqueous methanol, colorless plates, m.p. 49–51°, were obtained.

The methyl ester picrate, long chocolate-brown prisms, m.p. 118.5–120° (lit. 121–122° (7*a*)) was obtained from the ester with picric acid in wet ether.

The methyl ester, regenerated from the picrate with ether and aqueous sodium bicarbonate, melted at 50–53° (lit. 57° (7*a*)) after sublimation.

α-Carbethoxyhemopyrrole-dicarboxylic Acid, IIIa

The triethyl ester II*e* (1.94 gm.) in 20 ml. of ethanol and 14.2 ml. of 0.889 *N* sodium hydroxide (2.2 equiv.) was heated for two hours in an open flask on the steam bath. After it was taken to dryness *in vacuo*, the residual gum was dissolved in 9 ml. of water and the product precipitated with sulphur dioxide at 0° and washed with ice-water. After it was suspended in 12 ml. of water at 100° for 15 min., filtered at 0° and washed, the cream colored product (1.16 gm., 72%) melted at 232–234° (decomp.). For analysis, it was recrystallized four times from acetone (thimble) giving very light brown elongated prisms, m.p. 237–238° (decomp.), Ehrlich's reaction very weak cold but strongly

positive hot. Found in material dried *in vacuo* at 60°: C, 55.49; H, 5.82; N, 5.09%. Eq. wt. 140.6. Calc. for $C_{13}H_{17}O_6N$: C, 55.12; H, 6.05; N, 4.94%. Eq. wt. 141.6.

2-Methyl-3-carbobenzoxy-4-(2-carbomethoxyethyl)-5-carbomethoxypyrrole, Va

Sodium nitrite (45 gm.) in water (75 ml.) was slowly added at $\leqslant 8°$ with stirring to methyl β-ketoadipate (101.3 gm.) in acetic acid (350 ml), and the excess nitrite was destroyed with ammonium sulphamate. This solution and zinc dust (300 gm.) were added slowly with stirring and cooling to benzyl acetoacetate (121 gm.) and ammonium acetate (100 gm.) in acetic acid (250 ml.) at 60–70°. After one hour at 90° the solution was decanted into ice-water (6 liters) and the zinc washed with hot acetic acid (50% then glacial). After the oil which separated had solidified, it was filtered off, well washed with water, and dried *in vacuo*, m.p. 120–126°. Recrystallization from ethanol (400 ml.) gave the product as pale yellow crystals (118 gm., 61%), m.p. 128–130°. For analysis, it was recrystallized three times from ethanol giving nearly colorless rectangular plates, m.p. 130–130.5°, Ehrlich's reaction positive hot. Found in material dried at 60° *in vacuo*: C, 63.71; H, 5.56; N, 3.74%. Calc. for $C_{19}H_{21}O_6N$: C, 63.50; H, 5.89; N, 3.90%.

2-Methyl-3-carboxy-4-(2-carbomethoxyethyl)-5-carbomethoxypyrrole, Vb

The benzyl ester V*a* (112 gm.) in 800 ml. of ethanol was hydrogenated for eight hours at 130° and 1100 lb. per sq. in. over 10 ml. of Raney nickel. When filtered off and washed with ethanol, the product (87 gm., containing nickel) was suitable for decarboxylation. A portion (14 gm.) was ground and filtered with 1 liter of ice-cold *N*/10 sodium carbonate, the product precipitated from the filtrate with carbon dioxide, filtered, and washed, giving 9 gm., m.p. 243–244° (decomp.). After two recrystallizations from ethanol and one from methanol, it formed colorless plates, melting point unchanged, Ehrlich's reaction positive hot. Found in material dried *in vacuo*: C, 53.76; H, 5.87; N, 5.36%. Calc. for $C_{12}H_{15}O_6N$: C, 53.53; H, 5.62; N, 5.20%.

2-Methyl-4-(2-carbomethoxyethyl)-5-carbomethoxypyrrole, Vc

The crude acid V*b* (73 gm., containing nickel) was distilled in two portions under the vacuum of a water pump at 230° rising to 245° (air-bath temperature) into an air condenser. The pale yellow waxy product was recrystallized from pentane (thimble) to give pink prisms (39 gm. 66% from the benzyl ester), m.p. 71–72°. This was suitable for the next stage. Two further recrystallizations gave the pyrrole as cream colored prisms, m.p. 72.5–73.5°. Ehrlich's reaction was slowly positive in the cold. Found in material dried *in vacuo*: C, 58.64; H, 6.86; N, 6.45%. Calc. for $C_{11}H_{15}O_4N$: C, 58.65; H, 6.71; N, 6.22%.

2-Methyl-5-carboxypyrrole-3-(glyoxylic acid)-4-(propionic acid), VIb

The ethyl ester II*d* (5.295 gm.) was heated in an open flask on the steam bath for two and one-half hours with 60 ml. of ethanol and 60 ml. of 10% sodium hydroxide. After removal of the residual solvent *in vacuo*, the gum was dissolved in 50 ml. of water, filtered, and the product precipitated with excess hydrochloric acid at 0°. The tricarboxylic acid VI*b* (2.81 gm., 70%) obtained

as a white powder by washing the precipitate with water and drying it *in vacuo* had a melting point of 197–198° (decomp.), which was depressed by admixture of 2-methyl-5-carbethoxypyrrole-3-(glyoxylic acid)-4-(propionic acid) VI*a* (see below). Ehrlich's reaction was slowly positive in the cold.

Precipitation by sulphur dioxide instead of hydrochloric acid gave a product containing sodium.

2-Methyl-5-carboxypyrrole-3-(glyoxylic acid)-4-(propionic acid) Trimethyl Ester, Vd

(*i*) *From the Triethyl Ester IId by Hydrolysis and Re-esterification*

The glyoxylic acid VI*b* (2 gm.) was added in portions to diazomethane (from 14 gm. of nitrosomethylurea) in ether. After it had stood for three hours, the ethereal solution was washed with dilute hydrochloric acid, with aqueous sodium bicarbonate, and with water, dried over sodium sulphate, and evaporated to dryness. The residue, which crystallized slowly at 0°, was recrystallized from methanol (12 ml.) – water (18 ml.), and had the melting point 106–107.5° (1.82 gm., 78%). After three recrystallizations from aqueous methanol, it formed long colorless prisms, m.p. 108–109° or, with slow heating, 114–115°. The Ehrlich's reaction was positive hot. Found in material dried *in vacuo* at 60°: C, 53.63; H, 5.10; N, 4.57%. Calc. for $C_{14}H_{17}O_7N$: C, 54.01; H, 5.51; N, 4.50%.

Subsequent preparations gave only the higher melting form, colorless rectangular plates, m.p. 114.5–115°, and undepressed by admixture of the lower melting form. Ehrlich's reaction was positive hot. Found: C, 54.22; H, 5.48; N, 4.69%.

(*ii*) *From 2-Methyl-4-(2-carbomethoxyethyl)-5-carbomethoxypyrrole, Vc (Preparative Method)*

The pyrrole V*c* (32.6 gm.) was dissolved in 35 ml. of methyl cyanoformate (b.p. 97.5–98.5°), 38 ml. of chloroform (dry and alcohol free), and 120 ml. of dry ether, cooled in ice-salt with the exclusion of moisture, stirred, and treated with a rapid stream of dry hydrogen chloride for three hours. Solid separated during the reaction; the mixture was evaporated to dryness by a stream of dry air passed into the mixture, without cooling, for four hours. Dry ether (120 ml.) was added and, after 12 hr. at 0°, the ketimine hydrochloride was collected as a yellow powder, washed with ether, and dried under water pump vacuum. The hydrochloride was powdered and added portionwise, with stirring, to ice-water (3 liters). The glyoxylic ester was collected, washed with water, and dried *in vacuo* after the initially clear yellow solution had been allowed to stand for four hours at 0°. The crude product was dissolved in methanol (160 ml.), warmed with charcoal, filtered, and recrystallized by the addition of water, giving colorless plates (39.0 gm., 86.5%) m.p. 111°-113°, sufficiently pure for hydrogenation.

2-Methyl-5-carboxypyrrole-3-(acetic acid)-4-(propionic acid) Trimethyl Ester, Ve

(*i*) *By Reduction of the Glyoxylic Ester (Preparative Method)*

The glyoxylic ester V*d* (36.4 gm., m.p. 111–113°, prepared by method (*ii*))

in acetic acid (120 ml.) and sulphuric acid (6.49 ml.) with palladium black (2.3 gm., freshly prepared) was shaken at 28° under hydrogen (60 lb. per sq. in.) for four hours. After the theoretical uptake in two hours, absorption nearly ceased. The filtrate and acetic acid washings from the catalyst were evaporated to dryness under reduced pressure on the steam bath after the addition of anhydrous sodium carbonate (13.5 gm.). The residue was taken up in dry benzene (320 ml.), which was distilled, initially at atmospheric pressure, and finally to dryness under water pump vacuum. The rapidly solidifying gum was dissolved in dry methanolic hydrogen chloride (160 ml. of 10%), warmed to 55° in a water bath, and allowed to cool in the bath overnight. The crystals that rapidly separated when the solution was poured into ice-water (2.5 liters) were collected after one hour at 0°, well washed with water, and dried *in vacuo*. The crude product was recrystallized from methanol (180 ml.) – water (320 ml.) to give the pyrrole (27.0 gm., 78%) as pale pink plates, m.p. 92°.

(*ii*) A sample prepared in the same way by reducing glyoxylic ester (m.p. 114–115°, prepared by method (*i*)) and recrystallized twice from aqueous methanol formed colorless plates, m.p. 92°, giving a positive Ehrlich's reaction (hot). Found in material dried *in vacuo*: C, 56.32; H, 6.41; N, 4.93%. Calc. for $C_{14}H_{19}O_6N$: C, 56.56; H, 6.44; N, 4.71%.

The melting point of this specimen was not depressed by admixture of material prepared by method (*i*).

(*iii*) *From the Ethyl Ester IIe Via the Tricarboxylic Acid IIIb*

The tricarboxylic acid III*b* (0.116 gm., m.p. 144–145°) was esterified with diazomethane (from 2 gm. of nitrosomethylurea). After one hour the ether was washed with dilute hydrochloric acid, with aqueous sodium bicarbonate, and with water, and dried over sodium sulphate. The gum which remained after evaporation of the ether rapidly crystallized. Recrystallization from methanol (2 ml.) – water (9 ml.) gave the product (64 mgm., 47%), m.p. 91–92°. The melting point was unchanged after recrystallizations from aqueous ethanol and aqueous methanol. Found, in material dried *in vacuo*: N, 4.81%. The identity of this product and the analytical sample of (*ii*) above was confirmed by their mixed melting point and by their infrared spectra in carbon disulphide.

2-Methyl-5-carbethoxypyrrole-3-(glyoxylic acid)-4-(propionic acid), VIa

The triethyl ester II*d* (7 gm.) in ethanol (45 ml.) and 0.889 *N* sodium hydroxide (50 ml., 2.23 equiv.) was heated in an open flask on the steam bath for 35 min. The solvent was removed *in vacuo* and the partially crystalline residue dissolved in water (25 ml.) and made strongly acid with hydrochloric acid at 0°. The crude product was filtered off and washed with ice-water. Two recrystallizations from water (20 ml.) gave 2.17 gm. (37%), m.p. 195–196° (decomp.), eq. wt. 148.0 (calc. 148.6). Large pale pink prisms, m.p. 198–199°, Ehrlich's reaction positive hot, were obtained after two further recrystallizations. Found in material dried *in vacuo*: C, 52.20; H, 5.16; N, 5.03%. Calc. for $C_{13}H_{15}O_7N$: C, 52.52; H, 5.09; N, 4.71%.

As in the case of VI*b*, the crude product contained sodium when precipitated by sulphur dioxide.

Diethyl β-Ketoadipate

(*i*) To diethyl β-keto-α-carbethoxyadipate (809.5 gm.) (14) cooled in an ice–salt bath, sulphuric acid (810 ml.) was added at $\leqslant 20°$ with stirring. After 12 hr. at 27°, absolute ethanol (1500 ml.) was added with stirring, together with solid carbon dioxide to keep the temperature at $\leqslant 10°$. After 20 hr. at room temperature, the solution was poured into ice-water (8 liters) and extracted with benzene (3 × 500 ml.). The extracts were washed twice with dilute sulphuric acid, thrice with dilute sodium bicarbonate, twice with water, and dried over sodium sulphate. Distillation through a Vigreux column gave the diester (330 gm. 54%), b.p. (0.4 mm.) 112–120°, η_D^{25} 1.4390.

(*ii*) Three liters of water and 1406 gm. of ethyl β-keto-α-carbethoxyadipate were gently boiled with vigorous stirring under a 12 in. Vigreux column for four and one-half hours. A hydrometer showed 180 gm. (theory 225 gm.) of ethanol in the 1.8 liters of distillate. The undistilled residues from two such runs were combined. The ester was separated and combined with the ether wash (1 liter) of the water layers, washed with saturated sodium bicarbonate, four times with water, and with 4 × 250 cc. of cold saturated sodium carbonate which was then back-washed with ether. The organic layer was clarified with anhydrous sodium sulphate, washed three times with water, three times with dilute sulphuric acid, and four times with water, clarified with an anhydrous sodium sulphate, filtered, the ether removed on the steam bath, and the residue distilled to 150° at 0.2 mm. The fractionation of the distillate at 0.2 mm. with a 12 in. lagged Vigreux column was followed refractometrically; the product (1367 gm., 65%, η_D^{26} 1.4390) consisted of the main fraction (1280 gm., b.p. 108–119°, nearly all 117–119°) together with that obtained by refractionating the 95–108° cut.

Methyl δ,δ-Dicarbethoxylevulinate

The ester (214 gm., 81%) b.p. 140° (0.4 mm.) was obtained according to the method used for the triethyl ester (14) from 145.5 gm. of β-carbomethoxypropionyl chloride, 162 gm. of malonic ester, and 23.4 gm. of magnesium. For analysis, it was slowly distilled through a 3 in. Vigreux column and collected at 115° (0.25 mm.), as a colorless liquid, η_D^{27} 1.4486, giving a violet-brown color with ferric chloride. Found: C, 52.60; H, 6.51%. Calc. for $C_{12}H_{18}O_7$: C, 52.55; H, 6.61%.

Dimethyl β-Ketoadipate

β-Ketoadipic acid (281.5 gm.) from the above ester and hydrochloric acid (cf. (5)) gave the dimethyl ester (3) (126 gm., 38%) b.p. (0.6 mm.) 100–104°, η_D^{27} 1.4416, when esterified with 250 ml. of methanol containing 93 gm. of hydrogen chloride.

5,5′-Dimethylpyrromethene-3,3′-(diacetic acid)-4,4′-(dipropionic acid) Hydrobromide, VIIa

The tricarboxylic acid I*b* (1 gm., crude m.p. 143°) (10) was heated on the steam bath with 98% formic acid (5 ml.) and 30% hydrogen bromide in acetic acid (2.5 ml.) under reflux for 40 min. After two hours at 10° the product

was filtered off and washed with cold formic acid. The brown powder, 0.535 gm. (53%), m.p. 200–201° (decomp.), gave orange-yellow micro needles (0.385 gm.), melting point unchanged, on recrystallizing from formic acid (8 ml.). Found in material dried *in vacuo*: C, 49.22; H, 5.08; N, 5.45; Br, 15.39%. Calc. for $C_{21}H_{25}O_8N_2Br$: C, 49.13; H, 4.91; N, 5.46; Br, 15.57%.

It is stable when kept *in vacuo* over phosphorus pentoxide and protected from light.

5,5′-Dimethylpyrromethene-3,3′-(dipropionic acid)-4,4′-(diacetic acid) Hydrobromide, VIIb

The crude tricarboxylic acid III*b* (1.02 gm., m.p. 145°) was heated under reflux on the steam bath with 98% formic acid (5 ml.) and 30% hydrogen bromide in acetic acid (2.5 ml.) for one hour. The reaction mixture was evaporated to dryness under reduced pressure and acetic acid (15 ml.) added to the rapidly crystallizing brown residue. After one hour at 0°, the methene hydrobromide was collected, washed with cold acetic acid, and dried *in vacuo*. The orange-powder (0.641 gm., 62%), m.p. 217°–218° (decomp.), was recrystallized from formic acid (4 ml.) to give small orange elongated prisms (0.405 gm.), m.p. 218–218.5° (decomp.). The melting point was unchanged by further recrystallization. Found in material dried *in vacuo*: C, 49.38; H, 4.95; N, 5.36; Br, 15.55%. Calc. for $C_{21}H_{25}O_8N_2Br$: C, 49.13; H, 4.91; N, 5.46; Br, 15.57%.

The hydrobromide was stored *in vacuo* over phosphorus pentoxide, and protected from light.

REFERENCES

1. ADKINS, H., BURGOYNE, E. E., and SCHNEIDER, H. J. J. Am. Chem. Soc. 72: 2626. 1950.
2. BAKER, B. R., SCHAUB, R. E., and WILLIAMS, J. H. J. Org. Chem. 17: 116. 1952.
3. BARDHAN, J. C. J. Chem. Soc. 1851. 1936.
4. BERNHARD, A. Ann. 282: 166. 1894.
5. EISNER, U., ELVIDGE, J. A., and LINSTEAD, R. P. J. Chem. Soc. 2223. 1950.
6. FISCHER, H. and ANDERSAG, H. Ann. 458: 117. 1927.
7. FISCHER, H. and ORTH, H. Chemie des Pyrrols. Leipzig. 1934. Band I: (*a*) p. 282. (*b*) p. 289. (*c*) p. 235. Band II/i: (*d*) p. 3.
8. FISCHER, H., WEISS, B., and SCHUBERT, M. Ber. 56: 1194. 1923.
9. KINDLER, K., METZENDORF, W., and DSCHI-YIN-KUOK. Ber. 76: 308. 1943.
10. MACDONALD, S. F. Chemistry & Industry, 759. 1951. J. Chem. Soc. 4176, 4184. 1952.
11. MACDONALD, S. F. and STEDMAN, R. J. J. Am. Chem. Soc. 75: 5448. 1953.
12. MOZINGO, R., SPENCER, C., and FOLKERS, K. J. Am. Chem. Soc. 66: 1859. 1944.
13. OTT, W. Thesis, Technische Hochschule, Munich. 1953. p. 51. TREIBS, A. and HINTERMEIER, K. Chem. Ber. 87: 1167. 1954.
14. RIEGEL, B. and LILIENFELD, W. M. J. Am. Chem. Soc. 67: 1273. 1945.
15. SINAIGO, F. K. and ADKINS, H. J. Am. Chem. Soc. 58: 709. 1936.
16. STEDMAN, R. J. and MACDONALD, S. F. Can. J. Chem. 33: 468. 1955.
17. TAUSZ, J. and VON PUTNOKY, M. Ber. 52: 1573. 1919.

SIMPLE PYRROLES AS BASES[1]

By R. J. Stedman[2] and S. F. MacDonald

ABSTRACT

Some simple pyrroles form stable hydrobromides. Their formation may interfere with some reactions, but offers analytical possibilities.

Although the basic nature of dipyrromethenes and of porphyrins is well-known, that of simple pyrroles has been largely ignored. Discussions have been limited to rationalizing the instability of salts of pyrrole itself (1, 10). However, the acidic (7) and basic properties of simple pyrroles are very dependent on the substituents present. Solubility in mineral acid has been noted (13), shown spectroscopically to be due to salt formation (3), and used to separate mixtures by partition (9). Chloroaurates and chloroplatinates (13, 2) as well as picrates are known, but apparently only two salts of simple pyrroles with mineral acids have been described: the deliquescent or unstable hydrochloride of cryptopyrrole (2,4-dimethyl-3-ethylpyrrole) (6), and an unstable hydrobromide of 2-bromomethyl-3-methyl-4-ethyl-5-carbethoxypyrrole (8).

When the preparation of a dipyrromethene from I*b* was attempted with formic acid and hydrogen bromide at 55° (12), the product which separated was the hydrobromide of I*a*, cryptopyrrole-dicarboxylic acid. The hydrobromide could also be prepared directly from I*a* in ether, to which it again reverted with aqueous pyridine. α-Carboxy-hemopyrrole-dicarboxylic acid, II*b*, behaved like I*b*, and both hemopyrrole-dicarboxylic acid, II*a*, and cryptopyrrole-carboxylic acid, III, behaved like I*a*. The hydrobromides were stable to recrystallization and to drying in vacuum. The behavior of other pyrroles with hydrogen bromide has not been studied.

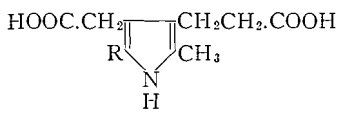

I*a*, R = H
b, R = COOH

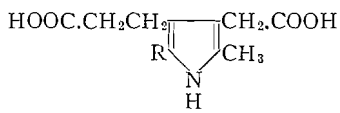

II*a*, R = H
b, R = COOH

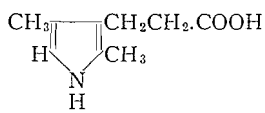

III

These hydrobromides should prove useful analytically, for pyrroles such as I*a* are very soluble in water and neither the acids nor the methyl esters are

[1]*Manuscript received November 8, 1954.*
Contribution from the Division of Pure Chemistry, National Research Council of Canada, Ottawa. Issued as N.R.C. No. 3507.
[2]*National Research Council of Canada Postdoctorate Fellow, 1952–1954.*

precipitated by picric acid, the classical reagent for separating pyrrole mixtures. In a preliminary experiment the pyrrole mixture resulting on the reduction of uroporphyrin, previously obtained as an oil (5), was readily precipitated from ether with hydrogen bromide in acetic acid, and the hydrobromides converted into a solid mixture of pyrroles.

EXPERIMENTAL

Hydrobromide of Cryptopyrrole-dicarboxylic Acid

(*i*) *From Cryptopyrrole-dicarboxylic Acid, Ia*

The pyrrole (0.192 gm.) was dissolved in acetic acid (2 ml.) and dry ether (5 ml.). The addition of hydrogen bromide (0.5 ml. of a 30% solution in acetic acid) caused the separation of an oil which crystallized on scratching. More ether was added, and the product (0.231 gm., 87%), m.p. 134–136° (decomp.), filtered off and washed with ether. By recrystallization from acetic acid (2 ml.) – ether (2 ml.), it was obtained as pale pink plates, m.p. 137–138° (decomp.), unchanged on further recrystallization. Ehrlich's reaction was strongly positive cold. Found in material dried *in vacuo*: C, 41.11; H, 4.61; N, 4.70; Br, 27.59%. Calc. for $C_{10}H_{14}O_4NBr$: C, 41.11; H, 4.83; N, 4.80; Br, 27.36%.

(*ii*) *From α-Carboxycryptopyrrole-dicarboxylic Acid, Ib*

The crude tricarboxylic acid (4 gm., m.p. 140.5°) was suspended in 98% formic acid (8 ml.) and warmed at 55° with hydrogen bromide (4 ml. of a 30% solution in acetic acid) to solution and cessation of effervescence (*ca.* 20 min.) (cf. (12)). The solvent was removed *in vacuo* at 50°, the partially crystalline residue shaken with acetic acid (140 ml.) at 50° and, after two hours at 25°, some dipyrromethene removed by filtration and washed with acetic acid. The pyrrole hydrobromide (3.18 gm., 69%), a yellow powder m.p. 136–138° (decomp.), was precipitated from the combined filtrate and washings by dry ether (200 ml.) and washed with acetic acid – ether (1:1). After recrystallization from acetic acid (25 ml.) – ether (25 ml.) it formed pale tan plates (2.71 gm.), m.p. 137–138° (decomp.), undepressed by admixture with the hydrobromide obtained under (*i*). Ehrlich's reaction was strongly positive cold. Found in material dried *in vacuo*: C, 41.24; H, 4.87; N, 4.67; Br, 27.27%. The infrared spectra in Nujol mull of the products obtained under (*i*) and (*ii*) confirmed their identity.

The material (0.246 gm., 6%), insoluble in acetic acid, was recrystallized from formic acid to give the yellow 5,5′-dimethyl pyrromethene-3,3′-diacetic acid-4,4′-dipropionic acid hydrobromide, m.p. 200–200.5° (decomp.), undepressed by admixture with authentic material (12).

Cryptopyrrole-dicarboxylic Acid, Ia, from its Hydrobromide

The pyrrole hydrobromide (292 mgm., 1 millimole) was dissolved in aqueous pyridine (0.5 ml. of a 16.5% w/v solution, 1.05 millimole). After one hour at 0°, the pale pink plates (86 mgm., 41%) were filtered off and washed with a little ice cold water. The m.p. (128–129°) was undepressed by authentic cryptopyrrole-dicarboxylic acid of m.p. 128–129° (11), and identity was confirmed by infrared spectra in Nujol mull.

Hydrobromide of Hemopyrrole-dicarboxylic Acid

(*i*) *From Hemopyrrole-dicarboxylic Acid, IIa*

This hydrobromide (0.716 gm., 95%) m.p. 158–159°, was obtained as a gray powder from 0.545 gm. of the pyrrole II*a* in 5 ml. of acetic acid with 1 ml. of hydrogen bromide in acetic acid, as was the isomer above. After two recrystallizations from 7 ml. of acetic acid it formed violet prisms, m.p. 160–161°. Ehrlich's reaction was strongly positive cold. Found in material dried *in vacuo*, C, 41.18; H, 5.01; N, 4.57; Br, 24.81%. Calc. for $C_{10}H_{14}O_4NBr.\frac{1}{2}CH_3.COOH$: C, 41.01; H, 5.01; N, 4.35; Br, 24.81%.

The distillate from a solution of the hydrobromide (30 mgm., subjected to prolonged drying *in vacuo*) in 0.75 ml. of water gave a positive test for acetic acid when treated with lanthanum nitrate, iodine, and ammonia (4).

(*ii*) *From α-Carboxyhemopyrrole-dicarboxylic Acid, IIb*

The crude tricarboxylic acid II*b* (0.5 gm., m.p. 149°) was heated at 70° for a few minutes with 1 ml. of formic acid and 0.5 ml. of hydrogen bromide in acetic acid. The solvent was removed *in vacuo* at 25°, leaving a gum which rapidly crystallized. Recrystallization from 7 ml. of acetic acid gave a yellow powder (0.278 gm., 48%), m.p. 157–159°. After two further crystallizations it formed pale yellow prisms, m.p. 159–160.5°. Contamination by dipyrromethene was detected by the visible spectrum. Ehrlich's reaction was strongly positive in the cold. Found in material dried *in vacuo*: C, 41.40; H, 5.04; N, 4.66; Br, 24.64%. The melting point was undepressed by the product of (*i*) above, and the infrared spectra in Nujol mull confirmed their identity.

Hydrobromide of Cryptopyrrole-carboxylic Acid

Cryptopyrrole-carboxylic acid, III, (0.501 gm., m.p. 140–141°) in 10 ml. of dry ether was treated with hydrogen bromide (1 ml. of a 30% solution in acetic acid). The oil which was immediately deposited rapidly crystallized and the product (0.716 gm., 96%) was collected after one hour at room temperature, washed with dry ether, and dried *in vacuo*. The crude material, a greenish powder, m.p. 148–150° (decomp.) was recrystallized from 7 ml. of acetic acid, giving small green prisms (0.365 gm.), m.p. 151–151.5°. The color persisted after two further recrystallizations and the melting point was unchanged. The Ehrlich's reaction was strongly positive in the cold. Found in material dried *invacuo*: C, 43.86; H, 5.90; N, 5.83; Br, 32.28%. Calc. for $C_9H_{14}O_2NBr$: C, 43.56; H, 5.69; N, 5.65; Br, 32.21%.

Cryptopyrrole-carboxylic Acid, III, from its Hydrobromide

The pyrrole hydrobromide (193 mgm.; 0.78 millimole) was dissolved in 1 ml. of water and treated with pyridine (0.80 ml. of a 7.9% w/v aqueous solution, 0.80 millimole). The free pyrrole was immediately deposited and was collected after one hour at 0° as a brown powder (95.5 mgm., 73%), washed with cold water, and dried *in vacuo*. Sublimation at 100° in a high vacuum gave a colorless product, m.p. 141–142°, undepressed by admixture of authentic cryptopyrrole-carboxylic acid.

REFERENCES

1. BAMBERGER, E. Ber. 24: 1758. 1891.
2. CIAMICIAN, G. Ber. 37: 4200. 1904.
3. COOKSON, G. H. J. Chem. Soc. 2789. 1953.
4. FEIGL, F. Spot tests. Vol. 2. 4th English ed. Elsevier Publishing Co., Inc., Amsterdam. 1954. p. 247.
5. FISCHER, H. Z. physiol. Chem. 95: 58. 1915; 98: 78. 1916. FISCHER, H. and ANDERSAG, H. Ann. 458: 117. 1927. FISCHER, H. and ZERWICK, W. Z. physiol. Chem. 137: 243. 1924.
6. FISCHER, H., BAUMANN, E., and RIEDL, H. J. Ann. 475: 205. 1929.
7. FISCHER, H. and ELHARDT, E. Z. physiol Chem. 257: 61. 1939. FISCHER, H. and ERNST, P. Ann. 447: 139. 1926.
8. FISCHER, H. and STANGLER, G. Ann. 459: 53. 1927.
9. FISCHER, H. and TREIBS, A. Ann. 450: 132. 1926.
10. INGOLD, C. K. Structure and mechanism in organic chemistry. Cornell Univ. Press, Ithaca, N.Y. 1953. pp. 160, 174.
11. MACDONALD, S. F. J. Chem. Soc. 4184. 1952.
12. MACDONALD, S. F. and STEDMAN, R. J. Can. J. Chem. 33: 458. 1955.
13. ZANETTI, C. U. and LEVI, E. Ber. 27. Ref. 585. 1894.

PHOTOLYSIS OF ACETONE IN THE PRESENCE OF MERCURY DIMETHYL[1]

By H. G. Oswin, R. Rebbert, and E. W. R. Steacie

ABSTRACT

The reactions between $CH_3+CH_3—Hg—CH_3$ were investigated in a system in which acetone was used as the source of CH_3 radicals. Similarly d_6-acetone was used to investigate the reactions of CD_3 radicals and $CH_3—Hg—CH_3$. Activation energies for the hydrogen abstraction reactions were calculated, and no significant difference was found between the CD_3 and CH_3 reactions, being respectively 10.0 and 10.2 kcal./mole. Under conditions of constant intensity and acetone concentration, reaction rates appear to be dependent on mercury dimethyl concentrations. In the case of the acetone-d_6 system, quantities of $C_2D_3H_3$ were found in the reaction products. This is discussed as possible evidence of such a reaction as:

$$CD_3+CH_3—Hg—CH_3 \rightarrow CD_3—CH_3+Hg+CH_3.$$

INTRODUCTION

The photolysis of mercury dimethyl was recently investigated (4) and an activation energy for the reaction

$$CH_3+Hg(CH_3)_2 \rightarrow CH_4+CH_3—Hg—CH_2 \qquad [1]$$

was derived. The work presently described was carried out to determine whether this value is in fact independent of the source of methyl radicals.

Acetone and deuterated acetone are suitable sources of methyl radicals, and can be photolyzed in a wavelength region above 2800 Å, where mercury dimethyl does not absorb. Under these conditions there will be two competing reactions producing methane,

$$CH_3+Hg(CH_3)_2 \rightarrow CH_4+CH_3—Hg—CH_2 \qquad [1]$$

$$CH_3+CO(CH_3)_2 \rightarrow CH_4+CH_3—CO—CH_2. \qquad [2]$$

To obtain the rate of reaction [1], the rate of reaction [2] is subtracted from the over-all rate of formation of methane. The disadvantage of this method is that the rate constant of reaction [2] is considerably larger than [1], and consequently contributes far more to the over-all methane formation rate.

Deuterated acetone has been used successfully to investigate similar reactions (3, 6), and under the circumstances should give a clearer picture of the two competing reactions; in this case:

$$CD_3+Hg(CH_3)_2 \rightarrow CD_3H+CH_3—Hg—CH_2 \qquad [3]$$

$$CD_3+CO(CD_3)_2 \rightarrow CD_4+CD_3—CO—CD_2. \qquad [4]$$

Hence the ratio of CD_4 to CD_3H (determined mass spectrometrically) should give a more accurate measure of the relative rates. A correction can be made for CD_3H formed by reactions of the type

[1]*Manuscript received November 9, 1954.*
Contribution from the Division of Pure Chemistry, National Research Council, Ottawa, Canada. Issued as N.R.C. No. 3508.

$$CD_3+HCD_2—CO—CD_3 \rightarrow CD_3H+CD_2—CO—CD_3 \quad [4a]$$

and $$CD_2H+CD_3—CO—CD_3 \rightarrow CD_3H+CD_2—CO—CD_3 \quad [4b]$$

from the rates found in the photolysis of the deuterated acetone sample alone.

EXPERIMENTAL TECHNIQUE

A conventional high-vacuum apparatus was employed, containing a suitable cell, mixing bulb, and micro-gas analysis equipment. All stopcocks were lubricated with silicone grease to minimize the amount of mercury dimethyl dissolving.

A suitable filter (Corning 0/53) was used to absorb radiation of shorter wavelength than 2800 Å. This eliminates direct energy absorption by mercury dimethyl, a fact which was established by carrying out a few preliminary blank runs with only mercury dimethyl present.

Mercury dimethyl was prepared in the previously described manner (4). Reagent grade acetone was first dried and distilled *in vacuo* before using.

A sample of deuterated acetone was prepared (3) and analyzed mass spectrometrically. It was found that the total hydrogen content of the sample consisted of 96% of the deuterium isotope.

In the case of the experiments with deuterated acetone, the various fractions of the reaction products were analyzed mass spectrometrically. By this method, CO, CD_4, and CD_3H can be determined in the C_1 fraction. In the C_2 fraction only C_2D_6 can be analyzed accurately, estimates of the succeeding compounds C_2D_5H, $C_2D_4H_2$ etc. becoming progressively less accurate.

RESULTS

(a) *"Light" Acetone and Mercury Dimethyl*

The case of "light" acetone will be considered first.

The temperature range investigated here was restricted between 433° and 511°K., the lower limit being imposed by small rates of reaction [1] at low

TABLE I

No.	Temp., °C.	Acetone (mm.)	Mercury dimethyl (mm.)	Rates of formation of products (molecules/cc./sec. × 10^{11}) CH_4	C_2H_6	CO	$(k_2/k_5^{\frac{1}{2}}) \times 10^{13}$
Photolysis of acetone alone							
174	126	41.7		5.65	15.0	20.1	4.57
176	144	42.4		8.24	13.8	21.4	7.18
172	178	46.0		17.5	11.0	25.2	17.0
175	212	49.3		27.0	6.1	25.8	35.4
177	238	52.6		34.4	3.74	27.4	56.5
Photolysis of acetone in presence of mercury dimethyl							
186	160	43.3	42.3	11.4	8.69	16.5	1.81
180	178	45.6	45.0	18.9	9.71	22.3	2.63
185	195	48.1	47.7	22.6	6.42	19.6	4.26
184	212	49.2	48.2	29.4	5.18	20.6	6.59
181	238	51.4	50.9	45.5	4.92	24.2	10.4

temperatures. The upper limit is determined by the increased thermal decomposition of mercury dimethyl above this temperature range.

Table I lists the reaction rates for pure acetone and acetone–mercury dimethyl mixtures. Values of log $(k_1/(k_5)^{\frac{1}{2}})$ were calculated where k_5 is the rate constant for methyl recombination.

$$CH_3+CH_3 \rightarrow C_2H_6 \qquad [5]$$

These values are shown plotted against $10^3/T°K.$ in Fig. 1.

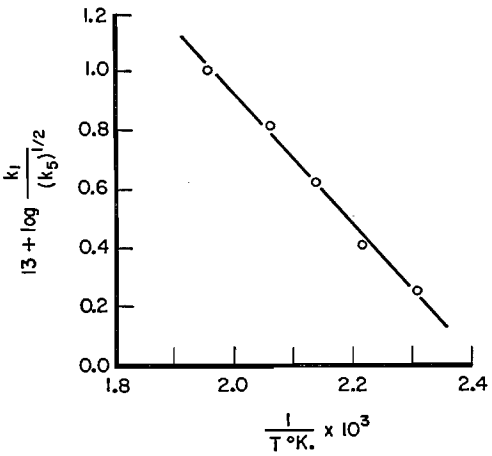

FIG. 1

The regression equation of log $(k_1/(k_5)^{\frac{1}{2}})$ on T is

$$\log (k_1/(k_5)^{\frac{1}{2}}) = -(2238/T°K.)-7.59$$

from which it is found that

$$E_1-\tfrac{1}{2}E_5 = 10.2\pm1.0 \text{ kcal. per mole.}$$

TABLE II

EFFECT OF MERCURY DIMETHYL ON PRODUCTS AT CONSTANT INTENSITY

No.	Temp., °C.	Pressure of acetone (mm.)	Pressure of $Hg(CH_3)_2$ (mm.)	R_{CO}	$\frac{1}{2}R_{C_1}+R_{C_2}$
176	144	42.4	0	2.32	1.94
182	144	41.5	40.7	2.12	1.84
187	144	40.9	41.4	2.08	1.83
172	178	46.0	0	2.71	2.12
180	178	45.6	45.0	2.44	2.09
175	212	49.3	0	2.85	2.18
184	212	49.2	48.2	2.57	2.49
177	238	52.6	0	2.99	2.27
181	238	51.4	50.9	2.73	3.11

Table II shows various rates measured under conditions of constant intensity at different temperatures. The apparent dependence of these rates on mercury dimethyl concentrations will be discussed later.

(*b*) *Deuterated Acetone and Mercury Dimethyl*

The rates of formation of the various reaction products are listed in Table III. The column headed R_{CD_3H} lists the corrected values allowing for the CD_3H formation from acetone.

TABLE III

No.	Temp., °C.	d_6-acetone (mm.)	Mercury dimethyl (mm.)	Rates of formation of products (molecules/cc./sec. × 10^{11})			
				CD_4	CD_3H	C_2D_6	$C_2D_3H_3$
18	202	84	25	7.63	3.66	3.29	4.39
17	200	79	46	5.81	4.08	1.78	3.38
16	200	89	—	16.7	1.50	11.6	—
6	200	75	26	10.2	4.77	11.3	5.72
5	197	87	49	10.9	9.88	8.58	7.38
7	182	82	54	7.92	7.63	9.45	7.18
13	172	83	—	8.84	1.01	11.6	0.2
14	172	71	44	3.85	4.64	6.72	4.4
15	172	89	22	8.08	3.19	15.6	5.08
12	155	76	52	3.23	4.48	10.5	5.07
2	153	80	—	6.95	1.53	39.8	—
3	153	69	45	4.64	4.19	20.9	6.06
4	148	77	30	4.04	2.26	20.7	3.34
11	135	89	25	3.36	1.59	13.8	1.57
10	134	85	44	2.99	2.74	10.0	2.0
19	126	88	—	2.44	0.33	11.8	—
20	125	85	33	1.81	1.09	11.0	4.39
21	125	78	49	1.10	1.29	7.58	6.24
8	125	88	53	2.08	2.05	18.8	4.97

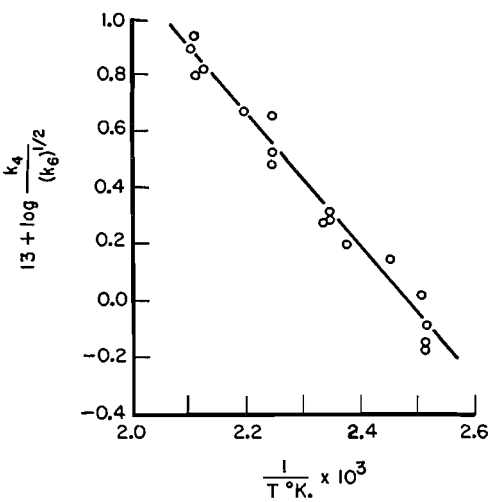

FIG. 2

Very small quantities of C_3 products were found, but these were too small to allow accurate analysis, and would probably contain appreciable proportions

of C_2 compounds. By volume this fraction usually amounted to between one per cent and three per cent of the C_2 fraction.

A preliminary check on the conditions of the experiment can be obtained from a calculation of the activation energy for the reaction:

$$CD_3 + (CD_3)_2CO \rightarrow CD_4 + CD_3—CO—CD_2. \qquad [4]$$

Fig. 2 shows a plot of log $(R_{CD_4}/(R_{C_2D_6})^{\frac{1}{2}})$ [acetone] against $10^3/T°K$.

The regression equation of this relationship is given by

$$\log (k_4/(k_6)^{\frac{1}{2}}) = -(2373/T°K.) - 9.254,$$

where k_6 is the rate constant for the methyl recombination:

$$2CD_3 \rightarrow C_2D_6. \qquad [6]$$

From the above expression

$$E_4 - \tfrac{1}{2}E_6 = 10.9 \pm 1.0 \text{ kcal. per mole.}$$

The activation energy for reaction [3]

$$CD_3 + CH_3—Hg—CH_3 \rightarrow CD_3H + CH_3—Hg—CH_2$$

was calculated from a plot of

$$\log (R_{CD_3H}/(R_{C_2D_6})^{\frac{1}{2}}) \text{ [mercury dimethyl] versus } 10^3/T°K.$$

The plot shown in Fig. 3 may be represented by

$$\log (k_3/(k_6)^{\frac{1}{2}}) = -(2196/T°K.) - 7.336.$$

Hence $E_3 - \frac{1}{2}E_6 = 10.0 \pm 1.0$ kcal. per mole.

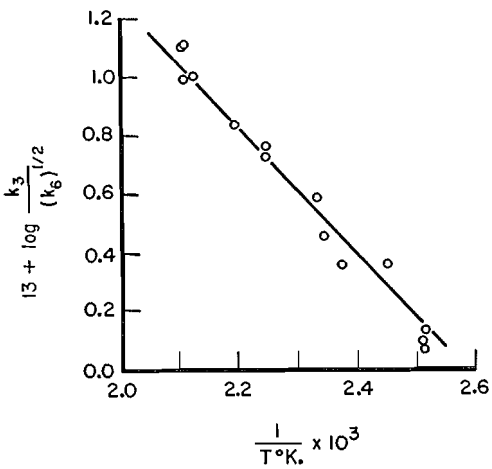

FIG. 3

Also listed in Table III are the rates of formation of $C_2D_3H_3$. Although the accuracy of these figures may be no better than $\pm 50\%$, the quantities are still

too large to be accounted for by such reactions as

$$CD_2H + CH_2D \rightarrow C_2D_3H_3.$$

The presence of $C_2D_3H_3$ will be discussed later.

DISCUSSION

The value of 10.9 kcal./mole found for E_4 lies between the previous values of 10.6 and 11.6 kcal./mole obtained respectively by Majury and Steacie (3) and Whittle and Steacie (6). In view of the different experimental conditions, the present value of 10.9 is probably not as accurate as these others. However, Whittle and Steacie in support of the higher value suggest that the lower value of 10.6 kcal./mole is due to non-linearity of the Arrhenius plot at lower temperatures; since the present work was carried out at the lower temperatures also, it is not surprising that it agrees more with the value of 10.6 kcal./mole.

The recent figures of McNesby and Gordon (2) for the acetone–acetone-d_6 photolysis indicate that there is no measurable difference in activation energy for the abstraction of hydrogen from acetone by CH_3 and CD_3 radicals. It seems reasonable to assume therefore that there should be no significant difference between the activation energies for reactions [1] and [3], as is indicated by the values of 10.2 ± 1.0 and 10.0 ± 1.0 kcal./mole presently obtained.

Activation energies previously obtained (5) for hydrogen abstraction reactions, using mercury dimethyl as a source of methyl radicals, are generally in good agreement with those obtained in acetone systems. It was assumed in this work that the only sources of CH_4 and C_2H_6 were by hydrogen abstraction and recombination of methyl radicals. However, several features of the present work with acetone and mercury dimethyl must be considered in this respect.

(1) In the presence of an equal amount of mercury dimethyl, the rate of formation of CO from acetone is reduced by 10% over the range 144°–238°C. (see Table II).

(2) Table II also indicates that the quantum yield of methyl radicals recovered as CH_4 and C_2H_6, in the presence of mercury dimethyl, is decreased at the lower temperatures and increased at the higher temperatures, eventually exceeding two CH_3 radicals per CO formed.

(3) Mixtures of deuterated acetone and mercury dimethyl yield appreciable quantities of $C_2D_3H_3$ (see Table III), although only CD_3 radicals are formed in appreciable amount by direct light absorption.

Holroyd and Noyes (1), investigating the photolysis of mercury dimethyl alone at 2600 Å, established these points:

(4) At 175°C., there is an increase in $R_{CH_4}/R_{C_2H_6}^{\frac{1}{2}}[DM]$ with increasing light absorption.

(5) At 175°C., more than two methyls appear as methane and ethane per quantum absorbed.

(6) The quantum yield of ethane formation is nearly independent of the amount of methane formed, and is approximately the same at 30°C. and 175°C. There is a slight increase with decreasing light absorption.

In reference to point (1), there are two possible causes of a decrease in CO formation:

(*a*) decreasing extinction coefficient of acetone, in the presence of mercury dimethyl; but in view of the pressures used, it is unlikely that this effect would be appreciable;

(*b*) transfer of energy from an excited acetone molecule or CH_3CO radical; this may or may not induce decomposition of the mercury dimethyl molecule.

Both of these possibilities would result in an increased or decreased primary production of methyl radicals, but would not affect the modes of formation of methane and ethane. If the transfer of energy to mercury dimethyl resulted in subsequent decomposition, it would explain the presence of CD_3–CH_3 in the reaction products, but could not account for all of it.

Observation (5), that more than two methyls appear per quantum absorbed, has been offered by Holroyd and Noyes as evidence of the reaction:

$$CH_3+CH_3—Hg—CH_3 \rightarrow C_2H_6+CH_3+Hg. \qquad [7]$$

The observed formation of CD_3–CH_3 in the present work also indicates that reaction [7] may occur. This reaction together with the suggested explanations of the R_{CO} decrease could explain qualitatively the reported observations. In view of the possibility of energy transfer, the quantities of CD_3–CH_3 formed cannot be used for an accurate estimation of the importance of reaction [7].

If reaction [7] is an additional mode of formation of ethane, then the relation holds

$$\frac{k_1}{k_5^{\frac{1}{2}}}[DM] = \frac{R_{CH_4}}{R_{C_2H_6}\beta^{\frac{1}{2}}} - \frac{k_8}{k_5^{\frac{1}{2}}}[RH]$$

$$= 1 - \frac{k_7}{k_1}\frac{R_{CH_4}}{R_{C_2H_6}}\left(1+\frac{k_8}{k_1}\frac{[RH]}{[DM]}\right)$$

where k_8 is the rate constant for the abstraction of hydrogen from an added hydrocarbon RH. Hence from the photolysis of mercury dimethyl alone, it is possible to determine the two parameters $k_1/k_5^{\frac{1}{2}}$ and k_7/k_1 from variations in the formation of CH_4 and C_2H_6 over an extensive range of light absorption. From Holroyd and Noyes data, k_7/k_1 would be between zero and unity at 175°C. At room temperature no methane is formed and

$$C_2H_6 = 1+\frac{k_7}{k_5^{\frac{1}{2}}}\frac{[DM]}{I_a^{\frac{1}{2}}}$$

which is in qualitative agreement with the drift with light absorption observed by Holroyd and Noyes.

Inasmuch as reaction [7] does occur, it should have a very low activation energy and an unusually small steric factor; unfortunately no more than these qualitative conclusions can be drawn.

Analysis of the present and previous (4) data, assuming reaction [7] occurs, shows that in view of the amounts of CH_4 and C_2H_6 found at higher temperatures, k_7 can have no more than a slight temperature coefficient. Arbi-

trarily taking $E_1 - E_7 = 10$ kcal. and $k_7/k_1 = 0.37$ at 175°C., it is found that values of $k_1/k_5^{\frac{1}{2}}$ and $E_1 - \frac{1}{2}E_5$ become practically identical for mercury dimethyl alone, and the present experiments with acetone – mercury dimethyl mixtures. Other values for hydrogen-abstraction reactions remained virtually unaffected by this treatment.

Although this treatment has no more than a qualitative significance, it would seem that a second mode of ethane formation could exist in the mercury dimethyl photolysis without affecting the observed agreement with the acetone work.

ACKNOWLEDGMENT

We should like to thank Miss F. Gauthier, Miss J. Fuller, and Dr. F. P. Lossing for the mass-spectrometer analysis, and Dr. R. J. Cvetanovic for very helpful discussions.

REFERENCES

1. HOLROYD, R. A. and NOYES, W. A., JR. J. Am. Chem. Soc. 76: 1583. 1954.
2. MCNESBY, J. R. and GORDON, A. S. J. Am. Chem. Soc. 76: 1416. 1954.
3. MAJURY, T. and STEACIE, E. W. R. Can. J. Chem. 30: 800. 1952.
4. REBBERT, R. E. and STEACIE, E. W. R. Can. J. Chem. 31: 631. 1953.
5. REBBERT, R. E. and Steacie, E. W. R. J. Chem. Phys. 21: 1723. 1953.
6. WHITTLE, E. and STEACIE, E. W. R. J. Chem. Phys. 21: 993. 1953.

STUDIES ON CARRAGEENIN: COMPARISON OF FRACTIONS OBTAINED WITH POTASSIUM CHLORIDE AND BY SUCCESSIVE EXTRACTION AT ELEVATED TEMPERATURES[1]

By D. A. I. Goring and E. Gordon Young

ABSTRACT

Carrageenin was fractionated with potassium chloride and by successive extractions at elevated temperatures. Measurements were made of sulphate content, optical rotation, gel strength, intrinsic viscosity, sedimentation rate, and ionic mobility. The results indicated three components extractable at 30°C., 60°C., and 100–120°C. The 60°C. extract had a high gel strength while the components extracted at 30°C. and 100–120°C. showed low gelling tendencies. The two non-gelling components were concentrated in the supernatant liquid when fractionated with potassium chloride.

INTRODUCTION

Carrageenin, the polysaccharide extractable from the red alga Irish moss (*Chondrus crispus*), has been shown to consist mainly of D-galacto-4-sulphate residues joined in the 1–3 position (11). Other monosaccharides have been found in carrageenin as usually prepared (2, 9, 11, 19, 24). The chemical individuality of these preparations however was not established. Cook, Rose, and Colvin (3) observed in the ultracentrifuge two components in commercial carrageenin. Smith and Cook (21) and Smith, Cook, and Neal (22) were able to separate these components in aqueous solution with potassium chloride. They applied the term κ-carrageenin to the precipitated component and λ-carrageenin to the component remaining in solution. These components differed in sulphate content, optical activity, rates of sedimentation and of diffusion, and intrinsic viscosity. Neither Cook *et al.* (3) nor Goring (6) could detect any clear separation of components electrophoretically.

Rose (18) found no evidence for chemically distinct components but cold and hot water extracts have been reported to differ in optical rotation and gelling tendencies (15). The usual hot water extract of carrageenin will act as a suspending agent in milk only when mixed at 60°–70°C. Hess and Siehrs (10) noted that when the residues of a hot water extraction were re-extracted with steam at 105°–120°C., a substance was obtained which suspended cocoa in milk when mixed at 10°–20°C.

These observations indicated that fractionation of the polysaccharides in Irish moss was feasible and that these fractions differed in certain properties. The purpose of the present work was to compare the properties of fractions separated by (*a*) potassium chloride and (*b*) re-extraction of the plant at increasing temperatures. Measurements were made of sulphate content, optical rotation, gel strength, intrinsic viscosity, sedimentation rate, and electrophoretic mobility.

[1]*Manuscript received October 4, 1954.*
Contribution from the Maritime Regional Laboratory, National Research Council, Halifax, Nova Scotia. Issued as N.R.C. No. 3515.

PREPARATION AND FRACTIONATION

All preparations were made from one lot of *Chondrus crispus* harvested at Prospect, Nova Scotia, in September, 1952. The plants were washed, air-dried, and milled to pass a 40-mesh screen. Manipulations were carried out as quickly as possible and toluene was added as a preservative when necessary. Samples were stored at −13°C. No excessive bacterial contamination was found at any time either microscopically or by plating.

The solvent used throughout for extraction and fractionation was aqueous sodium acetate of ionic strength (I) 0.02.

The various fractions were studied exclusively as the sodium salt. A 0.5% solution of the crude polysaccharide was dialyzed with internal mechanical stirring against aqueous sodium acetate for 24 hr. at 10°C. The acetate was then removed by dialysis against a solution of 50–100 mgm./liter sodium hydroxide in distilled water. If the concentration of sodium hydroxide was 1% of the concentration of carrageenin in the solution, the final pH of the dialyzate was 8–9. Dialysis against distilled water caused the pH to fall and degradation to occur which brought about a marked drop in viscosity.

Sodium carrageenate was obtained by freeze-drying the dialyzed solution. The water content of this material was 1–4%.

Fractionation with Potassium Chloride

Following the method of Smith *et al.* (21, 22), potassium chloride was added to the solutions of carrageenin. On centrifugation a gel separated and the supernatant liquid was decanted. These fractions are subsequently termed *gel* and *sol* respectively. Fractionation was difficult with carrageenin of high intrinsic viscosity because of more or less complete gelation. A more effective fractionation was possible after the solutions had been heated to 90°C. for 15 min. and cooled. The intrinsic viscosity of the purified polysaccharide was unchanged by this treatment.

Preliminary fractionations confirmed in general the results of Smith and co-workers (21, 22). The fractionation with potassium chloride, which was studied in detail, is shown in Fig. 1. Dried, ground *Chondrus crispus* was extracted with 0.02 M aqueous sodium acetate at 100°C. for five minutes in a Servall Dumore blendor. The solution was clarified by centrifugation and the crude polysaccharide was precipitated by pouring into five volumes of ethanol. The yield on the basis of dry weight was 65%.

The crude polysaccharide was redissolved at a concentration of 0.5% and the solution heated to 90°C. for 15 min. Part of the solution was dialyzed and freeze-dried to give the unfractionated material (Fig. 1). The remainder was fractionated by adding a 10% solution of potassium chloride dropwise with vigorous stirring until a concentration of 0.4% was established. This caused the separation of a *sol* fraction, S1, and a *gel* fraction, G1. Part of G1 was dialyzed and refractionated to give S2 and G2. Fractions were finally dialyzed and freeze-dried to give the sodium salt. The ratio G1/S1 was 2.36 and G2/S2 was 2.43. These *gel*/*sol* ratios were considerably larger than the values reported by Smith *et al.* (21, 22). The higher concentration of carrageenin used by us

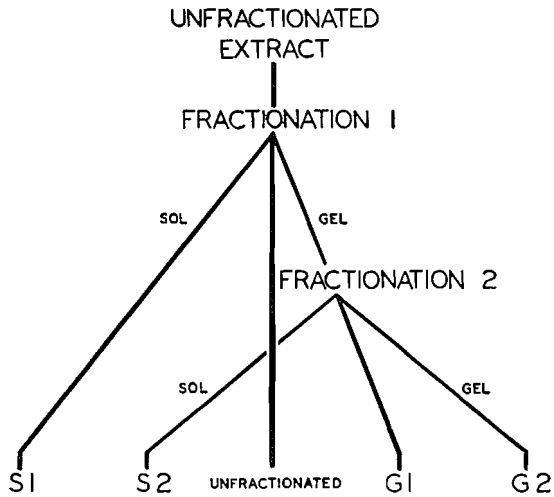

FIG. 1. Fractionation with potassium chloride.

(0.5% compared to 0.05–0.2%) could account for this difference. The equality of G1/S1 and G2/S2 showed that the fractionation was not as clean-cut as that obtained by Smith *et al.* (22) with more dilute solutions.

Successive Extraction at Increasing Temperature

Two series of extractions were made. These are designated Extraction E and Extraction F.

Extraction E.—Forty grams of dried, ground *Chondrus crispus* were stirred in 1400 cc. of aqueous sodium acetate at 30°C. for two hours. After centrifuging the clear supernatant liquid was dialyzed and freeze-dried. The residue was re-extracted at 60°C. for 15 min. After separation, a further extraction was made at 120°C. for 15 min. The final residue was discarded. As controls, portions of the 30°C. and 60°C. extracts were subjected to identical treatment at 120°C. Notation of the extracts and yields expressed as percentages of the total yield are given in Table I.

TABLE I

EXTRACTION E. SUCCESSIVE EXTRACTIONS OF IRISH MOSS AT 30°C., 60°C., AND 120°C.

	Temp., °C.	Time, min.	Yield, % of total	Notation of fraction
	30	120	25	E 30
	60	15	55	E 60
	120	15	20	E 120
Controls	30–120	15	—	EC 30–120
	60–120	15	—	EC 60–120

Extraction F.—Extraction F was similar to Extraction E except that temperatures were 60°C., 100°C., and 120°C. Portions of the 60°C. extract were subjected to the higher temperatures to provide controls. Notation and yields are given in Table II.

TABLE II

EXTRACTION F. SUCCESSIVE EXTRACTIONS OF IRISH MOSS AT 60°C., 100°C., AND 120°C.

	Temp., °C.	Time, min.	Yield, % of total	Notation of fraction
	60	60	77.5	F 60
	100	60	16.0	F 100
	120	25	4.2	F 120-A
	120	60	2.3	F 120-B
Controls	100	60	—	FC 100
	120	25	—	FC 120-A

ANALYTICAL PROCEDURES

Measurement of Concentration

The concentration, c, was based on the weight of purified material dried at 50°C. *in vacuo*. For sulphate content, gel strength, optical rotation, and refractive increment, concentrations were computed by direct weighing. For viscosity, sedimentation, and electrophoresis a refractometric determination was made with a Bellingham and Stanley refractometer. The mean value of dn/dc at 5461 Å for six different samples was 0.132 ($\pm$0.002) gm.$^{-1}$ cm.^{3}

Optical Rotation

The specific rotation was measured at a concentration of 0.3% in a 20 cm. tube at room temperature (23°C.) in a Rudolph polarimeter with a sodium lamp.

Sulphate

Sodium carrageenate was hydrolyzed by refluxing for three hours in 6 N hydrochloric acid. The solution was diluted and filtered. Sulphate was determined in the filtrate as barium sulphate. Measurements were done in duplicate and the mean deviation was $\pm$0.7%.

Ionic Mobility

Electrophoresis was observed at 25°C. in a Tiselius apparatus fitted with the Longsworth scanning device. The buffer was sodium acetate (pH = 5.5, I = 0.05) made up according to Green (7). The usual technique was modified as previously described (6). The mobility, U, was the mean for the rates of migration of ascending and descending boundaries.

Viscosity

The intrinsic viscosity, $[\eta]$, was determined with Ubbelohde capillary viscometers as previously described (6). A correction for degradation on storage was not necessary because it was found that the viscosity was constant over long periods for the sodium salt obtained from a solution at pH 8–9. Measurements were made at 25°C. in acetate buffers (pH = 5.5; I = 0.05).

Some variation of intrinsic viscosity with rate of shear has been observed in carrageenin of high molecular weight (14). The intrinsic viscosity observed must, therefore, be considered to obtain only for the mean rate of shear for solvent flow (1100 sec.$^{-1}$) in the viscometers used.

Gel Strength

Gel strength was measured with the apparatus shown in Fig. 2. A motor-driven cylindrical plunger (0.8 cm. in diameter) descended at 0.15 cm./sec. on the surface of the gel contained in a 5 ml. beaker as used in the Beckman

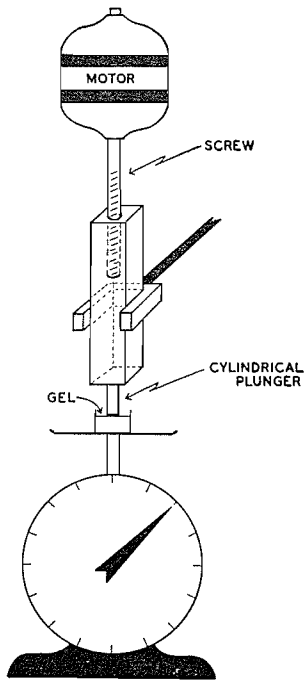

FIG. 2. Apparatus for measurement of gel strength.

pH meter. The beaker rested on a 500 gm. dietary spring balance. The breaking point was the maximum reading of the balance before penetration. This point was quite sharp and readily determined.

The solvent was a solution of potassium chloride ($I = 0.05$) in acetate buffer (pH = 5.5; $I = 0.05$). Gels were made by allowing a 2% solution of the polysaccharide to set overnight at a temperature of 20°C. Immediately before measurement the gel was inverted in the beaker, exposing a fresh surface. A stainless steel disk placed initially in the bottom of the beaker facilitated this operation. Measurements were done in triplicate and the mean deviation was $\pm 5\%$.

Sedimentation

Sedimentation was observed in an analytical Spinco ultracentrifuge at 42°C. to inhibit gelation. The rotor and cells were kept at 50°C. overnight. The filled cells and the rotor were then equilibrated at 50°C. for one hour. In the machine, the rotor was equilibrated under vacuum for one hour. At intervals during the run the temperature was taken with the fixed couple. The difference between the readings for the fixed and free couples was taken at

the end of the run. On an average the free couple reading exceeded the fixed couple reading by 0.6°C. By this method excellent temperature control was achieved. The range of fixed couple readings in any one run was 0.8°C. and the average temperature was 42.3 (±0.4)°C. for 66 runs. Thus, the range during any one run was small and the temperature for a series of runs was essentially constant.

As shown in Fig. 3, the graphs of $\log_{10} r$ vs. time were linear for all concentrations studied. Although the concentrated solutions were gel-like, no variation of the sedimentation constant, s, with time occurred as reported for thymus nucleoprotein (20).

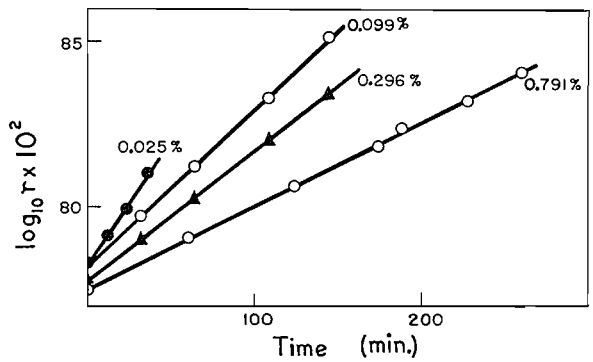

FIG. 3. Graphs of $\log_{10} r$ vs. time for S1.

Sedimentation constants were corrected (1) to water at 40°C. This correction implies that the molecular shape in the buffer is unaltered in water. With a polyelectrolyte such as sodium carrageenate this is not the case. Therefore the s°_{40} value gives the rate of sedimentation in water for a molecule having the same shape as sodium carrageenate in the buffer used.

Areas of the peaks were measured on enlargements with a planimeter. For the two components observed, dn/dc was assumed equal and relative concentrations were assumed to be proportional to areas. The relative area of the fast "shoulder" varied with the total concentration of carrageenin and was sometimes difficult to estimate. To permit comparison, all measurements of area were done on runs at the same concentration of carrageenin (0.007 gm. cm.$^{-3}$).

The variation of s°_{40} with c was studied for the fractions shown in Fig. 1 and Table II. As may be seen in Fig. 6, s°_{40} usually increased rapidly for low values of the concentration. Graphs of $\sqrt{s}$, $1/s$, and $\log_{10} s$ vs. c and sc vs. s failed to give a straight line. The graph of $\sqrt{(1/s)}$ vs. c was linear but the intercept was too near the origin to permit interpretation. The method of Jullander as used by Greenwood (8) was found to be applicable. On the same graph s°_{40} vs. c and $s^\circ_{40}\,\eta_{rel}$ vs. c are plotted. As shown in Fig. 4, the double extrapolation permits a reasonably unambiguous determination of $(s^\circ_{40})_{c=0}$. For these fractions the values of $(s^\circ_{40})_{c=0}$ were also obtained by the method of Newman, Loeb, and Conrad (16). Agreement between the two methods was ±1%.

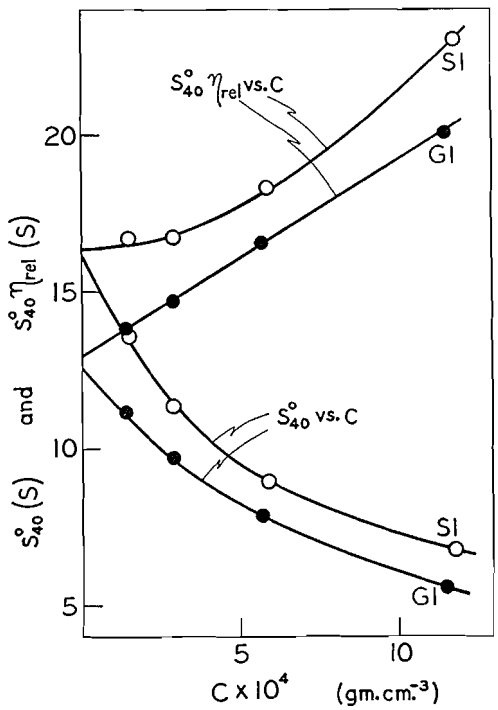

FIG. 4. Graphs of s°_{40} vs. c and $s^{\circ}_{40}\,\eta_{rel}$ vs. c for S1 and G1.

The molecular weight, M, was computed by the method of Mandelkern and Flory (12) from

$$[1] \qquad M = \left(\frac{(s^{\circ}_{40})_{c=0}\,[\eta]^{\frac{1}{3}}\,\eta_0 N}{2.5 \times 10^6(1-\bar{v}\rho)}\right)^{3/2}$$

where η_0 is the viscosity of the solvent, N is Avogadro's number, $\bar{v}$ is the partial specific volume of the solute, and ρ is the density of the solvent. The partial specific volume determined by Cook *et al.* was used (3).

Certain experimental factors limited the validity of the absolute values of M. The intrinsic viscosity was measured at 25°C. in an ionic strength of 0.05 whereas sedimentation was observed at 40°C. in an ionic strength of 0.2. Cook *et al.* (3) have noted that $[\eta]$ does not change markedly for such a range in ionic strength and temperature. Also, for one of the undegraded fractions studied, the decrease in $[\eta]$ for rates of shear from 100 sec.$^{-1}$ to 1000 sec.$^{-1}$ was 13%. However since $[\eta]$ occurs in Equation 1 only as a cube root such errors are small.

As noted by Smith *et al.* (22) a more serious discrepancy lies in the assumption of a random, uncharged coil implicit in the Mandelkern-Flory treatment. The carrageenin molecule is charged and although its shape in solution is not known with certainty, viscometric (13) and light scattering (4) results suggest

that it is rod-like. However, experimental conditions were identical for all fractions and therefore the relative values of M were considered to indicate the approximate changes in molecular weight from fraction to fraction.

RESULTS

Fractionation with Potassium Chloride

The electrophoretic and ultracentrifugal diagrams of the fractions (Fig. 1) are shown in Tables III and IV respectively. The corresponding values for the sulphate content, $[\eta]$, gel strength, M, and $[\alpha]_D$ are given in Table V. Included in Table IV are the relative concentrations of the minor component observed in sedimentation.

Successive Extraction at Increasing Temperature

The ultracentrifugal data for Extractions E and F (Tables I and II) are given respectively in Tables VI and VIII. The corresponding values of $[\alpha]_D$, gel strength, $[\eta]$, and sulphate content are given in Tables VII and IX.

TABLE III

ELECTROPHORESIS FOR THE FRACTIONS OBTAINED WITH POTASSIUM CHLORIDE SHOWN IN FIG. 1. IN THE DIAGRAMS, THE MEAN TIME AND DISTANCE OF MIGRATION OF THE ASCENDING BOUNDARIES WERE RESPECTIVELY 110 (±3) MIN. AND 63 (±3) MM.; THESE WERE 58 (±5) MIN. AND 28 (±2.5) MM. FOR THE DESCENDING BOUNDARIES

Fraction	Diagram	$U \times 10^4$, cm.^{2} sec.$^{-1}$ volt^{-1}
	ASCENDING → DESCENDING ←	
S1	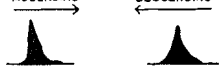	3.1
S2		3.0
Unfrac.		2.9
G1	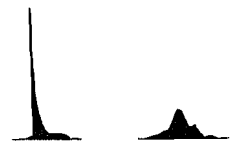	2.9
G2	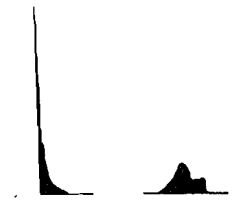	2.8

TABLE IV

SEDIMENTATION CONSTANTS AND DIAGRAMS FOR THE FRACTIONS OBTAINED WITH POTASSIUM CHLORIDE SHOWN IN FIG. 1. IN THE DIAGRAMS THE BAR ANGLE WAS 70° AND THE MEAN DISTANCE OF SEDIMENTATION WAS 6.9 (±0.8) MM.

Fraction	Diagram $c = 0.007$ gm. cm.$^{-3}$	Percentage of minor component	$(s^{\circ}_{40})_{c=0}$ S
S1	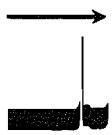	16	16
S2		10	13
Unfrac.		7	14
G1		4	13
G2	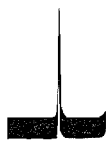	0	11

TABLE V

DATA FOR FRACTIONATION WITH POTASSIUM CHLORIDE SHOWN IN FIG. 1
ELECTROPHORESIS AND ULTRACENTRIFUGE DIAGRAMS ARE IN TABLES III AND IV RESPECTIVELY

Fraction	Sulphate, % SO_4	$[\eta] \times 10^{-2}$, gm.$^{-1}$ cm.^{3}	Gel strength, gm. cm.$^{-2}$	$[\alpha]_D$	$M \times 10^{-5}$
S1	24.1	15	<20	+29.0	14
S2	24.9	18	60	+41.3	11
Unfrac.	23.6	18	150	+48.5	12
G1	22.9	16	290	+50.7	10
G2	22.6	18	470	+60.3	8

TABLE VI

SEDIMENTATION CONSTANTS AND DIAGRAMS FOR SUCCESSIVE EXTRACTIONS AT INCREASING TEMPERATURE SHOWN IN TABLE I. IN THE DIAGRAMS THE BAR ANGLE WAS 70° AND THE MEAN DISTANCE OF SEDIMENTATION WAS 6.9 (±0.6) MM.

Extract	Diagram c = 0.007 gm. cm.$^{-3}$	Percentage of minor component
E 30		9
E 60	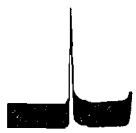	10
E 120		18
EC 30–120		0
EC 60–120		5

TABLE VII

DATA FOR SUCCESSIVE EXTRACTIONS AT INCREASING TEMPERATURE DESCRIBED IN TABLE I. ULTRACENTRIFUGE DIAGRAMS ARE SHOWN IN TABLE VI

Extract	Sulphate, % SO_4	$[\eta] \times 10^{-2}$, gm.$^{-1}$ cm.^{3}	Gel strength, gm. cm.$^{-2}$	$[\alpha]_D$
E 30	26.4	10	0	+45.7
E 60	25.9	14	240	+47.9
E 120	25.0	11	50	+32.4
EC 30–120	25.9	8	0	+45.1
EC 60–120	24.7	11	210	+46.2

TABLE VIII

SEDIMENTATION CONSTANTS AND DIAGRAMS FOR SUCCESSIVE EXTRACTIONS AT INCREASING TEMPERATURE SHOWN IN TABLE II. IN THE DIAGRAMS THE BAR ANGLE WAS 70° AND THE MEAN DISTANCE OF SEDIMENTATION WAS 7.0 (±0.5) MM.

Extract	Diagram c = 0.007 gm. cm.$^{-3}$	Percentage of minor component	$(s^{\circ}_{40})_{c=0}$ S
F 60		9	13
F 100		14	13
FC 100		8	12
F 120-A		6	10
FC 120-A	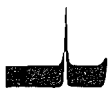	0	8
F 120-B		0	8

TABLE IX

DATA FOR SUCCESSIVE EXTRACTIONS AT INCREASING TEMPERATURE DESCRIBED IN TABLE II. ULTRACENTRIFUGE DIAGRAMS ARE SHOWN IN TABLE VIII

Extract	Sulphate, % SO_4	$[\eta] \times 10^{-2}$, gm.$^{-1}$ cm.^{3}	Gel strength, gm. cm.$^{-2}$	$[\alpha]_D$	$M \times 10^{-5}$
F 60	25.3	13	210	+50.4	10
F 100	22.8	11	50	+47.3	8
FC 100	25.4	12	210	+49.0	8
F 120-A	18.4	8	10	+40.3	5
FC 120-A	24.7	7	150	+49.1	3
F 120-B	—	5	—	+25.1	3

DISCUSSION

In families of polymeric substances there are two major categories of molecular differences. In the first the molecules of any single polymer may differ in chain length to give a polydispersity of molecular weight. In the second the difference is of molecular type. For example, sulphated polysaccharides may differ in type of linkage, sugar residues, branching, or degree of sulphation. In the present work we are concerned mainly with the second category, i.e. with components rather than polydispersity of molecular weight. Therefore

properties independent of molecular weight were most important in identifying components.

As mentioned previously, the fractionations were probably not sharp and it is likely that all the fractions were, to some extent, mixtures of components. However, marked differences were noted in some of the properties from fraction to fraction. It was therefore possible to infer that in some fractions a component with certain physical properties predominated. The results indicated three components. The differences in the various properties of these components are discussed in detail in the sections below.

Gel Strength

Large differences were noted in the gel strengths of different fractions compared with the relatively small decrease in the controls (EC 60–120 in Table VII and FC 100 and FC 120-A in Table IX). Further S1, with a molecular weight twice as great as the strongly gelling G2, had nearly zero gel strength. Thus it appeared that the gel strength depended more on structural factors than on molecular weight.

For successive extractions at increasing temperatures (Tables VII and IX) a pronounced maximum in gel strength was noted in the 60°C. extracts. This supports the early reports (15) of a non-gelling cold extract. The decrease in gel strength for re-extractions at 100–120°C. agrees with the findings of Hess and Siehrs (10). These results suggest that there are three components extractable at approximately 30°C., 60°C., and 100–120°C., the 60°C. extract having a strong gelling tendency.

The extract fractionated with potassium chloride was made at 100°C. and therefore would contain some of each of the three components. The fractionation would be expected to concentrate the single gelling component in the *gel* fractions while the *sol* fractions would contain the two non-gelling components. Provisionally the components extractable at 30°C., 60°C., and 100–120°C. will be called respectively Components A, B, and C.

Sedimentation

In nearly all the fractions (Tables IV, VI, and VIII) a varying proportion of a minor fast-moving component was noted. A similar component has been noted by Cook *et al.* (3) and Smith *et al.* (21, 22). Usually the minor component was more concentrated in extracts made at 100°–120°C. (Tables VI and VIII) and, as later discussed, F 120-B was composed largely of this material. Its proportion was not increased in the controls and thus it probably did not originate from heat treatment of the other components.

The minor component was probably the non-gelling Component C. This is supported by the increased concentration of the minor component in the sol fractions (Table IV). However, its proportion was small. Thus, the main component of the *sol* fractions would be A.

Differences in the three components are further illustrated by the concentration dependence of s°_{40}. As shown in Fig. 5, the graphs of s°_{40} vs. c for F 60 and F 120-A were coincident from $c = 0.002$ to $c = 0.01$ gm. cm.$^{-3}$ despite the marked decrease in $[\eta]$ and M on degradation. Below $c = 0.002$ gm. cm.$^{-3}$

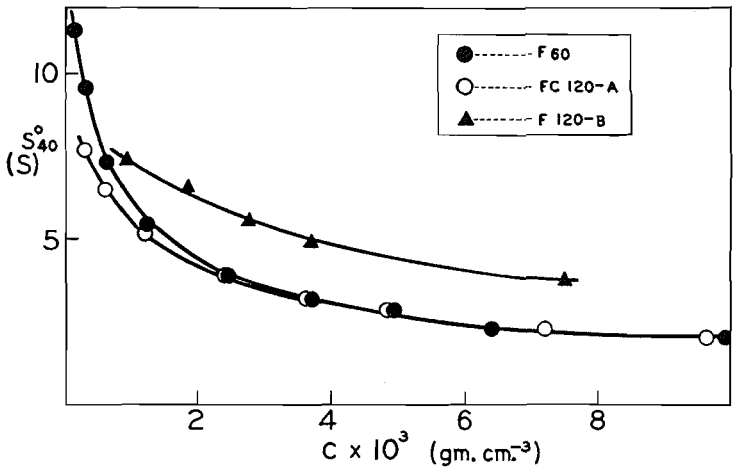

FIG. 5. Graphs of s°_{40} vs. c for F 60, FC 120-A, and F 120-B (Table IX).

the heavier molecule sedimented more quickly. However, F 120-B shows a faster sedimentation over most of the concentration range with a smaller dependence of s°_{40} on c. A similar though smaller effect was noted for F 120-A. These results suggest that F 120-A and F 120-B are composed largely of the quickly sedimenting Component C. The molecular weight of F 120-B is considerably less than that of F 60. The difference in sedimentation behavior must therefore be associated with a difference in shape or intermolecular interaction.

A lesser distinction in sedimentation is noted for G1 and the main component of S1, as shown in Fig. 6. The concentration dependence is similar but

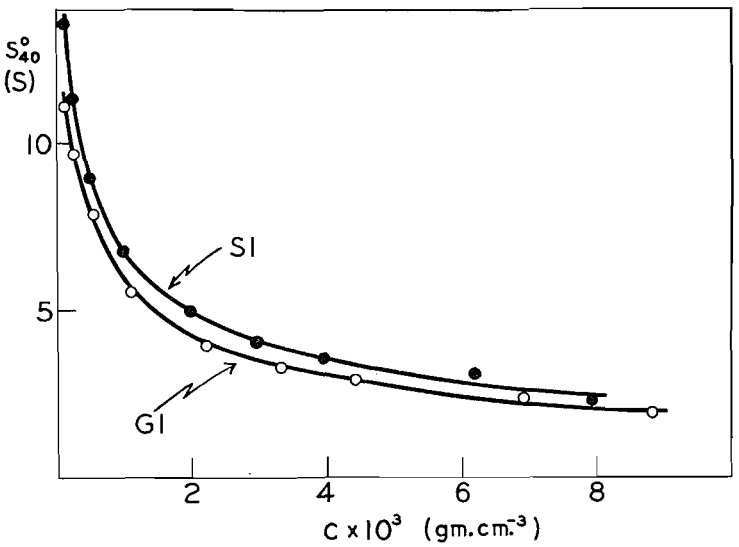

FIG. 6. Graphs of s°_{40} vs. c for S1 and G1 (Fig. 1).

s°_{40} for S1 is higher than that for G1. This small increase in s°_{40} occurred in all fractions rich in Component A. This might be expected since the molecular weights for the *sol* fractions (Table V) were greater than those for the *gel* fractions in agreement with the data of Smith *et al.* (21, 22). However, the coincidence of s°_{40} vs. c for F 60 and FC 120-A shows that a change in chain length alone does not alter s°_{40} at $c \geqslant 0.002$ gm. cm.$^{-3}$ Therefore, the slightly greater value of s°_{40} for Component A probably arises from a small structural variation in the polysaccharide rather than a difference in chain length.

Sulphate Content

The sulphate content was remarkably constant for most fractions at 23–26%. Also, the controls (Tables VII and IX) showed that a negligible loss in sulphate occurred on heating to 100–120°C. A decrease in sulphate content was noted for F 100 and F 120-A (Table IX). This suggests that a lower sulphate content was a property of Component C.

The sulphate contents of the *sol* fractions were higher than those of the *gel* fractions (Table V). This effect was smaller but in the same direction as that observed by Smith and Cook (21). The low sulphate content of Component C concentrated in the *sol* fractions could have masked the difference in sulphate between Components A and B.

Optical Rotation

On heating, the change in $[\alpha]_D$ for the controls was negligible (Tables VII and IX). But low values of $[\alpha]_D$ were observed in all fractions in which the quickly sedimenting component was concentrated (e.g. S1 in Table V or F 120-B in Table IX) indicating a low rotation for Component C.

The equality of $[\alpha]_D$ for E 30 and E 60 (Table VII) suggested that the rotations of Components A and B were essentially equal. The low rotation of the *sol* fractions could then be due to the increased concentration of Component C.

Electrophoresis

As observed by previous workers (3, 6) the electrophoretic diagrams (Table III) showed no clear indication of separate components. The peak asymmetry increased with gel strength. This effect was due to a non-classical distribution of concentration at the boundaries (described in detail elsewhere (5)) and could not definitely be associated with polydispersity. Because of the uncertainty in interpretation of the patterns, electrophoresis was not attempted on all the fractions.

The mobility of the *sol* fractions was slightly greater than that of the *gel* fractions. This trend was probably due to the smaller sulphate content (Table V) of the *gel* fractions.

Viscosity

The intrinsic viscosity of E 60 (Table VII) was greater than that of E 30 and a marked decrease in $[\eta]$ occurred for the extracts and controls of Extraction F at 100–120°C. (Table IX). As noted by Rose (18) this decrease is probably due to the degradation of the polysaccharide by the high tempera-

tures used. Because of the ease of degradation of carrageenin (6, 13) the intrinsic viscosity could not be used as a means of identifying components.

CONCLUSIONS

The results of the potassium chloride fractionation agree well with those of Smith *et al.* considering the different sources of material in the two investigations. In both, the *sol* fractions showed a higher molecular weight, sedimentation constant, and sulphate content and a lower specific rotation (Tables IV and V). The small divergences in detail from the results of these workers could be due to either (*a*) different degrees of degradation on preparation of the carrageenin or (*b*) different proportions of the two non-gelling components in the sol fractions.

The significant properties of the three components are summarized in Table X. Sulphate content and $[\alpha]_D$ were found to be independent of the

TABLE X

A SUMMARY OF THE PROPERTIES OF THE THREE COMPONENTS EXTRACTABLE FROM *Chondrus crispus*

Component	Temp. of extraction, °C.	Relative conc., % of extractable material*	Gelling tendency	$[\alpha]_D$	Sulphate content (%)
A	30	35	Nil	45–50	26
B	60	50	Strong	45–60	22–26
C	100–120	15	Weak	<30	<20

**The proportion of Component C was derived from the areas of the quickly sedimenting components in Extraction F. The remainder was assumed to consist entirely of Components A and B. An approximate A/B ratio was obtained by assuming the main component of S1 and S2 to be entirely A.*

decrease in molecular weight which occurred on extraction at higher temperatures. The gel strength showed some decrease on degradation but this was small compared with the large differences between the gelling and non-gelling extracts. These properties therefore pertain to the molecular *type* of the component. The figures given for the proportion of a component, $[\alpha]_D$, or the sulphate content obtain only for the sample of Irish moss examined although the trends noted may be general.

From the results it is clear that Components A and B made up the bulk of the extractable polysaccharide. The marked distinction between the two components lies in the ability of B to form a gel. The gelling tendency might be related to different degrees of branching in the molecules. An appreciable change in the concentration dependence of the sedimentation would then be expected. As shown in Fig. 6, the sedimentation behavior of the two components was similar. On the other hand, O'Neill (17) has recently discovered 24% of 3,6-anhydro-D-galactose in a *gel* fraction whereas the corresponding *sol* fraction contained considerably less (23). The gelling tendency may therefore be associated with this structural difference in the chain rather than a difference in shape due to branching.

The minor component, C, comprised only a small percentage of the extractable material although a greater proportion may be available with prolonged extraction. The low sulphate content suggests that it was a desulphated product of one of the major components. This could give rise to the small concentration dependence of s°_{40} due to the decrease in interaction (Fig. 5). However, the controls showed no loss in sulphate, which indicated that the material differed in this respect from Component A or B.

ACKNOWLEDGMENTS

The authors wish to thank Dr. A. N. O'Neill for his help in the measurements of optical rotation, and H. F. Roberts, F. G. Mason, and Miss M. C. Chepeswick for technical assistance.

REFERENCES

1. ALEXANDER, A. E. and JOHNSON, P. Colloid science. Oxford University Press, London. 1949.
2. BUCHANAN, J., PERCIVAL, E. E., and PERCIVAL, E. G. V. J. Chem. Soc. 51. 1943.
3. COOK, W. H., ROSE, R. C., and COLVIN, J. R. Biochim. et Biophys. Acta, 8: 595. 1952.
4. GORING, D. A. I. Can. J. Chem. 31: 1078. 1953.
5. GORING, D. A. I. Nature, 173: 734. 1954.
6. GORING, D. A. I. J. Colloid Sci. 9: 141. 1954.
7. GREEN, A. A. J. Am. Chem. Soc. 55: 2331. 1933.
8. GREENWOOD, C. T. Biochem. J. (London), 57: 151. 1954.
9. HAAS, P. and RUSSELL-WELLS, B. Biochem. J. (London), 23: 425. 1929.
10. HESS, M. P. and SIEHRS, A. E. U.S. Patent No. 2,462,398. 1949.
11. JOHNSTON, R. and PERCIVAL, E. G. V. J. Chem. Soc. 1994. 1950.
12. MANDELKERN, L. and FLORY, P. J. J. Chem. Phys. 20: 212. 1952.
13. MASSON, C. R. and CAINES, G. W. Can. J. Chem. 32: 51. 1954.
14. MASSON, C. R. and GORING, D. A. I. To be published.
15. MORI, T. Advances in Carbohydrate Chem. 8: 315. 1953.
16. NEWMAN, S., LOEB, L., and CONRAD, C. M. J. Polymer Sci. 10: 463. 1953.
17. O'NEILL, A. N. Abstr. of papers presented before the Div. of Carbohydrate Chem., Am. Chem. Soc. September, 1954.
18. ROSE, R. C. Can. J. Research, F, 28: 202. 1950.
19. RUSSELL-WELLS, B. Biochem. J. (London), 16: 578. 1922.
20. SHOOTER, K. V., DAVISON, P. F., and BUTLER, J. A. V. Biochim. et Biophys. Acta, 13: 192. 1954.
21. SMITH, D. B. and COOK, W. H. Arch. Biochem. and Biophys. 45: 233. 1953.
22. SMITH, D. B., COOK, W. H., and NEAL, J. L. Arch. Biochem. and Biophys. 53: 192. 1954.
23. SMITH, D. B., O'NEILL, A. N., PERLIN, A. S., and COOK, W. H. To be published.
24. YOUNG, E. G. and RICE, F. A. H. J. Biol. Chem. 164: 35. 1946.

THE PHOTO-OXIDATION OF AZOMETHANE[1]

By G. R. Hoey[2] and K. O. Kutschke

ABSTRACT

The photo-oxidation of azomethane has been studied at low oxygen pressures (0.02 to 1 mm.) in the temperature range *ca.* 25°C. to 161°C. The primary process in the normal photolysis of azomethane is essentially unaffected by the presence of oxygen. Carbon monoxide is probably a secondary product of the oxidation of methyl radicals. Carbon dioxide formation is quite small, and therefore neither methyl radicals nor $CH_3N{=}N{-}CH_2$ radicals are oxidized appreciably to carbon dioxide. Nitrous oxide, which is a major product of the oxidation, is most likely formed from the oxidation of $CH_3N{=}NCH_2$ radicals. The suggested mechanism of N_2O formation is:

$$CH_3N{=}N{-}CH_2+O_2 = CH_3N{=}NCH_2O_2$$
$$CH_3N{=}N{-}CH_2O_2 = CH_3+N_2O+H_2CO.$$

The reaction of methyl radicals with oxygen was found to proceed with a negligible activation energy and a steric factor of the order of 10^{-2}. Evidence for the occurrence of the reactions

$$2CH_3O_2 = 2CH_3O+O_2$$
$$2CH_3O = CH_3OH+H_2CO$$

at room temperature was obtained.

INTRODUCTION

The photolysis of azomethane has been studied extensively, and the mechanism appears to be well established. The main reactions involved in the photolysis are (15, 23):

$$CH_3N{=}NCH_3+h\nu = 2CH_3+N_2$$
$$CH_3+CH_3N{=}NCH_3 = CH_4+CH_3N{=}NCH_2$$
$$CH_3+CH_3N{=}NCH_3 = (CH_3)_2N{-}NCH_3$$
$$CH_3+CH_3 = C_2H_6$$
$$CH_3+CH_3N{=}NCH_2 = CH_3N{=}NC_2H_5$$
$$CH_3+(CH_3)_2N{-}NCH_3 = (CH_3)_2N{=}N(CH_3)_2.$$

The quantum yield of nitrogen formation is close to unity at the longer wavelengths, and independent of temperature. Since Φ_{N_2} is independent of the pressure of azomethane, and unaffected by the presence of carbon dioxide, the possibility of an excited molecule mechanism is unlikely (23). There is no evidence for a stable $CH_3N{=}N$ radical. Azomethane has been shown to be a convenient source of radicals for reactions of the type

$$CH_3+RH = CH_4+R$$

where RH is a hydrogen donor compound (1, 15). In view of these features of the photolysis, azomethane would be expected to be a convenient source of radicals for a study of the reaction of methyl radicals with oxygen.

Marcotte and Noyes (18) have investigated the photolysis of acetone in the presence of oxygen at low oxygen pressures and low light intensities. Their

[1]*Manuscript received November 18, 1954.*
Contribution from the Division of Pure Chemistry, National Research Council, Ottawa, Canada. Issued as N.R.C. No. 3514.
[2]*National Research Laboratories Postdoctorate Fellow 1952–1954.*

results indicated that the reaction between a methyl radical and oxygen, which they assumed to yield a formyl radical and a water molecule, proceeds with negligible activation energy and a low steric factor (*ca.* 10^{-4}). Christie (8), working in Noyes' laboratories, has since shown that, for experimental conditions similar to those of Marcotte and Noyes, methyl radical oxidation leads to formaldehyde and water with a further acetone molecule supplying the additional hydrogen. On the basis of Christie's results, the earlier scheme must be considered oversimplified; in particular the products of methyl radical interaction with oxygen postulated by Marcotte and Noyes seem rather doubtful.

Martin and Noyes (19) have extended the study to mixtures of mercury dimethyl and oxygen, and methyl iodide and oxygen. The relative amounts of CO and CO_2 were different than for acetone. Formaldehyde is a major product with methyl iodide – oxygen mixtures at room temperature (2, 19) and with acetone at temperatures above 120°C. (8, 14), whereas with mercury dimethyl with temperatures above 100°C., it does not seem to be a major product (19). It would be interesting to compare results obtained with azomethane and oxygen with those obtained by Noyes and co-workers using similar experimental conditions.

There has been no study reported in the literature on the thermal oxidation of azomethane. Scheer and Taylor (22) photolyzed azomethane in the presence of propane and oxygen. They observed a slow oxidation of propane in the temperature range 35° to 200°C., and cool flames at 250°C.

EXPERIMENTAL

PART I

The azomethane was prepared by Mr. R. Renaud of these laboratories (21). It was purified by a trap to modified Ward still (16) distillation, and the fraction collected between −78°C. and −110°C. was stored as a gas in a blackened flask behind a mercury cutoff. The oxygen was prepared by heating potassium permanganate and purified by passage through two traps at liquid nitrogen temperature. Commercial carbon dioxide was degassed at −196°C. Carbon monoxide was prepared by heating a $ZnO–CaCO_3$ mixture (27) and purified by passage through a trap at −196°C.

A Hanovia S-500 mercury arc was used as the light source. The beam, which was collimated by a quartz lens, completely filled the reaction cell. A Corning violet ultra filter No. 586, 6 mm. in thickness, was used in all the experiments. This filter limited the incident intensity mainly to the 3340 Å and 3660 Å wavelengths. The relative extinction coefficients of these wavelengths are such that the absorbed light intensity is effectively the 3660 Å wavelength (15). The incident light intensity was varied by the use of neutral density filters.

The quartz cell was 10 cm. long and 5 cm. in diameter with a volume of 180 cc. The cell was surrounded by an aluminum block furnace, and the temperature was controlled manually to ±1°C. The total volume of the reaction system, including reaction cell, U-tube manometer, stirrer, and McLeod gauge, was 400 cc.

Oxygen pressures as low as 0.02 mm. were used in this work. An oxygen consumption of at least 0.15 mm. was necessary for analysis of the products. Since constant oxygen pressures were desired at pressures less than 0.15 mm., small oxygen doses (0.003 mm.) were added during the run as frequently as necessary to maintain constancy of pressure. The number of doses required was determined in trial runs.

The run was interrupted at regular intervals (two to five minutes), at which time a premeasured oxygen dose was pumped into the reaction mixture through an iron, glass-enclosed float, and sufficient time allowed for mixing of the gases. The rate of oxygen disappearance was found to depend on the temperature and on the oxygen pressure. To compensate for this, the number of doses per run, and consequently the exposure time per dose (rather than the size of the oxygen dose), was varied. Mixing of the gases was effected by a glass propeller type stirrer with a glass-enclosed copper core at the bottom; the stirrer was driven by an induction motor. At oxygen pressures greater than 0.15 mm., 0.02 mm. doses were added during the exposure without interrupting the run.

Gas analyses were carried out for N_2, CH_4, CO, O_2, CO_2, and N_2O. After each run the reaction mixture was passed through a modified Ward still at -196°C. The non-condensables, N_2, CH_4, CO, and O_2, were analyzed by means of a Cu–CuO furnace at a temperature of about 230°C. The oxygen formed CuO. The CO was oxidized to CO_2 and was frozen out at a cold finger. The remainder, N_2 and CH_4, was collected and analyzed for N_2 and CH_4 mass spectrometrically. The CO_2 and the N_2–CH_4 mixture were measured directly, and the oxygen was determined by difference. The CO_2 and N_2O were distilled from the Ward still at -160°C., and were collected for mass spectrometric analysis. Ethane was not detected in any of the experiments in which oxygen was present.

Azomethane was used as an actinometer. A value of unity (23) for the quantum yield of nitrogen formation in the absence of oxygen was used for the temperature range 25° to 161°C. The data in the literature are in accord (4, 7, 15) with such a value although the individual values are quite often less than unity and nearer 0.9. If, in fact, $\Phi_{N_2} < 1$ in the absence of oxygen, the values of the quantum yields quoted here are too large by about 10%.

Formaldehyde was not detectable at the Ward still or by mass spectrometric analysis. This, however, is not conclusive evidence that formaldehyde is not a major product of the oxidation as the formaldehyde may have polymerized. To check this point, an amount of formaldehyde roughly comparable to that expected in the experiments described in Part II was introduced into the reaction system in the presence of azomethane. Polymerization of the formaldehyde evidently occurred as formaldehyde was not detected by the two methods mentioned above. Analysis of formaldehyde in the presence of azomethane in aqueous media was not accomplished since an acid catalyzed hydrolysis forms formaldehyde and methyl hydrazine from azomethane (28). Methods which were unsuccessful owing to this interference by azomethane were Lebbin's resorcinol test, Schiff's test, and the polarographic method (25). Thus, it

cannot be stated whether or not formaldehyde is a major product of the reaction.

The products remaining after distilling off the azomethane at −90°C. were analyzed mass spectrometrically. Water and methanol were identified positively and formed most of the fraction.

PART II

Experiments of long duration were performed at room temperature in order to collect sufficient products for chemical analysis. Large oxygen pressures were used and oxygen was not added during the run. The azomethane pressure was maintained constant during the run at 6.6 mm. by circulating the gases through two traps in the reaction system held at the temperature of dry ice.

After the run, the gases were passed to the Ward still. The non-condensables and CO_2 were analyzed as described in Part I. N_2O was not detected by mass spectrometric analysis. The azomethane was separated from the Ward still at −90°C.; no product was detected between these fractions. This fraction was shown to be azomethane with trace quantities of methanol and water by mass spectrometric analysis. These results were verified by the infrared absorption of the fraction. The remainder, which will be designated as the "liquid products", was separated from the Ward still at room temperature.

The liquid products were analyzed by the following methods. Mass spectrometric analysis showed the presence of methanol and water only. The methanol was analyzed by the method of Elving and Warshowsky (10) and by infrared analysis. The two methods agreed to within 20%. The acid, which was shown to be formic acid by its infrared absorption, was titrated directly using phenolphthalein as the indicator. Peroxides were determined by the method of Nozaki (20).

The liquid products were also placed in contact with metallic sodium. The hydrogen given off was a measure of the total active hydrogen present (amount of $H_2 = \frac{1}{2} \times$ amount of active hydrogen). The quantum yield of water formation was assumed to be

$$\Phi_{H_2O} = (\Phi_{\text{active hydrogen}}) - (\Phi_{CH_3OH} + \Phi_{HCOOH} + \Phi_{\text{peroxides}}).$$

RESULTS AND DISCUSSION

The lack of variation of Φ_{N_2} with the experimental conditions of temperature and oxygen pressure (Fig. 1) and of azomethane pressure (Table I) strongly suggests that nitrogen is formed solely in a primary process. Since ethane was not detected at any temperature at an oxygen pressure as low 0.02 mm., the possibility of a direct molecular rearrangement into ethane and nitrogen (6) may be discounted. This is in agreement with the conclusion reached by Davis, Jahn, and Burton (9) who observed complete suppression of hydrocarbon products and no inhibition of the nitrogen yield when the photolysis was carried out in the presence of nitric oxide (10 mm.). On the basis of this evidence, the primary process is taken as [1], proceeding with a quantum efficiency close to unity in the presence of oxygen.

$$CH_3N_2CH_3 + h\nu \rightarrow 2CH_3 + N_2. \qquad [1]$$

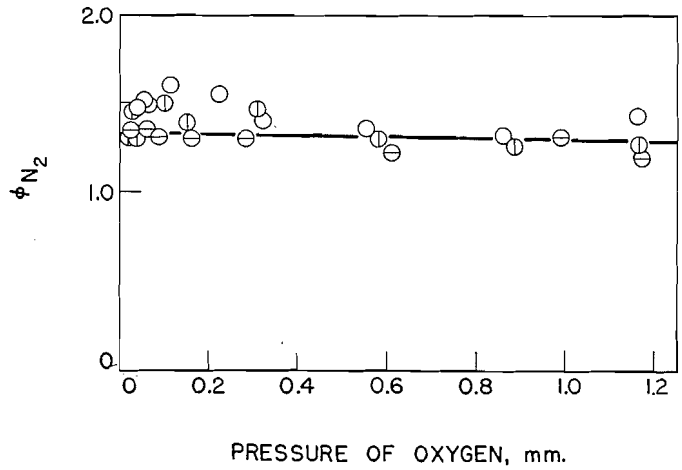

FIG. 1. Dependence of Φ_{N_2} on oxygen pressure:
$I_a = 5 \times 10^{11}$ quanta/cc./sec.; pressure of azomethane, 101 mm.; ○, 161°C.; ◑, 123°C.; ⊖, *ca.* 25°C.

TABLE I

EFFECT OF AZOMETHANE PRESSURE ON THE REACTION

Pressure (mm.) Azomethane	Total	Φ_{N_2}	Φ_{CO}	Φ_{N_2O}	$-\Phi_{O_2}$
102	103	1.25	0.22	0.51	3.0
6.6	100[a]	1.21	0.36	—	2.2
6.6	100[b]	—	—	0.10	—
6.6	8	1.11	0.31	0.06	2.0

Pressure of oxygen = 0.9±0.1 mm.; temp. = 123°C.; $I_a = 10^{12}$ quanta/cc./sec.
[a]*CO_2 added.*
[b]*CO added.*

The photo-oxidation, under conditions such that methane is found, is postulated to proceed in part through the following steps:

$$CH_3 + A \rightarrow CH_4 + CH_3N_2CH_2 \quad [2]$$
$$CH_3 + A \rightarrow CH_3A \quad [3]$$
$$CH_3 + O_2 \rightarrow CH_3O_2 \quad [4]$$
$$CH_3A + O_2 \rightarrow CH_3AO_2 \quad [5]$$
$$CH_3N_2CH_2 + O_2 \rightarrow CH_3N_2CH_2O_2. \quad [6]$$

Reaction [2] has been well substantiated (1, 15, 23) and reaction [3] has been shown to proceed at a somewhat greater rate (15). Reaction [5] has been included to account for $-\Phi_{O_2} \geqslant 2$ at low oxygen pressure Fig. 2; i.e. every methyl radical must, directly or indirectly, lead to the consumption of one molecule of oxygen. The sole fate of methyl radicals produced in the primary process must be reaction with oxygen when Φ_{CH_4} is negligible. This condition is met at all oxygen pressures studied at room temperature, and at a progressively higher oxygen pressure as the temperature is increased (Fig. 3). A similar phenomenon is observed in the photo-oxidation of acetone (8, 14, 18).

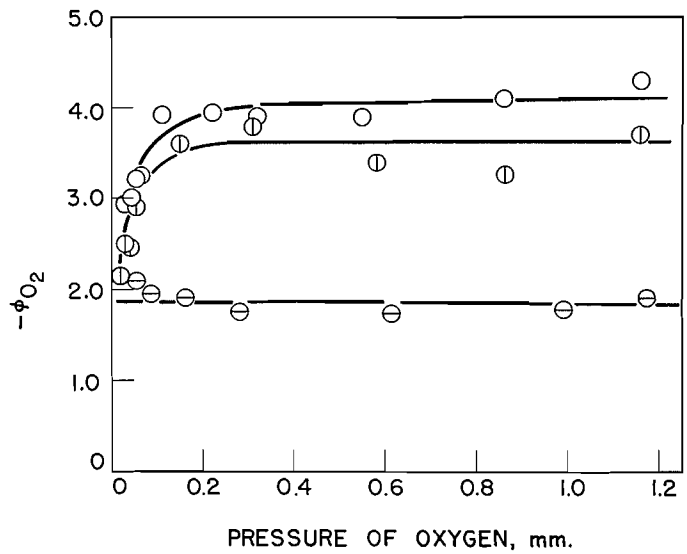

FIG. 2. Dependence of $-\Phi_{O_2}$ on oxygen pressure:
$I_a = 5 \times 10^{11}$ quanta/cc./sec.; pressure of azomethane, 101 mm.; ○, 161°C.; ⊕, 123°C.; ⊖, *ca.* 25°C.

Nitrous oxide is a major product at the higher temperatures employed. An upper limit to Φ_{N_2O} is attained at oxygen pressures such that Φ_{CH_4} is negligible (Figs. 3 and 4); the value of this limit is temperature dependent (Fig. 3). At

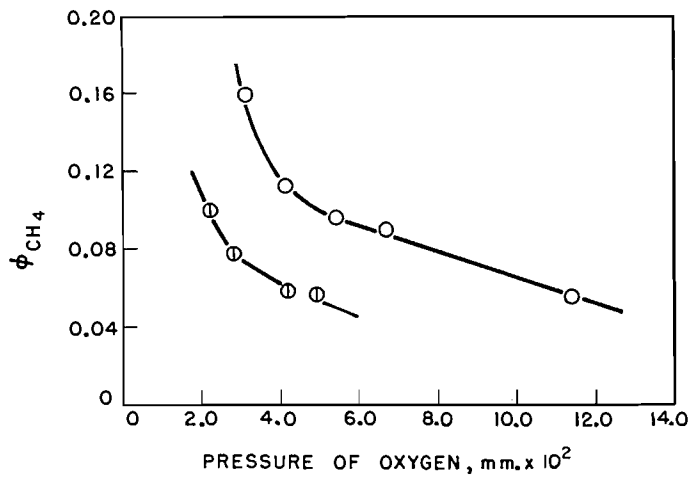

FIG. 3. Dependence of Φ_{CH_4} on oxygen pressure:
$I_a = 5 \times 10^{11}$ quanta/cc./sec.; pressure of azomethane, 101 mm.; ○, 161°C.; ⊕, 123°C.

oxygen pressures such that this limit is attained, a radical resulting from the oxidation of a methyl radical must initiate a sequence of reactions which eventually produces nitrous oxide. A plausible scheme is

$$CH_3O_2 \rightarrow R + ? \quad [7]$$
$$R + CH_3N_2CH_3 \rightarrow RH + CH_2N_2CH_3 \quad [8]$$
$$CH_3N_2CH_2 + O_2 \rightarrow CH_3N_2CH_2O_2 \quad [6]$$
$$CH_3N_2CH_2O_2 \rightarrow CH_3 + N_2O + H_2CO \quad [9]$$
$$R \rightarrow \text{no } N_2O \quad [10]$$

where R is some oxygenated radical. Reaction [10], a chain termination not involving azomethane or oxygen, is included to account for the dependence of Φ_{N_2O} on the concentration of azomethane (Table I). Insufficient data are available to determine whether [10] is of the first or second order in radical concentration. Since [8] and possibly [9] will probably require an activation energy, the temperature dependence of Φ_{N_2O} is qualitatively explained.

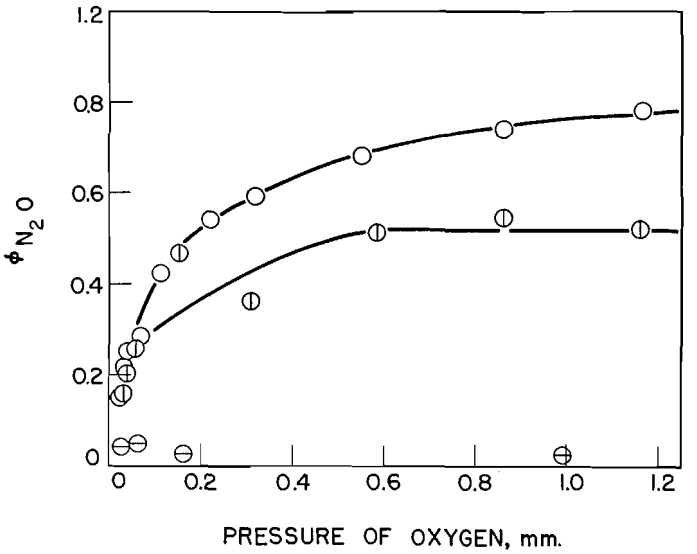

FIG. 4. Dependence of Φ_{N_2O} on oxygen pressure:
$I_a = 5 \times 10^{11}$ quanta/cc./sec.; pressure of azomethane, 101 mm.; ○, 161°C.; ◑, 123°C.; ⊖, *ca.* 25°C.

Although it has been assumed that nitrous oxide is produced in a chain propagating reaction, [9], which may occur in steps, the over-all yield of this product is low, $\Phi_{N_2O} < 1$. Unless fates other than [6] and [9] are postulated for $CH_3N_2CH_2$ and $CH_3N_2CH_2O_2$ respectively, it seems necessary to employ efficient chain termination reactions for the radicals R. Methyl radicals disappear rapidly in a system containing azomethane, presumably by addition to the nitrogen–nitrogen double bond to form tetramethyl hydrazine (15). It is, therefore, conceivable that azomethane acts as a sink for oxygenated radicals in a two stage addition process; the over-all reaction may be written

$$2R + CH_3N_2CH_3 \rightarrow CH_3NRNRCH_3. \quad [11]$$

The correct general form of $-\Phi_{O_2}$, Φ_{CH_4}, and Φ_{N_2O} as a function of (O_2) and of $(CH_3N_2CH_3)$ is obtained from a steady state treatment of the mechanism.

Under conditions such that Φ_{CH_4} is negligible, i.e. Φ_{N_2O} and $-\Phi_{O_2}$ have attained their limiting values, the mechanisms predict that

$$-\Phi_{O_2} = 2+2\Phi_{N_2O}.$$

Substitution of the observed values of Φ_{N_2O} leads, at 123°C., to $-\Phi_{O_2} = 3.1$ (experimental = 3.6), and at 161°C. to $-\Phi_{O_2} = 3.6$ (experimental = 4.0). The proposed mechanism, though obviously oversimplified, is in near accord with the data.

The relative rates of [2] and [4] may be determined from a relationship between Φ_{CH_4} and Φ_{N_2O} derived from the following assumptions: (i) two methyl radicals are produced in the primary process; (ii) methyl radicals are consumed only by [2], [3], and [4]; (iii) each methyl radical formed in other than the primary process is accompanied by the production of one molecule of nitrous oxide.

$$(2+\Phi_{N_2O})/\Phi_{CH_4} = (k_2+k_3)/k_2+k_4(O_2)/k_2(A)$$

In Fig. 6 a linear relation is shown between $(2+\Phi_{N_2O})/\Phi_{CH_4}$ and (O_2) at constant (A) for two temperatures. The slopes of these lines lead to $k_4/k_2 = 6.8 \times 10^4$ at 123°C. and 3.3×10^4 at 161°C. Extrapolation to $(O_2) = 0$ yields $(k_2+k_3)/k_2 = 5.0$ at 123° and 6.5 at 161°C.; the values obtained from the data of Jones and Steacie (15) for these intercepts are 6.2 and 6.0 respectively. This degree of agreement is considered adequate. The Arrhenius activation energy difference, E_2-E_4, is equal to 6.9 kcal./mole and the collision theory steric factor ratio, p_4/p_2, is 17; $E_2 - \frac{1}{2}E_E$ equals 7.3 kcal./mole and $p_2/p_E^{\frac{1}{2}}$ equals 4×10^{-4} (1), where the subscript E refers to the combination of two methyl radicals producing ethane, the latter proceeding with negligible activation energy and approximately unit collision efficiency (11). Hence $E_4 \backsim 0.4$ kcal./mole and $p_4 \backsim 7 \times 10^{-3}$.

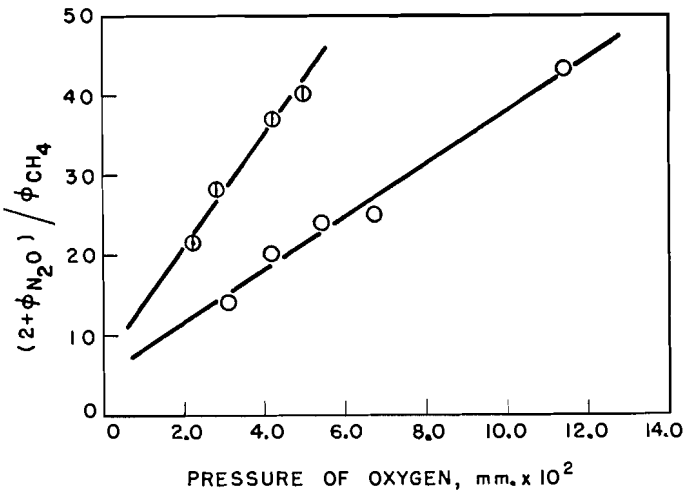

FIG. 6. Dependence of $(2+\Phi_{N_2O})/\Phi_{CH_4}$ on oxygen pressure:
$I_a = 5 \times 10^{11}$ quanta/cc./sec.; pressure of azomethane, 101 mm.; ○, 161°C.; ◑, 123°C.

Using acetone photolysis as a source of methyl radicals, Marcotte and Noyes (18) obtained $E_4 \backsim 0$ and $p_4 \backsim 10^{-1}$ by a method essentially similar to that employed here. The general agreement of the present determination with the earlier work in which more extensive data were reported at four temperatures is taken as support for the over-all reaction [9]. From an investigation of the photo-oxidation of methyl iodide, Blaedel, Ogg, and Leighton (5) estimated $E_4 \sim 3$ kcal./mole, while van Tiggelen (24) obtained an approximate value $E_4 \sim 1.5$ kcal./mole in a study of the acetone photosensitized oxidation of methane. Thus, there is general agreement that reaction [4] is rapid and that both the activation energy and steric factor are low.

The identity of the primary products of the oxidation of methyl radicals is still a matter of conjecture, however; thus [7] has been explicitly written as

$$CH_3O_2 \rightarrow HCO + H_2O \qquad [12]$$
$$\rightarrow HCHO + OH. \qquad [13]$$

Other reactions of peroxymethyl radicals which have been suggested are (12, 17, 26)

$$CH_3O_2 + R'H \rightarrow CH_3O_2H + R' \qquad [14]$$
$$CH_3O_2 + CH_3O_2 \rightarrow 2CH_3O + O_2. \qquad [15]$$

Reaction [12] is now considered unlikely (8, 14, 19) and reaction [15] should not be of great importance in the low concentration range under discussion at present. The positive identification of methanol and water among the liquid products suggests that R radicals may be identified tentatively with CH_3O_2, CH_3O, and OH. Further speculation regarding the detailed reactions of these radicals are, on the basis of the present data, unwarranted.

Small quantities of carbon monoxide and dioxide are found, the latter in almost insignificant amounts and apparently independent of conditions ($\Phi_{CO_2} < 0.1$). The carbon monoxide yield roughly parallels that of nitrous oxide as a function of oxygen pressure (Figs. 4 and 5) but is smaller by a factor

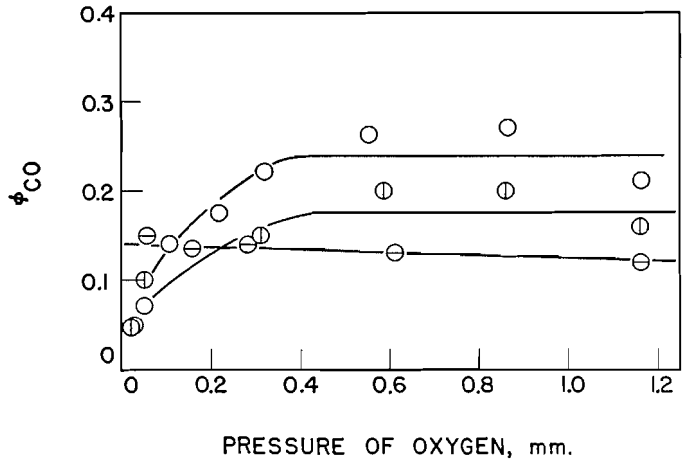

FIG. 5. Dependence of Φ_{CO} on oxygen pressure:
$I_a = 5 \times 10^{11}$ quanta/cc./sec.; pressure of azomethane, 101 mm.; ○, 161°C.; ◑, 123°C.; ⊖, *ca.* 25°C.

of approximately two. The variation of Φ_{CO} as azomethane concentration is decreased by a factor of 15 with a constant rate of production of radicals is small and in the opposite direction to that of Φ_{N_2O} in the same circumstances (Table I). This suggests that carbon monoxide arises from an oxidation of methyl radicals and that the intermediate stages do not involve the substrate. The variability (18, 19) in the CO/CO_2 ratio when various methyl radical sources are used suggests that both these products arise in an indirect manner (14). This is supported by Hentz (13) who observed an induction period for the production of carbon monoxide in the acetone–oxygen system. It might be pointed out that the low yield of carbon dioxide observed here is compensated by the production of nitrous oxide. Indeed, if the acetonyl radical were to react with oxygen in the manner postulated here for $CH_3N_2CH_2$ (i.e. [6] and [9]), the product would be carbon dioxide.

The experiments described in Part II of the Experimental section are reported in Table II as averages taken over a number of experiments. The salient facts are: (i) Φ_{N_2} and $-\Phi_A$ do not differ significantly from unity; (ii) $-\Phi_{O_2}$ lies

TABLE II

PRODUCTS OF AZOMETHANE PHOTO-OXIDATION

	Φ		Φ
N_2	1.1	"Liquid products"	1.1
CO	0.06	HCOOH	0.1
CO_2	0.09	"Peroxides"	0.02
CH_3OH	0.7[a]	O_2 disappearance	1.3
H_2O	0.1–0.2	Azo disappearance[b]	1.1

Partial pressure of azomethane, 6.6 mm.; average pressure of oxygen, 10 mm.; room temperature; $I_a \sim 10^{14}$ quanta/cc./sec.; exposure time, 48 hr.; volume of reaction system, 420 cc.

[a]*Average of the two analytical methods used.*

[b]*About one-half (9 mm.) of the azomethane originally present was reacted.*

between one and two; (iii) methanol, water, and formic acid are major products; (iv) a material balance is not even approximately attained if one nitrogen molecule is accompanied by the production of two single carbon radicals; (v) the oxygen concentration and the absorbed intensity, and hence the radical concentration, were high, while the temperature and azomethane concentration were low.

As pointed out previously, the experimental arrangement was such that formaldehyde probably could not have been detected as a product. If the total apparent decrement in the carbon balance is assumed to be formaldehyde, $\Phi_{H_2CO} \sim 1$. It is not readily apparent how an explanation of the results can be advanced if Φ_{H_2CO} is not at least as great as Φ_{CH_3OH} since the nearly unit yield of azomethane disappearance renders abstraction reactions unimportant. If this assumption is made, however, the mechanism might be expected to reduce to the radical–radical interactions suggested by Vaughan *et al.* (3), viz. [1], [4], and [15] followed by

$$2CH_3O \rightarrow CH_3OH + H_2CO. \qquad [16]$$

This is in qualitative accord with the data if it is noted that small amounts of oxygen will be required to oxidize some of the products of [16] to the water, acid, and carbon oxides found.

ACKNOWLEDGMENTS

The authors are indebted to Dr. E. W. R. Steacie for advice and encouragement throughout this work. They also wish to thank Dr. L. C. Leitch and Mr. R. Renaud for azomethane samples, Miss F. Gauthier and Miss M. J. Fuller for the mass spectrometric analyses, and Mr. R. Lauzon for the infrared absorption measurements.

REFERENCES

1. Ausloos, P. and Steacie, E. W. R. Can. J. Chem. 32: 593. 1954.
2. Bates, J. R. and Spence, R. J. Am. Chem. Soc. 53: 1689. 1931.
3. Bell, E. R., Raley, J. H., Rust, F. F., Seubold, F. H., and Vaughan, W. E. Discussions Faraday Soc. 10: 242. 1950.
4. Blacet, F. E. and Taurog, A. J. Am. Chem. Soc. 61: 3024. 1939.
5. Blaedel, W., Ogg, R. A., and Leighton, P. A. J. Am. Chem. Soc. 64: 2499, 2500. 1942.
6. Burton, M., Davis, T. W., and Taylor, H. A. J. Am. Chem. Soc. 59: 1038. 1937.
7. Cannon, C. V. and Rice, O. K. J. Am. Chem. Soc. 63: 2900. 1941.
8. Christie, M. I. J. Am. Chem. Soc. 76: 1979. 1954.
9. Davis, T. W., Jahn, F. P., and Burton, M. J. Am. Chem. Soc. 60: 10. 1938.
10. Elving, P. J. and Warshowsky, B. Ind. Eng. Chem., Anal. Ed. 19: 1006. 1947.
11. Gomer, R. and Kistiakowsky, G. B. J. Chem. Phys. 19: 85. 1951.
12. Gray, J. A. J. Chem. Soc. 3150. 1952.
13. Hentz, R. R. J. Am. Chem. Soc. 75: 5810. 1953.
14. Hoare, D. E. Trans. Faraday Soc. 49: 1292. 1953.
15. Jones, M. H. and Steacie, E. W. R. J. Chem. Phys. 21: 1018. 1953.
16. LeRoy, D. J. Can. J. Chem. 28: 492. 1950.
17. Lewis, B. and von Elbe, G. Combustion, flames and explosions in gases. Academic Press, Inc., New York. 1951.
18. Marcotte, F. B. and Noyes, W. A., Jr. Discussions Faraday Soc. 10: 236. 1951. J. Am. Chem. Soc. 74: 783. 1952.
19. Martin, R. B. and Noyes, W. A., Jr. J. Am. Chem. Soc. 75: 4183. 1953.
20. Nozaki, K. Ind. Eng. Chem., Anal. Ed. 18: 583. 1946.
21. Renaud, R. and Leitch, L. C. Can. J. Chem. 32: 545. 1954.
22. Scheer, M. D. and Taylor, H. A. J. Chem. Phys. 20: 653. 1952.
23. Steacie, E. W. R. Atomic and free radical processes. 2nd ed. Reinhold Publishing Corporation, New York. 1954. p. 376.
24. van Tiggelen, A. Ann. mines Belg. 43: 117. 1942.
25. Walker, J. F. Formaldehyde. 2nd ed. Reinhold Publishing Corporation, New York. 1953.
26. Walsh, A. D. Trans. Faraday Soc. 43: 297. 1947.
27. Weinhouse, S. J. Am. Chem. Soc. 20: 442. 1948.
28. Whitmore, F. C. Organic chemistry. 2nd ed. D. Van Nostrand Company, Inc., New York. 1951.

THE PREPARATION OF DICYANODIACETYLENE

By F. J. Brockman

ABSTRACT

The preparation of dicyanodiacetylene as reported by Moureu and Bongrand has been investigated more fully and a procedure developed whereby yields as high as 36% have been obtained.

INTRODUCTION

In 1920 Moureu and Bongrand (1) reported what was undoubtedly the first synthesis of dicyanodiacetylene. By the action of aqueous potassium ferricyanide on the cuprous derivative of propriolonitrile (cyanoacetylene) they obtained trace quantities of a solid with characteristic properties. This preparation has been investigated more fully and a procedure developed whereby yields as high as 36% have been obtained. The product was characterized as dicyanodiacetylene (C_6N_2) by elementary analysis and molecular weight determinations and by conversion on hydrogenation to hexamethylenediamine. Although the yield of hexamethylenediamine (isolated as the picrate) was low (8.5%), this low yield appeared to be due to decomposition of the dicyanodiacetylene in the presence of the hydrogenation catalyst (Adams' platinum oxide).

Dicyanodiacetylene is an unstable, volatile, white solid with a marked irritating odor. By sublimation in a stream of carbon dioxide gas it may be obtained as fine, elongated crystals melting at 64.5–65.5°C. X-ray diffraction lines obtained from a single crystal rotation pattern are listed in Table I, together with their estimated relative intensities.

TABLE I

X-RAY* DIFFRACTION PATTERN DATA ON DICYANODIACETYLENE

Spacing, d (Å)	Intensity, I/I_1	Spacing, d (Å)	Intensity, I/I_1
5.10	30	2.62	10
4.09	60	2.57	10
3.98	5	2.39	20
3.52	5	2.35	10
3.43	30	2.16	10
3.24	100	2.09	20
3.19	80	2.05	10
3.10	80	1.88	10
3.05	80	1.84	20
2.88	20	1.76	10
2.83	20	1.58	10

*Wave length 1.5418 Å.

Attention should be drawn to the unusual composition and structure of dicyanodiacetylene. Being composed solely of carbon and nitrogen it can be

[1]Manuscript received September 27, 1954.
Contribution from the Central Research Laboratory, Canadian Industries (1954) Ltd., McMasterville, Quebec.

considered as a subnitride of carbon. It is also one of the longest, completely linear molecules described and should be a very interesting compound for structural study.

EXPERIMENTAL

Preparation of Cuprous Propriolonitrile

Cuprous chloride (9.9 gm., 0.10 mole) was dissolved in 10 cc. of 14% aqueous ammonia under an atmosphere of nitrogen and diluted with 900 ml. of water. To this solution at approximately 25°C. was added with agitation propriolonitrile (1) (1.5 gm., 0.029 mole) over a three minute period. After being stirred for an additional five minutes the olive green precipitate was separated by decantation and filtration and washed twice with 30 ml. of 1.5% aqueous ammonia. The product after drying under vacuum, first over sulphuric acid and finally over phosphorus pentoxide, weighed 3.7 gm. (110% yield on propriolonitrile). Cuprous propriolonitrile is subject to detonation by heat and shock.

Preparation of Dicyanodiacetylene

A solution of 7.8 gm. (0.0234 mole) potassium ferricyanide in 20 ml. of water was added over a five minute period to a stirred suspension of cuprous propriolonitrile (1.5 gm., 0.012 mole) in 25 ml. of water and 25 ml. of benzene. The temperature of the reaction mixture was maintained at 5 to 6°C. throughout. Agitation was continued for two minutes after addition was complete and the reaction mixture then centrifuged, the centrifuge bottles and cups being chilled before use in an ice-water bath. After centrifuging for five minutes at 2000 r.p.m., the benzene layer (17 ml.) was removed. The lower aqueous layer and a heavy sludge-like precipitate were again cooled, extracted with a further 20 ml. of benzene, and the centrifuging procedure repeated. Owing to the formation of a fine black precipitate at this stage, only 10 ml. of benzene extract could be separated by this means. By filtration of the residual mixture through filter-aid, a further 15 ml. of extract was obtained. The combined benzene extracts were dried over sodium sulphate and most of the benzene removed by fractionation at atmospheric pressure through a short (8 cm.) Vigreux column. The resulting dark brown concentrate (2 ml.) was taken to dryness in a slow stream of carbon dioxide, the condensate being collected in a small ice-cooled receiver. After removal of all the benzene, dicyanodiacetylene was sublimed from the residue by continuing the volatization procedure. The sublimate was further purified by resublimation in a stream of carbon dioxide. The white crystalline product thus obtained, m.p. 64.5–65.5°C., weighed 0.180 gm. (30.5% yield). Calc. for C_6N_2: C, 72.0; N, 28.0; mol. wt., 100. Found: C, 72.15; N, 27.42; mol. wt. (depression of f.p. of benzene) 97. An additional 0.035 gm. of product, m.p. 64–64.5°C., was obtained by distilling most of the solvent from the benzene distillates using a column packed with glass spirals and working up the concentrate as described above. The total yield isolated was 0.215 gm. (36% yield on cuprous propriolonitrile).

Dicyanodiacetylene gradually turns brown at room temperature, but may be stored at 0°C. This discoloration is more rapid in the presence of water or

in ether solution and occurs at once in alcohol. Petroleum ether, b.p. 28–35°C., may be used as an extraction solvent in place of benzene. Ether is unsatisfactory owing to the instability of dicyanodiacetylene in this medium and chloroform is not recommended since it is difficult to separate from the by-product sludge.

Hydrogenation of Dicyanodiacetylene to Hexamethylenediamine

The hydrogenation was carried out in a small high pressure hydrogenation unit equipped with a 110 ml. glass liner. Dicyanodiacetylene (0.27 gm., 0.0027 mole) was dissolved in 20 ml. of acetic anhydride and Adams' platinum oxide (0.10 gm.) added just prior to the sealing up of the mixture in the hydrogenation unit. (Although dicyanodiacetylene is reasonably stable in acetic anhydride solution, decomposition occurs in the presence of Adams' catalyst as evidenced by the gradual appearance of a dark brown color.) After being flushed out with hydrogen, the apparatus was charged to a pressure of 800 p.s.i. and the shaker started. The pressure fell off to 725 p.s.i. in 15 min. and more slowly to 710 p.s.i. over a three and one-half hour period. No further drop in pressure had occurred at the five hour mark and the reaction was stopped. The reaction temperature remained at approximately 30°C. throughout the hydrogenation. The solvent was removed from the dark brown reaction mixture by vacuum distillation, and the residual oily gum, containing acetylated hexamethylenediamine, was hydrolyzed by refluxing for five hours with 20% aqueous sulphuric acid (5 gm.). The hydrolyzate was made alkaline to a pH of 13–13.5 with 20% aqueous sodium hydroxide to liberate hexamethylenediamine from its salt and the resulting solution distilled to dryness under aspirator vacuum. To the distillate was added 1.4% aqueous picric acid (40 ml.) and the precipitate of hexamethylenediamine picrate removed by filtration. The product, m.p. 219°C., weighed 0.13 gm. (8.5% yield on dicyanodiacetylene). After recrystallization from water, the material melted at 221–222°C. (lit. 220°C.). It was further identified as hexamethylenediamine

TABLE II

X-RAY* DIFFRACTION PATTERN DATA ON HEXAMETHYLENEDIAMINE PICRATE

Spacing, d (Å)	Intensity, I/I_1	Spacing, d (Å)	Intensity, I/I_1
11.3	50	2.89	2
8.25	2	2.70	2
7.47	80	2.58	5
6.40	15	2.50	3
5.54	20	2.44	3
5.20	15	2.31	2
4.64	40	2.25	2
4.37	30	2.13	2
4.21	80	2.06	2
3.91	20	1.97	2
3.54	100	1.92	2
3.35	40	1.86	2
3.30	40	1.76	2
3.17	50		

*Wave length 1.5418 Å.

picrate by X-ray diffraction analysis (see Table II for list of diffraction lines from powder diagram and their relative intensities).

ACKNOWLEDGMENT

The author wishes to thank Dr. A. O. McIntosh for the X-ray diffraction work and Mr. R. J. Fabris for the elementary analyses.

REFERENCE

1. MOUREU, C. and BONGRAND, J. Ann. chim. 14: 47. 1920.

ALLOYS OF INDIUM: THE SYSTEM INDIUM–LEAD–TIN[1]

By A. N. Campbell, R. M. Screaton,[2]
T. P. Schaefer,[3] and C. M. Hovey[4]

ABSTRACT

There is no ternary eutectic in the system: indium–lead–tin: the eutectic trough extends from the lead–tin eutectic to the tin–indium eutectic. The liquidus surface has been outlined. The structures of all alloys of the above system have been investigated, at room temperature, by the X-ray and microscopic techniques. A one-phase region extends across the ternary diagram from the limits of the β-phase in the indium–tin system to the limits of the β-phase in the lead–indium system. This indicates that the intermetallic β-phases of the two systems (lead–indium and tin–indium) have the same lattice structure, viz. face-centered tetragonal. Heterogeneity has been detected by direct experiment in the system lead–indium, whereas it had previously only been deduced. Hardness tests, both Brinell and Vickers, have been made on the alloys.

The only previous work that has been reported on the above system is that of Grymko and Jaffee (5), who dealt primarily with the corrosion-resistance properties of the indium–lead–tin solders; they state, however, that the liquidus of one alloy containing 37.5 weight per cent lead, 37.5 weight per cent tin, and 25 weight per cent indium, lies at 181° C. and the solidus at 134° C. The component binary systems, viz.: lead–tin, indium–lead, and indium–tin, have all been investigated and very little remains in doubt. To save unnecessary discussion, the equilibrium diagrams are given in Figs. 1, 2,

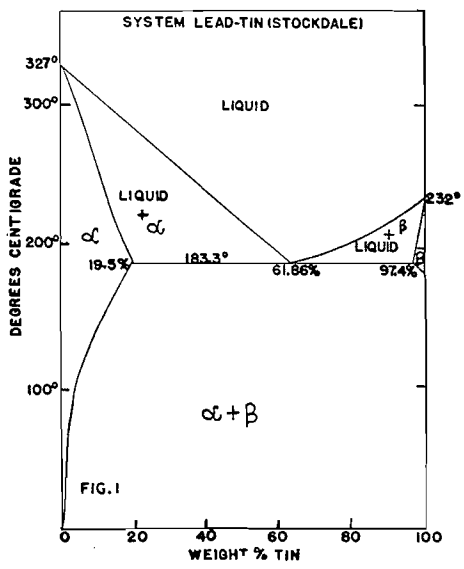

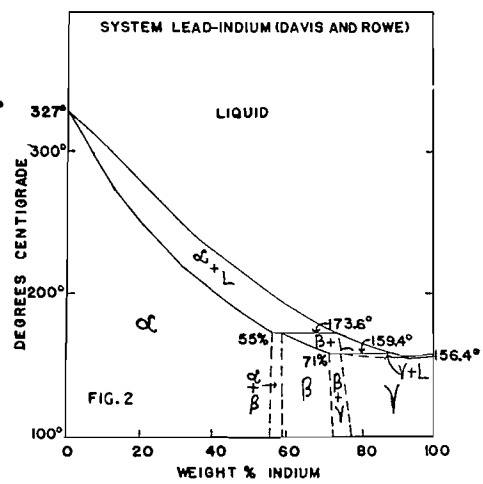

[1]*Manuscript received November 8, 1954.*
Contribution from Department of Chemistry, University of Manitoba, Winnipeg, Manitoba.
[2]*Cominco Fellow, 1953–54.*
[3]*Holder of an N.R.C. Bursary, 1954–55.*
[4]*Professor of Civil Engineering, The University of Manitoba, Winnipeg, Man.*

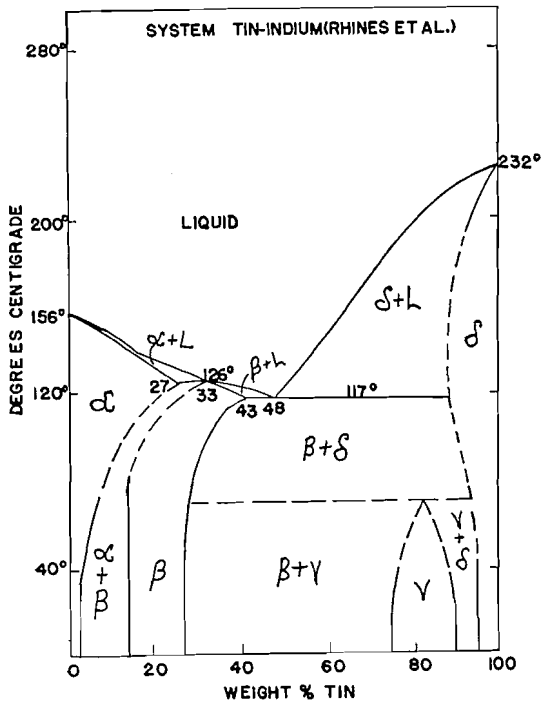

FIG. 3.

and 3. Fig. 1 is due to Stockdale (11) and represents the system lead–tin. The only point of interest in this system is a mysterious evolution of heat at 150° C., which occurs in all lead rich alloys; this is not due to any ordinary phase change.

Fig. 2 represents the system indium–lead: it is due to Davis and Rowe (1). This system shows a minimum freezing temperature, lying 1° C. below the melting point of pure indium, and three solid phases, an α-phase with the lead structure, a γ-phase with the indium structure, and an intermediate β-phase, for which Klemm (7) claims a face-centered tetragonal structure; further discussion of this structure is reserved until the discussion of our own work. The most complicated system is that of indium–tin (Fig. 3) due to Rhines (9). It is seen that this system exhibits four solid structures, one of which, however, the γ-phase, exists only at relatively low temperatures and therefore cannot be in equilibrium with melt. The α-phase possesses the structure of indium, the δ-phase that of tin, while the β-phase, according to Orlamunder (7) has a tetragonal, face-centered lattice. For the low-temperature γ-phase, Valentiner (12) proposed a body-centered tetragonal structure, but Fink (4) thought this phase was simple hexagonal: however, Ferguson and Screaton (3) believe it to be simple hexagonal with one atom per unit cell.

PART 1. THE LIQUIDUS SURFACE

Materials Used

The lead contained the following impurities:

Antimony	0.005%
Silver	0.002%
Total foreign metals	0.05%

The indium was given to us by the Consolidated Mining and Smelting Company of Canada Limited and had the following impurities:

Tin	0.015%
Nickel	0.0015%
Lead	0.015%
Copper	0.002%
Cadmium	0.001%
Iron	0.0005%

The tin analysis gave:

Iron	0.0020%
Antimony	0.0023%
Lead	Trace
Copper	Trace
Tin	99.9957% (by difference)

Methods of Chemical Analysis

The method of sampling differed in the study of the liquidus from that used in the study of the completely solid system. In no case did we rely on the original weighed composition since oxidation, though slight, is preferential, occurring chiefly to the lead. For the study of the liquidus, samples of liquid alloy were drawn up into a 1/16 in. diameter alundum tube. The alloy solidified in the tube after mounting a short distance; the tube was then broken and the whole of the sample analyzed, in case there should have been segregation of the alloy during solidification. Alloys with low indium content were dissolved, with the help of platinum foil, in hydrochloric acid, and the tin content determined by titration with iodine (10). Lead was estimated by the standard method of precipitation as sulphate. Prolonged attempts were made to determine indium directly, both polarographically and by precipitation with 8: 4 hydroxyquinoline but neither method was satisfactory in the presence of lead and tin. In the end, therefore, indium was obtained by difference. This may seem a doubtful procedure when the indium content is small but it should be remembered that the composition never differed much from that of the original weight composition. In alloys of high indium content, tin was determined as metastannic acid, which was subsequently ignited to the dioxide and weighed as such. All these analytical methods are well known.

Determination of Equilibrium Curves and Surfaces

The method of thermal analysis was used to determine these. The melts

were contained in alundum crucibles and temperature was measured with a mercury-in-glass thermometer, reading from 0 to 201° C. in 1/10°. The thermometer was calibrated against a standard platinum resistance thermometer: temperature was therefore accurate to ± 0.2° C.

The method of linear cooling was used, the rate of cooling being 1° per 1.5 minutes. The molten alloys were well stirred and kept at a temperature at which they were entirely liquid, for two hours, to ensure homogeneity. Starting with the composition of the lead–tin eutectic, as given by Stockdale (11), indium was added progressively and a cooling curve taken and an analysis made after each addition. An examination of the cooling curve showed whether or not the mixture had the trough composition. If it did not have, there was primary crystallization of a single phase and a preliminary point of inflection on the cooling curve. This was corrected, when necessary, by adding small quantities of tin (lead was never necessary). It soon became apparent that the eutectic trough, starting from the lead–tin eutectic, was heading smoothly for the indium–tin eutectic. Therefore, this was checked by starting from the indium–tin eutectic and adding lead. In this way, we were able to show that even the smallest addition of lead raised the solidification temperature of the indium–tin eutectic and therefore the possibility of a ternary eutectic lying very close to the indium–tin eutectic was excluded.

We thought it advisable to check the statement that there is a minimum freezing point in the lead–indium system, lying, according to the literature, 1° below the melting point of indium. For this purpose, we used a Beckmann thermometer with which we determined the freezing point of pure indium. Small weighed quantities of lead were then added and the freezing point determined each time. The procedure was repeated until a minimum freezing temperature was obtained. The freezing temperature of the lowest freezing alloy was then determined absolutely on the 200° thermometer. We obtained a depression of about 0.15° C. (constant) after the addition of 2.5 weight per cent lead.

Because of the occurrence of one peritectic in the lead–indium system and two in the indium–tin system, we expected peritectic halts along the eutectic trough of the ternary system. We first investigated the binary peritectics but we found the heat effects slight and difficult to observe, at least by our technique. When the third metal was added to these binary peritectic compositions, the heat effect was quenched entirely. Experimentally, then, we found no peritectic halt on the eutectic trough. Our investigation of the completely solid alloy at room temperature shows that there must be one, and only one, peritectic halt on the trough, but we do not know its temperature and composition.

To complete the study of the liquid surface, some points on the areas representing equilibrium of liquid with single solid phases were necessary (chiefly in the region where α-lead separates from the melt) and these were obtained by making up alloys of suitable composition and applying thermal analysis, using, however, a chromel–alumel thermocouple, since the temperatures involved were somewhat higher.

Experimental Results

TABLE I

DETERMINATION OF EUTECTIC TROUGH

Alloy No.	Solidification temperature (° C.)		Composition by weight		
	Start	Finish	Sn, %	In, %	Pb, %
Pb–Sn eutectic	183.3	183.3	61.9	—	38.1
1	177.6	174.8	59.5	2.9	37.6
2	170.7	164.5	57.0	5.8	37.2
3	164.7	159.1	56.1	7.7	36.2
4	147.7	134.9	54.1	17.3	28.6
7	135.9	130.8	51.8	25.9	22.3
8	134.3	129.4	51.5	27.4	21.1
9	132.7	128.0	51.1	28.9	20.0
10	131.2	126.4	50.9	30.3	18.8
11	130.0	126.0	51.1	31.1	17.8
12	129.0	126.0	50.7	32.2	17.1
13	128.3	125.7	50.2	33.5	16.3
14	127.1	125.1	50.1	34.6	15.3
15	125.9	124.5	50.3	36.6	13.1
16	124.9	123.6	49.8	38.0	12.2
17	124.5	121.5	49.4	38.9	11.7
18	118.7	118.7	48.7	51.3	—
19	118.9	118.7	48.4	51.1	00.5
20	119.6	118.8	47.4	50.0	2.6
21	120.3	119.6	46.8	49.3	3.9
22	121.7	120.0	45.8	48.3	5.9
23	122.6	121.4	48.1	42.8	9.1
25	123.9	122.5	48.2	42.0	—
26	118.8	118.8	48.7	51.3	—
27	118.8	118.8	48.7	51.2	0.1
30	150.3	133.3	53.2	15.8	31.0
31	147.1	133.8	53.4	18.2	28.4
32	144.6	132.8	53.5	20.0	26.5
33	142.0	131.9	53.6	21.8	24.6

TABLE II

EFFECT OF SMALL QUANTITIES OF LEAD ON THE MELTING POINT OF INDIUM

Alloy No.	Composition by weight		Freezing point
	In, %	Pb, %	
53	100.00	0	3.431
54	99.59	0.41	3.374
55	98.87	1.13	3.353
56	97.95	2.05	3.289
57	96.83	3.17	3.281
58	95.30	4.70	3.331
59	93.57	6.43	3.422

Beckmann setting of 3.422° = 156.5°C.
Melting point of pure indium was therefore = 156.5° C.

TABLE III

INVESTIGATION OF LIQUIDUS

Alloy No.	Solidification begins	Solidification ends	Trough temp.	Composition by weight % Sn	In	Pb
39	157.9° C.	132.3° C.	145.6° C.	62.2	17.0	20.8
40	179.6	129.0	140.7	70.8	12.5	16.7
42	154.7	125.6	143.7	35.7	34.7	29.6
43	131.6	128.8	—	28.6	65.6	5.8
44	140.4	133.7	—	25.4	58.0	16.6
45	152.3	136.6	—	22.6	51.8	25.6
46	172.3	137.7	153.8	20.1	46.0	33.9
47	177.5	138.5	152.3	19.3	44.4	36.3
48	123.6	121.5	—	38.0	61.9	0.1
49	125.9	123.4	—	36.4	59.3	4.3
50	127.5	125.6	—	34.0	62.0	4.0
51	128.9	126.6	—	31.6	64.7	3.7
52	130.6	127.8	—	29.0	67.6	3.4
61	155.4	145.2	—	10.1	67.0	22.9
62	241.0	—	—	21.5	14.2	64.3

Discussion of the Liquidus Surface

The experimental results show that there is no ternary eutectic in this system; the eutectic trough extends from the lead–tin eutectic to the tin–indium eutectic.

Our value for the eutectic temperature of the binary system lead–tin, 183.3° C., is in good agreement with Stockdale's value (11). We have, however,

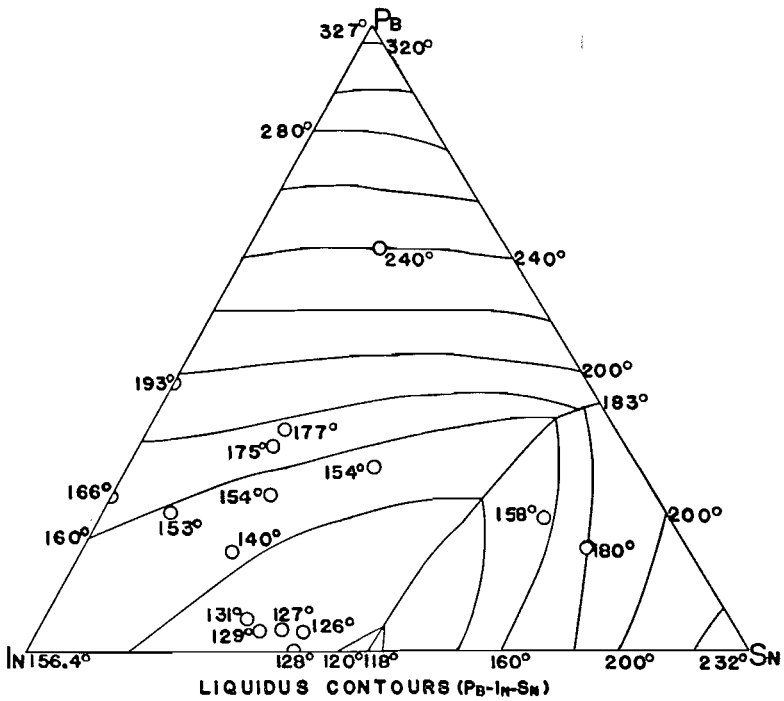

FIG. 4.

repeated the eutectic of the tin–indium system several times, using the composition given by Rhines (9) and we obtain values for this eutectic temperature lying between 118.7° C. and 118.9° C., as against Rhines's own value of 117° C. This may be due to our having had at our disposal very pure indium. In the lead–indium system, we confirm the existence of a minimum freezing temperature lying, however, only 0.15° C. below the melting point of pure indium.

Fig. 4 is a projection diagram of the liquid surface, with isothermal lines.

PART 2. ROOM TEMPERATURE ISOTHERM

The structure of the completely solidified alloy was studied by the X-ray and microscopic techniques. As a subsidiary aid in the study of structure and because of its intrinsic practical importance, the hardness was determined in various regions of the composition triangle: both Brinell and Vickers hardness tests were applied.

Experimental

All alloys were heat-treated by cooling them gradually over a period of twenty-four hours, from a temperature at which they were completely liquid down to room temperature. This was achieved by coupling a slow, constant speed, electric motor through a system of gears to a "Variac", which governed the input to the furnace. After the potential fell to zero, an automatic switch cut out the circuit. Twenty-three hours were required to rotate the Variac through its complete range. Obviously, such an apparatus does not decrease temperature linearly since the power input is proportional to the square of the voltage; in other words, cooling was more rapid at higher than at lower temperatures, but this is rather a desirable feature.

The purity of the materials is described under the first Section, where, also, it is stated that all alloys were analyzed and the methods of analysis are given. The method of treatment of alloys for the study of the solid system was as follows: A total weight of 40 gm. of the desired composition was charged into a crucible and preheated to about 60° above the liquidus temperature, as read from the appropriate equilibrium diagram (see preceding section). After fusion and repeated stirring with an alundum rod, the melt was cooled to roughly three degrees above the temperature of the liquidus surface, the whole process occupying about three hours. The continuous cooling mechanism was now set in motion and the alloy annealed down to room temperature.

From the ingot prepared as above the oxide film was removed with a lathe. A specimen for microscopic examination, approximately 7 mm. in width and 4 mm. thick, was also prepared on the lathe. Turnings for chemical analysis were taken from the immediate vicinity of the prepared surface. No demarcation marks, denoting gross phase separation during cooling, could ever be detected by a vertical saw-cut; moreover, the general agreement between final analysis and original composition of charge favors this conclusion.

A strip for X-ray examination was cut from the surface of the prepared specimen, with a sharp thin-bladed knife: it was possible to reduce the thickness of this strip as low as 0.2 mm. Powder pictures of such strips were taken on a North American Phillips X-ray unit, using a simple Debye camera of

57.3 mm. diameter. Copper radiation and a nickel filter were used. The exposure time varied from one to three hours depending on the composition and size of the specimen. The above procedure was necessary because indium and alloys rich in indium are almost as soft as putty. Filings could not be prepared readily because of the "smearing" properties of these alloys. The small degree of cold-working by the knife-edge would only cause a slightly preferred orientation of the grains and this effect was neutralized by rotation of the specimen during exposure to X rays.

Our treatment of the specimens prior to microscopic examination is described in detail, because no satisfactory methods of polishing and etching the indium alloys in question are to be found in the literature. Preparatory to polishing, the surface was lightly rubbed on a fine mill-file, held stationary, the teeth being cleaned after each stroke. The final polish was given on a wheel-driven silk cloth (selvyt), using the "light" variety of powdered magnesium oxide as polishing agent. If the sample contained large quantities of lead, tarnishing tended to occur but it was found that this could be prevented by the use of soap. Too much water on the cloth increased the tarnishing but a heavily tarnished layer could be removed by dabbing the surface with glacial acetic acid. Polishing was carried on close to the center of the wheel until the surface had a lustrous appearance, as far as possible scratch-free.

An etching reagent consisting of seven parts of glycerol, two parts of concentrated nitric acid, and one part of glacial acetic acid gave the best results over the whole concentration range, but the nitric acid content was varied for different samples to achieve the best effect. This reagent was described by Villela and Beregekoff (13) for lead alloys. Etching took place by immersion for 5 to 30 sec. at approximately 40° C. To ensure that the true structure of the sample did not remain latent, the specimen was alternately lightly polished and etched. This also decreased the danger of cold-working from overpolishing and the deterioration of a delicate microstructure from overetching.

Hardness tests were made by the Brinell ball and Vickers' diamond hardness tests. Because of the softness of these alloys, a special Brinell machine was constructed, which had a unit ratio of load in kgm. to the square of the diameter of the ball in mm., as specified in "Metals Handbook" (8). A load of 5.5 kilograms was applied to a steel ball of 2.35 mm. diameter, for 30 sec. The Vickers-Armstrong machine was of a standard type.

The method of procedure was as follows: Alloys, some fifteen in number, representing both the pure phases and the heterogeneous regions, of the binary systems, were prepared and, after heat-treatment in the manner described, the powder pattern and microstructure of each alloy were determined. A small quantity of third component was then added to each alloy; the alloy was then remelted, heat-treated, and examined by the two techniques mentioned, attention being directed to the appearance of a new phase. Because of the great similarities in lattice structure of β-lead–indium and β-tin–indium, it was thought that a continuous series of solid solutions might exist, forming a band over the diagram, and this was found to be the case.

Experimental Results

Table IV contains the compositions of all alloys studied, together with their hardness figures, on both scales. Table V gives approximate figures which will permit the single-phase, two-phase, and three-phase areas to be plotted.

TABLE IV

COMPOSITION AND HARDNESS

Sample No.	Composition by weight			Hardness	
	Pb	Sn	In	Bhn	DPH
1	—	100	—	3.9	5.8
1a	—	98.6	1.4	8.4	7.9
2	—	93.7	6.3	10.0	12.8
3	—	64.7	35.3	3.8	7.1
4	—	79.1	20.9	10.1	11.4
5	—	25.5	74.5	1.01	1.04
6	—	5.6	94.4	1.3	1.9
7	—	5.1	94.9	0.89	1.7
8	100.0	—	—	2.6	4.3
9	15.1	—	84.9	3.5	4.4
10	27.4	—	72.6	5.5	7.7
11	35.9	—	64.1	8.1	10.2
12	44.7	—	55.3	8.4	11.4
13	89.7	—	10.3	7.3	7.8
14	51.4	—	48.6	9.2	13.4
15	4.6	75.3	20.1	10.1	13.8
16	1.8	77.8	20.4	8.5	11.0
17	2.0	18.2	79.8	1.8	2.1
18	9.5	14.8	75.7	2.3	3.1
19	20.2	9.9	69.9	4.2	5.2
20	27.0	5.4	67.6	5.9	6.9
21	9.9	7.1	83.0	2.7	3.3
22	21.3	19.1	59.6	4.3	5.1
23	34.8	11.2	54.0	8.4	9.7
24	49.8	5.1	45.1	10.9	13.3
25	35.8	1.0	63.2	7.9	9.4
26	15.9	8.8	75.3	3.7	4.4
27	9.9	4.1	86.0	2.9	3.5
28	27.1	16.6	56.3	6.0	7.7
30	51.5	15.8	32.7	9.0	12.4
31	57.8	23.3	18.9	10.9	13.6
32	50.2	34.1	15.7	10.0	13.0
33	60.9	32.3	6.8	10.4	13.2
34	49.8	47.6	2.6	10.5	14.5
35	36.0	8.1	55.9	7.1	8.2
36	77.9	4.4	17.7	10.1	11.6
37	24.2	66.3	9.5	7.4	11.4
38	24.9	49.8	25.3	10.0	12.8
39	64.3	21.5	14.2	10.8	13.4

Fig. 5 is a graphical representation of these data—the room temperature isotherm. We give no X-ray data since no new phase occurs in the three component alloy and the X-ray data for all binary phases are now to be found in the literature. We reproduce, however, certain photomicrographs since, without them, a paper of this kind is practically valueless to workers in the field: the etching reagent was always that described previously, unless other-

wise stated. It will be noted on Fig. 5 that a single phase region extends across the isotherm from β-indium–tin to β-indium–lead. This is the most interesting of the results and it indicates that the two phases (of the binary systems) are of closely similar structure. The invariant triangle in which β-indium–tin, γ-indium–tin, and α-lead are in equilibrium occupies a large part of the isotherm.

In Fig. 6, the hardness numbers, both DPH and Bhn, are plotted for the binary systems designated. For the indium–tin system there is no indication of the formation of the intermediate β-phase but in the plot of the indium–tin alloys a maximum appears at the composition of the γ-phase. Fig. 7 is a plot of hardness contours for the ternary system.

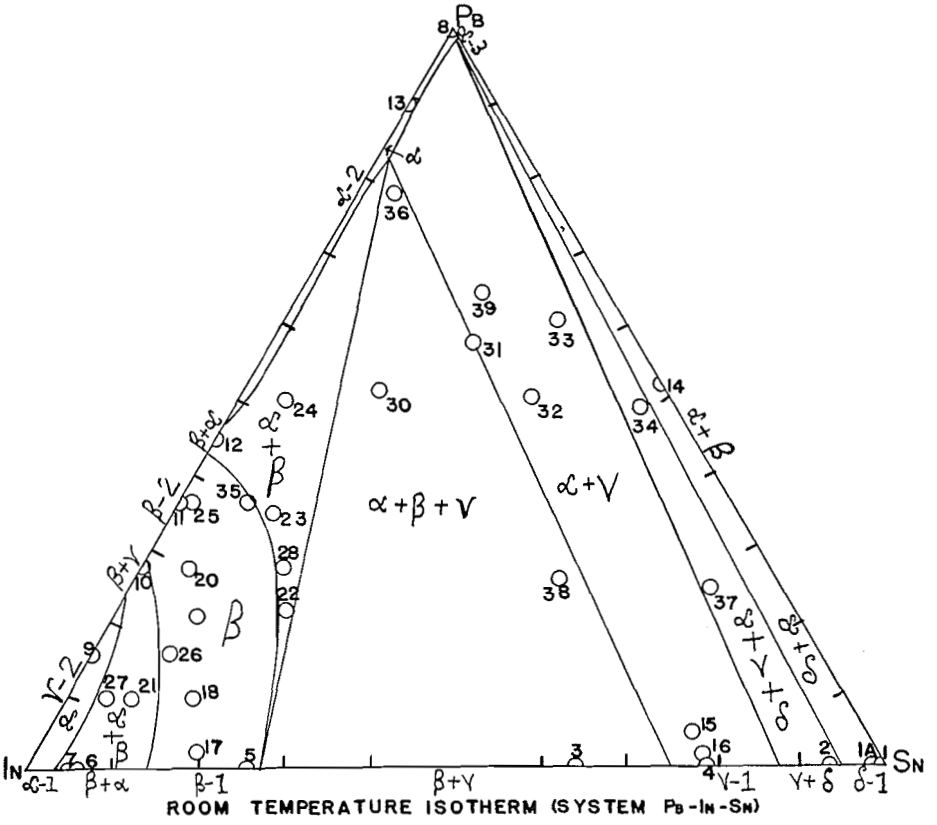

FIG. 5.

There follows a description of the individual photomicrographs. To facilitate discussion the phases designated by Greek letters are distinguished by Arabic numerals, thus, 1 for In–Sn, 2 for Pb–In, and 3 for Pb–Sn.

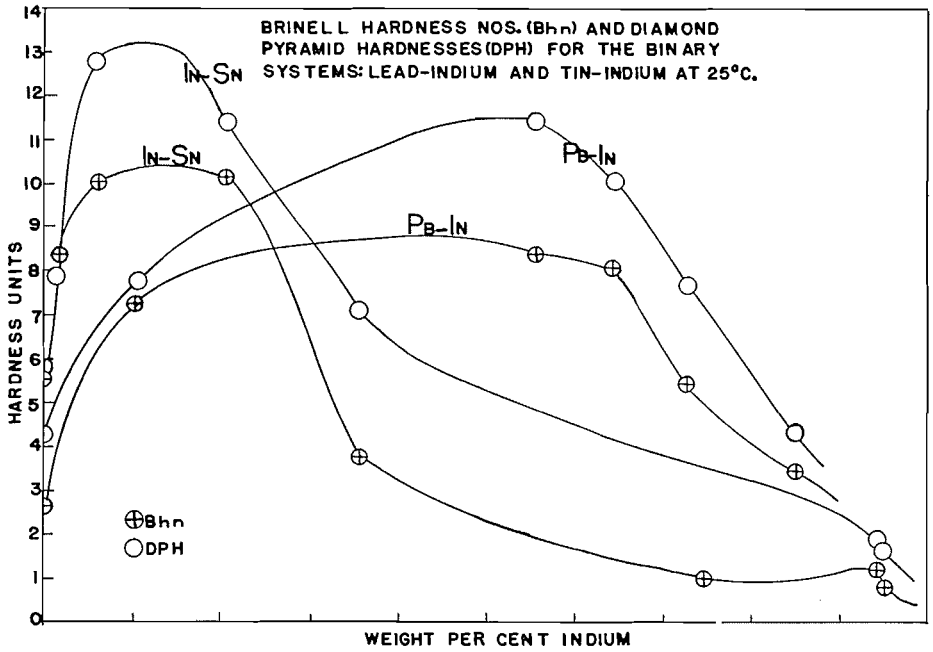

FIG. 6.

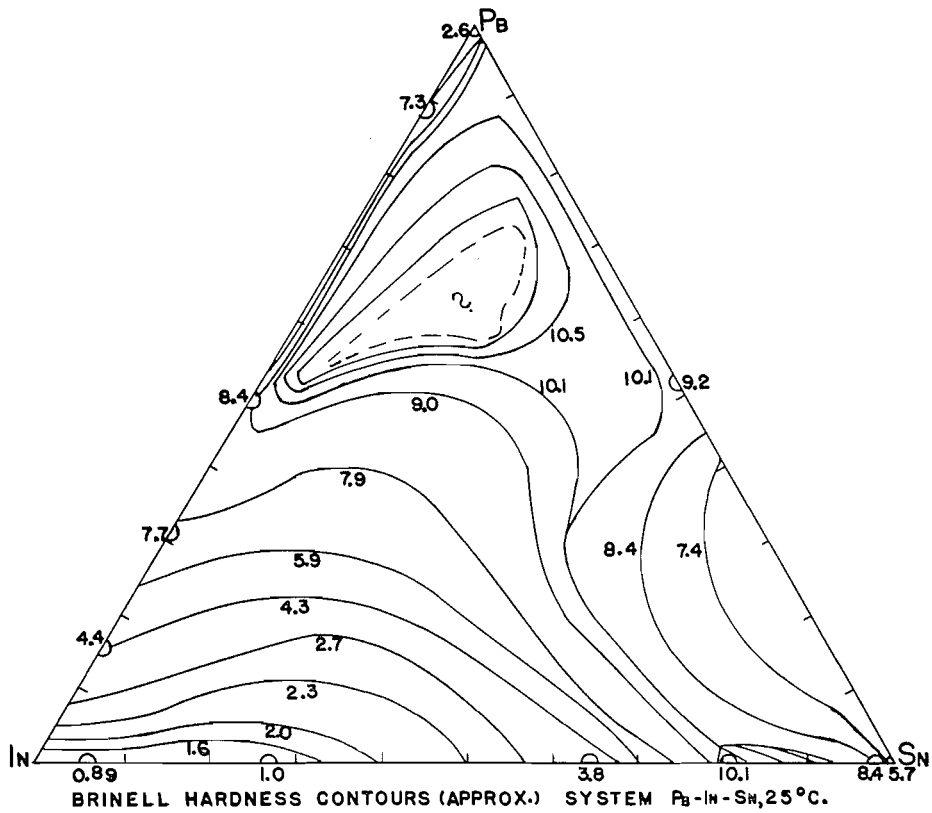

FIG. 7.

TABLE V

Nature of phase	Type of lattice	Composition of points defining area
Single-phase areas		
α-Lead	Face-centered cubic	(1) 1.5% Sn, 98.5% Pb (2) 53.1% In, 46.9% Pb (3) 1% Sn, 25% In, 74% Pb
δ-Tin	Body-centered tetragonal	Does not occur as a single phase in the ternary system; stable up to 5% In in In–Sn system
α-In	Face-centered tetragonal	(1) 3% Sn, 97% In (2) 23% Pb, 77% In (3) 3% Sn, 10% Pb, 87% In
γ-Tin–indium	Simple hexagonal	Does not occur as a single phase in the ternary system: (1) 75% Sn, 25% In (2) 88% Sn, 12% In
β-Lead-indium	Face-centered tetragonal	This phase extends down to β-In–Sn and is isostructural with it. The following points define the band: (1) 28% Pb, 72% In (2) 43% Pb, 57% In (3) 78% In, 13% Pb, 9% Sn (4) 14% Sn, 86% In (5) 27% Sn, 73% In (6) 61% In, 19% Sn, 20% Pb (7) 45% In, 8% Sn, 37% Pb
β-Tin–indium	Face-centered tetragonal	
Two-phase areas		
α-Lead + δ-Tin		(1) 100% Sn (2) 95% Sn, 5% In (3) 1.5% Sn, 97.5% Pb, 1% In
α-Lead + γ-Tin–indium		(1) 1.5% Sn, 97.5% Pb, 1.0% In (2) 95% Sn, 5% In (3) 88% Sn, 12% In (4) 16% In, 1% Sn, 83% Pb
α-Lead + β-Lead–tin		(1) 27% Sn, 73% In (2) 43% Pb, 57% In (3) 47% Pb, 53% In (4) 16% In, 1% Sn, 83% Pb
α-Indium + β-Lead–tin		(1) 14% Sn, 86% In (2) 3% Sn, 97% In (3) 3% Sn, 10% Pb, 87% In (4) 23% Pb, 77% In (5) 28% Pb, 72% In (6) 8% Sn, 77% In, 15% Pb
Three-phase areas		
α-Lead + δ-Tin + γ-Tin–indium		(1) 88% Sn, 12% In (2) 95% Sn, 5% In (3) 1.5% Sn, 97.5% Pb, 1% In
α-Lead + β-Lead–indium + γ-Tin–indium		(1) 75% Sn, 25% In (2) 27% Sn, 73% In (3) 23.5% Sn, 19% In, 57.5% Pb (4) 16% In, 1% Sn, 83% Pb

Interpretation of Photomicrographs

A number of representative photomicrographs are given, in order to indicate the type of microstructure obtained, and particularly such as are not to be found in the literature. Fig. 8 shows the difference in etching characteristics

between the γ-1 and δ-1 phases, the γ-1 being light, i.e. not attacked to the same extent as the δ-1 phase. Fig. 9 shows the grain boundaries in the γ-1 phase (the dark spots are probably spurious effects arising from polishing). That the γ-phase is the one actually present is proved by the powder photograph of this sample, which was identical with that obtained by Ferguson

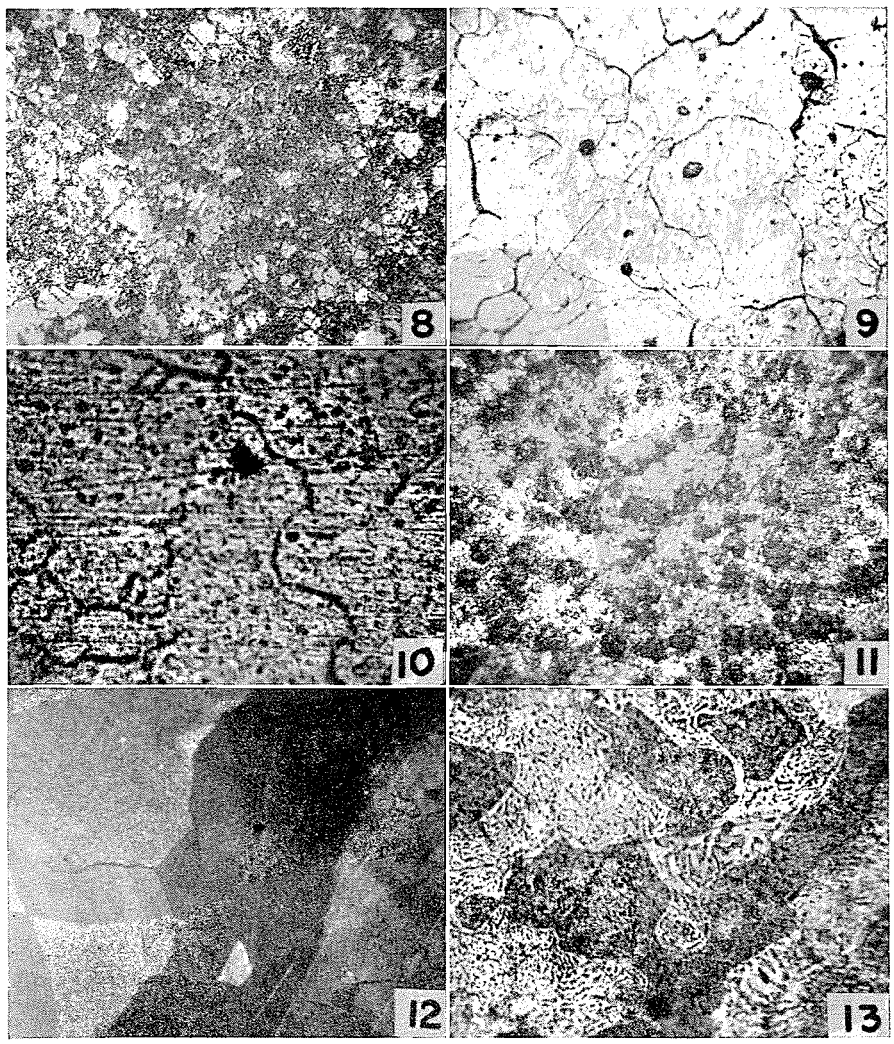

FIG. 8. Alloy 2, × 250. Note the difference in etching characteristics of γ-1 (light) and δ-1 (dark).
FIG. 9. Alloy 4, × 135. Grain boundaries in γ-1; black spots are probably spurious, although some β-1 may be present.
FIG. 10. Alloy 5, × 135. Grain boundaries in β-1, exhibiting the characteristic pitted appearance of this phase.
FIG. 11. Alloy 10, × 250. Repolished and re-etched after three months at room temperature; β-2 in a background of γ-2.
FIG. 12. Alloy 11, × 135. Repolished and re-etched after three months at room temperature; grain boundaries in β-2.
FIG. 13. Alloy 14, × 250. Lead grains (dark) in the Pb–Sn eutectic.

and Screaton (3) and showed the lines of the simple hexagonal lattice of γ-1. Grain boundaries in the β-1 phase are visible in Fig. 10 and were obtained by polishing in an electrolyte consisting of equal parts of 70% perchloric acid and

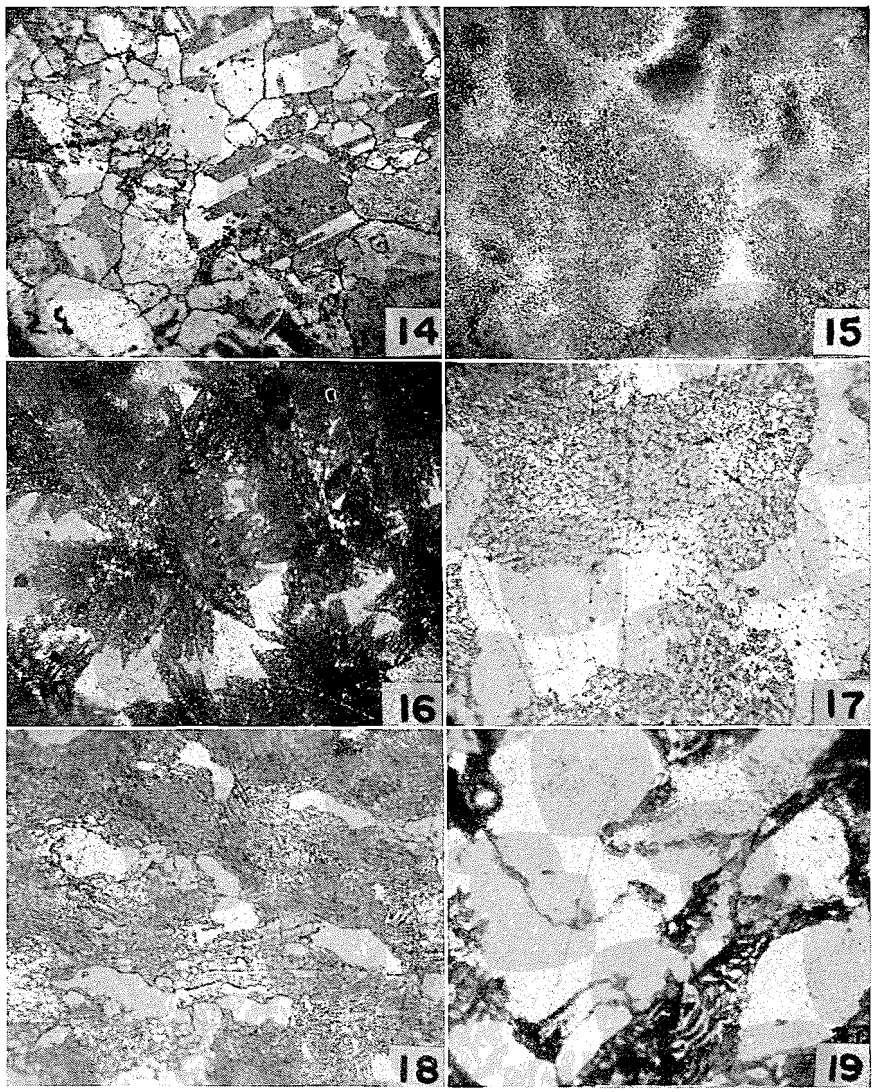

FIG. 14. Alloy 25, × 250. Repolished and re-etched after one month at room temperature; grains of β with twinning bands.
FIG. 15. Alloy 23, × 135. Repolished and re-etched after one month at room temperature; showing α-2 and β.
FIG. 16. Alloy 30, × 250. The dendritic growth of β is here well marked; α-2 and γ-1 are also present (light areas) as proved by X-ray photograph.
FIG. 17. Alloy 32, × 250. A region of the alloy where α-2 is present with eutectic of α-2 and δ-1; now breaking up with the disappearance of δ-1 and appearance of γ-1.
FIG. 18. Alloy 39, × 250. As cast; α-2 (light) in a eutectic matrix of α-2, and δ-1. Note difference (Fig. 13) in appearance of lead crystals when indium is present.
FIG. 19. Alloy 38, × 250. α-2 (light), β-(black), γ-1 (gray).

glacial acetic acid, the sample being made the anode with an aluminum plate serving as cathode (current density 0.3 amp. per cm.^{2}), followed by the usual etch. Note the pitted appearance of the surface. Fig. 11 shows the heterogeneity in alloy 10, Fig. 12 the grain boundaries in alloy 11. The eutectic in the lead–tin system (Fig. 13) has a lamellar structure, the lead etching darkly in the absence of indium. Twinning bands are to be seen in the grains of alloy 25, shown in Fig. 14: they arose from the cold-working caused by polishing. In Fig. 15, the microstructure of an alloy defining the phase boundary between the one- and two-phase regions, as seen on the isotherm, is exhibited. The interpretation is obvious, when one notes that the α-2 phase, lead structure, etches very weakly (appearing light) in the presence of indium. The X-ray photographs substantiate this argument. With alloy 30, Fig. 16, we enter the invariant triangle. The dendritic growth of the β-phase here manifests itself clearly, and this explains the difficulty in distinguishing it from certain other phases in the binary systems, as found by Davis and Rowe (9, in discussion). Such a growth can apparently produce interfluence between the phases. The γ-1 (gray) and α-2 (light) phases are also present and this is corroborated by the X-ray photograph.

As we leave the invariant triangle and enter the adjacent two-phase region where γ-1 and α-2 are stable, the microstructures take on the appearance of Fig. 17 which depicts a region of alloy 32 in which the eutectic (δ-1 and α-2) is in the process of breaking up into α-2 and γ-1. The structure of a cast alloy in this region is portrayed in Fig. 18, alloy 39; the X-ray photograph shows lines for α-2 and δ-1. Note that the lead phase appears light and is delineated by the dark structure of the eutectic. The three phases β (black), γ-1 (light gray), and α-2 (light) occur in Fig. 19, representing alloy 38.

DISCUSSION

Ferguson and Screaton (3) do not agree with Valentiner (12) on the structure of β-indium–tin but, since the lattice of β-indium–lead is established as face-centered tetragonal and since this is the stable lattice right across the diagram, it appears as if Valentiner's view is correct.

Previous workers have failed to detect, by microscopic examination, any evidence of heterogeneity in the lead–indium system, although they had deduced the existence of an intermediate β-phase from X-ray data. Our photomicrograph of alloy 10 (Fig. 11) shows the heterogeneity. The trouble is due to the fact that both α-indium and β-indium–lead have face-centered tetragonal lattices. Davis and Rowe (9, in discussion) do not state their etching reagent. It is probable that the acetic acid in ours was the factor of success, since it tends to remove tarnished films.

For stable intermetallic phases in an alloy the rule is that the intermetallic compound is usually harder than the hardest of its components. This is exemplified by the graph of hardness vs. composition for the indium–tin system, where the peak on the curve lies in the γ region: the β-phase is softer than pure tin and just slightly harder than pure indium. In general, an intermetallic "compound" has some composition within the boundaries of its stable

existence and corresponding to a definite chemical formula. Since compounds, according to Hume-Rothery (6) correspond to definite valence electron to atom ratios, one can hence attribute much of their hardness to their tendency to form homopolar bonds. The results support this view. The γ-phase, of simple hexagonal structure, is almost twice as hard as the body-centered tetragonal lattice of pure tin. Since the hexagonal lattice would have more planes for deformation slipping than the tetragonal, some other forces must be operative, e.g. homopolar bonding.

Alloys containing the γ-indium–tin phase could not be dissolved completely in acids, unless platinum was used to promote solution by galvanic action. Whatever the cause of this passivity, the phenomenon is interesting from the point of view of corrosion studies.

ACKNOWLEDGMENT

We are indebted to Professor R. B. Ferguson, Associate Professor of Crystallography, for much helpful advice in carrying out the X-ray measurements.

REFERENCES

1. Davis, H. M. Trans. Am. Soc. Metals, 39: 712. 1947.
2. Eyring, H. J. Phys. Chem. 57: 942. 1953.
3. Ferguson, R. and Screaton, R. Acta Cryst. 7: 364. 1954.
4. Fink, C. J., Jette, E. R., Katz, S., and Schnettler, F. S. Trans. Electrochem. Soc. 75: 463. 1939; 88: 229. 1945.
5. Grymko, S. M. and Jaffee, R. I. Materials & Methods, p. 59. March 1950.
6. Hume-Rothery, W. J. Inst. Metals, 35: 295. 1926.
7. Klemm, W., Klemm, Li, Hohmann, E., Volk, E., Orlamunder, E., and Klein, H. A. Z. anorg. Chem. 256: 239. 1948.
8. Metals handbook. American Society for Metals. p. 93. 1948.
9. Rhines, F. N., Urquhart, N. M., and Hoge, H. R. Trans. Am. Soc. Metals, 39: 694. 1947.
10. Scott, W. W. Standard methods of chemical analysis. D. Van Nostrand Company, Inc., New York. 1927. p. 536.
11. Stockdale, D. J. Inst. Metals, 49: 267. 1932.
12. Valentiner, S. Z. Metallkunde, 32: 31. 1940.
13. Villela, J. R. and Beregekoff, D. Ind. Eng. Chem. 19: 1049. 1927.

HYDROGEN PEROXIDE AND ITS ANALOGUES

VI. INFRARED SPECTRA OF H_2O_2, D_2O_2, AND HDO_2 [1]

By Osias Bain[2] and Paul A. Giguère

ABSTRACT

The absorption spectrum of hydrogen peroxide was re-examined with a prism instrument in the region 1.5 to 25μ. A pair of well-resolved perpendicular bands arising from torsional oscillation of the OH groups were found centered about 460 and 575 cm.$^{-1}$. The overtone band at 3.8μ was shown to be a hybrid with prominent rotational structure and some indications of doubling. Its assignment to the combination $\nu_2+\nu_6$ implies a positive anharmonicity. Four new overtone bands were observed in liquid hydrogen peroxide. The infrared spectrum of deuterium peroxide was measured for the first time in the solid and vapor states. The vapor bands are quite different in appearance from those of hydrogen peroxide. One of the fundamentals, the asymmetric O—D stretching at 2661 cm.$^{-1}$, was resolved sufficiently to allow calculation of the rotational constants of the isotopic molecule. Mixtures of the two peroxides containing around 40% of HDO_2 were also investigated; from the results the frequency of the as yet unobserved symmetric modes ν_1 and ν_2 could be estimated with fair certainty. The O—O stretching vibration at 11μ was too weak to be located definitely in the spectra of the gaseous peroxides. The structural parameters of the H_2O_2 molecule are now established as follows:

$$r_{O—O} = 1.49\pm0.01 \text{ Å}$$
$$r_{O—H} = 0.97\pm0.01 \text{ Å}$$
$$\alpha_{OOH} = 100°\pm2°$$

The O—H and O—D stretching bands were studied in solutions of the three isotopic peroxides in carbon tetrachloride.

Previous investigations of the molecular spectrum of hydrogen peroxide (2, 6, 10, 30, 34) have served to confirm the structure now accepted for that molecule but, otherwise, they have left unanswered a number of important questions, such as the assignment of the weak band at 3.8μ and the frequency of the four symmetric modes, especially ν_4 the torsional oscillation. In an effort to solve some of these problems the infrared spectrum of that compound was measured again under a wider range of conditions than covered heretofore. In addition, the completely deuterated peroxide was prepared and its spectrum in the vapor state was recorded for the first time. Mixtures of these two isotopic peroxides were used to obtain valuable information on the hybrid molecule HDO_2. Unfortunately, study of the latter was severely limited by interference from the parent molecules H_2O_2 and D_2O_2, always present in large proportions, in addition to traces of H_2O, D_2O, and HDO. Finally the spectra of the three peroxides dissolved in a non-polar solvent have helped elucidate the region of the O—H and O—D stretching fundamentals. While the subject remains far from exhausted the new results have made possible calculation of the force constants of the molecule (11) and an appreciable refinement in our knowledge of the structural parameters.

EXPERIMENTAL

The material used for obtaining the spectra was prepared as described before;

[1]*Manuscript received November 22, 1954.*
Contribution from the Department of Chemistry, Laval University, Quebec, with financial assistance from the National Research Council of Canada.
[2]*Present address: C.A.R.D.E., Valcartier, Que.*

the hydrogen peroxide, 99.5%, by fractional distillation of Becco's 90% commercial product, and the deuterium peroxide, 90–93%, by dissociation of heavy water vapor, 99.6% pure, in the electrodeless discharge (16). The tendency of these peroxides to decompose spontaneously gave rise to numerous difficulties in selecting suitable containers and window material. For the latter, plates of highly polished silver chloride were found to be quite satisfactory. Spectra of the solid peroxides were studied without too much difficulty because of the slower decomposition rate at low temperature. An absorption cell of the type described by Wagner and Hornig (31) was used. One drop of liquid peroxide was squeezed between two precooled silver chloride plates and the whole was quickly inserted in the holder. After the cell was evacuated the temperature was lowered further with dry ice and acetone. Atmospheric humidity had to be kept low enough to prevent condensation on the windows.

The liquid peroxides could not be studied so easily. Even with very smooth silver chloride plates some slight decomposition always occurred at room temperature and the oxygen produced forced out the thin film of liquid. In the overtone region glass spacers were used and the thickness, measured by an interference method (28), was about 0.1 mm. Below 1μ a glass cell 1 cm. thick was used so that four new combination bands could be detected in both hydrogen and deuterium peroxides (Table I). Solutions in carbon tetrachloride could only be studied in the near infrared up to approximately 4μ where the solvent is still sufficiently transparent. A very thick absorption cell was needed then because of the low solubility of the peroxides. (No data are available on the solubility of hydrogen peroxide in carbon tetrachloride but, from the relative intensity of the various absorption bands, it seems to be of the same magnitude as that of water (7), namely 8–10 mgm. per 100 gm. of solvent.) A glass tube, 10 cm. long, closed by silver chloride windows made tight by means of Koroseal gaskets was entirely satisfactory. For the vapor a Perkin-Elmer 1-meter multiple reflection cell made of cast aluminum was tried at first. In practice the sample of liquid peroxides could not be heated much above 70°C., where the vapor pressure is of the order of 30 mm. Hg. To prevent condensation on the mirrors and windows the cell had to be kept at 90°C. Under such conditions, decomposition was so rapid, even with a flow system, that a steady concentration of peroxide could not be secured and the water vapor produced blotted large sections of the spectrum. Therefore a glass cell of 1.25 meter path-length was built as shown in Fig. 1.

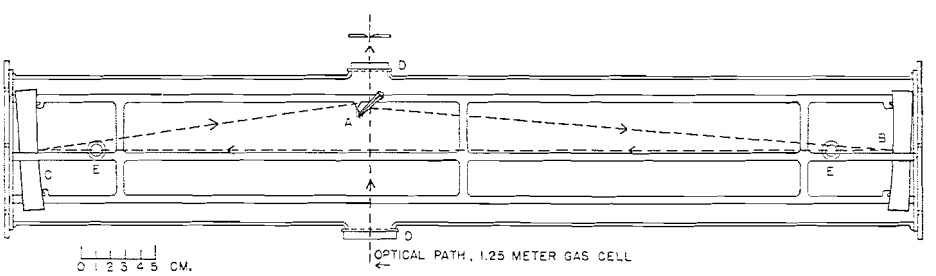

FIG. 1. Diagram of the 1.25 meter absorption cell made of Pyrex glass.

TABLE I

INFRARED SPECTRA OF HYDROGEN AND DEUTERIUM PEROXIDES

H_2O_2				D_2O_2				
Vapor		Liquid, cm.$^{-1}$	Solid, cm.$^{-1}$	Vapor		Liquid, cm.$^{-1}$	Solid, cm.$^{-1}$	Assignment
cm.$^{-1}$	(a)*			cm.$^{-1}$	(a)*			
465 575	0.07	635 m.†	472 v.w.† 660 s. 792 w.			538 m.†	480 m.	$\nu_4(a)$
890(?)	0.007	878 m.w.	878 m.w.			878 m.w.†	880 m.w.	$\nu_3(a)$
1266	0.38	1350 s.	1380 s.	923 947	0.45	1004 s.†	1000 s.	$\nu_6(b)$
			1430 w.†	1007(?)				$\nu_2(a)$
2647	0.065	2780 m.	2840 m. 2930 w.	1985	0.02	2087 m.w.†	2090 m.w.	$\nu_2+\nu_6(B)$
3610	0.24	3360 v.s.†	3320 v.s.†	2661	0.25	2482 v.s.†	2470 v.s.	$\nu_5(b)$
4465	0.004	4290 v.w.						$\nu_3+\nu_5(B)$
4835 4955	0.007	4770 w.	4595 v.w.†			3430 w.		$\nu_1+\nu_6(B)$ $\nu_2+\nu_5(B)$
		6100 v.w.						
7036.6 7041.6		6805 w.		5240	0.03	4980 v.w.		$\nu_1+\nu_5(B)$
		8040 v.w.				6110 v.w.		$2\nu_5+\nu_6(B)$
10283.7 10291.1		9950 v.w.				7215 v.w.		$2\nu_1+\nu_5(B)$, $3\nu_5(B)$

*$(a) = (1/pl) \log I_0/I$, with p in atm. and l in cm.
†From reference (30).

The cell proper is made out of a 60 cm. length of Pyrex tube 10 cm. diameter. The ends, slightly flared and ground flat, are closed by disks of 1S aluminum, 3 mm. thick and well polished. (Very pure aluminum, when properly cleaned, is fairly inert towards hydrogen peroxide.) The two front-aluminized, spherical mirrors, B and C, 8 cm. diameter and 117.5 cm. focal length (such as used in the Perkin-Elmer spectrometer) are mounted in a frame of three thick glass rods held together by rings of bent glass rods. Light, stainless steel springs press the spherical mirrors against lumps of glass fused onto the main rods. Two small plane mirrors, 1.8 × 2.5 cm. cut from microscope slides and bevelled on one side, are mounted diagonally and back-to-back in a holder of thin glass rods fused onto the glass frame. (They could be replaced by a single wedge-shape piece.)

The optical alignment proved to be a delicate operation, but once made it was permanent. To that end the optical assembly was taken out of the glass tube and placed at right angle in the convergent beam of the spectrometer. Mirrors A and B were first lined up so that the reflected beam was collimated and centered about the main axis of the cell. This was achieved by a trial and error method. The lumps of glass, against which the spherical mirrors rest, were softened with a torch and "worked" to the correct position. Mirror C was then similarly adjusted so as to focus the reflected beam on the entrance slit of the monochromator after reflection on the other face of the "wedge" mirror, A. Such an arrangement does not alter appreciably the convergence of the infra-red beam. With the optimum alignment of the mirrors, as much as 80% of the incident light was transmitted after traversing the cell. The openings of the cell, closed either by the aluminum disks or by silver chloride windows, D, could be made tight without difficulty by means of Koroseal gaskets. However, this material is somewhat troublesome in that the plasticizer (a mixture of tritolyl phosphates) distills off on heating *in vacuo*. These esters were identified by their infrared spectra (8) in the 11–15μ region. By keeping the pressure above 15 mm. Hg in the cell at all times this undesirable phenomenon could be reduced appreciably.

To keep the cell at 85–90°C. it was wrapped with insulated nichrome wire and covered with asbestos paper and aluminum foil. The extent of decomposition of the peroxide vapor after one passage through this cell was of the order of 15%, as compared with 85% with the all-metal cell. Various techniques were tried to introduce the peroxide vapor. A static system with the liquid peroxide in a side tube and the absorption cell evacuated was unsatisfactory on account of decomposition. Continuous pumping of the cell through a dry-ice trap and a reducing valve adjusted so that the pressure in the cell remained at 15 mm. Hg resulted in a steady state as indicated by the reproducibility of the intensity spectra. Evacuation of the absorption cell was not necessary, however. The device shown in Fig. 2 was found useful: the sample of liquid peroxide in tube A is surrounded by a vapor jacket B in which a suitable liquid (for instance carbon tetrachloride) is boiled under atmospheric pressure. A regulated stream of dry nitrogen is bubbled through a small tube closed by a fritted glass disk. The stream of gas saturated with peroxide vapor is passed at constant rate

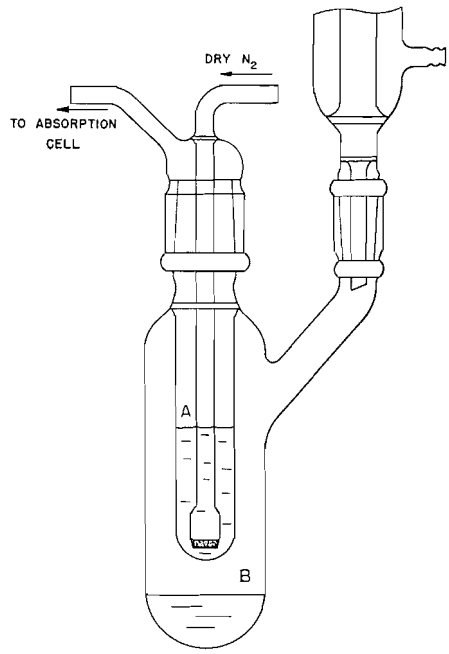

FIG. 2. Device for filling the absorption cell with peroxide vapor.

through the absorption cell and then through a dry-ice trap. The infrared spectrometer was a Perkin-Elmer, model 12C, with automatic scanning and recording on a Speedomax. During this investigation the monochromator was converted to double-pass with notable increase of resolving power and reduction of scattered light. Absorption by atmospheric gases was kept at a tolerable level by circulation of dry nitrogen through the two housings of the instrument.

INTERPRETATION OF THE SPECTRA

From the structural point of view the molecules H_2O_2 and D_2O_2 may be described as slightly asymmetric, prolate tops. The degree of prolateness is characterized by the function

$$\beta = (I_{B,C}/I_A) - 1, \qquad [1]$$

where $I_{B,C}$ is the harmonic mean of the two large moments of inertia and I_A is the minor moment of inertia of the molecule. The rotational constants of H_2O_2 have been measured previously (10, 34) and from these, β turns out to be 11.2. Similar calculations for D_2O_2, assuming the same structural parameters, lead to $\beta = 6.4$. As for their asymmetry (I_B/I_C), it cannot be evaluated with the same certainty because of insufficient data, but estimates of the individual moments of inertia (3, 10) show that it must be less than 5%, even in the case of D_2O_2, unless the azimuthal angle ϕ is very different from 90°. The spectra of these molecules will therefore exhibit two different types of band structures; (*a*) perpendicular bands, corresponding to the symmetric vibrations, ν_1 to ν_4, (10) for which the change of electric moment is essentially perpendicular to the

top axis, and, (*b*) hybrid bands of predominantly parallel character arising from the asymmetric vibrations ν_5 and ν_6. The former, presumably rather weak in infrared, will have a single broad maximum with a rotational structure easily resolvable under the dispersion of a prism instrument. Indeed, the spacing of their rotational levels is 18 cm.$^{-1}$ for H_2O_2 and about half as much for D_2O_2.

On the other hand, the strong parallel component of the hybrid bands will show separate *P*, *Q*, and *R* branches but the rotational structure will not be perceptible because of too fine spacing: 1.65 cm.$^{-1}$ for H_2O_2 and 1.47 cm.$^{-1}$ for D_2O_2. The contour of these bands may be predicted from the equation of Gerhard and Dennison (9). Thus the separation of the *P* and *R* maxima, dependent on the various moments of inertia and the temperature, is calculated to be 43 and 45 cm.$^{-1}$ respectively for H_2O_2 and D_2O_2 at 70°C. Similarly the intensity of the zero *Q* branch relative to the total intensity of the parallel band should be 9% for H_2O_2 and 12% for D_2O_2. Finally, the perpendicular component of these hybrid bands may be expected to alter the over-all intensity distribution, particularly near the center, with more or less definite indications of a coarse rotational structure.

Spectra of the Vapor

(A) *The Torsional Oscillation Mode*

The outstanding feature in the present study of hydrogen peroxide vapor is certainly the band system of medium intensity extending from 16μ to beyond the transmission limit of KBr optics. For deuterium peroxide the corresponding band lies mostly outside the present range of our instrument; we hope to investigate it soon with CsBr optics. The tracing shown in Fig. 3 was recorded with a

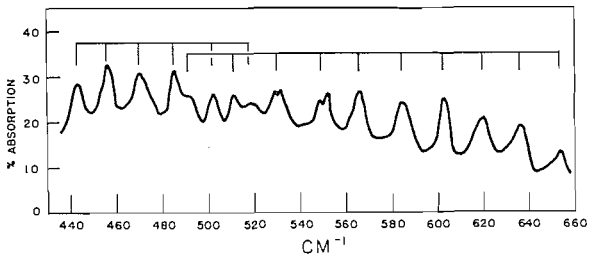

FIG. 3. The torsional oscillation band in hydrogen peroxide vapor.

slit equivalent to a resolved width of frequency band ranging from 4.4 to 6.7 cm.$^{-1}$. On the basis of location and relative intensity there is little doubt that this band arises from the torsional oscillation, or hindered internal rotation, mode ν_4. Qualitatively this oscillation may be expected to result in a fairly large change of the electric moment of the molecule perpendicular to the top axis. Analysis of the rotational structure (Table II) shows a spacing averaging 18 cm.$^{-1}$ on the short wavelength side, dropping suddenly to 16–15 cm.$^{-1}$ somewhere around 480 cm.$^{-1}$. This convergence is in opposite direction to that in the second (10) and third harmonics (34) of the O—H stretching vibrations and, for that reason, it is unlikely that we have here a single, or unsplit

TABLE II

APPROXIMATE FREQUENCIES AND TENTATIVE ASSIGNMENTS OF THE PRINCIPAL MAXIMA IN THE 17–22μ BANDS OF HYDROGEN PEROXIDE

	High frequency band				
K	${}^{P}Q_K$	${}^{R}Q_K$	$\frac{{}^{R}Q_K - {}^{P}Q_K}{4K}$	$\frac{{}^{R}Q_{K-1} - {}^{P}Q_{K+1}}{4K}$	Low frequency band
	cm.$^{-1}$	cm.$^{-1}$	cm.$^{-1}$	cm.$^{-1}$	cm.$^{-1}$
0		585			519
1	567	603	9.0	8.5	503
2	551	620	8.6	9.1	486
3	530	637	8.9	9.1	470
4	511	653	8.8	9.1	456
5	492				443

vibrational transition. This, coupled with the irregular spacing observed between 485 and 520 cm.$^{-1}$, points strongly to the presence of two separate bands. From intensity distribution the center of the short wavelength component is tentatively located at 575 cm.$^{-1}$ and the other, around 465 cm.$^{-1}$. Obviously these figures, especially the latter, are rather uncertain because of the low intensity of incident radiation and the small number of maxima observed.

That this band is doubled confirms the previous interpretation of a similar feature in overtone bands namely, a double minimum in the torsional oscillation. Indeed, the other explanations considered seem most unlikely. For instance, it is doubtful that one of the two bands could be due to transition from an excited state such as $2\nu_4 - \nu_4$ because both components have about the same intensity and "borrowing" by coupling of levels is not expected in this case. Also, the high-frequency band is too intense to be an harmonic of some fundamental situated in the far infrared. The large doublet splitting, about 110 cm.$^{-1}$, is not surprising as the torsional oscillation is much more closely associated with the double minimum than the other vibrational levels. (Compare the inversion splitting of ν_1 and ν_2 in NH_3 (18) for instance.) It also confirms that one of the potential barriers must be fairly low. According to the model of Penney and Sutherland (26) rotation of the two O—H groups about the O—O bond is restricted by an asymmetric potential function having a high and low barrier in the *cis*- and *trans*-positions respectively. The height of the first, V_1, was estimated by them at 1 electron volt and that of the second V_2, at about half of that value. No complete theoretical treatment of the asymmetric potential function has been reported yet although various approximations have been suggested (22, 27). From electron density calculations Lassettre and Dean (19) arrived at values of 94° to 113° for ϕ, the azimuthal angle, with heights of potential barriers ranging from 8 to 21 kcal./mole for V_1 and from 2 to 10 kcal./mole for V_2. Therefore, the potential function generally assumed for the torsional oscillation in molecules such as ethylene,

$$V = \tfrac{1}{2}V_0(1-\cos 2\phi), \qquad [2]$$

where V_0 is the barrier of periodicity π, is not strictly applicable to the case of

hydrogen peroxide. If a periodicity of 2π is to be preserved, then a cosine function of the following form is the simplest possible one:

[3] $$V = \tfrac{1}{2}(V_1 - V_2)\cos\phi + \tfrac{1}{2}(V_1 + V_2)\cos^2\phi.$$

From this the position of the minima is given by

[4] $$\phi \text{ min.} = 2n\pi \pm \cos^{-1}[(V_2 - V_1)/2(V_2 + V_1)],$$

and a ratio of V_1/V_2 of about 3 is required to make $\phi = 105°$, the average estimated by Lassettre and Dean. In principle the energy levels could be found by replacing the potential function in the Schrödinger equation by V from [3], and would be given by the periodic eigenvalues of "a" in the following Mathieu-type equation:

[5] $$(d^2M/dx^2) + (a - b\cos 2x - c\cos^2 2x)M = 0,$$

[6] where $$a = 32\pi^2 I_r E/h^2,$$

[7] $$b = (16\pi^2 I_r/h^2)(V_1 - V_2),$$

[8] and $$c = (16\pi^2 I_r/h^2)(V_1 + V_2).$$

At present the lengthy calculations to determine how the eigenvalues of "a" depend on V_1 and V_2 do not seem justified for lack of enough accurate data.

Pending rigorous solution of the wave equation for the asymmetric function [3] various simplifications are necessary in correlating the experimental results. Thus, assuming a symmetrical twofold barrier [2], an average value of 520 cm.$^{-1}$ for the torsional frequency leads, through solution of the Mathieu equation, to a value of $V_0 = 6$ kcal./mole. About the same value was obtained from the perturbed oscillator treatment (20). A recent investigation of the microwave spectrum of hydrogen peroxide (24) has yielded a much lower value, *ca.* 320 cal./mole, also on the assumption of a symmetrical potential function. It is possible that this spectrum could be interpreted as well in terms of a function with a high and a low barrier.

On the other hand the difference between the calorimetric entropy at 25°C. and the calculated statistical entropy of hydrogen peroxide (13) corresponds to an hypothetical barrier $V_0 = 3.5$ kcal./mole. On the same basis the treatment suggested by Pitzer (27) for molecules with slightly asymmetric tops attached to a rigid frame yields the more reliable value 4.7 kcal./mole. Thus it appears fairly certain that the *trans*-barrier is appreciably lower than the *cis*-one. However, it could hardly be as low as suggested by the microwave spectrum because then an important fraction of the H_2O_2 molecules would possess a torsional energy greater than V_2 at moderate temperatures, and their symmetry would be effectively C_{2h} (23). In that respect it is unfortunate that the low volatility and thermal unstability of hydrogen peroxide make it impossible to measure the infrared spectrum or the heat capacity of the vapor as a function of temperature.

(*B*) *The O—O Stretching Mode*

Repeated scrutiny of the 11μ region in the spectrum of H_2O_2 vapor has failed to reveal any definite indication of the O—O vibration ν_3. Under the maximum

equivalent path-length attainable, absorption amounted to less than 3% in the range 830–920 cm.$^{-1}$ while it was complete for ν_6, the OH bending mode. (In D_2O_2 and HDO_2 the situation is less favorable because of the strong ν_6 band near by.) This remarkable fact, which, alone, is sufficient to rule out any tautomeric form of the molecule such as H_2O—O, has not been fully appreciated in previous investigations. One of us (10) reported a very weak maximum "hardly noticeable" in the vapor and assigned to it a value of 877 cm.$^{-1}$ largely on the faith of the corresponding Raman shift (6). As for the band of medium intensity found by Bailey and Gordon at 870 cm.$^{-1}$ (2), it must have resulted from condensation on the windows of the absorption cell as confirmed otherwise (10) by the resemblance of their spectra in both phases.

Indeed, it is a peculiarity of this frequency that it is much stronger, relatively speaking, in the condensed states than in the vapor. Such enhanced activity must be due to strong molecular association as it is not likely that the configuration of the free molecule is appreciably different from that in the liquid or the solid. X-ray investigations of the crystal structure of hydrogen peroxide (1) and its addition compound with urea (21) have shown azimuthal angles of about 94° and 106° respectively. Even when the hydrogen atoms of H_2O_2 are replaced by much heavier groups, as in SF_5—O—O—SF_5, the azimuthal angle remains nearly the same (107°±5° (17) from electron diffraction by the vapor). According to the C_2 model of H_2O_2 ν_3 must yield a perpendicular band with a single maximum, which makes its location still more problematic. The intensity, at any rate relatively low, would depend on the azimuthal angle, becoming zero for $\phi = 180°$. A consequence of this situation is that the frequency of ν_3 is not yet known accurately, having been measured so far only in the liquid and solid where it may be altered slightly by molecular interaction. Cf. the case of hydroxylamine (12). For that reason measurement of the Raman spectrum of hydrogen peroxide vapor would be a desirable, if difficult investigation.

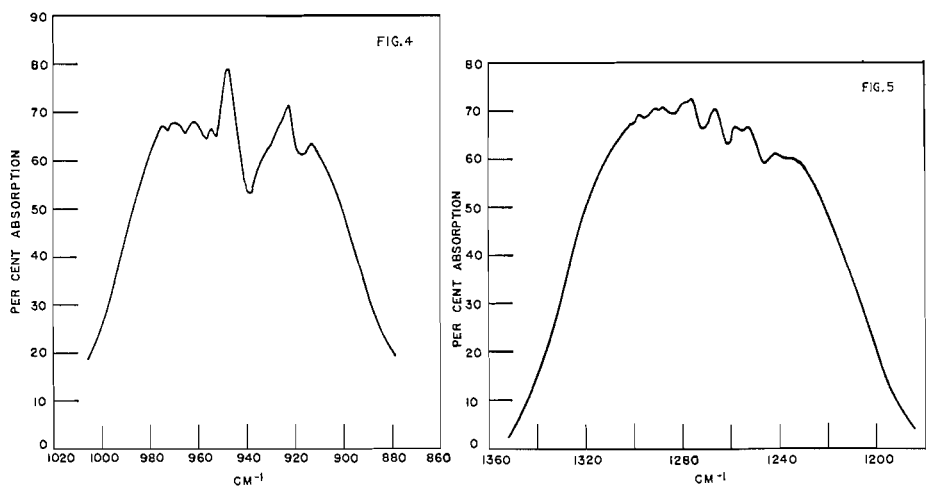

FIG. 4. The asymmetric OD bending frequency in deuterium peroxide vapor.
FIG. 5. The OH bending vibration ν_6 in gaseous hydrogen peroxide.

(C) The OH and OD Bending Modes

The asymmetric bending modes ν_6 are the most intense in the spectra of both peroxides, their central Q branch occurring at 1266 cm.$^{-1}$ in H_2O_2 and 947 cm.$^{-1}$ in D_2O_2. The first one was recorded with a fluorite prism and the second, with a rock salt prism; in both cases the resolution was about 4 cm.$^{-1}$. As predicted by the equation of Gerhard and Dennison (9) the Q branch is much stronger in D_2O_2 (Fig. 4) than in H_2O_2 (Fig. 5). It was not possible to evaluate the separation of the P and R maxima because of some coarse structure arising presumably from the perpendicular component. No regularity could be detected in this rotational structure, possibly on account of doubling of the bands. The prominent maxima on the low frequency side, specially in the case of D_2O_2, at 923 cm.$^{-1}$, resemble the satellite bands reported by Williams (32) in his study of formic acid. In general appearance both bands show pronounced asymmetry, the intensity gap between the P and Q branches missing in D_2O_2. Since other bands of both peroxides feature the same unequal intensity distribution it is doubtful if it arises from another coincident vibration, ν_2 in this case. Rather we believe there is an appreciable frequency difference between ν_2 and ν_6 on the basis of the following indirect evidence.

The spectrum of HDO_2 measured in that region showed very clearly the Q branch of the OOD bending vibration at 981 cm.$^{-1}$. By analogy with the

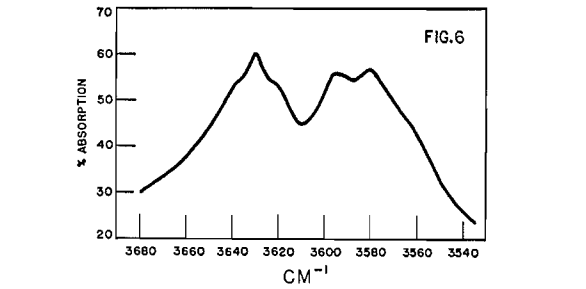

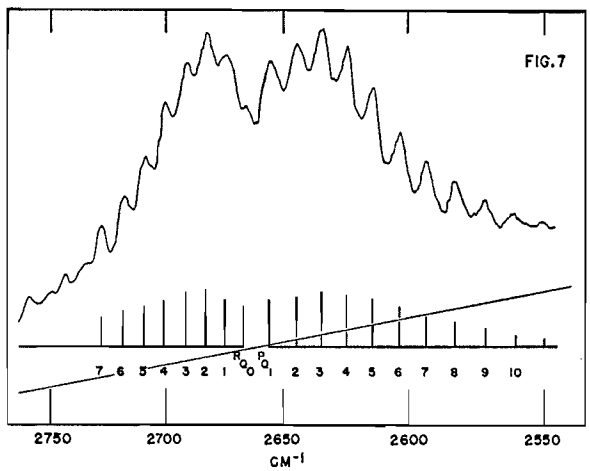

FIG. 6. The O—H stretching band ν_5 in hydrogen peroxide vapor.
FIG. 7. Rotational structure of the stretching band ν_5 in deuterium peroxide. (The sloping line corresponds roughly to the background.)

bending frequency in HDO, which occurs about halfway between those in H_2O and D_2O, we infer that ν_2 should be around $981+(981-947) = 1015$ cm.$^{-1}$ in D_2O_2. In fact a slight absorption was noticeable at 1007 cm.$^{-1}$ in the vapor of both D_2O_2 and HDO_2. The corresponding OOH bending mode could not be identified with certainty in H_2O_2 but, from the isotope shift, it may be expected to lie around 1350 cm.$^{-1}$ in that molecule. Consideration of various combination bands leads to the same conclusion, as explained below.

(D) The O—H and O—D Stretching Modes

Recording of the asymmetric stretching bands ν_5 was done under medium absorption with a LiF prism and a spectral half-width resolution of 9.7 cm.$^{-1}$ for H_2O_2 (Fig. 6) and 4.9 cm.$^{-1}$ for D_2O_2 (Fig. 7). Here the two peroxides show still greater differences than for the bending modes. While both bands have the same parallel contour, the coarse rotational structure of the perpendicular component is prominent in D_2O_2 but is missing completely in H_2O_2 although the resolution was sufficient to bring it out. This situation is reminiscent of the overtone band of hydrogen peroxide $\nu_1+\nu_5$ under high dispersion (10) in contrast with the corresponding band finely resolved in hydrogen persulphide (33). Still, the present circumstance may be fortuitous—overlapping by water vapor bands or doublet splitting—as there is no obvious reason why the perpendicular component should be much stronger in D_2O_2 than in H_2O_2.

The frequencies of the various maxima in Fig. 7 are listed in Table III together with the calculated rotational constants A′ and A″. The accuracy of these figures is estimated to be 4%. The band center was found from the equation of Dieke and Kistiakowsky (5) to be at 2661 cm.$^{-1}$. For the H_2O_2 band the center was taken at the absorption minimum, 3610 ± 5 cm.$^{-1}$. Like the others these values are not corrected for vacuum.

TABLE III

ROTATIONAL ANALYSIS OF THE 2661 CM.$^{-1}$ BAND OF D_2O_2

K	^PQ_K	^RQ_K	$\frac{^RQ_K-{}^PQ_K}{4K}$	$\frac{^RQ_{K-1}-{}^PQ_{K+1}}{4K}$	ν_0
	cm.$^{-1}$	cm.$^{-1}$	cm.$^{-1}$	cm.$^{-1}$	cm.$^{-1}$
0		2667.6			
1	2657.6	2676.5			
2	2646.6	2685.1	4.81	5.13	2662.4
3	2635.5	2693.5	4.84	4.98	2660.7
4	2625.4	2702.5	4.82	4.91	2660.6
5	2614.9	2711.2	4.81	4.94	2661.5
6	2603.7	2720.3	4.86	4.90	2658.7
7	2593.7	2729.4	4.85	4.92	2660.2
8	2582.6			4.95	
9	2571.2	Average	4.83	4.93	2661.
10	2560.0				

(E) Overtone Bands

An interesting result of this investigation is the resolution of the hybrid band at 3.8μ in H_2O_2 vapor, the origin of which had remained uncertain until

now. With its definite parallel-type contour and prominent rotational structure (Fig. 8) it can only arise from combination of the two bending modes $\nu_2+\nu_6$ since both $2\nu_2$ and $2\nu_6$ would be predominantly perpendicular. Besides

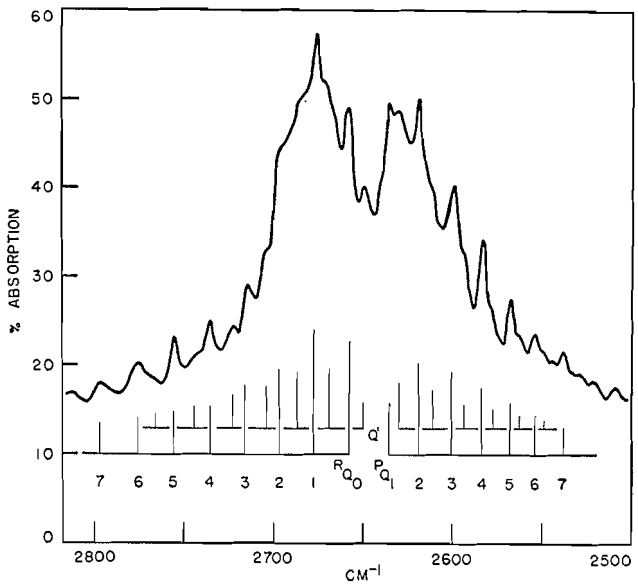

FIG. 8. Overtone band at 3.8μ in gaseous hydrogen peroxide.

they should be very weak, and for different reasons: $2\nu_6$, because even harmonics of unsymmetrical frequencies are usually missing in non-linear molecules, and $2\nu_2$, because of the weakness of its first harmonic. The present assignment leads to an unexpected anharmonicity as the frequency of the combination band, 2647 cm.$^{-1}$, is higher, instead of lower, than the sum of its components, about 2615 cm.$^{-1}$ if the above deduced value for ν_2 is correct. The difference cannot be due entirely to uncertainty in the latter estimate. Indeed, an increase of more than 30 cm.$^{-1}$, making ν_2 greater than 1380 cm.$^{-1}$, would hardly leave any shift for this frequency in the condensed phases. In fact it has been observed at 1400 cm.$^{-1}$ in the Raman effect of the pure liquid (29). That the unusual anharmonicity associated with $\nu_2+\nu_6$ is real is further confirmed by the frequency of this band in the Raman spectrum, *ca.* 2815 cm.$^{-1}$ (29).

Recordings of this band made under maximum absorption revealed some secondary peaks between the main ^PQ and ^RQ sub-bands particularly at 2650 and 2723 cm.$^{-1}$. These could be due to absorption from the first excited level of ν_4 although we are inclined to consider them as indications of doubling in view of their fair intensity and the presence of the same feature in the other two resolved overtones. The separation of the doublet at the center, 10 cm.$^{-1}$ from the minima of intensity, seems plausible in that conjecture. The irregular convergence of the rotational structure (Table IV) is probably exaggerated by the low resolving power available. Consequently the rotational constants derived therefrom would be much less accurate than those from the two over-

TABLE IV

FREQUENCIES OF THE PRINCIPAL MAXIMA IN THE 3.8μ BAND OF H_2O_2

K	^PQ_K	^RQ_K	$^PQ'_K$	$^RQ'_K$
	cm.$^{-1}$	cm.$^{-1}$	cm.$^{-1}$	cm.$^{-1}$
0		2658		2650
1	2636	2678	2630	2670(?)
2	2619	—	2612(?)	2686(?)
3	2601	2716	2593(?)	2704
4	2584	2736	2577(?)	2723
5	2568	2755	2562(?)	2744
6	2554	2776	2545(?)	2766(?)
7	2538.5	2797.5		

Note: The primed symbols refer to the secondary band.

tones of the O—H stretching frequencies (10, 34). Incidentally when the latter are compared with the present band the difference in general appearance is striking. In particular no ^PQ or ^RQ branches are missing near the center (Fig. 8). The reason for such differences is not clear at present. For the corresponding band in D_2O_2 at 5μ absorption was too low to reveal any structure. Similarly, the combination $\nu_1+\nu_5$ appeared as a hybrid band at 5240 cm.$^{-1}$. Finally a few very weak maxima were noticed in H_2O_2 vapor at 4465, 4835, and 4955 cm.$^{-1}$. The first of these can be assigned unambiguously to $\nu_3+\nu_5$ which gives a reasonable anharmonicity, 35 cm.$^{-1}$. As for the other two, their separation is far too great for the P and R branches of a single band, so that they must arise from different combinations among the various possibilities listed in Table I.

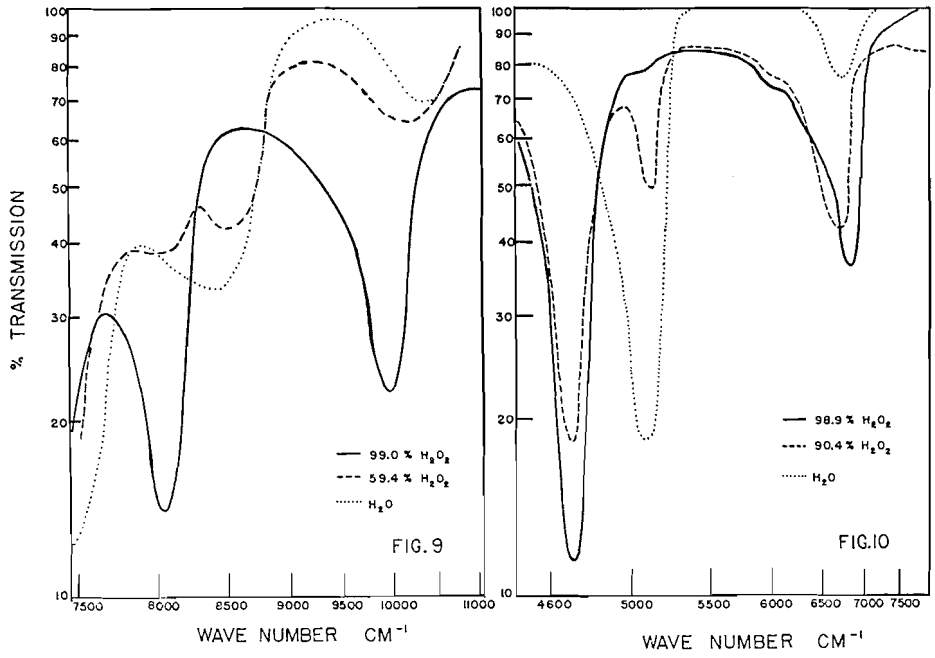

FIG. 9. Absorption spectra of aqueous hydrogen peroxide solutions in the 1μ region.
FIG. 10. Infrared spectra of liquid hydrogen peroxide and water between 1.2 and 2μ.

Spectra of the Condensed States

(F) Liquid and Solid

Strong molecular association in the peroxides makes a spectroscopic study of their condensed states of special interest. On the other hand, and for the same reason, little information may be expected from it in connection with the structure of the free molecule. In the region covered by the LiF prism six weak maxima were found in liquid H_2O_2 (Figs. 9 and 10) and four in liquid D_2O_2 (Table I). Of the latter, two are rather uncertain (at 6110 and 7215 cm.$^{-1}$) as they were observed in a dilute solution (15–20%) and the maxima are probably shifted appreciably by dilution (compare Figs. 9 and 10). For crystalline H_2O_2 the present measurements agree quite well with those of Taylor (30) except for the combination band reported by him at about 2740 cm.$^{-1}$ which we found at a higher frequency and resolved into two peaks at 2840 and 2930 cm.$^{-1}$. Thus the temperature shift is really in the same direction as for the fundamentals ν_2 and ν_6 so there is no objection to an assignment to that combination; this leads to a positive anharmonicity as for the vapor band. The weaker component at 2930 cm.$^{-1}$ may be due to $2\nu_2$ and/or to a ternary combination with a lattice mode. In crystalline D_2O_2 the frequency of ν_4 shows the normal isotope shift with the low-frequency band in H_2O_2. Therefore it is likely that the value given by Taylor for this mode in liquid D_2O_2, (538 cm.$^{-1}$) is too high. Attempts to check this point were unsuccessful. No splitting of the bending OD frequencies could be detected contrary to H_2O_2, although the peak at 1000 cm.$^{-1}$ (Fig. 11) appears slightly asymmetric.

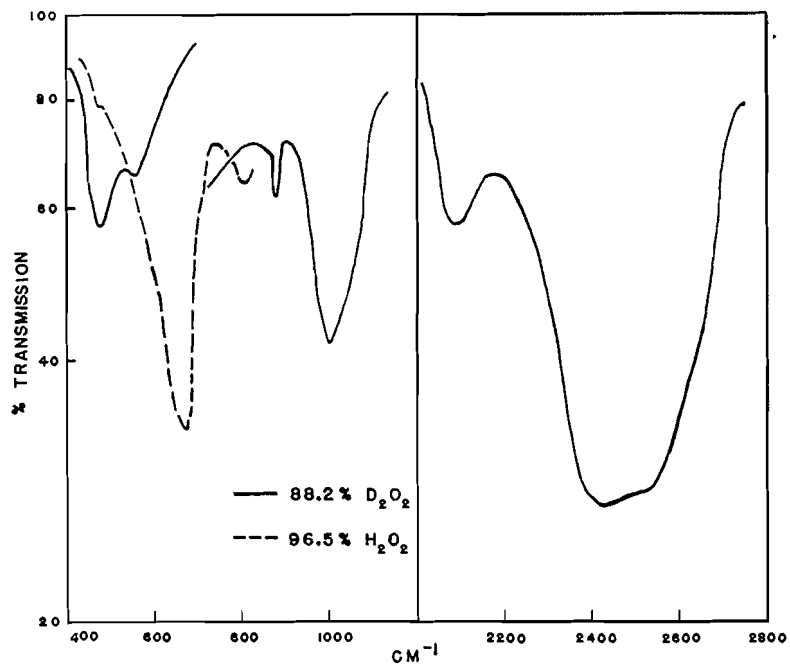

FIG. 11. Absorption spectra of crystalline H_2O_2 and D_2O_2.

(G) Solutions in Carbon Tetrachloride

Just as in the case of water (7) the absorption spectra of H_2O_2 and D_2O_2 dissolved in a non-polar solvent have provided valuable information on the O—H and O—D stretching modes. Mixtures of the two peroxides were particularly useful in that respect. It must be remembered here that an equimolar mixture of H_2O_2 and D_2O_2 will contain approximately 25 mole % of each constituent along with the hybrid compound HDO_2. In addition the molecular species H_2O, D_2O, and HDO will also be present in various amounts depending on the initial concentration of the peroxides. The H_2O_2 used was over 99% pure and the D_2O_2, about 50% in D_2O; the CCl_4 always contained some H_2O.

The results, shown in Table V and Figs. 12 and 13, lead to some interesting correlations the most striking of which is the exact coincidence of the O—H stretching frequency in HDO_2 with ν_5 in H_2O_2 and similarly, of the O—D

TABLE V

INFRARED BANDS OF ISOTOPIC WATER AND PEROXIDE MOLECULES IN SOLUTION IN CCl_4

cm.$^{-1}$	H_2O_2	D_2O_2	HDO_2	H_2O	D_2O	HDO
2628 v.s.		ν_5, (ν_1)	ν_{O-D}			
2646†	$\nu_2+\nu_6$				ν_1	
2696 s.						ν_{O-D}
2753 s.					ν_3	
3554 v.s.	ν_5, (ν_1)	$\nu_5+\nu_6$	ν_{O-H}			
3565 v.w.		$\nu_1+\nu_6$				
3615 w.				ν_1		
3666 s.		$\nu_2+\nu_5$(?)				ν_{O-H}
3714 s.				ν_3		
4414 v.w.	$\nu_3+\nu_5$					
4818 v.w.	$\nu_1+\nu_6$					
4919 v.w.	$\nu_2+\nu_5$					
5172 v.w.		$\nu_1+\nu_5$				

†*Weak in solutions of D_2O, and medium in solutions of H_2O_2.*

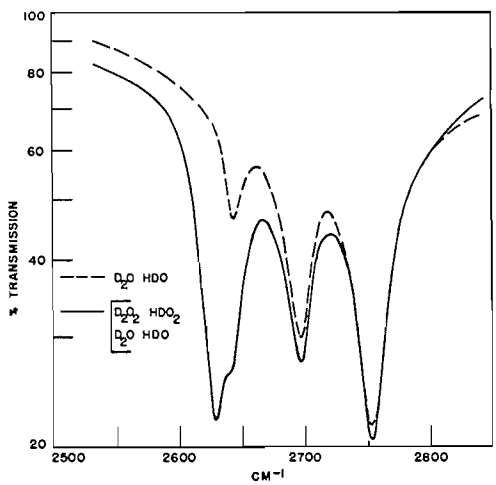

FIG. 12. Absorption by water and peroxide molecules in solution in carbon tetrachloride.

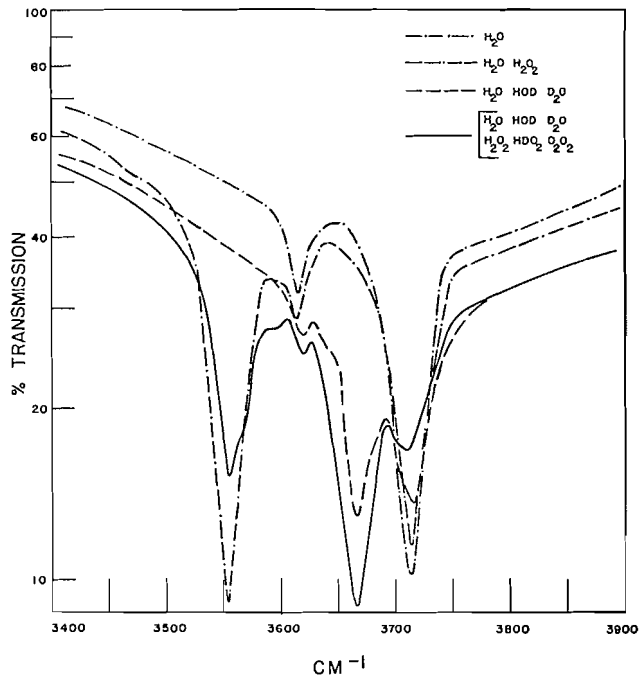

FIG. 13. Absorption bands due to various peroxide and water molecules in carbon tetrachloride solutions.

frequency in HDO_2 with ν_5 in D_2O_2. In HDO the O—H and O—D frequencies occur midway between the symmetric and asymmetric vibrations of the corresponding parent molecules.* By analogy the same relationship may be expected to abide in the peroxide molecules from which, therefore, it follows that the symmetric and asymmetric modes ν_1 and ν_5 should have nearly the same frequency. This conclusion, in harmony with the loose coupling between these two modes, explains why only one O—H stretching vibration has been observed so far, even in the crystal at low temperatures. The weak band found by Taylor (30) shifted some 135 cm.$^{-1}$ from the main O—H band in the Raman spectrum of the crystal was correctly assigned by him to a combination with a lattice vibration since the same difference appears between other frequencies in the solid. It may be noted here that assignment of the two H_2O_2 bands at 4818 and 4919 cm.$^{-1}$ to combination of one stretching with one bending mode is consistent with the previous conclusions, $\nu_1 \approx \nu_5$ and $\nu_2 \approx \nu_6 + 90$ cm.$^{-1}$.

It is instructive to compare the shifts of the various frequencies in the condensed states of the peroxide molecules with those of water. The figures summarized in Table VI are only approximate on account of the width of the absorption maxima. That the shifts of the O—H stretching frequency in peroxides are only half of those in water molecules might be considered an indication of weaker hydrogen bonds in the former. Other physical properties

**The present results for D_2O and HDO dissolved in carbon tetrachloride agree with those of a recent investigation of HDO vapor (4) as regards the frequency of ν_3 in that molecule.*

TABLE VI

FREQUENCY SHIFTS (IN CM.$^{-1}$) FOR WATER AND PEROXIDE MOLECULES IN CONDENSED PHASES

	H_2O_2	D_2O_2	H_2O	D_2O
Vapor – crystal (at −70°C.)				
ν bend.	−115	−53	−55	−30
ν stretch.	290	190	515	350
Vapor – solution in CCl_4				
ν stretch.	56	50	37	30

have been interpreted in the sense of nearly equal energy of these bonds in both compounds (15, 25). Judging from the shortest O—H · · · O distances in the crystals the difference cannot be very large since these distances are 2.78 Å in solid H_2O_2 (1) and 2.76 Å in ice. However, whereas in the latter all the hydrogen bonds are of equal length and tetrahedrally oriented, in H_2O_2 there are two slightly longer O—H · · · O distances per molecule, namely 2.90 Å. Comparison between the two types of molecules is further complicated by the fact that the shifts of the bending frequency are about twice as great in peroxides as in water. On the other hand the shifts in a non-polar solvent involve mainly van der Waals forces and this is confirmed by the observation that for peroxide and water solutions in carbon tetrachloride the shifts are roughly in the same ratio as the polarizability of the two molecules, 2.31 and 1.48 × 10^{-24} cm.^{3} (15).

Structural Parameters

The above data were used to calculate the force constants and bond lengths and angles in the peroxide molecule. All these have been published elsewhere (11) except for the two following points: First, the resolution of the rotational structure of a D_2O_2 band (Table III) makes possible some refinement of the molecular parameters. Thus the locus of points corresponding to the X_{01}

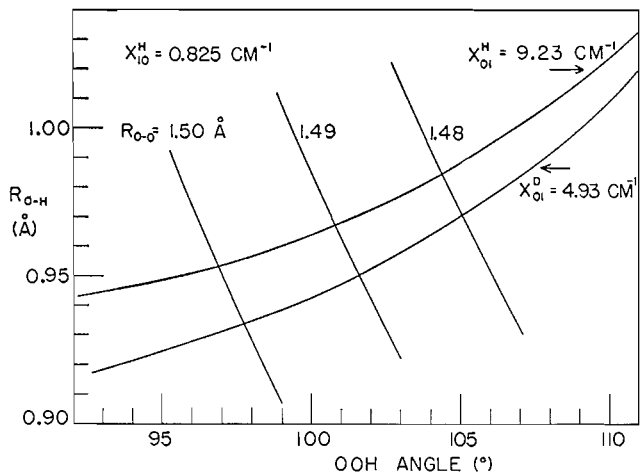

FIG. 14. Locus of O—H distances and OOH angles fitting the rotational constants of H_2O_2 and D_2O_2.

rotational constant for D_2O_2, 4.93 cm.$^{-1}$, has been added to the already published graph in Fig. 14. From the nearness of loci for the two isotopic molecules it is clear that more accuracy is needed for the D_2O_2 constant X_{01} in order to improve the situation significantly. The other point concerns the second rotational constant of H_2O_2 in the ground state, $X_{10} = 0.825$ cm.$^{-1}$ (34) contribution of which was not included in the published calculations. Since it corresponds to the harmonic mean of the two large moments of inertia it is very sensitive to changes in the O—O distance. Calculated values of this constant for $r_{O-O} = 1.48$, 1.49, and 1.50 Å have been plotted in Fig. 14 against r_{O-H} and α_{OOH}, the azimuthal angle being taken as 90°. The intersection of these curves shows that $r_{O-O} = 1.49 \pm 0.01$ Å in exact agreement with the X-ray data on the crystal (1) and within the limits of accuracy of the electron diffraction results (14). This datum is of special interest in connection with the single bond covalent radius of oxygen.

RÉSUMÉ

Le spectre infrarouge du peroxyde d'hydrogène a été mesuré de nouveau avec un appareil à prisme couvrant la région de 1.5 à 25μ. Une bande double, dont les centres sont situés aux environs de 460 et 575 cm.$^{-1}$, apparaît dans la vapeur due à la torsion des groupes OH. La bande rapportée précédemment à 3.8μ a été résolue; elle est attribuée à la combination des modes de déformation $\nu_2+\nu_6$, ce qui implique une anharmonicité positive. Dans le spectre d'absorption du liquide on a observé quatre nouvelles bandes.

On a également mesuré le spectre du peroxyde de deutérium dans les mêmes conditions. On a réussi à résoudre la structure fine d'une des fondamentales, ν_5, à 2661 cm.$^{-1}$, ce qui a permis de calculer les constantes de rotation de la molécule isotopique. Des mélanges des deux peroxydes contenant environ 45% de la molécule hybride HDO_2 ont aussi été étudiés. Enfin on a mesuré l'absorption de ces trois molécules en solutions diluées dans un solvant non polaire. A partir des nouvelles données on a obtenu les constantes de force des diverses liaisons ainsi que les paramètres suivants:

$$r_{O-O} = 1.49 \pm 0.01 \text{ Å},$$
$$r_{O-H} = 0.97 \pm 0.01 \text{ Å},$$
$$\alpha_{OOH} = 100 \pm 2°.$$

REFERENCES

1. Abrahams, S. C., Collin, R. L., and Lipscomb, W. N. Acta Cryst. 4: 15. 1951.
2. Bailey, C. R. and Gordon, R. R. Trans. Faraday Soc. 34: 1133. 1938.
3. Bain, O. Ph.D. Thesis, Laval University, Quebec. 1953.
4. Benedict, W. S., Gailar, N., and Plyler, E. K. J. Chem. Phys. 21: 1302. 1953.
5. Dieke, G. H. and Kistiakowsky, G. B. Phys. Rev. 45: 4. 1934.
6. Fehér, F. Ber. 72: 1778. 1939.
7. Fox, J. J. and Martin, A. E. Proc. Roy. Soc. (London), A, 174: 234. 1940.
8. Ganz, E. Helv. Chim. Acta, 28: 1580. 1945.
9. Gerhard, S. L. and Dennison, D. M. Phys. Rev. 43: 197. 1933.
10. Giguère, P. A. J. Chem. Phys. 18: 88. 1950.
11. Giguère, P. A. and Bain, O. J. Phys. Chem. 56: 340. 1952.
12. Giguère, P. A. and Liu, I. D. Can. J. Chem. 30: 948. 1952.
13. Giguère, P. A., Liu, I. D., Dugdale, J. S., and Morrison, J. A. Can. J. Chem. 32: 117. 1954.

14. GIGUÈRE, P. A. and SCHOMAKER, V. J. Am. Chem. Soc. 65: 2025. 1943.
15. GIGUÈRE, P. A. and SECCO, E. A. Can. J. Chem. 32: 550. 1954.
16. GIGUÈRE, P. A., SECCO, E. A., and EATON, R. S. Discussions Faraday Soc. 14: 104. 1953.
17. HARVEY, R. B. and BAUER, S. H. J. Am. Chem. Soc. 76: 859. 1954.
18. HERZBERG, G. Infrared and Raman spectra of polyatomic molecules. D. Van Nostrand Company, Inc., New York. 1945.
19. LASSETTRE, E. N. and DEAN, L. B. J. Chem. Phys. 17: 317. 1949.
20. LIU, I. D. Ph.D. Thesis, Laval University, Quebec. 1954.
21. LU, C. S., HUGHES, E. W., and GIGUÈRE, P. A. J. Am. Chem. Soc. 63: 1507. 1941.
22. LUFT, N. W. J. Chem. Phys. 21: 179. 1953.
23. LUFT, N. W. Private communication.
24. MASSEY, J. T. and BIANCO, D. R. J. Chem. Phys. 22: 442. 1954.
25. PAULING, L. Nature of the chemical bond. Cornell Univ. Press, Ithaca, N.Y. 1939.
26. PENNEY, W. G. and SUTHERLAND, G. B. B. M. J. Chem. Phys. 2: 492. 1934.
27. PITZER, K. S. J. Chem. Phys. 14: 239. 1946.
28. SUTHERLAND, G. B. B. M. and WILLIS, H. A. Trans. Faraday Soc. 41: 174. 1945.
29. TAYLOR, R. C. Ph.D. Thesis, Brown University, Providence, R.I. 1947.
30. TAYLOR, R. C. J. Chem. Phys. 18: 898. 1950.
31. WAGNER, E. L. and HORNIG, D. F. J. Chem. Phys. 18: 296. 1950.
32. WILLIAMS, V. Z. J. Chem. Phys. 15: 243. 1947.
33. WILSON, M. K. and BADGER, R. M. J. Chem. Phys. 17: 1232. 1949.
34. ZUMWALT, L. R. and GIGUÈRE, P. A. J. Chem. Phys. 9: 458. 1941.

A COMPARATIVE STUDY OF THE DEHYDRATION KINETICS OF SEVERAL HYDRATED SALTS[1]

By R. C. Wheeler[2] and G. B. Frost

ABSTRACT

Rates of dehydration under full vacuum, and also as the pressure of water vapor due to the dehydration process was allowed to increase, have been determined for a number of hydrated salts. The dehydration of manganous sulphate tetrahydrate, zinc sulphate heptahydrate, nickel sulphate hexahydrate, and magnesium sulphate heptahydrate has been found to proceed through the formation of amorphous intermediates, the last two of these being very stable. The dehydration of nickel nitrate hexahydrate, magnesium nitrate hexahydrate, and probably of ferrous sulphate heptahydrate and cobalt chloride hexahydrate at very low pressures takes place with the formation of crystalline intermediates. The results obtained are discussed in relation to the dependence of rate of dehydration on water vapor pressure previously reported for copper sulphate pentahydrate and for manganous oxalate dihydrate.

INTRODUCTION

It has been shown in an earlier paper (3) that when powdered samples of copper sulphate pentahydrate are dehydrated under vacuum at moderate temperatures, the dehydration proceeds to the monohydrate stage with a gradual decrease in rate. The product is amorphous in the sense that it does not diffract X-rays. However, if similar samples are placed in a closed and initially evacuated space, and the water vapor pressure due to the dissociation of the hydrate allowed to increase in the vessel, the rate of dehydration at first decreases to a minimum value, then increases to a value much larger than the minimum rate, this being followed, in turn, by a decline. The end product formed under these conditions is crystalline.

The minimum in rate occurs at a water vapor pressure of approximately 0.25 mm. and the periods of acceleration and decline, over a range in pressure of only a few millimeters, these pressures being far below those corresponding to possible phase equilibria. This marked effect of water vapor in a very narrow region of pressure has been observed also by carrying out dehydrations at a series of controlled pressures. The dehydration curves obtained for pressures below 0.25 mm. are quite different than for those above this value, the former showing a gradual loss in weight with time, while the latter show induction periods, the duration of which depends on the pressure.

The behavior of copper sulphate pentahydrate in this respect is similar to that of manganous oxalate dihydrate (6, 7), which for many years was regarded as unique in the dependence of its rate of dehydration on water vapor pressure. On vacuum dehydration this salt hydrate also yields a product which does not diffract X-rays.

Explanations of the form of these rate curves have been discussed elsewhere (1, 3, 4). The initial fall in rate is probably due to the retarding effect of water

[1]*Manuscript received November 16, 1954.*
Contribution from the Department of Chemistry, Queen's University, Kingston, Ontario.
[2]*Present address: Imperial Oil Fellow in Chemistry, Cambridge University.*

vapor on diffusion through a transition layer of amorphous material formed during the initial stages of dehydration, and the intermediate acceleration in rate, to an increase in porosity occurring on crystallization of the amorphous product in the presence of adsorbed water. The final decline is probably due to the gradually increasing impedance of the crystalline layer.

The purpose of the present work has been to survey the dehydration kinetics of a number of hydrated salts in order to obtain information regarding the generality of these effects. Rate determinations have been carried out for dehydrations at pressures of 10^{-5} mm. or less (designated as vacuum dehydrations in the following) and also while the pressure due to the liberated water vapor increased. For convenience, these latter are referred to as "increasing pressure" dehydrations. Determinations of rates of dehydration at externally controlled and constant pressures of water vapor have not been made in this work, although they give much more detailed information regarding the nature of the processes involved. However, such experiments are very time consuming, and it was desired to obtain comparative data for as many salts as possible.

EXPERIMENTAL METHOD

The salts used were reagent grade materials, recrystallized twice, air-dried, and screened, the "through 60 mesh on 80 mesh" fraction being used.

The essential features of the apparatus have been described (3). Powdered samples were placed in a small basket made of 100-mesh copper gauze, and suspended from a quartz spiral. The water vapor pressure in the system was measured by means of an oil manometer which had a conventional vertical arm and also an inclined arm for fine sensitivity in low pressure ranges. Readings of spiral extension and of pressure were made with a rigidly mounted cathetometer.

Vacuum dehydrations were carried out by allowing small samples (approximately 50 mgm. in most cases) to dehydrate while the pumps were in operation. Readings were plotted as weight-loss versus time. For several salts these curves were found to present points of interest, but they also served to establish the composition of the dehydration product. Increasing pressure dehydrations were carried out in the following manner. The samples were nucleated by allowing dehydration to proceed under vacuum to 10% of the total possible weight loss as determined by vacuum dehydration. The spiral case was then closed off from the pumps and the samples allowed to dehydrate and slowly build up a pressure of water vapor in the system. Readings of weight-loss were commenced at the beginning of the nucleation period, and those of pressure, at the time of closing off the spiral case, both of these being continued at a series of times for several hours. Determinations of rates of dehydration were made by evaluating tangents to the weight-loss versus time curves at a series of time values.

X-ray powder photographs were made using copper K_α radiation. For convenience, the term "X-ray amorphous" is used to describe products for which no diffraction lines were observed.

RESULTS

(1) *Manganous Sulphate Tetrahydrate*

Vacuum dehydration at 40°C. resulted in the smooth continuous weight-loss versus time curve shown in Fig. 1 (lower curve) the end product being of the monohydrate composition.

The results obtained on dehydration at 50°C. as the pressure of water vapor in the system increased are shown in Fig. 2.

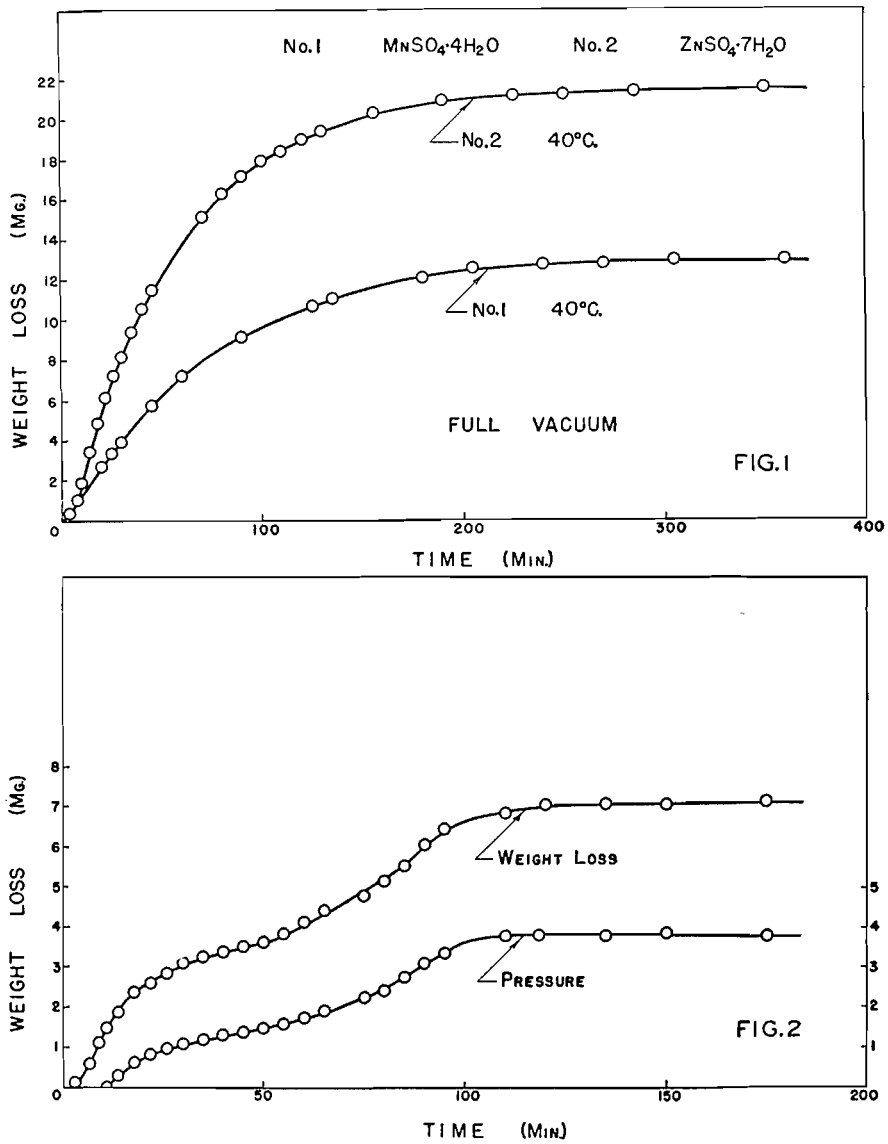

FIG. 1. The dehydration of zinc sulphate heptahydrate and of manganous sulphate tetrahydrate under vacuum.

FIG. 2. The dehydration of manganous sulphate tetrahydrate with increasing pressure of water vapor.

Following the period of nucleation under vacuum, the slope of the weight-loss curve gradually decreases as the pressure in the system becomes greater. The curve flattens somewhat at a weight-loss of about 3.5 mgm. which corresponds roughly to the trihydrate composition. An accelerated rate is then observed followed by a decline, the slope becoming zero at the dihydrate stage. These rates of dehydration plotted against the pressure, are shown in Fig. 3. Although the decline in rate to a minimum value, followed by an accelerated period, is similar to that reported for copper sulphate pentahydrate and for manganous oxalate dihydrate, the actual weight-loss versus time curve (Fig. 2) is slightly different in that a fairly rapid weight-loss persists for some time after the sample is exposed to water vapor, whereas with copper sulphate pentahydrate an induction period occurs almost immediately.

Unfortunately, X-ray data could not be obtained for this salt with the copper target available, since the absorption of the radiation was strong, resulting in fluorescent radiation.

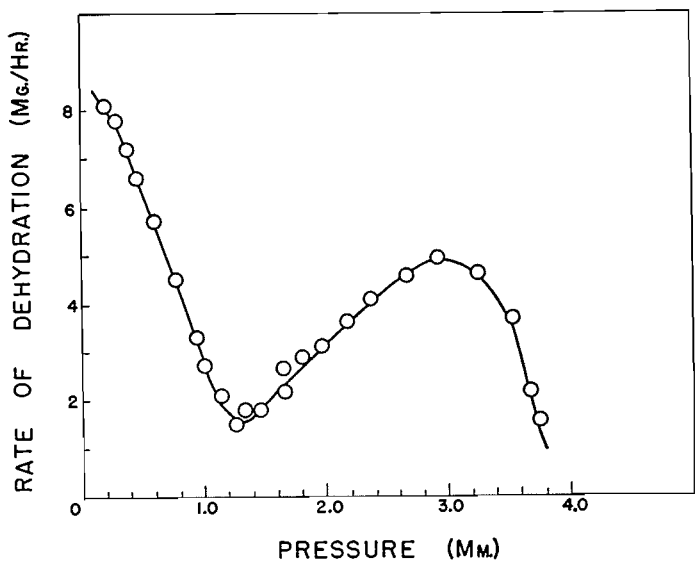

FIG. 3. The change in rate of dehydration of manganous sulphate tetrahydrate with pressure increase.

(2) *Zinc Sulphate Heptahydrate*

Vacuum dehydration at 40°C. again resulted in a smooth continuous curve (upper curve, Fig. 1), the end product being stoichiometrically of the monohydrate composition, and X-ray amorphous.

Measurements made at increasing pressure, and at 40°C., are shown in Fig. 4.

A small but reproducible induction period occurred immediately after nucleation, corresponding to the longer induction period observed for copper sulphate pentahydrate. Following this, the weight-loss curve has a slightly concave portion followed by a slightly convex portion, there being no clearly

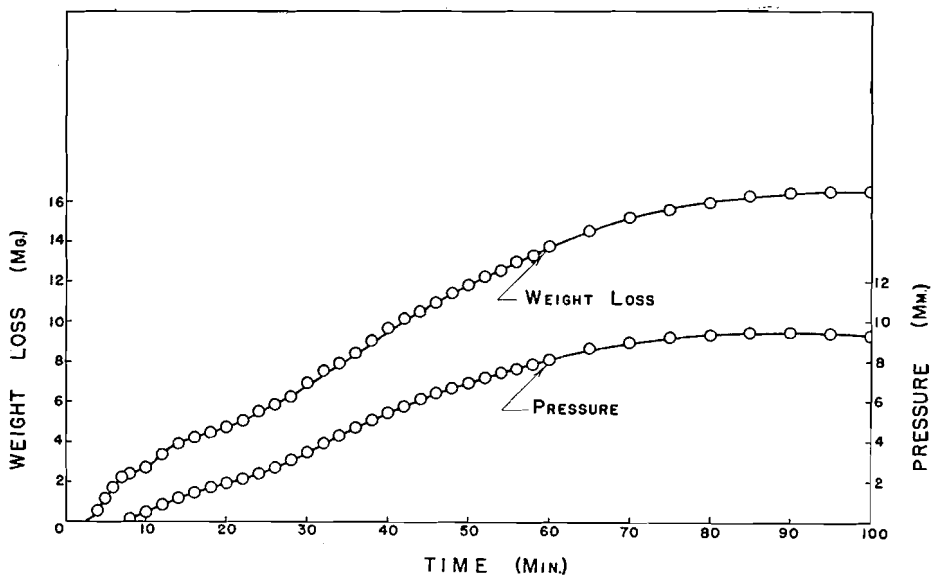

FIG. 4. The dehydration of zinc sulphate heptahydrate with increasing pressure of water vapor.

defined induction period. This resulted in two minima being obtained when the rate of dehydration was plotted against the pressure, as shown in Fig. 5.

X-ray powder photographs of the products obtained from these increasing pressure dehydrations showed a clearly defined diffraction pattern of monohydrate lines. Patterns identical with these were obtained when sealed samples of the amorphous product formed on vacuum dehydration were allowed to stand for several days.

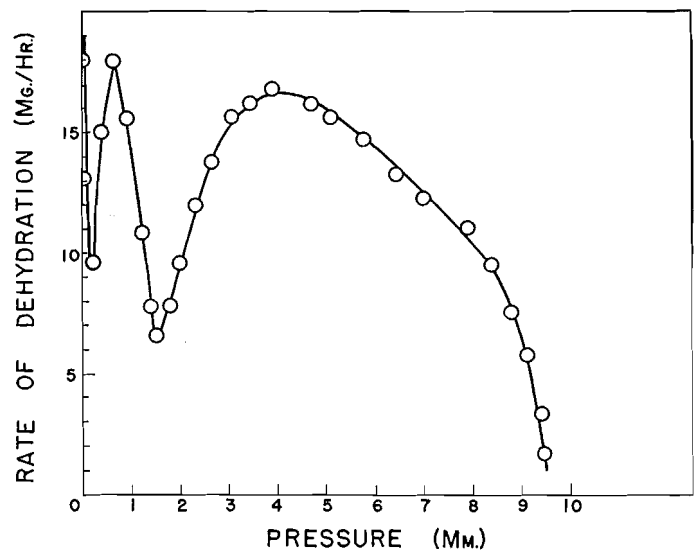

FIG. 5. The change in rate of dehydration of zinc sulphate heptahydrate with pressure increase.

(3) *Ferrous Sulphate Heptahydrate*

Dehydration under vacuum again exhibited a continuous loss of water from the heptahydrate to the monohydrate, the curve being similar to those shown in Fig. 1.

The weight-loss curve obtained on dehydration at increasing pressure at 60°C. is shown in Fig. 6.

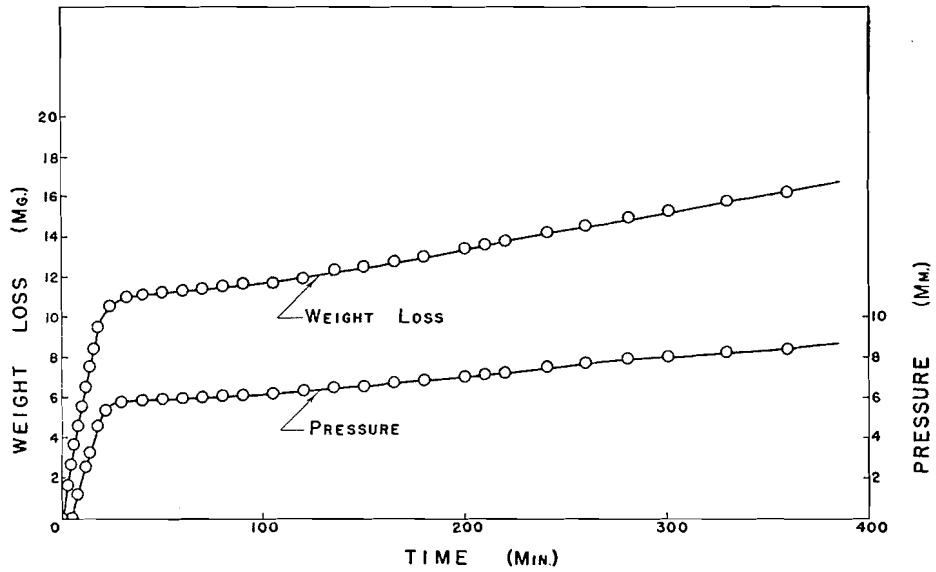

FIG. 6. The dehydration of ferrous sulphate heptahydrate with increasing pressure of water vapor.

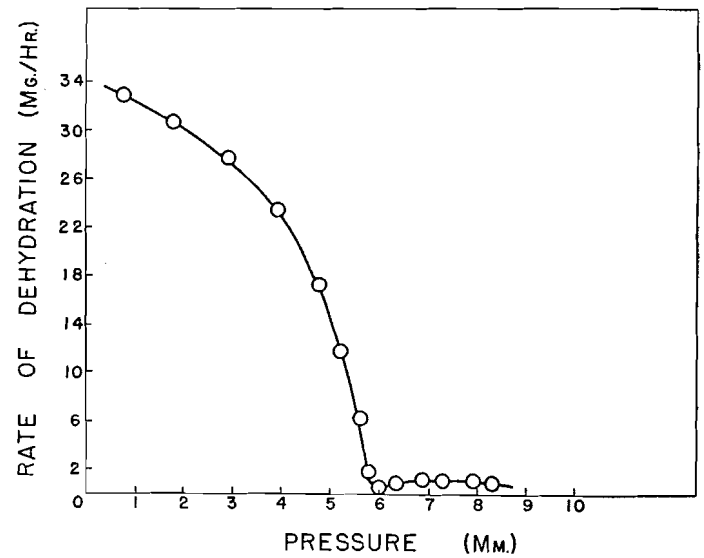

FIG. 7. The change in rate of dehydration of ferrous sulphate heptahydrate with pressure increase.

Following nucleation, rapid dehydration continued to somewhat beyond the tetrahydrate composition where an induction period set in followed by a slow increase in rate. This increase was diminished as the dehydration temperature was lowered, no increase being observed in a 21 hr. period at 40°C. The rate of dehydration at 60°C., plotted against the water vapor pressure, is shown in Fig. 7.

The curve is similar in character to that shown in Fig. 3, although the secondary increase in rate is much smaller, and the minimum occurs at a much higher pressure. It was not possible to obtain X-ray diffraction patterns for this salt for the reason that has been mentioned for manganous sulphate.

(4) *Nickel Nitrate Hexahydrate*

Vacuum dehydrations at several temperatures resulted in curves of different character than those described in the foregoing; the curve obtained at 40°C. is shown in Fig. 8, those obtained at other temperatures being similar. The initial loss of water is rapid and the rate nearly linear. After a weight-loss of about 6 mgm., the curve transforms to a second region which is also nearly linear, and then declines. If the two linear sections are extended to point A (Fig. 8), the point of intersection is found to be at approximately the tetrahydrate composition. The slopes of these linear portions were found to increase with temperature.

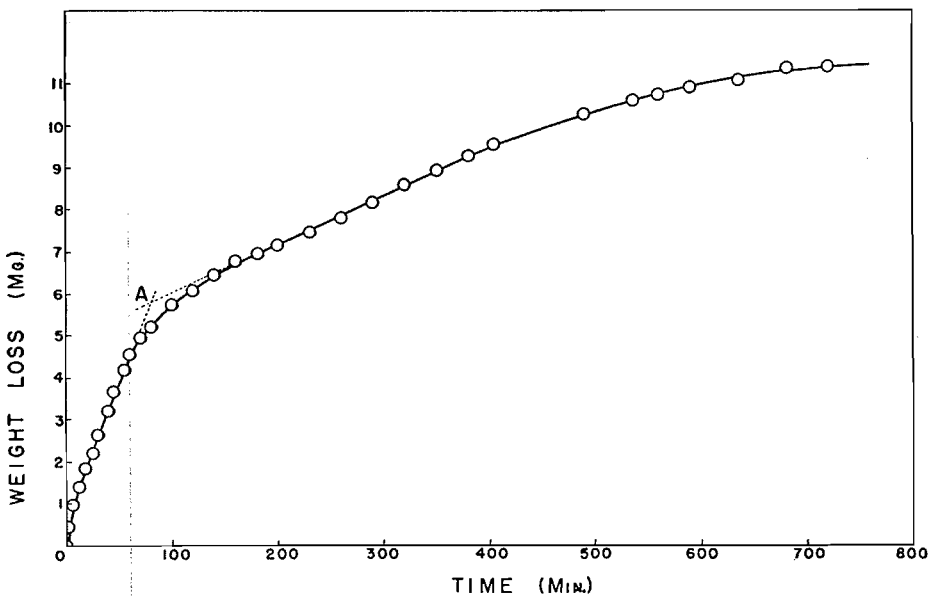

FIG. 8. The dehydration of nickel nitrate hexahydrate under vacuum.

The end product had the dihydrate composition. It appears, therefore, that under vacuum, dehydration takes place fairly rapidly to the tetrahydrate state, followed by the dehydration of this intermediate product to the dihydrate.

Unlike the examples reported in the foregoing, the end product of vacuum dehydration gave a definite X-ray diffraction pattern. However, if the time of preparation for the exposure were made as short as possible, the diffraction lines were very faint. It is possible that an amorphous material of very low stability was produced, subsequent handling being sufficient to cause the commencement of crystallization.

For dehydrations carried out at increasing pressure, an induction period was observed at the tetrahydrate stage followed by a slow and gradual increase in rate, the curves resembling closely those obtained for ferrous sulphate heptahydrate. Close examination of X-ray diffraction patterns obtained indicated the presence of tetrahydrate and dihydrate lines. It appears therefore that the first step in this process is the formation of crystalline tetrahydrate which then nucleates and forms crystalline dihydrate at a much slower rate. The rate of dehydration plotted against pressure is shown in Fig. 9, the curve again resembling that obtained for ferrous sulphate heptahydrate.

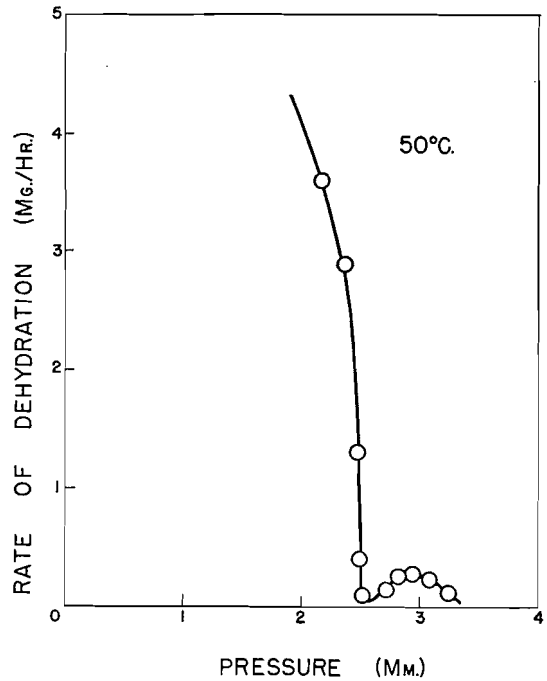

FIG. 9. The change in rate of dehydration of nickel nitrate hexahydrate with pressure increase.

The possibility of the formation of a basic salt in the dehydration process has been disregarded since it was found that the product formed both on vacuum and increasing pressure dehydration gave a pattern of only hexahydrate lines after standing in the room atmosphere for a few hours.

(5) *Magnesium Nitrate Hexahydrate*

Preliminary experiments with this salt indicated that effects occurred which were quite different from those observed for the other salts studied. Conse-

quently a number of dehydrations were carried out at several temperatures. The details of the experiments are given in Table I.

TABLE I

DEHYDRATION DATA FOR MAGNESIUM NITRATE HEXAHYDRATE

Expt. No.	Temp., °C.	Type of dehydration	Time of dehydration, min.	Sample wt., mgm.	Moles water lost per formula-wt.
1	30	Vacuum	1150	34.7	3.80
2	35	Vacuum	1166	40.2	3.92
3	40	Vacuum	1300	39.8	4.05
4	45	Vacuum	580	37.1	3.93
5	50	Vacuum	772	37.0	3.70
6	50	Vacuum	1370	37.3	3.98
7	55	Vacuum	510	38.9	2.39
8	40	Increasing pressure	1230	40.8	1.95
9	50	Increasing pressure	1415	35.4	3.42
10	40	Vacuum	35	32.3	1.89

Weight-loss versus time curves for the vacuum dehydration experiments Nos. 1, 3, 5, and 7 of Table I are shown in Fig. 10.

These dehydrations all displayed an induction period setting in at the tetrahydrate composition. These vacuum dehydration curves are, therefore, of the type which has been previously associated with dehydrations at increasing pressure. Furthermore, the period of acceleration following the induction period shows an interesting temperature dependence, the rate at 40°C. being higher than that at 30°C. and then declining as the temperature is raised.

Rate curves plotted against time, for these temperatures, are shown in Fig. 11. These curves show the minima and accelerated rates associated with increasing pressure dehydrations in the foregoing.

The end product of the vacuum dehydrations was found to be crystalline dihydrate, well defined and characteristic diffraction patterns being obtained. Clearly defined tetrahydrate lines were obtained with samples (Expt. 10) partially dehydrated to this stage. It appears quite definite, therefore, that on vacuum dehydration this salt forms crystalline tetrahydrate which then nucleates and forms crystalline dihydrate at rates which are markedly temperature dependent.

Experiments 8 and 9 of Table I were carried out at increasing pressure. Dehydration was observed to take place rapidly to the tetrahydrate stage at which an induction period set in, followed at 50°C. by a slow increase in rate, while at 40°C. no increase could be detected. The rate versus pressure curve obtained at 50°C. was found to be similar to that reported above for nickel nitrate hexahydrate.

Although many basic hydrated salts of magnesium have been reported, the formation of these takes place at dehydration temperatures exceeding 150°C. When the crystalline products obtained in the present experiments were allowed to stand in the humidity of the ordinary room atmosphere reversion to the hexahydrate crystalline form occurred.

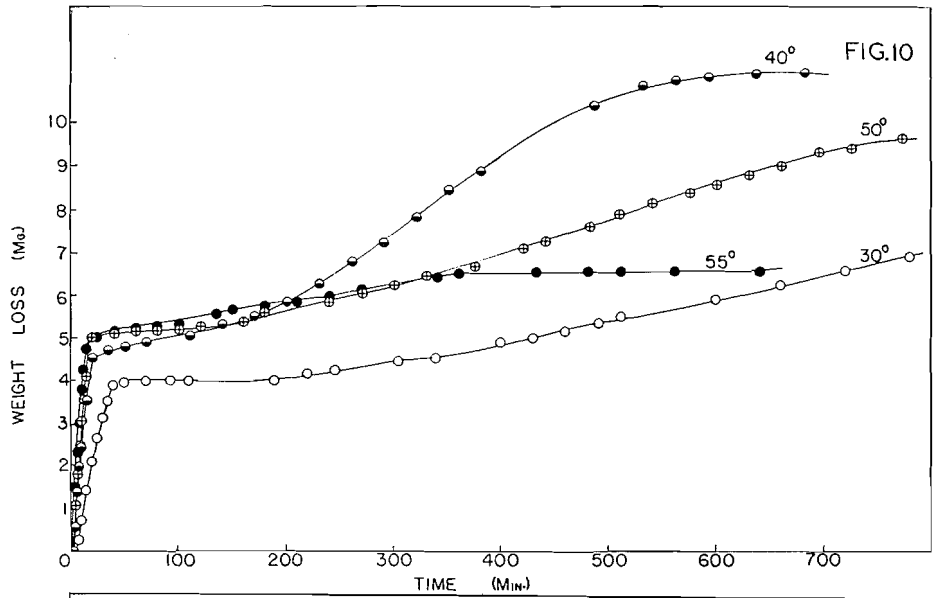

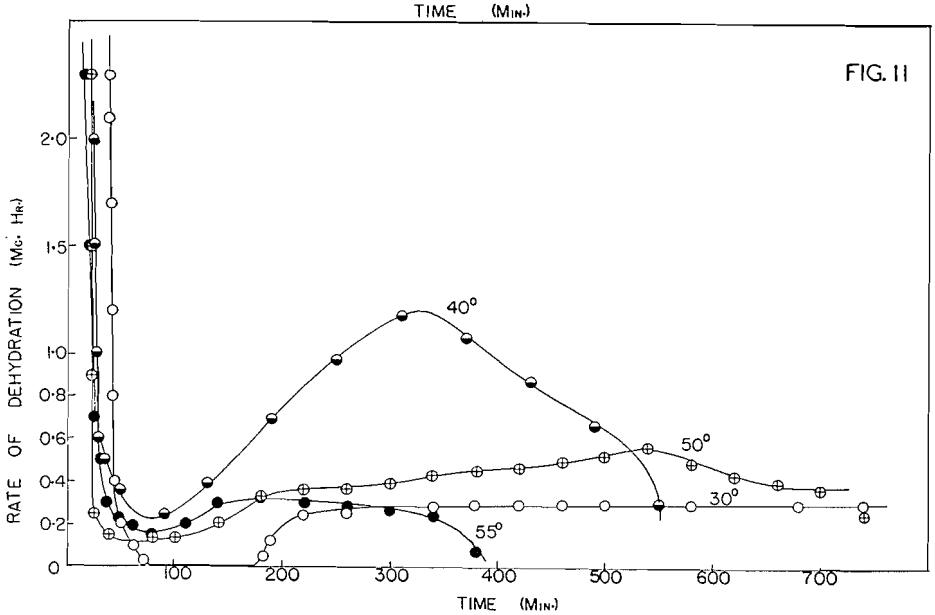

FIG. 10. The dehydration of magnesium nitrate hexahydrate under vacuum at several temperatures.

FIG. 11. The change in rate of dehydration of magnesium nitrate hexahydrate at several temperatures.

Since the dehydration from the tetrahydrate to the dihydrate stage has a temperature coefficient exhibiting a maximum in the region of 40°C., a careful survey of the rates in the temperature range from 30°C. to 55°C. was carried out. In order to make a comparison, the maximum rate of dehydration was found from the rate versus time curves (or from rate versus percentage decomposition curves) and converted to a rate per milligram of sample. (The com-

parison of maximum rates rather than rates obtained at the same percentage decomposition has been made in view of a suggestion by Colvin and Hume (1) that the maximum rates correspond to approximately the same interfacial conditions.) The results of these calculations are given in Table II and are

TABLE II

CALCULATED MAXIMUM RATES

Expt. No.	Temp., °C.	Maximum rate, mgm./hr./mgm.	Point Fig. 12
1	30.4	10.06	A
2	35.1	44.62	B
3	40.2	48.20	C
4	45.0	37.81	D
5	49.0	21.10	E
6	50.1	22.70	F
7	55.1	12.06	G

plotted in Fig. 12. From this figure it is clear that at temperatures above approximately 40°C., the mechanism of the dehydration process is in some way adversely affected by increase in temperature, the rate of dehydration becoming negligible above approximately 55°C.

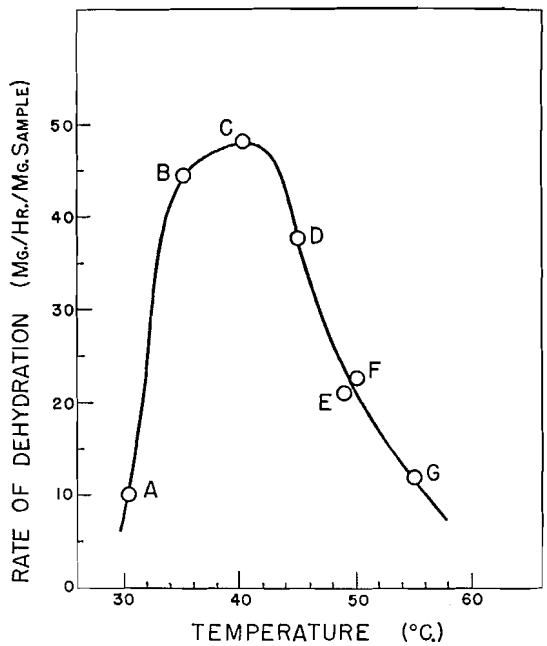

FIG. 12. The dependence of the second stage of the rate process on temperature for magnesium nitrate hexahydrate.

(6) *Magnesium Sulphate Heptahydrate*

Vacuum dehydration of this salt resulted in a smooth continuous curve of the same type as those shown in Fig. 1. The end product had the monohydrate

composition and was X-ray amorphous. Lines characteristic of the crystalline monohydrate appeared when amorphous samples were sealed and heated for two days at 130°C.

However, the behavior of this salt on dehydrating at increasing pressure was very different from that of any of the salts mentioned in the foregoing. It was found that the rate of dehydration gradually decreased with corresponding increase in pressure, no induction periods being observed. The product obtained was X-ray amorphous. The change of rate with pressure increase is shown in Fig. 13.

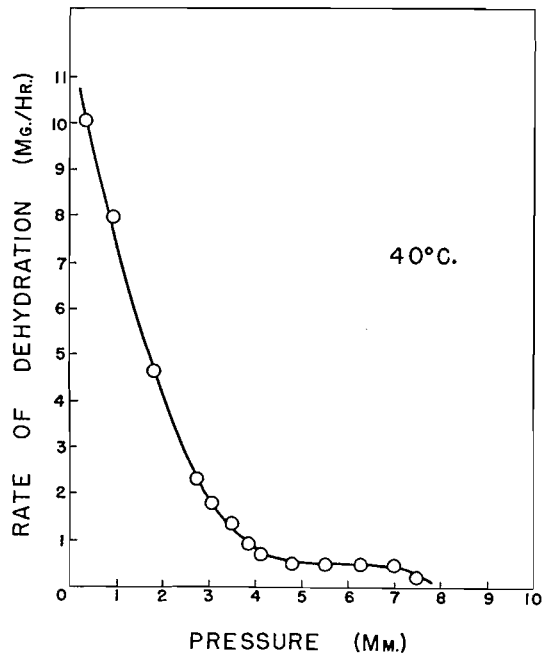

FIG. 13. The change in rate of dehydration of magnesium sulphate heptahydrate with pressure increase.

(7) *Nickel Sulphate Hexahydrate*

This salt was found to behave in similar manner to magnesium sulphate heptahydrate. The product of vacuum dehydration had the monohydrate composition and was X-ray amorphous. The effect of increasing water vapor pressure on the dehydration rate is similar to that shown in Fig. 13. Faint hexahydrate lines were obtained in this sample, indicating incomplete dehydration.

(8) *Cobalt Chloride Hexahydrate*

Vacuum dehydration resulted in curves similar to those obtained for nickel nitrate hexahydrate. These are shown in Fig. 14.

The rate of dehydration proceeds rapidly to the dihydrate stage followed by a much slower rate. Prolonged dehydration yields a product having the mono-

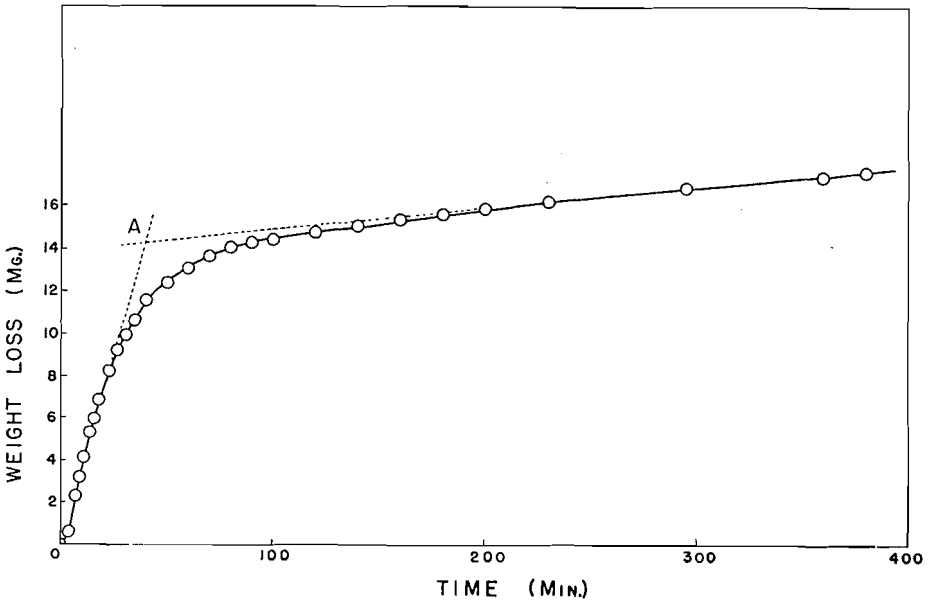

FIG. 14. The dehydration of cobalt chloride hexahydrate under vacuum.

hydrate composition. Unfortunately, the crystalline or amorphous character of the end product could not be definitely determined by X-ray diffraction for reasons which have been mentioned.

On dehydrating at increasing pressure, a rapid loss of water occurred to approximately the dihydrate composition, beyond which no change was observed. The change in rate with pressure increase is shown in Fig. 15.

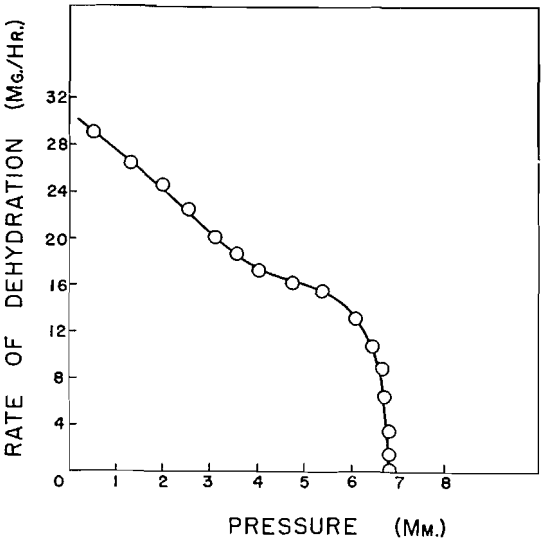

FIG. 15. The change in rate of dehydration of cobalt chloride hexahydrate with pressure increase.

DISCUSSION

Although it has not been possible to determine from X-ray evidence whether or not the product obtained from the vacuum dehydration of manganous sulphate tetrahydrate is amorphous, the similarity of the dehydration curves to those previously reported for copper sulphate pentahydrate (3) and for manganous oxalate dihydrate (6, 7) suggests that the dehydration process is the same in each case and is subject to the same interpretation. However, the minimum in the rate curve for the manganous salt occurs at about 1.2 mm., whereas for copper sulphate pentahydrate it occurs at about 0.25 mm., and for manganous oxalate dihydrate at less than 0.2 mm.

The dehydration process for zinc sulphate heptahydrate is more complex. Since an X-ray amorphous product is formed on vacuum dehydration, it is certain that this forms during the nucleation period. It is possible that the short induction period following nucleation (or therefore the first minimum in the rate curve) is due to the crystallization of this product at very low pressure. No adequate interpretation can be made of the second minimum at higher pressure on the basis of the present data and a more comprehensive study of the dehydration kinetics of this salt hydrate should be made.

Magnesium sulphate heptahydrate is of particular interest in that the dehydration curves obtained indicate that an X-ray amorphous product is formed not only on vacuum dehydration but also in the presence of water vapor at a pressure much higher than those observed for the other salts. The amorphous product is therefore very stable. This result suggests that this salt might be found to behave in a manner similar to copper sulphate pentahydrate if investigated over a wide range of controlled and constant pressures of water vapor. Experiments of this type are being carried out in this laboratory and will be reported in a later paper. The data given for nickel sulphate hexahydrate suggest a similar type of behavior.

The formation of crystalline products in the vacuum dehydration of nickel nitrate hexahydrate and magnesium nitrate hexahydrate indicates that if an amorphous product is formed at all, it must crystallize at extremely low water vapor pressures. Although the decomposition products obtained from ferrous sulphate heptahydrate could not be characterized by X-ray diffraction, the similarity of the dehydration curves to those obtained for nickel nitrate hexahydrate suggests that these products may be also crystalline. The minima observed in the rate versus pressure curves for these salts must be interpreted therefore in a somewhat different manner than has been done for copper sulphate pentahydrate. Instead of a process involving the crystallization of amorphous material, it must be assumed that as nuclei develop on the surfaces of the crystalline intermediates, the development of macrocrystalline aggregates is catalyzed by adsorbed water molecules.

The curves obtained for the dehydration of cobalt chloride hexahydrate are also similar to those obtained for nickel nitrate hexahydrate and it is probable that this dehydration also proceeds through the formation of a crystalline intermediate. However, with this salt the dehydration at increasing pressure does not proceed past the dihydrate stage, the corresponding pressure being

much lower than the equilibrium pressure reported by Derby and Yngve (2) for the hexahydrate – dihydrate – water vapor equilibrium. The behavior of this salt is of interest in comparison with that of magnesium sulphate heptahydrate, and a more comprehensive study of its dehydration kinetics is in progress.

The dehydration of magnesium nitrate hexahydrate is of particular interest, since the sequence of changes occurring on vacuum dehydration is that which is observed for other salts as the pressure of water vapor increases. Dehydration takes place rapidly with the formation of crystalline tetrahydrate which then nucleates and forms crystalline dihydrate. If it is assumed that the development of macrocrystals from these nuclei is catalyzed by water vapor, then this process must occur at the very low pressures prevailing in the transition layer as the water molecules liberated from the hexahydrate lattice pass through the crystalline tetrahydrate layer into the external evacuated space. The rate of escape of water molecules from the dehydrating tetrahydrate lattice will increase with temperature. However, any slight adsorption in the transition layer will decrease with the temperature. The opposition of these two effects may qualitatively explain the over-all dependence of rate on temperature which has been observed. However, any such explanation must be regarded as highly tentative in view of the lack of more comprehensive data. It will be observed from Fig. 10 that the rate of dehydration of the primary hexahydrate lattice increases with temperature in the normal manner, as also does both the primary and secondary rate for nickel nitrate hexahydrate.

It is clear from all the data presented in the foregoing that the effect of water vapor in first decreasing and then accelerating the over-all rate of dehydration, first observed by Topley and Smith for the decomposition of manganous oxalate dihydrate, is quite general and is always associated with an induction period in which a crystalline lower hydrate is formed from an intermediate. The intermediate may be an X-ray amorphous product or it may be crystalline. The nature of the X-ray amorphous product is, therefore, of interest. It may consist of an aggregate of microcrystals with dimensions of only a few unit cells, these being below the limiting size required for X-ray diffraction (about 100 Å). If this is so, the nature of the process whereby macrocrystals are formed in the presence of water molecules from X-ray amorphous intermediates does not differ in any essential way from that in which macrocrystals of the end product are formed from a nucleated crystalline intermediate. However, the heats of transition from the X-ray amorphous to the crystalline states which have been reported for the monohydrates of copper and zinc sulphate (4) are higher than might be expected from consideration of surface energy only, and it is possible that, for these salts at least, some condition other than high state of division results from low pressure dehydration of the primary lattices. The determination of such heats of transition for other salts is in progress.

The limiting pressure of water vapor above which amorphous products crystallize varies greatly from one salt hydrate to another, being virtually zero for nickel nitrate, magnesium nitrate, and cobalt chloride, and ranging to

presumably relatively high values for magnesium sulphate and nickel sulphate. Experiments carried out in this laboratory suggest that this effect is related to differences in the surface areas and capillary structures of the transition layer, although the nature of the amorphous material itself may also be a factor (5).

ACKNOWLEDGMENTS

Financial assistance given by the National Research Council of Canada during the progress of this work is gratefully acknowledged. One of the authors (R. C. W.) wishes to thank the Research Council of Ontario for a Scholarship held during part of this work.

REFERENCES

1. COLVIN, J. and HUME, J. Trans. Faraday Soc. 34: 969. 1938.
2. DERBY, I. H. and YNGVE, V. J. Am. Chem. Soc. 38: 1439. 1916.
3. FROST, G. B. and CAMPBELL, R. A. Can. J. Chem. 31: 107. 1953.
4. FROST, G. B., MOON, K. A., and TOMPKINS, E. H. Can. J. Chem. 29: 604. 1951.
5. QUINN, H. W., MISSEN, R. W., and FROST, G. B. Can. J. Chem. 33: 286. 1955.
6. TOPLEY, B. and SMITH, M. L. J. Chem. Soc. 321. 1935.
7. VOLMER, M. and SEYDEL, G. Z. physik. Chem. A, 179: 153. 1937.

NOTES

INTERDIFFUSION OF POLYISOBUTYLENE AND CYCLOHEXANE

By J. Kelly and A. T. Hutcheon

Prior to a more extensive study of the diffusion in dilute solutions of polyvinylacetate in acetone, results are reported here for one sample of polyisobutylene in interdiffusion with cyclohexane. The measurements were intended to be an experimental test for this system of the equation (5).

$$[1] \qquad D = \frac{RTP^{-1}\Phi^{\frac{1}{3}}}{\eta_0 N(M[\eta])^{\frac{1}{3}}}$$

in which the product $P^{-1}\,\Phi^{\frac{1}{3}}$ is claimed to be a constant for all polymer systems and the other symbols have their usual significance. Furthermore, the dependence of the diffusion coefficient on concentration serves as a test of the equation (4).

$$[2] \qquad Y = \frac{1+2\Gamma_2 c+3\Gamma_3 c^2}{D} = \frac{1+k_s c}{D_0}$$

since Γ_2 has been obtained from osmotic pressure measurements (2), and k_s from sedimentation (6) data assuming a linear dependence of the frictional coefficient on concentration.

EXPERIMENTAL

The diffusion was carried out in a Neurath cell (7) at 30°C. ±0.02 in a constant temperature air bath on a vibration-free mounting. The diffusion coefficients were calculated by the area-maximum ordinate method (3) from measurements of the refractive index gradient obtained by the scale method of Lamm (10).

The diffusion coefficient was measured at three different initial concentrations and at time intervals of several hours for each concentration, as shown in Table I. Average values of D_A are given for concentrations 0.2636 and 0.3660 gm./100 ml. For the concentration 0.5676 gm./100 ml., there was a decided gradual decrease in the value of D_A with time and for this experiment a corrected value of D was obtained by extrapolation to infinite time of the plot of D versus 1/time. This procedure is necessary when the boundary is not initially sharp (8).

The average and corrected values of D_A and the value of $\Gamma_2 = 0.63$ (2) were used in plotting the function

$$Y = (1+2\Gamma_2 c+3\Gamma_3 c^2)/D$$

against the mean concentration $c_0/2$ in Fig. 1 for $\Gamma_3 = \frac{5}{8}\,.\,\Gamma_2^2$ and $\Gamma_3 = \frac{1}{4}\,.\,\Gamma_2^2$. From the intercept, $1/D_0$, D_0 is calculated to be 3.3×10^{-7} cm.^{2} sec^{-1}.

TABLE I

DIFFUSION COEFFICIENTS, D_A, FOR POLYISOBUTYLENE IN CYCLOHEXANE AT 30°C.—MOLECULAR WEIGHT 86,700

Concentration, gm./100 ml.	Time (sec.)	$D_A \times 10^7$, cm.²/sec. (Area-maximum ordinate method)
0.2636	63,270	3.31
0.2636	122,550	3.23
		Average value 3.27±0.04
0.3660	22,350	3.27
0.3660	30,177	3.23
0.3660	58,895	3.28
0.3660	86,430	3.23
		Average value 3.25±0.03
0.5676	28,020	3.48
0.5676	41,516	3.41
0.5676	82,183	3.35
0.5676	104,940	3.34
		Corrected value 3.29

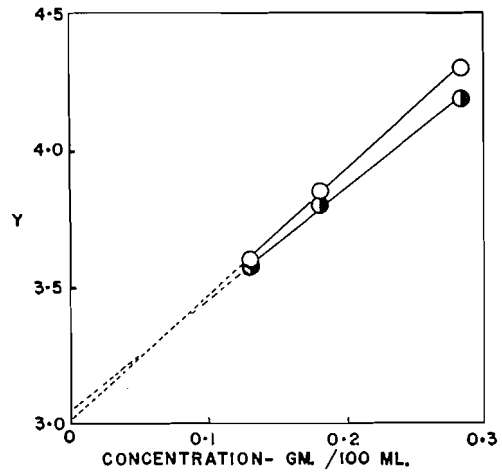

FIG. 1. $Y = (1+2\Gamma_2 c+3\Gamma_3 c^2)/D = (1+k_s c)/D_0$ as a function of concentration $c_0/2$, in gm./100 ml.

○ — $\Gamma_3 = \frac{5}{8}.\Gamma_2^2$
◑ — $\Gamma_3 = \frac{1}{4}.\Gamma_2^2$

DISCUSSION

This experimental value may be compared with that calculated from equation 1. Using Flory's data (6)—$\eta_0 = 9.7 \times 10^{-3}$ poises, $[\eta] = 2.76\times10^{-4} M^{0.69}$, $M = 86{,}700$, and $P^{-1}\Phi^{\frac{1}{3}} = 2.65 \times 10^{-6}$ for this particular fraction—D_0 is calculated to be 2.8×10^{-7} cm.²/sec. at 20°C. The value of $D_0 = 3.4 \times 10^{-7}$ cm.²/sec. at 30°C. is obtained from the relation (7)

$$D_0^{30} = D_0^{20} \frac{T_{30}\eta_{20}}{T_{20}\eta_{30}}$$

where T is the absolute temperature and η the viscosity of the solvent. This is in good agreement with the experimental value and better agreement would be obtained using the average value of $P^{-1}\,\Phi^{\frac{1}{3}}$ reported as 2.5×10^6 (1).

From equation 2, the slope of the plot of Y versus concentration is equal to k_s/D_0. From the data of Flory *et al.* on sedimentation (2), k_s is equal to 1.28 for this fraction of polyisobutylene, hence, using the calculated value of D_0, the predicted slope would be $1.28/(3.4 \times 10^{-7}) = 3.8 \times 10^6$. If the observed value of D_0 equal to 3.3×10^{-7} were used, the slope would be 3.9×10^6. The observed slopes in Fig. 1 are 4.6×10^6 for $\Gamma_3 = \frac{5}{8}.\Gamma_2^2$ and 4.1×10^6 for $\Gamma_3 = \frac{1}{4}.\Gamma_2^2$ when Y is plotted against $c_0/2$ from Table II. The suggestion

TABLE II

VALUES OF $Y = (1+2\Gamma_2 c+3\Gamma_3 c^2)/D = (1+k_s c)/D_0$ AS A FUNCTION OF CONCENTRATION

Concentration $c_0/2$, gm./100 ml.	$D_0 \times 10^7$ cm.^{2}/sec.	$Y \times 10^{-6}$ for $\Gamma_3 = \frac{5}{8}.\Gamma_2^2$	$Y \times 10^{-6}$ for $\Gamma_3 = \frac{1}{4}.\Gamma_2^2$
0.132	3.27	3.61	3.58
0.183	3.25	3.86	3.81
0.284	3.29	4.31	4.20

that the third virial coefficient should be less than $\frac{5}{8}.\Gamma_2^2$ (9) and that it is $\frac{1}{4}.\Gamma_2^2$ (2) is therefore supported by these data.

The values of D at the concentration of 0.2636 gm./100 ml. were least precise and if the other values at 0.3660 and 0.5676 gm./100 ml. are weighted more in drawing the lines in Fig. 1, the slope of the line for $\Gamma_3 = \frac{1}{4}.\Gamma_2^2$ would be 3.96×10^6 and D_0 would be 3.23×10^{-7} cm.^{2}/sec., which corresponds to $P^{-1}\,\Phi^{\frac{1}{3}} = 2.5 \times 10^6$ in equation 1, in agreement with Flory's best average value (1). The data are not sufficiently precise to contend for exact values of $P^{-1}\,\Phi^{\frac{1}{3}}$ or Γ_3, but the conclusion that $\Gamma_3 = \frac{1}{4}.\Gamma_2^2$ is more nearly correct than $\Gamma_3 = \frac{5}{8}.\Gamma_2^2$ is inescapable and that it *may* be exactly $\frac{1}{4}.\Gamma_2^2$ is not contradicted by these results.

The above good agreement between theory and experiment is for the diffusion coefficient calculated by the area-maximum ordinate method; there is some discrepancy, in these experiments, between D_A and D_σ (second moment method (6)) unlike the results of Schulz and Meyerhoff (8). The D_σ values generally lie *below* those for the area-maximum ordinate method. The reasons for this discrepancy are not known and will be discussed more fully in a future publication.

ACKNOWLEDGMENT

The authors are much indebted to Doctors Krigbaum and Flory for the sample of polyisobutylene and to the National Research Council of Canada for financial assistance.

1. FLORY, P. J. Principles of polymer chemistry. Cornell Univ. Press, Ithaca, N.Y. 1953. p. 628.
2. KRIGBAUM, W. R. and FLORY, P. J. J. Am. Chem. Soc. 75: 1775. 1953.
KRIGBAUM, W. R. Private communication.

3. LAMM, O. Nova Acta Regiae Soc. Sci. Upsaliensis, 10(4): 6. 1937.
4. MANDELKERN, L. and FLORY, P. J. J. Chem. Phys. 19: 984. 1951.
5. MANDELKERN, L. and FLORY, P. J. J. Chem. Phys. 20: 212. 1952.
6. MANDELKERN, L., KRIGBAUM, W. R., SCHERAGA, H. A., and FLORY, P. J. J. Chem. Phys. 20: 1392. 1952.
7. NEURATH, H. Chem. Revs. 30: 357. 1942.
8. SCHULZ, G. V. and MEYERHOFF, G. Makromol. Chem. 7: 294. 1952.
9. STOCKMAYER, W. H. and CASASSA, E. F. J. Chem. Phys. 20: 1560. 1952.
10. SVEDBERG, T. The ultracentrifuge. Oxford University Press, Toronto. 1940. p. 253.

RECEIVED NOVEMBER 3, 1954.
DEPARTMENT OF CHEMISTRY,
MCMASTER UNIVERSITY,
HAMILTON, ONTARIO.

UNIT CELL, SPACE GROUP, AND INDEXED X-RAY DIFFRACTION POWDER DATA FOR CERTAIN NARCOTICS
VII. MORPHINE HYDROCHLORIDE TRIHYDRATE, AND THE DIHYDRATES OF MORPHINE HYDROBROMIDE, MORPHINE HYDRIODIDE, CODEINE HYDROCHLORIDE, CODEINE HYDROBROMIDE, CODEINE HYDRIODIDE[1]

BY W. H. BARNES AND JUNE M. LINDSEY[2]

Morphine hydrochloride (anhydrous, and trihydrate) and morphine hydriodide dihydrate were the only hydrohalide salts of morphine or of codeine included in the collection of X-ray diffraction powder data completed in this laboratory some time ago as an aid to the identification of certain narcotics (1, 3). It was realized at the time of this survey that morphine hydrobromide, and the hydrochloride, hydrobromide, and hydriodide of codeine should be examined at some future date. Through the kindness of Dr. C. G. Farmilo, specimens of all four hydrohalide salts (in the form of the dihydrates) were obtained in due course, and their unit cell constants, space groups, and powder patterns (indexed for $d > \backsim 3$ Å), together with single-crystal data for morphine hydrochloride trihydrate and for morphine hydriodide dihydrate, have now been determined. At the same time the powder patterns for the last two salts, which are recorded in full elsewhere (3), have been indexed for those reflections corresponding to $d > \backsim 3$ Å. The experimental methods have been described in detail previously (1, 2, 3).

Of the various narcotics studied during the powder-data survey (3), morphine, codeine, and thebaine were selected as the first to be considered for complete structural investigation because of the widespread interest in their stereochemical configuration (11). In view of the fact, however, that their molecules are asymmetric, it was decided to use the corresponding hydrohalide salts in an application of the isomorphous-replacement method to the problem. This eliminated thebaine for which only the free base and the hydrochloride were immediately available.

The six salts of morphine and codeine, which are the subject of the present note, crystallized from water in rosettes, and in sheaves, of needles, elongated

[1]*Issued as N.R.C. No. 3524.*
[2]*National Research Laboratories Postdoctorate Fellow.*

3. LAMM, O. Nova Acta Regiae Soc. Sci. Upsaliensis, 10(4): 6. 1937.
4. MANDELKERN, L. and FLORY, P. J. J. Chem. Phys. 19: 984. 1951.
5. MANDELKERN, L. and FLORY, P. J. J. Chem. Phys. 20: 212. 1952.
6. MANDELKERN, L., KRIGBAUM, W. R., SCHERAGA, H. A., and FLORY, P. J. J. Chem. Phys. 20: 1392. 1952.
7. NEURATH, H. Chem. Revs. 30: 357. 1942.
8. SCHULZ, G. V. and MEYERHOFF, G. Makromol. Chem. 7: 294. 1952.
9. STOCKMAYER, W. H. and CASASSA, E. F. J. Chem. Phys. 20: 1560. 1952.
10. SVEDBERG, T. The ultracentrifuge. Oxford University Press, Toronto. 1940. p. 253.

RECEIVED NOVEMBER 3, 1954.
DEPARTMENT OF CHEMISTRY,
MCMASTER UNIVERSITY,
HAMILTON, ONTARIO.

UNIT CELL, SPACE GROUP, AND INDEXED X-RAY DIFFRACTION POWDER DATA FOR CERTAIN NARCOTICS
VII. MORPHINE HYDROCHLORIDE TRIHYDRATE, AND THE DIHYDRATES OF MORPHINE HYDROBROMIDE, MORPHINE HYDRIODIDE, CODEINE HYDROCHLORIDE, CODEINE HYDROBROMIDE, CODEINE HYDRIODIDE[1]

BY W. H. BARNES AND JUNE M. LINDSEY[2]

Morphine hydrochloride (anhydrous, and trihydrate) and morphine hydriodide dihydrate were the only hydrohalide salts of morphine or of codeine included in the collection of X-ray diffraction powder data completed in this laboratory some time ago as an aid to the identification of certain narcotics (1, 3). It was realized at the time of this survey that morphine hydrobromide, and the hydrochloride, hydrobromide, and hydriodide of codeine should be examined at some future date. Through the kindness of Dr. C. G. Farmilo, specimens of all four hydrohalide salts (in the form of the dihydrates) were obtained in due course, and their unit cell constants, space groups, and powder patterns (indexed for $d > \backsim 3$ Å), together with single-crystal data for morphine hydrochloride trihydrate and for morphine hydriodide dihydrate, have now been determined. At the same time the powder patterns for the last two salts, which are recorded in full elsewhere (3), have been indexed for those reflections corresponding to $d > \backsim 3$ Å. The experimental methods have been described in detail previously (1, 2, 3).

Of the various narcotics studied during the powder-data survey (3), morphine, codeine, and thebaine were selected as the first to be considered for complete structural investigation because of the widespread interest in their stereochemical configuration (11). In view of the fact, however, that their molecules are asymmetric, it was decided to use the corresponding hydrohalide salts in an application of the isomorphous-replacement method to the problem. This eliminated thebaine for which only the free base and the hydrochloride were immediately available.

The six salts of morphine and codeine, which are the subject of the present note, crystallized from water in rosettes, and in sheaves, of needles, elongated

[1]*Issued as N.R.C. No. 3524.*
[2]*National Research Laboratories Postdoctorate Fellow.*

in the direction of the *c*-axis. Individual crystals of the codeine hydrohalides, however, were somewhat larger, and of better form, than those of the corresponding salts of morphine. They were of almost square cross-section and could be cut readily to cubical shape of suitable size for single-crystal study. Primarily for these reasons, therefore, codeine hydrobromide dihydrate was selected for the investigation of the structure of the codeine molecule, and the isomorphous codeine hydriodide dihydrate was employed to provide data of assistance in the allocation of signs to the observed structure amplitudes. A brief account of the results of this investigation has been given elsewhere (7) and full details will be published later (8).

An interesting feature of the hydrohalide salts of morphine and of codeine is that the phase normally available from commercial sources (and obtained by crystallization from water or dilute alcohol at ordinary temperatures) is the dihydrate in all cases with the exception of morphine hydrochloride, which crystallizes as the trihydrate. The existence of other hydrates, and of the anhydrous salts, has been reported in the literature (10), and an extensive series of hydration–dehydration studies is now in progress in this laboratory. It is hoped to report X-ray diffraction data for some of these other hydrate phases in a subsequent note in order to supplement existing powder data for *anhydrous* morphine hydrochloride (3).

Single-crystal data, obtained from precession photographs (Cu K_α, λ = 1.5418 Å), for morphine hydrochloride trihydrate, morphine hydrobromide dihydrate, morphine hydriodide dihydrate, and the dihydrates of codeine hydrochloride, hydrobromide, and hydriodide, are summarized in Table I;

TABLE I

SINGLE CRYSTAL DATA (M = MORPHINE, $C_{17}H_{19}O_3N$; C = CODEINE, $C_{18}H_{21}O_3N$)

	M.HCl.3H$_2$O	M.HBr.2H$_2$O	M.HI.2H$_2$O	C.HCl.2H$_2$O	C.HBr.2H$_2$O	C.HI.2H$_2$O
a(Å)	13.04	12.75	13.04	12.93	13.10	13.44
b(Å)	20.78	20.04	20.34	20.47	20.86	21.38
c(Å)	6.92_1	6.92_3	6.87_4	6.82_5	6.81_8	6.83_5
S.G.	$P2_12_12_1$	$P2_12_12_1$	$P2_12_12_1$	$P2_12_12_1$	$P2_12_12_1$	$P2_12_12_1$
Z(mols. per cell)	4	4	4	4	4	4
ρ(gm./ml.)						
(calc.)	1.335	1.511	1.637	1.368	1.483	1.568
(obs.)	1.334	1.518	1.641	1.368	1.489	1.565

the accuracy of the unit cell dimensions is about $\pm 0.3\%$. The powder data (Co K_α, λ = 1.790 Å; camera diameter, 114.6 mm.) for the six salts are given in Table II, where B and BB identify lines that were broader and much broader, respectively, than the general average for a particular film, and an asterisk (under d(Obs.)) indicates the probable presence of a line the intensity of which was too low ($I/I_1 < 1$) for accurate measurement. Only the indexed data are shown for morphine hydrochloride trihydrate and for morphine hydriodide dihydrate because a complete list of observed spacings and relative intensities for each of these salts has already been recorded (3). The powder photographs of morphine hydrobromide dihydrate, codeine hydrochloride

dihydrate, codeine hydrobromide dihydrate, and codeine hydriodide dihydrate are reproduced in Fig. 1 for comparison with those of morphine hydrochloride

TABLE II

X-RAY DIFFRACTION POWDER DATA (INDEXED FOR $d > \sim 3$ Å)

I/I_1	d(Å) Obs.	d(Å) Calc.	hkl	I/I_1	d(Å) Obs.	d(Å) Calc.	hkl	I/I_1	d(Å) Obs.	d(Å) Calc.	hkl
			Morphine hydrochloride trihydrate								
1	11.1	11.0	110			4.63	211		*	3.35	160
85	10.4	10.4	020	1	4.59	4.58	131			3.34	102
75	8.11	8.12	120	20	4.32	4.32	221	10	3.33	3.33	340
	*	6.57	011	—	—	4.25	310			3.30	112
		6.52	200	20	4.15	4.15	041			3.28	022
		6.22	210		*	4.06	240		*	3.26	400
100	6.11	6.12	130	—	—	4.01	320			3.25	331
		6.11	101	100	3.95	3.96	141,150	—	—	3.22	410
85	5.80	5.86	111			3.91	231	10	3.19	3.18	122
		5.76	021			3.68	301,330			3.13	251
	*	5.52	220	10B	3.63	3.62	311	70	3.11	3.11	420
50	5.22	5.27	121			3.56	051			3.10	032,061
		5.19	040	60	3.50	3.50	241,250	—	—	3.06	202,260
40	4.87	4.90	031			3.47	321			3.02	212
		4.83	140			3.46	002,060	50	3.01	3.01	132,161
50	4.76	4.75	230	30B	3.42	3.44	151			3.00	341,350
		4.74	201			3.41	012				
			Morphine hydrobromide dihydrate								
3	10.8	10.8	110		*	3.47	051	15	2.25		
20	10.0	10.0	020			3.46	002	25	2.23		
30	7.87	7.88	120			3.42	241	25	2.19		
2	6.50	6.54	011	75	3.41	3.41	012,321	25	2.15		
25	6.37	6.38	200			3.39	250	10	2.12		
40	6.11	6.08	101	1	3.35	3.35	151	20	2.09		
		6.07	210			3.34	060,102	1	2.07		
60	5.89	5.92	130			3.29	112	20	2.03		
		5.82	111	20B	3.26	3.27	022	3	2.01		
60	5.69	5.69	021			3.24	340	2	1.94		
1	5.38	5.38	220			3.23	160	30	1.90		
50	5.21	5.20	121			3.19	400	5	1.88		
20	5.03	5.01	040	20	3.17	3.18	331	3BB	1.82		
	*	4.81	031			3.17	122	3	1.76		
60	4.70	4.69	201			3.15	410	5	1.74		
		4.66	140	—	—	3.07	032	5	1.71		
		4.61	230	45	3.05	3.05	251	3	1.70		
30B	4.59	4.57	211			3.04	202,420	10	1.66		
		4.50	131		*	3.01	061,212	2BB	1.61		
25	4.25	4.25	221			2.99	132	5	1.58		
	*	4.16	310	50	2.91			2	1.56		
15	4.06	4.06	041	10	2.89			3	1.54		
	*	3.94	240	20	2.79			3	1.52		
		3.91	320	15	2.69			2	1.50		
100	3.87	3.87	141	15	2.63			2	1.45		
		3.84	231	15	2.59			1	1.43		
	*	3.82	150	5B	2.48			1	1.42		
—	—	3.62	301	30	2.38			3	1.40		
30	3.57	3.59	330	15	2.33						
		3.56	311	10	2.28						
			Morphine hydriodide dihydrate								
50	11.0	11.0	110	3	4.57	4.61	211	30	3.38	3.39	012,060
	*	10.2	020			4.53	131			3.38	151
1	8.04	8.02	120	10	4.27	4.29	221			3.32	102
35	6.49	6.52	200			4.25	310			3.30	340
		6.51	011	1	4.10	4.09	041	10B	3.27	3.28	112,160
—	—	6.21	210		*	4.01	240			3.26	022,400
60	6.03	6.08	101			4.00	320			3.23	331
		6.02	130	100	3.89	3.90	141			3.22	410
20B	5.75	5.83	111			3.88	150,231	5	3.15	3.16	122
		5.70	021	—	—	3.67	301			3.10	420
1	5.47	5.49	220			3.66	330	40	3.09	3.08	251
60	5.21	5.22	121	20	3.60	3.61	311			3.07	032
	*	5.09	040	—	—	3.50	051				
—	—	4.83	031			3.46	241				
		4.74	140	40	3.45	3.45	250,321				
70	4.72	4.73	201			3.44	002				
		4.70	230								

TABLE II (*Concluded*)

I/I_1	d(Å) Obs.	d(Å) Calc.	hkl	I/I_1	d(Å) Obs.	d(Å) Calc.	hkl	I/I_1	d(Å) Obs.	d(Å) Calc.	hkl
			Codeine hydrochloride dihydrate								
10	11.0	10.9	110	—	—	3.64	301,330	5	2.67		
30	10.2	10.2	020	5	3.58	3.59	311	5B	2.57		
70	8.04	8.03	120	—	—	3.51	051	5	2.48		
—	—	6.47	011,260	5	3.45	3.46	241,250	10	2.42		
—	—	6.16	210			3.43	321	5B	2.35		
55	6.03	6.03	101,130	—	—	3.41	002,060	1	2.28		
—	—	5.79	111			3.39	151	2	2.24		
75	5.68	5.68	021	20	3.36	3.36	012	5	2.20		
	*	5.47	220	2	3.30	3.30	102,160	1	2.16		
30	5.17	5.20	121				340	10	2.13		
		5.12	040			3.26	112	2	2.11		
		4.82	031	2	3.24	3.24	022	10	2.05		
30B	4.75	4.76	140			3.23	400	2B	2.01		
		4.69	201,230	—	—	3.21	331	20	1.97		
1	4.54	4.57	211			3.19	410	1	1.93		
		4.52	131	10	3.13	3.14	122	1	1.90		
2	4.27	4.27	221	25	3.08	3.08	251,420	2	1.88		
—	—	4.22	310		*	3.05	032,061	10	1.84		
2	4.10	4.09	041	—	—	3.02	202,260	1	1.78		
	*	4.01	240	20	2.97						
		3.97	320	8	2.89						
100	3.91	3.90	141,150	1	2.84						
		3.87	231	20	2.76						
			Codeine hydrobromide dihydrate								
	*	11.1	110	—	—	3.70	330	15	2.90		
25	10.4	10.4	020			3.68	301	2	2.84		
20	8.16	8.16	120	20	3.61	3.62	311	25B	2.78		
5	6.52	6.55	200	—	—	3.56	051	25	2.71		
		6.48	011			3.52	250	25	2.59		
5	6.24	6.25	210			3.50	241	2	2.51		
—	—	6.14	130	20	3.48	3.48	060	5B	2.44		
45	6.04	6.05	101			3.47	321	15	2.38		
30B	5.75	5.81	111		*	3.43	151	1	2.35		
		5.71	021			3.41	002	2	2.23		
—	—	5.55	220	46	3.35	3.36	012,160	1	2.21		
75	5.22	5.23	121			3.35	340	18	2.13		
		5.21	040			3.30	102	5	2.08		
25	4.84	4.87	031			3.28	400	5	2.04		
		4.85	140	5B	3.25	3.26	112	20	1.99		
—	—	4.77	230			3.25	331	5	1.90		
40	4.71	4.72	201			3.24	022,410	10	1.86		
5	4.58	4.61	211			3.15	122	5	1.78		
		4.56	131	35	3.13	3.13	251,420	5	1.76		
	*	4.30	221			3.10	061	2B	1.71		
		4.27	310	1	3.06	3.07	260	1	1.47		
10	4.14	4.14	041			3.06	032	1	1.42		
—	—	4.08	240			3.02	202,350				
1	4.03	4.03	320			3.01	161,341				
		3.98	150	15B	2.99	2.99	212				
100	3.95	3.95	141			2.98	132				
		3.91	231			2.96	430				
			Codeine hydriodide dihydrate								
30	11.5	11.4	110			3.57	241	15	2.61		
10	10.7	10.7	020	30	3.56	3.56	060	1	2.57		
5	8.34	8.37	120			3.54	321	5	2.52		
—	—	6.72	200		*	3.50	151	2B	2.46		
		6.51	011	—	—	3.44	160	20	2.43		
25	6.43	6.41	210			3.43	340	5B	2.38		
—	—	6.30	130	25	3.42	3.42	002	20	2.29		
45	6.09	6.09	101			3.37	012	1	2.26		
50	5.86	5.86	111	30	3.36	3.36	400	15	2.24		
1	5.76	5.76	021		*	3.32	331,410	30	2.14		
—	—	5.69	220			3.31	102	20	2.02		
—	—	5.34	040		*	3.27	112	1	1.99		
85	5.29	5.29	121			3.26	022	5	1.95		
		4.97	140			3.20	420	5	1.93		
25	4.94	4.93	031	25B	3.18	3.19	251	15	1.89		
	*	4.89	230			3.16	061,122	2	1.82		
75	4.78	4.79	201			3.15	260	2	1.80		
—	—	4.68	211			3.09	350	1BB	1.73		
10	4.64	4.63	131	20	3.08	3.08	032,161	1BB	1.68		
		4.38	310			3.07	341	5	1.63		
5	4.37	4.37	221	—	—	3.05	202	5B	1.59		
		4.21	041			3.04	430	1	1.56		
5	4.20	4.18	240			3.02	212	1	1.54		
		4.13	320			3.01	401	1	1.51		
5	4.10	4.07	150	10B	3.00	3.00	132	1	1.49		
		4.02	141			2.99	411	1	1.47		
100	4.01	3.98	231			2.98	170	2	1.44		
—	—	3.79	330	20	2.92						
—	—	3.75	301	25	2.85						
30	3.68	3.69	311	25BB	2.78						
	*	3.62	051	1	2.72						
		3.61	250	15	2.66						

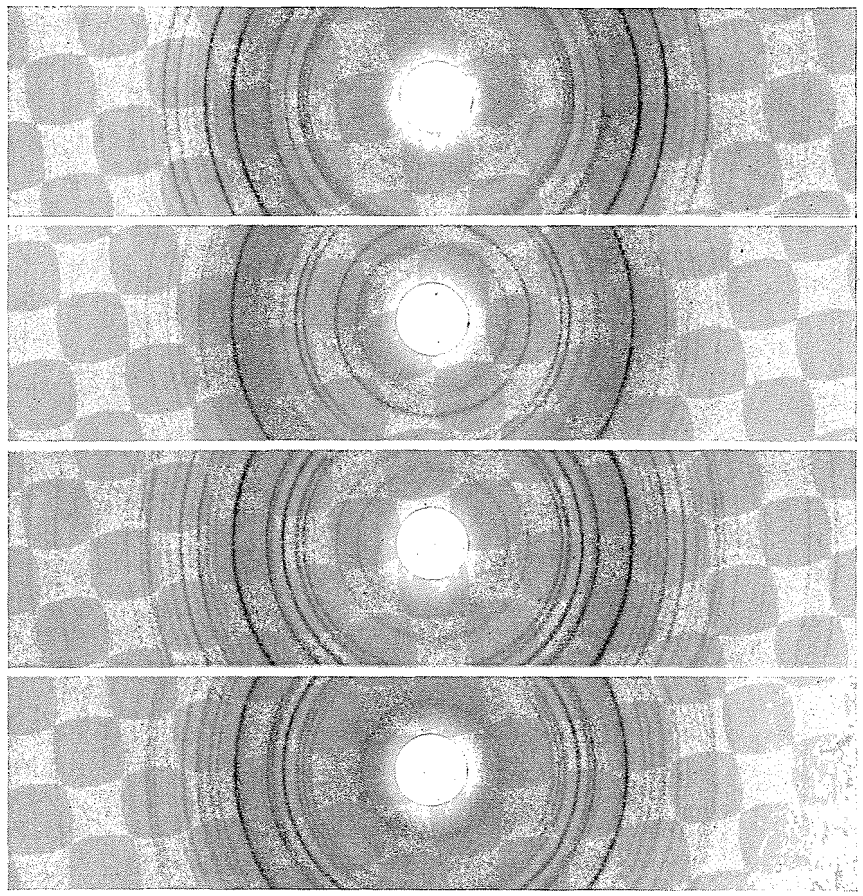

FIG. 1. X-ray diffraction powder photographs of A, morphine hydrobromide dihydrate; B, codeine hydrochloride dihydrate; C, codeine hydrobromide dihydrate; D, codeine hydriodide dihydrate. (Camera diameter: 114.6 mm.; radiation: $Co_{\alpha}K_{\alpha}$, $\lambda = 1.790$ Å).

trihydrate and morphine hydrobromide dihydrate, which will be found elsewhere (3).

It should be mentioned that the orientation chosen for the unit cells is $c < a < b$ in conformity with the convention recommended in Dana's *System of Mineralogy* (4) and in *Crystal Data* (5), and with that adopted for codeine (anhydrous free base) and for codeine monohydrate (free base) in *Barker's Index* (9) and by Groth (6).

Mr. B. J. Cowick assisted with the powder investigations.

1. BARNES, W. H. Bull. Narcotics U.N. Dept. Social Affairs, 6(1): 20. 1954.
2. BARNES, W. H. and FORSYTH, W. J. Can. J. Chem. 32: 984. 1954.
3. BARNES, W. H. and SHEPPARD, H. M. Bull. Narcotics U.N. Dept. Social Affairs, 6(2): 27. 1954.
4. DANA, J. D. and DANA, E. S. System of mineralogy. 7th ed. Vol. 1. *By* C. Palache, H. Berman, and C. Frondel. John Wiley & Sons, Inc., New York. 1944. p. 6.

5. DONNAY, J. D. H. and NOWACKI, W. Crystal data. Geol. Soc. Amer., Mem. No. 60. 1954. p. 138.
6. GROTH, P. Chemische Krystallographie. Vol. 5. W. Engelmann, Leipzig. 1919. pp. 964, 965.
7. LINDSEY, J. M. Acta Cryst. 7: 651. 1954.
8. LINDSEY, J. M. and BARNES, W. H. Acta Cryst. In press.
9. PORTER, M. W. and SPILLER, R. C. The Barker index of crystals. W. Heffer and Sons, Ltd., Cambridge, England. 1951. Index Nos. O.2059, O.2060.
10. SMALL, L. F. Chemistry of the opium alkaloids. Suppl. No. 103. Public Health Service, Washington. 1932. pp. 150, 189.
11. STORK, G. *In* The alkaloids. Vol. 2. *Edited by* R. H. F. Manske and H. L. Holmes. Academic Press, Inc., New York. 1952. p. 171. Rapoport, H. and Lavigne, J. B. J. Am. Chem. Soc. 75: 5329. 1953. Ginsburg, D. Bull. Narcotics U.N. Dept. Social Affairs, 6(1): 32. 1954.

RECEIVED NOVEMBER 17, 1954.
DIVISION OF PHYSICS,
NATIONAL RESEARCH COUNCIL,
OTTAWA, CANADA.

THE IDENTITY OF CRYPTOCAVINE AND CRYPTOPINE[1]

BY A. F. THOMAS,[2] LÉO MARION, AND R. H. F. MANSKE

Cryptocavine ($C_{21}H_{23}O_5N$) has been reported to occur in various fumariaceous plants (2) and to be different from, but isomeric with and closely related to cryptopine I. Its structure IV was deduced (3) from the Emde reduction of the methosulphate followed by dehydration with acetyl chloride which gave anhydrotetrahydromethylcryptocavine, very similar to anhydrotetrahydromethylcryptopine II obtained in the same way from cryptopine (4). Both anhydrotetrahydro derivatives, on oxidation with potassium permanganate, gave the same products, i.e., 5,6-methylenedioxy-*o*-toluic aldehyde and 4,5-dimethoxy-2-β-dimethylaminoethylbenzaldehyde. The slight difference between the anhydrotetrahydro compounds was ascribed to geometrical isomerism (3).

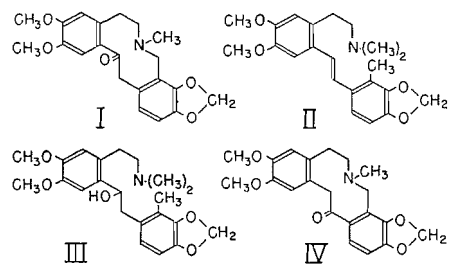

Construction of models of II showed that the *cis*-form would be highly strained with the aromatic rings partly overlapping. Examination, however, of the specimen originally obtained from cryptocavine and one freshly prepared from pure cryptopine showed that the two were identical. Both crystallized from dilute methanol as long colorless silky needles, m.p. 110°, undepressed on

[1]*Issued as N.R.C. No. 3522.*
[2]*National Research Council of Canada Postdoctorate Fellow.*

5. DONNAY, J. D. H. and NOWACKI, W. Crystal data. Geol. Soc. Amer., Mem. No. 60. 1954. p. 138.
6. GROTH, P. Chemische Krystallographie. Vol. 5. W. Engelmann, Leipzig. 1919. pp. 964, 965.
7. LINDSEY, J. M. Acta Cryst. 7: 651. 1954.
8. LINDSEY, J. M. and BARNES, W. H. Acta Cryst. In press.
9. PORTER, M. W. and SPILLER, R. C. The Barker index of crystals. W. Heffer and Sons, Ltd., Cambridge, England. 1951. Index Nos. O.2059, O.2060.
10. SMALL, L. F. Chemistry of the opium alkaloids. Suppl. No. 103. Public Health Service, Washington. 1932. pp. 150, 189.
11. STORK, G. *In* The alkaloids. Vol. 2. *Edited by* R. H. F. Manske and H. L. Holmes. Academic Press, Inc., New York. 1952. p. 171. Rapoport, H. and Lavigne, J. B. J. Am. Chem. Soc. 75: 5329. 1953. Ginsburg, D. Bull. Narcotics U.N. Dept. Social Affairs, 6(1): 32. 1954.

RECEIVED NOVEMBER 17, 1954.
DIVISION OF PHYSICS,
NATIONAL RESEARCH COUNCIL,
OTTAWA, CANADA.

THE IDENTITY OF CRYPTOCAVINE AND CRYPTOPINE[1]

BY A. F. THOMAS,[2] LÉO MARION, AND R. H. F. MANSKE

Cryptocavine ($C_{21}H_{23}O_5N$) has been reported to occur in various fumariaceous plants (2) and to be different from, but isomeric with and closely related to cryptopine I. Its structure IV was deduced (3) from the Emde reduction of the methosulphate followed by dehydration with acetyl chloride which gave anhydrotetrahydromethylcryptocavine, very similar to anhydrotetrahydromethylcryptopine II obtained in the same way from cryptopine (4). Both anhydrotetrahydro derivatives, on oxidation with potassium permanganate, gave the same products, i.e., 5,6-methylenedioxy-*o*-toluic aldehyde and 4,5-dimethoxy-2-β-dimethylaminoethylbenzaldehyde. The slight difference between the anhydrotetrahydro compounds was ascribed to geometrical isomerism (3).

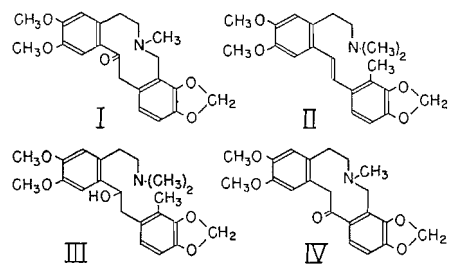

Construction of models of II showed that the *cis*-form would be highly strained with the aromatic rings partly overlapping. Examination, however, of the specimen originally obtained from cryptocavine and one freshly prepared from pure cryptopine showed that the two were identical. Both crystallized from dilute methanol as long colorless silky needles, m.p. 110°, undepressed on

[1]*Issued as N.R.C. No. 3522.*
[2]*National Research Council of Canada Postdoctorate Fellow.*

admixture, and both possessed the same absorption in the ultraviolet ($\lambda_{max.}$ 330 mμ, log ϵ, 4.38; $\lambda_{min.}$ 264 mμ, log ϵ, 3.91) and in the infrared. It is perhaps significant that at no time were we able to crystallize Perkin's tetrahydromethylcryptopine III although several preparations were made, and it is noteworthy that Perkin states that II contains solvent of crystallization when freshly prepared, and that the melting points of both II and III were the same (4).

The apparent confirmation of structure IV for cryptocavine (3) made it of interest to examine the *trans*-annular amide formation of this molecule. The perchlorate was prepared (crystallized from aqueous methanol, m.p. 226–228°, dec. Calc. for $C_{21}H_{23}O_5N.HClO_4$: Cl, 7.55. Found: Cl, 7.36, 7.42%), but was found to have an infrared absorption spectrum identical with that of cryptopine perchlorate. The free bases had the same pK_a value (8.09) which was higher than expected in view of the fact that cryptopine had been reported to be a weak base (1). Debye-Scherrer powder photographs of the two bases were the same, as were the infrared absorption spectra in various media. The melting point of a mixture of cryptocavine and cryptopine was not lowered provided that pure cryptopine was used, but it was found that any mixture of the pure bases with the cryptopine sample originally used (3) was indeed liquid at 205° as reported (3). Furthermore, both the Debye-Scherrer photograph and the infrared absorption spectrum of this sample contained all the characteristics of the corresponding photograph and spectrum of pure cryptopine, together with a few minor additional lines and peaks. The latter were all present in the Debye-Scherrer photograph and the infrared spectrum of protopine. Hence the sample of cryptopine originally used for comparison was contaminated with protopine. The melting point of this sample was taken again and found to be not 221°, but 204–208°. It must, therefore, be concluded that cryptocavine is identical with cryptopine, and the designation cryptocavine should be deleted from the literature.

ACKNOWLEDGMENTS

The pure cryptopine used in this work was obtained from the Dyson Perrins Laboratory, through Dr. A. S. Bailey whose courtesy we acknowledge. Our thanks are also due to Mr. R. Lauzon and Dr. R. N. Jones for the infrared spectra and to Dr. Maria Przybylska for the Debye-Scherrer photographs.

1. Anet, F. A. L., Bailey, A. S., and Robinson, R. Chemistry & Industry, 944. 1953.
2. Manske, R. H. F. Can. J. Research, B, 15: 274. 1937; B, 16: 438. 1938; B, 17: 51. 1939; B, 18: 75. 1940.
3. Manske, R. H. F. and Marion, L. J. Am. Chem. Soc. 62: 2042. 1940.
4. Perkin, W. H. J. Chem. Soc. 109: 815. 1916.

Received December 9, 1954.
Division of Pure Chemistry,
National Research Council,
Ottawa, Canada.

Canadian Journal of Chemistry

Issued by THE NATIONAL RESEARCH COUNCIL OF CANADA

VOLUME 33 APRIL 1955 NUMBER 4

THE SYNTHESIS OF OPSOPYRROLE-DICARBOXYLIC ACID[1]

BY D. M. MACDONALD[2] AND S. F. MACDONALD

ABSTRACT

The methyl groups of the pyrroles I*a* and II*a* react with sulphuryl chloride to give dichloromethyl derivatives which hydrolyze to aldehydes. The pyrrole I*a* also forms a trichloromethyl derivative which hydrolyzes to the corresponding acid. Alkaline decarboxylation of the latter gives opsopyrrole-dicarboxylic acid, IV*a*.

To obtain further pyrroles related to the uroporphyrins, we have studied the halogenation of the methyl groups of I*a* and II*a*, and further transformations analogous to those which had been carried out on an isomeric pyrrole (6, 9). The bromination of both I*a* (13) and II*a* (unpublished) proceeds normally giving the α-bromomethyl pyrroles.

With two moles of sulphuryl chloride, both I*a* and II*a* presumably gave dichloromethyl derivatives, which were not purified but hydrolyzed directly to the corresponding aldehydes I*b* and II*b*. The former has also been obtained from I*a* with lead tetraacetate (16). The latter, II*b*, was hydrolyzed to V*a* which was converted to the oxime V*b*.

With three moles of sulphuryl chloride, I*a* presumably gave a trichloromethyl derivative, which hydrolyzed to I*c*. The pyrrole I*d* was obtained from I*c* by thermal decarboxylation, and hydrolysis then gave III, one of the pyrroles which have been postulated as intermediates in the biosynthesis of hemin (12). Opsopyrrole-dicarboxylic acid IV*a*, one of the hypothetical reduction products of the uroporphyrins, was obtained from I*c* by alkaline decarboxylation. The method was not quite parallel to the analogous synthesis of opsopyrrole-carboxylic acid (7), for the greater solubility of the product here necessitated the release of the free acid by ion-exchange rather than by acidification. The dimethyl ester IV*b* was an oil which did not give a crystalline picrate. The structure of IV*a* was confirmed by its degradation to opsopyrrole-carboxylic acid (3-methylpyrrole-4-propionic acid). Further, although the usual methods for converting opsopyrroles to porphyrins failed here, when IV*a* was boiled with formaldehyde and dilute hydrochloric acid, then aerated, a mixture of uroporphyrins resulted, which was shown by paper chromatography to contain octacarboxylic acids only.

[1]*Manuscript received November 23, 1954.*
Contribution from the Division of Pure Chemistry, National Research Council, Ottawa, Canada. Issued as N.R.C. No. 3511.
[2]*National Research Council Postdoctorate Fellow.*

Several analogous chlorinations with sulphuryl chloride in ether, including those of the 3-methyl (5), 3-ethyl (10), and 3-propionic acid (7) derivatives of 2,4-dimethyl-5-carbethoxypyrrole, have not been sufficiently stepwise and complete to give good yields of aldehydes or acids. The influence of impurities in the ether there and in the preparations of I*b* and I*c* is unknown. In the case of II*b*, however, whether or not freshly dried ether was used, when the preliminary drying of the solvent ether was with phosphorus pentoxide rather

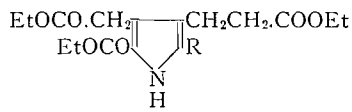

I*a*, R = CH_3
b, R = CHO
c, R = COOH
d, R = H

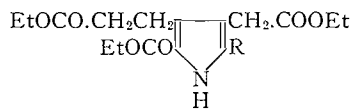

II*a*, R = CH_3
b, R = CHO

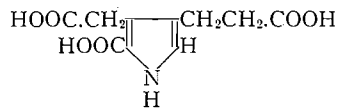

III

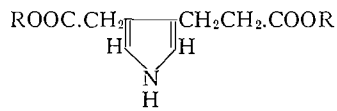

IV*a*, R = H
b, R = CH_3

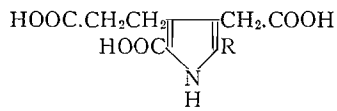

V*a*, R = CHO
b, R = CH=N.OH

than with sulphuric acid, the chlorination of II*a* with two moles of sulphuryl chloride was incomplete.[3] The main product, repeatedly isolated after the hydrolysis in 70–90% yield, was 3,3′-di-(carbethoxymethyl)-4,4′-di-(2-carbethoxyethyl)-5,5′-dicarbethoxydipyrromethane. This was identified by melting point and mixed melting point with the methane, m.p. 146°, obtained by boiling II(R = CH_2Br) with water (unpublished).

An improved preparation based on that of Pinner (1, 17, 18) has been worked out for the ethyl acetone-dicarboxylate required in the preparation of I*a*.

EXPERIMENTAL

The ether had been distilled with sulphuric acid and dried over sodium (2). Acetone had been distilled over potassium carbonate, and water had been boiled and cooled under nitrogen.

2-Carboxy-3-(2-carbethoxyethyl)-4-carbethoxymethyl-5-carbethoxypyrrole (*Ic*)

Sulphuryl chloride (10 ml.) was added slowly to a stirred solution of I*a*

[3]*This observation is due to Dr. A. H. Jackson.*

(12.95 gm.) in 200 ml. of absolute ether maintained at $\leqslant 4°$ and protected from moisture. Stirring was continued for 5 min., then for 30 min. with the cooling bath removed. The ether was evaporated *in vacuo* at $\leqslant 20°$, and three 100-cc. portions of ether successively added and evaporated in the same way. Hydrated sodium acetate (40 gm.) in 650 ml. of boiling water was added to the residual oily trichloromethyl derivative, the mixture boiled for three minutes with vigorous stirring and cooled quickly, sodium bicarbonate added to dissolve the precipitate, the solution extracted three times with ether, and the ether washed with 5% sodium bicarbonate (twice with 100 ml.). The combined aqueous layers were filtered, saturated with sulphur dioxide at 20°, and, after one hour at 0°, the crystalline product filtered off and washed with water (twice with 100 ml.). It was dissolved in 500 ml. of boiling ethanol, and water (3.5 liters, heated to 80°) added. After standing overnight the colorless needles were filtered off (8.76 gm., 62%), dried to constant weight over sulphuric acid at 10 mm., m.p. 140–141°, Ehrlich's reaction negative (cold), red (hot). Found in material recrystallized several times from ethanol–water and dried (18 hr., 56°, 0.1 mm.): C, 55.58, 55.62; H, 6.43, 6.25; N, 3.79%. Calc. for $C_{17}H_{23}NO_8$: C, 55.27; H, 6.28; N, 3.47%.

2-Carbethoxy-3-carbethoxymethyl-4-(2-carbethoxyethyl)-pyrrole (Id)

The acid Ic (3.154 gm.) was heated at 240° under nitrogen until the evolution of carbon dioxide ceased, then sublimed (160–220°, 10 mm.). The sublimate was crystallized three times from ether–hexane to remove oil, giving 590 mgm., m.p. 51–51.5°. An additional 120 mgm. (total, 25%) was obtained from the mother liquors by evaporating, subliming, dissolving in ether, filtering with charcoal, evaporating, putting onto an alumina column in a little methanol, eluting with ether until the cold Ehrlich's reaction was negative, washing the eluate with aqueous sodium bicarbonate, drying it with sodium sulphate, evaporating, and recrystallizing five times from ether–hexane. For analysis, it was recrystallized five times from pentane (Soxhlet), and the colorless plates dried (20 hr., 20°, 10^{-5} mm.), m.p. 51–52°, Ehrlich's reaction bluish-red (cold) (slow). Found: C, 59.29, 59.18; H, 7.14, 7.18; N, 4.60%. Calc. for $C_{16}H_{23}NO_6$: C, 59.06; H, 7.12; N, 4.31%.

2-Carboxy-3-carboxymethyl-4-(2-carboxyethyl)-pyrrole (III)

The ester Id (407 mgm.) was refluxed for one hour with 5% potassium hydroxide in 50% ethanol (10 ml.). The cooled solution was put through Amberlite IR–120 (H^+ form, from 20 gm. wet Na^+ form) and eluted with water until the Ehrlich's reaction was negative (cold). The eluate (150 ml.) was concentrated *in vacuo* at *ca.* 20° by swirling on the steam bath until the product crystallized. Filtration and washing with 1 ml. of water gave radiating clusters of thick rods (272 mgm.). A colorless product was obtained after two recrystallizations from acetone (Soxhlet) (143 mgm., 47%), m.p. 178° (decomp.), Ehrlich's reaction bluish-red (cold). For analysis, it was recrystallized four times from acetone and dried overnight (56°, 0.1 mm.). Found: C, 50.08; H, 4.72; N, 6.03%. Calc. for $C_{10}H_{11}NO_6$: C, 49.78; H, 4.60; N, 5.81%.

3-Carboxymethyl-4-(2-carboxyethyl)-pyrrole (Opsopyrrole-dicarboxylic Acid) (IVa)

The pyrrole Ic (0.5 gm.) in 3 ml. of 10% sodium hydroxide was heated under nitrogen in a sealed tube for two hours at 175–180°. The filtered contents of four such tubes were passed through Amberlite IR-120 (H^+ form, from 30 gm. wet Na^+ form), eluting with water (*ca.* 300 ml.) until the Ehrlich's reaction was weak in the cold. The eluate was concentrated (10 mm. *ca.* 20°) by swirling on the steam-bath, then freeze-dried. The colorless residue was extracted into ether (Soxhlet), the ether concentrated to 50 ml., filtered warm, and the product precipitated with hexane as colorless poorly formed needles (882 mgm., 83%), m.p. 139–140°, Ehrlich's reaction bluish-red (cold). For analysis the product was recrystallized four times from ether–hexane and dried (18 hr., 56°, 0.1 mm.). Found: C, 54.79, 54.90; H, 5.69, 5.70; N, 6.94%; eq. wt. 100.3. Calc. for $C_9H_{11}NO_4$: C, 54.81; H, 5.62; N, 7.10%; eq. wt. 98.5.

3-Carbomethoxymethyl-4-(2-carbomethoxyethyl)-pyrrole (Methyl Opsopyrrole-dicarboxylate) (IVb)

Opsopyrrole-dicarboxylic acid (210 mgm.) in ether was allowed to react with excess ethereal diazomethane for 15 min., the ether evaporated, and the residue distilled in a collar flask (138–147° bath temp., 10^{-4} mm.). The yellowish oily product (215 mgm., 90%) was redistilled and the colorless oily middle fraction (135–137° bath temp., 10^{-4} mm.) analyzed, Ehrlich's reaction bluish-red (cold). Found: C, 58.78, 58.67; H, 6.59, 6.39; N, 6.14%. Calc. for $C_{11}H_{15}NO_4$: C, 58.64; H, 6.71; N, 6.22%.

Degradation of Opsopyrrole-dicarboxylic Acid to 3-Methylpyrrole-4-propionic Acid (Opsopyrrole-carboxylic Acid)

The pyrrole IVa (275 mgm.) was heated in a sealed tube for two hours at 150° with 3 ml. of water. The solid left on freeze-drying the combined filtrate and washings from the contents of the tube was extracted with ether (Soxhlet). The ether was concentrated to 20 ml., then replaced by boiling while hexane was added, red amorphous material being filtered off periodically until a slightly cloudy colorless solution was obtained. The product separated, on cooling, as colorless aggregates. After three recrystallizations, 65 mgm. were obtained, m.p. 116°, raised to 117° by sublimation (95–103°, 10^{-2} mm.). Found: C, 62.89, 62.94; H, 7.01, 6.98; N, 9.02%; eq. wt. 148. Calc. for $C_8H_{11}NO_2$: C, 62.73; H, 7.24; N, 9.14%; eq. wt. 153.

Another preparation, after four recrystallizations from chloroform–hexane, had m.p. 115–116°, raised to 118.5–120° after sublimation (Lit.: 119° (not sharp) (11*a*, 4, 7), 117° (8)).

Mixture of Uroporphyrins from Opsopyrrole-dicarboxylic Acid

Opsopyrrole-dicarboxylic acid (100 mgm.) was refluxed for 20 min. in 200 ml. of 0.5% hydrochloric acid and 40 ml. of 1% formaldehyde, cooled, and aerated overnight. The porphyrin was precipitated, filtered off, washed, esterified with methanolic hydrogen chloride, and brought into chloroform in the usual way. The chloroform was washed with 50% aqueous resorcinol (14*b*)

which was subsequently washed with chloroform. The combined chloroform layers were washed free of resorcinol with water, and filtered through a column of alumina (grade V), the porphyrin being eluted with chloroform containing 5% of methanol. After washing with dilute sodium hydroxide and with water, the chloroform was replaced with methanol at the boil, and the solution concentrated to *ca.* 1 ml. giving a mixture of uroporphyrin methyl esters as rods (9 mgm.). Recrystallized six times, it had m.p. 252–258° (4.5 mgm.). Found in 1.5 mgm. sample: C, 60.40; H, 6.84%. Calc. for $C_{48}H_{54}N_4O_{16}$: C, 61.14; H, 5.77%.

A sample was hydrolyzed, and chromatographed on paper with 2,4-lutidine-water in an atmosphere of ammonia (15); the only spot had the same R_f as the uroporphyrin I marker.

Opsopyrrole-dicarboxylic acid did not give porphyrins with chloromethyl ether in alcohol, either on standing or on refluxing (cf. 3) or with formic acid at 100° (cf. 11*a*, 11*b*).

2-Formyl-3-(2-carbethoxyethyl)-4-carbethoxymethyl-5-carbethoxypyrrole (*Ib*)

Sulphuryl chloride (0.477 ml.) was slowly added to the pyrrole I*a* (1 gm.) in 10 ml. of ether, the solution being vigorously stirred, protected from moisture, and kept below 4°. After five minutes, the cooling bath was removed and stirring continued for 30 min. The ether was removed *in vacuo* below 20°, and three 10-ml. portions of ether were successively added and evaporated in the same way. Hydrated sodium acetate (2 gm.) in 50 ml. of boiling water was added to the oily residue of the dichloromethyl derivative, the mixture boiled for three minutes, cooled quickly to 0°, and the crystalline aldehyde filtered off. It was dissolved in 50 ml. of boiling ethanol, and 200 ml. of water (heated to 80°) added. On cooling, the product separated (800 mgm., 77%), m.p. 82–83°. For analysis it was recrystallized three times from ethanol–water and dried (18 hr., 56°, 0.1 mm.) giving nearly colorless needles, m.p. 83.5–84° (Lit.: 84.5° (16)), Ehrlich's reaction red (hot). Found: C, 58.01, 58.00; H, 6.70, 6.39; N, 4.25, 3.88%. Calc. for $C_{17}H_{23}O_7N$: C, 57.76; H, 6.56; N, 3.96%.

2-Formyl-3-carbethoxymethyl-4-(2-carbethoxyethyl)-5-carbethoxypyrrole (*IIb*)

As described for the isomer I*b* above, 10.8 gm. of II*a* (14*a*) in 120 ml. of ether was treated with 5.35 ml. of sulphuryl chloride, the oil evaporated three times with 30 ml. of ether, and boiled with 30 gm. hydrated sodium acetate in 500 ml. of water. The aldehyde was obtained as long needles, m.p. 80–81° (9.87 gm., 88%), after recrystallizing from 500 ml. of ethanol and 2250 ml. of water as for the isomer. For analysis, it was recrystallized five times from ethanol–water and dried (18 hr., 56°, 0.1 mm., nearly colorless needles), m.p. 80.5–81°, Ehrlich's reaction red (hot). Found: C, 57.69, 57.98; H, 6.56, 6.43; N, 4.15%. Calc. for $C_{17}H_{23}NO_7$: C, 57.76; H, 6.56; N, 3.96%.

2-Formyl-3-carboxymethyl-4-(2-carboxyethyl)-5-carboxypyrrole (*Va*)

The corresponding ester II*b* (16 gm.) was heated for two hours with 200 ml. of 10% sodium hydroxide on the steam bath under nitrogen. The cooled solution was passed through Amberlite IR–120 (H^+ form, from 400 gm. wet

Na^+ form) and eluted with water. The eluate (3 liters) was concentrated to 60 ml. (10 mm., bath temp. 60°), and the first crop of the product (10.02 gm.) filtered off. Second and third crops were obtained by concentrating the mother liquors to 20 ml. and filtering (0.37 gm.), then freeze-drying the last liquors. The first crop was extracted into 450 ml. acetone (Soxhlet), the solution concentrated to 150 ml., cooled slightly, and 300 ml. ether added; after colored material was filtered off warm, the first lot crystallized at 0° and was filtered off. The combined second and third crops were treated in the same way with 450 cc. acetone and 300 ml. of ether, colored material separated, and the filtrate combined with the mother liquors from the first lot. Amorphous material was precipitated by adding ether, the solution filtered, and the ether evaporated. The remaining acetone solution was decolorized with charcoal, and two further lots of crystals successively obtained by concentration and cooling. The combined three lots were extracted into 900 ml. of acetone, 2 liters of ether added, and the ether evaporated from the filtered solution while acetone was added to keep the product in solution. After the concentrate was filtered with charcoal, concentrated to 300 ml., and cooled, the product (7.2 gm.) separated as fine needles. The mother liquors were concentrated to 75 ml., giving 1.8 gm. more (total 74%).

For analysis, the product was recrystallized four times from acetone and dried (18 hr., 56°, 0.1 mm.) giving cream-colored needles, decomposing at about 240°, Ehrlich's reaction red (hot). Found: C, 49.45, 49.00; H, 4.22, 4.32; N, 5.02%; eq. wt. 86.3. Calc. for $C_{11}H_{11}NO_7$: C, 49.07; H, 4.12; N, 5.20%; eq. wt. 89.7.

2-Oximinomethyl-3-carboxymethyl-4-(2-carboxyethyl)-5-carboxypyrrole (*Vb*)

A solution of the aldehyde V*a* (8.99 gm.), 8.4 gm. of sodium hydroxide, and 4.7 gm. of hydroxylamine hydrochloride in 500 ml. of water was kept for 18 hr. at room temperature, then heated one and one-half hours on the steam bath. The cooled solution was passed through Amberlite IR-120 (H^+ form, from 200 gm. wet Na^+ form) and eluted with water. The eluate (3 liters) was adjusted to pH 4 with sodium hydroxide and concentrated to 200 ml. on the steam bath under nitrogen at 10 mm., the pH being kept above 2. The first crop, which separated on cooling as radiating needles (6.96 gm.), was recrystallized twice from acetone; a second crop was obtained by concentrating the acetone mother liquors and recrystallizing the solid from acetone. A third crop was obtained by evaporating the aqueous mother liquors to dryness *in vacuo* by swirling on the steam bath, extracting the residue with acetone (Soxhlet), concentrating, extracting the solid which separated with ether (Soxhlet), evaporating the ether until the solution was cloudy, and leaving at 0° overnight. The combined three lots were recrystallized from acetone (Soxhlet) giving 6.64 gm., m.p. 204° (decomp.); concentrating the mother liquor gave 1.68 gm., m.p. 201° (total 86%). For analysis, 120 mgm. were dissolved in 3 ml. acetic acid on the steam bath and 5 ml. of benzol added. The oxime which crystallized after 12 hr. at 0° was recrystallized in the same way giving cream-colored aggregates (17 mgm.), dried (30 hr., 56°, 10^{-3} mm.), m.p. 201° (de-

comp.). Ehrlich's reaction was violet (hot). Found: C, 46.67; H, 4.47; N, 9.75%. Calc. for $C_{11}H_{12}N_2O_7$: C, 46.48; H, 4.26; N, 9.86%.

Although the oxime takes up two moles of hydrogen over palladium black (19) in dilute ammonia, the product has not given consistent analyses.

Ethyl Acetone-dicarboxylate

To 550 gm. of anhydrous citric acid, free of large lumps, in a 5-liter round-bottomed flask protected by a calcium chloride tube, 1100 gm. of 15–18% oleum was added in portions with frequent shaking so that the temperature did not exceed 40°. After standing for three hours at 35–40° with frequent shaking, the solution was cooled below −15° by adding dry ice, and 1 liter of similarly cooled absolute alcohol added in portions with shaking and stirring, the temperature being kept below 0° by adding more dry ice. The mixture was allowed to stand until a clear solution resulted; this required two hours, the temperature rising to 15°. After standing at 0° overnight, the solution was poured into 3.5 liters of ice and water. Three such lots were worked up together. The first was extracted four times with 250 ml. of benzene, the last two extracts being used to extract the second lot, being followed by two extractions with 250 ml. of benzene also used to extract the third lot which was then extracted twice with 250 ml. of fresh benzene. The combined extracts were washed with water, with four lots of 250 ml. of saturated sodium bicarbonate, and with water. After clearing with sodium sulphate and filtering, they were washed twice with 250 ml. of 2% sulphuric acid, four times with 250 ml. of water, cleared with sodium sulphate, filtered, and fractionated through a 12 in. lagged Vigreux column. Yield: 1180 gm. (68%), b.p. (0.8 mm.) 93–96°, η_D^{25} 1.4391.

By the same procedure, except that the initial mixture stood four hours at 40–45°, three lots of 550 gm. of powdered citric acid monohydrate gave 984 gm. (62%) of the ester.

REFERENCES

1. BAKER, B. R., SCHAUB, R. E., QUERRY, M. V., and WILLIAMS, J. H. J. Org. Chem. 17: 97. 1952.
2. FIESER, L. F. Experiments in organic chemistry. 2nd ed. D. C. Heath and Company, New York. 1941. p. 361.
3. FISCHER, H. and ALDER, E. Z. physiol. Chem. 197: 237. 1931.
4. FISCHER, H. and ANDERSAG, H. Ann. 458: 117. 1927.
5. FISCHER, H. and HIERNIS, J. Ann. 492: 21. 1932.
6. FISCHER, H. and HOFMANN, H. J. Z. physiol. Chem. 246: 15. 1937.
7. FISCHER, H. and LAMATSCH, W. Ann. 462: 240. 1928.
8. FISCHER, H., MERKA, A., and PLÖTZ, E. Ann. 478: 283. 1930.
9. FISCHER, H. and STAFF, C. E. Z. physiol Chem. 234: 97. 1935.
10. FISCHER, H., STURM, E., and FRIEDRICH, H. Ann. 461: 244. 1928.
11. FISCHER, H. and TREIBS, A. (*a*) Ann. 450: 132. 1926. (*b*) Ber. 60: 377. 1927.
12. LEMBERG, R. and LEGGE, J. W. Hematin compounds and bile pigments. Interscience Publishers, Inc., New York. 1949. p. 639 ff.
13. MACDONALD, S. F. J. Chem. Soc. 4184. 1952.
14. MACDONALD, S. F. and STEDMAN, R. J. (*a*) J. Am. Chem. Soc. 75: 5448. 1953. Can. J. Chem. 33: 458. 1955. (*b*) Can. J. Chem. 32: 896. 1954.
15. NICHOLAS, R. E. H. and RIMINGTON, C. Biochem. J. (London), 48: 306. 1951.
16. OTT, W. Thesis. Technische Hochschule, Munich. 1953. pp. 31, 54.
17. PINNER, A. Ber. 28: 473. 1895.
18. SCHROETER, G. Ber. 49: 2697. 1916.
19. TAUSZ, J. and VON PUTNOKY, N. Ber. 52: 1573. 1919.

THE MERCURY PHOTOSENSITIZED HYDROGENATION OF PROPYLENE AND THE ACTIVATION ENERGY OF THE REACTION $C_3H_7+H_2 = C_3H_8+H$ [1]

By G. R. Hoey[2] and D. J. Le Roy

ABSTRACT

The reactions initiated in hydrogen–propylene mixtures by $Hg(^3P_1)$ atoms were studied over the temperature range from room temperature to 320°C. At 260° and above, the rate of formation of propane and the rate of pressure decrease are linear functions of the hydrogen pressure. This effect is attributed to the reaction $C_3H_7+H_2 = C_3H_8+H$ and its activation energy is estimated to be equal to or slightly greater than 12.5 kcal. per mole. This is 1.2 kcal. per mole greater than the corrected value for the activation energy of the analogous reaction $C_2H_5+H_2 = C_2H_6+H$. The ratio $k_{combination}/k_{disproportionation}$ is estimated to be approximately 2.0 at room temperature in the case of isopropyl radicals.

INTRODUCTION

Kinetic data are now available for the reaction of methyl (10, 17, 14) and ethyl (18, 9) radicals with hydrogen as well as for the reverse reactions of atomic hydrogen with methane (2) and ethane (1). The present investigation was undertaken for the purpose of obtaining data on the reaction of propyl radicals with hydrogen,

$$C_3H_7+H_2 = C_3H_8+H.$$

The method chosen was similar to that used by Le Roy and Kahn (9) in their study of the analogous reaction,

$$C_2H_5+H_2 = C_2H_6+H. \qquad [a]$$

Their method can be described briefly.

At temperatures below approximately 200°C. the mercury ($^3P_1$) photosensitized hydrogenation of ethylene was interpreted in terms of the following reactions:

$$Hg(^3P_1)+H_2 = 2H+Hg(^1S_0) \qquad [b]$$

$$H+C_2H_4 = C_2H_5 \qquad [c]$$

$$2C_2H_5 = C_4H_{10} \qquad [d]$$

$$2C_2H_5 = C_2H_6+C_2H_4. \qquad [e]$$

In agreement with this mechanism, the rate of pressure decrease was independent of hydrogen pressure. At high temperatures, however, the rate of pressure decrease and the rate of formation of ethane increased linearly with the hydrogen concentration. This effect was attributed to reaction [*a*]. When this reaction is incorporated into the mechanism the predicted slope of the *rate* vs. (H_2) curve is proportional to $k_a/(k_d+k_e)^{\frac{1}{2}}$. From the effect of tempera-

[1]*Manuscript received November 22, 1954.*
Contribution from the Department of Chemistry, University of Toronto, Toronto, Ontario.
[2]*Present address: Division of Applied Chemistry, National Research Council of Canada, Ottawa.*

ture on the slope Le Roy and Kahn obtained a minimum value of 10.5 kcal. per mole for E_a by neglecting the effect of temperature on $(k_d+k_e)^{\frac{1}{2}}$. Their result was in good agreement with the value of 11.5 ± 1 kcal. per mole subsequently obtained by Wijnen and Steacie (18) from experiments on the photolysis of diethyl ketone in the presence of deuterium.

Moore and Taylor (12), in their investigation of the mercury photosensitized hydrogenation of propylene, confined their measurements to room temperature. Moore (11) later studied the reaction at temperatures up to 200°C., but he did not investigate the effect of hydrogen pressure. In the present investigation we have studied the effect of hydrogen pressure on the mercury photosensitized hydrogenation of propylene over the temperature range from room temperature to 320°C. and we have been able to apply the method of Le Roy and Kahn to obtain a minimum value for the activation energy of the reaction of isopropyl radicals with hydrogen.

EXPERIMENTAL

Two different types of reaction system were used. The first (I) involved a quartz annular cell and furnace and a lamp arrangement similar to that used previously (9). Pressures were measured on a wide bore U-tube manometer. This apparatus was used to obtain a considerable fund of analytical data for 300° and 320°C. but it was not suitable for accurate pressure measurements or for reproducible light intensities.

The second reaction system (II) was particularly well adapted for the determination of rates at constant incident light intensity. The cylindrical quartz cell, 5 cm. in diameter and 10 cm. long, had a plane window at one end; the other end of the cell was tapered down to a quartz-to-pyrex graded seal which was sealed to the inner member of a 19/38 standard taper joint. During an experiment gas was circulated through the cell by a mercury piston pump; the gas entered through a 6 mm. tube ring-sealed to the outer part of the 19/38 joint and extending to within a few millimeters of the window. The cell was surrounded by a close fitting aluminum block furnace with a quartz window placed about 7.5 cm. beyond the cell window. The upper half of the furnace could be taken off to remove and clean the cell. The temperature of the furnace was controlled to within ±0.5°C. The lamp used in connection with this cell was of the usual type with rare gas carrier, but since it was entirely outside the heated zone its output was independent of the reaction temperature. With this reaction system more accurate pressure measurements were made possible by using a modified form of the differential manometer described previously (7) with a multiplication ratio of approximately nine. Of the total volume of the system 64.2% was outside the furnace.

Commercial electrolytic hydrogen was purified by passage through platinized asbestos at 500°C. and through silica gel at the temperature of liquid air. The propylene (Ohio Chemical Company) was said to have a purity of 99.5%; it was subjected to several trap-to-trap distillations before being placed in the storage reservoir. The hydrocarbons used for infrared identification were standard samples obtained from the United States Bureau of Standards.

The products were separated into fractions by low temperature distillation (8). The methane in the non-condensable fraction was separated from hydrogen by diffusion of the latter through palladium (8). The olefin content of the C_2, C_3, and C_4 fractions was determined by the method of Pyke, Kahn, and Le Roy (13). Infrared spectra of the C_5 and C_6 fractions were taken. Insufficient C_5 material was obtained for identification except at high temperatures; experiments at 300°C. showed this fraction to contain 2-methyl butene-1 to the extent of approximately 40%, the remainder was an unidentified paraffin. The C_6 fraction was found to contain 2,3-dimethyl butane and 4-methyl pentene-1, as well as an unidentified material comprising, on the average, about 8% of the fraction. No evidence was found for *n*-hexane or 2-methyl pentane; this is in agreement with the observations of Moore (11) and suggests that only isopropyl radicals are formed by the addition of atomic hydrogen to propylene.

RESULTS

A series of experiments was done at room temperature, using cell II, for the purpose of identifying products and studying their possible dependence on hydrogen pressure. In these experiments, and in those described subsequently, the pressure drop was not allowed to exceed 50% of the initial propylene pressure; preliminary experiments had shown that the rate of pressure drop was constant until the pressure drop reached approximately 75% of the initial propylene pressure. For propylene pressures from 10 to 53.6 mm. and hydrogen pressures from 115 to 380 mm. the proportions of the various products, with the exception of 4-methyl pentene-1, were independent of the initial composition of the reaction mixture within the accuracy of the measurements. The average composition of the products was: 2,3-dimethyl butane 46.0%, propane 36.6%, methane 4.9%, unidentified C_6 fraction 4.5%, C_5 2.3%, butane 1%, butene 1%.

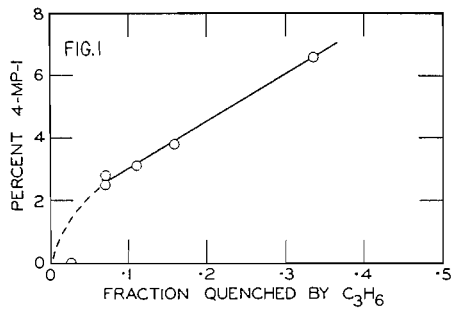

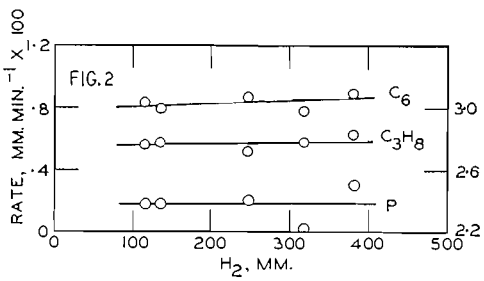

FIG 1. Effect of quenching of $Hg(^3P_1)$ atoms by propylene on the yield of 4-methyl pentene-1.
FIG. 2. Effect of hydrogen pressure on the rate of formation of the C_6 fraction and of propane (left hand scale) and on the rate of pressure decrease (right hand scale) at room temperature. Initial pressures of propylene were from 9.9 to 27.8 mm.

The percentage of 4-methyl pentene-1 increased considerably with the ratio of propylene to hydrogen. In Fig. 1 this percentage is plotted against the fraction of $Hg(^3P_1)$ atoms quenched by propylene, F. The value of F was calculated from the average concentrations of propylene and hydrogen, the

molecular weights of these two gases and of mercury, and the quenching cross sections for collisions of the two gases with $Hg(^3P_1)$ atoms. The quenching cross section for propylene was assumed to be 50×10^{-16} cm.^{2}, i.e. slightly greater than the value found by Steacie (16) for ethylene. The value taken for hydrogen was 8.9×10^{-16} cm.^{2} (16). Since only the ratio of these two quantities is involved in the calculation of F, the numbers would not be changed appreciably by using Darwent's suggested values of 31.0×10^{-16} and 6.0×10^{-16} for propylene and hydrogen, respectively (5).

The form of the curve in Fig. 1 suggests that 4-methyl pentene-1 probably arises through the quenching of $Hg(^3P_1)$ atoms by propylene. No 4-methyl pentene-1 could be detected in the experiment for which F was 0.028 (initial propylene 10 mm., initial hydrogen 380 mm.), which affords some justification for extrapolating the curve through the origin.

The rate of production of C_6 and propane and the rate of pressure drop are shown as functions of the hydrogen pressure in Fig. 2. This graph does not include the data for the experiment for which F was equal to 0.336 (*vide* Fig. 1); because of the considerable amount of quenching by propylene in this experiment the rate of pressure drop was only 1.68×10^{-2} mm. min.$^{-1}$.

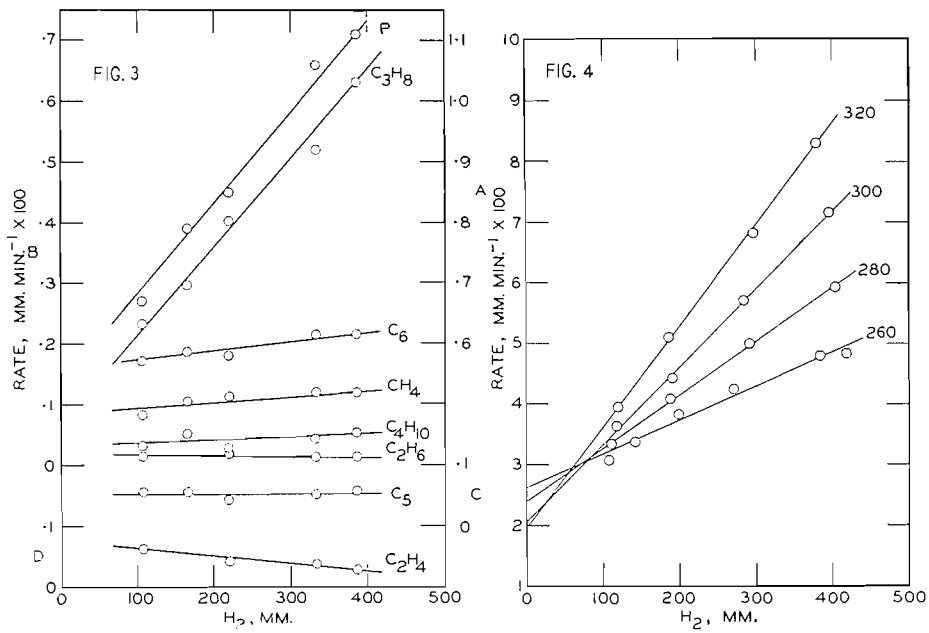

FIG. 3. Effect of hydrogen pressure at 320°C. Scale A: rate of pressure decrease; Scale B: rate of formation of methane, ethane, propane, butane, and C_6; Scale C: rate of formation of C_5; Scale D: rate of formation of ethylene. Initial pressures of propylene were in the range 17.7 to 18.2 mm.

FIG. 4. Effect of hydrogen pressure on the rate of pressure decrease at 260°, 280°, 300° and 320°C., using system II. In most cases the ratio hydrogen : propylene was of the order of 20 : 1 or greater. The ordinates refer to pressures corrected to 25°C., the abscissae to observed pressures at the reaction temperature.

In Fig. 3 are shown the results of a series of experiments using cell I at 320°C. The rate of production of propane and the rate of pressure drop are strongly

dependent on the hydrogen pressure at this temperature, while the rates of formation of the other products are not. Also, the rates of formation of ethane and ethylene are appreciable at 320°, although neither of these products could be detected at 25°C. A small amount of a product higher than C_6 was found at 320°C.; its rate of formation was independent of hydrogen pressure and equal to approximately 0.02×10^{-2} mm. min.$^{-1}$. At 25°C. the rates of formation of butane and butene were the same; at 320°C. the rate of formation of butene (*ca.* 0.012×10^{-2} mm. min.$^{-1}$) was considerably less than that of butane.

Quantitative comparison of the rates of formation of the various products at the two temperatures cannot be made with certainty because different lamps and cells were used. However, relative to the rate of formation of C_6, the rate of formation of methane is 6.3 times as great and of butane 11.5 times as great at 320° as at 25°C. The ratio of C_6 to propane for "zero hydrogen pressure" is 1.5 for 25°, 2.4 for 320°C. Since the C_6 fraction is largely 2,3-dimethyl butane, and since reaction [5] would not be expected to occur at low hydrogen pressures (see below) it would appear that there is little difference in activation energy for the combination and disproportionation of isopropyl radicals.

When a correlation had been established between the rate of pressure drop and the rate of formation of propane at high temperatures, a series of experiments was done to determine with some precision the rate of pressure drop as a function of hydrogen pressure and temperature. These measurements were made with cell II and the differential manometer; the results are shown in Fig. 4.

DISCUSSION

Even at the highest temperatures used, propane and 2,3-dimethyl butane are the major products. In view of the results shown in Figs. 2 and 3 it would appear that the most important reactions leading to their formation are the following:

$$Hg(^3P_1)+H_2 = 2H+Hg(^1S_0) \quad [1]$$

$$H+C_3H_6 = C_3H_7 \quad [2]$$

$$2C_3H_7 = C_6H_{14} \quad [3]$$

$$2C_3H_7 = C_3H_8+C_3H_6. \quad [4]$$

$$C_3H_7+H_2 = C_3H_8+H. \quad [5]$$

From the effect of hydrogen pressure on the rate of formation of propane it is clear that reaction [5] is negligible at room temperature but of increasing importance as the temperature is raised. Although at higher temperatures the rates of formation of methane and butane are greater, and ethane and ethylene appear in appreciable quantities, the formation of these products does not seem to be strongly influenced by hydrogen pressure. Furthermore, in the experiments at 320°C. in which propane was measured there was a good correlation between the rate of formation of propane and the rate of pressure drop. It therefore seems justifiable to interpret the slopes of the curves in Fig. 4 as showing the effect of hydrogen pressure on the rate of formation of propane.

Since, to a good approximation, all the products are saturated it follows that the rate of consumption of propylene will be almost identical with the rate of pressure drop.

The basic mechanism, reactions [1] to [5], inclusive, will be referred to as I. According to I the rate equation for the consumption of propylene is

$$-d(C_3H_6)/dt = I_a\left\{1+\frac{k_3}{k_3+k_4}\right\}+\frac{k_5 I_a^{\frac{1}{2}}}{(k_3+k_4)^{\frac{1}{2}}}(H_2). \qquad [i]$$

The curves in Fig. 4 satisfy an equation of the same form as [i], although mechanism I takes no account of the formation of methane, ethylene, or butane, to mention only three of the additional products found at higher temperatures. Also, mechanism I does not allow for the instability of the propyl radical at high temperatures (4) or for the possible occurrence of reaction [6],

$$H+C_3H_7 = C_3H_8. \qquad [6]$$

The analogous reaction between H atoms and ethyl radicals has been shown to be of some importance, under certain conditions, in the mercury photosensitized hydrogenation of ethylene (15).

If reaction [6], which may involve a third body, is included it is found that [i] still applies provided $k_2(k_3+k_4)(C_3H_6)/(k_5k_6(H_2))$ is appreciably greater than unity. From a consideration of the probable magnitudes of the quantities involved and from our analogous experiments with ethylene (15), it would appear that this condition obtains.

It is easily shown that if the propyl radical decomposes according to reaction [7],

$$C_3H_7 = C_3H_6+H, \qquad [7]$$

this will have no effect on the validity of [i].

If the propyl radical decomposes according to reaction [8],

$$C_3H_7 = C_2H_4+CH_3, \qquad [8]$$

and this is followed by [9],

$$CH_3+H_2 = CH_4+H, \qquad [9]$$

methane and ethylene will be formed at the same rate, viz. $k_8 I_a^{\frac{1}{2}}/(k_3+k_4)^{\frac{1}{2}}$ and a term of this same magnitude will be *added* to [i]; for brevity this term will be referred to as A.

If [8] is followed by [10],

$$CH_3+C_3H_7 = C_4H_{10}, \qquad [10]$$

it can be shown that [i] will be valid provided $(2I_a/A)^2$ is appreciably greater than unity. This condition undoubtedly obtains at the temperatures and light intensity used. Ethylene and butane will each be formed at a rate equal to A.

If [8] is followed by [11],

$$CH_3+H = CH_4, \qquad [11]$$

and if $(2I_a/A)^2$ is appreciably greater than unity it can be shown that the term A must be *subtracted* from [i]. Methane and ethylene will then each be formed at the rate A.

In all of the above cases the mechanisms predict that the steady state H atom concentration should increase with the concentration of H_2. The secondary reaction,

$$H+C_2H_4 = C_2H_5, \qquad [12]$$

would therefore be expected to become more important at high pressures of hydrogen. This probably accounts for the decrease in the yield of ethylene shown in Fig. 3.

Reactions [1] to [11] account in an adequate manner for all of the major products. In addition, some butane will be formed by the combination of ethyl radicals formed in [12]. The 4-methyl pentene-1, formed at low hydrogen concentrations, undoubtedly arises by the combination of propyl radicals with allyl radicals formed in the quenching of propylene by $Hg(^3P_1)$ atoms.

Bywater and Steacie (4) considered reaction [13],

$$H+C_3H_7 = CH_3+C_2H_5, \qquad [13]$$

to be the source of methyl radicals in the mercury photosensitized decomposition of propane at temperatures below 300°C. This reaction could occur if the excited propane formed in [6] were not deactivated. Reaction [6] would be more probable than [13] at the pressures used in these experiments, and since it has been shown that the occurrence of [6] is not likely to affect the validity of $[i]$ it seems justifiable to interpret the slopes of the curves in Fig. 4 in terms of $[i]$.

The logarithms of the slopes of the curves in Fig. 4 are plotted against $1000/T$ in Fig. 5. Least squares plots were used in each case. Since the ordinates in Fig. 4 refer to pressures measured with the whole system at 298°K., and the abscissae to pressures measured with the cell at the reaction temperature, T°K., it follows that the slopes, S, are given by the expression

$$S = \{298 V_c k_5 I_a^{\frac{1}{2}}\}/\{T(V_c+V_b)(k_3+k_4)^{\frac{1}{2}}\}, \qquad [ii]$$

in which V_c is the volume of the cell and V_b that of the rest of the system. Hence,

$$E_5 = -R\, d\{\ln S+\ln(k_3+k_4)^{\frac{1}{2}}+\ln T\}/d(1/T). \qquad [iii]$$

From Fig. 5 the first term is 11.4 kcal. per mole. The second term will be

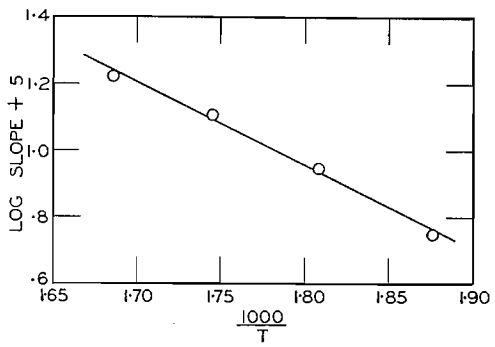

FIG. 5. Arrhenius plot of the slopes of Fig. 4.

neglected; the third is equal to RT. Using the average reaction temperature, 290°C., $E_5 = 12.5$ kcal. per mole.

For the analogous reaction,

$$C_2H_5+H_2 = C_2H_6+H \qquad [14]$$

Le Roy and Kahn found $-R\,d\ln S/d(1/T)$ to be 10.5 kcal. per mole (9). However, they plotted values of $-dP/dt$ reduced to 25°C. against values of P_{H_2} reduced to 25°C. In this case the third term is $RT^2V_b/(298V_c+TV_b)$, rather than RT. In their experiments V_c/V_b was 0.87, and for an average reaction temperature of 290°C. the correction term is 0.8 kcal. per mole. The corrected value of E_{14} is then 11.3 kcal. per mole, in good agreement with the value 11.5±1 kcal. per mole obtained by Wijnen and Steacie (18).

The errors introduced by neglecting the effect of temperature on combination and disproportionation in evaluating E_5 and E_{14} are probably less than 1 kcal. per mole.

An estimate of the value of k_3/k_4 may be obtained from the present data. The experiments of Moore and Taylor (12) suggest a value of 2.5 for this quantity at room temperature. Blacet and Calvert (3) and Durham and Steacie (6) found it to be *ca.* 2.0 at room temperature, while the latter obtained a value of 2.7 at 121°C. If we equate the ratio of hexane to propane at "zero hydrogen pressure" to k_3/k_4 the present results yield the value 1.3 at room temperature, *ca.* 2.1 at 320°C. The increase with temperature is in line with the results of Durham and Steacie. However, our experiments with ethylene (15) have shown that (product of combination)/(product of disproportionation) only approaches $k_{comb.}/k_{disp.}$ when the concentration of olefin is high, because of the influence of reaction [6] or its analogue. Moore and Taylor used a propylene pressure of 40 mm., which should be sufficient to yield a good value of k_3/k_4, but the ratio of propylene to hydrogen was only 1:6 which, in our experience, would result in the presence of a considerable amount of 4-methyl pentene-1 in the C_6 fraction. Their value of 2.5 at room temperature is probably too high for this reason. Our value is probably too low. A value close to 2.0 at room temperature would therefore seem to be established for the ratio of the rate of combination to the rate of disproportionation of isopropyl radicals.

ACKNOWLEDGMENT

The authors are grateful to the National Research Council for supporting this research and for granting a Fellowship to one of us (G. R. H.).

REFERENCES

1. BERLIE, M. R. and LE ROY, D. J. Discussions Faraday Soc. 14: 50. 1953.
2. BERLIE, M. R. and LE ROY, D. J. Can. J. Chem. 32: 650. 1954.
3. BLACET, F. E. and CALVERT, J. G. J. Am. Chem. Soc. 73: 661. 1951.
4. BYWATER, S. and STEACIE, E. W. R. J. Chem. Phys. 19: 319. 1951.
5. DARWENT, B. DE B., PHIBBS, M. K., and HURTUBISE, F. G. J. Chem. Phys. 22: 859. 1954.
6. DURHAM, R. W. and STEACIE, E. W. R. Can. J. Chem. 31: 377. 1953.
7. LE ROY, D. J. Ind. Eng. Chem. Anal. Ed. 17: 652. 1945.
8. LE ROY, D. J. Can. J. Research, B, 28: 492. 1950.
9. LE ROY, D. J. and KAHN, A. J. Chem. Phys. 15: 816. 1947.

10. MAJURY, T. G. and STEACIE, E. W. R. Can. J. Chem. 30: 800. 1952.
11. MOORE, W. J. J. Chem. Phys. 16: 916. 1948.
12. MOORE, W. J. and TAYLOR, H. S. J. Chem. Phys. 8: 504. 1940.
13. PYKE, R., KAHN, A., and LE ROY, D. J. Ind. Eng. Chem. Anal. Ed. 19: 65. 1947.
14. REBBERT, R. E. and STEACIE, E. W. R. Can. J. Chem. 32: 113. 1954.
15. SMITH, M. J., BEATTY, P. M., PINDER, J. A., and LE ROY, D. J. Can. J. Chem. In press. 1955.
16. STEACIE, E. W. R. Can. J. Research, B, 18: 44. 1940.
17. WHITTLE, E. and STEACIE, E. W. R. J. Chem. Phys. 21: 993. 1953.
18. WIJNEN, M. H. J. and STEACIE, E. W. R. J. Chem. Phys. 20: 205. 1952.

COMPRESSIBILITY OF GASES AT HIGH TEMPERATURES

IX. SECOND VIRIAL COEFFICIENTS AND THE INTERMOLECULAR POTENTIAL OF NEON[1]

By G. A. Nicholson[2] and W. G. Schneider

ABSTRACT

The second virial coefficients of neon have been determined in the temperature range 0° to 700°C. and the pressure range 10 to 80 atmospheres. These data were combined with published low temperature (−150° to 0°C.) second virial data, to investigate the intermolecular potentials of neon using both a Lennard-Jones potential, with a 9th and 12th power repulsion term, and also a modified Buckingham exponential–six potential. The agreement between observed and calculated values of $B(T)$ was excellent for both the exponential–six and the Lennard-Jones 12:6 potentials and slightly less satisfactory for the Lennard-Jones 9:6 potential.

VIRIAL COEFFICIENT DETERMINATION

Introduction

The determination of the second virial coefficients of neon consisted essentially of the accurate measurement of the pressure of gas in a pipette followed by the expansion of the gas into a smaller pipette, both pipettes being maintained at constant temperature, and the measurement of the final pressure. A series of experiments were carried out with different initial pressures and at different temperatures, and from the data obtained it was possible to calculate the virial coefficient at any of the experimental temperatures. Full details of the method have already been described in previous papers (10, 11, 14, 6).

Experimental

Stainless steel pipettes with volumes of approximately 220 and 50 ml. were used. Both vessels were maintained at constant temperature in a thermostat: oil was used as thermostat liquid up to 100°C. and a molten eutectic mixture of lithium, potassium, and sodium nitrates for temperatures above 100°C. Temperatures were controlled automatically to ±0.005°C. or better, using a photocell–amplifier–relay circuit in conjunction with a platinum resistance thermometer. A second platinum resistance thermometer was used to measure the temperature of the thermostat liquid.

Pressure measurements were made with a Keyes type of dead weight piston gauge which had been calibrated against the vapor pressure of carbon dioxide at 0°C. This instrument and the corrections to be applied to the measured pressure have already been described (10).

The neon used in these determinations was supplied by Linde Air Products as spectroscopically pure neon. Mass spectroscopic examination of the gas did not reveal any impurities, and subsequent analyses carried out at the beginning and end of each isotherm confirmed this.

[1]*Manuscript received December 6, 1954.*
Contribution from the Division of Pure Chemistry, National Research Council, Ottawa, Canada. Issued as N.R.C. No. 3535.
[2]*National Research Council of Canada Postdoctorate Fellow, 1953–54.*

Isotherms of neon were determined at 0°, 50°, 100°, and at 100° intervals up to 700°C. From these data second virial coefficients and intermolecular potentials have been calculated.

Interpretation of Experimental Results

If both pipettes are at a temperature T, their respective volumes are V_1 and V_2, and the number of molecules present initially in the large pipette at a pressure P_1 is n, then since we are dealing with a permanent gas at high temperatures and relatively low pressures, the isotherms can be fitted to simple virial expressions of the form

$$[1] \qquad P_1V_1/n = A_T+B_TP_1+C_TP_1^2.$$

On expanding the gas into the second pipette, the pressure is reduced to P but n remains constant

$$[2] \qquad P_2(V_1+V_2)/n = A_T + B_TP_2 + C_TP_2^2.$$

Combining equations [1] and [2] and eliminating n we get

$$[3] \qquad \frac{P_1}{P_2} = N+(N-1)\frac{B_T}{A_T}P_1+(P_1N-P_2)\frac{C_T}{A_T}P_1$$

where $N = (V_1+V_2)/V_1$.

The isotherms of neon are linear above 50°C. and the contribution due to the term involving the third virial coefficient can therefore be neglected in equation [3]. It must be considered, however, in calculating virial data for the 0° and 50°C. isotherms because these isotherms were found to have a slight curvature.

Considering the simple case

$$[4] \qquad \frac{P_1}{P_2} = N+(N-1)\frac{B_T}{A_T}P_1,$$

N is the intercept when the pressure ratio P_1/P_2 is plotted against P_1 and the value of B_T/A_T can therefore be derived from the slope of the graph. In order to calculate B_T for each isotherm, A_T must be known. If A_T and B_T are expressed in amagat units, then for the 0°C. isotherm

$$A_0+B_0 = 1.$$

Thus A_0 and B_0 can be determined and A_T is then calculated from the expression

$$A_T = A_0T/273.16.$$

Results

Experimental results are shown in Fig. 1 where the pressure ratio, P_1/P_2 is plotted against the pressure in the large pipette before expansion, P_1.*

**It should be noted that the experimental pressures P_1 along the abscissa are not equally spaced, but become progressively more closely spaced at lower pressures, approximately in the ratio $1/N$, as is obvious from equation [4]. This crowding together of the experimental points at low pressures is of great advantage in determining the limiting slope of the curve since from it the second virial coefficient is derived.*

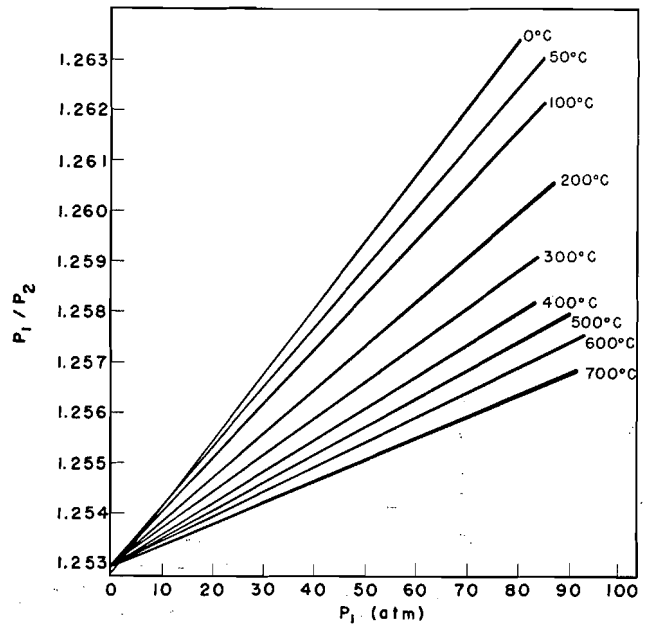

FIG. 1. Plot of pressure-ratios, P_1/P_2, vs. pressure, P_1, for neon.

The scatter of the individual points about the lines would not be noticeable on this scale and so all experimental points have been omitted. In every case, the scatter obtained was of the same order as the accuracy of the pressure measurement. At each temperature at least three expansion runs were carried out, each run usually consisting of eight expansions. The best line to represent the experimental results for each isotherm was fitted by a method of least mean squares (12) and the virial coefficients obtained from these are given in Table I. These data, expressed in amagat units of volume, are converted to cm.^{3}/mole units by multiplying by the normal volume V_N where

$$V_N = 22414.6/A_0 \text{ cm.}^3$$

The variation of the second virial coefficient, B, with temperature is shown graphically in Fig. 2. This graph also shows the results of other measurements carried out on neon (3, 4, 8, 5) and the data are recorded in Table II. There is

TABLE I

VIRIAL DATA AT DIFFERENT TEMPERATURES
(amagat units)

Temperature (°C.)	A_T	B_T ($\times 10^3$)	C_T ($\times 10^6$)
0	0.999514	0.4865	0.1996
50	1.182467	0.5494	0.0459
100	1.365375	0.5690	
200	1.731270	0.5987	
300	2.097165	0.6107	
400	2.463061	0.6143	
500	2.828956	0.6125	
600	3.194851	0.6192	
700	3.560747	0.6235	

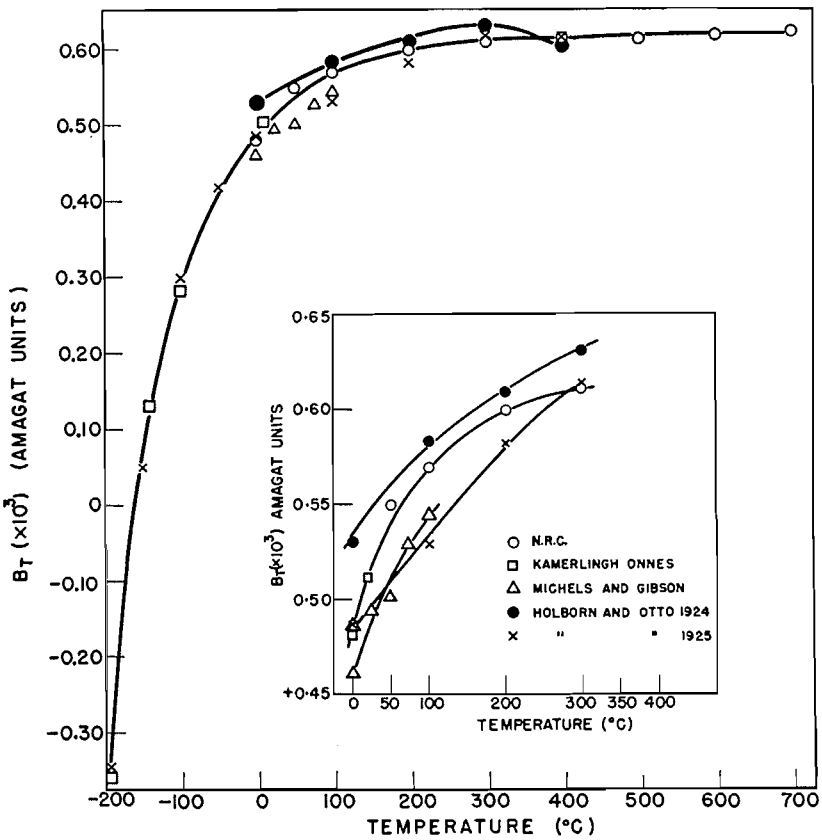

FIG. 2. Plot of second virial coefficients, B_T, vs. temperature.

TABLE II

COMPARISON OF MEASURED SECOND VIRIAL COEFFICIENTS WITH PREVIOUS VIRIAL DATA (×10³) (AMAGAT UNITS)

Temp. (°C.)	N.R.C.	Michels and Gibson	Holborn and Otto 1924	Holborn and Otto 1925	Kamerlingh-Onnes *et al.*
−182.5	—	—	—	—	−0.362
−150.0	—	—	—	0.055	—
−141.22	—	—	—	—	0.130
−103.01	—	—	—	—	0.281
−100.0	—	—	—	0.301	—
−50.0	—	—	—	0.418	—
0.0	0.4865	0.4612	0.5302	0.486	0.481
20.0	—	—	—	—	0.5114
24.47	—	0.4940	—	—	—
50.0	0.5494	—	—	—	—
50.40	—	0.5017	—	—	—
72.83	—	0.5292	—	—	—
100.0	0.5690	—	0.5834	0.529	—
100.83	—	0.5429	—	—	—
200.0	0.5987	—	0.6090	0.582	—
300.0	0.6107	—	0.6308	0.614	—
400.0	0.6143	—	0.6071	0.613	—
500.0	0.6125	—	—	—	—
600.0	0.6192	—	—	—	—
700.0	0.6235	—	—	—	—

good agreement between all the second virial data for neon except those results obtained in the temperature range 0° to 200°C. The data of Michels, Kamerlingh-Onnes, Holborn, and Otto (4), and N.R.C. agree quite closely at 0°C. but the Holborn and Otto (3) result is much higher. However, all the other Holborn and Otto (3) results are in fairly good agreement with N.R.C. results, while those of Michels, Kamerlingh-Onnes, and Holborn and Otto (4) in the temperature range 25° to 200°C. are much lower. It is interesting to note the sudden changes of curvature of the line joining the results of Holborn and Otto (4) at about 0°C. and 200°C. There appears to be no apparent explanation for the discrepancies in the data over the range 0° to 200°C. although the presence of impurities in the gas may be one of the most probable reasons.

ON THE INTERMOLECULAR POTENTIAL OF NEON

The second virial coefficient is related to the energy of interaction between pairs of molecules by the expression

$$B(T) = 2\pi N \int_0^\infty r^2(1-e^{-E(r)/kT})\,dr$$

where $B(T)$ is the second virial coefficient,

N is Avogadro's number,

$E(r)$ is the potential energy of interaction as a function of distance r.

Using this expression it is easy to calculate values for the second virial coefficients provided the potential $E(r)$ is known. The reverse process is not so easy, however, unless a fairly simple expression is used for the term $E(r)$. One such expression is the Lennard-Jones inverse power potential:

$$E(r) = 4\epsilon[(r_0/r)^n - (r_0/r)^6],$$

the special case of this being when $n = 12$, i.e. a 12th power of repulsion and a sixth power of attraction. In the above expression ϵ is the energy at the minimum of the potential energy curve and r_0 is the low-velocity collision diameter. The value of r at the minimum will be designated as r_m. An exp: 6 intermolecular potential

$$E(r) = \frac{\epsilon}{1-6/\alpha}\left[\frac{6}{\alpha}e^{\alpha(1-r/r_m)} - \left(\frac{r_m}{r}\right)^6\right],$$

where ϵ is the depth of the potential energy minimum,

r_m is the position of the minimum,

α is a parameter which measures the steepness of the repulsion energy, has also been used successfully, and it has also been used to predict data on transport properties with fair accuracy.

The experimental results were fitted with a Lennard-Jones 12:6 and 9:6 potential and also an exp:6 potential. For the Lennard-Jones 12:6 potential, integration of the above expression for B leads to $B(T) = b_0\,\beta(\tau)$ where $b_0 = \frac{2}{3}\pi N r_0^3$ and $\tau = kT/\epsilon$. Tables for the function $\beta(\tau)$ have been compiled by Hirschfelder, Bird, and Spotz (9). A method of least mean squares (13) was

used to calculate the best potential parameters. Two sets of virial data were used:

(i) N.R.C. data only.

(ii) N.R.C. data together with the low temperature (0° to −150°C.) data of Holborn and Otto (4) and Kamerlingh-Onnes. Quantum mechanical corrections (2) were applied to all virial data at temperatures of 0°C. and lower before they were used in the calculations. All values shown in Table III have already been corrected.

Good agreement was obtained between the two sets of data for the potential parameters (see Table III) and therefore in subsequent calculations, N.R.C.

TABLE III

COMPARISON OF EXPERIMENTAL AND CALCULATED SECOND VIRIAL COEFFICIENTS

		Lennard-Jones potential				Buckingham exp : 6 potential	
		12 : 6		9 : 6			
		r_0 2.756 Å r_m 3.093 Å ϵ/k 33.74°K. ± 0.18 ϵ 46.55 × 10^{-16} erg		r_0 3.326 Å r_m 3.806 Å ϵ/k 25.42°K. ± 0.01 ϵ 35.07 × 10^{-16} erg		r_0 2.758 Å r_m 3.084 Å ϵ/k 37.36°K. ± 0.19 ϵ 51.55 ± 10^{-16} erg α 15	
Temp. (°K.)	Exptl. 2nd virial coefficient (cm.³/mole)	Second virial coefficient (cm.³/mole)					
		Calc.	Exp.−calc.	Calc.	Exp.−calc.	Calc.	Exp.−calc.
123.16	1.23	1.36	−0.13	1.31	−0.08	1.30	−0.07
131.94	2.92	2.65	+0.27	2.66	+0.26	2.62	+0.30
170.15	6.30	6.54	−0.24	6.68	−0.38	6.59	−0.29
173.16	6.75	6.77	−0.02	6.90	−0.15	6.81	−0.06
223.16	9.37	9.46	−0.09	9.66	−0.29	9.52	−0.15
273.16	11.12	11.07	+0.11	11.21	−0.09	11.09	+0.03
323.16	12.32	11.97	+0.35	12.17	+0.15	12.05	+0.27
373.16	12.76	12.61	+0.15	12.77	−0.01	12.68	+0.08
473.16	13.43	13.35	+0.08	13.44	−0.01	13.39	+0.04
573.16	13.70	13.71	−0.01	13.72	−0.02	13.70	0.00
673.16	13.78	13.88	−0.10	13.83	−0.05	13.86	−0.08
773.16	13.74	13.96	−0.22	13.84	−0.10	13.92	−0.18
873.16	13.89	13.97	−0.08	13.79	+0.10	13.91	−0.02
973.16	13.98	13.94	+0.04	13.72	+0.26	13.85	+0.13

data were combined with the low-temperature data of previous workers. Second virial coefficients were calculated from the potential parameters and these are compared with experimental values in Table III. It is apparent from the comparison that the deviations for the 12:6 potential and the exp:6 potential are very similar and neither potential appears to be superior to the other. This is perhaps not surprising in view of the close similarity of the two types of potential energy curves, which are shown plotted in Fig. 3. The 9:6 potential gives a slightly poorer fit to the experimental data in that the sum of squares of the deviations is somewhat higher than for the other two potentials. The over-all fit is nevertheless surprisingly good in view of the rather large difference of this potential (also shown in Fig. 3) compared with the 12:6 and exp:6 potentials.

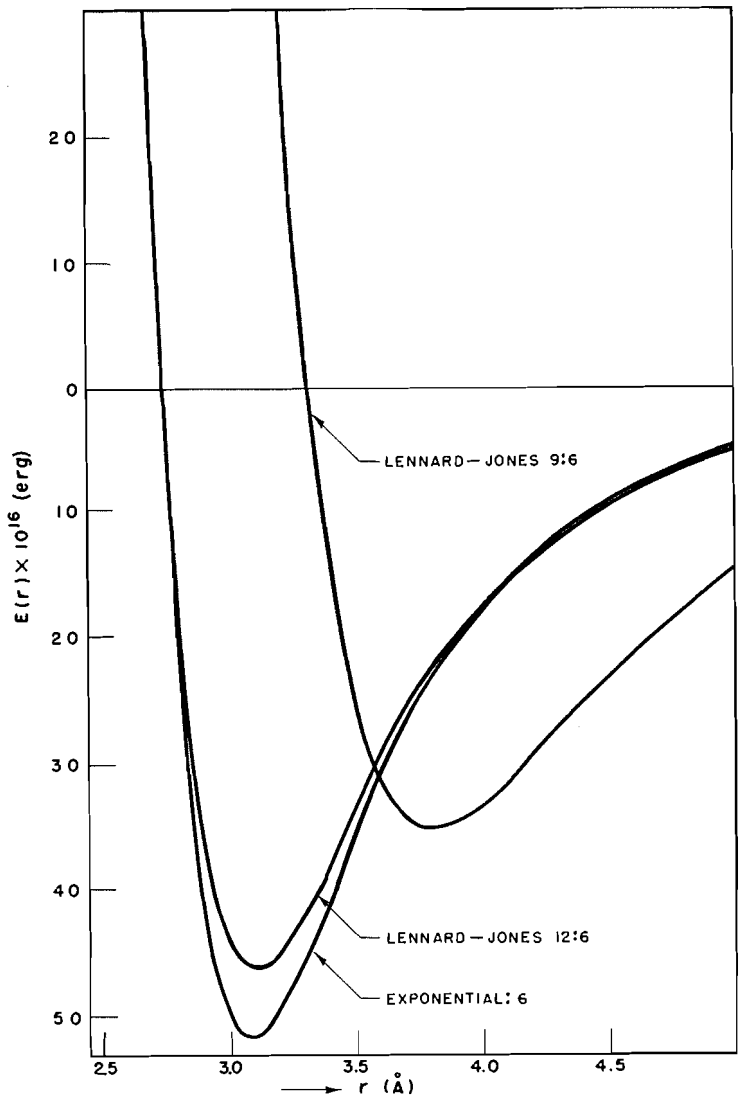

FIG. 3. Comparison of potential energy curves for neon.

Corner (1) has shown recently how calculations of intermolecular potentials may be improved by the use of crystal data in addition to gas property data. He used this method to determine the potentials of neon with repulsion of an exponential type from crystal, second virial, and Joule-Thomson coefficient data. Mason and Rice (7) extended the application of Corner's method to include experimental transport property results for the evaluation of the intermolecular potentials of a number of simple non-polar molecules, including neon. For comparison, the potential parameters obtained by Corner (1) are given in Table IV together with those of Mason and Rice (7) and N.R.C.: these are for an exp:6 potential only. The over-all agreement is very satisfactory.

TABLE IV

COMPARISON OF POTENTIAL PARAMETERS FOR AN EXP : 6 POTENTIAL

	α	r_m, Å	ϵ/k, °K.
N.R.C.	15	3.084	37.36
Corner	13.6	3.16	37.1
Mason and Rice	14.5	3.147	38.0

ACKNOWLEDGMENT

The authors wish to express their thanks to Mr. W. A. Stevenson for assisting in the construction of the apparatus, and to Mr. G. David for helping with the intermolecular potential calculations.

REFERENCES

1. CORNER, J. Trans. Faraday Soc. 44: 914. 1948.
2. HIRSCHFELDER, J. O., CURTISS, C. F., and BIRD, R. B. Molecular theory of gases and liquids. John Wiley & Sons, Inc., New York. 1954. p. 422.
3. HOLBORN, L. and OTTO, J. Z. Physik, 23: 77. 1924.
4. HOLBORN, L. and OTTO, J. Z. Physik, 33: 1. 1925.
5. KAMERLINGH-ONNES, H. *et al.* Commun. Phys. Lab. Univ. Leiden, 147d. 1915; 154a. 1919.
6. MACCORMACK, K. E. and SCHNEIDER, W. G. J. Chem. Phys. 18: 1269. 1950; 19: 845. 1951.
7. MASON, E. A. and RICE, W. E. J. Chem. Phys. 22: 843. 1954.
8. MICHELS, A. and GIBSON, R. O. Ann. Physik, 87: 850. 1928.
9. Publication CM-5999, University of Wisconsin. May 1950.
10. SCHNEIDER, W. G. Can. J. Research, B, 27: 339. 1949.
11. SCHNEIDER, W. G. and DUFFIE, J. A. H. J. Chem. Phys. 17: 751. 1949.
12. WHALLEY, E., LUPIEN, Y., and SCHNEIDER, W. G. Can. J. Chem. 31: 722. 1953.
13. WHALLEY, E. and SCHNEIDER, W. G. J. Chem. Phys. In press. 1955.
14. YNTEMA, J. L. and SCHNEIDER, W. G. J. Chem. Phys. 18: 641. 1950.

THE DEGRADATION OF CARRAGEENIN

I. KINETICS IN AQUEOUS SOLUTION AT pH 7[1]

By C. R. Masson

ABSTRACT

The degradation of carrageenin in buffered aqueous solution at pH 7.0 has been studied over the temperature range 60° to 101°C. by following the change in viscosity and reducing properties. Kinetic analysis indicates the occurrence of two reactions: (*a*) an initial rapid degradation representing only about 0.3% of the complete hydrolysis, followed by (*b*) a first-order random degradation having $k = 2.75 \times 10^{13}\ e^{-29,200/RT}$ hr^{-1}. The latter reaction becomes important at temperatures above 60°C. The results indicate that carrageenin is more unstable than would be expected of a simple 1–3 galactan, and that two types of weak linkage are involved in the structure of the polysaccharide.

INTRODUCTION

The polysaccharide carrageenin is a well known naturally-occurring hydrocolloid which, by virtue of its gelling and stabilizing properties in aqueous solution, is of commercial importance (12). Black (1) has recently reviewed the literature on the structure of this polysaccharide. The main units are D-galactose residues joined through carbon atoms 1 and 3 and carrying a half-ester sulphate group on carbon 4. The polysaccharide is obtained by extracting with water the red alga *Chondrus crispus*. In the commercial process, heat is generally employed at some stage during extraction and drying, but, although it has long been known (3) that carrageenin solutions are thermally unstable, no systematic study of the degradation has been reported. Such a study might not only yield results of practical value but might also help to elucidate some aspects of the structure of the macromolecule.

EXPERIMENTAL

Materials

In this Part, only one extract was employed. It was extracted from the dried *Chondrus* at approximately 80°C., decolorized with carbon at 60°C., and precipitated with ethanol from a slightly saline solution. As shown previously (4) it had a number average molecular weight not greater than 74,500. This extract was chosen on account of its relatively low molecular weight, as it was desired to employ reducing end-group titrations as a means of following the degradation. The material is referred to as extract F.

Solutions were prepared as required by "tumbling" at room temperature until homogeneous, and were clarified by means of Selas No. 02 porcelain filters. The sodium salt of the polysaccharide, which was used in all experiments, was prepared by passing the solutions through a column of Amberlite IR 100 exchange resin. Solutions were stored in the refrigerator at 4°C., but even at this temperature a slight decrease in viscosity occurred on standing. Experi-

[1]*Manuscript received December 6, 1954.*
Contribution from the Maritime Regional Laboratory, National Research Council, Halifax, N.S. Issued as N.R.C. No. 3531.

ments were therefore made as soon as possible after the solutions had been prepared.

Measurements

An iodometric method (11) was employed for the titrations of total reducing power.

Viscosities were measured at 25°C. in Ostwald viscosimeters with the characteristics given previously (4). All viscosities were independent of the rate of shear.

Preliminary experiments showed that the decrease in viscosity which occurred on heating an unbuffered solution of carrageenin was accompanied by a decrease in pH. This catalyzed further degradation so that the reaction became quite rapid in the later stages. Buffered solutions were therefore employed in studying the kinetics. *M*/30 sodium phosphate was chosen since the ionic strength was sufficiently high for adequate buffering capacity but low enough to avoid excessive suppression of the viscosity due to the cation effect.

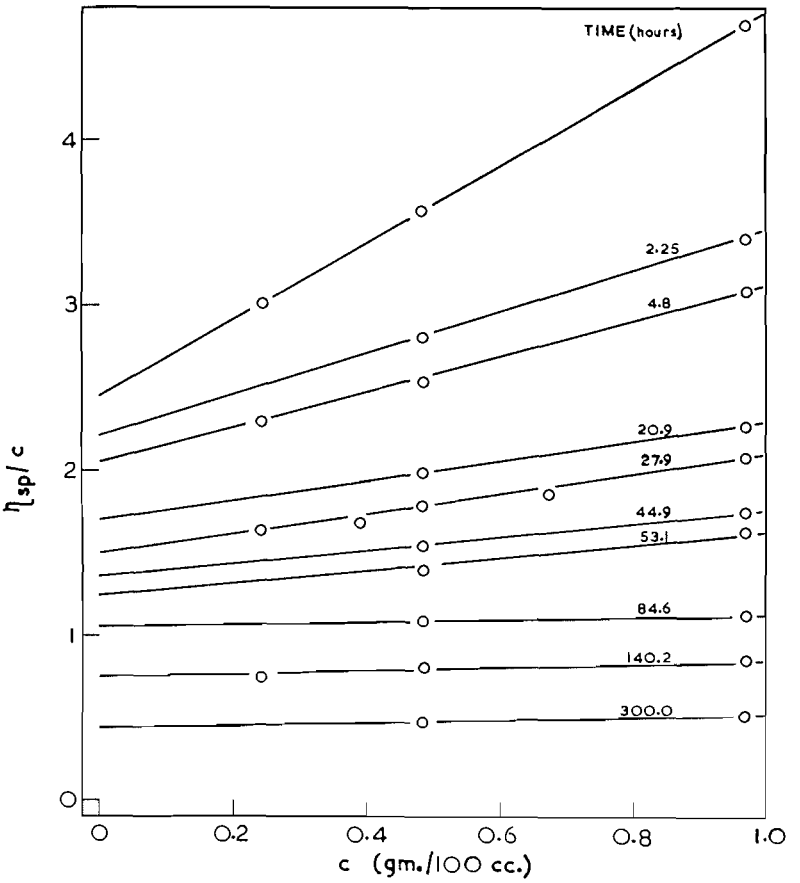

FIG. 1. η_{sp}/c vs. c for a carrageenin solution after various times of heating at 90°C. (Viscosities at 25°C.)

The degradation was studied by heating solutions, of concentration 0.944 gm./100 ml., at various temperatures and measuring the reducing property and intrinsic viscosity of samples withdrawn at various times. The flasks containing the solutions were equipped with reflux condenser, thermometer, and stopper to allow withdrawal of samples, and were placed in baths controlled to within ±0.1°C. Thermal equilibrium was established within one half hour. The experiment at 101°C. was made in an oil bath under gentle reflux and the temperature rose by about 0.5°C. during this experiment. All solutions darkened in color on prolonged heating, although this was slight at 60°C. In addition, small particles of a brown solid occasionally appeared and the solutions were filtered, if necessary, before viscosity measurements were made.

RESULTS

Fig. 1 illustrates the results of a typical experiment. The specific viscosities of the individual samples were measured at various concentrations in $M/30$ phosphate buffer. Extrapolation of the linear plots of η_{sp}/c against c to zero concentration gave values of $[\eta]$ at various times during the experiment. Table I shows the values of $[\eta]$ and of the total reducing power (expressed as

TABLE I

INTRINSIC VISCOSITIES AND END-GROUP TITRATIONS

Time (hr.)	$[\eta]$	mgm. galactose/ 5 ml.	$M \times 10^{-4}$ from equation [1]	Time (hr.)	$[\eta]$	mgm. galactose/ 5 ml.	$M \times 10^{-4}$ from equation [1]
Run 1, Temp. = 90°C.				*Run 2, Temp. = 60°C.*			
0	2.45	0.24	3.926	0	2.29	0.17	3.715
2.25	2.22	0.29	3.614	8.5	2.18	0.20	3.565
4.8	2.06	0.30	3.404	18.8	2.10	—	3.451
20.9	1.70	0.30	2.897	48.0	2.07	—	3.412
27.9	1.50	—	2.612	69.3	1.91	—	3.192
44.9	1.35	0.32	2.388	97.6	2.00	0.25	3.311
53.1	1.24	0.37	2.226	122	1.92	0.33	3.206
84.6	1.05	0.47	1.938	146	1.87	0.34	3.133
140.2	0.75	0.55	1.465	217	1.81	—	3.055
300.0	0.445	1.59	0.948	288	1.78	0.31	3.006
				382	1.74	—	2.958
				478	1.71	—	2.911
Run 3, Temp. = 75°C.				*Run 4, Temp. = 101°C.*			
0	2.29	0.17	3.715	0	2.19	0.23	3.573
3.75	2.10	0.24	3.451	1.95	1.94	0.25	3.236
18.6	1.85	0.29	3.105	5.8	1.79	—	3.027
48.0	1.78	0.32	3.006	11.1	1.56	—	2.698
69.3	1.75	0.24	2.972	20.4	1.32	0.42	2.350
97.6	1.62	0.25	2.786	34.8	0.96	0.46	1.799
122	1.55	—	2.680	45.8	0.84	0.53	1.611
146	1.54	—	2.668	59.3	0.59	0.70	1.199
217	1.41	0.45	2.478	81.8	0.42	0.75	0.904

mgm. galactose/5 ml. of solution) for experiments at different temperatures. Comparison with the titer obtained on complete hydrolysis showed that the degradation was less than 5% in all experiments.

Attempts to measure the molecular weights of some of the samples by their osmotic pressure were unsuccessful as appreciable quantities of low molecular-weight material passed through the cellophane membranes. Molecular weight

TABLE II

COMPARISON OF MOLECULAR WEIGHTS

Polymer	End-group titration (as mgm. galactose/gm. polymer)	Molecular weight from titration	Osmotic molecular weight
FA	3.04	59,000 ± 13,000	42,900
FB	4.92	37,000 ± 6000	30,100
FC	8.85	20,000 ± 1000	21,800

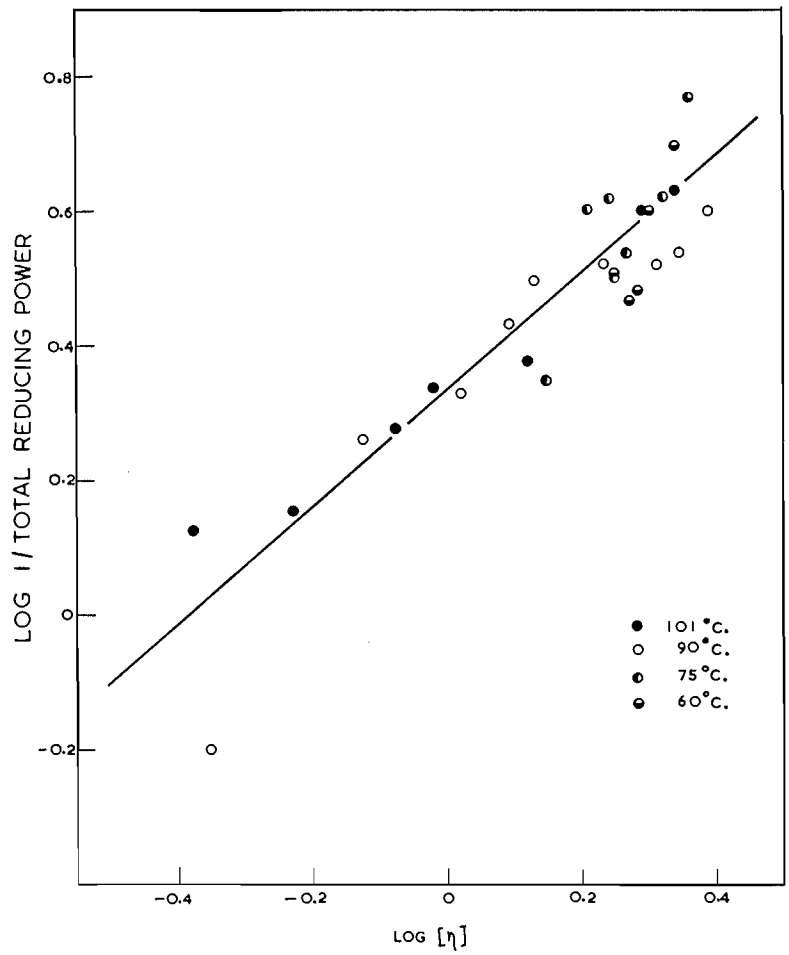

FIG. 2. log [η] vs. log (1/total reducing power) for all runs.

measurements have, however, been performed on dialyzed fractions of the degraded polysaccharide (4). End-group titrations on these fractions showed that the molecular weights calculated on the basis of one reducing end-group per molecule were in reasonable agreement with the accurate values obtained osmometrically. This is illustrated in Table II.

On the basis of this agreement, the titration values shown in Table I have been used to obtain a relationship between $[\eta]$ and M. In Fig. 2 log $[\eta]$ is plotted against log (1/total reducing power) for all the measurements. The scatter is large on account of the insensitivity of the chemical method in this region. For most points, however, the scatter is no greater than expected for an error of ± 0.1 ml. in the titrations. The line through the points corresponds to the relationship

[1] $$[\eta] = 7.59 \times 10^{-6} M^{1.20}.$$

Molecular weights calculated from the intrinsic viscosities by equation [1] are listed in Table I. These values are approximate only, but the relative values may be used to obtain a fairly accurate representation of the course of the degradation.

DISCUSSION

For a first-order, random degradation (2) the velocity constant k is given by the expression

[2] $$1/M_t - 1/M_0 = k\,t/m$$

where M_0 and M_t are the molecular weights at zero time and time t respectively, and m is the molecular weight of the monomer. In Fig. 3, $1/M_t - 1/M_0$ is plotted against t for the four runs. A sharp decrease in molecular weight is observed in the early stages of degradation. After this the plots become linear, indicating random degradation. The initial, non-linear portion of the reaction is exhibited most clearly in the runs at the lower temperatures and does not appear at 101°C. It represents only about 0.3% of the total degradation on the basis of complete hydrolysis.

The slopes of the linear portions of the curves in Fig. 3 give values of k/m. If a tentative value of $m = 250$ is adopted, the following values of k are obtained for the random degradation:

Temp. (°C.)	60	75	90	101
$k \times 10^5$ (hr.$^{-1}$)	0.15	1.13	6.48	20.5

From these data a good Arrhenius plot is obtained, which yields $E = 29.2$ kcal. for the activation energy and $A = 2.75 \times 10^{13}$ (hr.$^{-1}$) for the temperature-independent factor in the equation for the random degradation.

The value of E is of the same order of magnitude as the values found for the degradation of other polysaccharides. Thus Moelwynn-Hughes (8) has reported a value of $E = 30.97$ kcal. for the hydrolysis of maltose polysaccharides. A value of $E = 29$ kcal. has been found (7) for amylose, while for pectin $E = 28 \pm 6$ has been obtained (6).

The values of k are high for a polysaccharide in neutral solution. The labile nature of carrageenin suggests that the observed degradation does not corre-

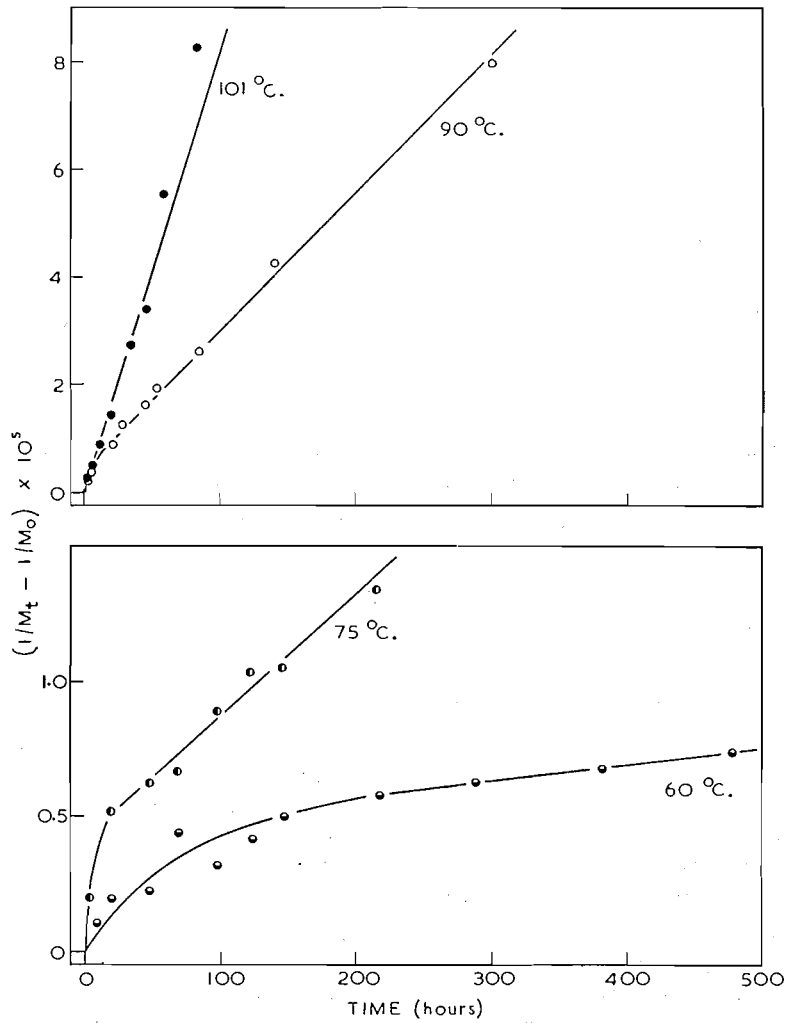

FIG. 3. $1/M_t - 1/M_0$ vs. t for runs at various temperatures.

spond to the scission of 1–3 linked D-galactose residues, but must be attributed to the presence of weaker bonds in the structure. Recent work (9) has revealed the presence of 3,6-anhydro-D-galactose as a constituent of the κ fraction (10) of carrageenin, and strong evidence is available that this compound is split off in the early stages of degradation (5, 9). The high velocity constants may therefore be attributed to this cause.

The random degradation may be interpreted on the basis that the anhydro-D-galactose residues are incorporated either at random or in a regular repeating sequence throughout the structure. The results indicate that long chains of 1–3 linked D-galactopyranose residues are not present in the structure of this extract as the degradation proceeds linearly to low values of $[\eta]$.

At temperatures below 60°C. the rate of random degradation becomes inappreciable. The decrease in viscosity observed for carrageenin solutions at lower temperatures is therefore ascribed to the non-random process noted above. The nature of the weaker linkages responsible for this aspect of the kinetics is at present unknown. A possible interpretation is that bonds responsible for chain-branching or cross-linking are broken in the early stages of degradation, but further work would be required to decide this.

ACKNOWLEDGMENTS

The author wishes to thank Dr. A. N. O'Neill for supplying the carrageen extract and Mr. G. W. Caines for technical assistance.

REFERENCES

1. BLACK, W. A. P. Ann. Repts. on Progr. Chem. (Chem. Soc. London), 50: 322. 1953.
2. EKENSTAM, A. Ber. 69, B: 540, 553. 1936. (Cf. Mark, H. and Tobolsky, A. V. *In* High polymers. Vol. 2. Interscience Publishers, Inc., New York. 1950. p. 462.)
3. GUTBIER, A. and HUBER, J. Kolloid-Z. 30: 20. 1922.
4. MASSON, C. R. and CAINES, G. W. Can. J. Chem. 32: 51. 1954.
5. MASSON, C. R., SANTRY, D., and CAINES, G. W. To be published.
6. MERRILL, R. C. and WEEKS, M. J. Am. Chem. Soc. 67: 2244. 1945.
7. MEYER, K. H., HOPFF, H., and MARK, H. Ber. 62, B: 1103. 1929.
8. MOELWYNN-HUGHES, E. A. Trans. Faraday Soc. 25: 81. 1929.
9. O'NEILL, A. N. J. Am. Chem. Soc. In press. 1955.
10. SMITH, D. A. and COOK, W. H. Arch. Biochem. and Biophys. 45: 232. 1953.
11. SOMOGYI, M. J. Biol. Chem. 195: 19. 1952.
12. TSENG, C. K. *In* Colloid chemistry. Vol. VI. Reinhold Publishing Corporation, New York. 1946. p. 629.

THE REACTION OF DIETHYL AZODICARBOXYLATE WITH DIHYDROGELSEMINE[1]

By Thelma Habgood and Léo Marion

ABSTRACT

Dihydrogelsemine reacts with diethyl azodicarboxylate yielding a carbinolamine which forms a methyl ether. Both this ether and the carbinolamine base can be oxidized by chromic acid to the same neutral lactam. That there has been no rearrangement of the carbon skeleton during these reactions is shown by reduction of the methyl ether of the carbinolamine with sodium borohydride to dihydrogelsemine and by reduction of the lactam with lithium aluminum hydride to tetrahydrodesoxygelsemine. It is concluded that both dihydrogelsemine and gelsemine contain a methylene group adjacent to $N_{(b)}$, and from the infrared spectrum of the lactam of dihydrogelsemine, $N_{(b)}$ appears to be part of a five-membered ring.

In the course of the investigation of the demethylation of dihydrogelsemine by means of cyanogen bromide (6), the use of diethyl azodicarboxylate as a demethylating agent was explored as an alternate route to dihydro-N-*nor*-gelsemine. It was observed, however, that the action of this reagent on dihydrogelsemine followed a different course. It gave rise to an intermediate which failed to produce formaldehyde when heated with dilute hydrochloric acid, contrary to what was expected from the observations of Diels and Fischer (2) in the preparation of *nor*codeine. The products of the hydrolytic reaction were a new base I and diethyl hydrazodicarboxylate. This seemed to indicate that the azo ester had attacked not the hydrogens of the N-methyl group, but the hydrogen on a carbon adjacent to $N_{(b)}$, and thus afforded a tool with which the alicyclic part of the molecule (5, 7) could be breached.

Because of its unstable character it was not possible to purify the new base I, but on standing in methanol solution in the presence of mild alkali, it was converted into a crystalline methoxy-base II ($C_{21}H_{26}O_3N_2$). The infrared absorption spectrum of this base II (Fig. 1, curve 1) contained two bands (1095 and 1115 cm.$^{-1}$) attributable to ether linkages, together with a band in the NH region and a strong peak at 1713 cm.$^{-1}$ due to the oxindole carbonyl. The base I formed a crystalline perchlorate, $C_{20}H_{23}O_2N_2 \cdot ClO_4$ corresponding to the anhydro-base III, and the infrared absorption spectrum of the salt (Fig. 1, curve 2) indeed showed an absorption band at 1668 cm.$^{-1}$ which has been shown to occur in the spectra of salts containing the $>C{=}N^+<$ grouping (3). The methoxy-base II when treated with perchloric acid gave rise to the same anhydro salt as base I. These facts can be interpreted on the assumption that base I is a dihydrogelsemine carbinolamine, and in support of this, the methoxy-base II gives the silver mirror test, reduces Fehling's solution, and within a few minutes gives a dark orange color with 2,4-dinitrophenylhydrazine. This interpretation was confirmed by the reduction of the methoxy base II

[1]*Manuscript received December 13, 1954.*
Contribution from the Division of Pure Chemistry, National Research Council, Ottawa, Canada. Issued as N.R.C. No. 3536.

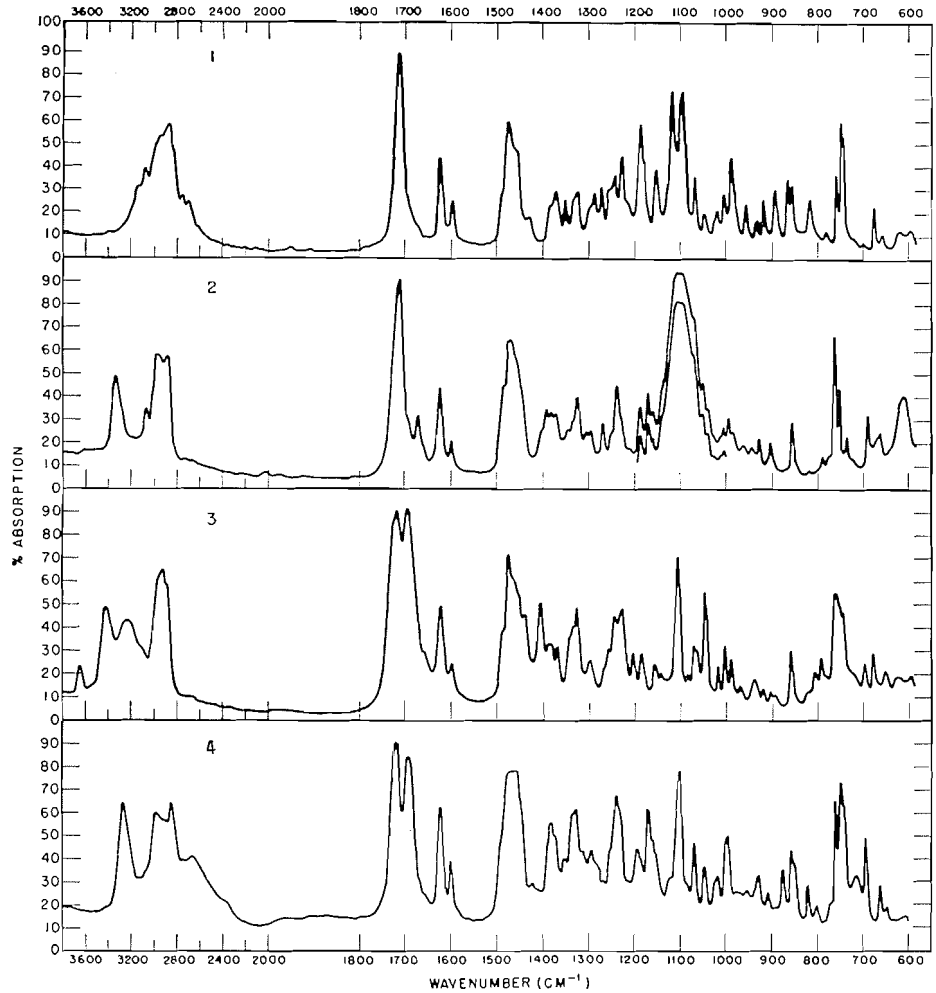

FIG. 1. Infrared absorption spectra in nujol mulls taken on a double beam Perkin-Elmer spectrophotometer, model 21. Curve 1, methoxy base II. Curve 2, perchlorate of base I. Curve 3, dihydrogelsemine lactam. Curve 4, dihydrogelsemine.

with sodium borohydride which converted it to dihydrogelsemine. Hence the above reactions can be represented by the partial formulae I–III.

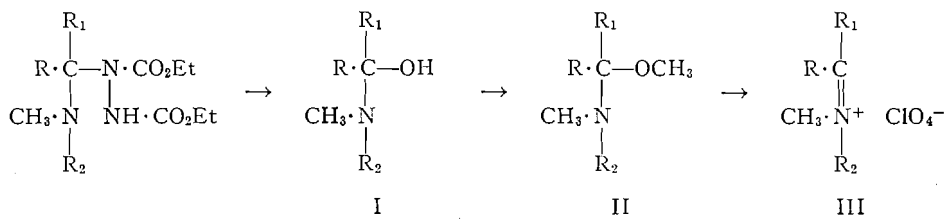

Oxidation of either base I or the methoxy-base II with chromic anhydride in acetic acid gave rise to a neutral product IV ($C_{20}H_{22}O_3N_2$). This product

differed from dihydrogelsemine in having two hydrogens less and one oxygen more. Its neutral properties suggested that it was a lactam, and its infrared absorption spectrum (Fig. 1, curve 3) supported this deduction. It showed a strong absorption band at 1718 cm.$^{-1}$ due to the oxindole carbonyl, and another still stronger peak at 1693 cm.$^{-1}$ attributable to a carbonyl present in a cyclic lactam[2]. The absorption of the new carbonyl in the infrared shows it to be part of a five-membered lactam since the carbonyl of six-membered lactams absorbs at lower frequencies. The lactamic nature of the new carbonyl was confirmed by the action of lithium aluminum hydride which converted product IV into tetrahydrodesoxygelsemine, $C_{20}H_{26}ON_2$, identical with that obtainable directly from dihydrogelsemine (7). Product IV, therefore, contains a carbonyl next to $N_{(b)}$ and dihydrogelsemine must contain a methylene group adjacent to the basic nitrogen. The lactam was hydrolyzed by barium hydroxide, but the resulting amino acid recyclized as soon as its aqueous solution was evaporated to dryness.

Since gelsemine is known to contain an exocyclic methylene group (4), and since the conversion of gelsemine to dihydrogelsemine has been shown to involve the saturation of this double bond (4), it is legitimate to assume that this reduction does not cause any alteration of the carbon-nitrogen skeleton. Hence, gelsemine also must contain a methylene group adjacent to $N_{(b)}$. Although the action of diethyl azodicarboxylate on gelsemine did not yield any crystalline substance, the amorphous reaction product was converted back to gelsemine by reduction with sodium borohydride, and this lends support to the foregoing conclusion.

In the light of these results, the structures suggested by Robinson (4) and by Prelog and his co-workers (5) to represent gelsemine are untenable. Of the six rings present in gelsemine the nature of three is now established and the base can be represented by one of the partial structures V or VI of which for biogenetic considerations V is preferred. Since one carbon is required for the exocyclic methylene group and one ring is a cyclic ether, a remnant C_7H_{10} is

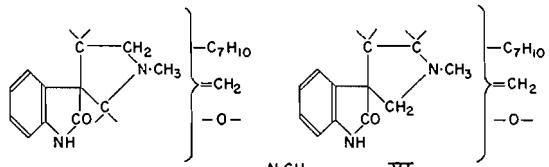

V

VI

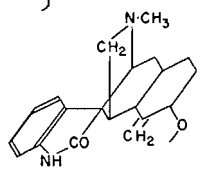

VII

[2]*In this connection it is noteworthy that the infrared spectrum of dihydrogelsemine (in a mull) shows a double peak in the carbonyl region although this base contains only one carbonyl group (Fig. 1, curve 4). The infrared spectrum of N-cyano-*norgelsemine *also contains a double peak in the carbonyl region whereas the spectra of gelsemine and N-cyanodihydro*norgelsemine *show a single absorption band in that region. In the spectrum of the lactam, however, the second peak is stronger than that of the oxindole carbonyl (Fig. 1, curve 3).*

left with which to form the two remaining rings. To represent gelsemine, formula VII is tentatively suggested. It can be derived from one molecule of tryptamine and one of tyrosine which together account for the carbon-nitrogen skeleton of the base. The known reactions of gelsemine can be explained on the basis of this formula in which, however, only one point of attachment of the ether oxygen is suggested, there being no evidence so far as to the size of the cyclic ether.

EXPERIMENTAL[3]

Dihydrogelsemine Carbinolamine

To a solution of dihydrogelsemine (3.643 gm.) in a mixture of acetone (100 ml.) and methanol (10 ml.) diethyl azodicarboxylate (4.0 ml.) (prepared according to the method of Curtius (1)) was added dropwise with swirling. A slight amount of gas was evolved and the solution became warm. After 2.5 hr. the solvent was removed under reduced pressure, and the gummy residue was heated on the steam bath for one hour with 10% hydrochloric acid. No smell of formaldehyde was detected. When cool, the acidic solution was extracted with chloroform to remove neutral compounds consisting of unreacted diethyl azodicarboxylate and of diethyl hydrazodicarboxylate, m.p. 133.2–133.7, either alone or in admixture with an authentic specimen. The acidic solution was alkalized with dilute sodium hydroxide and the precipitated base was extracted with chloroform. On evaporation, the extract left a pale yellow glass difficultly soluble in methanol (3.005 gm.). The basic fraction was benzoylated in chloroform solution with benzoyl chloride (1.6 gm.) under Schotten-Baumann conditions. The chloroform layer was washed with dilute sulphuric acid and the tertiary amine (1.829 gm.) was isolated by alkalization and extraction with chloroform. The tertiary base dissolved in methylene dichloride was chromatographed on alumina. Elution with methylene dichloride and chloroform gave a colorless glass (1.533 gm.). A portion of this base was allowed to stand overnight with methanol, potassium carbonate, and methyl iodide. The mixture was then filtered and the filtrate evaporated to dryness. A residue was left which crystallized from methanol as colorless prisms, softening at 262°, m.p. 264.5–267.5° (decomp.). After two recrystallizations from methanol, the product softened at 258.5° and decomposed at 262.5–264°. It gave no precipitate with silver nitrate solution, was soluble in dilute acids, and could be precipitated from solution by addition of alkali. Calc. for $C_{21}H_{26}O_3N_2$: C, 71.16; H, 7.39; N, 7.91; OCH_3, 8.8; $N\cdot CH_3$, 4.24; one active H, 0.28%. Found: C, 71.17; H, 7.30; N, 7.83; OCH_3, 9.17; $N\cdot CH_3$, 4.28; active H, 0.23%.

Later it was found that the methyl ether could be prepared simply by allowing the tertiary amine fraction to stand overnight in methanol in the presence of potassium carbonate.

The basic methyl ether formed a perchlorate which after two recrystallizations from methanol gave colorless prisms, m.p. 295–295.5°, (dec.) Calc. for $C_{20}H_{23}O_2N_2 \cdot ClO_4$: C, 56.79; H, 5.48; N, 6.63. Found: C, 56.85; H, 5.47; N, 6.72%. It is the perchlorate of the anhydro base and its formation involved

[3]*All melting points are corrected.*

the loss of the elements of methanol. The same salt could be obtained directly from the amorphous unmethylated base.

Reduction of Dihydrogelsemine Carbinolamine Methyl Ether

A solution of the carbinolamine methyl ether (72 mgm.) in methanol (5 ml.) was treated with powdered sodium borohydride (110 mgm.) and allowed to stand for one hour at room temperature. The solvent was evaporated under diminished pressure and the residue was taken up in water and extracted with chloroform. The extract was washed with dilute sulphuric acid, the washings were made alkaline with dilute sodium hydroxide and extracted with chloroform. The base obtained by evaporation of the chloroform (50 mgm.) crystallized on addition of a few drops of acetone, m.p. 219–221°, undepressed by admixture with dihydrogelsemine. The infrared absorption spectrum of the product was exactly superimposable on that of dihydrogelsemine.

Dihydrogelsemine Lactam

The carbinolamine methyl ether (338 mgm.) dissolved in glacial acetic acid (15 ml.) was treated with a solution of chromic anhydride (132 mgm.) in water (1 ml.) and acetic acid (5 ml.). A brown complex was precipitated at first which redissolved. After 18 hr. the excess oxidizing agent was destroyed by addition of a few milliliters of ethanol, and the solution was alkalized with dilute sodium hydroxide. The suspension was extracted with chloroform and the extract washed with dilute sulphuric acid. Evaporation of the chloroform left the neutral lactam (252 mgm.) as a pale yellow foam which was dissolved in benzene and chromatographed on alumina. Elution with ether gave the lactam (186 mgm.) which crystallized as long prisms from methanol. Undried material when heated slowly sintered at 152° and effervesced from 172–180°. When dried at 110° for 10 hr., the lactam had m.p. 157–159.5°. Calc. for $C_{20}H_{22}O_3N_2$: C, 70.98; H, 6.55; N, 8.28. Found: C, 70.70; H, 6.46; N, 8.23%.

Oxidation of Base I

The amorphous base I (338 mgm.) was dissolved in glacial acetic acid (15 ml.) and treated with a solution of chromic anhydride (132 mgm.) in acetic acid (5 ml.) and water (1 ml.). After 18 hr. at room temperature a little ethanol was added to destroy the excess of chromic acid, the solution was diluted with water, alkalized with sodium hydroxide, and extracted with chloroform. The chloroform extract was washed with dilute sulphuric acid and with water, and evaporated to dryness. The neutral product (252 mgm.) was dissolved in benzene and chromatographed on alumina (activity IV) and eluted with ether. A crystalline fraction (116 mgm.) was obtained which after recrystallization from methanol consisted of colorless prisms. After drying it melted at 157–159.5° either alone or in admixture with the dihydrogelsemine lactam obtained by oxidation of the carbinolamine methyl ether.

Reduction of Dihydrogelsemine Lactam

A solution of dihydrogelsemine lactam (260 mgm.) in dry dioxane (12 ml.) was added dropwise to a suspension of lithium aluminum hydride (650 mgm.) in freshly distilled ether (1 ml.). After the vigorous reaction had abated, the

mixture was refluxed for two hours and afterwards the excess reagent was destroyed by the cautious addition of 1:1 methanol–water. The precipitated hydroxides were centrifuged and washed with methanol, the decantate and washings were evaporated under diminished pressure, and the residue dissolved in chloroform. Evaporation of the filtered chloroform solution left a yellow gum (414 mgm.), the benzene-soluble portion of which was chromatographed on alumina. Elution with benzene yielded a colorless oil (190 mgm.) which crystallized from ether as colorless flat prisms, m.p. 142–142.5°, undepressed on admixture with an authentic specimen of tetrahydrodesoxygelsemine (7).

Saponification of the Lactam

Refluxing dihydrogelsemine lactam with potassium hydroxide in ethanol, or with aqueous dilute hydrochloric acid or concentrated hydrochloric acid did not hydrolyze the lactam. Heating with concentrated hydrochloric acid in a sealed tube at 160–180° also failed to bring about hydrolysis.

The lactam (375 mgm.) was heated in a sealed tube for five hours at 150–160° with saturated aqueous barium hydroxide solution (10 ml.). After cooling, the solution was filtered and to the filtrate small pieces of dry ice were added to precipitate the barium. The barium carbonate was centrifuged and washed with hot water. Evaporation of the combined decantate and washings almost to dryness gave 315 mgm. of long platelets which became brown above 200° but did not melt below 310°. Evaporation to complete dryness transformed the solid into a chloroform-soluble substance (185 mgm.) which crystallized from methanol as prisms softening at 155–168°, shown by its infrared absorption spectrum to be identical with the original lactam. The lactam was inert to 95% hydrazine at 125–135°.

Reaction of Gelsemine with Diethyl Azodicarboxylate

Gelsemine (2.569 gm.) in methanol solution was allowed to stand for 18 hr. with diethyl azodicarboxylate (1.754 gm.), and the product worked up exactly as described for dihydrogelsemine. It consisted of a colorless glass which did not crystallize from any of the usual solvents.

A quantity of the product (103 mgm.) dissolved in methanol (15 ml.) was treated with sodium borohydride (302 mgm.) exactly as described above. The product after chromatography on alumina consisted of a colorless foam (34 mgm.) which crystallized from acetone, m.p. 178.5–179°, undepressed on admixture with gelsemine.

ACKNOWLEDGMENT

The authors wish to express their thanks to Dr. R. N. Jones and Mr. R. Lauzon who determined the infrared absorption spectra.

REFERENCES

1. CURTIUS, T. and HEIDENREICH, K. J. prakt. Chem. (2) 52: 454. 1895.
2. DIELS, O. and FISCHER, E. Ber. 47: 2043. 1914.
3. EDWARDS, O. E., CLARKE, F. H., and DOUGLAS, B. Can. J. Chem. 32: 235. 1954.
4. GIBSON, M. S. and ROBINSON, R. Chemistry & Industry, 93. 1951.
5. GOUTAREL, R., JANOT, M.-M., PRELOG, V., SNEEDEN, R. P. A., and TAYLOR, W. I. Helv. Chim. Acta, 34: 1139. 1951.
6. HABGOOD, T. and MARION, L. Can. J. Chem. 32: 606. 1954.
7. KATES, M. and MARION, L. Can. J. Chem. 29: 37. 1951.

DISINTEGRATION-RATE DETERMINATION BY 4π-COUNTING
PART I[1]

By B. D. Pate[2] and L. Yaffe

ABSTRACT

The response probability of a 4π-counter has been examined and conditions determined for which the response probability is unity to within $\pm 0.1\%$ for a range of nuclides. Variables examined have been the effect of polarization potential, discriminator bias, source location, counting rate, counter gas purity, thickness of conductor on source mount, for particles of various energies and from various modes of disintegration.

GENERAL INTRODUCTION

The determination of absolute disintegration rates in a precise manner is of fundamental importance in nuclear physics and nuclear chemistry. It is also of some application in other fields, e.g. radiobiology, where radioactive tracers are used as a research tool. The experimental methods available have been reviewed a number of times (8, 18, 25, 26). All with the exception of 4π-counting and coincidence counting are subject to sources of error which limit the accuracy attainable to several per cent. Recent results (31) with β–γ and γ–γ coincidence measurements indicate that an accuracy of better than one per cent may be possible. The method, however, is limited to nuclides which emit gamma radiation and whose decay schemes are well known.

4π-Counting, up to this time used mainly in the standardization of material for therapeutic use, has considerably wider applicability and greater potential precision than the majority of other techniques. However, the results of international intercomparison of standards (31) show a scatter of a few per cent, and the limits of error assumed by individual workers are of the same order of magnitude (16, 18, 26, 31, 33).

Errors of this magnitude are certainly not inherent in the method and the present paper is the first of a series which will describe work aimed at improving the accuracy attainable with 4π-counting techniques. While some of the information we shall present is strictly applicable only to the design of chamber we have used, most of it is of interest in connection with any form of 4π gas-ion counting.

4π-Counting in the present form originated in 1944, when Simpson (32) described a counter with a geometry approaching 4π steradians. What was probably the first true 4π-counter was designed by L. Meyer-Schützmeister and described in 1948 by Haxel and Houtermans (17). Since that time a number of counting chambers of a variety of designs have been described (1, 2, 4–7, 16–18, 22, 23, 27, 28, 30, 32, 33, 35–37). A counter system with a geometry of 4π steradians can be achieved in several ways, e.g. with a gaseous source as part of the filling of a gas counter, or with the source dispersed

[1]*Manuscript received November 17, 1954.*
Contribution from the Radiochemistry Laboratory, Department of Chemistry, McGill University, Montreal, Quebec, with financial assistance from the National Research Council of Canada and Atomic Energy of Canada Ltd.
[2]*Holder of a National Research Council Studentship.*

throughout the phosphor of a scintillation counter. We have confined our attention to a system which has obvious advantages for routine radiochemical work—a chamber composed of two 2π gas-ion counters arranged face to face. The source material is placed between them, in solid form.

The particular advantages of a counter that will respond to radiation emitted over a solid angle of 4π steradians have been appreciated for some years. Since every charged particle that is emitted is registered by the counter system, any event subsequent to charged particle emission which occurs within the resolution time of the instrument will not be registered separately. This has two desirable consequences.

(i) Provided the primary events of the nuclear transition studied include charged particle emission with a total probability of unity, one count will be registered per distintegration. This remains undisturbed by the emission of secondary particles, nuclear gamma radiation, or annihilation radiation, when this occurs within the counter resolving time, as is usually the case. Cases for which some data from the decay scheme are required include those when particle emission occurs with a probability of less than unity (which includes orbital electron capture) and transitions leading to a metastable excited state of the product nucleus. In such cases, the accuracy of the disintegration-rate determination will clearly depend on the accuracy of the nuclear data employed, in addition to that inherent in the counting procedure.

(ii) Scattering of radiation either by source material, source mount, gas, or counter walls is without effect on the observed disintegration rate, since any discharges (subsequent to that corresponding to the primary event) caused by repeated scattering of one particle will occur within the counter resolving time. The same is true of secondary radiation production due to interaction of primary particles with gas, wall, or other material within the counter.

Thus most of the large corrections (38) of uncertain accuracy required to correct data from conventional counter systems (where the geometry is much less than 2π steradians) are eliminated. The only sources of error still to be corrected for in the calculation of disintegration rates from counter data are due to:

(*a*) Failure of the counter to respond once to every ionizing particle, arising from a nuclear disintegration, that reaches the counter gas.

(*b*) Absorption of radiation by the mount on which the source is deposited.

(*c*) Absorption of radiation by the source material itself ('self-absorption').

(*d*) Statistical fluctuations in the disintegration rate of the source and in the background counting rate of the counter. This error can clearly be reduced to within any desired limits by extension of the number of events observed.

This paper considers the first of the above items. Subsequent publications will deal with (*b*) and (*c*) and certain theoretical topics relating to counter behavior.

INTRODUCTION

For the present discussion, it is convenient to define a quantity which we shall call the *response probability* of the counter. This is the probability that a

discharge triggering the recorder be produced when a charged particle or photon originating from a nuclear disintegration reaches the counter gas. (The term "efficiency" is avoided since it has been used by different workers in various contexts.) This probability will have a certain value for a specific form of radiation (e.g. for charged particles ideally it will be unity) but under given conditions however it may deviate from this value. It is the purpose of the remainder of this paper to describe an examination of the variation of the response probability of the counter system used by us.

The response probability is found to be a function of several variables in the conditions under which the counter is operated. Some of these variables can be adjusted to ensure that no deleterious effect on the response probability occurs. Others cannot be controlled in this fashion and one must determine, to the desired degree of precision, the value of response probability as a function of the variable considered. Corrections for the departure from unit probability in the final calculation of disintegration rate can then be made.

The response probability of the counter may be less than unity if:

(*a*) the gas multiplication of the chamber is less than a minimum value;

(*b*) the "effective geometry" of the chamber is less than 4π steradians;

(*c*) the counting rate is so high that the apparatus is unable to resolve successive discharges, and "coincidence-losses" occur.

It may be more than unity, i.e. more than one count be registered per disintegration, when:

(*d*) at higher anode voltages, the discharge phenomena become more energetic. Then photon emission from the excited gas molecules and positive ion bombardment producing secondary and photoelectron emission from the cathode may lead to multiple discharging over a time interval greater than the counter resolution time.

(*e*) the counter gas contains more than a limiting concentration of impurities with an electron affinity. This may lead to the formation of slow moving negative ions which, collected after the electron pulse, may also lead to spurious pulses being observed.

(*a*) *Gas Multiplication*

In order that the passage of an ionizing entity through the chamber shall register a count, the ionization produced, after gas multiplication, collection at the counter anodes, and external amplification, must produce a pulse at the output of the amplifier system larger than the discriminator bias potential applied to the signal. Whether this condition is satisfied depends on the value of the multiplication factor, amplifier gain, capacitance of the chamber anode system and amplifier input, and the bias potential. These quantities may all be measured, but, aside from the discriminator bias, which cannot be reduced below a minimum value, the only one normally varied in the system is the gas-multiplication factor. This must be adjusted, by increasing the polarization potential for example, until the situation described above is obtained. However, the polarization potential cannot be raised indefinitely since above a limiting value the secondary processes described under (*d*) above set in.

Thus it is important to determine whether the gas multiplication can be raised sufficiently to bring the response probability of the chamber close to a value of unity for the radiation producing the least amount of ionization in the chamber. (This is clearly particularly important when beta radiation is to be examined, since the energy spectrum includes a proportion of particles with very low energies, a proportion which increases with decreasing spectrum energy end point.)

One may determine in two ways whether this state of affairs can be brought about.

(i) The change in counting rate as the gas multiplication is varied within the range available may be observed.

(ii) The various quantities described above, including the gas multiplication (as a function of polarization potential), may be measured and the total response probability of the counter under given conditions may be calculated for those energies where specific ionization is at a minimum.

Both these methods have been used in the present investigation.

In addition to being a function of the polarization potential, the gas multiplication is also dependent on several other variables.

(iii) The polarization field strength is a function of position inside the chamber, and therefore the ion collection will be a function of source position both within the normal source-mount plane, and for movements at right angles to this plane. However, at certain polarization potentials, it is expected that a region will exist in the center of the chamber over which the response probability is constant at a value of unity. The operation of the counter will then be insensitive to small movements of the source within this region.

(iv) Since the efficiency of ion collection within the chamber is a rapidly varying function of field strength it is important to ensure that in the vicinity of the source the field strength is at a maximum. This is especially true for soft β emitters which will have a short range in the gas and thus most of the ionization is produced in the immediate source vicinity. The counter design ensures this maximum field strength provided the source mount is conducting to the cathode surface. An insulating mount will disturb the field strength in such a manner that a position of zero field strength occurs at the source position and hence poor ion collection results.

Seliger and Cavallo (30) claimed that the loss in efficiency due to the use of a non-conducting film mounted over an aperture in an aluminum diaphragm was negligible provided the aperture diameter was limited to minimize the field disturbance. However, a later paper (22) agreed with most observers that, for reliable results, the film had to be rendered conducting. This is satisfactorily accomplished by distillation of gold *in vacuo* on to the film. A rapid routine method for estimating the thickness of the gold layer has been described in a previous publication (24). It is of considerable importance to reduce the superficial density of the source mount used as far as possible in order to reduce absorption of radiation (see the next paper in this series). It is thus essential to know the minimum superficial density of gold required for satisfactory counter operation, since it is fruitless to reduce the film super-

ficial density much below this figure. Little quantitative information is available on this point, or on whether one or both sides of the film need be coated. Hawkings (16) has used 25 μgm./cm.^{2} of gold on both sides of a 100 μgm./cm.^{2} Formvar film with success.

(v) The electron-collection process will clearly be affected to some extent if the counter gas contains a significant proportion of electron-accepting impurities. It is therefore of importance to determine the limiting concentration which can be tolerated without the counter operation being affected.

(*b*) *Counter "Geometry"*

The response probability will be reduced from a value of unity if conditions are such that a proportion of the emitted radiation is absorbed (other than by source material, or the mounting film) before it can produce the necessary minimum number of ions required to trigger the recorder. It must, therefore, be verified that, with the aperture sizes used by us, this effect is not serious.

(*c*) *Coincidence Losses*

Operation of the chamber as a proportional counter serves to increase the value of the response probability at high counting rates, by making possible a reduction in the resolution time of the apparatus, compared with that obtained with the counter operated as a Geiger-Müller counter for instance. The use of the 4π-counter over a wide range of counting rates nevertheless demands that the coincidence loss be accurately known as a function of counting rate. Owing to the variety of processes which may cause coincidence losses in the proportional counter and associated electronic equipment this function is best obtained empirically. The availability of thin films, described in a previous publication (24), has made possible a very precise determination of the coincidence loss function by a modification of the conventional multiple source technique.

EXPERIMENTAL PROCEDURES, RESULTS, AND DISCUSSION

The counter chamber used in these experiments is essentially that described by Hawkings *et al.* (16) and is reproduced in Fig. 1. It consists basically of two hemispherical brass cathodes of 7 cm. diameter and two ring-shaped anodes of 0.001 in. diameter tungsten wire. The source mount, which is continuous with the cathodic surface, consists of a plastic film of superficial density 5–10 μgm./cm.^{2} rendered conducting by a layer of gold (2 μgm./cm.^{2}) applied by distillation *in vacuo* to either surface of the film. The film is mounted over an aperture in an aluminum plate 1 mm. thick. The aperture diameter is usually 5 cm. and occasionally 2.5 cm.

The chamber is used in conjunction with a Nicholls high voltage supply (AEP 1007B). The anodes of the chamber are connected in parallel to an Atomic Instrument Co. preamplifier (205-B) which has been modified to obtain a low noise level. The output from this is fed into an Atomic Energy of Canada Ltd. amplifier (AEP 1448) which has non-overload characteristics, and thence after discrimination into a Marconi scaling unit of 1000 (AEP 908).

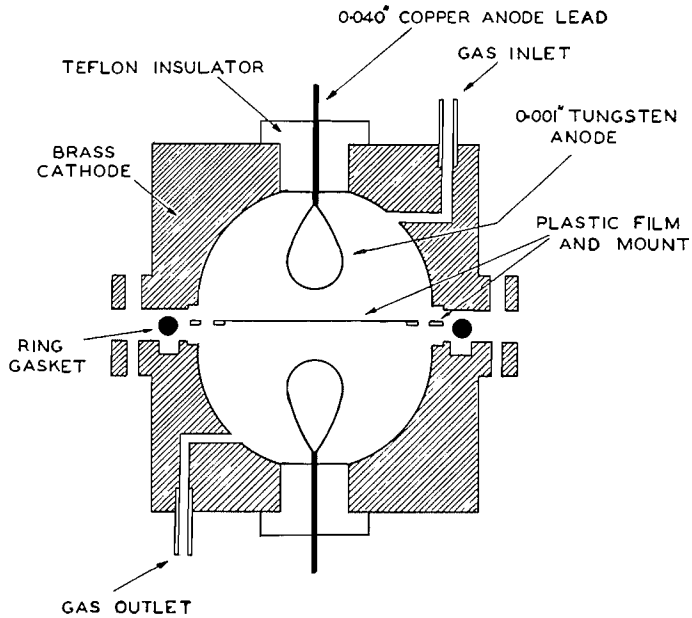

FIG. 1. The 4π-counting chamber.

The over-all gain of the amplifying system is 30,000 and a bias voltage up to 50 v. can be applied by the discriminator to the output signal.

The counter chamber is operated in the proportional region. The counting gas used is C.P. methane at atmospheric pressure dried by passage over silica gel. After insertion of the sample the counter is flushed for about five minutes at a rapid flow rate and the rate then moderated to a standard rate of 0.5 ml. methane per sec.

The stability of the equipment, which was checked with a standard RaD-E-F source and a Ni^{63} source, is excellent. This can also be attested to by the reproducibility of results obtained at different times.

The sources of radioactivity used were all of so high specific activity that source thickness did not affect the results quoted in this paper. Samples approximating "point-sources" were prepared by evaporation of a suitably sized aliquot of stock solution on the mounting film using infrared radiation. One exception to this procedure was the case of Tc^{99m}. This nuclide was co-separated with rhenium in the normal fission product procedure (14) up to the final stage when the Re–Tc mixture was precipitated as the sulphide. The sulphide was slurried with water and a portion evaporated on the film.

The half life, mode of decay, radiation characteristics, and source of supply of the nuclides used are shown in Table I.

(*a*) *Gas Multiplication*

(i) *High Voltage Characteristics of the Counter*

High voltage characteristic curves were obtained in the usual way for a series of sources of β radiation of increasing maximum energy, at a constant

TABLE I

CHARACTERISTICS AND SOURCE OF SUPPLY OF RADIOACTIVE NUCLIDES

Nuclide	Half life	Mode of decay	Maximum energy of particle (Mev.)	Source of supply
Ni^{63}	80 yr.	β^-, no γ	0.067	A.E.C.L.
S^{35}	87 days	β^-, no γ	0.167	A.E.C.L.
Ca^{45}	152 days	β^-, no γ	0.254	A.E.C.L.
Tl^{204}	4.0 yr.	β^-, no γ	0.765	A.E.C.L.
Bi^{210}	5.0 days	β^-, no γ	1.17	Separated from RaD-E-F from A.E.C.L.
P^{32}	14.4 days	β^-, no γ	1.70	A.E.C.L.
La^{140}	40.3 hr.	β^-, γ	2.26	Separated from fission products of uranium irradiated in BEPO, A.E.R.E. Harwell, England
Po^{210}	138 days	α	5.30 (mono-energetic)	Separated from RaD-E-F from A.E.C.L.
Na^{22}	2.6 yr.	β^+, γ	1.8	A.E.C.L.
Co^{60}	5.3 yr.	β^-, γ	0.319	A.E.C.L.
Tc^{99m}	6.0 hr.	IT	0.142 (mono-energetic)	Separated from fission products of uranium irradiated in NRX, Chalk River, Ont.

discriminator bias level. The nuclides employed, with the exception of La^{140} all emit β^- particles without accompanying γ radiation. Their nuclear properties are described in the top half of Table I. Fig. 2 indicates the response of the counter to pure β radiation. Standard deviations on the quantities measured lie within the areas of the points as plotted (as for all succeeding figures in this paper unless otherwise indicated).

The data shown in Fig. 2 indicate that the chamber used in this work is suitable for measurements of β^- emitters with maximum energies at least down to 0.067 Mev. The plateaus obtained in no case show any perceptible slope. The maximum figure which can be calculated on a basis of the statistics of the measurements concerned is less than 0.1% per 100 v. There is, therefore, little ambiguity as to the correct counting rate figure to be used as a basis for calculating the disintegration rate, and little doubt of the fact that substantially all of the particles in the spectrum are being registered. At polarization potentials of about 100 v. in excess of the threshold value, the response probability approximates very closely to unity. However, obviously, any polarization potential on the plateau may equally well be used if for any reason this is desirable.

The displacement observed with increasing particle energy is due to the reduced amount of ionization produced in the region of maximum polarization field strength by the more energetic radiation. The effect is less marked at the

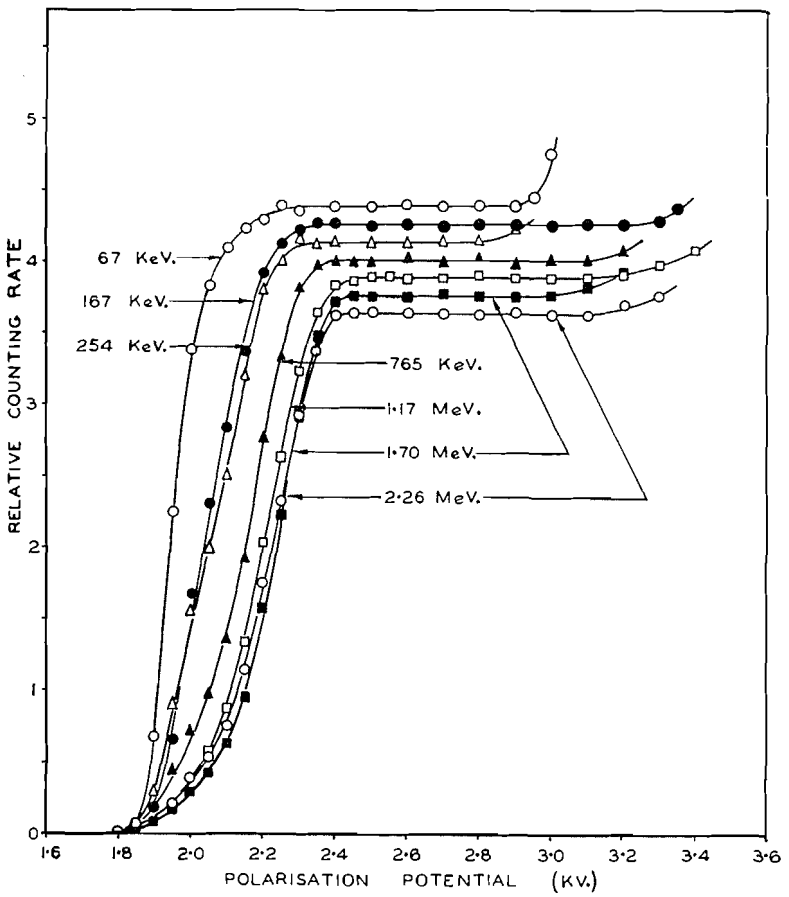

FIG. 2. High voltage characteristics for β radiation of varying maximum energies.

higher end of the energy scale since there is very little variation of specific ionization with energy in this region.

The length of the plateaus observed with β^- emitters is never less than 400 v. and may be as much as twice this. The polarization potential at which multiple pulsing sets in is dependent on many factors such as condition of source and temperature of the chamber.

Fig. 3 shows a series of characteristics obtained using Ni^{63} (maximum energy 0.067 Mev.) taken at increasing discriminator bias values. Fig. 4 shows a similar series using La^{140} (maximum energy 2.26 Mev.). Plateaus taken at increasing bias values are displaced to higher polarization potential values but otherwise are exactly superimposable. Fig. 5 shows characteristics obtained with nuclides decaying by the emission of alpha particles, positrons, negative electrons with gamma radiation, and by isomeric transition. These data indicate that the present chamber makes a satisfactory counter for many forms of radiation. Absolute measurements with α- and β^+- and β^--emitting nuclides with or without accompanying γ radiation are clearly straightforward.

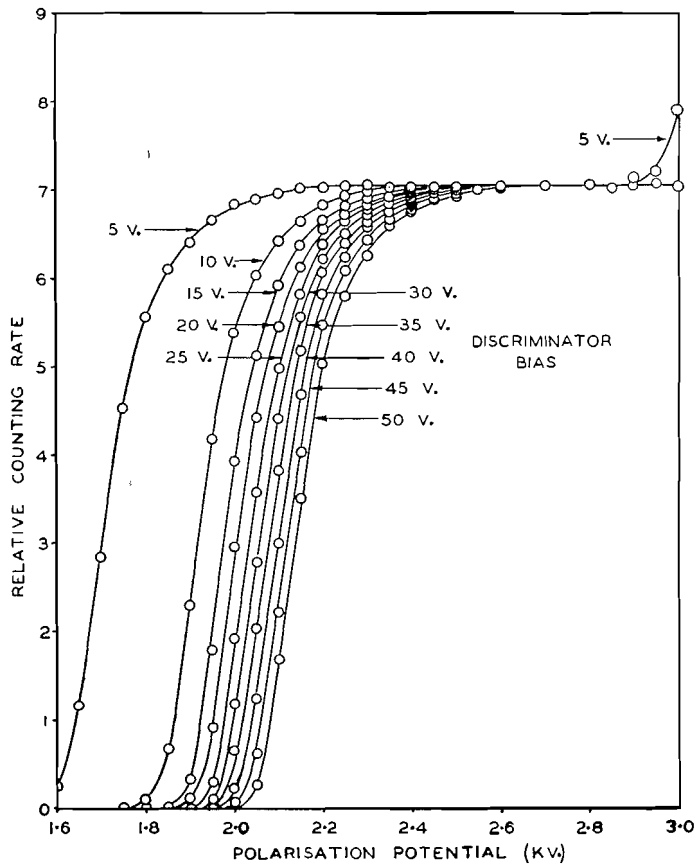

FIG. 3. High voltage characteristics for Ni^{63} β radiation as a function of applied discriminator bias.

With nuclides decaying by means of isomeric transition the same is true if the pertinent nuclear data are available.

Fig. 6 shows the variation of the characteristic with increasing disintegration rate. A series of P^{32} sources of known strength was prepared on 5–10 μgm./cm.^{2} films. The disintegration rates (about 500 d.p.s.) were below the region where coincidence losses were significant. A series of secondary sources was then prepared from these by lamination, the total disintegration rates being calculated by summing those of the component sources. (It will be shown in a forthcoming publication that the absorption of radiation from P^{32} even with 10 or more of these component films can be neglected.) The results of measurements at two values of discriminator bias are shown. The calculated rate for each source used is shown for comparison purposes.

These results show clearly that satisfactory characteristics are retained with our apparatus at least up to a counting rate of 3×10^3 counts per second. The irregular shape of the curves above this figure show that it is meaningless to quote a coincidence loss for a counting arrangement unless this loss is given

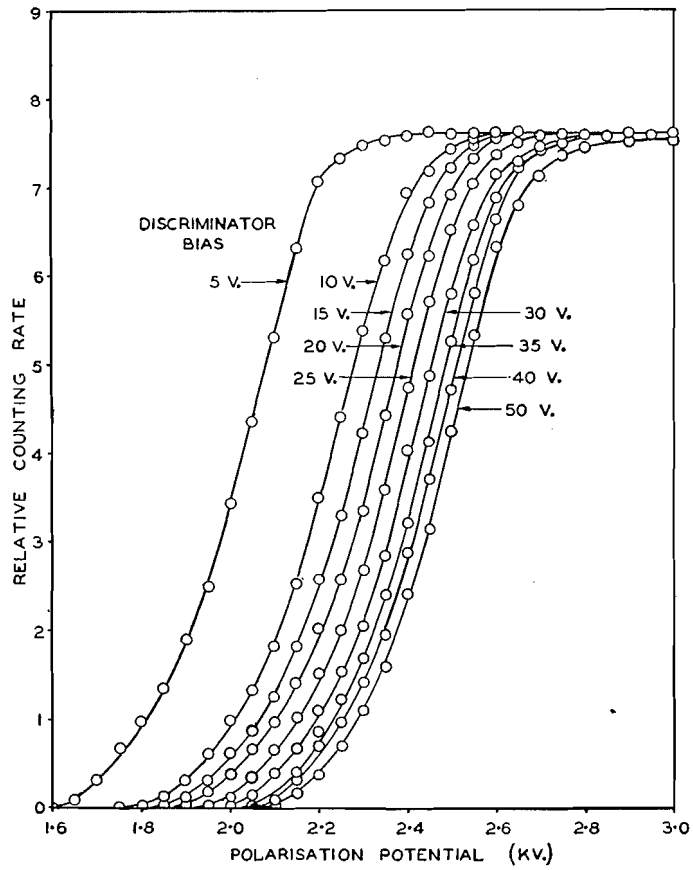

FIG. 4. High voltage characteristics for La^{140} β radiation as a function of applied discriminator bias.

for definite polarization conditions, since coincidence losses in proportional counting are due to a variety of reasons. For example, since the discharge mechanism results in a local and partial reduction of the polarizing field, the counter may enter into successive discharge processes with the effective counter field at different stages of recovery. Also, at higher counting rates, the slow migration of positive ions to the cathode may substantially reduce the polarization field and thus the gas multiplication. In addition to this losses in the electronic circuit may also occur.

(ii) *Response Probability to Charged Particles as a Function of Their Energy*

The ionization produced by most charged particles is more than adequate to ensure a response probability of unity under normal operating conditions. With low energy particles and electrons of about 2 Mev. (where the specific ionization is at a minimum (3)) this may not be so. For example, a small low energy fraction of any spectrum of β radiation will not count with unit probability. This fraction increases as the maximum energy of the spectrum decreases.

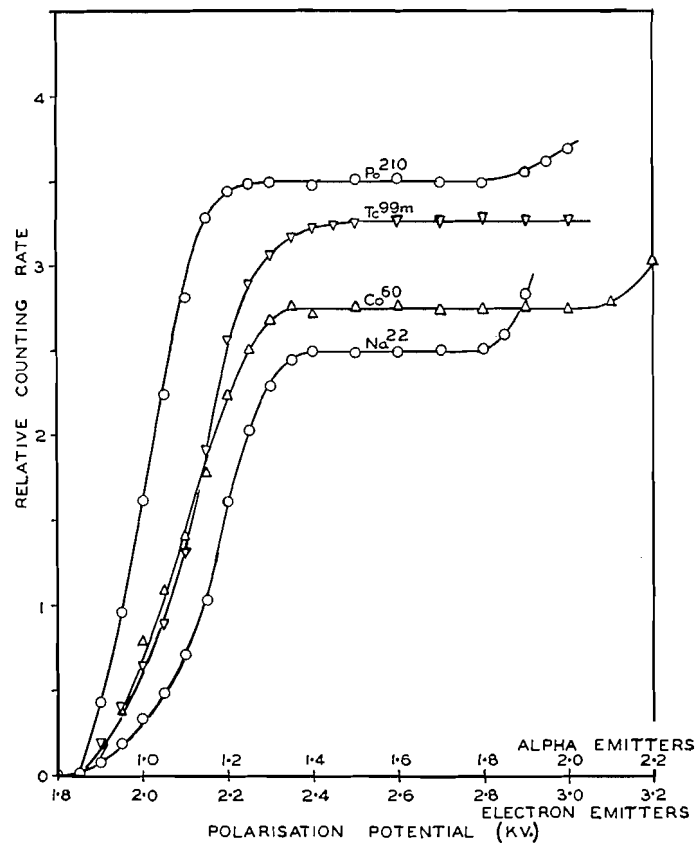

FIG. 5. High voltage characteristics for various forms of radiation.

We have calculated the response probabilities of the counter towards the entire spectrum of the β radiation of Ni^{63} and S^{35} since these were the softest β radiations studied. The calculations are conveniently made in three stages. *First*, the minimum total charge pulse arriving at the counter anode system which will trigger the recording mechanism is calculated from the measured electronic parameters. The corresponding original ionization is then computed.

Amplifier gain	$= 3 \times 10^4$	(measured with a calibrated pulse generator and oscilloscope)
Minimum bias level	= 3 v.	(i.e. a pulse greater than this will trigger the scaler circuit)
Minimum input	= 0.1 mv.	(calculated from above)
Capacitance of chamber anode system and amplifier input	= 25 $\mu\mu$f.	(measured by resonance bridge method)

Therefore, the 0.1 mv. input signal corresponds to a charge arriving at the anode of 2.5×10^{-15} coulombs or 1.6×10^4 electronic charges.

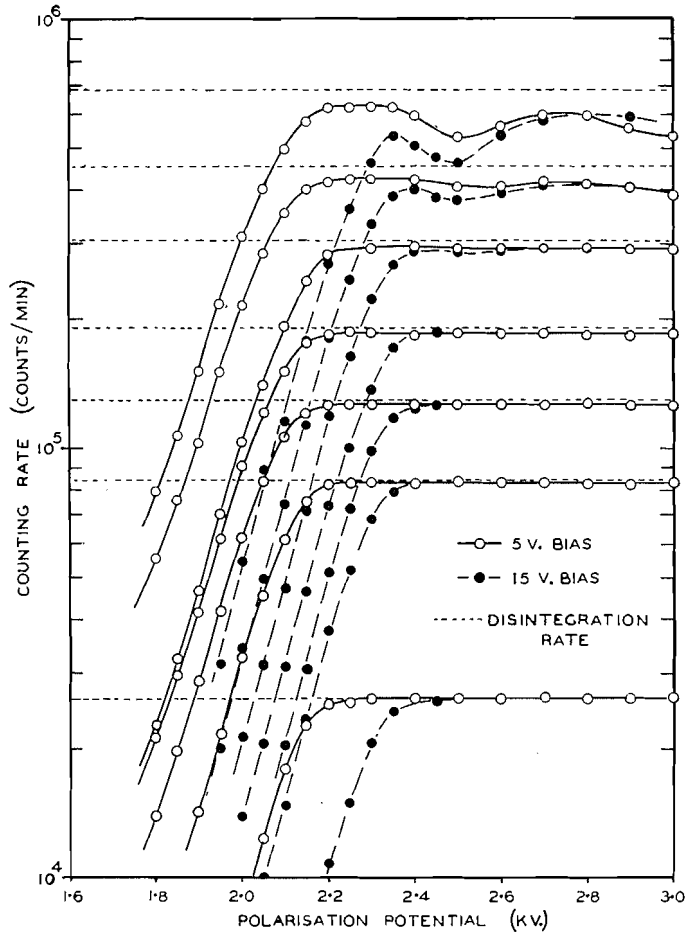

FIG. 6. High voltage characteristics as a function of disintegration rate.

The mean gas multiplication was determined in the following way. Using the alpha particles from Po^{210} the maximum pulse height obtained at the chamber anode system was measured with a cathode ray oscilloscope. Care was taken that pulses were not large enough to produce amplifier saturation or proportional counter distortion. The observed pulse amplitude was independent of polarization potential between 250 and 500 v. Here the chamber is acting as a saturated ion chamber and the gas multiplication is unity. Readings, taken at increasing potentials, were normalized to this value. When the danger of saturation or distortion became apparent a Ni^{63} source was substituted for the Po^{210}. A large range existed where both could be used so that no errors were introduced by the substitution.

The results are shown in Fig. 7. At 2.6 kv. the mean gas multiplication (A) has a value of 2.6×10^3 and at 2.9 kv., $A = 1.6 \times 10^4$. Therefore, at these polarization potentials, the counter will respond to a mean of six and one ion pairs respectively.

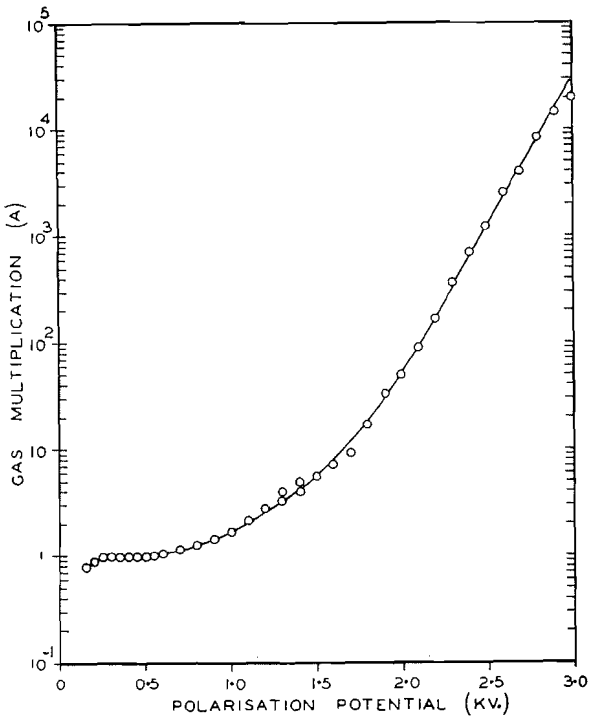

FIG. 7. Gas multiplication function of counter.

Secondly, the probability that a given particle energy will produce a certain minimum number of ion pairs should be calculable if the appropriate data are available. Curran *et al.* (9) note that the mean energy (W) necessary to produce one ion pair increases with particle energy at low energies, but give no quantitative data. They also note that W for both argon and nitrogen (both non-electron acceptors like methane) is substantially independent of energy down to 500 ev. This confirms theoretical predictions made by Fano (11). As a first approximation (adequate for present purposes) one can assume that the value due to Schmeider (29) of $W \sim 30$ ev. applies in the region of interest.

Both the ionization and gas multiplication obtained under given conditions are subject to variance. Let J_0 be the mean number of ion pairs produced in the chamber ($= E/W$ where E is the particle energy dissipated in the gas). The variance of J and of the gas multiplication A have been studied by a number of workers. Fano (12) has shown, on theoretical grounds, that the variance of J, $V_J = FJ_0$ where F (a constant for the particular gas) is found to be equal to 0.3 for atomic H where necessary data for calculation are available.

The variance of A was examined theoretically by Snyder (34) and Frisch (13) who found that $V_A = A$. Thus the total variance V of the output pulse amplitude of a counter expressed as an equivalent variance of the original ionization J will be $V = FJ_0 + J_0$. The observations of Hanna *et al.* (15) at

250 ev., 2.8 kev., and 17.4 kev. indicate that a value of $V = J_0$ describes the experimental results more exactly. Since F is not expected to be very small, the variance of the gas multiplication factor must be less than J_0, confirming the observations of Curran *et al.* (10).

Thus the distribution of pulse amplitudes at the chamber anode for a given energy will be approximately a Poisson distribution. On this basis, then, one can calculate the probability P that at least one or at least six ion pairs be produced, as a function of particle energy, corresponding to the polarization potential values mentioned above.

The probability functions are shown in Fig. 8. Since a minimum of one ion pair will trigger the counter at 2.9 kv., the curve for $J = 1$ represents the counter response probability function under this condition. Similarly, the curve for $J = 6$ gives the response probability at 2.6 kv. Clearly, at low E values these calculations are in error, but certainly show at worst an order of magnitude for P at these energies.

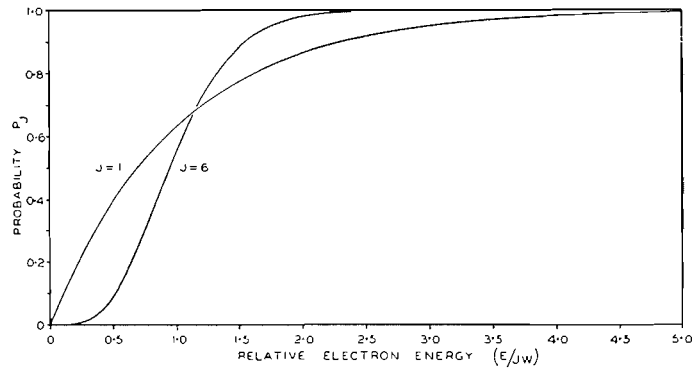

FIG. 8. Counter response probability as a function of electron energy for mean ionizations of one and six ion pairs.

Thirdly, from the probability curves of Fig. 8 it is now possible to obtain a mean response probability for a radiation of any known energy distribution. We have calculated the values for Ni^{63} and S^{35} at applied potentials of 2.6 and 2.9 kv. The relevant probability function has been integrated using energy values from the spectrometer data of Langer *et al.* (21) for S^{35} and Kobayashi *et al.* (19) together with the modified beta decay theory for $\Delta J = 2$, yes transitions (20) in the case of Ni^{63}. The results of the calculations are shown in Table II.

TABLE II

COUNTER RESPONSE PROBABILITY

Nuclide	Applied voltage (kv.)	Mean no. of ion pairs detected	Probability
Ni^{63}	2.6	6	0.9953
Ni^{63}	2.9	1	0.9992
S^{35}	2.6	6	0.9998
S^{35}	2.9	1	0.9999

Owing to their low energy emission Ni^{63} and S^{35} are the two nuclides we have studied which are most likely to have a low response probability. The response probability in the two cases is seen to be very close to unity. This conclusion is also, of course, corroborated by the observations recorded in Fig. 2. The counting rates obtained with all energies remained essentially unchanged even when for example, in the case of S^{35}, the applied potential was increased from 2.4 to 3.2 kv., corresponding to a change in the gas multiplication by a factor of about 160. A minimum in the specific ionization also occurs at a particle energy of about 2 Mev. The specific ionization at this point is about 40 ion pairs per cm. per atmosphere of methane (3) which corresponds to a production of at least 100 ion pairs in the chamber. This is clearly sufficient to ensure a response probability of unity.

(iii) *Response Probability as a Function of Source Position*

We have examined the variation of response probability of the counter for sources of radiation as a function of their location in the source-mount plane in a manner essentially similar to that employed by Hawkings *et al.* (16) for P^{32}. We have determined this for β emitters of varying energy from 0.067 Mev. to 2.26 Mev. at various polarization potentials and bias voltages.

The source was mounted on a small area of 5–10 μgm./cm.^{2} film supported over an aperture of 5 mm. diameter in a slide of aluminum foil. The slide was arranged to move between two parallel wires so that the source could be adjusted to any position along a diameter of the source-mounting diaphragm. This movement, combined with the rotation of the diaphragm, allowed the source to be brought to any point within the plane of the source mount. The whole was screened electrostatically from the electrode system by being sandwiched between two gold-coated 10 μgm./cm.^{2} films. Attenuation of the β radiation by absorption in the small layer of gas trapped between the films could be neglected for purposes of this experiment. The counting rate was observed with the source in 90 different positions, each at two values of polarization potential and two discriminator bias settings. Typical contours of qual response probability are shown in Figs. 9 and 10.

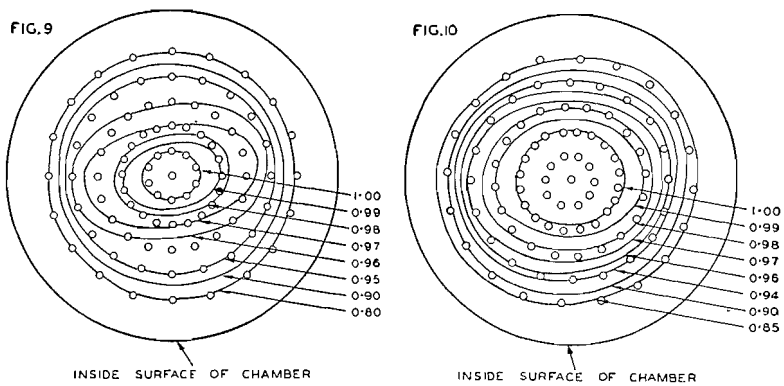

FIG. 9. Contours of equal response probability for Ni^{63} β radiation.
FIG. 10. Contours of equal response probability for La^{140} β radiation.

The contours are essentially similar to those obtained by Hawkings *et al.* (16) for P^{32}. The area over which the response probability is unity for a particular applied voltage and bias level can be seen to be smaller for Ni^{63} than for La^{140}, because of the reduced range of the weaker radiation in the counter gas. Other curves, similar in nature, have been obtained with varying polarization and bias level but are not shown here for reasons of brevity. These curves show an expansion of the contours with increasing polarization and decreasing bias voltage.

From these data it is clear that a source diameter of up to at least 1 cm. can be tolerated by the counter for all particle energies studied without a significant drop in response probability.

It will be seen from Fig. 1 that the counting chamber is constructed in such a manner that both hemispheres are recessed to accommodate an aluminum source-mount diaphragm. This allowed us to investigate the variation of response probability when a source of S^{35} was moved 1 mm. from the medial position towards each anode. (The source-mounting film is customarily affixed to one side of the aluminum diaphragm, and the source material deposited on the side of the film away from the diaphragm.) The results, as shown in Table III, show that a displacement of at least 1 mm. in either direction (the maximum allowed by the counter design) may occur without adversely affecting the counting rate.

TABLE III

EFFECT ON RESPONSE PROBABILITY OF VERTICAL SOURCE DISPLACEMENT

Position	Observed counting rate (counts/min.)
Source central facing upwards	39,070 ± 140
Source displaced 1 mm. towards top anode facing upwards	39,170 ± 140
Source central facing downwards	39,240 ± 140
Source displaced 1 mm. towards bottom anode facing downwards	39,280 ± 140

(iv) *Effect of Variation of Gold Thickness of Source-mount Films*

The effect on counter response probability of variation of gold thickness on films has been investigated in two sets of experiments, one each for Ni^{63} and P^{32} radiation. Sets of VYNS films (all of 5–10 μgm./cm.^{2} superficial density and mounted over diaphragm apertures of 5 cm. diameter) were coated on one side with a range of gold thicknesses. The superficial density of gold applied was measured spectrophotometrically as described previously (24). For each film, a source was applied centrally to the side of the film on which the gold had been deposited. The high voltage characteristic at a constant discriminator bias setting obtained with this arrangement was recorded. A diaphragm with aperture diameter of 2.5 cm. was then placed over the first, forming effectively a system in which a film with the same gold superficial density was mounted over a smaller aperture. The characteristic curve was again determined. The film, on the original diaphragm, was then removed from the counter and 10 μgm./cm.^{2} gold distilled on to it. In one half of the experiments the gold was

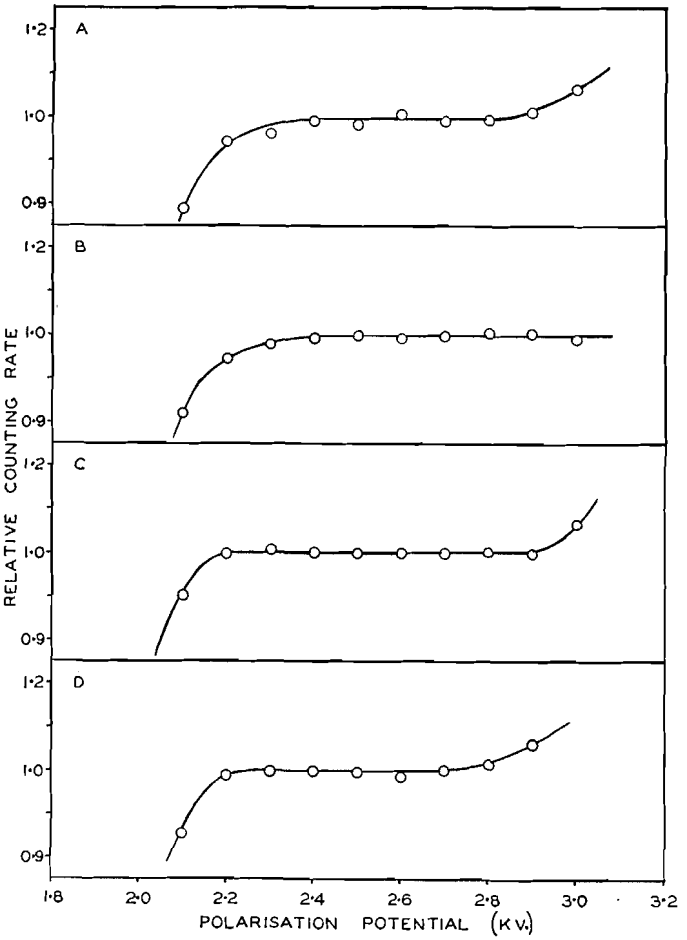

FIG. 11. High voltage characteristics as a function of side of mount to which gold is applied.
A. 5 μgm./cm.² of gold on source side. Ni^{63}
B. 5 μgm./cm.² of gold on reverse side. Ni^{63}
C. 5 μgm./cm.² of gold on source side. P^{32}
D. 5 μgm./cm.² of gold on reverse side. P^{32}

applied to the side of the film carrying the source and in the other half to the reverse side. The voltage characteristic was again determined. Finally, a further 10 μgm./cm.² of gold was applied, this time to the opposite side to the above (both sides now had at least 10 μgm./cm.² of gold) and a fourth characteristic was measured.

The results of the effect of gold thickness are as follows:

1. In all cases the last two characteristics were identical. Identical voltage characteristics were obtained regardless of whether the gold was on the source side, reverse side, or both sides. Representative characteristic curves are shown in Fig. 11.

2. The appearance of the characteristics obtained with increasing thicknesses of gold is shown in Fig. 12 for Ni^{63} and Fig. 13 for P^{32}. In order to render

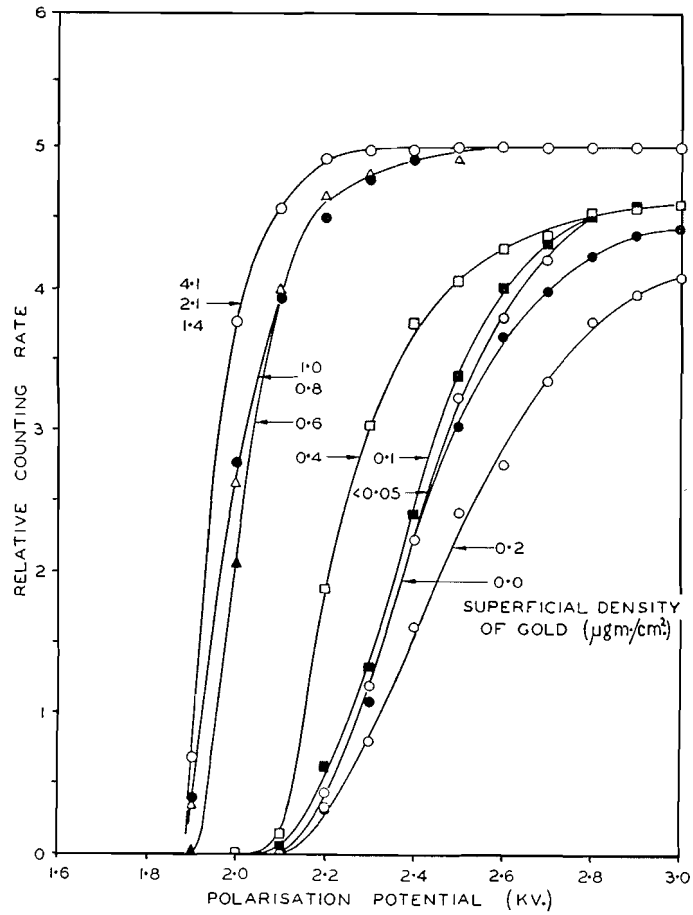

FIG. 12. High voltage characteristics for Ni^{63} as a function of gold thickness on source mount.

the data comparable the counting rates are expressed as a fraction of that found for the source after application of 10 μgm./cm.² of gold to the source mount. The figures plotted apply to a diaphragm aperture of 5 cm. The smaller aperture of 2.5 cm. had the effect of displacing the characteristic for a given gold thickness to a higher polarization potential. However, the gold thickness at which normal characteristics occurred (> 2 μgm./cm.²) was the same for both aperture sizes.

(v) *Effect of Purity of Counting Gas*

The effect of using a counter gas of inferior quality is shown in Fig. 14. This shows a series of characteristics using Ni^{63} as the radioactive source and Technical grade methane as the counting gas. The mass spectrometric analysis of a sample of C.P. methane, giving normal performance, is shown in Table IV. We do not give an analysis for Technical grade methane as this varies from one cylinder to another; the variation in quality is such that some samples may be found to give satisfactory characteristics.

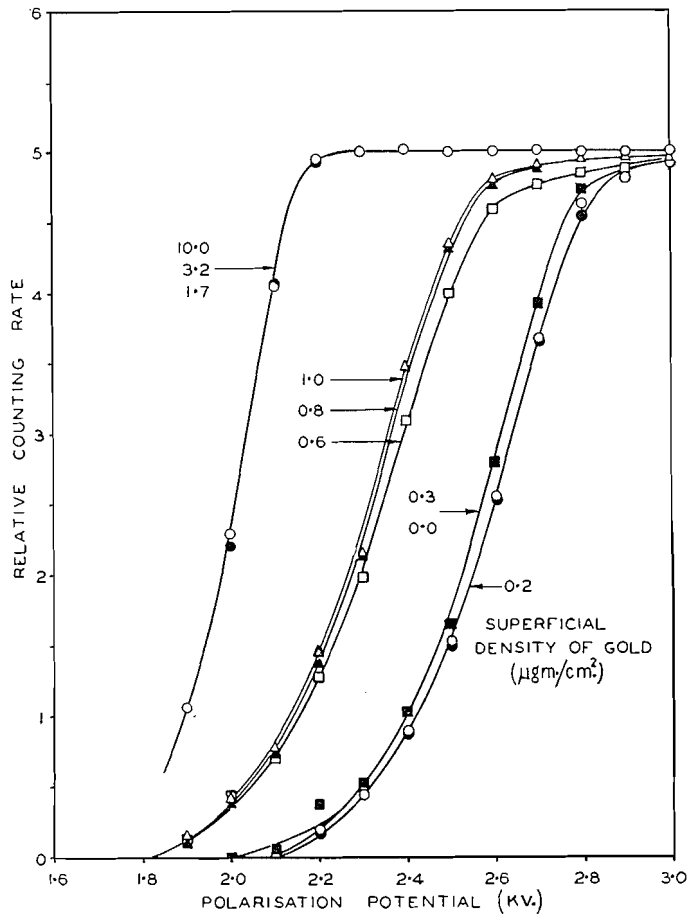

FIG. 13. High voltage characteristics for P^{32} as a function of gold thickness on source mount.

TABLE IV

MASS SPECTROMETRIC ANALYSIS OF C.P. METHANE*

Constituent	Concentration (% by weight)
H_2	0.1
C_2H_4	0.01
C_2H_6	0.59
N_2	0.5
O_2	0.01
CO_2	0.15
C_3, C_4	0.01
CH_4	Remainder

*The authors wish to thank Dr. H. I. Schiff for having performed this analysis.

Experiments performed with synthetically prepared gas mixtures showed that the counter is relatively insensitive to the presence of higher saturated

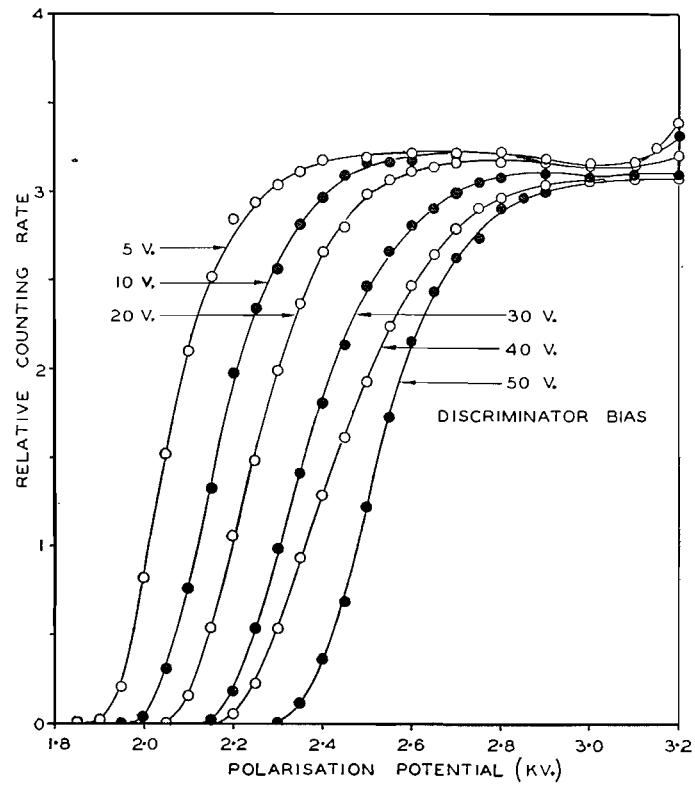

FIG. 14. High voltage characteristics obtained with impure methane for Ni^{63} β radiation.

and unsaturated hydrocarbons in the gas mixtures. The presence of small quantities of air or oxygen, however, is injurious, possibly owing to the electron affinity of the latter.

(*b*) "*Counter Geometry*"

Experimental techniques for determining effect of "counter geometry" are described in section (iv) of (*a*).

Characteristics for Ni^{63} and P^{32} are shown in Fig. 15 for both large and small diaphragm apertures. The gold thicknesses used in this experiment were greater than the limit at which regular behavior commenced.

Several workers (16, 23) have discussed the effect of using a relatively thick metal diaphragm in order to support the source-mounting film or foil. Calculations have been made of the fraction of particles emitted which will be "lost" owing to collision with the diaphragm aperture wall. Experiments have also been performed at a single value of the polarization potential to determine the effect of reduction of aperture size.

Fig. 15 shows clearly that no decrease in counter response occurs when the diaphragm aperture diameter normally used is decreased by one half. Provided that a particle produces the necessary minimum number of ions before being absorbed in the aperture wall, no loss in counts will occur. As the

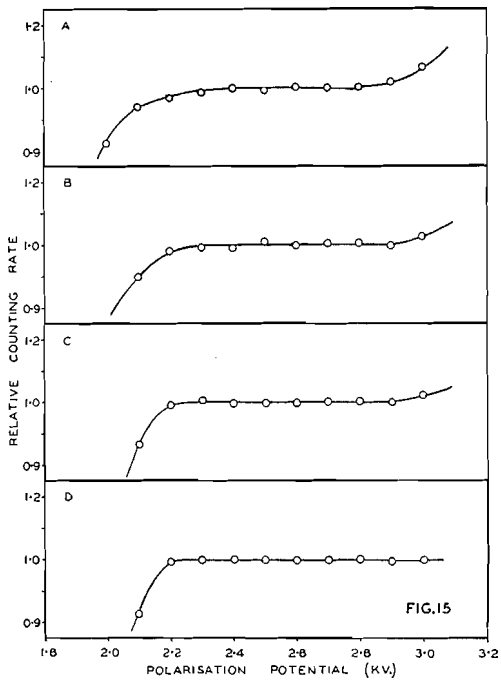

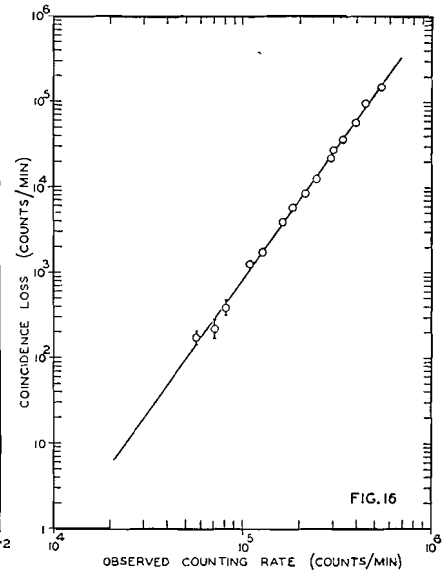

FIG. 15. High voltage characteristics obtained with varying size of diaphragm aperture.
A. 2.5 cm. diameter aperture. Ni^{63}
B. 5.0 cm. diameter aperture. Ni^{63}
C. 2.5 cm. diameter aperture. P^{32}
D. 5.0 cm. diameter aperture. P^{32}

FIG. 16. Coincidence loss function of the counter, at 2.6 kv. high voltage and 15 v. discriminator bias.

polarization potential is increased, the probability of this minimum number being produced approaches unity. Thus, the effect of a reduced aperture size is to displace the polarization characteristic to higher polarization potentials and does not reduce the effective counter geometry from 4π steradians.

(*c*) *Response Probability at Higher Counting Rates*

The coincidence loss function of the counting arrangement has been determined using the method previously described to examine the effect of disintegration rate on the characteristic curve of the counter. A series of 12 sources of P^{32} with disintegration rates ranging from between 3×10^2 and 10^4 d.p.s. was prepared and the counting rates of the single and laminated sources obtained. The results, expressed as "coincidence loss" as a function of the observed counting rate, are shown in Fig. 16 plotted on a log–log scale. Some points for the curve were also obtained by studying the departure from exponential decay of a source of Na^{24}.

The results obtained in Fig. 16 clearly illustrate the loss in counting rate of this counter assembly with increasing disintegration rate. The presentation of the data on a log–log plot results in a curve which is linear and thus facilitates extrapolation to lower counting rates. This correction curve can be used with

confidence for our arrangement up to an apparent counting rate of 6×10^5 c.p.m. It is highly probable that most of the losses which occur are not primarily due to the counter but due to the electronic equipment.

SUMMARY

On the basis of the experimental work discussed in this paper, it is estimated that the error due to the departure of the response probability of a 4π-counter from a value of unity may be reduced to less than 0.1%. For our apparatus, the conditions under which this is realized are the following: source-mounting film of 5–10 μgm./cm.^{2} VYNS resin mounted over a diaphragm aperture of 2.5 or 5.0 cm. and coated with at least 2 μgm./cm.^{2} of gold, counting gas C.P. methane, polarization potential 2.6 kv., and discriminator bias 15 v.

The absence of perceptible slope on the high voltage characteristics of the chamber when functioning correctly allows a considerable latitude in the conditions under which the system may be satisfactorily operated. It further allows a rapid verification that the system is so operating. If an increase of 200 v. in the polarization potential or 10 v. decrease in the discriminator bias causes no change in counting rate observed, then a response probability close to a value of unity is indicated.

ACKNOWLEDGMENTS

The authors wish to thank the National Research Council of Canada and Atomic Energy of Canada Ltd. for grants-in-aid. We would also like to express our appreciation to Dr. J. D. Jackson, Dr. R. E. Bell, and Mr. R. C. Hawkings for valuable discussions during the work and in the preparation of the manuscript. One of us (B.D.P.) wishes to thank the National Research Council for assistance received in the form of a studentship.

REFERENCES

1. Beyster, J. R. and Wiedenbeck, M. L. Phys. Rev. 79: 490. 1950.
2. Borkowski, C. J. Conference on absolute β counting. Preliminary Rept. No. 8. Nuclear Science Ser., N.R.C. Washington, D.C. p. 55. 1950.
3. Brode, R. B. Revs. Mod. Phys. 11: 222. 1939.
4. Charpak, G. and Suzor, F. Compt. rend. 231: 1471. 1950.
5. Charpak, G. and Suzor, F. Compt. rend. 232: 322. 1951.
6. Cohen, R. Compt. rend. 229: 356. 1949.
7. Cohen, R. Ann. phys. (12), 7: 185. 1952.
8. Conference on absolute β counting. Preliminary Rept. No. 8. Nuclear Science Ser., N.R.C. Washington, D.C. 1950.
9. Curran, S. C., Angus, J., and Cockroft, A. L. Phil. Mag. 40: 36. 1949.
10. Curran, S. C., Cockroft, A. L., and Angus, J. Phil. Mag. 40: 929. 1949.
11. Fano, U. Phys. Rev. 70: 44. 1946.
12. Fano, U. Phys. Rev. 72: 26. 1947.
13. Frisch, O. R. Statistics of multiplicative processes. 1948. Unpublished.
14. Glendenin, L. E. Paper 259. Natl. Nuclear Energy Ser. Vol. 9. Div. IV. McGraw-Hill Book Company, Inc., New York and London. 1951.
15. Hanna, G. C., Kirkwood, D. H. W., and Pontecorvo, B. Phys. Rev. 75: 985. 1949.
16. Hawkings, R. C., Merritt, W. F., and Craven, J. H. Proceedings of symposium: maintenance of standards. May 1951. National Physical Laboratory, H.M. Stationery Office, London. 1952.
17. Haxel, O. and Houtermans, F. G. Z. Physik, 124: 705. 1948.
18. Houtermans, F. G., Meyer-Schützmeister, L., and Vincent, D. H. Z. Physik, 134: 1. 1952.
19. Kobayashi, Y., Miyamoto, G. and Mori, S. J. Phys. Soc. Japan, 8: 684. 1953.
20. Konopinski, E. J. and Uhlenbeck, G. E. Phys. Rev. 60: 308. 1941.

21. LANGER, L. M., MOTZ, J. W., and PRICE, H. C., JR. Phys. Rev. 77: 798. 1950.
22. MANN, W. B. and SELIGER, H. H. J. Research Natl. Bur. Standards, 50: 197. 1953.
23. MEYER-SCHÜTZMEISTER, L. and VINCENT, D. H. Z. Physik, 134: 9. 1952.
24. PATE, B. D. and YAFFE, L. Can. J. Chem. 33: 15. 1955.
25. PUTMAN, J. L. Brit. Atomic Energy Rept. A.E.R.E. N/R 318. 1949.
26. PUTMAN, J. L. Brit. J. Radiol. 23: 46. 1950.
27. ROSSI, B. B. and STAUB, H. H. Ionization chambers and counters. Natl. Nuclear Energy Ser. Vol. 2. Div. V. McGraw-Hill Book Company, Inc., New York and London. 1949.
28. SAWYER, G. A. and WIEDENBECK, M. L. Phys. Rev. 79: 490. 1950.
29. SCHMEIDER, K. Ann. Physik, 35: 445. 1939.
30. SELIGER, H. H. and CAVALLO, L. J. Research Natl. Bur. Standards, 47: 41. 1951.
31. SELIGER, H. H. and SCHWEBEL, A. Nucleonics, 12 (No. 7): 54. 1954.
32. SIMPSON, J. A., JR. Rev. Sci. Instr. 15: 119. 1944.
33. SMITH, D. B. Brit. Atomic Energy Rept. A.E.R.E. I/R 1210. 1953.
34. SNYDER, H. S. Phys. Rev. 72: 181. 1947.
35. SUZOR, F. and CHARPAK, G. Compt. rend. 232: 720. 1951.
36. SUZOR, F. and CHARPAK, G. Compt. rend. 234: 720. 1952.
37. SUZOR, F. and CHARPAK, G. J. phys. radium, 13: 1. 1952.
38. ZUMWALT, L. R. U.S. Atomic Energy Comm. Rept. M.D.D.C. 1346. 1947.

THE COMPRESSIBILITY OF GASES AT HIGH TEMPERATURES

X. XENON IN THE TEMPERATURE RANGE 0° TO 700°C. AND THE PRESSURE RANGE 8 TO 50 ATMOSPHERES[1]

By E. Whalley, Y. Lupien, and W. G. Schneider

ABSTRACT

The virial coefficients of xenon have been measured in the temperature and pressure range described. The results are compared with previous measurements.

The compressibility and the virial coefficients of a number of gases have been previously measured over a wide temperature range using an expansion technique (5). In the present paper measurements of the virial coefficients of xenon from 0° to 700°C. are reported. Temperatures up to 700°C. were employed in the present measurements in order that the virial coefficients could be extended well above the Boyle point. The pressure ranges covered by the measurements were approximately 4 to 20 atm. at 0°C., 8 to 30 atm. at 50°C., and 8 to 50 atm. at the higher temperatures. The xenon gas used in the measurements was supplied by the Linde Company and contained no krypton or other impurities above the limit of detection by a mass spectrometer (about 0.01%). Frequent checks on its purity were made during the runs. The procedure and method of measurement were the same as described previously (5).

RESULTS

The experimental measurements were fitted to the equation of state

$$PV = A+BP+CP^2 \qquad [1]$$

by the method of least squares described previously (6). The values of the virial coefficients A, B, and C, and their standard errors, are summarized in Table I. The units are amagat units. The standard error of the derived coefficients has been defined previously (6) and it is perhaps worth pointing out that it does not necessarily represent the absolute error. The total number of gas expansions carried out in the measurements at each temperature are also given in the table.

At 0°C. the vapor pressure of xenon is approximately 41 atm. (3). It was not possible to fit the measured data above 20 atm. to a virial equation including the fourth virial coefficient, so only measurements below 20 atm. were retained in the final analysis. At 50°C. only measurements below 30 atm. were retained for the same reason. At higher temperatures the maximum pressure was 50 atm. and at all temperatures except for the 0° isotherm the lowest pressure was 8 atm. or lower. For the 0° isotherm, which presented the greatest difficulty in fitting a series equation, the measured pressures were extended down to 4 to 5 atm. This was accomplished with an auxiliary piston

[1]*Manuscript received December 29, 1954.*
Contribution from the Division of Pure Chemistry, National Research Council of Canada, Ottawa. Issued as N.R.C. No. 3537.

TABLE I

VIRIAL COEFFICIENTS OF XENON

	N.R.C. values					M.I.T. values		Amsterdam values	
T,°C.	A	Standard error of A ($\times 10^5$)	10^3B, amagat	10^6C, amagat atm.$^{-1}$	No. of expansions	10^3B, amagat	10^6C, amagat atm.$^{-1}$	10^3B, amagat	10^6C, amagat atm.$^{-1}$
0	1.00667	7	-6.614 ± 0.063	-60.5 ± 2.5	40			-6.952	-34.4_4
25						-5.846	-19.9_6		
50	1.19094	8	-4.840 ± 0.020	-19.00 ± 0.41	18	-4.967	-11.7_3	-4.985	-12.3_2
75						-4.243	-6.7_4	-4.273	-7.1_8
100	1.37520	10	-3.748 ± 0.026	-3.44 ± 0.25	17	-3.646	-3.6_3	-3.679	-4.0_4
125						-3.148	-1.6_1	-3.173	-2.10
150	1.55947	11	-2.811 ± 0.025	$+0.95 \pm 0.20$	17	-2.728	-0.28	-2.742	-0.979
200	1.74373	12	-2.127 ± 0.034	$+1.69 \pm 0.30$	16	-2.038	$+1.12$		
300	2.11226	15	-1.126 ± 0.010	$+1.93 \pm 0.10$	24	-1.058	$+1.78$		
400	2.48079	17	-0.484 ± 0.020	$+1.80 \pm 0.17$	26				
500	2.84932	20	-0.006 ± 0.014	$+0.80 \pm 0.12$	30				
600	3.21785	22	$+0.357 \pm 0.011$	—	24				
700	3.58638	25	$+0.638 \pm 0.022$	—	24				

gauge which was designed to operate in the pressure range from 3 to 15 atm. The additional low pressure data, which are very essential for obtaining accurate second virials for highly imperfect gases, greatly facilitated the fitting of the data to a series equation. Moreover, for the isotherms between 0° and 150°, where the curvature of the pressure-ratio vs. pressure plots was greatest, the value of N, the volume ratio of the gas pipettes, was determined separately at each temperature by measurements with helium in the usual way. This further simplified the fitting of the data since the intercept on the zero pressure axis of the pressure-ratio vs. pressure plots is then fixed, and the uncertainty of extrapolation of the data from higher pressures is greatly reduced.

COMPARISON WITH PREVIOUS MEASUREMENTS

The compressibility of xenon has been measured by Beattie, Barriault, and Brierley (1) at M.I.T. in the temperature range 16.65–300°C. and pressure range 20–400 atm., and by Michels, Wassenaar, and Louwerse (4) at Amsterdam in the temperature range 0–150°C. and pressure range 16–2800 atm.

The M.I.T. measurements were fitted (2) to the equation of state

$$[2] \qquad PV = RT+\frac{B_V}{V}+\frac{C_V}{V^2}+\frac{D_V}{V^4}.$$

The second and third virial coefficients B_V and C_V were converted to the corresponding pressure virial coefficients of equation [1] by the relations

$$[3] \qquad A = RT/V_N, \quad B = B_V/RTV_N, \quad C = \frac{C_V-B_V^2/RT}{V_NR^2T^2},$$

where V_N is the normal volume. The Amsterdam measurements below a density of 50 amagat units were fitted to the equation

$$[4] \qquad PV = A_\rho+B_\rho\rho+C_\rho\rho^2+D_\rho\rho^4.$$

The second and third virial coefficients were converted to the corresponding virial coefficients of equation [1] by the relations

$$[5] \qquad B = B_\rho/A_\rho, \quad C = \frac{C_\rho-B_\rho^2/A_\rho}{A_\rho^2}.$$

Both sets of values are compared with the present measurements in Table I. Both quoted values of the virial coefficients to several figures more than justified by their accuracy. They have been rounded off to the values quoted in the table.

The normal volumes of xenon deduced from the three sets of measurements are listed in Table II.

Our results are not in very good agreement with either the M.I.T. or the Amsterdam values, though these agree very well with each other. Apart from the 0° and 50° measurements, our second virial coefficients are uniformly about 0.1×10^{-3} amagat units higher than the others. This would appear to

TABLE II

NORMAL VOLUME OF XENON

Beattie *et al.**	22.2652 l./mole (corrected for 0.14% Kr content)
Michels *et al.*	22.2585 l./mole } from measured
This work	22.2654 ± l./mole } 0°C. isotherms

**Calculated by using the Beattie–Bridgeman equation of state which had been fitted to the isotherm measurements at higher temperatures. No measurements at 0°C. were carried out by these authors. Less weight should be placed on this value than on the others.*

indicate that there is some systematic difference between the measurements. In both the Amsterdam and the M.I.T. measurements the lowest pressures measured were rather high, being from 16.5 to 27.7 atm. for the Amsterdam isotherms, and 20.7 to 46.1 atm. for the M.I.T. isotherms, whereas the lowest pressure used in the present measurements was never greater than 8 atm. Since the second virial coefficient is obtained from a zero pressure slope it would seem that greater accuracy could be obtained from measurements extending to lower pressures. Because xenon is a rather imperfect gas, particularly at the lower temperatures, the measurements should preferably not extend to a too high pressure. The deviations of the experimental from the observed values of $V(PV-RT)$ at constant temperature of Beattie's measurements are not random (Table I, Ref. 2). We have not reported our pressure measurements since they are partly functions of the apparatus, but care was taken in the analysis that the deviations of the calculated from the observed pressure ratios were random, indicating that equation [1] was a good fit to the data. Another contributing cause of the different virial coefficients may be the use of an inverse volume series for the equation of state in the M.I.T. and the Amsterdam measurements, whereas we have used a pressure series.

ACKNOWLEDGMENTS

We wish to thank Mr. W. A. Stevenson for assistance in constructing the apparatus, and Mr. G. David for assistance with the computations.

REFERENCES

1. BEATTIE, J. A., BARRIAULT, R. J., and BRIERLEY, J. S. J. Chem. Phys. 19: 1219. 1951.
2. BEATTIE, J. A., BARRIAULT, R. J., and BRIERLEY, J. S. J. Chem. Phys. 19: 1222. 1951.
3. MICHELS, A. and WASSENAAR, T. Physica, 16: 253. 1950.
4. MICHELS, A., WASSENAAR, T., and LOUWERSE, P. Physica, 20: 99. 1954.
5. SCHNEIDER, W. G. Can. J. Research, B, 27: 339. 1949. And subsequent papers.
6. WHALLEY, E., LUPIEN, Y., and SCHNEIDER, W. G. Can. J. Chem. 31: 722. 1953.

IDENTIFICATION OF SPRUCE SULPHITE LIQUOR COMPONENTS[1]

By E. A. Kvasnicka and R. R. McLaughlin

ABSTRACT

Spruce sulphite liquor was extracted with butyl acetate. By means of solvent fractionation, chromatography, and countercurrent distribution, vanilloyl methyl ketone, vanillin, dihydroconiferyl alcohol, 3,3′-dimethoxy-4,4′-dihydroxystilbene, and a new phenolic compound, $C_{20}H_{24}O_5$, were isolated and identified.

In the field of lignin chemistry, the oxidation of sulphite waste liquor has aroused considerable interest. A large amount of work has been carried out for the purpose of isolating and identifying the low molecular weight fragments of lignin in such oxidized liquors (22). However, no such comparable effort has been made to investigate the original sulphite waste liquor, though a few constituents have been noted (8, 16, 21, 28). The amount of such compounds is much smaller than in oxidized liquor and consists mainly of degradation products of lignin together with some materials derived from the wood, or their reaction products (32, 35). It follows that the identification of these components could be an important link between the studies of wood extractives and the examination of the constituents of oxidized liquors, and might indicate technical uses of the compounds so identified, or of compounds that could be derived from them.

These considerations induced a thorough investigation of the solvent-extractable components of spruce sulphite liquor in this laboratory. The present paper describes the first part of the results obtained.

Spruce sulphite liquor was extracted with butyl acetate, which removes a larger amount of solids than benzene or ether (11). The extract contains three main groups of components: tannins and conidendrin, other phenols, and neutral compounds (hydrocarbons and esters). It was necessary to perform a crude separation into these groups by solvent fractionation before the further work was done. Conidendrin was separated by its low solubility in ethanol. Extraction of the ethanol-soluble part with ether left a minor amount of conidendrin and the tannins as residue. Extraction of the ether-soluble part with petroleum ether removed mainly hydrocarbons and left as residue the main part of the other phenolic compounds.

The next step was the separation of these groups into the bisulphite-soluble compounds (extraction with 21% sodium bisulphite), acids (10% sodium bicarbonate), and phenols (6% sodium hydroxide). The neutral compounds and a very small amount of phenols with extreme pK values (2) remained after these extractions.

The large number of components in these fractions made separations difficult and required an efficient method to check the course and extent of

[1]*Manuscript received November 30, 1954.*
Contribution from the Department of Chemical Engineering, University of Toronto, Toronto 5, Ontario.

the subsequent steps. Paper chromatography was used extensively for this purpose.

The bisulphite-soluble material was separated by chromatography. Vanillin and 1-(3-methoxy-4 hydroxyphenyl)-propanedione-1,2 were isolated. The latter compound has not yet been reported in spruce sulphite liquor. Its presence in the aqueous filtrates of lignin ethanolysis mixtures (3, 14) shows some relation between the degradation processes during ethanolysis and sulphite cooking.

The alkali-soluble material was separated by fractional acidification, utilizing the difference of the pK values. Further separation was obtained by countercurrent distribution which yielded dihydro-coniferyl alcohol (3-(3-methoxy-4-hydroxyphenyl)-propanol-1) as a new component of spruce sulphite liquor. Hibbert (13) and Schuerch (30) found this compound in the hydrogenolysis products of maple lignin. Kawai (17) isolated it as a degradation product of egonol.

From the same fraction, a new phenolic compound, $C_{20}H_{24}O_5$, m.p. 134°C., was isolated. Its spectrum (UV, IR) is closely related to dihydroconiferyl alcohol and the investigation of its structure is under way.

In addition to the previously reported compounds, a small amount of 3,3′-dimethoxy-4,4′-dihydroxystilbene was isolated by chromatography of the alkali-soluble fraction. Richtzenhain (26) found this stilbene in oxidized sulphite liquors and reported its absence in untreated liquors.

It can be seen that the compounds now isolated from spruce sulphite liquor are known as reaction products of quite different lignin degradation procedures: ethanolysis, hydrogenolysis, and oxidation.

Further investigations will be concerned with the identification of the remaining compounds of the extracts and with the origin of the isolated products.

EXPERIMENTAL PART

1. *Extraction*

Spruce sulphite waste liquor (SWL) (Cook No. 3001/48, Ontario Paper Co., Thorold, Ont.) was extracted with *n*-butyl acetate by a 21-ft. fast spray type extraction column (4) (countercurrent flow, flow ratio 2: 1/BuOAc–SWL (continuous phase)). This extract was concentrated and the last part of the solvent was removed in a 3-liter glass still under reduced pressure (12 mm., 40°C. bath temp.). Several such extractions gave an average of 1.38 gm. dry extract per liter of sulphite liquor. This amount can be increased at lower flow rates.

2. *Solvent Fractionation* (See Table I)

Fifty grams of dry extract was dissolved in 500 ml. ice-cold dry ethanol. The insoluble material (fraction I) was filtered off. The ethanol was removed under reduced pressure (12 mm.). The residue was shaken twice with 100 ml. portions of ether (30 min.). The insoluble part (fraction IV) was separated. The ether was distilled off under reduced pressure. The residue was extracted

TABLE I

SOLVENT FRACTIONATION OF BUTYL ACETATE EXTRACT

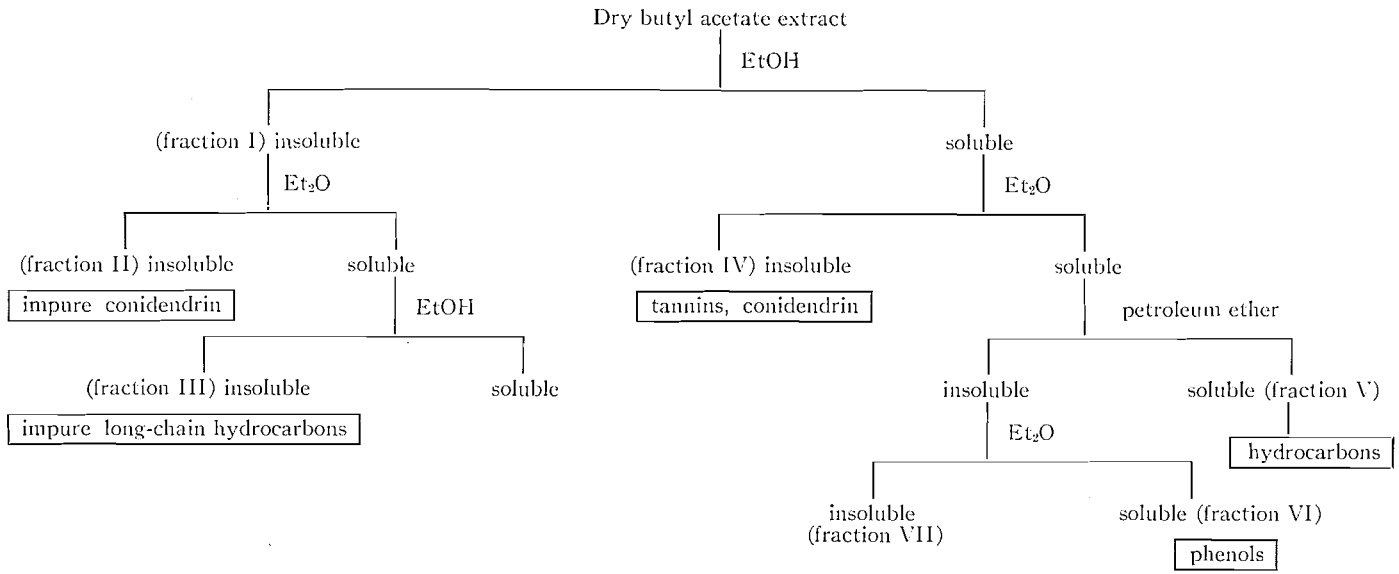

NOTE: Fraction	II	III	IV	V	VI	VII	others and loss
Weight (as % of the dry butyl acetate extract)	12.6	1.3	27.9	17	37.9	0.7	2.6

twice with 100 ml. portions of petroleum ether (b.p. 30–60°C.). The insoluble part (fraction V) was separated and extracted twice with 75 ml. portions of ether. The residue (fraction VII) was filtered off. Fraction I, the ethanol-insoluble material, was shaken with 200 ml. ice-cold ether (five minutes) and filtered. The residue was impure conidendrin (fraction II). The ether filtrate was concentrated to 50 ml. under reduced pressure, cooled to 0°C., and 150 ml. ice-cold dry ethanol added. The resulting precipitate was impure melene (28) (fraction III).

The extractions and separations reported under parts 1 and 2 are based on parts of the theses submitted by Sacks (28) and Kenyon and Kerr (18) in partial fulfillment of the requirements for the M.A.Sc. degree and B.A.Sc. degree at this University.

3. *Group Separation*

After evaporation fractions V and VI were each dissolved in 20 times their volume of butyl acetate. A small amount of conidendrin (1.6 gm.) separated from fraction VI after this procedure.

The solution was extracted successively with sodium bisulphite solution (21%), sodium bicarbonate solution (10%), and sodium hydroxide solution (6%).

The sodium bisulphite extract was acidified with sulphuric acid, heated, aspirated, and cooled. It was extracted with chloroform.

The bicarbonate and sodium hydroxide solutions were also acidified and extracted with chloroform.

The remaining butyl acetate solution was distilled under reduced pressure until the solvent was removed.

The chloroform solutions of the other groups were also evaporated and the weights of extracted materials determined, as shown in Table II.

TABLE II

GROUP SEPARATION OF FRACTIONS V AND VI

Group:	Bisulphite-soluble	Bicarbonate-soluble	Sodium-hydroxide-soluble	Remaining fraction
Fraction V	0.09	0.21	0.42	16.3%
Fraction VI	3.0	0.9	24.0	10 %

NOTE: *All numbers represent per cent by weight of the original dry butyl acetate extract.*

4. *Bisulphite-soluble Compounds*

Paper chromatography (see part 6) was used to give a preliminary indication of the composition of the fraction. No significant differences were found between the bisulphite-soluble components of fractions V and VI. Both contain two principal compounds (compound A—R_F: 0.53, compound B—R_F: 0.73) and minor amounts of other compounds.

Compound A was isolated from a series of paper chromatograms on Whatman No. 3 paper with the same solvent system (see part 6). The position of the spots was detected under the UV lamp, the spot area was marked, and was

cut out. Elution of the spots obtained by chromatography of a total amount of 12 mgm. bisulphite fraction gave 2.5 mgm. of a yellow oil. UV and IR spectra indicated a diketo-compound of the guaiacyl group. A larger quantity of bisulphite-soluble material (200 mgm.) was used for a chromatogram on a 2 × 15 cm. column of 100 mesh silica gel (Mallinckrodt). After development with 600 ml. benzene–methanol (250: 1, v/v), the column material was cut into zones. The material in the yellow zones was eluted with methanol and checked by paper chromatography. The combination of the material of the corresponding zones gave after recrystallization from ethanol–water (1: 3), 21 mgm. of yellow crystals, m.p. 72.5°C.[2]

The mixed melting point with authentic vanilloyl methyl ketone was not depressed. The spectra of the compounds were identical and both gave the same R_F values, color reactions with spray reagents, and the same characteristic nickel salt of the dioxime.

IR spectrum:[3] Maxima at 1720, 1664, 1593, 1510, 1463, 1430, 1376, 1350, 1297, 1262, 1227, 1202, 1172, 1139, 1125, 1117, 1033 cm.$^{-1}$ (CS_2, CCl_4)

The UV spectrum of compound B and its R_F value were identical with those of vanillin. Sublimation of a 50 mgm. sample of bisulphite-soluble material under reduced pressure gave 20 mgm. of crystalline sublimate, identified as vanillin by mixed melting point and paper chromatography.

5. *Sodium-hydroxide-soluble Compounds*

Paper chromatography (see part 6) revealed only minor quantitative differences in the composition of the sodium hydroxide extracts of fractions V and VI. Aside from conidendrin, two principal components (compound C—R_F: 0.20, compound D—R_F: 0.55) and smaller amounts of about 20 other phenolic compounds were indicated.

The course of all the following separation steps was checked by paper chromatography.

Half of the alkali-soluble part of fraction VI was dissolved in 200 ml. 2 *N* sodium hydroxide and the pH adjusted to 12.0 by addition of sodium dihydrogen phosphate. After extraction with chloroform (50 ml.), the water phase was acidified further in steps of 0.25 pH units and extracted again after each step with 50 ml. chloroform, until pH 5 was reached.

Isolation of Compound D

The five chloroform extracts made between pH 12.0 and 11.0 contained almost all of compound D and also some other phenols. These extracts were concentrated to a volume of 15 ml. The further separation was effected by countercurrent distribution between chloroform–ethanol – phosphate buffer solution (pH 12) (29) in a 24 stage circular type Craig apparatus (5). (Volume relation 7.7: 12 (buffer phase)). After 24 transfers, compound D had migrated from tube 1 to tubes 6–9 and these fractions contained only minor amounts of impurities. The solvent of these fractions was removed under reduced pressure

[2]*All melting points are uncorrected.*

[3]*We are grateful to Miss E. M. Kirby of the Ontario Research Foundation for the determination of all infrared spectra.*

(bath temperature below 50°C.) and the residue dissolved in the minimum amount of hot benzene. After cooling, crystals separated (240 mgm.). Recrystallization from benzene gave colorless prismatic crystals, m.p. 134°C.

Analysis: Found: C: 69.98, 69.95; H: 7.05, 6.96; CH_3O: 17.83, 17.90
Calc. for $C_{20}H_{24}O_5$: C: 69.74; H: 7.03; CH_3O: 18.1

Mol. wt.: Found: (Rast): 340
Calc.: 344.39

UV spectrum: (95% EtOH): Max. 229 mμ, 283 mμ
(95% EtOH, 1 mole KOH/l.): max. 247 mμ, 299 mμ

IR spectrum: Maxima at: 1604, 1516, 1453, 1430, 1366, 1266, 1231, 1202, 1180, 1149, 1120, 1094, 1030 cm.$^{-1}$ (melt, supercooled)

The mother liquors of these crystallizations yielded further quantities of compound D after chromatography on Magnesol–Celite (5: 1) (23) with benzene–methanol (250: 1) as eluent.

Isolation of Compound C

The chloroform extracts made between pH 10.75 and 9.75, containing the principal amount of compound C, were concentrated to 15 ml. and subjected to countercurrent distribution in a manner similar to that described above. Solvent system: chloroform – phosphate buffer (pH 11) – ethanol–water (29): volume relation 7.7: 14 (buffer phase). After 34 transfers, the compound had migrated from tubes 1–2 to tubes 18–28. The purest fractions were combined, the solvent removed under reduced pressure, and the residue purified further by chromatography on a Magnesol–Celite (5: 1) column (23) using benzene–methanol (250: 1, v/v) as eluent. The fractions were combined according to the results of paper chromatography. The solvent was removed under reduced pressure and a colorless oil remained (400 mgm.). Its IR spectrum was very similar to the spectrum of eugenol.

The compound was now benzoylated. A sample, 365 mgm., was dissolved in 10 ml. pyridine, cooled, and 0.5 ml. benzoyl chloride added. After 24 hr. at room temperature, the mixture was heated on the steam bath for five minutes, diluted with water, and extracted with chloroform. After drying, the solvent was removed and 720 mgm. crude benzoyl compound isolated. Recrystallization from petroleum ether – benzene yielded white needles, m.p. 62–63°C. A synthesized sample of dihydroconiferyl alcohol dibenzoate gave no depression of the mixed melting point.

Comparison of compound C with a synthesized sample of dihydroconiferyl alcohol (30) gave identical R_F values, spectra, refraction indices, and color reactions.

UV spectrum: (95% EtOH): Max. 228 mμ, 281.6 mμ

IR spectrum: Maxima at 1608, 1513, 1464, 1431, 1368, 1266, 1231, 1202, 1183, 1149, 1119, 1050, 1037 cm.$^{-1}$ (CS_2, CCl_4)

Isolation of 3,3′-Dimethoxy-4,4′-dihydroxystilbene

The alkali-soluble part (5 gm.) of fraction VI was chromatographed on a Magnesol–Celite (5: 1) column (23) (size: 3 × 40 cm.) using benzene–methanol

(200: 1) as eluent. The effluent was collected in 15-ml. portions. In addition to the compounds reported above a strongly fluorescent compound was found in the first fractions (Nos. 6–10) of the effluent. Another chromatogram was made on silica gel (Mallinckrodt, 100 mesh), using the same eluent. The zone with a strong violet fluorescence was cut out, eluted with ethanol, and concentrated. The resulting crystals were collected and recrystallized from ethanol, giving 20 mgm. colorless needles, m.p. 213°C. The mixed melting point with 3,3′-dimethoxy-4,4′-dihydroxystilbene (26) was not depressed. The color reactions were also identical.

6. *Paper Chromatography*

The solvent systems: butanol – 2% ammonia (24), butanol–water and benzene – petroleum ether – water (19) were used to some extent. However, the major part of paper chromatography in this work was carried out with the solvent system: tetrahydrofuran – petroleum ether (b.p. 65–110°C.) – water (3: 7: 5) because of the short travel time for this solvent (about 10 cm. per hour) and the good separation of a large number of compounds (see Table III). Descending chromatography was used.

TABLE III

IDENTIFICATION OF PHENOLIC COMPOUNDS BY PAPER CHROMATOGRAPHY

Compound (Reference)	$100 \times R_F$	Color reaction: Diazotized sulphanilic acid	Color reaction: Diazotized *p*-nitraniline	UV fluorescence on pH 11 paper
Acids				
Vanillic	13	Orange	Purple	
Homovanillic (7)	9	Red	Gray-blue	
Hydroferulic (6)	20	Red	Gray-blue	
Ferulic (27)	11	Purple	Lilac	Blue
Syringic	4	Pink	Blue	
Keto compounds				
Vanillin	53	Pale orange	Purple	Dark violet
Acetovanillone	48	Pale orange	Purple	Bright violet
Propiovanillone (10)	67	Pale orange	Purple	Bright violet
R—CO—CO—CH_3 (14)	73	Orange-brown	Red-brown	Dark brown
α-Hydroxy-propiovanillone (15)	32	Orange		Blue
R—CH_2COCH_3 (33)	52	Orange-red		
Alcohols				
Vanillyl alcohol	6	Orange		
Apocynol (9)	17	Orange		
R—$CH(OH)C_2H_5$ (31)	39	Orange		
R—$CH_2.CH(OH).CH_3$ (31)	26	Red	Gray-lilac	
R—$(CH_2)_3OH$ (30)	20	Red	Gray-lilac	
Coniferyl alcohol (1)	7	Purple	Lilac	

(*R* = *3-MeO-4-HO—C_6H_2-*)

Paper: Whatman No. 1

Spray reagents: 2,4-dinitrophenylhydrazine (0.4% in 2 *N* hydrochloric acid)
ferric chloride (1%) – potassium ferricyanide (1%), 1:1
phosphomolybdic acid (4%), followed by treatment with ammonia vapors
diazotized sulphanilic acid (12)
diazotized *p*-nitraniline (34)

Buffered papers: sheets of Whatman No. 1 paper were sprayed with 2% phosphate buffer solutions of pH values between 4 and 10 and dried at room temperature. These papers made possible separations of acids and acidic phenols from each other and from other phenolic compounds with similar R_F values. The R_F values of acidic compounds decrease on the papers with increasing alkalinity gradually to zero, depending on their pK values (20). This method can be used to distinguish between vanillin, acetovanillone, and vanillyl methyl ketone or between hydroferulic acid and dihydroconiferyl alcohol. The method of Reid and Newcombe (25) was also used to distinguish between vanillin and acetovanillone.

ACKNOWLEDGMENTS

The authors wish to thank the Research Council of Ontario for financial support of this research for the past eighteen months; the Advisory Committee on Scientific Research, University of Toronto, for earlier financial support; the Spruce Falls Power and Paper Company for a Fellowship held by W. Sacks (28); and Dr. H. B. Marshall of the Ontario Research Foundation for helpful discussions.

REFERENCES

1. Allen, C. F. H. and Byers, J. R. J. Am. Chem. Soc. 71: 2683. 1949.
2. Aulin-Erdtman, G. Svensk Papperstidn. 56: 287. 1953.
3. Bondi, A. and Meyer, H. Biochem. J. (London), 43: 248. 1948.
4. Bryson, M., Millard, J. W., and Ripley, F. D. B.A.Sc. Thesis, Dept. of Chemical Engineering, University of Toronto, Toronto, Ontario. 1950.
5. Craig, L. C. Anal. Chem. 21: 500. 1949.
6. Dean, W. L., Whaley, W. M., and Meadow, M. J. Org. Chem. 19: 1024. 1954.
7. Douglas, R. L. and Gulland, J. M. J. Chem. Soc. 2893. 1931.
8. Emde, H. Cellulosechemie, 16: 13. 1935.
9. Finnemore, H. J. Chem. Soc. 93: 1521. 1908.
10. Fodor, G., Kiss, J., and Szekerke, M. J. Org. Chem. 15: 227. 1950.
11. Hall, R. H. M.A.Sc. Thesis, Dept. of Chemical Engineering, University of Toronto, Toronto, Ontario. 1950.
12. Hanke, M. T. and Koessler, K. K. J. Biol. Chem. 50: 235. 1922.
13. Hibbert, H., Brewer, C. P., and Cooke, L. M. J. Am. Chem. Soc. 70: 57. 1948.
14. Hibbert, H., Brickman, L., and Hawkins, W. L. J. Am. Chem. Soc. 62: 2149. 1940.
15. Hibbert, H. and Cramer, A. B. J. Am. Chem. Soc. 61: 2205. 1939.
16. Holmberg, B. and Sjorberg, M. Ber. 54: 2406. 1921.
17. Kawai, S., *et al.* Ber. 72: 367. 1939.
18. Kenyon, G. H. and Kerr, W. D. B.A.Sc. Thesis, Dept. of Chemical Engineering, University of Toronto, Toronto, Ontario. 1950.
19. Leopold, B. Acta Chem. Scand. 6: 39. 1952.
20. Lindberg, J., Hästbacka, K., and Enkvist, T. Finska Kemistsamfundets Medd. 62: 25. 1953; Chem. Abstr. 48: 1000. 1954.
21. McLaughlin, R. R. Pulp & Paper Mag. Can. 50: 91. 1949.
22. Marshall, H. B. Pulp & Paper Mag. Can. 50: 123. 1949.
23. Pearl, I. A. J. Am. Chem. Soc. 73: 863. 1951.
24. Pearl, I. A. and Beyer, D. L. J. Am. Chem. Soc. 76: 2224. 1954.
25. Reid, S. G. and Newcombe, A. G. Nature, 172: 455. 1953.

26. RICHTZENHAIN, H. and VON HOFE, C. Ber. 72: 1890. 1939.
27. ROBINSON, R. and SHINODA, J. J. Chem. Soc. 127: 1973. 1925.
28. SACKS, W. M.A.Sc. Thesis, Dept. of Chemical Engineering, University of Toronto, Toronto, Ontario. 1949.
29. SCHUERCH, C. J. Am. Chem. Soc. 72: 3842. 1950.
30. SCHUERCH, C., *et al.* J. Am. Chem. Soc. 75: 707. 1953.
31. SHORYGINA, N. N. Doklady Akad. Nauk S.S.S.R. 64: 689. 1949; Chem. Abstr. 45: 1536. 1951.
32. Tappi Monograph Ser. No. 6. Nature of the chemical components of wood. Tappi, New York. 1948.
33. WACEK, A. v. Ber. 77: 85. 1944.
34. WHITE, K., BRAY, H. G., and THORPE, W. V. Biochem. J. (London), 46: 271. 1950.
35. WISE, L. E., ISENBERG, I. H., and BUCHANAN, M. A. Paper Ind. and Paper World, 28: 8. 1946.

A NEW TYPE OF CELLULOSE ETHER

THE PREPARATION AND PROPERTIES OF THE ω-(*p*-AMINOACETOPHENONE) ETHER OF CELLULOSE[1]

By R. R. McLaughlin and D. B. Mutton[2]

ABSTRACT

With the object of preparing a cellulose ether containing diazotizable amino groups, seven different forms of cellulose, or cellulose derivatives, were treated with 10 different reagents under a variety of conditions. Reasons why only one reagent under one set of conditions gave a product with a substantial degree of substitution (0.35) and with satisfactory physical properties are presented. This resulting ether, the ω-(*p*-aminoacetophenone) ether of cellulose, was prepared by the reaction between ω-chloro-*p*-aminoacetophenone and ethanol-washed soda-cellulose (from wood pulp, cotton, paper, or rayon). It can be (*a*) diazotized and coupled with any of the usual reagents to yield cellulose-azo colors, (*b*) xanthated, before or after coupling, and spun as rayon filament; if uncoupled at this point it can be diazotized and coupled, (*c*) dyed directly with acid dyes, (*d*) rendered organo-soluble by nitration, and (*e*) carboxymethylated after coupling to yield colored, water-soluble derivatives. It is insoluble in the usual cellulose reagents, and is as stable to acid and alkaline hydrolysis as cellulose.

INTRODUCTION

The purpose of the work described in this paper was the preparation of cellulose ethers containing primary aromatic amino groups. On diazotization and coupling such ethers should produce azo compounds in which the chromophore groups form part of the molecule of the cellulose derivatives, which should be as stable as cellulose to most reagents. Analogous nitro compounds, because they may be reduced to the corresponding aromatic amines, are also of interest. Ethers rather than esters were investigated because the former are more resistant to hydrolysis.

A number of attempts to prepare colored cellulose derivatives have been reported. In 1926 Peacock (42) obtained what he regarded as a superficial coloring of cotton by treating it with *m*-nitrobenzyl-phenyldimethyl-ammonium chloride, diazotizing, and coupling. A similar result was obtained by Kursanov and Solodkov (33). Charles Gränacher (19, 20, 21, 22, 23) obtained diazotizable cellulose fibers by a superficial etherification of swollen cellulose (alkali cellulose washed free of alkali with water) with such reagents as *p*-nitrobenzyl chloride and 2,4-dinitrochlorobenzene in the presence of lithium carbonate. Repetition of this work by us failed to give a degree of substitution (D.S.) greater than 0.01. A modification of this method applied by Pancirolli (41) to cellulose and starch yielded a *p*-nitrobenzyl ether of starch with a D.S. of 0.04. Repetition of Pancirolli's work led to the successful method described later in this paper.

The usual etherification reaction between alkali cellulose and an organic halide forms the basis for a number of patents (7, 8, 9, 10, 11, 28) wherein

[1]*Manuscript received May 31, 1954.*
Contribution from the Department of Chemical Engineering, University of Toronto, Toronto, Ontario. Abstracted from the Ph.D. thesis of D. B. Mutton.
[2]*Present address: Industrial Cellulose Research Ltd., Hawkesbury, Ontario.*

reaction conditions are usually described only vaguely, and analytical data are usually lacking. Such an attempt by Niethammer and Konig (39) with 2,4-dinitrochlorobenzene yielded a product with nitrogen content below 1% (D.S. <0.06). Reduction, diazotization, and coupling gave colors that were not intense. Repetition of this work by Andrews, Hyer, and Ray (1), in this laboratory, failed to give any product with a D.S. above 0.04, and variation of the reaction conditions with this reagent by us gave essentially the same results.

Recently Guthrie (25) colored cotton by treating it with an alkaline solution of a dye containing the chloroethyl or sulphatoethyl group, but concluded from the colors obtained that the D.S. was very low (26).

Seiberlich (49), Dinklage (9), and others (28) have reported the formation of a diazotizable cellulose derivative by the nitration of benzyl cellulose and reduction of the product, but the nitrogen content was not given. Our repetition of this work gave inconclusive analytical results and no intensely colored products.

Several other patents (12, 13, 50) refer to diazotizable cellulose ethers but no analytical results are cited.

Though the present work was confined to ethers, it ought to be recorded here that colored cellulose esters have been reported by a number of workers (3, 9, 10, 13, 24, 29, 30, 45), also a diazotizable aminocellulose (47, 48), and several derivatives prepared from oxycellulose (38, 46).

This survey indicates that no well-defined cellulose ether containing aromatic amino or nitro groups with a D.S. > 0.05 has hitherto been prepared. Apparent degrees of substitution below 0.05 might well be ascribed to adsorption.

RESULTS AND DISCUSSION

Preliminary Experiments

Several different forms of cellulose were treated with a number of etherifying agents under a variety of conditions. The etherifying agents used were 2,4-dinitrochlorobenzene, *p*-nitrochlorobenzene, picryl chloride, *p*-chloroaniline, *p*-bromoaniline, *p*-nitrobenzyl chloride, *p*-nitrobenzyl bromide, β-(*o*- and *p*-nitrophenyl) ethyl bromide, γ-(*p*-nitrophenyl) propyl bromide, *p*-amino-ω-chloroacetophenone, and *p*-nitrobenzyl chloromethyl ketone.

Three principal forms of cellulose were used. (1) Cellulose activated by swelling or solution was treated with an etherifying agent in the presence of some acid-binding reagent or solvent. This group included "activated cellulose", prepared according to Gränacher (19, 20, 21, 22, 23), and organo-soluble cellulose acetate, D.S. (of acetyl groups) 1.75 to 2.67. (2) Benzyl cellulose (D.S. 1.0 in benzyl groups, remaining hydroxyl groups blocked by acetylation) was nitrated according to Seiberlich (49) and Dinklage (9). (3) An etherifying agent was treated with an alkali derivative of cellulose such as ordinary alkali cellulose; sodium cellulosate according to the methods of Gaver (17, 18), and of Sugihara and Wolfrom (51); sodium cellulosate from sodium in liquid ammonia (15, 16, 43); and ethanol-washed alkali cellulose, modified after Pancirolli (41). The most commonly used conditions consisted in refluxing a solution (ether,

benzene, dioxan, ethanol, pyridine, or acetone) of the etherifying agent with the particular form of cellulose in use. Some experiments were carried out in the molten etherifying agent, and some at room temperature, with and without shredding, with and without solvent.

Purification of the products was effected by extraction of the unused reagents and the by-products with suitable solvents.

The only cases in which degrees of substitution consistently above 0.05 were obtained were those in which (*a*) molten *p*-nitrobenzyl chloride was reacted with sodium cellulosate (method of Sugihara and Wolfrom) (51), and (*b*) *p*-nitrobenzyl chloride and bromide, and *p*-amino-ω-chloroacetophenone, were reacted with ethanol-washed alkali cellulose.

The reaction with sodium cellulosate produced erratic results, and the products were amorphous powders of low D.P. Using ethanol-washed alkali cellulose, *p*-nitrobenzyl chloride and bromide produced degrees of substitution averaging 0.07–0.10. *p*-Amino-ω-chloroacetophenone, on the other hand, consistently gave products having D.S. between 0.20 and 0.35. This was by far the most successful combination.

In any etherification reaction the driving force, and the solubility, reactivity, and molecular size of the etherifying agent determine the result. For a successful reaction, a sufficient driving force must be available (40) (usually determined by the alkali concentration); the solubility of the reagent must be high enough to permit substantial diffusion to the reaction centers at the cellulose hydroxyl groups; and the reactivity of the reagent must be such that the extremes of a negligible rate of reaction and complete saponification to useless by-products are avoided.

The reason for the negative results obtained with most of the methods and reagents used in this work is probably that all the above conditions were not simultaneously fulfilled in such cases.

When alkali cellulose is washed with ethanol, much of the excess sodium hydroxide is removed, although the sodium hydroxide and water which are bound or preferentially absorbed by the cellulose are not affected to the same extent. Thus, while the proportion of hydroxyl groups in equilibrium with the sodium salt will be slightly decreased (making a lower D.S. possible), the excess alkali which is responsible for the hydrolysis of the etherifying agent will be sharply reduced. This, together with the higher water solubility of *p*-amino-ω-chloroacetophenone (hereinafter referred to simply as "ω"), is likely the reason for the success of the reaction of "ω" with ethanol-washed alkali cellulose.

ω-(p-Aminoacetophenone) Ether of Cellulose

This new ether of cellulose was prepared with D.S. up to 0.35 by reacting ethanol-washed alkali cellulose with an ethanol solution of "ω" (cf. Experimental). The purified product was usually light-yellow and fibrous.

The ratio of sodium hydroxide to the anhydro-glucose units of cellulose was varied by increasing the number of ethanol washings. The effect that this has upon the degree of substitution of the ω-cellulose is shown in Fig. 1, and indicates that the optimum molar ratio is about 1:1.

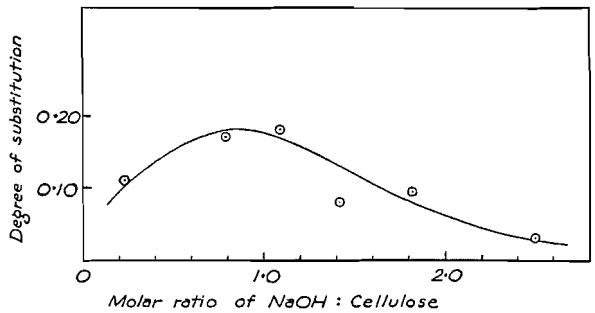

FIG. 1. The effect of the molar ratio of sodium hydroxide to anhydro-glucose units of cellulose upon the degree of substitution of ω-cellulose.

Twenty-eight per cent potassium hydroxide was used for steeping, in place of sodium hydroxide, and the resulting alkali cellulose was washed with ethanol to a potassium hydroxide: anhydro-glucose units molar ratio of 0.66: 1. When treated in the usual way with "ω", the product obtained had a D.S. of 0.20, showing, as was expected, that potassium hydroxide may be used in this reaction.

Since we had concluded that no well-defined cellulose ether containing aromatic amino or nitro groups with a D.S. > 0.05 had previously been prepared, we wished to establish definitely that ω-cellulose was actually a cellulose ether. No one experiment proved this unequivocally. However, the evidence given by the properties of the compound, as described below, make any other interpretation extremely unlikely.

Because of the adsorptive properties of cellulose it was necessary to demonstrate that ω-cellulose is neither a mechanical mixture of cellulose and "ω", nor an adsorption complex. A mechanical mixture of cellulose and "ω" was dialyzed with hot acetone, and the residue was found to be nitrogen-free. On the other hand, the nitrogen content of a sample of ω-cellulose (D.S. 0.28) was unchanged after dialysis for one week with hot acetone.

The stability of ω-cellulose (D.S. 0.21) to alkali with respect to time, temperature, and alkali concentration is shown in Figs. 2, 3, and 4. The levelling-off of all curves at D.S. 0.18 indicates that the ether linkage in ω-cellulose is quite stable to alkali. The slight decrease observed may be due to the removal of some lower molecular weight fractions having a slightly higher-than-average D.S.

In another experiment, boiling with 1% sodium hydroxide solution for six hours lowered the D.S. only from 0.30 to 0.26. The same treatment with 1% sodium carbonate solution had no effect.

The stability of ω-cellulose (D.S. 0.21) to acid with respect to time, temperature, and acid concentration is shown in Figs. 5, 6, and 7. These curves do not level off at a constant D.S. as in the case of the alkaline treatment, but slope gently downward. This indicates that the ether linkage in ω-cellulose is slowly cleaved by acid in a manner analogous to the acid hydrolysis of cellulose. The samples represented by the last two points in Fig. 7 were visibly degraded and could be crumbled to a powder when dry. This experiment indicates either that the ether linkage in ω-cellulose is as stable as the glycosidic linkages

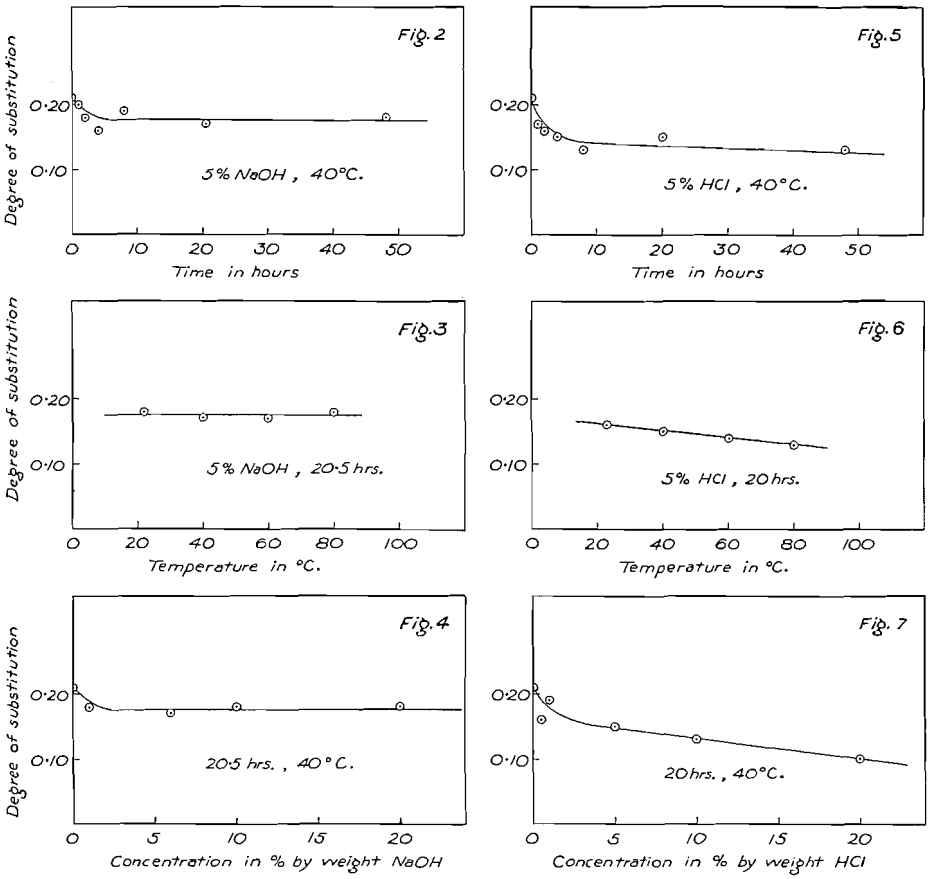

FIG. 2. The effect of time of hydrolysis in 5% sodium hydroxide at 40°C. upon the degree of substitution of ω-cellulose.

FIG. 3. The effect of temperature of hydrolysis in 5% sodium hydroxide for 20.5 hr. upon the degree of substitution of ω-cellulose.

FIG. 4. The effect of concentration of sodium hydroxide during hydrolysis at 40°C. for 20.5 hr. upon the degree of substitution of ω-cellulose.

FIG. 5. The effect of time of hydrolysis in 5% hydrochloric acid at 40°C. upon the degree of substitution of ω-cellulose.

FIG. 6. The effect of temperature of hydrolysis in 5% hydrochloric acid for 20 hr. upon the degree of substitution of ω-cellulose.

FIG. 7. The effect of hydrochloric acid concentration in the hydrolysis at 40°C. for 20 hr. upon the degree of substitution of ω-cellulose.

in cellulose, or else that the low molecular weight portions of the cellulose ether, which probably have a higher D.S., are being hydrolyzed and made water-soluble by the acid treatment.

In another experiment, boiling with 1% hydrochloric acid for six hours did not lower the D.S. (0.30) of a sample of ω-cellulose.

During purification of several batches of ω-cellulose, continued washing with acetone provided a colorless extract. On changing to hot water the washings were again slightly colored (yellow) but presently became colorless.

On changing to acetone the first washings were colored, but also, presently, became colorless. This process could be repeated, apparently indefinitely. During this treatment, the D.S. of the ω-cellulose decreased gradually, in one case from 0.28 to 0.19 over a period of six days' washing. It seems likely that some of the lower-molecular-weight and more highly substituted fraction of the ω-cellulose was slightly soluble in the solvent combination existing when a change of solvent was made.

Samples of ω-cellulose (D.S. 0.33) and the corresponding coupled products were examined by Industrial Cellulose Research, Limited, Hawkesbury, Ont., for the purpose of making viscosity measurements, but were found to be insoluble in cuprammonium or cupriethylene–diamine solutions. Were the product an adsorption complex this behavior would be very unlikely.

It could be envisaged that an initial small D.S. of "ω" groups in cellulose could be followed by a polymerization reaction between the excess "ω" and the amino groups present in the cellulose ether, thus:

Cellulose—O—CH_2.CO.C_6H_4.NH.CH_2.CO.C_6H_4.NH. . . . etc. An analysis for nitrogen would thus indicate a high D.S. whereas it might, in fact, be small. To clarify this point a sample of ω-cellulose (1.53% nitrogen, D.S. 0.21) was treated with nitrous acid at room temperature, heated to boiling, washed, and dried. The product contained 0.52% nitrogen (D.S. 0.07). It thus appears that at least two thirds of the original nitrogen was present as primary amino groups, i.e. that the original D.S. was at least 0.14. This is a minimum value, as it would be higher if there were any introduction of nitroso groups during the treatment with nitrous acid. This point is being further investigated.

Several attempts were made to hydrolyze ω-cellulose and to isolate ω-glucose. Neither the acetolysis procedure of Dickey and Wolfrom (6) nor the methanolysis procedure of Sugihara and Wolfrom (51) produced significant hydrolysis of the ω-cellulose. These failures, however, indicate a significant difference in structure between cellulose and ω-cellulose. Hydrolysis with 72% sulphuric acid was more successful. The hydrolyzate was purified and chromatographed. No ω-glucose was isolated, but a low-molecular-weight carbohydrate fragment containing an aromatic amino group was detected. Investigation of this problem is continuing.

Dr. A. W. Pross of the Central Research Laboratory of Canadian Industries, Limited, McMasterville, Quebec, carried out some work comparing the infrared spectra of cellulose, ω-cellulose, and carboxymethyl cellulose in an attempt to demonstrate compound formation. The results gave some indication that such was the case, but the experimental difficulties involved in these measurements made it impossible to draw any definite conclusions.

ω-Cellulose was diazotized and coupled by standard procedures to form colored azo derivatives. Using β-naphthol, the color of the product varied from a light pink, from ω-cellulose of D.S. 0.01 or less, to a very deep and brilliant red, from ω-cellulose of D.S. 0.20. At high magnification under a microscope the colors appeared to be uniform. Neither alkaline hypochlorite solution, 3% and 30% hydrogen peroxide, nor an acid solution of sulphur dioxide had any visible effect on the color of these derivatives.

An obvious possible application of ω-cellulose-azo compounds is their xanthation and spinning as molecularly-colored rayon. Viscose prepared from coupled ω-cellulose (D.S. 0.01) was spun into isotropic filaments by the method of Hermans (27). The thread, uniform, light red in color, could be stretched more than 100% and was of fair strength. Several yards of filament could be spun without a break, and under the microscope appeared smooth, uniform, and evenly colored. The same procedure was carried out with uncoupled ω-cellulose (D.S. 0.01). Almost colorless filaments were obtained, which could then be diazotized and coupled, or dyed directly with suitable acid dyes. A colored derivative prepared from ω-cellulose (D.S. 0.21) was also xanthated. The product dissolved only with difficulty in 6% sodium hydroxide solution and had to be diluted with more 6% sodium hydroxide solution before being filterable by suction. An attractive, bright-red filament was obtained by spinning the viscose solution as before. As mentioned previously, Industrial Cellulose Research, Limited, found that xanthated ω-cellulose of D.S. 0.33 was insoluble in sodium hydroxide solution. It thus appears that the solubility of the xanthate falls off sharply as the D.S. of ω-cellulose increases. It is possible, however, that this might be at least partially offset by increasing the D.S. of the xanthate groups. This point is being investigated.

It was found possible to render ω-cellulose-azo compounds water-soluble by carboxymethylation. The reaction was carried out on samples ranging in D.S. from 0.01 to 0.33. After purification by dialysis (34), the products were analyzed for D.S. of carboxymethyl group by the method of McLaughlin and Herbst (35). For ω-celluloses of D.S. 0.21 and 0.33, the D.S. of carboxymethyl groups had to be greater than 1.0 to make the product water-soluble. Degrees of substitution up to 1.7 were obtained. Whereas ordinary sodium carboxymethyl cellulose of a low D.S. is soluble in water, a considerably higher degree of substitution seemed to be required to confer complete solubility on the sodium carboxymethyl cellulose prepared from colored ω-cellulose.

Direct dyeing of cellulose is difficult because, unlike wool and silk, it contains no strongly polar groups such as the amino or carboxyl. ω-Cellulose, on the other hand, should possess direct-dyeing properties. A sample of ω-cellulose (D.S. 0.21) was dyed with a number of acid dyes such as croceine scarlet 3BX, croceine orange G, fast light green, and intensive blue. The dyeing procedures were adapted from those of Cain and Thorpe (4) and yielded attractive, intense, uniform colors which were fairly fast to washing. Controls run with shredded cellulose and absorbent cotton gave products from which the dyes were readily and completely removed by washing.

Nitration of ω-cellulose using standard techniques produced a material which was soluble in acetone. On evaporation of the filtered acetone solution a thin, opaque, yellow-brown, brittle film was obtained.

Samples of rayon yarn, paper towelling, surgical gauze, and factory cotton were soaked in 18% sodium hydroxide solution, pressed, washed with ethanol, and subjected to the usual etherification procedure. The D.S. of the samples were: ω-rayon, 0.01; ω-paper, 0.08; ω-gauze, 0.01; ω-cotton, 0.02. Diazotizing

and coupling with β-naphthol gave bright colored materials. The paper was red, the others orange. Direct dyeing with acid dyes was also effective, as before. Tensile strength tests on the rayon by Industrial Cellulose Research, Limited, revealed that, as expected, the tensile strength had been reduced by more than half. However, if the rayon derivative were required this effect can be avoided by etherifying before xanthation and regeneration. The low D.S. shows that the etherification conditions would need to be altered if the high D.S. obtained with shredded cellulose were desired, though intense, uniform colors are produced even with the low D.S. reported.

EXPERIMENTAL

Materials and Methods

For preparing alkali cellulose and for carrying out some of the reactions a Baker-Perkins Model No. 4–AN2 Werner-Pfleiderer shredder was used. A very much smaller model of this machine, having inside dimensions 2 × 2 × 4 in. (1/10th volume), was made later when some of the desired reagents proved to be difficult and expensive to make in the quantities required by the larger machine.

The only practical method of purifying the reaction products was by extraction of the unused reagents and by-products with suitable solvents. The extent of extraction necessary could often be judged by color since most of the reagents and their products of hydrolysis yield colored extracts. Therefore, when several consecutive extracts were colorless, purification was considered complete. In doubtful cases this was confirmed by establishing the constancy of the D.S. during the later stages.

The most convenient method for determining the extent of etherification was to analyze the products for nitrogen introduced as amino or nitro groups. The semimicro-Kjeldahl apparatus and procedure of Redemann (44) was used, with minor modifications. This involved 50 mgm. samples; reduction of any nitro groups with dextrose, according to Elek and Sobotka (14); selenium as a catalyst for digestion; collection of the ammonia evolved in 4% boric acid solution, and titration with 0.02 *N* hydrochloric acid, using a mixed indicator of methyl red and bromocresol green (31).

The *p*-amino-ω-chloroacetophenone used in this work was prepared by the method of Kunckell (32). Acetanilide was subjected to a Friedel and Crafts reaction with chloroacetyl chloride using aluminum chloride as a catalyst. The acetyl group was then removed by hydrolysis with aqueous hydrochloric acid. Pale, lemon-yellow crystals were obtained after repeated recrystallization from ethanol.

p-Nitrobenzyl chloromethyl ketone is a new compound. It was prepared by the chloromethylation of *p*-nitrophenylacetyl chloride after the method of McPhee and Klingsberg (36). Faintly yellow needles were obtained after recrystallization from ethanol (m.p. 94.0–94.5°C.; % nitrogen: calc. for $C_9H_8O_3NCl$: 6.56%; found: 6.59%).

ω-(p-Aminoacetophenone) Ether of Cellulose

Preparation

Ten grams of dry, shredded cellulose were steeped in 20% sodium hydroxide solution, pressed to a press-factor of three, slurried with just enough 95% ethanol to cover the mass, allowed to stand for one minute, and filtered. The ethanol washing was repeated as often as required (usually twice) (see Fig. 1). The product was refluxed for eight hours with 400 cc. of ethanol containing 15 gm. of *p*-amino-ω-chloroacetophenone. The light-yellow fibrous product was filtered, washed with hot acetone, water, and finally with acetone until the extract was colorless.

Hydrolysis with 72% Sulphuric Acid

Hydrolysis by sulphuric acid (37, 52, 53) was carried out as follows: Eight grams of ω-cellulose (D.S. 0.20) was covered with 100 cc. of cold 72% sulphuric acid, and the mixture, which soon became very dark colored, was allowed to stand at room temperature for 18 hr. The mixture was added to 3400 cc. of distilled water and refluxed for five hours. The dark-brown flocculent precipitate that separated on cooling was filtered off, and the red filtrate was neutralized with a hot aqueous solution of barium hydroxide. After removal of the barium sulphate, the yellow filtrate was concentrated to 175 cc. by evaporation at 50 mm. and 50°C. The concentrate was dialyzed through cellophane against three 225 cc. portions of distilled water and the combined dialyzates were reduced in volume to 150 cc. Unsubstituted glucose was removed from the concentrate by fermentation according to the method of Chen *et al.* (5). After the resulting mixture was centrifuged and filtered, the filtrate was evaporated to dryness, yielding a dark-red sirup. This was extracted with 30 cc. of dry, acetone-free methanol and treated with activated carbon to give a dark-red extract. A fraction obtained from this extract by chromatography on a Magnesol: Supercel column (2) (this column freely passed glucose and *p*-amino-ω-hydroxyacetophenone) gave a positive test for primary aromatic amino groups and a positive Molisch's test for carbohydrates. The nitrogen content (1.94%) was, however, too low for ω-glucose (4.47%).

Diazotization and Coupling

Ten grams of ω-cellulose suspended in 300 cc. of water was cooled to 5°C., 50 cc. of 1:1 hydrochloric acid was added, and the mixture cooled to 0°C. Two grams of sodium nitrite in 20 cc. of water was added, and the whole was allowed to stand for five minutes. The diazotized ω-cellulose was filtered off and washed with ice water. It was then added to a cooled solution (5°C.) made by dissolving 7.5 gm. of β-naphthol in 50 cc. of ethanol and adding 30 cc. of 20% sodium hydroxide solution and 300 cc. water. The mixture was vigorously stirred and then allowed to warm to room temperature and stand for half an hour. The colored ω-cellulose was filtered and thoroughly washed with water and ethanol.

Xanthation and Spinning

Five grams of ω-cellulose (D.S. 0.01) diazotized and coupled with β-naphthol was treated as in making alkali cellulose and then xanthated with 1.66 cc.

carbon bisulphide for 2.5 hr. in a small shredder. After the resulting 14 gm. of the red xanthate was added to 40 cc. of 6% sodium hydroxide solution, the mixture was kneaded for one hour. The resulting viscose solution was filtered without much difficulty through a thick, cotton pad and yielded a filtrate containing no undissolved fibers visible under the microscope. Isotropic filaments were spun by the method of Hermans (27) by forcing the viscose solution by low pressure through a fine glass capillary below the surface of a 14% ammonium sulphate solution.

Carboxymethylation

Five grams of ω-cellulose (D.S. 0.21) coupled with β-naphthol was mixed in the small shredder for 30 min. with 1.25 gm. of sodium hydroxide in 6.5 cc. of water; 3.5 gm. of powdered sodium chloroacetate was added, the mixture was shredded for 2.5 hr. and allowed to stand overnight; 1.25 gm. of flake sodium hydroxide was added and shredding was carried out for 30 min.; 3.5 gm. of sodium chloroacetate was added, shredding was continued for two hours, and the mixture was allowed to stand overnight. A sample was removed for analysis, and a third carboxymethylation step was carried out. The sticky, dark-red product was removed from the shredder and dissolved in water. The solution was purified by dialysis, using a cellophane membrane (34).

ACKNOWLEDGMENTS

We are indebted to the Advisory Committee on Scientific Research of the University of Toronto for financial assistance. One of us (D.B.M.) is also indebted to the Spruce Falls Power and Paper Company for fellowships held during the 1949–50 and 1950–51 academic sessions, and to the University of Toronto for the Wallberg Research Fellowship held during the 1951–52 session.

We should also like to thank Industrial Cellulose Research, Limited, Hawkesbury, Ont., for supplying raw materials and carrying out certain tests; and Dr. A. W. Pross, Canadian Industries Limited, McMasterville, Que., for the work on the infrared spectrum of ω-cellulose.

REFERENCES

1. ANDREWS, T., HYER, R. N., and RAY, G. B.A.Sc. Thesis, University of Toronto, Toronto, Ont. 1949.
2. BINKLEY, W. W. and WOLFROM, M. L. Chromatography of sugars and related substances. Sugar Research Foundation, (N.Y.)., Sci. Rept. Ser. No. 10. 1948.
3. BRIGGS, J. F. Z. angew. Chem. 26: 256. 1913.
4. CAIN, J. C. and THORPE, J. F. The synthetic dyestuffs. 7th ed. Charles Griffin & Co. Ltd., London. 1933.
5. CHEN, C. Y., MONTONNA, R. E., and GROVE, C. S. Tappi, 34: 420. 1951.
6. DICKEY, E. E. and WOLFROM, M. L. J. Am. Chem. Soc. 71: 825. 1949.
7. DINKLAGE, R. Fr. Patent No. 735,343. April 18, 1932. *Abstracted in* Chem. Abstr. 27: 1166. 1933.
8. DINKLAGE, R. Brit. Patent No. 398,279. September 14, 1933. *Abstracted in* Chem. Abstr. 28: 1531. 1934.
9. DINKLAGE, R. U.S. Patent No. 2,136,377. November 15, 1938. *Abstracted in* Chem. Abstr. 33: 1507. 1939.
10. DREYFUS, H. Brit. Patent No. 344,420. November 28, 1929. *Abstracted in* Chem. Abstr. 26: 304. 1932.
11. DREYFUS, H. Fr. Patent No. 704,280. October 23, 1930. *Abstracted in* Chem. Abstr. 25: 4705. 1931.
12. DREYFUS, H. Brit. Patent No. 486,527. June 3, 1938. *Abstracted in* Chem. Abstr. 32: 8778. 1938.

13. DREYFUS, H. Brit. Patent No. 486,564. June 7, 1938. *Abstracted in* Chem. Abstr. 32: 8778. 1938.
14. ELEK, A. and SOBOTKA, H. J. Am. Chem. Soc. 48: 501. 1926.
15. FREUDENBERG, K. and BOPPEL, H. Ber. 70, B: 1542. 1937.
16. FREUDENBERG, K., PLANKENHORN, E., and BOPPEL, H. Ber. 71, B: 2435. 1938.
17. GAVER, K. M. Ph.D. Dissertation. Ohio State University, Columbus, Ohio. 1945.
18. GAVER, K. M. U.S. Patent No. 2,397,732. April 2, 1946. *Abstracted in* Chem. Abstr. 40: 3620. 1946.
19. GRÄNACHER, C. Brit. Patent No. 346,385. December 28, 1928. *Abstracted in* Chem. Abstr. 26: 2051. 1932.
20. GRÄNACHER, C. Brit. Patent No. 347,117. April 17, 1929. *Abstracted in* Chem. Abstr. 26: 2862. 1932.
21. GRÄNACHER, C. Fr. Patent No. 687,298. December 27, 1929. *Abstracted in* Chem. Abstr. 25: 812. 1931.
22. GRÄNACHER, C. Brit. Patent No. 347,263. January 23, 1930. *Abstracted in* Chem. Abstr. 26: 2876. 1932.
23. GRÄNACHER, C. and MEIER, K. U.S. Patent No. 1,973,478. September 11, 1934. *Abstracted in* Chem. Abstr. 28: 7012. 1934.
24. GUENTHER, F. Ger. Patent No. 433,147. 1926. *Abstracted in* Chem. Zentr. II: 2232. 1926.
25. GUTHRIE, J. D. Am. Dyestuff Reptr. 41: 13 and 30. 1952.
26. GUTHRIE, J. D. Private communication.
27. HERMANS, P. H. Physics and chemistry of cellulose fibres. Elsevier Publishing Co., New York. 1949.
28. I.G. Farbenindustrie Akt.-Ges. Ger. Patent No. 492,062. September 26, 1919. *Abstracted in* Chem. Abstr. 24: 2599. 1930.
29. I.G. Farbenindustrie Akt.-Ges. Brit. Patent No. 322,556. September 15, 1928. *Abstracted in* Chem. Abstr. 24: 2883. 1930.
30. I.G. Farbenindustrie Akt.-Ges. Brit. Patent No. 458,684. December 21, 1936. *Abstracted in* Chem. Abstr. 31: 3690. 1937.
31. KOLTHOFF, I. M. and STENGER, V. A. Volumetric analysis. Vol. II. 2nd ed. Interscience Publishers, Inc., New York. 1947.
32. KUNCKELL, F. Ber. 33: 2644. 1900.
33. KURSANOV, D. N. and SOLODKOV, P. A. J. Appl. Chem. (U.S.S.R.), 16: 551. 1943.
34. MCLAUGHLIN, R. R. and HERBST, J. H. E. Can. J. Research, B, 28: 731. 1950.
35. MCLAUGHLIN, R. R. and HERBST, J. H. E. Can. J. Research, B, 28: 737. 1950.
36. MCPHEE, W. D. and KLINGSBERG, E. Org. Syntheses, 26: 13. 1946.
37. MONIER-WILLIAMS, G. H. J. Chem. Soc. 119: 804. 1921.
38. MÜLLER, F. Helv. Chim. Acta, 29: 130. 1946.
39. NIETHAMMER, H. and KONIG, W. Cellulosechemie, 10: 203. 1929.
40. OTT, E. Cellulose and cellulose derivatives. Interscience Publishers, Inc., New York. 1943.
41. PANCIROLLI, F. Boll. reparto fibre tessili vegetali regia staz. sper. ind. carta e fibre tessili vegetali, 32: 314. 1937.
42. PEACOCK, D. H. J. Soc. Dyers Colourists, 42: 53. 1926.
43. PETERSON, F. C. and BARRY, A. J. U.S. Patent No. 2,157,083. May 2, 1939. *Abstracted in* Chem. Abstr. 33: 6595. 1939.
44. REDEMANN, C. E. Anal. Chem. 11: 635. 1939.
45. RIESZ, E. Bull. soc. ind. Mulhouse, 99: 349. 1933.
46. ROGOVIN, Z. A., YASHUNSKAYA, A. G., and BOGOSLOVSKY, B. M. J. Appl. Chem. (U.S.S.R.), 23: 631. 1950.
47. SCHERER, P. C. and FEILD, J. M. Rayon Textile Monthly, 22: 607. 1941.
48. SCHERER, P. C. and GREEN, A. J. Rayon Textile Monthly, 25: 461. 1944.
49. SEIBERLICH, J. Rayon Textile Monthly, 18: 775. 1937.
50. Soc. Anon. Pour l'Ind. Chim. à Bâle. Fr. Patent No. 39,792. February 20, 1931. Addition to Fr. Patent No. 687,301. December 27, 1929. *Abstracted in* Chem. Abstr. 26: 4950. 1932.
51. SUGIHARA, J. M. and WOLFROM, M. L. J. Am. Chem. Soc. 71: 3509. 1949.
52. SUNDMAN, J., SAARNIO, J., and GUSTAFSSON, C. Finnish Paper Timber J. 31: 467. 1949.
53. SUNDMAN, J., SAARNIO, J., and GUSTAFSSON, C. Finnish Paper and Timber, 33: 115. 1951.

A 27°C. ISOTHERMAL CALORIMETER[1]

By Paul A. Giguère, B. G. Morissette,[2] and A. W. Olmos[3]

ABSTRACT

The need for a Bunsen-type isothermal calorimeter operating as close as possible to the standard thermochemical reference temperature, 25°C., was fulfilled by means of diphenyl ether (m.p. 26.9°C.) as the working substance. The instrument was calibrated electrically by comparison with the ice calorimeter and the constant was found to be 19.01±0.02 cal. per gm. of mercury. From this and other known properties of diphenyl ether the density of the solid at the melting point was estimated at 1.188 gm. per ml. Check determinations based on the heat of vaporization of water showed that for such measurements the mantle of solid ether must first be melted inside by an amount equivalent to the heat to be measured. The calorimeter was operated in a large water-thermostat kept constant to within 0.001°C. With highly purified diphenyl ether there was no noticeable temperature drift during the measurements. Quantities of heat up to 600 cal. could be measured with a reproducibility of the order of 0.2%. The new calorimeter is simpler to operate than the ice calorimeter and its sensitivity is more than three times as great.

INTRODUCTION

As part of a research program on hydrogen and deuterium peroxides (9) it was required to measure some thermochemical properties of these compounds such as the heats of vaporization, heats of solution, and heats of decomposition. Preliminary measurements of these quantities made in this laboratory with the ice calorimeter were reported a few years ago (5). Although generally satisfactory for this kind of work the ice calorimeter suffers from certain drawbacks such as low sensitivity and tedious operation. Furthermore, it is necessary to correct the results to 25°C., the standard temperature for thermochemical data. To minimize the uncertainty of such corrections it would be desirable to work as near as possible to that temperature. A number of Bunsen-type calorimeters operating with various organic compounds have been described in the literature. Coffin (1, 2) has reviewed the question and discussed the requirements for a suitable working substance. Diphenyl methane, m.p. 24.5°C. (11), and diphenyl ether, m.p. 26.9°C. (8, 10), have been used in the past for that purpose. On the basis of availability and stability towards oxidation the second was selected as more promising, a choice vindicated by recent investigations at the National Bureau of Standards (6).

In fact three or four distillations of a commercial product, followed by an equal number of crystallizations, were sufficient to obtain the ether in such a degree of purity that no "premelting" could be detected during the measurements. Another convenient feature of the diphenyl ether calorimeter is that it operates so near the average temperature of the laboratory that all thermal leaks are reduced to a minimum and a simple water-thermostat provides an

[1]*Manuscript received December 13, 1954.*
Contribution from the Department of Chemistry, Laval University, Quebec, Que., with financial assistance from the National Research Council.
[2]*Holder of a National Research Council Bursary, 1951–52.*
[3]*Holder of a Scholarship under the Bureau of Scientific Research of the Province of Quebec, 1952–54.*

entirely satisfactory surrounding. After more than three years of trouble-free operation we are convinced that this simple isothermal calorimeter is ideally suited for the measurement of heat effects accompanying physical or chemical changes at ordinary temperature.

EXPERIMENTAL

Two slightly different calorimeters were built in the course of this investigation. The most successful one will be described here together with suggestions for future improvements.

Construction of the Calorimeter

The calorimeter itself was made entirely of Pyrex glass although the use of a metal tube with appropriate seal for the central well, as suggested by some authors, would no doubt improve the heat transfer to the mantle. The dimensions shown in Fig. 1 are considered optimum; they are by no means

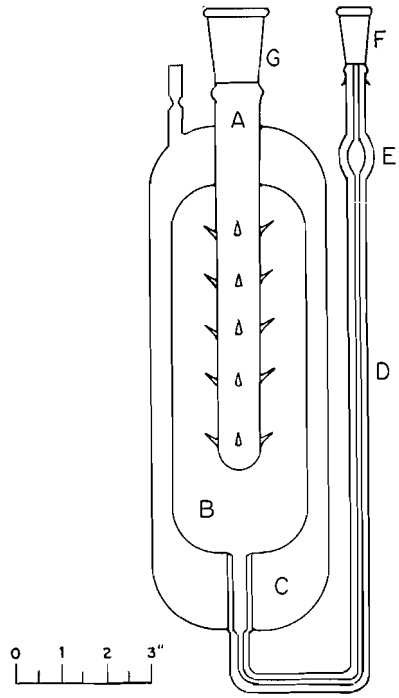

FIG. 1. Optimum dimensions for a diphenyl ether isothermal calorimeter of some 600 cal. capacity.

critical except, possibly, for the glass studs outside the central tube A which are needed to keep the mantle of frozen ether from slipping down. If made too short, they will not allow measurement of large enough amounts of heat; if too long, there is the danger of puncturing the mantle, with resulting heat loss, because the thermal conductivity of glass is appreciably higher than that of diphenyl ether. From the experience gained, 15 to 20 glass studs $\frac{3}{8}$ in. long would be adequate for a calorimeter of the size shown here.

The tube connecting the middle chamber B with the outside was first made S-shaped between the two jackets for greater elasticity. However, the inner seal soon broke merely on heating in an air-oven for drying. On the advice of a professional glass blower that section was replaced by a straight, thick-walled tube which, indeed, gave no trouble thereafter. The small bulb E, $\frac{1}{2}$ in. diameter blown on the capillary tube near the top, was found useful for trapping air bubbles before they reach the middle chamber. After cleaning thoroughly by the standard procedures the outside jacket C was evacuated down to 10^{-5} mm. Hg by means of a diffusion pump while the whole calorimeter was heated to about 100°C. in an oven. Just before sealing off the connecting tube a charcoal trap connected to the line was cooled in liquid air. In the first calorimeter the vacuum jacket had been silvered inside, except for a middle strip, but this was later found unnecessary. An outer shield of aluminum foil with opposite rectangular windows is sufficient to stop any radiant energy. It also affords a clearer view of the inside of the calorimeter, which is of great convenience, and it can be removed to speed up melting of the mantle when necessary.

Purification of the Diphenyl Ether

The starting product, Eastman's C.P., was first crystallized twice and then distilled four or five times under reduced pressure, 1.5 mm. Hg at about 102°C. Each time generous head- and tail-fractions were discarded until finally the distillation temperature remained constant to ±0.5°C. for the whole 800 ml. batch. To fill the calorimeter some 50 ml. of twice-distilled mercury were first introduced into chamber B. Then the calorimeter was mounted in an inverted, inclined position and the capillary tube was connected through the standard joint F to an "adapter tube" similar to those used in vacuum distillation apparatus. The lower end of that tube, reaching near the bottom of a 2-liter flask containing the pure ether, was bent so that it connected both the middle chamber of the calorimeter and the space above the ether to a vacuum pump and a cold trap. First the ether was rid of all dissolved gases by three successive freezings and meltings under reduced pressure. The solubility of air in diphenyl ether is so great that on the first freezing *in vacuo* the liquid seemed to boil violently. After three such operations no more dissolved gas was liberated. Then the bent tube was rotated by 180° about the ground joint and air was admitted above the liquid ether forcing it up into the calorimeter. A small residual bubble of vapor was expelled by blowing steam into the central well and then turning up the calorimeter while still heating it with steam until the mercury had filled the capillary tube up to the ground joint F.

Operation of the Calorimeter

The device for measuring the mercury was of the type developed for the ice calorimeter at the National Bureau of Standards (7). However, a steel needle-valve was not available so that an ordinary glass stopcock had to be used. This was somewhat unsatisfactory because only very little grease could be used on it and frequent cleaning was necessary. The calibrated capillary tube also required repeated cleaning as it was so fine (0.6 mm. diameter) that

mercury tended to stick in it. This part of the measuring device served only occasionally to obtain information on the thermal leak. Weighing of the displaced mercury in tiny beakers was done to the nearest 0.1 mgm. A mantle of solid ether was formed slowly by immersing a cold rod in the central well half-full of mineral oil for better heat transfer. In general one mantle could serve for two or three determinations. Before making a new mantle the old one was always melted completely. An infrared lamp was found very useful for this purpose. Apparently the manner of forming a mantle was of no great importance. Either ordinary ice or dry ice could be used, with rates varying from 20 min. to one hour. Usually it took five hours for a new mantle to come to equilibrium with the liquid ether.

The water-bath surrounding the calorimeter was a large aquarium made of plate-glass. Adequate temperature control was secured by means of a continuously adjustable "Magna-Set" mercury regulator and an electronic relay actuating a 500-watt immersion heater. A Cenco centrifugal stirrer provided efficient agitation. An auxiliary heater, hand-controlled through a Variac, was added for cold periods whereas a circulation of tap water was occasionally needed for operation in the summer. With such an arrangement the temperature could be kept constant indefinitely to within 0.03°C. but this was not quite sufficient. For a better temperature control and a more regular heat leak the principle of "internal insulation" suggested by Tian (12) was resorted to. The calorimeter proper was enclosed in a square box of Plexiglass which, effectively, provided an insulation of three inches of water between the calorimeter and the surrounding thermostat. As a result temperature fluctuations inside the box became smaller than 0.001°C. and the thermal leak of the calorimeter remained constant for a whole day instead of changing from hour to hour. What is important, indeed, is not so much the absolute value of this leak as its constancy, as has been pointed out by other investigators. As a matter of fact it was found preferable throughout this investigation to work with a steady, measurable thermal leak rather than with a vanishingly small one.

The temperature of the water-bath that gave the smallest leak (less than 0.2 cal. per hr.) was 26.90°C., as measured with a Leeds and Northrup certified platinum-resistance thermometer. In order to minimize fluctuations in the melting temperature of the diphenyl ether and, consequently, variations in the heat leak, the level of mercury in the measuring device was kept as constant as possible throughout a run. Another minor source of error stemmed from the small electric bulb used to light the calorimeter from behind. This energy amounted to only 0.3 cal. per hr. and could easily be accounted for.

Calibration of the Calorimeter

Usually such calibrations are carried out by absolute electric measurements. Since an ice calorimeter was available and since the factor of this instrument is known with great accuracy (7) it was decided to use it as reference for calibrating the diphenyl ether calorimeter. Two resistances R_1 and R_2 of about the same value were immersed in the central well of each calorimeter and connected in series. On passing an electric current in the circuit the amount

of heat dissipated in each calorimeter is obviously proportional to the values of R_1 and R_2. Therefore the electric energy need not be measured exactly; even the exact values of R_1 and R_2 are not required. Indeed, if a second series of experiments is made with the resistances interchanged then the calibration factors f of the two calorimeters are related thus,

$$f_e\sqrt{W_e \cdot W_e'} = f_i\sqrt{W_i \cdot W_i'},$$

where W and W' are the weights of mercury displaced in each set of determinations in each calorimeter.

The two resistances were made of 10-ohm windings of No. 34 Advance wire wound on thin glass tubes and connected to leads of No. 26 copper wire. In order to reduce the heat leak, particularly in the ice calorimeter, the leads were connected directly to "thermal shunts" made of sections of insulated brass foil immersed in the surrounding ice-bath. In spite of this precaution the leak of the ice calorimeter was nearly three times greater than normal which, in fact, represented the major uncertainty in these measurements. From the results collected in Table I and the factor for the ice calorimeter,

TABLE I

CALIBRATION OF THE DIPHENYL ETHER CALORIMETER BY COMPARISON WITH THE ICE CALORIMETER

Run. No.	Thermal leak (cal./hr.)				Approximate energy supplied (cal.)	W_e/W_i
	Ice calorimeter		Ether calorimeter			
	Initial	Final	Initial	Final		
First series						
1	1.27		1.43		430	3.0850
2	1.15	1.06	1.60	1.55	430	3.0890
3	1.41	1.48	2.39	2.45	280	3.0897
4	1.48		2.01		430	3.0881
5	1.13		0.35		200	3.0917
					Average	3.0887
Second series						
6	1.32	1.45	0.29	0.19	230	3.7434
7	1.34		0.24		150	3.7444
8	2.21		0.06		280	3.7431
9	2.05	1.99	0.44	0.31	380	3.7403
10	1.67		0.07		380	3.7422
11	2.22	1.76	0.38	0.13	400	3.7427
12	2.37	1.33	0.28	0.43	330	3.7450
13	2.08	1.37	1.37	1.70	380	3.7409
14	1.70	2.10	0.08	0.13	250	3.7405
15	1.84	3.51	0.28	0.19	320	3.7428
					Average	3.7425

$f_i = 64.640 \pm 0.007$ cal. per gm. of mercury (7), one finds for f_e 19.01 cal. per gm. of mercury with a standard deviation of 0.02 unit. Thus the diphenyl ether calorimeter has a sensitivity 3.4 times that of the Bunsen ice calorimeter. Holmberg (8) had obtained a slightly higher factor, 20.49, and Sachse (10),

a much greater one, 27.20 cal. per gm. of mercury, but the ether used by the latter must have been impure as shown by the melting point, 26.55°C. From the equation

$$f_e = L/\Delta v \,.\, d_m,$$

where L is the heat of fusion of the ether, 24.176 cal./gm. (6), and d_m is the density of mercury, we get 0.08574 for Δv, the change of specific volume of the ether on melting. The density of the liquid is 1.06611 at 30°C. and 1.06117 at 35° (4). Extrapolation to the melting point gives 1.0692 and from the above value of Δv the density of the solid at that temperature is calculated to be 1.188 while the coefficient dt/dp for the melting curve is 0.025° per atm. On the other hand, the triple point of diphenyl ether is known accurately: 26.87±0.01°C. from the measurements at the National Bureau of Standards. Therefore the melting point is 26.89_5°C. Adding to this the pressure effect of the mercury column above the mantle of solid ether (30 cm.) we arrive at the exact value 26.90° observed for the temperature of minimum leak, which confirms the high purity of the ether in the calorimeter. Dodd and Hu Pak Mi (3) found 26.85°C. by direct measurement and a slightly higher value, 26.95°C., from the break in the curve of viscosity vs. temperature.

A first series of calibrations of the new calorimeter based on the heat of vaporization of water had given a somewhat greater factor, 19.10 cal. per gm. of mercury. Since previous investigators have recommended that isothermal calorimeters be calibrated in the same way they are to be used, the cause of this discrepancy was investigated in order to apply it to measurements of the heat of vaporization of hydrogen and deuterium peroxides. For these check measurements a weighed 0.5 gm. sample of distilled, deaerated water in a thin glass tube was immersed in the calorimeter well and connected through a standard joint with a vacuum pump and a cold trap. The calibration factors thus obtained seemed to depend on the rate of evaporation of the water. As a high value of the factor indicates a loss of heat, it was suspected that the vapor left the calorimeter at a temperature lower than 26.9°C. No such difficulty had been encountered in similar measurements with the ice calorimeter so the explanation was thought to rest with the lower thermal conductivity of diphenyl ether. (No data are available on this compound in particular but organic liquids and solids generally have thermal conductivity about ten times smaller than that of ice.) To check this point a few determinations were carried out after first premelting the mantle of solid ether by an amount at least equal to the heat effect to be measured. The results in Table II seem to bear out the above contention, specially the first run where no premelting led to an abnormally high factor, and the second one, where only partial premelting gave an intermediate value. Still, the factors obtained by that method were always appreciably higher than by the more reliable electrical method, an indication that premelting does not provide exact compensation. At any rate the average value of f_e from these determinations, 19.04±0.04 cal. per gm. of mercury, was used only in measurements of heats of vaporization.

TABLE II

CALIBRATION OF DIPHENYL ETHER CALORIMETER BASED ON THE HEAT OF VAPORIZATION OF WATER

Run No.	Heat absorbed, cal.	Premelting, cal.	Thermal leak		Calibration factor, f_e
			Initial, cal./hr.	Final, cal./hr.	
20	345	Nil	0.213	0.217	19.17
21	135	90	0.308	0.308	19.08
22	223	250	0.275	0.216	19.07
23	283	320	0.217	0.192	19.07
24	312	320	1.18	0.776	18.99
25	264	400	0.125	0.038	19.08
26	246	380	1.15	0.845	19.04
27	321	330	0.61	0.55	19.03

CONCLUSION

The diphenyl ether isothermal calorimeter has proved to be a reliable and useful research instrument for measuring thermal phenomena at room temperature. It has the advantage of great simplicity of construction and operation. For over three years it has remained constantly in working condition with very little attention. Operation near room temperature reduces to a minimum, not only the thermal leaks, but also the correction of results to the accepted temperature for thermochemical data. The use of a water-thermostat means considerable simplification over the ice calorimeter. Diphenyl ether is currently available and easily purified; once in the calorimeter it seems indefinitely stable.

The aim of this investigation was to determine some calorimetric properties of hydrogen and deuterium peroxides (to be published in a following paper). Lack of time and equipment did not allow an exhaustive study of the possibilities of the diphenyl ether calorimeter. This is particularly true of the calibration, which should be repeated by an absolute electrical method to take full advantage of the greater sensitivity of the instrument.

RÉSUMÉ

On a mis au point un calorimètre isotherme du type de Bunsen fonctionnant avec l'oxyde de phényle dont le point de fusion est 26.9°C. Le facteur de calibration, 19.01 ± 0.02 cal./g. de mercure, a été déterminé électriquement par comparaison avec le calorimètre à glace. Le nouveau calorimètre est très simple de construction et de manipulation; il est contenu dans un thermostat à eau. Avec le modèle décrit on a pu mesurer jusqu'à 600 cal. avec une précision de l'ordre de 0.2%. Les fuites et corrections sont réduites au minimum parce que la température de fonctionnement est assez voisine de celle du laboratoire.

REFERENCES

1. CAULE, E. J. and COFFIN, C. C. Can. J. Research, B, 28: 639. 1950.
2. COFFIN, C. C., DEVINS, J. C., DINGLE, J. R., GREENBLATT, J. H., INGRAHAM, I. R., and SCHRAGE, S. Can. J. Research, B, 28: 579. 1950.
3. DODD, C. and HU PAK MI. Proc. Phys. Soc. (London), B, 62: 454. 1949.

4. DREISBACH, R. R. and MARTIN, R. A. Ind. Eng. Chem. 41: 2877. 1949.
5. FOLEY, W. T. and GIGUÈRE, P. A. Can. J. Chem. 29: 895. 1951.
6. FURUKAWA, G. T., GINNINGS, D. C., MCCOSKEY, R. E., and NELSON, R. A. J. Research Natl. Bur. Standards, 46: 195. 1951.
7. GINNINGS, D. C. and CORRUCCINI, R. J. J. Research Natl. Bur. Standards, 38: 583. 1947.
8. HOLMBERG, T. Soc. Sci. Fennica Commentationes, Phys.-Math. 9 (No. 17): 8 pp. 1938. *In* Chem. Abstr. 32: 6107. 1938.
9. PHIBBS, M. K. and GIGUÈRE, P. A. Can. J. Chem. 29: 173. 1951.
10. SACHSE, H. Z. physik. Chem. A, 143: 94. 1929.
11. SREERANGACHAR, H. B. and SREENIVASAYA, M. Biochem. J. (London), 29: 294. 1935.
12. TIAN, A. J. chim. phys. 20: 132. 1922.

REACTIONS BETWEEN SOLID CALCIUM CARBONATE AND ORTHOPHOSPHATE SOLUTIONS[1]

By J. S. Clark and R. C. Turner

ABSTRACT

Studies of the reactions between solid calcium carbonate and orthophosphate solutions at low partial pressures of carbon dioxide indicated that hydroxyapatite was the stable product formed in these systems. Hydroxyapatite precipitated directly even though dicalcium phosphate formed initially under certain conditions. The reactions with orthophosphate did not seriously disturb the normal calcium carbonate equilibrium with the solution.

INTRODUCTION

Owing to the importance of calcium carbonate in phosphate fixation (the conversion of soluble phosphates to less soluble forms) in calcareous soils, considerable attention has been given to reactions between phosphate in solution and solid calcium carbonate. Boischot *et al.* (2) and Cole *et al.* (4) showed that, at relatively low concentrations, phosphate was adsorbed on the surface of the calcium carbonate crystals. At higher concentrations there was apparently chemical precipitation of a calcium phosphate. Cole and his co-workers presented evidence that dicalcium phosphate was precipitated and they implied that this compound was an intermediate in the formation of hydroxyapatite ($Ca_{10}(PO_4)_6(OH)_2$).

The object of the work reported here was (*a*) to show the effect of the surface reaction between phosphate and calcium carbonate on the equilibrium between the solution and solid calcium carbonate, and (*b*) to obtain more information on the kind of reaction which takes place.

EXPERIMENTAL

Equilibration and rate studies of the reactions between solid calcium carbonate and solutions of phosphates at various initial concentrations were made at two partial pressures of carbon dioxide. The partial pressures of carbon dioxide in the systems were obtained by constantly bubbling through the suspensions either air piped in from just outside the laboratory window or a commercial mixture of 5% CO_2 and 95% N_2. The versene method (1) was used for the determination of calcium concentrations except in the rate studies where the flame photometer was found to be more convenient. The molybdenum blue method (5) was used for phosphorus and the glass electrode for pH. The activities of the ions were estimated by means of the Debye Huckel equation (7).

RESULTS

The results of the equilibration experiments are plotted as points in Fig. 1 in which the solubility lines are calculated from published data (6, 8). The

[1]*Manuscript received September 2, 1954.*
Contribution No. 264, Chemistry Division, Science Service, Department of Agriculture, Ottawa, Canada.

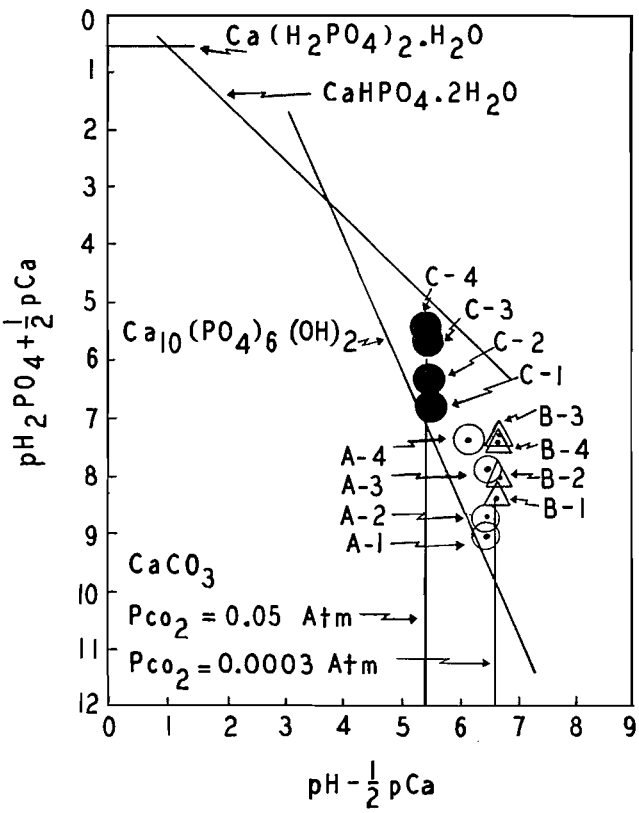

FIG. 1. Solubility diagram.
Legend:
P_{CO_2} = 0.0003 atm. Series A and B, 0.05 atm. Series C.
Initial phosphate concentrations:

A—1 10^{-6} M KH_2PO_4	B—1 5×10^{-6} M H_3PO_4	C—1 10^{-5} M H_3PO_4
A—2 5×10^{-6} M KH_2PO_4	B—2 10^{-5} M H_3PO_4	C—2 2×10^{-5} M H_3PO_4
A—3 10^{-5} M KH_2PO_4	B—3 5×10^{-5} M H_3PO_4	C—3 10^{-4} M H_3PO_4
A—4 10^{-4} M KH_2PO_4	B—4 10^{-4} M H_3PO_4	C—4 2×10^{-4} M H_3PO_4

solubility diagram is discussed fully elsewhere (3); however, a brief explanation of the diagram is included in the appendix.

After the 5% CO_2 and 95% N_2 mixture was bubbled through the suspensions for two weeks, the values of $pH - \frac{1}{2}pCa$, regardless of the initial concentration of phosphate, were reasonably close to the line in the diagram for calcium carbonate at P_{CO_2} (partial pressure of carbon dioxide) equal to 0.05 atmosphere. When air was bubbled through the suspensions for two to five weeks, the average value of $pH - \frac{1}{2}pCa$ was 6.5 compared with a calculated value of 6.6 for P_{CO_2} = 0.0003 atmosphere which is the average partial pressure of CO_2 in the air. There was more variation within a series when air was bubbled through the suspensions but this is probably the result of variations in the carbon dioxide content of the air. As the solubility product of $CaCO_3$ was generally satisfied, it seems unlikely that contamination from the atmosphere, e.g. NH_3 or SO_2, was serious.

The experimental data plotted on Fig. 1 show that although the solutions were virtually at equilibrium with solid calcium carbonate, they were not at equilibrium with a calcium phosphate compound. The fact that the experimental points are above the hydroxyapatite line indicates that equilibrium was reached slowly in these systems; therefore experiments were made to study the progress of the reactions towards equilibrium.

In Table I are presented results of experiments in which samples were removed at intervals while the carbon dioxide – nitrogen mixture was bubbled

TABLE I

EFFECT OF TIME ON REACTION AT P_{CO_2} APPROXIMATELY 0.05 ATMOSPHERE

Reaction time, min.	pH	$pH-\frac{1}{2}pCa$	$pH_2PO_4+\frac{1}{2}pCa$	Total P, moles/l. $\times 10^3$	$a_{Ca^{++}}$. $a_{HPO_4}=\times 10^{7*}$
(*a*) Initial solution approximately 2.5×10^{-2} *M* H_3PO_4					
20	5.56	4.42	2.86	22.50	22.90
100	5.90	4.55	3.55	7.30	6.31
225	6.61	5.21	4.44	1.40	3.71
460	6.70	5.31	4.60	0.97	3.24
1440	6.69	5.32	4.63	0.89	3.09
1860	6.79	5.32	4.63	0.89	3.09
(*b*) Initial solution approximately 2.2×10^{-3} *M* H_3PO_4					
20	6.60	5.26	4.18	2.13	7.59
390	6.66	5.32	4.25	1.85	7.42
1440	6.56	5.20	4.47	1.10	3.39
1860	6.56	5.28	4.71	0.68	2.34
2820	6.59	5.21	5.10	0.28	0.83
3120	6.70	5.32	5.12	0.28	1.00
(*c*) Initial solution approximately 1.7×10^{-3} *M* KH_2PO_4					
65	6.73	5.38	4.33	1.64	7.08
240	6.64	5.20	4.56	1.11	2.75
1860	6.70	5.36	4.72	0.66	2.75
4440	6.76	5.37	4.95	0.44	1.66
11280	6.86	5.47	5.17	0.31	1.26
(*d*) Initial solution approximately 2.4×10^{-4} *M* H_3PO_4					
70	6.76	5.41	5.21	0.23	1.00
260	6.82	5.46	5.21	0.23	1.12
500	6.84	5.31	5.21	0.23	0.80
1440	6.76	5.42	5.29	0.18	0.85
6240	6.84	5.50	5.48	0.13	0.66

**a designates the ion activity. Solubility product of dicalcium phosphate is 2.19 × 10⁻⁷.*

through phosphated suspensions of calcium carbonate. In each experiment 20 gm. of $CaCO_3$ was mixed with slightly less than 1 liter of water for 24 hr. by bubbling the gas through the suspensions. A sufficient volume of relatively concentrated phosphate solution was added to give the desired initial concentration and the solution was made up to 1 liter with water. Samples were taken at frequent intervals but only sufficient data to show the progress of the reactions are included in Table I.

It is seen from the second column of Table I that the solution was close to equilibrium with calcium carbonate within 20 min. except at the highest initial concentration of phosphate. With the highest concentration of phosphate, 2.5×10^{-2} *M* H_3PO_4, the values of $pH-\frac{1}{2}pCa$ did not approach that

required for P_{CO_2} equal to 0.05 atmosphere until after about four hours. There was a rapid initial precipitation of phosphate in this system. During the process of rapid precipitation the solution was supersaturated with respect to dicalcium phosphate. This can be seen by plotting the values of $pH_2PO_4 + \frac{1}{2}pCa$ and $pH - \frac{1}{2}pCa$ on the solubility diagram of Fig. 1 or more conveniently by comparing the values of $a_{Ca^{++}}.a_{HPO_4^=}$ in the last column of Table I with the solubility product of dicalcium phosphate. After the rapid precipitation, the phosphate concentration gradually reached a constant value for the remainder of the experiment and the solution was apparently at virtual equilibrium with dicalcium phosphate. With the intermediate initial concentrations of phosphate, 2.2×10^{-3} *M* H_3PO_4 and 1.7×10^{-3} *M* KH_2PO_4, the early rapid decrease in phosphate concentration was followed by a slower prolonged precipitation. Again the rapid precipitation occurred while the solution was supersaturated with respect to dicalcium phosphate, but the solution was definitely not supersaturated with respect to this solid during the slower precipitation. With the lowest initial concentration of phosphate, 2.4×10^{-4} *M* H_3PO_4, the solution was never supersaturated with respect to dicalcium phosphate and there was only a slow rate of decrease of the phosphate concentration during the whole experiment.

In Table II are reported data for experiments in which air was bubbled through the suspensions. For these experiments calcium carbonate was added directly to solutions of the various phosphates. When the phosphate solution

TABLE II

EFFECT OF TIME ON REACTION AT P_{CO_2} APPROXIMATELY 0.0003 ATMOSPHERE

Reaction time, min.	pH	$pH - \frac{1}{2}pCa$	$pH_2PO_4 + \frac{1}{2}pCa$	Total *P*, moles/l. $\times 10^3$	$a_{Ca^{++}}.a_{HPO_4^=} \times 10^{7*}$
(*a*) Initial solution approximately 1.56×10^{-3} *M* H_3PO_4					
20	7.40	5.95	4.79	1.50	9.13
65	7.56	6.02	5.10	1.10	5.25
100	7.80	6.33	6.19	0.17	0.87
360	8.00	6.38	6.57	0.10	0.41
4320	8.08	6.45	7.19	0.03	0.12
(*b*) Initial solution approximately 1.02×10^{-3} *M* KH_2PO_4					
50	7.80	6.16	5.57	0.72	2.46
120	8.04	6.30	6.13	0.33	0.93
300	8.15	6.47	6.67	0.12	0.40
4560	8.23	6.51	7.02	0.068	0.20
7200	8.25	6.53	7.11	0.058	0.17
(*c*) Initial solution approximately 1.01×10^{-3} *M* K_2HPO_4					
5	8.37	6.66	6.03	0.90	2.69
80	7.97	6.29	5.62	0.93	2.95
150	8.00	6.36	5.64	0.85	3.31
470	8.30	6.50	6.64	0.20	0.46
1380	8.30	6.47	6.81	0.16	0.29
(*d*) Initial solution approximately 0.5×10^{-3} *M* K_2HPO_4					
5	8.85	6.50	6.91	0.47	0.25
90	8.30	6.49	6.20	0.48	1.23
360	8.12	6.40	6.08	0.47	1.32
2880	8.31	6.52	7.08	0.081	0.17
7200	8.42	6.61	7.44	0.048	0.09

**a designates the activity of the ion. Solubility product of dicalcium phosphate is 2.19×10^{-7}.*

was either H_3PO_4 or KH_2PO_4, about two hours were required for the solution to approach equilibrium with solid calcium carbonate. With K_2HPO_4 solutions, the values of $pH-\frac{1}{2}pCa$ were always reasonably close to the equilibrium value. The values of $pH-\frac{1}{2}pCa$, however, decreased gradually during the early part of these experiments but this was followed by a slow increase. The behavior of the systems in which the initial phosphate concentrations were 1.56×10^{-3} M H_3PO_4 and 1.02×10^{-3} M KH_2PO_4 was similar to that of the intermediate concentrations reported in Table I; the values of $a_{Ca^{++}}.a_{HPO_4^=}$, however, decreased more rapidly at P_{CO_2} equal to 0.0003 atmosphere. When the initial phosphate concentration was 1.01×10^{-3} M K_2HPO_4 there was apparently no reaction for the first two hours even though the solution was supersaturated with respect to dicalcium phosphate. After two hours there was a rapid decrease in the phosphate concentration followed by a slower reaction. With the lowest phosphate concentration, 0.5×10^{-3} M K_2HPO_4, the value of $a_{Ca^{++}}.a_{HPO_4^=}$ never exceeded that for dicalcium phosphate and there was only a slow precipitation, which began after about six hours.

The rate of decrease of the phosphate concentration in the rate experiments reported in Tables I and II was extremely slow after the first rapid reaction. A long reaction period would be required for the solutions to reach equilibrium with hydroxyapatite. There are two possible reasons for this apparently slow reaction: one, that the solution was approaching equilibrium with some calcium phosphate other than hydroxyapatite; two, that it was simply a rate process, the rate being highly dependent on the phosphate concentration. The results in Fig. 2 suggest that the latter possibility is more probably correct

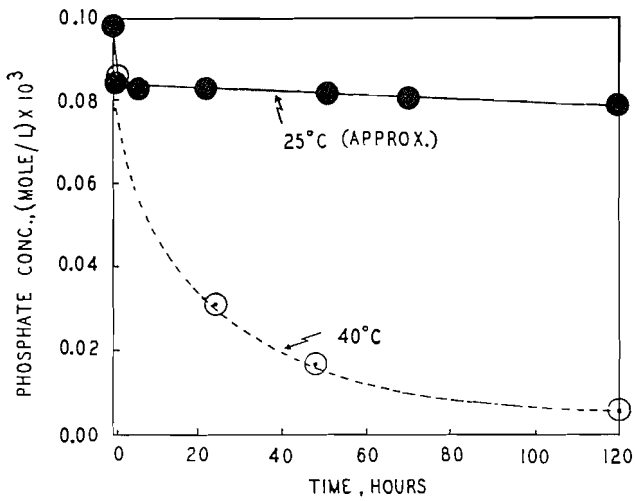

FIG. 2. Effect of temperature on rate of reaction at P_{CO_2} approximately 0.0003 atmosphere.

because the rate of decrease of the phosphate concentration was faster at 40°C. than at room temperature (about 25°C.) when the initial phosphate concentration was 0.098×10^{-3} M K_2HPO_4. The rate of decrease of the phosphate concentration at 40°C. was very slow after five days and, even

though the phosphate concentration was about one-tenth that of the lowest concentration obtained at room temperature, the solution was still supersaturated with respect to hydroxyapatite. In an experiment at 80°C., however, the solution was close to equilibrium with hydroxyapatite within 24 hr.

DISCUSSION

Regardless of the mechanism of the reaction between solid calcium carbonate and dilute solutions of phosphate, the calcium carbonate exerts its normal effect on the solution equilibrium.

It is seen from the diagram of Fig. 1 that, under the conditions prevailing in these experiments, dicalcium phosphate is not thermodynamically stable. As it is generally agreed that tricalcium phosphate does not exist in nature, the thermodynamically stable form is probably hydroxyapatite. If the solution is supersaturated with respect to dicalcium phosphate, however, this compound precipitates because hydroxyapatite forms at a much slower rate. This conclusion is based on the results reported under (*a*) in Table I which shows that about 21×10^{-3} mole of phosphorus was precipitated in less than eight hours, yet the solution was apparently supersaturated with respect to dicalcium phosphate after 31 hr. When the initial concentrations of phosphate were intermediate, (*b*) and (*c*) in Tables I and II, dicalcium phosphate was apparently precipitated in small quantities. The small quantities remained only for a short time, the length of time apparently depending on the quantity present and the rate of precipitation of hydroxyapatite. Judging by the results under (*d*) of Tables I and II, there seems little doubt that hydroxyapatite precipitated directly without the necessity of having to form dicalcium phosphate as an intermediate.

It was mentioned above that the values of the product $a_{Ca^{++}}.a_{HPO_4^{=}}$ decreased more rapidly when air was bubbled through the suspensions than when the 5% carbon dioxide mixture was used, indicating a more rapid approach to equilibrium in the former case. A possible explanation of this is that the rate of precipitation of hydroxyapatite is dependent on the concentration of $PO_4^{\equiv}$ ions which would be lower in the more acid suspensions through which the CO_2–N_2 mixture was passed. This observation along with the resulting increase in the rate of phosphate precipitation with increasing temperature indicates the advisability of making a thorough study of the kinetics of precipitation of hydroxyapatite.

APPENDIX

The solubility diagram of Fig. 1 is based on the fact that the equilibrium formation of a number of solid calcium orthophosphates in aqueous systems may be expressed by the equation

$$m\mathrm{Ca(OH)_2} + n\mathrm{Ca(H_2PO_4)_2} = \text{solid} + y\mathrm{H_2O} \qquad [1]$$

where m and n represent the number of moles of $Ca(OH)_2$ and $Ca(H_2PO_4)_2$, respectively, forming 1 mole of solid and y moles of H_2O. In relatively dilute solutions, $Ca(OH)_2$ and $Ca(H_2PO_4)_2$ may be assumed to be completely dis-

sociated. It follows, therefore, that

$$-m(\mathrm{pH}-\tfrac{1}{2}\mathrm{pCa})+n(\mathrm{pH_2PO_4}+\tfrac{1}{2}\mathrm{pCa}) = k \qquad [2]$$

where "p" represents the negative logarithm of the ion activity, k is a constant, and the activity of OH^- ions is expressed in terms of the ionic product of water, K_W, and the H^+ ion activity. With $(\mathrm{pH}-\frac{1}{2}\mathrm{pCa})$ and $(\mathrm{pH_2PO_4}+\frac{1}{2}\mathrm{pCa})$ as the two co-ordinates, equation 2 represents a straight line with slope m/n.

The constant k in equation 2 can be evaluated from the solubility product of the solid, the second and third dissociation constants of phosphoric acid, K_2 and K_3, and the ionic product of water. For hydroxyapatite, monocalcium phosphate, and dicalcium phosphate equation 2 becomes, respectively, equations 3, 4, and 5 below,

$$-7(\mathrm{pH}-\tfrac{1}{2}\mathrm{pCa})+3(\mathrm{pH_2PO_4}+\tfrac{1}{2}\mathrm{pCa}) = \tfrac{1}{2}(\mathrm{p}K_{sp}{}^{I}-6\mathrm{p}K_2K_3-2\mathrm{p}K_W) \qquad [3]$$

$$(\mathrm{pH_2PO_4}+\tfrac{1}{2}\mathrm{pCa}) = \tfrac{1}{2}\mathrm{p}K_{sp}{}^{II} \qquad [4]$$

$$-\tfrac{1}{2}(\mathrm{pH}-\tfrac{1}{2}\mathrm{pCa})+\tfrac{1}{2}(\mathrm{pH_2PO_4}+\tfrac{1}{2}\mathrm{pCa}) = \tfrac{1}{2}(\mathrm{p}K_{sp}{}^{III}-\mathrm{p}K_2) \qquad [5]$$

where $K_{sp}{}^{I}$, $K_{sp}{}^{II}$, and $K_{sp}{}^{III}$ are the solubility products of the appropriate solid phases. The solubility lines in Fig. 1 were drawn from equations 3, 4, and 5 using published values (8) for the right-hand side of the equation. In the figure, the co-ordinates are arranged so that the chemical potential of $Ca(H_2PO_4)_2$ increases upwards and that of $Ca(OH)_2$ to the right. If the solution is in equilibrium with a given solid phase, the solubility points must lie along the solubility line for that compound. A solubility point to the right or above a solubility line indicates supersaturation or the existence of a metastable solid phase.

If the solution is at equilibrium with solid calcium carbonate, it can be shown that

$$-(\mathrm{pH}-\tfrac{1}{2}\mathrm{pCa}) = \tfrac{1}{2}(\mathrm{p}K_{sp}{}^{IV}-\mathrm{p}K_1{}^{I}K_2{}^{I}-\mathrm{pC}-\mathrm{p}P_{CO_2})$$

where $K_{sp}{}^{IV}$ is the solubility product of $CaCO_3$, $K_1{}^{I}$ and $K_2{}^{I}$ are the first and second dissociation constants of carbonic acid, P_{CO_2} is the partial pressure of CO_2 in the system, and C is the total molal concentration of CO_2 in solution when P_{CO_2} is unity.

REFERENCES

1. Bersworth Chemical Co. The versenes. Tech. Bull. No. 2. 6th ed. Bersworth Chemical Co., Framingham, Mass. 1953.
2. Boischot, P., Coppenet, M., and Hebert, J. Plant and Soil, 2: 311. 1950.
3. Clark, J. S. and Peech, M. Solubility criteria for the existence of calcium and aluminum phosphates in soils. Soil. Sci. Soc. Amer. Proc. In press.
4. Cole, C. V., Olsen, S. R., and Scott, C. O. Soil Sci. Soc. Amer. Proc. 17: 352. 1953.
5. Dickman, S. R. and Bray, R. H. Ind. Eng. Chem. Anal. Ed. 12: 665. 1940.
6. Frear, G. L. and Johnston, J. J. Am. Chem. Soc. 51: 2082. 1929.
7. Glasstone, S. Introduction to electrochemistry. D. Van Nostrand Company, Inc., New York. 1942.
8. Tennessee Valley Authority. Phosphorus, properties of the element and some of its compounds. Chem. Eng. Rept. No. 8. 1950.

THE TERTIARYBUTYLBENZENES

I. ALKYLATION OF 1,4-DI-*t*-BUTYLBENZENE WITH *t*-BUTYL CHLORIDE[1]

By L. Ross C. Barclay and Eileen E. Betts[2]

ABSTRACT

The alkylation of *p*-di-*t*-butylbenzene with excess *t*-butyl chloride in the presence of aluminum chloride in the cold produces a new aromatic hydrocarbon, m.p. 218.5–219°. Evidence is given for the presence of an alicyclic nucleus in this hydrocarbon which analyzes for $C_{22}H_{34}$. The preparation of nitro and amino derivatives from this hydrocarbon is described. The alkylation of benzene under similar conditions yielded some 1,3,5-tri-*t*-butylbenzene, and an improved method of preparation of this hydrocarbon from *p*-di-*t*-butylbenzene is given.

INTRODUCTION

For some time we have been interested in synthesizing 1,3,5-tri-*t*-butylbenzene and in preparing derivatives of this compound required in a study of the influence of the bulky *t*-butyl group on functional group reactions. Recently Bartlett (1) showed that the reaction of *t*-butyl chloride and aluminum chloride with *p*-di-*t*-butylbenzene yields *m*-di-*t*-butylbenzene, 1,3,5-tri-*t*-butylbenzene, and a hydrocarbon of melting point 209–210°. This excellent communication prompted us to publish some of the work conducted in our laboratory on *t*-butylbenzenes.

We found that not only *p*-di-*t*-butylbenzene but also benzene is converted to a mixture of 1,3,5-tri-*t*-butylbenzene and a hydrocarbon of melting point 218–219°, when treated with excess *t*-butyl chloride and aluminum chloride. Bartlett's preparation of 1,3,5-tri-*t*-butylbenzene could not be repeated but an improved method is given in the experimental section (Run II). In these alkylations, 1,3,5-tri-*t*-butylbenzene is formed rapidly, but under the influence of excess aluminum chloride and prolonged reaction time it is converted to the higher melting hydrocarbon. Some interesting properties of this hydrocarbon are reported.

A New High Melting Hydrocarbon and Some Derivatives

A high melting (218.5–219°) aromatic hydrocarbon which analyzed for $C_{22}H_{34}$ was isolated by adding aluminum chloride in portions to a cold (below −5°) solution of *p*-di-*t*-butylbenzene in excess *t*-butyl chloride. This compound was nitrated and the nitro compound reduced to an amine. Attempts to convert the amine into a phenol whose properties could be compared with those of the known 2,4,6-tri-*t*-butylphenol (12) produced a pale yellow compound possessing an ultraviolet absorption intensity much higher than that of phenols. The properties of these derivatives indicate that they are highly hindered. For example, the nitro compound does not show the large increase in absorption in the near ultraviolet characteristic of nitro derivatives of

[1]*Manuscript received November 17, 1954.*
Contribution from the Department of Chemistry, Mount Allison University, Sackville, New Brunswick.
[2]*Recipient of a National Research Council Bursary.*

benzene and in this respect is similar to the sterically hindered nitro compounds studied by Brown and Reagan (4). In addition, the amine derivative does not dissolve in concentrated acid.

Certain general conclusions can be made concerning the structure of the high melting hydrocarbon from the ultimate and spectral analyses. The higher carbon values (or lower hydrogen values) of this compound compared to those of the butylbenzenes suggest a second ring fused onto the benzene ring in the alkylation. This might also explain the high melting point. The infrared spectrum (Fig. 1) shows the presence of *t*-butyl groups. The most characteristic feature is the strong band at 891 cm.$^{-1}$ and the absence of any strong band below this. In this respect it resembles the spectrum of pentamethylbenzene, which may indicate that the hydrocarbon contains a penta-substituted ring. The ultraviolet absorption of this hydrocarbon is very interesting in that it shows similarities to that of certain alicyclics, for example indan. The latter shows characteristic bands at 273.6, 267, and 260 mμ compared to 278, 271, and an inflection at 262 mμ for this hydrocarbon. In addition the very weak band for indan at 291 suggested by Morton and de Gouveia (9) as being due to impurities is present in this compound at 298 mμ.

It should be noted that tetralin also has similar absorption with bands at 274 and 267 and an inflection at 261 mμ but the weak band near 290 mμ is not reported (9). It is possible that this weak band may be of use in identifying the indan nucleus in the high melting hydrocarbon.

Early Research on the Poly-t-butylbenzenes

In 1890 Senkowski (10) reported tri-*t*-butylbenzene, m.p. 128°, along with *p*-di-*t*-butylbenzene, m.p. 70°, and a liquid hydrocarbon from the alkylation of benzene with isobutyl chloride. Smith (11) obtained some of Senkowski's hydrocarbon, m.p. 128°, by the rearrangement of isobutylphenyl ether in benzene solution with aluminum chloride.

In a study of various complexes formed by the Friedel-Crafts reaction, Gustavson (5) found that the action of *t*-butyl chloride and benzene on aluminum chloride at −10° led to the formation of a yellow crystalline compound, aluminum chloride ditributylbenzene hydrochloride, $Al_2Cl_5[C_6H_3-[(CH_3)_3C]_3]HCl$, which was also formed by the reaction of *p*-di-*t*-butylbenzene and powdered aluminum chloride with *t*-butyl chloride.

Ipatieff (6) and co-workers reported mono-, di-, and tri-*t*-butylbenzene (a liquid) from the reaction of isobutylene with a mixture of sulphuric acid and benzene. Koch and Steinbrink (7) alkylated benzene by the method described by Ipatieff and co-workers and obtained *p*-di-*t*-butylbenzene but were unable to prepare a tri-substituted product by this method. Legge (8) attempted to prepare tri-*t*-butylbenzene by the reaction of isobutylene with aluminum chloride or sulphuric acid on benzene but obtained instead a considerable number of unexpected alkylbenzenes and suggested an electronic explanation for the results obtained.

Bartlett and co-workers (1) found small quantities of Senkowski's hydrocarbon (m.p. 129.5–130°) in some residues from the preparation of *p*-di-*t*-

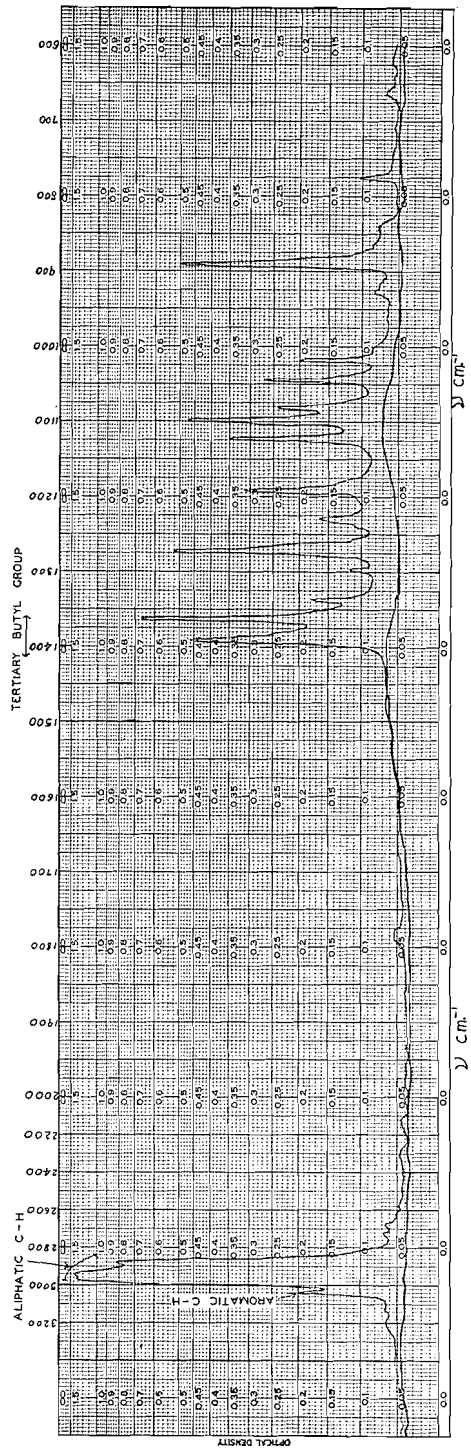

FIG. 1. Infrared spectrum of the high melting (218.5–219°) hydrocarbon in carbon disulphide.

butylbenzene by the Standard Oil Company of Indiana. However, these workers did not establish the structure of this hydrocarbon. It seems unlikely that the structure given to this compound by Smith (11), that is 1,2,4-tri-*t*-butylbenzene, is correct because of the improbability that two *t*-butyl groups can occupy adjacent positions in the benzene ring. Brown and co-workers (3) investigated homomorphs of *o*-di-*t*-butylbenzene and support this view.

EXPERIMENTAL

The melting points recorded were obtained with a Fisher-Johns type apparatus and are uncorrected. Ultraviolet spectra were measured on a Beckmann DU spectrophotometer with cyclohexane, free from aromatics, as solvent.

Alkylation of Benzene and Isolation of 1,3,5-Tri-t-butylbenzene

A solution of pure benzene (36 ml., 0.41 mole) in *t*-butyl chloride (189 ml., 1.7 moles) was cooled to −5° and 59 gm. of aluminum chloride added in small portions over a period of two hours. Aliquots removed after one and three-quarter hours and after all the aluminum chloride was added yielded colorless crystalline material mixed with some liquid on decomposition in ice. On crystallization from ethanol, these aliquots yielded a total of 14 gm. of crystalline material (m.p. 60–65°) consisting of a mixture of *p*-di-*t*-butylbenzene and 1,3,5-tri-*t*-butylbenzene. Careful crystallization from ethanol yielded some of the tri-substituted product, m.p. 73°, which did not depress the melting point of an authentic sample. The remainder of the reaction was decomposed in ice water after a total of six hours' reaction. The hydrocarbon layer was extracted with ether and the ether removed on the steam cone. The viscous residue was placed in a refrigerator overnight and some crystalline material (3 gm.) formed. Crystallization from benzene–ethanol yielded colorless crystals which consisted mainly of the high melting hydrocarbon and which melted at 195–200°.

Alkylation of p-Di-t-butylbenzene

Run I—Preparation of the High Melting Hydrocarbons

p-Di-*t*-butylbenzene (47 gm., 0.25 mole) was dissolved in 300 ml. of *t*-butyl chloride and the solution cooled to −5°, causing much of the hydrocarbon to precipitate. Powdered aluminum chloride (66 gm., 0.5 mole) was added in small portions over a two-hour period to this mixture with vigorous stirring. After about five minutes the hydrocarbon redissolved and there was copious evolution of hydrogen chloride. At the end of six hours' reaction in the cold, the evolution of hydrogen chloride subsided and two layers appeared—a yellow liquid layer on top and a thick dark amorphous mass at the bottom of the flask. The reaction mixture was decomposed in crushed ice and the hydrocarbon layer distilled with steam until oily droplets ceased coming over into the distillate. The solid residue was separated from adhering polymeric liquid products on the suction pump by washing with ethanol to yield 20 gm. of colorless crystalline material, m.p. 205–210°. In later runs it was found more convenient to extract the decomposed reaction product directly with ether and proceed with the isolation by concentration of the ether until the hydro-

carbon crystallized. Repeated crystallizations from 1:1 benzene–ethanol yielded colorless needles, m.p. 218.5–219°.

Anal. Found: C, 88.51, 88.63; H, 11.54, 11.45.
C, 88.45, 88.41; H, 11.28, 11.34.
C, 88.47, 88.58; H, 11.35, 11.31.
Molecular weight, 311.6, 309.5, 309.3.
Calc. for $C_{22}H_{34}$: C, 88.51; H, 11.49. Molecular weight 298.5.

Run II—Improved Synthesis of 1,3,5-Tri-t-butylbenzene

Seventy-five grams of *p*-di-*t*-butylbenzene was dissolved in 350 ml. of *t*-butyl chloride and the solution cooled to −3°, causing much of the hydrocarbon to precipitate. Seven grams of aluminum chloride was added during the first half hour to the stirred mixture, the temperature being maintained below 0°. Twenty grams of aluminum chloride was then added in 10 min. causing the semisolid reaction mixture to become liquid and the temperature to lower to −7°. After an additional 10 min., the reaction mixture was carefully decomposed in cold water. The organic layer was extracted with ether, which was removed with excess *t*-butyl chloride on the steam cone. The residue solidified on cooling with an ice–salt mixture to yield 70 gm. (75% yield) of colorless solid. After five recrystallizations from ethanol, this material melted at 74.8–75°. The ultraviolet absorption spectrum (Fig. 2) of this product was practically identical to that of authentic 1,3,5-tri-*t*-butylbenzene prepared in small yield in this laboratory by the condensation of pinacolone.

Anal. Found: Molecular weight 247.7, 245.5, 248.8.
Calc. for tri-butylbenzene 246.4.

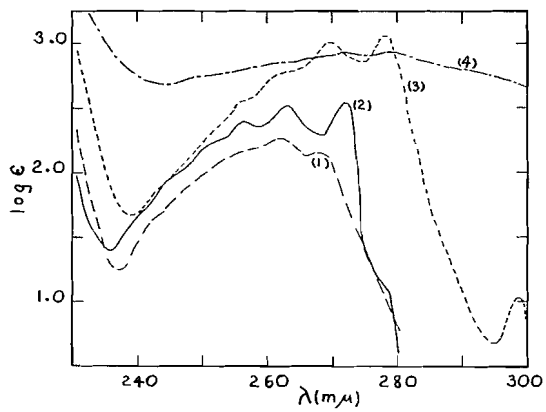

FIG. 2. Ultraviolet spectra.
(1) 1,3,5-Tri-*t*-butylbenzene (m.p. 74.8–75°).
(2) *p*-Di-*t*-butylbenzene (78.5–79°).
(3) The high melting hydrocarbon (m.p. 218.5–219°).
(4) Nitro derivative of the high melting hydrocarbon (m.p. 266.5–267°).

Run III—Intermediates in the Preparation of the High Melting Hydrocarbon

Essentially the same procedure with the same amounts of reagents as in Run II was used except that additional aluminum chloride (7.5 gm.) was added and the reaction was continued for six hours. Aliquots of the reaction

mixture were removed when the mixture became fluid (after 30 min.) and after 45 min. These were decomposed in water and recrystallized from ethanol. The first aliquot contained a mixture of *p*-di-*t*-butylbenzene and 1,3,5-tri-*t*-butylbenzene. The second aliquot (after 45 min.) contained 1,3,5-tri-*t*-butylbenzene, which after one crystallization melted at 73°. At the end of six hours, the remaining reaction mixture was decomposed, extracted with ether, and the excess *t*-butyl chloride removed with the ether on the steam cone. On standing, the liquid residue deposited some crystalline material which yielded 6 gm. of colorless crystals after crystallization from benzene–ethanol, m.p. 211–212°.

Nitration of the High Melting Hydrocarbon

The hydrocarbon (12.6 gm., m.p. 216–218°) was dissolved in a mixture of glacial acetic acid (580 ml.) and acetic anhydride (345 ml.) at 65°. Fuming nitric acid (5 ml., sp. gr. 1.5) was added drop by drop and the reaction mixture was heated at 90° for three hours. On cooling, the product crystallized as pale yellow crystals, 7.3 gm., m.p. 261–262°. Repeated crystallization from benzene–ethanol changed the melting point to 266.5–267°.

Anal. Found: C, 77.75, 77.52; H, 9.57, 9.49; N, 4.04.
Molecular weight, 335.9, 333.9, 334.5.
Calc. for $C_{22}H_{33}NO_2$: C, 76.91; H, 9.68; N, 4.08.
Molecular weight, 343.5.

Preparation and Attempted Hydrolysis of an Amino Derivative

A solution of 5 ml. of concentrated hydrochloric acid in 5 ml. of ethanol was added to a mixture of 0.5 gm. of the nitro derivative with 1 gm. of granulated tin. This mixture was heated on the steam cone under reflux and enough ethanol, saturated with dry hydrogen chloride, was added to give a clear solution. This solution was refluxed for five hours and then allowed to stand for a day. At the end of this time, no crystallization had taken place so that the product was worked up in the usual way by precipitation in water, addition of alkali to dissolve the tin, and extraction with ether. On evaporation of the ether colorless crystals formed, m.p. 247–248°. Crystallization from benzene–ethanol yielded colorless crystals, m.p. 249.2–249.7°.

Anal. Found: C, 85.00, 85.09; H, 11.27, 11.11; N, 4.01.
Calc. for $C_{22}H_{35}N$: C, 84.28; H, 11.26; N, 4.47.

This amine appeared to be almost completely insoluble in concentrated hydrochloric acid but the ultraviolet spectrum, with general absorption maxima at 292($E^{1\%}$ 71.3), 248($E^{1\%}$ 205), and 214 mμ ($E^{1\%}$ 1460), is typical of aromatic amines.

Two grams of this amine was dissolved in 180 ml. of a 1: 5 sulphuric acid – acetic acid solution. The solution was cooled in an ice bath and a solution of 22 gm. of sodium nitrite in 90 ml. of water was added. The reaction mixture was then warmed on the steam cone until evolution of nitrogen ceased, cooled, and extracted with ether. After washing with 10% sodium bicarbonate solution, the excess ether was removed and pale orange crystals formed, m.p. 208–209°. Unsuccessful attempts were made to remove the color from this

product by chromatography on alumina and crystallization with charcoal. The ultraviolet absorption, λ_{max} 265 mμ, $E^{1\%}$ 377, of this compound is much more intense than expected for a phenol and a more detailed study is required before a structure can be suggested for this product.

The Action of Oxidizing Agents on the High Melting Hydrocarbon

Tertiary-butyl groups are known to oxidize with difficulty; for example, Boedtker (2) obtained mainly di-*t*-butylquinone on attempted oxidative degradation of *p*-di-*t*-butylbenzene. Using increased pressure and temperature, Legge (8) succeeded in obtaining terephthalic acid by nitric acid oxidation of *p*-di-*t*-butylbenzene.

Attempts to oxidize the high melting hydrocarbon to a known benzenecarboxylic acid have not been successful. Oxidation with nitric acid in pressure tubes at elevated temperatures yielded acidic material but yields were very small and nitration accompanied oxidation. The use of such oxidizing agents as chromic acid or potassium permanganate in solvents such as acetone, acetic acid, or pyridine has not produced any identifiable benzenecarboxylic acid. It was found, however, that *p*-di-*t*-butylbenzene could be oxidized to terephthalic acid in small yield by heating a powdered mixture of the hydrocarbon with an oxidizing agent such as potassium permanganate in a nitrogen atmosphere at 220°. This procedure has yielded some polycarboxylic acid from the high melting hydrocarbon and, although the degradation was not complete in this case, seems the most promising approach.

ACKNOWLEDGMENTS

This work was conducted with the aid of a grant from the National Research Council of Canada, Ottawa, and in addition one of us (E.E.B.) gratefully acknowledges financial assistance provided by a National Research Council Bursary.

The authors wish to thank Dr. L. Marion for having ultimate analyses done for us at the National Research Council Laboratories. We also thank Dr. R. N. Jones and Mr. R. Lauzon for measuring and interpreting the infrared spectrum.

We are indebted to Dr. R. A. Friedel of the United States Bureau of Mines, Pittsburgh, for his assistance in the interpretation of the ultraviolet spectra and to Dr. S. H. Langer of the same laboratory for measuring the molecular weights.

REFERENCES

1. Bartlett, P. D., Roha, M., and Stiles, R. M. J. Am. Chem. Soc. 76: 2349. 1954.
2. Boedtker, E. Bull. soc. chim. [3] 31: 969. 1904.
3. Brown, H. C. and Nelson, K. L. J. Am. Chem. Soc. 75: 24. 1953.
4. Brown, W. G. and Reagan, H. J. Am. Chem. Soc. 69: 1032. 1947.
5. Gustavson, G. J. prakt. Chem. [ii] 72: 57. 1905.
6. Ipatieff, V. N., Corson, B., and Pines, H. J. Am. Chem. Soc. 58: 919 and 1056. 1936.
7. Koch, H. and Steinbrink, H. Brennstoff-Chem. 19: 277. 1938.
8. Legge, D. I. J. Am. Chem. Soc. 69: 2079. 1947.
9. Morton, R. H. and de Gouveia, A. J. A. J. Chem. Soc. 911. 1934.
10. Senkowski, M. Ber. 23: 2412. 1890.
11. Smith, R. A. J. Am. Chem. Soc. 55: 3718. 1933.
12. Stillson, G. H., Sawyer, D. W., and Hunt, C. K. J. Am. Chem. Soc. 67: 303. 1945.

THE SYNTHESIS OF C^{14}-CARBOXYL-LABELLED ω-THIOETHYL FATTY ACIDS[1]

By Anne E. Almond, Anna Mary Burditt, D. E. Douglas,[2] and Jean Eccles

ABSTRACT

Syntheses on a semimicro scale of thioethyl acetic, ω-thioethyl propionic, and ω-thioethyl butyric acids labelled with carbon-14 in the carboxyl group are described. The compounds were chromatographed on filter paper with butanol–water–ammonia as the developing solvent, and the R_F values determined.

In the course of an investigation, at this Institute, of ω-thioalkyl fatty acids as metabolic inhibitors in isolated tissues, carbon-14-carboxyl-labelled thioethyl acetic, ω-thioethyl propionic, and ω-thioethyl butyric acids were required. Experimental details for the synthesis of these labelled molecules on a semimicro scale are described in this communication.

Although ω-thioalkyl acetic acids have been prepared by alkylation of sodium thioglycollate with the appropriate alkyl halide (6) and these and other ω-thioalkyl fatty acids from the sodium salt of a thiol and a ω-halo fatty acid (3, 7) this latter method was only employed for the preparation of thioethyl acetic acid-1-C^{14}.

A more convenient synthetic method for higher homologues involves cyanidation of an ethyl ω-haloethyl sulphide followed by hydrolysis of the resulting nitrile to the acid. This method is not satisfactory when ethyl chloromethyl sulphide is a reactant, owing to the instability of this molecule (2). Ethyl γ-bromopropyl sulphide forms a Grignard reagent, which may be carbonated to yield ω-thioethyl butyric acid. Ethyl β-chloroethyl sulphide, however, failed to form a Grignard reagent.

A method for the paper chromatography of the acids described has been worked out, to assess the radiopurity of the labelled compounds.*

EXPERIMENTAL

Thioethyl Acetic Acid-1-C^{14}

Acetic acid was liberated from 4.8 mM. of sodium acetate-1-C^{14} (199,700 counts total activity) with hydrogen chloride gas according to a previously described high-vacuum procedure (4), and condensed into a reaction flask fitted with a micro dropping funnel and cold-finger condenser. The acetic acid was brominated in the presence of acetyl chloride (0.1 ml.), red phosphorus (20 mgm.), and a crystal of iodine with bromine (0.5 ml.). The latter was added dropwise, while the mixture was heated under reflux (4).

[1]*Manuscript received January 4, 1955.*
Contribution from the Division of Atomic Chemistry, Montreal General Hospital Research Institute, Montreal, P.Q.
[2]*In charge, Division of Atomic Chemistry.*
**Recently, a communication (J. Am. Chem. Soc. 76: 3860. 1954) from another laboratory has appeared regarding the antituberculosis activity of some ethylmercapto compounds, including several thioalkyl-fatty acids. No details are given regarding synthetic methods, and presumably carbon-14-labelled compounds were not employed in this investigation.*

After two hours the reaction mixture was hydrolyzed with 2 to 3 ml. of water, and the unreacted bromine removed in a stream of nitrogen. The last traces of bromine were removed with 1 *N* sodium bisulphite. The resulting solution was neutralized to pH 8 with dilute sodium hydroxide, and evaporated *in vacuo*. The residue was dissolved in the minimum amount of water, and 0.62 *M* sodium ethanethiolate (10 ml.) in ethanol was added. The mixture was shaken several times and allowed to stand for 24 hr. and then heated under reflux for three hours, and finally concentrated to dryness *in vacuo*.

The residue was dissolved in water and the aqueous solution extracted continuously with ether for four to five hours. The aqueous layer was acidified to pH 2 with dilute sulphuric acid and extracted continuously overnight with ether. The ethereal solution was dried over sodium sulphate, and evaporated in a stream of nitrogen. The oily residue was distilled from a Späth bulb (bath temperature 100°C.) on the high-vacuum system yielding 0.1555 gm. (21%) of a colorless oil. Specific activity 200 counts per min. per mgm. with 50% counter geometry. $\eta_D^{22°} = 1.4800$.

ω-Thioethyl Propionic Acid-1-C^{14}

Barium carbonate-C^{14} (1 mc. per mM.) was converted to sodium cyanide-C^{14} by Adamson's method (1). To 0.4 mM. of this radiocyanide were added 5 mM. (0.245 gm.) of carrier sodium cyanide, 8 ml. of 80% ethanol, and 5.4 mM. (0.65 ml.) of ethyl β-chloroethyl sulphide. The mixture was heated under reflux for four hours and the solvent was removed *in vacuo*. The remaining oil was hydrolyzed with a solution of 6 *N* hydrochloric acid (5 ml.) and glacial acetic acid (2.5 ml.) in a sealed tube at 100° for 12 hr. The acetic and hydrochloric acids were removed *in vacuo*, and the product dissolved in a few milliliters of water, and extracted exhaustively with chloroform. The chloroform solution was shaken several times with an excess of dilute sodium hydroxide, then with water. The combined alkaline extracts and washings were acidified to pH 2 and extracted four times with chloroform. The combined chloroform solutions were dried over sodium sulphate and filtered. The filtrate was concentrated and the remaining oil was distilled under high vacuum from a Späth bulb. Yield 0.2612 gm. (36%, based on ethyl β-chloroethyl sulphide). Colorless oil. Activity yield: 15.9% from barium carbonate-C^{14}. Specific activity 87,400 c.p.m./mgm. with 50% counter geometry. Calc. for $C_5H_{10}O_2S$: C, 44.76; S, 23.90. Found: C, 44.5; S, 23.8. $\eta_D^{21.5} = 1.4805$.

ω-Thioethyl Propionamide

A sample of non-radioactive ω-thioethyl propionic acid was treated with a slight excess of thionyl chloride, and the mixture heated at 80°C. for 10 min. to complete the reaction. Excess concentrated ammonium hydroxide was added carefully to the resulting acid chloride. The reaction mixture was evaporated to dryness *in vacuo*, and the amide dissolved in isopropyl ether, and recrystallized from the same solvent. Colorless plates, m.p. 64–65°C. Calc. for $C_5H_{11}NOS$: C, 45.08; N, 10.52; S, 24.07. Found: C, 44.3; N, 10.7; S, 24.5.

ω-Thioethyl Butyric Acid-1-C^{14}

(*a*) *Cyanidation of Ethyl γ-Chloropropyl Sulphide and Hydrolysis of the Nitrile*

A mixture of sodium cyanide (0.3 gm.), water (0.5 ml.), ethanol (5 ml.), and ethyl γ-chloropropyl sulphide (0.693 gm.) (5) was heated under reflux for six hours. The ethanol was evaporated *in vacuo*, the residue shaken with water to dissolve salts and then extracted with ether. The ethereal solution was dried with sodium sulphate and evaporated in a bomb tube under a stream of nitrogen. The oily residue was heated with a mixture of 1.5 ml. each of glacial acetic acid and concentrated hydrochloric acid for about three hours at 110°C. The acetic and hydrochloric acids were removed *in vacuo*, and the crude acid purified by the method described above for the preparation of ethyl thioacetic acid. After high-vacuum distillation, the product weighed 0.090 gm. Yield 12%, based on ethyl γ-chloropropyl sulphide. $\eta_D^{22°} = 1.4805$.

(*b*) *Carbonation of the Ethyl γ-Bromopropyl Sulphide Grignard Reagent*

Although ethyl γ-chloropropyl sulphide formed a Grignard reagent only in the presence of ethyl bromide added as promoter, the corresponding bromo-compound was active alone.

Ethyl γ-bromopropyl sulphide was prepared from ethyl γ-hydroxypropyl sulphide and phosphorus tribromide in carbon tetrachloride.

The Grignard reagent was prepared from ethyl γ-bromopropyl sulphide (2.2 gm.), magnesium (0.3 gm.), and dry ether (30 ml.). Carbonation was carried out according to the usual high-vacuum technique with carbon dioxide liberated from 0.9048 gm. (4.6 mM.) of barium carbonate-C^{14} (5.08×10^5 counts total activity) by means of concentrated sulphuric acid. The mixture was allowed to warm slowly to room temperature with occasional shaking after the carbonation at approximately −20°C. was assumed to be complete. The magnesio complex was carefully decomposed with excess of dilute sulphuric acid, and the ether layer was removed. The aqueous phase was extracted four times with ether and the combined ethereal solutions were washed with three portions of 0.5 *N* sodium hydroxide (total 15 ml.) then four times with water. The combined alkaline solution and washings were saturated with sodium sulphate, acidified to pH 2, and extracted with ether.

The ethereal solution was dried over sodium sulphate, and the ether removed leaving an oily residue. This residue was distilled in a Späth bulb under high vacuum at a bath temperature of 100° yielding 0.362 gm. of a colorless oil. Specific activity 570 c.p.m./mgm. Yield 53%, based on barium carbonate. Calc. for $C_6H_{12}O_2S$: C, 48.65; S, 21.60. Found: C, 48.7; S, 21.8. $\eta_D^{22.0°} = 1.4805$; mixed R.I. with the product prepared by the previous method $\eta_D^{22°} = 1.4805$. The identity of the compounds obtained by the two procedures was further established by chromatography on filter paper.

A crystalline amide could not be obtained from this compound with thionyl chloride and ammonia.

Paper Chromatography of the Thioethyl Fatty Acids

Approximately 0.1 mgm. quantities of the labelled acids in excess ammonium

hydroxide were chromatographed on Whatman No. 1 filter paper with butanol–water–ammonia by the ascending technique. Butanol (100 ml.) was shaken with water (25 ml.) and ammonium hydroxide (2 ml.) below room temperature, and the butanol layer separated. An open beaker containing concentrated ammonium hydroxide was placed under the battery jar containing the chromatogram. After approximately 15 hr., the chromatograms were removed and dried.

The paper was sprayed with 0.1% aqueous chloramine-T, dried, and sprayed immediately with starch – potassium iodide solution (0.1 gm. soluble starch and 0.1 gm. potassium iodide per 100 ml.). White spots on a blue background indicated the presence of the thio-acids. Radioautographs were obtained by placing the dried chromatograms before treatment with chloramine-T in contact with Eastman No-Screen X-ray film for approximately two weeks.

The following relative R_F values were observed for the regions of maximum concentration:

R_F $C_2H_5SCH_2COOH = 0.34$

$$\frac{R\ C_2H_5S(CH_2)_2COOH}{R\ C_2H_5SCH_2COOH} = 1.30$$

$$\frac{R\ C_2H_5S(CH_2)_3COOH}{R\ C_2H_5SCH_2COOH} = 1.55$$

A trace of radioactive contaminant with an R_F of 0.12 was present in the ω-thioethyl propionic and ω-thioethyl butyric acids.

ACKNOWLEDGMENT

The authors wish to thank Dr. Wm. Brown, formerly of this Institute, for samples of inactive thioethyl acetic and ω-thioethyl propionic acids.

REFERENCES

1. ADAMSON, A. W. J. Am. Chem. Soc. 69: 2564. 1947.
2. BÖHME, H. Ber. 69, B: 1612. 1936.
3. BROWN, W. Ph.D. Thesis, McGill University, Montreal, Que. September, 1954.
4. HUGHES, D. M., OSTWALD, R., and TOLBERT, B. M. U.S. Atomic Energy Comm. Document, URCL-704. 1950.
5. KRETOV, A. E. and TOROPOVA, E. M. J. Gen. Chem. (U.S.S.R.), 7: 2009. 1937. Chem. Abstr. 32: 518. 1938.
6. LARSSON, E. Ber. 63: 1347. 1930.
7. RAMBERG, L. Ber. 40: 2588. 1907.

OXIDE COMPLEXES FORMED IN THE SYSTEMS PLATINUM METALS : ALKALI CARBONATES : OXYGEN[1]

By J. J. Scheer, A. E. van Arkel, and R. D. Heyding[2]

ABSTRACT

On heating mixtures of a platinum metal with an alkali carbonate in different ratios and at different temperatures in an oxygen stream, two kinds of compounds are formed:

(1) the cubic compounds $Na_xPt_3O_4$ and $Na_xPd_3O_4$,

and

(2) a series of oxide complexes with compositions ABO_2 or A_2BO_3, both isomorphous with Na_2SnO_3.

Although all metals of the platinum group form oxides, anhydrous complexes of their oxides have not been described. The observation that at high temperatures platinum crucibles are readily attacked by lithium oxide in the presence of air (1) was the first indication that such complexes might be prepared. On investigating the reactions of lithium oxide – platinum black mixtures in oxygen at 1000°C., Bright reported the formation of a product with the approximate formula Li_2PtO_3 (3). Further study of the X-ray pattern has shown that this product was actually a mixture of two or more compounds.

We have found that lithium oxide and platinum react in oxygen even at 400°C. to form single compounds, and that the same products are obtained from lithium carbonate – platinum mixtures. Because of the ease with which carbonate–platinum mixtures could be handled in comparison to those of the oxide (2), all subsequent reactions were restricted to the carbonate. Like the oxide, the carbonate attacks most crucible materials, and it was necessary to use crucibles cut from fused polycrystalline blocks of magnesium oxide.

By replacing the platinum black in the reaction mixtures by other finely divided platinum metals, a number of lithium complexes with Pd, Rh, and Ir were prepared, and by the substitution of Na_2CO_3 for Li_2CO_3, analogous sodium complexes have been obtained.

EXPERIMENTAL

The platinum metals were used in the form of platinum black, prepared by the procedure described in Gmelin (5) (i.e., reduction with sodium formate); palladium black (5); rhodium and iridium sponge, both 99.95% pure, from British Drug Houses Ltd.

Analytically pure sodium carbonate and lithium carbonate (May and Baker) were preheated in oxygen at 400°C. for about five hours.

Portions of metal and carbonate were weighed into a magnesium oxide boat and mixed intimately. This mixture was heated under a slow stream of oxygen which had been dried over sulphuric acid, silica gel, sodium hydroxide, and,

[1]*Manuscript received December 28, 1954.*
Contribution from the Department of Physical and Inorganic Chemistry, University of Leiden, The Netherlands.
[2]*National Research Council Postdoctorate Overseas Fellow 1953–54. Present address: Division of Applied Chemistry, National Research Council, Ottawa, Canada.*

finally, phosphorous pentoxide. Heating was continued until no further change in weight could be observed.

Debye–Scherrer diagrams of the products were taken in a 9 cm. Unicam camera with Cu K_α radiation.

RESULTS AND DISCUSSION

In the systems Na–Pt–O and Na–Pd–O, the first compounds formed were the cubic phases $Na_xPt_3O_4$ and $Na_xPd_3O_4$ (a_0 = 5.67 Å and 5.64 Å, respectively), the first of which has been described by Waser and McClanahan (8). Experimental and calculated values of $\sin^2\theta$ and of line intensities for one of these structures are given in Table I.

TABLE I

DEBYE–SCHERRER DIAGRAM OF $Na_xPd_3O_4$ (CUBIC)
vs, very strong; s, strong; m, moderate; w, weak; vw, very weak

hkl	$\sin^2\theta$ (calc.)	$\sin^2\theta$ (obs.)	*I* (calc.)	*I* (obs.)
110	0.0371	0.0387	16.0	m–s
200	0.0742	0.0769	15.5	m–s
210	0.0928	0.0944	100.0	vs
211	0.111	0.113	31.9	s
220	0.149	0.151	0.3	w
300, 221	0.167	0.169	0.2	vw
310	0.186	0.188	7.6	m
222	0.223	0.225	35.5	s
320	0.241	0.244	39.1	s
321	0.260	0.262	25.3	s
400	0.297	0.299	27.0	s
411, 330	0.334	0.336	6.3	m
420	0.371	0.374	3.9	m
421	0.390	0.393	50.1	vs
510, 431	0.4826	0.4850	10.8	m
520, 432	0.5383	0.5407	67.0	vs
521	0.5568	0.5583	16.0	m
440	0.5939	0.5951	39.0	s
530, 433	0.6311	0.6327	7.8	m
600, 442	0.6682	0.6678	5.0	m
610	0.6867	0.6875	26.1	m–s
611, 532	0.7053	0.7054	28.2	m–s

On heating mixtures of the molecular proportions metal : carbonate ::1:1 for about 20 hr. at 600°–1000°C., the A_2BO_3 compounds Li_2RhO_3, Na_2IrO_3, Na_2PtO_3, and Li_2PtO_3 were obtained. These compounds are isomorphous with a series of complexes of quadrivalent elements, Li_2TiO_3, Na_2TiO_3, Na_2SnO_3, and Na_2PbO_3, investigated by Lang (6). Typical X-ray data are given in Table II.

It was not possible to prepare Na_2PdO_3 by this method, although quadrivalent palladium appears to exist in the phase Li_2PdO_3.

TABLE II
DEBYE–SCHERRER DIAGRAM OF Na_2PtO_3 (ORTHORHOMBIC)

hk l	$\sin^2\theta$ (calc.)	$\sin^2\theta$ (obs.)	*I* (calc.)	*I* (obs.)
00 6	0.0212	0.0209	58.3	s
02 0	0.0286	0.0283	3.5	w
0012	0.0850	0.0845	81.7	s
20 $\bar{2}$	0.0837			
20 4	0.0907	0.0922	56.8	s
20 $\bar{8}$	0.119	0.120	100.0	s
2010	0.140	0.141	38.3	m
0018	0.191	0.193	16.0	w
20$\bar{1}$4	0.197	0.197	15.1	w
2016	0.232	0.233	46.7	s
06 0	0.244	0.244	73.6	s
06 $\bar{6}$	0.2653	0.2663	65.9	s
20$\bar{2}$0	0.3173	0.3176	23.4	w–m
40 2	0.3277	0.3287	76.9	s
06$\bar{1}$2				
40 $\bar{4}$	0.3347	0.3341	9.6	w
0024	0.3398	0.3400	18.9	w
40 $\bar{8}$	0.3631	0.3624	25.5	m
20$\bar{2}$2	0.3669			
40$\bar{1}$0	0.3843	0.3845	6.7	w

The rhodium mixtures first formed the compounds $LiRhO_2$ and $NaRhO_2$, and it seems probable that the latter compound is also transformed into the A_2BO_3 compound Na_2RhO_3, but its crystal structure has not yet been established.

It has been found that both ABO_2 compounds are isomorphous with the A_2BO_3 compounds (Table III). The lattice of the compound $LiRhO_2$ consists of alternating layers of lithium and rhodium atoms separated by oxygen layers. From this structure the crystal of the A_2BO_3 type is formed by the

TABLE III
DEBYE–SCHERRER DIAGRAM OF $NaRhO_2$

hk l	$\sin^2\theta$ (calc.)	$\sin^2\theta$ (obs.)	*I* (calc.)	*I* (obs.)
00 6	0.0220	0.0232	34.1	s
20 $\bar{2}$	0.0854	0.0865	35.8	s
0012	0.0880	0.0896	27.6	m–s
20 4	0.0928	0.0947	49.6	s
20 $\bar{8}$	0.122	0.123	100.0	s
20$\bar{1}$0	0.144	0.145	29.1	m–s
20$\bar{1}$4	0.2028	0.204	21.7	m–s
0018	0.199			
2016	0.240	0.242	44.8	s
06 0	0.250	0.250	74.2	s
06 $\bar{6}$	0.2723	0.2728	29.5	m–s
20$\bar{2}$0	0.3275	0.3292	21.2	m
40 2	0.3344	0.3375	65.7	s
06$\bar{1}$2	0.3383			
0024	0.3520	0.3481	14.1	w
40 $\bar{8}$	0.3711	0.3705	15.1	m
20$\bar{2}$2	0.3788	0.3817	6.8	w–m
40$\bar{1}$0	0.3931	0.3924	5.5	w
0618	0.4483	0.4490	42.8	m–s
40$\bar{1}$4	0.4518			
40$\bar{1}$6	0.4885	0.4884	13.0	w–m
20$\bar{2}$6	0.4962	0.4978	13.7	w–m

substitution of one lithium and two quadrivalent rhodium ions for three trivalent rhodium ions in the lattice, leading to the formula $Li_{4/3}\,Rh_{2/3}\,O_2 = 2/3\,Li_2RhO_3$. A very similar substitution has been observed in fluorides of the $NaLaF_4$ type, which may be written as $Na_{3/2}\,La_{3/2}\,F_6$ or $(Na_{3/2}\,La_{1/2})LaF_6$, and are isomorphous with Na_2ThF_6 (9).

According to Lang (6), the structure of Na_2SnO_3 can be described by reference to a monoclinic cell, as well as to a larger orthorhombic cell, three times the volume of the former. In Table IV the parameters of both cells are given for the isomorphous ABO_2 and A_2BO_3 complexes; whether the symmetry is orthorhombic or pseudorhombic will be left undecided.

TABLE IV

LATTICE CONSTANTS OF THE ABO_2 AND A_2BO_3 COMPOUNDS EXPRESSED IN ANGSTROM UNITS
rh = orthorhomic; mo = monoclinic; $h\,k\,(3l+h)_{rh} = h\,k\,l_{mo}$

	Na_2SnO_3*	Na_2PtO_3	Na_2IrO_3	$NaRhO_2$	Li_2SnO_3*	Li_2PtO_3	Li_2RhO_3	$LiRhO_2$
a	5.50	5.39	5.39	5.34	5.29	5.17	5.12	5.23
b	9.53	9.34	9.33	9.22	9.19	8.96	8.87	9.07
c_{rh}	32.51	31.67	31.59	31.11	29.61	28.86	28.73	28.52
c_{mo}	10.99	10.71	10.68	10.32	10.03	9.77	9.73	9.66
c/a	5.93	5.88	5.86	5.83	5.59	5.58	5.61	5.45
β	99°6′	99°40′	99°41′	99°44′	100°1′	100°10′	100°6′	100°22′

*Cf. *Lang* (6).

The structure of these compounds is closely related to that of the hexagonal complexes of one of the iron metals, i.e. $LiNiO_2$ (high temperature modification) and $NaNiO_2$ (4), the difference lying in the relative positions of the metal layers. Both groups can be derived from a cubic close packed arrangement of oxygen ions, with the metal ions in the octahedral interstices. By a slightly different arrangement of the metal atoms the cubic structure of $LiFeO_2$ is obtained.

In all of these groups the metal ions are surrounded by six oxygen ions, and in this respect are completely different from the compounds of the $Na_xPt_3O_4$ type, in which all platinum atoms are in the center of square PtO_4 groups. There can be no doubt that the Pt—O bonds are due to dsp^2 hybridization, as in PtO (7); however there are two kinds of platinum ions in the lattice according to the formula $Na_xPt^{2+}_{1+x}Pt^{3+}_{2-x}O_4$. The range of the parameter x has not yet been determined.

We intend to continue this investigation by including the remaining metals of the iron and platinum groups as well as other alkali metals.

REFERENCES

1. VAN ARKEL, A. E., FLOOD, E. A., and BRIGHT, N. F. H. Can. J. Chem. 31: 1009. 1953.
2. VAN ARKEL, A. E., SPITSBERGEN, U., and HEYDING, R. D. Can. J. Chem. 33: 446. 1955.
3. BRIGHT, N. F. H. Interim Report on an Investigation into the Lithium Oxide: Platinum and Lithium Oxide: Rhodium Systems. Natl. Research Council Can., Ottawa. 15 pp. 1953.
4. DYER, L. D., BORIE, B. S., JR., and SMITH, G. P. J. Am. Chem. Soc. 76: 1499. 1954.
5. GMELIN, L. Handbuch der anorg. Chem. 68, A: 395. 1951.
6. LANG, G. Z. anorg. u. allgem. Chem. 276: 77. 1954.
7. MOORE, W. J. and PAULING, L. J. Am. Chem. Soc. 63: 1392. 1941.
8. WASER, J. and MCCLANAHAN, E. D. J. Chem. Phys. 19: 413. 1951; 20: 199. 1952.
9. ZACHARIASEN, W. H. J. Am. Chem. Soc. 70: 2147. 1948. Acta Cryst. 1: 265. 1948.

THE PURIFICATION OF SEDOHEPTULOSE[1]

By L. Ujejski[2] and E. R. Waygood[3]

ABSTRACT

Methods involving paper and cellulose column chromatography are described for the purification of sedoheptulose phosphate from the mother liquor obtained from *Sedum spectabile* by the procedure of LaForge and Hudson. The beginnings of crystallization with subrectangular arrangement of rod-like longulites of free sedoheptulose have been obtained by chromatographic separation in phenol from an equilibrium mixture of sedoheptulosan and sedoheptulose prepared by treating the former with 3 *N* hydrochloric acid at room temperature. A spraying reagent for carbohydrates containing ketose units is described.

The 7-carbon sugar sedoheptulose has been known since 1917 when it was isolated by LaForge and Hudson (7) from *Sedum spectabile* in the form of a syrup. Ettel (4) in 1932 established its configuration as D-altroheptulose. The free ketose has not yet been obtained in crystalline form, but Pratt *et al.* (9) in 1952 established the formula of the crystalline non-reducing anhydride, sedoheptulosan, as 2,7-anhydro-β-D-altroheptulopyranose.

The intermediate role of the sugar and its phosphorylated derivative in the metabolic processes of plants and animals has been recently investigated in many laboratories (5, 11). The subject matter of the present communication is, however, concerned solely with the purification of the free ketose and its phosphorylated derivative.

The previous assumption that sedoheptulosan and sedoheptulose may be determined by the same color reactions (10) has been proved correct and this also applies to sedoheptulose phosphate.

Sedoheptulose phosphate has been isolated from the 'mother liquor' obtained from leaves of *S. spectabile* by the method of LaForge and Hudson (7). The yellow-green dense liquid was chromatographed on filter paper and most of the yellow impurities remained at the starting line. Sedoheptulose phosphate was detected by orcinol reagent (1) and corresponding spots were eluted and determined spectrophotometrically by the cysteine–sulphuric and the carbazole – sulphuric acid reactions (3). The former reagent gave a transient yellow color which changed to orange after 48 hr., maximum density being at 510 mμ, characteristic of sedoheptulosan (10). Carbazole–sulphuric produced the expected red color, but the mixture did not show the constant ratio D490/D400 = 1.90 characteristic of the anhydride, indicating the presence of impurities. A second chromatographic separation, using 100 spots each containing 200 μgm. initially, produced a glassy yellow-product after elution and evaporation *in vacuo*. Larger amounts were purified on cellulose column

[1]*Manuscript received August 27, 1954.*
Contribution from the Department of Botany, McGill University, Montreal, Quebec. Grateful acknowledgment is made to the Charles F. Kettering Foundation, Yellow Springs, Ohio, which provided generous financial support.
[2]*Research Associate.*
[3]*Professor of Botany, University of Manitoba, Winnipeg, Manitoba, formerly Associate Professor of Botany, McGill University, Montreal, Quebec.*

and this procedure also produced a glassy product that, after drying, could be ground to a yellowish white powder, which became sticky on exposure to air. Determination of bound phosphate indicated that this substance was sedoheptulose monophosphate.

Free sedoheptulose was not isolated directly from the mother liquor; however this sugar was separated chromatographically from the equilibrium mixture produced by incubating sedoheptulosan with 3 N hydrochloric acid for 12 hr. at room temperature. Difficulties were encountered since no spraying reagent could be found for sedoheptulosan. Of numerous solvents tried, phenol was found to be preferable for the separation of sedoheptulose from the equilibrium mixture. Chromatographic development in this manner produced two spots with the orcinol reagent. Similar spots were obtained by developing a solution of the equilibrium mixture in ethanol – butanol – $N/20$ hydrochloric acid (110: 10: 20).

It is known that the behavior of phenol as a solvent (6) in paper chromatography differs from other organic solvents giving greater R_f values than could be expected from the water content. "The explanation probably lies in the fact that phenols can form compounds with sugars analogous to these formed by water, so that the distribution of a sugar between the aqueous phenolic solvent and water–cellulose complex will depend not only on the water present in each phase but also on the phenol." (6).

When sedoheptulose phosphate and sedoheptulosan were developed in phenol each gave one spot in different positions with the orcinol reagent, whereas the equilibrium mixture gave two spots in corresponding positions (Fig. 1). The explanation for this lies in the fact that performed sedoheptulose

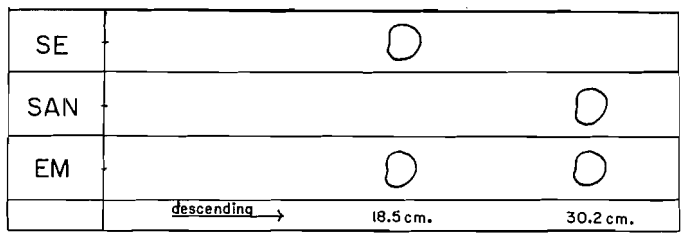

FIG. 1. Paper chromatogram showing the movement of sedoheptulose (SE), sedoheptulosan (SAN), and the equilibrium mixture (EM) in phenol.

in the equilibrium mixture moves slower in this solvent than sedoheptulosan, but the anhydride forms a new equilibrium mixture in its position on the paper in the presence of phenol. The newly formed free sugar is detected by the orcinol reagent but it does not separate from the anhydride during development. Therefore the two spots correspond to sedoheptulose and the newly formed equilibrium mixture of sedoheptulosan and sedoheptulose. This property of separation of sedoheptulose from the equilibrium mixture has served as a basis for its isolation in pure form.

Spots corresponding to free sedoheptulose were cut out, eluted with water, passed through Amberlite anion exchange resin, and evaporated to dryness *in vacuo*. A crystalline substance was obtained which was identified as sedo-

heptulose by its osazone. Complete crystallization of a large quantity of sedoheptulose was not obtained, but only the beginnings of crystallization of sedoheptulose (Fig. 2). The experiments indicated that in order to obtain larger amounts of the substance it would be advantageous to combine both cellulose column and ion exchange chromatography.

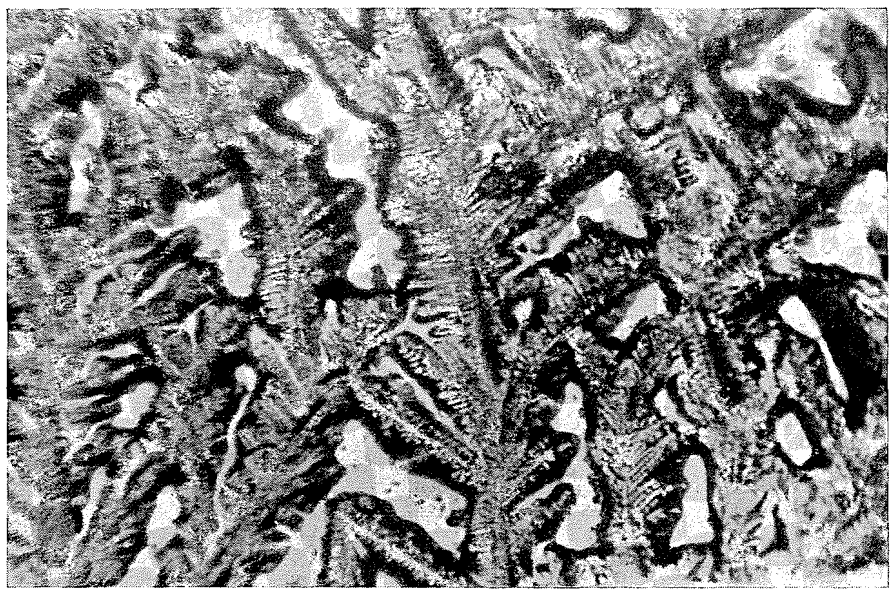

FIG. 2. The subrectangular arrangement of rod-like longulites of free sedoheptulose crystals.

Dische (2) prepared the equilibrium mixture by treating sedoheptulosan with 1% hydrochloric acid on a steam bath for 30 min. and obtained three different spots with the orcinol reagent on his chromatograms in phenol. Noggle (8) used 0.2 *N* hydrochloric acid on a steam bath for 30 min. and detected four spots under the same conditions. He suggested that the first two R_f 0.45 and 0.70 represented sedoheptulose and sedoheptulosan and the other two spots unknown carbohydrates.

It is possible that the heat treatment may produce other anhydrides of sedoheptulose (9). This is supported by Noggle's (8) use of Dowex 50 in the hydrogen form to prepare the equilibrium mixture in place of hot 0.2 *N* hydrochloric acid. Under these conditons he detected only sedoheptulose and sedoheptulosan in the equilibrium mixture. Our separations were concerned only with mixtures produced at room temperature.

In the course of studying various spraying reagents for sedoheptulosan, Dische's reagent (3) was modified and adapted for use on paper. Cysteine and carbazole dissolved in butanol and trichloracetic acid gave a brownish spot with sedoheptulose. This spray had a wide application and gave distinctly colored spots with reducing and non-reducing mono- and poly-saccharides containing ketose units. It was found also that phloroglucinol gave a bluish green spot with sedoheptulose.

EXPERIMENTAL

Purification of Sedoheptulose Phosphate by Chromatography

The purification of sedoheptulose syrup was accomplished either by paper or cellulose column chromatography.

In the former procedure, 20 mgm. of the syrup was dissolved in 1 ml. of water and aliquots of 10 μl. were placed on Whatman No. 1 filter paper and developed for 36 hr. in butanol–ethanol–water (10:1:2). The resulting spots, located by orcinol, were cut out and eluted with 400 ml. water. This solution was evaporated *in vacuo*, redissolved in 1 ml. water, and chromatographed again in butanol – acetic acid – water (4:1:2). Near to the end of the evaporation a yellow-white precipitate appeared which formed a glassy product when dry. Recovery was 80%. The filter papers were previously washed with 0.03 *N* hydrochloric acid, then with water to neutrality, and afterwards with 0.5 *N* sodium hydroxide followed by water to neutrality.

In the latter procedure, 20 ml. of a yellow solution of 1% sedoheptulose sirup in methanol was passed through a column (25 cm. $\times$ 1.5 cm.) of Whatman No. 1 cellulose. The yellow ring that remained on the column was eluted with water until the orcinol reaction became negative. The solution was evaporated *in vacuo* and a glassy yellow-white powder was obtained.The product was readily pulverized in a mortar but eventually became sticky during exposure to air.

In solution, free phosphate was formed after hydrolysis with *N* hydrochloric acid for three hours on a steam bath. The phosphate produced corresponded to a monophosphoric ester of sedoheptulose. Further purification of this material by paper chromatography did not alter its physical properties.

The first methyl alcoholic effluent was colorless and gave no orcinol reaction. After evaporation to dryness a small amount (1%) of amorphous white product was obtained. The substance was sparingly soluble in water, m.p. 138°C., and gave no reaction for sugars. The nature of this product is as yet unknown.

Separation of Crystalline Sedoheptulose from the Equilibrium Mixture

Crystalline sedoheptulosan was used as the starting material using descending paper chromatography with a 90% solution of freshly distilled phenol as the solvent. Sixty milligrams of sedoheptulosan were treated with 0.5 ml. of 3 *N* hydrochloric acid at room temperature for 12 hr., 3.5 ml. water were added; thus 1 ml. contained 15 mgm. of the equilibrium mixture (sedoheptulose and sedoheptulosan). Aliquots of 10 μl. of this solution were developed for 30 hr. on paper. The components of the equilibrium mixture were identified by running parallel spots of sedoheptulose phosphate and sedoheptulosan. Two spots were observed on the path of the equilibrium mixture, one corresponding to sedoheptulose and the other to sedoheptulosan. Apparently sedoheptulose phosphate and sedoheptulose move at the same rate. The identification of sedoheptulosan by the orcinol spray is due to the formation of a new equilibrium mixture in this spot.

Elutions of spots from 3 ml. of a solution containing 45 mgm. of the equilibrium mixture in hydrochloric acid were combined and passed through

Amberlite IR4B(OH) and evaporated *in vacuo*. Fig. 2 shows the beginnings of crystallization and the subrectangular arrangement of rod-like longulites of free sedoheptulose obtained by this separation. Seven milligrams of the free ketose was obtained corresponding to approximately 20% of sedoheptulose in the equilibrium mixture assuming 80% recovery.

Aliquots of 10 μl. of sedoheptulose phosphate as well as the equilibrium mixture were also developed in butanol – ethanol – $N/20$ hydrochloric acid (100:10:20). As with phenol one spot was obtained with sedoheptulose phosphate and two with the equilibrium mixture using the orcinol reagent.

New Spraying Reagent for Carbohydrates Containing Ketose Units

Dische's reagent, a mixture of cysteine, carbazole, and sulphuric acid, was modified as follows:

Cysteine hydrochloride, 1.5 gm., was dissolved in 6 ml. of water, 15 gm. of trichloracetic acid were added, made up to 100 ml. with butanol, and 0.12 gm. of carbazole was added. The sprayed papers were heated for 10 min. at 85°.

The following carbohydrates containing ketose units show brown spots: dihydroxyacetone, fructose, sorbose, hexosediphosphate, ascorbic acid, sedoheptulose, sucrose, turanose, melizitose, stachyose (two spots), and inulin.

REFERENCES

1. BENVENUE, A. and WILLIAMS, K. T. Arch. Biochem. and Biophys. 34: 225. 1951.
2. DISCHE, Z. J. Biol. Chem. 204: 983. 1953.
3. DISCHE, Z. and BORENFREUND, E. J. Biol. Chem. 192: 583. 1951.
4. ETTEL, V. Collection Czechoslov. Chem. Communs. 4: 513. 1932.
5. HORECKER, B. L., SMYRNIOTIS, P. Z., and KLENOW, H. J. Biol. Chem. 205: 661. 1953.
6. ISHERWOOD, F. A. and JERMYN, M. A. Biochem. J. (London), 48: 515. 1951.
7. LAFORGE, F. B. and HUDSON, C. S. J. Biol. Chem. 30: 61. 1917.
8. NOGGLE, G. R. Arch. Biochem. and Biophys. 43: 238. 1953.
9. PRATT, J. W., RICHTMYER, N. K., and HUDSON, C. S. J. Am. Chem. Soc. 74: 2200. 1952.
10. UJEJSKI, L. and WAYGOOD, E. R. Can. J. Chem. 32: 14. 1953.
11. VICKERY, H. B. J. Biol. Chem. 205: 369. 1953.

THE REACTION OF ACTIVE NITROGEN WITH HYDRAZINE[1]

By G. R. Freeman and C. A. Winkler

ABSTRACT

Hydrazine was completely destroyed by active nitrogen, at both 150°C. and 480°C., up to a hydrazine flow rate of about 22×10^{-6} mole per sec., whereas ammonia production was small at hydrazine flow rates below about 12×10^{-6} mole per sec. Thus it appears that ammonia is formed in secondary reactions only. The results indicate that NH_2 radicals rather than hydrogen atoms may be prominent in secondary reactions. Comparison of the rate of hydrazine destruction with the rate of production of hydrogen cyanide from ethylene indicates that excited nitrogen molecules do not make a large contribution to the chemical reactivity of active nitrogen.

INTRODUCTION

The reaction of active nitrogen with ammonia (5) gave strong indication that more than one chemically reactive species exists in active nitrogen.* It was therefore of interest to study the analogous reaction with the related compound, hydrazine.

EXPERIMENTAL

The apparatus used was essentially the same as that described in earlier papers (3, 6) with one modification. Since hydrazine is a liquid (b.p. 113°C.) with a vapor pressure of 10 mm. at 20°C., it was not convenient to store it as a gas. It was stored as a liquid in a cylindrical bulb (cross sectional area = 28 sq. cm.) which was connected to the flowmeter through a 7 liter ballast volume. The storage bulb was immersed in a thermostat regulated at 20.95 ± 0.05°C. The rate of flow of hydrazine into the reaction vessel was varied by placing jets of different sizes in the flowmeter.

The molecular nitrogen flow rate was 9.2×10^{-5} mole/sec., corresponding to a pressure of 1.5 mm. Hg in the reaction vessel. In some experiments, where hydrogen atoms replaced active nitrogen, the molecular hydrogen flow rate was 8.0×10^{-5} mole per sec., which gave an operating pressure of 1.0 mm. Hg.

Anhydrous hydrazine (99%) was very kindly contributed by the Mathieson Chemical Corp.

The only products from the reactions of hydrazine with either active nitrogen or hydrogen atoms are nitrogen, hydrogen, and ammonia. The condensable products were collected in a trap containing standard sulphuric acid, immersed in liquid nitrogen. After the solution had been melted, the total amount of base in the products was determined by titration to methyl red end point. The hydrazine content of the solution was then determined by

[1]*Manuscript received December 24, 1954.*
Contribution from the Physical Chemistry Laboratory, McGill University, Montreal, Quebec, with financial assistance from the National Research Council of Canada.
**It seems probable that one active species is nitrogen atoms, while some other component such as N_2^* or N_3 might also contribute to the activity.*

titration with iodate (1). The difference between the amounts of total base and hydrazine gave the amount of ammonia.

Some comparative experiments were also made with the ethylene – active nitrogen system. In these, hydrogen cyanide was analyzed by the Liebig–Dénigès method (7).

RESULTS AND DISCUSSION

The yellow afterglow of active nitrogen was observable in the tube leading from the reaction vessel to the cold trap at all hydrazine flow rates until that corresponding to the maximum rate of decomposition of hydrazine was approached (up to about 20×10^{-6} mole per sec.). In the ethylene – active nitrogen reaction, the yellow afterglow was gradually replaced by the cyanogen flame; at 420°C., no nitrogen afterglow could be observed at flow rates of ethylene above about 1×10^{-6} mole per sec. However, at this temperature the cyanogen flame was observable in the tube leading from the reaction vessel to the cold trap at all ethylene flow rates until that corresponding to the maximum rate of production of hydrogen cyanide was approached (up to about 13×10^{-6} mole per sec.). Thus the presence, in the tube leading to the cold trap, of the nitrogen afterglow in the hydrazine reaction, and the cyanogen flame in the ethylene reaction, seem to indicate the persistence of active nitrogen in the two reactions. Since active nitrogen reacts with ammonia to only about 15% the extent to which it reacts with ethylene (5) or hydrazine, the persistence of the yellow afterglow in the ammonia reaction up to flow rates much higher than that corresponding to the maximum rate of destruction

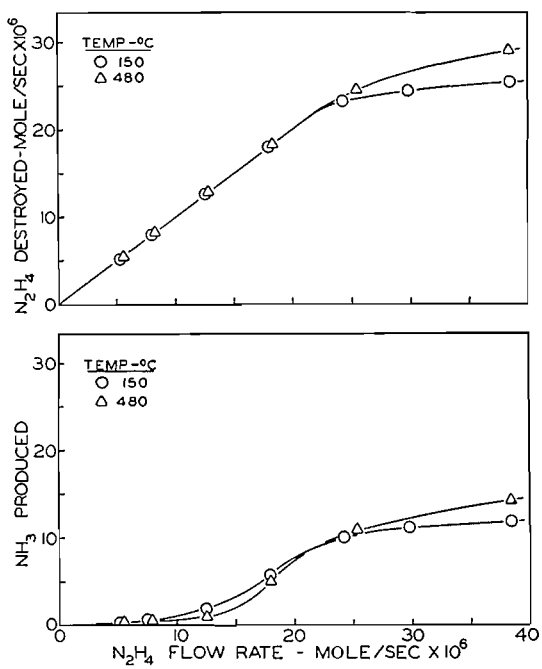

FIG. 1

of ammonia may be taken as further indication of the presence of two active species in active nitrogen.*

The relations between the hydrazine flow rate, the amount of hydrazine destroyed, and the corresponding amount of ammonia produced are shown in Fig. 1 for different temperatures. At both 150°C. and 480°C. hydrazine was completely destroyed up to a flow rate of about 22×10^{-6} mole per sec. The maximum rate of destruction increased by about 14% when the temperature was increased from 150°C. to 480°C.

From the shape of the ammonia production curves, it would appear that ammonia is formed only by reaction of hydrazine with a product of the hydrazine – active nitrogen reaction. The amount of ammonia produced at 480°C. was smaller than the amount produced at 150°C. in the range of lower flow rates, but the reverse was true at the higher flow rates (above about 20×10^{-6} mole per sec.). This was probably due to a greater increase in the rate of the active nitrogen – hydrazine reaction than in the rates of the secondary reactions. Thus there would be less hydrazine available for secondary reactions until all the active nitrogen was consumed. The possibility that ammonia was produced in the initial reaction, and destroyed by subsequent reaction with excess active nitrogen is ruled out because the maximum rate of destruction of ammonia by active nitrogen in the absence of any other reactant would be about 3×10^{-6} mole per sec. under similar conditions (5). It is

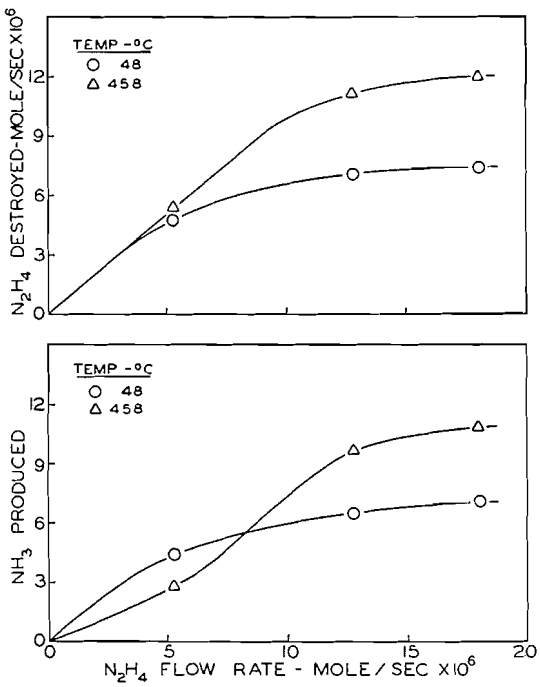

FIG. 2

**This persistence of the yellow afterglow implies the persistence of a species of nitrogen which contains at least 170 kcal. of energy, i.e. a species with sufficient energy to generate $N_2B^3\Pi_g$ molecules.*

probable, also, that the component in active nitrogen capable of reacting with ammonia would be rapidly removed by reaction with hydrazine.

There was a possibility that hydrogen atoms might be formed from the attack of active nitrogen on hydrazine. Although the hydrogen atom – hydrazine reaction has been studied (2, 4), some experiments were made in the present apparatus to permit a more direct estimate of the extent to which hydrogen atom reactions might contribute to the over-all active nitrogen – hydrazine reaction.

The hydrazine – hydrogen atom reaction was studied at 48°C. and 458°C., and the results are shown in Fig. 2. At 48°C., one mole of ammonia was produced for each mole of hydrazine destroyed. At 458°C., $(1-\alpha)$ mole of ammonia was formed for each mole of hydrazine destroyed, where $0 < \alpha < 1$. The value of α decreased, i.e. ammonia production increased, as the hydrazine flow rate was increased, probably in parallel with a decrease in hydrogen atom concentration available for secondary reactions as the hydrazine flow rate was increased (due to direct reaction between H and N_2H_4). This would imply that the decrease in yield of ammonia with increase of temperature was due to attack of hydrogen atoms on ammonia, or on an intermediate from which ammonia might be derived. The results can be explained by the following reactions:

		ΔH(kcal.)*	
$H+N_2H_4$	$\rightarrow H_2+N_2H_3$	$-(8$ to $13)$	[1*a*]
	$\rightarrow NH_3+NH_2$	-39	[1*b*]
$2N_2H_3$	$\rightarrow N_2+2NH_3$	$-(144$ to $154)$	[2]
$H+NH_3$	$\rightarrow H_2+NH_2$	$+4$	[3]
$NH_2+N_2H_3$	$\rightarrow N_2+H_2+NH_3$	$-(117$ to $122)$	[4]
$2NH_2$	$\rightarrow N_2+2H_2$	-90	[5*a*]
$2NH_2+M$	$\rightarrow N_2H_4+M$	-68	[5*b*]
$2H+M$	$\rightarrow H_2+M$	-102.7	[6]
$H+N_2H_3+M$	$\rightarrow N_2H_4+M$	$-(90$ to $95)$	[7*a*]
$H+N_2H_3$	$\rightarrow N_2+2H_2$	$-(113$ to $118)$	[7*b*]

**To calculate heats of reactions, the following dissociation energies and heats of formation were used:*
D_{N_2} = 9.765 ev. = 225.0 kcal. (Hendrie, J. M. J. Chem. Phys. 22: 1503. 1954).
D_{H_2} = 4.455 ev. = 102.7 kcal. (Beutler, H. Z. physik. Chem. B29: 315. 1935).
D_{H-NH_2} = 4.65 ev. = 107 kcal. (Devins, J. C. and Burton, M. J. Am. Chem. Soc. 76: 2618. 1954).
$\Delta H_f(NH_3) = -10.94$ kcal. (Handbook of chemistry and physics).
$\Delta H_f(N_2H_4) = 22.7$ kcal. (Reference (1), this paper).
From these values, the following were calculated:
Average N—H bond energy in NH_3 = 92.5 kcal.
Average N—H bond energy in NH_2 = 85.3 kcal.
Total bond energy in N_2H_4 = 407.7 kcal.
$D_{H_2N-NH_2}$ = 67.7 kcal.
Total bond energy in NH_3 = 277.5 kcal.
If it is then assumed that the average $H_2N—NH_2$ bond energy = 60 kcal., the average $H—N_2H_3$ bond energy = 87 kcal. Therefore, it was assumed that $D_{H-N_2H_3}$ = 90 to 95 kcal. It was also assumed that D_{H-NH} = 90 kcal., and D_{H-N} = 81 kcal. (these values were approximated from the total bond energy in NH_3 and D_{H-NH_2}).

If reaction [1*b*] were the predominant initial reaction, one ammonia molecule

would be formed from each hydrazine molecule destroyed. This would prohibit the reaction

$$NH_2+N_2H_4 \rightarrow NH_3+N_2H_3 \qquad \Delta H = -(12 \text{ to } 17)\text{kcal.} \quad [8]$$

since ammonia production never exceeded hydrazine consumption on a mole basis. At 458°C. and low hydrazine flow rates a large proportion of the ammonia formed by reaction [1*b*] would have to be subsequently destroyed by hydrogen atoms (see Fig. 2). This would seem to require that the ammonia so formed be excited, since the rate of destruction previously observed with hydrogen atoms at 440°C. (5) was much too small to explain the large value of α found at 458°C. and low hydrazine flow rates.

Although reaction [1*a*] is less favorable energetically than reaction [1*b*], its occurrence might be expected by analogy with the corresponding hydrogen atom reaction with ethane,*

$$C_2H_6+H \rightarrow C_2H_5+H_2 \qquad \Delta H = -4.7 \text{ kcal.} \quad [9a]$$

which is generally accepted over the more energetically favorable reaction

$$C_2H_6+H \rightarrow CH_4+CH_3 \qquad \Delta H = -18 \text{ kcal.} \quad [9b]$$

If reaction [1*a*] were the predominant initial reaction, the high value of α at 458°C. and low hydrazine flow rates could be explained readily by the combined effect of reactions [3] and [7*b*]. It is also possible that some N_2H_3 radicals are destroyed on the walls at high temperatures to yield nitrogen and hydrogen but no ammonia. Although the NH_2 radicals might have a significant concentration at high temperatures and low hydrazine flow rates, the hydrazine concentration should be very low because of reaction [1*a*]; hence reaction [8] following upon [1*a*] should not occur to any appreciable extent.

There are two possible exothermic reactions between nitrogen atoms and hydrazine,

$$N+N_2H_4 \rightarrow N_2+H_2+NH_2 \qquad \Delta H = -91 \text{ kcal.} \quad [10a]$$
$$\rightarrow N_2+H_2+NH+H \qquad \Delta H \approx -1 \text{ kcal.} \quad [10b]$$

If N_3 were an active species, it would react in the same manner as N, but the corresponding reactions would be less exothermic by the amount of the N_2—N bond energy in N_3. Since hydrazine reacts rapidly with active nitrogen the most probable mechanism for the reaction, if N and N_3 are assumed to be the reactive species, would seem to be:

		ΔH(kcal.)	
$N+N_2H_4$	$\rightarrow N_2+H_2+NH_2$	-91	[10*a*]
$NH_2+N_2H_4$	$\rightarrow NH_3+N_2H_3$	$-(12 \text{ to } 17)$	[8]
$2N_2H_3$	$\rightarrow N_2+2NH_3$	$-(144 \text{ to } 154)$	[2]
$NH_2+N_2H_3$	$\rightarrow N_2+H_2+NH_3$	$-(117 \text{ to } 122)$	[4]
$2NH_2$	$\rightarrow N_2+2H_2$	-90	[5*a*]
$2NH_2+M$	$\rightarrow N_2H_4+M$	-68	[5*b*]

**The bond strengths involved here were taken from a paper by Szwarc, M. Chem. Revs. 47: 75. 1950.*

If N_2^* were a reactive species, it could react with hydrazine without producing ammonia directly, or it might react to produce ammonia in a secondary reaction with the N_2H_3 radical derived from N atom attack on hydrazine:

$$N_2^* + N_2H_4 \rightarrow 2NH_2 + N_2 \quad [11]$$
$$N_2^* + N_2H_3 \rightarrow NH_3 + N_2 + N. \quad [12]$$

Reaction [12] would be followed by [10*a*]. Each N_2^* would result in the decomposition of only one hydrazine molecule.

Since ammonia is a product of secondary reactions only, it is possible to separate the effect of the secondary reactions from that of the total reaction. The ethylene – active nitrogen reaction at 451°C. was used to estimate the total active nitrogen concentration because hydrogen cyanide production from other hydrocarbons studied thus far has never been found to exceed that from ethylene. The maximum amount of hydrogen cyanide produced was 19.0×10^{-6} mole per sec. It may be assumed that if N_3 were a reactive species, each N_3 would yield one molecule of hydrogen cyanide, and if N_2^* were a reactive species, each N_2^* would yield two molecules of hydrogen cyanide. Therefore, if N_3 and N were the reactive species, the maximum amount of hydrazine decomposed without the production of ammonia should be approximately equal to the maximum amount of hydrogen cyanide produced from ethylene. If, however, N_2^* makes a predominant contribution to the activity of active nitrogen, the maximum amount of hydrazine decomposed without the production of ammonia should be much smaller than the maximum amount of hydrogen cyanide produced from ethylene.

The only product of the active nitrogen hydrazine reactions considered above which could react further with hydrazine is the NH_2 radical. Therefore, each hydrazine molecule decomposed in a secondary reaction (reaction [8], followed by reactions [2] and [4]) would yield two molecules of ammonia. Since, in the hydrogen atom – hydrazine reaction, at low temperature, little, if any, N_2H_3 was destroyed without production of ammonia, it is reasonable to assume that the same is true for the active nitrogen reaction at 150°C. Therefore, by subtracting one half of the amount of ammonia formed at 150°C. from the total amount of hydrazine destroyed at this temperature, for hydrazine flow rates of 24×10^{-6} mole per sec. and higher, it was estimated that 18.8×10^{-6} mole per sec. of hydrazine was destroyed by direct reaction with active nitrogen. This estimate must be increased by an amount corresponding to the amount of hydrazine regenerated by reaction [5*b*]. It was not possible to calculate from the present results the extent to which reaction [5*b*] occurred under the conditions of the reaction reported in this paper. Therefore, it may be concluded only that the maximum rate of destruction of hydrazine by active nitrogen was at least 18.8×10^{-6} mole per sec. The close agreement of this figure with that for hydrogen cyanide production in the ethylene – active nitrogen reaction indicates that N_2^* makes, at best, only a small contribution to the chemical reactivity of active nitrogen, and therefore, that reactions [11] and [12] only occur to a small extent or not at all.

The increase in the maximum amount of hydrazine destroyed when the temperature was increased from 150°C. to 480°C. was presumably due to an increased rate of decomposition of hydrazine in reaction [8].

The long "induction period" in the ammonia production curves (1) indicates that reaction [10*a*] is much faster than reaction [8], which would be expected.

The ammonia production curves tend to level off at a value corresponding to only about 35% of the NH_2 radicals reacting according to reaction [8]. This indicates that the NH_2 radicals are removed quite rapidly by the combined effects of reactions [4], [5*a*], and [5*b*].

REFERENCES

1. AUDRIETH, L. F. and OGG, B. A. The chemistry of hydrazine. John Wiley & Sons, Inc., New York. 1951.
2. BIRSE, E. A. B. and MELVILLE, H. W. Proc. Roy. Soc. (London), A, 175: 164. 1940.
3. BLADES, H. and WINKLER, C. A. Can. J. Chem. 29: 1022. 1951.
4. DIXON, J. K. J. Am. Chem. Soc. 54: 4262. 1932.
5. FREEMAN, G. R. and WINKLER, C. A. J. Phys. Chem. In press.
6. GREENBLATT, J. H. and WINKLER, C. A. Can. J. Research, B, 27: 721. 1949.
7. KOLTHOFF, I. M. and SANDELL, E. B. Textbook of quantitative inorganic analysis. The MacMillan Co., New York. 1946. p. 478.

THE REACTION OF METHYL RADICALS WITH ACETALDEHYDE[1]

By R. E. Dodd[2]

ABSTRACT

The rates of formation of methane and ethane in the photodecomposition of acetaldehyde have been measured between 391 and 564°K. The rate constant for the reaction

$$CH_3+CH_3CHO \rightarrow CH_4+CH_3CO$$

was found to be

$$k = 10^{10.8}\, T^{\frac{1}{2}}\, e^{-8000/RT} \text{ moles}^{-1} \text{ cm.}^{+3} \text{ sec}^{-1}.$$

The abstraction of hydrogen from acetaldehyde by methyl radicals, reaction [1], was first proposed by Leermakers (10) as a step in the photolysis of acetaldehyde

$$CH_3+CH_3CHO \rightarrow CH_4+CH_3CO. \qquad [1]$$

Undoubtedly it makes an important contribution to the rate of formation of methane, R_M, in the photolysis, and at high temperatures it predominates. For some time the activation energy, E_1, for reaction [1] was identified with the over-all activation energy, E_p, for the high-temperature photolysis. It is now clear that this involved the assumption of too simple a mechanism for the photolysis for which the reported values (1, 8, 10, 11) of E_p lay in the range 8.3–10.0 kcal./mole.

Under conditions where reaction [1] is the only source of methane $R_M = k_1[CH_3][CH_3CHO]$ but any attempt to state the methyl radical concentration in terms of the light absorption involves specific assumption about the possible reactions of the methyl radicals. For an estimate of k_1 it is safer to derive the methyl radical concentration from the rate of formation of ethane, R_E. This involves the one assumption that any ethane formed arises solely from reaction [2]

$$CH_3+CH_3 \rightarrow C_2H_6. \qquad [2]$$

Then $[CH_3] = k_2^{-\frac{1}{2}} R_E^{\frac{1}{2}}$ and hence

$$k_1k_2^{-\frac{1}{2}} = R_M R_E^{-\frac{1}{2}} [CH_3CHO]^{-1}.$$

Since, however, under the conditions of low light intensity which were used, reaction [1] is so much faster than reaction [2] ethane was not detected in the products of photolysis without the aid of the mass spectrometer. Volman and Brinton (13) were able to attain a higher concentration of methyl radicals by the thermal decomposition of di-*t*-butyl peroxide in the presence of acetaldehyde and were thus able to measure R_E and hence $k_1k_2^{-\frac{1}{2}}$. With $E_2 = 0$ (7) they obtained $E_1 = 7.5$ kcal. per mole over a narrow temperature range

[1]*Manuscript received November 29, 1954.*
Contribution from the Division of Pure Chemistry, National Research Council, Ottawa, Canada. Issued as N.R.C. No. 3543.
[2]*National Research Council of Canada Postdoctorate Fellow, 1952–53. Present address: The Chemical Laboratories, King's College, University of Durham, Newcastle-upon-Tyne, England.*

and with a rather large percentage conversion of reactant. Ausloos and Steacie (2) have now extended the temperature range using methyl radicals from the photolysis of azomethane and obtained a value $E_1 = 6.8$ kcal. per mole.

Although ethane was first detected by mass spectrometer in the products of the photolysis of acetaldehyde (3, 4, 6) it was not measured so as to give absolute values of R_E to allow calculation of $k_1k_2^{-\frac{1}{2}}$ (with the possible exception of one point (12) at 300°C.). During the course of work on the photolysis of acetone at low pressures (5) it became evident that the right conditions could be obtained for the formation of ethane from acetaldehyde in amount sufficient for measurement in a gas burette. Thus $k_1k_2^{-\frac{1}{2}}$ could be accurately measured in the direct photolysis. The results of experiments under these conditions are presented in this paper. Although it is somewhat higher than the value of E_1 (6.8 kcal. per mole) obtained from further measurements on the direct photolysis by Ausloos and Steacie, a value ($E_1 = 8.0$ kcal. per mole) lower than the over-all activation energy, E_p, is favored.

EXPERIMENTAL

The apparatus used is described in detail elsewhere (5). The reaction cell was of quartz, 100 cm. in length and 1185 cm.^{3} in effective volume. All experiments were with about 10 mm. of aldehyde. The length of vessel allowed sufficient absorption of light at this pressure of aldehyde, and the volume allowed the accumulation of sufficient products without going beyond about five per cent decomposition.

Two sets of experiments were performed: experiments 57–66 with a Corning 9700 filter, whose transmission exceeds 50% at wave lengths greater than 2900 Å; experiments 79–85 with Corning 9863 and 7740 filters, where the transmission exceeds 50% only above 3100 Å. The reduction in intensity in the second set is thus largely at the expense of higher energy quanta between 2900 and 3100 Å. For each set a separate calibration of the photometer was made using, as standard, the carbon monoxide yield from acetone above 125°C. Carbon monoxide, hydrogen, and methane were separated from ethane by a liquid nitrogen trap. Carbon monoxide and hydrogen were burnt on hot copper oxide. The resultant carbon dioxide was measured after the water was trapped with dry ice. The water, representing hydrogen, was measured by difference.

RESULTS AND DISCUSSION

The results are listed in Table I. The ratio $\rho = R_M R_E^{-\frac{1}{2}}[CH_3CHO]^{-1}$ is shown as a function of temperature in Fig. 1, which also includes the similar measurements reported by Ausloos and Steacie (2) for 35 mm. of aldehyde. It is evident that the three sets approach, with increasing temperature, a line of slope corresponding to about 8 kcal. per mole.

The curvature at low temperatures indicates that other sources of methane are becoming significant by comparison with the reduced rate of reaction [1]. Although more possibilities will have to be considered, it is convenient first to discuss the curvature in terms of a primary intramolecular rearrangement

TABLE I

SUMMARY OF RESULTS

Expt.	°K.	Pressure, mm.	I_a	R_{CO}	R_M	R_{H_2}	R_E	ρ	$k_1k_2^{-\frac{1}{2}}$
Corning 9700; 2900–3300 Å; $k_0' = 0.4$									
59	406	9.18	42.3	37.7	26.3	3.33	9.29	23.8	8.34
60	406	9.22	43.0	37.4	28.3	3.37	9.08	25.9	9.95
57	430	9.67	39.1	52.5	37.0	3.22	10.7	31.3	17.4
58	430	9.69	42.7	50.8	36.9	3.51	10.5	31.6	16.6
61	471	10.64	40.4	92.5	72.0	7.68	13.3	54.4	40.8
62	482	10.85	43.1	112.2	88.2	12.5	14.6	63.8	49.5
63	505	11.2	36.9	146.8	119.2	17.0	16.0	83.4	70.3
64	537	12.0	45.7	263	224	28.0	21.3	135	119
66	562	12.7	37.8	393	340	32.0	24.8	188	172
65	564	12.7	40.4	438	356	—	24.4	198	180
Corning 9860 and 7740; 3130 Å; $k_0' = 0.1$									
79	391	10.00	24.5	7.8	5.8	0.30	1.39	12.1	6.85
72	412	9.83	28.5	10.6	8.4	0.57	1.56	17.6	11.3
74	420	10.35	28.2	12.8	10.1	0.63	1.85	18.9	13.3
76	438	10.05	22.3	16.3	13.5	0.66	1.83	27.0	21.9
78	451	11.15	22.7	22.5	18.9	1.08	2.21	31.9	27.3
81	461	11.21	21.9	28.5	23.9	1.63	2.71	37.1	32.7
84	469	9.44	16.4	26.9	22.7	1.19	2.43	45.0	40.3
85	480	10.40	16.1	36.2	31.1	1.38	2.79	53.4	48.9

Units: aldehyde pressure, mm.; I_a, 10^{-12} Nhv cm.$^{-3}$ sec.$^{-1}$; rates, 10^{-12} moles cm.$^{-3}$ sec.$^{-1}$; and $k_1k_2^{-\frac{1}{2}}$, mole$^{-\frac{1}{2}}$ cm.$^{3/2}$ sec$^{-\frac{1}{2}}$.

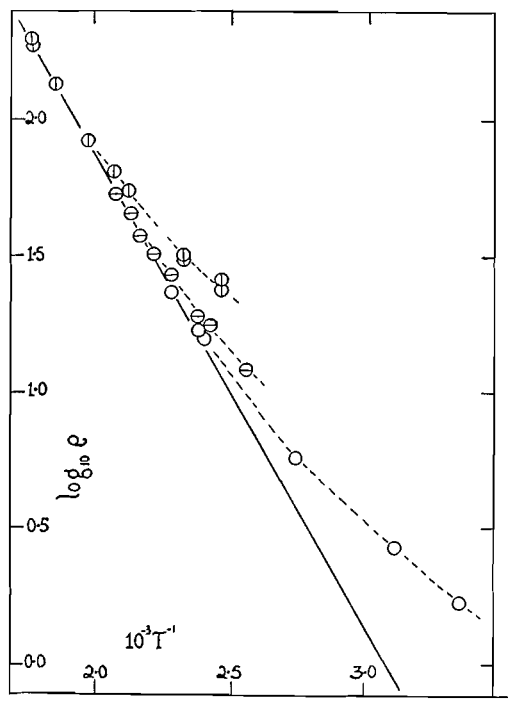

FIG. 1. The temperature dependence of $R_M/R_E^{\frac{1}{2}}$ [CH_3CHO].
⊕ Expts. 57–66; ⊖ Expts. 72–85; ○ Ausloos and Steacie, direct photolysis.

(quantum yield, k_0') so that the relevant steps in the mechanism are:

$$\begin{aligned} &CH_3CHO+h\nu \rightarrow CH_4+CO, && k_0'I_a \\ &CH_3CHO+h\nu \rightarrow CH_3+CHO, && k_0I_a \\ &CH_3+CH_3CHO \rightarrow CH_4+CH_3CO, && k_1 \\ &CH_3+CH_3 \rightarrow C_2H_6. && k_2 \end{aligned}$$

These lead to the equation:

$$\rho = k_1k_2^{-\frac{1}{2}}+k_0'I_aR_E^{-\frac{1}{2}}[CH_3CHO]^{-1}$$

in which, evidently, the last term becomes relatively smaller at high temperatures. The Arrhenius plot for ρ should tend with increasing temperature towards a straight line corresponding to that for $k_1k_2^{-\frac{1}{2}}$, as is the case. Further support is given to this interpretation of the curvature in Fig. 1 by the fact that, so far as my experiments are concerned, the curvature is proportionately less (i.e., commences at lower temperatures) in the set of experiments in which, other things being equal, the light intensity was lower. Furthermore it is possible to estimate the values of the quantum yield, k_0', which will give a straight line Arrhenius plot for $k_1k_2^{-\frac{1}{2}}$. Thus, $k_0' = 0.4$ for the experiments with light of wave length down to 2900 Å and 0.1 for those more closely limited to 3130 Å. These are reasonable values in accordance with the view that k_0' is greater at shorter wave lengths. It is not possible to make the same assessment for the experiments done on the direct photolysis by Ausloos and Steacie (2) since they did not measure I_a: it is probable that the intensities lay between those of the two sets of experiments reported here.

If account is taken of the fact that the formation of ethane is pressure dependent (5, 9) a correction must be applied to k_2 since these experiments were performed at 10 mm. pressure. This amounts to depressing the curves by 0.05 logarithmic units throughout. The two sets of corrected numbers are shown in Fig. 2 where they lie well on the line:

$$\log_{10}(k_1k_2^{-\frac{1}{2}}) = 4.65+\tfrac{1}{4}\log_{10}T-8000/2.3\,RT.$$

With the accepted value for k_2 (at high pressures) (7) this gives:

$$k_1 = 6.3 \times 10^{10}.T^{\frac{1}{2}}.e^{-8000/RT} \text{ moles}^{-1} \text{ cm.}^3 \text{ sec}^{-1}.$$

Included in Fig. 2 are results obtained by Volman and Brinton (13) and by Ausloos and Steacie (2) using methyl radicals derived from the thermal decomposition of di-*t*-butyl peroxide and from the photolysis of azomethane. The agreement in the overlapping temperature range is very good. On the other hand Ausloos and Steacie's figures, taken independently, lie on a line yielding $E_1 = 6.8$ kcal./mole, a difference from 8.0 kcal. which probably lies outside systematic experimental error. But the points at 27 and 51°C. lie above this line and the extra methane has been attributed to wall reactions. It may be suggested that any reaction leading to such amounts of additional methane at these temperatures would still make a significant contribution to the methane formation at higher temperatures and may thus explain the whole of the discrepancy between the two sets of data.

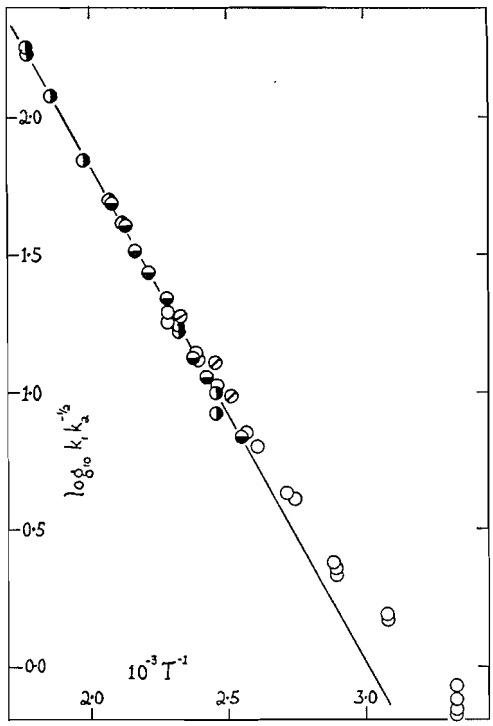

FIG. 2. The temperature dependence of $k_1 k_2^{-\frac{1}{2}}$.
◑ Expts. 57–66; ◒ Expts. 72–85; ○ Ausloos and Steacie, methyls from azomethane; ⊘ Volman and Brinton, methyls from di-*t*-butyl peroxide.

Production of methane at the walls may make some contribution to the curvature in Fig. 1, though this becomes less likely at higher temperatures. The reaction [3]

$$CH_3 + CHO \rightarrow CH_4 + CO \qquad [3]$$

is, however, an important alternative to the primary rearrangement as an explanation of the curvature. The values given to k_0' are thus upper limits. The occurrence of reaction [3] might be tested by high intensity flash experiments with mixtures of $CH_3.CHO$ and $CD_3.CDO$: under conditions where only radical–radical reactions occur the presence of CH_3D and of CD_3H in the products would confirm reaction [3].

The confirmation of a low value of E_1 (and, consequently, of a more reasonable frequency factor, A_1) in experiments on the photolysis of acetaldehyde itself makes it certain that the photolysis mechanism is complex. Since at high temperatures reaction [1] is nevertheless the principal methane-producing reaction the complications probably lie in other reactions which affect the relationship between the methyl radical concentration and the light intensity.

ACKNOWLEDGMENT

I am greatly indebted to Dr. E. W. R. Steacie, for his continual help and encouragement during my tenure of a National Research Council Post-

doctorate Fellowship; to Dr. P. Ausloos for valuable discussion and correspondence; to them both for allowing me to see their manuscript (2) before publication; and to King's College in the University of Durham for leave of absence.

REFERENCES

1. AKEROYD, E. I. and NORRISH, R. G. W. J. Chem. Soc. 890. 1936.
2. AUSLOOS, P. and STEACIE, E. W. R. Can. J. Chem. 33: 31. 1955.
3. BLACET, F. E. and BRINTON, R. K. J. Am. Chem. Soc. 72: 4715. 1950.
4. DANBY, C. J., BUCHANAN, A. S., and HENDERSON, I. H. S. J. Chem. Soc. 1426. 1951.
5. DODD, R. E. and STEACIE, E. W. R. Proc. Roy. Soc. (London), A, 223: 283. 1954.
6. DODD, R. E. and WALDRON, J. D. Nature, 167: 655. 1951.
7. GOMER, R. and KISTIAKOWSKY, G. B. J. Chem. Phys. 19: 85. 1951.
8. GRAHAME, D. C. and ROLLEFSON, G. K. J. Chem. Phys. 8: 98. 1940.
9. KISTIAKOWSKY, G. B. and ROBERTS, E. K. J. Chem. Phys. 21: 1637. 1953.
10. LEERMAKERS, J. J. Am. Chem. Soc. 56: 1537. 1934.
11. MITCHELL, J. W. and HINSHELWOOD, C. N. Proc. Roy. Soc. (London), A, 159: 32. 1937.
12. PRITCHARD, G. O., PRITCHARD, H. O., and TROTMAN-DICKENSON, A. F. J. Chem. Phys. 21: 748. 1953.
13. VOLMAN, D. H. and BRINTON, R. K. J. Chem. Phys. 20: 1764. 1952.

THE HYDROLYSIS OF PHOSPHATE DIESTERS WITH BARIUM HYDROXIDE[1]

By C. W. Helleiner[2] and G. C. Butler

ABSTRACT

The rate of alkaline hydrolysis of diphenyl phosphate has been found to be increased by the presence of barium. Similarly, desoxyribonucleate (DNA), which is not hydrolyzed rapidly by hot sodium hydroxide, is hydrolyzed by barium hydroxide. Only a very small proportion of the total phosphorus of either diphenyl phosphate or DNA is converted to inorganic phosphate during this hydrolysis. In addition to hydrolysis of the phosphate ester bonds of DNA, hot alkali also causes the deamination of desoxycytidylic acid residues and probably of the amino-purine nucleotides as well.

INTRODUCTION

For the study of nucleotide sequences in desoxyribonucleate (DNA) it seemed desirable to use a nonspecific hydrolytic agent to bring about partial degradation of the polymer to fragments whose identity could be established. Statements by Bredereck and Müller led us to believe that in hot alkaline solution, DNA would be degraded to tetranucleotides. Preliminary experiments showed that such degradation did not occur, but the work of Cherbuliez and Leber (9, 10) suggested that the reaction might proceed more readily if barium hydroxide were used instead of sodium hydroxide. It was found that barium hydroxide did apparently catalyze the hydrolysis of phosphate esters, and a more detailed study of the reaction with a model compound was undertaken.

EXPERIMENTAL

Materials and Methods

DNA was prepared from calf thymus glands by the method of Hammarsten (12).

Diphenyl phosphoric acid was prepared by hydrolysis of diphenyl phosphoryl chloride, which was kindly supplied by Dr. E. Baer. The product was recrystallized by dissolving it in hot water, acidifying the solution, and chilling.

Desoxycytidylic acid was prepared by the method described by Hurst, Marko, and Butler (14).

Desoxyuridylic acid was kindly given to us by Mr. I. G. Walker, who made it by deaminating desoxycytidylic acid with nitrous acid.

Determinations of phenol were done by the method of Folin and Ciocalteu (11) as modified by Kunkel and Tiselius (16).

Determinations of total phosphorus and inorganic phosphate were done by the method of King (15).

Hydrolysis of Diphenyl Phosphate

The hydrolysis of diphenyl phosphate was studied because this compound resembles DNA in containing a doubly-esterified phosphate group. The rate

[1]*Manuscript received November 26, 1954.*
Contribution from the Department of Biochemistry, University of Toronto, Toronto, Ontario.
[2]*National Research Council Fellow.*

of appearance of phenol and inorganic phosphate was determined in a solution containing 0.025% diphenyl phosphoric acid, sodium hydroxide, and barium chloride in the concentrations shown in Figs. 1 and 2. For each determination

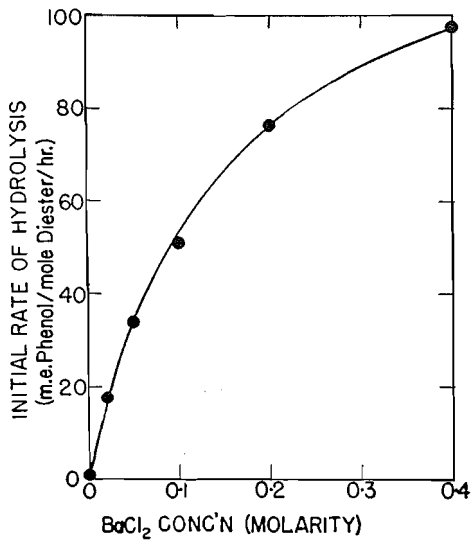

FIG. 1. Initial rate of release of phenol from diphenyl phosphate (0.025% solution) in the presence of 0.1 *N* sodium hydroxide and various concentrations of barium chloride.

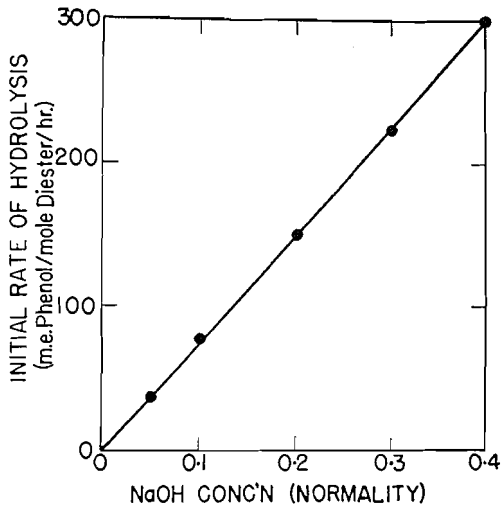

FIG. 2. Initial rate of release of phenol from diphenyl phosphate (0.025% solution) in the presence of 0.2 *M* barium chloride and various concentrations of sodium hydroxide.

a 3 ml. sample was cooled, acidified with 10% hydrochloric acid, and the barium precipitated by adding 0.5 ml. of saturated sodium sulphate solution. The barium sulphate was removed by centrifugation and total phosphorus, inorganic phosphate, and phenol were measured in the supernatant liquid. Most experiments were carried out in a boiling water bath; for the experiment

to investigate the effect of temperature on the reaction, the reaction mixture was sealed into glass tubes, which were heated in an oil bath.

The release of inorganic phosphate was in every case very slow compared to the release of phenol. The inorganic phosphate in various experiments amounted to from 0.1 to 0.4% of the total phosphorus after five hours' heating. Phenol, on the other hand, was released rapidly. Fig. 1 shows the effect of varying the concentration of barium chloride in the reaction mixture on the initial rate of appearance of free phenol. It can be seen that only very slow hydrolysis took place in the absence of barium chloride; as more barium was added to the digest, the rate of hydrolysis became greater. Fig. 2 shows the effect of varying the concentration of sodium hydroxide in the reaction mixture. The initial rate of appearance of free phenol was found to be directly proportional to the concentration of sodium hydroxide for concentrations up to 0.4 *N*. Evidently diphenyl phosphate was hydrolyzed to phenol and monophenyl phosphate, but very little hydrolysis of the resulting monophenyl phosphate occurred.

TABLE I

EXTENT OF HYDROLYSIS OF DIPHENYL PHOSPHORIC ACID (FINAL CONCENTRATION 0.025%) BY VARIOUS HYDROLYTIC AGENTS AFTER FIVE HOURS AT 100°

Hydrolytic agent	Extent of hydrolysis	
	Moles free phenol per mole diester	Moles inorganic phosphate per mole diester
0.01 *N* NaOH, plus:		
0.1 *M* Na_3AlO_3	0.176	0.004
0.43 *M* NH_4OH	0.006	—
approx. 0.01 *M* $Ca(OH)_2$ (saturated)	0.039	—
approx. 0.007 *M* $Mg(OH)_2$ (saturated)	0.012	—
0.1 *M* $BaCl_2$	0.260	0.003
no addition	0.0103	0.008

TABLE II

EXTENT OF HYDROLYSIS OF DIPHENYL PHOSPHORIC ACID (FINAL CONCENTRATION 0.025%) BY 0.1 *N* SODIUM HYDROXIDE, 0.2 *M* BARIUM CHLORIDE AFTER ONE HOUR AT VARIOUS TEMPERATURES

Temperature, (degrees C.)	Moles free phenol (per mole diester) released
90	0.039
100	0.102
110	0.224
120	0.446

Table I shows the effect of other di- and tri-valent cations on the hydrolysis of diphenyl phosphate. None of these was found to be as effective as barium in accelerating the reaction. The effect of temperature on the reaction, shown in Table II, conforms to the relation of Arrhenius.

Hydrolysis of DNA

The progress of the hydrolysis of DNA was followed by measuring the rate of increase in solubility in 10% trichloroacetic acid of the phosphorus-containing compounds of the mixture (17). Solutions containing 5 mgm. per ml. of DNA and the concentrations of sodium hydroxide and barium hydroxide shown in Table III were heated on a boiling water bath. Samples were treated as described for diphenyl phosphate to remove the barium, with precautions to avoid precipitation of DNA. To the solution from which the barium had been removed was added an equal volume of ice-cold 20% trichloroacetic acid. After filtration, the phosphorus contents of the original solution and of the filtrate were determined. This gave a measure of the solubility of the alkali-treated material in 10% trichloroacetic acid. Inorganic phosphate was also determined on the filtrate.

Table III shows that the hydrolysis of DNA apparently proceeds in accordance with expectations based on the findings with diphenyl phosphate. DNA is degraded to acid-soluble fragments with the production of only a little inorganic phosphate, and the reaction is accelerated by increasing the concentration of either barium or hydroxide. It was also found that the reaction could be speeded up by conducting it at 110°C. in a sealed reaction vessel.

TABLE III

EXTENT OF HYDROLYSIS OF DNA BY VARIOUS CONCENTRATIONS OF SODIUM AND BARIUM HYDROXIDE AFTER TWO HOURS AT 100°

NaOH conc'n, *N*	$Ba(OH)_2$ conc'n, *N*	% acid-soluble	% inorganic phosphate
Constant hydroxide concentration			
0.30	0.30	43	1.0
0.50	0.10	43	1.1
0.55	0.05	35	1.8
0.58	0.02	26	1.3
0.60	0.00	7.5	2.4
Constant barium chloride concentration (0.05 M)			
1.0		58	3.3
0.5		30	1.4
0.2		10	1.5
0.1		9	0.6

Deamination of Desoxycytidylic Acid

It seemed probable that the drastic conditions employed for hydrolyzing DNA would not only cleave phosphodiester linkages but would also deaminate the purine and pyrimidine bases. This possibility was investigated by subjecting desoxycytidylic acid to the same conditions as those required to hydrolyze

DNA, and measuring the rate of deamination of this compound to desoxyuridylic acid.

Shugar and Fox (18) showed that uracil has an isosbestic point at 235 mμ, i.e., changes in pH of solutions of uracil from values of about 1 to 7 do not affect the extinction at this wavelength. Cytosine, on the other hand, exhibits a large change in the extinction at 235 mμ when the pH of the solution is changed from 1 to 7. Therefore any difference in the extinction at 235 mμ between pH 1 and 7 of a solution containing only desoxycytidylic and desoxyuridylic acids should be proportional to the quantity of desoxycytidylic acid present, and independent of that of desoxyuridylic acid. This relationship was verified experimentally by adjusting the pH of solutions containing varying proportions of desoxycytidylic and desoxyuridylic acids to 1.0 and 7.0 using a Beckman model G pH meter. The optical densities of the solutions were read at 235 mμ on a Beckman model DU spectrophotometer. It was found that

$$58.8\ \Delta\epsilon = \mu\text{gm. of desoxycytidylic acid per ml.}$$

where $\Delta\epsilon$ is the difference in optical density of two solutions containing the same quantity of desoxycytidylic and desoxyuridylic acids, adjusted to pH 1 and 7 respectively. $\Delta\epsilon$ is independent of the concentration of desoxyuridylic acid.

The extent of deamination of desoxycytidylic acid (final concentration 0.05%) under various conditions, as measured by this method, is shown in Table IV. It is evident that under no conditions could DNA be hydrolyzed by

TABLE IV

DESTRUCTION OF DESOXYCYTIDYLIC ACID (FINAL CONCENTRATION 0.05%) UNDER VARIOUS CONDITIONS

Time of digestion	Temp. (°C.)	Hydrolytic agent 0.05 *M* $BaCl_2$ plus:	NH_4OH conc'n, *N*	% destruction of desoxycytidylic acid
5 hr.	91	0.2 *N* NaOH	—	59
5 hr.	91	0.1 *N* NaOH	—	34
90 min.	110	0.1 *N* NaOH	—	77
45 min.	110	0.1 *N* NaOH	—	32
60 min.	110	0.1 *N* NaOH	0.4	67

alkali without considerable deamination of desoxycytidylic acid, and probably of the other nucleotides as well. This finding is in keeping with that of Hurst (13), who found that all the nucleotides are readily deaminated in hot alkaline solution. It was thought that speeding up the hydrolytic reaction by raising the temperature, or adding a large amount of ammonium hydroxide to the reaction mixture might reduce the amount of deamination, but neither of these measures brought about any appreciable reduction.

DISCUSSION

The catalysis of hydrolysis of phosphate esters, as well as anhydrides of phosphoric acid by di- and tri-valent cations in alkaline solution, has been reported by several groups of investigators. Bamann *et al.* (1–7) have noted this type of effect with hydroxides of lanthanum and other rare earths; their

results are difficult to assess, however, since the insolubility of these hydroxides makes it impossible to state their concentration in the system. These workers have interpreted their findings as "phosphatase models". They have compared the specificities and pH optima of various rare earth hydroxides in hydrolyzing a large number of esters and anhydrides of phosphoric acid.

Cherbuliez and Leber (10) studied the effect of calcium hydroxide on the hydrolysis of esters of phosphoric acid, though without quantitative analysis of the products of the reaction. They observed a catalytic effect with calcium, but not with barium hydroxide.

The statement of Bredereck and Müller (8) concerning the lability of DNA to sodium hydroxide has been shown to be misleading. Weygand, Wacker, and Dellweg (19) have reported the hydrolysis of DNA by lead hydroxide; these workers isolated desoxyribosides from the hydrolyzate in yields ranging from 1–6%.

Although we have demonstrated that increasing the concentration of barium hydroxide leads to more rapid hydrolysis of phosphate esters, we have not found any explanation for the phenomenon. We see no virtue in making analogies with the equally poorly understood phenomenon of enzymic catalysis. Cherbuliez and Leber (10) propose a mechanism which involves the formation of phosphonium ions, but if it were valid, monovalent cations should also catalyze the hydrolysis of phosphate esters, and we have demonstrated that they do not.

The fact that an increase of sodium hydroxide concentration in the absence of barium does not appear to lead to any acceleration of the hydrolysis, while an increase of either barium or sodium hydroxides when both are present does lead to such an acceleration, suggests that the true catalytic agent may be undissociated barium hydroxide. In order to be certain of this it would be necessary to have measurements of the degree of dissociation of barium hydroxide at high temperatures and hydroxyl ion concentrations.

ACKNOWLEDGMENT

The authors wish to acknowledge the financial support of the National Research Council of Canada.

REFERENCES

1. Bamann, E., Fischler, F., and Trapmann, H. Biochem. Z. 325: 413. 1954.
2. Bamann, E. and Meisenheimer, M. Ber. 71: 1711. 1938.
3. Bamann, E. and Meisenheimer, M. Ber. 71: 1980. 1938.
4. Bamann, E. and Meisenheimer, M. Ber. 71: 2086. 1938.
5. Bamann, E. and Meisenheimer, M. Ber. 71: 2233. 1938.
6. Bamann, E. and Nowotny, E. Ber. 81: 451. 1948.
7. Bamann, E. and Nowotny, E. Ber. 81: 455. 1948.
8. Bredereck, H. and Müller, G. Ber. 72: 115. 1939.
9. Cherbuliez, E. and Leber, J.-P. Helv. Chim. Acta, 35: 2589. 1952.
10. Cherbuliez, E. and Leber, J.-P. Helv. Chim. Acta, 36: 537. 1953.
11. Folin, O. and Ciocalteu, V. J. Biol. Chem. 73: 627. 1927.
12. Hammarsten, E. Biochem. Z. 144: 383. 1924.
13. Hurst, R. O. Chemistry in Can. 6 (No. 5): 50. 1954.
14. Hurst, R. O., Marko, A. M., and Butler, G. C. J. Biol. Chem. 204: 847. 1953.
15. King, E. J. Biochem. J. (London), 26: 292. 1932.
16. Kunkel, H. G. and Tiselius, A. J. Gen. Physiol. 35: 89. 1951.
17. Little, A. J. and Butler, G. C. J. Biol. Chem. 188: 695. 1951.
18. Shugar, D. and Fox, J. J. Biochim. et Biophys. Acta, 9: 199. 1952.
19. Weygand, F., Wacker, A., and Dellweg, H. Chem. Abstr. 46: 7052*a*. 1952.

SYNTHESIS AND CHARACTERIZATION OF D-XYLOFURANOSE-5-PHOSPHATE[1]

By J. L. Barnwell, W. A. Saunders, and R. W. Watson

ABSTRACT

Phosphorylation of 1,2-*O*-isopropylidene-D-xylose with diphenylphosphorochloridate yielded crystalline 1,2-*O*-isopropylidene-D-xylofuranose-5-diphenylphosphate. Subsequent hydrogenolysis in glacial acetic acid over Adams' catalyst quantitatively removed phenyl groups as shown by infrared analysis. Mild hydrolysis in acetic acid for two hours at 80°C. removed the isopropylidene grouping, and D-xylose-5-phosphate was isolated as an amorphous barium salt. A yield of 81% of theoretical was obtained from 1,2-*O*-isopropylidene-D-xylose, or an over-all yield of 72% from xylose. The product was characterized through its amorphous barium, disodium, and dipotassium salts, and its crystalline dibrucine and distrychnine salts.

One of the earliest observations on phosphoryl group migration in sugar phosphates was that of Levene and Raymond (10). In attempts to prepare xylose-3-phosphoric acid (8, 9, 10, 11) as a basis for testing Robinson's suggestion that xylose was the pentose component of nucleic acid (13), 5-acetyl-, 5-benzoyl-, and 5-benzyloxycarbonyl-1,2-*O*-isopropylidene-D-xylose were separately phosphorylated with phosphorus oxychloride (10, 11). After removal of the acyl and isopropylidene groups by hydrolysis, the only product obtained was D-xylose-5-phosphate. Migration of the phosphoryl group from carbon-3 to carbon-5 at some stage of the synthesis was explained by postulating the formation of a cyclic intermediate (11). The possible significance of this exchange reaction in biological systems, as well as fundamental interest in the mechanism, have indicated the need for more complete investigation. In the present communication a revised synthesis for the preparation of D-xylose-5-phosphate is reported.

The only previously reported synthesis of D-xylose-5-phosphate was that of Levene and Raymond (10, 11). Phosphorylation of 1,2-*O*-isopropylidene-D-xylose (20 gm.) with phosphorus oxychloride in dry pyridine at −30°C., followed by drastic hydrolysis in 2 *N* sulphuric acid at 80°C. for two hours yielded 5.5 gm. of barium D-xylose-5-phosphate. This represented 14.3% of the theoretical yield from 1,2-*O*-isopropylidene-D-xylose, or approximately 12% from xylose. In the present study substitution of diphenylphosphorochloridate as the phosphorylating agent in dry 2,6-lutidine followed by hydrogenolysis and mild hydrolysis in acetic acid has increased the yield from 1,2-*O*-isopropylidene-D-xylose to 81%. The over-all yield of barium-D-xylose-5-phosphate from xylose in a typical synthesis was 72%.

The phosphorylation product, 1,2-*O*-isopropylidene-D-xylose-5-diphenylphosphate, may be obtained pure by recrystallization from carbon tetrachloride. Its elementary analysis conforms to the theoretical, and it has an extremely sharp melting point (within 0.2°). Infrared analysis of finely ground crystals

[1]*Manuscript received January 4, 1955.*
Contribution from the Division of Applied Biology, National Research Laboratories, Ottawa, Canada. Issued as N.R.C. No. 3547.

in a nujol mull shows characteristic phenyl absorption bands and a strong hydroxyl peak. The sharp melting point suggests the absence of isomeric phosphates and the greater reactivity of the primary hydroxyl indicates preferential phosphorylation in the 5-position. The assumption that phenyl groups would prevent double phosphorylation through hindrance is borne out by the elementary and infrared analyses.

If the phosphorylated product is homogeneous, acid conditions during hydrogenolysis and hydrolysis would favor retention of the phosphoryl group in position 5. The final product in the form of its barium salt has no inorganic or acid-labile phosphate, and it consumes 3.0 moles of oxidant when reacted with sodium periodate at pH 4.7. Barium, phosphorus, and pentose are close to theoretical for a monophosphorylated compound. However, when subjected to periodate oxidation either in 0.05 *N* sulphuric acid or at pH 4.7, samples prepared by different methods release from 3 to 7% of formaldehyde. The amount of formaldehyde released may be correlated with the pH during acetic acid hydrolysis. No exact estimate of the purity of the product may be made at present, although the samples used for characterization probably contain 97% D-xylose-5-phosphate.

Crystalline derivatives of D-xylose-5-phosphate have not previously been reported. Levene and Raymond (10) performed an elementary analysis on the barium salt and determined specific rotations for the barium and disodium salts. In the present study attempts to prepare crystalline metal salts were unsuccessful. Dilithium, disodium, dipotassium, as well as the barium salts precipitated from water and ethanol in amorphous form. In order to place identification on a crystalline basis the dibrucine and distrychnine salts were prepared and their constants determined.

EXPERIMENTAL

*Preparation of 1,2-O-Isopropylidene-*D*-xylose and Diphenylphosphorochloridate*

Pure 1,2;3,5-di-*O*-isopropylidene-D-xylose (115 gm.) was prepared from pure xylose in 87% yield (6). Hydrolysis of this product gave 1,2-*O*-isopropylidene-D-xylose in 99% yield (12). By molecular distillation this compound was obtained as colorless crystals with $[\alpha]_D^{26} = -19.3$ ($c = 5.70$ in water) (14). Diphenylphosphorochloridate in essentially pure form (212 gm.) was prepared from 1.1 moles of freshly distilled phosphorus oxychloride and 2 moles of redistilled phenol (79% yield) (3, 4).

*Phosphorylation of 1,2-O-Isopropylidene-*D*-xylose*

Crystalline 1,2-*O*-isopropylidene-D-xylose (5.25 gm.) was mixed with reagent benzene and the benzene distilled to remove traces of water. After removal of the benzene freshly distilled anhydrous 2,6-lutidine (60 gm.) (2) was added, the mixture shaken until solution was complete, and cooled to −20°C. with dry ice. Dry diphenylphosphorochloridate (15 gm.) was added dropwise over a period of 10 min. from a separatory funnel fitted with a drying tube. After standing for two days at 5°C. the reaction mixture was filtered, and the crystalline 2,6-lutidine–hydrochloride washed several times with cold 2,6-lutidine. After evaporation of the filtrate to a thick sirup water was added

and the distillation to dryness repeated to remove 2,6-lutidine. The resulting sirupy residue was dissolved in 100 ml. of chloroform, washed nine times with 100-ml. portions of water, and the washings discarded. The chloroform solution was evaporated to a sirup *in vacuo* at 35°C., the last traces of chloroform being removed by azeotropic distillation after addition of ethanol. Colorless needles were obtained by crystallization from ether. (Yield 10.8 gm., 93% of theoretical.) After it was recrystallized from carbon tetrachloride, washed with petroleum ether, and dried *in vacuo* at 50°C., the pure 1,2-*O*-isopropylidene-D-xylose-5-diphenylphosphate had m.p. 102.2°–102.4°: $[\alpha]_D^{20} = +10.8$ ($c = 2.21$ in chloroform). (Found: C, 56.10; H, 5.38. Calc. for $C_{20}H_{23}O_8P$: C, 56.84; H, 5.49.) The compound was soluble in chloroform and acetone, slightly soluble in ether, ethanol, and carbon tetrachloride, and insoluble in water and petroleum ether.

*Hydrogenolysis and Hydrolysis of 1,2-O-Isopropylidene-*D*-xylose-5-diphenylphosphate*

Low pressure hydrogenation of the crystalline phosphorylation product (2.0 gm.) over 0.20 gm. of Adams' catalyst (1) in 60 ml. of glacial acetic acid was complete in 115 min. The solution was filtered and the filtrate, after adjustment to pH 1.5 ± 0.2 with water, was hydrolyzed at 80 ± 2°C. for two hours. Acetic acid was removed by vacuum distillation, the sirup dissolved in 90 ml. of water, and 0.3 *N* barium hydroxide added until the pH reached 8.5. Removal of inorganic phosphate was effected by centrifuging the slightly turbid aqueous solution before the addition of four volumes of ethanol. After standing at 5°C. for two hours the colorless barium salts were separated by centrifugation and washed with 75% ethanol and ether before drying *in vacuo* over anhydrone. (Yield, 1.33 gm.) Concentration of the supernatant liquid to 20 ml. on a Craig evaporator at 30°C., readjustment of the pH to 8.5 with saturated aqueous barium hydroxide, and reprecipitation with four volumes of ethanol recovered 0.245 gm. for a total yield of 1.575 gm. (90% of theoretical).

Characterization of D-*Xylose-5-phosphate*

Data obtained by analysis of the barium salt isolated from the reaction mixture agreed with theoretical values calculated for a monophosphorylated pentose. (Found: Ba, 37.51; P, 8.54; pentose 40.2. Calc. for $C_5H_9O_8PBa$: Ba, 37.59; P, 8.58; pentose 41.0.) Pentose was estimated by the modified method of Cohn and Volkin (5). A series of analyses at different time intervals showed maximum color development with D-xylose-5-phosphate in 15 min. so that the heating period was reduced from 20 min. to 15 min.

Free xylose-5-phosphoric acid had $[\alpha]_D^{20} = +25.0$ ($c = 2.00$ in water) and the specific rotation remained unchanged for two days. The disodium salt, prepared by addition of a stoichiometric quantity of dilute sodium carbonate solution to the barium salt, had an initial $[\alpha]_D^{20}$ of +10.0 ($c = 2.00$ in water, pH 7.2) which changed with time in a levorotatory direction to +7.0°, +4.4°, +1.9°, 0.0°, and −1.0° after one two, three, four, and five days respectively. The dipotassium salt had $[\alpha]_D^{20} = +13.4$ ($c = 2.09$ in water, pH 8.9). In

half-saturated sodium tetraborate solution the specific rotation of the disodium salt increased gradually in a dextrorotatory direction. After two, three, four, and five days the initial rotation of $[\alpha]_D^{20} = +5.5$ ($c = 2.00$ in water) had changed to +6.8°, +8.5°, +10.1°, and +10.6° respectively. Several attempts were made to prepare crystalline metal salts of xylose-5-phosphoric acid. Under the conditions explored, the dilithium, disodium, dipotassium, and barium salts were always obtained in amorphous form from either water or ethanol.

Acid-labile phosphate, measurable by King's method (7), was not released by hydrolysis of the barium salt for seven minutes in *N* hydrochloric acid at 100°C. Oxidation with 0.1 *M* sodium periodate at pH 4.7 consumed 3.0 moles of oxidant in 58 hr. However oxidation of various samples of the barium salt either with 0.1 *M* periodic acid in 0.05 *N* sulphuric acid or with an equivalent concentration of sodium periodate at pH 4.7 released from 3 to 7% formaldehyde, measured colorimetrically using chromotropic acid.

To identify D-xylose-5-phosphate on a crystalline basis, dibrucine and distrychnine salts were prepared and their constants determined. The former was prepared by adding a stoichiometric amount of brucine sulphate heptahydrate in 15 ml. of water to 100 mgm. of barium xylose-5-phosphate dissolved in water. Barium sulphate was removed by filtration and the filtrate evaporated to dryness *in vacuo* at 35°C. The crude dibrucine salt weighed 262.8 mgm. (90% yield). When recrystallized from ethanol by rapid evaporation, it formed long colorless needles of a hydrate from which water of crystallization was completely removed by heating for two hours *in vacuo* at 50°C. The degree of hydration of the dibrucine salt varied with the conditions during its formation. On standing in room air overnight the anhydrous salt took up water exactly equivalent to an octahydrate. When equilibrated over a water – sulphuric acid solution (sp. gr. 1.420, relative humidity = 35) in a closed vessel, it combined with 6.5 moles of water. Recrystallization from absolute ethanol gave a hydrate with 3.5 H_2O. Analyses were therefore performed on the anhydrous salt. (Found: P, 3.06; pentose 14.02. Calc. for $C_{51}H_{63}N_4O_{16}P$: P, 3.04; pentose 14.72.) Pentose was determined by the modified Cohn–Volkin procedure (5) after titration of the dibrucine salt in water to pH 10 with *N*/10 sodium hydroxide. The anhydrous salt had $[\alpha]_D^{20} = -37.8$ ($c = 2.02$ in chloroform) and it decomposed without melting above 150°C.

The distrychnine salt was prepared by the same procedure followed for the dibrucine salt. Recrystallized from ethanol and ether it formed a tetrahydrate on standing in room air. (Found: P, 3.07; pentose 15.15. Calc. for $C_{47}H_{55}N_4O_{12}P.4H_2O$: P, 3.20; pentose 15.46.) The pure compound had $[\alpha]_D^{20} = -33.2$ ($c = 1.02$ in water) and like the dibrucine salt it decomposed above 150°C. without melting.

ACKNOWLEDGMENT

The authors wish to thank Dr. Morris Kates for his kindly interest and advice, and acknowledge their indebtedness to Mr. F. Rollin for preparing the infrared spectrograms.

REFERENCES

1. ADAMS, R., VOORHEES, V., and SHRINER, R. L. Org. Syntheses, Collective, 2nd ed. 1: 463. 1941.
2. ATHERTON, F. R., HOWARD, H. T., and TODD, A. R. J. Chem. Soc. 1106. 1948.
3. BAER, E. Biochem. Preparations, 1: 51. 1949.
4. BRIGL, P. and MÜLLER, H. Ber. 72: 2121. 1939.
5. COHN, W. E. and VOLKIN, E. *In* Methods of biochemical analysis. Vol. I. *Edited by* D. Glick. Interscience Publishers, Inc., New York. 1954. p. 298.
6. GRUNENBERG, H. V., BREDT, C., and FREUDENBERG, W. J. Am. Chem. Soc. 60: 1507. 1938.
7. KING, E. J. Biochem. J. (London), 26: 292. 1932.
8. LEVENE, P. A. and RAYMOND, A. L. J. Biol. Chem. 102: 317. 1933.
9. LEVENE, P. A. and RAYMOND, A. L. J. Biol. Chem. 102: 331. 1933.
10. LEVENE, P. A. and RAYMOND, A. L. J. Biol. Chem. 102: 347. 1933.
11. LEVENE, P. A. and RAYMOND, A. L. J. Biol. Chem. 107: 75. 1934.
12. MÜLLER, H. VON and REICHSTEIN, T. Helv. Chim. Acta, 21: 255. 1938.
13. ROBINSON, R. Nature, 120: 44. 1927.
14. SVANBERG, O. and SJÖBERG, K. Ber. 56: 863. 1923.

GLYCERIDE SYNTHESIS

I. SYNTHESIS OF SYMMETRICAL DIGLYCERIDES FROM DIHYDROXY ACETONE AND ALLYL ALCOHOL[1]

By P. J. Barry[2] and B. M. Craig

ABSTRACT

1,3-Distearoxy acetone and 1,3-dipalmitoxy acetone were prepared by interesterification of the methyl esters of the fatty acids with 1,3-dipropionoxy acetone diethyl mercaptal. The 1,3-diglycerides were obtained by hydrogenation of the ketone group. Allyl tetrahydropyranyl ether was oxidized to 1-tetrahydropyranyl glycerol which was acetylated and interesterified with methyl esters of fatty acids to produce 1,3-diglycerides.

Numerous references may be found in the literature for the synthesis of symmetrical and unsymmetrical diglycerides (11). The methods used involve blocking a primary hydroxyl group as an acetal or ether, i.e. trityl, reacting the glycerol derivative with 2 moles of the particular fatty acid chloride, and subsequent hydrolysis or hydrogenolysis to yield the desired diglyceride. Clocker and other workers (2, 1, 7) have synthesized simple triglycerides readily and in good yield by the interesterification of triacetin and the methyl ester of the fatty acid with sodium methoxide as a catalyst. The advantages of interesterification are (*a*) the mild conditions for the reaction and (*b*) the use of the methyl ester directly which is the usual derivative by which the fatty acids are purified through fractional distillation and fractional crystallization. A side reaction has been found in the interesterification of triacetin and methyl esters but the product has not been identified. The present work describes the preparation of symmetrical diglycerides by interesterification using dihydroxy acetone or allyl alcohol as starting materials.

Schlenk, Lamp, and DeHaas (12) have synthesized a number of fatty acid mono- and di-esters of dihydroxy acetone using glycolic acid chloride as a starting material. The diglycerides were produced from these products by hydrogenation over Raney nickel. Dihydroxy acetone (3) and mono fatty-acid derivatives of dihydroxy acetone (12) will undergo monomer–dimer interconversions.

In the present work the ketone group was protected as a mercaptal to eliminate this difficulty. The series of reactions at the top of page 717 outline the synthesis of diglycerides from dihydroxy acetone.

The yield of 1,3-dipropionoxy acetone diethyl mercaptal was much higher than the diethyl ketal. The 1,3-distearoxy acetone diethyl mercaptal was easily separated from the interesterification and the yields were almost quantitative in the remaining steps to the diglyceride. The method represents a direct preparation of 1,3-diglycerides without a β–α shift which is usually encountered due to an initial blocking of a primary hydroxyl group in the glycerol. Dipalmitin was also prepared in the same manner. The preparation

[1]*Manuscript received December 16, 1954.*
Contribution from the National Research Council of Canada, Prairie Regional Laboratory, Saskatoon, Sask. Issued as Paper No. 184 on the Uses of Plant Products and as N.R.C. No. 3546.
[2]*National Research Council of Canada Postdoctorate Fellow 1953–54.*

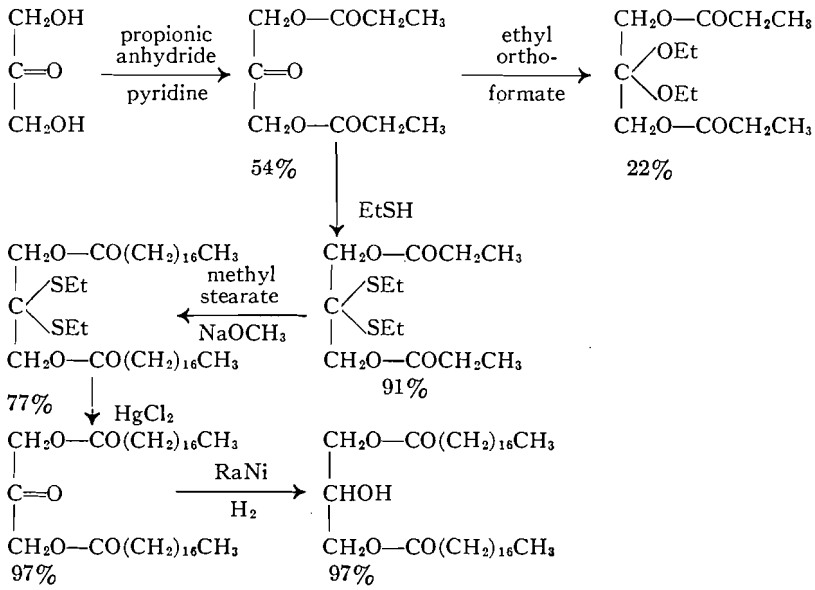

of unsaturated diglycerides would require a different procedure for reduction of the ketone group to an alcohol.

The synthesis of diglycerides from allyl alcohol required the formation of an acetal of allyl alcohol. The use of 2,3-dihydropyran for the preparation of acetals of alcohols has been investigated by Paul (10), Ott *et al.* (8), and Parham and Anderson (9). The reaction proceeds smoothly and in good yield and the acetal is readily cleaved by a mineral acid. Parham and Anderson (9) found it difficult to obtain the monoacetal of ethylene glycol. Preliminary work in this laboratory showed that it was difficult to obtain a monoacetal of glycerol. However allyl alcohol readily forms an acetal with 2,3-dihydropyran and oxidation of the ethylenic bond would yield the required monoacetal of glycerol.

The following series of reactions were followed for the synthesis of diglycerides from allyl alcohol.

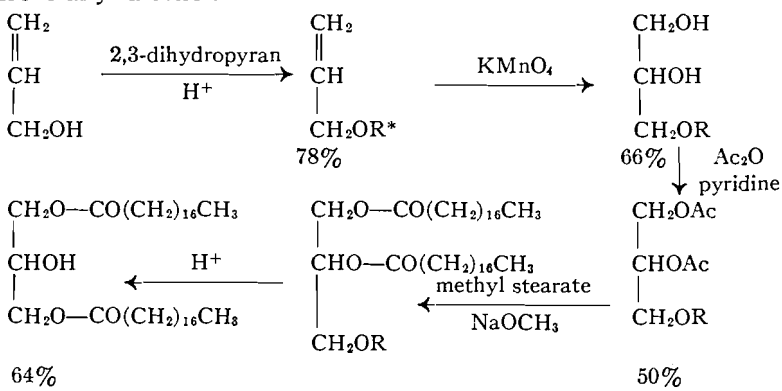

Dipalmitin, 64%.

R*, tetrahydropyranyl group.

The oxidation of the allyl tetrahydropyranyl ether by $KMnO_4$ in aqueous solution at 5°C. proceeded smoothly and in fair yield. Acetylation of the 1-tetrahydropyranyl glycerol gave a low yield which may have been due to the conditions of isolation of the diacetyl derivative. The interesterification with methyl stearate produced a gel which is likely responsible for the relatively low yield of distearin. This series of reactions for the synthesis of symmetrical diglycerides merits further study, since the number of steps involved is considerably reduced as compared to conventional procedures.

EXPERIMENTAL

I. *Preparation from Dihydroxy Acetone*

(*a*) *1,3-Dipropionoxy Acetone*

1,3-Dipropionoxy acetone was prepared according to the method given by Fischer and Mildbrand (3). Five grams of (0.55 mole) dihydroxy acetone* was added to a solution of 100 ml. of dry pyridine and 120 gm. (0.923 M.) propionic anhydride, then shaken for 15 min., and allowed to stand at room temperature for two days. The solution was poured into ice water and extracted with ethyl ether. The ethereal solution was washed successively with dilute hydrochloric acid, 5% sodium bicarbonate, and water and was dried over anhydrous sodium sulphate. The ether was removed and the 1,3-dipropionoxy acetone was crystallized from petroleum ether (Skellysolve "F"). Yield, 54%; m.p., 60–60.5°C. Analysis for $C_9H_{14}O_5$: C, 53.67%; H, 6.909%. Calc.: C, 53.46%; H, 6.978%.

(*b*) *1,3-Dipropionoxy Acetone Diethyl Ketal*

The procedure used by Hurd and Pollack (4) was followed for the preparation of the diethyl ketal. Four grams of dipropionoxy acetone, 3.9 gm. of ethyl orthoformate, 5.8 gm. of ethyl alcohol, and 60 mgm. of *p*-toluene sulphonic acid were refluxed for eight hours and allowed to stand for 24 hr. The solution was neutralized with sodium ethoxide and made up to 40 ml. with water. Extraction of the aqueous solution with petroleum ether (Skellysolve "F") yielded 1.2 gm. of a yellow oil (yield 22%) which was distilled *in vacuo* to give a colorless oil, n_D^{25} 1.4296.

(*c*) *1,3-Dipropionoxy Acetone Diethyl Mercaptal*

Five grams of dipropionoxy acetone was dissolved in 50 ml. ethyl mercaptan followed by the addition of 2.5 gm. anhydrous zinc chloride. The mixture stood in a salt–ice bath for 24 hr. and was poured into a saturated aqueous solution of sodium bicarbonate. The aqueous solution was filtered and extracted with ethyl ether. The ethereal solution was dried and distilled. A colorless liquid, b.p. 157–158 at 6 mm., was obtained in 91% yield. The product was purified by distillation to yield 5.7 gm. of 1,3-dipropionoxy acetone diethyl mercaptal, n_D^{25} 1.4966. Analysis for S: found, 20.58%; calc., 20.75%.

(*d*) *1,3-Distearoxy Acetone Diethyl Mercaptal*

Three grams of dipropionoxy acetone diethyl mercaptal, 6 gm. of methyl stearate, and 0.3 ml. of a saturated solution of $NaOCH_3$ in methanol were

Supplied by Dr. A. C. Neish, Prairie Regional Laboratory, National Research Council, Saskatoon, Sask.

placed in a flask and heated on a rotary evaporator in a steam bath under vacuum. The mixture was extracted with ethyl ether and crystallized to yield 5.6 gm. (77%) of 1,3-distearoxy acetone diethyl mercaptal, m.p. 49.1–49.4°C. Analysis for S: found, 8.74%; calc., 8.79%.

(*e*) *1,3-Dipalmitoxy Acetone Diethyl Mercaptal*

Two grams of dipropionoxy acetone diethyl mercaptal, 3.55 gm. of methyl palmitate, and 0.2 ml. of a saturated $NaOCH_3$ in methanol solution were treated as in (*d*). The 1,3-dipalmitoxy acetone diethyl mercaptal was crystallized from acetone. Yield, 3.53 gm. (81%); m.p., 39.5–40.0°C. Analysis for S: 9.48%; calc., 9.52%.

(*f*) *1,3-Distearoxy Acetone*

One gram of distearoxy acetone diethyl mercaptal was dissolved in 9.5 ml. of hot acetone and 0.5 ml. of water was added. Then 2.5 gm. of $HgCl_2$ in 10 ml. of acetone was added and the mixture was refluxed for four hours. A further 25 ml. of acetone was added and the mixture was refluxed for 20 min. and filtered while hot. The residue was washed carefully with hot acetone and the 1,3-distearoxy acetone was crystallized from the acetone. Yield, 97%; m.p., 87–87.5°C.

(*g*) 1,3-Dipalmitoxy acetone was prepared in the same manner in a 97% yield with a m.p. 82–82.5°C. (reported m.p. 77–78°C. (12)).

(*h*) *1,3-Distearin and 1,3-Dipalmitin*

1,3-Distearoxy acetone, 0.67 gm., was dissolved in 75 ml. of tetrahydrofuran and was hydrogenated over Raney nickel at 50 p.s.i. for three hours at room temperature. The 1,3-distearin was recrystallized from acetone. Yield, 0.65 gm.; m.p., 78.5–79°C. (reported m.p. 79.5°C. (6)).

1,3-Dipalmitin was prepared in the same manner in a similar yield, m.p. 72.0°C. (reported m.p. 72.5 (6)). Analysis for $C_{35}H_{68}O_5$: C, 74.07%; H, 12.17%. Calc.: C, 73.89%; H, 12.04%.

II. *Preparation from Allyl Alcohol*

(*a*) *Allyl Tetrahydropyranyl Ether*

Allyl alcohol, 11.5 gm., 2,3-dihydropyran, 17 gm., and one drop of concentrated HCl were mixed at room temperature. The reaction mixture was shaken in a wrist action shaker for three hours at room temperature and was then neutralized with $NaHCO_3$. The product was distilled over $NaHCO_3$ at b.p. 165–167°C. in 78% yield, n_D^{25} 1.4421.

(*b*) *1-Tetrahydropyranyl Glyceryl Ether*

Allyl tetrahydropyranyl ether, 106.5 gm., was suspended in 450 ml. water and cooled to 5°C. in an acetone – dry ice bath. One hundred and twenty grams of $KMnO_4$ in 2550 ml. of water was added with stirring at a rate that maintained the temperature of the mixture at 5°C. ±1°C. After the addition was completed the mixture was allowed to stand in the cooling bath for two hours and was then heated for one hour on a steam bath. The solution was filtered, cooled to room temperature, and saturated with K_2CO_3. The oil was separated from the aqueous mixture, dried, and dissolved in ethyl ether.

The ethereal solution was dried over K_2CO_3 and the ether was removed to yield 102 gm. (66.5% yield) of crude product. The product distilled at 146–149°C. at 4 mm. pressure, n_D^{25} 1.4736. Oxidation of 1-tetrahydropyranyl glycerol ether with periodic acid (5) was quantitative showing a monoether of glycerol.

(*c*) *2,3-Diacetoxy-1-tetrahydropyranyl Glycerol*

Twenty five grams of tetrahydroglyceryl ether was added to a solution of 150 ml. of pyridine and 80 ml. acetic anhydride and shaken for one hour at room temperature. The mixture was allowed to stand at room temperature for two days, poured into ice water, and allowed to stand for two hours. The aqueous solution was extracted twice with ethyl ether and the ethereal solution was washed successively with water, 10% HCl, water, 5% $NaHCO_3$ solution, and water. After the solution was dried over anhydrous Na_2SO_4, the ether was removed and the product was distilled. The 2,3-diacetoxy-1-tetrahydropyranyl ether was obtained in 50% yield, n_D^{25} 1.4456, saponification value 426.5, calculated 430.7.

(*d*) *1,3-Distearin by Acyl Chlorides*

Tetrahydropyranyl glyceryl ether, 4.6 gm., was dissolved in 10 ml. of dry pyridine and 25 ml. of dry $CHCl_3$ and 10 gm. of stearyl chloride (2) dissolved in 10 ml. of dry $CHCl_3$ was added slowly to the reaction vessel. The mixture was allowed to stand at room temperature for one hour and was then refluxed for 12 hr. The product was extracted with petroleum ether (Skellysolve "F") which was washed with water, dilute hydrochloric acid, and water and was dried over anhydrous sodium sulphate. Dry HCl gas was bubbled into the petroleum ether solution for one-half hour. The solution was allowed to stand at room temperature for one hour and filtered. The 1,3-distearin was recrystallized from acetone, yield 12.6 gm. (72% of theoretical), with a m.p. 78.5–79°C. (reported m.p. 79.5 (3)). Analysis for $C_{39}H_{76}O_5$: C, 73.56%; H, 12.06%. Calc.: C, 73.55%; H, 12.10%.

(*e*) *1,3-Distearin by Interesterification*

2,3-Diacetoxy-1-tetrahydropyranyl glyceryl ether, 2.6 gm., was reacted with 6.0 gm. methyl stearate and 0.2 ml. of saturated solution of $NaOCH_3$ in methanol under vacuum at 90–95°C. Petroleum ether (Skellysolve "F") was added to the mixture and the soaps were removed by filtration. The solution was dried over anhydrous Na_2SO_4 and the salt was then removed by filtration. Dry HCl gas was passed into the solution for one-half hour and allowed to stand for one hour at room temperature. The precipitate was filtered and crystallized from acetone to yield 3.95 gm. (64% yield) of 1,3-distearin, m.p. 78–79°C. (reported 79.5°C.). Analysis for $C_{39}H_{76}O_5$: C, 73.41%; H, 12.07%. Calc. for C, 73.55%; H, 12.10%.

(*f*) 1,3-Dipalmitin, m.p. 72.5–73.5°C. (reported m.p. 72.5°C. (6)), was prepared in a similar manner in 63% yield.

REFERENCES

1. BAUR, F. J. and LANGE, W. J. Am. Chem. Soc. 73: 3926. 1951.
2. CRAIG, B. M., LUNDBERG, W. O., and GEDDES, W. F. J. Am. Oil Chemists' Soc. 29: 128. 1952.

3. FISCHER, H. O. L. and MILDBRAND, H. Ber. 57: 707. 1924.
4. HURD, W. C. and POLLACK, M. A. J. Am. Chem. Soc. 60: 1909. 1938.
5. JACKSON, E. L. Organic reactions. II. John Wiley & Sons, Inc., New York. 1946. p. 341.
6. JACKSON, F. L., DAUBERT, B. F., KING, C. G., and LONGENECKER, H. E. J. Am. Chem. Soc. 66: 289. 1944.
7. LUNDBERG, W. O. and CHIPAULT, J. R. Hormel Inst. Univ. Minn., Ann. Rept. 1947–48.
8. OTT, A. C., MURRAY, M. F., and PEDERSON, R. L. J. Am. Chem. Soc. 74: 1239. 1952.
9. PARHAM, W. E. and ANDERSON, E. L. J. Am. Chem. Soc. 70: 4187. 1948.
10. PAUL, R. Bull. soc. chim. Mém. 1: 971. 1934.
11. RALSTON, A. W. Fatty acids and their derivatives. John Wiley & Sons, Inc., New York. 1948.
12. SCHLENK, H., LAMP, B. G., and DEHAAS, B. W. J. Am. Chem. Soc. 74: 2550. 1952.

NOTES

TETRAETHYL PYROPHOSPHATE LABELED WITH PHOSPHORUS-32

By J. R. Robinson

A supply of P^{32}-labeled tetraethyl pyrophosphate (TEPP) was required for research at this laboratory and, as no details of its synthesis[1] were found in the literature, the method described here was developed. The specific activity of the product was low, 65 microcuries per gram, but this could be increased by altering the ratio of active to inactive phosphorus and no major modification of the technique would be required.

EXPERIMENTAL

Labeled phosphoric acid,[2] suitably diluted with inactive orthophosphoric acid, was converted *via* silver phosphate to triethyl phosphate using reactions reported by Baldwin and Higgins (1).

$$PO_4^{\equiv} + 3Ag^+ \xrightarrow{\text{pH 7}} Ag_3PO_4$$

$$Ag_3PO_4 + 3C_2H_5Br \xrightarrow{\text{Heat}} (C_2H_5)_3PO_4 + 3AgBr$$

The final step of the synthesis utilized a reaction reported by Bell (2).

$$2(C_2H_5)_3PO_4 + SOCl_2 \xrightarrow{\text{Heat}} (C_2H_5)_4P_2O_7 + 2C_2H_5Cl + SO_2$$

Since the experimental technique is novel the details are reported in full.

Tetraethyl Pyrophosphate

Labeled triethyl phosphate (13.29 gm., 72.4 millimoles, 47 μc. per gm.) was placed in a Hickman vacuum still[3] and treated with 4 ml. (6.6 gm., 55.6 millimoles) of thionyl chloride. The still was fitted with a receiver and a calcium chloride tube. The system was suspended about one-half inch above a small hot plate and a thermometer was fixed in a horizontal position with its bulb touching the center point of the bottom of the still. Heating was adjusted until the thermometer was steady at 70–75° and this temperature was maintained for 24 hr. The temperature was then raised to 140° for half an hour to ensure completion of the reaction. During the total reaction time 1.5 ml. of excess thionyl chloride collected in the receiver while the sulphur dioxide and ethyl chloride passed off through the calcium chloride tube. The still was allowed to cool and then was fitted to a vacuum manifold. With the pressure at 10 mm. and the thermometer indicating 120° the last traces of reactants

[1]*The use of radioactive TEPP has been reported (3, 4, 5, 6, 7). References (3) and (4) were concerned with labeled hexaethyl tetraphosphate (HETP) which probably contained TEPP as the active principle.*

[2]*One millicurie of P^{32} as phosphoric acid, obtained from Atomic Energy of Canada Limited, Chalk River, Ontario.*

[3]*Fisher Scientific Co., Cat. No. 9–124, modified by the addition of two ground-glass joints.*

and by-products were removed. After one-half hour the pressure was lowered to 0.002 mm. and the tetraethyl pyrophosphate was distilled into weighed receivers. A forerun of 1.5 ml. (optimum quantity determined by inactive runs) was discarded and 6.4 gm. (61%) of TEPP was collected, b.p. 95–100°/ 0.002 mm., n_D^{25} 1.4174. (The boiling point and refractive index were determined on inactive samples produced in the same manner.) The corrected specific activity was 65 μc. per gm., representing a recovery of 41% of the initial radioactivity. The over-all chemical yield, also based on phosphoric acid, was 49%.

1. BALDWIN, W. H. and HIGGINS, C. E. J. Am. Chem. Soc. 74: 2431. 1952. Document 3563. American Documentation Institute, Washington, D.C. 1951.
2. BELL, A. U.S. Patent No. 2,495,220. Jan. 24, 1950. British Patent No. 652,632. Apr. 25, 1951.
3. BRAUER, R. W. J. Pharmacol. Exptl. Therap. 92: 162. 1948.
4. BRAUER, R. W. and PESSOTTI, R. L. Science, 110: 395. 1949.
5. FERNANDO, H. E., ROAN, C. C., and KEARNS, C. W. Ann. Entomol. Soc. Amer. 44: 551. 1951.
6. ROAN, C. C. Abstract of Thesis, Univ. of Illinois, Chicago, Ill. 1950.
7. ROAN, C. C., FERNANDO, H. E., and KEARNS, C. W. J. Econ. Entomol. 43: 319. 1950.

RECEIVED DECEMBER 6, 1954.
CONTRIBUTION NO. 41,
SCIENCE SERVICE LABORATORY,
CANADA DEPARTMENT OF AGRICULTURE,
UNIVERSITY SUB POST OFFICE,
LONDON, ONTARIO.

IDENTIFICATION OF DIHYDROCONIFERYL ALCOHOL

BY E. A. KVASNICKA, R. R. MCLAUGHLIN, AND S. REID

Dihydroconiferyl alcohol (3-(3-methoxy-4-hydroxyphenyl)-1-propanol) (7) is an important degradation product of lignin. It has been found not only in hydrogenolysis reaction mixtures (3, 9) but also after degrading naturally occurring related products (5).

Recently, this compound was found to be present in spruce sulphite liquor (6). At the same time, dihydroconiferyl alcohol was also found in the oxidized sulphite liquors (8).

During these investigations, extensive use has been made of the available methods of identification which are described in these papers. However, an important fact is reported here because of its special interest for those working at present in this field.

The UV spectra of dihydroconiferyl alcohol and similar compounds were reported by Schuerch (9), who found an absorption maximum of 265 mμ (determined in butanol). This value appeared to be in disagreement with the known rule that hydroxy groups in the γ-position in the side chain cause only negligible shifts of the UV absorption curve of the parent hydrocarbon (2). The UV absorption maximum of this hydrocarbon, coerulignol, is 281 mμ (1, 4).

and by-products were removed. After one-half hour the pressure was lowered to 0.002 mm. and the tetraethyl pyrophosphate was distilled into weighed receivers. A forerun of 1.5 ml. (optimum quantity determined by inactive runs) was discarded and 6.4 gm. (61%) of TEPP was collected, b.p. 95–100°/ 0.002 mm., n_D^{25} 1.4174. (The boiling point and refractive index were determined on inactive samples produced in the same manner.) The corrected specific activity was 65 μc. per gm., representing a recovery of 41% of the initial radioactivity. The over-all chemical yield, also based on phosphoric acid, was 49%.

1. BALDWIN, W. H. and HIGGINS, C. E. J. Am. Chem. Soc. 74: 2431. 1952. Document 3563. American Documentation Institute, Washington, D.C. 1951.
2. BELL, A. U.S. Patent No. 2,495,220. Jan. 24, 1950. British Patent No. 652,632. Apr. 25, 1951.
3. BRAUER, R. W. J. Pharmacol. Exptl. Therap. 92: 162. 1948.
4. BRAUER, R. W. and PESSOTTI, R. L. Science, 110: 395. 1949.
5. FERNANDO, H. E., ROAN, C. C., and KEARNS, C. W. Ann. Entomol. Soc. Amer. 44: 551. 1951.
6. ROAN, C. C. Abstract of Thesis, Univ. of Illinois, Chicago, Ill. 1950.
7. ROAN, C. C., FERNANDO, H. E., and KEARNS, C. W. J. Econ. Entomol. 43: 319. 1950.

RECEIVED DECEMBER 6, 1954.
CONTRIBUTION NO. 41,
SCIENCE SERVICE LABORATORY,
CANADA DEPARTMENT OF AGRICULTURE,
UNIVERSITY SUB POST OFFICE,
LONDON, ONTARIO.

IDENTIFICATION OF DIHYDROCONIFERYL ALCOHOL

BY E. A. KVASNICKA, R. R. MCLAUGHLIN, AND S. REID

Dihydroconiferyl alcohol (3-(3-methoxy-4-hydroxyphenyl)-1-propanol) (7) is an important degradation product of lignin. It has been found not only in hydrogenolysis reaction mixtures (3, 9) but also after degrading naturally occurring related products (5).

Recently, this compound was found to be present in spruce sulphite liquor (6). At the same time, dihydroconiferyl alcohol was also found in the oxidized sulphite liquors (8).

During these investigations, extensive use has been made of the available methods of identification which are described in these papers. However, an important fact is reported here because of its special interest for those working at present in this field.

The UV spectra of dihydroconiferyl alcohol and similar compounds were reported by Schuerch (9), who found an absorption maximum of 265 mμ (determined in butanol). This value appeared to be in disagreement with the known rule that hydroxy groups in the γ-position in the side chain cause only negligible shifts of the UV absorption curve of the parent hydrocarbon (2). The UV absorption maximum of this hydrocarbon, coerulignol, is 281 mμ (1, 4).

In view of this discrepancy, we re-examined the spectrum of dihydroconiferyl alcohol. A sample was synthesized according to the procedure of Schuerch (9) and characterized by the refractive index and the preparation of the known derivatives (5).

We found absorption maxima of 281.6 mμ (solvent: 95% ethanol) and 281.8 mμ (solvent: *n*-butanol).

Therefore, dihydroconiferyl alcohol cannot be regarded as an exception to the above-mentioned rule.

EXPERIMENTAL PART

The sample of dihydroconiferyl alcohol was prepared by reduction of ethyl hydroferulate with lithium aluminum hydride according to the literature (9). The compound was characterized by the preparation of the benzoate and *p*-nitrobenzoate and the purity was checked by the refractive index and paper chromatography (6).

The spectra were determined with a Beckman model DU spectrophotometer, and the resulting data appear in Table I.

TABLE I

ULTRAVIOLET SPECTRUM OF DIHYDROCONIFERYL ALCOHOL

Solvent	Concentration, mgm./l.	Maximum, mμ	Molar extinction
95% ethanol	27	281.6	2871
95% ethanol + 0.5 mole KOH/l.	27	297	3845
n-butanol	30	281.8	
n-butanol + 0.5 mole KOH/l.	30	297	

NOTE: *Equal extinction values for both neutral and alkaline solutions: 268.6 mμ.*

1. AULIN-ERDTMAN, G. Svensk Papperstidn. 47: 91. 1944.
2. BRAUNS, F. E. Chemistry of lignin. Academic Press, Inc., New York. 1952. p. 219.
3. HIBBERT, H., BREWER, C. P., and COOKE, L. M. J. Am. Chem. Soc. 70: 57. 1948.
4. HILLMER, A. and SCHORNING, P. Z. physik. Chem. A, 167: 407. 1933; 168: 81. 1934.
5. KAWAI, S. *et al.* Ber. 72: 367. 1939.
6. KVASNICKA, E. A. and MCLAUGHLIN, R. R. Can. J. Chem. 33: 637. 1955.
7. NOMURA, H. and HOTTA, S. Science Repts. Tôhoku Imp. Univ. 17: 693. 1928.
8. REID, S. To be published.
9. SCHUERCH, C. and GRANATH, M. J. Am. Chem. Soc. 75: 707. 1953.

RECEIVED NOVEMBER 30, 1954.
DEPARTMENT OF CHEMICAL ENGINEERING,
UNIVERSITY OF TORONTO, TORONTO 5, ONTARIO,
AND
ONTARIO RESEARCH FOUNDATION,
43 QUEENS PARK,
TORONTO 5, ONTARIO.

Canadian Journal of Chemistry

Issued by THE NATIONAL RESEARCH COUNCIL OF CANADA

VOLUME 33 MAY 1955 NUMBER 5

STUDIES IN THE POLYOXYPHENOL SERIES

IX. THE SYNTHESIS OF PAPAVERINE AND PAPAVERALDINE BY THE POMERANZ-FRITSCH METHOD[1]

BY DONALD A. GUTHRIE,[2] ARLEN W. FRANK,[3] AND C. B. PURVES

ABSTRACT

Fritsch's cyclization of N-(α-veratrylveratrylidene)-aminoacetal in sulphuric acid was shown to give 1.1% of papaverine and 23% of an isomer, m.p. 164.5–165.5°C.; hydrochloride, m.p. 212°C. decomp., which was supposed to be 4,5-bis(3,4-dimethoxyphenyl)-2*H*-pyrrolenine, produced by an internal condensation of the acetal or the corresponding aldehyde with the reactive methylene group. A similar structure was proposed for another unidentified isomer prepared by Schlittler and Müller. Hydrogenation of Fritsch's acetal gave N-(α-veratryl-veratryl)-aminoacetal, m.p. 69.5–70°C., which was cyclized to a base, m.p. 155.5–156°C.; N-acetyl derivative, m.p. 203.5–204°C., formulated as 2,3-bis(3,4-dimethoxyphenyl)-3-pyrroline. Substances presumed to be the intermediate aldehyde and aldol were isolated as colorless oils. Condensation of the diketone veratril with aminoacetal, followed by cyclization of the crude product, constituted a new two-step synthesis of papaveraldine in 8% yield, and the reduction of the latter to papaverine was known.

Other crystalline compounds prepared incidentally and thought to be new were veratril monoanil, m.p. 172–173°C.; α,α′-biveratrylideneaminoacetal, m.p. 101–102°C.; a compound formulated as 2,3-bis(3,4-dimethoxyphenyl)-4-ethylmercaptopyrrolidine hydrochloride, m.p. 184–185°C.; from this an unidentified mercury complex, m.p. 109°C. decomp.; 4,4′dibenzyloxy-3,3′-dimethoxydesoxybenzoin, m.p. 141–142°C.; and its oxime, m.p. 137.5°C.

INTRODUCTION

The opium alkaloid papaverine is now produced in about 15% yield from vanillin by the Bischler-Napieralski isoquinoline synthesis (3, 4), but the possible application of the less familiar Pomeranz-Fritsch synthesis is still of interest because the product would in theory be obtained in fewer steps. Pomeranz (15) was the first to plan this application, but the attempts of Allen and Buck (1), Fritsch (8), and Schlittler and Müller (17) to put it into effect gave disappointing results. The present article reveals some of the factors that caused these attempts to fail, and describes modifications that lead to syntheses of papaverine and papaveraldine. Manske (14) reviewed the general methods available for the synthesis of isoquinolines.

[1]*Manuscript received December 31, 1954.*
Contribution from the Division of Industrial and Cellulose Chemistry, McGill University, and from the Wood Chemistry Division, Pulp and Paper Research Institute of Canada, Montreal, Que. Abstracted from Ph.D. theses submitted to the University in May 1952 by D.A.G. and in August 1954 by A.W.F.

[2]*Present address: Esso Laboratories, Standard Oil Development Co., P.O. Box 51, Linden, N.J., U.S.A.*
[3]*Present address: Division of Pure Chemistry, National Research Council, Ottawa, Canada.*

Fritsch (8) reported in 1903 that N-(α-veratrylveratrylidene)-aminoacetal (I), prepared by condensing desoxyveratroin with aminoacetal, was cyclized with 75% sulphuric acid at room temperature to give a 13% yield (based on desoxyveratroin) of a yellow compound melting at 162°C., or 15°C. higher than papaverine (III). Found: C, 70.7; H, 6.4; N, 4.8%. Calc. for papaverine, $C_{20}H_{21}O_4N$: C, 70.7; H, 6.2; N, 4.1%. Like papaverine, the yellow compound was soluble in acetone and sparingly soluble in ethanol and ether. On the basis of these results, Fritsch claimed that the compound was isomeric with papaverine, but he did not attempt to establish its structure.

As a preliminary to repeating Fritsch's synthesis, it was noted that one mole of water was expelled and one mole of aminoacetal was retained when benzoin was boiled with an excess of the acetal, and formation of the Schiff base was presumably complete. A new compound, the desoxybenzoin from O-benzylvanillin, was incidentally prepared in crystalline form. Desoxyveratroin was then condensed with aminoacetal by distilling a mixture of the two substances at atmospheric pressure and up to 245°C. until the water and the excess of aminoacetal were removed. Several attempts to carry out the condensation under milder conditions failed. The product, the Schiff base (I),

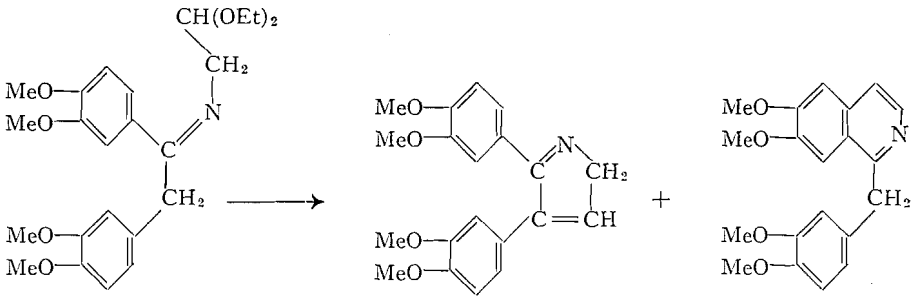

I II III

was an uncrystallized, viscous yellow oil, just as described by Fritsch (8). Cyclization of the Schiff base in 83% sulphuric acid gave an 18–23% yield of yellow needles melting at 164.5–165.5°C., whose composition confirmed the supposition that the compound was an isomer of papaverine. A small amount of papaverine (1.1%) was isolated from the mother liquor by chromatography on an alumina column.

One possible isomer, 5,6-dimethoxy-1-veratrylisoquinoline, which might have arisen by cyclization at position 2 rather than position 6 in the veratryl nucleus, could be dismissed immediately, since this isomer had been prepared unambiguously by the Bischler-Napieralski method as a white crystalline solid, m.p. 89–91°C. (13). Another possibility was the isomer 4,5-bis(3,4-dimethoxyphenyl)-2*H*-pyrrolenine (II), formed by an internal aldol condensation of the acetal, or of the aldehyde produced by hydrolysis, with the reactive methylene group in (I). A mass of evidence was assembled in support of this structure. The absence of active hydrogen (Zerewitinoff) and an inability to prepare an acetyl or benzoyl derivative indicated the absence of the N—H

group. The base formed no methiodide, but a solution in hydrochloric acid and acetone deposited an orange-colored crystalline hydrochloride which was somewhat unstable to hot solvents and was sparingly soluble in water. Further support for structure (II) was gained from the infrared absorption spectrum of the base. The presence of two very close bands at 805–810 cm.$^{-1}$, corresponding to two unsymmetrical triply-substituted benzene rings, excluded the isoquinoline ring structure (papaverine has only one band in this region). A C=N band at 1566 cm.$^{-1}$ and the absence of the N—H band showed that, if a pyrrole ring were present, the hydrogen atoms would have to be distributed around the ring in an abnormal manner.

In accord with structure (II), we would like to propose a structure for another unidentified isomer of papaverine, obtained by Schlittler and Müller in 1948 (17). The Schiff base N-(α-veratrylveratryl)-iminoacetal (IV), prepared by condensing 1,2-bis(3,4-dimethoxyphenyl)-ethylamine with glyoxal semiacetal, was cyclized with 75% sulphuric acid in 10% yield to a white crystalline compound melting at 222–223°C. and with the carbon and hydrogen content required for $C_{20}H_{21}O_4N$. The product was probably 2,3-bis(3,4-

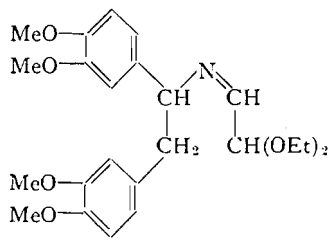

IV

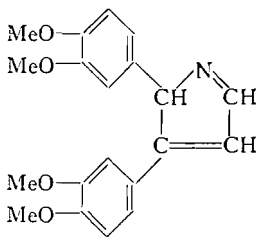

V

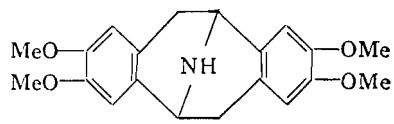

VI

dimethoxyphenyl)-2*H*-pyrrolenine (V), differing from (II) only in the position of the C=N bond.

An attempt was made by Allen and Buck (1) in 1930 to synthesize papaverine by the Fischer-Rügheimer modification of the Pomeranz-Fritsch synthesis. This modification, which was the subject of a recent paper (7), consisted of cyclizing N-benzylaminoacetals with sulphuric acid in the presence of an oxidizing agent such as arsenic pentoxide. Allen and Buck found that condensation of 1,2-bis(3,4-dimethoxyphenyl)-ethylamine with bromoacetal at 150°C. yielded a red oil, presumably N-(α-veratrylveratryl)-aminoacetal (VII), which could not be crystallized and which gave no crystalline derivatives. When the oil was treated with arsenic pentoxide in sulphuric acid solutions of various strengths, nothing but black amorphous material was obtained. In the present work, attempts were made to condense the amine with excess chloroacetal in boiling xylene, or with a slight excess of bromoacetal in cold benzene, but the first experiment yielded a black gum, and the second a white amorphous solid containing almost no nitrogen. In both cases much of the original amine could not be recovered. Allen and Buck (1) apparently employed the dimethyl acetal of bromoacetaldehyde instead of the more common

diethyl acetal used in the above experiments, and a direct comparison with their results was not possible.

It was then discovered that the desired secondary amine, N-(α-veratryl-veratryl)-aminoacetal (VII), could be prepared in good yield as a white crystalline solid by hydrogenation of the Schiff base (I) over Raney nickel. Cyclization of this crystalline amine (VII) under the conditions of the Rügheimer synthesis gave a white crystalline solid, m.p. 155.5–156°C., in yields of up to 56%. The product had the composition of dihydropapaverine, $C_{20}H_{23}O_4N$, but differed from the known substances 3,4-dihydropapaverine, m.p. 97–98°C., and pavine (VI), m.p. 201–202°C. (2, 18). Analogy with the cyclization of the Schiff base (I) suggested that the new substance was either the hitherto unknown 1,2-dihydropapaverine, or 2,3-bis(3,4-dimethoxyphenyl)-3-pyrroline (IX), formed by an internal aldol condensation of the acetal (or aldehyde) with the reactive methylene group. The former, however, was shown to be an unstable intermediate in the reduction of papaverine with tin and hydrochloric acid, cyclizing spontaneously in the acid solution to pavine (VI) (18). The absence of pavine in the acidic reaction mixture from the cyclization of (VII) was, therefore, an indication that no 1,2-dihydropapaverine was produced.

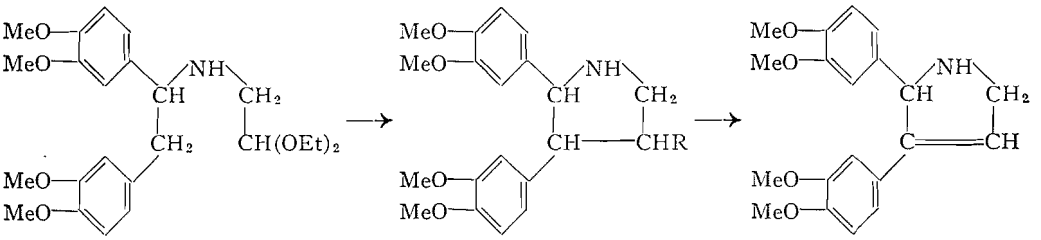

VII VIII, R = OH or SC_2H_5 IX

The over-all pattern of the infrared spectrum of the new base favored a structure similar to the pyrrolenine (II). A double band at 799–808 $cm.^{-1}$ indicated, as in the pyrrolenine, the presence of two unsymmetrical triply-substituted benzene rings. The presence of an N—H group was established by the presence of the N—H stretching frequency and by the preparation of a crystalline acetyl derivative. The base was, however, completely destroyed when attempts were made at dehydrogenation to the pyrrolenine with selenium at 250°C., with palladium-on-charcoal at 190°C., or with palladium black in boiling decalin.

Other experiments on the cyclization of the secondary amine (VII) at 20°C. showed that sulphuric acid of 20 to 65% strength was capable of hydrolyzing the acetal, but was unable to convert the product (aldehyde or aldol; see below) to the pyrroline (IX). At an acid strength of 75 or 83%, fair yields of the pyrroline were obtained, with or without arsenic pentoxide, but the duration of the reaction was critical (Fig. 1) because the product was unstable toward the condensing agent. When samples of the crystalline pyrroline were

dissolved in 83% sulphuric acid at room temperature and worked up in the usual manner after 2 and 18 hr., the recovery of the pyrroline was only 48% and 18%, respectively. The fact that the conditions of cyclization were so narrowly defined constituted another reason why Allen and Buck (1) failed to isolate the pyrroline.

The hydrolysis of N-(α-veratrylveratryl)-aminoacetal (VII) to the free aldehyde was studied in the hope that this procedure would reduce the time required for the subsequent cyclization. When the hydrolysis was carried out with 2 *N* hydrochloric acid for seven hours at 100°C. there was obtained, as anticipated, a product exhibiting a very strong positive dinitrophenylhydrazine test for the carbonyl function, and 92% of the theoretical amount of ethanol was recovered. The crude, gummy product was cyclized in 83% sulphuric acid over a four-hour period to the pyrroline (IX) in 32% yield (based on the acetal). When the acetal was hydrolyzed with concentrated hydrochloric acid at 20°C. for 0.5, 3, 6, 24, and 51 hr., the ethanol recovered amounted to 14, 71, 98, 100, and 99%, respectively, of the theoretical amount. Even after six hours, when the hydrolysis was complete, the colorless gum which formed the product gave a negative dinitrophenylhydrazine test for the carbonyl function. This product was probably the intermediate aldol, 2,3-bis(3,4-dimethoxyphenyl)-4-pyrrolidinol (VIII, R = OH). Concentrated hydrochloric acid, then, was presumably capable of cyclizing the acetal or aldehyde to the aldol, but not of dehydrating the aldol to the pyrroline.

Support for this argument was unintentionally provided by the results of an attempt to prepare the free aldehyde, N-(α-veratrylveratryl)-aminoacetaldehyde, by conversion of the acetal (VII) to the thioacetal, followed by cleavage of the thioacetal with mercuric chloride and cadmium carbonate (22). Instead of the expected thioacetal, the crystalline product, isolated from the reaction of the acetal with ethyl mercaptan in concentrated hydrochloric acid, had the composition of the sulphide, 2,3-bis(3,4-dimethoxyphenyl)-4-ethylmercaptopyrrolidine hydrochloride (VIII, R = SC_2H_5). The concentrated hydrochloric acid had effected, at some stage in the reaction, an aldol condensation.

Treatment of the sulphide with mercuric chloride and cadmium carbonate, under the conditions normally employed for the hydrolysis of a thioacetal to the corresponding aldehyde (22), gave a brilliant yellow mercury complex, m.p. 109°C. decomp., which contained nitrogen atoms, methoxyl groups, and mercury atoms in the ratio 2:8:1. When the complex was decomposed with hydrogen sulphide a colorless oil resulted, which was probably the aldol (VIII, R = OH), since tests for halogen and carbonyl groups were negative, and the oil yielded up to 34% of the pyrroline (IX) when aliquots were treated with 83% sulphuric acid.

In retrospect, it appeared that a major obstacle to the completion of the synthesis of papaverine by the Pomeranz-Fritsch method was the reactivity of the methylene group in N-(α-veratrylveratrylidene)-aminoacetal (I), and that this obstacle might be removed by replacing the group with, for example, a hydroxyl or keto group. Veratroin was not a suitable starting material,

because it was difficult to purify (12), and would probably not withstand the drastic conditions required for condensation with aminoacetal. On the other hand, the diketone veratril was a stable, crystalline compound, readily prepared by mild oxidation of veratroin (10, 12), or by methylation of vanillil, a substance now isolated from oxidized waste sulphite liquor and of potential commercial importance. It was found advantageous to methylate the vanillil in the form of its bright yellow crystalline disodium salt.

Many attempts were made to prepare the desired mono-Schiff base, N-(α-veratroylveratrylidene)-aminoacetal (X), by condensing veratril with various proportions of boiling aminoacetal. The conditions finally employed were slightly milder than those for the similar condensation of desoxyveratroin, but efforts to employ a lower temperature resulted only in the quantitative recovery of the veratril. After isolation, the product soon deposited a substantial quantity of the disubstituted compound, α,α'-biveratrylideneaminoacetal (XI), as white crystals. Since this compound yielded veratril on hydrolysis with dilute acid, no further internal condensation, such as formation of an imidazole (11), had occurred. The remainder of the product was a yellow oil which resisted attempts at purification by chromatography on Magnesol or cellulose columns. A paper chromatogram of the oil, developed with petroleum ether saturated with water, and sprayed with acid 2,4-dinitrophenyl-

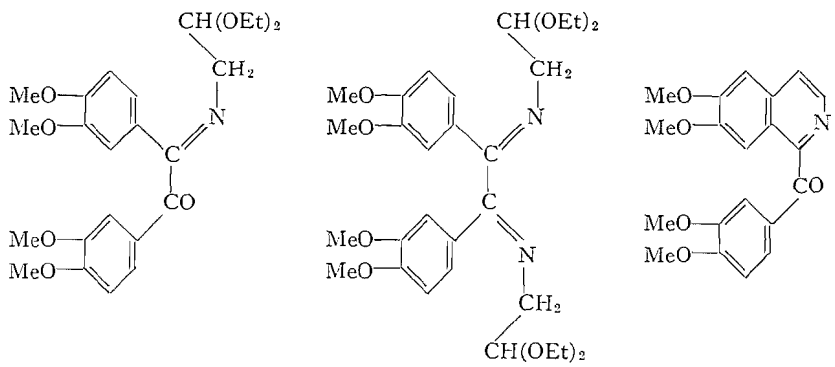

X XI XII

hydrazine, showed a yellow spot at R_f 0.79 and a red spot at R_f 0.68. Reference chromatograms with veratril and the crystalline di-Schiff base showed yellow spots at the base line and at R_f 0.79, respectively. The oil therefore contained some of the di-Schiff base and also a carbonyl compound which was assumed to be the sought-for mono-Schiff base (X). The oil, however, could not be crystallized, and repeated attempts to isolate the mono-Schiff base ended in failure. Attempts to reach the same goal by partial hydrolysis of the di-Schiff base were also fruitless. These failures were unexpected, because a preliminary condensation of veratril with boiling aniline readily gave the pale yellow crystalline monoanil in good yield.

An attempt was also made to isolate the secondary amine corresponding to the mono-Schiff base (X). The Schiff base mixture, or the pure di-Schiff base

alone, consumed no hydrogen when shaken with Adams' platinum oxide catalyst and 30–40 p.s.i. of hydrogen for 25 hr. at room temperature. Hydrogenation of the Schiff base mixture over freshly prepared Raney nickel at 1500 p.s.i. for three hours at 80–90°C. gave an oil which slowly deposited 2% of the unchanged di-Schiff base, but none of the desired secondary amine. Only 7% of veratril was recovered after hydrolysis of the residual oil with dilute hydrochloric acid, and neutralization of the acidic mother liquor caused the separation of a red ether-soluble oil (83% of the original veratril) which was not examined in detail.

In default of the pure mono-Schiff base (X), the experiments on cyclization were carried out on the original crude mixture. No papaveraldine (XII) was isolated from attempted cyclizations in 83% sulphuric acid for 20 hr. at room temperature, or in concentrated sulphuric acid for three minutes at 150°C., but an 8% yield, based on veratril, resulted from a cyclization carried out with 72% acid at room temperature or less. This result amounted to a new synthesis of papaverine (III), for papaveraldine was known to be reduced to papaverine with zinc dust and acetic anhydride (5, 19), as well as in a less direct way (5).

EXPERIMENTAL

Melting points were not corrected. The infrared spectra were obtained from Nujol mulls.

Materials

Veratroin was prepared from veratraldehyde by the benzoin condensation, and was reduced to desoxyveratroin substantially as described by Kubiczek (12). After the observation of Fritsch (8) that desoxyveratroin could not be separated from traces of veratril by crystallization had been confirmed, the crude product, 11.3 gm., was boiled for two hours under reflux with 100 ml. of anhydrous ethanol, 10 ml. of glacial acetic acid, and 6.7 gm. of Girard's "T" reagent for carbonyl compounds (the hydrochloride of N-trimethylaminoacethydrazide) (9). When cool, the solution was poured into 300 gm. of ice and water containing 21.5 gm. of potassium carbonate and was extracted with benzene until the extracts were colorless. The adduct was decomposed by acidifying the aqueous residue to pH 1 with hydrochloric acid, and an hour later the precipitated desoxyveratroin, 4.6 gm., was collected. The best overall yield was 18%, and m.p. 103.5–104.5°C., the recorded values being 106°C. (12, 21) or 107°C. (1).

Desoxyveratroin oxime, melting correctly at 128.5–129°C. (1, 12), was obtained in 99% yield by stirring a slurry of desoxyveratroin, hydroxylamine hydrochloride, and sodium acetate in aqueous ethanol for three days at room temperature. A yield of only 67% was obtained when the hydrochloride was used in pyridine solution (1). This oxime was reduced to 1,2-bis(3,4-dimethoxyphenyl)-ethylamine in 78% yield by sodium amalgam (1, 10), and in 69% yield by hydrogenation for 50 min. at 80–100°C. and 1300 p.s.i. over a Raney nickel catalyst. This catalyst was apparently more suitable than palladium-on-charcoal, which recently failed to give the expected result (21).

To prepare veratril, a mixture of 30.2 gm. (0.1 mole) of vanillil, m.p. 233–233.5°C. (diacetate, m.p. 139–140°C.), 24 gm. of sodium hydroxide, and 200 ml. of water was shaken rapidly until solution was complete. In a few minutes the red solution began to deposit in practically quantitative yield the bright yellow needles of the disodium salt of vanillil, which was washed with ethanol and dried *in vacuo* over solid potassium hydroxide. This salt melted above 265°C., was insoluble in all common organic liquids, but dissolved readily in water to give a yellow solution. A mixture of the dry, powdered salt with 28 ml. of dimethyl sulphate and 500 ml. of toluene was heated for five hours under reflux, and was then cooled. The next day the solid product, 55 gm., was freed from sodium salts by being ground in a mortar with 10% sodium carbonate, and the residue of almost pure veratril weighed 26.6 gm. (80.5%). One recrystallization from glacial acetic acid raised the melting point to 224–225°C., the recorded value being 223°C. (12). Veratril was also obtained by methylating vanillil with dimethyl sulphate and aqueous sodium carbonate or methanolic sodium hydroxide, but the yields were only 31% and 66%, respectively. Oxidation of the crude veratroin described above with copper sulphate in pyridine (10), or by air and alkali (12), gave veratril in over-all yields of 10% or less from veratraldehyde.

Aminoacetaldehyde diethyl acetal was prepared in 35% yield from chloroacetal as described by Richmond and Wright (16); the colorless product had the right composition, boiled correctly at 160–165°C., and yielded a picrate melting correctly at 142–143°C. When the chloroacetal was replaced by bromoacetal the yield of aminoacetal decreased to 14% or less; none was obtained from chloroacetal and sodamide suspended in boiling liquid ammonia, ether, or toluene.

4,4′-Dibenzyloxy-3,3′-dimethoxydesoxybenzoin

In accord with Kubiczek's general procedure (12), a solution of 35 gm. of O-benzylvanillin, m.p. 61°C., and 5.2 gm. of potassium cyanide in 100 ml. of ethanol was boiled under reflux for four and one-half hours in an atmosphere of hydrogen. The gum which precipitated when the solution was poured into 400 ml. of cold water was dissolved in 400 ml. of ether, and the ethereal solution was washed with dilute sodium carbonate, dilute sodium bisulphite, and finally with water. After the solution had been dried, evaporation of the ether left the benzoin as a crude oil, which was then dissolved in a boiling mixture of methanol, 300 ml., acetic acid, 150 ml., and water, 75 ml., and reduced by the gradual addition of 39 gm. of zinc dust during one and one-half hours. The white solid that separated when the solution cooled was extracted with acetone from excess zinc dust, and the extract was poured into water. The long white needles that separated weighed 9.5 gm. (28%) and their melting point of 141–142°C. was not changed by recrystallization from ethanol. Found: OCH_3, 13.0, 13.2%. Calc. for $C_{30}H_{28}O_5$: OCH_3, 13.2%. The oxime could not be prepared by stirring the desoxybenzoin with hydroxylamine hydrochloride and sodium acetate in 80% ethanol, but an 85% yield resulted when the substance was boiled for five and one-half hours with a solution of

the hydrochloride in pyridine. After three recrystallizations from ethanol, the melting point of the oxime was 137–137.5°C., depressed to 124–133°C. by admixture with the original desoxybenzoin.

Cyclization of N-(α-Veratrylveratrylidene)-aminoacetal (I)

A 125 ml. distillation assembly containing 25 gm. (0.079 mole) of desoxyveratroin and 30 gm. (0.225 mole) of aminoacetal was swept out with nitrogen and the heating was adjusted from time to time to give slow, uniform distillation of the excess aminoacetal. The temperature of the liquid rose steadily over the course of one hour from 165°C. to 245°C., as the last traces of the excess aminoacetal were carried over. The light yellow still residue of crude Schiff base (I) weighed 29.8 gm. (calc. 34.1 gm.).

Part of this oil (15.0 gm.) was dissolved in 160 ml. of chilled 83% sulphuric acid, the crimson solution was stirred for 20 hr. at room temperature, and was then mixed with 500 gm. of chopped ice. The slurry was made alkaline with aqueous sodium hydroxide and extracted with benzene. Extraction of the benzene solution with 0.1 *N* hydrochloric acid and addition of excess aqueous sodium hydroxide to the aqueous extract gave a slightly brown solid, which was then taken up in hot ethanol, decolorized with charcoal, and filtered. On cooling, there separated 2.89 gm. (21.5% based on desoxyveratroin) of yellow needles melting at 164–165°C. The melting point was raised slightly to 164.5–165.5°C. by recrystallization from ethanol. Found: C, 70.5, 70.8; H, 6.3, 6.2; N, 4.01, 4.02; OCH_3, 35.9, 36.1%; mol. wt., determined cryoscopically in benzene, 354, 336. Calc. for $C_{20}H_{21}O_4N$: C, 70.7; H, 6.2; N, 4.13; OCH_3, 36.6%; mol. wt., 339. Determinations made in anisole by the Zerewitinoff method showed the presence of only 0.12, 0.07 gm. of active hydrogen per mole. The compound was very soluble in chloroform, pyridine, glacial and aqueous acetic acid, sparingly soluble in acetone, methanol, and ethanol, and insoluble in water and ether.

The hydrochloride, prepared by adding a little concentrated hydrochloric acid to an acetone solution of the base, melted with decomposition at 212°C. Found: Cl, 9.36, 9.33%. Calc. for $C_{20}H_{22}O_4NCl$: Cl, 9.46%. This orange-colored substance was only sparingly soluble in water, and was rather unstable to recrystallization from hot solvents.

The brown ethanol filtrate, from which the yellow base had been removed, was evaporated to dryness and the residue digested exhaustively with boiling petroleum ether. Filtration and evaporation of the extract left 0.39 gm. of a pale yellow solid melting over the range 134–138°C. This solid was dissolved in dry benzene and chromatographed on an alumina column; the yellow base, $C_{20}H_{21}O_4N$, washed through the column weighed 0.17 gm. (1.3%) and melted at 164–165°C. The column was then extruded and all but the upper 0.5 cm., which was deep brown in color, was extracted with 5% pyridine in methanol. This extract yielded, on filtration and evaporation, 0.15 gm. (1.1%) of papaverine, m.p. 146.5–147.5°C. The base was converted to its hydrochloride, m.p. 221–222°C. The melting points of the base and its hydrochloride were identical with those of authentic papaverine and its hydrochloride, respectively, and no depression in the melting points was observed on admixture.

N-(α-Veratrylveratryl)-aminoacetal (VII)

The crude Schiff base (I), obtained as a pale yellow oil from a condensation of 20.0 gm. of desoxyveratroin with 33.7 gm. of aminoacetal, was dissolved in 100 ml. of ethanol and hydrogenated with 2 gm. of Raney nickel in a 300 ml. steel bomb at 1300 p.s.i. and 80–100°C. for 80 min. The yellow oil remaining after filtration and evaporation of the bomb contents was dissolved in 150 ml. of *N* hydrochloric acid and the solution was extracted several times with ether. A small amount (1.8 gm.; 9%) of desoxyveratroin was recovered from the ether extract. Neutralization of the acidic aqueous solution with sodium hydroxide caused the deposition of a mass of white crystals, which after washing and drying weighed 16.5 gm. (61% based on desoxyveratroin) and melted at 66–68°C. Repeated crystallization from methanol gave fine white felted needles and raised the melting point to 69.5–70°C. Found: C, 66.5, 66.5; H, 8.3, 8.3; N, 3.25, 3.29; OCH_3, 42.6, 42.2%. Calc. for $C_{24}H_{35}O_6N$: C, 66.5; H, 8.2; N, 3.24; OCH_3 (OC_2H_5 calc. as OCH_3), 43.0%. The product was very soluble in dilute mineral acids, ether, ethyl acetate, chloroform, and benzene, was only slightly less soluble in ethanol and methanol, and was insoluble in water.

In subsequent preparations under apparently identical conditions the yield of N-(α-veratrylveratryl)-aminoacetal (VII) was only 20–25% of the desoxyveratroin used.

2,3-Bis(3,4-dimethoxyphenyl)-3-pyrroline (IX) (Fig. 1)

The following experiment was typical of the series. A solution of 1.0 gm. of the acetal (VII) in 11 ml. of chilled 83% sulphuric acid was allowed to stand for seven hours at room temperature, and was then poured into ice water. After extraction with benzene, the acid solution was made alkaline and

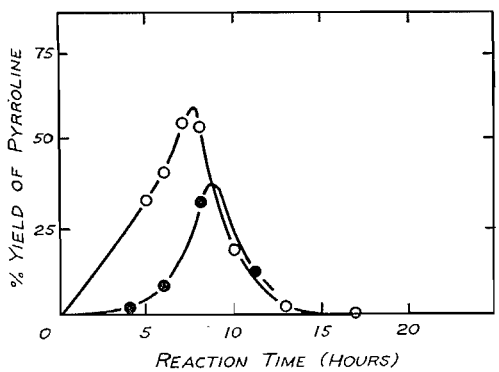

FIG. 1. Per cent yield of 2,3-bis(3,4-dimethoxyphenyl)-3-pyrroline (IX) from cyclization of N-(α-veratrylveratryl)-aminoacetal (VII) in sulphuric acid at 20°C. for various times; ○ in 83% acid, ● in 75% acid.

filtered. The acid-soluble white precipitate weighed 0.44 gm. (56%) and melted at 150–154°C. The melting point was raised to 155.5–156°C. by successive precipitation from hydrochloric acid solution with alkali. Found:

C, 70.3, 70.2; H, 6.9, 6.8; N, 4.05, 4.11, 4.02; OCH_3, 35.7, 35.5%. Calc. for $C_{20}H_{23}O_4N$: C, 70.3; H, 6.8; N, 4.10; OCH_3, 36.4%.

Treatment of the base with acetic anhydride in pyridine for three days at room temperature gave a 94% yield of the N-acetyl derivative melting at 203.5–204°C. Found: N, 3.56, 3.60; OCH_3, 32.1, 32.2%. Calc. for $C_{22}H_{25}O_5N$: N, 3.66; OCH_3, 32.4%.

2,3-Bis(3,4-dimethoxyphenyl)-4-ethylmercaptopyrrolidine Hydrochloride (VIII, R = SC_2H_5)

The acetal (VII), 3.65 gm. (0.0084 mole), was added to a stirred suspension of 15 ml. (0.20 mole) of ethyl mercaptan in 100 ml. of concentrated hydrochloric acid. After 24 hr., the mixture was poured into 100 ml. of water and the solution was washed with benzene. The solution was made alkaline with aqueous sodium hydroxide and again extracted with benzene. The benzene extract, on drying over anhydrous sodium sulphate and evaporating, yielded 1.98 gm. of a colorless oil. This oil was dissolved in acetone and converted to the hydrochloride by treatment with a few drops of the concentrated acid; the gum left on evaporation of the solution slowly crystallized when heated at 60°C. *in vacuo* for two hours. The product, washed with dry acetone and dry ether and then dissolved in a little methanol, was precipitated into dry ether. Weight, 1.38 gm. (37.5%), and m.p. 184–185°C. Found: C, 60.0; H, 5.9; N, 3.08, 2.99; S, 6.90, 7.08; OCH_3, 28.0, 27.9%. Calc. for $C_{22}H_{30}O_4NSCl$: C, 60.0; H, 6.9; N, 3.18; S, 7.28; OCH_3, 28.2%. The base, prepared from the hydrochloride by treatment with alkali, was an oil which appeared to decompose.

A solution of 1.29 gm. (0.003 mole) of the crystalline hydrochloride in water was made alkaline and extracted with benzene. The colorless oil left after evaporation of the dried extract was dissolved in 70 ml. of acetone to which had been added 3.75 gm. of mercuric chloride, 4.8 gm. of cadmium carbonate, and 1.0 ml. of water. The mixture was stirred for 24 hr. at room temperature, and was then filtered. The residue left after evaporation of the filtrate was dissolved in a large volume of chloroform and was washed with dilute aqueous potassium iodide followed by water. Evaporation of the dried chloroform solution left 1.17 gm. of a brilliant yellow solid melting with decomposition at 85°C. The melting point was raised to 109°C. by repeated solution in acetone and precipitation with ether. Found: N, 1.88, 1.90; OCH_3, 16.9, 17.2; Hg, 13.8%. These figures were in the ratio 1.96 N: 8.0 OCH_3: 1.0 Hg.

A solution of 0.800 gm. of this mercury complex in aqueous acetone containing a few drops of acetic acid was treated with hydrogen sulphide until no further precipitation of black mercuric sulphide occurred. This precipitate was dried and weighed to yield the analytical figure for mercury quoted above. The acetone solution was diluted with water, made alkaline, and extracted with benzene. Evaporation of the dried extract left 0.468 gm. of a colorless oil which was negative to tests for halogen and carbonyl groups; yield as the aldol (VIII, R = OH) based on the sulphide (VIII, R = SC_2H_5), 65%.

This oil was treated with 5 ml. of 83% sulphuric acid at room temperature. Aliquots were removed at various intervals and the pyrroline (IX) was

isolated as outlined previously. After 1.5, 3, 5, 7, and 15 hr. the yields of *IX* (based on the oil) were 22, 30, 34, 19, and 2% respectively. The authenticity of these products was established by mixed melting point with samples of the pyrroline (IX).

Condensation of Veratril with Aminoacetal

A mixture of 16.5 gm. (0.05 mole) of veratril and 25.0 gm. (0.17 mole) of aminoacetal was boiled gently under reflux in a nitrogen atmosphere until all of the veratril was dissolved. After cooling, the viscous red product was dissolved in ether and the solution was filtered to remove the unchanged veratril, which in this run weighed only 0.1 gm. The ethereal solution was extracted several times with water to remove the excess aminoacetal, then was dried over anhydrous potassium carbonate and evaporated. On rubbing with a little ethanol, the residue partly crystallized in well-formed white hexagonal plates, which weighed 3.3 gm. (12%) and melted at 98.5–100°C. after one recrystallization from ethanol–water. Two more recrystallizations from ethanol–water raised the melting point to 101–102°C., unchanged by recrystallization from ligroin. Found: C, 64.3, 63.8; H, 7.8, 7.7; N, 4.82, 4.84, 4.89, 4.84; OCH_3, 43.3, 43.4%. Calc. for α,α'-biveratrylideneaminoacetal (XI), $C_{30}H_{44}O_8N_2$: C, 64.3; H, 7.9; N, 5.00; OCH_3 (OC_2H_5 calc. as OCH_3), 44.3%. Another 1.2 gm. of this di-Schiff base was recovered from the eluates of the experiments on column chromatography, bringing the total yield up to 16%. The product was very soluble in methanol, ethanol, ether, chloroform, and benzene, less soluble in hot ligroin, and insoluble in water.

A solution of 47.6 mgm. of the di-Schiff base, 2 ml. of ethanol, and 10 ml. of *N* hydrochloric acid was kept for 10 hr. at room temperature and then filtered. The veratril weighed 6.5 mgm. (23%) and melted at 223.5–224°C. (mixed m.p. undepressed). The recovery of veratril was increased to 42% when the reaction was carried out on the steam bath for six hours under reflux.

Papaveraldine (XII)

Condensation of 3.30 gm. of veratril with 5.0 gm. of aminoacetal as described above gave 6.6 gm. of a partly crystalline red oil, and 0.33 gm. of veratril was recovered. Part of this mixture of Schiff bases, 4.7 gm., was dissolved cautiously in 50 ml. of 72% sulphuric acid and kept for two days at 5°C. and for another three days at room temperature. The dark red solution was poured onto 50 gm. of chopped ice, filtered, and extracted twice with ether. When the aqueous portion was neutralized with 10% sodium carbonate an amorphous buff-colored solid separated, together with much black gummy material. A solution of the solid in benzene was combined with a benzene extract of the filtrate, and applied to a 6 in. alumina column. The black material remained at the top of the column. The benzene eluates were separately evaporated, the residues taken up in dilute hydrochloric acid, and the solutions distilled to dryness under reduced pressure. Some of the fractions yielded a crystalline hydrochloride, m.p. 189–192°C. These fractions were combined, taken up in hot water, and neutralized with concentrated ammonia. The

base which separated, when collected on a filter and washed thoroughly with water, weighed 0.177 gm. (8%) and melted at 205–207°C. One recrystallization from methyl ethyl ketone gave 0.135 gm. of papaveraldine melting at 208–209°C., not depressed on admixture with an authentic sample, m.p. 208–209°C., prepared by oxidation of papaverine with selenium dioxide as described by Taylor (20).

The hydrochloride, prepared by covering the base with 10% hydrochloric acid, heating the mixture on a steam bath, and adding water dropwise until solution was complete, crystallized on cooling in fine yellow needles, m.p. 198–199°C., undepressed on admixture with a sample similarly prepared from authentic papaveraldine. Papaveraldine was reported to melt at 210°C. corr., and its hydrochloride at 200°C. corr. (6, 20).

Veratril Monoanil

A mixture of 3.30 gm. (0.01 mole) of veratril and 4.65 gm. (0.05 mole) of freshly distilled aniline was heated under nitrogen for three hours with steady reflux (bath temp. 230°C.). The mixture partly crystallized on cooling. After being triturated with ether in a mortar, the mixture left a residue of 1.75 gm. which was identified as veratril (52% recovery).

The ethereal mother liquor was evaporated to dryness and the residual oil was mixed with 5 ml. of ethanol. A crop of yellow crystals, 0.757 gm., slowly separated. Further dilution with ethanol yielded two more crops of 0.826 gm. and 0.476 gm. Recrystallization of the middle crop from ethanol gave a product, m.p. 172–173°C. with strong sintering at 159°C., which appeared to be a mixture of two crystalline substances, one pale yellow and the other golden yellow. Recrystallization from ethyl acetate removed the golden yellow impurity, and the veratril monoanil then melted at 172–173°C. Found: C, 70.8, 70.7; H, 5.7, 5.8; N, 3.33, 3.36; OCH_3, 30.5, 30.5%. Calc. for $C_{24}H_{23}O_5N$: C, 71.1; H, 5.7; N, 3.45; OCH_3, 30.6%. The anil was very soluble in chloroform, soluble in benzene, ether, and hot ethyl acetate, slightly soluble in ethanol, and insoluble in water and hexane.

A solution of 30.2 mgm. of veratril monoanil, 2 ml. of ethanol, and 5 ml. of *N* hydrochloric acid was heated on the steam bath for six hours under reflux. After cooling, the mixture was poured into water, allowed to stand undisturbed for several hours, and filtered. The veratril weighed 22.8 mgm. (93%) and melted at 223.5–224°C. (mixed m.p. undepressed).

ACKNOWLEDGMENTS

We wish to thank Mr. A. W. Pross of Canadian Industries (1954) Limited, McMasterville, Que. for determining and interpreting the infrared spectra, and Dr. C. A. Sankey of the Ontario Paper Company, Thorold, Ont. for a generous gift of vanillil. Two of us are grateful for assistance in the form of scholarships from Canadian Industries Limited (D.A.G.), from the Spruce Falls Power and Paper Company (A.W.F.), from the Pulp and Paper Research Institute of Canada (A.W.F.), and from the National Research Council of Canada (D.A.G. and A.W.F.).

REFERENCES

1. ALLEN, I. and BUCK, J. S. J. Am. Chem. Soc. 52: 310. 1930.
2. BATTERSBY, A. R. and BINKS, R. Chemistry & Industry, 1455. 1954.
3. BISCHLER, A. and NAPIERALSKI, B. Ber. 26: 1903. 1893.
4. British Intelligence Objectives Subcommittee, Final Rept. 766: 119. 1945; 1774: 1. 1947.
5. BUCK, J. S., PERKIN, W. H., JR., and STEVENS, T. S. J. Chem. Soc. 127: 1462. 1925.
6. DOBSON, B. and PERKIN, W. H., JR. J. Chem. Soc. 99: 135. 1911.
7. FRANK, A. W. and PURVES, C. B. Can. J. Chem. 33: 365. 1955.
8. FRITSCH, P. Ann. 329: 37. 1903.
9. GIRARD, A. and SANDULESCO, G. Helv. Chim. Acta, 19: 1095. 1936.
10. HARTWELL, J. L. and KORNBERG, S. R. L. J. Am. Chem. Soc. 67: 1606. 1945.
11. JAPP, F. R. and DAVIDSON, W. B. J. Chem. Soc. 67: 32. 1895.
12. KUBICZEK, G. Monatsh. 76: 55. 1945.
13. LINDENMANN, A. Helv. Chim. Acta, 32: 69. 1949.
14. MANSKE, R. H. F. Chem. Revs. 30: 145. 1942.
15. POMERANZ, C. Monatsh. 14: 116. 1893.
16. RICHMOND, H. H. and WRIGHT, G. F. Can. J. Research, B, 23: 158. 1945.
17. SCHLITTLER, E. and MÜLLER, J. Helv. Chim. Acta, 31: 914. 1948.
18. SCHÖPF, C. Experientia, 5: 201. 1949.
19. STUCHLIK, L. Monatsh. 21: 813. 1900.
20. TAYLOR, E. P. J. Pharm. and Pharmacol. 2: 324. 1950.
21. WALKER, G. N. J. Am. Chem. Soc. 76: 3999. 1954.
22. WOLFROM, M. L. J. Am. Chem. Soc. 51: 2188. 1929.

THE VAPOR PHASE PHOTOLYSIS OF HEXAFLUOROACETONE IN THE PRESENCE OF METHANE AND ETHANE[1]

By P. B. Ayscough,[2] J. C. Polanyi,[3] and E. W. R. Steacie

ABSTRACT

The photolytic decomposition of hexafluoroacetone by light of wavelength 3130 Å has been used to produce trifluoromethyl radicals for a study of their reactions with methane and ethane. It has been shown that these radicals abstract hydrogen with greater facility than do methyl radicals. The activation energies for the two reactions

$$CF_3 + CH_4 \rightarrow CF_3H + CH_3$$

and

$$CF_3 + C_2H_6 \rightarrow CF_3H + C_2H_5$$

are found to be 10.3 ± 0.5 kcal./mole and 7.5 ± 0.5 kcal./mole respectively, if one can assume zero activation energy for the recombination of trifluoromethyl radicals.

INTRODUCTION

Relatively few kinetic studies have been made on the reactions of fluoroalkyl radicals and most of those so far reported have not yielded very precise data about the elementary reactions of these radicals. In part this is the result of analytical difficulties in handling the mixtures of fluorinated compounds in the reaction products. Further difficulties have arisen because of low quantum yields (as in the photolysis of trifluoromethyl iodide (2, 4, 6)), side reactions caused by the necessity of using high temperatures for pyrolyses (as in the pyrolysis of tristrifluoromethyl arsine (1)), or the production of more than one type of radical in the primary breakdown (as in the photolysis of trifluoroacetone (12)). Some exploratory work on the photolysis of hexafluorodimethyl mercury (11) showed that trifluoromethyl radicals were produced by straightforward fission of the mercury–carbon bonds but the total yield was small on account of the low volatility of the substrate.

During a preliminary study of the photolysis of hexafluoroacetone it was found that this compound fulfills most of the requirements of a source of trifluoromethyl radicals and that a simple analytical procedure can be devised for estimating the products. It was therefore decided to begin a study of the elementary reactions of these radicals with an investigation of their reactions with the simpler hydrocarbons, using the photolysis of hexafluoroacetone as the source of the radicals.

Between 80° and 300°C. hexafluoroacetone yields on photolysis only hexafluoroethane and carbon monoxide, in the stoichiometric proportions. The quantum yield is independent of light intensity and is only slightly affected by pressure in the range used (20–100 mm.). In the presence of hydrocarbons fluoroform is found in the products and under certain conditions replaces the hexafluoroethane almost completely. For instance when 25 mm. hexafluoroacetone is photolyzed at 120°C. in the presence of an equal amount of isobutane

[1]*Manuscript received November 30, 1954.*
Contribution from the Division of Pure Chemistry, National Research Council, Ottawa, Canada. Issued as N.R.C. No. 3554.
[2]*National Research Council of Canada Postdoctorate Fellow, 1953–55.*
[3]*National Research Council of Canada Postdoctorate Fellow, 1952–54.*

over 99% of the fluorine appears in the products as fluoroform. It therefore seems that above 80°C. the primary decomposition is a simple split into radicals

$$CF_3COCF_3 \rightarrow 2\ CF_3 + CO$$

and that these radials can abstract hydrogen or dimerize according to the composition of the reaction mixture. Above 300°C. some attack on the walls of the vessel takes place with the formation of silicon tetrafluoride and carbon dioxide, though the rate of this reaction can be considerably reduced by placing on the inside of the vessel a thin coating of calcium fluoride. No carbon tetrafluoride was found even at the highest temperatures used (about 350°C.) so it appears that the activation energy for reactions such as

$$CF_3 + CF_3COCF_3 \rightarrow CF_4 + CF_3COCF_2$$

is quite high.

A more detailed report on the photolysis of hexafluoroacetone will be presented elsewhere. The present paper describes experiments in which this compound was photolyzed in the presence of methane and ethane.

EXPERIMENTAL

Apparatus

The apparatus was essentially the same as that used in experiments on the photolysis of acetone described in earlier papers from this laboratory. The light source was a B.T.H. high pressure mercury lamp (type ME/D, 250 watts) operated on 220 v. d-c. This lamp gives a concentrated beam of light which was easily collimated by a single quartz lens and a stop. The quartz reaction vessel (10 cm. long, 5 cm. diam.) had a volume of about 190 ml. It was found desirable to use a beam of light of smaller diameter than the vessel in order to reduce attack on the walls by fluorinated radicals at high temperatures, so the illuminated volume was only 62 ml. A layer of calcium fluoride a few wavelengths in thickness was sputtered on to the inside of the vessel to further prevent access of the radicals to the quartz. (It should be stated that there is no proof that these precautions are necessary at the lower temperatures used in studying hydrogen-abstraction reactions such as those reported here. The vessel and optical system were designed for experiments at high temperatures at which this form of attack is troublesome.) The reaction cell was heated in an aluminum block furnace, the temperature of which could be controlled to within 1°C.

All the runs described in this paper were carried out using a combination of 5 cm. nickel sulphate (200 gm./l.), 1 cm. potassium chromate (0.2 gm./l.), 1 cm. potassium hydrogen phthalate (5 gm./l.), and a 3 mm. C.S. 7–54 (9863) filter to isolate the 3130 Å line.

Materials

Two samples of hexafluoroacetone were presented by the Minnesota Mining and Manufacturing Co., to whom we are greatly indebted. Further samples were prepared in collaboration with Dr. L. C. Leitch and Mr. A. T. Morse by the permanganate oxidation of perfluoroisobutene (3, 10). The final sample

after drying over P_2O_5 was distilled in a Podbielniak column and a small middle cut taken for use. This material had a b.p. of −27.8°C. at 754 mm. pressure, and when analyzed on the mass spectrometer showed a spectrum which could be completely identified with that expected from CF_3COCF_3. It was stored in a blackened bulb at liquid air temperature because some decomposition was observed at room temperature. The methane and ethane were Phillips Research Grade and were found by mass spectrometric analysis to contain less than one per cent impurity (mainly higher hydrocarbons).

Procedure

Hexafluoroacetone was admitted to the heated reaction vessel and its pressure measured on a mercury manometer. When methane was to be added the hexafluoroacetone was condensed in a cold finger close to the cell at −180°C. while the methane was admitted. After allowing the hexafluoroacetone to warm up to cell temperature the total pressure was measured. From this the pressure of methane could be obtained. After the reactants were mixed for at least five minutes by means of a Toepler type pump the reaction vessel was isolated by closing a cutoff valve and the light switched on. When ethane was used the two reactants were condensed separately into the cold finger and then mixed as before. The photolyses were allowed to proceed until the amount of decomposition was about five per cent. No correction for pyrolysis was necessary in the experiments described.

Analytical Methods

The products were analyzed by means of two LeRoy stills in conjunction with a mercury diffusion pump and a combined Toepler and gas burette. The bulk of the hexafluoroacetone was condensed in the first still at −145°C. while the second still was maintained at −210°C. to retain all the products except CO (and CH_4 in reactions with this gas). Mixtures of CO and CH_4 were estimated mass spectrometrically. The second still was then raised to −155°C. to collect the C_2F_6, CF_3H, C_2H_6, and SiF_4 and CO_2 if present. Two methods were used to analyze this fraction; the mass spectrometer was used when an approximate estimate of all the components was needed, but in most of the experiments described here C_2F_6 and CF_3H accounted for at least 95% of this fraction and it was found more convenient and probably more accurate to use the infrared absorption of these compounds for the estimation. Both have very strong and sharp bands in the region 1300 cm.$^{-1}$ to 1100 cm.$^{-1}$ and there is very little overlapping. In the presence of a large excess of ethane correction must be made for the pressure broadening of the CF_3H band. When mass spectrometric and infrared analyses were made on the same mixtures the agreement was excellent. The hexafluoroacetone remaining was examined mass spectrometrically for the presence of other products such as CF_3CH_3 and $CF_3CH_2CH_3$, but quantitative analysis for such substances is very uncertain.

RESULTS

In Table I are presented the results of experiments in which hexafluoroacetone was photolyzed in the presence of methane or ethane, together with a

TABLE I

Temp., °K.	Press. CF_3COCF_3, mm.	Press. RH, mm.	Time, sec.	Products, moles/sec. × 10^{10}			$\frac{R_{CF_3H}}{R^{\frac{1}{2}}_{C_2F_6}[RH]} \times 10^{12}$ (molecules/cc.)$^{-\frac{1}{2}}$ sec.$^{-\frac{1}{2}}$
				C_2F_6	CF_3H	CO	
Hexafluoroacetone alone							
394	51.0	—	3600	24.7	—	25.4	—
406	49.0	—	1800	25.3	—	27.1	—
433	25.0	—	2700	18.4	—	19.5	—
494	24.7	—	2400	16.3	—	17.4	—
RH = methane							
395	25.1	92.5	5100	10.72	2.11		0.282
400	24.6	89.7	6600	11.8	2.62		0.348
407	24.7	84.0	3600	10.72	2.74		0.415
409.5	25.0	93.6	3300	12.52	3.12	17.8	0.394
416	23.4	46.6	4200	10.7	1.77	12.4	0.494
433	24.6	85.2	4200	10.9	5.08	15.2	0.801
441.5	25.0	72.8	4500	10.2	5.61		1.09
451	25.8	56.3	3600	10.85	5.00		1.25
451	24.8	94.5	6000	10.75	8.79		1.31
457.5	23.0	55.0	3000	9.74	5.08	13.8	1.385
469	24.9	43.0	3600	7.97	5.48	10.3	2.17
477.5	24.5	54.9	3000	8.42	9.11		2.79
485	25.4	55.9	3600	9.39	10.95	15.5	3.07
491.5	24.3	58.0	3600	7.20	12.4		4.01
503	25.2	48.5	4200	8.86	13.5	18.9	4.80
510	25.0	50.6	3300	8.39	16.0		5.67
524	24.7	42.5	2430	8.10	17.4		7.71
RH = ethane							
353.5	25.4	27.2	6000	0.88	2.16	2.78	2.61
362.5	25.7	26.5	6000	1.53	3.42	4.66	3.74
366	24.0	25.4	6000	2.02	4.06	5.01	3.68
385	25.5	24.7	5400	2.96	7.18	7.68	6.17
391	24.5	23.9	3600	1.88	6.67	5.98	8.18
403	25.2	56.6	3600	0.59	11.95	8.00	11.3
421.5	25.8	25.4	3900	2.66	14.35	9.78	14.9
428.5	24.1	25.8	3600	1.86	13.95		17.4
439	25.6	26.0	3000	1.32	15.8	9.20	23.7
443.5	24.5	24.1	2400	1.42	18.65	10.0	29.5
454	38.0	25.2	2400	1.99	22.4	13.0	29.3
471.5	39.5	24.0	2400	2.03	27.5	16.9	38.9
489	25.1	25.4	2400	0.59	24.7	12.2	63.3

few runs without hydrocarbon. The runs were carried out in several series with different light intensities to show that the value of the ratio $R_{CF_3H}/R^{\frac{1}{2}}_{C_2F_6}$ (CH_4) is not affected by changes in intensity. This method of grouping the results also had the effect of showing that there was none of the progressive change in rate constants due to surface effects that had been a feature of previous investigations (1).

Hexafluoroethane and fluoroform are major products at all temperatures and these clearly result from dimerization and hydrogen-abstraction reactions of trifluoromethyl radicals. The following reaction scheme will account for these products.

$$CF_3COCF_3 \rightarrow 2\ CF_3 + CO \qquad [1]$$

$$2\ CF_3 \rightarrow C_2F_6 \qquad [2]$$

$$CF_3 + CH_4 \rightarrow CF_3H + CH_3 \qquad [3]$$

$$CF_3+C_2H_6 \rightarrow CF_3H+C_2H_5. \quad [3']$$

Since CF_3CH_3 and C_2H_6 were found in appreciable amounts in the products from experiments with methane as substrate it is reasonable to assume that the methyl radicals produced in reaction [3] disappear by reactions such as

$$CH_3+CF_3 \rightarrow CF_3CH_3 \quad [4]$$

and

$$2\ CH_3 \rightarrow C_2H_6. \quad [5]$$

The disappearance of the ethyl radicals produced in reaction [3'] can be accounted for by the analogous reactions

$$C_2H_5+CF_3 \rightarrow CF_3C_2H_5 \quad [4']$$

and

$$2\ C_2H_5 \rightarrow C_4H_{10}. \quad [5']$$

The amount of CF_3CH_3 and C_2H_6 increases markedly with temperature as would be expected from this mechanism. Further support for this reaction scheme can be provided by evaluating the functions

$$R_1 = [2(C_2F_6)+(CF_3H)+(CF_3CH_3)]/CO \text{ and } R_2 = [2(C_2H_6)+(CF_3CH_3)]/CO$$

which should both be equal to unity if all the radicals can be accounted for in this way. For three runs in which complete analyses were made the values were, for R_1, 0.97, 0.95, 0.97 and for R_2, 0.85, 0.90, 1.05. This is considered satisfactory in view of the difficulty of estimating small quantities of CF_3CH_3 in the presence of excess hexafluoroacetone.

If the reaction mechanism suggested is substantially correct, the rate of formation of C_2F_6 can be expressed by

$$R_{C_2F_6} = k_2[CF_3]^2$$

and the rate of formation of CF_3H by

$$R_{CF_3H} = k_3[CF_3][CH_4]$$

or

$$k_3'[CF_3][C_2H_6].$$

From these equations it follows that

$$k_3/k_2^{\frac{1}{2}} = R_{CF_3H}/R_{C_2F_6}^{\frac{1}{2}}[CH_4] = A_3/A_2^{\frac{1}{2}}.e^{-(E_3-\frac{1}{2}E_2)/RT}$$

and

$$k_3'/k_2^{\frac{1}{2}} = R_{CF_3H}/R_{C_2F_6}^{\frac{1}{2}}[C_2H_6] = A_3'/A^{\frac{1}{2}}.e^{-(E_3'-\frac{1}{2}E_2)/RT}.$$

Reference to Fig. 1 will show that the Arrhenius plots for both reactions are straight lines within the experimental error, in the temperature range used. The values obtained by the method of least squares for the differences in activation energy are

$$E_3-\tfrac{1}{2}E_2 = 10.3 \text{ kcal./mole}$$
$$E_3'-\tfrac{1}{2}E_2 = 7.5 \text{ kcal./mole.}$$

Assuming an effective cell volume of 62 ml., the ratios of rate constants at 182°C. (455°K.) are

$$k_3/k_2^{\frac{1}{2}} = 1.52 \times 10^{-12} \text{ (molecule/cc.)}^{-\frac{1}{2}}\text{sec.}^{-\frac{1}{2}}$$
$$k_3'/k_2^{\frac{1}{2}} = 3.18 \times 10^{-11} \text{ (molecule/cc.)}^{-\frac{1}{2}}\text{sec.}^{-\frac{1}{2}}$$

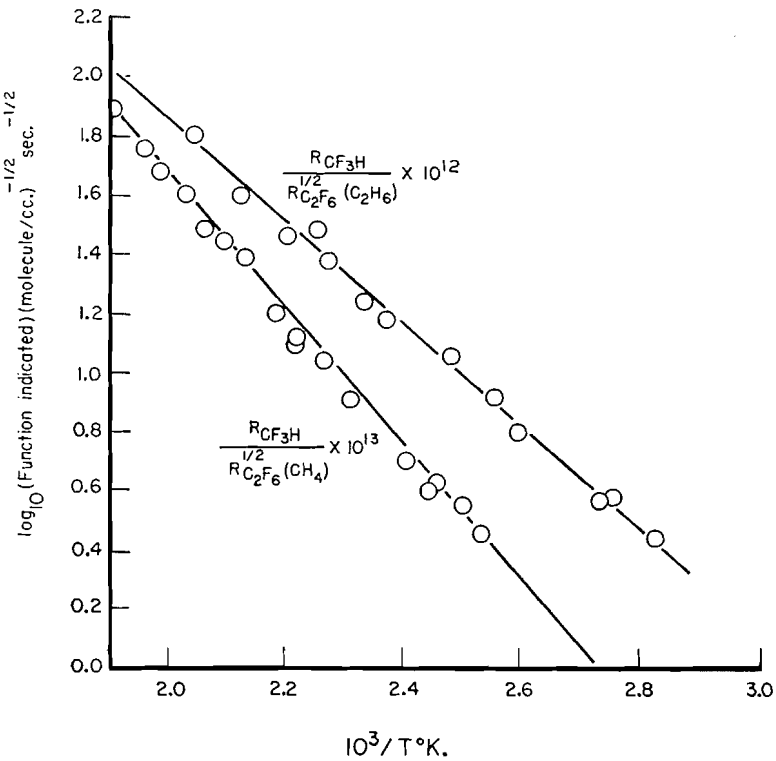

FIG. 1. Arrhenius plots for the photolysis of hexafluoroacetone.

and the ratio of steric factors

$$P_3/P_2^{\frac{1}{2}} = 5 \times 10^{-3}$$
$$P_3'/P_2^{\frac{1}{2}} = 3 \times 10^{-3}.$$

For these calculations the collision diameters assumed were as follows: CH_3, 3.5 Å; CH_4, 3.5 Å; C_2H_6, 4.5 Å; CF_3, 4.0 Å. The mean square deviation of the values of the activation energies is 0.22 kcal./mole in each case, but the systematic errors in the analyses are probably greater and the error is more likely to be about 0.5 kcal./mole.

DISCUSSION

It has been shown that hexafluoroacetone is a convenient source of trifluoromethyl radicals and that the technique used for studies of the reactions of methyl radicals may be applied in a very similar manner to these radicals. At the moment lack of sufficient quantitative data makes a close comparison between methyl and trifluoromethyl radicals rather speculative. In order to use the available data it is necessary to make certain assumptions about the steric factors and activation energies for the dimerization reactions of methyl and trifluoromethyl radicals. It is now reasonably certain that the steric factor for the recombination of methyl radicals is about unity and the activa-

tion energy zero or very nearly so (5, 7, 8), and there seems to be no reason to suppose that the steric factor is markedly different for the dimerization of trifluoromethyl radicals. This suggestion is supported by the fact that the steric factors obtained in this study are "normal" (compare the value 6×10^{-4} obtained by Trotman-Dickenson, Birchard, and Steacie (13) for the reaction $CH_3+C_2H_6 \rightarrow CH_4+C_2H_5$). However, it does not appear to be entirely justifiable to assume zero activation energy for the dimerization of trifluoromethyl radicals. Sieger and Calvert (12) have mentioned this possibility, basing their suggestion on configurational differences between methyl and trifluoromethyl radicals. It seems to us that even if there is no important difference in configuration the marked polarity of the carbon–fluorine bonds will result in dipole–dipole interaction at some stage of the reaction which may cause an energy barrier of significant proportions. However, it is extremely unlikely that it would be as high as 5–6 kcal. which would be necessary to bring the values of E_3 and E_3' into line with the currently accepted values for the analogous reactions $CH_3+CH_4 \rightarrow CH_4+CH_3$ (13–14 kcal.) (14, 9), and $CH_3+C_2H_6 \rightarrow CH_4+C_2H_5$ (about 10.4 kcal.) (13). Thus there is little doubt that trifluoromethyl radicals do abstract hydrogen with greater facility than do methyl radicals, though it would not be wise to suggest that the observed differences in activation energies for abstraction by methyl and trifluoromethyl radicals have any great quantitative significance. On the basis of present information the difference appears to be about 3 kcal./mole, assuming for the moment zero activation energy for the reaction $2\ CF_3 \rightarrow C_2F_6$. Sieger and Calvert give a value of 2.3 kcal./mole for this difference in the case of abstraction of hydrogen from trifluoroacetone (12). It is, however, clearly desirable to determine the rate constants of the dimerization reaction with sufficient accuracy to evaluate the activation energy and pre-exponential factors before discussing this question further.

ACKNOWLEDGMENT

We are indebted to Mr. R. Lauzon for assistance in the infrared analyses and to Miss F. Gauthier and Miss J. Fuller for the mass spectrometric analyses.

REFERENCES

1. Ayscough, P. B. and Emeleus, H. J. J. Chem. Soc. 3381. 1954.
2. Banus, J., Emeleus, H. J., and Haszeldine, R. N. J. Chem. Soc. 3041. 1950.
3. Brice, T. J., Lazerte, J. D., Hals, L. J., and Pearlson, W. H. J. Am. Chem. Soc. 75: 2698. 1953.
4. Dacey, J. R. Discussions Faraday Soc. 14: 84. 1953.
5. Gomer, R. and Kistiakowsky, G. B. J. Chem. Phys. 19: 85. 1951.
6. Haszeldine, R. N. Discussions Faraday Soc. 14: 134. 1953.
7. Ingold, K. U. and Lossing, F. P. J. Chem. Phys. 21: 368. 1953.
8. Ingold, K. U. and Lossing, F. P. J. Chem. Phys. 21: 1135. 1953.
9. McNesby, J. R. and Gordon, A. S. J. Am. Chem. Soc. 76: 4196. 1954.
10. Morse, A. T., Ayscough, P. B., and Leitch, L. C. Can. J. Chem. 33: 453. 1955.
11. Polanyi, J. Unpublished work.
12. Sieger, R. A. and Calvert, J. G. J. Am. Chem. Soc. 76: 5197. 1954.
13. Trotman-Dickenson, A. F., Birchard, J. R., and Steacie, E. W. R. J. Chem. Phys. 19: 163. 1951.
14. Trotman-Dickenson, A. F. and Steacie, E. W. R. J. Chem. Phys. 19: 329. 1951.

FREE RADICAL RECOMBINATION IN THE PHOTOLYSIS OF ACETONE[1]

By S. N. Naldrett[2]

ABSTRACT

$(CH_3CO)_2$-1-C^{14} (I) was prepared by irradiating $(CH_3)_2CO$ in the presence of CH_3I-C^{14}. Acetone was then irradiated at room temperature with light of 2537 Å in the presence of (I). Radioactivity was found in all products which contained methyl groups but not in any carbon monoxide product. The amount of carbon-14 ultimately found in acetone confirms that the quantum efficiency of the primary photolytic process is nearly unity and that extensive recombination of methyl and acetyl radicals to form acetone is responsible for the low over-all quantum efficiency of decomposition.

INTRODUCTION

The photolysis of acetone has been exhaustively investigated. (For reviews see Dorfman and Noyes (2) and Steacie (7).) One important feature of the mechanism is the explanation of the low quantum yield at low temperatures by the recombination reaction:

$$CH_3 + CH_3CO \rightarrow CH_3COCH_3.$$

It seemed of value to make a direct check of this reaction by the use of radioactive carbon.

EXPERIMENTAL

The Photolysis System

Irradiations were carried out in a cylindrical quartz vessel 45 mm. in diameter and 108 mm. long with polished plane parallel windows. Illumination was supplied by a neon-mercury resonance lamp in a quartz envelope with a filter of chlorine gas so that the light was mostly 2537 Å. Three different lamps were used in the course of the experiments. All irradiations were carried out at room temperature.

Measurement of Radioactivity

All samples were counted in Geiger-Mueller tubes as gases, so that no counts were lost because of self-absorption or window absorption and only a geometry correction was necessary. The counting efficiency of each gas mixture was checked by the response given to an external radioactive standard. Usually no external quench was required, but if necessary a Neher-Harper type of electronic quenching circuit was used. Sufficient counts were observed so that the uncertainty in the count rate recorded was less than other errors such as measurement of sample size, loss by adsorption, or in stopcock grease, etc.

Preparation of Biacetyl-1-C^{14}

Active $(CH_3CO)_2$ was prepared by irradiating a mixture of CH_3COCH_3 and CH_3I-C^{14} in the vapor phase. In the first attempt a mixture of 2.7×10^{-3}

[1]*Manuscript received October 22, 1954.*
Contribution from Division of Chemistry, National Research Council, Ottawa, Canada, and Royal Military College, Kingston, Canada.
[2]*Present address: Royal Military College, Kingston, Canada.*

moles acetone and 8.6×10^{-5} moles of active methyl iodide with an activity of 1.9×10^{7} disintegrations per minute was irradiated for 110 hr. with a current of 30 ma. through the lamp in the irradiation system described. Less than 0.5% of the activity was recovered as $(CH_3CO)_2$-C^{14} and since the amount was not sufficient, the preparation was repeated. For the second preparation a mixture of 5.6×10^{-3} moles of acetone and 2.3×10^{-5} moles of CH_3I-C^{14} with an activity of 8.5×10^{7} d.p.m. was irradiated for 690 hr. with a lamp current of 100 ma. The light absorbed in the cell was of the order of 10^{19} quanta/hour. A tubulation which had been added to the irradiation cell was kept at 0°C. and served to reduce the amount of biacetyl vapor in the light beam, so that reaction to carbon monoxide and ethane was reduced. The 3.8×10^{-4} moles of biacetyl recovered had an activity of 7.4×10^{6} d.p.m. This amounts to 9.1% of the total methyl groups and 8.7% of the total activity in the reaction cell. Although neither of these figures is very reliable, the similarity between them seems to indicate that there has been a very high degree of exchange of methyl radicals amongst the molecules CH_3I, CH_3COCH_3, and $(CH_3CO)_2$.

Purification of Biacetyl-1-C^{14}

Radioactive tracers and also mass spectrometer analysis showed that biacetyl and acetone were not separated by low pressure fractionation in a Ward type still to the extent expected from their relative vapor pressures. However, for the purpose of this project the presence of acetone in the biacetyl was not a disadvantage, provided that the acetone was not radioactive. To ensure this, bulk amounts of inactive biacetyl (about 0.75 gm.) and of inactive acetone (about 0.3 gm.) were added to the micro amount of active biacetyl product, and the acetone fraction was then separated in the Ward type still. Further additions of inactive acetone and fractionations were made until the process had been repeated seven times. No further changes in the specific radioactivities of either the biacetyl or acetone fractions were observed in the last three fractionations, indicating that the removal of radioactive acetone was complete. Mass spectrometer analysis showed that there was about 14% inactive acetone in the active biacetyl sample.

Analysis of the Products

After the irradiation the products were separated into fractions by means of a Ward-Savelli still (5). The temperatures of the four condensers were set at −183°; −140°; −78°; −60° respectively, and the fractions as separated consisted largely of (1) CH_4 and CO; (2) C_2H_6; (3) $(CH_3)_2CO$, and (4) $(CH_3CO)_2$. The carbon monoxide was removed from the methane fraction by oxidation over hot copper oxide and absorption in Ascarite. No measurable amount of hydrogen was found in preliminary runs and attempts to estimate it separately from the carbon monoxide were discontinued. The volumes of the fractions were measured and the quantities are shown in Table I as moles $\times 10^{5}$. The analysis of the products of Photolyses Nos. 6 and 7 was made by means of a mass spectrometer.

TABLE I

PHOTOLYSIS OF ACETONE AND BIACETYL-1-C^{14}

Photolysis number	Irradiation conditions: Lamp	Irradiation conditions: Quanta $\times 10^{-20}$ estimated from CO	Substance	Reactants: Moles $\times 10^5$	Reactants: CH_3-C^{14} / CH_3-C^{12} $\times 10^7$	Products: Moles $\times 10^5$	Products: CH_3-C^{14} / CH_3-C^{12} $\times 10^7$	Degree of exchange in acetone	Quanta absorbed / Molecules reactant
1	B	2.8	$(CH_3CO)_2$	15.2	36.0	7.35	35.4		
			$(CH_3)_2CO$			2.25	33.2		
			C_2H_6			3.73	32.6		
			CO			9.25			
			CH_4			0.55	34.0		
			Total or av.	15.2	36.0		34.1		
2	B	1.9	$(CH_3CO)_2$			14.5			
			$(CH_3)_2CO$	167.2		130.2			
			C_2H_6			17.5			
			CO			6.35			
			CH_4			0.69			
			Total or av.	167.2					
3	A	0.95	$(CH_3CO)_2$	10.3	2.95	9.06	1.53		
			$(CH_3)_2CO$	22.0		15.90	0.61	0.59	0.5
			C_2H_6			5.00	1.37		
			CO			3.08			
			CH_4			1.12	1.90		
			Total or av.	32.3	0.94		1.03		
4	C	3.4	$(CH_3CO)_2$	26.8	35.9	19.6	7.80		
			$(CH_3)_2CO$	119.9		116.0	1.30	0.59	0.37
			C_2H_6			13.8	1.49		
			CO			11.1			
			CH_4			4.15	2.84		
			Total or av.	146.7	6.57		2.19		
5	C	4.7	$(CH_3CO)_2$	25.3	36.0	30.4	12.0		
			$(CH_3)_2CO$	206.6		156.2	1.39	0.45	0.34
			C_2H_6			27.4	3.83		
			CO			15.6			
			CH_4			1.28	2.9		
			Total or av.	231.9	3.92		3.11		
6	C	3.8	$(CH_3CO)_2$	15.2	36.0	26.6	4.38		
			$(CH_3)_2CO$	158.7		104.4	0.86	0.49	0.37
			C_2H_6			20.6	2.59		
			CO			12.6			
			CH_4			1.36	3.3		
			Total or av.	173.9	3.15		1.75		
7	C	3.0	$(CH_3CO)_2$	16.7	36.0	28.3	7.71		
			$(CH_3)_2CO$	313.2		281.9	0.44	0.40	0.30
			C_2H_6			26.8	1.01		
			CO			19.7			
			CH_4			2.74	2.61		
			Total or av.	329.9	1.82		1.09		
8	A	0.8	$(CH_3CO)_2$	9.25	36.2	16.4	10.9		
			$(CH_3)_2CO$	263.3		241.6	0.17	0.20	0.049
			C_2H_6			7.85	0.54		
			CO			2.58			
			CH_4			1.61	1.24		
			Total or av.	272.6	1.23		0.84		

The radioactivity of each of the fractions was measured directly in Experiments 1, 3, and 5. In the other experiments each fraction was further treated after the volume was measured, by addition of carriers and hold-back carriers and refractionated until radiochemical purity was attained. For example, after the volume of the acetone product had been measured, there was added to it convenient amounts of ethane, acetone, and biacetyl, and the acetone fraction was again recovered by fractionation in the Ward-Savelli still. The process was repeated, usually three times, until it was assured that the radioactivity was definitely associated with the substance being determined and not with a contaminant. Some of the product was sacrificed to the more volatile and to the less volatile carriers at each fractionation, and in the end the total radioactivity recovered in all of the products was only about one half the total activity of the reactants.

OBSERVATIONS AND DISCUSSIONS

The results of some typical experiments are listed in Table I. Experiment No. 2 shows results which are typical of the behavior of pure acetone when irradiated in this system; the results are quite similar to what has been reported by others. Experiment No. 1 shows typical behavior of pure biacetyl; these observations also are similar to what has been reported by others (1). The remainder of the table indicates what was observed when mixtures of radioactive biacetyl and inactive acetone were irradiated. The products obtained in these experiments are not far different from the composite which would result from the separate irradiation of the biacetyl and the acetone. The addition of biacetyl therefore does not seem to have any particular effect on the decomposition of acetone and the conclusions can probably be applied to the photolysis of pure acetone.

The most significant feature of the observations is that after irradiation, radioactivity is present in every substance which contains methyl radicals, but no radioactivity was found in the carbon monoxide fraction in any experiment. This confirms the fact that free radicals play a major role in the photolysis reactions and that recombination of free radicals to acetone occurs.

The next to the last column in the table shows an estimate of the degree of exchange of radicals amongst acetone and the other substances. This figure is simply the ratio of the specific activity of the methyl groups in acetone to the average specific activity of all methyl groups recovered. However, for some experiments only about half of the original radioactivity was recovered, and in using this figure as a measure of the extent of exchange, it is assumed that the fraction of active acetone lost between the first measurement of volume and the counting after purification is the same as the average loss of the other active compounds. Of course this assumption may be in error; the only justification for it is that it gives results which are consistent with those obtained in experiments in which nearly all of the radioactivity was recovered, and in which this assumption does not enter. It would appear that exchange was from one fifth to three fifths completed by the irradiation given in these experiments.

The results indicate that the exchange increased with irradiation, although a precise measurement of the number of quanta absorbed was not made. The dimensions and the intensity of the light beam in these experiments were not carefully controlled since the irradiations extended over several days and had to be left unattended. However, an estimate of limited value can be made from the yield of carbon monoxide. The quantum efficiency for the production of carbon monoxide in the photolysis of acetone at room temperature by light of 2537 Å was determined by Herr and Noyes (3) to be 0.22 for somewhat similar light intensities and pressures of acetone. The validity of this figure for the conditions of the experiments described here was established by determining the amount of hydrolysis of a solution of monochloroacetic acid (6) under the same experimental conditions before and after Photolysis No. 6. The light absorbed by the cell from Lamp C during Photolysis No. 6 was thereby determined to be 2.8×10^{18} quanta per hour, and the quantum efficiency of carbon monoxide production from these data is 0.20. This figure was used to calculate the total quanta absorbed, and the quanta per molecule for each photolysis as shown in the table. The differences in the absorption coefficients of biacetyl and acetone for the radiation involved is certainly less than 10% (4) and therefore equal absorption has been assumed in making the calculations.

On the simplest assumption that one quantum per molecule will produce free radicals and permit exchange, it would be expected that the figure for degree of exchange would be similar to the figure for quanta absorbed per molecule. These figures are reasonably similar except for Photolysis No. 8, and for this experiment the estimate of quanta absorbed from carbon monoxide production seems too low by comparison with Photolysis No. 3 in which the same lamp was used for a shorter irradiation. These observations are confirmatory evidence that the quantum efficiency is close to unity for the primary process: $CH_3COCH_3+h\nu = CH_3+CH_3CO$ and that the recombination of radicals to reform acetone accounts for the low over-all quantum efficiency of decomposition of acetone.

The behavior of $C^{12}H_3$ and $C^{12}H_3CO$ will, of course, not be quite the same as that of the C^{14} compounds. The isotope effect will, however, be negligible as far as our present purpose is concerned.

ACKNOWLEDGMENT

The author is grateful to Dr. F. P. Lossing for the mass-spectrometer analyses, and to Dr. E. W. R. Steacie for generous assistance with the photochemical technique, and many helpful discussions.

REFERENCES

1. Anderson, H. W. and Rollefson, G. K. J. Am. Chem. Soc. 63: 816. 1941.
2. Dorfman, L. M. and Noyes, W. A., Jr. J. Chem. Phys. 16: 557. 1948.
3. Herr, D. S. and Noyes, W. A., Jr. J. Am. Chem. Soc. 62: 2052. 1940.
4. Lardy, G. C. Compt. rend. 176: 1548. 1923.
5. Savelli, J. J., Seyfried, W. D., and Filbert, B. M. Ind. Eng. Chem. Anal. Ed. 13: 868. 1941.
6. Smith, R. N., Leighton, P. A., and Leighton, W. G. J. Am. Chem. Soc. 61: 2299. 1939.
7. Steacie, E. W. R. Atomic and free radical reactions. 2nd ed. Reinhold Publishing Corporation, New York. 1954.

THE DETERMINATION OF MOLECULAR WEIGHT[1]

By A. F. Sirianni and I. E. Puddington

ABSTRACT

The molecular weights of organic compounds of known constitution have been determined with satisfactory accuracy, using milligram quantities of materials, by a static measurement of the vapor pressure difference between pure solvents and solutions of the compounds. The method may be used over a considerable temperature range. The suitability of solvents is governed by their chemical stability and vapor pressure. Results obtained using compounds in the molecular weight range of 600–1000 are reported.

INTRODUCTION

A previous publication (4) indicated some success in using static measurements of the difference in vapor pressure between pure solvents and solutions to estimate the molecular weights of non-ionizing solutes. The procedure utilized a mercury micromanometer that was relatively insensitive to the vibration normally encountered in laboratories. In the previous work compounds having molecular weights below about 350 were used and the measurements were all made at 20°C., using solvents to which a hydrocarbon base stopcock lubricant was substantially inert.

Since the method appeared to be applicable to the measurement of the molecular weights of polymers with relatively low degrees of polymerization, it seemed desirable to extend the temperature range of the instrument and to increase the number of usable solvents, by eliminating the possible contamination from stopcock grease. As this has involved considerable modification in the construction and operation of the apparatus, the present communication is intended to record some of the more essential refinements that have been suggested as the result of several years of use and to indicate results that have been obtained. Compounds of molecular weight up to about 1000 that had known constitutions, with a variety of solvents, concentrations, and temperatures, have now been used successfully.

APPARATUS AND EXPERIMENTAL

The apparatus that was eventually adopted is shown in Fig. 1. Part *A* was built in such a way that it could be enclosed by a thermostat constructed of "aluminum foil backed masonite" and "ten test", equipped with heaters, fans, and thermoregulators to give temperatures that varied not more than ±1°C. in various locations within the box and ±0.1°C. in any one location, over the range 30° to 100°.

Continuous resistance heaters controlled by variacs were located on the side walls of the thermostat and a low power intermittent heater controlled by the thermoregulator was located in the slip stream of a 10 in. fan. The manometer and burette were enclosed in a secondary ten-test box, open at

[1]*Manuscript received January 6, 1955.*
Contribution from the Division of Applied Chemistry, National Research Council, Ottawa, Canada. N.R.C. No. 3555.

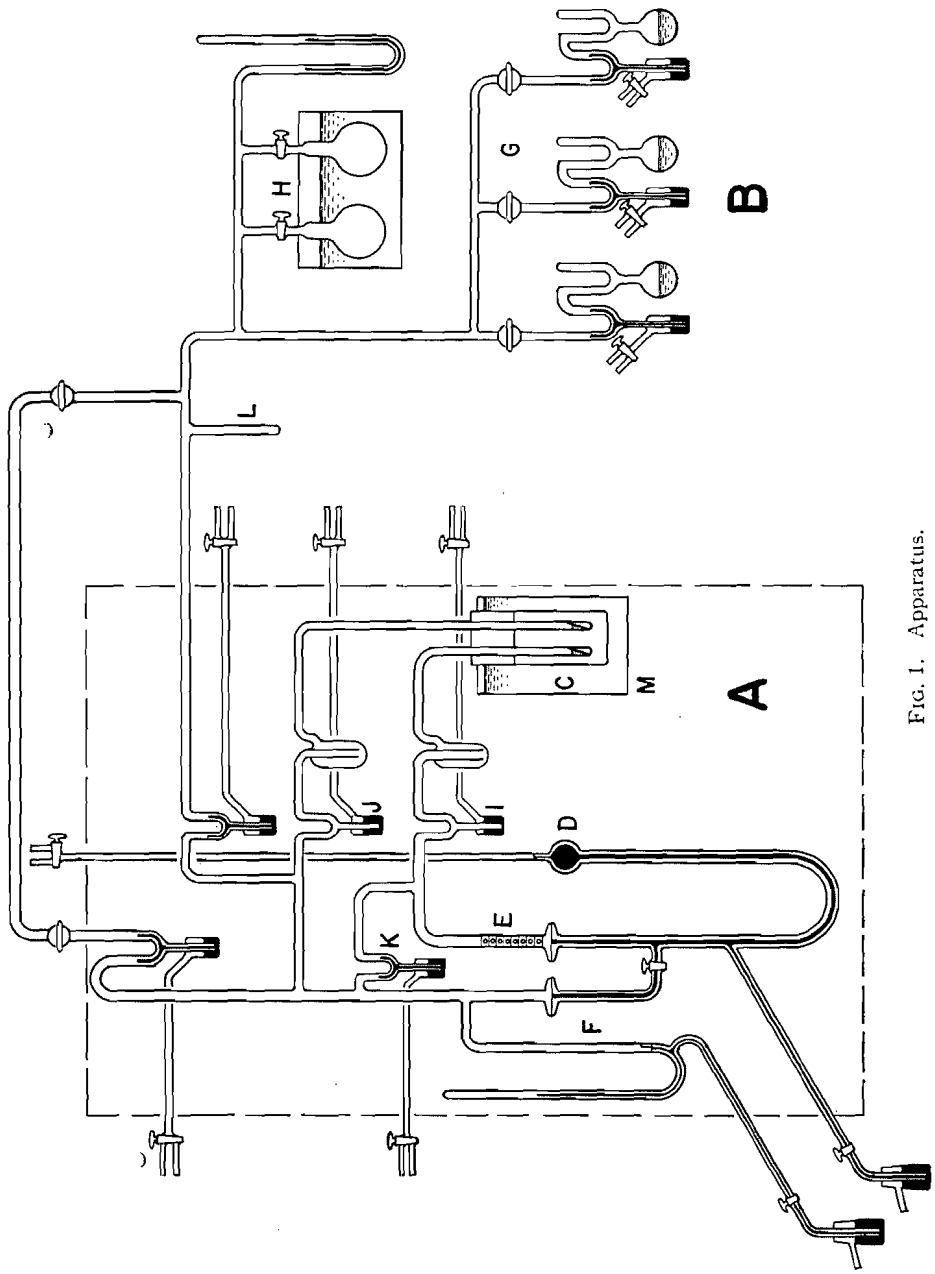

FIG. 1. Apparatus.

the top and containing an 8 in. fan blowing outward, located in one side near the bottom, to give a continuous downward flow of air through the box. The temperature within this box did not vary by more than 0.2°C. Thermostat "*C*" contained the solution and solvent holders enclosed in a copper block, the details of which are shown in Fig. 2. This thermostat consisted of a

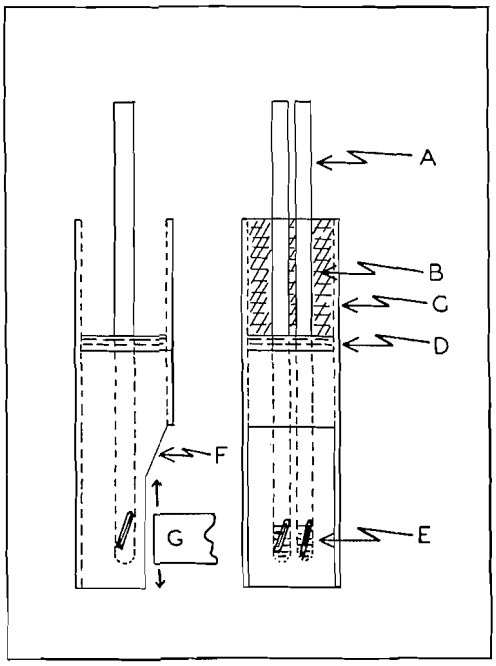

FIG. 2. Enlarged view of copper block. *A*, sample holders; *B*, glass wool insulation; *C*, cellulose acetate sleeve; *D*, mercury film; *E*, stirrers; *F*, recessed portion of copper block; *G*, magnet.

2 liter, wide mouth, dewar flask. It was maintained at 10–30° below the air thermostat to prevent solvent condensation in the connecting tubing. The temperature of the oil contained in the thermostat was controlled to ±0.0005°C. Good thermal contact was maintained between the sample holders and the copper block with a film of mercury and the copper block itself was partially insulated from the bath with a piece of cellulose acetate tubing and a heavy coat of shellac. Both solution and solvent were stirred with glass sheathed bars of iron, actuated by an alnico magnet that oscillated in a vertical direction with a frequency of about 20–25 cycles per minute.

As suggested in the earlier paper, etching of the inside of the two bulbs forming the arms of the U tube was found desirable to give reproducible contact angles at the mercury–glass–vapor interface. This is important since the operation of the manometer assumes that the volume of mercury transferred between the arms of the U tube is proportional to the pressure change. Experiments have indicated that the contact angle is quite sensitive to temperature changes, changes in the type of vapor contained in the bulb, and probably to large differences in the pressure of any one vapor. No pair of

bulbs yet used seems to behave in an identical fashion and while the zero point of the instrument has remained constant to ± 0.001 mm. for periods up to 10 days, if conditions are kept reasonably constant, it may change substantially if, for example, alcohol vapor is substituted for benzene or the vapor pressure of the solvent is raised by several centimeters with mercury cutoff K open. These effects obviously become more important as the magnification factor of the instrument is increased. The behavior of the manometer was invariably good if the contact angle was sufficiently diffuse that no sharp line of contact was visible at the mercury–glass interface. It could frequently be improved by contaminating the mercury surface with about 10^{-7} to 10^{-9} gm. of lithium stearate added in distilled methanol. Contact angles rarely gave any trouble, however, at temperatures above about 30°C.

The most convenient method found for etching the bulbs to the desired degree consists in placing a few grams of 200–325 mesh carborundum in the bulbs along with a few cubic centimeters of water and sections of flattened lead shot. The bulbs are then rotated for 16–24 hr. at a speed just below that required to carry the pieces of lead around with the rotating bulb. This must be followed by a thorough cleaning and steaming before the bulbs are fixed into the rest of the apparatus. Final traces of grinding residues were sometimes removed by reducing the pressure suddenly when the glass surface was wet with methanol.

All of the stopcocks within the thermostat in contact with the solvent vapor were replaced with short arm mercury cutoffs equipped with glass check valves. The cutoffs could be controlled by two way stopcocks located outside the thermostat. The stopcock separating the two arms of the U tube was lubricated with a film of dried aquadag* plus a very thin film of heavy lithium stearate grease. This tap was operated by a felt lined stirrup attached to an iron rod extending through the top of the thermostat. It did not have to be relubricated more frequently than once in two years. It was exposed to temperatures up to 90°C. A mercury sealed 4 mm. pyrex stopcock similar to Corning 7500 was found quite satisfactory for this valve. The large bulbs and the stopcock were set in plaster of Paris to ensure rigidity.

In order to increase the range of the manometer, a series of small bulbs about equal to the measuring capillary in volume were located in the short piece of capillary (E) above the right hand arm of the U tube. These bulbs were marked volumetrically with etches. If, during a measurement, the tail end of the mercury thread was off scale when the advancing end reached the first etch, it was merely pushed on to the etch that allowed a reading to be made on the measuring capillary. In the present case three bulbs were used to give a total range of about two millimeters pressure difference, with a magnification of approximately 2000. The diameters of the bulbs that formed the arms of the U tubes were about 5 cm.

A change in manometer design was examined wherein the essential difference was the reversal of the positions of the measuring capillary and bulb D.

**A dispersion of graphite in water prepared by the Acheson Colloids Corp., Port Huron, Michigan, U.S.A.*

The expansions in capillary *E* were then placed below the bulb forming the right hand arm of the U tube. In this model the volume of mercury in the right hand arm was measured by withdrawing it into the empty bulb *D* and again noting the location of the mercury thread in the measuring capillary when the tail end of the mercury was at a convenient etch. While this design offered the advantages at high magnifications of using much less mercury and of a considerable saving of time, during readings, owing to the fact that only a small thread of mercury rather than a large volume had to pass through the measuring capillary, the older model was quite satisfactory for most work.

In making a molecular weight determination, the solute in amounts varying from 0.1 to about 2 mgm. was weighed into a 3 to 4 mm. i.d. pyrex tube. After placing the stirrer within the tube, it was sealed to the apparatus and the pressure reduced to about 10^{-5} mm. Pure solvents, previously deaired by refluxing *in vacuo* until a sample of the vapor could be condensed into a 1 mm. capillary to give a thread of liquid containing no bubbles, were stored in the bulbs *B* outside of the air thermostat.

A cold finger containing dry ice made a satisfactory reflux condenser for the deairing procedure. Although slightly different methods were used with the various solvents, the Reagent Grade compounds were usually passed through a chromatographic column packed with silica gel and alumina, and dried with calcium hydride (1, 2) wherever practicable, prior to degassing. The amount of solvent to be used was measured in the vapor state in the calibrated volumes *H* contained in a thermostat. After the solvent vapor in the connecting tubing was condensed into the reservoir, the vapor in one of the bulbs "*H*" was quantitatively condensed on the solute sample. The requirement on the solvent side could then be supplied from the other bulb, and the solvent and solution connected to their respective sides of the manometer. If the determination was the first after the interior of the apparatus had been exposed to the air, it was flushed with solvent vapor, to displace residual air or water vapor adsorbed on the glass walls, and re-evacuated.

In the early operation of the apparatus it was learned that the manometer provided a sensitive means of testing the purity of the solvent. If pure solvent was condensed in about the same volume in both the solvent and solution holders, no vapor pressure difference should be detectable after successive portions were removed from one of the containers. Solvents of this purity are not infrequently difficult to obtain, however, and in order to reduce any fractionation of solvent that might occur to a minimum during a determination, two closely similar volumes were used at *H*. The dead space on either side of the U tube was made the same, the final adjustment being made by selection of the position in *F* to which the mercury was adjusted to read the vapor pressure of the pure solvent. Small compensating adjustments in volume required by the use of different size sample holders could be made by changing slightly the position of the mercury level in the necks of cutoffs *I* and *J* before a vapor pressure difference was measured. Since the apparatus was contained in a thermostat, thermal expansion of the mercury was not a problem. The zero point of the manometer needed to be checked only in-

frequently, usually after a series of readings for one concentration. The null point not infrequently varied from run to run but this appeared to be due to the distillation of mercury within the system when no solvent vapor was present. There was no indication of a zero point change during a run.

As observed by Frazer and his associates (3) the attainment of vapor pressure equilibrium required only about 30 min. provided the solvent was air free; a trace of air increased this time considerably, however. When high vapor pressures were used, it was necessary to know the dead space on the solution side of the manometer accurately since the concentration of the solution was determined by making the appropriate dead space correction on the amount of solvent measured in *H*.

By condensing the solvent in side arm *L* after a determination was completed, the solvent could be used over again to prepare a slightly more concentrated solution for a second determination. It was thus possible to measure the vapor pressure difference on a rather wide range of solution concentration on a single solute sample and with a minimum expenditure of pure solvent. A usual solution contained between 15 and 90 mgm. of solvent.

Consecutive readings of vapor pressure lowering on the same sample normally did not vary by more than one per cent.

RESULTS

The results of the determination of molecular weight of sucrose octaacetate (mol. wt. = 678), raffinose hendecaacetate* (mol. wt. = 967), and three samples of bitumen† in various solvents and at a number of temperatures are shown in the accompanying graphs. Variations from the mean are normally

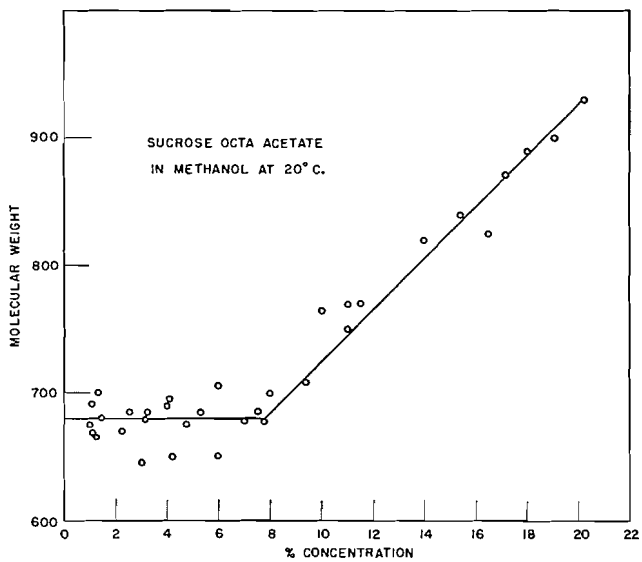

FIG. 3. Variation in molecular weight of sucrose octaacetate with concentration in methanol at 20°C.

*Kindly supplied by Dr. R. P. A. Sims.
†Kindly supplied by Dr. D. S. Montgomery.

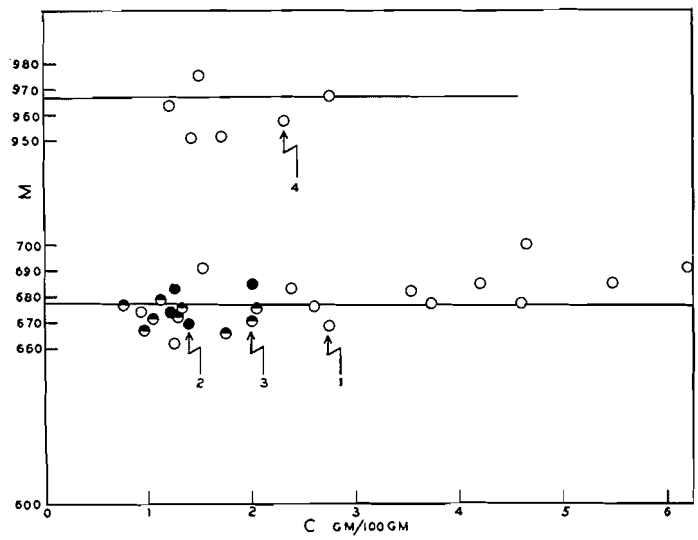

FIG. 4. Molecular weight of sucrose octaacetate and raffinose hendecaacetate in benzene at various temperatures: (1) sucrose octaacetate at 30°C., (2) sucrose octaacetate at 50°C., (3) sucrose octaacetate at 55°C., (4) raffinose hendecaacetate at 55°C. Solid lines in each case represent theoretical molecular weight.

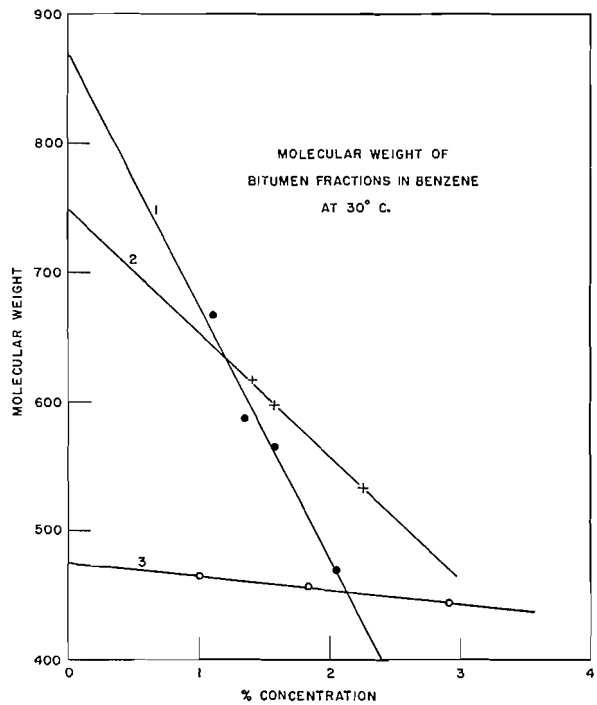

FIG. 5. Molecular weight vs. concentration for three samples of bitumen in benzene at 30°C.

not more than two per cent. With the crystalline materials dependence of molecular weight on concentration over the range examined was noted only with sucrose octaacetate in methanol at 20°C. and in concentrations in excess of 8% by weight. This is probably due to association of the solute. The bitumen samples on the other hand behaved like polymers. The weight of solute used in all cases was between 0.3 and 1.1 mgm. The method has been used successfully to determine the molecular weights of polymers up to about 20,000. The results of this work will be presented in a future publication.

ACKNOWLEDGMENT

It is a pleasure to acknowledge the substantial contributions made by G. Stainsby and R. A. Campbell to this work.

REFERENCES

1. BROWN, A. S., LEVIN, P. M., and ABRAHAMSON, E. W. J. Chem. Phys. 19: 1226. 1951.
2. DAVIS, R. T. and SCHIESSLER, R. J. Phys. Chem. 57: 966. 1953.
3. FRAZER, J. W. C. and LOVELACE, B. F. J. Am. Chem. Soc. 36: 2439. 1914.
4. PUDDINGTON, I. E. Can. J. Research, B, 27: 151. 1949.

PARTICLE MOTIONS IN SHEARED SUSPENSIONS

III. FURTHER OBSERVATIONS ON COLLISIONS OF SPHERES[1]

By R. St. J. Manley[2] and S. G. Mason

ABSTRACT

Two-body interactions between glass spheres of diameters a_1 and a_2 caused by velocity gradients vary with a_1/a_2. When $1 < a_1/a_2 < 2$, well-defined collisions similar to those previously reported for spheres of equal size can be observed. Fair agreement is found between the experimentally observed and calculated collision frequencies over a range of particle concentrations and velocity gradients. When $a_1/a_2 > 2$ the particles are separated at all times and the phenomena of interaction are more complex. Single air bubbles rotate at the same angular velocity as rigid spheres. When two air bubbles of equal size are brought into collision a doublet is formed; instead of the mirror-image separation observed with neutral rigid spheres, the doublet continues to rotate for as many as 60 rotations before coalescence occurs. Less frequently a doublet with distinct particle separation is observed. Periods of rotation of both types of doublet and certain details of the rotational orbit of a doublet of touching air bubbles have been measured and compared with values predicted from Jeffery's theoretical equations for rigid ellipsoids. Apart from their intrinsic interest, the phenomena described are of importance in theories of viscosity and coagulation of suspensions and colloidal dispersions.

INTRODUCTION

In an earlier paper (5), the two-body collisions of rigid neutral spheres of equal size suspended in a liquid subjected to a velocity gradient were described in some detail. It was shown experimentally that in a simple field of fluid shear described by

$$u = Gy, \qquad v, w = 0 \tag{1}$$

where u, v, and w are the respective velocities along the X-, Y-, and Z-axes and G is the rate of shear, two spheres can approach one another along an undisturbed rectilinear path parallel to the X-axis until they come into apparent collision at the rate

$$f = 4a^3nG/3 \tag{2}$$

$$= 8cG/\pi\,. \tag{3}$$

Here, f denotes the number of collisions per particle per unit time, a the particle diameter, n the number of particles per unit volume of suspension, and c the volume of particles in the suspension.

The doublet formed by two colliding spheres rotates about the Z-axis at a constant angular velocity

$$\omega = G/2 \tag{4}$$

until it reaches the mirror image through the Y–Z plane of the initial position of contact; the two particles then separate.

[1]*Manuscript received January 17, 1955.*
Contribution from Pulp and Paper Research Institute of Canada and the Department of Chemistry, McGill University, Montreal, Que.
[2]*Holder of a Fellowship from the National Research Council of Canada.*

The measured values of the mean and maximum doublet lives and the distribution function of doublet lives were shown to be in good agreement with values calculated from the experimentally established mechanism of doublet behavior. Most of the experimental evidence suggested that the contact between the spheres of the doublet is real, resulting from a force which is generated by distortion of the local field of fluid motion and which operates to push the particles together. In one set of experiments, however, in which the motion was interrupted by a period of quiescence, the behavior of the doublets suggested that the particles do not come into true contact (5).

Equations [2] and [3] are readily derived (5, 8) by calculating the number of particle centers which are carried in unit time along rectilinear paths parallel to the X-axis, at the translational velocities given by equation [1], into a "collision sphere" of radius a drawn about the center of a reference sphere. For simplicity the reference sphere is placed at the origin of the coordinate system. If two spheres of different diameters a_1 and a_2 approach one another in a similar manner until they collide, the binary collision frequency is obtained by substituting $(a_1+a_2)/2$ for a in equation [2], i.e.

[5] $$f_{12} = (a_1+a_2)^3 n_2 G/6$$

where f_{12} is the number of collisions per unit time suffered by a type-1 sphere with type-2 spheres, and n_2 is the number concentration of the latter. If c_2 is the volume fraction of type-2 spheres in the suspension, $\pi a_2^3 n_2/6 = c_2$, whence by substitution in equation [5]

[6] $$f_{12} = \frac{(a_1+a_2)^3}{a_2^3} c_2 G.$$

The present paper deals with an experimental study of interactions in binary suspensions of rigid spheres of different diameter ratios and in suspensions of air bubbles of approximately equal size. These experiments were carried out to extend the earlier observations (5), to test equation [6], and to attempt to resolve the question of whether or not the two spheres of a doublet come into true physical contact. Although the question of contact remains incompletely answered, a number of interesting and, it is believed, significant observations were made which have application to theories of viscosity and coagulation of suspensions and colloidal dispersions.

EXPERIMENTAL PART

The experiments were conducted in the concentric cylinder apparatus previously described (9). Single particles and doublets were observed at the origin of a field of motion as defined by equation [1], through a microscope directed along the Y-axis of the coordinate system so that the particles were viewed as their projections on the X–Z plane (Fig. 1). The velocity gradient G could be calculated with a precision of 0.1% from the measured speeds of rotation and could be varied continuously from 0 to 2.5 sec^{-1}.

Binary suspensions of rigid spheres were prepared by suspending glass spheres ranging from 5μ to 180μ in diameter in corn sirup having a viscosity of about 50 poises and a density of 1.3 gm./cc. The experimental methods for

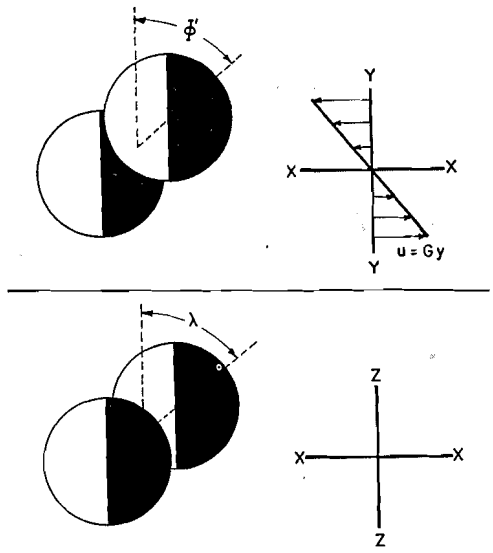

FIG. 1. Coordinate system for describing velocity gradients and motions of spherical doublets. Experimental observations are made along Y-axis so that particles are viewed as projections on the X–Z plane. ϕ' is the azimuthal angle referred to Z as the polar axis, and λ the azimuthal angle referred to Y as polar axis. The angular velocity $\omega = -d\phi'/dt$.

uniform dispersion and deaeration previously employed with monodisperse systems were used (5). For measurements of the collision frequency f_{12}, a supply of two sizes of glass spheres having a narrow size distribution was prepared by screen fractionation of bulk samples. The size spectra are given in Table I. Suspensions of volume concentration c_2 from 0.4 to 1.6% were prepared; each of these suspensions contained about 0.02 volume per cent of type-1 spheres which were used as reference particles.

TABLE I

SIZE DISTRIBUTION OF SPHERES

Diameter a_1, μ	% of diameter $< a_1$	Diameter a_2, μ	% of diameter $< a_2$
160	0.91	107	2.5
165	17.3	112	28.6
175	49.0	117	74.0
185	91.0	122	95.0
190	100.0	127	100.0
Number average diameter = 179μ		Number average diameter = 117μ	
Standard deviation = 9.0μ		Standard deviation = 4.4μ	

Attempts to produce suitable uniform dispersions of fluid drops were only partly successful. However, dilute "foams" of air bubbles of unknown and variable concentration were prepared by vigorous mechanical stirring of viscous liquids such as corn sirup and glycerine. After agitation, the systems were allowed to stand so that larger bubbles rose to the surface leaving behind bubbles of fairly uniform diameter of about 150μ.

RESULTS

1. *Glass Spheres*

General

The type of interaction between two spheres of diameters a_1 and a_2 (where $a_1 > a_2$) was found to depend upon the ratio a_1/a_2. In systems in which $a_1/a_2 < 2$ approx., collisions were easily recognizable and, indeed, were similar to those of equal-sized spheres (5). The doublet formed by the two colliding particles appeared to rotate as a rigid dumbbell until a position was reached which was a mirror image about the Y–Z plane of the point of initial contact; separation then occurred and each sphere was restored to the same y-coordinate existing before the onset of collision.

When $a_1/a_2 > 2$, the interactions were much more complex and the particles could be seen to be separated at all times. One striking type which was repeatedly observed was as follows: upon approaching a large sphere, a small sphere began to describe the type of planetary motion around the large one as illustrated in Fig. 2, moving in a gradually widening spiral path past the

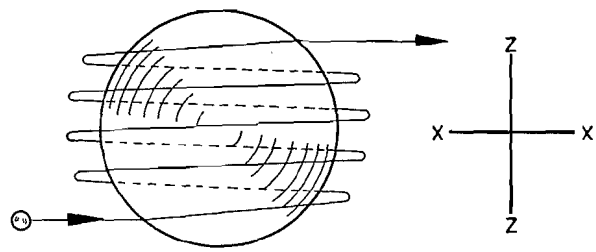

FIG. 2. Planetary motion of a sphere moving in an upward spiral path around a larger reference sphere (schematic).

equatorial plane until it attained a latitude roughly equivalent to that at which it started. It then separated from the large sphere at a velocity which appeared to be equal to that with which it approached. Upon reversal of the field of fluid motion (by reversing the directions of rotation of the two concentric cylinders), it was found that the smaller sphere continued to move upwards. In a number of instances, a "zig-zag" motion of the small sphere upwards in a roughly constant X–Z plane was also observed.

Collision Frequency

These measurements were made using spheres having the dimensions given in Table I. The collision frequency f_{12} was determined over a range of values of c_2 and G in the same manner as for monodisperse spheres (5). The results together with the values calculated from equation [6] are summarized in Table II. For a total of 857 observed collisions the ratio $f_{obs}/f_{calc} = 1.08$; since the standard deviation of this ratio is estimated to be 16% from the spreads in particle diameters given in Table I and 3% from the random sampling error of 900 collisions, the agreement may be considered satisfactory.

TABLE II

COMPARISON OF OBSERVED AND CALCULATED COLLISION FREQUENCIES

Volume fraction, $c_2 \times 10^3$	G, sec.$^{-1}$	N^*	f_{12}, Obs./Calc.
4.1	0.580	53	1.28
8.1	0.580	64	1.21
12.1	0.580	60	0.97
16.2	0.580	57	0.81
8.1	0.826	35	0.88
12.1	0.826	57	1.07
16.2	0.826	71	1.20
4.1	0.826	46	1.05
16.2	0.826	81	0.99
8.1	1.260	65	1.05
12.1	1.260	63	0.95
16.2	1.260	64	1.20
8.1	0.973	75	1.30
8.1	1.349	66	1.22
	Total	857	Mean 1.08

**Number of collisions counted.*

2. *Air Bubbles*

General

Single air bubbles were not visibly deformed up to the highest velocity gradients attempted (2.5 sec.$^{-1}$) and were found to spin about the Z-axis in the same manner as rigid spheres (9). Two bubbles, upon approaching one another, formed a doublet which rotated about the Z-axis; however, instead of rotating through the angle 2ϕ, where ϕ ($< \pi/2$) is the azimuthal angle corresponding to the point of initial contact (Fig. 1), and then separating at the mirror image of the initial position of contact ($-\phi$) as was observed with equal-sized glass spheres (5), the doublet continued to rotate for as many as 60 complete rotations over a period as long as one-half hour, *until the pair suddenly coalesced into a single bubble.* During the interval between initial contact and coalescence, the doublet rotated about the Z-axis in a manner qualitatively similar to that of a rigid cylindrical particle, i.e. somewhat like

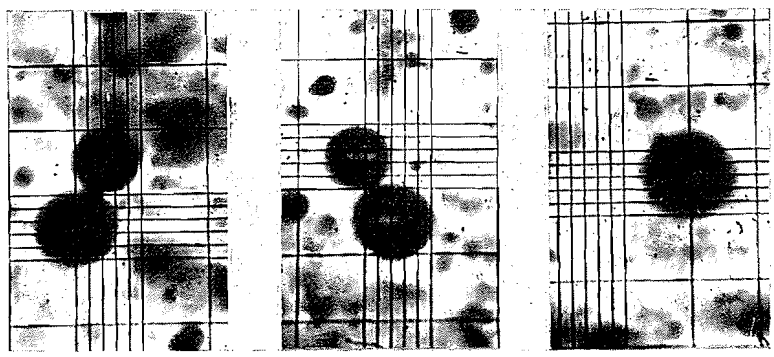

FIG. 3. Photomicrographs of a doublet of air bubbles (of different diameters) at $\lambda > 0$ (No. 1), $\lambda < 0$ (No. 2), and after coalescence to a single sphere (No. 3).

a precessing gyroscope (9). A doublet in two positions before and one position after coalescence to a single sphere is shown in the photomicrographs in Fig. 3.

Practically all of the interactions observed were as described above, i.e. the bubbles came into apparent contact and after a time coalesced. In many instances, a doublet of bubbles in contact collided with a singlet to form a triplet of which a pair eventually coalesced, thus forming a doublet which eventually coalesced into a singlet. In a number of cases doublets were formed in which the bubbles were clearly separated, but which executed a number of complete rotations as a pair and then separated.

Rotation of Single Bubbles

It has been shown theoretically (4, 11) and confirmed experimentally (9) that a single rigid sphere spins about the Z-axis at the angular velocity given by equation [4], i.e. with a period

$$[7] \qquad T_1 = 4\pi/G.$$

It was considered to be of interest to see how closely equation [7] was followed by air bubbles.

Although the bubbles were opaque in the directly illuminated microscope field, their rotational motion could be followed by observing particles of carbon 2μ to 5μ in diameter which were dispersed in the liquid medium and became lodged at the air/liquid interface during the agitation process. One of these particles suitably chosen could be used as a convenient reference point. The time required by the particle to make two successive crossings of the X–Z plane (Fig. 1) was taken to be the half-period of rotation. The precision of these measurements was not as high as with glass spheres (5, 9); the latter were transparent in the microscope field and reference marks on the surface or inside of the particle could be seen throughout the rotation.

Table III contains the observed periods of rotation of an air bubble over a range of velocity gradients. For purposes of comparison the periods calculated from equation [7] are also given. The agreement is seen to be reasonably good considering the difficulty in making accurate measurements.

TABLE III

PERIODS OF ROTATION OF SINGLE AIR BUBBLES

G, sec.$^{-1}$	T_1, sec. Observed	Mean observed	Calculated	Observed / Calculated
0.625	22.4, 23.6, 19.2, 22.8	22.0	20.1	1.09
0.737	18.6, 17.4, 18.0, 18.0	18.0	17.1	1.05
0.985	12.0, 11.8, 12.4, 12.4	12.1	12.8	0.94
1.34	8.4, 8.2, 9.0, 8.8	8.6	9.4	0.91
2.33	4.8, 6.2, 7.0, 7.2, 5.0	6.0	5.4	1.11
				Mean 1.02

These results show that over the range of velocity gradients studied here, the air bubbles rotate like rigid spheres. This observation accords with Garner's

observation that at low Reynolds numbers sedimenting fluid spheres behave as though they were solid, i.e. they fall at the Stokes velocity without the expected circulation of fluid inside the drop (3).

Periods of Rotation of Air Doublets

A series of measurements of the periods of rotation T_2 about the Z-axis of the doublet formed by two colliding spheres which ultimately coalesced was made over a range of shear rates. The experimental method was similar to that previously described for cylindrical particles (9). In these experiments care was taken to select doublets having bubbles of equal size. Table IV shows

TABLE IV

PERIODS OF ROTATION OF DOUBLETS FORMED BY THE COLLISION OF FLUID SPHERES

G, sec.$^{-1}$	Mean T_2, sec.	$T_2G/2\pi$
Doublet No. 1		
0.581	40.4	3.74
0.846	27.6	3.72
1.12	20.8	3.72
1.44	16.0	3.68
1.87	11.9	3.55
Doublet No. 2		
0.566	41.0	3.70
0.733	32.2	3.76
1.07	21.6	3.68
1.41	16.4	3.69
2.17	10.4	3.60
	Mean	3.68

typical results for two doublets over a range of shear rates. It will be noted from values shown in the last column that T_2 varies inversely with the velocity gradient.

Periods of rotation of two doublets of separated and hence non-coalescing bubbles were also measured; these are given in Table V.

TABLE V

PERIODS OF ROTATION OF AIR DOUBLETS WITHOUT BUBBLE CONTACT

G, sec.$^{-1}$	Mean T_2, sec.	$T_2G/2\pi$
1.776	16.4	4.64
2.020	22.4	7.20

According to Jeffery (4), the period of rotation about the Z-axis of a rigid prolate spheroid of axis ratio r is given by

$$T_2 = 2\pi[r+(1/r)]/G \qquad [8]$$

which for $r = 2$ yields a value $T_2G/2\pi = 5/2$. It is seen from Table IV that

the period of rotation of a doublet of contacting spheres is greater than that of a spheroid of corresponding axis ratio. The "equivalent ellipsoidal axis ratio" r_e may be calculated from equation [8] by inserting the *measured* value of $T_2G/2\pi$. This yields a value of $r_e/r = 1.69$ for contacting bubbles; this is considerably higher than the corresponding values of 0.5 for a doublet of neutral rigid spheres (equation [4]), and 0.6 to 0.7 for rigid cylindrical particles having r's ranging from 130 to 20 (9).

Details of Orbit

It has been previously shown (9) that the spherical elliptical orbit of a prolate spheroid predicted by Jeffery (4) may be transformed to the form

$$\tan \lambda = \tan \lambda_{max} \cdot \sin 2\pi t/T \qquad [9]$$

where t is time, λ is the angle between the Z-axis and the X–Z projection of the major axis of the particle (Fig. 1), and λ_{max} is the maximum value of λ achieved in a particular orbit. Equation [9], which describes the rocking to and fro between the angles $\pm\lambda_{max}$ of the X–Z projection of the particle, has been confirmed experimentally for rigid cylindrical particles (9).

The variation of λ with time of a doublet of touching air bubbles was measured using a goniometric ocular on the microscope in the same manner as with cylindrical particles (9). The results, which are shown plotted over a half-rotation in Fig. 4, show excellent agreement with equation [9].

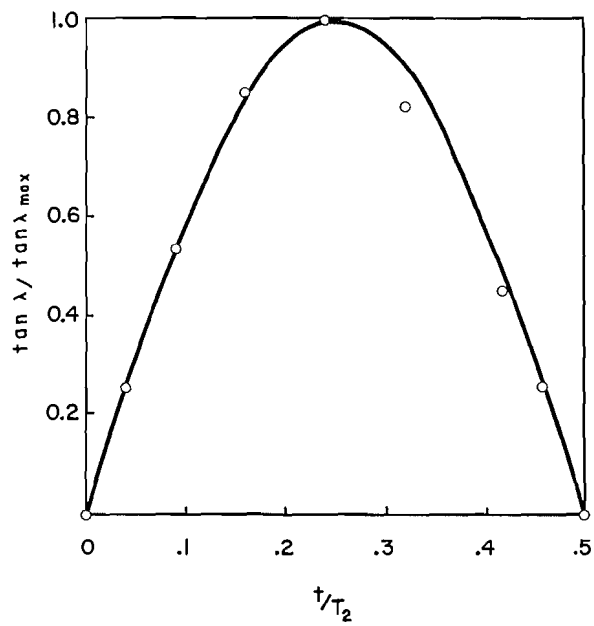

FIG. 4. Variation of the azimuthal angle λ (Fig. 1) with time for a semirotation of a doublet formed by the collision of two air bubbles of equal size. The points are calculated from measured values of λ and T_2 and the curve from Jeffery's equation for a rigid ellipsoid in the form of equation [9].

DISCUSSION

General

Except when $a_1/a_2 > 2$, when the particles can be seen to be separated at all times, the evidence of true contact between glass spheres from these experiments and from the more detailed experiments reported and discussed previously (5) is inconclusive.

The planetary motion observed when $a_1/a_2 > 2$, and which became more marked as the ratio was increased, is complex in nature but may be a manifestation of streamlines around the larger of the two spheres; circular streamlines in the X–Y plane around an isolated rigid sphere may be expected, but the details have not yet been worked out from theory. No explanation can be offered for the "zig-zag" motion. The upward motion of the smaller sphere relative to the larger, which has been shown to occur independent of the direction of rotation of the spheres, is most probably due to differential sedimentation, since a downward sedimentation of the glass spheres in the less dense liquid medium is to be expected.

The coalescence of the air bubbles, while not positive proof of contact, suggests an initial approach of the two spheres close enough so that they adhere with sufficient force to prevent separation in the mirror-image position observed with glass spheres. Owing to the uncertain nature of the long range London – van der Waal's attraction forces, and of the electrostatic repulsion and electroviscous effects existing in thin liquid films which are revealed in the experiments of Derjaguin (1), Elton (2), and others, caution must be exercised in interpreting the significance of the observations on coalescence until additional experiments are carried out.

The formation of air bubble doublets with complete separation cannot be explained although it is possible that it may be related to the planetary motion observed in the binary systems of glass spheres.

Steady State Concentration of Doublets

The persistence of a doublet of neutral rigid spheres for a finite period between collision and separation causes a steady state concentration of doublets to be built up when the suspension is stirred, caused to flow, or otherwise subjected to a velocity gradient. At statistical equilibrium, the number formed per unit time equals the number which die by separation. Thus if F is the total number of doublets formed in unit volume per unit time, and $\bar{\tau}$ is the mean doublet life, then the steady state number of doublets n' per unit volume is given by

$$n' = \bar{\tau}F. \qquad [10]$$

For equal-sized spheres, $F = fn/2$ and $\bar{\tau} = \pi/G$ (5). It readily follows that the volume fraction of doublets (c') in the steady state becomes

$$c' = 8c^2 \qquad [11]$$

where c is the total volume concentration of singlets. Equation [11] can be valid only at low concentrations since the depletion of the system of singlets and the formation of triplets, etc., have been ignored. Several values from

equation [11] are shown in Table VI where it is seen that even at low concentrations an appreciable fraction of neutral spheres can exist in doublet form.

TABLE VI

STEADY STATE CONCENTRATION OF DOUBLETS IN A SUSPENSION OF NEUTRAL SPHERES

c, volume %	c', volume %	100 c'/c
2	0.3	15
4	1.3	32
8	5.1	64

We wish next to consider the doublet concentration in a binary system where $a_1/a_2 < 2$. Equation [6] gives the collision frequency per particle; the collision frequency per unit volume F_{12} is given by $f_{12}n_1$. Thus for collisions between k different species uniformly dispersed, the total number of two-body collisions of all types in unit time and unit volume is given by

$$F = \tfrac{1}{2}\sum_{j=1}^{k}\sum_{j=1}^{k} f_{ij}n_i, \qquad [12]$$

the factor $\frac{1}{2}$ appearing since each collision has been counted twice under the summation sign. This reduces to

$$F = \frac{G}{12}\sum\sum (a_i+a_j)^3 n_i n_j. \qquad [13]$$

For a binary system, i.e. $k = 2$, this yields

$$F = \frac{24G}{\pi^2}\left[\frac{c_1^2}{a_1^3}+\frac{c_2^2}{a_2^3}+\frac{(a_1+a_2)^3}{4a_1^3a_2^3}\right]c_1c_2, \qquad [14]$$

the first two terms corresponding to 1–1 and 2–2 collisions respectively, and the third to 1–2 collisions. Assuming that the doublet life for unequal spheres is the same as that for equal spheres, it follows that the steady state concentration of doublets is given by

$$c' = 8c_1^2+8c_2^2+(1+a_1/a_2)^3(1+a_2^3/a_1^3)c_1c_2. \qquad [15]$$

It is readily shown that c' is a minimum when $a_1 = a_2$; it follows therefore that polydispersity may increase the steady concentration of doublets.

Recently we have shown (6) how doublet formation as described above in monodisperse and polydisperse suspensions may be used to modify a theoretical equation due to Vand (11); this modification gives good agreement with measured values of the relative viscosity of rigid spheres at concentrations up to 18% by volume.

The interaction phenomena are of interest in connection with the well-known increase in rate of coagulation of hydrosols and aerosols caused by stirring, turbulent flow, etc. The theory of this effect, which is based upon the increase in collision frequency due to velocity gradients (orthokinetic collisions)

over the normal Brownian (perikinetic) collisions, was first developed by Smoluchowski (8) and has since been extended by Tuorilla (10), Muller (7), and others.

ACKNOWLEDGMENT

We are indebted to A. P. Arlov for the preparation of the photomicrographs shown in Fig. 3.

REFERENCES

1. DERJAGUIN, B. V. Discussions Faraday Soc. In press.
2. ELTON, G. A. H. Proc. Roy. Soc. (London), A,194: 275. 1948.
3. GARNER, F. H. Trans. Inst. Chem. Engrs. (London), 28: 88. 1950.
4. JEFFERY, G. B. Proc. Roy. Soc. (London), A,102: 161. 1922.
5. MANLEY, R. ST. J. and MASON, S. G. J. Colloid Sci. 7: 354. 1952.
6. MANLEY, R. ST. J. and MASON, S. G. Can. J. Chem. 32: 763. 1954.
7. MULLER, H. Kolloidchem. Beih. 27: 223. 1928.
8. SMOLUCHOWSKI, M. VON. Z. Physik. Chem. 92: 129. 1917.
9. TREVELYAN, B. J. and MASON, S. G. J. Colloid Sci. 6: 354. 1951.
10. TUORILLA, P. Kolloidchem. Beih. 24: 1. 1927.
11. VAND, V. J. Phys. & Colloid Chem. 52: 277, 300. 1948.

THE RECIPROCAL SALT-PAIR SYSTEM: SODIUM CHLORIDE – AMMONIUM SULPHITE – SODIUM SULPHITE – AMMONIUM CHLORIDE – WATER AT 20°C. AND 60°C.

PART I. TERNARY SYSTEMS[1]

By J. A. Labash[2] and G. R. Lusby

ABSTRACT

Solubility data have been obtained at 20°C. and 60°C. for the following ternary systems:

(1) $NaCl–NH_4Cl–H_2O$ (2) $NH_4Cl–(NH_4)_2SO_3–H_2O$
(3) $Na_2SO_3–(NH_4)_2SO_3–H_2O$ (4) $NaCl–Na_2SO_3–H_2O$

No evidence of the formation of double salts or of solid solutions in the first three systems was obtained. Ammonium sulphite monohydrate does not appear to dehydrate at 60°C. in solutions saturated with sodium sulphite or ammonium chloride. In the study of the $NaCl–NH_4Cl–H_2O$ system, the data agree with average values obtained from the literature and some discrepancies in the published data have been noted. In the $NaCl–Na_2SO_3–H_2O$ system some anomalous results can be explained on the basis of the existence of solid solutions of the hydrated and anhydrous forms of sodium sulphite and sodium sulphate.

INTRODUCTION

The work described in the present paper and in a following paper was carried out for the purpose of obtaining data necessary for the development of a process for making sodium sulphite and ammonium chloride directly from sodium chloride, sulphur dioxide, and ammonia. The carrying out of such a process industrially requires careful control of liquor compositions in order that products of high purity may be obtained. Because the solubility data in the literature were insufficient for such control of the proposed process, a phase rule study was made of the reciprocal salt-pair system: $NaCl–(NH_4)_2SO_3–Na_2SO_3–NH_4Cl–H_2O$, at 20°C. and 60°C., and of the four associated ternary systems.

EXPERIMENTAL

(1) *Chemicals*

Analytical reagent (A.R.) ammonium sulphite was found to contain a relatively high percentage of sulphate and its use was abandoned after a series of preliminary experiments. Ammonia and sulphur dioxide gases were added in place of solid ammonium sulphite wherever possible. When the solid [$(NH_4)_2SO_3.H_2O$] was needed, it was freshly prepared from the constituent gases; the solid, thus prepared, was found to contain much less sulphate than the reagent chemical. Ammonium sulphite was used in some cases in the form of a thick slurry, in order to avoid the oxidation which occurs during filtering and drying operations.

Sodium sulphite heptahydrate for the 20°C. work was freshly prepared by cooling a saturated solution of anhydrous sodium sulphite. It, also, was used in the form of a slurry when it was possible to do so.

[1]*Manuscript received January 17, 1955.*
Contribution from Central Research Laboratory, Canadian Industries (1954) Limited, McMasterville, Quebec.
[2]*Present address*: *Canadian Industries (1954) Limited, Hamilton, Ontario.*

The ammonium chloride, sodium chloride, and anhydrous sodium sulphite were of A.R. grade. The latter contained about 1% of sodium sulphate.

(2) *Procedure*

A constant temperature bath was used, of which the temperature was controlled to ±0.1°C. For most of the work, solutions were stirred in three-necked flasks using glass propeller-type stirrers. In earlier work it was found that the sulphate content of the solution increased considerably over a period of a few days, particularly at 60°C. In most of the present work therefore the air was displaced with nitrogen in order to keep oxidation at a minimum. It was also found that ammonia has quite an appreciable vapor pressure over these solutions. Loss of ammonia therefore occurred and this resulted in the formation of bisulphite ion. Solutions were analyzed frequently for bisulphite, which was then neutralized by the addition of ammonia gas.

A solution was sampled by allowing salts to settle and then quickly drawing a sample up into a pipette. A short length of glass tubing containing a wad of absorbent cotton was attached by a rubber tube to the lower end of the pipette to prevent any salts being drawn up into the pipette. In the case of solutions above room temperature the pipette and filter tube were heated. The sample was run into a weighing bottle which was then stoppered and weighed. The sample was diluted in a volumetric flask and suitable aliquots were taken for analysis.

The procedure used in studying the ternary systems consisted in preparing a saturated solution of a single salt, to which portions of the second salt were then added, and the solution was stirred in the presence of an excess of the first salt. After time was allowed for equilibrium to be reached, the solution was analyzed. Additions of the second salt were continued until the composition of the solution became constant. When it was desired to determine the composition of the solid phase, the "rest" method of Schreinemakers was followed. Use was also made of the microscope for identification of solids.

Duplicate analyses were not usually carried out on solutions representing points on lines of ternary (or quaternary) systems. The data for solutions at points of intersections of lines (univariant points), however, are averages of two or more analyses.

(3) *Analytical Methods*

(*a*) *Bisulphite*

Owing to the buffering action of the sulphites, these solutions could not be analyzed accurately for bisulphite or free ammonia by a direct titration with standard alkali or acid respectively. The sulphite was therefore oxidized to sulphate and bisulphite to bisulphate by the addition of neutral hydrogen peroxide (A.R.). This oxidation was carried out at room temperature because the hydrogen peroxide contained a stabilizer which developed acidity in a hot solution. The oxidized solution was then titrated with standard alkali in the presence of methyl red to determine bisulphite, now in the form of bisulphate. Excess ammonia, when present, was titrated with standard acid in the presence of phenolphthalein, after oxidation of the sulphite.

(*b*) *Sulphite*

In order to minimize oxidation an aliquot was taken immediately after dilution of the sample and was added to $N/10$ iodine solution, the excess of which was then titrated with $N/10$ thiosulphate solution using starch indicator. The sulphite concentration was calculated in the usual way and a correction was made when bisulphite was present.

(*c*) *Sulphate*

An aliquot was oxidized with bromine water and the total sulphate was determined gravimetrically as barium sulphate. The actual sulphate content of the solution was then determined by subtracting from the total sulphate, the sulphate equivalent to the sulphite and bisulphite in the liquor.

(*d*) *Chloride*

A fourth aliquot was analyzed for chloride by the standard volumetric method using $N/10$ silver nitrate in excess and back-titrating with $N/10$ ammonium thiocyanate, using ferric alum indicator.

(*e*) *Ammonium*

Ammonium was determined by the method of Ronchèse (11), which is based on the fact that formaldehyde reacts with the ammonia contained in ammonium salts to form hexamethylene tetramine. The liberated acid can then be titrated to give a measure of the combined ammonia. Because formaldehyde reacts with sulphites, however, the solution used for the ammonium determination was that in which the sulphite had already been oxidized with iodine as described above (*b*). Methyl red was added to this solution at the end of the thiosulphate back-titration and the acid was exactly neutralized with sodium hydroxide solution. An excess of neutral 20% formaldehyde solution was added and the solution was heated to about 50°C. for a few minutes. The acid liberated by the reaction between ammonia in the ammonium salts and the formaldehyde was then titrated with standard sodium hydroxide solution using phenolphthalein indicator. The sodium hydroxide was standardized by the same procedure using dried A.R. ammonium chloride.

The neutralization of 20% formaldehyde solution was done by taking a measured quantity, diluting it with water to about the same extent as in a regular analysis, and then titrating it with sodium hydroxide, using phenolphthalein indicator. From the volume of sodium hydroxide used in this titration was calculated the amount to be added to the bottle containing the 20% formaldehyde. Alternatively, an electrometric titration was also found to be useful in exactly neutralizing the acidity of the 20% formaldehyde solution, which otherwise is difficult because of buffering action.

(*f*) *Sodium*

Sodium was determined by the standard method of converting all sodium salts to the sulphate, evaporating the solution to dryness, and heating the residue to constant weight.

The accuracy of the analytical methods was such that duplicate analyses checked within 2 parts per 1000 in the case of the sulphite, ammonium, and

chloride determinations, and within 4 parts per 1000 for sodium and total sulphate determinations.

EXPERIMENTAL RESULTS AND DISCUSSION

(1) *NH_4Cl–$NaCl$–H_2O System*

The data obtained in the present work at 20°C. and 60°C. are presented in Tables I and II.

TABLE I

SOLUBILITY DATA IN THE SYSTEM: NH_4Cl–$NaCl$–H_2O at 20°C. and 60°C.

(*a*) Temp. 20°C.			(*b*) Temp. 60°C.		
Composition of solution, weight %		Solid phases	Composition of solution, weight %		Solid phases
NaCl	NH_4Cl		NaCl	NH_4Cl	
26.36	0	NaCl	0	35.37	NH_4Cl
23.10	5.32	NaCl			
20.94	8.92	NaCl			
18.30	13.78	NaCl			
17.66	14.79	NaCl			
17.63	14.87	NaCl+NH_4Cl	13.60	24.70	NH_4Cl+NaCl
13.57	17.38	NH_4Cl			
8.41	20.96	NH_4Cl			
4.27	24.02	NH_4Cl	27.03	0	NaCl
0	27.26	NH_4Cl			

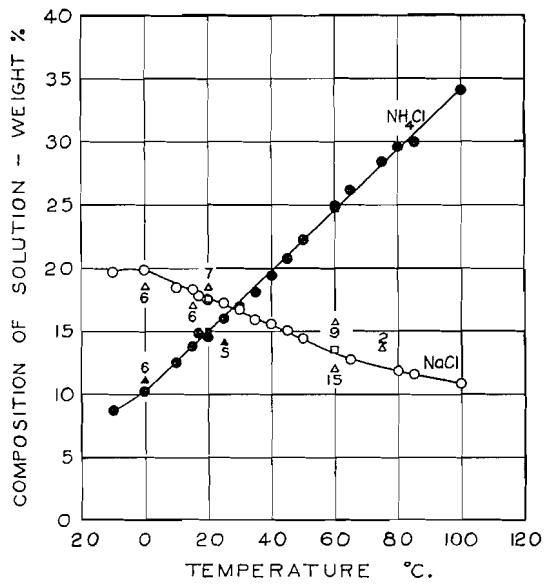

FIG. 1. Mutual solubilities of sodium chloride and ammonium chloride.
○ ● Published data, averaged where possible.
△ ▲ Published data, differing considerably from average values. Numeral indicates literature reference.
□ ■ Data obtained in present work.

TABLE II

SUMMARY OF PUBLISHED SOLUBILITY DATA FOR AQUEOUS SOLUTIONS SATURATED WITH BOTH NaCl AND NH_4Cl

Temp., °C.	Composition of solution, weight %		Authors
	NaCl	NH_4Cl	
−10	19.70	8.75	Yarlikov (14)
0	19.99	10.20	Fedotiev (1)
	19.78	10.26	Gerassimov (2)
	19.94	10.20	Lauffenburger and Brodsky (5)
	18.39*	11.06*	Mondain-Monval (6)
	19.9	10.2	Rivett (9)
	19.58	10.22	Sborgi and Franco (10)
	19.58	10.08	Yarlikov
10	18.27	12.49	Sborgi and Franco
	18.55	12.65	Yarlikov
15	18.20	13.56	Fedotiev
	17.04*	14.00	Mondain-Monval
	18.44	13.76	Toporescu (12)
17	17.78	14.88	Karsten (4)
20	18.52*	14.32	Rengade (7)
	17.52	14.78	Gerassimov
	17.54	14.50	Yarlikov
	17.63*	14.87*	Present work (Table I)
25	17.60	14.07*	Lauffenburger and Brodsky
	17.28	15.86	Restaino (8)
	17.10	15.9	Rivett
	16.83	16.16	Sborgi and Franco
30	16.55	16.97	Fedotiev
35	16.04	17.99	Toporescu
	15.82	18.29	Yarlikov
40	15.5	19.4	Rivett
45	15.03	20.70	Fedotiev
50	14.30	22.42	Gerassimov
	14.43	22.33	Restaino
	14.44	22.09	Toporescu
	14.48	21.98	Yarlikov
60	15.7*	24.4	Rivett
	11.96*	25.30	Zil'berman and Ivanov (15)
	13.60*	24.70*	Present work (Table I)
65	12.65	26.18	Yarlikov
75	13.57*	28.39	Gerassimov
80	12.0	29.5	Rivett
	11.55	29.76	Yarlikov
85	11.57	29.94	Zil'berman and Ivanov
100	10.82	34.13	Restaino
	10.77	33.98	Wurmser (13)

**Not used in averaging the data, and plotted separately in Fig. 1.*

It was noted that there were quite large differences between the present data and those in the literature, for solutions saturated with both sodium and ammonium chlorides at 60°C. Consideration of these differences led to a survey of all the available literature data on the mutual solubilities of these two salts. The original papers, the International Critical Tables and the handbooks of Seidell and Landolt-Bornstein, were consulted. The data thus found are summarized in Table II and plotted in Fig. 1. In those cases where two or more sets of data were available at a given temperature, the average values were plotted. However, data differing considerably from the average were not included in the average but were plotted separately. In addition to these larger discrepancies which are shown in Fig. 1, several smaller ones are apparent from a study of the data in Table II.

An explanation of some of these discrepancies may be that sufficient time of agitation was not allowed for equilibrium to be reached. In some cases, the explanation may be the occurrence of typographical errors. For example, Yarlikov (14) gives the same value for NaCl at 35°C. and 50°C. The 50°C. value is evidently a typographical error as it can be calculated from other data which he gives in Table II of his paper that the value at 50°C. should be 22.8 instead of 23.9 gm. NaCl/100 gm. of H_2O. The 50°C. value of Yarlikov (14.48%), given in Table II of the present paper was calculated using the value of 22.8 gm./100 gm. of H_2O.

Data obtained in the present work at 20°C. and 60°C. for solutions saturated with both salts appear to be in quite good agreement with curves representing average values of the published data, as indicated in Fig. 1.

(2) *NH_4Cl–$(NH_4)_2SO_3$–H_2O System*

(*a*) *20°C. Data*

The data are given in Table III and Fig. 2.

Ishikawa and Murooka (3) showed that ammonium sulphate does not form solid solutions with ammonium sulphite and there is no evidence in the

TABLE III

SOLUBILITY DATA IN THE SYSTEM: NH_4Cl–$(NH_4)_2SO_3$–H_2O AT 20°C.

Point in Fig. 2	Composition of solution, weight %			Composition of rest, weight %			Solid phases
	NH_4Cl	$(NH_4)_2SO_3$	$(NH_4)_2SO_4$	NH_4Cl	$(NH_4)_2SO_3$	$(NH_4)_2SO_4$	
S	27.26	0	0	—	—	—	NH_4Cl
	24.70	5.25	0.45	75.97	1.13	0.82	NH_4Cl
	22.45	10.00	1.06	70.70	2.90	1.54	NH_4Cl
	20.08	15.52	—	—	—	—	NH_4Cl
	18.39	19.13	—	—	—	—	NH_4Cl
F	16.61	23.57	1.20	52.28	24.20	0.28	$NH_4Cl+(NH_4)_2SO_3.H_2O$
F	16.57	23.64	1.15	16.79	62.26	2.12	$NH_4Cl+(NH_4)_2SO_3.H_2O$
	15.36	24.55	0.90	3.39	72.24	1.30	$(NH_4)_2SO_3.H_2O$
	9.66	28.85	—	2.29	71.56	1.78	$(NH_4)_2SO_3.H_2O$
	5.13	32.63	—	0.78	74.82	1.84	$(NH_4)_2SO_3.H_2O$
R	0	37.34	0.49	—	—	—	$(NH_4)_2SO_3.H_2O$

literature for the existence of solid solutions of ammonium chloride and ammonium sulphate. The sulphate content of a given rest could therefore only be due to ammonium sulphate in the adhering mother liquor and to oxidation of the sulphite by air during filtration. Because the sulphate content of the rest was usually much higher than that which could be accounted for by the adhering mother liquor, a correction was made by converting the ammonium sulphate in the rest to ammonium sulphite and adding this value to the $(NH_4)_2SO_3$ value before the rest composition was plotted in Fig. 2.

The data in Table III and Fig. 2 show no evidence of double salt or solid solution formation between ammonium chloride and ammonium sulphite at 20°C.

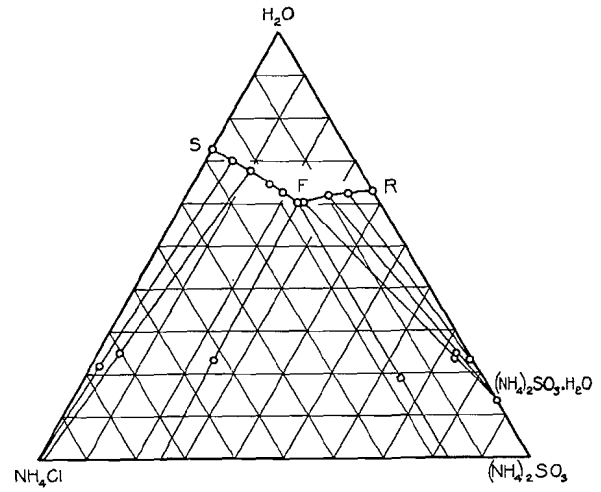

FIG. 2. Ammonium chloride – ammonium sulphite – water system at 20°C.

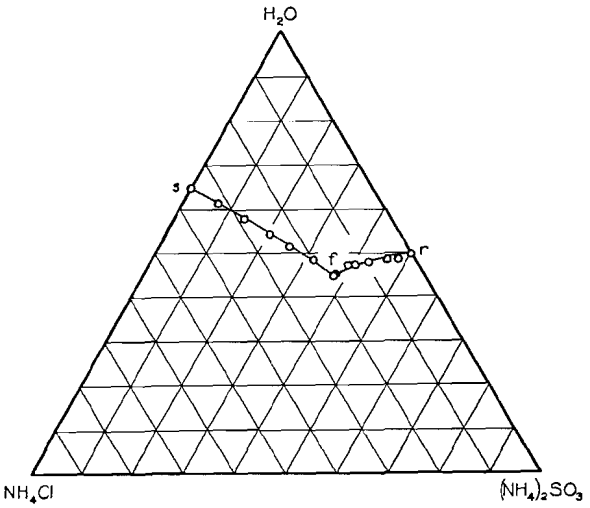

FIG. 3. Ammonium chloride – ammonium sulphite – water system at 60°C.

(b) 60°C. Data

The data in Table IV and in Fig. 3 show no evidence of the formation of a double salt or of solid solutions of ammonium chloride and ammonium sulphite at 60°C. The results also indicate that ammonium sulphite monohydrate does not dehydrate at 60°C. in solutions containing ammonium chloride, although no rest analyses were made to confirm this point.

The composition of the solution saturated with both salts is considerably different from that found by Zil'berman and Ivanov (15).

TABLE IV

SOLUBILITY DATA IN THE SYSTEM: NH_4Cl–$(NH_4)_2SO_3$–H_2O AT 60°C.

Point in Fig. 3	Composition of solution, weight %					Solid phases
	NH_4Cl	$(NH_4)_2SO_3$	$(NH_4)_2SO_4$	NH_4HSO_3	NH_3	
s	35.37	0	0	0	0	NH_4Cl
	32.04	6.95	—	—	—	NH_4Cl
	28.56	13.97	—	0.23	0	NH_4Cl
	25.35	20.75	—	0.09	0	NH_4Cl
	22.98	25.75	—	0.22	0	NH_4Cl
	19.82	32.06	—	0.43	0	NH_4Cl
f	17.84	37.72	0.91	—	—	$NH_4Cl+(NH_4)_2SO_3.H_2O$
	(16.74	35.82)*	—	—	—	$NH_4Cl+(NH_4)_2SO_3.H_2O$
f	17.82	37.86	0.99	—	—	$NH_4Cl+(NH_4)_2SO_3.H_2O$
	17.71	37.7	—	0.17	—	$(NH_4)_2SO_3.H_2O$
	16.90	37.6	—	0	0.22	$(NH_4)_2SO_3.H_2O$
	13.82	39.6	—	0	0.02	$(NH_4)_2SO_3.H_2O$
	15.64	38.5	—	—	—	$(NH_4)_2SO_3.H_2O$
	12.29	40.7	0.89	—	—	$(NH_4)_2SO_3.H_2O$
	9.05	43.1	—	0	0.02	$(NH_4)_2SO_3.H_2O$
	5.35	46.2	—	0	0.05	$(NH_4)_2SO_3.H_2O$
	3.14	48.6	—	0.51	—	$(NH_4)_2SO_3.H_2O$
r	0	50.48	—	0.13	0	$(NH_4)_2SO_3.H_2O$

**Zil'berman and Ivanov (15).*

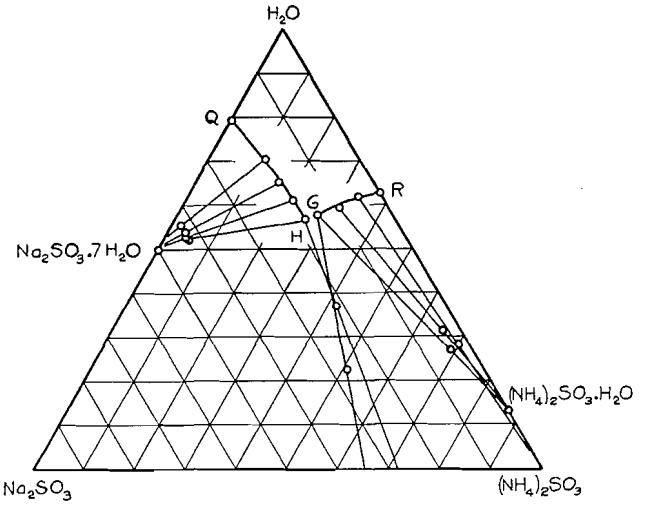

FIG. 4. Sodium sulphite – ammonium sulphite – water system at 20°C.

(3) *Na_2SO_3–$(NH_4)_2SO_3$–H_2O System*

(a) 20°C. Data

When portions of each salt were added to a saturated solution of the other salt, it was found that the two final compositions at 20°C. were not the same (Table V and Fig. 4). This result indicates the formation of a new solid phase between *G* and *H*, but sufficient work was not done to establish its nature.

TABLE V

SOLUBILITY DATA IN THE SYSTEM: Na_2SO_3–$(NH_4)_2SO_3$–H_2O AT 20°C.

Point in Fig. 4	Composition of solution, weight %			Composition of rest, weight %			Solid phases
	Na_2SO_3	$(NH_4)_2SO_3$	$(NH_4)_2SO_4$	Na_2SO_3	$(NH_4)_2SO_3$	$(NH_4)_2SO_4$	
R	0	37.34	0.49	—	—	—	$(NH_4)_2SO_3.H_2O$
	4.74	33.52	1.10	2.14	69.65	1.72	$(NH_4)_2SO_3.H_2O$
	9.91	30.91	0.62	3.78	64.60	0.41	$(NH_4)_2SO_3.H_2O$
	14.79	27.55	1.00	4.60	67.82	0.92	$(NH_4)_2SO_3.H_2O$
G	14.98	27.43	0.96	26.95	50.51	0.95	$(NH_4)_2SO_3.H_2O$ +unknown solid
H	17.26	25.75	1.30	21.56	41.24	1.95	Undetermined
	17.21	25.70	0.80	42.79	4.82	0.85	$Na_2SO_3.7H_2O$
	17.97	20.87	0.88	43.03	3.77	0.87	$Na_2SO_3.7H_2O$
	18.65	15.95	0.84	42.73	3.25	0.79	$Na_2SO_3.7H_2O$
	19.34	10.44	0.87	42.79	1.57	1.44	$Na_2SO_3.7H_2O$
Q	20.58	—	(Na_2SO_4) 0.77	—	—	—	$Na_2SO_3.7H_2O$

60°C. Data

Little work was done on this system at 60°C. and only the data for two solutions saturated with both salts are given in Table VI. These solutions

TABLE VI

SOLUBILITY DATA IN THE SYSTEM: Na_2SO_3–$(NH_4)_2SO_3$–H_2O AT 60°C.

Composition of solution, weight %					Solid phases
Na_2SO_3	$(NH_4)_2SO_3$	Na_2SO_4	NH_4HSO_3	NH_3	
(8.35	45.08)*	—	—	—	$(NH_4)_2SO_3.H_2O$, Na_2SO_3
7.76	44.7	0.74	0	0.08	Not determined
7.69	45.0	0.71	0.08	0	Not determined

**Zil'berman and Ivanov (15).*

were obtained by starting with solutions saturated with sodium sulphite and with ammonium sulphite respectively, and adding portions of the other salt until the compositions became constant. It is seen from Table VI that these compositions are practically identical, but these data do not show whether there is formation of a double salt or a solid solution at 60°C. or if dehydration of ammonium sulphite monohydrate occurs. The data obtained, however, are

in fair agreement with those of Zil'berman and Ivanov (15) for a solution saturated with respect to $(NH_4)_2OS_3.H_2O$ and Na_2SO_3.

(4) *NaCl–Na_2SO_3–H_2O System*

(*a*) *20°C. Data*

The data obtained are given in Table VII and are shown plotted in Fig. 5. Between *P* and *C*, the solid phase is NaCl, and between *Q* and *L* it is $Na_2SO_3.7H_2O$. The space between *L* and *C* indicates the existence of an undetermined solid phase.

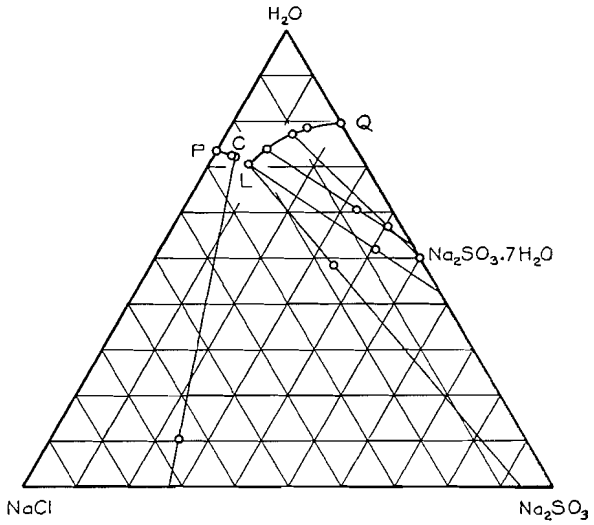

FIG. 5. Sodium chloride – sodium sulphite – water system at 20°C.

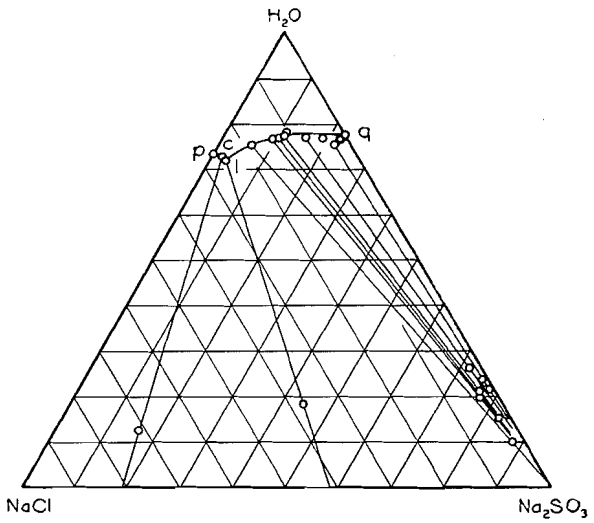

FIG. 6. Sodium chloride – sodium sulphite – water system at 60°C.

TABLE VII

SOLUBILITY DATA IN THE SYSTEM:
$NaCl$–Na_2SO_3–H_2O AT 20°C. AND AT 60°C.

Point in figure	Composition of solution, weight %			Composition of rest, weight %			Solid phases
	NaCl	Na_2SO_3	Na_2SO_4	NaCl	Na_2SO_3	Na_2SO_4	
At 20°C.							
Fig. 5							
P	26.36	0		—	—	—	NaCl
	24.22	3.26	0.22		—	—	NaCl
C	23.68	4.35	0.21	65.25	24.28	1.75	Undetermined
L	21.10	7.41	1.24	16.86	34.65	1.18	Undetermined
	21.19	7.61	1.23	7.34	40.60	1.60	Undetermined
	16.73	9.13	1.14	2.95	42.13	2.59	$Na_2SO_3.7H_2O$
	16.89	9.20	0.71	6.59	32.78	1.48	$Na_2SO_3.7H_2O$
	10.27	12.46	1.04	2.39	40.65	1.24	$Na_2SO_3.7H_2O$
	6.76	14.87	0.86	—	—	—	$Na_2SO_3.7H_2O$
Q	0	20.58	0.77	—	—	—	$Na_2SO_3.7H_2O$
At 60°C.							
Fig. 6							
p	27.03	—	—				NaCl
c	25.77	1.89	0.30	71.8	16.02	0.68	Apparently NaCl+Na_2SO_3
	(24.23	2.36)*					NaCl+Na_2SO_3
l	25.14	3.04	0.16	37.58	44.60	1.12	Apparently NaCl+Na_2SO_3
	18.85	5.98	0.93	2.16	88.3	3.10	Na_2SO_3
	14.03	9.57	0.70	3.34	77.2	2.22	Na_2SO_3
	12.75	10.64	1.05	2.16	83.01	2.66	Na_2SO_3
	11.69	11.46	2.40	2.86	76.50	1.47	Na_2SO_3
	10.88	11.27	1.06	—	—	—	Na_2SO_3
	7.55	15.80	2.04	2.11	72.00	5.40	Na_2SO_3
	4.45	18.90	1.32	0.99	75.75	3.40	Na_2SO_3
	2.98	21.90	1.02	0.76	78.00	6.21	Na_2SO_3
	1.29	22.50	0.65	0.41	76.30	4.43	Na_2SO_3
q	0	22.86	0.67	—	—	—	Na_2SO_3

**Zil'berman and Ivanov (15).*

(*b*) *60°C. Data*

Sodium chloride was added to a solution saturated with sodium sulphite (*q*) until a constant composition was reached at *l* (Table VII and Fig. 6). Similarly, when sodium sulphite was added to a solution saturated with sodium chloride the point *c* was obtained. The experiment was repeated several times with the same result being obtained each time. That is, the compositions of the two solutions stopped at *l* and *c* respectively, solid sodium chloride at *l*, and solid sodium sulphite at *c* having little effect on the compositions even after several days' stirring. Thus, there appeared to be an undetermined solid phase present in this system at 60°C. as well as at 20°C.

The following attempts were made to obtain solutions between *c* and *l*, since analysis of the rests from such solutions should give the identity of the solid phase in the region between *c* and *l*. Portions of a filtered solution at *l* were added to three bottles of 150 ml. capacity. To each bottle were added 0.1 gm. of sodium sulphite and 1.0 gm. of sodium chloride. Similarly, a solution

at c was filtered and portions of it were placed in three bottles. To these were added 0.1 gm. of sodium chloride and 1, 2, and 3 gm. of sodium sulphite respectively. These bottles were closed with glass stoppers (greased) and rotated, so that the solids fell from top to bottom of each bottle and vice versa, during a revolution, for seven weeks in a constant temperature bath. At the end of that time the bottles were removed, and analyses were made on the solutions and rests.

The data obtained are given in Table VIII. It will be noted that the sulphate content in solutions c_3 is very low and is evidently in error. The sodium sulphite content in solutions c, c_1, c_2, and c_3 shows comparatively little change except

TABLE VIII

$NaCl$–Na_2SO_3–H_2O SYSTEM AT 60°C.
EXPERIMENTS IN ROTATING BOTTLES

Solution	Solution, weight %			Rest, weight %			Remarks
No.	NaCl	Na_2SO_3	Na_2SO_4	NaCl	Na_2SO_3	Na_2SO_4	
c	25.77	1.89	0.30	71.8	16.02	0.68	
c_1	25.20	1.97	0.62	1.70	87.3	4.70	Soln. c+0.1 gm. NaCl and 1.0 gm. Na_2SO_3
c_2	25.25	2.08	0.70	1.66	88.6	3.99	Soln. c+0.1 gm. NaCl and 2.0 gm. Na_2SO_3
c_3	25.55*	2.54	0.04	11.77	79.9	3.25	Soln. c+0.1 gm. NaCl and 3.0 gm. Na_2SO_3
l	25.14	3.04	0.16	37.58	44.60	1.12	
l_1	25.03	2.93	0.30	66.00	18.37	5.96	Soln. l+0.1 gm. Na_2SO_3 and 1.0 gm. NaCl
l_2	23.36	2.68	0.56	—	—	—	Soln. l+0.1 gm. Na_2SO_3 and 1.0 gm. NaCl
l_3	24.72	3.00	0.56	31.99	39.79	4.46	Soln. l+0.1 gm. Na_2SO_3 and 1.0 gm. NaCl

Calc. by diff.

in the case of solution c_3 but even in this case it is still considerably below the value for the solution at l. Two grams of sodium sulphite would have been sufficient, had it all dissolved, to move the composition of the solution from c to l. In the case of the experiments in which sodium chloride and a small proportion of sodium sulphite were added to solutions at l (Table VIII), there was no significant decrease in the sulphite content nor increase in the chloride content during seven weeks, for the first and third solutions (l_1 and l_3). In the case of solution l_2, the decrease in the contents of both sodium chloride and sodium sulphite and the fact that there was insufficient rest for and analysis indicate that water leaked into this bottle.

Because a series of solutions with compositions lying between l and c was not obtained, the results of these experiments do not indicate the nature of the unknown solid phase. A possible explanation of the results may be the formation of solid solutions of sodium sulphate in sodium sulphite, as several such solid solutions are known. It might be, for example, that sodium chloride is in equilibrium with one solid solution of sodium sulphate in sodium sulphite

at *c* (60°C. diagram) and with a different solid solution at *l*. In a second paper dealing with the quaternary system the nature of the solid phase between *L* and *C* (20°C. data) and between *l* and *c* (60°C. data) will be discussed further.

REFERENCES

1. FEDOTIEV, P. P. Z. physik. Chem. 49: 162. 1904.
2. GERASSIMOV, I. Z. anorg. u. allgem. Chem. 187: 321. 1930.
3. ISHIKAWA, F. and MUROOKA, H. *Cited by* J. W. Mellor. A comprehensive treatise on inorganic and theoretical chemistry. Vol. X. Longmans, Green and Co., London, New York, Toronto. 1930. p. 258.
4. KARSTEN. *Cited by* A. Seidell. Solubilities of inorganic and metal organic compounds. Vol. I. 3rd ed. D. Van Nostrand Company, Inc., New York. 1940. p. 1223.
5. LAUFFENBURGER, R. and BRODSKY, M. Compt. rend. 206: 1383. 1938.
6. MONDAIN-MONVAL, P. Compt. rend. 174: 1014. 1922; 175: 162. 1922.
7. RENGADE, E. Chimie & industrie, 7: 1090. 1922.
8. RESTAINO, S. Atti 10th congr. intern. chim. Rome, 2: 761. 1938.
9. RIVETT, A. C. D. J. Chem. Soc. 121: 379. 1922.
10. SBORGI, U. and FRANCO, C. Gazz. chim. ital. 51 (II): 1. 1921.
11. SUTTON, F. Volumetric analysis. 12th ed. P. Blakiston's Son & Co., Inc., Philadelphia. 1935. p. 75.
12. TOPORESCU, E. Compt. rend. 174: 870. 1922; 175: 268. 1922.
13. WURMSER, MLLE. Compt. rend. 174: 1466. 1922.
14. YARLIKOV, M. M. Zhur. Priklad. Khim. 7: 902. 1934.
15. ZIL'BERMAN, YA. I. and IVANOV, P. T. Zhur. Priklad. Khim. 14: 939. 1941.

THE RECIPROCAL SALT-PAIR SYSTEM: SODIUM CHLORIDE – AMMONIUM SULPHITE – SODIUM SULPHITE – AMMONIUM CHLORIDE – WATER AT 20°C. AND 60°C.

PART II: THE QUATERNARY SYSTEM[1]

By J. A. Labash[2] and G. R. Lusby

ABSTRACT

In the above quaternary system at 60°C., besides those representing the four salts at the corners of the Janecke diagram two other saturation areas were found. At 20°C. there are three, and possibly more than three additional areas. In the course of the present work it was not possible to establish the nature of the solid phases in these additional areas of the quaternary system. However, the data of Lewis and Rivett suggest that at least some of these unknown areas may indicate the presence of different solid solutions of sodium sulphate in sodium sulphite. This quaternary system appears to be a rather complex one and much further work remains to be done in order to complete the knowledge of it at 60°C. and 20°C., particularly at the latter temperature.

INTRODUCTION

Zil'berman and Ivanov (6) made a study of the reciprocal salt-pair system: $NaCl$–$(NH_4)_2SO_3$–Na_2SO_3–NH_4Cl–H_2O at 60°C. and 85°C., and of the system: $NaCl$–NH_4HSO_3–$NaHSO_3$–NH_4Cl–H_2O at 25°C. and 60°C. The ultimate purpose of their work was the same as that of the present work, namely, the industrial preparation of sodium sulphite and ammonium chloride from sodium chloride, sulphur dioxide, and ammonia.

The process as developed in this laboratory and used in the plant at Hamilton, Ont. (1), consists essentially in adding sulphur dioxide and ammonia gases to a mother liquor containing sodium chloride in suspension, and centrifuging off the precipitated sodium sulphite at 60°C. The mother liquor is cooled to 20°C., the ammonium chloride which crystallizes out is centrifuged off, and the mother liquor is used for the next cycle.

Such a cyclic process as outlined above is the subject of several German patents dating from 1887. Zil'berman and Ivanov point out that these patents are very vague in regard to the details of the process and that they found it necessary to carry out solubility studies in order to define more precisely the operating conditions. It was for the same reason that the present work was undertaken.

In the previous paper (2) data were given on the four ternary systems associated with the reciprocal salt-pair system: $NaCl$–$(NH_4)_2SO_3$–Na_2SO_3–NH_4Cl–H_2O at 20°C. and 60°C. The present paper contains data on the quaternary system.

The experimental methods were essentially the same as those used for the ternary systems.

[1]*Manuscript received January 17, 1955.*
Contribution from Central Research Laboratory, Canadian Industries (1954) Limited, McMasterville, Quebec.
[2]*Present address: Canadian Industries (1954) Limited, Hamilton, Ontario.*

EXPERIMENTAL

The presence of sulphate ion as an impurity presents a difficulty in the accurate plotting of the data according to the method of Janecke for reciprocal salt-pairs. Because it was usually not known how the sulphate was distributed between the ammonium and sodium ions, the ionic ratios of these two ions were based on the total sodium and ammonium values.

(1) *60°C. Data*

In Fig. 1 it will be noted that there are two saturation areas where the solid phase has not been identified, namely, (*a*) the area between the lines *cb* and *le*, and (*b*) the area between the lines *ej* and *do*.

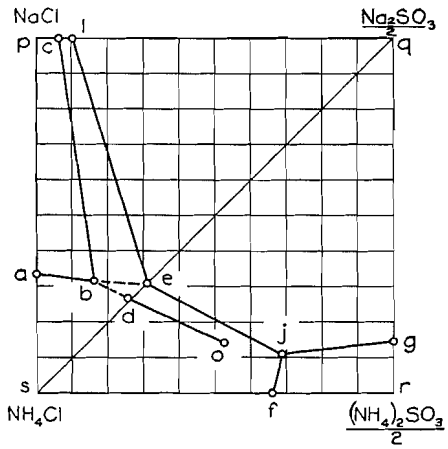

FIG. 1. Sodium chloride – ammonium sulphite – sodium sulphite – ammonium chloride – water system at 60°C.

(*a*) Area between *cb* and *le* at 60°C.

The points *c* and *l* at the top of this area have already been discussed under the $NaCl–Na_2SO_3–H_2O$ system (2). Ammonium chloride was added in portions to a solution at *c*, in the presence of excess sodium chloride and sodium sulphite, and the solution was analyzed after each addition. In this way several points were obtained along the line *cb*. At *b* the solids were filtered off and each of the three salts sodium chloride, ammonium chloride, and sodium sulphite was added singly, to the filtered solution, which was stirred for several hours in each case. No change in composition occurred and it thus seemed that the solution at *b* was saturated with these three salts. Points along *cb* were also obtained by adding sodium sulphite to solutions plotting to the left of *cb*.

To a solution at *a*, in the presence of excess sodium and ammonium chlorides, sodium sulphite was added and points were obtained along *ab*. The composition became constant at *b*, and was practically the same as that obtained by starting from *c* (Table I).

The point *e* was obtained by adding ammonium chloride to a saturated solution of sodium sulphite and then, after the composition had become

constant, adding sodium chloride. No change in composition occurred when the latter salt was added so the solution at *e* was also apparently saturated with the three salts, sodium chloride, ammonium chloride, and sodium sulphite. Points along the line *le* were obtained by adding sodium chloride to solutions which plotted to the right of this line. In some cases the composition did not stop at this line, but moved into the *cbel* area. The addition of ammonium chloride to a solution on the lower part of the line *le* always caused the composition to move towards the corner *s* of the diagram until the line *be* was reached.

Points on *be* were also obtained by adding sodium chloride to solutions plotting below *be*. Once the composition reached a point on *be*, however, the presence of an excess of solid sodium chloride did not cause the composition to move towards *b*. Also, no noticeable change in composition occurred in a few hours on adding the three salts sodium chloride, ammonium chloride, and sodium sulphite separately to solutions represented by points on the line *be*. There was no difficulty, however, in moving the composition from *b* to *e* by adding ammonium sulphite to a filtered solution at *b*.

(*b*) Area between *ej* and *do* at 60°C.

When ammonium chloride was added to a saturated sodium sulphite solution, the composition moved along the diagonal from *q* to *e*, where the composition became constant. Similarly, when sodium sulphite was added to a saturated ammonium chloride solution, the composition moved from *s* to *d*. The existence of the two points *d* and *e* indicates the presence of another solid phase, which could be a double salt or a solid solution. Points *d* and *e* were also obtained when these experiments were repeated using solutions which were slightly ammoniacal. This was done because the only known double salt containing sodium and ammonium sulphites has the formula $2Na_2SO_3.(NH_4)_2S_2O_5.10H_2O$ (4). This double salt was encountered in the present work in certain solutions containing bisulphite ion, but it dissolved readily when the solution was neutralized with ammonia. The possibility of its formation was therefore assumed to have been eliminated by avoiding acidic conditions in the above experiments at the points *d* and *e*, and the existence of the area between *d* and *e* is presumably not due to formation of this double salt.

Chemical analysis and microscopic examination of the rests indicated the presence of sodium chloride, ammonium chloride, and sodium sulphite at *e* and ammonium chloride and sodium sulphite at *d*. The microscopic technique, however, would not have revealed the presence of solid solutions if these had differed only slightly in optical properties from the pure salts. It was decided to investigate the nature of the unknown solid phase by attempting to obtain points between *d* and *e* in the pseudoternary system: NH_4Cl–Na_2SO_3–H_2O in the following manner.

All solids were filtered from a solution at *e*, which was then divided into five portions. To each portion (about 150 gm.) was added 0.1 gm. of sodium sulphite and 1.0 to 2.5 gm. of ammonium chloride, the latter quantity being more than sufficient to move the composition to *d* if it dissolved. Similarly, to each of five portions of filtered liquor at *d* were added 0.2 gm. of ammonium

TABLE I

RECIPROCAL SALT-PAIR SYSTEM: $NaCl$-$(NH_4)_2SO_3$-Na_2SO_3-NH_4Cl-H_2O AT 60°C. AND 20°C.

	Line	Composition of solution, weight %							Solid phases
		NaCl	NH_4Cl	$(NH_4)_2SO_3$	Na_2SO_3	Na_2SO_4	NH_4HSO_3	NH_3	
At 60°C.									
Point in Fig. 1									
a	—	13.60	24.70	0	0	0	0	0	$NaCl$, NH_4Cl
b	*cb*	5.96	27.17	0	7.24	1.73	0	0.01	NH_4Cl, Na_2SO_3, $NaCl$*
	ab	6.00	27.43	0	7.64	0.80	0.16 ($NaHSO_3$)	0	
c	—	25.77	0	0	1.89	0.30	0	0	$NaCl$, Na_2SO_3*
d	—	0	30.48	0	12.42	0.76	—	—	NH_4Cl, Na_2SO_3*
		(0	30.84	0.52	12.84)†	—	—	—	NH_4Cl, Na_2SO_3, $NaCl$
e	—	0	29.20	0.41	14.77	0.62	0.07	—	NH_4Cl, Na_2SO_3, $NaCl$*
f	—	0	17.84	37.72	0	0.91 ($(NH_4)_2SO_4$)	—	—	NH_4Cl, $(NH_4)_2SO_3.H_2O$
g	—	0	0	45.0	7.69	0.71	0.08	0	Na_2SO_3, $(NH_4)_2SO_3.H_2O$
	fj	0	16.87	34.5	5.23	1.26	0.37	0	NH_4Cl, Na_2SO_3, $(NH_4)_2SO_3.H_2O$*
	gj	0	16.87	34.4	5.55	0.64	0.79	0	
	ej	0	15.89	34.3	6.24	2.29	—	—	
		(0	15.79	35.11	4.25)†				NH_4Cl, Na_2SO_3, $(NH_4)_2SO_3.H_2O$
l	—	25.14	0	0	3.04	0.16	0	0	$NaCl$, Na_2SO_3*
o	—	0	22.18	20.22	6.68	1.48	—	—	NH_4Cl, Na_2SO_3*
p	—	27.03	0	0	0	0	0	0	$NaCl$
q	—	0	0	0	22.86	0.67	0	0	Na_2SO_3
r	—	0	0	50.48	0	—	0.13	0	$(NH_4)_2SO_3.H_2O$
s	—	0	35.37	0	0	0	0	0	NH_4Cl

At 20°C.

Point in Fig. 2									
A	—	17.63	14.87	0	0	0	0	0	NaCl, NH_4Cl
B	*AB*	10.24	16.54	0	8.20	0.65	—	—	NH_4Cl, Na_2SO_3, NaCl*
	CB	10.47	16.50	0	8.51	0.46	—	—	
C	—	23.68	0	0	4.35	0.21	—	—	Undetermined
D	—	0.35	21.52	0	16.61	0.44	—	—	NH_4Cl, Na_2SO_3*
E	—	3.86	18.55	0	16.36	0.59	—	—	NH_4Cl, Na_2SO_3, NaCl*
F	—	0	16.59	23.61	0	1.17 $((NH_4)_2SO_4)$	—	—	NH_4Cl, $(NH_4)_2SO_3.H_2O$
G	—	0	0	27.43	14.98	0.96 $(NH_4)_2SO_4$	—	—	Undetermined
H	—	0	0	25.75	17.26	1.30 $(NH_4)_2SO_4$	—	—	Undetermined
I	*FI*	0	14.58	17.23	11.60	1.51	0	0	NH_4Cl, Na_2SO_3, $(NH_4)_2SO_3.H_2O$*
	DI	0	13.88	17.88	10.71	2.91	—	—	
J	—	0	13.80	15.78	15.18	0.89	—	—	NH_4Cl, Na_2SO_3, $(NH_4)_2SO_3.H_2O$*
K	—	0	17.33	1.68	22.25	0.71	—	—	NaCl, $Na_2SO_3.7H_2O$, Na_2SO_3
L	—	21.43	0	0	7.44	0.86	—	—	Undetermined
N	—	0	19.95	0	18.92	1.45	—	—	NH_4Cl, Na_2SO_3*
P	—	26.36	0	0	0	0	0	0	NaCl
Q	—	0	0	0	20.58	0.77	—	—	$Na_2SO_3.7H_2O$
R	—	0	0	37.34	0	0.49 $(NH_4)_2SO_4$	—	—	$(NH_4)_2SO_3.H_2O$
S	—	0	27.26	0	0	0	0	0	NH_4Cl

**Apparent solid phases.*
†*Zil'berman and Ivanov (6).*

TABLE II

NH_4Cl–Na_2SO_3–H_2O SYSTEM AT 60°C. EXPERIMENTS IN ROTATING BOTTLES

Test sol'n (Fig. 1)	Solution, weight %						Rest, weight %			Remarks
	NaCl	NH_4Cl	$(NH_4)_2SO_3$	Na_2SO_3	Na_2SO_4	NH_4HSO_3	Na_2SO_3	NH_4Cl	Na_2SO_4	
e	0	29.18	0.41	14.90	0.80	0.02	69.4	18.7	1.26	Clear solution divided into five 150 gm. portions and treated as indicated below, for 7 weeks
e_1	0	29.04	0.52	14.66	0.75	—	2.16	89.4	4.54	*e*+0.1 gm. Na_2SO_3+1.0 gm.NH_4Cl
e_2	0	29.15	0.29	14.31	0.80	0.04	Not enough for analysis			*e*+0.1 gm. Na_2SO_3+2.0 gm.NH_4Cl
e_3	0	28.80	0.87	14.32	0.84	—	2.30	88.7	—	*e*+0.1 gm. Na_2SO_3+2.0 gm.NH_4Cl
e_4	0	29.08	0.29	14.75	0.59	—	4.50	74.9	0.86	*e*+0.1 gm. Na_2SO_3+2.5 gm.NH_4Cl
e_5	0	28.98	0.41	14.59	0.98	—	8.14	58.4	1.14	*e*+0.1 gm. Na_2SO_3+2.5 gm.NH_4Cl
d	0	30.40	0	12.57	0.71	—	25.05	69.0	0.43	Clear solution divided into five 150 gm. portions and treated as indicated below, for 7 weeks
d_1	0	29.35	0	12.31	0.86	—	92.0	1.71	4.29	*d*+0.3 gm. NH_4Cl+2.0 gm.Na_2SO_3
d_2	0	30.20	0	12.88	0.56	—	87.8	3.56	1.75	*d*+0.2 gm. NH_4Cl+4.0 gm.Na_2SO_3
d_3	0.23	29.98	0	12.59	0.84	0.04	65.7	19.51	1.88	*d*+0.2 gm. NH_4Cl+4.0 gm.Na_2SO_3
d_4	0	29.40	0	12.84	0.49	—	93.1	2.17	2.12	*d*+0.2 gm. NH_4Cl+6.0 gm.Na_2SO_3
d_5	0	29.82	0.17	12.36	1.35	—	67.9	23.58	1.57	*d*+0.2 gm. NH_4Cl+6.0 gm.Na_2SO

chloride and 2 to 6 gm. of sodium sulphite. These solutions and their respective solids were placed in bottles and rotated in the constant temperature bath at 60°C. for six to seven weeks. At the end of that time the solutions and rests were analyzed. In all cases except two (d_1 and d_4), the solution compositions were found not to have changed appreciably and the rests, as indicated by analysis, were mostly ammonium chloride at *e* and mostly sodium sulphite at *d* (Table II). Because points were not obtained between *d* and *e*, these experiments did not result in the identification of the solid phase between the lines *ej* and *do*.

The areas between *b* and *d*, and between *o* and *j* were not explored; *d* and *o* do not represent univariant points but simply the last points determined along the line *do*. The line *do* was explored by adding ammonium sulphite to a liquor at *d*. It was noticed that the composition had a tendency to move across the area between *ej* and *do*, so that when one analysis showed the composition to be on *do*, the analysis after another addition of ammonium sulphite frequently showed the composition to be on *ej*. To avoid this difficulty, solutions were made up whose compositions were represented by points below *do*. On addition of anhydrous sodium sulphite in excess, the compositions moved to points on *do*.

It is interesting to note that the composition found by Zil'berman and Ivanov (6) for the solution saturated with sodium chloride, ammonium chloride, and sodium sulphite corresponds with the composition of the solution at *d*, which in the present work was found to be not saturated with sodium chloride (Table I and Fig. 1). This difference may be due to a difference in the sulphate content of the two solutions.

When sodium sulphite was added to a solution at *f*, points were obtained along *fj*, and the composition became constant at *j*. Ammonium chloride was added to a solution at *g* and the composition was followed along *gj* until *j* was again reached, as indicated in Table I. Analysis of the rest indicated the presence of anhydrous sodium sulphite, ammonium chloride, and ammonium sulphite, but it was not determined whether the latter was in the form of the hydrate or not.

When ammonium sulphite hydrate was added to a solution at *e*, along with excesses of sodium sulphite and ammonium chloride, points were obtained along *ej* until the solution reached a constant composition. It will be seen that the final composition *j* in this case is somewhat different from the other two compositions, particularly in respect to the ammonium chloride value (Table I). This difference may be due to the higher content of sodium sulphate in this particular solution. The difference between the composition of the solution at *j*, obtained by Zil'berman and Ivanov, and the present values may also be due to differences in the sulphate contents.

(2) *20°C. Data*

The 20°C. data are given in Table I and Fig. 2.

The points *C* and *L* have already been mentioned in connection with the ternary system $NaCl$–Na_2SO_3–H_2O at 20°C. (2). To a solution at *C* in the

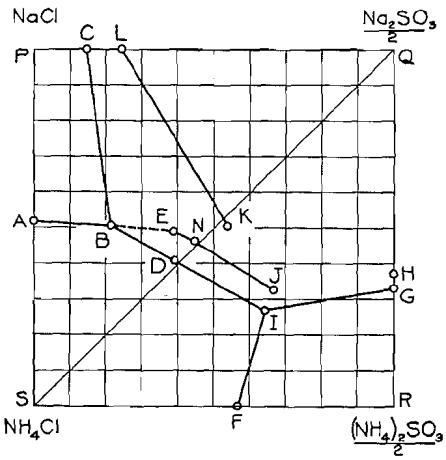

FIG. 2. Sodium chloride – ammonium sulphite – sodium sulphite – ammonium chloride – water system at 20°C.

presence of excess sodium chloride and sodium sulphite, portions of ammonium chloride were added. Analyses gave solution compositions which plotted along the line *CB*. Finally the point *B* was reached where the solid phases appeared to be sodium chloride, anhydrous sodium sulphite, and ammonium chloride. Several points on *CB* were also obtained by adding anhydrous sodium sulphite to solutions to the left of *CB* in the sodium chloride area. Similarly, by adding sodium sulphite to a solution at *A*, the composition followed the line *AB* until it became constant at *B*. The two compositions thus obtained agree quite well (Table I).

Points were obtained along *LK* by adding sodium chloride to solutions in the sodium sulphite heptahydrate area to the right of *LK*. Such solutions were analyzed after each addition of sodium chloride until their compositions became constant and remained so for several days. The apparent solid phases were sodium chloride and sodium sulphite heptahydrate.

Several solutions were obtained, which plotted along a line between *CB* and *LK*, and which appeared to be in equilibrium with sodium chloride and anhydrous sodium sulphite but sufficient work was not done to establish definitely the position of this line.

The point *K* was obtained by adding ammonium chloride in portions to a solution saturated with sodium sulphite heptahydrate (*Q*). The composition of the solution moved along the diagonal *QS* until it approached *K*, when it left the diagonal and became constant at *K*, where the solid phases appeared to be sodium sulphite heptahydrate, anhydrous sodium sulphite, and sodium chloride. After further portions of ammonium chloride had been added, the composition returned to the diagonal and moved to the point *N*, where the solid phases were apparently ammonium chloride and anhydrous sodium sulphite.

Several solutions were obtained which were apparently in equilibrium with sodium sulphite heptahydrate and anhydrous sodium sulphite in the region

between K and H but this area was not studied sufficiently to establish the boundary line between the hydrated and anhydrous forms of sodium sulphite. The procedure followed in these experiments was to add ammonium chloride to solutions in contact with excess sodium sulphite heptahydrate. The results were inconsistent, possibly because of metastable states of equilibria. No data are given therefore.

The point I was obtained by adding anhydrous sodium sulphite to a liquor at F in equilibrium with solid ammonium chloride and ammonium sulphite hydrate. The composition became constant at I where the solid phases were apparently ammonium chloride, anhydrous sodium sulphite, and ammonium sulphite monohydrate. Points on the line IG were obtained by adding anhydrous sodium sulphite to solutions whose compositions plotted below IG.

The point I was apparently reached also by adding ammonium sulphite monohydrate to a solution at D and following the line DI. The difference in composition between the two solutions at I (Table I) is possibly due to the difference in sulphate content. Several points along BI were obtained by adding anhydrous sodium sulphite to solutions below this line. Solutions plotting between B and D usually moved slowly towards BE in the presence of an excess of anhydrous sodium sulphite. In some cases the compositions changed quite quickly on the addition of sodium sulphite, to points between D and E. On the other hand solutions along DI showed little tendency to change even after a week's stirring.

The addition of sodium chloride to solutions along the line BD caused the compositions to move immediately to points on BE. For example, on taking a solution at D in contact with excess ammonium chloride and anhydrous sodium sulphite and adding sodium chloride to it, the new composition corresponded to E. The solids were filtered off and the clear solution was stirred separately with each of the three salts. No significant change in composition was observed, which indicated that the solution at E was apparently saturated with ammonium chloride, sodium chloride, and anhydrous sodium sulphite.

Solutions along BE behaved similarly to those along be in the 60°C. diagram. That is, the addition of sodium chloride to a solution on BE in the presence of excess ammonium chloride and anhydrous sodium sulphite did not have any noticeable effect on its composition. On the other hand, ammonium sulphite added to solutions along BE caused their compositions to move along BE to E.

By adding ammonium sulphite (in the form of ammonia and sulphur dioxide gases) to a solution on NJ, a constant liquor composition was reached at J. The filtered solution was tested singly with the three salts—anhydrous sodium sulphite, ammonium chloride, and ammonium sulphite (added in the form of the two gases), but no appreciable change in the liquor composition was noted in any case.

The present data at 20°C. as plotted in Fig. 2 indicate that there are at least three unknown saturation areas one of which, within the region of the points K, H, G, I, and J may represent solutions in equilibrium with anhydrous

sodium sulphite. A possible explanation of the presence of these unknown saturation areas is discussed below.

GENERAL DISCUSSION

In the 60°C. diagram (Fig. 1), the existence of unknown saturation areas could indicate the presence of double salts or solid solutions of either sodium chloride and sodium sulphite or ammonium chloride and sodium sulphite. It would seem more reasonable, however, to base an explanation of the results on the formation of solid solutions of sodium sulphite and sodium sulphate. (Sulphate was an impurity in the present work.) Such solid solutions are well known as a result of the work of Lewis and Rivett (3, 5). Thus, the line *cb* may represent solutions in equilibrium with sodium chloride and one solid solution of sodium sulphate in sodium sulphite, while in the case of the line *le* the solids may be sodium chloride and a different solid solution. The area between the lines *cb* and *le* (and similarly the area between *bdo* and *ej*) would then be due to the overlapping of two areas which represent solutions saturated with respect to two different solid solutions of sodium sulphate in sodium sulphite. In a similar manner may be explained the existence of unknown saturation areas in the 20°C. diagram. The tendency of sodium sulphate and sodium sulphite to form metastable solid solutions may explain some apparently metastable states of equilibrium encountered in the present study.

The quaternary system is obviously more complicated at 60°C. than the results of Zil'berman and Ivanov indicate, and it is still more complex at 20°C. It is not the intention of the present authors to continue the study of this system of salts but it is hoped that the information presented in these two papers will be of assistance to others in future studies. Much work remains to be done on the quaternary system at 20°C. and 60°C. particularly on the identification of the solid phases, and X-ray diffraction techniques should be very useful in such studies. Literature data on the three ternary systems containing sulphites are also rather scanty, so that salt systems containing sulphites present a large field for phase rule investigations.

REFERENCES

1. Cook, E. J. R. Can. Chem. Process Ind. 29: 221. 1945.
2. Labash, J. A. and Lusby, G. R. Can. J. Chem. 33: 774. 1955.
3. Lewis, N. B. and Rivett, A. C. D. J. Chem. Soc. 125: 1156, 1162. 1924.
4. Mellor, J. W. A comprehensive treatise on inorganic and theoretical chemistry. Vol. X. Longmans, Green and Co., London, New York, Toronto. 1930. p. 270.
5. Rivett, A. C. D. and Lewis, N. B. Rec. trav. chim. 42: 954. 1923.
6. Zil'berman, Ya. I. and Ivanov, P. T. Zhur. Priklad. Khim. 14: 939. 1941.

ON THE INTERMOLECULAR FORCE FIELD OF NITRILES[1]

By F. E. Murray[2] and W. G. Schneider

ABSTRACT

The nature of the intermolecular force field of the nitriles is considered on the basis of the electron orbital structure and charge distribution of the nitrile group. The directional nature of the force field is due to a well-directed lone pair orbital on the N atom, which may be expected to exhibit strong donor properties, and two π-orbitals which may exhibit weak donor properties. Accordingly with good acceptor molecules such as chloroform and hydrogen chloride, simple 1:1 molecular addition compounds should occur. The existence of molecular complexes of this type was confirmed with the aid of binary freezing-point diagrams which were determined for aceto-, propio-, butyro-, and benzo-nitrile with chloroform and hydrogen chloride. The 1:1 association complex was absent, however, in the system acetonitrile–chloroform. This is accounted for by the stronger association occurring in acetonitrile itself, the nature of which is discussed. The structure of the 1:1 molecular complexes is considered. Additional molecular complexes with lower nitrile mole ratios are indicated in the freezing-point diagrams. Of particular interest are the well-defined compounds appearing in the nitrile – hydrogen chloride systems with the composition RCN.5HCl. The possibility that the π-orbitals of the nitrile group may function as donors in these compounds is discussed, and a tentative structure is suggested.

INTRODUCTION

Because of its highly directional character, the intermolecular force field of the nitrile group is of particular interest. Although the nitriles, as for example the alkyl nitriles, RCN, have high dipole moments, the strong molecular association of such molecules cannot in general be attributed primarily to dipole interaction. The charge distribution which gives rise to the strongly polar force field is made up of two π-orbitals which are directed at right angles to each other and centered mainly in the region between the C and N atoms, and of a lone pair orbital centered on the N atom. The latter can be represented approximately by a digonally hybridized *sp* orbital directed along the CN axis, and it is accordingly an excellent "donor" (7). Thus boron trifluoride, a typical vacant orbital acceptor, forms stable addition compounds with nitriles (4) and hydrogen cyanide associates into linear chains by hydrogen bonding (1). Because the lone pair orbital on the N atom is directed along the molecular axis, it is largely responsible for the high dipole moment of the nitrile group. Moreover, because of the greater electronegativity of the N atom relative to C, the π-orbitals will be displaced somewhat toward the N atom. Accordingly the over-all charge distribution will be such as to make the N atom considerably more negative than the C atom, which may be roughly represented as follows:

$$R—\overset{+}{C}\equiv\overset{-}{N}- - -$$

the dotted line indicating the direction of the lone pair orbital.

[1]*Manuscript received January 21, 1955.*
Contribution from the Division of Pure Chemistry, National Research Council, Ottawa, Canada, and the Department of Chemistry, University of Manitoba, Winnipeg, Manitoba. Issued as N.R.C. No. 3562.
[2]*Summer Research Associate, Division of Pure Chemistry, National Research Council, 1954. Present address: Department of Chemistry, University of Manitoba, Winnipeg, Manitoba.*

Molecular association in acetonitrile vapor has been studied by Lambert *et al.* (3). From measurements of the second virial coefficient as a function of temperature, it was concluded that dimerization occurs, with a heat of dimerization of approximately 5200 cal./mole. Dimerization was considered to be due to dipole interaction resulting from a parallel orientation of dipoles as shown in (I). This configuration would, however, appear to be extremely

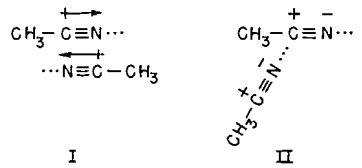

I II

unlikely, since the mutual repulsions of the high charge densities in the region of the CN triple bond would make it unfavorable. The configuration shown in II in which the N lone pair orbital is directed at the C atom of the second molecule would appear to be a more probable one. This structure is closely related to the configuration observed in the crystal of the linear molecule dicyanoacetylene (2); instead of a parallel arrangement of the rod-shaped molecules, the structure is an open one in which the closest approach between neighboring molecules is between the N atom of one molecule and one of the innermost C atoms of the second molecule.

Apart from molecular interactions involving a "donor" action of the N lone pair orbital, there is also the possibility of a similar role by the two π-orbitals of the CN group. Such interaction to form the so-called π-complexes has been observed for the ethylenic and aromatic π-electrons. It is very probable, however, that the "donor" action of the π-electrons in the nitrile group is much weaker than that of the N lone pair orbital and may become significant only in the presence of very strong electron acceptors (acids).

The present work was undertaken in order to obtain a better understanding of the nature of the force field of the nitriles and their molecular associations. It was desired to investigate particularly those molecular associations of the nitriles which will lead to definite compound formation in the solid, the configuration of which can later be established by X-ray methods. Accordingly, the freezing-point diagrams of aceto-, propio-, butyro-, and benzo-nitrile with chloroform and with hydrochloric acid have been determined. Both chloroform and hydrochloric acid may be expected to function primarily only as acceptors, and hence if only the N lone pair orbital of the nitrile group interacts strongly with these reagents, simple 1:1 addition compounds may be expected to appear in the freezing-point diagram.

EXPERIMENTAL

A modified Beckmann freezing-point apparatus was used to obtain cooling curves. The inner glass cell, which contained the mixture being studied, was joined to a vacuum system. A glass stirrer into which was sealed a small iron slug was moved up and down by mechanically driven magnets. Cooling was effected by conduction to liquid nitrogen and the rate could be altered by

changing the pressure in the space between the inner cell and the outer glass tube.

A glass thermocouple well was sealed into the inner cell and temperatures were measured using two copper–constantan junctions. The thermocouple voltage (reference junctions in ice) was recorded continuously during cooling with a recording potentiometer. A platinum resistance thermometer was used to obtain a calibration of the thermocouple–recorder arrangement.

Compositions of the binary liquid mixture were changed by addition of one of the components, either from a pipette or by condensation from a weighing bulb attached to the vacuum system. Hydrogen chloride was added to the nitrile by condensing it into the cell with liquid nitrogen. The amount of gas condensed was obtained by measuring the pressure change in a calibrated volume. Reagent grade chemicals were used throughout without further purification. Interpretation of cooling curves was based on the analysis by Mair *et al.* (5). Temperature measurements were accurate within ±0.5° C.

RESULTS

The freezing-point diagrams for chloroform with each of the four nitriles studied are plotted in Fig. 1. In Fig. 2 the corresponding binary diagrams for hydrogen chloride with each of the three alkyl nitriles are shown. The melting points of the addition compounds appearing in these diagrams are collected in Table I.

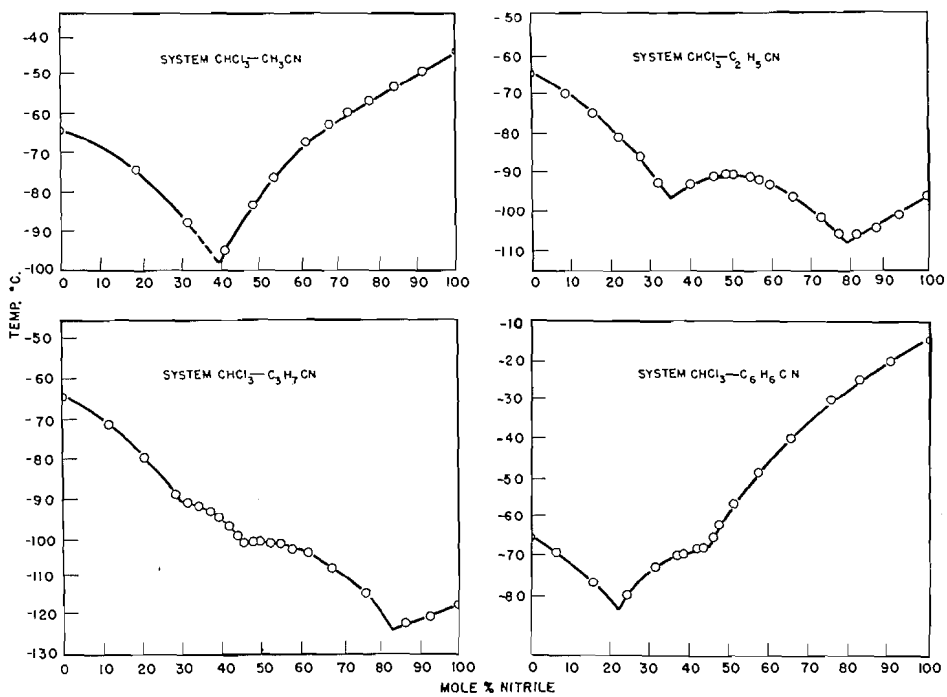

FIG. 1. Freezing-point diagrams for some nitrile–chloroform systems.

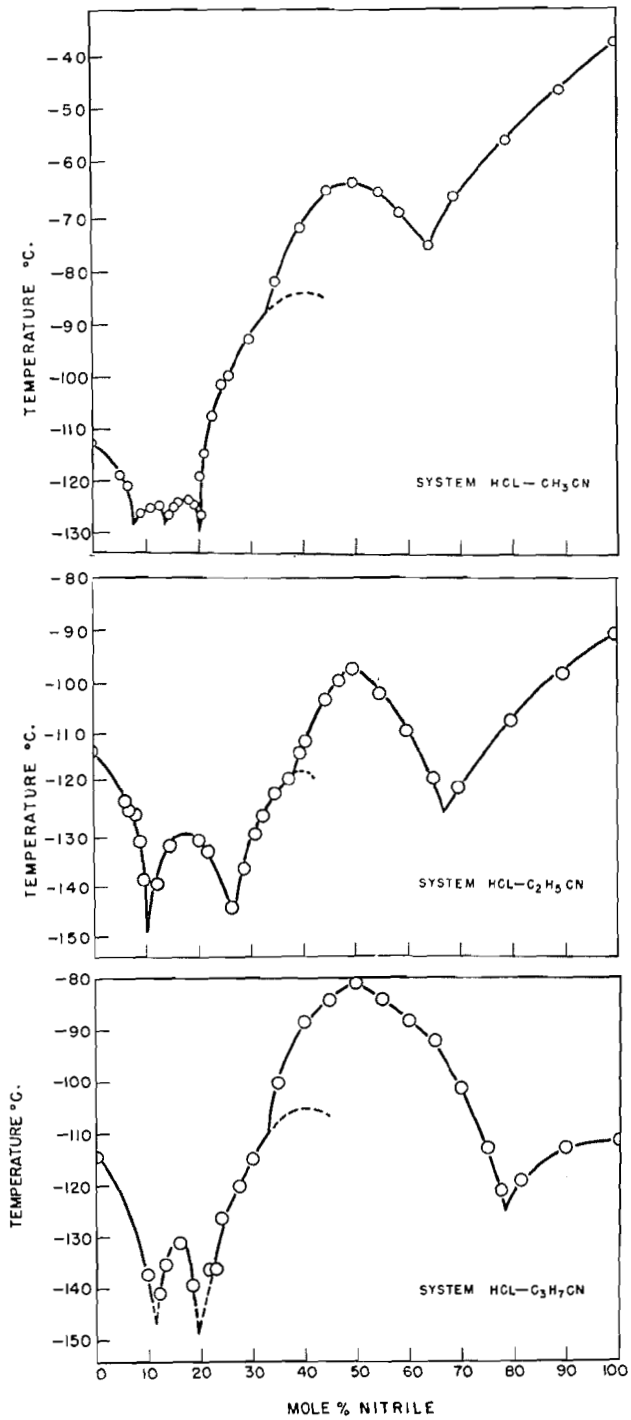

FIG. 2. Freezing-point diagrams for some nitrile – hydrogen chloride systems.

TABLE I

MELTING POINTS OF MOLECULAR ADDITION COMPOUNDS

Compound	M.p. (° C.)	Compound	M.p. (° C.)
$C_2H_5CN.CHCl_3$	− 90.5	$CH_3CN.7HCl$	−125.0
$C_3H_7CN.CHCl_3$	−101.5	$C_2H_5CN.HCl$	− 97.2
$C_3H_7CN.3CHCl_3$	(− 91.5)*	$2C_2H_5CN.3HCl$	(−117)*
$C_6H_6CN.CHCl_3$	(− 67.5)*	$C_2H_5CN.5HCl$	−129
		$C_3H_7CN.HCl$	− 80.6
$CH_3CN.HCl$	− 63.2	$2C_3H_5CN.3HCl$	(−109)*
$2CH_3CN.3HCl$	(− 88)*	$C_3H_5CN.5HCl$	−130
$CH_3CN.5HCl$	−123.6		

**Melts incongruently.*

DISCUSSION OF RESULTS

The occurrence of intermolecular complexes of both chloroform and hydrogen chloride with the nitriles in a 1:1 mole ratio had been anticipated. The considerations underlying this expectation have been outlined above and the results amply confirm the basic concepts of the nature of the molecular interaction put forward. However, the absence of the 1:1 complex in the chloroform–acetonitrile system was unexpected. The most probable explanation of this anomaly is that acetonitrile is capable of associating with itself more strongly than with chloroform. The nature of the mutual association of acetonitrile molecules has already been referred to; it does not appear likely that this is due to dipole association but results from the positive character of the C atom of the nitrile group. The latter accordingly acts as an acceptor to the donor lone pair orbital on the N atom of a neighboring molecule. In the higher nitriles the positive character of the nitrile C atom is less pronounced owing to the greater inductive effect of the larger alkyl groups. In these nitriles the C atom is now a weaker acceptor than the H atom of the chloroform molecule, with which they accordingly form the 1:1 compound.

If the above explanation for the absence of the 1:1 compound in the acetonitrile–chloroform system is correct, we may expect that with a much stronger acceptor (acid) than chloroform, such as HCl, the mutual association in acetonitrile would be disrupted in favor of the more stable addition compound $CH_3CN.HCl$. This is confirmed by the freezing-point diagram shown in Fig. 2.

Since the donor lone pair orbital on the N atom of the nitrile group is directed out along the C–N axis the 1:1 addition compounds of the nitriles with chloroform and hydrogen chloride can be assigned the following structures:

$$R—C{\equiv}N- - -H—CCl_3 \qquad R—C{\equiv}N- - -H—Cl$$

where the dotted line indicates the direction of the lone pair orbital. The latter forms a hydrogen bond with the H atom of chloroform and with that of hydrogen chloride. These structures presumably involve a completely linear configuration of nuclei* as follows: C—C≡N- - -H—C in the first com-

**This statement assumes a collinear configuration of the lone pair orbital direction and the H—X acceptor in the hydrogen bond (see Ref. (7)).*

pound, and C—C≡N- - -H—Cl in the second, where in each case the first C atom is part of the alkyl group. A determination of the crystal structure of these compounds, which may be expected to have a somewhat open structure, would therefore be of interest.

The 1:1 addition compounds of the nitriles with hydrogen chloride cannot be regarded as salts. The low melting point of these compounds is not compatible with such a structure. On the other hand there is some evidence that in the presence of moisture the addition compound may slowly change to the corresponding salt. Thus if acetonitrile is saturated with hydrogen chloride and allowed to stand at room temperature in the presence of water vapor, white crystals, presumably the salt, are observed to separate from the solution after several days. The transition from a molecular addition compound, in which the binding forces are primarily the electrostatic forces of a hydrogen bond, to that of the corresponding salt may be expected to be favored by the presence of a high dielectric medium such as water. Hydrolysis of the nitrile under these conditions (room temperature) to the corresponding carboxylic acid may however occur to some extent.

The fact that the nitriles do not readily form salts with hydrogen chloride, whereas the corresponding amines do, is of some interest in connection with the relative donor properties exhibited by the nitrogen lone pair orbital in these two classes of compounds. From considerations of the degree of *sp* hybridization occurring in the N lone pair orbital in amines (or ammonia) and in the nitriles, it was previously concluded (7) that the latter should exhibit stronger donor properties. This conclusion is, however, not confirmed by the present results. An alternative relative measure of donor strength of lone pair orbitals is the ionization potential since, for molecules of the type under consideration here, ionization involves removal of an electron from the lone pair orbital. Hence the lower the ionization potential the stronger should be the donor property of the lone pair electrons. The ionization potentials for acetonitrile and methylamine are 12.4 ev. and 9.4 ev. respectively (6), which thus appear to represent more nearly the relative donor strengths indicated by the present experiments.

Additional molecular compounds other than the 1:1 compounds also occur in some of the freezing-point diagrams at lower nitrile concentrations. A number of these have incongruent melting points. Thus butyronitrile forms an incongruent melting compound with chloroform having the probable composition $C_3H_7CN.3CHCl_3$. The three alkyl nitriles studied all form incongruent melting compounds with hydrogen chloride with the probable composition 2RCN:3HCl.

Of particular interest are the well-defined compounds occurring in the alkyl nitrile – HCl systems with the composition RCN:5HCl (a further compound with even lower nitrile concentration appears in the acetonitrile–HCl system). From the general shape of the freezing-point diagrams, these compounds are evidently much less stable than the corresponding 1:1 compounds. Since they appear in all three nitrile systems, the alkyl group, R, is not a determining factor, and hence the additional donor "centers" which

are evidently brought into play must be attributed to the nitrile group. Apart from the lone pair orbital on the N atom, the only other possible donor "centers" available are the two π-orbitals of the C–N triple bond. Since these orbitals are orthogonal to each other and are directed at right angles to the C–N axis, the configuration shown in Fig. 3 would appear to be the most

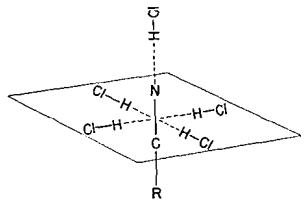

Fig. 3.

probable structure for the 1:5 compounds. One HCl molecule is bonded to the N lone pair, while four HCl molecules are accommodated in a plane at right angles to the molecular axis. It is assumed that each π-orbital can act as donor to two HCl molecules which are directed in the plane at an orientation of 180°. Little is known about the donor properties of π-orbitals, and particularly about those of the "triple" bond. However, if such donor action, even though it is weak, is possible at all, one might expect it to be manifest under the conditions of the present experiments, that is to say at low temperatures and in the presence of a strong small-molecule acceptor such as HCl. Moreover, if the above-postulated structure is correct one might expect analogous structures to occur with hydrogen chloride and acetylene or its derivatives. This possibility is now being investigated.

ACKNOWLEDGMENT

We wish to thank Mr. Yves Lupien for assistance in some of the experimental measurements.

REFERENCES

1. DULMADGE, W. J. and LIPSCOMB, W. N. Acta Cryst. 4:330. 1951.
2. HANNAN, R. B. and COLLIN, R. L. Acta Cryst. 6:350. 1953.
3. LAMBERT, J. D., ROBERTS, G. A. H., ROWLINSON, J. S., and WILKINSON, V. J. Proc. Roy. Soc. (London), A, 196:113. 1949.
4. LAUBENGAYER, A. W. and SEARS, D. S. J. Am. Chem. Soc. 67:164. 1945.
5. MAIR, B. J., GLASGOW, A. R., and ROSSINI, F. D. J. Research Natl. Bur. Standards, 26:591. 1941.
6. MORRISON, J. D. and NICHOLSON, A. J. C. J. Chem. Phys. 20:1021. 1952.
7. SCHNEIDER, W. G. J. Chem. Phys. 23:26. 1955.

HYDROGEN PEROXIDE AND ITS ANALOGUES

VII. CALORIMETRIC PROPERTIES OF THE SYSTEMS $H_2O - H_2O_2$ AND $D_2O - D_2O_2$[1]

By Paul A. Giguère, B. G. Morissette[2], A. W. Olmos[3], and O. Knop[4]

ABSTRACT

The heat of mixing of hydrogen peroxide and water and the heat of vaporization of the mixtures were measured over a wide concentration range at 0° C. with a Bunsen ice calorimeter and at 26.9° with a diphenyl ether calorimeter. The heat capacities of the solutions were determined between these two temperatures. Similar measurements were carried out on the corresponding deuterium compounds. The heat of decomposition of hydrogen peroxide catalyzed by colloidal platinum was also measured at 26.9° as a function of concentration. Correlation of all the results leads to the following recommended values for the thermochemical properties of the pure peroxides in the liquid state at 25° C.

		H_2O_2	D_2O_2
Heat of decomposition	(kcal./mole)	23.44 ± 0.02	23.41 ± 0.02
Heat of vaporization	(kcal./mole)	12.34 ± 0.03	12.51 ± 0.05
Heat of mixing	(cal./mole)	819 ± 2	807 ± 2
Heat capacity	(cal./deg. mole)	21.35 ± 0.05	22.9 ± 0.1

A number of related functions are given for convenience in recalculating these quantities to other temperatures. Apart from their practical value the new data are of interest in connection with molecular association and hydrogen bonds.

INTRODUCTION

A previous paper in this series (5) reported measurements of some thermal properties of hydrogen peroxide made at 0° C. in an ice calorimeter. Among these were preliminary results on the heat of decomposition of the liquid at various concentrations, which showed serious discrepancies with other published values. In view of the importance of such data in thermochemical equations involving hydrogen peroxide it was felt desirable to repeat the measurements using a more reliable technique. In order to minimize the importance of corrections to 25° C., the standard temperature, an isothermal calorimeter working with diphenyl ether (m.p. 26.9°) was used as described elsewhere (7). This calorimeter also has the advantages of greater sensitivity and easier operation than the ice calorimeter.

Calculation of the heat of formation of gaseous hydrogen peroxide from the heat of decomposition of the liquid requires knowledge of the heat of vaporization. Therefore, this quantity was also measured at the same temperature as a function of concentration. Comparison of the results with those previously found at 0° C. revealed a strong temperature dependence of the heat of mixing of hydrogen peroxide and water. As only scanty data on this property were available in the literature, the present measurements were extended to include

[1]*Manuscript received January 14, 1955.*
Contribution from the Department of Chemistry, Laval University, Quebec, Que., with financial assistance from the National Research Council of Canada.
[2]*Holder of a National Research Council Bursary, 1951–52.*
[3]*Holder of a Scholarship under the Bureau of Scientific Research of the Province of Quebec, 1952–54.*
[4]*On leave of absence from the Nova Scotia Technical College, Halifax, N.S.*

direct determinations of the heat of mixing at both 0° and 26.9° C. from 99% down to fairly low concentrations of peroxide.

The importance of these measurements is twofold. First, they make possible a more exact correlation between the various sets of thermochemical data and a more accurate extrapolation to arrive at the properties of pure hydrogen peroxide. Secondly, they provide much-needed experimental material for testing the validity of proposed theories of solutions of non-electrolytes. Indeed, the system hydrogen peroxide – water is of special interest in that connection as it is probably the simplest binary system with extensive hydrogen bonding. The only systematic investigation of sufficient accuracy to warrant calculation of the relevant thermodynamic functions dealt with vapor pressure of the mixtures (14). However, the results had to be extrapolated considerably beyond the temperature range of the measurements. Even if the present results are only of a modest degree of precision they are valuable in that they provide a direct source of information on the associative properties of the system hydrogen peroxide – water. In the meantime, the availability of mixtures of deuterium peroxide and heavy water was an incentive to extend the investigation to the isotopic system of compounds.

THE SYSTEM $H_2O - H_2O_2$

So far the heat of decomposition, the latent heat of vaporization, and the heat of mixing of mixtures of hydrogen peroxide and water have been investigated and reported in the literature (cf. (15) for a review). Of these quantities the last one is by far the smallest. It may be obtained indirectly from the other two but the calculations involve differences between two large quantities. To arrive at reasonably precise values the heats of decomposition or vaporization would have to be measured with much greater accuracy than has been done until now. Therefore, it seemed more logical to determine experimentally the heat of mixing of hydrogen peroxide and water and then to use the results to obtain accurate values of the heats of decomposition and vaporization from pertinent data for the pure components.

The temperature dependence of these quantities could be ascertained either directly, by measurements at two or more different temperatures, or indirectly through Kirchhoff's equation. For the latter method the heat capacities of the solutions are needed, and since no reliable data could be found in the literature for this quantity, it was determined at a number of concentrations.

Heat Capacity

The method and experimental details were essentially the same as used previously for measuring the heat capacity of pure liquid hydrogen peroxide (5), except that the initial temperature of the sample was 26.9° C. instead of 25°. The results listed in Table I give an idea of the precision of the measurements. In particular, the average of three determinations with pure water agrees to better than 0.1% with the accepted values of the mean specific heat c_p over the same temperature interval. Extrapolation leads to 0.628 cal./deg. gm. or 21.35 cal./deg. mole for pure H_2O_2, a value considered fairly accurate on account of the short extrapolation and the practically straight-line

TABLE I

ENTHALPY CHANGES BETWEEN 0° AND 26.9° OF H_2O–H_2O_2 MIXTURES

Concentration, 100 w_p	Weight of solution, gm.	Heat effect measured, cal./gm. solution	c_p, cal./deg. gm.
0	4.1654	26.92	
0	4.2987	27.02	1.002
0	4.0239	26.95	
21.2	4.7556	24.13	
21.2	4.7556	23.97	0.893
21.2	4.7077	23.97	
41.0	4.8261	22.00	
41.0	4.8261	21.98	0.817
60.1	5.2702	20.37	
60.1	5.2702	20.36	0.757
79.1	5.7391	18.73	0.696
79.1	5.7391	18.73	
98.6	5.9067	17.07	
98.6	5.9067	17.03	
98.6	6.6162	16.93	0.632
98.6	5.9879	17.01	
98.6	5.9879	17.00	

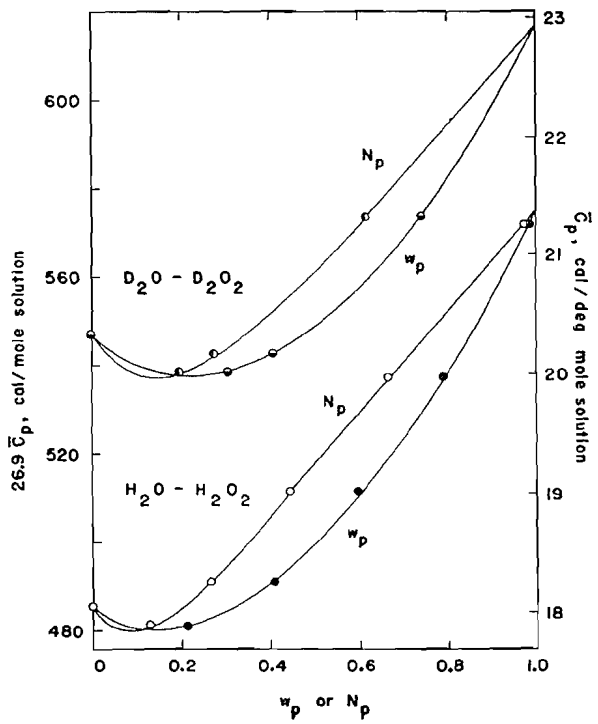

FIG. 1. Molar enthalpy changes and average heat capacities between 0° and 26.9° for H_2O–H_2O_2 and D_2O–D_2O_2 mixtures.

relationship in that range. A slightly higher value, 0.632 cal./deg. gm., has been reported by Foley and Giguère; the discrepancy was traced to a small error in the calibration of the mercury thermometer used by these authors. For the present work a platinum resistance thermometer (Leeds and Northrup, certified at the National Bureau of Standards) was employed.

A plot of the molar enthalpy change of the solutions from 0° to 26.9° C. is shown in Fig. 1 as a function both of the weight fraction w_p and mole fraction N_p of hydrogen peroxide. From a large-scale graph smoothed values were obtained and from these various related properties were derived for convenience in calculating other thermochemical quantities of the peroxide–water mixtures as illustrated below. These derived functions are defined in Table II and their numerical values are given in concentration steps of $10w_p$. For these calculations the following constants were used: oxygen, $C_p = 6.97$; water vapor, $C_p = 7.98$; hydrogen peroxide vapor, $C_p = 10$ cal./deg. mole (11).

TABLE II

SMOOTHED VALUES OF THE AVERAGE HEAT CAPACITIES AND RELATED PROPERTIES OF H_2O–H_2O_2 MIXTURES BETWEEN 0° AND 26.9°

Concentration		C_p	$\Delta_m C_p$ [a]	ΔC_p, [b]	$D_m C_p$ [c]	$\theta_m C_p$ [d]	θC_p, [e]
$100\,w_p$	$100\,N_p$	cal./deg. mole solution		cal./deg. mole H_2O_2	cal./deg. mole solution		cal./deg. mole H_2O_2
0	0	18.06	0	−8.90	-10.0_8	0	9.1
10	5.6	17.87	−0.38	−6.72	-9.7_8	0.39	6.92
20	11.7	17.88	−0.57	−4.84	-9.6_6	0.59	5.04
30	18.5	18.04	−0.63	−3.41	-9.6_9	0.66	3.57
40	26.1	18.27	−0.65	−2.50	-9.7_7	0.70	2.68
50	34.6	18.61	−0.59	−1.71	-9.9_4	0.66	1.91
60	44.3	19.00	−0.52	−1.18	-10.1_4	0.60	1.35
70	55.3	19.48	−0.40	−0.73	-10.3_9	0.51	0.92
80	67.9	19.99	−0.31	−0.46	-10.6_5	0.44	0.65
90	82.7	20.62	−0.16	−0.19	-10.9_9	0.32	0.38
100	100	21.35	0	0	-11.3_8	0.19	0.19

[a] $\Delta_m C_p = C_p(\text{solution}) - N_w C_p(H_2O, l) - N_p C_p(H_2O_2, l) = N_p \Delta C_p$.
[b] $\Delta C_p = (1+n) C_p(\text{solution}) - n C_p(H_2O, l) - C_p(H_2O_2, l)$.
[c] $D_m C_p = N_w C_p(H_2O, g) + N_p C_p(H_2O_2, g) - C_p(\text{solution})$.
[d] $\theta_m C_p = C_p(H_2O, l) + \frac{1}{2} N_p C_p(O_2, g) - C_p(\text{solution}) = N_p \theta C_p$.
[e] $\theta C_p = (1+n) C_p(\text{solution}) - (1+n) C_p(H_2O, l) - \frac{1}{2} C_p(O_2, g)$.

Heat of Mixing

Previous measurements of this quantity reported in the open literature are, in chronological order, those of de Forcrand (3), of Roth, Grau, and Meichsner (13), of Evans and Uri (4), and of Kubaschewski and Weber (10). However they covered only a narrow concentration range and the experimental conditions were not always fully stated. For the present work two different experimental techniques were tried in succession. In the first one (experimenter M.) two small test tubes, one fitting inside the other, were used. The inner tube containing the peroxide solution had a very thin bottom so that it could easily be broken with a glass rod that also served as a stirrer. It was

noticed that the thermal leak was always slightly greater after the mixing owing to a slight decomposition of the peroxide by the glass fragments. However, the difference was small (of the order of 0.5 cal./hr.) and the correction was applied from the instant of mixing.

In the second method (experimenter K.), which was applied only to measurements in the diphenyl ether calorimeter, the water was added to the peroxide solution in a small test tube from a long pipette fitted with a rubber bulb. Care was taken that the tip of the pipette did not touch the inside walls of the test tube nor the peroxide solution. The tip of the pipette was formed into a thick-walled capillary and it was coated with a thin film of Halocarbon grease to reduce the size of the drops and prevent them from creeping up the outer wall of the pipette. The amount of water added was determined by difference weighing. To prevent drops of water from falling prematurely into the peroxide solution the pipette was warmed a little before it was filled with water and weighed. Stirring was achieved by means of a small glass-enclosed magnet (Alnico alloy) resting in the peroxide solution. A similar magnet was placed in the bottom of the calorimeter well and so oriented that it repelled the magnet in the test tube. Raising and lowering the latter provided sufficient

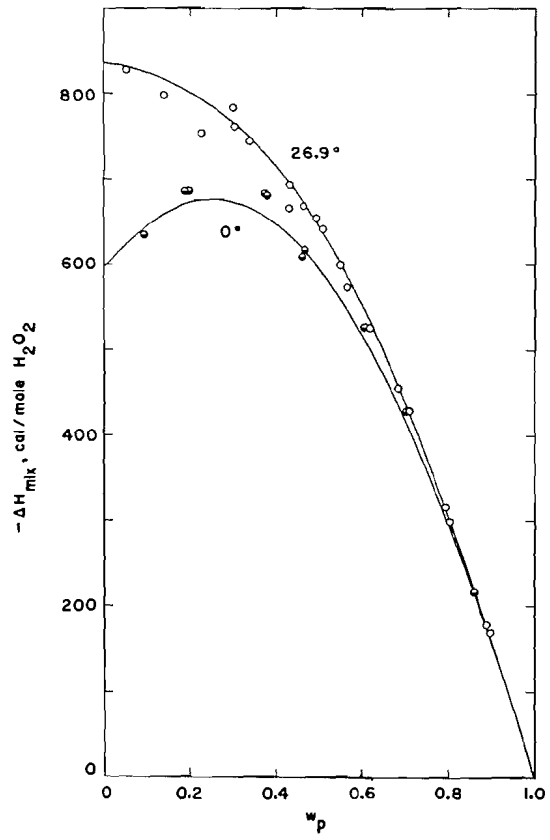

FIG. 2. Heat of mixing of hydrogen peroxide and water at 0° and 26.9° C.

stirring. The progress of the mixing operation could be followed visually to some extent by observing the "schlieren" in the solution but the only safe indication that the mixing was complete was the thermal leak of the calorimeter as shown by the movement of the mercury in the capillary (7).

A run lasted about two hours including the determination of the heat leak of the calorimeter after the reaction. The final concentration of the solution was checked by means of the refractive index; the agreement with the calculated composition was always good. The maximum amount of liquid that could be accommodated in the test tube was only 3 ml. For that reason most of the determinations were carried out with concentrated solutions of peroxide in order to have a good precision on the calorimetric measurements. This had the advantage of minimizing the importance of extrapolation to 100% hydrogen peroxide. On the other hand, it increased the uncertainty at low concentrations because the curve flattens out then (Fig. 2) and the differential heat effect becomes progressively smaller. On recalculating to one mole of peroxide the

TABLE III

EXPERIMENTAL DATA ON THE HEAT OF MIXING OF HYDROGEN PEROXIDE AND WATER

Concentration, 100 w_p		Weight of initial solution, gm.	Heat effect measured cal./mole	Correction applied H_2O_2	$-\Delta H_{mix}$, cal./mole H_2O_2	$-\Delta_m H_{mix}$, cal./mole solution
Initial	Final					
At 0°						
98.7	86.0	2.3589	195	21	216	165
99.4	70.2	1.4583	417	11	428	238
99.4	60.5	0.9868	515	11	526	236
98.7	46.3	2.0358	594	21	615	193
99.4	45.9	0.7660	597	11	608	188
99.4	38.1	0.4854	669	11	680	167
99.4	37.2	0.8316	670	11	681	163
99.4	19.7	0.9546	672	11	683	79
99.4	19.1	0.6033	672	11	683	76
24.5	9.3	1.5709	−42	675	633	33
At 26.9°						
98.7*	89.7	4.9856	148	21	169	139
98.7*	88.9	5.2199	158	21	179	145
97.6†	80.3	1.5465	257	42	299	205
98.7*	79.4	3.0715	297	21	318	213
98.7*	71.0	2.7033	408	21	429	242
88.3†	68.2	1.5431	263	190	453	241
98.7*	62.0	1.8583	504	21	525	244
68.2†	56.5	1.9985	107	465	572	233
98.7*	54.9	1.8496	578	21	599	235
98.7*	50.3	1.8718	622	21	643	224
98.7*	49.6	2.1562	631	21	652	224
99.4†	46.2	0.8782	657	12	669	209
99.4†	42.9	0.7754	653	12	665	189
98.7*	42.8	1.5030	672	21	693	197
99.3†	33.9	0.8103	734	12	746	160
98.7*	30.1	1.1420	740	21	761	142
99.3†	30.0	0.5437	775	12	787	146
99.3†	22.6	0.4621	739	12	751	101
98.7*	14.0	0.6854	777	21	798	63
98.7*	5.3	0.2939	807	21	828	24

*Observer M. †Observer K.

experimental error is magnified gradually, so that it is quite large at zero concentration of peroxide.

The experimental results given in Table III refer to both one mole of peroxide, ΔH_{mix}, and one mole of solution, $\Delta_m H_{mix} = N_p \cdot \Delta H_{mix}$, as is customary. Graphical extrapolation led to 834 cal./mole for the heat of mixing of the pure peroxide to infinite dilution at 26.9° C. and from this, the correction to be applied to each determination was computed. The results at 26.9° were taken as the basis of the correlation for the following reasons. They are twice as numerous as those at 0° and they were obtained by two different experimenters using two different techniques in one of which, at least, errors due to decomposition of the peroxide were successfully eliminated. Then the measurements were made at a later stage when more experience had been gained. Finally the diphenyl ether calorimeter is more than three times as sensitive as the ice calorimeter and its performance has also been found to be somewhat more regular and reliable.

A set of smoothed values of the heat of mixing at 26.9° were obtained by interpolation and extrapolation from the composite aggregate. As may be seen in Fig. 2 the majority of experimental points fit very closely to the smoothed curve. By means of the equations

[1] $$\Delta H_{mix}(T° \text{ C.}) = \Delta H_{mix}(26.9° \text{ C.}) - \Delta C_p \cdot \Delta T$$

and

[2] $$\Delta_m H_{mix}(T° \text{ C.}) = \Delta_m H_{mix}(26.9° \text{ C.}) - \Delta_m C_p \cdot \Delta T,$$

where ΔT is the temperature interval from 26.9° and the terms ΔC_p and $\Delta_m C_p$ are taken from Table II, the smoothed values of the heat of mixing given in Table IV were obtained. It may be pointed out here that recalculation of the

TABLE IV

SMOOTHED VALUES OF THE HEAT OF MIXING OF H_2O AND H_2O_2 AT 0° AND 25°

Concentration, 100 w_p	ΔH_{mix}, cal./mole H_2O_2		$\Delta_m H_{mix}$, cal./mole solution	
	0°	25°	0°	25°
0	597	819	0	0
10	644	812	36	45
20	671	792	79	93
30	671	757	124	140
40	645	707	168	185
50	598	641	207	222
60	518	548	230	243
70	419	438	232	242
80	297	308	202	209
90	158	163	130	135
100	0	0	0	0

data to 0° C. involves no great uncertainty since it does not require knowledge of the instantaneous values of the heat capacity of the solutions, the enthalpy changes having been measured directly between the two very same temperatures. The fit of experimental points to the calculated curve at 0° is not especially good (Fig. 2). In particular it is strange that the two points showing the

greatest discrepancy were duplicated closely. A similar situation occurred in previous measurements of the heat of decomposition (5) and must have originated in the performance of the ice calorimeter.

A plot of the heat of mixing per mole of solution shows that the curve for 26.9° is nearly symmetrical with respect to the axis $N = 0.5$ (Fig. 4). In fact a general second-degree equation derived from all the experimental results in Table III exhibited no significant departure from a symmetrical form. Considering the exceptional nature of the hydrogen peroxide – water mixtures this property is interesting. The dotted line in Figs. 3 and 4 refers to the equation derived by Scatchard, Kavanagh, and Ticknor (14) from their vapor pressure measurements. Their expression

$$[3] \qquad \Delta_m H_{mix} = N_p N_w[-1017+85(N_p-N_w)+13(N_p-N_w)^2]$$

leads to much too high values, especially for dilute peroxide solutions, but this is not surprising as the numerical coefficients were chosen in such a way as to give an equation independent of temperature. These authors felt that the accuracy of their measurements did not warrant calculation of the variation of the heat of mixing with temperature. They pointed out that their equation

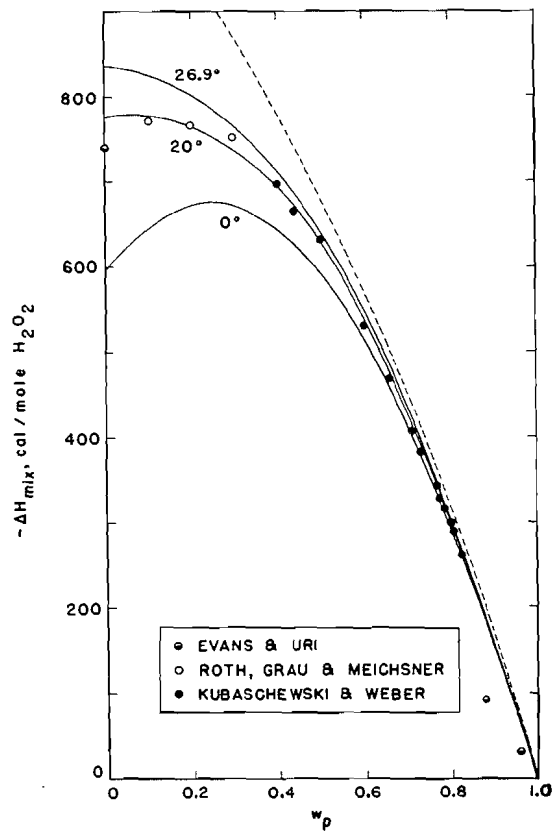

FIG. 3. Comparison of various published data for the heat of mixing of hydrogen peroxide and water with the present ones recalculated to 20° (solid curve).

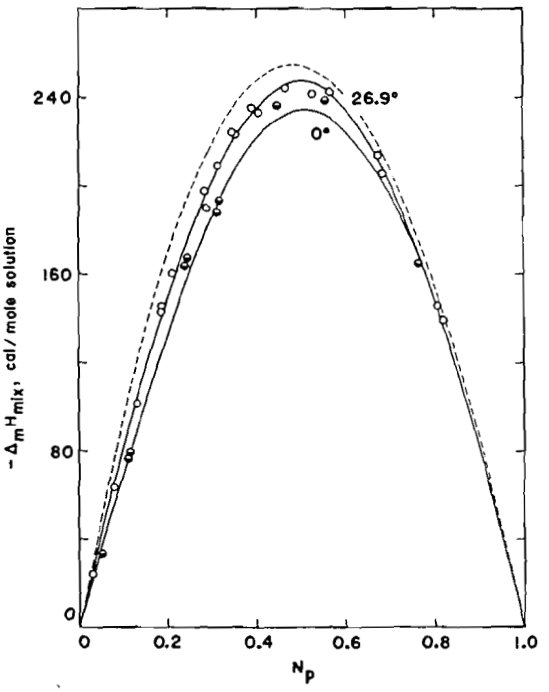

FIG. 4. Heat of mixing, per mole of solution, of hydrogen peroxide and water at 0° and 26.9° C.

should yield more correct values of the heat of mixing in the temperature range of their vapor pressure measurements, namely 60° to 90° C., and this is borne out by the trend of the curves in Fig. 3.

Heat of Vaporization

Measurements of the heat of vaporization at 26.9° were carried out as described before (5) and mostly with concentrated solutions in order to secure a reliable value for the pure peroxide. The quantity obtained by extrapolation, 12,315 cal./mole, was combined with the heat of mixing to obtain the heat of vaporization at various concentrations. Agreement with the experimental results (in Table V) is very good in all cases, the maximum deviation (at

TABLE V

HEAT OF VAPORIZATION OF H_2O–H_2O_2 MIXTURES MEASURED AT 26.9°

Concentration, 100 w_p	$\Delta_m H_{vap}$ (expt.), cal./gm. solution	$\Delta_m H_{vap}$ (expt.) kcal./mole solution	$\Delta_m H_{vap}$ (calc.) kcal./mole solution
99.3	363.7*	12.30	12.30
98.4	366.5†	12.29	12.28
87.4	394.9	12.08	12.08
74.2	428.4	11.86	11.82
48.1	485.3	11.20	11.30

Average of three determinations.
†*Average of four determinations.*

74.2% H_2O_2) being less than 0.3%. From these data smoothed values were obtained for 0° and 25° by means of the equation

$$[4] \qquad \Delta_m H_{vap}(T°\ C.) = \Delta_m H_{vap}(26.9°\ C.) - D_m C_p \,.\, \Delta T.$$

Here again (Table VI) excellent agreement is found with the quantity previously reported for pure hydrogen peroxide at 0°, 12.59 kcal./mole (5).

TABLE VI

CALCULATED VALUES OF THE HEAT OF VAPORIZATION OF H_2O–H_2O_2 MIXTURES

Concentration, 100 w_p	$\Delta_m H_{vap}$, kcal./mole solution	
	0°	25°
0	10.76	10.51
10	10.90	10.66
20	11.06	10.81
30	11.23	10.99
40	11.41	11.17
50	11.61	11.36
60	11.81	11.56
70	12.02	11.76
80	12.23	11.96
90	12.43	12.15
100	12.62	12.34

Heat of Decomposition

In view of the difficulties encountered previously with a solid catalyst a colloidal solution of platinum was used this time. It allows a better control of the reaction rate, especially at the beginning, and complete decomposition is more easily achieved. Any dilution effect of the platinum sol must be entirely negligible in the present conditions. The colloidal suspension was prepared after the classical method of Bredig (1) in which an electric arc is struck between platinum wires immersed in distilled water. The circuit comprised a 150-volt battery in series with a 90-ohm shunt and a 22-henry inductance. Because the latter was too low for stable performance the arc lasted only 15–20 sec. at a time. The brownish suspension of platinum was filtered to remove all coarse particles and diluted to a suitable concentration. Then it was placed in a small pipette closed by a stopcock and protected by a tiny glass tube over the tip to prevent drops of the catalyst from falling prematurely in the peroxide solution. The latter was contained in a small test tube in the central well of the calorimeter. Once thermal equilibrium was reached the pipette was taken out of the protective tube and the colloidal solution was added dropwise, very slowly at first, to secure a reasonable reaction rate. Analysis of the residue confirmed that in all cases decomposition was complete. In between runs it was necessary to clean the test tube with aqua regia as otherwise the sample of peroxide decomposed spontaneously owing to traces of platinum adsorbed on the glass.

The results of seven determinations (by experimenter M.) are compared in Table VII with values calculated from the heat of mixing and the heat of

TABLE VII

HEAT OF DECOMPOSITION OF H_2O–H_2O_2 MIXTURES MEASURED AT 26.9°

Concentration, 100 w_p	$-\Delta H_{dec}$(expt.)	$-\Delta H_{dec}$(calc.)* kcal./mole peroxide	$-\Delta H_{dec}$(calc.)†	$-\Delta_m H_{dec}$, kcal./mole solution
24.64	22.66	22.65	23.45	3.35
24.72	22.64	22.65	23.43	3.37
25.10	22.66	22.65	23.45	3.42
49.6	22.79	22.79	23.44	7.83
74.2	23.01	23.05	23.39	13.94
98.5	23.44	23.42	23.46	22.77
98.6	23.42	23.42	23.43	22.82
100	—	Average	23.44±0.02	—

*Of solution at initial concentration w_p.
†Of pure hydrogen peroxide.

decomposition of the pure peroxide averaged from extrapolations of each experimental result (in the fourth column). The latter quantities agree among themselves to within ±20 cal. except for that at 74.2% H_2O_2 for which the rate of reaction was too fast. When the present results are compared with those of previous authors (5, 12, 13) the only serious discrepancies arise from some of the preliminary measurements of Foley and Giguère considered doubtful at the time. As was done for the other calorimetric properties smoothed values of the heat of the chemical reaction

$$[N_p\ H_2O_2 + N_w\ H_2O](l) \rightarrow H_2O(l) + \tfrac{1}{2}N_p\ O_2(g)$$

were calculated for 0° and 25° C. by means of the equations

[5] $$\Delta H_{dec}(T°\ C.) = \Delta H_{dec}(26.9°\ C.) - \theta C_p\ .\ \Delta T$$

and

[6] $$\Delta_m H_{dec}(T°\ C.) = \Delta_m H_{dec}(26.9°\ C.) - \theta_m C_p\ .\ \Delta T;$$

these values are shown in Table VIII. The quantities thus found for 0° were deemed more reliable that any obtainable from direct determinations with the

TABLE VIII

HEAT OF DECOMPOSITION OF H_2O–H_2O_2 MIXTURES AT 0° AND 25° CALCULATED FROM EXPERIMENTAL DATA AT 26.9°

Concentration, 100 w_p	$-\Delta H_{dec}$, kcal./mole H_2O_2		$-\Delta_m H_{dec}$, kcal./mole solution	
	0°	25°	0°	25°
0	22.84	22.62	0.0	0.0
10	22.80	22.62	1.28	1.27
20	22.77	22.64	2.66	2.65
30	22.77	22.68	4.21	4.20
40	22.80	22.73	5.95	5.93
50	22.84	22.80	7.90	7.89
60	22.92	22.89	10.15	10.14
70	23.02	23.00	12.73	12.72
80	23.14	23.13	15.71	15.70
90	23.28	23.27	19.26	19.25
100	23.44	23.44	23.44	23.44

ice calorimeter. As has been remarked before (6) the heat of decomposition of pure hydrogen peroxide in the liquid state is practically temperature-independent.

THE SYSTEM $D_2O - D_2O_2$

The same general pattern was followed in measuring the thermochemical properties of the deuterium compounds except that no determinations of the heat of decomposition were carried out because the amount of isotopic material needed would have been prohibitive. Instead, this quantity was calculated from the corresponding one for hydrogen peroxide and the zero-point energy difference of the two molecules (11). This method (details to be published later) leads, no doubt, to more reliable results than could be achieved experimentally at present. On the whole the calorimetric measurements for the deuterium system of compounds were fewer and less accurate than for the hydrogen compounds because of the difficulty and cost of preparation of deuterium peroxide. In fact this compound has been available in convenient quantities only since the application of the electrodeless discharge method (8).

TABLE IX

ENTHALPY CHANGES, BETWEEN 0° AND 26.9°, OF D_2O–D_2O_2 MIXTURES

Concentration, 100 w_p	Weight of solution, gm.	Heat effect measured, cal./gm. solution	c_p, cal/deg. gm. solution
0	5.0822	27.33	1.016
0	5.0822	27.30	
30.46	3.6664	23.25	0.864
40.7	4.5892	22.17	0.825
40.7	4.5892	22.18	
74.2	4.5865	19.21	0.714
74.2	4.5865	19.20	

TABLE X

SMOOTHED VALUES OF THE AVERAGE HEAT CAPACITIES OF D_2O–D_2O_2 MIXTURES BETWEEN 0° AND 26.9°

Concentration, D_2O_2					
100 w_p	100 N_p	C_p cal./deg. mole solution	$\Delta_m C_p$ [a] cal./deg. mole solution	$\Delta C_{p,}$ [b] cal./deg. mole D_2O_2	$D_m C_{p,}$ [c] cal./deg. mole solution
0	0	20.3_5	0	−9.00	-12.2_2
10	5.81	20.1_0	−0.40	−6.88	-11.8_1
20	12.19	19.9_9	−0.67	−5.50	-11.5_3
30	19.23	20.0_2	−0.83	−4.32	-11.3_7
40	27.02	20.1_6	−0.88	−3.26	-11.3_9
50	35.71	20.3_9	−0.87	−2.44	-11.2_9
60	45.45	20.7_0	−0.82	−1.80	-11.3_2
70	56.45	21.1_1	−0.69	−1.22	-11.4_4
80	68.96	21.6_2	−0.51	−0.74	-11.6_1
90	83.33	22.2_5	−0.24	−0.29	-11.8_5
100	100	22.9_2	−0	0	-12.0_7

[a,b,c] *See Table II for definitions.*

Heat Capacity

Three solutions only were measured (Table IX) as the highest concentration of deuterium peroxide available at the time was about 75%. Two determinations with liquid heavy water (99.6% D_2O) gave a value within 1% of that extrapolated from the most recent data (2). As could be expected the experimental points fall on a curve nearly parallel to that for the hydrogen compounds (Fig. 1). This property was relied upon to extrapolate the curve to 100% D_2O_2. A set of smoothed values of C_p (Table X) were obtained from a large-scale plot. The mean heat capacity of heavy water vapor was taken as 8.13 (9), and that of deuterium peroxide vapor, as 11 cal./deg. mole (11).

Heat of Mixing

The second of the above-described methods was followed for measuring the heat of mixing of deuterium peroxide and heavy water at 26.9° C. As shown in Table XI and Fig. 5 the data are quite extensive, covering the composition range from 98.3% D_2O_2 (the highest concentration ever obtained) for the initial solution, to 7.1% for the most dilute solution. Smoothed values of the heat of

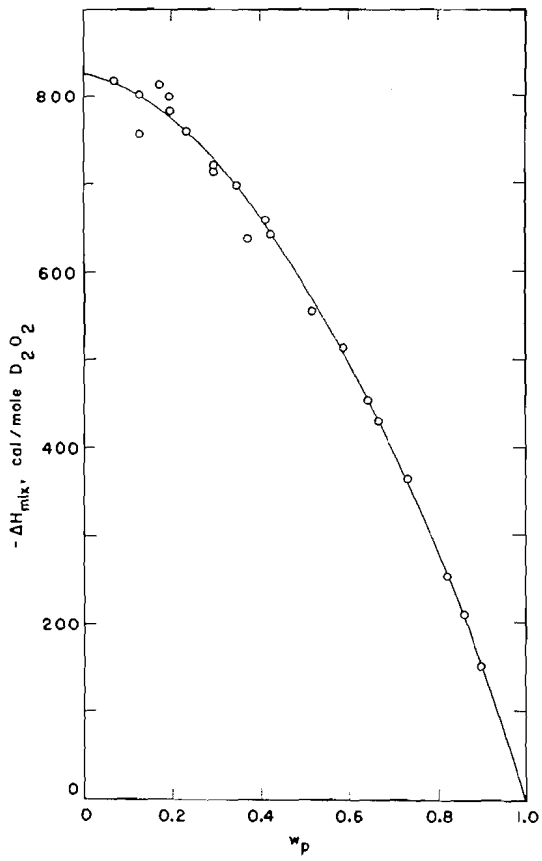

FIG. 5. Heat of mixing at 26.9° C. for the system D_2O–D_2O_2.

TABLE XI

HEAT OF MIXING OF DEUTERIUM PEROXIDE AND HEAVY WATER AT 26.9°

Concentration, $100\,w_p$		Weight of initial solution, gm.	Heat effect measured	Correction applied cal./mole H_2O_2	$-\Delta H_{mix}$	$-\Delta_m H_{mix}$, cal./mole solution
Initial	Final					
98.3	89.8	2.5190	116	35	151	125
96.6	86.2	2.5689	151	60	211	164
97.0	82.3	2.3050	206	47	253	182
96.6	73.7	1.3482	305	60	365	222
91.0	66.8	1.5401	290	140	430	227
97.0	64.7	1.5836	407	47	454	229
91.0	59.1	1.2938	372	140	512	228
91.0	52.0	1.4379	414	140	555	208
91.0	42.3	1.0702	502	140	642	186
91.0	41.7	0.9641	526	140	660	188
91.0	37.3	0.7956	498	140	638	158
92.6	35.0	0.9318	571	130	701	161
91.0	29.5	0.7595	575	140	715	135
92.0	29.5	0.7509	587	135	722	136
91.2	23.5	0.6828	622	138	760	111
92.0	19.8	0.4617	647	135	782	84
92.0	19.5	0.5502	665	135	800	95
91.2	17.6	0.4828	674	138	812	86
91.2	13.1	0.3359	620	138	758	58
91.2	12.6	0.3286	665	138	803	59
91.2	7.1	0.1749	681	138	819	34

TABLE XII

SMOOTHED VALUES OF THE HEAT OF MIXING OF D_2O AND D_2O_2 AT 0° AND 25°

Concentration, $100\,w_p$	ΔH_{mix}, cal./mole D_2O_2		$\Delta_m H_{mix}$, cal./mole solution	
	0°	25°	0°	25°
0	582	807	0	0
10	625	797	36	46
20	630	767	77	94
30	612	720	118	138
40	573	655	155	177
50	519	580	186	207
60	447	493	203	223
70	363	394	205	223
80	262	281	180	193
90	142	150	118	125
100	0	0	0	0

mixing were calculated as in the case of the hydrogen peroxide – water system; obviously, the uncertainty of these quantities (Table XII) is greater than for the hydrogen compounds. It is interesting to note that the heat of mixing of the $D_2O - D_2O_2$ system is smaller than that of the $H_2O - H_2O_2$ system contrary to the other calorimetric properties. The difference is particularly marked for the $\Delta_m H_{mix}$ function (Fig. 6). The significance of this situation will be considered later in the light of other associative properties of the two binary systems.

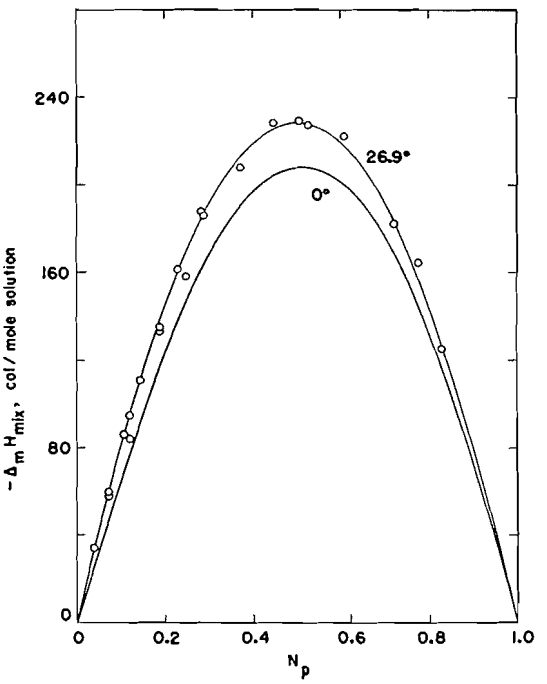

FIG. 6. Heat of mixing, per mole of solution, for D_2O–D_2O_2 mixtures.

Heat of Vaporization

This quantity was the only one measured both at 0° and 26.9° C. for the deuterium compounds. The latter set of data (Table XIII) were used for

TABLE XIII

HEAT OF VAPORIZATION OF D_2O–D_2O_2 MIXTURES MEASURED AT 0° AND 26.9°

Concentration, 100 w_p	$\Delta_m H_{vap}$(expt.), cal./gm. solution	$\Delta_m H_{vap}$(expt.) kcal./mole solution	$\Delta_m H_{vap}$(calc.) kcal./mole solution
At 0°			
93.0	371.8	12.69	12.70
93.0	368.1	12.56	12.70
49.2	461.8	11.84	11.93
22.2	514.4	11.43	11.48
8.1	541.0	11.24	11.26
At 26.9°			
96.5	354.6	12.43	12.43
94.4	359.5	12.40	12.40
81.0	388.4	12.15	12.18
55.0	442.0	11.71	11.71
53.9	442.2	11.65	11.69
47.0	454.9	11.51	11.57
22.2	498.8	11.09	11.15
8.1	526.4	10.94	10.94

TABLE XIV

SMOOTHED VALUES OF THE HEAT OF VAPORIZATION OF D_2O–D_2O_2 MIXTURES

Concentration, 100 w_p	$\Delta_m H_{vap}$, kcal./mole solution	
	0°	25°
0	11.15	10.84
10	11.28	10.98
20	11.43	11.14
30	11.58	11.30
40	11.75	11.47
50	11.93	11.64
60	12.10	11.82
70	12.29	12.00
80	12.47	12.18
90	12.65	12.35
100	12.81	12.51

calculating the smoothed values at 0° and 25° (Table XIV) from the heat of mixing and the heat of vaporization of pure deuterium peroxide found by extrapolation. As in the case of water, isotopic substitution by deuterium raises the heat of vaporization of hydrogen peroxide, the effect (170 cal./mole) being about half of that for water (330 cal./mole).

CONCLUSIONS

The present thermochemical data for hydrogen peroxide and its mixtures with water are recommended as superseding previous values because they are based on extensive series of calorimetric measurements closely intercorrelated. The heat of decomposition and heat of vaporization were determined directly on very concentrated solutions in order to arrive at accurate values of these quantities for the pure peroxide. Numerous determinations of the heat of mixing enabled interpolation over the whole concentration range. Finally, from the heat capacities of the mixtures it is possible to recalculate the various properties with fair accuracy over a moderate temperature interval. Although, in general, the calorimetric measurements were executed in such a way as to yield the maximum of internal consistency, it must be remembered, in using the new data, that they are not all known to the same degree of accuracy.

As for the system D_2O–D_2O_2, the above measurements provide us not only with the thermodynamic properties of the pure peroxide, but also with comprehensive data on an isotopic system of compounds, the only one, no doubt, thus investigated so far. In a following paper of this series we intend to present a discussion of these two binary systems from the point of view of the existing theories of solutions of non-electrolytes, together with recalculated values of the excess functions and other associative properties.

ACKNOWLEDGMENT

The authors are grateful to the National Research Council for financial assistance and to Mr. R. L. Wentworth of the Massachusetts Institute of Technology for helpful suggestions.

RÉSUMÉ

On a mesuré à 0° C. dans un calorimètre à glace, et à 26.9° dans un calorimètre à oxyde de phényle les propriétés thermochimiques suivantes de mélanges de peroxyde d'hydrogène et d'eau à différentes concentrations: chaleur spécifique, chaleur de vaporisation, et chaleur de mélange. Des mesures semblables ont ensuite été effectuées sur les composés isotopiques, peroxyde de deutérium et eau lourde. La chaleur de décomposition du peroxyde d'hydrogène catalysée par le platine colloïdal a été déterminée de nouveau avec précision. Par corrélation interne de ces données on est arrivé à un système de fonctions et d'équations permettant de calculer les quantités thermochimiques à toute concentration et sur un intervalle de température modéré.

Outre leur intérêt pratique les nouveaux résultats sont importants du point de vue de la théorie des solutions de liquides associés.

REFERENCES

1. Bredig, G. Z. Elektrochem. 4: 514. 1898.
2. Cockett, A. H. and Ferguson, A. Phil. Mag. 29: 185. 1940.
3. De Forcrand, R. Ann. chim. et phys. 15(8): 433. 1908.
4. Evans, M. G. and Uri, N. Trans. Faraday Soc. 45: 224. 1949.
5. Foley, W. T. and Giguère, P. A. Can. J. Chem. 29: 895. 1951.
6. Giguère, P. A. Can. J. Research, B, 28: 485. 1950.
7. Giguère, P. A., Morissette, B. G., and Olmos, A. W. Can. J. Chem. 33: 657. 1955.
8. Giguère, P. A., Secco, E. A., and Eaton, R. S. Discussions Faraday Soc. No. 14: 104. 1953.
9. Kirschenbaum, I. Physical properties and analysis of heavy water. McGraw-Hill Book Company, Inc., New York. 1951.
10. Kubaschewski, O. and Weber, W. Z. Elektrochem. 54: 200. 1950.
11. Liu, I. D. Ph.D. Thesis, Laval University, Quebec, Que. 1954.
12. Matheson, G. L. and Maass, O. J. Am. Chem. Soc. 51: 674. 1929.
13. Roth, W. A., Grau, R., and Meichsner, R. Z. anorg. u. allgem. Chem. 193: 161. 1930.
14. Scatchard, G., Kavanagh, G. M., and Ticknor, L. B. J. Am. Chem. Soc. 74: 3715. 1952.
15. Schumb, W. C., Satterfield, C. N., and Wentworth, R. L. Hydrogen peroxide. Mass. Inst. Technol. Rept. No. 43. 1953.

COMBINATION AND DISPROPORTIONATION OF ETHYL RADICALS: INFLUENCE OF THE REACTION $H+C_2H_5 = C_2H_6$[1]

By Moyra J. Smith,[2] Patricia M. Beatty,[3] J. A. Pinder, and D. J. Le Roy

ABSTRACT

The mercury ($^3P_1$) photosensitized hydrogenation of ethylene has been studied at room temperature as a function of ethylene concentration, mercury concentration, and light intensity. In addition to combination and disproportionation, ethyl radicals have been shown to take part in the reaction

$$H+C_2H_5 = C_2H_6.$$

The conditions favoring this reaction have been established and anomalous values previously found for the ratio of ethane to butane have been explained. The value obtained for the ratio of the rate constants for the disproportionation and combination of ethyl radicals, $0.15\pm.01$, is in excellent agreement with the values obtained by other methods. Hexane formation is of some importance at low light intensities and high ethylene concentrations, and is adequately accounted for by the reactions

$$C_2H_5+C_2H_4 = C_4H_9$$
$$C_4H_9+C_2H_5 = C_6H_{14}.$$

INTRODUCTION

It is now generally agreed that in systems containing ethyl radicals both combination and disproportionation will take place. From the variety of data discussed by Steacie (13) it is clear that in some instances it is not justifiable to equate the ratio of the rate constants for disproportionation and combination, k_4/k_3, to $(C_2H_6)/(C_4H_{10})$, $(C_2H_4)/(C_4H_{10})$, or to $\frac{1}{2}((C_2H_6)+(C_2H_4))/(C_4H_{10})$ because of the occurrence of secondary reactions which consume ethylene or because the products may be formed in some other way. When these factors are taken into account both reactions appear to have small or negligible activation energies and steric factors not greatly different from unity (6). Nevertheless, in the case of the mercury photosensitized hydrogenation of ethylene there are differences in the apparent value of k_4/k_3 at room temperature which are greater than the experimental errors.

There is little doubt that the basic mechanism of the reaction at room temperature is the following:

$$Hg^*+H_2 = 2H+Hg \quad [1]$$
$$H+C_2H_4 = C_2H_5 \quad [2]$$
$$2C_2H_5 = C_4H_{10} \quad [3]$$
$$2C_2H_5 = C_2H_6+C_2H_4. \quad [4]$$

However, from the amounts of ethane and butane formed Moore and Taylor (11) found k_4/k_3 to be 0.17, while Le Roy and Kahn (9) found values ranging from 0.22 to 0.61. In their recent study of the mercury photosensitized hydrogenation of acetylene Cashion and Le Roy (4) found evidence for reactions [3] and [4], although the ratio $(C_2H_6)/(C_4H_{10})$ varied from 0.77 to 1.25.

[1]*Manuscript received January 27, 1955.*
Contribution from the Department of Chemistry, University of Toronto, Toronto, Ontario.
[2]*Present address: Somerville College, Oxford.*
[3]*Present address: Division of Applied Chemistry, National Research Council, Ottawa, Ontario.*

The latter authors suggested that in systems containing atomic hydrogen, as well as ethyl radicals, "high" values of the ratio might be obtained because of the following reactions:

$$H+C_2H_5 = C_2H_6^* \quad [5]$$
$$C_2H_6^* = 2CH_3 \quad [6]$$
$$C_2H_6^*+M = C_2H_6+M. \quad [7]$$

This set of reactions was first postulated by Darwent and Steacie (5) in order to explain their results on the mercury photosensitized decomposition of ethane. The over-all reaction

$$H+C_2H_5 = C_2H_6 \quad [8]$$

would be more likely to occur at high pressures, while the over-all reaction

$$H+C_2H_5 = 2CH_3 \quad [9]$$

would be more likely to occur at low pressures. Nevertheless, even at the low pressures (*ca.* 0.5 mm.) used in the Wood-Bonhoeffer discharge method there is some evidence that D atoms will add to ethyl radicals by the analogue of reaction [8] (14, 15). Berlie and Le Roy (2) studied the reaction of H atoms with ethane in a manner which made it possible to detect the occurrence of reaction [8], and their results indicate that it takes place to some extent at pressures as low as 5 mm.

In the present investigation we have been able to show that reaction [8] is of considerable importance in the mercury photosensitized hydrogenation of ethylene at room temperature and that when it is taken into account a value of k_4/k_3 may be obtained which is in good agreement with the most reliable values obtained by other methods.

The following *local* rate equations are obtained for the mechanism consisting of reactions [1], [2], [3], and [4]:

$$d(C_2H_6)/dt = k_4I_a/(k_3+k_4) \quad [i]$$
$$d(C_4H_{10})/dt = k_3I_a/(k_3+k_4). \quad [ii]$$

It follows that the ratio of the final concentrations, $(C_2H_6)_f/(C_4H_{10})_f$, should be independent of light intensity and the concentrations and equal to k_4/k_3.

If reactions [5], [6], and [7] are included in the mechanism the *local* rate equations cannot be solved explicitly unless certain approximations are made. Most of the present experiments were carried out with total pressures of the order of 220 mm., and the carbon balances indicated that reaction [6] was of no importance. The net effect of reactions [5] and [7] will be the consumption of H atoms and ethyl radicals by reaction [8]. Two limiting conditions then arise: (*A*) the rate of reaction [8] is sufficiently small that the relative concentrations of H atoms and ethyl radicals are not appreciably affected by its occurrence, and (*B*) the rate of [8] is sufficiently large that it controls the ethyl radical concentration.

For the limiting condition (*A*) it can be shown that

$$\frac{d(C_2H_6)/dt}{d(C_4H_{10})/dt} = \frac{k_4}{k_3}+\frac{2k_8(k_3+k_4)^{\frac{1}{2}}I_a^{\frac{1}{2}}}{k_2k_3(C_2H_4)}. \quad [iii]$$

This equation applies to *local* rates and cannot be integrated rigorously without a knowledge of the spatial distribution of I_a and of the radical concentrations. It is possible to calculate I_a as a function of the distance from the front window of the cell from a knowledge of the mercury concentration and the extinction coefficients for the absorption of 2537 Å radiation (which vary across the width of the absorption line), but the calculation can only be carried out for an assumed form for the emission line from the lamp. The rates of diffusion of the various species would also have to be taken into account. The spatial integration of [iii] is therefore fraught with a considerable amount of difficulty. Nevertheless, if a number of experiments are carried out with the same lamp, and using the same mercury concentration, the spatial distribution of I_a will remain constant, and under these conditions it will probably be justifiable to integrate [iii] with respect to time, viz.,

$$\frac{(C_2H_6)_f}{(C_4H_{10})_f} = \frac{k_4}{k_3} + \frac{4.606\ k_8(k_3+k_4)^{\frac{1}{2}} I_e^{\frac{1}{2}}}{-\Delta(C_2H_4)\ k_2k_3} \log\frac{(C_2H_4)_0}{(C_2H_4)_f}. \qquad [iv]$$

The quantity I_e in this expression will be the effective average value of I_a.

The expression analogous to [iv] for the limiting condition (B) is

$$\frac{(C_2H_6)_f}{(C_4H_{10})_f} = \frac{3\ k_8{}^2 I_e}{k_2{}^2 k_3} \cdot \frac{-\Delta(C_2H_4)}{(C_2H_4)_0{}^3 - (C_2H_4)_f{}^3}. \qquad [v]$$

If we set $(C_2H_4)_0/(-\Delta(C_2H_4)) = \sigma$, equation [v] may be written in the more convenient form,

$$\frac{(C_2H_6)_f}{(C_4H_{10})_f} = \frac{k_8{}^2 I_e}{k_2{}^2 k_3} \cdot \frac{1}{-\Delta(C_2H_4)\ .\ (C_2H_4)_0(\sigma - 1 + 1/3\sigma)}. \qquad [vi]$$

For example, if a constant conversion of 50% is used in each experiment $(\sigma - 1 + 1/3\sigma)$ will be equal to 7/6.

EXPERIMENTAL

A number of exploratory experiments showed that $(C_2H_6)_f/(C_4H_{10})_f$ decreased when either the incident light intensity or the concentration of mercury in the cell was reduced. In both cases this would amount to a reduction of I_a which, in its rigorous definition, is the number of quanta absorbed per unit volume per unit time at a point in the reaction vessel. It was also found that the ratio of ethane to butane increased when the ethylene concentration was decreased at constant hydrogen pressure. Previous work had shown that below 200°C. the ratio was not sensitive to hydrogen pressure over the range from approximately 100 to 300 mm. (9).

Since the preliminary experiments appeared to bear out the predictions of the theory outlined above, a number of experiments were carried out to study in detail the effect of incident light intensity, mercury concentration, and ethylene pressure. In addition, some experiments were performed using a cell with an optical path length of approximately two millimeters. With such a cell the amount of surface exposed to H atoms and ethyl radicals would be

approximately doubled and surface reactions, if they occurred, would be enhanced.

All of the experiments were carried out at room temperature and all pressures were corrected to 25°C. Products were fractionated by low temperature distillation (8) and the C_2 fraction was analyzed for ethylene and ethane by the method of Pyke, Kahn, and Le Roy (12). For the experiments reported here the lamps were of the low pressure type with rare gas carrier; for such lamps the half-width of the emission line is somewhat greater than for a true resonance lamp (10) and the effective reaction zone will penetrate farther into the cell.

EFFECT OF INCIDENT LIGHT INTENSITY

These experiments were carried out in a static system using a 1 liter spherical cell with a plane Vicor window. Initial hydrogen pressures were approximately 180 mm., initial ethylene pressures were approximately 20.5 mm., and the average pressure drop was 10.7 mm. The incident light intensity was varied simply by changing the distance between the lamp and the cell; in this way the rate of pressure drop was varied from 1.42×10^{-3} to 163×10^{-3} mm. min^{-1}.

The values of I_e were unknown and hence the results could only be expressed in relative terms. The inverse square law would not be valid for a finite source and thus the distances from lamp to cell could not be used to obtain relative values of I_e. However, since all of the products are saturated $-\Delta(C_2H_4)$ will be equal to $-\Delta P$, and the rate of pressure drop will be equal to the rate of consumption of ethylene. The latter is equal to $(1+k_3/(k_3+k_4))I_e$ for the limiting condition (A), and to I_e for the limiting condition (B).

In Fig. 1 a plot of $(C_2H_6)_f/(C_4H_{10})_f$ against $[(-\Delta P)^{\frac{1}{2}}t^{\frac{1}{2}}]^{-1}\log[(C_2H_4)_0/(C_2H_4)_f]$ is shown; this corresponds to the use of equation [iv], i.e. to the limiting condition (A). It is seen that as I_e approaches zero $(C_2H_6)_f/(C_4H_{10})_f$ becomes linear in $I_e^{\frac{1}{2}}$. The intercept at $I_e = 0$ is 0.14_5, in good agreement with the values

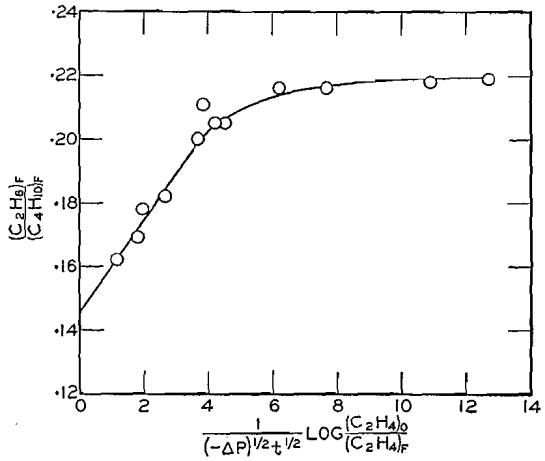

FIG. 1. Test of equation [iv] for variations in incident light intensity.

of k_4/k_3 obtained at room temperature by other methods (*vide* Table I). The decrease in slope which sets in at high light intensities (large values of the abscissa) is not predicted by the present mechanism; the curvature in Fig. 1 is opposite to that predicted on the assumption that the limiting condition (*B*) obtains at high light intensities. Because of the assumptions involved in the spatial integration of I_a this is not surprising. However, regardless of detailed mechanisms, it is obvious that reaction [8] should become negligible at low light intensities and that under these conditions $(C_2H_6)_f/(C_4H_{10})_f$ should approach k_4/k_3.

EFFECT OF MERCURY CONCENTRATION

Even though we do not know the spatial distribution of I_a it is clear that a reduction in the mercury concentration in the cell will cause a decrease in the number of quanta absorbed in unit time in any unit volume. According to the present mechanism this should cause a decrease in $(C_2H_6)_f/(C_4H_{10})_f$. A number of experiments were performed with a circulating system in which the gases were passed through a trap containing mercury at temperatures ranging from 27°C. to −12°C. before entering the cell. In each case hydrogen pressures of approximately 220 mm. and ethylene pressures of approximately 17.5 mm. were used. The pressure decreases were not kept as close to 50% of the initial ethylene pressure as in the other experiments and ranged from 5.7 to 14 mm. The incident light intensity was kept constant by fixing the position of the lamp with respect to the cell window. As shown in Fig. 2, the ratio

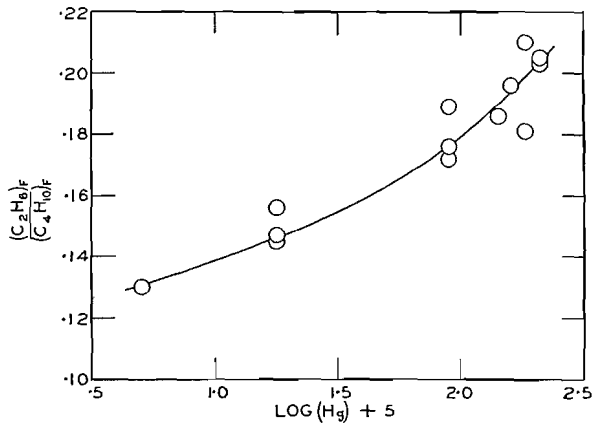

FIG. 2. Influence of the mercury concentration in the cell on the ethane/butane ratio.

$(C_2H_6)_f/(C_4H_{10})_f$ decreases as the mercury concentration is lowered, in agreement with the predictions of the present mechanism. It would be expected, of course, to approach a constant value, k_4/k_3, as I_e tends toward zero.

EFFECT OF OPTICAL PATH LENGTH

Since, in a mercury photosensitization experiment, most of the light is absorbed very close to the entrance window, an increase in the ratio of the surface to the effective volume of the reaction zone can best be accomplished

by using a cell with a short optical path. The cell was constructed by blowing a bulb in the middle of a piece of quartz tubing and then heating and sucking in one side to form a concave cell with more or less parallel sides approximately two millimeters apart. The side arms of the cell were painted black.

A series of three experiments using this cell and four with a cell having an optical path length of about 10 cm. were made using a circulating system. The same distance between lamp and cell was used in each case. Initial hydrogen pressures were approximately 205 mm.; initial ethylene pressures were approximately 17.5 mm. With the small cell $(C_2H_6)_f/(C_4H_{10})_f$ was $0.22_9 \pm .00_6$; with the large cell it was $0.22_7 \pm .00_7$. It would therefore appear that surface reactions, if they do occur, have no influence on this ratio.

EFFECT OF ETHYLENE CONCENTRATION

A series of experiments was performed in which the initial ethylene pressure was varied from 0.75 mm. to 17.9 mm. using a constant hydrogen pressure of approximately 218 mm. To provide sufficient products for analysis at the lower ethylene pressures a circulating system containing a buffer volume was used. The average fraction of ethylene consumed in any experiment was $0.52 \pm .05$. The results are plotted in Fig. 3 according to equation [iv]. The

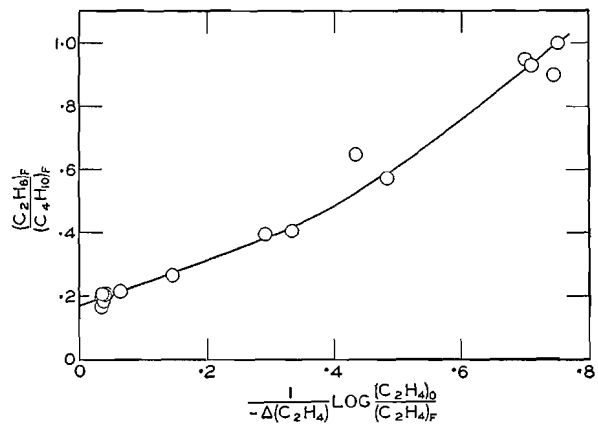

FIG. 3. Influence of ethylene concentration on the ethane/butane ratio. Since approximately 50% of the initial ethylene was used in each experiment, the abscissae are, roughly, $0.6/(C_2H_4)_0$.

value of I_e should be constant for the series, at least to a first approximation, since both the position of the lamp and the mercury concentration in the cell were fixed. The range of values of $(C_2H_6)_f/(C_4H_{10})_f$ shown in this figure is greater than any obtained previously by the method of mercury photosensitization and illustrates the important effect of ethylene concentration.

The value of k_4/k_3 obtained from the intercept of Fig. 3 is approximately 0.16. Accepting this value, it follows that for initial ethylene pressures of the order of 1 mm., and with the light intensities used in these experiments, approximately four times as much ethane is produced by reaction [8] as by reaction [4].

Fig. 3 shows an appreciable curvature upwards at low ethylene pressures (large values of the abscissa). Such a curvature would be expected if the limiting condition (B) were to come into play. However, it is believed that at least part of this curvature is due to the fact that the rate of circulation of the gases becomes important at low ethylene concentrations.

The circulating pump used had a displacement of 30 cm.^{3} min^{-1}. At high ethylene pressures this would be sufficient to ensure that the partial pressure of ethylene in the gas leaving the cell would not be much less than in the gas entering the cell. But at low ethylene pressures most of the ethylene entering the cell would be consumed. Because these experiments were of short duration much of the gas never left the buffer volume and as a result, although only approximately 50% of the total ethylene was consumed a considerably larger figure would apply to the gas which actually passed through the cell. If this effect could be allowed for the points for low ethylene pressures in Fig. 3 would be moved to the right, thus prolonging the range of linearity of the curve.

HEXANE FORMATION

At low light intensities, particularly at the higher ethylene concentrations, low temperature distillation indicated a product having a vapor pressure in the hexane range. Under the most favorable conditions for its formation it amounted to only 2.1% of the saturated products. Its vapor pressure was determined in the range $-52°$ to $-72°$ using the low temperature still (8) and the values agreed within a range of approximately 5°C. with those calculated for n-hexane from the data of International Critical Tables; the thermocouple used had not been calibrated. The vapor pressure at 27°C., determined as the condensation pressure in a McLeod gauge, was 155 mm., compared to 163 mm. calculated for n-hexane.

The most probable method of formation of n-hexane is by the sequence

$$C_2H_5+C_2H_4 = C_4H_9 \qquad [10]$$
$$C_4H_9+C_2H_5 = C_6H_{14}. \qquad [11]$$

The conditions which were found to be the most favorable for the formation of hexane are the least favorable for the occurrence of reaction [8] and hence it is unlikely that any hexane would be formed by the addition of H atoms to hexyl radicals.

For the limiting condition (A),

$$\frac{d(C_6H_{14})/dt}{d(C_4H_{10})/dt} = \frac{k_{10}(k_3+k_4)^{\frac{1}{2}}(C_2H_4)}{k_3 I_a^{\frac{1}{2}}}. \qquad [vii]$$

It was pointed out previously that the rate of pressure drop should be proportional to the effective average value of I_a, and hence, to a first approximation, $(C_6H_{14})_f/(C_4H_{10})_f$ should be directly proportional to $(C_2H_4)_0/(-\Delta P/\Delta t)^{\frac{1}{2}}$. The data plotted in Fig. 4 show that this is approximately true. Because of the small amounts involved, hexane could not be measured with very great accuracy.

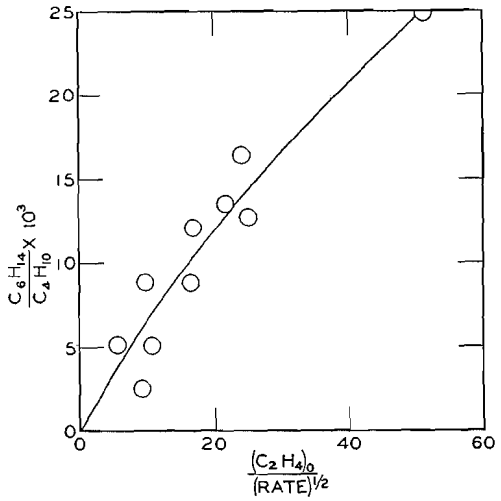

FIG. 4. Correlation of hexane formation with equation [vii]. The effective average value of I_a is assumed to be proportional to the rate of pressure drop.

DISCUSSION

From the present data the most probable value of k_4/k_3 is 0.15±.01. This is in good agreement with most of the recent work based on other methods, as shown in Table I.

TABLE I

VALUES OF k_4/k_3 OBTAINED BY DIFFERENT METHODS
(Room temperature)

Method	k_4/k_3	Ref.
Photolysis of diethyl mercury	0.35	(6)
Photolysis of propionaldehyde	0.1	(3)
Photolysis of diethyl ketone	0.12 ± .02	(7)
Photolysis of 2,2′,4,4′ tetradeuterodiethyl ketone	0.1	(16)
Photolysis of azoethane	0.13 ± .02	(1)
This research	0.15 ± .01	

The discrepancies among the values of the ratio $(C_2H_6)_f/(C_4H_{10})_f$ obtained by the method of mercury photosensitization can now be understood. Moore and Taylor (11) used an initial ethylene pressure of 40 mm. and their value of 0.17 would therefore be expected to be only slightly larger than k_4/k_3. Le Roy and Kahn (9), using the full intensity of the lamp and an initial ethylene pressure of 13.3 mm., obtained 0.61 and 0.44 for the ratio; from the pressure drops they observed the final pressures of ethylene would be approximately 1.0 and 1.3 mm., respectively. Using a lower light intensity, initial ethylene pressures of 15.7 mm., and final ethylene pressures of 5.3 and 5.9 mm., they obtained 0.22 and 0.28 for the ratio. Their results are therefore not out of line with those obtained in the present investigation.

Cashion and Le Roy (4) found ethane and butane to be important products in the mercury photosensitized hydrogenation of acetylene and attributed their origin to ethyl radicals produced in the reactions

$$C_2H_3+H_2 = C_2H_5 \quad [12]$$
$$H+C_2H_4 = C_2H_5. \quad [2]$$

However, since they found the ethane/butane ratio to be in the range 0.77 to 1.25 they concluded that ethane must be formed in some reaction in addition to [4], namely [8]. An examination of their results shows that for conditions in which [12] would be negligible compared to [2] (i.e. $(H_2) \rightarrow 0$, their Fig. 2) the ethane/butane ratio would be approximately 1.4. The ethylene concentration in this case would have been zero at the beginning of the experiment and about 0.2 mm. at the end. The large values of the ratio obtained by them can be adequately explained in terms of the present mechanism. They were reluctant to attribute ethane/butane ratios of almost ten times the accepted value of k_4/k_3 solely to the influence of reaction [8] and suggested the additional reaction

$$C_2H_5+C_2H_3 = C_2H_6+C_2H_2. \quad [13]$$

It is clear, however, that the last postulate is unnecessary.

ACKNOWLEDGMENT

The authors are grateful to the National Research Council for financial assistance.

REFERENCES

1. Ausloos, P. and Steacie, E. W. R. Bull. soc. chim. Belges, 63: 87. 1954.
2. Berlie, M. R. and Le Roy, D. J. Discussions Faraday Soc. No. 14: 50. 1953.
3. Blacet, F. E. and Pitts, J. N. J. Am. Chem. Soc. 74: 3382. 1952.
4. Cashion, J. K. and Le Roy, D. J. Can. J. Chem. 32: 906. 1954.
5. Darwent, B. de B. and Steacie, E. W. R. J. Chem. Phys. 16: 381. 1948.
6. Ivin, K. J. and Steacie, E. W. R. Proc. Roy. Soc. (London), A, 208: 25. 1951.
7. Kutschke, K. O., Wijnen, M. H. J., and Steacie, E. W. R. J. Am. Chem. Soc. 74: 714. 1952.
8. Le Roy, D. J. Can. J. Research, B, 28: 492. 1950.
9. Le Roy, D. J. and Kahn, A. J. Chem. Phys. 15: 816. 1947.
10. Mitchell, A. G. and Le Roy, D. J. J. Chem. Phys. 21: 2075. 1953.
11. Moore, W. J. and Taylor, H. S. J. Chem. Phys. 8: 396. 1940.
12. Pyke, R., Kahn, A., and Le Roy, D. J. Ind. Eng. Chem. Anal. Ed. 19: 65. 1947.
13. Steacie, E. W. R. Atomic and free radical reactions. Reinhold Publishing Corporation, New York. 1954.
14. Trenner, N. R., Morikawa, K., and Taylor, H. S. J. Chem. Phys. 5: 203. 1937.
15. Trost, W. R. and Steacie, E. W. R. J. Chem. Phys. 16: 361. 1948.
16. Wijnen, M. H. J. and Steacie, E. W. R. Can. J. Chem. 29: 1092. 1951.

THE RELATIVE ABUNDANCES OF NEODYMIUM AND SAMARIUM ISOTOPES IN THE THERMAL NEUTRON FISSION OF U^{235} AND U^{233} [1]

By E. A. Melaika, M. J. Parker, J. A. Petruska,[2] and R. H. Tomlinson

ABSTRACT

The relative fission yields of neodymium and samarium isotopes have been measured with a mass spectrometer for samples of natural uranium and U^{233} that had been irradiated with moderated neutrons. The cross sections for neutron capture by Sm^{149} and Sm^{151} have been determined to be $66{,}200 \pm 2500$ barns and 12,000 barns respectively, relative to the cross section of a B^{10} monitor. The half-lives of Pm^{147} and Sm^{151} have been evaluated to be 2.52 ± 0.08 yr. and $\sim$93 yr., respectively, from samarium fission yield data for samples differing in age by seven years.

INTRODUCTION

Inghram, Hayden, and Hess (5) have reported a mass spectrometric determination of the relative abundances of rare earth isotopes separated from fission products in uranium fuel rods. The values obtained were considered to represent relative fission yields of U^{235}, although the previously accepted mass–yield curve (9) for the thermal neutron fission of U^{235} was considerably different in this mass region. Inghram *et al.* pointed out, however, that the mass spectrometric values represent yields for the neutron energy distribution found in thick uranium slugs and do not necessarily correspond to those for the thermal neutron fission of U^{235}. Likewise, the various pile neutron capture cross sections reported by Inghram *et al.* need not be applicable for a thermal neutron energy distribution.

This paper reports the mass spectrometric determination of the relative yields of neodymium and samarium isotopes for the thermal neutron fission of U^{235} and U^{233}. The amount of neutron capture by Sm^{149} and Sm^{151} was large in a sample of uranium for which the integrated neutron flux was monitored with BF_3. From the observed ratios of the samarium isotopes in this sample, the measured fission yields of samarium isotopes, and the change in the B^{10}/B^{11} ratio for the BF_3, the neutron capture cross sections of Sm^{149} and Sm^{151} relative to that of B^{10} were obtained. Since the relative abundances of the samarium isotopes were measured at different times after irradiation for the various samples, it was possible to evaluate the half-lives of Sm^{151} and Pm^{147}.

EXPERIMENTAL

For the study of the fission yields for U^{235}, four samples of normal uranium metal were irradiated in the NRX reactor at Chalk River and one at Oak Ridge. A 50 mgm. sample of UO_3, in which the uranium content was 14.4 atom % U^{233}, 0.6 atom % U^{235}, and 85.0 atom % U^{238}, was irradiated in the

[1]*Manuscript received January 17, 1955.*
Contribution from the Department of Chemistry, Hamilton College, McMaster University, Hamilton, Ontario.
[2]*Holder of a Research Council of Ontario scholarship, 1953–54.*

TABLE I

IRRADIATION DATA

Sample	Form	Reactor	Neutron flux, $n/cm.^2/sec.$	t_1,* days	t_2,† days
A	Uranium metal 20 gm.	NRX, Chalk River thermal column	5.0×10^{10}	81	618
B	Uranium metal 1.6 gm.	NRX, Chalk River	7.0×10^{12}	31	590
C	Uranium metal 30 gm.	Oak Ridge	6.0×10^{11}	18	2950
D	Uranium metal 3.0 gm.	NRX, Chalk River	2.30×10^{12}	36	910
E	50 mgm. UO_3 14.4% U^{233}	NRX, Chalk River	1.23×10^{13}	31	517

**Time of irradiation.*

†Time from beginning of irradiation until time of chemical separation and analysis by mass spectrometer.

NRX reactor for the study of U^{233} fission. The irradiation data are summarized in Table I. In no case was the integrated flux greater than 2×10^{19} neutrons/cm.^{2}, and hence Pu^{239} did not contribute more than 0.1% to the fission products of either U^{235} or U^{233}. In sample *D*, the contribution from fast neutron fission of U^{238} was estimated from pile data to be 2.5%; it was probably comparable in samples *B* and *C*. Sample *A*, which was irradiated in a thermal column, had essentially no U^{238} fission. Unfortunately, in the case of sample *A*, the time of irradiation was divided into three periods so that the time between periods could not be neglected. Since several determinations of fission yields were made for sample *A* at widely different times, and since there are three corresponding values of t_2 for each of these determinations, the value of t_2 tabulated for sample *A* is only an approximate average.

The uranium, after dissolution in nitric acid, was separated from the fission products either by ion exchange or by precipitation from solution at pH 7 with hydrogen peroxide. The ion exchange method permitted a separation of the neodymium from the samarium and other fission products, whereas the peroxide precipitation method did not. It was found, however, that separation of the rare earths prior to mass spectrometric analysis was not necessary. The peroxide precipitation method was preferred since a much higher chemical yield of neodymium and samarium could be obtained.

The mass spectrometer that was used was a 90° sector instrument with magnetic scanning and a hot filament ion source (2). When a platinum-plated tungsten filament was used, neodymium and samarium samples of 0.01 μgm. were adequate. The neodymium yields were measured from the NdO^+ ion spectrum at a relatively low filament temperature; the samarium was measured from the Sm^+ ion spectrum which occurred only at a higher filament temperature. The SmO^+ ions also appeared at this higher temperature and were used for the determination of the Sm^{152}/Sm^{154} ratio since a LaO^+ peak at mass 155 tended to interfere with the Sm^{154} metal ion peak when the fission products were not separated from each other. Since, in each case, only mass spectra of

the expected fission isotopes were observed, and since no changes in the ratios were observed with time, it was assumed that no other elements contributed to the mass spectrum of either the samarium or the neodymium.

RESULTS

The relative abundances of the samarium isotopes obtained from the thermal neutron fission in four samples of normal uranium and one sample of uranium containing 14.4% U^{233} are given in Table II. The fission samarium

TABLE II

THE RELATIVE ABUNDANCES OF NEODYMIUM AND SAMARIUM ISOTOPES IN THE THERMAL NEUTRON FISSION OF U^{235} AND U^{233}

Sample	Relative abundances of isotopes					
Neodymium isotopes for U^{235} fission						
	Nd^{143}	Nd^{144}	Nd^{145}	Nd^{146}	Nd^{148}	Nd^{150}
A Observed	1.000	(0.713)	0.663	0.502	0.280	0.109
Relative yield	1.000	(0.912)	0.663	0.502	0.280	0.109
B Observed	1.000	0.723	0.665	0.506	0.282	0.112
Relative yield	1.000	0.943	0.665	0.506	0.282	0.112
C Observed	1.000	0.923	0.666	0.507	0.282	0.110
Relative yield	1.000	0.923	0.666	0.507	0.282	0.110
D Observed	1.000	0.820	0.665	0.504	0.280	0.110
Relative yield	1.000	0.923	0.665	0.504	0.280	0.110
Average	1.000	0.930	0.665	0.505	0.281	0.110
S.D.		±0.012	±0.001	±0.002	±0.001	±0.002
Inghram *et al.*	1.000	0.860	0.670	0.520	0.304	0.122
Samarium isotopes for U^{235} fission						
	Sm^{147}	Sm^{149}	Sm^{150}	Sm^{151}	Sm^{152}	Sm^{154}
A Observed	0.724	0.987	0.013	0.393	0.250	0.068
Relative yield	(2.05)	1.000	0.000	0.398	0.250	0.068
C Observed	1.864	0.979	0.021	0.374	0.251	0.068
Relative yield	2.10	1.000	0.000	0.398	0.251	0.068
D Observed	1.025	0.797	0.203	0.373	0.267	0.068
Relative yield	2.10	1.000	0.000	0.398	0.251	0.068
Average	2.10	1.000	0.000	0.398	0.251	0.068
S.D.	±0.04				±0.001	±0.000
Inghram *et al.*	1.96	1.000	0.000	0.405	0.254	0.083
Neodymium isotopes for U^{233} fission						
	Nd^{143}	Nd^{144}	Nd^{145}	Nd^{146}	Nd^{148}	Nd^{150}
E Observed	1.000	0.543	0.587	0.441	0.224	0.089
Relative yield	1.000	0.779	0.587	0.441	0.224	0.089
Samarium isotopes for U^{233} fission						
	Sm^{147}	Sm^{149}	Sm^{150}	Sm^{151}	Sm^{152}	Sm^{154}
E Observed	0.846	0.405	0.595	0.327	0.373	0.061
Relative yield	2.81	1.000	0.000	0.422	0.278	0.061

abundances reported as the observed values have been corrected for contamination by natural samarium. The contamination corrections, which were about two to three per cent of the total samarium present, were based on the natural abundances of the samarium isotopes and the measurement of the Sm^{148} which is not formed in fission. In order to obtain the relative cumulative fission yields shown in Table II, it was necessary to take into account several known nuclear processes which occur in the various fission chains which form samarium isotopes. The equations relating the observed ratios to the cumulative fission yields of the samarium isotopes have been given by Inghram *et al.* (5).

Since beta decay in the mass 150 chain from fission terminates at Nd^{150}, the observed Sm^{150} is the result of neutron capture by Sm^{149}. The total relative yield for the mass 149 chain was obtained by direct addition of the Sm^{149} and Sm^{150} abundances. The ratio of the observed Sm^{149} to Sm^{150} is given by equation [1].

$$[1] \qquad \frac{N_{149}}{N_{150}} = \frac{1-\exp(-{}_{62}\sigma^{149}\phi t_1)}{{}_{62}\sigma^{149}\phi t_1 - 1 + \exp(-{}_{62}\sigma^{149}\phi t_1)}$$

where N_{149}/N_{150} = the observed ratio of Sm^{149} to Sm^{150},
${}_{62}\sigma^{149}$ = the neutron capture cross section for Sm^{149},
ϕ = the neutron flux,
t_1 = the time of irradiation.

For samples *A* and *C*, the amount of Sm^{149} capture was small and the flux could be estimated only from pile operation data. For sample *D*, however, there was a large amount of Sm^{150} formed, and the flux was accurately determined from the change in the B^{10}/B^{11} ratio in a sample of BF_3 that was irradiated simultaneously. The ratio of the B^{10}/B^{11} ratio before irradiation to the B^{10}/B^{11} ratio after irradiation was found to be 1.029 ± 0.001. The value of ${}_5\sigma^{10}\phi t_1$, where ${}_5\sigma^{10}$ is the neutron absorption cross section for B^{10}, was calculated to be 0.0286 ± 0.0010 assuming that all of the change in the ratio of the boron isotopes was due to the $B^{10}(n, \alpha)Li^7$ reaction. From the observed ratio N_{149}/N_{150} for sample *D*, a value of 0.472 ± 0.007 was calculated with equation [1] for ${}_{62}\sigma^{149}\phi t_1$. Thus, the ratio ${}_{62}\sigma^{149}/{}_5\sigma^{10}$ is 16.5 ± 0.6 at an estimated neutron temperature of 57°C. This ratio corresponds to a neutron capture cross section of $66{,}200 \pm 2500$ barns if a value of 755 barns (1) is used for the neutron capture cross section of natural boron and 18.83% (4) is used for the natural abundance of B^{10}.

The fission yield of Sm^{151} relative to that of Sm^{149} is given by equation [2] as a function of the observed samarium ratios and the time.

$$[2] \qquad \frac{N_{151}}{(N_{149}+N_{150})} = \frac{f_{151}[1-\exp(-{}_{62}\lambda^{151}t_1 - {}_{62}\sigma^{151}\phi t_1)][\exp(-{}_{62}\lambda^{151}t_2 + {}_{62}\lambda^{151}t_1)]}{f_{149}({}_{62}\lambda^{151} + {}_{62}\sigma^{151}\phi)t_1}$$

where $N_{151}/(N_{149}+N_{150})$ = the ratio of Sm^{151} to Sm^{149} plus Sm^{150} observed at time t_2,
f_{151}/f_{149} = the ratio of the cumulative yields of mass chains 151 and 149,

$_{62}\lambda^{151}$ = the decay constant of Sm^{151},
$_{62}\sigma^{151}$ = the neutron capture cross section for Sm^{151},
ϕ = the neutron flux,
t_1 = the time of irradiation,
t_2 = the time from the beginning of irradiation until the time of chemical separation and isotopic analysis.

If the time of irradiation is short compared to the time of the analysis, and if t_1 is small compared to the half-life of Sm^{151}, equation [2] reduces to equation [3].

$$[3] \qquad \frac{N_{151}}{(N_{149}+N_{150})}=\frac{f_{151}\exp(-{}_{62}\lambda^{151}t_2)[1-\exp(-{}_{62}\sigma^{151}\phi t_1)]}{f_{149}\,{}_{62}\sigma^{151}\phi t_1}.$$

In the case of samples A and C, the contribution to mass 150 resulting from neutron capture by Sm^{149} is only 1 to 2%, and, therefore, neutron capture by Sm^{151} will be negligible provided its cross section is less than that of Sm^{149}. Thus, for samples A and C, equation [3] reduces to equation [4].

$$[4] \qquad \frac{N_{151}}{(N_{149}+N_{150})}=\frac{f_{151}\exp(-{}_{62}\lambda^{151}t_2)}{f_{149}}.$$

The observed relative yield at mass 152 is given by equation [5], and its simplified forms, comparable to equations [3] and [4], are given by equations [6] and [7].

$$[5] \qquad \frac{N_{152}}{(N_{149}+N_{150})}=\frac{f_{152}}{f_{149}}+\frac{f_{151}\,{}_{62}\sigma^{151}\phi t_1}{f_{149}({}_{62}\lambda^{151}+{}_{62}\sigma^{151}\phi)^2t_1^2}$$
$$\times[({}_{62}\lambda^{151}+{}_{62}\sigma^{151}\phi)t_2-1+\exp(-{}_{62}\lambda^{151}t_1-{}_{62}\sigma^{151}\phi t_1)]$$

$$[6] \qquad \frac{N_{152}}{(N_{149}+N_{150})}=\frac{f_{152}}{f_{149}}+\frac{f_{151}}{f_{149}\,{}_{62}\sigma^{151}\phi t_1}[{}_{62}\sigma^{151}\phi t_1-1+\exp(-{}_{62}\sigma^{151}\phi t_1)]$$

$$[7] \qquad \frac{N_{152}}{(N_{149}+N_{150})}=\frac{f_{152}}{f_{149}}.$$

Thus, for samples A and C, the observed Sm^{152} ratios are the actual relative fission yields as shown by equation [7]. The yield of Sm^{151} for these samples, however, is dependent on the half-life of Sm^{151} as shown by equation [4]. From the observed ratios for these two samples, it was possible to solve this equation for both f_{151}/f_{149} and $_{62}\lambda^{151}$. For sample A, the uncertainty of the value of t_2 in this calculation is not significant. The value obtained for f_{151}/f_{149} is 0.398 and for $_{62}\lambda^{151}$ is 0.00747 $yr.^{-1}$ which corresponds to a half-life of 93 yr.

The yields of Sm^{151} and Sm^{152} for sample D have been set equal to the values obtained from samples A and C. For sample D, $_{62}\sigma^{151}\phi t_1$ may then be calculated from either the observed ratio $Sm^{151}/(Sm^{149}+Sm^{150})$ and equation [3], or the observed ratio $Sm^{152}/(Sm^{149}+Sm^{150})$ and equation [6]. These equations give values of 0.090 and 0.080, respectively, for $_{62}\sigma^{151}\phi t_1$. From the value of $_5\sigma^{10}\phi t_1$, the cross section of natural boron, and the natural abundance of B^{10} given

above, values of 12,500 and 11,200 barns are obtained for the neutron capture cross section of Sm^{151}.

The amount of Sm^{147} relative to the amount of Sm^{149} plus Sm^{150} is given by equation [8].

$$[8] \quad \frac{N_{147}}{(N_{149}+N_{150})} = \frac{f_{147}[{}_{61}\lambda^{147}t_1 - \exp(-{}_{61}\lambda^{147}t_2 + {}_{61}\lambda^{147}t_1) + \exp(-{}_{61}\lambda^{147}t_2)]}{f_{149}\ {}_{61}\lambda^{147}t_1}$$

where ${}_{62}\lambda^{147}$ = the decay constant of Pm^{147}.

In equation [8], there are two unknowns, ${}_{61}\lambda^{147}$ and f_{147}/f_{149}, and these can be evaluated using the observed data from samples *C* and *D* if it is assumed that f_{147}/f_{149} is the same for both samples. A value of 0.275 ± 0.007 yr.$^{-1}$ was obtained for ${}_{61}\lambda^{147}$ which corresponds to a half-life of 2.52 ± 0.08 yr. The ratio, f_{147}/f_{149}, was found to be 2.10 ± 0.04. The limits of error assigned to the above values are obtained only from the standard deviations of the mass spectrometric results for samples *C* and *D*. Data for sample *A* were not used for this calculation because of the uncertainty introduced by the three-period irradiation.

Since the samarium yields were determined for only one set of irradiation conditions with U^{233}, the relative fission yields could not be obtained in the same manner as above for U^{235}. In this case, it was necessary to assume a smooth fission mass–yield curve, which gave 0.422 for the ratio f_{151}/f_{149} and 0.278 for the ratio f_{152}/f_{149}.

For this U^{233} sample, neutron capture by Sm^{149} was considerable, and equation [1] was used to solve for ${}_{62}\sigma^{149}\phi t_1$. A value of 2.19 ± 0.09 was obtained. Also, equation [3] may be used to solve for ${}_{62}\sigma^{151}\phi t_1$ if the value of 0.422, interpolated from a smooth yield–mass curve, is taken for the relative yield of mass chain 151 to 149. A value of 0.229 is obtained for ${}_{62}\sigma^{151}/{}_{62}\sigma^{149}$. If a value of 66,200 barns is taken for the value of ${}_{62}\sigma^{149}$, then a value of 15,200 barns is is obtained for ${}_{62}\sigma^{151}$.

The results for the relative abundances of the neodymium isotopes in the fission of U^{235} and U^{233} have been given in Table II. The abundances reported as the observed values have already been corrected for contamination by a small amount of natural neodymium. The contamination corrections, which were about 0.5% of the total neodymium present, were based on the natural abundances of the neodymium isotopes and the measurement of Nd^{142}, which is not formed in fission. The relative fission yields take into account the amount of 282-day Ce^{144} which had not decayed to Nd^{144} at the time of analysis. The Ce^{144} correction for sample *C* was negligible.

DISCUSSION

Table II shows that the relative fission yields of the neodymium and samarium isotopes resulting from the thermal neutron fission of U^{235} decrease more rapidly with increasing mass than the yields obtained by Inghram *et al.* (5). The difference (e.g. 11% at mass 150) appears to be real since the precision of either set of data is better than one per cent. This may be the result of different neutron energy distributions, since the fission products analyzed by Inghram *et al.* were obtained from a fuel rod where a large fraction of the

neutrons would have energies of several Mev., whereas in the present work neutron energies were essentially thermal. When fission is induced by particles of very high energy, it is well known that the fission yield curve tends to become more symmetrical. Some evidence of this change has been shown to occur even with fast (fission) neutrons. For example, in the case of Pu^{239}, the relative yield of masses 153/140 was found to be 0.074 for thermal neutrons, whereas the same relative yield was 0.096 for fast (fission) neutrons (12). Whereas the neutron energy may account for the greater part of the difference between the relative yields reported by Inghram *et al.* and those obtained in this work, it is also necessary to consider that fission products contributed by the fast neutron fission of U^{238} and to a smaller extent from the thermal neutron fission of Pu^{239} may have influenced the values obtained by Inghram *et al.*

Apart from the general increase in the slope of the mass–yield curve, the present results indicate that the yield of mass 144 is about 7% greater than the value obtained by Inghram *et al.* and hence could not fall on a smooth curve such as Inghram *et al.* have drawn. The apparently high yield at mass 144 may be taken as evidence for the fine structure predicted for this mass by Pappas (8).

Table II also shows the relative fission yields of the neodymium and samarium isotopes resulting from the thermal neutron fission of U^{233}. These relative yields are probably accurate to within one per cent except at mass 154 where a combination of a low yield and a comparable contamination correction make this particular yield uncertain.

A further correction must be made for the contribution to the fission products from the 0.6 atom % U^{235} present in the sample. The largest correction would occur at Nd^{150} where the relative yield would be reduced by about one per cent if it is assumed that the cross section for the formation of the neodymium isotopes is approximately the same for U^{233} and U^{235} fission. Comparison of the relative yields of neodymium and samarium for U^{233} with those for U^{235} show that the former decrease more rapidly with increase in mass of the fission product. By radiochemical methods, Steinberg *et al.* (13) have obtained yields at masses 144 (3.4%) and 153 (0.078%) while Grummitt and Wilkinson (3) have obtained yields at masses 144 (2.2%) and 147 (0.6%) for thermal neutron fission in U^{233}. Although the agreement between these groups at mass 144 is poor, the relative values obtained by each group confirm the steeper slope of the U^{233} mass–yield curve when compared to the U^{235} mass–yield curve given by Coryell and Sugarman (10).

The value of the half-life of Pm^{147} found in this work is 2.52 ± 0.08 yr. which is longer than the value of 2.26 yr. obtained by Inghram *et al.* (5). The 2.52 yr. value, however, is based on relative abundances measured at different times rather than an assumed yield as was used by Inghram *et al.* The value of 2.52 ± 0.08 yr. compares favorably with the value of 2.6 ± 0.2 yr. obtained by a counting-rate decay method (11).

The half-life of Sm^{151} based on changes in the relative abundances of Sm^{151} in fission products differing in age by about seven years is found to be 93 yr.

Whereas no limit has been set on the accuracy of this value it is considered in reasonable agreement with a value of 73^{+25}_{-14} yr. found by Karraker *et al.* (6) from the change in Sm^{151} abundances over a 3.8 yr. period.

The 66,200±2500 barn value obtained for the neutron capture cross section of Sm^{149} is based on a 755 barn cross section for natural boron. Nuclear Data (7) have reported a value of 65,000 barns for the cross section of Sm^{149} averaged for a maxwellian distribution of neutron energies at a temperature of 20.4°C. A value of 47,000 barns for pile neutrons has been reported by Inghram *et al.* (5). This value, however, is not strictly comparable to the other values without more specific information about the neutron energies. A cross section of 12,000 barns has been found for Sm^{151} relative to a 755 barn cross section for natural boron. It is difficult to set a limit of accuracy on this value since the observed changes in the isotopic abundances from which this value was calculated were small. The value of 15,200 barns obtained from the U^{233} data is based on assumed fission yields and hence has unknown reliability. Inghram *et al.* (5) have obtained a cross section of 7200 barns for the pile neutron cross section of Sm^{151} based on assumed fission yields for U^{235}.

Absolute fission yields may be obtained from the relative thermal neutron fission yields of the U^{235} and U^{233} when suitable normalization values are obtained either by radiochemical or isotope dilution methods.

ACKNOWLEDGMENTS

We wish to thank Atomic Energy of Canada Limited for supplying the U^{233} and uranium metal and arranging for the irradiation of samples. The financial support of the National Research Council of Canada and Atomic Energy of Canada Limited is gratefully acknowledged. The authors are indebted to Dr. H. G. Thode and Dr. W. H. Fleming for helpful discussions and the isotopic analysis of the BF_3.

REFERENCES

1. Atomic Energy Commission. Neutron Cross Section Advisory Group AECU-2040. May 15, 1952.
2. GRAHAM, R. L., HARKNESS, A. L., and THODE, H. G. J. Sci. Instr. 24: 119. 1947.
3. GRUMMITT, W. E. and WILKINSON, G. Nature, 158: 163. 1946.
4. INGHRAM, M. G. Phys. Rev. 70: 653. 1946.
5. INGHRAM, M. G., HAYDEN, R. J., and HESS, D. C. Phys. Rev. 79: 271. 1950.
6. KARRAKER, D. G., HAYDEN, R. J., and INGHRAM, M. G. Phys. Rev. 87: 901. 1952.
7. National Bureau of Standards. Nuclear Data. N. B. S. Circular 499. United States Department of Commerce. 1950.
8. PAPPAS, A. C. Lab. for Nuclear Science Tech. Rept. No. 63. Mass. Inst. Technol. September 15, 1953.
9. Plutonium Project "Nuclei Formed in Fission". Revs. Mod. Phys. 18: 513. 1946.
10. Radiochemical Studies: The Fission Products. Book 3, Appendix B. *Edited by* Coryell, C. D. and Sugarman, N. McGraw-Hill Book Company, Inc., New York and London. 1951.
11. SCHUMAN, R. P. and CAMILLI, A. Phys. Rev. 84: 158. 1951.
12. STEINBERG, E. P. and FREEDMAN, M. S. Radiochemical Studies: The Fission Products. Book 3, Paper 219. *Edited by* Coryell, L. D. and Sugarman, N. McGraw-Hill Book Company, Inc., New York and London. 1951.
13. STEINBERG, E. P., SEILER, J. A., GOLDSTEIN, A., and DUDLEY, A. MDDC-1632. United States Atomic Energy Commission. 1947.

CATALYSIS ON FILMS OF ARSENIC, ANTIMONY, AND GERMANIUM[1]

By Sir Hugh Taylor

ABSTRACT

Arsenic, antimony, and germanium films laid down on glass surfaces by decomposition of the hydrides have been studied from the standpoint of reaction kinetics in three sets of reactions: the decomposition of hydrides and deuterides, the interaction of hydrides and molecular deuterium, and the exchange reaction of hydrogen and deuterium. Only in the first of these have the surfaces marked catalytic activity. The orders of reaction and the activation energies have been determined. The accelerated catalytic influence of foreign elements, notably antimony in arsine decomposition, has been established. The results obtained contrast strikingly with the properties of clean filaments and evaporated films among the transition elements. The results emphasize the basic importance of chemical factors and de-emphasize the importance of surface cleanliness as a controlling factor in problems of chemisorption and surface catalysis.

It is a pleasant opportunity to outline, in tribute to a lifetime devoted to academic teaching and research by Professor Otto Maass in physical chemistry, some results in an area of physical chemical investigation which, while remote from the area which Professor Maass has so diligently and successfully cultivated, nevertheless has been contemporaneous with that work and has brought to the writer a large measure of the same satisfactions which research and the educational effort bring.

It is proposed to present a summary of some results recently obtained in the Princeton laboratories by a group of postdoctoral students and concerned with the catalytic properties of arsenic, antimony, and germanium films laid down on glass surfaces by the decomposition of the corresponding hydrides at appropriate temperatures. The deposited films act catalytically in the decomposition of the hydrides. Comparative experiments can also be performed on the decomposition of the deuterides. It has also been possible to study the interactions of the hydrides and deuterides among themselves and with molecular hydrogen and deuterium. The exchange reaction between hydrogen and deuterium on the several surfaces has also been examined. The results have a definite bearing on the properties of evaporated metal films which have been intensively studied in recent years in elucidation of the catalytic properties of technical metal catalysts.

Researches by Roberts (3) on the chemisorption of gases on clean flashed tungsten filaments and by Beeck (1) on the adsorption of gases on clean evaporated films of a variety of metals including nickel, iron, tungsten, rhodium, and platinum had emphasized that the activation energy of chemisorption of hydrogen on such clean surfaces was negligible, since it was demonstrably occurring at temperatures in the neighborhood of liquid hydrogen. Such observations gave rise to a very prevalent generalization that if

[1]*Manuscript received January 26, 1955.*
Contribution from the Frick Chemical Laboratory, Princeton University, Princeton, New Jersey, U.S.A.

the metal surfaces were clean the chemisorption of gases might occur without any activation energy. The determination of activation energies of chemisorption of hydrogen on a variety of technical catalysts led to the view that the cause of the activation energy might lie in the impurities present on the surfaces of all technical catalysts.

Such a point of view tended to obscure an obvious fact in the science of catalysis, namely, the very specific activity of particular elements in bringing about catalytic change. The examples of such specificity which could be quoted are legion. It may suffice, however, to recall that whereas iron and osmium surfaces are excellent catalysts in the synthesis of ammonia, nickel, and platinum are obviously inferior. Since all of these metals readily chemisorb hydrogen even down to quite low temperatures, the differences between them in respect to ammonia synthesis would seem to lie in the capacity of these surfaces to chemisorb nitrogen.

Quite recently Trapnell (5) published some comparative data on the interaction of nitrogen, hydrogen, carbon monoxide, ethylene, acetylene, and oxygen with clean evaporated films of some twenty metals between 0 and −183°C. Oxygen chemisorption is universal among the metals studied save in the case of gold. Chemisorption of both nitrogen and hydrogen is limited to transition metals, W, Ta, Mo, Ti, Zr, Fe, and alkaline earth metals such as Ca and Ba. The metals Ni, Pd, Rh, Pt, Cu, Al, K, Zn, Cd, In, Sn, Pb, Ag, and Au do not chemisorb nitrogen in this temperature range but Ni, Pd, Rh, and Pt chemisorb hydrogen. Chemisorption of carbon monoxide, ethylene, and acetylene occurs on the metals which chemisorb both nitrogen and hydrogen and in addition to these Al, Cu, and Au. The metals Zn, Cd, In, Sn, Pb, and Ag do not chemisorb carbon monoxide, ethylene, and acetylene. It is the particular virtue of this study with clean evaporated films that it emphasizes the necessity for activation energy of chemisorption even on clean surfaces.

Dr. M. Boudart in Princeton pointed out that it was possible to expand the area of our knowledge of the chemisorption of hydrogen by a study of the production of films of arsenic, antimony, and germanium by decomposition of the respective hydrides and that the nature of the isotopic hydrogen produced by decomposition of mixtures of hydrides and deuterides of these elements would give clues with respect to the interaction between hydrogen and such surfaces. Further, the constant deposition of fresh elemental product of the reaction, As, Sb, or Ge, on the surface ensured a continuous cleanliness of the surface provided the purity of the original hydrides was secured. A series of researches dealing with these topics is now in process of publication. The present occasion permits a summary survey of the results obtained.

Antimony Surfaces

Dr. K. Tamaru has studied the decomposition of stibine by a static method in the temperature range of 10 to 45°C. The rate is dependent only on the stibine pressure and independent of the hydrogen pressure. The order of reaction in stibine is unity at 45°C. and decreases with decreasing temperature

reaching 0.75 at 10°C. At 40 cm.-Hg stibine pressure the activation energy of the reaction is 8.8 kcal./mole, with lower values at lower pressures. The rate of decomposition of deuterostibine is slightly lower than that for stibine under similar conditions.

A feature common to all three surfaces can now be indicated. Stibine decomposition in presence of deuterium at 25°C. did not produce any hydrogen deuteride which shows that no exchange reaction between hydrogen and deuterium occurs at that temperature on the antimony surface. Decomposition of a mixture of stibine and deuterostibine produced a large proportion of hydrogen deuteride.

Stibine decomposes very slowly on the glass surface of a clean vessel but as antimony is deposited on the glass the rate accelerates until after 200 cm.-Hg of stibine have been decomposed the rate becomes reproducible. When a small amount of oxygen is introduced into the stibine there is a small acceleration in reaction rate but very considerably less than that to be noted subsequently in the decomposition of germane.

The evidence indicates that at the higher temperature limit of 45°C. in the measurements the chemisorption of stibine on the surface determines the rate of reaction. As the temperature is lowered the desorption of hydrogen, resulting from the decomposition of the stibine, from the antimony surface becomes slow enough to be comparable with the chemisorption process. The order of the reaction decreases and at sufficiently low temperatures where desorption of hydrogen became determinant the order would be zero. The data indicate a transition over the temperature range employed between the two kinds of rate process.

Arsenic Surfaces

The decomposition of arsine can be studied only in a much higher temperature range, between 218 and 278°C. Dr. Tamaru overcame a difficulty which had prevented good kinetic measurements by van't Hoff and Kooj (2) and by Stock and co-workers (4). This difficulty lay in the inability to form a coherent arsenic film on the surface of glass. Tamaru solved this problem by first laying down on the glass surface a coherent film of antimony on which by subsequent decomposition of arsine a coherent film of arsenic was formed. These experiments demonstrated that arsine decomposes slowly on glass even at 350°C. but decomposes more rapidly on antimony surfaces than it does on arsenic surfaces. On the antimony surface the original rate of arsine decomposition is relatively rapid, the rate decreasing as the antimony becomes covered with arsenic, constant rates of decomposition being secured after some ten experiments, this rate being assumed to be characteristic of a coherent arsenic film. In such a manner the kinetics and the activation energy of arsine decomposition on such arsenic films have been successfully obtained. We hope to be able to characterize the surfaces by electron diffraction studies.

The reaction is first order with respect to arsine and independent of hydrogen concentration. The apparent activation energy on arsenic surfaces is 23.2 kcal./mole. In the decomposition of a mixture of arsine and deuteroarsine at

255°C. intermolecular exchange occurs as revealed by infrared spectroscopy. The decomposition product contains a high percentage of hydrogen deuteride. When arsine is decomposed with molecular deuterium at this temperature no hydrogen deuteride is found, indicating no exchange between hydrogen and deuterium on the arsenic surface. Analysis of the experimental data indicates that the chemisorption of arsine is the rate determining step on arsenic surfaces.

Germanium Surfaces

Dr. P. J. Fensham who initiated this whole experimental program found that the decomposition of germane and deuterogermane on germanium films did not differ significantly in velocity. He demonstrated that the product from the decomposition of mixtures of germane and deuterogermane contained considerable amounts of hydrogen deuteride in the product hydrogen. On the other hand, germane–deuterium mixtures and molecular hydrogen – deuterium mixtures contained minimal amounts of hydrogen deuteride after reaction.

Dr. Tamaru examined the kinetics of the decomposition in greater detail and succeeded in showing that a zero order surface-catalyzed decomposition of germane occurs simultaneously with a first-order homogeneous decomposition in the gas phase in the temperature range 230 to 330°C. The kinetic expression in cylindrical vessels with surface to volume ratios from 1 to 7.5 cm.$^{-1}$ was expressible by an equation

$$v = k_0 + k_1 p$$

where v is the observed velocity, k_0 and k_1 the zero and first order constants respectively. For the two reactions the activation energies were 41.2 and 51.4 kcal./mole respectively. By filling the reaction vessel with glass wool and thus enhancing the zero order reaction some 30-fold the surface zero order reaction became dominant and the first order reaction negligible. Even in the unpacked cylindrical vessels the ratios of k_0 to $k_1 p$ were such that below 10 cm. working pressure of germane the reaction was kinetically closely zero order.

The surface reaction evidently occurs on a surface practically covered with chemisorbed GeH_x radicals and adsorbed hydrogen atoms, the evaporation of which in the steady state determines the rate of the surface reaction. That Fensham did not observe marked hydrogen deuteride formation in his experiments with germane–deuterium mixtures means either that his surface reaction was dominant in his experimental conditions over the homogeneous reaction or that this latter, if it were occurring, proceeds via GeH_2+H_2 rather than via GeH_3+H. The presence of H atoms in the latter type of decomposition would ensure considerable formation of hydrogen deuteride via the homogeneous chain-reaction exchange process $H+D_2 = HD+D$, followed by $D+H_2 = HD+H$.

Some interesting added facts emerged from the kinetic measurements. Arsine decomposes very slowly on germanium surfaces at 302°C., much more slowly than on antimony and arsenic surfaces. Nevertheless, in presence of minor amounts of arsine the rate of decomposition of germane is measurably

accelerated. Apparently, the deposition of As atoms in the germanium surface enhances the catalytic activity for germane decomposition.

Much more striking effects resulted from the introduction of small amounts of oxygen into the germane. Rapid reaction between the two gases occurs. The decomposition of residual germane on the oxygen-contaminated germane surface was markedly greater than on a pure germanium surface. Further, the accelerating influence persists through successive runs with pure germane. This indicates that the oxygen impurity retains its position and effect in the germanium *surface* in spite of further deposition of germanium in the decomposition process. The accelerating action of oxygen contamination in the germanium surface contrasts strikingly with the pronounced inhibitory effects of oxygen contamination on iron-synthetic ammonia catalysts.

DISCUSSION

The obvious conclusion from these researches is that while clean arsenic, antimony, and germanium surfaces activate the X—H bond in the several hydrides they none have any marked activation efficiency with respect to the H—H bonds in the temperature range 10 to 330°C. It follows that chemistry is involved in the process of chemisorption and that cleanliness of the elemental surface cannot substitute for the chemical factors involved. The influence of arsenic and oxygen impurities in the hydride decomposition processes on these surfaces is additional evidence in the same direction. It is expected that further studies, now in progress, will correlate these catalytic data with the growing body of data on the solid state physics of germanium.

The experience gained in the present studies makes it possible to approach the general problem of chemisorption of gases on these surfaces. Such work is in progress and will permit a correlation with the data that are being accumulated on the adsorption of gases on single crystals, notably of germanium, of such importance in the modern use of transistors.

ACKNOWLEDGMENTS

My thanks are due to Drs. Boudart, Fensham, and Tamaru for permission to make use of the data that are in process of detailed publication elsewhere. These postdoctoral workers have been assisted either by the fellowship provided to Princeton University by the Shell Fellowship Committee of the Shell Companies Foundation, Inc., of New York City, or by a research project sponsored by the Office of Naval Research, N6onr-27018 on Solid State Properties and Catalytic Activity. To both these sources of support I wish to express the indebtedness of Princeton University for their generous assistance.

REFERENCES

1. BEECK, O. Advances in catalysis. Academic Press, Inc., New York. 1950. p. 151.
2. Etudes de dynamique chimique. Muller and Co., Amsterdam. 1884. p. 83.
3. ROBERTS, J. K. Proc. Roy. Soc. (London), A, 152: 477. 1935.
4. STOCK, A., GOMOLKA, F., and HEYNEMANN, H. Ber. 40: 532. 1907.
   STOCK, A., ECHEANDIA, E., and VOIGT, P. R. Ber. 41: 1319. 1908.
5. TRAPNELL, B. M. W. Proc. Roy. Soc. (London), A, 218: 566. 1953.

PRELIMINARY STUDY OF PHOTOCHEMICAL BEHAVIOR IN THE SYSTEM NITROGEN DIOXIDE – ETHANE[1]

By T. M. Rohr[2] and W. Albert Noyes, Jr.

ABSTRACT

The addition of ethane to nitrogen dioxide either during exposure to radiation transmitted by pyrex, or afterwards, reduces the amount of oxygen formed. At room temperature this is apparently due to the effectiveness of ethane in promoting the reverse reaction of nitric oxide and oxygen to form nitrogen dioxide. At temperatures over 100° there is a reaction which uses oxygen atoms produced in the primary process. Nitroethane (or nitrosoethane) is formed along with carbon monoxide, carbon dioxide, and some methane. The results suggest that acetaldehyde is an intermediate, but acetaldehyde could not be detected because it would react thermally with nitrogen dioxide. It is not possible to give a complete explanation of the results, but suggestions can be made which might form the basis for later work.

The photochemical reaction between nitrogen dioxide and methane has been studied, but no evidence for reaction found (4). The oxygen atoms almost certainly produced in the primary process might react either with nitrogen dioxide or with methane, and the rate of the former reaction seemed to be sufficiently great to obscure the latter. Harteck and Kopsch (5) showed that oxygen atoms produced in a discharge tube react with ethane with an estimated activation energy of 7 kcal.

It was hoped in starting this investigation to obtain information both about the reactions of oxygen atoms with ethane and possibly also about the reactions of hydroxyl radicals. As so often happens, the course of the reaction is complex, and only suggestions can be made about some of the steps. A few semiquantitative estimates of relative rates can be made.

EXPERIMENTAL

Nitrogen dioxide was prepared by heating lead nitrate in a stream of oxygen, condensation by dry ice – acetone, and fractional distillation. The middle third was retained and stored at the temperature of liquid nitrogen. Stopcocks were lubricated with Myvacene-S (Dow-Corning) which proved not to be attacked by nitrogen dioxide as far as could be ascertained.

Ethane (Phillips Petroleum Company, Research Grade) appeared upon hydrogenation to contain traces of ethylene. It was mixed with nitrogen dioxide at 160° to remove ethylene and the ethane was distilled from a trap at −150°.

Mercury vapor was mostly kept out of the reaction cell by a trap immersed in dry ice – acetone. Final traces were eliminated by admission of nitrogen dioxide and evacuation just before a run. Initial pressures of reactants were measured by a Bourdon gauge.

[1]*Manuscript received January 7, 1955.*
Contribution from the Department of Chemistry, University of Rochester, Rochester, N.Y.
[2]*Postdoctoral Fellow 1952–54 under a grant made to the Department of Chemistry, of the University of Rochester, by the Doctors Camille and Henry Dreyfus Foundation.*

A Hanovia Alpine burner Type S-100 was used, and the radiation (except in the first series of runs) passed through Corning Filter No. 7740 to remove radiation below 3000 Å. The beam was collimated by a quartz lens and completely filled the cell which was 2.5 cm. in diameter and 20 cm. in length. A magnetically driven glass stirrer largely prevented the development of local concentration gradients.

Owing to the nature of the products the complete analysis proved to be difficult, and not all products have been completely identified.

The gases were condensed immediately after reaction to eliminate the reverse reaction

$$2NO+O_2 = 2NO_2. \qquad [1]$$

The products not condensed by supercooled liquid nitrogen at −210° were removed by a Toepler pump. These would consist of oxygen, nitrogen (if any), carbon monoxide, methane, and possibly traces of nitric oxide. The latter would, however, mainly be held back by formation of nitrogen trioxide with nitrogen dioxide. In a few runs when the nitrogen dioxide was nearly used up, nitric oxide might appear in this fraction.

Oxygen, carbon monoxide, and methane were determined by methods previously described (8).

The separation of condensable products proved to be difficult. Carbon dioxide could not be separated from the large amount of ethane present. After removal of the ethane at −155°, the residue was condensed in a cold finger subsequently filled with mercury. After a few hours' standing nitrogen dioxide was reduced to nitric oxide which could be pumped off at −150°. The remaining products were volatilized and burned to carbon dioxide over a copper oxide furnace at 650° and the pressure of carbon dioxide measured. Blank runs showed that nitroethane could be quantitatively determined in this way.

RESULTS

Blank runs showed no thermal reaction between nitrogen dioxide and ethane to occur at temperatures up to 160°, the highest temperature used in these experiments.

The results may be summarized briefly as follows:

(*a*) The addition of carbon dioxide (120 mm.) to nitrogen dioxide (5 mm.) did not affect the rate of production of gas uncondensed at −210°. Ratio of amounts with carbon dioxide to blanks at 108°: 1.03, 1.00.

(*b*) The addition of ethane (100 mm.) to nitrogen dioxide (5 mm.) reduces the amount of gas uncondensed at −210° (mainly oxygen) by the following ratios: 25° (1.09); 108° (0.54, 0.59); 160° (0.57).

In a series of experiments at 25° the oxygen yield was about the same whether or not ethane was added, and it was not influenced by variation in ethane pressure. The formation of condensable products in these experiments is probably due to impurities in the ethane, because with each successive run the amount diminished and it became zero after the sixth run.

In experiments at 108° and at 160° the decrease of the oxygen yield in the presence of ethane, compared to that either without ethane or merely with addition of carbon dioxide, cannot be explained by postulating that the missing oxygen is used for the oxidation of ethane even if one assumes the formation of products which escape detection by analysis. The presence of ethane favors the reaction of oxygen with nitric oxide as the following experiments showed.

If after radiation of 5 mm. of nitrogen dioxide at 160° for four hours the products were condensed immediately after turning off the light, one obtained 4.88×10^{-6} moles of oxygen. If the gases were condensed 30 min. after turning off the light, one obtained only 4.39×10^{-6} moles of oxygen. One tenth of the oxygen therefore was used by reacting with nitric oxide during this period of time. Addition of 50 mm. of ethane, immediately after radiation, greatly accelerated this reverse reaction since only 2.46×10^{-6} moles of oxygen were left after 30 min. Thus 50% was used in the same period.

(*c*) Nitroethane shows continuous absorption below about 3000 Å (2, 13), but no observable products were formed when the gas was irradiated under the conditions of the present experiments. Moreover there was no observable thermal reaction between nitroethane and nitrogen dioxide at temperatures up to 160°.

(*d*) When mixtures of nitrogen dioxide (5 mm.) and nitroethane (0.04 mm.) were irradiated, the rate of production of gas not condensed at −210° was unaffected by the presence of the nitroethane. When nitroethane was present at pressures of 27–35 mm., the yield of non-condensables was reduced to about half that in the blank runs. The non-condensables were oxygen and carbon monoxide. Products not volatile at −150° would not have been detected.

(*e*) When mixtures of ethane (usually 100 mm.) and of nitrogen dioxide (5 mm.) were irradiated at 160°, the gas uncondensed at −150° (measured as carbon dioxide, see above) was formed at a constant rate. In four runs of 4,

TABLE I

RESULTS WITH NITROGEN DIOXIDE – ETHANE MIXTURES
(P_{NO_2} = 5 mm., $P_{C_2H_6}$ ≈ 100 mm., T = 160°, Alpine burner, pyrex filter)

Time, hours	Products not condensable at −210° moles × 10^6			Products condensable at −150° (measured as CO_2)
	O_2	CO	CH_4 (or N_2)	
4	2.49	0.49	—	1.24
4	2.15	0.40	—	0.78
12	1.96	0.23	0	2.4
18	0.35	0.19	0.004	3.3
25.5	0.35 (total)			Not measured
42	0	0.45	0.013	Not measured
52.7	0	0.48	0.017	Not measured
52.7*	0	0.65	0.013	Not measured

**0.035 mm. oxygen added. This shows oxygen to disappear.*

12, 18, and 52.7 hr., the moles $\times 10^6$ formed per hour were 0.19, 0.20, 0.19, and 0.17, respectively. On the other hand, oxygen was formed in short runs but could not be detected at the end of long runs. Carbon monoxide was formed to an increasing extent along with small amounts of methane (or nitrogen). Table I shows the results.

(*f*) Some experiments were made with mixtures of nitrogen dioxide and of acetaldehyde as shown in Table II.

TABLE II

RESULTS WITH NITROGEN DIOXIDE – ACETALDEHYDE MIXTURES

(T = 160°, P_{NO_2} = 5 mm., P_{CH_3CHO} = 1.5 mm., Time: 4 hr., Alpine burner, pyrex filter)

Moles of products × 10^6				
O_2	CO	CH_4 (or N_2)	NO	CO_2
0[a]	0	0	0	0
			4.59	>9.0[b]
0[d]	0.22	0	>7.2	3.1
0	0.47	0	4.1	>9.0
[e]	0.89	0	0	>9.0
0[c]	0.20	0		

[a] *Blank with no nitrogen dioxide.*
[b] *Thermal reaction.*
[c] *100 mm. ethane also present.*
[d] P_{NO_2} = *2.5 mm.*
[e] P_{NO_2} = *10 mm.*

It is evident that there is a thermal reaction between nitrogen dioxide and acetaldehyde even at room temperature but that this reaction does not lead to methane formation.

DISCUSSION

The absorption characteristics of the system nitrogen dioxide – nitrogen peroxide have been carefully studied by Hall and Blacet (3). Since this mixture had a total pressure of 5 mm. in the present work, it can be shown from the data of Giauque and Kemp (1) that the pressure of nitrogen peroxide at 25° would be 0.17 mm. At wave lengths of 3130 and 3650 Å the absorption will be almost exclusively by nitrogen dioxide and not by nitrogen peroxide even at room temperature, and absorption by the latter will be entirely negligible at the higher temperatures used (1, 3).

The photochemistry of nitrogen dioxide has been carefully studied (7, 10). The primary process is undoubtedly

$$NO_2 = NO + O \qquad [2]$$

and this is followed by

$$O + NO_2 = O_2 + NO. \qquad [3]$$

The yield of the primary process must be high, and in the absence of foreign gases Equation [3] must occur nearly quantitatively. When foreign gases are added, Equation [3] will compete with other reactions of oxygen atoms. The latter, under conditions of the present experiments, are almost certainly

formed in the normal (^3P) state. Kinetic energies of the oxygen atoms after primary dissociation might be equivalent to 4 kcal. at 3650 Å and 8 kcal. at 3130 Å provided dissociation proceeds immediately before vibrational energy can be lost by collision. Unless steric factors are high for hot oxygen atom reactions, one would not expect to find noticeable "hot atom" effects.

If ethane is added to nitrogen dioxide, the first reaction of oxygen atoms should be

$$O+C_2H_6 = C_2H_5+OH. \quad [4]$$

The data show this reaction to be negligible at 25° compared to Equation [3] since (*a*) the amount of oxygen formed is almost the same in the presence and in the absence of ethane; (*b*) products condensed at −150° but not at −210° are negligible if the ethane has been previously exposed to radiation in the presence of nitrogen dioxide. Apparent reaction is due therefore to impurities in the ethane at this temperature.

The rate of the reaction

$$OH+C_2H_6 = C_2H_5+H_2O \quad [5]$$

is not known with precision but may have a low activation energy (12). The first reaction of ethyl radicals formed from either Equation [4] or Equation [5] should be

$$C_2H_5+NO_2 = C_2H_5NO_2 \quad [6]$$

where $C_2H_5NO_2$ is probably nitroethane but might be ethyl nitrite. Mass spectrographic analysis tends to favor the latter.

It is not possible to obtain a precise estimate of the activation energy of Equation [4]. From the results at 160° $E_4-E_3 \sim 3$ kcal. if Equation [3] and Equation [4] have the same steric factors. This result is probably low since with such a low activation energy and similar steric factors reaction [4] should compete more successfully than it does with reaction [3] at 25°. On the other hand if one takes 'condensables at −150°' divided by 'non-condensables at −210°' as a measure of the ratio of rate of Equation [4] to rate of Equation [3], one obtains from the results at 108° and at 160° a value of 8 kcal. This is based on results with considerable scatter and is not a reliable figure. One may merely say that probably the activation energy of Equation [4] is less than 10 kcal. in agreement with the work of Harteck and Kopsch (5). An activation energy of 5 kcal. or more is compatible with the results at 25°.

Oxygen atoms evidently do react with nitroethane but at a somewhat slower rate than with ethane. Hirschlaff and Norrish (6) suggest a reaction of oxygen atoms with nitroethane to give ethylene and the latter in the present system would give dinitroethane and would escape analysis by the procedure used. The probable formation of small amounts of methane and of larger amounts of carbon monoxide suggests that acetaldehyde is an intermediate. This could be formed easily from ethyl nitrite (11). This would disappear rapidly either by thermal reaction with nitrogen dioxide or by a reaction with radicals or excited molecules.

One of the striking points is the formation of oxygen during the early stages of the reaction and its subsequent disappearance. This would indicate that as

reaction proceeds, some radical or atom is produced which reacts much more rapidly with oxygen than with nitrogen dioxide and other molecules present. Not over 20% of the nitrogen dioxide would have disappeared during even the longest run. Thus this radical or atom must have a rate of reaction with oxygen of the order of magnitude of 10 to 100 times as fast as with nitrogen dioxide. Alkyl radicals may fulfill this requirement and so might possibly oxygen atoms.

The amount of carbon monoxide produced was not affected markedly by varying (*a*) the ethane pressure; (*b*) the nitrogen dioxide pressure; (*c*) the time. Blank runs showed that this lack of variation with conditions is not due to impurities.

Oxygen atoms react much less readily with carbon monoxide than with oxygen (9), but carbon monoxide may react with ozone or with peroxy radicals in the system. A detailed study of the reason why carbon monoxide apparently reaches a steady state might prove of interest.

ACKNOWLEDGMENT

This work was supported in part by contract with the Office of Naval Research, United States Navy. We wish to thank Mr. R. C. Wilkerson, Celanese Corporation of America, Clarkwood, Texas, for mass spectrographic analyses.

REFERENCES

1. GIAUQUE, W. F. and KEMP, J. D. J. Chem. Phys. 6: 40. 1938.
2. GOODEVE, J. W. Trans. Faraday Soc. 30: 504. 1934.
3. HALL, T. C., JR. and BLACET, F. E. J. Chem. Phys. 20: 1745. 1952. This article gives references to earlier work.
4. HARRIS, L. and SIEGEL, B. M. J. Am. Chem. Soc. 63: 2520. 1941.
5. HARTECK, P. and KOPSCH, U. Z. physik. Chem. B, 12: 327. 1931.
6. HIRSCHLAFF, E. and NORRISH, R. G. W. J. Chem. Soc. 1580. 1936.
7. HOLMES, H. H. and DANIELS, F. J. Am. Chem. Soc. 56: 630. 1934.
8. MARCOTTE, F. B. and NOYES, W. A., JR. Discussions Faraday Soc. No. 10. 236. 1951.
9. NOYES, W. A., JR. and LEIGHTON, P. A. The photochemistry of gases. Reinhold Publishing Corporation, New York. 1941. p. 253 gives a review of this subject.
10. NOYES, W. A., JR. and LEIGHTON, P. A. The photochemistry of gases. Reinhold Publishing Corporation, New York. 1941. p. 400 gives a review of this subject.
11. STEACIE, E. W. R. Atomic and free radical reactions. Vol. 1. Reinhold Publishing Corporation, New York. 1954. p. 239.
12. STEACIE, E. W. R. Atomic and free radical reactions. Vol. 2. Reinhold Publishing Corporation, New York. 1954. p. 607.
13. THOMPSON, H. W. and PURKINS, T. F. Trans. Faraday Soc. 32: 674. 1936.

FURTHER DEGRADATION REACTIONS OF ANNOTININE[1]

By F. A. L. Anet[2] and Léo Marion

ABSTRACT

Both the hydroxylactone obtained by the action of chromous chloride on annotinine chlorohydrin, and the unsaturated lactone B prepared by the action of the same reagent on the hydroxylactone, contain a secondary nitrogen and a vinyl group. The unsaturated lactone A which accompanies the hydroxylactone is a cyclic allylamine which on oxidation with potassium permanganate yields an amino acid $C_{14}H_{19}O_4N$. These facts make it possible to explain the reaction of chromous chloride with annotinine chlorohydrin. The amino acid can be dehydrogenated to an acid containing a free carboxyl and a lactamic grouping ($C_{14}H_{15}O_3N$) but no longer containing a lactone ring. The lactamic acid which seems to contain a benzene ring is readily decarboxylated to a neutral substance $C_{13}H_{15}ON$, showing color reactions and ultraviolet absorption similar to those of strychnine.

Annotinine, $C_{16}H_{21}O_3N$, was found (9) to react with hydrochloric acid to form annotinine chlorohydrin, $C_{16}H_{22}O_3NCl$, which was reduced (10) with chromous chloride to a mixture of "unsaturated lactone A", $C_{16}H_{21}O_2N$, and "hydroxylactone", $C_{16}H_{23}O_3N$. The latter compound on more vigorous treatment (10) with chromous chloride in strongly acidic solution gave "unsaturated lactone B", $C_{16}H_{21(23)}O_2N$. The two unsaturated lactones each contained a readily reducible double bond and gave two different dihydro-derivatives (10). The relationship of these compounds has now been clarified and affords supporting evidence for MacLean and Prime's suggestion (8) of the presence of the system 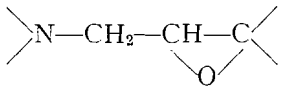 in annotinine and also for the modification of this scheme to 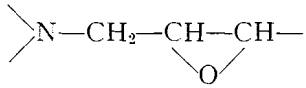 suggested by Wiesner *et al.* (6).

Following MacLean and Prime we can write 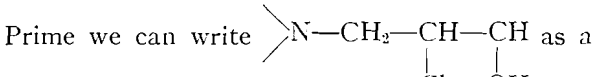 as a grouping in annotine chlorohydrin instead of 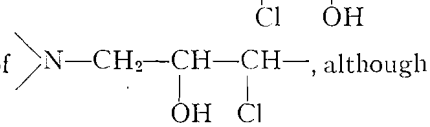 , although the evidence adduced by these authors for the former arrangement is meager. It does allow, however, of a simple interpretation for the chromous chloride reduction products, which is not possible with the alternate cleavage of the oxide ring of annotine (see below).

Chromous chloride is known to reduce various chlorinated derivatives of the senecio alkaloids, e.g., chloroisoheliotridene (i) by replacement of the halogen by hydrogen. Julian *et al.* (7) found that chromous chloride reduced

[1]*Manuscript received January 25, 1955.*
Contribution from the Division of Pure Chemistry, National Research Council, Ottawa, Canada. Issued as N.R.C. No. 3570.
[2]*National Research Council of Canada Postdoctorate Fellow. Present address: Department of Chemistry, University of Ottawa, Ottawa.*

steroid *vic*-dihalides to the corresponding unsaturated compounds. In both of these reductions, chromous chloride behaves in much the same way as does zinc in neutral or acidic conditions. Fieser and Ettore (5) found that zinc and acetic acid converted certain steroid *vic*-chlorohydrins to the olefins and therefore it would be anticipated that chromous chloride could effect the same reaction. Furthermore, it is only a simple extension to consider β-chloroamines which could react as below (see also Fig. 1)

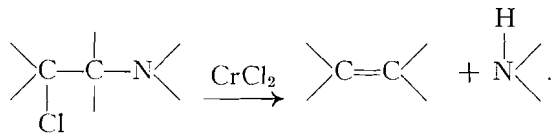

That this extension is not unjustified is shown by the work of Paul (11) who showed that the reduction by metallic sodium of cyclic ethers of *vic*-chlorohydrin and of β-chloro*tert*.amine proceeds analogously, e.g., in the case of tetrahydrofurfuryl chloride and β-chloroethyldiethylamine,

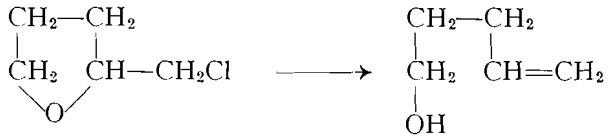

$$(C_2H_5)_2N{-}CH_2{-}CH_2Cl \rightarrow (C_2H_5)_2NH + CH_2{=}CH_2\,.$$

It was found in the present work that the hydroxylactone was unsaturated and yielded a dihydro-derivative on hydrogenation and formaldehyde on ozonolysis. Although the action of acetyl chloride failed to give the expected product (10), treatment of the hydroxylactone with acetic anhydride produced a neutral O,N-diacetyl derivative (infrared bands 1740 and 1678 $cm.^{-1}$ in Nujol). The hydroxylactone was obviously not formed by simple replacement of the chlorine of annotinine chlorohydrin by hydrogen, but its formation could be readily explained by analogy to the reactions outlined above.

The unsaturated lactone A would be expected to be the olefin VIII (Fig. 1) corresponding to annotinine chlorohydrin, and this was substantiated by the reactions of the unsaturated lactone A which behaved as a cyclic allylamine. Its pK_a was 7.06 whereas that of its dihydro-derivative was 8.48 (cf. Ref. 14), and it gave a methosulphate which was smoothly hydrogenolized in the presence of Adams' catalyst with the uptake of two moles of hydrogen and the formation of a tertiary base X ($C_{17}H_{27}O_2N$). Oxidation of the unsaturated lactone A with potassium permanganate yielded an amino acid XV isolated as the sulphate, $C_{14}H_{19}O_4N \cdot \frac{1}{2}H_2SO_4$, which was identical with the oxidation

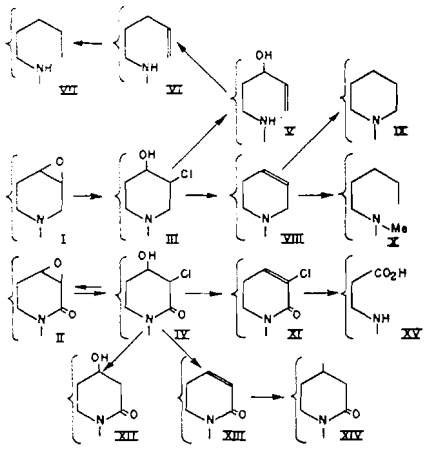

FIG. 1. Partial formulae of degradation products.

product obtained as described by Wiesner *et al.* (6) from the anhydro derivative of annotinine lactam chlorohydrin XI (8).

The relation of the unsaturated lactone B to the other products was obscured by the fact that its infrared spectrum showed no NH band although that of its dihydro-derivative did contain such a band. Yet it formed a neutral N-acetyl derivative (infrared band at 1762 cm.$^{-1}$) which yielded formaldehyde on ozonolysis. The easy reduction of the unsaturated lactone B to its dihydro-derivative, and the low intensity of its ultraviolet absorption at short wave lengths also indicated the presence of a terminal methylene group. The dihydrolactone B also gave a N-acetyl derivative (infrared band at 1755 cm.$^{-1}$).

The infrared spectra in carbon disulphide of the unsaturated lactone B and its dihydro-derivative were very similar and were consistent with the presence of a vinyl group in the former. We therefore assign the partial formulae VI and VII to these compounds respectively. This is also consistent with a re-investigation of the empirical formulae of this series which showed that the unsaturated lactone B was definitely $C_{16}H_{23}O_2N$ and not $C_{16}H_{21}O_2N$.

Annotinine lactam chlorohydrin (IV) which can be prepared either by oxidation (10) of annotinine chlorohydrin, or by treatment (8, 10) of annotinine lactam with hydrochloric acid gave two main products on chromous chloride reduction. These were identical with the compounds $C_{16}H_{21}O_4N$ and $C_{16}H_{19}O_3N$ prepared previously (8) by MacLean and Prime. Since the compound $C_{16}H_{21}O_4N$ was dehydrated (8) with phosphorus oxychloride to the second compound $C_{16}H_{19}O_3N$, the two products may be allotted the partial structures XII and XIII respectively. It may be noted that XIII is produced in the chromous chloride reduction under conditions that are not sufficient to dehydrate XII, which agrees with the mechanism proposed above. MacLean and Prime (8) found that catalytic or Clemmensen reduction of annotinine lactam chlorohydrin gave XII and XIV (Fig. 1). It is most probable that XII and XIII are the primary reduction products and that XIII is further reduced

to XIV. Indeed, as expected, XII could not be hydrogenated (8). The action of phosphorus oxychloride, or prolonged treatment with boiling hydrochloric acid convert (8) annotinine lactam chlorohydrin to a compound $C_{16}H_{18}O_3NCl$ which may be represented by XI (Fig. 1). Confirmation of the structures of XI and XIII is given by their ultraviolet spectra shown in Fig. 2 with those of

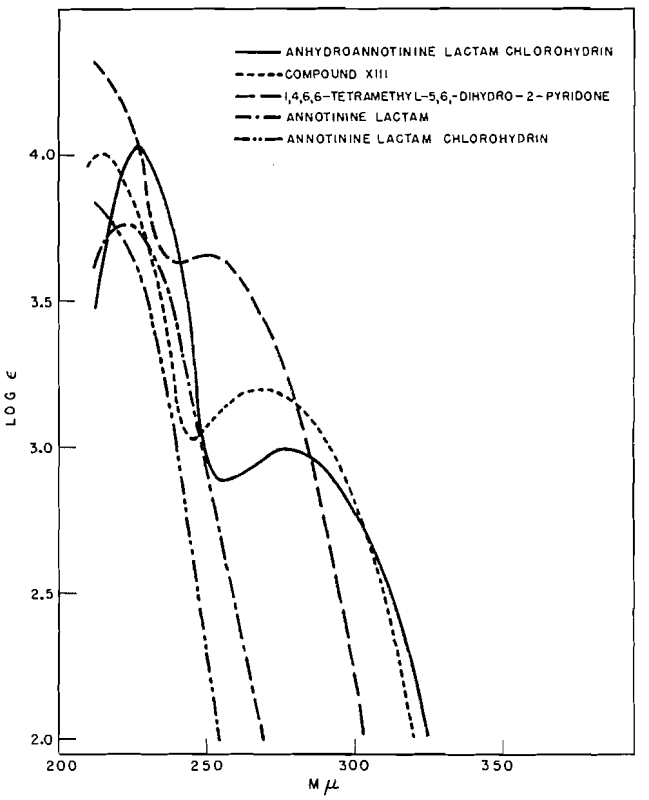

FIG. 2. Ultraviolet spectra in alcohol.

1,4,6,6-tetramethyl-5,6-dihydro-2-pyridone (12), annotinine lactam, and annotinine lactam chlorohydrin. The absorption bands of XI and XIII are at a longer wave length than would be expected when compared with the model compound, but there seems to be no doubt that a conjugated system is present. An $\alpha\beta$-unsaturated lactam system is also indicated by the infrared absorption spectra of XI and XII which contain two bands in the carbonyl region whereas the spectra of the saturated lactams contain only one band (cf. Edwards and Singh (4)). The spectra of all the compounds in Fig. 1 had a band at about 1780 cm.$^{-1}$ indicative of a γ-lactone group.

The amino acid XV, $C_{14}H_{19}O_4N$, was dehydrogenated in the presence of palladium on barium sulphate at 200–250° to an acid XVI, $C_{14}H_{13}O_3N$. The new acid no longer showed the γ-lactone band in its infrared spectrum but showed bands at 1715, 1620, and 1575 cm.$^{-1}$ in Nujol (curve 1, Fig. 4) and at

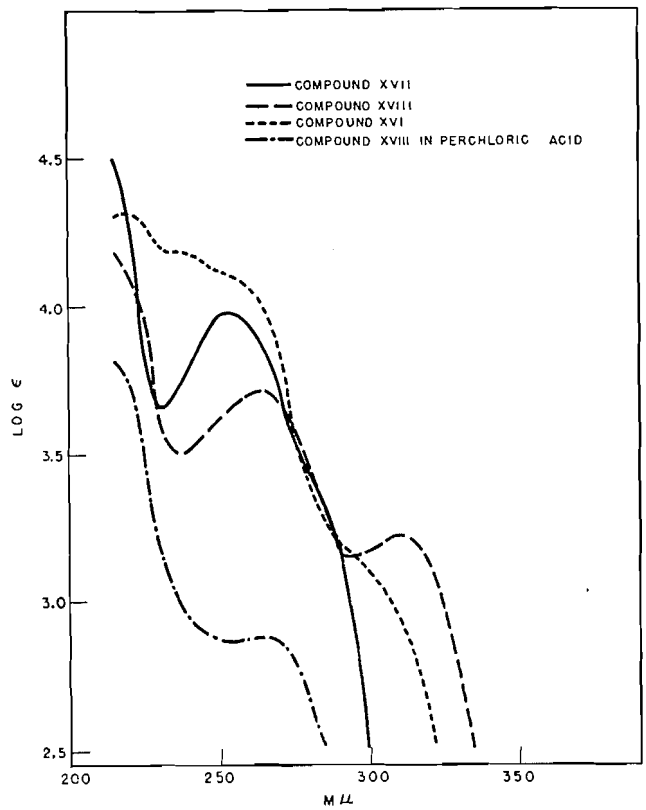

FIG. 3. Ultraviolet spectra.

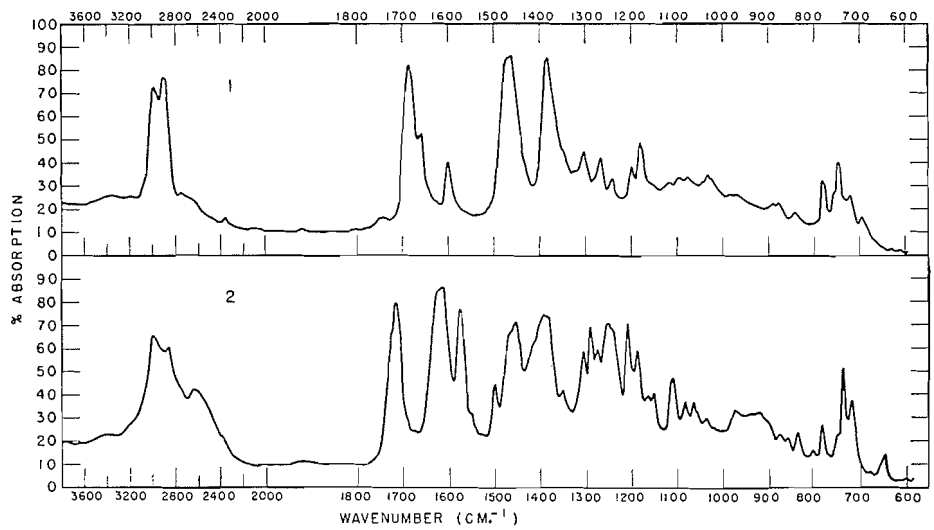

FIG. 4. Infrared absorption spectra: curve 1, compound XVI; curve 2, compound XVII.

1692, 1665, 1610, and 1575 cm.$^{-1}$ in chloroform solution which are consistent with the presence of a carboxyl, an amide group, and a benzene ring. The ultraviolet spectrum is shown in Fig. 3. The dehydrogenated acid was decarboxylated by heating with copper powder to a neutral compound XVII, $C_{13}H_{15}ON$ (m.p. 70°). The ultraviolet spectrum of XVII is shown in Fig. 3 and the difference from that of the acid indicates that the carboxyl group is directly attached to the chromophoric system in the acid. The infrared spectrum in Nujol contained no bands in the NH region, but bands at 1685 and 1660 cm.$^{-1}$ (weak) assigned to an amide group and at 1600 cm.$^{-1}$ (benzene ring) (curve 2, Fig. 4). The bands were shifted in chloroform solution to 1655 and 1600 cm.$^{-1}$. Although the compound appears not to contain an NH band it is probable that an NH group is present, for if a benzene ring is present, as is almost certain (see also below) the dehydrogenated acid must contain one less ring than the acid XV. A carbon–nitrogen fission seems more likely than a carbon–carbon fission, and would result in the formation of a NH group. The ultraviolet spectrum of XVII is very similar to that of strychnine (13) and like this alkaloid, XVII gave an intense violet color with 80% sulphuric acid and a trace of chromic acid (Otto reaction).

Unfortunately, we have not been able to secure more than very small amounts of XVII. Reduction of XVII with lithium aluminum hydride in ether solution gave a weak base, which formed a crystalline picrate, m.p. 172° (decomp.). The base XVIII gave an intense red color with nitric acid or with ferric chloride and its ultraviolet spectrum, shown in Fig. 3, is roughly similar to that of strychnidine (13). In strong acid the spectrum changed to that of an isolated benzene ring.

More drastic dehydrogenation of annotinine itself at 300° over palladium gave a small amount of 7-methylquinoline, isolated as the picrate. Wiesner *et al.* (3) have recently studied the selenium dehydrogenation of annotinine and have isolated 8-*n*-propylquinoline as well as another base and a neutral nitrogen-containing substance. The formation of both 7-methyl-and 8-*n*-propylquinoline in the dehydrogenation of annotinine under different conditions is puzzling. With reference to the neutral nitrogen containing substance obtained in the selenium dehydrogenation, it may be stated that the structure XIX suggested by Wiesner *et al.* (3) for this substance seems highly unlikely

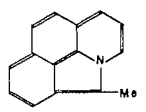

XIX

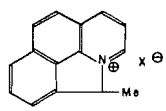

XX

as it is the anhydro base of XX and, therefore, would be expected to revert to the quaternary salt XX in the presence of acid.

On the other hand, the structure XXI that we suggested for annotinine in our preliminary note (2) does not explain the formation of 8-*n*-propylquinoline by dehydrogenation. According to the views of Wiesner *et al.* (6) on the relactonization of various annotinine derivatives to compounds containing a new γ-lactone, the acid XV should contain the grouping

O—C(=O)—C—C—CO_2H. Hence, the dehydrogenation of XV should give an *o*-phthalic acid derivative, because one of the carboxyl groups has been shown to be attached to a benzene ring. This is not so, however, for the other carboxyl group becomes involved in amide formation with the nitrogen atom that is attached to the benzene ring. Thus, the relactonization theory, although attractive, presents difficulties which can only be surmounted by assuming either a change in the carbon skeleton in the formation of XVI, or that the lactone ring in some of the derivatives of annotinine is larger than five-membered in spite of the infrared evidence.

It appears plausible that one of the rings in annotinine may be larger than six-membered and that the formation of quinoline derivatives in the dehydrogenations involves a rearrangement. However, formula XXI which we have tentatively suggested earlier (2) to represent annotinine possesses the merit

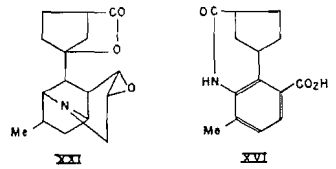

XXI XVI

that it permits the representation of the dehydrogenated acid XVI by a structure which is consistent with its ultraviolet absorption and its color reactions.

EXPERIMENTAL

Optical rotations were determined in a 1 dcm. tube. Ultraviolet absorption spectra were determined on a Beckmann spectrophotometer, Model D.U. Infrared absorption spectra were measured on a Perkin-Elmer double beam instrument, Model 21. Values of pK_a were determined in 50% methanol–water with a Beckmann pH meter (Model G) fitted with a glass and a calomel electrode; 0.1 *N* hydrochloric acid used for the titration was delivered from a microburette.

Unsaturated Lactone B

The compound prepared as described earlier (10) was twice crystallized from *n*-hexane from which it was obtained as colorless glistening prisms, m.p. 135–136°. Calc. for $C_{16}H_{23}O_2N$: C, 73.53; H, 8.87; 1 act. H, 0.386%. Found: C, 73.82; H, 8.86; (on sample sublimed at 10^{-4} mm.) C, 73.70, 73.79; H, 8.93, 8.82; act. H (at room temp.) 0.00%, (at 100°), 0.448%. $pK_a = 8.44$.

Dihydro Lactone B

The compound prepared as described before (10) was recrystallized from *n*-hexane and dried *in vacuo* at room temperature. Calc. for $C_{16}H_{25}O_2N$: C, 72.96; H, 9.57. Found: C, 73.12; H, 9.34%. $pK_a = 8.44$.

Acetyl Unsaturated Lactone B

Unsaturated lactone B (25 mgm.) in acetic anhydride (5 ml.) was heated on a steam bath for half an hour. The mixture was poured into water and after

hydrolysis of the excess acetic anhydride, made alkaline with sodium hydroxide and extracted with ether. The ether extract was washed with acid and then with water, dried, and evaporated. The residue, after recrystallization from *n*-hexane, had m.p. 137–138°, depressed to 125° by the starting product. Calc. for $C_{18}H_{25}O_3N$: C, 71.25; H, 8.31. Found: C, 70.96; H, 8.17.

Acetyl Dihydro Lactone B

This compound was prepared as described above for the unsaturated analogue and after recrystallization from *n*-hexane it formed fine needles, m.p. 141–142°. Calc. for $C_{18}H_{27}O_3N$: C, 70.79; H, 8.91. Found: C, 71.11, 71.44; H, 8.92, 8.86.

Unsaturated Lactone A

The compound (10) after sublimation *in vacuo* had m.p. 130–132°; pK_a, 7.06; $[\alpha]_D^{24} = -70°$ (*c*, 2.6 in ethanol).

Dihydro Lactone A

The compound (10) after sublimation *in vacuo* had m.p. 110°; pK_a, 8.48; $[\alpha]_D^{24} = -35°$ (*c*, 1.4 in ethanol).

Hydroxylactone

A sample of hydroxylactone (10) was sublimed *in vacuo* after which it had m.p. 174°; pK_a, 8.21; $[\alpha]_D^{22}$ −30° (*c*, 1.42 in ethanol).

Dihydro Hydroxylactone

Hydroxylactone (0.25 gm.) in methanol (15 ml.) was hydrogenated in the presence of Adams' catalyst (20 mgm.). Absorption of 23.4 ml. of hydrogen (*ca.* 1 mole) was complete after 2.5 minutes. The platinum was filtered off and the filtrate evaporated to dryness. Recrystallization of the residue from *n*-hexane gave long brittle needles, m.p. 141–142°. For analysis the compound was sublimed *in vacuo*. Calc. for $C_{16}H_{25}O_3N$: C, 68.78; H, 9.02. Found: C, 68.97; H, 9.26%. pK_a, 8.00; $[\alpha]_D^{22}$ −65° (*c*, 1.47 in ethanol). The dihydroxylactone was unaffected by prolonged boiling with chromous chloride in concentrated hydrochloric acid.

Ozonolysis of Hydroxylactone

Hydroxylactone (80 mgm.) in pure carbon tetrachloride (15 ml.) was ozonized at −10° for about two minutes. Water (10 ml.) and hydrochloric acid (1 ml.) were added, followed by a hot saturated solution of 2,4-dinitrophenylhydrazine in 15% hydrochloric acid (5 ml.). The mixture was refluxed for 15 min., cooled, and extracted with benzene (twice). The dried extract was evaporated to 20 ml. and the yellow solution passed through a short column of neutral alumina (activity II–III), which was then washed with a little benzene. The eluate was evaporated to dryness *in vacuo* and the residue crystallized from hexane. Yellow needles (14.6 mgm. 24%), m.p. 162–163°, were obtained. There was no depression of melting point with authentic formaldehyde 2,4-dinitrophenylhydrazone of m.p. 163–164°, and the infrared absorption spectra of the two compounds were identical.

Ozonolysis of Acetyl Unsaturated Lactone B

The lactone (63 mgm.) was ozonized in carbon tetrachloride solution (10 ml.) at 0° until ozone appeared from the guard tube containing water (10 ml.). The combined water and carbon tetrachloride solution was boiled for half an hour and then mixed with a solution of 2,4-dinitrophenylhydrazine in hydrochloric acid. The cooled mixture was extracted three times with benzene, and the combined dried extract passed through a column of alumina which was then washed with benzene. The benzene eluate gave on evaporation formaldehyde 2,4-dinitrophenylhydrazone (3.5 mgm.), m.p. 160–161°, undepressed by the authentic compound. Elution of the column with benzene containing methanol (3%) gave a fraction which, after two crystallizations from methanol, was obtained as yellow needles, m.p. 218–219°, and was not further investigated.

Unsaturated Lactone A Methosulphate

Unsaturated lactone A (200 mgm.) was dissolved in benzene (5 ml.) and allowed to stand 40 hr. with freshly distilled dimethyl sulphate (0.2 gm.). The faintly yellow prisms which separated were collected and recrystallized from methanol–ether. The methosulphate formed colorless prisms, m.p. 234–235°. Calc. for $C_{16}H_{21}O_2N\cdot(CH_3)_2SO_4$: C, 56.09; H, 7.06. Found: C, 56.28; H, 7.23.

Reduction of Unsaturated Lactone A Methosulphate

Unsaturated lactone A methosulphate (72 mgm.) was hydrogenated in water (10 ml.) in the presence of Adams' catalyst (7 mgm.). Absorption of 2 moles of hydrogen took 15 min. The filtered solution was made alkaline with ammonia and the glistening needles which separated were collected. The base was recrystallized from *n*-pentane and for analysis was sublimed *in vacuo*, m.p. 90–91°. Calc. for $C_{17}H_{27}O_2N$: C, 73.60; H, 9.81. Found: C, 73.67; H, 9.89%.

O,N-diacetyl Hydroxy Lactone

Hydroxylactone (60 mgm.) was heated at 100° with acetic anhydride (4 ml.) for three hours and the mixture then diluted with water (10 ml.) and kept for two hours. The mixture was extracted three times with ether and the combined extracts were washed with aqueous sodium carbonate and then with water. The residue obtained after evaporation of the ether from the dried extract crystallized from hexane in prisms, m.p. 124–126°. After several crystallizations the melting point was raised to 132–133°. Calc. for $C_{20}H_{27}O_5N$: C, 66.46; H, 7.53. Found: C, 66.62; H, 7.85%.

Chromous Chloride Reduction of Annotinine Lactam Chlorohydrin

Annotinine lactam (1.69 gm.) was boiled with concentrated hydrochloric acid (40 ml.) for 40 min. To the mixture was added, in an atmosphere of nitrogen, a filtered solution of chromous chloride, prepared from chromic chloride (30 gm.), concentrated hydrochloric acid (40 ml.), water (60 ml.), and amalgamated zinc (25 gm.). The mixture was refluxed under nitrogen for

2.5 hr., diluted with water (500 ml.), and the cold solution extracted with chloroform four times (total volume: 200 ml.). The dried extract was evaporated to dryness *in vacuo*. The residue (0.84 gm.) was triturated with benzene, filtered, and crystallized from aqueous ethanol from which it separated as prisms, m.p. 300° (decomp.), undepressed by the compound $C_{16}H_{21}O_4N$ prepared as described by MacLean and Prime (8). The benzene solution was chromatographed on alumina (activity II–III). Elution with benzene gave a small amount of low melting product, followed by a main fraction (0.4 gm.), m.p. 174–175° after crystallization from acetone–pentane. It was identical (mixed m.p.) with the compound $C_{16}H_{19}O_3N$ prepared as described by MacLean and Prime (8). Hydrogenation of this compound (0.1 gm.) with Adams' catalyst (20 mgm.) in ethanol (20 ml.) resulted in the uptake of 1 mole of hydrogen and the substance isolated had m.p. 176–177° identical with the compound $C_{16}H_{21}O_3N$ of MacLean and Prime.

Oxidation of Unsaturated Lactone A

The unsaturated lactone A (1 gm.) was dissolved in acetone (100 ml.) and treated with powdered potassium permanganate until the pink color was unchanged for five minutes. The filtered manganese dioxide was suspended in water and brought into solution by passing sulphur dioxide through the solution. Continuous ether extraction of the mixture gave after evaporation of the ether a viscous liquid containing some crystals. The product was crystallized from methanol–ether to yield colorless prisms (0.25 gm.), m.p. 232° (decomp.); $[\alpha]_D^{25}$ −31° (*c*, 1.7 in water) of the sulphate of XV. Calc. for $C_{14}H_{19}O_4N \cdot \frac{1}{2}H_2SO_4$: C, 53.48; H, 6.41. Found: C, 53.67; H, 6.64%. The compound was identical as shown by infrared spectra and mixed melting point with the amino acid sulphate prepared as described by Wiesner *et al.* (6) (see below). The compound showed only end absorption in the ultraviolet (log ϵ, 2.58 at 210 mμ).

Oxidation of Anhydro Annotinine Lactam Chlorohydrin (XI)

Annotinine lactam chlorohydrin (10) (1.83 gm.) was dissolved in dry pyridine (80 ml.) and mixed with phosphorus oxychloride (3 ml.). The mixture became warm and was kept for five hours at room temperature. It was poured into water, the pyridine neutralized with hydrochloric acid, and the mixture extracted with chloroform (four times). The combined extract was dried and evaporated to dryness. The residue was crystallized from methanol giving a total of 1.53 gm. of product, m.p. 186–187°. This modification gave a much better yield of XI than MacLean and Prime's method (8). Anhydro annotinine lactam chlorohydrin (0.95 gm.) in acetone (200 ml.) was oxidized with potassium permanganate (1.35 gm.). The mixture was worked up as described above and gave 0.3 gm. of the sulphate of XV, m.p. 232° (decomp.).

Dehydrogenation of $C_{14}H_{19}O_4N$ (XV)

The above amino-acid sulphate (0.13 gm.), barium carbonate (0.04 gm.), and 5% palladium – barium sulphate (0.5 gm.) were mixed and stirred with water (0.5 ml.). The dried mixture was heated in an atmosphere of nitrogen at 200° for one hour and the temperature was gradually raised to 250° during the

course of three hours. The product was extracted with ether several times, and the ether extract washed with acid. The ether was then extracted with 5% sodium carbonate solution. The ether solution generally contained a small amount of XVII formed by decarboxylation of XVI. The aqueous extract was acidified with hydrochloric acid and extracted with ether. Evaporation of the dried extract left a residue, crystallizing from benzene–pentane in colorless needles (0.018 gm.), m.p. 250° (decomp.); $[\alpha]_D^{25}$ +47° (*c*, 0.9 in ethanol). Calc. for $C_{14}H_{15}O_3N$: C, 68.55; H, 6.16; N, 5.71; equiv. wt. 245.3. Found: C, 68.90, 68.71; H, 6.35, 6.19; N, 5.87; equiv. wt. 250.

Decarboxylation of the Acid $C_{14}H_{15}O_3N$ (XVI)

The acid $C_{14}H_{15}O_3N$ (10 mgm.) was mixed with copper powder (20 mgm.) in a tube. The mixture was heated with a free flame, when a colorless oil distilled on the cooled parts of the tube. The oil crystallized on cooling and was purified by repeated sublimation *in vacuo*. The colorless prisms then had m.p. 70° and gave an intense violet color when a trace of the compound in 80% sulphuric acid was treated with a few drops of dilute chromic acid. Calc. for $C_{13}H_{15}ON$: C, 77.58; H, 7.51. Found: C, 77.40; H, 7.45%.

Lithium Aluminum Hydride Reduction of $C_{13}H_{15}ON$ (XVII)

The neutral compound $C_{13}H_{15}ON$ (10 mgm.) in dry ether was refluxed with a large excess of lithium aluminum hydride in ether for three hours. The mixture was decomposed with water and sodium hydroxide, and the ether layer separated and mixed with ethereal picric acid. The precipitate was recrystallized from methanol–ether when it was obtained as yellow prisms, m.p. 172° (decomp.). The regenerated base was obtained as an oil which gave an intense red color with ferric chloride solution and with concentrated nitric acid. There was insufficient pure material for elementary analysis.

Dehydrogenation of Annotinine

Annotinine (1.2 gm.) was mixed with 5% palladium – barium sulphate (1 gm.) and heated to 310° during the course of two hours. The cooled mixture and distillate was extracted twice with ether (10 ml. in all). The ether solution was extracted three times with dilute hydrochloric acid and the combined extract made strongly alkaline with sodium hydroxide. The mixture was distilled until 10 ml. of distillate had collected. The distillate was extracted with ether, and the ether evaporated. The residue was mixed with picric acid in methanol (3 ml.), and the crystals, which formed gradually, were collected by centrifugation. Three more crystallizations from methanol gave long yellow needles, m.p. 238–240°, and in admixture with 7-methylquinoline picrate of m.p. 240–241°, 239–241°. The infrared spectra of the two samples were virtually identical. The original ether extract containing the neutral products from the dehydrogenation gave a strong Ehrlich reaction in the cold and possibly contained indole derivatives, but no crystalline picrate was obtained.

ACKNOWLEDGMENT

The authors wish to express their gratitude to Dr. R. Norman Jones and Mr. R. Lauzon of these laboratories for taking the infrared absorption spectra.

REFERENCES

1. ADAMS, R. and MAHAN, J. G. J. Am. Chem. Soc. 65: 2009. 1943.
2. ANET, F. A. L. and MARION, L. Chemistry & Industry, 1232. 1954.
3. BANKIEWICZ, C., HENDERSON, D. R., STONNER, F. W., VALENTA, Z., and WIESNER, K. Chemistry & Industry, 1068. 1954.
4. EDWARDS, O. E. and SINGH, T. Can. J. Chem. 32: 683. 1954.
5. FIESER, L. F. and ETTORE, R. J. Am. Chem. Soc. 75: 1700. 1953.
6. HENDERSON, D. R., STONNER, F. W., VALENTA, Z., and WIESNER, K. Chemistry & Industry, 544. 1954; 852. 1954.
7. JULIAN, P. L., COLE, W., MAGNANI, A., and MEYER, E. W. J. Am. Chem. Soc. 67: 1728. 1945.
8. MACLEAN, D. B. and PRIME, H. C. Can. J. Chem. 31: 543. 1953.
9. MANSKE, R. H. F. and MARION, L. J. Am. Chem. Soc. 69: 2126. 1947.
10. MEIER, H. L., MEISTER, P. D., and MARION, L. Can. J. Chem. 32: 268. 1954. MEIER, H. L. and MARION, L. Can. J. Chem. 32: 280. 1954.
11. PAUL, R. and TCHELITCHEFF, S. Compt. rend. 238: 2089. 1954; PAUL, R. and RIOBE, O. Compt. rend. 224: 475. 1947.
12. PICCINI, G. Atti accad. sci. Torino, 43: 554. 1907.
13. PRELOG, V. and SZPILFOGEL, S. Helv. Chim. Acta, 28: 1169. 1945.
14. VEXLEARSCHI, G. and RUMPF, P. Compt. rend. 236: 939. 1953.

FREE RADICALS BY MASS SPECTROMETRY

VII. THE IONIZATION POTENTIALS OF ETHYL, ISOPROPYL, AND PROPARGYL RADICALS AND THE APPEARANCE POTENTIALS OF THE RADICAL IONS IN SOME DERIVATIVES[1]

By J. B. Farmer[2] and F. P. Lossing

ABSTRACT

The ionization potentials of ethyl, isopropyl, and propargyl radicals have been measured by electron impact on radicals produced by thermal decomposition of appropriate compounds. The values are: ethyl 8.78±0.05 ev., isopropyl 7.90±0.05 ev., and propargyl 8.25±0.08 ev. From the appearance potentials of these ions in various compounds, the following values of bond dissociation energies were obtained:

$D(C_2H_5—H) = 98.5\pm2.3$, $D(s\text{-}C_3H_7—H) = 86.7\pm2.3$,
$D(s\text{-}C_3H_7—I) = 42.4\pm2.3$, $D(s\text{-}C_3H_7—Br) = 58.8\pm2.3$,
$D(s\text{-}C_3H_7—Cl) = 73.3\pm2.3$, $D(CH{:}C.CH_2—I) = 45.7\pm3.2$,
$D(CH{:}C.CH_2—Br) = 57.9\pm3.2$ kcal./mole, assuming no kinetic energy of the products.

INTRODUCTION

The ionization potential of the ethyl radical was measured by Fraser and Jewitt (5) by directing a beam of ethyl radicals and other products from the decomposition of lead tetraethyl into an ionization gauge detector. They found $I(C_2H_5) = 10.6\pm0.8$ ev., a value which was undoubtedly too high because of the presence of reaction products such as ethylene. Hipple and Stevenson (7) measured the ionization potential of the ethyl radical by electron impact on radicals produced by the thermal decomposition of lead tetraethyl in a quartz capillary furnace opening into the ionization chamber of a mass spectrometer. By this means they found $I(C_2H_5) = 8.67\pm0.1$ ev., a value which, taken in conjunction with the appearance potential of $C_2H_5^+$ in the mass spectrum of ethane, 12.92±0.1 ev. (23), led to a dissociation energy of the C_2H_5—H bond of 4.25±0.2 ev. or 98.0±4.6 kcal./mole. This is in good agreement with the average electron impact value of 4.20±0.04 ev. (96.9±1 kcal./mole) recently quoted by Stevenson (21) and the value of 98±2 kcal./mole obtained by photobromination (1).

The ionization potential of the isopropyl radical has not previously been measured directly, but a value of 7.45±0.1 ev. has been derived from the appearance potentials of $C_3H_7^+$ in the mass spectra of isobutane, isopentane, and 2,3-dimethyl butane, the heats of formation of these compounds, and the bond dissociation energies of CH_3—H and C_2H_5—H (20). This value, together with the appearance potential of the $C_3H_7^+$ ion in the mass spectrum of propane, 11.67±0.1 ev. (24), leads to a dissociation energy for the s-C_3H_7—H bond of 4.22±0.2 ev. (97.3±4.6 kcal./mole). This appears to be high by comparison with Stevenson's electron impact average of 4.09±0.09 ev.

[1]*Manuscript received January 14, 1955.*
Contribution from the Division of Pure Chemistry, National Research Council, Ottawa, Canada. Issued as N.R.C. No. 3571.
[2]*N.R.C. Postdoctorate Fellow 1953–1955.*

(94.3±2 kcal./mole) and with the Butler and Polanyi pyrolysis value of ~89 kcal./mole (19).

As far as the authors are aware, no published measurements or predictions of the ionization potential of the propargyl radical ($CH{:}C.CH_2$) have been made. The radical does not appear to have been identified previously, although it has been suggested that its thermal stability might be high (27).

EXPERIMENTAL

Production of the Radicals

The fact that ethyl and isopropyl radicals are much less stable thermally than methyl, allyl, or benzyl radicals, whose ionization potentials were reported in an earlier paper (13), required a modification of the reactor used previously. In a reactor of the type described in earlier papers (14, 15) the residence time was sufficiently long to allow the disappearance of an appreciable fraction of the radicals at the temperature (~660°C.) at which mercury diethyl or azoisopropane decomposed. Although these radicals were found in considerable abundance under these conditions (12), the presence of appreciable amounts of the decomposition, disproportionation, and combination products caused serious interference at the parent peak of the radical. In order to reduce this interference a furnace was constructed in which the residence time would be shorter. This furnace was similar in design to that used by Hipple and Stevenson (7) and consisted of a quartz tube of 1.5 mm. internal diameter surrounded at the end by a heater, 2 cm. in length, cut from tantalum sheet in the shape previously described (15). The heater was enclosed in a quartz sheath sealed to the end of the quartz tube. A cylindrical radiation shield of Nichrome V surrounded the sheath. The furnace was mounted coaxially with the hole in the top plate of the ionization chamber, at a distance of about 1 mm. The compound was admitted to the reactor through a molecular-flow leak without the use of helium as a carrier. With this arrangement the pressure in the reactor was very low (~10^{-3} mm.) and second-order products were considerably reduced. The dissociation products of the radicals were still present but in reduced amounts.

(*a*) *Ethyl Radicals*

The decomposition of mercury diethyl at about 800°C. gave rise to ethyl radicals, butane, ethane, ethylene, and hydrogen. A small amount of undecomposed mercury diethyl was also present. Out of a combined peak height of 497 cm. at mass 29 using 50 ev. electrons, a net peak height of 249 cm. for the ethyl radical was obtained after subtraction of the contributions from ethane, butane, $C^{12}C^{13}H_4$, and mercury diethyl. The ratio of ethane to butane at 800°C. was 0.36:1. This ratio of disproportionation (k_1) to combination (k_2) (0.36) is not greatly different from that found ($k_1/k_2 = 0.1$ to 0.3) at lower temperatures (2, 10). If significant, this result would suggest that

$$E_{\text{combination}} \simeq E_{\text{disproportionation}}.$$

However, at the very low pressures involved (~10^{-3} mm.) it is questionable whether the ethane and butane arise from homogeneous disproportionation

and combination reactions rather than from surface reactions. Some butane may also be formed directly from mercury diethyl under these conditions.

(*b*) *Isopropyl Radicals*

As in the case of ethyl, the production of a high concentration of isopropyl radicals presented experimental difficulties owing to the thermal instability of the radicals. In the high pressure reactor, the decomposition of azoisopropane in a stream of helium at 6.5 mm. was almost complete at 665°C. The increase in the mass 43 peak at low electron energies showed the isopropyl radical to be present. At this temperature some isopropyl radicals were decomposing, the products being propylene and hydrogen almost exclusively (12). By the use of a retractable furnace (9) in the high pressure reactor, the product of dimerization of the radicals was found to be mainly 2,3-dimethyl butane with a small amount of another hexane, possibly 2-methyl pentane, showing that the radicals were indeed isopropyl radicals. In the low pressure reactor, azoisopropane was 90% decomposed at 655°C. At this temperature the mass 43 peak height was 1030 cm. After subtracting the contributions from 2,3-dimethyl butane, propane, and undecomposed azoisopropane, a peak height of 329 cm. for the isopropyl radical remained.

(*c*) *n-Propyl Radicals*

Attempts to produce the *n*-propyl radical in quantities sufficient for ionization potential measurements were unsuccessful. The decomposition of azo-*n*-propane at 665°C. in the high pressure reactor resulted in the formation of methyl radicals and ethylene in approximately equal amounts, together with nitrogen, *n*-hexane, propane, propylene, and some ethane formed from the combination of the methyl radicals (12). The mode of decomposition of *n*-propyl appears to be almost entirely by

$$n\text{-}C_3H_7 \rightarrow CH_3 + C_2H_4$$

and not by

$$n\text{-}C_3H_7 \rightarrow C_3H_6 + H.$$

This is in agreement with conclusions drawn from kinetic studies (19).

(*d*) *Propargyl Radicals*

The decomposition of propargyl iodide at 1000–1100°C. in either the high-pressure or the low-pressure reactor resulted in a good yield of propargyl radicals. The dimer, 1,5-hexadiyne, was also formed.

Measurement of the Ionization Potentials

The method of calibrating the voltage scale using a number of standards was the same as that used previously (13). In this case the calibration line was found to have a slope of unity within the precision of measurement. Krypton was added to the gas stream as a reference standard, and the difference between the appearance potential of the radical peak and the appearance potential of the krypton mass 84 peak was determined by the method of extrapolated voltage differences (28). The net peak height for the radical ion at 50 ev. was determined by subtracting the contributions from dimers and other prod-

ucts as described above. Ionization efficiency curves for the radical ions from these products were measured to ensure that no contributions to the peaks could occur at the low electron energies at which the voltage difference measurements were made. The only correction of this kind found to be necessary was a small correction to the krypton mass 84 peak as a result of the 2,3-dimethyl butane formed from isopropyl radicals. This correction was evaluated from measurements of the mass 84 peak in the absence of krypton, other conditions being the same.

Measurement of the Appearance Potentials

As found by Stevenson and Hipple (23) a significant correction to the mass 29 peak was required in the measurement of $A(C_2H_5^+)$ from ethane. The appearance potential of $C_2H_4^+$ from ethane is appreciably lower than that of $C_2H_5^+$ (23). Consequently the mass 28 peak is many times as high as the mass 29 peak at electron energies a few volts above $A(C_2H_5^+)$. The isotopic $C^{12}C^{13}H_4^+$ peak from $C_2H_4^+$ was found to account for almost one-third of the mass 29 peak under these conditions. The correction to mass 29 was calculated from the natural abundance of C^{13} assuming that no difference in the ionization efficiency curves of $C^{12}C^{12}H_4^+$ and $C^{12}C^{13}H_4^+$ or in the ratio of formation of the ions would occur as a result of isotopic factors. This correction raised the observed value of $A(C_2H_5^+)$ by about 0.2 ev. as was found by Stevenson and Hipple (23).

The ionization efficiency curves for $A(C_2H_5^+)$ from the halides showed curved δV vs. I plots and the extrapolated values being apparently low by 0.4 to 0.6 ev. are not reported here. The cause of this discrepancy is not obvious. I^- ions from the iodide were found, but only to the extent of about one part in 6000 of the $C_2H_5^+$ ion. This amount should not appreciably lower the appearance potential, and in any case the ion may arise by a secondary process. The formation of ethyl radicals by pyrolysis on the filament followed by diffusion back into the ionization chamber would lower the observed appearance potential. However, it is difficult to see, in view of the thermal instability of ethyl, why this effect should be larger than for the more stable methyl or allyl radicals.

The appearance potential of the mass 39 ion from propyne was not measured since this ion may arise by two different processes

$$CH{:}C.CH_3 + e \rightarrow CH{:}C.CH_2^+ + H + 2e \quad [1]$$
$$CH{:}C.CH_3 + e \rightarrow C{:}C.CH_3^+ + H + 2e \quad [2]$$

depending on which hydrogen atom is lost. In order to find out the extent to which process [2] occurs, the mass spectrum of a sample of $CH{:}C.CD_3$, kindly prepared by Dr. L. C. Leitch, was examined. The isotopic purity of the sample was determined from the mass spectrum obtained with electrons of energy sufficient to form the molecular ion but insufficient to form dissociation products (25). As shown in Table I, the sample was about 80% $CH{:}C.CD_3$.* In the 50-volt spectrum, after the parent ions have been subtracted in the

**The improbable rearrangement product $CD{:}C.CD_2H$ was assumed to be absent.*

ratio of their abundance, the fragment ion at mass 42 can arise only by

$$CH{:}C.CD_3 + e \rightarrow C{:}C.CD_3^+ + H + 2e \quad [3]$$

and that at mass 41 mainly by

$$CH{:}C.CD_3 + e \rightarrow CH{:}C.CD_2^+ + D + 2e \quad [4]$$

with a small contribution from the impurity

$$CH{:}C.CD_2H + e \rightarrow CH{:}C.CD_2^+ + H + 2e. \quad [5]$$

TABLE I

MASS SPECTRA OF TRIDEUTEROPROPYNE

Mass No.	Peak height at low energy	Mole %	Peak height at 50 ev.	Parent ions	Fragment ions
44	0.2	1.1	—	—	—
43	15.0	79.4	2015	2015	—
42	2.8	14.8	798	376	422
41	0.5	2.7	1482	69	1413
40	0.35	2.0	—	—	—

If the contribution from process [5] is ignored, the ratio H loss/D loss from $CH{:}C.CD_3$ is then 422/1413 = 0.30. It is possible, however, to correct for process [5] on the assumption that its probability is one half the sum of the probabilities of process [1] and process [2]. The contribution of process [5] to the mass 41 peak is then $376 \times \frac{1}{2} \times$ ratio mass 39/mass 40 in propyne (0.859). The fragment peak at mass 41 resulting from process [4] is then $1413 - (376 \times \frac{1}{2} \times 0.859) = 1252$, and the corrected ratio of H loss/D loss is 422/1252 or 0.337. This is almost exactly $\frac{1}{3}$, suggesting that after a propyne molecule has been struck by a 50-volt electron, the four hydrogens in the excited ion are equivalent and the loss of a hydrogen atom from either end occurs on a statistical basis. Unfortunately the isotopic purity of the sample was not sufficiently high to give appearance potentials for processes [3] and [4] free from interference.

The same inherent ambiguity exists in the mass 43 peak from propane. It has, however, been reported that this ion is mainly $s\text{-}C_3H_7^+$ (18, 26). In addition, it is possible to say that the process

$$C_3H_8 + e \rightarrow s\text{-}C_3H_7^+ + H + 2e \quad [6]$$

will have a lower appearance potential than the process

$$C_3H_8 + e \rightarrow n\text{-}C_3H_7^+ + H + 2e \quad [7]$$

since (21) $I(n\text{-}C_3H_7) > I(s\text{-}C_3H_7)$ and $D(n\text{-}C_3H_7\text{—}H) > D(s\text{-}C_3H_7\text{—}H)$. In view of these considerations it is very probable that $A(C_3H_7^+)$ corresponds to process [6] and that the derived dissociation energy can be assigned to the $s\text{-}C_3H_7\text{—}H$ bond.

RESULTS AND DISCUSSION

The individual and average values obtained for the ionization potentials of the three radicals are given in Table II, together with some measured and calculated values from the literature. The appearance potentials of the radical ions from the derivatives are given in Table III. The dissociation energies for the radical–atom bonds, derived on the assumption that no kinetic energy term is involved, are also given in Table III for comparison with values from the literature. The limits of error shown should be regarded as limits of precision and not of absolute error.

TABLE II

IONIZATION POTENTIALS OF THE FREE RADICALS ETHYL, ISOPROPYL, AND PROPARGYL

		Ionization potential (ev.)				
Radical	Source	Individual values	Average	Literature value	Method	
Ethyl	Mercury diethyl	8.80 8.79 8.76 8.78	8.78±0.05	8.67±0.1	Direct electron impact (7)	
Isopropyl	Azoisopropane	7.91 7.93 7.88 7.90	7.90±0.05	7.43±0.1 7.73 7.81	$A(s\text{-}C_3H_7^+)$ from isoalkanes Calculated Calculated	(20) (4) (22)
Propargyl	Propargyl iodide	8.23 8.23 8.28	8.25±0.08			

Ethyl

The average value for the ionization potential of the ethyl radical, 8.78 ±0.05 ev., agrees with that of 8.67±0.1 ev., measured by Hipple and Stevenson, within the combined limits of error. The appearance potential of $C_2H_5^+$ from ethane, 13.05±0.05 ev., lies within the estimated limits of error of the three previous measurements. Using the present data for $I(C_2H_5)$ and $A(C_2H_5^+)$, $D(C_2H_5—H)$ = 4.27±0.10 ev. (98.5±2.3 kcal./mole). This result is perhaps just significantly higher than the average value from electron impact data (21), and within the limits set by the photobromination data (1).

As described above, the appearance potentials of the ethyl ion from the halides were anomalously low, and no reliable values for the dissociation energies of the ethyl–halide bonds could be obtained. It would be interesting to study the ionization efficiency curves for the ethyl ion from these compounds using some means of detecting fine structure (3, 17).

Isopropyl

The measured ionization potential of the isopropyl radical, 7.90±0.05 ev., is considerably higher than the 7.43±0.1 ev. derived from the appearance potentials of $s\text{-}C_3H_7^+$ in the mass spectra of isoalkanes and from the relevant heats of formation (20). It is, in fact, very close to the 7.94±0.1 ev. derived in the same way for the *n*-propyl radical (21). As discussed in a previous section, there appeared to be no doubt of the identity of the isopropyl radical on the basis of the dimer formed. Even if some *n*-propyl radicals were initially

TABLE III

APPEARANCE POTENTIALS AND BOND DISSOCIATION ENERGIES

		Appearance potential (ev.)			Bond dissociation energy (kcal./mole)		
Substance	Ion	This work	Literature	Reference	This work	Literature	Reference
Ethane	Ethyl	13.05±0.05	12.92±0.1 12.81±0.2 12.71±0.4	(23) (11) (16)	98.5±2.3	98±2 96.9±1	(1) (21)
Propane	Isopropyl	11.66±0.05	11.67±0.1 11.5 ±0.3 11.76±0.1	(24) (11) (16)	86.7±2.3	∽89 94.3±2	(19) (21)
Isopropyl iodide	Isopropyl	9.74±0.05	—	—	42.4±2.3	46	(19)
Isopropyl bromide	Isopropyl	10.45±0.05	—	—	58.8±2.3	—	—
Isopropyl chloride	Isopropyl	11.08±0.05	—	—	73.3±2.3	—	—
Propargyl iodide	Propargyl	10.23±0.06	—	—	45.7±3.2	—	—
Propargyl bromide	Propargyl	10.76±0.06	—	—	57.9±3.2	—	—

formed, they would decompose very rapidly at the temperature of the reactor as was found in the attempt to produce the *n*-propyl radical. With the present method of plotting the ionization efficiency curves, the measured ionization potential would be high if some contribution to the 50 ev. peak at mass 43 had been neglected in calculating the net radical peak height at 50 ev. A decrease of 10% in the net 50 ev. peak height would lower the ionization potential by only 0.05 ev. The four individual values for $I(s\text{-}C_3H_7)$ given in Table III were obtained in two separate experiments separated by an interval of a few days.

The appearance potential of mass 43 from propane (11.66±0.05 ev.) is in good agreement with previously measured values (11, 16, 24). However the value of $D(s\text{-}C_3H_7\text{—}H)$ from the present data

$$A(s\text{-}C_3H_7^+) - I(s\text{-}C_3H_7) = 11.66 - 7.90 = 3.76 \pm 0.10 \text{ ev.},$$

or 86.7±2.3 kcal./mole, would appear to be considerably too low by comparison with the electron impact average of 94.3±2 kcal. The derived dissociation energies for the isopropyl–halide bonds also appear to be low, although the absence of reliable kinetic data for these bonds makes comparison difficult. The appearance potential data for the isopropyl ion would suggest that the measured ionization potential is too high by about 0.3 ev. It is interesting to note that two values of the ionization potential calculated by Franklin and Field (4) (7.73 ev.) and by Stevenson (22) (7.81 ev.) on the basis of a simplified molecular orbital method, both lie between the presently measured value and the average electron impact value. The calculated value of Franklin and Field, 7.73 ev., was based on $I(CH_3) = 10.07$ ev. and $I(C_2H_5) = 8.67$ ev., that of Stevenson on the later value for methyl $I(CH_3) = 9.96$ ev. and $I(C_2H_5) = 8.67$ ev. Using $I(CH_3) = 9.96$ and $I(C_2H_5) = 8.78$ as measured in this work, the same calculation of the ionization potential of the isopropyl radical gives 7.97 ev. In view of the assumptions and simplifications necessary in such a calculation, it is doubtful whether this result can be considered as support for the high value for $I(s\text{-}C_3H_7)$ found here. It would appear that further work is necessary to resolve the discrepancy.

Propargyl

The ionization potential of the propargyl radical, 8.25±0.08 ev., is only slightly higher than the 8.16±0.03 ev. found for the allyl radical (13). This difference is considerably smaller than that between the ionization potentials of propyne (10.43±0.1 ev.) (6) and propylene (9.84 ev.) (8).

The dissociation energies of the propargyl–halide bonds are not known from other sources for comparison purposes, but the derived values seem rather low in view of the high temperature required to dissociate propargyl iodide.

REFERENCES

1. ANDERSON, H. C. and VAN ARTSDALEN, E. R. J. Chem. Phys. 12: 479. 1944.
2. AUSLOOS, P. and STEACIE, E. W. R. Bull. Soc. chim. Belges, 63: 87. 1954.
3. FOX, R. E., HICKAM, W. M., and KJELDAAS, T. Phys. Rev. 89: 555. 1953; 90: 386. 1953.
4. FRANKLIN, J. L. Private communication.
5. FRASER, R. G. J. and JEWITT, T. N. Proc. Roy. Soc. (London), A, 160: 563. 1937. Phys. Rev. 50: 1091. 1936.

6. GAUTHIER, F. and PILON, J. R. Unpublished work.
7. HIPPLE, J. A. and STEVENSON, D. P. Phys. Rev. 63: 121. 1943.
8. HONIG, R. E. J. Chem. Phys. 16: 105. 1948.
9. INGOLD, K. U. and LOSSING, F. P. J. Chem. Phys. 21: 1135. 1953.
10. IVIN, K. J., WIJNEN, M. H. J., and STEACIE, E. W. R. J. Phys. Chem. 56: 967. 1952.
11. KOFFEL, M. B. and LAD, R. A. J. Chem. Phys. 16: 420. 1948.
12. LOSSING, F. P., INGOLD, K. U., and HENDERSON, I. H. S. Applied Mass Spectrometry, Institute of Petroleum, London 1954.
13. LOSSING, F. P., INGOLD, K. U., and HENDERSON, I. H. S. J. Chem. Phys. 22: 621. 1954.
14. LOSSING, F. P., INGOLD, K. U., and TICKNER, A. W. Discussions Faraday Soc. No. 14: 34. 1953.
15. LOSSING, F. P. and TICKNER, A. W. J. Chem. Phys. 20: 907. 1952.
16. MITCHELL, J. J. and COLEMAN, F. F. J. Chem. Phys. 17: 44. 1949.
17. MORRISON, J. D. J. Chem. Phys. 19: 1305. 1951.
18. SCHISSLER, D. O., THOMPSON, S. O., and TURKEVICH, J. Discussions Faraday Soc. No. 10: 46. 1951.
19. STEACIE, E. W. R. Atomic and free radical reactions. Reinhold Publishing Corporation, New York. 1954.
20. STEVENSON, D. P. Discussions Faraday Soc. No. 10: 35. 1951.
21. STEVENSON, D. P. Trans. Faraday Soc. 49: 867. 1953.
22. STEVENSON, D. P. Abstracts A.C.S. Meeting. Kansas City. April 1954.
23. STEVENSON, D. P. and HIPPLE, J. A. J. Am. Chem. Soc. 64: 1588. 1942. (Corrected to I(argon) = 15.77 ev.)
24. STEVENSON, D. P. and HIPPLE, J. A. J. Am. Chem. Soc. 64: 2769. 1942.
25. STEVENSON, D. P. and WAGNER, C. D. J. Am. Chem. Soc. 72: 5612. 1950.
26. STEVENSON, D. P. and WAGNER, C. D. J. Chem. Phys. 19: 11. 1951.
27. SZWARC, M. Discussions Faraday Soc. No. 10: 143. 1951.
28. WARREN, J. W. Nature, 165: 810. 1950.

THE HYDRATION OF PLASTER OF PARIS[1]

By Fraser W. Birss[2] and T. Thorvaldson

ABSTRACT

The hemihydrate of calcium sulphate labelled with calcium-45 or sulphur-35 was hydrated in a supersaturated solution of calcium sulphate at 21°C. The distribution of the radioactive isotope between the solution and the solid phases and the concentration of the solution throughout the period of hydration were measured. The exchange of calcium ions between crystalline gypsum and its solution was also studied. The experimental results are discussed from the viewpoint of the mechanism involved. They are found to be in agreement with a mechanism which postulates a single passage of the structural units of the solid hemihydrate through the solution and not consistent with one of direct hydration without temporary independent existence of the products in the liquid phase.

INTRODUCTION

The availability of radioactive isotopes provides a new method for the study of reactions between slightly soluble substances and aqueous solutions. A paper by Graham, Spinks, and Thorvaldson (1) on the hydrolysis and hydration of tricalcium silicate and β-dicalcium silicate illustrates some of the possibilities of the method. The experimental results obtained by these workers are readily interpreted on the basis of the theory of Le Chatelier, that the anhydrous silicates pass into solution and react to form less soluble hydrated silicates, which then separate out of the supersaturated solution. They are not so readily interpreted on the basis of the direct hydration of the silicate in the solid state, with only calcium hydroxide splitting off to enter the hydrating liquid.

As the study of the hydration of these silicates is complicated by the variable lime–silica ratio and the gel-like nature of the hydrated silicates, it was considered desirable to apply the method to a simpler system. The hydration of plaster of Paris was selected because of its historical and scientific interest in relation to the chemistry of cements.

There are several points of difference between the hydration of tricalcium silicate and of plaster of Paris. In the case of the silicate labelled with calcium-45 two methods are available for following the progress of the reaction, i.e. the determination of (i) the alkalinity and (ii) the activity[3] of the liquid phase, while in the case of plaster of Paris labelled with calcium-45 or sulphur-35 only the second method is available. The solubility of the hydrated silicate in solutions of calcium hydroxide is extremely small while the solubility of gypsum in water is much higher and supersaturation of the order of fourfold with respect to the hydration product may be obtained during hydration of the hemi-

[1]*Manuscript received January 25, 1955.*
Contribution from the Department of Chemistry, University of Saskatchewan, Saskatoon, Sask., with financial support from the National Research Council of Canada. This paper represents a part of a thesis submitted by one of us (F. W. B.) as partial requirement for the degree of Master of Arts.
[2]*Holder of a bursary from the National Research Council of Canada.*
[3]*The terms "active", "inactive", and "activity" will be used to refer to radioactivity and not to the chemical activity of the materials under discussion.*

hydrate. The ratio of lime to silica in the silicate changes during the hydration and this ratio in the product varies with the concentration of lime in the solution, while the corresponding stoichiometric ratio of the calcium sulphate remains unchanged. Furthermore, the hydrolysis of the silicate is a comparatively long process, starting off fairly rapidly with the rate tapering off with time, while the hydration of the hemihydrate of calcium sulphate begins very slowly and continues at a steadily accelerating rate.

Assuming a "through-solution" mechanism for the conversion of the hemihydrate to the dihydrate, a mathematical expression for the progressive change in the activity of the liquid phase may readily be developed in a similar manner to that used in the case of the hydration of tricalcium silicate (1). Two complicating factors may enter: (i) substantial changes in the concentration of the hydrating liquid due to the formation of supersaturated solutions with subsequent precipitation of gypsum, and (ii) exchange of Ca^{45} or $S^{35}O_4$ ions between the solution and the hydration product after precipitation. These must be considered in applying the theoretical equation to the experimental data.

EXPERIMENTAL

Materials

Calcium sulphate dihydrate was prepared from reprecipitated "alkali-free" calcium carbonate. The latter was dissolved in hot dilute hydrochloric acid, calcium sulphate precipitated slowly with ammonium sulphate, washed, and dried over plaster of Paris. The radioactive samples were prepared by addition of a suitable amount of $Ca^{45}Cl_2$ or $H_2S^{35}O_4$, obtained from Atomic Energy of Canada, to the solution before the precipitation. The sample of gypsum labelled with calcium-45 was completely crystalline, composed mainly of thin prisms varying in thickness from 0.002 to 0.01 mm. with an occasional crystal as much as 0.025 mm. thick. The loss on dehydration agreed well with the theoretical value for the dihydrate.

The gypsum was dehydrated in an oven at 85–87°C. in a slow current of air. The time required to reduce the moisture content to that of the hemihydrate was about eight hours when further dehydration almost stopped. The Ca^{45}-labelled sample used for the hydration appeared to be mainly in the form of elongated fibrous plates, composed of aggregates of small crystals. The sample labelled with $S^{35}O_4$ ions was composed of smaller particles. The water content of the samples was close to the theoretical value for the hemihydrate.

Determination of the Activity of the Solutions

The activity of the solutions was determined on 0.500-ml. portions, at least in triplicate, after precipitation of the calcium as oxalate and evaporation to dryness, using an end window Geiger–Mueller tube (window thickness 1.7 mgm. per sq. cm.; scale of 64 scaler) and an electric timer. The geometry was kept constant and enough counts were made to reduce the probable error to less than 2%. Corrections were made for background, for self-absorption when necessary, and for the resolving time error of the tube-scaler assembly above counting rates of 25 registers per min.

Exchange of Calcium Between Gypsum Crystals and Solution

Freshly precipitated gypsum crystals were digested for a long period of time, first at 38°C. and then at 21°C., and after filtration were dried over plaster of Paris. The sample was composed of long prisms of fairly uniform thickness of from 0.004 to 0.007 mm. with an occasional crystal measuring 0.003 mm. In the exchange experiments 0.05-gm. samples were shaken in pyrex centrifuge tubes with 9 ml. water at 21°C. for four weeks, 1 ml. of a saturated solution of calcium sulphate labelled with calcium-45 was then added, the shaking was continued, and individual tubes were removed from time to time for counting the solution. The ratio of solid to dissolved calcium sulphate in the system was about 1:1. The room was thermostatted at 21°C.

The calculated activity at time of mixing, assuming no exchange, was 15.16 registers per min. for 0.5 ml. of solution. Counts were made on separate tubes at 30 sec.; 20, 40, and 60 min.; two, four, and six hours after adding the calcium-45 activity. The values obtained were (reg./min./0.5 ml.) 15.08, 15.12, 15.22, 15.21, 15.13, 15.07, and 15.03, respectively. For the conditions and duration of these experiments it appears that exchange of calcium ions between the solid and solution does not significantly affect the activity within the accuracy of counting.

In our hydration experiments with plaster of Paris one might expect greater exchange owing to smaller crystals and higher specific surface. A second series of experiments was therefore made to attempt to determine exchange rates with very small crystals. These were prepared by shaking together in pyrex centrifuge tubes weighed quantities of precipitated calcium carbonate and equivalent amounts of 0.1 molar sulphuric acid. Within two minutes the calcium carbonate had completely dissolved, followed by the formation of a voluminous precipitate of hydrated calcium sulphate. After rapid centrifuging, samples of the clear supersaturated liquid were removed for analysis to determine the concentration of the solution and the weight of solid (by difference). A standard solution of calcium sulphate labelled with calcium-45 was immediately added to each tube and the tubes shaken to allow exchange to take place. The total time required for these manipulations up to the beginning of the exchange shaking was approximately six minutes. From time to time tubes were centrifuged and the solution counted. The concentration of the solution was determined in each case and corrections applied to the count for self-absorption on the basis of previously determined values for the concentrations found.

The crystals formed by the action of the acid on the carbonate, separated from the mother liquor by rapid filtration two minutes after mixing, were fine prisms mostly less than 0.0015 mm. in diameter. At this stage the mother liquor was highly supersaturated with respect to gypsum, containing as much as five times the saturation value. The concentration after dilution with the active solution was still three to four times the saturation value. After an additional period of shaking with the mother liquor for 12 min. (i.e. the period required for complete hydration in the experiments described below) the crystals had grown considerably; many of them were more than 0.002 mm. in diameter and the solution was approaching saturation.

The experimental conditions were in some ways similar to those of the hydrations described below. The total weight of calcium sulphate in the system and the volume used were the same. The concentrations of the solutions at the beginning of the exchange shaking were of the same order as those at the beginning of the hydration runs. On the other hand in the exchange experiments the activity of the solution and the specific activity of the solute were at the maximum at the beginning when the size of the crystals was at a minimum while in the hydration runs the total and specific activities of the solute were at a minimum at the beginning when the crystals of gypsum were of minimum size. Thus the conditions were more favorable to high exchange in the present experiments than in the hydration runs.

The per cent exchange of calcium was calculated, correction being made for the activity removed from the solution by precipitation. This correction, which was based on the mean specific activity of the solute during the exchange period, is probably too small, since most of the precipitation occurred during the first half of the time interval when the specific activity is near the maximum, thus making the value attributed to exchange too large. The average value obtained for exchange was 2.2% in 10 min. and 4.8% in 20 min. This amounts to about 3% for a 12-min. period, the time required for the hydration runs. The great increase in the size of the crystals during this period suggests that the exchange is mainly due to recrystallization of the original inactive finely divided precipitate. As long as there are a large number of small crystals present subject to recrystallization, the rate of this process probably increases as the concentration of the solution falls giving proportionally greater exchange during the longer periods. While we were mainly interested in what happened during the first 12 min., the experiments were continued up to 24 hr. The approximate values obtained for the per cent exchange for the longer periods indicated that the rate of exchange increased up to a maximum in about one hour, then fell slowly, and that 100% exchange was approached in 24 hr. The question of exchange in the hydration experiments will be discussed later.

The Hydration of Plaster of Paris Labelled With Calcium-45

If one brings the active solid hemihydrate into contact with a saturated solution of gypsum it dissolves, producing, before any precipitation occurs, an active solution which is highly supersaturated with respect to the dihydrate. To reduce such dissolution of the active sulphate it is necessary to prepare an inactive supersaturated solution and to use this as the hydrating liquid.

The hydrating solution was prepared by adding successive portions of the inactive hemihydrate to freshly boiled and cooled redistilled water until apparently no further solution occurred on vigorous shaking. Five-milliliter portions of the centrifuged solution were placed in a number of 15-ml. centrifuge tubes each containing 44.0 mgm. of the radioactive plaster of Paris. These were immediately stoppered with serum bottle caps and shaken vigorously for a definite period of time. After centrifuging, three 0.500-ml. samples of the solution were withdrawn for determination of concentration (evaporation and weighing on a microbalance) and three samples for counting. Three

series of runs were made. The experimental values for the initial concentration of the hydrating liquid of the three series of runs were 4.42, 4.40, and 4.41 mgm. (expressed as the hemihydrate) per 0.5 ml. The average value 4.41 mgm./0.5 ml. was used in all the calculations. The maximum activity in the solution was, in each case, recorded at 11.7 min. The data for one of the series of runs are recorded in Table I. All the determinations of the activity for the three runs and the corresponding values for the concentration of the hydrating liquid are plotted in Fig. 1.

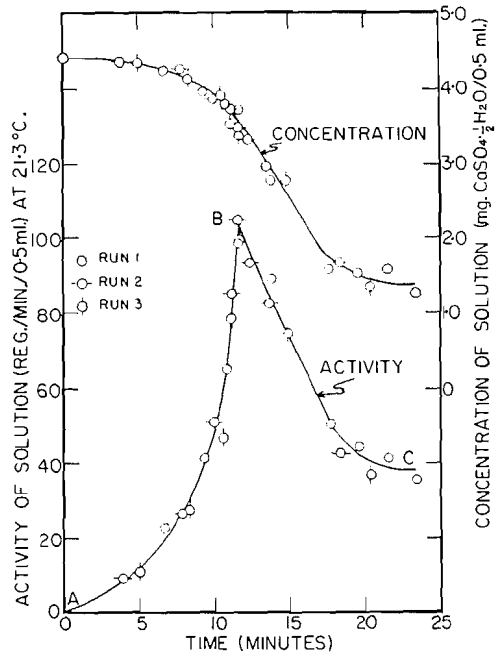

FIG. 1. The liberation of activity to the solution and the changes in concentration when 44 mgm. of the hemihydrate of calcium sulphate, labelled with calcium-45 (specific activity 43.1 reg./min./mgm.), were hydrated in 5 ml. of inactive calcium sulphate solution.

TABLE I

HYDRATION OF 44.0 MGM. Ca^{45}-LABELLED PLASTER OF PARIS* IN 5 ML. SUPERSATURATED SOLUTION OF INACTIVE CALCIUM SULPHATE AT 21.3°C.

Shaking period, min.	Centrifuging period, min.	Concentration of solution†	Count,‡ reg./min./0.5 ml.
0	0	4.40	0
3.8	3.0	4.37	9.7
7.8	3.1	4.28	26.5
10.0	2.8	3.88	50.7
11.2	2.9	3.74	85.0
11.7	3.1	3.50	105.0
12.35	2.7	3.32	93.6
13.6	2.9	2.98	82.5
18.4	3.2	1.68	42.4

**Specific activity of the plaster of Paris = 43.1 reg./min./mgm.*

†Expressed as milligrams of plaster of Paris per 0.5 ml. of solution.

‡Corrected for background, self-absorption, and resolving time but not for changes in concentration of the solution.

The Hydration of Plaster of Paris Labelled with Sulphur-35

Three similar runs were made with the sample of plaster of Paris labelled with sulphur-35. The same types of curves were obtained both for the development of activity in the hydrating liquid and for changes in concentration. The maximum activity in the liquid was attained in a shorter time (approximately nine minutes) possibly owing to the smaller particles of the sample or to presence of more gypsum nuclei. There was somewhat greater variability in the experimental results. Otherwise there was no essential difference between the curves obtained for the hydration of the two samples of hemihydrate labelled with calcium-45 and sulphur-35.

DISCUSSION

Derivation of the Theoretical Expression for the Activity of the Solution

An expression for the relation between the extent of hydration and the activity of the hydrating solution may be derived on the basis of a through-solution mechanism. The derivation given below assumes:

(i) Constant concentration of the solution, i.e. that the rate of precipitation of gypsum is at all times equivalent to the rate of solution of the hemihydrate.

(ii) No exchange of the active ion between the solution and the hydrate after precipitation.

(iii) Rapid enough shaking so that the dissolved radioactive isotope is at all times essentially uniformly distributed throughout the solution.

Let a = moles of inactive $CaSO_4$ in the original solution,
m = moles of labelled solid hemihydrate placed in the system,
b = the specific activity per mole of the hemihydrate,
x = moles of labelled hemihydrate which have passed into the solution,
$f(x)$ = the specific activity of the calcium sulphate in the liquid phase.

Consider the hydration of dx moles of active plaster of Paris, releasing an activity bdx to give a solution of specific activity $f(x)$. The sulphate precipitates as gypsum carrying down an activity $f(x)dx$ from the solution. The net activity liberated to the solution during the process is $bdx-f(x)dx$. When x moles of the plaster of Paris have thus passed through the solution the activity in the solution becomes

$$\int_0^x (bdx-f(x)\,dx) = bx-\int_0^x f(x)\,dx.$$

One can evaluate $f(x)$ in terms of a, b, and x and integrate this expression by a method similar to that used by Graham, Spinks, and Thorvaldson (1), thus obtaining the expression for the activity in solution $= ab(1-e^{-x/a})$. Dividing by mb the total activity in the system and multiplying by 100 one obtains the percentage of total activity in the solution $= (100a/m)(1-e^{-x/a})$.

In place of "moles $CaSO_4$" one may use the weight of $CaSO_4$, $CaSO_4 \cdot \frac{1}{2}H_2O$, or $CaSO_4 \cdot 2H_2O$ in the system, or weight of any of these per unit volume of solution provided the basis of reference is the same for all quantities. In the discussion of the hydration experiments in this paper the concentration of

calcium sulphate in solution is always expressed in terms of milligrams of the hemihydrate per 0.5 ml. of solution.

The End Point of the Hydration

In each series of the hydration runs with the Ca^{45}-labelled sample, the maximum activity of the hydrating liquid was attained in 11.7 min. The question presents itself: was the hydration complete at this point or was an increase in activity due to subsequent hydration masked by a lowering due to precipitation? This question is answered by consideration of the specific activity of the calcium sulphate in the solution after the 11.7-min. point (Fig. 1, curve BC). If the specific activity of the solute remains constant, then precipitation is the only process taking place.[4] Calculation of the specific activity at points between 11.7 and 20.0 min. gave a constant value, i.e.,

$$[\text{activity (reg./min./0.5 ml.)}]/[\text{concentration (mgm./0.5 ml.)}] = 29.$$

This indicates that after the 11.7-min. point the only factor affecting the activity of the solution was precipitation and that the hydration was therefore essentially complete at this point.

The Correction for Changes in Concentration of the Hydrating Liquid

Before comparing the experimental values for the activity of the hydrating liquid during the period of hydration (Fig. 1, curve AB) with those calculated by use of the theoretical equation, correction must be made for changes in concentration. The gradual decrease in the concentration of the solution indicated in Fig. 1 corresponds to the removal of continually increasing amounts of activity. For the ascending portion (AB) of the hydration curve the change in concentration is comparatively small while after the end point of the hydration it is much more rapid until the solution approaches saturation with respect to gypsum.

An approximate value for the lowering of the activity of the solution due to the decrease in concentration during any small time-interval is given by the expression

$$(w_i - w_f)[\tfrac{1}{2}(a_i/w_i + a_f/w_f)]$$

where w_i and w_f are the concentrations at the beginning and end, respectively, of the interval, and a_i and a_f are the corresponding activities of the solution. The expressions a_i/w_i and a_f/w_f represent the specific activities of the calcium sulphate in the hydrating liquid at the beginning and end, respectively, of the time interval.

The calculated corrections for the period of hydration, using nine time-intervals, are given in Table II. Doubling the number of intervals does not change the corrected final a_f value materially.

The corrected experimental value for the activity of the solution at the end of the hydration period (i.e. at 11.7 min.) is 116 reg./min./0.5 ml. or 61% of the total activity of the system. The corresponding value for complete hydration calculated from the theoretical equation is 63% of the total activity.[5]

[4]*An exception to this statement would be the unlikely case where two or more compensating processes in addition to precipitation occur in the system.*

[5]*For total exchange the calculated value for the activity of the solution at the end point of the hydration, for our experimental conditions, is 76 reg./min./0.5 ml., or 40% of the total activity of the system.*

TABLE II

HYDRATION OF PLASTER OF PARIS
Correction of experimental activities for changes in concentration

Time interval (min.)	0–5	5–7	7–8	8–9	9–10	10–10.5	10.5–11	11–11.5	11.5–11.7
Activity* at beginning of interval (a)	0	11.8	20.5	28.5	38.2	50.5	57.5	73	95
Activity at end of interval (a_f)	11.8	20.5	28.5	38.2	50.5	57.5	73.0	95	105
Conc.† of soln. at beginning of interval (w_i)	4.41	4.36	4.25	4.20	4.10	3.95	3.87	3.76	3.62
Conc. of soln. at end of interval (w_f)	4.36	4.25	4.20	4.10	3.95	3.87	3.76	3.62	3.57
Decrease in conc.	0.05	0.11	0.05	0.10	0.15	0.08	0.11	0.14	0.05
Calc. activity removed by change in conc.	0.1	0.4	0.3	0.8	1.7	1.1	1.9	3.2	1.4
a_f correction for change in conc. of soln.	11.9	21.0	29.3	39.8	53.8	61.9	79.3	105	116
Per cent of total activity in soln.	6.3	11.1	15.5	21.0	28.3	32.6	41.8	55	61

**All activities are expressed as registers per minute per 0.5 ml.*
†All concentrations are expressed as milligrams plaster of Paris per 0.5 ml.

These values may be considered to be in good agreement as any lack of thorough mixing of the solution during the hydration would tend to cause precipitation of gypsum in regions of high activity and thus lower unduly the activity of the solution. There is likely to be some lowering of activity due to this cause near the end of the hydration when the rate of reaction is very high and the diffusion of the calcium ions through a film adhering to the solid may become the limiting factor. Furthermore, the experimental values obtained at the 11.7-min. point are likely to be below the true maximum, as a slight displacement along the time axis, either way, from the true end point (which is not necessarily exactly 11.7 min.) would give lower values for the activity. For these reasons the maximum experimental value at 11.7 min. was used in the calculation of the final corrected maximum instead of the average for the three series of runs. The close reproducibility of the three series of experimental runs is an indication of the clock-like regularity of the hydration process under given conditions.

The Question of Exchange

The theoretical equation gives a measure of the exchange of the radioactive isotope between the solid and the solution, resulting from the dissolution of the active hemihydrate and the essentially simultaneous precipitation of an equivalent amount of an active dihydrate. Exchange of calcium occurring during the hydration period but after separation of the solid hydration product would reduce the experimental value for the activity of the solution below those values calculated by the equation. Recrystallization during the period of hydration through the solution of very small crystals with redeposition on larger ones, which means a second passage of the calcium sulphate through the solution, would also lower unduly the activity of the solution.

There is considerable evidence indicating that the effect of these processes on the experimental values for the activity of the hydrating liquid is small. The experiments described above indicate that the rate of exchange of the calcium ion between gypsum and its saturated solution, after the system has attained equilibrium, is negligible for the time of exposure involved in our experiments. During the hydration the surfaces of the growing crystals are continually in radioactive exchange equilibrium with the calcium sulphate in the solution. For further exchange the radioactive ion must pass from the surface to the zone of lower radioactivity inside the crystal. The very low rate of diffusion of the calcium ion in the crystalline solid therefore determines the rate of exchange.

The gypsum prisms formed in the hydration runs were of fairly uniform size, mainly 0.003 to 0.004 mm. in diameter, with very few less than 0.002 mm. This suggests a regular growth of the crystals during the hydration period and indicates that near the end of the hydration there were very few crystals small enough to take part in a recrystallization process. Such recrystallization would also be inhibited by the very high supersaturation of the solution right up to the end of the hydration period.

During the early part of the hydration period when both exchange through diffusion, due to the high specific surface, and exchange through recrystalliza-

tion, due to the small size of the crystals of gypsum, would be at a maximum, both the rate of hydration and the activity of the solution are very low. Less than 5% of the plaster of Paris is hydrated during the first third and less than 10% during the first half of the hydration period (see Fig. 3) thus favoring the growth of the gypsum nuclei present in the solution to a size where the tendency for recrystallization is reduced or eliminated. Even if there were considerable exchange during this early period the over-all effect for the hydration of the whole sample would be small.

The constancy of the specific activity of the dissolved solid in the post-hydration period is perhaps the strongest evidence for the absence of appreciable exchange effects through diffusion or recrystallization during the period of hydration, for such processes, if operating, would be expected to carry beyond the end point.

The experimental findings are therefore in agreement with the assumption that the structural units of crystalline plaster of Paris pass through the solution during the hydration and that the theoretical equation is applicable to the process.

The Rate of Hydration

From the corrected experimental values for the per cent of total activity found in the solution (Table II) one may calculate, by means of the theoretical equation, the percentage of the plaster of Paris hydrated (i.e. $100x/m$) corresponding to any given activity or the end of any time interval. Fig. 2 gives the calculated per cent hydration vs. the corrected activity of the solution and Fig. 3 the rate curve for the hydration at 21.3°C. under the conditions of our experiments.

Another approximation of the extent of hydration may be derived directly from the experimental data if the through-solution mechanism is assumed. In any interval, x_i moles of labelled hemihydrate pass into solution releasing an activity bx_i to the solution. If no concurrent precipitation took place the activity of the solution would become a_i+bx_i and the concentration w_i+x_i. Upon precipitation the solution assumes an activity a_f which is directly proportional to the final concentration attained, w_f.

$$a_f = [w_f/(w_i+x_i)](a_i+bx_i)$$

and

$$x_i = (a_i w_f - a_f w_i)/(w_f b - a_f).$$

Calculations based on this approximation yield results in good agreement with those given in Figs. 2 and 3 if the intervals are sufficiently small.

It is of interest to note that the shape of our rate curve, which was obtained with a very low ratio of the hemihydrate to solution, is in general agreement with the thermal curve obtained by Weiser and Moreland (2) with a very high ratio of plaster to water (50 gm. to 30 ml.). The period of slow hydration at the beginning ("inhibition period") is attributed by these authors to dearth of crystal nuclei of the hydration product and was found to be shortened or eliminated by the addition of small amounts of finely crystalline gypsum to the plaster.

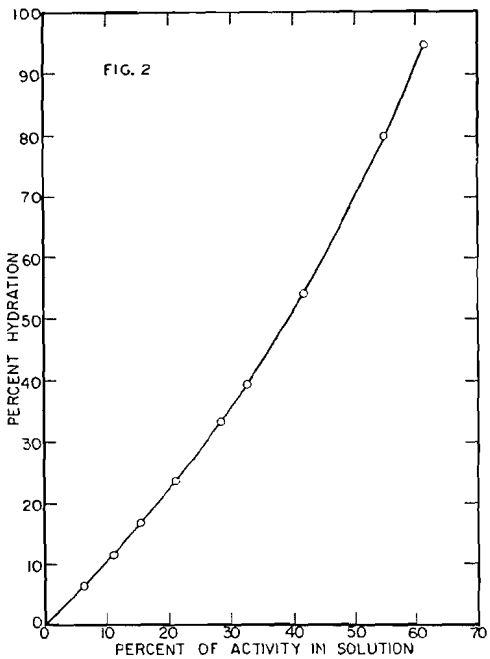

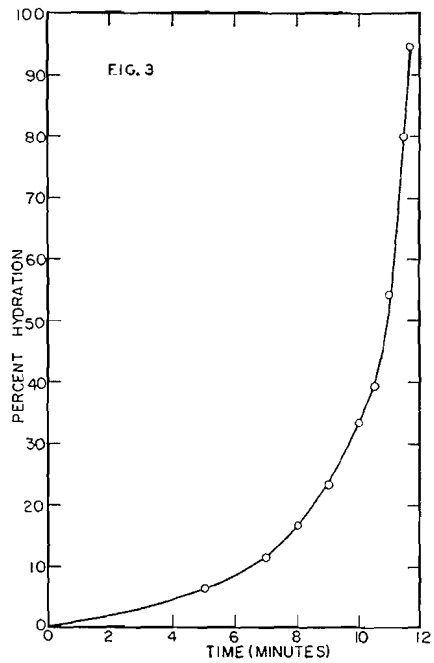

FIG. 2. The relation between the per cent of active plaster of Paris hydrated and the per cent of the total activity found in the hydrating liquid.
FIG. 3. The rate curve for the hydration of plaster of Paris at 21.3°C.

The Hydration of Plaster of Paris Labelled with Sulphur-35

The above discussion also applies to the data obtained with the sample of plaster of Paris labelled with S^{35}. The final value for the activity corrected for the effect of precipitation was 62% of the total activity in the system as compared to 64%, the value required by the theory for hydration by a through-solution mechanism under our experimental conditions.

GENERAL CONCLUSION

The experimental results for the hydration of plaster of Paris are in agreement with those calculated for a through-solution mechanism, while they are not consistent with the assumption of any mechanism of direct hydration without the solid passing into solution. Direct hydration alone would not give rise to activity in the solution. If one assumes that the first step of the process is a surface reaction between the crystals of the hemihydrate and water one would have to postulate that the dihydrate formed passes into solution and maintains the high supersaturation of the solution with respect to gypsum crystals during the period of hydration.

REFERENCES

1. GRAHAM, W. A. G., SPINKS, J. W. T., and THORVALDSON, T. Can. J. Chem. 32: 129. 1954.
2. WEISER, H. B. and MORELAND, F. J. Phys. Chem. 36: 1. 1932.

THE MECHANISM OF THE HYDRATION OF CALCIUM OXIDE[1]

By Fraser W. Birss[2] and T. Thorvaldson

ABSTRACT

Three samples of calcium oxide, designated as A, B, and C, were prepared from calcium carbonate labelled with calcium-45. A was heated to constant weight at 700°C.; B was heated an additional three hours at 1400 to 1550°C.; and C was heated six hours at the same temperature. The samples were hydrated in a supersaturated lime solution at 21°C., the development of activity and the changes in concentration of the solution being determined. The activity entering the solution accounted, according to theory, for the following percentages of the samples passing through the solution during the hydration: A, 27%; B, 57%; C, 94%. These results indicate that sample C ("dead-burnt" lime) hydrated by a "through-solution" mechanism, but that A and B either hydrated partly according to some other mechanism, such as a vapor phase process in the pores of the particles of lime, or the calcium ions failed to reach the bulk of the hydrating liquid before precipitation as calcium hydroxide.

INTRODUCTION

Three cases of hydration, namely of tricalcium silicate, β-dicalcium silicate, and the hemihydrate of calcium sulphate, have been studied by the newly developed method of using radioactive elements as tracers (1, 2). The experimental evidence available on the mechanism of the hydration of the two silicates has in the past been rather inconclusive. However, it is generally considered that when plaster of Paris is brought into contact with a large excess of water, the solid passes into solution and then crystallizes out as gypsum. The results of the experiments with the hemihydrate of calcium sulphate labelled with calcium-45 or sulphur-35 (1) were found to be compatible with such a "through-solution" mechanism, thus giving, when combined with the previous findings (2), indirect support to the theory of a similar mechanism for hydration of the silicates.

Calcium oxide was selected for similar experiments because of the violence of its reaction with water. It was thought that the tracer method applied to this reaction might give support to the alternative theory that some solids react directly with water, hydrating without passing through the solution in the process. It is well known that when calcium oxide is brought into contact with water, solutions highly supersaturated with respect to crystalline calcium hydroxide are formed, and that these solutions shed the excess hydroxide rather slowly. Thus it is evident that, at least in part, the solid passes through the solution. However, if the predominant reaction is a direct one between water and solid lime without the latter passing into solution, then the tracer method should disclose this and might show that the hydration goes completely by this path if a highly supersaturated solution of lime is used as the hydrating liquid.

[1]*Manuscript received January 25, 1955.*
Contribution from the Department of Chemistry, University of Saskatchewan, Saskatoon, Sask., with financial support from the National Research Council of Canada. This paper represents a part of a thesis submitted by one of us (F. W. B.) as partial requirement for the degree of Master of Arts.
[2]*Holder of a bursary from the National Research Council of Canada.*

EXPERIMENTAL

The experimental procedures were very similar to those described in the preceding paper (1) by Birss and Thorvaldson on the hydration of plaster of Paris. The methods and the precautions used to ensure accuracy of the measurements of radioactivity were the same. The work was done in a room thermostatted at 21±0.1°C.

Three samples of calcium oxide, A, B, and C, were prepared from calcium carbonate of high purity, labelled with calcium-45, by the various heat treatments indicated in Table I.

Supersaturated solutions containing from 1.26 to 1.35 gm. of inactive[3] calcium oxide per liter were used as the hydrating liquids so as to reduce, as far as possible, further increase in concentration through solution of active lime during the hydration. Fifty-milliliter aliquots of the supersaturated calcium hydroxide solution were shaken with freshly ignited 0.05-gm. samples (±1%) of active calcium oxide in sealed 100-ml. gold or silver lined steel tubes. At intervals tubes were centrifuged, 25 ml. of the clear liquid titrated with 0.06 *N* hydrochloric acid, and five 0.500-ml. samples counted. Duplicate series of hydrations were run with each sample of calcium oxide.

RESULTS

The three samples of lime showed considerable differences in their behavior on hydration. In each case the concentration of the supersaturated hydrating liquid increased; with samples B and C to a much greater extent than with sample A. Sample C, which gave the highest supersaturation, required the longest time for complete hydration. Some observations on the hydrations follow.

Sample A.—The concentration of the hydrating liquid rose rapidly from an initial 1.26 to 1.33 gm. CaO/liter (10 min.), then more slowly to 1.35 gm./liter (30 min.). The same value was obtained at 60 min., with a slight decrease during the next 60 min. The activity of the solution reached a maximum in 30 to 50 min. The duplicate series were not in close agreement.

Sample B.—The concentration rose from 1.29 to 1.44 gm. CaO/liter in five minutes, reached 1.46 to 1.47 gm./liter at 20 min., then remained almost constant until the two-hour test. The activity of the solution reached a maximum in 60 min., and showed very slight decrease at the two-hour test.

Sample C.—The concentration rose from the initial of 1.34 gm. CaO/liter to as high as 1.52 gm./liter in 5 to 10 min., then fell rapidly, reaching 1.30 gm./liter at four hours and 1.28 gm./liter at eight hours. The activity of the solution increased rapidly during the first 10 min., then slowly up to the four-hour test, and then fell slightly during the next four hours. The duplicate determinations of the two series with this sample were in fairly good agreement.

The apparent times required for complete hydration were:

Sample A, 30–50 min.; Sample B, one hour; Sample C, four hours.

[3]*The terms "inactive", "active", and "activity" will be used to refer to radioactivity and not to the chemical activity of the materials under discussion. The* Ca^{45} *was supplied by Atomic Energy of Canada.*

"Through-solution" Hydration of Lime

A theoretical expression for the liberation of radioactivity by a labelled sample of the hemihydrate of calcium sulphate when hydrated in a solution of inactive calcium sulphate has been developed in the preceding paper (1). The expression holds also for the case of the through-solution hydration of lime labelled with Ca^{45} in a solution of inactive calcium hydroxide, namely:

Per cent of total activity in the solution $= (100a/m)(1-e^{x/a})$

where a = moles of inactive lime in the original solution,

m = moles of labelled calcium oxide placed in the system,

x = moles of labelled calcium oxide which have passed into solution during the hydration.

The limitations in the application of the expression to the experimental data have been discussed in the preceding paper (1).

The experimental results obtained with sample C will be considered first. Fig. 1 gives the plot for the changes in the activity of the hydrating liquid with time, and the corresponding changes in the concentration of the solution. It also gives the plot of the experimental values of the activity in the solution corrected for the changes in the concentration, by the method described in the preceding paper (1). The corrected experimental activity at the maximum is 67.4% of the total activity of the system as compared with 70.5%, the theoretical value for complete hydration by a through-solution mechanism. This may be considered to be reasonable agreement because of probable errors which would tend to lower the experimental activity. Assuming complete radioactive exchange equilibrium between the lime in the solid and solution at the end of the hydration would give only 55% of the activity in the solution.

Discussion of Errors

The errors affecting the experimental results have been discussed at length in the preceding paper, and will therefore be considered only briefly here. The rapid reaction at the beginning of the hydration may result in incomplete mixing and consequent precipitation of the hydrated lime in regions of high

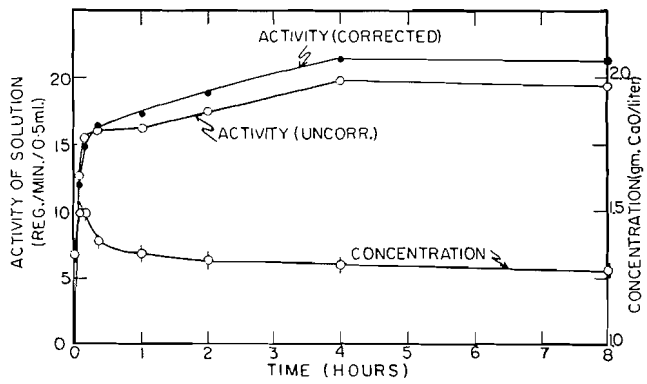

FIG. 1. The liberation of activity to the solution and the changes in concentration when 0.05-gm. samples of calcium oxide (heated six hours at 1400–1550°C.) labelled with calcium-45 (specific activity 63.2 reg./min./mgm.) were hydrated in 50 ml. of inactive lime solution 1.34 gm. CaO/liter).

activity. This would lower the observed activity in the liquid. In the hydration of plaster of Paris a similar danger was present near the end of the hydration period. The experimental measurement of activity at the four-hour point (Sample C, Fig. 1), which was taken as the maximum value, is not necessarily the true peak, thus possibly giving too low a maximum. However, as the slope of the curve at this point is small, the error is probably not large.

Exchange of calcium ions between the liquid and solid after the precipitation of the calcium hydroxide would lower the activity but the error is probably not large since the drop in activity, after correction for precipitation, from the four-hour to the eight-hour value is within the probable experimental error of counting. Direct determination of exchange by shaking inactive calcium hydroxide crystals with a solution of labelled calcium hydroxide (ratio of solid to dissolved calcium hydroxide six to one) gave a marked drop in the activity of the solution on mixing, probably owing to exchange of calcium ions between the liquid and the large area of surface of the thin calcium hydroxide plates. This was followed by a slow decrease in the activity of the solution. Surface exchange does not affect the results in the hydration experiments as the surface of the crystals is at all times in exchange equilibrium with the solution. When the initial drop in activity observed in the exchange experiments is eliminated and correction is made for the ratio of calcium hydroxide in the solid and liquid phase (0.8 to 1 in the hydration runs), the direct experiments give an estimated drop in activity of about 0.1% per hour for the conditions of the hydration experiments. This is of the order of the drop observed between four and eight hours in the hydration of sample C.

During the very rapid hydration of sample C in the first 10 min. when, by calculation, about 60% of the sample was hydrated, very small crystals of calcium hydroxide were probably formed. These would be subject to recrystallization, thus depressing the activity of the solution. During the 10–60 min. period (Fig. 1) the activity (lower curve) is depressed by the drop in the concentration of the solution. This correction has been made in the upper curve. However, the apparently low values for the one and two hour points on the "corrected" curve are probably due to recrystallization and the low experimental value for activity of 67.4 instead of the theoretical 70.5% may be mainly due to this factor.

Thus one must conclude that in the case of sample C there is no evidence of direct hydration of the solid calcium oxide without passage of the solid into solution during the over-all hydration process.

Comparison of the Hydration of Samples A, B, and C

The activity values obtained for the hydration liquids were corrected for changes in concentration (1). From the figures obtained the proportion of the calcium oxide apparently hydrated by a through-solution mechanism was calculated by means of the theoretical equation. The results are given in Fig. 2 and in Table I.

The marked difference in the behavior of the three samples is apparently due to the heat treatments. The sample of calcium carbonate was composed

TABLE I

COMPARISON OF DATA FOR CaO SAMPLES A, B, AND C

Sample		A	B	C
Heat treatment		20 hr. at 700°C.	3 hr.* at 1400–1550°C.	6 hr.* at 1400–1550°C.
Maximum activity of liquid (corr.) (as % of total activity)	{	31.0	45.4	67.3
	{	26.1	46.1	67.4
	Mean	28.6	45.8	67.4
Calc. % CaO hydrated "through-solution" (mean)		32	57	94

**After 20 hr. at 700°C. The samples were ground lightly to break up aggregates and ignited two hours at 950°C. before use.*

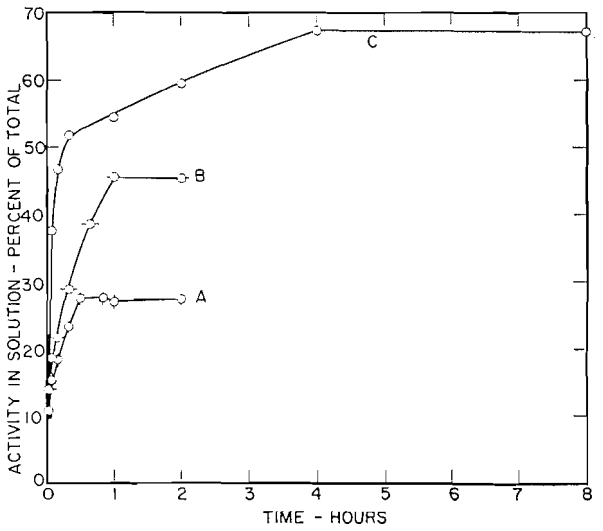

FIG. 2. Comparison of the activity liberated to the solution on hydration of three samples of calcium oxide labelled with calcium-45 (see Table I).

of crystals mainly 0.022 to 0.04 mm. in diameter. Sample A retained the shape of the original crystals and microscopic measurements indicated only slight shrinkage. The particles of samples B and C had to a great extent lost their original shape, were smaller, and some sintering had occurred.

Hedin and Thorén (3) have made a very thorough study of volume changes during the ignition of calcium carbonate at various temperatures. They have concluded that ignition at low temperatures produces particles of oxide of extremely loose structure composed of very small crystals of calcium oxide and having a large amount of internal pore space, but that progressive heating at higher temperatures gives closer packing and finally a compact crystalline material. They consider that the high rate of slaking of soft burnt lime is due to a large area of internal surface at which slaking can take place, while dead-burnt lime slakes only at the external surface of the particles. Hedin and

Thorén have further concluded from their studies on the hydration of calcium oxide that the first step of slaking is merely the dissolution of the oxide and that this solution presumably occurs by direct formation of ions. However, they do not exclude the possible formation of hydroxide in the solid but consider that the supersaturation is due to the direct dissolution of calcium oxide.

The results obtained with sample A could be explained on the assumption that the particles possess a large amount of internal surface and that a large proportion of the hydration of the oxide and precipitation of the hydroxide occurs in the capillaries and pores of the particles. This would, in part, prevent the radioactive ions of calcium from entering the bulk of the hydrating liquid. The average activity developed in the solution by this sample corresponded to a 32% hydration, through-solution. One would then assume that internal hydration occurs to a much lesser extent in sample B, which gave a calculated 57% through-solution hydration, while it is absent in sample C, where the normal through-solution mechanism becomes evident with sufficient time lag between solution and precipitation for approaching complete uniformity of concentration in the hydrating liquid.

On the basis of the above one might perhaps assume that essentially the mechanism of the hydration of the three samples is the same. There is, however, the question of the mechanism of the "internal" hydration. Does water, as liquid, enter the pore space, in which case the hydration might occur in liquid films, or does only water vapor pass into the capillaries giving a vapor phase reaction with the solid? Our experiments do not answer these questions but they indicate that sample C, which probably corresponds to "dead-burnt" lime, hydrates by a "through-solution" mechanism. While the "ionic" solution of the calcium oxide seems probable, the possibility that calcium hydroxide is first formed and then dissolves is not excluded.

REFERENCES

1. BIRSS, F. W. and THORVALDSON, T. Can. J. Chem. 33: 870. 1955.
2. GRAHAM, W. A. G., SPINKS, J. W. T., and THORVALDSON, T. Can. J. Chem. 32: 129. 1954.
3. HEDIN, R. and THORÉN, Å. Swed. Cement Concrete Inst. Stockholm, Bull. No. 16. 1949.

THE ELECTRICAL CONDUCTANCE OF STRONG ELECTROLYTES: A TEST OF STOKES' EQUATION[1]

By A. N. Campbell and E. M. Kartzmark

ABSTRACT

The equation recently put forward by Wishaw and Stokes, purporting to reproduce the equivalent conductance of concentrated solutions of strong electrolytes, has been tested by applying it to the experimental data of Campbell, Kartzmark *et alii*. The agreement between the calculated and observed values of Λ is astonishingly good, in the case of lithium nitrate up to a concentration of 7 molar. The deviations found for silver nitrate and ammonium nitrate are attributed to ion-pair formation and a dissociation "constant" deduced (for silver nitrate) which does show approximate constancy; a similar calculation by Stokes for ammonium nitrate shows even better constancy. Since the Stokes' equation is fully theoretical and contains only quantities to which physical meaning can be attached, it is to be preferred to any empirical, or semiempirical, equation. The Stokes' equation, being merely an extension of the Debye–Hückel–Onsager concept, cannot be expected to apply to concentrations greater than, say, 5 N. Attention is again drawn to the empirical observation that in the region of very high concentration the plot of Λ versus log C is a true straight line.

For a number of years, the present authors in collaboration with others (1) have been determining the equivalent conductances of concentrated solutions of strong electrolytes, at various temperatures and at concentrations up to that of the molten salt (at sufficiently high temperature). This they have done in a purely experimental manner, since they lacked any theoretical equation which could be tested by their results, and there was no picture of the mechanism of conduction in strong solutions. The Debye–Hückel–Onsager equation, which requires a straight line relation between Λ and $\sqrt{C}$, is only valid in the extremely dilute region, say up to 0.01 N; at high concentrations it even gives negative values for Λ. It is unnecessary here to go into detail, since the situation is summarized by Harned and Owen in their well-known book (4, pp. 144–158). Suffice it to say that attempts have been made to extend the Debye–Hückel–Onsager equation by the addition of further terms to the $\sqrt{C}$ term. The best known of these are the equations of Onsager and Fuoss (7) and of Shedlovsky (8); the latter, however, is purely empirical. At best, these equations represent the variation of equivalent conductance with concentration only up to, say, 1.0 N.

Quite recently, Wishaw and Stokes (9) have produced an equation which is an extension of Onsager's equation, taking into account the effect of finite ionic size[2] (and Falkenhagen's evaluation of the relaxation effect (3)). The Wishaw–Stokes equation is

$$\Lambda = \left(\Lambda^\circ - \frac{B_2\sqrt{C}}{1+B\mathring{a}\sqrt{C}}\right)\left(1 - \frac{B_1\sqrt{C}.F}{1+B\mathring{a}\sqrt{C}}\right)\frac{\eta^\circ}{\eta}.$$

[1]*Manuscript received January 17, 1955.*
Contribution from the Department of Chemistry, University of Manitoba, Winnipeg, Manitoba.

[2]"*The term* å *[distance of closest approach of the ions] is not the sum of the crystallographic radii of the appropriate ions (probably owing to the increase in effective radius of the ions due to their solvation sheaths), and must therefore be determined empirically.*" *Kortüm-Bockris (5).*

The symbols have the following meaning:

Λ = equivalent conductance at concentration C,
Λ° = limiting equivalent conductance,
$B_1 = 8.20\times10^5/(\epsilon T)^{3/2}$, where ϵ = dielectric constant of solvent,
$B_2 = 82.5/\eta^\circ(\epsilon T)^{\frac{1}{2}}$, where η° = viscosity of solvent,
$B = 50.29/(\epsilon T)^{\frac{1}{2}}$,
η = viscosity of solution,
å = mean distance of closest approach of ions, (Å),

$F = \dfrac{(e^{0.2929Ka}-1)}{0.2929Ka}$ where K = quantity in Debye–Hückel theory given by $K^2 = \left[\dfrac{4\pi Ne^2}{1000\epsilon kT}\right] C(\nu_1 z_1^2+\nu_2 z_2^2)$ and a = mean distance of closest approach (cm.).

Other symbols have their usual meanings.

Wishaw and Stokes have tested their equation using their own data for ammonium chloride and for ammonium nitrate (the latter data are identical with our own). For ammonium chloride they find good agreement up to 5 N ($\pm$1 mho), while the discrepancies observed with the ammonium nitrate results are attributed to ion-pair formation, and a dissociation constant is evaluated which is reasonably constant up to 6 N.

As our results are more extensive than those of Wishaw and Stokes and apply at different temperatures, it seems appropriate to test their very interesting equation using our results. Before doing so, however, some comment is necessary. In a letter from Dr. Stokes he makes use of the following words: "I am rather sorry that your extensive conductivity measurements refer to nitrates; the behaviour of these is less simple and respectful towards the theory than that of chlorides, etc. . . . I believe the ion-pair formation in nitrates is genuine—it ties up with the thermodynamic data and the diffusion fairly convincingly. . . For silver nitrate I should suggest an å something between 3.5 and 4 Å; not the crystallographic value. According to Bjerrum, one should really take å = 3.57 for the ionized part of a one: one electrolyte which forms ion-pairs, but this parameter is fairly elastic. The greatest difficulty in applying the theory to ammonium nitrate or silver nitrate at temperatures other than 25° is that we have no activity coefficient data to use in calculating the ion-pair dissociation-constant K. However, the theory may still be used to estimate α, the degree of dissociation of the ion-pairs, and to compare it at different temperatures. It is quite possible that α will be nearer to unity at your higher temperatures; the behaviour of the function $e^2/\epsilon kT$ ought to correlate with the amount of ion-pair formation at a given concentration at various temperatures. This function has the values 7.135 at 25°; 7.225 at 35°; 7.935 at 95°; all $\times$ 10^8."

We have applied the Stokes equation to our data for silver nitrate and ammonium nitrate, at 25°, 35°, and 95°, and to potassium chloride (6) at 25°, and to lithium nitrate at 25° (unpublished data by Dr. G. Debus, working in this laboratory).

In using Stokes' equation, the quantities which may require arbitrary selection are å and Λ°; F is not such a quantity. Λ° is well known or can be found from the ionic conductances, for all common electrolytes at 25°, but at other temperatures it becomes a matter of guesswork (in the absence of further experimental work). å is occasionally known (at 25°) but usually again only a probable value can be assigned. According to Bjerrum, å should have a fixed value of 3.57 for the ionized part of a 1:1 electrolyte which forms ion-pairs. This value, however, can be altered within reasonable limits and still retain its physical meaning but it must not vary with temperature. In other words, such a value of å is chosen (varying, say, between 3 and 4 Å) as fits the data for 25° (Λ° is known without ambiguity for this temperature) and this value of å is used for calculations at other temperatures.

There remains what Stokes calls "the vexed question" of a viscosity correction. While admitting that a viscosity correction is necessary, and that this correction is not given by the ordinary bulk viscosity, he is nevertheless forced to use this bulk viscosity. Stokes thinks there is "some justification" for this. The particular substances investigated by him, ammonium chloride and ammonium nitrate, exhibit anomalous viscosity, that is, up to quite high concentrations, the viscosity is somewhat less than that of water and never, even at the highest concentrations, much greater. Silver nitrate and lithium nitrate, which are used in our calculations, form very viscous solutions at high concentrations. It is fair to point out that some of the deviation observed may be due to the use of a viscosity correction which may be only approximate.

CALCULATIONS

Our calculations are contained in Tables I to IV. It should be emphasized once again that the choice of å and Λ° (except at 25°) is only guesswork but this does not detract from the value of Stokes' equation; it merely requires further experimental work. Ion-pair formation has been assumed with silver nitrate and a dissociation constant calculated using the activity coefficients given in Harned and Owen (4). The calculation was not carried beyond the point at which $\alpha(=\Lambda_{exp}/\Lambda_{calc})$ appeared to increase with further concentration. A similar calculation has already been made for ammonium nitrate by Wishaw and Stokes (10). The results for Λ_{exp} and Λ_{calc} are graphed in Figs. 1 to 5.

DISCUSSION

Obviously, the values of Λ obtained are dependent on the values of å chosen (and of Λ° if this is not known) but the general behavior is the same, whatever value of å is chosen. For example, a value of å may be chosen (e.g. 2.30 for silver nitrate) which may reproduce rather well the observed results over the initial range (up to 3 N for silver nitrate) and then give systematically decreasing values of Λ up to the limit of saturation. If it is objected that the value of 2.30 is too low to have physical significance and the more reasonable value of 4.35 assumed, then the initial calculated values are somewhat too high and later values finally become too low. In other words, the behavior is qualitatively the same. We have used a number of alternative å values in the case

TABLE I

C	Λ_{exp}	Λ_{calc} å = 2.3	Λ_{calc} å = 4.35	α (for å = 4.35)	K
		I. Silver nitrate at 25°, Λ° = 133.36			
0.0005	131.36	131.36	131.39	0.999	—
0.001	130.51	130.57	130.62	0.999	—
0.005	127.20	127.31	127.56	0.997	—
0.01	124.76	125.00	125.32	0.996	2.41
0.02	121.41	121.93	122.52	0.991	2.07
0.05	115.24	116.36	117.55	0.980	2.08
0.1	109.14	109.84	112.81	0.967	2.98
1.004	77.82	78.69	89.20	0.872	2.52
1.998	64.20	63.90	76.29	0.842	2.74
3.028	54.97	53.21	65.63	0.838	3.10
4.000	48.50	44.69	56.46	0.859	3.96
5.029	43.14	37.77	48.64	0.887	
6.006	38.55	31.87	41.58	0.927	
7.012	34.70	26.79	35.36	0.981	
8.011	31.20	22.46	30.09		
9.010	27.99	18.21	24.44		
9.709	26.1	16.09	21.67		
		*II. Silver nitrate at 35°, Λ° = 158.43**			
0.986	132.5	129.7	133.2	0.995	
1.4023	85.37	83.0	97.1	0.879	
1.7757	79.55	76.8	91.6	0.868	
3.0322	65.41	60.5	75.6	0.865	
3.8230	58.91		66.8	0.882	
4.2306	56.06		62.9	0.892	
		*III. Silver nitrate at 95°, Λ° = 340.6**			
0.0534	298.3		295.2		
0.1	278.0		281.4	0.988	
1.220	172.7		199.9	0.864	
2.189	147.8		165.8	0.891	
2.967	130.8		141.2	0.926	
4.829	103.1		104.1	0.990	
6.591	84.88		77.57		
8.830	48.12		54.27		
9.906	61.28		45.60		
11.876	50.35		39.0		

**Calculated using the temperature coefficients of conductance from (1).*

The constants B, B_1, B_2 at 95° were calculated using the dielectric constant data of Wyman and Ingalls (10), and viscosity data from I.C.T.

TABLE II

C	Λ_{exp}	Λ_{calc}	α	C	Λ_{exp}	Λ_{calc}	α
I. Ammonium nitrate at 25°, $\Lambda°$ = 144.84; å = 4.35							
0.001	142.0	142.01	—	1.004	101.32	110.35	0.918
0.002	141.4	140.93	—	1.993	91.95	104.62	0.879
0.005	138.7	138.87	—	2.982	84.28	97.79	0.862
0.01	136.2	136.84	—	4.020	76.78	91.58	0.838
0.02	133.3	134.20	—	5.014	70.00	84.68	0.827
0.05	128.0	129.80	0.986	6.036	63.12	76.49	0.825
0.07	125.5	127.98	0.981	7.015	56.73	69.31	0.819
0.10	122.7	125.82	0.975	8.011	50.36	61.26	0.822
0.20	116.9	121.02	0.966	9.043	43.93	53.37	0.823
0.50	108.0	113.64	0.950	10.004	38.19	45.05	0.848
				11.282	31.3	35.90	0.872
II. Ammonium nitrate at 35°, $\Lambda°$ = 171.78; å = 4.35							
0.0538	153.1	152.03		2.450	103.2	114.2	0.904
1.023	119.4	125.8	0.949	7.671	59.84	68.65	0.872
1.694	111.0	120.3	0.923	9.409	47.46	52.52	0.904
1.9104	108.2	118.7	0.912				
III. Ammonium nitrate at 95°, $\Lambda°$ = 365; å = 4.35							
0.0878	306.2	307.0	0.997	6.632	116.0	125.2	0.927
0.194	275.3	285.4	0.965	7.95	97.81	105.3	0.929
0.9963	234.8	237.6	0.988	8.74	88.04	95.4	0.923
1.525	213.6	222.4	0.960	10.12	72.44	74.0	0.979
2.576	185.6	203.8	0.912	11.13	61.99	63.4	0.978
3.600	166.9	182.7	0.914	13.31	42.07	41.4	—
4.221	154.7	162.2	0.954	14.81	28.71	35.92	0.799

NOTE. *K values (for 25°) have been calculated by Wishaw and Stokes (9), whose experimental results are in close agreement with ours.*

TABLE III

POTASSIUM CHLORIDE AT 25°, $\Lambda°$ = 149.86; å = 4.6

C	Λ_{exp}	Λ_{calc}	$\frac{\Lambda_{exp}}{\Lambda_{calc}}$
0.0005	147.81	147.78	
0.001	146.95	146.91	
0.005	143.55	143.71	0.999
0.01	141.27	141.68	0.997
0.02	138.34	138.91	0.996
0.05	133.37	134.19	0.994
0.10	128.96	129.88	0.993
0.20	123.9	125.0	0.991
0.50	117.2	117.29	0.999
1.00	111.9	111.96	0.999

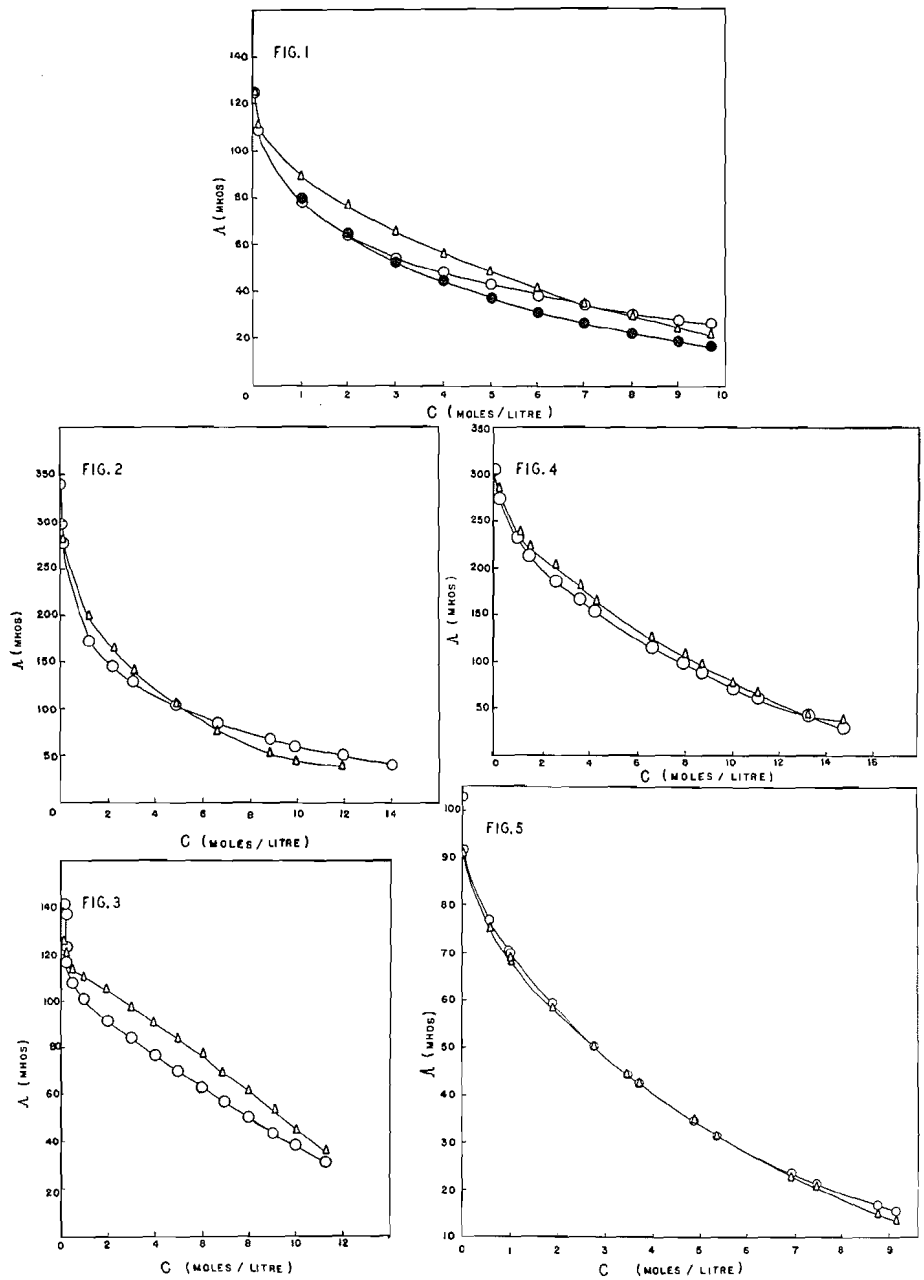

FIG. 1. $AgNO_3$ at 25°C. ○ experimental; △ calculated, å = 4.35; ● calculated, å = 2.30, Λ° = 133.36.
FIG. 2. $AgNO_3$ at 95°C. ○ experimental; △ calculated, å = 4.35, Λ° = 340.6.
FIG. 3. NH_4NO_3 at 25C°. ○ experimental; △ calculated, å = 4.35, Λ° = 144.84.
FIG. 4. NH_4NO_3 at 95°C. ○ experimental; △ calculated, å = 4.35, Λ° = 365.
FIG. 5. $LiNO_3$ at 25°C. ○ experimental; △ calculated, å = 4.5, Λ° = 110.13.

TABLE IV

LITHIUM NITRATE AT 25°; $\Lambda^\circ = 110.13$

			Λ_{calc}				
C	η/η_0	Λ_{exp}	å = 3.5	å = 4.0	å = 4.5	å = 5.0	å = 6.0
0.00997	1.005	102.79	101.94	102.04	102.3	102.5	102.47
0.09902	1.013	91.74	90.42	91.05	90.88	91.46	92.45
0.5526	1.063	76.86	75.52	—	75.18	76.82	79.04
0.9579	1.109	70.26	70.01	—	68.75	70.15	
0.9951	1.111	69.78			68.33	69.86	
1.8855	1.221	58.95			58.22	59.44	
2.7401	1.351	50.60	56.66		50.41	52.02	
3.4560	1.490	44.72			44.44	45.96	
3.6980	1.534	42.81			42.78	44.26	
4.857	1.826	34.69			34.89	35.86	
5.337	1.984	31.66			31.43	32.58	
6.916	2.637	23.52			22.69	23.50	
7.427	2.914	21.24			20.31	20.99	
8.725	3.849	16.51			14.86	15.40	
9.130	4.218	15.20			13.34	13.93	

of lithium nitrate, to demonstrate this. In view of Dr. Stokes' remark that nitrates are liable to ion-pair formation, in general we have preferred those values of å which give a calculated Λ greater than that we have observed, and from the α-value thus obtained we have calculated a dissociation constant; for silver nitrate it is reasonably constant. The agreement between Λ_{exp} and Λ_{calc} for lithium nitrate, using an å value of 4.5 Å, is so close, i.e. $\alpha \sim 1$, that we prefer these results and therefore we have not attempted to calculate a dissociation constant. This means that we believe there is no ion-pair formation in lithium nitrate solutions up to at least 7 N. Such deviations as do occur may be due to the viscosity correction being uncertain (*vide supra*, p. 889). This leaves the problem of explaining why lithium nitrate should not form ion-pairs, while other nitrates do, but a ready explanation offers itself in the well-known fact, or supposition, that the lithium ion is highly hydrated, in comparison with other univalent ions.

The equation of Stokes seems to us to constitute a major advance, in that it carries the Debye–Hückel–Onsager concepts up to a concentration of from 3 to 5 N. It is of course true that the figures obtained are far from exhibiting that close correspondence with the experimental results which an empirical equation might give but this is not the point. A similar objection might be made to van der Waals' equation of state, as contrasted with other empirical and semiempirical equations, but van der Waals' equation is still the best for teaching and theoretical purposes, because of the clear and relatively simple picture it gives of the structure of a compressed gas. The same may be said of Stokes' equation; it supplies a mechanism of conductance up to a region of truly high concentration.

The essential virtue of Stokes' equation is that it is entirely free from empiricism, every quantity contained in it having a clear physical meaning. It may be objected that å, the distance of closest approach of the ions, is really only an empirical constant, but against this there are the strong objections that

it is always of the order of magnitude that would be expected and, above all, is independent of temperature. We note that, in agreement with Stokes' suggestion, the α-values are larger at the higher temperatures (using of course the same å values), that is, ion-pair formation is less. As would be expected, the calculated results, measured in terms of so-called α-values, become meaningless above a concentration of about 5 N.

For solutions of the highest concentration and for anhydrous melts it may be that an entirely new theory is called for. In this connection, we cannot help referring again to an observation made by Mr. John Herron (2), when working with us, viz. that from the region of, say, 5 N (where the Stokes' equation begins to break down) the plot of Λ against log C is a rigorously straight line. This has recently been confirmed by Debus' observations on lithium nitrate (up to 9N). To say that any quantity plotted against log C would be a straight line or that the curve is merely approaching a straight line is incorrect; the curve is absolutely straight by any test with which we are acquainted. The observation is quite empirical but, if it is accepted, any proposed theory will have to account for this.

REFERENCES

1. CAMPBELL, A. N. and KARTZMARK, E. M. Can. J. Research, B, 28: 43, 161. 1950; Can. J. Chem. 30: 128. 1952. CAMPBELL, A. N., KARTZMARK, E. M., BISSETT, D., and BEDNAS, M. E. Can. J. Chem. 31: 303. 1953. CAMPBELL, A. N., GRAY, A. R., and KARTZMARK, E. M. Can. J. Chem. 31: 617. 1953. CAMPBELL, A. N., KARTZMARK, E. M., BEDNAS, M. E., and HERRON, J. T. Can. J. Chem. 32: 1051. 1954.
2. CAMPBELL, A. N., KARTZMARK, E. M., BEDNAS, M. E., and HERRON, J. T. Can. J. Chem. 32: 1051. 1954.
3. FALKENHAGEN, H., LEIST, M., and KELBG, G. Ann. Physik, 6(II): 51. 1952.
4. HARNED, H. S. and OWEN, B. B. The physical chemistry of electrolytic solutions. Reinhold Publishing Corp., New York. 1943.
5. KORTÜM-BOCKRIS. Textbook of electrochemistry, Vol. 1. Elsevier Publishing Company, Maastricht. 1951. p. 191.
6. MACINNES, D. A. Principles of electrochemistry. Reinhold Publishing Corp., New York. 1939. p. 339.
7. ONSAGER, L. and FUOSS, R. M. J. Phys. Chem. 36: 2689. 1932.
8. SHEDLOVSKY, T. J. Am. Chem. Soc. 54: 1405. 1932.
9. WISHAW, B. F. and STOKES, R. H. J. Am. Chem. Soc. 76: 2065. 1954.
10. WYMAN, J., Jr. and INGALLS, E. N. J. Am. Chem. Soc. 60: 1182. 1938.

STUDIES ON CARRAGEENIN: THE EFFECT OF SHEAR RATE ON VISCOSITY[1]

By C. R. Masson and D. A. I. Goring

ABSTRACT

The viscosity of aqueous solutions of carrageenin of high molecular weight was markedly dependent on the rate of shear. The shear-dependence increased with decrease in the concentration of added electrolyte. Because of curvature, extrapolation of $[\eta]$ to zero rate of shear was not possible. The Huggins interaction coefficient, k', increased with decrease in rate of shear; k' also increased with increase in concentration of added electrolyte. In water, maxima of η_{sp}/c were observed at concentrations of carrageenin equivalent to the ionic impurities in the distilled water used. At higher concentrations the data fitted the Fuoss equation at rates of shear of 200 and 100 sec.$^{-1}$ but not below 100 sec.$^{-1}$ The constants A and D both increased with decrease in rate of shear.

INTRODUCTION

The polysaccharide carrageenin, a water-soluble extract of the red alga *Chondrus crispus*, is of interest as a naturally occurring polyelectrolyte of high molecular weight. Solutions of carrageenin show a wide range in viscosity (2, 6, 8, 9) depending on the method of preparation and treatment of the extract. The intrinsic viscosity, $[\eta]$, is important as a means of characterizing any given sample.

It has been shown previously (8) that the viscosity of solutions of carrageenin of relatively low molecular weight is similar to that of other polyelectrolytes, while for extracts of higher molecular weight the viscosity becomes shear-dependent. The present work is part of an attempt to establish some general measurement of viscosity independent of rate of shear or intermolecular interaction. This paper describes the effect of shear rate on the viscosity of aqueous solutions of carrageenin, both in the presence and absence of added salts.

EXPERIMENTAL

Preparation of Extract

Carrageenin was extracted with water at 80°C. from the residue of a preliminary extraction at 30°C.–40°C. In order to obtain a product of high molecular weight care was taken to avoid undue degradation or bacterial contamination.

The extract was filtered through a No. 10 "Selas" porcelain filter and precipitated in four volumes of 95% ethanol. The white fibrous material was washed in absolute ethanol and ether, dried *in vacuo*, ground to pass a 20-mesh screen, and stored at −13°C. This extract is referred to in this and subsequent work as "Extract G". A preliminary osmometric determination of its molecular weight gave a value of 2,500,000.

Recent work (6, 12, 13) has shown that carrageenin contains at least two components, distinguishable mainly by their gelling tendencies. Although no

[1]*Manuscript received January 17, 1955.*
Contribution from the Maritime Regional Laboratory, National Research Council, Halifax, Nova Scotia. Issued as N.R.C. No. 3569.

attempt was made in the present investigation to separate these components, recent results (6) indicated that a hot extract prepared in the above manner consists largely of the gelling fraction.

Preparation of Solutions

Solutions were made up as required by tumbling at room temperature. The sodium salt of the polyelectrolyte was used in all experiments. This was prepared by passing a solution of concentration 0.1 to 0.2 gm. dl.$^{-1}$ down a column of Amberlite IR 100 ion exchange resin. Final clarification was achieved with a No. 02 Selas filter element.

Buffering salts were added by mixing known volumes of the carrageenin with a stronger salt solution. The three ionic conditions studied were (1) distilled water, (2) $M/30$ sodium phosphate at pH 7.0 (referred to as $M/30$ phosphate), (3) $M/30$ sodium phosphate plus $M/20$ sodium chloride at pH 7.0 (referred to as $M/12$ phosphate/NaCl).

Viscosity Measurements

Capillary viscometers, each equipped with a series of bulbs to provide different hydrostatic heads, were employed. Various designs were tried in order to cover as wide a range of shear gradients as possible.

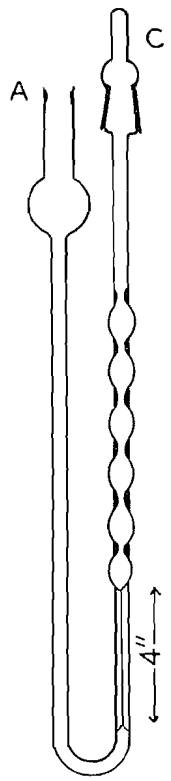

FIG. 1. Viscometer for checking on the possibility of drainage errors.

Three of the viscometers were similar to the one described by Schurz and Immergut (11). By using various lengths of capillary tubing a range of shear gradients for water between 221 and 2135 sec.$^{-1}$ was obtained. Where measurements were taken with different viscometers over the same range of shear gradients, the difference between the results was less than two per cent.

The design of a fourth viscometer, shown in Fig. 1, was such as to allow the liquid to flow into the dry bulbs, thus providing a check on the possibility of drainage errors. The viscometer was filled through A with cap C closed. Sufficient time was allowed for temperature equilibrium to be established, cap C was then removed, and the time required to fill each bulb in turn was noted. The range of shear gradients covered was 607 to 2061 sec.$^{-1}$ Results obtained with this instrument for a highly viscous aqueous solution agreed within experimental error with data from one of the other viscometers. Thus drainage errors were inappreciable.

Measurements were made at 25°C. in thermostats controlled to ±0.05°C. or better. Kinetic energy corrections were applied to all the results. Viscometers were calibrated by measuring the flow times of glycerol–water mixtures of known density and viscosity. Kinetic energy corrections were calculated for each bulb by the usual method. In one viscometer the correction for water in the bulb with the highest shear was 6% of the flow time and the correction decreased with increasing time of flow. All other corrections were lower than this and in several viscometers were negligible. The intrinsic viscosity, $[\eta]$, was obtained from the specific viscosity, η_{sp}, by the usual relationship

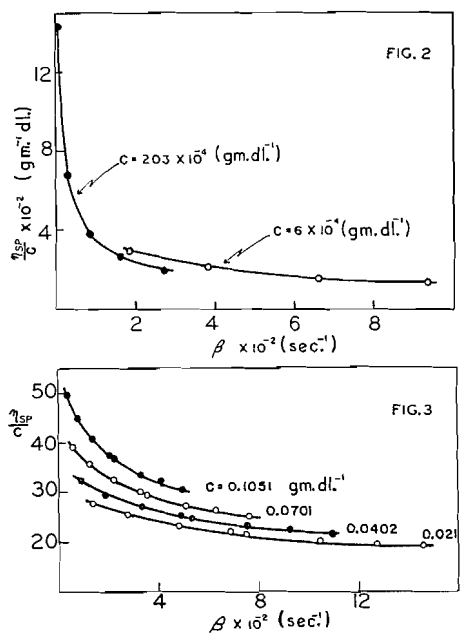

FIG. 2. η_{sp}/c vs. β for Extract G in water.
FIG. 3. η_{sp}/c vs. β for Extract G in $M/12$ phosphate/NaCl.

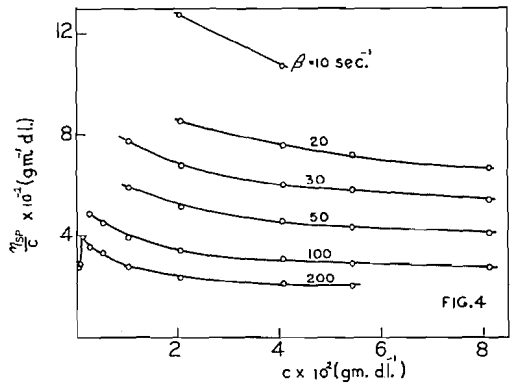

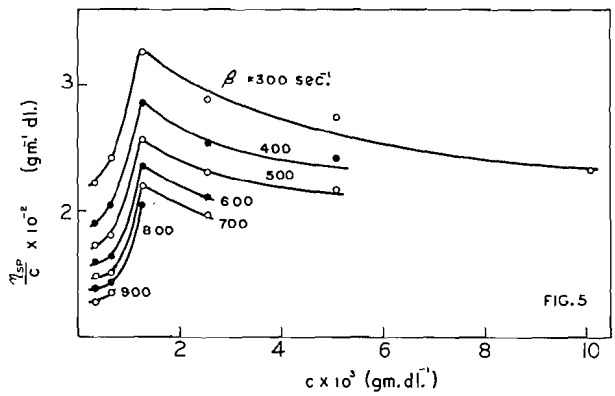

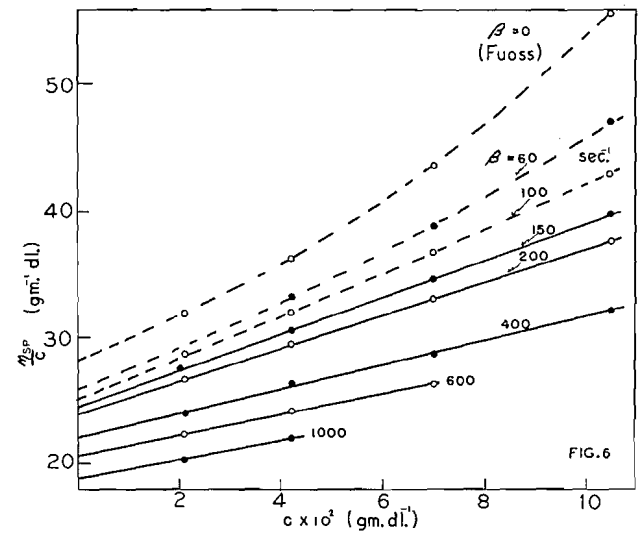

FIG. 4. Isoshear graphs of η_{sp}/c vs. c for Extract G in water. Values of β are from 10–200 sec.$^{-1}$

FIG. 5. Isoshear graphs of η_{sp}/c vs. c for Extract G in water. Values of β are from 300–900 sec.$^{-1}$

FIG. 6. Isoshear graphs of η_{sp}/c. vs. c for Extract G in $M/12$ phosphate/NaCl.

[1] $$[\eta] = (\eta_{sp}/c)_{c\to 0}$$

The average shear gradient, β, was calculated from

[2] $$\beta = 8V/3\pi r^3 t$$

where V is the volume of bulb, r is the radius of capillary, and t is the time of flow.

RESULTS

Experimental curves of η_{sp}/c vs. β for various concentrations of Extract G in water and $M/12$ phosphate/NaCl are given in Figs. 2 and 3. From such curves, values of η_{sp}/c at constant shear were derived and isoshear graphs of η_{sp}/c vs. c (Figs. 4, 5, and 6) were drawn. In $M/12$ phosphate/NaCl, as shown in Fig. 6, η_{sp}/c varied linearly with c except for the slight curvature at $\beta = 60$ sec.$^{-1}$ Extrapolation to $c = 0$ gave values of $[\eta]$ corresponding to definite shear rates. Similar results were obtained with $M/30$ phosphate; $[\eta]$ is plotted against β in Fig. 7 for both sets of measurements.

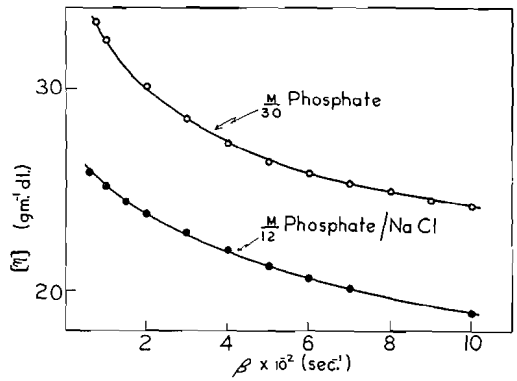

FIG. 7. Intrinsic viscosity vs. shear rate for Extract G in $M/30$ phosphate and $M/12$ phosphate/NaCl.

The isoshear graphs for Extract G in water did not permit extrapolation to zero concentration. At low shear rates (Fig. 4) the plots were curved upwards; at higher shear rates, where measurements could be carried to very low concentrations, distinct maxima in the plots were observed (Fig. 5).

DISCUSSION

The results fit the general pattern of polyelectrolyte behavior. Solutions containing added electrolyte behave like those of uncharged polymers, with the exception that curvature is noted in the plots of η_{sp}/c against c at low rates of shear (Fig. 6). This makes it difficult to obtain accurate values of $[\eta]$ at low shear rates. In addition, since the plot of $[\eta]$ vs. β (Fig. 7) is also curved, the value of $[\eta]$ at zero rate of shear can not be determined by extrapolation with any degree of accuracy.

An interesting feature of these measurements concerns the magnitude of the Huggins (7) interaction coefficient, k'. As shown in Table I, k' increases with

TABLE I

VALUES OF k' AT VARIOUS SHEAR GRADIENTS FOR EXTRACT G IN $M/30$ PHOSPHATE AND $M/12$ PHOSPHATE/NaCl

β	$k' \times 10^3$,	
sec.$^{-1}$	$M/30$ phosphate	$M/12$ phosphate/NaCl
1000	117	
700	140	193
600	147	193
500	153	196
400	156	198
300	161	208
200	169	232
150		248
100		281

decreasing shear rate. Solutions of high molecular weight carrageenin have been shown to have a yield point which increases at higher concentration (8). Thus an increase in the concentration dependence of η_{sp}/c at low rates of shear might be expected. A similar dependence of k' on shear gradient has recently been noted (10) for solutions of cellulose and cellulose nitrate.

It is also of interest that the values of k' are higher with $M/12$ phosphate/NaCl than with $M/30$ phosphate, when comparison is made at the same rate of shear or the same intrinsic viscosity. This is the opposite behavior to that anticipated if the effect of adding salt is to cause a further coiling of the molecule in solution. A possible explanation is that neutralization of the charges on the polymer chain by the addition of electrolyte results in a decrease in electrostatic repulsion between neighboring chains thereby allowing an increase in some structure-forming tendency. In the case of carrageenin, the latter effect may predominate under the conditions studied. This interpretation is consistent with the gelling tendency of solutions of certain fractions of carrageenin (6) on the addition of electrolytes. A detailed interpretation of this anomaly must await the development of an adequate theory of polyelectrolyte solutions.

Regarding the measurements in the absence of added salts (Figs. 4 and 5), the occurrence of maxima similar to those observed here has been noted by Conway and Butler (1) for dilute solutions of thymus nucleic acid. Fuoss and Cathers (4) have shown that for solutions containing traces of added salt, such maxima are to be expected when the concentration of ions from the polyelectrolyte and salt are roughly equivalent. The specific conductance of the distilled water was approximately 2×10^{-6} mho cm.$^{-1}$ This could be attributed to sodium chloride in a concentration of 2×10^{-5} M. The maxima in the curves occur at a carrageenin concentration of 0.0012 gm. dl.$^{-1}$ The sulphate content (as OSO_3^-) of carrageenin is approximately 25% giving a value of 384 for the equivalent weight. The "molar" concentration of carrageenin was therefore 3×10^{-5} M. The occurrence of maxima in the viscosity curves in this region is thus probably due to the suppression of ionization by foreign cations in roughly equivalent concentration. Such effects have been

predicted by Flory and Osterheld (3) but can only be observed with polyelectrolytes of high molecular weight where viscosity measurements are still practicable at very low concentrations.

The curves shown in Fig. 4 have been plotted according to the equation of Fuoss and Cathers (4)

$$[3] \qquad z = \eta_{sp}/c = \frac{A}{1+Bc^{\frac{1}{2}}} + D.$$

Previous work (8) has shown that this equation adequately fits the viscosity–concentration relationship for carrageenin of low molecular weight. In the present work, the occurrence of maxima at $c = 0.0012$ gm. dl.$^{-1}$ makes the shape of the curves of η_{sp}/c vs. c uncertain at low concentrations. It was assumed, however, that this would not influence η_{sp}/c at concentrations above 0.01 gm. dl.$^{-1}$

From the linear plots of η_{sp}/c vs. $c^{-\frac{1}{2}}$, values of D were obtained at various shear rates. As shown in Fig. 8, D is markedly shear-dependent, increasing rapidly at low values of β. Since D represents the reduced specific viscosity at $c = \infty$, this means that even in concentrated solutions the molecule is rod-shaped. Values of D are higher than the corresponding intrinsic viscosities in salt solutions indicating that the coiling effect of a high concentration of polyelectrolyte is not as great as that of small quantities of added salt.

In Fig. 9, plots of $1/(z-D)$ vs. $c^{\frac{1}{2}}$ at various shear rates are shown. The plots are linear for shear rates of 200 and 100 sec.$^{-1}$ but become curved at lower shear. For $\beta = 200$ and 100 sec.$^{-1}$, A was respectively 800 and 1240 gm.$^{-1}$ dl. also

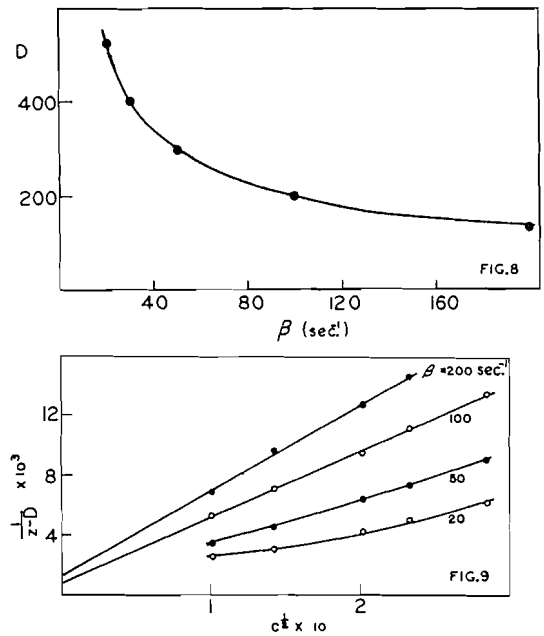

FIG. 8. Variation of D with rate of shear for Extract G in water.
FIG. 9. Graph of $1/(z-D)$ vs. $c^{\frac{1}{2}}$ for Extract G in water.

showing marked shear-dependence. Values of 46 (±5) and 55 (±8) were obtained for the constant B at 200 and 100 sec.$^{-1}$ respectively. These values are similar to those obtained previously with a low molecular weight sample (8).

The data have also been analyzed by the method of Goldberg and Fuoss (5), in which $1/\eta$ is plotted against $\eta\beta$. For Extract G in water (Fig. 10) the results are similar to those obtained by these authors for aqueous solutions of poly-*n*-N-butyl-4-vinylpyridine. At high concentrations the relationship is linear, but extrapolation yields apparently negative values of $1/\eta$, indicating curvature near the origin. At lower concentrations the relationship is non-linear and extrapolation is uncertain.

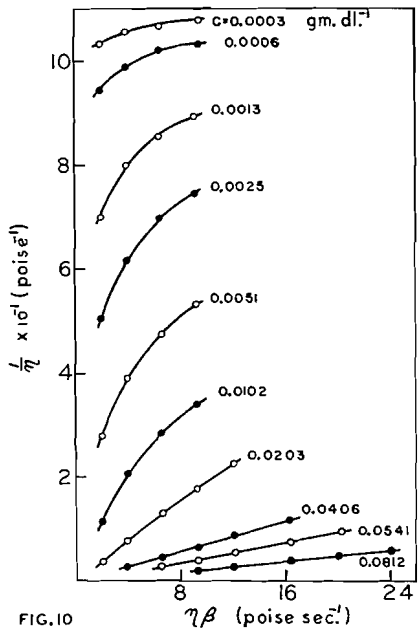

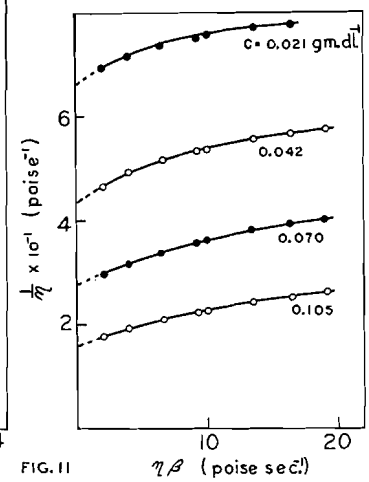

FIG. 10. Graph of $1/\eta$ vs. $\eta\beta$ for Extract G in water.
FIG. 11. Graph of $1/\eta$ vs. $\eta\beta$ for Extract G in $M/12$ phosphate/NaCl.

For the results in $M/12$ phosphate/NaCl, the curvature in these plots was not so pronounced (Fig. 11), and the method was applied to obtain a rough estimate of the value of $[\eta]$ at zero rate of shear. The curve of η_{sp}/c vs. c at zero rate of shear which is obtained in this way is included in Fig. 6.

Other empirical methods which have been described in the literature have been applied to the above results in attempts to extrapolate to zero rate of shear. All methods tried were unsuccessful; for characterization of the polyelectrolyte it appears best at present to use the value of $[\eta]$ at some arbitrary shear rate above 100 sec.$^{-1}$

ACKNOWLEDGMENTS

The authors are indebted to Dr. E. Gordon Young for help and advice in preparing the manuscript, and also to Messrs. G. W. Caines and J. MacAulay for technical assistance.

REFERENCES

1. CONWAY, B. E. and BUTLER, J. A. V. J. Polymer Sci. 11: 277. 1953.
2. COOK, W. H., ROSE, R. C., and COLVIN, J. R. Biochim. et Biophys. Acta, 8: 595. 1952.
3. FLORY, P. J. and OSTERHELD, J. E. J. Phys. Chem. 58: 653. 1954.
4. FUOSS, R. M. and CATHERS, G. I. J. Polymer Sci. 4: 97. 1949.
5. GOLDBERG, P. and FUOSS, R. M. J. Phys. Chem. 58: 648. 1954.
6. GORING, D. A. I. and YOUNG, E. G. Can. J. Chem. 33: 480. 1955.
7. HUGGINS, M. L. J. Am. Chem. Soc. 64: 2716. 1942.
8. MASSON, C. R. and CAINES, G. W. Can. J. Chem. 32: 51. 1954.
9. ROSE, R. C. Can. J. Research, F, 28: 202. 1950.
10. SCHURZ, J. J. Polymer Sci. 10: 123. 1953.
11. SCHURZ, J. and IMMERGUT, E. H. J. Polymer Sci. 9: 279. 1952.
12. SMITH, D. B. and COOK, W. H. Arch. Biochem. and Biophys. 45: 232. 1953.
13. SMITH, D. B., COOK, W. H., and NEAL, J. L. Arch. Biochem. and Biophys. 53: 192. 1954.

THE HEAT OF WETTING OF SILK FIBROIN BY WATER[1]

By H. Brian Dunford[2] and John L. Morrison[3]

ABSTRACT

The heats of wetting by water of silk fibroin initially containing various amounts of adsorbed and desorbed water have been measured. These measurements along with the water vapor adsorption isotherm of Hutton and Gartside have been used to calculate the integral and differential heats, free energies, and entropies of adsorption. In contrast with cellulose, silk containing desorbed water evolves less heat than that containing adsorbed water. This fact suggests that any contribution by a heat of swelling term is very small for silk fibroin, so that the calculated thermodynamic properties probably can be assigned almost entirely to the adsorption process. The changes in the heats and entropies of adsorption appear to parallel the sequence of changes in film formation as revealed by surface area calculations.

Bull (2) determined the water vapor adsorption isotherms of a large number of proteins including silk fibroin at 25° and 40°C. Dole and McLaren (4) and Davis and McLaren (3) corrected and extended Bull's thermodynamic calculations of the water–protein systems. In these calculations, isosteric heats of adsorption were obtained by applying the Clausius–Clapeyron equation to the adsorption isotherms at the two different temperatures. Much uncertainty in this method of determining heats of adsorption occurs in the low and high water vapor pressure regions, yet it is these regions that are very important in understanding the nature of the adsorption process.

Direct measurement of the heats of wetting of water by silk fibroin over the whole range of vapor pressures are reported here. With these data and the adsorption isotherm of Hutton and Gartside (11), the thermodynamic functions have been calculated. The only reported similar measurements that have come to our attention were made at four initial water contents by Hedges (8).

EXPERIMENTAL

Rotating Adiabatic Calorimeter

A rotating adiabatic calorimeter as originally designed by Lipsett, Johnson, and Maass (13, 14) was used with some small modifications (1, 5).

The heat capacity of the calorimeter was obtained by the method used for the original apparatus (13). This consisted of measuring the heat of solution of sodium chloride in water, using sets of two determinations with the same salt–water ratios but differing absolute amounts of reactants. The average heat capacity for seven sets of determinations was within 0.08 calories of the calculated value of 13.09 calories. Although this is an error of 0.6% for the metal container, it is only 0.1% for the total heat capacity when the 50 ml. of accurately weighed water used for all heat of wetting measurements is included.

[1]*Manuscript received January 18, 1955.*
Contribution from the Department of Chemistry, University of Alberta, Edmonton, Alberta. Based on a thesis submitted to the School of Graduate Studies, University of Alberta, in partial fulfillment of the requirements for the M.Sc. degree. Presented in part to the Annual Conference of the Chemical Institute of Canada, Windsor, Ontario, June 4–6, 1953.
[2]*Present address: Department of Chemistry, McMaster University, Hamilton, Ontario.*
[3]*Associate Professor, Department of Chemistry, University of Alberta, Edmonton, Alberta.*

Evacuated Glass Calorimeter

The heat of wetting measurements were carried out in air. To determine the magnitude of the heat effect arising from the desorption of the air by water, some heat of wetting measurements were made in a simple vacuum calorimeter.

The glass reaction cell of the calorimeter was similar to that of Howard and Culbertson (10) and consisted of two compartments, one of about 20 ml. volume to hold the evacuated silk sample, and the other of about 50 ml. to hold the water. Upon breaking the hook-shaped thin glass partition between the two compartments, the water came in contact with the silk. The whole assembly, including glass cell, Beckmann thermometer, 50 ohm resistance wire, and glass stirring rod, was immersed in xylene (low heat capacity liquid) contained in a Dewar flask (inside dimensions: 6.7 cm. diameter by 28 cm. height). The top was sealed as completely as possible by a waxed cork. The glass cell was discarded after an experiment.

The temperature rise of the wetting process was simulated electrically so that it was unnecessary to determine the heat capacity of the calorimeter.

Silk Fibroin

Japanese raw silk was kindly supplied by Belding-Corticelli Ltd., Montreal. It was degummed by the method of Sookne and Harris (19).

Drying and Moistening Procedures

Most samples were dried by a procedure similar to that of Hedges (8). A stream of compressed air was passed successively through absorbent cotton, sulphuric acid scrubbers, sodium hydroxide pellets, and magnesium perchlorate towers. The dry air entered a copper coil and desiccator inside an oven at $105\pm1°C$. After it was dried for two hours in the oven desiccator, the sample was placed in a specially designed desiccator (16) over phosphorus pentoxide for 30 min. to cool.

If the sample was being used to determine the heat of wetting at the above dryness, the container for drying the sample was the inner box of the calorimeter. If, however, the sample was being prepared for heats of wetting measurements at finite initial moisture contents, the drying container was a weighing bottle. After the dry weight of the silk was obtained, the weighing bottle was placed over an aqueous sulphuric acid solution of concentration necessary to give the required initial moisture content. Then, after at least three days, the sample was transferred as rapidly as possible to the inner box of the calorimeter, covered by the weighed greased lid, and reweighed to determine the moisture content.

Some heat of wetting measurements were made on samples from which water had been partially desorbed. First, the samples were placed over distilled water, and then over various aqueous sulphuric acid solutions.

Bull's data as well as the present measurements are on a vacuum-dry basis. Three samples which had been previously dried by the above method were dried for two hours in an Aberhalden vacuum drying apparatus which uses boiling water as a heat source. These determinations showed that the oven-

dried samples contained 0.20% moisture on the vacuum-dry basis. The heat of wetting of one of these samples was determined.

Finally, for the heat of wetting measurements of evacuated samples, the silk was dried *in vacuo* at 105°C. by an electric furnace.

RESULTS AND CALCULATIONS

Net Heat of Adsorption

The heats of wetting of silk fibroin at 25°C. and equilibrated with various amounts of water, both adsorbed and desorbed, are given in Table I and Fig. 1. For comparison, Hedges' four determinations (8) are included in Fig. 1. A comparison of the degree of precision of our calorimetry with that of Hedges may be shown by the fact that, in our case, the mean deviation of three determinations at 0.20% moisture content is ± 0.03 cal. gm.$^{-1}$, while the mean deviation of Hedges' four values for the heat of wetting of dry wool is ± 0.4 cal. gm.$^{-1}$.

The measurements of the heat of wetting of seven evacuated samples in the Dewar calorimeter gave an average of 15.94 ± 0.11 cal. gm.$^{-1}$. Since these values agree with the result obtained in the presence of air, the air has no measurable effect. Also, the value of the initial, vacuum-dried sample (15.93) was confirmed by a different type of calorimeter.

The integral net heats of adsorption, ΔH, in calories per 100 gm. silk fibroin (above the heat of condensation of water vapor to liquid) have been calculated from the heats of wetting by the method of Dole and McLaren (4) (See also Wahba (21)).

In our case, the *heat of wetting*, q_0, of 100 gm. dry protein is evolved by Process 1.

(1) Protein (dry at $p = 0$) + excess liq. H_2O (at p_0) $\rightarrow$ Protein (with excess liq. H_2O at p_0), in which p_0 is the vapor pressure of pure water at 25°C.

TABLE I

HEATS OF WETTING OF SILK FIBROIN CONTAINING ADSORBED AND DESORBED WATER VAPOR

Adsorption		Adsorption		Desorption	
Water content, %	Heat of wetting, cal.	Water content, %	Heat of wetting, cal.	Water content, %	Heat of wetting, cal.
0.00	15.93	8.38	4.03	1.24	12.47
0.20	15.71	8.45	3.70	1.45	11.72
0.54	14.64	9.73	2.98	3.82	8.83
0.71	14.40	10.39	2.51	5.64	6.31
0.86	14.09	11.87	1.83	7.59	4.36
1.11	13.24	12.11	1.68	9.98	2.48
2.52	10.92	14.19	1.13		
2.56	10.78	14.20	1.03		
4.14	8.51	16.4	0.69		
4.23	8.37	23.9	0.34		
5.80	6.42	25.2	0.19		
5.90	6.39				

Note: Water content is in per cent of the dry weight of fibroin. The heats of wetting are given in calories per gram of dry fibroin.

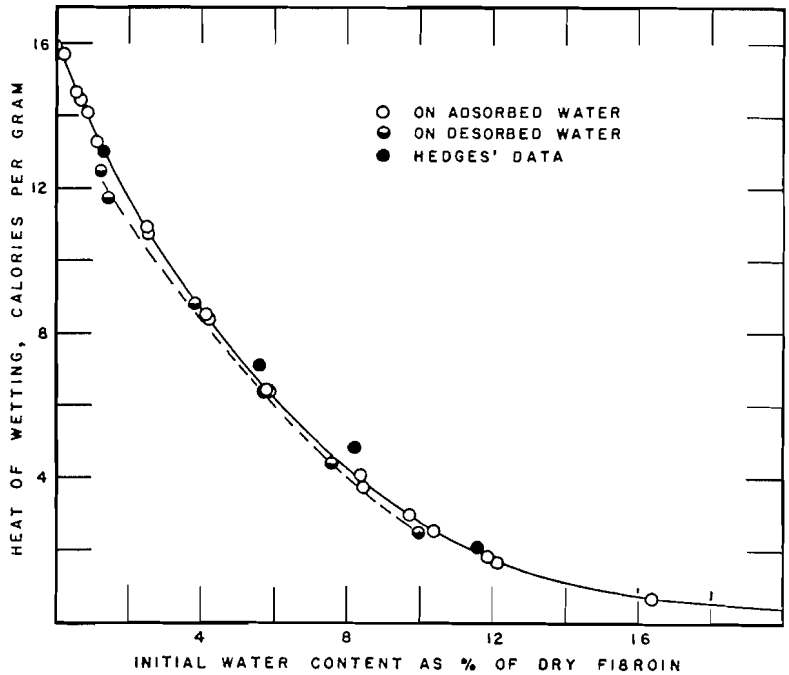

FIG. 1. The heats of wetting by water of silk fibroin containing various amounts of adsorbed and desorbed water.

When 100 gm. protein has been equilibrated in water vapor at pressure p and has taken up n moles of water, the *heat of wetting*, q, is evolved by Process 2.

(2) Protein (with n H_2O at p) + excess liq. H_2O (at p_0) → Protein (with excess liq. H_2O at p_0).

TABLE II

CALCULATED THERMODYNAMIC PROPERTIES OF THE SILK–WATER SYSTEM AT 25°C.

n	P/P_0	$-\Delta H$	$-\Delta F$	$-\Delta S$	$-\overline{\Delta H}$	$-\overline{\Delta F}$	$-\overline{\Delta S}$
0	0	0	0	0	4665	—	—
0.05	.015	215	151	0.22	3880	~2400	~4.97
0.10	.040	390	265	0.42	3170	1820	4.53
0.20	.150	660	414	0.83	2460	1125	4.48
0.30	.300	900	503	1.33	2230	705	5.12
0.35	.377	1010	535	1.59	2160	575	5.32
0.40	.452	1105	561	1.88	1750	475	4.28
0.50	.588	1255	600	2.20	1210	320	2.99
0.60	.703	1360	625	2.47	870	210	2.21
0.70	.777	1435	642	2.66	600	150	1.51
0.80	.830	1490	655	2.80	440	110	1.11
0.90	.868	1520	665	2.87	270	85	0.62
1.00	.898	1545	672	2.93	155	65	0.30
1.20	.938	1560	683	2.94	50	35	0.05
1.40	.965	1570	688	2.96	—	—	—

Note on units: n, moles per 100 gm. fibroin; ΔH and ΔF, calories per 100 gm. fibroin; $\overline{\Delta H}$ and $\overline{\Delta F}$, calories per mole of water; ΔS, entropy units per 100 gm. fibroin; $\overline{\Delta S}$, entropy units per mole of water.

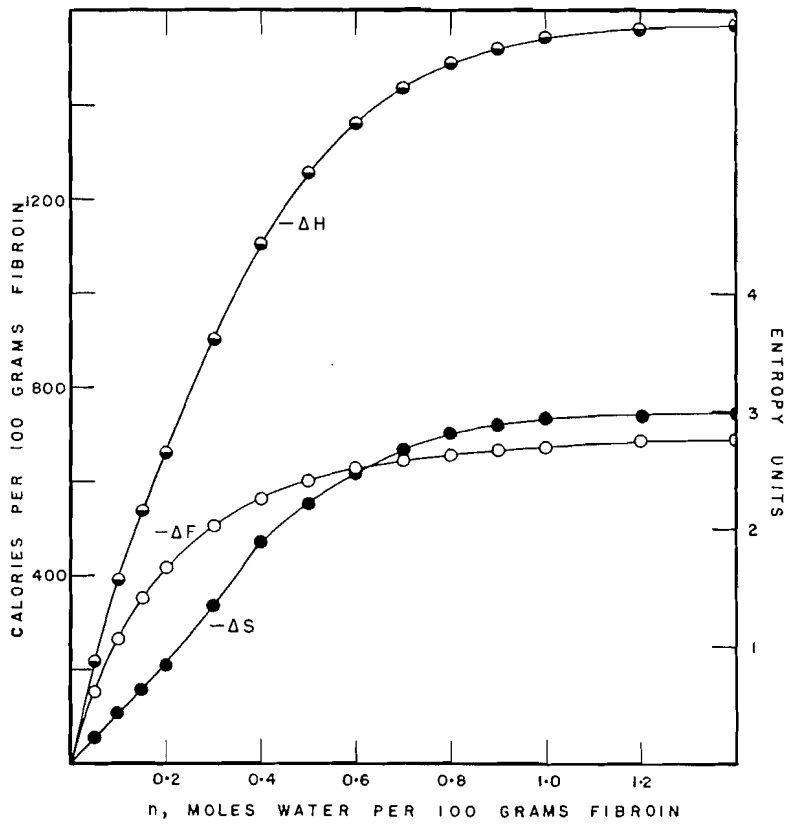

FIG. 2. The integral heat, free energy, and entropy of adsorption of water by silk fibroin.

Subtraction of Process 2 from Process 1 gives Process 3:

(3) Protein (dry at $p = 0$)$+n$ H_2O (at p_0) $\rightarrow$ Protein (with n H_2O at p), with the evolution of (q_0-q) calories/100 gm. dry protein, or ΔH, the integral net heat of adsorption.

Our Process 3 is the same as Dole and McLaren's Process (4). Values of ΔH are given in Table II and Fig. 2.

The differential net heats of adsorption, $\overline{\Delta H}$, given in Table II and Fig. 3, were obtained by careful graphical differentiation of the plot of ΔH vs. n, the number of moles of water adsorbed per 100 gm. fibroin.

Free Energy of Adsorption

The integral and differential free energies of adsorption of water on a protein are obtained from the vapor adsorption isotherm. Following Dole and McLaren (4), the differential free energy, $\overline{\Delta F}$, is given by

$$\overline{\Delta F} = RT \ln (P/P_0)$$

and the integral free energy, ΔF, of *our* Process 3 is given by

$$\Delta F = -RT \int_0^1 n d \ln(P/P_0) + nRT \ln(P/P_0).$$

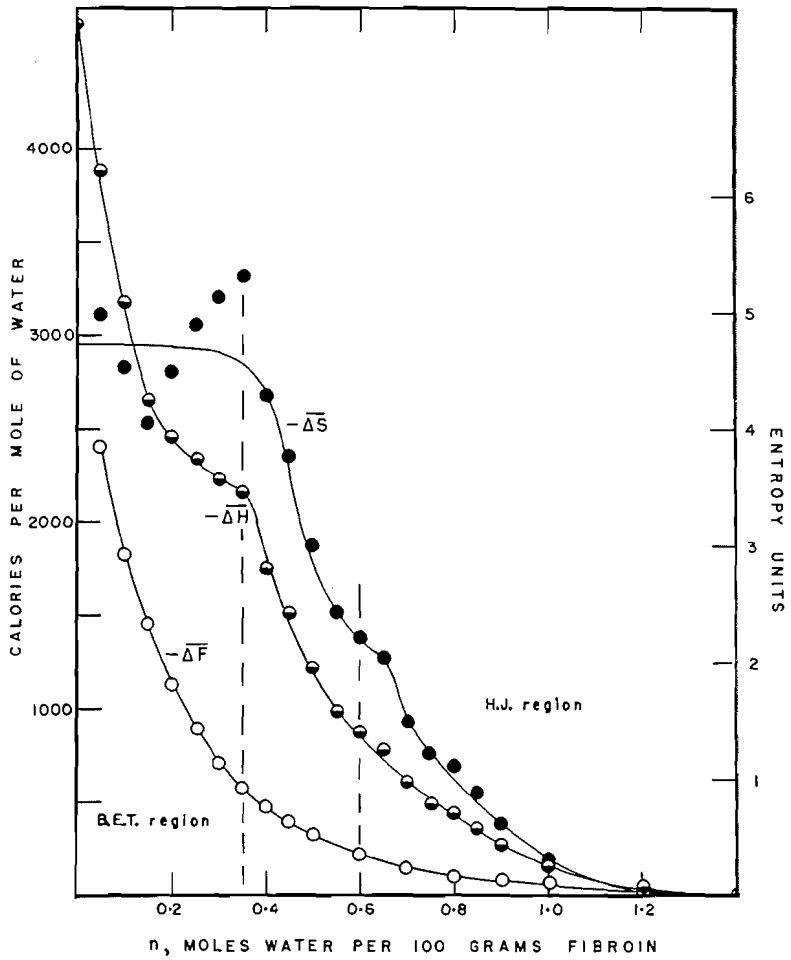

FIG. 3. The differential heat, free energy, and entropy of adsorption of water by silk fibroin.

A number of attempts were made to obtain a reproducible adsorption isotherm with a vacuum apparatus like that used by Wiig and Juhola (22) for charcoal. Although the middle and upper pressure parts of the adsorption branch matched the corresponding parts of the isotherm of Hutton and Gartside (11), the amount adsorbed in the low pressure region was lower than that obtained by them and others (2, 18). It was realized that the determination of the correct isotherm is a major project in itself.

Fortunately, Hutton and Gartside (11) have carried out an exhaustive study of the water isotherm on silk at 25°C. They found that degummed silks of Japanese, Chinese, and Italian origins gave practically the same isotherm, and by both the vacuum and the desiccator methods.

Dunford and Morrison (6) have shown that the Brunauer, Emmett, and Teller equation and the Harkins–Jura equation, although applying to the opposite extremes of Bull's water–protein systems, gave the same monolayer

adsorption for each protein. Liang's method (12) was used to correlate the two equations. These equations were applied to the isotherm of Hutton and Gartside. The B.E.T. plot gave a straight line over the relative pressure range 0.07 to 0.35, with a monolayer content, X_m, of 4.49 gm. water per 100 gm. silk fibroin. The H.J. plot gave a straight line over the relative pressure range 0.60 to 0.97 (and probably to 1.00), with $X_m = 4.46$ gm. It is considered that this coincidence of X_m values further validates the isotherm. The same test applied to our isotherm failed to produce a straight line for the B.E.T. plot, while it gave a value of $X_m = 4.48$ gm. for the H.J. plot.

Thus, the water vapor adsorption isotherm of Hutton and Gartside was used to calculate ΔF and $\overline{\Delta F}$, the results of which are given in Table II and Figs. 2 and 3.

Entropy of Adsorption

The integral and differential net entropies of adsorption, calculated by the well known equations

$$\Delta S = (\Delta H - \Delta F)/T$$
$$\text{and} \quad \overline{\Delta S} = (\overline{\Delta H} - \overline{\Delta F})/T,$$

are given in Table II and Figs. 2 and 3.

DISCUSSION

Comparison with Calculations of Davis and McLaren

The results shown in Figs. 2 and 3 may be compared with the corresponding calculations of Davis and McLaren (3), based on Bull's data (2). In contrast with their results, the present integral heats and entropies in Fig. 2 reach higher values and approach maximum values as saturation vapor pressure is reached.

The differential heats and entropies in Fig. 3 show similar general features to those of Davis and McLaren except at the extremes of the vapor pressure range. In the low pressure range, a mean value of about -4.7 e.u. is suggested for $\overline{\Delta S}$, the differential entropy change. Entropy values of this order of magnitude are maintained until appreciably above a B.E.T. monolayer film content. The value of -4.7 e.u., which is much less than the value of nearly -8 obtained by Davis and McLaren, is still sufficient to suggest chemisorption of water as proposed by Pauling (17). The fact that the entropy does not fall off until a film content 40% above the monolayer is reached suggests that some water in the second layer is very tightly held.

In the region of high vapor pressure, the upswing in the negative differential heats and entropies calculated by Davis and McLaren are not found in the present calculations; instead, $-\overline{\Delta H}$ and $-\overline{\Delta S}$ decrease regularly to those of liquid water. However, Davis and McLaren doubt the reality of their upswings.

Heat of Wetting Hysteresis

In interpreting thermodynamic calculations of adsorption systems, the question of how much of the changes arise from the adsorbate and the adsorbent respectively must be determined. This is particularly true of protein–water systems, in which swelling phenomena and even solution may occur.

The silk fibroin – water system appears to be a relatively simple one, so that the thermodynamic changes can be fairly definitely identified with purely adsorption phenomena. The fact that fibroin is very accessible to water, independently of its structure, so that its water vapor adsorption isotherm is unaffected by solution and reprecipitation (15) does not in itself eliminate the possibility of swelling phenomena. Wool, which shows swelling properties, behaves similarly to silk in that its adsorption isotherm is largely unaffected by the destruction of its structure. However, while the *amounts* adsorbed may be unaffected, the energy relations may be profoundly affected.

No comparison of silk with wool is possible because Hedges (8) who measured the heats of wetting of wool by water did not make measurements on "desorbed" samples. However, Argue and Maass (1) made measurements for cellulose and found that the heats of wetting on the 'desorbed' samples were significantly *higher* than for the corresponding 'adsorbed' samples. This is generally explained by including a heat of swelling term in the net heat of wetting on an 'adsorbed' sample, part of which would not be included in the heat of wetting of a 'desorbed' sample. In our case, if there is any heat of swelling, it is probably very small because the desorption heats of wetting are *below* the adsorption heats.

It must be remembered that both silk fibroin and cellulose give the same type of sorption isotherm hysteresis. At equal moisture contents, water is more tightly held on the desorption branch. Therefore we would expect the heat of wetting to be *less* for the desorption side if there are no phenomena occurring other than pure adsorption.

Adsorption Areas

Adsorption area measurements assist in the interpretation of the thermodynamic properties of adsorption systems. In the case of the silk fibroin – water system, it was shown (6) in common with all Bull's data that the B.E.T. and H.J. area equations when applied to the two parts of the adsorption isotherm gave coincident monolayer values (X_m = 4.48 gm. H_2O per 100 gm. fibroin). This confirms the observation of Mellon, Korn, and Hoover (15) that swelling phenomena do not appear to affect the accessibility of water molecules to the molecular chains of fibrous proteins. The coincidence of monolayer areas has been interpreted by Dunford and Morrison (6) to indicate that the upper part of the isotherm involves the formation of a condensed film above the monolayer laid down in the first part of the isotherm. This interpretation confirms the observations of Hoover and Mellon (9) who, by applying a polarization theory to protein–water sorption isotherms, showed "that sorption on active sites occurs at low vapor pressures and that sorption at higher vapor pressure is due to this prior sorption".

Finally, let us consider what happens when vapor saturated silk fibroin is immersed in liquid water. An attempt was made to measure the area of the protein by the absolute method of Harkins and Jura (7). A sample was kept above pure water for three days attaining 25.2% moisture content before being immersed in the calorimeter. The heat of wetting was 0.19 cal. gm.$^{-1}$. However,

the saturation moisture content of silk fibroin is 36% (11) and extrapolation to this water content gave a value of less than 0.10 cal. (Wahba (20) found 0.30 cal. gm.$^{-1}$ for cellulose under the same conditions). Assuming that the heat of immersion of the vapor saturated fibroin does not include swelling energy, the Harkins and Jura 'absolute' area is less than 3.5 sq. meters gm.$^{-1}$, compared with the isotherm area of 158 sq. meters gm.$^{-1}$. This suggests that near the relative vapor pressure of unity, the spaces between the molecular protein chains are completely filled with water and that the area 3.5 sq. meters gm. may correspond to the external area of the fibrils.

Conclusion

The area and thermal measurements and calculations of the silk fibroin – water system are consistent; in Fig. 3, the differential heat and entropy curves indicate a transition from monolayer and multilayer formation to a condensed film, which in turn becomes indistinguishable from liquid water. If swelling occurs, its effect is not reflected in either the amounts or energies of adsorption.

ACKNOWLEDGMENTS

We wish to thank Dr. H. W. Habgood of the Alberta Research Council, Edmonton, for helpful discussions. Acknowledgments are also made to the National Research Council and the General Research Committee of the University of Alberta for grants in aid of this work.

REFERENCES

1. ARGUE, G. H. and MAASS, O. Can. J. Research, 12: 564. 1935.
2. BULL, H. B. J. Am. Chem. Soc. 66: 1499. 1944.
3. DAVIS, S. and MCLAREN, A. D. J. Polymer Sci. 3: 16. 1948.
4. DOLE, M. and MCLAREN, A. D. J. Am. Chem. Soc. 69: 651. 1947.
5. DUNFORD, H. B. Thesis, University of Alberta, Edmonton, Alta. 1952.
6. DUNFORD, H. B. and MORRISON, J. L. Can. J. Chem. 32: 558. 1954.
7. HARKINS, W. D. and JURA, G. J. Am. Chem. Soc. 66: 1362. 1944.
8. HEDGES, J. J. Trans. Faraday Soc. 22: 178. 1926.
9. HOOVER, S. R. and MELLON, E. F. J. Am. Chem. Soc. 72: 2562. 1950.
10. HOWARD, F. L. and CULBERTSON, J. L. J. Am. Chem. Soc. 72: 1185. 1950.
11. HUTTON, E. A. and GARTSIDE, J. J. Textile Inst. Trans. 40: T161. 1949.
12. LIANG, S. C. J. Phys. & Colloid Chem. 55: 1410. 1951.
13. LIPSETT, S. G., JOHNSON, F. M. G., and MAASS, O. J. Am. Chem. Soc. 49: 925. 1927.
14. LIPSETT, S. G., JOHNSON, F. M. G., and MAASS, O. J. Am. Chem. Soc. 49: 1940. 1927.
15. MELLON, E. F., KORN, A. H., and HOOVER, S. R. J. Am. Chem. Soc. 71: 2761. 1949.
16. MORRISON, J. L., CAMPBELL, W. B., and MAASS, O. Can. J. Research, B, 15: 447. 1937.
17. PAULING, L. J. Am. Chem. Soc. 67: 555. 1945.
18. ROWEN, J. W. and BLAINE, R. L. Ind. Eng. Chem. 39: 1659. 1947.
19. SOOKNE, A. M. and HARRIS, M. J. Research Natl. Bur. Standards, 23: 299. 1939.
20. WAHBA, M. J. Phys. & Colloid Chem. 52: 1197. 1948.
21. WAHBA, M. J. Phys. & Colloid Chem. 54: 1148. 1950.
22. WIIG, E. O. and JUHOLA, A. J. J. Am. Chem. Soc. 71: 561. 1949.

THE ADSORPTION OF NITROGEN, OXYGEN, AND ARGON BY GRAPHITE[1]

By H. L. McDermot and J. C. Arnell

ABSTRACT

The adsorption of nitrogen, oxygen, and argon by three Acheson graphites has been measured at liquid nitrogen and liquid oxygen temperatures. The isotherms were Type II in the B.E.T. classification and displayed two kinds of hysteresis. The first kind was attributed to the presence of pores in the graphite and the second kind to intercrystalline swelling.

INTRODUCTION

This paper describes an investigation of three artificial graphites manufactured by the Acheson Colloids Corporation. Very little detailed adsorption work has been done with graphites of this type with a view to elucidating their structure. Barrer (2) has measured the adsorption of nitrogen, argon, and hydrogen by an Acheson graphite over a considerable temperature range and has calculated isosteric heats from the isotherms. He found that the graphite was energetically heterogeneous to all three gases and that the heats in the case of nitrogen were unaffected by the addition of chemisorbed oxygen to the surface of the graphite. He concluded therefore that the heterogeneity was a property of the carbon structure. In the opinion of the authors, the weakness of this work lies in the fact that very few adsorption points were measured at each temperature and no desorption points at all were determined. Bartell and Dodd (4) measured the adsorption of nitrogen at liquid nitrogen temperatures by a number of carbons which included two Acheson graphites. The purpose of the work was to measure the surface area of the carbons so that only a small number of points were determined and only in the case of the diamond powder were desorption points taken. It is stated that no desorption points were measured for the graphite because reversibility for nitrogen adsorption had been established at liquid oxygen temperatures. Bartell and Dodd do not indicate to what pressures these measurements were carried, but it will be shown in the present paper that reversibility of the nitrogen isotherm at 90°K. is by no means a criterion for reversibility unless pressure measurements are extended to well over an atmosphere. Because of the lack of data on these graphites, it was decided to undertake a detailed study of three typical artificial graphites. The first step was to measure isotherms at low temperatures using as adsorbates nitrogen, oxygen, and argon. Unusual hysteresis effects were encountered and therefore a detailed study was made on one graphite using nitrogen as the adsorbate. For comparative purposes the nitrogen isotherm of a nonporous carbon black was also determined.

[1]*Manuscript received January 17, 1955.*
Contribution from the Defence Research Chemical Laboratories, Ottawa, Canada. Issued as DRCL Report No. 184.

EXPERIMENTAL AND RESULTS

Samples of three graphites of surface areas up to 100 $m.^2/gm.$ were supplied by the Acheson Colloid Corporation. They were designated as Lot 6226, Lot 6131, and No. 39. For the purpose of this paper they have been designated as G-1, G-2, and G-3, respectively.

Nitrogen was supplied by the Canadian Liquid Air Co. It was stated to be 99.5% nitrogen and was used without further purification.

Oxygen was also supplied by the Canadian Liquid Air Co. and specified as 99.9% oxygen.

The argon used was Matheson Research Grade and was rated as 99.9% pure.

The adsorption isotherms were measured by means of a standard volumetric adsorption apparatus. For the isotherms at 77.5°K. and 90.0°K., open baths of liquid nitrogen and liquid oxygen were used. The maximum variation in the temperature of these baths was ±0.2°. For the isotherm at 70.6°K., a cryostat was used the temperature of which was controlled and measured by a nitrogen thermometer. The temperature of the cryostat was regulated to better than ±0.02°. Before commencing adsorption measurements the samples of graphite were outgassed by evacuation at 120°C. for at least 12 hr.

The isotherm for the adsorption of nitrogen by G-1 is shown in Fig. 1. The isotherm is Type II in the B.E.T. classification and displays a normal hysteresis loop from saturation down to a relative pressure of 0.45. Several scanning curves are also shown illustrating the effect of desorption from pressures below saturation. Below a relative pressure of 0.45, an unusual desorption curve

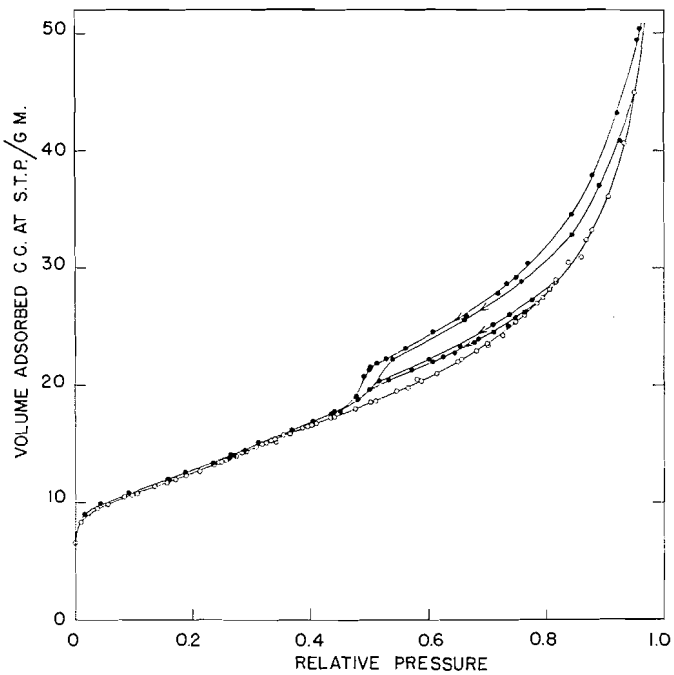

FIG. 1. Isotherm of nitrogen sorbed by G-1 at 77.5°K.

approximately parallel to the adsorption curve and slightly above it was found. The separation of the curves at this part of the isotherm is small, but is nevertheless believed to be real. Over ten separate adsorption–desorption cycles were carried out with this system and in every case the desorption points were observed to lie slightly above the adsorption points despite the fact that desorption was begun from a variety of relative pressures (all above the inception of the hysteresis loop). If for example a cumulative error existed, a different separation would be anticipated for each relative pressure chosen for the commencement of desorption. This was not found to be the case. However when desorption was carried out at pressures below the inception of the hysteresis loop then no hysteresis at all was observed. This point is illustrated by Fig. 2, which shows the isotherm of nitrogen adsorbed by G-1 at

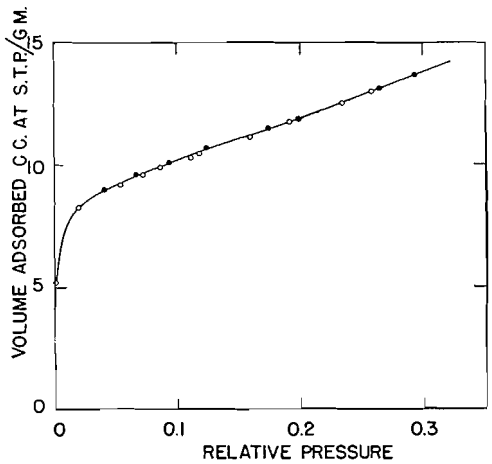

FIG. 2. Isotherm of nitrogen sorbed by G-1 at 90.0°K.

90.0°K. The characteristics outlined for the adsorption isotherm of nitrogen on G-1 were found to be typical of the nitrogen isotherms of all these graphites.

As the initial measurements with G-1 revealed the unusual hysteresis effects referred to above, experiments were conducted to discover if these effects stemmed from the packing of the powder in the adsorption cell. In the first of these experiments, the nitrogen isotherm was remeasured using 1 gm. of graphite instead of 10 gm. The results are plotted in Fig. 3 along with the original isotherm. There is no discernible difference between the two sets of data. In a second experiment, a 1 gm. sample was spread out (approximately 1 mm. in depth) on circular trays arranged on a vertical rod and separated from each other by washers. Before filling with graphite, the trays were washed with organic solvents to remove machining compounds and were thoroughly dried. The adsorption of nitrogen was then measured. The isotherm is shown in Fig. 4 along with that determined for a 1 gm. sample in bulk. Although the adsorption is somewhat greater for the sample on trays at high relative pressures, the hysteresis effects remained substantially unchanged. It was concluded therefore that the unusual hysteresis effects were real. No explana-

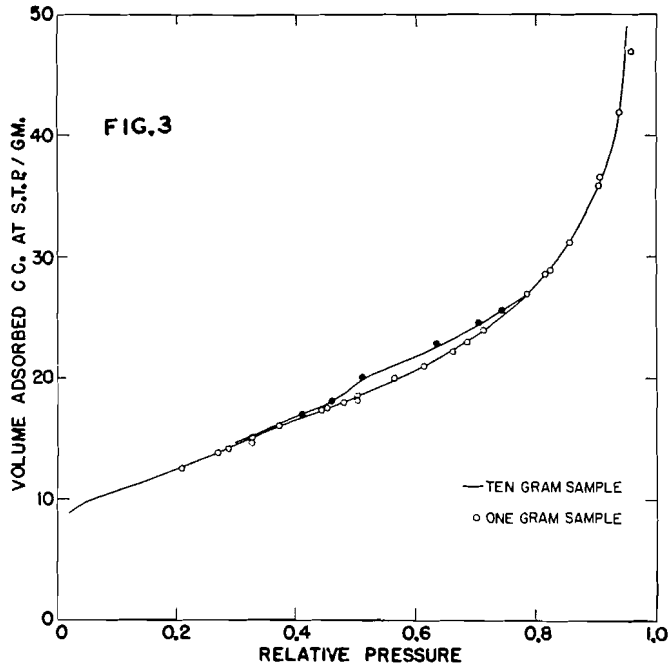

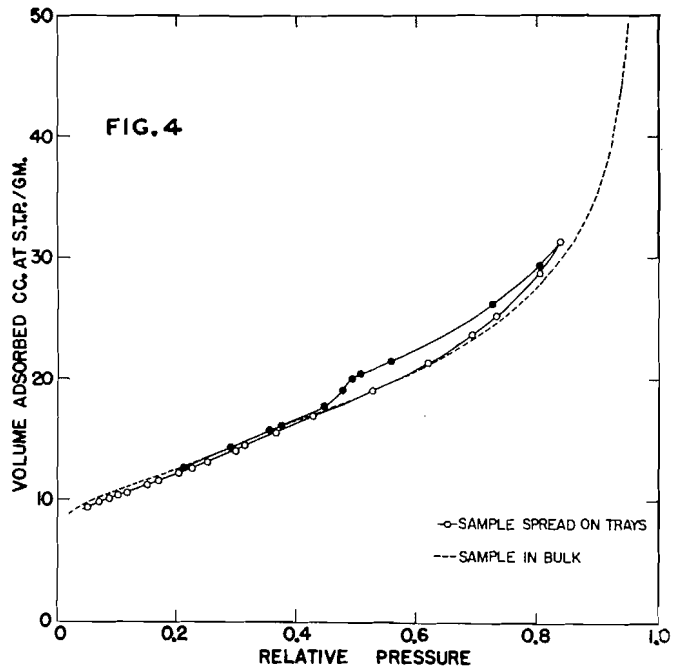

FIG. 3. Sorption isotherms of nitrogen by G-1 at 77.5°K. showing the effect of variations in sample size.

FIG. 4. Sorption isotherms of nitrogen by G-1 at 77.5°K. showing the effect of sample dispersion.

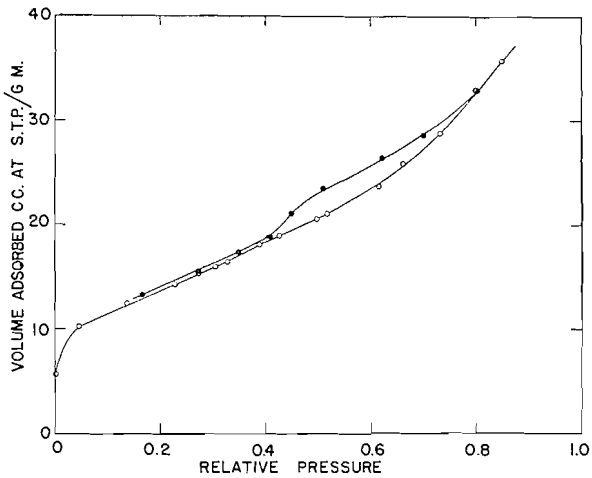

FIG. 5. Isotherm of oxygen sorbed by G-1 at 90.0°K.

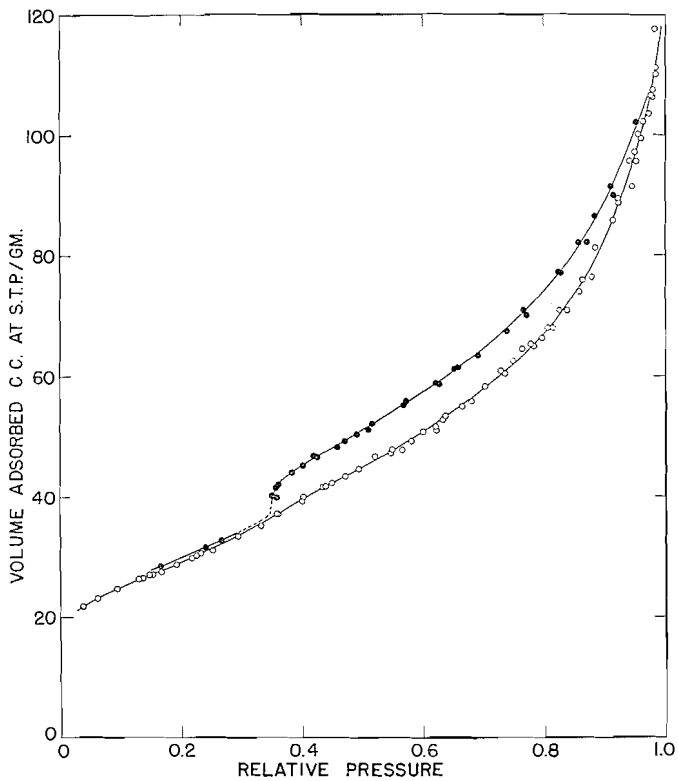

FIG. 6. Isotherm of argon sorbed by G-2 at 77.5°K.

tion has been found for the difference between the isotherms of the "bulk" sample and the "dispersed" sample. The reproducibility of the measurements indicates that the effect is real and not due to experimental error. An obvious speculation is that some packing is occurring in the "bulk" sample which hinders adsorption at higher relative pressures.

It was then suspected that the hysteresis phenomena observed in the adsorption isotherms of nitrogen by these graphites were due to the graphite structure. To confirm this suspicion, measurements were made with two other gases, oxygen and argon. Fig. 5 shows the adsorption isotherm of oxygen on G-1 at 90.0°K. and Fig. 6 the isotherm of argon on G-2 at 77.5°K. These isotherms clearly display the features previously described for the nitrogen isotherms.

Finally, a closer investigation of these phenomena was made utilizing the G-3 nitrogen system. This system was chosen because the separation of the lower part of the desorption curve from the adsorption curve was found to be greater for G-3 than for the other graphites. The isotherms for the adsorption

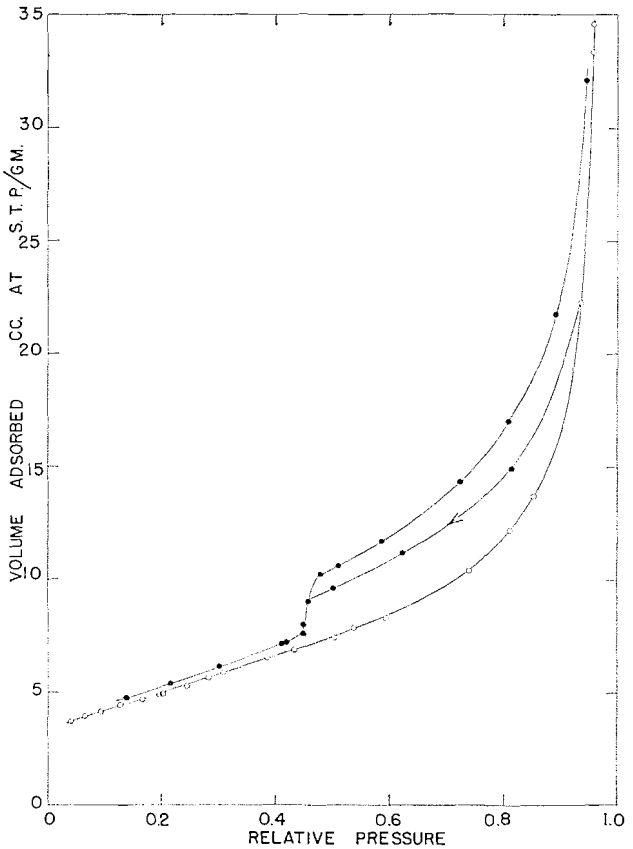

FIG. 7. Isotherm of nitrogen sorbed by G-3 at 77.5°K.

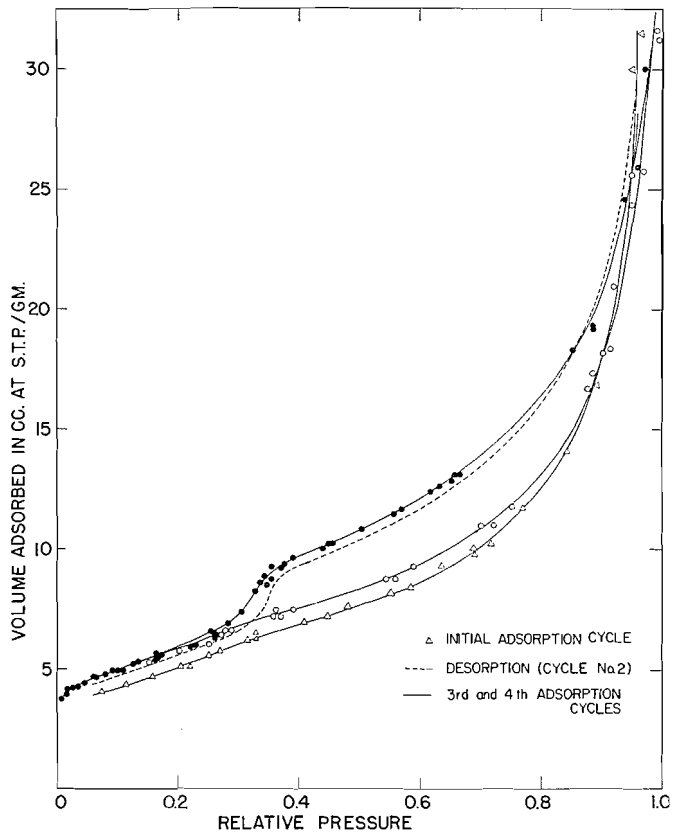

FIG. 8. Isotherm of nitrogen sorbed by G-3 at 70.6°K.

of nitrogen by G-3 at 77.5°K. and at 70.6°K. are shown in Figs. 7 and 8 respectively. It will be observed that the form of the isotherm at 77.5°K. is qualitatively similar to that for G-1 which is depicted in Fig. 1.

The data plotted in Fig. 8 are taken from these series of runs, with up to four successive adsorption cycles for a series. Except for the first cycle of a series, a typical adsorption cycle was begun by readsorption from the lowest desorption point of the previous cycle, without altering the bath temperature. Between each series the graphite was given the standard outgassing treatment. The initial adsorption curve is seen to be considerably below the subsequent ones. After the second adsorption cycle, the hysteresis loop closes completely and a reversible section of the isotherm is observed below the beginning of the loop. The dotted line and the points just below the upper of the two adsorption curves represent data from the second adsorption cycle, which appears to be a transition cycle between the first and final adsorption cycles. It can be seen from Figs. 7 and 8 that the separation of the adsorption curves is greater at 70.6°K. than it is at 77.5°K. This is partly the effect of the extra cycling at 70.6°K. and partly the effect of the lower temperature.

DISCUSSION

The foregoing results have shown that the low temperature isotherms of the three graphites considered are Type II with hysteresis.

The adsorption curves obey the B.E.T. equation from $p/p_0 = 0.08$ to $p/p_0 = 0.30$. The values of V_m derived from the B.E.T. plots and the surface areas calculated from them are given in the following table. In every case the data used were taken from the initial adsorption isotherm.

Graphite	Adsorbate	Temperature, °K.	V_m, cc. at S.T.P.	Area, m.²/gm.
G-1	Nitrogen	77.5	10.35	45.3
G-1	Nitrogen	90.0	9.86	41.6
G-1	Oxygen	90.0	11.49	43.4
G-2	Nitrogen	77.5	21.97	96.2
G-2	Argon	77.5	23.92	82.0
G-3	Nitrogen	77.5	4.21	18.4
G-3	Nitrogen	70.6	4.44	17.3

Closer examination has revealed two distinct types of hysteresis. The first type is represented by a wide loop extending from saturation down to a relative pressure of approximately 0.45. It is illustrated by a closed loop in Fig. 8. The second hysteresis effect is a much smaller one which takes the form of a slight elevation of the desorption curve above the adsorption curve at relative pressures below the beginning of the main hysteresis loop. This effect is most clearly shown in Fig. 8, which also shows that readsorption without evacuation follows the desorption branch until the main hysteresis loop is reached after which a new path is taken.

The first type of hysteresis is believed to be evidence that these graphites are porous. Moreover in agreement with the ideas of Wheeler (7) and of Barrett, Joyner, and Halenda (3) on the mechanism of the sorption of vapors in pores, it is believed that the loops are a result of the presence of pores greater than four to six molecular diameters. These arguments have been previously advanced by McDermot and Arnell (6) to explain the presence of hysteresis loops in the isotherms of wide-pored charcoals and their absence in narrow-pored charcoals. Thus the hysteresis loops are thought to be similar for the charcoals and for the graphites though the similarity may be masked by the widely different surface areas and porosities. The postulated mechanism of adsorption and desorption is briefly as follows: layer adsorption occurs on the walls of the pores until the layers build up to a point where they coalesce to form a meniscus after which capillary condensation may occur in that pore. Thus capillary condensation is occurring in the small pores while layer adsorption is taking place in larger pores which have not yet formed a meniscus. Hysteresis arises because adsorption takes place by a mixture of layer adsorption and capillary condensation, whereas desorption occurs by evaporation from pores that are initially full of liquid. An adsorbed layer is left on the walls as capillary evaporation proceeds, but the process is not the reverse of the adsorption process owing to delay in meniscus formation on the adsorption branch. This mechanism does not of course exclude any contributions to hys-

teresis that may be made by pore constrictions, but these are only important when an attempt is made to evaluate pore distributions. Further support for these ideas is offered by Carman (5), who has measured the isotherm of CF_2Cl_2 on Linde silica powder and on the same powder compressed into a plug of known porosity. A hysteresis loop was obtained for sorption by the plug and a reversible isotherm for the powder. More vapor was sorbed on the adsorption branch of the isotherm by the plug than by the powder until the plug was filled with liquid at which point sorption ceased. This behavior is in accord with the postulated hypothesis, because at a given relative pressure layer adsorption would be greater on a curved surface than on a plane one. In order to demonstrate that the hysteresis loops discussed here are characteristic of sorption by a porous material, an experiment similar to Carman's was performed using as a porous carbon a sample of G-2 and as a nonporous carbon a sample of Spheron 9 supplied by the Godfrey L. Cabot Co. Arnell and Henneberry (1) calculated the surface area of this carbon black from adsorption, permeability, and electron microscope data and found approximate agreement by all three methods. This is taken to be good evidence that Spheron 9 is nonporous. The adsorption of nitrogen at 77.5°K. by G-2 and by Spheron 9 is compared in Fig. 9. As Spheron 9 has a slightly larger surface area than G-2 the data are plotted as V/V_m versus p/p_0 rather than directly on the basis of volumes adsorbed. It will be observed that although the curves coincide initially the adsorption curve for the graphite rises above that of the carbon black. These results are qualitatively similar to those of Carman (5), and are considered sufficient proof that G-2 is porous.

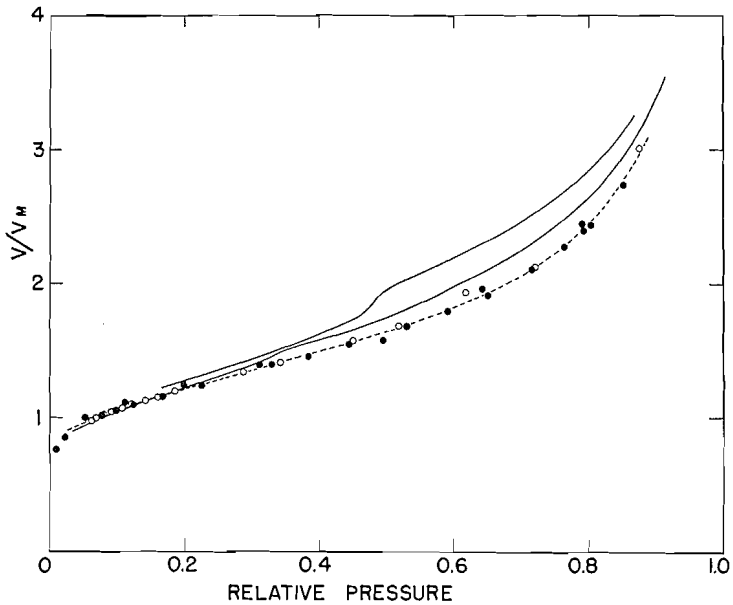

FIG. 9. Comparison between the sorption of nitrogen by G-2 and Spheron 9 at 77.5°K. Solid line represents the isotherm of G-2 and the dashed line that of Spheron 9.

The second hysteresis effect is most clearly observed in the adsorption isotherm of nitrogen on G-3 at 70.6°K. which is plotted in Fig. 8. It has been found that if one proceeds along the lower adsorption curve to a pressure at which the two curves are still well separated and then desorbs a reversible isotherm is obtained. If however adsorption is taken to a point where the two adsorption curves merge, then on desorption the upper curve is attained on completion of the main hysteresis loop. Moreover readsorption then takes place along the upper curve. Once the upper curve has been reached, it is only possible to regain the lower curve by warming the sample to the point where virtually all the nitrogen is desorbed. To sum up, the transition to the upper curve is only possible after the sorption of a considerable quantity of nitrogen, but once it has occurred it cannot be reversed. This type of behavior is characteristic of a sorption system which swells, and indeed the upper and lower adsorption branches in Fig. 8 are very similar in form to the isotherm of water sorbed by cellulose. It will be instructive to review the cellulose–water system and show that the resemblance noted above is not merely superficial. In the cellulose–water system swelling takes place along the adsorption branch and is only complete at saturation when the water has completely penetrated the structure. On desorption the path followed lies above the adsorption path because water which was able to enter the structure when it was swollen is trapped and can only be removed by completely drying the cellulose. Thus the initial adsorption curve can only be retraversed by completely drying the cellulose or in part by adding enough water to reswell the cellulose. By analogy it is believed that when sufficient gas is adsorbed by the graphite, the crystallites swell because of intercrystalline penetration. Once this penetration has occurred, some molecules are trapped and can only be removed by warming the graphite and desorbing all the gas. The analogy is not perfect because it is possible to scan the loop of the cellulose–water isotherm, but not the two adsorption curves of Fig. 8. The explanation is believed to be the following: on the sorption of water, cellulose swells gradually and continuously over the whole course of the adsorption loop and similarly on desorption water is lost gradually from the interior of the fiber. Hence the fiber can be reswollen from the partially dried state or dried from the partially swollen state, the amount of trapped water depending on the degree of swelling. In contradistinction, the graphite swells only when a critical quantity of nitrogen is sorbed and the process is sudden and irreversible. Once swelling has occurred, the quantity of trapped nitrogen is fixed and the lower curve cannot be attained without complete desorption.

REFERENCES

1. ARNELL, J. C. and HENNEBERRY, G. O. Can. J. Research, A, 26: 29. 1948.
2. BARRER, R. M. Proc. Roy. Soc. (London), A, 161: 476. 1937.
3. BARRETT, E. P., JOYNER, L. G., and HALENDA, P. P. J. Am. Chem. Soc. 73: 373. 1951.
4. BARTELL, F. E. and DODD, C. G. J. Phys. & Colloid Chem. 54: 114. 1950.
5. CARMAN, P. C. and RAAL, F. A. Proc. Roy. Soc. (London), A, 209: 59. 1951.
6. MCDERMOT, H. L. and ARNELL, J. C. Can. J. Chem. 30: 177. 1952.
7. WHEELER, A. Presentations at Catalysis Symposia, Gibson Island A.A.A.S. Conferences. June 1945 and June 1946.

THE MANNICH CONDENSATION OF COMPOUNDS CONTAINING ACIDIC IMINO GROUPS[1]

By Caurino Cesar Bombardieri[2] and Alfred Taurins

ABSTRACT

The synthesis of several new Mannich bases was accomplished by the condensation of secondary amines and formaldehyde with the following compounds: (1) 2-pyrrolidone, (2) 2,4-thiazolidinedione, (3) hydantoin, (4) 5,5-dimethylhydantoin, (5) uracil, (6) ethylnitramine, and (7) *n*-butylnitramine.

INTRODUCTION

While much work has been done on the Mannich condensation of compounds containing acidic hydrogen on carbon, considerably fewer data are available on the Mannich reaction of substances possessing active hydrogens on nitrogen, as it can be seen from this historical introduction.

Feldman and Wagner (6) prepared piperidinomethyl derivatives of succinimide, phthalimide, and carbazole. In their study of morpholinomethyl derivatives of urea and substituted ureas, Weaver, Simons, and Baldwin (13) condensed morpholinomethanol with phthalimide and succinimide. N-(Morpholinomethyl)- and N-(piperidinomethyl)-phthalimide were also synthesized by Moore and Rapala (12). The condensation of benzothiazole-2-thione and related compounds with formaldehyde and secondary amines was described in the German patent 575,114 in 1933. The purpose of the latter work was to prepare methylenediamine derivatives for use in the rubber industry.

Bachman and Heisey (1) condensed benzimidazole and benzotriazole with formaldehyde and secondary amines. Baker, Querry, Kadish, and Williams (2) prepared two Mannich bases of 4-quinazolone in reactions with formaldehyde, piperidine, and morpholine respectively. The Mannich condensation of pyrazole was studied by Huttel and Jochum (9). Butenandt and Hellmann (3) studied the reaction of hydantoin with formaldehyde and piperidine. However, they did not investigate the reaction product further. The most recent work on the synthesis of N-Mannich bases has been published by Hellmann and Löschmann (8). They describe the condensation of isatin, phthalimide, succinimide, and carbazole and give a few references on the previous publications of other authors.

That the alkylnitramines undergo a condensation with piperidinomethanol was observed by Franchimont (7) as early as 1910. However, he did not give any data on analysis and properties of the reaction product.

The objective of this work was to investigate the Mannich condensation of the cyclic imino compounds containing one or two imino groups in addition to the carbonyl groups as the hydrogen activators. We also studied the condensation of alkylnitramines in which the nitro group activates the hydrogen atom of the imino group.

[1]*Manuscript received January 18, 1955.*
Contribution from the Organic Chemistry Laboratory, McGill University, Montreal, Quebec, with the financial assistance of the National Research Council of Canada, Ottawa.
[2]*Holder of a National Research Council Studentship 1953–1954.*

DISCUSSION

We consider the replaceability of a hydrogen of the imino group by halogens or by metals, or by both, as the guiding principle enabling us to indicate the compounds possessing the ability to react in the Mannich condensation. On the bases of a similar behavior of ketones and imides in the reactions of halogenation and salt formation via enolization, we can assume that the Mannich condensation in both groups of compounds must follow the same course. Lieberman and Wagner (11) postulated the formation of a carbanion from a C—H acid compound as a necessary step in this reaction. It is reasonable to assume that the N—H acidic substance undergoes an analogous change to give a mesomeric anion in which the negative charge is located in the group N—C=O. The formation of the Mannich base may be visualized as the addition of the intermediate methylene-ammonium cation or the protonated dialkylaminomethanol at the mesomeric anion, as in the example of the reaction of 2-pyrrolidone.

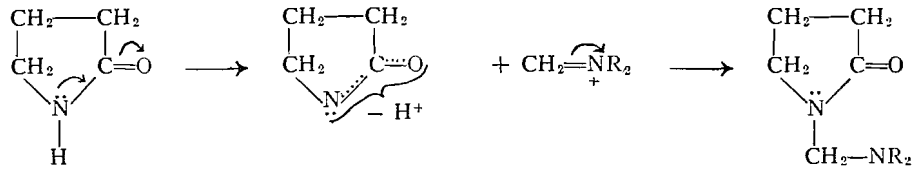

Most of the condensations of imino carbonyl compounds were carried out using free secondary bases, but not their salts because of the sensitivity of the N—CH_2—N bond towards acids. However, in a few cases the condensation was successful using even secondary amino hydrochlorides. Thus 2-pyrrolidone [2-pyrrolidinone] was successfully condensed with morpholine and piperidine bases, and dimethylamine hydrochloride as well.

2,4-Thiazolidinedione (4, 14) possesses acidic properties and forms alkali and silver salts. It reacted very easily at 0° with morpholine, piperidine, and dimethylamine. Even methylamine reacted with two molecules of the 2,4-thiazolinedione to give (VII). Both hydantoin [2,4-imidazolidinedione] and 5,5-dimethylhydantoin [5,5-dimethyl-2,4-imidazolidinedione] demonstrated their ability to react in the Mannich condensation with two molecules of formaldehyde and two molecules of morpholine. No reaction products were obtained in the attempted condensations of both hydantoins with piperidine and dialkylamines respectively.

We found that uracil [2,4-(1H, 3H)-pyrimidinedione] reacted with morpholine and formaldehyde to give 1-(morpholinomethyl)uracil. Despite the close resemblance to uracil, dihydrouracil did not react in the Mannich reaction.

In this work, alkylnitramines were prepared by the procedure of Curry and Mason (5). The attempted condensations of alkylnitramines with formaldehyde and secondary amines under reflux gave no desired products. However, the condensation succeeded when the reaction mixture was kept at 0° for 12 hr. It was found that dimethylamine and diethylamine did not undergo the Mannich condensation with *n*-butyl- and ethyl-nitramine. All attempts to form Mannich bases using methylnitramine were unsuccessful.

For the purpose of identification, the ultraviolet spectra of alkylnitramines and their derivatives were determined in absolute alcohol (DU Beckman spectrophotometer).

Compound	λ_{max}, $m\mu$	ϵ_{max}
Methylnitramine	230	14010
Ethylnitramine	227–232	28230
n-Butylnitramine	231–233	9727
N-(Morpholinomethyl)-ethylnitramine	232	6603
N-(Morpholinomethyl)-*n*-butylnitramine	234	2931

Although the observed values of λ_{max} are in agreement with the reported absorption spectra (10), the values of the molecular extinction coefficients are considerably higher than those given for methyl- and *n*-butyl-nitramine.

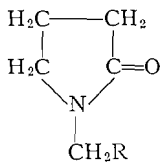

I: R = NC_4H_8O
II: R = NC_5H_{10}
III: R = $N(CH_3)_2$

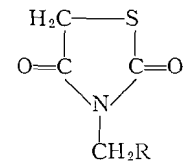

IV: R = NC_5H_{10}
V: R = NC_4H_8O
VI: R = $N(CH_3)_2$

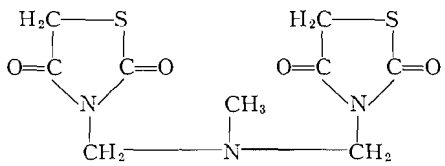

VII

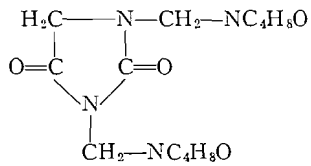

VIII

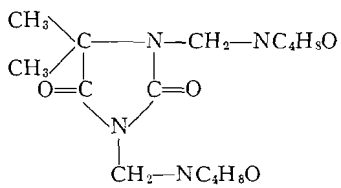

IX

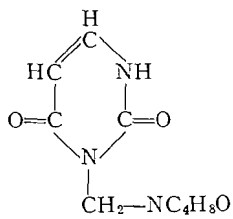

X

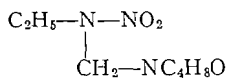

XI

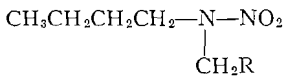

XII: R = NC_5H_{10}
XIII: R = NC_4H_8O

EXPERIMENTAL

1-(Morpholinomethyl)-2-pyrrolidone (I)

In a 50 ml. three-necked flask, a solution containing 2.55 gm. (0.03*M*) of 2-pyrrolidone in 20 ml. of water and 2.8 gm. (0.03*M*) of morpholine was placed. The mixture was stirred and 2.7 ml. (0.03*M*) of 35% formaldehyde was added slowly. The reaction mixture was refluxed at 100° for one hour. Upon cooling, the solution was extracted with chloroform and the extract was concentrated by distillation on a water bath. To this residue, 25 ml. of ethanol was added and the solution was concentrated by further distillation. After 12 hr., solid white crystals of I appeared which, after several crystallizations, melted at 68.5–69.5°. The total yield was 1.5 gm. (27.2%). The yield of I was increased to 2.1 gm. (37.8%) when the reaction time was extended to two hours.

Anal. Calc. for $C_9H_{16}N_2O_2$: N, 15.26%. Found: N, 15.12%.

1-(Piperidinomethyl)-2-pyrrolidone (II)

The compound II was prepared by refluxing the mixture of 2.55 gm. of 2-pyrrolidone, 2.7 ml. of 35% formaldehyde, 2.7 ml. of piperidine, and 20 ml. of water at 100° for one-half hour in the same manner as described for the above experiment. A precipitate was crystallized from ethanol and yielded 1.5 gm. (27.4%) of white crystals which melted at 47.5–49°.

Anal. Calc. for $C_{10}H_8N_2O$: N, 15.37%. Found: N, 15.25%.

1-(Dimethylaminomethyl)-2-pyrrolidone (III)

The reaction mixture of equimolar amounts (0.03*M*) of 2-pyrrolidone, 35% formaldehyde, dimethylamine hydrochloride, and 20 ml. of water was heated at 68° for one-half hour with constant stirring. The solution was cooled, made alkaline with 20% solution of potassium carbonate, and extracted with chloroform. The extract was evaporated and fractionally distilled to yield 1.5 gm. (37.4%) of a liquid product (III), b.p. 64–67° at 1 mm. pressure.

Anal. Calc. for $C_7H_{14}N_2O$: N, 19.7%. Found: N, 19.72%.

3-(Piperidinomethyl)-2,4-thiazolidinedione (IV)

To the solution of 3.5 gm. of 2,4-thiazolidinedione in 15 ml. of ethanol, an equimolar amount of formaldehyde and piperidine was added at 0°. In short time, crystals of IV appeared. After crystallization from absolute ethanol 6.17 gm. (95.9%) of white crystals, m.p. 76–77°, was obtained.

Anal. Calc. for $C_9H_{14}N_2O_2S$: C, 50.44; H, 658; N, 13.02%.
Found: C, 50.69; H, 6.55; N, 13.04%.

3-(Morpholinomethyl)-2,4-thiazolidinedione (V)

This substance was formed with great ease by the interaction of 2,4-thiazolidinedione, formaldehyde, and morpholine and was obtained as white crystals, m.p. 147°, in 99.9% yield.

Anal. Calc. for $C_8H_{12}N_2O_3S$: N, 12.95%. Found: 13.05%.

3-(Dimethylaminomethyl)-2,4-thiazolidinedione (VI)

The condensation product VI was obtained by a similar procedure in a yield

of 71.5%. It gave white crystals which after crystallization from absolute alcohol melted at 82°.

Anal. Calc. for $C_6H_{10}N_2O_2S$: C, 41.36; H, 5.79; N, 16.08%.

Found: C, 41.60; H, 5.92; N, 16.05%.

N-Methyl-N,N-bis(2,4-thiazolidinedionomethyl)amine (VII)

A mixture of 3.5 gm. of 2,4-thiazolidinedione dissolved in 15 ml. of ethanol and 2.7 ml. of 35% formaldehyde was cooled to 0° and 4.85 ml. of 25% methylamine solution was added dropwise. The reaction product was crystallized from absolute ethanol to yield 4.34 gm. (50%) of soft white crystals, m.p. 144–145°.

Anal. Calc. for $C_9H_{11}N_3O_4S_2$: N, 14.52%. Found: N, 14.59%.

The above experiment was repeated using a 2:2:1 mole ratio of 2,4-thiazolidinedione, formaldehyde, and methylamine respectively. The yield was increased to 7.1 gm. (83%).

1,3-Di(morpholinomethyl)hydantoin (VIII)

To the heated solution of 3 gm. (0.03*M*) of hydantoin in 20 ml. of water, 5.6 ml. of morpholine was added and 5.4 ml. of 35% formaldehyde was introduced dropwise. The mixture was stirred and heated at 85° for 15 min. The reaction product was extracted from the cold solution with chloroform. After recrystallization from ethanol VIII yielded 2 gm. (22%) of white crystals, m.p. 144–145.5°.

Anal. Calc. for $C_{13}H_{22}N_4O_4$: N, 18.84%. Found: 18.76%.

Acid Hydrolysis of VIII

Dry hydrogen chloride gas was bubbled through the solution of 0.3 gm. of VIII in 25 ml. of absolute ethanol. A white precipitate of hydantoin, m.p. 218°, separated (lit. m.p. 220°).

1,3-Di(morpholinomethyl)-5,5-dimethylhydantoin (IX)

The condensation of 5,5-dimethylhydantoin with morpholine and formaldehyde in molar ratio 1:2:2 respectively, was carried out at 90° for 30 min. The product was recrystallized from ethanol to yield 3.9 gm. (39.8%) of white crystals, m.p. 134–134.5°.

Anal. Calc. for $C_{15}H_{26}N_4O_4$: N, 17.1%. Found: N, 17.02%.

1-(Morpholinomethyl)uracil (X)

Uracil (3.4 gm.) dissolved in 40 ml. of water and morpholine (2.8 ml.) were cooled to 0° and 2.7 ml. of 35% formaldehyde was slowly added. A precipitate was formed which after crystallization from alcohol yielded 2.16 gm. (56%) of white crystals, m.p. 208–209°.

Anal. Calc. for $C_9H_{13}N_3O_2$: N, 19.89. Found: N, 19.92%.

N-(Morpholinomethyl)ethylnitramine (XI)

The reaction mixture of ethylnitramine, morpholine, and formaldehyde in molar ratio 1:1:1 respectively, was allowed to stand for 12 hr. at 4°. The product XI was crystallized from petroleum ether (b.p. 65–110°). The yield

of white plates, m.p. 86–87°, of XI was 92%.

Anal. Calc. for $C_7H_{15}N_3O_3$: C, 44.43; H, 7.99; N, 22.2%.

Found: C, 44.61; H, 8.0; N, 21.97%.

N-(Piperidinomethyl)-n-butylnitramine (XII)

A solution of 7.1 gm. of *n*-butylnitramine in 20 ml. of alcohol was cooled to 0° and 5.4 ml. of 35% formaldehyde was added dropwise. To this mixture, 5.4 ml. of piperidine was slowly introduced and the flask was kept at 0° for 12 hr. The alcohol was evaporated and the residue fractionally distilled. The total yield of XII was 4.6 gm. (35.7%; b.p. 97–100°) at 1 mm.

Anal. Calc. for $C_{10}H_{21}N_3O_2$: C, 55.78; H, 9.83; N, 19.52%. Found: C, 55.34; H, 10.08; N, 18.79%.

N-(Morpholinomethyl)-n-butylnitramine (XIII)

The substance XIII was prepared by the method described as above, with the exception that the reaction product was crystalline and it separated from the solution. It was crystallized from petroleum ether (b.p. 30–60°) and obtained as white crystals, m.p. 53–53.5°, in 97.6% yield.

Anal. Calc. for $C_9H_{19}N_3O_3$: N, 19.34%. Found: N, 19.62%.

REFERENCES

1. BACHMAN, G. B. and HEISEY, L. V. J. Am. Chem. Soc. 68: 2496. 1946.
2. BAKER, B. R., QUERRY, M. V., KADISH, A. F., and WILLIAMS, J. H. J. Org. Chem. 17: 35. 1952.
3. BUTENANDT, A. and HELLMANN, H. Z. physiol. Chem. 284: 168. 1949.
4. CLAESSON, P. Ber. 10: 1346. 1877.
5. CURRY, H. M. and MASON, J. P. J. Am. Chem. Soc. 73: 5041, 5043. 1951.
6. FELDMAN, J. R. and WAGNER, E. C. J. Org. Chem. 7: 31. 1942.
7. FRANCHIMONT, M. A. P. N. Rec. trav. chim. 29: 296. 1910.
8. HELLMANN, H. and LÖSCHMANN, I. Chem. Ber. 87: 1684, 1690. 1954.
9. HUTTEL, R. and JOCHUM, P. Ber. 85: 820. 1952.
10. JONES, R. N. and THORN, G. D. Can. J. Research, B, 27: 828. 1949.
11. LIEBERMAN, S. V. and WAGNER, E. C. J. Org. Chem. 14: 1001. 1949.
12. MOORE, M. B. and RAPALA, R. T. J. Am. Chem. Soc. 68: 1657. 1946.
13. WEAVER, W. I., SIMONS, J. K., and BALDWIN, W. E. J. Am. Chem. Soc. 66: 222. 1944.
14. WHEELER, H. L. and BARNES, B. Am. Chem. J. 24: 60. 1900.

DISINTEGRATION-RATE DETERMINATION BY 4π-COUNTING

PART II. SOURCE-MOUNT ABSORPTION CORRECTION[1]

By B. D. Pate[2] and L. Yaffe

ABSTRACT

The various methods in use for determining the correction for absorption due to the source mount used in a 4π-counter are discussed, and experiments conducted to test the validity of the correction, arising from these methods, for β emitters of varying end-point energies. The methods all give erroneous corrections for low energy β emitters and possible reasons for the errors introduced by the 'sandwich method' are discussed. An 'absorption curve' type method is proposed which is shown to give more accurate correction factors.

A. INTRODUCTION

In a previous publication (8), we have discussed the principles of 4π-counting and described the design of counting chamber used in this laboratory. We also discussed the errors to which the final disintegration-rate value is subject and the conditions under which the first of these—departure from unit counter response probability—is minimized. In the present paper, we shall discuss corrections for the second of the sources of error, namely absorption of radiation in the mounting film on which the source is deposited.

For determinations involving nuclides emitting monoenergetic radiation, such as α radiation and conversion electrons, of such an energy that the range of the particle in the source-mount material is greater than its path length in the film used, no source-mount absorption correction is necessary. As long as a sufficient number of ion pairs are produced by the ionizing particle to trigger the counting circuit, each disintegration will be recorded. The majority of determinations for which a 4π proportional counter will be employed, however, involve β radiation with a continuous distribution of particle energies; in this case a fraction of the emitted particles will always be absorbed by the film, the fraction being larger the smaller the end point of the beta spectrum.

We have already (7) described techniques developed in this laboratory for the production of films, for use in 4π-counters, of a superficial density of 5–10 μgm./cm^2. For disintegration-rate determinations of moderate precision with β radiation of moderate or high energy, the use of films of this thickness allows absorption of radiation in the source mount to be neglected. For work of the greatest precision, however, and particularly that with the weaker β emitters, the absorption loss must be accurately evaluated and a correction made. The use of very thin films is nevertheless still of considerable advantage, since the magnitude of the correction is reduced, and the final disintegration-rate value less sensitive to errors in the correction.

[1]*Manuscript received January 17, 1955.*
Contribution from the Radiochemistry Laboratory, Department of Chemistry, McGill University, Montreal, Quebec, with financial assistance from the National Research Council of Canada and Atomic Energy of Canada Ltd.
[2]*Holder of a National Research Council Studentship.*

Three methods of determining the absorption correction have been described in the literature: the so-called "sandwich" procedure, calculation from 2π and 4π counting rates, and the use of absorption curves.

(i) The "sandwich" procedure has been described by Hawkings *et al.* (3). The counting rate given by a source mounted on a known thickness of mounting film is determined, and then a second determination made with an identical film superimposed over the first so as to sandwich the source. The observed reduction of counting rate was applied as a correction to the single film value to arrive at the source disintegration rate, and the validity of this procedure was taken to be apparent "from a consideration of the contribution to the counting rate from each hemisphere". However, Smith (11) found that applying the sandwich procedure to similar sources of, for instance, S^{35} using sets of films of differing superficial density lead to results for the disintegration rate differing by as much as seven per cent. The results should of course be independent of the thickness of films used.

(ii) Seliger and co-workers (5, 9) have attempted to develop mathematical relationships which would allow calculation of the source disintegration rate from measured 2π- and 4π-, single and sandwiched film counting rates. The resulting formulae as quoted in the second and more rigorous of the two papers (5) were:

$$(a) \qquad (N_t - N_b)/(N_T - N_b) = 2\beta_f + \tau \approx \tau$$

where N_t and N_b are the counting rates observed in the top and bottom half-counters respectively, N_T is the counting rate observed from both halves combined, β_f is the fractional back-scattering factor, and τ the fractional absorption factor for the film used as source mount.

$$(b) \qquad (N_T - N_S)/(2N_T - N_S) = \tau/2$$

where N_S is the counting rate obtained with the source sandwiched between two similar films. The value of τ obtained from these equations was then to be substituted into

$$N_0 = N_T/(1 - \tau/2)$$

to obtain N_0, the true disintegration rate of a source where no self-absorption corrections have to be made.

As is common with calculations of this sort (11), the combination of a continuous distribution of beta energies with energy-dependent scattering and absorption coefficients and a complex geometrical arrangement make the problem analytically very difficult without the adoption of several simplifications. For example: Among those employed by Seliger *et al.* were the supposition that the absorption and scattering characteristics of β radiation were unaffected by the scattering process (e.g. degradation of the energy spectrum was neglected) and, in several places in the derivation, the assumption that β_f and τ were small compared to unity.

The latter may be true in the region of beta energies and film thicknesses where the absorption correction is in any case insignificant, but with lower beta energies where an accurate correction is required, both coefficients are

by no means negligible, and vary rapidly with changing beta energy. In particular, the back-scattering effect observed in a 4π geometry is found to be considerably larger than in conventional counter systems. The 4π-counter will respond to particles having undergone scattering at low angles to the source mount, and low angle scattering is evidently important even with thin films made from a material of low average atomic number. Using a 4π-counter, Meyer-Schützmeister and Vincent (6) have reported an 8% back-scattering for S^{35} β particles from 30–40 μgm./cm.^{2} cellulose films, Houtermans *et al.* (4) reported similar results for P^{32}, and Borkowski (1) found 5% back-scattering of Na^{24} β radiation from 50 μgm./cm.^{2} of Formvar.

Thus the over-all 2% accuracy claimed by Mann and Seliger (5) for their absorption correction is probably over-rated when one is using β emitters of low energy (e.g. Ni^{63}, C^{14}, S^{35}, etc.).

(iii) The 'absorption curve method' used to correct the results obtained from end-window counters for the absorption of radiation suggests itself as a corrective technique applicable to this case. A procedure of this sort was used by the workers at Göttingen (4, 6). They made a series of counting-rate measurements with a source mounted on a film, and with increasing thicknesses of aluminum foil placed *over* the source, and used the curves obtained to correct the original counting rate. However, such a procedure would appear to be open to the same objections as the ordinary sandwich procedure.

A study of the variation of counting rate as a function of the actual mount thickness was first carried out by Smith (11). He commenced with a source mounted on aluminum of 260 μgm./cm.^{2} and took measurements of the counting rates obtained with the source backed by increasing thicknesses of this material. The curve obtained on plotting the results was observed to be approximately linear, and Smith assumed that the value obtained by extrapolating back to zero mount thickness represented the source disintegration rate. However, this value was found to be low compared with the counting rate observed with a similar source mounted on 30 μgm./cm.^{2} of cellulose acetate, by 3% in the case of S^{35}, and 1.5% in the case of Co^{60}. The discrepancy probably arose from a change of slope in the absorption curve below 260 μgm./cm.^{2} superficial density, such as was observed by Suzor and Charpak in another connection (12). Provided sufficiently thin films and a suitable technique were used, this type of procedure would be expected to produce the most accurate means of correcting for mount absorption, the results being independent of any assumptions regarding counter mechanisms and so on. The anomalous back-scattering effects observed by Yaffe and Justus (13) and Glendenin and co-workers (2) would not be expected to cause any disturbing effects.

B. EXPERIMENTAL PROCEDURE AND RESULTS

For the following experiments, we have used the chamber and ancillary equipment described in the previous publication (8), operating under the conditions found to give unit response probability. We have performed two sets of experiments:

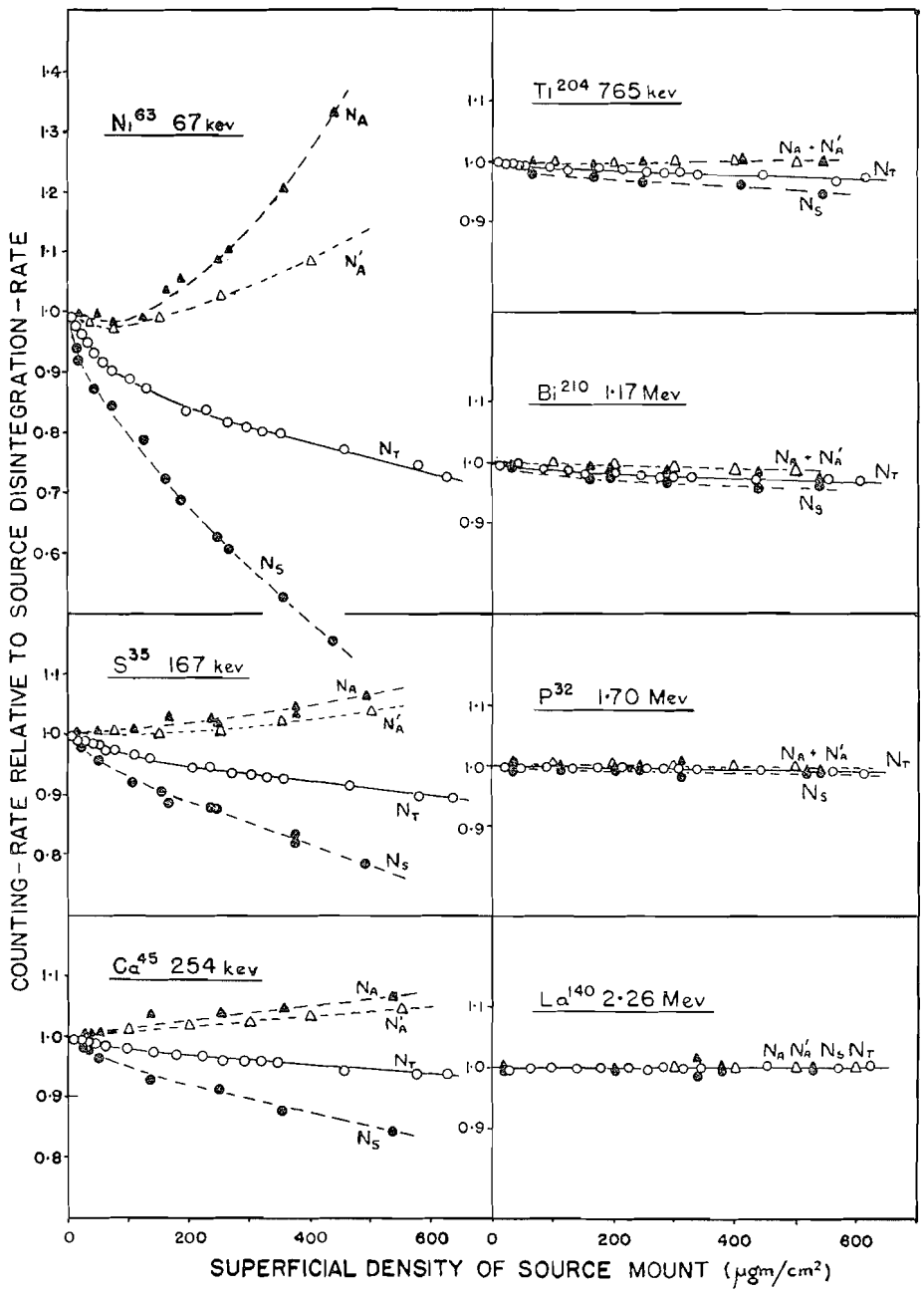

FIG. 1. Source-mount absorption characteristics for a series of beta emitters.

(i) *Single Film Source-mount Absorption Characteristics*

A series of counting-rate measurements was taken for each nuclide of the series of seven β emitters of increasing end-point energy, and four emitters of differing forms of radiation, whose nuclear characteristics were described earlier (8). For each of a series of increasing source-mount superficial densities, we have measured the total counter counting rate (N_T) with the anodes connected in parallel to the amplifying system. The source mounts used were of gold-coated VYNS film (7) mounted on a 1 mm. aluminum diaphragm of aperture 2.5 cm. in diameter. The thinnest films employed were of 5 to 10 μgm./cm.^{2} superficial density, and increasing thickness was obtained:

(*a*) up to about 70 μgm./cm.^{2} by allowing a series of films of known superficial density to adhere to the back of the initial mount;

(*b*) above 70 μgm./cm.^{2} by temporarily placing in contact with the back surface of the mount, in position in the chamber, each of a series of standardized films of increasing superficial density.

The results of these experiments are shown plotted in Figs. 1 and 2. Data as shown are for "weight-less" sources. Experiments with Ni^{63} have shown that identical results are obtained even for source thicknesses where self-absorption of the order of 80 to 90% occurs.

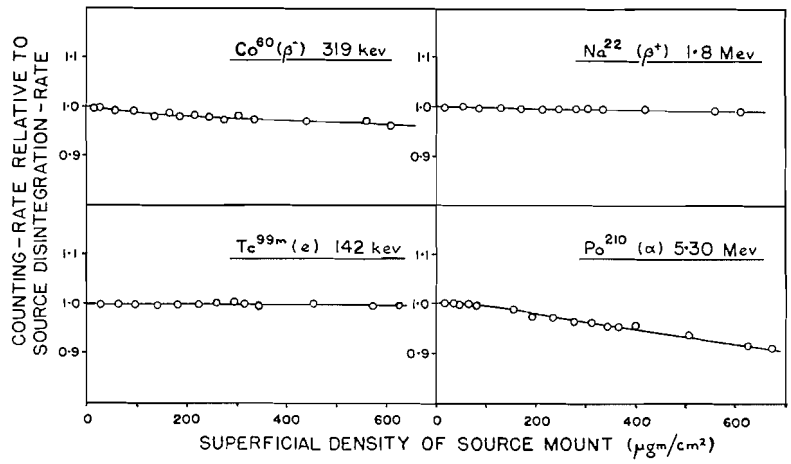

FIG. 2. Source-mount absorption characteristics for emitters of other forms of radiation.

(ii) *Sandwich Characteristics*

A second series of measurements was taken using the series of seven β emitters described above as shown in Fig. 1. In this case sources of each nuclide were prepared on a series of films of increasing superficial density and the following quantities measured: the total counting rate with the anodes in parallel with a single mount (N_T), and the total counting rate with a second identical sandwiching film added (N_S). From these values the expected disintegration rate of the sources used has been calculated by the procedure of Hawkings *et al.* (N_A) and by the more rigorous of the procedures of Seliger and co-workers (N_A'). The results are shown plotted as a function of source-mount

superficial density in Fig. 1, with the true source disintegration rates normalized to a common value for each nuclide using the curves for N_T obtained in the first series of experiments.

C. DISCUSSION

(*a*) *The Sandwich Procedure*

The results shown in Fig. 1 give a fairly complete picture of the accuracy of the sandwich procedure as a function of mount thickness and β end-point energy, whether applied by the method of Hawkings *et al.* (3) or by the NBS method (5, 9, 10), and are in accord with those found by Smith (11). Though the procedure may be said to work fairly well at higher particle energies, where the mount absorption is small in any case, at lower energies, where accurate information is desirable, it becomes progressively less and less useful. The fact that the calculation of the disintegration rate leads to results that vary considerably (for example in the case of Ni^{63}) with source mount thickness would indicate that the mathematical treatment was oversimplified.

(*b*) *The Absorption Curve Procedure*

The anomalous results obtained by this method by Smith (11) using mounts with a superficial density in excess of 260 μgm./cm.^{2} are readily understood on

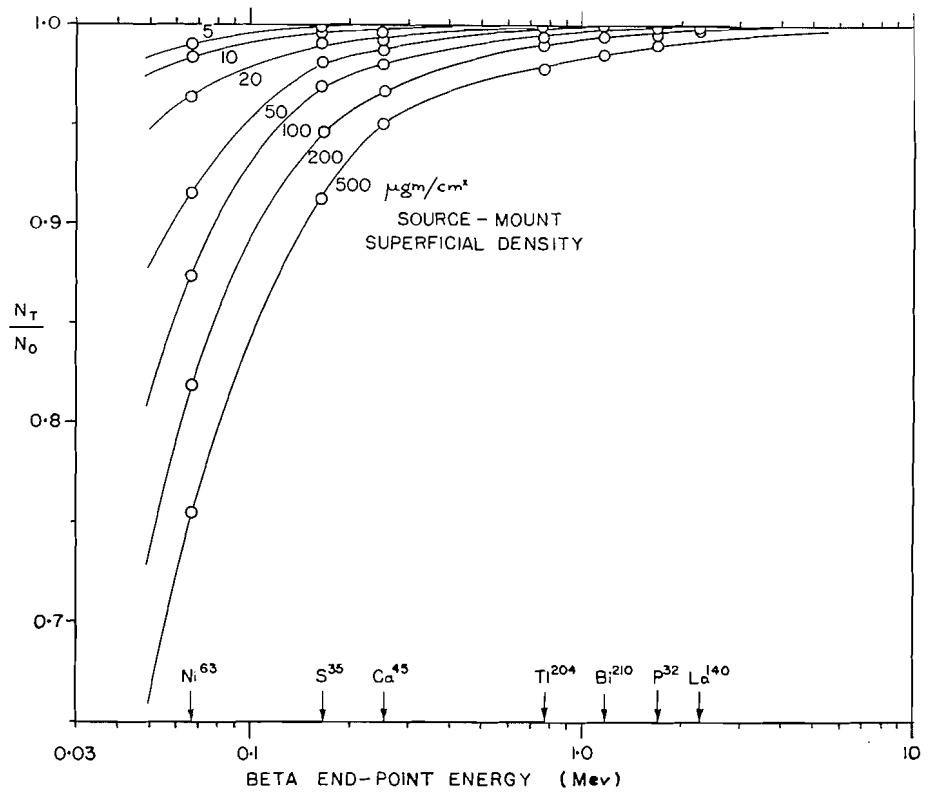

FIG. 3. Absorption parameter (N_T/N_0) as a function of beta end-point energy, for a series of film thicknesses.

a basis of the curves for N_T shown in Fig. 1. Extrapolation of the approximately linear portion of the curves obtained at higher mount thicknesses would take no account of the initial fall in counting rate, particularly pronounced at low β end-point energies, due to progressive absorption by the source mount of the softest radiation in the beta energy spectrum.

For work of moderate precision the data in Fig. 1 may be used directly to correct observed single-film results for source-mount absorption. In order to allow interpolation to intermediate β energies, the data are replotted in Fig. 3 with the absorption parameter (N_T/N_0) as a function of beta end-point energy for a series of film thicknesses. Clearly several approximations are introduced by use of the data in this way, including a neglect of variation in the form of the beta energy spectrum with nature of the beta transition (degree of forbiddenness etc.) and of the additional complication of nuclear gamma emission when this is present. Also, obviously the transition must be recognized as a beta transition and the end-point energy known.

For work of maximum precision, the procedure adopted to obtain our experimental results is recommended. In this case, the source material is mounted on the thinnest film available, and the counting rate N_T measured as a function of increasing mount thickness as outlined above. The disintegration rate is obtained by extrapolating to zero mount thickness.

The accuracy of the disintegration-rate value, arrived at in this way, can also be judged from Fig. 1. It is limited by the statistical deviation of the counting rates measured, and by the accuracy with which the superficial density values are known (7). No error of significance should be introduced by the technique of allowing additional films to adhere to the original mount, and we estimate that the error in the final disintegration-rate value can be reduced to about $\pm 0.2\%$ in the case of the weakest beta radiation studied, and probably to less than this at higher particle energies. We find this method satisfactory in routine use, the necessary measurements and manipulations taking very little more time than those required for the conventional sandwich procedure.

In the case of a beta emitter of unknown energy, once the disintegration rate is known from the absorption curve procedure, Fig. 3 may be used to derive from the observed value of N_T/N_0 a crude but nevertheless useful estimate of the end-point energy of the spectrum. This technique replaces those commonly used with end-window counters, which are inapplicable in a 4π steradian-geometry.

It is of interest to consider why the value of source disintegration rate predicted by the sandwich procedure should vary with increasing source-mount thickness, and in general differ (widely at low beta energies) from the figure unequivocally indicated by the absorption curve method. The reasons for variations in the separate counting rates of the hemispheres above and below the source mount, and in the rate of coincidences between the two half-counters, are various and will be discussed in the fourth paper of this series. However, the change in total counting rate (N_T) can only be due to increased absorption of radiation in the mounting film or reduction of particle energy to below that

required to trigger the counter. It has been shown in paper one of this series (8) that, under the adopted operating conditions, substantially all particles entering the counter gas produce the necessary minimum ionization and trigger the counter.

It is proposed to leave the quantitative analysis of the relative contribution of the various scattering and absorption processes to paper four of this series, in which a more complete set of data for the half-counter counting rates and coincidence rates observed with different forms and energy of radiation under different conditions will be presented.

One should, however, perhaps consider the data for N_T for Po^{210} shown in Fig. 2. Po^{210} is an α emitter of 5.30 Mev. energy which has a range of $\sim$5.1 mgm./cm.^{2} in air, and therefore using known atomic stopping powers one can compute the range in the film to be 4.9 mgm./cm.^{2} Hence, with film superficial densities of up to at least 600 μgm./cm.^{2} no fall in N_T with increasing d might be expected, whereas an approximately linear decrease is observed. One observes in this case (α emission) that the rate of coincidences between the two half-counters is very small ($<0.1\%$ of N_0) and that N_T is substantially the sum of the counting rates of the upper hemisphere (which is constant with increasing d) and of the lower hemisphere (which decreases linearly with increasing d). Thus, the observed effect is due solely to absorption of α particles in the film, which at the film thicknesses used should be small in view of the monoenergetic nature of the emission.

However, if the film thickness is again d and the range of the radiation in film material is R, as in Fig. 4, then of those α particles emitted in the 2π steradian angle towards the film, only those inside the cone of half-angle

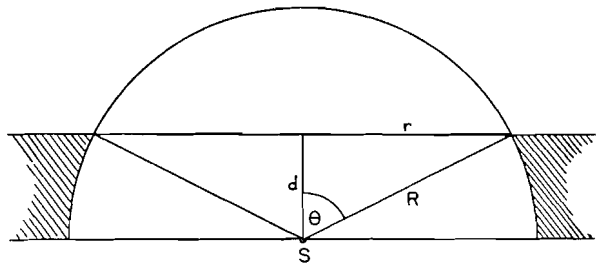

FIG. 4. Film absorption of α radiation (schematic).

subtended by the radius r will emerge into the gas volume and register. The proportion of the total radiation emitted outside this cone and totally absorbed in the film can be shown to be $(2\pi rd)/4\pi R^2$ for large values of θ

$$= rd/2R^2$$
$$\simeq d/2R$$

in agreement with the observed linearity with d. In a film thickness corresponding to 600 μgm./cm.^{2}, the loss by absorption is found to be 6.5% compared to an observed value of 7.5%. The agreement is fair considering the assumptions made regarding the range of Po^{210} α particles in the film material.

The absence of apparent decrease of N_T with d in the case of the (monoenergetic) conversion electrons from Tc^{99m} (Fig. 2) is presumably due to their longer range (26 mgm./cm.^{2}) and the influence of back-scattering.

ACKNOWLEDGMENTS

The authors wish to thank the National Research Council of Canada and Atomic Energy of Canada Ltd. for grants-in-aid. We would also like to express our appreciation to Dr. R. E. Bell for valuable discussions. One of us (B. D. P.) wishes to thank N.R.C. for assistance in the form of a Studentship.

REFERENCES

1. BORKOWSKI, C. J. Conference on Absolute β Counting. Prelim. Rept. Nuclear Sci. Ser. N.R.C., Washington, D.C. No. 8: 55. 1950.
2. GLENDENIN, L. E. Conference on Absolute β Counting. Prelim. Rept. Nuclear Sci. Ser. N.R.C., Washington, D.C. No. 8: 20. 1950.
3. HAWKINGS, R. C., MERRITT, W. F., and CRAVEN, J. H. Proceedings of Symposium: Maintenance of Standards. Natl. Phys. Lab. May, 1951. H.M. Stationery Office, London. 1952.
4. HOUTERMANS, F. G., MEYER-SCHÜTZMEISTER, L., and VINCENT, D. H. Z. Physik, 134: 1. 1952.
5. MANN, W. B. and SELIGER, H. H. J. Research Natl. Bur. Standards, 50: 197. 1953.
6. MEYER-SCHÜTZMEISTER, L. and VINCENT, D. H. Z. Physik, 134: 9. 1952.
7. PATE, B. D. and YAFFE, L. Can. J. Chem. 33: 15. 1955.
8. PATE, B. D. and YAFFE, L. Can. J. Chem. 33: 610. 1955.
9. SELIGER, H. H. and CAVALLO, L. J. Research Natl. Bur. Standards, 47: 41. 1951.
10. SELIGER, H. H. and SCHWEBEL, A. Nucleonics, 12 (No. 7): 54. 1954.
11. SMITH, D. B. Brit. Atomic Energy Rept. A.E.R.E. I/R 1210. 1953.
12. SUZOR, F. and CHARPAK, G. Compt. rend. 234: 720. 1952.
13. YAFFE, L. and JUSTUS, K. M. J. Chem. Soc. Suppl. S. 341. 1949.

SIMULTANEOUS SURFACE EXCHANGE STUDIES USING BOTH CATION AND ANION[1]

By R. M. Stow[2] and J. W. T. Spinks

ABSTRACT

Labelled Sr^{++} and $SO_4^{=}$ have been used simultaneously to measure the apparent surface area of a $SrSO_4$ precipitate by the direct radioactive method. The values found differ by about 90%. By contrast, when labelled Pb^{++} and $SO_4^{=}$ are used to measure the apparent surface area of $PbSO_4$, the values found are in close agreement. The results are discussed with reference to the kinetics of surface exchange reactions.

INTRODUCTION

The heterogeneous exchange between the ions on the surface of a solid and the ions in a solution has been widely used as the basis for the radioactive method for determining the "active" surface area of a solid. The method was introduced by Paneth and Vorwerk (4), and has been the subject of numerous investigations (for recent summaries, see (3, 8)). There appears to be a very rapid primary exchange, involving only the surface layer of the solid, followed by a much slower secondary exchange which may involve penetration of ions into the crystal. In the primary exchange, equilibrium is reached in a few minutes. According to Paneth, at equilibrium $N_S^1/N_S = N_L^1/N_L$ where N_S^1 = number of tracer atoms (or ions) on the surface, N_S = total number of this species of atoms (or ions) on the surface, N_L^1 = number of tracer atoms (or ions) in the bulk of the solution, and N_L = total number of this species of atoms (or ions) in the bulk of the solution. N_S is readily calculated knowing N_S^1, N_L^1, and N_L, and from this the surface area, $S = N_S l^2$, can be calculated. l^2 is the effective area of the tagged atom (or ion) on the surface and is given by $l^2 = (\text{M.W.}/aNd)^{2/3}$ where M.W. = the formula weight of the solid, a = number of gram atoms (or gram ions) of the tagged species of atoms per formula weight of solid, N = Avogadro's number, and d = density.

Using Paneth's method, tracers isotopic with either cation or anion of the precipitate should, on the basis of simple theory, yield the same surface area. However, Imre (1, 2) has suggested that surface exchange may not be quite so simple as Paneth suggests. He suggests rather that for the surface exchange equilibrium $(N_S^1/N_S)(N_L/N_L^1) = K$, where $K = K_0\, e^{-E/RT}$ and is not necessarily unity. K_0 is a symmetry factor which is equal to unity for self-adsorption systems (e.g. Pb^{++} on $PbSO_4$). For self-adsorption, $K = e^{-E/RT}$, K being called the 'activation' factor and E the 'activation energy'. This terminology is perhaps unfortunate since it seems to imply that we are dealing with kinetics of exchange reactions whereas in fact we are dealing with measurements of exchange equilibrium. Imre states that different K values result for the exchange of Pb^{++} and $CrO_4^{=}$ on $PbCrO_4$ but suggests that the K values will

[1]*Manuscript received January 10, 1955.*
Contribution from the Department of Chemistry, University of Saskatchewan, Saskatoon, Saskatchewan, with financial assistance from the National Research Council of Canada.
[2]*Died while a student in Cambridge, England, 1951.*

be the same for the exchange of Pb^{++} and $SO_4^{=}$ on $PbSO_4$. The availability of S^{35}, Sr^{90}, and Pb^{212} has made it possible to test this hypothesis with precipitates of $SrSO_4$ (7) and $PbSO_4$. In some experiments surface exchange was carried out with either cation or anion labelled; in other experiments, both cation and anion were labelled in the same experiment.

EXPERIMENTAL

Radioactive Materials

S^{35} was obtained from Chalk River in the form of an aqueous solution of sulphuric acid. Tests showed that all the S^{35} was in the form of $SO_4^{=}$ and that the half life and absorption half thickness were in agreement with published values (6). Sr^{90}, obtained from Chalk River as $SrCO_3$[3], was converted to the acetate to form a stock solution (5). Immediately prior to a surface exchange experiment, the Y^{90} daughter was separated from the Sr^{90} by adding yttrium holdback carrier and precipitating Sr as the sulphate. The precipitated $SrSO_4$ was washed with a small amount of saturated $SrSO_4$ solution.

Pb^{212} was obtained from the emanation from thorium hydroxide (5). No attempt was made to remove the 60.5-min. half life daughter, Bi^{212}.

Strontium Sulphate

The strontium sulphate used was that prepared in 1946 by Singleton (5) and kept in contact with strontium sulphate solution since that time.

Lead Sulphate, Suspension S (Precipitate Prepared Using Excess Sulphate)

The first precipitate was prepared using 5% excess sulphate. A solution of 250 gm. reagent grade lead nitrate in 650 ml. distilled water was added with stirring to 300 ml. of a sulphuric acid solution. The addition took place over a period of one hour. When the addition was complete, a test of the filtrate showed it to contain excess sulphate ion. The precipitate was washed, with accompanying stirring, with 15 1-liter portions of distilled water over a period of one month.

Lead Sulphate, Suspension L (Precipitate Prepared Using Excess Lead)

This precipitate was prepared in a manner similar to that described for Suspension S except that the chemicals were added in the reverse order, and a 5% excess of lead, instead of sulphate, was used. A test of the filtrate, after the mixing of the chemicals, showed an excess of lead ion.

The washing scheme for this precipitate was identical to that for Suspension S.

Saturated Solutions of the Precipitates in Water

The individual washings of a precipitate were accomplished by agitating the precipitate for 24 hr., with 1-liter portions of distilled water, by means of an electrically driven stirrer. When the last agitation of a precipitate in any particular set of washings had been completed, the suspension was allowed to settle and some of the solution decanted, filtered, and saved. The solution

[3]*The more convenient Sr^{89} was not readily available at that time (1949–50).*

obtained was thus a saturated solution of the precipitate compound in water at room temperature, as given by the precipitate at that stage of washing.

Solutions Containing Sr^{90}

A small amount of highly active strontium sulphate precipitate, freed from yttrium, was stirred with a quantity of saturated inactive strontium sulphate solution. As exchange between the precipitate and solution occurred, activity entered the solution. After approximately one hour, when the solution had attained a sufficient degree of activity,[4] the mixture was allowed to settle and the solution decanted and filtered. Solutions containing Sr^{90} were thus obtained without introducing additional strontium or foreign ions.

Solutions Containing $S^{35}O_4^{=}$

One-tenth of a milliliter of the stock solution of $S^{35}O_4^{=}$ obtained from Chalk River was diluted to 1 ml. with distilled water. To approximately 400 ml. of saturated inactive strontium or lead sulphate solution a sufficient quantity (0.15 ml.) of the diluted stock solution was added to give an activity of 80 counts per sec. per 5 ml.

Solutions Containing ThB

After the platinum foil in the emanation apparatus had been collecting activity for two days, the foil was removed and rinsed in a quantity of saturated inactive lead sulphate solution. After 15 min. the platinum foil was removed and the solution was ready for use.

Measurement of Radioactivity

Counting equipment consisted of an Atomic Instrument Company Scale of 64 scaler and an end-window Geiger tube. The usual corrections for resolving time and background were made. Backscattering corrections were avoided by always using identical 1 ml. Pt dishes, diameter 2.2 cm., for counting. Statistical counting errors were reduced to about 1% by recording 10,000 counts. Self-absorption corrections were eliminated by preparing all samples containing a given radionuclide in such a way that they contained the same weight of absorbing agent. Thus, samples from experiments with the strontium sulphate precipitate were all counted with the residue left upon evaporation of 5 ml. of saturated strontium sulphate solution. This residue weighs approximately 0.62 mgm., equivalent to 0.2 mgm. per sq. cm. when evaporated on dishes of 2.2 cm. diameter. Similarly, samples from experiments with the lead sulphate precipitates have been counted with the residue, weighing approximately 0.20 mgm., from 5 ml. of saturated lead sulphate solution.

Miscellaneous Equipment

A mechanical shaker was used to keep samples agitated during the absorption experiments.

Thirty-milliliter glass stoppered flint glass bottles were used as shaking bottles, the same as in previous experiments (5).

Suspensions were stirred with an electrically driven stirrer.

[4]*Radioactivity.*

Experimental Procedure

The procedure was essentially the same as that used in the previous work on strontium sulphate (5, 6). After the precipitate suspension had been agitated by a mechanical stirrer for at least five minutes, an aliquot of the suspension, usually 5 ml., was withdrawn by pipette and placed in a shaking bottle. An aliquot, usually 15 ml., of the appropriate active solution was then pipetted into the bottle and shaking on the mechanical stirrer was begun immediately. The temperature was room temperature, approximately 20°C. Shaking time was measured from the time the solution had completely drained into the shaking bottle. When shaking was complete the bottle was removed and centrifuged for approximately one minute. Five milliliters of the supernatant liquid was then withdrawn by pipette and evaporated in successive portions in a 1-ml. platinum dish on a semimicro water bath.

The radioactivity of the sample in the Pt dish was then measured under an end-window Geiger tube.

It is necessary to know the starting activity of the active solution before admixture with the precipitate, as well as the activity after mixing, if the amount adsorbed by the precipitate in an exchange experiment is to be obtained by difference. The procedure used in measuring the starting activity of an aliquot of active solution was such that the starting activity samples went through all experimental operations except the actual addition of the precipitate. The effects of adsorption, if any, of tracer ions on equipment were thus made to cancel out. The starting activity samples were made by transferring an aliquot of inactive solution to a shaking bottle and adding the same volume of active solution as used in the exchange experiment. The solution was shaken for a time, then a portion was withdrawn and evaporated on a sample dish. The aliquot of inactive solution to which active solution was added was equal in volume to the volume occupied by liquid in an aliquot of the precipitate suspension. For example, the volume occupied by liquid in a 5 ml. aliquot of strontium sulphate suspension was $(5-0.24) = 4.76$ ml., the volume of the solid precipitate being 0.24 ml.

The amount of precipitate suspension and the amount of active solution used in each experiment were so chosen that roughly 50% adsorption or exchange of activity would occur. At 50% adsorption the accuracy of the experiment is at a maximum.

The weight of precipitate in an aliquot of suspension was determined by transferring a number of aliquots to a Gooch filter crucible, filtering, drying in an oven (105°C.) overnight, and weighing.

Corrections for the Growth of Y^{90} from Sr^{90}

The sample was measured first without an absorbing screen and then with an absorbing screen of thickness 231 mgm./sq. cm. between it and the Geiger tube. This reduced the Sr^{90} count to less than 0.2% but transmitted 39% of the Y^{90} count. Multiplying the second count by 100/39 and subtracting this from the first count gave the count due to Sr^{90}.

Counting of S^{35} in the Presence of Sr^{90} Plus Y^{90}

By counting the sample through a screen of 17.4 mgm./sq. cm. thickness all the S^{35} radiations were cut out. Combining this count with a knowledge of the fraction of the Sr–Y radiations transmitted by this screen and a measurement of the amount transmitted by a 231 mgm./sq. cm. screen allowed the calculation of both S^{35} and Sr^{90} activities in a given sample.

Counting of S^{35} in the Presence of ThB

The ThB was measured by counting the sample behind a 17.4 mgm./sq. cm. screen which absorbed the S^{35} radiations. The S^{35} was measured six days later when all the ThB had decayed.

Method of Calculation

The starting activity and the activity of the exchange samples belonging to a particular set of experiments were first corrected for background. They were then brought to the same basis by taking into account any dilution that had occurred as a result of the experimental procedure.

When dealing with Sr^{90} the next step in the calculations was the correction for growth of daughter activity.

After applying these corrections the quantity of activity adsorbed by the precipitate was obtained by difference. Substitution was then made in the ratio on the left side of the fundamental equation:

$$\frac{\text{No. tracer anions or cations in soln.}}{\text{No. tracer anions or cations in surf.}} = \frac{\text{No. of anions or cations in soln.}}{\text{No. of anions or cations in surf.}}.$$

The quantity "number of anions or cations in solution" is calculated from the solubility of the precipitate in water. For strontium sulphate, formula weight 183.7 and solubility in water 0.1233 gm. per liter (7), the number of strontium or sulphate ions per milliliter of saturated solution is

$$0.1233\times6.02\times10^{23}/1000\times183.7 = 4.04\times10^{17} \text{ ions per ml.}$$

For lead sulphate, formula weight 303.3 and solubility in water 2.56×10^{-4} moles per liter at 20°C., the corresponding figure is 1.54×10^{17} ions per ml. Using the formula given in the Introduction, the area per molecule is, for strontium sulphate (density 3.96 gm. per ml.), $(183.7/3.96\times6.02\times10^{23})^{2/3} = 1.81\times10^{-15}$ sq. cm. The corresponding area for lead sulphate (density 6.2 gm. per ml.) is 1.88×10^{-15} sq. cm.

Typical Calculations

(*a*) *Exchange of Sr^{90} at the Surface of a Strontium Sulphate Precipitate*

Five milliliters of a suspension of strontium sulphate was added to 15 ml. of saturated strontium sulphate solution containing Sr^{90}. The mixture was shaken for 10 min. and then centrifuged. Five milliliters of the centrifugate was evaporated and counted. After correcting for yttrium, the activity was 23.65 registers/min. (1 reg. = 64 counts). Five milliliters of the original solution gave 52.9 reg./min. Thus, the percentage activity adsorbed or exchanged $= (1-23.65/52.9)\ 100 = 55.3\%$. The weight of $SrSO_4$ in the suspension was

1.1315 gm. and the total volume of solution was 19.76 ml. Thus, the number of ions in the surface per gram of precipitate equals

$$\frac{55.3}{44.7} \times \frac{19.76 \times 4.04 \times 10^{17}}{1.1315} = 8.55 \times 10^{18}.$$

The surface area per gram, corresponding to 8.55×10^{18} ions in the surface, is equal to $8.55 \times 10^{18} \times 1.81 \times 10^{-15} = 15{,}500$ sq. cm.

(*b*) *Combined Sr^{90} and $S^{35}O_4^{=}$ Experiment*

An experiment was conducted in which 5 ml. of a suspension of strontium sulphate were shaken with 15 ml. saturated strontium sulphate solution containing approximately equal activities of Sr^{90} and $S^{35}O_4^{=}$. Shaking time was 10 min. The results are recorded in Table I.

TABLE I

EXCHANGE EXPERIMENT USING BOTH S^{35} AND Sr^{90}

	Activity, registers/min., corrected for background	
	Starting activity sample	Exchange sample
1. No screen	61.7	33.4
2. 17.4 mgm./sq. cm. screen	20.1	9.56
3. 231 mgm./sq. cm. screen	0.53	0.50
4. Calculated Sr^{90} activity passing 231 mgm./sq. cm. screen	0.04	0.02
5. Y through 231 mgm./sq. cm. screen ((3)−(4))	0.49	0.48
6. Y, no screen ((5).100/39)	1.25	1.23
7. Y through 17.4 mgm./sq. cm. screen (0.95(6))	1.19	1.17
8. Sr^{90} through 17.4 mgm./sq. cm. screen ((2)−(7))	18.91	8.39
9. Sr^{90}, no screen ((6)/0.56)	33.8	14.95
10. S^{35}, no screen ((1)−(9)−(6))	26.7	17.2

% Sr adsorbed = [(33.8−14.95)/33.8]100 =55.8 ;
% S^{35} adsorbed = [(26.7−17.2)/26.7]100 = 35.5.
These figures correspond to areas of 16,200 and 7050 sq. cm. per gram of precipitate, respectively.

RESULTS

$SrSO_4$

The effect of time of shaking on percentage adsorption of $S^{35}O_4^{=}$ on $SrSO_4$ is shown in Fig. 1, together with the corresponding figures for the exchange of Sr^{++} by the same precipitate (see Ref. (5)) in experiments done two years earlier. As before, there is a very rapid primary exchange followed by a much slower secondary exchange. The primary exchange is essentially complete in about ten minutes, and as a consequence this time of shaking has been rather arbitrarily chosen as the point at which to calculate surface area in most experiments.

Shaking time, 10 min.

(*a*) Using Sr^{90} only, average area per gm. = 15,000 sq. cm. (cf. Singleton, 12,800 sq. cm., in 1947).

(*b*) Using Sr^{90} and S^{35} simultaneously; based on Sr^{90}, area per gm. = 16,200 sq. cm.; based on $S^{35}O_4^{=}$, area per gm. = 7050 sq. cm.

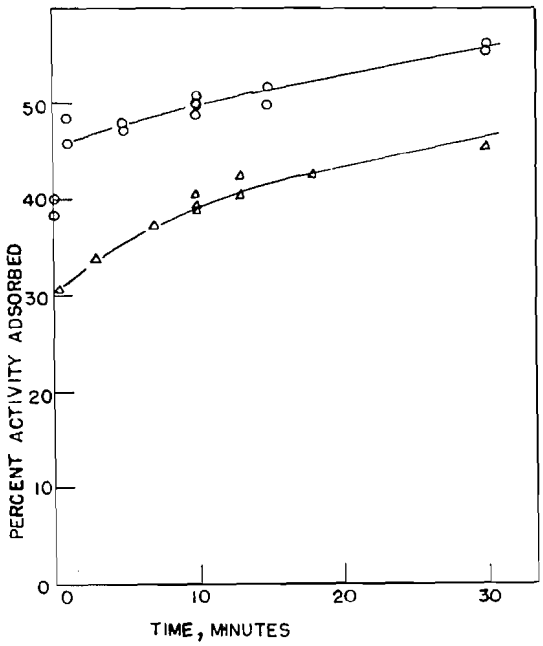

FIG. 1. Variation of percentage adsorption of ions on a strontium sulphate precipitate, with time of shaking; ○, Sr^{90} (Singleton 1947), △, $S^{35}O_4^{=}$ (Stow 1949).

The precipitate was then washed with six 1-liter portions of distilled water and the exchange experiments repeated with the following results:
Based on $S^{35}O_4^{=}$, average area per gm. = 7830 sq. cm.
Based on Sr^{90}, average area per gm. = 14,400 sq. cm.
Washing the precipitate thus had very little effect on the apparent surface area.

Celestine

A single, well-formed crystal of celestine[5] was reduced to a fine powder using an agate mortar and pestle. The powder was washed by stirring with 10 successive 300-ml. portions of water over a period of 40 hr. and then used in exchange experiments with labelled Sr^{++} and $SO_4^{=}$. Shaking 8.5 gm. powdered celestine with 8.5 ml. saturated $SrSO_4$ solution for 20 min. resulted in 65.5% adsorption of $SO_4^{=}$ and 75% adsorption of Sr^{++}. The relative surface areas as measured by Sr^{++} and $SO_4^{=}$ were thus in the ratio (75/25)(34.5/65.5) = 1.58 (cf. 1.9 for $SrSO_4$ prepared in the laboratory). The surface area per gram as measured by Sr^{++} was 2140 sq. cm.

$PbSO_4$; Suspensions S and L

Results for time of shaking experiments with $PbSO_4$ suspensions are recorded in Figs. 2 and 3.

In four of the experiments both $SO_4^{=}$ and Pb^{++} were labelled; in the remainder, one ion only was labelled. For Suspension S the percentage adsorptions of $SO_4^{=}$ and Pb^{++} were not significantly different and the difference was only

[5]*Obtained from Ward's Natural Science Establishment.*

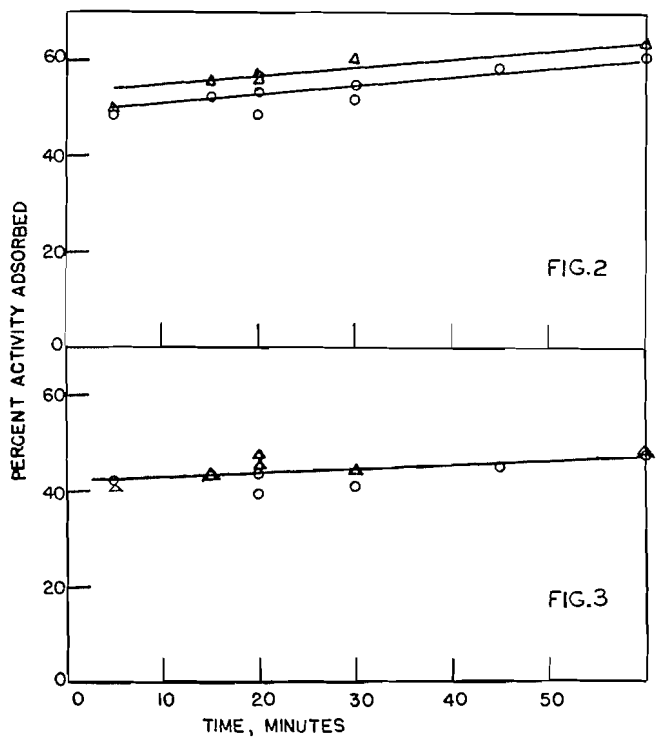

FIG. 2. Variation of percentage adsorption of ions on a lead sulphate precipitate, Suspension L, with time of shaking; ○, ThB; △, $S^{35}O_4^{=}$.

FIG. 3. Variation of percentage adsorption of ions on a lead sulphate precipitate, Suspension S, with time of shaking; ○, ThB; △, $S^{35}O_4^{=}$.

slight for Suspension L. The mean surfaces per gram of precipitate (20 min. shaking) are 2160 and 3650 sq. cm. for S and L, respectively.

The precipitate was then washed with six 1-liter portions of distilled water and the exchange experiment repeated. Again the percentage adsorptions for a given suspension were not significantly changed by the washing for either ThB or $S^{35}O_4^{=}$. Thus washing the precipitate had little effect on the surface area.

DISCUSSION

The foregoing experiments, in which two labelled ions have been used simultaneously to measure the degree of exchange at a surface consisting of the two ions, indicate that the degree of exchange is not necessarily the same for the two ions. The statistical mechanical approach of Imre has indicated that factors other than those considered by Paneth may sometimes be involved. It is of particular interest that his prediction that the degrees of exchange for Pb^{++} and $SO_4^{=}$ on $PbSO_4$ would be the same is borne out by the present experiments. It is also of some interest that the degrees of exchange for Sr^{++} and $SO_4^{=}$ on $SrSO_4$ differ markedly from one another, both for artificially prepared $SrSO_4$ and for the naturally occurring celestine. While altogether too few experiments have been done to warrant any speculation concerning the origin of the differ-

ence, it might possibly be due to differing hydration energies of the Sr^{++} and $SO_4^{=}$ ions. However the present experiments do indicate that this method, and possible extensions of it, does provide a powerful tool for investigating the behavior of ions at surfaces. Further experiments have been planned.

ACKNOWLEDGMENT

We are grateful to the National Research Council of Canada for financial aid.

REFERENCES

1. IMRE, L. Kolloid-Z. 99: 147. 1942.
2. IMRE, L. Kolloid-Z. 106: 39. 1944.
3. PANETH, F. A. J. chim. phys. 45: 205. 1948.
4. PANETH, F. A. and VORWERK, W. Z. physik. Chem. 101: 445. 1922.
5. SINGLETON, R. H. and SPINKS, J. W. T. Can. J. Research, B, 27: 238. 1949.
6. STOW, R. M. *Thesis, University of Saskatchewan, Saskatoon, Sask.* 1950.
7. STOW, R. M. and SPINKS, J. W. T. J. Chem. Phys. 17: 744. 1949.
8. WAHL, A. C. and BONNER, N. A. Radioactivity applied to chemistry. John Wiley & Sons, Inc., New York. 1951.

INTERFACIAL POTENTIALS[1]

By J. T. Davies and Sir Eric Rideal

ABSTRACT

A new relation between interfacial distribution potentials and interfacial surface (contact) potentials is presented. By a suitable choice of experimental system either distribution potentials or surface potentials may be measured separately; results are in good agreement with theory. Surface potentials are shown to be made up of several independent components. The rates of decay of surface potentials are also discussed.

The origin of interfacial potentials between oil and water, important as biological analogies, has long been a matter of some controversy. Many of the early experiments were conducted with salicylaldehyde or *o*-toluidine as the oil phase, and the potential differences measured when different organic salts were added changed slowly with time during the experiments. Beutner (4, 5) believed that the potential differences arise from the free charge at the interface due to an unequal distribution of the various cations and anions across the interface. The distribution potential difference caused by this process may be termed after Lange the ψ or outer potential. Baur (3) on the other hand believed the changes were due to selective ionic adsorption at the oil–water interface. Such surface or interfacial potentials may be represented by ΔV or by $\delta\chi$ in Lange's nomenclature.

After much controversy Baur accepted Beutner's explanation as to their origin. Some years later Dean, Gatty, and Rideal (15) showed theoretically that if one or more types of ions can dissolve in both oil and water no *stable* interfacial potential ΔV can be measured.

Whether the older potential differences were distribution or surface potentials has been summed up by Adam (1):

> "It seems quite likely, however, that both (Beutner and Baur) were right, according to circumstances; although the final potential when thermodynamic equilibrium is attained is not an adsorption potential, the establishment of this equilibrium probably takes a very long time".

Indeed, since the paper of Dean, Gatty, and Rideal (15), it has become clear that the time for decay of the surface potential ΔV determines whether we measure $\Delta\psi$ or ΔV when different organic salts are added. In this paper we shall estimate such times, and confirm that with polar oils at equilibrium only $\Delta\psi$ is measured. Although ψ may take a considerable time to reach equilibrium, owing to the slow diffusion of the salts, and although a diffusion potential (6) may also be measured while this occurs, the surface potential ΔV must decay to zero extremely rapidly in the systems of Beutner and Baur.

Further, by a suitable choice of oils, it has now become possible to measure potential changes ascribable wholly to ψ or to V.

[1]*Manuscript received February 7, 1955.*
Contribution from Department of Physical Chemistry, University of London, King's College, London, England.

(*a*) DISTRIBUTION POTENTIALS

According to Nernst's theory of distribution potentials, these are measured when the salt has an appreciable solubility in the oil and they arise from the different solubilities of the positive and negative ions in the two phases. We can express this in the following manner:

$$B_+ = \exp[({}_w\mu_+^0 - {}_o\mu_+^0)/RT] \text{ or } RT \ln B_+ = {}_w\mu_+^0 - {}_o\mu_+^0,$$

$$B_- = \exp[({}_w\mu_-^0 - {}_o\mu_-^0)/RT] \text{ or } RT \ln B_- = {}_w\mu_-^0 - {}_o\mu_-^0,$$

where $B_\pm$ refers to the ionic distribution coefficients, and μ^0 the standard chemical potential. Subscripts o and w refer to the oil and water phases respectively.

These different solubilities of the two ions cause a potential between the two phases, as shown in Fig. 1.

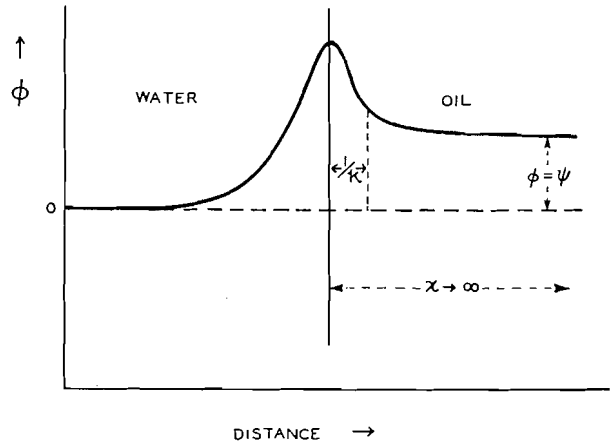

FIG. 1. Variation of ϕ (relative to the interior of the water phase) near an oil–water interface. The oil is assumed polar. The distance from the interface is represented by x, and measurements are made where $x \longrightarrow \infty$ compared with the ionic double layer thickness $1/\kappa$.

The water phase is generally assigned zero potential, while the oil phase has a potential in Lange's notation ϕ (sometimes termed the inner or Galvani potential). If positive ions (e.g. tetramethylammonium) dissolve preferentially in the oil phase, while (say) chloride ions tend to remain in the water, ϕ is positive. The potential ϕ includes both ψ and V thus: $\phi = \psi + V$, or in Lange's notation, $\phi = \psi + \chi$.

We now relate ϕ to B_+ and B_- by means of their electrochemical potentials, $\bar{\mu}$. The Faraday unit is written F.

[1] $${}_w\bar{\mu}_+ = {}_w\mu_+^0 + RT \ln {}_wc_+$$

[2] $${}_o\bar{\mu}_+ = {}_o\mu_+^0 + RT \ln {}_oc_+ + \phi F$$

[3] $${}_w\bar{\mu}_- = {}_w\mu_-^0 + RT \ln {}_wc_-$$

[4] $${}_o\bar{\mu}_- = {}_o\mu_-^0 + RT \ln {}_oc_- - \phi F$$

At equilibrium:

[5] $$ {}_w\bar{\mu}_+ = {}_o\bar{\mu}_+ $$

and

[6] $$ {}_w\bar{\mu}_- = {}_o\bar{\mu}_- . $$

Further, each phase must be electrically neutral, therefore

[7] $$ {}_wc_+ = {}_wc_- $$

and

[8] $$ {}_oc_+ = {}_oc_- . $$

By substitution of equations [1] to [4] into equations [5] and [6], we find:

$$ {}_w\mu_+^0 + RT \ln {}_wc_+ = {}_o\mu_+^0 + RT \ln {}_oc_+ + \phi F $$

and

$$ {}_w\mu_-^0 + RT \ln {}_wc_- = {}_o\mu_-^0 + RT \ln {}_oc_- - \phi F . $$

If we subtract, remembering equations [7] and [8], we obtain:

$$ ({}_w\mu_+^0 - {}_o\mu_+^0) - ({}_w\mu_-^0 - {}_o\mu_-^0) = +2\phi F $$

or

$$ RT \ln B_+ - RT \ln B_- = 2\phi F $$

or

[9] $$ \phi = \phi_{x=\infty} = (RT/2F)\ln(B_+/B_-) . $$

Here $\phi_{x=\infty}$ is defined as in Fig. 1, ϕ being measured far from the interface when x is great compared with the Debye–Hückel term $1/\kappa$. Equation [9] is the required relation between ϕ, B_+, and B_-. If B_+ is large compared with B_-, ϕ is positive.

It can easily be shown that if S is the ratio (conc. salt in oil)/(conc. salt in water),

[10] $$ S = (B_+ . B_-)^{\frac{1}{2}} . $$

Hence, from equations [9] and [10],

$$ \phi = (RT/2F)\ln(S^2/B_-^2) . $$

Although the absolute potentials ϕ are not measurable, we can determine differences in ϕ for (say) NaI and KI. Then B_- is constant, and

$$ \Delta\phi = (RT/F)\ln(S_{NaI}/S_{KI}) . $$

Since ΔV should theoretically not contribute to $\Delta\phi$ in such systems (15), and since $\Delta\phi = \Delta\psi + \Delta V$, if x tends to infinity,

[11] $$ \Delta\phi = \Delta\psi = (RT/F)\ln(S_{NaI}/S_{KI}) . $$

Further, as we may see from inspection of equation [9], $\Delta\phi$ is independent of the common ion. Thus $\Delta\phi$ or $\Delta\psi$ is the same if chlorides are considered instead of iodides in equation [11], since

[12] $$ \Delta\phi = (RT/2F)\ln(B_{Na^+}/B_{K^+}) . $$

Karpfen and Randles (18) have recently set up the cell shown in Fig. 2. They found good agreement between theory, as given by equation [11], and experiment.

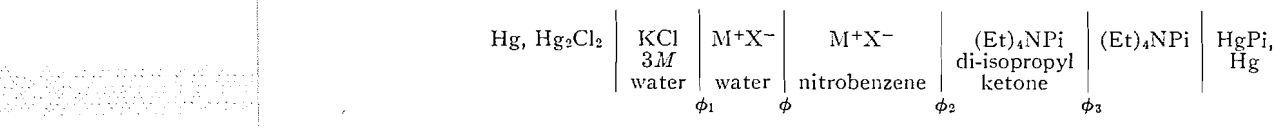

FIG. 2. Cell for measuring $\Delta\phi$ at interface of water and a polar oil such as nitrobenzene (18). Salt bridges are chosen so that when the salt MX is changed, the measured potential change is $\Delta\phi$, i.e. ϕ_1, ϕ_2, and ϕ_3 remain constant. In such an experiment $\Delta\phi$ is measured across thicknesses of solvent great compared with the thickness of the interfacial electrical double layers. Pi is picrate.

Results are shown in Table I, the distribution coefficients for simple salts in nitrobenzene having been found by Davies (7). The agreement is strong support for the validity of equation [11] if the oil is polar. Similar evidence in favor of equation [11] has recently been forthcoming from Göttingen, where Dr. Strehlow and his colleagues have been working along similar lines.

TABLE I

System (see Fig. 2)	$\Delta\phi$ calculated from distribution experiments (7), using equations [11] and [12]. Quoted from (18)	$\Delta\phi$ (observed) (18)
K^+ replaced by $(Et)_4N^+$	−124 mv.	−126 mv.
K^+ replaced by Na^+	− 50 mv.	− 53 mv.
Cl^- replaced by I^-	+ 95 mv.	+102 mv.

(*b*) SURFACE POTENTIALS IN RELATION TO DISTRIBUTION POTENTIALS

If now an oil is chosen in which practically no salt can dissolve (e.g. a paraffinic oil such as decane), an ionic double layer cannot build up completely in the thickness of oil (e.g. 1 mm.) available. Hence equation [8] does not apply to measurements with this oil, although, since the system is by definition at equilibrium in that the free energy is minimal for this thickness of oil, equations [1] to [7] still hold.

Dividing the potential at the oil side of the interface into V (due either to a dipole array formed by spreading or by adsorption or to a charged film) and $\psi_{x=\infty}$ (see Fig. 3) we shall show that if the oil solubilities of the interfacial film and of the salt present are very small, only ΔV contributes to the measured change in ϕ when a film is spread.

From the above equations, if equation [8] is no longer true, equation [9] is extended to:

$$[13] \qquad \phi = \frac{RT}{2F}\ln\left(\frac{B_+}{B_-}\right) - \frac{RT}{2F}\ln\left(\frac{{}_oc_+}{{}_oc_-}\right)$$

in which ${}_oc_+$ and ${}_oc_-$ refer to ionic concentrations in the oil at the point where

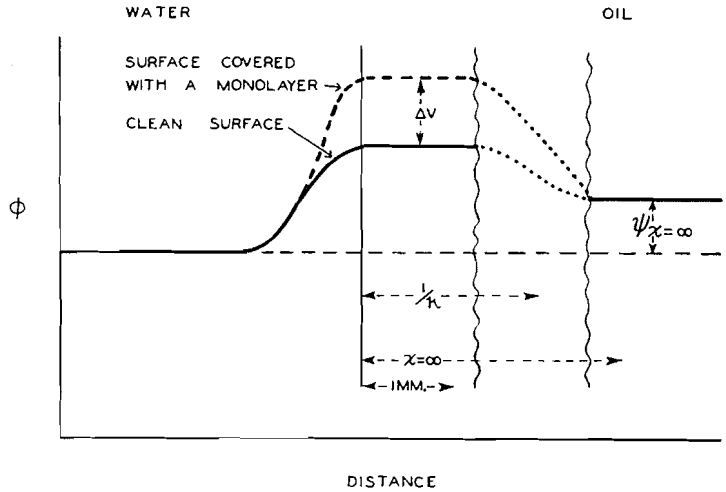

FIG. 3. Variation of ϕ (relative to the interior of the water phase) at the interface with a paraffinic oil. Measurements are made with $x(\sim 1$ mm.) less than $1/\kappa$.

ϕ is measured. To express these concentrations in terms of measurable quantities, we apply the equations of Boltzmann in the form:

[14] $$ {}_oc_+ = ({}_oc_+)_{x=\infty} \times \exp[-e(V - \psi_{x=\infty})/kT] $$

and

[15] $$ {}_oc_- = ({}_oc_-)_{x=\infty} \times \exp[+e(V - \psi_{x=\infty})/kT] $$

and, in the hypothetical region of oil at $x = \infty$, where the electrical double layer is complete,

[16] $$ ({}_oc_+)_{x=\infty} = ({}_oc_-)_{x=\infty}. $$

Hence equation [13] becomes:

$$ \phi = \frac{RT}{2F} \ln\left(\frac{B_+}{B_-}\right) - \frac{RT}{2F} \ln \exp[-2e(V - \psi_{x=\infty})/kT]. $$

The double layer is complete at $x = \infty$, so $\phi_{x=\infty} = \psi_{x=\infty}$ and hence, according to equation [9],

$$ \psi_{x=\infty} = \frac{RT}{2F} \ln\left(\frac{B_+}{B_-}\right). $$

Therefore

$$ \phi = \psi_{x=\infty} + \frac{2RTe}{2kTF}(V - \psi_{x=\infty}) $$

or

$$ \phi = \psi_{x=\infty} + (V - \psi_{x=\infty}) $$

or

$$ \phi = V. $$

Here ϕ is independent of B_+ and B_-, and

[17] $$ \Delta\phi = \Delta V (= \delta\chi, \text{ Lange nomenclature}). $$

From the above considerations we note that with a polar oil in a cell of the type shown in Fig. 2, we can make measurements with direct current (18) to test equation [11]:

[11] $$\Delta\phi = \Delta\psi = (RT/F)\ln(S_{NaI}/S_{KI}) .$$

With a non-conducting oil, the vibrating plate method (8, 9) must be employed. This is a capacity method, and depends upon alternating current, since no measurable direct current can pass through a non-conducting oil, in which salts are effectively insoluble. To such potentials, equation [17] applies:

[17] $$\Delta\phi = \Delta V.$$

To test the theories we thus require different oils: if the oil is polar, $\Delta\phi$ should depend only on the distribution coefficients, and not on ΔV; but if the oil is paraffinic, $\Delta\phi$ should depend on ΔV and not on S, the distribution coefficient.

If the non-aqueous phase is so non-polar that ions cannot appreciably dissolve in it, the interfacial potential will alter only if an interfacial film is formed—the partition coefficients being assumed to be unaltered by the interfacial monolayer. Ions are unstable in air near a water surface, and no double layer can therefore form above a water surface; thus the measurement (23) of film potentials at the air–water surface is rendered possible and equation [17] can be tested, where ΔV is the difference of potential between the clean water surface and one on which a film has been spread, as shown in Fig. 3. Such potential changes are perfectly stable with time, no decrease ever having been observed with insoluble films. Exactly similar results are obtained, though the experimental technique is different (8, 9, 12), with paraffinic oils, as shown in Fig. 4. The petrol-ether used in this experiment is made up of decane and near homologues.

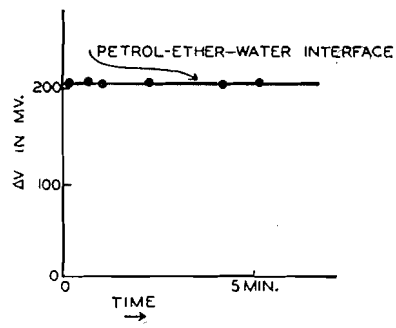

FIG. 4. Surface potential for monolayer of $C_{18}H_{37}N(CH_3)_3^+$ spread to 92 Å² per chain between petrol-ether and water. The latter contained 1.0 *N* NaCl. The potential does not change with time (12).

Again, if the paraffinic oil be replaced by a fairly polar oil there should, by equation [11] which is now applicable, be no change in potential between the system with a clean interface and one with a monolayer at the interface. Only if the distribution coefficient is changed will the potential alter. This is in full accord with experiment.

If, however, we study a very slightly polar oil, spreading a film and measuring the potential difference $\Delta\phi$ (equation [17]), this should now slowly decrease to zero, since, if the oil is slightly polar, ions from the water will redistribute themselves and set up a new double-layer in the oil. During this process of ionic redistribution (Fig. 5) we pass from the region of applicability

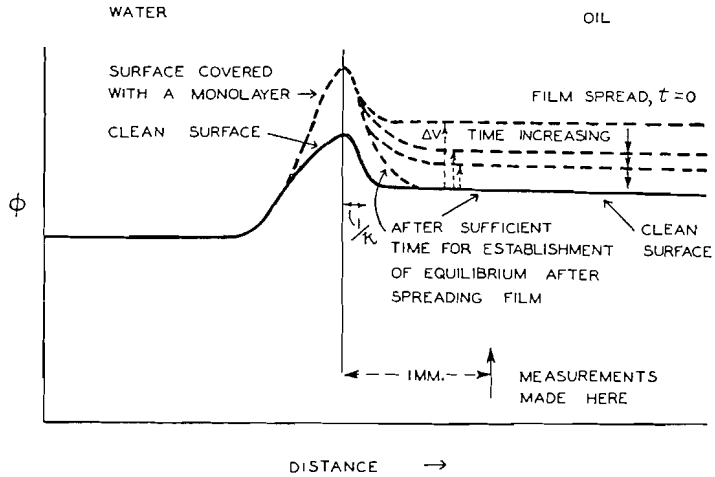

FIG. 5. Potential redistribution on oil side of interface after spreading a film if the oil is slightly polar. The (negatively charged) ionic atmosphere slowly builds up in the oil till ΔV has decreased to zero, provided that the thickness of oil used is sufficient to dissolve the necessary ions.

of equation [17] to that of equation [11]. The latter predicts $\Delta\phi$ should be zero, since a monolayer will not appreciably affect the distribution coefficients. Thus the potential difference $\Delta\phi$ due to the spread film should decrease with time and, if a complete double layer can form in the oil, will eventually become zero. This is borne out by experiment (Fig. 6).

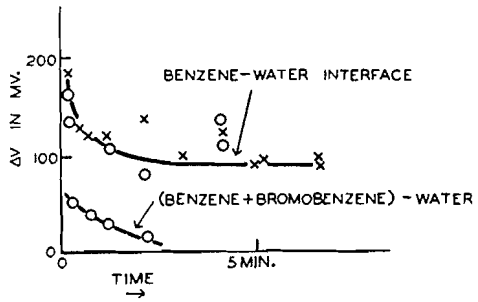

FIG. 6. Interfacial potentials of film of $C_{18}H_{37}N(CH_3)_3^+$ spread to 92 Å^2 per chain between water and slightly polar oils. The decrease in ΔV with time reflects the change from the region of applicability of equation [17] to that of equation [11]. Crosses denote potentials measured with the vibrating plate apparatus (8, 9) and circles those found with the radioactive source method (2).

We can now proceed further and observe that if the times for the potential to decay to one half its initial value are found, a rough correlation with the

TABLE II

Non-aqueous phase	Calculated concentration of Cl^- in non-aqueous phase	Depth of ionic atmosphere, i.e. $1/\kappa$	Time calculated for Cl^- to reach equilibrium positions after film was spread	Observed time of decay of ΔV to $1/e$ of original value
Air	$10^{-65}N$	10^{24} cm.	10^{54} sec.	∞
Petrol-ether (decane)	$10^{-33}N$	10^{8} cm.	10^{21} sec.	∞
Benzene	$10^{-11}N$	5×10^{-3} cm.	$\sim$1 sec.	60 sec.
Benzene + bromobenzene	$10^{-8}N$	5×10^{-4} cm.	$\sim$0.01 sec.	$\sim$1 sec.

rates of diffusion of the counter-ions from the water into the oil (to build up the new double layer) might be expected. In Table II this is shown, the calculated times (12) being functions of the polarity of the oil, i.e. of the equilibrium concentration of chloride ions immediately on the oil side of the interface. From here the ions must diffuse through the oil to a mean distance of $1/\kappa$ (the Debye–Hückel function) away from the interface. Although benzene is only slightly more polar than paraffins, it dissolves more water, so that ions in benzene can be at least partly hydrated and in consequence more ions can dissolve in benzene than in petrol-ether. Thus interfacial potentials at the benzene–water interface decrease with time, although those at the paraffin–water interface are stable.

(c) COMPONENTS OF ΔV, THE SURFACE POTENTIAL

Throughout this paper the orientation of the dipoles at the water surfaces has been neglected, and by definition $\phi_{H_2O} = 0$. If ψ, the free charge, is zero in the water, the absolute potential ϕ_{H_2O} is V or χ, the potential of the water dipoles. Although questions of absolute potentials have been avoided in the present work, it is interesting to note that V has been estimated for the air–water surface. The figures range, however, from -0.5 volts to $+0.4$ volts (21).

If, however, a monolayer is spread on a clean water surface, the water dipoles will be reoriented about the film-forming molecules, because of the new dipoles introduced into the surface. This change, for each molecule spread

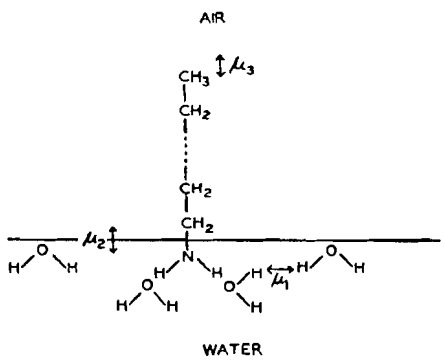

FIG. 7. Components μ_1, μ_2, and μ_3 of the surface potential ΔV for an electrically neutral monolayer.

in the monolayer, will be denoted μ_1. The dipoles of the film-forming molecules (e.g. C—NH_2 in a long-chain amine) will also contribute to ΔV by an amount depending on the dipole moment μ_2. A third component of ΔV for electrically neutral films spread at the air–water surface is μ_3, the moment of the bond (e.g. C—H) at the upper limit of the monolayer (Fig. 7). If we apply the Helmoltz formula for an array of n dipoles per cm.^{2}, and if they are all vectorially additive in the vertical direction (Eucken), we obtain:

$$[18] \qquad \Delta V = 4\pi n\mu = 4\pi n\mu_1 + 4\pi n\mu_2 + 4\pi n\mu_3$$

where μ is an over-all dipole moment including all components.

Unfortunately μ_1 cannot be measured, so it is usual to combine this term with μ_2, especially since the reorientation of the water dipoles, given by μ_1, probably depends on μ_2, as in Fig. 7.

The term μ_3 is normally constant since paraffinic chains are usual in surface active molecules, so that then equation [18] becomes for an electrically neutral film:

$$[19] \qquad \Delta V = 4\pi n\mu = 4\pi n\mu_D$$

where $\mu_D = \mu_1 + \mu_2 + \mu_3$, characteristic of the dipole of the head-group (e.g. C═O, C—NH_2) of the molecules in the monolayer.

In recent years there has been added interest in substituted hydrocarbon chains, and to investigate these we use [18] in the form:

$$[20] \qquad \Delta(\Delta V) = 4\pi n(\Delta\mu_3) \ .$$

Thus by comparing films with the same numbers of molecules per cm.^{2}, spread at the same interface, and having the same polar head groups, we measure the difference in potential due to substitution of the —CH_3 group at the upper

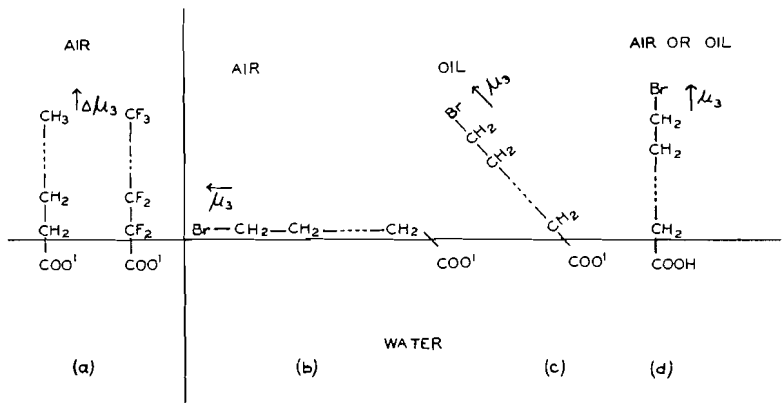

FIG. 8. (*a*) Anions of an aliphatic acid and of a perfluoro acid spread at the air–water interface. The difference in ΔV is due to the change in μ_3, the vertical dipole moment of the uppermost bond (19).

(*b*) Anion of ω-bromohexadecanoic acid at air–water interface. The vertical component of μ_3 is zero (13).

(*c*) Anions of ω-bromohexadecanoic acid at decane–water interface. Vertical component of μ_3 now appreciable, as the ω-bromo group is easily lifted into the oil (13).

(*d*) Molecule of ω-bromohexadecanoic acid in close-packed film at pH 4 at air–water surface. The dipole μ_3 is now relatively large (17).

limit of the film by (say) —CH_2Br or —CF_3, as shown in Fig. 8. Some results are shown in Table III. That $\Delta\mu_3$ is less than the dipole of the carbon–halogen link suggests that there is mutual polarization of the dipoles in condensed films (first and last examples in Table III). Further, the dipoles of such ω-halogen links are unlikely to be oriented vertically, but rather at half the tetrahedral angle (17).

TABLE III

VARIATIONS IN μ_3 FOR DIFFERENT FILMS AT THE AIR–WATER AND OIL–WATER INTERFACES

Film	ΔV	$\Delta(\Delta V)$	$\Delta\mu_3$ (vertical component of dipole differences in ω-bonds)	Difference in μ for ω-bond and C—H bond from bulk measurements
Myristic acid with carboxyl group ionized (25 Å², air–water)	−50 mv.	−900 mv. (19)	−600 mD. (see Fig. 8*a*)	−1800 mD.
Perfluorodecanoic acid with carboxyl group ionized (25 Å², air–water	−950 mv.			
Hexadecanoic acid on 1 *N* NaOH at 66 Å², air–water	−28 mv.	0 (13)	0 (see Fig. 8*b*)	−1900 mD.
ω-Bromohexadecanoic acid on 1 *N* NaOH at 66 Å², air–water	−28 mv.	−132 mv. (13)	−230 mD. (see Fig. 8*c*)	−1900 mD.
ω-Bromohexadecanoic acid on 1 *N* NaOH at 66 Å², oil–water	−160 mv.			
Hexadecanoic acid pH4 air–water (20 Å²)	+390 mv.	−1260 mv. (17)	−660 mD. (see Fig. 8*d*)	−1900 mD.
ω-Bromohexadecanoic acid, pH4, air–water (20 Å²)	−870 mv.			

If now we consider a charged film of $C_{18}H_{37}N(CH_3)_3^+$ ions, an additional term ψ_0 for the electrostatic potential of the interface relative to the subjacent layers of liquid is necessary. Thus equations [18] and [19] become:

$$[21] \qquad \Delta V = 4\pi n\mu = 4\pi n\mu_1 + 4\pi n\mu_2 + 4\pi n\mu_3 + \psi_0,$$

$$[22] \qquad \Delta V = 4\pi n\mu = 4\pi n\mu_D + \psi_0,$$

or

$$[23] \qquad \mu = \mu_D + \mu_0$$

where μ_0 is the dipole contribution of the electrical double layer.

At low surface coverages, ψ_0 may be expected to contribute to μ a dipole moment (Fig. 9) given by the product of the mean thickness of the ionic double layer (the Debye–Hückel term $1/\kappa$) and the charge thus separated per molecule, i.e. one electron. Both these quantities are large (e.g. $1/\kappa$ may be

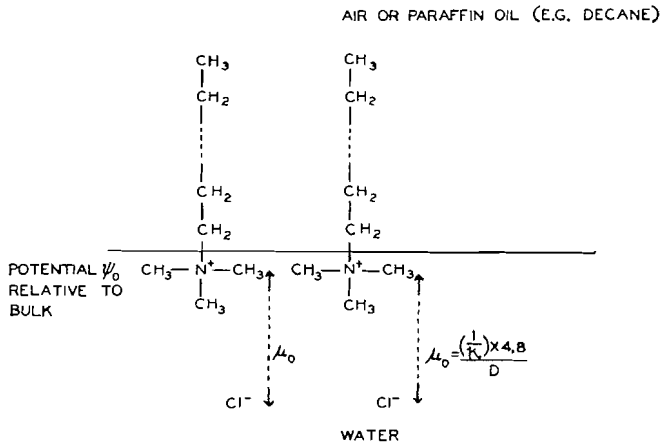

FIG. 9. A monolayer of $C_{18}H_{37}N(CH_3)_3^+$ at air–water or decane–water interface. The mean depth of the Cl^- counter-ions is $1/\kappa$, and this makes possible very large dipole contributions if the ionic strength is low (Table IV). The electrostatic potential at the interface is ψ_0 relative to the bulk of the aqueous phase.

several hundred Angstrom units), so very large dipole moments may be expected. To treat the double layer as an array of dipoles in this manner we have assumed that the dielectric constant D of the water is always 80 in the electrical double layer, and that the charges are far enough apart in the surface for their mutual interactions to be neglected. Thus:

[24] $$\underset{n\to 0}{\mu_0} = \frac{(1/\kappa) \times 4.8}{D}$$

and hence, by [23],

[25] $$\underset{n\to 0}{\mu} = \mu_D + \frac{(1/\kappa) \times 4.8}{D}.$$

Comparison of μ thus calculated with the experimental results at different ionic strengths (8) is made in Table IV. The value of μ_D is 400 mD. throughout (11). Although the dipole moments, especially on 10^{-4} N solution ($1/\kappa$ = 300 Å), are very high, the potentials at 1000 Å (Table IV) are not very great. However, since n is then only 10^{13}, μ is large by equation [22]. At greater surface concentrations (n increasing), ΔV increases only slightly, and μ falls steeply owing to mutual interaction of the electrical charges (8).

Equation [22] can also be tested (10) using the Gouy equations for ψ_0:

[26] $$\psi_0 = \frac{2kT}{e} \sinh^{-1}\left(\frac{134 \times 10^{-16} \times n}{\sqrt{c}}\right).$$

Comparison with experiment is made in Table V, combining equations [22] and [26]:

[27] $$\Delta V = 4\pi n\mu_D + \frac{2kT}{e} \sinh^{-1}\left(\frac{134 \times 10^{-16} \times n}{\sqrt{c}}\right).$$

These considerations all apply to the air–water or decane–water interface. If, however, a polar oil is used, ΔV for charged films is found (see above) to

TABLE IV

CALCULATED AND MEASURED DIPOLE MOMENTS μ FOR COMPLETELY IONIZED FILMS OF $C_{18}H_{37}N(CH_3)_3^+$ AT THE AIR–WATER OR DECANE–WATER INTERFACES. THE DISTANCE $1/\kappa$ IS GIVEN BY $3/\sqrt{c}$ Å, WHERE c IS THE SALT CONCENTRATION

NaCl concentration, c	μ (calculated)*	μ (measured (8))	Potential ΔV at $n = 10^{13}$ (1000 Å² per chain)
2 N ($1/\kappa$ = 2.1 Å)	528 mD.	500 mD. as $n \rightarrow 0$	22.5 mv.
10^{-1} N ($1/\kappa$ = 9.5 Å)	970 mD.	1026 mD. as $n \rightarrow 0$	43 mv.
10^{-2} N ($1/\kappa$ = 30 Å)	2200 mD.	2700 mD. as $n \rightarrow 0$	86 mv.
10^{-3} N ($1/\kappa$ = 95 Å)	6100 mD.	6170 mD. as $n \rightarrow 0$	124 mv.
10^{-4} N ($1/\kappa$ = 300 Å)	18,400 mD.	19,300 mD. as $n \rightarrow 0$	220 mv.

*$\mu = 400 + \frac{(1/\kappa) \times 4.8}{D}$; *the figure of 400 mD. for μ_D is from Ref. 11.*

TABLE V

TEST OF EQUATION [27]. DATA FOR $C_{18}H_{37}N(CH_3)_3^+$ (11, 10). AS BEFORE, μ_D = 400 MD.

Function of ΔV	Calculated	Experimental
$\left(\frac{\partial(\Delta V)}{\partial \log c}\right)_n$	-59 mv. $= \frac{2.303kT}{e}$ if c not too high	-57 mv. to -62 mv.
$\left(\frac{\partial(\Delta V - 4\pi n \times 400)}{\partial \log n}\right)_c$	$+118$ mv. $= \frac{2 \times 2.303kT}{e}$ if n not too low	$+110$ mv.
$\Delta V - 4\pi n \times 400 = \psi_0$ ($n = 3.33 \times 10^{13}$)	$+108$ mv.	$+112$ mv.
$\Delta V - 4\pi n \times 400 = \psi_0$ ($n = 6.67 \times 10^{13}$)	$+142$ mv.	$+145$ mv.

be zero at equilibrium, in agreement with the theory of Dean, Gatty, and Rideal (15). They pointed out that a compensative electrical double layer must also be set up in a polar oil (whether or not ψ_0 is zero), and this, represented here as ψ_{oil}, must at equilibrium be given by:

$$\Delta V = 4\pi n\mu_D + \psi_0 + \psi_{oil} = 0. \quad [28]$$

GENERAL DISCUSSION

That the Gouy equations, based on the assumption of a uniformly charged and impenetrable film in contact with counter-ions which are point charges, predict so accurately ψ_0 up to high ionic strengths had been interpreted (14) in terms of compensation of the effects of the finite sizes of the counter-ions with the penetration of some of the counter-ions between the charged groups

constituting the film. This conclusion has been supported by studying the surface viscosity and interfacial reaction kinetics as ψ_0 changes.

In the last few years various authors have measured interfacial potentials with cells of the type shown in Fig. 2. Thus McMullen (20) found that the introduction of cetyltrimethylammonium bromide into an octyl alcohol – water system caused a potential $\Delta\phi$ of about 130 mv. although this decayed rapidly. Similar results were found with amyl-acetate. On the other hand Dupeyrat and Guastalla (16), using nitrobenzene as oil, found $\Delta\phi$ to be constant at 400 mv. when a myristyl-trimethylammonium salt was added. We consider that distribution potentials ($\Delta\psi$ of equation [11]) and diffusion potentials are responsible for all these results, the very thin layers of oil used by McMullen eventually making possible distribution potentials at *both* oil–water interfaces ($\Delta\phi_2 \sim \Delta\phi$ in Fig. 2, owing to diffusion). The potential of Dupeyrat and Guastalla is certainly a stable $\Delta\psi$, though rather higher than found by Powell and Alexander (22), whose measurements are more difficult to interpret. They used the contact potential method, ionizing the air gap above the oil layer (and possibly the oil itself) with a mesothorium source. Interfacial potentials due to cetyltrimethylammonium bromide added to the water were usually constant after the first few minutes, and then it was found that $\Delta\phi$ varied in the order:

$$\Delta\phi(\text{air}) \gg \Delta\phi(\text{amyl acetate}) > \Delta\phi(\text{octyl alcohol}) .$$

This sequence is in the reverse order of the dielectric constants. Powell and Alexander interpret these $\Delta\phi$ measurements as ΔV potentials, though by comparison with the results of Fig. 6 and Table II this seems unlikely, especially as they claim that the equilibrium postulated by Dean, Gatty, and Rideal (15) must be very slow in attainment since their potentials are stable with time after a few minutes. We consider that Powell and Alexander's oil–water results are probably distribution potentials or may sometimes be due to diffusion to and adsorption at the upper (oil–air) interface. Distribution potentials would be expected to decrease with increasing dielectric constant of the oil, since B_+ depends on ${}_o\mu_+^0$.

Our considerations concerning the adsorption and ion partition potential differences which may develop at liquid–liquid interfaces and the effects of an added electrolyte on their magnitude can evidently be extended to the case in which, for example, a lipoid-like membrane is inserted between two aqueous phases. The best known method of estimating the various components of a membrane potential into phase boundary and diffusion potentials has been laid on a sure foundation by the investigations of Kurt Meyer and T. Teorell.

CONCLUSION

In general $\Delta\phi = \Delta\psi + \Delta V$, but by choosing polar and paraffinic oils, we can separate $\Delta\psi$ and ΔV thus:

$$\Delta\phi \begin{cases} \Delta\psi = f(B_+, B_-) & \text{polar oil,} \\ \Delta V = f(n, \mu) & \text{paraffinic oil.} \end{cases}$$

From our results we conclude that Beutner was indeed correct—Baur's adsorption potentials (surface potentials) either cannot be detected or are very transient for polar oils. Only with recent techniques for investigating interfacial potentials between water and pure paraffinic oils can stable oil–water interfacial potentials (ΔV or $\delta\chi$) be measured (8, 9). This lends strong support to the theory of Dean, Gatty, and Rideal (15).

Surface potentials have been analyzed into components from the dipoles of the polar "head groups" of film-forming molecules, from the dipoles at the upper end of the carbon chain, and from ionic redistributions if the film is electrically charged.

REFERENCES

1. ADAM, N. K. The physics and chemistry of surfaces. Oxford University Press, Oxford. 1944. p. 361.
2. ALEXANDER, A. E. Trans. Faraday Soc. 37: 117. 1941.
3. BAUR, E. *et al.* Z. Elektrochem. 19: 590. 1913; 32: 547. 1926.
4. BEUTNER, R. *et al.* Z. Elektrochem. 19: 319, 467. 1913.
5. BEUTNER, R. *et al.* Science, 104: 569. 1946.
6. BONHOEFFER, K. F., KAHLWEIT, M., and STREHLOW, H. Z. physik. Chem. 1: 21. 1954.
7. DAVIES, J. T. J. Phys. & Colloid Chem. 54: 185. 1950.
8. DAVIES, J. T. Nature, 167: 193. 1951.
9. DAVIES, J. T. Z. Elektrochem. 55: 559. 1951.
10. DAVIES, J. T. Proc. Roy. Soc. (London), A, 208: 224. 1951.
11. DAVIES, J. T. Trans. Faraday Soc. 48: 1052. 1952.
12. DAVIES, J. T. Trans. Faraday Soc. 49: 683. 1953.
13. DAVIES, J. T. Trans. Faraday Soc. 49: 949. 1953.
14. DAVIES, J. T. and RIDEAL, SIR ERIC. J. Colloid. Sci. Suppl. 1: 1. 1954.
15. DEAN, R. B., GATTY, O., and RIDEAL, E. K. Trans. Faraday Soc. 36: 161. 1940.
16. DUPEYRAT, M. and GUASTALLA, J. Colloque sur les composes superficiellement actifs. Paris. 1955.
17. GEROVICH, M. and FRUMKIN, A. J. Chem. Phys. 4: 624. 1936.
18. KARPFEN, F. M. and RANDLES, J. E. B. Trans. Faraday Soc. 49: 823. 1953.
19. KLEVENS, H. and DAVIES, J. T. J. Am. Chem. Soc. In press.
20. MCMULLEN, A. I. Ph.D. Thesis, Cambridge. 1948.
21. PARSONS, R. *In* Modern aspects of electrochemistry. *Edited by* J. O'M. Bockris and B. E. Conway. London. 1954. p. 124.
22. POWELL, B. D. and ALEXANDER, A. E. J. Colloid. Sci. 7: 482, 493. 1952.
23. SCHULMAN, J. H. and RIDEAL, E. K. Proc. Roy. Soc. (London), A, 130: 259. 1931.

CYSTINE AS AN ADDITION AGENT IN THE ELECTRODEPOSITION OF COPPER[1]

By A. J. Sukava[2] and C. A. Winkler

ABSTRACT

The steady state polarization of 100 mv. in acid copper sulphate electrolyte, at 2 amp./dm.^{2}, appears to consist of 45 to 50 mv. activation overpotential to deposit aquo–copper complexes, 20 to 25 mv. concentration polarization, and about 30 mv. polarization due to hydrogen ion interference. The presence of cystine in the electrolyte gave rise to polarization–time curves similar to those observed previously with gelatine. The increase of polarization caused by cystine appears to be due to an obstructive effect of adsorbed cystine (or its copper complex), together with an increase of concentration polarization. Cystine alone probably does not affect the activation overpotential. Addition of sufficient chloride virtually eliminated the polarization due to obstruction by cystine, possibly by acting as an electron bridge or by forming more readily dischargeable chloro–cystine–copper complexes. Chloride also eliminated the increment in concentration polarization caused by cystine. Attainment of a minimum total steady state polarization of about 40 mv. in the presence of cystine and chloride appeared to reflect an increase of surface, hence a decrease of true current density with time of deposition. The addition agent behavior of methionine was, in most respects, similar to that of cystine. The behavior of thiourea at low concentrations appeared to be complicated, but the effects of chloride were similar to those observed with gelatine.

INTRODUCTION

Since gelatine is probably the most commonly used addition agent in the electrodeposition of copper, much work has been done in this laboratory and elsewhere to study its behavior in this capacity. An understanding of its action is clouded, however, by the complex structure of the gelatine molecule, and it has seemed desirable to find, if possible, a simple amino acid with which the addition agent effect of gelatine might be closely simulated. A previous study with glutamic acid (1) indicated that this substance was not a satisfactory substitute for gelatine. The present paper recounts similar studies with some simple thioamino acids.

EXPERIMENTAL

Polarization measurements were made with the equipment and procedure outlined in earlier papers (1, 10). All chemicals were reagent grade, and water was twice distilled from alkali. The standard electrolyte contained 125 gm./liter $CuSO_4.5H_2O$ and 100 gm./liter H_2SO_4. The composition of other electrolytes used in the study will be specified as required. The Haring cell contained 150 ml. of electrolyte in all experiments, and measurements were made at 24.5° C. throughout the study.

Each cathode surface was brought to a standard condition by electrodeposition from standard electrolyte at 24.5° C. at 3 amp./dm.^{2} for 30 min.,

[1]*Manuscript received January 14, 1955.*
Contribution from the physical chemistry laboratory, McGill University, Montreal, with financial assistance from the National Research Council, Ottawa, and the Consolidated Mining and Smelting Co., Trail, B.C.
[2]*Holder of a Cominco Research Fellowship. Present address: Department of Chemistry, University of Western Ontario, London, Ontario.*

followed by deposition at 2 amp./dm.^{2} until steady state polarization (100 $\pm$ 5 mv.) was attained (4).

RESULTS

Initial Cathode Polarization in Absence of Addition Agent

In an earlier study (10) it was observed that, at 2 amp./dm.^{2}, the polarization rose almost instantaneously to about 100 mv. in the standard electrolyte, and then increased slowly to a slightly higher steady state value. A more detailed study of the behavior with the cathode ray oscilloscope or the Brush recorder has shown that a zero time* polarization of 85 to 90 mv. was followed by an increase to about 115 mv. after one to two minutes, and a subsequent decrease during about 30 min. to the steady state value. Typical results are shown in Fig. 1. Transition from the behavior represented in Fig. 1B to that of Fig. 1C was essentially complete after interruption of the current for one to two minutes. This indicates that the time for dissipation of the cathode film is about the same as that for attainment of the initial maximum polarization and for formation of the cathode film (2).

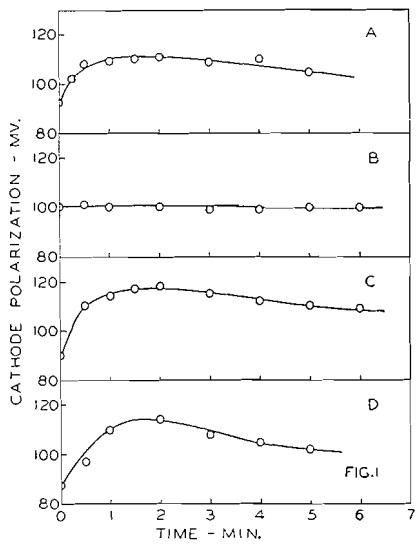

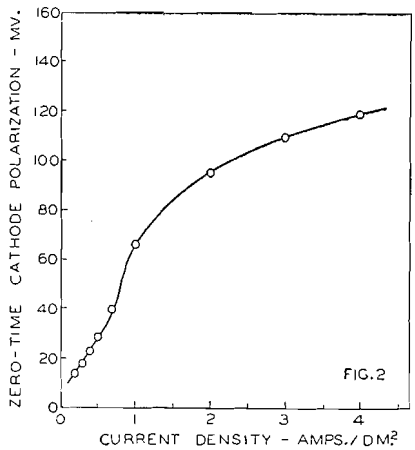

FIG. 1. Initial cathode polarization–time relation for standard electrolyte and standard cathode surface.
A. Cathode film absent at zero time (new standard electrolyte).
B. Cathode film present at zero time (current switched off and immediately re-established).
C. Cathode film absent at zero time (current switched off and cell left undisturbed for four hours).
D. Cathode film absent at zero time (current switched off and solution stirred for one minute).
FIG. 2. Zero-time cathode polarization – current density relation with standard electrolyte and standard cathode surface.

The concentration polarization at the steady state was found to range from 20 to 25 mv. Hence the true zero time polarization presumably should have been 75–80 mv. It is probable that the higher value recorded includes

Zero time is taken as the time at which a first polarization value could be identified.

some initial build-up of concentration polarization before the first reading was obtained on the C.R.O. or Brush recorder.

The effect of current density on the zero time polarization (Brush recorder) in the absence of cathode film is shown in Fig. 2. The linear relation at low current densities is similar to that observed for other polarization values under different conditions (3, 11, 12); at current densities above 0.6 amp./dm.^{2} the polarization was, within experimental error, linear with the logarithm of the current density.

Cathode Polarization in the Presence of Cystine

The initial polarization pattern observed when cystine was added to the standard electrolyte resembled that previously observed with gelatine (10). The presence of cystine caused the polarization to pass through an early maximum, P_{max} (after a fraction of a second), then through a minimum, P_{min} (after about two seconds), followed by a gradual rise to the steady state value, P_s. As with gelatine, the values of P_{max} and P_{min} increased with immersion time, i.e. the time the electrode was in contact with the electrolyte before electrolysis was begun. The following data were obtained with 50 mgm./liter cystine and 2 amp./dm.^{2}:

Immersion time (min.)	Initial polarization (mv.) (maximum at 0–0.05 sec.)	(minimum at 1–2 sec.)
1	150	120
5	177	122
10	205	125
15	235	145
30	270	155
50	275	155
85	292	157

The time to attain P_{max} showed no definite dependence on immersion time. A constant immersion time of five minutes was adopted for routine purposes, and is applicable to the remainder of the discussion.

The value of P_{max}, and to a lesser extent that of P_{min}, was found to increase steadily with increased cystine concentration (Fig. 3A). The times to P_{max} and to P_{min} decreased with increased concentration of cystine. Both P_{max} and P_{min} always exceeded the lowest zero-time polarization (80 mv.) measured in the absence of addition agent.

The steady state polarization was found to be related to cystine concentration as shown in Fig. 3B. The values for concentrations of cystine below about 10 mgm./liter are approximate only, since there was a continued slight decrease of polarization even after five to seven hours electrolysis. The concentration polarization at the steady state, obtained with the C.R.O. (13), also showed a definite, though somewhat erratic, increase with increased cystine concentration (Fig. 3C).

Effect of Chloride on the Polarization in the Presence of Cystine

Addition of various amounts of chloride ion to standard electrolyte containing 20 mgm./liter cystine showed that the depolarizing effect of chloride

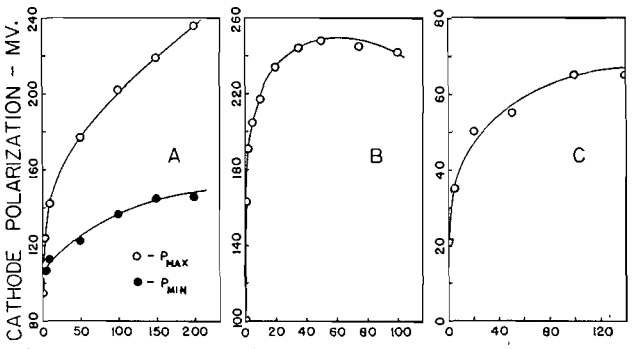

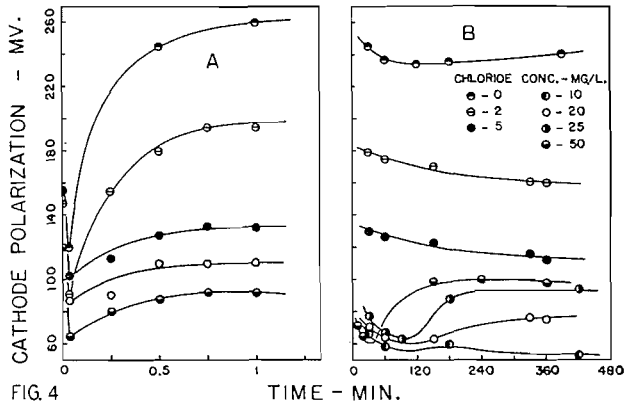

FIG. 3. Cathode polarization – cystine concentration relations.
A. Initial maximum and minimum polarizations.
B. Steady state polarization.
C. Concentration polarization at steady state.

FIG. 4. Cathode polarization–time relations in the presence of 20 mgm./liter cystine and different amounts of chloride.
A. Initial polarization–time pattern.
B. Polarization–time pattern after prolonged electrolysis.

was immediate (Fig. 4A). Concentrations of chloride higher than about 15 mgm./liter eliminated the influence of cystine to give a behavior, during the first minute, almost identical with that observed in the absence of addition agent. Much higher chloride concentrations (50 to 100 mgm./liter) reduced the initial polarization further by 15 to 20 mv. Following upon the immediate depolarization due to chloride were the slower changes shown in Fig. 4B. These were not due to chemical changes other than electrode processes, since aging the solutions prior to electrolysis had no effect.

The steady state polarization as a function of chloride concentration is shown in Fig. 5A. The minimum polarization (about 50 mv. at 12 mgm./liter chloride) was always accompanied by a coarse, irregular deposit.

The effect of cystine concentration on the position of the minimum in the steady state polarization – chloride concentration curve is shown in Fig. 5B.

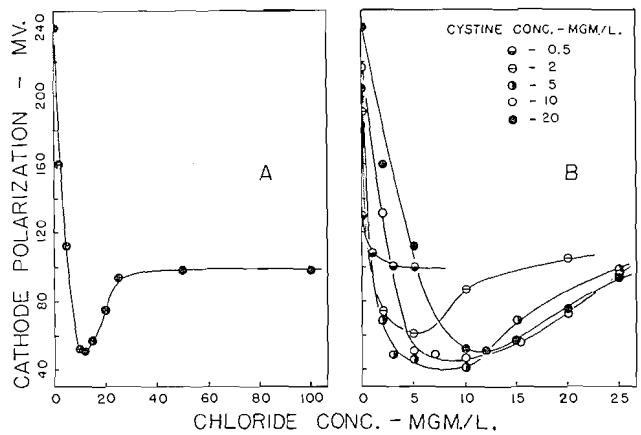

FIG. 5. Steady state cathode polarization – chloride concentration relations for different concentrations of cystine.
A. Effect of wide range of chloride concentrations with 20 mgm./liter cystine.
B. Effects of low chloride concentrations with different amounts of cystine.

It would seem that approximately 40 mv. represents the lower limit to which the polarization may be reduced by chloride in the presence of cystine for the conditions of electrolysis used.

The initial polarization in the presence of cystine and chloride is determined largely by the surface condition of the electrode. This was shown by the following experiment: A solution containing 5 mgm./liter cystine and 10 mgm./liter chloride was electrolyzed (starting with a standard surface electrode), at 2 amp./dm.^{2}, to the steady state polarization of 40 mv. The solution was removed from the cell and the cell thoroughly rinsed with water and standard electrolyte to remove as much adsorbed cystine and chloride as possible. Electrolysis was then resumed with fresh electrolyte of the same composition as in the first electrolysis. During the first electrolysis with a standard surface cathode a sharp decrease in polarization from 92 mv. to a minimum at 65 mv. occurred after two seconds. This was followed by an increase during the next half minute to 110 mv. and a subsequent decrease to the steady state value after about three hours. The second electrolysis showed a small decrease in polarization (55 mv. to 50 mv.) during the first two seconds, which was succeeded by an increase to 70 mv. after 1.5 min., and thereafter by a decrease to the steady state value in about the same time as the first electrolysis. Repetition of the experiment with a steady state surface obtained at a polarization of 105 mv. in electrolyte containing 2 mgm./liter cystine and 20 mgm./liter chloride gave initial polarization values in the second electrolysis that were within 5 mv. of those in the first electrolysis. Evidently, the steady state and standard electrode surfaces were essentially identical in this last experiment.

Concentration polarization at 2 amp./dm.^{2} in the presence of different concentrations of cystine and chloride had the following values:

Cystine conc. (mgm./liter)	Chloride conc. (mgm./liter)	Concentration polarization (mv.)
0.5	1	20
2	20	20
5	5	20
5	10	20
10	50	20
20	0	50
20	1	35
20	10	25
20	12	25
20	20	20
20	50	20
20	100	20

It would appear that the presence of amounts of chloride above the concentrations corresponding to the minima in the steady state polarization – chloride concentration curves reduced the concentration polarization effectively to the value observed in the absence of addition agent.

The effect of acid concentration of the electrolyte on the initial polarization maximum was determined in the absence and presence of cystine, at 2 amp./dm.^{2}, with a standard cathode surface. Not only was the initial maximum polarization a linear function of acid concentration in both systems, but the increase of polarization in the presence of cystine over that in its absence was virtually constant at the different acid concentrations, thus:

Cystine conc. (mgm./liter)	Acid conc. (gm./liter)	Polarization (mv.)		
		Initial max.	Steady state	Concentration
0	25	60	—	
0	50	70	64	25
0	75	77	87	25
0	100	85	99	25
0	150		107	25
20	50	128	203	50
20	75	137	233	50
20	100	146	234	50
20	150	—	235	50

While the steady state polarizations indicate roughly parallel behavior with acid concentration in the presence and absence of addition agent, changes in surface characteristics at the cathode undoubtedly influence these values somewhat. For example, the surface corresponding to the steady state polarization with 50 gm./liter acid, in the absence of cystine, showed microscopically a rough, irregular structure, in contrast to the smoother texture of the initial standard surface.

If the relation between initial maximum polarization and acid concentration is assumed to be linear down to zero acid concentration, the contribution made by acid of a given concentration to the total polarization may be estimated by extrapolating to zero acid concentration and noting the difference between the polarization for zero acid and that at the given acid concentration. This treatment of the data yields a value of about 30 mv. for the contribution by acid to the polarization at a standard cathode surface in electrolyte containing 100 gm./liter acid.

Cathode Polarization in the Presence of Methionine

With methionine alone as addition agent, the initial polarization–time relations, the variation of initial polarization maximum with methionine concentration, and the relations of steady state total and concentration polarization values with methionine concentration, were all quite similar to the corresponding relations when cystine was the addition agent.

When chloride was added in conjunction with methionine, the depolarizing action was immediate, as it was with cystine. However, prolonged electrolysis revealed some differences in the behavior of the two addition agents. In particular, with higher chloride concentrations (5 to 25 mgm./liter) there were no minima in the polarization–time curves with methionine, while at all chloride concentrations the change of polarization to the steady state was slower. The steady state polarization showed the same type of relation with chloride ion concentration as that observed with cystine. The only difference appeared to be that the minimum polarization (again, about 40 mv.) was obtained with 5 mgm./liter, instead of 12 mgm./liter, chloride ion concentration, when the concentrations of the addition agents were 20 mgm./liter.

Cathode Polarization in the Presence of Thiourea

The cathode polarizations obtained with concentrations of thiourea of 3 mgm./liter and lower, though not those with higher concentrations, were found to be very irreproducible. Moreover, they were found to vary considerably with age of the stock solution of electrolyte containing the addition agent, possibly as a result of oxidation by cupric ion. After about 10 days, the solution contained a yellowish precipitate, apparently free sulphur.

Regardless of the age of the electrolyte and with concentrations of thiourea up to 3 mgm./liter, the polarization–time curves consisted of an early low polarization stage (70–90 mv.) followed by an increase, perhaps due to an anodic oxidation product, to a higher value (200–220 mv.) after about one hour electrolysis. The polarization during the initial stage increased at first with age of solution, then decreased to a limiting low value of about 70 mv. after eight days. The higher second stage value was practically eliminated by such aging when the thiourea concentration was 2 mgm./liter or less. When the electrolyte containing 3 mgm./liter thiourea was treated with hydrogen peroxide at room temp, then warmed to decompose excess peroxide, the resulting solution decreased the polarization to a steady state value of 70 mv., unaltered by further electrolysis.

Addition of chloride to freshly prepared electrolyte containing 10 mgm./liter thiourea gave steady state polarization values with a minimum at about 160 mv., corresponding to a chloride concentration of about 2 mgm./liter. (The polarization with 10 mgm./liter thiourea alone was about 240 mv.) With higher chloride concentrations, the deposits had a very rough and nodular structure. The behavior, including the high value of the minimum polarization, is reminiscent of the previous observations with gelatine as the addition agent.

DISCUSSION

The increase in initial polarization maximum, P_{max}, with increased immersion time in the presence of cystine is strong evidence for the prior adsorption of cystine on the copper cathode. The time required to attain a steady state in respect of adsorption is probably increased by simultaneous corrosion at the copper surface. Adsorption prior to electrolysis should, of itself, result in an increase of zero time polarization values with increase of cystine concentration in accordance with an adsorption isotherm type of relation. On the other hand, P_{max} might be expected to include additional polarization due to cataphoretic migration to the cathode of positively charged cystine (or cysteine) when electrolysis is begun. (It may be assumed that cysteine is formed by cathodic reduction.) This, too, should increase with increase of cystine concentration. Hence, the sustained increase of P_{max} in Fig. 3A appears to be reasonable. On the other hand, a maximum in P_{max} with immersion time might be expected, since in these experiments a constant addition agent concentration was used, and the contribution due to cataphoresis should be substantially constant.

The presence of subsequent minimum and steady state polarizations as electrolysis is continued may be explained in the manner suggested previously for the similar behavior with gelatine (10).

The rapid increase of steady state polarization as the cystine concentration is increased might be attributed to adsorption of cystine, with consequent decrease of active area and increase of true current density. Alternatively, it might be due to adsorption of copper–cystine complexes from which copper is discharged with difficulty or not at all. For standard electrolyte and a standard surface, the activation overpotential of 45 to 50 mv.* presumably corresponds to discharge of the aquo-complex. Only by consideration of the effect of chloride does it seem possible to suggest a reason for the increase of polarization in the presence of cystine over that observed in its absence.

From the data presented, it is evident that all but 40 to 50 mv. of the total steady state polarization in the presence of cystine can be overcome by addition of an appropriate amount of chloride. It seems reasonable to assume that this residual polarization is due mainly to concentration polarization plus an overpotential caused by hydrogen ions, acting perhaps as a barrier to approach of the copper ions to the cathode.† Values of these polarizations somewhat less than the 20 mv. and 30 mv. respectively estimated for the standard surface might be expected if the rougher surfaces laid down in the presence of cystine are of larger active area and the true current density therefore less. In this event, there would remain some (probably small) activation polarization at the steady state.

The amount of chloride necessary to give the 40–50 mv. minimum steady state polarization in the presence of cystine reduced the *initial* (one to two

**Determined as the difference between the total polarization (100 mv.) and the sum of the concentration polarization (20 to 25 mv.) and that due to hydrogen ion (30 mv.).*

†Since the increase of polarization due to increased acid concentration was essentially the same in the absence and presence of cystine, it seems doubtful that adsorption of hydrogen ions on the copper surface is responsible for the contribution to polarization made by hydrogen ions.

minutes) polarization to approximately the level (100 mv.) obtained in the absence of addition agent. Since the concentration and hydrogen ion contributions to the 100 mv. polarization are essentially the same (20 mv. and 30 mv. respectively) in the standard electrolyte and in the presence of cystine, the remaining 50 mv. in both cases probably also represents the same activation overpotential for discharge of aquo-complexes. It seems significant that the levels of the initial polarizations, with amounts of chloride capable of yielding minimum steady state polarizations, were but little influenced by the amount of cystine present. This would indicate that the activation overpotential involved is independent of cystine, and this would be true if it involved the aquo-complex.

With a chloride concentration much larger than that necessary to give a minimum steady state polarization (50 mgm./liter chloride with 20 mgm./liter cystine) the *initial* polarization (i.e. after one to two minutes) was some 15 mv. lower than the value for standard electrolyte. This lowering presumably represents a decrease in activation overpotential to about 30–35 mv. This cannot correspond to facilitated deposition from a chloro–aquo-complex since chloride ion (5 to 10 mgm./liter) in the absence of other addition agents increases the steady state polarization by about 15 mv. for the conditions of the present experiments (9). It might, however, represent discharge of a chloro–cystine–copper complex.

On the basis of the data and analysis presented above, the steady state polarization *in excess of about 100 mv.*, due to cystine alone, might reasonably be attributed to an increment (about 30 mv.) in concentration polarization, plus a component of the polarization arising from the obstructive influence of adsorbed cystine or cystine–copper complexes. Virtual elimination of this component of the polarization by chloride might be explained by facilitated electron transfer through an electron bridge, in the manner suggested by Heyrovsky (5), or by the formation of more readily dischargeable chloro–cystine–copper complexes, in accordance with Lyons' views (6, 7). The tendency for the initial activation overpotential in the cystine–chloride system to attain, with excess chloride, a lower value than that corresponding to discharge of the aquo-complex, as discussed previously, gives some support, perhaps, to the second suggestion.

The increment in concentration polarization caused by cystine may be explained if the cystine–copper complex is less readily discharged than the aquo-complex. A reaction of the type

$$\mathrm{Cu(Cystine)}_m^{+2} + 4\ \mathrm{H_2O} = \mathrm{Cu(H_2O)_4^{+2}} + m\ \mathrm{Cystine}$$

would then proceed to the right under kinetic conditions of current flow and be restored to equilibrium when the current is stopped only by further hydrolysis of the cystine complex, corresponding to the observed increment in concentration polarization. Rapid formation of directly dischargeable chloro–cystine complexes on addition of chloride would render formation of aquo-complexes by the above reaction less significant as a factor in maintaining current flow, hence in determining the magnitude of the concentration polar-

ization. With sufficient chloride, the limiting concentration polarization of 20 mv. probably reflects diffusion and convection effects only.

The increase in polarization caused by increasing the chloride concentration above the point of minimum polarization with cystine and methionine may be attributed to accumulation and adsorption of colloidal cuprous chloride on the cathode, as discussed previously for gelatine (8). The delay of about one hour, after electrolysis is begun, before the rise in polarization is noted suggests that the cuprous chloride originates at the anode (1). The magnitude of the overpotential caused by adsorption of cuprous chloride may be estimated by taking advantage of the observation that the surface laid down at 100 mv. *steady state* overpotential in the presence of cystine plus excess chloride was microscopically similar to that obtained at 100 mv. steady state overvoltage in standard electrolyte. If this be taken to indicate that the true current densities were approximately equal in the two systems, a hydrogen ion contribution of about 30 mv. may be ascribed to both polarizations. Also, the activation overpotential for discharge of chloro-cystine complexes at the 100 mv. steady state polarization should have about the same value as that estimated previously (30–35 mv.) for these complexes at a standard surface in the absence of adsorbed cuprous chloride, i.e. from the initial polarization values. These polarization values, together with 20 mv. concentration polarization give, by subtraction from the 100 mv. total steady state polarization, a value of 15–20 mv. for the overpotential due to adsorption of cuprous chloride at the steady state. A similar value is obtained from McConnell's value of 115 mv. for the effect of chloride alone (9), by introducing the hydrogen ion and concentration polarization values given above, together with the previously estimated activation overpotential of 45–50 mv. for discharge of aquo-complexes.

REFERENCES

1. Adamek, S. and Winkler, C. A. Can. J. Chem. 32: 931. 1954.
2. Brenner, A. Proc. Am. Electroplaters' Soc. 28. 1941.
3. Gardam, G. E. Discussions Faraday Soc. No. 1: 182. 1947.
4. Gauvin, W. and Winkler, C. A. Can. J. Research, A, 21: 37. 1943.
5. Heyrovsky, J. Discussions Faraday Soc. No. 1: 212. 1947.
6. Lyons, E. H. J. Electrochem. Soc. 101: 363. 1954.
7. Lyons, E. H. J. Electrochem. Soc. 101: 376. 1954.
8. Mandelcorn, L., McConnell, W. B., Gauvin, W., and Winkler, C. A. J. Electrochem. Soc. 99: 84. 1952.
9. McConnell, W. B. Ph.D. Thesis, McGill University, Montreal, Que. 1949.
10. Parsons, B. I. and Winkler, C. A. Can. J. Chem. 32: 581. 1954.
11. Shreier, L. L. and Smith, J. W. Trans. Faraday Soc. 50: 393. 1954.
12. Taft, R. and Messmore, H. E. J. Phys. Chem. 35: 2585. 1931.
13. Turner, R. C. and Winkler, C. A. J. Electrochem. Soc. 99: 78. 1952.

MICROCALORIMETRIC DETERMINATION OF THE CRITICAL CONCENTRATION AND THE MOLECULAR DIMENSIONS OF POLYVINYL ACETATE IN SOLUTION[1]

By Michel Parent[2] and Marcel Rinfret

ABSTRACT

Heats of mixing of polyvinyl acetate fractions with *s*-tetrachloroethane and methanol have been determined for the low concentration region. At the lowest concentrations the graphs of ΔH vs. volume fraction are linear as predicted by the van Laar, Scatchard, and Hildebrand theory. As the concentration increases, an inflection point appears, the enthalpy increment being smaller for a short concentration interval and then resuming its former value up to the limit of the range studied. The position of the critical interval depends on the solvent employed and on the molecular weight of the fraction. An equation, based on Flory's theory, has been developed for predicting the critical concentration from intrinsic viscosity. Assuming that, at the critical concentration, the molecules are just coming into contact, it is possible to calculate the diameter of the sphere equivalent to a molecule. Comparison of the dimensions obtained from the critical concentration and the root-mean-square end-to-end distance of the molecule calculated by the Flory equation leads to agreement within 10%.

INTRODUCTION

The existence in high polymer solutions of a critical concentration, above which the macromolecules are entangled, was first postulated by Staudinger (9). More recently, Boyer and Spencer (1) have made a survey of the literature on the subject and Streeter and Boyer (10) have demonstrated its existence by viscosity measurements on highly dilute solutions of polystyrene. Further microcalorimetric studies of heats of mixing by Daoust and Rinfret (2) and determinations of partial molal volumes by Horth and Rinfret (5) give results in accord with the findings of Boyer and co-workers. The purpose of this paper is to show the dependence of the critical concentration on the nature of the solvent and the molecular weight of the solute. Moreover it will be shown that it is possible to deduce the dimensions of the macromolecule in solution from the critical concentration.

Most high polymers are amorphous and are often considered as very viscous liquids. The enthalpy change in mixing with a solvent is therefore given by the van Laar, Scatchard, and Hildebrand theory (4),

$$[1] \qquad \Delta H_M \doteq \Delta E_M = V_M B \Phi (1 - \Phi) ,$$

V_M being the total volume of mixture, and Φ the volume fraction of the solute. B is a parameter characterizing the net heat of interaction between solute and solvent. According to Scatchard (8),

$$[2] \qquad B = C_{11} + C_{22} - 2C_{12}$$

where C_{11}, C_{22}, and C_{12} are the interaction energies per milliliter (also called

[1]*Manuscript received January 28, 1955.*
Contribution from the Department of Chemistry, University of Montreal, Montreal, Quebec. This paper is taken in part from the Ph.D. thesis of Michel Parent.
[2]*Holder of the C.I.L. Fellowship 1952–54. Present address: Centre de Recherches sur les Macromolécules, Strasbourg, France.*

cohesive energy densities) between similar and dissimilar molecules. It can be shown that for similar molecules, the cohesive energy density per milliliter is given by:

[3] $$C_{11} = (\Delta E_v/V)_1 \quad \text{and} \quad C_{22} = (\Delta E_v/V)_2$$

where ΔE_v is the energy of vaporization per mole and V, the molar volume of species 1 and 2 respectively. It has not been possible to calculate C_{12} for dissimilar molecules, and it has been postulated by Scatchard that:

[4] $$C_{12} = (C_{11} \cdot C_{22})^{\frac{1}{2}}.$$

Using [2], [3], and [4] equation [1] can be rewritten:

[5] $$\Delta H_M = V_M\left[\left(\frac{\Delta E}{V}\right)_1^{\frac{1}{2}} - \left(\frac{\Delta E}{V}\right)_2^{\frac{1}{2}}\right]^2 \Phi(1-\Phi).$$

Equation [5] indicates that all heats of mixing are positive. That many mixtures are accompanied by a negative heat evolution shows that the Scatchard postulate [4] is only valid for limiting cases. Where C_{12} is much different from the value given in [4] because of specific interaction between solute and solvent, B can take negative as well as positive values but is still a measure of the net heat of solute–solvent interaction.

Since polymer–solvent interactions take place between a molecule of solvent and an adjacent short segment of polymeric chain, the net energy of interaction should be independent of chain length. This will be shown to be true by the constancy of parameter B over a large range of molecular weights for a given polymer–solvent pair.

EXPERIMENTAL

A polyvinyl acetate fraction of molecular weight 29,000 was available from a previous investigation (2). A sample of Gelva-15, from Canadian Resins and Chemicals Co., of average molecular weight 60,000 was dissolved in 2% acetone solution and precipitated by water into seven main fractions using a method derived from Flory (3). Fractions were kept under vacuum over phosphoric anhydride.

The *s*-tetrachloroethane was of Eastman grade, stored over "Drierite", and distilled before use. Methanol was an acetone-free sample from Brickman Co. and was distilled, at high reflux ratio, in a 35 theoretical plates fractionating column. The microcalorimetric technique was essentially the same as already described (2). An improvement over the results obtained previously was effected by an even greater elimination of evaporation losses and the metallization of the Pyrex calorimeter cells to promote better heat conduction to the thermocouples. These cells were first chemically silvered and then a thin coat of copper was deposited by electrolysis. Intrinsic viscosities were determined with modified Ubbelohde viscometers as described elsewhere (2).

RESULTS

Table I together with Figs. 1–3 shows the heats of mixing of polyvinyl acetate fractions of various molecular weights in methanol and *s*-tetrachloro-

TABLE I

HEATS OF MIXING OF POLYVINYL ACETATE IN METHANOL AND *s*-TETRACHLOROETHANE AT 25° C.

Fraction mol. wt.	$\Phi(1-\Phi) \times 10^2$	ΔH_M, cal.	V_M, ml.	$\Delta H_M/V_M$	B, cal. per ml.
Methanol					
536,000	4.38	.217	7.141	$.030_4$	6.9
	5.01	.221	6.584	$.033_5$	6.7
	6.44	.299	6.406	$.046_7$	7.3
	7.56	.317	6.305	$.050_2$	6.6
	8.82	.354	6.289	$.056_3$	—
	11.98	.458	6.184	$.074_1$	6.9
	15.93	.637	6.086	.105	7.1
	19.32	.747	5.983	.125	6.9
	23.5	.996	6.400	.156	7.0
255,000	4.02	.203	7.001	$.029_0$	7.2
	7.06	.361	7.309	$.049_4$	7.0
	7.99	.399	7.354	$.054_3$	6.8
	9.92	.447	6.319	$.070_7$	7.1
	11.03	.594	7.758	$.076_5$	6.9
	11.98	.544	7.005	$.077_7$	—
	12.91	.627	7.375	$.085_0$	—
	14.20	.564	6.199	$.090_9$	6.9
	15.70	.774	7.680	.101	6.9
	19.58	.849	6.546	.130	7.0
29,000	7.93	.403	7.128	$.056_6$	7.1
	11.98	.575	6.709	$.085_7$	7.1
	15.67	.690	6.082	.113	7.2
	16.95	.626	5.081	.123	7.3
	18.09	.875	6.654	.132	7.3
	19.28	.662	5.133	.129	—
	19.82	.525	3.825	.137	7.2
s-Tetrachloroethane					
536,000	1.04	— .148	6.526	$-.022_7$	−21.9
	1.53	— .196	6.511	$-.030_1$	−19.7
	1.75	— .237	6.441	$-.036_8$	−21.0
	2.03	— .332	8.014	$-.041_5$	—
	2.13	— .326	7.598	$-.043_0$	—
	2.52	— .222	4.834	$-.045_9$	−21.0
	3.52	— .532	8.028	$-.066_3$	−20.9
	4.69	— .799	8.764	$-.091_2$	−20.9
	5.70	— .821	7.394	−.111	−20.7
	6.49	— .978	7.625	−.128	−20.8
	6.84	— .893	6.484	−.138	−21.2
255,000	1.26	— .215	8.072	$-.026_6$	−21.1
	2.01	— .347	8.269	$-.041_9$	−20.9
	2.44	— .366	7.493	$-.048_8$	−21.5
	2.99	— .321	5.319	$-.060_3$	−21.4
	3.63	— .630	8.715	$-.072_2$	−20.9
	3.95	— .593	7.454	$-.079_5$	−21.1
	4.95	— .752	7.320	−.103	−21.5
	5.04	— .783	7.650	−.102	−21.0
	6.43	−1.03$_4$	7.881	−.131	−21.0
191,000	1.02	— .147	6.932	$-.021_2$	−20.8
	2.02	— .317	7.856	$-.040_2$	−19.9
	2.52	— .372	7.149	$-.052_0$	−20.6
	3.00	— .416	6.624	$-.062_8$	−21.0
	3.49	— .524	7.319	$-.071_6$	−20.5
	3.79	— .554	7.278	$-.076_1$	−21.1
	4.61	— .595	7.396	$-.080_5$	−20.9
	5.07	— .794	7.725	−.103	−20.9
	6.01	— .966	7.898	−.122	−20.9
29,000	2.49	— .436	8.278	$-.052_6$	−21.2
	3.50	— .551	7.364	$-.074_8$	−21.4
	4.53	— .728	7.363	$-.098_8$	−21.8
	5.04	— .784	7.246	−.108	−21.5
	5.98	−1.03	7.857	−.131	−21.9
	6.96	−1.09	7.243	−.150	−21.5
	9.96	−1.26	5.854	−.214	−21.5
	10.87	−1.50	6.547	−.230	−21.5
	12.14	−1.62	6.268	−.259	−21.7

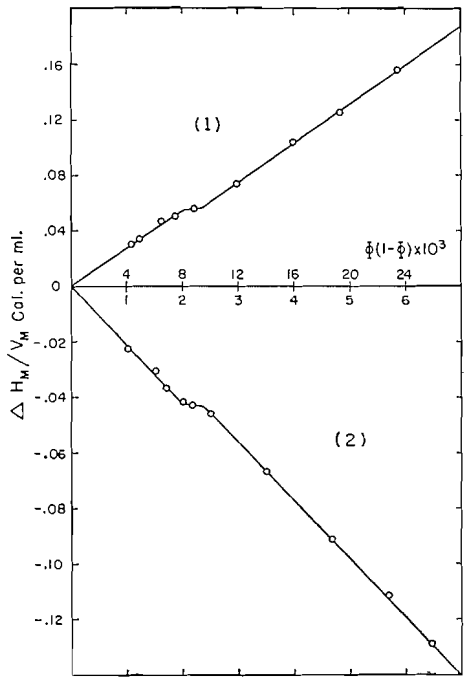

FIG. 1. Heats of mixing at 25° C. of polyvinyl acetate (mol. wt. 536,000) in: (1) methanol, (2) *s*-tetrachloroethane.

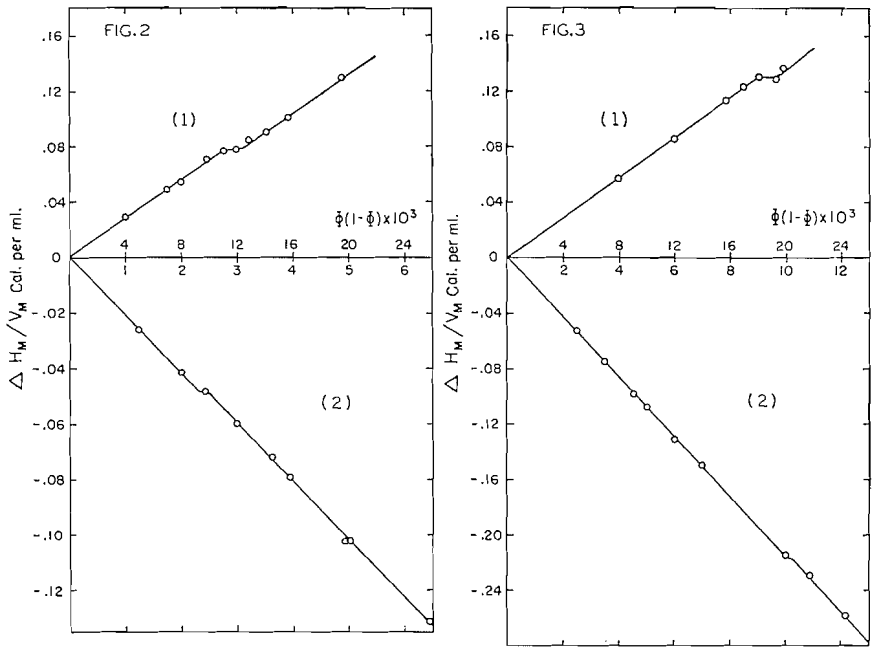

FIG. 2. Heats of mixing at 25° C. of polyvinyl acetate (mol. wt. 255,000) in: (1) methanol, (2) *s*-tetrachloroethane.

FIG. 3. Heats of mixing at 25° C. of polyvinyl acetate (mol. wt. 29,000) in: (1) methanol, (2) *s*-tetrachloroethane.

ethane. The values of B given in the table are derived from equation [1] below the critical concentration and from the following equation above the inflection point:

$$[6] \qquad \Delta H_M/V_M = B\Phi(1 - \Phi) + C$$

where C is the parallel displacement of the curve before and after the inflection point, along the $\Delta H_M/V_M$ axis.

The molecular weights of the fractions M_v were calculated from an equation given by Wagner (11) for polyvinyl acetate in solution in acetone at 25° C.:

$$[7] \qquad \log M_v = 1.47 \log[\eta] + 5.519.$$

Table II gives the intrinsic viscosities, at 25° C., of the various fractions of polymer in the two solvents used in this study.

TABLE II

INTRINSIC VISCOSITIES OF POLYVINYL ACETATE FRACTIONS IN METHANOL AND *s*-TETRACHLOROETHANE AT 25° C.

M_v	$[\eta]$ in methanol	$[\eta]$ in *s*-tetrachloroethane
536,000	0.79	2.10
255,000	0.62	1.54
191,000	—	1.00
29,000	0.25	0.42

DISCUSSION

When the results given here are compared with those of Daoust and Rinfret (2) a great improvement is noticed. This must be ascribed to a more elaborate experimental technique, as described above, and to a greater care in reducing impurities in polymer and solvent such as elimination of all trace of moisture. A relatively slight increase in accuracy has shown that the curves of $\Delta H_M/V_M$ vs. Φ such as that of Fig. 4 (of Reference 2, above) were actually straight lines. With this knowledge it was possible to make a better choice of concentrations to be investigated and to reject spurious results due to losses by evaporation and other causes.

Figs. 4 and 5 show the displacement of the inflection point with molecular weight for a poor solvent, methanol, and a very good solvent, *s*-tetrachloroethane. The values of the parameters B and C together with the critical concentration are given in Table III. The accuracy of positioning of the inflection point for the low molecular weight fraction (Fig. 3) is lower than that of the other fractions, but the experimental results (Table I) show that the inflection points are real even if their final position is subject to slight revision. A remarkable feature is that after the inflection point the slope of the curves, B, resumes its former value. Parameter B is also quite constant over the range of molecular weight; any slight change with molecular weight might be ascribed to previous history of the polymer fraction. Similar remarks can be made about C, although here there may be a real effect in the higher value found in both solvents with the 536,000 molecular weight fraction.

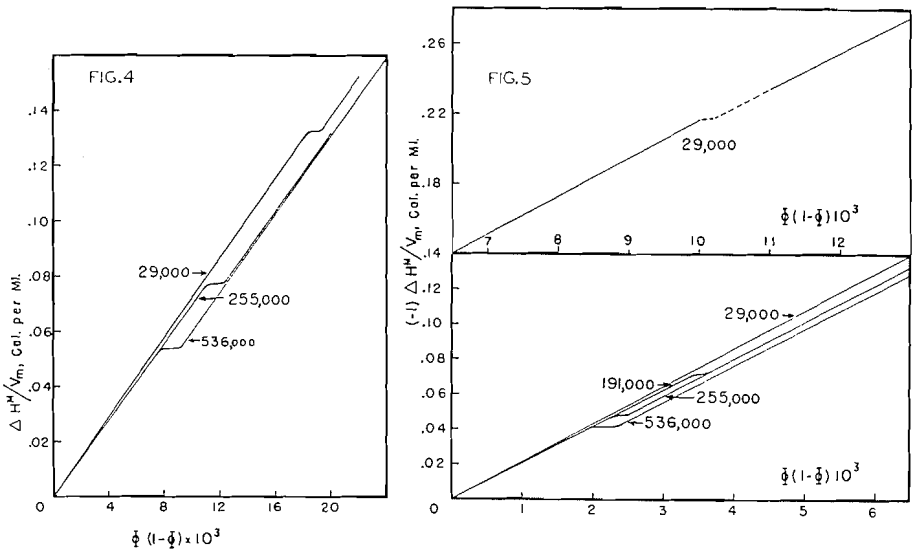

FIG. 4. Heats of mixing at 25° C. of various polyvinyl acetate fractions in methanol.
FIG. 5. Heats of mixing at 25° C. of various polyvinyl acetate fractions in *s*-tetrachloroethane.

TABLE III

PARAMETERS B AND C AND THE CRITICAL CONCENTRATION FOR VARIOUS FRACTIONS IN METHANOL AND *s*-TETRACHLOROETHANE

Solvent	Fraction mol. wt.	Critical volume fraction $\times 10^2$	B, cal. per ml.	C, cal. per ml. $\times 10^2$
Methanol	536,000	0.86	+ 6.9	−0.9
	255,000	1.2_1	+ 7.0	-0.7_5
	29,000	1.9_2	+ 7.2	−0.6
s-Tetrachloroethane	536,000	0.22	−20.9	+0.7
	255,000	0.24	−21.1	+0.4
	191,000	0.35	−20.7	$+0.3_5$
	29,000	1.05	−21.6	$+0.4_5$

As stated in the introduction, parameter B measures the net heat of interaction per contact of polymer segment – solvent molecule times the number of such contacts per segment. Although the total number of contacts between polymer and solvent increases with concentration, B will be essentially constant at low concentrations. At the moment of critical concentration Weissberg, Simha, and Rothman (12) have shown that the random polymer coils would be compressed because of the tendency of a polymer molecule to exclude all others from the space it occupies. Since this phenomenon occurs at only one concentration, it appears as a parallel displacement of the curves and parameter C is not affected by concentration. This effectively amounts to a new spatial distribution of polymer and solvent in the solution. An interesting property of the critical concentration lies in its use in the calculation of the dimension of the polymer molecule in solution. By making the assumption

that at this point each molecule occupies a sphere that has a diameter equal to the end-to-end distance of the chain, this dimension can be calculated. Given A the side of a cube occupied by N_s spheres of diameter D one finds for closed-packed spheres:

$$N_s = 1.41\ A^3/D^3. \quad [8]$$

If $A = 10$ cm. the number of spheres becomes the number per liter. This number N_S is also given by:

$$N_S = (m_c \times N)/M \quad [9]$$

where N is Avogadro's number, m_c, the critical concentration in grams per liter, and M, the molecular weight of the polymer. From [8] and [9], it is found that:

$$D = 13.3(M/m_c)^{\frac{1}{3}}\ \text{Å}. \quad [10]$$

The dimensions obtained from equation [10] are given in Table IV where they are compared with the value of $(\overline{r^2})^{\frac{1}{2}}$, the root-mean-square separation of

TABLE IV

MOLECULAR DIMENSIONS OF POLYVINYL ACETATE IN SOLUTION AT 25° C.

Solvent	Fraction mol. wt.	D in Å equation [10]	$(\overline{r^2})^{\frac{1}{2}}$ in Å equation [11]
Methanol	536,000	500	580
	255,000	350	420
	29,000	140	150
s-Tetrachloroethane	536,000	790	810
	255,000	600	570
	191,000	480	450
	29,000	180	180

polymer chain ends from Flory's equation:

$$(\overline{r^2})^{\frac{1}{2}} = (M[\eta]/\phi)^{\frac{1}{3}}\ \text{cm}. \quad [11]$$

where ϕ is a universal constant derived by Kirkwood and Riseman (6), who found the value 3.6×10^{21}, and recently determined experimentally by Newman, Krigbaum, Laugier, and Flory (7). Their best value is given as 2.5×10^{21}.

Concordance of the two methods in Table IV for calculating molecular dimensions is good enough to suggest equating D and $(\overline{r^2})^{\frac{1}{2}}$ to give:

$$13.3(M/m_c)^{\frac{1}{3}} = (M[\eta]/\phi)^{\frac{1}{3}} \times 10^8 \quad [12]$$

and therefore:

$$m_c = 5.9/[\eta] \quad \text{and} \quad [13]$$

$$\Phi_c = 5.9 \times 10^{-3}/(d_p \times [\eta]) \quad [14]$$

where Φ_c is the critical volume fraction and d_p the density of the polymer.

Because of the differences between D and $(\overline{r^2})^{\frac{1}{2}}$ in Table IV, this equation should be taken as a semiquantitative guide to the value of the critical concentration, until further investigation.

ACKNOWLEDGMENTS

We wish to express our thanks to Canadian Industries Limited for providing a Fellowship to one of us (M.P.). We are also grateful to the National Research Council for grants in aid of research and summer assistance.

REFERENCES

1. BOYER, R. F. and SPENCER, R. S. J. Polymer Sci. 5: 375. 1950.
2. DAOUST, H. and RINFRET, M. Can. J. Chem. 32: 492. 1954.
3. FLORY, P. J. J. Am. Chem. Soc. 65: 372. 1943.
4. HILDEBRAND, J. H. and SCOTT, R. L. The solubility of nonelectrolytes. 3rd ed. Reinhold Publishing Corporation, New York. 1950.
5. HORTH, A. and RINFRET, M. J. Am. Chem. Soc. 77: 503. 1955.
6. KIRKWOOD, J. G. and RISEMAN, J. J. Chem. Phys. 16: 565. 1948.
7. NEWMAN, S., KRIGBAUM, W. R., LAUGIER, C., and FLORY, P. J. J. Polymer Sci. 14: 451. 1954.
8. SCATCHARD, G. Chem. Revs. 8: 321. 1931.
9. STAUDINGER, H. Die hochmolekularen Verbindungen. Verlag von Julius Springer, Berlin. 1932. p. 128.
10. STREETER, D. J. and BOYER, R. F. J. Polymer Sci. 14: 5. 1954.
11. WAGNER, R. H. J. Polymer Sci. 2: 21. 1947.
12. WEISSBERG, S. G., SIMHA, R. S., and ROTHMAN, S. J. Research Natl. Bur. Standards, 47: 298. 1951.

SOME THERMODYNAMIC CONSIDERATIONS OF SURFACE REGIONS

SURFACE TENSION, ADSORPTION, AND ADSORPTION HYSTERESIS[1]

By E. A. Flood

ABSTRACT

Thermodynamic conditions for equilibrium between bodies which exert forces upon one another are discussed. The two bodies are treated as assemblies of infinitesimal volumes of pure components and the influence of the mutual potential fields examined. The results provide a thermodynamic description of surface tension and certain types of adsorption phenomena, as well as throwing considerable light on adsorption hysteresis.

INTRODUCTION[2]

In general where any two bodies are in contact with one another, they exert forces upon each other, usually only the very short range forces being of importance thermodynamically. As a consequence of these short range forces, when considering equilibria within the interfacial region, we cannot "regard as immaterial the position . . . of the various homogeneous parts of which . . ." each body is composed, as done by Gibbs (7) in deducing the phase rule. In general, these short range forces give rise to potentials of position.

The influence of these potentials on the thermodynamic conditions for equilibrium may be treated formally, in much the same way as the influence of the gravitational potential is treated. However, in the case of the gravitational potential, the force function of the field is treated as though it is independent of the state of the substance, while in the case of the interaction between two bodies, the "potential" is almost certainly influenced by the state

[1]*Manuscript received January 21, 1955.*

Contribution from the Division of Pure Chemistry, National Research Council, Ottawa, Canada. Issued as N.R.C. No. 3581. An Abstract of this paper was presented at the Symposium on Problems Relating to Adsorption of Gases by Solids at Kingston, Ontario, September 10–11, 1954. The text of the paper presented at the Symposium appears in the special issue of the Canadian Journal of Chemistry covering the Symposium (5).

[2]*A primary object of this enquiry is to obtain some insight into the physical factors which control rates of flow of fluids through porous adsorbents. The author is greatly indebted to Dr. Otto Maass of McGill University for encouragement and assistance in the pursuit of this problem.*

In the case of adsorption of condensable gases, liquid–vapor interfaces as well as solid–vapor interfaces are to be expected. Accordingly, it is necessary to know something of the natures of these surface regions in order to discuss "surface" flow mechanisms.

Evidence has been presented previously that where adsorbates are contained within pores which are fairly large compared with molecular dimension (10^{-7} to 10^{-5} cm.) adsorbates may be regarded as Polanyi compressed films, and that flow mechanisms of such films are essentially those of classical laminar flow, but flow rates are controlled by density and pressure gradients (both normal and parallel to the direction of flow) that are functions of the surface forces. These adsorbate gradients are very different from the directly observable or applied "gradients" of the gas outside the range of the surface forces. Generally adsorbate gradients are not directly observable and must be measured indirectly or inferred from measurements of adsorbate densities, surface tensions, surface energies, or other measurable average properties. Where we can determine adsorbate density gradients and can assume that the adsorbate behaves as a single substance, we can calculate corresponding pressure gradients, and make considerable progress in relating net flow rates to the physical structure of these fine grained porous adsorbents; while where the adsorbate cannot be regarded as a single component fluid the problem of correlating the permeability with the structure of an adsorbent, if at all possible in any literal sense, is much more complex.

of the bodies in contact (i.e., the potential of position may be a function of the density, pressure, and temperature as well as of the mass).

When two bodies of different kinds of matter are in contact with one another, the different kinds of material will eventually diffuse into one another to a greater or lesser degree, and the whole system everywhere must be regarded ultimately as a two component system. However, there are many cases where these diffusive processes are so slow, or where the equilibrium states are such, that the two bodies, including the interfacial regions, may be regarded as two distinct volumes each consisting of a single component. Evidently we must assume in such cases that the surface "potential" is such that, as the "boundary" of one of these volumes of pure component is approached, very strong repulsive forces are called into play ultimately limiting the density of this component to vanishing values (i.e. preventing interpenetration). When the two bodies in contact are more or less rigid solids, the short range surface forces acting between the bodies will give rise to states of stress in the interfacial regions which differ from those prevailing throughout the bulk phases. These states of stress will be accompanied by deformations, or states of strain, in the interfacial region which will result in small over-all deformations of the two bodies as they are brought into contact. If, however, one of the bodies is a highly compressible fluid, the density of the fluid in the interfacial region will be very materially influenced by the surface forces, resulting in comparatively large changes in volume of the compressible fluid as a result of its being brought into contact with the solid, i.e., adsorption will occur.

Thus we may consider the whole of the volume of the compressible fluid (or gas) as constituting a single component system bounded by regions of complex potential fields which are functions of the pressure, temperature, and natures of the gas and solid.

We confine our interest to cases where all the material of the compressible component in the interfacial region is fluid, and we shall inquire into the thermodynamic conditions for equilibrium which must prevail in such complex single component fluid systems. While the thermodynamic conditions for equilibrium in constant potential fields are discussed in standard texts, the thermodynamics of the more general case where the force function of the field may depend on the density, pressure, and temperature of the fluid has been largely ignored.

In Part I of what follows, we present some general thermodynamic considerations of the equilibrium conditions which must prevail in complex single component fluid systems; in Part II, these ideas are applied to surface tension problems; and in Part III, they are applied to gas adsorption problems.[3]

It is shown that these ideas lead to a plausible detailed thermodynamic description of surface tension phenomena, and that in the case of adsorption phenomena, they predict results capable of experimental verification.

[3]*When applied to adsorption theory, the thermodynamic considerations lead to what is essentially a Polanyi (14) adsorption potential theory, but where the "potential" of the surface is variable, i.e., is a function of the equilibrium pressure of the gas, the density of the adsorbate, etc., thus providing for so-called "co-operative effects".*

I. SINGLE COMPONENT COMPLEX FLUIDS

Thermodynamics is, strictly, a science of observable quantities and hence is a science dealing with the properties of matter in bulk. Accordingly, the validity of the assigning of thermodynamic properties to elementary volumes of material is open to question.

Tolman (19) in his theory of surface tension treats elementary laminar volumes as thermodynamic systems and discusses the validity of such treatments. When we consider the pressure gradients, energy gradients, etc. of a gas in a gravitation field, we assume that such gradients are continuous. Thus we tacitly assume that laminae of infinitesimal dimensions have thermodynamic properties. It is evident that when we deal with helium we may take as the thickness of a lamina a dimension considerably less than that of the diameter of the spherical molecule, only those molecules whose centers of mass lie within the lamina being considered as "contained" within the elementary laminar volume. In this way it is quite possible to construct statistical model fluids that are very accurate descriptions of real gases, and which are equally applicable to infinitesimal volumes and to large finite volumes, equally applicable to volumes small or large compared with molecular dimensions. If the fluid molecules are dipoles and may be subject to orientation in a field, the situation is somewhat more complex and it might seem that we must consider adjacent laminae as consisting of different "kinds of material" as would be the case in an ionic crystal. In the latter case the long range order is a permanent condition, a state of the system, and even after very long periods of time, neighboring elementary laminar volumes cannot be regarded as consisting of the same substance, i.e., they are not reversibly convertible into one another by any ordinary sort of thermodynamic process (e.g., layers containing almost wholly chloride ions and layers containing sodium ions are not thermodynamically interconvertible). If, however, any orientation forces can be resolved into forces and couples acting on and about molecular mass centers, a statistical model fluid can be constructed such that elementary volumes regardless of size can be regarded as elementary thermodynamic systems containing the same component as the whole assembly of elementary volumes. Without looking more closely into statistical details of such problems, we shall define a single component fluid complex as follows: an assembly of elementary fluid volumes, where every elementary volume is thermodynamically identical with an equal elementary volume of a single fluid in some bulk state, the bulk state being in reversible equilibrium with externally applied forces no matter how bizarre these forces may be. Thus the state of each elementary volume corresponds exactly to a bulk state of a single substance under specific external forces. All the elementary volumes are thus inherently capable of reversible thermodynamic conversion into another. Since we will be mainly concerned with fluids, we shall assume that pressures of elementary volumes are equal in all directions and that all pressure, energy, density gradients, etc. are continuous. The forces transmitted across boundaries of adjacent elementary volumes are necessarily equal.

Thermodynamic Equilibria in Single Component Complexes

When two bodies exert forces upon one another, the energy associated with separating them is not strictly a property of either body alone. However, we may arbitrarily fix the energy of one of these bodies and consider it as being in a reference state and accordingly assign the energy of separation to the second body. This is the normal procedure when considering equilibrium in a force field. Since in the usual derivations of the conditions for equilibrium in force fields the force field is assumed independent of the state of the body, it is necessary to re-examine the equilibrium when the potential of position of unit mass may be a function of the volume of the mass.

The condition that changes in thermodynamic states of a system under the action of external forces shall be reversible is that the heat received by the system during such changes shall be equal to the change in the energy of the system plus the maximum work which the system can do against the external forces if such a maximum exists. When no potential of position is involved and the only work is associated with a change in volume, this condition for reversibility is expressed by the well-known equation

$$dE_0 = TdS - pdv + \mu_0 dm$$

where E_0 is the intrinsic energy, T the temperature, S the entropy, p the pressure, v the volume, μ the intrinsic thermodynamic potential, and m the mass.

When a "potential" of position is involved we can write
where

$$[1] \quad dE = dE_0 + d\omega = TdS - pdv + \mu_0 dm + d\omega$$
$$= TdS - pdv + \mu_0 dm + \Omega dm$$
$$= TdS - pdv + \mu_0 dm + \frac{\partial}{\partial m}\int_{x_0}^{x} f(x)\, dx \,.\, dm$$
$$= TdS - pdv + \mu dm$$

where
$$d\omega = \Omega dm = \frac{\partial}{\partial m}\int_{x_0}^{x} f(x)\, dx \,.\, dm,$$

and $(\partial/\partial m)\int_{x_0}^{x} f(x)dx$ represents the maximum or reversible work associated with moving unit mass at constant S and v from the initial position x_0 to the final position x. This work is assumed dependent only on the initial and final positions in the potential field. Such fields are sometimes referred to as scalar fields. It is implied that in the reference state corresponding to x_0, $f(x)$ is zero. Other relations expressed by the equations are self-explanatory.

By definition of the single component complex, Equation [1] is applicable to every element of volume of the assembly, and accordingly an equation of similar form is applicable to assemblies of these volumes. The conditions for equilibrium between these volumes will depend upon the physical conditions assumed applicable within the complex, or between elements of the complex and a reference volume. Since the complex is essentially a fluid mass, heat and

matter may be assumed to be in a state of flux between the various parts. Accordingly we assume the following physical conditions: (*a*) increments of heat-energy and mass, independently, may flow in to or out of any of the volumes concerned, (*b*) no work is involved in the transport of entropy through finite distances, (*c*) the transport of mass through finite distances involves performance of work against the force function of the field. With these conditions, following exactly the method of Gibbs, it can readily be shown that the necessary and sufficient conditions for equilibrium throughout the complex are: (*a*) uniformity of temperature, (*b*) uniformity of total potential per unit mass, μ or $\mu_0+\Omega$. Evidently the existence of potentials of position that may be functions of the volume as well as of the mass of the substance concerned does not change the basic equilibrium conditions applicable to systems in constant potential fields.

Equation [1] may be written in the form

$$\begin{aligned} dF &= -SdT+vdp+\mu_0 dm+\frac{\partial}{\partial m}\int_{x_i}^{x} f(x)\,dx\,.\,dm \\ &= -SdT+vdp+\mu dm \end{aligned}$$

where $F = E-TS+pv$ and $\mu = \partial F/\partial m = \partial E/\partial m$, etc.

Assuming that $F(T, p = 0, x, m = 0) = 0$ and that $\int_{x_0}^{x} f(x)dx = 0$ when $m = 0$, we can write for the potential F of any mass m of fluid at any position x under any pressure p,

$$F = \int_{p=0,m=0}^{p,m} (vdp+\mu dm),$$

the path of integration corresponding to increasing the mass of material at some position x while v, p, and μ take particular values for various values of m.

We suppose that the complex is in equilibrium with a bulk reference fluid of uniform properties, and that the complex remains in reversible equilibrium with the bulk reference fluid throughout a path where the density and pressure of the reference fluid vary from zero to specified values.

Assigning the value x_0 to the bulk reference state and the value x_{ai} to the ith element of the complex, we can write for equal masses of material at x_0 and x_{ai}

$$F_0(p_1, m_i, x_0) = \int_{p=0,m=0}^{p=p_1,m=m_i} (vdp+\mu_0 dm),$$

$$F_{ai}(p_{ai}, m_i, x_{ai}) = \int_{p=0,m=0}^{p=p_{ai},m=m_i} (vdp+\mu_{ai}dm),$$

and $F_0 = F_{ai}$ and $\mu_0 = \mu_{ai}$ throughout the path of integration. Also we may write

$$F_{ai} = \int_{p=0,m=0}^{p=p_1,m=m_i} (vdp+\mu_0 dm)+\int_{p_1,x_0}^{p_{ai},x_0} vdp+\int_{x_0,p_{ai}}^{x_{ai},p_{ai}} f(x)\,dx$$

where

$$\int_{p_1,x_0}^{p_{ai},x_0} vdp + \int_{x_0,p_{ai}}^{x_{ai},p_{ai}} f(x)\,dx = \int_{p_1,x_{ai}}^{p_{ai},x_{ai}} vdp + \int_{x_0,p_1}^{x_{ai},p_1} f(x)\,dx.$$

It will be noted that $\int_{p_1,x_0}^{p_{ai},x_0} vdp$ is not necessarily equal to $\int_{p_1,x_{ai}}^{p_{ai},x_{ai}} vdp$. When they are equal, the equation of state (v of p, T constant) is independent of the field. When the integrals are not equal, the force function of the field is a function of v.

We may suppose the uniform reference fluid broken up into elementary volumes δv_i of mass δm_i equal to the mass of each elementary volume of the complex δv_{ai} at x_{ai}. For the equilibrium between these elementary volumes, the x coordinates remaining constant while δm_i and the pressures vary, we have

$$\delta v_{1i} \cdot \delta p_1 + \mu_0 dm_i = \delta v_{ai} \cdot \delta p_{ai} + \mu_{ai} dm_i,$$

and since $\mu_0 = \mu_{ai}$,

$$\sum_i \delta v_{ai} \cdot \delta p_{ai} = \delta p_1 \cdot \sum_i \delta v_{1i} = \frac{\delta p_1}{\rho_1} \sum_i \delta v_{ai} \cdot \rho_{ai}.$$

Therefore

$$v_a \delta \bar{p}_a^{\,v} = v_a \bar{\rho}_a \cdot \frac{\delta p_1}{\rho_1}$$

where the density of the uniform reference fluid is ρ_1, and $\rho_1 = \delta m_i/\delta v_{1i}$. Hence

$$[2] \qquad \bar{p}_a^{\,v} = \int_{p=0,m=0}^{p=p_1,m=m} \bar{\rho}_a/\bar{\rho}_1 \cdot dp_1.$$

Thus the volumetric mean pressure $\bar{p}_a^{\,v}$ can be determined if the volumetric mean density $\bar{\rho}_a$ is known as a function of p_1, i.e., if m and v_a are known functions of the pressure, p_1, of the reference gas along a path of thermodynamic reversibility where the equilibrium pressures vary from zero to p_1 while m varies from 0 to m.

It will be noted that since $\bar{\rho}_a$ and ρ_1 are positive, $\bar{p}_a^{\,v}$ is necessarily positive for any path of thermodynamic reversibility where the equilibrium pressure increases from zero to p_1. If, however, other paths of thermodynamic reversibility intersect this path at points below p_1, say at p_1', so that if the pressure of reference fluid is raised from zero to p_1 and then reduced to p_1'' below p_1', the system may follow the second path from p_1' to p_1'' and

$$\bar{p}_a^{\,v} = \int_0^{p_1} \frac{\bar{\rho}_a}{\rho_1} \cdot dp_1 + \int_{p_1}^{p_1'} \frac{\bar{\rho}_a}{\rho_1} dp_1 + \int_{p_1'}^{p_1''} \frac{\bar{\rho}_a'}{\rho_1} dp_1$$

$$= \int_0^{p_1'} \frac{\bar{\rho}_a}{\rho_1} \cdot dp_1 - \int_{p_1''}^{p_1'} \frac{\bar{\rho}_a'}{\rho_1} \cdot dp_1.$$

If the second integral is larger than the first, $\bar{p}_a^{\,v}$ may be negative.

When $\bar{\rho}_a > \rho_1$, $\bar{p}_a^{\,v} > p_1$ and the potential of position of the reference fluid is greater than the average potential per unit mass of the complex.

The mean "potential" difference between the complex and the reference fluid may be expressed by

$$\sum_i \frac{p_{ai}-p_1}{\overline{\rho_{ai}}|_{p_1-p_{ai}}} \cdot \rho_{ai} \cdot \delta v_{ai} = -\omega$$

where $\overline{\rho_{ai}}|_{p_1-p_{ai}}$ is the mean density of the reference fluid over the pressure interval p_1 to p_{ai}. Thus

$$\omega = cv_a(p_1-\bar{p}_a{}^v)$$

where c is a dimensionless positive quantity. If $\bar{p}_a{}^v > p_1$, $c \geqslant 1$. If the material is incompressible in all of the ranges p_1 to p_{ai}, $c = 1$. In general ω will be dependent on the distribution function, $v(\omega)$, of the complex and upon the equation of state of the reference fluid. It will be noted that $\Omega(x_{ai}-x_0, p_1)$ is not necessarily the same as $\Omega(x_{ai}-x_0, p_{ai})$. Thus in general we cannot determine ω when $\bar{p}_a{}^v$ can be determined unless the fluid is incompressible in the various pressure intervals p_1 to p_{ai}. If the reference fluid is a condensable gas and p_1 is above the saturation pressure, that is p_1 is the pressure of the reference liquid, then if the liquid is practically incompressible, we can obtain a measure of ω, i.e., $\omega = v_a(p_1-\bar{p}_a{}^v)$.

Phase Rule Considerations

We have assumed that each elementary volume or lamina is thermodynamically identical with equal elementary volumes of the fluid in some bulk state. Accordingly elementary volumes having the same p, T, and μ but different densities are to be regarded as different phases in the sense of the phase rule. However, the fundamental thermodynamic equation has in addition to S, v, and m one more variable, namely, that measuring the force function of the field, $f(x)$. When v of p (T and m constant) is not influenced by $f(x)$, if the potential of position $\Omega(x-x_0, p_1)$ vanishes at three values of x in the surface region, and the corresponding laminae have three different densities for given values of T, p, and μ, the system will be invariant in the sense of the phase rule. But if the relation between v and p is influenced by $f(x)$, then where $f(x)$ is not zero, the density of a fluid lamina for given values of p may differ from the density where $f(x)$ is zero. Since $\Omega(x-x_0, p_1)$ may vanish for some value of x for which $f(x)$ does not vanish, we may have $\Omega(x-x_0, p_1)$ zero for three values of x, while $f(x)$ is zero for only two of these values. Under these circumstances, we may have two density states corresponding, say, to normal liquid and vapor, and a third density state where $f(x)$ is large, while the system is still monovariant in the phase rule sense.

We cannot, in general, suppose a fluid divided into laminae and treat the "spreading pressure" of each layer as an independent variable in order to calculate the phase "variance". However, when a force field is involved p_{at} will in general differ from p_1 and may be regarded as constituting a measure of the potential of the field and of $f(x)$ (cf. Rowley and Innes (16)).

In Part II of this paper the interface between a liquid and vapor of a single substance will be treated as a single component complex and in Part III the boundary of a fluid or gas in contact with a solid of a different kind of substance will be similarly treated. While both cases are essentially similar, in the former

case both bulk phases consist of a single component while in the latter case the two bulk phases are different components. In both cases surface forces are assumed to be classical.[4]

II. SURFACE TENSION

The Liquid–Vapor Interface, A Single Component Complex Fluid

Consider a liquid separated from its vapor by a flat interface. Far from the interface the net hydrostatic pressures of the liquid and of the vapor are the same and are, of course, positive. The interfacial region, however, exhibits a tension, and accordingly negative pressures or negative stress intensities are to be expected in this region. If following Tolman (19) we think of the interface as made up of very thin laminae parallel with the surface and if we suppose the material constituting these laminae to be fluid so that stress intensities acting on elementary volumes (i.e., laminae) are equal in all directions, we must suppose a sharp pressure gradient to exist along the normal to the surface, the gradient vanishing within the body of the liquid and within the vapor.

Let $p(x)$ be the pressure of the fluid as a function of x, where x is the distance along a normal to the surface, measured from liquid to gas. If h is the thickness of the interface, the thickness of the region wherein $p(x)$ varies with x, then $\int_x^{x+h} p(x)\,dx \equiv \bar{p}(x)\cdot h$ is the net parallel surface force exerted by unit area of the surface region, and $\bar{p}(x)$ is the mean value of the stress intensities exerted by the various laminae parallel with the surface. If $\bar{p}(x)$ is negative, $-\bar{p}(x)\cdot h$ is literally a positive "surface tension". The work done by the surface system when the surface of area σ is increased by $d\sigma$, the thickness remaining constant, is, of course, $\bar{p}(x)\cdot h\cdot d\sigma$. Hence the corresponding Helmholtz free energy change is given by $(\partial A/\partial\sigma)_{T,h} = -\bar{p}(x)\cdot h = \gamma$. Thus, this "surface tension", γ, is unambiguously the Helmholtz free energy per unit surface.

It may be remarked that considerable confusion (18) exists in the literature dealing with the relations between "surface tension" and "surface free energy". This confusion arises partly from following Lewis and Randal (11) and equating the change in Gibbs free energy, F (where $F = E - TS + pv$), of the surface to the work of stretching the film, i.e., in writing $dF_T = \gamma d\sigma$ instead of

[4]*If the energy states of molecules of the fluid with respect to the surface force field are continuous and the distribution of these states largely classical in character, the detailed structure of all of the energy states at a given temperature will be largely characteristic of the fluid in some bulk state. Accordingly, fluid laminae under the influence of such fields will behave as a single substance in the sense that laminae of the bulk states of fluid can exist in equilibrium with external forces in states that are thermodynamically practically identical with corresponding laminae in the force field. However, when the energy states of the molecules in the surface layers are quantized and the surface forces large, the detailed structure of the energy states at any given temperature may be quite different from those of any bulk state of the pure fluid. Accordingly, laminae under the influence of such potential fields will not behave as the same substance, thermodynamically, as the bulk fluid, and the assembly of surface laminae cannot be treated as an assembly of volumes of a single component.*

A pure component of a chemical compound or of a solution is, in general, capable of reversible transformation with the same substance in the compound or solution. For such a process $\Delta F = 0$, but ΔA, ΔE, $\Delta S \neq 0$. For the special case of an ideal gas solution where each gas behaves as a vacuum to each other gas ΔF, ΔA, ΔE, $\Delta S = 0$ but $\Delta v \neq 0$, $\Delta\bar{p}^v \neq 0$. When ΔF, ΔA, ΔE, ΔS, Δv, $\Delta\bar{p}^v$, etc. $= 0$ the forces of interaction between the bodies in the combined system take the place of the external forces of the pure components. The latter case may be called "mechanical" or "physical" interaction, as distinct from the first case of "chemical" interaction and from the second case of pure "solution".

equating the Helmholtz free energy to this work, i.e., instead of writing $dA_T = \gamma d\sigma$.[5] However, these difficulties are due mainly to the fact that some authors treat the surface as an isolated thermodynamic system distinct from the material lying on either side of it, while others define surface tension by $(\partial A/\partial\sigma)_{T,v} = \gamma$ where the operation $(\partial A/\partial\sigma)_{T,v}$ is applied to systems containing surfaces and bulk material. Thus in the latter case, a distortion of a solid at constant volume would yield a "surface free energy" or "surface tension" quite different from the "surface tension" that would be obtained if the process $(\partial A/\partial\sigma)_{T,v}$ corresponded to increasing the number of crystals while decreasing their size, their shapes remaining constant. In the case of liquids with flat surfaces, if $(\partial A/\partial\sigma)_{T,v}$ corresponds to the process of changing the shape of the container of a liquid–gas system so that the surface area of the interface is increased while the volume remains constant,

$$(\partial A/\partial\sigma)_{T,v} = [\bar{p}(x) - p_0]\, h$$

where p_0 is the vapor pressure of the liquid. Evidently the operation $(\partial A/\partial\sigma)_{T,v}$ applied to a system containing surfaces and bulk material does not in general constitute a measure of a definite quantity, the operation being capable of yielding a variety of "surface tensions" depending upon further particulars not specified by the operation.

In the case of a liquid the actual net force of the surface tension is one of its most striking characteristics and is directly measurable. In most cases the methods of measurement of the surface tension of a liquid correspond closely to the operation $(\partial A/\partial\sigma)_T$ applied to the surface layer only. Accordingly, in what follows we shall consider that surface tension is the net parallel mechanical force actually exerted by the surface. Thus we put $-\bar{p}(x) \cdot h = \gamma$.[6]

In general, if a surface has an energy per unit surface area, under equilibrium conditions the surface energy will be a minimum consistent with its entropy. Thus the flat surface will not be quite smooth, but will have a somewhat greater area than the flat surface, the excess area corresponding to the thermal energy of motion of the surface as a whole. In the absence of gravitational and other external fields, changes in position of the interface will have no effect on the equilibrium within the systems. If we suppose the surface region divided into geometrically flat elementary laminae parallel with the mean position of the surface region and of area equal to the apparent area of the "flat" interface separating a liquid from its vapor, the assembly of laminar

[5] *Replacing pv by $\bar{p}(x).h.\sigma$ then for the surface system only, $dw = \bar{p}(x).h.d\sigma$, $dA_T = -\bar{p}(x).hd\sigma$, $dF_T = h.\sigma.d\bar{p}(x)$, and if $\bar{p}(x)$ is constant, $dF_T = 0$. Thus increasing the area of a flat surface is, formally, exactly equivalent to increasing the volume of a phase in equilibrium with other phases. If a system consists of bulk phases and surface phases so that the potential per unit mass is given by $\mu = E - TS + pv - \gamma\sigma$, etc., we should write $dF = -SdT + vdp - \sigma d\gamma$, and when T, p, and γ are constant, $dF = 0$ irrespective of any work done when stretching the surface or when increasing the volume.*

[6] *Some writers regard the "surface tension" as a fiction but regard the surface free energy as real. This is much like regarding the pressure of a gas as a fiction but its thermodynamic potential as real (1). In the case of ionic substances "surface free energy" phenomena might be exhibited by very marked gradients in electrical charge density and corresponding gradients in mass density. In this case mechanical stress gradients in the surface regions might be quite negligible and the actual "surface tension" practically zero.*

volumes will constitute, thermodynamically, a single component complex as defined in Section I above. Evidently all of the thermodynamic relations applicable to the single component fluid complex are applicable to liquid–vapor systems including the interfacial regions when these interfacial regions are fluid throughout.

It will be noted that, in general, the mean pressure of laminae within the interfacial region will be negative if the surface tension is positive. If we regard the vapor as the reference fluid and the interfacial region as the complex, the interfacial region cannot be formed reversibly along a constant temperature path of increasing pressure of the reference gas. Thus if we fill a fixed volume with vapor of a condensable substance and increase the pressure until a liquid–vapor interface is formed, if the interface is of finite dimensions and has a positive surface tension, some irreversibility is involved in the process (cf. p. 984). However, we may suppose the volume filled with vapor above the critical temperature and then cooled reversibly so that the meniscus can form reversibly. Along this path $\bar{p}_a{}^v$ and $\bar{p}(x)$ can become negative reversibly. To form a strictly flat interface by such a process in the absence of other sources of potential, it would appear necessary that the fixed volume be of infinite size. Accordingly, in the absence of condensing surfaces the formation of the flat meniscus by a strictly reversible process would appear to be experimentally unattainable. However, a spherical drop could be formed by such a process at constant volume. Of course, as pointed out by Gibbs (7) curved surfaces of tension cannot be in, strictly, stable reversible equilibrium with any source of constant pressure, in the absence of condensing surfaces or other sources of potential.

Thermodynamic Description of a Fluid Liquid–Vapor Interface

Writing $\Omega(x)$ as the potential of position as a function of the distance x along the normal to the surface, we may take $\Omega(x)$ as zero within the body of the liquid far from the interface. Evidently $\Omega(x)$ must become positive in regions of negative pressure and finally vanish in the interior of the vapor. Accordingly, $\Omega(x)$ must have at least one maximum. Since

$$\frac{dF}{dx} = v\frac{dp}{dx} + \frac{d\Omega}{dx} = 0,$$

$$v\frac{dp}{dx} = -\frac{d\Omega}{dx} = f(x)$$

everywhere along the normal to the surface. When $\Omega(x)$ is a maximum or a minimum $f(x)$ and dp/dx are necessarily zero. Further, as before, taking h as the thickness of the surface region, i.e., the region where $\Omega(x)$ may differ from zero,

$$\int_0^h \frac{dp}{dx}\,dx = \overline{\frac{dp}{dx}} \cdot h = 0$$

for flat surfaces, and also

$$\int_0^h f(x)\,dx = \int_0^h v\frac{dp}{dx}\,dx \equiv \overline{v \cdot \frac{dp}{dx}} \cdot h = 0.$$

The latter two necessary conditions impose a considerable constraint on possible forms of $\Omega(x)$, $p(x)$, and $v(x)$. Thus, if $\Omega(x)$ has only one extreme value and that a maximum at x_m, $0 < x_m < h$. Then since the specific volume $v(x)$ increases by large factors as the vapor is approached from the liquid and the mean value of $v(x)$ on the liquid side of x_m (i.e., in the range 0 to x_m) is less than that on the vapor side of x_m, it follows that the specific volume on the liquid side of x_m must rise to greater values than on the vapor side. Hence, the rapid increase in volume must occur mainly on the liquid side of x_m. The point x_m is the point at which $\Omega(x)$ is a maximum and $p(x)$ a minimum; accordingly in this case the minimum pressure must occur in the region where $v(x)$ is large, i.e., in regions where densities are comparable with vapor densities. The relations are illustrated in Fig. 1. From physical considerations dilute gases cannot exert negative pressures. Accordingly, the relations illustrated in Fig. 1 could only apply to systems where gas densities were relatively high and/or surface tensions small or negative. (If $\bar{p}(x)$ is less than p_0, the system will exhibit "surface tension" behavior, but if $\bar{p}(x)$ is positive the surface tension is negative.) Evidently, in cases where surface tensions are high and vapor densities much less than liquid densities $\Omega(x)$ cannot have the simple form indicated in Fig. 1. In the case of the flat interface where the bulk liquid and vapor have equal pressures, if $\Omega(x)$ has more than one extreme value in the interval $0 < x < h$, there must be at least three equal values of $p(x)$ in this interval. Thus, there must be at least three laminae having different densities but equal values of T, p, and μ. Accordingly, $(\partial F/\partial p)_x$ must be a function of x; i.e. the "equation state" must be influenced by the force field. Otherwise the system would be invariant in the sense of the phase rule (cf. I, p. 985). In Fig. 2*A* the relations between the various functions are shown, assuming $\Omega(x)$ to have the simplest form consistent with a positive surface tension, and $v(x)$ to have a plausible maximum and minimum.

It will be noted that whatever the shape of the curve $\Omega(x)$, if $f(x)$ is positive for any value of x in the interfacial region it must also have negative values. Thus, if material is attracted toward the liquid on the liquid side of the x_{m_1}, it must be repelled from the liquid somewhere in the region $x_{m_1} \leqslant x \leqslant h$. Some authors treat the surface forces as though a net thermodynamic potential difference existed between the liquid and its vapor.

The relations indicated in Fig. 2*A* correspond physically with a case where the "interface" adsorbs its own vapor, i.e., both the density and pressure rise as the interface is entered from the vapor. These relations are consistent with some statistical mechanical descriptions of an interface (20). It is not, of course, necessary from thermodynamic considerations alone that $v(x)$ have a maximum and a minimum.

The $v(x)$ curve as drawn is intended to suggest that in order for molecules to enter the more or less close packed liquid structure some selection is involved resulting in a reduction in density of the "transition" laminae. In the case of very dense liquids this "surface" might behave very much like a solid surface and allow only limited penetration, i.e., a comparatively large percentage of the molecules "striking the surface" would be reflected.

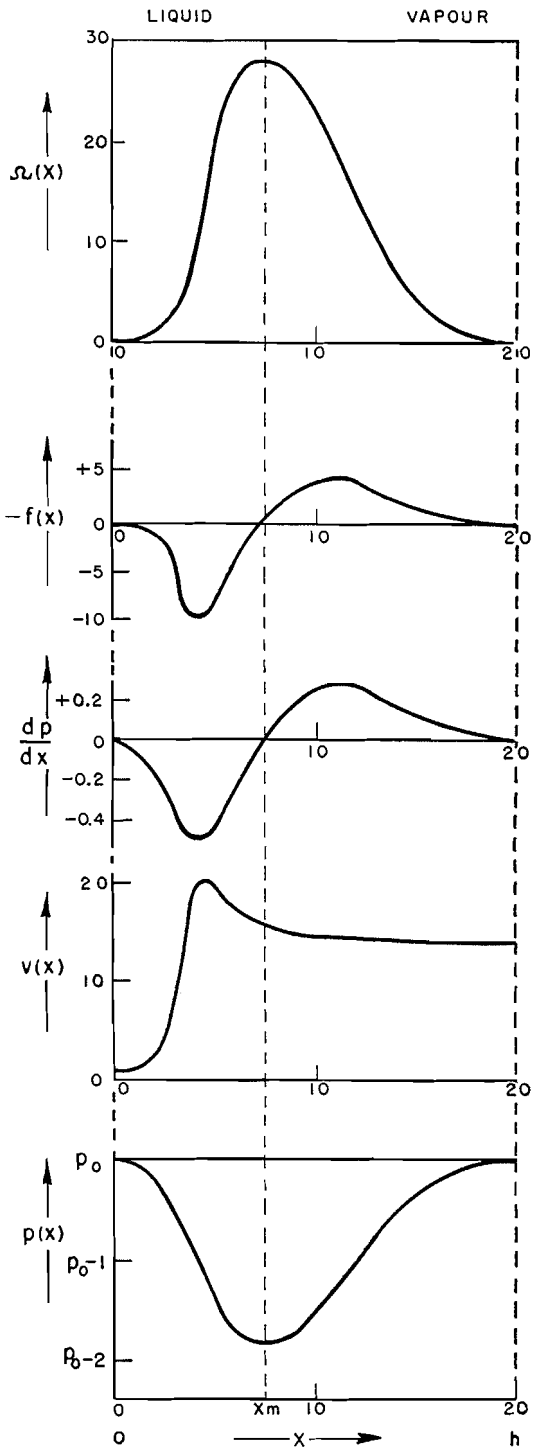

FIG. 1.

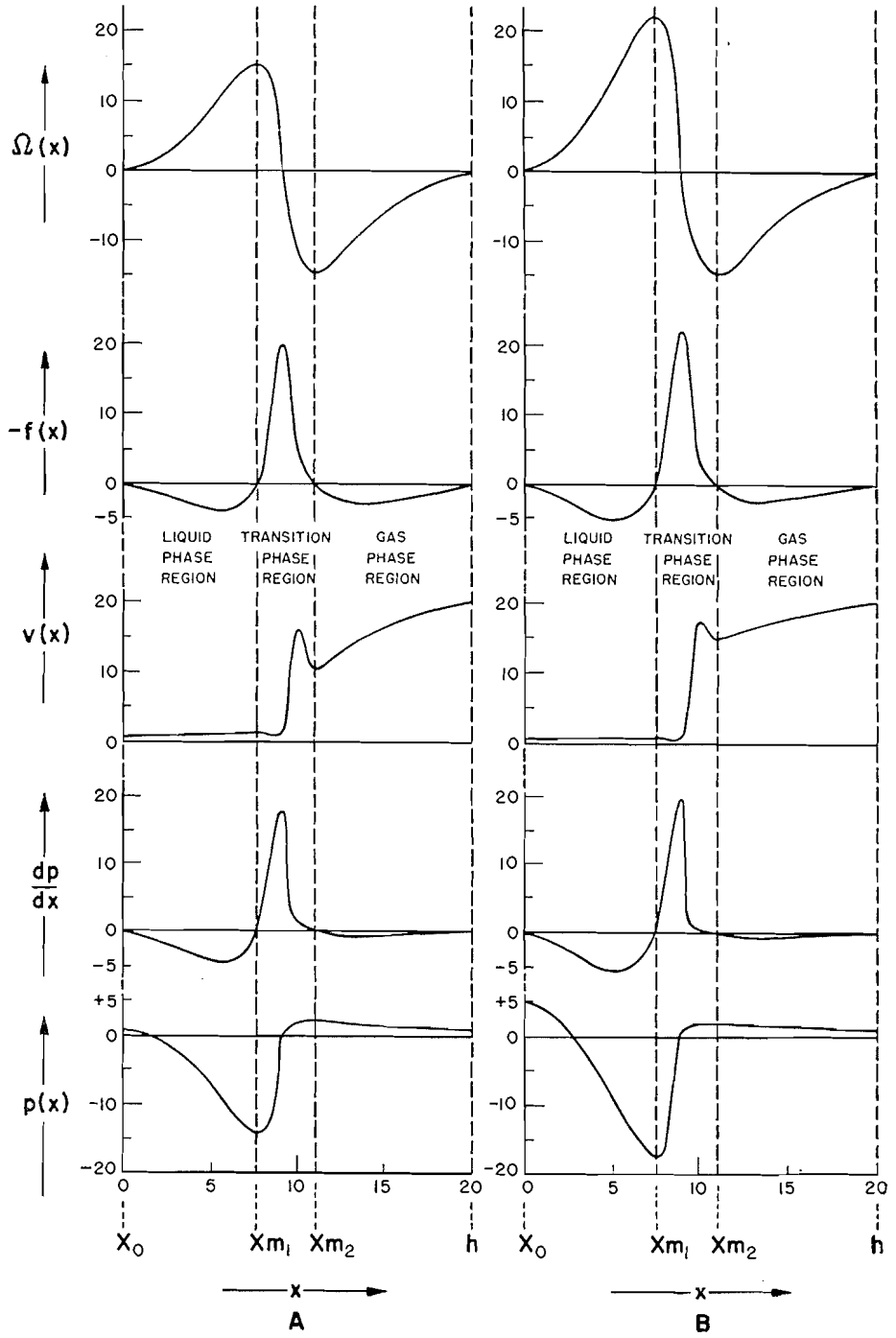

FIG. 2.

Referring to Fig. 2*A*, at the maximum of $\Omega(x)$, $f(x) = 0$ and $v(x)$ must be that corresponding to normal bulk liquid under the corresponding negative stress. Thus in the region $0 \leqslant x \leqslant x_{m_1}$, we regard the fluid as being essentially normal liquid under negative hydrostatic stress; in the region $x_{m_2} \leqslant x \leqslant h$ the fluid is normal gas; while in the intermediate region the equation of state v of p is materially influenced by the force field. Thus in the region where $\Omega(x) \rightarrow 0$ but $f(x)$ approaches a maximum, the fluid is neither normal liquid nor normal gas but is in a transition state.

Capillary Rise and Depression

As a variation of the "flat" interface illustrated by Fig. 2*A* we may suppose the whole system raised or lowered in a potential field independent of surface potential fields. If we impose the condition $dF = 0$ for this variation the conditions are analogous to capillary rise or depression.

In order that $dF = 0$, the relative changes in liquid and gas pressures will be more or less proportional to densities. Accordingly, the $p(x)$ curve must be distorted so that $\int_0^h (dp/dx)\, dx \neq 0$. However, for small rises or depressions $\bar{p}(x)$ and $\bar{\Omega}(x)$ will not be changed appreciably, since the magnitudes of $\bar{p}(x)$, $p(x_m)$, etc. are large compared with the pressure changes introduced by the rise or depression. For large depressions, analogous to the effect of curvature on very small droplets, the pressure changes may be comparable with $\bar{p}(x)$. In such cases to retain constancy of surface tension either $\Omega(x)$ must change or the surface thickness, h, or both must change. A natural assumption is that the tendency of the surface to adsorb its own vapor becomes less on surfaces concave toward the dense phase and hence that $\Omega(x)$ is changed. Fig. 2*B* illustrates a "capillary depression" of the hypothetical system illustrated by Fig. 2*A*, the values of $\bar{p}(x)$ and h being unchanged, but $v(x)$, $p(x)$, and $\bar{\Omega}(x)$ distorted so that there is a net pressure difference between liquid and vapor. The surface tensions and the surface thicknesses are the same for the two cases, but $\Omega(x)$ is greater for the depressed curved surface. Rice (17) has pointed out that γ might be expected to increase with increasing pressure, in view of the Lewis (11) relation,

$$(\partial\gamma/\partial p)_{\sigma,T} = (\partial v/\partial\sigma)_{p,T}.$$

Since γ is essentially a mean volumetric stress intensity, the interpretation of this equation, if valid at all, is obscure. In general one would expect $\Omega(x)$ to be due largely to the density gradient in the surface region and consequently that changes in the vapor–liquid equilibrium conditions which tended to make the density and compressibility differences vanish would also tend to make $\Omega(x)$ vanish. Both large increases or decreases in vapor pressures would tend toward reducing density and compressibility differences between liquid and vapor. Accordingly, we should expect $\Omega(x)$ to be a maximum for nearly flat surfaces. Thus for exceedingly minute gas bubbles or drops γ should be materially less than that corresponding to the flat surface and the pressure differences across small spheres reach a maximum and finally practically vanish as the radius diminishes.

Thickness of the Interface

For convenience of illustration the difference between the specific volumes of liquid and vapor has been taken much less than is the case with liquid–vapor systems such as water. The magnitudes of the negative pressures are also much smaller with respect to vapor pressures than is the case in ordinary systems of appreciable surface tension.

In the case of the water interface $-\bar{p}(x) \cdot h \simeq 70$ dynes cm.$^{-1}$ at room temperature. If the thickness of the interface, h, lies between 10 and 1 Å, the mean negative pressure or mean stress intensity must lie between 7 and 70 hundred atmospheres. Evidently such large tensile stresses cannot be sustained in the more dilute regions of the fluid interface and hence practically the whole contribution to $\bar{p}(x)$ must come from the region where the fluid has high tensile strengths, high densities, and low compressibilities, i.e., from the liquid region of the interface. The maximum tensile stress in this region will exceed the mean tensile stress by factors depending on the relative thicknesses of these regions, the factors being the greater, the smaller the ratio of the thickness of the dense region to the thickness of the whole interface. In the case illustrated in Fig. 2*A* this factor is about five and correspondingly, the maximum tensile stress is between 35 and 3.5 thousand atmospheres for total film thicknesses between 1 and 10 Å. The film thickness as measured by the Rayleigh method will be the region of rapid change of refractive index and thus will be the region of rapid increase in specific volume. The thickness of the water interface as measured by Raman and Ramdas (15) using the Rayleigh method is about 1 Å. If the relative thicknesses of the various regions are as illustrated, the total film thickness is somewhat less than 10 Å and the maximum tensile stress of the order of 4×10^3 atmospheres. It seems very improbable that this figure can be much too low since it is comparable with the measured tensile strength of some metals.

The Laplace (10) method of calculating the tensile strength of liquids, neglecting the quite appreciable heat of "evaporation" of monomolecular layers, leads to values of the order of 25×10^3 atmospheres which are almost certainly too high. Further, owing to relaxation effects, it seems unlikely that the maximum negative stress sustained in the surface layers of a free surface will be as large as the tensile strength of the bulk liquid.

Thus it would appear that the maximum tensile stress in the surface region of liquid water is of the order of 10^3 atmospheres or less and hence that the thickness is of the order of 10 Å or more.

Surface Potential

Finally a word may be said concerning the factors giving rise to the surface potential $\Omega(x)$. The energy of a vapor is, of course, in general much greater than the energy of the corresponding liquid. The heat energy or TS energy change from liquid to vapor is somewhat greater than the internal energy change (i.e., by $p_0 \Delta v$). In order that a positive potential of position exist $\Delta(E+p_0v)/\Delta x$, p_0 constant, must exceed $T\Delta S/\Delta x$. We may ascribe the positive potential of position as being, in the main, due to an increase in energy without

a compensating increase in entropy. In the dense part of the interface where the fluid compressibility is small, any increase in volume, i.e., a small increase in mean distance of nearest neighbors, will give a large energy increase with little change in entropy. Proceeding further toward the gas the region is reached where fluid extensibility is large and the rapid increase in volume is accompanied by a large increase in entropy. In the case indicated in Fig. 2*A* the negative potential of position corresponds to a condition where the entropy of the nearly gaseous layers is larger with respect to their energy than prevails in the body of the gas. Ultimately these laminae correspond to states of "supersaturation" of the vapor. While laminae near the liquid or vapor side may be expected to have the normal equation of state of bulk liquid or gas, in the intermediate regions the relations between p, T, and μ or E, S, and v (per unit mass) will depend upon $f(x)$.

We may express the total potential of the surface, ω, as follows (cf. p. 985):

$$\omega = -\sum_{\delta v_{ai}} \frac{p_{ai}-p_0}{\overline{\rho_{ai}}|_{p_0-p_{ai}}} \cdot \rho_{ai} \cdot \delta v_{ai},$$

and since in this case $\delta v_{ai} = \sigma \delta x_i$ and $p_{ai} = p(x)$, we may write

$$\omega = \sigma \int_0^h \frac{[p_0-p(x)]}{\overline{\rho(x)}|_{p_0-p(x)}} \cdot \rho(x)\, \delta x$$

$$= c\sigma[p_0-\bar{p}(x)] \cdot h = c\sigma[poh+\gamma]$$

where $c \geqslant 1$. Since in cases where the surface tension is large, by far the greater mass of material lies in the regions where fluid compressibilities are small (i.e., where $c = 1$) and the pressures are of large negative magnitudes, ω is very nearly equal to $\gamma\sigma$. Thus γ is practically energy per unit surface. Where compressibilities are high throughout the surface region (near the critical temperature) ω will be greater than $\gamma\sigma$. Further, we should expect ω to consist partially in a decrease in entropy as well as an increase in energy. Thus near the critical region γ will not constitute a measure of surface energy.

III. ADSORPTION AND ADSORPTION HYSTERESIS

If in adsorption processes adsorbates and adsorbents retain their own individual properties, adsorbates at suitable temperatures and equilibrium pressures may be regarded as single component complex fluids as defined in Part I of this paper. In such cases all of the thermodynamic relations applicable to the single component complex are applicable to the adsorbates. Thus we have at once a method of calculating the mean volumetric pressures of the adsorbates from isotherm data, provided that the relevant isotherms represent paths of thermodynamic reversibility.

From Part 1, the mean volumetric adsorbate pressure will be given by

$$\bar{p}_a{}^v = \int_0^t \frac{\bar{p}_a}{\rho_1}\, dp_1 = \alpha p_1$$

and α can be calculated from isotherm data (6). The corresponding change in

reversible (elastic) volumetric mean state of stress of the solid can be shown to be related to the adsorbate stress by the following equation,

$$[3] \qquad v_a \cdot \bar{p}_a{}^v + v_c \bar{p}_c{}^v = (v_a + v_c) p_1$$

where v_a and v_c are the volumes of adsorbate and solid; v_a+v_c is the total volume of the porous body; $\bar{p}_a{}^v$ and $\bar{p}_c{}^v$ are the changes in volumetric mean states of stress of the void volume v_a and solid volume v_c, respectively, while p_1 is the change in hydrostatic state of stress of the whole porous body.

From Equation [3] we get at once

$$\bar{p}_c{}^v = (1+\phi-\phi\alpha)p_1$$

where $\phi = v_a/v_c$, $\bar{p}_a{}^v = \alpha p_1$, and $\bar{p}_c{}^v$ refers to the actual change in elastic state of stress of the adsorbent as a result of the adsorption reaction.[7]

If we are interested in comparing changes in linear dimensions of an adsorbent due to adsorption of gas, we can expect a correlation between these dimensional changes and its change in state of stress. The change in linear dimension per unit length will be a function of the change in linear average state of stress. If $\bar{p}_c{}^v$, the mean volumetric change of stress, were a measure of a change of hydrostatic stress (as would be the case if $\bar{p}_a{}^v$ were a uniform hydrostatic pressure equal to p_1), $\bar{p}_c{}^v$ would be the same as the change in linear average stress, $\bar{p}_c{}^l$. If in a given direction the solid were perfectly uniform in cross section and its surface field uniform in this direction, then $\bar{p}_c{}^v$ and $\bar{p}_c{}^l$ would be the same. However, in general, these quantities are not equal. Let us write

$$\bar{p}_c{}^v = p_1 + (\bar{p}_c{}^v)',$$
$$\bar{p}_c{}^l = p_1 + (\bar{p}_c{}^l)',$$

where $\bar{p}_c{}^v$ is considered as consisting of the hydrostatic stress p_1 due to the gas pressure and the additional stress $(\bar{p}_c{}^v)'$ due to interaction with the gas, i.e., due to its surface field. Similarly, $(\bar{p}_c{}^l)'$ is the additional linear stress due to interaction. While in the general case $(\bar{p}_c{}^l)'$ may be greater or less than $(\bar{p}_c{}^v)'$, if the surface forces are more or less uniform but the cross section variable, the ratio $(\bar{p}_c{}^l)'/(\bar{p}_c{}^v)'$ will be greater than unity and the ratio will be a constant descriptive of the structure of the adsorbent. Putting $(\bar{p}_c{}^l)' = K(\bar{p}_c{}^v)'$ we get $\bar{p}_c{}^l = (1+K\phi-K\phi\alpha)p_1$. Hence for isotropic solids which obey Hooke's law we can write

[7] *Following Gibbs (7) we can write for a solid or for an assembly of solid systems*

$$[A] \qquad dE = TdS = \sum\sum'[X_x' \, \delta(dx/dx') \, dxdydz$$
$$= TdS - \bar{p}_c{}^v.dv$$

where $\sum\sum'[X_x' \, \delta(dx/dx')]$ *and* $-\bar{p}_c{}^v$ *represent the generalized state of stress of the element of volume dxdydz. Thus* $-\bar{p}_c{}^v$ *represents the volumetric mean adiabatic strain energy per unit volumetric strain. The variation in Gibbs free energy corresponding to a variation in reversible state of strain, all other independent variables remaining constant, may be written* $dF = v_c d\bar{p}_c{}^v$ *where* v_c *is the total volume of the assembly of solid volumes. It is important to note that these relations imply that release of the stress (i.e. putting* $\bar{p}_c{}^v = 0$*) will be accompanied by the spontaneous release of the strain, the elements dxdydz becoming identical with the reference elements dx'dy'dz'. Thus Equation [A] cannot be used to describe strains beyond the elastic limit or irreversible strains. In the case of a so-called self-strained body, the state of strain of the body as a whole is to be taken as zero when the matter comprising the body is everywhere statistically at rest and no external forces are operative.*

[4] $$\delta l/l = -\tfrac{1}{3}\beta(1+K\phi-K\phi\alpha)p_1,$$

where l is the length of the sample and β[8] its compressibility. Where the dilation (or contraction) is isotropic we do not need to introduce the Poisson ratio. If the adsorbent is not isotropic both "β" and K will differ in different directions. In very extreme cases where K is very different in different directions, corrections of the Poisson contraction type will be necessary, and must be known or inferred for accurate correlation of experimental results.

It has been shown (6) that Equation [4] can be used to describe experimental data fairly well.[9] Accordingly the view that the adsorbate may be regarded as a single component complex appears to have considerable validity. The factor K in so far as it is determined by the solid structure will be a constant and thus have the same value for different gases at various temperatures. However, if the mechanism of adsorption changes, the value of K will change. Thus as we have shown (6) K will have different values for a given solid structure when the void volume is filled with liquid under a uniform pressure (e.g. extreme cases of capillary condensation) as compared with the case where the adsorbate is condensed in layers upon the surface.

Adsorption and Adsorption Hysteresis

In general when considerable adsorption occurs, the apparent potential of the surface is modified by molecular interactions of the adsorbate, i.e., the "potential" is a function of the equation of state of the gas. If the gas is condensable, liquid–gas interfaces will form and these interfaces introduce additional "potentials" of position which must be combined with the surface potentials. However, as long as the isotherm represents a path of thermodynamic reversibility, the mean volumetric pressure of the adsorbate will be given by Equation [2] of Part I.

The formation of adsorbate liquid–gas interfaces may lead to irreversible adsorption. The adsorption mechanism commonly referred to as "capillary condensation" is inherently a thermodynamically irreversible process. While the thermodynamics of hysteresis and reversible and irreversible adsorption have been treated by Hill (8) and others using statistical mechanical models, there are a number of inferences that can be drawn from purely thermodynamic considerations which are important and quite independent of any models.

The usual method of measuring adsorption isotherms is to expose the initially evacuated adsorbent to sources of constant gas pressure. When equilibrium is attained at each pressure, the thermodynamic potentials of the gas and adsorbate are the same, thus $\partial F/\partial m_1$, the partial molar free energy or thermodynamic potential of the adsorbate, equals dF/dm_1, the thermodynamic potential of the gas, and in each case,

$$\Delta F = \int_{m_1=0,m_2}^{m_1,m_2} \frac{\partial F}{\partial m_1}\,dm_1 = \int_{m_1=0}^{m_1} \frac{dF}{dm_1}\,.\,dm_1$$

[8]*This assumes that the compressibility of the solid is uniform and not changed by the adsorption. Even where the fundamental equations are strictly applicable, i.e., where the adsorbent changes* only *in state of stress, if the accompanying change in volume is large, β will be neither uniform nor constant.*

[9]*The validity of Equation [4] may be considered as a criterion for judging the validity of the potential theory of adsorption. If Equation [4] is valid the surface forces behave as a "potential".*

and in the case of the gas,

$$\Delta F = \int_0^{p_1} v_1 dp_1.$$

If the adsorbate behaves as a single component complex so that the volume of the adsorbate has a physical meaning,

$$\Delta F = \int_{\bar{p}_0{}^v=0}^{\bar{p}_0{}^v} v_a d\bar{p}_0{}^v.$$

However, all of these relations assume that v_1 or m_1 (the mass adsorbed) and hence that F and μ are known as functions of p_1 or that p_1 is known as a function of m_1. If the equilibrium gas pressure is anywhere a decreasing function of m_1, say at m_1', the system would be mechanically unstable when containing the mass m_1' and would spontaneously fill irreversibly to some value m_1''. The equilibrium pressures and hence the potentials corresponding with the filling would not be observable in this case under ordinary experimental conditions. Such mechanisms as the "Cohan" (3) or any other "capillary condensation" mechanism would lead to such results.

Suppose, for example, that the equilibrium gas pressure as a function of the mass adsorbed has the form shown in Fig. 3.[10] The line CF is the only line[11]

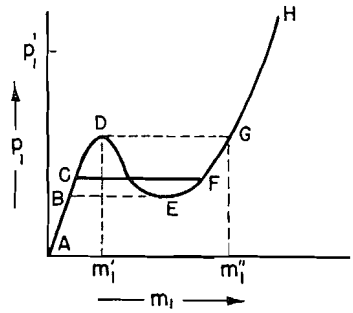

FIG. 3.

along which the mass may increase at constant pressure and give the correct value of ΔF. If the filling is premature, i.e., occurs at lower pressures along the line BE, the apparent observed value of ΔF from $p_1 = 0$ to some point $p_1 = p_1'$ will be too large, while if the filling occurs at higher pressures, e.g. along DG, the apparent value of ΔF will be too small.

If $p_1(m_1)$ has the form shown above, and the adsorbate behaves as a single component complex regardless of mechanism of adsorption, $\bar{p}_a{}^v$, the adsorbate pressure, will be a function of p_1 having the form shown in Fig. 4.[12] The point C of Fig. 4 corresponds with the line CF of Fig. 3. If the adsorption actually

[10] *$p_1(m_1)$ is assumed as measured in a small constant volume apparatus. $p_1(m_1)$ cannot, of course, have any such form when exposed to sources of m_1 at constant pressure.*

[11] *The position of CF is obtained from a plot of v_1 against p_1 using Maxwell's rule of equal areas (cf. Hill (8)).*

[12] *Assuming suitable relative magnitudes of corresponding gas and adsorbate densities.*

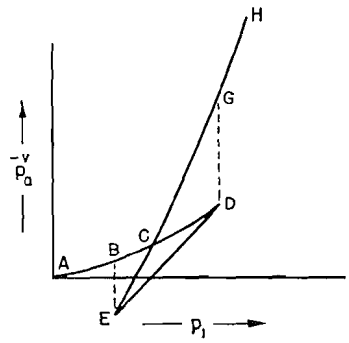

FIG. 4.

followed the curve of Fig. 3 the corresponding adsorbate pressures would follow the curves *AD*, *DE*, *EH* in Fig. 4. If the adsorption follows the path *ABEH* of Fig. 3 the corresponding path in Fig. 4 will be *ABEH*. If the adsorption follows *ADGH* of Fig. 3 the adsorbate pressure will follow *ADGH* of Fig. 4. In the former of the irreversible cases the adsorbate pressures will become negative, while in the latter case they will be positive throughout.

It is to be emphasized that $\bar{p}_a{}^v$, the adsorbate pressure, can only become negative on *adsorption* if the filling occurs at equilibrium pressures below the line *CF*. If the filling occurs along *CF* or at pressures above *CF*, $\bar{p}_a{}^v$ will be positive. In order that the adsorbent, if reasonably isotropic, contract on adsorption, i.e., on increasing the equilibrium pressures, the net adsorbate pressure must become negative and this can only occur if the filling occurs irreversibly along a path lying below *CF*. The fact that in some cases quite appreciable contractions are observed in the lower pressure regions of increasing pressure indicates that $p_1(m_1)$ is a decreasing function of m_1 in these lower pressure regions. This may be construed as evidence of the existence of "capillary condensation" or of some equivalent mechanism such as the "two-dimensional condensation" of Pierce (13).

When the filling of the adsorbate volume is irreversible whether above or below the line *CF* the observed "ΔF" (i.e. $\int_0^{p_1} v_1\, dp_1$) is not an accurate measure of the actual ΔF of the adsorbate and the application of thermodynamic relations based on such values of ΔF will be in error. Such errors are to be expected when liquid–vapor surface tensions are high.

While as pointed out by Hill (8) we would normally expect that irreversible transitions would be delayed (i.e. occur above *CF* of Fig. 3) the fact that contractions are observed on increasing pressure paths indicates that these transitions are premature (i.e., occur below *CF*). The absence of appreciable hysteresis in these regions together with the fact that contractions on desorption and adsorption are of much the same magnitude indicates that on *desorption* the transition is *delayed*. This apparently anomalous behavior may be due to the difference in sign of the temperature effect of adsorption and

desorption. Thus if the hypothetical constant pressure (p_s') line at the higher temperature lies below that at the lower temperature (e.g. if $\partial p_s'/\partial t$ is negative in these regions (cf. Coolidge (4)) the transition may occur, as expected, above the line corresponding to the actual temperature of the adsorbent, the adsorbate pressures being positive at the adsorbent temperature but becoming negative on cooling to the isothermal bath temperature. The reverse temperature effect would be expected on desorption and thus tend to equalize the adsorption and desorption states actually obtained.

In general, if the actual quantity of material per "site" "area" or "pore" for which $p_1(m_1)$ has the form of Fig. 3 is very small, filling of these sites irreversibly may be controlled by minor differences in experimental procedures. In addition there may be little apparent difference between adsorption and desorption isotherms, depending on the distribution of pressures corresponding to CF lines for the various sites. If, however, the quantity of material is large so that there are large differences in mass m_1 per site as CF is traversed, filling of these sites will in general occur at pressures above CF and the emptying (desorption) occur below CF. This will, in general, lead to marked hysteresis. In the extreme case of the filling of large void volumes, such volumes will fill with liquid only at pressures above saturation but the liquid will persist considerably below saturation if separated from the equilibrium gas by small pores. If appreciable areas of liquid–vapor surfaces having appreciable positive tensions are formed along paths of increasing pressures some irreversibility must be involved. Where a considerable mass of adsorbate is under a net negative pressure due, say, to capillary condensation and where this condition is reached along a path of increasing gas equilibrium pressures, the irreversibility will be large and ΔF quite different from the observed value of $\int_0^{p_1} v_1\, dp_1$. Under these circumstances $\bar{p}_0^v$ as measured by the observed value of αp_1 will be seriously in error and is apt to be of the wrong sign. The mean adsorbate pressure, in some cases, may be estimated by adding "Kelvin" adsorption and "reversible" adsorption, but in general these pressures are not additive quantities.

It is quite possible for the adsorption isotherm to represent a path of almost perfect thermodynamic reversibility from zero gas pressures up to saturation, and that a considerable part of the desorption branch also represents such a path even when the hysteresis is large, so that the two thermodynamically reversible branches are widely different. In this case ΔF and $\bar{p}_a^v$ can be correctly calculated from the observed data along the two reversible branches. Of course, the desorption curve must eventually meet the adsorption curve at lower relative pressures and hence involve considerable irreversibility in these regions of the desorption branch.

In general where the theoretically reversible continuous curve p_1 (m_1) has negative values of $\partial p_1/\partial m_1$, observed reversible isotherms will be stepwise.

Finally if p_1 (m_1) is nowhere for any site (area or pore) a decreasing function of m_1, ΔF will be given accurately by $\int_0^{p_1} v_1\, dp_1$ applied to the equilibrium gas

and $\bar{p}_a{}^v$ by $\int_0^{p_1} \bar{\rho}_a/\rho_1 \cdot dp_1$, or αp_1, quite regardless of whether liquid–vapor interfaces of any form are present or not. In such cases the "tension" of any liquid–vapor interfaces must be negative, i.e., pressures in these surfaces must be positive.

Adsorption Isotherm

The validity of the Polanyi (14) potential theory of adsorption is commonly based on the ability to calculate adsorption isotherms of a variety of gases at various temperatures from the characteristic curve for one representative gas. This, of course, involves the assumptions that the "potential" of the surface is the same for each gas and is independent of the temperature. It assumes that the equations of state of the gases concerned are known reasonably well. Although there are many exceptions, it is indeed surprising to what an extent these rather violent assumptions have been confirmed. Without any reservations concerning the nature of the potential field, if Equation [4] above is valid it constitutes strong evidence of the essential validity of the Polanyi theory. Thus our previously reported experimental results may be taken as confirmation of Polanyi's compressed film hypothesis. McBain's (12) "disproof" of the potential theory was based on considerations of adsorbate pressures. Some of the fallacies in McBain's "disproof" have been pointed out by Brunauer (2). Our results indicate that such considerations instead of contributing to a "disproof" of the compressed film hypothesis" lend very considerable support to it. Adsorption equilibrium is, of course, thermodynamic equilibrium. Accordingly, in its broadest sense, the "potential" theory is necessarily correct. We usually limit the "potential" theory of adsorption to processes where the adsorbate may be regarded as a single substance and thus distinguish "physical adsorption" from chemical reaction, and from solution. In its most restricted sense the "potential theory" is limited further to those cases where the "surface potential" is constant. The principal weakness of the potential theory of adsorption lies in its generality, since even in its most restricted form almost any type of adsorption isotherm can be consistent with it, as has been shown by many authors. Even if we assume that a condensable gas obeys the ideal gas law exactly, below the saturation pressure, and that above saturation it is an incompressible liquid of density unity, ignoring liquid–vapor interfaces a great variety of isotherm shapes can be generated depending on the form of the volumetric distribution of the "potential" of the surface region as well as upon the magnitude of the mean potential with respect to RT.[13]

[13]*Let $V(\Omega)\,d\Omega$ be the volume of the surface region having a potential lying between Ω and $d\Omega$, and let*

$$V(\Omega) = v_a/h)\ \Omega\, e^{-h\Omega}, \qquad 0 \leqslant \Omega \leqslant \infty.$$

Taking v_a as ½ cc. per gram of adsorbent and neglecting the concentration of vapor, one gets

$$x/m = \tfrac{1}{2}(p/p_s)^a[1 - \log(p/p_s)^a]$$

where $a = 2RT/\mu\bar{\Omega}$. Fig. 5 shows a plot of this equation for various values of a. Evidently to determine whether or not experimental points fall on such curves or on, say, a Freundlich curve, we must be very sure of the experimental data and resort to rather elaborate mathematical analysis of these data (cf. Honig (9)).

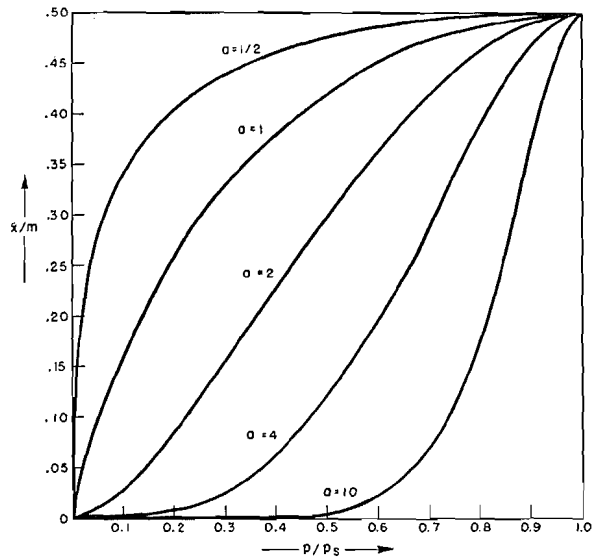

FIG. 5.

Since we cannot deduce an equation of state of a single homogeneous substance from purely thermodynamic considerations, it is evident that we cannot deduce an adsorption isotherm from such considerations. All so-called "thermodynamic" derivations of adsorption isotherms are based either directly or indirectly on assumed equations of state of both the equilibrium gas and the corresponding adsorbed material.

REFERENCES

1. BROWN, R. C. Proc. Phys. Soc. (London), 59: 429. 1947.
2. BRUNAUER, S. The adsorption of gases and vapors. Princeton University Press, Princeton, N.J. 1943.
3. COHAN, L. H. J. Am. Chem. Soc. 60: 433. 1938.
4. COOLIDGE, A. S. J. Am. Chem. Soc. 49: 708. 1927. (cf. S. Brunauer Ref. (2)).
5. FLOOD, E. A. and HUBER, M. Can. J. Chem. 33: 203. 1955.
6. FLOOD, E. A. and HEYDING, R. D. Can. J. Chem. 32: 660. 1954.
7. GIBBS, J. W. Collected works. Yale University Press, New Haven, Conn. 1948.
8. HILL, T. L. J. Chem. Phys. 15: 767. 1947.
9. HONIG, J. M. and ROSENBLOOM, P. C. Can. J. Chem. 33: 193. 1955.
10. LAPLACE. *In* J. R. Partington's An advanced treatise on physical chemistry. Vol. II. Longmans, Green and Co., London. 1951.
11. LEWIS, G. N. and RANDAL, M. Thermodynamics, McGraw-Hill Book Company, Inc., New York. 1923.
12. MCBAIN, J. W. and BRITTON, G. T. J. Am. Chem. Soc. 52: 2198. 1930.
13. PIERCE, C. and SMITH, R. J. Phys. & Colloid Chem. 54: 784. 1950.
14. POLANYI, M. Verhandl. deut. physik. Ges. 15: 55. 1916.
15. RAMAN, C. V. and RAMDAS, L. A. Phil. Mag. 3: 220. 1927.
16. ROWLEY, H. H. and INNES, W. B. J. Phys. Chem. 46: 537. 1942.
17. RICE, O. K. J. Chem. Phys. 15: 333. 1947.
18. SHUTTLEWORTH, R. Proc. Phys. Soc. (London), A, 62: 167. 1949.
19. TOLMAN, R. C. J. Chem. Phys. 16: 758. 1948.
20. WYLLIE, G. Proc. Roy. Soc. (London), A, 197: 383. 1948.

OXIDATION OF ALKENES BY MERCURIC SALTS[1]

By D. A. Shearer and George F Wright

ABSTRACT

The α-oxymercurials of cyclohexene, 2-methyl-1-phenylpropene-1, and the geoisomers of stilbene have been shown to be the intermediates in the oxidation of these alkenes by mercuric nitrate and other salts, usually in methanol. These intermediates are stable in the oxidation environment and their alkoxy groups appear intact in the oxidation product; indeed organomercurials without vicinal alkoxy groups are likewise oxidized. The reaction products from alkenes in methanol are 1,2-dimethoxyethanes, 1,1-dimethoxyethanes, and (with mercuric nitrate) 1-methoxy-2-nitroxyethanes, formation of the latter being most rapid. The oxidation is stereospecific, each geoisomer yielding its characteristic diastereomeric products. It is catalyzed by acids such as nitric acid but not by nitrate ion, though neither affect the ratio of products. This over-all second-order reaction, first-order in organomercurial and first-order in mercuric salt, becomes over-all first-order with mercuric acetate when it is catalyzed by boron fluoride. Combination of the catalyst with the organomercurial must be rate-controlling. The similarity of the oxidation and the acid decomposition reactions of organomercurials is discussed.

The oxidation of alkenes by mercuric salts is not a new reaction (3, 2, 25) but interest has recently been revived because of its application to sterol dehydrogenation (4, 5, 38, 39). A mechanism for the sterol dehydrogenation has been proposed involving a "mercurinium ion" (33) but it seems to be inconsistent with the observed formation of mercurous salts rather than metallic mercury. On the other hand, another mechanism has been suggested (11) for the oxidation of cycloalkene by mercuric salts (20, 36, 37) which does not take into account the equilibration: $2HgOAc \rightleftarrows Hg + Hg(OAc)_2$. Neither mechanism is consistent with the earlier observations that two equivalents of mercuric salt are involved in the oxidation of an alkene to an alkadiene or an alkenyl ester as well as to a glycol derivative (7) or rearrangement product (10, 30).

The consumption of two equivalents of mercuric salt per equivalent of alkene was confirmed by Brook and Wright (10) who also proposed a mechanism for the conversion of cyclohexene to formylcyclopentane not involving the intermediacy of an oxymercurial. These workers thought that an oxymercurial could not be involved because "hydroxymercuration with mercuric nitrate is not a significant reaction in water". We have now found this statement to be incorrect.

The error of Brook and Wright lay in dilution of their reaction aliquots with excess aqueous sodium chloride. The hydrochloric acid generated in this way decomposed the mercurial. Alternatively if cyclohexene is mixed with an equivalent each of mercuric nitrate and nitric acid (1 molar) and diluted after 10 min. into *one equivalent* of cold aqueous sodium chloride a maximal 80% yield of 2-hydroxy-1-chloromercuricyclohexane may be isolated. The equilibrium is shifted to afford a 63% yield when the system is 2 molar in nitric acid.

[1]*Manuscript received January 21, 1955.*
Contribution from the Chemical Laboratory, University of Toronto, Toronto, Ontario.

Kinetic studies* show that the oxidation of cyclohexene by two equivalents of aqueous mercuric nitrate proceeds through the intermediate mercurial, and that the over-all second-order kinetics are first-order in respect of mercurial and of mercuric nitrate, *i.e.* the oxymercuration of the alkene is so fast that the subsequent oxidation is rate-controlling. Table I shows, by comparison of Expt. 1 with Expts. 2, 3, and 4, that the rate is enhanced by addition of nitric acid, but the effectiveness does not increase in direct proportion to the concentration. Expt. 5 has been carried out with an excess of mercuric nitrate and the rate has been calculated by the expression

$$kt = [2.303/(a-b)] \log [b(a-x)/\{a(b-x)\}], \qquad [i]$$

where a is the concentration of mercuric salt *after mercuration is assumed to have occurred*, and b is the concentration of mercurial assumed to form instantly at zero time while $a-x$ and $b-x$ are corresponding values after certain time

TABLE I

REACTION OF CYCLOHEXENE WITH AQUEOUS MERCURIC NITRATE AT 25.0±0.1°C.

Expt. No.	Initial molarities			Molarities after mercuration			Second-order rate constant k(l. moles^{-1} min.$^{-1}$)	% Investigated
	$Hg(NO_3)_2$	C_6H_{10}	HNO_3	$Hg(NO_3)_2$	Mercurial	HNO_3		
1	.50	.25	—	.25	.25	0.25	.0259±.0008	71.8
2	.50	.25	1.0	.25	.25	1.25	.0473±.0041	60.6
							.0476±.0017	57.7
							.0489±.0036	60.1
3	.50	.25	1.5	.25	.25	1.75	.0505±.0014	62.0
4	.50	.25	2.0	.25	.25	2.25	.0520±.0043	69.8
5	.50	.125	1.0	.375	.125	1.125	.0447±.0043	75.0

intervals. Agreement of this rate constant with that obtained from systems containing a comparable amount of nitric acid (Expt. 2) shows that the rates are independent of cyclohexene concentration because the alkene is very rapidly converted to the mercurial. These results are valid for about 60% of the reaction, after which the rate falls off markedly. The deviation from simple second-order kinetics is not unexpected since the isolable yield of product, formylcyclopentane, has never exceeded 45% of theoretical.

This oxidation of cyclohexene is not limited to use of aqueous mercuric nitrate alone. The reaction proceeds in methanolic mercuric nitrate solution (two equivalents with one equivalent of both cyclohexene and nitric acid, each 0.25 molar) but 41 hr. are required for 65% of oxidation, in contrast to two hours for 60% of oxidation in the aqueous system. It may be significant that the intermediate methoxymercurial is a more stable compound than the hydroxymercurial which is intermediate in the aqueous system. The product from the methanolic system seems to be the dimethylacetal of formylcyclo-

**A referee has adversely but correctly questioned the value of kinetic data based on this complex reaction which is not in stoichiometric balance, and in which the limited analytical precision precludes wide variation in reagent concentration. Indeed the kinetic studies only have value in so far as the same conclusions can be drawn from experiments using four different alkenes.*

pentane according to the sluggish reaction with 2,4-dinitrophenylhydrazine. The same product is obtained when 2-methoxycyclohexylmercuric nitrate is treated with mercuric nitrate in methanol.

The conversion of cyclohexene to formylcyclopentane is not limited to use of the nitrate salt. A 45% combined yield of the aldehyde and cyclopentanecarboxylic acid is obtained with mercuric sulphate and molar sulphuric acid; the reaction is comparable in rate with that of the nitrate salt, but is difficult to follow kinetically because mercurous sulphate precipitates during the reaction. The reaction is much slower in aqueous mercuric benzenesulphonate containing benzenesulphonic acid, but the same products are obtained. Thus the anion can be varied within limitations (chloride is ineffective and acetate is unduly slow). But the mercury is necessary. Nitrate salts of barium, cadmium, copper II, iron III, lead, zinc, and bismuth are ineffective in the oxidation either of cyclohexene or of its oxymercurials.

The oxidation study has been extended to 2-methyl-1-phenylpropene-1 (I). This compound has previously been methoxymercurated. The 2-methoxy-2-methyl-1-phenylethylmercuric salt thus obtained has been converted by means of iodine or bromine to substances which essentially are oxidation products of the alkene (6). The action of methanolic mercuric nitrate on 2-methyl-1-phenylpropene-1 or 2-methoxy-2-methyl-1-phenylethylmercuric nitrate (VI) does not produce two of these products (3-phenylbutanone-2 and 2-methyl-2-phenylpropanal) but the third, 1,2-dimethoxy-1-methyl-2-phenylpropane (II), is obtained in fair yield. Additionally the mercuric nitrate oxidation yields a higher boiling compound, seemingly 2-methoxy-2-methyl-1-phenylpropyl nitrate (III), since it gives a positive diphenylamine test for nitrate and is reduced by zinc and acetic acid to a 71% yield of 2-methoxy-2-methyl-1-phenylpropanol-1 (IV, characterized as its *p*-nitrobenzoate). Although previously reported (35) this alcohol actually was unknown (6). However it has

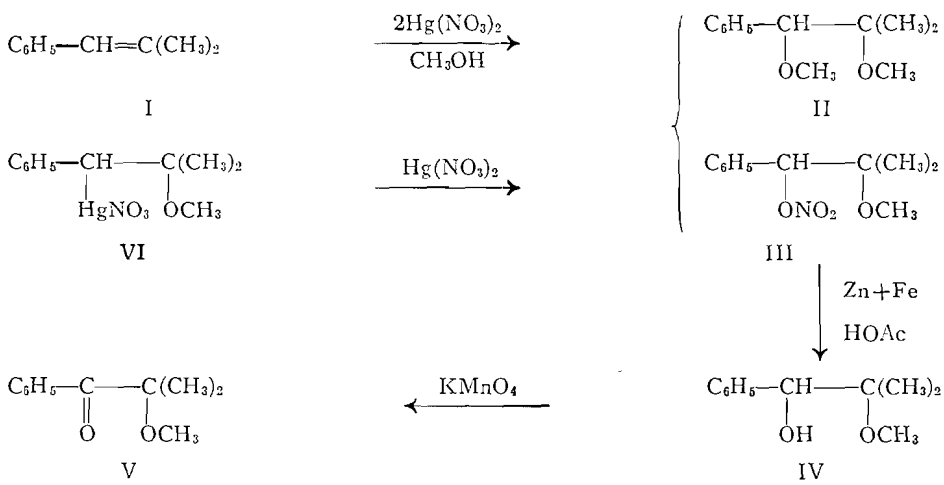

TABLE II

REACTION OF 1-PHENYL-2-METHYLPROPENE AND OF 1-PHENYL-2-METHOXY-2-METHYL-PROPYLMERCURIC NITRATE WITH MERCURIC NITRATE IN METHANOL

Expt. No.	Initial molarities				Time (hr.)	Yields, %			Ratio, nitrate ester: total yield
	Alkene	Mercurial	$Hg(NO_3)_2$	70% HNO_3		Dimethyl ether	Nitrate ester	Total	
1	.25	—	.52	.5	0.5	31	25	56	.45
2	.25	—	.52	—	20	50	28	78	.36
3	—	.25	.26	—	48	54	30	84	.36

now been identified by oxidation to the known 2-methoxy-2-methyl-1-phenyl-propanone (V).

The relative yields of II and III from either the alkene I or its mercurial VI are shown in Table II. The apparent augmentation of III is due to incompleteness of Expt. 1 and not to presence of nitric acid. It is shown clearly in Fig. 1 that the ratio of II to II+III is related to duration of reaction; i.e. nitroxylation is faster than methoxylation. Although nitric acid is ineffective in changing

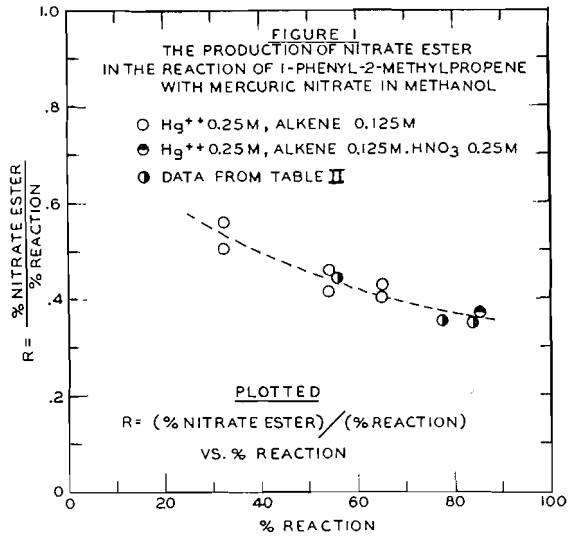

the ratio of nitrate ester to ether, it does increase the rate of reaction. This effect is shown by the first four experiments in Table III in which the rates have been calculated on the assumption that formation of the oxymercurial VI is virtually complete at the onset of oxidation. Then if b is the initial concentration of this mercurial VI and a is the initial concentration of mercuric

nitrate after mercuration, the rate may be calculated according to equation [i] where x is extent of oxidation at time t. The comparable rates of Expts. 3 and 4 indicate that this assumption is approximately true; further the data show that the oxidation is first-order in mercurial and first-order in mercuric nitrate. The effectiveness of nitric acid may be due to its acidity since the over-all second-order rate is enhanced markedly by addition of water to the system

TABLE III

REACTION OF 1-PHENYL-2-METHYLPROPENE WITH MERCURIC NITRATE IN METHANOL AT 25°C.

Expt. No.	Initial molarities			Molarities after mercuration			Molarity of other reagents	Second-order specific rate k (l. moles^{-1} min.$^{-1}$)	% Investigated
	$Hg(NO_3)_2$	Alkene	HNO_3	$Hg(NO_3)_2$	Mercurial	HNO_3			
1	.125	.0625	—	.0625	.0625	.0625	—	.103±.008	66.0
2	.25	.125	—	.125	.125	.125	—	.114±.010	68.6
3	.25	.125	.125	.125	.125	.250	—	.130±.010	62.5
4	.25	.083	.125	.167	.083	.208	—	.123±.016	86.6
5	.25	.125	—	.125	.125	.125	H_2O 5.6	.420±.020	83.6
6	.25	.125	—	.125	.125	.125	NO 0.01	.092±.013	51.5

(Expt. 5). It may be noted (Expt. 6) that nitric oxide is ineffective in alteration of the rate.

The complexity of the reaction is indicated by oxidation of 2-methyl-1-phenylpropene-1 with two equivalents of other mercuric salts. Aqueous mercuric sulphate in two days gives a 70% yield of 2-methyl-1-phenylpropanediol-1,2 and no sulphate ester although aqueous mercuric nitrate seems to yield a compound not the diol (to be reported in detail in the future). Methanolic mercuric trifluoroacetate in two days gives 50% of 1,2-dimethoxy-1-phenyl-2-methylpropane contaminated with a trace of 3-phenylbutanone-2. Methanolic mercuric acetate does not react appreciably with 2-methyl-1-phenylpropene-1 until 0.5 equivalent of boron trifluoride etherate is added. After the rapid oxymercuration is complete the subsequent formation of 1,2-dimethoxy-1-phenyl-2-methylpropane is first-order over-all ($k = 1.16 \times 10^{-3}$ min.$^{-1}$), as if co-ordination with the boron fluoride were the rate-determining step.

Some years ago the oxidation of the 2-methoxy-1,2-diphenylethylmercuric chlorides was reported (7) and these studies have now been elaborated by use of pure *cis*- and *trans*-stilbenes* as well as their oxymercurials. Each of the geoisomeric alkenes yields, besides the original alkene, three characteristic crystalline products as well as a common oil, 1,1-dimethoxy-2,2-diphenylethane (XIII), when each is treated with two equivalents of methanolic mercuric nitrate.

**The question of cis-stilbene purity has always been vexing. Although this geoisomer has usually been thought to melt below 0°, Brackman and Plesch recently (8) reported the melting point to be 5–6°, decreasing to 0.62° with age. Many years ago material of high melting point was available in our laboratory but subsequently could not be obtained. Now we have found that pure (40) cis-stilbene (which is best obtained without distillation of the mercurial decomposition product) is dimorphic. The form most readily obtained melts at −24 to −23° (uncorr.) but when this melt is seeded with cis-stilbene, m.p. 1.5–3.0° (uncorr.), it resolidifies and then melts entirely at the higher temperature.*

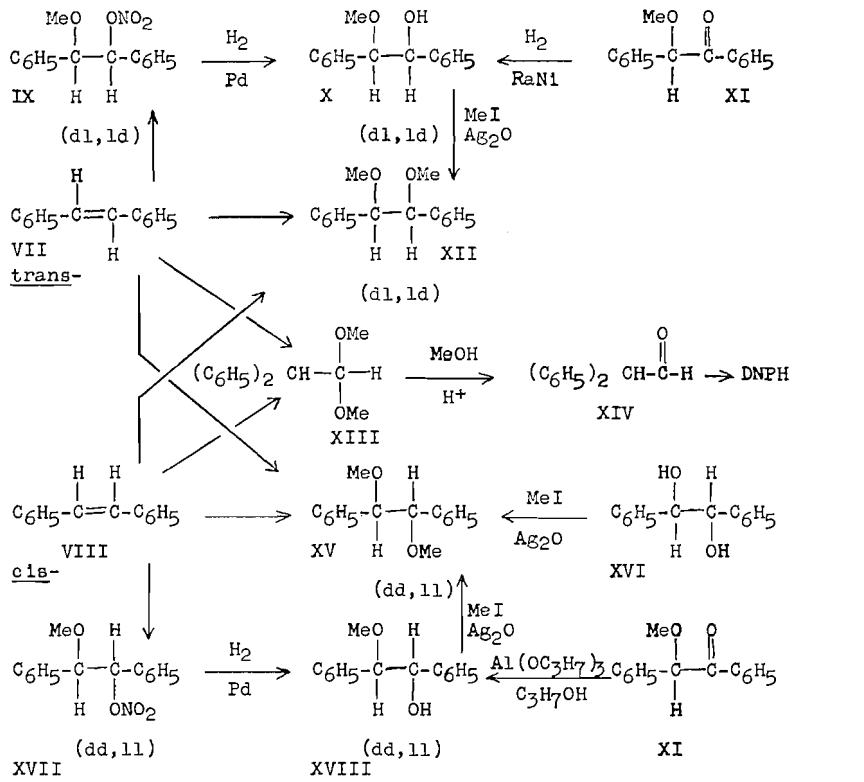

These products are listed below in the order that they are separated by elution from an alumina column by frontal displacement:

From *cis*-stilbene			From *trans*-stilbene
(VIII)	*cis*	(1) stilbene	*trans* (VII)
(XVII)	*dd,ll*	(2) 2-methoxy-1,2-diphenylethyl nitrate	*dl,ld* (IX)
(XII)	*dl,ld*	(3) 1,2-dimethoxy-1,2-diphenylethane	*dl,ld* (XII)
(XIII)		(4) diphenylacetaldehyde dimethylacetal	(XIII)
(XV)	*dd,ll*	(5) 1,2-dimethoxy-1,2-diphenylethane	*dd,ll* (XV)

The *cis*-stilbene is conveniently identified by methoxymercuration with mercuric acetate while *trans*-stilbene is identified by mixture melting point. The two diastereomeric nitrate esters, only one of which is obtained from each geoisomeric stilbene, were hitherto unknown. They have been identified by analysis and by catalytic hydrogenation with palladium-on-charcoal (24) to the diastereomeric 2-methoxy-1,2-diphenylethanols which in turn have been configurationally characterized. The (*dl,ld*)-methoxydiphenylethanol (X) (19), which also is obtained almost quantitatively by Raney nickel reduction of benzoin methyl ether (XI), is converted by Purdie methylation to the configurationally-known (*dl,ld*)-1,2-dimethoxy-1,2-diphenylethane (XII) (19). The (*dd,ll*)-methoxydiphenylethanol (XVIII), which may also be obtained by

fractional crystallization of the diastereomeric mixture from aluminum isopropoxide reduction of benzoin methyl ether (XI), is likewise related by methyl iodide – silver oxide methylation to the known (*dd,ll*)-1,2-dimethoxy-1,2-diphenylethane (XV) (13). Finally the 1,1-dimethoxy-2,2-diphenylethane (XIII), which obviously arises by 1,2-rearrangement in these systems, is identified by analysis and by conversion to the 2,4-dinitrophenylhydrazone of 2,2-diphenylethanal (XIV).

TABLE IV

A COMPARISON OF THE REACTIONS OF *cis*- AND *trans*- STILBENES WITH MERCURIC NITRATE IN METHANOL

Alkene	Time (hr.)	Per cent yields of products					Recovered alkene, %	Fraction of total products			
		dl,ld Ether	*dd,ll* Ether	Nitrate ester	Acetal	Total		*dl,ld* Ether	*dd,ll* Ether	Nitrate ester	Acetal
				(*dd,ll*)							
cis-	48	2.5	16.7	37.8	39.0	96.0	1.2	.025	.17	.39	.41
	11	1.0	19.1	34.2	34.6	88.9	3.7	.011	.21	.38	.39
				(*dl,ld*)							
trans-	40	21.8	2.3	33.6	20.6	78.3	10.9	.28	.029	.43	.26
	41	22.4	1.0	35.3	24.4	83.1	14.7	.27	.012	.42	.29

The yields of these oxidation products from *cis*- and *trans*-stilbenes are shown in Table IV. The stereospecificity which completely gives *dd,ll*-2-methoxy-1,2-diphenylethyl nitrate (XVII) from *cis*-stilbene and the *dl,ld* diastereomer (IX) from *trans*-stilbene is also preponderant for the 1,2-dimethoxy-1,2-diphenylethanes although a yield of 2–3% of the *dl,ld* diether (XII) arises from VIII. Also 1–2% of *dd,ll* diether (XV) arises from *trans*-stilbene. Both render stereospecificity incomplete. However in large part these oxidation products are characteristic of over-all apex–base (*trans*) addition to the geoisomers.

Recovery of alkene as shown in Table IV is much greater when *trans*-stilbene is oxidized, by contrast to the *cis* geoisomer. But this might be expected if the methoxymercurials are intermediates in these oxidations since the oxymercuration of *trans*-stilbene has been shown (40) to be less complete than that of *cis*-stilbene. Finally one may note in Table IV that the ratio (0.68) of acetal yields for *trans*- versus *cis*- stilbene is roughly inversely proportional to the ratio (0.72) of the diether yields from *cis*- versus *trans*- stilbene. By contrast the ratio of nitrate ester yields is 0.9. This contrast may be due to the more rapid formation of nitrate ester versus diether if methoxylation must compete with relatively slow 1,2-rearrangement.

Addition of nitric acid to the system comprising methanolic mercuric nitrate and each of the stilbenes accelerates reaction with the *cis* geoisomer and retards it with the *trans* form although, as is shown in Table V, the ratios of product yield are essentially unchanged. It is probable then that nitric acid exerts a dual effect by accelerating the oxidation of the intermediate oxymercurial but also by decreasing the equilibrium concentration of the oxymercurial. The favorable equilibrium of the *cis*-stilbene system favors the first effect, while the adverse equilibrium in the *trans*-stilbene system is accentuated owing to the latter effect.

TABLE V

ADDITION OF NITRIC ACID TO METHANOLIC SYSTEMS 0.26 MOLAR IN MERCURIC NITRATE AND 0.125 MOLAR IN STILBENES

Geo-isomer	Molarity HNO_3	Time, hr.	% Yield of products				Recovered stilbene, %	% of total product		
			Ether	Ester	Acetal*	Total		Ether	Ester	Acetal
cis	0	11	19	34	36	89	4	21	39	40
cis	0.25	4	19	34	35	88	6†	22	38	40
trans	0	40	22	34	23	79	11	28	43	29
trans	0.25	88	16	31	18	65	14	24	48	28
trans	0.50	88	14	27	19	60	14	24	45	31

**The small yield of nonpreponderant ether has been included with the acetal.*
†Recovered stilbene half trans.

TABLE VI

REACTION OF *trans*-STILBENE WITH MERCURIC NITRATE IN METHANOL EFFECT OF VARYING THE CONCENTRATION OF REAGENTS

Initial molarities		Time, hr.	Per cent yield of products				Recovered alkene, %	% of total product		
$Hg(NO_3)_2$	*trans*-Stilbene		Ether	Ester	Acetal	Total		Ether	Ester	Acetal
.13	.0625	47	22	32	22	76	14	29	42	29
.26	.125	40	22	34	23	79	11	28	43	29
.52	.25	46	21	32	25	78	5	26	42	32
.39	.125	48	24	33	21	78	2	31	42	27

The data of Table VI show that the ratios of products are practically unaffected by fourfold variation in the concentrations of *trans*-stilbene and mercuric nitrate in methanol. Likewise the augmentation of ionic strength by inclusion of lithium nitrate (Table VII) does not affect the yield of *dl,ld*-2-methoxy-1,2-diphenylethyl nitrate (IX) until the concentration is very large, but it does alter markedly the ratio of diether (XII) to acetal (XIII). This effect is not unexpected when a 1,2-rearrangement is involved, and the relatively slow methoxylation ought to be affected more than the rapid nitroxylation. The effect of added lithium nitrate does seem to show that methoxylation and, especially, nitroxylation are not directly dependent on the ionic species.

TABLE VII

REACTION OF 0.625 MOLAR *trans*-STILBENE AND 0.13 MOLAR MERCURIC NITRATE IN METHANOL WITH ADDED LITHIUM NITRATE

Molarity $LiNO_3$	Time, hr.	Per cent yields of products				Recovered alkene, %	% of total product		
		Ether	Ester	Acetal	Total		Ether	Ester	Acetal
0	40	22	34	23	79	11	28	43	29
0.0625	47	20	29	20	69	9	30	41	29
0.25	48	12	29	29	70	7	17	42	41
0.75	48	17	34	30	81	9	21	41	37
1.25	47	10	23	20	53	13	19	43	38
3.50	46	13	28	38	79	8	16	36	48

Before kinetic studies of the stilbene oxidation are considered it seems advisable to establish unequivocally that the oxymercurials are intermediate in the reaction. This has been done in three different ways of which the first is a

demonstration that organomercurials in general are oxidized by mercuric salts of oxy acids. When benzylmercuric nitrate in methanol is shaken with an equivalent of mercuric nitrate for 40 hr. the products are mercurous nitrate, a 46% yield of benzyl methyl ether, and a 15% yield of benzyl nitrate. Toluene in this environment is unaffected, so the reaction does not involve hydrolytic decomposition of the mercurial. Actually hydrolysis may be deleterious to the oxidation since the less stable *sec*-butylmercuric nitrate gives only a 5% yield of *sec*-butyl nitrate and no other product.

Secondly it can be shown that the oxymercurial is formed rapidly under the conditions of oxidation. When *cis*-stilbene is treated with two equivalents of a 0.125 molar methanolic solution of mercuric nitrate for 10 min. and then drowned in cold dilute aqueous sodium chloride the mercurous salt which is formed indicates that 8–9% of oxidation already has occurred, but the remainder of the precipitate (washed with hexane to remove stilbene) is 2-methoxy-1,2-diphenylethylmercuric chloride in 78% yield. It is believed that this yield represents an equilibrium concentration since it is depressed to 74% and to 73% by inclusion into the reaction system of two or four equivalents of nitric acid; these additions only increase the amount of oxidation to 10%.

Thirdly we have demonstrated that the oxymercurial rather than the alkene is the species which undergoes oxidation. When α-2-methoxy-1,2-diphenylethylmercuric nitrate (XIX) is treated with mercuric nitrate in ethanol a 39% yield of (*dd*,*ll*)-2-methoxy-1,2-diphenylethyl nitrate (XVII) is obtained, as compared with the 35% yield of this diastereomer obtained by oxidation of *cis*-stilbene from which the α mercurial is derived. If oxidation of the mercurial

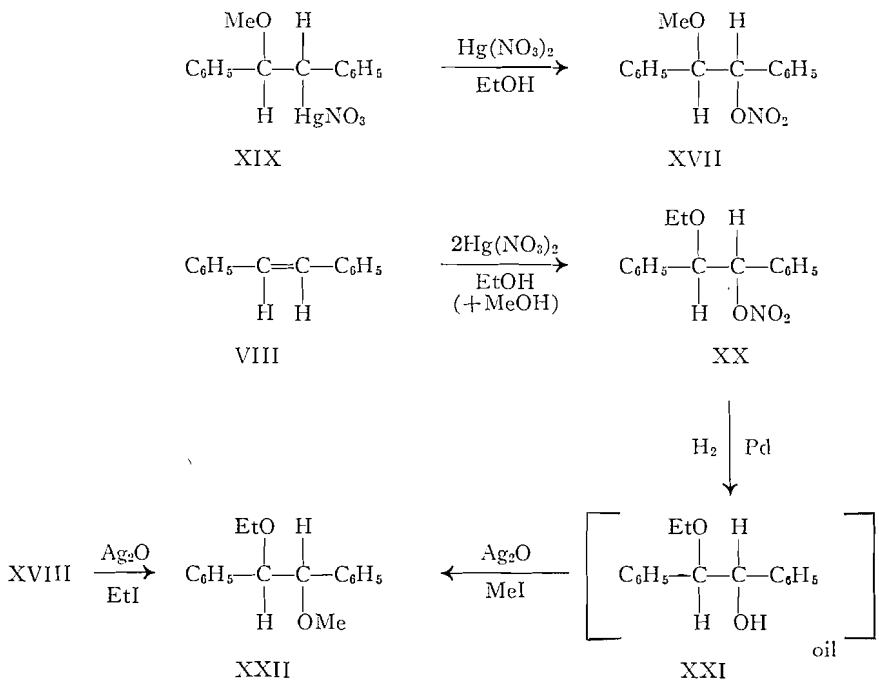

had involved appreciable reversion to the alkene the product would have been the ethoxy nitrate (XX). The proof is valid unless the single equivalent of methanol which would be formed by decomposition of the methoxymercurial to the alkene were to be selected for the oxidation process from a large excess of ethanol. This doubt has been dispelled by treatment of *cis*-stilbene with two equivalents of mercuric nitrate in ethanol containing one equivalent of methanol. The product in 25% yield is evidently (*dd,ll*)-2-ethoxy-1,2-diphenylethyl nitrate (XX) since it is reduced by palladium-on-charcoal to ammonia and an oil. This oil must be (*dd,ll*)-2-ethoxy-1,2-diphenylethanol (XXI) since treatment with methyl iodide and silver oxide produces (*dd,ll*)-1-ethoxy-2-methoxy-1,2-diphenylethane (XXII), identical according to mixture melting point with that prepared by ethylation with silver oxide and ethyl iodide of (*dd,ll*)-2-methoxy-1,2-diphenylethanol (XVIII). Therefore it seems to be definite that the alkene reacts with two equivalents of mercuric nitrate, first to form the oxymercurial, the carbon–metal linkage of which is replaced by nitroxylation (and presumably by alkoxylation) without involvement of the vicinal oxy linkage.

Thus for kinetic study the oxidation of *cis*-stilbene by alcoholic mercuric nitrate may be described by two equations:

$$\underset{\text{VIII}}{\text{Alkene}} + \underset{A}{\text{Hg(NO}_3)_2} + \text{ROH} \underset{k_1}{\overset{k_2}{\rightleftharpoons}} \underset{\text{XIX}}{\text{mercurial}} + \text{HNO}_3 \qquad \text{[ii]}$$

$$\text{XIX} + \underset{A'}{\text{Hg(NO}_3)_2} + \text{ROH} \xrightarrow{k} \underset{B}{\text{Hg}_2\text{(NO}_3)_2} + (\gamma)\text{HNO}_3 + \begin{pmatrix}\text{XIII}\\ \text{XV}\\ \text{XVII}\end{pmatrix} \qquad \text{[iii]}$$

where γ is the fraction of nitrate ester (XVII) to total products. No general integrated equation has been devised (29) to express the kinetic behavior of such a reacting system, especially in consideration of the observed catalytic effect of nitric acid. However the knowedge that $k_1 \gg k_2 \gg k$ in the reaction with *cis*-stilbene makes this system amenable to study if the effect of nitric acid is neglected by examination of the early stages of reaction. This expedient is probably workable because the catalytic effect of nitric acid opposes its equilibrium-depressant effect in the first reaction. Then the kinetics may be described in terms of [iii] and if a is the initial concentration of A' and b is the concentration of XIX (or A) the second-order relationship of equation [i] is applicable.

However since k_1 is not infinitely larger than k_2 it is apparent that analytically it is better to follow the appearance of mercurous salt rather than the disappearance of mercuric salt. This preference is exemplified in Fig. 2 (see also Table XIII) wherein the combined rate of oxymercuration (reaction [ii]) and oxidation (reaction [iii]) is not apparent as a second-order relationship in $1/M$ but may be so interpreted in $1/P$. But this expedient is ineffective in the oxidation of *trans*-stilbene in methanol for several reasons. Firstly the system is not initially homogeneous. Secondly it is probable that k_2 actually is larger than k_1 and both are comparable with k. Nevertheless a roughly determined rate constant (0.017 l. moles^{-1} min.$^{-1}$) has been calculated showing

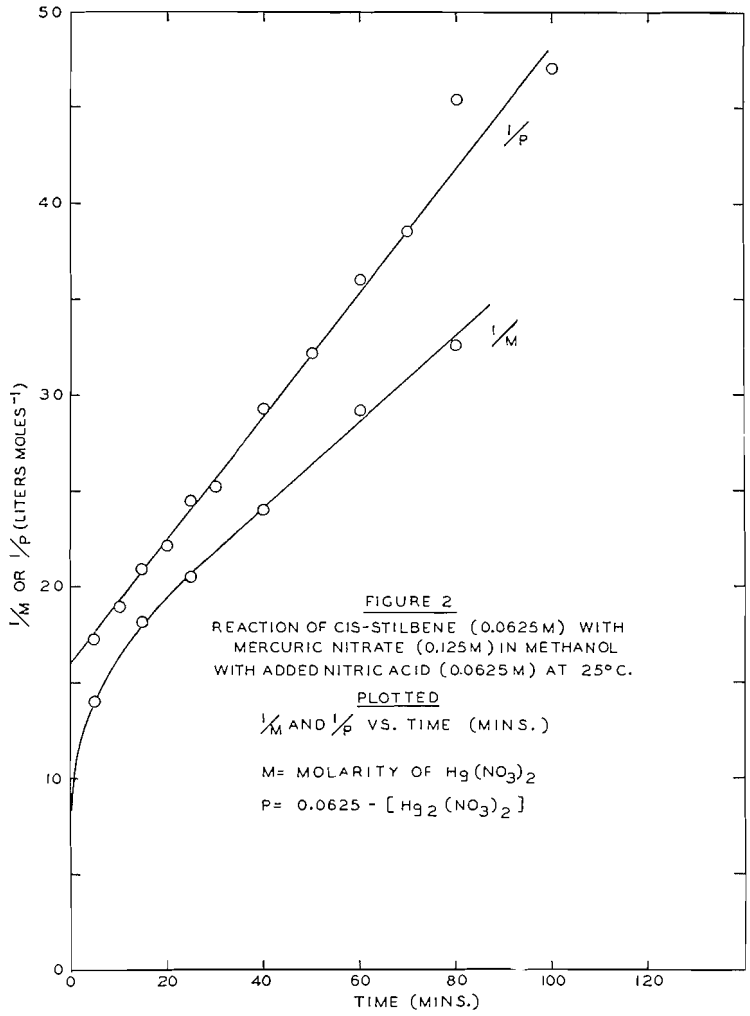

FIGURE 2
REACTION OF CIS-STILBENE (0.0625 M) WITH MERCURIC NITRATE (0.125 M) IN METHANOL WITH ADDED NITRIC ACID (0.0625 M) AT 25°C.
PLOTTED
$1/M$ AND $1/P$ VS. TIME (MINS.)
M= MOLARITY OF $Hg(NO_3)_2$
P= 0.0625 - $[Hg_2(NO_3)_2]$

at least that the over-all oxidation of the *trans*-isomer is slower than that of the *cis* form. Since mercurials easily decomposed according to reaction [ii] are usually oxidized more easily according to reaction [iii] it would seem that the slow rate of *trans*-stilbene oxidation is due to an especially unfavorable equilibrium in reaction [ii].

Probably because the reaction becomes more quickly homogeneous, and possesses a more favorable equilibrium in the mercuration step (like reaction [ii]), the kinetics of the oxidation of *trans*-stilbene by mercuric acetate in methanol (7) are more amenable for study than oxidation with mercuric nitrate though both mercurous nitrate and acetate are separable from mercuric salt. Titration of unchanged mercuric acetate after chloroform extraction of mercurial (41) provides concentration values of A' (reaction [iii]) from which reciprocals are plotted versus time (Curve A, Fig. 3). Despite the marked initial curvature characterizing the slow attainment of a steady-

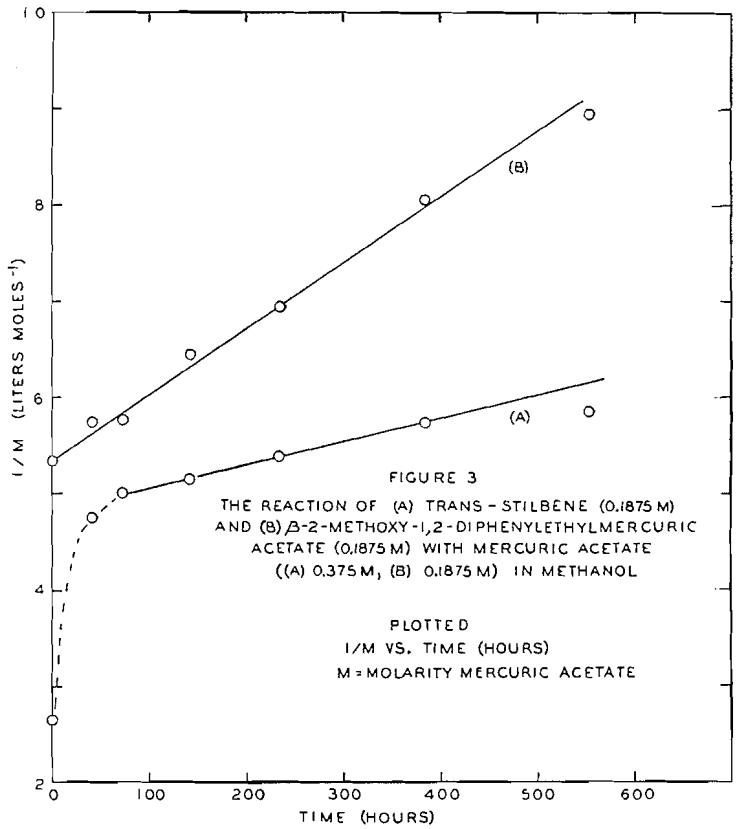

state concentration of β-2-methoxy-1,2-diphenylethylmercuric acetate the remainder of the curve is sufficiently linear for calculation of 0.39×10^{-4} l. moles^{-1} min.$^{-1}$ as a second-order specific rate constant. However a better evaluation is possible since it is realized that the mercurial is an intermediate in the oxidation. Direct reaction of β-2-methoxy-1,2-diphenylethylmercuric acetate (from the chloromercurial and silver acetate) with one equivalent of methanolic mercuric acetate occurs according to Curve *B*, Fig. 3, the slope of which gives a realistic second-order rate constant of 1.2×10^{-4} l. moles^{-1} min^{-1}.

The products of the reactions of *cis*- and *trans*-stilbenes, as well as their characteristic oxymercurials, with methanolic mercuric acetate (containing boron fluoride etherate) are shown in Table VIII. The results, obtained by chromatographic separation, resemble those obtained with mercuric nitrate since *trans*-stilbene (VII) yields chiefly (*dl*,*ld*)-1,2-dimethoxy-1,2-diphenylethane (XII) together with a small amount of the (*dd*,*ll*)-diastereomer (XV), while the converse distribution of diastereomeric diethers is obtained from *cis*-stilbene. However it is notable that the ratio (*ca.* 4 : 1) of (*dd*,*ll*) to (*dl*,*ld*) diastereomer obtained from *cis*-stilbene is somewhat smaller than the ratio (*dl*,*ld*) to (*dd*,*ll*) (*ca.* 21 : 1) of these diastereomers obtained from *trans*-stilbene and methanolic mercuric acetate. Similar but lesser differences (diastereo-

meric ratios of *ca.* 7 : 1 for *cis*-stilbene and *ca.* 15 : 1 for *trans*-stilbene) are found (Table IV) for reactions of comparable duration with methanolic mercuric nitrate. Since the reactions with mercuric acetate are slower than those

TABLE VIII

REACTION OF *cis*- AND *trans*-STILBENES AND OF α- AND β-2-METHOXY-1,2-DIPHENYLETHYLMERCURIC ACETATES IN METHANOL WITH 0.02 *M* BORON FLUORIDE ETHERATE

Initial molarities			Time, hr.	% Yields of products				Recovered alkene, %	% of total products		
$Hg(OAc)_2$	Mercurial	Stilbene		(*dl*,*ld*) Diether	(*dd*,*ll*) Diether	Acetal	Total		(*dl*,*ld*) Diether	(*dd*,*ll*) Diether	Acetal
cis-Stilbene											
.10	—	.05	58	5.2	22.6	8.0	35.8	6.6	15	63	22
.05	.05	—	118	6.2	28.4	13.6	48.2	8.3	13	59	28
trans-Stilbene											
.10	—	.05	117.5	44.4	2.1	14.0	60.5	12.2	73	35	24
.05	.05	—	146	41.2	1.9	22.7	65.8	6.4	63	3	34

utilizing mercuric nitrate, and (as will be explained below) when the highly acidic methoxytrifluoboric acid is present, the systems described in Table VIII will suffer *cis–trans* isomerism (9). Although the exact position of the *cis–trans* equilibrium between the stilbenes is still in doubt (12) it is at least 95% *trans*. It might then be expected that, despite the faster rate of *cis*-stilbene mercuration, the preponderance of *trans*-stilbene following small extents of geoisomerization would tend to accentuate the diastereomeric ratio of (*dl*,*ld*) to (*dd*,*ll*). Evidence for some geoisomerization during the oxidation is provided by the observation that *cis*-stilbene recovered from the oxidations contains some *trans*-isomer. In consequence of these observations it is conceivable that the oxidation reaction is entirely stereospecific, and the nonstereospecific product is a consequence of side-reaction during experiments of long duration. Significant to this argument are the yields of 1,1-dimethoxy-2,2-diphenylethane (Table VIII) which are about the same for *cis*- and *trans*-stilbenes in these slow reactions with mercuric acetate, although they are quite different for the more rapid reactions with mercuric nitrate (Table IV).

It has been noted that the experiments described in Table VIII include boron trifluoride etherate (the methylate behaves identically) which has been shown previously (7) to accelerate oxidation of alkenes and their mercurials by mercuric acetate. The type, if not ratios, of products is the same if the catalyst is not used, but of course the yields are meager and are contaminated with products of side-reactions caused, for example, by the slow oxidation of methanol by mercuric acetate which takes place in absence of alkenes. However we have necessarily assumed, because of experimental difficulties of isolation, that the kinetic results of the uncatalyzed reaction of stilbenes with mercuric acetate give about the same amounts of products as those which have been isolated from reactions which are catalyzed with boron fluoride.

The kinetic behavior of the boron-fluoride-catalyzed reaction is quite different from that of the uncatalyzed reaction. In presence of the catalyst the reaction is first-order over-all up to at least 70% of completion. This behavior

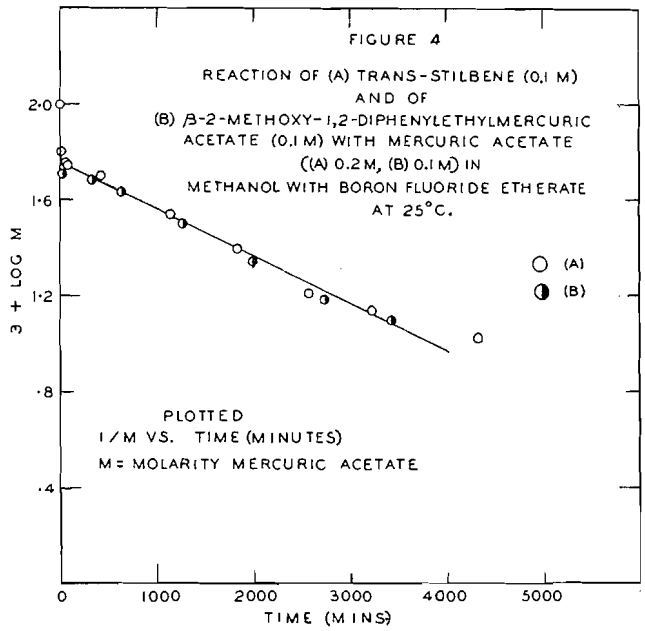

is evident in Fig. 4 where the logarithm of mercuric acetate concentration has been plotted against time of reaction with *trans*-stilbene (Curve *A*) and its mercurial (Curve *B*) in presence of boron fluoride. The linearity is that expected of a first-order reaction although the initial stages indicate that oxymercuration, though rapid, does not go to completion; conversely the oxymercurial when used initially seems to decompose reversibly so as to regenerate mercuric acetate. This behavior is shown more clearly in Fig. 5, describing reaction of β-2-methoxy-1,2-diphenylethylmercuric acetate in methanol with boron fluoride alone. Disappearance of mercuric and appearance of mercurous salt have been determined simultaneously. At first there is a rapid appearance of mercuric acetate which then remains relatively constant at a ratio of 2 $Hg(OAc)_2$: 8 oxymercurial until, after about five hours, it begins to increase. The increase undoubtedly is due to shifting equilibrium caused by acetic acid generated by the oxidation which, according to the generation of mercurous salt, is proceeding continually.

The significance of the catalyst in respect of the first-order kinetics is shown in Table IX, where the rate is found to be directly proportional to the boron fluoride concentration. Also significant is the fact that the first-order oxidation rate of either *cis*-stilbene or its derivative, α-2-methoxy-1,2-diphenylethylmercuric acetate, is approximatey the same as that of *trans*-stilbene or the β-methoxymercurial. This similarity is shown by comparison of Expts. 1 and 2, Table X, with the rate constant (5.56×10^{-4}) for the comparable experiment with β-2-methoxy-1,2-diphenylethylmercuric acetate in Table IX. Expts. 3 and 4, Table X, also are comparable, although the recorded rate constants are different because Expts. 3–7 were analyzed for mercurous salt

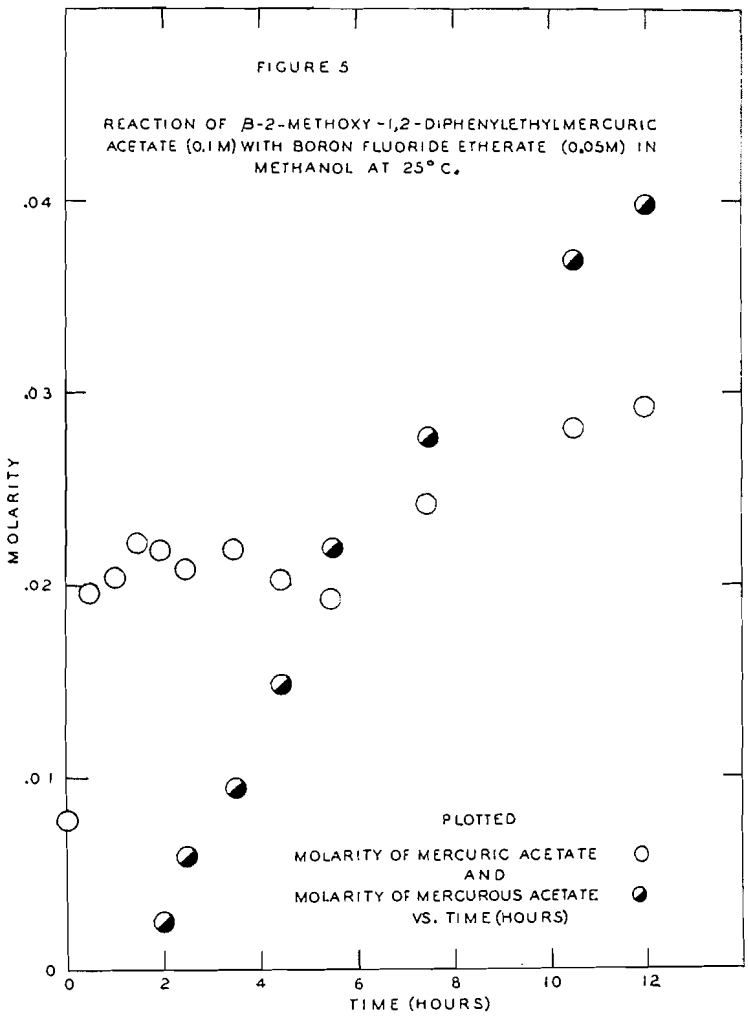

TABLE IX

REACTION OF β-2-METHOXY-1,2-DIPHENYLETHYLMERCURIC ACETATE (0.1 *M*) WITH MERCURIC ACETATE (0.1 *M*) IN METHANOL WITH BORON FLUORIDE ETHERATE AT 25°C.

Molarity of BF_3.etherate(M_{BF_3})	First-order spec. rate k (min.$^{-1}$)	k/M_{BF_3}
.03	3.22×10^{-4}	.0107
.04	5.56	.0139
.06	7.76	.0129
.08	9.29	.0116

TABLE X

REACTION OF *cis*-STILBENE WITH MERCURIC ACETATE IN METHANOL CATALYZED BY BORON FLUORIDE AT 25°C.

Expt. No.	Initial molarities			Molarities after mercuration			First-order k (min.$^{-1}$)	Per cent investigated
	$Hg(OAc)_2$	*cis*-Stilbene	$BF_3.Et_2O$	$Hg(OAc)_2$	Mercurial	HOAc		
1	—	—*	.02	.05	.05	—	$5.05\pm.25\times10^{-4}$	79
2	.1	.05	.02	.05	.05	.05	$5.68\pm.30$	75
3	.2	.1	.02†	.1	.1	.1	$3.95\pm.05$	66
4	.2	.1	.02	.1	.1	.1	$4.08\pm.10$	69
5	.1	.05	.02	.05	.05	.05	$4.62\pm.11$	72
6	.25	.1	.02	.15	.1	.1	$4.70\pm.17$	70
7	.20	.05	.02	.15	.05	.05	$6.77\pm.36$	88

**Mercurial used instead of alkene.*
†BF_3 gas in methanol.

while mercuric acetate was determined in the first two experiments. The rate constants are more accurate when calculated from mercurous salt analyses.

Inspection of Expt. 7, Table X, shows that first-order kinetics no longer are valid when the molar ratio of mercuric acetate to *cis*-stilbene becomes large. The same type of deviation is observed when the ratio of mercuric acetate to β-2-methoxy-1,2-diphenylethylmercuric acetate is 2 : 1 rather than 1 : 1 (k = 5.35 versus 4.9×10^{-4} min.$^{-1}$). Additionally the apparent rate seems to increase as the reactions with excess of mercuric acetate proceed. These behaviors are exemplified by comparison of the detailed kinetic data of Expt. 4 (and Expts. 6 and 7 are similar) with Expt. 7 in Table X. The comparison is delineated in Table XI in terms of calculated first- and second-order rate constants. No satisfactory integral order can be defined for Expt. 7, in contrast to the first-order kinetic agreement for Expt. 4.

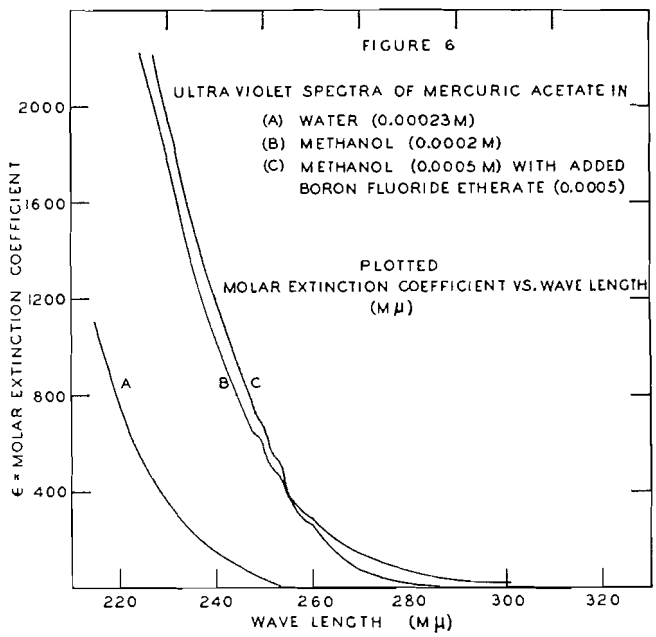

TABLE XI

THE REACTION OF *cis*-STILBENE WITH MERCURIC ACETATE IN METHANOL WITH ADDED BORON FLUORIDE ETHERATE AT 25°C.

Expt. 4 Mercuric acetate, 0.1 *M*; mercurial, 0.1 *M*			Expt. 7 Mercuric acetate, 0.15 *M*; mercurial, 0.05 *M*		
Time (min.)	k_1 (min.$^{-1}$)	k_2(l. moles^{-1} min.$^{-1}$)	Time (min.)	k_1 (min.$^{-1}$)	k_2 (l. moles^{-1} min.$^{-1}$)
130	4.61×10^{-4}	4.82×10^{-3}	120	4.13×10^{-4}	4.06×10^{-3}
250	4.33	4.59	240	6.53	4.41
380	4.24	4.56	370	6.44	4.45
460	4.05	4.45	465	6.50	4.56
590	4.01	4.53	695	6.32	4.51
710	4.01	4.64	870	6.61	4.76
880	3.92	4.69	1420	6.90	5.25
1430	3.94	5.30	1780	7.34	5.75
1790	4.09	6.02	2850	7.50	6.26
2865	4.10	7.83			

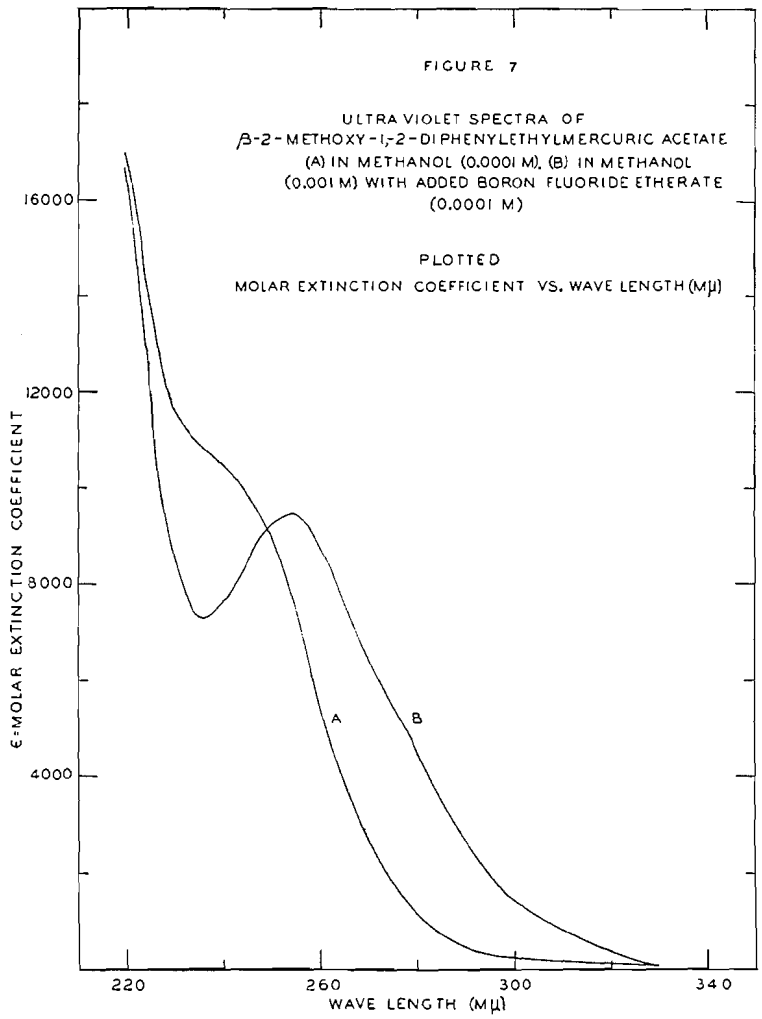

In order to evaluate these results the ultraviolet spectra of some of these systems have been examined. It may be seen in Fig. 6 that aqueous mercuric acetate (0.00023 *M*) is as transparent as water at wavelengths longer than 255 mμ but methanolic mercuric acetate (0.0005 *M*) begins to absorb at 300 mμ and is completely opaque at 220 mμ. The addition of boron fluoride etherate (0.0005 *M*) to this latter solution does not change its absorption. On the other hand it is seen in Fig. 7 that methanolic β-2-methoxy-1,2-diphenylethylmercuric acetate (0.0001 *M*) begins to absorb at about 340 mμ and the absorption rises steadily until a single inflection is found (E_{molar} = 11,000) at 240 mμ. Addition of boron fluoride etherate (0.001 *M*) to this solution has a profound effect. The absorption rises more steeply from 340 mμ to a peak at 253 mμ (E_{molar} = 9500) and then dips to a trough of transmission (E_{molar} = 7000) at 235 mμ. The α-2-methoxy-1,2-diphenylethylmercuric acetate in methanol shows essentially the same behavior (Fig. 8). However its solution containing

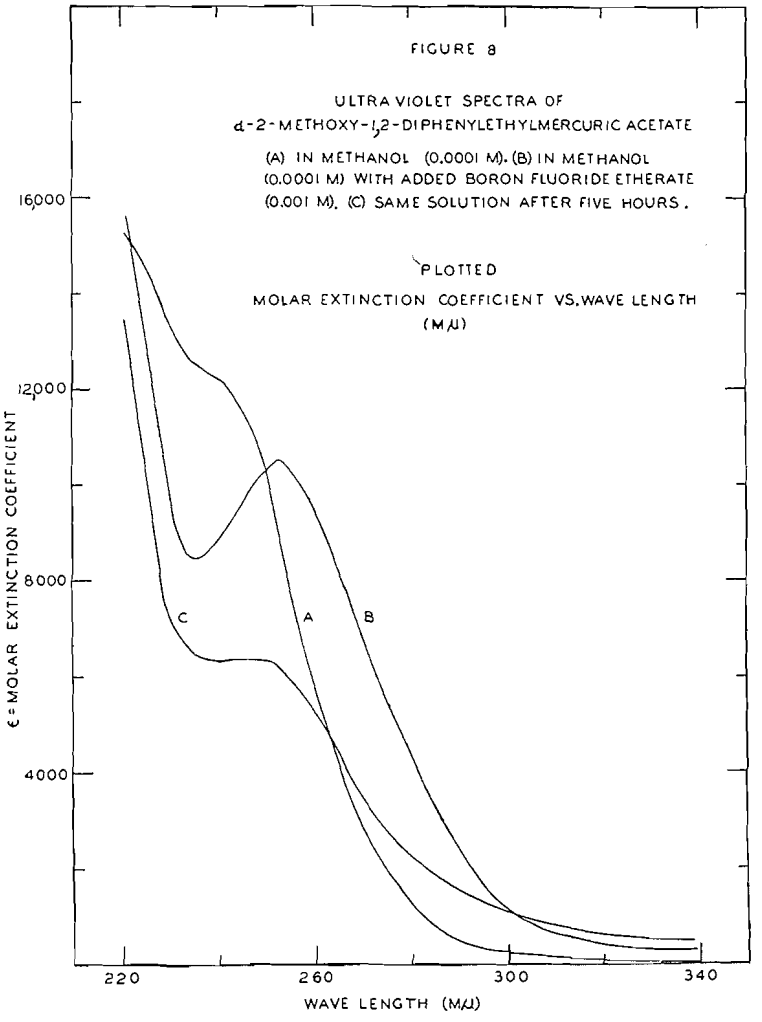

10 equivalents of boron fluoride has been examined further, with respect to time. After five hours it is found that the peak has almost disappeared, as if a complex were decomposing to give substances of greater transparency than those contained in the original system. These substances cannot include appreciable amounts of the stilbenes since the *cis*-isomer absorbs strongly at 270 mμ while the *trans* form absorbs at 300 mμ.

It would seem from these data that the combination of boron fluoride with acetate involves the rate-controlling step, which should then be first-order. Furthermore, since the ease of oxidation of alkenes (and of course the intermediate oxymercurial) is greater with salts of strong acids rather than weak ones, the boron fluoride must be creating a salt of a strong acid. The creation of an u.v. absorption region when boron fluoride is added to the oxymercurial, and the disappearance of this band at a rate commensurate with that of oxidation, indicates the reaction:

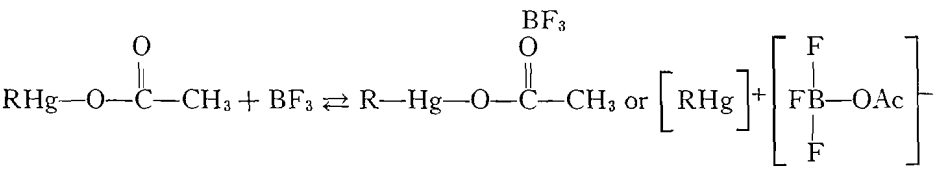

but the deviation from first-order kinetics with consequent acceleration when mercuric acetate is in large excess ought to involve the reaction:

$$AcOHgOAc + BF_3 \rightleftarrows [AcOHg]^+ [BF_3OAc]^-.$$

Thus the rate of oxidation by mercuric salts seems to depend on the acid involved with the mercury and, especially, with the intermediate organomercurial. However it is doubtful that the acid is functioning in an ionic form. The effectiveness of acids (HNO_3, H_2SO_4 > $HClO_4$ > $C_6H_5SO_3H$, CF_3COOH) does not correspond with the dissociation of these acids in water. Certainly in media such as ethanol, nitric acid is largely non-dissociated (15, 16, 21, 28). The ion concentration would have to be very low, but in this circumstance the reaction would have to be very sensitive to added ions. It has been shown (Table VII) that the oxidation as such is unaffected by addition of lithium nitrate. From these considerations it would seem that the acid and its salts were not active in the oxidation as free ions.

The effect of acid in the oxidation has an additional significance. It is known, and has further been demonstrated in the present report, that acids cause decomposition of oxymercurials, which then revert to the parent alkene. But those oxymercurials which are most stable toward acid decomposition are also most difficult to oxidize. For example, hydroxyethylmercuric nitrate and 2,2′-dinitratomercuridiethyl ether (which actually can be prepared from ethylene in acid solutions of mercuric salts) are recovered unchanged after treatment with mercuric nitrate in methanol.

Of course the hydrolytic decomposition and the oxidation of oxymercurials have other characteristic resemblances. Both seem to be stereospecific in the

sense that diastereomeric oxymercurials tend to revert by acid decomposition to the geoisomer from which they were originally derived, while oxidation gives derivatives characteristic of this geoisomer. This would seem to preclude the postulation of a carbonium ion intermediate in either reaction. The demonstration in the present report that the vicinal alkoxy group is not involved directly in the oxidation renders improbable the participation of an epoxonium ion. It would seem likely that molecular species are operative in both reactions either by ion-pair exchange (giving HgX^+ and X^- in the acid decomposition versus HgX^- in the oxidation) or by homopolar exchange giving HgX radicals from which mercuric or mercurous salts could be formed.

EXPERIMENTAL*

Acidic Hydroxymercuration of Cyclohexene

A solution 0.5 molar in mercuric nitrate and 1.0 molar in nitric acid was treated with cyclohexene equivalent to the mercuric salt. After 10 min. the system was poured into 0.1 molar aqueous sodium chloride equivalent to the cyclohexene. The yield of α-2-hydroxycyclohexylmercuric chloride, m.p. 145–147°, was 79%. A 20-min. experiment gave the identical yield. When the reaction system was 1.0 molar in mercuric nitrate and 2.0 molar in nitric acid the otherwise identical experiment gave a 63% yield.

Formylcyclopentane and Its Derivatives

(*a*) *From Mercuric Nitrate – Cyclohexene*

To a solution of 68.6 gm. (0.2 mole) of mercuric nitrate monohydrate in 400 ml. of water containing 12.6 ml. (0.2 mole) of 70% nitric acid was added with vigorous stirring 10.1 ml. (0.1 mole) of cyclohexene. After 84 hr. the system (which contained 0.8 gm. of free mercury) was extracted with four 50-ml. portions of chloroform. Distillation yielded 2.22 gm. (23%) of formylcyclopentane, b.p. 40–50° (8 mm.), n_D^{20} 1.4460, and 1.54 gm. (14%) of cyclopentanecarboxylic acid, b.p. 94° (8 mm.) n_D^{20} 1.4597. The residue, separated from 0.11 gm. of mercurous salt, was crystallized from 95% ethanol, 1.20 gm. (12%) of 2,4,6-tricyclopentyl-1,3,5-trioxane, m.p. 123–125°, identified by mixture melting point.

(*b*) *From Mercuric Nitrate and 2-Hydroxycyclohexylmercuric Nitrate*

When 8.38 gm. (0.025 mole) of 2-hydroxycyclohexylmercuric chloride was shaken with 50 ml. of water containing 4.25 gm. (0.025 mole) of silver nitrate and 5 ml. of methanol for 70 min. the precipitate of silver chloride weighed 3.71 gm. (92%). To the filtrate was added 8.54 gm. (0.026 mole) of mercuric nitrate in 50 ml. of water. The system was azeotropically distilled at 8 mm. and 35° for two hours. No cyclohexene was found in the ice-cooled or dry-ice-cooled receivers but 0.93 gm. (38%) of formylcyclopentane, b.p. 75–85° (94 mm.), was obtained by distillation of the ether extract. No cyclopentanecarboxylic acid was found.

**Melting points have been corrected against reliable standards. X-ray diffraction patterns were determined using Cu K_α (Ni filtered) radiation at relative intensities I/I_1 and d spacings in Angstrom units.*

(*c*) *From Methanolic Mercuric Nitrate – Cyclohexene*

A system containing 6.86 gm. (0.02 mole) of mercuric nitrate, 0.63 ml. (0.01 mole) of 70% nitric acid, and 1.01 ml. (0.01 mole) of cyclohexene in 40 ml. of methanol was studied kinetically by removal of 10-ml. aliquots into 40 ml. of 5% aqueous sodium chloride. After 17.5, 41.5, and 114 hr. the mercurous chloride weighed 0.28, 0.77, and 0.89 gm. respectively, representing oxidation to the extent of 24, 65, and 76%. The filtrate from the third aliquot on treatment with a solution of 2,4-dinitrophenylhydrazine in 2 *N* hydrochloric acid yielded 0.12 gm. of formylcyclopentane dinitrophenylhydrazone (17% based on cyclohexene), m.p. 148–152°, with X-ray diffraction pattern [10] 4.05; [6] 5.12; [5] 7.48; [4] 3.20; [1] 3.40; [0.5] 3.05, 2.44, 2.03, identical with an authentic specimen.

(*d*) *From Mercuric Nitrate and 2-Methoxycyclohexylmercuric Nitrate*

A quantitative yield of silver chloride was obtained when 3.49 gm. (0.01 mole) of α-2-methoxycyclohexylmercuric chloride was treated with 1.70 gm. (0.01 mole) of silver nitrate. The remainder of the system after three days with 3.25 gm. (0.01 mole) of mercuric nitrate was diluted with 100 ml. of water and extracted with 125 ml. of ether in four portions. This extract, washed with alkali and with water and dried with magnesium sulphate, was distilled to yield only 0.54 gm. (55%) of formylcyclopentane, n_D^{20} 1.4495, identified as the dinitrophenylhydrazone. The extracted aqueous dilution liquor yielded mercurous chloride quantitatively upon treatment with aqueous sodium chloride.

(*e*) *From Cyclohexene and Mercuric Sulphate*

After 11 hr. a system comprising 43.4 gm. (0.2 mole) of mercuric oxide in 50 ml. of 6 molar sulphuric acid (0.3 mole), 340 ml. of water, and 10.1 ml. (0.1 mole) of cyclohexene gave a negative test for mercuric salt. The suspension was flash-distilled at 10–12 mm. into receivers at −15° and −80°. Extraction of the distillate yielded 3.5 gm. (37%) of formylcyclopentane, b.p. 65–68° (75–76 mm.), identified as the dinitrophenylhydrazone. Extraction of the 96% yield of mercurous sulphate with chloroform gave an oil which, combined with the residue from distillation of the aldehyde, yielded about 0.8 gm. (7%) of cyclopentanecarboxylic acid, b.p. 80–90° (9 mm.).

(*f*) *From Cyclohexene and Other Mercuric Salts*

After five days a system comprising 9.48 gm. (0.06 mole) of benzenesulphonic acid, 4.34 gm. (0.02 mole) of mercuric oxide, and 1.01 ml. (0.01 mole) of cyclohexene was filtered to remove 0.12 gm. (3%) of free mercury. Treatment of the filtrate with sodium chloride followed by extraction with ether gave successively 3.65 gm. (77%) of mercurous chloride and 0.39 gm. of oil which gave the dinitrophenylhydrazone of formalcyclopentane. By contrast no trace of the aldehyde was obtained from mercuric phosphate.

2-Methyl-1-phenylpropene (I) Purification

The preparation according to Tiffeneau and Orékoff (35) gave a product in 90% yield, b.p. 75–86° (15–17 mm.), redistilled for 75% over-all yield, b.p. 75–79° (12–14 mm.), n_D^{20} 1.5376, d_4^{20} 0.903, m.p. −66 to −63°. After conversion

to 2-methoxy-2-methyl-1-phenylethylmercuric chloride (6), m.p. 78.5–80°, which was crystallized, the alkene was recovered by decomposition of the mercurial with 1 : 1 methanol – concentrated hydrochloric acid, aqueous dilution, and petroleum ether extraction. The distilled product boiled at 65.5–66° (12 mm.) or 75–77° (18 mm.), n_D^{20} 1.5405, and seemed to exist in polymorphic forms. Crystallization by rapid cooling gave a melting point of about −56°; if maintained at this temperature the sample resolidified, then melted at −50° to −48°.

2-*Methyl*-1-*phenylpropene with Mercuric Salts*

(*a*) *With Mercuric Nitrate in Methanol*

The addition of 17.0 gm. (0.052 mole) of mercuric nitrate to 100 ml. of methanol produced a yellow precipitate, principally mercuric oxide, but it redissolved within two minutes when 3.65 ml. (0.025 mole) of 2-methyl-1-phenylpropene was added. After 20 hr. the system was filtered from 4.74 gm. of mercurous nitrate. The filtrate, diluted with 200 ml. of water and thrice extracted with a total of 200 ml. of ether, was then treated with sodium chloride to precipitate mercurous chloride. Since the remaining liquor with hydrogen sulphide gave 0.6 gm. of mercuric sulphide, the total recovery of mercury is 98%.

The ether solution, washed with water, 5% alkali, and water, then dried with magnesium sulphate, contained 4.66 gm. of oil which was distilled (8 mm.) to yield two lots of impure (40%) 1,2-dimethoxy-2-methyl-1-phenylpropane (II), b.p. 94–100° (n_D^{20} 1.4966), m.p. 0–6°, and b.p. 100–106° (n_D^{20} 1.4980), finally purified by fractional freezing of the 2.11 gm. total, m.p. 8–11.5°, identified by mixture melting point (6). After an intermediate fraction, b.p. 106–122°, 0.57 gm. (n_D^{20} 1.5027), there distilled 1.30 gm. (23%) at 124–126° (n_D^{20} 1.5083) 2-methoxy-2-methyl-1-phenylpropyl nitrate (III). Anal.: Calc. for $C_{11}H_{15}O_4N$: N, 6.22. Found: N, 5.96. The intermediate and final fractions were contaminated with small amounts of benzaldehyde or its acetal, identified by preparation of its dinitrophenylhydrazone, m.p. 237–238°, with unchanged mixture melting point. The amount of benzaldehyde was enhanced by addition of nitric acid to the original system. Essentially the same yields of principal products were obtained (according to refractive indices) when 2-methoxy-2-methyl-1-phenylpropylmercuric nitrate replaced the 2-methyl-1-phenylpropene in the original system, although contamination with benzaldehyde was diminished.

In order to demonstrate that the nitrate ester is formed more rapidly than the 1,2-dimethoxy-2-methyl-1-phenylpropane a system comprising 2.029 gm. (0.00625 mole) of finely ground mercuric nitrate and 0.459 ml. (0.00313 mole) of 2-methyl-1-phenylpropene made up to 25 ml. with methanol was maintained at 25°. One series of 1-ml. aliquots was withdrawn periodically and analyzed according to kinetic methods outlined below. Another set of 5-ml. aliquots was periodically diluted with 10 ml. of 0.1 *N* nitric acid. The ether extract (40 ml.) of this diluate was extracted with two 10-ml. portions of 5% sodium sulphate, then diluted to exactly 50 ml. with ether. Two 10-ml. aliquots

of this solution were evaporated, treated with *m*-xylenol and sulphuric acid (42), and examined through a blue filter in the Klett Summerson colorimeter using potassium nitrate as a standard. A second experiment was performed with inclusion of 0.262 ml. (0.00625 mole) and at 29°. A single analysis was performed after 130 min. Results are outlined in Table XII.

TABLE XII

RATE OF NITRATE ESTER FORMATION IN REACTION OF MERCURIC NITRATE WITH 2-METHYL-1-PHENYLPROPENE

Expt.	Time, min.	% Reaction (*Y*)	% Nitrate ester (*X*)	Ratio *X*/*Y*
1	30	32	17	0.53
1	70	54	24	0.44
1	120	66	27	0.42
2	130	86	30	0.35

(*b*) *With Mercuric Trifluoroacetate in Methanol*

Mercuric trifluoroacetate was prepared by solution of 10.83 gm. (0.05 mole) of mercuric oxide in 10 ml. (0.147 mole) of trifluoroacetic acid. After the initial evolution of heat a further 5-ml. portion of trifluoroacetic acid was added, and the whole was heated on the steam bath until solution was almost complete. The hot suspension was filtered through sintered glass and chilled to 0°. The white crystals were filtered off and vacuum dried, 10.9 gm. (53%), m.p. 164–168° with softening at 158°. The X-ray diffraction pattern was: [20] 10.00; [18] 10.64; [16] 15.49, 13.71; [14] 4.90; [12] 7.82, 4.18; [10] 4.07, 3.40, 3.15; [8] 4.48, 3.53; [6] 5.27, 3.91, 2.98, 2.66, 2.28; [4] 6.91, 3.76, 2.93, 2.36, 2.23, 2.03; [2] 6.44, 5.49, 4.76, 3.33, 2.77, 2.00, 1.96, 1.93; [1] 7.49, 5.71, 2.59, 2.48. Anal.: Calc. for $Hg(CF_3COO)_2$: Hg, 47.0. Found: Hg, 46.7.

To a solution of 4.27 gm. (0.01 mole) of mercuric trifluoroacetate in 20 ml. of methanol was added 0.73 ml. (0.005 mole) of 2-methyl-1-phenylpropene. Dilution with 25 ml. of water after two days and extraction with 20 ml. of chloroform gave a solution which, washed with water, 2 *N* hydrochloric acid, 5% aqueous alkali and water, then dried, was distilled at 16 mm. giving 0.45 gm., b.p. 106–111°, n_D^{20} 1.4999, and 0.17 gm., b.p. 110–120, $_D^{20}$ 1.5080, and 0.21 gm. of residue. The first fraction (m.p. −16 to −6°) was converted in part to 3-phenylbutanone-2 dinitrophenylhydrazone with the methanolic hydrochloride reagent and was identified by mixture melting point. According to the 1.98 gm. of mercurous chloride obtained from the diluted reaction liquor by hydrochloric acid treatment the oxidation reaction was 84% complete.

(*c*) *With Mercuric Sulphate in Water*

To the bright yellow precipitate obtained when 21.7 gm. (0.1 mole) of mercuric oxide was shaken with 200 ml. (0.2 mole) of molar sulphuric acid was added 7.31 ml. (0.05 mole) of 2-methyl-1-phenylpropene. After shaking for two days 23.5 gm. (95%) of mercurous sulphate was filtered off and washed with methanol and ether. The filtrate was extracted with this ether and with three more 25-ml. portions of ether and three 50-ml. portions of chloroform.

Evaporation of the combined, dried extract left 5.80 gm. (70%) of 2-methyl-1-phenylpropanediol-1,2 which crystallized slowly, m.p. 47–62°. Crystallization from diethyl ether and petroleum ether (b.p. 40–50°) gave 4 gm., m.p. 63–63.5°, identified by mixture melting point with an authentic sample.

2-Methoxy-2-methyl-1-phenylpropanol-1 (IV)

A solution of 0.78 gm. (0.0035 mole) of 2-methoxy-2-methyl-1-phenylpropyl nitrate in 7 ml. of acetic acid was warmed gently while small amounts of zinc dust and iron powder were added until a test sample no longer gave a blue color with diphenylamine and sulphuric acid. The dark-brown mixture was filtered into 30 ml. of water containing 15 gm. of potassium carbonate (pH 8). A triple extraction with 40 ml. total of ether removed an oil, b.p. 118–124° (12 mm.), 0.44 gm. (70%), n_D^{20} 1.5177, m.p. 17–23° (actual yield probably only half this apparent 70%). A repeated partial freezing raised this melting point to 36–39°. This alcohol, still impure, was identified by preparation of derivatives.

After oxidation of 0.08 gm. of the impure alcohol with one equivalent of alkaline permanganate at 0° the mixture was extracted with ether and the extract evaporated. The oil was dissolved in methanol and the dried solution was treated with 2,4-dinitrophenylhydrazine to yield 0.03 gm. of α-methoxyisobutyrophenone dinitrophenylhydrazone, m.p. 124–127°, which, crystallized from methanol and from 20 : 1 petroleum ether – benzene, melted at 139–140° (0.01 gm.). The X-ray powder diagram was: [10] 10.97, 3.54; [9] 3.09; [7] 9.25, 4.13; [6] 6.21, 3.97; [5] 6.75, 5.53, 3.23; [4] 4.87; [3] 4.31, 2.82; [2] 2.97. Comparison with this powder diagram and by mixture melting point showed that this derivative was identical with that obtainable from the known ketone (1).

trans-Stilbene with Methanolic Mercuric Nitrate

A clear solution was obtained after one hour from 0.90 gm. (0.005 mole) of *trans*-stilbene and 3.41 gm. (0.0105 mole) of mercuric nitrate in 40 ml. of methanol. Dilution with 100 ml. of water after 38 hr. gave a mixture which was thrice extracted with a total of 70 ml. of ether. Treatment of the aqueous layer with 10 ml. of saturated sodium chloride precipitated 2.28 gm. (92%) of mercurous chloride.

The etherous extract, washed with 5% alkali and water, then dried with sodium sulphate, was evaporated leaving 1.19 gm. of semisolid, of which a benzene solution of 339 mgm. was chromatographed on non-activated 80–200 mesh Alcoa alumina in a column 29 × 1.6 cm. Elution with benzene gave 10 fractions: 1, 10 ml. (29 mgm.), m.p. 110–119°; 2, 11 ml. (131 mgm.), m.p. 85–89°; 3, 10 ml. (42 mgm.), m.p. 120–135°; 4, 10 ml. (27 mgm.), m.p. 139.5–140.5°; 5, 10.5 ml. (11 mgm.), oily solid; 6, 10 ml. (32 mgm.), oil; 7, 11 ml. (21 mgm.), oil; 8, 16 ml. (12 mgm.), oil; 9, 15.5 ml. (1 mgm.); 10, 40 ml. (9 mgm.), m.p. 89–91°.

Fraction 1, crystallized from ethanol, was *trans*-stilbene (VII), m.p. 121–123°, identified by mixture melting point. Fraction 2 was crystallized four times from methanol, m.p. 91.4–92.0°, and this (*dl,ld*)-2-methoxy-1,2-diphenylethyl nitrate (IX) gave a positive test with diphenylamine and sulphuric acid.

Anal.: Calc. for $C_{15}H_{15}O_4N$: C, 65.9; H, 5.50; N, 5.13. Found: C, 66.2; H, 5.69; N, 5.09. X-Ray diffraction pattern: [10] 3.79; [7] 9.25, 3.39; [5] 5.65, 5.50, 5.18; [4] 7.62, 6.13, 3.97; [3] 4.29, 4.16; [2] 3.26, 3.02; [1] 4.79, 2.90, 2.79. Fraction 3 is an impure specimen of fraction 4, which is almost-pure (*dl,ld*)-1,2-dimethoxy-1,2-diphenylethane (XII) as was authenticated by mixture melting point and by X-ray diffraction pattern: [10] 5.21; [9] 4.98; [8] 4.76, 3.50; [7] 5.96; [6] 4.01; [4] 9.45, 4.53, 4.44; [3] 6.91, 6.53, 3.37, 3.28; [2] 3.21; [1] 3.13, 3.03, 2.99, 2.81, 2.76. Disregarding fraction 5, the next three, 6, 7, and 8, were combined (n_D^{20} 1.5280) and evidently comprised in large part diphenylacetaldehyde dimethyl acetal (XIII) since it gave no active hydrogen and no carbonyl addition in the Grignard machine, yet slowly yielded the 2,4-dinitrophenylhydrazone of diphenylacetaldehyde (m.p. 143–146°) when it was treated with the methanolic hydrochloride reagent. Two crystallizations from ethanol or chloroform–petroleum ether (b.p. 60–70°) or from methanol–ethyl acetate raised this melting point to 150.2–150.5°. Anal.: Calc. for $C_{20}H_{14}O_4N_4$: C, 63.8; H, 4.29; N, 14.9. Found: C, 63.7; H, 4.24; N, 14.6. The X-ray diffraction pattern was: [10] 15.6; [8] 5.20, 3.65, 3.18; [7] 4.60, 3.94; [6] 6.93; [5] 7.73; [4] 5.64, 5.40. When this derivative was prepared from authentic diphenylacetaldehyde, b.p. 165–166° (12 mm.), n_D^{20} 1.5878, d_4^{20} 1.09, it was found to be identical with the analyzed sample. Fraction 10 was shown by mixture melting point to be (*dd,ll*)-1,2-dimethoxy-1,2-diphenylethane. Its X-ray diffraction pattern was: [10] 6.30, 3.55; [9] 5.01, 4.95; [6] 7.28; [5] 8.58, 4.26, 4.13; [4] 3.32; [3] 5.43, 4.74; [2] 5.88, 3.76; [1] 3.96, 3.06, 2.90.

(*dl,ld*)-2-*Methoxy*-1,2-*diphenylethanol* (*X*)

(*a*) *From Benzoin Methyl Ether*

The procedure of Irvine and Weir (19) was altered by reduction with Raney nickel in ethanol at 27° and 1–2 atmospheres. The product (97%) melted at 100–102°, X-ray diffraction pattern: [10] 5.14; [9] 3.63, 3.42; [7] 8.66, 3.90; [6] 4.66; [4] 12.7, 6.39, 5.64, 4.27, 3.98; [3] 4.88, 3.82, 3.74; [1] 3.34. The configuration was demonstrated by treatment of 1.14 gm. (0.005 mole) with 7.10 gm. (0.05 mole) of methyl iodide and 4.35 gm. (0.016 mole) of fresh gradually-added silver oxide under reflux for five hours. The product (83%) m.p. 140–142° after crystallization was identical (mixture melting point) with that obtained by methylation of hydrobenzoin.

(*b*) *From* (*dl,ld*)-2-*Methoxy*-1,2-*diphenylethyl Nitrate* (*IX*)

A solution of the nitrate ester (27 mgm., 0.0001 mole) in 4 ml. of 1 : 1 dioxane–ethanol was hydrogenated at atmospheric pressure over 0.1 gm. of palladium-on-charcoal (17). The system, containing ammonia, was filtered and evaporated, 19 mgm. (83%), m.p. 97.5–100°. Crystallization from ethanol–water raised the melting point to 100.5–101.8°. The compound was identical with that obtained by procedure (*a*).

(*c*) *From Stilbene Oxide and Methyl Nitrate – Nitric Acid*

When 0.196 gm. (0.001 mole) of stilbene oxide (34) (m.p. 68–69°) in 10 ml. of methanol was treated with 0.154 gm. (0.002 mole) of methyl nitrate (b.p.

65–66°, n_D^{20} 1.3754, d_4^{20} 1.192) at 27° for 29 hr. it was recovered unchanged. However when 0.105 ml. (0.0025 mole) of absolute nitric acid was added the system upon vacuum evaporation after 42 hr. yielded 0.226 gm. of yellow solid, m.p. 40–90°. Chromatography on alumina did not yield any methoxy nitrate ester or dimethoxy compound but 97 mgm., m.p. 91–96°, was obtained, from which (*dl,ld*)-2-methoxy-1,2-diphenylethanol, m.p. 99.5–100.5°, was identified (after crystallization from petroleum ether (b.p. 60–70°) and ethanol–water) by mixture melting point. Both (*dl,ld*)-1,2-dimethoxy-1,2-diphenylethane and (*dl,ld*)-2-methoxy-1,2-diphenylethyl nitrate were found to be stable in the reaction system.

cis-Stilbene with Methanolic Mercuric Nitrate

A shaken suspension of 3.41 gm. (0.0105 mole) of mercuric nitrate and 0.43 gm. (0.0024 mole) of *cis*-stilbene (40) in 40 ml. of methanol was clear after five minutes. After 48 hr. the system was diluted into 80 ml. of water. The diluate, extracted with three 10-ml. portions of chloroform, was then treated with 10 ml. of saturated aqueous sodium chloride to precipitate 1.33 gm. (0.0055 mole) of mercurous chloride. Addition of ammonia to the filtrate then precipitated 1.09 gm. (0.0043 mole) of aminomercuric chloride to give a total of 93% of the original mercury.

The chloroform extract, washed with 5% alkali and with water and dried over sodium sulphate, was evaporated to leave 0.703 gm., semicrystalline, of which 0.242 gm. in benzene was chromatographed as was described for the oxidation of *trans*-stilbene. Fraction 1, 3 mgm., was *cis*-stilbene; 2, 94 mgm., m.p. 87–93°; 3, 6 mgm., m.p. 115–138°; 4, 81 mgm., oil; 5, 31 mgm., m.p. 85–91°. Fraction 2 was twice crystallized from methanol and once from ethanol, m.p. 93.6–93.9°. The X-ray diffraction pattern of this (*dd,ll*)-2-methoxy-1,2-diphenylethyl nitrate (XVII, which gave a blue color with diphenylamine and sulphuric acid) was measured: [10] 10.77, 10.39, 4.08, 4.04; [9] 6.94, 6.73; [8] 7.43, 7.25; [7] 5.18, 5.09, 2.78; [5] 3.64, 3.36; [4] 3.19; [3] 8.07, 7.79, 6.15, 5.30, 4.98. A mixture melting point with the (*dl,ld*)-diastereomer was depressed. Anal.: Calc. for $C_{15}H_{14}NO_4$: C, 65.9; H, 5.50; N, 5.13. Found: C, 65.9; H, 5.80; N, 5.02. Fraction 3, when crystallized from methanol, melted at 138–140°, identified as (*dl,ld*)-1,2-dimethoxy-1,2-diphenylethane by mixture melting point and X-ray diffraction pattern. Fraction 4 was converted to diphenylacetaldehyde 2,4-dinitrophenylhydrazone, m.p. 145–146°, with the methanolic hydrochloride reagent. After crystallization (m.p. 150°) it was authenticated by mixture melting point. Fraction 5 was identified by mixture melting point and X-ray diffraction pattern as (*dd,ll*)-1,2-dimethoxy-1,2-diphenylethane (XV).

(*dd,ll*)-2-*Methoxy*-1,2-*diphenylethanol* (*XVIII*)

(*a*) *From Benzoin Methyl Ether and Aluminum Isopropoxide*

A mixture of 2.12 gm. (0.01 mole) of benzoin methyl ether, 4.0 gm. (0.02 mole) of aluminum isopropoxide, and 35 ml. of isopropyl alcohol in a Hahn apparatus (14) was slowly distilled (28 ml.) until acetone (dinitrophenylhydrazine test) no longer was produced. The cooled residue, diluted with 35 ml.

of 7% hydrochloric acid, was twice extracted with ether. The extract (washed with 5% alkali and water, and sodium-sulphate-dried) was evaporated, 1.88 gm., m.p. 55–59°. By fractional crystallization from petroleum ether (b.p. 60–70°) the more soluble component was separated, m.p. 54.5–55.5°; X-ray diffraction pattern: [10] 5.21; [7] 8.66, 5.71; [6] 4.77; [5] 6.65; [3] 5.01; [2] 4.35, 4.07, 4.00, 3.85, 3.74, 3.49; [1] 13.4, 3.69. Anal.: Calc. for $C_{15}H_{16}O_2$: C, 78.9; H, 7.07. Found: C, 78.4; H, 7.16. The configuration was confirmed by methyl iodide – silver oxide methylation; 0.094 gm. (99%), m.p. 80–88°, was crystallized from 0.5 ml. of methanol, m.p. 92–93°. This (*dd,ll*)-1,2-dimethoxy-1,2-diphenylethane (XV), identical with that obtained by methylation of isohydrobenzoin, was compared by mixture melting point and X-ray diffraction pattern.

(*b*) *By Reduction of* (*dd,ll*)-2-*Methoxy*-1,2-*diphenylethyl Nitrate* (*XVII*)

The procedure used for the (*dl,ld*)-diastereomer gave a 75% yield, m.p. 50–52°. After crystallization from petroleum ether (b.p. 60–70°) this (*dd,ll*) isomer, m.p. 54.3–55.5°, was identified by mixture melting point and X-ray diffraction pattern.

α-2-*Methoxy*-1,2-*diphenylethylmercuric Chloride*

After about four minutes a strongly shaken mixture of 1.07 gm. (0.0033 mole) of mercuric nitrate and 0.281 gm. (0.0016 mole) of *cis*-stilbene in 25 ml. of methanol at 25° was clear. After 10 min. of reaction time the system was added to 25 ml. of cold 0.4 *N* aqueous sodium chloride. The precipitate, 0.737 gm., was extracted with chloroform, then with methanol to remove mercuric chloride, leaving 0.129 gm. (17%) of mercurous chloride.

The evaporated chloroform solution (0.584 gm.) was washed with 1 ml. of petroleum ether (b.p. 60–70°) to leave 0.548 gm., m.p. 132–139°. After crystallization from ethanol the product (m.p. 141–143°) was identified by mixture melting point.

α-2-*Methoxy*-1,2-*diphenylethylmercuric Nitrate* (*XIX*) *with Ethanolic Mercuric Nitrate*

After 1.118 gm. (0.0025 mole) of α-2-methoxy-1,2-diphenylethylmercuric chloride and 0.425 gm. (0.0025 mole) of silver nitrate in 10 ml. of anhydrous ethanol was shaken for 35 min. and the silver chloride (0.354 gm. or 0.0025 mole) was filtered and washed with 10 ml. of anhydrous ethanol, the combined filtrate and washings were shaken with 0.845 gm. (0.0026 mole) of mercuric nitrate for 72 hr. Filtration removed 1.047 gm. (0.004 mole) of mercurous nitrate; the filtrate, diluted with an equal volume of water, was thrice extracted with 5-ml. portions of chloroform and was treated then with dilute hydrochloric acid. The precipitated mercurous chloride weighed 0.31 gm. (0.001 mole).

The water-washed chloroform extract was dried and evaporated, leaving 0.633 gm. This product was partially chromatographed, as outlined above, to yield two fractions. The first was crystallized from petroleum ether (b.p. 60–70°), 0.237 gm. (39%), identified as (*dd,ll*)-2-methoxy-1,2-diphenylethyl

nitrate, m.p. 93.5–94°, by mixture melting point. The second fraction, which was oily and weighed 0.290 gm., was treated with hot methanolic 2,4-dinitrophenylhydrazine hydrochloride reagent, yielding the derivative, m.p. 133–138°. After crystallization from ethyl acetate – methanol, m.p. 150–151°, this diphenylacetaldehyde dinitrophenylhydrazone was identified by mixture melting point. If the oil is the diethyl acetal the yield is 43% of theoretical.

(dd,ll)-2-Ethoxy-1,2-diphenylethyl Nitrate

To a mixture of 1.69 gm. (0.0052 mole) of mercuric nitrate in 20 ml. of anhydrous ethanol containing 0.080 gm. (0.0025 mole) of methanol (shaken until the solid had disintegrated) was added 0.4506 gm. (0.0025 mole) of *cis*-stilbene and the mixture was shaken vigorously for 48 hr. After dilution with water the system was thrice extracted with a total of 20 ml. of chloroform. The aqueous layer yielded 0.0049 mole of mercurous chloride when it was treated with aqueous sodium chloride.

The water-washed chloroform extract was dried and evaporated to leave 0.658 gm. of an oil. Chromatography of 258 mgm. of this oil by the method outlined above yielded 29 mgm., m.p. 48–68°, and 80 mgm., m.p. 67–73°, as well as 117 mgm. of an oil. The 80 mgm. portion was crystallized from petroleum ether (b.p. 60–70°), 52 mgm., m.p. 74–75°. Recrystallization raised this melting point to 74.8–75.5°; X-ray diffraction pattern: [10] 3.88; [5] 10.04, 4.82; [4] 4.58, 4.13; [3] 2.94. Anal.: Calc. for $C_{16}H_{17}NO_4$: C, 66.9; H, 5.97; N, 4.88. Found: C, 67.3; H, 6.14; N, 4.68. The residue from the evaporated crystallization liquors melted at 57–69°, 27 mgm.

(dd,ll)-1-Ethoxy-2-methoxy-1,2-diphenylethane (XXII)

(a) From (dd,ll)-2-Methoxy-1,2-diphenylethanol (XVIII)

Gradual addition of 0.46 gm. (0.002 mole) of fresh silver oxide to 83 mgm. (0.0036 mole) of the alcohol in 2.0 ml. (0.0025 mole) of boiling ethyl iodide during four hours gave a mixture which was filtered and evaporated; 89 mgm. slowly crystallized, m.p. 51–54°. A benzene solution, passed through 10 gm. of Alcoa alumina in a column, gave a fraction (79 mgm.), m.p. 54–55°, which was crystallized from 0.3 ml. of petroleum ether (b.p. 40–50°), m.p. 55.2–55.5°, with X-ray diffraction pattern: [10] 6.48; [9] 5.24; [5] 9.16, 7.13, 4.20; [4] 3.81, 3.57, 3.44. Anal.: Calc. for $C_{17}H_{20}O_2$: C, 79.7; H, 7.86. Found: C, 79.7; H, 7.97.

(b) From (dd,ll)-2-Ethoxy-1,2-diphenylethyl Nitrate (XX)

Hydrogenation of 36 mgm. (0.00125 mole) of the nitrate ester with palladium-on-charcoal as outlined earlier yielded 30 mgm. of oil which was methylated with silver oxide and methyl iodide. The crude product in benzene was passed through 2 gm. of Alcoa alumina in a column and the main fraction upon evaporation slowly crystallized, m.p. 53–54.5°. A mixture melting point with product prepared by procedure (*a*) was not lowered.

β-2-Methoxy-1,2-diphenylethylmercuric Acetate

After shaking 5.0 gm. (0.0112 mole) of β-2-methoxy-1,2-diphenylethylmercuric chloride and 1.87 gm. (0.012 mole) of silver acetate in 40 ml. of

methanol for one hour in the dark the mixture was filtered from silver chloride (100%). Vacuum evaporation of the filtrate left 5.35 gm. (100%), m.p. 100–104°. Solution in 15 ml. of methanol followed by dilution with 8 ml. of water gave 4.22 gm., m.p. 103.5–105°. After crystallization from 95% ethanol the X-ray diffraction pattern of the compound, m.p. 104.5–105.5°, was determined: [10] 11.04; [9] 4.16; [8] 3.43; [6] 4.38; [5] 5.79, 4.58; [3] 3.73; [1] 7.59, 5.27, 4.95. Anal.: Calc. for $C_{17}H_{18}HgO_3$: Hg, 42.6. Found: Hg, 42.4. The product was identified by reconversion to the chloromercurial by treatment of a methanolic solution with aqueous sodium chloride.

cis- or trans-Stilbene or the Corresponding Methoxymercurials with Methanolic Mercuric Acetate and Boron Fluoride Etherate at 25°

The reaction with *trans*-stilbene is typical. A solution of 0.90 gm. (0.005 mole) of *trans*-stilbene, 3.19 gm. (0.01 mole) of mercuric acetate (crystallized from acetic acid), and 0.28 gm. (0.002 mole) of boron fluoride etherate was made up to 100 ml. with dry methanol. The reaction was followed by titration of 2-ml. aliquots with thiocyanate solution after they had been diluted with water and extracted with chloroform. After five days the system was filtered to remove 1.70 gm. (65%) of mercurous acetate. The filtrate, evaporated and diluted with water, was thrice extracted with chloroform. The extract, washed with 5% alkali, water, and then dried and evaporated, yielded 1.055 gm. of semisolid. Chromatography of 277 mgm. as described before yielded 26 mgm. of stilbene, 130 mgm. of impure (*dl,ld*)-1,2-dimethoxy-1,2-diphenylethane, m.p. 137–139° (mixture melting point at 140–141.5° after crystallization from ethanol), 40 mgm. of diphenylacetaldehyde acetal, converted to its 2,4-dinitrophenylhydrazone, m.p. 145–147°, purified 149–150°, m.m.p., and finally 6 mgm. of impure (*dd,ll*)-1,2-dimethoxy-1,2-diphenylethane, crystallized from methanol to melt at 90–91°, m.m.p.

Benzylmercuric Nitrate and Methanolic Mercuric Nitrate

A mixture of 6.54 gm. (0.02 mole) of benzylmercuric chloride (22), m.p. 105–105.5°, and 3.40 gm. (0.02 mole) of finely-ground silver nitrate in 20 ml. of methanol was vigorously shaken for several hours, then filtered to remove 2.75 gm. (0.019 mole) of methanol-washed silver chloride. Then 6.83 gm. (0.021 mole) of mercuric nitrate was added and the system was shaken nine hours and let stand 30 hr. After filtration to remove 0.17 gm., infusible, the system was diluted with an equal volume of water and four times extracted with 50 ml. total of chloroform. The extract, washed with cold 5% aqueous sodium hydroxide and water, then dried over sodium sulphate, was distilled, yielding two discreet fractions. The first one (0.90 gm., 46%) was benzyl methyl ether, b.p. 62–70° (15 mm.), n_D^{20} 1.5042; redistilled at 168–171° (750 mm.), n_D^{20} 1.5040, m.p. −61 to −56°, it was identified by mixture melting point with an authentic sample, b.p. 170.5°, n_D^{20} 1.5034, m.p. −56 to −54° (31).

The second fraction, b.p. 65–75° (1.5 mm.), n_D^{20} 1.5212 (0.47 gm., 15%), was redistilled at 66–72° (1–2 mm.), n_D^{20} 1.5204, m.p. −21 to −19°, and then frozen fractionally, m.p. −19.5 to −15°. Anal.: Calc. for $C_7H_7NO_3$: NO_3, 40.5. Found: NO_3, 40.0. This benzyl nitrate was identified by mixture melting point

with an authentic sample (26), b.p. 99–100° (16 mm.), n_D^{20} 1.5211, m.p. −17 to −15° (uncorr.). When toluene was subjected to the same reaction conditions used for the mercurial neither of the products was detected and no mercurous salt was formed.

sec-Butyl Nitrate

A mixture of 5.86 gm. (0.02 mole) of *sec*-butylmercuric chloride (27), m.p. 128.5–129.3°, and 3.40 gm. (0.02 mole) of finely-ground silver nitrate in 25 ml. of methanol was shaken for 30 min. After filtration from 2.93 gm. of silver chloride the filtrate with 20 ml. of methanolic washings was shaken with 6.83 gm. (0.021 mole) of mercuric nitrate for 10 hr., then filtered to remove 3.33 gm. (30%) of mercurous nitrate. The filtrate diluted with water was ether extracted and the extract, water and alkali washed, was dried and distilled to yield a fraction, b.p. 120–123° (750 mm.), 0.12 gm. (5%), n_D^{20} 1.4006. This product was identified as *sec*-butyl nitrate by its physical constants (23), by a positive test with diphenylamine – sulphuric acid, and by uptake of hydrogen over palladium-on-charcoal to the extent of 96% of that expected for *sec*-butyl nitrate with consequent formation of ammonia.

2,2′-Dinitratomercuridiethyl Ether with Methanolic Mercuric Nitrate

Both this compound and hydroxyethylmercuric nitrate were prepared by the method of Hoffmann and Sand (18) and both were stable toward 10% nitric acid although they were decomposed by hydrochloric acid. When a methanolic solution of dinitratomercuridiethyl ether was shaken for five days with mercuric nitrate there was no evidence for mercurous salt formation, even when some water was added to the system.

Methods of Analysis for Kinetic Studies

When analysis for mercuric salts in absence of chlorides was possible the method of thiocyanate titration following chloroform extraction (41) was used. However the interference by mercurous salt frequently made this method unusable and the procedure of Personne (32) was refined for our purpose. By this refinement a 1 or 2 ml. aliquot (which might be about 0.5 molar in total inorganic mercury I and II) was added to 10 ml. of water in a separatory funnel and 1 ml. of 1 *N* nitric acid was added to prevent hydrolysis of the inorganic mercury salts. Three extractions with 5-ml. portions of chloroform were made for removal of organomercurial, then the aqueous layer was rinsed into 10 ml. of 2 *N* hydrochloric acid. The resulting precipitate of mercurous chloride was filtered off after 20 or 30 min. with celite as filter-aid, and washed at least four times. Filtrate and washings were combined and treated with 10 ml. of 0.19 *N* potassium iodide solution. The clear solution was diluted to a volume of about 80 ml. and was titrated with standardized (against red mercuric oxide in nitric acid) 0.1 *N* mercuric nitrate solution to the first appearance of a permanent red color due to mercuric iodide. Best results are obtained using a dark background and side-lighting. The titer value was subtracted from a blank carried out similarly on the potassium iodide solution. It is important that the final volume of each analyzed solution be nearly the same.

$$\text{Molarity of } Hg^{++} = \frac{\text{normality}}{2} \cdot \frac{\text{(vol. of blank titer} - \text{vol. of sample titer)}}{\text{volume of aliquot}}$$

Since 2-hydroxycyclohexylmercuric salts cannot be extracted quantitatively by chloroform the kinetic study of cyclohexene oxidation by aqueous mercuric nitrate does not include the extraction step and the aliquot is added directly to dilute hydrochloric acid which decomposes the hydroxymercurial and precipitates the mercurous salt at the same time. In this event the rate must be calculated on the assumption that the oxymercuration has gone rapidly to completion (see equation [i]).

The determination of mercurous salt above, or of both mercurous and mercuric salt, is obviously better suited to a kinetic study of oxidation by mercuric salt than is a determination of the mercuric salt alone, especially since the organomercurial is involved as an intermediate. Two methods have been employed.

In the first method, after extraction of the organomercurial the mercurous salt is precipitated but then filtered and washed by suction on a micro filtering crucible from which it is dissolved and oxidized by warming with 2 ml. of *aqua regia* until solution is complete. This solution is diluted, treated with potassium iodide, and titrated as described before,

$$Hg_2^{++} = \frac{\text{normality}}{4} \cdot \frac{\text{blank titer} - \text{sample titer}}{\text{volume of aliquot}},$$

while the mercuric salt is determined as before.

The second method is iodometric. After extraction of the organomercurial the aqueous layer is rinsed into a solution of 0.5 gm. of potassium iodide in 10 ml. of 2 *N* hydrochloric acid plus 5 ml. of 0.1 *N* standard iodine solution. Titration is then carried out with 0.1 *N* standard thiosulphate using a starch endpoint because of a tendency for the final solution to be slightly yellow.

Kinetic studies based on this determination of mercurous salt are shown in Table XIII, depicting the reaction of *cis*-stilbene with mercuric nitrate in methanol at 25°. Rates calculated from data corresponding to the $1/P$ curve, Fig. 2, show (Expts. 1 and 2, 3 and 4, 5 and 6) a satisfactory second-order relationship dependent on the concentration of nitric acid, which exerts an accelerating effect.

TABLE XIII

REACTION OF *cis*-STILBENE WITH MERCURIC NITRATE IN METHANOL AT 25°±0.1°C.

Expt. No.	Initial molarities			Molarities after mercuration			Second-order specific rate constant, l. moles^{-1} min.$^{-1}$	% Investigated
	$Hg(NO_3)_2$	*cis*-Stilbene	HNO_3	$Hg(NO_3)_2$	Mercurial	HNO_3		
1	.0937	.0313	.125	.0625	.0313	.156	.293±.012	73
2	.125	.0313	.125	.0938	.0313	.156	.294±.009	88
3	.125	.0625	.125	.0625	.0625	.188	.338±.009	68
4	.156	.0625	.125	.0938	.0625	.188	.335±.007	84
5	.125	.0625	.250	.0625	.0625	.312	.402±.006	72
6	.125	.0625	.375	.0625	.0625	.437	.413±.006	74

REFERENCES

1. ASTON, J. G., CLARKE, J. T., BURGESS, K. A., and GREENBERG, R. B. J. Am. Chem. Soc. 64: 300. 1942.
2. BALBIANO, L. Gazz. chim. ital. 36, I: 237. 1906. Ber. 42: 1503. 1909.
3. BALBIANO, L. and PAOLINI, V. Ber. 35: 2994. 1902; 36: 3575. 1903.
4. BARTON, D. R. H. J. Chem. Soc. 516. 1946.
5. BARTON, D. R. H. and ROSENFELDER, W. J. J. Chem. Soc. 2381. 1951.
6. BERMAN, L., HALL, R. H., PYKE, R. G., and WRIGHT, G. F. Can. J. Chem. 30: 541. 1952.
7. BIRKS, A. M. and WRIGHT, G. F. J. Am. Chem. Soc. 62: 2412. 1940.
8. BRACKMAN, D. S. and PLESCH, P. H. J. Chem. Soc. 2188. 1952.
9. BRACKMAN, D. S. and PLESCH, P. H. J. Chem. Soc. 1289. 1953.
10. BROOK, A. G. and WRIGHT, G. F. Can. J. Chem. 29: 308. 1951.
11. COPE, A. C., NELSON, N. A., and SMITH, D. S. J. Am. Chem. Soc. 76: 1100. 1954.
12. DOWNING, D. C. and WRIGHT, G. F. J. Am. Chem. Soc. 68: 141. 1946.
13. FISCHER, H. O. L. and TAUBE, C. Ber. 59: 855. 1926.
14. HAHN, A. Ber. 43: 420. 1910. *Cf.* Org. Syntheses, 20: 27. 1940.
15. HARTLEY, W. N. J. Chem. Soc. 81: 556. 1902.
16. HARTLEY, W. N. J. Chem. Soc. 83: 221. 1903.
17. HARTUNG, W. H. J. Am. Chem. Soc. 50: 3373. 1928.
18. HOFFMANN, K. A. and SAND, J. Ber. 33: 1340. 1900.
19. IRVINE, J. C. and WEIR, J. J. Chem. Soc. 91: 1390. 1907.
20. JEFFRIES, P. R., MACBETH, A. K., and MILLIGAN, B. J. Chem. Soc. 705. 1954.
21. JONES, R. N. and THORN, G. D. Can. J. Research, B, 27: 580. 1949.
22. KHARASCH, M. S., PINES, H., and LEVINE, H. J. Org. Chem. 3: 347. 1938.
23. KORNBLUM, N., PATTON, J. T., and NORDMANN, J. B. J. Am. Chem. Soc. 70: 746. 1948.
24. KUHN, L. J. Am. Chem. Soc. 68: 1761. 1946.
25. LEYS, A. Bull. soc. chim. [4] 1: 262, 633. 1907.
26. LUCAS, G. R. and HAMMETT, L. P. J. Am. Chem. Soc. 64: 1928. 1942.
27. MARVEL, C. S. and CALVERY, H. O. J. Am. Chem. Soc. 45: 820. 1923.
28. MEEN, R. H. and WRIGHT, G. F. J. Org. Chem. 19: 391. 1954.
29. MEYER, J. Z. physik. Chem. 67: 257. 1909.
30. MORTON, A. A. and PENNER, H. P. J. Am. Chem. Soc. 73: 3300. 1951.
31. OLSON, W. T. *et al.* J. Am. Chem. Soc. 69: 2451. 1947.
32. PERSONNE, J. Compt. rend. 56: 951. 1863.
33. RUYLE, W. V. *et al.* J. Am. Chem. Soc. 76: 2604. 1953.
34. TIFFENEAU, M. and LEVY, J. Bull. soc. chim. [4] 39: 781. 1926.
35. TIFFENEAU, M. and OREKOFF, A. Bull. soc. chim. [4] 29: 816. 1921.
36. TRIEBS, W. and BAST, H. Ann. 561: 165. 1948.
37. TRIEBS, W., LUCIUS, G., KOGLER, H., and BRESLAUER, H. Ann. 581: 59. 1953.
38. WINDAUS, A. Ann. 552: 135, 142. 1942.
39. WINDAUS, A. and LINSERT, O. Ann. 465: 157. 1928.
40. WRIGHT, G. F. Can. J. Chem. 30: 268. 1952.
41. WRIGHT, G. F. J. Am. Chem. Soc. 57: 1993. 1935.
42. YAGODA, H. Ind. Eng. Chem. Anal. Ed. 15: 27. 1943.

THE PHOTOINITIATED ADDITION OF MERCAPTANS TO OLEFINS

II. THE KINETICS OF THE ADDITION OF *n*-BUTYL MERCAPTAN TO 1-PENTENE[1,2]

By M. Onyszchuk[3] and C. Sivertz[4]

ABSTRACT

The detailed kinetics involved in the photoinitiated addition of *n*-butyl mercaptan to 1-pentene is presented. It has been shown that side reactions such as propagation and α-dehydrogenation are relatively negligible and the principal mechanism comprises attack by thiyl radical followed by transfer with mercaptan by the alkyl radical. The velocity constant of the attack step is estimated to be 7×10^6 and that of the transfer step 1.4×10^6 liters/mole-sec. These values together with approximate termination velocity constants are shown to explain the kinetics over a wide range of concentration.

INTRODUCTION

In the first study (2) rates were observed for only *equal* concentrations of mercaptan and olefin. This preliminary work emphasized the need for a more general formulation of the kinetics and the inadmissability of simplifying assumptions with regard to terminations. The mechanism previously proposed (2) involved an attack step followed by a transfer step but the isolation of each of these was not accomplished. It was therefore the principal object of this work to vary the concentrations of reagents over a wide range and test the proposed reaction scheme in terms of a more general kinetic description, and if possible to measure both the attack and transfer velocity coefficients.

BASIC REACTIONS: UNCONJUGATED VINYLS

The basic reactions and consequent steady state equations are presented in considerable detail in this paper to form a foundation of symbolism and theory for subsequent papers. Some estimates of incidental velocity coefficients at 30°C. are included to help in forming a judgment of the reactions which need to be considered.

In this paper we discuss only the photoinitiated addition of *n*-butyl mercaptan to unconjugated vinyls, and proceed to break the over-all process up into the various steps involved. Velocity constants are in liters moles^{-1} sec^{-1}.

Origin of Radicals

As in previous work (2) the origin of radicals is through the photolysis of 2,2′-azo-bis-isobutyronitrile designated Q_2, using a filter system which forbids activation of reactants:

(1) $\quad Q_2 + h\nu = 2\dot{Q} \qquad\qquad k(I)$

where $k(I)$ is the rate of origin of kinetic chains (moles/liter-sec.). In the

[1]*Manuscript received January 13, 1955.*
Contribution from the Department of Chemistry, University of Western Ontario, London, Ont. This work was supported by funds provided by the National Research Council of Canada.
[2]*The first paper of this series is Reference (2).*
[3]*Graduate student 1952. Present address—University of Cambridge, Cambridge, England.*
[4]*Associate Professor of Chemistry, University of Western Ontario, London, Ontario.*

present treatment we will assume that $\dot{Q}$ radicals have negligible concentration compared to all others and that they disappear by transfer with mercaptan:

(2) $\dot{Q}+RSH = QH+R\dot{S}$ k_3^0

Initiation

The thiyl radical attacks monomer to produce an unconjugated radical designated $\dot{X}$, e.g. $RSCH_2\dot{C}HCH_2CH_2CH_3$ results from an attack on 1-pentene. That the addition was counter Markovnikov was proved by product analysis.

(3) $R\dot{S}+M = \dot{X}_1$ k_1 2.5×10^6 (2)

Propagation

Nothing much is known of the propagation of $\dot{X}$ radicals into monolefins in the liquid phase. If we extrapolate James and Steacie's (5) values to 30° for the gas phase propagation of C_2H_5 radicals into 1-heptene and also their dehydrogenation constant, it may be shown that the kinetic chain would be of the order of unity, owing to degradative transfer, even in the absence of mercaptan. Consequently we can neglect propagation.

(4) $\dot{X}_1+M = \dot{X}_2$ $k_2 = 0$

Chain Transfer

In the presence of sufficient mercaptan the principal transfer reaction is

(5) $\dot{X}+RSH = P+R\dot{S}$ k_{3X} 2.5×10^6(2)

where P is addition product.

At low mercaptan concentrations we have reason to believe that there may be significant α-hydrogen transfer with the production of the strongly stabilized allylic radical designated $\dot{A}$.

(6) $\dot{X}+M = P+\dot{A}$ $k_{3\alpha}$ 150 (5)

This value for $k_{3\alpha}$ is that for the dehydrogenation of 1-heptene in the gas phase determined by James and Steacie (5).

(7) $R\dot{S}+M = RSH+\dot{A}$ $k_{3\alpha}'$

Finally reaction (7) is reversible, hence

(8) $\dot{A}+RSH = M+R\dot{S}$ k_{3A} 100

Since $k_{3\alpha}'/k_{3A} = K$, the equilibrium constant for (7), we can estimate K through bond energies to be somewhat less than unity. The value of $k_{3A} = 100$ is about the transfer constant of isoprenyl radical previously reported (2).

Termination

(9)	$2R\dot{S} = RSSR$	k_4'	6×10^{11}	(2)*
(10)	$R\dot{S}+\dot{X} = RSX$	k_5		
(11)	$2\dot{X} = X_2$	k_6'	10^{11}	(2)*
(12)	$\dot{X}+\dot{A} = X\dot{A}$	k_7		
(13)	$2\dot{A} = A_2$	k_8'	10^9	
(14)	$R\dot{S}+\dot{A} = RSA$	k_9		

In the light of the experimental results to be reported we have found it expedient to deal with the system:

**Recent work in this laboratory indicates that the value 6×10^{11} previously reported is an average for $R\dot{S}$ and $\dot{X}$ with $k_4' > k_6'$.*

(1) assuming the geometric mean for the crossed terminations and including the α-dehydrogenation,

(2) neglecting α-dehydrogenation and making no simplifying assumption with regard to cross terminations.

Total Radical Termination

With the assumption of the geometric mean for crossed termination two added constants suffice to express all termination constants in terms of one. Let $k_4 = u^2k_6$, $k_8 = \sigma^2k_6$, then all terminations may be expressed as $k_6(u\dot{RS}+\sigma\dot{A}+\dot{X})^2$.

Here we write $k_4 = 2k_4'$, $k_6 = 2k_6'$, $k_8 = 2k_8'$, and $k_5 = 2\sqrt{k_4'k_6'} = \sqrt{k_4k_6}$. Such a definition of the crossed termination k_5 is suggested by elementary collision theory since the collision number for unlike species is twice that for single. With this convention the expression $k_6[u\dot{RS}+\sigma\dot{A}+\dot{X}]^2$ is equal to the rate of disappearance of *all* radicals. We may note that in terms of the approximate values of k_4, k_6, and k_8 given above $u \div 2$, $\sigma \div 0.1$.

STEADY STATE EQUATIONS

The radical whose steady state is described is shown on the left. Since all terminations except those for $\dot{Q}$ radicals are included, the rate detail for terminations is implied by the letters T. For example

$T_{II} = k_4(\dot{RS})^2+k_5(\dot{RS})(\dot{X})+k_9(\dot{RS})(\dot{A})$.

I	$\dot{Q}$	$k(I) = k_3^0(RSH)(\dot{Q})$
II	$\dot{RS}$	$k_3^0(RSH)(\dot{Q})+k_{3A}(RSH)(\dot{A})+k_{3X})RSH)(\dot{X}) = k_1(\dot{RS})(M)+k_{3\alpha}'(\dot{RS})(M)+T_{II}$
III	$\dot{A}$	$k_{3\alpha}'(RS)(M)+k_{3\alpha}(\dot{X})(M) = k_{3A}(RSH)(\dot{A})+T_{III}$
IV	$\dot{X}$	$k_1(\dot{RS})(M) = k_{3X}(RSH)(X)+k_{3\alpha}(M)(\dot{X})+T_{IV}$.

Summation to infinity yields

$$[1] \qquad k(I) = \Sigma T = k_6[u\dot{RS}+\sigma\dot{A}+\dot{X}]^2.$$

The reaction rate measured dilatometrically is

$$[2] \qquad R = k_1(\dot{RS})(M) = k_{3X}(RSH)(\dot{X})$$

providing we neglect T_{IV} and $k_{3\alpha}(M)$ compared to $k_{3X}(RSH)$. The former is not permissible, as $RSH \neq 0$. For *long* kinetic chains we can express $(\dot{RS})$ and $(\dot{A})$ in terms of $(\dot{X})$ through IV and III. This value of $(\dot{X})$ substituted in [2] yields

$$[3] \qquad R = k_{3X}(RSH)\omega_6 \Big/ \left[1+u\frac{k_{3X}(RSH)}{k_1(M)}+\sigma\frac{k_{3\alpha}(M)}{k_{3A}(RSH)}\right]$$

after elimination of insignificant terms. In [3], $\omega_6 = \sqrt{k(I)/k_6}$. Owing to the last term in the denominator of [3] this equation predicts *lower* rates at *low mercaptan* than would be the case if $k_{3\alpha} = 0$. If α-dehydrogenation is neglected equation [3] can take a linear form, viz.,

$$[4] \qquad \frac{1}{R} = \frac{1}{k_{3X}(RSH)\omega_6}+\frac{u}{k_1(M)\omega_6},$$

from which on varying RSH at constant (M_0)

[5] $$u\,k_{3X}/k_1 = \text{Intercept}(M_0)/\text{slope}.$$

By the same procedure the rate may be expressed in terms of the RṠ radical (equation [2]).

[6] $$R = k_1(M)\omega_6/[u+k_1(M)/k_{3X}(RSH)\{1+k_{3\alpha}(M)/k_{3A}(RSH)\}].$$

No sigmoidal form of R vs. M such as that implied in [3] for R vs. RSH is now apparent, but the rate should fall at high M values owing to $k_{3\alpha}$. Again if $k_{3\alpha} = 0$ [6] can be written in a similar form to [4]

[7] $$R = k_1(M)\omega_6/u[1+k_1(M)uk_{3X}(RSH)]$$

which in linear form yields

[8] $$uk_{3X}/k_1 = \text{slope/intercept}(RSH_0).$$

Cross Termination

If the cross termination is not given by the geometric mean we can represent it quite generally thus: $k_5 = \phi\sqrt{k_4k_6}$ in which ϕ may have any value from 0 upwards. When this is included in the solution for the steady states it readily follows that equation [3] neglecting α-hydrogen reactions now becomes:

[9] $$R_1 = k_{3X}(RSH)\omega_6/[1+2\phi br+b^2r^2]^{\frac{1}{2}}$$

where $b = uk_{3X}/k_1$ and $r = (RSH)/(M)$. Similarly [7] becomes

[10] $$R_2 = k_1(M)\omega_6 br/u[1+2\phi br+b^2r^2]^{\frac{1}{2}}.$$

As rates R_1 are measured, varying RSH at constant M_0 a limiting value of [9] is implied at $(r \div \infty)$ $R_1^\infty = k_1(M_0)\omega_6/u$. Similarly $R_2^\infty = k_{3X}(RSH_0)\omega_6$ $(r \div 0)$. Consequently we can write [9] and [10] in terms of the two constants b and ϕ, and the limiting rates R_1^∞ and R_2^∞ viz.,

[11] $$R_1 = R_2^\infty r/[1+2\phi br+b^2r^2]^{\frac{1}{2}},$$

[12] $$R_2 = R_1^\infty b/[1+2\phi br+b^2r^2]^{\frac{1}{2}}.$$

METHODS

In general the methods employed were those described in the first paper (2) except that a new apparatus was constructed employing a series of four quartz lenses to collimate and focus the mercury arc light in a manner similar to that of Bartlett *et al.* (3).

The ultraviolet light source was a Hanovia A H-8, 85-watt lamp. The *photosensitizer* was again 2,2-azo-isobutyronitrile (AIN) employed in such concentration as to absorb not more than 20% of the light in the cell. Corning *filters* 9863 and 5840 were used to isolate radiation capable of photolyzing the AIN alone. Dilatometer technique was identical with that previously described (2).

EXPERIMENTAL

1-*Pentene*—Phillips Petroleum Research Grade was used without further purification.

Normal butyl mercaptan—Eastman Kodak's white label was distilled under an atmosphere of nitrogen through a 40-plate Todd column. The middle cut retained had the following properties: b.p. 98.0°C. at 750 mm., $n_D^{26} = 1.4410$. *Benzene*—Merck's Reagent Grade Thiophene-free was used without further purification.

Azo-isobutyronitrile was prepared by the method of Overberger *et al.* (7); m.p. 102.5–103.5°C.

The following series of experiments were carried out. All concentrations are expressed in moles/liter. *n*-Butyl mercaptan is represented as BuSH. Temperature was constant at 25°C.

TABLE I

	(AIN)10^3	(1-Pentene)	(*n*-BuSH)	$10^7k(I)$
Series I	3.15	1.59	1.61	1.1
Series II	3.15	4.8	0.803(const.)	1.1
Series III	3.15	0.797(const.)	4.8	1.1

k(I) values were determined by the method of Reference (1).

RESULTS AND DISCUSSION

Series I was designed to show the reproducibility of rate measurements, which is shown in Fig. 1. The measured rates are 0.159, 0.161, 0.161, and 0.16 mm./sec.

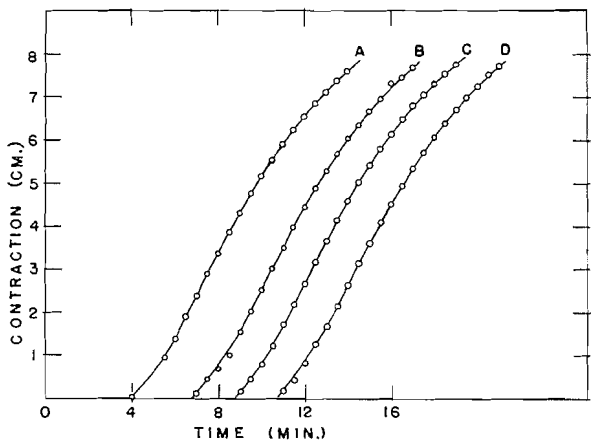

FIG. 1. Dilatometric measurement of the rate of addition of *n*-butyl mercaptan to 1-pentene, showing reproducibility of rate measurements. Series I.

Butyl Mercaptan and 1-Pentene

Series II—Analysis of the data plotted in Fig. 2, in the light of the theory, proceeded by attempting first to fit equation [6]. This suggested that the last term in the denominator was so small that it could not be distinguished from possible effects due to the considerable changes in environment as the composition was altered. In general the shape of the curve in Fig. 2 is that anticipated

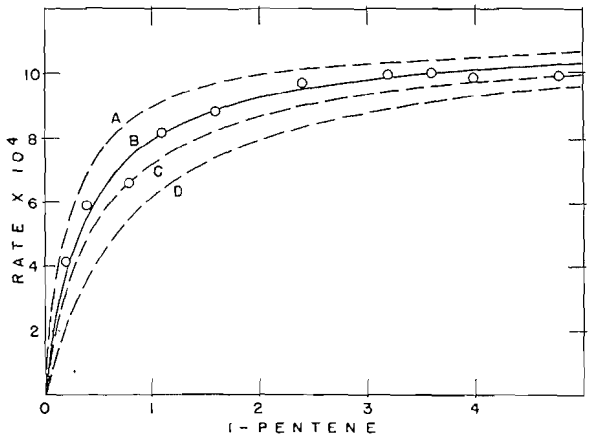

FIG. 2. Rate of addition of mercaptan as a function of 1-pentene at constant mercaptan (0.803 moles/liter). Series II. Curve A: $b = 0.3$, $\phi = 1$; Curve B: $b = 0.5$, $\phi = 1$; Curve C: $b = 0.5$, $\phi = 1.5$; Curve D: $b = 1.0$, $\phi = 1$.

by equation [7] or [12]. We could then proceed to apply equation [7] which assumes the geometric mean or equation [12] which does not. The result of the first alternative in terms of the linear form of equation [7], Fig. 3, yields an intercept $1/k_{3X}(\mathrm{RSH})_0\,\omega_6 = 900$ liter sec./mole, and a slope $u/k_1\omega_6 = 360$ sec., and hence a value of $u\,k_{3X}/k_1 = b \div 0.5$. The application of equation [12] is discussed below.

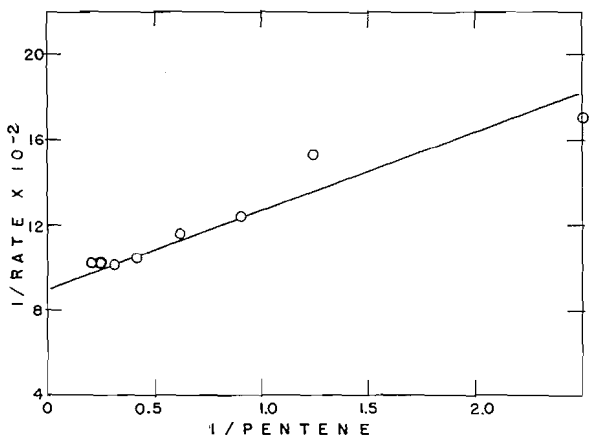

FIG. 3. Plot of data in Fig. 2 according to linear form of equation [7]. Intercept = 900 liter-sec./mole, slope = 360 sec.

Series III—The data are plotted in Fig. 4. From Series II we have values for $k_{3X}\omega_6$ and $u\,k_{3X}/k_1$, and hence "calculated" rates neglecting α-dehydrogenation can be determined. These are shown in Fig. 2*B* and 4*B*. A glance at the latter shows that the rates are lower than calculated in both low and high mercaptan regions. It is hence obvious that the linear form [4] cannot apply to

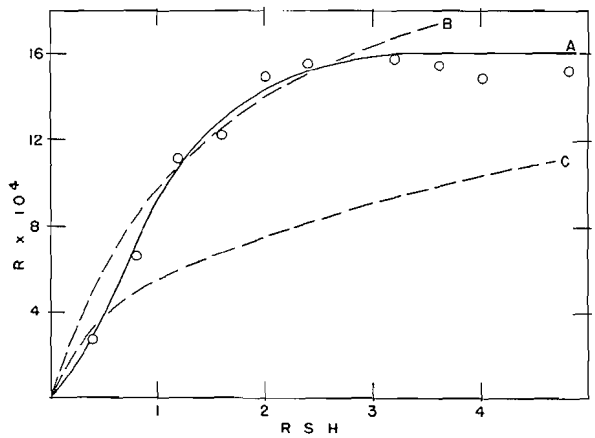

FIG. 4. Rate of addition of mercaptan as a function of mercaptan, 1-pentene constant (0.797 moles/liter). Series III. Curve A: smoothed experimental curve. Curve B: $b = 0.5$, $\phi = 1$; Curve C: $b = 0.5$, $\phi = 6$.

all values of mercaptan. Nevertheless the *general form* is that anticipated by [3] or [11] proceeding from a region where rates are dependent on mercaptan through a *transition* region to one in which rate is independent of mercaptan. Moreover the relative value of constants, viz., $u\ k_{3X}/k_1 = 0.5$ determined from Series II, does locate the position of the transition region. The deviation at low mercaptan may be partly imputed to some α-dehydrogenation (equation [3]). Another obvious reason for low rates could be the neglect of termination by Q radicals (basic reaction (2)) which cannot be valid at low mercaptan concentrations. There is nothing in the kinetics which anticipates the sharp levelling off of rates at *high* mercaptan and we can only surmise that this is due to the considerable changes in environment. Also shown are curves A and D, Fig. 2, which indicate the sensitivity to $b = u\ k_{3X}/k_1$ values when $\phi = 1$. Fig. 4 shows in curve C the effect of $\phi = 6$, $b = 0.5$.

Application of Equations [11] *and* [12]: *Non-geometric Termination*

Considering that α-dehydrogenation appears to be close to negligible we may with more confidence apply equations [11] and [12]. It should be noted that only unique values of ϕ and b will satisfy both equations. It was found that when $b = 0.5$ and $\phi = 0.5$ a reasonably good fit of the data is again obtained (Fig. 5). However the data can hardly discriminate between this interpretation and that of the geometric mean. Our main conclusions are (*a*) the cross termination is close to the geometric mean, (*b*) the value of $u\ k_{3X}/k_1$ appears to be quite closely given as 0.5 at 25°C., (*c*) deviations from the anticipated rate curves at high mercaptan values are probably due to environmental effects on the mechanism, but the general form is that predicted by the basic reactions given.

Estimation of Absolute Velocity Constants

While it was not the object of this work to determine the velocity coefficients and no half-life measurements were made, we may estimate these by taking

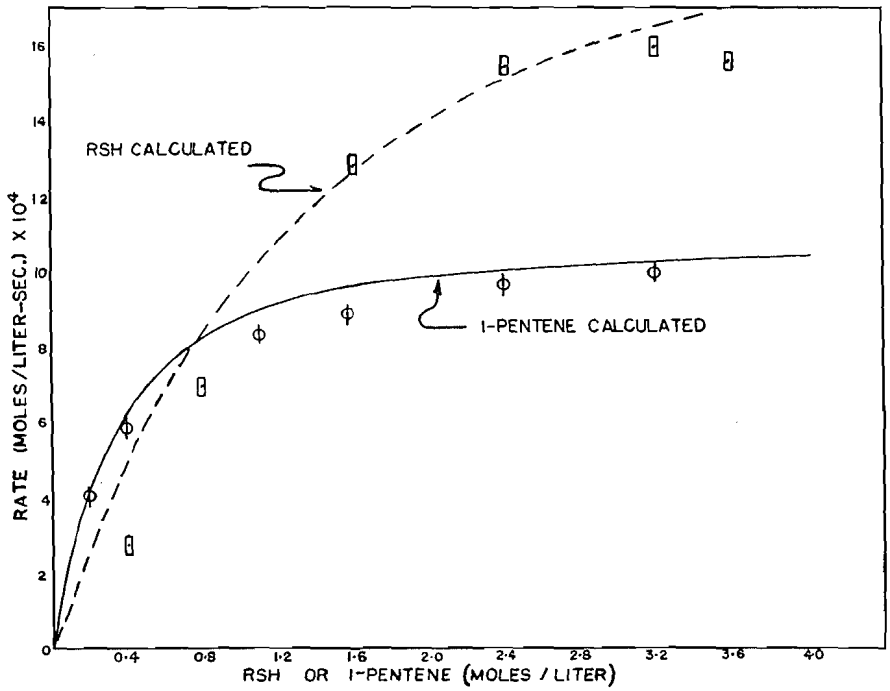

FIG. 5. Plot of equations [11] and [12] with $b = 0.5$, $\phi = 0.5$, showing agreement with measured rates.

$k_6 = 10^{11}$ which corresponds to 5×10^{10} for k_6', the recombination constant of $\dot{X}$ radicals. This value is somewhat lower than that previously reported (2) and higher than Ivin and Steacie (4) report for C_2H_5 radicals in the gas phase, viz., 1.56×10^{10}. This value for k_6 together with the $k(I)$ (Table I) for the series yields $\omega_6 \div 10^{-9}$. From Fig. 3 we found $1/k_{3X}(RSH_0)\omega_6 = 900$ or alternatively that $R_2^{\infty} = k_{3X}(RSH_0)\omega_6$ (Fig. 2) $= 1.1 \times 10^{-3}$. Therefore since $(RSH_0) = 0.8$, $k_{3X} = 1.1 \times 10^{-3}/0.8 \times 10^{-9} = 1.4 \times 10^6$ liter/mole-sec. If we take k_4 for the $R\dot{S}$ radical as 6×10^{11} (2), then $u = 2.45$ and hence $k_1 = 7 \times 10^6$. This happens also to yield for $u\,k_{3X}/k_1$ the value $2.45 \times 1.4 \times 10^6/7 \times 10^6 = 0.52$, which is hence consistent with the direct experimental value.

GENERAL CONCLUSIONS

(1) The "calculated" curves shown in Fig. 5 are seen to be in substantial agreement with the experimental results except for high mercaptan concentrations. In consequence we can presume that the mechanism of the photoinitiated addition of mercaptan to 1-pentene does in fact take place in two independent steps: an attack step ($k_1 = 7 \times 10^6$) and a mercaptan transfer step ($k_{3X} = 1.4 \times 10^6$).

(2) With regard to equation [7] it should be noted that the last term in the denominator $k_1(M)/uk_{3X}(RSH)$ is equal to $(\dot{X})/u(R\dot{S})$ and hence measures the relative abundance of these radicals. On the plateau of Fig. 2 we may

hence presume that $(\dot{X}) > (R\dot{S})$, and a half life in this region may be assigned to the $\dot{X}$ radical. In a similar manner we might isolate the $R\dot{S}$ radical. Melville, Robb, and Tutton (6) were the first to point out that when such measurements of half lives are combined with one made in a region of obvious cross-termination the cross-termination velocity constant k_5 could be measured. It is concluded here that such a procedure is valid only (*a*) if it has been shown that such side reactions as α-dehydrogenation are negligible, (*b*) if no propagation occurs, (*c*) provided the regions where radicals may be taken as isolated have been defined experimentally such as shown in this paper.

ACKNOWLEDGMENTS

We are grateful for financial assistance from the National Research Council and one of us, M. Onyszchuk, for a scholarship from the Ontario Research Council and also for permission to publish these results from the Associate Committee of the National Research Council on Synthetic Rubber.

REFERENCES

1. Back, R. and Sivertz, C. Can. J. Chem. 32: 1061. 1954.
2. Back, R., Trick, G., McDonald, C., and Sivertz, C. Can. J. Chem. 32: 1078. 1954.
3. Bartlett, P. D. and Kwart, H. J. J. Am. Chem. Soc. 72: 1051. 1950.
4. Ivin, K. J. and Steacie, E. W. R. Proc. Roy. Soc. (London), A, 208: 25. 1951.
5. James, D. G. L. and Steacie, E. W. R. Private communication.
6. Melville, H. W., Robb, J. C., and Tutton, R. C. Discussions Faraday Soc. 10: 5595. 1951.
7. Overberger, C. G., O'Shaughnessy, M. T., and Shalit, H. J. J. Am. Chem. Soc. 71: 2161. 1949.

Canadian Journal of Chemistry

Issued by THE NATIONAL RESEARCH COUNCIL OF CANADA

VOLUME 33 JUNE 1955 NUMBER 6

SEDIMENTATION AND VISCOSITY STUDIES OF BOVINE SERUM ALBUMIN IN UREA SOLUTION[1]

BY P. A. CHARLWOOD

ABSTRACT

Sedimentation and viscosity measurements were made on bovine serum albumin during denaturation at pH 9.9 in 8.0 *M* urea in the presence of sodium-*p*-chloromercuribenzoate. The results suggested that the urea caused a rapid initial increase in the axial ratio and equivalent volume of the protein molecule. A subsequent slower increase in asymmetry was attributed to the effect of the mercury compound.

INTRODUCTION

The action of strong urea solutions on proteins is an example of "denaturation", a subject recently reviewed by Putnam (34). For many proteins the primary change in denaturation is believed to be a rearrangement of the secondary-bonded structure (21, 34). At this stage molecular weight is unaltered (5, 35), but changes in molecular shape will occur. The present work was undertaken to study the gross changes which occur in the shape of the bovine serum albumin molecule in the presence of urea.

The dynamic characteristics of a protein will reflect changes of molecular shape, but there are many difficulties involved in establishing the precise relation (13). To avoid some of these difficulties Scheraga and Mandelkern (39) related the observed characteristics of the protein molecule to a hypothetical "hydrodynamically equivalent ellipsoid", through a function, β, which depends only on the axial ratio of the (prolate or oblate) ellipsoid.

For the calculation of β, accurate measurements of several quantities should be made (in the same solvent, under the same conditions) and extrapolated to infinite dilution of protein. One combination consists of the sedimentation constant, s, intrinsic viscosity, $[\eta]$ (10), partial specific volume, $\bar{v}$, and molecular weight, M. From these characteristics $\beta = Ns[\eta]^{1/3}\eta_0 / M^{2/3}(1-\bar{v}\rho_0)$, where η_0 and ρ_0 are respectively the viscosity and density of the solvent, and N is Avogadro's number. Recently Champagne (6) applied a similar method of Sadron (36). However, Sadron (36) attempted to attribute a portion of the equivalent volume to hydration expressed in terms of $\bar{v}$, a procedure which Scheraga and Mandelkern (39) deprecate.

Measurements of s and $[\eta]$ made here have been used to follow the changes in β which occur when urea acts on bovine serum albumin in aqueous solution.

[1]*Manuscript received January 6, 1955.*
Contribution from the Division of Applied Biology, National Research Laboratories, Ottawa, Canada. Issued as N.R.C. No. 3557.

Viscosity measurements under different conditions were made to obtain information about the intramolecular changes responsible for the alterations in β.

EXPERIMENTAL

Stock solutions of bovine serum albumin (Armour, batch 66706) were made up, and their concentrations determined by diluting samples for measurements in the differential refractometer (4). A specific refractive increment of 0.00186 (32) was assumed at the wavelength used (5890 Å).

Chemicals were reagent grade. Further purification of the urea was considered unnecessary (42). It was, however, dried by heating *in vacuo* for six hours at 55°C. (16). The solvent used for the main group of experiments contained urea (8.0 *M*), sodium borate (borax) (0.05 *M*), and sodium *p*-chloromercuribenzoate* (0.005 *M*), the last constituent being added to prevent aggregation (15). The pH, measured on a Beckman model G pH meter, was about 9.9, varying slightly (±0.03) from batch to batch and with time for a given protein solution. In some experiments phosphate buffers (pH 7.0 and 8.3, ionic strength 0.2) were used.

In the main group of experiments series of measurements were made at each of six protein concentrations in the range 0.25–1.5%. The stock solutions of protein and solvent were respectively 11 and 1.1 times the concentrations required in the mixture. Coarse sintered glass filters were used to eliminate dust. At the start of each series, the stock solutions were mixed. At intervals, samples were removed from the mixture for ultracentrifuge runs. In each series seven runs were made, extending to about six days after mixing. A standard schedule was followed so that, in corresponding runs at different protein concentrations, photographs were taken at the same time after mixing. Replicate mixtures were used to avoid the necessity of doing runs during the night. Concurrently with the ultracentrifuge runs, viscosity measurements were made every 30–60 min. in triplicate, extending to about 27 hr. after mixing. Different viscosimeters contained the various replicate mixtures, so that each relative viscosity – time graph was composite, providing information on reproducibility.

A slight opalescence developed in the mixtures at pH 9.9 after 24 hr., more particularly at the higher protein concentrations. One solution (1% protein) was left standing for a week. Some gross particles were removed by passage through a coarse sintered glass filter, and part of the filtrate was centrifuged in the preparative ultracentrifuge. Comparative viscosity measurements were made on the solution which was centrifuged and that which was not. Some of the centrifuged solution was dialyzed exhaustively against 0.2 ionic strength phosphate buffer (pH 7.0), and examined in the analytical ultracentrifuge.

A solution of about 1% bovine serum albumin, 8.0 *M* urea, 0.2 ionic strength phosphate buffer (pH 8.3), and 0.00015 *M* PCMB, after three days at 25°C., was redialyzed against phosphate buffer (pH 7.0, ionic strength 0.2) containing 0.00015 *M* PCMB. Sedimentation and viscosity measurements were made using this protein solution and several dilutions of it (in the same buffer). Similar measurements were made on albumin not exposed to urea.

**This will be referred to subsequently as PCMB.*

Various viscosity experiments were done in urea at several PCMB concentrations, at a lower pH (8.3), and in the presence of silver nitrate. Additional measurements were made in 0.005 *M* PCMB at pH 9.65 in the absence of urea.

Sedimentation constants were measured at 59,780 r.p.m. in the Spinco ultracentrifuge in the usual way (7). The 3-mm. cell was employed for protein concentrations above 0.9%, the 12-mm. cell for the rest. Eight photographs were taken at 16-min. intervals during each run. Because of the slow separation of the peak from the meniscus, the first exposure could not be made until the rotor had been at top speed for about an hour. Since even a slight leak would introduce a large relative error in the distance moved by the peak, the position of the meniscus was determined with particular care during measurement of the photographs. The rotor temperature immediately prior to each run was adjusted so that the rise of about 2°C. during the run ensured a mean temperature of approximately 25°C. The temperature at the middle of the time interval between first and last exposures was estimated in the manner of Kegeles and Gutter (22), taking into account the 1°C. correction indicated by Waugh and Yphantis (44) and Biancheria and Kegeles (3). Sedimentation constants were corrected to water at 20°. The viscosity of solvent, rather than solution, was used (20, 24). Solvent density, determined from weighings of the volumetric flask used, agreed closely with that expected from the data of Gucker, Gage, and Moser (17). As urea solutions have no exceptional compressibility (33), no correction was applied for this.

Viscosity determinations were made in Ostwald-Fenske type viscosimeters (ASTM No. 100), giving a flow time of 70–120 sec. at the temperature of the thermostat (25.1°C.). In experiments not involving urea, ASTM No. 50 viscosimeters were used to keep the flow times sufficiently long. The ratio of flow times for protein solution and solvent was taken as the relative viscosity (10). However, for measurements in the absence of urea, when the relative viscosity was low, the effect of the protein on the solution density was taken into account.

RESULTS

In the main group of sedimentation measurements, values at finite concentrations decreased with time (Table I). The concentration dependence (Table I) was several times greater than for the original albumin (22). Regression lines were calculated at each time, the intercepts giving the extrapolated values shown in Table II. The mean deviation of points from these lines amounted to about 1.7%, and about 15% of the points showed deviations of over 3%. These unusually large errors were probably due to the small distances moved by the boundaries in the rather viscous and dense solvent. For two reasons, the points were not weighted in the calculation of the regression lines. Firstly, the greater sharpness of the maxima of peaks at the higher concentrations was less pronounced when the short cell was used. Secondly, the boundaries moved more rapidly at lower concentrations.

Viscosity measurements in the main group were plotted as reduced viscosity (10), η_{red}, against time at each protein concentration. The derived curves,

TABLE I

SEDIMENTATION CONSTANTS OF BOVINE SERUM ALBUMIN AT pH 9.9 IN 8.0 *M* UREA, 0.005 *M* PCMB, 0.05 *M* BORAX

Time after mixing (min.)	Protein concentration (gm./100 ml.)					
	0.245%	0.497%	0.728%	0.967%	1.20_6%	1.45_7%
150	2.48	2.41	2.36	2.10	1.95	1.85
388	2.43	2.31	2.10	1.95	1.83	1.73
622	2.34	2.30	2.06	1.97	1.81	1.67
960	2.38	2.28	2.00	1.96	1.76	1.64
1290	2.33	2.18	1.97	1.91	1.78	1.57
1636	2.41	2.25	1.94	1.92	1.68	1.63
8798	2.29	2.04	1.79	1.51	1.55	1.32

NOTE: *Measurements were made at about 25°C. All values are corrected to water at 20°C. and expressed in Svedberg units.*

TABLE II

AXIAL RATIOS AND VOLUMES OF EQUIVALENT ELLIPSOIDS FOR BOVINE SERUM ALBUMIN

	Time (min.)	$s^0_{20,w}$ (Svedberg units)	$[\eta]$ (gm./100 ml.)$^{-1}$	$\beta \times 10^{-6}$	Axial ratio, a/b	$V_e \times 10^{19}$ (ml.)
Untreated albumin in phosphate buffer, pH 7.0, ionic strength 0.2		4.40	0.042	2.15	2.6	1.4
Albumin in 8.0 *M* urea, borate buffer, pH 9.9, plus 0.005 *M* PCMB	150	2.67	0.208	2.22	4.6	4.3
	388	2.57	0.241	2.24	5.2	4.3
	622	2.52	0.261	2.26	5.8	4.1
	960	2.54	0.278	2.32	7.5	3.3
	1290	2.47	0.293	2.30	7.0	3.8
	1636	2.53	0.305	2.39	9.2	2.7
	8798	2.40				
Recovered albumin in phosphate buffer, pH 7.0, ionic strength 0.2, plus 0.00015 *M* PCMB		4.62	0.041	2.24	5.2	0.8

which resembled those obtained at 30°C. by Frensdorff, Watson, and Kauzmann (15), were of the same type as obtained in the presence of silver (Fig. 4, upper curves). A few points fell so far off the curves as to indicate errors of ±0.3 sec., but usually the deviations were much smaller.

From the viscosity curves values of η_{red} were read at times corresponding to the middle of the ultracentrifuge runs. These figures were plotted as η_{red} against protein concentration at six different times (Fig. 1). Regression was linear within experimental error, the deviations of points at the lowest concentration corresponding to a systematic difference of only 0.1 sec. Extrapolation to zero protein concentration showed the intrinsic viscosity increasing with time (Fig. 1 and Table II). The slopes of the lines also increased steadily with time, indicating increased intermolecular influences. In the fitting of the regression lines shown, weights were assigned to the points, based approximately on the relative errors in η_{red} produced at different concentrations by

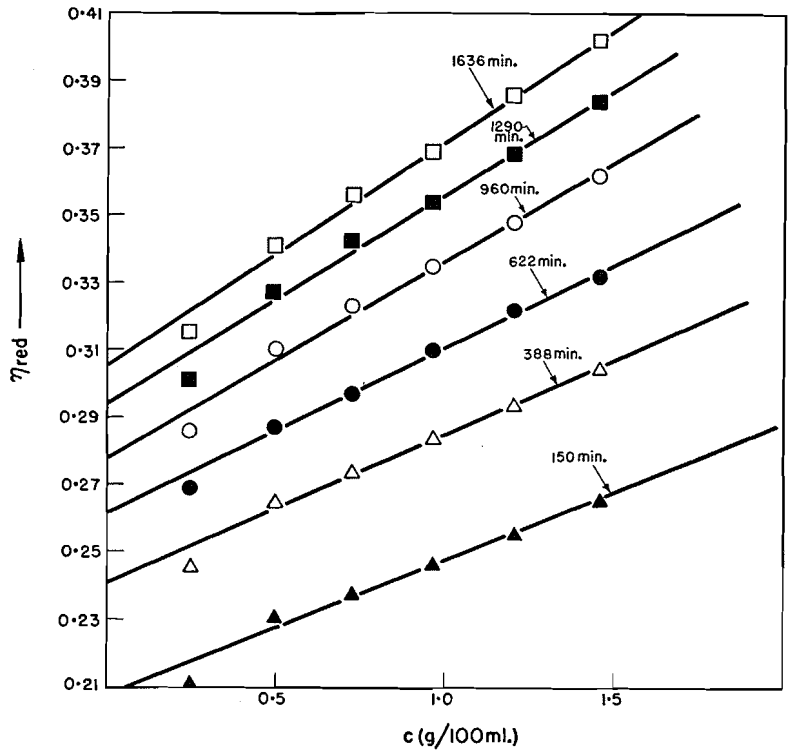

FIG. 1. Reduced viscosity of bovine serum albumin after various times at pH 9.9 in 8.0 M urea, 0.05 M borax, 0.005 M PCMB.

the same absolute error in timing. Experiments in which the head was varied confirmed that flow was Newtonian.

In the calculations of β from $s^0_{20,w}$ and $[\eta]$, $\bar{v}$ was taken as 0.734 (12) and M as 66,000 (see Discussion). In urea solution, β increased with time (Table II). Since the first six values of $s^0_{20,w}$ in urea solution did not show a statistically significant trend, this increase was due to the rise in intrinsic viscosity. However, when the value at 8798 min. was included, the whole series showed time dependence ($p \sim 0.02$).

In each series of ultracentrifuge runs (except the one at the highest concentration) the areas under the peaks showed no measurable decrease. The peaks showed no obviously abnormal degree of spreading, although no quantitative measurements of the spread were attempted. There was only a very slight difference in viscosity between the sample from the preparative ultracentrifuge and that which was not centrifuged. This evidence indicates that the material responsible for the opalescence is rendered insoluble without prior formation of soluble aggregates.

Removal of urea by dialysis against pH 7.0 phosphate buffer caused extensive aggregation. There was some precipitation, and the ultracentrifuge revealed an asymmetric peak which moved several times faster than normal, and spread quickly. In the absence of PCMB, urea caused s to increase with

time and the boundary spread rather rapidly (cf. 34). The material recovered from solution in 8.0 *M* urea, 0.00015 *M* PCMB at pH 8.3 gave a clear solution on redialysis. In pH 7.0 phosphate buffer in the ultracentrifuge it gave one peak moving only slightly faster than normal (Table II). There was a trace of a heavier component, but no more than in the untreated albumin.

Under all conditions 8.0 *M* urea caused a rapid initial increase in the viscosity of bovine serum albumin. Subsequent behavior depended on the composition of the solution. At pH 9.9 (in 0.05 *M* borax) there was always a slow secondary increase. At the protein concentration used, the minimum secondary effect occurred at about 0.0005 *M* PCMB (Fig. 2). At pH 8.3 (0.2 ionic strength

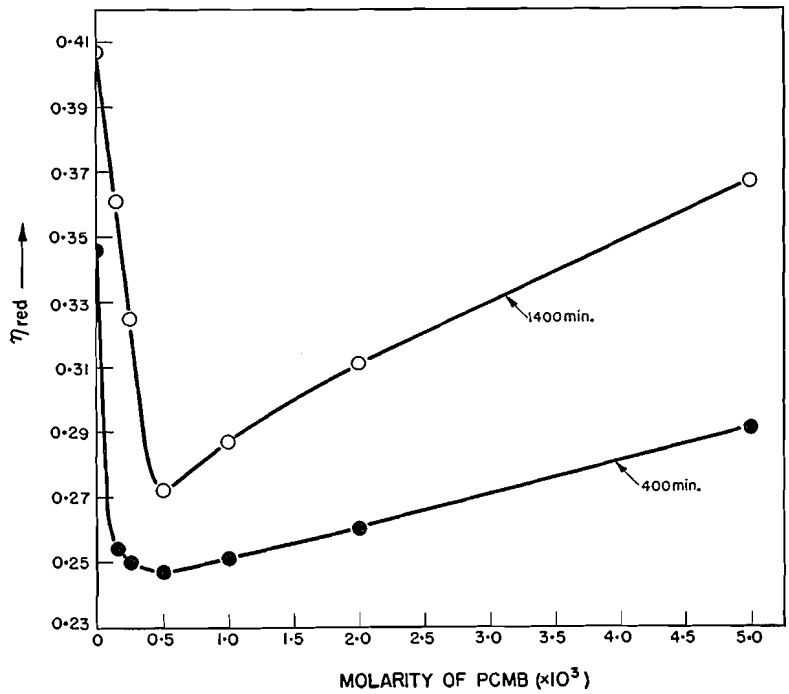

FIG. 2. Effect of PCMB concentration on the reduced viscosity of bovine serum albumin at pH 9.9 in 8.0 *M* urea, 0.05 *M* borax. Protein concentration 0.97%.

phosphate) in 0.00015 *M* PCMB (about one mole per mole of protein), the viscosity remained constant for a day after the initial increase (Fig. 3). At higher concentrations of PCMB there was a detectable secondary increase, illustrated in Fig. 3 by the behavior at 0.005 *M*.

At pH 8.3 (phosphate buffer) one mole of silver nitrate per mole of protein prevented a secondary increase in viscosity. This increase reappeared in the presence of 0.005 *M* PCMB (Fig. 4). At pH 9.9 (borate buffer) silver nitrate failed to eliminate the secondary effect, either in the absence, or in the presence, of PCMB (Fig. 4).

At pH 9.65 (borate buffer), in the absence of urea, 0.005 *M* PCMB caused no detectable variation in the viscosity of the protein solution over the course of 48 hr.

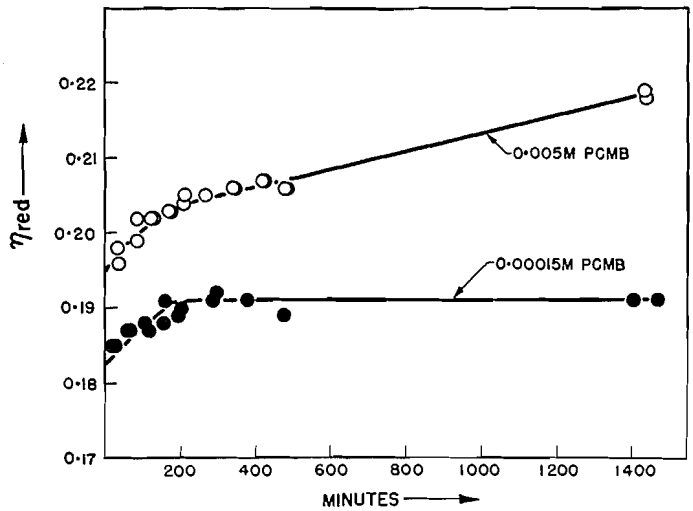

FIG. 3. Effect of PCMB concentration on the time dependence of the reduced viscosity of bovine serum albumin in 8.0 *M* urea at pH 8.3 (0.2 ionic strength phosphate). Protein concentration 0.97%.

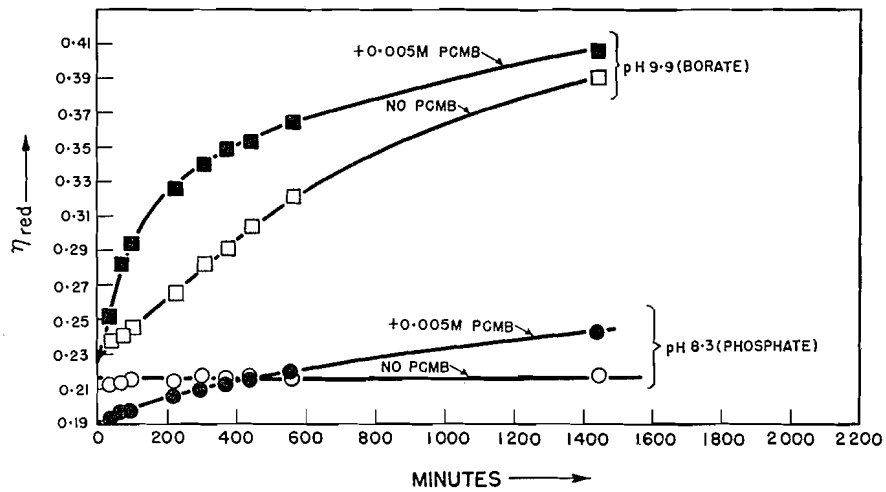

FIG. 4. Reduced viscosity of bovine serum albumin in 8.0 *M* urea with one equivalent of silver nitrate added. Protein concentration 0.97%.

DISCUSSION

As Scheraga and Mandelkern (39) emphasized, quite high experimental accuracy must be attained for successful application of their method, as axial ratio is critically dependent on β. It is evident, from the discrepancies between measurements on the same protein by different workers, that such accuracy is uncommon in available data. It was hoped to circumvent this problem by choice of suitable conditions, and by the use of a series of comparative measurements.

The solvent used was chosen because the work of Frensdorff, Watson, and Kauzmann (15) showed that η_{red} would be reasonably high, and would give measurable variations with time.

Although it is known that crystalline bovine serum albumin contains impurities of higher molecular weight (1), similar or other important objections could be raised to the use of alternative proteins. Moreover, as this albumin has been widely studied, it presented some advantages. Recent determinations of M by independent methods have given 65,400 (11), 66,100 (26), and about 66,000 (18) and for human albumin 65,600 (25). If the 1°C. temperature correction is applied to the sedimentation measurements of Creeth (11), and the most recent value of $\bar{v}$ (12) substituted for that he used, the value of M is increased, but only slightly. In the calculations in the present paper M was taken as 66,000.

Since no method presented itself for following possible changes in molecular weight, conditions were chosen under which there is believed to be little alteration (5). Incorporation of PCMB in the solution should not only prevent much aggregation (15), but also help to prevent autoxidation, which might otherwise occur at pH 9.9 (27). At a concentration of 0.005 M, this reagent is equivalent to albumin present at about 1.1%, even if all the sulphur in the protein were to exist in the form of —SH groups.

Although enhanced intermolecular influences were evident from the magnitude of the concentration dependence of s (Table I; cf. 22 for native albumin), any aggregation must have been slight in extent, as there was no curvature of the η_{red} regression lines (Fig. 1; cf. 15). Extrapolation to zero concentration should eliminate complications introduced by intermolecular effects, including any aggregation. The values of β should, therefore, not contain errors due to these causes.

According to Frensdorff, Watson, and Kauzmann (14), the ionic strength of the borax is high enough to suppress anomalies in viscosity measurements. There is no curvature of the sedimentation regression lines to suggest that the ionic strength was not sufficiently high for these experiments. In any case, extrapolation should eliminate any small anomalies which persist.

Since s, when measured at finite concentrations, decreases with time (Table I), the usual method of computation is not strictly accurate. Analogous problems have been recently discussed. Schwert (40) has considered the effect of increasing temperature, and Alberty (2) the effect of variations in s due to concentration changes in the ultracentrifuge cell. A treatment similar to that of Alberty (2), based on a Taylor expansion, showed that the errors involved in using the ordinary method of calculation were negligible. This conclusion was not surprising, because the total variation of s during a run (from all causes) was never more than double the error of a determination, and there was no significant curvature of the $\log x$ vs. t lines.

Several points relating to ultracentrifuge measurements were discussed earlier (7, 8). One very important factor, which influences the values of β, is the density factor, $\bar{v}\rho$. This has been discussed by Longsworth (24) and by Schachman and Lauffer (37). The magnitude of β in urea solution (Table II)

is consistent with the assumption that $\bar{v}$ in these solutions is not greatly different from normal (29). The trend of β would be the same even if $\bar{v}$ were different. Only a decrease of $\bar{v}$ with time in urea solution might invalidate the conclusions.

In so far as the bovine serum albumin molecule may be identified with the equivalent ellipsoid, the results suggest that initial exposure to the urea solution increases both the axial ratio and the volume of the protein molecule. Subsequently the axial ratio continues to increase with time, but the volume may decrease. This secondary change may be due to the PCMB. Frensdorff, Watson, and Kauzmann (15) have suggested that under alkaline conditions intramolecular —S—S— bridges undergo some hydrolysis, liberating —SH groups. Reaction of these with PCMB would accentuate the splitting and produce a more extended molecule.

The secondary increase which occurs in the viscosity of bovine serum albumin in urea solution (in the absence of inhibitors) was ascribed by Hospelhorn, Cross, and Jensen (19) to aggregation resulting from a chain reaction. Ultracentrifuge experiments under these conditions also strongly suggested aggregation (see Results). The chain reaction was believed to be initiated by the free —SH group of the albumin molecule. At pH 8.0 (phosphate buffer) Hospelhorn, Cross, and Jensen (19) found that incorporation of one or two equivalents of silver nitrate in the urea solution eliminated the secondary increase in viscosity. This they ascribed to the blockage of the free —SH group.

The effects of one equivalent of silver nitrate and one of PCMB were similar at pH 8.3 in phosphate buffer (Figs. 3, 4). Probably, therefore, the PCMB under these conditions merely blocks the free —SH group. Much higher concentrations of PCMB restored the secondary increase (Figs. 3, 4), presumably by splitting the —S—S— bridges, as discussed above.

The failure of silver nitrate at pH 9.9 (borate buffer) to prevent the secondary effect (Fig. 4) might be accounted for by some hydrolysis, either of the silver derivative or of the —S—S— bridges. Both processes would liberate —SH groups capable of starting aggregation. The further increase in viscosity at pH 9.9 when PCMB was also incorporated (Fig. 4) could be due to its effect on the splitting of the —S—S— bridges.

To account for the shape of the curves in Fig. 2 it may be assumed that at very low molarities there is insufficient PCMB to block all —SH groups, and aggregation can occur. As the concentration increases, there is enough to react with the —SH groups, and to promote the splitting of —S—S— links, causing an increase in viscosity. The minima in the curves of Fig. 2 will occur when aggregation has been largely suppressed, but the concentration of PCMB is not yet great enough to exert much influence on the hydrolysis of the intramolecular —S—S— links. The lack of effect of PCMB in the absence of urea seems to indicate that it can act only after a preliminary opening up of the protein molecule. All the phenomena are thus explicable in terms of the complementary propositions of Frensdorff, Watson, and Kauzmann (15) and Hospelhorn, Cross, and Jensen (19).

The basis of the concept of Scheraga and Mandelkern (39) has been challenged (43) on the grounds that the sedimentation constant and intrinsic viscosity of an actual protein (bovine serum albumin being quoted as a possible example) might lead to a value of β less than 2.12 ($\times 10^6$), which is inconsistent with the theory. The sedimentation constant used by Tanford and Buzzell (43) does not include the 1°C. correction. Careful determination of the intrinsic viscosity (Table II) gave 0.042, in agreement with 0.042 obtained by Oncley, Scatchard, and Brown (31) and 0.041_3 by Koening and Perrings (23). Using 0.042 for $[\eta]$ and increasing s to 4.4 units in the data used for computing β gives 2.15 from sedimentation and viscosity, or 2.13 from diffusion and viscosity. The example given by Tanford and Buzzell (43) does not, therefore, provide unequivocal verification of their general hypothesis. Nevertheless, a quantitative theoretical investigation of their ideas is highly desirable.

Scheraga and Mandelkern (39) applied their theory to measurements by Neurath and Saum (29) of the viscosity and diffusion of horse serum albumin in the presence of urea (pH 5.2). They remarked that β values obtained, 1.98–2.07, were within experimental error of 2.12, but that a value of 2.23 for the native protein was not. These conclusions seem inconsistent. Moreover, it has been suggested (35) that an empirical correction factor should be applied to diffusion measurements made in solutions of high viscosity. Recently Scheraga *et al.* (38), using diffusion and viscosity data, calculated $\beta = 2.15$ (± 0.10) and 2.35 (± 0.07) for untreated and urea-denatured fibrinogen respectively. They did not regard these figures as differing significantly, in view of the probable errors shown in brackets, and were of the opinion that their results did not provide evidence of any gross unfolding on denaturation.

Ogston (30) and Shulman (41) have compared the method of Scheraga and Mandelkern (39) with earlier, more conventional ones. Agreement in some instances was poor. Generally, lower axial ratios (and higher equivalent volumes) were given by the newer theory. This is only to be expected, because the older methods are based on assumptions which may sometimes be far from correct (39).

It has been suggested (21) that the molecules of bovine serum albumin denatured in urea may approximate to random coils rather than to rigid ellipsoids. For flexible chain molecules forming a random coil, Mandelkern and Flory (28) gave a treatment similar to, but not identical with, that of Scheraga and Mandelkern (39). They deduced that a function $\Phi^{1/3}P^{-1}$, which is formally the same as β, should be constant. The value they found experimentally for this constant was about 2.5 ($\times 10^6$). Although β (Table II) does not become as large as this, it is increasing, and might well attain 2.5 at later times. Thus, although the results quoted are consistent with the ellipsoidal model, it is possible that at later times a random coil might be a better approximation. If that is so, the actual shape of the molecule will probably combine some characteristics of both types, the relative importance altering with time.

It appears from the viscosity experiments that the first, rapid change in the protein is due to the urea, but the secondary change is brought about by the combined action of the urea and PCMB. The recovered albumin had been submitted to conditions in which only the first type of change occurred. The figures (Table II) show that the molecule returned to a more symmetrical shape, but was less symmetrical than untreated material.

The general conclusion from this work is that the Scheraga–Mandelkern (39) theory gives a very reasonable account of the changes observed. Chernyak and Pasynsky (9), using figures for the adsorption of urea by horse serum albumin as a measure of solvation, attempted to evaluate the relative contributions of volume and shape changes to the observed viscosities of the protein in urea solutions. Their method is based essentially on the older type of treatment. Moreover, since they used a different albumin under different conditions, no comparison can be made with the present results.

ACKNOWLEDGMENTS

The author wishes to thank Dr. W. H. Cook for his interest and helpful advice, and Drs. J. R. Colvin, E. O. Hughes, M. E. Reichmann, and D. B. Smith for criticism of the manuscript. The technical assistance of Mr. D. Muirhead is gratefully acknowledged.

REFERENCES

1. Akeley, D. F. and Gosting, L. J. J. Am. Chem. Soc. 75: 5685. 1953.
2. Alberty, R. A. J. Am. Chem. Soc. 76: 3733. 1954.
3. Biancheria, A. and Kegeles, G. J. Am. Chem. Soc. 76: 3737. 1954.
4. Brice, B. A. and Halwer, M. J. Opt. Soc. Amer. 41: 1033. 1951.
5. Burk, N. F. J. Biol. Chem. 98: 353. 1932.
6. Champagne, M. Compt. rend. 237: 521. 1953.
7. Charlwood, P. A. Biochem. J. (London), 51: 113. 1952.
8. Charlwood, P. A. Biochem. J. (London), 56: 259. 1954.
9. Chernyak, R. and Pasynsky, A. Colloid J. (U.S.S.R.), 14: 204. 1952. English Translation by Consultants Bureau, 152 West 42nd St., New York 18, N.Y.
10. Cragg, L. H. J. Colloid Sci. 1: 261. 1946.
11. Creeth, J. M. Biochem. J. (London), 51: 10. 1952.
12. Dayhoff, M. O., Perlmann, G. E., and MacInnes, D. A. J. Am. Chem. Soc. 74: 2515. 1952.
13. Edsall, J. T. *In* The proteins. Vol. I, Part B. *Edited by* H. Neurath and K. Bailey. Academic Press, Inc., New York. 1953.
14. Frensdorff, H. K., Watson, M. T., and Kauzmann, W. J. Am. Chem. Soc. 75: 5157. 1953.
15. Frensdorff, H. K., Watson, M. T., and Kauzmann, W. J. Am. Chem. Soc. 75: 5167. 1953.
16. Gosting, L. J. and Akeley, D. F. J. Am. Chem. Soc. 74: 2058. 1952.
17. Gucker, F. T., Jr., Gage, F. W., and Moser, C. E. J. Am. Chem. Soc. 60: 2582. 1938.
18. Gutfreund, H. Trans. Faraday Soc. 50: 628. 1954.
19. Hospelhorn, V. D., Cross, B., and Jensen, E. V. J. Am. Chem. Soc. 76: 2827. 1954.
20. Jullander, I. Arkiv. Kemi Mineral. Geol. 21, A (No. 8). 1945.
21. Kauzmann, W. *In* A symposium on the mechanism of enzyme action. *Edited by* W. D. McElroy and B. Glass. The Johns Hopkins Press, Baltimore, Md. 1954.
22. Kegeles, G. and Gutter, F. J. J. Am. Chem. Soc. 73: 3770. 1951.
23. Koenig, V. L. and Perrings, J. D. Arch. Biochem. and Biophys. 41: 367. 1952.
24. Longsworth, L. G. Proc. Natl. Acad. Sci. U.S. 36: 502. 1950.
25. Low, B. W. J. Am. Chem. Soc. 74: 4830. 1952.
26. McClure, L. E., Schieler, L., and Dunn, M. S. J. Am. Chem. Soc. 75: 1980. 1953.
27. Macheboeuf, M. and Robert, B. Bull. soc. chim. biol. 35: 399. 1953.
28. Mandelkern, L. and Flory, P. J. J. Chem. Phys. 20: 212. 1952.
29. Neurath, H. and Saum, A. M. J. Biol. Chem. 128: 347. 1939.

30. OGSTON, A. G. Trans. Faraday Soc. 49: 1481. 1953.
31. ONCLEY, J. L., SCATCHARD, G., and BROWN, A. J. Phys. & Colloid Chem. 51: 184. 1947.
32. PERLMANN, G. E. and LONGSWORTH, L. G. J. Am. Chem. Soc. 70: 2719. 1948.
33. PERMANN, E. P. and URRY, W. D. Proc. Roy. Soc. (London), A, 126: 44. 1929.
34. PUTNAM, F. W. *In* The proteins. Vol. I, Part B. *Edited by* H. Neurath and K. Bailey. Academic Press, Inc., New York. 1953.
35. PUTNAM, F. W., ERICKSON, J. O., VOLKIN, E., and NEURATH, H. J. Gen. Physiol. 26: 513. 1943.
36. SADRON, C. Cahiers phys. (2) No. 12: 26. 1942.
37. SCHACHMAN, H. K. and LAUFFER, M. A. J. Am. Chem. Soc. 72: 4266. 1950.
38. SCHERAGA, H. A., CARROLL, W. R., NIMS, L. F., SUTTON, E., BACKUS, J. K., and SAUNDERS, J. M. J. Polymer Sci. 14: 427. 1954.
39. SCHERAGA, H. A. and MANDELKERN, L. J. Am. Chem. Soc. 75: 179. 1953.
40. SCHWERT, G. W. Arch. Biochem. and Biophys. 48: 310. 1954.
41. SHULMAN, S. J. Am. Chem. Soc. 75: 5846. 1953.
42. SIMPSON, R. B. and KAUZMANN, W. J. Am. Chem. Soc. 75: 5139. 1953.
43. TANFORD, C. and BUZZELL, J. G. J. Am. Chem. Soc. 76: 3356. 1954.
44. WAUGH, D. F. and YPHANTIS, D. A. Rev. Sci. Instr. 23: 609. 1952.

INTERNAL ROTATION

VIII. THE INFRARED AND RAMAN SPECTRA OF FURFURAL[1]

By G. Allen[2] and H. J. Bernstein

ABSTRACT

The Raman spectrum of furfural has been obtained photoelectrically in the liquid over a temperature range of 50° and in solution. The infrared spectrum has been obtained for the solid, the liquid (over a temperature range of 90°), and in dilute solution over a 50° temperature range. The vibrational spectrum is interpreted in terms of an equilibrium mixture of two rotational isomers with planar configuration. The isomer with higher electric moment is the more stable form in the liquid and in the solid.

Mirone (5) has summarized the observed Raman and infrared data for furfural in a recent article and reported intense doublets at 2800, 1670, 1420, and 1370 cm^{-1}. Further, for solutions of furfural in organic solvents the distribution of intensity in the doublets at 1670 $cm.^{-1}$ and 1470 $cm.^{-1}$ is a function of concentration and is also dependent on the particular solvent used (5). This indicates that the doublets arise in one of three ways. A doublet arising from a Fermi type of resonance interaction might behave in this manner, on the other hand these observations could be interpreted in terms of the existence of two rotational isomers. Another alternative is that the doublets might occur because of the high degree of association usually encountered in this type of compound. We have established that there are at least four doublets in the infrared and Raman spectra of furfural which behave in a similar manner for temperature and environmental changes and find that the spectrum can best be explained in terms of the existence of two rotational isomers 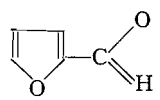 and 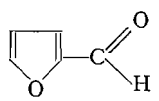 . Conjugation of the carbonyl group with the furane ring will exclude nonplanar configurations.

EXPERIMENTAL

Purification of Furfural

Furfural was purified by distillation through a Stedman column to give a colorless oily liquid (b.p. 160° C.). The pure compound oxidizes to a yellow liquid when in contact with air. In the 30 min. required to obtain a Raman spectrum no appreciable change in color was observed, but if the furfural was irradiated over a period of an hour the liquid became amber in color. The $NaNO_2$ filter used in obtaining the Raman spectra retarded the discolorization. Pure furfural could be kept in vacuo for a period of days before becoming colored.

[1]*Manuscript received January 11, 1955.*
Contribution from the Division of Pure Chemistry, National Research Council, Ottawa. Issued as N.R.C. No. 3558.
[2]*National Research Council Postdoctorate Research Fellow, 1952–1954.*

The Raman spectra were recorded photoelectrically (cf. Fig. 1) using a White spectrometer (8). Depolarization ratios (ρ) were obtained by the method of Edsall and Wilson (3) and corrected for convergence by the method

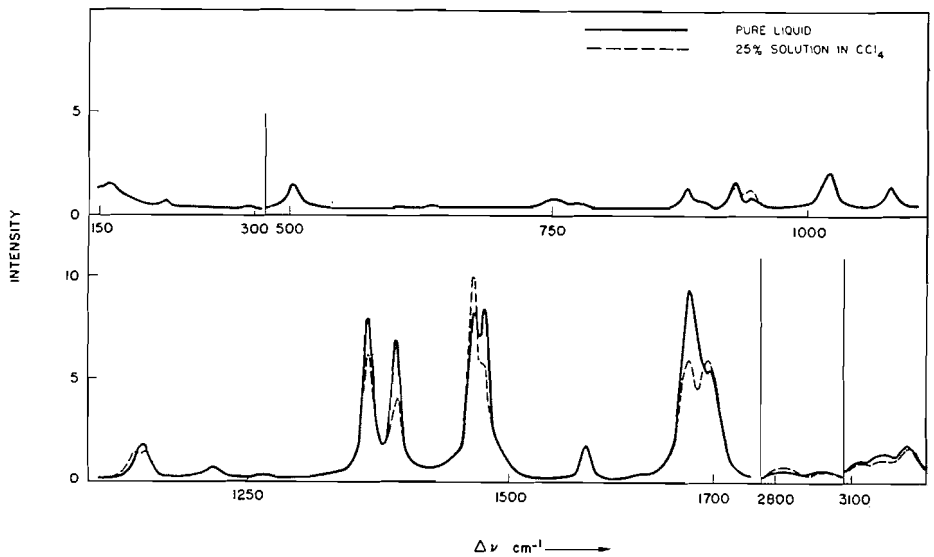

FIG. 1. Raman spectrum of furfural.

of Rank and Kagarise (7). These data are recorded in Table I. Scattering coefficients ($\tilde{S}$) referred to the 458 cm.$^{-1}$ band in CCl_4 and corrected for convergence error, viz.:—

$$\tilde{S} = I/I_{458} \cdot \sigma_{\Delta\nu}/\sigma_{458} \times [(1+\rho_{458})/(1+\rho_{obs})],$$

have been obtained for the Raman bands in the mixture of the two isomers of furfural. In the expression (1) for $\tilde{S}$, I is the integrated intensity and $\sigma_{\Delta\nu}$ is the spectral sensitivity of the photomultiplier tube at the wavelength corresponding to a Raman shift $\Delta\nu$. Standard Raman intensities per molecule could not be obtained since it was not possible to obtain a Raman spectrum of a pure sample of one isomer. The temperature dependence of the Raman spectrum has been studied over a range of 10–60° C. for the pure liquid. The Raman spectra of 25, 50, and 75% solutions of furfural in CCl_4 were also obtained to determine the effect of the dielectric constant of the medium on the relative concentration of the two isomers (cf. Fig. 1).

The infrared spectra were obtained with a Perkin-Elmer Model 12C spectrometer. The infrared spectrum of the pure liquid at 20° C. and of the solid at $\sim -70°$ C. were investigated in the region 3000–700 cm.$^{-1}$ using LiF, CaF_2, and NaCl optics. The results are shown in Fig. 2 and Table I. The temperature dependence of the intensity of the infrared doublet at 2800 cm.$^{-1}$ was studied over a range of 20–70° C. for a 0.001 M solution of furfural in CCl_4 and over a range of 20–110° C. for a thin film of the pure liquid (cf. Fig. 3). The temperature dependence of other doublets could not be studied accurately

TABLE I

INFRARED AND RAMAN SPECTRUM OF FURFURAL

Raman			Infrared			
Liquid[a]			Liquid[b]	Solid[c]	Approximate character	Isomer
Wave No.	ρ_{true}	$\tilde{S}$	Wave No.			
			~3160 m			
3150	0.22	0.34	3140 s	3135 m	ν_{CH}, ring	*B*
3127	0.80	0.15	~3120 m			
3107	0.48	0.11		3090 s	ν_{CH}, ring	*A*
				~3060 m		
				~3030		
2858	0.46	0.04	2854 m	2856 m	ν_{CH}, aldehyde	*A*
2813	0.46	0.04	2817 m	~2814	ν_{CH}, aldehyde	*B*
1693	~0.55	3.60	~1690 s	~1695	$\nu_{C=O}$	*B*
1676	~0.50		~1675 s	1665 s		*A*
1572	0.65	0.32			ring vibration	
1479	0.44	2.49	1476 s	1476 s	$\nu_{C=C}$	*A*
1469	0.44		1466 s	~1465		*B*
~1440						
1397	0.50	1.02	1393 s	1393 s		
1371	0.37	1.39	1369 m	1363 m		
1340		~0.01				
1328		~0.01				
1280		~0.01	1279 m	1281 m		
			1244			*B*
1226	~0.5	0.11	1223	1226		*A*
1206	~0.5	~0.03				
1160	0.44	0.43	1159	~1160		*A*
~1155	~0.4			1157		*B*
1081	0.82	0.18	1081 m	~1076 m		
1024	0.36	0.39	1020 s	1014 s		
948	0.28	0.08	947			*B*
932	0.20	0.24	930 m	930 m		*A*
885	0.85	0.13	884	884		
773	0.85	0.10	~ 770 m	770 s	δ_{CH}	*A*
756	0.85		755 s	756 s		*B*
630	~0.86	0.03				
598	~0.86	~0.01			ring deformations	
505	0.32	0.31				
295	0.86	~0.01				
217	0.86	0.02			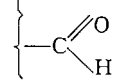 deformations	
166	~0.86	0.07				

s = strong, m = medium, unclassified infrared bands are weak.
[a]*Pure liquid at 27° C. (cf. Fig. 1)*
[b]*Pure liquid at 20° C. (cf. Fig. 2)*
[c]*Solid at ~ −70° C.*

because they were not well resolved and because of strong water vapor absorption in the region where the most intense doublets occur.

The infrared spectrum of solid furfural (Fig. 2) was obtained by condensing the vapor onto a transparent NaCl window which was suspended in vacuum and cooled externally. If the vapor at room temperature was condensed rapidly to a solid (No. 1) deposit then an infrared spectrum could be obtained which was similar to the spectrum of the liquid at room temperature. However if this solid No. 1 is allowed to melt the resulting liquid has a different spectrum

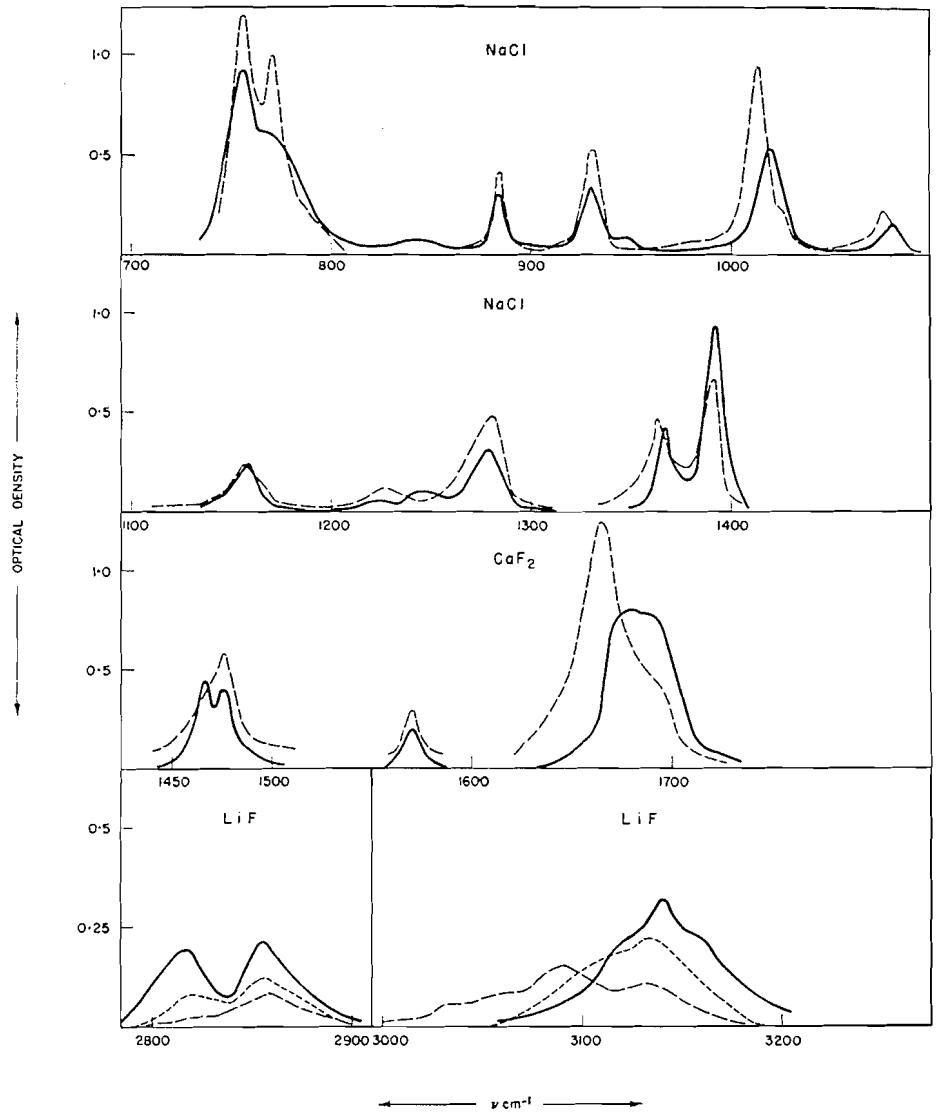

FIG. 2. Infrared spectrum of furfural.
——— liquid at 20° C. - - -liquid at −37° C.
— — — solid at −70° C.

and the most noticeable changes occur in the intensity distribution within the doublets previously discussed. Fig. 4 shows these changes for the doublet at 2800 cm^{-1}. If the liquid is then cooled slowly a crystalline modification (solid No. 2) is obtained in which one component of the 2800 $cm.^{-1}$ doublet almost disappears (Fig. 4). The infrared spectrum of solid No. 2 is shown in Fig. 2 and it is readily seen that other bands at 1690, 1466, 1244, 947 $cm.^{-1}$ disappear on solidification and the contours of the bands at 3100, 1369, 1160, and 770 $cm.^{-1}$ undergo an appreciable change.

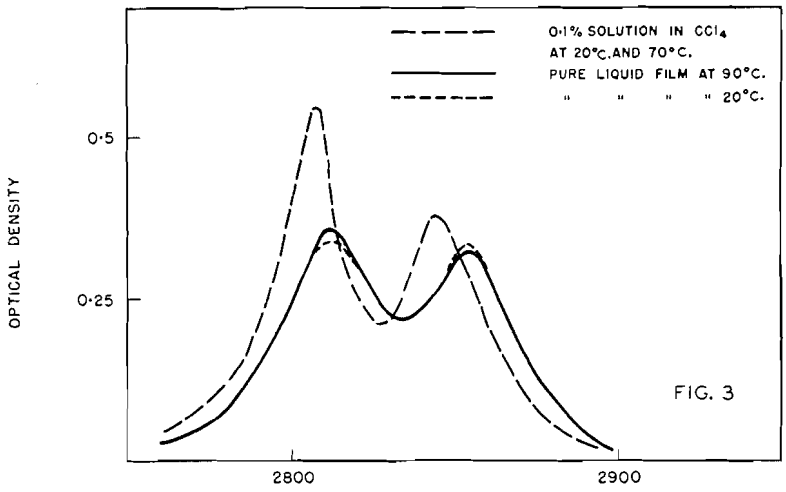

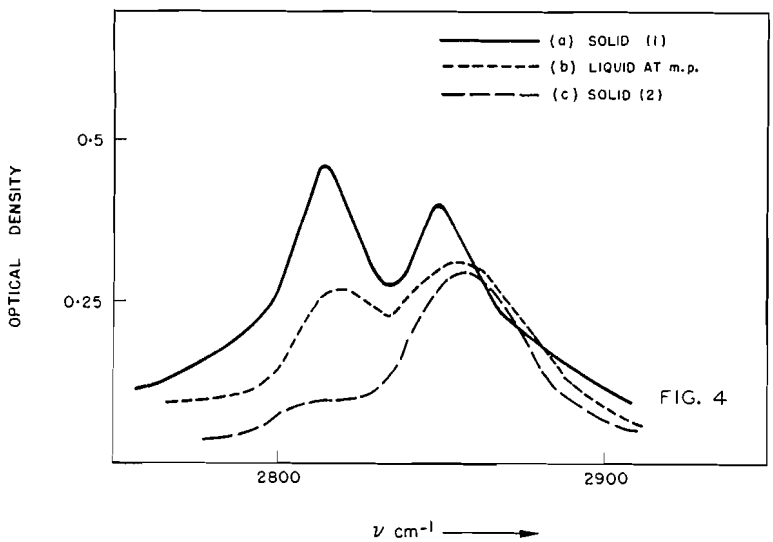

FIG. 3. Temperature dependence of the 2800 cm.$^{-1}$ doublet in the infrared spectrum of furfural. Optical density scale for the pure liquid is twice that for the solution.

FIG. 4. Infrared spectrum of furfural in the 2800 cm.$^{-1}$ region.
(*a*) Solid No. 1 obtained by rapidly freezing the vapor.
(*b*) Liquid obtained from melting solid No. 1.
(*c*) Solid No. 2 obtained by slow cooling of liquid (*b*).

DISCUSSION OF RESULTS

Fermi resonance can be ruled out as a possible explanation for the doublets in the furfural spectrum since it is extremely unlikely that there would be so many (~6), and furthermore the intensity distributions in the doublets would not all have the same dependence on environmental changes (see for example the effect of dilution, Fig. 1, and solidification, Fig. 2). On the other

hand the type of behavior observed on solidification of furfural is well known for solids containing rotational isomers (2, 4). Further a mixture of rotational isomers could also account for the intensity changes observed on dilution.

The spectra shown in Figs. 1 and 2 might also be explained in terms of molecular association. To exclude this possibility the temperature dependence of the doublet at 2800 cm.$^{-1}$ was investigated for a dilute solution ($\sim$0.001 M) of furfural in CCl_4. The doublet has exactly the same contour at 20° and 70° C. and is shown in Fig. 3. The fact that both components of the doublet are intense at very high dilution and also the absence of any temperature dependence of intensity renders unlikely an explanation of the doublet in terms of molecular association. Molecular association would however be expected to broaden some bands which arise from vibrations in associating groups.

The gross features of the Raman and infrared spectra can now be interpreted in terms of two rotational isomers (A and B) of furfural. From Fig. 2 the change in the infrared spectra on solidification indicates that the bands at 2854, 1675, 1476, 1225, and 930 cm.$^{-1}$ belong to one isomer (A) and the bands at 2815, 1690, 1466, 1244, 947 cm.$^{-1}$ belong to the other isomer (B). Configurations can be assigned to isomers A and B from a comparison of the Raman spectrum of the pure liquid with the Raman spectrum of a solution of furfural in CCl_4 (Fig. 1). The pure liquid has a dielectric constant of $\sim$45 whereas the dielectric constant of a 25% solution in CCl_4 is in the region of 5–10, consequently the isomer with the larger dipole will be more stable in the pure liquid than in the solution (6). From Fig. 1 it will be seen that pronounced changes in the spectrum do occur when furfural is diluted with CCl_4. The bands which do not disappear on solidification (isomer A) decrease in intensity and those which disappear on solidification (isomer B) increase in intensity. Hence isomer A is identified with the configuration having the higher dipole moment, viz.:— 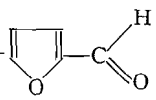 and the configuration of isomer B is then 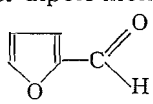 .

The intensities of the 2853 and 2815 cm.$^{-1}$ infrared bands were studied over a range of temperature in an attempt to measure the energy difference between the rotational isomers. No temperature dependence was observed for the vapor (10–110° C.), or for the 0.1% solution in CCl_4, indicating that the isomeric energy difference is small. A small temperature dependence was observed in the pure liquid for these bands over the range −37° to 110° C. corresponding to an energy of isomerization of the order of one kcal. This was confirmed in a qualitative manner for other doublets at 1680 and 1470 cm.$^{-1}$ in the Raman spectrum of the pure liquid.

Some of the bands in the spectrum of furfural may now be assigned to the isomers A and B (last column of Table I) and the approximate character of the mode of vibration has been tentatively assigned in some cases. The identification of the doublet at 1380 cm.$^{-1}$ is uncertain. From Fig. 2, the bands at 1393 cm.$^{-1}$ and 1363 cm.$^{-1}$ in the solid may be assigned to the A isomer. The shift to 1369 cm.$^{-1}$ in the liquid suggests that this band is a superposition of a band from A and one from B. This would account also for the change in

relative intensity of the bands at 1371 cm.$^{-1}$ and 1397 cm.$^{-1}$ in the Raman spectrum of the CCl_4 solution (Fig. 1). A similar doubt exists for the doublet at 760 cm.$^{-1}$; the intensity change on solidification is not very pronounced but it appears that the 770 cm.$^{-1}$ band belongs to the isomer *A*. The doublet observed in both the infrared and Raman spectrum at 1160 cm.$^{-1}$ could be the ν C—CHO mode since this would not be expected to be very different for the two isomers. In the ν CH region of the spectrum, the strong band observed at ~3140 cm.$^{-1}$ in the infrared spectrum of the liquid is associated with a ν CH ring vibration in isomer *B*, the corresponding mode probably occurs at ~3090 cm.$^{-1}$ in isomer *A* since this band increases in intensity on solidification. A shift in frequency is to be expected for the hydrogen stretching mode (of the ring) nearest to the aldehyde group.

Finally it will be noticed that there is a small shift (~5 cm.$^{-1}$) for some bands in the spectrum of solid furfural. A tentative explanation for this is that the bands are unresolved doublets in which the positions change as the relative intensities of the bands change on solidification.

REFERENCES

1. BERNSTEIN, H. J. and ALLEN, G. J. Opt. Soc. Amer. In press.
2. BROWN, J. K. and SHEPPARD, N. J. Chem. Phys. 19: 976. 1951.
3. EDSALL, J. T. and WILSON, E. B. J. Chem. Phys. 6: 124. 1938.
4. MALHERBE, F. E. and BERNSTEIN, H. J. J. Chem. Phys. 19: 1607. 1951.
5. MIRONE, P. Atti accad. nazl. Lincei Rend. Classe sci. fis. mat. e nat. 351: 483. 1954.
6. MIZUSHIMA, MORINO, KURATANI, and KATAYAMA. J. Chem. Phys. 18: 754. 1950.
7. RANK, D. H. and KAGARISE, R. E. J. Opt. Soc. Amer. 40: 89. 1950.
8. WHITE, J. U. and ALPERT, N. J. Opt. Soc. Amer. In press.

THE PHOTOLYSIS OF METHYL ETHYL KETONE[1]

By P. Ausloos[2] and E. W. R. Steacie

ABSTRACT

Methyl ethyl ketone has been photolyzed at temperatures between 25° and 240°C., at varying pressures and intensities. Azomethane has also been photolyzed in the presence of methyl ethyl ketone. It is concluded that the ratio of disproportionation to recombination for a methyl and an ethyl radical is of the order of 0.04. The activation energy for the abstraction of hydrogen from the ketone by methyl is 7.4 ± 0.1 kcal., and by ethyl it is 8.0 ± 0.1 kcal.

INTRODUCTION

The purpose of the present work was to make a study of a system in which both methyl and ethyl radicals were present. Methyl ethyl ketone has therefore been photolyzed over a range of temperature. In addition, the photolysis of azomethane has been used to produce methyl radicals in the presence of methyl ethyl ketone. Because of the complexity of the system the results are not as clean cut as might have been hoped. The results do, however, furnish some interesting information on certain elementary processes.

Several workers (11, 13) have investigated the photolysis of methyl ethyl ketone in the presence of iodine in order to determine the ratio of the two primary steps:

$$CH_3COC_2H_5 + h\nu \rightarrow CH_3CO + C_2H_5 \qquad (A)$$
$$CH_3COC_2H_5 + h\nu \rightarrow C_2H_5CO + CH_3. \qquad (B)$$

A gradual increase in the ratio A/B has been observed with decrease in wave length. At 3130 Å the ratio is over 10, so that process (B) is not of much importance. After the primary step the CH_3CO and C_2H_5CO radicals may further decompose, either spontaneously by energy carried over from the primary step or by normal thermal decomposition.

On the basis of previous work the following secondary reactions may be proposed to account for the noncondensable reaction products:

$$CH_3 + CH_3COC_2H_5 \rightarrow CH_4 + CH_3COC_2H_4 \qquad [1]$$
$$C_2H_5 + CH_3COC_2H_5 \rightarrow C_2H_6 + CH_3COC_2H_4 \qquad [2]$$
$$CH_3 + CH_3 \rightarrow C_2H_6 \qquad [3]$$
$$C_2H_5 + C_2H_5 \rightarrow C_2H_6 + C_2H_4 \qquad [4]$$
$$C_2H_5 + C_2H_5 \rightarrow C_4H_{10} \qquad [5]$$
$$CH_3 + C_2H_5 \rightarrow CH_4 + C_2H_4 \qquad [6]$$
$$CH_3 + C_2H_5 \rightarrow C_3H_8. \qquad [7]$$

It may be assumed that it is mainly secondary hydrogen atoms in the ketone which are abstracted by methyl or ethyl. Although the fate of the $CH_3COC_2H_4$ radical has not been investigated, it can safely be assumed by

[1]*Manuscript received January 20, 1955.*
Contribution from the Division of Pure Chemistry, National Research Council, Ottawa, Canada. Issued as N.R.C. No. 3588.
[2]*National Research Council of Canada Postdoctorate Fellow, 1952–54.*

analogy with $C_2H_5COC_2H_4$ that it may undergo one of the following reactions:

$$CH_3COC_2H_4+CH_3 \rightarrow CH_3COC_3H_7 \quad [8]$$
$$CH_3COC_2H_4+C_2H_5 \rightarrow CH_3COC_4H_9 \quad [9]$$
$$2\,CH_3COC_2H_4 \rightarrow (CH_3COC_2H_4)_2 \quad [10]$$
$$CH_3COC_2H_4 \rightarrow CH_3+CH_3CH{=}CO \quad [11]$$
$$CH_3COC_2H_4 \rightarrow CH_3CO+C_2H_4. \quad [12]$$

At low temperatures other products may be formed from acetyl and propionyl radicals.

EXPERIMENTAL

The apparatus has been previously described (5). The light source was a Hanovia S-500 medium pressure mercury arc. For the photolysis of azomethane in the presence of methyl ethyl ketone a Corning filter No. 7380 was used to cut off radiation below 3400 Å. For the photolysis of methyl ethyl ketone itself the full arc was used.

The analysis of the products was done as described previously (5), both a mass spectrometer and a LeRoy–Ward still being used.

RESULTS

If methane, ethane, ethylene, propane, and butane are formed only by reactions [1] to [7], the following relationships exist:

$$R_M = k_6[CH_3][C_2H_5]+k_1[CH_3][K]$$
$$R_E = k_3[CH_3]^2+k_4[C_2H_5]^2+k_2[C_2H_5][K]$$

or

$$R_M = \frac{k_6}{k_7}\cdot R_P+\frac{k_1k_5^{\frac{1}{2}}}{k_7}\cdot\frac{R_P}{R_B^{\frac{1}{2}}}[K] \quad [I]$$

$$R_E = \frac{k_4}{k_5}R_B+\frac{k_3k_5}{k_7^2}\cdot\frac{R_P^2}{R_B}+\frac{k_2}{k_5^{\frac{1}{2}}}\cdot R_B^{\frac{1}{2}}[K] \quad [II]$$

where R_M, R_E, R_P, and R_B represent the rates of formation of methane, ethane, propane, and butane, and $[K]$ represents the concentration of methyl ethyl ketone.

The Disproportionation and Recombination of Methyl and Ethyl

Recent work on the photolysis of diethyl ketone (7, 9, 10) gives accurate information on the relative rates of reactions [4] and [5], i.e. $k_4/k_5 = 0.125$. Whence, assuming reaction [12] to be negligible,

$$k_6/k_7 = (R_{C_2H_4}-0.125\,R_B)/R_P. \quad [III]$$

This relationship may be expected to be valid only at lower temperatures and higher intensities where reaction [12] is unimportant.

The values calculated from equation [III] are given in the last column of Table I. The values of k_6/k_7 increase at high temperatures, because of the occurrence of reaction [12]. They also increase at low temperatures. The low temperature increase is probably due to the occurrence of the reaction

$$C_2H_5+CH_3CO \rightarrow C_2H_4+CH_3CHO. \quad [13]$$

TABLE I

PHOTOLYSIS OF METHYL ETHYL KETONE

Run	Temp., °C.	Press., cm.	Time, min.	Rate, cc./min. $\times 10^4$						$k_1k_5^{\frac{1}{2}}/k_7$ $\times 10^{13}$ molecules$^{-\frac{1}{2}}$ cm.$^{3/2}$ sec.$^{-\frac{1}{2}}$	$k_2/k_5^{\frac{1}{2}}$	k_6/k_7
				CO	CH_4	C_2H_4	C_2H_6	C_3H_8	C_4H_{10}			
1	26	4.95	1260	0.633	0.0855	0.134	0.248	0.287	0.645	0.64	0.53	0.185
2	27	4.85	29	15.60	0.590	5.08	5.32	8.20	29.0	0.56	0.67	0.177
3	28	3.40	30	5.65	0.227	1.73	1.93	2.60	9.85	0.695	0.79	0.192
4	28	1.82	35	3.80	0.125	1.12	1.14	1.82	6.33	0.635	0.70	0.179
5	79	5.15	40	31.2	4.25	2.00	7.60	13.2	10.25	3.25	2.32	0.051
6	87	3.1	20	28.5	3.22	1.50	6.60	12.15	9.25	4.20	2.90	0.028
7	88	6.2	12	53.0	8.10	2.77	13.15	20.8	15.0	4.15	3.33	0.043
8	104	5.3	20	75.1	12.9	3.84	21.5	34.5	23.4	6.2	4.55	0.026
9	110	5.0	110	13.15	4.64	0.553	3.85	3.55	2.23	7.4	5.35	0.077
10	110	5.1	16	107.4	16.6	5.00	29.0	42.8	25.6	7.0	6.0	0.042
11	114	5.5	20	58.0	13.0	2.11	15.65	20.5	11.9	7.7	5.75	0.030
12	114	3.15	21	38.6	6.90	1.57	10.42	14.4	8.05	8.2	6.90	0.039
13	130	5.0	16	98.0	22.0	3.80	25.9	32.5	20.5	12.4	9.90	0.038
14	144	5.1	15	124.0	32.0	5.40	37.3	39.6	22.0	15.6	15.4	0.067
15	144	5.15	30	44.8	18.2	1.75	13.65	11.6	7.00	17.0	12.85	0.076
16	161	5.05	15	120.0	39.4	5.85	37.65	33.7	18.7	22.0	21.0	0.104
17	174	5.25	20	107.0	45.0	4.48	34.5	27.0	16.0	30.0	24.2	0.092
18	188	5.05	17	109.0	53.0	5.02	36.7	21.8	13.5	49.5	34.5	0.145
19	203	4.9	25	86.0	49.3	4.35	31.25	13.0	7.95	55.0	43.5	0.260
20	215	5.1	18	113.0	60.0	5.70	4.43	14.20	11.95	74.5	56.2	0.295
21	222	1.6	255	22.6	12.35	1.24	8.10	3.67	2.05	74.0	64.0	0.270
22	234	2.25	30	56.0	29.5	2.89	18.81	8.00	4.66	97.0	78.0	0.287

There is much evidence (2, 3, 4) for the analogous reactions

$$CH_3+CH_3CO \rightarrow CH_4+CH_2{=}CO$$

and

$$CH_3CO+CH_3CO \rightarrow CH_3CHO+CH_2{=}CO.$$

The analogous reaction

$$C_2H_5+C_2H_5CO \rightarrow C_2H_6+C_2H_4CO$$

will be of less importance since $[CH_3CO] \gg [C_2H_5CO]$.

In the range from 78° to 130°C. the ratio k_6/k_7 remains approximately constant with a mean value of about 0.04. This value also is consistent with other aspects of the kinetics. It appears reasonably safe, therefore, to assume that k_6/k_7 is equal to 0.04 ± 0.02.

Wijnen (14) has recently investigated the photolysis of mixtures of CD_3COCD_3 and $C_2H_5COC_2H_5$. For CD_3 and C_2H_5 radicals he arrives roughly at the value $k_6/k_7 < 0.08$ in agreement with the present results.

The Abstraction Reaction $CH_3+CH_3COC_2H_5 \rightarrow CH_4+CH_3COC_2H_4$

If the ratio k_6/k_7 is known, it is possible to calculate $k_1k_5^{\frac{1}{2}}/k_7$, and thus obtain some information about the abstraction reaction [1]. A value of 0.04 has been used for k_6/k_7. As discussed above, there is some uncertainty in this value. However, except at high intensities and low temperatures, the methane formed by reaction [6] is negligible, and hence k_6/k_7 does not have to be known accurately. The only experiments in which this is not so are 2, 3, and 4. Since the results for these agree well with 1, further support is furnished for the value $k_6/k_7 = 0.04$.

In Fig. 1, $\log k_1 k_5^{\frac{1}{2}}/k_7$ is plotted against $1/T$. A good straight line is obtained. There are some indications of a deviation from linearity at room temperature. The results are not accurate enough, however, to establish this with certainty. From the slope of the Arrhenius plot in Fig. 1 a value of 7.4 ± 0.1 kcal. is obtained for $E_1+\frac{1}{2}E_5-E_7$. E_5 and E_7 are almost certainly zero since they apply to radical combination reactions. Hence $E_1 = 7.4 \pm 0.1$ kcal.

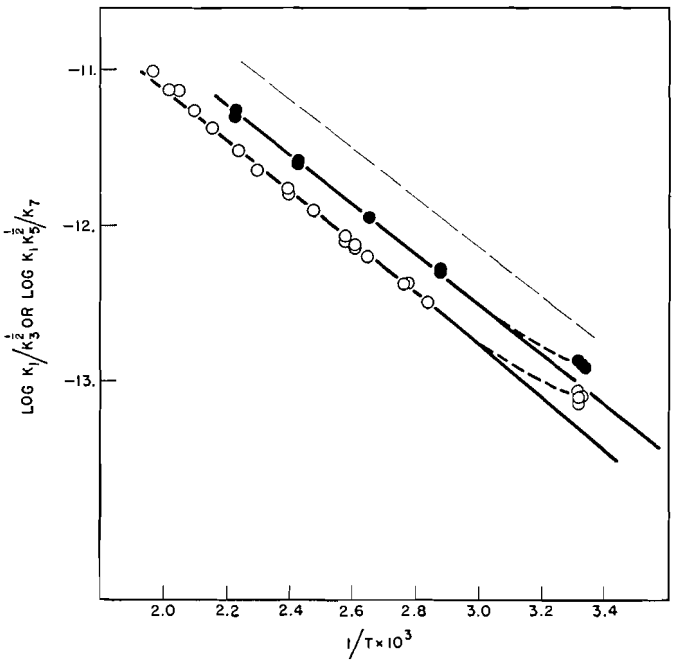

FIG. 1. The reaction of methyl radicals with methyl ethyl ketone.
○ Photolysis of methyl ethyl ketone.
● Photolysis of azomethane – methyl ethyl ketone mixtures.

As a check on this value, azomethane was photolyzed in the presence of methyl ethyl ketone, using light of wave length greater than 3400 Å. Under these conditions methane is also produced by

$$CH_3 + CH_3N_2CH_3 \rightarrow CH_4 + CH_3N_2CH_2 \qquad [14]$$

so that

$$\frac{k_1}{k_3^{\frac{1}{2}}} = \frac{R_{CH_4}/R_{C_2H_6}^{\frac{1}{2}} - k_{14}/k_3^{\frac{1}{2}}[CH_3N_2CH_3]}{[CH_3COC_2H_5]}.$$

The values of $k_{14}/k_3^{\frac{1}{2}}$ have been taken from an experimental plot for azomethane alone (1). The results for $k_1/k_3^{\frac{1}{2}}$ are given in the last column of Table II, and an Arrhenius plot is given in Fig. 1. The slope of the line corresponds to an activation energy of 7.4 ± 0.1 kcal. Hence $E_1 = 7.4$ kcal., in exact agreement with the value obtained from the direct photolysis of methyl ethyl ketone. Some curvature is present in the plot at low temperatures, as is the

TABLE II

PHOTOLYSIS OF MIXTURES OF AZOMETHANE AND METHYL ETHYL KETONE

Temp., °C.	Pressure, cm.		Time, min.	Rate, cc./min. $\times 10^4$			$k_1/k_3^{\frac{1}{2}}$ $\times 10^{13}$
	Azomethane	Ketone		N_2	CH_4	C_2H_6	
26	1.6	2.73	50	13.4	0.87	12.0	1.20
27	2.92	3.33	55	9.9	1.01	8.38	1.28
28	3.05	3.78	148	4.06	0.70	2.92	1.36
74	3.68	2.60	50	12.5	3.10	7.10	5.05
74	2.65	3.37	50	9.13	2.87	5.04	5.30
104	3.22	3.40	45	10.0	4.75	2.98	11.2
138	3.55	2.80	40	27.6	12.4	5.50	26.4
138	4.60	3.42	65	12.1	7.30	1.30	25.2
175	2.68	2.52	25	18.7	11.9	2.22	50.0
175	3.07	2.75	35	18.3	13.4	2.00	55.5

case in the photolysis of methyl ethyl ketone alone. Analogous curvature has been found in the case of acetone, and has been ascribed (2) to wall reactions.

In principle it should be possible to estimate $k_7/k_3^{\frac{1}{2}}k_5^{\frac{1}{2}}$ from the displacement of the two curves in Fig. 1. In this way a value of about 1.8 was obtained. This is rather rough. However, it is of interest that a similar value (1.84), also rather rough, has recently been obtained (14) from the photolysis of mixtures of CD_3COCD_3 and $C_2H_5COC_2H_5$.

For comparison Fig. 1 also gives the results obtained in a previous investigation for the reaction

$$CH_3+C_2H_5COC_2H_5 \rightarrow CH_4+C_2H_4COC_2H_5.$$

It will be seen that the curves are nearly parallel. Abstraction is, however, approximately twice as fast from diethyl ketone which contains two ethyl groups.

The Abstraction Reaction $C_2H_5+CH_3COC_2H_5 \rightarrow C_2H_6+CH_3COC_2H_4$

It can be seen from equation [II] that it is possible to calculate $k_2/k_5^{\frac{1}{2}}$ if k_4/k_5 and k_7^2/k_3k_5 are known. It is probable that k_4/k_5 is known with sufficient accuracy. The calculation is quite sensitive to the value of k_7^2/k_3k_5 especially at low temperatures, and this is only known approximately. It can therefore be expected that the values of $k_2/k_5^{\frac{1}{2}}$ will be reliable at high temperatures, but uncertain at low temperatures. If the value of 1.84 is used for $k_7/k_3^{\frac{1}{2}}k_5^{\frac{1}{2}}$, an Arrhenius plot of $k_2/k_5^{\frac{1}{2}}$ gives a reasonably good straight line at higher temperatures, but shows a downward break at low temperatures. A value of 2.0 gives a good straight line over most of the temperature range. Results calculated in this way are given in Table I, and are plotted in Fig. 2. The curve leads to a value of $E_2-\frac{1}{2}E_5 = E_2 = 8.0 \pm 0.1$ kcal. The uncertainty is, of course, somewhat greater than the stated precision because of the approximate nature of the calculation.

In Fig. 2, results for mixtures of azoethane and diethyl ketone are also given for comparison. These apply to the reaction

$$C_2H_5+C_2H_5COC_2H_5 \rightarrow C_2H_6+C_2H_4COC_2H_5. \qquad [15]$$

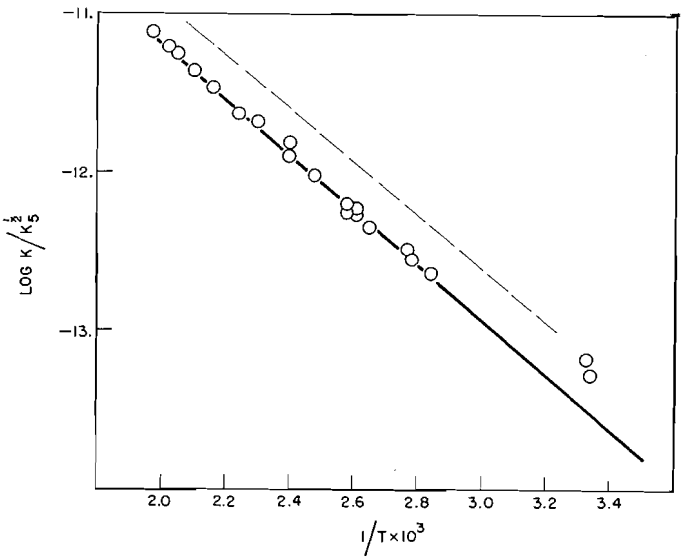

FIG. 2. The reaction of ethyl radicals with methyl ethyl ketone.

The activation energies of [5] and [15] are about the same but the steric factor appears to be twice as great for [15], as might be expected.

DISCUSSION

The above results clearly indicate that the ratio of the rate of disproportionation to that of combination for a methyl and an ethyl radical is considerably smaller than the ratio for two ethyls, i.e.

$$k_6/k_7 \sim 0.04$$
$$k_4/k_5 = 0.125 \pm 0.01.$$

All the reactions probably have activation energies of zero, so that the degree of exothermicity is not the rate determining factor. This is confirmed by the above results where the most exothermic disproportionation reaction gives the smallest ratio.

There are a number of other cases, which are similar in that the more exothermic disproportionation reaction appears to occur to the smaller extent. Thus for the reactions (2)

$$CH_3CO+CH_3CO \rightarrow CH_3CHO+CH_2CO \quad [16]$$
$$CH_3CO+CH_3CO \rightarrow CH_3COCOCH_3 \quad [17]$$
$$CH_3+CH_3CO \rightarrow CH_4+CH_2CO \quad [18]$$
$$CH_3+CH_3CO \rightarrow CH_3COCH_3 \quad [19]$$

the ratio k_{18}/k_{19} is apparently considerably less than k_{16}/k_{17}, although reaction [18] is considerably more exothermic than [16].

Similarly for the reactions

$$CH_3CH_2CH_2+CH_3CH_2CH_2 \rightarrow CH_3CH_2CH_3+CH_3CH{=}CH_2 \quad [20]$$

$$CH_3CH_2CH_2+CH_3CH_2CH_2 \rightarrow C_6H_{14} \quad [21]$$

$$CH_3CHCH_3+CH_3CHCH_3 \rightarrow CH_3CH_2CH_3+CH_3CH{=}CH_2 \quad [22]$$

$$CH_3CHCH_3+CH_3CHCH_3 \rightarrow C_6H_{14} \quad [23]$$

k_{20}/k_{21} has been found to be in the range 0.1 to 0.17 (6, 12) while k_{22}/k_{23} is about 0.5 (6, 8) although [20] is more exothermic than [22].

It is possible to explain all these cases on purely steric grounds if it is assumed that the rates of the recombination reactions are not greatly different. There is definite evidence (7) that the rates of recombination of methyl and of ethyl radicals are not greatly different. Also, it can be shown from the present data at 114°C., where acetyl will be almost completely decomposed, that after correction for C_2H_6 formed by abstraction, the relative amounts of ethane, propane, and butane are very nearly in the ratio 1:2:1 as would be the case if the rate constants for all three recombination reactions were equal.

We will therefore assume that the differences in the ratio of disproportionation to recombination are mainly to be ascribed to the disproportionation reactions. In reaction [6] there are three primary hydrogens in the ethyl radical which may be abstracted in the disproportionation reaction, while in reaction [4] there are six. On this basis [4] may be expected to be of the order of twice as fast as [6]. Similarly one would expect [16] to be faster than [18] in the ratio 6/3, and [22] to be faster than [20] in the ratio 12/4. While this is all very rough and somewhat naive it does explain rather puzzling results in all three cases.

The difference in activation energy between the abstraction reactions [1] and [2] amounts to 0.6 ± 0.2 kcal. This is the same as the difference previously found for the corresponding reactions of diethyl ketone.

REFERENCES

1. Ausloos, P. and Steacie, E. W. R. Can. J. Chem. 32: 593. 1954.
2. Ausloos, P. and Steacie, E. W. R. Can. J. Chem. 33: 31. 1955.
3. Ausloos, P. and Steacie, E. W. R. Can. J. Chem. 33: 39. 1955.
4. Ausloos, P. and Steacie, E. W. R. Can. J. Chem. 33: 47. 1955.
5. Ausloos, P. and Steacie, E. W. R. Bull. soc. chim. Belges, 63: 87. 1954.
6. Blacet, F. E. and Calvert, J. G. J. Am. Chem. Soc. 73: 661. 1951.
7. Brinton, R. B. and Shepp, H. Unpublished.
8. Durham, R. W. and Steacie, E. W. R. Can. J. Chem. 31: 377. 1953.
9. James, D. G. L. and Steacie, E. W. R. Proc. Roy. Soc. (London). In press.
10. Kutschke, K. O., Wijnen, M. H. J., and Steacie, E. W. R. J. Am. Chem. Soc. 74: 714. 1952.
11. Martin, G. R. and Sutton, H. C. Trans. Faraday Soc. 48: 823. 1952.
12. Masson, C. R. J. Am. Chem. Soc. 74: 4731. 1952.
13. Pitts, J. N. and Blacet, F. E. J. Am. Chem. Soc. 72: 2810. 1950.
14. Wijnen, M. H. J. J. Chem. Phys. 22: 1631. 1954.

THE STRUCTURE AND PROPERTIES OF DL-1,2-*O*-CYCLOHEXYLIDENEGLYCEROL[1]

By A. J. E. Porck[2] and B. M. Craig

ABSTRACT

DL-1,2-*O*-Cyclohexylideneglycerol was prepared by reacting cyclohexanone and glycerol in the presence of sulphuric acid. It is miscible with all common organic solvents and is slightly soluble in water. It is not affected by hydrogenolysis at 25°C. over palladous oxide at 50 p.s.i. for 24 hr. The DL-1,2-*O*-cyclohexylidene-3-*O*-*p*-nitrobenzoylglycerol is readily cleaved by mineral acids to yield 3-*O*-*p*-nitrobenzoylglycerol. Proof of the 1,2 ketal structure was obtained by (*a*) preparation of the monomethyl derivative, acid hydrolysis, and periodic acid oxidation of the resultant 1-monomethyl ether of glycerol and (*b*) treatment of the tosyl derivative with sodium iodide which gave a 93% yield of sodium *p*-toluenesulphonate.

O-Cyclohexylideneglycerol was first prepared by Kühn (3) in 1940 but the structure was not established. The compound was most likely a 1,2 ketal similar to DL-1,2-*O*-isopropylideneglycerol. Since *O*-cyclohexylideneglycerol can be prepared readily in large quantities it seemed desirable to investigate the structure and the chemical properties to evaluate the compound as a possible starting material for the synthesis of glycerides.

O-Cyclohexylideneglycerol was prepared in 58% yield by reacting glycerol with cyclohexanone in the presence of sulphuric acid. It is miscible with all common organic solvents, slightly soluble in water, and is not affected by catalytic hydrogenolysis at 25°C. over palladous oxide at 50 p.s.i. for 24 hr. It is readily cleaved by mineral acids.

Evidence of the 1,2 cycloketal structure was obtained by preparation of the monomethyl derivative and subsequent acid hydrolysis. Periodic acid oxidation of the resultant monomethylglycerol showed consumption of 1 mole of oxidant. The DL-1,2-*O*-cyclohexylidene-3-*O*-*p*-toluenesulphonylglycerol was prepared and reacted with sodium iodide in acetic anhydride at 100°C. Sodium *p*-toluenesulphonate was obtained in 93% yield and constituted proof that the tosyl group was at a terminal position in the glycerol. DL-1,2-*O*-Cyclohexylidene-3-*O*-*p*-nitrobenzoylglycerol was prepared and the ketal was cleaved with dilute sulphuric and dilute hydrochloric acids to give 1-*O*-*p*-nitrobenzoylglycerol in yields of 70 and 73% respectively.

The DL-1,2-*O*-cyclohexylideneglycerol appears to be similar to DL-1,2-*O*-isopropylideneglycerol and could be used in glyceride synthesis. It offers an advantage in the ease of preparation.

EXPERIMENTAL

(1) DL-*1,2-O-Cyclohexylideneglycerol*

A mixture of 665 gm. (700 ml.) of anhydrous cyclohexanone, 330 gm. (262 ml.) of anhydrous glycerol, and 46 ml. of concentrated sulphuric acid

[1]*Manuscript received January 4, 1955.*
Contribution from the Prairie Regional Laboratory, National Research Council, Saskatoon, Saskatchewan. Issued as Paper No. 186 on the Uses of Plant Products and as N.R.C. No. 3591.
[2]*National Research Council of Canada Postdoctorate Fellow 1954.*

was shaken at room temperature for 20 min. Anhydrous $CuSO_4$ (160 gm.) was added and shaking was continued for 30 min., whereupon the mixture was filtered by suction. The filtrate was dissolved in 400 ml. of ethyl ether and was stirred vigorously with a solution of 200 gm. K_2CO_3 in 3000 ml. of water for 30 min. The ethereal layer was separated, washed once with water, and dried over anhydrous K_2CO_3. After evaporation of the ether the product was distilled in a Podbielniak Heligrid distillation column to yield 360 gm. (58% of the theoretical amount) of analytically pure ketal, b.p. 137° at 17 mm., 252° at 714 mm., $n_D^{25} = 1.47645$, reported b.p. 133–135° at 15 mm. (3).

The DL-1,2-*O*-cyclohexylideneglycerol is miscible with all common organic solvents. It is soluble in water at 26°C. to the extent of 6.5% and the solubility of water in the cyclohexylideneglycerol at 26°C. is 30%.

The ketal is stable to hydrogenolysis by catalytic hydrogenation at 25°C. over palladous oxide at 50 p.s.i. for 24 hr. with methanol as a solvent.

(2) DL-*1,2-O-Cyclohexylidene-3-O-p-nitrobenzoylglycerol*

p-Nitrobenzoyl chloride, 43.2 gm., was added to a solution of 40 gm. of DL-1,2-*O*-cyclohexylideneglycerol in 200 ml. of anhydrous pyridine. The mixture was shaken at room temperature for 18 hr., poured into 1000 ml. of ice water, and stirred. The crystals were filtered off, dried in a desiccator, and recrystallized once from *n*-butanol. Yield, 50 gm. (67% of the theoretical amount). Further recrystallizations from ethanol, Skellysolve "B", and methanol gave the pure compound, m.p. 49.5–50.0°C. (stout prisms with a slightly yellow color). Analysis for $C_{16}H_{19}O_6N$: C, 59.92%; H, 5.99%; N, 4.35%. Calc. for C, 59.80%; H, 5.96%; and N, 4.36%.

The compound is very soluble in acetone and chloroform, soluble in methanol, benzene, ethanol, and carbon tetrachloride, slightly soluble in ethyl ether, and nearly insoluble in water.

(3) DL-*1,2-O-Cyclohexylidene-3-O-methylglycerol*

Acetone, 1500 ml., and DL-1,2-*O*-cyclohexylideneglycerol, 200 gm., were placed in a 3 liter flask equipped with a stirrer, reflux condenser, and two dropping funnels. The solution was heated to 50°C., 370 gm. (278 ml.) of dimethyl sulphate and a 50% aqueous solution of NaOH (272 gm.) in the dropping funnels were added simultaneously at a rate sufficient to maintain reflux and an alkaline medium. After the addition of the alkylating agents was completed, the bulk of the acetone was distilled off with continuous stirring. The remaining liquid was stirred with 400 ml. of 30% NaOH solution at 100°C. for three hours. The nonaqueous layer was separated and distilled on the Podbielniak distillation column. Yield, 184 gm. (85% of the theoretical amount), b.p. 106° at 12 mm., 226° at 714 mm., n_D^{25} 1.4539. Analysis for $C_{10}H_{18}O_3$: C, 64.03%; H, 9.70%. Calc. for C, 64.48%; H, 9.74%.

The compound is miscible with common organic solvents, and is insoluble in water and glycerol.

(4) *Hydrolysis of* DL-*1,2-O-Cyclohexylidene-3-O-methylglycerol*

Sixty milliliters of DL-1,2-*O*-cyclohexylidene-3-*O*-methylglycerol and 60 ml. of 10% sulphuric acid were refluxed for four hours. The aqueous layer

was neutralized with sodium carbonate solution, separated from the cyclohexanone and distilled. A second distillation of the product yielded 30 gm. of 1-*O*-methylglycerol, b.p. 135° at 40 mm. (reported b.p. 135.5–136°C. at 40 mm.) (2). The product was oxidized with periodic acid in aqueous solution at room temperature. Periodic acid, 0.99 moles, was consumed after one hour and no change was observed after an additional 20 hr.

(5) DL-*1,2-O-Cyclohexylidene-3-O-p-toluenesulphonylglycerol*

p-Toluenesulphonyl chloride, 4.5 gm., was added to a solution of 4 gm. of DL-1,2-*O*-cyclohexylideneglycerol in 20 ml. of anhydrous pyridine cooled in an ice-water mixture. The mixture was allowed to stand at room temperature for 48 hr. and was then poured into 110 ml. of ice water and stirred. The DL-1,2-*O*-cyclohexylidene-3-*O*-*p*-toluenesulphonylglycerol, which crystallized, was filtered and dried. Yield of crude material, 6.5 gm. (86% of the theoretical amount), m.p. 49°. Several recrystallizations from Skellysolve "B" – amyl alcohol (1: 1) gave the analytically pure compound in the form of prisms, m.p. 48.5–49.0°C. Analysis for $C_{16}H_{22}O_5S$: C, 59.05%; H, 6.76%; S, 9.88%. Calc. for C, 58.87%; H, 6.79%; and S, 9.82%.

The compound is very soluble in acetone, chloroform, benzene, ethyl acetate, and ethyl ether, soluble in methanol, ethanol, and carbon tetrachloride, slightly soluble in Skellysolve "F", and almost insoluble in water.

(6) *Reaction of* DL-*1,2-O-Cyclohexylidene-3-O-p-toluenesulphonylglycerol with Sodium Iodide*

One gram of the tosyl derivative and 1.2 gm. of anhydrous sodium iodide were dissolved in 15 ml. of acetic anhydride and the solution was heated at 100°C. on a steam bath. Precipitation of sodium *p*-toluenesulphonate began after 15 min. and heating was continued for five hours. The precipitate was collected, dried, and weighed. Yield, 0.55 gm. (93% of the theoretical amount).

(7) *Acid Hydrolysis of* DL-*1,2-O-Cyclohexylidene-3-O-p-nitrobenzoylglycerol with Mineral Acids*

(*a*) *Sulphuric Acid*

Two grams of the compound was added to a solution of 38 ml. of acetone and 5 ml. of 1.0 *N* H_2SO_4 and the mixture was refluxed for four hours. The solution was diluted with an equal volume of water, neutralized by passing through a column of Amberlite IR-4B, and evaporated to a volume of 25 ml. The oil which separated was taken up in 60 ml. of hot chloroform; the chloroform layer was separated and evaporated to a volume of 15 ml. The 1-*O*-*p*-nitrobenzoylglycerol was crystallized from this solution. Yield, 1.05 gm. (70% of the theoretical amount), m.p. 107° (reported m.p. 107°) (1).

(*b*) *Hydrochloric Acid*

Acid hydrolysis was carried out in the same manner with 1.0 *N* hydrochloric acid. Silver oxide was used to neutralize the acid after hydrolysis. Yield, 1.1 gm. (73% of the theoretical amount), m.p. 107°.

ACKNOWLEDGMENT

The microanalyses were made by J. A. Baignee of the Prairie Regional Laboratory.

REFERENCES

1. FAIRBOURNE, A. and FOSTER, G. E. J. Chem. Soc. 127: 2759. 1925.
2. FAIRBOURNE, A., GIBSON, G. P., and STEPHENS, D. W. Chemistry & Industry, 49: 1021. 1930.
3. KÜHN, M. J. prakt. Chem. 156: 103. 1940.

OLIGOSACCHARIDES OF XYLOSE FROM WHEAT STRAW HEMICELLULOSE[1]

By C. T. Bishop

ABSTRACT

A series of oligosaccharides were prepared by autoclaving wheat straw hemicellulose at 120°C. in distilled water. The di- to the hepta-saccharide inclusive were shown to be members of the (1 → 4)-β-D-xylopyranose series. The octasaccharide was shown to be doubly branched. Certain aspects of the structure of wheat straw hemicellulose are discussed on the basis of these results.

The structure of a polysaccharide is usually determined by identifying and estimating hydrolysis products of the methylated polysaccharide. This procedure gives a picture of the gross structure of the polysaccharide, but, because of uncertainty of complete methylation or difficulty in separating the hydrolysis products, finer details may be missed. With the advent of chromatographic methods (9, 11) it is now possible to isolate oligosaccharides produced by partial hydrolysis of unsubstituted polysaccharides. Finer details in the structure of the parent polysaccharide are often revealed by characterization of oligosaccharides. A large number of these compounds have already been investigated (12).

A previous report (3) described the preparation of a crystalline xylan and a mixture of mono- and oligo-saccharides from wheat straw hemicellulose. The purpose of the present investigation was to characterize the oligosaccharides and relate the results to the gross structures previously proposed for wheat straw hemicellulose (1, 2).

Individual components in the mixture of mono- and oligo-saccharides obtained by the autoclaving of wheat straw hemicellulose were isolated by successive displacement from charcoal columns (11) and by repeated chromatography on large paper sheets. The monosaccharides consisted of D-xylose and L-arabinose. The oligosaccharides were separated into seven, chromatographically-pure components which appeared to constitute a polymeric homologous series. Table I records the yields and properties of these components. Molecular weights of the compounds corresponded to the calculated values for a series of pentose oligosaccharides ranging from a di- to an octasaccharide. Hydrolysis of each oligosaccharide released only D-xylose. These results suggested that the compounds were members of the (1 → 4)-β-D-xylopyranose series first isolated, up to the heptasaccharide, by Whistler and Tu (13, 14, 15) from corncob xylan. The di- and tri-saccharides were crystallized and identified as xylobiose and xylotriose by their physical properties and those of their crystalline acetates (Table II). The tetra-, penta-, and hexasaccharides could not be crystallized but yielded crystalline acetates (Table

[1]*Manuscript received February 9, 1955.*
Contribution from the Division of Applied Biology, National Research Council, Ottawa, Canada. Issued as N.R.C. No. 3592.

TABLE I

OLIGOSACCHARIDES OF XYLOSE FROM WHEAT STRAW HEMICELLULOSE

	Yield, % of hemicellulose	Molecular weight (alkaline iodine)		$[\alpha]_D^{25}$ ($c = 1-2\%$ in water)		Melting point, °C.	
		Found	Calculated*	Found	Reported* (13)	Found	Reported*
Disaccharide	6.18	284	282	−24.8	−25.5	188–190	185–186 (13)
Trisaccharide	5.56	450	423	−44.4	−47.0	204–205	205–206 (13) 214 (8)
Tetrasaccharide	6.82	533	546	−57.8	−60.0	—	
Pentasaccharide	6.74	711	678	−62.4	−66.0	—	
Hexasaccharide	6.80	842	810	−70.0	−72.8	—	
Heptasaccharide	4.94	953	942	−71.3	−74.0 (15)	—	
Octasaccharide	6.24	1069	1074	−25.2	—	—	

**For the (1 → 4)-β-D-xylopyranose series.*

TABLE II

ACETATES OF OLIGOSACCHARIDES OF XYLOSE FROM WHEAT STRAW HEMICELLULOSE

	Melting point, °C.		$[\alpha]_D^{25}$ (c = 1–2% in chloroform)	
	Found	Reported* (14)	Found	Reported* (14)
Disaccharide	155.5–156	155.5–156	−74.3	−74.47
Trisaccharide	109 – 110	109 – 110	−85.0	−85.0
Tetrasaccharide	199 – 201	201 – 202	−93.6	−93.7
Pentasaccharide	248 – 249	248 – 249	−97.5	−97.5
Hexasaccharide	257 – 259	260 – 261	−103	−102
Heptasaccharide	—	—	−105	—
Octasaccharide			−56.8	—

**For the (1 → 4)-β-D-xylopyranose series.*

II) having physical constants identical with those reported (14) for the acetates of xylotetraose, xylopentaose, and xylohexaose. The hepta- and octa-saccharides could not be crystallized, nor did they yield crystalline acetates. Characterizations of these two compounds were therefore based on optical rotations and oxidations with periodate.

In a polymeric homologous series, if the linkages are identical, $[M]_{n/n}$ plotted against $(n-1)/n$ yields a straight line where $[M]_n$ is the molecular rotation (specific rotation × molecular weight/100) and n is the degree of polymerization (7, 14). When molecular rotations of the acetates of the present series of oligosaccharides were plotted in this way a linear relationship was found to exist from the di- to the hepta-saccharide inclusive (Fig. 1). These results indicated that the heptasaccharide was most likely xyloheptaose, a member of the (1 → 4)-β-D-xylopyranose series, the lower members of which were positively identified. The octasaccharide, however, must have contained some linkages different from the (1 → 4)-β-D-type.

Some structural details of carbohydrates can often be revealed by periodate oxidation. Members of the present series of oligosaccharides were oxidized by periodate using the micromethod developed by Perlin (10), in which the oxidation can be followed by continuous measurement of the formic acid

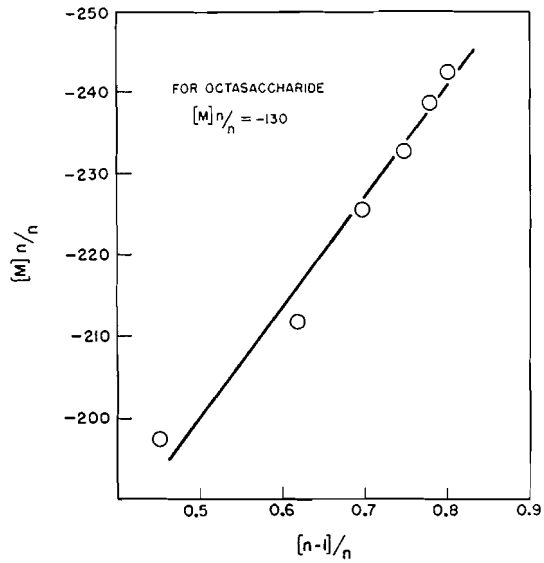

FIG. 1. Relation between molecular rotations and degrees of polymerization of oligosaccharide acetates.

produced, without stopping the reaction. Theoretically, each member of a (1 → 4)-β-D-xylopyranose oligosaccharide series should consume $n+2$ moles of periodate with the production of three moles of formic acid. Results of the oxidations are shown in Fig. 2. All members of the present series consumed the theoretical $n+2$ moles of periodate and all except the octasaccharide produced 3 moles of formic acid. The octasaccharide produced almost five (4.82) moles of formic acid indicating that it was doubly branched, i.e. it possessed one reducing and three non-reducing xylopyranose units. In such an octasaccharide two of the eight xylopyranose units would be protected, by

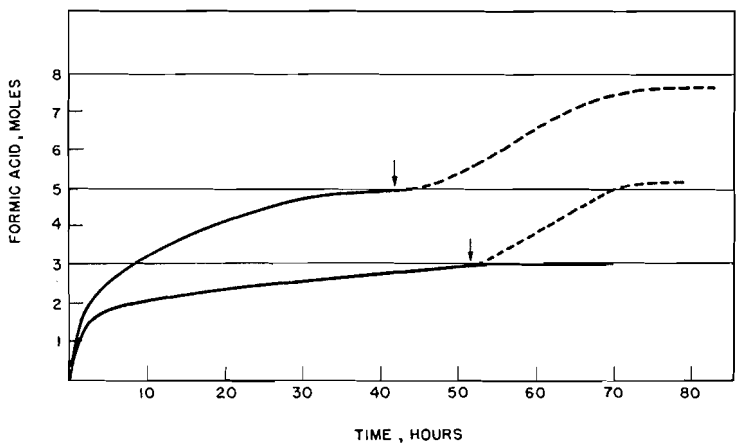

FIG. 2. Periodate oxidation of oligosaccharide series. Upper curve, octasaccharide. Lower curve, tri-, tetra,- penta-, hexa-, and hepta-saccharides. Broken lines, overoxidations of octa- and hepta-saccharides.

the branching, from oxidation by periodate. The oxidized octasaccharide was therefore hydrolyzed and recovery of 2 moles of xylose confirmed the presence of the doubly branched structure. It should be mentioned that following the initial oxidations of the hepta- and octa-saccharides there was a time lag in the reactions after which overoxidation occurred (Fig. 2, broken lines). No difficulty was experienced in distinguishing between the two phases of oxidation.

The results presented here are in reasonable agreement with those of previous investigations on wheat straw hemicellulose (1, 2, 3) in which the same predominance of $(1 \rightarrow 4)$-β-D-xylopyranose linkages were found. However, isolation of the doubly branched octasaccharide showed that at least 1.56% of the xylose units in the polysaccharide were joined by another type of linkage. Detection of this branching illustrates the advantage of examining oligosaccharides formed by partial hydrolyses of polysaccharides. It should also be mentioned that D-xylose, autoclaved under the same conditions, showed no evidence of syntheses. Investigations of the gross structure of wheat straw hemicellulose by methylation techniques have been reported by Adams (1) and by Aspinall and Mahomed (2). Adams (1) found that all of the 2-*O*-methyl-D-xylopyranose could be accounted for by 2,3,5-tri-*O*-methyl-L-arabofuranose, thus obviating any possibility of branching in the xylan chain. However, it is doubtful whether the analytical methods available are sensitive enough to estimate differences in the quantities of these two sugars to account for a small amount of branching. Aspinall and Mahomed (2) obtained 3.4% of 2-*O*-methyl-D-xylopyranose which was attributed to incomplete methylation and demethylation during hydrolysis. In the light of our present work it seems probable that part of this 2-*O*-methyl-D-xylopyranose was due to branching in the xylan chain. The work reported here shows that some of the xylan chains in wheat straw hemicellulose have a structure similar to that of esparto (4) and pear cell-wall (5) xylans, in which single branch points were found every 75 and 115 units respectively.

EXPERIMENTAL

The following solvents (v/v) were used to separate sugars on paper chromatograms: (*A*) pyridine: ethyl acetate: water—1: 2: 2; (*B*) butanol: pyridine: water—6: 4: 3; (*C*) butanol: pyridine: water—5: 5: 3. Specific rotations were measured in a 1 dm. tube and are equilibrium values. Evaporations were done at 35°C. or less and molecular weights were estimated by the alkaline iodine method (15). All melting points are corrected.

Formation of Oligosaccharides

Wheat straw hemicellulose (32 gm.) was autoclaved in distilled water at 120°C. and the resulting mixture of soluble sugars was isolated as previously described (3). This mixture, dried to constant weight over phosphoric anhydride at 0.03 mm., was a yellow, friable solid (24.3 gm., 76% of the hemicellulose). D-Xylose autoclaved under the same conditions yielded no oligosaccharides.

Separation on Charcoal Columns

One-third (8.09 gm.) of the sugar mixture, dissolved in water (100 ml.), was adsorbed on a column (170 × 34 mm.) consisting of a mixture of equal parts by weight of Darco G-60 and Celite 535 (11). The mixture of adsorbed sugars was resolved into four fractions by successive displacement with water (900 ml.), 5% ethanol (1100 ml.), 15% ethanol (800 ml.), and 30% ethanol (900 ml.). The course of desorption was followed by anthrone spot tests. The remaining two-thirds of the mixture was fractionated in the same way and the corresponding eluates were combined. Examination of the four fractions by paper strip chromatography (solvent *A*) showed that they could be designated as the monosaccharide, disaccharide, trisaccharide, and higher oligosaccharide fractions, respectively.

Monosaccharide Fraction

The water eluates were evaporated to dryness leaving a sirup (6.5 gm., 20% of the hemicellulose), part of which was redissolved in water and chromatographed on large sheets of Whatman 3MM paper (solvent *A*). Extraction of appropriate portions of the chromatograms yielded D-xylose, m.p. and mixed m.p. 144–145°C., $[\alpha]_D^{25} = +19.5$ ($c = 3.2$ in water), and L-arabinose, identified by formation of its crystalline benzoylhydrazone, m.p. and mixed m.p. 185–186°C.

Purification of Oligosaccharides

The 5%, 15%, and 30% ethanol eluates from the charcoal columns were evaporated separately and the residues were purified by chromatography on Whatman 3MM paper (solvent *B* for the 5% and 15% ethanol fractions, solvent *C* for the 30% ethanol fractions). Extraction of appropriate portions of the papers yielded a disaccharide from the 5% ethanol eluate, a trisaccharide from the 15% ethanol eluate and tetra-, penta-, hexa-, hepta-, and octa-saccharides from the 30% ethanol eluate. The last five oligosaccharides were purified by rechromatography in the same way. Table I gives yields, molecular weights, and physical properties of all the oligosaccharides together with the corresponding reported or calculated values for the (1 → 4)-β-D-xylopyranose series. The di-, and tri-saccharides were crystallized from methanol and 85% ethanol respectively. Attempts to crystallize the other oligosaccharides were unsuccessful.

The oligosaccharides were acetylated by the sodium acetate – acetic anhydride method so that all anomeric hydroxyl groups were in the β-D-configuration. Table II lists the physical properties of these acetates and the corresponding values reported for acetates of the (1 → 4)-β-D-xylopyranose oligosaccharide series.

Hydrolysis of Oligosaccharides

A portion (10 mgm.) of each oligosaccharide was heated at 97°C. for five hours with *N* hydrochloric acid (0.5 ml.). At one hour intervals samples were removed from each hydrolysis and chromatographed on Whatman No. 1

paper in solvent *A*. The developed chromatograms showed that all hydrolyses were completed in the first hour and that xylose was the only sugar produced.

Periodate Oxidations

Each oligosaccharide except xylobiose was oxidized by periodate in the Warburg respirometer by the method of Perlin (10) which permitted the use of small samples (2—4 mgm.). Fig. 2 gives the results of the oxidations which were done in duplicate at 20°C. and pH 5.7. When production of formic acid first reached a constant value, one set of samples was removed for estimation of periodate (arrows in Fig. 2). Periodate consumption by the tri-, tetra-, penta-, hexa-, hepta-, and octa-saccharides were respectively 4.9, 6.0, 6.86, 7.91, 8.96, and 9.88 moles.

For oxidation of the octasaccharide 2.73 mgm. samples were taken. If the octasaccharide was double-branched then the oxidized samples should release 0.756 mgm. of xylose when hydrolyzed. The two octasaccharide oxidations (after estimation of periodate), together with two blanks to which 0.76 mgm. of D-xylose had been added, were deionized with Amberlite IR 120 and Dowex-2 (carbonate form). The deionized solutions were evaporated to 1 ml. and were boiled under reflux for two and one-half hours with 12% hydrochloric acid (0.25 ml.). The hydrolyzates were neutralized with Dowex-2 (carbonate form) and the xylose present in each of them was estimated by quantitative (6) paper chromatography (solvent *A*). Average recoveries of xylose were 0.544 mgm. from the blanks, 0.579 mgm. from the oxidized octasaccharides.

ACKNOWLEDGMENTS

The author wishes to thank Dr. A. S. Perlin, Prairie Regional Laboratory, National Research Council, Saskatoon, for assistance with the periodate oxidations. The careful technical assistance of R. W. Rowsome is gratefully acknowledged.

REFERENCES

1. ADAMS, G. A. Can. J. Chem. 30: 698. 1952.
2. ASPINALL, G. O. and MAHOMED, R. S. J. Chem. Soc. 1731. 1954.
3. BISHOP, C. T. Can. J. Chem. 31: 793. 1953.
4. CHANDA, S. K., HIRST, E. L., JONES, J. K. N., and PERCIVAL, E. G. V. J. Chem. Soc. 1289. 1950.
5. CHANDA, S. K., HIRST, E. L., and PERCIVAL, E. G. V. J. Chem. Soc. 1240. 1951.
6. FISHER, R. B., PARSONS, D. S., and MORRISON, G. A. Nature, 161: 764. 1948.
7. FREUDENBERG, K. Tannin, cellulose and lignin. Verlag von Julius Springer, Berlin. 1933. pp. 90, 104.
8. JONES, J. K. N. and WISE, L. E. J. Chem. Soc. 2750. 1952.
9. PARTRIDGE, S. M. Nature, 158: 270. 1946.
10. PERLIN, A. S. J. Am. Chem. Soc. 76: 4101. 1954.
11. WHISTLER, R. L. and DURSO, D. F. J. Am. Chem. Soc. 72: 677. 1950.
12. WHISTLER, R. L. and MCGILVRAY, D. I. Ann. Rev. Biochem. 23: 82. 1954.
13. WHISTLER, R. L. and TU, C. C. J. Am. Chem. Soc. 74: 3609. 1952.
14. WHISTLER, R. L. and TU, C. C. J. Am. Chem. Soc. 74: 4334. 1952.
15. WHISTLER, R. L. and TU, C. C. J. Am. Chem. Soc. 75: 645. 1953.

FREQUENCY SPECTRA OF FREE LATTICES AND PARTICLE SIZE EFFECTS ON THE HEAT CAPACITY OF SOLIDS[1]

By D. Patterson[2]

ABSTRACT

The effect of particle size on the heat capacity of solids has been investigated using lattices with free boundaries as models. A monatomic lattice shows a low temperature effect associated with the acoustic modes. This can be compared with results obtained from a continuum model. With a diatomic lattice, however, an effect is also associated with the optical modes and is apparent at higher temperatures. The possibility that this latter effect can explain some recent experimental results is examined.

The continuum model of the solid has been used to predict an effect of particle size on the specific heat which would be observable at low temperatures (4, 12, 17); such an effect has recently been found with NaCl (14). However, an effect at higher temperatures which had not been predicted has also been found using TiO_2 in the rutile form (5), and a theoretical explanation is required. The frequency spectrum of rutile contains both acoustic and optical modes, as is shown by the fact that the specific heat is fitted with a combination of Einstein and Debye functions (16). The continuum (Debye) model must therefore be inadequate in this case and it seemed worth while to investigate the particle size effect using simple lattice models. These have the advantage of giving a more adequate picture of the acoustical modes and of also being able to show the optical (Einstein) modes when the lattice contains atoms of differing mass. Although a simple model of nearest neighbor interactions only is employed in the three-dimensional case, the essential features of the effect are displayed and an extension to more elaborate models may be made when warranted by the sensitivity of the experiments. The effect of particle size on the specific heat of a monatomic lattice is treated in Part I and thus only the acoustic modes are considered there. It is shown that at low enough temperatures the continuum model gives the same results as the lattice model, as might be expected.

Part II goes on to consider lattices containing atoms of differing mass. It is shown that particle size effects are associated with the optical modes as well as the acoustic modes and should be observable at high temperatures. A calculation assuming a simple cubic structure for TiO_2 gives about one-fifth of the effect actually observed at higher temperatures. Although a calculation for the actual TiO_2 lattice should produce a larger result, it is thus possible that some other effect occurs.

While the only thermodynamic property dealt with explicitly is the specific heat, it is apparent that once the effect of particle size on the frequency spectrum is known the corresponding effects on the other thermodynamic proper-

[1]*Manuscript received November 30, 1954.*
Contribution from the Division of Pure Chemistry, National Research Laboratories, Ottawa, Canada. Issued as N.R.C. No. 3589.
[2]*National Research Laboratories Postdoctorate Fellow.*

ties may be obtained by the conventional methods of statistical thermodynamics.

I. EFFECT OF PARTICLE SIZE ON SPECIFIC HEAT (MONATOMIC LATTICES)

The frequencies of vibration of free chains and free lattices have already been discussed to some extent, the former particularly in connection with long chain molecules (10, 15). Born (3) remarks that the frequencies of the free monatomic chain should be given by

$$[1] \qquad \pi\nu = \sqrt{\frac{a}{m}} \sin \phi_l; \quad \phi_l = \pi l/2N, \qquad l = 0, 1, \ldots (N-1).$$

Here a is the Hooke's Law constant for the interatomic interactions, m the mass of the atoms, and N the number of atoms in the linear chain. This is to be compared with the case of a chain where consideration of the boundary has been obviated by the adoption of periodic boundary conditions. Then

$$[2] \qquad \phi_l = \pi l/N, \qquad l = 0, 1, \ldots (N-1).$$

Halford (7) has obtained [1] for the free chain and has generalized it to a three-dimensional lattice, taking into account nearest neighbor interactions only. For vibrations parallel to the x direction

$$[3] \qquad \pi^2\nu^2 = \frac{a}{m}\sin^2\phi_x + \frac{b}{m}\sin^2\phi_y + \frac{b}{m}\sin^2\phi_z,$$
$$\phi_x = \pi l/2N_x, \quad \phi_y = \pi m/2N_y, \quad \phi_z = \pi n/2N_z;$$

$l = 0, 1, \ldots (N_x-1)$, $m = 0, 1, \ldots (N_y-1)$, $n = 0, 1, \ldots (N_z-1)$ where N_x, N_y, N_z are the numbers of atoms in the linear dimensions of the particle and a and b are the Hooke's Law interactions in the direction of vibration and perpendicular to it. The spectrum of frequencies in the other two directions is obtained by interchanging x, y, z so that the total number of modes is $3N_xN_yN_z$. For the case of periodic boundary conditions

$$\phi_x = \pi l/N_x, \qquad \phi_y = \pi m/N_y, \qquad \phi_z = \pi n/N_z.$$

The validity of the model has already been discussed to some extent (7). It may be shown further that at low temperatures the model becomes equivalent to a consideration of nearest neighbor interactions as well, provided this interaction is small, as is usually the case. When these conditions are fulfilled, the spectrum with next nearest neighbors is given by Blackman (2) to be

$$[4] \qquad 4\pi^2\nu^2 = \frac{(\alpha+4\gamma)}{m}\phi_x^2 + \frac{2\gamma}{m}\phi_y^2 + \frac{2\gamma}{m}\phi_z^2$$

where α and γ are the constants for nearest and next nearest interactions. [4] may be compared with [3], putting

$$[5] \qquad (\alpha+4\gamma) = a,$$
$$2\gamma = b.$$

The specific heat associated with the lattice vibrations may be obtained as the sum of Einstein terms over the frequency spectrum, i.e.

$$[6] \qquad C = \sum_{\nu} E(\nu) = \sum_{\nu} k \frac{(h\nu/2kT)^2}{\sinh^2(h\nu/2kT)}.$$

The specific heat of the linear chain will first be considered. According to [1] ν may be taken as a function of ϕ evaluated at equal intervals between ϕ_0 and ϕ_{N-1}. The summation [6] may therefore be replaced by an integration through the use of the Euler–Maclaurin series (R. B. Dingle, private communication). Thus if

$$h = \phi_1 - \phi_0 = \phi_2 - \phi_1 = \ldots = \phi_{l+1} - \phi_l,$$

$$[7] \qquad h \sum_{\phi=\phi_0}^{\phi=\phi_{N-1}} E(\phi) = h \sum_{\phi=\phi_0}^{\phi=\phi_N} E(\phi) - E(\phi_N)$$
$$= \int_{\phi_0}^{\phi_N} E(\phi)\, d\phi + \tfrac{1}{2}\{E(\phi_0) - E(\phi_N)\}$$
$$+ h \sum_{m=0}^{N-1} \int_{m}^{m+1} (\phi - m - \tfrac{1}{2}) \frac{dE}{d\phi} d\phi$$

(see Jeffreys and Jeffreys (8), for instance). The error in replacing the summation by the integral is given by the last term of [7] which is quite negligible if

$$h\nu_0/2kT \ll 2N/\pi \quad \text{where } 2\pi\,\nu_0 = (4\alpha/m)^{\frac{1}{2}},$$

the maximum frequency of the spectrum. For the chain with free boundary conditions, then

$$h = \pi/2N, \quad \phi_0 = 0, \quad \phi_N = \tfrac{1}{2}\pi, \quad \text{and}$$

$$[8] \qquad C = (2N/\pi) \int_0^{\frac{1}{2}\pi} E(\phi)\, d\phi + \tfrac{1}{2}\{E(0) - E(\tfrac{1}{2}\pi)\}$$
$$= (2N/\pi) \int_0^{\frac{1}{2}\pi} E(\phi)\, d\phi + \tfrac{1}{2}\{k - E(\tfrac{1}{2}\pi)\}.$$

Thus C contains a term proportional to N, the number of atoms in the chain, plus a constant term due to an "end effect" on the frequencies. At low temperatures $\sin\phi \sim \phi$ and $E(\frac{1}{2}\pi) \sim 0$. [7] may be integrated to give

$$C = \tfrac{1}{2}k + \frac{2N}{\pi}\left(\frac{2kT}{h\nu_0}\right) \int_0^{\infty} \frac{u^2 du}{\sinh^2 u}$$

of the form

$$[9] \qquad C = \tfrac{1}{2}k + AT.$$

Such a constant contribution does not arise when periodic boundary conditions are assumed, i.e. the frequencies are given by [2] and $\phi_0 = 0$, $\phi_N = \pi$. The constant term then becomes $\frac{1}{2}\{E(0) - E(\pi)\}$, which is zero since $E(0) = E(\pi) = 0$. Thus, although [1] and [2] show the frequency density of modes to be the same whether or not the free boundary is considered, the frequencies associated with ϕ_N are different, producing a particle size effect in one case and not in the other. As will be seen, the same holds for a diatomic chain and

in the three-dimensional case. Born (3) shows that in the former case the density of modes is the same whether free or periodic boundary conditions are chosen. For the three-dimensional case Ledermann (11) has proved quite generally that the difference in the density of modes due to considering the boundary is one which tends to zero with increasing size of the solid. However, in these cases a particle size effect exists for a particular model at least and arises from the behavior of the frequency spectrum when $\phi \sim 0$.

The specific heat of the three-dimensional lattice may be dealt with in a manner analogous to the one-dimensional case, the summation [6] over the frequency spectrum [4] being evaluated by means of the Euler–Maclaurin approximation applied three successive times. There are then contributions to the specific heat which may be associated with the volume, surface, and edges of the lattice, and finally with the translation of the lattice. Of these, the first two are most important, whence

$$C = k\left(\frac{2}{\pi}\right)^3 N_x N_y N_z \int_0^{\frac{1}{2}\pi}\int_0^{\frac{1}{2}\pi}\int_0^{\frac{1}{2}\pi} E(\phi_x, \phi_y, \phi_z)\, d\phi_x\, d\phi_y\, d\phi_z$$
$$+k\left(\frac{2}{\pi}\right)^2 (N_xN_y+N_yN_z+N_zN_x) \int_0^{\frac{1}{2}\pi}\int_0^{\frac{1}{2}\pi} \tfrac{1}{2}\{E(\phi_x, \phi_y, 0)-E(\phi_x, \phi_y, \tfrac{1}{2}\pi)\}\, d\phi_x d\phi_y \qquad [10]$$

plus corresponding terms for the vibrations in the other two directions. In the case of periodic boundary conditions, the integrand of the surface contribution is

$$\tfrac{1}{2}\{E(\phi_x, \phi_y, 0)-E(\phi_x, \phi_y, \pi)\}$$

and vanishes.

It may be noted that in both the one- and three-dimensional cases the Euler–Maclaurin approximation requires correction through the final term of [7] when $h\nu_0/2kT \sim 2N/\pi$, where N is the linear dimension of the lattice. In the one-dimensional case as $T \rightarrow 0$ the correction term $\rightarrow \frac{1}{2}k$, so that $C \rightarrow k$ instead of $\frac{1}{2}k$ as would be expected from [8]. In the three-dimensional case the contribution of particle size to the specific heat ceases to be extensive in the surface area as in [10]. It has been suggested (9) that the excess specific heat be considered as a surface thermodynamic quantity. It is seen, however, that the particle size and the temperature must be of sufficient magnitude for these surface thermodynamics properties to be extensive.

At high temperatures the full integration of [10] would be difficult. At low temperatures, however, the approximation becomes valid. Blackman (2) has shown that in this case the specific heat follows a T^3 law and an analogous treatment of the surface contribution in [10] shows that it follows a T^2 law. In fact [10] reduces to

$$C = 464(T/\theta)^3+B(T/\theta)^2 \text{ cal./deg.-mole where}$$
$$B = \frac{(36\pi)^{\frac{1}{3}}}{2}\frac{N_s}{N_v}\frac{a^{\frac{1}{2}}+b^{\frac{1}{2}}}{a^{\frac{1}{2}}b}\int_0^\infty \frac{u^3 du}{\sinh^2 u} \qquad [11]$$

with N_s/N_v as the proportion of atoms on the surface of the solid. There is an exact correspondence between [11] and the low temperature form of the

expression given by Montroll (12) for the specific heat of small particles, provided the factor $(a^{\frac{1}{2}}+2b^{\frac{1}{2}})/a^{\frac{1}{2}}b$ of the lattice model compares with $3^{2/3}c_3^{2/3}/c_2$ in the Montroll continuum model.

II. EFFECT OF PARTICLE SIZE ON THE SPECIFIC HEAT (OPTICAL MODES)

If now alternate atoms of a free chain of $2N$ atoms are of differing masses m_1 and m_2 there are $2N$ equations of motion whose compatibility is assured by the following secular equation

$$[12] \qquad \begin{vmatrix} \frac{a}{m_1}-4\pi^2\nu^2 & \frac{a}{m_1} & & & \\ \frac{a}{m_2} & \frac{2a}{m_2}-4\pi^2\nu^2 & \frac{a}{m_2} & & \\ & \cdot & & & \\ & & \cdot & & \\ & & & \frac{a}{m_1} & \frac{2a}{m_1}-4\pi^2\nu^2 \quad \frac{a}{m_1} \\ & & & \frac{a}{m_2} & \frac{a}{m_2}-4\pi^2\nu^2 \end{vmatrix} = 0.$$

By means of a diagonal expansion it may be shown that the determinant

$$[13] \qquad C = \begin{vmatrix} \frac{a}{m_1}-4\pi^2\nu^2 & \frac{a}{m_1} \\ \frac{a}{m_2} & \frac{a}{m_2}-4\pi^2\nu^2 \end{vmatrix}$$

is a factor. Thus, two of the frequencies of the chain are given by the secular equation for a free pair of atoms, $C = 0$, leading to a translation of zero frequency and the vibration

$$[14] \qquad 4\pi^2\nu^2 = a\left(\frac{m_1+m_2}{m_1m_2}\right).$$

The remaining modes are those of a chain of $(N-1)$ pairs of atoms given by

$$[15] \qquad 4\pi^2\nu^2 = \frac{a(m_1+m_2) \pm a\sqrt{m_1^2+m_2^2+2m_1m_2\cos 2\phi_l}}{m_1m_2}$$

$$\phi_l = \frac{\pi l}{2N}, \quad l = 1, 2, \ldots (N-1).$$

The frequencies may be compared with those found for a chain with periodic boundary conditions in which the $2N$ frequencies are given by [15] but with $\phi_l = \pi l/N$ and $l = 0, 1, \ldots (N-1)$. In the free case the modes lie along two branches but that corresponding to $l = 0$ of the optical branch has been displaced downwards, as shown in Fig. 1. The significance of the position of this mode becomes apparent if $m_1 \ll m_2$. In this case, the $(N-1)$ frequencies

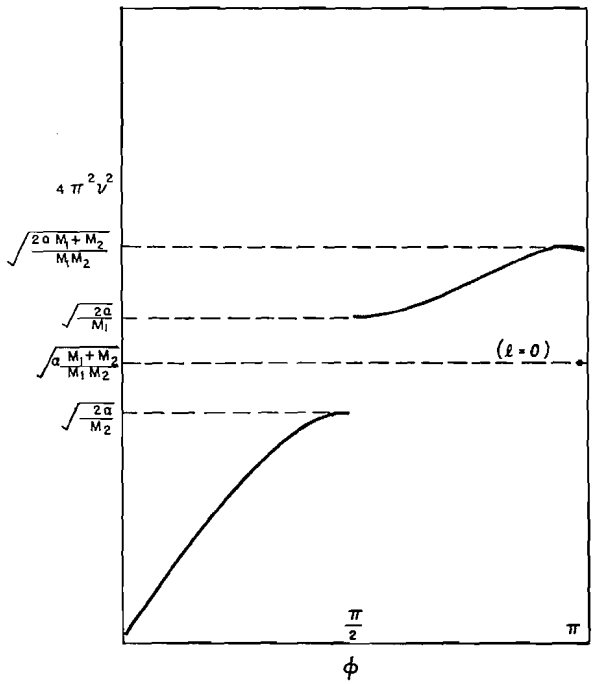

FIG. 1. Acoustic and optical modes for a free diatomic chain.

of the optical branch given by [15] may be approximated by the single Einstein frequency $4\pi^2\nu^2 = 2a/m_1$ and the remaining mode is of frequency $4\pi^2\nu^2 = a/m_1$. In the case of periodic boundary conditions, all N optical modes would have $4\pi^2\nu^2 = 2a/m_1$. Here each atom is identical in interacting with two neighbors, while in the free boundary case the end atoms have only one neighbor. This result may be obtained directly from [12]. As $m_2 \rightarrow \infty$, $a/m_2 \rightarrow 0$, so that in [12] the off-diagonal elements in alternate rows reduce to 0 and the diagonal elements each become $-4\pi^2\nu^2$. The determinant is then easily expanded to give

$$[16] \qquad (-4\pi^2\nu^2)^N\left(\frac{2a}{m_1}-4\pi^2\nu^2\right)^{N-1}\left(\frac{a}{m_1}-4\pi^2\nu^2\right)$$

or the product of the diagonal elements. Thus the frequency spectrum comprises an N-fold root at 0 (the acoustic modes), $(N-1)$ roots at $2a/m_1$, and a root at a/m_1. In the periodic case the N optical modes fall at $2a/m_1$.

The integration of [6] is now performed separately over the acoustic $(-)$ and optical $(+)$ modes in order to obtain the specific heat. In the periodic case

$$[17] \qquad C = \frac{N}{\pi}\int_0^{\pi} E_+(\phi)\,d\phi + \tfrac{1}{2}\{E_+(0)-E_+(\pi)\} + \frac{N}{\pi}\int_0^{\pi} E_-(\phi)\,d\phi + \tfrac{1}{2}\{E_-(0)-E_-(\pi)\}.$$

Now $E_+(0) = E_+(\pi) = E_-(0) = E_-(\pi) = 0$, whence

$$C = \frac{N}{\pi}\int_0^{\pi} E_+(\phi)\,d\phi + \frac{N}{\pi}\int_0^{\pi} E_-(\phi)\,d\phi.$$

In the case of the free boundary the frequency of the optical mode at $l = 0$ has been replaced by half the value in the periodic case or the term $E_+(0)$ must be replaced by $\mathscr{E}_+(0)$. The specific heat then becomes

$$\begin{aligned} C &= \frac{2N}{\pi}\int_0^{\frac{1}{2}\pi} E_+(\phi)\,d\phi - \tfrac{1}{2}\{E_+(0)+E_+(\tfrac{1}{2}\pi)\} + \mathscr{E}_+(0) \\ &\quad + \frac{2N}{\pi}\int_0^{\frac{1}{2}\pi} E_-(\phi)\,d\phi + \tfrac{1}{2}\{E_-(0)-E_-(\tfrac{1}{2}\pi)\} \\ &= \frac{N}{\pi}\int_0^{\pi} E_+(\phi)\,d\phi - \tfrac{1}{2}\{E_+(0)+E_+(\tfrac{1}{2}\pi)\} + \mathscr{E}_+(0) \\ &\quad + \frac{N}{\pi}\int_0^{\pi} E_-(\phi)\,d\phi + \tfrac{1}{2}\{E_-(0)-E_-(\tfrac{1}{2}\pi)\} \end{aligned} \qquad [18]$$

and the effect of free ends is to add the bracketed terms to the specific heat. It may be noted that when $m_1 = m_2$ the second bracket is zero and the contribution reduces to

$$\tfrac{1}{2}\{k - E_+(0)\}.$$

Since enumeration of the optical modes starts with $l = 0$ corresponding to the highest frequency, $E_+(0)$ is the same as $E(\frac{1}{2}\pi)$ for the chain of equal masses. Thus [18] reduces to [8] when the masses are equal.

The contribution to the specific heat given by [18] is plotted in Fig. 2 as a function of $2kT/h\nu_0$ for mass ratios $m_1/m_2 = 1, 9, 16$. Thus if the masses are

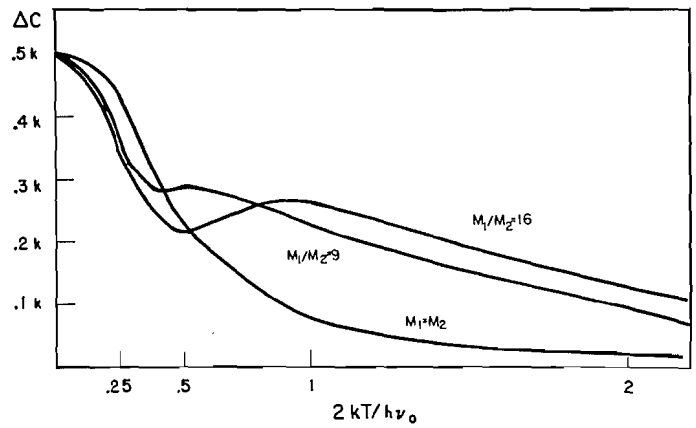

FIG. 2. Contribution of "end effect" to specific heat of a free diatomic chain.

quite different and there is a gap between the acoustic and optical modes, the effect associated with the acoustic modes may die away before that associated with the optical modes becomes prominent.

In the three-dimensional case the effect of the free boundary is easily evaluated when one of the masses is much greater than the other, say as

$m_2 \rightarrow 0$. The secular determinant corresponding to [12] may then be expanded as the product of its diagonal elements, from which the roots are found immediately. If the lattice is of dimensions $2N_x \times 2N_y \times 2N_z$ atoms the roots fall into groups associated with the acoustic ($\nu^2 \sim 0$) and the optical modes which are further subdivided into groups associated with atoms in the bulk of the material, on the surface, along the edges, and finally at the corners. Of these, the most important are the bulk and surface groups. There are $4(N_x-1)(N_y-1)(N_z-1)$ of the former with $4\pi^2\nu^2 = 2(a+2b)/m_1$ and $4(N_x-1)(N_y-1)$ of the latter with $4\pi^2\nu^2 = 2(a+b) = 2(a+b)+b/m_1$, and similarly modes found by interchanging $x, y; y, z; z, x$.

Since the modes associated with the surface atoms have a lower frequency of vibration than those associated with the bulk, a higher contribution to the specific heat will result. The excess specific heat due to the surface modes may be found by taking the Einstein functions of the frequencies involved. In most cases $\gamma/\alpha \sim 0.1$ or, using [5], $b/a \sim 0.14$ so that the frequencies of vibration of surface atoms perpendicular to the surface are considerably different from the frequency of an interior atom, while vibrations in the plane of the surface are not greatly different. With $\gamma/\alpha = 0.1$ the mode of vibration perpendicular to the surface has 0.78 of the frequency of an interior atom and at a temperature one-half of the characteristic Einstein temperature the contribution to the specific heat of the modes is 25% higher than from an interior atom. Thus with small particles which may have 10% of their atoms on the surface it should be quite feasible to observe the effect.

Obviously it cannot be correct to apply these considerations to the complex rutile structure since a simple cubic lattice is assumed. Nevertheless, the order of magnitude of the particle size effect may be obtained. It appears that only about one-fifth of the observed specific heat difference between the small particles and the bulk crystal (3% at 270°K.) can be accounted for in this way. It should be noted, however, that the predominant rutile surface ({110}) is covered with chains of relatively exposed oxygen atoms producing a rougher surface than the predominant {100} of the simple cubic structure, and hence a larger surface effect.

SUMMARY

The lowered frequency spectrum of a monatomic lattice with free boundaries results in an increased specific heat as shown by equation [10]. At low temperatures the expression [11] results which compares with the result found using a continuum model. If atoms of differing mass are present in the lattice, a particle size effect is associated with the optical modes and appears at high temperatures. It is evident that although the model chosen is a simple one, refinements such as the introduction of next nearest neighbors and lattice defects may be introduced into the lattice model in order to give a better picture of the particle size effect.

ACKNOWLEDGMENT

I should like to thank Dr. J. A. Morrison and Dr. J. S. Dugdale for their assistance through much invaluable discussion.

REFERENCES

1. BAUER, S. H. J. Am. Chem. Soc. 75: 1004. 1953.
2. BLACKMAN, H. Proc. Roy. Soc. (London), A, 148: 384. 1935.
3. BORN, M. Proc. Phys. Soc. (London), 54: 362. 1942.
4. BRAGER, A. and SCHUCHOWITZKY, A. Acta Physicochim. U.R.S.S. 21: 1001. 1946.
5. DUGDALE, J. S., MORRISON, J. A., and PATTERSON, D. Proc. Roy. Soc. (London), A, 224: 228. 1954.
6. GIAUQUE, W. F. J. Am. Chem. Soc. 71: 3192. 1949.
7. HALFORD, J. O. J. Chem. Phys. 19: 1375. 1951; 20: 822. 1952.
8. JEFFREYS, H. and JEFFREYS, B. S. Methods of mathematical physics. Cambridge University Press, London. 1950. p. 280.
9. JURA, G. and GARLAND, C. W. J. Am. Chem. Soc. 71: 3192. 1952.
10. KIRKWOOD, J. G. J. Chem. Phys. 7: 506. 1939.
11. LEDERMAN, W. Proc. Roy. Soc. (London), A, 182: 362. 1944.
12. MONTROLL, E. W. J. Chem. Phys. 18: 183. 1950.
13. PARKS, G. S. and KELLEY, K. K. J. Phys. Chem. 30: 47. 1926.
14. PATTERSON, D., MORRISON, J. A., and THOMPSON, F. W. Can. J. Chem. 33: 240. 1955.
15. PITZER, K. S. J. Chem. Phys. 8: 711. 1940.
16. SHOMATE, C. H. J. Am. Chem. Soc. 69: 218. 1947.
17. STRATTON, R. Phil. Mag. 44: 519. 1953.

THE DEGRADATION OF CARRAGEENIN

II. INFLUENCE OF FURTHER VARIABLES[1]

By C. R. Masson, D. Santry, and G. W. Caines

ABSTRACT

A further study has been made of the degradation of carrageenin in aqueous solution. An 80°C. extract of *Chondrus crispus* degraded more rapidly than a preparation from which a 30°C. extract had been first removed. The latter preparation could be degraded to a lower limiting intrinsic viscosity under suitable conditions. Degradation was mainly random, but a more rapid initial degradation was observed under all conditions studied. The presence of dissolved oxygen accelerated the reaction above 60°C. Maximum stability was observed in an inert atmosphere at pH 9 in the presence of salts. Hydroxymethylfurfural and formic acid were identified as products, the yield of the former being higher than from D-galactose alone. The results have been discussed in the light of recent work on the constitution of the polysaccharide.

INTRODUCTION

In Part I (8) the kinetics of degradation of carrageenin of low molecular weight were described. It is of interest to observe if similar kinetics are obtained with an extract of high molecular weight, and to examine the effect of other variables, such as concentration, pH, and atmospheric oxygen, on the reaction. It is also important to establish the nature of the products. These aspects are investigated in the present work.

EXPERIMENTAL

Materials

The carrageenin used for the kinetic experiments was an 80°C. extract of dried Irish moss which had been previously extracted at 30°C. The significant details are given elsewhere (9). It had a number average molecular weight, determined osmometrically, of approximately 2.5×10^6. It is referred to as extract G.

In the experiments designed to identify the products of degradation, an 80° extract was employed, no attempt being made to remove the 30° extract separately. This extract is designated H. Both extracts were stored at −13°C.

Solutions were prepared as described previously (8). For all experiments with extract G the sodium salt was used.

Oxygen-free nitrogen was prepared by passing gas from a cylinder through heated copper turnings.

Measurements

Experiments in the presence of air were carried out exactly as described previously (8). For experiments in the absence of oxygen, two techniques were employed. In the first, carrageenin solutions were contained in sealed

[1]*Manuscript received January 25, 1955.*
Contribution from the Maritime Regional Laboratory, National Research Council, Halifax, Nova Scotia. Issued as N.R.C. No. 3593.

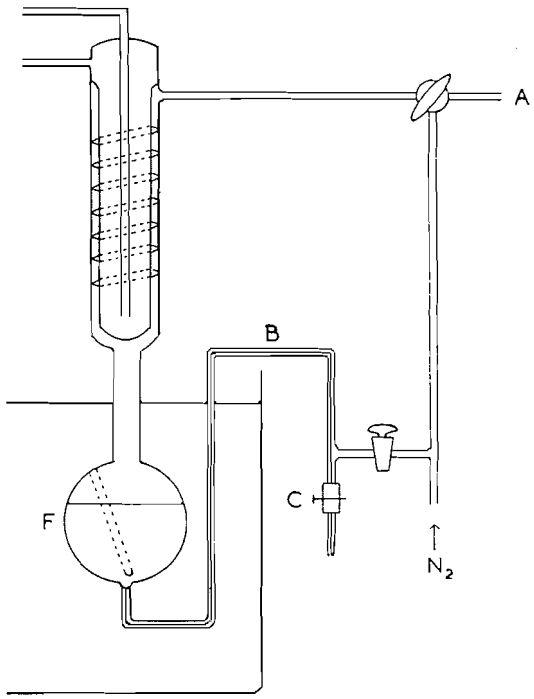

FIG. 1. Apparatus for studying degradation in nitrogen.

pyrex tubes which had been either flushed thoroughly with nitrogen or degassed by repeated freezing and thawing of the contents *in vacuo*. Tubes were immersed simultaneously in a bath at the appropriate temperature and removed at various intervals. This method was later discontinued and the apparatus shown in Fig. 1 was constructed for studying the degradation in an atmosphere of nitrogen. The solution was introduced into flask F *via* clip C, by applying suction at A. During an experiment, nitrogen was passed through the solution *via* capillary B. By suitable manipulation of the stopcocks a pressure of nitrogen could be applied to the surface of the solution and samples removed *via* C without the introduction of air.

It has recently been shown (9) that the viscosity of solutions of carrageenin of high molecular weight is markedly dependent on the rate of shear. For each sample, therefore, the viscosity was measured at various rates of shear as well as at various concentrations. Capillary viscosimeters similar to those described elsewhere (9) were employed. The shear-dependence decreased, as expected, during an experiment and became negligible when the intrinsic viscosities had fallen to 5.5 gm.$^{-1}$ 100 cm.^{3} Lower viscosities were therefore measured in a simple Ostwald viscosimeter, with a flow time for water of 179.2 sec.

Polarograms were obtained with a Sargent-Heyrovsky No. XII instrument. Aqueous 0.1 *N* KCl, with or without buffer, was used as supporting electrolyte, and gelatin in 0.01% concentration was used to suppress undesired maxima.

RESULTS

Degradation in Air at pH 7.0

A 0.1314% solution of extract G in $M/30$ sodium phosphate buffer (pH 7.0) was heated at 90°C. in the presence of air, and samples were withdrawn at various times for viscosity measurements. Inspection of the results showed that all measurements could be referred to a common shear rate of 700 sec.$^{-1}$. Linear plots of η_{sp}/c against c at this shear rate were extrapolated to yield values of $[\eta]_{S=700}$ for various times during the run. The results are presented in Table I.

TABLE I

DEGRADATION OF EXTRACT G IN AIR AT pH 7.0

Time (hours)	$[\eta]$ at 700 sec.$^{-1}$	Time (hours)	$[\eta]$ at 700 sec.$^{-1}$
0	23.15	35.8	8.25
2.0	17.2	57.4	5.7
5.2	14.6	145.1	2.92
10.0	13.1	219.2	2.35
20.3	10.4	313.7	2.15
27.5	9.4	381.5	2.15

Comparison of Results for Extracts F and G

For comparison with previous work, the results are plotted as $1/[\eta]_t - 1/[\eta]_0$ against t, where $[\eta]_0$ and $[\eta]_t$ are the intrinsic viscosities at zero time and time t respectively. This plot is chosen as no relationship between $[\eta]$ and M is at present available at high molecular weights. Trial shows, however, that the nature of the above plot is not greatly influenced by the value of the exponent

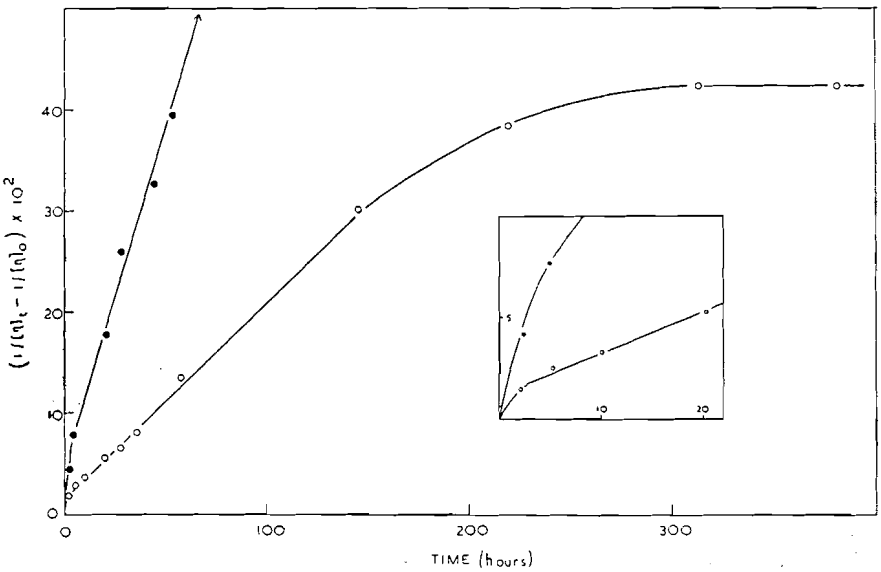

FIG. 2. Rate curves for extracts F and G in air at pH 7.
● Extract F; ○ Extract G.
Insert (same ordinates), showing early stages of degradation.

α in the equation $[\eta] = KM^{\alpha}$, so that the main features of the degradation are adequately depicted in this way.

Fig. 2 shows this plot for the present results and for the degradation of the low-molecular-weight extract F studied previously (8). Three features are observed: (*a*) Extract G is degraded more slowly than extract F under the same conditions. (*b*) Both extracts show an initial sharp decrease in viscosity, followed by random degradation. The initial change is slight for extract G, and is complete in about two hours as compared with five hours for extract F. (*c*) With extract G, the rate of random degradation eventually decreases until, after 300 hr., a lower limiting viscosity of $[\eta] = 2.15$ is reached. This value of $[\eta]$ is only slightly lower than the initial intrinsic viscosity of extract F.

Effect of Oxygen

Initial experiments (extract G) showed that, at temperatures below 55°C., the rate of fall in viscosity was unaffected by passing oxygen, nitrogen, or air through the solutions.

At higher temperatures, however, the rate is slower *in vacuo* or in nitrogen than in the presence of air. Fig. 3 shows the results of experiments in sealed tubes at 90°C. and pH 7.0. The experiments were performed at various

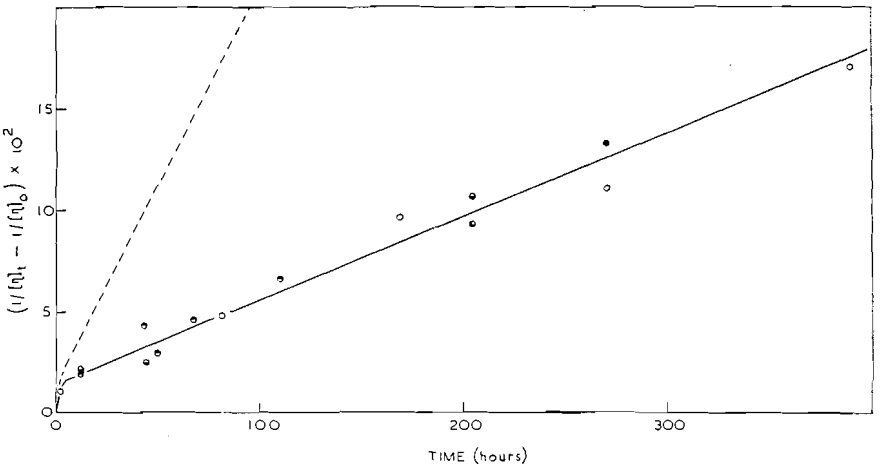

FIG. 3. Effect of dissolved oxygen on degradation of extract G at pH 7.
- - - - - - in air; —— in absence of oxygen.
● $c = 0.0936\%$ *in vacuo*; ◐ $c = 0.0702\%$ *in vacuo*;
○ $c = 0.0936\%$ in nitrogen; ◓ $c = 0.0468\%$ *in vacuo*;
◒ $c = 0.0468\%$ *in nitrogen*.

concentrations to check that the reaction is truly first-order. The scatter in the points is due to the difficulty of determining the true initial viscosity for each sample, as the viscosity of the blank solution dropped appreciably during the time required for degassing the solutions. The effect of oxygen is, however, obvious. The slopes of the lines indicate that the rate of random degradation in air is approximately 4.6 times that *in vacuo* or in nitrogen.

In unbuffered solution, as noted previously (8), the degradation of carrageenin in the presence of air is accompanied by a decrease in pH. In one experiment the pH decreased from 6.15 to 2.88 on heating for 102 hr. at 90°C. In the presence of nitrogen, however, the decrease in pH is less pronounced, although the viscosity of the solution still drops markedly. The pH of an unbuffered solution of extract G, for example, decreased only from 6.50 to 6.10 on heating for 265 hr. at 90°C. The specific conductance of this solution remained constant at 1.740±.04, while the value of $(\eta_{sp})_{\beta=200}$ at c = 0.052 gm./100 ml. fell from 9.27 to 0.03.

This result shows also that the rate of degradation is considerably retarded by the presence of salts. Thus the intrinsic viscosity of a buffered solution of extract G, after heating for 265 hr. in nitrogen, is $[\eta]_{\beta=700}$ = 6.05. This may be compared with the value of (η_{sp}/c) = 0.58 obtained for the unbuffered solution above. The difference in salt concentration and shear rate in the two sets of measurements would, if taken into account, further accentuate this difference. It is evident also that, in the absence of salts, the viscosity falls well below the limiting value attained in buffered solution in the presence of air.

Effect of $[H^+]$

Experiments were done to determine the pH for optimum stability of carrageenin in the presence of nitrogen. Portions of a 0.396% solution of extract G in 0.05 *M* sodium chloride were brought to different pH values by the addition of a few drops of 1 *N* NaOH or 1 *N* HCl. The solutions were then heated at 90°C. for four hours in nitrogen, quenched in ice water, and the viscosities measured. A shear rate of 100 sec.$^{-1}$ was common to the measurements. The specific viscosities of the heated solutions, at this rate of shear, are plotted against pH in Fig. 4. $(\eta_{sp})_{\beta=100}$ for the unheated blank was 18.65. Maximum stability is observed around pH 9, although even at this pH a significant decrease in viscosity has occurred.

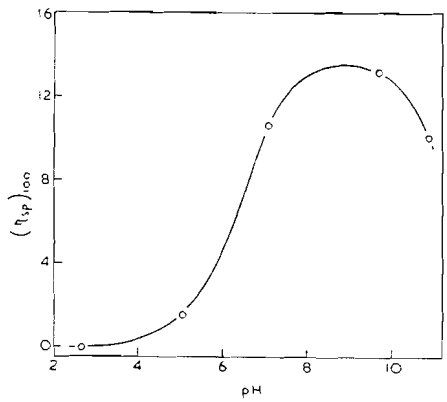

FIG. 4. Effect of $[H^+]$.

The course of the degradation at pH 10 in 0.5 *M* sodium carbonate – bicarbonate buffer was studied at 90°C. in nitrogen. The results could be compared

over a range of shear rates. Measurements at three shear rates are given in Table II. The plot of $1/[\eta]_t - 1/[\eta]_0$ against t was found to be independent of the rate of shear and showed the initial rapid degradation illustrated previously.

TABLE II

DEGRADATION OF EXTRACT G IN CARBONATE–BICARBONATE BUFFER AT pH 10.0 IN NITROGEN

Time (hours)	$[\eta]$ at 100 sec.$^{-1}$	$[\eta]$ at 200 sec.$^{-1}$	$[\eta]$ at 300 sec.$^{-1}$
0	22.2	21.6	20.7
2.7	16.0	15.7	15.4
17.0	12.0	11.6	11.5
48.25	9.6	9.3	9.1
126.0	6.45	6.4	6.4

Products of Degradation

Attempts were made to identify some of the products of degradation using polarographic and spectrophotometric methods. The only products conclusively identified were 5-hydroxymethyl-2-furaldehyde (HMF) and formic acid. The presence of the former was established by comparison of its ultraviolet absorption spectrum and polarograms with those of an authentic sample, and of the latter by chemical tests supplemented by its polarographic behavior.

Three hundred milliliters of a 1% solution of extract H in water was autoclaved for three hours at 127°C. and 21 lb. The resulting light brown solution (pH 5) was extracted with ethyl acetate. The absorption spectrum of the extract (λ_{max} = 2750 Å) was not identified. The solution, after extraction, was boiled under reflux for a further 36 hr. The pH dropped to 2 and the solution darkened further in color. This solution was extracted continuously with ether for eight hours. The ether extract, which was light brown in color and highly acidic, had a strong penetrating odor resembling that of formic or acetic acid. On distilling off the ether under reduced pressure and allowing the vapors to pass through an ice trap, a few milliliters of a colorless liquid were collected. This gave the usual tests for formic acid. Polarograms in dilute buffered and unbuffered solution were exactly similar to those obtained using dilute formic acid. In unbuffered solution, well-defined waves having half-wave potentials $E_{\frac{1}{2}}$ of −1.61 v. and −1.57 v. (vs. S.C.E.) were obtained at pH 3.6 and 2.9 respectively. In buffered solution (pH 6.3) the waves were less clearly defined and had $E_{\frac{1}{2}}$ = −1.80 v. From the magnitude of the diffusion currents the yield of formic acid was estimated to be approximately 3% of the weight of carrageenin.

The brown residue remaining after removal of the ether dissolved only partly in water. The absorption spectrum of the dilute filtered solution was identical with that of HMF prepared by the method of Haworth and Jones (6). In addition, polarograms of this solution and of HMF showed identical half-wave potentials under the same conditions. This solution also gave positive tests with Fehling's solution, α-naphthol – sulphuric acid and resorcinol–HCl reagents, indicating that this compound is most probably

responsible for the positive ketose tests so often reported for carrageenin (3, 4, 5, 12, 14).

After extracting with ether, the solution of degraded carrageenin was still brown in color and still acidic. Attempts to isolate further low-molecular-weight products, however, were unsuccessful. A sensitive photometric test (1) for furfural was applied to further extracts of degraded carrageenin with negative results. Control tests showed that furfural could have been detected in 0.002% concentration. Tests for reductic acid, using sodium-2,6-dichlorobenzenoneindophenol (2) on several acid fractions, were also negative.

Origin of HMF

The yield of HMF from carrageenin was found to be 31 times larger than from D-galactose under the same conditions. A 10% gel of carrageenin and a 10% solution of D-galactose each in 1% HCl were heated on a steam bath for one and one-half hours. After neutralizing the solutions with NaOH, buffering with phosphate, and diluting, the absorption spectra were compared. The ratio of the peak heights at λ 2825 Å gave the relative yields of HMF.

That HMF did not originate from the liberation of ketose residues or from 2-keto gluconic acid was indicated by heating solutions of inulin and calcium-2-ketogluconate under the same conditions as carrageenin and comparing the absorption spectra. This was further verified by the absence of spots due to these compounds on paper chromatograms of various solutions of degraded carrageenin (11).

Yield of HMF from Extract G

(*a*) *In Air*

A 0.0856% aqueous solution of extract G was heated at 90°C. in air for 102 hr. The pH dropped from 6.18 to 2.88. The solution was titrated potentiometrically with 0.005 *N* NaOH. Found: pK = 3.79. Alkali, 15.8 ml., neutralized 20 ml. solution. The absorption spectrum of the neutral solution was similar to HMF and had an optical density of 1.13 at λ 2825 Å. A test for free sulphate was positive.

To calculate the total yield of HMF, it was first assumed that all the sulphate groups in the polymer had been hydrolyzed. Taking a value of 25% for the sulphate content (as SO_4) of the polymer, the acidity due to this cause was calculated. The remaining acidity may then be attributed to organic acids. On the basis that these consisted of formic and levulinic acids arising from the decomposition of HMF, the yield of HMF required to account for this was calculated to be 0.01083 gm./100 ml. From its extinction coefficient (7) at λ 2825 Å, the yield of free HMF was found to be 0.00152 gm./100 ml. The total HMF calculated in this way represents a maximum yield of 14.4% of the weight of carrageenin.

(*b*) *In Nitrogen*

A 0.104% aqueous solution of extract G was heated in nitrogen at 90°C. Examination of the absorption spectrum at various times showed that HMF was formed considerably more slowly than in air. Slight absorption (λ_{max}

2600 Å, $D = 0.23$; λ_{min} 2420 Å, $D = 0.195$) appeared after 164 hr., but the spectrum of HMF was not observed until later. The yield of HMF after 264.5 hr. was only 1.05%, the rate of formation being approximately 1/35 of that in the presence of air.

DISCUSSION

It is apparent that the decrease in viscosity which occurs on mild hydrolysis of carrageenin is associated with the liberation of HMF, and that this does not arise from the galactan portion of the molecule nor from ketose residues in the chain. The negative furfural test indicated that the degradation was not due to the liberation of pentose sugars.

Recent work (13) has revealed the presence in carrageenin of two distinct components, the relative amounts of which vary in different preparations according to the method of extraction. It has also been found (10) that 3,6-anhydro-D-galactose is a constituent of the so-called κ-, or gelling, component. Several features of the present results may be interpreted in the light of these observations.

O'Neill has pointed out (10) that 3,6-anhydro-D-galactose would be expected to yield HMF readily on heating, particularly in acid solution, and the formation of this compound is thus accounted for. The yield of HMF is high in unbuffered solution in air on account of the drop in pH, which catalyzes its formation. The value of 14.4% found for the yield from extract G may be compared with the value of 18.7% for the pure κ fraction (10). This indicates a high percentage of κ-carrageenin in this extract.

The random degradation may thus be attributed to the splitting out of 3,6-anhydro-D-galactose residues from the polysaccharide. The difference in rate observed for extracts F and G may be due to a higher proportion of these residues in the former extract. If the degradation is attributed to the instability of the κ fraction, the result indicates a higher percentage of this fraction in extract F. This is in accord with the results of Smith and Cook (13) who showed that a 60°C. extract contained a greater proportion of the κ fraction than an extract of the residue at higher temperatures.

Previous results (8) indicated the absence in extract F of long chains of 1–3 linked D-galactose residues, as this extract could be degraded randomly to very low viscosities. For extract G, however, the limiting viscosity reached on degradation at pH 7.0 (Fig. 2) may correspond to the presence of such residues. Whether this is an actual portion of the molecule or a separate component is not at present known.

The rate of random degradation of extract G will, of course, be lower than that of extract F by virtue of the presence of this stable residue. Allowance has therefore been made for this by plotting the quantity $[1/([\eta]_t - 2.15)] - [1/([\eta]_0 - 2.15)]$ against time for the early stages of random degradation of extract G, and comparing the rate curve with that obtained for extract F. The correction is, however, insufficient to account for the difference in rates for the two extracts. This indicates that the component responsible for random degradation in extract G is not identical with that in extract F. Further

studies, using separate fractions of carrageenin, are obviously necessary to explain this difference in rate.

From a practical aspect, the results indicate that for extraction of carrageenin with minimum of degradation, best results are to be obtained at pH 9 in the presence of salts, and with the exclusion of dissolved oxygen if the temperature exceeds 60°C.

ACKNOWLEDGMENTS

Our thanks are due to Dr. E. Gordon Young for his interest in this work and for helpful suggestions concerning the manuscript. We wish also to thank our colleagues in these laboratories for useful discussions.

REFERENCES

1. ADAMS, G. A. and CASTAGNE, A. E. Can. J. Research, B, 26: 314. 1948.
2. BIRCH, I. W., HARRIS, L. J., and RAY, S. N. Biochem. J. 27: 590. 1933.
3. BUCHANAN, J., PERCIVAL, E. E., and PERCIVAL, E. G. V. J. Chem. Soc. 51. 1943.
4. HAAS, P. and RUSSELL-WELLS, B. Biochem. J. 23: 425. 1929.
5. HADECKE, J., BAUER, R. W., and TOLLENS, B. Ann. 238: 302. 1887.
6. HAWORTH, W. N. and JONES, W. G. M. J. Chem. Soc. 667. 1944.
7. MACKINNEY, G. and TEMMER, O. J. Am. Chem. Soc. 70: 3586. 1948.
8. MASSON, C. R. Can. J. Chem. 33: 597. 1955.
9. MASSON, C. R. and GORING, D. A. I. Can. J. Chem. 33: 895. 1955.
10. O'NEILL, A. N. J. Am. Chem. Soc. In press. 1955.
11. O'NEILL, A. N. and MASSON, C. R. Unpublished work.
12. SEBOR, J. Oesterr. Chem.-Ztg. 3: 441. 1900.
13. SMITH, D. B. and COOK, W. H. Arch. Biochem. and Biophys. 45: 232. 1953.
14. YOUNG, E. G. and RICE, F. A. H. J. Biol. Chem. 156: 781. 1944.

SULPHATED DERIVATIVES OF LAMINARIN[1,2]

By A. N. O'Neill

ABSTRACT

The polysaccharide, laminarin, was prepared from the marine alga, *Laminaria digitata*, and was sulphated with chlorosulphonic acid in pyridine and in liquid sulphur dioxide at temperatures below 0°. Derivatives containing both O-sulphate and N-sulphate groups were prepared by sulphating β-aminoethyl ethers of laminarin obtained by the reaction of laminarin with ethylenimine. These derivatives were found to act as anticoagulants for blood *in vitro*. The preparations with highest sulphate were most active, and for equivalent sulphate that with both O-sulphate and N-sulphate groups was more active than the one containing only the former.

INTRODUCTION

A naturally occurring blood anticoagulant was isolated in 1916 by McLean (15) from liver and bovine heart. It was named heparin by Howell and Holt (9). Structural studies (25, 6, 12) have shown that it is a polysaccharide composed of D-glucuronic acid and D-glucosamine residues (1:1). Extensive work has indicated that the anticoagulant activity of heparin is dependent largely upon the degree of sulphation (11.3% S). Recently it has been shown (13, 17, 24, 26) that the amino groups in the molecule are sulphated and that these are readily removed by mild hydrolysis resulting in essentially complete inactivation. The molecular weight of heparin has been reported to be 15,000–20,000 (16, 26).

In 1935 Bergström (2) discovered that polysaccharides which contained sulphate groups had anticoagulant activity while similar derivatives of mono- and di-saccharides were inactive. Since that time a number of synthetic anticoagulants have been prepared by sulphating such polysaccharides as chondroitin sulphuric acid (2, 14), cellulose (14, 5, 1), inulin (10), starch (1), chitin (14, 1), alginic acid (19), and dextran (21). These sulphated derivatives had the disadvantage of possessing a much lower anticoagulant activity and a much higher toxicity than heparin. In view of recent work (26, 27, 7) the low activity can be attributed to their lack of sulphamic acid groups and the toxicity to their high molecular weights.

Laminarin, a water-soluble polysaccharide composed of D-glucopyranose units joined through C_1 and C_3 by β-glucosidic linkages, is found in some brown marine algae. It occurs in greatest amount in the fronds of *Laminaria*, and comprises 30–50% of the dry plant. The molecular weight of laminarin has been reported (20) to be about 4000–8000, and hence this polysaccharide should be suitable for the preparation of anticoagulants without recourse to partial hydrolysis and fractionation as has been found necessary for other polysaccharides.

[1]*Manuscript received February 11, 1955.*
Contribution from the National Research Council, Maritime Regional Laboratory, Halifax, Canada. Issued as N.R.C. No. 3598.
[2]*Patent applied for.*

RESULTS AND DISCUSSION

Since it was desirable that sulphation be accomplished without serious degradation of the polysaccharide, attempts were made to carry out the reaction of laminarin with chlorosulphonic acid in pyridine at -5 to $-15°$. This, however, was not completely satisfactory since the maximum sulphate content obtained was only 35% or about one sulphate half-ester group per glucose unit. The degree of sulphation below this value could be varied by changing the proportion of chlorosulphonic acid in the reaction mixtures. By increasing the temperature to 65–70° preparations could be obtained with higher sulphate but these were severely degraded as noted from their color and reducing properties.

The derivatives with highest sulphate were prepared by treating laminarin with a solution of chlorosulphonic acid in liquid sulphur dioxide at $-20°$. By this procedure preparations were obtained containing 1.7 sulphate groups per glucose unit. These were white in color and nonreducing and showed no noticeable degradation. Liquid sulphur dioxide is an excellent solvent for chlorosulphonic acid and it may be readily removed by simple evaporation. The reaction is heterogeneous since the polysaccharide is not soluble in this solvent. The use of sulphur dioxide as a solvent was proposed previously for preparing arylsulphonic acids (4, 22), and was used by Meyer (18) for the sulphation of chondroitin sulphuric acid with sulphur trioxide.

Derivatives of laminarin containing primary amino groups which could be sulphated to the corresponding sulphamic acid residues at first proved difficult to prepare. All attempts to replace tosyl groups by amino in a derivative in which the primary alcohol groups had been tosylated were not successful. However the introduction of such groups was readily accomplished with ethylenimine, whereby a β-aminoethyl ether derivative was obtained. This is a general reaction for polysaccharides and was carried out in a closed flask in the presence of an emulsifying agent at 80–90°. The degree of substitution was controlled by varying the proportion of ethylenimine in the reaction and preparations containing from 0.5 to 1.0 β-aminoethyl residues per monosaccharide unit were obtained. Several side reactions may occur such as the formation of a polyethylenimine ether and a hydroxyethylimine of laminarin. However agreement between the nitrogen analyses by the Kjeldahl and Van Slyke methods indicated that essentially all of the nitrogen was in the form of primary amino groups and hence the derivatives were the β-aminoethyl ethers. These derivatives formed very basic and highly viscous solutions in warm water. They were sulphated with chlorosulphonic acid in liquid sulphur dioxide to give products containing both sulphamic acid and half-ester sulphate groups.

The neutral sodium salts of all these derivatives were tested for their anticoagulant activities in comparison with a standard heparin by the method of Howell as modified by Charles and Scott and described by Jaques and Charles (11). The only modification was that freshly drawn human venous blood was used instead of that from the cannulated carotid artery of a cat.

TABLE I

COMPARISON OF THE ANTICOAGULANT ACTIVITIES OF SULPHATED DERIVATIVES OF LAMINARIN WITH THAT OF A STANDARD HEPARIN BY *in vitro* ASSAY

Preparation	Description of material	Sulphate, %	Activity, I.U. per mgm.
Heparin	Standard from Connaught Medical Research Laboratories		100
1	Laminarin sulphated at −20° with chlorosulphonic acid in liquid sulphur dioxide	46.5	25
2	β-aminoethyl ether of laminarin (7.28% N) sulphated at −20° with chlorosulphonic acid in liquid sulphur dioxide	46.2	40
3	β-aminoethyl ether of laminarin (3.2% N) sulphated at −20° with fluorosulphonic acid in liquid sulphur dioxide	43.8	20
4	Laminarin sulphated at −10° with chlorosulphonic acid in pyridine	32.8	6
5	Laminarin sulphated at −5° with chlorosulphonic acid in pyridine	35.0	6
6	Laminarin sulphated at −15° with chlorosulphonic acid in pyridine	29.6	6
7	β-aminoethyl ether of laminarin (7.28% N) sulphated at 90° with chlorosulphonic acid in pyridine. Highly degraded	39.1	6

The apparent potency of the sulphated laminarins, assuming the standard heparin to contain 100 I.U. per mgm., is shown in Table I. In general, preparations with highest sulphate groups per glucose residue had an anticoagulant activity of 25–30% that of a standard heparin. The material prepared by sulphating a β-aminoethyl ether of laminarin, which contained 7.28% nitrogen, had an activity of 35–40% that of heparin. This derivative contained both sulphamic acid and half-ester sulphate groups.

These results have been confirmed by *in vivo* studies in rats and dogs and are to be reported elsewhere (8).

EXPERIMENTAL

Preparation of Laminarin

The soluble form of laminarin was prepared from local *Laminaria digitata* (3). The yield from 500 gm. of dried plant was 85 gm.; $[\alpha]_D^{24} -12.2°$ (*c* 3.0, water), ash 0.8%.

Sulphation of Laminarin

(*a*) *With chlorosulphonic acid in pyridine.*—Dried, finely powdered laminarin (5.0 gm.) was dissolved in 50 ml. of pyridine and 20 ml. of formamide and the solution cooled to −5°. The pyridine had been freshly distilled over phosphorus pentoxide. Freshly distilled chlorosulphonic acid (6.0 ml.) was dissolved in dry chloroform (25 ml.) and added dropwise over a period of 30 min. to the solution of laminarin. The mixture was rapidly stirred at −5° for three hours and then allowed to stand at this temperature overnight. Sufficient ice and water were added to dissolve the precipitated derivative followed by sodium bicarbonate until the evolution of carbon dioxide ceased.

The solution was exhaustively extracted with ether, and the resulting aqueous solution neutralized to phenolphthalein with dilute sodium hydroxide and dialyzed until free from sulphate. The sulphated derivative was precipitated by the addition of ethyl alcohol and a little sodium chloride. It was washed with absolute ethanol and ether and finally dried to a white powder. Yield, 8.6 gm.; sulphate, 35.0%.

(*b*) *With chlorosulphonic acid in liquid sulphur dioxide.*—Commercial gaseous sulphur dioxide from a cylinder was dried by passage through three drying towers containing respectively silica gel, sulphuric acid, and phosphorus pentoxide. It was condensed in a flask which was protected from atmospheric moisture and was immersed in a bath of dry ice and acetone. The liquid sulphur dioxide (120 ml.) was cooled in an ice–salt bath to −20°. Freshly distilled chlorosulphonic acid (3 ml.) was added followed by 2.0 gm. of dry laminarin. The mixture was continuously stirred at −20° for six hours and then the sulphur dioxide was allowed to evaporate. On completion of the evaporation 100 ml. of *N* sodium hydroxide at −5° were added to dissolve the solid residue. The solution was neutralized with sodium hydroxide. It was dialyzed against running water for two days and against distilled water for one day. The dialyzed solution was concentrated *in vacuo* to 200 ml. and the sulphated laminarin precipitated by pouring the solution into 1000 ml. of 95% ethanol containing a small amount of sodium chloride. The precipitate was centrifuged, washed with absolute ethyl alcohol, with ether, and dried. Yield, 4.0 gm.; sulphate, 46.5%.

Preparation of Ethylenimine

Ethylenimine was prepared from β-aminoethyl sulphuric acid by heating with sodium hydroxide (23). It was purified by distilling over potassium hydroxide through a 15 in. Widmer column and collecting the fraction boiling between 56° and 58°. It was stored in the refrigerator over solid sodium hydroxide.

Reaction of Laminarin with Ethylenimine

Air-dried laminarin (5.0 gm.) and 0.5 ml. of a 1% solution of emulsifier BRIJ 35 (Atlas Powder Co.—polyoxyethylene lauryl alcohol) were mixed to a paste and 4.8 ml. (4.0 gm.) of ethylenimine were added. The mixture was stirred in a closed reaction flask at 80–90° for four hours. The resulting material was dissolved with some difficulty in 200 ml. of warm water. After cooling, the viscous solution was filtered through a sintered glass funnel of medium porosity and poured with stirring into 1000 ml. of ethyl alcohol. The precipitate was recovered by centrifugation, washed with aqueous methyl alcohol acidified with hydrochloric acid, absolute ethanol, and finally with ether. It was dried *in vacuo*. Yield, 7.7 gm.; N (Kjeldahl) 7.28%, (Van Slyke) 6.9%.

Sulphation of the β-Aminoethyl Ether

An amount of 1.6 gm. of the above material was sulphated in 100 ml. of liquid sulphur dioxide with 2.6 ml. of chlorosulphonic acid in the same manner as described for laminarin. Yield, 2.5 gm.; sulphate, 46.2%.

REFERENCES

1. ASTRUP, T., GALSMAR, I., and VOLKERT, M. Acta Physiol. Scand. 8: 215. 1944.
2. BERGSTRÖM, S. Naturwiss. 23: 706. 1935. Z. physiol. Chem. 238: 163. 1936.
3. BLACK, W. A. P., CORNHILL, W. J., DEWAR, E. T., and WOODWARD, F. N. J. Appl. Chem. (London), 1: 505. 1951.
4. BURKHARDT, G. N. and LAPWORTH, A. J. Chem. Soc. 684. 1926.
5. CHARGAFF, E., BANCROFT, F., and STANLEY-BROWN, M. J. Biol. Chem. 115: 155. 1936.
6. CHARLES, A. F. and SCOTT, D. A. Biochem. J. 30: 1927. 1936.
7. DOCZI, J., FISCHMAN, A., and KING, J. A. J. Am. Chem. Soc. 75: 1512. 1953.
8. HAWKINS, W. W. and O'NEILL, A. N. Can. J. Biochem. Physiol. In press. 1955.
9. HOWELL, W. H. and HOLT, E. Am. J. Physiol. 47: 328. 1918.
10. INGELMANN, B. Arkiv Kemi Mineral. Geol. 24: 4. 1946.
11. JAQUES, L. B. and CHARLES, A. F. Quart. J. Pharm. and Pharmacol. 14: 1. 1941.
12. JORPES, J. E. and BERGSTRÖM, S. Z. physiol. Chem. 244: 253. 1936.
13. JORPES, J. E., BOSTRÖM, H., and MUTT, V. J. Biol. Chem. 183: 607. 1950.
14. KARRER, P., KOENIG, H., and USTERI, E. Helv. Chim. Acta, 26: 1296. 1943.
15. MCLEAN, J. Am. J. Physiol. 41: 250. 1916.
16. MEYER, K. H. *In* Natural and synthetic high polymers. 2nd ed. Interscience Publishers, Inc., New York. 1950. p. 456.
17. MEYER, K. H. and SCHWARTZ, D. E. Helv. Chim. Acta, 33: 1651. 1950.
18. MEYER, K. H., PIROUÉ, R. P., and ODIER, M. E. Helv. Chim. Acta, 35: 574. 1952.
19. MOLHO, I. and COTTE, J. Bull. soc. chim. biol. 33: 312. 1951.
20. PERCIVAL, E. G. V. and ROSS, A. G. J. Chem. Soc. 720. 1951.
21. RICKETTS, C. R. Biochem. J. 51: 129. 1952.
22. ROSS, J., PERCY, J. H., BRANDT, R. L., GEBHART, A. J., MITCHELL, J. E., and JOLLES, S. Ind. Eng. Chem. 34: 924. 1942.
23. WENKER, H. J. Am. Chem. Soc. 57: 2328. 1935.
24. WOLFROM, M. L. and MCNEELY, W. H. J. Am. Chem. Soc. 67: 748. 1945.
25. WOLFROM, M. L. and RICE, F. A. H. J. Am. Chem. Soc. 68: 532. 1946.
26. WOLFROM, M. L., MONTGOMERY, R., KARABINOS, J. V., and RATHGEB, P. J. Am. Chem. Soc. 72: 5796. 1950.
27. WOLFROM, M. L., SHEN, T. M., and SUMMERS, C. G. J. Am. Chem. Soc. 75: 1519. 1953.

CARBOHYDRATE THIOETHERS

I. 6-DEOXY-6-THIOETHYL-D-GALACTOSE[1]

By Samuel B. Baker

ABSTRACT

A thioalkyl derivative has been synthesized by two distinct methods. One of these methods left no doubt as to the structural configuration. It is suggested that the other method of synthesis yields first an epoxy anhydro derivative which on further reaction leads to the thioalkyl carbohydrate, namely, 6-deoxy-6-thioethyl-D-galactose.

Thioalkyl substituted carbohydrates in which the sulphur atoms were not linked to the glycosidic carbon atoms were first obtained by Raymond (6) and by Brigl and Schinle (1).

Levene and Raymond (4) synthesized 3,5-anhydro-1,2-isopropylidene-D-xylofuranose (II) and, unequivocally, determined the structure of this substance. Hot methanolic sodium methylate led to the formation of a monomethyl pentose, after removal of the isopropylidene group. This methyl pentose, being different from the known 3-methyl-D-xylose, was assumed to be 5-methyl-D-xylofuranose (IV).

Raymond (6) then synthesized a substance which he considered to be 5-deoxy-5-thioethyl-D-xylose (III) by treating 1,2-isopropylidene-5-*O*-*p*-tolylsulphonyl-D-xylofuranose (I) with two molecular equivalents of dry potassium ethanethiolate followed by hydrolysis of the isopropylidene group. Owing to the fact that the C-3 position had an hydroxyl group, it is probable that under the conditions of the experiment anhydridization would occur and the anhydro derivative (II) would cleave in the presence of the second molecular equivalent of potassium ethanethiolate (3) to yield the product 1,2-isopropylidene-5-deoxy-5-thioethyl-D-xylofuranose.

In similar manner, this worker (6) obtained 6-deoxy-6-thiomethyl-D-glucose from 1,2-isopropylidene-6-*O*-*p*-tolylsulphonyl-D-glucofuranose and two molecular equivalents of dry potassium methanethiolate. The intermediate 5,6-anhydro-1,2-isopropylidene-D-glucofuranose would be formed and this would then cleave to yield the glucose thioether.

The present publication pertains to a third ω-thioalkyl aldose, namely 6-deoxy-6-thioethyl-D-galactose (XII) that was obtained by two methods, one of which left no doubt as to the configuration. In the first method, 1,2-3,4-diisopropylidene-6-*O*-*p*-tolylsulphonyl-D-galactose (V) was treated with concentrated hydrochloric acid and ethanethiol. The isopropylidene groups were cleaved and the tolylsulphonyl aldose reacted with the ethanethiol to yield 6-*O*-*p*-tolylsulphonyl-D-galactose diethyl thioacetal (VI). This product was then treated with two molecular equivalents of dry sodium ethanethiolate to give the substance VII, 6-deoxy-6-thioethyl-D-galactose diethyl thioacetal. In addition, when VI was treated with one molecular equivalent of sodium

[1]*Manuscript received November 19, 1954.*
Contribution from the Research Institute, Montreal General Hospital, Montreal, Quebec.

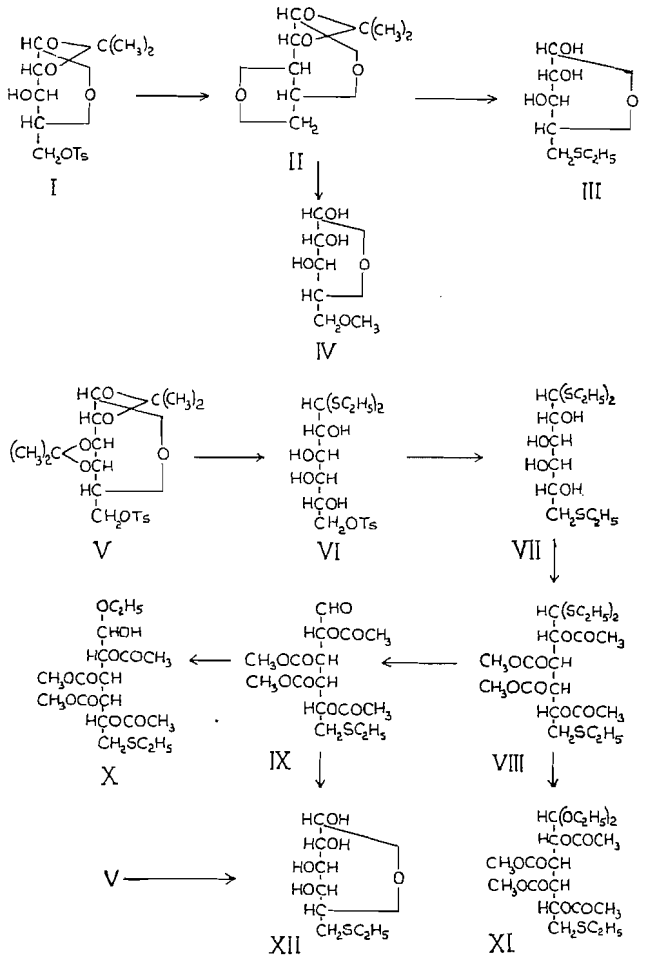

methylate and the reaction product acetylated, a sirup was obtained. Treating the sirup with one molecular equivalent of sodium ethanethiolate yielded VII.

The second method of preparation of 6-deoxy-6-thioethyl-D-galactose (XII) left no doubt about its structural configuration. One molecular equivalent of 1,2-3,4-diisopropylidene-6-*O*-*p*-tolylsulphonyl-D-galactose (V) was heated in a suitable solvent with one molecular equivalent of sodium ethanethiolate. The sirupy product, after hydrolysis to remove the two isopropylidene groups, yielded XII. Possibly the tolylsulphonyloxy group was cleaved to yield a carbonium ion and since there were no free or potential hydroxyl groups under the reaction conditions employed, anhydro ring formation could not occur. The nucleophilic thioethyl group reacted with the electrophilic carbonium center.

Acetylation of VII, 6-deoxy-6-thioethyl-D-galactose diethyl thioacetal, yielded the tetraacetate VIII. This latter substance (VIII) formed *aldehydo-*

2,3,4,5-tetraacetyl-6-deoxy-6-thioethyl-D-galactose (IX) on reaction with mercuric chloride and cadmium carbonate in methanol-free acetone. The *aldehydo* derivative (IX) reacted directly with ethanol to yield the hemiacetal (X). This phenomenon appears to be general for *aldehydo* acetyl sugars (2, 8). Mercuric chloride and cadmium carbonate, on reaction with VIII, in the presence of absolute methanol and absolute ethanol yielded the dimethyl and diethyl acetals, respectively, of 2,3,4,5-tetraacetyl-6-deoxy-6-thioethyl-D-galactose.

EXPERIMENTAL

1,2-3,4-*Diisopropylidene*-6-*deoxy*-6-*thioethyl*-D-*galactose*

1,2-3,4-Diisoproylidene-6-*O*-*p*-tolylsulphonyl-D-galactose (7) (V) (60 gm.) and freshly prepared dry sodium ethanethiolate (16 gm.) were dissolved in N,N-dimethylformamide (275 cc.). The reaction mixture was heated at 100° for two hours and after cooling to room temperature it was poured into cold water (2000 cc.). A sirup separated, and after it had been left to stand for two hours at 5°, it was taken up in ether. The ethereal solution was dried over sodium sulphate, filtered, and the filtrate concentrated *in vacuo*. The resulting viscous sirup weighing 39 gm. (89%) did not crystallize from any solvent and it was distilled at 123–126°/0.12 mm. yielding 33.4 gm. (76%). A portion was redistilled at 124–126°/0.12 mm. yielding a colorless viscous sirup which was insoluble in water but soluble in all common solvents including petroleum ether. The refractive index was $\eta_D^{24°}$ 1.4795 and $[\alpha]_D^{22°}-85.7°$ ($CHCl_3$; *c*, 6.5052). Anal.: Calc. for $C_{14}H_{24}SO_5$: C, 54.28; H, 7.89; S, 10.52. Found: C, 54.06; H, 7.96; S, 10.6.

6-*Deoxy*-6-*thioethyl*-D-*galactose* (*XII*)

The sirupy 1,2-3,4-diisopropylidene-6-deoxy-6-thioethyl-D-galactose (30 gm.) was dissolved in 95% ethanol (250 cc.). Water (100 cc.) containing sulphuric acid (5 cc.) was added and the solution was heated for two hours at 70°. The hot solution was then diluted with hot water (350 cc.) and neutralized with an excess of barium carbonate. The barium salts were removed by centrifugation and the clear supernatant was concentrated *in vacuo* at 40°. Traces of water were removed by three codistillations with absolute ethanol and the dry, somewhat turbid, sirup was dissolved in absolute ethanol (125 cc.) and the solution was treated with charcoal to remove the turbidity and a trace of color. Ether was added to the colorless solution until it became slightly turbid, and crystallization occurred on extended cooling at −20°. The product was recrystallized from a small volume of absolute ethanol and the yield was 14.7 gm. (67%), m.p. 98–100°, and $[\alpha]_D^{22°}+73.8°$ equil. (water; *c*, 1.3536). Anal.: Calc. for $C_8H_{16}SO_5$: C, 42.85; H, 7.14; S, 14.28. Found: C, 42.78; H. 7.21; S, 14.19.

6-*O*-*p*-*Tolylsulphonyl*-D-*galactose Diethyl Thioacetal* (*VI*)

1,2-3,4-Diisopropylidene-6-*O*-*p*-tolylsulphonyl-D-galactose (V) (25 gm.) was dissolved in ethanethiol (30 cc.). Concentrated hydrochloric acid (25 cc.) was added and the mixture was agitated on the shaking machine for one hour.

The colorless reaction mixture became milky with the partial separation of reaction product and after cooling to 5° the mixture was cautiously neutralized with cold ammonium hydroxide. Petroleum ether (30–60°) was added and the heterogeneous mixture stirred well and allowed to stand at 5° for about one hour. The mixture was filtered and the reaction product washed with cold water and finally with petroleum ether (30–60°). The yield was 15 gm. (64%) and, after one recrystallization from hot acetone, the melting point was 114–115° and $[\alpha]_D^{21°}+7.5°$ (pyridine; *c*, 8.6314). Further recrystallization did not alter these constants. The literature (5) reports m.p. 115° and $[\alpha]_D^{20°}+7.66°$ (pyridine).

6-*Deoxy*-6-*thioethyl*-D-*galactose Diethyl Thioacetal* (*VIII*)

(1) 6-*O*-*p*-Tolylsulphonyl-D-galactose diethyl thioacetal (VI) (3.5 gm.) and sodium ethanethiolate (1.4 gm., 2 mol. equiv.) were dissolved in anhydrous N,N-dimethylformamide (40 cc.). The mixture warmed spontaneously and it was then heated at 100° for two hours, cooled to 15°, and the sodium *p*-toluenesulphonate was removed by filtration. The filtrate was added to cold water and the separated feathery mass was filtered, washed with a small volume of cold water, and then air-dried. It was recrystallized from acetone and an additional crop was obtained from the mother liquor. The combined yield was 2.2 gm. (90%), the melting point was 157–158°, and the optical rotation $[\alpha]_D^{24°}-6.2°$ (pyridine; *c*, 4.0292). Anal.: Calc. for $C_{12}H_{26}S_3O_4$: C, 43.63; H, 7.87; S, 29.1. Found: C, 43.6; H, 7.94; S, 29.1.

(2) 6-*O*-*p*-Tolylsulphonyl-D-galactose diethyl thioacetal (VI) (4 gm.) was suspended in anhydrous methanol (50 cc.). A solution (10 cc.) of sodium methylate, containing 0.2 gm. (1 mol. equiv.) of sodium, was added. Solution occurred rapidly and, after the reaction mixture had been allowed to stand for six hours at 22°, carbon dioxide was passed into it to destroy any unreacted sodium methylate. The reaction mixture was then concentrated *in vacuo* at 40° and the dry residue containing sodium *p*-toluenesulphonate was acetylated with pyridine and acetic anhydride. The reaction mixture was poured into cold water and after it had stood for 24 hr. at 22° the sirup did not crystallize. The sirup was taken up in ether and the ethereal solution was dried over sodium sulphate and the solvent removed *in vacuo*. The resulting sirup, probably 5,6-anhydro-D-galactose diethyl thioacetal triacetate, was dissolved in N,N-dimethylformamide (50 cc.) and dry sodium ethanethiolate (0.8 gm.) was added. The solution was allowed to stand overnight at 5°, heated one hour at 100°, cooled to room temperature, and then added to cold water (150 cc.). The product that separated was air-dried and recrystallized from acetone. The yield was 2 gm. (66%) and the melting point, 157–158°, was not depressed when a sample was admixed with 6-deoxy-6-thioethyl-D-galactose diethyl thioacetal.

(3) 6-Deoxy-6-thioethyl-galactose and 1,2-3,4-diisopropylidene-6-deoxy-6-thioethyl-D-galactose were each mercaptalated by the usual hydrochloric acid – ethanethiol method and the products that were isolated in each case were recrystallized from acetone and melted at 157–158°. Mixed melting point

determinations with authentic samples of 6-deoxy-6-thioethyl-D-galactose diethyl thioacetal showed identity.

2,3,4,5-*Tetrabenzoyl*-6-*deoxy*-6-*thioethyl*-D-*galactose Diethyl Thioacetal*

6-Deoxy-6-thioethyl-D-galactose diethyl thioacetal (VII) (7.8 gm.) was dissolved in anhydrous pyridine (50 cc.). The solution was cooled to $-10°$ and benzoyl chloride (14.8 gm.) was added dropwise with stirring. The reaction mixture was then allowed to stand overnight at room temperature and finally poured into water. Solid potassium bicarbonate was added to dissolve benzoic acid that arose from the excess benzoyl chloride used. The sirupy product did not crystallize and it was extracted with chloroform. The chloroform solution was dried over anhydrous sodium sulphate, filtered, and then concentrated *in vacuo*. The light yellow sirup was dissolved in 99% ethanol and petroleum ether (30–60°) was added until the solution became slightly turbid. The solution was cooled to $-20°$ and an oil separated. More 99% ethanol was added so that the oil was just redissolved and further cooling caused the deposition of a crystalline product. The material was again recrystallized from a small volume of absolute ethanol. The yield was 11.7 gm. (71%) and the substance melted at 90–91°. The substance rotated $[\alpha]_D^{23°}+5.8°$ ($CHCl_3$; *c*, 5.5592). Anal.: Calc. for $C_{40}H_{42}S_3O_8$: C, 64.34; H, 5.63; S, 12.87; C_6H_5CO, 56.3. Found: C, 64.28; H, 5.71; S, 12.9; C_6H_5CO, 56.1.

2,3,4,5-*Tetraacetyl*-6-*deoxy*-6-*thioethyl*-D-*galactose Diethyl Thioacetal* (*VIII*)

6-Deoxy-6-thioethyl-D-galactose diethyl thioacetal (VII) (23 gm.) was suspended in anhydrous pyridine (75 cc.) and acetic anhydride (50 cc.). The reaction mixture was allowed to stand overnight at room temperature and the colorless solution was poured into a large volume of cold water. A sirup separated and it solidified within 30 min. The solid was broken up, filtered, and washed to remove pyridine. The substance was dissolved in ether and the solution dried over anhydrous sodium sulphate and then filtered. The filtrate was concentrated to about 50 cc. and petroleum ether (30–60°) was added until the solution became turbid. The turbidity was cleared with several drops of ether and after cooling for 48 hr. at $-20°$ large colorless hexagonal crystals separated. The product melted at 77.5–78° and rotated $[\alpha]_D^{22°}-4.9°$ ($CHCl_3$; *c*, 7.6792). The yield was 30.5 gm. (88%). Anal.: Calc. for $C_{20}H_{34}S_3O_8$: C, 48.19; H, 6.82; S, 19.27; CH_3CO, 34.54. Found: C, 48.06; H, 7.02; S, 19.2; CH_3CO, 34.4.

Aldehydo-2,3,4,5-*tetraacetyl*-6-*deoxy*-6-*thioethyl*-D-*galactose* (*IX*)

2,3,4,5-Tetraacetyl-6-deoxy-6-thioethyl-D-galactose diethyl thioacetal (VIII) (5 gm.) was dissolved in methanol-free acetone (100 cc.) and cadmium carbonate (20 gm.) was added, followed by mercuric chloride (11 gm.). The mixture was heated under reflux for five hours, filtered hot into fresh cadmium carbonate, and the filter washed twice with hot methanol-free acetone. The combined filtrates were concentrated to dryness in the presence of cadmium carbonate. The residue was refluxed with three portions of absolute reagent

diethyl ether (containing not more than 0.01% ethanol) and the combined ether solutions were washed with 10% aqueous potassium iodide solution to remove the mercury compounds. The washed ether solution was dried over anhydrous sodium sulphate, filtered, and then concentrated to about 20 cc. Cooling at −15° caused precipitation of the product and after filtration it was washed once with pure absolute diethyl ether (5 cc.) at −15°. The yield was 3.2 gm. (82%) and the substance melted at 102–103° and rotated $[\alpha]_D^{26°} -28.7°$ ($CHCl_3$—ethanol free; *c*, 1.772). Mutarotation occurred in USP chloroform probably owing to the direct combination with the ethanol found in USP chloroform to form the hemiacetal (X). Anal.: Calc. for $C_{16}H_{24}SO_9$: C, 48.98; H, 6.12; S, 8.16; CH_3CO, 43.8. Found: C, 48.91; H, 6.41; S, 8.2; CH_3CO, 43.6.

2,3,4,5-*Tetraacetyl*-6-*deoxy*-6-*thioethyl*-D-*galactose Ethyl Hemiacetal* (*X*)

A sample of the aldehydo derivative (IX) (2 gm.) above was dissolved in hot absolute ethanol (5 cc.). The solution was allowed to stand overnight at room temperature when crystallization occurred. The product was recrystallized from toluene, m.p. 129.5–130° and $[\alpha]_D^{24°} -3.05°$ ($CHCl_3$; *c*, 5.0728). Anal.: Calc. for $C_{18}H_{30}SO_{10}$: C, 49.31; H, 6.82; S, 7.3. Found: C, 49.24; H, 6.98; S, 7.3. The semicarbazones were made from IX and from the hemiacetal (X) by the usual method of water and potassium acetate and after recrystallization from hot water the melting points and mixed melting points were 202–204°. Anal.: Calc. for $C_{17}H_{27}SN_3O_9$: N, 9.35; S, 7.12. Found: N, 9.28; S, 7.1.

2,3,4,5-*Tetraacetyl*-6-*deoxy*-6-*thioethyl*-D-*galactose Dimethyl Acetal*

2,3,4,5-Tetraacetyl-6-deoxy-6-thioethyl-D-galactose diethyl thioacetal (VIII) (11.2 gm.) was dissolved in anhydrous methanol (150 cc.). Powdered cadmium carbonate (50 gm.) and mercuric chloride (26 gm.) were added and the mixture was refluxed vigorously for four hours. The reaction mixture was allowed to stand overnight at room temperature. Additional quantities of cadmium carbonate (30 gm.) and anhydrous methanol (150 cc.) were added and the mixture refluxed for three hours. The hot mixture was filtered into some cadmium carbonate in a distilling flask and the filtrate was concentrated to dryness *in vacuo* at 40°. Chloroform (200 cc.) was added, the solution filtered, and the filtrate extracted twice with 10% potassium iodide solution to remove soluble mercury compounds. The chloroform solution was dried over anhydrous sodium sulphate, the mixture filtered, and the filtrate concentrated to dryness *in vacuo* at 40°. The resulting sirup was dissolved in a small volume of ether, and petroleum ether (30–60°) was added to turbidity. Cooling at −15° caused precipitation. The product was recrystallized twice from ether – petroleum ether and once from a large volume of hot petroleum ether (65–110°). The yield was 6.8 gm. (69%) and the melting point 89–90° and rotation $[\alpha]_D^{23°} +6.1°$ ($CHCl_3$; *c*, 4.0592). Anal.: Calc. for $C_{18}H_{30}SO_{10}$: C, 49.31; H, 6.82; S, 7.3; CH_3CO, 40.1. Found: C, 49.11; H, 6.88; S, 7.3; CH_3CO, 39.8.

2,3,4,5-*Tetraacetyl*-6-*deoxy*-6-*thioethyl*-D-*galactose Diethyl Acetal* (*XI*)

2,3,4,5-Tetraacetyl-6-deoxy-6-thioethyl-D-galactose diethyl thioacetal (XIII) (5 gm.) was dissolved in absolute ethanol (100 cc.). Cadmium carbonate (25 gm.) was added followed by mercuric chloride (11 gm.). The mixture was refluxed for two hours, filtered into fresh cadmium carbonate, then concentrated to dryness. The residue was extracted with three portions (50 cc.) of hot chloroform and after filtration, the chloroform solution was washed twice with 10% potassium iodide solution to remove soluble mercury compounds. The solution was dried over sodium sulphate, filtered, and concentrated *in vacuo* to a thick sirup, which crystallized on standing. The solid mass of crystals was recrystallized twice from 60% ethanol and it did not reduce Fehling's solution prior to acid hydrolysis. The yield was 3.6 gm. (76%) and the melting point was 94.5–95.5° and it rotated $[\alpha]_D^{20°}+4.1°$ ($CHCl_3$; *c*, 4.8468). Anal.: Calc. for $C_{20}H_{34}SO_{10}$: C, 51.50; H, 7.29; S, 6.86; CH_3CO, 39.05. Found: C, 51.42; H, 7.31; S, 6.9; CH_3CO, 38.8.

6-*Deoxy*-6-*thioethyl*-D-*galactose Diethyl Acetal*

The solution, above, from the optical rotation determination (1.2117 gm.) was cooled to −15° and sodium methylate solution (0.5 cc. of 0.3 *N*) was added. The clear solution was allowed to stand at room temperature and within two hours a thin gel formed. The reaction mixture, after it had been left to stand 24 hr. at room temperature, was added to anhydrous ether (100 cc.) and the crystalline product washed with a small volume of anhydrous ether. The crude product was twice recrystallized from a small volume of hot water and it melted at 143.5–144° and rotated $[\alpha]_D^{19°}+11.1$ (pyridine; *c*, 2.464). The yield was 0.6 gm. (80%). Anal.: Calc. for $C_{12}H_{26}SO_6$: C, 48.32; H, 8.72; S, 10.73. Found: C, 48.2; H, 8.91; S, 10.69.

The above substance (0.5 gm.) was acetylated with pyridine and acetic anhydride and after isolation and one recrystallization from 60% ethanol, the product, weighing 0.58 gm. (75%), had a melting point of 94–95°. The melting point of a sample mixed with 2,3,4,5-tetraacetyl-6-deoxy-6-thioethyl-D-galactose diethyl acetal, obtained previously, was 94–95°.

ACKNOWLEDGMENT

The author wishes to thank the Sugar Research Foundation for kind financial assistance.

REFERENCES

1. BRIGL, P. and SCHINLE, R. Ber. 65: 1890. 1932.
2. DIMLER, R. J. and LINK, K. P. J. Am. Chem. Soc. 62: 1216. 1940.
3. JEANLOZ, R., PRINS, D. A., and REICHSTEIN, T. Helv. Chim. Acta, 29: 371. 1946.
4. LEVENE, P. A. and RAYMOND, A. L. J. Biol. Chem. 102: 331. 1933.
5. MICHEEL, F. and RUHKOPF, H. Ber. 70: 850. 1937.
6. RAYMOND, A. L. J. Biol. Chem. 107: 85. 1934.
7. RAYMOND, A. L. and SCHROEDER, E. F. J. Am. Chem. Soc. 70: 2785. 1948.
8. WOLFROM, M. L., KONIGSBERG, M., and MOODY, F. B. J. Am. Chem. Soc. 62: 2343. 1940.

GEOMETRICAL CORRECTIONS TO THE BRAGG-GRAY RELATION APPLIED TO ABSOLUTE CHEMICAL DOSIMETRY[1]

By P. J. Dyne

ABSTRACT

The γ-ray irradiation conditions for the valid application of the Bragg-Gray relation, which relates the energy deposition in a solid to the ionization in an air-filled cavity, are examined with particular reference to some published experiments on the yield of the radiation-induced oxidation of ferrous sulphate. It is pointed out that experiments in which divergent radiation is used will give a higher oxidation yield than the relation indicates. A quantitative treatment is advanced which accounts for the discrepancies between certain experimental results.

White, Marinelli, and Failla (10) have shown that the Bragg-Gray relation will give erroneous results if applied to ion chambers which are irradiated by divergent radiation and have given a method for estimating the error. Weiss, Bernstein, and Kuper (9) suggested that this was the reason for some of the discrepant results reported by different experimenters on the G value (No. of ions oxidized per 100 ev. absorbed) for the radiation-induced oxidation of ferrous sulphate. Earlier work in which the energy absorption was obtained from ion chamber measurements, using the Bragg-Gray relation, gave a G of about 20 which is considerably higher than the now well-established value of about 16 (3, 5, 7, 9). This paper will describe explicitly the reason for the failure of the Bragg-Gray relation in these earlier experiments and will show that the treatment given by White, Marinelli, and Failla can be extended to give a semiquantitative explanation of the anomalous high G values.

For this purpose we shall discuss a set of experiments in which the energy deposition in a solution was obtained from the ionization in an identical volume of air. All these experiments were carried out with polystyrene vessels using hard γ or X rays and differ only in the geometrical arrangement of source and solution. "Edge" effects, which arise because the solution near the polystyrene wall is being irradiated by secondary electrons generated in the wall, can be shown, from the relative stopping powers and electron densities of polystyrene and 0.8 N H_2SO_4, to be negligible.

The chosen set comprises the experiments of Miller (6), Hardwick (2), Hochanadel and Ghormley (3), and Weiss, Bernstein, and Kuper (9). The G values which they reported are shown in column A of Table I. As different values were used in their calculations for the energy per ion pair and the ratio of the stopping powers of air and polystyrene we have recalculated their results using the values used by Weiss, Bernstein, and Kuper. These are shown in column B. It can be seen that there is a discrepancy of about 15% between the first two experiments and the last two.

The Bragg-Gray relation (1, 8) states that the rate of energy deposition per unit volume, E, in a mass of solid material is given by $E = JW\rho$ where J

[1]*Manuscript received January 26, 1955.*
Contribution from the Research Chemistry Branch, Atomic Energy of Canada Limited, Chalk River, Ontario. Issued as A.E.C.L. No. 169.

TABLE I

G VALUES FOR THE OXIDATION OF FERROUS SULPHATE

	A	B
Miller	20.3	18.5
Hardwick	20.7	18.5
Hochanadel and Ghormley	16.7	15.5
Weiss, Bernstein, and Kuper	15.9	15.9

is the rate of formation of ion pairs per unit volume in an air-filled cavity in the solid, W is the energy per ion pair for air, and $\rho = n_S S_S / n_A S_A$ where n_S and n_A are the electron densities in the solid and air respectively and S_S, S_A are the stopping powers of the solid and air respectively. For this relation to hold it is required that the dimensions of the cavity be small compared with the range of the secondary (Compton recoil) electrons in air. Apart from this restriction, the relation is independent of the geometry of the cavity, provided that the radiation field is strictly uniform over the whole volume of the chamber. This is demonstrated most clearly in the treatment given by Laurence (4).

This requirement of uniform irradiation may be fulfilled experimentally either by a uniform parallel beam of gamma or X rays or by isotropic irradiation which could be realized, for example, by placing the sample at the center of a spherical shell of material which emitted gamma rays. The former configuration was used by Weiss, Bernstein, and Kuper, the latter was approached by Hochanadel and Ghormley whose irradiation cell was placed on the axis of a cylindrical source of Co^{60}. Both of these values may be taken to be in agreement with $G \simeq 16$.

The irradiation apparatus used by Miller and by Hardwick is shown diagrammatically in Fig. 1. The radioactive source (*S*) is placed on the axis

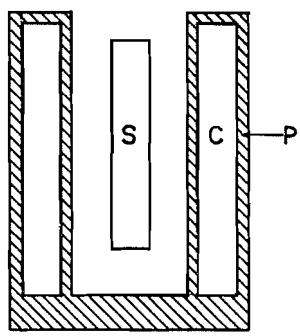

FIG. 1. Cylindrical ion chamber as used by Miller and by Hardwick. *S*, source; *C*, cavity; *P*, polystyrene wall.

of a cylindrical shell (*C*) of solution or air which is enclosed by polystyrene walls (*P*). The experimental volume is being irradiated by a divergent, nonuniform field and we cannot apply the Bragg-Gray relation to the ion current to obtain the energy deposition in the liquid.

The energy deposition in the liquid can be calculated for divergent radiation by a modification of the method of White (11) and White, Marinelli, and Failla (10). These workers discussed the case of a cavity between two concentric spherical shells with a point source of radiation at the center. In Fig. 2

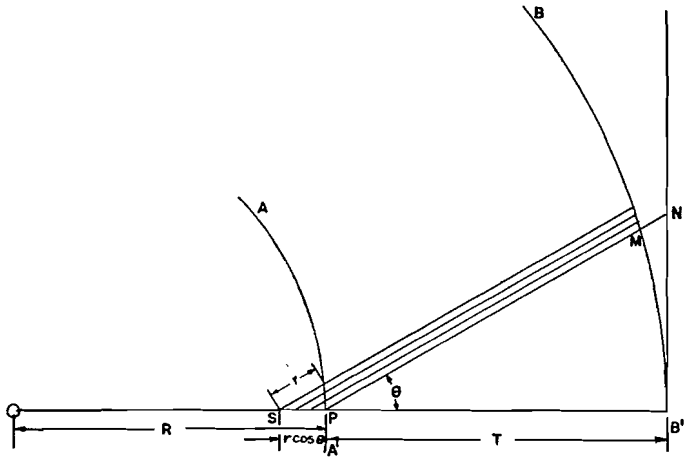

FIG. 2. Paths of secondary electrons crossing a spherical shell.

we show the paths of secondary electrons generated by γ rays originating from the point O crossing the walls of the spherical chamber, AA', BB'. Let the γ rays generate n secondary electrons per cm. having a range r cm. in the solid, which are scattered through an angle θ from the direction of the incident γ ray. Since the range of the secondaries in air is very much greater than that in the wall, secondaries which are formed up to a distance $r \cos \theta$ inside the wall will be able to cross the air cavity. The number of secondaries crossing the air cavity is, therefore, $nr \cos \theta$. Since $r \ll T$, the thickness of the air cavity, these secondaries have path lengths which are all effectively equal to PM. We put $PM = PN/\lambda = T/\lambda \cos \theta$. If these secondary electrons produce τ ions per cm. in air, losing W ev. per ion pair, the total energy deposition in the gas is $E_G = nr \cos \theta$. $(T/\lambda \cos \theta)\tau W = (nrT\tau W)/\lambda = JW$, where J is the ion current.

When the air cavity is filled with liquid (or any condensed medium) the energy deposition is due entirely to secondaries generated in the liquid. The γ rays cross T cm. of liquid and will produce nT secondaries of range r cm. if the wall and liquid are equivalent. Each secondary will deposit $r\tau\rho W$ ev. where $\rho = n_L S_L / n_A S_A$ as before, the subscripts referring to the liquid and air respectively. The energy deposition in the liquid is $E_L = nrT\tau\rho W$ ev. Combining the equations for E_L and E_G and noting that $E_G = JW$ we find

$$E_L = E_G \rho \lambda = JW\rho\lambda, \qquad [1]$$

which is a form of the Bragg-Gray relation modified by the introduction of the geometric factor λ. It can be seen from Fig. 1 that λ is appreciably greater than unity. Application of the unmodified Bragg-Gray relation will, therefore,

underestimate E_L and consequently will overestimate the G value for a radiation-induced reaction.

White, Marinelli, and Failla showed that for a cavity in the shape of a spherical shell

$$\lambda = T/\{[(R\cos\theta)^2+2RT+T^2]^{\frac{1}{2}}\cos\theta - R\cos^2\theta\}.$$

This formula was applied to measurements on a set of ion chambers of different dimensions. For $\theta \simeq 60°$ a satisfactory agreement was obtained between their measurements and earlier independent measurements on the specific gamma ray output from radium. It should be noted that θ is an empirical parameter.

The calculation of the energy deposition in a cylindrical cavity follows precisely the same steps. The paths of secondary electrons crossing the cavity are shown in Fig. 3. The lines MQ and OQ are in the YOZ plane. The source

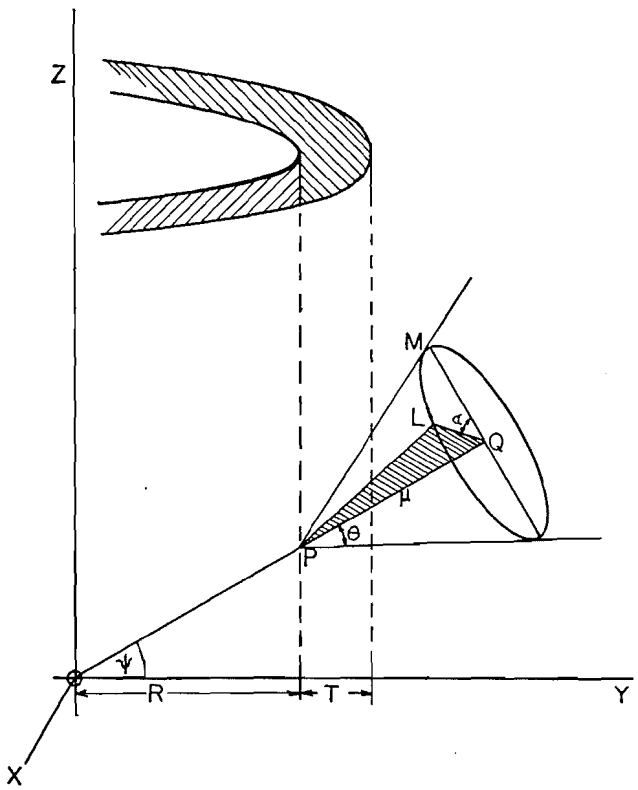

FIG. 3. Paths of secondary electrons crossing a cylindrical cavity.

is at the origin, halfway along the length of the cylindrical cavity. A γ ray follows the path OPQ making an angle ψ with the Y axis and generates secondary electrons which emerge, in effect, at the point P at the edge of the inner wall. The paths of all the secondaries crossing the air cavity, scattered through an angle θ, generate a cone, semiangle θ with an axis OPQ, vertex at P.

The coordinates (x, y, z) of the point L shown in the diagram are

$$[2] \qquad x = \mu \tan\theta \sin\alpha,$$
$$[3] \qquad y = R+\mu(\cos\psi-\tan\theta\cos\alpha\sin\psi),$$
$$[4] \qquad z = R\tan\psi+\mu(\sin\psi+\tan\theta\cos\alpha\cos\psi).$$

These may be taken as the parametric equations of the line LP which is the path of an individual secondary electron specified by the angles ψ, θ, and α.

For the cylindrical ion chamber the equation of the outer cylinder which terminates the paths of the secondary electrons is

$$[5] \qquad x^2+y^2 = (R+T)^2.$$

The path length D of the secondary electron crossing the cylindrical cell is $\mu/\cos\theta$ when, from equations [1], [2], and [5],

$$\mu^2[\tan^2\theta\sin^2\alpha+(\cos\psi-\tan\theta\cos\alpha\sin\psi)^2] +2\mu R(\cos\psi-\tan\theta\cos\alpha\sin\psi)+R^2-(R+T)^2 = 0;$$

whence

$$[6] \qquad D = \frac{+R\beta+\sqrt{(R+T)^2(\tan^2\theta\sin^2\alpha+\beta^2)-R^2\tan^2\theta\sin^2\alpha}}{\cos\theta(\tan^2\theta\sin^2\alpha+\beta^2)}$$

where $\beta = (\tan\theta\cos\alpha\sin\psi-\cos\psi)$.

A secondary electron whose path is defined by ψ, θ, and α has the path length $D(\alpha)$ and will deposit $D(\alpha)\tau W$ ev. in the cavity. To obtain the total energy deposition for gamma rays having the direction ψ we first multiply this energy by the number of secondary electrons having this path and then integrate over all values of α. The paths of secondary electrons inside the wall, near the edge of the cavity, are shown in Fig. 4. The points P and S correspond to the points

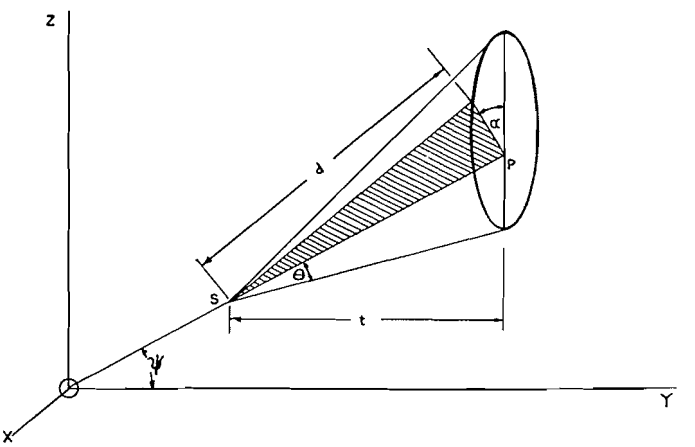

FIG. 4. Paths of secondary electrons inside the wall, at the edge of the cavity.

P and S in Figs. 2 and 3. The paths of secondary electrons in the wall are terminated by a vertical *plane* (since $r \ll R$). It can be shown using equations

[2], [3], and [4] above that a secondary of path length d is generated a distance t inside the wall where $t = d(\cos\theta - \tan\theta \sin\psi \cos\alpha)\cos\theta = -d\beta\cos\theta$. All secondaries generated along the path $SP = t/\cos\psi$ when $d = r$ will cross the cavity. Using our previous notation the number of secondary electrons $N(\alpha)$ specified by the direction α which cross the cavity is given by

$$N(\alpha) = -nr\beta\cos\theta/\cos\psi.$$

The total energy deposition from secondaries generated by γ rays having the direction ψ is E_G where

$$[7] \qquad E_G = \int_0^{2\pi} N(\alpha)D(\alpha)\tau W d\alpha \Big/ \int_0^{2\pi} d\alpha.$$

When the cavity is filled with liquid the γ rays cross $T/\cos\psi$ cm. of this medium and consequently the energy deposition in the liquid E_L is given by

$$[8] \qquad E_L = nTr\tau\rho W/\cos\psi,$$

whence we find

$$[9] \qquad E_L = -E_G\rho T \int_0^{2\pi} (1/\beta\, D(\alpha))d\alpha \Big/ \cos\theta \int_0^{2\pi} d\alpha,$$

which we may rewrite, noting that $E_G = JW$, as $E_L = JW\rho\eta$. This is similar to equation [1], the factor η corresponding to the factor λ defined for spherical cavities. The quantity η may be evaluated numerically.

Since η is a function of ψ the factor required to correct the experimental results is the value of η, weighted for the distribution of γ rays as a function of ψ averaged over ψ. Since in the experiment which we are discussing the source of γ rays was a cylinder of length and diameter comparable with those of the cell itself (not a point source by any means) we do not know this distribution function. All we shall do is to discuss the values which η make take for chosen values of ψ.

In our calculations we used a value of $\theta = 60°$ as found experimentally by White, Marinelli, and Failla. This describes the average path of electrons generated by a gamma ray whose path is normal to a spherical wall. For small angles of ψ we would expect θ to be unchanged for the cylindrical wall since the radius of curvature of the wall is large compared with the path length of the secondaries in the wall. For $R = 10$ mm., $T = 4$ mm., dimensions corresponding to the Miller and the Hardwick cell, and for $\psi = 0°$, $10°$, and $15°$, η has the values of 1.16, 1.18, and 1.19 respectively. The G values, as they were originally calculated, would be about 18% higher than the true value if the averaged value of η was of this magnitude.

When $\psi > 15°$ we cannot use equation [7] for, with the experimental cells, some of the secondary electrons crossing the air cavity are not terminated by the cylindrical wall but by the plane end of the cell. The geometrical correction will therefore be greater than the value of η given by equation [9]. The calculation is further complicated when $\psi > 30°$ for, with $\theta = 60°$, only part of the cone of secondary electrons cross the air cavity at all. The value

of η is still however appreciably greater than unity. For small values of ψ, η is in the range 1.15–1.20.

These calculations are based on an idealized model and too much weight should not be placed on the numerical values we have quoted. In addition to the fact that the angular distribution of gamma rays is not known, we have assumed a single value of θ. The value chosen was that found experimentally for electrons generated by a gamma ray whose path is normal to the edge of the cavity. When the incident γ ray intersects the cavity obliquely we should not expect the average scattering angle to be quite the same. This will not alter the conclusion of the last paragraph, namely that the correction is always appreciably greater than unity, but the possible range of values for the correction should be extended.

We can say, in conclusion, that the Bragg-Gray relation applied to cylindrical ion chambers as used by Miller and by Hardwick will give energy depositions in a condensed medium which are low by 10–20%. This observation is offered as an explanation of the high G values obtained by these experimenters compared with those obtained by Hochanadel and Ghormley and by Weiss, Bernstein, and Kuper.

ACKNOWLEDGMENTS

I should like to acknowledge many helpful discussions with Dr. R. W. Attree; in particular the generous help and guidance I received from him on the mathematical derivations in this paper. I should also like to acknowledge helpful correspondence with Dr. N. Miller and Dr. T. N. White.

REFERENCES

1. GRAY, L. H. Proc. Roy. Soc. (London), A, 122: 647. 1929; A, 156: 578. 1936.
2. HARDWICK, T. J. Can. J. Chem. 30: 17. 1952.
3. HOCHANADEL, C. J. and GHORMLEY, J. A. J. Chem. Phys. 21: 880. 1953.
4. LAURENCE, G. C. Can. J. Research, A, 15: 67. 1937.
5. LAZO, R. M., DEWHURST, J. A., and BURTON, M. J. Chem. Phys. 22: 1370. 1954.
6. MILLER, N. J. Chem. Phys. 18: 79. 1950.
7. SALDICK, J. and ALLEN, A. O. J. Chem. Phys. 22: 438. 1954.
8. WANG, T. J. Nucleonics, 7: 55. 1950.
9. WEISS, J., BERNSTEIN, W., and KUPER, J. B. H. J. Chem. Phys. 22: 1593. 1954.
10. WHITE, T. N., MARINELLI, L. D., and FAILLA, G. Am. J. Roentgenol. Radium Therapy, 44: 889. 1940.
11. WHITE, T. N. Gamma rays: measurement. *In* Medical physics. *Edited by* O. Glasser. Year Book Publishers Inc., Chicago, 1950. p. 339.

A SYNTHESIS OF D-TAGATOSE FROM D-GALACTURONIC ACID[1]

By P. A. J. Gorin,[2] J. K. N. Jones,[2] and W. W. Reid[3]

ABSTRACT

D-Tagatose has been synthesized by a series of reactions from D-galacturonic acid.

INTRODUCTION

D-Tagatose is generally prepared by the isomerization of D-galactose with very dilute alkali (1) or hot pyridine (4). However, the yields from these reactions are small and the isolation of the product tedious. D-Tagatose has also been prepared by the biochemical oxidation of the rare sugar derivative D-talitol using *Acetobacter suboxydans* (5).

We now describe a preparation of D-tagatose from D-galacturonic acid. This material is readily prepared by the enzymic hydrolysis of pectic acid (3). Isomerization of D-galacturonic acid (I) with lime water gave the calcium salt of 5-keto-L-galactonic acid (II; 2) which on treatment with an acetone–sulphuric acid mixture followed by esterification with ethereal diazomethane

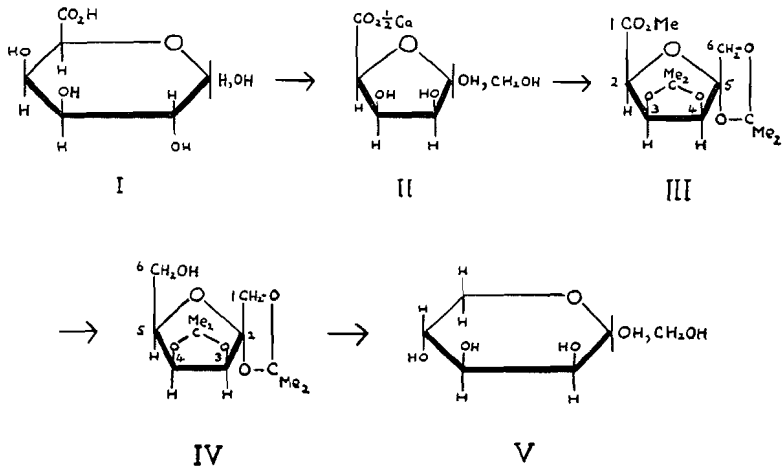

yielded 3,4;5,6-di-*O*-*iso*propylidene-5-keto-L-galactofuronic acid methyl ester (III). An ethereal solution of this material was reduced with lithium aluminum hydride to 1,2;3,4-di-*O*-*iso*propylidene-D-tagatose (IV) which was identical with an authentic specimen prepared from D-tagatose. Acid hydrolysis of (IV) gave a material indistinguishable from D-tagatose (V) in 25% over-all yield from the calcium salt of 5-keto-L-galactonic acid.

[1]*Manuscript received February 14, 1955.*
Contribution from the Department of Chemistry, Queen's University, Kingston, Ontario, and the Research Department, H. W. Carter and Company Limited, Coleford, Gloucester, England.
[2]*Department of Chemistry, Queen's University, Kingston, Ontario.*
[3]*Research Department, H. W. Carter and Company Limited, Coleford, Gloucester, England.*

EXPERIMENTAL

Evaporations were carried out under reduced pressure. Optical rotations were measured at 16±2°C. Melting points are uncorrected.

3,4;5,6-*Di-O-isopropylidene*-5-*keto*-L-*galactofuronic Acid Methyl Ester* (III)

The calcium salt of 5-keto-L-galactonic acid (II; 620 mgm.), prepared by the isomerization of D-galacturonic acid (I) by alkali, was shaken in dry acetone (12 ml.) containing sulphuric acid (0.5 ml.) for four hours. The solution, which contained a suspension of calcium sulphate, was neutralized by rapid addition to aqueous lime. The alkaline solution was then neutralized with carbon dioxide, filtered, and the filtrate evaporated to a white solid (the calcium salt of 3,4;5,6-di-*O-iso*propylidene-5-keto-L-galactofuronic acid). The free acid was obtained from the salt by the addition of dilute sulphuric acid to an emulsion of ether and a solution of the calcium salt in ice-cold water. The ethereal extract was washed with water (four times), dried (sodium sulphate), filtered, and esterified by addition of an excess of ethereal diazomethane. After 30 min. the solution was evaporated to a sirup which crystallized. Two recrystallizations from ethanol gave white needles (353 mgm.) with m.p. 60°C. and $[\alpha]_D$ +22° (*c*, 1.0 in chloroform). Found: C, 54.4; H, 7.0%. Calc. for $C_{13}H_{20}O_7$: C, 54.2; H, 6.9%.

1,2;3,4-*Di-O-isopropylidene*-D-*tagatose* (*IV*)

3,4;5,6-Di-*O-iso*propylidene-5-keto-L-galactofuronic acid methyl ester (III; 848 mgm.) was added with stirring to an excess of lithium aluminum hydride (500 mgm.) in ether (20 ml.). After five hours, excess of reagent was destroyed by addition of ethyl acetate. Water (50 ml.) was added and organic solvents evaporated. The solution was neutralized with acetic acid, filtered, and the filtrate extracted with an equal volume of chloroform. The extract was washed once with water, dried (sodium sulphate), filtered, and evaporated to a sirup (674 mgm.) which crystallized. Two recrystallizations from light petroleum (b.p. 30–60°C.) gave white needles which had m.p. 63–64°C. not depressed on admixture with an authentic specimen of 1,2;3,4-di-*O-iso*propylidene-D-tagatose which had been prepared from D-tagatose and $[\alpha]_D$ +64° (*c*, 0.80 in chloroform). Found: C, 55.1; H, 7.5%. Calc. for $C_{12}H_{20}O_6$: C, 55.4; H, 7.6%.

D-*Tagatose* (*V*)

1,2;3,4-Di-*O-iso*propylidene-D-tagatose (IV; 173 mgm.) was hydrolyzed by heating in 0.05 *N* sulphuric acid (5 ml.) at 100° for one hour. The reaction mixture was neutralized (aqueous barium hydroxide, then barium carbonate), filtered, and evaporated to a sirup (115 mgm.). The product was crystallized twice from ethanol to give white crystals (71 mgm.) which had m.p. 131–132°C. undepressed on admixture with authentic D-tagatose prepared by isomerization of D-galactose and $[\alpha]_D$ +2° (2 min.) → −3° (30 min.; constant value) (*c*, 1.0 in water). Found: C, 40.3; H, 7.0%. Calc. for $C_6H_{12}O_6$: C, 40.0; H, 6.7%.

ACKNOWLEDGMENT

The authors are grateful to the National Research Council for financial assistance.

REFERENCES

1. De Bruyn, C. A. L. Rec. trav. chim. 14: 150. 1895.
2. Ehrlich, F. and Guttmann, R. Ber. B, 67: 573. 1934.
3. Henglein, F. A. and Hann, M. Makromol. Chem. 2: 289. 1948.
4. Reichstein, T. and Bosshard, W. Helv. Chim. Acta, 17: 753. 1934.
5. Totton, E. L. and Lardy, H. A. J. Am. Chem. Soc. 71: 3076. 1949.

THE SYNTHESIS OF D,L-SERINE BY SELECTIVE REDUCTION OF N-SUBSTITUTED AMINOMALONIC AND CYANOACETIC ESTERS[1,2]

By Louis Berlinguet[3]

RÉSUMÉ

L'étude de la réduction sélective de l'amino malonate d'éthyle libre ou substitué sur l'azote par des radicaux acylés et de l'acétamido cyano acétate d'éthyle, par les hydrures $LiAlH_4$, NaH_4B, KH_4B, et $LiBH_4$ dans différents solvants et différentes conditions expérimentales a été faite. Une nouvelle synthèse de la D,L-sérine, à la fois rapide et facile, a ainsi été effectuée. Par réduction sélective des esters N-substitués des acides amino malonique et amino cyanoacétique, au moyen de l'hydrure de sodium et de bore dans l'eau et l'éthanol, suivie d'hydrolyse acide, on obtient la D,L-sérine avec de bons rendements.

INTRODUCTION

Serine is an important amino acid. One of its derivatives, azaserine, has been used with success in cancer research. However, most of the general methods for the synthesis of D,L-serine are not convenient. The starting materials for some of them are difficult, laborious, or expensive to prepare, and the over-all conversion to serine is not particularly good by any of them.

The best method published so far is by King (9) who condensed quantitatively formaldehyde with ethyl acetamidomalonate (I). However, acid hydrolysis of the intermediate gave no serine but ammonium chloride and pyruvic acid. Owing to the instability of the condensation product in acid, it had to be first monosaponified with one equivalent of normal alkali, acidified, decarboxylated, and then hydrolyzed to D,L-serine, with an over-all yield of 65%. With the condensation product of formaldehyde and ethyl acetamidocyanoacetate (II), no serine could be obtained either by acid or by alkaline hydrolysis.

Both ethyl acetamidomalonate (I) and ethyl acetamidocyanoacetate (II) contain the three-carbon skeleton of serine and are easily available. It was felt that a better synthesis of serine could be worked out from these starting materials if the condensation with formaldehyde and the subsequent hydrolysis were avoided.

The availability of powerful reducing agents such as the hydrides and their recent use in the synthesis of 2-amino alcohols (1) have prompted us to study the selective reduction of N-substituted aminomalonic esters, and ethyl acetamidocyanoacetate, products easily available in large quantities. Three possibilities were to be expected in the reduction of ethyl acetamidomalonate (I): (1) No reduction, in which case, the unchanged starting material would yield glycine (III) by acid hydrolysis. (2) Reduction at both ester groups to

[1]*Manuscript received in original form September 13, 1954, and, as revised, January 21, 1955. Contribution from the Department of Biochemistry, Faculty of Medicine, Laval University, Quebec, P.Q.*

[2]*Presented before the annual meeting of the Chemical Institute of Canada, Toronto, June 20–23, 1954.*

[3]*Holder of a Fellowship of the National Cancer Institute of Canada.*

give after hydrolysis 2-amino-1,3-propanediol (IV). (3) Selective reduction at one ester group which would form ethyl N-acetyl serine ester, from which D,L-serine (V) would be obtained by hydrolysis.

REDUCTION OF N-SUBSTITUTED AMINOMALONIC ESTER

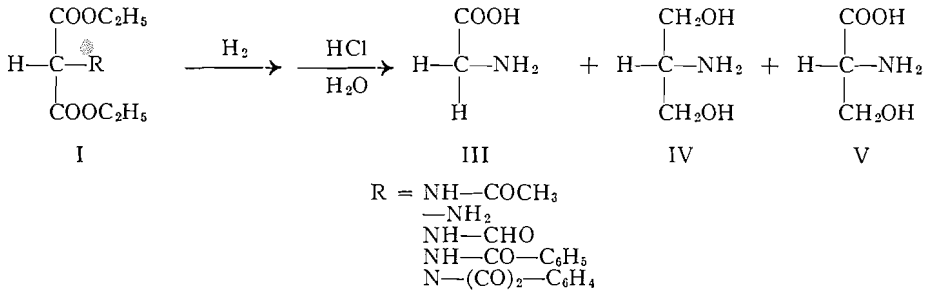

It was highly improbable that the amide group would be reduced to the secondary amine since Bory and Mentzer (3) had shown that this reduction required very drastic reducing conditions, which were not found in our experiment.

It was hoped that suitable conditions would be found in which possibilities (1) and (2) would be absent or reduced to a minimum, with the reduction proceeding only on one ester group to give D,L-serine.

In the reduction of ethyl acetamidocyanoacetate only two products were possible. In fact, no reduction was to be expected at the nitrile or at the amide groups since the reducing conditions were not drastic enough. Hence, only glycine and serine could be produced.

REDUCTION OF ETHYL ACETAMIDOCYANOACETATE

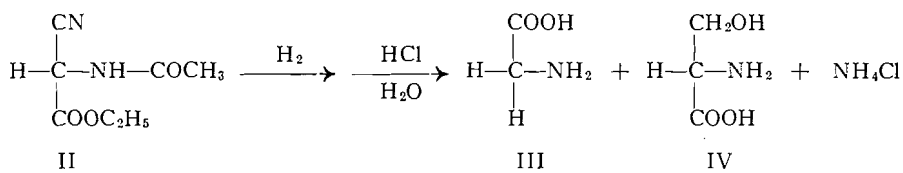

Several N-acyl derivatives of ethyl aminomalonate were reduced and subsequently were hydrolyzed to give serine, some glycine, and a trace of amino alcohol (Table I). No significant differences were found between N-acetamido, N-formamido, N-phthalimido, and N-benzamido ethyl malonates, except a slight decreasing yield in serine, probably due to the lower solubilities of the latter esters. In the case of N-unsubstituted ethyl aminomalonate, practically no serine and no glycine were found but free ammonia was abundant, apparently produced by the decomposition of the ester molecule.

As expected the reduction of ethyl cyanoacetate gave serine, no amino alcohol, but here again glycine was produced, though in a small yield.

Experimental conditions used during these reductions were studied in order to minimize the yield of glycine and 2-aminopropanediol.

Effect of Solvent (Table I)

When the ester to be reduced is water soluble, an aqueous medium gives the highest yield in serine. If the reduction is carried out in alcohol, a more complete reduction takes place at both ester groups with a subsequent greater formation of propanediol at the expense of serine and glycine.

Ethyl acetamidocyanoacetate does not give propanediol and, therefore, reduction in alcohol gives a slightly better yield of serine on account of the better solubility of this ester in alcohol than in water.

Nature of the Hydride (Table I)

Sodium borohydride gives the best yield in D,L-serine. Potassium borohydride also gives serine but is of slightly inferior reducing power. Lithium borohydride does not improve the yield. Lithium aluminum hydride in ether or in tetrahydrofuran at different temperatures does not reduce selectively any of the esters. In all cases no serine could be detected on paper chromatograms.

It is significant to note that it has been claimed previously that sodium and potassium borohydrides could not reduce esters, especially in water.

The concentration of the hydride, the order of addition, the pH of the medium, and the surface of contact between the hydride and the ester have no effect on the yield of the reduction. An increase of temperature, however, decreases the yield of serine (Table II).

From these studies, a new direct synthesis of serine has been worked out by reduction of ethyl acetamidomalonate or by reduction of ethyl acetamidocyanoacetate with sodium borohydride in aqueous medium.

EXPERIMENTAL PART

Compounds

Sodium borohydride, potassium borohydride, and lithium aluminum hydride were obtained from Metal Hydrides Inc., Beverly, Mass., and were used without purification.

Ethyl isonitrosomalonate was prepared according to Cerchez (4). The oxime has been described as an oil. However, when it was dissolved in benzene, a crystalline product was obtained in the cold. Melting point: 87°C.* Calc. for $C_7H_{11}O_5N$: N, 7.41%. Found: N, 6.87%. Subsequent recrystallizations from benzene did not raise the nitrogen content. This solid product, which seemed to be the oxime, was transformed into ethyl acetamidomalonate with the same yield as the ordinary oil.

Ethyl aminomalonate was obtained by reducing diethyl isonitrosomalonate with aluminum amalgam, according to Cerchez (5). The product was obtained as an oil. From this oil, the hydrochloride, m.p. 162°C., and the oxalate, m.p. 138°C., were prepared, as described by Cerchez (5), in yields of 45% and 55% respectively, calculated from the diethyl isonitrosomalonate. Calc. for $C_7H_{14}O_4NCl$: N, 6.56%. Found: N, 6.45%. Calc. for $C_9H_{15}O_8N$: N, 5.28%. Found: N, 5.20%.

**Melting points are not corrected.*

Some oximes have been reduced to amines with $LiAlH_4$ (18) but we have tried unsuccessfully to reduce diethyl isonitrosomalonate with $LiAlH_4$ and NaH_4B. No positive test to ninhydrin was obtained and free ammonia was present.

Ethyl formylaminomalonate was prepared according to Galat (7). Yield: 50%. Melting point 47°C. Calc. for $C_8H_{13}O_5N$: N, 6.90%. Found: N, 6.78%.

Ethyl phthalimidomalonate was obtained by reaction of ethyl bromomalonate with potassium phthalimide as described in *Organic Syntheses* (12). Melting point: 73°C. Yield: 70%. Calc. for $C_{15}H_{15}O_6N$: N, 4.59%. Found: N, 4.55%.

Ethyl benzamidomalonate was prepared according to Redeman and Dunn (15) by reacting benzoyl chloride and diethyl aminomalonate in pyridine. Melting point: 55°C. (from benzene and ligroin). Yield: 80%. Calc. for $C_{14}H_{17}O_5N$: N, 5.02%. Found: N, 5.10%.

Ethyl acetamidomalonate was prepared from isonitrosomalonic ester which was hydrogenated and acetylated with zinc dust in acetic anhydride and acetic acid. Melting point: 96°C. (from ether or ethyl acetate). Yield: 71%. Calc. for $C_9H_{15}O_5N$: N, 6.45%. Found: N, 6.52%.

Ethyl acetamidocyanoacetate was prepared by reducing isonitroso ethyl cyanoacetate with sodium hydrosulphite in acetic anhydride (19). Melting point: 129°C. (from acetic acid). Yield: 65%. Calc. for $C_7H_{10}O_3N_2$: N, 16.48%. Found: 16.58%.

Analytical Procedures

In order to study the relative yields of glycine and serine in the reduction experiments, methods of analysis for these products had to be found.

Paper Chromatography

Paper chromatography has been widely used for the analysis of amino acids and amino alcohols. However, glycine and serine, having very similar R_f values in most solvents, are difficult to separate. In our case pyridine and water (80:20) have been used with great success. In this system, the R_f values for glycine and serine are respectively 0.19 and 0.30. 2-Amino-1,3-propanediol has a much higher value at 0.75.

Glycine and serine were determined quantitatively with standard methods of paper chromatography. The simplified procedure used was as follows: Weighed drops of the calibrated solution obtained after reduction were placed on a paper chromatogram. The ascending chromatograms were run in pyridine and water (80:20) and were dried at room temperature. They were sprayed with 0.5% ninhydrin in acetone and were dried in the oven at 110°C. for 10 min. When allowed to dry at room temperature, serine appeared first, giving a bright bluish color, with glycine appearing later with a reddish color. The color due to aminopropanediol is rather slow to appear and is always weak. The two spots of serine and glycine were cut, placed in a test tube, triturated with 4 ml. of warm water, and filtered on a fritted disk. The filter paper was further washed with 1 ml. of warm water and the optical density of the clear filtrate was read at 540 mμ in a Beckman spectrophotometer.

Standard molar solutions of serine, glycine, and serine plus glycine were analyzed as above. As expected, equivalent molecular quantities of serine and glycine gave the same intensity when sprayed with 0.1% ninhydrin in butanol. However with 0.5% ninhydrin in acetone, serine gave a much deeper color than glycine.

The relative yields of serine and glycine were of primary importance in this study. For this reason, the amounts of serine and glycine in the reaction mixtures were determined colorimetrically from the ninhydrin color developed and eluted after chromatography. The "comparative" yield of serine was expressed as the number of moles of serine in 100 moles of amino acids (serine and glycine) in the reaction mixture. Since in most cases the amounts of aminopropanediol and other secondary products were negligible, the "comparative yield" approximated the true yield.

To reveal serine and the amino alcohol, a useful identification test has been used. The chromatogram was dipped in a watch glass containing a 10% solution of periodic acid. Then, it was dipped in Nessler reagent. Ten to twenty seconds later, a yellow spot developed which rapidly turned brown, then black. If this yellow color develops in Nessler reagent without having first dipped the paper in periodic acid, ammonia is present. The R_f values obtained in pyridine–water (80:20) with this test were respectively: 0.30 for serine, 0.52 for ammonium chloride, and 0.75 for aminopropanediol.

This test for serine was first described by Consden, Martin, and Gordon (6). We have found that it can be very useful in detecting 2-amino alcohols on paper chromatograms.

Periodate Estimation

When no amino alcohol was present, as in the reduction of ethyl acetamidocyanoacetate, for instance, the direct estimation of D,L-serine could be made by the method of Rees (16). In this method the amino acid is oxidized with periodic acid and the formaldehyde produced is titrated with bisulphite. Glycine was found by difference.

This procedure measures serine, threonine, glycols, and 2-amino alcohols. Thus if it is to be used to determine serine in presence of aminopropanediol, care must be taken to remove the latter before carrying out the oxidation.

Methods of Isolating Serine

The isolation of serine can be carried out by different procedures.

(1) Owing to the much higher solubility of glycine as compared to serine, the two amino acids can be separated by two or three recrystallizations from water–alcohol mixtures, serine crystals separating first. The hydrochloric acid used during hydrolysis can be removed from the amino acid by one of the following: (*a*) silver carbonate, (*b*) deacidite column, or (*c*) neutralization with an equivalent of lithium hydroxide forming LiCl which is soluble in alcohol.

(2) When small quantities are involved, the ideal separation would appear to be the chromatographic procedure used by Moore and Stein (8, 11) on Dowex-50 columns. An excellent method of isolation of serine by adsorption

on Zeo-Karb has been described by Partridge (13). Another chromatographic procedure has been used with success. When the amino acids are adsorbed on Permutit S-1 and eluted with 0.1 *N* acetic acid, glycine appears first, followed by a mixture of serine and glycine. Then serine alone is eluted.

(3) For larger batches of serine, the selective removal of glycine is made using classical methods (2), such as distillation of the ethyl ester of glycine or selective precipitation of glycine with 5-nitronaphthalene-sulphonic acid (17).

Separation of Glycine and Serine on Permutit S-1

A solution of D,L-serine (1.0 gm.) and glycine (1.0 gm.) was slowly passed through a column of Permutit S-1 (35 × 180 mm.). The amino acids were retained on the column. Elution was made with 0.1 *N* acetic acid. Aliquots from each 25 ml. of the eluate were analyzed with paper chromatography.

The first 250 ml. contained no amino acid. In the next 150 ml. only glycine was present. The solution was evaporated and the residue recrystallized from ethanol and water. Yield of pure glycine: 0.4 gm. (40%). Calc. for $C_2H_5O_2N$: N, 18.66%. Found: N, 18.50%.

The following 225 ml. contained a mixture of glycine and serine. When evaporated, the total weight of the residue was 0.6 gm.

Aliquots from the next 200 ml. gave only the serine spot on paper chromatograms. The solution was evaporated to dryness and the residue was recrystallized from aqueous ethanol. Yield of D,L-serine: 0.8 gm. (80%). Calc. for $C_3H_7O_3N$: N, 13.32%. Found: N, 13.55%.

Conditions Used During the Reductions

Different experimental conditions were used in the reductions of different esters in order to find out the best synthesis of serine. Results are summarized in Tables I and II.

The standard conditions used for the reductions were as follows: One gram of the ester was dissolved in the selected solvent system, water, methanol, ethanol, tetrahydrofuran, ether, or mixtures of them. Two grams of the hydride in solution or in solid form were then added at a chosen rate, with vigorous agitation. After one or two hours, the mixture was first acidified with dilute hydrochloric acid to pH 1.0 and then hydrolyzed by boiling for four to six hours for substituted aminomalonates and 12 to 17 hr. for acetamidocyanoacetate.

After hydrolysis, the solution was evaporated to dryness and the residue was dissolved in distilled water to a calibrated volume of 100 ml. Aliquots were analyzed for their glycine and serine contents as described.

Some of the reductions were carried out in the refrigerator, some in boiling water. When the surface of contact was studied, the above standard procedure for the reduction was carried out in a column (300 mm. × 20 mm.) packed with glass beads.

When lithium aluminum hydride was used, drops of water were carefully added to the reduction mixture at the end of the reaction to decompose any unreacted hydride.

In order to obtain lithium borohydride, equivalent quantities of potassium borohydride and lithium chloride were mixed in ethanol prior to the addition of the ester (10, 14).

TABLE I

YIELDS OF SERINE AS COMPARED TO THE TOTAL YIELD OF SERINE AND GLYCINE

	Hydride									
	NaH_4B					KH_4B	LiH_4B	LiH_4Al		
	Solvent									
	Ethanol–water	Ethanol	Water			Ethanol–water	Ethanol	Tetrahydrofuran		
			1*	1½	2			0°	20°	65°
Ethyl acetamidomalonate	68	50†	54	69	70	50	65	0		0
Ethyl formamidomalonate	70	50	66	68	62	50	26	0	Traces	0
Ethyl phthalimidomalonate	62	49	35	57	44	50	24	0		
Ethyl benzamidomalonate	60									
Ethyl aminomalonate	Traces	Traces				Traces		0		
Ethyl acetamidocyanoacetate	67	72	45	55	66	35	50	0		

Grams of NaH_4B per gram of ester.
†*When the yield is underlined, the amount of amino alcohol produced was larger than usual.*

Reductions of Ethyl Aminomalonates

Reduction of Ethyl Aminomalonate

With LiH_4Al, no ninhydrin test was obtained after hydrolysis. Free ammonia was formed, indicating decomposition of the aminomalonate.

With NaH_4B, and KH_4B, slight traces of glycine, serine, ammonia, and aminopropanediol were detected on paper chromatograms.

These reductions were carried out on the free amino ester. When the oxalate or the hydrochloride were reduced, the yields of 2-aminopropanediol and serine seemed to increase a little.

Reduction of Ethyl Phthalimidomalonate

As was to be expected, reduction with $LiAlH_4$ gave no serine but a mixture of glycine, free ammonia, and several unknown products.

When NaH_4B was used, serine was produced in good or poor yields, depending on the solvent used. In water, the ester is too insoluble to react with the hydride; hence, glycine is produced by acid hydrolysis. With ethanol and water, paper chromatography has shown that serine and glycine are produced in relative yields of 60% and 40%.

Reduction with KBH_4 gave about the same results as with $NaBH_4$.

Reduction of Ethyl Benzamidomalonate

In a mixture of water and ethanol, the reduction with NaH_4B gave "comparative" yields of 60% serine and 40% glycine.

Reduction of Ethyl Formamidomalonate

In this case, the reduction with $LiAlH_4$ in tetrahydrofuran gave in low yield some serine, with glycine, ammonia, and unknown products.

Ethyl formamidomalonate (5.0 gm.), treated with 3.0 gm. NaH_4B in aqueous methanol or ethanol, gave after hydrolysis 1.29 gm. (50%) of D,L-serine. Silver carbonate was used to liberate the amino acid from hydrochloric acid. After recrystallization from aqueous alcohol, transparent platelets, characteristic of D,L-serine, were obtained. Calc. for $C_3H_7O_3N$: N, 13.32%. Found: N, 13.37%. No glycine was found on paper chromatograms from this isolated serine.

In the reductions with KBH_4, equal quantities of serine and glycine were found on paper chromatograms.

Reduction of Ethyl Acetamidomalonate

Reductions in different experimental conditions were studied. The results are presented in Tables I and II.

In tetrahydrofuran or ether, the reduction with $LiAlH_4$ gave no serine but glycine and free ammonia.

When ethyl acetamidomalonate was monosaponified with an equivalent of sodium hydroxide before reduction with $NaBH_4$, the yield of serine was only about 30%.

With KBH_4, the reduction gave about the same yield in glycine and serine as with $NaBH_4$.

TABLE II

YIELDS OF SERINE AS COMPARED TO THE TOTAL YIELD OF SERINE AND GLYCINE

Reduction of ethyl acetamidomalonate in water with NaH_4B; at room temperature, except where specified

Conditions used	Yields, %
Hydride into ester	67
Ester into hydride	71
Temperature: 0°C.	74
Temperature: 100°C.	44
Surface (glass beads)	67
pH (Dowex 50)	50

Reduction of Ethyl Acetamidocyanoacetate

After reduction with $LiAlH_4$ and hydrolysis, the residue gave on a paper chromatogram a spot at 0.17 (glycine), a very weak spot at 0.48 (NH_4Cl), and a very strong blue spot at 0.68 (unknown product). No serine was present.

When $NaBH_4$ was used to reduce the ester, the yields in D,L-serine obtained from the periodate analysis were around 70%, irrespective either of the solvent or of the acid used during the hydrolysis (Table III).

With KBH_4, the yields in serine were much lower (35%).

TABLE III

PERIODATE ANALYSIS OF THE REDUCTION PRODUCTS OF ETHYL ACETAMIDOCYANOACETATE

Solvent	Hydride used	Hydrolysis with	Mgm. of serine		% yield	"Comparative" yield
			Found	Calc.		
Blank (no reduction)	—	HCl	0	0	—	—
Ethanol–water	$NaBH_4$	HCl	416	618	67	70
Ethanol–water	$NaBH_4$	HCl	443	618	72	80
Water	$NaBH_4$	10% H_2SO_4	810	1235	66	76
Ethanol	$NaBH_4$	10% H_2SO_4	433	618	70	75
Ethanol–water	$NaBH_4$	10% H_2SO_4	395	618	65	73
Water	KBH_4	10% H_2SO_4	371	772	48	—
Ethanol–water	KBH_4	10% H_2SO_4	208	772	27	—
Ethanol–water	KBH_4	HCl	292	772	38	—
Ethanol	KBH_4	HCl	242	772	31	—

Typical Synthesis of Serine

From Ethyl Acetamidomalonate

From these studies, a new direct synthesis of serine has been worked out.

The best conditions found for ethyl acetamidomalonate are to reduce it with an excess of $NaBH_4$ in water or water–alcohol (80: 20) solution in the cold, with a subsequent two-hour hydrolysis with dilute acid. In this case, propanediol is produced in a negligible quantity and glycine is reduced to a minimum. Paper chromatograms indicated a proportion of serine over glycine of 4 to 1. Depending on the various methods used in the isolation of serine, D,L-serine was obtained in yields ranging from 40% to 60%.

To a solution of 43.4 gm. of ethyl acetamidomalonate (0.2 mole) in 200 ml. of methanol and water (1: 1) were added, over a period of an hour with vigorous stirring and cooling, 12.0 gm. of solid sodium borohydride. The mixture was stirred for an additional hour, 200 ml. of concentrated HCl were added, and the mixture was boiled for three hours.

The solution was evaporated to dryness *in vacuo*, and the residue was leached with boiling ethanol. The insoluble inorganic salts were removed by filtration and the filtrate was evaporated. The residue was dissolved in water and divided in four equal portions.

(*a*) The first solution was neutralized to pH 6.0 with lithium hydroxide and concentrated to a small volume (25 ml.). Warm ethanol (500 ml.) was slowly added and D,L-serine crystallized. It was recrystallized from aqueous ethanol and dried. Yield: 3.1 gm. (59%).

(*b*) The second portion was neutralized with ammonium hydroxide to pH 6.5 and concentrated to a small volume. Methanol was added and after cooling, the crystalline amino acid was filtered, recrystallized, and dried. Yield: 2.8 gm. (53%).

(*c*) The third solution was treated with an excess of silver carbonate, filtered, saturated with hydrogen sulphide, and filtered again. After treatment with charcoal, warm ethanol was added to the clear filtrate. D,L-Serine crystallized in the cold. The amino acid was recrystallized and dried. Yield: 2.6 gm. (49.5%).

(*d*) Finally, the last portion was passed through a column of Permutit S-1. The amino acids were retained and eluted with 10% acetic acid. The eluate was evaporated to dryness and the residue was recrystallized from ethanol and water. Yield: 2.4 gm. (46%).

The four samples of D,L-serine thus obtained were mixed, recrystallized, and analyzed. At the microscope, the crystals appeared as transparent platelets which had a melting point of 244°C. (decomp.) on the Fisher-Johns block. No sublimate was observed on the upper glass slide, whereas commercial glycine has been found to give such a sublimate. When a paper chromatogram of the sample was run in pyridine-water, no glycine was present. Chloride was absent. Calc. for $C_3H_7O_3N$: N, 13.32%. Found: N, 13.30%.

D,L-Serine ethyl ester hydrochloride.—Dry HCl was bubbled through a suspension of 4.05 gm. of the above D,L-serine in ethanol. The ester hydrochloride was recrystallized from methanol–ether. Yield: 5.15 gm. (86%). Melting point: 133°C. Lit.: 134°C. (9). Calc. for $C_4H_9O_3N$. HCl: N, 9.01%, Cl, 22.8%. Found: N, 9.00%. Cl, 22.7%.

From Ethyl Acetamidocyanoacetate

Similar and even better is the synthesis of serine from the reduction of ethyl acetamidocyanoacetate with NaH_4B in ethanol at room temperature, followed by hydrolysis for six hours with concentrated HCl. No propanediol was produced and the yield of serine was around 70%, as shown by both quantitative analysis and paper chromatography.

A solution of ethyl acetamidocyanoacetate containing 10.0 gm. of the ester in 25 ml. ethanol was reduced by adding slowly 6.0 gm. of sodium borohydride, while vigorous agitation was maintained. After the addition, the solution was further mixed for an hour, 200 ml. of concentrated HCl were added, and the mixture was boiled for eight hours.

The amino acid hydrochlorides were treated with silver carbonate and D,L-serine was isolated as described for ethyl acetamidomalonate. Yield: 3.6 gm. (58%). Calc. for $C_3H_7O_3N$: N, 13.32%. Found: N, 13.10%.

No glycine was detected on paper chromatograms obtained from this serine.

CONCLUSIONS

D,L-Serine can be prepared directly by reducing ethyl acetamidocyanoacetate or ethyl acetamidomalonate with sodium borohydride.

Sodium and potassium borohydrides are capable of reducing certain esters even in water.

ACKNOWLEDGMENTS

To the National Cancer Institute of Canada, the author expresses his gratitude for a Fellowship. He is also grateful to the Permutit Company for a sample of Permutit S-1. His thanks are also due to Mr. Bertin Girard for technical assistance.

REFERENCES

1. BERLINGUET, L. Can. J. Chem. 32: 31. 1954.
2. BLOCK, J. R. and BOLLING, D. The amino acid composition of proteins and food. Charles C. Thomas, Publisher, Springfield, Ill. 1951. p. 343.
3. BORY, MLLE and MENTZER, M. C. Bull. soc. chim. France, 815. 1953.
4. CERCHEZ, M. V. Bull. soc. chim. France, 47: 1279. 1930.
5. CERCHEZ, M. V. Bull. soc. chim. France, 47: 1282. 1930.
6. CONSDEN, R., MARTIN, A. J. P., and GORDON, A. H. Biochem. J. 40: 33. 1946.
7. GALAT, A. J. Am. Chem. Soc. 69: 965. 1947.
8. HIRS, C. H. W., MOORE, S., and STEIN, W. S. J. Biol. Chem. 195: 669. 1954.
9. KING, J. A. J. Am. Chem. Soc. 69: 2738. 1947.
10. KOLLONITSH, J., FUCHS, O., and GABOR, V. Nature, 173: 126. 1954.
11. MOORE, S. and STEIN, W. H. J. Biol. Chem. 192: 663. 1951.
12. OSTERBERG, A. E. Organic syntheses, Collective Vol. 1. John Wiley & Sons, Inc., New York. 1941. p. 271.
13. PARTRIDGE, B. Biochem. J. 51: 628. 1953.
14. PAUL, R. and JOSEPH, N. Bull. soc. chim. France, 550. 1952.
15. REDEMAN, C. E. and DUNN, M. S. J. Biol. Chem. 130: 341. 1939.
16. REES, M. W. Biochem. J. 40: 632. 1946.
17. STEIN, W. H., MOORE, D., STAMN, G., CHOU, C., and BERGMANN, M. J. Biol. Chem. 143: 121. 1942.
18. WALTER, R. C. J. Am. Chem. Soc. 74: 5185. 1952.
19. Winthrop Chemical Company. Brit. Patent No. 601,184. April 29, 1948. Chem. Abstr. 42: 7325g. 1948.

BENZYL 2-CHLOROETHYL ETHERS[1]

By Marshall Kulka and F. G. Van Stryk

ABSTRACT

The solvolysis reaction between benzyl chlorides and ethylene chlorohydrin has been employed for the synthesis of a series of benzyl 2-chloroethyl ethers (III) required in insecticide screening tests. This method is limited to the synthesis of III which possesses a partially deactivated nucleus. Several new benzyl chlorides are recorded.

Several classes of compounds including derivatives of chlorobenzenesulphonic acid (8, 10), 2-hydroxybenzophenones (9), and phenoxymethyl 2-chloroethyl ethers (11) have been synthesized in this laboratory and screened for insecticidal value by Musgrave and Kukovica (14) at the Ontario Agricultural College. In continuation of the joint program of insecticide research this report deals with a class of compounds possessing the grouping $-CH_2OCH_2CH_2Cl$.

Genzer, Huttrer, and van Wessem (5) developed a method for the synthesis of benzyl 2-chloroethyl ether (III) and its *ortho* chloro-derivative which comprises treatment of benzyl chloride (I) with the monosodium salt of ethylene glycol (IV) followed by conversion of the resulting benzyl 2-hydroxyethyl ether (V) to III (Method B). Although this method was satisfactory in many cases, a more direct method was sought. The solvolysis reaction between benzyl halides (I) and ethylene chlorohydrin (II) to form III and hydrogen

$$\underset{\text{I}}{X{-}C_6H_4CH_2Cl} + \underset{\text{II}}{HOCH_2CH_2Cl} \rightarrow \underset{\text{III}}{X{-}C_6H_4CH_2OCH_2CH_2Cl} \qquad \text{(A)}$$

$$\underset{\text{I}}{X{-}C_6H_4CH_2Cl} + \underset{\text{IV}}{NaOCH_2CH_2OH} \xrightarrow{SOCl_2,\ C_6H_5N(CH_3)_2} \underset{\text{V}}{X{-}C_6H_4CH_2OCH_2CH_2OH} \qquad \text{(B)}$$

chloride under the influence of heat (Method A) was found to be of preparative value though of limited scope. The failure of Method A in some cases can be attributed to the fact that benzyl halides are susceptible to polymerization under the influence of heat and acid catalyst and the extent of this side reaction is governed by the reactivity of the benzene nucleus. The following benzyl halides (I) gave polymers almost exclusively when heated with II: 2,4-dimethyl- (7), 2,4-dimethyl-5-chloromethyl (7), 3,4-dimethoxy- (12), 3-bromo-4-methoxy- (15), 2-nitro-4,5-dimethoxy-, 2-(2-chloroethoxy)-5-chloro-, 2,4-bis(chloromethyl)- (7), and *p*-nitrophenoxy- (17) benzyl chlorides

[1]*Manuscript received February 23, 1955.*
Contribution from the Dominion Rubber Company Limited Research Laboratories, Guelph, Ontario.

as well as 6-chloro-8-chloromethyl-1,3-benzodioxane (1) and 1-chloromethylnaphthalene (2). The nuclei of the majority of these compounds are activated by alkyl or alkoxyl substituents. Benzyl halides (I) possessing nuclear deactivating substituents such as chloro or nitro polymerized to a lesser extent when heated with ethylene chlorohydrin and formed the benzyl 2-chloroethyl ethers (III) (Table I). The reaction between I and II to form III was complete after heating under reflux for 24 to 48 hr. except in one case. Much of *p*-nitrobenzyl chloride remained unchanged after heating with II for four days.

The benzyl chlorides required for this investigation were prepared by chloromethylation of the appropriate aromatic compounds. It is interesting to note that 2-nitro-4,5-dimethoxybenzyl chloride, which was obtained from 3,4-dimethoxybenzyl chloride (12) by nitration, unlike the parent compound, is stable at room temperature. However it decomposes rapidly when warmed with alcoholic solutions of alkali or potassium cyanide to form resinous materials. Heating with ethanolic thiourea produced stable 2-nitro-4,5-dimethoxybenzyl isothiuronium chloride.

TABLE I

PREPARATION OF BENZYL 2-CHLOROETHYL ETHERS ($X—C_6H_4CH_2OCH_2CH_2Cl$, III) FROM THE CORRESPONDING BENZYL HALIDES (I)

III X=	Method of prep.	Yield, %	B.p. or m.p., °C.	n_D^{20}	Analyses			
					Calc.		Found	
					C	H	C	H
H	B (5)	77	b_{13} = 115	1.5200	63.33	6.45	63.26	6.15
	A	60						
o-Chloro (5)	B	49	b_{12} = 132–136	1.5344				
p-Chloro	B	40	b_{12} = 138–142	1.5348	52.69	4.88	52.35	4.84
2,4-Dichloro	A	40	b_{12} = 158–161	1.5483	45.09	3.76	44.99	3.93
2,5-Dichloro	A	47	b_{12} = 155–160	1.5362	45.09	3.76	44.83	4.36
3,4-Dichloro	B	61	b_{12} = 155–160	1.5498	45.09	3.76	45.36	3.69
	A	45						
2,3,4,5,6-Pentachloro	B	81	m.p. 71–72		31.49	1.75	31.90	1.97
p-β-Chloroethyl	A	40	b_{12} = 170–175		56.65	6.01	56.72	5.80
p-Nitro	A	23	b_{12} = 190–195		50.12	4.64	49.92	4.63
3-Nitro-4-methoxy	A	80	b_1 = 175–177	1.5535	48.88	4.88	49.30	4.81
3-Nitro-4-*n*-butoxy	A	78	$b_{0.2}$ = 160–163	1.5315	54.26	6.26	54.25	6.20
3-Nitro-4-*n*-dodecyloxy	A	82	$b_{0.2}$ = 235–240	1.5088	63.08	8.51	63.24	8.28
3-Chloro-6,β-chloroethoxy	A	24	b_{12} = 205–207	1.5452	46.56	4.58	46.82	4.46
	B	85						
3-Nitro-4-methyl	A	44	b_{12} = 189–194	1.5452	52.29	5.23	52.49	5.09
3-Bromo-4-methoxy	B	84	b_{12} = 186–188	1.5622	42.93	4.29	43.34	4.38
α-Naphthylmethyl 2-chloroethyl ether	B	85	b_{12} = 188	1.5990	70.75	5.89	70.32	5.75

The benzyl 2-chloroethyl ethers (III) suffer degradation in the presence of acidic reagents. An attempt to chloromethylate benzyl 2-chloroethyl ether (III, X = H) resulted only in low-boiling materials. Similar results were obtained in attempts to chlorinate and nitrate III. The alkyl chlorine of III is far less reactive than the chlorine in bis(2-chloroethyl) sulphide (mustard gas), but like bis(2-chloroethyl) ether will react with alcoholic potassium thiocyanate after prolonged heating.

TABLE II

PREPARATION OF BENZYL 2-HYDROXYETHYL ETHERS (X—$C_6H_4CH_2OCH_2CH_2OH$, V) FROM THE CORRESPONDING BENZYL HALIDES (I) AND ETHYLENE GLYCOL

V, X=	Yield, %	B.p. or m.p., °C.	n_D^{20}	Analyses			
				Calc.		Found	
				C	H	C	H
H (5)	81	$b_{0.25}$ = 95	1.5209				
o-Chloro (5)	84	$b_{0.03}$ = 84	1.5348				
p-Chloro	52	b_{12} = 151–154	1.5330	57.91	5.90	57.56	5.99
3,4-Dichloro	51	b_{12} = 176–179	1.5502	48.87	4.52	48.65	4.34
2,3,4,5,6-Pentachloro*	20	m.p. 83–84		33.28	2.16	33.44	2.33
3-Chloro-6,β-chloroethoxy	64	$b_{0.1}$ = 148–150	1.5500	49.81	5.28	50.95	5.30
3-Bromo-4-methoxy	83	b_{12} = 201	1.5655	45.98	4.98	46.07	4.87
α-Naphthylmethyl 2-hydroxyethyl ether	82	b_{12} = 198	1.6045	77.23	6.93	77.24	6.93

**In the preparation of this compound it was necessary to heat the reaction mixture for 18 hr. instead of 2 hr.*

EXPERIMENTAL

2-*Nitro*-4,5-*dimethoxybenzyl Chloride*

To a solution of 3,4-dimethoxybenzyl chloride (12) (46 gm.) in acetic acid (120 ml.) kept at 8–10° was added dropwise with stirring concentrated nitric acid (d = 1.42) (37 gm.) over one-half hour. After the reaction mixture was stirred at 8–10° for two hours it was poured into cold water. The yellow precipitate was filtered, washed, and crystallized from methanol. The yellow prisms weighed 26 gm. (50%) and melted at 87–88°. Anal. calc. for $C_9H_{10}NO_4Cl$: C, 46.65; H, 4.32; N, 6.05. Found: C, 47.08, 46.86; H, 4.43, 4.42; N, 6.23. Heating with thiourea in methanol under reflux produced *S*-2-*nitro*-4,5-*dimethoxybenzyl isothiuronium chloride* in 90% yield. The light-yellow needles melted at 215–216° with decomposition. Anal. calc. for $C_{10}H_{14}N_3O_4ClS$: C, 39.03; H, 4.55. Found: C, 38.64; H, 4.82.

3-*Nitro*-4-*n*-*butoxybenzyl Chloride*

This is essentially the method previously used for the preparation of 3-nitro-4-methoxybenzyl chloride (4). Into a suspension of trioxymethylene (16 gm.), zinc chloride (25 gm.), and acetic acid (350 ml.) dry hydrogen chloride was passed until saturated. Then *o*-nitro-*n*-butoxybenzene (100 gm.) was added and the resulting solution was heated at 75–80° for 72 hr. The

solution was added to water, extracted with benzene, and the benzene extract washed with water, with aqueous sodium bicarbonate, and with water. Removal of the solvent and distillation of the residue yielded a yellow oil (80 gm. or 64%) boiling at 140° (0.3 mm.) or 200° (12 mm.), $n_D^{20} = 1.5450$. Anal. calc. for $C_{11}H_{14}NO_3Cl$: C, 54.21; H, 5.75. Found: C, 54.66; H, 5.70.

3-*Nitro*-4-(*β-bromoethoxy*)*benzyl Chloride*

This was prepared in 54% yield by the same method as was 3-nitro-4-*n*-butoxybenzyl chloride above from *o*-nitro-*β*-bromoethoxybenzene which was obtained from *o*-nitrophenol and ethylene dibromide. The product distilled at 150–170° (0.3 mm.) and crystallized from methanol as white needles melting at 78–79°. Anal. calc. for $C_9H_9NO_3ClBr$: C, 36.67; H, 3.06. Found: C, 36.57; H, 3.09.

3-*Nitro*-4-*n-dodecyloxybenzyl Chloride*

This was prepared in 56% yield by the same method as was 3-nitro-4-*n*-butoxybenzyl chloride above from *o*-nitrododecyloxybenzene. It crystallized as white needles from methanol and from ethyl acetate and melted at 55–56°. Anal. calc. for $C_{19}H_{30}NO_3Cl$: C, 64.13; H, 8.44. Found: C, 64.01; H, 8.58.

3-*Chloro*-6-(*β-chloroethoxy*)*benzyl Chloride*

This was prepared in 65% yield by the method used for the preparation of 3-nitro-4-*n*-butoxybenzyl chloride above from *β*-chloroethyl *p*-chlorophenyl ether (3). In this case it was not necessary to heat for 72 hr.; 20 hr. was sufficient and the amount of zinc chloride should be reduced by 30%. The product distilled at 165–175° (12 mm.), crystallized as white prisms from methanol, and melted at 34–35°. Anal. calc. for $C_9H_9Cl_3O$: C, 45.09; H, 3.76. Found: C, 45.25, 45.26; H, 3.79, 3.85.

p-(*β-Chloroethyl*)*benzyl Chloride*

Into a stirred reaction mixture of *β*-chloroethylbenzene (50 gm.), ethylene dichloride (100 ml.), paraformaldehyde (10 gm.), and zinc chloride (10 gm.) hydrogen chloride was passed for three hours. The temperature was maintained at 40° by cooling at first and warming later. After standing overnight, the reaction mixture was washed with water, with aqueous sodium bicarbonate, and with water. The solvent was removed and the residue was distilled and the fraction (32 gm.) boiling at 140° (12 mm.), $n_D^{20} = 1.5550$, was collected. Anal. calc. for $C_9H_{10}Cl_2$: C, 57.14; H, 5.29. Found: C, 57.39, 57.14; H, 5.39, 5.14.

3-*Nitro*-4-*methylbenzyl Chloride*

This was prepared by a method similar to that of Matsukawa and Shirakawa (13). To stirred 20% oleum (475 gm.) was added dropwise a solution of *o*-nitrotoluene (137 gm.) and crude methyl chloromethyl ether (100 gm.) over one and a half hours, the temperature being kept at 5–10° by cooling. After it was stirred for an additional two hours at 5–10° the dark reaction mixture was poured onto cracked ice. The precipitated oil was extracted with benzene, the extract washed with water, and the solvent removed. The residue was

distilled and the fraction (39 gm.) boiling at 140–150° (12 mm.) was collected. This solidified on standing and was crystallized from methanol, m.p. 44–45°; literature (18) m.p. 45°.

2,5-Dichlorobenzyl Chloride and 2,5-Dichloro-p-xylylene Dichloride

To stirred 20% oleum (500 gm.) kept at 0–5° by cooling was added dropwise a solution of *p*-dichlorobenzene (74 gm.) in 150 gm. of crude methyl chloromethyl ether over one hour. The reaction mixture was stirred at 0–5° for two hours, let stand overnight at 8–10°, and then poured on cracked ice. The reaction mixture was extracted with chloroform, the extract was washed with water, and the solvent was then removed. The residue was fractionally distilled and two main fractions were collected. The first fraction, a colorless liquid (14 gm.) which was *2,5-dichlorobenzyl chloride*, boiled at 122–124° (15 mm.), $n_D^{20} = 1.5750$. Anal. calc. for $C_7H_5Cl_3$: C, 42.97; H, 2.56. Found: C, 42.29; H, 2.61.

The second fraction boiled at 165–180° (15 mm.) and the distillate (16 gm.) which solidified was crystallized from ethanol. The colorless rhombohedrans of *2,5-dichloro-p-xylylene dichloride* (13 gm.) melted at 98–99°. Anal. calc. for $C_8H_6Cl_4$: C, 39.35; H, 2.46. Found: C, 39.68; H, 2.48.

The *S,S'-2,5-dichloro-p-xylylene bis-isothiuronium chloride* was prepared by boiling the 2,5-dichloro-*p*-xylylene dichloride with thiourea in ethanol. It melted at 289–292° (with decomposition) after crystallization from water. Anal. calc. for $C_{10}H_{14}N_4Cl_4S_2$: C, 30.30; H, 3.54. Found: C, 30.02; H, 3.72.

Preparation of Benzyl 2-Chloroethyl Ethers by Method A

Some of the benzyl 2-chloroethyl ethers listed in Table I were prepared by a method used for the preparation of *p-xylylene bis-2-chloroethyl ether* which follows: A solution of *p*-xylylene dichloride (7) (20 gm.) in dry ethylene chlorohydrin (100 ml.) was heated under reflux for 24 hr. The hydrogen chloride gas was allowed to escape through a condenser kept at about 60°. The excess ethylene chlorohydrin was removed and the residue distilled. The colorless liquid boiled at 200–203° (12 mm.), $n_D^{20} = 1.5260$. The yield was 26 gm. or 85%. Anal. calc. for $C_{12}H_{16}O_2Cl_2$: C, 54.75; H, 6.08. Found: C, 55.12, 55.13; H, 5.97, 5.99.

o-Xylylene bis-2-chloroethyl ether.—This was prepared in 68% yield by Method A from *o*-xylylene dichloride (7). The colorless liquid boiled at 190–195 (14 mm.). Anal. calc. for $C_{12}H_{16}O_2Cl_2$: C, 54.75; H, 6.08. Found: C, 54.44, 54.49; H, 5.53, 5.60.

Preparation of Benzyl 2-Chloroethyl Ethers by Method B

Some of the benzyl 2-chloroethyl ethers listed in Table I were prepared by Method B. This method, which was used by Genzer *et al.* (5), is further exemplified by the preparation of *2,5-dichloro-p-xylylene bis-2-chloroethyl ether.*

(*a*) *2,5-Dichloro-p-xylylene bis-2-hydroxyethyl ether.*—To a solution of dry ethylene glycol (50 ml.), xylene (25 ml.), and sodium (2.5 gm.) was added a solution of 2,5-dichloro-*p*-xylylene dichloride (12 gm.) in xylene (25 ml.).

The reaction mixture was heated under reflux for two hours, most of the xylene and glycol were removed *in vacuo*, and the residue was treated with water. The white solid was filtered and crystallized from methanol. The white crystals (12 gm.) melted at 120–121°. Anal. calc. for $C_{12}H_{16}O_4Cl_2$: C, 48.82; H, 5.42. Found: C, 49.32; H, 5.47.

(*b*) 2,5-*Dichloro-p-xylylene bis*-2-*chloroethyl ether*.—To a stirred suspension of 2,5-dichloro-*p*-xylylene bis-2-hydroxyethyl ether (10 gm.), dimethylaniline (10 ml.), and dry chloroform (25 ml.) was added dropwise with cooling a solution of thionyl chloride (6 ml.) in chloroform (10 ml.), the temperature being kept at 20–30°. The dark reaction mixture was heated under reflux for one-half hour and then poured into cold dilute hydrochloric acid. This was extracted with chloroform, the extract was washed with dilute hydrochloric acid and with water, and the solvent was removed. The residue was crystallized from methanol and from petroleum ether (30–60°) yielding 9 gm. (80%) of white needles which melted at 70–71°. Anal. calc. for $C_{12}H_{14}O_2Cl_4$: C, 43.38; H, 4.22. Found: C, 43.81, 43.77; H, 4.33, 4.32.

p,p′-Dichlorobenzhydryl 2-*Chloroethyl Ether*

A method simpler than A or B which was employed by Kato *et al.* (6) was followed in this case.

To a hot solution of *p,p′*-dichlorobenzhydrol (16) (10 gm.) in ethylene chlorohydrin (40 ml.) was added a solution of concentrated sulphuric acid (2 ml.) in water (10 ml.) and the resulting solution was heated at 80° for six hours. The reaction mixture containing a precipitated oil was poured into water, extracted with benzene, the benzene extract washed with water, and the solvent removed. The residue distilled at 167–170° (0.2 mm.) giving a colorless liquid (15 gm.), $n_D^{20} = 1.5830$. Anal. calc. for $C_{15}H_{13}OCl_3$: C, 57.06; H, 4.12. Found: C, 57.00; H, 4.14.

o,p′-Dichlorobenzhydryl 2-*Chloroethyl Ether*

This was prepared in 90% yield as above from *o,p′*-dichlorobenzhydrol. The colorless liquid distilled at 155–160° (0.2 mm.), $n_D^{20} = 1.5835$. Anal. calc. for $C_{15}H_{13}OCl_3$: C, 57.06; H, 4.12. Found: C, 57.52; H, 4.25.

3-*Nitro*-4-*methoxybenzyl* 2-*Thiocyanatoethyl Ether*

A solution of 3-nitro-4-methoxybenzyl 2-chloroethyl ether (13 gm.) in ethanol (150 ml.) and potassium thiocyanate (6 gm.) was heated under reflux for 40 hr. The precipitated potassium chloride was filtered and the ethanol was distilled off from the filtrate. The residue was dissolved in benzene and washed with water. The solvent was removed and the residue distilled yielding a malodorous yellow liquid (8 gm.), b.p. = 165–170 (1 mm.). Anal. calc. for $C_{11}H_{12}N_2O_4S$: C, 49.25; H, 4.48. Found: C, 48.82, 48.78; H, 4.81, 4.74.

p-Chlorobenzyl 2-*Thiocyanatoethyl Ether*

This was prepared in 65% yield as above. It boiled at 187–192° (12 mm.), $n_D^{20} = 1.5358$. Anal. calc. for $C_{10}H_{10}NOClS$: C, 52.75; H, 4.39. Found: C, 52.45; H, 4.83.

ACKNOWLEDGMENT

The analyses of all compounds were provided by Gisela von Stritzky.

REFERENCES

1. BUEHLER, C. A., BASS, B. C., DARLING, R. B., and LUBS, M. E. J. Am. Chem. Soc. 62: 890. 1940.
2. CAMBRON, A. Can. J. Research, B, 17: 10. 1939.
3. COLEMAN, G. H. and STRATTON, G. B. U.S. Patent No. 2,186,367. 1940; Chem. Abstr. 34: 3281. 1940.
4. DARZENS, G. Compt. rend. 208: 818. 1939; Chem. Abstr. 33: 4587. 1939.
5. GENZER, J. D., HUTTRER, C. P., and VAN WESSEM, G. C. J. Am. Chem. Soc. 73: 3159. 1951.
6. KATO, N. *et al.* Japanese Patent No. 1304. 1950; Chem. Abstr. 47: 2212. 1953.
7. KULKA, M. Can. J. Research, B, 23: 106. 1945.
8. KULKA, M. J. Am. Chem. Soc. 72: 1215. 1950.
9. KULKA, M. J. Am. Chem. Soc. 76: 5469. 1954.
10. KULKA, M. Can. J. Chem. 32: 598. 1954.
11. KULKA, M. Can. J. Chem. 33: 1. 1955.
12. LIVSHITS, R. S., BAINOVA, M. S., BAZILEVSKAYA, G. I., GENKIN, E. I., PREOBRAZENSKII, N. A., RAZANOVA, YU. M., and BARANOVA, Z. A. Zh. Obsch. Khim. 21: 1354. 1951; Chem. Abstr. 46: 5050. 1952.
13. MATSUKAWA, T. and SHIRAKAWA, K. J. Pharm. Soc. Japan, 70: 25. 1950; Chem. Abstr. 44: 4435. 1950.
14. MUSGRAVE, A. J. and KUKOVICA, I. Ann. Rept. Entomol. Soc. Ontario, 84: 63. 1953.
15. NAIK, R. G. and WHEELER, T. S. J. Chem. Soc. 1780. 1938.
16. SMITH, W. T. and RYAN, J. W. J. Am. Chem. Soc. 75: 749. 1953.
17. SOUTHWICK, P. L., FOLTZ, G. E., and MCINTYRE, W. E. J. Am. Chem. Soc. 75: 5877. 1953.
18. STEPHEN, H., SHORT, W. F., and GLADDING, G. J. Chem. Soc. 117: 510. 1920.

INTENSITY IN THE RAMAN EFFECT

III. THE EFFECT OF DEUTERIUM SUBSTITUTION ON THE INTENSITY OF RAMAN BANDS OF BENZENE[1]

By G. Allen[2] and H. J. Bernstein

ABSTRACT

Standard intensities of the Raman bands of C_6H_6, 1,3,5,-$C_6H_3D_3$, and C_6D_6 have been obtained photoelectrically. An ambiguity in the vibrational assignment for 1,3,5,-$C_6D_3H_3$ has been removed, and the assumption of the invariance of the polarizability and anisotropy derivatives upon isotopic substitution has been tested. A sum rule for depolarization ratios of Raman bands in isotopic homologues has been derived subject to the same assumptions used for obtaining the intensity sum rules.

The Raman shifts and normal mode assignments are well known (1, 6, 7) both for C_6H_6 and C_6D_6 and the relative intensities of the Raman bands have been obtained photographically (1). Rank (10) has reported integrated intensities for C_6H_6 obtained with an electronically recording spectrometer but there are no corresponding data for C_6D_6. The Raman intensities are of interest because Lord and Teller (8) have calculated the intensities of the a_{1g} modes in C_6D_6 in terms of the intensities of the a_{1g} modes in C_6H_6 and Crawford (3) has derived a sum rule for intensities in isotopically substituted molecules which applies to the a_{1g} and the e_{2g} modes in these molecules.

1,3,5-Trideuterobenzene has been studied by Langseth and Lord (7) and also by Ingold *et al.* (1). There is disagreement on the assignment of the e'-type fundamentals which are associated with the C—H and C—D stretching modes. The two reports also disagree in the assignment of one of the e''-type modes. Langseth and Lord have calculated the intensities of the a'_1-type vibrations in 1,3,5-$C_6H_3D_3$ relative to the intensities of the a_1'-type vibrations in C_6H_6.

We have obtained standard intensities with a photoelectric spectrometer for the three benzene molecules in the liquid phase and have cleared up the ambiguity in the assignment for $C_6H_3D_3$, and have tested the assumption of the invariance of the polarizability derivatives for isotopic substitution.

EXPERIMENTAL

The Raman spectra and depolarization ratios were obtained at 27°C. using a White Raman spectrometer (12). Standard intensities of scattering per molecule referred to the 458 cm.$^{-1}$ band of CCl_4 were obtained by a method previously described (2). The expression used to obtain the standard intensities is (2):

$$[1]\quad S = \frac{I}{I_{458}} \cdot \frac{1+\rho_{458}}{1+\rho} \cdot \frac{n^2}{n^2_{CCl_4}} \cdot \frac{\sigma}{\sigma_{458}} \cdot \frac{R(n)}{R(n)_{CCl_4}} \times \frac{M}{d}\left(\frac{d}{M}\right)_{CCl_4} \cdot \frac{\Delta\nu}{458}\left(\frac{\nu-458}{\nu-\Delta\nu}\right)^4 \cdot \frac{1-e^{-1.44\Delta\nu/T}}{1-e^{-1.44\times 458/T}} = \frac{45(\alpha')^2+7(\gamma')^2}{[45(\alpha')^2+7(\gamma')^2]_{458}}$$

[1]*Manuscript received January 18, 1955.*
Contribution from the Division of Pure Chemistry, National Research Council, Ottawa. Issued as N.R.C. No. 3602.
[2]*National Research Council Postdoctorate Fellow, 1952–1954.*

where I = integrated intensity, ρ = observed depolarization ratio for natural light, n = refractive index of compound, σ = spectral sensitivity of phototube, $R(n)$ = reflection loss, M = molecular weight, d = density, $\Delta\nu$ = Raman shift, $\nu = 22938$ cm.$^{-1}$, the frequency of the exciting line, T = absolute temperature, $\alpha' = \partial\alpha/\partial Q$ = derivative of the average polarizability with respect to the normal coordinate at the equilibrium position, $\gamma' = \partial\gamma/\partial Q$ = derivative of the anisotropy with respect to the normal coordinate at the equilibrium position.

The results for C_6H_6 and C_6D_6 are given in Table I, the experimental error is of the order of $\pm 2\%$ in $\bar{S}$ ($\bar{S} = \{I/I_{458}\} \cdot \{\sigma/\sigma_{458}\}$) and $\pm 10\%$ in S. Depolarization ratios were obtained by the method of Edsall and Wilson (5) and

TABLE I

RAMAN INTENSITIES IN C_6H_6 AND C_6D_6

	$\Delta\nu$, cm.$^{-1}$	Symmetry type	ρ_{obs}	ρ_{true}	$\bar{S}$	S
C_6H_6	606	e_{2g}	0.98	0.86	0.212	0.181
	849	e_{1g}	0.95	0.86	0.079	0.105
	992	a_{1g}	0.24	0.11	1.756	4.406
	1178	e_{2g}	0.97	0.86	0.300	0.584
	1584, 1606	e_{2g}	0.98	0.86	0.382	1.084
	3045	e_{2g}	0.96	0.86	0.633	4.608
	3061	a_{1g}	0.34	0.21	1.537	16.505
C_6D_6	577	e_{2g}	0.98	0.86	0.169	0.146
	661	e_{1g}	1.00	0.86	0.200	0.204
	867	e_{2g}	1.00	0.86	0.214	0.305
	945	a_{1g}	0.26	0.12	1.610	4.041
	1560	e_{2g}	1.00	0.86	0.333	0.979
	2264	e_{2g}	1.00	0.86	0.505	2.470
	2292	a_{1g}	0.34	0.21	1.035	7.702

Reflection loss = 1.04.

corrected for convergence to ρ_{true} by the method of Rank and Kagarisse (11). In order to obtain

$$\frac{45(\alpha')^2+13(\gamma')^2}{[45(\alpha')^2+13(\gamma')^2]_{458}},$$

the theoretical quantity given for transverse scattering, S should be multiplied by $(1+\rho_{obs})$.

Two samples of C_6D_6 were investigated. The intensities reported in Table I were obtained from a sample loaned by Professor Langseth. The second sample was prepared by Dr. Leitch and good agreement for the intensities of all bands except 867 and 661 cm.$^{-1}$ was obtained. In the sample obtained from Dr. Leitch the two anomalous bands had "shoulders" which were due to an impurity and which prevented an accurate estimation of the integrated intensities of these bands.

The sample of 1,3,5,-$C_6H_3D_3$ was obtained from Professor Langseth. In this case the estimation of standard intensities was complicated by the presence of about 17.5% of 1,3-$C_6H_4D_2$ in the sample. 1,3-$C_6H_4D_2$ has bands which

overlap all the fundamentals in 1,3,5-$C_6H_3D_3$ with the exception of 955 cm.$^{-1}$. In order to estimate the amount (17.5%) of 1,3-$C_6H_4D_2$ in the sample (and hence to correct the observed intensities to correspond to pure 1,3,5-$C_6H_3D_3$) we assume:

(*a*) the 955 cm.$^{-1}$ band in $C_6H_3D_3$ and the 968 cm.$^{-1}$ band in $C_6H_4D_2$ have the same standard intensity,

(*b*) where bands from each molecule overlap then the observed intensity is equal to the intensity in pure 1,3,5-$C_6H_3D_3$.

The first assumption is not unreasonable because the standard intensities of the corresponding bands in C_6H_6 and C_6D_6 differ only by $\backsim$10%. The second assumption means that the maximum error in the intensities is 17.5%. In Table II, therefore, the intensities of the 955 cm.$^{-1}$ and 1576 cm.$^{-1}$ bands

TABLE II

RAMAN INTENSITIES IN $C_6D_3H_3$[a]

$\Delta\nu$	Symmetry type	ρ_{obs}	ρ_{true}	$\bar{S}$	S_{obs}	S_{corr}
374	e''	1.00	0.86	0.030	0.013	0.013
594	e'	1.00	0.86	0.160	0.180	0.180
710	e''	1.00	0.86	0.094	0.101	0.101
832	e'	0.98	0.86	0.101	0.133	0.133
955	a_1'	0.26	0.12	0.931	2.279	2.785[c]
968	Impurity[b]	0.26	0.12	0.197	0.490	
1003	a_1'	0.25	0.11	0.305	0.804	0.804
1102	e'	1.00	0.86	0.092	0.169	0.169
1396	e'	1.00	0.86	0.020	0.049	0.049
1576	e'	1.00	0.86	0.266	0.767	0.925[c]
2273	e'	1.00	0.86	0.110	0.523	0.523
2283	a_1'	0.36	0.22	0.342	2.422	2.422
3054	$a_1'+e'$	0.51	0.36	0.772	7.730	7.730

[a] *Raman spectrum of liquid, reflection loss* $R(n) = 1.04$.
[b] *m-*$C_6H_4D_2$ *impurity band. The intensity of this band indicates that it is present to the extent of* $\backsim$*17.5%.*
[c] *Corrected for 17.5% m-*$C_6H_4D_2$ *impurity.*

are accurate within the limits of the first approximation, since these bands could be obtained without overlap. The intensities of the remaining bands are subject to the validity of the second assumption.

The intensities obtained photographically by Ingold *et al.* (1) should be compared with the intensities listed under $\bar{S}$.

DISCUSSION

A comparison of our results for C_6H_6 and C_6D_6 shows the same general features as the photographic intensities. For the a_{1g} and the e_{2g} modes there is a slight decrease in intensity on deuteration. For the e_{1g} mode however both investigations show that there is an increase in intensity on deuteration. This anomaly has been successfully explained by Lord and Teller (8).

Lord and Teller have also calculated the relative intensities of the a_{1g} modes in C_6H_6 and C_6D_6 assuming that the polarizability and anisotropy derivatives with respect to internal coordinates do not change on deuterium substitution. The intensities of the a_{1g} vibrations in C_6D_6 (a'^{CC}_{1g} and a^{CD}_{1g})

are expressed as linear superpositions of the a_{1g} vibrations in C_6H_6, viz.:

$$a'^{CC}_{1g} = \xi_1 a^{CH}_{1g} + \eta_1 a^{CC}_{1g}; \qquad a^{CD}_{1g} = \xi_2 a^{CH}_{1g} + \eta_2 a^{CC}_{1g}.$$

The coefficients ξ and η have been evaluated by Lord and Teller from the amplitudes of vibration obtained from the equations of motion using a complete quadratic potential function. Since our standard intensity S is defined in terms of the normal coordinate Q, it cannot be substituted directly into these equations. It must be transformed as shown below into S', viz.:

$$[2] \qquad S' = S \cdot \frac{458}{\Delta\nu} = \frac{[45(\alpha')^2 + 7(\gamma')^2]}{[45(\alpha')^2 + 7(\gamma')^2]_{458}} \cdot \frac{Q^2_{\Delta\nu}}{Q^2_{458}}.$$

The experimental values for S' are given in Table III. Using our data for S' and ρ we have followed through the calculations of Lord and Teller. The results of the calculations are also given in Table III. This represents a more satisfactory test of Lord and Teller's treatment than the one given in their original paper.

TABLE III

CALCULATED RAMAN INTENSITIES

	$\Delta\nu$, cm.$^{-1}$	Observed		Calculated	
		S'	ρ_{true}	S'	ρ_{true}
C_6H_6	992	2.034	0.11		
	3062	2.569	0.21		
C_6D_6	945	1.965	0.11	2.17±0.35[a]	0.11
	2292	1.511	0.21	1.25±0.20[a]	0.23
$C_6D_3H_3$	955	1.35	0.12	1.44	0.12
	1003	0.37	0.11	0.95	0.11
	2283	0.49	0.22	1.24	0.19
	3054	1.16	0.36	1.22	0.21

[a] *The errors arise from the experimental errors in the observed S' for the C_6H_6 bands.*

If the coefficients ξ and η derived for a simple valence force potential function by Lord and Langseth (7) are used to calculate the intensities of the a_1' modes in $C_6H_3D_3$ from the experimental data for C_6H_6, the results given in the lower field of Table III are obtained. The calculation for the intensity of the band at 955 cm.$^{-1}$ is satisfactory but the disagreements between the calculated and observed intensities for the bands at 1004 cm.$^{-1}$ and 2283 cm.$^{-1}$ are well outside the experimental error. The observed and calculated intensities for the Raman band at 3054 cm.$^{-1}$ cannot be compared directly. There is some doubt about the assignment of this band. Langseth and Lord assign the band as a superposition of the a_1' and e' νCH modes. Ingold *et al.* observe the e'-type νCH mode at 3082 cm.$^{-1}$ in the infrared spectrum of $C_6H_3D_3$ vapor and they conclude that the Raman band observed at 3054 cm.$^{-1}$ in the spectrum of the liquid arises solely from the a_1'-type mode. We have investigated the infrared spectrum of liquid $C_6H_3D_3$ using LiF optics, and find bands at 3055 and 2273 cm.$^{-1}$; these bands are assigned to the

e'-type νCH and νCD modes respectively. It appears then that the assignment given by Lord and Langseth is correct for the spectrum of liquid $C_6H_3D_3$. This is supported by the fact that the depolarization ratio for this band is higher than that for the other a_1-type bands in the Raman spectra of $C_6H_3D_3$, C_6H_6, and C_6D_6. All the other a_1-type νCH or νCD modes reported in this paper have depolarization ratios in the region of 0.22, but the depolarization ratio for the 3054 cm.$^{-1}$ band is 0.36. The observed intensity (S') of the a_1-type band at 3054 cm.$^{-1}$, is therefore <1.16, and the calculated value is too high.

This over-all poor agreement between observed and calculated intensities for the totally symmetrical modes of 1,3,5-$C_6H_3D_3$ may be due to the fact that only a simple valence force potential function (7) has been used to evaluate the ξ's and η's and the calculation of intensities is very sensitive to the values of force constants employed.

SUM RULES FOR RAMAN INTENSITY

Recently Crawford (3) derived intensity sum rules for Raman bands in isotopic molecules. The intensity of the a^{th} fundamental of Raman shift $\Delta\nu_{1a}$ in the gas phase is given by the following expression according to Placzeck (9):

$$[3] \qquad I_{1a} = \frac{K_{1a}N}{\Delta\nu_{1a}} \cdot [P_\alpha(\bar{a}_{1a})^2 + P_\beta(\bar{\beta}^2_{1aa})].$$

In this expression a universal constant is included in I, N is the number of scattering molecules, $K_{1a} = (\nu - \Delta\nu_{1a})^4(1 - e^{-1.44\Delta\nu_{1a}/T})^{-1}$, where ν is the frequency of the exciting line and T is the absolute temperature. The notation in the square bracket is that used by Crawford. Here P_α and P_β are constants depending only on the conditions of observation. Equation [3] is used for the intensity in the liquid phase also, since whatever changes occur in passing from gas to liquid might be expected to be very nearly the same for isotopic homologues. The temperature dependent term is included in the intensity expression since it is very nearly independent of phase and indeed has been shown to give the correct Stokes/anti-Stokes intensity ratio in liquid CCl_4 (2). Following Crawford we write his Σ^F rule in the form

$$[4] \qquad \sum_a \frac{I_{1a}}{K_{1a}\Delta\nu_{1a}} = \sum_a \frac{[P_\alpha(\bar{a}_{1a})^2 + P_\beta(\bar{\beta}^2_{1aa})]}{\Delta\nu^2_{1a}} = (F^{-1})^{kj}[P_\alpha(\bar{a}_{1k})(\bar{a}_{1j}) + P_\beta(\bar{\beta}^2_{1kj})]$$

and his Σ^G rule* in the form

$$[5] \qquad \sum_a \frac{I_{1a}\Delta\nu_{1a}}{K_{1a}} = (G_1)^{kj}[P_\alpha(\bar{a}_{1k})(\bar{a}_{1j}) + P_\beta(\bar{\beta}^2_{1kj})].$$

In these equations K_{1a} has been included in the summation and not considered to be constant (3) and the number of molecules N has been assumed constant since the same volume of the isotopic homologues is used to obtain the Raman spectra.

**There is a misprint in equation (26) in Crawford's paper. The L.H.S. should read $\Sigma_a I_{1a}{}^R\omega_{1a}$ instead of $\Sigma_a I_{1a}{}^R/\omega_{1a}$. Prof. Crawford (private communication, Feb. 11, 1955) suggested that this might be a suitable way in which to record this correction.*

TABLE IV

SUM RULES FOR RAMAN INTENSITIES

C_6H_6				C_6D_6				$1,3,5\text{-}C_6H_3D_3$	
$\Delta\nu$, cm.$^{-1}$	$\frac{\bar{S}\times 10^{21}}{K\Delta\nu}$	S	$\frac{S\times 10^{6}}{\Delta\nu^2}$	$\Delta\nu$, cm.$^{-1}$	$\frac{\bar{S}\times 10^{21}}{K\Delta\nu}$	S	$\frac{S\times 10^{6}}{\Delta\nu^2}$	$\Delta\nu$, cm.$^{-1}$	S
992 (a_{1g})	7.56	4.41	4.48	945 (a_{1g})	7.20	4.06	4.54	955 (a_1')	2.78
[a]3062 (a_{1g})	3.22	16.51	1.76	[b]2292 (a_{1g})	2.50	7.56	1.46	1003 (a_1')	0.80
	10.78	20.92	6.24		9.70	11.62	6.00		
								2283 (a_1')	2.42
								3053 (a_1')	7.73
									13.73
			L.H.S. of equation [6] = 10.78, R.H.S. = 9.70						
			L.H.S. of equation [11] = 6.24, R.H.S. = 6.00						
			L.H.S. of equation [12] = 32.54, R.H.S. = 2 × 13.73 = 27.46						
606 (e_{2g})	1.33		0.49	577 (e_{2g})	1.10		0.44		
1178 (e_{2g})	1.12		0.42	867 (e_{2g})	1.03		0.41		
1584, 1606 (e_{2g})	1.15		0.43	1560 (e_{2g})	1.02		0.40		
[a]3045 (e_{2g})	1.33		0.50	[b]2264 (e_{2g})	1.22		0.48		
	4.93		1.84		4.37		1.73		
			L.H.S. of equation [6] = 4.93, R.H.S. = 4.37						
			L.H.S. of equation [11] = 1.84, R.H.S. = 1.73						

[a,b] *These bands are doublets which were only partially resolved. The experimental error in determining their intensity is about* $\pm 10\%$.

The R.H.S. of equation [4] is invariant with isotopic substitution when (i) the force constants of the most general quadratic potential function do not change with isotopic substitution, (ii) the polarizability and anisotropy derivatives with respect to internal coordinates do not change with isotopic substitution, (iii) anharmonicity effects may be neglected. Assumption (ii) is valid only for symmetry types for which there is no molecular rotation which changes the equilibrium polarizability.

As long as the conditions of irradiation and observation are the same for the isotopic molecules, integrated intensities observed with any experimental arrangement may be used to verify equation [4] in the form

$$[6] \qquad \sum_a \frac{I_{1a}}{K_{1a}\Delta\nu_{1a}} = \sum_a \frac{I_{2a}}{K_{2a}\Delta\nu_{2a}}.$$

Here subscripts $_1$ and $_2$ refer to the two isotopic species. In Table IV, $\bar{S}$, the integrated intensity of the Raman bands of the a_{1g} and e_{2g} symmetry species of C_6H_6 and C_6D_6, referred to the intensity of the 458 cm.$^{-1}$ band in CCl_4 and corrected for the sensitivity of the photomultiplier tube, has been used to form the sums of equation [6]. The disagreement between the L.H.S. and R.H.S. of this equation is within the experimental error because of the difficulty in measuring accurately the intensity of the components of the partially resolved doublets at 3050 cm.$^{-1}$ and 2280 cm.$^{-1}$ in C_6H_6 and C_6D_6 respectively.

For parallel transverse irradiation $P_\alpha = 45$ and $P_\beta = 13$ in equations [3], [4], and [5]. The depolarization ratio under these experimental conditions is given by

$$[7] \qquad \rho_{1a} = \frac{6(\bar{\beta}^2_{1aa})}{45(\bar{\alpha}_{1a})^2 + 7(\bar{\beta}^2_{1aa})}.$$

Substituting from equation [7] in equation [3], the following expressions may be derived in the same manner as given by Crawford for equations [4] and [5]:

$$[8] \qquad \sum_a \frac{I_{1a}}{K_{1a}\Delta\nu_{1a}(1+\rho_{1a})} = (F^{-1})^{kj}[45(\bar{\alpha}_{1k})(\bar{\alpha}_{1j}) + 7(\bar{\beta}^2_{1kj})],$$

$$[9] \qquad \sum_a \frac{I_{1a}\Delta\nu_{1a}}{K_{1a}(1+\rho_{1a})} = (G_1)^{kj}[45(\bar{\alpha}_{1k})(\bar{\alpha}_{1j}) + 7(\bar{\beta}^2_{1kj})].$$

Equation [8] gives the intensity sum rule

$$[10] \qquad \sum_a \frac{I_{1a}}{K_{1a}\Delta\nu_{1a}(1+\rho_{1a})} = \sum_a \frac{I_{2a}}{K_{2a}\Delta\nu_{2a}(1+\rho_{2a})}$$

in which the intensities to be used in forming the sum are those observed under conditions of parallel transverse irradiation. Equation [10] then is a sum rule for depolarization ratios on isotopic substitution. In the simple case when there is only one vibration in the symmetry species (e.g. H_2, the a_{1g} mode in CH_4) it is apparent from equations [6] and [10] that the depolarization ratio is unchanged for complete isotopic substitution. If there are several modes of vibration in the symmetry species, the depolarization ratios of corresponding bands may still be the same but are not required to be so.

It has been shown (2) that the ratio $I/(1+\rho)$ is independent of experimental conditions provided that under the usual conditions of irradiation the incident beam may be considered to make an average angle with the direction of observation. Since this assumption has been shown to be valid (2) within the experimental error equation [10] may be written in terms of the standard intensity defined in equation [1], viz.:

$$[11] \qquad \sum_a \frac{S_{1a}}{\Delta\nu_{1a}^2} = \sum_a \frac{S_{2a}}{\Delta\nu_{2a}^2}.$$

A satisfactory experimental verification of this equation is shown for the a_{1g} and e_{2g} modes of C_6H_6 and C_6D_6 in Table IV.

Similarly one may write $\Sigma_a S_{1a}$ instead of the L.H.S. in equation [9].

Decius (4) has shown that the same relations are valid upon isotopic substitution for the L.H.S. of equation [9] and $\Sigma_a \Delta\nu_a{}^2$. Thus for example for the a_{1g} and b_{1u} modes of C_6H_6 and C_6D_6, and the a_1' modes of 1,3,5-$C_6H_3D_3$, one should have

$$[12] \qquad \sum S_{(C_6H_6)} + \sum S_{(C_6D_6)} = 2\sum S_{(1,3,5\text{-}C_6H_3D_3)}.$$

Since the b_{1u} modes for C_6H_6 and C_6D_6 are inactive in the Raman effect their contribution to the sums is zero. In Table IV the experimental data for verification of equation [12] are given. Again within the experimental error the rule has been verified.

It is readily seen from application of equations [8] and [9] to the molecules H_2, HD, and D_2 that the depolarization ratio is constant.

REFERENCES

1. Angus, W. R., Ingold, C. K., and Leckie, A. H. J. Chem. Soc. 925. 1936.
2. Bernstein, H. J. and Allen, G. J. Opt. Soc. Amer. 45: 237. 1955.
3. Crawford, B. J. Chem. Phys. 20: 977. 1952.
4. Decius, J. C. J. Chem. Phys. 20: 1039. 1952.
5. Edsall, J. T. and Wilson, E. B. J. Chem. Phys. 6: 124. 1938.
6. See, for example, Herzberg, G. Infrared and Raman spectra. D. Van Nostrand Company Inc., New York. 1945.
7. Langseth, A. and Lord, R. C., Jr. Kgl. Danske Videnskab. Selskabs, 16: 6. 1938.
8. Lord, R. C. and Teller, E. J. Chem. Soc. 1728. 1937.
9. Placzeck, G. Handb. Radiol. VI: (2). Leipzig. 1934.
10. Rank, D. H. J. Opt. Soc. Amer. 37: 798. 1947.
11. Rank, D. H. and Kagarisse, R. E. J. Opt. Soc. Amer. 40: 89. 1950.
12. White, J. U. and Alpert, N. J. Opt. Soc. Amer. 45: 154. 1955.

LIGHT ABSORPTION STUDIES

PART I. ULTRAVIOLET ABSORPTION SPECTRA OF SUBSTITUTED ACETOPHENONES[1]

By W. F. Forbes and W. A. Mueller

ABSTRACT

The steric hindrance postulated by Arnold and co-workers to account for anomalous reaction rates of some substituted acetophenones has been verified by means of ultraviolet light absorption data. The spectra of a number of other substituted acetophenones have been discussed in terms of the electronic and steric effects of substituents.

INTRODUCTION

Acetophone exhibits an intense band near 240 mμ, $\epsilon \sim 10$–15,000, which also appears in benzaldehyde, propiophenone, and butyrophenone (see Table I). This band, which is typical of $\pi-\pi$ conjugation, is ascribed to an N $\rightarrow$ V transition, and is found in a variety of phenyl derivatives containing unsaturated side-chains (styrenes, aromatic amines, benzoic acids, benzamidines, etc.), as also in biphenyls and cyclohexene derivatives. In acetophenone, therefore, the allowed transition from a state having a non-ionic wave function to one having an ionic wave function can be represented by Ph—C=O $\rightarrow$ Ph^+ =C—O^-. As has previously been pointed out elsewhere (6), whilst in benzaldehyde, *m*- and *p*-methyl groups cause a small increase in ϵ, and *o*-methyl groups produce a small decrease, in the acetophenones, *m*- and *p*-methyl groups also cause small increases in ϵ, but *o*-methyl groups produce very marked decreases in ϵ. A similar effect is observed for *o*- and *p*-methyl substituted propiophenones (see Table I). This effect is ascribed to steric overlap between the *o*-methyl groups and the keto-methyl or keto-ethyl group setting up appreciable interference and thus preventing the attaining of a uniplanar configuration. Steric inhibition of electronic interaction thus raises the energy level of the ground state, but since the phenyl-carbon link in the postulated polar excited state contains a larger amount of double bond character, and since the energy required to twist a double bond is considerably in excess of that required to twist a single bond, and further since the interplanar angle cannot from theoretical considerations (Franck–Condon principle) change during a transition, therefore the energy-level of the excited state will be raised even more than that of the ground state. Thus the transition energy is increased, which results in a hypsochromic shift of the band, and also in a reduced transition probability, which results in a loss of absorption intensity (ϵ).

ULTRAVIOLET ABSORPTION SPECTRA

Propiophenone itself, compared to acetophenone, gives rise to a slight steric effect of the type referred to above, presumably because the replacement of a

[1]*Manuscript received January 20, 1955.*
Contribution from the Department of Chemistry, Memorial University of Newfoundland, St. John's, Newfoundland.

hydrogen atom by a methyl group gives rise to further steric overlap between the additional hydrogen atoms and the carbonyl group and/or the ortho-positioned hydrogen atom of the benzene ring. *n*-Butyrophenone has an absorption spectrum almost entirely similar, which is as expected—from steric considerations alone—since the additional methyl group is too far removed to interfere effectively with the rest of the molecule. It is somewhat surprising though that the reported value of isobutyrophenone (9) does not indicate additional steric interference, since one would expect the additional methyl group to exert further steric overlap. One would expect the change from acetophenone, propiophenone, and isobutyrophenone, i.e. the successive replacement of two hydrogen atoms by two methyl groups, to be accompanied by first a slight, and then by a more pronounced steric effect, since in each case the molecule will assume the sterically most favorable position—there being no, or very little, restriction to the free rotation of the methyl group. Thus accommodation of the second methyl group—the molecule having attained the sterically most favorable position after the introduction of the first methyl group—would be at least equally, but probably more, difficult and hence involve more appreciable steric overlap. The spectra of propio- and isobutyrophenone, however, are reported to be the same (9); our own values indicate a slight, though definite, change of absorption intensity as expected from the above hypothesis (see Table I).

A further point of interest is that the change in spectral properties between 4-methylacetophenone and 2-methylacetophenone is almost identical with the change observed between 4-methylpropiophenone and 2-methylpropiophenone. For the first pair there is a bathochromic shift of 10 mμ and the ratio of the molar extinction coefficients is 0.57 (8500/15,000), whilst for the second pair the shift is 9 mμ, and the corresponding ratio is 0.57 (8000/14,000) (see Table I). This is reasonably conclusive evidence that the preferred planar configuration of 2-methylacetophenone and 2-methylpropiophenone is IA rather than IB, since if IB were correct, the replacement of the methyl group by the ethyl group in 2-methylpropiophenone would increase the steric overlap

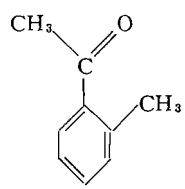

IA

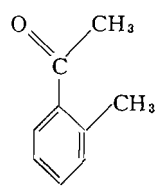

IB

already caused by the 2-methyl group (relative to 4-methylacetophenone), which would be in a position directly adjoining the more bulky ethyl group. This argument is verified by the absorption spectra of pairs of compounds, where the replacement of a methyl by an ethyl group normally causes additional steric effects (see, for example, Table I, for spectra of pentamethyl- and pentaethyl-acetophenones).

For 4-methylbenzaldehyde and 2-methylbenzaldehyde there is no bathochromic shift and the ratio of the molar extinction coefficients is 0.87 (13,000/15,000). Thus whilst in acetophenone and propiophenone the intensity of absorption is approximately halved by the introduction of a 2-methyl group, in benzaldehyde the intensity of absorption remains approximately constant. This type of steric effect has previously been discussed (5) and has been shown to be prevalent in conjugated systems which can exist in at least one unhindered or only weakly hindered uniplanar configuration, and has been ascribed to transitions involving non-planar ground states and planar excited states (6). Thus the fraction of molecules which are in a sufficiently planar ground state to be able to be raised to the postulated planar excited state governs the observed intensity of absorption. Therefore in 2-methylbenzaldehyde, the number of permitted near-planar vibrational states is only very slightly reduced, whilst in 2-methylacetophenone or in 2-methylpropiophenone it is approximately halved, indicating that structures of type IB can no longer contribute appreciably to the absorption band. This hypothesis is confirmed for 2,6-dimethylacetophenone where the absorption band has almost completely disappeared (see Table I).

The band under consideration is clearly sensitive to *para*-substituents and has on account of this previously been provisionally assigned to electronic transitions associated with *para*-resonance forms of type IC (7).

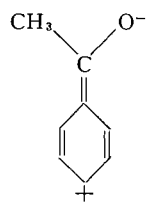

IC

Thus 4-methyl substituents will increase the *para*-resonance contributions to the hybrid of the ground—and even more so its contributions to the excited—states, giving rise to a bathochromic shift and an increased probability of absorption. An *ortho*-methyl group will likewise tend to exert a similar bathochromic shift accompanied by increased intensity of absorption, but in this instance, these effects are counterbalanced by the previously described steric effects. Hence the steric effect of the *ortho*-methyl group is larger than it appears to be, since it has to overcome the electronic effect associated with resonance forms of type IC. This is why it is necessary to compare the *ortho*-substituted compounds with the *para*-substituted analogues, rather than with the unsubstituted parent compounds. Also, it may be noted that this electronic effect of the *ortho*-methyl group becomes more evident in certain compounds, such as 2-methylbenzaldehyde and 4-acetylhydrindacene (II). In the latter, the second *ortho*-methylene group (which is comparable to a methyl group) gives rise to a bathochromic shift of about 10 mμ, which is similar to the

bathochromic shift observed between acetophenone and *p*-methylacetophenone.

In 2,6-dimethylacetophenone, the molecule can no longer take up a more favorable steric configuration (as is the case for 2-methylacetophenone, where the molecule takes up the more favorable configuration IA) and the interplanar angle is considerably increased resulting in an almost total loss of the conjugation band (see Table I).

Introduction of a third methyl group in the *para*-position gives rise to a slight bathochromic shift accompanied by increased transition probability, evidently due to the increased double bond character between the carbonyl group and the benzene ring caused by greater contributions of resonance forms of type IC. This decreases the interplanar angle and gives rise to the observed effect. It may further be noted that a similar difference is observed between 2,3,5,6-tetramethyl- and 2,3,4,5,6-pentamethyl-acetophenones (see Table I).

To account for the spectrum of 4-acetylhydrindacene (II) it must be noted that here both positions corresponding to structures IA and IB are equally possible. The observed maximal absorption at 252 mμ is approximately as expected for two *ortho*-alkyl substituents, but the intensity of absorption indicates a certain amount of steric hindrance of the type described above, i.e. corresponding to non-planar ground states and planar excited states. Since there is a decrease of intensity of absorption relative to acetophenone and an increase in intensity of absorption relative to 2,6-dimethylacetophenone, the

TABLE I

ABSORPTION SPECTRA OF ORTHO-SUBSTITUTED ACETOPHENONES AND RELATED COMPOUNDS IN ABSOLUTE ETHANOL

Wave-lengths and intensities of the main maxima (values in italics represent inflections)

Compound	λ_{max}, mμ	ϵ_{max}	λ_{max}, mμ	ϵ_{max}
Benzaldehyde	244	13,000	279	950
Acetophenone	240	12,500	276	1000
Propiophenone	240	12,000	276	1000
n-Butyrophenone	240	11,500	276	1000
Isobutyrophenone	240	10,500	276	850
4-Methylbenzaldehyde (6)	251	15,000	—	—
2-Methylbenzaldehyde (6)	251	13,000	—	—
4-Methylacetophenone (6)	252	15,000	*278*	*850*
2-Methylacetophenone (6)	242	8500	283	1250
2,4-Dimethylacetophenone (6)	251	13,000	282	1250
2,6-Dimethylacetophenone (12)	*241*	*2100*	—	—
2,4,6-Trimethylacetophenone (12)	*245*	*2300*	—	—
2,3,5,6-Tetramethylacetophenone	*212*	*11,500*	277	850
2,3,4,5,6-Pentamethylacetophenone	*216*	*12,000*	*280*	*600*
2,3,4,5,6-Pentaethylacetophenone	*218*	*14,000*	*280*	*500*
4-Methylpropiophenone	249	14,000	—	—
2-Methylpropiophenone	240	8000	282	1200
4-Acetylhydrindacene (II)	252	7000	308	3000
4-Acetyl-5,6-dimethylindane (III)	246	3000	280	1700
9-Acetyloctahydroanthracene (IV)	*220*	*10,000*	282	1500
5-Acetyl-6,7-dimethyltetralin (V)	*218*	*11,000*	278	1100
2,3,5,6-Tetramethylbenzene	*214*	*8500*	268	600

ortho-methylene group in the cyclopentyl ring offers steric resistance intermediate to that of an *ortho*-hydrogen atom and an *ortho*-methyl group, which is indeed as would be expected from an examination of scale models.

In 9-acetyloctahydroanthracene (IV), the steric effect due to the methylene group, as indicated by the location of maximal absorption, is considerably more pronounced, in agreement with the observation of Arnold and Craig (1), who found from reactivity measurements and in part from the values of carbonyl Raman frequencies that the steric hindrance around the carbonyl group decreases in the order V > IV > III > II. Thus the methylene group, held in a position where there is considerable interaction between the methyl group of the —$COCH_3$ group and the hydrogen atoms of the methylene group, increases the transition energy which results in the observed hypsochromic shift of the band. The observed intensity of absorption can be con-

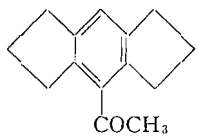

II

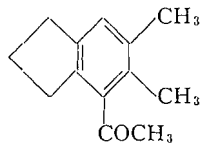

III

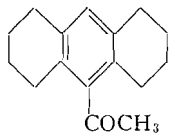

IV

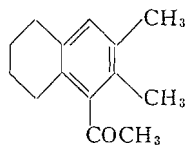

V

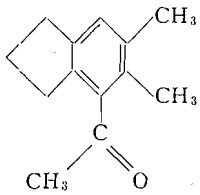

IIIA

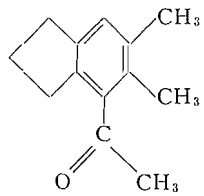

IIIB

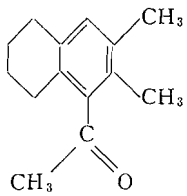

VA

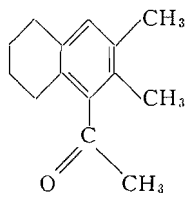

VB

sidered to be largely due to the superposition of absorption due to the "tetramethylbenzene" band at 214 mμ.

For 4-acetyl-5,6-dimethylindane (III) two structures (IIIA) and (IIIB) are possible. The tendency for coplanarity between the carbonyl group and the rest of the molecule—which is due both to contributions of resonance forms to the ground-state hybrid and possibly to steric effects of the *ortho*-methylene group—will be opposed by the usual steric effect.

If structure IIIA predominates, the location and intensity of the absorption band should be similar to that of 2,6-dimethylacctophenone, although two secondary effects will be operating in opposite directions. Thus the molecule will be more hindered since the additional methyl group in the meta-position increases the steric effect (cf., for example, Table I, the spectra of 2,6-dimethyl- and 2,3,5,6-tetramethyl-acetophenones), but this effect will be opposed by the substitution of the cyclopentyl group for the second *ortho*-methyl group, which, as has been noted above, will reduce steric hindrance. If structure IIIB predominates, the location and intensity of the absorption band should again resemble that of 2,6-dimethylacetophenone, but having undergone further steric hindrance due to the "buttressing" effect of the methyl group in the *meta*-position. Since it has been shown that the pronounced steric effect in 2,6-dimethylacetophenone is due to the interference of the α- and *ortho*-methyl groups, the cyclopentyl group in IIIB would not be expected to affect the amount of steric hindrance obtained. Therefore, if structure IIIB were correct, a further steric effect relative to 2,6-dimethylacetophenone should occur. From Table I it is seen that only structure IIIA can fit the observed spectrum. This is also what would have been expected from scale models, since the C=O group has a smaller interference radius than the methyl group and would more readily be accommodated in the arrangement as represented by IIIA.

On applying a similar argument to the spectrum of 5-acetyl-6,7-dimethyltetralin (V), the data at first sight seem to point to a structure VB rather than to a structure VA, since the observed spectrum closely resembles the spectrum of 9-acetyloctahydroanthracene (IV), and also exhibits an absorption intensity more than twice as high as that of 4-acetyl-5,6-dimethylindane (IIIA); this is an argument that the two structures are probably dissimilar, since if they were similar, the absorption intensity of VA would be smaller than that of the corresponding five-membered ring compound IIIA. However, if the observed intensity of IV and V is almost wholly due to "tetramethylbenzene" absorption, as is indicated by the spectrum of tetramethyl benzene, the argument clearly becomes invalid and the question of the preferred configuration remains open. It should be remembered that for compounds IV and V, the interplanar angle approaches 90°, and since conjugation is hence almost completely inhibited, one would not expect to be able to draw conclusions about preferred configurations of these compounds, from a study of *this* particular band.

The spectrum of 2,3,5,6-tetramethylacetophenone (Table I) is of interest as it illustrates the "buttressing" effect of the *m*-methyl group, which may

be regarded as preventing bending away of the *o*-methyl group (5). That the pronounced effect in the spectrum is chiefly of a steric, rather than electronic, nature is indicated since in 4-acetylhydrindacene (II), no similar effect (i.e. a very pronounced hypsochromic shift) is observed, although in that compound both the *m*-positions are also occupied.

The secondary band, near 280 mμ, which may be regarded as derived from the low intensity band of benzene near 255 mμ and which is benzenoid in character (4), is not sensitive to the steric influences discussed in the present communication. The effect of substituents on this band, together with the effect of different solvent systems and temperature variations, will be the subject of a separate communication.

The absorption spectra of the 2,4-dinitrophenylhydrazones of some of the sterically hindered acetophenones, together with those of some reference compounds, are listed in Table II. The dinitrophenylhydrazones of acetophenones and propiophenones which absorb maximally at 372 and 374 mμ indicate interaction between the hydrazine group and the benzene ring, which is enhanced in *para*-substituted acetophenones as evidenced by a further bathochromic shift and increased intensity of absorption. In the dinitrophenylhydrazone of 2-methylpropiophenone this interaction is inhibited and the spectrum closely resembles that of the 2,4-dinitrophenylhydrazone of cyclohexanone, in which no cross-conjugation is possible, and must be ascribed to the $\rangle C{=}N{-}NH{-}R$ (R = 2,4-dinitrophenyl chromophore). The spectrum of the 2,4-dintrophenylhydrazone of isobutyrophenone is entirely similar and therefore indicates that in this instance, the change from propiophenone to isobutyrophenone brings about a change from a planar or near-planar to a non-planar configuration. The 2,4-dinitrophenylhydrazones of 4-acetylhydrindacene (II) and 4-acetyl-5,6-dimethylindane (III) absorb maximally at 366 mμ and 362 mμ respectively, indicating an increasing amount of steric inhibition of conjugation. 9-Acetyloctahydroanthracene (IV), 5-acetyl-6,7-dimethyltetralin (V), tetramethyl-, pentamethyl-, or pentaethyl-acetophenones do not form 2,4-dinitrophenylhydrazones, oximes, or semicarbazones under

TABLE II

ABSORPTION SPECTRA OF 2,4-DINITROPHENYLHYDRAZONES OF ACETOPHENONES AND RELATED COMPOUNDS IN CHLOROFORM

Wave-lengths and intensities of the main maxima

Carbonyl compound	λ_{max}, mμ	ϵ_{max}	Color
Benzaldehyde	372	29,000	Orange-red
Acetophenone	372	25,000	Red
Propiophenone	374	25,000	Red
4-Methylpropiophenone	380	25,500	Red
2-Methylpropiophenone	362	23,500	Red
Isobutyrophenone	362	23,500	Yellow
Cyclohexanone	362	23,500	Yellow
4-Acetylhydrindacene	366	24,000	Orange
4-Acetyl-5,6-dimethylindane	362	22,000	Orange

the usual conditions. The amount of steric hindrance can also sometimes be estimated in the above-mentioned 2,4-dinitrophenylhydrazones by their color (see Table II).

EXPERIMENTAL PART

The ultraviolet spectra were determined by standard methods using a Unicam SP 500 spectrophotometer. ϵ represents the molecular extinction coefficient defined by $\epsilon = [\log_{10}(I_0/I)]/cl$, where I_0 and I = intensity of incident and of transmitted light, respectively, c = concentration in moles/liter, and l = cell thickness in centimeters.

Melting points are uncorrected; analyses were carried out in the microanalytical laboratory (Mr. F. H. Oliver) of the Department of Organic Chemistry, Imperial College, London, England.

Benzaldehyde, Acetophenone, Propiophenone, Isobutyrophenone

The commercially available compounds were redistilled to constant refractive index and intensity of absorption. Light absorption in ethanol: see Table I. The 2,4-dinitrophenylhydrazones of these, as well as of the other carbonyl compounds described below, were chromatographed on alumina from chloroform–benzene and crystallized, unless otherwise stated, from ethanol – ethyl acetate mixtures. Benzaldehyde 2,4-dinitrophenylhydrazone crystallized from glacial acetic acid as red needles, melting point 241–242° (Johnson (10) gives melting point 239–240°); acetophenone 2,4-dinitrophenylhydrazone crystallized from glacial acetic acid as red needles, melting point 250° (Johnson (10) gives melting point 247–248°); propiophenone 2,4-dinitrophenylhydrazone crystallized as red plates, melting point 196–197° (with decomposition) (Johnson (10) gives melting point 193–194°); isobutyrophenone 2,4-dinitrophenylhydrazone crystallized as yellow monoclinic prisms, melting point 165–166° (Johnson (10) gives melting point 161–162°). Light absorption in chloroform: see Table II.

4-Methylpropiophenone

Anhydrous aluminum chloride (9.1 gm.) was added to toluene (100 ml.), and propionyl chloride (6.3 gm.) was added dropwise with stirring at 0°C. After stirring for one hour, the mixture was hydrolyzed and isolated in the usual manner. The product distilled at 110°, 12 mm., yield 5.5 gm. (55%), $n_D^{22.5}$ 1.5264 (Birch *et al.* (3) give boiling point 135°, 30 mm.; n_D^{20} 1.5278). Light absorption in ethanol: see Table I. The 2,4 dinitrophenylhydrazone crystallized from ethyl acetate as red monoclinic prisms, melting point 209° with decomposition (Cullinane *et al.* (8) give melting point 201°). Light absorption in chloroform: see Table II.

2-Methylpropiophenone

2-Methylpropiophenone was prepared according to the method of Birch *et al.* (3), and was obtained as a colorless liquid, boiling point 100° at 18 mm., n_D^{22} 1.5243 (Birch *et al.* (3) give n_D^{20} 1.5250), yield 9.2 gm. (62%). Light absorption in ethanol: see Table I. The 2,4-dinitrophenylhydrazone crystallized from ethanol as red plates, melting point 115°. Anal.: Calc. for $C_{15}H_{14}O_4N_4$:

C, 57.3; H, 4.5; N, 17.8%. Found: C, 57.3; H, 4.5; N, 17.7%. Light absorption in chloroform: see Table II.

2,3,5,6-Tetramethylacetophenone

Durene (4 gm.), prepared from xylene by the method of Smith (13), was dissolved in carbon disulphide (40 ml.) at 0°. Aluminum chloride (4 gm.) was added to the stirred mixture in small portions followed by the dropwise addition of acetyl chloride (2.4 gm.) over a period of 10 min. Stirring was continued for three hours at 0°, and the mixture was then allowed to stand overnight at room temperature. It was then poured onto an ice – hydrochloric acid mixture and extracted with ether. After drying, removal of ether afforded the acetophenone in 55% yield, which crystallized from petroleum ether (boiling range 40–60°) as colorless plates, melting point 75° (Meyer (11) gives melting point 73°). No oxime, semicarbazone, or 2,4-dinitrophenylhydrazone could be obtained under the usual conditions. Light absorption in ethanol: see Table I.

2,3,4,5,6-Pentamethylacetophenone

Pentamethylbenzene (2 gm.), prepared by the method of Smith (13), was dissolved in carbon disulphide (50 ml.) and treated with aluminum chloride (1.8 gm.) and acetyl chloride (1.1 gm.) as described above. The product, which crystallized from methanol as colorless needles, melting point 87°, was obtained in 90% yield. Anal.: Calc. for $C_{13}H_{18}O$: C, 82.1; H, 9.5%. Found: C, 82.1; H, 9.7%. No oxime, semicarbazone, or 2,4-dinitrophenylhydrazone could be obtained under the usual conditions. Light absorption in ethanol: see Table I.

2,3,4,5,6-Pentaethylacetophenone

Pentaethylbenzene (5.1 gm., n_D^{25} 1.5130), prepared by the method of Smith and Guss (14), was treated with aluminum chloride (3.2 gm.) and acetyl chloride (2.7 gm.) as described above. The product which crystallized from 95% ethanol as colorless needles, melting point 143.5–144°, was obtained in 80% yield. Anal.: Calc. for $C_{18}H_{28}O$: C, 83.0; H, 10.9%. Found: C, 83.0; H, 11.0%. No oxime, semicarbazone, or 2,4-dinitrophenylhydrazone could be obtained under the usual conditions. Light absorption in ethanol: see Table I.

4-Acetyl-5,6-dimethylindane (III)

5,6-Dimethylindane (1.9 gm., $n_D^{26.5}$ 1.5318), prepared by the method of Arnold and Craig (1), in carbon disulphide (30 ml.) was treated with aluminum chloride (1.7 gm.) and acetyl chloride (1 gm.) as described above. Fractionation at 3 mm. afforded the indane as a pale yellow oil, which solidified on standing and crystallized from petroleum ether (boiling range 40–60°) as monoclinic prisms, melting point 42.5°. Arnold and Craig (1) report melting point 43° for this compound. Light absorption in ethanol: see Table I. The 2,4-dinitrophenylhydrazone crystallized from benzene as yellow plates, melting point 196–197°. Anal.: Calc. for $C_{19}H_{20}O_4N_4$: C, 61.9; H, 5.5; N, 15.2%. Found: C, 61.9; H, 5.5; N, 15.1%. Light absorption in chloroform: see Table II.

4-Acetylhydrindacene (II), 9-Acetyloctahydroanthracene (IV), and 5-Acetyl-6,7-dimethyltetralin (V)

These compounds were crystallized to constant melting point and constant intensity of absorption. Their preparation has previously been described (1, 2) and we are grateful to Professor R. T. Arnold for very kindly providing us with the required specimens. The last two compounds do not form any oximes, semicarbazones, or 2,4-dinitrophenylhydrazones. The 2,4-dinitrophenylhydrazone of 4-acetylhydrindacene crystallized from ethanol as orange needles, melting point 185°. Anal.: Calc. for $C_{20}H_{20}O_4N_4$: C, 63.15; H, 5.3; N, 14.7%. Found: C, 63.2; H, 5.3; N, 14.6%. Light absorption in chloroform: see Table II.

ACKNOWLEDGMENTS

The authors are greatly indebted to Dr. E. A. Braude for a number of invaluable discussions, and to the National Research Council of Canada for a research grant. They also wish to thank two students of the University for determining some of the absorption spectra (Mr. N. Coates) and for assisting in the preparation of the manuscript (Miss R. M. Gosine).

REFERENCES

1. Arnold, R. T. and Craig, P. N. J. Am. Chem. Soc. 70: 2791. 1948.
2. Arnold, R. T. and Rondestvedt, E. J. Am. Chem. Soc. 68: 2176. 1946.
3. Birch, S. F., Dean, R. A., Fidler, F. A., and Lowry, R. A. J. Am. Chem. Soc. 71: 1362. 1949.
4. Bowden, K. and Braude, E. A. J. Chem. Soc. 1068. 1952.
5. Braude, E. A. and Forbes, W. F. J. Chem. Soc. In press. 1955.
6. Braude, E. A., Sondheimer, F., and Forbes, W. F. Nature, 173: 117. 1954.
7. Cram, D. J. and Cranz, F. W. J. Am. Chem. Soc. 72: 595. 1950.
8. Cullinane, N. M., Chard, S. J., and Leyshon, D. M. J. Chem. Soc. 376. 1952.
9. Hedden, G. D. and Brown, W. G. J. Am. Chem. Soc. 75: 3744. 1953.
10. Johnson, G. D. J. Am. Chem. Soc. 75: 2720. 1953.
11. Meyer, V. Ber. 29: 847. 1896.
12. Schwartzman, L. H. and Corson, B. B. J. Am. Chem. Soc. 76: 781. 1954.
13. Smith, L. I. Organic syntheses. Collective Vol. II. John Wiley & Sons, Inc., New York. 1943. p. 248.
14. Smith, L. I. and Guss, C. O. J. Am. Chem. Soc. 62: 2625. 1940.

GROWTH RATES OF SINGLE CRYSTALS OF ETHYLENE DIAMINE TARTRATE[1]

By A. H. Booth[2] and H. E. Buckley[3]

ABSTRACT

Single crystals of ethylene diamine tartrate were grown under controlled conditions and the growth rate of the faces measured directly in the solution at short intervals by means of a travelling microscope. For the $(\bar{1}10)$ $(1\bar{1}0)$ pair of faces, the fastest growing form, steady growth at constant supersaturation was interrupted by occasional short periods of more rapid growth. Rejecting these erratic "spurts", reasonably reproducible values could be obtained, and the dependence upon supersaturation plotted. The equivalent faces at the opposite end of the polar axis of the crystal grew, at low supersaturation, with erratic starts and stops, so that reproducible growth-rate values could not be obtained. The results are discussed in relation to existing crystal growth theories.

INTRODUCTION

Plates cut from large crystals of ethylene diamine tartrate (EDT) have been used instead of quartz in the filter circuits needed for carrier telephone systems (9). Growing EDT crystals large enough for this purpose requires careful control (7). In order to study the influence of solution conditions on the growth of a single crystal it was desired, as a first step, to determine the growth rates of the various faces as a function of supersaturation. This paper describes an attempt to do this. A later paper reports the use made of the method in a search for possible growth "improvers".

At the outset it was not known whether reproducible growth-rate measurements could be obtained on single crystals. Rates of crystalline precipitation are usually reproducible, but they represent merely the mean growth rate of the large number of crystals involved. Corresponding studies have rarely been made on single crystals, and the little information available was confusing. It has been observed by many that visibly flawed crystals grow two or three times as fast as clear flawless ones, but it seems to have been rather generally assumed that crystals free from obvious flaws would grow at the same rate. However, no data to support this could be found in the literature. There is, in fact, some evidence against it. Berg (1) and others (2, 5) determined growth rates of the cube faces of sodium chlorate in a thin film of solution under the microscope, while measuring concentration gradients continuously by an optical interference method. They found that the growth rates of equivalent faces of the same crystal varied widely and that occasionally a face completely stopped growing for a while even though it was in contact with a strongly supersaturated solution.

The reason for this behavior is not clear. A possible explanation is that the faces studied were so minute that the nucleation centers at which growth

[1]*Manuscript received March 15, 1955.*
Contribution from the Crystallography Department, University of Manchester, Manchester, England. Part of a Ph.D. Thesis, University of Manchester, Manchester, England, 1952. Presented before the Chemical Institute of Canada, June 5, 1953, at Windsor, Ontario.
[2]*Present address: Atomic Energy of Canada Limited, Chalk River, Ontario.*
[3]*Present address: University of Manchester, Manchester, England.*

layers started were few or zero. Their distribution would then be of critical influence on the growth rate. It seemed possible that by working with moderate sized crystals more reproducible growth rates might be obtained. Diffusion effects would, of course, have to be eliminated or held constant. On this point Egli and Zerfoss (3) state that usually only moderate stirring is needed to eliminate diffusion as a rate controlling factor. Van Hook (6) found this to be so for sucrose and concluded that the reaction at the crystal face is a slower process than transport toward it.

EXPERIMENTAL

The apparatus is shown in Fig. 1. It consisted of a crystallizing chamber enclosed by a water jacket, both made of transparent plastic. The volume of the crystallizing cell was made large enough in relation to the crystal seed so that as the crystal grew, the supersaturation remained constant during the

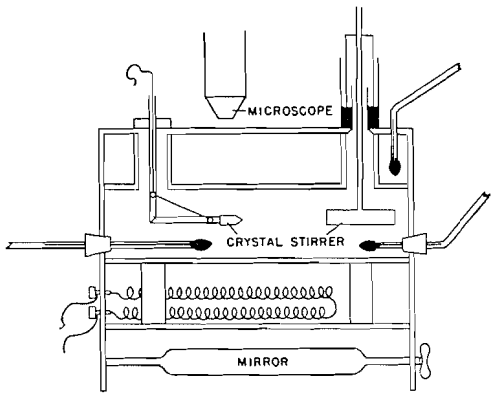

FIG. 1. Crystal growth-rate apparatus.

measuring period. The temperature could be held constant within 0.1°C. The shaft of the stirrer operated through a mercury seal to prevent evaporation. The crystal was viewed and measured with a low power travelling microscope, the transit of which read directly to 0.001 mm.

Solutions were prepared by dissolving recrystallized EDT-monohydrate in water. (The monohydrate is the stable form below 40.6°C.) The solutions were used only until they became slightly colored by decomposition products and then were discarded. The crystal seeds were about 4–12 mm.^{2} in cross section, and were free from visible flaws. They were cemented on a hinged plastic rod which was inserted in the cell and the hinged part then drawn up into position with a wire. Solutions saturated at the required temperature were prepared in a separate water bath; but after the cell was filled the saturation temperature was checked in the following way. The crystal was allowed to grow somewhat and then the temperature was raised very slowly until the first sign of rounding of the sharp edges was seen. This method was found to be accurate to within 0.2°C. The saturation temperature was checked frequently throughout the life of the solution to ensure that the supersaturation had not been lowered appreciably by the growth of the crystal.

Normally most rapid growth is on the wedge shaped $(\bar{1}\bar{1}0)$ $(1\bar{1}0)$ pair of faces which cap the negative end of the *y*-axis. Generally, the edge of the wedge was taken as the marker, and measurements were made of the growth along the axis. The recorded values therefore do not represent directly the growth rates of any real face, but if they are multiplied by cos 45° 30′ (one half the interfacial angle) they give the average for the two members of the pair. The two were always nearly equal unless one of the faces was visibly flawed. In such a case the flawed face grew more quickly so that its area decreased relative to the other, and the crystal became asymmetric.

The equivalent faces at the positive end of the *y*-axis, (110) $(\bar{1}10)$, are reportedly "non-growing" under the conditions in the industrial crystallizer. They are said to grow appreciably only when visibly flawed (7). Measurements at this end of the crystal were made in the same way. The top and side faces (001) and (100) were not studied in detail. Their growth behavior seemed similar to that of the (110) $(\bar{1}10)$ pair.

The settings of the microscope cross hairs against the crystal point were reproducible to about 0.003 mm. Growth rates were recorded for equal increments of added length, usually 0.02 mm. The average of at least 10 readings was taken in each case.

The effect of stirring speed was studied first. With quite moderate agitation a maximum growth rate was reached; then the stirring speed could be doubled without any further increase. All subsequent work was done with stirring speeds that were well over the necessary minimum. Unfortunately, with such agitation it was not possible to work at undercoolings of more than 4 or 5°C. (supersaturations of 1.5%) without great danger of spontaneous crystallization.

Growth rates covering the practical supersaturation range were measured. The reproducibility for different individual crystals and the dependence upon solution composition and temperature were then studied.

RESULTS

(*a*) *The Negative End of the y-Axis*

At constant supersaturation the measured value of the growth rate, when the crystal was growing with its normal habit faces and without visible flaws, was nearly constant. However, occasionally a sudden jump to a value erratically higher was noted. This was commonly about twice as great as the steady value, the deviation being quite outside the combined errors of temperature and length measurement. The rate usually dropped back to the steady value in a short time, often on the next reading. The irregularities seemed greater when the temperature was changing than when it was held nearly constant. It was found better to measure the growth rates at each supersaturation separately, holding the temperature constant for a time and dropping it stepwise, rather than by interpolating the values from a continuous cooling curve.

These erratic periods of more rapid growth left no visible mark in the crystal. However, sometimes when the supersaturation was high the enhanced rate of growth continued for a much longer time before dropping back to the

normal rate. Then a visible "veil" appeared. Veils were more frequent when the stirring was inefficient. They could be produced almost at will on a given face by orienting the face so that it was in the lee of the current. Presumably, dead spots in the circulation leading to irregularities in the supersaturation of the solution at various points along the face promoted the disordered growth.

Despite the complication caused by the erratic jumps, it was quite feasible to evaluate "normal" growth rates. The jumps were usually well-defined and not too close together, and so could be rejected unambiguously. The rate values quoted later always refer to these corrected values, not to the gross average rates.

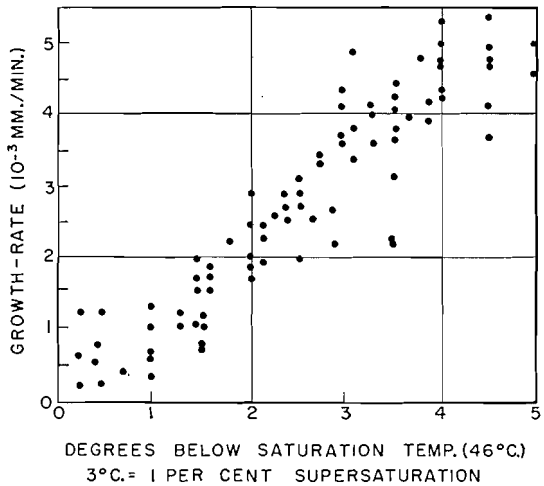

FIG. 2. Growth rates at negative end of y-axis.

Even with this limitation, some variation outside experimental error was found in measurements made under apparently identical conditions. First with the same crystal in position, measurements were taken up and down the supersaturation scale several times. Then four other crystals successively were treated in the same way in the same solution. Later in the work, four other crystals were measured at various times in similar solutions. The differences between the values obtained in different runs with the same crystal were just as great as those between different individual crystals. In Fig. 2 all the values obtained are shown without distinguishing separate cases. Although not good, the reproducibility was sufficient to allow study of some factors which might be presumed to affect the growth rate.

The effect of temperature was studied first. A series of curves for the same crystal over different temperature ranges was plotted. These were replotted by interpolation as rate curves at different fixed temperatures. It will be seen in Fig. 3 that the rates increase appreciably with increase in temperature. On the other hand, the rate was found to be not very sensitive to the presence of those substances which normally occur as impurities in EDT solutions. Variations

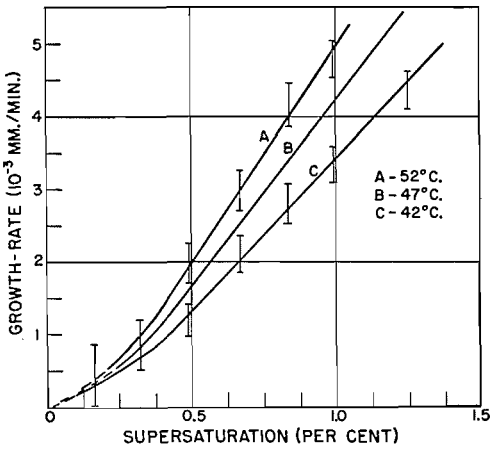

FIG. 3. Growth rates at various temperatures.

in pH over the range 5.0 to 8.0, due to excess of either tartaric acid or ethylene diamine, gave no change sufficiently large to be observable. The decomposition products* of EDT also had little effect, at least when in low concentration. Solutions aged at 40–55°C. for periods up to four months produced no detectable change in the growth curve. One very much older solution gave erratic values, but this effect was not studied further.

Variation of the size of the crystal from 1 to 10 mm.^{2} cross section did not affect the rate of growth. Moreover, the values obtained are of the same order of magnitude as those observed with the larger crystals (100 times greater facial area) which are grown industrially. Most likely the rate is independent of the size of the face.

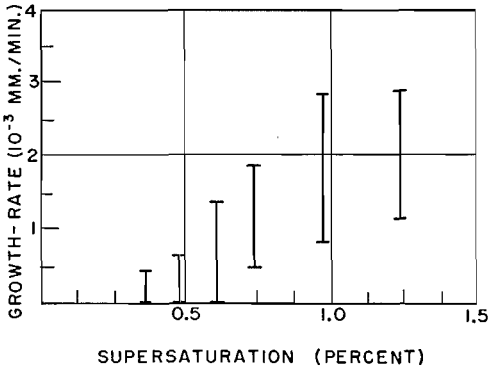

FIG. 4. Growth rates at positive end of y-axis.

*Walker (7) states that "heat and sunlight both cause brownish decomposition products", but it was found that the color is entirely a result of atmospheric oxidation, heat accelerating the reaction. The solutions remained colorless when under an inert atmosphere or when sodium sulphite was added.

(b) The Positive End of the y-Axis

Growth at the positive end of the y-axis of the crystal was quite different from that at the negative end discussed above. It proceeded discontinuously except when the supersaturation was high. There were long pauses, during which no growth at all occurred, intermingled with periods of activity. This is represented diagrammatically in Fig. 4 where the markers delimit the highest and lowest values observed in a series of tests.

DISCUSSION

The marked difference between the growth at the positive and negative ends of the crystal makes it necessary to discuss the two separately.

(a) The Negative End

It is well established that crystals grow by the spreading out of thin layers which start from growth centers on the faces. The irreproducibility of the growth-rate determinations under apparently identical conditions must be caused by differences in the surface structure, leading to differences in the pattern of developing layers. The nature of the growth centers is still under discussion. In the Frank dislocation theory (4) they are the points where screw dislocation lines emerge at the surface. Growth is controlled by a few of the most active ones. Variations in the growth rate would then be caused by the shifting of dominant screw dislocations under the influence of slight stresses.

However the erratic "spurts" may be associated with grosser changes in the surface structure caused by the interference of slightly disoriented layer systems with each other— an idea rather similar to that suggested by Yamamoto (10) to explain skeletal growth. Disoriented junctions between layer systems would serve as strong growth centers and lead to more rapid growth. Probably there are then two opposing tendencies. One is for a group of active centers to become dominant, bridge over gaps, and heal the surface. The other is for the disordered structure to spread, and to become less amenable to healing; for the gaps between disoriented layers will become larger as growth proceeds outward. Consequently, the surface either heals quickly or not at all. In the latter event a visible veil appears. It is interesting that a veil usually covers a face completely but does not spread to adjacent faces. No doubt, this follows from the observed fact that spreading layers usually end at the edge of the face on which they start. That veils can frequently be induced to heal at low supersaturation may be evidence of the ability of the most active growth center to dominate the others.

(b) The Positive End

The peculiar growth behavior of the (110) ($\bar{1}$10) faces is similar to that described for the cube faces of microscopic sodium chlorate crystals (1). This raises the possibility that the phenomenon may be a rather common one and the smoother increase with supersaturation shown by the ($\bar{1}\bar{1}$0) (1$\bar{1}$0) faces exceptional. Since data for other crystals are lacking, this remains speculation.

The complete stopping and sporadic restarting of growth is difficult to explain. Blockage of nucleation centers by adsorption of impurities is a possibility. More probably, however, the solvent itself interacts with these crystal faces in such a way as to inhibit growth. The likelihood of this can be seen by considering an experiment of Wells (8). He found that resorcinol grown from benzene solution grows equally well at the two ends of the polar axis but from water solution most of the growth takes place at one end. He was able to explain this convincingly as caused by the interaction of water molecules with the non-growing end, the structure of which exposes hydroxylic groups at the surface. It will be of interest to determine whether a similar correlation can be made in the case of EDT when its structure is fully determined.

REFERENCES

1. BERG, W. F. Proc. Roy. Soc. (London), A, 164: 79. 1938.
2. BUNN, C. W. Discussions Faraday Soc. No. 5: 132. 1949.
3. EGLI, P. H. and ZERFOSS, S. Discussions Faraday Soc. No. 5: 61. 1949.
4. FRANK, F. C. Discussions Faraday Soc. No. 5: 112. 1949.
5. HUMPHREYS-OWEN, S. P. F. Proc. Roy. Soc. (London), A, 197: 218. 1949.
6. VAN HOOK, A. Ind. Eng. Chem. 36: 1042. 1944.
7. WALKER, A. C. J. Franklin Inst. 250: 481. 1950.
8. WELLS, A. F. Discussions Faraday Soc. No. 5: 197. 1949.
9. WILLIS, E. S. Trans. AIEE, 65: 134. 1946.
10. YAMAMOTO, T. Sci. Papers Inst. Phys. Chem. Research (Tokyo), 35: 228. 1939.

THE EFFECT OF BORIC ACID ON THE GROWTH OF ETHYLENE DIAMINE TARTRATE CRYSTALS[1]

By A. H. Booth[2] and H. E. Buckley[3]

ABSTRACT

When present in ethylene diamine tartrate (EDT) solutions in small concentration boric acid produces many crystallographic phenomena associated with specific adsorption on crystal faces; especially habit modification and growth inhibition. These effects are typical of those given, incidentally, by "growth improvers", and it is concluded that boric acid would be a logical choice for intensive testing as a flaw suppressor in the solutions from which large single crystals of EDT are grown.

INTRODUCTION

To be useful in fabricating channel filters for carrier telephone systems crystals of ethylene diamine tartrate must be free from flaws, at least from those of visible size. The most common type of flaw is a "veil", an opaque region in the otherwise clear crystal caused by disordered growth (also called skeletal, disoriented, porous, or rotten growth). To prevent the appearance of such veils the crystal must be grown very slowly and uniformly. In industrial practice a growing period of several months is required to obtain the desired size, which is about one pound in weight. In the present work methods for speeding up the growth of flawless crystals were sought.

It appears to be a general principle of crystal growth, first established by Yamamoto (4), that for any crystal there is a critical growth rate which, if exceeded, results in skeletal rather than clear compact growth. The critical rate depends greatly on the size of the face, being lower for large than for small faces, and this makes it all the more difficult to grow perfect crystals of large size. The critical rate can, however, be greatly raised by the presence in the solution of specific impurities, often in very small amount. Such additives have been used successfully in several cases for improving the growth of large crystals (1, 2), and the principles involved in selecting a suitable additive are becoming clear. Presumably they owe their effect to selective adsorption on the crystal faces, which restrains the initiation of new layers. This limits the number of layer series existing contemporaneously and so prevents them from interfering with one another.

The adsorption is usually revealed by a number of other crystallographic effects. The most important of these are a change of crystal habit, a slowing down of the growth rate, and an increase in the supersaturation range in which spontaneous crystallization does not occur. A *decrease* in growth rate compared with a pure solution of equal supersaturation is thus connected with an *increase* in the critical rate (the maximum rate for clear growth). To evaluate the worth

[1]*Manuscript received March 15, 1955.*
Contribution from the Crystallography Department, University of Manchester, Manchester, England. Part of a Ph.D. Thesis, University of Manchester, Manchester, England, 1952.
[2]*Present address: Atomic Energy of Canada Limited, Chalk River, Ontario.*
[3]*Present address: University of Manchester, Manchester, England.*

of an "improver" directly is a difficult and time consuming problem, so that an attempt was made to make a preliminary selection of likely substances by a study of these associated effects.

EXPERIMENTAL

Habit modification effects were studied by crystallizing single crystals in test tubes, or in a cell under the microscope. Growth inhibition was studied in the apparatus described in the preceding paper. In addition a few tests were made in an apparatus similar to that used in industrial practice, as described by Walker (3). The crystallizing vessel was a 5 liter beaker. Large seeds about 2 in. wide were mounted on a "spider" which rotated in the solution with a reciprocating motion, the direction of stirring being reversed every 30 sec.

RESULTS

The crystals were for the most part quite unaffected by the presence of small amounts of foreign substances introduced into the solution. This applies to common inorganic ions, surface active agents, and some arbitrarily chosen organic compounds. However, a very powerful and striking effect was found with small quantities of boric acid.

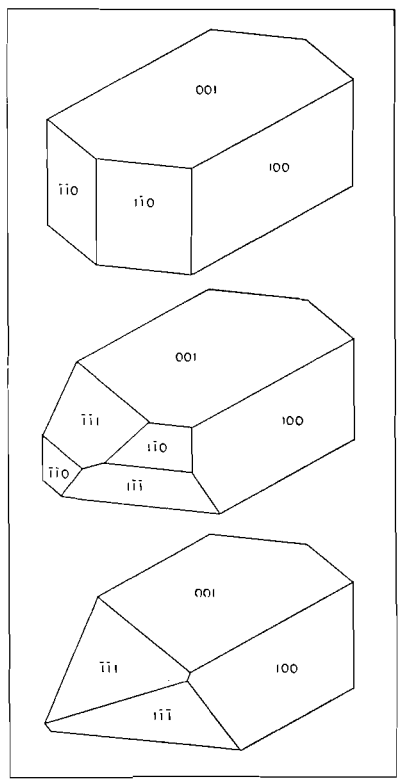

FIG. 1. Crystal habits of EDT: (top) normal; (center and bottom) modified by presence of boric acid in the solution.

(*a*) *Habit Modification*

Quite small amounts of boric acid suppress the development of the $(\bar{1}\bar{1}0)$ $(1\bar{1}0)$ faces. The $(\bar{1}\bar{1}1)$ $(1\bar{1}\bar{1})$ pair, not normally present, appears in their stead. It has no such effect at the positive end of the *y*-axis. The actual concentration required depends on the rate of growth. At very slow rates maintained for long times, as in the industrial type crystallizer, concentrations over 0.04 gm. per liter invariably produced an appreciable development of the $(\bar{1}\bar{1}1)$ $(1\bar{1}\bar{1})$ faces, and at concentrations over 0.1 gm. per liter they completely replaced the $(\bar{1}\bar{1}0)$ $(1\bar{1}0)$ pair. If both pairs were coexisting and the growth rate was then increased the $(\bar{1}\bar{1}1)$ $(1\bar{1}\bar{1})$ faces became smaller and finally disappeared. In the growth rate measurement apparatus the crystals were mostly growing at somewhat higher rates than in the larger crystallizer, so that appreciable development of the $(\bar{1}\bar{1}1)$ $(1\bar{1}\bar{1})$ faces was not observed below concentrations of about 0.5 gm. per liter, with complete replacement of the other pair at about 1.0 gm. per liter. The normal and modified forms are shown in Fig. 1.

(*b*) *Growth Inhibition*

The rate curves for several concentrations of boric acid are shown in Fig. 2. Below 0.2 gm. per liter there was no detectable change. From 0.2 to 0.6 gm. per liter there was a progressive slowing down of the rate. This was accompanied by an apparent decrease in the number of the sudden erratic "spurts" discussed in the preceding paper. The tendency toward spontaneous crystallization was also lessened. The temperature could be lowered several degrees below that at which "snow-storm" crystallization usually occurs.

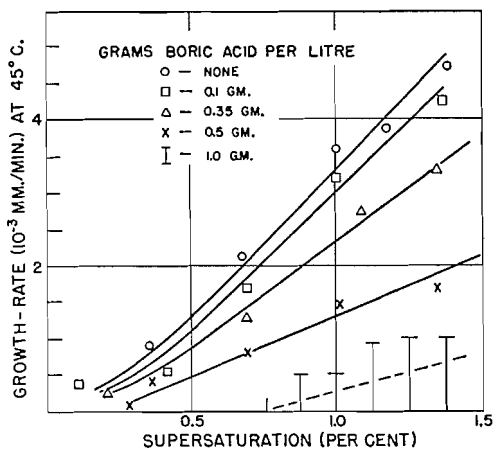

FIG. 2. Growth rates with boric acid additive.

At concentrations of about 1.0 gm. per liter a rounded (partially dissolved) seed grew out to form plane faces and then stopped growing completely. This was with a supersaturation of 1.0%. The temperature was then lowered, but growth did not start again until the supersaturation was about 2.0%. The crystal then grew slowly for a short time but soon stopped growing again and remained completely stopped for several hours.

The behavior with even larger amounts of boric acid in the solution is interesting. The crystals will grow only at high supersaturations and the faces appear warped or rounded. Above about 10 gm. per liter a rounded seed does not grow out to form plane faces. Instead, a mass of extremely small crystals form over the surface. These crystals drift off into the solution and start a dense microcrystalline precipitation. Apparently under these conditions it is easier for new crystals to form than for growth to proceed on existing ones. At yet higher concentrations nuclei formation is so inhibited that the solution can be evaporated to a sirup which sets to a glass on cooling.

This behavior appears to be similar to that observed with substances that have been used as growth improvers in other cases. For instance, Egli and Zerfoss (1), speaking generally, say that "if concentrations beyond the optimum are used habit is modified, flaws are induced and spontaneous nuclei occur more readily than from pure solution".

On the evidence of these effects, then, which point to an adsorption of the desired kind, boric acid would appear to be a logical choice for intensive testing as a flaw suppressor in EDT crystallizer solutions. The optimum concentration would probably be below that needed for habit modification.

ACKNOWLEDGMENTS

The encouragement given by Mr. C. E. Richards of the Post Office Research Department of Great Britain is gratefully acknowledged. One of us (A.H.B.) is indebted to the National Research Council of Canada for a grant and special leave.

REFERENCES

1. EGLI, P. H. and ZERFOSS, S. Discussions Faraday Soc. No. 5: 61. 1949.
2. JAFFE, H. and KJELLGREN, B. R. F. Discussions Faraday Soc. No. 5: 319. 1949.
3. WALKER, A. C. J. Franklin Inst. 250: 481. 1950.
4. YAMAMOTO, T. Sci. Papers Inst. Phys. Chem. Research (Tokyo), 35: 228. 1939.

STEROIDS

III. THE EPIMERIC N-ACETYL-3-AMINOCHOLEST-4- AND -5-ENES[1]

By R. A. B. Bannard and A. F. McKay[2]

ABSTRACT

Lithium aluminum hydride reduction of the oximes of 3-ketocholest-4- and -5-enes gave mixtures of amines. These amines on acetylation and separation gave respectively N-acetyl-3(α)-aminocholest-5-ene, N-acetyl-3(β) aminocholest-5-ene, N-acetyl-3(α)-aminocholest-4-ene, and N-acetyl-3(β)-aminocholest-4-ene. The N-acetyl-3(α)-aminocholest-5-ene (m.p. 184.5°C.) was shown to be identical with the cholesterylacetamide obtained by the acetylation of the degradation product from N-benzyl-3(α)-aminocholest-5-ene (m.p. 90–91°C.).

It was previously (6) shown that benzylamine and 3(β)-chlorocholest-5-ene heated together at 180°C. gave a mixture of 3(β)-benzylaminocholest-5-ene (m.p. 116.5–117.5°C., $[\alpha]_D^{25}$ −23°) and 3(α)-benzylaminocholest-5-ene (m.p. 90–91°C., $[\alpha]_D^{25}$ −9°). Julian *et al.* (5) had degraded the 3(β)-benzylaminocholest-5-ene to 3(β)-aminocholest-5-ene which they converted into 3(β)-acetylaminocholest-5-ene (m.p. 243°C.). The same 3-cholesterylacetamide (m.p. 243°C.) was prepared by Windaus and Adamla (7) by heating 3(β)-chlorocholest-5-ene with ammonia solution in a sealed tube and by reduction of cholest-4-ene-3-one oxime with sodium in alcohol. Two other isomeric cholesterylacetamides melting at 190°C. and 216°C. were isolated also from the latter reaction. When 3(α)-benzylaminocholest-5-ene was degraded (6) to the corresponding amine and converted to 3(α)-acetamidocholest-5-ene (m.p. 184.5°C.[3]), it was thought that this cholesterylacetamide might correspond to the one melting at 190°C. isolated by Windaus and Adamla (7). However since there was no way of confirming this by direct comparison of the cholesterylacetamides from the two different reactions, the four epimeric N-acetyl-3-aminocholest-4- and -5-enes were synthesized.

Cholest-5-ene-3-one oxime (m.p. 184.5–186.5°C.) on reduction with lithium aluminum hydride gave a mixture of epimeric 3-aminocholest-5-enes. The free amines on conversion to their acetyl derivatives and chromatographic separation gave a 46.6% yield of pure N-acetyl-3(β)-aminocholest-5-ene (m.p. 243°C.; $[\alpha]_D^{24.8}$ −44.9°) and a 23% yield of pure N-acetyl-3(α)-aminocholest-5-ene (m.p. 184.5°C.; $[\alpha]_D^{24.8}$ −59.4°). The identity of this N-acetyl-3(α)-aminocholest-5-ene with the cholesterylacetamide (m.p. 184.5°C.) obtained from the degradation of 3(α)-benzylaminocholest-5-ene (6) was established by a mixed melting point determination.

The configurations of the epimeric 3-benzylaminocholest-5-enes were deduced (6) from their rotations in agreement with the rule that the 3(α) form of a steroid will have a higher positive rotation than the 3(β) form (1). If this

[1]*Manuscript received March 7, 1955.*
Contribution from Defence Research Chemical Laboratories, Ottawa, Ontario. Issued as D.R.C.L. Report No. 172.
[2]*Present address: Monsanto Canada Limited, Ville LaSalle, Quebec.*
[3]*This melting point was previously (6) reported as 189°C. but the substance melted at 184.5°C. in the Hershberg melting point apparatus used in these studies.*

rule applies to the N-acetyl-3-aminocholest-5-enes then the higher melting compound (243°) having the more positive rotation will have to be assigned a 3(α) configuration. This would reverse the assignments given above for these cholesterylacetamides. Thus one must conclude that degradation of the 3-benzylaminocholest-5-enes is accompanied by an unexpected (6) Walden inversion at the C_3—N bond or the above rotation rule does not apply to the N-acetyl-3-aminocholest-5-enes. The purity and rotations of the epimeric N-acetyl-3-aminocholest-5-enes were checked repeatedly to confirm the given rotations.

The reduction of cholest-4-ene-3-one oxime (m.p. 158°C.) with lithium aluminum hydride gave a mixture of epimeric 3-aminocholest-4-enes. This mixture was acetylated and the acetamides were separated by chromatography. This procedure gave a 27% yield of pure N-acetyl-3(β)-aminocholest-4-ene (m.p. 223.5°C.; $[\alpha]_D^{24.8}$ +6.2°) and a 28% yield of pure N-acetyl-3(α)-aminocholest-4-ene (m.p. 163–164°C.; $[\alpha]_D^{24.8}$ +105.5°). This is the first time that the latter acetamide (m.p. 164°C.) has been described. The rotations of the epimeric N-acetyl-3-aminocholest-4-enes agree with the rule that the 3(α) epimer should possess the higher positive rotation.

This work confirms the structure originally (6) assigned to the new N-benzyl-3(α)-aminocholest-5-ene (m.p. 90–91°C.).

EXPERIMENTAL[4,5]

Cholest-5-ene-3-one

Cholest-5-ene-3-one (m.p. 122–124°C.) was prepared in 54% yield from cholesterol via cholesterol dibromide and 5(α), 6(β)-dibromocholestan-3-one following the procedure of Fieser (4).

Cholest-5-ene-3-one Oxime

Cholest-5-ene-3-one (2.96 gm.; 0.0077 mole), hydroxylamine hydrochloride (0.71 gm.; 0.01 mole), and fused sodium acetate (0.83 gm.; 0.01 mole) in 95% ethanol (90 cc.) were heated under reflux for six hours. After the reaction mixture had cooled to room temperature, the resultant crystalline slurry was poured slowly into 300 cc. of water with stirring and the colorless crystalline precipitate (m.p. 165–169°C.) was removed by filtration and dried, yield 3.04 gm. (98.6%). Three recrystallizations from methanol raised the melting point to 184.5–186.5°C. with decomposition, yield 1.79 gm. (58.1%). Butenandt and Schmidt-Thomé (2) report the melting point of cholest-5-ene-3-one oxime as 188°C. with decomposition.

Reduction of Cholest-5-ene-3-one Oxime with Lithium Aluminum Hydride

Cholest-5-ene-3-one oxime (1.00 gm.; 0.0025 mole) was placed in a glass extraction thimble consisting of a glass tube with a sealed-in fritted-glass disk. For hot extraction the thimble was placed in a tube which was attached to the center neck of a three-neck 300-cc. round-bottom flask equipped with an

[4]*All melting points are uncorrected and were observed in a Hershberg melting-point apparatus using a temperature rise of 2°C. per minute.*

[5]*Microanalyses by Micro-Tech Laboratories, Skokie, Illinois.*

Allihn condenser set for reflux and protected from entry of moisture with a calcium chloride guard tube. A second neck of the flask was fitted with a dropping funnel, and the third neck was closed by means of a glass stopper. The flask was equipped with a "glascol" heating mantle and a magnetic stirrer. The entire apparatus was swept with "oxygen-free" dry nitrogen as for a Grignard reaction. Lithium aluminum hydride (0.862 gm.; 0.023 mole), which was weighed in a nitrogen-swept dry-box, was added to the reaction flask along with 75 cc. of anhydrous ether. The mixture was heated under reflux with stirring until the oxime had all been extracted from the thimble (one hour). After the solution had been refluxed for a further period of six hours, it was allowed to cool and stand overnight at room temperature. During this time the reaction mixture was maintained under an atmosphere of nitrogen. The stirred suspension was hydrolyzed after addition of a further 100 cc. of anhydrous ether by dropwise addition of water until evolution of hydrogen ceased and the precipitate became colorless and granular (5 cc.). Stirring was continued for a further hour after which the precipitate was collected by filtration and washed with anhydrous ether (6 × 25 cc.). The combined ethereal solutions were concentrated to a volume of 125 cc. and dried over anhydrous sodium sulphate (15 gm.). The dry ether solution was evaporated to dryness first at atmospheric pressure and then *in vacuo* at 60°C. The resultant colorless, porous, solid residue weighed 0.975 gm.

No attempt was made to separate this mixture of cholesterylamines but the residue was heated with 5 cc. of acetic anhydride at 70°C. for 10 min., cooled, treated with 20 cc. of anhydrous ether, and heated under reflux for one hour in an apparatus protected from entry of moisture. The mixture was poured into 100 cc. of water with stirring and a colorless precipitate separated at the ether–water interface. Stirring was continued for 30 min. to complete the hydrolysis after which the colorless solid (m.p. 233–236°C.) was removed by filtration and dried, yield 250 mgm. The residual aqueous phase was neutralized to pH 6 by addition of 10% sodium hydroxide solution followed by 5% sodium bicarbonate solution, extracted with "peroxide-free" ether (6 × 50 cc.), and the combined ethereal solutions evaporated to a volume of 200 cc. and dried over anhydrous sodium sulphate (15 gm.). The dried solution was decanted and evaporated to a volume of 25 cc. on the steam-bath, whereupon colorless platelets (m.p. 234–237°C.) separated, yield 202 mgm. The ether solution failed to yield more of this substance so was evaporated to dryness. The residual pale yellow oil was heated *in vacuo* at 60°C. in the presence of potassium hydroxide to remove a trace of acetic acid, whereupon the oil slowly crystallized, yield 675 mgm. The latter material, on boiling with 30–60° petroleum ether, partially dissolved, leaving behind 42 mgm. of insoluble substance melting at 222–232°C. The filtrate was evaporated to dryness, the residue (578 mgm.) dissolved in 25 cc. of anhydrous 56–67° petroleum ether and transferred to a column for chromatographic analysis (diam. 20 mm.) packed with alumina (neutralized, reactivated, activity II, 17 gm.). The column was eluted with 50-cc. portions of solvent. The benzene–ether (1 : 1) eluates furnished two crops of crystalline material, the first and larger amount of which

on recrystallization from methanol yielded 248 mgm. (23.2%) of fine colorless needles, $[\alpha]_D^{24.8}$ −59.4° (103.1 mgm. substance dissolved in chloroform, 10 cc., 1 dm. tube); m.p. 183–184.5°C. alone and in admixture with an authentic specimen of N-acetyl-3(α)-aminocholest-5-ene of m.p. 184.5°C. previously (6) prepared.

The smaller quantity of crystalline material, m.p. 235°C., (60 mgm.) from the chromatogram proved to be identical with the higher melting crops (250 mgm., 202 mgm., and 46 mgm. respectively) previously obtained at various stages in the purification of the mixture of N-acetylcholesterylamines. This substance on recrystallization from acetone furnished 498 mgm. (46.6%) of N-acetyl-3(β)-aminocholest-5-ene as colorless platelets, m.p. 242–243°C.; $[\alpha]_D^{24.8}$ −44.9° (104.2 mgm. substance dissolved in chloroform, 10 cc., 1 dm. tube). Anal.: Calc. for $C_{29}H_{49}NO$: C, 81.45; H, 11.54; N, 3.27%. Found: C, 81.49; H, 11.59; N, 3.71%. This substance is undoubtedly the N-acetylcholesterylamine of m.p. 244°C. and 238–240°C. reported by Windaus and Adamla (7) and by Julian *et al.* (5) respectively.

Cholest-4-ene-3-one

Cholest-4-ene-3-one of m.p. 81–82°C. was prepared in 94% yield from cholest-5-ene-3-one by Fieser's (4) procedure.

Cholest-4-ene-3-one Oxime

Cholest-4-ene-3-one (10.0 gm.; 0.0260 mole) was heated under reflux for six hours with hydroxylamine hydrochloride (2.80 gm.; 0.0403 mole) and anhydrous sodium acetate (3.20 gm.; 0.0390 mole) in 350 cc. of 95% ethanol, allowed to stand overnight, and poured slowly into 2500 cc. of water with stirring. The colorless flocculent precipitate which separated was collected by suction filtration and dried to constant weight in a vacuum desiccator in the presence of phosphorus pentoxide. The crude cholest-4-ene-3-one oxime weighed 10.3 gm. and exhibited a double melting point of 88–90°C. and 149–151°C. This substance was dissolved in boiling ethyl acetate (75 cc.) and the filtered solution allowed to stand in a desiccator in the presence of phosphorus pentoxide. Slow adsorption of the solvent by the desiccant caused long clusters of colorless needles (m.p. 157–158°C.) to separate. In this manner, over a period of four weeks, four crops of crystals of the above melting point were obtained, yield 8.90 gm. (85.6%). Diels and Abderhalden (3) report the melting point of cholest-4-ene-3-one oxime as 152°C.

Reduction of Cholest-4-ene-3-one Oxime with Lithium Aluminum Hydride

The apparatus and procedure were the same as described for the reduction of cholest-5-ene-3-one oxime except that 2.00 gm. (0.005 mole) of cholest-4-ene-3-one oxime, 1.70 gm. (0.045 mole) of lithium aluminum hydride, and 150 cc. of anhydrous ether were used. The crude mixture of cholesterylamines (1.81 gm.) which resulted from hydrolysis of the complex followed by ether extraction was acetylated with acetic anhydride (10 cc.) by the same procedure as described for the mixture of cholesterylamines resulting from reduction of cholesten-5-one-3 oxime.

The cholesterylacetamides proved to be entirely ether extractable. The ether extract on evaporation to dryness *in vacuo* furnished 2.00 gm. of pale yellow solid. This material was refluxed with 58–64° petroleum ether (25 cc.), the suspension filtered, and the solid residue (m.p. 221.5–223°C.) on the filter washed with 2 × 10 cc. of boiling petroleum ether, yield 262 mgm. This substance proved to be identical with a second crop of material (m.p. 221–223°C.) which separated from the petroleum ether solution on cooling, yield 298 mgm. The petroleum ether solution failed to yield any further crystalline substance on slow evaporation and was consequently evaporated to dryness *in vacuo* and brought to constant weight. The resultant pale yellow oily solid (1.45 gm.) was dissolved in 58–64° petroleum ether and transferred to a column (diam. 24 mm.) packed with alumina (neutralized, reactivated, activity II, 46 gm.) for chromatographic analysis. The column was eluted with 100-cc. portions of solvent.

Elution with benzene–ether (1 : 1) gave 143 mgm. of crystalline substance which, after recrystallization from methanol, gave 71 mgm. of flat colorless needles which proved to be identical with the substance of m.p. 221–223°C. previously obtained. The three crops of this substance (262 mgm., 298 mgm., and 71 mgm. respectively) were combined and recrystallized from methanol (35 cc.) yielding 592 mgm. (27.7%) of N-acetyl-3(β)-aminocholest-4-ene, m.p. 222.5–223.5°C., $[\alpha]_D^{24.8}$ +6.2° (104.2 mgm. substance dissolved in chloroform, 10 cc., 1 dm. tube), as long flat needles. Calc. for $C_{29}H_{49}NO$: C, 81.45; H, 11.54; N, 3.27%. Found: C, 81.22; H, 11.71; N, 3.27%.

Elution with ether containing 0.5% methanol gave 801 mgm. of colorless crystalline substance, which on recrystallization from *n*-pentane (35 cc.) yielded 615 mgm. (28.8%) of colorless feathery needles melting at 160–161°C. Two more recrystallizations from the same solvent raised the melting point to 163–164°C., $[\alpha]_D^{24.8}$ +105.5° (103.1 mgm. substance dissolved in chloroform, 10 cc., 1 dm. tube). Anal.: Calc. for $C_{29}H_{49}NO$: C, 81.45; H, 11.54; N, 3.27%. Found: C, 81.16; H, 11.30; N, 3.64%. The latter substance is the hitherto unreported N-acetyl-3(α)-aminocholest-4-ene.

ACKNOWLEDGMENTS

The authors wish to thank Mr. R. O. Braun for assistance with some of the chromatography.

REFERENCES

1. Bernstein, S., Hicks, E. M., Clark, D. M., and Wallis, E. S. J. Org. Chem. 11: 646. 1946.
2. Butenandt, A. and Schmidt-Thomé, J. Ber. 69: 882. 1936.
3. Diels, O. and Abderhalden, E. Ber. 37: 3092. 1904.
4. Fieser, L. F. J. Am. Chem. Soc. 75: 2421. 1953.
5. Julian, P. L., Magnani, A., Meyer, E. W., and Cole, W. J. J. Am. Chem. Soc. 70: 1834. 1948.
6. Vavasour, G. R., Bolker, H. I., and McKay, A. F. Can. J. Chem. 30: 933. 1952.
7. Windaus, A. and Adamla, J. Ber. 44: 3051. 1911.

THE INFRARED AND RAMAN SPECTRA OF *cis* AND *trans* DIBROMOETHYLENE, TRIBROMOETHYLENE, AND AN APPLICATION OF THE FREQUENCY SUM RULE[1]

By J. C. Evans[2] and H. J. Bernstein

ABSTRACT

Complete vibrational assignments have been obtained for tribromoethylene and *cis* dibromoethylene and thermodynamic functions calculated. Ten of the twelve fundamentals of *trans* dibromoethylene have been assigned and the approximate frequency of the missing pair evaluated by application of the frequency sum rule. The heat capacity of *trans* dibromoethylene has been calculated.

Satisfactory spectroscopic data exist for vinyl bromide (6) and 1,1-dibromoethylene (9), while the infrared active fundamentals of tetrabromoethylene below 300 cm.$^{-1}$ remain to be observed (11). Previous investigations did not enable complete vibrational assignments to be made for tribromoethylene, or for *cis* and *trans* dibromoethylene. The Raman spectrum of tribromoethylene has been obtained (15), but in the absence of values for the depolarization ratios only a very limited assignment was attempted. More extensive work has been done on the *cis* and *trans* dibromoethylenes (8, 10, 17), but for both molecules the assignments are incomplete.

In this investigation, the Raman spectra of the liquids with depolarization ratios and the infrared spectra of the liquids and their vapors were obtained for tribromoethylene and *cis* and *trans* dibromoethylene. Complete assignments for tribromoethylene and *cis* dibromoethylene, and an assignment of all but two modes (Raman inactive, infrared active lying below 250 cm.$^{-1}$) for the *trans* molecule, have been made.

EXPERIMENTAL

The sample of C_2HBr_3 (Eastman Kodak) was fractionally distilled under reduced pressure. A mixture of *cis* and *trans* $C_2H_2Br_2$ (Eastman Kodak) was redistilled and a partial separation of the isomers was achieved by fractional distillation with absolute alcohol (18).

A White photoelectric recording grating spectrometer (20) and a Perkin Elmer Model 12C double pass infrared spectrometer (LiF, CaF, NaCl, KBr, and CsBr optics) were used to obtain the spectra. Depolarization ratios were measured (7) and corrected for convergence error (16). The Raman spectra of liquid mixtures of *cis* and *trans* dibromoethylene were obtained at several temperatures between 0° and 85°C., the temperature variation of the *cis* $\rightleftharpoons$ *trans* equilibrium being sufficient over this range to enable the identification of the Raman bands of the *cis* and the *trans* species to be made. The spectra of the *cis*-enriched and the *trans*-enriched samples at room temperature made the identification unequivocal.

[1]*Manuscript received January 21, 1955.*
Contribution from the Division of Pure Chemistry, National Research Council, Ottawa. Issued as N.R.C. No. 3606.
[2]*National Research Council Postdoctorate Research Fellow, 1953–1955.*

Under conditions of optimum resolution with the NaCl prism it was possible to resolve only partially the rotational structure of the perpendicular a_u band of *trans* dibromoethylene at 899 cm^{-1}. Complications from hot bands may account for this.

Figs. 1, 2, and 3, respectively, illustrate the Raman spectrum of the liquid, the infrared spectra of the liquid and solution, and the infrared spectrum of the

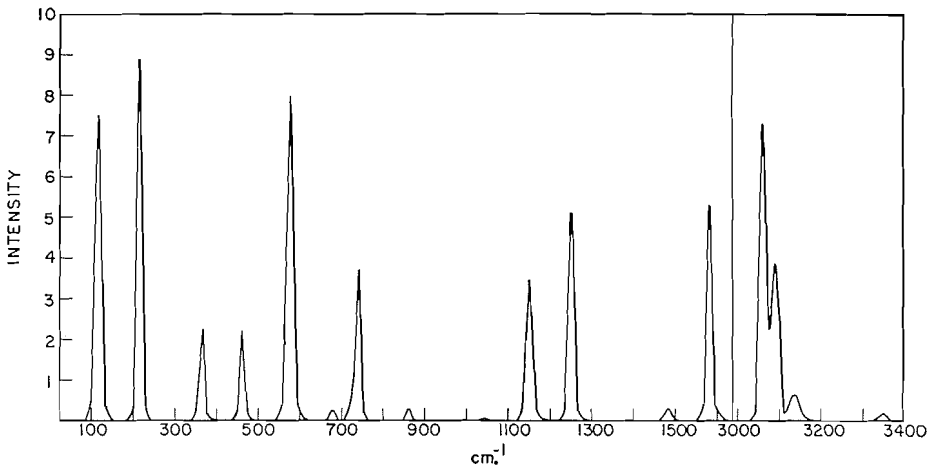

FIG. 1. Observed Raman spectrum of equilibrium mixture of *cis* and *trans* dibromoethylene at 27°C.

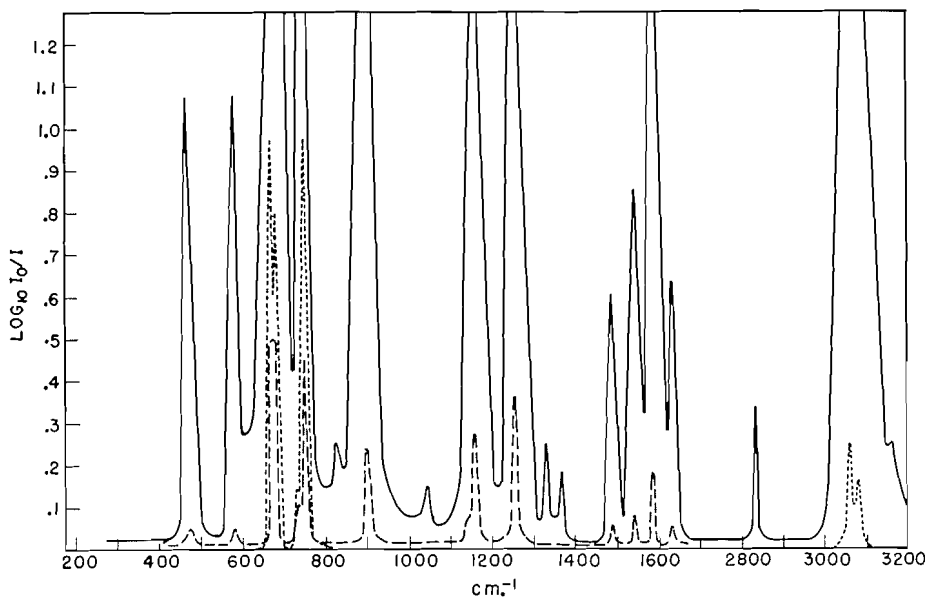

FIG. 2. Infrared spectrum of an equilibrium mixture of *cis* and *trans* dibromoethylene at 20°C.

——— 0.1 mm. liquid film; – – – – capillary liquid film; - - - - - - - ~1% solution in CS_2, 0.1 mm. cell.

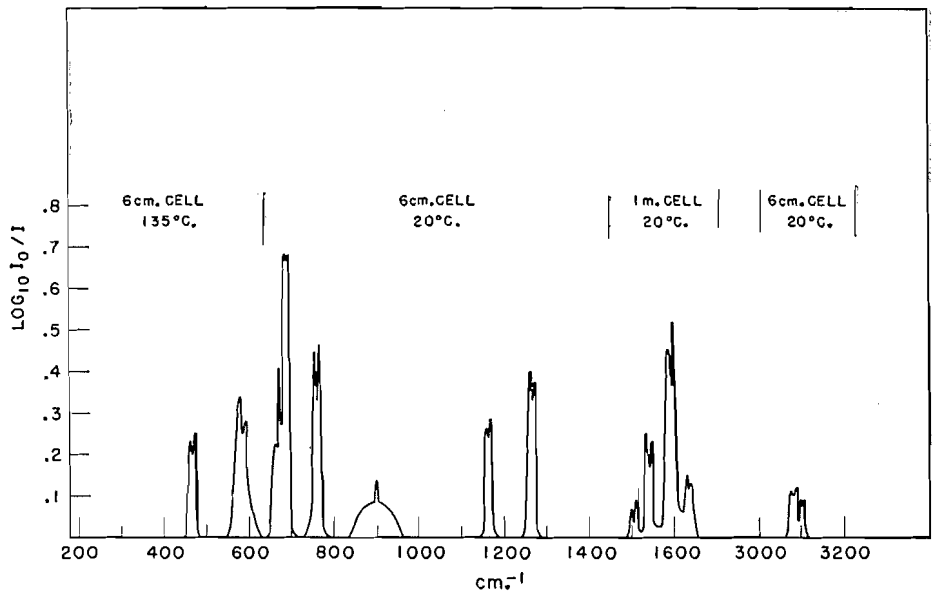

Fig. 3. Infrared spectrum of an equilibrium mixture of *cis* and *trans* dibromoethylene vapor spectrum.

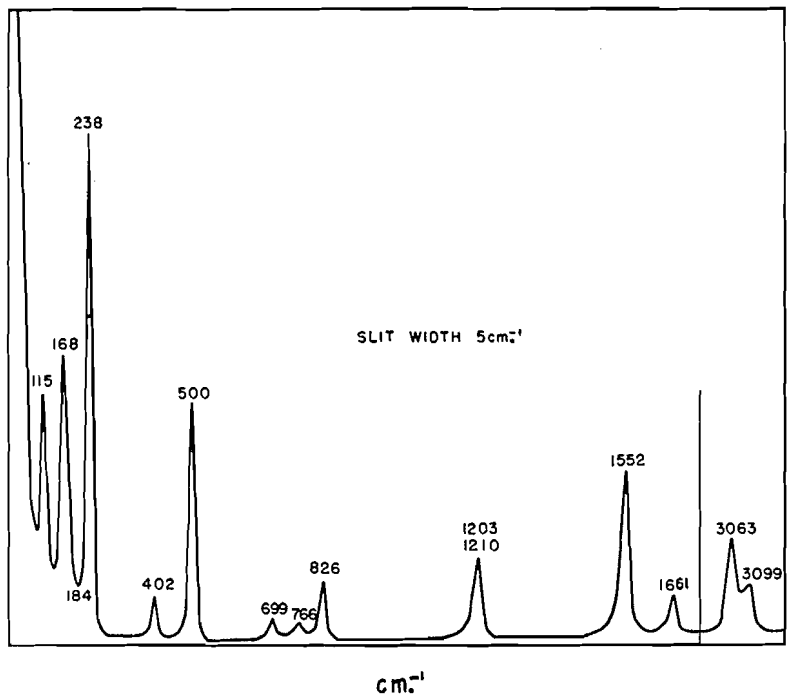

FIG. 4. Raman spectrum of liquid tribromoethylene.

vapor of the *cis–trans* dibromoethylene equilibrium mixture at room temperature. Tables I and II summarize the assignment for the *cis* and *trans* molecules.

Fig. 4, the Raman spectrum of liquid tribromoethylene, is a direct reproduction of a chart taken at high scanning speed, and some of the features which are obvious at slower scanning speeds are not apparent. Fig. 5 shows the infrared spectrum of tribromoethylene. Tables III and IV summarize the assignments of all the observed bands of tribromoethylene, while in Table V the assignments of the fundamental modes of tribromoethylene and trichloroethylene are compared.

TABLE I

INFRARED AND RAMAN FREQUENCIES FOR *cis* $C_2H_2Br_2$

Infrared		Raman		Assignment
Vapor	Liquid	cm.$^{-1}$	$\rho_{corr.}$	
	3161 w	3158 w	P	$2\nu_2 = 3170$ (A_1)
3084 3081 3076	3064 s			ν_8 (b_1)
		3061 s	~0.4	ν_1 (a_1)
	2826 w			$\nu_2+\nu_9 = 2839$ (B_1)
	2727 vw			$\nu_2+\nu_3 = 2735$ (A_1)
	2630 vvw			$2\nu_{10}+\nu_3 = 2646$ (A_1)
	2166 vw			$\nu_2+\nu_4 = 2165$ (A_1)
	2001 vvw			$\nu_9+\nu_{10} = 2002$ (A_1)
1595 1587 1584	1585 s	1581 s	P	ν_2 (a_1)
1543 1539 1535	1540 m			$\nu_6+\nu_{12} = 1533$ (B_1)
1508 1498	1489 m	1485 vw		$\nu_{10}+\nu_{10} = 1496$ (A_1)
	1369 w			$\nu_5+\nu_9 = 1372$ (B_1)
	1328 w			$\nu_4+\nu_{10} = 1328$ (B_1); $\nu_6+\nu_{11} = 1327$ (B_2)
1268 1264 1260	1254 s			ν_9 (b_1)
	1150 vw	1150 s	0.68	ν_3 (a_1)
	1044 vvw	1044 vw		$\nu_4+\nu_{11} = 1045$ (B_1); $\nu_7+\nu_{12} = 1038$ (B_1)
	867 vvvw			$\nu_5+\nu_{10} = 866$ (B_1)
		862 w	0.86	ν_6 (a_2)
	830 v			$\nu_7+\nu_{11} = 833$ (B_2)
762 757 753	748 vs			ν_{10} (b_1)
	738 sh. m.			$\nu_7+\nu_7 = 736$ (A_1)
679 670 662	670 vs	~670 w	0.86	ν_{12} (b_2)
590 577	580 s	580 vs	0.12	ν_4 (a_1)
471 ? 461	465 s	462 m	0.86	ν_{11} (b_1)
		368 m	0.86	ν_7 (a_2)
		118 vs	0.5	ν_5 (a_1)

TABLE II

INFRARED AND RAMAN FREQUENCIES FOR *trans* $C_2H_2Br_2$

Infrared		Raman (liquid)		Assignment
Vapor	Liquid	cm.$^{-1}$	$\rho_{corr.}$	
		3158 w	P	$2\nu_2 = 3162$ (A_g)
		3089 s	0.22	ν_1 (a_g)
3102, 3096	3081 s			ν_9 (b_u)
	2727 vw			$\nu_2+\nu_{10} = 2741$ (B_u)
	2396 vw			$\nu_3+\nu_{10} = 2411$ (B_u)
	1927 vw			$\nu_3+\nu_{11} = 1931$ (B_u)
	1905 sh. vvw			$\nu_4+\nu_{10} = 1903$ (B_u)
1636, 1629	1628 m.			$\nu_6+\nu_8 = 1635$ (B_u)
		1581 s	P	ν_2 (a_g)
		1251 s	0.30	ν_3 (a_g)
1166, 1160	1160 s			ν_{10} (b_u)
900(center)	899 vs			ν_6 (a_u)
		743 m	0.22	ν_4 (a_g)
		736 w	0.86	ν_8 (b_g)
691, 686	681(CS_2 sol.)	vs		ν_{11} (b_u)
		218 vs	0.39	ν_5 (a_g)

TABLE III

RAMAN SPECTRUM OF C_2HBr_3 (LIQUID)

cm.$^{-1}$	Corrected depolarization ratio	Intensity*	Assignment
3099	0.30	1.44	$2\nu_2 = 3100$ } Fermi resonance
3063	0.39	2.33	ν_1 } Fermi resonance
1661	0.30	0.41	$\nu_2+\nu_9 = 1667$
1640			$2\nu_4 = 1652$
1552	0.43	1.35	ν_2
1531	0.40	0.31	$2\nu_{10} = 1536$; $\nu_4+\nu_5 = 1533$ } Fermi resonance
1499			$\nu_5+\nu_5+\nu_9 = 1513$
1210	0.49	0.64	ν_3 } Fermi resonance
1203	0.49	0.64	$\nu_5+\nu_6$ } Fermi resonance
1176			$\nu_{10}+\nu_{11} = 1168$
826	0.48	0.26	ν_4
811 sh.			$2\nu_{11} = 808$; $\nu_5+\nu_9 = 814$
766	0.86	0.084	ν_{10}
699	0.17	0.12_5	ν_5
500	0.16	0.052	ν_6
469			$2\nu_7 = 476$
442		vvw	$2\nu_{12}+\nu_9 = 251$
402	0.86	0.050	ν_{11}
238	0.28	0.36	ν_7
184 sh.	0.69	0.025	ν_8
168	0.86	0.074	ν_{12}
115	0.61	0.031	ν_9

**Intensities quoted are the standard intensities relative to the CCl_4 band at 458 cm^{-1}. A correction for the reflection loss should be applied to these values. The method for determining these intensities has been described (3).*

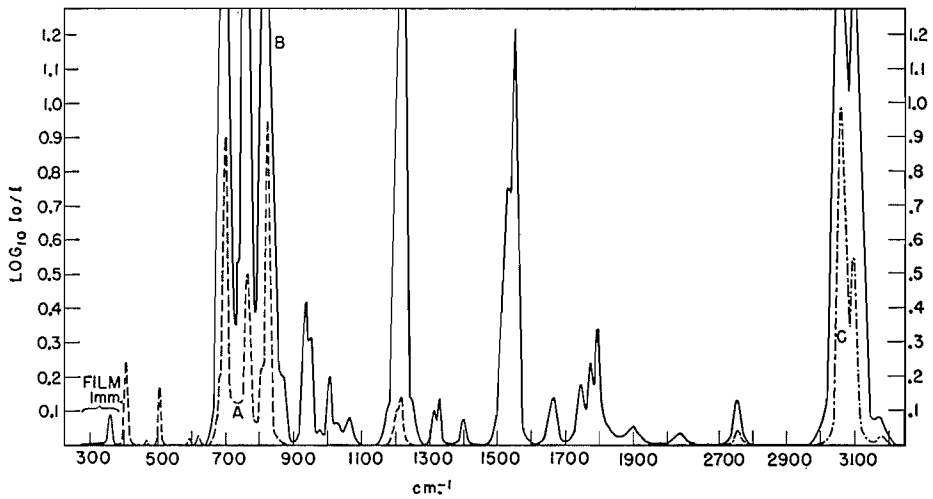

FIG. 5. Infrared spectrum of tribromoethylene.
A Capillary film of the liquid;
B 0.1 mm. film of the liquid;
C Capillary film of the liquid.

TABLE IV

INFRARED SPECTRUM OF C_2HBr_3

Liquid	Vapor	Assignment
3180 vw		$\nu_1+\nu_9 = 3178$
3101 vs		$2\nu_2 = 3100$ } Fermi resonance
3065		ν_1 }
2756 vw		$\nu_2+\nu_3 = 2765$
2037 vw		$\nu_3+\nu_4 = 2036$
1900 vw		$\nu_3+\nu_5 = 1910$
1796 w		$\nu_2+\nu_7 = 1793$
1775 w		$\nu_2+2\nu_9 = 1787$
1747 vw		$\nu_2+\nu_8 = 1739$
1665 w		$\nu_2+\nu_9 = 1672$
1557 m		ν_2
1538 m		$2\nu_{10} = 1536$; $\nu_4+\nu_5 = 1533$ } Fermi reso-nance
1401 vw		$\nu_5+\nu_5 = 1404$
1329 vw		$\nu_4+\nu_8 = 1331$
1318 vw		$\nu_3+\nu_9 = 1323$
1240 vvw sh.		$\nu_4+\nu_{11} = 1233$
1215 } s		ν_3 }
1206 }		$\nu_5+\nu_6 = 1205$ } Fermi resonance
1180 vvw sh.		$\nu_{10}+\nu_{11} = 1172$
1065 vw		$\nu_4+\nu_7 = 1066$
1030 vvw		$2\nu_{12}+\nu_5 = 1038$; $2\nu_{11}+\nu_7 = 1048$
1008 vw		$2\nu_5 = 1008$; $\nu_7+\nu_{10} = 1005$
		$\nu_4+\nu_8 = 1012$
977 vvvw		$\nu_6+2\nu_7 = 979$
952 w		$\nu_8+\nu_{10} = 951$
940 w		$\nu_4+\nu_9 = 943$; $\nu_{10}+\nu_{12} = 935$; $\nu_5+\nu_7 = 940$
870 vw sh.		$\nu_5+\nu_{12} = 870$; $\nu_9+\nu_{10} = 882$
829 vs	843 838	ν_4
814 w		$2\nu_{11} = 816$; $\nu_5+\nu_9 = 817$
768 s	776 771 766	ν_{10}
744 vw sh.		$\nu_6+\nu_7 = 741$
704 vs	711	ν_5
688 vw sh.		$\nu_6+\nu_8 = 687$
621 vw		$\nu_6+\nu_9 = 618$
593 vw		$\nu_8+\nu_{11} = 589$
506 m		ν_6
465 vw		$2\nu_7 = 476$
408 m		ν_{11}
364 vvw		$2\nu_8 = 368$

TABLE V

ASSIGNMENT OF THE FUNDAMENTAL MODES OF C_2HBr_3

		C_2HBr_3		C_2HCl_3[a]	
ν	Approximate description	Wave number	Corrected depolarization ratio	Wave number	Corrected depolarization ratio
1	ν_a' (CH)	f 3100, 3064	P	3080	P
2	ν_a' (C=C)	f 1555, 1535	P	1589	P
3	δ_a' (CH)	f 1212, 1204	P	1242	0.56
4	ν_a' (C—X)	828	0.48	932	0.65
5	ν_a' (C—X)	702	0.17	840	0.24
6	ν_a' (C—X)	503	0.16	628	0.16
7	a' skeletal	238	0.28	381	0.35
8	a' skeletal	184	0.69	274	0.77
9	a' skeletal	115	0.61	172	0.60
10	δ_a'' (CH)	767	0.86	780	0.86
11	a'' skeletal	402	0.86	450	0.86
12	a'' skeletal	168	0.86	211	0.86

f = Fermi resonance.
[a]*Allen, G. and Bernstein, H. J. Can. J. Chem. 32:1044. 1954.*

DISCUSSION

cis and trans Dibromoethylene

The assignments are consistent with the selection rules, the depolarization ratios, the vapor band contours,* and with the assignments for the corresponding chloroethylenes (5). The missing *trans* fundamentals, ν_7 and ν_{12}, lie beyond the CsBr prism limit but a rough estimate of their sum may be made from the vapor phase equilibrium data obtained by Noyes and Dickenson (14). For the equilibrium *cis* $\rightleftharpoons$ *trans*, these authors determined the heat of isomerization to be -130 ± 300 cal./mole. Assuming $\Delta E_0^\circ \approx 0\pm300$ cal./mole, and using the moments of inertia quoted in the footnote and the equilibrium constant at 158°C. of 0.98, it is found by a calculation analogous to that described for the chloroethylenes (5) that $\nu_7+\nu_{12} = 340\pm90$ cm^{-1}.

Another estimate of each missing frequency will be described below.

Tribromoethylene

The 12 fundamental modes are distributed between the symmetry species a' and a'' as $9a'+3a''$. The three depolarized Raman bands are assigned to the $3a''$ modes and, in the case of the highest and strongest ν_{10}, the infrared vapor band contour provides confirmation. The nine polarized a' modes fall readily into the approximate descriptions given in Table V.

**Assuming bond lengths for both cis and trans molecules: C=C = 1.34Å, C—Br = 1.84Å, C—H = 1.07Å, and all angles 120°, the following moments of inertia were determined: trans $I_A = 9.3$, $I_B = 1344$, $I_C = 1353$ gm. cm.$^2 \times 10^{-40}$ (approximates to a symmetric top); cis $I_A = 106$, $I_B = 679$, $I_C = 785$ gm. cm.$^2 \times 10^{-40}$; $S = -0.95$, $\rho = 5.6$ for the cis molecule(1).*

The Frequency Sum Rule

It has been shown that the frequency sum rule is applicable to the chloroethylenes (4) and that the five parameters of Table VI describe the relations between the sums adequately. Here n is the number of substituted halogen atoms in the series $C_2H_{4-n}H_n$. To apply the sum rule to the bromoethylenes

TABLE VI

n	Molecule	$\Sigma\nu$
0	C_2H_4	a
1	C_2H_3X	$a+b$
2	1 : 1—$C_2H_2X_2$	$a+2b+c$
2	*cis* $C_2H_2X_2$	$a+2b+d$
2	*trans* $C_2H_2X_2$	$a+2b+e$
3	C_2HX_3	$a+3b+c+d+e$
4	C_2X_4	$a+4b+2(c+d+e)$

the data given in Table VII have been used. Just as for the chloroethylenes the sum rule should apply to the in-plane modes and out-of-plane modes as well as for all the modes. In Table VIII the sums for *trans* dibromoethylene and C_2Br_4 have been calculated from the experimental sums for ethylene, vinyl bromide, *cis*- and *asym*-dibromoethylene and tribromoethylene. In this

TABLE VII

C_2H_4[a]	C_2H_3Br[b]	*cis* $C_2H_2Br_2$[c]	*trans*[c]	*asym*[d]	C_2HBr_3[c]	C_2Br_4[e]
In-plane						
3108	3103	3064	3089	3108	3070	1532
3106	3075	3060	3081	3023	1547	885
3020	3014	1581	1581	1593	1206	767
2990	1596	1254	1251	1373	826	631
1623	1370	1150	1160	1065	699	267
1443	1253	748	743	696	503	211
1342	1004	580	681	467	238	144
1236	601	465	218	322	184	—
810	348	118	—	184	115	—
Out-of-plane						
1027	942	862	899	886	766	464
949	906	670	736	688	402	—
943	583	368	—	405	168	—

[a]*Arnett, R. H. and Crawford, B. L. J. Chem. Phys. 18: 118. 1950; with the new value for* ν_5 (b_{1g}) *found by Stoicheff, B. P. J. Chem. Phys. 21: 755. 1953.*
[b]*Reference 6.*
[c]*This work.*
[d]*Reference 9.*
[e]*Reference 11.*

way $\nu_7(a_u)$ and $\nu_{12}(b_u)$ are calculated as 194 ± 63 cm.$^{-1}$ and 154 ± 130 cm.$^{-1}$ respectively for *trans* dibromethylene; $\nu_4+\nu_7 = 265\pm45$ cm.$^{-1}$ and $\nu_{10}+\nu_{12} = 303\pm100$ cm.$^{-1}$ are calculated for tetrabromoethylene. The quoted uncertainties are maximum values based on assuming an error of ±25 cm.$^{-1}$ in the sum of the 12 observed frequencies for each molecule.

TABLE VIII

	Total		In-plane		Out-of-plane	
	Calc.	Obs.	Calc.	Obs.	Calc.	Obs.
C_2H_4		21597[a]		18678[a]		2919[a]
C_2H_3Br		17795[b]		15364[b]		2431[b]
cis $C_2H_2Br_2$		13920[c]		12020[c]		1900[c]
asym		13810[d]		11831[d]		1979[d]
trans	13787[f]	13439[e]	11957[f]	11803[e]	1830[f]	1636[e]
	13730[g]	$+\nu_7+\nu_{12}$	11939[g]	$+\nu_{12}$	1791[g]	$+\nu_7$
C_2HBr_3		9730[e]		8394[e]		1336[e]
C_2Br_4	5467[f]	4900[e]	4738[f]	4435[e]	729[f]	464[e]
	5460[g]	$+\nu_4+\nu_7$	4750[g]	$+\nu_{10}+\nu_{12}$	710[g]	$+\nu_4+\nu_7$
		$+\nu_{10}+\nu_{12}$				

[a,b,c,d,e] *Same footnotes as in Table VII.*
[f] *From parametric equations.*
[g] *From linear plots.*

The frequency sum rule may be applied in a graphical manner and possibly less uncertain values may be obtained. From Table VI it is readily seen that the values of $\sum\nu$ for $n = 0$, 1, the average for $n = 2$, $n = 3$, and 4 lie on a parabola. The sums then for two homologous series such as the chloroethylenes $C_2H_{4-n}Cl_n$ and bromoethylenes $C_2H_{4-n}Br_n$ are given by two quadratic equations, viz.:

$$\sum\nu C_2H_{4-n}Cl_n = a+n\left(b-\frac{c+d+e}{6}\right)+n^2\left(\frac{c+d+e}{6}\right)$$

and

$$\sum\nu C_2H_{4-n}Br_n = a+n\left(b'-\frac{c'+d'+e'}{6}\right)+n_2\left(\frac{c'+d'+e'}{6}\right).$$

In general there will be a relation between $\sum\nu\ C_2H_{4-n}Cl_n$ and $\sum\nu\ C_2H_{4-n}Br_n$ of the type

$$\sum\nu\ C_2H_{4-n}Cl_n = A+B(\sum\nu\ C_2H_{4-n}Br_n)+C(\sum\nu\ C_2H_{4-n}Br_n)^2.$$

However, this will be linear if C, which is proportional to

$$[(c'+d'+e')/b']-[(c+d+e)/b],$$

is very small.

In the case of the above-mentioned series the three points corresponding to $n = 0$, 1, and 3 plotted for the sums of the chloro- and bromo-ethylenes lie within the experimental uncertainty on a straight line (Fig. 6). Similarly, straight lines are obtained from the plots of the in-plane and out-of-plane sums. Interpolation from the known value of the average of the sums of the three disubstituted chloroethylenes gives a value for the average of the three disubstituted bromoethylenes and extrapolation to the value for C_2Cl_4 allows the corresponding values for C_2Br_4 to be estimated.

In Table VIII the calculated sums for *trans* dibromoethylene and C_2Br_4 obtained from linear plots of corresponding sums are also shown. In Table IX

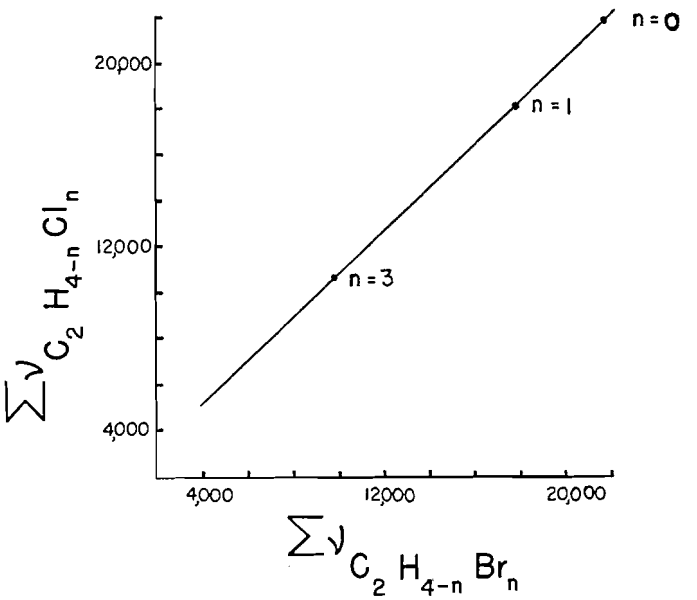

FIG. 6. Frequency sums (cm.$^{-1}$) of the chloro- and the bromo-ethylenes.

the calculated values for missing frequencies in these molecules have been collected. The usefulness of the sum rule for estimating low lying frequencies may be judged from the uncertainties for these values given in Table IX.

TABLE IX

CALCULATED MISSING FREQUENCIES

		From linear plots	From relations of Table VI	From equilibrium data	Mean value
trans $C_2H_2Br_2$	ν_7	154±30	194±63		164±50
	ν_{12}	135±94	154±130		145±110
	$\nu_7+\nu_{12}$	289±124	348±193	340±90	320±135
C_2Br_4	$\nu_4+\nu_7$	246±10[a]	265±45		255±40
	$\nu_{10}+\nu_{12}$	315±70[a]	303±100		309±100

[a] *Using the assignment for C_2Cl_4 given by Mann, Acquista, and Plyler (12). Somewhat different values are obtained if the assignment of Bernstein (2) is used.*

Thermodynamic Functions

The vibrational contributions were computed from tables by Miller, West, and Bernstein (13), while the formulae given by Rossini *et al.* (19) were used to determine the rotational and vibrational contributions. The moments of inertia of the dibromoethylenes have been quoted earlier. Using the same values for bond lengths and angles, the product of the moments of tribromoethylene was determined as $I_A I_B I_C = 1.210 \times 10^{-111}$ gm.^{3} cm^6.

TABLE X

CALCULATED THERMODYNAMIC FUNCTIONS

T	C_p°	S°	$-\frac{F^\circ - E_0^\circ}{T}$
C_2HBr_3 as an ideal gas			
300	20.51	85.69	70.94
400	22.79	91.92	75.43
500	22.44	97.18	79.27
600	25.68	101.76	82.65
cis $C_2H_2Br_2$ as an ideal gas			
300	16.53	75.80	64.07
400	19.17	80.93	67.65
500	21.17	85.43	70.77
600	22.71	89.44	73.55
trans dibromoethylene as an ideal gas			
300	17.00		
400	19.40		
500	21.30		
600	22.80		

The thermodynamic functions have been given for a few temperatures only since liquid data have been used for many of the vibrational frequencies. Furthermore, only C°_p was calculated for *trans* dibromoethylene since large uncertainties arise in calculating the other thermodynamic functions from the uncertainties in the values for ν_7 and ν_{12}. It may be shown numerically that for two modes ν_a and ν_b, the contribution to the vibrational heat capacity from ν_a plus the contribution from ν_b is very nearly equal to twice the contribution from $(\nu_a+\nu_b)/2$ (at the same temperature). The best estimate for $\nu_7+\nu_{12}$, 320 cm.$^{-1}$, was used in the computation, and the error in C°_p is determined by the error in estimating $\nu_7+\nu_{12}$.

The results for the three molecules are given in Table X.

The authors have appreciated helpful correspondence with Professor M. de Hemptinne who has been investigating the vibrational spectra of *cis* and *trans* dibromoethylene and their deuterated analogues at the same time as the present work was done.

REFERENCES

1. BADGER, R. M. and ZUMWALT, L. R. J. Chem. Phys. 17: 711. 1938.
2. BERNSTEIN, H. J. J. Chem. Phys. 18: 478. 1950.
3. BERNSTEIN, H. J. and ALLEN, G. J. Opt. Soc. Amer. 45:237. 1955.
4. BERNSTEIN, H. J. and PULLIN, A. D. E. J. Chem. Phys. 21: 2188. 1953.
5. BERNSTEIN, H. J. and RAMSAY, D. A. J. Chem. Phys. 17: 556. 1949.
6. CHARETTE, J. and DE HEMPTINNE, M. Bull. classe sci., Acad. roy. Belg. 38: 934. 1952.
7. EDSALL, J. T. and WILSON, E. B., JR. J. Chem. Phys. 6: 124. 1938.
8. EMSCHWILLER, G. and LECOMTE, J. J. phys. radium, 8: 130. 1937.
9. DE HEMPTINNE, M. Trans. Faraday Soc. 42: 7. 1946.
10. KOHLRAUSCH, K. W. F. Ramanspektren. J. W. Edwards, Ann Arbor, Michigan. 1943. Table 15, p. 127.
11. MALHERBE, F. E., ALLEN, G., and BERNSTEIN, H. J. Can. J. Chem. 31: 1223. 1953.
12. MANN, D. E., ACQUISTA, N., and PLYLER, E. K. J. Research Natl. Bureau Standards, 52: 67. 1954.

13. MILLER, E., WEST, K., and BERNSTEIN, H. J. Natl. Research Council Can. Bull. No. 1. 1951.
14. NOYES, R. M. and DICKINSON, R. G. J. Am. Chem. Soc. 65: 1427. 1943.
15. PRILEZHAEVA, E. N., SYRKIN, YA. K., and VOL'KENSHTEIN, M. V. Acta Physicochim. U.R.S.S. 12: 176. 1940.
16. RANK, D. H. and KAGARISSE, R. E. J. Opt. Soc. Amer. 40: 89. 1950.
17. TORKINGTON, P. J. Chem. Phys. 17: 1279. 1949.
18. VAN DER WALLE, H. Bull. soc. chim. Belges, 27: 209. 1913.
19. WAGMAN, D. D., KILPATRICK, J. E., TAYLOR, W. J., PITZER, K. S., and ROSSINI, F. D. J. Research Natl. Bureau Standards, 34: 143. 1945.
20. WHITE, J. U., ALPERT, N., and DeBELL, A. G. J. Opt. Soc. Amer. 45:154. 1955.

NOTES

THE SYNTHESIS OF ETHANOLAMINE-1-C^{14}

By D. E. Douglas and Anna Mary Burditt

Pilgeram *et al.* (4) have reported a synthesis of uniformly labelled ethanolamine-C^{14} from barium carbonate-C^{14} via acetylene and ethylene oxide, yielding di- and tri-ethanolamine as by-products.

We have synthesized ethanolamine-1-C^{14} from radiocyanide through the formation of (C^{14}-cyano)methyl benzoate (1, 3) and its subsequent reduction with lithium aluminum hydride to ethanolamine in 30% over-all yield. This method involves only two stages and yields solely primary amine. The reactions are as follows:

$$H_2O+HCHO+NaC^{14}N \rightleftarrows HOCH_2C^{14}N+NaOH$$

$$NaOH+HOCH_2C^{14}N+C_6H_5COCl \rightarrow C_6H_5COOCH_2C^{14}N+NaCl$$

$$C_6H_5COOCH_2C^{14}N \xrightarrow{LiAlH_4} C_6H_5CH_2OH+HOCH_2C^{14}H_2NH_2.$$

EXPERIMENTAL

(C^{14}-Cyano)methyl benzoate was prepared by the method of Aloy and Rabaut (1) on a semimicro scale as follows: To 0.154 gm. (2.9 mM.) of sodium cyanide-C^{14} (3.28×10^7 counts/min. total activity) in 0.5 ml. of water cooled in an ice-bath and stirred with a magnetic stirrer was added 0.24 ml. of 37% formalin (2.7 mM. of formaldehyde). After one hour, 0.30 ml. (2.6 mM.) of benzoyl chloride was added, and stirring at 0° C. continued three hours longer. After the addition of 3 ml. of 5% sodium bicarbonate, the reaction mixture was extracted continuously with ether for two to three hours. The ether extract was dried thoroughly, first over calcium chloride, then over Drierite.

The cyanomethyl benzoate was reduced without isolation by the gradual addition of the dried ether solution to 3.5 ml. of an ethereal solution of lithium aluminum hydride (approximately 2.6 mM. per ml.). The complex was decomposed by stirring with 30 ml. of water, added slowly, the ether was removed by evaporation, and the aqueous phase was saturated with carbon dioxide. The aluminum hydroxide was centrifuged off and washed thoroughly with several portions of hot water. The supernatant and washings were combined, 1 ml. of ethylene glycol monobutyl ether (2) and 5 ml. of 0.5 *N* sodium hydroxide added, and the ethanolamine and water removed by lyophilization and condensed into a trap cooled with dry ice – isopropyl alcohol. The residue remaining was taken up in water, 1 ml. of ethylene glycol monobutyl ether added, and lyophilization repeated. This process was carried out four times altogether. The ethanolamine was recovered as hydrochloride by evaporation

of the combined condensates from the cold trap with excess hydrochloric acid, and the salt recrystallized from isopropyl alcohol – ether. Yield: 0.0946 gm. (30.9%, based on sodium cyanide). The material was recrystallized for activity and melting point determinations. Specific activity: 132,000 counts per min. per mgm. Melting point: 79.8–82° C. Mixed melting point with authentic ethanolamine hydrochloride: 79.8–83° C.

Thirty-seven per cent of the initially added radiocyanide activity was found in the aqueous phase after ether extraction of the cyanomethyl benzoate.

To check the radiopurity, ethanolamine hydrochloride prepared by the above procedure was chromatographed on paper, with water-saturated phenol as the developing solvent. Radioautography indicated that the material was essentially free from radioactive contaminants. The R_f was 0.76.

1. ALOY, J. and RABAUT, C. Bull. soc. chim. France, (4) 13: 457. 1913.
2. HORSLEY, L. H. Anal. Chem. 21: 838. 1949.
3. MOWRY, D. T. J. Am. Chem. Soc. 66: 371. 1944.
4. PILGERAM, L. O., GAL, E. M., SASSENRATH, E. N., and GREENBERG, D. M. J. Biol. Chem. 204: 367. 1953.

RECEIVED DECEMBER 15, 1954.
DIVISION OF ATOMIC CHEMISTRY,
THE MONTREAL GENERAL HOSPITAL, RESEARCH INSTITUTE,
MONTREAL, P.Q.

A SELF PUMPING DROPPING MERCURY ELECTRODE FOR USE WITH STIRRED SOLUTIONS[1]

BY D. M. MILLER

The theory of polarography assumes the formation of a polarized layer around one electrode in an electrolysis cell. If through agitation of the solution this layer is disturbed the current passing through the cell is no longer diffusion dependent and the Ilkovic equation does not apply. Wilson and Smith (12) studied the effect of increasing flow rate of solution on the dropping mercury electrode (DME) and found first of all a deviation from diffusion controlled current and finally a complete disruption of the regular drop formation. By employing a slow rate of flow in a horizontal direction they were able to monitor continuously sulphur dioxide in industrial solutions by a polarographic method (13). This principle has been used by a number of workers (1, 11) while others have employed baffles (4, 5, 6, 7, 14) and some have even abandoned the ordinary DME in favor of the vibrating DME (2), or solid electrodes (3, 9, 10).

This paper describes a cell in which the DME is situated in a side arm and the solution is circulated past the electrode by the pumping action of the detached drops descending through a capillary. Basically the cell consists of a Lingane-Laitinen H cell (8) to which a side arm has been attached

[1]*Contribution No. 45, Science Service Laboratory, London, Ontario.*

of the combined condensates from the cold trap with excess hydrochloric acid, and the salt recrystallized from isopropyl alcohol – ether. Yield: 0.0946 gm. (30.9%, based on sodium cyanide). The material was recrystallized for activity and melting point determinations. Specific activity: 132,000 counts per min. per mgm. Melting point: 79.8–82° C. Mixed melting point with authentic ethanolamine hydrochloride: 79.8–83° C.

Thirty-seven per cent of the initially added radiocyanide activity was found in the aqueous phase after ether extraction of the cyanomethyl benzoate.

To check the radiopurity, ethanolamine hydrochloride prepared by the above procedure was chromatographed on paper, with water-saturated phenol as the developing solvent. Radioautography indicated that the material was essentially free from radioactive contaminants. The R_f was 0.76.

1. ALOY, J. and RABAUT, C. Bull. soc. chim. France, (4) 13: 457. 1913.
2. HORSLEY, L. H. Anal. Chem. 21: 838. 1949.
3. MOWRY, D. T. J. Am. Chem. Soc. 66: 371. 1944.
4. PILGERAM, L. O., GAL, E. M., SASSENRATH, E. N., and GREENBERG, D. M. J. Biol. Chem. 204: 367. 1953.

RECEIVED DECEMBER 15, 1954.
DIVISION OF ATOMIC CHEMISTRY,
THE MONTREAL GENERAL HOSPITAL, RESEARCH INSTITUTE,
MONTREAL, P.Q.

A SELF PUMPING DROPPING MERCURY ELECTRODE FOR USE WITH STIRRED SOLUTIONS[1]

BY D. M. MILLER

The theory of polarography assumes the formation of a polarized layer around one electrode in an electrolysis cell. If through agitation of the solution this layer is disturbed the current passing through the cell is no longer diffusion dependent and the Ilkovic equation does not apply. Wilson and Smith (12) studied the effect of increasing flow rate of solution on the dropping mercury electrode (DME) and found first of all a deviation from diffusion controlled current and finally a complete disruption of the regular drop formation. By employing a slow rate of flow in a horizontal direction they were able to monitor continuously sulphur dioxide in industrial solutions by a polarographic method (13). This principle has been used by a number of workers (1, 11) while others have employed baffles (4, 5, 6, 7, 14) and some have even abandoned the ordinary DME in favor of the vibrating DME (2), or solid electrodes (3, 9, 10).

This paper describes a cell in which the DME is situated in a side arm and the solution is circulated past the electrode by the pumping action of the detached drops descending through a capillary. Basically the cell consists of a Lingane-Laitinen H cell (8) to which a side arm has been attached

[1]*Contribution No. 45, Science Service Laboratory, London, Ontario.*

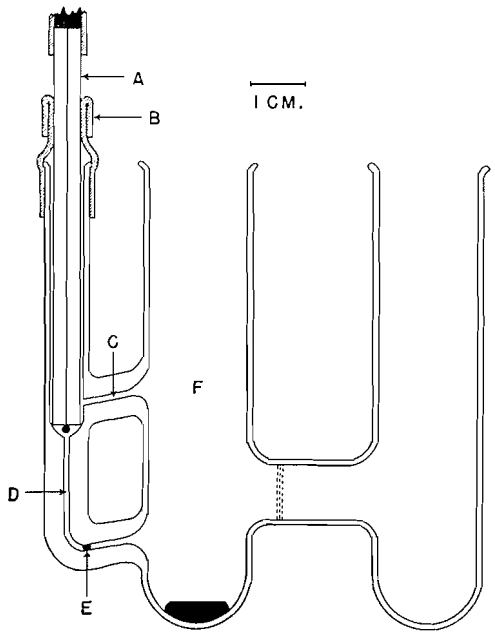

FIG. 1. Polarographic cell assembly.

as shown in Fig. 1. The DME capillary *A* is inserted through rubber tubing *B* into the top part of the side arm, the mercury drops falling into capillary *D*. The diameter of *D* is slightly smaller than that of the detached mercury drops (approximately one millimeter) so that the drop seals the capillary and forces the solution downward as it falls. This draws fresh solution into the side arm through *C* and because of the small volume of liquid in the side arm the solution is completely changed with every two or three drops. Each drop comes to rest at *E*, the lowest point in *D*, where it remains until forced out by the succeeding drop and thus temporarily seals the side arm against disturbances in the main body of the solution *F*. Since the drop descends to *E* in less than a second, the solution is in motion for only a short time at the beginning of each drop formation, and for drop times of four seconds or greater the effect on the polarogram is negligible.

To test the response of the DME to changes in solution composition, 10 ml. of a 0.1 *N* KCl solution saturated with air were placed in the cell and the polarogram recorded by a Sargent Model XXI Visible Recording Polarograph. The applied e.m.f. was constant at −0.75 v. vs. S.C.E., the sensitivity set at 0.030 μamp./mm., the damping switch in the off position, and the drop time 4.55 sec. The polarogram obtained under these and the following conditions is shown in Fig. 2. For the first minute the diffusion current due to oxygen is recorded. At point *L* a fritted glass gas dispersion tube was plunged into *F* and nitrogen bubbled through the solution at about 100 ml./min. The rapid drop in the oxygen concentration is indicated by the fall in the current between one and three minutes. Two drops of cadmium sulphate

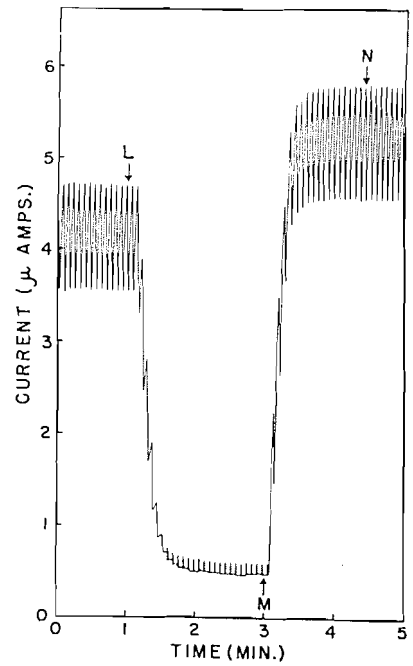

FIG. 2. Response of polarograph cell:
L—nitrogen bubbled through cell.
M—cadmium sulphate solution added.
N—bubbler withdrawn.

solution were introduced at *M* and the subsequent rise in current demonstrates a 98% response in 30 sec. following a change in concentration in *F*. At point *N* the dispersion tube was withdrawn with no visible effect on the polarogram.

The cell as depicted in Fig. 1 has proved very useful for general polarographic work. If clamped into a water bath and cleaned by suction it provides the added advantage that the position of the DME is fixed and reproducible. Certain precautions must be observed however in the building of this cell or design of other assemblies based on the same principle. The length of *C* must not be too great because of its high resistance (this was 1200 ohms in the cell used by the author with 0.1 *N* KCl as ground electrolyte). Further, the agitation in *F* must not be violent enough to cause vibration of the DME or to dislodge the mercury drop prematurely from its position at *E*. Actually, stirring by the means described here is preferable since it is thorough, smooth, and rapidly deoxygenates any added reagents. The DME is undisturbed by the gas flow, even to the point at which the solution foams over the top of the cell.

1. BECKMANN, P. Chemistry & Industry, 791. 1948.
2. BERMAN, D. A., SAUNDERS, P. R., and WINZLER, R. J. Anal. Chem. 23: 1040. 1951.
3. COOKE, W. D. Anal. Chem. 25: 215. 1953.
4. JURA, W. H. Anal. Chem. 26: 1121. 1954.
5. LAITINEN, H. A. and BURDETT, L. W. Anal. Chem. 22: 833. 1950.

6. LAITINEN, H. A., HIGUCHI, T., and CZUHA, M. J. Am. Chem. Soc. 70: 561. 1948.
7. LARCHAR, T. B. and CZUHA, M. Anal. Chem. 26: 1351. 1954.
8. LINGANE, J. J. and LAITINEN, H. A. Ind. Eng. Chem. Anal. Ed. 11: 504. 1939.
9. MARPLE, T. L. and ROGERS, L. B. Anal. Chem. 25: 1351. 1953.
10. MÜLLER, O. H. J. Am. Chem. Soc. 69: 2992. 1947.
11. SPOOR, W. A. Science, 108: 421. 1948.
12. WILSON, L. D. and SMITH, R. J. Anal. Chem. 25: 218. 1953.
13. WILSON, L. D. and SMITH, R. J. Anal. Chem. 25: 334. 1953.
14. WISE, W. S. Chemistry & Industry, 37. 1948.

RECEIVED FEBRUARY 7, 1955.
SCIENCE SERVICE LABORATORY,
CANADA DEPARTMENT OF AGRICULTURE,
UNIVERSITY OF WESTERN ONTARIO SUB POST OFFICE,
LONDON, ONTARIO.

Canadian Journal of Chemistry

Issued by THE NATIONAL RESEARCH COUNCIL OF CANADA

VOLUME 33 JULY 1955 NUMBER 7

THE NATURE OF THE INTERACTION FORCES BETWEEN PARTICLES IN SUSPENSIONS OF GLASS SPHERES IN ORGANIC LIQUID MEDIA[1]

BY P. G. HOWE,[2] D. P. BENTON,[2] AND I. E. PUDDINGTON

ABSTRACT

Electrostatic agglomeration can be induced in suspensions of glass beads in organic liquid media. The stability of the agglomerates is markedly dependent on temperature. The influence of surface roughness and the presence of small quantities of water on the interparticle interaction is discussed. Assuming a simple model the observed relationship between yield value and particle size for systems containing the same concentration of solid phase is derived.

INTRODUCTION

The behavior of suspensions of solids in liquid media is of considerable importance owing to the numerous practical applications of systems of this type which exhibit non-Newtonian behavior. Basically, the behavior of such a system is determined by the interparticle interaction, which is, in turn, determined by the nature and composition of the supporting medium. Suspensions of inert solids in organic liquids have been investigated by a number of workers (5, 12) and the presence of small amounts of water as an immiscible liquid has recently been shown to be of profound importance (9, 10).

Eggleton and Puddington (4) investigated the effect of temperature on suspensions of glass beads in toluene containing various amounts of water. Although the suspensions containing large amounts of water behaved as expected, showing a minimum yield value below the freezing point of water, the anhydrous suspension and that containing 0.1% water showed an unexpected and steady increase in sedimentation volume and yield value as the temperature was lowered to $-60°$ C. This work is concerned with a further investigation of this phenomenon and a consideration of other factors involved in systems of this type.

EXPERIMENTAL

Glass beads, -275 mesh, were supplied by the Flexolite Manufacturing Corporation. The beads were fractionated dry in a current of air by means of an Aminco Roller Particle Size Analyzer. A fraction of average diameter 41 μ

[1]*Manuscript received March 8, 1955.*
Contribution from the Division of Applied Chemistry, National Research Council, Ottawa, Canada. Issued as N.R.C. No. 3613.
[2]*N.R.L. Postdoctorate Fellow, 1953–55, National Research Council, Ottawa, Canada.*

was used in all experiments. Fig. 1 shows the distribution of bead sizes. This fraction was selected to conform with that of 43 μ obtained by Eggleton and Puddington by wet fractionation. The main impurity in the beads was a ferromagnetic dust, the bulk of which was removed by flowing the aqueous

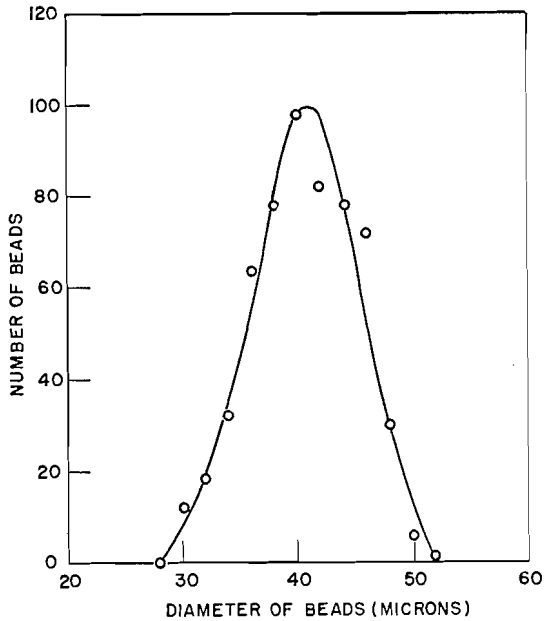

FIG. 1. Size distribution of glass beads.

suspension of beads through a glass tube placed between the poles of a powerful magnet. The beads were then cleaned in aqua regia and extracted with hot distilled water by decantation to remove acid. End washings were strongly alkaline and analysis of the supernatant liquor for Na and Ca showed considerable solution of the soft glass. It is possible that the glass beads used in similar work (4, 13) were considerably etched by solution of the glass. The beads were finally oven-dried before use.

The reagent grade organic liquids were purified as follows. Toluene was dried over calcium hydride and refluxed *in vacuo*. Chloroform was washed several times with distilled water, dried over silica gel, and refluxed *in vacuo*. Methyl alcohol was partially dried over calcium oxide, was distilled into a vacuum reservoir containing magnesium turnings, and after solution of the magnesium was degassed by refluxing *in vacuo*. The required amount of beads was weighed into a calibrated 12 mm. tube attached to the vacuum line. The glass beads were then baked out *in vacuo* at 350° C. until a stick vacuum in the McLeod gauge was obtained, and were allowed to cool. The required organic liquid was then further degassed by repeated distillation between two traps and finally distilled into the tube containing the beads. The tube was then immersed in liquid nitrogen and sealed off at a preformed constriction. A similar tube containing beads with no supporting liquid was also prepared.

Copper spheres, 100–200 mesh, were substituted for the glass spheres in one tube. These were reduced at 350° C. in an atmosphere of hydrogen and the water reaction product was frozen out in a liquid nitrogen trap. The system was then degassed at 350° C. and filled with toluene as described above.

RESULTS AND DISCUSSION

(*a*) *The Behavior of Glass and Copper Spheres in Anhydrous Media*

It was found that the sedimentation volume of the glass beads in toluene was a minimum (the same as for the beads *in vacuo*) and virtually independent of temperature, as long as the suspension was not subjected to too vigorous or sustained agitation. Observations were carried out in an air thermostat capable of regulation to 0.3° C. between room temperature and −60° C. Gentle agitation by inversion of the tube would eventually cause agglomeration and the time required was shortened to a few seconds by vigorous shaking. The maximum sedimentation volume so obtained (about 2 ml./gm. compared with about 0.67 ml./gm. minimum) also appeared to be independent of the temperature, but at room temperature the subsequent collapse of the settled agglomerate to the minimum volume was very rapid, whereas at lower temperatures the agglomerate appeared to be very stable and showed no tendency to collapse over periods of some six hours. Similar behavior was observed for the beads in chloroform but in methyl alcohol no increase in sedimentation volume was observed.

Gallay and Puddington (6) have shown that an attractive force between particles causes an increase in the sedimentation volume by preventing the close packing of the particles. It is apparent from the above observations that the agglomeration observed in the anhydrous toluene and chloroform is caused by the build-up of electrostatic charges which exert a strong attraction between the beads. The formation of the charges is probably owing to the collisions which take place between the beads during agitation or to the relative motion of the glass beads and the supporting liquid. The formation of electrostatic charges by the relative motion of two dielectrics is a well-known phenomenon. It appears that the presence of the liquid phase is important in that it allows for relative motion of the beads with respect to each other or to the liquid medium. The agitation of the glass beads *in vacuo* did not give any agglomeration since there is no resistance to flow.

The reduced copper spheres in anhydrous toluene showed no agglomeration at all from room temperature to −60° C. The resistance of the settled beads measured between two sealed-in tungsten electrodes about 1 cm. apart was less than 1 ohm. This value was obtained immediately after settling and did not alter with time of standing. An adsorbed layer of toluene would be expected to give an appreciably higher resistance since the resistance of the original oxide coated beads was of the order of 5 megohms.

The agglomeration of the glass beads in anhydrous toluene and chloroform and the absence of any such aggregation in anhydrous methanol can be considered in the light of the electrical conductivities of these liquids. Both toluene and chloroform are good dielectrics; toluene has a volume resistivity

of about 10^{-14} ohm-cm. whereas that of methanol is about 10^{-6}. No appreciable adsorption of toluene on glass would be expected but methanol should be chemisorbed and give a suitably conducting surface, thus preventing the formation of localized charge centers during agitation. At room temperature the surface conductance of the glass in toluene is apparently sufficient to cause a rapid collapse of the charged agglomerate.

It is surprising that the agglomerates are so stable at lower temperatures. At contact points the behavior of the liquid can be compared to that of a liquid in a capillary of molecular dimensions. The temperature coefficients of surface resistivity and of liquid viscosity in such a system are not known but are possibly of an order which will explain the observed properties. There is little doubt that adsorption energies and electroviscous forces in such a system are very high compared with normal bulk properties.

The copper beads in toluene showed no agglomeration, and in this case no *localized* charges are capable of existing on the surface of the bead. It should be noted that if the glass beads all possessed a uniform surface charge of the same sign, no agglomeration would be expected since the existence of a uniform surface potential would tend to stabilize a suspension by repulsion between the particles in the same way as an electrical double layer stabilizes aqueous suspensions. The glass beads may, however, possess *localized* surface charges all of the same sign, and agglomerate by electrostatic induction. Alternatively, the beads may possess both positive and negative localized surface charges which would cause the observed flocculation. The existence of a stable charge mosaic on the surface of glass has been suggested elsewhere (3).

The actual mechanism of the electrostatic agglomeration is important in connection with the stabilization of suspensions of inert materials in organic liquid media. Garner and co-workers (7) have shown that an electrical charge is present at the surface of particles of carbon black dispersed in organic liquids and that the particles may be either positive or negative according to the nature of the supporting medium. Toluene was found to give a negatively charged suspension and chloroform a positively charged one. It is possible that this phenomenon and that of the electrostatic agglomeration of the glass beads are related and the same basic phenomenon may cause both stabilization and agglomeration of a suspension according to the nature of the suspended material. When this is sufficiently conductive the charge will distribute itself over the whole surface and stabilization of the suspension will result. The stability of a double layer on a conducting particle of this type may be owing to the seat of the charge not being confined to the periphery of the solid but being smeared out throughout the whole particle. In the case of the glass suspensions, charges may be localized at points on the surface and the adsorption of oppositely charged solvent molecules could take place at other surface locations.

The electrostatic agglomeration of the beads is not affected by small amounts of water although this is more apparent below 0° C., when the water is frozen out on the beads. However, the indication is that the electrostatic behavior is inherent in such suspensions and is not owing to the presence of ionic im-

purities. Suspensions of various materials in organic and aqueous solutions in which the particles are capable of hydrogen bonding with the liquid medium are generally stabilized against flocculation (8). Thus, suspensions of copper sulphide in water and ether are stabilized by the addition of hydrogen sulphide which allows for such bonding to occur. Such bonding would also be expected in suspensions of glass beads in methanol and water and, in fact, these suspensions do not flocculate. However, it might also be expected that in such systems stabilization is brought about by the formation of a continuous double layer on the surface owing to the adsorption of one of the ionic dissociation products of the stabilizing medium.

(*b*) *Minimum Sedimentation Volumes*

The settled volumes of the glass spheres in various liquids are shown in Table I. The minimum volumes are the same in methanol, toluene, water, and

TABLE I

MINIMUM SEDIMENTATION VOLUMES OF GLASS SPHERES IN DIFFERENT LIQUIDS

Supporting medium	Sedimentation volume, ml./gm.		
	Settled under gravity	Tapped down while settling	Centrifuged
Water	0.67	0.67	0.67
Methanol	0.66	0.66	—
Vacuum	—	0.68	—
Toluene	0.67	0.67	—
Chloroform*	0.70	0.70	—

**Higher values in chloroform may be due to small amounts of decomposition products of the chloroform.*

in vacuo indicating that electrostatic agglomeration is absent. In all these cases it is to be noted that the minimum volume is well above that expected for a closest packing of the spheres and since the spheres cover a small but definite fraction range it would be expected that the close packed volume would be still smaller. Table II shows the void fraction for various theoretical types of packing (2) of uniform spheres.

Taking a density of 2.32 for soft glass and 0.67 ml./gm. as the minimum sedimentation volume observed, the calculated porosity is about 0.36. This lies between the orthorhombic and tetragonal-sphenoidal porosities and

TABLE II

THEORETICAL CLOSE PACKING OF PERFECT SPHERES (2)

Packing orientation	Porosity*	Contacts per sphere
Cubic	0.476	6
Orthorhombic	0.395	8
Tetragonal-sphenoidal	0.302	10
Rhombohedral	0.260	12

**Porosity = volume of void space per total volume.*

corresponds to about 9 contacts per sphere compared with the theoretical maximum of 12 contacts per sphere. This may well be the closest packing which can be obtained experimentally but no dilatancy is apparent and there is some evidence that all these suspensions possess a small residual yield value, which would prevent closer packing owing to the force of interaction between the beads. This might be due to a small London – van der Waals interaction between the beads.

(*c*) *The Influence of Water and Surface Roughness*

For suspensions of glass beads in toluene the results of Eggleton and Puddington show that the influence of the electrostatic effect is still apparent in the presence of small amounts of water below a certain concentration. The behavior of the beads with 0.1% water is the same as in the anhydrous suspensions between −60° C. and +30° C., but with 0.28% water only weak electrostatic forces are apparent below 0° C. This is probably owing to the surface roughness of the beads. Preferential adsorption of water would be expected in the surface depressions leaving the surface peaks exposed. Localized charge build-ups would then be able to take place at these peaks. This is in keeping with general electrostatic phenomena.

With 0.28% water the surface depressions will be filled leaving only a few high points exposed. Below 0° C. only weak electrostatic forces are present and the yield value is low. Above 0° C. enough of the surface is covered with water to allow some water necks to form between some of the beads, which causes the yield value to increase sharply. However, the yield value falls off quickly as the temperature is raised owing to the increasing solubility of water in the toluene. The small apparent residual yield value obtained with larger amounts of water below 0° C. might be attributed to a small residual electrostatic effect on a better conducting ice surface or, since surface discontinuities will have been smoothed out by filling the depressions with water, it might also be attributed to increased London – van der Waals forces.

The B.E.T. area of the water-etched beads was shown by Thompson (13) to be as much as 21 times the value for unetched beads. This corresponds to a monolayer coverage by about 0.04% water. At 0.28% water, where coverage is practically complete, about seven monolayers would appear to be sufficient to fill up the surface depressions. Assuming that the volume of the depressions is equal to the volume of the peaks, an approximate mean height of the surface peaks can be estimated as being equal to the thickness of a film of water composed of 14 monolayers, i.e., *ca.* 50 Å. This is probably a low estimate but indicates that the maximum surface irregularities may be of the order of 100 Å.

(*d*) *Yield Value of Suspensions Containing Water*

The high maximum yield value and the large sedimentation volumes of inert suspensions containing water immiscible with the organic liquid medium are owing to the formation of water "necks" between the particles. Bloomquist and Shutt (1) related the sedimentation volumes of glass spheres in various organic liquids to their interfacial tension against water. Those with the largest values gave the largest sedimentation volumes. Kruyt and van Selms (9,

10) found that the yield value of starch and quartz suspensions in organic liquids depended on the care taken in drying the materials and the amount of water subsequently added.

McFarlane and Tabor (11) have shown that the force between a bead and a plate owing to the neck of liquid between them is given by the expression

$$F = 4\pi R\gamma \cos\alpha \quad [1]$$

where F is the force in dynes, R the radius of the bead, γ the interfacial tension, and α the contact angle. The equation applies strictly only for small amounts of water and when the contact angle is very small, but, essentially, for small amounts of water the adhesion is independent of the amount of water in the neck. It has been observed by the present authors that as the water in the neck is increased to large amounts, the adhesion decreases somewhat.

For the adhesion between two spheres the same equation will hold where γ is the interfacial tension between water and the organic liquid. For quartz suspensions Kruyt and van Selms (9, 10) have shown that the yield value is constant over the range 2–12% water and then begins to fall off until the point is reached where the quartz and water separate out as a second phase. This behavior is consistent with that expected for the adhesion between the beads. Below 2% water, where the sigmoid characteristic of the yield value versus water content appears, several factors probably account for the shape of the curve. This could be influenced, for example, by the solubility of water in the organic liquid, the extent of adsorption of water from the organic liquid when below saturation, or the filling of surface discontinuities by water and the consequent continuous increase in neck formation up to the maximum possible.

Kruyt and van Selms also showed that for the same concentration of solid phase the maximum yield value is inversely proportional to the radius of the spheres. They arrived at a relationship between the yield value and the water content of the suspension by calculating the *work* required to separate a pair of glass beads with a known quantity of water in the neck joining them. Eggleton and Puddington noted that the yield value has the dimensions of a force, rather than of work, and that the adhesion between the beads is the important factor.

The observed proportionality between particle size and yield value can be derived by considering the following simple model. Systems in which the interparticle interaction is strong will form a continuous network in the supporting medium composed of chains of particles. The force required to break down this network and cause flow is the yield value of the suspension. Consider an ideal system of uniform spheres which interact strongly when supported in a liquid medium. Let a unit volume of the system contain x chains, each of which is composed of n spheres of radius r. For two such systems containing the same weight of solid but with spheres of radius r_1 and r_2, then the ratio of the total numbers of spheres in the two systems is given by

$$n_1x_1/n_2x_2 = r_2^3/r_1^3. \quad [2]$$

The ratio of the chain lengths is given by

[3] $$n_1 r_1 = n_2 r_2.$$

Combining equations [2] and [3] gives the ratio of the number of chains

[4] $$x_1/x_2 = r_2^2/r_1^2.$$

For any plane of the same area intersecting the volume element the number of chains cutting the plane will be Px where P is some constant allowing for the random orientation of the chains. Therefore, the ratio of the number of chains intersecting such a plane is given by

[5] $$Px_1/Px_2 = r_2^2/r_1^2.$$

The yield value θ is assumed to be proportional to the force across the plane, i.e., the force required to break all the chains intersecting the plane. The force F required to break any one chain will be the force between any two beads in the chain. From equation [1] it is seen that the maximum force between two beads of radius r with a connecting water neck is given by $F = 4\pi r\gamma \cos\alpha$, i.e., $F \propto r$. It follows therefore that

[6] $$\theta_1/\theta_2 = F_1 Px_1/F_2 Px_2 = r_2/r_1.$$

Thus for the same concentration of solid phase, the yield value is inversely proportional to the radius of the spheres, which is the experimentally observed proportionality.

REFERENCES

1. BLOOMQUIST, C. R. and SHUTT, R. S. Ind. Eng. Chem. 38: 827. 1940.
2. BROWN, G. G. (*Editor*). Unit operations. John Wiley & Sons, Inc., New York. 1950. p. 215.
3. DERJAGUIN, B. V. Discussions Faraday Soc. In press. September, 1954.
4. EGGLETON, A. E. J. and PUDDINGTON, I. E. Can. J. Chem. 32: 86. 1954.
5. FREUNDLICH, H. and RODER, H. L. Trans. Faraday Soc. 34: 511. 1938.
6. GALLAY, W. and PUDDINGTON, I. E. Can. J. Research, B, 21: 171. 1943.
7. GARNER, F. H., MOHTADI, M. F., and NUTT, C. W. J. Inst. Petroleum, 38: 974. 1952.
8. GLASMAN, U. M. *In* Report of the Federal Conference on Colloid Chemistry, Kiev, 1952. p. 349.
9. KRUYT, H. R. and VAN SELMS, F. G. Rec. trav. chim. 62: 407. 1943.
10. KRUYT, H. R. and VAN SELMS, F. G. Rec. trav. chim. 62: 415. 1943.
11. MCFARLANE, J. S. and TABOR, D. Proc. Roy. Soc. (London), A, 202: 224. 1950.
12. OSTWALD, W. and HALLER, W. Kolloid-Beih. 29: 354. 1929.
13. THOMPSON, J. B., WASHBURN, E. R., and GUILDNER, L. A. J. Phys. Chem. 56: 979. 1952.

THE REACTION OF NITRAMINES WITH HYDROCHLORIC ACID[1]

By A. F. McKay, W. G. Hatton, and M. Skulski

ABSTRACT

A facile process for the conversion of N-(β-nitraminoethyl)-N′-substituted-N″-nitroguanidines into the reactive N-(β-chloroethyl)-N′-substituted-N″-nitroguanidines has been developed. N-(β-Nitraminoethyl)-N′-phenyl-N″-nitroguanidine on standing in concentrated hydrochloric acid solution gives a mixture of N-(β-chloroethyl)-N′-phenyl-N″-nitroguanidine and 1-nitro-2-phenylamino-2-imidazoline. N-(β-Chloroethyl)-N′-diethyl-N″-nitroguanidine, which is prepared in a similar manner, is unstable at room temperature and it slowly cyclizes to give 1-nitro-2-diethylamino-2-imidazoline. Some new nitroguanidine derivatives formed from the reaction of amines with methylnitrosonitroguanidine also are described.

It was previously (2) shown that alkyl nitramines in dilute acid solutions decomposed to give alkyl cations. Thus methylnitramine in dilute hydrochloric acid solution gave a 50% yield of methyl chloride from the reaction of the intermediate methyl cation with the chloride ion. The mechanism of this reaction indicated the possibility of substituting the chloro group for a nitramino group in good yield by treating an aliphatic nitramine with an excess of concentrated hydrochloric acid. This assumption was realized (8) with N-β-nitraminoethyl-N′-nitroguanidine on treatment with concentrated hydrochloric acid when a 92.6% yield of the expected N-β-chloroethyl-N′-nitroguanidine was obtained. Since this reaction provided a simple method of obtaining the reactive and highly substituted N-β-chloroethyl-N′-nitroguanidines, it was investigated further.

N-(β-Nitraminoethyl)-N′-phenyl-N″-nitroguanidine (I) in concentrated hydrochloric acid solution gave a 74.2% yield of N-(β-chloroethyl)-N′-phenyl-N″-nitroguanidine (III). The filtrate after neutralization in the cold with sodium hydroxide solution gave a 20.4% yield of 1-nitro-2-phenylamino-2-imidazoline (or the tautomeric 1-nitro-2-phenyliminoimidazolidine) (IV). These products are easily explained on the basis of the formation of an intermediate alkyl cation II as shown below. The similarity of the reactions depicted here to those previously outlined for the reaction of acetyl chloride with N-(β-nitraminoethyl)-N′-substituted-N″-nitroguanidines (4, 7, 9, 10) will be apparent. As stressed before (7) the main reason for the complexity ascribed to some of the acetyl chloride – nitramine reactions was the variety of products isolated. Some of these products undoubtedly arose from secondary reactions during the involved isolation procedures. The products from the reaction of the N-(β-nitraminoethyl)-N′-substituted-N″-nitroguanidine with concentrated hydrochloric acid solution can be separated with ease, which eliminates this difficulty.

The structure of N-(β-chloroethyl)-N′-phenyl-N″-nitroguanidine (III) was

[1]*Manuscript received March 21, 1955.*
Contribution from Defence Research Chemical Laboratories, Ottawa, Ontario, and L. G. Ryan Research Laboratory of Monsanto Canada Limited, Ville LaSalle, Quebec. Issued as D.R.C.L. Report No. 140.

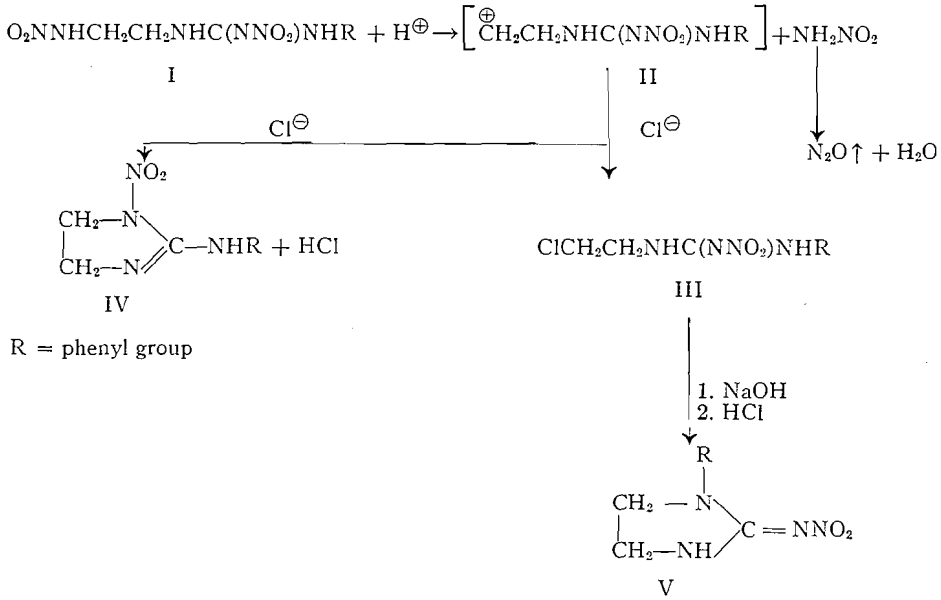

confirmed by its infrared spectrum and by its conversion to the known 1-phenyl-2-nitriminoimidazolidine (V) (12). 1-Phenyl-2-nitriminoimidazolidine was previously (12) referred to as the tautomeric 1-phenyl-2-nitramino-2-imidazoline. The reason for this change in nomenclature has been discussed recently (13).

A more highly substituted compound N-(β-nitraminoethyl)-N′-diethyl-N″-nitroguanidine also was allowed to stand at room temperature in hydrochloric acid solution. The product from this reaction melted at 96–97° C. and it was identified as N-(β-chloroethyl)-N′-diethyl-N″-nitroguanidine by analysis and by its chemical properties. When N-(β-chloroethyl)-N′-diethyl-N″-nitroguanidine was heated with water it cyclized to 1-nitro-2-diethylamino-2-imidazoline. The latter compound was isolated as its picrate. On standing in a vial the crystalline N-(β-chloroethyl)-N′-diethyl-N″-nitroguanidine changed into a viscous oil with entrained gas bubbles. This oil was dissolved in water and then treated with a saturated solution of picric acid. A 69% yield of 1-nitro-2-diethylamino-2-imidazolinium picrate was obtained. Thus the original crystalline N-(β-chloroethyl)-N′-diethyl-N″-nitroguanidine cyclized on standing at room temperature. The presence of gas bubbles in the viscous oil suggests that some decomposition also occurred.

Some new nitroguanidine derivatives have been prepared by the reaction of amines with methylnitrosonitroguanidine (6, 14). These are described in the Experimental section.

EXPERIMENTAL[2]

N-Methyl-N-nitroso-N′-nitroguanidine

This compound (m.p. 118° C. with decomp.) was prepared as previously described (11).

[2]*All melting points were taken on a Kofler block. Microanalyses by Micro-Tech Laboratories, Skokie, Illinois.*

N-Acetyl Ethylenediamine

N-Acetyl ethylenediamine was prepared by the method of Hill and Aspinall (1, 5). Ninety-five per cent ethylenediamine (570 gm., 9.0 moles) was mixed with 264 gm. (3.0 moles) of ethyl acetate and left at room temperature for eight days. The ethyl alcohol and excess amine were removed by distillation *in vacuo*. The residue on distillation *in vacuo* gave 233.3 gm. (69.9%) of N-acetyl ethylenediamine, b.p. 99–103° C. (0.5 mm.). This distillate soon solidified after which it melted at 49.5° C. The melting point given in the literature (5) is 51° C. The residual solid (62.6 gm.) in the distillation flask melted sharply at 173–174.5° C. after one crystallization from 95% ethanol (2.4 cc./gm.). A melting point of 175° C. is given in the literature (5) for N,N′-diacetyl ethylenediamine.

N-(β-Acetylaminoethyl)-N′-nitroguanidine

To 32.7 gm. (0.032 mole) of monoacetylethylenediamine in 35 cc. of water was added portionwise 15.7 gm. (0.0107 mole) of methylnitrosonitroguanidine over a period of 25 min. During the addition period the temperature was held at 22–27° C. A creamy-white solid separated which was removed by filtration and washed with water, yield 11.24 gm. (56.2%). One crystallization from 95% ethanol (9 cc./gm.) raised the melting point from 134° C. to 150.5–151.5° C. Calc. for $C_5H_{11}N_5O_3$: C, 31.75; H, 5.82; N, 37.03%. Found: C, 31.54; H, 5.87; N, 37.28%.

Monocarbethoxyethylenediamine

Monocarbethoxyethylenediamine (b.p. 135–137°C. (23 mm.); ($n_D^{24.8}$ 1.455; $d_4^{24.8}$ 1.029) was prepared in 40% yield by the method of Moore *et al.* (15).

N-(N-Carbethoxy-β-aminoethyl)-N′-nitroguanidine

To 7.5 gm. (0.0568 mole) of monocarbethoxyethylenediamine in 30 cc. of water was added gradually with stirring 2.79 gm. (0.019 mole) of methylnitrosonitroguanidine over a period of 32 min. During the addition period and an additional half hour of stirring, the temperature was held at 30–35° C. The white solid (m.p. 165.0° C.) was removed by filtration and washed with water, yield 3.34 gm. (80.2%). One crystallization from absolute ethanol (44.3 cc./gm.) raised the melting point to 165.5° C. Calc. for $C_6H_{13}N_5O_4$: C, 32.88; H, 5.93; N, 31.96%. Found: C, 33.05; H, 6.22; N, 32.22%.

N-(β-Nitraminoethyl)-N′-diethyl-N″-nitroguanidine

Five grams (0.029 mole) of 1-nitro-2-nitriminoimidazolidine were covered with 20 cc. of diethylamine and then allowed to stand at room temperature for three days. This reaction mixture was acidified and then placed in the refrigerator for two days. The crystals were removed by filtration and washed with ether and ethanol, yield 3.05 gm. (43.1%). Two crystallizations from 95% ethanol raised the melting point from 133–135° C. with decomposition to 152.5° C. with decomposition. The Franchimont test using dimethylaniline was negative. Calc. for $C_7H_{16}N_6O_4$: C, 33.85; H, 6.45; N, 33.85%. Found: C, 33.86; H, 6.48; N, 33.81%.

N-(β-Nitraminoethyl)-N'-phenyl-N''-nitroguanidine

N-(β-Nitraminoethyl)-N'-phenyl-N''-nitroguanidine (m.p. 139.5–140.5° C.) was prepared in 96% yield as previously described (10).

Reaction of N-(β-Nitraminoethyl)-N'-phenyl-N''-nitroguanidine with Hydrochloric Acid Solution

N-(β-Nitraminoethyl)-N'-phenyl-N''-nitroguanidine (4.97 gm., 0.018 mole) was suspended in 10 cc. of concentrated hydrochloric acid solution and left at room temperature for 48 hr. After the reaction mixture was diluted with 10 cc. of water, it was placed in the refrigerator for 12 hr. The crystals (m.p. 101–102° C., resolidified at 112° C. and then decomposed at 160–163° C.) were removed by filtration and washed with water, yield 3.245 gm. (74.2%). Two crystallizations from methanol at room temperature by the addition of water increased the melting point to 112–113° C. with resolidification at 117–118° C. and decomposition at 160–163° C. Calc. for $C_9H_{11}Cl\,N_4O_2$: C, 44.54; H, 4.56; Cl, 14.62; N, 23.09%. Found: C, 44.75; H, 4.65; Cl, 14.92; N, 22.80%. This product possessing a double melting point was further identified as N-(β-chloroethyl)-N'-phenyl-N''-nitroguanidine by cyclization to the known 1-phenyl-2-nitriminoimidazolidine (12). N-(β-Chloroethyl)-N'-phenyl-N''-nitroguanidine (500 mgm., 0.002 mole) was refluxed for one minute with 117 mgm. (0.0027 mole) of potassium hydroxide in 2 cc. of 95% methanol. On cooling, colorless crystals (m.p. 164–168° C.) separated, yield 394 mgm. (92.7%). One crystallization from 95% methanol raised the melting point to 168–168.5° C. The melting point was unchanged on admixture with an authentic sample of 1-phenyl-2-nitriminoimidazolidine (m.p. 168–169° C.).

The mother liquor from the N-(β-chloroethyl)-N'-phenyl-N''-nitroguanidine gave 140 mgm. of the original N-(β-nitraminoethyl)-N'-phenyl-N''-nitroguanidine (m.p. 138–139° C.). The latter compound was identified by a mixed melting point determination with an authentic sample of N-(β-nitraminoethyl)-N'-phenyl-N''-nitroguanidine (m.p. 139.5–140.5° C.).

The original filtrate from the first crop of crystals on neutralization with 10% sodium hydroxide solution gave 602 mgm. (20.45%) of crystals (m.p. 129–130° C.). One crystallization from ethanol raised the melting point to 138–139° C. (m.p. 132.5–133.5° C. by the capillary method). This compound gave a deep green color with dimethylaniline in the Franchimont test (3). Calc. for $C_9H_{10}N_4O_2$: C, 52.42; H, 4.89; N, 27.17%. Found: C, 52.49; H, 4.99; N, 27.00%. This compound gave a picrate (m.p. 146–147° C.) when treated in the usual manner, yield 80.5%. This picrate was identified as 1-nitro-2-phenylamino-2-imidazolinium picrate by a mixed melting point determination with an authentic sample (10).

Reaction of N-(β-Nitraminoethyl)-N'-diethyl-N''-nitroguanidine with Hydrochloric Acid Solution

N-(β-Nitraminoethyl)-N'-diethyl-N''-nitroguanidine (5.0 mgm., 0.020 mole) was covered with 15 cc. of concentrated hydrochloric acid solution and left at room temperature for 19 hr. The clear solution was diluted with one volume of water and then placed in the refrigerator for several hours. During neutral-

ization of the cold solution with 10% sodium hydroxide solution, colorless crystals separated, yield 2.53 gm. (53.51%). Another 534 mgm. (total yield 66.39%) of crystalline material was obtained from the mother liquor on evaporation. The melting point (96–97° C.) of the crude material was not changed by crystallization from absolute methanol. Calc. for $C_7H_{15}ClN_4O_2$: C, 37.76; H, 6.74; Cl, 15.94; N, 25.18%. Found: C, 38.02; H, 6.66; Cl, 16.15; N, 25.00%.

A sample (377 mgm., 0.0015 mole) of this N-(β-chloroethyl)-N′-diethyl-N″-nitroguanidine was converted to 1-nitro-2-diethylamino-2-imidazoline by refluxing for 15 min. with 10 cc. of water. The aqueous solution on addition of a saturated aqueous picric acid solution gave a yellow picrate, yield 337 mgm. (47.9%). The picrate melted at 128.5° C. Calc. for $C_{13}H_{17}N_7O_9$: C, 37.58; H, 4.12; N, 23.60%. Found: C, 37.43; H, 4.01; N, 23.20%.

The crystalline N-(β-chloroethyl)-N′-diethyl-N″-nitroguanidine changed into a viscous liquid containing gas bubbles on standing for a few weeks at room temperature. A sample (207 mgm., 0.0009 mole) of this oil gave a 69.9% yield of the picrate melting at 128.5° C. on treatment with an alcoholic solution of picric acid. This picrate did not depress the melting point of the above-described picrate of 1-nitro-2-diethylamino-2-imidazoline.

REFERENCES

1. ASPINALL, S. R. J. Am. Chem. Soc. 63: 852. 1941.
2. BARROTT, J., DENTON, I. N., and LAMBERTON, A. H. J. Chem. Soc. 1998. 1953.
3. FRANCHIMONT, A. P. N. Rec. trav. chim. 16: 213. 1897.
4. HALL, R. H. and WRIGHT, G. F. J. Am. Chem. Soc. 73: 2208. 1951.
5. HILL, A. J. and ASPINALL, S. R. J. Am. Chem. Soc. 61: 822. 1939.
6. McKAY, A. F. J. Am. Chem. Soc. 71: 1968. 1949.
7. McKAY, A. F. Chem. Revs. 51: 301. 1951.
8. McKAY, A. F. J. Am. Chem. Soc. 77: 1057. 1955.
9. McKAY, A. F. and HATTON, W. G. J. Am. Chem. Soc. 75: 963. 1953.
10. McKAY, A. F., HATTON, W. G., and TAYLOR, G. W. J. Am. Chem. Soc. 75: 1120. 1953.
11. McKAY, A. F., OTT, W. L., TAYLOR, W. G., BUCHANAN, M. N., and CROOKER, J. F. Can. J. Research, B, 28: 683. 1950.
12. McKAY, A. F., PARK, W. R. R., and VIRON, S. J. J. Am. Chem. Soc. 72: 3659. 1950.
13. McKAY, A. F., WEINBERGER, M. A., PICARD, J. P., HATTON, W. G., BEDARD, M., and ROONEY, H. E. J. Am. Chem. Soc. 76: 6371. 1954.
14. McKAY, A. F. and WRIGHT, G. F. J. Am. Chem. Soc. 69: 3028. 1947.
15. MOORE, T. S., BOYLE, M., and THORN, V. M. J. Chem. Soc. 39. 1929.

THE STRUCTURE OF MONO-*O*-METHYLENE- AND DI-*O*-METHYLENE-D-GLUCOSE[1]

By W. P. Shyluk, John Honeyman, and T. E. Timell

ABSTRACT

The structure of 1,2-*O*-methylene-α-D-glucofuranose has been proved by preparing the 3,5,6-trimethanesulphonate and the 3,5,6-tri-*p*-toluenesulphonate derivatives of this compound from the corresponding derivatives of 1,2-*O*-isopropylidene-α-D-glucofuranose. The results also constitute an additional proof for the recently established structure of the 1,2;3,5-di-*O*-methylene-α-D-glucofuranose.

Brownell (1), who was interested in proving the structure of di-*O*-methylene-D-glucose, obtained by its partial hydrolysis a crystalline, non-reducing mono-*O*-methylene-D-glucose. Before his work was completed, however, Schmidt, Distelmaier, and Reinhard (5) established the constitution of the di-*O*-methylene derivative. The present study of the structure of mono-*O*-methylene-D-glucose also confirmed that for the di-*O*-methylene derivative deduced by Schmidt *et al.*

The presence of a furanose ring and the location of the methylene group in the 1,2-position in mono-*O*-methylene-D-glucose were shown by the following reaction sequence. Treatment of 1,2-*O*-isopropylidene-α-D-glucofuranose[2] (I) with methanesulphonyl chloride gave the trimethanesulphonate (II), which had previously been prepared by Helferich and Gnüchtel (2). The isopropylidene group was replaced by a methylene group giving 1,2-*O*-methylene-α-D-glucofuranose 3,5,6-trimethanesulphonate (III), identical with the compound obtained by esterification of mono-*O*-methylene-α-D-glucofuranose (IV). Similarly, 1,2-*O*-isopropylidene-α-D-glucofuranose was converted into 1,2-*O*-methylene-α-D-glucofuranose 3,5,6-tri-*p*-toluenesulphonate, also obtained directly from mono-*O*-methylene-D-glucose.

The above results also prove the structure of the di-*O*-methylene-D-glucose. Hough, Jones, and Magson (3) have shown that the hydroxyl group on C_6 is free. Since one methylene group is in the 1,2-position and there is a furanose ring, the second methylene group must be in the 3,5-position.

Ohle and Wilcke (4) prepared the 3,5,6-tri-*p*-toluenesulphonate from 1,2-*O*-isopropylidene-α-D-glucofuranose and from its 3-*p*-toluenesulphonate in 15 and 30% yields, respectively. In the present study, preparation of the tri-*p*-toluenesulphonate has been found to present no inherent difficulty, since direct esterification of 1,2-*O*-isopropylidene-α-D-glucofuranose gave the triester in a yield of 82% after one recrystallization from ethanol.

EXPERIMENTAL

1,2;3,5-Di-O-methylene-α-D-glucofuranose

Di-*O*-methylene-D-glucose was obtained by deacetylation with barium methylate in methanol of the di-*O*-methylene-D-glucose 6-acetate, which was

[1]*Manuscript received March 25, 1955.*
Contribution from the Division of Industrial and Cellulose Chemistry, McGill University, and the Wood Chemistry Division, Pulp and Paper Research Institute of Canada, Montreal, Quebec.
[2]*The more likely α configuration is assumed throughout.*

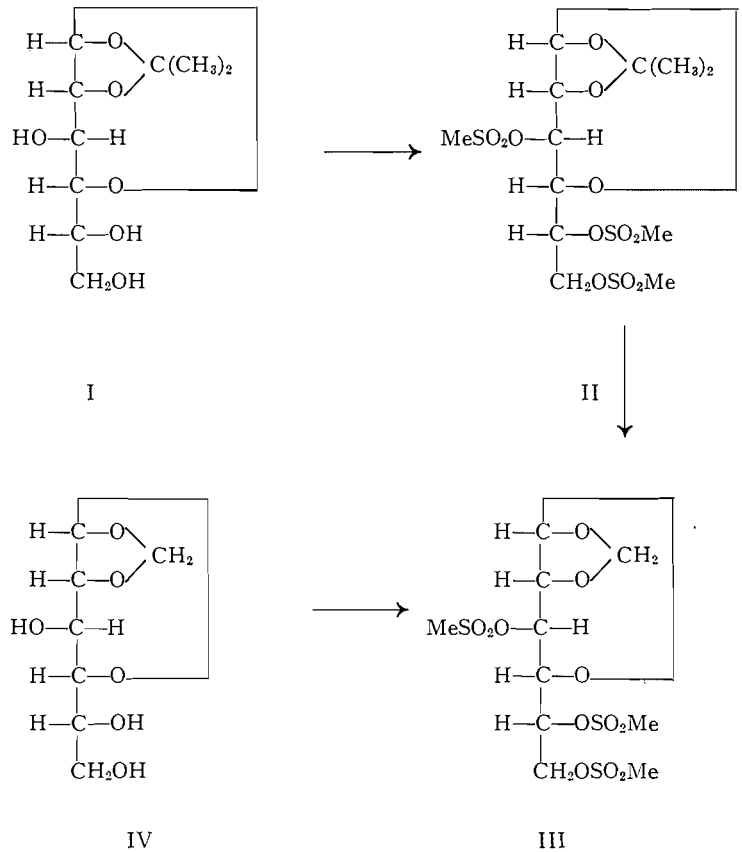

prepared according to the method of Hough *et al.* (3). The sirup was crystallized and its melting point and specific rotation were identical with those reported by Schmidt *et al.* (5).

1,2-O-Methylene-α-D-glucofuranose

A solution of 1,2;3,5-di-*O*-methylene-α-D-glucofuranose, 13.0 gm., in 2.0% aqueous hydrochloric acid, 175 ml., was kept at 100° C. for one hour, then deacidified by passage through a column of anion exchange resin (Amberlite IR-4B) and evaporated *in vacuo* to 42 ml. The neutral solution was extracted eight times with 70-ml. portions of ethyl acetate and evaporated *in vacuo* to a sirup, 2.73 gm. Glucose was removed by fermentation of its aqueous solution with baker's yeast for 36 hr. at 30° C., after which Super-Cel was added and the mixture was filtered. The clear filtrate was deionized with Amberlite IR-4B and Amberlite IR-120 exchange resins and concentrated *in vacuo* to a sirup, 1.95 gm., which partly crystallized on standing. The crystalline material weighed 0.24 gm. and melted at 145–146° C. Recrystallization from 1.5 ml. of ethanol gave pure 1,2-*O*-methylene-α-D-glucofuranose, m.p. 147–148° C., $[\alpha]_D^{22}$ −6.2° (*c*, 1.2 in water). Calc. for $C_7H_{12}O_6$: C, 43.8; H, 6.30%. Found:

C, 43.7; H, 6.21%. The material was non-reducing to the copper reagent of Shaffer and Somogyi (6).

Crude di-*O*-methylene-D-glucose, 6.8 gm., was recovered by evaporation of the first four ethyl acetate extracts. The other four extracts were evaporated *in vacuo* to a sirup, 3.6 gm., which was dissolved in 10 ml. of water and extracted twice with 10-ml. portions of ethyl acetate. The glucose was removed by fermentation and the solution evaporated to a sirup, which was dissolved in a small amount of ethanol and seeded with pure 1,2-*O*-methylene-α-D-glucofuranose, crystallization occurring slowly at room temperature. The crude material was recrystallized from ethanol to yield 0.09 gm. of 1,2-*O*-methylene-α-D-glucofuranose, m.p. 147–148° C. The total yield of the mono-*O*-methylene-D-glucose was 0.34 gm. or 5.8% of theory.

1,2-O-Isopropylidene-α-D-glucofuranose 3,5,6-Trimethanesulphonate

Monoacetone glucose, 4.4 gm., was dissolved in 9 ml. of pyridine with slight heating, after which methanesulphonyl chloride, 5.5 ml., was added and the mixture cooled while shaking. After 42 hr. at room temperature a few drops of water were added to the reaction mixture followed after 15 min. by a few more drops. An additional amount of water, 30 ml., was added after some time, at which point the sirup crystallized while the mixture was being stirred. The crude product amounted to 8.0 gm., corresponding to a yield of 90.5%. The material was recrystallized twice from chloroform and *n*-pentane at room temperature to give 6.3 gm. of 1,2-*O*-isopropylidene-α-D-glucofuranose 3,5,6-trimethanesulphonate, m.p. 162.5–163.5° C., $[\alpha]_D^{22}$ −20.4° (*c*, 1.8 in pyridine). Helferich and Gnüchtel report m.p. 165° C., $[\alpha]_D$ −24.2° in pyridine for this compound.

1,2-O-Isopropylidene-α-D-glucofuranose 3,5,6-Tri-p-toluenesulphonate

Monoacetone glucose, 4.4 gm., was dissolved in 10 ml. of pyridine and 16 gm. of *p*-toluenesulphonyl chloride was added gradually while cooling, after which the mixture was kept at room temperature for four days. Water was added dropwise with cooling and stirring; the thick sirup crystallized while being ground in a mortar with more water. The crystals were collected and washed with water. The crude product weighed 14.1 gm., m.p. 118–123° C. Recrystallization from ethanol at room temperature gave 1,2-*O*-isopropylidene-α-D-glucofuranose 3,5,6-tri-*p*-toluenesulphonate, 11.1 gm., in 81.6% yield, m.p. 129–130° C., $[\alpha]_D^{22}$ −4.3° (*c*, 1.4 in chloroform). Ohle and Wilcke (4) report m.p. 129° C., $[\alpha]_D$ −5.4° in chloroform for this compound.

Conversion of 1,2-O-Isopropylidene-α-D-glucofuranose 3,5,6-Trimethanesulphonate into the Methylene Analogue

Paraformaldehyde, 2.75 gm., and 1,2-*O*-isopropylidene-α-D-glucofuranose trimethanesulphonate, 2.5 gm., were dissolved in 10 ml. of glacial acetic acid by heating on a steam bath. Concentrated sulphuric acid, 0.75 ml., was slowly added and the reaction mixture kept on a steam bath for 80 min. Water, 20 ml., was added to the cooled reaction mixture, which was subsequently extracted twice with 20-ml. portions of chloroform. The combined chloroform solut-

ions were washed with 20 ml. of water, then another 20-ml. portion of water, to which solid sodium bicarbonate was added until no more reaction was evident. After further washing with two 20-ml. portions of saturated aqueous sodium bicarbonate and three 20-ml. portions of water, the chloroform solution was dried over anhydrous sodium sulphate and concentrated *in vacuo* at 50°C. to a partially crystallized sirup. Crystallization from chloroform and *n*-pentane gave 1,2-*O*-methylene-α-D-glucofuranose 3,5,6-trimethanesulphonate, 1.4 gm. in 60% yield, m.p. 92.5–100° C. Two more recrystallizations from the same solvents yielded 0.8 gm. of a pure product, m.p. 104.5–105.5° C., $[\alpha]_D^{22}$ −13.4° (*c*, 1.4 in pyridine). Calc. for $C_{10}H_{18}O_{12}S_3$: C, 28.3; H, 4.24%. Found: C, 27.8; H, 4.18%.

Conversion of 1,2-O-Isopropylidene-α-D-glucofuranose 3,5,6-Tri-p-toluenesulphonate into the Methylene Analogue

Paraformaldehyde, 2.75 gm., and 1,2-*O*-isopropylidene-α-D-glucofuranose 3,5,6-tri-*p*-toluenesulphonate, 2.5 gm., were suspended in 10 ml. of glacial acetic acid and the mixture cooled in an ice-bath. Concentrated sulphuric acid, 0.75 ml., was slowly added and the mixture was kept on a steam bath for 80 min. The product was isolated as described for the trimethanesulphonate and amounted to 2.1 gm. in 84% yield, m.p. 120–128° C. after one recrystallization from chloroform and *n*-pentane at room temperature. Two more recrystallizations from the same solvents gave 0.8 gm. of 1,2-*O*-methylene-α-D-glucofuranose 3,5,6-tri-*p*-toluenesulphonate, m.p. 134.5–135° C., $[\alpha]_D^{22}$ +9.8° (*c*, 1.2 in chloroform). Calc. for $C_{28}H_{30}O_{12}S_3$: C, 51.4; H, 4.59%. Found: C, 51.3; H, 4.47%.

1,2-O-Methylene-α-D-glucofuranose 3,5,6-Trimethanesulphonate

Methanesulphonyl chloride, 0.2 ml., was added to a solution of 0.152 gm. of 1,2-*O*-methylene-α-D-glucofuranose in 0.32 ml. of pyridine and the mixture was kept at room temperature for 40 hr. Excess mesyl chloride was decomposed by addition of a few drops of water. After the addition of 2 ml. of water, the sirup crystallized while being stirred; the solid, after washing with two 2-ml. portions of water, amounted to 0.32 gm. Two recrystallizations from chloroform and *n*-pentane at room temperature gave 1,2-*O*-methylene-α-D-glucofuranose 3,5,6-trimethanesulphonate, 0.16 gm., m.p. 106–107° C., $[\alpha]_D^{22}$ −12.8° (*c*, 1.3 in pyridine). No depression of melting point was detected when this material was mixed with the product from the replacement of the isopropylidene by a methylene group in 1,2-*O*-isopropylidene-α-D-glucofuranose 3,5,6-trimethanesulphonate.

1,2-O-Methylene-α-D-glucofuranose 3,5,6-Tri-p-toluenesulphonate

p-Toluenesulphonyl chloride, 0.55 gm., was slowly added to a solution of 1,2-*O*-methylene-α-D-glucofuranose, 0.15 gm., in 0.35 ml. of pyridine. The solution was allowed to stand at room temperature for three days, after which a few drops of water were added to decompose the excess tosyl chloride. The sirup was stirred with 2.5 ml. of water and the crystals formed were separated and again treated with 2.5 ml. of water. The crude product, 0.50 gm., was recrystallized twice from chloroform and *n*-pentane to yield 0.18 gm. of

1,2-*O*-methylene-α-D-glucofuranose 3,5,6-tri-*p*-toluenesulphonate, m.p. 135.5–136° C., $[\alpha]_D^{22}$ +10.0° (*c*, 1.4 in chloroform). No depression of the melting point was noted when this material was mixed with the product from the replacement of the isopropylidene group by a methylene group in 1,2-*O*-isopropylidene-α-D-glucofuranose 3,5,6-tri-*p*-toluenesulphonate.

ACKNOWLEDGMENT

The authors wish to express their gratitude to Professor C. B. Purves, Head of this Division, for his kind interest in the present study.

REFERENCES

1. BROWNELL, H. H. Ph.D. Thesis, McGill University, Montreal, Quebec. 1953.
2. HELFERICH, B. and GNÜCHTEL, A. Ber. 71: 712. 1938.
3. HOUGH, L., JONES, J. K. N., and MAGSON, M. S. J. Chem. Soc. 1525. 1952.
4. OHLE, H. and WILCKE, H. Ber. 71: 2316. 1938.
5. SCHMIDT, O. T., DISTELMAIER, A., and REINHARD, H. Ber. 86: 7.41. 1953.
6. SHAFFER, P. A. and SOMOGYI, M. J. Biol. Chem. 100: 695. 1933.

REACTIONS OF ARYLSULPHONIC ESTERS

II. THE ALKYL GROUP[1]

By P. M. Laughton[2] and R. E. Robertson

ABSTRACT

As part of the project outlined in Paper I of this series, we report kinetic data, including Arrhenius parameters, for the solvolysis of a number of alkyl benzene- and toluene-sulphonates in ethanol and in water. The alkyl groups include the α- and β-methylation series: methyl, ethyl, isopropyl, *n*-propyl, isobutyl, and neopentyl; the straight chain series *n*-butyl and *n*-amyl; and a small group of oxygen-containing chains. The observed rates for the α-methylation series parallel those for the bromides and nitrates, and for the β-methylation, those for the bromides. However, it is evident that current interpretations of rate differences observed in the straight chain and oxygenated series cannot be applied with confidence to the benzenesulphonates since the changes in the Arrhenius parameters are larger than the observed differences in the rate.

In connection with our survey of the behavior of alkyl arylsulphonates in solvolysis, we have examined the effect of changing the structure of the alkyl group. Since this work was undertaken, Winstein's laboratory has reported data on many alkyl groups, mostly in acetic acid and in formic acid and from the point of view of rearrangements. Our work is chiefly concerned with nucleophilic solvents—water and alcohols—and with less complicated alkyl groups.

In particular we hope to be able to characterize the system

$$ROH + ArSO_3R' \rightarrow R{-}O{-}R' + ArSO_3H$$

sufficiently comprehensively that our data may be used in an attack on the problem of the detailed picture of solvent participation in this apparently very simple reaction.

The analysis of the mechanism of displacement reactions has reached a point where most of the large rate-controlling effects have yielded to a semi-quantitative treatment. Hammett's (17) free energy relationship, $\log k/k^\circ = \rho\sigma$, where σ is a measure of the relative effect of substituents in rigid molecules, has recently been extended by Swain (33) to some nucleophilic displacement reactions in the aliphatic series, $\log k/k^\circ = sn$, where s is a measure of the sensitivity of substrate to the nucleophility of the attacking agent. Swain also points out that this equation and that of Winstein, Grunwald, and Jones (39) $\log k/k^\circ = Ym$ (where Y = "solvent ionizing power") may both be special cases of the more general case, $\log k/k^\circ = sn + s'e$, where s' is a measure of substrate sensitivity to electrophilicity in a generalized termolecular displacement. Even the very difficult problem of steric effects seems to be approaching quantitative treatment (cf. Dostrovsky, Hughes, and Ingold (10); Newman (26); Brown (4); Taft (35), among many others).

[1]*Manuscript received March 2, 1955.*
Contribution from the Division of Pure Chemistry, National Research Council, Ottawa, Canada. Issued as N.R.C. No. 3626.
[2]*National Research Council Summer Research Assistant, 1952 and 1954. Present address: Department of Chemistry, Carleton College, Ottawa, Canada.*

This leaves as a major unknown variable the problem of the detailed participation of the medium. While an approach to this problem can be made by considering the solvent as a bulk dielectric, this can only be a first approximation. Taft (34) and Evans and Hamann (13) have interpreted relative rates using the concept of interference with solvation by groups about the reaction site. Yet, as Swain (33) comments, few precise kinetic data are available for treating the effect of different solvents on relative rates of substrates. A further complication is that most of the data available, for solubility reasons, are in a variety of mixed solvent systems. Also, much of the work has been reported at single temperatures because, in the words of Ingold (19, pp. 255–56), as "kinetic effects become smaller, the first quantity to show unintelligible irregularities is the Arrhenius energy of activation".

While we are by no means certain what lines of attack will solve the problem of solvent participation, we hope that our consistent body of kinetic data may provide information useful in this respect. We are certainly going to exercise due caution about attaching any simple significance to small differences in activation energy (19); however, we are sanguine enough to provide temperature coefficients in the hope that what we cannot ourselves interpret may prove useful to others.

RESULTS AND DISCUSSION

α-Methylation Series

The survey reported here covers a number of alkyl groups of recurring interest in other systems. Since this work was undertaken, two communications from Tommila's laboratory have appeared, dealing with some of these systems (37, 38). Table I shows relative rates and Arrhenius parameters ($k = pZ\,e^{-E_A/RT}$) for the series of increasing α-methylation in ethanol and water. (We also (11, 37) have found *t*-butyl sulphonates too unstable for isolation.) This series shows the minimum at the ethyl compound to be expected (19, pp. 317–18) for a shift in mechanistic category from S_N2 toward S_N1. It is noteworthy that the increased rate for the isopropyl derivative in both solvents is due to a more favorable entropy term which outweighs an increase in activation energy. One factor which should result in a more positive entropy for isopropyl is the probability that the solvent is more highly ordered about the initial state, in which ionic contributions to the structure are favored. This increase would, however, have to be larger than any corresponding change in ordering about the more nearly ionized transition state.

In water the anticipated shift towards S_N1 is apparent, the ethyl compound drawing up to the methyl, and isopropyl greatly increasing.[3] These relationships are dealt with in detail in the previous paper in this series (28) in which the benzenesulphonates are compared with the bromides and the nitrates.

β-Methylation Series

The second series of wide interest is that of β-methylation. Table II records

[3]*That the solvolysis of the primary esters must be stereochemically S_N2 is, however, established by the elegant work of Streitwieser on active butanol-1-d p-Br benzenesulphonate (J. Am. Chem. Soc. 77: 1117. 1955).*

our data in ethanol and water for the series ethyl, *n*-propyl, isobutyl, and neopentyl.

TABLE I

SOLVOLYTIC RATE CONSTANTS FOR THE REACTION OF BENZENESULPHONATES WITH ETHANOL AND WATER

$C_6H_5SO_3R + R'OH$; R′ = ethyl, 0.01 *M*; R′ = H, 0.2 gm./l.

R′	R	*T*, °C.	$k \times 10^5$ sec.$^{-1}$	E_A, kcal./mole*	$\log_{10}pZ$
Et	Me	70.00	7.04 ± 0.03		
		80.00	16.73 ± 0.09	20.40 ± 0.45	8.847
		90.00	36.6 ± 0.3		
	Et	70.00	3.06 ± 0.02		
		80.00	7.53 ± 0.03	21.38 ± 0.27	9.107
		90.00	17.22 ± 0.10		
	*i*Pr	50.00	1.262 ± 0.012		
		60.00	3.71 ± 0.04	22.95 ± 0.12	10.627
		70.10	10.24 ± 0.08		
H	Me	50.003	19.66 ± 0.08		
		60.026	52.66 ± 0.13	20.52 ± 0.47	10.181
		74.906	193.4 ± 0.4		
	Et	50.125	18.99 ± 0.12		
		60.026	50.11 ± 0.10	21.04 ± 0.06	10.500
		74.892	195.2 ± 0.2		
	*i*Pr	0.092	1.952 ± 0.008		
		20.010	34.58 ± 0.03	22.78 ± 0.42	13.513
		30.122	124.3 ± 0.6		
		50	(1270)		

**The "errors" reported for the Arrhenius energies of activation may be partially attributed to the ΔC_p of activation for these systems, which is of the order of 30 cal./mole degree in water (29). For example, such a C_p would be equivalent to a curvature of ±0.4 kcal./mole for a 25° range. Known or estimated ΔC_p's are capable of accounting for most of the small discrepancies between our work and the Arrhenius parameters recently reported by Tommila et al. (37, 38).*

TABLE II

SOLVOLYTIC RATE CONSTANTS FOR THE REACTION OF ALKYL BENZENESULPHONATES WITH ETHANOL AND WATER

$C_6H_5SO_3R + R'OH$; R′ = ethyl, 0.01 *M*; R′ = H, 0.2–0.05 gm./l.

R′	R	*T*, ° C.	$k \times 10^5$ sec.$^{-1}$	E_A	$\log_{10}pZ$
Et	Et	80.00	7.60	21.38	9.107
	Pr	50.00	0.248 ± 0.003		
		80.00	4.41 ± 0.05	21.45 ± 0.60	8.906
		90.00	9.84 ± 0.09		
	*i*Bu	50.00	0.0178 ± 0.0005		
		80.00	0.383 ± 0.004	23.16 ± 0.03	8.918
		90.00	0.949 ± 0.011		
	NeoPen*	110.0	0.0984 ± 0.0014		
		120.0	0.255 ± 0.008	28.50	10.260
		80.00	(0.0043)**		
H	Et	60.026	50.1	21.04	10.500
	Pr	50.125	13.09 ± 0.09		
		60.026	35.59 ± 0.11	21.09 ± 0.37	10.376
		74.953	135.9 ± 0.3		
	*i*Bu	59.989	11.75 ± 0.07		
		74.902	55.40 ± 0.06	23.67 ± 0.40	11.60
		83.926	129.1 ± 0.6		
	NeoPen	59.998	5.48 ± 0.04		
		74.900	26.8 ± 0.02	24.98 ± 0.45	12.13
		83.932	68.8 ± 0.7		

**Tosylate.* ***Extrapolated.*

In alcohol we see again the slight jump of about 1 kcal./mole in activation energy for the isobutyl derivative, followed by the large jump of 7 kcal./mole for the neopentyl compound, as noted before in the case of the bromides (10).

Winstein (40, 41) shows that changing the solvent from ethanol through acetic acid to formic acid steadily increases the rate of neopentyl tosylate, indicating a cationic intermediate in all three. He also presents evidence for some anchimeric participation by the β-methyls. This probable difference in mechanism together with the possibility that solvent may assist the ionization by an attack on the β-carbon discourages detailed speculation about the rise in the entropy factor. The possible explanation for the similar increase with isopropyl, based on a more polar initial state, is not available for this compound.

The neopentyl tosylate was prepared in order to check the data of Winstein (40, 41) but the benzenesulphonate was used for the work in water because of solubility difficulties. Winstein's value for the solvolysis of neopentyl tosylate in alcohol touches our two-temperature Arrhenius plot, although his extrapolated value at 75° implies a somewhat different activation energy.

The relative rates for our series in water at 60° (Me: Et: *i*Bu: NeoPen: :10: 9.6: 2.2: 1.0) are similar to the corresponding series for the tosylates in acetic acid (10: 9.1: 2.8: 1) although there is a difference in rate between the two series of more than three powers of ten. Since there is also a difference in the range of activation energies (9 kcal./mole in acetic acid and $4\frac{1}{2}$ kcal./mole in water) one must recognize that the similarity in relative rate sequences here results from fortuitous choice of temperatures for comparison.

Straight-chain Series

Because of the appearance, among the more usual monotonously decreasing rate series (13; 19, p. 319), of the occasional report of straight-chain anomalies in the butyl–pentyl region, we have also examined the series: methyl, ethyl, propyl, butyl, and pentyl in both ethanol and water. Data are recorded in Tables III and IV. Adsorption effects, which begin to become important at very low solubilities (*ca.* 0.0002 *M* for the pentyl compound), have impeded an extension of the series in water. *n*-Hexyl benzenesulphonate in water, on the basis of less precise data, (judging from scatter in the Guggenheim rate plots) solvolyzes more slowly than *n*-pentyl.

There is a minimum rate at propyl in water, but the differences both in rates and in activation parameters are very small. We have no explanation for this minimum which could be generalized for other cases, some of which show peculiar fluctuations.

For example, the following orders of reactivity may be found in the literature for primary amines: Me > Et < Pr < Bu < Pen (5); Me < Et > Pr < Bu < Pen (5); Me > Et > Pr < Bu > Pen (1, 22). Brown (5) has suggested that a break in the series should occur for the first member for which the free rotation of the end of the chain is reduced or increased by changes at the reaction site in the product or transition state. This concept by itself implies

TABLE III

SOLVOLYTIC RATE CONSTANTS FOR THE REACTION OF ALKYL BENZENESULPHONATES IN DRY ETHANOL, 0.01 *M*

R	*T*, ° C.	$k \times 10^5$ sec.$^{-1}$	E_A	$\log_{10}pZ$
Me*	80.00	16.7	20.40	8.847
Et*	80.00	7.60	21.38	9.107
Pr**	80.00	4.41	21.45	8.906
Bu	80.00	4.23 ± 0.04		
	90.00	9.06 ± 0.08	20.98	8.611
	100.00	21.0 ± 0.3		
Pen	77.42	3.70 ± 0.03		
	79.97	4.07 ± 0.11	21.56 ± 0.80	8.954
	90.00	10.8 ± 0.2		
	100.00	22.5 ± 0.6		
$EtO(CH_2)_2$***	100.00	3.88 ± 0.06		
	105	5.46 ± 0.06	19.62 ± 0.37	7.081
	110	7.79 ± 0.05		
$EtO(CH_2)_3$***	90.00	4.20 ± 0.07		
	(100)	(8.61)	21.07	8.277
	105.00	1.254 ± 0.006		
	110.0	17.9 ± 0.3		
$(EtO)_2C(CH_2)_2$***	100.00	6.35 ± 0.05		
	110.00	12.49 ± 0.08	19.74 ± 0.65	7.366
	119.9	24.4 ± 0.4		
$NC(CH_2)_2$***	99.9	1.28 ± 0.01	(21)	(7.5)
	110.0	2.72 ± 0.03		

**From Table I.* ***From Table II.* ****p-Toluenesulphonate.*

TABLE IV

SOLVOLYTIC RATE DATA FOR THE REACTION OF ALKYL BENZENESULPHONATES IN WATER, 0.2 GM./L. OR LESS

R	*T*, ° C.	$k \times 10^5$ sec.$^{-1}$	E_A	$\log_{10}pZ$
Me	50.003	19.66	20.52	10.181
Et	50.125	18.99	21.04	10.500
Pr	50.00	23.09	21.09	10.376
Bu	39.869	5.09 ± 0.04		
	49.904	14.38 ± 0.04	20.53 ± 0.30	10.040
	60.026	37.5 ± 0.5		
Pen	39.870	5.275 ± 0.007		
	50.125	15.6 ± 0.3	20.70 ± 0.60	10.173
	60.026	39.5 ± 0.4		
Hex	49.991	15.23 ± 0.07		
$MeO(CH_2)_2$	50.009	0.9095 ± 0.00		
	59.993	2.610 ± 0.00	22.84 ± 0.23	10.399
	74.901	11.58 ± 0.05		
$EtO(CH_2)_2$	50.009	0.966 ± 0.006		
	60.173	2.69 ± 0.05	22.45 ± 0.77	10.149
	74.900	11.77 ± 0.07		
$EtO(CH_2)_3$	49.904	3.336 ± 0.014		
	60.026	10.18 ± 0.16	21.93 ± 0.17	10.396
	74.900	42.30 ± 0.46		

a vertical displacement at the critical chain length in an otherwise monotonously increasing or decreasing series, an effect which seems intuitively reasonable although its order of magnitude is difficult to evaluate, especially in a condensed phase. However, this cannot be the whole story where the series passes through a minimum as it does in the case of Table IV, or where the curve has a zig-zag character (13).

Anomalies similar to our own have been reported for displacements by ions. Segaller's (31) results for the displacement of alcoholic phenoxide on alkyl iodides show a dip at pentyl. Crowell's (9) work on the attack of alcoholic thiocyanate on alkyl bromides shows a rise to octyl from a minimum at butyl. McKay (23) also found a minimum at butyl for the iodide exchange reaction, pentyl being slightly faster than propyl. On the other hand, the data of Conant and Hussey (6) for iodide displacement on chlorides in acetone show upward displacements in a decreasing curve at pentyl and octyl.

Oxygen-containing Alkyl Groups

Because of the peculiarity reported by Rabinovitch and Schramm (27) for the alkaline hydrolysis in aqueous acetone of β-ethoxyethyl acetate (k_2 twice that for ethyl acetate, but E_A 15.4 kcal./mole versus 11.7 for the ethyl ester), we examined several β- and γ-substituted derivatives in alcohol.[4] All three compounds, β-ethoxyethyl, γ-ethoxypropyl, and β-carbethoxyethyl *p*-toluenesulphonate were an order of magnitude *less* reactive than the simple alkyl esters. (The β-chloroethyl and β-cyanoethyl compounds also reacted very slowly, but the second functional group in each reacted at comparable rates.) However, the activation energies are slightly lower than others in the series, the drop in rate arising from the entropy factor.

This decrease in rate corresponds to that noted for solvolysis of β-ethoxyethyl chloride in aqueous dioxane versus butyl (2), and the very slow solvolysis of β-ethoxyethyl iodide in water (21) as compared with ethyl iodide. In this latter note (21) and in an earlier paper from the same laboratory (8), the suggestion made by Hinshelwood, Laidler, and Timm (18) is used to relate the polar effect of substituents on the heat of activation in displacement reactions. Although this relation should hold only for ΔH_A^0, not for ΔH_A^T, these authors base their discussion on a value of E_A for methyl iodide in water, a reaction which has the large ΔC_p of -67 cal./mole degree (15), and one for ethyl iodide which is in doubt because of a side reaction (25). Further, they assume that the only changes in E_A that are significant arise from polar effects of the substituents, although whatever changes in the ordering of solvent are responsible for the large changes in $\Delta S^{\ddagger}$ must surely make substantial concomitant contributions to E_A.

Although both electron-releasing (12, 14) and electron-withdrawing (3) substituents may facilitate S_N2 displacements by anions, evidently those involving neutral molecules are hindered by electron-withdrawing groups. One might expect the electrophilicity of the carbon undergoing substitution to be more important for the weaker nucleophilics.

EXPERIMENTAL

Materials

Properties of the esters are given in Table V. Methyl and ethyl benzenesulphonate were purified as used by fractional freezing of Eastman Kodak

[4]*We later became aware of the paper by Salmi and Leimu (30) reporting data for the acetates and a number of other esters in pure water and aqueous dioxane. In both solvents the rate of the Cellosolve esters is again roughly twice that of the ethyl esters, but activation energies calculated from their rates are only about 1 kcal./mole higher for the β-ethoxyethyl esters.*

TABLE V

PROPERTIES OF BENZENESULPHONIC ESTERS

Ester	n_D^{25}	N.E.	Analysis obtained		Calculated	
			%C	%H	%C	%H
Pr *p*-H[a]	1.5035	202.2				
Bu *p*-H[b]	1.4998	215.6				
*i*Bu	1.4962	214.7	56.15	6.55	56.05	6.59
Pen *p*-H[b]	1.4987	229.7				
NeoPen *p*-H[a]	1.4932	227.3	57.95	6.95	57.87	7.06
Hex *p*-H[b]	1.4945	244				
$MeO(CH_2)_2$ *p*-H	1.5072	218.7	50.12	5.16	49.99	5.59
$EtO(CH_2)_2$ *p*-H[a]	1.5009	231.2	52.17	6.11	52.16	6.13
$EtO(CH_2)_3$ *p*-H	1.4962	243.0	53.95	6.55	54.08	6.60
$EtO(CH_2)_2$ *p*-Me[a]	1.5039 (26° C.)	246	m.p. 15–16° C.			
$EtO(CH_2)_3$ *p*-Me	1.4960 (27° C.)	253	55.88	7.06	55.78	7.05
$EtO_2(CH_2)_2$ *p*-Me[a]	1.5011 (28° C.)	solidifying and decomposing on standing				
$NC(CH_2)_2$ *p*-Me[a]	m.p. 64.0–64.5° C.					
NeoPen *p*-Me[c]	m.p. 47.0–48.0° C.	243	59.50	7.34	59.48	7.49

[a]*Ref. 32.* [b]*Ref. 11.* [c]*Ref. 41.*

white label material. β-Cyanoethyl and β-ethoxycarbonylethyl *p*-toluenesulphonate were prepared according to the published methods (32). The remaining esters were synthesized by the Tipson method (36) using the appropriate alcohols. Of the alcohols, propyl, isopropyl, butyl, isobutyl, methoxyethyl, ethoxyethyl, β-cyanoethyl, and β-chloroethyl were refractionated from the best available commercial products. All liquid esters were repurified before each series of runs by redistillation from a molecular still, giving colorless products.

γ-Ethoxypropyl alcohol was prepared by reduction of refractionated Eastman Kodak β-ethoxypropionaldehyde with either lithium aluminum hydride or hydrogen and Raney nickel catalyst. After fractionation under reduced pressure its properties correspond to those given by Karvonen (20). The alkoxyalkanols were redistilled just before use because of peroxide formation.

Since analytical grade *n*-pentyl alcohol proved to be a mixture on fractionation, both it and neopentyl alcohol were prepared by Grignard reactions with formaldehyde (7), using *n*-butyl bromide and *t*-butyl chloride respectively.

n-Hexyl alcohol, d_{20}^{20} 0.8178, n_D^{20} 1.4159, was purified from Eastman Kodak practical grade by repeated recrystallization of the *p*-hydroxybenzoate, m.p. 52.0–2.8°, (from petroleum ether) followed by saponification and fractionation.[5]

Ethanol was purified by distillation from sodium and diethyl phthalate (24). Conductance water was prepared by passing distilled water through an Amberlite MB-1 mixed bed resin.

Methods

The work in alcohol as a solvent was done as described in Paper I (28).

In water, rates were followed by conductance methods to be described in Paper III of this series. The Guggenheim method of treatment of data was

[5]*This purification was carried out by Mr. A. Rayner of Carleton College.*

used (16). Precisions recorded in the tables are within runs for the work in ethanol and between runs for the work in water.

For the work in alcohol, temperature was controlled to ±0.01–0.02 C.° using tenth degree thermometers calibrated by the Heat Section of the Division of Physics. For the conductance work, temperature was controlled to ±0.001–0.003 C.°, measured by a platinum resistance thermometer and a Leeds and Northrup G-1 Mueller bridge.

We were initially disturbed by the fact that ethyl benzenesulphonate in water gave a consistently higher value by conductance than by titration according to Tommila's procedure (38). However, there appeared to be appreciable hydrolysis of the ester during the titration. Accordingly, we carried out a titration run in an early model of a continuous titration device. This result confirmed that obtained by conductance. Except for the least soluble esters, adsorption did not appear to interfere with the conductance measurements, since results were indistinguishable for the variety of sizes and shapes of cells which were used in many of the runs. For the *n*-butyl and the pentyl esters, cells with small surface to volume ratios had to be used.

ACKNOWLEDGMENT

Thanks are due to Mr. P. Tymchuck and to Mr. A. Relf for careful technical assistance in the course of this investigation.

REFERENCES

1. ARNETT, E. M., MILLER, J. G., and DAY, A. R. J. Am. Chem. Soc. 72: 5635. 1950.
2. BÖHME, H. and SELL, K. Chem. Ber. 81: 123. 1948.
3. BORDWELL, F. G. and COOPER, G. D. J. Am. Chem. Soc. 73: 5184. 1951.
4. BROWN, H. C. *et al.* J. Am. Chem. Soc. 75: 1. 1953.
5. BROWN, H. C., TAYLOR, M. D., and SUJISHI, S. J. Am. Chem. Soc. 73: 2464. 1951.
6. CONANT, J. B. and HUSSEY, R. E. J. Am. Chem. Soc. 47: 476. 1925.
7. CONANT, J. B., WEBB, C. N., and MENDUM, W. C. J. Am. Chem. Soc. 51: 1246. 1929.
8. COWAN, H. D., MCCABE, L., and WARNER, J. C. J. Am. Chem. Soc. 72: 1194. 1950.
9. CROWELL, T. I. J. Am. Chem. Soc. 75: 6046. 1953.
10. DOSTROVSKY, I., HUGHES, E. D., and INGOLD, C. K. J. Chem. Soc. 173. 1946.
11. EMLING, B. L. J. Am. Chem. Soc. 74: 4702. 1952.
12. EVANS, A. G. Nature, 157: 438. 1946.
13. EVANS, A. G. and HAMANN, S. D. Trans. Faraday Soc. 47: 40. 1951.
14. FELDSTEIN, A. and VANDER WERF, C. A. J. Am. Chem. Soc. 76: 1626. 1954.
15. GLEW, D. N. and MOELWYN-HUGHES, E. A. Proc. Roy. Soc. (London), A, 211: 254. 1952.
16. GUGGENHEIM, E. A. Phil. Mag. [7] 2: 538. 1926.
17. HAMMETT, L. P. Physical organic chemistry. McGraw-Hill Book Company, Inc., New York. 1940. Chap. VII.
18. HINSHELWOOD, C. N., LAIDLER, H. J., and TIMM, E. W. J. Chem. Soc. 848. 1938.
19. INGOLD, C. K. Structure and mechanism in organic chemistry. Cornell Univ. Press, Ithaca, N.Y. 1953.
20. KARVONEN, A. Ann. Acad. Sci. Fennicae, Ser. A (No. 9) 10: 7. 1918.
21. KLEMPERER, W., MCCABE, L., and SINDLER, B. J. Am. Chem. Soc. 74: 3425. 1952.
22. KOOB, R. P., MILLER, J. G., and DAY, A. R. J. Am. Chem. Soc. 73: 5775. 1951.
23. MCKAY, H. A. C. J. Am. Chem. Soc. 65: 702. 1943.
24. MANSKE, R. H. F. J. Am. Chem. Soc. 53: 1104. 1931.
25. MOELWYN-HUGHES, E. A. Proc. Roy. Soc. (London), A, 164: 295. 1938.
26. NEWMAN, M. S. J. Am. Chem. Soc. 74: 3929. 1952.
27. RABINOVITCH, B. and SCHRAMM, C. H. J. Am. Chem. Soc. 72: 627. 1950.
28. ROBERTSON, R. E. Can. J. Chem. 31: 589. 1953.
29. ROBERTSON, R. E. Paper III. To be published.
30. SALMI, E. J. and LEIMU, R. Suomen Kemistilehti, B, 20: 43. 1947.
31. SEGALLER, D. J. Chem. Soc. 105: 106. 1914.
32. SUTER, C. M. Organic chemistry of sulfur. John Wiley & Sons, Inc., New York. 1944. Chap. V.

33. SWAIN, C. G. and SCOTT, C. J. Am. Chem. Soc. 75: 141. 1953.
34. TAFT, R. W., JR. J. Am. Chem. Soc. 75: 4534. 1953.
35. TAFT, R. W., JR. J. Am. Chem. Soc. 75: 4538. 1953.
36. TIPSON, R. S. J. Org. Chem. 9: 235. 1949.
37. TOMMILA, E. and JUTILA, J. Acta Chem. Scand. 6: 844. 1952.
38. TOMMILA, E. and LINDHOLM, M. Acta Chem. Scand. 5: 647. 1951.
39. WINSTEIN, S., GRUNWALD, E., and JONES, H. W. J. Am. Chem. Soc. 73: 2700. 1951.
40. WINSTEIN, S. and MARSHALL, H. J. Am. Chem. Soc. 74: 1120. 1952.
41. WINSTEIN, S., MORSE, B. K., GRUNWALD, E., SCHREIBER, K. C., and CORSE, J. J. Am. Chem. Soc. 74: 1113. 1952.

A NEW METHOD FOR THE PREPARATION OF D-ERYTHROSE AND OF L-GLYCERALDEHYDE[1]

By A. S. Perlin and Carol Brice

ABSTRACT

D-Glucose is degraded selectively to di-*O*-formyl-D-erythrose by oxidation with two moles of lead tetraacetate. The ester groups are easily hydrolyzed, giving D-erythrose in an over-all yield of at least 80% of theory. In like manner oxidation of L-arabinose, followed by hydrolysis, affords L-glyceraldehyde. It is suggested that D-erythrose can readily associate intermolecularly, a property previously ascribed among sugars only to the trioses.

INTRODUCTION

Among monosaccharides the tetroses constitute probably the most poorly characterized group. Only one preparation of a crystalline tetrose, that of D-threose, has been reported (6), but subsequent investigations by Hockett (9, 10) and Hockett *et al.* (11) have cast serious doubt on the identity of this preparation. The current importance of the tetroses is illustrated by the use of D-erythrose as a starting point for synthesis of 2-deoxy-D-ribose (20, 29) and of ribose-1-C^{14} (7, 18).

At least seven methods for preparing D-erythrose are recorded in the literature. Five of these have been evaluated by Overend, Stacey, and Wiggins (20), who recommended the Ruff procedure (26) as modified by Hockett and Hudson (12), and two additional methods have since been reported (30, 25, 16, 14). All of these procedures involve degradation of an appropriate sugar derivative—the acid, glucal, acetal, or mercaptal—which, however, is itself sometimes not obtained readily or in good yield. This communication now reports a convenient preparation of D-erythrose in high yield directly from D-glucose.

When aldohexoses are treated with lead tetraacetate they rapidly consume two moles of oxidant, after which the reaction becomes very slow (13, 24). Applied to D-glucose it is found that the initial rapid stage of the reaction corresponds to virtually complete conversion of the hexose to D-erythrose. With one mole of oxidant, D-arabinose as well as D-erythrose is obtained (23). The oxidation is carried out in acetic acid solution by the addition of two moles of the powdered oxidant per mole of glucose. Removal of the divalent lead and distillation of the solvent affords a clear, colorless sirup, in 90 to 95% yield, which exhibits the properties of a diformate ester of D-erythrose (24). The ester groups are easily hydrolyzed by heating in water or dilute acid, giving a product which has an equilibrium specific rotation of about $-30°$ and which is uncontaminated by hexose or pentose sugars (paper chromatogram). The infrared absorption spectrum of the free sugar, using the potassium bromide

[1]*Manuscript received March 28, 1955.*
Contribution from the National Research Council of Canada, Prairie Regional Laboratory, Saskatoon, Saskatchewan. Issued as Paper No. 191 on the Uses of Plant Products and as N.R.C. No. 3628.
Presented in part before the 38th Annual Conference of the Chemical Institute of Canada, Quebec City, Quebec, 1955.

window technique (27), is identical with that of D-erythrose prepared from 4,6-*O*-ethylidene-D-glucose (25), and gives no indication of the presence of other compounds. The compound has been further characterized as D-erythrose by hydrogenation to erythritol, by oxidation with bromine to D-erythrono-γ-lactone, and by preparation of the crystalline 2,5-dichlorophenylhydrazone.

On paper chromatograms the new preparation of D-erythrose and the sample prepared from ethylidene glucose behave in identical fashion but show complex properties. For example, each gives a single equally-fast-travelling spot when the solvent is ethyl acetate/acetic acid/water (3/1/3) (15), but in butanol/ethanol/water (4/1/5) (2) much streaking from the origin almost to the solvent front is observed. When an aqueous solution of either preparation is frozen, then thawed, and examined on the chromatogram with the use of methyl ethyl ketone/water (4), at least two spots are found, the major component having an R_f of 0.22 and the other remaining close to the origin. The proportion of slow-moving component is, however, less if the solution is first heated on the boiling-water bath before chromatographing. This behavior may be related to gross changes in optical rotation which have been observed when a solution of the sugar is frozen and thawed. Thus, a solution of D-erythrose having an equilibrium specific rotation of $-31°$, after freezing for 18 hr. and thawing, had a specific rotation of about $-6°$, reverting to the original value during a period of four hours at room temperature. The specific rotation changed to $+2°$ when the solution was stored in the frozen state for 48 hr. These results suggest that D-erythrose in solution readily enters into loose intermolecular association possibly with formation of a dimer or other complex. Such behavior has long been recognized with glyceraldehyde (35), but appears not to have been reported for tetroses. The observed mutarotation changes might therefore correspond to a polymer ↔ monomerfuranose interconversion together with attainment of an α,β-anomer equilibrium for the latter. Perhaps this complexity in part accounts for the wide variation in specific rotations reported for erythrose, such as $-14.5°$ for the D-isomer and $+32.7°$ for the L-isomer (33). Further, the tendency of D-erythrose to associate or dimerize may explain why attempts to crystallize the compound have been unsuccessful.

Pentoses also quickly consume two moles of lead tetraacetate and it was therefore to be expected, by analogy with hexoses, that the degradation should yield the corresponding triose. D-Glyceraldehyde, first prepared by Wohl and Momber (34), is readily obtainable through the elegant method of Fischer and Baer (5), which involves periodate or lead tetraacetate oxidation of 1,2;5,6-di-*O*-isopropylidene-D-mannitol, and, more directly, through the procedure recently reported by Schöpf and Wild (28) in which D-glucose is oxidized with three moles of periodate. By contrast, L-glyceraldehyde is not as easily obtained since the methods just noted require the corresponding but rare L-sugars. Thus Baer and Fischer (2) prepare L-glyceraldehyde from 1,2;5,6-di-*O*-isopropylidene-L-mannitol which is first synthesized from L-arabinose *via* the cyanohydrin reaction and reduction. With lead tetraacetate oxidation, however, L-arabinose is degraded directly to L-glyceraldehyde in high yield. As with D-erythrose the product is recovered from the reaction as

a sirupy formate ester (24), which yields the free glyceraldehyde upon hydrolysis in water or dilute acid. The compound gives an elongated spot on the chromatogram (ethyl acetate/acetic acid/water solvent) with a rate of travel slightly smaller than D-erythrose, possibly due to its existence as a dimer. Traces of arabinose and erythrose were detected in some preparations. The butanol solvent causes much streaking of material on the chromatogram and several spots are discernible, but these are attributed at present to the various modifications possible for glyceraldehyde (2). It will be remembered that erythrose also behaved atypically with this solvent. The equilibrium specific rotation of the compound in water, $[\alpha]_D^{25}$ $-7°$, is close to the value of $+9°$ reported for a freshly-prepared solution of the D-isomer (3). The relatively high purity of the preparation is indicated by the fact that it gave a 73% yield of the L-glyceraldehyde dimedon, which agreed well with the yield of 75% obtained by Baer and Fischer from pure L-glyceraldehyde (2). The product was characterized further as the crystalline 2,4-dinitrophenylhydrazone.

Since oxidation of other aldohexoses and aldopentoses by lead tetraacetate parallels the foregoing oxidations, it is seen, for example, that D-threose may readily be prepared directly from D-galactose and D-glyceraldehyde from D-xylose. A description of their preparation is included in another communication (24), which considers the mechanism of the lead tetraacetate oxidation of reducing sugars.

EXPERIMENTAL

Lead tetraacetate was prepared according to the procedure of Vogel (31). A commercial sample (Matheson Co., Inc.) was also used. All other chemicals were reagent grade.

Spray reagents used for chromatography were triphenyltetrazolium chloride (32), silver nitrate (21), and aniline (22).

Solutions were concentrated *in vacuo* at 35° C.

*Di-O-formyl-*D*-erythrose*

D-Glucose (1.50 gm., 8.3 mM.) dissolved in 3 ml. of water was taken up in 150 ml. of glacial acetic acid. Lead tetraacetate[2] (7.7 gm., 17.4 mM.) was added over a period of three to four minutes to the rapidly stirred solution. Within five minutes' reaction time the lead tetraacetate had dissolved and the solution gave a faint potassium iodide – starch test. Oxalic acid dihydrate (1.9 gm.), dissolved in glacial acetic acid, was added,[3] and the suspension was stirred for an additional 30 min. The precipitate was filtered and washed with acetic acid and the filtrate was concentrated to a volume of a few milliliters. Ethyl acetate was added and the precipitate which formed was triturated with several portions of ethyl acetate. The extracts were combined, filtered, and concentrated to a sirup which was further purified twice by extraction with ethyl acetate. The product was a clear, pale yellow oil. Weight, 1.30 gm. This

[2]*If the compound was dark it was recrystallized before use from acetic acid. Or, it was dissolved in glacial acetic acid and the solution was filtered and added to the glucose solution.*

[3]*Excess lead tetraacetate was thereby decomposed and the divalent lead precipitated.*

compound, which is described in greater detail elsewhere (24), is found to contain two formate ester groups.

D-*Erythrose*

Di-*O*-formyl-D-erythrose (0.201 gm.) was dissolved in 20 ml. of 0.05 *N* hydrochloric acid (a slight turbidity was removed by filtering) and the solution was heated at 50° C., the hydrolysis being followed polarimetrically: $[\alpha]_D$ +0.55° (initial) → −0.40° (two hours, constant). The reducing power of the hydrolyzate, measured by hypoiodite oxidation (8), was equivalent to 0.122 gm. of tetrose (91%); $[\alpha]_D^{27}$ −32.7°. Acid was removed by use of a column (1 cm. × 10 cm.) of Amberlite IR4B resin with some loss of reducing power. The calculated weight of D-erythrose was 0.114 gm., an over-all yield from D-glucose of 80% of theory. $[\alpha]_D^{27}$ −30.0° (equilibrium) (*c*, 0.64).

Erythritol

Di-*O*-formyl-D-erythrose (1.0 gm.) was dissolved in absolute alcohol (40 ml.) and was hydrogenated at ambient temperature and pressure using reduced platinum oxide catalyst (1). Fifty milliliters of hydrogen was taken up, corresponding approximately to one mole per mole of erythrose, and the solution was then only faintly reducing to Fehling's solution. The catalyst was filtered and the filtrate concentrated to a colorless sirup which quickly crystallized. After washing with alcohol and drying the product weighed 0.25 gm. (73%); m.p. 114–116° C. Recrystallization from alcohol raised the melting point to 118° C.; the mixed melting point with an authentic specimen of erythritol (m.p. 118.5° C.) was 118–118.5° C. The X-ray diffraction pattern was identical with that of erythritol.

D-*Erythrono-γ-lactone*

Barium carbonate (10 gm.) was suspended in an aqueous solution of D-erythrose (2.0 gm. in 30 ml.), and bromine (3.4 ml.) was added dropwise with stirring. After three hours' reaction time excess bromine was removed by aeration, and there were added in succession silver carbonate to remove bromide, hydrogen sulphide gas to remove excess silver, and dilute sulphuric acid to precipitate excess barium. The final colorless solution was concentrated, giving a sirup which solidified when dried in high vacuum at 60° C. Weight, 1.3 gm. (65%). After one recrystallization from alcohol, m.p. 103–104° C., $[\alpha]_D^{27}$ −72.1° (*c*, 1, water); (m.p. 103° C., $[\alpha]_D$ −73.3° (26)).

D-*Erythrose 2,5-Dichlorophenylhydrazone*

D-Erythrose sirup (0.44 gm.), prepared by concentrating an aliquot of the neutral solution described above, was taken up in 20 ml. of methanol in an evaporating dish. 2,5-Dichlorophenylhydrazine (0.65 gm.) was added and the methanol was rapidly distilled on the steam bath (procedure of Mandl and Neuberg (17)). The product was dissolved in ether, filtered, and the ether was distilled. The residue was dissolved in ethyl acetate, treated with charcoal, and an equal volume of benzene was added. Crystallization was rapid in the cold. Weight, 0.68 gm. (68%), m.p. 101–105° C. Recrystallized twice from

ethyl acetate – benzene (1: 1), m.p. 110–112° C., $[\alpha]_D^{27}$ −12.5° (*c*, 1, methanol). (m.p. 110° C. (19)). Calc. for $C_{10}H_{12}O_3N_2Cl_2$: N, 10.04%; found: N, 10.06%.

By using an excess of the hydrazine reagent (1.6 moles per mole) and distilling off three successive additions of methanol containing a few drops of acetic acid, an osazone was obtained. Melting point after recrystallization from ethyl acetate – benzene (1: 1), 219–220° C. Calc. for $C_{16}H_{14}O_2N_4Cl_4$: N, 12.81%; found: N, 12.85%.

L-*Glyceraldehyde*

The method for preparation of the L-glyceraldehyde formate ester was the same as for di-*O*-formyl-D-erythrose differing only in the quantities of oxidant and oxalic acid used. L-Arabinose (1.5 gm.) was oxidized with 9.0 gm. of lead tetraacetate and most of the lead was removed by the addition of 2.5 gm. of oxalic acid dihydrate dissolved in acetic acid. The product obtained by ethyl acetate extraction was a clear, pale yellow oil. Weight, 1.2 gm. This compound, which is described in greater detail elsewhere (24), is found to contain about 1.5 formate ester groups.

The ester (0.201 gm.) was hydrolyzed to constant rotation in 10% acetic acid at 50° C. (7.5 hr.), and the acid was removed by distillation. The quantity of sugar estimated by hypoiodite oxidation was 0.102 gm., corresponding to a yield of L-glyceraldehyde from the ester of 83% $[\alpha]_D^{27}$ −7.15° (equilibrium) (*c*, 2).

Dimedon-L-*glyceraldehyde*

L-Glyceraldehyde formate ester (1.02 gm.) in 100 ml. of phosphate buffer (containing 10 ml. of 1 *M* monopotassium phosphate and 5.9 ml. of 1 *N* sodium hydroxide) was treated with 2.0 gm. of dimedon at room temperature. After 18 hr. reaction time the solution was concentrated and the crystalline product was recovered by filtration. Weight, 1.73 gm. (73%), m.p. 191–200° C. Two recrystallizations from 50% alcohol raised the melting point to 196.5–198.5° C.; $[\alpha]_D^{27}$ −208° (*c*, 0.5, ethanol), (m.p. 198° C., $[\alpha]_D$ −198° (2)). Calc. for $C_{19}H_{26}O_5$: C, 68.24%; H, 7.84%; found: C, 67.97%; H, 7.86%.

L-*Glyceraldehyde-2,4-dinitrophenylhydrazone*

To a solution of L-glyceraldehyde (0.71 gm.) in 25 ml. of water, cooled in an ice-bath, was added a slightly warm solution of 2,4-dinitrophenylhydrazine (1.6 gm.) in 2 *N* hydrochloric acid (90 ml.) over a period of 30 min. The reaction mixture was maintained at 0° C. for an additional 30 min. A copious yellow precipitate which formed was filtered, then washed with dilute hydrochloric acid and water, and dried. Weight, 0.97 gm., m.p. 120–140° C. Recrystallized three times from 50% alcohol, m.p. 146–148° (m.p. 147–148° (2)). Calc. for $C_9H_{10}O_6N_4$: C, 40.00%; H, 3.73%; found: C, 40.09%; H, 3.83%.

ACKNOWLEDGMENT

The technical assistance of Mr. J. Giroux is gratefully acknowledged. The authors express their gratitude to Dr. A. C. Neish for the gift of a sample of D-erythrose, to Mr. J. Baignee for analyses, to Miss A. Epp for preparation of infrared spectra, and to Dr. W. H. Barnes for X-ray diffraction analyses.

REFERENCES

1. ADAMS, R., VOORHEES, V., and SHRINER, R. L. Organic syntheses, Collective Vol. 1. John Wiley & Sons, Inc., New York. 1932. p. 452.
2. BAER, E. and FISCHER, H. O. L. J. Am. Chem. Soc. 61: 761. 1939.
3. BAER, E., GROSHEINTZ, J. M., and FISCHER, H. O. L. J. Am. Chem. Soc. 61: 2607. 1939.
4. BOGGS, L., CUENDET, L. S., EHRENTHAL, I., KOCH, R., and SMITH, F. Nature, 166: 520. 1950.
5. FISCHER, H. O. L. and BAER, E. Helv. Chim. Acta, 17: 622. 1934.
6. FREUDENBERG, W. Ber. 65: 168. 1932.
7. FRUSH, H. L. and ISBELL, H. S. J. Research Natl. Bur. Standards, 51: 307. 1953.
8. HINTON, C. L. and MACARA, T. Analyst, 49: 2. 1924.
9. HOCKETT, R. C. J. Am. Chem. Soc. 57: 2260. 1935.
10. HOCKETT, R. C. J. Am. Chem. Soc. 57: 2265. 1935.
11. HOCKETT, R. C., DEULOFEU, V., SEDOFF, A. L., and MENDIVE, J. R. J. Am. Chem. Soc. 60: 278. 1938.
12. HOCKETT, R. C. and HUDSON, C. S. J. Am. Chem. Soc. 56: 1632. 1934.
13. HOCKETT, R. C. and ZIEF, M. J. Am. Chem. Soc. 72: 2130. 1950.
14. HOUGH, L. and TAYLOR, T. J. Chemistry & Industry, 575. 1954.
15. JERMYN, M. A. and ISHERWOOD, F. A. Biochem. J. 44: 402. 1949.
16. MACDONALD, D. L. and FISCHER, H. O. L. J. Am. Chem. Soc. 74: 2087. 1952.
17. MANDL, I. and NEUBERG, C. Arch. Biochem. and Biophys. 35: 326. 1952.
18. NEISH, A. C. Can. J. Chem. 32: 334. 1954.
19. NEISH, A. C. Private communication.
20. OVEREND, W. G., STACEY, M., and WIGGINS, L. F. J. Chem. Soc. 1358. 1949.
21. PARTRIDGE, S. M. Nature, 158: 270. 1946.
22. PARTRIDGE, S. M. Nature, 164: 443. 1949.
23. PERLIN, A. S. J. Am. Chem. Soc. 76: 2595. 1954.
24. PERLIN, A. S. and BRICE, C. Chemistry in Can. (Abstr.), 7(No. 5): 55. 1955.
25. RAPPAPORT, D. A. and HASSID, W. Z. J. Am. Chem. Soc. 73: 5524. 1951.
26. RUFF, O. Ber. 32: 3672. 1899.
27. SCHIEDT, O. and REINWEIN, H. Z. Naturforsch. 76: 270. 1952.
28. SCHÖPF, C. and WILD, H. Ber. 87: 1571. 1954.
29. SOWDEN, J. C. J. Am. Chem. Soc. 71: 1897. 1949.
30. SOWDEN, J. C. J. Am. Chem. Soc. 72: 808. 1950.
31. VOGEL, A. I. Practical organic chemistry. Longmans, Green and Co., Inc., New York. 1948.
32. WALLENFELS, K. W. Naturwiss. 37: 491. 1950.
33. WOHL, A. Ber. 32: 3666. 1899.
34. WOHL, A. and MOMBER, F. Ber. 47: 3346. 1914.
35. WOHL, A. and NEUBERG, C. Ber. 33: 3095. 1900.

MECHANISM FOR THE FORMATION OF GUANIDINE FROM UREA AND AMMONIUM SULPHAMATE[1]

By Jean L. Boivin and A. L. Lovecy

ABSTRACT

The over-all mechanism of the formation of guanidine from urea and ammonium sulphamate is briefly discussed. Experimental results are presented, indicating that primary formation of the ammonium salt of ureasulphonic acid and subsequent dissociation into cyanamide and ammonium sulphate, which further react to form guanidine in the known manner, constitute the main steps in the process.

The essential process of conversion of urea to guanidine may be described as the ammonolysis of urea:

[1] $$\begin{matrix} NH_2 \\ | \\ C{=}O \\ | \\ NH_2 \end{matrix} \rightleftharpoons \begin{matrix} NH \\ \| \\ C{-}OH \\ | \\ NH_2 \end{matrix} + NH_3 \rightleftharpoons \begin{matrix} NH \\ \| \\ C{-}NH_2 \\ | \\ NH_2 \end{matrix} + H_2O\,.$$

Although this equilibrium reaction has been stated to occur in liquid ammonia, there is no reliable evidence that an acceptable yield is obtainable. Blair (2) obtained a 23% yield; Sander (6) using aluminum, aluminum chloride, or phosphorus pentoxide to remove the water formed reported yields of 90%.

In considering possible dehydrating agents to remove the water formed and so assist the completion of the equilibrium reaction (Eq. [1]), sulphur trioxide or its reaction products with ammonia are attractive (5) from the viewpoint of economy and availability:

[2] $$H_2N{-}SO_3NH_4 + H_2O \rightarrow (NH_4)_2SO_4.$$

Combining equation [2] with [1] gives the following over-all equation:

[3] $$\begin{matrix} NH_2 \\ | \\ C{=}O \\ | \\ NH_2 \end{matrix} + H_2N{-}SO_3NH_4 \rightarrow \begin{matrix} NH_2 \\ | \\ C{=}NH\,. \\ | \\ NH_3.NH_4SO_4 \end{matrix}$$

Whilst in fact urea does react with sulphamic acid to produce guanidine the reaction is not adequately described by the simple dehydration process indicated above (Eq. [3]), since the following facts must be explained: The fusion of equimolar quantities of urea and sulphamic acid yields traces of guanidine; substitution of ammonium sulphamate gives a pronounced increase in yield mainly when an excess of the former is used (5). Ammonium sulphamate does not in fact react readily with water (3).

In view of these facts, there is no evidence that the reaction-sequence involves an initial dehydration of urea (Eq. [1]) with subsequent or simultaneous interaction of ammonium sulphamate with the water formed (Eq. [2]).

[1]*Manuscript received March 2, 1955.*
Contribution from the Organic Section of Canadian Armament Research and Development Establishment, Valcartier, Quebec. Issued as C.A.R.D.E. Report No. 43, August 1950.

In seeking an alternative mechanism, it is reasonable to consider the elimination of ammonia rather than water as the primary step, particularly in view of the observation that ammonia is liberated at a temperature of 140° C.

There are two ways in which this might occur when urea and ammonium sulphamate are fused together:

[4] $$\begin{array}{l} NH_2 \\ | \\ C{=}O \\ | \\ NH_2 \end{array} + H_2N{-}SO_3NH_4 \rightarrow \begin{array}{l} NH_2 \\ | \\ C{=}O \\ | \\ NH_2.HO_3S{-}NH_2 \end{array} + NH_3,$$

[5] $$\begin{array}{l} NH_2 \\ | \\ C{=}O \\ | \\ NH_2 \end{array} + H_2N{-}SO_3NH_4 \rightarrow \begin{array}{l} NH_2 \\ | \\ C{=}O \\ | \\ NHSO_3NH_4 \end{array} + NH_3.$$

As regards equation [4], attempts to prepare a definite urea salt of sulphamic acid were unsuccessful. When an aqueous solution containing equimolar quantities of the base and acid was evaporated to dryness, and the solid obtained was extracted with alcohol, a solution of urea and a residue of sulphamic acid were obtained.

Attention was therefore turned to the second alternative (Eq. [5]), i.e. the formation of ammonium ureasulphonate. Ureasulphonic acid itself has been prepared by the sulphonation of urea with sulphur trioxide and is an intermediate in the formation of sulphamic acid as described by Baumgarten (1). It has now been prepared in 60% yield by treatment of urea with sulphuric acid and acetic anhydride at low temperature, whereby a viscous product separates, believed to be the urea salt of ureasulphonic acid. By dissolving this material in absolute ethanol and passing in gaseous ammonia a crystalline compound was obtained, m.p. 168–170° C.; this was the ammonium salt of ureasulphonic acid, described by Linhard (4).

By fusion of this salt alone at 240° C. a yield of guanidine equivalent to 43–45% of the theoretical was obtained (estimated as the picrate). Melamine was also shown to be present in 22% yield. This result indicates that ureasulphonic acid may be involved in the conversion of urea to guanidine. Heating under a pressure of ammonia was tried, the ammonia being introduced as liquid. At a pressure of 1500 p.s.i. and 295° C., the yield of guanidine obtained after one and one-quarter hours was 63%, and at a pressure of 200 p.s.i. and 300° C., the yield of guanidine was only 10% but melamine was formed in 77% yield.

A reaction based on the formation of cyanic acid from urea would also explain the mechanism:

[6] $$NH_2{-}CO{-}NH_2 \rightleftharpoons NH_4OCN \rightleftharpoons NH_3 + HOCN,$$

[7] $$HOCN + NH_2SO_3NH_4 \rightarrow NH_4SO_3{-}NH{-}CO{-}NH_2.$$

The formation of cyanic acid takes place at temperatures upwards of 140° C. and it seems that this active fragment reacts with sulphamic acid to form ureasulphonic acid. Actually, a 57% yield of the latter compound has been

isolated from a melt of urea with ammonium sulphamate, carried out at a temperature not exceeding 140° C. under reduced pressure.

Assuming the primary formation of ammonium ureasulphonate as probable, its subsequent conversion to guanidine is still by no means obvious. It is conceivable that a further dissociation and rearrangement is involved, particularly since a temperature in the region of 290° C. seems necessary in order to obtain a good yield.

By analogy with the fusion of amides with ammonium sulphamate or the intermediate product, ammonium N-alkylsulphamates, which are transformed into high yields of nitriles (3), it seems that ammonium ureasulphonate should produce the corresponding nitrile which is cyanamide (Eq. [8]).

[8] $$\begin{matrix} NH_2 \\ | \\ C{=}O \\ | \\ NHSO_3NH_4 \end{matrix} \rightarrow \begin{matrix} NH_2 \\ | \\ C{\equiv}N \end{matrix} + NH_4HSO_4$$

[9] $$\begin{matrix} NH_2 \\ | \\ C{\equiv}N \end{matrix} + (NH_4)_2SO_4 \rightarrow \begin{matrix} NH_2 \\ | \\ C{=}NH \\ | \\ NH_3.NH_4SO_4 \end{matrix}$$

It is well known that cyanamide in the presence of ammonium salt is quickly transformed into guanidine (Eq. [9]) or its trimer, melamine.

EXPERIMENTAL

Ammonium Ureasulphonate

To a cold solution (−20° C.) of acetic anhydride (250 ml.) and sulphuric acid (95%, 48 gm., 0.5 mole) was added a solid feed of finely powdered urea (60 gm., 1.0 mole). The temperature of the mixture was allowed to rise slowly to 15° C. with occasional stirring. Urea dissolved completely, and at 15–18° C. a viscous product was formed which was decanted. This oily material was dissolved in absolute ethanol (500 ml.) (methanol is not suitable). The solution was chilled to −30° C. and saturated with gaseous ammonia. A crystalline compound separated out. It was filtered, washed thoroughly with ether, and dried, m.p. 167.5–168° C. with decomposition. Yield, 47 gm. (60% from sulphuric acid). The urea in excess may be recovered by evaporation of the filtrate.

This ammonium ureasulphonate was hydrolyzed quantitatively with dilute nitric acid to urea nitrate and sulphuric acid. By treatment of this substance with concentrated sulphuric acid, sulphamic acid is obtained (1).

Guanidine from Ammonium Ureasulphonate

(*A*) This ammonium salt (5.1 gm.) was heated at 225–230° C. for one-half hour. The residue was dissolved in water and analyzed for guanidine and melamine. Guanidine: 0.8 gm. (42%); melamine: 22%.

(*B*) The same ammonium salt (5.3 gm., 0.03 mole) and liquid ammonia (20 ml.) were heated in a closed vessel at 295° C. for 75 min. at a pressure of 5100 p.s.i.g. Guanidine: 63%; melamine was absent.

(*C*) The same reaction was effected as above, but conditions were the following: temp.: 300° C.; heating time: 17 hr.; pressure: 200 p.s.i.; melamine: 77%; guanidine: 10%.

Preparation of Ammonium Ureasulphonate from Urea and Ammonium Sulphamate

Urea (6.0 gm., 0.1 mole) and ammonium sulphamate (11.7 gm., 0.1 mole) were heated at 135–140° C. under reduced pressure (15 mm.) in order to eliminate the ammonia formed in the reaction. The heating was effected during six hours. The reaction mixture was boiled with 85% ethanol. On cooling, a crystalline compound separated out. It was filtered and dried, m.p. 165–166° C. By working up the filtrate, it was possible to isolate 9.1 gm. of this material (57%). A portion of this solid was recrystallized from ethanol. It melted at 167–168° C. A mixed melting point with an authentic sample was not depressed.

REFERENCES

1. BAUMGARTEN, P. Ber. B, 64: 301. 1931.
2. BLAIR, J. S. J. Am. Chem. Soc. 48: 87. 1926.
3. BOIVIN, J. L. Can. J. Research, B, 28: 671. 1950.
4. LINHARD, M. Ann. 525: 267. 1938.
5. MACKAY, J. S. U.S. Patent No. 2,515,244. July 18, 1950.
6. SANDER, F. Ger. Patent No. 527,237. Jan. 1, 1928.

INFRARED AND RAMAN SPECTRA OF 1-CHLOROPROPYNE AND 1-CHLOROPROPYNE-d_3[1]

By D. W. Davidson[2] and H. J. Bernstein

ABSTRACT

The infrared spectra of 1-chloropropyne and 1-chloropropyne-d_3 have been investigated in the vapor state, in solution, and, in part, in the liquid over the spectral region 3 to 35μ. Intensities of the infrared bands have been measured from the spectra of the solutions. The Raman spectra of the compounds in the liquid state, together with standard intensities and depolarization ratios of the Raman bands, were obtained. A complete assignment, based on a normal coordinate calculation of the fundamentals, has been made. Coriolis coupling coefficients of three of the perpendicular-type fundamentals of $CH_3C{\equiv}CCl$ were determined and those of the other two shown to be near unity. Two coupling coefficients for $CD_3C{\equiv}CCl$ were obtained. The potential function and isotope effects on Raman intensity and Raman displacement of the CCl stretching vibration are discussed.

INTRODUCTION

1-Chloropropyne (methylchloroacetylene: $CH_3C{\equiv}CCl$) has been investigated previously by Cleveland and Murray (5), who obtained the Raman spectrum of the liquid, as prepared by a Grignard reaction from methylacetylene. These Raman bands were tentatively assigned by Meister (14), with the aid of a normal coordinate treatment. Parts of the chloropropyne spectrum were obscured, however, by lines arising from the presence of ethyl bromide in considerable quantity in the sample. Morse and Leitch (15) have recently reported a more efficient synthesis and have provided us with a sample both of $CH_3C{\equiv}CCl$ and of the completely deuterated form $CD_3C{\equiv}CCl$ (1-chloropropyne-d_3). We have investigated the vibrational spectra of these molecules and confirm Meister's assignment of fundamentals for $CH_3C{\equiv}CCl$.

Methylchloroacetylene belongs to the C_{3v} symmetry point group and possesses five normal vibrations of symmetry type A_1 and five doubly degenerate E-type vibrations. With the exception of $\nu_{10}(e)$, all the fundamentals in both molecules have been observed. Assignments have been made for the combination bands, although in some cases it has not been possible to choose between alternative assignments. Sum and difference bands involving $\nu_{10}(e)$ have been used to fix approximately the frequency of this mode.

An attempt has been made to measure the intensities of prominent bands in both the infrared and Raman spectra and the depolarization ratios of the stronger Raman bands. The Coriolis coupling coefficients were determined for the fundamental bands of the perpendicular type, wherever these were resolved.

EXPERIMENTAL METHODS

The infrared data were obtained with a single beam double pass Perkin-Elmer spectrometer (Model 112) using LiF, CaF_2, NaCl, KBr, and CsBr

[1]*Manuscript received January 18, 1955.*
Contribution from the Division of Pure Chemistry, National Research Council, Ottawa, Canada. Issued as N.R.C. No. 3643.
Presented at the Symposium on Molecular Structure, Columbus, Ohio, June 1954.
[2]*National Research Council Postdoctorate Research Fellow 1951–1953.*

prisms. Window materials were KBr, except for the CsBr region where windows of KI-TlI were used. Except for a few strong bands, which were examined also at lower pressures, vapor spectra were obtained at the vapor pressure of the liquid at 22°C. For $CH_3C{\equiv}CCl$ and $CD_3C{\equiv}CCl$ these pressures were approximately 530 and 560 mm., respectively.[3] Band intensities were determined for spectra obtained in solutions in CS_2 or CCl_4. The solution spectra were useful also for resolving bands which overlap in the vapor spectra, and, together with the liquid spectra recorded at low frequencies, for detecting weak bands.

Raman spectra of $CH_3C{\equiv}CCl$ were recorded by two methods. In the first, as in previous work (2), a double-prism photographic instrument (f/3.5, dispersion 29 Å/mm. at 5000 Å) was used. The second instrument was a new photoelectric-recording grating spectrometer (21), constructed by the White Development Corporation, Stamford, Connecticut. The photoelectric instrument has the advantage of speed and simplicity in the determination of relative intensities and depolarization ratios. The method of Edsall and Wilson (8) was used to measure depolarization ratios. The Raman spectrum of $CD_3C{\equiv}CCl$ was obtained with the photoelectric instrument only. Both liquids turned yellowish under mercury radiation, although the effect was considerably reduced when a filter consisting of a saturated aqueous solution of $NaNO_2$ was placed between the mercury source and the Raman tube. This filter also practically eliminated excitation by the Hg > 4047 line.

RESULTS

The infrared spectra are shown in Figs. 1 and 2 and the observed bands listed in Tables I and II. The photoelectrically-recorded Raman spectra are reproduced in Fig. 3 and the data given in Tables III and IV.

Most of the observed infrared and Raman bands could be satisfactorily ascribed to $CH_3C{\equiv}CCl$ or $CD_3C{\equiv}CCl$. Near 800 cm.$^{-1}$, however, absorption occurred in solution spectra of both molecules, although it was absent in the vapor spectra. It was greatly reduced by distillation and is attributed to traces of grease.

The results of Cleveland and Murray (5) are included in Table III. The band observed by them at 184 cm.$^{-1}$ was not observed directly in the present work, probably because of its weakness and interference from grating ghosts in this part of the spectrum. Nor was the corresponding band in the spectrum of $CD_3C{\equiv}CCl$ observed.

INTENSITIES OF INFRARED BANDS

Integrated extinction coefficients (ϵ) for the solution bands (Tables I and II) were calculated from the maximum optical density ($d_{max.} = \log_{10} I_0/I$) and the band width ($\Delta\nu_{\frac{1}{2}}$) at half-maximum intensity, assuming the Lorentz band shape. The small correction for finite spectral slit width (s) was incorporated in ϵ by multiplying $d_{max.} \cdot \Delta\nu_{\frac{1}{2}}/c.l$ by the factor K, usually not quite $\pi/2$, as tabulated by Ramsay (16). The concentration c has been expressed in moles

[3]*These values were derived by an extrapolation of the vapor pressure vs. temperature curves of Morse and Leitch (15).*

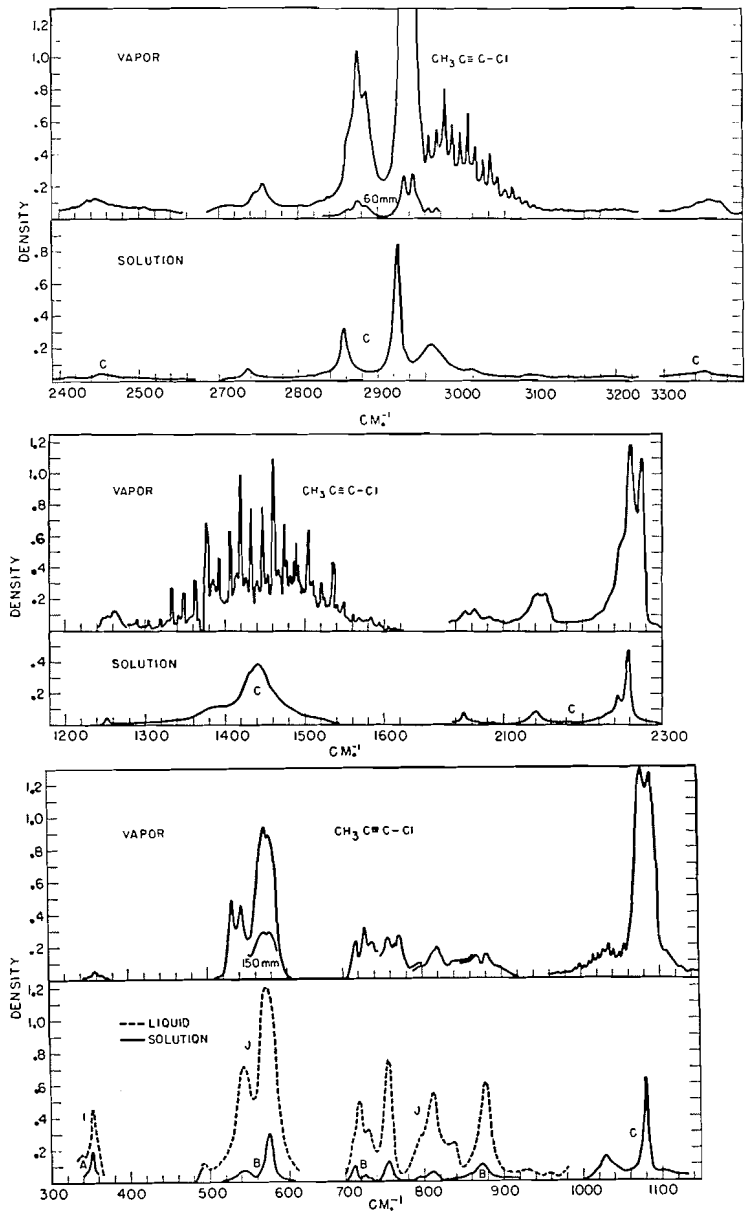

FIG. 1. Infrared spectra of $CH_3C\equiv C—Cl$.

per liter and the cell thickness l in centimeters. The value of s was taken to be half the spectral slit width for single pass optics.

DEPOLARIZATION RATIOS AND INTENSITIES OF RAMAN BANDS

Because of the convergence of light from the source on the Raman tube, the observed depolarization ratio ρ has been corrected to give the true value

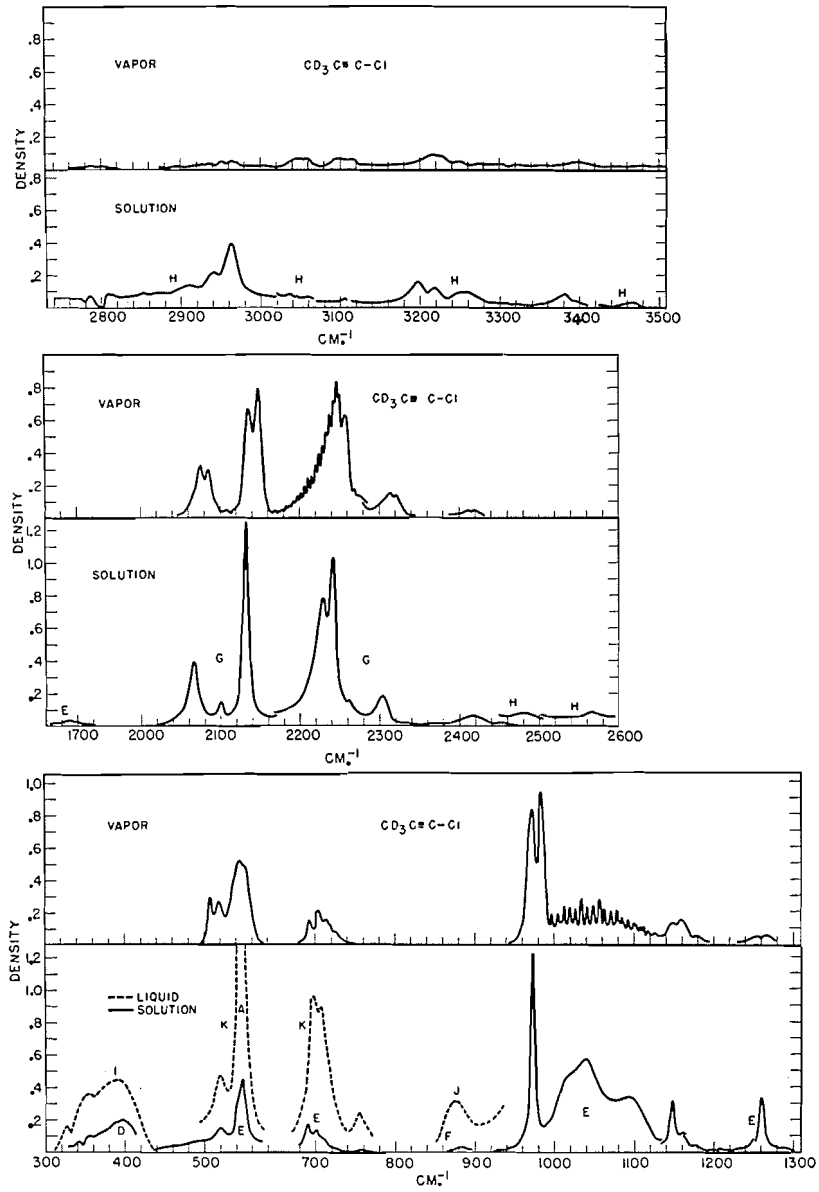

FIG. 2. Infrared spectra of $CD_3C{\equiv}C{-}Cl$.

ρ_t essentially according to the method of Rank and Kagarise (17). Values of ρ and ρ_t are given in Tables III and IV.

These tables include also the peak intensity (i) relative to that of the $\nu_1(a_1)$ band (taken as $i = 100$) which includes the correction for the spectral sensitivity of the IP21 photomultiplier. The observed half-band widths ($\Delta\nu_{\frac{1}{2}}$) and spectral slit width s are also given and the standard intensity S referred to the 458 cm.$^{-1}$ band in CCl_4 for each band obtained from the equation (1).

[1] $$S = \frac{I}{I_{458}} \frac{1+\rho_{458}}{1+\rho} \frac{n^2}{n^2_{CCl_4}} \frac{\sigma_{\Delta\nu}}{\sigma_{458}} \frac{R(n)}{R_{CCl_4}} \frac{M}{d} \left(\frac{d}{M}\right)_{CCl_4} \times \frac{\Delta\nu}{458} \left(\frac{\nu-458}{\nu-\Delta\nu}\right)^4 \frac{1-e^{-1.44\Delta\nu/T}}{1-e^{-1.44\times458/T}}.$$

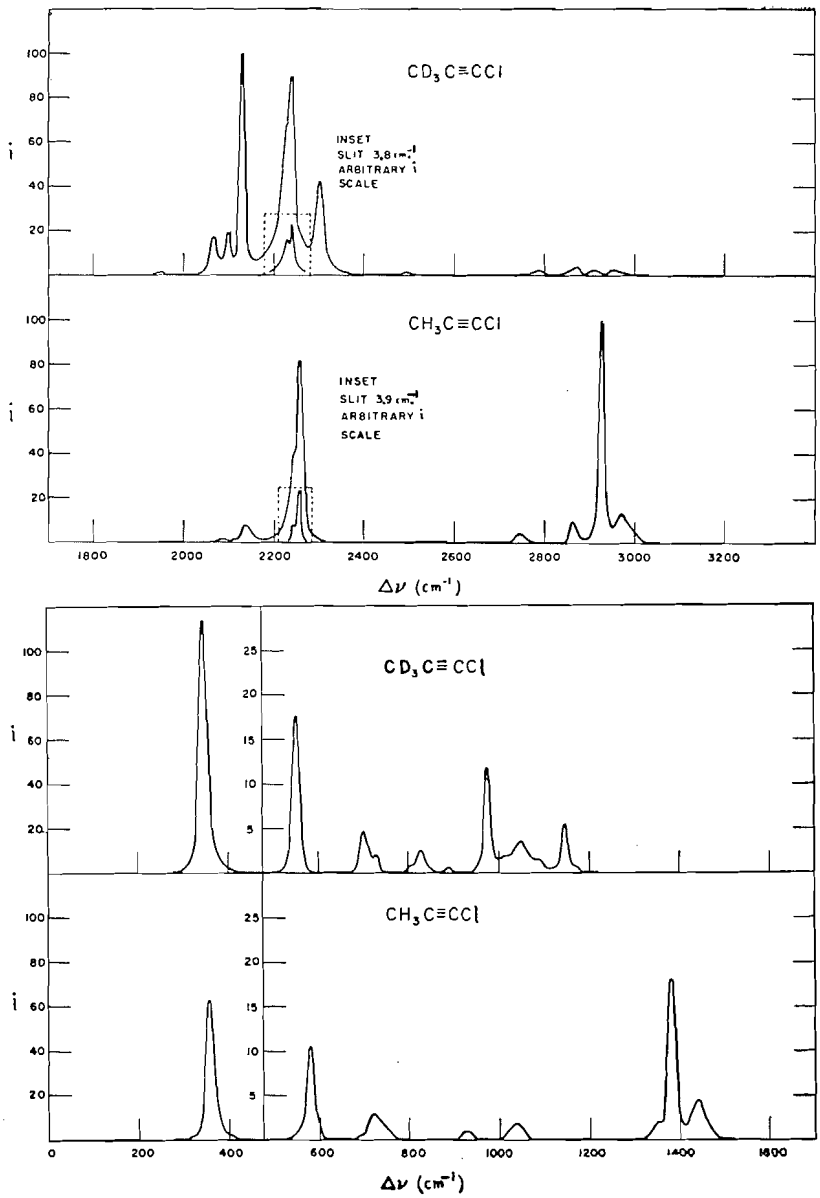

FIG. 3. Raman spectra of liquid $CH_3C{\equiv}C{-}Cl$ and $CD_3C{\equiv}C{-}Cl$.

TABLE I

INFRARED DATA FOR $CH_3C{\equiv}CCl$

Vapor			Solution						Liquid		
$\nu_{vac.}$, cm.$^{-1}$	s, cm.$^{-1}$	Band character	$\nu_{vac.}$, cm.$^{-1}$	Conditions	$d_{max.}$	$\Delta\nu_{\frac{1}{2}}$, cm.$^{-1}$	s, cm.$^{-1}$	ϵ*	$\nu_{vac.}$, cm.$^{-1}$	Conditions	Assignments
358	2.1		351.8	*A*	0.193	8.5	4.2	35	353.2	*I*	$\nu_9(e)$
536.8	2.1	Doublet	544	A_1	0.58	28	1.9	157	544	*J*	$\nu_9(e)+\nu_{10}(e) = 542$
575.3	2.1	Doublet	576	*B*	0.32	12	2.6	180	573	*J*	$\nu_6(a_1)$
721	2.5	Doublet	713	*B*	0.090	~10	4.1	~ 40	718	*J*	$\{2\nu_9(e)=716; \nu_9(e)+2\nu_{10}(e)=726\}$
734.2	2.6	Doublet	725	*B*	0.030	~ 9	2.7	~ 13	729	*J*	$\{\nu_4(a_1)-\nu_9(e)=726\}$
765	2.5	Triplet	755.6	*B*	0.116	10	3.1	55	754.8	*J*	$\nu_5(a_1)+\nu_{10}(e) = 759$
819	3.1	Single pk.?	811	*B*	0.054	13	2.6	30	810	*J*	$\nu_3(a_1)-\nu_5(a_1) = 820$
840	3.1								836	*J*	$\nu_8(e)-\nu_{10}(e) = 849$
874.8	2.4	Doublet	871.5	*B*	0.097	14	3.3	65	876	*J*	$\nu_7(e)-\nu_5(a_1) = 878$
1033.0	3.1	*K*-structure	1029.3	*C*	0.155	21	3.7	157	1025.5	*J*	$\nu_8(e)$
1083.6	3.8	Doublet	1080.3	*C*	0.63	8.7	4.5	250	1074.5	*J*	$\nu_4(a_1)$
1257.5	3.4	Doublet	1252.2	*C*	0.046		4.2	w			$\nu_7(e)-\nu_{10}(e) = 1270$
~1395	3.8	Doublet	~1379	*C*	~0.041		5.8	w			$\nu_3(a_1)$
1453.7_8	2.7	*K*-structure	1440.0	*C*	0.385	~48	6.7	~890			$\nu_7(e)$
2058.5	1.6	Doublet	2050.5	*C*	0.075	8.5	2.8	30			$2\nu_8(e) = 2066$
2089	1.8	Doublet	2079	*C*	0.060		1.2				$\nu_2(a_1)-\nu_{10}(e) = 2084$
2149	2.0	Doublet	2141	*C*	0.085	17	3.2	69			$2\nu_4(a_1) = 2168$
~2222	2.0	Single pk.?	2219	*C*	~0.030		3.5				$\{\nu_2(a_1)+n\nu_1(e)$
~2233	2.0	Single pk.?	2231	*C*	~0.030		3.5				$\{-n\nu_1(e)\}$
2252	2.0	Doublet	2245	*C*	0.14	~15	3.6	~100			
2267.7	2.0	Doublet	2258	*C*	0.48	7.6	3.7	165			$\nu_2(a_1)$
2444.5	2.2		2451	*C*	~0.030		3.4				$\nu_2(a_1)+\nu_{10}(e) = 2452$
2749	3.0	Doublet	2736	*C*	0.065	~19	4.7	~ 58			$\nu_1(a_1)-\nu_{10}(e)=2755$; $2\nu_3(a_1) = 2790$
2875.5	3.5	Triplet?	2857.5	*C*	0.320	14	5.4	207			$2\nu_7(e) = 2906$
2939.2	3.7	Doublet	2924.8	*C*	0.837	10.3	5.8	396			$\nu_1(a_1)$
2980.0	2.9	*K*-structure	2967.3	*C*	0.225	43	6.1	466			$\nu_6(e)$
~3198	3.5	Broad pk.									$\nu_6(e)+\nu_{10}(e)=3164$; $\nu_1(a_1)+\nu_9(e) = 3297$
~3357	4.1	Broad pk.	~3351	*C*	~0.030	~21	6.1	~ 30			$\nu_2(a_1)+\nu_4(a_1) = 3352$

Letters under "Conditions" identify the solvent, concentration, and cell in the case of solutions and the cell in the case of liquids:

A 2.7 M./l. in CS_2, 0.25 mm. KI-TlI cell,
A_1 same solution in 0.60 mm. KBr cell,
B 1.35 M./l. in CS_2, 0.24 mm. KBr cell,
C 1.35 M./l. in CCl_4, 0.24 mm. KBr cell,
I liquid in 0.25 KI-TlI cell,
J in 0.24 mm. KBr cell,
**ϵ is the integrated extinction coefficient in mole^{-1} liters cm^{-2}.*

TABLE II

INFRARED DATA FOR $CD_3C{\equiv}CCl$

Vapor			Solution						Liquid		
$\nu_{vac.}$, cm.$^{-1}$	s, cm.$^{-1}$	Band character	$\nu_{vac.}$, cm.$^{-1}$	Conditions	$d_{max.}$	$\Delta\nu_{\frac{1}{2}}$ cm.$^{-1}$	s, cm.$^{-1}$	ϵ	$\nu_{vac.}$, cm.$^{-1}$	Conditions	Assignments*
			$\sim$ 341	D	$\sim$0.050	$>$20	1.9	$>$ 8	327	I	$\nu_3(a_1)-\nu_8(e)$ = 326
			$\sim$ 355	D	$\sim$0.10	Broad	2.3	$\sim$ 15	352	I	$2\nu_{10}(e)$ = 354
			$\sim$ 396	D	$\sim$0.20	$>$35	2.7	$\sim$ 54	388	I	$\nu_9(e)$
512.8	1.25	Doublet	519.6	E	0.110	20	2.1	70	519.8	K	$\nu_9(e)+\nu_{10}(e)$ = 520
546.8	1.50	Doublet	548.2	E	0.146	14.5	2.4	207	547.3	K	$\nu_5(a_1)$
698.6	1.55	Doublet	689.4	E	0.173	$\sim$10	2.0	$\sim$ 55	696	K	$2\nu_9(e)$ = 686
$\sim$ 714	1.6		701.5	E	$\sim$0.09	$\sim$24	2.1	$\sim$ 69	706	K	$\nu_7(e)-\nu_9(e)$ = 704
? 726	2.1		728	E	$\sim$0.015		2.3				$\nu_5(a_1)+\nu_{10}(e)$ = 724
888	1.6		882	F	0.030		4.1		875	J	$\nu_5(a_1)+\nu_9(e)$ = 890
977.2	1.4	Doublet	972.7	E	1.22	5.5	2.1	214			$\nu_4(a_1)$
			$\sim$1013	E		Broad	2.4				$3\nu_9(e)$ = 1029; $\nu_8(e)+\nu_{10}(e)$ = 1002
1050.8	1.7	K-structure	1038	E	$\sim$0.57	$\sim$27	2.6	$\sim$492			$\nu_7(e)$
$\sim$1107	2.2	Doublet	1095	E	$\sim$0.27	$\sim$35	2.8	$\sim$303			$2\nu_5(a_1)$ = 1094; $\nu_2(a_1)-\nu_3(a_1)$ = 1101
1151	2.4	Doublet	1148	E	0.360	9.0	2.0	103			$\nu_3(a_1)$
$\sim$1159	2.4	Shoulder	1162	E	$\sim$0.060		2.0				$\nu_8(e)+\nu_9(e)$ = 1168; $\nu_4(a_1)+\nu_{10}(e)$ = 1154
?1178	2.1	Single pk.	?$\sim$1177	E	$\sim$0.030		2.1				$\nu_6(e)-\nu_7(e)$ = 1184
$\sim$1260	5.7	Doublet	1260	E	0.34	9.6	1.6	105			$\nu_2(a_1)-\nu_4(a_1)$ = 1275; $\nu_6(e)-\nu_4(a_1)$ = 1258
2080.4	1.7	Doublet	2061	H	0.86	17	3.2	161			$2\nu_7(e)$ = 2102; $\nu_2(a_1)-\nu_{10}(e)$ = 2075
$\sim$2113	1.8	Doublet	2100	G	0.146	10	3.5	45			$\nu_3(a_1)+\nu_4(a_1)$ = 2128
2142.4	1.9	Doublet	2134.8	G	1.26	8.6	3.7	345			$\nu_1(a_1)$
2235.4	2.1	K-structure	2229.3	G	$\sim$0.60	$\sim$28	3.3	$\sim$538			$\nu_6(e)$
2252	2.1	Doublet	2242	G	$\sim$0.60	$\sim$ 6	3.3	$\sim$107			$\nu_2(a_1)$

2273	2.2	Doublet	2262	*G*	~0.05		3.4		$\nu_2(a_1)+\nu_{10}(e)-\nu_{10}(e)$?
2318	2.3	Doublet?	2303	*G*	0.180	20	3.6	115	$2\nu_3(a_1) = 2302$; $\nu_1(a_1)+\nu_{10}(e) = 2319$
2414	1.9	Doublet?	2416	*H*	0.170	~14	3.1	~ 26	$\nu_6(e)+\nu_{10}(e) = 2412$; $\nu_2(a_1)+\nu_{10}(e) = 2429$
			~2480	*H*	~0.030		3.2		$\nu_1(a_1)+\nu_9(e) = 2485$
			~2566	*H*	~0.030		3.0		$\nu_6(e)+\nu_9(e) = 2578$; $\nu_2(a_1)+\nu_9(e) = 2595$
~2795	2.9	Doublet	2785	*H*	~0.080		3.8		$\nu_2(a_1)+\nu_5(a_1) = 2799$
			~2907	*H*	~0.060		4.3		$\nu_6(e)+2\nu_9(e) = 2921$
? 2952	2.5	May together	~2939	*H*	0.13		4.4		$\nu_2(a_1)+2\nu_9(e) = 2938$
? 2966	2.5	form a doublet	2963	*H*	0.39	22	4.6	94	$\nu_1(a_1)+\nu_8(e) = 2967$
3057		Doublet	3042	*H*	w		3.4		$\nu_6(e)+\nu_8(e) = 3060$; $\nu_2(a_1)+\nu_8(e) = 3077$
3105		Doublet	3106	*H*	0.056		3.6		$\nu_1(a_1)+\nu_4(a_1) = 3119$
3213	3.1	Broad pk.	3197	*H*	0.160	~24	4.0	42	$\nu_4(a_1)+\nu_6(e) = 3212$
			3219	*H*	~0.09		4.0		$\nu_4(a_1)+\nu_2(a_1) = 3229$
3248	3.3		3255	*H*	~0.10	Broad	4.4		$\nu_6(e)+\nu_7(e) = 3286$; $\nu_1(a_1)+\nu_3(a_1) = 3293$; $\nu_2(a_1)+\nu_7(e) = 3302$
3396	9.3		3380	*H*	0.080	~18	4.7	~ 16	$\nu_2(a_1)+\nu_3(a_1) = 3403$
			~3466	*H*	~0.034		5.1		$\nu_1(a_1)+\nu_4(a_1)+\nu_9(e) = 3462$

D *2.03 M./l. in CCl_4, 1 mm. cell,*
E *2.03 M./l. in CS_2, 0.24 mm. cell,*
F *4.06 M./l. in CCl_4, 0.24 mm. cell,*
G *2.03 M./l. in CCl_4, 0.24 mm. cell,*
H *2.03 M./l. in CS_2, 0.70 mm. cell,*
I *liquid in 0.25 mm. KI-TlI cell,*
J *0.24 mm. KBr cell,*
K *0.12 mm. KBr cell,*

**Raman values of $\nu_9(e) = 343$ cm.$^{-1}$ and $\nu_8(e) = 825$ cm.$^{-1}$ are used in evaluating combination bands.*

TABLE III

RAMAN SPECTRUM OF $CH_3C{\equiv}CCl$

Photoelectric instrument							Photographic instrument	Assignments[a]	Observed by Cleveland and Murray
$\Delta\nu_{vac.}$, cm.$^{-1}$	i	$\Delta\nu_{\frac{1}{2}}$, cm.$^{-1}$	s, cm.$^{-1}$	ρ	ρ_t	S	$\Delta\nu_{vac.}$, cm.$^{-1}$		$\Delta\nu_{vac.}$, cm.$^{-1}$
								$\nu_{10}(e) = 184$	184
355	63	19	10.9	0.93	0.78	0.22	±352	$\nu_9(e) = 354$	±353
								$\nu_8(e) - \nu_5(a_1) = 452$	439
579	11	19	10.7	0.32	0.19	0.12	577	$\nu_5(a_1) = 578$	
718	3	∼28	10.6	(0.5)[c]		∼0.06	725	$2\nu_9(e) = 708$	
								$\nu_8(e) - \nu_{10}(e) = 846$	842[b]
∼ 926	∼ 0.8	∼32	10.3	(0.9)[c]		∼0.03		$\nu_5(a_1) + \nu_9(e) = 932$	
∼1037	∼ 2		10.2				1030	$\nu_8(e) = 1030$	1029
1378	18	20.5	9.8	0.72	0.58	0.47	1380	$\nu_3(a_1) = 1379$	1380
1437	3.6	∼28	9.8	∼1.0	∼0.85	∼0.13	1444	$\nu_7(e) = 1443$	1449
∼2090	∼ 1	∼15	9.3			∼0.03		$\nu_4(a_1) + \nu_8(e) = 2114$	2102[b]
2138	8.3	20	9.2	0.38	0.24	0.48	2137	$2\nu_4(a_1) = 2168$	2134[b]
2244	∼15	∼20	3.9	∼1.0	∼0.85	∼0.66	2243	$\nu_2(a_1) + \nu_{10}(e) - \nu_{10}(e)$	2235
2257	69	18	3.9	0.44	0.30	3.99	2259	$\nu_2(a_1) = 2259$	2263
2450	∼ 5						2448	$\nu_2(a_1) + \nu_{10}(e) = 2443$	
2740	4	25	8.7	(0.5)[c]		0.38	2734	$2\nu_3(a_1) = 2758$	2733
2862	10	19.5	8.6	0.50	0.36	0.82	2859	$2\nu_7(e) = 2886$	2864[b]
2926	100	14.4	8.5	0.23	0.10	7.00	2926	$\nu_1(a_1) = 2926$	2926[b]
2971	8	∼32	8.5	0.93	0.78	1.80	2968	$\nu_6(e) = 2970$	2971[b]
∼3117	∼ 6		8.3				∼3115	$\nu_1(a_1) + \nu_{10}(e) = 3110$	

[a] *Fundamental frequencies given are those regarded as "best" from the Raman data. Wherever possible, the numbers given for the combination bands are evaluated from the "best" values of Raman fundamentals.* $\nu_4(a_1)$ *is taken to be 1084 cm*$^{-1}$.

[b] *These bands observed by Cleveland and Murray correspond approximately to ethyl bromide bands and may be affected by their presence.*

[c] *Parenthesized* ρ*'s are assumed values for the purpose of estimating S.*

TABLE IV

RAMAN SPECTRUM OF $CD_3C{\equiv}CCl$

$\Delta\nu_{vac.}$, cm.$^{-1}$	i	$\Delta\nu_{\frac{1}{2}}$, cm.$^{-1}$	s, cm.$^{-1}$	ρ	ρ_t	S	Assignments[a]
343	132	22.4	10.9	0.90	0.76	0.66	$\nu_9(e)$
551	19.9	18.7	10.7	0.32	0.19	0.22	$\nu_6(a_1)$
701	4.4	~29	10.6	(0.5)[b]		~0.09	$2\nu_9(e) = 686$; $\nu_7(e)-\nu_9(e) = 705$
~ 731	1.4						$\nu_5(a_1)+\nu_{10}(e) = 728$
825	2.9	23	10.4	~1	~0.85	0.05_3	$\nu_8(e)$
890	1.0			~0.6	~0.4_6		$\nu_5(a_1)+\nu_9(e) = 894$
974	11.7	16.8	10.3	0.77	0.63	0.17	$\nu_4(a_1)$
~1012	v.w.						$\nu_8(e)+\nu_{10}(e) = 1002$; $3\nu_9(e) = 1029$
1048	2.6	Broad					$\nu_7(e)$
1090	~ 1						$2\nu_5(a_1) = 1102$; $\nu_2(a_1)-\nu_3(a_1) = 1094$
1146	5.5	18.1	10.1	0.87	0.73	0.11	$\nu_3(a_1)$
1947	1.4						$2\nu_4(a_1) = 1948$
2068	25	21.3	9.3	0.31	0.18	1.80	$2\nu_7(e) = 2096$
2100	22	16.2	9.3	0.36	0.22	1.14	$\nu_2(a_1)+\nu_4(a_1) = 2120$
2131	100	13.5	9.2	0.30	0.17	4.31	$\nu_1(a_1)$
2229	33	~25.8	3.8	~1.0	~0.85	~2.2	$\nu_6(e)$
2240	57	15.2	3.8	0.4 to 0.5	0.26 to 0.36	~3.2	$\nu_2(a_1)$
2302	43	22.6	9.0	0.45	0.31	3.50	$2\nu_3(a_1) = 2292$
~2490	2		8.9				$\nu_1(a_1)+\nu_9(e) = 2474$
2786	2.8		12.9				$\nu_1(a_1)+\nu_6(e) = 2780$; $\nu_1(a_1)+\nu_2(a_1) = 2791$
2868	3.8		12.7				$\nu_1(a_1)+\nu_5(a_1)+\nu_{10}(e) = 2859$
~2909	2.7	~23	12.7	(0.5)[b]		~0.26	$\nu_6(e)+2\nu_9(e) = 2915$; $\nu_2(a_1)+2\nu_9(e) = 2926$
~2949	2.8	~22	12.7	(0.9)[b]		~0.22	$\nu_1(a_1)+\nu_8(e) = 2956$; $\nu_5(a_1)+\nu_6(e)+\nu_{10}(e) = 2957$

[a]*See footnote a, Table III.* $\nu_{10}(e)$ *is taken to be 177 cm*$^{-1}$.
[b]*See footnote c, Table III.*

Here I is the integrated intensity of the band in question,
ρ is the observed depolarization ratio,
n is the refractive index of the material,
$\sigma_{\Delta\nu}$ is the spectral sensitivity of the IP21 tube at the wavelength corresponding to $\Delta\nu$,
$R(n)$ is the reflection loss,
M is the molecular weight and d the density of the material,
$\Delta\nu$ is the wave number of the Raman band,
ν is the wave number of the exciting radiation,
and T is the absolute temperature.

The subscript CCl_4 indicates the corresponding quantities for the reference substance CCl_4, and the subscript 458 refers to the band at 458 cm.$^{-1}$ in CCl_4. In Reference (1) it has been shown that

$$S = \frac{[45(\partial\alpha/\partial Q)^2+7(\partial\gamma/\partial Q)^2]_{\Delta\nu}}{[45(\partial\alpha/\partial Q)^2+7(\partial\gamma/\partial Q)^2]_{458}}$$

where α and γ are the average polarizability and anisotropy respectively and Q is the normal coordinate for the band whose Raman shift is $\Delta\nu$. In obtaining a standard intensity from this formula the integrated intensity has been obtained by using the product of the peak intensity and the observed half-band width and then correcting for the effect of the finite slit width by means of the curves calculated by Bernstein and Allen (1) to give the true integrated intensity. In the above equation the observed intensity has been corrected also for convergence of the incident beam, spectral sensitivity of the detector, the amount of light the spectrometer sees, the amount of light incident on the sample tube; and then expressed as scattering intensity per molecule. The intensities determined in this way are probably accurate to $\pm 10\%$ for the strong isolated bands at 343 cm.$^{-1}$ and 551 cm.$^{-1}$ in $CD_3C{\equiv}CCl$ and at 355 cm.$^{-1}$ and 579 cm.$^{-1}$ in $CH_3C{\equiv}CCl$. Because of overlapping in the region 2000–2400 cm.$^{-1}$ the standard intensities are considerably less accurate.

For $CH_3C{\equiv}CCl$ and $CD_3C{\equiv}CCl$ values of n are given by Morse and Leitch (15). A rough determination of the density gave 1.008 for $CH_3C{\equiv}CCl$ at 25°C. The molecular volume of $CD_3C{\equiv}CCl$ was assumed to be the same as that for $CH_3C{\equiv}CCl$.

CALCULATION OF THE FREQUENCIES

Meister (14) has calculated the fundamental frequencies of methylacetylene-type molecules, $CH_3C{\equiv}C{-}X$, from a potential energy function which includes all eight bond-stretching and -bending force constants and five interaction constants. In our treatment, we have adopted the same potential function and the same symbols for the force constants and the molecular dimensions.

Some of the E elements in the G matrix used by Meister are in error.[4] For the symmetry coordinate R_{1a}, R_{1b}, R_{2a}, . . . R_{5b} chosen by Meister, the values of G_{14}, G_{24}, G_{25}, and G_{34} are to be multiplied by -2. The changes in

[4]*These corrections were pointed out by A. V. Golton in correspondence with A. G. Meister, who has kindly communicated them to us.*

these elements arise from the necessity of choosing $\mathbf{S}^t_{4a}$ and $\mathbf{S}^t_{5a}$ for all t to lie in the same plane through the symmetry axis as the other $\mathbf{S}^t_{ja}$ (the Wilson $\mathbf{S}$ vectors for the atom t and the symmetry coordinate R_{ja}) and the new values are readily verified. The F matrix elements and the remaining G matrix elements are unchanged.

Following Meister, we have transferred most of the force constants from methylacetylene to methylchloroacetylene. Golton [5] has recalculated the force constants of methylacetylene, taking into account the G matrix changes mentioned above. The potential constants that appear in the F matrix for the A_1 vibration are the same as those of Meister. Of the remainder, k_α, k_β, and $k_{\alpha\beta}$ are not greatly altered, but the change in the value of k_ϕ is considerable. Both sets of values are listed in Table V, together with the set we have adopted for use in the present calculations.

TABLE V

FORCE CONSTANTS FOR METHYLCHLOROACETYLENE (10^5 DYNES/CM.)

	Meister's value	Golton's value	Adopted value
k_H	4.8384	Same	Same
k_c	5.1296	Same	Same
k_a	15.799	Same	Same
k_X	5.3008	Same	Same
k_{ca}	0.47059	Same	Same
$k_{c\gamma}$	−0.26186	Same	Same
k_{Xa}	0	0	0
k_α	0.45342	0.4515	0.4515
k_β	0.56207	0.5636	0.5636
$k_{\alpha\beta}$	0.01285	0.0108	0.0108
k_ϕ	0.12714	0.1524	0.1524
k_θ	0.09729		0.09624
$k_{\phi\theta}$	0.045303		0.05244

It is worth noting that all force constants except k_H, k_X, k_θ, and $k_{\phi\theta}$ have been taken over from methylacetylene. The value of k_H is that calculated by Meister from the frequencies of $\nu_6(e)$ in all three methylhaloacetylenes investigated in the Raman effect by Cleveland and Murray (5); Meister evaluated k_X from the observed frequency of $\nu_2(a_1)$. We have calculated k_θ and $k_{\phi\theta}$ by taking $\nu_9(e)$ = 353 cm.$^{-1}$ and $\nu_{10}(e)$ = 184 cm.$^{-1}$ for $CH_3C{\equiv}CCl$. No frequencies of $CD_3C{\equiv}CCl$ were used to evaluate force constants.

The atomic masses and molecular dimensions used in the calculation were the same as those employed by Meister. The calculated fundamental frequencies, shown in Table VI (second and last columns), are explicit solutions of the fifth power secular equations. Table VI also includes fundamental frequencies calculated by Meister (third column).

ASSIGNMENTS

Fundamentals

With the exception of $\nu_{10}(e)$ all fundamentals in each molecule were observed in either the infrared or Raman spectrum.

The A_1 fundamental bands in the infrared have the doublet structure

[5] *Private communication to the authors.*

TABLE VI

FUNDAMENTAL FREQUENCIES (CM.$^{-1}$)

$CH_3C{\equiv}CCl$				$CD_3C{\equiv}CCl$	
$\nu_{vac.}$ (exp.)**	ν (calc.)	ν (M.)*		$\nu_{vac.}$ (exp.)**	ν (calc.)
2939	2899	2894	$\nu_1(a_1)$	2142	2095
2268	2264	2261	$\nu_2(a_1)$	2252	2266
1380[1]	1385	1391	$\nu_3(a_1)$	1151	1154
1084	1085	1078	$\nu_4(a_1)$	977	977
575	578.5	579	$\nu_5(a_1)$	547	548
2980[2]	3017	3010	$\nu_6(e)$	2235[2]	2257
1453[2]	1453	1456	$\nu_7(e)$	1051[2]	1047
1033[2]	1041	1036	$\nu_8(e)$	825[1]	822
358	353[3]	353[3]	$\nu_9(e)$	343[1]	335
—	184[3]	184[3]	$\nu_{10}(e)$	—	177

*As calculated by Meister.

**Vapor infrared values, unless otherwise noted.

[1] Liquid Raman value.

[2] ν_0 as determined by perpendicular sub-band analysis.

[3] Assumed in order to calculate k_θ, $k_{\phi\theta}$.

characteristic of parallel-type bands of symmetric top molecules, with P–R peak separations approximately as predicted by the Gerhard–Dennison formula (9), viz., 11.2_3 cm.$^{-1}$ for $CH_3C{\equiv}CCl$ and 10.6_7 cm.$^{-1}$ for $CD_3C{\equiv}CCl$. The half widths of the corresponding solution bands are comparatively small ($\sim$8 to 12 cm.$^{-1}$). Likewise, the Raman bands are comparatively sharp, with half widths of the order of 15 cm^{-1}. The depolarization ratios are considerably less than 6/7, except for $\nu_3(a_1)$ in $CD_3C{\equiv}CCl$ which is not strong enough for accurate depolarization measurements.

The spacing between the sub-bands of the doubly degenerate perpendicular fundamental depends on the strength of the Coriolis coupling between degenerate modes. Sub-bands were resolved from one another in $\nu_6(e)$ and $\nu_7(e)$ for both molecules and in $\nu_8(e)$ for $CH_3C{\equiv}CCl$. The latter fundamental was not observed in the vapor spectrum of $CD_3C{\equiv}CCl$, even with a path length of 1 meter. In neither molecule was $\nu_9(e)$ strong enough in the vapor to stand out well among the water bands in the region near 350 cm.$^{-1}$, despite considerable reduction of the water vapor content of the spectrometer by flushing dry nitrogen through a specially constructed housing. In the solution spectra, the perpendicular fundamentals were broad bands with half widths usually greater than 20 cm^{-1}. The Raman bands are likewise comparatively broad with the exception of $\nu_9(e)$. The depolarization ratios which could be measured for the E-type fundamental were found to be 6/7 within experimental error.

It is worth noting that for these molecules the magnitude of the half-band width of the fundamentals appearing in the infrared and Raman spectra of the liquids and solutions provides a criterion for dividing the bands into A_1 and E types. This is true also for the bands in the infrared spectrum of liquid methyl iodide.[6]

The observation by Cleveland Murray (5) of $\nu_{10}(e)$ at 184 cm.$^{-1}$ in the light molecule was approximately confirmed by the frequencies of combination

[6] As may be seen by examination of the spectra recorded by Irving L. Mador and Ruth S. Quinn (J. Chem. Phys. 20: 1837. 1952).

bands in which $\nu_{10}(e)$ appears, as is also the calculated value 177 cm.$^{-1}$ for the frequency of this fundamental in the heavy molecule (see below).

The value of $\nu_{10}(e)$ in $CD_3C{\equiv}CCl$ may also be obtained from the Teller–Redlich product rule for the E-type fundamentals (11); viz.,

$$[2] \qquad \nu_{10}(e) = \frac{\prod_{i=6}^{10} \nu_i(e)}{\prod_{i=6}^{9} \nu_i'(e)} \cdot \left(\frac{m_H}{m_D}\right)^{3/2} \cdot \left(\frac{M'}{M}\,\frac{I'_B}{I}\right)^{1/2} = 171 \text{ cm}^{-1}.$$

This value is in good agreement with the values calculated in Table VI and estimated from combination tones. In equation [2] the primed quantities refer to $CD_3C{\equiv}CCl$ and the other symbols have their usual meanings.

The product rule for the fundamentals of the A_1 type is

$$[3] \qquad \prod_{i=1}^{5} \nu_i(a_1) \Big/ \prod_{i=1}^{5} \nu_i'(a_1) = \left(\frac{m_H}{m_D}\,\frac{M'}{M}\right)^{\frac{1}{2}}.$$

The theoretical ratio of the frequencies is 1.946, and the observed value of the left-hand side is 1.930.

COMBINATION AND DIFFERENCE BANDS

$CH_3C{\equiv}CCl$

The remaining bands in the spectra of $CH_3C{\equiv}CCl$ may be readily assigned, as indicated in Tables I and III, on the basis of binary sums or differences. Ternary combinations of the type $\nu_2(a_1)+n\nu_i(e)-n\nu_i(e)$, however, appear to account best for the series of infrared bands lying just below the C≡C stretching fundamental $\nu_2(a_1)$. Meister (14) has made the assignment $[\nu_2(a_1)+\nu_9(e)]-\nu_9(e)$ to the band that occurs on the low frequency side of $\nu_2(a_1)$ in the Raman spectra of 1-chloro, 1-bromo, and 1-iodo acetylene, with $\nu_1(a_1)-2\nu_9(e)$ an alternative assignment. In 1-chloropropyne, however, $\nu_1(a_1)-2\nu_9(e)$ ($=2223$ cm.$^{-1}$) appears to lie too low to account for any of the strong bands in this region. The band occurring at 2252 cm.$^{-1}$ in the infrared and at 2244 cm.$^{-1}$ in the Raman spectrum is probably $\nu_2(a_1)+\nu_{10}(e)-\nu_{10}(e)$. "Hot" transitions of the form $\nu_2(a_1)+n\nu_i(e)-n\nu_i(e)$ have previously been assigned to bands occurring on the low frequency side of the C≡C stretching fundamental (which corresponds to $\nu_2(a_1)$ in methylchloroacetylene) in the Raman (12) and infrared (4) spectra of methylacetylene.

Fermi resonance with $\nu_5(a_1)$ may account for the high intensity in the infrared spectrum of the band assigned as $\nu_9(e)+\nu_{10}(e)$ (A_1+A_2+E). The fundamental $\nu_7(e)$ gives rise to a very strong overtone (A_1+E) in the infrared, whose intensity is probably enhanced by Fermi interaction with $\nu_1(a_1)$. Similarly, in the Raman spectrum, the $2\nu_7$ band is stronger than the ν_7 band.

Since the strong band at 2749 cm.$^{-1}$ appears to be stronger than the $\nu_3(a_1)$ fundamental, it is more likely to arise from $\nu_1(a_1)-\nu_{10}(e)$ rather than $2\nu_3(a_1)$.

A value of 184 cm.$^{-1}$ for $\nu_{10}(e)$, as mentioned above, appears satisfactory, although examination of the frequencies of the combination and difference

bands in which $\nu_{10}(e)$ occurs suggests that a higher value (190 to 195 cm.$^{-1}$) is to be preferred, at least for the molecule in the vapor.

The assignment of the infrared band at 819 cm.$^{-1}$ is not completely satisfactory.

$CD_3C{\equiv}CCl$

In spite of the presence of strong atmospheric water and solvent absorption, the infrared spectrum of $CD_3C{\equiv}CCl$ appears to show at least three bands below 400 cm^{-1}. Besides $\nu_9(e)$, the binary combinations $[\nu_3(a_1)-\nu_8(e)]$ (E), $2\nu_{10}(e)$ (A_1+E), and $[\nu_5(a_1)-\nu_{10}(e)]$ (E) may occur in this region, and $2\nu_{10}$ has the correct symmetry for resonance with $\nu_9(e)$.

More than one assignment is possible for many of the weaker bands of $CD_3C{\equiv}CCl$. Some of these involve ternary combinations in which $\nu_9(e)$ or $\nu_{10}(e)$ occur. In general, wherever $\nu_9(e)$ occurs in a combination assignment (Table II), an alternative assignment in which $2\nu_{10}(e)$ replaces $\nu_9(e)$ may be made. There appears to be only one band, that at 2318 cm.$^{-1}$ in the infrared spectrum of the vapor, to which may be unequivocally assigned a transition involving $\nu_{10}(e)$. With due regard to anharmonicity the assignment $\nu_1(a_1)+\nu_{10}(e)$ to this band leads to a value of $\nu_{10}(e) > 176$ cm^{-1}. The infrared band at 513 cm.$^{-1}$ gives $\nu_{10}(e) > 170$ cm.$^{-1}$ if assigned to $\nu_9(e)+\nu_{10}(e)$, and $\nu_{10}(e) > 171$ cm.$^{-1}$ if assigned to $3\nu_{10}(e)$. The actual value of $\nu_{10}(e)$ therefore appears to be close to the calculated frequency of 177 cm^{-1}.

There is good evidence for the existence of strong Fermi interaction between $\nu_2(a_1)$ and the band that occurs with a Raman shift of 2302 cm.$^{-1}$ in the liquid and at 2318 cm.$^{-1}$ in the infrared spectrum of the vapor. This band has been assigned to $2\nu_3(a_1)$. In both the Raman and infrared spectra it has an intensity about equal to that of the $\nu_2(a_1)$ fundamental. In the second place, the Raman band is strongly polarized. Thirdly, the experimental value of the frequency of $\nu_2(a_1)$ is lower than would have been expected while that of $2\nu_3(a_1)$ is higher. If one compares, for the data of Table VI, the calculated value of $\delta\nu$, the change in frequency of a fundamental in going from $CH_3C{\equiv}CCl$ to $CD_3C{\equiv}CCl$, with the observed change, one finds that $\delta\nu_{\text{obs.}}-\delta\nu_{\text{calc.}}$ has values from $+1$ to $+15$ cm.$^{-1}$ for all fundamentals, with the exception of $\nu_2(a_1)$, for which this quantity is -18 cm^{-1}. It therefore seems likely that Fermi interaction has reduced the frequency of the $\nu_2(a_1)$ fundamental by about 20 cm.$^{-1}$, while raising that of $2\nu_3(a_1)$ to about the same extent (observed value of $2\nu_3(a_1)=$ 2318 cm.$^{-1}$ vs. $\nu_3(a_1) = 1151$ cm.$^{-1}$).

Band Contours

The contours of the combination bands in the infrared spectra of the vapors tend to resemble those of the parallel fundamentals, even when the symmetry class of the transition is A_1+E or, as in a few cases, solely E. Possibly a diffused E component would be expected to be less pronounced than an A_1 component of equal intensity, and E bands with large ζ values (see Rotational Structure of Perpendicular Bands, below) take on the appearance of parallel bands under conditions of low resolution. Large ζ_{ij}'s are expected for transitions $\nu_i(a_1)+\nu_j(e)$ in which ζ_j is itself large (3). For both molecules, ζ_9 and ζ_{10} are near

unity (see below). The $CH_3C{\equiv}CCl$ band at 765 cm.$^{-1}$ [$\nu_5(a_1)+\nu_{10}(e)$] shows the type of contour expected under these conditions. The sharpness (for a perpendicular band) of the corresponding band in the solution spectrum may perhaps also be attributed to a large ζ value.

ROTATIONAL STRUCTURE OF THE PERPENDICULAR BANDS

The rotational structure of several of the E-type fundamentals was resolved. The Q-branches of the sub-bands that arise from $\Delta K = +1$, $\Delta J = 0$ transitions are given by

$$[4] \quad \nu_0^{sub} = \nu_0 + A'(1-\zeta)^2 - B' \pm 2[A'(1-\zeta) - B']K + [(A'-B') - (A''-B'')]K^2$$

which is identical with the expression given by Herzberg (13) except for the factor $(1-\zeta)^2$ instead (4) of $(1-2\zeta)$ which shifts the band origin ν_0 for large ζ. To determine ζ from equation [4], dimensions of the chloropropyne molecule were assumed. Except for the C—Cl bond distance, the dimensions were taken to be the same as those obtained for 1-bromo- and 1-iodo-propyne by Sheridan and Gordy (19); $r_{CH} = 1.092$ Å, $r_{C{\equiv}C} = 1.207$ Å, $r_{C-C} = 1.459$ Å and $\measuredangle$ HCH = 109°8′. The value of the C—Cl distance was taken to be 1.632 Å, the same as that in chloroacetylene as determined from the microwave spectrum (20). Reciprocal moments are then $A'' = 5.281$, $B'' = 0.075$ cm.$^{-1}$ for $CH_3C{\equiv}CCl$ and 2.661 and 0.067 cm.$^{-1}$, respectively, for $CD_3C{\equiv}CCl$.

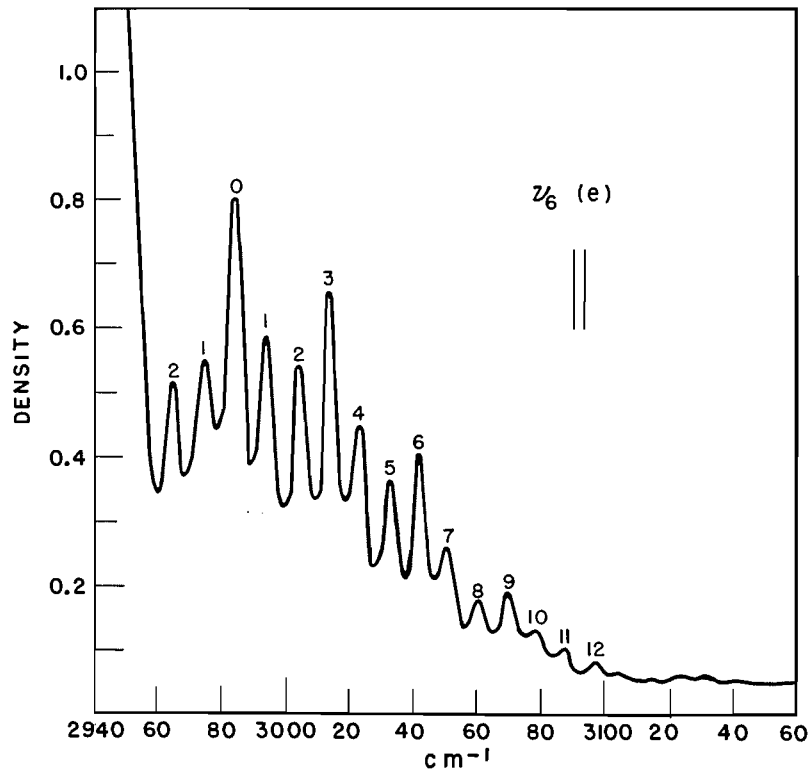

FIG. 4. $\nu_6(e)$ band of $CH_3C{\equiv}C{-}Cl$. The spectral slit width is shown.

In making the K assignments to the sub-bands, one is greatly assisted by the strong, weak, weak, strong, . . . intensity sequence imposed by the nuclear spin of the H (or D) atoms. The strongest peak corresponds to the transition in which K goes from 0 to 1.

The sub-band frequencies observed in $\nu_6(e)$ of $CH_3C{\equiv}CCl$ (Fig. 4) are given in Table VII. The ^PQ branch for large K's is obscured by $\nu_1(a_1)$. By least

TABLE VII

SUB-BAND FREQUENCIES IN $\nu_6(e)$ OF $CH_3C{\equiv}CCl$

$\nu_{vac.}$, cm.$^{-1}$	Value of K in ^PQ_K	$\nu_{vac.}$, cm.$^{-1}$	Value of K in ^RQ_K
2964.6	2	2984.6	0
2974.8	1	2994.5	1
		3004.3	2
		3014.0	3
		3023.5	4
		3033.2	5
		3042.4	6
		3051.4	7
		3060.7	8
		3070.1	9
		3079.0	10
		3087.5	11
		3096.9	12
		—	
		(3114)	
		(3123)	
		(3131)	

squares the observed peaks have been fitted to equation [4] (with an average deviation of ± 0.13 cm.$^{-1}$) to give

$$[5] \qquad \nu_0^{sub} = 2984.7_0 \pm 9.884\,K - 0.0460\,K^2.$$

Since $A'' \gg B''$, $(A'-B')-(A''-B'')$ can be set nearly equal to $A'-A''$, whence $A' = 5.235$ cm.$^{-1}$, $B' = B''$, $\nu_0 = 2979.9$ cm.$^{-1}$, and $\zeta_6 = 0.042$.

The intensity distribution among the sub-bands of $\nu_7(e)$ of $CH_3C{\equiv}CCl$ (Fig. 5) permits a choice of either 1419 or 1461 cm.$^{-1}$ for the 0–1 transition. That the latter is probably the correct assignment is shown by the occurrence of the solution peak at 1440 cm^{-1}. Besides the intensity distribution, many of the sub-band frequencies are apparently affected by the presence of overlapping and perturbing bands: $\nu_3(a_1)$ at *ca.* 1395 cm.$^{-1}$, $(\nu_3(e)-\nu_{10}(e))$ (A_1+E) at 1258 cm.$^{-1}$, at least one "hot" transition (see below), and probably a band at about 1510 cm.$^{-1}$ (most likely $(\nu_3(a_1)+\nu_{10}(e))$ (E). The ^RQ_K sub-bands for K greater than 2 appear to be perturbed, especially in the region between 1500 and 1580 cm^{-1}. The frequencies in Table VIII assigned to ^PQ_K and ^RQ_K transitions (the latter up to $K = 2$) may be fitted with a mean deviation of ± 0.3 cm.$^{-1}$ by

$$[6] \qquad \nu_0^{sub} = 1460.81 \pm 13.901\,K - 0.0276\,K^2.$$

Thus $A' = 5.253$ cm.$^{-1}$, $\nu_0 = 1453.78$ cm.$^{-1}$, and $\zeta_7 = -0.337$.

$\nu_8(e)$ (Fig. 6) is a comparatively weak band, with most of the ^RQ sub-bands obscured by $\nu_4(a_1)$ and some irregularity in the ^PQ spacings (see Table IX).

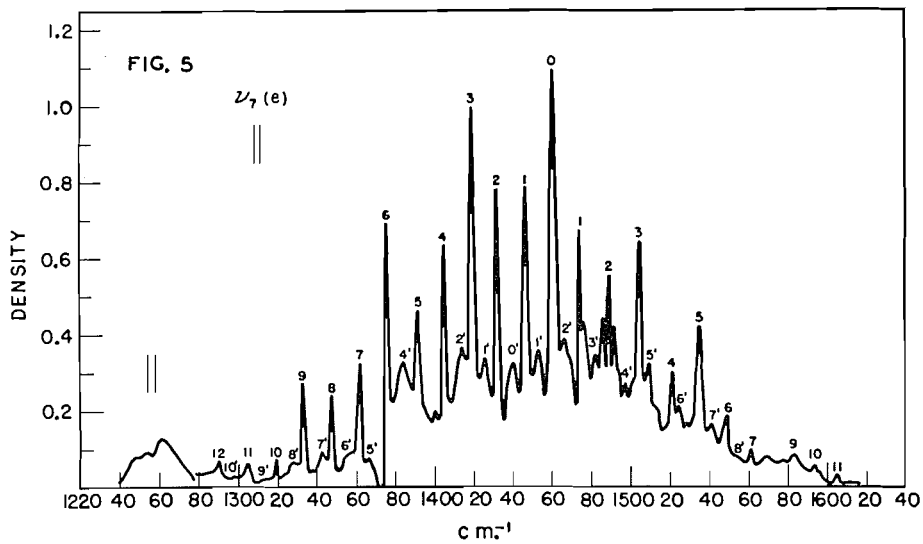

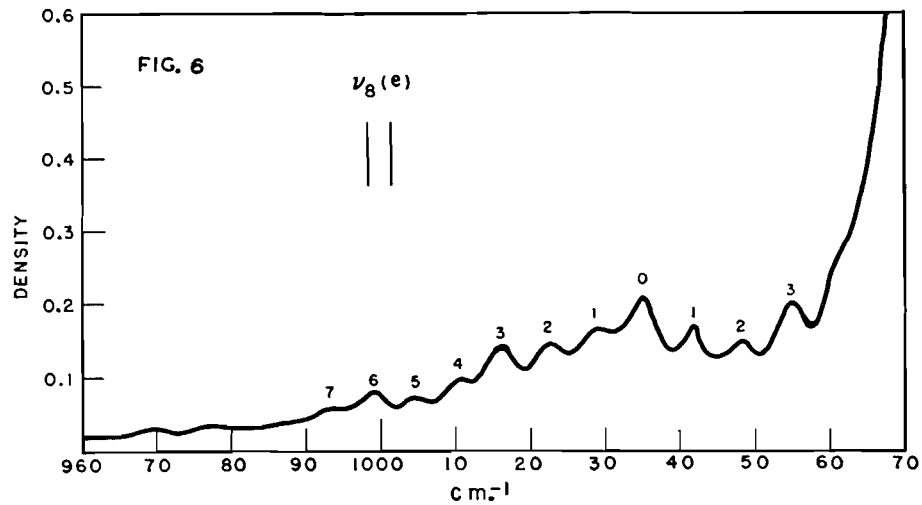

FIG. 5. $\nu_7(e)$ band of $CH_3C{\equiv}C{-}Cl$. The spectral slit width is shown.
FIG. 6. $\nu_8(e)$ band of $CH_3C{\equiv}C{-}Cl$. The spectral slit width is shown.

TABLE VIII

SUB-BAND FREQUENCIES IN $\nu_7(e)$ OF $CH_3C{\equiv}CCl$

$\nu_{vac.}$, cm.$^{-1}$	K in ^PQ_K	$\nu_{vac.}$, cm.$^{-1}$	K in ^RQ_K
1290.1	12	1460.7	0
1304.8	11	1474.7	1
1319.0	10	1489.1	2
1333.1	9	1505.2	3
1347.6	8	1521.2	4
1362.3	7	1535.0	5
1375.7	6	1548.2	6
1391.6	5	1560.8	7
1405.1	4	—	8
1418.7	3	1583.0	9
1432.1	2	1593.3	10
1446.8	1	1604.6	11

TABLE IX

SUB-BAND FREQUENCIES IN $\nu_8(e)$ OF $CH_3C{\equiv}CCl$

$\nu_{vac.}$, cm.$^{-1}$	K in ^PQ_K	$\nu_{vac.}$, cm.$^{-1}$	K in ^RQ_K
992.5	7	1035.0	0
998.8	6	1041.4	1
1004.0	5	1048.0	2
1010.2	4	1054.7	3
1016.1	3		
1022.2	2		
1028.7	1		

In it, with the rotational constants assumed the same in the ground and excited states, ζ_8 was determined from the average spacing (excluding $^PQ_7$ and $^PQ_6$) to be 0.40 and $\nu_0 = 1034.5$ cm^{-1}.

In neither $CH_3C{\equiv}CCl$ nor $CD_3C{\equiv}CCl$ was the structure of $\nu_9(e)$ or $\nu_{10}(e)$ resolved.

The sub-bands (Table X) on the high frequency side of $\nu_6(e)$ in $CD_3C{\equiv}CCl$

TABLE X

SUB-BAND FREQUENCIES IN $\nu_6(e)$ OF $CD_3C{\equiv}CCl$

$\nu_{vac.}$, cm.$^{-1}$	K in ^PQ_K	$\nu_{vac.}$, cm.$^{-1}$	K in ^RQ_K
2192.2	10	2237.9	0
2197.0	9	2242.0	1
2201.6	8	2245.9	2
2206.1	7	2249.7	3
2210.4	6		
2214.9	5		
2219.5	4		
2223.8	3		
2228.6	2		
2233.8	1		

(Fig. 7) are obscured by $\nu_2(a_1)$. The intensity distribution in the rest of the band makes it uncertain whether $^RQ_0$ is 2224 or 2238 cm^{-1}. Since the solution frequency (here 2229 cm.$^{-1}$) is ordinarily lower than that of the vapor band center, $^RQ_0$ is probably 2238 cm^{-1}. By least squares (average deviation ± 0.4 cm.$^{-1}$),

$$[7] \qquad \nu_0^{sub} = 2237.41 \pm 4.619\,K + 0.01385\,K^2,$$

with the result that $A' = 2.675$ cm.$^{-1}$, $\zeta_6 = 0.112$, and $\nu_0 = 2235.3_7$ cm^{-1}.

Frequencies in the $\nu_7(e)$ band (Fig. 8) are shown in Table XI. Two spurious

TABLE XI

SUB-BAND FREQUENCIES IN $\nu_7(e)$ OF $CD_3C{\equiv}CCl$

$\nu_{vac.}$, cm.$^{-1}$	K in ^PQ_K	$\nu_{vac.}$, cm.$^{-1}$	K in ^RQ_K
997.8	8	1056.5	0
1004.8	7	1063.6	1
1012.1	6	1070.7	2
1019.3	5	1078.1	3
1026.5	4	1085.2	4
1033.8	3	1093.0	5
1041.3	2	1100.2	6
1048.8	1	(1102.6)*	
		1108.0	7
		(1111.6)*	

**Spurious to this band (see text).*

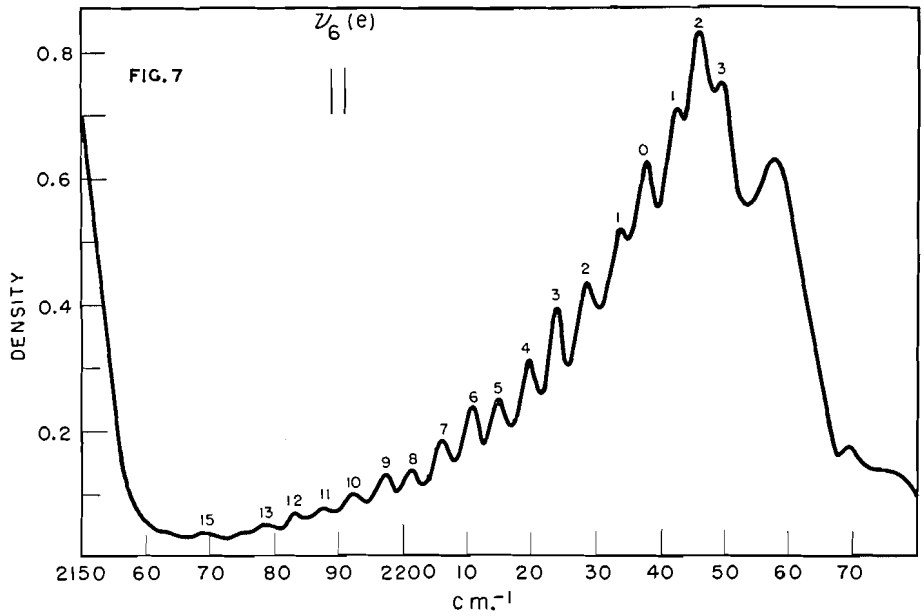

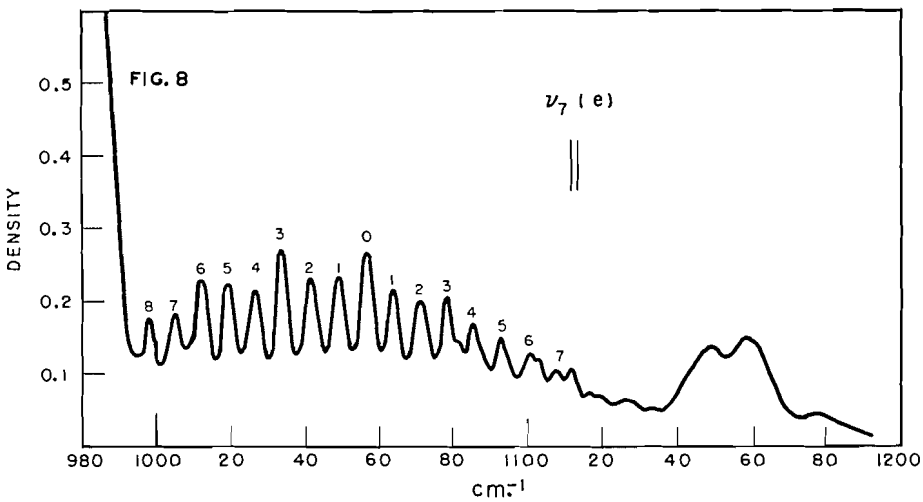

FIG. 7. $\nu_6(e)$ band of $CD_3C{\equiv}C{-}Cl$. The spectral slit width is shown.
FIG. 8. $\nu_7(e)$ band of $CD_3C{\equiv}C{-}Cl$. The spectral slit width is shown.

peaks appear at 1103 and 1112 cm^{-1}. These have been attributed (see Assignments) to the parallel contour of a combination band. The remaining subbands are expressed (with an average deviation of ± 0.16 cm.$^{-1}$) by

$$[8] \qquad \nu_0^{sub} = 1056.00 \pm 7.361\,K + 0.0049\,K^2$$

with $A' = 2.666$ cm.$^{-1}$, $\nu_0 = 1050.8$ cm.$^{-1}$, and $\zeta_7 = -0.406$.

Table XII summarizes the ζ's and compares them with the values obtained for the corresponding vibrations in $CH_3C{\equiv}C{-}H_3$ and in $CH_3C{\equiv}C{-}D_{10}$.

As in the present case, the structure of the $\nu_9(e)$ and $\nu_{10}(e)$ bands in these molecules was not resolved. Boyd and Longuet-Higgins (3) have shown

TABLE XII

SUMMARY OF ζ'S

	$CH_3C{\equiv}CCl$	$CD_3C{\equiv}CCl$	$CH_3C{\equiv}CH$[1]	$CH_3C{\equiv}CD$[2]
$\zeta_6(e)$	0.042	0.112	0.074	0.071
$\zeta_7(e)$	−0.357	−0.406	−0.39	−0.37
$\zeta_8(e)$	0.40		0.387	0.40
$\zeta_9(e)$	$0.90 < \zeta < 1$		$0.96 < \zeta < 1$	$0.92 < \zeta < 1$
$\zeta_{10}(e)$	$0.90 < \zeta < 1$		$0.96 < \zeta < 1$	$0.92 < \zeta < 1$

[1]*Boyd–Thompson results.*
[2]*Grisenthwaite–Thompson results.*

generally that the sum rule for the ζ's of C_{nv} molecules, when there are n equivalent atoms symmetrically disposed about the symmetry axis and only one degenerate symmetry class E, is

$$[9] \qquad \sum_i \zeta_i = (\text{no. of axial atoms}) - 2 + B/2A,$$

to a first order approximation. For $CH_3C{\equiv}CCl$

$$[10] \qquad \zeta_9 + \zeta_{10} = 1.90_2,$$

which places each of the individual ζ values between 0.90 and 1. The corresponding range in methylacetylene is 0.96 to 1. For $CD_3C{\equiv}CCl$, where only ζ_6 and ζ_7 have been determined:

$$[11] \qquad \zeta_8 + \zeta_9 + \zeta_{10} = 2.30_7,$$

which is consistent with a value of ζ_8 not far from 0.4 and ζ_9 and ζ_{10} again near unity. The signs and magnitudes of the ζ's for chloropropyne are similar to those observed for similar degenerate vibrations in other molecules.[7]

In addition to the strong features in the $\nu_7(e)$ band of $CH_3C{\equiv}CCl$, there appear a large number of weak subsidiary peaks interspersed between the $\nu_7(e)$ peaks. Although the presence of water absorption and the occurrence of the doublet contour of $\nu_3(a_1)$ around 1400 cm.$^{-1}$ introduce uncertainties into the values of the frequencies, an attempt has been made to fit them by equation [4]. Eighteen of the twenty-four subsidiary peaks listed in Table XIII and shown in Fig. 5 can be fitted with success; the remainder, in the region of 1500 cm.$^{-1}$, may arise from other "hot" bands or from the effects of water absorption. The $\nu_7(e)$ sub-bands at 1535 cm.$^{-1}$ show an irregular intensity, and it and other features in this region may be associated with the presence of a weak solution band near 1510 cm^{-1}. The equation resulting from the assignment shown in Table XIII, viz.,

[7]*A rough empirical correlation may be seen between ζ values and vibrational type, as shown, for example, by the similarity in ζ's for corresponding vibrations in methylacetylene and chloromethylacetylene (Table XII). For CH_3CN and CH_3NC, where there is only one low-lying perpendicular bending mode, the ζ's are 0.068, −0.45, 0.42, and 0.99, and 0.08, −0.33, 0.36, and 0.92 respectively (Thompson, H. W. and Williams, R. L. Trans. Faraday Soc. 48: 502. 1952). In $H_3BC{=}O$, $\zeta_1 = 0.13$ and $\zeta_3 = 0.56$ (Cowan, R. D. J. Chem. Phys. 18: 1101. 1950).*

TABLE XIII

SUBSIDIARY PEAKS IN REGION OF $\nu_7(e)$ OF $CH_3C{\equiv}CCl$
(Most peaks approximate)

$\nu_{vac.}$, cm.$^{-1}$	Tentative K in ^PQ_K of hot band	$\nu_{vac.}$, cm.$^{-1}$	Tentative K in ^RQ_K of hot band
1297.7	10	1440.1	0
1312.5	9	1453.7	1
1328.7	8	1466.7	2
1341.8	7	1476.8	
1355	6	1482.0	3
1366.9	5	1491.8	
1384.1	4	1494.4	
1400.1	3	1497	4
1414.1	2	1500	
1425.8	1	1509.7	5
		1512.9	
		1524.8	6
		1529	
		1540.5	7
		1554.5	8

[12] $$\nu_0^{sub} = 1440.0 \pm 14.06\,K + 0.015\,K^2,$$

gives $A' = 5.296$ cm.$^{-1}$, $\nu_0 = 1430.5$ cm.$^{-1}$, and $\zeta = -0.34$ with much less accuracy than before. The K assignment is uncertain, since the intensity alternation is not clear, and it may be that the band origin should be shifted by one or more peaks. The solution spectrum shows a weak shoulder located at about 1428 cm^{-1}. Although the ν_0 value is therefore doubtful, the value of ζ will not be greatly dependent upon the assignment. It is, within experimental limits, identical with the value of ζ for $\nu_7(e)$, as is to be expected for a transition of the type $\nu_7(e)+n\nu_i(e)-n\nu_i(e)$. Our resolving power was not great enough to make the presence of hot bands in conjunction with other strong perpendicular fundamentals observable.

With the exception of the "hot" bands mentioned above, no combination band showed sufficiently well-defined perpendicular structure to make possible an estimation of ζ.

DISCUSSION

There are two aspects of the isotope effect on the vibrational spectrum of these molecules which require emphasis. Firstly there is a shift in frequency of the $\nu_5(a_1)$ band of 28 cm.$^{-1}$ which seems too large to anticipate for a C—Cl valence vibration so far removed from the C atom where isotopic substitution took place.[8] Secondly, this band doubles in intensity in the Raman effect on deuterium substitution and the $\nu_9(e)$ band for example is enhanced in intensity by about a factor of 3 whereas smaller intensity changes are observed for these bands in the infrared spectra. It is readily noticed that there is no simple relation between the observed intensities of corresponding Raman bands of $CD_3C{\equiv}CCl$ and $CH_3C{\equiv}CCl$. Nor do the intensities of the corresponding infrared bands of $CD_3C{\equiv}CCl$ and $CH_3C{\equiv}CCl$ change in any simple manner. However, for isotopic substitution Crawford has developed a sum rule (7)

[8]*The isotopic shift of the C—Cl vibration in CH_3Cl and CD_3Cl is 87 cm.$^{-1}$, cf. Ref. (11), page 315.*

which is applicable to the sum of I/ν^2 for the infrared bands and the sum of $S/\Delta\nu^2$ for the Raman bands of the A_1 modes. Unfortunately the measurement of both the infrared and Raman intensities of these modes is complicated by the fact that several bands overlap, by contributions from bands in Fermi resonance, and by uncertainty in placing the background for the Raman bands at $\sim$2925 cm^{-1}. The experimental errors introduced by these difficulties make it impossible to test quantitatively the validity of the intensity sum rules for these molecules.

The large changes in Raman intensity of corresponding bands of these molecules are probably due to the fact that here the molecular polarizability varies in a complicated manner with the normal coordinate whereas in 1-chloropropane, the saturated analogue of 1-chloropropyne, the intensity of the C—Cl mode for example is given approximately by polarizability changes in the C—Cl bond.

The necessity of dealing with the molecular polarizability in $CH_3C{\equiv}CCl$ rather than bond polarizabilities is further indicated by the presence of the abnormally short CH_3—C and C—Cl bonds in this molecule showing that strong interactions exist between all pairs of bonds between axial atoms. The explanation for the short C—Cl bond in $HC{\equiv}C{-}Cl$ has been given (18) in terms of resonance with the doubly bonded form $H\bar{C}{=}C{=}\overset{+}{Cl}$, whereas hyperconjugation has been involved to account for the short C—C bond in $CH_3C{\equiv}CH$ (6). Thus a realistic potential function for this type of molecule should include non-negligible interaction constants between adjacent bonds. Meister's function (14) for 1-chloropropyne might be criticized on these grounds since the C≡C, CCl interaction constant (K_{Xa}) is taken as zero.[9] However since the agreement between observed and calculated frequencies for $CH_3C{\equiv}CCl$ is quite good it must mean that the K_{Xa} interaction has been taken up in the values for the other constants. In this connection it is instructive to inspect the sets of force constants that Meister has tested for $CH_3C{\equiv}CBr$ (14). They are all about equally good from the point of view of closeness of fit between calculated and observed frequencies, yet one set differs from the others essentially by having a fairly large (0.65×10^5 dynes per cm.) value for the C≡C, CBr interaction constant. The resulting adjustment necessary in the other constants is only to change $K_{C\equiv C}$ by about 4%, K_{CCl} by about 8%, with minor changes in two interaction constants.

ACKNOWLEDGMENT

We are indebted to Dr. D. J. Boyd for helpful discussions.

REFERENCES

1. BERNSTEIN, H. J. and ALLEN, G. J. Opt. Soc. Amer. 45: 237. 1955.
2. BERNSTEIN, H. J. and PULLIN, A. D. E. Can. J. Chem. 30: 963. 1952.
3. BOYD, D. R. J. and LONGUET-HIGGINS, H. C. Proc. Roy. Soc. (London), A, 213: 55. 1952.
4. BOYD, D. R. J. and THOMPSON, H. W. Trans. Faraday Soc. 48: 493. 1952.
5. CLEVELAND, F. F. and MURRAY, M. J. J. Chem. Phys. 11: 450. 1943.
6. COULSON, C. A. Valence. The Clarendon Press, Oxford. 1952. p. 313.

[9] *A similar criticism has been made of the potential function for $CH_3C{\equiv}CH$. See Reference (10).*

7. CRAWFORD, B. L. J. Chem. Phys. 20: 977. 1952.
8. EDSALL, J. T. and WILSON, E. B., JR. J. Chem. Phys. 6: 124. 1938.
9. GERHARD, S. L. and DENNISON, D. M. Phys. Rev. 43: 197. 1953.
10. GRISENTHWAITE, A. J. and THOMPSON, H. W. Trans. Faraday Soc. 50: 212. 1954.
11. HERZBERG, G. Infrared and Raman spectra of polyatomic molecules. D. Van Nostrand Company, Inc., New York. 1945. p. 232.
12. HERZBERG, G. Infrared and Raman spectra of polyatomic molecules. D. Van Nostrand Company, Inc., New York. 1945. p. 338.
13. HERZBERG, G. Infrared and Raman spectra of polyatomic molecules. D. Van Nostrand Company, Inc., New York. 1945. p. 429.
14. MEISTER, A. G. J. Chem. Phys. 16: 950. 1948.
15. MORSE, A. T. and LEITCH, L. C. Can. J. Chem. 32: 500. 1954.
16. RAMSAY, D. A. J. Am. Chem. Soc. 74: 72. 1952.
17. RANK, D. H. and KAGARISE, R. E. J. Opt. Soc. Amer. 40: 89. 1950.
18. RICHARDSON, W. S. and GOLDSTEIN, J. H. J. Chem. Phys. 18: 1314. 1950.
19. SHERIDAN, J. and GORDY, W. J. Chem. Phys. 20: 735. 1952.
20. WESTENBERG, A. A., GOLDSTEIN, J. H., and WILSON, E. B. J. Chem. Phys. 17: 1319. 1949.
21. WHITE, J. U., ALPERT, N. L., and DEBELL, A. G. J. Opt. Soc. Amer. 45: 154. 1955.

MESYL* DERIVATIVES OF HYDRAZINE[1]

By Alan G. Newcombe[2]

ABSTRACT

Monomesylhydrazide, 1-acetyl,2-mesylhydrazide, and *sym*-dimesylhydrazide were obtained by means of the Schotten–Baumann reaction. For comparison with these compounds the hydrazinium dimesylate, hydrazinium monomesylate, monomesylhydrazide mesylate, and monoacetylhydrazide mesylate were prepared. The preparation of dimesyldiimide by the action of metallic sodium on N,N-dichloromesylamide was attempted.

INTRODUCTION

Although numerous hydrazides of aromatic and aliphatic carboxylic acids have been prepared, very little is known of the hydrazides of sulphonic acids. The few sulphonic acid hydrazides which have been prepared were chiefly derivatives of aromatic sulphonic acids. It seemed, therefore, of interest to ascertain whether aliphatic sulphonic acid hydrazides could be prepared.† Because of the ready availability of mesyl chloride the hydrazine derivatives of methanesulphonic acid were investigated first.

It was found that few of the reactions available for the preparation of the hydrazides of carboxylic acids can be used for the synthesis of the hydrazides of aromatic or aliphatic sulphonic acids. Curtius and Lorenzen (4) found that by treating hydrazine with either the anhydride or the ethyl ester of benzenesulphonic acid the hydrazine disulphonate salt, and not the *sym*-dibenzenesulphonylhydrazide, was formed. Similar results were obtained in this laboratory using the corresponding aliphatic sulphonic acid derivative (mesyl anhydride (1) or ethyl mesylate (1)) in attempts to prepare the *sym*-dimesylhydrazide.

Raschig's (16) method for the preparation of hydrazodisulphonic acid (HO—SO_2—NH—NH—SO_2—OH) was also found to be unsuitable for the preparation of the *sym*-dimesylhydrazide when mesyl chloride was used as the sulphonating agent. Very small quantities of *sym*-dimesylhydrazide were obtained, however, by using the method of Diels and Paquin (8), substituting mesyl chloride for the chloromethyl carbonate.

Considerably better, although still low, yields of *sym*-dimesylhydrazide were obtained by means of the Schotten–Baumann reaction under the conditions reported by Helferich *et al.* (10, 12) for the preparation of dimesylimide.

[1]*Manuscript received March 23, 1955.*

Contribution from the Banting and Best Department of Medical Research, University of Toronto, Toronto, Ontario.

This paper forms part of a thesis submitted to the Department of Chemistry of the University of Toronto, in partial fulfillment of the requirements for the Degree of Doctor of Philosophy.

[2]*Holder of a Research Council of Ontario scholarship in 1947–48. Holder of summer scholarships from the National Research Council in 1947 and 1948. Present address: Ontario Research Foundation, Toronto, Ontario.*

**The use of the word mesyl, which was first suggested by Helferich and Gnüchtel (11), in place of methanesulphonyl is followed throughout this paper.*

†*G. H. Stempel, Can. Patent No. 511,584, April 5, 1955, reports the preparation of aliphatic monosulphonylhydrazides by the use of the Schotten–Baumann reaction utilizing alkyl sulphonyl halides having at least four carbon atoms.*

Several changes in the procedure were made in order to increase the yield, but were unsuccessful.

Analysis of the material produced by the Schotten–Baumann reaction gave figures that agreed well with those calculated for *sym*-dimesylhydrazide. It was realized, however, that the reaction product might have been hydrazinium dimesylate, hydrazinium monomesylate, monomesylhydrazide mesylate, hydrazinium dimethanesulphinate,‡ or 1,1-dimesylhydrazide, since these materials possess similar or identical analytical figures. The possibility of the Schotten–Baumann product being identical with one of the first three compounds named was ruled out by comparing it with hydrazinium dimesylate, hydrazinium monomesylate, and monomesylhydrazide mesylate prepared by reliable methods (2). Since the Schotten–Baumann product did not react with benzaldehyde under conditions which resulted in the immediate formation of benzalmesylhydrazone and benzalazine from monomesylhydrazide hydrochloride and hydrazinium dimesylate, respectively, it could not have been hydrazinium dimethanesulphinate or 1,1-dimesylhydrazide.

In a similar manner it was shown that the Schotten–Baumann reaction of acetylhydrazide with mesyl chloride yielded the 1-acetyl,2-mesylhydrazide and not acetylhydrazide mesylate, acetylhydrazide methanesulphinate, or 1-acetyl,1-mesylhydrazide.

In attempting to prepare a monosubstituted hydrazide, namely the monomesylhydrazide, the methods for the preparation of the monohydrazides of carboxylic acids were investigated first. Following the method of Curtius and Struve (5) by heating the methane sulphonamide with hydrazine hydrate or anhydrous hydrazine yielded only the unchanged starting material. Heating the ethyl or butyl (14) mesylate with hydrazine hydrate or anhydrous hydrazine following the method of Curtius and Hofmann (3) yielded in every case the undesired hydrazinium monomesylate. These results are in line with those obtained by Curtius and Lorenzen (4) in their attempts to prepare the monobenzenesulphonylhydrazide. The monomesylhydrazide was readily obtained, and in excellent yield, by means of the Schotten–Baumann reaction. The monomesylhydrazide, a viscous oil, gave a solid hydrochloride and on treatment with benzaldehyde immediately formed the benzalmesylhydrazone.

It was thought that the diacylhydrazides (*sym*-dimesylhydrazide and 1-acetyl,2-mesylhydrazide) might be useful starting materials in the preparation of dimesyldiimide and acetylmesyldiimide. The preparation of these substances by the oxidation of the hydrazides with fuming nitric acid according to Diels *et al.* (7, 8) proved unsuccessful. The method of Stollé (17) was found not to be feasible since the mercury salts of *sym*-dimesylhydrazide and 1-acetyl,2-mesylhydrazide decomposed too readily to permit their isolation. Attempts to prepare the diimide derivatives by oxidation of the disubstituted hydrazides by means of lead tetraacetate in glacial acetic acid were also unsuccessful. While no reaction occurred with 1-acetyl,2-mesylhydrazide at either 0°, 25°, or the boiling point of the solution, the *sym*-dimesylhydrazide

‡*Dann and Davies (6) have shown that the production of sulphinate salts from hydrazine and sulphonic acid chlorides occurs rather easily.*

reacted vigorously, even in the cold, with the evolution of a gas and complete decomposition of the hydrazide. The oxidation of the similar diacetylhydrazide (*sym*) with lead tetraacetate in glacial acetic acid gave a reddish colored oil in a yield of 33% which, like the "diacetyl diimide" of Stollé(17) and Inhoffen, Pommer, and Bohlman (13), decomposed too rapidly to permit analysis.

Finally the possibility of preparing the dimesyldiimide via the action of sodium metal on a N,N-dihalomesylamide was investigated. For this purpose the unknown N,N-dichloromesylamide was prepared by the action of sodium hypochlorite on an aqueous solution of mesylamide at 0°. The N,N-dichloromesylamide was obtained in a pure state and a high yield. While this investigation was in progress Mel'nikov, Sukhareva, and Kavenoki (15) reported the preparation of N,N-dichloromesylamide by the same procedure. The bromination of mesylamide with sodium hypobromite gave a product which lost bromine on washing with ether or other organic solvents.

When a suspension of N,N-dichloromesylamide in ether or benzene was treated with sodium wire and the solvent removed, an orange colored mixture was obtained from which, however, no dimesyldiimide could be isolated.

EXPERIMENTAL

sym-Dimesylhydrazide

To an ice-cold solution of 5.48 gm. (80 mM.) of hydrazine hydrochloride in 10 ml. of water, 20.9 gm. (182 mM.) of mesyl chloride and 60.5 ml. of 4.34 *N* sodium hydroxide solution were added dropwise and at such a rate that the pH of the solution was in the proximity of 8.0. During the addition, which in general required 30 min., the temperature of the solution was kept at 6°. The stirring of the mixture was continued for 15 min. after the addition was completed. At the end of this time hydrochloric acid was added and the solid was filtered off, washed with water, and dried *in vacuo*. The dimesylhydrazide was obtained in yields ranging from 8 to 12%; m.p. 168.5–170° (with decomposition). Calc. for $C_2H_8O_4N_2S_2$ (186.2): C, 12.8; H, 4.25; N, 14.9; S, 34.05%. Found: C, 12.8; H, 4.21; N, 15.2; S, 33.80%.

Variations.—Using, instead of the 4.34 *N* sodium hydroxide, 2 *N* sodium hydroxide, 2 *N* potassium hydroxide, saturated barium hydroxide, or sodium bicarbonate solution, or adding the mesyl chloride at a faster rate did not improve the yield of the *sym*-dimesylhydrazide.

Hydrazinium Dimesylate

A solution containing 9.61 gm. (100 mM.) of methanesulphonic acid, dissolved in 10 ml. of water, was prepared and cooled to 0°. The solution was then added slowly to 2.5 gm. (50 mM.) of hydrazine hydrate. The resultant solution, on standing overnight at 6°, produced a crystalline precipitate, which was filtered off and air dried. Concentrating the mother liquor *in vacuo* yielded more material. The total yield of hydrazinium dimesylate was 8.31 gm. (74%). The material, after drying *in vacuo* at 100° to constant weight, melted at 202–203°. *Analyses*: Calc. for $C_2H_{12}O_6S_2N_2$ (224.3): C, 10.71; H, 5.39; N, 12.50; S, 28.59%. Found: C, 10.97; H, 5.29; N, 12.48; S, 28.89%.

The hydrazinium dimesylate was recovered unchanged by recrystallization

from 99% ethanol. On recrystallization from 95% ethanol only hydrazinium monomesylate, melting at 143.0–143.5°, was obtained. The decomposition of a hydrazine di-salt to the corresponding mono-salt is not uncommon (9).

Hydrazinium Monomesylate

To an ice-cold mixture of 5.0 gm. (100 mM.) of hydrazine hydrate and 22 ml. of ether in a flask equipped with a reflux condenser, was added slowly 9.61 gm. (100 mM.) of methanesulphonic acid. After the exothermic reaction ceased the ether was distilled off, and the white residue was recrystallized from a small amount of ethanol. The material thus obtained melted from 139 to 144°. For further purification it was dissolved in a small volume of hot water and precipitated by the addition of 99% ethanol to the point of turbidity; m.p. 143.0–143.5°. Calc. for $CH_8O_3SN_2$ (128.2): C, 9.37; H, 6.29; N, 21.85%. Found: C, 9.42; H, 6.46; N, 21.74%.

Monomesylhydrazide

A solution of 5.0 gm. (100 mM.) of hydrazine hydrate in 15 ml. of water was placed in a three-necked flask immersed in a salt–ice bath. To the solution, 11.5 gm. (100 mM.) of mesyl chloride and 50 ml. of a 2 *N* sodium hydroxide solution were added dropwise and with stirring in such a manner that the temperature did not rise above 8°. After the addition had been completed the solution was concentrated *in vacuo* with the occasional removal of sodium chloride. To the concentrate was added 99% ethanol and the solution again was concentrated *in vacuo*. The residue was taken up in anhydrous ether, centrifuged, and the solvent removed *in vacuo*. The residue, a clear, colorless, viscous oil weighed 10.31 gm. (93.5%). The monomesylhydrazide is moderately soluble in alcohol or ether; but readily soluble in chloroform or carbon tetrachloride. *Analyses*: Calc. for $CH_6O_2N_2S$ (110.1): C, 10.9; H, 5.50; N, 25.4%. Found: C, 10.7; H, 5.25; N, 25.1%.

Monomesylhydrazide Hydrochloride

The mesylation of 5.0 gm. (100 mM.) of hydrazine hydrate was carried out as described above. To the reaction mixture was added 25 ml. of concentrated hydrochloric acid, and the *sym*-dimesylhydrazide which was formed in a small amount was filtered off. The filtrate was concentrated *in vacuo*. The white residue was recrystallized twice from boiling 99% ethanol. The crystals of monomesylhydrazide hydrochloride, after drying *in vacuo*, weighed 10.79 gm. (73.7%) and melted at 152–153°. *Analyses*: Calc. for $CH_7O_2N_2SCl$ (146.6): C, 8.20; H, 4.82; N, 19.14%. Found: C, 8.24; H, 5.20; N, 19.21%.

Monomesylhydrazide Mesylate

This salt of monomesylhydrazide was best prepared by the following method. A solution of 1.10 gm. (10 mM.) of monomesylhydrazide in 10 ml. of water was added to a solution of 0.96 gm. (10 mM.) of methanesulphonic acid in 30 ml. of water and the mixture was concentrated *in vacuo*. The oil was dissolved in 99% ethanol and the solution again concentrated *in vacuo*. This operation was repeated once more. The white crystalline substance was recrystallized, after solution in a warm mixture of 20 ml. of 99% ethanol and

2 ml. of chloroform, by the addition of anhydrous ether to the point of turbidity. The substance (m.p. 137–138°) was recrystallized once more using a warm mixture of chloroform: absolute ethanol (1:1 v/v) and anhydrous ether. In this manner 0.24 gm. (11.7%) of the monomesylhydrazide mesylate was obtained; m.p. 144–145°. *Analyses*: Calc. for $C_2H_{10}O_5N_2S_2$ (206.2): C, 11.63; H, 4.88; N, 13.59%. Found: C, 11.43; H, 5.08; N, 13.67%.

Benzal Mesylhydrazone

A solution of 1.10 gm. (10 mM.) of monomesylhydrazide in 16 ml. of water was added to a solution of 1.06 gm. (10 mM.) of benzaldehyde in 30 ml. of hot 95% ethanol. The mixture was heated to the boiling point and alcohol was added until the precipitate was dissolved. The yellow precipitate which formed on cooling was filtered off, redissolved in hot ethanol, and precipitated by the addition of water. The colorless crystals were once more recrystallized from warm ethanol and water. The benzal mesylhydrazone weighed 1.11 gm. (56%); m.p. 150–151°. *Analyses*: Calc. for $C_8H_{10}O_2N_2S$ (198.2): C, 48.5; H, 5.07; N, 14.13%. Found: C, 48.4; H, 5.10; N, 14.19%.

1-*Acetyl,2-mesylhydrazide*

Acetylhydrazide was obtained by the method of Curtius and Hofmann (3) and mesylated in the following manner.

To a cooled solution of 5.0 gm. (67.5 mM.) of acetylhydrazide in 10 ml. of water were added dropwise and with gentle stirring 7.75 gm. (67.5 mM.) of mesyl chloride and 34 ml. of 2 *N* sodium hydroxide at such a rate that the pH was kept below 8.0. The temperature of the mixture was not allowed to rise above 8°. Towards the end of the addition the 1-acetyl,2-mesylhydrazide, a fine white crystalline solid, precipitated. The solid was collected with suction on a Büchner funnel, washed with a small volume of water, and dried *in vacuo*. Yield: 2.27 gm. (22.2%); m.p. 197–199°. *Analyses*: Calc. for $C_3H_8O_3N_2S$ (152.2): C, 23.65; H, 5.29; N, 18.40%. Found: C, 23.59; H, 5.22; N, 18.28%.

Acetylhydrazide Mesylate

To a solution of 0.77 gm. (6.8 mM.) of 95% methanesulphonic acid in 30 ml. of water was added a solution of 0.50 gm. (6.8 mM.) of acetylhydrazide in 4 ml. of water, and the mixture was concentrated *in vacuo*. The sirupy residue was taken up in 99% ethanol and the solvent removed *in vacuo*. This process was repeated twice using anhydrous ether followed by 99% ethanol. The dry material was then recrystallized from warm 99% ethanol by the addition of anhydrous ether. The acetylhydrazide mesylate was thus obtained in a yield of 1.06 gm. (90%), m.p. 114–116°. *Analyses*: Calc. for $C_3H_{10}O_4N_2S$ (170.2): C, 21.20; H, 5.92; N, 16.47%. Found: C, 21.10; H, 6.09; N, 16.35%.

Reactivity of Hydrazine Derivatives with Benzaldehyde

Hydrazinium Salts

To a solution of 5 mM. of hydrazinium monomesylate or hydrazinium dimesylate and equivalent amounts of sodium acetate in 2.2 ml. of water was

added 10 mM. of freshly distilled benzaldehyde. In each case, the formation of the well-known benzalazine took place immediately.

Monoacylhydrazide Salts

To a solution of acetylhydrazide mesylate (0.447 gm., 2.63 mM.) and 0.292 gm. (3.56 mM.) of anhydrous sodium acetate in 5 ml. of water was added 0.279 gm. (2.63 mM.) of benzaldehyde and the mixture was well shaken. The known benzalacetylhydrazone was formed.

In a similar experiment with monomesylhydrazide hydrochloride (2.63 mM.), but using 80% acetic acid as solvent (10 ml.), the known benzalmesylhydrazone was obtained.

Diacylhydrazides

Neither the 1-acetyl, 2-mesylhydrazide nor the *sym*-dimesylhydrazide reacted with benzaldehyde under conditions similar to the one immediately above. Both hydrazides were recovered unchanged.

N,N-Dichloromesylamide

To a solution of 0.64 gm. (16 mM.) of sodium hydroxide in 3.5 ml. of water cooled in ice was added 0.76 gm. (8 mM.) of mesylamide, and chlorine gas was passed through the solution for a period of 15 min. The white precipitate which formed immediately was filtered off, washed with a small amount of water, and dried *in vacuo*. The N,N-dichloromesylamide was obtained in a yield of 1.09 gm. (83.2%); m.p. 84–86°. Carbon, hydrogen, and nitrogen analyses were attempted but the substance exploded in the combustion tube. Iodometric analysis indicated a positive chlorine content of 43.1%. Theory, 43.2%.

ACKNOWLEDGMENTS

The author is grateful to the Research Council of Ontario and to the National Research Council for financial assistance during the course of this work.

REFERENCES

1. BILLETER, O. C. Ber. 38: 2018. 1905.
2. CURTIUS, T. and FRANZEN, H. Ber. 35: 3240. 1902.
3. CURTIUS, T. and HOFMANN, T. S. J. prakt. Chem. 53: 524. 1896.
4. CURTIUS, T. and LORENZEN, F. J. prakt. Chem. 58: 160. 1898.
5. CURTIUS, T. and STRUVE, G. J. prakt. Chem. 50: 295. 1894.
6. DANN, A. T. and DAVIES, W. J. Chem. Soc. 1050. 1929.
7. DIELS, O. and FRITZSCHE, P. Ber. 44: 3026. 1911.
8. DIELS, O. and PAQUIN, M. Ber. 46: 2007. 1913.
9. EPHRAIM, F. Inorganic chemistry. Revised 4th ed. Oliver and Boyd, Ltd., Edinburgh. 1943. p. 658.
10. HELFERICH, B. and FLECHSIG, H. Ber. 75: 532. 1942.
11. HELFERICH, B. and GNÜCHTEL, A. Ber. 71: 712. 1938.
12. HELFERICH, B. and GRÜNERT, H. Ann. 545: 178. 1940.
13. INHOFFEN, H. H., POMMER, H., and BOHLMANN, F. Chem. Ber. 81: 507. 1948.
14. MARVEL, C. S. and SEKERA, V. C. J. Am. Chem. Soc. 55: 345. 1933.
15. MEL'NIKOV, N. N., SUKHAREVA, N. D., and KAVENOKI, F. YA. Chem. Abstr. 40: 5696^{3}. 1946. J. Appl. Chem. (U.S.S.R.), 18: 568. 1945.
16. RASCHIG, F. Schwefel und Stickstoff Studien. Verlag Chemie, G.m.p.H. Leipzig, Berlin. 1904. p. 199.
17. STOLLÉ, R. Ber. 45: 273. 1912.

THE APPLICATION OF GAS–LIQUID PARTITION CHROMATOGRAPHY TO PROBLEMS IN CHEMICAL KINETICS[1]

By A. B. Callear[2] and R. J. Cvetanović

ABSTRACT

A gas–liquid partition chromatographic method for analysis of samples of the order of magnitude of a micromole is described. Examples of application are given.

INTRODUCTION

The analysis of 'liquid products', produced for example in photochemical reactions, has in the past been attempted by mass spectrometer analysis, by infrared analysis, and by specific tests for various functional groups. The liquid products are most frequently complex mixtures and in usual chemical kinetic investigations appear in quantities varying from a fraction to several micromoles. Their analysis has great significance for elucidating the mechanism of the process. Owing to the small size of the samples and their complexity, a complete mass spectrometric analysis can rarely be carried out. Other methods of analysis usually lead to an incomplete picture of the reaction products. The present paper describes the application of gas–liquid partition chromatography to these and some related problems.

Two types of gas chromatography have been considered in connection with the present problem: the displacement method (3, 7, 11) and the gas–liquid partition method (4, 5, 6). In the former, the mixture to be analyzed was first adsorbed on charcoal in a column, and was then displaced from the column by nitrogen containing a material such as bromobenzene or ethyl acetate. Separation occurred as a result of the difference in adsorption energies. In the latter method the stationary phase used was Celite 545 (kieselguhr) mixed with a liquid of low vapor pressure (silicones, liquid paraffin, glycerol, dinonyl phthalate, and others). The gases were eluted from the column with nitrogen, and separation occurred as a result of the different partition coefficients between the gas and liquid. This method was first used for the separation of organic acids (5) and amines (4, 6) and the analyzer was an automatic burette. Later Ray (12, 13) developed a more general method using thermal conductivity cells as the analyzer. He analyzed samples of about 10 mgm. and used a 6 ft. column containing 0.45 gm. dinonyl phthalate per gram of celite.

In the present work the partition method has been chosen for analysis of liquid products in preference to the displacement method because the same column can be used indefinitely and there is no contamination of the components with the displacing compound. There are also, in individual cases, the advantages of reversibility and greater selectivity. The method of Ray is

[1]*Manuscript received March 11, 1955.*
Contribution from the Division of Applied Chemistry, National Research Council, Ottawa, Canada. Issued as N.R.C. No. 3644.
[2]*N.R.L. Postdoctorate Fellow 1954–55.*

further developed in order to make it applicable to the extremely small quantities of material produced in chemical kinetic studies. The details of a gas–liquid partition chromatographic apparatus applicable to samples of the order of magnitude of a micromole are given with particular emphasis on a discussion of the factors of importance for its construction and use. Some examples of application are given. In some favorable cases as little as 2×10^{-9} moles of a gas can be detected. In general, the sensitivity is of the order of 1×10^{-8} moles and is, therefore, at least as good as that of a gas burette or of a mass spectrometer. Isolation of fractions from relatively large samples has been previously reported (7, 8). The possibility of the isolation of fractions from the extremely small samples used in the present work has been investigated and it has been found that chromatographic fractionation can be combined, with distinct advantage, with other analytical procedures. This is especially true in cases when the peaks overlap and some of the constituents cannot be isolated singly. The method has proved applicable both for quantitative analysis and for identification of components of unknown mixtures.

SENSITIVITY OF THE THERMAL CONDUCTIVITY MEASUREMENTS

The possibility of application of gas–liquid partition chromatography to the extremely small amounts of products encountered in kinetic studies depends on a high sensitivity of detection of these products in very large amounts of the eluent gas. Thermal conductivity measurements appear to be, at present, the most convenient means of achieving the necessary sensitivity, provided that a high sensitivity can be obtained while the general "noise" level is kept low. A number of factors affect both the sensitivity and the stability of thermal conductivity measuring devices.

In the present work two thermal conductivity cells, forming in the customary manner the adjacent arms of a Wheatstone bridge, were used. They were, however, both placed at the exit end of the column and separated from each other by a series of cold traps so that the substances eluted from the column affected only the first cell while pure eluent gas passed through the second cell. For the measurement of very small amounts of substances this arrangement was preferred to the usual one, with the "reference" cell preceding the column, because of the difficulty of completely eliminating fluctuations in the input pressure of the eluent gas. The bridge was balanced with the eluent gas alone in both cells. The temperature change of the platinum resistance wire in the conductivity cell due to the presence of an impurity is proportional to V^2, the square of the e.m.f. across the wire. A given resistance change of the wire produces an off-balance signal proportional to V. The sensitivity, i.e., the off-balance signal arising from the presence of a fixed percentage of an impurity, is, therefore, proportional to V^3. A very marked increase in sensitivity can, evidently, be achieved by increasing the e.m.f. across the resistance wire. However, it was found that if the wire temperature was increased to over 200°C., a permanent change in the zero position occurred at every peak, indicating either a physical change in the surface of the wire or a change of its position within the cell. The former would alter the tempera-

ture discontinuity (14) at the gas–solid interface and thus change the zero point. The platinum wires were actually maintained at about 100°C., as was established by observing resistance change with wattage dissipation. At the flow rates used, no appreciable difference in the wire temperature could be observed for stationary and flowing gas.

Platinum resistance wire of 10^{-3} in. diameter was used for the conductivity cells. Since the desired sensitivity was achieved, no experiments with different thicknesses of the wire were conducted. Thinner wires may offer some advantage in the greater response, but are more difficult to handle and in all probability would be more sensitive to pressure fluctuations because of greater temperature discontinuity.

The effect of an impurity on the thermal conductivity of a gas is given by Chapman and Cowling (1) for a special molecular model. If the impurity has a very high molecular weight compared to the bulk of the gas, this equation reduces to

$$\lambda(\text{impure mixture}) = \lambda - n_{21}\lambda^2(5-4B)/2F$$

where λ is the thermal conductivity of the pure gas, B is a constant and, under these conditions, F is inversely proportional to the molecular weight of the impurity. n_{21} is the ratio of the number of impurity molecules to the number of eluent gas molecules. Thus for this ideal case, the effect of a constant amount of impurity is proportional to the square of the thermal conductivity of the eluent gas and proportional to the first power of the molecular weight of the impurity. Though the practical case will only approximate to this relationship, it is clear that a gas of high thermal conductivity should be used. For this reason, hydrogen has been chosen for the eluent gas in preference to nitrogen. The use of hydrogen as eluent gas has recently been reported by Patton, Lewis, and Kaye (10).

A rough comparison of the performance of hydrogen and nitrogen gas eluents can be made. The thermal conductivity ratio is about 7 to 1. The changes in thermal conductivity of the gases on addition of the same percentage of a vapor of high molecular weight differ by at least a factor of 7 and possibly by a factor as high as 7^2. If the wire is to be at 100°C. for both gases, the ratio of the e.m.f.'s is $7^{1/2}$. It follows that the off-balance signal produced by the impurity in the nitrogen is between $7^{3/2}$ and $7^{5/2}$ times less than that for hydrogen. The small fluctuations in temperature between the two thermal conductivity cells would produce a "noise" $7^{1/2}$ times greater for hydrogen than for nitrogen, since the voltage is that much higher. Thus the ratios of signal to noise for the two cases would differ by a factor between 7 and 7^2 in favor of hydrogen. Apart from this fundamental difference in behavior, to obtain the same size "peak" for both gases on the recording chart, the amplification has to be very much higher for nitrogen, introducing further electrical noise and noise due to pressure variations, making stable working conditions more difficult to achieve.

Since each molecule of an impurity present in the eluent gas can be regarded as making its own contribution to the recorded peak and this contribution

is proportional to the time each molecule remains in the thermal conductivity cell, it can be expected that the area under the peaks should decrease with increasing rate of eluent gas flow. A marked variation in peak area with flow rate has been observed with the experimental arrangement used, though the flow rates were not known sufficiently accurately to establish a quantitative relationship.

GENERAL FEATURES OF THE APPARATUS AND THE PROCEDURE

The flow system is shown in Fig. 1. Hydrogen gas from a cylinder and reducing valves enters the apparatus at *A* at a pressure slightly greater than one atmosphere as regulated by the small buffer volume *B* (200 cc.) and the

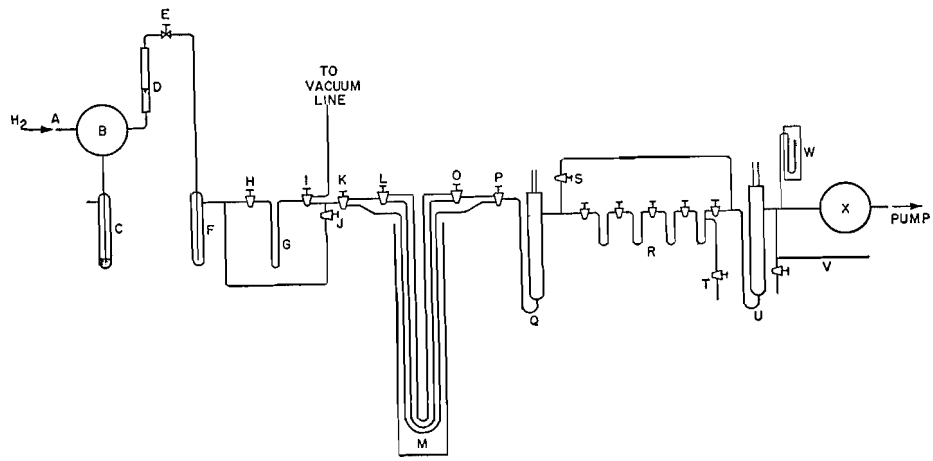

FIG. 1. General outlay of the apparatus.

bubbler *C* containing dibutyl phthalate. Through the latter, excess gas is allowed to bubble at a constant rate. The rotameter *D* gives an approximate value for the rate of flow and a polythene diaphragm valve *E* can be used to vary the pressure applied to the column. The liquid nitrogen trap *F* removes any condensable impurities from the hydrogen. The sampling trap *G* can be evacuated by closing the vacuum stopcock *H* and opening the two-way capillary vacuum stopcock *I* to the vacuum manifold. The sample is measured in a gas burette and is condensed in *G*, care being taken to raise finally the level of liquid nitrogen above the condensed sample. During introduction of sample, the hydrogen bypasses *G* by means of stopcock *J*. To introduce the sample to the column, *I* is closed and *H* is slowly opened to disturb the pressure as little as possible. With *G* full of hydrogen at one atmosphere, *I* is opened to the column and *J* is closed. It is usually necessary to pass hydrogen for a few minutes to restore stability of the analyzer. The sample is then evaporated into the gas stream by replacing the liquid nitrogen with hot water. The present apparatus incorporates three columns for different types of separation. The column is selected by operation of three-way capillary vacuum stopcocks *K*, *L*, *O*, and *P*. The sample passes through the column *M* which is contained

in a 6.5 cm. i.d. glass cylinder about 100 cm. long. A spiral of resistance wire placed inside the cylinder is used to heat the column to the desired temperature, as measured on a thermometer near the center of the cylinder. The 'dead space' between G and M is reduced as much as possible by using capillary tubing. After leaving M, the gas passes through about 20 cm. of 4 mm. i.d. thin-walled glass tubing, so that it is cooled to room temperature before entering the first thermal conductivity cell Q. After passing through Q, the sample can be removed from the hydrogen in a series of cold traps R, made of 4 mm. i.d. thin-walled glass tubing. The volume is kept as small as possible by using capillary stopcocks between the traps. The various components passing through the first thermal conductivity cell are recorded automatically in the form of peaks. They can usually be trapped out in successive liquid nitrogen traps R on the first run. In the case of an unknown mixture which gives overlapping peaks, it is sometimes necessary to observe the chromatographic spectrum on the first run and then send the sample through again, in order to effect the most favorable fractionation. The last trap is connected through stopcock T to the vacuum system so that the fractions can be successively removed and measured. While this is done the stream of hydrogen is bypassed through S. After the second thermal conductivity cell U the gas stream enters a 15 liter flask, serving as a buffer volume, and is then pumped out by a vacuum oil pump. The pressure is observed on the manometer W, and is maintained constant by bleeding in air through the $\frac{1}{2}$ mm. i.d. glass capillary tubing V. In some experiments the pressure was 40 mm. and in others 70 mm. Variations in pressure between these values had little effect on the separations. The flow rates were determined by observing the time taken for a small amount of air to pass between Q and U. The volume of the tubing and traps between Q and U was known. The flow rates in cc. (N.T.P.) per min. were

Column 1: 1.8; Column 2: 15.3; Column 3: 3.3.

CONSTRUCTION OF THE THERMAL CONDUCTIVITY CELLS

Fig. 2 shows one of the thermal conductivity cells. The gas enters the cell through the 4 mm. i.d. thin-walled glass tubing A. The platinum wire FG

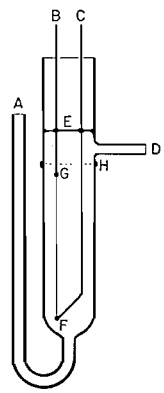

FIG. 2. Thermal conductivity cell.

(10^{-3} in. in diameter) is silver soldered to thick platinum crosspieces which, in turn, are silver soldered to tungsten rods *B* and *C*. Spot welded contacts used originally were found to be unsatisfactory. The tungsten leads are protected from the thermostatting water by extension of the 15 mm. i.d. glass tube of which the cell is made some 10 cm. above the seal *E*. The wire is mounted by breaking the cell at *H* and sealing back on when the wire has been attached. The gas exit is at *D*. The two cells are embedded side by side in paraffin wax contained in a glass cylinder 10 cm. in diameter. The whole is in a two liter beaker containing water which is stirred. The paraffin wax extends to *E* and the water level is about 5 cm. above this. A layer of oil is spread on the surface of the water to prevent evaporation. In early experiments, the inner cylinder contained mercury instead of paraffin wax. The performance was poor, becoming worse when the mercury was stirred. A gel was used successfully until, after a few weeks, it began to decompose and liquefy when it was replaced with paraffin wax.

The platinum wires formed two adjacent arms of a Wheatstone bridge network, the junction of the two wires being connected to the amplifier and the other ends of the wires to a 12 volt battery. A box of oil-immersed resistances formed the other arms of the bridge. In series with the battery was a 30 ohm resistance. All the connections in the bridge network were made with thick copper wire. The off-balance signal was amplified with a d-c. amplifier (Liston-Becker Model 14) and the output was fed to a pen recorder. Screening of the circuit was not necessary. The amplifier was not used on full gain and its "noise" level was far below that arising from temperature fluctuations between the two thermal conductivity cells. The resistance of the platinum wires was about 12 ohms at room temperature.

CONSTRUCTION AND EXPERIMENTS WITH DIFFERENT TYPES OF COLUMNS

A number of different columns were made and their performance with synthetic samples observed. In order to maintain the flow rates within suitable limits, columns of relatively small diameters were used. The dinonyl phthalate columns were $2\frac{1}{4}$ mm. i.d. glass capillary tubing, and the glycerol column was 4 mm. i.d. glass tubing. They were made in *U* shape, each arm of the *U* being 3 ft. They were filled by attaching small funnels to the open ends and the stationary phase was packed in by prolonged tapping of the curved portion on a solid floor. The packing was improved by heating the column to 100°C. during this operation, and seemed to result in a uniformly packed column. It was found that a certain amount of tailing was exhibited by the peaks as smaller and smaller samples were used. The following experiments were all carried out with a mixture of methyl and ethyl alcohol in order to test the separation and the tailing of the peaks with different column materials. (*a*) Since it has been suggested that the tailing occurs as a result of some adsorption on the solid (5), some columns were made containing celite which had been stirred in a solution of 10% dinonyl phthalate in methyl alcohol and acetone. The resulting solid was drained on a Büchner funnel and most of the alcohol and acetone was removed by drawing air through it. The resulting

column contained 4 gm. dinonyl phthalate to 10 gm. of celite. This treatment did not reduce the tailing of the peaks. (*b*) Varying amounts of sorbitol tristearate were added, in order to block the surface with strongly adsorbed polyfunctional groups. This had little effect. (*c*) Instead of celite some weaker adsorbents were tried as supporting materials. Oxidized copper spheres (200–325 mesh) proved unsatisfactory, as did powdered teflon. Glass spheres (passing 270 mesh) on the other hand proved to be advantageous from the point of view of tailing and the uniformity of column packing. Larger glass spheres were tried but were less successful. The glass spheres contained some iron oxide and attempts were made to remove this in aqua regia followed by washing with distilled water. Columns made from glass spheres prepared in this way gave very little separation of the two alcohols. The untreated glass spheres gave the most satisfactory columns. They were mixed with 4% dinonyl phthalate by weight in a beaker, and the resulting mixture packed uniformly and tightly into the glass tubing. As a result a suitable, relatively slow flow rate was obtained. Most of the work described below was carried out on columns constructed in this way. (*d*) It was found that addition of phosphoric acid to the columns reduced the tailing of organic acids (5). Addition of phosphoric acid to the dinonyl phthalate glass columns caused complete removal of alcohols, possibly through formation of non-volatile esters. This type of column might have use for some special problems, where small amounts of material are to be separated from an excess of alcohol. The three columns that were finally integrated into the apparatus were : (1) 1 part dinonyl phthalate and 25 parts glass spheres passing 270 mesh; (2) 20 parts of celite and 9 parts of dinonyl phthalate; (3) 1 part of glycerol and 100 parts glass spheres passing 270 mesh. Column 2 is used for the less volatile mixtures since it gives a higher flow rate. Column 3 has not yet been used to advantage since the separations have been successfully carried out on the dinonyl phthalate columns.

THE EFFECT OF TEMPERATURE ON SEPARATION

In a theoretical treatment of gas–liquid partition chromatography, James and Martin (5) have defined the retention volume of a substance as the product of the flow rate and the appearance time of the center of the peak. Both of these quantities are dependent on the pressures at the inlet and outlet of the column and if these pressures are varied, the retention volume changes. In the present work it was found more convenient to consider the appearance times rather than the less direct quantities, the retention volumes.

The results of James and Martin and later of Ray (12) showed that the appearance times of successive members of a homologous series are mutually related in a simple manner. Ray pointed out that separation of a mixture is impaired if the temperature of the column is too high. This was confirmed in the present work when it was shown that a sample of 10^{-6} mole of a mixture of methanol and ethanol gave overlapping peaks at 70°C. while a good separation was effected at room temperature. It was found to be of advantage in a number of cases to carry out separation of the more volatile components at

room temperature and to start heating the column part way through the experiment in order to avoid excessive appearance times for the less volatile components.

EXAMPLES OF APPLICATION

Liquid products formed by reaction of oxygen atoms with ethylene, reaction of oxygen atoms with acetaldehyde, and decomposition of ethylene oxide in the presence of ethylene have been analyzed by the present method in order to test its applicability. The details and kinetics of these reactions are given elsewhere (2). The detection of impurities in an ethylene cylinder was also carried out, since in some chemical reactions the ethylene gave rise to abnormal behavior.

Since aldehydes are important products in the reaction of oxygen atoms with ethylene, as well as in a large number of other reactions, experiments were carried out using synthetic mixtures of acetaldehyde, propionaldehyde, and butyraldehyde. Fig. 3*a* shows the separation obtained on column 1 at

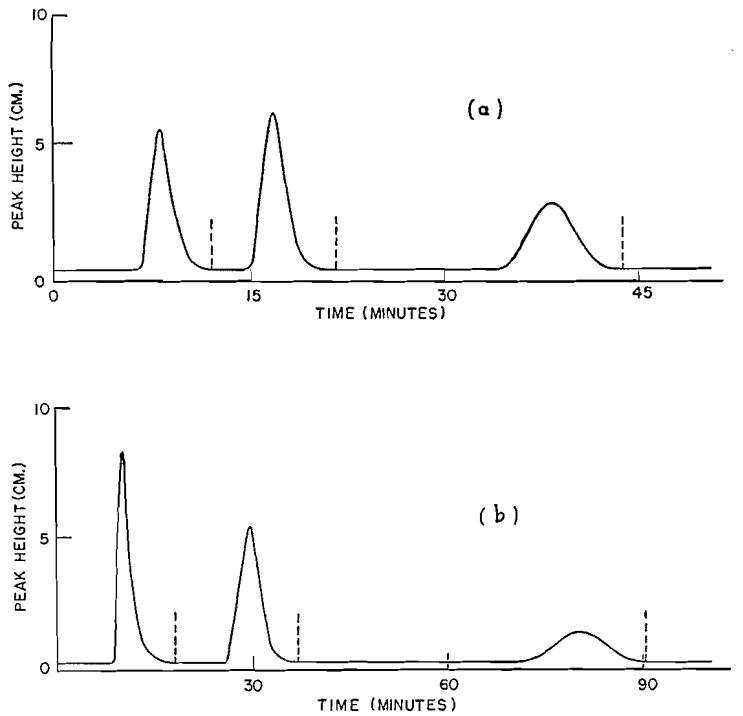

FIG. 3. (*a*) Chromatogram of a synthetic mixture of acetaldehyde, propionaldehyde, and butyraldehyde. (*b*) Chromatogram of −80°C. fraction from the reaction of O-atoms with ethylene.

50°C. The compounds were trapped out at points shown by the vertical dotted lines. Each component was measured before and after recovery with a gas burette, on a volume of 2.85 cc. Each burette reading on this quantity could be in error by 2%.

	Burette reading (pressure in mm. Hg)	
	Introduced	Recovered
Acetaldehyde	10.9	11.5
Propionaldehyde	13.6	13.7
Butyraldehyde	8.5	8.3

Fig. 4 shows the variation in peak height for acetone, with the size of the sample, demonstrating the linearity of the recording device, and the reproducibility of the method.

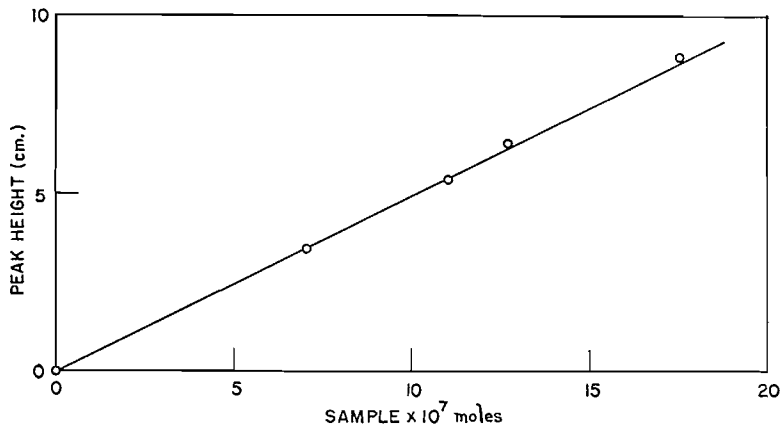

FIG. 4. Variation of peak height with varying amounts of acetone.

Fig. 3*b* shows the chromatogram obtained at 26°C. from the −80°C. Le Roy still (9) fraction from the oxygen atom and ethylene reaction. The peaks were trapped out and mass spectrometric analysis identified the first as acetaldehyde, the second as propionaldehyde, and the third as largely butyraldehyde. The rest of the third peak could have been accounted for as some compound isomeric with butyraldehyde. It was shown that under identical conditions methyl ethyl ketone separated only partially from the butyraldehyde. In another experiment, the third peak was split by trapping at the maximum point. The two halves had the same mass spectrum. With the column at 26°C. instead of 50°C. as used on the synthetic mixture of aldehydes, the ratio of the appearance times of the higher aldehydes to lower aldehydes has increased and the separation has considerably improved.

Fig. 5*a* shows the chromatogram obtained from the −80°C. fraction from the reaction of oxygen atoms and acetaldehyde carried out on column 1 at 26°C. The peaks were trapped out and identified by the mass spectrometer. The heater was switched on after 75 min. and the temperature of the column was 85°C. at the appearance of the third peak. The first peak is the excess acetaldehyde, the second peak is acetone, and the third is biacetyl. The acetone was present to the extent of 3% of the acetaldehyde. It is doubtful if it could have been identified by any conventional method since although the parent peak of the acetone would be observed in such a mixture on the mass spectrometer, the rest of the spectrum would be masked. As a check a

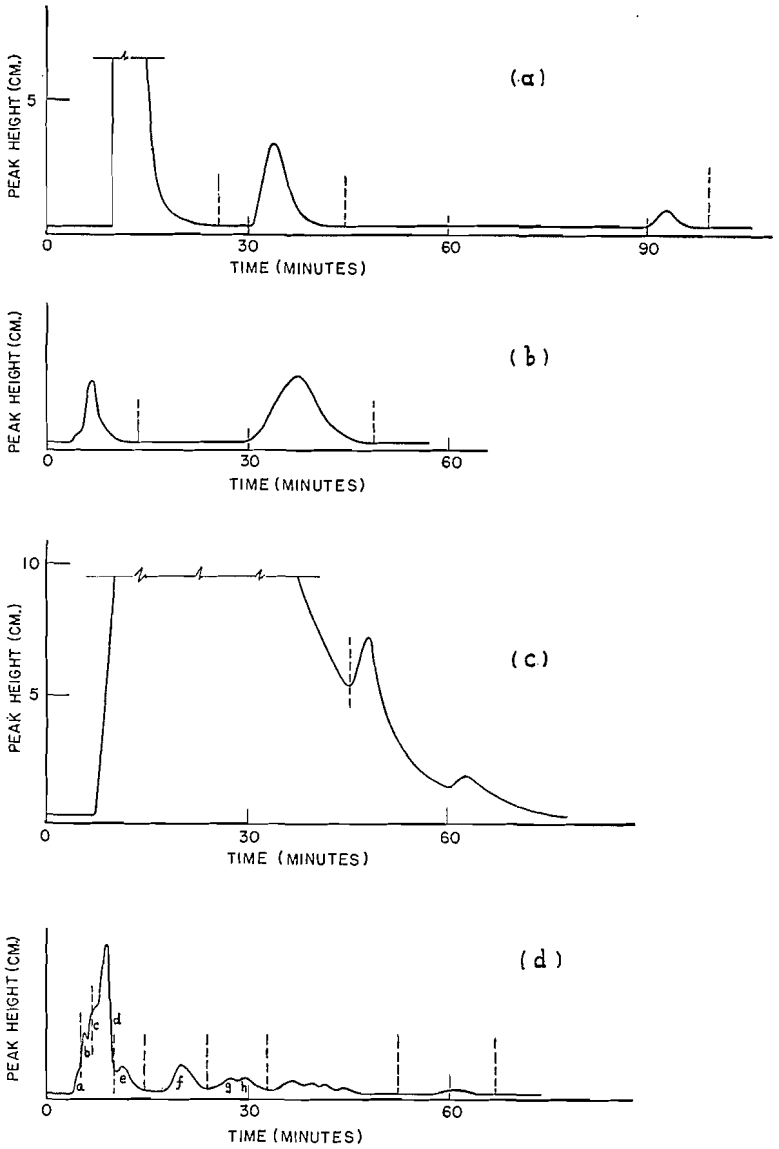

FIG. 5. (*a*) Chromatogram of −80°C. fraction from the reaction of O-atoms with acetaldehyde. (*b*) Chromatogram of room temperature fraction. (*c*) Chromatogram of −80°C. fraction from the mercury sensitized decomposition of ethylene oxide in the presence of small amounts of ethylene. (*d*) Chromatogram of the impurities in cylinder ethylene gas.

synthetic mixture of 30 parts of acetaldehyde and 1 part of acetone was run on the column and the same appearance times were observed. Fig. 5*b* shows the room temperature fraction from the same reaction separated on column 2 at 26°C. The peaks were trapped out and measured and analyzed as water and biacetyl. A sample of water was passed through the column and the position of the first peak was verified.

Fig. 5*c* shows the chromatogram of the −80°C. fraction obtained on column 1 at 26°C. for the decomposition of ethylene oxide in the presence of ethylene. The heater was switched on after 29 min. The sample was 1.5×10^{-3} moles consisting mainly of ethylene oxide which, in such a large quantity, appeared to saturate the column. The two small peaks on the tail of the ethylene oxide peak were trapped out as shown by the vertical line. At the appearance of the third peak the temperature was 102°C. The sample obtained from the tail of the ethylene oxide peak was rechromatographed and gave three separate peaks. The first was ethylene oxide, the second butyraldehyde, and the third pentaldehyde.

Fig. 5*d* shows the chromatogram obtained for the −60°C. fraction from a cylinder of ethylene prepared by dehydration of ethyl alcohol. Four hundred milliliters of impure ethylene at one atmosphere were condensed on a Le Roy still. The ethylene was removed at −175°C. and the −60°C. fraction yielded 1.04×10^{-5} moles of impurity. The chromatogram was started at 26°C. and the heater was switched on after 24 min. By trapping out according to the vertical lines, the impurities were identified by mass spectrometric analysis as (*a*) CO_2, (*b*) propylene, (*c*) isobutane, (*d*) butene-2, (*e*) isopentane, (*f*) diethyl ether and pentene-2, (*g*) hexane, (*h*) hexene (branched chain). The rest of the spectrum consisted of heptenes, heptanes, octenes, and octanes. No ethyl alcohol was detected.

The foregoing examples illustrate the applicability of the gas–liquid partition chromatography to the very small samples encountered, for example, in chemical kinetic and photochemical investigations. Good reversibility of the gas–liquid partition process is demonstrated by the observed quantitative recovery of the aldehydes. It should be mentioned at the same time that with the small samples used in the present work some compounds exhibit a partially irreversible adsorption. In some instances the reversibility is strongly temperature dependent. Thus, water and biacetyl show incomplete recoveries, especially at lower column temperatures. It is, therefore, necessary, when quantitative determinations are made, to establish the percentage recovery for each compound in the mixture at a particular column temperature.

ACKNOWLEDGMENT

Applicability of gas–liquid partition chromatography to chemical kinetic problems is being independently investigated in these laboratories by Dr. K. O. Kutschke and the authors are pleased to acknowledge some useful exchange of information and discussion. The authors are also thankful to Drs. J. E. Currah and R. R. Barefoot of Canadian Industries Ltd., McMasterville, P.Q., for some general information on the subject, to Dr. A. Tickner for mass spectrometer analysis, and to Mr. L. C. Doyle for valuable technical assistance.

REFERENCES

1. Chapman, S. and Cowling, T. G. Mathematical theory of non-uniform gases. Cambridge University Press, London, England. 1939. p. 242.
2. Cvetanović, R. J. To be published.
3. Griffiths, J., James, D., and Phillips, C. Analyst, 77: 897. 1952.
4. James, A. T. Biochem. J. 52: 242. 1952.
5. James, A. T. and Martin, A. J. P. Biochem. J. 50: 679. 1952.

6. JAMES, A. T., MARTIN, A. J. P., and SMITH, G. H. Biochem. J. 52: 238. 1952.
7. JAMES, D. H. and PHILLIPS, C. S. G. J. Chem. Soc. 1600. 1953.
8. JANAK, J. Collection Czechoslov. Chem. Communs. 18: 798. 1953.
9. LE ROY, D. J. Can. J. Research, B, 28: 492. 1950.
10. PATTON, H. W., LEWIS, J. S., and KAYE, W. I. Anal. Chem. 27: 170. 1955.
11. PHILLIPS, C. S. G. Discussions Faraday Soc. No. 7: 241. 1949.
12. RAY, N. H. J. Appl. Chem. (London), 4: 21. 1954.
13. RAY, N. H. J. Appl. Chem. (London), 4: 82. 1954.
14. SMOLUCHOVSKY, M. Ann. Physik, 35: 983. 1911.

NOTES

A NOTE ON THE ALKALOIDS OF *BUPHANE DISTICHA*

By L. G. Humber and W. I. Taylor

In the course of work which has been discontinued we had occasion to examine the alkaloidal content of some bulbs of *Buphane disticha* Herb. (*Haemanthus toxicarius* Herb.) and our results differ somewhat from those recorded by Tutin (8) and Lewin (4). The crude alkaloids were chromatographed over activated alumina to furnish in low yield lycorine (previously isolated by Tutin) and a new base which does not appear to have been characterized previously. The base, m.p. 189°, analyzed for $C_{17}H_{19}O_4N$, had one methoxyl, no N-methyl, one active hydrogen, and one readily hydrogenatable double bond which from infrared data must be trisubstituted. The infrared spectra of the free base and its perchlorate showed that the double bond could not be $\alpha\beta$ to the nitrogen atom. It gave a positive test for a methylenedioxy group with Labat's reagent and the ultraviolet spectrum (λ_{max} 285 mμ, log ϵ 3.2) suggested the presence of the aromatic moiety shown in (I) since it closely resembled safrole (5). The double bond was not conjugated with the aromatic nucleus since the ultraviolet absorption spectrum of the dihydro-compound was identical to that of the original base. The active hydrogen was present in a hydroxyl group since the dihydro-base gave an O-acetate (ν_{CO} 1710 cm.$^{-1}$) rather than a N-acetyl derivative. The nature of the hydroxyl group has not been determined but it is unlikely to be tertiary since it acetylated readily; however in an attempted chromic acid oxidation of the dihydro-compound only the starting material could be isolated in 50% yield.

I

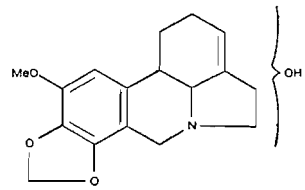

If this alkaloid resembles other members of this class of known constitution, e.g. lycorine (2, 7), homolycorine (3), and lycorenine (3), then the above results are compatible with the formula (I). The lack of material precludes further study at this time but we have shown by direct comparison and infrared spectra that our new base is not identical with crinamine, m.p. 193–194° (6), or haemanthamine, m.p. 200° (1), both of which have the formula $C_{17}H_{19}O_4N$ and contain a methylenedioxy and a methoxyl group.

EXPERIMENTAL[1]

Dried shredded bulbs of *Buphane disticha* (1500 gm.) were percolated with 95% alcohol (48 liters). The combined extracts were concentrated to dryness

[1]*All melting points are uncorrected and the infrared spectra are measured in potassium bromide mulls.*

and the residue triturated with dilute hydrochloric acid. The acid solution after several washings with chloroform was basified and the precipitated alkaloids taken up in chloroform. The dried extract on concentration afforded the crude bases (4.3 gm.) which were chromatographed over activated alumina (300 gm.). Most of the material was irreversibly adsorbed but a chloroform eluate (850 mgm.) and an ethanolic eluate (250 mgm.) were obtained.

Lycorine

In ethanol the ethanolic eluate slowly deposited needles (75 mgm.), m.p. 260°, which gave an undepressed melting point on admixture with an authentic sample of lycorine. Found: C, 66.9; H, 6.0. Calc. for $C_{16}H_{17}O_4N$: C, 66.9; H, 5.9%.

The Base

The chloroform eluate in ethanol slowly gave the base in large prisms (350 mgm.), m.p. 189°, unchanged on further crystallization. Found: C, 67.8; H, 6.4; N, 4.7; OMe, 10.6; act. H (Zerewitinow), 0.35. Calc. for $C_{17}H_{19}O_4N$: C, 67.7; H, 6.3; N, 4.7; OMe, 10.3; act. H, 0.33%. In microhydrogenation 4.6 mgm. took up 0.37 ml. (N.T.P.) and the theoretical for one double bond requires 0.35 ml. (N.T.P.). The ultraviolet absorption spectrum measured in 95% ethanol showed a maximum 285 mμ (log ε 3.17) and a minimum 260 mμ (log ε 2.59) and was unaltered in acidic or alkaline solution. The base gave a positive test for a methylenedioxy group with Labat's reagent.

Base Perchlorate

The salt was crystallized from water, m.p. 119°. Found: C, 47.6; H, 5.5. Calc. for $C_{17}H_{19}O_4N.HClO_4.1.5H_2O$: C, 47.5; H, 5.5%.

Dihydro-base

The base was hydrogenated in acetic acid using platinum oxide as a catalyst. The dihydro derivative had m.p. 200°, from acetone. Found: C, 67.3; H, 7.0. Calc. for $C_{17}H_{21}O_4N$: C, 67.3; H, 7.0%. The ultraviolet absorption spectrum showed a maximum at 285 mμ (log ε 3.2), and in the infrared the medium strength band present at 840 $cm.^{-1}$ in the original base had disappeared.

Monoacetyldihydro-base Perchlorate

The dihydro-base (50 mgm.) was acetylated in acetic anhydride (2 ml.) using a drop of perchloric acid as a catalyst. The free base after isolation could not be obtained crystalline and was converted into its perchlorate, which crystallized readily from water, m.p. 131–132°. Found on a sample dried at 60° for 12 hr. *in vacuo*: C, 45.8; H, 5.8. Calc. for $C_{19}H_{23}O_5N.HClO_4.3H_2O$: C, 45.6; H, 6.0%. The infrared showed ν_{CO} at 1710 cm^{-1}.

ACKNOWLEDGMENTS

We are indebted to the National Research Council of Canada for support and to Dr. S. Uyeo for a sample of crinamine and Dr. Hans-G. Boit for the haemanthamine. We thank Mr. W. Fulmor and Staff of Lederle Laboratories Division of American Cyanamid for the determination of the infrared spectra.

The *Buphane disticha* was obtained in the Belgian Congo through the facilities afforded by the Institut National pour L'Etude Agronomique at Keyburg.

1. BOIT, HANS-G. Ber. 87: 1339. 1954.
2. HUMBER, L. G., KONDO, H., KOTERA, K., TAKAGI, S., TAKEDA, K., TAYLOR, W. I., THOMAS, B. R., TSUDA, Y., TSUKAMOTO, K., UYEO, S., YAJIMA, H., and YANAIHARA, N. J. Chem. Soc. 4622. 1954.
3. KITAGAWA, T., TAYLOR, W. I., UYEO, S., and YAJIMA, H. J. Chem. Soc. 1066. 1955.
4. LEWIN, L. Arch. exptl. Pathol. Pharmakol. 68: 333. 1912.
5. PATTERSON, R. F. and HIBBERT, H. J. Am. Chem. Soc. 65: 1862. 1943.
6. TANAKA, K. J. Pharm. Soc. Japan, 57: 139. 1937.
7. TAYLOR, W. I., THOMAS, B. R., and UYEO, S. Chemistry & Industry, 929. 1954.
8. TUTIN, F. J. Chem. Soc. 99: 1240. 1911.

RECEIVED FEBRUARY 21, 1955.
CHEMISTRY DEPARTMENT,
UNIVERSITY OF NEW BRUNSWICK,
FREDERICTON, NEW BRUNSWICK.

THE VIBRATIONAL SPECTRUM OF THE SULPHITE ION IN SODIUM SULPHITE[1]

BY J. C. EVANS[2] AND H. J. BERNSTEIN

The Raman and infrared spectra of the sulphite ion in sodium sulphite have been reinvestigated. Hibben (3), on reviewing the work done prior to 1939, decided that the Raman spectrum of the sulphite ion required further examination. More recently, Siebert (7) has obtained the Raman spectra, without measuring the depolarization ratios, of aqueous solutions of three sulphites and has assigned the four bands observed in each spectrum to the four fundamental modes of the ion. In the infrared, Miller and Wilkins (4) included several sulphites in their study of the absorption spectra of solid salts, but confined their study to the region 3–16 μ. We have shown that measurement of the depolarization ratios of the Raman bands and an examination of the infrared spectrum between 3 and 33 μ confirm Siebert's assignment.

Two samples of sodium sulphite which gave identical spectra were examined. One was made available to us by Professor H. G. Thode and the other was C.P. grade (Fischer Scientific Company). The Raman spectrum of a saturated aqueous solution was obtained with a White photoelectric recording spectrometer (8), and depolarization ratios were measured (1) and corrected (5). A Perkin Elmer double-pass infrared spectrometer with LiF, NaCl, KBr, CsBr optics was used to obtain the infrared spectra of a saturated aqueous solution and of solid films of the sulphite. Nujol films and films obtained by evaporating aqueous solutions on AgCl were examined.

The results are tabulated in Table I. In some regions in the infrared, absorption by water or nujol made examination difficult or impossible.

X-Ray diffraction results (9) indicate that the sulphite ion is pyramidal (C_{3v}) with the sulphur atom at the apex. This model should have two sym-

[1]*Issued as N.R.C. No. 3619.*
[2]*National Research Council Postdoctorate Fellow, 1953–55.*

The *Buphane disticha* was obtained in the Belgian Congo through the facilities afforded by the Institut National pour L'Etude Agronomique at Keyburg.

1. BOIT, HANS-G. Ber. 87: 1339. 1954.
2. HUMBER, L. G., KONDO, H., KOTERA, K., TAKAGI, S., TAKEDA, K., TAYLOR, W. I., THOMAS, B. R., TSUDA, Y., TSUKAMOTO, K., UYEO, S., YAJIMA, H., and YANAIHARA, N. J. Chem. Soc. 4622. 1954.
3. KITAGAWA, T., TAYLOR, W. I., UYEO, S., and YAJIMA, H. J. Chem. Soc. 1066. 1955.
4. LEWIN, L. Arch. exptl. Pathol. Pharmakol. 68: 333. 1912.
5. PATTERSON, R. F. and HIBBERT, H. J. Am. Chem. Soc. 65: 1862. 1943.
6. TANAKA, K. J. Pharm. Soc. Japan, 57: 139. 1937.
7. TAYLOR, W. I., THOMAS, B. R., and UYEO, S. Chemistry & Industry, 929. 1954.
8. TUTIN, F. J. Chem. Soc. 99: 1240. 1911.

RECEIVED FEBRUARY 21, 1955.
CHEMISTRY DEPARTMENT,
UNIVERSITY OF NEW BRUNSWICK,
FREDERICTON, NEW BRUNSWICK.

THE VIBRATIONAL SPECTRUM OF THE SULPHITE ION IN SODIUM SULPHITE[1]

BY J. C. EVANS[2] AND H. J. BERNSTEIN

The Raman and infrared spectra of the sulphite ion in sodium sulphite have been reinvestigated. Hibben (3), on reviewing the work done prior to 1939, decided that the Raman spectrum of the sulphite ion required further examination. More recently, Siebert (7) has obtained the Raman spectra, without measuring the depolarization ratios, of aqueous solutions of three sulphites and has assigned the four bands observed in each spectrum to the four fundamental modes of the ion. In the infrared, Miller and Wilkins (4) included several sulphites in their study of the absorption spectra of solid salts, but confined their study to the region 3–16 μ. We have shown that measurement of the depolarization ratios of the Raman bands and an examination of the infrared spectrum between 3 and 33 μ confirm Siebert's assignment.

Two samples of sodium sulphite which gave identical spectra were examined. One was made available to us by Professor H. G. Thode and the other was C.P. grade (Fischer Scientific Company). The Raman spectrum of a saturated aqueous solution was obtained with a White photoelectric recording spectrometer (8), and depolarization ratios were measured (1) and corrected (5). A Perkin Elmer double-pass infrared spectrometer with LiF, NaCl, KBr, CsBr optics was used to obtain the infrared spectra of a saturated aqueous solution and of solid films of the sulphite. Nujol films and films obtained by evaporating aqueous solutions on AgCl were examined.

The results are tabulated in Table I. In some regions in the infrared, absorption by water or nujol made examination difficult or impossible.

X-Ray diffraction results (9) indicate that the sulphite ion is pyramidal (C_{3v}) with the sulphur atom at the apex. This model should have two sym-

[1]*Issued as N.R.C. No. 3619.*
[2]*National Research Council Postdoctorate Fellow, 1953–55.*

TABLE I

Assignment		Raman, aqueous solution			Infrared	
		cm.$^{-1}$	ρ_{obs}	ρ_{true}	Aqueous solution	Solid
$2\nu_1$	A	—			—	1995 (vw)
$\nu_1 + \nu_3$	E	—			—	1968 (vw)
$2\nu_3$	$A + E$	—			—	1932 (vw) 1912
$2\nu_2$	A	—			—	1213 (w)
$\nu_2 + \nu_4$	E	—			—	1135 (w)
ν_1	a	967 (s)	0.64	0.47	1002 (m)	1010 (m)
ν_3	e	933 (m)	1.05	0.86	954 (s)	961 (s)
$2\nu_4$	$A + E$	896 (vw)	?		—	—
ν_2	a	620 (w)	P		632 (w)	633 (s)
ν_4	e	469 (m)	1.06	0.86	—	496 (s)

metric modes of vibration ν_1 and ν_2 (a type) and two asymmetric doubly degenerate modes ν_3 and ν_4 (e type). All four modes are infrared and Raman active.

The observed Raman spectrum is immediately explained in terms of the four expected fundamental vibrations. The strong polarized Raman band at 967 cm.$^{-1}$ is assigned to ν_1, the symmetric stretching mode, while the other polarized weak band at 620 cm.$^{-1}$ is assigned to ν_2. The two depolarized bands of medium intensity at 933 and 469 cm.$^{-1}$ are assigned to ν_3 and ν_4 respectively. The remaining very weak band at 896 cm.$^{-1}$ may be 2 ν_4.

The infrared spectrum of the aqueous solution shows three bands which must be identified as ν_1, ν_2, and ν_3. ν_4 was not observed, the absorption of the water in this region being strong. The large discrepancies between the positions of the Raman and infrared bands must be ascribed to the strong intermolecular interaction, and, as is usually found in such cases, the infrared bands have higher frequencies (6).

The infrared spectrum of the solid shows several bands that are satisfactorily explained as combinations and overtones of the four fundamental modes.

Using the mean values of the Raman and infrared frequencies of the four modes in aqueous solution, the dimensions of the ion from X-ray data, and the equations derived from a four-constant potential function (2), the following values of the four constants were calculated: $K_1 = 5.49_6$, $K_1' = 0.64_3$, $K_\delta = 1.01_9$, and $K_\delta' = 0.31_0$ all in units of 10^5 dynes per cm. These constants were used to calculate the following frequencies of the fundamentals in the isotopic ion $S^{34}O_3^{16}$: $\nu_1 = 972$, $\nu_2 = 623$, $\nu_3 = 937$, and $\nu_4 = 457$, all in cm.$^{-1}$.

We wish to thank Professor H. G. Thode for suggesting this problem.

1. Edsall, J. T. and Wilson, E. B., Jr. J. Chem. Phys. 6: 124. 1938.
2. Herzberg, G. Infrared and Raman spectra of polyatomic molecules. D. Van Nostrand Company, Inc., New York. 1945. p. 188.
3. Hibben, J. H. Raman effect and its chemical applications. Reinhold Publishing Corporation, New York. 1939. p. 394.
4. Miller, F. A. and Wilkins, C. H. Anal. Chem. 24: 1253. 1952.
5. Rank, D. H. and Kagarise, R. E. J. Opt. Soc. Amer. 40: 89. 1950.

6. SHORYGIN, P. P. Zhur. Fiz. Khim. 23: 873. 1949.
7. SIEBERT, H. Z. anorg. u. allgem. Chem. 275: 235. 1954.
8. WHITE, J. U., ALPERT, N., and De Bell, A. G. J. Opt. Soc. Amer. 45: 154. 1955.
9. ZACHARIASEN, W. H. and BUCKLEY, H. E. Phys. Rev. 37: 1295. 1931.

RECEIVED MARCH 28, 1955.
DIVISION OF PURE CHEMISTRY,
NATIONAL RESEARCH COUNCIL,
OTTAWA, CANADA.

AN OSCILLOSCOPIC POLAROGRAPH

BY G. F. ATKINSON AND W. A. E. MCBRYDE

Polarographic half-wave potentials may be determined without the necessity of obtaining the whole polarographic wave by the use of several derivative techniques. Many of these are based on the introduction of a low-voltage alternating signal into the cell circuit, and observation of some change produced in this signal by its passage through the cell. We have extended the designs of Müller *et al.* (4) and Boeke and van Suchtelen (1) for an oscilloscopic polarograph (*i*) by the introduction of phase-shifting components so as to produce elliptical Lissajous patterns, and (*ii*) by the incorporation of an electronic switch in the oscilloscope's vertical input so as to provide a reference signal in addition to that observed for the polarographic cell. Since the apparatus was built we became aware of the circuit of Rodrequez and Sancho (5) which incorporates the first of the above features. As this type of determination requires the recognition of a distorted pattern on the oscilloscope screen, discrimination is made much easier by the presence of a second undistorted pattern at the same time, especially as the two images may be superimposed.

The circuit is shown in Fig. 1. The cell circuit proper, in which the polarizing direct current flows, is made up of the polarographic cell, the source of direct voltage, the coupling transformer to the detecting circuit, and the resistance across which the alternating signal is supplied. The source of alternating signal was a Heathkit Audio Oscillator, Model AO-1, which was operated to produce a sine wave at 200 c.p.s. The output of this was about 4.1 volts under normal load, and was fed directly to the horizontal input of the oscilloscope and through a resistor to the synchronizing terminal. The signal for the cell circuit was tapped from a 10,000-ohm linear carbon volume control across the oscillator output, and applied across one of a selection of small resistors in the cell circuit.

Direct voltage was supplied by a Fisher Elecdropode manual polarograph modified in two respects. In parallel with the 100-ohm "STD" control a 400-ohm control was added, with considerable gain in convenience in setting the slidewire span voltage. The main voltage divider was replaced by a 10-turn, 200-ohm Helipot potentiometer, Model A. The Model W Duodial used with this was marked to 1 mv., and could be read to 0.5 mv. without difficulty.

The alternating signal was detected by a filament transformer operated

6. SHORYGIN, P. P. Zhur. Fiz. Khim. 23: 873. 1949.
7. SIEBERT, H. Z. anorg. u. allgem. Chem. 275: 235. 1954.
8. WHITE, J. U., ALPERT, N., and De Bell, A. G. J. Opt. Soc. Amer. 45: 154. 1955.
9. ZACHARIASEN, W. H. and BUCKLEY, H. E. Phys. Rev. 37: 1295. 1931.

RECEIVED MARCH 28, 1955.
DIVISION OF PURE CHEMISTRY,
NATIONAL RESEARCH COUNCIL,
OTTAWA, CANADA.

AN OSCILLOSCOPIC POLAROGRAPH

BY G. F. ATKINSON AND W. A. E. MCBRYDE

Polarographic half-wave potentials may be determined without the necessity of obtaining the whole polarographic wave by the use of several derivative techniques. Many of these are based on the introduction of a low-voltage alternating signal into the cell circuit, and observation of some change produced in this signal by its passage through the cell. We have extended the designs of Müller *et al.* (4) and Boeke and van Suchtelen (1) for an oscilloscopic polarograph (*i*) by the introduction of phase-shifting components so as to produce elliptical Lissajous patterns, and (*ii*) by the incorporation of an electronic switch in the oscilloscope's vertical input so as to provide a reference signal in addition to that observed for the polarographic cell. Since the apparatus was built we became aware of the circuit of Rodrequez and Sancho (5) which incorporates the first of the above features. As this type of determination requires the recognition of a distorted pattern on the oscilloscope screen, discrimination is made much easier by the presence of a second undistorted pattern at the same time, especially as the two images may be superimposed.

The circuit is shown in Fig. 1. The cell circuit proper, in which the polarizing direct current flows, is made up of the polarographic cell, the source of direct voltage, the coupling transformer to the detecting circuit, and the resistance across which the alternating signal is supplied. The source of alternating signal was a Heathkit Audio Oscillator, Model AO-1, which was operated to produce a sine wave at 200 c.p.s. The output of this was about 4.1 volts under normal load, and was fed directly to the horizontal input of the oscilloscope and through a resistor to the synchronizing terminal. The signal for the cell circuit was tapped from a 10,000-ohm linear carbon volume control across the oscillator output, and applied across one of a selection of small resistors in the cell circuit.

Direct voltage was supplied by a Fisher Elecdropode manual polarograph modified in two respects. In parallel with the 100-ohm "STD" control a 400-ohm control was added, with considerable gain in convenience in setting the slidewire span voltage. The main voltage divider was replaced by a 10-turn, 200-ohm Helipot potentiometer, Model A. The Model W Duodial used with this was marked to 1 mv., and could be read to 0.5 mv. without difficulty.

The alternating signal was detected by a filament transformer operated

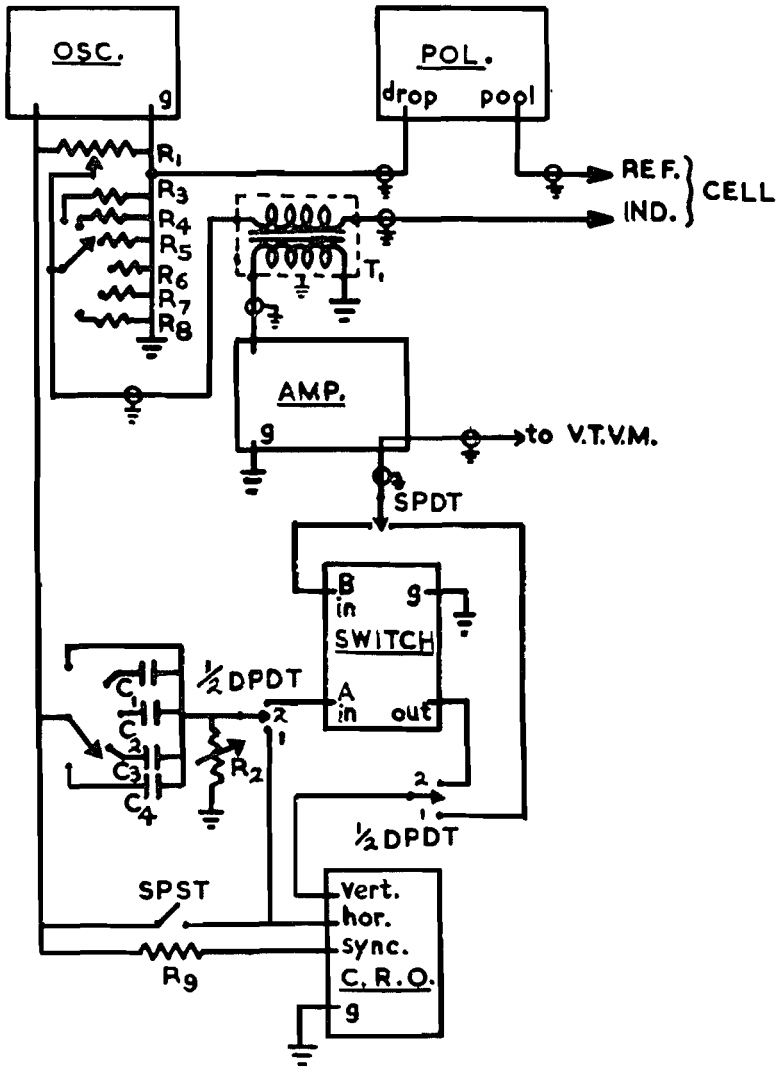

FIG. 1. Circuit diagram.

R_1 10,000-ohm linear carbon
R_2 500,000-ohm carbon
R_3 to R_8 7 to 400 ohm
R_9 470,000-ohm
C_1 to C_4 10 μf. to 0.015 μf.
T_1 Hammond 167 B 25 (6.3: 110)

backward, and was fed to a 6-watt amplifier built in the Department of Physics, University of Toronto. A 500-ohm output was used, and, at full gain with bass boost on, the gain was 700 for a 200-cycle signal. The noise level was 0.2 mv. at full gain, and there was no distortion of a sine wave up to 135 v. output. The cell signal and a reference signal were presented to the oscilloscope through a DuMont Electronic Switch, Model 185. The signals were observed on a Heathkit 5-in. oscilloscope, Model O-7, operated on its 400-v. range at very low vertical gain, to produce a trace as free from noise and visible tran-

sients as possible. Many leads were shielded, as shown, to prevent pickup of stray signals.

To observe the summit potential phenomenon described by Delahay and Adams (2), a Hewlett-Packard A.C. Vacuum Tube Voltmeter was connected as shown, and operated on its 3-v. range.

The characteristics of the components used led to the choice of the following operating conditions: (*i*) a high switching speed, with the pattern appearing as a line, (*ii*) relatively high gain on the amplifier before the switch, (*iii*) lowest possible gain in the switch and oscilloscope, (*iv*) low intensity setting to minimize halo.

Method of operation.—With the cell operating, the oscilloscope, electronic switch, and signal generator were turned on. This gave a pattern shown in Fig. 2*a*. This was adjusted by means of the "A" gain of the switch and the

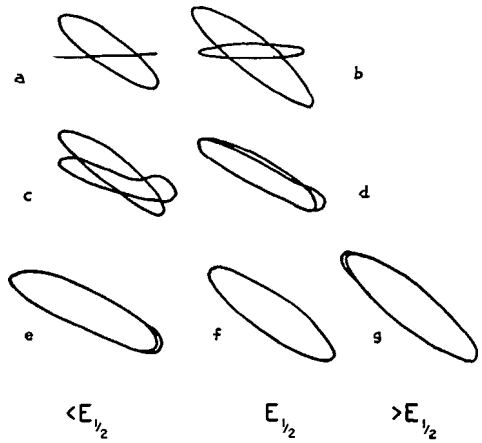

FIG. 2. Oscilloscopic traces.

horizontal gain of the oscilloscope to a suitable size, the phase-shifting resistance having first been set to tilt the figure at about 45°. Next, the amplifier and polarograph were turned on with the applied potential set at zero (Fig. 2*b*). The height of the cell signal was set by the "B" gain of the switch and the amplifier gain to a somewhat lower level. While observing the screen, the potential was increased until a point was reached at which the cell figure became elliptical (Fig. 2*c*). The phase-shifting circuit was used to place the reference signal at the same angle as the cell signal, and the balance and gain controls of the switch were used to superimpose the figures if desired (Fig. 2*d*). Then a short potential interval was investigated with the polarograph until the point of no deviation of the two ellipses was found. By using the sweep generator of the oscilloscope, two sine waves could be matched in the same way. It will be noted that the circuit provides for elimination of the electronic switch so that a single sine wave or ellipse can be projected if desired.

Measured half-wave potentials.—The following observations were made for solutions for which known half-wave potentials were available for comparison.

Solution	Supporting electrolyte	$E_{\frac{1}{2}}$ vs. N.C.E., volts Observed	Literature
0.001 *M* $CdSO_4$	0.1 *M* KCl	−0.661	−0.63 (3)
0.001 *M* $Cu(ClO_4)_2$	0.1 *M* KCl	−0.029	−0.03 (3)
0.001 *M* $Pb(NO_3)_2$	0.1 *M* KNO_3	−0.432	−0.46 (3)
			−0.43 (6)

In each case the reading was checked by resetting the potential dial several times. For cadmium there was found to be an interval of 4 mv. in which no distortion was visible, the middle of which could easily be located to 1 mv. For copper and lead the region of no distortion was about 10 mv. Bubbling with nitrogen for a period of two hours did not change the indication obtained for a fresh solution of cadmium ion.

We do not doubt that the details of this circuit could be improved; for instance, the use of a double-gun oscilloscope would obviate the electronic switch. The principal difficulty encountered was the elimination of stray noise, and it must be stressed that adequate shielding and grounding of the circuit are imperative for satisfactory operation.

We are greatly indebted to Professor J. M. Anderson of the Department of Physics, University of Toronto, for the loan of equipment and for much help with the design of the circuit. We also gratefully acknowledge financial assistance from the University's Advisory Committee on Scientific Research.

1. Boeke, J. and van Suchtelen, H. Philips Tech. Rev. 4: 213. 1939.
2. Delahay, P. and Adams, T. J. J. Am. Chem. Soc. 74: 5740. 1952.
3. Kortüm, G. and Bockris, J. O'M. Textbook of electrochemistry. Vol. II. Elsevier Publishing Co., Inc., Amsterdam. 1951. p. 765.
4. Müller, R. H., Garman, R. L., Droz, M. E., and Petras, J. Ind. Eng. Chem. Anal. Ed. 10: 339. 1938.
5. Rodrequez, A. and Sancho, J. Anales real soc. españ. fís. y quim. (Madrid), Ser. B, 49: 657. 1953.
6. Zuman, P. Collection Czechoslov. Chem. Communs. 15: 1107. 1950.

Received March 20, 1955.
Department of Chemistry,
University of Toronto,
Toronto 5, Ontario.

THE FORMATION OF MOLECULAR COMPLEXES BETWEEN SOLID UREA AND *n*-OCTANE VAPOR

By H. G. McAdie[1] and G. B. Frost

The formation of molecular complexes, called adducts, between urea and *n*-paraffins has been known for some time. Schlenk (3) has given a detailed account of their preparation from solution, and has reported an elucidation of their structure on the basis of X-ray evidence. He showed that when straight chain hydrocarbon molecules are added to a concentrated solution of urea, in a suitable solvent, crystallization of the urea occurs in such a way that each hydrocarbon molecule becomes imprisoned in a canal formed by a hexagonal arrangement of urea molecules, as contrasted with the normal closely packed

[1]*C.I.L. Fellow in Chemistry, 1954–55.*

Solution	Supporting electrolyte	$E_{\frac{1}{2}}$ vs. N.C.E., volts Observed	Literature
0.001 *M* $CdSO_4$	0.1 *M* KCl	−0.661	−0.63 (3)
0.001 *M* $Cu(ClO_4)_2$	0.1 *M* KCl	−0.029	−0.03 (3)
0.001 *M* $Pb(NO_3)_2$	0.1 *M* KNO_3	−0.432	−0.46 (3)
			−0.43 (6)

In each case the reading was checked by resetting the potential dial several times. For cadmium there was found to be an interval of 4 mv. in which no distortion was visible, the middle of which could easily be located to 1 mv. For copper and lead the region of no distortion was about 10 mv. Bubbling with nitrogen for a period of two hours did not change the indication obtained for a fresh solution of cadmium ion.

We do not doubt that the details of this circuit could be improved; for instance, the use of a double-gun oscilloscope would obviate the electronic switch. The principal difficulty encountered was the elimination of stray noise, and it must be stressed that adequate shielding and grounding of the circuit are imperative for satisfactory operation.

We are greatly indebted to Professor J. M. Anderson of the Department of Physics, University of Toronto, for the loan of equipment and for much help with the design of the circuit. We also gratefully acknowledge financial assistance from the University's Advisory Committee on Scientific Research.

1. Boeke, J. and van Suchtelen, H. Philips Tech. Rev. 4: 213. 1939.
2. Delahay, P. and Adams, T. J. J. Am. Chem. Soc. 74: 5740. 1952.
3. Kortüm, G. and Bockris, J. O'M. Textbook of electrochemistry. Vol. II. Elsevier Publishing Co., Inc., Amsterdam. 1951. p. 765.
4. Müller, R. H., Garman, R. L., Droz, M. E., and Petras, J. Ind. Eng. Chem. Anal. Ed. 10: 339. 1938.
5. Rodrequez, A. and Sancho, J. Anales real soc. españ. fís. y quim. (Madrid), Ser. B, 49: 657. 1953.
6. Zuman, P. Collection Czechoslov. Chem. Communs. 15: 1107. 1950.

Received March 20, 1955.
Department of Chemistry,
University of Toronto,
Toronto 5, Ontario.

THE FORMATION OF MOLECULAR COMPLEXES BETWEEN SOLID UREA AND *n*-OCTANE VAPOR

By H. G. McAdie[1] and G. B. Frost

The formation of molecular complexes, called adducts, between urea and *n*-paraffins has been known for some time. Schlenk (3) has given a detailed account of their preparation from solution, and has reported an elucidation of their structure on the basis of X-ray evidence. He showed that when straight chain hydrocarbon molecules are added to a concentrated solution of urea, in a suitable solvent, crystallization of the urea occurs in such a way that each hydrocarbon molecule becomes imprisoned in a canal formed by a hexagonal arrangement of urea molecules, as contrasted with the normal closely packed

[1]*C.I.L. Fellow in Chemistry, 1954–55.*

tetragonal lattice of urea. The hexagonal structure has now been worked out in detail (4) and the whole subject of urea adducts has been reviewed elsewhere (1, 5).

Schlenk (3) has also reported the slow formation of urea adducts by the mere contact of finely divided tetragonal urea crystals with certain pure liquid *n*-paraffins, and has also suggested the possibility of forming such adducts by exposure of tetragonal urea to the vapor of the lower boiling *n*-paraffins. Redlich and co-workers (2) have reported measurements of equilibrium pressures for various systems consisting of adduct, solid urea, and a long chain molecule. These measurements imply a reversibility between the reactions involving adduct decomposition and formation.

The present work was undertaken in an attempt to throw light upon the mechanism of this reaction between tetragonal urea and pure *n*-paraffin vapors, which is an interesting one from the standpoint of the molecular forces involved. The following is a report of some preliminary experimental findings, and an indication of some of the experimental work in progress.

Reagent grade urea was recrystallized, dried, and screened, the "through 60 mesh on 80 mesh" portion being used. Small samples (40 mgm.) were contained in a basket of 100-mesh copper gauze and suspended on a quartz spiral balance. The balance case was connected with the usual vacuum system and means were provided for the exposure of the suspended sample to *n*-octane vapor at its saturation vapor pressure at 25° C. Provision was also made for the addition of other gases.

On exposure of urea samples, prepared in this way, to *n*-octane vapor, no evidence of adduct formation was observed after 24 hr. It was found, however, that adduct formation took place rapidly in the presence of water vapor, and that if the adducts so formed were decomposed under vacuum, addition of *n*-octane vapor then occurred rapidly in the absence of water vapor, and that cycles of decomposition and absorption of hydrocarbon could be carried out. Adduct formation in the presence of water vapor has been confirmed by X-ray diffraction, the line patterns being identical with those obtained for adducts of several normal hydrocarbons and alcohols prepared from saturated solutions of urea in methanol. The nature of the products formed by the addition of *n*-octane vapor after the evacuation of the adduct and in the absence of water vapor has not as yet been definitely established.

The results of a typical experiment are shown in Fig. 1 where the weight increase, as obtained by readings of spiral extension, is plotted against the square root of the time in minutes. In this experiment, the urea sample was evacuated at 10^{-4} mm. and 25° C. for 24 hr., in order to remove traces of water vapor. It was then exposed to *n*-octane vapor at its saturation vapor pressure at 25° C. for 24 hr. No significant change in weight was observed during this period. Water vapor at a pressure of approximately 11 mm. was then admitted. The sample started to increase in weight immediately, and a gradual swelling occurred. Zero time in Fig. 1 is taken as the time of admission of water vapor.

When the reaction appeared to be approaching completion, vacuum was applied and the weight of the sample decreased rapidly to its initial value.

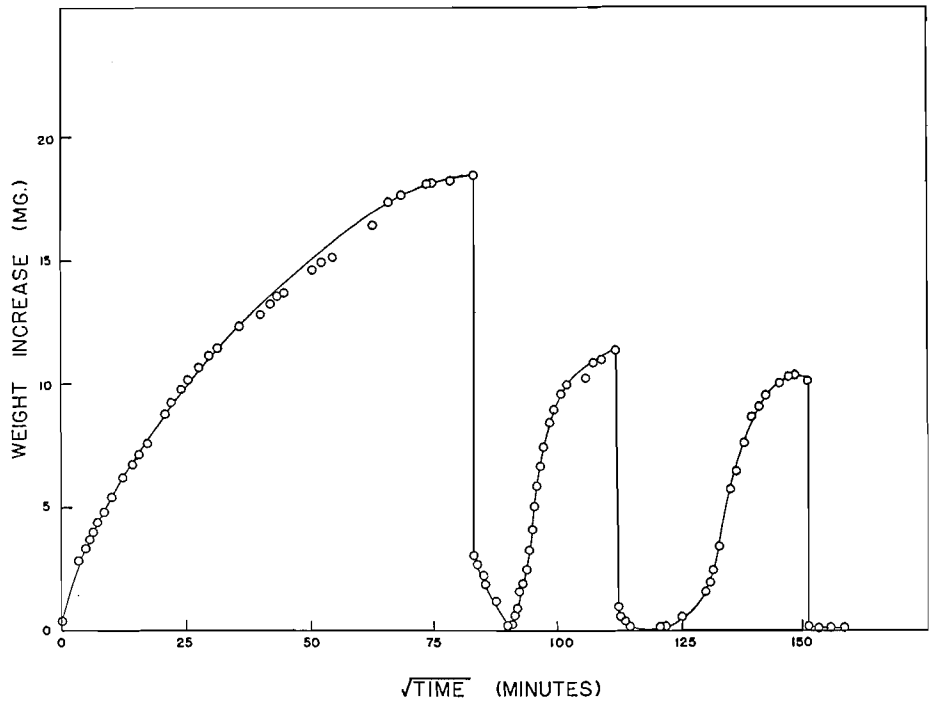

FIG. 1. Typical formation and decomposition curves for the urea–*n*-octane adduct.

Pure *n*-octane vapor at its saturation pressure was then admitted, but no water vapor. A rapid increase in weight occurred (the second rise shown in Fig. 1), the rate decreasing at a much lower uptake of the hydrocarbon. The reaction was allowed to proceed for a time and the cycle of operations repeated. Uptake of *n*-octane was again observed.

If adduct formation occurs during the second and third exposures, some stability of the hexagonal lattice after the withdrawal of the hydrocarbon chain may be indicated. It is also possible that the removal of the hydrocarbon at very low pressure may result in the collapse of the hexagonal lattice into an assembly of microcrystals of tetragonal urea, and that adduct formation takes place more readily on this material of high surface area. It is also possible that the observed uptake of *n*-octane in the absence of water vapor is due to adsorption. Experiments are being carried out with the purpose of deciding among these alternatives.

Adduct formation in the presence of water vapor was accompanied by a marked swelling of the sample. This is probably due to the increased volume of the hexagonal channel structure over the normal tetragonal crystals and has been reported by others (1). It is interesting to note that this swollen state persisted after the decomposition of the sample at low pressure.

While extensive quantitative results are not yet available, the rate of adduct formation appears to have a linear dependence on water vapor pressure over the range from 8 to 15 mm. There appears to be a lower limit of water vapor

pressure (approximately 7 mm.) below which adduct formation does not occur for crystals of the dimensions used in these experiments.

The reaction between urea crystals and *n*-octane vapor in the presence of water vapor was also observed by a photomicrographic technique. At water vapor pressures of 14 to 15 mm. the reaction was observed to proceed quite readily. This was shown by the loss of transparency of the urea crystal and the formation of a fuzzy, opaque, somewhat larger crystal.

Photomicrographic evidence appears to indicate that not all the urea crystals react at once. However, once initiation of reaction occurs on a given crystal, the reaction progresses rapidly through that crystal. When water vapor was present to the extent of 7 to 8 mm. no reaction occurred after 24 hr., indicating again the presence of a limiting water vapor pressure below which adduct formation does not occur.

The fact that water vapor promoted the adduct formation led to an investigation of other possible promoters. Methanol and ethanol, at pressures in the region of 10 to 15 mm., promoted the reaction after considerable time. There is some indication that nitromethane and ethylenediamine behave in a similar manner. The effect of other substances is being studied.

Work is being carried out on the adsorption of water vapor on urea, the determination of the change in surface area on removal of hydrocarbons at low pressure, and more extensive utilization is being made of X-ray techniques. The results will be reported in a subsequent paper.

1. KOBE, K. A. and DOMASK, W. G. Petroleum Refiner, No. 3: 106. 1952; No. 5: 151. 1952; No. 7: 125. 1952.
2. REDLICH, O., GABLE, C. M., DUNLOP, A. K., and MILLER, R. W. J. Am. Chem. Soc. 72: 4153. 1950.
3. SCHLENK, W., Jr. Ann. 565: 204. 1949.
4. SMITH, A. E. Acta Cryst. 5: 224. 1952.
5. TRUTER, E. V. Research (London), 6: 320. 1953.

RECEIVED MARCH 23, 1955.
DEPARTMENT OF CHEMISTRY,
GORDON HALL,
QUEEN'S UNIVERSITY,
KINGSTON, ONTARIO.

1-ALKYL-2-IMIDAZOLIDINETHIONES[1]

BY G. D. THORN[2]

For the study in this laboratory of the fungicidal activity of compounds containing the thiocarbamoyl grouping, it became necessary to have a series of 1-alkyl-2-imidazolidinethiones. Except for a paper by Rich and Horsfall (10) in which is reported the fungitoxicity of *n*-octyl-, *t*-octyl-, and *n*-octadecylethylenethiourea (for which no physical characteristics are given), no reference to simple 1-alkyl-2-imidazolidinethiones is to be found in the literature.

[1]*Contribution No. 51, Science Service Laboratory, London, Ontario.*
[2]*Senior Chemist.*

pressure (approximately 7 mm.) below which adduct formation does not occur for crystals of the dimensions used in these experiments.

The reaction between urea crystals and *n*-octane vapor in the presence of water vapor was also observed by a photomicrographic technique. At water vapor pressures of 14 to 15 mm. the reaction was observed to proceed quite readily. This was shown by the loss of transparency of the urea crystal and the formation of a fuzzy, opaque, somewhat larger crystal.

Photomicrographic evidence appears to indicate that not all the urea crystals react at once. However, once initiation of reaction occurs on a given crystal, the reaction progresses rapidly through that crystal. When water vapor was present to the extent of 7 to 8 mm. no reaction occurred after 24 hr., indicating again the presence of a limiting water vapor pressure below which adduct formation does not occur.

The fact that water vapor promoted the adduct formation led to an investigation of other possible promoters. Methanol and ethanol, at pressures in the region of 10 to 15 mm., promoted the reaction after considerable time. There is some indication that nitromethane and ethylenediamine behave in a similar manner. The effect of other substances is being studied.

Work is being carried out on the adsorption of water vapor on urea, the determination of the change in surface area on removal of hydrocarbons at low pressure, and more extensive utilization is being made of X-ray techniques. The results will be reported in a subsequent paper.

1. KOBE, K. A. and DOMASK, W. G. Petroleum Refiner, No. 3: 106. 1952; No. 5: 151. 1952; No. 7: 125. 1952.
2. REDLICH, O., GABLE, C. M., DUNLOP, A. K., and MILLER, R. W. J. Am. Chem. Soc. 72: 4153. 1950.
3. SCHLENK, W., Jr. Ann. 565: 204. 1949.
4. SMITH, A. E. Acta Cryst. 5: 224. 1952.
5. TRUTER, E. V. Research (London), 6: 320. 1953.

RECEIVED MARCH 23, 1955.
DEPARTMENT OF CHEMISTRY,
GORDON HALL,
QUEEN'S UNIVERSITY,
KINGSTON, ONTARIO.

1-ALKYL-2-IMIDAZOLIDINETHIONES[1]

BY G. D. THORN[2]

For the study in this laboratory of the fungicidal activity of compounds containing the thiocarbamoyl grouping, it became necessary to have a series of 1-alkyl-2-imidazolidinethiones. Except for a paper by Rich and Horsfall (10) in which is reported the fungitoxicity of *n*-octyl-, *t*-octyl-, and *n*-octadecylethylenethiourea (for which no physical characteristics are given), no reference to simple 1-alkyl-2-imidazolidinethiones is to be found in the literature.

[1]*Contribution No. 51, Science Service Laboratory, London, Ontario.*
[2]*Senior Chemist.*

The reaction of equimolar amounts of ethylenediamine and carbon disulphide was shown by Hofmann (4) to yield N-(β-aminoethyl)dithiocarbamic acid (I, R = H). Thermal decomposition of this inner salt gave 2-imidazolidinethione (II, R = H). These reactions were later extended to various N- and N,N′-substituted 2-imidazolidinethiones by van Alphen (1), Baum (2), Donia, Shotton, Bentz, and Smith (3), Hurwitz and Auten (5), Lob (7), Newmann (8), Schmidt (11), Vaugh and Bean (12), and Zienty (13).

Following the classical procedures, a series of 1-alkyl-2-imidazolidinethiones has been prepared.

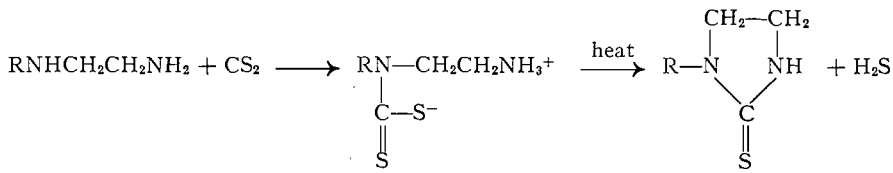

I II

EXPERIMENTAL[3]

The N-alkylethylenediamines were prepared either by reaction of the requisite alkylamine with 2-bromoethylamine (9) (R = ethyl through hexyl), or by reaction of an alkyl halide with 98% ethylenediamine (6) (R = heptyl through dodecyl).

The N-alkyl-2-imidazolidinethiones were prepared essentially according to the method given by Donia *et al.* (3). The reaction of the amine with carbon disulphide was carried out in ether to give a fine white precipitate of the dithiocarbamic acid inner salt. The use of acetone (3) as the reaction medium resulted in yellow gummy precipitates, which could however be triturated with ether to give more tractable material.

A typical preparation is described, in which the alkyl group is octyl: A solution of 10.1 gm. (0.059 mole) of N-octylethylenediamine in 80 ml. ether was cooled to 10° C. in an ice-bath, and stirred vigorously while 4.72 gm. (0.062 mole) of carbon disulphide in 30 ml. ether was added dropwise. Stirring was continued for 30 min. after addition was completed. The precipitate was removed by filtration, washed with ether, and air-dried. The yield was 14.3 gm. (98%). Found: N, 11.2%. Calc. for $C_{11}H_{24}N_2S_2$: N, 11.3%.

The inner salt was heated for two hours in a wide-mouthed Erlenmeyer flask immersed in an oil bath at 130° C. The dark residue was crystallized from hexane to give 9.7 gm. (77%) of 1-octyl-2-imidazolidinethione. The material was then recrystallized from hexane to constant melting point (Table I).

The yields given in Table I are calculated from the amount of material obtained after one crystallization of the crude imidazolidinethione. Hexane was the preferred solvent for recrystallization, except for the first three members of the series, where ether or hexane–acetone was used.

[3]*All melting points are uncorrected and were obtained on the Fisher-Johns block.*

TABLE I

1-ALKYL-2-IMIDAZOLIDINETHIONES

R in formula II	Yield, %, from I	m.p., °C.	Analyses			
			Found		Calc.	
			C	H	C	H
Ethyl	72	79–80	46.1	7.56	46.2	7.69
Butyl	70	78–79	53.3	8.87	53.2	8.87
Pentyl	81	68–68.5	55.8	9.35	55.8	9.30
Hexyl	90	71–72	57.9	9.57	58.1	9.68
Heptyl	81	69–70	60.0	10.15	60.0	10.00
Octyl	77	52–53	61.7	10.36	61.7	10.28
Nonyl	73	56–57	63.2	10.38	63.2	10.53
Decyl	81	64.5–65	65.0	10.38	64.5	10.74
Dodecyl	74	60–61	66.9	10.91	66.8	11.10

1. ALPHEN, J. VAN. Rec. trav. chim. 55: 412, 669, 835. 1936; 57: 265. 1938; 58: 544. 1939; 59: 31. 1940.
2. BAUM, A. A. to E. I. DU PONT DE NEMOURS AND CO. U.S. Patent No. 2,544,746. May 13, 1951.
3. DONIA, R. A., SHOTTON, J. A., BENTZ, L. O., and SMITH, E. P., Jr. J. Org. Chem. 14: 946. 1949.
4. HOFMANN, A. W. Ber. 5: 240. 1872.
5. HURWITZ, M. D. and AUTEN, R. W. to ROHM AND HAAS CO. U.S. Patent No. 2,613,211. Oct. 7, 1952; U.S. Patent No. 2,613,212. Oct. 7, 1952.
6. LINSKER, F. and EVANS, R. L. J. Am. Chem. Soc. 67: 1581. 1945.
7. LOB, G. Rec. trav. chim. 55: 859. 1936.
8. NEWMANN, H. E. Ber. 24: 2191. 1891.
9. O'GEE, R. C. and WOODBURN, H. M. J. Am. Chem. Soc. 73: 1370. 1951.
10. RICH, S. and HORSFALL, J. G. Science, 120: 122. 1954.
11. SCHMIDT, A. to the GOLDSCHMIDT, A.-G. Ger. Patent No. 812,317. Aug. 27, 1951.
12. VAUGH, R. S. and BEAN, F. R. to EASTMAN KODAK CO. U.S. Patent No. 2,596,742. May 13, 1952.
13. ZIENTY, F. B. J. Am. Chem. Soc. 68: 1388. 1946.

RECEIVED APRIL 4, 1955.
SCIENCE SERVICE LABORATORY,
CANADA DEPARTMENT OF AGRICULTURE,
LONDON, ONTARIO.

Canadian Journal of Chemistry

Issued by THE NATIONAL RESEARCH COUNCIL OF CANADA

VOLUME 33 AUGUST 1955 NUMBER 8

PYROLYSIS OF ETHYL MERCAPTAN[1]

BY JEAN L. BOIVIN AND RODERICK MACDONALD

ABSTRACT

The decomposition of ethyl mercaptan to ethylene and hydrogen sulphide was studied at various temperatures, with and without a catalyst. Metal sulphides (copper, nickel, and cadmium) proved to be the most efficient catalysts for cracking ethyl mercaptan into unsaturated end products, the optimum temperature being 500–600° C. When no catalyst was used a 40–50% yield of ethylene and a nearly quantitative conversion to hydrogen sulphide was observed between 600 and 700° C. Other products identified in the exit gas were carbon disulphide, carbonyl sulphide, methane, hydrogen, ethane, thiophene, diethyl sulphide, and free sulphur. Identification of these products was aided by infrared and mass spectral analysis of the gas. A tentative mechanism for the reaction justifying the presence of the above by-products is outlined.

INTRODUCTION

Sabatier and Mailhe (4) report that diethyl sulphide and hydrogen sulphide are formed when dry ethyl mercaptan is passed over a cadmium sulphide catalyst at 330° C. and that upon heating to 380° C. ethylene and hydrogen sulphide are quantitatively formed:

$$2CH_3CH_2{-}SH \xrightarrow[CdS]{330^\circ\ C.} (CH_3CH_2)_2S + H_2S \qquad [1]$$

$$CH_3CH_2{-}SH \xrightarrow[CdS]{380^\circ\ C.} CH_2{=}CH_2 + H_2S. \qquad [2]$$

The conditions reported by Sabatier and Mailhe were reproduced but no reaction product was obtained. Hydrogen sulphide was absent, which proved that even diethyl sulphide was not formed (Eq. [1]) at this temperature. A study was then undertaken to determine the optimum conditions for the preparation of ethylene and hydrogen sulphide from ethyl mercaptan.

APPARATUS

The reaction chamber consisted of a Pyrex or silica tube 24 in. in length and 1 in. in diameter mounted vertically in a cylindrical furnace. The bottom of the tube was connected through a ground-glass joint to a two-necked flask which served as the vaporization vessel. To the second neck was attached a measuring dropping funnel for the introduction of ethyl mercaptan. The products of the reaction were allowed to escape through an opening at the

[1]*Manuscript received April 4, 1955.*
Contribution from the Organic Section of Canadian Armament Research and Development Establishment, Valcartier, Quebec. Issued as C.A.R.D.E. Report No. 115–55.

top of the reaction chamber and passed through an upright water-cooled condenser. The gaseous fraction was led from the top of the condenser to a series of scrubbers (for H_2S and unsaturated compounds) while condensable materials were retained in a flask attached to the bottom of the condenser. In operation the reaction tube was packed with alternate layers of glass wool and catalyst, or glass wool only. The inside temperature was recorded by means of a thermocouple. The vaporization flask was heated by a glas-col mantle.

GENERAL METHOD

In operation a weighed quantity of ethyl mercaptan was added from the dropping funnel at the rate of 1 gm. per min. to the vaporization flask which was held at 150°C. The volatilized mercaptan entered the reaction tube (held at a constant temperature) and emerged as a mixture of gases and some condensable products. The gases were bubbled first through water to remove free sulphur, then through 30% sodium hydroxide to remove hydrogen sulphide, and finally through bromine (under water) to remove unsaturated material.

When a total analysis of the reaction products was required a sample was taken directly from the top of the condenser. Using an Orsat apparatus, the sample (100 ml.) was measured at equalized pressure and sent through an absorption pipette containing 30% sodium hydroxide until the volume of remaining gas remained constant. The loss in volume was measured as hydrogen sulphide. Unsaturated materials were removed with fuming sulphuric acid (20%) or bromine. The remaining portion was passed through hot copper oxide several times to determine its hydrogen content, and then the remainder was burned in the presence of oxygen and the volumes of carbon dioxide and water formed were measured. The latter measurements enable one to determine the amount of methane and ethane in a sample of gas when only the two are present.

RESULTS

Since cadmium sulphide was reported as a good catalyst by Sabatier, it was studied over a wide range of temperatures. One mole of ethyl mercaptan was used and samples were taken five to ten minutes after the reaction had begun, to ensure the absence of air.

With this catalyst, formation of ethylene (Table I) started at 400° C. with a yield of only 5.7% of the total gases coming out of the reactor. Also much liquid condensed, which was identified as diethyl sulphide with minor quantities of ethyl mercaptan.

A maximum yield was attained at 600° C. with 24.1% of ethylene in the gas mixture. As can be noted, the ethylene formation passed through a maximum at 600° C. The hydrogen sulphide formation was very high at the start and then decreased steadily with increasing temperatures. Sulphur was also formed in small amounts.

Hydrogen formation increased with the temperature of pyrolysis. This is undoubtedly due to the cracking of hydrocarbon or hydrogen sulphide. Also the mixture of gas B after ethylene, hydrogen sulphide, and hydrogen have

TABLE I

COMPOSITION OF EFFLUENT GASES

Catalyst	Temp., ° C.	C_2H_4, %	H_2S, %	H_2, %	B, %
CdS	300	Nil	Nil	Nil	Nil
	350	Nil	Nil	Nil	Nil
	400	5.7	88.4	Nil	5.9
	450	10.5	75.2	8.5	5.8
	500	16.3	58.7	14.0	11.0
	550	20.3	47.2	17.7	14.8
	600	24.1	44.5	16.9	14.5
	700	17.6	37.4	24.0	21.0
NiS	400	Nil	Nil	Nil	Nil
	450	20.2	64.8	1.0	14.0
	500	28.8	52.1	1.3	17.8
	550	27.0	51.5	1.3	20.2
	600	27.9	48.9	3.2	21.0
	700	26.8	43.0	6.8	23.4
$(Al_2O_3)_x(SiO_2)_y$	400	Nil	Nil	Nil	Nil
	450	29.5	0.5	0.5	2.0
	500	30.3	0.4	0.4	10.0
	550	30.6	0.4	0.4	15.0
	600	25.5	1.3	1.3	21.0
	700	19.6	9.0	9.0	26.0
None	450	Nil	Nil	Nil	Nil
	500	31.9	49.4	0.8	17.9
	550	30.9	49.0	0.9	19.2
	600	29.1	48.5	0.8	21.6
	650	28.1	46.3	2.4	23.2
	700	30.1	45.0	4.1	20.8

B refers to gases that could not be analyzed by the Orsat apparatus.

been removed increased with the temperature. This mixture of gases when burned in the Orsat apparatus could not be calculated as methane and ethane.

Following these results a search for a more efficient catalyst was made. Other sulphides were studied.

With nickel sulphide catalyst (Table I) results were similar to cadmium sulphide except that the formation of ethylene took place at a higher temperature (450° C. instead of 400° C.).

Other sulphides were used, namely those of cobalt, copper, and iron, and gave similar results to nickel sulphide with minor differences.

Aluminosilicate behaved like sulphides, except that less hydrogen was formed. The yield of ethylene was about 30% at 500° C.

Without a catalyst (Table I), ethylene was produced at 500° C. and the composition of the gas remained nearly constant from 500 to 700° C.

IDENTIFICATION OF PRODUCTS

The condensate obtained from the reaction products was quite large at low reaction temperatures. This was shown by a boiling point determination to be diethyl sulphide with a small amount of unreacted ethyl mercaptan.

A white colloidal material was noticed in the water scrubber after the reaction had proceeded for 30 min. Extraction with carbon disulphide removed this material. Upon evaporation sulphur was obtained.

(*a*) *Infrared Spectra*

The gas coming out of the reactor was sampled in a gas cell with sodium chloride windows. Another sample was usually taken after hydrogen sulphide and ethylene were removed.

Ethylene was easily identified by its broad and very intense band at 949 cm.$^{-1}$ and a triplet at 1860, 1889, 1910 cm.$^{-1}$ (3). Other bands may be common to other products.

After removal of ethylene and hydrogen sulphide, the spectrum also showed the presence of methane with an absorption band at 1306 cm.$^{-1}$ (3) and of ethane at 820 cm.$^{-1}$ (3).

The mixture also contained carbon disulphide as shown by the band at 2183 cm.$^{-1}$ (3).

Carbonyl sulphide was detected by its very intense absorption at 2050 cm.$^{-1}$, which in many cases has a dual nature under dilution (1). Another band which might be characteristic of thiophene was present at 710 cm.$^{-1}$ (2). The spectrum of the unscrubbed and scrubbed gases is fully explained and all bands were assigned to known gases.

(*b*) *Mass Spectrometry*

In order to know the relative amount of product present in one of these mixtures of gases mass spectral analysis was used. Since the Orsat apparatus could give reasonable accuracy for the estimation of ethylene, hydrogen sulphide, and hydrogen, the samples used for mass spectral analysis were free of hydrogen sulphide and ethylene.

Results obtained when using cadmium sulphide catalyst at 500° C. showed an average composition of 41% of ethane, 8.4% of methane, and 47% of hydrogen, and traces of other materials such as carbon disulphide, carbonyl sulphide, and thiophene. Therefore the proportion of ethane in this gas mixture is high and that of methane, low. The composition of this fraction of gas indicates cracking of ethane or ethylene.

DISCUSSION

The pyrolysis of ethyl mercaptan under flow conditions is very slightly catalytic if at all. With the best catalysts used, such as sulphides of copper, nickel, cobalt, and cadmium, the lowest temperature at which ethylene is produced is 450° C. The yield is small, and the best temperature for the optimum formation of ethylene, with catalysts, is 500° C. Moreover, from 500 to 700° C. without a catalyst, the yield of ethylene is practically constant. It is considered that temperatures of 500–600° C. would be efficient using Pyrex or silica tubes packed with glass wool.

MECHANISM

The basic reaction in the pyrolysis of ethyl mercaptan is analogous to the dehydration of ethyl alcohol. This dehydration reaction is reversible under certain conditions. Also the pyrolysis of ethyl mercaptan, which can be termed as a desulphurization process, is a reversible reaction:

$$CH_3CH_2{-}OH \underset{H_2SO_4}{\overset{Al_2O_3}{\rightleftharpoons}} CH_2{=}CH_2+H_2O \qquad [3]$$

$$2EtOH \longrightarrow Et_2O+H_2O \qquad [4]$$

$$CH_3CH_3SH \rightleftharpoons CH_2{=}CH_2+H_2S\,. \qquad [5]$$

At lower temperatures, when the hydrogen sulphide formation is high, some liquid is formed, which was identified as diethyl sulphide (Eq. [1]).

Since elemental sulphur is formed in the pyrolysis, it should come from the decomposition of hydrogen sulphide which is said to start at 400° C. Even if the dissociation of hydrogen sulphide is small, the equilibrium is shifted to the right by removal of sulphur or hydrogen, which are both present in the reaction products.

Ethane is found at all the temperatures studied as evidenced by the infrared spectra obtained. It is likely to be formed by the reduction of ethylene with the hydrogen generated from hydrogen sulphide. At higher temperatures methane is produced in greater proportion and the hydrogen content of the gaseous products is higher indicating that another pyrolysis is taking place.

Carbon disulphide, carbonyl sulphide, and thiophene are also formed in traces. The occurrence of carbon disulphide indicates that methane has reacted with sulphur vapor (Eq. [6]). This reaction is the basis of a commercial process to make carbon disulphide:

$$CH_4+4S \longrightarrow CS_2+2H_2S\,. \qquad [6]$$

The presence of carbonyl sulphide is due to some oxygen in the system, probably some oxide impurity in the catalyst, and the presence of thiophene is due to the dehydrogenation of diethyl sulphide or to the condensation of ethylene with hydrogen sulphide followed by dehydrogenation.

REFERENCES

1. BARTUNEK, P. F. and BARKER, E. F. Phys. Rev. 48: 516. 1935.
2. GODART, J. J. chim. phys. 34: 70. 1937.
3. HERZBERG, G. Infrared and Raman spectra of polyatomic molecules. Vol. II. 3rd printing. D. Van Nostrand Company, Inc., New York. 1947. pp. 271–369.
4. SABATIER, S. and MAILHE, C. R. Compt. rend. 150: 1571. 1910.

THE PAPILIONACEOUS ALKALOIDS

XXI. THE ALKALOIDS OF *LUPINUS PILOSUS* WALT. AND THE STRUCTURE OF TETRALUPINE[1]

By A. F. Thomas,[2] H. J. Vipond,[2] and Léo Marion

ABSTRACT

The alkaloidal extract from *Lupinus pilosus* Walt. was found to contain two alkaloids, one widely occurring one, *d*-lupanine, and one which had already been reported to occur in this plant, i.e., *d-epi*lupinine, but no lupinine. The alkaloid tetralupine has been found by direct comparison of the bases and their corresponding salts and by their infrared absorption spectra to be identical with *dl-epi*lupinine. A study of the infrared absorption spectra of lupinine and *epi*lupinine leads to the same conclusion as the chemical evidence, i.e., that in the former the hydroxymethylene group occupies the axial position whereas in *epi*lupinine this group is in the equatorial position.

Although *Lupinus pilosus* has been mentioned as a source of *l*-lupinine (2), White (11) reported *d-epi*lupinine as the only identifiable alkaloid in the plant. Since there was available a crude alkaloidal extract of *Lupinus pilosus* Walt. (*Lupinus villosus* Willd.) prepared and given to us by Dr. James F. Couch, the alkaloids were reinvestigated. The crude extract consisted of a thick dark syrup. A quantity of the syrup was dissolved in benzene, chromatographed on a column of alumina, and eluted with a number of solvents taken in the order benzene–ether–chloroform–methanol, the proportions of each being gradually changed. A trace of non-alkaloidal material was eluted first. Solvents containing benzene (40%) and ether (60%) to ether (95%) and chloroform (5%) eluted a colorless oil which behaved chromatographically on buffered paper as *d*-lupanine. This base formed a crystalline perchlorate, the melting point of which was undepressed on mixing with *d*-lupanine perchlorate. The identity of this salt was further confirmed by comparison of its Debye-Scherrer powder diagram with that of authentic *d*-lupanine perchlorate. This fraction composed about 15% of the crude mixture.

Fractions eluted in the solvent range ether (60%) – chloroform (40%) to ether (40%) – chloroform (60%) gave crystals, m.p. 76–78°, representing 35% of the original crude mixture. This crystalline substance on a paper chromatogram behaved like lupinine, but mixing with the latter lowered the melting point to 43–47°. The crystalline base, after recrystallization, melted at 78–79° and had $[\alpha]_D$ +37.1° (12), which agreed with the properties reported for *d-epi*lupinine, and the melting point was undepressed in admixture with a sample of the latter prepared as described by Schöpf, Schmidt, and Braun (10). The infrared absorption spectra of the two were superimposable (Fig. 1, curve 1) but different from that of lupinine (Fig. 1, curve 2).

[1]*Manuscript received April 15, 1955.*
Contribution from the Division of Pure Chemistry, National Research Council, Ottawa, Canada. Issued as N.R.C. No. 3649.
[2]*National Research Council of Canada Postdoctorate Fellow.*

NOTE ADDED IN PROOF: *After submission of the manuscript, a paper was published by W. D. Crow and N. V. Riggs (Australian J. Chem. 8: 136. 1955) reporting the occurrence of d-epilupinine and d-epilupinine-N-oxide in* Lupinus varius *L.*

In order to ascertain that *epi*lupinine did not arise on the column of alumina by epimerization of lupinine, some of the latter was chromatographed in the same way and eluted with ether containing increasing quantities (up to 10%) of chloroform. All the lupinine was recovered unchanged.

The remaining fractions from the main chromatogram yielded a dark brown glass which resisted all attempts at crystallization, and failed to give either a

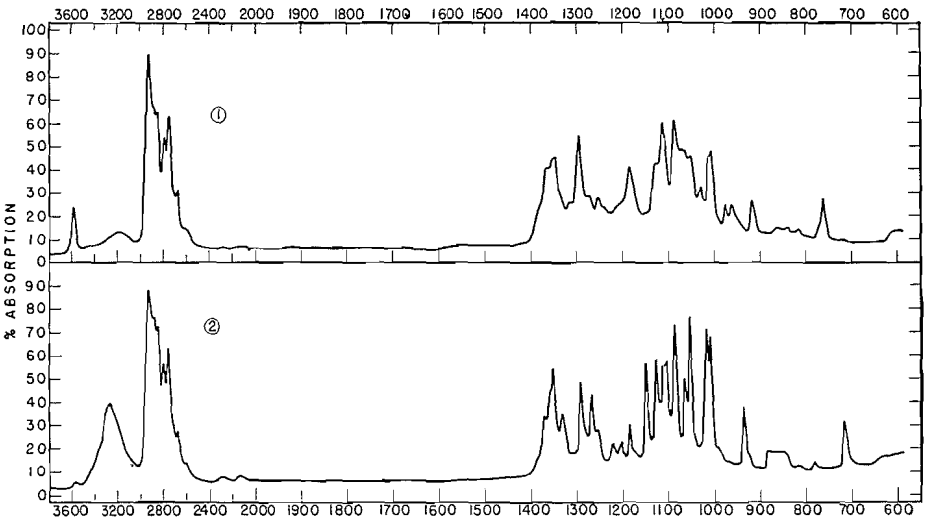

FIG. 1. Infrared absorption spectra taken in carbon disulphide solution on a Perkin-Elmer double beam spectrophotometer, model 21. Curve 1, *epi*lupinine; curve 2, lupinine.

crystalline picrate or perchlorate. When this glass was chromatographed on paper, it gave a number of indeterminate streaks. A paper chromatogram of the original crude alkaloidal extract had shown that there were only two major components which are, therefore, *d*-lupanine and *d-epi*lupinine.

As previously recorded (10, 12) *d-epi*lupinine showed a depression in melting point when mixed with the isomeric alkaloid tetralupine discovered by Couch[3] in 1934 (4). A sample of tetralupine was dissolved in benzene, chromatographed on a column of alumina, eluted, sublimed *in vacuo*, and recrystallized from petroleum ether. It then melted at 83° and was optically inactive (Couch had reported $[\alpha]_D$ +4.63°). It formed a picrolonate, a picrate, and a methiodide which were all crystalline. Comparison of tetralupine and its salts by melting point and mixed melting point with authentic samples of *dl-epi*lupinine and its corresponding salts, kindly supplied by Professor G. R. Clemo, showed the identity of the two bases. The identity was confirmed by the infrared absorption spectrum of tetralupine which was exactly superimposable on those of *d-epi*lupinine and *dl-epi*lupinine. It can, therefore, be concluded unambiguously that tetralupine is identical with *dl-epi*lupinine.

An examination of the infrared absorption spectra of lupinine and *epi*-

[3]*Dr. James F. Couch, about a year before his death, had most generously given to the senior author his entire supply of tetralupine.*

lupinine in nujol mulls shows that both contain a broad bonded OH band at *ca.* 3160 cm.$^{-1}$, but that in carbon disulphide solution the hydroxyl band in the spectrum of *epi*lupinine becomes sharp and is shifted to 3580 cm.$^{-1}$, while in the spectrum of lupinine the hydroxyl band moves only to 3270 cm.$^{-1}$ and remains broad.

This observation is indicative that in lupinine the hydroxyl group is hydrogen bonded, as previously inferred by Cookson (3), whereas it is not in *epi*lupinine. It is also significant that lupinine is eluted from an alumina column before *epi*lupinine. Consequently, lupinine must be assigned a conformation with the hydroxymethylene group occupying a position in which it may easily form a hydrogen bond to the nitrogen atom. Such hydrogen bonding is possible in the axial position I, but is impossible in the equatorial position II. Hence formula I must be assigned to lupinine while formula II must represent *epi*lupinine.

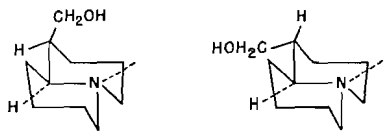

I LUPININE II EPILUPININE

This assignment of conformations from the absorption characteristics of the hydroxyl group in the infrared spectra of the two bases is in agreement with the conformations assigned recently by Galinovsky and Nesvadba (6) to lupinine and *epi*lupinine from the interpretation of the rearrangement readily undergone by the tosyl ester of lupinine and the stability of the tosyl ester of *epi*lupinine. Lupinine can be degraded to 2-*n*-butyl-3-methylpiperidine (12) and by an unambiguous synthesis of the isomers of this substance Leonard and Ryder (7) have correlated the stereochemistry of the degradation product with that of lupinine. Recently, Ratuský, Reiser, and Šorm (9) by a study of the dipole moments of lupinine and *epi*lupinine as well as of the two forms of 3-hydroxymethylquinolizidine have reached the same conclusion as to the conformations of the two alkaloids. Consequently, all the evidence points to formula I for lupinine and formula II for *epi*lupinine.

Paper chromatography has been shown to be a useful preliminary tool to examine the constituents of a crude alkaloidal mixture in the lupine series. When using sodium phosphate – citric acid buffers and saturated aqueous *n*-butanol as the developing agent, the R_F values obtained for a group of lupine alkaloids show that they can be separated easily. The spots were detected with the Munier-Dragendorff reagent (8). The papers were buffered by dipping in a buffer solution of appropriate strength, blotting, and allowing to dry completely (contrast Brindle *et al.* (1)).

EXPERIMENTAL

d-Lupanine

A quantity (1.0 gm.) of the crude alkaloidal extract was dissolved in dry benzene (100 ml.), the solution filtered, and chromatographed on alumina.

The column was eluted with benzene, ether, chloroform, and methanol, 98 fractions of 60 ml. each being collected. The initial fractions contained non-basic material. From fractions 26–43 (60% ether – 40% benzene to 95% ether – 5% chloroform) a colorless oil was obtained (150 mgm.) which with 60% perchloric acid gave a perchlorate $[\alpha]_D^{19}$ +46° (*c*, 1.0 in water), m.p. 207–210°, and after two recrystallizations from methanol, m.p. 211°, either alone or in admixture with an authentic sample of *d*-lupanine perchlorate. The literature (5) gives $[\alpha]_D$ +46.8°. The identity of the perchlorate was further confirmed by comparison of its Debye-Scherrer powder diagram with that of authentic *d*-lupanine perchlorate. Each fraction had been shown by paper chromatography at pH 7 to be the same, and to behave in the same way as *d*-lupanine with varying pH.

d-Epilupinine

Fractions 53 (60% ether – 40% chloroform) to 70 (40% ether – 60% chloroform) of the chromatogram yielded a crystalline substance, 350 mgm., m.p. 76–78°, which after two recrystallizations from petroleum ether melted at 78–79° and had $[\alpha]_D^{19}$ +37.1° (*c*, 1.0 in ethanol). Found: C, 71.4; H, 11.1. Calc. for $C_{10}H_{19}ON$: C, 71.0; H, 11.3%. The melting point of this base was unaffected by mixture with *d-epi*lupinine, but depressed to 68–78° by admixture with tetralupine, and to 43–47° by admixture with lupinine. Comparison of the infrared absorption spectra confirmed the identity of the base with *d-epi*lupinine.

Chromatography of Lupinine

Lupinine (390 mgm.) was dissolved in ether and chromatographed on alumina. It was eluted at once by the same solvent, the last traces being removed with ether – 10% chloroform.

Tetralupine

A quantity of tetralupine was chromatographed on alumina and eluted exactly as described for *d-epi*lupinine. The substance was sublimed in a high vacuum and recrystallized from petroleum ether from which it separated in small colorless prisms, m.p. 83°, and in admixture with an authentic sample of *dl-epi*lupinine, m.p. 82–83°, $[\alpha]_D$ 0 in ethanol. The infrared absorption spectrum of tetralupine was superimposable on that of *dl-epi*lupinine. Tetralupine formed a picrolonate, m.p. 231–232°, undepressed by admixture with *dl-epi*lupinine picrolonate (m.p. 225°). Found: C, 55.41; H, 5.97. Calc. for $C_{10}H_{19}ON \cdot C_{10}H_{27}O_6N_5$: C, 55.41; H, 6.28%. The picrate consisted of yellow needles, m.p. 145.5–147°, either alone or in admixture with synthetic *dl-epi*lupinine picrate. Found: C, 48.18, 48.41; H, 6.09, 5.46. Calc. for $C_{10}H_{19}ON \cdot C_6H_3O_7N_3$: C, 48.24; H, 5.57%. Tetralupine also formed a methiodide, m.p. 251–253°, either alone or in admixture with *dl-epi*lupinine methiodide (m.p. 248°). Found: C, 42.92; H, 7.31. Calc. for $C_{11}H_{22}ONI$: C, 42.44; H, 7.13%.

ACKNOWLEDGMENT

We wish to express our thanks to Professor G. R. Clemo, University of Durham, for his kindness in supplying us with authentic samples of *dl-*

*epi*lupinine and its salts, and to Mr. R. Lauzon and Dr. R. N. Jones of these laboratories for taking the infrared absorption spectra.

REFERENCES

1. Brindle, H., Carless, J. E., and Woodhead, H. B. J. Pharm. and Pharmacol. 3: 793. 1951.
2. Clemo, G. R. and Raper, R. J. Chem. Soc. 1927. 1929.
3. Cookson, R. C. Chemistry & Industry, 337. 1953.
4. Couch, J. F. J. Am. Chem. Soc. 56: 2434. 1934.
5. Edwards, O. E., Clarke, F. H., and Douglas, B. Can. J. Chem. 32: 235. 1954.
6. Galinovsky, F. and Nesvadba, H. Monatsh. 85: 1300. 1954.
7. Leonard, N. J. and Ryder, B. L. J. Org. Chem. 18: 598. 1953.
8. Munier, R. Bull. soc. chim. biol. 35: 1225. 1953.
9. Ratuský, J., Reiser, A., and Šorm, F. Chem. Listy, 48: 1795. 1954.
10. Schöpf, C., Schmidt, E., and Braun, W. Ber. 64: 683. 1931.
11. White, E. P. New Zealand J. Sci. Technol. 33: 50. 1951.
12. Winterfeld, K. and Holschneider, F. W. Ber. 64: 137. 1931.

THE SELECTIVE DEGRADATION OF WHEAT GLUTEN[1]

By L. Wiseblatt,[2] L. Wilson,[3] and W. B. McConnell

ABSTRACT

A method believed to hydrolyze peptide bonds of proteins selectively at the amino groups of serine was used to obtain polypeptides from wheat gluten. The procedure involved the use of strong acid and introduced appreciable amounts of sulphur into the products possibly as sulphonic acid groups. Most of the serine appeared at the amino termini of the peptides. The peptides displayed a striking electrophoretic homogeneity which may at least in part be accounted for by the acquired acid groups. Osmotic pressure measurements indicated an average molecular weight near 20,000 and terminal group estimates indicate that each molecule contained several N-terminal serine residues. There appeared to be strong association or chemical cross linking between peptide chains of the degraded gluten.

INTRODUCTION

In 1948 Desnuelle and Casal (8) showed that when proteins are hydrolyzed in 10 *N* hydrochloric acid at 30°C. the amino groups of the hydroxy amino acids, serine and threonine, are released much more rapidly than those of other amino acids. They suggested that the increased rate of rupture of these bonds involved a preliminary migration of the acyl part of the peptide bond from the amino group to the hydroxyl group of the hydroxy amino acid. The mechanism probably involves formation of an intermediate hydroxyoxazolidine structure as follows (1, 9):

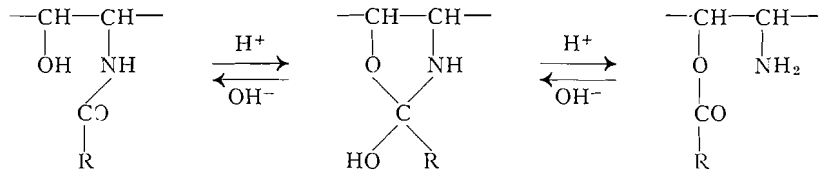

More recently Desnuelle and Bonjour (7) observed that a more specific hydrolysis at hydroxy amino acids could be obtained by pretreating the protein with cold anhydrous sulphuric acid according to the method of Reitz, Ferrel, Fraenkel-Conrat, and Olcott (19). Subsequent hydrolysis in 6 *N* hydrochloric acid at 18°C. released the amino groups of the hydroxy amino acids many times more rapidly than those of all other amino acids.

Elliott (9) utilized the above observations in an ingenious manner. Silk fibroin was treated with cold concentrated sulphuric acid to produce the N-peptidyl → O-peptidyl shift. The product was then acetylated to block the newly freed amino groups. Subsequent treatment with cold dilute barium hydroxide saponified the ester links yielding N-acetyl peptides. About 60%

[1]*Manuscript received March 30, 1955.*
Contribution from the National Research Council of Canada, Prairie Regional Laboratory, Saskatoon, Saskatchewan. Issued as Paper No. 194 on the Uses of Plant Products and as N.R.C. No. 3648. Taken in part from a thesis by L. Wiseblatt presented to the University of Saskatchewan n partial fulfillment of the requirements for the degree of Doctor of Philosophy.
[2]*Present address: American Institute of Baking, 400 E Ontario Street, Chicago 11, Illinois.*
[3]*National Research Council of Canada Postdoctorate Fellow, 1952–53. Present address: 4, Melbourne Rd., Saltcoats, Ayrshire, Scotland.*

of the serine and no threonine was N-terminal. The absence of terminal threonine was not considered very significant because of the very low percentage of that amino acid in silk. In a subsequent degradation of lysozyme Elliott (11) found that nearly all the serine and about one-third of the threonine was terminal. The amino groups of serine and threonine accounted for all of the amino nitrogen in the degradation products of lysozyme (11) whereas a small amount of non-specific hydrolysis of silk fibroin occurred.

This communication is a report of results obtained when Elliott's degradation scheme was applied to wheat gluten. The method seemed particularly attractive because serious solubility problems are encountered in almost all chemical investigations of native gluten. Thus denaturation occurs irreversibly in dilute alkali, the only aqueous medium which gives apparently monodisperse solutions, and aqueous acetic acid, sodium salicylate, and urea do not give molecular dispersions of the protein. If gluten could be specifically degraded to soluble products, these difficulties would be partly overcome. Information from a study of degradation products might well help elucidate the constitution of gluten.

EXPERIMENTAL METHODS AND RESULTS

Sulphuric Acid Treatment of Gluten

Ten grams of wheat gluten prepared by the method of Lusena (15) was suspended in 200 ml. of anhydrous sulphuric acid (sulphuric acid containing 10% by volume of 20% oleum). After 24 hr. at −20°C. the mixture was allowed to warm slowly to room temperature and was left to stand with occasional shaking for another five days. The resulting viscous brown liquid was poured with vigorous stirring into 2 liters of anhydrous ether at −35°C. The precipitate was collected by centrifugation, washed three times with dry ether, and finally added to 600 gm. of crushed ice on which it formed a sticky yellow mass.

Degradation of Gluten Sulphate

The suspension obtained above was adjusted to pH 5 with solid sodium acetate and treated over a period of two hours with 100 ml. of acetic anhydride. The temperature was not allowed to exceed 5°C. Sodium acetate was added as required to maintain pH at 5. The reaction products were dialyzed against water until they reached a constant low acidity as measured by titration or until the washings were acetate free as indicated by the sensitive lanthanum nitrate spot test (7, 13). The dialysis washings were discarded after they had been shown to be nitrogen free. The contents of the dialysis bag were reduced to about 100 ml. in a stream of air and the gluten derivative, which settled out as a spongy mass, was collected and added to 100 ml. of 0.1 *N* barium hydroxide. After two hours at room temperature all material dissolved to yield a yellowish brown solution. This was saturated with carbon dioxide and the precipitated barium carbonate discarded after it had been shown to be free of nitrogen. The supernatant solution was freeze dried to yield about 9 gm. of acetyl peptide.

In an attempt to remove acetyl groups 1 gm. of acetyl peptide was shaken with a mixture of 100 ml. of dry methanol and 1 ml. of concentrated hydro-

chloric acid for three days at 5°C. (In a few later experiments a 1% solution of anhydrous hydrochloric acid in dry methanol was used to reduce unspecific peptide bond hydrolysis.) The solid residue was filtered off, washed with methanol, then dissolved in water and freeze dried yielding a pale brown methanol insoluble peptide (hereinafter called MIP). The filtrate was evaporated at room temperature *in vacuo*, the residue taken up in water and freeze dried to yield the methanol soluble peptide (MSP). Both MSP and MIP were readily soluble in water, yielding solutions which foamed readily and which gave precipitates with trichloroacetic, tannic, and metaphosphoric acids.

MSP gave a strong color reaction with ninhydrin but both the original acetyl peptide and MIP were ninhydrin negative. It appeared therefore that deacetylation was incomplete and that only MSP contained free amino groups. This suggestion was supported by the qualitative detection of acetyl groups in MIP but not in MSP. A modification of the method of Clark (6) was used for acetyl determinations but as might be expected with N-acetyl derivatives of comparatively long chain peptides quantitatively reliable data could not be obtained. It was further observed that MIP did not contain amino groups detectable by either the formal titration or the Van Slyke nitrous acid method of deamination.

Reitz *et al.* (19) have shown that the preferential reaction of sulphuric acid with proteins is the formation of sulphuric esters with aliphatic hydroxyl groups of hydroxy amino acids followed by sulphonation of the aromatic ring of tyrosine and conversion of cystine and cysteine to thiosulphates. Some sulphur determinations were, therefore, done on the degradation products by the method of Sundberg and Royer (21). All analyses showed that sulphuric acid treated gluten contained about three times as much sulphur as the original gluten. For example, a preparation of acetyl peptide contained 3.5% sulphur whereas the gluten from which it was derived contained 1.1% sulphur. This is approximately equal to the addition of one mole of sulphur for each 12–14 amino acid residues. This amount would be expected to contribute in an appreciable way to the properties of the peptides.

Terminal Group Determinations

Sanger's method (20) of detecting N-terminal amino acids by reaction with 1-fluoro-2,4-dinitrobenzene (DNFB) was applied to the methanol soluble peptides. Seventy-five milligrams MSP were dissolved in 5 ml. of water, and 100 ml. of sodium bicarbonate and 250 mgm. of DNFB in 10 ml. of ethanol were added. The mixture was shaken for three hours, evaporated to dryness, and extracted with ether until no more of the yellow reagent could be removed. The residue was hydrolyzed by boiling in 6 *N* hydrochloric acid for eight hours and after evaporating to dryness *in vacuo* it was extracted with ether to dissolve any dinitrophenyl (DNP) amino acids produced from N-terminal amino acids.

The ether extracts were chromatographed on No. 1 Whatman filter paper impregnated with pH 6 phthalate buffer and were developed by both ascending and descending flow. The following solvent systems were used: 30 : 70

propanol–cyclohexane; 10 : 90 ethanol – benzyl alcohol and tertiary amyl alcohol (2). DNP acids for comparison were prepared as described by Porter (18). Except for spots due to the reagent and to 2,4-dinitroaniline the chief spot on all chromatograms corresponded to DNP serine. The yellow spots were extracted from the paper with ether and hydrolyzed in a sealed tube at 100°C. for two hours with concentrated aqueous ammonia. When these hydrolyzates were chromatographed on paper using 75% aqueous phenol as solvent they all gave ninhydrin positive spots with the same R_f value as serine.

The above results strongly suggest that serine is a major N-terminal amino acid residue in degraded gluten. Quantitative estimates of N-terminal serine and threonine in MSP were attempted by a microdiffusion method employing periodate oxidation (23). No N-terminal threonine was found but ammonia corresponding to 5.7 gm. serine per 16 gm. MSP nitrogen was obtained. Since Wiseblatt and McConnell (23) found by the same method that gluten contains 5.7 gm. serine per 16 gm. gluten nitrogen, the result indicates complete liberation of serine amino groups by the Elliott degradation. The value for terminal serine in degraded gluten is high compared to Elliott's yields of about 60% for silk fibroin. An experimentally reproducible value for N-terminal serine (7.7 gm. serine per 16 gm. nitrogen) was obtained with a colorimetric method in which formaldehyde from periodate oxidation was collected by distillation (4). Since carbohydrates, some of which could also have given formaldehyde, were shown (17) to be present only in trace amounts no explanation for the high results can be offered. Although the results may not be quantitatively acceptable they do support the qualitative suggestion that the degradation scheme used was effective in liberating much of the serine nitrogen in gluten.

Preliminary experiments were attempted to identify C-terminal amino acids present in the peptides. Because appreciable N-terminal serine appeared to be liberated the C-terminal residues may be assumed to be largely those bound to serine in the original gluten. Samples of both the MIP and MSP were refluxed for eight hours with equal weights of lithium aluminum hydride in 100 volumes of tetrahydrofuran. The products were hydrolyzed and the amino alcohols isolated by the methods of Fromageot, Jutisz, Meyer, and Penasse (12). Paper chromatography of the ether extract of each hydrolyzate with the recommended solvent systems gave mainly one ninhydrin positive spot. (R_f corresponded most closely to that of phenylalaninol.) Other spots were present in smaller quantities. It is emphasized that the results are not sufficient to show that there is one major C-terminal amino acid, but they suggest that there may be a relatively simple pattern of C-terminal residues. More experiments are required on this phase of the work before definite statements regarding the liberation of C-terminal amino acids can be made.

Electrophoretic Properties

The apparatus and procedure described by Kunkel and Tiselius (14) was used for paper electrophoresis of some products of the gluten degradation. Fig. 1 shows "ionograms" obtained from acetyl peptides, MIP, and MSP in acetate buffer at pH 4.5 and ionic strength 0.1. With each sample a single,

fairly well defined peak was obtained. There was no indication of a multiplicity of peaks or of marked spreading as ordinarily obtained with a heterogeneous substance. Paper ionograms were made with a number of different preparations of the gluten degradation products and it is significant that single peaks were obtained (Fig. 1). The results served to distinguish sharply between the MSP

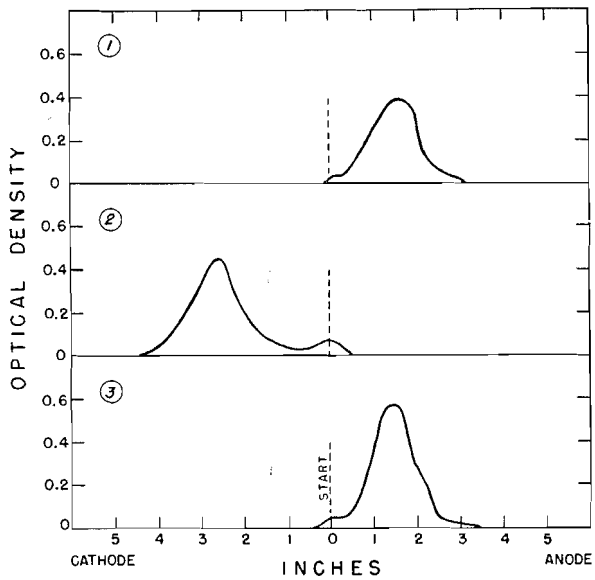

FIG. 1. Results of filter paper electrophoresis on gluten degradation products.

Acetate buffer	pH 4.5	ionic strength 0.1
1. Acetyl peptides	22 hr.	0.25 ma. per cm.
2. MSP	28 hr.	0.20 ma. per cm.
3. MIP	28 hr.	0.20 ma. per cm.

and MIP as derived from the deacetylation step and are in general accord with the earlier suggestion that the latter was not deacetylated.

A limited number of experiments were made with a moving boundary electrophoresis apparatus (Aminco Portable, American Instrument Co., Silver Springs, Maryland). MSP and MIP which had been kept in 0.1 *N* NaOH at 5°C. for 16 hr., freeze dried, taken up in the desired buffer, and filtered were used. Drawings of the patterns obtained with the treated MSP are given in Fig. 2. The alkali treatment had evidently changed the electrophoretic properties of MSP but, as with experiments on paper, the method failed to effect any separation of the material into fractions of different mobility. On the contrary, the sample displayed a striking electrophoretic homogeneity, and in buffers of pH 8.6, 6.0, and 4.5 it had mobilities of 2.08×10^{-4}, 1.91×10^{-4}, and 1.31×10^{-4} cm.^{2}/sec./volt, respectively. If acidic groups had been introduced perhaps during the sulphuric acid treatment, the movement toward the anode would have been expected. The MIP treated with sodium hydroxide as described above gave patterns of the same general character as shown in Fig. 2 for sodium hydroxide treated MSP.

The reason for the markedly different behavior of MSP before and after alkali treatment is not known. It is likely that many of the acidic groups on the dissolved material were converted to methyl esters during the treatment with methanolic hydrochloric acid and that before saponification at 5°C. deacetylated amino groups caused migration toward the cathode (Fig. 1). It would appear, therefore, that in the saponified peptides a preponderance of

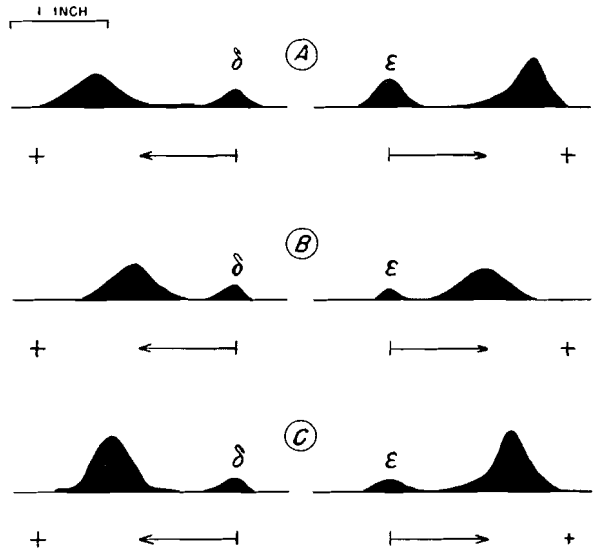

FIG. 2. Electrophoretic patterns of MSP obtained with Aminco Portable Electrophoresis Apparatus.

A. Barbitol buffer	pH 8.6	ionic strength 0.1	3130 sec. at 5.7 volts/cm.
B. Cacodylate buffer	pH 6	ionic strength 0.1	5680 sec. at 2.3 volts/cm.
C. Acetate buffer	pH 4.5	ionic strength 0.1	7850 sec. at 3.2 volts/cm.

acidic groups was effective in masking charge differences arising from different degrees of deacetylation of amino groups. If, as is reasonable to suppose, the sulphur acquired by the peptides during the degradation occurs as ionizable acid groups, and if, after treatment with sodium hydroxide the acid groups are free, the peptides would be expected to behave as anions. The contribution of the acidic groups to electrical properties of the material might well be large compared to that from amino groups and may account for the observed electrophoretic homogeneity.

By contrast, gluten is known to be heterogeneous according to physical chemical criteria. It seems unlikely, therefore, that the degradation is sufficiently systematic and the array of amino acids in gluten sufficiently regular to yield peptides with the degree of homogeneity suggested by the electrophoretic results. Because the contribution of sulphonic acid groups to the electrical properties is not known it is difficult to determine whether the degradation product is more or less homogeneous than gluten.

The introduction of acid groups into the degradation products may also

explain results obtained in attempts to fractionate them by selective adsorption on ion exchange resins. Samples were applied to 100 cm. columns of either 12% or 2% cross linked Dowex 50 and eluted according to procedures described by Moore and Stein (16). The bulk of the peptide nitrogen was quickly eluted from the column in pH 3.5 buffer. No other nitrogenous material was detected by nesslerization in eluates obtained with buffers of increasing pH.

Molecular Size Estimates

From the value of 5.7 gm. N-terminal serine per 16 gm. of MSP nitrogen given above it was calculated that the average molecular weight of MSP would be not more than 1400 (assuming single unbranched chains). Such a peptide would have been expected to pass freely through a dialyzing membrane. Experiments were therefore done to determine directly the molecular weight of MSP in pH 4.5 acetate buffer of ionic strength 0.1. Osmotic pressure measurements were made according to the method of Bull (5) except that semipermeable membranes of cellophane transfusion tubing were used instead of collodion bags. The average molecular weight was estimated to be 20,500. The value, although much larger than originally indicated by terminal amino acid analysis, was consistent with the physical behavior of MSP solutions upon dialysis.

The osmotic pressure equilibrium tended to drift slowly downward over a period of several days but the change did not represent a large increase in the molecular weight of the peptide. Redetermination of the terminal serine residues on MSP dialyzed in cellophane bags showed that, although appreciable material had passed through the membrane, the weight equivalent to each remaining terminal residue was not more than 3000. The results could be most readily explained by assuming that the degradation products consisted of branched chain structures with an average molecular weight of about 20,000. The number of free serine amino groups suggested that there are several chains in each molecule but the data were not considered sufficiently precise for a quantitative statement of the degree of branching.

Although MSP may possess branched chains it cannot also be assumed that undegraded gluten also possesses branched chains. For example, Elliott (11) found that lysozyme, which diffuses at an appreciable rate through a dialysis membrane, became non-diffusible after treatment with sulphuric acid and formic – acetic anhydride. A high proportion of the nitrogen was non-diffusible after alkaline hydrolysis. Elliott suggested that, since indoles polymerize under the influence of acid, cross linkages may have been formed through tryptophan residues and supported his suggestion with the observation that tryptophan could not be detected in the preparation by the Ehrlich color reaction. Although gluten probably contains no more than 1.5% tryptophan (22) a similar phenomenon may occur in its degradation.

Ultracentrifuge studies at 250,000 gravities for a period of 80 min. at 27°C. showed that the peptides were of "low" molecular weight—the "peak" had not completely separated from the meniscus after an hour. Also there was

sufficient broadening or spreading of the peak to indicate considerable heterogeneity and to render attempts at quantitative determination useless.

Formylation of Gluten Sulphate

One of the objectives of this study was to derive from gluten a uniform water soluble product suitable for further study. Incomplete deacetylation with resultant division of the product into MIP and MSP was therefore undesirable.

No other method for removal of blocking acetyl groups was known which would not also lead to fission of peptide chains. Experiments were done to test an alternative procedure for protecting amino acids exposed by the N-peptidyl → O-peptidyl shift. Carbobenzoxylation seemed attractive except that a relatively high sulphur content in the peptides might interfere with catalytic hydrogenolysis. Recourse was taken therefore to a formylation method suggested by Elliott (10). Boissonnas and Preitner (3) have demonstrated that this group can be removed with methanolic hydrochloric acid without hydrolysis of peptide chains. In this investigation it was observed that ninhydrin positive groups of sulphuric acid treated gluten were completely "formylated" by treatment at pH 5 with sodium formate and anhydrous formic acid for 12 hr. at room temperature. As with acetylated materials degradation to soluble products occurred upon saponification with 0.1 *N* $Ba(OH)_2$. Treatment with 1.5 *M* hydrogen chloride in methanol at 20°C. for 24 hr. gave a 90–95% yield of a ninhydrin positive material soluble in methanol. A comparison of the material with MSP has not been made but formylation appears superior to acetylation in experiments where recovery of peptides with unprotected terminal amino groups is required. Work to be described in a later publication suggests that deamination with nitrous acid can be used to prevent reversal of the acyl migration from peptide nitrogen to β-hydroxy group. Although the terminal amino acid is destroyed the method may sometimes be used to replace the blocking methods.

In the present work it was hoped to obtain a soluble derivative suitable for further chemical studies on the nature of gluten. In general the results give promise of meeting these objectives. Water soluble products were obtained apparently with a high degree of specificity. These should be amenable to study with experimental techniques not formerly applicable to gluten itself. The indication, for example, of a fairly simple pattern of C-terminal amino acid residue suggests that gluten may possess systematic structural features. This is particularly true because although gluten contains about 25% glutamic acid there was no evidence of appreciable amounts of C-terminal glutamic acid in the peptides. Changes may occur however which limit the usefulness of the peptides for further study. An unknown amount of cross linking of peptide chains may have occurred. If this is so it is impossible to estimate the degree of cross linking in gluten from the amount of chain branching observed in the degraded fractions. Furthermore, introduction of sulphonic acid groups may markedly alter the electrical properties of the material. The striking electrophoretic homogeneity of the peptides and the difficulty in fractionating them on a Dowex column may have been caused by this modification.

ACKNOWLEDGMENT

These studies were made possible by a National Research Council Studentship held by one of us (L. Wiseblatt). The authors are indebted to Dr. L. R. Wetter for advice and assistance with the electrophoretic work and to Drs. W. H. Cook and J. R. Colvin of the National Research Laboratories in Ottawa for measurements made with the ultracentrifuge.

REFERENCES

1. BERGMANN, M., BRAND, E., and WEINMANN, F. Hoppe-Seyler's Z. physiol. Chem. 131: 1. 1923.
2. BLACKBURN, S. and LOWTHER, A. G. Biochem. J. 48: 126. 1951.
3. BOISSONNAS, R. A. and PREITNER, G. Helv. Chim. Acta, 36: 875. 1953.
4. BOYD, M. J. and LOGAN, M. A. J. Biol. Chem. 146: 279. 1942. See also BLOCK, R. J. and BOLLING, D. The amino acid composition of proteins and foods. 2nd ed. Charles C. Thomas, Publisher, Springfield, Ill. 1951.
5. BULL, H. B. and CURRIE, B. T. J. Am. Chem. Soc. 68: 742. 1946.
6. CLARK, E. P. Ind. Eng. Chem. Anal. Ed. 8: 487. 1936; 9: 539. 1937.
7. DESNUELLE, P. and BONJOUR, G. Biochim. et Biophys. Acta, 7: 451. 1951.
8. DESNUELLE, P and CASAL, A. Biochim. et Biophys. Acta, 2: 64. 1948.
9. ELLIOTT, D. F. Biochem. J. 50: 542. 1952.
10. ELLIOTT, D. F. Chemistry & Industry, 86. 1952.
11. ELLIOTT, D. F. *In* A Ciba foundation symposium. The chemical structure of proteins. *Edited by* G. E. W. Wolstenholme and M. P. Cameron. J. & A. Churchill, Ltd., London, England. 1953.
12. FROMAGEOT, C., JUTISZ, M., MEYER, D., and PENASSE, L. Biochim. et Biophys. Acta, 6: 283. 1950.
13. KRÜGER, D. and TSCHIRCH, E. Ber. 62: 2776. 1929; 63: 826. 1930.
14. KUNKEL, H. G. and TISELIUS, A. J. Gen. Physiol. 35: 89. 1951.
15. LUSENA, C. V. Cereal Chem. 27: 167. 1950.
16. MOORE, S. and STEIN, W. H. J. Biol. Chem. 192: 663. 1951.
17. MORRIS, D. L. Science, 107: 254. 1948.
18. PORTER, R. R. Methods in medical research. Vol. 3. *Edited by* R. W. Gerard. Year Book Publishers, Inc., Chicago, Ill. 1950.
19. REITZ, H. C., FERREL, R. E., FRAENKEL-CONRAT, H., and OLCOTT, H. S. J. Am. Chem. Soc. 68: 1024. 1946.
20. SANGER, F. Biochem. J. 39: 507. 1945.
21. SUNDBERG, O. E. and ROYER, G. L. Ind. Eng. Chem. Anal. Ed. 18: 719. 1946.
22. WISEBLATT, L. Ph.D. Thesis, University of Saskatchewan, Saskatoon, Sask. October, 1952.
23. WISEBLATT, L. and MCCONNELL, W. B. Can. J. Chem. In press.

THE PHOTOLYSIS OF ACETONE IN THE LIQUID PHASE: THE GASEOUS PRODUCTS[1]

By R. Pieck[2] and E. W. R. Steacie

ABSTRACT

An investigation has been made of the photolysis of liquid acetone in the temperature range from 55° to −25°C. The quantum yields of all products are small, and decrease strongly with decreasing temperature. It is concluded that the low yields can be explained both on the basis of the 'cage effect', and by the deactivation of an excited molecule. At high temperatures and intensities the gaseous products can be accounted for on the assumption that radicals have escaped from the 'cage' and react analogously to the gas-phase mechanism. At low temperatures ethane formation in the 'cage' may be of importance.

INTRODUCTION

The photolysis of acetone in the gas phase has been extensively investigated. The photolysis in the liquid phase was investigated by Bowen and co-workers (1, 2, 3). They found practically no gaseous products with acetone alone, while tertiary alcohols were produced when they worked in hydrocarbon solvents. Frankenburg and Noyes (4) have also investigated the photolysis of the liquid systems acetone–oxygen and acetone–heptane–oxygen. Their work with pure acetone was confined to a rough determination of quantum yields.

It seemed of interest to investigate the photolysis of pure liquid acetone to obtain information about the behavior of radicals in the liquid phase, and to see how far the mechanism parallels that in the gas phase.

EXPERIMENTAL

Materials

Acetone (Merck) was dried over potassium carbonate and purified by a bulb-to-bulb distillation. Deutero-acetone was prepared for us by Dr. L. C. Leitch of these laboratories. *n*-Heptane was a "Phillips Pure Hydrocarbon" product. Special care was taken in degassing these reagents, in view of the sensitivity of the reaction to traces of oxygen.

Apparatus

The acetone was irradiated in a quartz cell of approximately 5 cm. diameter and 0.05 cm. thickness. The cell was provided with two outlets, one of which was sealed off after filling, while the other, closed by a break-seal, could be connected to the analytical system. Between experiments the cell was washed with acetone, attached to the filling system, heated *in vacuo* at 200°C. for two hours, and filled by distilling acetone into it.

Irradiation was carried out in a thermostat consisting of a brass cylinder with double walls, the space between the walls being evacuated. The cell was placed in an aluminum block which was located in the thermostat in such a

[1]*Manuscript received March 24, 1955.*
Contribution from the Division of Pure Chemistry, National Research Council, Ottawa, Canada. Issued as N.R.C. No. 3656.
[2]*National Research Council of Canada Postdoctorate Fellow, 1953–54.*

way that the cell was as close as possible to the innermost of two quartz windows through which the light beam entered the thermostat. The thermostat was filled with ethyl alcohol purified by the method of Leighton (7).

For experiments above room temperature the thermostat was heated electrically by an immersion heater. For low temperature experiments a copper coil was immersed in the alcohol. The coil was connected to a large container of alcohol which was cooled by a small refrigeration unit and kept automatically at the desired temperature. The temperature could be maintained constant to within ± 0.5°C.

Light Source

For most experiments the light source was a B.T.H. high pressure mercury lamp (type ME/D, 250 watts) operated on 220 v. d-c. The beam was roughly collimated by a quartz lens. A Corning filter (9-53) cut off wave lengths below 2800 Å. The beam thus consisted mainly of wave lengths around 3130 Å.

For experiments with light in the neighborhood of 2537 Å a Hanovia S500 lamp was used, together with a filter consisting of a quartz cell of 1 cm. thickness filled with a solution of diphenylbutadiene in ether (5).

The light intensity was reduced in some experiments by the use of quartz neutral density filters.

Analysis

A comparison of the infrared spectrum of pure acetone and that of a sample of irradiated acetone did not reveal the presence of any liquid products. However, in view of the large amount of acetone present, it is not surprising that small quantities of liquid products could not be detected. At temperatures below 0°C., however, a very small amount of liquid residue remained in the cell after acetone had been distilled off.

After an experiment the contents of the cell were distilled into a column, at the top of which was a "cold finger" maintained at -78°C. The acetone was refluxed continuously in the column to remove dissolved gases. The gaseous products were then fractionated by means of two modified Ward stills (8). The CO–CH_4 fraction was removed at -195°C., and the C_2H_6 fraction at -170°C. The amount of CO was determined by combustion of the CO–CH_4 fraction over hot copper oxide. In a number of cases check analyses were made with a mass spectrometer.

RESULTS

(A) Determination of the CO Quantum Yield

An estimate of the quantum yield of CO was made by comparing the photolysis in the liquid phase at 25°C. with the gas-phase photolysis at 164°C. A quantum yield of unity was assumed for the latter. Values obtained were:

$\lambda > 2800$ Å (mainly 3130 Å)	0.9×10^{-4}
$\lambda \sim 2537$ Å	2.3×10^{-4}.

The results are uncertain by a factor of about 2, and hence there is no certain

difference between the two wave lengths. The values are in agreement with the rough estimate of Frankenburg and Noyes (4).

(B) Variation of the Rate with Intensity

Table I gives the results of experiments at four different temperatures and at various light intensities. In view of the inhomogeneous nature of the light absorption, too much accuracy cannot be expected as far as kinetic constants are concerned, although the very short path length minimizes this effect. It is evident from the table that, although there is a decided drift in some of the constants, all products are formed at a rate proportional to the light intensity to within a factor of 3.

TABLE I

VARIATION OF RATE WITH INTENSITY

Temp., °C.	Time, min.	Relative light int.	Products, molecules/cc./sec. $\times 10^{-13}$			$\frac{R_{CH_4}}{R^{\frac{1}{2}}_{C_2H_6}} \times 10^{-7}$	$\frac{CH_4}{C_2H_6}$
			CO	CH_4	C_2H_6		
55	100	1.00	20.7	565	9.5	57.9	59.5
55	155	0.50	18.5	298	3.1	53.5	96
55	300	0.36	12.2	246	3.5	41.6	73
55	752	0.16	6.25	125	2.16	26.8	58
40	120	1.00	16.3	360	5.5	48.5	65
40.5	100	1.00	14.6	340	4.2	52.4	81
41	100	1.00	18.2	387	5.1	54.1	76
40	230	0.50	11.75	244.0	2.70	47.0	90
40	260	0.20	3.7	63.6	0.42	31.0	151
40	305	0.20	4.1	84.1	0.78	30.1	108
40	1140	0.14	2.08	51.7	0.74	19.0	70
40	1050	0.14	2.1	50.2	0.62	20.2	81
40	1020	0.05	0.66	8.6	0.15	7.1	57
40	1410	0.02	0.54	4.2	0.13	3.7	32
31	210	1.00	13.2	213	3.5	36.1	61
31	270	0.36	5.8	135	1.95	30.6	69
31	315	0.20	3.6	64	0.64	25.3	100
31	850	0.14	2.3	43	0.35	23.0	123
31	952	0.05	0.73	11.8	0.15	9.7	79
31	1650	0.02	0.44	6.5	0.10	6.5	65
15	245	1.00	6.41	84.0	2.1	18.3	40
15	350	0.14	1.86	31.0	0.37	16.1	84
15	630	0.05	0.34	5.2	0.15	4.2	35

The last two columns give the ratios $R_{CH_4}/R^{\frac{1}{2}}_{C_2H_6}$ and $R_{CH_4}/R_{C_2H_6}$. On the basis of the gas-phase mechanism methane arises by

$$CH_3 + CH_3COCH_3 \rightarrow CH_4 + CH_2COCH_3$$

and ethane by

$$2CH_3 \rightarrow C_2H_6.$$

This leads to the constancy of the former ratio. It is evident that this is not so in the liquid phase. The ratio $R_{CH_4}/R_{C_2H_6}$ remains roughly constant (to within a factor of about 2) over the intensity range. The ratio $R_{CH_4}/R^{\frac{1}{2}}_{C_2H_6}$, on the other hand, varies at 40°C. by a factor of about 12, and at all tem-

peratures shows a steady fall with decreasing intensity. However, there are definite indications that the ratio is approaching constancy at high intensities. (See Fig. 1).

(C) Variation of the Rate with Temperature

Table II gives the results of experiments at temperatures from 55°C. to −25°C. at constant intensity. To avoid side reactions the conversion was always kept below 5%.

A plot of log $R_{CH_4}/R^{\frac{1}{2}}_{C_2H_6}$ against $1/T$ (Fig. 2) gives a good straight line and an apparent activation energy of 8 kcal. as compared with 9.7 kcal. for the gas phase. In plotting the results only those at higher intensities were used,

TABLE II

VARIATION OF RATE WITH TEMPERATURE

Temp., °C.	Time, min.	[Ac], molecules/cc. $\times 10^{-21}$	Products, molecules/cc./sec. $\times 10^{-13}$			$\frac{R_{CH_4}}{R^{\frac{1}{2}}_{C_2H_6}[Ac]} \times 10^{14}$
			CO	CH_4	C_2H_6	
55	120	7.77	24.3	740	6.9	11.5
55	100	7.77	20.7	565	9.5	7.47
40	120	7.96	16.3	360	5.5	6.81
40.5	100	7.95	14.6	340	4.2	6.61
41	100	7.92	18.2	387	5.1	6.10
33	214	8.05	9.6	229	3.6	4.75
33	210	8.05	13.2	213	3.5	4.46
33	260	8.05	12.0	181	3.2	3.97
15	245	8.26	6.4	84	2.1	2.24
6.5	350	8.37	4.5	38.8	1.44	1.21
6.0	320	8.38	5.2	41.1	1.40	1.31
0.5	200	8.44	4.2	26.2	1.00	0.98
0.5	240	8.44	4.4	26.1	2.00	0.69
−15	1385	8.60	1.8	5.66	0.32	0.37
−16	1215	8.60	1.95	5.46	0.37	0.33
−24	1395	8.65	0.98	2.59	0.21	0.21
−25	1580	8.67	1.57	2.54	0.19	0.21

since the ratio $R_{CH_4}/R^{\frac{1}{2}}_{C_2H_6}$ falls off rapidly with decreasing intensity. Since in most cases the high intensity runs still do not give a quite constant ratio, the results are open to some uncertainty. In view of this the agreement with the gas-phase results is probably satisfactory.

If Arrhenius plots are made of R_{CH_4}, R_{CO}, or $R_{C_2H_6}$ reasonably good straight lines are obtained, from which *apparent activation energies* may be calculated, viz.

$$E_{CH_4} = 11.4 \text{ kcal.}$$
$$E_{CO} = 6 \text{ kcal.}$$
$$E_{C_2H_6} = 7 \text{ kcal.}$$

These have no simple meaning but indicate the order of magnitude of the variations in quantum yield with temperature.

Some experiments with a 1:1 mixture of CH_3COCH_3 and CD_3COCD_3 are shown in Table IIIA. The results agree well with those for light acetone. There is, however, one puzzling feature. In the gas phase it has been found

TABLE IIIA

RUNS WITH A MIXTURE $CH_3COCH_3+CD_3COCD_3$ IN RATIO 1/1

Temp., °C.	Molecules/cc./sec. $\times 10^{-13}$								$\frac{CH_4+CD_3H}{CD_4+CH_3D}$	
	CD_4	CD_3H	CD_2H_2	CDH_3	CH_4	C_2H_6	CO	CH_4 (total)	Calc.	Exp.
55	34.9	255	42.2	20.2	305	16.0	17.1	657	12.7	10.2
40	18.0	129	2.0	5.9	135	10.2	15.9	290	12.8	11.5
3	2.02	8.4	1.7	2.05	11.8	1.4	2.9	26.0	13.1	4.96
− 3	1.35	4.17	0.78	1.11	6.17	1.32	2.1	13.7	13.12	4.2
*− 3	0.26	1.29	0.23	0.29	1.66	0.26	0.69	3.8		5.4
−24	0.39	1.04	0.18	0.62	1.8	0.19	1.13	4.0	13.24	2.86
*−24	0.068	0.206	0.065	0.065	0.268	0.14	0.57	0.69		3.5

**Runs with 2537* Å.

that there is a higher activation energy for the abstraction of D, as compared with H. On this basis the ratio

$$(CH_4+CD_3H)/(CD_4+CH_3D)$$

should have the values given in the second to last column of Table IIIA. The actual values of the ratio are given in the last column. It will be seen that the ratio falls rapidly at lower temperatures, which is the reverse of the predicted behavior.

The two experiments at 2537 Å give lower rates because of lower light intensity, but show the same trend.

A few experiments were also made with pure CD_3COCD_3, and the results are given in Table IIIB.

TABLE IIIB

RUNS WITH CD_3COCD_3

Temp., °C.	Molecules/cc./sec. $\times 10^{-13}$		
	CD_4	C_2D_6	CO
55	380	47.4	30.7
20	55.9	6.37	3.3
5	26.5	2.48	0.75
−19	7.35	0.8	0.24

(*D*) *Runs with 2537* Å

The results of a few experiments with λ2537 Å are given in Table IV, and plotted in Fig. 2. The results are rather scattered because of the relatively weaker intensity and therefore smaller amounts of products. In general, however, the trend appears to be very similar. As pointed out above, the quantum yield is not appreciably different at 2537 Å. The results for methane are more accurate than the others because of the larger amounts of products,

and it is possible that the apparent activation energy is a trifle smaller. However, the accuracy of the results is not sufficient to justify any definite conclusion. There thus appears to be no direct evidence for hot radical effects.

TABLE IV

EXPERIMENTS WITH 2537 Å

Time, min.	Temp., °C.	Molecules/cc./sec. $\times 10^{-13}$			$\frac{R_{CH_4}}{R^{\frac{1}{2}}_{C_2H_6}[Ac]} \times 10^{14}$
		CO	C_2H_6	CH_4	
140	54	7.9	1.26	131	4.76
330	27	2.8	1.9	74.5	2.10
350	24	4.16	1.55	74	2.30
975	12	1.19	0.34	20.8	1.37
760	10	1.8	0.42	23.0	1.34
840	3	1.15	0.21	13.6	1.12
1580	−23	0.53	0.10	3.05	0.35

(E) Runs with a Solvent

A few experiments were made with water and *n*-hexane as solvents. The results are given in Tables V and VI. Experiments with D_2O showed that the methane formed was entirely CH_4.

TABLE V

EXPERIMENTS WITH ACETONE–WATER SOLUTIONS
Temp. = 40°C.

Molecules/cc. $\times 10^{-21}$		Molecules/cc./sec. $\times 10^{-13}$			$\frac{R_{CH_4}}{[Ac]} \times 10^{8}$	$\frac{R_{CH_4}}{R^{\frac{1}{2}}_{C_2H_6}[Ac]} \times 10^{14}$
[Ac]	$[H_2O]$	CO	CH_4	C_2H_6		
7.92	0	18.2	387	5.1	49.0	6.9
7.17	3.37	4.91	186	4.06	25.8	4.0
5.98	8.44	4.07	194	3.68	32.4	5.3
*3.99	16.8	4.75	181	2.86	45.6	8.5
3.99	16.8	1.29	143	2.30	36.1	7.5

**D₂O used in this run.*

TABLE VI

EXPERIMENTS WITH ACETONE–*n*-HEXANE SOLUTIONS
Temp. = 40°C.

Molecules/cc. $\times 10^{-21}$		Molecules/cc./sec. $\times 10^{-13}$			$\frac{R_{CH_4}}{[Ac]} \times 10^{8}$	$\frac{R_{CH_4}}{R^{\frac{1}{2}}_{C_2H_6}[Ac]} \times 10^{14}$
[Ac]	[Hexane]	CO	CH_4	C_2H_6		
7.92	0	16.3	360	5.5	45.5	6.2
7.92	0	18.2	387	5.1	49.0	6.9
7.85	0.05	5.46	263	4.6	33.5	5.0
7.85	0.05	5.95	256	4.2	32.6	5.1
7.85	0.05	5.74	276	4.5	35.2	5.4
6.4	0.64	2.37	130	2.8	20.2	3.8
5.7	1.29	1.30	65.9	1.6	11.5	2.9
5.7	1.29	1.35	64.0	1.9	11.2	2.6
2.27	3.22	0.76	20.2	0.80	8.9	3.2
1.13	3.86	0.52	8.06	0.74	7.1	2.6

DISCUSSION

There are a number of very puzzling features about the results. It should be emphasized that in view of the high absorption, the distribution of absorbed intensity is very inhomogeneous. As a result the kinetic data can only be assumed to have semiquantitative significance. The discussion will, therefore, be confined to a somewhat qualitative consideration of the main features of the reaction.

The Quantum Yield

The major difference between the present results and those of the gas-phase photolysis is the low quantum yields. Thus ϕ_{CO} is about 10^{-4} at 25°C. and about 10^{-5} at −25°C. $\phi_{C_2H_6}$ is still smaller. The values of ϕ_{CH_4} are somewhat larger, falling from about 2×10^{-3} at 25°C. to 2×10^{-5} at −25°C. Also, the yield of all reaction products increases very strongly with temperature. Thus over the range −25°C. to 55°C. ϕ_{CH_4} increases by a factor of about 300.

There are two possible explanations of the low quantum yields. In the first place, if the primary step in the gas phase is

$$CH_3COCH_3 + h\nu \rightarrow CH_3COCH_3^* \qquad [1]$$

followed by the decomposition of the excited molecule, it is possible that ϕ will be cut down largely by deactivation in the liquid phase. If this explanation holds deactivation must be strongly temperature dependent. It seems certain that the results are to be explained, at least partially, on the basis of deactivation. There is no question that active molecules play some role in the gas-phase reaction, as indicated by fluorescence studies. There seem to be two types of excited molecule one of which has a life of about 10^{-4} sec. Since there is considerable self quenching which is temperature dependent there seems to be not only collisional deactivation, but also an activation energy for the dissociation of active molecules. The low yields and the effect of temperature on the quantum yields can therefore be attributed at least to some extent to excited molecule deactivation.

The other explanation of the low value of ϕ is recombination because of the cage effect, i.e.

$$CH_3COCH_3 + h\nu \rightarrow CH_3CO + CH_3 \qquad [2]$$

followed by

$$CH_3 + CH_3CO \rightarrow CH_3COCH_3, \qquad [3]$$

the rate of [3] being greatly enhanced by the cage effect. The increase in the quantum yield with temperature is then explained by the increase in the rate of diffusion. A similar explanation has been suggested by Lampe and Noyes (6, 9) to explain the variation of the quantum yield of iodine dissociation in inert solvents. It may be mentioned that reaction [3] may also occur out of the cage. In view of the low quantum yield of ethane formation, however, this must be of minor importance. As mentioned above the apparent activation energy for methane production at 3130 Å is 11.4 kcal. Since methane is by far the largest product, this is approximately the temperature coefficient of the

quantum yield of the over-all decomposition. It is presumably to be related to the temperature coefficient of the diffusion process.

Experiments with a 1:1 mixture of CD_3COCD_3 and CH_3COCH_3 and with pure CD_3COCD_3 give results in general agreement with those with CH_3COCH_3.

The Dissociation of Acetyl by Energy Carry-over

In the gas-phase photolysis it is postulated that, depending on wave length, between 0.07 and 0.22 of the acetyl radicals formed dissociate spontaneously,

$$CH_3CO^* \rightarrow CH_3+CO. \qquad [4]$$

If this were so in the present case ϕ_{CO} could not be nearly as low as it is. This suggests either that deactivation of an excited molecule is the main cause of the low quantum yield, or else that in the liquid phase most hot acetyls are deactivated and that [4] rarely occurs. This is supported by the fact that ϕ_{CO} has a considerable temperature coefficient.

Disproportionation

In the gas phase there is evidence that reaction [5]

$$CH_3+CH_3CO \rightarrow CH_4+CH_2{=}CO \qquad [5]$$

occurs about 1/10 to 1/100 as often as [3], and also has an activation energy of about zero. If this were true in the liquid phase it would be impossible to obtain a very low value of ϕ_{CH_4}, unless this were due to deactivation. Also, reaction [5] would lead to E_{CH_4} approaching zero at low temperatures which is far from the case. It seems probable that in the liquid phase where the excited complex $CH_3COCH_3^*$ formed by [3] or [5] will have a very short life, disproportionation may well become negligible compared with recombination. These conclusions are, however, incompatible with those of the following paragraphs concerning deuterium exchange. It is therefore possible that the low quantum yields are due to deactivation of an excited molecule rather than to primary recombination.

It is also possible that disproportionation may occur outside the cage between radicals which have been formed from different molecules. As a check on this a 1:1 mixture of CH_3COCH_3 and CD_3COCD_3 was photolyzed. If the gas-phase mechanism holds almost all methane formed will arise from the abstraction reactions

$$CH_3+CH_3COCH_3 \rightarrow CH_4+R \qquad [6]$$

$$CH_3+CD_3COCD_3 \rightarrow CH_3D+R' \qquad [7]$$

$$CD_3+CH_3COCH_3 \rightarrow CD_3H+R'' \qquad [8]$$

$$CD_3+CD_3COCD_3 \rightarrow CD_4+R'''. \qquad [9]$$

In the gas phase there is little difference between the rates of abstraction by CH_3 and CD_3, but there is considerable difference between the abstraction of an H- or a D-atom. The ratio $(CH_4+CD_3H)/(CD_4+CH_3D)$ can be calculated from known rate constants, and will increase slightly at low temperatures as shown by the calculated values in Table IIIA. Actually there is a strong decrease at low temperatures. It should be noted that the ratio is not affected

by uncertainties in the relative ease of splitting off CD_3 or CH_3 from an active molecule. It depends solely on the relative ease of abstracting an H- or a D-atom in the subsequent abstraction reactions.

If methane is also formed by disproportionation between CH_3 or CD_3 radicals and CH_3CO and CD_3CO, since all the disproportionations occur with zero activation energy, the ratio of methanes from disproportionation will be unity. Hence the above ratio will tend toward unity at low temperatures where abstraction is negligible, and will rise rapidly with temperature and approach the 'calculated' values in Table IIIA. The observed behavior thus indicates that disproportionation is becoming more and more important at low temperatures.

The Abstraction Reaction

In the gas-phase photolysis of acetone the methane and ethane formed are almost all accounted for by the reactions:

$$CH_3+CH_3COCH_3 \rightarrow CH_4+CH_2COCH_3 \qquad [6]$$

$$CH_3+CH_3 \rightarrow C_2H_6 \qquad [10]$$

from which

$$R_{CH_4}/R^{\frac{1}{2}}_{C_2H_6}[\text{Acetone}] = k_6/k^{\frac{1}{2}}_{10}.$$

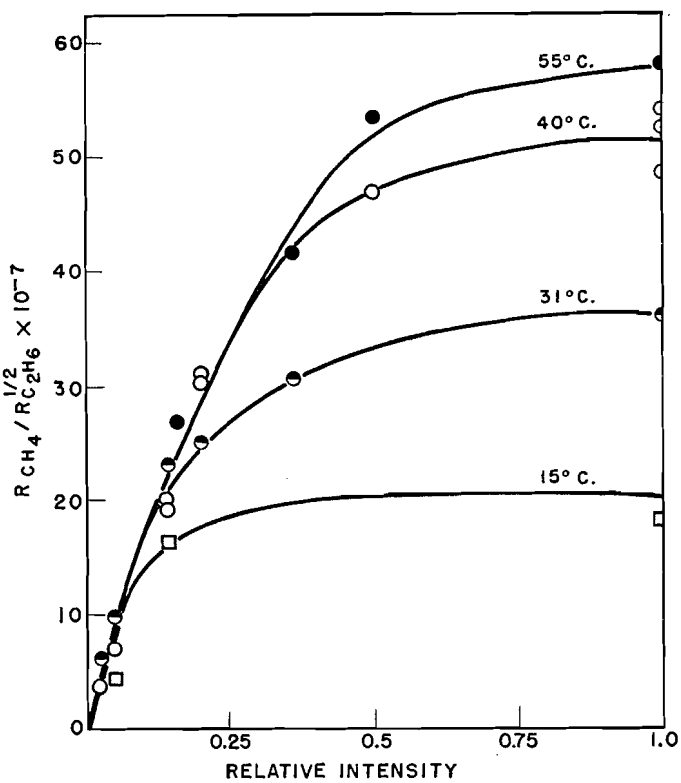

FIG. 1. The variation of $R_{CH_4}/R^{\frac{1}{2}}_{C_2H_6}$ with intensity.

If this relation holds in the liquid phase, $R_{CH_4}/R^{\frac{1}{2}}_{C_2H_6}$ should be independent of the absorbed intensity. In Fig. 1 $R_{CH_4}/R^{\frac{1}{2}}_{C_2H_6}$ has been plotted against the intensity for different temperatures. The figure shows that the ratio decreases sharply with intensity in the low intensity region, although it is tending towards constancy at high intensities. The results suggest that the formation of ethane at low intensity is mainly by some reaction dependent on the first power of the intensity, i.e. of the radical concentration. Possible explanations are formation of ethane to some extent in the cage, or by a direct intramolecular reaction.

The fact that $R_{CH_4}/R^{\frac{1}{2}}_{C_2H_6}$ is nearly independent of intensity at high intensities indicates that under these conditions most methane and ethane is formed by reactions [6] and [10], and that at high intensity inter-cage effects predominate. The photolysis of CD_3COCD_3 furnishes further proof that some ethane is formed by inter-cage effects. In this case the higher strength of C—D bonds reduces the effect of abstraction, and C_2D_6 is greater than CO. This would be impossible if all ethane were formed in the cage.

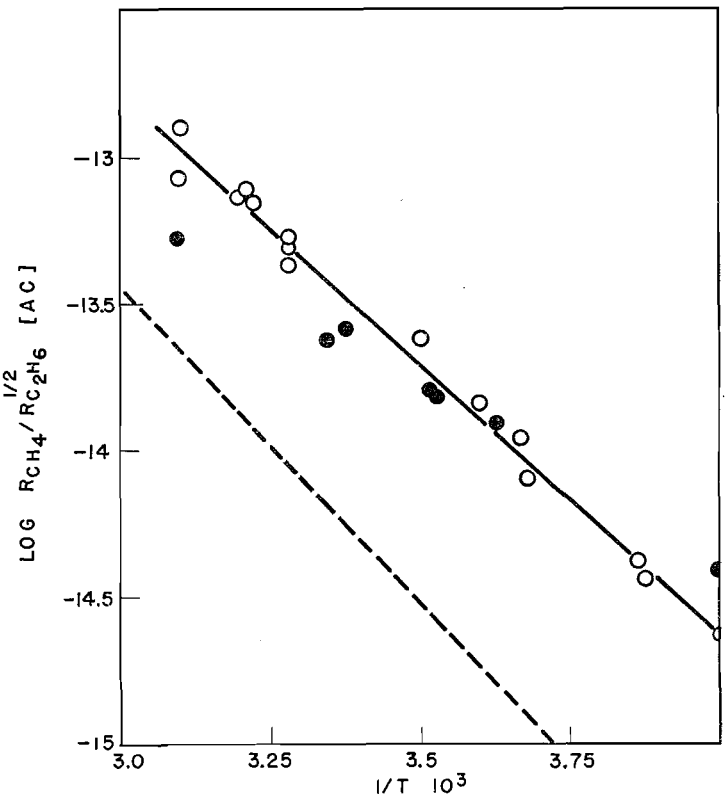

FIG. 2. Arrhenius plot of $R_{CH_4}/R^{\frac{1}{2}}_{C_2H_6}$ [Acetone] for liquid acetone.
○ wave length approximately 3130 Å.
● wave length approximately 2537 Å.
The dotted curve represents an extrapolation to low temperatures of results for gaseous acetone.

In Fig. 2 an Arrhenius plot is given of $R_{CH_4}/R^{\frac{1}{2}}_{C_2H_6}$ [Acetone] for runs with CH_3COCH_3 at 3130 Å and high intensities (i.e. in the region where the ratio is essentially independent of intensity). A good straight line is obtained, from which $E_6 - \frac{1}{2}E_{10} \sim E_6 = 8$ kcal. This agrees satisfactorily with the gas-phase value of 9.7 kcal., since the result will be approximate because of errors due to diffusion effects, to inhomogeneity of absorption, and to the formation of methane by disproportionation of CH_3 and CH_3CO at low temperatures. While the slopes of the two lines agree reasonably, the gas-phase line lies considerably below that for the liquid phase, corresponding to a difference of a factor of about 7 in the ratio. This has little significance, however, in view of the uncertain meaning of concentration in the liquid phase.

The results obtained by photolyzing CD_3COCD_3 are no doubt affected to a much greater extent by the occurrence of reaction [5], because of the slower rate of abstraction of D from CD_3COCD_3 as compared with H from CH_3COCH_3. The results lead to an apparent activation energy about 2 kcal. lower than those for CH_3COCH_3, but this is presumably complex and has no simple significance.

The data at 2537 Å are not sufficiently extensive to warrant detailed discussion.

A few experiments were made with acetone–water and acetone–*n*-hexane solutions, and are given in Tables V and VI. The results indicate:

(*a*) With water, no change larger than the rather considerable experimental error occurs in the $R_{CH_4}/[Ac]$, or $R_{CH_4}/R^{\frac{1}{2}}_{C_2H_6}$ [Ac] ratios. It is evident that water acts essentially as an inert solvent, as far as the production of gaseous products is concerned, and that the reaction

$$CH_3 + H_2O \rightarrow CH_4 + OH$$

does not occur to an appreciable extent. This is expected in view of the high H—OH bond dissociation energy (*ca.* 118 kcal.). Previous work (10) indicates that condensable products such as formaldehyde and acetic acid are formed.

(*b*) With acetone–hexane solutions there is a slight but significant drop in the ratio $R_{CH_4}/R^{\frac{1}{2}}_{C_2H_6}[Ac]$. Since the activation energy of the reaction

$$CH_3 + n\text{-}C_6H_{14} \rightarrow CH_4 + C_6H_{15} \qquad [11]$$

is less than that of

$$CH_3 + CH_3COCH_3 \rightarrow CH_4 + CH_2COCH_3 \qquad [12]$$

by 1.6 kcal. (11), while the steric factors are in the ratio $P_{11}/P_{12} = 0.3$, it would be expected that abstraction by [11] would be faster than by [12] by a factor of 3.3. A considerable increase in methane would therefore be expected. Actually there is a decrease. However, in view of the probable formation on irradiation of an addition compound between acetone and *n*-hexane (4) the situation is complex and further discussion is unwarranted.

It is apparent that many features of the results cannot be explained in detail. The above discussion at least points out the general problems involved.

It is hoped that further work on the more complex products, and on the reaction at still lower temperatures, may throw more light on the mechanism.

ACKNOWLEDGMENT

The authors are indebted to Dr. P. Ausloos for much advice and discussion.

REFERENCES

1. BOWEN, E. J. and HORTON, A. T. J. Chem. Soc. 1685. 1936.
2. BOWEN, E. J. and PRAUDIERE, E. L. A. E. DE LA. J. Chem. Soc. 1503. 1934.
3. BOWEN, E. J. and TIETZ, E. L. J. Chem. Soc. 234. 1930.
4. FRANKENBURG, P. E. and NOYES, W. A., JR. J. Am. Chem. Soc. 75: 2847. 1953.
5. KASHA, M. J. Opt. Soc. Amer. 38: 929. 1948.
6. LAMPE, F. W. and NOYES, R. M. J. Am. Chem. Soc. 76: 2140. 1954.
7. LEIGHTON, P. A., CRARY, R. W., and SCHIPP, L. T. J. Am. Chem. Soc. 53: 3017. 1932.
8. LEROY, D. J. Can. J. Research, B, 28: 492. 1950.
9. NOYES, R. M. J. Chem. Phys. 22: 1349. 1954.
10. QURESHI, U. and TAHER, N. A. J. Phys. Chem. 36: 2670. 1932.
11. TROTMAN-DICKENSON, A. F. and STEACIE, E. W R. J. Chem. Phys. 19: 329. 1951.

SUR L'OXYDATION LENTE DE L'ÉTHER DIÉTHYLIQUE EN PHASE GAZEUSE[1]

PAR ANDRÉ LEMAY[2] ET CYRIAS OUELLET

RÉSUMÉ

La réaction de l'éther diéthylique avec l'oxygène a été étudiée dans un récipient en Pyrex, dans l'intervalle de température 160–175° C., voisin de la limite inférieure de flamme froide. L'oxygène est consommé durant la baisse initiale de pression suivant une réaction d'ordre zéro, affectée d'une énergie d'activation d'environ 50 kcal./mole, durant laquelle il apparaît de l'eau, des peroxydes, des acides, et autres produits. La hausse de pression qui survient plus tard correspond à des réactions postérieures à l'oxydation proprement dite; elle peut avoir lieu en l'absence d'oxygène. Les taux d'oxydation tirés de la vitesse maximum d'accroissement de la pression sont ainsi remis en question. On discute quelques processus susceptibles d'intervenir dans chacune de ces deux phases de la réaction.

INTRODUCTION

Divers phénomènes caractéristiques de la combustion—oxydation lente, flamme froide, et explosion—peuvent être étudiés dans des conditions particulièrement avantageuses dans l'oxydation de l'éther diéthylique. Ils y sont observables à des pressions basses de l'ordre de 10 à 100 mm. Hg et dans un intervalle de températures allant de 150 à 250° C., tandis que la plupart des hydrocarbures ne subissent ces réactions qu'à des pressions et températures beaucoup plus élevées. Plusieurs aspects de la flamme froide de l'éther ont été étudiés dans notre laboratoire (18) en particulier au moyen du spectromètre de masse à échantillonnage continu de Léger (10, 11). Dans le but de mieux comprendre en quoi consiste le passage de l'oxydation lente à la flamme froide, nous avons cherché dans le présent travail à obtenir de nouvelles données sur la cinétique de l'oxydation lente de l'éther dans l'intervalle de 160 à 175° C. situé immédiatement en dessous de la limite de flamme froide.

L'oxydation des éthers semble occuper une place intermédiaire entre celle des hydrocarbures (5, 12, 15, 21) et celle des aldéhydes (12, 13) mais est moins bien connue que ces dernières. Walsh et ses collaborateurs (4, 14) ont fait une étude détaillée des domaines d'inflammation des éthers, surtout de l'éther diéthylique; mais pour ce qui concerne l'oxydation lente, ces auteurs se sont attachés surtout à celle de l'éther diisopropylique. Eastwood et Hinshelwood (7) ont comparé les oxydations lentes de cinq éthers aliphatiques. Dans le cas de l'éther diéthylique, le plus facilement oxydable de la série étudiée, la réaction débute par une baisse de pression suivie d'un accroissement de pression analogue à celui qui succède à la période d'induction classique des hydrocarbures. En se basant sur cette ressemblance, ces auteurs ont pris comme mesure du taux d'oxydation la pente maximum de cette montée de pression. Ils ont constaté que les peroxydes formés au début de la réaction sont relative-

[1]*Manuscrit reçu le 24 février, 1955.*
Contribution du Département de Chimie, Université Laval, Québec. Travail subventionné par un octroi (DRB–129) (Projet D44–50–01–09) du Comité de Recherches pour la Défense.
[2]*Boursier du Conseil National de Recherches. Adresse actuelle: Canadian Armament Research and Development Establishment, Valcartier, Québec.*

ment stables et survivent même au passage d'une flamme froide. Il se peut que cette propriété résulte uniquement du fait que la flamme froide de l'éther se produit à une température relativement basse, comparée, par exemple, à celle du butanone (1) durant laquelle les peroxydes accumulés disparaissent rapidement.

MÉTHODE EXPÉRIMENTALE

La réaction est étudiée en système statique en l'absence de vapeur de mercure. La chambre à réaction est un cylindre en Pyrex de 4.4 × 14 cm. et la pression est enregistrée électriquement.

Appareil

La figure 1 montre un dessin schématique de la chambre à réaction *C* et de ses principaux accessoires. Elle est enfermée dans un four en acier *F* chauffé

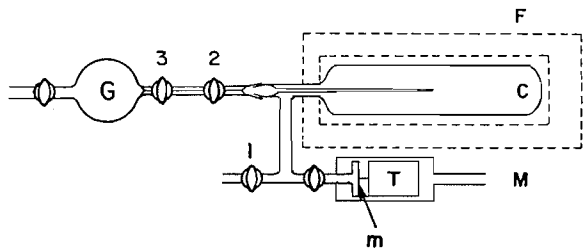

FIG. 1. Schéma montrant la chambre à réaction *C*, le manomètre à membrane *m*, et à transducer *T*, ainsi que le système *G*-3-2 pour l'injection de gaz étrangers.

électriquement et est entourée d'un manchon en laiton destiné à uniformiser la température. Un thermomètre pénètre dans le four et un couple thermo-électrique peut être déplacé sous le manchon, où le gradient de température ne dépasse pas 1° C. d'une extrémité à l'autre de la chambre à réaction. Un transformateur Sola à voltage constant et un Variac permettent de contrôler la température du four. Le robinet 1 sert à l'introduction des réactifs; il conduit d'une part au réservoir contenant le mélange de gaz et d'autre part à un piège à −80° C. suivi d'une pompe à diffusion utilisant de l'huile silicone et d'une pompe mécanique.

Les tubes qui vont de *C* aux premiers robinets sont chauffés à 100° C. pour empêcher une condensation qui se produit aux stages ultérieurs de la réaction et qui s'est manifestée dans plusieurs de nos expériences par une baisse considérable de la pression, vers la fin de la réaction.

L'injection, en plein centre de la chambre à réaction, de petites quantités dosées de gaz inhibiteurs, se fait au moyen du tube capillaire, précédé d'un petit volume calibré, inclus entre les robinets 2 et 3, et d'un réservoir *G*.

La pression est enregistrée au cours de la réaction au moyen d'un manomètre différentiel. Le déplacement d'une membrane *m* de duralumine de 0.07 mm. d'épaisseur, collée sur une capsule de verre, est transmis à un "transducer" *T* de type Statham G1-1.5-315, alimenté par une tension de 1.5 volt. Le signal de sortie est transmis à un enregistreur Brown qui trace la courbe de pression. La capsule manométrique et le transducer sont enfermés dans une boîte étanche

en laiton où règne la pression de référence mesurée sur le manomètre anéroide *M* de type Wallace & Tiernan. Dans la région de 100 mm. Hg qui nous intéresse, la valeur absolue de la pression est mesurée à 0.5 mm. près et les variations sont enregistrées à 0.1 mm. près avec une inertie de l'ordre d'une seconde.

Réactifs

L'éther diéthylique est distillé trois fois en contact avec une solution acide de permanganate, séché en présence de sodium, puis redistillé en rejetant les premières et les dernières fractions. On a aussi employé, avec des résultats identiques, la méthode de Dasler (6) suivant laquelle l'éther est libéré de peroxyde et d'eau par passage à travers une colonne d'alumine activée. Cet éther est conservé sous vide dans un ballon lié à l'appareil. Pour préparer un mélange, on en laisse évaporer une partie dans un ballon évacué, on ajoute la quantité d'oxygène requise, et on laisse reposer pendant quelques heures. Des mesures au spectromètre de masse ont révélé que l'oxygène, provenant directement d'un cylindre, contenait un peu d'azote, mais il a été vérifié que ce gaz n'affecte pas le cours de la réaction. Les robinets sont lubréfiés avec des graisses Apiezon T et L et silicone. Il a été vérifié par des mesures manométriques que ces graisses n'absorbent pas de quantité appréciable d'éther diéthylique, contrairement à ce qui se produit avec les éthers supérieurs.

Parmi les gaz injectés, le formaldéhyde est produit par chauffage de paraformaldéhyde, tandis que l'oxyde nitrique, le propylène, et l'acide bromhydrique sont de marque Mathieson; on les prélève directement des cylindres.

Analyses

On dose l'oxygène en mesurant sa pression partielle dans un analyseur magnétique de Pauling, modèle Beckman D. Au moment choisi, on aspire dans l'analyseur évacué un échantillon (environ 10 cc.) de gaz provenant de la chambre à réaction, après avoir balayé le gaz froid des canalisations en l'aspirant dans un récipient auxiliaire. La quantité de gaz ainsi prélevée est telle qu'il faut interrompre la réaction.

Pour doser les acides et les peroxydes, on évacue la chambre à réaction au moment choisi et on capte dans un piège les produits condensables à $-80°$ C. On extrait ces derniers au moyen de 20 cc. d'eau bidistillée. Les acides sont titrés immédiatement par la soude 0.01 *N* en présence de phénolphtaléine. Le dosage des peroxydes se fait dans une atmosphère d'azote en titrant par le thiosulfate, 0.01 *N* d'abord l'iode libéré en 15 min. en présence d'un excès d'iodure de potassium en milieu neutre et, ensuite, l'iode libéré en trois heures en milieu acide.

RÉSULTATS

Marche et produits de la réaction

La réaction est mesurable dans un intervalle de températures restreint; en dessous de 155° C., elle est trop lente, au-dessus de 175° C., elle est trop rapide et tend à dégénérer en flamme froide. La figure 2 montre l'allure générale des phénomènes pour une réaction produite dans des conditions moyennes. Les quantités d'acides et de peroxydes y sont représentées par les pressions

partielles que ces produits exerceraient dans les conditions de l'expérience. Les courbes de pression totale sont reproductibles à 3% près, sauf pour la première expérience d'une série.

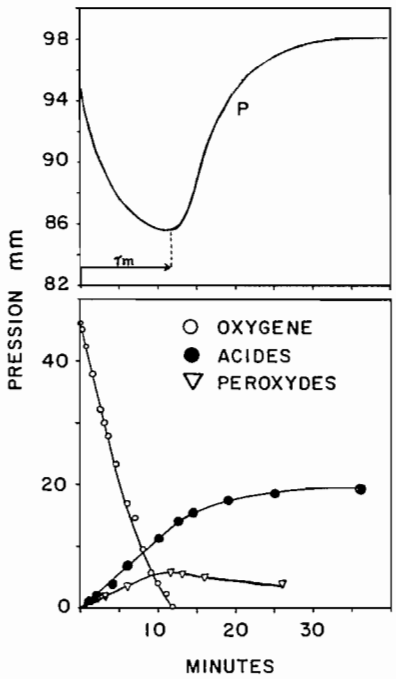

FIG. 2. Courbes de pression totale P et de pressions partielles au cours de la réaction à 168° C. d'un mélange équimoléculaire d'éther et d'oxygène.

Pour le cas typique représenté par la figure 2, la pression totale décroît au début jusqu'à un minimum atteint au bout d'environ 10 min. et se met ensuite à croître pour tendre vers un palier légèrement supérieur à la pression initiale. C'est durant la faible baisse initiale de la pression qu'a lieu la principale réaction d'oxydation, puisque l'oxygène est entièrement consommé durant cette période. Le taux de cette consommation est sensiblement d'ordre zéro. A mesure que l'oxygène disparaît, la pression partielle des produits acides croît linéairement à une vitesse égale à un quart de celle de la consommation de l'oxygène. La concentration des produits peroxydiques croît parallèlement à celle des acides, mais deux fois moins vite. Tout l'iode titrable est libéré rapidement en milieu neutre, ce qui est caractéristique du peroxyde d'hydrogène et des peracides. Après le minimum de pression, les acides augmentent lentement, à un taux sensiblement égal à celui de la diminution des peroxydes.

Des renseignements additionnels sur la variation de la composition du mélange au cours de la réaction ont été fournis par quelques expériences de M. L. P. Blanchard, qui a suivi cette oxydation au moyen d'un spectromètre de masse à échantillonnage continu (10). Les mesures faites avec des mélanges contenant 50 et 30% d'éther indiquent qu'il disparaît deux molécules d'oxygène

pour une d'éther. On observe aussi, dès le début, et jusqu'au moment où le minimum de pression est atteint, un accroissement d'abondance de la masse 18 attribuée à l'eau, et de la masse 43, attribuable à l'acide peracétique ou à l'acide acétique. Rien n'indique une accumulation appréciable de peroxyde d'hydrogène. Durant la montée de pression, on voit croître l'abondance de le masse 28 qui peut refléter, entre autres composés, l'oxyde de carbone. Les résultats de cette étude encore en cours seront publiés plus tard. Des courbes très différentes des précédentes ont été observées dans des expériences sur l'oxydation à 235° C. de l'éther diméthylique par une égale quantité d'oxygène; la réaction débute, sans période d'induction, par un faible accroissement de pression qui se poursuit linéairement jusqu'à un palier.

Influence de la température et de la composition du mélange

La figure 3 fait voir quelques familles de courbes de pression totale et de pression partielle d'oxygène obtenues avec des mélanges de trois compositions différentes, à diverses températures. On voit que le coefficient de température

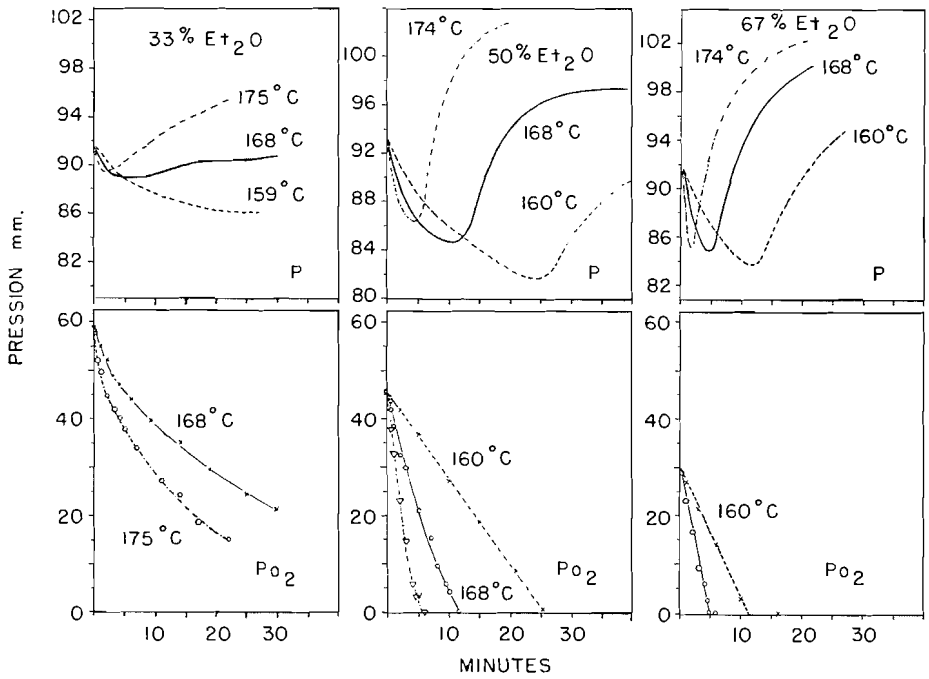

FIG. 3. Comparaisons de courbes de pression totale (haut) et de pression d'oxygène (bas) pour des mélanges contenant initialement 33%, 50%, et 67% d'éther en volume. (Les courbes de pression totale sont obtenues par enregistrement continu.)

est positif et grand à toutes ces compositions, tant par les taux de descente et de montée de la pression que pour celui de la consommation d'oxygène. Dans les mélanges contenant 50% d'éther ou plus, la consommation d'oxygène semble être d'ordre zéro et est complète au moment où la pression totale passe par le minimum. Les mélanges contenant, au départ, deux fois plus d'oxygène

que d'éther accusent deux particularités: la montée de pression est supprimée aux basses températures; à température plus élevée, la consommation d'oxygène, rapide et apparamment d'ordre zéro jusqu'au minimum, se poursuit ensuite plus lentement et suivant une loi du premier ordre. Cette loi est mise en évidence par la transposition à l'échelle logarithmique des deux courbes obtenues à 168° C. et 175° C.

Comme il n'est pas facile de mesurer sans ambiguité la pente initiale de pression, nous prenons, comme mesure de la vitesse de la première étape de la réaction, soit la pente de la courbe de l'oxygène, soit l'inverse du temps τ_m (figure 2) qui s'écoule entre l'instant initial et celui où le minimum de pression est atteint. La figure 4 montre les droites d'Arrhenius obtenues par ces deux

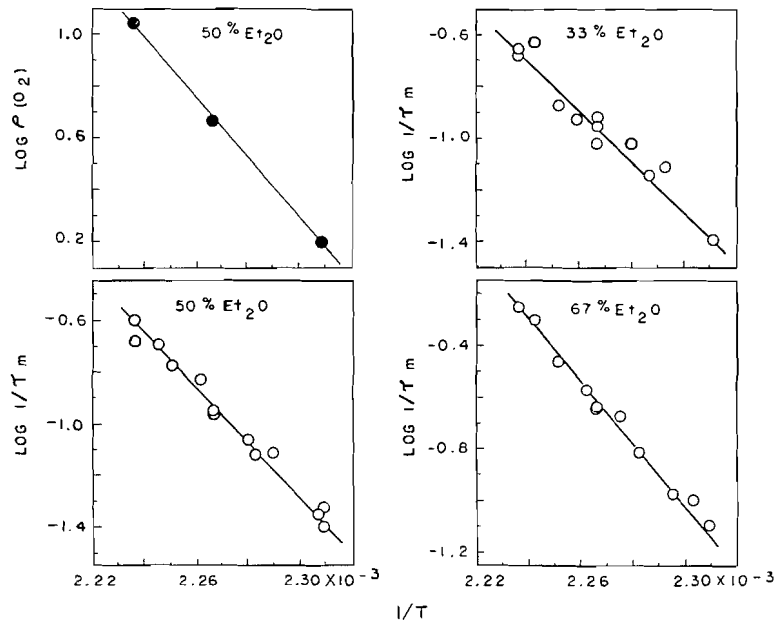

FIG. 4. Courbes de $1/T°$ K. contre les logarithmes de la vitesse initiale calculée d'après le taux de consommation d'oxygène (O_2) et d'après le temps τ_m écoulé au minimum de pression.

méthodes. On a pu vérifier, dans le cas du mélange à 50%, que le coefficient de température obtenu par les deux méthodes est le même, ce qui permet de considérer τ_m comme une grandeur significative. En prenant pour mesure de la vitesse de la seconde étape de la réaction la pente maximum ρ_m de la montée de pression, on obtient les droites d'Arrhenius de la figure 5.

Nos données permettent un calcul approximatif des énergies d'activation apparentes. Pour la phase initiale (figure 4), les valeurs obtenues pour 33%, 50%, 67%, et 90% d'éther sont de 44, 51, 55, et 48 kcal./mole respectivement. La valeur obtenue d'après le taux de consommation d'oxygène à 50% d'éther est 53 kcal./mole, en bon accord avec la valeur ci-dessus tirée de τ_m. Le taux maximum ρ_m d'accroissement de pression conduit à des valeurs de 32, 25, et 26 kcal./mole pour 50, 67, et 90% d'éther respectivement. Ces valeurs gros-

sières, obtenues sur un étroit intervalle de températures, peuvent néanmoins servir à caractériser le coefficient de température près de la limite de flamme froide.

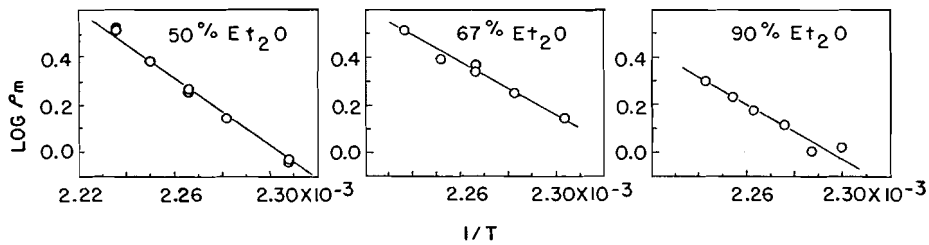

FIG. 5. Courbes de $1/T°$ K. contre le logarithme du taux maximum ρ_m de l'accroissement de pression.

L'influence de la proportion des réactifs sur les deux vitesses représentées par $1/\tau_m$ et ρ_m se voit dans la figure 6. On voit que ces grandeurs sont sensiblement indépendantes de la composition tant qu'il y a moins de 50% d'éther, mais qu'elles varient rapidement dans les mélanges pauvres en oxygène. On a aussi trouvé que, pour un mélange à 50% à 170° C., $1/\tau_m$ varie peu avec la pression totale entre 45 et 95 mm. Hg tandis que ρ_m est sensiblement proportionnel à cette pression. Des expériences effectuées dans le dessein de dégager l'influence de la pression partielle de chacun des réactifs ont abouti à des

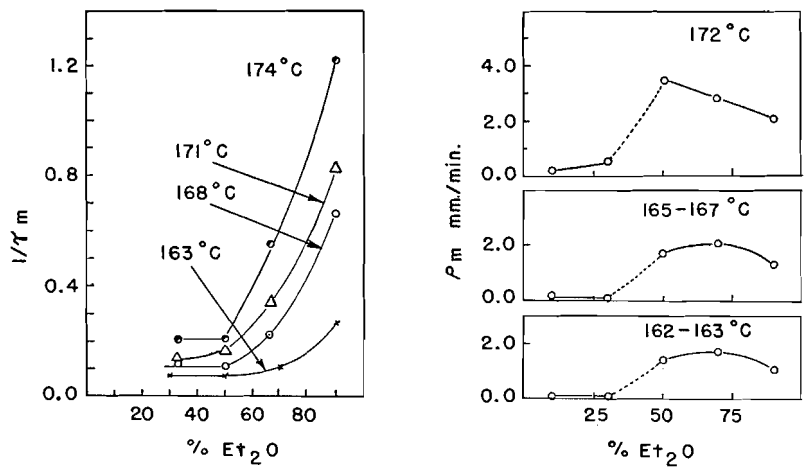

FIG. 6. Variations de la vitesse initiale $1/\tau_m$ min.$^{-1}$ et du taux maximum ρ_m de l'accroissement de pression, en fonction de la composition du mélange.

courbes présentant des maxima semblables à ceux de ρ_m dans la figure 6. Il semble donc que la proportion des réactifs soit le facteur le plus important. Dans l'ensemble, ces résultats concordent avec ceux de Eastwood et Hinshelwood (7) qui ont observé une inhibition considérable par l'oxygène; en effet, la figure 6 montre que la réaction est toujours plus lente aux fortes proportions d'oxygène.

Influence de la surface et de gaz étrangers

Un cylindre en quartz de mêmes dimensions que notre chambre à réaction en Pyrex a donné les mêmes courbes de pression et d'oxygène. Par contre, en traitant la paroi de Pyrex par une solution de chlorure de potassium, nous avons obtenu les courbes de la figure 7. Cet effet a déjà été observé par L. Ouellet et C. Ménard (17), qui nous ont suggéré ces expériences. On voit que, dans ces conditions, l'allure de la réaction ressemble à celle des oxydations d'hydrocarbures et de l'éther diisopropylique (4, 12, 14); une courte période d'induction est décelable sur la courbe de pression et sur celle de la consommation de l'oxygène, mais il n'y a plus de minimum de pression.

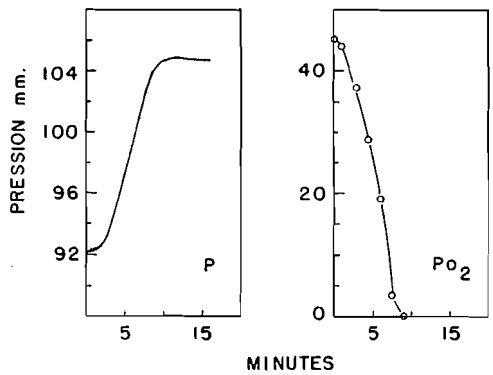

FIG. 7. Courbes de pression totale P et de pression d'oxygène P_{O_2} pour une réaction à 168° C. et 50% d'éther en volume, dans un récipient en Pyrex traité au chlorure de potassium.

L'injection de petites quantités d'oxyde nitrique à diverses époques avant ou durant la réaction inhibe dans tous les cas la consommation de l'oxygène et l'abaissement de la pression, mais n'agit pas toujours de la même façon sur l'accroissement de la pression. La vitesse est réduite d'environ 30 fois par 0.6% d'oxyde nitrique, ce qui donne une indication approximative de la longueur des chaînes. Ces effets et ceux qui résultent de l'addition de propylène, d'acide bromhydrique, et de formaldéhyde seront décrits dans une autre publication.

DISCUSSION

La réaction débute sans période d'induction appréciable, contrairement aux oxydations des hydrocarbures et de l'acétaldéhyde; les peroxydes formés n'exercent donc pas d'effet autocatalytique. On distingue deux phases assez nettement séparées dans le temps. La première phase correspond surtout à la consommation de l'oxygène et s'accompagne d'un abaissement de la pression. Sa forte inhibition par l'oxyde nitrique indique qu'il s'agit d'une réaction en chaînes longues. La seconde phase s'accompagne d'un accroissement de la pression; elle n'exige pas la présence d'oxygène libre. Cette seconde phase peut être accélérée, par traitement de la surface en chlorure de potassium, à tel point qu'elle n'est plus en retard sur la précédente; on retrouve alors la courbe de pression ascendante caractéristique des hydrocarbures (figure 7). La compa-

raison des figures 7 et 2 montre que le taux de la consommation de l'oxygène est peu affecté par ce changement de surface.

Cette séparation en deux phases semble constituer la principale différence entre l'oxydation de l'éther diéthylique et celle des hydrocarbures. On peut vraisemblablement l'attribuer à la température anormalement basse d'oxydation de l'éther, plutôt qu'à une différence essentielle de mécanisme; les réactions de la seconde phase seraient suffisamment lentes à cette température pour ne pas masquer la phase initiale d'oxydation. Si cette hypothèse est vraie, on devrait pouvoir reproduire cette séparation en oxydant un hydrocarbure sur une surface empoisonnée, ou la retrouver dans le cas d'hydrocarbures oxydables à température relativement basse. On sait (3) que certaines oléfines semblent se comporter comme l'éther aux basses températures et comme les paraffines aux températures élevées. Dans l'ensemble, l'oxydation lente de l'éther sur le Pyrex et le quartz ressemble beaucoup plus à celle de l'acétaldéhyde, qui débute aussi par une baisse de pression et a lieu dans le même domaine de températures (13), qu'à celle des hydrocarbures (5, 12). Remarquons que la coutume de prendre le taux maximum ρ_m de l'accroissement de pression comme mesure de la vitesse d'oxydation ne peut être suivie dans le cas de l'éther diéthylique; les comparaisons basées sur cette grandeur (7) réflètent plutôt les vitesses des réactions secondaires.

Bien que les faits connus actuellement ne permettent pas une analyse détaillée de la cinétique et du mécanisme de la réaction, il est utile de supposer que les processus en jeu dans chacune des phases sont de mêmes types que ceux qui ont été invoqués pour interpréter l'oxydation des hydrocarbures (2, 5, 12, 21). Appliquant la distinction développée systématiquement par Niclause, Combe, et Letort (15, 16), on peut penser qu'en gros l'abaissement de pression représente la partie de la réaction attribuable à l'oxydation proprement dite, et que la partie de l'oxygène consommé dont cet abaissement ne rend pas compte est engagée dans des dégradations oxydantes s'effectuant sans changement de pression. Enfin, l'accroissement de pression correspondrait à des pyrolyses induites par l'oxygène résiduel ou par la décomposition de peroxydes. L'importance relativement faible des variations de pression laisse supposer que la dégradation oxydante prédomine. L'ordre zéro par rapport à l'oxygène peut être considéré comme une manifestation de l'inhibition par un excès de ce réactif. Ce comportement, bien connu chez les réactions de ce type (2, 5, 7), a été attribué (2) à la prédominance d'un processus de rupture par recombinaison de radicaux peroxydiques.

Pour ce qui concerne la nature des produits intermédiaires au cours de la première phase, il faudra rendre compte de l'apparition hâtive de l'eau et d'un peracide. Il est peu probable que le peroxyde dihydroxyéthylique, produit connu (19) de l'oxydation de l'éther liquide à froid, joue un rôle à la température de notre réaction. Le mode d'initiation le plus vraisemblable est l'abstraction d'un hydrogène secondaire par l'oxygène et par les radicaux, en particulier les radicaux peroxydiques produits au cours de la chaîne.

$$C_2H_5OC_2H_5 + O_2 = CH_3\dot{C}HOC_2H_5 + HO_2^{\cdot} \qquad [1a]$$

$$C_2H_5OC_2H_5 + HO_2^{\cdot} = CH_3\dot{C}HOC_2H_5 + H_2O_2 \qquad [1b]$$

Ce gros radical peut capter une molécule d'oxygène pour former un radical peroxydique $CH_3CH(O\dot{O})OC_2H_5$ et éventuellement l'hydroperoxyde correspondant; il peut aussi se décomposer et donner lieu aux réactions suivantes:

$$CH_3\dot{C}HOC_2H_5 = CH_3CHO + C_2H_5^{\cdot} \qquad [2]$$

$$C_2H_5^{\cdot} + O_2 = C_2H_5OO^{\cdot} \qquad [3]$$

$$C_2H_5OO^{\cdot} = CH_3CHO + OH^{\cdot} \qquad [4a]$$

$$C_2H_5OO^{\cdot} = CH_3CO^{\cdot} + H_2O \qquad [4b]$$

$$CH_3CO^{\cdot} + O_2 = CH_3COOO^{\cdot} \qquad [5]$$

$$CH_3COOO^{\cdot} + RH = CH_3COOOH + R^{\cdot} \qquad [6]$$

où le rôle de RH sera joué au début par l'éther, mais de plus en plus par l'acétaldéhyde, dont l'hydrogène est plus facile à abstraire. Dans la mesure où [4*b*] est possible contre la concurrence de [4*a*] et de [7], on obtiendrait, dans les premiers temps de la réaction, le bilan

$$C_2H_5OC_2H_5 + 2O_2 = CH_3CHO + CH_3COOOH + H_2O \qquad [a]$$

qui correspond au rapport observé des taux de consommation de l'éther et de l'oxygène, mais ne comporte pas d'abaissement de pression. Par ailleurs, [4*a*] et [4*b*] seront vraisemblablement concurrencées par la réaction

$$C_2H_5OO^{\cdot} + RH = C_2H_5OOH + R^{\cdot}. \qquad [7]$$

On sait que l'hydroperoxyde d'éthyle se décompose sur la surface avec une demi-vie de l'ordre d'une minute, (9) vers 170° C., avec formation d'acétaldéhyde et d'eau

$$C_2H_5OOH \xrightarrow{S} CH_3CHO + H_2O \qquad [8]$$

et que cette décomposition est fortement catalysée par le chlorure de potassium. Par la voie [2-3-7-8], on obtiendrait deux molécules d'acétaldéhyde. Dans la région de 160 à 175° C., ce dernier s'oxyde, à une vitesse sensiblement égale (13) à celle de l'oxydation de l'éther, suivant:

$$CH_3CHO + O_2 = CH_3COOOH. \qquad [9]$$

Il est probable que le chlorure de potassium catalyse aussi la décomposition de l'acide peracétique. Ce dernier réagirait aussi dans une certaine mesure avec l'acétaldéhyde, suivant:

$$CH_3COOOH + CH_3CHO = 2CH_3COOH. \qquad [10]$$

Dans tous les cas envisagés, un fragment de la molécule d'éther donne immédiatement une molécule d'acétaldéhyde suivant (2). L'autre fragment peut être oxydé rapidement en acide peracétique par une seule chaîne [3-4*b*-5-6]. Ceci donnerait le bilan [*a*] ne comportant aucune variation de pression. Mais ce second fragment peut aussi donner d'abord une seconde molécule d'acétaldé-

hyde par l'une des voies [4*a*] ou [3-7-8] puis de l'acide peracétique par [9]. Le faible abaissement de pression réfléterait l'importance relative de la réaction [9]. Enfin, la réaction [10] expliquerait que la quantité d'acide dépasse nettement celle du peroxyde et s'accroît aux dépens de cette dernière.

Au début de la seconde phase, s'il reste beaucoup d'oxygène, la pression continue à décroître à cause de la réaction [9] si la température est assez basse (figure 3). Mais à température plus élevée ou dans un mélange pauvre en oxygène, les réactions de pyrolyse de l'acétaldéhyde (et autres produits) prédominent et la pression croît. Dans ces conditions, la réaction [5] cède le pas à la décomposition du radical acétyle, affectée d'une énergie d'activation de l'ordre de 15 kcal./mole (20):

$$CH_3CO^{\cdot} = CH_3^{\cdot} + CO.$$

Le radical méthyle pourra, en l'absence d'oxygène, former du méthane par abstraction et de l'éthane par recombinaison; en présence d'un peu d'oxygène, il sera surtout oxydé suivant l'un des schémas proposés par Grumer (8), avec formation d'oxyde de carbone, de méthanol, et d'eau.

Il est difficile de dire dans quelle mesure la décomposition d'un peroxyde contribue directement à l'accroissement de la pression. Il se peut qu'une telle décomposition gouverne la vitesse de la seconde phase, dont l'énergie d'activation globale est du bon ordre de grandeur, soit de 25 à 30 kcal./mole.

En somme, la première phase correspondrait dans l'ensemble à la dégradation en molécules à deux atomes de carbone, la seconde phase, à celle en molécules à un atome de carbone. En présence de chlorure de potassium (figure 7), la décomposition de l'acide peracétique et éventuellement de l'hydroperoxyde d'éthyle serait accélérée à tel point que la seconde phase ne serait plus en retard sur la première.

La comparaison du taux d'oxydation lente de l'éther à ceux d'autres substances est impossible du fait que la pente maximum ρ_m de la courbe d'accroissement de pression a été prise par plusieurs auteurs comme mesure des taux d'oxydation lente de diverses substances organiques. Or, dans le cas de l'éther et vraisemblablement dans plusieurs autres, cette grandeur n'a pas la signification qu'on lui avait prêtée.

REMERCIEMENTS

Nous adressons nos remerciements au Comité de Recherches pour la Défense pour un octroi (DRB-129) et au Conseil National de Recherches qui a accordé des bourses à l'un de nous (A.L.). Nous remercions aussi M. E. G. Léger de l'aide fréquente qu'il nous a prêtée au cours de ce travail, M. L. P. Blanchard qui nous a fourni les spectres de masses, ainsi que MM. P. Ausloos et L. Ouellet qui nous ont fait d'utiles suggestions.

SUMMARY

The reaction of diethyl ether and oxygen in a Pyrex vessel has been studied over the temperature range 160–175° C., below the lower limit of cool flame. During the initial pressure drop, oxygen is consumed in a zero order process with an activation energy of some 50 kcal./mole, giving rise to water, peroxides,

acids, and other products. The pressure rise which follows is secondary to the main oxidation reaction; it does not require the presence of oxygen. Oxidation rates derived from maximum rates of pressure rise are therefore questionable. A number of processes, which may account for these two reactions stages, are examined.

RÉFÉRENCES

1. BARDWELL, J. et HINSHELWOOD C. Proc. Roy. Soc. (London), A, 205: 375. 1951.
2. BATEMAN, L. Quart. Revs. (London), 8: 147. 1954.
3. BAWN, C. E. H. et SKIRROW, G. Abstr. Fifth Symposium on Combustion. Pittsburg. 1954. p. 82.
4. CHAMBERLAIN, G. H. N. et WALSH, A. D. Flame and Explosion Phenomena. Third Symposium on Combustion. The Williams & Wilkins Company, Baltimore. 1949. p. 368.
5. CULLIS, G. H. N. et HINSHELWOOD, C. N. Discussions Faraday Soc. No. 2: 117. 1947.
6. DASLER, W. et BAUER, C. D. Ind. Eng. Chem. Anal. Ed. 18: 52. 1946.
7. EASTWOOD, T. A. et HINSHELWOOD, C. J. Chem. Soc. 733. 1952.
8. GRUMER, J. Abstr. Fifth Symposium on Combustion. Pittsburg. 1954. p. 41.
9. HARRIS, E. J. Proc. Roy. Soc. (London), A, 173: 126. 1939.
10. LÉGER, E. G. Can. J. Phys. 33: 74. 1955.
11. LÉGER, E. G. et OUELLET, C. J. Chem. Phys. 21: 1310. 1953.
12. LEWIS, B. et VON ELBE, G. Combustion, flames and explosion of gases. Academic Press, Inc., New York. 1951.
13. MACDOWELL, C. A. et THOMAS, J. H. J. Chem. Soc. 2217. 1949.
14. MALHERBE, F. E. et WALSH, A. D. Trans. Faraday Soc. 46: 824. 1950.
15. NICLAUSE, M. et COMBE, A. Rev. inst. franç. pétrole, 8: 311. 1953.
16. NICLAUSE, M., COMBE, A., et LETORT, M. J. chim. phys. 49: 605. 1952.
17. OUELLET, L. et MÉNARD, C. Communication privée.
18. OUELLET, L. et OUELLET, C. Can. J. Chem. 29: 986. 1951.
19. RIECHE, A. Z. angew. Chem. 44: 896. 1931.
20. STEACIE, E. W. R. Atomic and free radical reactions. 2nd ed. Reinhold Publishing Corporation, New York. 1954.
21. WALSH, A. D. Trans. Faraday Soc. 43: 305. 1947.

POLYMERIZATION OF 2-FLUOROBUTADIENE-1,3 AND PROPERTIES OF POLYMERS[1]

By R. J. Orr and H. Leverne Williams

ABSTRACT

Fluorobutadiene has been copolymerized with styrene in emulsion at 5°C. The rate of mercaptan consumption, rate of conversion, copolymer composition, and the intrinsic viscosity of the copolymer have been measured. Reactivity ratios and regulating indices were calculated for this temperature. Copolymerization reactions at 50°C. were studied in solution, and the reactivity ratios calculated. These were, for the following monomers as monomer 2: styrene at 5°C., $r_1 = 1.61 \pm 0.24$ and $r_2 = 0.16 \pm 0.08$; styrene at 50°C., $r_1 = 1.55 \pm 0.10$ and $r_2 = 0.50 \pm 0.10$; acrylonitrile at 50°C., $r_1 = 0.59 \pm 0.10$ and $r_2 = 0.07 \pm 0.03$; isoprene at 50°C., $r_1 = 2.05 \pm 0.19$ and $r_2 = 0.19 \pm 0.10$; α-methyl styrene at 50°C., $r_1 = 1.77 \pm 0.19$ and $r_2 = 0.38 \pm 0.11$; and methyl methacrylate at 50°C., $r_1 = 1.54 \pm 0.08$ and $r_2 = 0.64 \pm 0.08$. Polyfluorobutadiene has a cohesive energy density of 90–100 cal./cc., a second order transition point of −62.5°C., and some units formed by 1,2 or 3,4 addition.

INTRODUCTION

There are few data on the polymerization of 2-fluorobutadiene or on the physical properties of its polymers. The patent literature contains information on preparation of the polymers in emulsion and their properties (8, 9, 10, 16, 17, 18, 19, 24). Other papers have appeared summarizing the properties and preparations of the polymers (21, 33).

Fluorobutadiene lies between butadiene and chlorobutadiene in its properties. It polymerizes nearly as rapidly as chlorobutadiene, but unlike the latter copolymerizes with many monomers readily. Homopolymers have been found to be resistant to crystallization on stretching but require reinforcement for development of high tensile properties. Methods of synthesis of the monomer have been reported in a number of patents (2, 11, 12, 25, 26, 27, 28, 29).

EXPERIMENTAL RESULTS

Copolymerization Rates

The rate of conversion was measured as a function of monomer ratio for copolymerization with styrene at 5°C.; the results are given in Table I. The conversion rate is unaffected by the per cent diene in the charge. The time–conversion relation is quite linear, showing a rate of conversion considerably more rapid than during the polymerization of butadiene.

Chain Transfer Reactions

The intrinsic viscosities of the polymers prepared to different conversions, from various charge ratios and mercaptan contents, were measured in benzene and ethylene dichloride. The mercaptan used was a mixture of tertiary mercaptans of an average molecular weight 220. The data are in Table II. The disappearance of mercaptan (RSH) over the course of the polymerization was determined by amperometric titration. The results are in Table III.

[1]*Manuscript received April 6, 1955.*

Contribution from Research and Development Division, Polymer Corporation Limited, Sarnia, Ontario, Canada.

Study conducted under Defence Research Board Grant X-9, Project D4-75-50-01. Presented at the Sixth Canadian High Polymer Forum, St. Catharines, Ontario, April, 1955.

TABLE I

CONVERSION RATES FOR STYRENE–FLUOROBUTADIENE COPOLYMERIZATION

% Diene in charge	Hours	% Conversion
100	3.75	43
78	1.00	11
	2.50	40
60	1.00	18
	1.50	26
	2.25	36
	3.25	49
20	1.00	10
	3.00	40

TABLE II

INTRINSIC VISCOSITIES OF FLUOROBUTADIENE POLYMERS AND COPOLYMERS

% Diene in charge	Mercaptan parts	% Conv.	Solvent	$[\eta]$
100	0	18	Ethylene dichloride	0.49
		23		0.50
		30		0.49
		36		0.67
		38		0.50
		45		0.50
		48		0.84
		58		0.43
		43		0.3
	0.9	46		0.6
	2.0	40		0.7
78	2.3	18	Benzene	0.90
		34		0.88
		48		0.65
60	2.3	21		0.80
		38		0.79
		49		0.80
20	2.3	14		0.4
		36		1.0
		42		0.7

TABLE III

MERCAPTAN DISAPPEARANCE IN STYRENE–FLUOROBUTADIENE COPOLYMERIZATION

% Diene	% Conversion	$[RSH]/[RSH]_0$
78	18	0.79
	34	0.31
	48	0.36
60	21	0.85
	38	0.61
	49	0.33

Polymer Compositions from Emulsion and Solution Polymerizations

Polymers from polymerizations in emulsion and solution, at 5° and 50°C. respectively, were analyzed for per cent diene.

Styrene was the comonomer at 5°C. and the comonomers at 50°C. were styrene, acrylonitrile, isoprene, α-methyl styrene, and methyl methacrylate.

The emulsion polymers were obtained at varying conversions. The polymers prepared in solution were as low conversion as possible. The results of the analyses are in Table IV.

TABLE IV

POLYMER COMPOSITIONS FOR FLUOROBUTADIENE (M_1) COPOLYMERS

Weight % M_1 in initial monomer		% Conv.	Weight % diene	Weight % diene at 0 % conv. (calc.)
78	M_2 = styrene at 5°C.	33	87.5	87.2
		47	87.0	
60		11	72.0	72.5
		15	71.5	
		38	73.0	
		49	73.0	
30		6.5	53.5	53.5
		30	53.5	
		50	51.2	
20		14	41.0	41.0
		36	33.0	
		42	31.0	
60	M_2 = styrene at 50°C.	<3	73.9	75.3
		<3	74.6	
		<3	78.6	
50		<3	62.2	61.3
		<3	60.5	
40		<3	55.8	52.7
		<3	48.1	
20		<4	38.0	37.4
		<4	36.8	
68	M_2 = α-methyl styrene at 50°C.	6.36	81.9	80.0
		13.78	78.0	
52		2.66	67.9	68.5
		11.37	69.0	
36		2.20	47.9	50.8
		8.55	43.8	
20		1.19	31.2	36.0
		5.28	40.6	
68	M_2 = methyl methacrylate at 50°C.	8.12	76.2	78.1
		11.60	80.0	
52		10.17	50.3	56.9
		11.23	63.5	
36		9.97	48.2	49.5
		15.27	50.8	
20		15.60	20.5	27.3
		17.36	34.2	
68	M_2 = isoprene at 50°C.	<4	85.7	83.8
		12.7	81.9	
52		6.8	73.7	73.7
36		5.3	65.2	65.2
20		<4	38.4	40.8
		<4	43.2	
60	M_2 = acrylo-nitrile at 50°C.	4.7	67.6	67.6
50		2.3	63.6	63.6
40		5.0	61.1	61.1
20		6.9	50.4	50.4

Effect of Solvents on Vulcanized Polyfluorobutadiene

The tendency of this polymer to swell in a series of solvents of varying cohesive energy densities was determined. The per cent swell was determined by soaking a strip of the rubber in the solvent and determining the weight increase. The equilibrium weight was used to determine the amount of swelling.

Some of the cohesive energy density values were taken from publications (14, 31). Those unavailable were calculated from the relation c.e.d. $= \Delta H_{vap} - RT$. In Table V are given the results.

TABLE V

SWELL BEHAVIOR OF VULCANIZED POLYFLUOROBUTADIENE

Solvent	c.e.d. (Ref.)	% Swell
Toluene	80 (14)	115
Benzene	82 (14)	110
Methyl ethyl ketone	86	93
Ethylene dichloride	96	219
Carbon disulphide	97	134
Acetone	100 (14)	110
Pyridine	100 (31)	203
Dioxane	100 (14)	199
Dimethyl formamide	140 (31)	100
Nitromethane	160 (31)	183

Second Order Transition Temperature

This was determined by a dilatometric method as being −62.5°C. There was no evidence of crystallization at this temperature.

Infrared Spectra of Polyfluorobutadiene

All infrared spectroscopic work had to be done on the solid films since the polymers were insoluble in carbon disulphide. No quantitative conclusions were possible but qualitative results could be obtained. In Fig. 1 are curves for polyfluoro- and polychloro-butadiene. These are compared with the spectra of polybromoprene (20). Since all spectra were determined in polyethylene, no data were obtained below 7.8 microns where polyethylene begins to interfere.

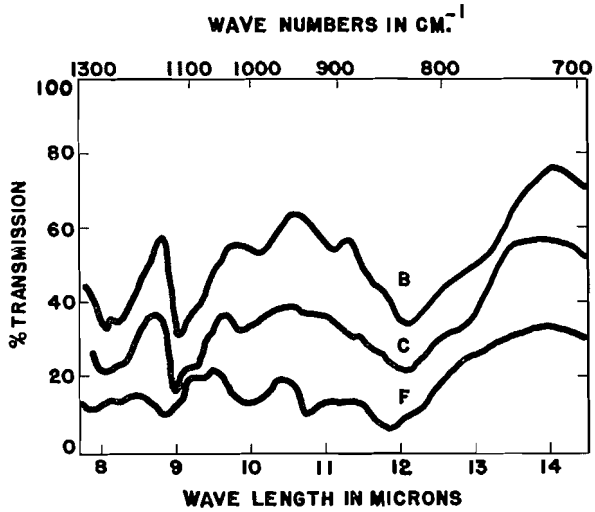

FIG. 1. Infrared spectra of polyfluorobutadiene (F), polychlorobutadiene (C), and polybromobutadiene (B).

DISCUSSION

Emulsion Polymerizations

Emulsion copolymerization rates are quite rapid compared to butadiene (3, 6) indicating either efficient utilization of initiating radicals or a high solubilization of monomers by soap. The independence of rate with per cent fluorobutadiene in the charge suggests polymerization rates similar to those of styrene. The low intrinsic viscosities of the polymers may be due to low molecular weight, a highly gelled polymer, or an improper choice of solvent. Since the values did not change markedly for measurements using two liquids of a different cohesive energy density, the choice of solvent could not have been responsible. There seems little possibility that the polymers were gelled since the intrinsic viscosity of polyfluorobutadiene prepared in the absence of mercaptan did not show the peak characteristic of gelation, even at very low conversion. The low intrinsic viscosities must be characteristic of low molecular weights due to chain transfer reactions. These cannot be due to mercaptan since the intrinsic viscosity is independent of the mercaptan content of the original charge. Either the fluorobutadiene itself, or some impurity difficult to remove, such as difluorobutene, must be responsible. The mercaptan does react during polymerization at a rate indicating the same reactivity toward the fluorobutadienyl radical as toward butadienyl (6). If this reaction is first order with respect to mercaptan over the first part of the reaction, the regulating indices would be 1.8 and 0.6 for 78/22 and 60/40 fluorobutadiene–styrene charge ratios respectively.

Structure of Polyfluorobutadiene

The dominant band in the spectra near 12 microns must be due to the C–H on the CH=CF group. This completely obscures that portion of the spectra which would give a measure of the proportion of *cis* 1,4 addition (by analogy with the spectrum of Hevea). Some 1,2 or 3,4 addition is indicated by the band at 10.75 microns. This is different from polychlorobutadiene which is 100% 1,4 (20).

Solubility of Polyfluorobutadiene

One method of determining the cohesive energy density (c.e.d.) of a polymer is to find the liquid in which the swelling of the vulcanized polymer is a maximum (31). From the data in Table V, the cohesive energy density of polyfluorobutadiene was estimated as 90–100 cal./cc. Acetone and nitromethane gave anomalous results. The cohesive energy density is of the order of that for polyvinyl chloride and is larger than the value for polychlorobutadiene and 75/25 butadiene–acrylonitrile copolymers. Fluorine changed the cohesive energy density of the polymer in the same direction but to a greater extent than did chlorine. This does not correlate well with the low values obtained with other fluorine containing polymers (31). The structure of the polymer chain may affect the part that fluorine plays in determining the cohesive energy density.

Reactivity Ratios of Fluorobutadiene in Copolymerization

The reacted monomer data from the emulsion polymerizations were extra-

polated to zero conversion. Solution polymerizations were stopped at low conversions and the polymer composition assumed to be identical with that formed at zero conversion. These values, with the corresponding charge ratio, were substituted in the copolymerization equation, the r_1–r_2 lines calculated, and the values of r_1 and r_2 determined. The error was estimated from the size of the triangle of intersection. A typical r_1–r_2 plot is shown in Fig. 2. In Table VI are the values which were determined.

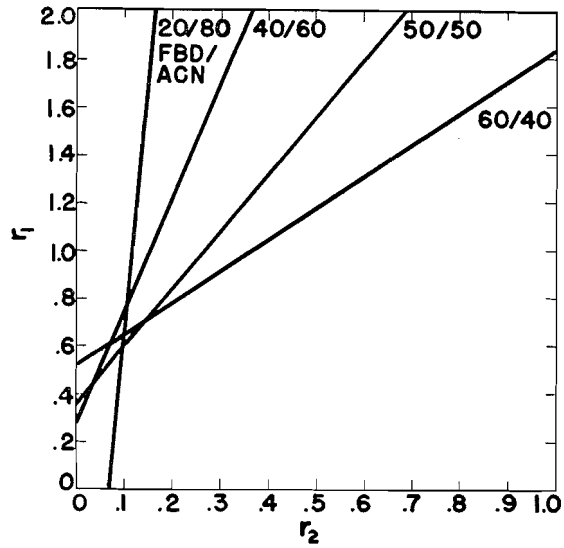

FIG. 2. r_1–r_2 lines for fluorobutadiene–acrylonitrile copolymerization at 50°C.

TABLE VI

REACTIVITY RATIOS OF FLUOROBUTADIENE WITH COMONOMERS

Comonomer (M_2)	T (°C.)	r_1	r_2	$r_1 \times r_2$
Styrene	5	1.61±0.24	0.16±0.08	0.26
Styrene	50	1.55±0.10	0.50±0.10	0.78
Acrylonitrile	50	0.59±0.10	0.07±0.03	0.04
Isoprene	50	2.05±0.19	0.19±0.10	0.39
Alpha methyl styrene	50	1.77±0.19	0.38±0.11	0.67
Methyl methacrylate	50	1.54±0.8	0.64±0.08	0.99

The influence of temperature on r_2 seems much more pronounced than on r_1. There is a strong tendency to alternate in the copolymers, reaching a maximum with acrylonitrile and a minimum with methyl methacrylate. The ratio of r_1 and r_2 indicates a general tendency to enter the copolymer more rapidly than the comonomer.

The Q and e Values of Fluorobutadiene

These values were calculated from the Alfrey-Price equation and are in Table VII. The values for fluorobutadiene were determined using styrene as the primary standard with $Q = 1.0$ and $e = -0.8$. Those for the other comonomers were determined using the fluorobutadiene as a secondary standard.

TABLE VII

Q AND e VALUES FOR FLUOROBUTADIENE AND THE COMONOMERS

Monomer	T (°C.)	Q	e
Fluorobutadiene	5	1.39	+0.36
Fluorobutadiene	50	1.32	−0.30
Methyl methacrylate	50	0.85	−0.30
Acrylonitrile	50	2.5	+1.5
Isoprene	50	0.86	−1.27
Alpha methyl styrene	50	0.98	−0.93

Agreement with the values reported previously (1) is within experimental error except for the e value of methyl methacrylate which was reported as 0.4. The Q and e values for isoprene at 50°C. were not previously reported but the deviation from butadiene at this temperature is in accord with that observed at −18°C. (22, 23).

It is of interest to compare the relative effects of chlorine and fluorine substitution on the polarity of the double bond and the resonance stabilization of the dienyl free radical. The reactivity ratios for chlorobutadiene have been reported as $r_1 = 3.41$, $r_2 = 0.59$ for butadiene and $r_1 = 3.65$, $r_2 = 0.133$ for isoprene (chlorobutadiene being monomer-1) at 50°C. (30). Using butadiene as a secondary standard with $Q = 1.33$ and $e = -0.8$, then Q and e for chlorobutadiene are 1.5 and −0.24 respectively. It may be seen that the change in Q and e caused by the substitution of the fluorine group is in the same direction, but not as pronounced as it was for the chlorine. Fluorobutadienyl radical is less resonance stabilized and the double bond of the monomer is poorer in electrons than that of the chlorobutadiene.

EXPERIMENTAL METHODS

The recipe was similar to one developed previously for butadiene copolymerization (6) and is:

Monomers	100 parts by weight, active material
Water	180
Potassium fatty acid soap flakes	5.0
Mixed tertiary mercaptans	Variable
Cumene hydroperoxide	0.10
Ferrous sulphate heptahydrate	0.14
Potassium pyrophosphate	0.177

An emulsion of ditertiary butyl hydroquinone was used as the stopping agent.

Fluorobutadiene was prepared by the Defence Research Chemical Laboratory through the courtesy of Dr. H. Sheffer. It was subjected to simple distillation before use. Other monomers were commercial materials which were fractionated, taking the center fraction. All polymerization chemicals were standard Commercial grade. Analytical reagents were C.P. grade.

The mercaptan in the latex was determined by amperometric titration (13). Intrinsic viscosities were measured at 30.0°C. by dissolving the latex directly in an 80:20 benzene–ethanol or ethylene dichloride – ethanol solution. Dilutions were made with pure benzene (or ethylene dichloride) so that intrinsic viscosities could be calculated (4, 7, 15).

The polyfluorobutadiene was synthesized at 5°C., coagulated in brine acid, stabilized with BLE, compounded in the test recipe, and vulcanized. Swelling indices were done on the vulcanized stock. Second order transition points were determined on uncured samples by a dilatometric technique. Polymers were purified for analysis by swelling in benzene and extracting in methanol.

A normal Parr bomb combustion using 50 mgm. polymer, 15 gm. sodium peroxide, and 0.5 gm. benzoic acid was used. The ignition was electrical and it was found that the position of the fuse wire in respect to the top of the combustion mixture was critical. Potassium perchlorate was omitted from the combustion mixture since it was found to have a deleterious effect in the subsequent colorimetric analysis for fluoride ion.

Fluoride was determined on aliquots of the solution containing the soluble combustion products by the extent of bleaching brought about by the addition of fluoride ions to a ferric thiocyanate solution (5, 32). The amount of bleaching is definite and reproducible but not a linear function of fluoride ion concentration. There is a slow but distinct decrease in the colorimeter reading with time and the color varies considerably with pH. The combustion mixture was brought to pH = 7.0 with nitric acid and further adjusted to 2.0 with hydrochloric acid. The method was standardized against sodium fluoride solution with readings taken on a Klett-Summerson colorimeter and a Beckman DU ultraviolet spectrophotometer set at 4900 Å wavelength. Analysis of polyfluorobutadiene indicated complete recovery and identification of organic fluorine.

ACKNOWLEDGMENT

Mr. G. Turner (Polymer Corporation Limited) measured and interpreted the infrared spectra. Dr. L. Breitman determined the second order transition temperature. Messrs. S. J. Butler and C. Freeman assisted with the work. The authors appreciate the permission to publish this paper extended by the Defence Research Board and Polymer Corporation Limited.

REFERENCES

1. ALFREY, T. and PRICE, C. C. J. Polymer Sci. 2: 101. 1947.
2. COFFMAN, D. D. and SALISBURY, L. F. (duPont) U.S. Patent No. 2,451,612. Oct. 19, 1948.
3. EMBREE, W. H., SPOLSKY, R., and WILLIAMS, H. L. Ind. Eng. Chem. 43: 2553. 1951.
4. FORDHAM, J. W. L., O'NEIL, A. N., and WILLIAMS, H. L. Can. J. Research, F, 27: 119. 1949.
5. FOSTER, M. D. Ind. Eng. Chem. Anal. Ed. 5: 234. 1933.
6. GILBERT, R. D. and WILLIAMS, H. L. J. Am. Chem. Soc. 74: 4114. 1952.
7. HENDERSON, D. A. and LEGGE, N. R. Can. J. Research, B, 27: 666. 1949.
8. HILL, F. B., Jr. (duPont) U.S. Patent No. 2,436,213. Feb. 17, 1948.
9. HILL, F. B., Jr. (duPont) Can. Patent No. 459,661. Sept. 13, 1949.
10. IMPERIAL CHEM. INDUSTRIES Brit. Patent No. 591,086. Aug. 6, 1947.
11. IMPERIAL CHEM. INDUSTRIES Brit. Patent No. 603,855. June 24, 1948.
12. JOHNSON, F. W. (duPont) U.S. Patent No. 2,398,181. April 9, 1946.
13. KOLTHOFF, I. M. and HARRIS, W. E. Ind. Eng. Chem. Anal. Ed. 18: 161. 1949.
14. MARK, H. and TOBOLSKY, A. V. Physical chemistry of high polymeric systems. Vol. 2. Interscience Publishers, Inc., New York. 1940. p.261.
15. MITCHELL, J. M. and WILLIAMS, H. L. Can. J. Research, F, 27: 35. 1949.
16. MOCHEL, W. E. (duPont) U.S. Patent No. 2,426,560. Aug. 26, 1947.
17. MOCHEL, W. E. (duPont) U.S. Patent No. 2,429,838. Oct. 28, 1947.
18. MOCHEL, W. E. (duPont) U.S. Patent No. 2,446,382. Aug. 3, 1948.
19. MOCHEL, W. E. (duPont) Can. Patent No. 459,955. Sept. 27, 1949.

20. MOCHEL, W. E. and HALL, M. B. J. Am. Chem. Soc. 71: 4082. 1949.
21. MOCHEL, W. E., SALISBURY, L. F., BARNET, A. L., COFFMAN, D. D., and MIGHTON, C. J. Ind. Eng. Chem. 40: 2285. 1948.
22. ORR, R. J. and WILLIAMS, H. L. Can. J. Chem. 29: 270. 1951.
23. ORR, R. J. and WILLIAMS, H. L. Can. J. Chem. 30: 108. 1952.
24. SALISBURY, L. F. (duPont) U.S. Patent No. 2,416,456. Feb. 25, 1947.
25. SALISBURY, L. F. (duPont) U.S. Patent No. 2,426,792. Sept. 2, 1947.
26. SALISBURY, L. F. (duPont) U.S. Patent No. 2,437,307. Mar. 9, 1948.
27. SALISBURY, L. F. (duPont) U.S. Patent No. 2,437,308. Mar. 9, 1948.
28. SALISBURY, L. F. (duPont) U.S. Patent No. 2,469,948. May 10, 1949.
29. SALISBURY, L. F. (duPont) U.S. Patent No. 2,519,199. Aug. 14, 1950.
30. SIMHA, R. and WALL, L. A. J. Research Natl. Bur. Standards, 41: 521. 1948.
31. SMALL, P. A. J. Appl. Chem. (London), 3: 71. 1953.
32. SMITH, H. V. Ind. Eng. Chem. Anal. Ed. 7: 23. 1935.
33. STARKWEATHER, H. W., BARE, P. O., CARTER, A. S., HILL, F. B., Jr., HURKA, V. R., MIGHTON, C. J., SANDERS, R. A., WALKER, H. W., and YOUKER, M. A. Ind. Eng. Chem. 39: 210. 1947.

STUDIES ON THE HETEROGENEITY OF CARRAGEENIN[1]

By David B. Smith,[2] A. N. O'Neill,[3] and A. S. Perlin[2,4]

ABSTRACT

The carbohydrate residues in κ-carrageenin are 3,6-anhydro-D-galactose and D-galactose which are present in nearly equal amounts. Tests following fractional precipitation of κ-carrageenin indicate general chemical homogeneity but physical heterogeneity. κ-Carrageenin is not susceptible to oxidation with periodate. Fractional precipitation of λ-carrageenin separates a main fraction which contains only D-galactose and a trace of 3,6-anhydro-D-galactose. This polysaccharide is susceptible to periodate oxidation. It is polydisperse on a mass basis. Materials containing glucose, xylose, and L-galactose segregate into minor fractions of λ-carrageenin and hence cannot be integral parts of the principal polysaccharides of carrageenin. L-Galactose has been isolated from carrageenin by a simple procedure.

Carrageenin is the polysaccharide complex which is extracted with water from certain red seaweeds, in particular, *Chondrus crispus* and *Gigartina stellata* (26). D-Galactose comprises about two-thirds of the organic matter. The principal remaining organic constituent is 3,6-anhydro-D-galactose recently identified by O'Neill (17, 18). The presence of small amounts of glucose, pentose, and L-galactose has been established (2, 13). Carrageenin contains also about 30% of monoesterified sulphuric acid and consequently, in neutral solution, exists as a salt.

Chemical evidence (4, 13, 15) bearing on the structure of carrageenin has usually been interpreted on the basis of a monotypical substance though the possibility of greater complexity has been admitted (13). Differences in degree of gel formation and other properties among fractions obtained by extraction at successively higher temperatures (7, 9, 10, 20) have been taken to indicate different polysaccharides. However, the principal chemical difference reported in the earlier literature has been in cation ratios and it has been suggested that the polysaccharides are otherwise essentially identical (2).

The development of a new method of fractionation (23) based on the gelatinizing effect of potassium ions on carrageenin has opened a new approach to the structure of this material. This fractionation, provided it is performed on sufficiently dilute carrageenin solutions, permits a sharp separation into potassium-sensitive material which is precipitated by potassium ions and potassium-insensitive material which remains in solution (23, 24).

This paper describes some analytical and physical characterization of subfractions of these two materials. The suggestion made previously (24) that the potassium-sensitive fraction (κ-carrageenin) would be more chemically homogeneous than the potassium-insensitive material (λ-carrageenin) is confirmed.

[1]*Manuscript received May 11, 1955.*
Contribution from the National Research Laboratories, Ottawa, Canada. Issued as N.R.C. No. 3666.
[2]*Division of Applied Biology, National Research Council, Ottawa, Canada.*
[3]*Maritime Regional Laboratory, National Research Council, Halifax, Nova Scotia.*
[4]*Present address: Prairie Regional Laboratory, National Research Council, Saskatoon, Saskatchewan.*

MATERIALS AND METHODS

Preparation of Carrageenin and Its κ- and λ-Components

Dried *Chondrus crispus* was ground coarsely, washed briefly with cold water, and extracted in 1% suspension for one hour at 90°C. in water containing 0.2% NaCl and 0.1% Na_2CO_3. Insoluble material was filtered out and re-extracted for one hour at 90°C. using one-third the first volume of extractant. The combined extracts were dialyzed against several changes of 0.2 *M* NaCl to remove ions other than Na^+. The dialyzed solution was clarified by centrifugation at 2000 *g*. The carrageenin was precipitated from a portion of this solution with three volumes 95% ethanol and was washed and dried with ethanol and ether. This sample was designated CL3.

The remaining carrageenin solution was diluted with water to 0.24% solids. Solid KCl was added slowly with stirring to a concentration of 0.25 *M*. The crude κ-carrageenin precipitate was separated by centrifugation at 2000 *g*. The precipitate was dialyzed first against 0.1 *M* NaCl to remove potassium ions and then against water to remove NaCl. The κ-carrageenin dissolved and was diluted to about 0.2%. Potassium chloride was added to 0.25 *M* and the κ-carrageenin again separated by centrifugation. Dialysis with solution of the κ-carrageenin and its reprecipitation were repeated once more. The final κ-carrageenin precipitate was suspended in 0.5 *M* NaCl, dialyzed free of potassium ions, and precipitated with three volumes of ethanol. After the precipitate was washed free of chloride ion with 80% ethanol followed by absolute ethanol and ether, it was dried over $CaCl_2$. This sodium κ-carrageenate preparation was designated CL3 κ-1.

The supernatants from the foregoing centrifugations (with the exception of the last which contained a negligible amount of polysaccharide) were combined and evaporated at 35°C. to one-tenth the initial volume. The λ-carrageenin (CL3 λ-1) was precipitated from this solution, and washed and dried in the same manner as the previous preparations.

Fractionation of κ- and λ-Carrageenins

κ-Carrageenin (CL3 κ-1) was fractionated by precipitation from dilute solution (0.2% in 0.25 *M* NaCl) by the graded addition of ethanol at 20–25°C. The precipitate was removed after each addition of ethanol by centrifugation. The fractions were washed free of chloride ion and dried over $CaCl_2$ after absolute ethanol and ether washes. The ethanol concentration ranges used for fractionation and the yields obtained are shown in Table I. (Considerable loss of material, particularly of Fraction 2*a*, attended the first fractionation.)

The fractionation of λ-carrageenin (preparation C5 λ-2) has been described before (24). Particulars and yields are reproduced, for reference, in Table I.

Physical Measurements

Viscosity at 25°C. and sedimentation rates were measured in the manner already described (24). For extrapolation of the sedimentation results to zero concentration the method of Newman, Loeb, and Conrad (16) was used.

TABLE I

SUBFRACTIONATION OF CARRAGEENIN FRACTIONS

Fractionation No.	Fraction obtained	Ethanol concentration range, %	Yield (% of original sample)
1	CL3 κ-1 Fr. 1*a*	0–30	2
	Fr. 2*a*	30–45	35
	Fr. 3*a*	45–75	16
2	CL3 κ-1 Fr. 1*b*	0–35	4
	Fr. 2*b*	35–45	64
	Fr. 3*b*	45–75	25
3	C5 λ-2 Fr. 1	0–12	1.4
	Fr. 2	12–24	2
	Fr. 3	24–36	62
	Fr. 4	36–48	11
	Fr. 5	48–60	1.4

Analytical Methods

Sulphate was determined after refluxing for 24 hr. in 0.5 *N* HCl followed, after tenfold dilution, by precipitation as $BaSO_4$.

For chromatographic analyses, samples (1% in 0.5 *N* H_2SO_4) were hydrolyzed in sealed tubes for 10–15 hr. on a boiling water bath. After neutralization of the hydrolyzates with $BaCO_3$ and filtration, the filtrates were examined by descending paper chromatography (12, 19). For quantitative chromatographic analysis, the method of Flood *et al.* (5) was used. Isolation of galactose as the crystalline α-methyl-α-phenylhydrazone was also employed for galactose estimation.

L-Galactose was taken to be the galactose remaining after treatment of the neutral hydrolyzate with a suspension of a galactose fermenting yeast, *Saccharomyces cerevisae*, strain N.R.C. No. 824, (16 hr. culture from D-galactose agar) at 37°C. for 3.5 hr. The activity of the culture was simultaneously tested with a 1% solution of D-galactose. After incubation, the yeast, together with added charcoal, was separated by centrifugation and the supernatant liquor examined on the chromatogram. D-Galactose was completely fermented as was glucose, but xylose was unaffected.

3,6-Anhydro-D-galactose cannot be determined directly because of its instability during acid hydrolysis. The following procedure takes advantage of its degradation under such conditions to 5-hydroxymethyl-2-furaldehyde which can be determined spectrophotometrically. Samples (25 mgm.) were weighed into tubes containing 2 ml. 0.15 *N* H_2SO_4. After they were sealed, the tubes were placed in a bath at 100°C. At intervals tubes were removed, their contents neutralized with $BaCO_3$ and filtered quantitatively into 10 ml. volumetric flasks which were made to volume. The optical densities at 2850 Å (the characteristic absorption maximum for 5-hydroxymethyl-2-furaldehyde) were determined on suitable dilutions. Since 5-hydroxymethyl-2-furaldehyde undergoes a first order decomposition under the above conditions to formic and levulinic acids (25), the logarithms of the optical densities were plotted against time and the curves extrapolated to zero time (Fig. 1). From these extrapolated values and the molar extinction coefficient (16,500) of 5-hydroxymethyl-2-furaldehyde, the initial amounts of the latter were estimated and recalculated as 3,6-anhydro-D-galactose.

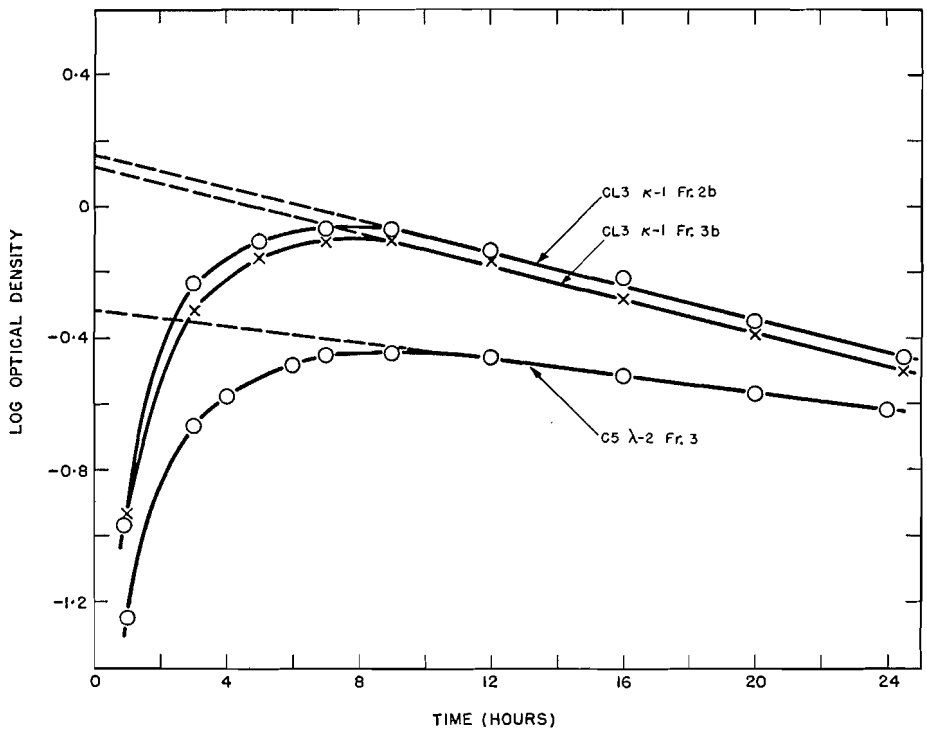

FIG. 1. Course of the formation and disappearance of 5-hydroxymethyl-2-furaldehyde.

Isolation and Identification of L-*Galactose*

Carrageenin (sample C5 (24), 8 gm.) was hydrolyzed in 800 ml. 0.3 N H_2SO_4 for four hours at 100°C. The hydrolyzate was neutralized with $BaCO_3$, decolorized with charcoal, and incubated at 37°C. for four hours with a suspension of *S. cerevisae* cells (strain N.R.C. No. 824) from a 16 hr. culture in D-galactose broth. After the cells were precipitated with charcoal and the solution concentrated, the sirup (1.3 gm.) was chromatographed on a cellulose column using *n*-butanol saturated with water as the developing solvent (11). Those portions of the eluate containing galactose were combined and dried *in vacuo* at 50°C. The residue (0.11 gm.) was extracted with water and the extract was incubated with yeast cells, as above. The product recovered from this second fermentation by extraction into alcohol readily crystallized in the cold. Amount obtained was 0.09 gm., m.p. 162–163°C. Two recrystallizations raised the melting point to 167°C. The X-ray powder diagram was identical with that of D-galactose, but the optical rotation was negative, $[\alpha]_D^{27}$ −96° (15 min.) → −76° (eqm.) (*c* 2.0, water). This product was, therefore, α-L-galactose.

Oxidation with Periodate

Samples (100 mgm.) of carrageenin fractions were dissolved in 25 ml. water (solution was neutral to methyl red) at 16.6°C. and 250 mgm. sodium metaperiodate was added. Formic acid was estimated on aliquots removed from

the reaction mixture at intervals by titration in the presence of potassium iodide with thiosulphate after the addition of excess ethylene glycol. Periodate consumption was measured iodometrically on similar aliquots after the addition of sodium bicarbonate, arsenite, and potassium iodide (8).

RESULTS AND DISCUSSION

Paper chromatograms of hydrolyzates of κ-carrageenin showed only two principal components, identified as galactose and 5-hydroxymethyl-2-furaldehyde. The latter has been shown to be a decomposition product of 3,6-anhydro-D-galactose which can be isolated from κ-carrageenin as the crystalline diethylmercaptal obtained after mercaptolysis of the polysaccharide (17, 18). A trace of xylose could also be detected.

Chromatography of hydrolyzates of λ-carrageenin revealed galactose as the main component, lesser amounts of glucose and xylose, and only a trace of 5-hydroxymethyl-2-furaldehyde. Examination of the fractions of λ-carrageenin indicated that Fraction 3 contained predominantly galactose with a trace of 5-hydroxymethyl-2-furaldehyde, that Fraction 4 contained mostly galactose but also glucose and xylose, and that Fraction 5 also contained these three sugars but that galactose had become a minor constituent. Fraction 5 gave a red color with iodine. These results suggest that xylose and glucose polymers are not integral components of carrageenin but represent small amounts of xylan and floridean starch coextracted by the isolation procedure. From this point of view, the trace of xylose found in κ-carrageenin could also be ascribed to contamination.

A small proportion of the galactose residues in carrageenin was reported by Johnson and Percival (13) to consist of L-galactose. In the present study, however, it became evident that the component containing L-galactose was separable by fractional precipitation from the D-galactose polymers which comprise the bulk of carrageenin. After fermentation with a yeast strain capable of utilizing D-galactose, a reference solution of D-galactose and a hydrolyzate of κ-carrageenin were found to contain no galactose, a hydrolyzate of C5 λ-2 Fraction 3 showed only a trace of galactose, but hydrolyzates of C5 λ-2 Fractions 4 and 5 gave strong tests for galactose. The "tail" fractions of λ-carrageenin thus account for most of the L-galactose. This sugar therefore is not associated with the polysaccharides which make up the greater part of carrageenin.

The validity of these fermentation tests was assessed by the isolation of L-galactose from the nonfermented residue of a large-scale fermentation. Although the yield of L-galactose was low (about 2% of the sugars present in carrageenin), the availability of the starting material and the ease of isolation of the L-galactose make carrageenin a ready source of this rare sugar. May and Weinland (14) have recently isolated L-galactose from snail galactogen by a similar procedure.

After 220 hr. reaction time, there was no detectable consumption of periodate by κ-carrageenin. This result conforms with the formulation of κ-carrageenin as consisting of D-galactose-4-sulphate residues glycosidically linked through

carbon atoms 1 and 3 (2) and with the presence of 3,6-anhydro-D-galactose residues (17, 18). The possibility of branching (1, 4, 13) is not precluded, but the terminal units of such branches must be 3,6-anhydro-D-galactose since end units of D-galactose-4-sulphate would consume periodate at the 2,3-glycol configuration. The lack of effect of periodate on κ-carrageenin is in agreement with the previous finding (23) that after treatment of whole carrageenin with sodium periodate, the κ-fraction could still be precipitated by potassium chloride.

In a parallel experiment, the main fraction of λ-carrageenin (C5 λ-2 Fr. 3) consumed, per mole of sugar residue, 0.30 moles of periodate in 165 hr. and 0.31 moles in 220 hr. At the same reaction times 0.12 and 0.13 moles respectively of formic acid were produced. Since, therefore, one unit in five must have at least one free diol group and one unit in eight, a free triol group, this fraction cannot consist only of a chain of 1,3-linked D-galactose-4-sulphate residues. A model involving branching could account for the periodate consumption with some residues unesterified. It would be necessary that some of the latter be end groups to yield formic acid. Johnson and Percival (13) and Dillon and O'Colla (4) have presented evidence of branching from methylation studies.

The reaction of C5 λ-2 Fraction 3 with periodate raises doubts about the use of this oxidant in the method whereby Dillon and O'Colla (4) "purified" carrageenin. These workers ascribed the consumption of periodate to oxidation of floridean starch and cellulose. Fraction 3 contained neither of these materials.

The results of analyses of some of these carrageenin preparations are given in Table II. Though the sum of the residues found totals only about 90% in

TABLE II

ANALYTICAL RESULTS

Material	Galactose, %	3,6-Anhydro-D-galactose, %	SO_3Na, %	Total recovery, %	Molar ratio, galactose / SO_3Na
CL3 κ-1	38.1	24.0	28.2	90.3	1.03
CL3 κ-1 Fr. 2*b*	35.0	28.1	28.1	91.2	0.95
CL3 κ-1 Fr. 3*b*	—	25.9	28.8	—	—
C5 λ-2 Fr. 3	46.3	1.8	37.9	89.4[a]	0.90

[a]*Contains 3.4% of contaminating NaCl.*

both the κ-carrageenin and the principal fraction of λ-carrageenin, this discrepancy is believed to represent the sum of determination errors since, with the exception of a trace of xylose in the κ-carrageenin preparation, no components other than those listed could be found. The content of 3,6-anhydro-D-galactose is much lower in the principal fraction of λ-carrageenin than in κ-carrageenin while the galactose content is higher. The slightly smaller amount of 3,6-anhydro-D-galactose found in unfractionated κ-carrageenin compared with the mean content of its two major subfractions suggests that the small first fraction may be low in the anhydro sugar. Unfortunately

insufficient amounts of the first fraction were available for analysis. The amount of sulphate nearly parallels the galactose content with molar ratios of galactose to sulphate of about unity with κ-carrageenin and about 0.9 with λ-carrageenin. The sulphate contents recorded in Table II confirm those reported earlier (23).

The results of viscosity and sedimentation rate measurements on carrageenin preparation CL3, its κ-component, and the fractions of the κ-carrageenin are shown in Table III. Also included are molecular weights computed using a random coil model by the Mandelkern–Flory equation and using an ellipsoid model by the Perrin and Simha equations (24).

TABLE III

VISCOSITY, SEDIMENTATION, AND MOLECULAR WEIGHT DETERMINATIONS

Material	$[\eta]$, dl./gm.	$S^{\circ}_{20} \times 10^{13}$ $c \rightarrow 0$	Mol. wt. $\times 10^{-5}$ (Mandelkern and Flory)	Mol. wt. $\times 10^{-5}$ (Perrin and Simha)
CL3	13.2±0.57	8.3	9.5	5.4
CL3 κ-1	12.6±0.78	7.2	7.5	4.3
CL3 κ-1 Fr. 1*a*	7.9±0.19	4.7	3.1	1.8
Fr. 2*a*	11.4±0.29	6.2	5.7	3.3
Fr. 3*a*	10.8±1.35	7.7	7.7	4.4
Fr. 1*b*	9.5±0.09	5.9	4.8	2.8
Fr. 2*b*	10.0±0.30	5.9	5.0	2.9
Fr. 3*b*	8.5±0.51	7.2	5.3	3.7

If the fractionation of the κ-carrageenin had been based solely on size, $[\eta]$, S, and M should have decreased as the mean alcohol concentration required for the precipitation of the fractions increased. However, this simple pattern, adhered to in the subfractionation of C5 λ-2 Fraction 3 (24), was not found in the fractionation of κ-carrageenin. Hence the differences in solubility responsible for the fractionation must reflect (besides size differences) differences in structure, composition, or both. Since the analytical data (Table II) suggest general similarity of composition, it is likely that the solubility differences may be partly explained by structural differences (varying degrees and types of branching).

CONCLUSIONS

Previous physical investigations of carrageenin and carrageenin extracts obtained at different temperatures by viscosity, sedimentation, diffusion, osmotic, and electrophoretic methods (3, 6, 7, 20, 21) have provided evidence that these materials are heterogeneous on a mass basis. Some of this heterogeneity is due to the differences between κ- and λ-carrageenins. However, both of these components, particularly λ-carrageenin (24), have been shown to be polydisperse.

The differences between κ- and λ-carrageenin in response to potassium and similar ions, in sulphate content, optical rotation (23), effect on milk viscosity (22), shape, and size (24), have a chemical basis in the greatly differing D-galactose: 3,6-anhydro-D-galactose ratios. Bayley (1) has used these compositional data in conjunction with measurements of intramolecular spacings from

X-ray diffraction studies to put forward a tentative explanation of the potassium sensitivity of κ-carrageenin.

Probably many of the differences in behavior between carrageenin extracts obtained at different temperatures are due to differing contents of κ- and λ-carrageenins (23). Other factors must include the average size and nature of the mass polydispersity of these components within the extracts, the chemical heterogeneity, and the cation content.

At the present stage in the investigation of the structure of carrageenin, two major and several minor components can be discerned.

1. One of these major components contains D-galactose and 3,6-anhydro-D-galactose residues in a ratio of approximately 1.4 : 1 together with about 25% esterified sulphate. Since fractionation studies have provided evidence of both mass and structural polydispersity, it is not inconceivable that considerable variation in the relative amounts of these residues may be found if the material is fractionated more narrowly. The greater part (perhaps all) of this component is aggregated or gelled by the addition of potassium ions. Though nearly all the material that may be precipitated from dilute (0.1%) aqueous solutions by potassium chloride is precipitated at 0.15 *M*, a small additional amount is precipitated between 0.15 *M* and 0.25 *M* (24). It may be that small quantities of this component are not readily precipitated by potassium ions and would consequently be left in the supernatant after centrifugation. The small amount of 3,6-anhydro-D-galactose found in C5 λ-2 Fraction 3 (Table II) may have arisen in this way.

The extension of the original definition of κ-carrageenin (23, 24) from the material affected by potassium ions to include all of the component consisting of D-galactose, considerable amounts of 3,6-anhydro-D-galactose, and esterified sulphate is proposed.

2. In the second major component of carrageenin, D-galactose together with about 35% esterified sulphate greatly predominates over the small amount of 3,6-anhydro-D-galactose which may be an impurity. It is suggested that the term λ-carrageenin, hitherto (24) referring to all the material not precipitable by potassium, be restricted to this polysaccharide.

3. Minor amounts of various polysaccharides are found in carrageenin preparations and may be regarded as impurities. On hydrolysis, these give rise to glucose (possibly from floridean starch), xylose (possibly from a xylan), and L-galactose.

The similarities between the two principal types (κ- and λ-carrageenins) suggest that intergrading material may exist. However, in those samples of carrageenin so far tested, the sharp fractionation achieved indicates that the amount of such intermediate material must be small.

ACKNOWLEDGMENTS

The authors wish to thank Dr. W. H. Cook for his interest and encouragement. They are also grateful to Dr. W. H. Barnes for an X-ray diffraction diagram, to Miss M. T. Clement for supplying yeast cultures, and to Messrs. J. Giroux, J. Labelle, and D. R. Muirhead for technical assistance.

REFERENCES

1. BAYLEY, S. T. Biochim. et Biophys. Acta. In press.
2. BUCHANAN, J., PERCIVAL, E. E., and PERCIVAL, E. G. V. J. Chem. Soc. 51. 1943.
3. COOK, W. H., ROSE, R. C., and COLVIN, J. R. Biochim. et Biophys. Acta, 8: 595. 1952.
4. DILLON, T. and O'COLLA, P. Proc. Roy. Irish Acad. 54: 51. 1951.
5. FLOOD, A. E., HIRST, E. L., and JONES, J. K. N. J. Chem. Soc. 1679. 1948.
6. GORING, D. A. I. J. Colloid Sci. 9: 141. 1954.
7. GORING, D. A. I. and YOUNG, E. G. Can. J. Chem. 33: 480. 1955.
8. GRANGAARD, D. H., GLADDING, E. K., and PURVES, C. B. Paper Trade J. 115 (No. 7): 41. 1942.
9. HAAS, P. and HILL, T. G. Ann. Appl. Biol. 7: 352. 1921.
10. HESS, M. P. and SIEHRS, A. E. U.S. Patent No. 2,462,398. 1949.
11. HOUGH, L., JONES, J. K. N., and WADMAN, W. H. J. Chem. Soc. 2511. 1949.
12. JERMYN, M. A. and ISHERWOOD, F. A. Biochem. J. (London), 44: 402. 1949.
13. JOHNSTON, R. and PERCIVAL, E. G. V. J. Chem. Soc. 1944. 1950.
14. MAY, F. and WEINLAND, H. Z. physiol. Chem. 296: 154. 1954.
15. MORI, T. Advances in Carbohydrate Chem. 8: 315. 1953.
16. NEWMAN, S., LOEB, L., and CONRAD, C. M. J. Polymer Sci. 10: 463. 1953.
17. O'NEILL, A. N. Abstracts of Papers. 126th meeting, Am. Chem. Soc. Sept. 1954. p. 9D.
18. O'NEILL, A. N. J. Am. Chem. Soc. 77: 2837. 1955.
19. PARTRIDGE, S. M. Nature, 158: 270. 1946.
20. ROSE, R. C. Can. J. Research, F, 28: 202. 1950.
21. ROSE, R. C. and COOK, W. H. Can. J. Research, F, 27: 323. 1949.
22. SMITH, D. B. Can. J. Technol. 31: 209. 1953.
23. SMITH, D. B. and COOK, W. H. Arch. Biochem. and Biophys. 45: 232. 1953.
24. SMITH, D. B., COOK, W. H., and NEAL, J. L. Arch. Biochem. and Biophys. 53: 192. 1954.
25. TEUNISSEN, H. P. Rec. trav. chim. 49: 784. 1930; 50: 1. 1931.
26. TSENG, C. K. Science, 101: 597. 1945.

SOME NEW REACTIONS AND DERIVATIVES OF KOJIC ACID[1]

By Andrew Beélik[2] and C. B. Purves

ABSTRACT

The stability of the ring structure in kojic acid toward various reagents was investigated. Cleavage to an open-chain, dienol derivative in *N* sodium hydroxide at 25°, or fragmentation of the structure, was very slow. The benzoyl group in the fifth (phenolic) position of dibenzoylkojic acid was removed by hydroxylamine hydrochloride in pyridine so selectively that the method was of value in synthesizing certain new derivatives. Although catalytic hydrogenation readily reduced the pyrone ring in kojic acid to undefined substances, zinc dust in glacial acetic acid reduced the hydroxymethyl group in the dibenzoate to a methyl group and yielded benzoylallomaltol. The ring in dibenzoylkojic acid was apparently opened, with retention of both benzoyl groups, by semicarbazide hydrochloride and pyridine to yield two isomeric "disemicarbazones", $C_{22}H_{22}N_6O_7$, decomp., 215° and 172–173°, respectively. The higher-melting isomer when boiled with dilute acid gave a compound $C_{21}H_{15}N_3O_5$, m.p. 244°, which was apparently cyclic; the same isomer with nitrous acid yielded two isomeric, apparently open-chain "monosemicarbazones", $C_{21}H_{19}N_3O_7$, decomp., 215° and 178–179°, respectively. The structures of these five compounds were not determined. The following substances were thought to be new: sodium kojate, a white powder, and its crystalline tetrahydrate; 5-hydroxy-2-(methoxymethyl)-γ-pyrone, m.p. 75–76°, and its crystalline aluminum salt, decomp. 270–271°; molecular addition compound of dibenzoylkojic acid and benzoic acid, m.p. 120–121°; 2-(acetoxymethyl)-5-benzoxy-γ-pyrone, m.p. 144°; 2-(benzoxymethyl)--5-hydroxy-γ-pyrone, m.p. 180–181°; and 2-(benzoxymethyl)-5-methoxy-γ-pyrone, m.p. 110–111°. A more convenient synthesis was discovered for 5-benzoxy-2-(hydroxymethyl)-γ-pyrone, and the published melting point was revised from 136° to 143–144°; the melting point of 5-benzoxy-2-(triphenylmethoxymethyl)-γ-pyrone was revised from 206–208° to 213–214°.

INTRODUCTION

Kojic acid, (5-hydroxy-2-(hydroxymethyl)-γ-pyrone) (I), is a crystalline substance which can be produced in good yield by the action of many molds of the *Aspergillus* family on a wide range of carbohydrates. This biological synthesis has been studied extensively because it is the simplest example of the conversion of a sugar to a γ-pyrone. The possibility of utilizing industrial carbohydrate by-products by converting them to kojic acid has also stimulated interest in the chemical properties of this compound. Barham and Smits

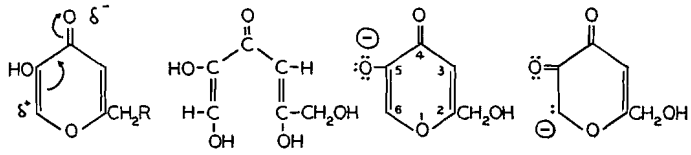

I, R = OH
II, R = H
III, R = Cl

Ia Ib Ic

[1]*Manuscript received March 29, 1955.*
Contribution from the Division of Industrial and Cellulose Chemistry, McGill University, and the Wood Chemistry Division, Pulp and Paper Research Institute of Canada, Montreal, Que. Abstracted from a Ph.D. thesis submitted by A. B. to the University in September, 1954.
[2]*Present address: Department of Chemistry, Royal Military College of Canada, Kingston, Ontario.*

(4) have summarized the earlier literature, and a new review is to appear elsewhere (6).

Practically all the known derivatives of kojic acid were formed by reactions involving the two hydroxyl groups, by nuclear substitutions at position 6, or by the replacement of the ring oxygen atom with the nitrogen of ammonia or amines to give γ-pyridones (6, 11, 12). A few γ-pyrones other than kojic acid, however, were cleaved at the ring oxygen atom by cold dilute aqueous alkalies to yield open-chain derivatives. With the possible exception of Haitinger and Lieben's "xanthochelidonic acid" (10), the dienolic compounds initially produced underwent further changes to more stable ketonic forms (19). Acidification (10), or heating with dilute acid (19), usually regenerated the original γ-pyrone. Willstätter and Pummerer (20) prepared stable derivatives of the dienolic cleavage product of γ-pyrone itself by methylation and benzoylation in the alkaline reaction mixture. The similar open-chain form (I*a*) was assumed as the final intermediate in the biosynthesis of kojic acid (6), but the only experimental evidence for its existence was the fact that kojic acid in warm dilute alkali resembled other α-carbonyl dienol structures in reducing Tillman's reagent (2,6-dichlorophenol-indophenol) (18). When the alkali was more concentrated, or was heated, the pyrone ring was fragmented; thus Yabuta (22, 23), and more recently Arnstein and Bentley (3), found that dimethylkojic acid was degraded to formic acid, methoxyacetic acid, and methoxyacetone by boiling aqueous barium hydroxide. The present research had the object of studying the action of bases on kojic acid under milder conditions, and of isolating open-chain derivatives in an unfragmented state.

One-gram samples of kojic acid were accordingly dissolved in approximately 1.2 *N* sodium hydroxide and the clear yellow solutions were acidified with 20% sulphuric acid after various times. Table I, column 4, records the amount

TABLE I

STABILITY OF KOJIC ACID IN APPROXIMATELY 1.2 *N* AQUEOUS SODIUM HYDROXIDE AT 25°

NaOH, mM.[a]	Water, ml.	Time, hr.	Kojic acid recovered			Formic acid, mM. %[a]
			Fract. 1, gm.	Fract. 2, gm.	Total, %	
2	11.3	1.2	0.76	0.13	89	—
2	11.3	3.0	0.73	0.15	88	—
2	11.3	13.5	0.77	—	—	1.0
2	11.3	32	0.74	—	—	2.5
3	16.9	1.0	0.66	0.19	85	—
3	16.9	32	0.74	—	—	3.2
5	28.2	1.0	0.56	0.25	81	—

[a]*Per mM. of kojic acid, 1 gm. or 7.06 mM. of which was used in all cases.*

of kojic acid which crystallized when the acidified liquor was kept at −3°; in some experiments the mother liquors were concentrated to recover a second fraction, and in others 60% of the volume was distilled at atmospheric pressure in order to estimate any formic acid produced. Even after 32 hr. in an excess of the alkali, more than 80% of the kojic acid could be recovered as such,

and only a few per cent had been decomposed to formic acid. Kojic acid was therefore either nearly stable in these conditions, or its hypothetical open-chain enolic form (I*a*) recyclized almost quantitatively when the solution was acidified.

In attempts to methylate or benzoylate any enolic compound formed, dimethyl sulphate or benzoyl chloride was added to solutions of kojic acid in aqueous alkali. The methylation was carried out with a molar ratio of 1:6:3.7 for kojic acid, potassium hydroxide, and dimethyl sulphate, respectively, but the only product, obtained in low yield, was a new, crystalline monomethyl ether of kojic acid itself. This ether imparted a deep wine color to ferric chloride solution and therefore contained a free phenolic hydroxyl group; methylation with diazomethane gave the known 5-methoxy-2-(methoxymethyl)-γ-pyrone. Hence the new monomethyl ether was 5-hydroxy-2-(methoxymethyl)-γ-pyrone (IV). In the process of purification, IV reacted with the alumina in a chromatograph column to give a pale yellow, crystalline derivative in which three moles were substituted by one atom of aluminum; that is, the derivative had the composition of the aluminum phenoxide. The isomeric monomethyl ether, 2-(hydroxymethyl)-5-methoxy-γ-pyrone (VIII), was obtained in a crude yield of 72% by Campbell and his co-workers (8) from kojic acid, potassium hydroxide, and dimethyl sulphate in a 1:1:1 molar ratio. Heyns and Vogelsang (11) prepared the dimethyl ether from the same reagents, using a molar ratio of 1:8:9.

Two methods were used for the benzoylations, differing mainly in the excess of sodium hydroxide present throughout the reaction. When this excess was considerable, the products were the known, crystalline dibenzoylkojic acid (5-benzoxy-2-(benzoxymethyl)-γ-pyrone) (22, 23) and a new, crystalline addition compound, m.p. 120–121°, between equimolecular amounts of this dibenzoate and benzoic acid. The infrared spectrum of a benzene solution of the adduct was identical with that given by an equimolecular mixture of its compon-

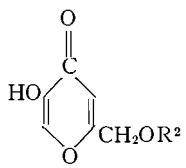

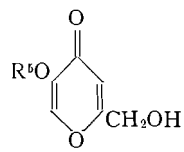

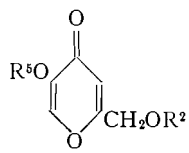

IV R^2 = methyl
V R^2 = benzoyl
VI R^2 = acetyl
VII R^2 = trityl

VIII R^5 = methyl
IX R^5 = benzoyl
X R^5 = sodium

XI R^2 = trityl; R^5 = benzoyl
XII R^2 = benzoyl; R^5 = methyl
XIII R^2 = acetyl; R^5 = benzoyl

ents, a Perkin-Elmer Model 21 spectrophotometer fitted with a rock salt prism being used for the determination. This addition compound could be recrystallized without change from hydrocarbon solvents, but dissociated into its constituents when dissolved in polar liquids. When the excess of alkali used in the benzoylation was small, the product consisted of the above adduct, together with a monobenzoyl derivative of kojic acid which melted at 142–143°. This melting point was 7° higher than a value reported by Yabuta for a mono-

benzoate prepared from kojic acid and benzoyl chloride in ether (22, 23), or from 5-benzoxy-2-(triphenylmethoxymethyl)-γ-pyrone (XI) by detritylation (25). The latter unequivocal synthesis was repeated, the proper melting point of the resulting 5-benzoxy-2-(hydroxymethyl)-γ-pyrone (IX) was found to be 142–143°, and identity with the monobenzoate under discussion was proved.

Other attempts to isolate a derivative of I*a* involved the complete evaporation of aqueous solutions of kojic acid containing one or two molecular equivalents of sodium hydroxide. The product was the new sodium kojate, which occurred either as a crystalline tetrahydrate or in the anhydrous condition. This "salt" was presumably the 5-sodio derivative (X). The tetrahydrate reacted with benzoyl chloride in dry benzene to give the 5-monobenzoate (IX); the yield of the latter rose to 79.5% when anhydrous sodium kojate was used. These observations, together with the results of the methylations and benzoylations, seemed to indicate the absence of an open-chain form like I*a* from solutions of kojic acid in dilute aqueous alkali.

As was expected from the inert nature of the carbonyl group, no derivatives could be isolated when kojic acid was treated with hydroxylamine hydrochloride or with semicarbazide hydrochloride. The customary procedures for oximation, however, produced from dibenzoylkojic acid in up to 90% yield a crystalline substance which proved to be a new monobenzoate and not an oxime. Benzoylation in dry pyridine gave back the dibenzoate, and the presence of a free phenolic function in the monobenzoate was indicated by the wine color it produced with ferric chloride. Methylation with diazomethane yielded another new crystalline substance which was identified as 2-(benzoxymethyl)-5-methoxy-γ-pyrone (XII) by a synthesis from VIII and benzoyl chloride. The monobenzoate was therefore the 2-derivative (V).

The selective deacylation displayed by hydroxylamine in the above reaction was also illustrated by the smooth debenzoylation of the 5-benzoxy derivatives of 2-acetoxymethyl- (XIII) and 2-(triphenylmethoxymethyl)-γ-pyrone (XI), and of benzoylallomaltol to the corresponding 5-hydroxy derivatives (VI, VII, and II). The method should thus be useful for preparing derivatives of kojic acid monosubstituted in the generally less reactive 2-position, especially when a substituent such as acetyl or trityl offers but little resistance to conventional methods of hydrolysis. Although the cleavage of esters by hydroxylamine in the presence of a strong base is frequently used for the preparation of substituted hydroxamic acids (26), the method has not hitherto been employed for selective deacylations. Ingold and Shoppee (15), however, incidentally observed that their oximation of 2-benzoxy-4,4,5,5-tetramethyl-2-cyclopenten-1-one (XIV) was accompanied by debenzoylation, although the benzoyl group in the analogous saturated ketone was unaffected under identical conditions. The results support the view that enolic and phenolic ester groups adjacent to a carbonyl group are cleaved with particular ease by hydroxylamine. It therefore seems probable that the same method might prove useful in other compounds containing the same grouping; for example, in the selective deacylation of flavonols at position 3.

Another selective debenzoylation, this time involving the group in the

second instead of the fifth position of dibenzoylkojic acid, was brought about by reduction with zinc dust in glacial acetic acid. The products included nearly one mole of benzoic acid and a crystalline substance which was proved to be the benzoate of allomaltol (II) (5-benzoxy-2-methyl-γ-pyrone). This proof consisted of repeating Yabuta's reduction (24) of 2-(chloromethyl)-5-hydroxy-γ-pyrone (III) to the 2-methyl derivative (II) and benzoylating the latter. The primary alcohol unit in dibenzoylkojic acid thus resembled that in benzyl ethers in its tendency to undergo reductive fission. In accord with this inference, the dibenzoate yielded 0.6 mole of benzoic acid when hydrogenated at room temperature and atmospheric pressure over a platinum catalyst. This hydrogenation probably involved hydrogenolysis, since hydrolysis was not likely in the glacial acetic acid used as a solvent. The other product of the hydrogenation was a sirup which was not studied in detail because numerous earlier catalytic hydrogenations of kojic acid, its ethers and esters, gave sirups of indefinite composition (6). Ingold and Shoppee (15) observed that the enolic benzoyl group in (XIV) was unaffected by zinc or sodium amalgam in glacial acetic acid, while the double bond was readily reduced (with retention of the benzoyl group) by hydrogenation.

Dibenzoylkojic acid failed to form a benzoylhydrazone and a 2,4-dinitrophenylhydrazone, but condensation occurred with semicarbazide hydrochloride in boiling ethanol–pyridine. The product consisted of two white, neutral, microcrystalline isomers, but the one with the lower melting point was formed in too small yield to be examined in detail. The molecular formula of these isomers, $C_{22}H_{22}N_6O_7$, corresponded to disemicarbazones of an open-chain form of dibenzoylkojic acid, and structures such as XV were tentatively assigned to them. The higher-melting isomer was readily saponified by cold dilute alkali,

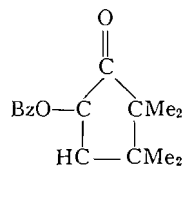

XIV

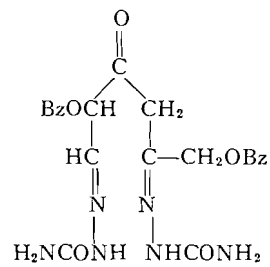

XV

but the only product identified was benzoic acid in nearly quantitative yield. These structures were unusual, for the initial open-chain products from other γ-pyrones and hydrazines invariably lost one additional molecule of water to give cyclic end products. Bedekar and co-workers (5) represented these end products as pyridones, but Ainsworth and Jones (1) recently found very good evidence in favor of pyrazole structures. No carboxylic acid derived from a pyridone or pyrazole, however, could be recovered when the higher-melting isomer was oxidized with potassium permanganate, only benzoic and benzoyl-

glycolic acids being identified. When the same isomer was boiled in 10% hydrochloric acid, the yellow-white, microcrystalline substance which formed in small yield had the molecular formula $C_{21}H_{15}N_3O_5$, which corresponded to the loss of one semicarbazide unit and two molecules of water. Cyclization probably occurred in this case, but the point could not be definitely proved owing to lack of material.

The higher-melting "disemicarbazone" lost one semicarbazide group on treatment with nitrous acid (9, 21), and two neutral, microcrystalline "monosemicarbazones" resulted. The lower-melting, or "β", form was the main product (69%), and the "α-isomer" was isolated only when a larger quantity of nitrous acid was employed. Since an excess of nitrous acid did not convert the β- to the "α-monosemicarbazone" the two were perhaps position isomers. To judge from the composition of these two products, $C_{21}H_{19}N_3O_7$, both were open-chain derivatives and no cyclization occurred during the treatment with nitrous acid. No carboxylic acids other than benzoic and benzoylglycolic could be isolated when the β-isomer was oxidized with aqueous potassium permanganate. An attempt to regenerate the "disemicarbazone" from the "β-monosemicarbazone" by treating the latter with semicarbazide hydrochloride and pyridine in boiling methanol failed, the starting material being recovered unchanged. Hydroxylamine hydrochloride likewise had no effect. These results were surprising, because the presence of a carbonyl group created by the fission of a semicarbazone unit could reasonably have been assumed (21); the negative outcome with hydroxylamine also suggested that neither of the two benzoyl groups was of the phenolic type present in dibenzoylkojic acid. At this point, attempts to elucidate the structures of the "monosemicarbazones" had to be abandoned.

The failure of *N* sodium hydroxide to open the ring of kojic acid stood in sharp contrast to the apparent cleavage of the ring in the dibenzoate by semicarbazide, a much weaker base. Cleavage of γ-pyrone rings was presumably initiated by a nucleophilic reagent at position 6, where the drift of electrons toward the carbonyl group would create an electrophilic center. This might happen in the case of dibenzoylkojic acid, as indicated in I, when semicarbazide was the attacking nucleophile (14). In sodium hydroxide, kojic acid would be present as the kojate anion (I*b*), and an important contribution to the resonance hybrid of this anion could be expected from the diketo form (I*c*) with the full negative charge located at position 6. This nucleophilic center would face the nucleophilic hydroxyl ion, and no cleavage would result. If this explanation was correct, the production of open-chain forms of kojic acid by basic cleavage required either the use of very weak bases or the blocking of the hydroxyl group in position 5 by a substituent stable to alkali.

EXPERIMENTAL

All melting points were corrected. All of the nitrogen analyses, and two carbon and hydrogen analyses marked by an asterisk, were by Schwarzkopf Microanalytical Laboratory, Woodside, N.Y., U.S.A. Reactants were always weighed to the nearest 10 mgm.

5-Hydroxy-2-methoxymethyl-γ-pyrone (IV) and Its Aluminum "Salt"

Dimethyl sulphate, 47 gm. (0.373 mole), was slowly added over a period of three hours and at room temperature to a stirred solution of 15 gm. (0.106 mole) of kojic acid and 37.5 gm. (0.6 mole) of potassium hydroxide in 315 ml. of water. The mixture slowly warmed to 37°, but was then kept below 30°. The alkaline liquor, having been concentrated at 50° *in vacuo* to 250 ml., was extracted continuously with benzene to remove any dimethylkojic acid, but the yellow extract yielded only traces of an oil. The aqueous liquor was then acidified to pH 2 with 50% sulphuric acid and was re-extracted continuously with benzene for 21 hr. This dark red extract was treated with activated carbon, concentrated to small volume, and diluted with ligroin. The red oil which separated solidified on chilling to a yellow-brown substance, 6.85 gm. melting between 55° and 66°. Crystallization from ethyl acetate left 1.85 gm. (11.2%), m.p. 75–76°, unchanged by recrystallization from toluene–hexane. Found: C, 53.7, 53.8; H, 5.3, 5.2; OCH_3, 20.4, 20.4%. Calc. for $C_6H_5O_3(OCH_3)$: C, 53.9; H, 5.1; OCH_3, 19.9%.

The combined mother liquors from the above crystallizations were evaporated, and a concentrated solution of the residue in benzene was applied to a short column of alumina. Elution with benzene, evaporation of the eluates, and recrystallization of the orange products from ethanol gave 0.71 gm. (4%) of pale yellow crystals melting with decomposition at 270–271°. A qualitative test demonstrated the presence of aluminum. Found: Ash, 10.4; Al, 5.5; OCH_3, 18.6%. Calc. for Al $[C_6H_4O_3(OCH_3)]_3$: Ash, 10.4; Al, 5.5; OCH_3, 18.9%.

A solution of 0.15 gm. of these crystals in water was adjusted to pH 2 with dilute sulphuric acid and evaporated cautiously to a sirup. Extraction of this sirup with toluene yielded 0.09 gm. (63%) of 5-hydroxy-2-(methoxymethyl)-γ-pyrone with the proper melting point, undepressed by admixture with an authentic sample.

A 0.5 gm. sample of the monomethyl ether was kept dissolved in 20 ml. of dry benzene containing about 0.56 gm. of diazomethane (2) for 12 hr. at room temperature. Evaporation of this solution, and crystallization of the yellow residue from benzene–hexane, yielded 0.33 gm. (60.5%) of white needles melting at 89–90°, undepressed by admixture with an authentic sample of dimethylkojic acid (11).

Sodium Kojate and Its Crystalline Tetrahydrate

A solution of 3.0 gm. (21 mM.) of kojic acid and 0.88 gm. (21 mM.) of sodium hydroxide in 15 ml. of water was evaporated to dryness *in vacuo* at 40°. The residual solid was recrystallized twice from 5 ml. of hot water, and the white crystals were dried in air at 25°. Yield, 2.62 gm. or 53%. Found: Na, 10.3; loss of weight at 110°, 30.3, 30.2; at 25° over phosphorus pentoxide, 29.7%. Calc. for $C_6H_5O_4Na.4H_2O$: Na, 9.8; water, 30.5%.

The water of crystallization was determined by drying samples either for about six hours at 110° or for about 18 hr. *in vacuo* over phosphorus pentoxide at 25°. Anhydrous sodium kojate was a white powder when prepared by the latter method, and a tan powder by the former.

A New Synthesis of 5-Benzoxy-2-(hydroxymethyl)-γ-pyrone

Crude sodium kojate was prepared from 2 gm. (14 mM.) of kojic acid as just described, and was rendered anhydrous by drying *in vacuo* over phosphorus pentoxide. The product was shaken in the original tightly-stoppered flask with 50 ml. of dry benzene and 2.5 gm. (18 mM.) of benzoyl chloride at room temperature for 26 hr. It was necessary to interrupt the shaking to loosen solid material which adhered initially to the walls of the flask. After adding 30 ml. of benzene, the white suspension was heated to boiling and was filtered while hot. The residual solid was re-extracted with hot benzene, then with water, and again with benzene. The combined benzene solutions, when dried and evaporated, deposited 2.53 gm. of white needles melting at 143–144°, together with a second fraction which was recrystallized from aqueous acetone to give 0.22 gm. with the proper melting point. Total yield, 79.5%. A mixed melting point with authentic 5-benzoxy-2-(hydroxymethyl)-γ-pyrone (see below) was not depressed.

The authentic sample was prepared from 5-benzoxy-2-(triphenylmethoxymethyl)-γ-pyrone, (XI), which when recrystallized from aqueous dioxane melted at 213–214°, and not at 206–208° as recorded by Yabuta and Anno (25). The removal of the trityl group with boiling 80% acetic acid, followed by the separation of triphenylcarbinol, left a product which was crystallized from benzene. Yield, 55%, and melting point 140–141°. Further recrystallizations from benzene raised the melting point to 142–143°, the value quoted by Yabuta being 135–136°.

Dibenzoylkojic Acid – Benzoic Acid Addition Compound

(*a*) *Benzoylation in Sodium Hydroxide*

A solution of 5 gm. (35 mM.) of kojic acid and 7.3 gm. (177 mM.) of sodium hydroxide was prepared in 177 ml. of water. Benzoyl chloride, 19.7 gm. (140 mM.), was added slowly, with stirring and at room temperature, during two and three-quarter hours, and the granular solid which separated was recovered. A solution of 5.8 gm. (140 mM.) of sodium hydroxide in 50 ml. of water was added to the acidic filtrate, and the benzoylation was repeated with another 140 mM. of benzoyl chloride. After one hour more of stirring, a second crop of the solid was recovered from the liquor, which again had become acid. The two crops when combined and crystallized from dry benzene–hexane yielded 1.55 gm. (18%) of a less soluble fraction which consisted of white crystals with the composition and melting point, 142–143°, of 2-(hydroxymethyl)-5-benzoxy-γ-pyrone (IX). A mixed melting point with an authentic sample was not depressed.

The more soluble fraction was composed of 5.88 gm. (35.5%) of matted white needles melting at 117–118°, raised by further recrystallizations to m.p. 120–121°. Mixtures of this molecular addition compound with dibenzoylkojic acid and with benzoic acid showed depressions in melting point. Found: C, 68.8, 69.0; H, 4.4, 4.4%. Calc. for $C_{20}H_{14}O_6.C_7H_6O_2$: C, 68.6; H, 4.2%.

A solution of 0.50 gm. of the addition compound in 5 ml. of warm acetone was diluted with an equal volume of cold water; the mixture was cooled and the

white precipitate which had immediately formed was recovered. The precipitate melted correctly for dibenzoylkojic acid at 134–135°, a mixed melting point with an authentic sample was not depressed, and the yield of 0.37 gm. was 100% of theory. The clear filtrate when concentrated to half-volume deposited 0.12 gm. (92.5%) of benzoic acid melting at 117–119°, raised to the proper value of 122° by recrystallization from water. A mixed melting point was not depressed. Dibenzoylkojic acid also crystallized from solutions of the adduct in dioxane (on dilution with water), 95% ethanol, ethyl acetate, absolute methanol, and pyridine. The benzoic acid was extracted selectively by aqueous 5% sodium carbonate from a solution of the adduct in benzene. On the other hand, the adduct could be recrystallized substantially without change from benzene, benzene–hexane, toluene, and glacial acetic acid.

(*b*) *Benzoylation in Pyridine*

Five grams (36 mM.) of benzoyl chloride was added in several increments to a solution of 2 gm. (14 mM.) of kojic acid in dry pyridine. Next day the pyridine was evaporated in a current of dry air, with gentle heating, to leave a moist pulp. The product in this pulp was separated from the pyridine salts by extraction with hot benzene, and was recovered from the extract in several fractions. The less soluble fractions yielded 3.45 gm. (70%) of pure dibenzoylkojic acid, which was carefully identified as such. Recrystallization of the more soluble fractions from benzene–ligroin gave 0.66 gm. (10%) of white matted needles whose melting point of 120–121° was not depressed by admixture with the dibenzoylkojic acid – benzoic acid addition compound.

The product from a similar benzoylation was isolated in the customary way by pouring the mixture into chilled 5% aqueous sulphuric acid. A 98.5% yield of pure dibenzoylkojic acid was obtained.

2-(Benzoxymethyl)-5-hydroxy-γ-pyrone (*V*)

A solution of 0.30 gm. (0.86 mM.) of dibenzoylkojic acid and 0.12 gm. (1.7 mM.) of hydroxylamine hydrochloride in 4 ml. of pyridine was kept for 12 hr. at room temperature, then diluted with 20 ml. of cold water. After the suspension had been kept cold for a few hours, the white precipitate was recovered. Yield, 0.19 gm. (90%); m.p. 179–180°, increased to 180–181° by recrystallization from ethanol. Found: C, 63.5, 63.6; H, 4.1, 4.2; COC_6H_5, 41.7, 41.0%. Calc. for $C_6H_5O_4(COC_6H_5)$: C, 63.4; H, 4.1; COC_6H_5, 42.7%.

The same product was obtained in 83% yield by boiling dibenzoylkojic acid with three equivalents each of hydroxylamine hydrochloride and pyridine in 95% ethanol for 30 min.; also by replacing the pyridine with sodium acetate and using 80% ethanol. In the latter case the pure product crystallized in 74% yield when the solution cooled. Three equivalents of either sodium acetate or hydroxylamine hydrochloride alone had no appreciable effect on dibenzoylkojic acid in boiling ethanol.

A 15% excess of benzoyl chloride was slowly added to an ice-cold solution of the above monobenzoate in dry pyridine. An 89% yield of dibenzoylkojic acid was recovered, melting at 135°, after crystallization from aqueous acetone. A mixed melting point was undepressed.

2-(Benzoxymethyl)-5-methoxy-γ-pyrone (XII)

One gram (4.1 mM.) of finely powdered 2-(benzoxymethyl)-5-hydroxy-γ-pyrone was added to 18 ml. of benzene containing about 0.5 gm. of diazomethane (2). Practically all of the solid dissolved within six hours, and the product was isolated by concentrating and cooling the solution. The yield was 0.52 gm. (49%) of near-white crystals melting at 109–110°; the use of absorbent charcoal in ethanol, and recrystallization from benzene–ligroin, gave a snow-white product melting at 110–111°. Found: C, 64.7, 64.9; H, 4.6, 4.8; OCH_3, 12.0, 12.1%. Calc. for $C_{13}H_9O_4(OCH_3)$: C, 64.6; H, 4.6; OCH_3, 11.9%.

The same product was obtained when 2-(hydroxymethyl)-5-methoxy-γ-pyrone (VIII), prepared according to Campbell and co-workers (8), was esterified with benzoyl chloride in dry pyridine. A mixture of the two samples showed no depression in melting point.

2-(Acetoxymethyl)-5-benzoxy-γ-pyrone (XIII)

A solution of 2.8 gm. (11 mM.) of 5-benzoxy-2-(hydroxymethyl)-γ-pyrone (IX) in 24 ml. of dry pyridine was chilled, mixed with 4.1 gm. (40 mM.) of acetic anhydride, and kept overnight at room temperature. Precipitation of the solution into 200 ml. of cold water yielded 3.06 gm. (93%) of crystals melting at 143–144°. Recrystallizations from benzene and from aqueous acetone left the melting point of the white plates at 144°, and a mixed melting point with the starting material was depressed to 120–127°. Found: C, 62.8, 62.5; H, 4.3, 4.5%. Calc. for $C_{15}H_{12}O_6$: C, 62.5; H, 4.2%.

A solution of 0.96 gm. (3.3 mM.) of XIII and 0.46 gm. (6.6 mM.) of hydroxylamine hydrochloride in 13 ml. of pyridine was kept at room temperature for 12 hr. before being diluted with six volumes of cold water. After being extracted with benzene, the aqueous liquor was evaporated to dryness *in vacuo* at 50° and the solid, yellow residue was extracted with boiling benzene. The combined benzene extracts yielded a total of 0.47 gm. (77%) of white needles melting at 134–135°, plus a second fraction (6%) of slightly less pure material. 2-(Acetoxymethyl)-5-hydroxy-γ-pyrone (VI), whose published melting point was 133.5° (12) and 137° (17), gave a wine color with aqueous ferric chloride. When acetylated in the presence of sodium acetate (13), the substance yielded 5-acetoxy-2-(acetoxymethyl)-γ-pyrone which was carefully identified by comparison with an authentic sample.

Debenzoylation of 5-Benzoyl-2-(triphenylmethoxymethyl)-γ-pyrone (XI)

The debenzoylation was accomplished as just described, except that an 8.4 molar equivalent of hydroxylamine hydrochloride was used. After recrystallizations from benzene–ligroin, dioxane–water, and carbon tetrachloride – isopropyl ether, 66% of pure 5-hydroxy-2-(triphenylmethoxymethyl)-γ-pyrone (VII) remained, melting at 180–182° (25).

Benzoylallomaltol from Dibenzoylkojic Acid

Thirty grams of technical grade zinc dust was added to a hot solution of 5 gm. (14.3 mM.) of dibenzoylkojic acid in 125 ml. of glacial acetic acid; the mixture was vigorously stirred on the steam bath, and eight drops of concen-

trated sulphuric acid were added during five minutes. Stirring was stopped after one hour, the hot mixture filtered, the residual zinc rinsed with hot glacial acetic acid, and the combined liquors were evaporated completely *in vacuo*. The residual brown oil was treated with an excess of solid sodium carbonate, the resulting mixture was extracted with boiling benzene, and the benzene extract was washed with dilute aqueous sodium carbonate and with water. Pure benzoic acid, 1.31 gm. (75%), was recovered from the benzene-insoluble solid residue and the sodium carbonate washings. The golden brown benzene solution was completely evaporated and the residual tan solid was recrystallized twice from isopropyl ether, using a small amount of decolorizing charcoal. The yield was 1.48 gm. (45%) of benzoylallomaltol as off-white, flat needles melting at 125–126°. An analytical sample, recrystallized from the same solvent, melted at 126–127°, undepressed when mixed with an authentic sample (24). Found: C, 67.9*, 67.8; H, 4.8*, 4.8%. Calc. for $C_{13}H_{10}O_4$: C, 67.8; H, 4.4%.

A solution of 2.4 gm. (10 mM.) of benzoylallomaltol and 0.95 gm. (14 mM.) of hydroxylamine hydrochloride in 25 ml. of pyridine was kept at room temperature for 11 hr., and was then evaporated *in vacuo*. After being dried over solid potassium hydroxide in a vacuum desiccator, the residual brown oil was extracted several times with boiling benzene. The combined benzene extracts yielded a total of 1.05 gm. of crude allomaltol as white crystals melting at 143–149°; recrystallization from a mixture of isopropyl ether and ethyl acetate left 0.93 gm. (71%) melting at 150–151°. This substance was soluble in water and gave a wine color with ferric chloride. Benzoylation with benzoyl chloride in dry pyridine gave back benzoylallomaltol. An authentic sample of allomaltol prepared by Yabuta's method (24) also melted at 150–151°, not at 166° as reported, and a mixed melting point was undepressed. The present value confirmed that recently given by Looker and Okamoto (16).

Dibenzoylkojic Acid "Disemicarbazone"

(*a*) A mixture of 14 gm. (40 mM.) of dibenzoylkojic acid, 14 gm. (125 mM.) of semicarbazide hydrochloride, 14 ml. (174 mM.) of pyridine, 40 ml. of water, and 350 ml. of ethanol was boiled under reflux for 50 min. and then kept at room temperature for six days. The crop of yellow-white crystals deposited from the clear solution was extracted in succession with hot ethyl acetate, water, and dioxane, and the residual microcrystalline white solid, 6.04 gm., melted at 212° with decomposition. A second crop, recovered from the original mother liquor 15 days later, increased the yield to 7.96 gm. or to 41.5%. This "disemicarbazone" was sparingly soluble in glacial acetic acid but insoluble in all other liquids tried. The sample for analysis was dissolved in much glacial acetic acid by warming to not more than 70° and was reprecipitated by adding five volumes of cold water. The melting point was then 215° with decomposition. Found: C, 54.8, 54.8; H, 4.7, 4.8; N, 16.9%. Calc. for $C_{22}H_{22}N_6O_7$: C, 54.8; H, 4.6; N, 17.4%.

(*b*) The above condensation was repeated with 5 gm. of dibenzoylkojic acid, 3.2 gm. of semicarbazide hydrochloride, 5 ml. of pyridine, 10 ml. of water, and

60 ml. of ethanol, the molar ratio of the first three substances being about 1:2:4 instead of about 1:3:4. The yellow solution deposited a yellow-white solid decomposing at 179–181° when concentrated on the steam-bath, and a soft solid separated when the mother liquor was diluted with water and chilled. Extraction of the latter fraction with boiling ethyl acetate removed 0.33 gm. of a solid, m.p. 183–184°, which was combined with the previous fraction of similar melting point. These fractions were purified by extraction with hot ethyl acetate and water to yield 1.65 gm. (24%) of the "disemicarbazone" noted in (*a*) and melting at 213°.

On cooling overnight, the red ethyl acetate extract deposited 0.61 gm. of white crystals melting at 121° with decomposition. Recrystallizations from ethyl acetate and from ethanol–methanol left 0.4 gm. (6%) of this isomeric "disemicarbazone" and raised the melting point to 172–172.5° with decomposition. Found: C, 54.6, 54.5; H, 5.0, 4.9; N, 16.6%. Calc. for $C_{22}H_{22}N_6O_7$: C, 54.8; H, 4.6; N, 17.4%.

Experiments with the Higher Melting "Disemicarbazone"

(*a*) *Action of Dilute Alkali*

Two grams of the above "disemicarbazone" dissolved almost completely when stirred at room temperature for 30 min. with 20 ml. of 10% potassium hydroxide. The clear filtrate contained no substances that could be extracted by ether or chloroform. When acidified with hydrochloric acid, the filtrate deposited 0.95 gm. (95%) of benzoic acid with the correct melting point and mixed melting point.

(*b*) *Action of Dilute Acid*

A suspension of 1.5 gm. of the "disemicarbazone" in 25 ml. of 10% hydrochloric acid was boiled under reflux for three and one-half hours. The sticky brown residue was separated from the acidic filtrate (which yielded 0.31 gm., or 41%, of benzoic acid) and was crystallized from methanol–ethanol–benzene, from dioxane–water, and from acetone. The pure product, 0.11 gm. or 9%, was a white, microcrystalline solid melting at 244°. Found: C, 64.3, 64.5; H, 4.1, 4.2; N, 10.8%; mol. wt. (Rast), 423. Calc. for $C_{21}H_{15}N_3O_5$: C, 64.8; H, 3.9; N, 10.8%; mol. wt. 389.

(*c*) *Oxidation with Potassium Permanganate*

A mixture of 5.61 gm. (11.6 mM.) of the "disemicarbazone", 10 gm. (63 mM.) of potassium permanganate, 4 ml. (70 mM.) of glacial acetic acid, and 370 ml. of water was kept at 90° for 30 min. After removing the manganese dioxide, the weakly acid filtrate was concentrated to 250 ml. *in vacuo*, was adjusted to pH 2, and was continuously extracted with benzene. The residue from the extract, when fractionally crystallized from benzene–hexane, yielded 0.38 gm. (27%) of pure benzoic acid, and 0.24 gm. (11.5%) of benzoylglycolic acid melting correctly (7) at 111–112°. Found for the latter: C, 60.0; H, 4.8%*; neut. equiv., 179.7. Calc. for $C_9H_8O_4$: C, 60.0; H, 4.4%; neut. equiv., 180.

Dibenzoylkojic Acid "α-Monosemicarbazone"

A suspension of 3.05 gm. (6.33 mM.) of the "disemicarbazone" in 70 ml.

of glacial acetic acid was stirred at room temperature, while a concentrated aqueous solution of 10.8 gm. (157 mM.) of sodium nitrite was added very slowly during six hours. Stirring was discontinued one hour later, and next day the yellow-green solution was filtered from 0.3 gm. of the starting material. Dilution of the filtrate with an equal volume of cold water precipitated 2.03 gm. of a white solid melting at 173–174°. This solid contained several components, but only one could be isolated in a pure form by recrystallizing the mixture from benzene–methanol (1 vol. : 4 vol.). The product, 0.24 gm. (9%), was a white microcrystalline powder melting with decomposition at 212–213°, increased to 215° by recrystallizations from acetone–methanol. A mixed melting point determination with the original "disemicarbazone" (m.p. also 215°) was markedly depressed. Found: C, 59.6, 59.0; H, 4.7, 4.6; N, 10.1%. Calc. for $C_{21}H_{19}N_3O_7$: C, 59.3; H, 4.5; N, 9.9%.

Dibenzoylkojic Acid "β-Monosemicarbazone"

The preparation for the α-isomer was repeated with 7.2 gm. (104 mM.) of sodium nitrite instead of 10.8 gm., and with 60 ml. instead of 70 ml. of glacial acetic acid. The filtered liquor on dilution with 240 ml. of cold water deposited 2.41 gm. of a white solid decomposing at 166–170°. This product was extracted with 120 ml. of boiling methanol to remove a small amount of unchanged "disemicarbazone". The filtered extract, when diluted with 500 ml. of water, deposited 1.82 gm. (69%) of a white, microcrystalline solid whose decomposition point at 178–179° was not altered by recrystallization from benzene–methanol–ligroin. Found: C, 59.3, 59.2; H, 5.1, 4.9; N, 9.8%. Calc. for $C_{21}H_{19}N_3O_7$: C, 59.3; H, 4.5; N, 9.9%. A sample was recovered unchanged after its suspension in glacial acetic acid had been treated with an excess of aqueous sodium nitrite at room temperature.

Another sample, 0.60 gm. (1.4 mM.), was heated on the steam bath with 1.1 gm. (7 mM.) of potassium permanganate and 40 ml. of water for one and three-quarter hours. The reaction mixture, when worked up as already described for the oxidation of the "disemicarbazone", yielded 0.05 gm. (19.5%) of benzoylglycolic acid melting at 106–110°. Recrystallization raised the melting point to 111–112°, undepressed by admixture with the previous sample. The other product of the oxidation was benzoic acid, which was recrystallized until pure.

ACKNOWLEDGMENTS

One of us (A. B.) wishes to thank the National Research Council of Canada for a Studentship, and the Pulp and Paper Research Institute of Canada for a summer stipend. We acknowledge gratefully the determination of the infrared spectra of the dibenzoylkojic acid – benzoic acid adduct by Mr. A. W. Pross of Canadian Industries (1954) Limited, McMasterville, Que.; also a generous gift of kojic acid from the Corn Products Refining Company, Argo, Ill.

REFERENCES

1. AINSWORTH, C. and JONES, R. G. J. Am. Chem. Soc. 76: 3172. 1954.
2. ARNDT, F. Organic syntheses. Vol. XV. John Wiley & Sons, Inc., New York. 1935. p. 4, Note 7.

3. ARNSTEIN, H. R. V. and BENTLEY, R. J. Chem. Soc. 3436. 1951.
4. BARHAM, H. N. and SMITS, B. L. Trans. Kansas Acad. Sci. 37: 91. 1934.
5. BEDEKAR, D. N., KAUSHAL, R. P., and DESHAPANDE, S. S. J. Indian Chem. Soc. 12: 465. 1935.
6. BEÉLIK, A. *In* Advances in carbohydrate chemistry. Vol. 11. *Edited by* M. L. Wolfrom. John Wiley & Sons, Inc., New York. To be published in 1956.
7. BRIGL, P. and GRÜNER, H. Ber. 65: 641. 1932.
8. CAMPBELL, K. N., ACKERMAN, J. F., and CAMPBELL, B. K. J. Org. Chem. 15: 221. 1950.
9. GOLDSCHMIDT, S. and VEER, W. L. C. Rec. trav. chim. 65: 796. 1946.
10. HAITINGER, L. and LIEBEN, A. Monatsh. 5: 339. 1884.
11. HEYNS, K. and VOGELSANG, G. Ber. 87: 1377. 1954.
12. HEYNS, K. and VOGELSANG, G. Ber. 87: 1440. 1954.
13. HURD, C. D. and SIMS, R. J. J. Am. Chem. Soc. 71: 2440. 1949.
14. INGOLD, C. K. Structure and mechanism in organic chemistry. Cornell Univ. Press, Ithaca, N.Y. 1953. pp. 206, 214.
15. INGOLD, C. K. and SHOPPEE, C. W. J. Chem. Soc. 1868. 1928.
16. LOOKER, J. H. and OKAMOTO, T. T. Abstr. of Papers, Am. Chem. Soc. 125: 9N. 1954.
17. MAURER, K. Ber. 63: 25. 1930.
18. PETUELY, F. and KÜNSSBERG, U. Monatsh. 83: 80. 1952.
19. SCHÖNBERG, A. and SINA, A. J. Am. Chem. Soc. 72: 1611. 1950.
20. WILLSTÄTTER, R. and PUMMERER, R. Ber. 38: 1461. 1905.
21. WOLFROM, M. L. Rec. trav. chim. 66: 238. 1947.
22. YABUTA, T. J. Chem. Soc. Japan, 37: 1185. 1916. Chem. Abstr. 17: 1475. 1923.
23. YABUTA, T. J. Chem. Soc. Japan, 37: 1234. 1916. Chem. Abstr. 17: 1475. 1923.
24. YABUTA, T. J. Chem. Soc. 125: 575. 1924.
25. YABUTA, T. and ANNO, K. J. Agr. Chem. Soc. Japan, 23: 104. 1949. Chem. Abstr. 44: 3492. 1950.
26. YALE, H. L. Chem. Revs. 33: 209. 1943.

Canadian Journal of Chemistry

Issued by THE NATIONAL RESEARCH COUNCIL OF CANADA

VOLUME 33 SEPTEMBER 1955 NUMBER 9

LONDON – VAN DER WAALS ATTRACTIVE FORCES BETWEEN GLASS SURFACES[1]

BY P. G. HOWE,[2,3] D. P. BENTON,[2] AND I. E. PUDDINGTON

ABSTRACT

The attractive force between a pyrex glass bead and plate has been measured using a sensitive pendulum-type apparatus. The force required for separation of the bead from the plate has been shown to be strongly time dependent, a phenomenon which appears not to have been reported previously for adhesions in gaseous media. The observed results have been shown to be consistent with the theoretical London – van der Waals interaction. The estimated value of the London force constant is compared with that obtained by other workers.

INTRODUCTION

Many workers have shown the existence of attractive forces between solid surfaces. Tomlinson (11) demonstrated the adhesion between quartz fibers and between equal glass spheres. Bradley (1) confirmed this adhesion between quartz spheres and improved the method to measure the adhesion between sodium pyroborate spheres and quartz spheres of unequal size. He also established experimentally the theoretical dependence of adhesion on the ratio of the bead diameters. McFarlane and Tabor (9) attempted to measure the interaction between a suspended glass bead and a glass plate by means of a pendulum-type apparatus. With this apparatus adhesions as low as 10^{-6} *g* could theoretically be measured but in clean dry air no adhesion was observed. Courtney-Pratt (3) found considerable adhesion when freshly cleaved mica sheets were placed in contact. Spaarnay and Overbeek (10) found the existence of long range attractive forces between highly polished parallel glass plates and that the calculated force constant was of the expected magnitude. Derjaguin (4) has also shown the existence of adhesion between various glasses but disagrees with the magnitude of those obtained by Spaarnay and Overbeek. In this paper the existence of time-dependent attractive forces between glass surfaces has been demonstrated. These have been attributed to London – van der Waals attractive forces and have been shown to be consistent with theoretical considerations.

[1]*Manuscript received March 24, 1955.*
Contribution from the Division of Applied Chemistry, National Research Council, Ottawa, Canada. Issued as N.R.C. No. 3669.
[2]*N.R.L. Postdoctorate Fellow, 1953–55, National Research Council, Ottawa, Canada.*
[3]*Present address: American-Marietta Company, Adhesives and Resin Division, Seattle 4, Washington, U.S.A.*

EXPERIMENTAL

Measurements have been made of the adhesion between pyrex glass surfaces using various pendulum-type apparatuses, both *in vacuo* and in small pressures of nitrogen. In the main these apparatuses have consisted of a glass bead, about 1 mm. diameter, formed on the end of a very fine pyrex fiber which was suspended by sealing into a 25 mm. pyrex tube. Contact surfaces were variously a flame-polished glass plate, a convex surface drawn in from the wall of the container tube and approximately equivalent to a sphere of radius 25 mm., or the concave inner wall of the glass tube itself, preheated to the melting point of the glass. Both bead and contact surfaces were formed just prior to assembly and evacuation of the apparatus. The apparatus was then degassed at about 350°C. and mounted on an electrically driven slow-motion rotor arm. When not continuously attached to the vacuum line, the apparatus was sealed off or closed with a vacuum stopcock. Some tubes were coated externally with electrically conducting silver paint and effectively earthed.

The measurement of adhesion was carried out as follows. The bead was allowed to make contact with the plate for a certain time and then the deflection, α, of the bead suspension from the vertical at the break point was measured. As the fiber suspensions used were practically weightless compared with the weight of the bead, calculation of the adhesion was made assuming a rigid pivoted assembly, using the equation

$$F = mg.\sin\alpha \qquad [1]$$

where m is the weight of the bead.

The results obtained show that adhesion exists but that the interaction is strongly time dependent. Very large instantaneous adhesions were found with the freshly degassed apparatus. The time of contact required for maximum adhesion increased, while the maximum adhesion itself fell, as the initial hard vacuum decayed in the closed system to *ca.* 10^{-3} mm. The adhesion then fell off more slowly over a period of days until some reproducible lower maximum was obtained.

Fig. 1 shows the *typical* slow build-up of the adhesion which was consistently encountered. The decay of adhesion after separation of the bead from the plate was very rapid, as is also shown in Fig. 1. Measurement of this decay of adhesion was carried out as follows. After a required separation time a quick measurement of adhesion was made within the minimum time necessary to bring the bead up to the plate and rotate to find the angle of break. The contact time required for this operation was about 10 sec. and the residual adhesion in the decay curve is due to this short contact time. This is also shown in Fig. 2, which is essentially a detail from Fig. 1. Fig. 2 further shows the reproducibility of the adhesion build-up in successive determinations.

DISCUSSION

1. The time dependency is possibly determined by the viscous flow of the gaseous or adsorbed medium from the gap between the approaching bead and plate, since with the freshly degassed surfaces the adhesion is very large and

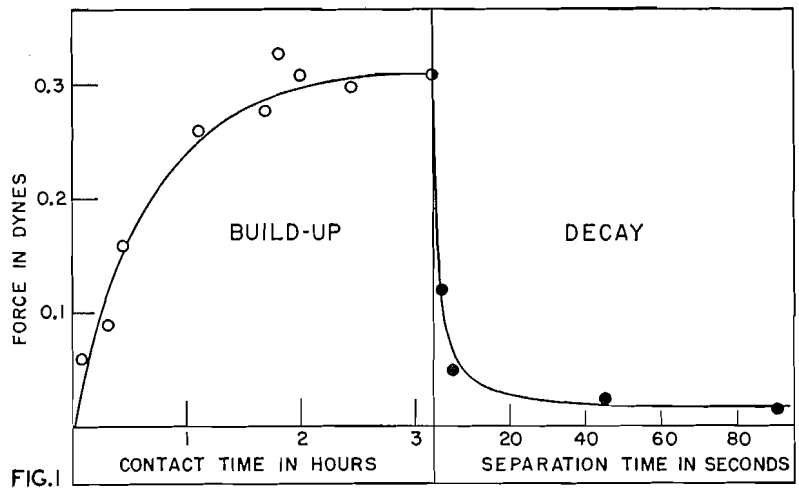

FIG. 1

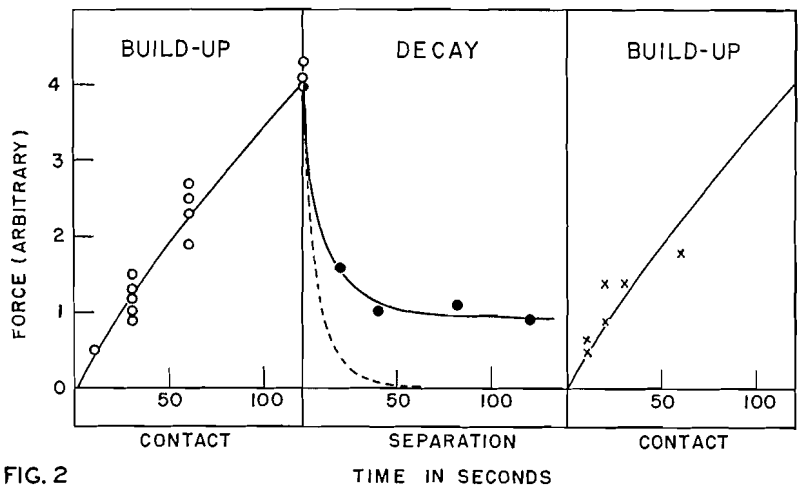

FIG. 2

FIG. 1. Adhesion build-up and decay for 0 7 mm. diameter bead and convex surface in decayed vacuum.

FIG. 2. Adhesion build-up and decay for 0.7 mm. diameter bead and convex surface in decayed vacuum. Residual adhesion of decay curve is due to short contact times required for force measurement.

instantaneous. If the movement over molecular distances of the bead towards the plate is responsible for the increase in adhesion with time, the time dependency of the decay may be explained by the reorientation of the molecules adsorbed on the surface. The initial rapid fall off in the maximum adhesion may be caused by this adsorption on the glass surface. The subsequent gradual fall off in the maximum adhesion might be attributed, in part, to the shock abrasion of the surfaces by repeated impact of the bead. Fig. 3 shows the decrease in the maximum adhesion over a period of several days in an apparatus containing 1 mm. of dry nitrogen. No very large adhesions were observed in atmospheres of nitrogen. The time required for the maximum adhesion

was very similar to that observed in a decayed vacuum although much greater than that required in freshly evacuated systems. This is consistent with the observed fall of the large maximum adhesions observed with freshly degassed and evacuated systems. The lower adhesions in atmospheres of nitrogen and the time dependence of the adhesion build-up might explain why McFarlane and Tabor (9) found no adhesion between glass surfaces in air. It is interesting to note that the adhesion kinetics reported in this paper are similar to those found by Derjaguin (4) for the interaction between quartz fibers in aqueous solution. The significance of this phenomenon in relation to the properties of suspensions is discussed elsewhere (7).

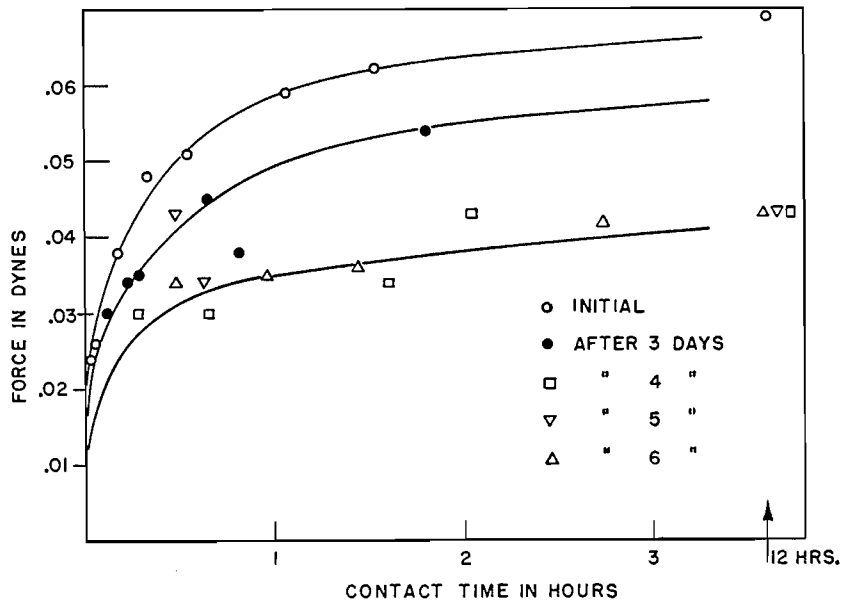

FIG. 3. Adhesion in 1 mm. nitrogen; 0.5 mm. diameter bead and convex surface.

In the course of the various experiments over a period of one year it was noted that the behavior of the bead was considerably affected by the induction of electrostatic charges. However, these decayed fairly rapidly and the consistent reproducibility of the adhesion and the adhesion kinetics points to the existence of attractive forces inherent in the system rather than spurious electrostatic charges. It seems unlikely that the mere 'contact' of the bead with the plate should induce electrostatic charge build-up. Also, the order of magnitude of the adhesion was found to be consistently the same in all experiments and with the various apparatuses used. In connection with this point it is interesting to refer to the behavior of glass spheres in anhydrous toluene (8). Agitation of the glass spheres in toluene apparently induces electrostatic charges which cause the beads to adhere to one another. Quite vigorous or prolonged agitation of the beads is required to produce agglomeration at room temperatures and the agglomerate collapses fairly rapidly in this temperature

region. Agitation of the beads alone, *in vacuo*, did not give any agglomeration, showing that the motion of the beads due to the supporting medium is important. In itself, this suggests that the contact of a bead with a plate is not sufficient to cause the build-up of an electrostatic attractive force. Furthermore, no indication of any increase in interparticle adhesion with time was obtained in the case of the uncharged sediments of glass spheres in various anhydrous liquids and with the glass beads *in vacuo*. If the observed time-dependent adhesion with the bead and the plate were electrostatic in origin, such an increase, of considerable magnitude, might be expected.

When the bead was brought into contact with the plate, it was allowed to rest under a small positive force. The application of larger positive forces did not seem to affect the observed adhesions. However, this was difficult to ascertain owing to the experimental difficulty of bringing the bead to the same position on the contact surface, since very small tangential forces would cause the bead to move in an arc, dictated by the fiber suspension, on the contact surface. Derjaguin (4) also observed the small dependence of the adhesion on the applied pressure in aqueous media.

McFarlane and Tabor (9) have shown that the elastic forces in the solid are important and that as the applied force is removed, contact points causing adhesion can break one by one. The measured adhesion is then the same as that without any applied load. In the above experiments it did not appear that elastic recovery prevented the measurement of adhesion. This is not surprising for two reasons; in the first place it is doubtful, except in the case of rigorously outgassed and freshly evacuated systems, whether the surfaces of the bead and plate in the above experiments ever were in true contact (continuous lattice formation) and secondly, elastic recovery at contact points implies an interaction between two irregular surfaces whereas in this case contact between the opposing lattices would be virtually at a single 'point' of molecular dimensions, if it occurred at all. It will be shown that the observed adhesion is consistent with the theoretical interaction expected for the close approach of the bead and the contact surface.

2. For the London – van der Waals force of interaction between a sphere and a plate Hamaker (5) obtains

$$F = AD/12d^2 \qquad [2]$$

where F is the force in dynes, $A = \pi^2 q^2 \lambda$, λ is the London constant, D is the diameter of the sphere in cm., d is the shortest distance of separation between the sphere and the plate in cm., and q is the number of atoms per cm^3.

This expression is not greatly affected by the curvature of the contact surface (the 'plate') as long as the radius of curvature of the plate is large compared with that of the bead. In the above experiments the curvature ratio was about 50 and any correction is of negligible importance, Fig. 4 shows the variation of F with d for a 1 mm. diameter bead, calculated from equation [2]. For a mean distance of close approach of 3–10 Å, which may be considered a reasonable range to assume for the approach between fused glass surfaces, it is seen that the attractive force would be in the vicinity of 10–100

dynes, taking the value of the A constant as 10^{-11} to 10^{-12} erg. This is consistent with the observation that the force of adhesion between freshly formed and rigorously degassed surfaces was well beyond the upper limit of force measurement of the apparatus which was about 1 dyne. The maximum adhesion measured with surfaces aged after evacuation and in atmospheres of nitrogen was generally of the order 0.1–0.2 dyne for beads of 1 mm. diameter. Taking the theoretical value of 10^{-12} for the force constant A, this corresponds

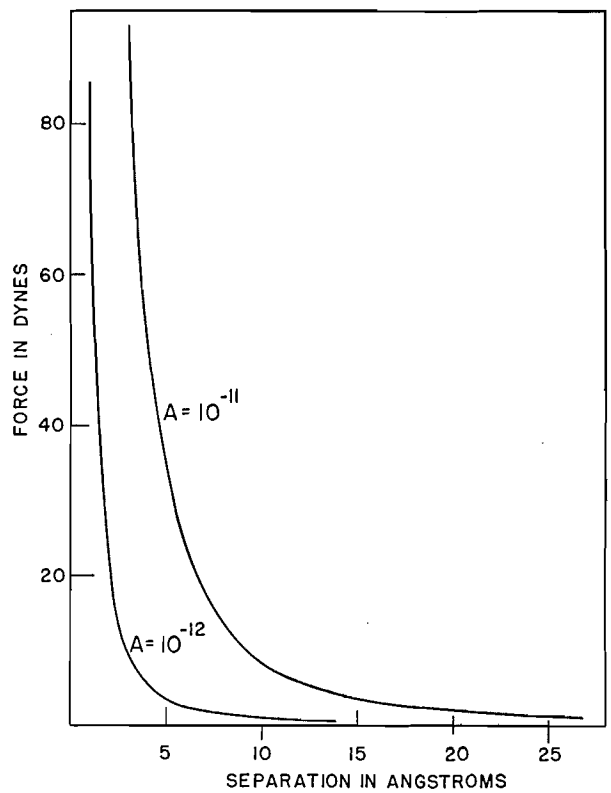

FIG. 4. Calculated interaction for 1 mm. diameter bead and plate.

to a distance of separation of 20–29 Å. This is a reasonable order for the effective separation in the presence of adsorbed foreign molecules in view of the separation considered *in vacuo*, and the fact that two solid surfaces are involved.

Table I shows the calculated variation in d, the closest distance of approach for perfect surfaces using the observed *maximum residual* forces of interaction. Using these values the selection of a value for the force constant A, which is consistent with the experimental evidence, will be considered. These residual forces were at least 10–100-fold less than the forces observed with freshly prepared and degassed systems *in vacuo*. This implies that the lower values of A, viz. 10^{-13} and 10^{-14}, can probably be eliminated since a 10–100-fold

TABLE I

CALCULATED SEPARATION BETWEEN 1 MM. DIAMETER BEAD AND PLATE FOR SELECTED VALUES OF THE A CONSTANT

A constant (ergs)	Separation d (Å)	
	F = 0.1 dyne	F = 0.2 dyne
10^{-10}	290	200
10^{-11}	91	65
10^{-12}	29	20
10^{-13}	9	7
10^{-14}	3	2

increase in the adhesion from the residual value would lead to a very unlikely value for the distance of closest approach, i.e., to within less than the diameter of an adsorbed gas molecule. Also, although fused glass surfaces are among the smoothest types of solid surfaces that can be obtained, surface undulations and discontinuities will possibly be of the order of 10–20 Å and this will tend to reduce the interaction. Calculated values of d will therefore tend to be too high, which favors the elimination of the lower values of the force constant.

For the residual adhesion it appears that the bead and the plate may be separated by adsorption products which prevent their approaching to within an atomic distance. It is unlikely that this adsorbed layer of gas could extend to over 50 Å from the surface of the solid, i.e., 10 or more molecular diameters. In view of this it is suggested that the values of 10^{-10} and 10^{-11} for A are too high. Adsorption studies in general indicate that after a few monolayers, adsorption energies are weak for physically adsorbed gases and approach normal bulk gaseous interactions. The observed results are therefore consistent with the adsorption of gaseous material and, with due allowance made for surface irregularities, the most favorable value of the A constant is about 10^{-12}, which agrees very well with the theoretical value.

3. The magnitude of the London – van der Waals interaction will depend on the value of the London constant, λ, which is included in the constant A. The direct experimental verification of the value of A is exceptionally difficult and the experimental results of different workers are conflicting. Table II shows the estimated values of A from the experimental data of other workers. These vary from about 10^{-10} to 10^{-14}, scattering about the theoretical estimate (2, 12) of 10^{-12} erg. For close approach between the surfaces a value of about 10^{-12} is general but Spaarnay and Overbeek (10) and Derjaguin (4), for wider distances of separation, give values which differ very considerably from one another. Unfortunately, the extreme sensitivity of the attraction to small changes of separation at close approach does not allow for a precise estimation of the force constant owing to the indeterminancy of the actual distance of separation, quite apart from other factors involved.

Derjaguin has suggested that the results of Spaarnay and Overbeek are too high owing to the inadequate removal of electrostatic mosaics from the glass surfaces. If this were the case it would seem surprising that the presence of water vapor or the coating of the glass plates with an evaporated silver layer

TABLE II

Author	Gaseous medium	Material	Minimum separation (Å)	A constant (ergs) ($\times 10^{12}$)
Bradley	Vacuum	Borate spheres	Close approach (3)	4.7*
	Vacuum	Quartz spheres	Close approach (3)	2.2*
Courtney-Pratt (3)	Air	Cleaved mica	Close approach (5–25)	0.1–10†
Spaarnay and Overbeek	Air	Glass plates 1	Close approach (200)	0.01–22
		Glass plates 2	Close approach (200)	0.015–15
		Glass plates 1	2500	1.1–30
		Glass plates 2	5000	60–230
		Quartz plates	3000	11–30
		Silvered quartz	8000	39–78
Derjaguin (4)	Air	Quartz sphere and plate	1000	0.05
Present authors	Vacuum and nitrogen	Pyrex glass bead and plate	Close approach	0.1–10†
Theoretical (2, 12)	Vacuum			1

**After Hamaker (6).*
†Estimates only. Calculated by present authors.

did not affect the measured interaction. It appears that the important question of the electrical neutrality of the surface, either on a molecular or on a macro scale, has not yet been settled. If a charge mosaic were capable of stable existence on such surfaces then it might be expected that such a phenomenon might also be a dominant factor in many types of suspensoidal systems. For glass type solids, the major part of the London interaction has been attributed to the highly polarizable oxygen atoms. In view of this, it is perhaps surprising that freshly sheared dispersions of paraffin wax in methanol coagulate spontaneously on standing. Vold (13) has offered an explanation of the interparticle adhesion in soap greases based on the polarizability of the oxygen atoms in the predominantly hydrocarbon fiber matrix. It is interesting to note, however, that comparable interparticle attraction apparently exists in polyethylene greases, in which the solid particles are totally hydrocarbon in composition and are embedded in a hydrocarbon liquid. This might suggest that such attractions are predominantly electrostatic in nature rather than London-type interactions. Alternatively, the application of the London additivity theorem to the interaction between solids might be inadequate, as suggested by Spaarnay and Overbeek, and much higher interactions than calculated from the London theory might be possible. Apart from the possibility of charged surface mosaics, the existence of induced like charges on two interacting glass-type surfaces might also be possible and thus account for the reduced interactions observed by Derjaguin. However, the present authors obtained reproducible adhesions in systems where there was no introduction of ionizing contaminants. The reproducibility of the observed adhesions suggests that the attractive force is an inherent property of the system and not due to electrostatic forces. The observed adhesion kinetics support this inference and are, in themselves, extremely important in the understanding and evaluation of colloidal and other aggregative phenomena.

REFERENCES

1. BRADLEY, R. S. Phil. Mag. 13: 853. 1932.
2. CASIMIR, H. B. G. and POLDER, D. Phys. Rev. 73: 360. 1948.
3. COURTNEY-PRATT, J. S. Proc. Roy. Soc. (London), A, 202: 505. 1950.
4. DERJAGUIN, B. V. *et al.* Discussions Faraday Soc. No. 18: 24. 1954.
5. HAMAKER, H. C. Physica, 4: 1058. 1937.
6. HAMAKER, H. C. Rec. trav. chim. 57: 61. 1938.
7. HOWE, P. G. and BENTON, D. P. To be published.
8. HOWE, P. G., BENTON, D. P., and PUDDINGTON, I. E. Can. J. Chem. 33: 1189. 1955.
9. MCFARLANE, J. S. and TABOR, D. Proc. Roy. Soc. (London), A, 202: 224. 1950.
10. OVERBEEK, J. T. G. and SPAARNAY, M. J. Discussions Faraday Soc. No. 18: 12. 1954.
11. TOMLINSON, G. A. Phil. Mag. 6: 695. 1928.
12. VERWEY, E. J. W. and OVERBEEK, J. T. G. Theory of the stability of lyophobic colloids. Elsevier Publishing Co., Inc., New York. 1948. p. 32.
13. VOLD, M. J. N.L.G.I. Spokesman, 19: 24. April, 1955.

THE MESOMORPHIC BEHAVIOR OF ANHYDROUS SOAPS

PART I. LIGHT TRANSMISSION BY ALKALI METAL STEARATES[1]

By D. P. Benton,[2] P. G. Howe,[2] and I. E. Puddington

ABSTRACT

The anhydrous salts of the long chain fatty acids are known to pass through a number of well-defined mesomorphic forms between the true crystalline solid and the isotropic liquid. The nature of some of these mesomorphic forms has been investigated by a study of their optical properties, electrical conductivity, density, and viscosity. In this paper, results obtained by an optical method are presented for phase transition temperatures of the alkali metal stearates and a number of sodium stearates having substituents in the hydrocarbon chain.

INTRODUCTION

The extensive and varied studies that have been made, in the past two or three decades, of the mesomorphic forms of salts of the long chain fatty acids have included a number of optical methods. The majority of the optical work has involved the use of hot stage microscopes; many photographs have been made of the different mesomorphic forms, particularly with the use of polarized light (10). The "hot wire" technique, used by Vold (7), has been very useful in the determination of phase transition temperatures. Relations between the transitions in different soaps have been investigated by Vold by a systematic microscopic study of the mesomorphic forms of the sodium salts of the *n*-fatty acids containing an even number of carbon atoms from C_6 to C_{22} (9) and also those of the series of alkali metal palmitates (11).

The optical methods have depended, in general, on the visual observation of change in appearance, usually by transmitted light, produced by the transition from one mesomorphic form to another. The experimental technique to be described here consists essentially of following the changes in intensity of light transmitted through the material under investigation, as a function of temperature, by means of a sensitive photometer. Besides confirming transitions which are observable to the eye without difficulty, this technique has enabled many less well defined changes from one mesomorphic form to another to be followed easily and speedily without camera work and without uncertainties caused by eye fatigue.

In this paper are given results obtained by the application of the light transmission technique to a study of the phase transitions in the alkali metal stearates and in a number of sodium stearates having substituents in the hydrocarbon chain. The density, viscosity, and electrical conductivity of these soaps have also been investigated in some detail and the results will be presented in subsequent papers in this series.

EXPERIMENTAL

Apparatus

The apparatus is shown diagrammatically in Fig. 1. The cell (*A*) consisted of a 3 in. length of precision molded Pyrex tubing, rectangular in cross-section,

[1]*Manuscript received March 24, 1955.*
Contribution from the Division of Applied Chemistry, National Research Council, Ottawa, Canada. Issued as N.R.C. No. 3673.
[2]*National Research Council Postdoctorate Fellow, 1953–55.*

supplied by H. S. Martin & Co. It was sealed at the lower end and fitted with a standard ground glass joint, for connection to the vacuum line, at the upper end. The internal dimensions of the cell were 10 mm.×2 mm. The cell fitted into a dural block furnace (*F*) which was bored so that light entering the tube (*B*) passed through the 2 mm. dimension of the cell. The block was

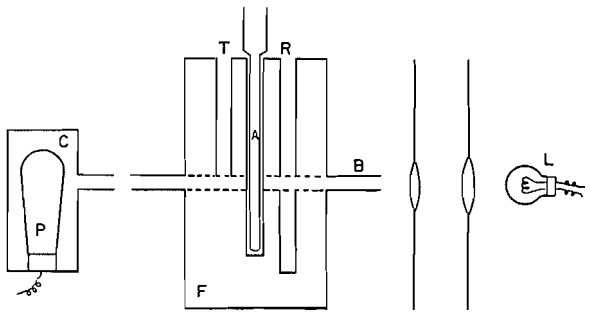

FIG. 1. Arrangement of apparatus (diagrammatic).

also bored to receive a thermocouple or thermometer at *T* and a mercury regulator at *R*. It was heated electrically by a Chromel winding and heavily lagged with asbestos. Temperature control was better than ±0.5°C. Light from an incandescent lamp (*L*) passed via a system of converging lenses through the tube (*B*) and was received by a phototube (*P*), mounted in the casing (*C*). The 12 volt lamp was usually run at 9 or 10 volts, this voltage being supplied from the mains, stabilized by a Sorenson regulator, and reduced by a Variac.

The maximum in the relative energy distribution curve for the lamp was in the wavelength region 7000–10,000 Å and the phototube selected was an RCA No. 917, giving maximum response in the region 7000–9000 Å. The phototube was operated in conjunction with a two-stage d-c. amplifier, this being a modification of a circuit appearing in Phototubes Form PT20R1 by RCA. The plate current of the second-stage amplification, a function of the light intensity and wavelength, was metered. A 1 ma. graphic meter was used, suitably shunted to give a recordable range of 0–20 ma. in the photoelectric current.

Preparation of Materials

The stearic acid used was the Eastman Kodak White Label material (m.p. 69–70°C.). 12-Hydroxystearic acid (m.p. 75°C.) was supplied by the Baker Castor Oil Co. 10-Methylstearic acid (tuberculostearic acid) (m.p. 26°C.) and 9-keto-10-methylstearic acid (m.p. 25°C.) were prepared by the method of Schmidt and Shirley (4). Phenylstearic acid was prepared from oleic acid by Friedel-Crafts reaction with benzene in presence of aluminum trichloride. This material was undoubtedly a mixture of the 9- and 10-phenylstearic acids.

The alkali metal salts (soaps) were prepared by titration of a hot solution of the acid in ethyl alcohol with an alcoholic solution of the appropriate alkali metal hydroxide, using phenolphthalein as indicator. The resultant gel (Na,

Rb, Cs stearates; Na 9-CO-10-Me stearate) or precipitate (Li, K stearates; Na 12-OH stearate; Na 10-Me stearate; Na phenyl stearate) was dried in an air oven at 105°C. In each case the soap was then fused under vacuum to remove last traces of water and alcohol. The opinion has been expressed, by Ralston (3) and Lawrence (1), that this treatment is insufficiently drastic to remove last traces of water associated with soaps. However, it has been shown (5) that the dilatometric behavior of sodium stearate prepared in the above manner is identical to that of sodium stearate prepared from sodium and stearic acid under anhydrous conditions. It would therefore seem most likely that fusion of the soap under vacuum will render it anhydrous.

Experimental Procedure

The soap was crushed and placed in the cell, which was then evacuated, and the temperature raised above the "final melting point" of the soap—this term being used to signify the temperature at which the soap becomes optically transparent. Nitrogen at a pressure of one atmosphere was then admitted to the cell. In the absence of this positive gas pressure slight degassing of the glass cell took place at higher temperatures and gas bubbles rising through the soap affected the measurement of the transmitted light intensity. This effect could be considerably reduced by prior degassing of the cell but was more conveniently eliminated by the presence of the nitrogen.

The temperature was then lowered in stages of about 5°C. and in each case time was allowed for the system to come to equilibrium, the criterion taken being a steady reading of the graphic meter for at least 15 min. Each substance investigated was run twice on a cooling curve and also checked on a heating curve. The equilibrium photoelectric current readings, being a measure of the intensity of light transmitted through the soap, were plotted as a function of temperature.

RESULTS AND DISCUSSION

The intensity of light transmitted through the 2 mm. thickness of soap decreased as cooling proceeded. A series of marked discontinuities occurred in the curve obtained by plotting the photoelectric current as a function of temperature. The results obtained are shown in Figs. 2 and 3. In these figures the degree of translucency of the soap, as measured by the photoelectric current, has been expressed as a percentage of the transparency of the liquid above the final melting point, i.e.,

$$\%\ \text{transmission at } T°\text{C.} = \frac{\text{photoelectric current at } T°\text{C.} \times 100}{\text{photoelectric current above final melting point.}}$$

While it is not presumed that the absolute values of the photoelectric current can have much significance in this experimental arrangement, the above function provides a convenient means of comparing the discontinuities in the change of translucency with temperature, for the different soaps. The temperatures at which these discontinuities appear have been found to be very accurately reproducible (virtually within 1°C.), both on cooling and on heating. The actual values of the photoelectric current were fairly reproducible on

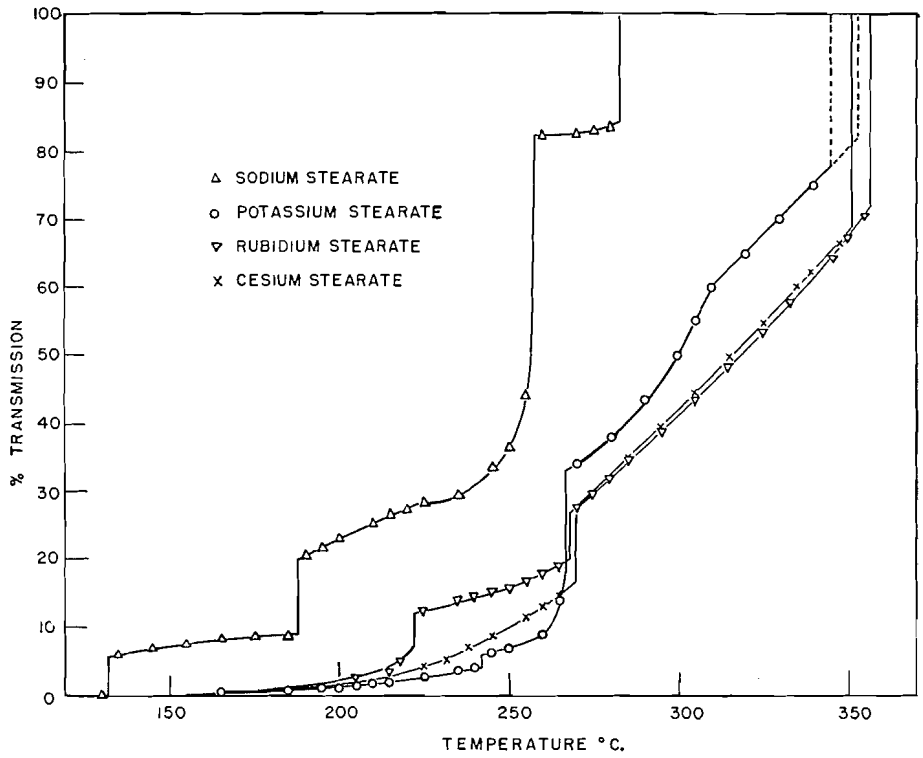

FIG. 2. Light transmission of alkali metal stearates as a function of temperature.

cooling curves but rather lower and less reproducible on heating curves, particularly at the lower temperatures. The reason for this is not perfectly clear but, in view of the excellent agreement between temperatures of discontinuities obtained on cooling and on heating, it would appear that supercooling is not responsible. One possible explanation may be that, on cooling from one phase to another where an appreciable density change is involved, microscopic cracking or vacuole formation may occur in the soap which will increase the light scattering and decrease the light transmission. On reheating it is to be expected that a hysteresis will exist in the closing of these cracks, leading to lower transmissions at any given temperature than those on cooling. Further, it is to be expected that the effect will be most marked in the lower temperature, more crystalline phases.

It should be mentioned here that one example of supercooling was observed in the case of lithium stearate. No results could be obtained for this soap below the temperature at which it melted to an optically clear liquid. The melting point was reproducible at 229°C. on heating. However, freezing occurred at temperatures between 229°C. and 218°C., depending on the rate of cooling. Below 229°C. the photoelectric current was irreproducible and no equilibrium was observed, even after two days had been allowed at each temperature.

A rather different phenomenon occurs in the case of potassium stearate

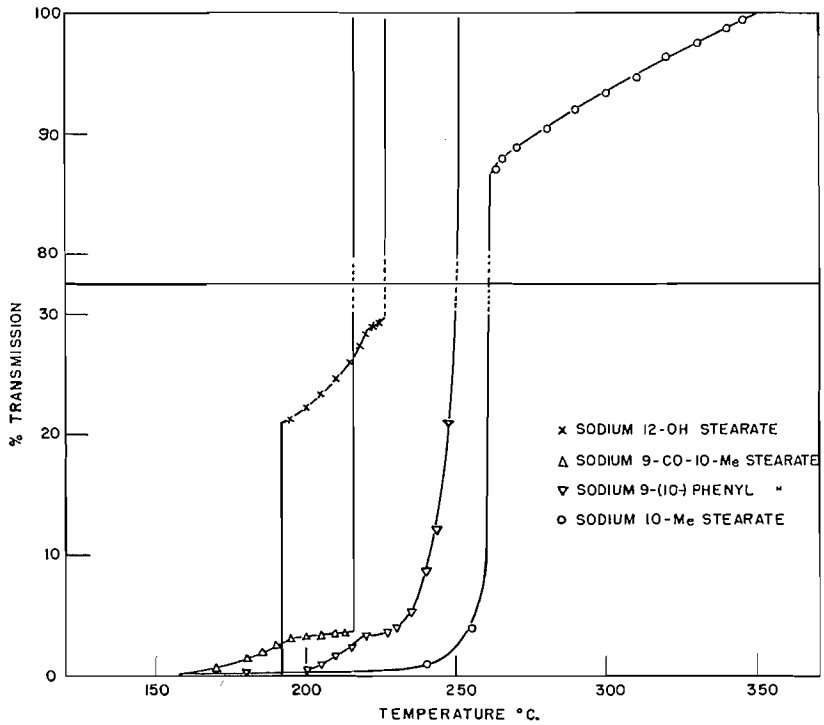

FIG. 3. Light transmission of some substituted sodium stearates as a function of temperature.

in the region of final melting. Between 345°C. and 353°C. two phases appear to be present, in stable equilibrium, and discrete lumps are visible to the naked eye. Above 353°C. the soap is optically clear and a maximum photoelectric current is obtained. Below 345°C. the homogeneous neat phase gives reproducible photoelectric current readings. Between these two temperatures, however, the reading depends on the position of the discrete lumps with respect to the optical path. For this reason, the final melting of potassium stearate is represented in two stages in Fig. 2.

A large non-equilibrium decrease in the intensity of transmitted light sometimes took place while a change was in progress. This was most probably caused by increased light scattering in the material while two phases were present.

A summary of the data obtained is given in Table II and comparison of the data for sodium stearate with those of Vold (8) and of Stross and Abrams (6) is given in Table I. It should be mentioned here that transition temperatures indicated by the optical method may not *necessarily* be true thermodynamic transition temperatures, since a change in translucency may be due to causes other than a phase transition. This may explain the discontinuity in the curve for sodium stearate at 188°C., which though doubtless a manifestation of the transformation from the superwaxy to the subneat phase is,

TABLE I

TRANSITION TEMPERATURES FOR SODIUM STEARATE

Transition	Temperature			
	Vold (8)	Vold (8)	Stross and Abrams (6)	This work
Curd–curd	89	90	88–96	—
Curd–subwaxy	114	117	112–118	—
Subwaxy–waxy	134	132	129–130	132
Waxy–superwaxy	—	167	—	165
Superwaxy–subneat	208	205	198	188 220
Subneat–neat	238	257	243–251 271–273	258
Neat–isotropic	280	288	280	283

TABLE II

SUMMARY OF OPTICAL TRANSITION TEMPERATURES

Soap	Final m.p., °C.					
Li stearate	229					
Na stearate	283	258	220†	188	165	132
K stearate	353, 345, 310†	267	242		160–165*	
Rb stearate	357	268	222		160–165*	
Cs stearate	351	270			160–165*	
Na 12-OH stearate	226		220†	192		
Na 9-(10-)phenyl stearate	250		220†		160–165*	
Na 10-Me stearate	*ca.* 350†	261			160–165*	
Na 9-CO-10-Me stearate	216		195†		160–165*	

**Temperature at which soap becomes opaque.*
†Minor transitions.

nevertheless, 10–15° lower than the previously reported temperatures of this transition. However, in general and where comparable, the agreement between the present data and transition temperatures determined by observation of other properties is very close.

It is apparent from Figs. 2 and 3 that the present transition data may be divided into two types, i.e. those transitions where an abrupt change occurs in the intensity of the transmitted light and those manifested by a change of slope in the light transmission – temperature curves. It is believed that the temperatures at which these latter minor changes occur are very much more accurately determined by the present technique than by the usual microscopic methods.

The final melting points of the alkali metal stearates are seen to rise from lithium to rubidium and then fall slightly in the case of cesium. This parallels the behavior of the palmitates (11). For sodium stearate in the neat phase the light transmission is nearly constant throughout the range of existence but shows a very large decrease at the transition neat to subneat at 258°C. In potassium, rubidium, and cesium stearates it decreases steadily as the neat phase is cooled and shows a very much smaller abrupt decrease at the transition neat to subneat. A small, but very definite and reproducible change is indicated within the neat phase, at 310–315°C., in the case of potassium stearate. Below the neat–subneat transition, the behavior of potassium,

rubidium, and cesium stearates is less closely similar. Between this transition and 165°C., where all three soaps become opaque, potassium stearate shows a transition at 242°C., rubidium stearate at 222°C., and cesium stearate none at all. A corresponding variation in sodium stearate,within the subneat phase, is found at 220°C., confirming the observation of Powell and Puddington (2) from viscosity determinations.

Below 165°C. only sodium stearate retains any degree of translucence and shows a minor transition at this temperature. The soap finally becomes abruptly opaque at 132°C., the accepted transition from the waxy to the subwaxy phase.

Turning to a consideration of the results obtained for the sodium salts of the substituted stearic acids, it is found that, with the exception of sodium 10-methyl stearate, a very much greater decrease in intensity of light transmitted through these soaps takes place at the melting point. A very large decrease does, in fact, occur in the sodium 10-methyl stearate at 261°C. but this temperature is not the final melting point. Optically clear liquid does not exist below about 340–350°C. It has not been found possible to fix a definite temperature; the photoelectric current starts to decrease slowly at approximately 350°C. Between 350°C. and 261°C. this soap definitely possesses considerable rigidity and will not, for example, flow under its own weight. The introduction of the methyl group into sodium stearate thus considerably strengthens the structure. The introduction of the phenyl group weakens it, (sodium phenyl stearate m.p. 250°C.). The methyl group has approximately the same dimensions as the cross-sectional area of the hydrocarbon chain and its presence might conceivably allow these chains to interlock instead of standing end to end, as is considered the case in the unsubstituted stearates. Such interlocking would not only increase the interaction between chains but would also increase the interaction between polar carboxylic end groups, in successive polar planes, since these would be brought closer together. The very much larger phenyl group would be more likely to affect the lateral chain spacings to such a degree that the result may be a reduction of chain interaction and probably even of polar interaction if similar over-all packing is exhibited.

The introduction of the carbonyl group in the 9-CO-10-Me stearate lowers the melting point to 216°C. and the 12-OH stearate melts at 226°C. This effect caused by the introduction of a second distal polar group in the molecule is consistent with the behavior of compounds such as octadecane dicarboxylates, although the strength and position of the second polar groups in the above compound is insufficient to eliminate the mesomorphic properties.

It is interesting to note that small discontinuities of the same type as that shown by sodium stearate are apparent at 220°C. in the 12-OH stearate and the phenyl stearate. Furthermore the 12-OH stearate shows an abrupt decrease in transmitted light at 192°C. to be compared with that in sodium stearate at 188°C.

Vold (11) has pointed out that, with the exception of lithium soaps, the temperature of formation of neat soap is essentially constant, being very nearly independent both of the nature of the cation, in the series of palmitates,

and of the length of the hydrocarbon chain. This is also seen to be true for the stearates. Vold concludes that the forces of interaction between the chains are therefore all important and it is especially interesting in this connection to consider the results obtained here for the substituted stearates.

In the neat phase of the unsubstituted soaps some type of micellar structure would seem to be involved. This micellar structure may still be possible in the case of the sodium methyl stearate, accounting for the transition at 261°C., but the large phenyl group is likely not to allow its formation, by virtue of both entropic and polar interactions. Also it is difficult to imagine a stable micellar structure in the cases where a second distal polar group is present in the hydrocarbon chain. The subneat–neat transition is that at which the soaps become appreciably electrically conducting and a study of this property, in progress at the moment, seems likely to give useful information regarding the structure of soaps in the high temperature phases. The results of this work will be given in a later paper in this series.

ACKNOWLEDGMENTS

We are indebted to Mr. J. K. Waterman for photometer construction and to Dr. A. M. Eastham for preparation of the substituted stearic acids.

REFERENCES

1. LAWRENCE, A. S. C. Trans. Faraday Soc. 34: 660. 1938.
2. POWELL, B. D. and PUDDINGTON, I. E. Can. J. Chem. 31: 828. 1953.
3. RALSTON, H. W. Fatty acids and their derivatives. John Wiley & Sons, Inc., New York. 1948. p. 889.
4. SCHMIDT, G. A. and SHIRLEY, D. A. J. Am. Chem. Soc. 71: 3804. 1949.
5. STAINSBY, G., FARNAND, R., and PUDDINGTON, I. E. Can. J. Chem. 29: 838. 1951.
6. STROSS, F. H. and ABRAMS, S. T. J. Am. Chem. Soc. 73: 2825. 1951.
7. VOLD, M. J. J. Am. Chem. Soc. 63: 160. 1941.
8. VOLD, R. D. J. Am. Chem. Soc. 63: 2915. 1941.
9. VOLD, R. D., MACOMBER, M., and VOLD, M. J. J. Am. Chem. Soc. 63: 1168. 1941.
10. VOLD, R. D. and VOLD, M. J. J. Am. Chem. Soc. 61: 808. 1939.
11. VOLD, R. D. and VOLD, M. J. J. Phys. Chem. 49: 32. 1945.

THE ACTION OF PYRIDINE ON DULCITOL HEXANITRATE[1]

By G. G. McKeown and L. D. Hayward

ABSTRACT

A pyridine solution of dulcitol hexanitrate evolved gas and became highly colored when warmed to 50°C.; dilution with water caused the precipitation of 67% of the theoretical amount of a dulcitol pentanitrate. The product was characterized as D,L-galactitol-1,2,4,5,6-pentanitrate by methylation to a monomethyl dulcitol pentanitrate, denitration of the latter, and periodate oxidation of the monomethyl dulcitol obtained. The hexitol derivatives were all obtained in a pure crystalline form. The significance of the data now available on the selective partial denitration by pyridine of hexitol hexanitrates is briefly discussed.

INTRODUCTION

In a previous research (5) it was shown that excess pyridine at 35°C. selectively removed the third (or equivalent fourth) nitrate group from D-mannitol hexanitrate to give D-mannitol-1,2,3,5,6-pentanitrate in 73% yield. This reaction was first described in 1903 by Wigner (14) who also reported a good yield of a mannitol pentanitrate from the action of alcoholic pyridine on mannitol hexanitrate. Wigner also nitrated dulcitol (I) to obtain a hexanitrate melting at "about 95°" (3, 4, 13) and found that alcoholic pyridine had almost no effect on this product even at the boiling point. Warming a solution of the dulcitol hexanitrate in pure pyridine, however, caused a reaction accompanied by evolution of a gas, and, on pouring the reaction mixture into water, Wigner obtained a crystalline product which "sintered at 71° and melted at about 75°" after three recrystallizations from aqueous alcohol. Analysis indicated this product to be a dulcitol pentanitrate.

In the present research Wigner's results were confirmed and the dulcitol pentanitrate was characterized as the racemic D- and L-galactitol-1,2,4,5,6-pentanitrate (III) by a series of reactions parallel to that previously described (5) for the characterization of D-mannitol-1,2,3,5,6-pentanitrate.

Dulcitol hexanitrate (D- or L-galactitol-1,2,3,4,5,6-hexanitrate) (II) was prepared in 92% yield by direct nitration of dulcitol (galactitol) (I) with nitric–sulphuric acid mixture, and the pure, crystalline, optically inactive compound melted at 98–99°C. and had the correct nitrate nitrogen content. Hydrogenolysis of a sample of the hexanitrate produced dulcitol quantitatively (5, 6). The hexanitrate dissolved readily in pure pyridine at 30°C. to give an initially colorless solution which became orange-colored in five minutes. No gas evolution was observed until the solution was warmed to 50°C., whereupon an exothermic reaction commenced, brown fumes were observed in the open vessel, and fine, colorless, needle-like crystals appeared on the inner walls of the flask above the solution. The vigorous reaction subsided within a few minutes and after 24 hr. the dark-red solution was poured into

[1]*Manuscript received May 30, 1955.*
Contribution from the Department of Chemistry, University of British Columbia, Vancouver, B.C. This paper constitutes part of a thesis submitted by G. G. McKeown in partial fulfillment of the requirements of the degree of Master of Science in Chemistry, September 1952.

water which caused the separation of crystalline dulcitol pentanitrate (III) in 63–72% yield. The pure pentanitrate melted at 85–86°, was optically inactive, and did not reduce Fehling's solution (13). Hydrogenolysis again gave a nearly quantitative yield of dulcitol thus proving that the pyridine caused no structural or configurational changes in the hexitol skeleton. The pentanitrate was stable to the further action of pyridine under conditions which caused the partial denitration of the hexanitrate.

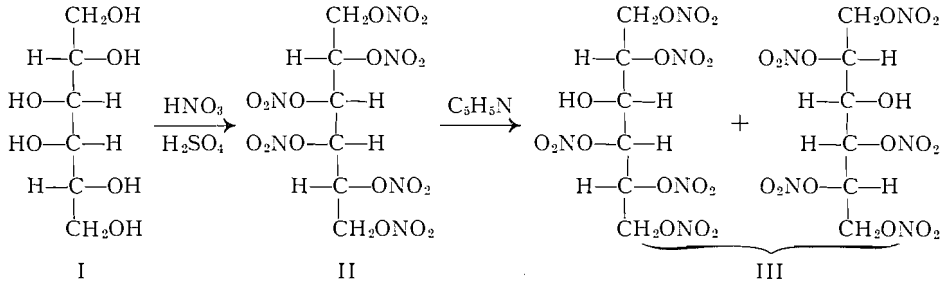

I II III

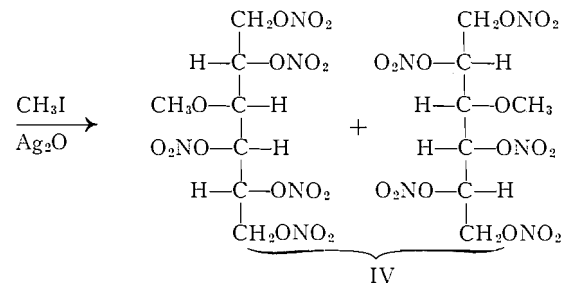

IV

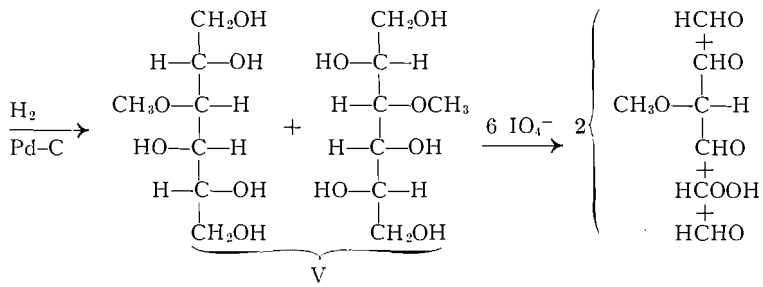

V

II or III $\xrightarrow{H_2,\ Pd\text{–}C}$ I (quantitative) III + C_5H_5N ⟶ 94% recovery

V $\xrightarrow[H_2SO_4]{HNO_3}$ IV (75%) IV + C_5H_5N ⟶ 89% recovery

Methylation of the pentanitrate gave a 67% yield of a new methyl dulcitol pentanitrate (IV), m.p. 99–100°C., with correct methoxyl and nitrogen analyses and this compound was also stable to pyridine at room temperature. Catalytic hydrogenolysis of the methylated pentanitrate yielded a crystalline

monomethyl dulcitol (V) melting at 149–150°. A sample of (V) was renitrated with mixed acids at −10°C. to give a 75% yield of the original methyl dulcitol pentanitrate (IV).

A literature search revealed no previous report of monomethyl derivatives of dulcitol and, apart from an independent synthesis, periodate oxidation appeared to be the most reliable means of locating the position of the methyl group. Taking account of the meso configuration of dulcitol our monomethyl hexitol was one of three possible compounds: a racemate of (1) D- and L-1-*O*-methyl galactitol, (2) D- and L-2-*O*-methyl galactitol, or (3) D- and L-3-*O*-methyl galactitol. The theoretical behavior of these compounds toward periodate oxidation is summarized in Table I.

TABLE I

THEORETICAL PRODUCTS OF THE PERIODATE OXIDATION OF HEXITOL MONOMETHYL ETHERS

	Position of OCH_3 group	Periodate consumed (moles)	Oxidation products (moles)		
			HCHO	HCOOH	Other
Case 1	1 or 6*	4	1	3	CHO | CH_2OCH_3
Case 2	2 or 5*	3	1	2	CH_2OH | H—C—OCH_3 | CHO
Case 3	3 or 4*	3	2	1	CHO | H—C—OCH_3 | CHO

**Pairs of structural isomers although each compound has a unique configuration. Of the mannitol and iditol derivatives only one compound of the* D*-configuration and one of the* L*-configuration can exist in each case. For dulcitol and allitol derivatives the pair in each case is racemic.*

Oxidation of the monomethyl dulcitol with aqueous sodium periodate at room temperature showed a consumption of 4.9 moles of oxidant with the production of 2.1 moles of formic acid and 2.0 moles of formaldehyde per mole of methyl ether. Dulcitol under the same conditions gave the nearly theoretical values of consumption of oxidant (4.95 moles), formic acid (3.68 moles), and formaldehyde (1.98 moles). Comparison of the results for the monomethyl dulcitol with Table I showed Case 1 to be ruled out and that either Case 2 or Case 3 could have given these values if an additional oxidation requiring 2 moles of oxidant occurred with the concomitant formation of an extra mole of formaldehyde or of formic acid respectively. The rate of the periodate oxidation was therefore studied to determine the possibility of "overoxidation" at room temperature. The rates of oxidant consumption, and aldehyde and acid production at 23°C. for the monomethyl dulcitol (Fig. 1, Curves A, B, and C) indicated a rapid initial consumption of 3 moles of oxidant producing 2 moles of formaldehyde and approximately 1 mole of formic acid. The results at this stage conformed to Case 3. An hour later the aldehyde value was the same but the amount of

formic acid had increased to 2 moles and that of oxidant consumed to 5. A rate reaction run at 0°C. (Fig. 1, Curve D) in order to slow or halt the overoxidation clearly showed the rapid initial formation of 1 mole of formic acid followed by a slower secondary oxidation in which further quantities of

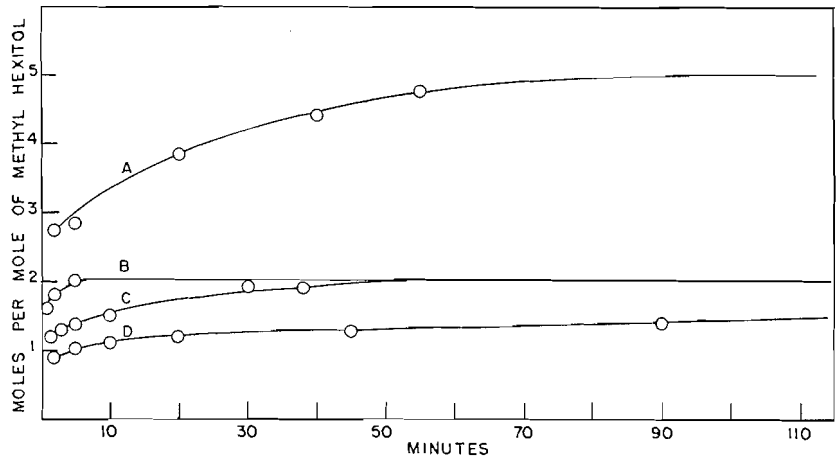

FIG. 1. Periodate oxidation of 3-*O*-methyl-D,L-galactitol.
A: Periodate consumption at 23°C.
B: Formaldehyde production at 23°C.
C: Formic acid production at 23°C.
D: Formic acid production at 0°C.

acid were produced to the final total of 2.0 moles of acid at 11 hr. These data indicated Case 3 to be involved and that the dialdehyde formed (Table I) in the first stages of the oxidation was oxidized further to produce a mole of formic or other acid. A similar reaction of the dialdehyde of malonic acid

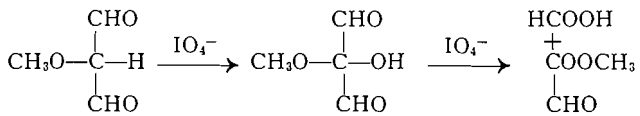

VI

(VII) was reported by Huebner, Ames, and Bubl (7) in which 3 moles of formic acid was produced with oxidant consumption of 3 moles. The methyl

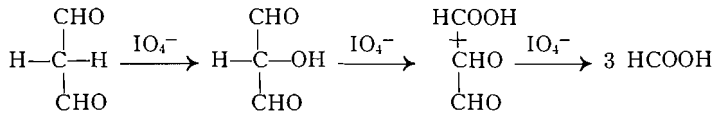

VII

ester of glyoxylic acid (VI) presumably formed in Case 3 could be expected to be comparatively stable to further oxidation. The unique correlation of the periodate oxidation data was for the monomethyl dulcitol to be the racemate,

3-*O*-methyl-D- and L-galactitol (V), and hence the structures and configurations of the compounds (III) and (IV) which preceded it were also established.

The reactions of mannitol and dulcitol hexanitrates with pyridine were analogous and consisted in the replacement of a nitric acid ester group by hydrogen at the 3 (or equivalent 4) position in about 70% of the hexanitrate molecules. No inversion of configuration occurred at the asymmetric center attached to the nitrate group and it may therefore be assumed that the O—N bond was cleaved through some type of nucleophilic attack of pyridine on the nitrate nitrogen (1, 2).

The selectivity of the reaction for one particular nitrate group among six in each molecule is intriguing. To test the hypothesis that this group must occupy a unique spatial environment we plan to treat the nitrates of other polyols with pyridine. Urbanski and Kwiatkowska (12) reported partial denitration of sorbitol hexanitrate when it was heated with alcoholic pyridine; however, the viscous product was not characterized.

EXPERIMENTAL

Materials and Methods

Since dulcitol hexanitrate and its partially nitrated derivatives are explosives (11), the scale of the preparations was restricted to 5 gm. or less and all evaporations were under reduced pressure with bath temperatures not exceeding 50°C.

Pure dulcitol (galactitol (I)) (m.p. 187–188°, optically inactive) (8) when nitrated with fuming nitric and concentrated sulphuric acids at −10°C., as described by Bechamp (3) and Patterson and Todd (9), gave a 92% yield of the crystalline dulcitol hexanitrate (II). After recrystallization from aqueous ethanol the colorless, needle-like crystals of hexanitrate were optically inactive and melted at 98–99°C. (corr.). The melting point was not altered by further recrystallizations. Previous workers (3, 13, 14) reported a melting point of 95°C. Found: N (nitrometer), 18.4, 18.8%. Calc. for $C_6H_8(NO_3)_6$: N, 18.6%. Hydrogenolysis of 0.685 gm. of the hexanitrate over palladized charcoal at 20–30 p.s.i. and room temperature as previously described (5, 6) yielded 0.289 gm. of crude product. Recrystallization from aqueous ethanol gave thick, colorless crystals melting at 185–187°C. A mixed melting point with authentic dulcitol showed no depression.

The analytical procedures for nitrate nitrogen, methoxyl, and periodate oxidation products were previously described (5, 6, 10).

Action of Pyridine on Dulcitol Hexanitrate

A 500 ml. Erlenmyer flask containing 3.11 gm. of pure dry dulcitol hexanitrate was immersed in a water-bath at 30°C. The hexanitrate dissolved immediately on addition of 25 ml. of pyridine (B.D.H. analytical reagent grade) to form a clear, colorless solution which became orange-colored within five minutes. No further change was observed until the water-bath was heated to 50°C. when the solution rapidly evolved small bubbles of gas and fine, colorless crystal-needles appeared on the neck of the flask. After the first vigorous reaction had subsided, the now dark-red solution was allowed to stand at room temperature for 24 hr. and was then poured with stirring into

300 ml. of water. The colorless sirup which separated crystallized readily and was recovered on a glass filter, washed thoroughly with water, and dried to constant weight *in vacuo*; yield 1.81 gm. (65%). Yields obtained in similar denitrations were 63, 65, 69, and 72%. Recrystallization of the product from aqueous ethanol, ether – petroleum ether, or carbon tetrachloride yielded colorless needles of pure dulcitol pentanitrate (D,L-galactitol-1,2,4,5,6-pentanitrate) (III); m.p. 85–86°C., optically inactive, soluble in alcohol, ether, benzene, and chloroform, insoluble in water and petroleum ether. The pentanitrate did not reduce Fehling's solution (13, 14). Found: N (nitrometer), 16.9, 17.0%. Calc. for $C_6H_8(OH)(NO_3)_5$: N, 17.2%.

A sample of the dulcitol pentanitrate (0.63 gm.) when treated with pyridine (4.0 ml.) under the conditions which caused denitration of the hexanitrate produced no gas, although the solution became dark-red in color. Unchanged pentanitrate, 0.59 gm. (94%), was recovered when the solution was worked up as described above. A 0.240 gm. sample of dulcitol pentanitrate yielded 0.110 gm. (100%) of crude dulcitol when hydrogenolyzed as described for the hexanitrate. The pure product melted at 185–188°C. and caused no depression in the melting point of pure dulcitol.

Methyl Dulcitol Pentanitrate (*3-O-Methyl*-D,L-*galactitol-1,2,4,5,6-pentanitrate*) (*IV*)

Dulcitol pentanitrate, 0.730 gm., was dissolved in 11 ml. of methyl iodide and 4 ml. of methanol and treated with 5 gm. of Drierite and 5 gm. of freshly-prepared silver oxide. After being refluxed for nine hours the mixture was filtered and the solids washed with dry acetone. Evaporation of the filtrate and washings and recrystallization of the colorless solid residue from aqueous ethanol yielded 0.508 gm. (67%) of monomethyl dulcitol pentanitrate (3-*O*-methyl-D,L-galactitol-1,2,4,5,6-pentanitrate) (IV); m.p. 99–100°C., soluble in alcohol, ether, acetone, and dioxane, insoluble in water. Found: N, 16.6, 16.5%; OCH_3, 7.34, 7.37%. Calc. for $C_6H_8(OCH_3)(NO_3)_5$: N, 16.6%; OCH_3, 7.37%. A sample of the methylated dulcitol pentanitrate was recovered unchanged in 89% yield from a pyridine solution after two days at room temperature.

Monomethyl Dulcitol (*3-O-Methyl*-D,L-*galactitol*) (*V*)

Monomethyl dulcitol pentanitrate, 1.42 gm., dissolved in 30 ml. dioxane diluted with 45 ml. ethanol and 5 ml. of water was hydrogenated at room temperature over 1 gm. of palladized charcoal at 45 p.s.i. After one hour the pressure became constant and the solution was free of nitrate by the diphenylamine test. The catalyst was filtered off, and evaporation of the solution left a colorless crystalline product. Recrystallization from boiling absolute alcohol gave 0.552 gm. (83%) of thick, colorless crystals; m.p. 149–150°C. Recrystallization from isoamyl alcohol or from water yielded the same product. Found: OCH_3, 16.1, 16.0%. Calc. for $C_6H_8(OCH_3)(OH)_5$: OCH_3, 15.8%. The monomethyl dulcitol did not react with Fehling's solution or bromine water.

Nitration of a sample of the monomethyl dulcitol with sulphuric–nitric acid mixture gave a 75% yield of the original 3-*O*-methyl-D,L-galactitol-

1,2,4,5,6-pentanitrate, identified by a mixed melting point and methoxyl analysis. Found: OCH_3, 7.39, 7.20%.

Periodate Oxidation of Monomethyl Dulcitol (3-O-Methyl-D,L-galactitol) (V)

Forty to fifty milligram samples of the monomethyl dulcitol were oxidized with aqueous sodium periodate solution by procedures previously described (6) which revealed the amount of periodate consumed and the amounts of formic acid and formaldehyde formed. At room temperature the amounts of formic acid obtained per mole of methyl dulcitol were 1.20, 1.30, 1.38, 1.51, 1.91, 2.06, and 2.11 moles after 1.5, 3, 5, 10, 38, 130, and 900 min. respectively. At 960 min. 4.93 moles of periodate had been consumed and at 1020 min. the formaldehyde production was found to be 1.98 moles. In two other runs under the same conditions the consumption of 2.76, 2.83, 3.86, 4.43, and 4.77 moles of periodate at 2, 5, 20, 40, and 55 min. was observed while the molar production of formaldehyde amounted to 1.61, 1.81, 2.02, 1.92, and 1.98 after 1, 2, 5, 30, and 1020 min. Oxidation of pure dulcitol under the same conditions formed 3.53, 3.63, and 3.68 moles of formic acid after 5, 15, and 25 hr. At 25 hr. the periodate consumption was found to be 4.95 moles and formaldehyde production 1.98 moles.

An oxidation of methyl dulcitol conducted in an ice bath revealed formic acid production as 0.91, 1.04, 1.12, 1.20, 1.27, 1.40, 1.70, 2.06, and 2.11 moles after 2, 5, 10, 20, 45, 90, 300, 660, and 1440 min.

The data for the oxidation of the monomethyl dulcitol are plotted in Fig. 1; theoretical values for the different structural isomers are listed in Table I.

ACKNOWLEDGMENT

The authors wish to thank the National Research Council of Canada for Grant G249 which helped to defray the cost of this research. One of them (G.G.M.) also thanks the Standard Oil Company of British Columbia Limited for a Fellowship which enabled him to complete the work.

REFERENCES

1. ANBAR, M., DOSTROVSKY, I., SAMUEL, D., and YOFFE, A. D. J. Chem. Soc. 3603. 1954.
2. BAKER, J. W. and NEALE, A. J. J. Chem. Soc. 608. 1955.
3. BECHAMP, A. Compt. rend. 51: 255. 1860.
4. CHAMPION, P. Compt. rend. 78: 1150. 1874.
5. HAYWARD, L. D. J. Am. Chem. Soc. 73: 1974. 1951.
6. HAYWARD, L. D. and PURVES, C. B. Can. J. Chem. 32: 19. 1954.
7. HUEBNER, C. F., AMES, S. R., and BUBL, E. C. J. Am. Chem. Soc. 68: 1621. 1946.
8. LOHMAR, R. and GOEPP, R. M., JR. *In* Advances in carbohydrate chemistry. Vol. 4. *Edited by* W. W. Pigman and M. L. Wolfrom. Academic Press, Inc., New York. 1949. p. 219.
9. PATTERSON, T. S. and TODD, A. R. J. Chem. Soc. 2876. 1929.
10. SEGALL, G. H. and PURVES, C. B. Can. J. Chem. 30: 860. 1952.
11. TAYLOR, C. A. and RINKENBACH, W. H. J. Franklin Inst. 204: 369. 1927.
12. URBANSKI, T. and KWIATKOWSKA, S. Roczniki Chem. 25: 312. 1951.
13. VIGNON, L. and GERIN, F. Compt. rend. 133: 540. 1901.
14. WIGNER, J. H. Ber. 36: 794. 1903.

COEXISTENCE PHENOMENA IN THE CRITICAL REGION

III. COMPRESSIBILITY OF ETHYLENE AND XENON FROM LIGHT SCATTERING[1]

By F. E. Murray[2] and S. G. Mason

ABSTRACT

Turbidity measurements in the region immediately above the critical temperature are used to calculate values of $(\partial p/\partial v)_T$. These results show that $(\partial p/\partial v)_T$ is a continuously variable function of the density to within 0.02°C. above the critical temperature. The experiments indicate that there exists no region above T_c throughout which $(\partial p/\partial v)_T = 0$ in ethylene or xenon.

INTRODUCTION

In 1938 Mayer and Harrison (9, 10) concluded from a statistical treatment of a real gas that the phase transition at the critical point did not occur in the manner proposed by Andrews (1, 2). Their prediction of a "derby hat" region between two characteristic temperatures has stimulated a great deal of experimental work.

Maass (6) has summarized the evidence for the existence of anomalous behavior. Zimm (19), from a series of light-scattering measurements, concluded that the region predicted by McMillan and Mayer (8) did not exist in the case of a binary liquid system. From a theoretical viewpoint, Zimm (20) has discussed the probability of a single critical temperature. Weinberger and Schneider (16, 17) and Habgood and Schneider (4) found no evidence of a "derby hat" region in xenon. Other results observed in unstirred systems are of questionable value in settling this question, as it is doubtful if equilibrium can be attained without mechanical mixing. The experimental work described here was undertaken to obtain information regarding the validity of conclusions by Mayer and Harrison.

To account for the turbidity in the critical region of a pure gas, Smoluchowski (15) and Einstein (3) derived an equation from the theory of density fluctuations which may be written

$$[1] \qquad \frac{I_\theta}{I_0'} = \frac{A T \rho^3}{\lambda^4}\left[\frac{1+\cos^2\theta}{-(\partial p/\partial v)_T}\right].$$

Here I_θ is the intensity of the radiation scattered at angle θ from the incident beam, I_0' is the incident intensity, and λ the wavelength of the incident light beam. A is a constant for a particular gas and a fixed distance of observation, T is the absolute temperature, ρ is the density, and p and v are the pressure and specific volume of the fluid.

When the angular dependence of I_θ is given by the factor $(1+\cos^2\theta)$, the turbidity τ is related to the transversely scattered light by the equation

$$[2] \qquad \tau = b\, I_{90°}/I_0',$$

[1]*Manuscript received May 9, 1955.*
Contribution from the Chemistry Department, McGill University, Montreal, Quebec.
[2]*Holder of a Fellowship from the National Research Council of Canada. Present address: Chemistry Department, University of Manitoba, Winnipeg, Manitoba.*

where b is a constant. Equations [1] and [2] may be combined to yield:

$$[3] \qquad \tau = \frac{BT\rho^3}{\lambda^4} \Big/ -\left(\frac{\partial p}{\partial v}\right)_T.$$

Equation [3] predicts that I_θ becomes infinite when $(\partial p/\partial v)_T = 0$, i.e. at the classical critical point. This result is obtained because the derivation predicts infinite density fluctuations at the critical point. Physically, it is of course impossible for I_θ to be infinite. In a modified treatment of the problem by Ornstein and Zernicke (12, 13), the density fluctuations at the critical point are infinite, but I_θ is kept finite owing to optical interference between wavelets scattered from different volume elements in the fluid.

In a more detailed analysis, which neglects optical interference, Rocard (14) derived the equation

$$[4] \qquad \tau = \frac{BT\rho^3}{\lambda^4} \Big/ \left(-\left(\frac{\partial p}{\partial v}\right)_T + c\right),$$

where c is a constant for any particular gas and light source.

In the development of Eq. [4], both the density fluctuations and the value of I_θ are kept finite when $(\partial p/\partial v)_T$ becomes zero. Klein and Tisza (5) have shown that both Eq. [3] and Eq. [4] as well as that of Ornstein and Zernicke follow from their work.

At constant λ and over a small temperature range, Eq. [4] may be rearranged to the form

$$[5] \qquad \tau^{-1} = \frac{K}{\rho^3}\left[-\left(\frac{\partial p}{\partial v}\right)_T + c\right],$$

where K is virtually constant.

From Eq. [5] it follows that

$$[6] \qquad -\left(\frac{\partial p}{\partial v}\right)_T = \frac{\rho^3\tau^{-1}}{K} - c.$$

If K and c are known, $(\partial p/\partial v)_T$ may be calculated using Eq. [6]. In any case, $(\partial p/\partial v)_T$ is a linear function of $\rho^3\tau^{-1}$ over the temperature range in which K may be considered constant. Equation [6] indicates that if $(\partial p/\partial v)_T$ becomes zero, $\rho^3\tau^{-1} = Kc$, i.e. $\rho^3\tau^{-1}$ should be constant within the "derby hat" region predicted by Mayer and Harrison (9, 10).

In this investigation, the turbidity τ was calculated from measurements of transmitted light using the relation (for 1 cm. light path in the fluid)

$$\tau = 2.30 \log(I_0'/I'),$$

where I' is the intensity of the transmitted beam.

A polychromatic light source was used to give high intensity illumination which could be measured with a 929 photocell. Since the total intensity of such a beam may be written as the sum of intensities at various wavelengths in the incident light, then the total intensity is

$$I_0' = \sum I_0'(\lambda),$$

where the sum is taken over all wavelengths in the spectrum of the incident beam. $I_0'(\lambda)$ is the incident intensity over a small wavelength interval. For the scattered intensity in a single wavelength interval, Rocard's equation predicts that

$$I_\theta(\lambda) = \frac{I_0'(\lambda)}{\lambda^4} AT\rho^3 \left[\frac{1+\cos^2\theta}{-(\partial p/\partial v)_T + c}\right].$$

For the total intensity scattered from the polychromatic beam at angle θ,

[7] $$\sum I_\theta(\lambda) = \sum \frac{I_0'(\lambda)}{\lambda^4} AT\rho^3 \left[\frac{1+\cos^2\theta}{-(\partial p/\partial v)_T + c}\right].$$

When both sides of [7] are divided by $\sum I_0'(\lambda)$, the intensity of transversely scattered light becomes

[8] $$\frac{I_{90°}}{I_0'} = \frac{AT\rho^3}{\sum I_0'(\lambda)} \sum \frac{I_0'(\lambda)}{\lambda^4} \left[\frac{1}{-(\partial p/\partial v)_T + c}\right].$$

Combining equations [2] and [8] yields

[9] $$\tau = \frac{BT\rho^3}{I_0'} \sum \frac{I_0'(\lambda)}{\lambda^4} \left[\frac{1}{-(\partial p/\partial v)_T + c}\right].$$

For any stable light source, where the distribution of $I_0'(\lambda)$ remains constant throughout the spectrum of the beam, $\sum I_0'(\lambda)/\lambda^4$ is constant and equation [9] may be written

[10] $$\tau = DT\rho^3/(-(\partial p/\partial v)_T + c)$$

or in a form similar to Eq. [6],

[11] $$-\left(\frac{\partial p}{\partial v}\right)_T = \frac{\rho^3 \tau^{-1}}{K'} + c.$$

Equation [11] is the form applicable to the following experimental results.

T_c is defined as the highest temperature (°C.) at which visible droplets form on slow cooling of the fluid; $\Delta T = (T - T_c)$ and may be positive or negative. The mean density $\bar{\rho}$ equals total mass of gas divided by volume of bomb.

EXPERIMENTAL

Apparatus

Except for modifications made to obtain transmission measurements, the apparatus was the same as that previously described (11). These modifications included the addition of a 929 photocell to the optical measuring assembly of Fig. 2 in Reference (11) to measure the intensity of the transmitted light. Except for a small round opening (about $\frac{1}{4}$ in. diameter) upon which the incident beam was aligned, the glass envelope of the photocell was painted black. The entire optical assembly could be moved to any desired level along the glass bomb.

The fluid sample was contained in a long (about 35 cm.) glass bomb (11). The bomb used in these experiments was sealed off at a point approximately

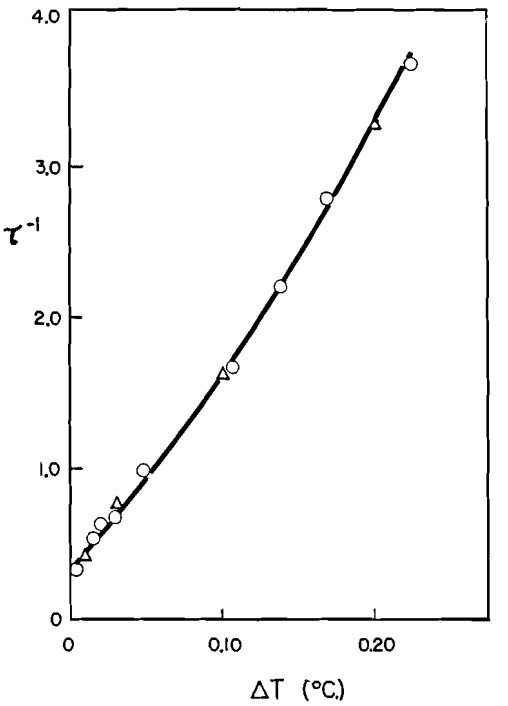

FIG. 1. Variation of τ^{-1} with $\Delta T = T - T_c$ at the density of maximum turbidity of xenon. The circles are measured values and the triangles values calculated from $(\partial p/\partial v)_{\min}$ values of Habgood and Schneider (4) using the Rocard equation.

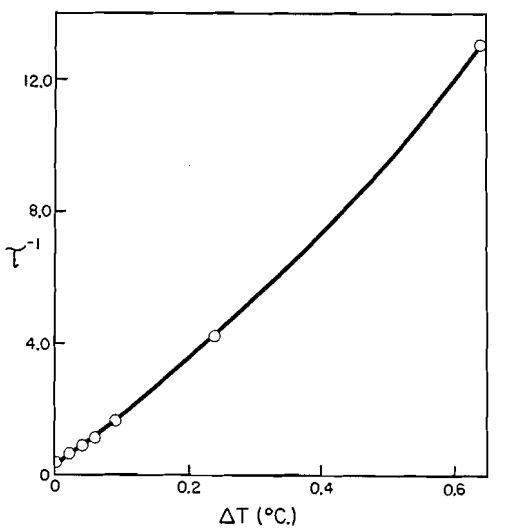

FIG. 2. Variation of τ^{-1} with ΔT at the density of maximum turbidity in ethylene.

10 cm. from the extreme top. This sealed-off portion was filled with methanol and was used at one fixed point to check and maintain a constant incident light intensity. The light source and 929 photocell combination had extremely good stability.

Procedures

The ethylene sample was Phillips research grade and contained 99.9 mole per cent ethylene before fractionation in the glass filling apparatus. The xenon was obtained from Linde Air Products and showed only the xenon spectrum when analyzed in a mass spectrometer. The xenon and ethylene samples were purified and distilled into the glass bomb in the manner previously described (11).

All transmission measurements were obtained immediately after vigorous stirring of the fluid and at one level near the center of the bomb. In this way,

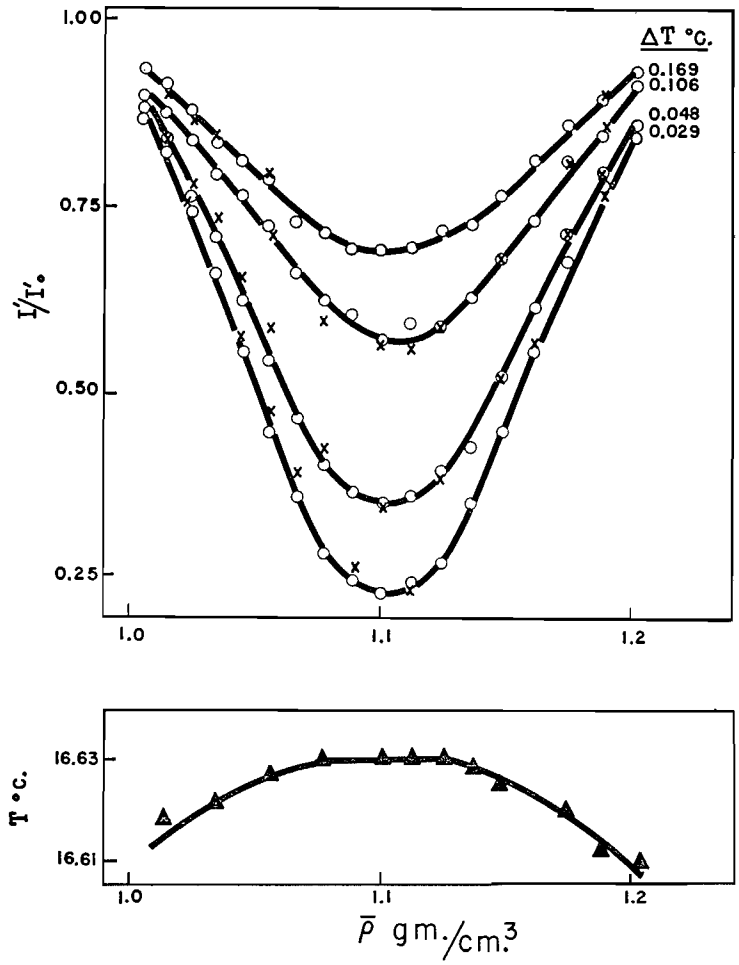

FIG. 3. Variation of transmittance with density along isothermals above T_c (upper curves) and liquid–vapor coexistence curve (lower curve) of xenon.

no appreciable time was allowed for establishment of a vertical density gradient and the density at the point of observation was virtually equal to the mean density. Under these conditions, the mean density $\bar{\rho}$ was used in the calculations from equation [11].

Points on the coexistence curves (lower parts of Figs. 3 and 5) were obtained by observing the first formation of visible droplets when the quiescent system was slowly cooled from above T_c as previously described (11, 18). The observed temperatures at any value of the average density were reproducible within ± 0.002°C. on a Beckmann thermometer.

RESULTS

Variation of Turbidity with Temperature

Xenon

Fig. 1 shows the variation of τ^{-1} with ΔT in xenon. All measurements were taken at the density of maximum turbidity ($\bar{\rho} = 1.100$ gm./cc.) and after the fluid had been efficiently stirred.

Using the equation

$$[12] \qquad \tau^{-1} = \frac{45.1}{\rho^3}\left[-\left(\frac{\partial p}{\partial v}\right)_T + 0.0059\right],$$

values of τ^{-1} were calculated from the $(\partial p/\partial \rho)_{\text{min}}$ data of Habgood and Schneider (4). K' and c in Eq. [12] were chosen to give best correspondence between these calculated values and those obtained from our transmission measurements.

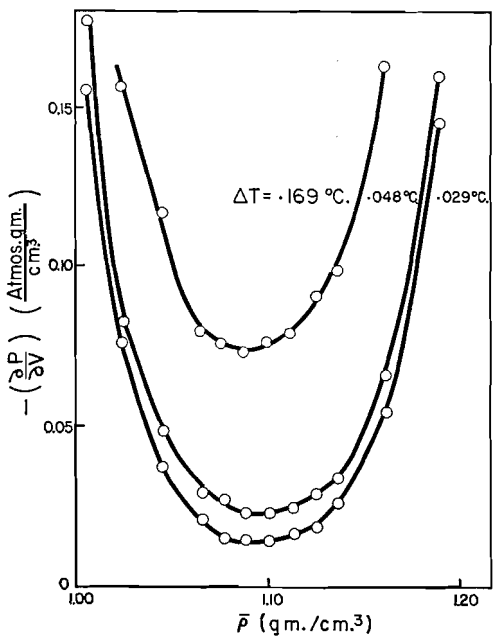

FIG. 4. Variation of $-(\partial p/\partial v)_T$ with density in xenon on isotherms immediately above T_c. Temperatures shown are values of ΔT.

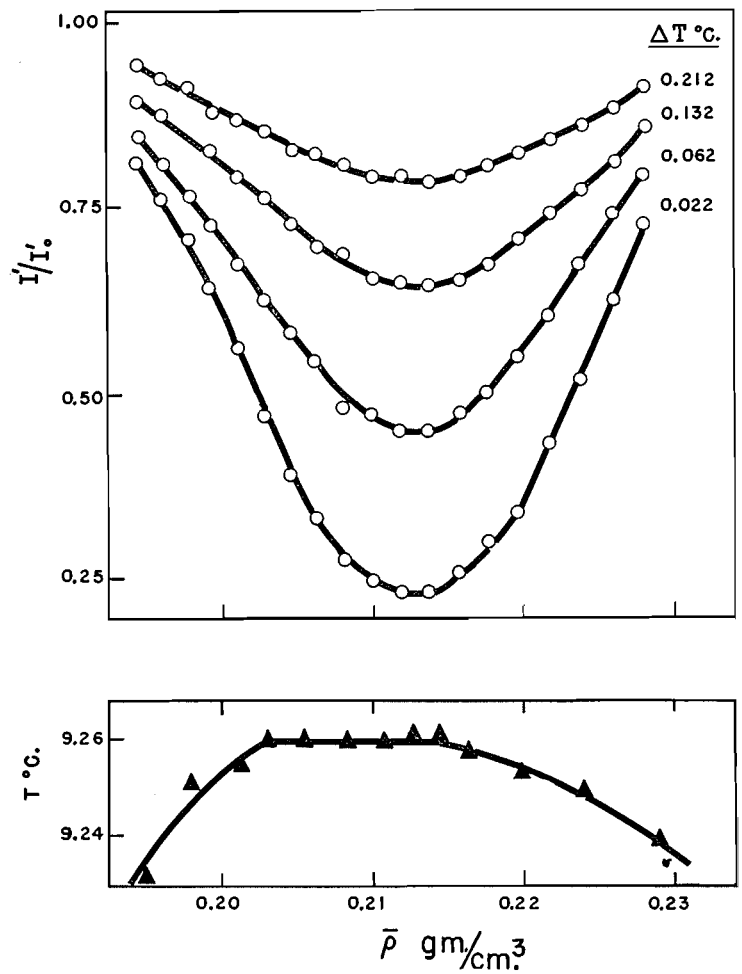

FIG. 5. Variation of transmittance with density along isothermals above T_c (upper curves) and liquid–vapor coexistence curve (lower curve) of ethylene.

Having, in this manner, established the values of K' and c for xenon, Eq. [12] was used to obtain $(\partial p/\partial v)_T$ from transmission measurements at other densities.

Ethylene

Fig. 2 shows values of τ^{-1} as a function of ΔT in ethylene. The curve obtained is almost identical with that obtained for xenon. The available PVT data on ethylene (7) are not sufficiently accurate for comparison of calculated and experimental values of τ^{-1}; consequently K' and c cannot be evaluated in this case.

Transmittance Isothermals

Figs. 3 and 5 show variation of transmittance with density in the systems xenon and ethylene and, in the lower portions, coexistence curves for these two

systems. The value of T_c observed for ethylene was 9.26±0.02°C. and that for xenon 16.63±0.02°C. The flat apexes on the coexistence curves have been attributed to gravity gradients by Weinberger and Schneider (17) and Mason *et al.* (11, 18).

The transmittance data are well fitted by continuous curves which show no indication of a discontinuity in τ.

Calculated $(\partial p/\partial v)_T$ *Isotherms*

Fig. 4 shows values of $(\partial p/\partial v)_T$ calculated from Eq. [12] at various densities in xenon.

Since K' and c of Eq. [11] could not be obtained for ethylene, $\tau^{-1}\rho^3$ is shown as a function of density in Fig. 6.

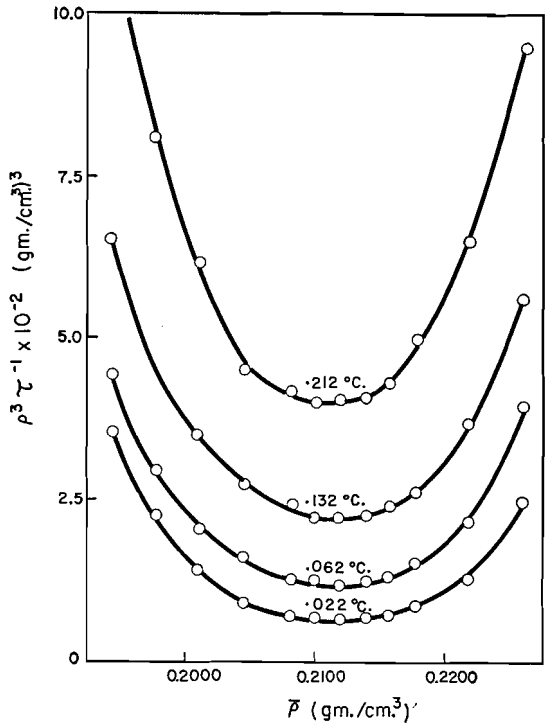

FIG. 6. Variation of $\rho^3\tau^{-1}$ with density in ethylene on isotherms immediately above T_c. Temperatures shown are values of ΔT.

CONCLUSIONS

The results of these experiments indicate that $(\partial p/\partial v)_T$ is a continuous function of the density and not equal to zero within 0.02°C. above T_c in ethylene and to within 0.03°C. above T_c in xenon.

Our results for xenon confirm the conclusion of Habgood and Schneider (4) based on PVT measurements. They are in disagreement with the conclusions of McIntosh, Dacey, and Maass (7) which were based on rather insensitive PVT data obtained for ethylene.

It appears that the "derby hat" region predicted by Mayer and Harrison

(9, 10) does not exist for the two systems studied. Other experiments, which are discussed in the following paper, indicate, however, that considerable molecular clustering may occur above T_c. This extensive molecular clustering is predicted by Mayer and Harrison (9, 10) at low values of $(\partial p/\partial v)_T$ and follows more rigorously from their theory than does the "derby hat" region.

ACKNOWLEDGMENTS

The authors are indebted to Dr. H. I. Schiff of McGill University for analyses of xenon in the mass spectrometer.

REFERENCES

1. ANDREWS, T. Trans. Roy. Soc. (London), A, 159: 583. 1869.
2. ANDREWS, T. J. Chem. Soc. 23: 74. 1870.
3. EINSTEIN, A. Ann. Physik, 33: 1275. 1910.
4. HABGOOD, H. W. and SCHNEIDER, W. G. Can. J. Chem. 32: 98. 1954.
5. KLEIN, M. J. and TISZA, L. Phys. Rev. 76: 1861.. 1949.
6. MAASS, O. Chem. Rev. 23: 17. 1938.
7. MCINTOSH, R. L., DACEY, J. R., and MAASS, O. Can. J. Research, B, 17: 241. 1939.
8. MCMILLAN, W. G. and MAYER, J. E. J. Chem. Phys. 13: 276. 1945.
9. MAYER, J. E. and HARRISON, S. F. J. Chem. Phys. 6: 87. 1938.
10. MAYER, J. E. and HARRISON, S. F. J. Chem. Phys. 6: 101. 1938.
11. MURRAY, F. E. and MASON, S. G. Can. J. Chem. 30: 550. 1952.
12. ORNSTEIN, L. S. and ZERNICKE, F. F. Physik. Z. 19: 134. 1918.
13. ORNSTEIN, L. S. and ZERNICKE, F. F. Physik. Z. 27: 761. 1926.
14. ROCARD, Y. J. phys. radium, 4: 165. 1933.
15. SMOLUCHOWSKI, M. Ann. Physik, 25: 205. 1908.
16. WEINBERGER, M. A. and SCHNEIDER, W. G. Can. J. Chem. 30: 422. 1952.
17. WEINBERGER, M. A. and SCHNEIDER, W. G. Can. J. Chem. 30: 847. 1952.
18. WHITEWAY, S. G. and MASON, S. G. Can. J. Chem. 31: 569. 1953.
19. ZIMM, B. H. J. Phys. & Colloid Chem. 54: 1306. 1950.
20. ZIMM, B. H. J. Chem. Phys. 19: 1019. 1951.

COEXISTENCE PHENOMENA IN THE CRITICAL REGION

IV. TIME-DEPENDENT BEHAVIOR IN VERTICAL DISTRIBUTION OF THE CRITICAL OPALESCENCE IN ETHYLENE AND XENON[1]

By F. E. Murray[2] and S. G. Mason

ABSTRACT

The variation with height of the transmittance in the critical region at various heights in long columns of xenon and ethylene continued to change for several hours after stirring. This change with time is attributed to gravitational settling of large molecular clusters. Other experiments also indicate that a region in which extensive molecular clustering occurs is necessary for an adequate description of phase transitions in the critical region.

INTRODUCTION

In a previous paper (4), it was shown that vertical gradients in the intensity of scattered light occurred in the system ethane in the region of the critical temperature. These gradients in turbidity were destroyed by stirring and re-formed only after a considerable time lag. In the experiments to be described, these time lags were the subject of extensive study in the systems xenon and ethylene.

Mayer and Harrison (2, 3) considered a gas to be made up of a mixture of single molecules and molecular clusters formed by molecular attraction. The rate of change of pressure with volume for any gas is given, according to their work, by the relation

$$\left(\frac{\partial p}{\partial V}\right)_T = \frac{-kT}{V^2}\left(\sum_l l^2 V b_l Z^l\right)^{-1}. \qquad [1]$$

In this equation, l is the number of molecules in any cluster and the summation is taken over all values of l; b_l is the cluster integral for clusters of l molecules each; V is the average volume per molecule; and Z is defined by the relation

$$\sum l V b_l Z^l = 1.$$

When l in Eq. [1] is small, $(\partial p/\partial V)_T$ remains large, but when the large molecular clusters begin to form, l becomes large and $(\partial p/\partial V)_T$ becomes small as in the region of the critical point.

According to fluctuation theory, density deviations in small volume cells of a fluid give rise to critical opalescence. A large positive deviation in density results if the number of molecules in a volume cell is much greater than the average number in that volume. Such a deviation must bring the molecules close enough together to render important the intermolecular forces between them. In this way, a large positive deviation in density corresponds, from a physical viewpoint, to a mathematical cluster of the theory of Mayer and Harrison.

[1]*Manuscript received May 9, 1955.*
Contribution from the Chemistry Department, McGill University, Montreal, Quebec.
[2]*Holder of a Fellowship from the National Research Council of Canada. Present address: Chemistry Department, University of Manitoba, Winnipeg, Manitoba.*

Since there is no essential conflict between fluctuation and cluster theory one can obtain an expression for the turbidity in a "cluster" gas using an equation derived by fluctuation treatment. For the turbidity τ of a gas, in terms of $(\partial p/\partial V)_T$, Rocard (6) derived an equation which we have (5) expressed in the form

$$[2] \qquad \tau = \frac{BT\rho^3}{\lambda^4}[c-(\partial p/\partial V)_T]^{-1}$$

where B and c are constants for given fluid and optical arrangements, T is the absolute temperature, and ρ and v are respectively the density and specific volume of the gas. Combining Eqs. [1] and [2] for a cluster gas yields

$$[3] \qquad \tau = \frac{BT\rho^3}{\lambda^4}\left[c+\frac{kT}{V^2}\left(\sum l^2 V b_l z^l\right)^{-1}\right]^{-1}.$$

Eq. [3] indicates that the high turbidity in the region above T_c is caused by the formation of numerous large molecular clusters.

The following symbols are used to denote experimental quantities:

T_c = the highest temperature at which visible aggregates form when the fluid is cooled slowly,
$\Delta T = (T-T_c)$,
I'/I_0' = the optical transmittance of the fluid,
$(t-t_0)$ = time elapsed since cessation of stirring,
$\bar{\rho}$ = mean density, i.e. total mass/total volume,
$\bar{\rho}_m$ = mean density at which maximum turbidity was observed,
x = distance measured downward from the top of the fluid column.

EXPERIMENTAL

The apparatus and procedures were identical to those described in previous papers (4, 5). The xenon and ethylene systems were the same as those already described (5).

RESULTS

Transmittance Gradients in Xenon

Figs, 1, 2, and 3 show typical vertical gradients of transmittance in xenon. Results in Fig. 1 were observed at an average density less than $\bar{\rho}_m$. Results in Fig. 2 were obtained at average densities very near to $\bar{\rho}_m$ such that the transmittance was a minimum near the center of the fluid column. Fig. 3 shows gradients in transmittance at a density greater than $\bar{\rho}_m$.

To obtain these results, the fluid was well stirred and after cessation of stirring, measurements were recorded when the transmittance at various levels in the bomb remained virtually constant with time. Similar results were obtained with ethylene.

Time Lags after Stirring

When the fluid was stirred, the transmittance gradients such as shown in Figs. 1, 2, and 3 were destroyed. These gradients re-formed gradually during a period of at least one hour.

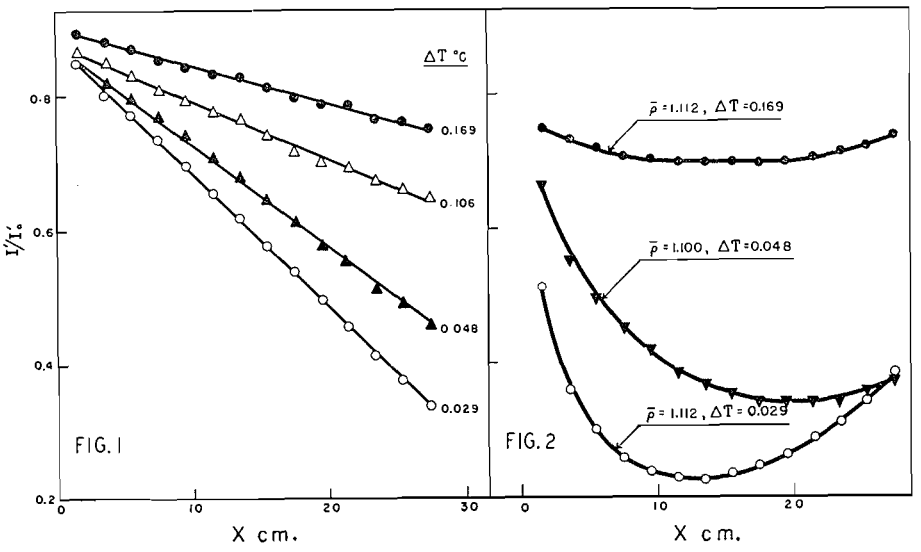

FIG. 1. Change in transmittance with distance (x) from top of vertical tube of xenon at various values of ΔT and at a mean density of 1.055 gm./cc., i.e. at $\bar{\rho} < \bar{\rho}_m$, $\bar{\rho}_m$ = 1.110 gm./cc.
FIG. 2. Transmittance–height curves in xenon at $\bar{\rho} = \bar{\rho}_m$ = 1.110 gm./cc.

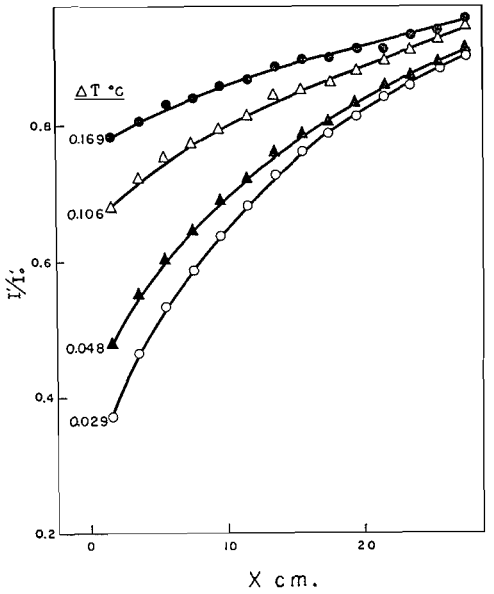

FIG. 3. Transmittance–height curves in xenon at $\bar{\rho}$ = 1.188 gm./cc., i.e. $\bar{\rho} > \bar{\rho}_m$.

Fig. 4 shows the change of transmittance with time after stirring in xenon. These diagrams typify results obtained from numerous observations. Similar behavior was observed in ethylene but the times to equilibrium were greater.

The upper diagram in Fig. 4 shows change of transmittance with time at a number of levels in the bomb, at ΔT = 0.048°C. and an average density less

than $\bar{\rho}_m$. The lower part of Fig. 4 shows results obtained at density greater than $\bar{\rho}_m$. These results illustrate the slow readjustment of the turbidity which appears visually to be due to a gravitational settling process.

Time Lags after a Turbidity Perturbation

When stirring in a fluid above T_c is stopped, rearrangement of material within the bomb takes place to establish the density gradients due to gravitational compression, which have been shown to exist (1, 4, 7, 8). The possibility of an extensive time lag in turbidity, not associated with redistribution of material, was investigated.

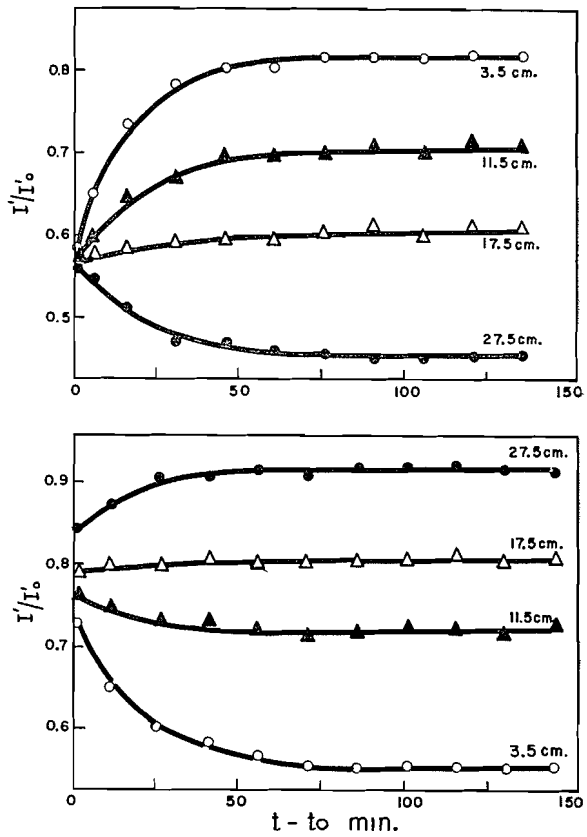

FIG. 4. Change in transmittance with time after cessation of stirring in xenon at $\bar{\rho}$ = 1.055 gm./cc., i.e. $\bar{\rho} < \bar{\rho}_m$ (upper diagram) and at $\bar{\rho}$ = 1.188 gm./cc., i.e. $\bar{\rho} > \bar{\rho}_m$ (lower diagram). Measurements made at various vertical heights indicated.

Xenon was allowed to attain vertical equilibrium, after stirring at $\bar{\rho}$ = 1.100 gm./cc. and ΔT = 0.048°C. The system was then rapidly compressed by means of the injector (4, 8) by a volume change of about 0.1%. This rapid compression caused a sharp increase in transmittance as shown in the lower part of Fig. 5. The transmittance was allowed to return to its precompression value and the system was rapidly expanded back to its original volume.

The rapid expansion caused a sharp decrease in transmittance. During the compression and expansion, the transmission was recorded continuously (at $x = 15.5$ cm.) on a Brush recording oscillograph.

Fig. 5 (lower part) shows a typical result of one of these experiments. The total perturbation by compression and expansion required slightly less than 1.5 min. In less than two minutes after the fluid was returned to its original volume, the turbidity had returned to its precompression value.

The upper portion of Fig. 5 shows the gradients observed at $\theta = 0$ min. (before the volume perturbation) and at $\theta = 10$ min. (after the volume

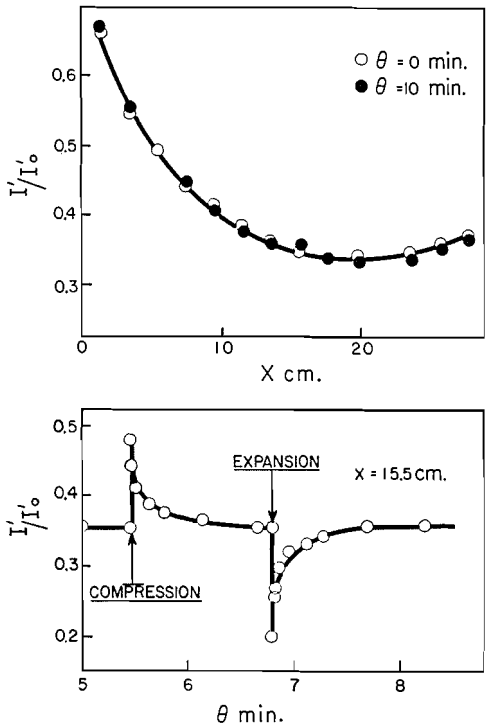

FIG. 5. The transmittance gradient in xenon immediately before (open circles) and after (solid circles) a rapid compression and expansion of xenon is shown in the upper curve. The lower curve shows the change in transmittance with time at $x = 15.5$ cm., $\bar{\rho} = \bar{\rho}_m = 1.100$ gm./cc., and $\Delta T = 0.048$°C.

perturbation). The total disturbance had no effect on the vertical transmittance gradient as shown by the coincidence of the open and closed circles.

From these results, it appears that the transmittance undergoes no protracted time lags when the vertical distribution of turbidity is not changing. Accordingly, the time lags after stirring must be associated with the slow redistribution of material in the gravitational field.

Miscellaneous Effects of Stirring

When a two phase system at $\bar{\rho} = \bar{\rho}_m$ is heated through T_c without stirring, the meniscus separating the two phases gradually becomes flat, but a visible

boundary persists over a positive interval of ΔT. A number of experiments were performed to show the result of stirring xenon after heating from below T_c without stirring. These experiments illustrate the increasing stability of a dispersion of the two phases as one approaches T_c from below. Above T_c, the two apparent phases are completely dispersible, by stirring, to a stable turbid fluid.

In the first of these experiments, xenon was heated, without stirring, from

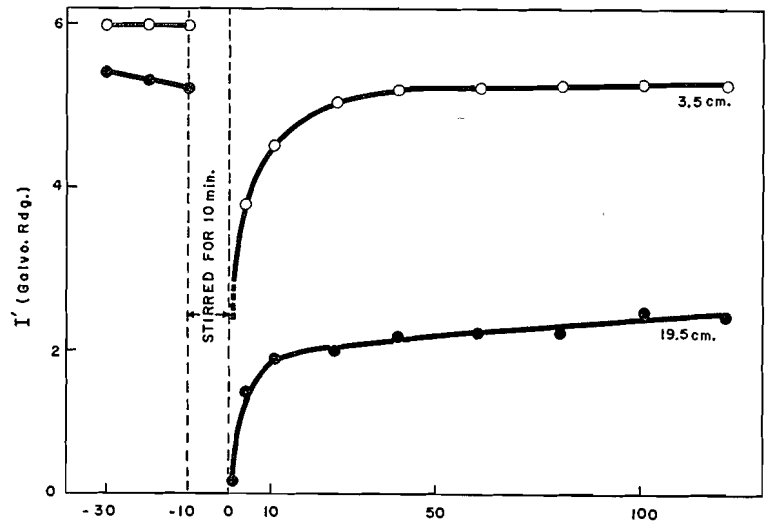

FIG. 6

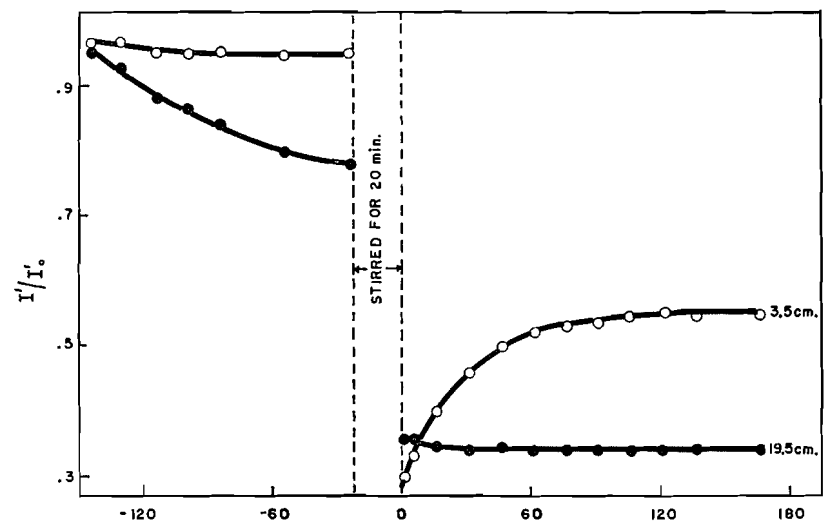

FIG.7

FIG. 6. Change in transmission readings before and after stirring xenon at $\bar{\rho} = \bar{\rho}_m = 1.100$ gm./cc. and $\Delta T = 0.027°C$.

FIG. 7. Change of transmittance before and after stirring xenon at $\bar{\rho} = \bar{\rho}_m$ and $\Delta T = 0.048°C$.

$\Delta T = -2$°C. and thermostatted at $\Delta T = -0.670$°C. No measurable change of transmission with time occurred at $\Delta T = -0.670$°C. and stirring was begun. Stirring caused complete mutual dispersion of the liquid and gas in the bomb. When stirring was stopped, the dispersion broke rapidly and the meniscus re-formed. There was no difference between transmission values observed before and after stirring.

As T_c was approached, the behavior of the dispersed system gradually changed. Fig. 6 shows the effect of stirring xenon, after heating without stirring from $\Delta T = -2$°C. to $\Delta T = -0.027$°C. Transmission readings, taken near the meniscus and near the top of the bomb, are shown as a function of $(t-t_0)$. When stirring was stopped, visible liquid droplets settled rapidly out of the gas phase to form a meniscus. This visible sedimentation was in progress during the observations at $(t-t_0) = 1$ and 4 min. At values of $(t-t_0)$ greater than five minutes, no discrete aggregates were visible above or below the meniscus and the opalescence which remained appeared visually to be identical in nature to that observed above T_c. At $(t-t_0) = 121$ min. a vertical gradient in transmission persisted throughout the fluid column.

In the experiment illustrated by Fig. 7, the xenon was heated from $\Delta T = -2$°C. through T_c, to $\Delta T = 0.048$°C. The fluid was thermostatted at this point. Before stirring, a clearly defined boundary persisted at the level $x = 20$ cm. During this time, the turbidity throughout the fluid column increased enormously. When stirring was stopped, the turbidity changed slowly throughout the bomb to reach an equilibrium distribution after about 90 min. The observed behavior resembled that which is seen when two liquid layers are dispersed by stirring to form a stable emulsion.

CONCLUSIONS

The experimental results discussed in this paper can be accounted for in terms of extensive molecular clustering in the region of T_c as was predicted by Mayer and Harrison (2, 3). The failure to observe any region within which $(\partial p/\partial V)_T$ remains zero (5) is not a serious contradiction of the more general cluster theory, but indicates that Mayer and Harrison (2, 3) may have made an erroneous assumption. This possibility is pointed out by Zimm (9) who contends that only one characteristic temperature is required to describe the phase change. In general, cluster theory, with the singular point modification of Zimm (9), seems best to describe the critical region.

REFERENCES

1. ATACK, D. and SCHNEIDER, W. G. J. Phys. & Colloid Chem. 54: 1323. 1950.
2. MAYER, J. E. and HARRISON, S. F. J. Chem. Phys. 6: 87. 1938.
3. MAYER, J. E. and HARRISON, S. F. J. Chem. Phys. 6: 101. 1938.
4. MURRAY, F. E. and MASON, S. G. Can. J. Chem. 30: 550. 1952.
5. MURRAY, F. E. and MASON, S. G. Can. J. Chem. 33: 1399. 1955.
6. ROCARD, Y. J. phys. radium, 4: 165. 1933.
7. WEINBERGER, M. A. and SCHNEIDER, W. G. Can. J. Chem. 30: 847. 1952.
8. WHITEWAY, S. G. and MASON, S. G. Can. J. Chem. 31: 569. 1953.
9. ZIMM, B. H. J. Chem. Phys. 19: 1019. 1951.

TEMPERATURE COEFFICIENTS IN HYDROCARBON OXIDATION[1]

By Nan-chiang Wu Shu and J. Bardwell

ABSTRACT

The oxidation of gaseous butane has been investigated in the range 260°C. to 540°C. with reaction vessels differing greatly in surface to volume ratio. Increased surface area retards the reaction. The rate–temperature relation shows a maximum and a minimum. At low temperatures the rate is very sensitive to temperature, the apparent activation energy being greater than 100 kcal. The abnormal temperature coefficients are shown to arise in part from the differing response to temperature of the branching reactions and the initiation reactions, and in part from the occurrence of competing reactions.

The unusual effect of temperature on the rates of oxidation reactions has been pointed out by many investigators. Bodenstein (7) found that the oxidation of gaseous nitric oxide is slightly retarded by increased temperature. A similar but more pronounced effect, over a limited temperature range, was discovered by Pease in the oxidation of propane (18). Here the rate of reaction was found to pass through a maximum at 330°C. and then to decline, passing through a minimum at 380°C. The results of Pease were confirmed by Newitt and Thornes (16) and by Mulcahy (14). Anomalous temperature coefficients in oxidation reactions have been reported by others, for example by Beatty and Edgar with heptane (6), by Chamberlain and Walsh with diisopropyl ether (8), and by Bardwell and Hinshelwood with butanone (3, 4). The intervention of cool flames in hydrocarbon oxidation at certain temperatures and their disappearance at higher temperatures are related phenomena (3, 18).

When experiments are done at temperatures well below that at which a maximum occurs in the rate–temperature relation, it is frequently found that temperature now has an unusually large effect. The length of the induction period is particularly sensitive to changes of temperature. Aivazov and Neumann (1) reported that with pentane the apparent activation energy is in excess of 100 kcal. Abnormally high temperature coefficients have also been reported by Prettre (19) and by Mulcahy (14) with other hydrocarbons.

The oxidation of gaseous butane exhibits temperature effects similar to those cited for other fuels. In this paper these relations will be analyzed from the viewpoint of the theory of branching chains.

EXPERIMENTAL

Apparatus

The reaction vessel was supported vertically in a furnace and was connected to a manometer and an appropriate vacuum system. Close control of temperature was achieved by use of a "Merc-to-merc" thermoregulator and a Sunvic relay. The reactant gases were admitted separately to the vessel and the course of combustion was followed by pressure measurements.

Two reaction vessels were used, one with a low surface to volume ratio, the

[1]*Manuscript received May 17, 1955.*
Contribution from the Department of Chemistry, University of Saskatchewan, Saskatoon, Saskatchewan. This work was supported by a grant from the National Research Council of Canada

other with a high ratio. Both vessels were made of clear silica and were cylindrical in shape, 6 cm. in external diameter and 9 cm. in length. The first vessel was empty; the second was packed with 25 silica tubes each of 0.6 cm. inside diameter. The surface to volume ratio of the packed vessel was therefore more than 10 times that of the empty vessel.

RESULTS

Analysis of Pressure–Time Curves

The autocatalytic character of the reaction between oxygen and gaseous hydrocarbons necessitates the use of some arbitrary criterion of reaction rate. Two such criteria have found extensive use in previous kinetic investigations (2, 9, 15):

(*a*) the maximum rate, ρ_{max}, i.e. the slope of the pressure–time curve at its inflection point,

(*b*) the reciprocal induction period, $1/\theta$, the induction period being the length of time between the entrance of the reactants to the vessel and the attainment of some defined rate, often the maximum rate.

Theoretical treatments of hydrocarbon oxidation, for example that of Semenov (21), have ascribed the autocatalytic nature of the reaction to a slow multiplication of reaction centers by chain branching of a degenerate type. In a reaction where chain branching occurs the number of chain centers x increases with time according to the equation

$$[1] \qquad dx/dt = B' + Ax.$$

B' is the rate of production of chain centers independent of the branching process, for example by direct interaction of fuel and oxygen. A is the branching factor. Insofar as it is permissible to consider A and B' constant in the early part of the reaction, equation [1] may be integrated to yield:

$$[2] \qquad x = (B'/A)(e^{At} - 1).$$

Thus chain centers multiply in an approximately exponential fashion, and reaction rate increases accordingly. If it is assumed that the observed rate of pressure increase dp/dt is a valid measure of reaction rate, the increase in pressure, Δp, will be proportional to $\int x dt$, i.e. proportional to:

$$(B'/A^2)(e^{At} - At - 1).$$

Combining the proportionality constant and B' to give a new term B, we obtain

$$[3] \qquad \Delta p = (B/A^2)(e^{At} - At - 1).$$

When At is considerably greater than unity the exponential term dominates and a plot of log Δp against time should be linear.

The oxidation of butane provides abundant confirmation of this prediction. Plots of log Δp against time show excellent linearity during the first third or so of the reaction; i.e. before the consumption of reactants becomes excessive. This is true both with the empty vessel and with the packed vessel, and with

wide variations of vessel temperature and reactant concentration. The precision with which the pressure–time data conform to the predicted exponential relation compares favorably with that observed in studies of the oxidation of other gaseous fuels (4, 21). For calculation it is convenient to neglect all but the exponential term in Eq. [3], i.e. to take

$$\Delta p = (B/A^2)e^{At}. \quad [4]$$

A is thus the slope of the linear portion of the plot of the natural logarithm of the pressure increase against time of reaction. B is calculated from the intercept and slope of this plot, and has the units of mm./min^2. B will henceforth be called the initiation factor, whereas A will be called the branching factor. The units of A are min^{-1}.

The use of Eq. [4] rather than the more exact Eq. [3] for estimating A and B introduces an approximation, the magnitude of which is exemplified by the following data for an experiment with the empty vessel at 270°C. using 100 mm. each of butane and oxygen. Here Δp increased from 5.8 mm. at 8 min. to 20.1 mm. at 10 min. Calculated values of A and B are given in Table I. The errors introduced by use of the approximate but much more convenient Eq. [4] are not serious for present purposes, since discrepancies are always in the same direction and are small compared with the alteration of A and B with temperature (see below).

TABLE I

CALCULATION OF A AND B FROM PRESSURE–TIME DATA

	A (min.$^{-1}$)	B (mm./min.^{2})
By Eq. [3]	0.622	0.0156
By Eq. [4]	0.608	0.0172

Effect of Temperature on Maximum Rate and Reciprocal Induction Period

The general effect of temperature on oxidation rate with butane may be seen in Figs. 1–3, in which the logarithms of the usual criteria of reaction rate, ρ_{max} and $1/\theta$, are plotted against the reciprocal of the absolute temperature. Fig. 1 shows that with the empty vessel, the reciprocal induction period, $1/\theta$, passes through a maximum at about 350°C. and a minimum at about 430°C. The corresponding results for the maximum rate ρ_{max} are shown in Fig. 2. The curves resemble those in Fig. 1 in that the minima again occur at about 430°C. However, with the pressures used slow combustion gives way to cool flames over a considerable range of temperature and the curves for ρ_{max} are therefore not continuous.

When the packed vessel was used instead of the empty vessel, the reaction was considerably slower and cool flames appeared only in exceptional circumstances. Measurements of ρ_{max} and $1/\theta$ in the range 314°C. to 540°C. yielded the results shown in Fig. 3, which are qualitatively similar to those obtained using the empty vessel and lower pressures. The results also illustrate the two unusual temperature effects with which we are here principally concerned:

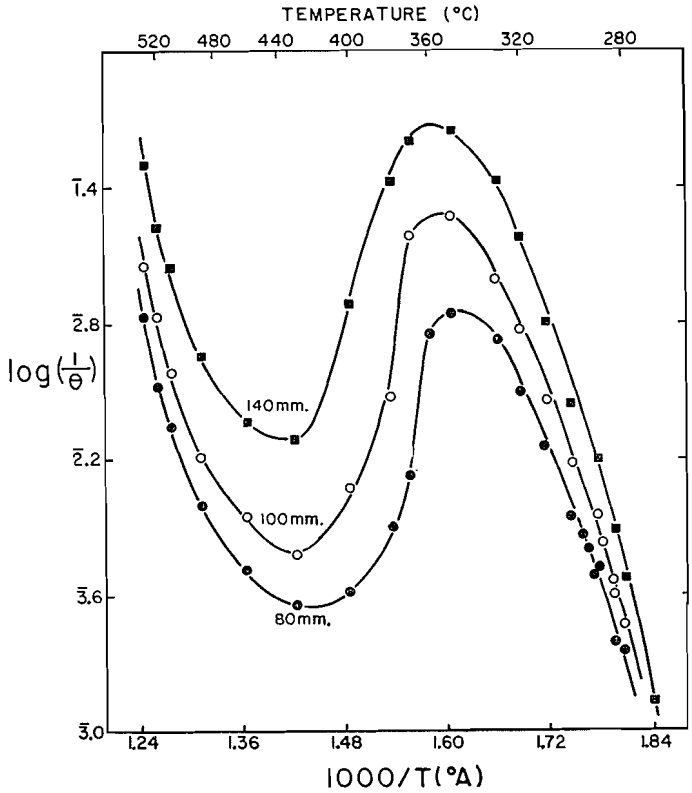

FIG. 1. Effect of temperature on the reciprocal induction period with equimolecular mixtures of butane and oxygen and an empty vessel 6 cm. in diameter. Total reactant pressure is shown.

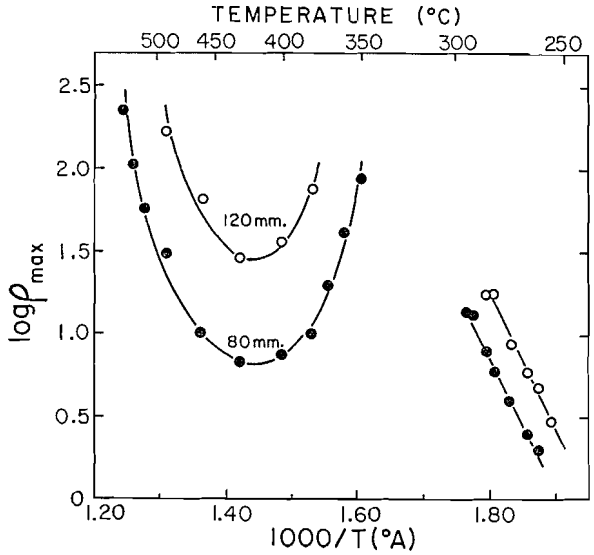

FIG. 2. Effect of temperature on the maximum rate of oxidation of butane with equimolecular mixtures of butane and oxygen and an empty vessel 6 cm. in diameter. Total reactant pressure is shown.

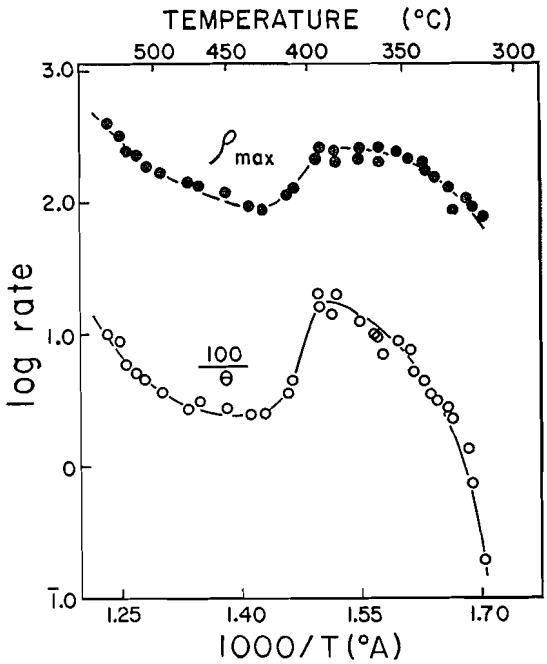

FIG. 3. Effect of temperature on the maximum rate of oxidation and on the reciprocal induction period using a packed vessel and equimolecular mixtures of butane and oxygen at a total pressure of 200 mm.

(*a*) The decline of reaction rate with rising temperature, which here occurs between 395°C. and 430°C. We shall henceforth refer to this negative effect of temperature as the anomalous temperature coefficient.

(*b*) The great sensitivity of the induction period to changes of temperature in the low temperature region. For example the data plotted in Fig. 3 show that on lowering the temperature from 324°C. to 314°C., the induction period increases from 50 sec. to 500 sec.

The Initiation Factor and the Branching Factor at Low Temperatures

Since the abnormal temperature coefficients noted above must arise from unusual sensitivity to temperature of the initiation factor, B, or of the branching factor, A, or of both, it is of interest to explore the effect of temperature on each of these factors. The exceptionally large temperature coefficient at low temperatures will be considered first.

When the pressure–time curves were analyzed by the method described above it was found that the initiation factor B was much more temperature-dependent than the branching factor A. For example, the results plotted in Fig. 3 in the temperature range 314°C. to 345°C. yield an apparent activation energy of 31 kcal. for A but a value of over 120 kcal. for B. In fact, the temperature coefficient of B becomes essentially infinite at about 314°C. with the pressure used.

The above relationships were investigated further in a series of experiments using 200 mm. each of butane and oxygen, again with the packed vessel. Convenient rates were obtained in the temperature range 260°C. to 305°C.

The results are shown in Fig. 4 and the calculated activation energies given in Table II. Of the four quantities plotted it is seen that the initiation factor B is by far the most sensitive to temperature, the values increasing by a factor of about 10^{13} for a temperature increase of 45°C. Considerable sensitivity to temperature is also shown by $1/\theta$, particularly in the range 260°C. to 270°C. In this 10-degree interval, $1/\theta$ increases by a factor of about five whereas ρ_{max} and A are approximately doubled. On the other hand B increases by a factor

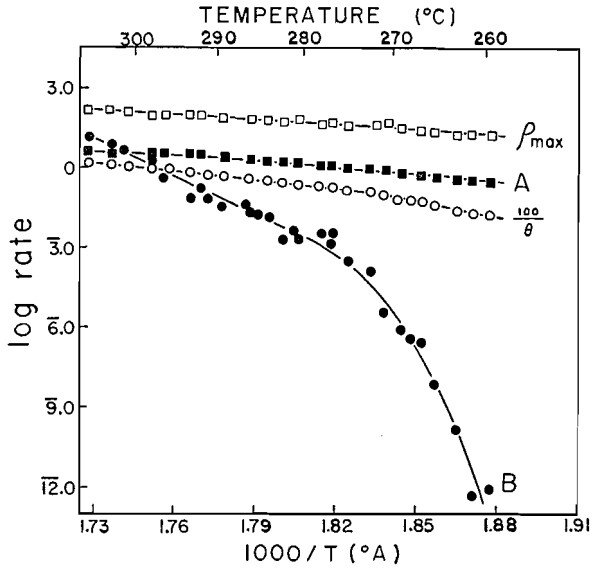

FIG. 4. Effect of temperature on maximum rate (ρ_{max}), reciprocal induction period ($100/\theta$), branching factor (A), and initiation factor (B) using a packed vessel and equimolecular mixtures of butane and oxygen at a total pressure of 400 mm.

of about 30 million. It may be concluded therefore that the large dependence of $1/\theta$ on temperature in this range is derived from the initiation factor rather than from the branching factor.

Experiments with the empty vessel gave results that confirmed the above conclusions for the packed vessel. For example, measurements in the temperature range 273°C. to 294°C. with 100 mm. each of butane and oxygen showed that the apparent activation energy of B was about 100 kcal. whereas that of A was about 68 kcal.

TABLE II

APPARENT ACTIVATION ENERGIES OF THE MAXIMUM RATE, RECIPROCAL INDUCTION PERIOD, BRANCHING FACTOR, AND INITIATION FACTOR

Butane pressure: 200 mm.; oxygen pressure: 200 mm.

Temperature range (°C.)	Activation energy (kcal.)			
	ρ_{max}	$1/\theta$	A	B
275° to 305°C.	30	49	38	220
260° to 270°C.	41	93	46	1000

Limiting Pressure for Finite Induction Periods

The large variation of induction period with temperature appears to be related to the existence of pressure limits in hydrocarbon oxidation. Here we shall not be concerned with the pressure limits delineating the regions of occurrence of slow combustion, cool flames, ignition, etc., but only with the low-pressure limit which marks the transition from finite to infinite induction periods. The existence of such a limit has been clearly demonstrated by Malherbe and Walsh (13) who showed that a plot at constant temperature of induction period against pressure yielded an asymptote of a definite positive pressure. Below this pressure the induction period was of infinite duration. Using a vessel with an effective diameter intermediate between those employed in the present investigation, Malherbe and Walsh showed that the low-pressure limit increased with decreasing temperature (13).

Our measurements have in general confirmed the above conclusions and have shown, furthermore, that the low-pressure limit increases with increasing surface to volume ratio (see Fig. 5). The low-pressure limit, P_c, is readily

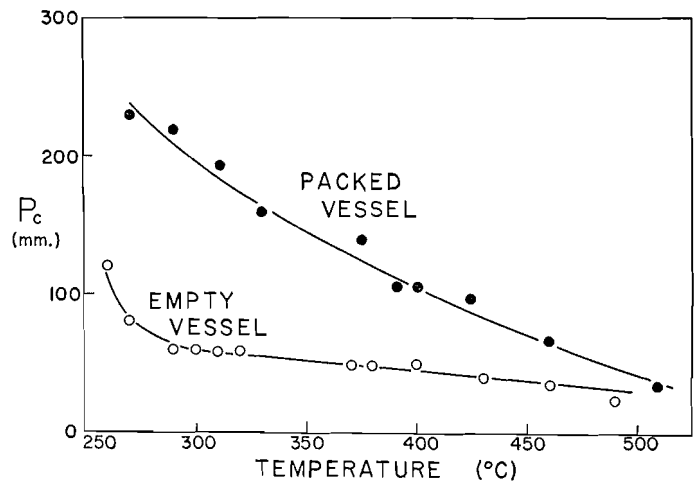

FIG. 5. Effect of temperature on the low-pressure limit. P_c is the total pressure of an equimolecular mixture of butane and oxygen at which the induction period becomes infinite.

determined by extrapolation of a plot of $1/\theta$ against pressure. Experiments with pressures slightly below this limit show that no perceptible reaction occurs even after many hours. Reaction can, however, be induced by the addition of a small amount of acetaldehyde (14) and it is of interest that the values of A and ρ_{max} then determined agree well with those obtained without acetaldehyde just above the pressure limit. Additions of acetaldehyde to reaction mixtures just above the low-pressure limit greatly increase B but have only a small effect on A. From these results it may be concluded that although favorable conditions for chain branching may still exist below the low-pressure limit the induction period is infinite because the effective rate of initiation is zero.

The Anomalous Temperature Coefficient

Attempts were made to analyze the sharp decline of reaction rate at about 400°C. by assessing the temperature coefficients of the branching factor and initiation factor. The empty vessel proved to be unsuitable for this purpose since the reaction rate was very high in the temperature range of interest (see Fig. 2). Even with the packed vessel where reaction was somewhat slower it was difficult to determine precise values of A and B over a considerable temperature range with any chosen constant pressure of reactants. The trends observed however are illustrated by the results given in Table III, which allow

TABLE III

EFFECT OF TEMPERATURE ON ρ_{max}, $1/\theta$, A, AND B IN THE REGION OF THE ANOMALOUS TEMPERATURE COEFFICIENT

Butane pressure: 70 mm.; oxygen pressure: 70 mm.

Temperature (°C.)	ρ_{max} (mm./min.)	$1/\theta$ (sec.$^{-1}$)	A (min.$^{-1}$)	B (mm./min.^{2})
368	83	0.030	8.9	6.7
382	20	0.0056	1.7	0.22

comparison of the behavior at 368°C. with that at 382°C. The latter temperature is approximately that for minimum reaction rate with the pressure employed. It is seen that here the sharp decline in ρ_{max} and $1/\theta$ is accompanied by substantial decreases in both A and B.

DISCUSSION

Temperature Coefficients

Although the experiments reported above have been confined to the oxidation of butane, comparison with other investigations shows that a wide range of temperature coefficient is a common property of the gas-phase oxidation of hydrocarbons (10, 12). Search for the origin of this behavior is considerably assisted by the exponential form of the pressure–time curve in butane oxidation, and by the opportunity thereby provided of estimating separately the branching rate and the initiation rate. It has been shown above that these two rates can differ greatly in their temperature dependence.

The large temperature coefficient of the induction period at low temperatures (Figs. 3 and 4) is apparently associated with the low-pressure limit (Fig. 5). Since this limit moves toward higher pressures as the temperature is lowered, it follows that when a series of experiments is done with constant pressures at successively lower temperatures the induction period will become infinite at (and below) some definite temperature. Comparison of Fig. 3 with Fig. 5 shows that it is just above this temperature that the induction period is most temperature-sensitive.

The Origin of the Low-pressure Limit

Malherbe and Walsh (13) have suggested that the low-pressure limit in hydrocarbon oxidation is similar in origin to that observed in the hydrogen–oxygen reaction, and represents the pressure above which the branching factor becomes positive and below which it is negative. Our results do not

support this explanation. Fig. 4 shows that the rapid lengthening of the induction period as the limit is approached, here by a decrease of temperature, is due to the approach to zero of the initiation factor B. It is also apparent from Fig. 4 and Table II that in this range the branching factor A is neither very small nor very temperature-sensitive. It seems very unlikely therefore that the branching factor would drop abruptly to zero when the temperature is lowered a few degrees more. The suggestion of Malherbe and Walsh also encounters difficulties in explaining the observed effect of adding small amounts of acetaldehyde along with the fuel and oxygen. As already noted, these additions to mixtures above the low-pressure limit greatly increase the initiation factor but have only a slight effect on the branching factor. The addition of acetaldehyde to mixtures just below the limit, i.e. where the induction period would normally be infinite, induces reaction which then displays a branching factor of substantial magnitude, and comparable to that observed just above the limit. These effects are not consistent with a vanishing of A at the limit but are quite in harmony with a vanishing of B.

The Anomalous Temperature Coefficient

It has been shown above that when the temperature approaches 400°C. the oxidation rate, as judged by either ρ_{max} or $1/\theta$, passes through a maximum and then declines. This behavior, as well as the resurgence of reaction at still higher temperatures, is similar to that reported in investigations of the combustion process with other paraffin hydrocarbons (18, 20). The customary interpretation is that at high temperatures the mechanism involves formaldehyde and relatively simple atoms and radicals, but that at lower temperatures complex molecules such as peroxides and higher aldehydes play an important part (11, 17). The decline of reaction rate with rising temperature at about 400°C. is taken as a sign of the decreasing importance of these compounds as combustion intermediates. Although the reactions responsible for this effect have not yet been firmly established, two reasonable possibilities exist:

(*a*) the combustion intermediate is wasted through its participation in reactions leading to inactive products (9, 20),

(*b*) the combustion intermediate is produced in smaller amounts because of pyrolytic destruction of one of its precursors in the chain sequence (22).

It has been shown in Table III that both the branching factor and the initiation factor are sharply reduced by a small rise of temperature in the region of the anomalous temperature coefficient. The decline of the initiation factor contributes to the lengthening of the induction period, but the decrease of the branching factor is more important since it affects both the induction period and the maximum rate, ρ_{max} (5).

Explanation by Competing Reactions

There remains the need for an explanation of the vanishing of the initiation factor and the branching factor at particular temperatures. For simplicity we may assume that a relatively stable combustion intermediate is formed which undergoes two modes of decomposition, one leading to its regeneration in increased quantity, the other leading to comparatively inert products. It may

be shown (5, 21) that when two such competing reactions occur the branching factor A is the difference of two terms, e.g. A_1-A_2. Each of these terms presumably increases with rising temperature, the rates of increase being determined by the respective activation energies E_1 and E_2. Now if $E_2 > E_1$, the variation of log (A_1-A_2) with $1/T$ will be as sketched in Fig. 6(*a*). At a sufficiently low temperature the apparent activation energy of the branching factor approaches that of A_1, but as the temperature is increased A_1-A_2 passes through a maximum and then falls off sharply. In this way the anomalous temperature coefficient at about 400°C. is accounted for, although the predicted vanishing of A is obscured by the intervention of the high-temperature mechanism of oxidation.

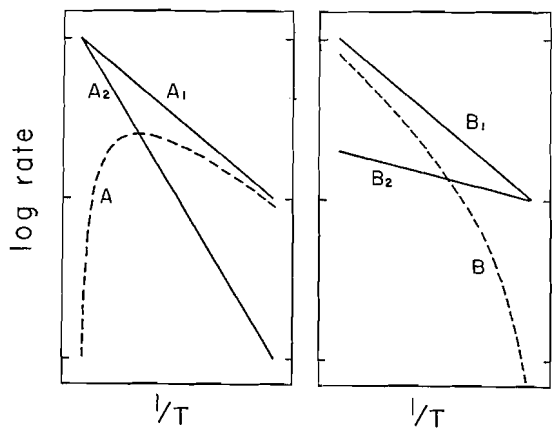

FIG. 6. Schematic diagrams explaining abnormal temperature coefficients.
Diagram (*a*), on left, $A = A_1-A_2$; activation energy of A_1 less than that of A_2.
Diagram (*b*), on right, $B = B_1-B_2$; activation energy of B_1 greater than that of B_2.

The extreme temperature-sensitivity of the initiation factor, B, at lower temperatures is explicable in a generally similar way. We may consider the measured initiation factor as being the difference of two terms, e.g. B_1-B_2, where B_2 represents inhibiting influences. If the activation energy of B_1 is greater than that of B_2 the variation of log (B_1-B_2) with $1/T$ will be as sketched in Fig. 6(*b*). The very large apparent activation energy of B (Table II) and the existence of a temperature below which the induction period is infinite (Fig. 5) are consistent with this diagram.

REFERENCES

1. AIVAZOV, B. and NEUMANN, M. Z. physik. Chem. B, 33: 349. 1936.
2. ANDREEV, E. A. Acta Physicochim. U.R.S.S. 6: 57. 1937.
3. BARDWELL, J. and HINSHELWOOD, C. N. Proc. Roy. Soc. (London), A, 205: 375. 1951.
4. BARDWELL, J. and HINSHELWOOD, C. N. Proc. Roy. Soc. (London), A, 207: 461. 1951.
5. BARDWELL, J. Proc. Roy. Soc. (London), A, 207: 470. 1951.
6. BEATTY, H. A. and EDGAR, G. J. Am. Chem. Soc. 56: 102. 1934.
7. BODENSTEIN, M. Z. physik. Chem. 100: 68. 1922.
8. CHAMBERLAIN, G. H. N. and WALSH, A. D. Third Symposium on Combustion, Flame and Explosion Phenomena. p. 368. 1949.
9. CULLIS, C. F. and HINSHELWOOD, C. N. Discussions Faraday Soc. No. 2: 117. 1947.
10. CULLIS, C. F. and SMITH, L. S. A. Trans. Faraday Soc. 46: 42. 1950.
11. EGERTON, A. C. Nature, 121: 10. 1928.

12. JOST, W. Explosion and combustion processes in gases. McGraw-Hill Book Company, Inc., New York. 1946. pp. 448–451.
13. MALHERBE, F. E. and WALSH, A. D. Trans. Faraday Soc. 46: 824. 1950.
14. MULCAHY, M. F. R. Trans. Faraday Soc. 45: 575. 1949.
15. MULCAHY, M. F. R. and RIDGE, M. J. Trans. Faraday Soc. 49: 1297. 1953.
16. NEWITT, D. M. and THORNES, L. S. J. Chem. Soc. 1669. 1937.
17. NORRISH, R. G. W. Discussions Faraday Soc. No. 10: 269. 1951.
18. PEASE, R. N. J. Am. Chem. Soc. 60: 2244. 1938.
19. PRETTRE, M. Compt. rend. 202: 1176. 1936.
20. PRETTRE, M. Compt. rend. 207: 576. 1938.
21. SEMENOV, N. Chemical kinetics and chain reactions. Oxford University Press, London, 1935.
22. WALSH, A. D. Trans. Faraday Soc. 43: 297. 1947.

SYNTHESES OF A SERIES OF 15-KETOGLYCOLS AND 15-KETO FATTY ACIDS FROM USTILIC ACID[1]

By A. T. Crossley[2] and B. M. Craig

ABSTRACT

Reaction of the methyl ester of ustilic acid A (15,16-dihydroxypalmitic acid) with a methyl Grignard, oxidation of the glycol grouping, bromination, and hydrogenolysis produced 15-methylhexadecanoic acid. A series of 15-keto acids resulted from reaction of the amide of ustilic acid A with the appropriate Grignard reagent followed by oxidation of the glycol grouping. Infrared absorption characteristics of these compounds are described.

Ustilagic acid has been produced by fermentation using a culture of *Ustilago zeae* (2). Ustilic acid A (15,16-dihydroxypalmitic acid) and ustilic acid B (2,15,16-trihydroxypalmitic acid) are produced by hydrolysis of ustilagic acid (4). These acids are easily separated from the remainder of the hydrolysis products and from one another and are potentially available in large quantities.

The ustilic acids possess a carboxyl group at one end of the molecule and an easily oxidizable glycol grouping at the other end and as such should constitute valuable starting materials for the synthesis of various new and naturally occurring long chain compounds. The present investigation deals with the synthesis of 15-methylhexadecanoic acid and a series of 15-keto acids.

A number of methyl branched fatty acids which are primarily concerned with the wool fats have been synthesized by a number of workers (1, 3, 7, 8, 9). These syntheses have involved the preparation of appropriate fragments followed by chemical coupling or anodic syntheses. Weitkamp (9) prepared 15-methylhexadecanoic acid from a lower homologue and Stenhagen *et al.* synthesized the same acid (1). Ustilic acid A is a convenient starting material for the synthesis of this acid by the following series of reactions:

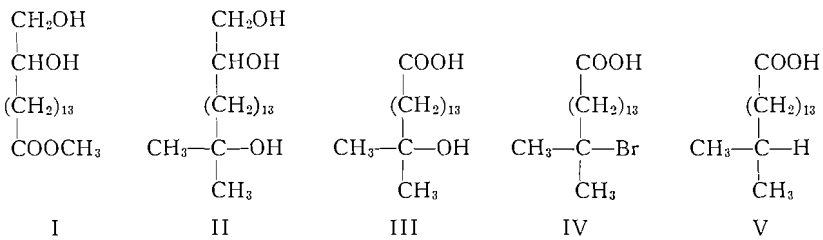

I II III IV V

Methyl ustilate A (I) was converted in almost theoretical yield into the tertiary alcohol II, m.p. 55.5–56.0° C., by using a large excess of methylmagnesium bromide. Reaction of methyl isopropylidene ustilate A with the Grignard reagent followed by removal of the isopropylidene grouping with

[1]*Manuscript received May 24, 1955.*
Contribution from the National Research Council of Canada, Prairie Regional Laboratory, Saskatoon, Saskatchewan. Issued as Paper No. 197 on the Uses of Plant Products and as N.R.C. No. 3696.
[2]*National Research Council of Canada Postdoctorate Fellow 1952.*

methanolic hydrochloric acid gave a very poor yield of II. Oxidation of II with chromic oxide in acetic acid at low temperature gave 15-methyl-15-hydroxyhexadecanoic acid III, m.p. 70.5–71.5° C., which yielded *p*-bromophenacyl derivative, m.p. 80.6–81.0° C. This oxidation was also carried out using lead tetraacetate and oxygen as described below. The hydroxy acid III was treated with hydrogen bromide in acetic acid to give the tertiary bromo derivative IV, m.p. 45–46° C., which, on treatment with hydrogen and Raney nickel in ethanolic sodium hydroxide, gave 15-methylhexadecanoic acid V, m.p. 60.7–61.3° C. (reported m.p. 59.3–59.9° C. (1) and 60.2° C. (9)).

The synthesis of a series of 15-keto acids was carried out by the series of reactions given below. To favor the formation of the ketoglycol rather than the tertiary alcohol derivative, the amide of ustilic acid A was used as a starting material in the Grignard reaction. The reaction of amides with Grignard reagents has been investigated by Whitmore *et al.* (10, 11). To increase solubility the isopropylidene derivative (VII) was used. Reaction of the latter with 1.1 moles of methylmagnesium bromide gave a poor yield of the ketone (VIII) (R = CH_3), m.p. 40.0–41.0° C., semicarbazone m.p. 123.5–124.0° C., but the yield was increased by the use of 100% excess of the Grignard reagent. A small amount of the tertiary alcohol formed was separated on alumina. The corresponding ethyl, propyl, and butyl homologues (VIII) were also prepared by using the appropriate Grignard reagents. These had melting points, respectively, of 37° C. (R = C_2H_5), 43° C. (R = C_3H_7), and 48.5° C. (R = C_4H_9). Removal of the isopropylidene group afforded the free ketoglycols (IX) which are described in Table I. Purification of the latter compounds was greatly facilitated by a treatment with warm alcoholic alkali before crystallization from benzene.

TABLE I

MELTING POINTS AND ELEMENTAL ANALYSIS OF KETOGLYCOLS AND KETO ACIDS

Compound	Formula	M.p., °C.	Found		Calculated	
			C (%)	H (%)	C (%)	H (%)
1,2-Dihydroxy-16-ketoheptadecane	$C_{17}H_{34}O_3$	83.0–83.7	71.34	12.07	71.28	11.96
1,2-Dihydroxy-16-ketooctadecane	$C_{18}H_{36}O_3$	93.8	72.43	11.48	72.44	11.51
1,2-Dihydroxy-16-ketononadecane	$C_{19}H_{38}O_3$	92.5	73.39	11.59	73.02	11.61
1,2-Dihydroxy-16-ketoeicosane	$C_{20}H_{40}O_3$	93.9	73.08	12.07	73.11	12.27
15-Ketohexadecanoic acid*	$C_{16}H_{30}O_3$	82.3	70.86	11.10	71.07	11.18
15-Ketoheptadecanoic acid	$C_{17}H_{32}O_3$	85.7–86.1	71.73	11.44	71.78	11.34
15-Ketooctadecanoic acid	$C_{18}H_{34}O_3$	83.4	72.44	11.51	72.43	11.48
15-Ketononadecanoic acid	$C_{19}H_{36}O_3$	85.7	73.39	11.59	73.03	11.61

**Semicarbazone, m.p. 129.6° C. (C, 62.57; H, 10.22; N, 12.82%. Calc. for $C_{17}H_{33}O_3N_3$: C, 62.35; H, 10.16; N, 12.83%.)*

These ketoglycols (IX) were converted to 15-keto fatty acids (X) by simultaneous oxidation with lead tetraacetate and oxygen at 50° C. according to the method of Mendel and Coops (6). The oxidation products were purified by distillation and crystallization from alcohol. The melting points of these four, hitherto unprepared, keto fatty acids are given in Table I.

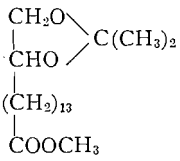

VI

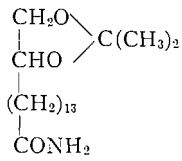

VII

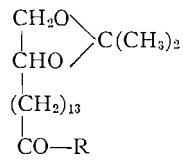

VIII

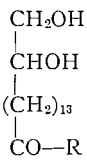

IX

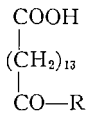

X

Infrared absorption determinations were made on all the compounds with a Perkin-Elmer Model 21 instrument equipped with a sodium chloride prism, and the crystalline samples were mounted in KBr. The 15-methyl-15-hydroxy-hexadecanoic acid showed OH absorption bands at 3440 and 1152 cm.$^{-1}$, and also several poorly resolved bands between 1390 and 1300 cm.$^{-1}$ which might be caused by the $(CH_3)_2C$— group. The 15-methylhexadecanoic acid showed two clearly resolved bands at 1385 and 1365 cm.$^{-1}$ which are characteristic for branched methyl groups. These bands were absent in the spectrum of pure hexadecanoic acid. The 1,2-dihydroxy-15-keto compounds showed the expected hydroxyl band between 3400 and 3200 cm.$^{-1}$ and also two absorption bands at 1100 and 1082 cm.$^{-1}$ which could be assigned to a secondary and a primary hydroxyl group respectively. They also showed the ketonic carbonyl absorption between 1710 and 1705 cm.$^{-1}$. The corresponding 15-keto acids showed absorptions in the 1700 cm.$^{-1}$ and the 900–700 cm.$^{-1}$ regions characteristic for carboxylic acids. Resolutions of the carboxyl C=O and ketone C=O were achieved in the 1720–1700 cm.$^{-1}$ region for 15-ketohexadecanoic and 15-ketoheptadecanoic acids but not for 15-ketooctadecanoic and 15-keto-nonadecanoic acids. The C=O absorption band in the latter was much wider than for the corresponding 15-keto-1,2-dihydroxy-nonadecane and -eicosane.

EXPERIMENTAL

NOTE: All melting points are corrected and determinations have been made in each case in the usual manner and also on a heating stage microscope.

Separation of the Ustilic Acids

A ustilic acid mixture (158 gm.), prepared by hydrolysis of ustilagic acid (4), was shaken for four hours with 1 liter of dry acetone containing 1% sulphuric acid. A small amount of inorganic material remained insoluble and the solution was filtered into a separatory funnel containing 3 liters of ice-cold water. The solution was extracted with 1.6 liters of petroleum ether (b.p. 60–80° C.) and the mother liquor was extracted with a further 1 liter. The combined petroleum ether extracts were washed three times with water. A cold solution of 60 gm. of potassium hydroxide in 420 ml. of water was then added and after

one minute's shaking, 450 ml. of 40% aqueous ethanol was added and the aqueous layer run off. The petroleum ether extract was then washed with 500 ml. of 3% aqueous potassium hydroxide and three times with 30% aqueous ethanol. The five aqueous ethanol washings were combined and diluted with 1 liter of water and re-extracted with 400 ml. petroleum ether, the extract being added to the main bulk of petroleum ether solution. The aqueous extract was acidified with sulphuric acid and extracted with chloroform to yield 163 gm. of crude isopropylidene ustilic acid A which was recrystallized from acetone to m.p. 64–65° C. The petroleum extracts gave 12 gm. of diisopropylidene ustilate B, m.p. 42–43° C., reported m.p. 42.5–43° C. (5).

The proportions of the ustilic acids in the mixture have been found to vary slightly and the present mixture represents the highest proportion of ustilic acid A which has been found. The amount may fall to about 70% of the mixture of acids.

Methyl Isopropylidene Ustilate A

Isopropylidene ustilate A (154 gm.) was esterified with diazomethane in dry ether to yield 160 gm. of the crude product as outlined in the procedure of Lemieux (5). Two crystallizations from acetone at 4° C. gave the pure methyl ester, m.p. 46.3–46.7° C., reported m.p. 46–47° C. (5).

Methyl Ustilate A

Isopropylidene ustilic acid A (20 gm.) was boiled under reflux with 4% methanolic HCl for two hours as outlined by Lemieux (5). The solution was poured into water and extracted with chloroform to give 16.2 gm. of crude methyl ustilate A, which after three crystallizations from ethanol had m.p. 85.2–86.1° C., reported m.p. 85.5–86.0° C. (5).

1,2,16-Trihydroxy-16-methylheptadecane

Methyl ustilate A (10 gm.) in 200 ml. of dry ether was added during one hour, with rapid stirring, to 23.5 gm. of methylmagnesium iodide in 300 ml. of ether, the mixture being allowed to reflux continuously during the addition. The semisolid reaction mixture was boiled under reflux for 10 hr. and was then decomposed with water and acetic acid. The crude tertiary alcohol, 10.1 gm., m.p. 54.0–55.0° C., was extracted with chloroform. The 1,2,16-trihydroxy-16-methylheptadecane purified by one crystallization from acetone had a m.p. 55.5–56.0° C. Calc. for $C_{18}H_{38}O_3$: C, 71.50; H, 12.60%. Found: C, 71.33; H, 12.50%.

15-Hydroxy-15-methylhexadecanoic Acid

The above tertiary alcohol (5.0 gm.) was dissolved in 140 ml. of acetic acid containing 7.0 gm. of chromic oxide and the solution allowed to stand for 12 hr. at 3° C., when it was diluted with ice-cold water (1 liter) and extracted with benzene. The benzene solution was washed with water until neutral and the benzene evaporated. The crude hydroxy acid was then taken up in 100 ml. of ether and the ether washed twice with 5% aqueous potassium hydroxide, and twice with water. The combined washings were acidified with sulphuric acid and extracted with ether to yield 2.63 gm. of 15-hydroxy-15-methyl-

hexadecanoic acid, which was purified by three crystallizations from acetone and crystallized as colorless needles, m.p. 70.5–71.5° C. Calc. for $C_{17}H_{34}O_3$: C, 72.10; H, 11.95%. Found: C, 72.45%; H, 12.06%.

15-Bromo-15-methylhexadecanoic Acid

The hydroxy acid (1.39 gm.) was dissolved in 10 ml. of a 50% solution of hydrobromic acid in acetic acid and left for 14 hr. at 22° C. The solution was then diluted with 100 ml. of ice-cold water and the product extracted with benzene. Yield, 1.71 gm.; m.p. 45.0–46.5° C. Calc. for $C_{17}H_{33}O_2Br$: Br, 22.6%. Found: Br, 22.5%.

15-Methylhexadecanoic Acid

The 15-bromo-15-methylhexadecanoic acid (1.65 gm.) was dissolved in 25 ml. of ethanol, and 50 ml. of ethanol containing 5 ml. of 4 *N* sodium hydroxide added, together with a small amount of Raney nickel. The mixture was shaken with hydrogen under a pressure of 25 p.s.i. for 14 hr. at 25° C. The solution was filtered, poured into dilute sulphuric acid, and the product extracted with ether. Unexpectedly this material contained a large proportion of unsaturated material (iodine value 40) and it was therefore hydrogenated, in a similar medium to that previously used, but at a temperature of 80° C. and a pressure of 800 p.s.i. of hydrogen, for four hours. The product was saturated (iodine value 0), and was purified by distillation followed by three crystallizations from ethanol. The pure 15-methylhexadecanoic acid had m.p. 60.7–61.3° C. (reported m.p. 59.3–59.9° C. (1) and 60.2° C. (9)). Calc. for $C_{17}H_{34}O_2$: C, 75.56; H, 12.59%. Found: C, 75.45; H, 12.72%. The *p*-bromophenacyl derivative had a m.p. 83.1–83.6° C. Calc. for $C_{25}H_{39}O_3Br$: C, 64.23; H, 8.41; Br, 17.1%. Found: C, 63.61; H, 8.64; Br, 17.4%.

Isopropylidene Ustilamide A

Methyl isopropylidene ustilate A (70 gm.), together with 1500 gm. of a 25% (wt.) solution of ammonia in methanol (prepared and kept below 0° C.), was heated to 180° C. in a sealed bomb for six and one-half hours. The product was poured into 3000 ml. of ice-cold water and the precipitated amide filtered off and washed with 1000 ml. of cold water. This material was dried and then boiled with 500 ml. of ether, and the slurry cooled to 5° C. when it was filtered. The precipitate was washed with 300 ml. of cold ether. Thirteen grams of unchanged methyl isopropylidene ustilate A were recovered from the ethereal filtrate and 55 gm. of crude amide were obtained, which crystallized from methanol as colorless plates, m.p. 99.7–100.3° C. Calc. for $C_{19}H_{37}O_3N$: C, 69.67; H, 11.39; N, 4.15%. Found: C, 69.62; H, 11.32; N, 4.17%.

Reaction of Isopropylidene Ustilamide A with Grignard Reagents

A solution of methylmagnesium bromide was prepared by slow addition of 236 gm. of a 17% solution of methyl bromide in dry ether (prepared by passing methyl bromide gas into dry ether at 0° C.) to 10.0 gm. of magnesium in 300 ml. ether. The Grignard reagent was allowed to settle, decanted, and its strength determined by titration.

A solution of methylmagnesium bromide in 440 ml. ether containing 47.5 gm.

(1.9 times theoretical) of the reagent was added to a solution of 33.9 gm. of isopropylidene ustilamide A, dissolved in 1500 ml. of a mixture of equal volumes of dry benzene and dry ether, with stirring, the solution being allowed to reflux during the addition. The solution was heated under reflux for a further eight hours, and the product was isolated in the usual manner. It was then dissolved in 50 ml. of ether and a small amount of unchanged amide was filtered off. The crude ketone (32.79 gm.) was dissolved in a small amount of benzene, transferred to an alumina column (14 cm. × 5 cm.), and eluted with benzene. The material in the first 150 ml. of eluate (0.3 gm.) was discarded and the pure ketone (25.0 gm.) was isolated from the next 8000 ml. of eluate. The isopropylidene ether of 1,2-dihydroxy-16-ketoheptadecane had m.p. 40.0–40.5° C. Calc. for $C_{20}H_{38}O_3$: C, 74.12; H, 11.74%. Found: C, 73.9; H, 11.85%. Its semicarbazone had m.p. 123.5–124.0° C. Calc. for $C_{21}H_{41}O_3N_3$: C, 65.75; H, 10.77; N, 10.96%. Found: C, 65.79; H, 10.71; N, 11.00%. Three homologous ketones were prepared in a similar manner by using ethyl-, propyl-, and butyl-magnesium bromide Grignard reagents. These were purified by recrystallization and the melting points were respectively 37.0° C. (R = C_2H_5), 43.0° C. (R = C_3H_7), and 48.5° C. (R = C_4H_9).

1,2-Dihydroxy-16-ketoheptadecane

The 1,2-isopropylidene ether of 16-ketoheptadecane (8.0 gm.) was dissolved in 70 ml. of chloroform and the solution cooled to 5° C. Thirty milliliters of a 20% (wt.) solution of hydrochloric acid in 85% aqueous methanol was added and the solution allowed to stand at 20° C. for two hours. Water (100 ml.) was added and the product (m.p. 72–76° C.) extracted with chloroform. It was then dissolved in 50 ml. of 3% alcoholic potassium hydroxide solution and kept at 50° C. for 20 min. The solution was poured into 300 ml. of cold water and the methyl ketoglycol, 5.5 gm., m.p. 78–81° C., was filtered off and recrystallized three times from benzene, the pure product having m.p. 83.0–83.7° C. The products from the reaction of the ethyl, propyl, and butyl Grignards were treated in a similar manner to prepare the three other homologues whose constants are given in Table I.

15-Ketohexadecanoic Acid

Lead tetraacetate (300 mgm.) was dissolved in 25 ml. of dry benzene in a 50 ml. three-necked flask fitted with a stirrer, dropping funnel, and a condenser through which a glass tube passed and projected below the surface of the solution in the flask. 1,2-Dihydroxy-16-ketoheptadecane (500 mgm.) dissolved in 10 ml. of benzene (solution was maintained by the use of an infrared lamp) was added over a period of six hours from a dropping funnel. During addition the reaction mixture was stirred and maintained at a temperature of 50° C. and a stream of dried oxygen saturated with benzene was passed through the solution. At intervals of 45 min. 450 mgm. of lead tetraacetate was added to the solution. After the addition of ketoglycol was complete, the mixture was maintained at 50° C. with stirring for a further one and one-half hours, when 100 mgm. of ethylene glycol was added. After a further 10 min.

the warm solution was filtered and 10 ml. 30% acetic acid and then 100 ml. of water was added to the filtrate and the product extracted with benzene.

The benzene layer was washed once with water and the washings discarded. The keto acid was then extracted from the benzene layer by one washing with 50 ml. of 10% aqueous potassium hydroxide solution and two washes with water, disregarding emulsions formed owing to the rather low solubility of the potassium salt. The combined aqueous washings were acidified with sulphuric acid and extracted with benzene to yield 310 mgm. of the crude ketohexadecanoic acid. This was purified by conversion to its methyl ester, which was distilled and then reconverted to the free acid, which was crystallized four times from 95% methanol.

The ethyl, propyl, and butyl keto acids (Table I) were prepared similarly except that it was found unnecessary to convert to the methyl ester for the distillation of the crude product. The yield was found to decrease slightly as the molecular weight of the product increased.

ACKNOWLEDGMENT

The authors wish to express their thanks to J. A. Baignee for the microanalyses and to Miss Agnes Epp for the infrared studies.

REFERENCES

1. ARSENIUS, K. E., STALLBERG, G., STENHAGEN, E., and TAGASTROM-EKETORP, B. Arkiv Kemi Mineral. Geol. 26A. 1948.
2. HASKINS, R. H. and THORN, J. A. Can. J. Botany, 29: 585. 1951.
3. HAUGEN, F. W., ILSE, D., SUTTON, D. A., and DE VILLIEAS, J. P. J. Chem. Soc. 98. 1953.
4. LEMIEUX, R. U. Can. J. Chem. 29: 415. 1951.
5. LEMIEUX, R. U. Can. J. Chem. 31: 396. 1953.
6. MENDEL, H. and COOPS, J. Rec. trav. chim. 58: 1133. 1939.
7. MILBURN, A. H. and TRUTER, E. V. J. Chem. Soc. 3344. 1954.
8. VELICK, S. F. J. Am. Chem. Soc. 69: 2317. 1947.
9. WEITKAMP, A. W. J. Am. Chem. Soc. 67: 447. 1945.
10. WHITMORE, F. C., POPKIN, A. H., WHITAKER, J. S., MATTIL, K. F., and ZECH, J. D. J. Am. Chem. Soc. 60: 2462. 1938.
11. WHITMORE, F. C., NOLL, C. I., and MEUNIER, V. C. J. Am. Chem. Soc. 61: 683. 1939.

THE REACTION OF 2-ALKYLTETRAHYDROPYRANS WITH ANILINE OVER ACTIVATED ALUMINA[1]

By H. P. Richards[2] and A. N. Bourns

ABSTRACT

The vapor-phase reaction over activated alumina of 2-ethyltetrahydropyran with aniline gave 1-phenyl-2-ethylpiperidine, 1-phenyl-2-propylpyrrolidine, N-phenyl-4-heptenylamine, and N-phenyl-5-heptenylamine. 2-Methyltetrahydropyran with aniline gave 1-phenyl-2-methylpiperidine, 1-phenyl-2-ethylpyrrolidine, N-phenyl-4-hexenylamine, and N-phenyl-5-hexenylamine. The structures of the cyclic amines were confirmed by independent syntheses. The unsaturated secondary amines were reduced to known N-alkylanilines and degraded by ozonolysis. A mechanism has been proposed to account for the formation of these products.

INTRODUCTION

In an earlier communication the results of an investigation of the reaction of tetrahydropyran with primary aromatic amines were reported (1). N-Arylpiperidines were formed in almost theoretical yields with aniline, *m*-toluidine, and *p*-toluidine, while a lower yield (65%) was obtained when *o*-toluidine was used as the amine component. The investigation has now been extended to the reaction of aniline with 2-ethyltetrahydropyran (I) and 2-methyltetrahydropyran (II). In contrast to the results obtained with the parent ether, the 2-alkyl homologues produced a mixture of amine products suggestive of a carbonium ion mechanism.

Reaction of 2-Ethyltetrahydropyran (I) with Aniline

Careful fractional distillation of the product formed by passing aniline and the cyclic ether, in a molar ratio of 2:1, over activated alumina at 300° C. gave three distinct fractions. These were identified as 1-phenyl-2-ethylpiperidine (III), 1-phenyl-2-propylpyrrolidine (IV), and a mixture (V) of N-phenyl-4-heptenylamine and N-phenyl-5-heptenylamine. The composition of the reaction product, the elemental analysis data, the boiling point and refractive index of each fraction, and the melting points of picrates prepared from the two cyclic amines are given in Table I.

TABLE I

PRODUCTS OF THE REACTION OF 2-ETHYLTETRAHYDROPYRAN WITH ANILINE

No.	Compound	Mole %[a]	b.p., ° C. at 8 mm.	n_D^{20}	Analyses[b]			Picrate m.p., ° C.
					Carbon	Hydrogen	Nitrogen	
III	1-Phenyl-2-ethylpiperidine	17	126–127	1.5502	82.67	10.36	7.16	178.2–178.8
IV	1-Phenyl-2-propylpyrrolidine	26	136–137	1.5518	82.65	10.40	6.95	137.0–137.5
V	N-Phenyl-4-heptenylamine and N-Phenyl-5-heptenylamine	57	145–146	1.5364	82.85	10.09	7.09	

[a]*The product composition figures are an average of three runs, the deviation of which did not exceed one per cent.*

[b]*Calculated for $C_{13}H_{19}N$, the molecular formula of all four compounds: C, 82.40; H, 10.11; N, 7.49.*

[1]*Manuscript received June 15, 1955.*
Contribution from the Department of Chemistry, McMaster University, Hamilton, Ontario.
[2]*Present address: Ontario Paper Company, Thorold, Ontario.*

The identity of the cyclic amines was established through independent syntheses involving reaction of dibromoheptanes with aniline. The reaction sequence and composition of products are shown in the following reaction scheme:

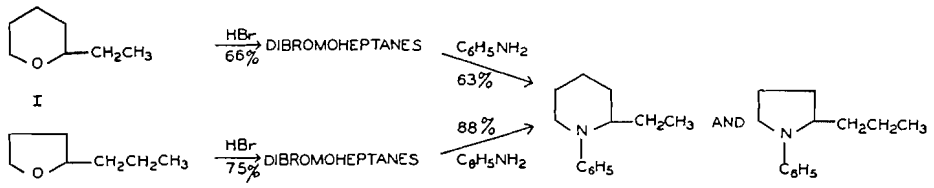

I VI III IV

PRODUCT COMPOSITION		
FROM I	70%	30%
FROM VI	17%	83%

Treatment of 2-ethyltetrahydropyran (I) with hydrogen bromide converted it into dibromoheptanes, which on reaction with aniline gave a product 70% of which was shown to be identical with the lowest-boiling component (III) of the product of the catalytic reaction. The remaining 30% was identical with IV, the component of intermediate boiling point. On the other hand, conversion of 2-propyltetrahydrofuran (VI) to dibromoheptanes followed by reaction with aniline gave a product consisting of 17% III and 83% IV. In each sequence, ether → dibromide → amine, the major product was considered to be that resulting from direct substitution of oxygen by nitrogen without rearrangement, that is, the substituted piperidine from 2-ethyltetrahydropyran and the pyrrolidine from 2-propyltetrahydrofuran. This conclusion is based on the reasoning that if the major product of one sequence was that formed through a rearrangement, then this same compound would also have been the major product of the other sequence, since in this case it would have been formed directly without requiring a proton shift. Such clearly was not the case; the major product of one synthesis was the minor product of the other.* On the basis of these results, the lowest-boiling amine product of the catalytic reaction is considered to be 1-phenyl-2-ethylpiperidine; the component of intermediate boiling point, 1-phenyl-2-propylpyrrolidine.

The highest-boiling component (V) gave solid benzenesulphonamide derivatives, but these could not be recrystallized to constant melting point. Hydrogenation over Raney nickel converted V to N-heptylaniline. Ozonolysis of the benzoate of V produced volatile aldehydes identified as acetaldehyde and propionaldehyde by means of their 2,4-dinitrophenylhydrazones, which were separated chromatographically. The third component of the reaction of 2-ethyltetrahydropyran with aniline, therefore, consisted of a mixture of N-phenyl-4-heptenylamine and N-phenyl-5-heptenylamine. A separation of these unsaturated secondary amines was not attempted.

**The small amount of rearrangement occurring at the secondary carbon in these syntheses is considered more likely to occur in the reaction of the cyclic ethers with hydrogen bromide rather than in the subsequent reaction of the dibromide product with aniline.*

Reaction of 2-Methyltetrahydropyran with Aniline

Fractional distillation of the product formed by the reaction of 2-methyltetrahydropyran with aniline gave three distinct fractions identified as 1-phenyl-2-methylpiperidine (VII), 1-phenyl-2-ethylpyrrolidine (VIII), and a mixture (IX) of N-phenyl-4-hexenylaniline and N-phenyl-5-hexenylaniline. The composition of the product, the elemental analysis data, the boiling point and refractive index of each fraction, and the melting points of the picrates are shown in Table II.

TABLE II

PRODUCTS OF THE REACTION OF 2-METHYLTETRAHYDROPYRAN WITH ANILINE

No.	Compound	Mole %[a]	b.p., ° C. at 8 mm.	n_D^{20}	Analyses[b]			Picrate m.p., ° C.
					Carbon	Hydrogen	Nitrogen	
VII	1-Phenyl-2-methylpiperidine	42	113–114	1.5528	81.72	9.72	8.00	166.8–167.2
VIII	1-Phenyl-2-ethylpyrrolidine	27	125.5–126.5	1.5590	81.83	9.61	7.89	120.6–121.2
IX	N-Phenyl-4-hexenylamine and N-Phenyl-5-hexenylamine	31	131.5–132.5	1.5412	81.90	9.62	7.92	

[a] *Based on a single run.*
[b] *Calculated for $C_{12}H_{17}N$, the molecular formula for all four compounds: C, 82.23; H, 9.78; N, 7.99.*

The identity of the two tertiary amines (VII and VIII) was established by an independent synthesis. 2-Methyltetrahydropyran was converted to dibromohexane, which on treatment with aniline gave a product 87% of which was identical with VII. The remaining 13% was identical with VIII. This result is entirely analogous to that obtained in the corresponding synthesis of 1-phenyl-2-ethylpiperidine (III) and 1-phenyl-2-propylpyrrolidine (IV), discussed in the preceding section. Furthermore, there is a similar relationship in boiling points, refractive indices, and picrate melting points of the isomeric tertiary amines in the two cases. (See Tables I and II.)

The highest-boiling component (IX) of the catalytic reaction was converted into N-hexylaniline on reduction over Raney nickel. Ozonolysis of the acetate of IX gave the volatile aldehydes, formaldehyde and acetaldehyde. It is therefore concluded that IX was a mixture of the two unsaturated secondary amines, N-phenyl-4-hexenylamine and N-phenyl-5-hexenylamine.

Reaction Mechanism Considerations

The reaction of aniline with tetrahydropyran, which involves the displacement of oxygen at two primary carbon centers, gives almost theoretical yields of 1-phenylpiperidine. In contrast, the corresponding reaction of 2-alkyltetrahydropyran, in which one of the two carbons joined to oxygen is secondary, gives a mixture of products suggestive of a process proceeding through an intermediate carbonium ion. The following mechanism is proposed:

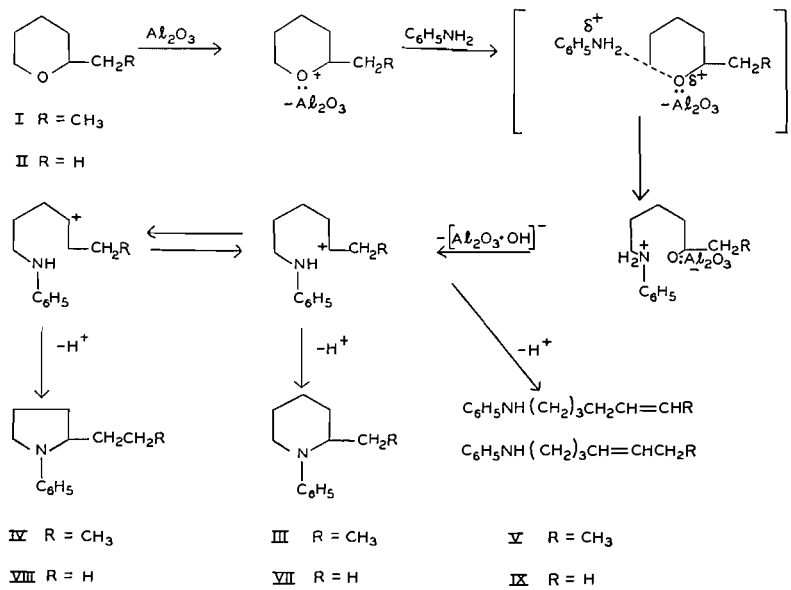

The alumina, acting as a Lewis acid, accepts a pair of electrons from oxygen, thus weakening the two carbon–oxygen bonds of the ether molecule (13).* Bimolecular attack of aniline at the primary carbon is followed by proton transfer from nitrogen to oxygen and then by unimolecular dissociation of the oxygen – secondary carbon bond. The resulting 'carbonium ion' may (*a*) interact with nitrogen to form the substituted piperidine, (*b*) rearrange to give a new 'carbonium ion', which on ring closure yields the pyrrolidine, or (*c*) lose a proton from a carbon atom adjacent to the center of electron deficiency and produce an unsaturated secondary amine.

It is possible that the initial cleavage occurs at the secondary rather than at the primary carbon. However, the fact that the 2-alkyltetrahydropyrans appear to be somewhat less reactive than tetrahydropyran itself would suggest that the bimolecular displacement at primary carbon is more facile, and therefore is the initial cleavage step. It is worthy of note in this connection that reaction of hydrogen iodide with *n*-butyl *sec*-butyl ether has been shown to give *n*-butyl iodide and *sec*-butyl alcohol (7). Ether fission in this reaction would appear to involve bimolecular attack of iodide ion at the primary carbon atom.

Reference to the composition data given in Tables I and II shows that there is a very much greater tendency for unsaturated secondary amine formation in the reaction of 2-ethyltetrahydropyran. It is suggested that hyperconjugation is one factor responsible for this. Of the two unsaturated amines formed in each of the two systems, one possesses the partial structure $-CH_2CH{=}CHCH_3$. The second unsaturated amine found in the product from 2-methyltetrahydropyran has the partial structure $-CH_2CH{=}CH_2$, and

**Although this is undoubtedly an oversimplification of the catalytic function (14), it seems reasonable to assume that it is in this capacity that alumina performs its key role in dehydration reactions.*

in the product from 2-ethyltetrahydropyran, $—CH_2CH{=}CHCH_2CH_3$. Since hyperconjugative stabilization is greater in the latter, the reaction of the 'carbonium ion' giving this product should compete more effectively with the ring closure forming the substituted piperidine. Analogous effects of hyperconjugation in determining product proportions have been observed in the solvolysis of alkyl bromides (3) and of sulphonium salts (5).

Steric effects (2) also may play a role in determining product proportions in the two cyclic ether – aniline reactions. Ring closure at the carbonium ion center, $—CH_2CH_2\overset{+}{C}HCH_3$, giving the substituted piperidine from 2-methyltetrahydropyran should have a somewhat higher entropy of activation, and therefore greater reaction rate, than closure at the center, $—CH_2CH_2\overset{+}{C}HCH_2CH_3$, required to produce a piperidine from the 2-ethyl homologue. On the other hand, the two reactions giving the substituted pyrrolidines involve the two ions of partial structures $—CH_2\overset{+}{C}HCH_2CH_3$ and $—CH_2\overset{+}{C}HCH_2CH_2CH_3$. These would be expected to show smaller differences in rate, since the increase in steric requirements resulting from the substitution of *n*-propyl for ethyl at the seat of displacement is not as great as that resulting from substitution of ethyl for methyl. This relationship between the steric requirements of *n*-alkyl groups has been demonstrated in bimolecular substitution reactions (6), and it might be expected to show up in processes involving interaction of a bulky nucleophilic reagent with carbonium ion centers.

If now it is assumed that the interconversion of the isomeric carbonium ions is rapid compared to their conversion to stable products, then these steric considerations lead to the prediction that more substituted piperidine and less unsaturated amines should be formed from 2-methyltetrahydropyran than from the 2-ethyl homologue. Reference to Tables I and II shows this to be the case.

A further factor which would tend to favor piperidine formation at the expense of the pyrrolidine from the 2-methyl ether is the somewhat greater stability and, if equilibrium between the isomeric carbonium ions is approached, greater concentration of $—CH_2CH_2\overset{+}{C}HCH_3$ compared to $—CH_2\overset{+}{C}HCH_2CH_3$, since in the former an extra C—H bond is available for hyperconjugation. The fact that the pyrrolidine is favored in the reaction of the 2-ethyl compound might be taken to mean a greater inherent stability of the five-membered heterocyclic system.

EXPERIMENTAL*†

Catalysis Procedure

The catalysis procedure has been described in detail in an earlier communication (1). The cyclic ethers and aniline, mixed in a molar ratio 1:2, were vaporized in a preheater and the vapors passed through 200 ml. of pretreated (1) Alcoa Activated Alumina (Grade F-1, 4-8 mesh) at 300° C. The

**All melting points are corrected; boiling points are uncorrected.*

†The microanalyses were performed at the Research Laboratories, Dominion Rubber Company, Guelph, Ontario, by Mr. Ralph Mills.

feed rate was 60 ml. of mixed liquid reactants per hour. A run consisted of 100 ml. of mixed reactants, following a prerun of 40 ml. during which temperature and feed rate were given final adjustment.

The organic product was separated from a water phase, dried over sodium hydroxide, and very carefully fractionated in a 30-plate modified Podbielniak column (8). A small amount of low-boiling alkadienes and unreacted cyclic ether was removed at atmospheric pressure, while excess aniline and the amine reaction products were distilled at 8 mm. pressure. Composition of amine products, properties, and elemental analysis data are given in Tables I and II. Combined yields of the amine products, based on cyclic ether charged, were 60% from 2-ethyltetrahydropyran and 76% from 2-methyltetrahydropyran.

2-Ethyl- and 2-Methyl-tetrahydropyran

The cyclic ethers were prepared from dihydropyran by the method of Paul (9) and purified by fractional distillation. 2-Ethyltetrahydropyran, b.p. 126.8–127.1° C., n_D^{20} 1.4262, was obtained in 63.4% yield, and 2-methyltetrahydropyran, b.p. 101.5–101.8° C., n_D^{20} 1.4180, in 76% yield.

Synthesis of 1-Phenyl-2-ethylpiperidine (III) from 2-Ethyltetrahydropyran (I) via 1,5-Dibromoheptane

2-Ethyltetrahydropyran, 30.0 gm., was added slowly to a cold mixture of 340 gm. of 48% hydrobromic acid and 18 ml. of concentrated sulphuric acid. Following a three-hour refluxing period, the reaction mixture was steam distilled, and the organic phase of the distillate extracted with ether, washed with sodium carbonate solution, and dried over calcium chloride. Fractionation gave 44.4 gm. (66.3%) dibromide, b.p. 112–116° C. (12 mm.), n_D^{17} 1.5010–1.5025. On the basis of the composition of the product formed in the subsequent reaction with aniline, this product is considered to consist of 70% 1,5-dibromoheptane and 30% 1,4-dibromoheptane.

A solution of 38.5 gm. (0.15 mole) of the dibromide and 62.2 gm. (0.68 mole) of aniline was warmed on a steam bath until it had formed into a brown cake. The reaction mixture was dissolved in hydrochloric acid and the free amines liberated by addition of sodium hydroxide solution. The organic phase was extracted with ether and dried over sodium hydroxide. Careful fractionation gave 12.5 gm. (44%) of 1-phenyl-2-ethylpiperidine (III), b.p. 125.5–126.0° C. (8 mm.), n_D^{20} 1.5505, picrate m.p. 177.6–178.2° C., and 5.3 gm. (19%) of 1-phenyl-2-propylpyrrolidine (IV), b.p. 132–136° C. (8 mm.), n_D^{20} 1.5534, picrate m.p. 135.6–136.1° C. A mixture of the picrate of III with the picrate formed from the lowest-boiling fraction of the product of the 2-ethyltetrahydropyran–aniline reaction showed no depression in melting point. Similarly, the melting point of the picrate of IV was not depressed in admixture with the picrate of the intermediate fraction of the catalysis product.

Synthesis of 1-Phenyl-2-propylpyrrolidine (IV) from 2-Propyltetrahydrofuran (VI) via 1,4-Dibromoheptane

Thirty-six grams (0.315 mole) of 2-propyltetrahydrofuran, b.p. 130–133° C., n_D^{20} 1.4215, prepared by the method of Paul (10, 11) from furfural in an over-all

yield of 65%, was dissolved in an equal volume of glacial acetic acid. The solution was saturated with anhydrous hydrogen bromide and heated in a sealed tube at 120° C. for three hours. The product was steam distilled and the organic phase extracted with ether and dried over anhydrous sodium sulphate. Fractionation gave 61 gm. (75%) dibromide, b.p. 108–110° C. (8 mm.), n_D^{20} 1.5010–1.5015. The results of the subsequent reaction with aniline indicated that this product consisted of 83% 1,4-dibromoheptane and 17% 1,5-dibromoheptane.

The dibromide, 57.6 gm. (0.22 mole), was treated with 84.3 gm. (0.91 mole) of aniline and the product worked up as described in the preceding section. Careful fractionation gave 30.7 gm. (73%) of 1-phenyl-2-propylpyrrolidine (IV), b.p. 137–138° C. (8 mm.), n_D^{20} 1.5518, picrate m.p. 136.0–136.5° C., and 6.3 gm. (15%) of 1-phenyl-2-ethylpiperidine (III), b.p. 126–129° C. (8 mm.), n_D^{20} 1.5502, picrate m.p. 177.2–177.6° C. Mixed melting point determinations on the picrates of these compounds with the picrates of corresponding fractions obtained from the catalysis reaction showed no depression.

Reduction of Mixed N-Phenylheptenylamines (V) to N-Heptylaniline

A solution containing 6.5 gm. of the highest-boiling fraction from the 2-ethyltetrahydropyrananiline reaction in 100 ml. of ethanol was treated with hydrogen in the presence of Raney nickel at room temperature and 50 p.s.i. pressure. Distillation, following removal of the catalyst, gave 5.1 gm. (79%) of product, b.p. 163–169° C. (24 mm.), n_D^{20} 1.5188, *p*-bromobenzenesulphonamide derivative m.p. 117–118° C. A mixture of this derivative with *p*-bromobenzenesulphonamide prepared from authentic N-heptylaniline showed no depression in melting point.

Ozonolysis of N-Benzoyl-N-phenylheptenylamines

To a solution of 3.8 gm. (0.02 mole) of the mixed heptenylanilines in 38 ml. of dry pyridine and 76 ml. of dry benzene was added dropwise 4.8 gm. (0.034 mole) of benzoyl chloride at 60–70° C. After an additional 30 min. at this temperature, the product was worked up in the usual way. Distillation gave 4.6 gm. (78.4%) of a thick straw-colored oil, b.p. 163–173° C. (0.3 mm.).

A stream of ozone (5%) was passed into a solution of 3.2 gm. of the benzoyl derivative in 50 ml. of aldehyde-free propionic acid until ozonization was complete. The ozonide was decomposed by hydrogenolysis for 10 hr. over palladium on calcium carbonate at room temperature and 63 p.s.i. pressure. Following removal of the catalyst, the volatile carbonyl products were swept out of the gradually-heated propionic acid solution and collected in ethanol cooled to dry-ice temperatures. These were then converted to 2,4-dinitrophenylhydrazones in the usual way and separated chromatographically on a silicic acid – Super Cel column (12). The less strongly absorbed hydrazone, on recrystallization from ethanol, melted at 153.3–154.8° C. and gave no melting point depression when mixed with authentic propionaldehyde 2,4-dinitrophenylhydrazone. The more strongly absorbed derivative, also recrystallized from ethanol, melted at 166–167° C., and did not depress the melting point of authentic acetaldehyde 2,4-dinitrophenylhydrazone.

Synthesis of 1-Phenyl-2-methylpiperidine (VII) from 2-Methyltetrahydropyran (II) via 1,5-Dibromohexane

2-Methyltetrahydropyran, 18.0 gm. (0.18 mole), was dissolved in glacial acetic acid and treated with anhydrous hydrogen bromide at 120° C., following the procedure previously described for the reaction of hydrogen bromide with 2-propyltetrahydrofuran. Fractionation of the product gave 35.7 gm. (82%) dibromide, b.p. 100.0–102.3° C. (12 mm.), $n_D^{13.5}$ 1.5077. The composition of the product formed in the subsequent reaction with aniline indicated that the dibromide consisted of 87% 1,5-dibromohexane and 13% 1,4-dibromohexane.

The conversion of the dibromide to cyclic amines by reaction with aniline was carried out following the procedure previously described. From 34.5 gm. of the dibromide was obtained 16.9 gm. (80%) of 1-phenyl-2-methylpiperidine (VII), b.p. 110.8–113.0° C. (8 mm.), n_D^{13} 1.5560, picrate m.p. 167.4–168.4° C., and 2.4 gm. (12%) of 1-phenyl-2-ethylpyrrolidine (VIII), b.p. 117.5–118.5° C. (8 mm.), n_D^{14} 1.5631, picrate m.p. 118–119° C. The melting points were not depressed when these picrates were mixed with picrates from corresponding fractions obtained from the reaction of 2-methyltetrahydropyran with aniline.

Reduction of Mixed N-Phenylhexenylamines (IX) to N-Hexylaniline

A sample of the mixed amines dissolved in ethanol was reduced at room temperature and 43 p.s.i. pressure over Raney nickel. Distillation gave a product, b.p. 163–165° C. (30 mm.), n_D^{20} 1.5230, *m*-nitrobenzenesulphonamide m.p. 79.6–80.2° C., and *p*-toluenesulphonamide m.p. 67–68° C. The melting points of these sulphonamides agree closely with literature values for the corresponding derivatives of N-hexylaniline (4). The *p*-bromobenzenesulphonamide melted at 96.2–97.2° C.

Ozonolysis of N-Acetyl-N-phenylhexenylamines

A solution of 4.5 gm. (0.026 mole) of mixed amines (IX) dissolved in 10.6 ml. (0.10 mole) of acetic anhydride and 70.8 ml. of piperidine was refluxed for one and one-half hours. Dilute sulphuric acid was added and the organic phase extracted with ether, dried, and distilled to give 4.75 gm. (85%) of liquid product, b.p. 115–120° C. (0.5 mm.), n_D^{21} 1.5223.

A stream of ozone (5%) was passed into a solution of 2 gm. of N-acetyl-N-phenylhexenylamines in 50 ml. of purified glacial acetic acid until ozonization was complete. The ozonide was decomposed by hydrogenolysis over palladium on calcium carbonate. Following removal of the catalyst, nitrogen was passed through the solution while its temperature was gradually raised. The aldehyde first swept from the solution was converted into *p*-nitrophenylhydrazone and 2,4-dinitrophenylhydrazone derivatives, the melting points of which corresponded to derivatives of acetaldehyde. Mixed melting point determinations showed no depression. The sweep gas passing through the solution at the higher temperatures was led into ethanol cooled in dry-ice, dimedone added, and the resulting derivative recrystallized from ethanol. Its melting point

corresponded to that of the dimedone of formaldehyde, and a mixed melting point determination with authentic compound gave no depression.

ACKNOWLEDGMENTS

Acknowledgment is made to the National Research Council of Canada for financial assistance which made this work possible.

REFERENCES

1. BOURNS, A. N., EMBLETON, H. W., and HANSULD, M. K. Can. J. Chem. 30: 1. 1952.
2. BROWN, H. C. and FLETCHER, R. S. J. Am. Chem. Soc. 72: 1223. 1950.
3. DHAR, M. L., HUGHES, E. D., and INGOLD, C. K. J. Chem. Soc. 2058. 1948.
4. HICKENBOTTOM, W. J. J. Chem. Soc. 1119. 1937.
5. HUGHES, E. D., INGOLD, C. K., and WOOLF, L. I. J. Chem. Soc. 2084. 1948.
6. IVANOFF, N. and MAGAT, M. J. chim. phys. 47: 914. 1950.
7. LIPPERT, W. Ann. 276: 148. 1893.
8. MITCHELL, F. W. and O'GORMAN, J. M. Anal. Chem. 20: 315. 1948.
9. PAUL, R. Compt. rend. 198: 1246. 1934.
10. PAUL, R. Compt. rend. 200: 1118. 1935.
11. PAUL, R. Bull. soc. chim. 5: 1053. 1938.
12. ROBERTS, J. D. and GREEN, C. Ind. Eng. Chem. Anal. Ed. 18: 335. 1946.
13. ROYALS, E. E. Advanced organic chemistry. Prentice-Hall, Inc., New York. 1954.
14. WALLING, C. J. Am. Chem. Soc. 72: 1164. 1950.

2,3-DIHYDROBENZO(*f*)-1,4-OXATHIEPIN AND DERIVATIVES[1]

By Marshall Kulka

ABSTRACT

A method has been developed for the synthesis of a new heterocyclic system III. When 2-β-chloroethoxybenzyl chloride (XI) was heated with thiourea in alcohol solution, S-(2-β-chloroethoxybenzyl)isothiuronium chloride (XII) was formed which on cleavage with aqueous alkali in high dilution yielded 2,3-dihydrobenzo(*f*)-1,4-oxathiepin (III). Derivatives of III with substituents such as methyl, *t*-butyl, chlorine, and nitro in the 7 and 9 positions were prepared in high yields from the corresponding substituted 2-β-chloroethoxybenzyl chlorides. The presence of substituents in the position ortho to the chloroethoxy group of XII had no retarding effect on the cyclization to XIV.

During the synthesis of aralkyl mercaptans required as intermediates in a synthetic insecticide research program, a new heterocyclic system, III, was discovered. The name for this new system is derived from oxepin (I) and 1,4-oxathiepin (II). The fusion of a benzene ring in the *f* position of 1,4-oxathiepin (II), followed by saturation of the 2,3-double bond, results in the new system, (III), for which the name 2,3-dihydrobenzo(*f*)-1,4-oxathiepin is appropriate.

The thiourea method for the preparation of alkyl (12) and aralkyl (8) mercaptans (VII) comprises heating the alkyl or aralkyl halide (IV) with thiourea (V) in alcohol solution followed by alkaline cleavage of the resulting isothiuronium chloride (VI). Sodium chloride, water, and cyanoguanidine (VIII) are formed along with the mercaptan (VII). It is well known (1,9) that mercaptans react with alkyl halides (IX) in the presence of aqueous or alcoholic alkali to form sulphides (X).

During the preparation of various benzyl mercaptans from the corresponding benzyl chlorides by the thiourea method, interest was aroused in regard to the behavior of 2-β-chloroethoxybenzyl chlorides (XI) in this reaction. Since phenyl 2-chloroethyl ether does not react with thiourea (V) under these conditions, the first product of the reaction between XI and V should be the S-(2-β-chloroethoxybenzyl)isothiuronium chloride (XII). This on treatment with alkali should yield the mercaptan XIII, which could theoretically undergo two reactions under these conditions. An intramolecular reaction would result in the 1,4-oxathiepin (XIV), while an intermolecular reaction would lead to the polymer (XV). Actually when an aqueous-alcoholic solution of S-(2-β-chloroethoxybenzyl)isothiuronium chloride (XII) was treated with excess sodium hydroxide in a small volume of hot water, the main product of

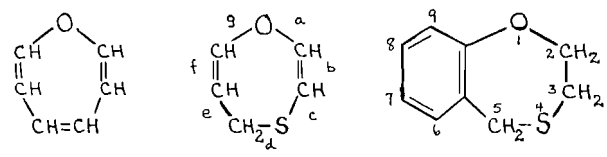

I II III

[1]*Manuscript received May 24, 1955.*
Contribution from the Dominion Rubber Company Limited Research Laboratories, Guelph, Ontario.

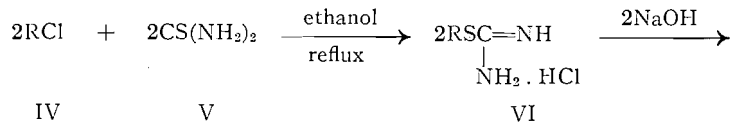

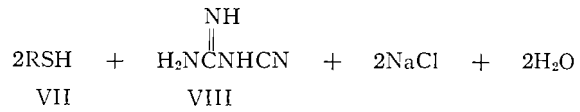

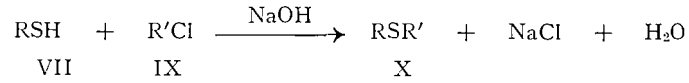

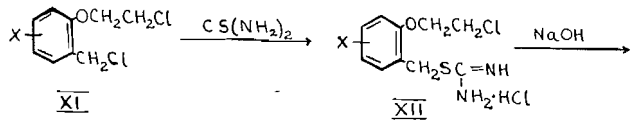

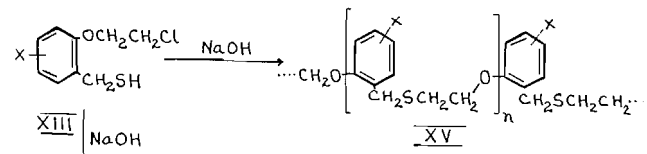

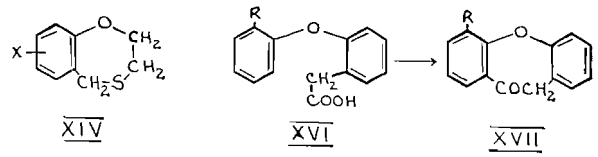

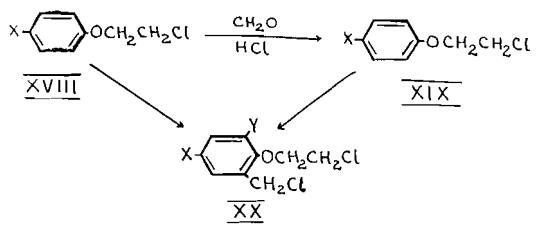

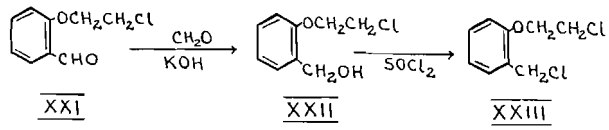

NOTE: The formula for compound XIX should read

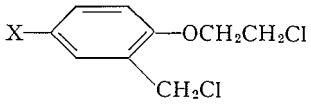

the reaction was the benzene-insoluble polymer (XV). On the other hand when the aqueous-alcoholic solution of XII was added dropwise to excess sodium hydroxide in a large volume of hot water, a benzene-soluble compound was obtained in high yield. This compound possessed a boiling point slightly lower than the corresponding 2-β-chloroethoxybenzyl chloride (XI), it was free of chlorine and contained a neutral sulphur which oxidized easily to the sulphone. On the basis of these properties together with analytic figures and molecular weight it must be presumed to be the intramolecular reaction product XIV.

The thiourea method has been successfully applied to the synthesis of several 2,3-dihydrobenzo(*f*)-1,4-oxathiepins (XIV) substituted in the benzene ring (Table II). These were oxidized to the corresponding sulphones (Table III). The method appears to have wide scope which is governed only by the availability of the benzyl chlorides (XI). Difficulties were expected in the preparation of nitroderivatives of XIV in view of the facts that S-(3-nitro-4-methoxybenzyl)isothiuronium chloride on treatment with aqueous alkali yields only resinous materials and no mercaptan and that *p*-nitrobenzyl mercaptan is sensitive to hot alkali (1). However XII (X = NO_2) was easily converted to XIV (X = NO_2) (Table II). A number of 3-substituted-5-alkyl-2-β-chloroethoxybenzyl chlorides (XI, X = 3-Cl, 3-NO_2, and 3-*t*-butyl) were also easily converted to the 1,4-oxathiepins (XIV, X = 9-Cl, 9-NO_2, and 9-*t*-butyl) via the corresponding isothiuronium chlorides (XII) showing that 3-substituents in XII have no retarding effect on the cyclization to XIV. This is in direct contrast to the behavior of 2-phenoxyphenylacetic acids (XVI) where substituents in the *ortho* position (R) sterically hinder the cyclization to the dibenzoxepinones (XVII) (6).

The 4-substituted-2-β-chloroethoxybenzyl chlorides (XIX) required in this investigation were prepared by chloroethylation of the phenols with ethylene dichloride according to the method of Harris and Stewart (4) followed by chloromethylation of the resulting 2-chloroethyl phenyl ethers (XVIII). A few failures were experienced when *p*-nitrophenol, 2,4-di-*t*-butylphenol (11), and 2-hydroxy-5-methylacetophenone (10) reacted poorly or not at all with ethylene dichloride and when 2,4,5-trichlorophenyl 2-chloroethyl ether failed to chloromethylate. The introduction by usual methods of such groups as chlorine, nitro, and *t*-butyl into the 4-substituted-phenyl 2-chloroethyl ethers (XVIII) either before or after chloromethylation yielded additional 2-β-chloroethoxybenzyl chlorides (XX) required in this investigation. *o*-β-Chloroethoxybenzyl chloride (XXIII) was prepared from salicylaldehyde by chloroethylation and reduction (crossed Cannizzaro) of the resulting aldehyde (XXI) to the benzyl alcohol (XXII) followed by thionyl chloride treatment. This compound (XXIII) proved to be extremely unstable and had to be used immediately without purification in the preparation of the isothiuronium salt.

EXPERIMENTAL

2-β-Chloroethoxybenzaldehyde (XXI)

A reaction mixture of *o*-hydroxybenzaldehyde (100 gm.), ethylene dichloride (100 ml.), and potassium hydroxide (50 gm.) in water (100 ml.) was heated

under reflux for five days. The organic layer was separated, diluted with ethylene dichloride, washed with aqueous sodium hydroxide and with water, and the solvent removed. The residue was distilled, the fraction boiling at 163–164° (12 mm.) being collected; yield, 61 gm. or 40%. The distillate crystallized from benzene as white prisms melting at 38–39°. Anal. Calc. for $C_9H_9O_2Cl$: C, 58.53; H, 4.88. Found: C, 58.34; H, 4.71.

2-β-Chloroethoxybenzyl Alcohol (*XXII*)

To a stirred solution of 2-β-chloroethoxybenzaldehyde (20 gm.), ethanol (100 ml.), and 40% formaldehyde (40 ml.) was added dropwise 50% aqueous potassium hydroxide (50 ml.), the temperature being kept at 35–40° by cooling. The reaction mixture was stirred at 40° for two hours and then about half the ethanol was removed *in vacuo*. The residue was extracted with ether, the ether solution was washed with aqueous sodium bisulphite, and the solvent was removed. The residue distilled at b.p. (12 mm.) = 166–167° as a colorless liquid, $n_D^{20} = 1.550$, yield, 17 gm. or 85%. Anal. Calc. for $C_9H_{11}O_2Cl$: C, 57.90; H. 5.89. Found: C, 57.34, 57.60; H, 5.76, 5.90.

2-β-Chloroethoxybenzyl Chloride (*XXIII*)

To a solution of 2-β-chloroethoxybenzyl alcohol (12 gm.) in dry benzene (50 ml.) was added portionwise thionyl chloride (10 gm.), the temperature being kept below 35° by cooling. The reaction mixture was allowed to stand at room temperature for five hours during which time hydrogen chloride and sulphur dioxide were evolved. About two-thirds of the benzene was removed *in vacuo without heat application* and the purple solution was used directly in the formation of the isothiuronium salt (see below). The 2-β-chloroethoxybenzyl chloride is extremely unstable and polymerizes on standing or on warming.

2-β-Chloroethoxy-5-methylbenzyl Chloride (*XIX*, $X = CH_3$)

A reaction mixture of *p*-tolyl 2-chloroethyl ether (100 gm.) (4), ethylene dichloride (150 ml.), concentrated hydrochloric acid (300 ml.), water (15 ml.), and paraformaldehyde (22 gm.) was stirred and heated at 55–60° for 24 hr. The organic layer was separated, washed with water, with aqueous sodium bicarbonate, and with water. The solvent was removed and the residue was distilled, yielding a colorless liquid (111 gm. or 88%) boiling at 158–160° (12 mm.) and melting at 25–27°. Anal. Calc. for $C_{10}H_{12}OCl_2$: C, 54.80; H, 5.48. Found: C, 54.77, 54.59; H, 5.70, 5.33.

2-β-Chloroethoxy-5-t-butylbenzyl Chloride (*XIX*, $X = C(CH_3)_3$)

This was prepared in 50% yield as above from *p-t*-butylphenyl 2-chloroethyl ether (2). The colorless liquid boiled at 170–173° (12 mm.), $n_D^{20} = 1.533$. Anal. Calc. for $C_{13}H_{18}OCl_2$: C, 59.80; H, 6.90. Found: C, 59.43, 59.48; H, 6.53, 6.60.

2-β-Chloroethoxy-3,5-dichlorobenzyl Chloride (*XX*, $X = Y = Cl$)

The preparation of this compound required considerably more drastic conditions than those used for the preparation of 2-β-chloroethoxy-5-chlorobenzyl chloride (7).

A suspension of paraformaldehyde (25 gm.), zinc chloride (150 gm.), and acetic acid (400 ml.) was saturated with hydrogen chloride. To the resulting solution was added 2,4-dichlorophenyl 2-chloroethyl ether (100 gm.) (2) and the solution was heated at 90–95° for four days. About half of the acetic acid was distilled off *in vacuo* from the reaction mixture, and the residue was treated with dilute hydrochloric acid and extracted with benzene. The benzene solution was washed with water, with aqueous sodium bicarbonate, and with water and the solvent was removed. The residue was fractionally distilled, yielding fraction 1 (52 gm.) boiling at 150–175° (12 mm.) and fraction 2 (18 gm.) boiling at 175–185° (12 mm.). Fraction 2 could not be purified further so the crude material was used in the preparation of the isothiuronium salt (see below).

2-β-Chloroethoxy-5-nitrobenzyl Chloride (*XIX*, $X = NO_2$)

This was prepared in 35% yield of crude material by the chloromethylation of *p*-nitrophenyl 2-chloroethyl ether (5) employing a method similar to that above except that 30 gm. of zinc chloride was used instead of 150 gm. The yellow liquid boiled at 170–175° (1 mm.). In view of the fact that this contained a small amount of difficultly separable *p*-nitrophenyl 2-chloroethyl ether, the crude material was used directly in the preparation of the isothiuronium salt where purification was easier.

2-Chloro-4-t-butylphenyl 2-Chloroethyl Ether

Into a solution of *p-t*-butylphenyl 2-chloroethyl ether (71 gm.) (2), sodium acetate (35 gm.), and acetic acid (200 ml.), chlorine gas was passed until 24 gm. were absorbed, the temperature being maintained at 35–40° by cooling. After it had been left at room temperature for 15 min., the reaction mixture was poured into water and extracted with benzene. The benzene extract was washed with water and the solvent was removed. The residue was distilled and the fraction boiling at 160–163° (12 mm.) collected. The yield of the colorless distillate was 56 gm. or 75%, $n_D^{20} = 1.532$. Anal. Calc. for $C_{12}H_{16}OCl_2$: C, 58.30; H, 6.48. Found: C, 58.72, 58.21; H, 6.60, 6.46.

2-β-Chloroethoxy-3-chloro-5-t-butylbenzyl Chloride (*XX*, $X = C(CH_3)_3$, $Y = Cl$)

Into a suspension of paraformaldehyde (10 gm.), zinc chloride (30 gm.), and acetic acid (250 ml.), hydrogen chloride was passed until saturated. To this was added 2-chloro-4-*t*-butylphenyl 2-chloroethyl ether (44 gm.) and the resulting solution was heated at 80–90° for three days. About half of the acetic acid was distilled off *in vacuo* and the residue was treated with dilute hydrochloric acid and extracted with benzene. The benzene extract was washed with water, with aqueous sodium bicarbonate, and with water. The solvent was removed and the residue was distilled, yielding 32 gm. (60%) of a colorless liquid, $n_D^{20} = 1.539$, boiling at 180–185° (13 mm.). Anal. Calc. for $C_{13}H_{17}OCl_3$: C, 52.80; H, 5.75. Found: C, 53.31, 53.17; H, 5.88, 5.61.

2-β-Chloroethoxy-3-nitro-5-t-butylbenzyl Chloride (*XX*, $X = C(CH_3)_3$, $Y = NO_2$)

To a solution of 2-β-chloroethoxy-5-*t*-butylbenzyl chloride (12 gm.) (XIX) in acetic acid (25 ml.) and acetic anhydride (10 ml.) was added dropwise fuming nitric acid (4 ml.) with stirring, the temperature being kept at 25–30° by

cooling. After it was allowed to stand at room temperature for two hours, the reaction mixture was poured into water and the precipitated oil was extracted with benzene. The benzene extract was washed with water and the solvent removed. The residue on crystallization from methanol yielded 9.8 gm. (70%) of white prisms melting at 77–78°. Anal. Calc. for $C_{13}H_{17}NO_3Cl_2$: C, 50.98; H, 5.55. Found: C, 50.93; H, 5.55.

2-t-Butyl-4-methylphenyl 2-Chloroethyl Ether

To a solution of *p*-tolyl 2-chloroethyl ether (150 gm.) (4) in *t*-butyl chloride (400 ml.) was added aluminum chloride (3 gm.) in three 1-gm. portions with cooling and swirling until dissolved. Then the reaction mixture was heated under gentle reflux for three hours. Because of the continuous evolution of hydrogen chloride the internal temperature remained at 35–40° for the first two hours and rose gradually to 50° during the last hour of the reaction. The dark red solution was washed with cold dilute hydrochloric acid, with water, with aqueous sodium bicarbonate, and with water. After the excess *t*-butyl chloride was distilled off, the residue was fractionally distilled, the fraction (106 gm.) boiling at 140–160° (13 mm.) being collected. This partially solidified on cooling and rubbing with a little methanol and was crystallized from methanol. The white prisms melted at 35–37° and weighed 58 gm. (30%). Anal. Calc. for $C_{13}H_{19}OCl$: C, 68.87; H, 8.39. Found: C, 68.94, 69.26; H, 8.16, 8.37.

2-β-Chloroethoxy-3-t-butyl-5-methylbenzyl Chloride ($XX, X = CH_3, Y = C(CH_3)_3$)

A suspension of 2-*t*-butyl-4-methylphenyl 2-chloroethyl ether (30 gm.), paraformaldehyde (6 gm.), and acetic acid (150 ml.) was saturated with hydrogen chloride and then heated at 78–80° for 18 hr. Most of the acetic acid was removed *in vacuo*, and the residue was treated with water and extracted with benzene. The benzene solution was washed with water, with aqueous sodium bicarbonate, and with water and the solvent was removed. The residue was distilled and the fraction boiling at 172–177° (13 mm.) collected. The yield of the colorless liquid was 20 gm. or 60%, $n_D^{20} = 1.534$. Anal. Calc. for $C_{14}H_{20}OCl_2$: C, 61.09; H, 7.25. Found: C, 61.48; H, 7.38.

2,4,5-Trichlorophenyl 2-Chloroethyl Ether

This was prepared in 72% yield from 2,4,5-trichlorophenol and ethylene dichloride according to the method of Harris and Stewart (4). The white needles melted at 52–53°. Anal. Calc. for $C_8H_6OCl_4$: C, 36.92; H, 2.31. Found: C, 37.37; H, 2.47.

2-Acetyl-4-methylphenyl 2-Chloroethyl Ether

This was prepared in 10% yield from 2-hydroxy-5-methylacetophenone (10) and ethylene dichloride (4). The white prisms melted at 61–62°. Anal. Calc. for $C_{11}H_{13}O_2Cl$: C, 62.14; H, 6.12. Found: C, 62.72; H, 6.24.

Preparation of S-Benzylisothiuronium Chlorides (XII) (Table I)

To a solution of the 2-β-chloroethoxybenzyl chloride (20 gm.) in ethanol (50 ml.) was added about 20% excess thiourea and the reaction mixture was

heated under reflux for three hours. The ethanol was removed *in vacuo* from the solution and the residual sirup was treated with hot water (20 ml.) (about twice as much water was required by the nitro derivatives of XII). The resulting solution was then extracted with benzene in order to remove any impurities, which were present only when crude 2-β-chloroethoxybenzyl chloride was used, and the aqueous solution was allowed to cool. The S-(2-β-chloroethoxybenzyl)isothiuronium chloride precipitated and could be crystallized from water or alcohol. Although S-benzylisothiuronium chloride is known to exhibit dimorphism (3), this was not observed with those chlorides listed in Table I.

TABLE I

THE PREPARATION OF S-(2-β-CHLOROETHOXYBENZYL)ISOTHIURONIUM CHLORIDES (XII) FROM THE CORRESPONDING BENZYL CHLORIDES (XI)

XII substituent(s)	Formula	M.p., °C.	Yield, %	Analyses			
				Calc.		Found	
				C	H	C	H
Unsubstituted	$C_{10}H_{14}N_2OCl_2S$		(Not purified)				
5-Chloro-	$C_{10}H_{13}N_2OCl_3S$	169–170	75	38.04	4.03	37.92	3.87
3,5-Dichloro-	$C_{10}H_{12}N_2OCl_4S$		(Not purified)				
5-Methyl-	$C_{11}H_{16}N_2OCl_2S$	180–181	82	44.75	5.42	44.76	5.13
5-*t*-Butyl-	$C_{14}H_{22}N_2OCl_2S$	199–200	69	49.85	6.53	49.93	6.30
5-Nitro-	$C_{11}H_{17}N_5O_3Cl_2S_2$[a]	158–159	80	32.84	4.23	33.02	4.29
3-Chloro-5-*t*-butyl-	$C_{14}H_{21}N_2OCl_3S$	194–195	79	45.22	5.65	45.28	5.50
3-Nitro-5-*t*-butyl-	$C_{14}H_{21}N_3O_3Cl_2S$	190–191	90	43.97	5.50	44.25	5.24
3-*t*-Butyl-5-methyl-	$C_{15}H_{24}N_2OCl_2S$	Sirup	(Not purified)				

[a]*Calc. N, 17.4. Found: N, 17.0. The analyses of this compound indicate that it possesses two molecules of thiourea instead of one.*

Preparation of the 2,3-Dihydrobenzo(f)-1,4-oxathiepins (XIV) (Table II)

The S-(2-β-chloroethoxybenzyl)isothiuronium chloride (30 gm.) (XII) was dissolved in ethanol (50 ml.) and water (100 ml.) and the solution was then

TABLE II

THE PREPARATION OF THE 2,3-DIHYDROBENZO(*f*)-1,4-OXATHIEPINS (XIV) FROM THE CORRESPONDING S-(2-β-CHLOROETHOXYBENZYL)ISOTHIURONIUM CHLORIDES (XII)

XIV substituents	Formula	M.p., °C.	B.p. (13 mm.)	Yield, %	Analyses			
					Calc.		Found	
					C	H	C	H
Unsubstituted	$C_9H_{10}OS$	35–36	130	47[a]	65.06	6.03	65.21	5.90
7-Chloro-	C_9H_9OClS[b]	70–71	160–162	80	53.84	4.49	54.15	4.35
7,9-Dichloro-	$C_9H_8OCl_2S$	114–115	*ca.* 180	10[a]	45.95	3.40	45.80	3.47
7-Methyl-	$C_{10}H_{12}OS$	45–46	146–147	90	66.66	6.67	66.67	6.55
7-*t*-Butyl-	$C_{13}H_{18}OS$	53–54	170	94	70.26	8.11	70.09	8.01
7-Nitro-	$C_9H_9NO_3S$	124–125		84	51.18	4.27	51.44	4.33
7-*t*-Butyl-9-chloro-	$C_{13}H_{17}OClS$		185–190	80	60.81	6.63	61.14	6.77
7-*t*-Butyl-9-nitro-	$C_{13}H_{17}NO_3S$	81–82		86	58.43	6.37	58.45	6.22
7-Methyl-9-*t*-butyl-	$C_{14}H_{20}OS$	61–62	175–180	53[a]	71.19	8.47	71.40	8.53

[a]*These yields are based on the 2-β-chloroethoxybenzyl chlorides and not on the corresponding isothiuronium salts as in the other cases.*

[b]*Molecular weight: calc., 200.5; found, 197 (Rast).*

added dropwise over one-half hour to a stirred solution of sodium hydroxide (20 gm.) in water (1 l.) heated on the steam bath. The stirring and heating was continued for another hour and the precipitated oil was then extracted with benzene. The benzene solution was washed with water and the solvent was removed. The residue was distilled and the almost odorless distillate crystallized from methanol. The results are shown in Table II.

Preparation of 2,3-Dihydrobenzo(f)-1,4-oxathiepin-4,4-dioxides (Table III)

To a solution of the 2,3-dihydrobenzo(*f*)-1,4-oxathiepin (XIV) (1 gm.) in acetic acid (5 ml.) was added 30% hydrogen peroxide (3 ml.). The reaction

TABLE III

THE PREPARATION OF 2,3-DIHYDROBENZO(*f*)-1,4-OXATHIEPIN-4,4-DIOXIDES BY THE OXIDATION OF XIV

2,3-Dihydrobenzo(*f*)-1,4-oxathiepin-4,4-dioxide substituent(s)	Formula	M.p., °C.	Analyses			
			Calc.		Found	
			C	H	C	H
Unsubstituted	$C_9H_{10}O_3S$	165–166	54.53	5.05	54.62	4.79
7-Chloro-	$C_9H_9O_3ClS$	194–195	46.45	3.87	46.56	4.00
7,9-Dichloro-	$C_9H_8O_3Cl_2S$	209–210	40.45	3.00	40.42	2.96
7-Methyl-	$C_{10}H_{12}O_3S$	175–176	56.60	5.66	56.77	5.64
7-*t*-Butyl-	$C_{13}H_{18}O_3S$	184–185	61.42	7.08	61.33	7.12
7-Nitro-	$C_9H_9NO_5S$	185–186	44.44	3.70	44.29	3.73
7-*t*-Butyl-9-chloro-	$C_{13}H_{17}O_3ClS$	158–159	54.07	5.89	54.43	6.03
7-*t*-Butyl-9-nitro-	$C_{13}H_{17}NO_5S$	187–188	52.17	5.68	52.31	5.80
7-Methyl-9-*t*-butyl-	$C_{14}H_{20}O_3S$	189–190	62.69	7.46	62.82	7.46

was exothermic and the temperature rose to about 80°. The solution was heated on the steam bath for one hour and then diluted with hot water and the sulphone allowed to crystallize. The white prisms were analytically pure and the yield was quantitative.

ACKNOWLEDGMENT

The author is indebted to Gisela von Stritzky for the microanalyses.

REFERENCES

1. BENNETT, G. M. and BERRY, W. A. J. Chem. Soc. 1666. 1927.
2. COLEMAN, G. H. and STRATTON, G. B. U.S. Patent No. 2,186,367. 1940. Chem. Abstr. 34: 3281. 1940.
3. DONLEAVY, J. J. J. Am. Chem. Soc. 58: 1004. 1936.
4. HARRIS, G. R. and STEWART, R. Can. J. Research, B, 27: 739. 1949.
5. KATRAK, B. N. J. Indian Chem. Soc. 13: 334. 1936. Chem. Abstr. 30: 7107. 1936.
6. KULKA, M. and MANSKE, R. H. F. J. Am. Chem. Soc. 75: 1322. 1953.
7. KULKA, M. and VAN STRYK, F. G. Can. J. Chem. 33: 1130. 1955.
8. LEWIS, T. R. and ARCHER, S. J. Am. Chem. Soc. 73: 2109. 1951.
9. PATTERSON, W. I. and DU VIGNEAUD, V. J. Biol. Chem. 111: 393. 1935. Chem. Abstr. 30: 80. 1936.
10. ROSENMUND, K. W. and SCHNURR, W. Ann. 460: 56. 1928.
11. STILLSON, G. H., SAWYER, D. W., and HUNT, C. K. J. Am. Chem. Soc. 67: 303. 1945.
12. URQUHART, G. G., GATES, J. W., JR., and CONNOR, R. Org. Syntheses, Collective Vol. III: 363. 1955.

NOTES

THE CRYSTAL STRUCTURE OF THE ALIPHATIC DIBASIC ACID $C_4H_4O_6.2H_2O$[1]

By M. P. Gupta[2]

The aliphatic dibasic acid $C_4H_4O_6.2H_2O$ has variously been described as having either the *cis*- or the *trans*- configuration. Chemical evidence against or in favor of either of these configurations has been presented by Hartree (2). In a previous communication, however, the present author (1) was able to show conclusively from X-ray diffraction data that the molecule in the crystalline state must have the *trans*-configuration since it crystallized in the monoclinic system, class $2/m$, space group $P2_1/c$ with two molecules in the unit cell of dimensions

$$a = 6.40, \quad b = 13.03, \quad c = 5.34 \text{ Å}, \quad \beta = 126.5°.$$

Thus the molecules were, tentatively, confirmed as molecules of dihydroxyfumaric acid and not dihydroxymaleic acid. The present note describes the results of a Fourier analysis of the X-ray diffraction data obtained from the crystals of dihydroxyfumaric acid dihydrate.

Reflections in the $\{0kl\}$ and the $\{h0l\}$ zones were obtained from Weissenberg photographs using Cu unfiltered radiation, and the intensities were estimated visually. Patterson projections were calculated for both these zones. The $\{h0l\}$ projection showed clearly the molecules to be lying in a plane perpendicular to the a axis which was the best axis for clear resolution of the atoms. The first Fourier map showed the rough orientation of the molecule as well as the position of the water molecule and this was refined in successive stages; the last Fourier map obtained is shown in Fig. 1 below. The figure shows the molecule as projected on a plane perpendicular to the a axis. Only one molecule is outlined together with parts of the neighboring molecules. All the atoms in this projection are clearly resolved. The structure has been confirmed by the $\{h0l\}$ projection in which, however, there is serious overlap—only two atoms out of the six in the asymmetric unit are clearly resolved in this projection.

There is no hydrogen bonding in the COOH groups of the adjacent molecules which form an extensive chain running roughly parallel to the [102] axis, and as in oxalic acid dihydrate, the crystal structure is held together mainly by the water molecules. No pronounced departure from a completely planar molecule is expected. The crystal structure is being refined using three-dimensional data, and full details of the intramolecular and intermolecular distances will be published later.

The author wishes to thank Dr. W. H. Barnes for providing all facilities for this research in his laboratory.

[1]*Issued as N.R.C. No. 3668.*
[2]*National Research Laboratories Postdoctorate Fellow.*

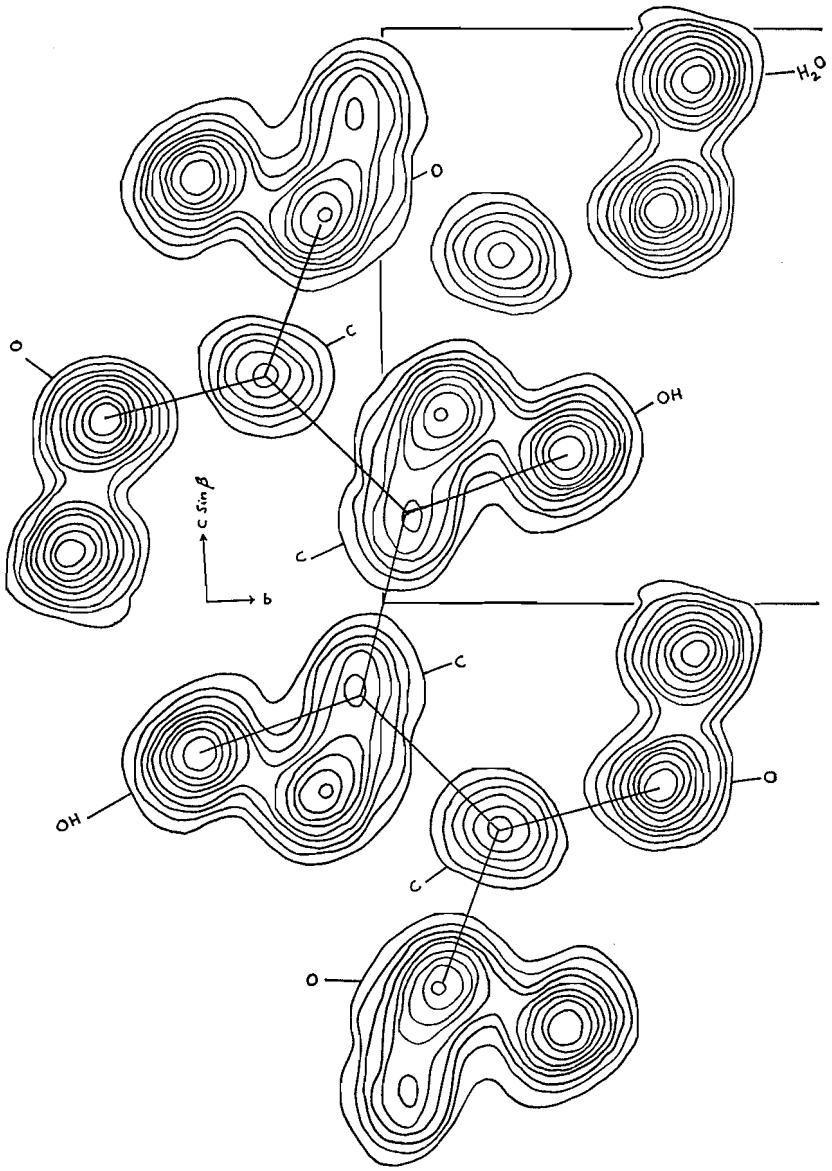

FIG. 1. Electron density projected on a plane perpendicular to the [100] axis. Contours drawn at arbitrary but equal levels of electron density.

1. GUPTA, M. P. J. Am. Chem. Soc. 75: 6312. 1953.
2. HARTREE, E. F. J. Am. Chem. Soc. 75: 6244. 1953.

RECEIVED MAY 17, 1955.
DIVISION OF PURE PHYSICS,
NATIONAL RESEARCH COUNCIL,
OTTAWA, CANADA.

THE ESTIMATION OF β-HYDROXY AMINO ACIDS BY A MICRODIFFUSION METHOD[1]

By L. Wiseblatt and W. B. McConnell

The periodic acid oxidation of β-hydroxy amino acids proceeds according to the following formula:

$$R—CHOH—CHNH_2—COOH \longrightarrow R—CHO + CHO—COOH + NH_3.$$

The reaction is rapid and quantitative and is used in analytical methods for determining serine and threonine (3, 5). It has also been used to estimate hydroxylysine, which occurs in a few proteins (6). Threonine yields acetaldehyde while serine and hydroxylysine give formaldehyde. Shinn and Nicolet (3) estimated threonine by aspirating the acetaldehyde into an excess of bisulphite, and Winnick (7) subsequently modified this to a microdiffusion method. Van Slyke, Hiller, and MacFadyen (6) have described a method for determining ammonia liberated by periodate oxidation (periodate ammonia) by aspirating it into boric acid and titrating in the usual way.

This communication describes a modified method for determining "periodate ammonia" which utilizes Conway Microdiffusion units (2).

To employ the method with protein hydrolyzates the following reagents are required:

1. Paraperiodic acid 0.5 *M* (114 gm. H_5IO_6 per liter).
2. Glycine solution (5% in *N* NaOH).
3. Potassium metaborate 5 *N* (410 gm. KBO_2 per liter).
4. Boric acid 2% containing 0.1% of bromcresol green – methyl red 2: 1.

One and one-half milliliters of boric acid solution are pipetted into the center well of a No. 1 Conway unit. One milliliter of sample solution, containing about 10 microequivalents of β-hydroxy amino acids, is added to the outer chamber. Immediately before the cell is sealed the following are added to the sample: 0.5 ml. periodic acid, 0.5 ml. glycine solution, 1.5 ml. potassium metaborate. After at least five hours at room temperature the contents of the center well are titrated with standard hydrochloric acid and the ammonia adsorbed is calculated. A control experiment with periodic acid omitted must be included to obtain a value for "preformed ammonia". Total ammonia less preformed ammonia is equal to periodate ammonia. Samples (10 microequivalents) of serine and threonine were analyzed as above. On individual determinations the percentage recoveries of the theoretical yield of ammonia were: serine—99.7, 100.4, 99.7, 100.1; threonine—99.5, 99.5, 100.3, 99.8. No interference from other common amino acids was found.

The total β-hydroxy amino acids in a protein hydrolyzate can be estimated in terms of periodate ammonia using the method outlined. If threonine is then estimated by Winnick's method (7) and "threonine ammonia" is subtracted from periodate ammonia, the difference should be a measure of serine content. Hydroxylysine glucosamine and ethanolamine give ammonia upon periodate oxidation and if present they would interfere with the estimation of serine.

[1]*Issued as N.R.C. No. 3692.*

Selected proteins were hydrolyzed for 20 hr. in refluxing 6 *N* hydrochloric acid. The hydrolyzates were freed from excess acid by repeated vacuum evaporation and dilution, made to suitable volumes, and 1-ml. aliquots were taken for "periodate ammonia" and threonine analyses. Aliquots were analyzed for total nitrogen by the micro-Kjeldahl method. Results are given in Table I.

TABLE I

SERINE AND THREONINE CONTENT OF PROTEIN
(In gm. per 16.0 gm. total nitrogen)

	Threonine			Serine		
	This investigation	Previously reported*		This investigation	Previously reported*	
Edestin	3.6	3.3	3.3	5.7	5.4	5.4
Casein	4.9	4.0 4.9	4.8 4.6	6.9	5.9 6.0	7.5 6.8
Ovalbumin	4.2	4.3 4.7	4.1	9.3†	7.6 9.5	8.3
Gluten	2.7	2.7	2.3	5.7	4.7‡	

**Taken from a compilation by Block and Bolling (1).*
†Hydrolyzates of ovalbumin are known to contain glucosamine.
‡Reported by Pence et al. (4).

Triplicate determinations of periodate ammonia agreed to within less than two per cent; this is slightly better than the agreement reported by Winnick (7) for the threonine estimations.

1. BLOCK, R. J. and BOLLING, D. The amino acid composition of proteins and foods. 2nd ed. Charles C. Thomas, Publisher, Springfield, Ill. 1951.
2. CONWAY, E. J. Microdiffusion analysis and volumetric error. Revised ed. Crosby, Lockwood & Son, London. 1947.
3. NICOLET, B. H. and SHINN, L. D. J. Biol. Chem. 139: 687. 1941.
4. PENCE, J. W., MECHAM, D. K., ELDER, A. H., LEWIS, J. C., SNELL, N. S., and OLCOTT, H. S. Cereal Chem. 27: 335. 1950.
5. REES, M. W. Biochem. J. 40: 632. 1946.
6. VAN SLYKE, D. D., HILLER, A., and MACFADYEN, D. A. J. Biol. Chem. 141: 681. 1941.
7. WINNICK, T. J. Biol. Chem. 142: 461. 1942.

RECEIVED MARCH 30, 1955.
PRAIRIE REGIONAL LABORATORY,
NATIONAL RESEARCH COUNCIL OF CANADA,
SASKATOON, SASKATCHEWAN.

A NEW TYPE OF OSMOMETER FOR AQUEOUS SOLUTIONS

BY J. L. GARDON[1] AND S. G. MASON

INTRODUCTION

Most osmometers for determining molecular weights of macromolecules have metal plate membrane supports and solvent-filled manometers. These units are not convenient for use in aqueous solutions, because the high surface tension causes air bubbles to be trapped at the metal surfaces and also leads to large capillarity errors in the manometer.

[1]*Holder of the Anglo-Paper Research Fellowship and of a Studentship from the National Research Council of Canada. Present address: Industrial Cellulose Research Ltd., Hawkesbury, Ontario.*

Selected proteins were hydrolyzed for 20 hr. in refluxing 6 *N* hydrochloric acid. The hydrolyzates were freed from excess acid by repeated vacuum evaporation and dilution, made to suitable volumes, and 1-ml. aliquots were taken for "periodate ammonia" and threonine analyses. Aliquots were analyzed for total nitrogen by the micro-Kjeldahl method. Results are given in Table I.

TABLE I

SERINE AND THREONINE CONTENT OF PROTEIN
(In gm. per 16.0 gm. total nitrogen)

	Threonine			Serine		
	This investigation	Previously reported*		This investigation	Previously reported*	
Edestin	3.6	3.3	3.3	5.7	5.4	5.4
Casein	4.9	4.0 4.9	4.8 4.6	6.9	5.9 6.0	7.5 6.8
Ovalbumin	4.2	4.3 4.7	4.1	9.3†	7.6 9.5	8.3
Gluten	2.7	2.7	2.3	5.7	4.7‡	

**Taken from a compilation by Block and Bolling (1).*
†Hydrolyzates of ovalbumin are known to contain glucosamine.
‡Reported by Pence et al. (4).

Triplicate determinations of periodate ammonia agreed to within less than two per cent; this is slightly better than the agreement reported by Winnick (7) for the threonine estimations.

1. BLOCK, R. J. and BOLLING, D. The amino acid composition of proteins and foods. 2nd ed. Charles C. Thomas, Publisher, Springfield, Ill. 1951.
2. CONWAY, E. J. Microdiffusion analysis and volumetric error. Revised ed. Crosby, Lockwood & Son, London. 1947.
3. NICOLET, B. H. and SHINN, L. D. J. Biol. Chem. 139: 687. 1941.
4. PENCE, J. W., MECHAM, D. K., ELDER, A. H., LEWIS, J. C., SNELL, N. S., and OLCOTT, H. S. Cereal Chem. 27: 335. 1950.
5. REES, M. W. Biochem. J. 40: 632. 1946.
6. VAN SLYKE, D. D., HILLER, A., and MACFADYEN, D. A. J. Biol. Chem. 141: 681. 1941.
7. WINNICK, T. J. Biol. Chem. 142: 461. 1942.

RECEIVED MARCH 30, 1955.
PRAIRIE REGIONAL LABORATORY,
NATIONAL RESEARCH COUNCIL OF CANADA,
SASKATOON, SASKATCHEWAN.

A NEW TYPE OF OSMOMETER FOR AQUEOUS SOLUTIONS

BY J. L. GARDON[1] AND S. G. MASON

INTRODUCTION

Most osmometers for determining molecular weights of macromolecules have metal plate membrane supports and solvent-filled manometers. These units are not convenient for use in aqueous solutions, because the high surface tension causes air bubbles to be trapped at the metal surfaces and also leads to large capillarity errors in the manometer.

[1]*Holder of the Anglo-Paper Research Fellowship and of a Studentship from the National Research Council of Canada. Present address: Industrial Cellulose Research Ltd., Hawkesbury, Ontario.*

The units described in this paper are inexpensive to construct, simple to operate, and have the following advantages:

(1) Measurements can be carried out reasonably fast, even with low porosity membranes, by making use of large membrane areas.

(2) In membranes as big as 200 sq. cm., membrane ballooning is eliminated.

(3) The membrane area per cc. half cell volume is 10 sq. cm., which compares favorably with other designs (2).

(4) The unit is transparent.

(5) Solutions can be changed readily without taking the unit apart.

The osmometer consists essentially of a cell and a manometer attachment. Two lucite disks and two rubber rings constitute the main body of the cell (Fig. 1). The membrane is clamped between two stainless steel screens and is

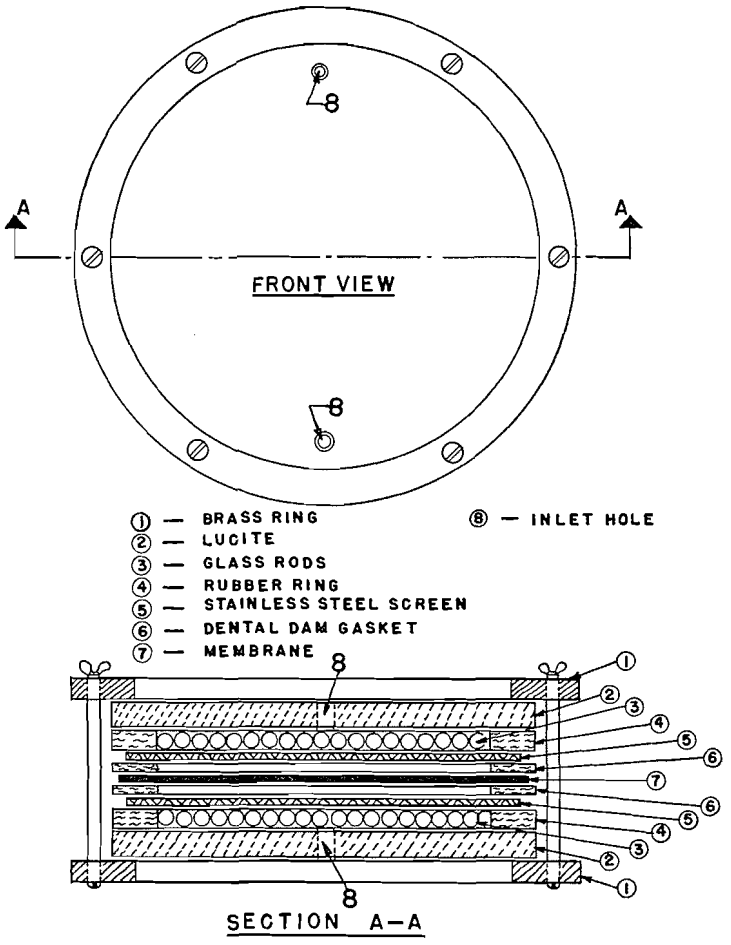

FIG. 1. Details of osmometer cell (exploded view).

supported by a layer of glass rods, closely packed parallel to one another in both cell compartments. The unit is sealed by means of the two rubber

rings mentioned above, which are compressed to the same thickness as the glass rods when the unit is assembled.

The osmotic pressure is measured in a capillary manometer which is connected to the solvent chamber. A syringe such as that from a glass syringe pipette acts as a levelling device.

All parts are individually clamped to a metal rod which forms the backbone of the unit.

CONSTRUCTION OF THE CELL

The stainless steel screens are placed between the rubber rings and the membrane. To avoid leakage through the screen meshes and to protect the membrane, two dental dam gaskets are placed between the screens and the membrane and the rubber rings are lubricated with silicone grease where they are in contact with the screens. As an additional precaution, Pyseal cement can be applied on the outside. If, for any reason, the use of silicone grease is to be avoided, four dental dam gaskets are used on each side of the screens, and Pyseal cement applied on the outside of the cell.

The components of three typical cells having active membrane areas of approximately 200, 60, and 20 sq. cm. are described in Table I. Standard

TABLE I

DIMENSIONS OF OSMOMETER CELL COMPONENTS

Active membrane area, sq. cm.	200	60	20
2 brass rings			
Inside diameter, cm.	18	11.5	6.5
Outside diameter, cm.	25.5	15	11.5
Number of holes for screws	8	6	4
2 lucite disks			
Thickness, 1 cm.			
Diameter, cm.	20.5	12.5	7.5
2 rubber rings			
Thickness, 3.1±0.1 mm.			
Inside diameter, cm.	15	10	5
Outside diameter, cm.	20.5	12.5	7.5
2 or 4 dental dam gaskets			
Inside diameter, cm.	15	10	5
Outside diameter, cm.	20.5	12.5	7.5
2 stainless steel screens			
125 mesh			
Diameter, cm.	16.5	11	6.0
Membrane			
Full diameter	17.5	11.5	6.5

pyrex rods with 3 mm. diameter are used as membrane supports. When these rods are initially packed into the cell, a 3 mm. clearance is left between them and the rubber rings to allow for expansion of the latter when the cell is tightened. The rods are vertical when the cell is in use.

There are two alternative methods of stabilizing the membrane and the stainless steel screen reinforcers.

(1) They can be supported by two disks of 12-mesh stainless steel screen instead of the glass rods. The diameters of these disks for the cells described in Table I are 14.5, 9.5, and 4.5 cm. The rubber rings for this design are cut

from sheets $\frac{1}{2}$ to 1 mm. thick, corresponding to the thickness of the 12-mesh screens.

(2) Disks of 5 mm. diameter, cut out of the same rubber sheet as used to prepare the body of the cell, can also be used as stabilizers. These disks are placed in pairs opposite to each other on both sides of the membrane, using two to three such pairs per 10 sq. cm. membrane area. This method does not provide as firm a membrane support as the two others and should be used only for small cells.

The cell is clamped to the metal rod backbone through two short metal rods pressed into drilled holes in one of the brass rings.

When the largest cell is assembled, there is a tendency for the lucite and consequently for the membrane to balloon, since the pressure is applied only at the edges of the lucite disks. This can be overcome by providing additional compression at the center of the disks by means of a suitable clamp which is independent of the brass rings.

The lucite disks are simply and tightly connected with the stopcocks and the glass parts leading to the manometer attachment by tygon tubing without any cement. This tubing, of 1.5 mm. wall thickness and 10 mm. outside diameter, is placed into 8 mm. bore holes in the lucite. To introduce the tubing into the smaller hole, a piece of end is cut off conically along the length and using the tongue thus formed, the tubing is pulled into the hole. The tongue is finally cut away.

The lucite disks are equipped with the connectors before the cell is assembled, and for this purpose, each lucite disk has two holes near the opposite ends of its vertical diameter.

THE MANOMETER

The design of the glass parts assembled with the cell is shown in Fig. 2 and, as can be seen, the cells can be changed without taking the manometer unit apart. The different glass parts are connected by spherical ground-glass joints of 12 mm. sphere diameter. These joints are lubricated with silicone grease and clamped together. The glass parts can also be connected by tygon tubing. All connecting capillaries have 1 mm. bore. To ensure a constant capillary rise effect, the measuring capillary (E) should be of uniform bore; it was found that the most satisfactory bore diameter was 0.3 ± 0.003 mm. The tubes (A) and (B) are 1 cm. in diameter and are cut from the same piece of tubing. The syringe is lubricated with silicone grease and its plunger is firmly wired to a levelling screw. The toluene–water interface is in the 1.5 cm. diameter bulb below the measuring capillary. The ground-glass joint (D) is lubricated with toluene-insoluble lubricant (e.g. Fisher's Nonaq Grease) and waterproofed by coating the outside with Pyseal cement. All stopcocks have 1 mm. bore.

OPERATION

The measuring capillary is attached to the unit after the other parts have been filled with water. The bulb (D) is then filled with toluene, the capillary is sealed in, the stopcock (C) is opened, and toluene is allowed to rise into the dry capillary.

The unit is filled with solution from a pipette which is connected to the stopcock (H) by rubber tubing. To change solutions, the solution chamber is emptied and rinsed several times with the new solution. If necessary the water in the solvent chamber can be changed without disturbing the toluene–water interface, through stopcocks (G) and (F).

The measurements are carried out slightly above room temperature in a water thermostat controlled to 0.001° C. Temperature equilibrium is established in the cell within 0.5 to 1.5 hr.

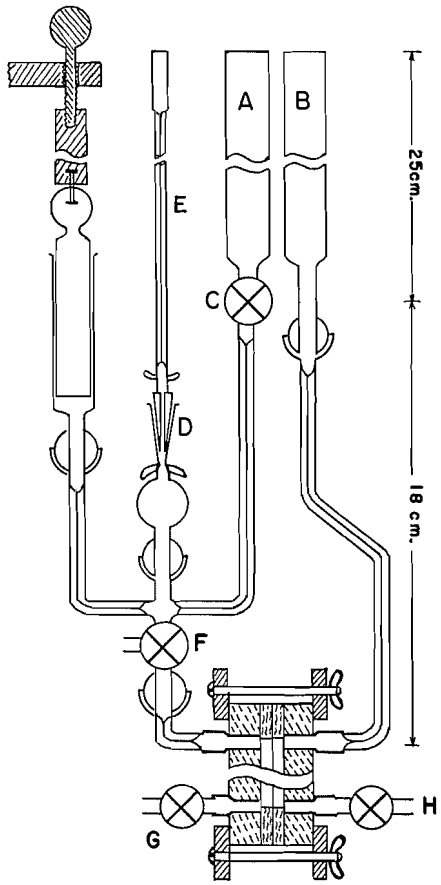

FIG. 2. Assembled osmometer unit showing details of the manometer system.

The readings are made on a scale with 0.5 mm. subdivisions behind the measuring capillary and are estimated to 0.01 cm. To avoid parallax, the scale is viewed through a cathetometer. The levels in tubes (A) and (B) are brought within 0.1 mm. of one another and the meniscus height in the measuring capillary is recorded. Stopcock (C) is then closed and the osmotic equilibrium is established by the half-sum method suggested by Fuoss and Mead (1). The difference between the original capillary meniscus reading and the one corresponding to the equilibrium is equal to the osmotic pressure

in centimeters toluene. No correction is necessary, since the density difference between water and the solution is negligible.

It is desirable to avoid excessive dilution of the solution by osmotic diffusion of solvent while the temperature equilibrium is being established. The measuring technique described above can be used only when the osmotic pressure of the solution is small, in our experience less than 3 cm. toluene. In the case of the larger osmotic pressures, it is preferable to adjust a level difference roughly corresponding to the expected osmotic pressure in tubes (A) and (B) when the instrument is being filled. Thus the driving pressure acting on the solvent is kept small until the actual measurement can be started. When temperature equilibrium is reached, stopcock (C) is closed and the osmotic equilibrium is established by the half-sum method. If the levels in tubes (A) and (B) are u and v respectively, and the meniscus levels in the capillary with stopcock (C) open and at equilibrium are w and z respectively, the osmotic pressure in gm./sq. cm. is given by

$$p = (v-u)d_{\text{solvent}}+(w-z)d_{\text{toluene}}$$

where d is the density.

The reproducibility of the capillary rise along the length of a 0.3 mm. bore capillary is ± 0.02 cm., if the precision of the bore is within 1%. If necessary, the accuracy can be improved by using larger capillaries; this however, can only be done at the expense of a longer time to osmotic equilibrium.

In addition, the accuracy of the measurements depends on the so-called "zero pressure", i.e. the finite apparent osmotic pressure existing when solutions of identical composition are placed on both sides of the membrane. In some instances, the solute may be adsorbed on the membrane thus leading to considerable difference in zero pressure before and after the measurement.

The speed of the measurements depends mainly upon the ratio of the capillary cross-section to membrane area. Using the small cell with 300 PT cellophane and the large cell with denitrated nitrocellulose and a capillary of 0.3 mm. bore, equilibrium osmotic pressures can be established to ± 0.02 cm. by the half-sum method within four hours after the temperature equilibrium is reached. This compares favorably with other designs of osmometer.

These units have been used for molecular weight determinations of fractionated samples of sodium ligninsulphonate; the results will be presented in a later communication.

1. Fuoss, R. M. and Mead, D. J. J. Phys. Chem. 47: 59. 1943.
2. Wagner, R. H. Technique of organic chemistry. Vol. I. Pt. I. *Edited by* A. Weissberger. Interscience Publishers, Inc., New York. 1949. pp. 518–540.

Received June 10, 1955.
Pulp and Paper Research Institute of Canada,
and
Chemistry Department,
McGill University,
Montreal, Quebec.

Canadian Journal of Chemistry

Issued by THE NATIONAL RESEARCH COUNCIL OF CANADA

VOLUME 33 | OCTOBER 1955 | NUMBER 10

CARBOHYDRATE THIOETHERS

1-DEOXY-1-THIOETHYL-D-FRUCTOSE[1]

BY SAMUEL B. BAKER

ABSTRACT

1-Deoxy-1-thioethyl-D-fructose was synthesized by two distinctly different methods. Less than the usual hindrance of the toluenesulphonyloxy group on the C-1 position in 2,3-4,5-diisopropylidene-1-*O*-*p*-toluenesulphonyl-D-fructose was found to occur in the presence of sodium ethanethiolate.

A previous (1) publication described the synthesis of a thioalkyl aldose, namely, 6-deoxy-6-thioethyl-D-galactose. Extension of this investigation into the ketose series resulted in the synthesis of 1-deoxy-1-thioethyl-D-fructose (III) by two distinctly different methods.

The first method employed 2,3-4,5-diisopropylidene-1-*O*-*p*-toluenesulphonyl-D-fructose (I). A solution of the latter substance in anhydrous N,N-dimethylformamide on treatment with freshly prepared sodium ethanethiolate yielded 2,3-4,5-diisopropylidene-1-deoxy-1-thioethyl-D-fructose (II), but only after heating at 100° for 30 hr. This latter reaction was exceedingly slow when compared with the reaction of sodium ethanethiolate and 1,2-3,4-diisopropylidene-6-*O*-*p*-toluenesulphonyl-D-galactose (I). The latter reaction was complete in two hours. The sluggishness of the ketose reaction is reminiscent of the nonreaction of the same fructose derivative with sodium iodide in acetone (4).

The second method of synthesis of III made use of so-called "glutose". This substance is essentially a mixture of fructose anhydrides (6, 7). Treatment of the amorphous "glutose" mixture with an excess of sodium ethanethiolate in anhydrous methanol yielded a small quantity of a substance that proved to be identical to that obtained from I.

EXPERIMENTAL

2,3-4,5-Diisopropylidene-D-fructose (3)

This substance was prepared according to the method of Glen, Myers, and Grant (3) with slight modification. A yield of 347 gm. (89%) was obtained from 270 gm. fructose. The melting point 96–97° and $[\alpha]_D^{22°}$ −32.6° (H_2O: *c*, 1.013) agreed with the constants reported in the literature (2) for 2,3-4,5-diisopropylidene-D-fructose.

[1]*Manuscript received May 13, 1955.*
Contribution from the Division of Organic Chemistry, Research Institute, Montreal General Hospital, Montreal, Que.

*2,3-4,5-Diisopropylidene-1-O-p-toluenesulphonyl-*D*-fructose* (*I*) (*5*)

2,3-4,5-Diisopropylidene-D-fructose (179 gm.) was tosylated with *p*-toluenesulphonyl chloride (135 gm.) in anhydrous pyridine. The reaction mixture was treated in the usual manner and the crude air-dried product was recrystallized from methanol yielding 192 gm. (66%). A second recrystallization from aqueous ethanol gave m.p. 81–82° and $[\alpha]_D^{22°}$ −27.2° (ethanol: *c*, 2.693). The literature (5) reports m.p. 83° and $[\alpha]_D$ −27.1° (ethanol).

*2,3-4,5-Diisopropylidene-1-deoxy-1-thioethyl-*D*-fructose* (*II*)

2,3-4,5-Diisopropylidene-1-*O*-*p*-toluenesulphonyl-D-fructose (I) (97.5 gm.) and freshly prepared sodium ethanethiolate (35 gm.) were dissolved in hot N,N-dimethylformamide (275 cc.). The mixture was heated on the steam bath for 30 hr. and then added to cold water (3000 cc.). An oil separated and the mixture was extracted twice with ether. The ethereal solution was dried over

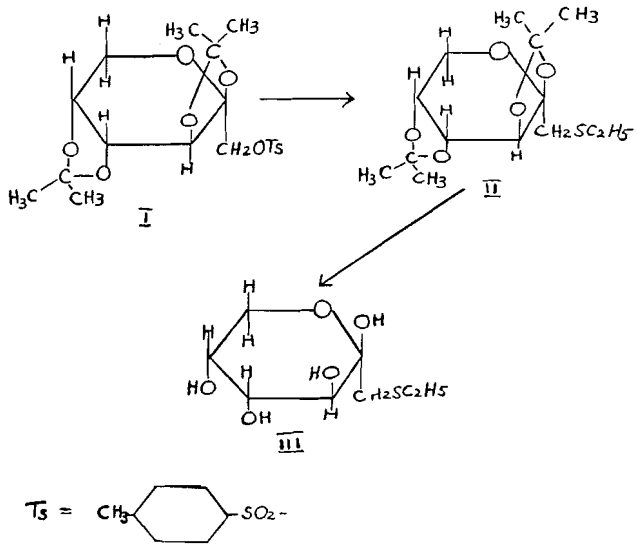

anhydrous sodium sulphate, filtered, and concentrated *in vacuo*. The residual sirup was then heated at 100° for six hours at 10 mm. pressure to remove any N,N-dimethylformamide. The main product was distilled at 96–100° and 0.04 mm. and the yield was 54.4 gm. (76%). A portion of the nearly colorless distillate was fractionally distilled through a 20 cm. Widmer column and practically all distilled at 107° and 0.07 mm. The constants were: $\eta_D^{26°}$ 1.4823 and $[\alpha]_D^{20°}$ −58.4° (chloroform: *c*, 9.4212). Anal.: Calc. for $C_{14}H_{24}SO_5$: C, 54.27; H, 7.89; S, 10.52. Found: C, 54.02; H, 7.93; S, 10.44.

*1-Deoxy-1-thioethyl-*D*-fructose* (*III*)

2,3-4,5-Diisopropylidene-1-deoxy-1-thioethyl-D-fructose (20 gm.) was added to 1 *N* sulphuric acid (1000 cc.). The mixture was stirred for 18 hr. at 50°, then cooled to room temperature and carefully neutralized with barium hydroxide – barium carbonate. The solution was not allowed to become alkaline

at any time. The barium sulphate and carbonate mixture was removed by filtration, the filter washed several times with hot water, and the combined filtrates and washings concentrated to a thick sirup *in vacuo* at 40°. The sirup, after it had been kept for three days in an evacuated desiccator over calcium chloride, crystallized. The hard mass was dissolved in a small volume of hot acetone and filtered. Slow cooling of the filtrate caused crystallization. The nearly pure product, having a melting point of 86–88°, was recrystallized once more from anhydrous acetone – ether mixture when the melting point was raised to 87.5–88.5° and it showed $[\alpha]_D^{22°}$ −71.3° → −62.8° (24 hr.) (water: *c*, 3.1548). Anal.: Calc. for $C_8H_{16}SO_5$: C, 42.85; H, 7.14; S, 14.29. Found: C, 42.66; H, 7.31; S, 14.3.

D-Glucose Phenylosazone from 1-Deoxy-1-thioethyl-D-fructose

1-Deoxy-1-thioethyl-D-fructose (2 gm.) was dissolved in water (20 cc.). Acetic acid (5 cc.) and redistilled phenylhydrazine (4 cc.) were added and the clear solution heated at 80° for 30 min. Ethanethiol was evolved and precipitation occurred. The reaction mixture was cooled to 20°, filtered, and the filter washed with cold water. The yield of air-dried material was 2.3 gm. (71%). A sample was recrystallized twice from hot dilute methanol and it melted at 205–207°. A mixed melting point determination with authentic D-glucose phenylosazone was 204–207°.

1-Deoxy-1-thioethyl-D-fructose from "Glutose" (6, 7)

Ethanethiol (40 cc.) was added to cold 0.7 *N* sodium methylate solution (500 cc.). "Glutose" (6, 7) (21 gm.) was added and the brown solution heated under reflux on the steam bath for two hours. The reaction mixture was cooled to 10°, neutralized carefully in the fume cabinet with 3 *N* hydrochloric acid, and then concentrated *in vacuo* at 30°. Final traces of water were removed by ethanol–benzene azeotropic distillation. The dry sirup was extracted with boiling anhydrous acetone and the filtrate was concentrated *in vacuo* to a thick sirup. The latter sirup was again extracted with hot acetone and the filtered solution was decolorized with activated charcoal. The yellow filtrate obtained was concentrated to approximately 50 cc., seeded with several crystals of 1-deoxy-1-thioethyl-D-fructose (III), and allowed to stand stoppered at room temperature for about three weeks. During this time crystallization occurred. The crystals were removed by filtration and the filter was washed with cold (0°) acetone. The crude product was twice recrystallized from acetone–ether and after drying it melted at 87–88.5°. The mixed melting point with 1-deoxy-1-thioethyl-D-fructose, obtained previously, was 86–88°. The yield was 0.36 gm.

Tetraacetyl-1-deoxy-1-thioethyl-D-fructose

1-Deoxy-1-thioethyl-D-fructose (5 gm.) was dissolved in anhydrous pyridine (25 cc.). The solution was cooled to −20° and acetic anhydride (25 cc.) was added. The reaction mixture was kept at −20° for one hour, allowed to stand at 22° for 22 hr., and finally added to cold water. The separated sirupy product did not crystallize and the aqueous mixture was extracted four times with ether (100 cc.). The combined ethereal solutions were washed with cold 2%

hydrochloric acid, water, and saturated potassium bicarbonate and then dried over anhydrous sodium sulphate. The ethereal solution, after filtration, was concentrated to dryness by slow evaporation in a desiccator and the sirupy mass solidified, in a yield of 5.9 gm. (68%). It was recrystallized twice from anhydrous ether and it melted at 133–134° and $[\alpha]_D^{22°}$ −47.6° (chloroform: *c*, 1.8492). Anal.: Calc. for $C_{16}H_{24}SO_9$: C, 48.98; H, 6.12; S, 8.19; CH_3CO, 43.9. Found: C, 48.60; H, 6.41; S, 8.2; CH_3CO, 43.74.

*Tetrabenzoyl-1-deoxy-1-thioethyl-*D*-fructose*

1-Deoxy-1-thioethyl-D-fructose (5 gm.) was dissolved in anhydrous pyridine (50 cc.). The mixture was cooled to −20° and benzoyl chloride (13 gm.) was added in one portion. The mixture was allowed to stand at −20° for two hours, then overnight at 22°. The reaction product was isolated as above and the resulting sirup was crystallized from methanol. The separated crystalline mass was recrystallized from hot methanol and the nearly pure product, 8.1 gm. (57%), after an additional recrystallization from a large volume of ether – petroleum ether (1: 1) melted at 103–104° and $[\alpha]_D^{22°}$ +61.9° (chloroform: *c*, 2.2844). Anal.: Calc. for $C_{36}H_{32}SO_9$: C, 67.5; H, 5.0; S, 5.0; C_6H_5CO, 65.62. Found: C, 67.34; H, 5.1; S, 4.96; C_6H_5CO, 65.6.

ACKNOWLEDGMENT

The author is indebted to the Sugar Research Foundation for a grant-in-aid.

REFERENCES

1. BAKER, S. B. Can. J. Chem. 33: 1102. 1955.
2. FISCHER, E. Ber. 28: 1164. 1895.
3. GLEN, W. L., MYERS, G. S., and GRANT, G. A. J. Chem. Soc. 2568. 1951.
4. LEVENE, P. A. and TIPSON, R. S. J. Biol. Chem. 120: 607. 1937.
5. OHLE, H. and KOLLER, I. Ber. 57: 1566. 1924.
6. SATTLER, L. and ZERBAN, F. W. Ind. Eng. Chem. 37: 1133. 1945.
7. WOLFROM, M. L. and BLAIR, M. G. J. Am. Chem. Soc. 70: 2407. 1948.

THE TERMINAL AMINO ACIDS OF WHEAT GLIADIN[1]

By L. K. Ramachandran[2] and W. B. McConnell

ABSTRACT

Wheat gliadin has been found by two different methods to contain three N-terminal histidine residues for each molecular weight of 27,000. Trace amounts of N-terminal aspartic acid, glutamic acid, alanine, valine, and serine were also detected in the preparation used. Hydrolysis in boiling hydrochloric acid partially destroyed the di-2,4-dinitrophenyl derivative of histidine. Losses of from 5% to 25% occurred depending upon the time and conditions of hydrolysis. Carboxypeptidase did not release free amino acids from wheat gliadin but qualitative evidence for the occurrence of C-terminal glutamic acid and C-terminal "leucine" was obtained.

It has been reported by Koroś (9) that wheat gliadin contains three free amino groups and that these belong to the three N-terminal histidine residues. Although doubt exists that gliadin is composed of a homogeneous and unique molecular species the observations of Koroś would point to the existence of at least one characteristic feature in gliadin. Because details of Koroś's work were unavailable independent experiments were done to determine the nature of the N-, and also of the C-, terminal amino acids of gliadin. Since the completion of the present work Koroś's results have been questioned (6) and it was reported that Sanger's method revealed one N-terminal tyrosine residue in gliadin from *Triticum durum*, and two N-terminal residues, one each of glutamic acid and tyrosine, in gliadin from *Triticum vulgare*; no N-terminal histidine was detected. Results recorded in the present communication support the earlier report (9) that histidine is the major N-terminal amino acid in gliadin. In addition, evidence presented indicates that glutamic acid and "leucine" occupy the C-terminal positions.

EXPERIMENTAL

Gliadin was prepared by the method of Blish and Sandstedt (4). The sample contained 17.64% nitrogen on a moisture and ash-free basis. The ninhydrin colorimetric procedure (8) and the Van Slyke nitrous acid method (11 min. reaction) indicated 3.18 and 3.32 free amino groups, respectively, for an assumed molecular weight of 27,000.

Identification of N-Terminal Groups Using 2,4-Dinitrofluorobenzene

DNP-gliadin was prepared using the reaction conditions described by Porter (14). Two grams of the protein and 2 gm. $NaHCO_3$ were suspended in 20 ml. water, 40 ml. of a 10% (w/v) solution of DNFB in ethanol were added, and the mixture was shaken for two hours at room temperature. The reaction mixture was exhaustively dialyzed against distilled water and the precipitated protein collected, washed, and dried (yield 2.0 gm.). It was calculated from

[1]*Manuscript received June 10, 1955.*
Contribution from the National Research Council of Canada, Prairie Regional Laboratory, Saskatoon, Saskatchewan. Issued as Paper No. 198 on the Uses of Plant Products and as N.R.C. No. 3706.
[2]*National Research Council of Canada Postdoctorate Fellow, 1953–55.*

the amide nitrogen content (14) that 119.9 mgm. of DNP-gliadin corresponded to 100 mgm. of the original gliadin. Samples of DNP-gliadin (100 mgm.) were hydrolyzed in 10 ml. of boiling 5.7 *N* hydrochloric acid for four hours or for 24 hr. Another sample was hydrolyzed in 12 *N* acid in a sealed tube at 105° C. for 24 hr. (14). The DNP-amino acids in the hydrolyzates were fractionated into ether-soluble and acid-soluble materials and the fractions were chromatographed by each of three previously used methods (2, 3, 13).

DNP-histidine was the only amino acid derivative found in the acid-soluble fraction. Trace amounts of DNP-aspartic acid, glutamic acid, alanine, valine, and serine were detected in the ether-soluble material and, although gliadin contains at least two residues of lysine per molecule, no ϵ-DNP-lysine was found. The identity of the DNP-histidine was established by hydrolyzing it with concentrated ammonia (12) in a sealed tube and chromatographing the resulting amino acid on paper.

The yields of various 2,4-dinitrophenyl derivatives obtained from the treated gliadin are recorded in Table I. The calculations for the histidine are

TABLE I

YIELD OF DNP-DERIVATIVES FROM ACID HYDROLYZATES OF DNP-GLIADIN

Derivative	Yield: moles/27,000 gm.	
	4 hr. hydrolysis	24 hr. hydrolysis
Di-DNP-histidine (N-terminal histidine)	3.1	2.9
Other DNP-amino acids*	0.17	0.11
Dinitrophenol, dinitroaniline, etc.†	1.3	1.0

**Calculated as DNP-aspartic acid.*
†Calculated as dinitrophenol.

based on optical density measurements at 360 mμ and reference to the calibration curve for di-DNP-histidine. The DNP-amino acids found in traces are calculated as DNP-aspartic acid. Values for histidine are corrected for hydrolytic losses by increasing them by 25% (see below). It was also found that only 71% of the expected histidine derivative could be estimated in a dinitrophenylation of histidine done under the same conditions as employed with gliadin. To compensate for this low recovery in dinitrophenylation the yields of di-DNP-histidine were also multiplied by the factor 1.41. Because of the large corrections the results in Table I are only approximate. Chromatography on a silicic acid column was used to separate trace amounts of DNP-amino acids from the relatively large amounts of dintrophenol and dinitroaniline found in the ether-soluble fraction (11). No corrections have been applied for hydrolytic losses of the latter materials.

Effect of Acid Hydrolysis on Di-DNP-histidine

Di-DNP-histidine, with the reported physical constants (15), was prepared according to the method of Porter. Twenty-five milligrams was hydrolyzed with 20 ml. of 5.7 *N* HCl. The hydrolyzates were extracted with ether to remove artifacts like dinitroaniline and dinitrophenol, and the di-DNP-histidine

remaining in the acid phase was determined by spectrophotometry. For time intervals of 3.5, 6.5, and 24.0 hr. the destruction observed was 0.0, 5.0, and 12.0% respectively. When the same weight of the pure derivative was hydrolyzed in the presence of 40 mgm. gliadin the destruction observed was 25.0% for 24 hr. The latter figure has been used to correct for hydrolytic losses.

Application of the Edman Method (7) to N-Terminal Residue Identification

One gram gliadin was dissolved in 4 ml. 50% pyridine, the pH was adjusted to 8.6 with 0.1 *N* alkali, and 0.2 ml. of phenylisothiocyanate was added with vigorous stirring. The temperature was maintained at 40° C., and alkali was added as required to keep the pH at 8.6. When consumption of alkali ceased, the reaction mixture was extracted twice with benzene and the protein precipitated with acetone. The dry phenylthiocarbamyl protein was then suspended in 9 ml. of anyhydrous nitromethane containing 4% HCl by weight. After an hour of agitation, the material was filtered and washed with a few milliliters of the solvent. The combined filtrates were evaporated *in vacuo* to remove all traces of solvents and HCl. The residue was dissolved in EtOH. Absorption at 270 mμ indicated a content of 3.2 M. of phenylthiohydantoin per 27,000 gm. of the protein. Paper chromatography of the material (10) showed that PTH-histidine was the major component. Its identity was confirmed by barium hydroxide hydrolysis to the free amino acid. Stepwise degradation of the residual protein was carried out but during the second and third treatments an abnormally high yield of phenylthiohydantoin (of the order of five moles) was obtained. No detailed identification of the material was attempted, but paper chromatography of barium hydroxide hydrolyzates indicated the presence of several ninhydrin positive spots.

C-Terminal Residues of Gliadin

Action of carboxypeptidase on gliadin.—One-half gram of gliadin was suspended in 20 ml. water, the pH was adjusted to 7.7 with 0.2 *N* NaOH, and the mixture was incubated with 0.2 ml. of carboxypeptidase suspension (12.6 mgm./ml. Armour). In another experiment the same weight of protein was suspended in 20 ml. of 1% (w/v) sodium bicarbonate. No liberation of amino *N* could be detected by the Van Slyke method during a seven-hour period, and no free amino acids could be detected in the reaction mixture by paper chromatography. It was therefore concluded that the C-terminal amino acid residues in gliadin, if any, were not susceptible to hydrolysis by carboxypeptidase under the conditions used.

Application of the method of Schlack and Kumpf (1) to gliadin.—One gram of the protein was mixed with 0.3 gm. of pulverized anhydrous ammonium thiocyanate in 77 ml. of an AcOH: Ac_2O (9: 1) mixture, and the reaction mixture was stirred at 45° C. for four hours. At the end of this period 30 ml. of HCl was added dropwise with stirring and the material heated on a steam bath for one hour. The product was dried *in vacuo*, the residue dissolved in 60 ml. of 0.25 *M* phosphate (pH 6.5) and extracted five times with equal volumes of ethyl acetate. The combined extracts were washed once with an equal volume of water and dried, and the residue was hydrolyzed with 2.5 ml.

of 1.25 *N* $Ba(OH)_2$ at 140° C. in a sealed tube. The hydrolyzate was neutralized with carbon dioxide and heated for 10 min. on a steam bath to destroy carbamic acids. Aliquots of the suspension were examined by paper chromatography (BuOH–AcOH–H_2O, 4:1:5). The only amino acids detected were glutamic acid and "leucine". The amounts of these amino acids were estimated by ninhydrin colorimetry using a standard curve for the two amino acids obtained under the same conditions. One-half mole of glutamic acid and 0.45 mole of "leucine" were found for each 27,000 gm. gliadin. No corrections were applied.

Application of the lithium borohydride reduction method of Chibnall (5) indicated the presence of glutamic acid and "leucine" in C-terminal positions. Appreciable traces of other amino acids were also detected. Using a nine-fold excess of diazomethane for esterification of the protein and a 13-fold excess of $LiBH_4$ for the reduction in tetrahydrofuran, the total yield of α-amino alcohols was 0.654 mole per 27,000 gm. protein.

DISCUSSION

The present work supports the observations of Koroś (9) that gliadin of molecular weight 27,000 contains three free amino groups and that these belong to histidine. From this result, it was expected that three C-terminal amino acids could be detected. It was surprising, therefore, that carboxypeptidase did not liberate any free amino acids from the protein; particularly in view of the finding that leucine and glutamic acid were detected as C-terminal residues by the chemical method (1). Recoveries by the latter method are known to be very poor, and since only about 0.5 mole of C-terminal leucine and glutamic acid was found the data were not adequate for evaluation of the amounts of C-terminal leucine and C-terminal glutamic acid in gliadin. It is to be noted that Baptist and Bull (1) could not identify glutamic acid in glutathione or recover glutamic acid from glutamine by the Schlack and Kumpf method. The present identification of the C-terminal acids would therefore be tentative.

REFERENCES

1. Baptist, V. H. and Bull, H. B. J. Am. Chem. Soc. 75: 1727. 1953.
2. Biserte, G. and Osteux, R. Bull. soc. chim. biol. 33: 50. 1951.
3. Blackburn, S. and Lowther, A. G. Biochem. J. 48: 126. 1951.
4. Blish, M. J. and Sandstedt, R. M. Cereal Chem. 3: 144. 1926.
5. Chibnall, A. C. and Rees, M. W. Ciba foundation. The chemical structure of proteins. *Edited by* G. E. W. Wolstenholme and M. P. Cameron. J. & A. Churchill, Ltd., London. 1953. p. 70.
6. Deutsch, T. Acta Phys. Acad. Sci. Hung. 6: 209. 1954. Chem. Abstr. 49: 4736*b*. 1955.
7. Edman, P. Acta Chem. Scand. 4: 283. 1950.
8. Harding, V. J. and MacLean, R. M. J. Biol. Chem. 24: 503. 1916.
9. Koroś, Z. Magyar Kém. Folyóirat, 56: 131. 1950. Chem. Abstr. 45: 7958*h*. 1951.
10. Landmann, W. A., Drake, M. P., and Dillaha, J. J. Am. Chem. Soc. 75: 3638. 1953.
11. Li, C. H. and Ash, L. J. Biol. Chem. 203: 419. 1953.
12. Lowther, A. G. Nature, 167: 767. 1951.
13. Mellon, E. F., Korn, A. H., and Hoover, S. R. J. Am. Chem. Soc. 75: 1675. 1953.
14. Porter, R. R. Methods in medical research. Vol. 3. *Editor-in-Chief* R. W. Gerard. Year Book Publishers, Inc., Chicago. 1950. p. 256.
15. Rao, K. R. and Sober, H. A. J. Am. Chem. Soc. 76: 1328. 1954.

THE PREPARATION OF GUANIDINE FROM UREA, AMMONIUM CHLORIDE, ALUMINUM SULPHATE, AND AMMONIA UNDER PRESSURE[1]

By Jean L. Boivin

ABSTRACT

Guanidine has been synthesized by heating under ammonia pressure an intimate mixture of finely powdered urea, ammonium chloride, and aluminum sulphate. Good yields of guanidine as the hydrochloride salt have been obtained over a wide range of conditions. The mechanism of this synthesis is briefly discussed.

INTRODUCTION

If urea is heated under ammonia pressure, it is much more stable at high temperature because of the stabilizing effect of ammonia (1). The preparation of guanidine about to be described makes use of aluminum sulphate to assist the removal of water from the reaction. This starting material can be produced cheaply from bauxite, clay, and similar materials containing aluminum.

DESCRIPTION OF METHOD

By heating urea, ammonium chloride, and aluminum sulphate together under ammonia pressure at 300° C. for some time, yields of guanidine as high as 70% have been obtained. The reaction product was boiled with ammoniacal water in order to precipitate aluminum hydroxide (Diagram 1). The clear filtrate, which contained guanidine hydrochloride, ammonium sulphate, and unreacted urea and ammonium chloride, was evaporated to dryness. The residue was treated with liquid ammonia and the mixture filtered free from ammonium sulphate. By evaporation of the liquid ammonia solution, a residue was left containing guanidine hydrochloride together with unreacted urea and ammonium chloride. This crude guanidine hydrochloride was transformed into guanidine nitrate by treating its saturated aqueous solution with a quantity of ammonium nitrate equivalent to its guanidine content. After guanidine nitrate was removed the filtrate was evaporated to dryness and the residue heated to 250° C. This material was nearly pure ammonium chloride, suitable for use in a subsequent cycle.

The aluminum hydroxide and ammonium sulphate, individually isolated from the reaction products as indicated above, were heated together at 350° C. to regenerate aluminum sulphate (5) according to the following equation:

$$2Al(OH)_3+3(NH_4)_2SO_4 \rightarrow Al_2(SO_4)_3+6H_2O+6NH_3. \qquad [1]$$

The ammonia evolved during heating can be dried and returned to the reactor.

EFFECT OF TEMPERATURE

In order to explore the effect of the temperature of heating, mixtures consisting of equimolar quantities of urea and ammonium chloride and various

[1]*Manuscript received June 2, 1955.*
Contribution from the Organic Section of Canadian Armament Research and Development Establishment, Valcartier, Quebec. Issued as C.A.R.D.E. Report No. 50/51, 1951.

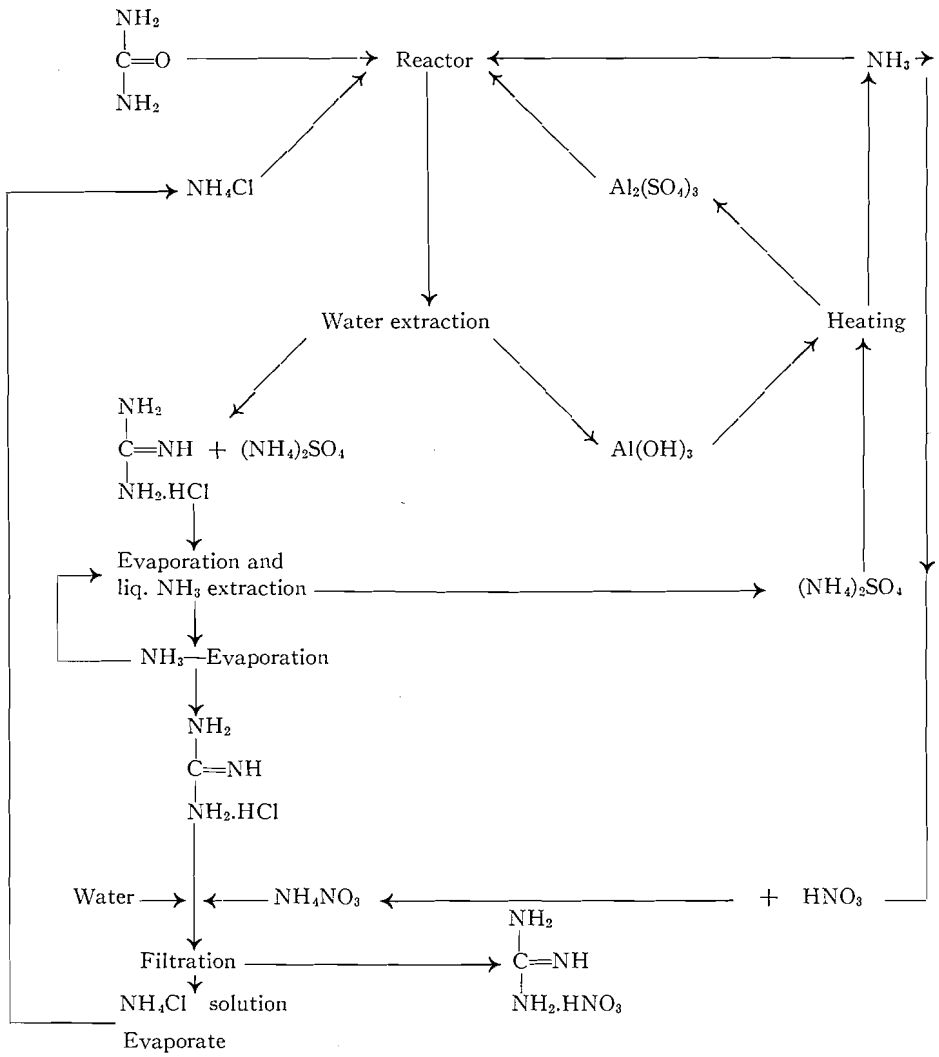

Diagram 1

amounts of aluminum sulphate were heated together under ammonia pressure. Table I shows the compositions of the mixtures and the conditions of the reaction. At high temperature, melamine is produced at the expense of guanidine. The yields of guanidine increase with temperature up to a maximum value, beyond which the formation of melamine becomes increasingly significant. The low yields shown here are ascribed to the fact that the ingredients were coarse and not thoroughly mixed. However, the table shows that increasing yields of guanidine were obtained with increasing amounts of aluminum sulphate.

TABLE I

EFFECT OF TEMPERATURE

Urea: 0.10 mole; NH_4Cl: 0.10 mole; time: 30 min.; pressure: 1000 p.s.i.g.

$Al_2(SO_4)_3$, mole	Temp., ° C.	Yield from urea, %	
		Guanidine	Melamine
0.0166	225	4	Nil
	250	10	Nil
	275	17	Nil
	300	36	10
	325	41	28
	350	29	35
0.033	250	14	Nil
	275	32	Nil
	300	45	Nil
	325	48	16
	350	38	20
0.05	225	Traces	Nil
	250	26	Nil
	275	40	Nil
	300	55	Nil
	325	63	37
	350	45	42

EFFECT OF CONCENTRATION OF UREA

By varying the molar quantities of urea added to a constant mixture of ammonium chloride and aluminum sulphate, as can be seen in Table II, the optimum yield was attained from equimolar amounts of urea and ammonium chloride. When urea was added in excess of this value, melamine was formed together with cyanuric acid.

TABLE II

EFFECT OF CONCENTRATION OF UREA

NH_4Cl: 0.10 mole; $Al_2(SO_4)_3$: 0.05 mole; temp.: 300° C.; time: 30 min.; pressure: 1000 p.s.i.g.

Urea, mole	Yield from urea, %	
	Guanidine	Melamine
0.05	43	Nil
0.10	55	Nil
0.15	34	23
0.20	31	22
0.30	22	20

EFFECT OF CONCENTRATION OF AMMONIUM CHLORIDE

It has been found (Table III) that increasing quantities of ammonium chloride give increasing yields of guanidine, melamine being absent under these conditions. There is a great increase in yield as ammonium chloride increases from 0.05 mole to the stoichiometric amount of 0.10 mole. The better yields obtained here are attributed to thorough mixing of solid ingredients before reaction took place.

TABLE III

EFFECT OF AMMONIUM CHLORIDE

Urea: 0.10 mole; $Al_2(SO_4)_3$: 0.033 mole; temp.: 300° C.; time: 30 min.; pressure: 1000 p.s.i.g.

NH_4Cl, mole	Guanidine yield from urea, %
0.05	39
0.10	68
0.15	70
0.20	75
0.25	68
0.30	65

EFFECT OF TIME OF HEATING

This reaction is dependent on the period of heating (Table IV). It is more complete when the reaction time is longer. The yields increase with time and also with temperature.

TABLE IV

Urea: 0.10 mole; NH_4Cl: 0.10 mole; $Al_2(SO_4)_3$: 0.033 mole; pressure: 1000 p.s.i.g.

Temp., ° C.	Time, min.	Guanidine yield from urea, %
275	30	58
	60	62
	90	64
	120	68
300	30	68
	45	70
	60	72
	90	79

EFFECT OF PRESSURE

The pressure factor is quite important in this reaction. There is evidence (Table V) that the yields are better at higher pressure. At atmospheric pressure, neither guanidine nor melamine was produced. At high pressure, yields were improved very significantly.

TABLE V

EFFECT OF PRESSURE

Urea: 0.10 mole; NH_4Cl: 0.10 mole; $Al_2(SO_4)_3$: 0.033 mole; temp.: 300° C.; time: 30 min.

Pressure, p.s.i.g.	Guanidine yield from urea, %
0	0
100	33
200	37
400	57
1000	68
2000	72

MECHANISM OF THE REACTION

Although the mechanism of this reaction, involving four starting materials, is not fully understood, some suggestions may be offered as to the possible

intermediate compounds. In the absence of ammonium chloride, the heating of urea with aluminum sulphate and ammonia failed to give guanidine under the same conditions. Likewise, urea, ammonium chloride, and ammonia gave low yields of guanidine under these conditions of temperature and time; even with the long period of heating employed by Blair (1), these reactants gave only 23% guanidine. When both ammonium chloride and aluminum sulphate are present, however, yields as high as 75% can be obtained in a period of only an hour or so.

It is believed that in the presence of ammonia vapor, as in the present reaction, ammonium chloride and aluminum sulphate react as in the following reaction:

$$6NH_4Cl + Al_2(SO_4)_3 \longrightarrow 2AlCl_3 + 2(NH_4)_2SO_4. \qquad [2]$$

If then urea is present (6) and a small conversion to guanidine takes place, liberating water, the latter can react with aluminum chloride:

$$2AlCl_3 + 3H_2O \longrightarrow Al_2O_3 + 6HCl. \qquad [3]$$

Accordingly, reaction is displaced towards the right, i.e. formation of guanidine is facilitated.

By analogy with the sulphamate synthesis of guanidine from urea (3) and also with the preparation of nitriles from amides by the action of sulphamates (2), it might be expected that an intermediate compound, comprising a substituted urea, could be involved.

Norris and Klemka (4) have shown that nitriles are obtained from amides and aluminum chloride through the formation of an intermediate compound, according to the following equation:

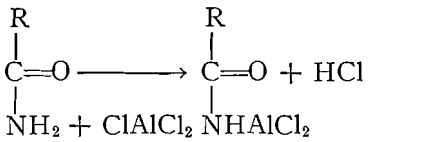

[4]

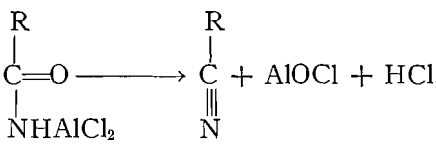

[5]

Urea, which is an amide, could react similarly giving cyanamide:

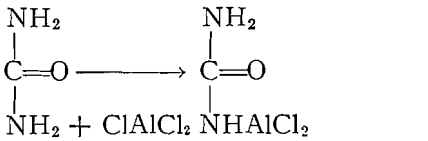

[6]

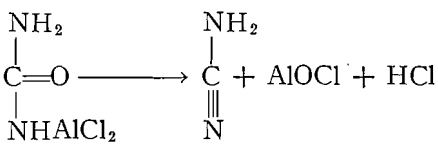

[7]

which under the actual condition should yield guanidine or melamine.

The above suggestions, though tentative, seem to offer an explanation of the observation that whereas neither ammonium chloride nor aluminum sulphate alone is effective, the two together produce a high yield of guanidine from urea and ammonia in a relatively short time of reaction.

It is believed that guanidine hydrochloride is formed from urea according to the following over-all equation:

$$3\,\underset{\underset{NH_2}{|}}{\overset{NH_2}{|}}C{=}O + 3NH_4Cl + Al_2(SO_4)_3 + 6NH_3 \rightarrow 3\,\underset{\underset{NH_2.HCl}{|}}{\overset{NH_2}{|}}C{=}NH + Al_2O_3 + 3(NH_4)_2SO_4. \qquad [8]$$

EXPERIMENTAL

Starting Materials

The urea used was commercial material previously dried at 110° C. Ammonium chloride used was Merck Reagent. Aluminum sulphate was the anhydrous material which had been heated at 500° C.

Procedure

An intimate mixture of finely powdered urea, ammonium chloride, and aluminum sulphate was placed in a glass liner. Enough ammonia (liquid) was added to the mixture to build the desired pressure. After the bomb was closed and the necessary connections were made, the reaction mixture was heated to the temperature of synthesis and in most cases vented to 1000 p.s.i.g. The period of heating was recorded from the time when the temperature of reaction was attained. After the mixture was cooled, the solid products were boiled with ammoniacal water. Aluminum hydroxide was filtered off and the filtrate was analyzed for guanidine and melamine contents.

Identification of Guanidine

(*A*) The picrate obtained from the solution presumed to contain guanidine was treated with an excess of dilute nitric acid and boiled. Then the mixture was exhaustively extracted with benzene to remove picric acid. By evaporation of the aqueous layer, a residue was obtained, m.p. 203–205° C. Recrystallizations from ethanol raised the melting point to 212–213° C. A mixed melting point with an authentic sample of guanidine nitrate was not depressed.

(*B*) A portion of the filtrate was evaporated to dryness and the residue dissolved in the minimum amount of water. Then ammonium nitrate was added, and the solution was heated to boiling and allowed to cool. Crystals separated out, m.p. 202–205° C. Recrystallizations from ethanol raised the melting point to 212–213° C.

REFERENCES

1. Blair, J. S. J. Am. Chem. Soc. 48: 87. 1926.
2. Boivin, J. L. Can. J. Research, B, 28: 671. 1950.
3. Boivin, J. L. and Lovecy, A. Can. J. Chem. 33: 1222. 1955.
4. Norris, J. F. and Klemka, A. J. Am. Chem. Soc. 62: 1432. 1940.
5. Rinman, E. L. Swedish Patent No. 15,590. 1906.
6. Sander, F. Ger. Patent No. 527,237. 1928.

SYNTHESIS OF γ-HYDROXYGLUTAMIC ACID (DIASTEREOMERIC MIXTURE)[1]

By Léo Benoiton and L. P. Bouthillier

ABSTRACT

γ-Hydroxyglutamic acid has been synthesized by two independent methods, namely the condensation of ethyl α-acetoxy-β-chloropropionate with diethyl acetamidomalonate, and the hydroxylation of glutamic acid. Chemical evidence is provided for the structure of the compound.

γ-Hydroxyglutamic acid has been proposed as an intermediate in the metabolism of hydroxyproline (3, 8). In 1941, Dakin (1) claimed to have prepared this dicarboxylic amino acid; however, the details of his synthesis were never published. As yet, there is no method available for the synthesis of this compound. We wish to report here the synthesis of γ-hydroxyglutamic acid by two independent methods.

For the first method, Fig. 1, ethyl α-acetoxy-β-chloropropionate (I) was condensed with diethyl acetamidomalonate (II) in the presence of sodium

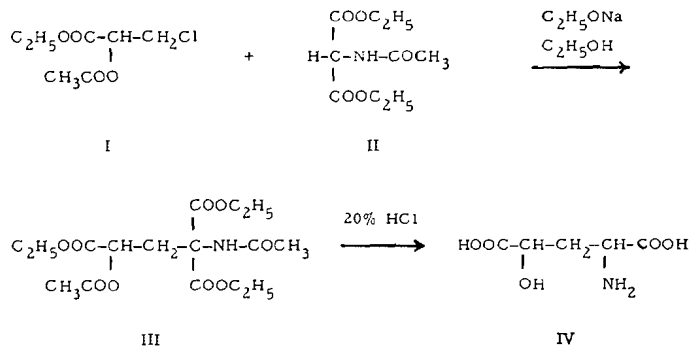

FIG. 1

ethoxide to form diethyl α-acetamido-α-carbethoxy-γ-acetoxyglutarate (III) which on acid hydrolysis gave γ-hydroxyglutamic acid (IV). The free amino acid crystallized as the monohydrate from an aqueous solution at pH 2.5. The same product was obtained by condensing diethyl acetamidomalonate with ethyl α-acetoxyacrylate instead of ethyl α-acetoxy-β-chloropropionate in the presence of a catalytic amount of sodium; however the yield was not any better.

The structure of the compound was confirmed by the fact that it is resistant to periodate oxidation, oxidized to aspartic acid by potassium permanganate, and reduced to glutamic acid by hydriodic acid. The formation of aspartic acid and glutamic acid was demonstrated by paper chromatography in several solvents.

[1]*Manuscript received June 27, 1955.*
Contribution from the Department of Biochemistry, Faculty of Medicine, University of Montreal, Montreal, Quebec.

For the second method, Fig. 2, N-phthaloyl-L-glutamic anhydride (V) was brominated and the γ-bromo-N-phthaloylglutamic acid (VI) thus obtained was hydroxylated to give γ-hydroxy-N-phthaloylglutamic acid (VII) which on hydrolysis gave γ-hydroxyglutamic acid (IV). The crystalline product obtained was contaminated with glutamic acid and could only be adequately purified by column chromatography. The pure amino acid coincided on paper

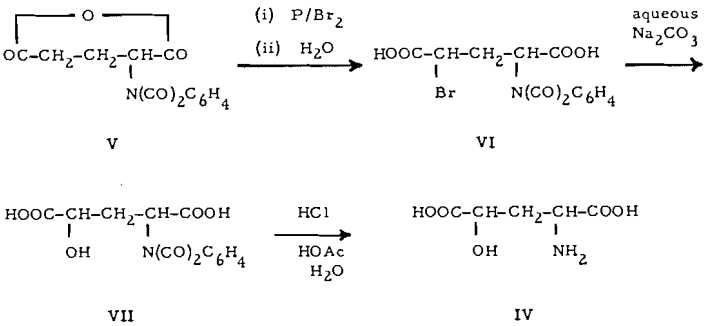

V VI VII IV

FIG. 2

chromatograms (Table I) with the γ-hydroxyglutamic acid prepared by the first method, and when submitted to the action of periodate, permanganate, and hydriodic acid, it gave results which were identical with those previously obtained.

EXPERIMENTAL*

1. *Preparation of γ-Hydroxyglutamic Acid*

(a) *Condensation of Ethyl α-Acetoxy-β-chloropropionate with Diethyl Acetamidomalonate*

To a solution containing 1.38 gm. (0.06 gm-atom) of sodium and 10.85 gm. (0.05 mole) of diethyl acetamidomalonate in 100 ml. of anhydrous alcohol was added dropwise 9.75 gm. (0.05 mole) of ethyl α-acetoxy-β-chloropropionate (4, 5). The reaction flask was placed on a mechanical shaker overnight and then the sodium chloride was removed by centrifugation and washed with alcohol. The combined supernatant and washings were freed of alcohol by distilling under reduced pressure and the remaining condensation product was refluxed for three hours in 100 ml. of 20% hydrochloric acid. The excess hydrochloric acid was removed by repeated distillation under reduced pressure and the residue was taken up with 25 ml. of water and decolorized with charcoal. The pH of the solution was adjusted to 2.5 with concentrated ammonia and the solution was cooled. The white crystalline mass obtained was filtered and recrystallized from water–alcohol. A further crop requiring several recrystallizations was obtained from the mother liquor by addition of alcohol. Total yield: 35%; m.p. 171–173° C. dec. Analysis for $C_5H_9NO_5 \cdot H_2O$: C, 33.89, 33.85; H, 6.23, 6.18; N, 7.81, 7.70. Calc.: C, 33.17; H, 6.12; N, 7.73.

When heated at 110° C. over phosphorus pentoxide *in vacuo*, the compound

**Analyses by the Geller Microanalytical Laboratories, Hackensack, N.J.; melting points by capillary method, uncorrected.*

loses two molecules of water to presumably give the lactam.* Analysis for $C_5H_7NO_4$: C, 42.23, 42.52; H, 4.78, 4.99; N, 9.80, 9.57. Calc.: C, 41.39; H, 4.86; N, 9.65.

(*b*) *Hydroxylation of* L-*Glutamic Acid*

N-Phthaloyl-L-glutamic anhydride was prepared by the method of Sheehan and Bolhofer (7). It was then brominated using a technique described by Eck and Marvel (2). Dry bromine, 146 gm., was added dropwise, with stirring, to a cooled mixture of 63 gm. of N-phthaloyl-L-glutamic anhydride and 9.4 gm. of red phosphorus. The mixture was then warmed on a water bath for six hours and the hot mixture was poured slowly into 500 ml. of water with vigorous stirring. The hydrolysis of the acyl bromide must be initiated by gentle warming, but it must then be controlled by cooling. The light yellow crystals obtained upon cooling were recrystallized from 500 ml. of hot water containing a few grams of bisulphite.

The product (35 gm.) was then refluxed in 250 ml. of 2 *N* sodium carbonate for three hours. The sodium ions were removed by adding sufficient Amberlite IR-120 to bring the pH down to 1, and the solution was concentrated under reduced pressure. The oily residue was refluxed for two hours in a mixture of 70 ml. of concentrated hydrochloric acid, 70 ml. of glacial acetic acid, and 70 ml. of water (6). The solution was cooled, the phthalic acid was filtered off, and the filtrate was evaporated to dryness under reduced pressure. The residue was taken up with 25 ml. of water, filtered, and treated successively with silver carbonate, hydrogen sulphide, and charcoal. The solution was concentrated to 25 ml. and alcohol was added. The white crystals which formed (8 gm.) were chromatographed in two portions on an 8×50 cm. column of Dowex 50 (200 to 400 mesh) in the acid form using *N* hydrochloric acid as the eluting agent. The fractions containing the γ-hydroxyglutamic acid were combined and evaporated to dryness under reduced pressure. The residue was dissolved in 25 ml. of water and the solution was adjusted to pH 2.5 and cooled. The yield was 10% based on the N-phthaloylglutamic anhydride employed. The decomposition point observed was ill-defined (about 150°), being lower than the one reported above. This might well be due to a difference in the relative amounts of the optical isomers in the products obtained by the two methods. Analysis for $C_5H_9NO_5 \cdot H_2O$: C, 34.02, 34.13; H, 6.08, 6.05; N, 7.78, 7.61. Calc.: C, 33.17; H, 6.12; N, 7.73.

2. Characterization of γ-Hydroxyglutamic Acid

(*a*) *Paper Chromatography*

Five-microgram quantities of γ-hydroxyglutamic acid dissolved in water were chromatographed on Whatman No. 1 filter paper in several solvent systems using the ascending technique. The amino acid spots were revealed by spraying the chromatograms with a 0.1% solution of ninhydrin in *n*-butanol, and by heating them at 70° for 15 min. The results appear in Table I. The gray spots obtained in the last three solvents change to purple in 24 hr.

**The ninhydrin reaction was positive only after prolonged heating of the dehydrated product in the presence of the reagent.*

TABLE I

CHROMATOGRAPHY DATA

Solvent system	R_f	Color
Phenol–water (80: 20)	0.13	Purple
n-Butanol – acetic acid – water (60: 12: 28)	0.17 and 0.19	Pink and purple
Pyridine–water (65: 35)	0.53	Gray
n-Butanol–methanol–benzene–water (2: 4: 2: 2)	0.26	Gray
n-Butanol – 95% ethanol – ammonia (8: 1: 3)	0.02	Gray

In butanol – acetic acid – water, γ-hydroxyglutamic acid gives two overlapping spots of different colors. This is most probably due to the presence of two diastereoisomers.

(*b*) *Permanganate Oxidation*

A warm solution of 50 mgm. of γ-hydroxyglutamic acid in 50 ml. of 2 *N* sulphuric acid was titrated with a solution of potassium permanganate until no more reagent was consumed. The amino acids were extracted from the solution by shaking one hour with 5 gm. of Dowex 50 (20 to 50 mesh), and then displaced from the resin with 25 ml. of 5 *N* ammonium hydroxide (9). The eluate was evaporated to dryness, the residue was taken up with water, and aliquots of the solution were chromatographed. The only amino acid present in the solution coincided with aspartic acid in the five solvent systems described in Table I.

(*c*) *Reduction with Hydriodic Acid*

Forty milligrams of γ-hydroxyglutamic acid, 50 mgm. of red phosphorus, and 3 ml. of 57% hydriodic acid were heated in an evacuated sealed tube at 150° C. for eight hours. The mixture was diluted to 30 ml. with water and the amino acids were extracted from the reaction medium as in the previous experiment. Chromatograms of the resulting solution gave only one spot which coincided with glutamic acid in the same five solvents.

(*d*) *Periodate Oxidation*

A mixture of 10 mgm. of γ-hydroxyglutamic acid in 15 ml. of water, 10 ml. of 0.5 *M* sodium periodate, and 5 ml. of *M* sodium bicarbonate was allowed to stand for one hour. Chromatograms of the desalted solution, obtained as previously described, indicated a quantitative recovery of the original amino acid.

ACKNOWLEDGMENT

The authors are indebted to the 'Fondation Joseph Rhéaume', Montreal, Quebec, for supporting this research.

REFERENCES

1. DAKIN, H. D. J. Biol. Chem. 140: 847. 1941.
2. ECK, J. C. and MARVEL, C. S. Org. Syntheses, 19: 18. 1939.
3. GIANETTO, R. and BOUTHILLIER, L. P. Can. J. Biochem. Physiol. 32: 154. 1954.
4. KENYON, W. O., UNRUH, C. C., and LAAKSO, T. T. M. U.S. Patent No. 2,499,393. March 7, 1950.
5. KOELSCH, C. F. J. Am. Chem. Soc. 52: 1105. 1930.
6. RATNER, S. and CLARKE, H. T. J. Am. Chem. Soc. 59: 200. 1937.
7. SHEEHAN, J. C. and BOLHOFER, W. A. J. Am. Chem. Soc. 72: 2470. 1950.
8. TAGGART, J. V. and KRAKAUR, R. B. J. Biol. Chem. 177: 641. 1949.
9. THOMSON, A. Nature, 169: 495. 1952.

PHYSICOCHEMICAL STUDIES OF LIGNINSULPHONATES

I. PREPARATION AND PROPERTIES OF FRACTIONATED SAMPLES[1]

By J. L. Gardon[2] and S. G. Mason

ABSTRACT

High molecular weight ligninsulphonates were separated from other constituents of spent sulphite liquor by a method of dialysis allowing continuous removal of the dialyzates and their replacement by distilled water. The process was controlled by continuous analysis of the residue and dialyzate. The lower molecular weight ligninsulphonates in the dialyzates were separated from the carbohydrates by precipitating their barium salts with ethanol; four fractions corresponding to different times of dialysis were prepared in this manner. The ligninsulphonates in the dialyzed liquor were separated into four additional fractions by ultrafiltration through membranes of different pore sizes. The methoxyl, sulphur, and phenolic hydroxyl contents, neutralization equivalent weights, reducing powers, ultraviolet absorption spectra, diffusion coefficients, and number-average molecular weights of the eight fractions were determined. The molecular weights of the fractions range from 3700 to 58,000 but the integral molecular weight distribution curve indicates the presence of ligninsulphonates with molecular weights as high as 100,000.

INTRODUCTION

The dissolved solids in spent sulphite liquor consist largely of ligninsulphonates, and the remainder of sugars and acidic degradation products of cellulose and lignin. Various methods of separating ligninsulphonates from the other constituents have been used (2, 14) including precipitation, dialysis, and ion exchange. Attempts have also been made to fractionate the highly polydisperse ligninsulphonates according to their molecular weights by fractional dialysis (6, 32), fractional extraction of the free acids by propanol (31), fractional precipitation of the barium salts by ethanol (23) or acetone (25), countercurrent butanol extraction of free acids and amine salts in water (22), differential sorption on swollen ion-exchange resins (18), and fractionation by the different solubilities of various amine salts (4, 5, 19, 25).

It has been found that the methoxyl content of the fractions increases with decreasing diffusion coefficient (23), i.e. with increasing molecular weight, while the sulphur content of the fractions, with few exceptions (18), decreases with increasing methoxyl content.

Various attempts have been made to determine the molecular weights of ligninsulphonates. Cryoscopic and ebullioscopic methods (17, 30) yielded apparent molecular weights in the range of 1000 to 6000, but owing to electrolytic dissociation of the ligninsulphonates these values are probably low. Estimates of molecular weights have also been made from the diffusion coefficients (6, 7, 16) and from the dialysis rates (31) either by comparison of the ligninsulphonates with various test substances or by assuming that the ligninsulphonate molecules are spherical and non-solvated, and that the

[1]*Manuscript received June 10, 1955.*
Contribution from the Pulp and Paper Research Institute of Canada and the Chemistry Department, McGill University, Montreal, Quebec.
[2]*Holder of the Anglo-Paper Research Fellowship and of a Studentship from the National Research Council of Canada. Present address: Industrial Cellulose Research, Ltd., Hawkesbury, Ontario.*

relation between the molecular radius and the diffusion coefficient given by the Sutherland–Einstein equation applies.

Molecular weights ranging from 2000 to 20,000 have thus been obtained. These values agree in order of magnitude with the more precise values calculated by McCarthy (22) from diffusion and sedimentation constants, and by Olleman, Pennington, and Ritter (25, 28) from diffusion and viscosity data. McCarthy (22) obtained molecular weights ranging up to 100,000.

The ultimate aim of our work was to investigate some of the basic physicochemical properties of ligninsulphonates. For this purpose relatively large quantities of chemically well-defined ligninsulphonate fractions were prepared by a combination of fractional dialysis and ultrafiltration of a spent sulphite liquor concentrate. The flow sheet of this procedure is presented in Fig. 1.

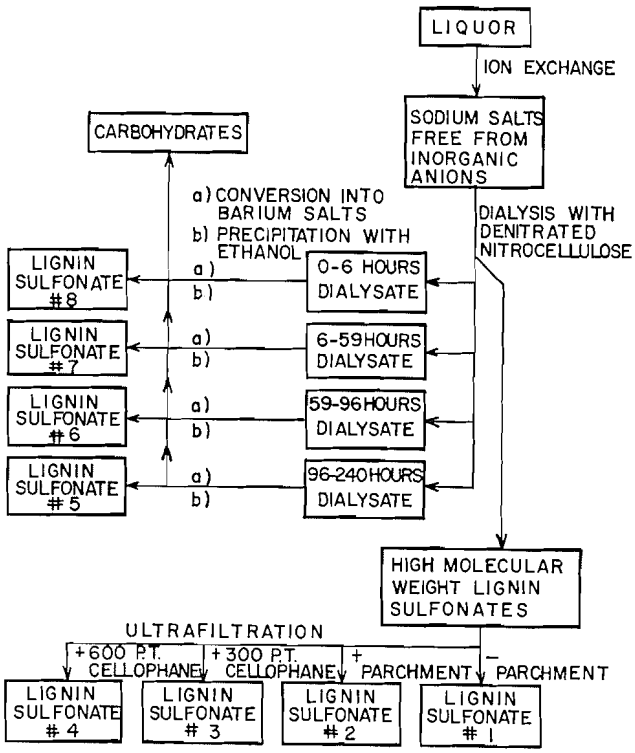

FIG. 1. Flow sheet for the fractionation of ligninsulphonates.

In this paper the fractionation techniques are described and the correlation between the analytical data and molecular weights of the samples is discussed. A number of other properties of the fractions are described in the following paper (10).

EXPERIMENTAL

Material

Spray-dried spent sulphite liquor marketed under the name of Lignosol B and supplied by Lignosol Chemicals Ltd. was used as the starting material.

The spent liquor was drawn from cooks of a mixture of balsam and spruce in approximately equal amounts.

About 700 gm. Lignosol was dissolved in 2 liters of water, filtered, passed through previously regenerated and well-washed Amberlite IR-4B (OH) anion- and IR-120 (H) cation-exchange resins to remove mineral acids and calcium respectively, and finally neutralized to pH 6.5 with sodium hydroxide. The resulting solution contained 633 gm. solids.

Fractionation

1. *Dialysis*

A Webcell Laboratory Model continuous countercurrent dialyzer (manufactured by Brosites Machine Corp., N.Y.) was used with denitrated nitrocellulose membranes. This dialyzer consists of 13 lucite rings, 17.5 cm. I.D. The membranes are clamped between these rings yielding seven water, and six solution chambers connected respectively in series through suitable channels. These channels were not used as it was found that the apparatus could be controlled better if the corresponding chambers worked in parallel. The design was accordingly altered by drilling holes in the top and bottom of each ring.

As shown in Fig. 2, the liquor was circulated from a reservoir through the dialyzer, with a continuous countercurrent flow of distilled water. A

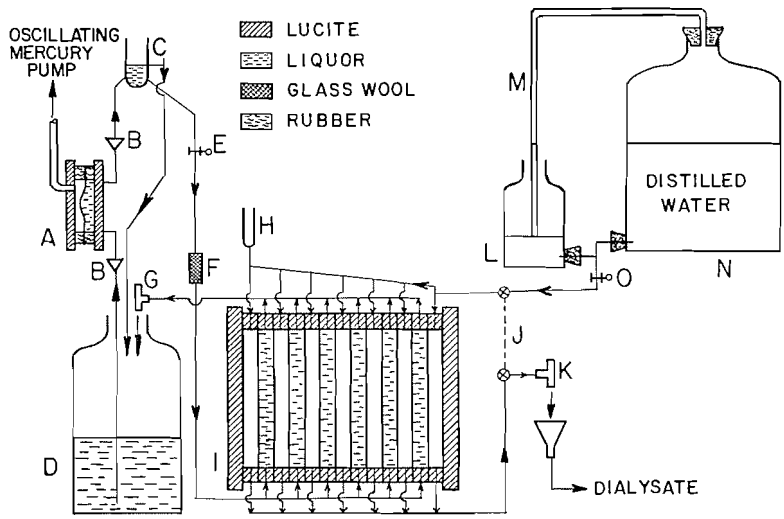

FIG. 2. The dialysis unit: (A) membrane pump, (B) valves, (C) liquor overflow, (D) liquor reservoir, (E) pinchcock to regulate liquor flow, (F) glass wool filter, (G) T tube, (H) air inlet, (I) dialysis cell, (J) bypass for initial filling of the water chambers, (K) T tube, (L) constant head device, (M) air inlet tube, (N) distilled water reservoir, (O) pinchcock to regulate water flow.

membrane pump (A) governed by an oscillating mercury pump was used for this purpose. The functioning of the pump is described in detail elsewhere (8).

To ensure steady flow the pump did not feed directly into the dialyzer, but passed through an overflow (C) and liquor flowed through the unit by gravity. The flow rate was regulated to 60 cc./min. by a pinchcock (E).

The distilled water came from a reservoir (N) and through a constant head device (L) at 3 cc./min. The free head of the water in the constant head device was maintained by the air inlet tube (M) which controlled the flow of air into and the flow of water from the reservoir (N). In this way the head of water was automatically maintained constant within 2 cm.

The volume of liquor was maintained between four and six liters. The volume increase due to osmosis amounted to about two liters per 12 hr.; this excess was periodically removed, neutralized with sodium hydroxide to avoid polymerization of the ligninsulphonic acids, concentrated by vacuum evaporation at 60°C., and reintroduced into the system.

To avoid growth of fungi during dialysis and the subsequent ultrafiltration, a small amount of toluene was added to the liquor.

The dialyzates produced every 12 hr. were handled as separate fractions. They were brought to pH 6.5 with sodium hydroxide or with cation-exchange resin as required. The content, reducing power, and neutralization equivalent weight of solids were determined. The reducing power of the solids in the residual liquor was calculated from these results by difference and checked by direct determination every 48 hr.

The dialysis was stopped after 19 days when the reducing power of the solids in both dialyzates and residual liquor became of the same order of magnitude (Fig. 3, curves F and G).

To separate the carbohydrates from the β-ligninsulphonates, i.e. the low molecular weight fractions, the barium salts were precipitated with ethanol as suggested by Erdtman (5). The dialyzates corresponding to 0 to 6, 6 to 59, 59 to 98, 98 to 240 hr. of dialysis were respectively combined to yield four separate fractions from which sodium was removed by cation exchange. The resulting free acids were neutralized with barium hydroxide, and the solutions were concentrated by vacuum evaporation at 60°C. to about 30% solid content and poured dropwise into four volumes of ethanol with vigorous stirring. The precipitates were twice dissolved in water and reprecipitated. The barium salts were passed through a cation exchanger and the free acids obtained were neutralized with sodium hydroxide and dried at 60°C. under vacuum, yielding fractions Nos. 5 to 8. The alcoholic mother liquors containing the carbohydrates were discarded; it should be noted, however, that in subsequent investigations it would be well worth while to study these constituents.

2. *Ultrafiltration*

Evidence presented later indicated that the residual liquor at the end of the dialysis contained pure ligninsulphonates. The residue was separated into four fractions (Nos. 1 to 4) by means of ultrafiltration using 600 P.T. cellophane, 300 P.T. cellophane, and No. 27 parchment membranes as supplied with the Webcell dialyzer.

It can be concluded from the results of the fractionation procedure that the

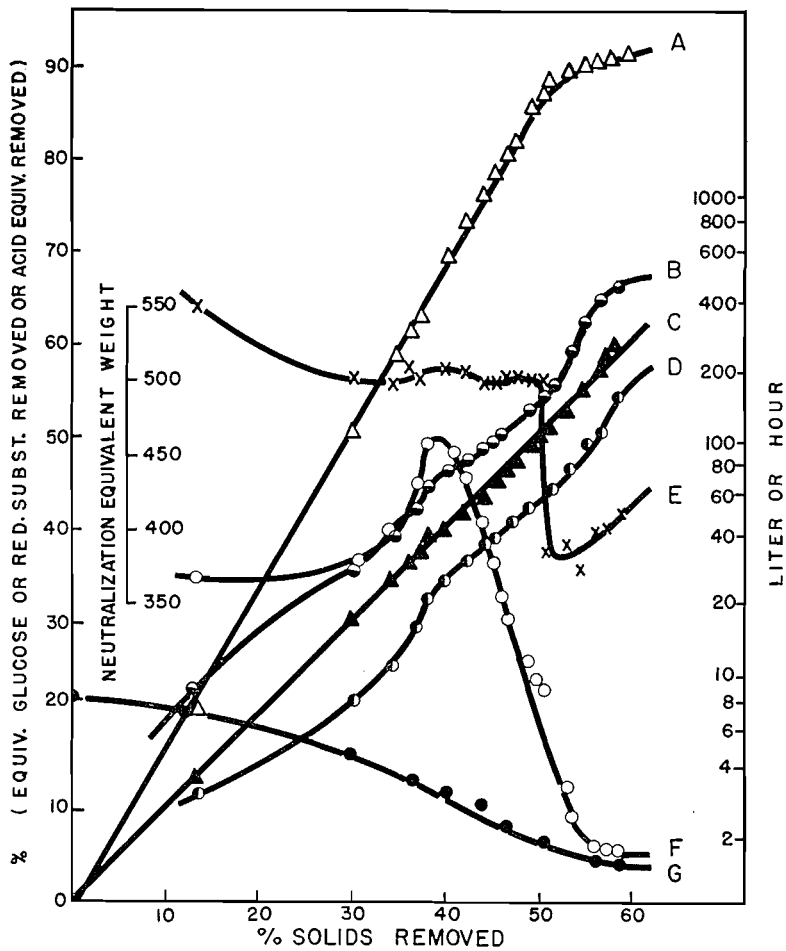

FIG. 3. Dialysis control diagrams showing per cent reducing substances removed (curve A), dialysis time (B), per cent acid equivalents removed (C), cumulative dialyzate volume (D), neutralization equivalent weight of the solids in the dialyzate (E), reducing power of the solids in the dialyzate (F), and reducing power of the solids in the dialyzed liquor (G).

denitrated nitrocellulose membranes used in dialysis have the smallest, and the parchment membranes the largest pore size.

The ultrafilter developed for the purpose of fractionating the lignin-sulphonates is described in detail in a separate publication (8); six ultrafilter cells each having a membrane area of 200 sq. cm. were used with cellophane and three with parchment membranes. The residual liquor was circulated in these cells and its volume was maintained constant at 1 liter. The ultrafiltration was stopped after 3, 7, and 12 days for the parchment, 300 P.T. cellophane, and 600 P.T. cellophane membranes respectively, the end points being determined as described later.

The ultrafiltrate of the 600 P.T. cellophane is fraction No. 4 and the fraction that did not pass the parchment is fraction No. 1. Before the solutions of the

different fractions were evaporated, they were adjusted to pH 6.5 by treatment with cation exchanger and addition of hydroxide as required.

All four of these fractions could be quantitatively precipitated with barium and alcohol.

Analytical Methods

To determine the neutralization equivalent weights, the sodium was removed by Amberlite IR-100 (H) cation exchanger and the free acid thus obtained was titrated with methyl red as indicator. Separate conductivity and pH titration experiments showed that all fractions have only one titration end point at pH 6.5. The titration curves were very similar to the ones presented by Peniston and McCarthy (26).

After the ligninsulphonates were oxidized with nitric acid the sulphur was determined as barium sulphate, as suggested by Yorston (34).

The methoxyl content was determined by the method of Peniston and Hibbert (27) adding red phosphorus, as suggested by Vjebock and Schwappach (33), instead of phenol to the hydriodic acid ligninsulphonate mixture.

The reducing power of the fraction was compared to that of glucose by means of Fehling solution and expressed as equivalent glucose, as described by Yorston (34).

Ultraviolet absorption spectra were measured in a Beckman Model DU spectrophotometer in pH 6 and pH 12 solutions with the buffers as blanks. It was shown that Beer's Law is valid for all fractions when ultraviolet light is used.

Diffusion Coefficients

The diffusion coefficients were evaluated in 0.5 *N* sodium chloride solution by the porous plate method (21, 24) in a modified apparatus described elsewhere (9). The diffusion cells were calibrated with 0.1 *N* potassium chloride, using Gordon's value (12) of 1.588 sq. cm./day for this solution. The ligninsulphonate concentrations were calculated by means of Beer's Law from the optical densities at 280 mμ.

Molecular Weights

The molecular weights were established from osmotic pressure measurements. To suppress dissociation 0.5 *N* aqueous sodium chloride was used as solvent. When necessary the results were corrected for membrane leakage as described in a separate paper (9). All data presented refer to neutral sodium salts.

RESULTS AND DISCUSSION

Dialysis

The main problem in fractionation of polydisperse materials by dialysis is to determine when the process is ended, since small amounts continue to diffuse through the membrane after long periods of dialysis. It was not possible to establish firm analytical criteria for the purity of ligninsulphonate fractions because their reducing power, sulphur content, neutralization equivalent weight, and methoxyl content change with the molecular weight. To complicate

matters further there are other acidic, reducing, sulphur-containing, and probably methoxyl-containing materials present in the liquor. These substances, mostly sugars and degradation products of cellulose and lignin, are believed, however, to have lower molecular weights than the bulk of the ligninsulphonates.

In Fig. 3 the control data of the dialysis are shown plotted against the cumulative percentage of the solids removed. Since the dialyzates contained materials with different diffusion rates, no theoretical relation could be derived for the time-dependence of the removal of the dialyzable solids. It was found that the concentration of the dialyzates was roughly inversely proportional to the dialysis time and cumulative dialyzate volume (Fig. 3, curves B and D).

The most significant curves are those of the reducing power of the solids in the dialyzate and in the residual liquor (curves *F* and *G*) and of the neutralization equivalent weights of the solids in the dialyzate (curve E). The following distinct stages of dialysis can be observed:

(1) The first 30% solids removed have a progressively increasing reducing power and decreasing neutralization equivalent weight as can be seen from curves F and G.

(2) In the next dialysis period 20% solids were removed. The reducing power of the solids in the dialyzate passed through a maximum while their neutralization equivalent weight remained constant.

(3) The reducing power and neutralization equivalent weight of the subsequent 2% solids removed decreased sharply and the neutralization equivalent weight passed through a minimum at 375. At this minimum the reducing power of the dialyzate was low, thus indicating that it contained little non-ionic sugar. Thus it is fair to assume that the previous dialyzates contained acids with neutralization equivalent of 375 and less.

(4) There is evidence that after the diffusion of 52% solids, the residual liquor consists of carbohydrate-free ligninsulphonates. This is indicated by the fact that the reducing power of the solids in the dialyzate and in the rest of the liquor is roughly the same and that, with increasing time of dialysis, the neutralization equivalent weight of the dialyzate increases; the neutralization equivalent weight of the ligninsulphonates increases with increasing molecular weight.

The reducing power of the diffusing and of the residual solids was roughly equal at the end of the dialysis indicating that the reducing power of the ligninsulphonates investigated was inherent and not due to impurities. In this connection the experiments of Peniston and McCarthy (26) are of interest. These authors plotted the reducing power of dialyzed ligninsulphonates, as obtained in a continuous countercurrent dialyzer, against the reciprocal of the time of dialysis and by extrapolating their data to a value corresponding to infinite time of dialysis concluded that really pure ligninsulphonates should not be reducing. The present experiments indicate that care must be taken in such an extrapolation. The curve G can be extrapolated to zero from the region of 30 to 52% solids removal but, on the other hand, it runs almost parallel to the horizontal axis.

Degree of Fractionation

Neither fractional dialysis nor ultrafiltration as employed allow absolute separation of the different molecular weight fractions; while this is self-evident in fractional dialysis, it needs further explanation for ultrafiltration.

The behavior of solutes in ultrafiltration depends on sizes of the molecules, and the membrane pores. Materials with relatively small molecules can pass through the membrane in unchanged concentration, intermediate molecular size materials pass through the membrane with a reduced concentration, and substances with relatively large molecules are retained by the membrane.

The concentration $c_i(t)$ of a fraction i in the solution after a period of ultrafiltration t can be calculated from an equation derived elsewhere (8):

$$c_i(t) = c_i(0).e^{-\gamma_i Kt/V_0}$$

where V_0 is the volume of the residual solution, constant under the experimental conditions, K is the volume of ultrafiltrate produced in unit time, and γ_i is the partition coefficient of the solute in question between the solutions in and outside of the membrane. To determine the time of ultrafiltration it was assumed that the solution to be filtered contained a component which could pass through the membrane in unchanged concentration, i.e. γ was unity. The values of V_0 and K were determined experimentally and the time necessary for the removal of 99.5% of this component was calculated. Consequently, besides really high molecular weight substances, a portion of the materials with $0 < \gamma_i < 1$ was left behind. Thus it is to be expected that there was some overlapping in the molecular weight distributions, even for higher fractions.

Despite the imperfections in the methods of fractionation, the fractions represent well-defined molecular weight ranges. In osmotic pressure measurements it was possible to follow the diffusion rates of fractions Nos. 2 to 6 continuously with time. Furthermore, in the diffusion coefficient determinations the diffusion times were varied up to threefold and it was found that the diffusion rates were independent of diffusion time; this indicates that the fractions cannot be very heterodisperse.

Analytical Data

It has already been mentioned that the dialysis method makes it probable that the four high molecular weight fractions are carbohydrate-free ligninsulphonates; further evidence is provided by the analytical data in Table I. The acid and sulphur contents are approximately equal, thus indicating that all acid groups are sulphonic. The reducing power of these fractions is low and the methoxyl content is high.

Some 60% of the total solids of the spent sulphite liquor from which the mineral acids were removed by ion exchange can be precipitated with ethanol as barium salts. It is, however, doubtful whether this technique in itself is adequate to separate the carbohydrates from the ligninsulphonates quantitatively. If not, there may be considerable impurities present in the low molecular weight fractions.

TABLE I

ANALYTICAL DATA OF SODIUM LIGNINSULPHONATE FRACTIONS

Frac. No.	% total of original solids	% total of fractions	% methoxyl	% S	% phenolic* acid	Reducing power, % eq. glucose	Neut. eq. wt.	Acid groups S / sulphur	Acid groups S / MeO	Mol. wt.	Diffusion coefficient, sq. cm./day
1	7.3	11.87	10.45	5.22	0.945	3.56	599	1.03	0.53	58000	0.0314
2	18.7	30.41	10.40	5.58	0.739	3.36	570	1.01	0.56	19200	0.0849
3	2.8	4.55	10.41	5.40	0.780	3.35	585	1.01	0.55	15500	0.113
4	10.2	16.58	9.82	5.98	0.870	3.79	535	1.00	0.64	8500	0.134
5	4.8	7.80	8.80	6.37	0.770	7.18	450	1.11	0.81	5200	0.178
6	9.5	15.45	7.24	6.25	0.696	9.20	375	1.36	0.89	4600	0.194
7	3.4	5.53	4.06	5.55	0.672	9.42	289	2.00	1.46	3700	0.219
8	4.8	7.80	2.25	5.02	0.530	8.47	227	2.81	2.38	3650	0.221
Total	61.5%	100%									

**Calculated from differential ultraviolet extinction coefficient (see text).*

Fractions 5 to 8 contain more acidic groups than calculated on the basis of their sulphur content. Freudenberg *et al.* (7) found similar analytical results and suggested that these were due to the presence of carboxyl groups in the ligninsulphonates. An alternative explanation is that the carboxyl groups belong to the contaminating carbohydrates.

The sulphur contents of the fractions increase with decreasing molecular weights up to fraction No. 5 and then decrease. This peculiar drop in sulphur contents after fraction No. 5 may be caused by the presence of sulphur-free impurities.

Even if the low molecular weight fractions are contaminated, there is no doubt that their bulk is made up of ligninsulphonates chemically similar to the higher fractions. The strongest evidence is furnished by ultraviolet absorption spectra.

It is well known that the ultraviolet absorption spectra of lignin preparations in neutral solution have maxima near 280 mμ and minima near 260 mμ. Not only do all of the fractions show the same pattern (Fig. 4, Table II) but

TABLE II

CHARACTERISTIC DATA OF THE ULTRAVIOLET ABSORPTION SPECTRA

	pH 6						pH 12			Differential spectrum	
Frac. No.	ϵ_{280}, cm.$^{-1}$ gm.$^{-1}$ liter	Optical density at 280 mμ	λ_{max}, mμ	λ_{min}, mμ	$\epsilon_{max}/\epsilon_{min}$	$\epsilon_{245}/\epsilon_{260}$	λ_{max}, mμ	λ_{min}, mμ	$\epsilon_{max}/\epsilon_{min}$	λ_{max}, mμ	$\Delta\epsilon_{max}$, cm.$^{-1}$ gm.$^{-1}$ liter
1	13.9	4200	282	263	1.32	2.28	282	266	1.13	300	2.28
2	13.3	4090	283	263	1.39	2.28	281	267	1.13	298	1.78
3	13.5	4150	282	262	1.38	2.23	281	267	1.12	301	1.88
4	12.4	4020	282	262	1.29	2.20	281	268	1.07	298	2.10
5	11.1	4100	283	263	1.39	2.15	281	268	1.09	299	1.86
6	8.8	3900	283	262	1.38	2.05	282	270	1.10	300	1.68
7	5.8	4200	277	261	1.34	1.89	281	270	1.16	299	1.62
8	4.2	6360	277	258	1.30	1.59	282	273	1.09	297	1.28

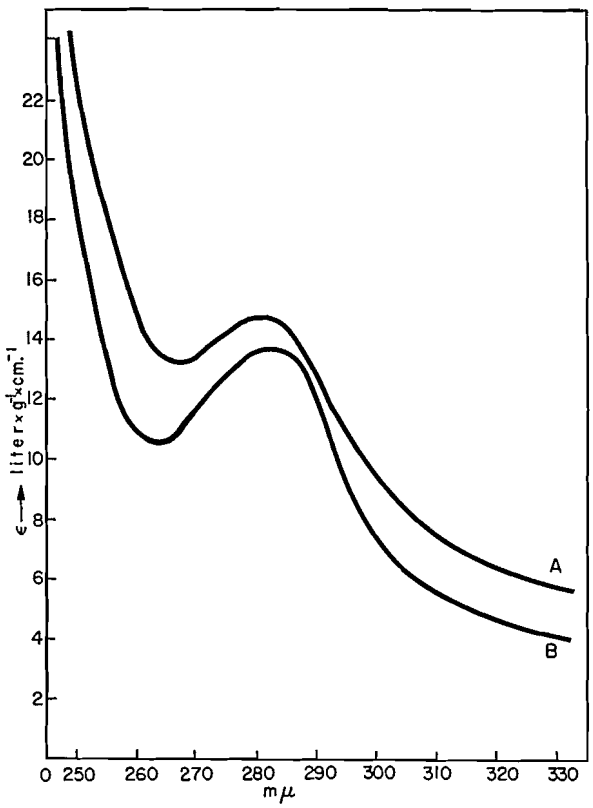

FIG. 4. Ultraviolet absorption spectra of fraction No. 1; curve A: pH 12, curve B: pH 6.

the ratio of the extinction coefficients (ϵ) at the maximum and minimum is approximately constant at 1.35 for all fractions. The only difference in the shapes of the curves is that the slopes in the lower wavelength region decrease with the molecular weights of the fractions. The ratios of extinctions at 245 and 260 mμ decrease from fraction No. 1 to fraction No. 8 (Table II).

The light-absorbing power decreases with the molecular weights of the fractions; this can be noticed by the visual observation of the color and is expressed quantitatively by the extinction coefficients for 0.1% solutions at 280 mμ (Table II). Nevertheless the ultraviolet light absorbing power per methoxyl bearing unit at 280 mμ is the same for all the fractions except the lowest, for which it is relatively high (Table II).

Aulin-Erdtman (1) found shifts in the characteristic ultraviolet spectra of lignin compounds when determined in neutral and in alkaline solutions, and attributed them to the ionization of the phenolic hydroxyl groups. The minima of the samples shifted from 263 to 266 mμ for the highest, and from 258 to 273 mμ for the lowest fraction. The values of λ_{max} decreased on the average by 1 mμ. The ratio $\epsilon_{max}/\epsilon_{min}$ was the same for all fractions, the mean value being 1.11, i.e. less than for neutral solutions.

Goldschmid (11) suggested that the phenolic hydroxyl contents of lignin

and analogous model compounds can be determined from the differential spectra of solutions with pH 6 and pH 12. These spectra were shown to have maxima around 250 and 300 mμ. With model substances Goldschmid determined the characteristic maximum extinction at 300 mμ ($\Delta\epsilon_{max}$) for 1 mole phenolic hydroxide per liter. According to this value the unknown phenolic hydroxyl content of a substance can be calculated from the following formula:

$$\%(\phi-OH) = (17/41)\ \Delta\epsilon_{max}.$$

The hydroxyl contents of the fractions (Table I) were determined from such differential spectra, characteristic data of which are shown in Table II and three of which are plotted in Fig. 5.

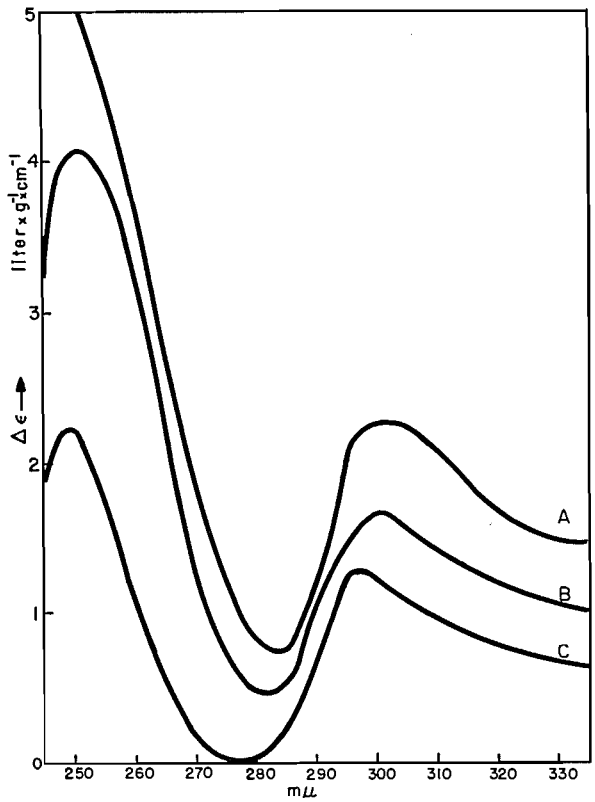

FIG. 5. Differential absorption spectra between solutions at pH 12 and pH 6; curve A: fraction No. 1, curve B: fraction No. 6, and curve C: fraction No. 8.

Molecular Weights

As described in a separate paper (9), molecular weights of all but the two lowest fractions were determined by the osmotic pressure method; these values are tabulated in Table II. When the logarithm of the molecular weight is plotted against the logarithm of the diffusion coefficient, the points corresponding to fractions Nos. 4, 5, and 6 fall on a straight line which can be extra-

polated to the measured diffusion coefficients of the lowest fractions, from which the molecular weights were calculated. It must be borne in mind that the ultraviolet extinction coefficients of the solutions were used to determine the concentrations in the diffusion experiments. Should the lower fractions be mixtures of ultraviolet light-absorbing ligninsulphonates and relatively transparent carbohydrates, the diffusion coefficients would be indicative of the ligninsulphonates alone.

In a homologous polymer series the following relation holds between the weight-average molecular weights M and diffusion coefficients D_1 (10):

$$D_1 = K\,M^{-b}$$

where b is a constant depending on the shape of the molecules and K is a constant characteristic for the homologous series. The error involved in using number-average molecular weights and the diffusion coefficients for estimating the molecular weights of the lowest ligninsulphonates should be small. As can be seen from the integral molecular weight distribution plot (Fig. 6) the degree of polydispersity of the fractions except the highest (No. 1) is relatively low. Hence there is only a slight difference between the weight-average and the number-average molecular weights.

The integral molecular weight distribution plot (Fig. 6) indicates that the

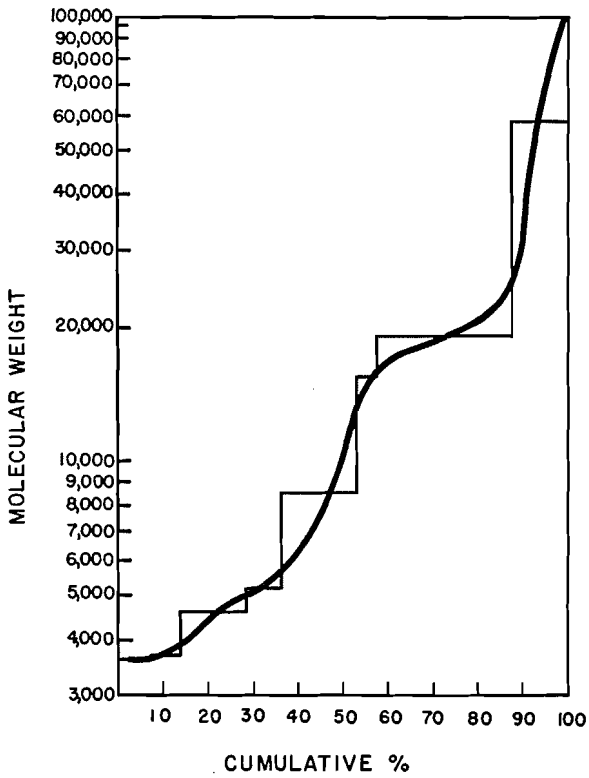

FIG. 6. Integral molecular weight distribution of the ligninsulphonates.

molecular weights of the ligninsulphonates investigated range from about 3700 to about 100,000. Around 30% of the material have molecular weights between 3700 and 5000 and also between 15,000 and 25,000.

It is beyond the scope of this paper to give a critical survey of the numerous attempts to determine the molecular weights of different lignin preparations. The accumulated data (2, 14) present a confusing picture because in the isolation of lignin or ligninsulphonates the original lignin in the wood can be considerably degraded or polymerized. Furthermore it is also possible that in the lower molecular weight region association may occur in the solutions (10); if this occurs the molecular weights obtained for the lower fractions would also be too high.

Nevertheless it is interesting to note that some investigators (3, 13, 20, 29) have found that lignin preparations isolated under mild conditions have molecular weights not lower than 3500 to 4000 which correspond well to the lower limit of the data presented here. According to Gralen (13) there is some indication that lignins with degrees of polymerization corresponding to the molecular weights 4000 and 8000 are the most stable. In the light of this, it is significant that 30% of our fractions have molecular weights in the 4000 range.

Considerably lower molecular weights of lignin, however, also have been reported (2, 15). Until a study is made of how the degree of polymerization of lignin is changed in the various isolation techniques it will be difficult to interpret the available data. Since the highest reported native lignin molecular weight is 27,000 (13), there is strong indication that during the sulphite cook at least part of the lignin becomes considerably polymerized.

REFERENCES

1. AULIN-ERDTMAN, G. Tappi, 32: 160. 1949.
2. BRAUNS, F. E. Chemistry of lignin. Academic Press, Inc., New York. 1952. pp. 114–125, 191–197.
3. CONNER, W. P. J. Chem. Phys. 9: 591. 1941.
4. ERDTMAN, H. Svensk Kem. Tidskr. 53: 201. 1941.
5. ERDTMAN, H. Svensk Papperstidn. 45: 374, 392. 1942.
6. ERNSBERGER, F. M. and FRANCE, W. C. J. Phys. Chem. 52: 647. 1942.
7. FREUDENBERG, K., LAUTSCH, W., and PIEZOLO, G. Cellulosechemie, 22: 97. 1948.
8. GARDON, J. L. and MASON, S. G. Can. J. Chem. 33: 1491. 1955.
9. GARDON, J. L. and MASON, S. G. Forthcoming publication.
10. GARDON, J. L. and MASON, S. G. Can. J. Chem. 33: 1491. 1955.
11. GOLDSCHMID, O. Anal. Chem. 26: 1421. 1954.
12. GORDON, A. R. Ann. N.Y. Acad. Sci. 46: 285. 1945.
13. GRALEN, N. J. Colloid Sci. 1: 453. 1946.
14. HAGGLUND, E. Chemistry of wood. Academic Press, Inc., New York. 1951.
15. HENGSTENBERG, J. Die Physik der Hochpolymeren. Vol. II. *Edited by* H. A. Stuart. Verlag von Julius Springer, Berlin. 1953. pp. 483–484.
16. IVARSSON, B. Svensk Papperstidn. 51: 1. 1951.
17. KLASON, P. Beitrage zur Kenntnis der Zusammensetzung des Fichtenholzes. p. 34. 1911.
18. LAUTSCH, W. Die Chemie, 57: 149. 1949.
19. LEOPOLD, B. Acta Chem. Scand. 6: 65. 1952.
20. LOUGHBOROUGH, D. L. and STAMM, J. J. Phys. Chem. 40: 1113. 1936; 45: 1137. 1941.
21. MCBAIN, J. W. and LIU, T. H. J. Am. Chem. Soc. 53: 59. 1933.
22. MCCARTHY, J. L. Private communication.
23. MARKHAM, A. E., PENISTON, Q. P., and MCCARTHY, J. L. J. Am. Chem. Soc. 71: 3599. 1949.
24. NORTHRUP, J. H. and ANSON, M. L. J. Gen. Physiol. 12: 543. 1929.
25. OLLEMAN, E. D., PENNINGTON, D. E., and RITTER, D. M. J. Colloid Sci. 3: 185. 1948.

26. PENISTON, Q. P. and MCCARTHY, J. L. J. Am. Chem. Soc. 70: 1324. 1948.
27. PENISTON, Q. P. and HIBBERT, H. Paper Trade J. 109: 231. 1939.
28. PENNINGTON, D. E. and RITTER, D. M. J. Am. Chem. Soc. 69: 665. 1941.
29. SAMEC, M. and PIRKENMEYER, B. Kolloid-Z. 72: 336. 1935.
30. SAMEC, M. and RIBERIC, I. Kolloidchem. Beih. 24: 157. 1927.
31. SCHWABE, K. and HAHN, E. Holzforschung, 2: 42. 1947.
32. SCHWABE, K. and HASNER, L. Cellulosechemie, 20: 61. 1952.
33. VJEBOCK, F. and SCHWAPPACH, A. Ber. 63: 2818. 1930.
34. YORSTON, F. H. Pulp & Paper Mag. Can. 47 (13): 74. 1947.

PHYSICOCHEMICAL STUDIES OF LIGNINSULPHONATES

II. BEHAVIOR AS POLYELECTROLYTES[1]

By J. L. Gardon[2] and S. G. Mason

ABSTRACT

Conductivity, dyestuff adsorption, and viscosity measurements on aqueous solutions of fractionated ligninsulphonate samples having various molecular weights indicate that they behave as flexible polyelectrolytes. There is evidence that ligninsulphonates of molecular weight less than 5000 associate in solution in a manner analogous to micelle formation in colloidal electrolytes. From the variation of intrinsic viscosity with molecular weight, it may be concluded that the degree of molecular branching of the high molecular weight ligninsulphonates is greater than that of the low molecular weight fractions.

INTRODUCTION

In the pulping of wood by the sulphite process, large quantities of lignin-sulphonic acids and salts appear in the spent liquor. Relatively large amounts of ligninsulphonate concentrates are now used as dispersants and adhesives (16, 26), although the mechanisms underlying these applications are not understood. The purpose of the investigation outlined in this paper and in subsequent papers was to study some of the physicochemical properties of the material which may be relevant to these applications.

While the exact structure of ligninsulphonates is not known, it is believed (2, 14, 16) that they are built of guaiacyl–propyl units with the sulphonate groups attached to the aliphatic chains. This molecular structure and the results of the experiments described in this paper indicate that the lignin-sulphonates can be considered as substances consisting of flexible chain molecules with ionizable groups attached to them, i.e. they are polyelectrolytes.

Recently considerable research has been carried out on polyelectrolytes, general accounts of which are given by Fuoss (10, 11), Flory (8), and Kat-chalsky (20). The most important characteristic is that in solution the molecular shape depends upon the net electrical charge of the molecule. In the uncharged state the molecule curls up. If the ionic groups are dissociated, the polyelectrolyte molecule extends owing to the electrostatic repulsion between neighboring groups.

The degree of ionization of the polyelectrolyte depends on its concentration and also upon the presence of simple electrolytes in the solution. At low polyelectrolyte concentrations, the molecules occupy only a small part of the available space in the solution; this favors the escape of the counter-ions, e.g. the sodium ions of the ligninsulphonates, from polymer molecules, leaving the latter charged. The equilibrium between the counter-ions associated with the polymer molecules and in the part of the solvent free of polymer molecules, i.e. in the free space, is analogous to a Donnan-type equilibrium. Consequently

[1]*Manuscript received June 10, 1955.*
Contribution from The Pulp and Paper Research Institute of Canada and the Chemistry Department, McGill University, Montreal, Quebec.
[2]*Holder of the Anglo-Paper Research Fellowship and of a Studentship from the National Research Council of Canada. Present address: Industrial Cellulose Research Ltd., Hawkesbury, Ontario.*

when the free space becomes smaller as the polyelectrolyte concentration is increased, the counter-ion concentration in this free space greatly increases, inhibiting further ionic dissociation. The polyelectrolyte molecules can also lose their charge, even at low concentrations, if the concentration of the counter-ions in the free space is increased by the addition of simple electrolytes containing the same counter-ion as the solution.

The dependence of the charge of the molecules of the polyelectrolyte on its concentration can be shown by conductivity measurements. As the molecules progressively lose their charge with increasing concentration, less and less current can be carried by each molecule. The specific conductivity/concentration (or reduced specific conductivity) decreases with increase of the square root of the concentration, but not linearly, as predicted by the Onsager equation for simple electrolytes. The corresponding plot is curved and is steep at low concentrations.

The flexible coiling of the molecules as they progressively lose their charge can be demonstrated by the dependence of the reduced viscosity (η_{sp}/c) on the concentration. As the effect of an extended molecule on the viscosity of the solution is greater than that of a molecular coil, the reduced viscosity of the polyelectrolyte decreases with increasing concentration. If, however, determinations are made of the viscosities of solutions containing different amounts of polyelectrolyte and always the same sufficiently large amount of simple electrolyte, the reduced viscosity of the polyelectrolyte, like the viscosity of uncharged polymers, increases linearly with concentration.

In the present paper, results of conductivity, dyestuff adsorption, and viscosity measurements carried out with ligninsulphonates of various molecular weights are presented. The method of preparation of these fractions, their analytical data, their diffusion coefficients D_1, and the determination of their molecular weights by osmotic pressure measurements are reported elsewhere (12, 13).

CONDUCTIVITY MEASUREMENTS

From the foregoing considerations variation of the reduced specific conductivity with concentration of ligninsulphonates may be expected to differ from that of simple electrolytes. This apparent anomaly has been observed but not adequately explained by a number of investigators (7, 22, 27, 30). The results obtained by Samec and Ribaric (30) and Koenig (22) did not conform with the pattern predicted for polyelectrolytes and, oddly enough, the reduced specific conductivity curves had maxima at very low concentrations.

The variation of the reduced specific conductivities of several sodium ligninsulphonate fractions with $\sqrt{c}$ at 25°C. is shown in Fig. 1. Curves A and B represent fractions having molecular weights of 58,000 and 19,200 respectively and are typical of polyelectrolytes. Curves C, D, and E obtained for fractions with molecular weights 5200, 3700, and 3650 show apparent breaks; these breaks may indicate association, as generally observed (1, 25) for colloidal electrolytes, but not for polyelectrolytes. The reduced specific conductivity vs. $\sqrt{c}$ plot for a colloidal electrolyte shows a sharp discontinuity at the critical micelle formation concentration. At lower colloidal electrolyte concentrations,

the plot is linear and descends slightly; at higher concentrations, it drops very markedly and quite often passes through a minimum (1, 25). The molecular weights of colloidal electrolytes, however, are in the range of several hundreds and about 20 to 200 molecules associate to form a micelle; abrupt changes are therefore shown in the properties at the critical concentration of micelle formation. Considerably higher molecular weights were found for the

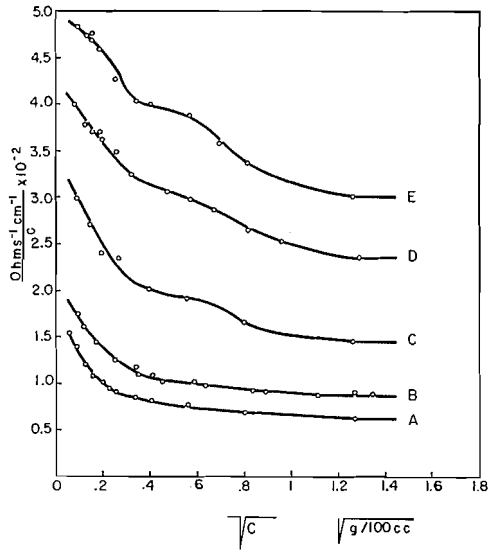

FIG. 1. Reduced specific conductivities of sodium ligninsulphonate fractions having molecular weights 58,000 (A), 19,200 (B), 4600 (C), 3700 (D), and 3650 (E).

ligninsulphonates investigated than for conventional colloidal electrolytes. Consequently it is improbable that aggregates consisting of a great number of ligninsulphonate molecules are formed. Hence the ligninsulphonate solutions do not show such sharp discontinuities as the solutions of colloidal electrolytes around the critical micelle formation concentration. The shape of curves C, D, and E may be considered as evidence that the low molecular weight ligninsulphonates are intermediate between polyelectrolytes and colloidal electrolytes. As will be shown, the reduced viscosity curves of all fractions and the dyestuff adsorption curves of all but the lowest molecular weight fraction were smooth. Hence the conductivity curves cannot be considered as absolute proof for association in the low molecular weight range; this matter requires further study.

DYESTUFF ADSORPTION MEASUREMENTS

It has been observed (15) that the optical absorption spectra of aqueous solutions of certain dyestuffs shift in the presence of micelles of colloidal electrolytes. According to Corrin and Harkins (4) this is due to adsorption or incorporation of the dyestuff on, or into, the micelle and to the different colors of the dyes in a polar medium, e.g. water, and in a non-polar medium,

as the non-charged micelle. They suggested the use of this phenomenon to detect the critical micelle formation concentration.

The influence of uncharged coiled polyelectrolyte molecules on the color of indicator dyes has not yet been investigated. The experiments here described indicate that, as was to be expected, they changed the absorption spectra of such dyes just as the micelles of the colloidal electrolytes.

Pinacyanole is blue when dissolved in pure water and green in the presence of uncharged aggregates (4). This cationic dyestuff was found to be suitable for experiments with ligninsulphonates. In Fig. 2 light-absorption curves of

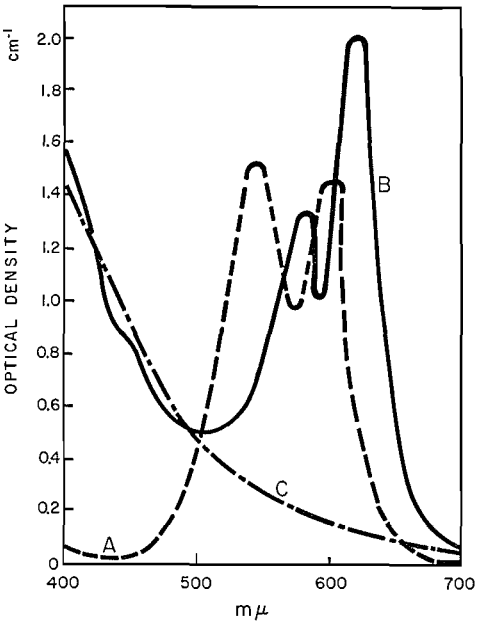

FIG. 2. Absorption curves of (A) 1.2 mgm./100 cc. pinacyanole, (B) 1.2 mgm./100 cc. pinacyanole and 0.5 gm./100 cc. ligninsulphonate (molecular weight 19,200), and (C) 0.5 gm./100 cc. ligninsulphonate.

solutions containing 1.2 mgm./100 cc. dye (A), the same amount of dye and 0.5 gm./100 cc. ligninsulphonate (B), and 0.5 gm./100 cc. ligninsulphonate alone (C) are shown. The maximum at 620 mμ in curve B is characteristic of the dyestuff – discharged aggregate complex, but the pure dyestuff solution also absorbs light at this wavelength appreciably. However, the light absorption of both pure dye and pure ligninsulphonate at 630 mμ wavelength is negligibly small. The optical density at 630 mμ can be considered as a measure of the amount of discharged aggregate – dye complex present in the solution.

The optical densities of solutions containing a fixed amount of dyestuff at various concentrations of ligninsulphonates, measured in a Beckman Model DU spectrophotometer at 630 mμ, are shown in Fig. 3.

As the molecules progressively lose their charge with increasing concentration, they adsorb increasing amounts of dyestuff. The high molecular weight

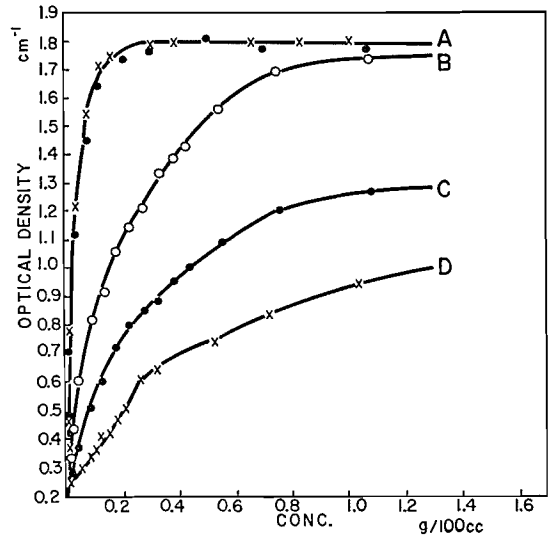

FIG. 3. Optical densities at 630 mμ of solutions containing 1.2 mgm./100 cc. pinacyanole and various amounts of ligninsulphonates. The molecular weights of the ligninsulphonates are 58,000 and 15,500 (A), 4500 (B), 3700 (C), and 3650 (D).

fractions adsorb all the dyestuff present in the solution at around 0.2% concentration. The shape of Curve A representing fractions with molecular weights 58,000 and 15,500 corresponds well to the pattern demonstrated by the conductivity and viscosity measurements.

The curves B, C, and D indicate that the ability of the lower molecular weight fractions to adsorb dye is smaller than that of the high molecular weight fractions. The uncharged particles of the low molecular weight fractions are probably smaller than those of the high molecular weight fractions and, if they contain associated molecules, the number of the molecules per aggregate is probably small. The break in curve D may indicate that lowest molecular weight fractions associate in solution.

VISCOSITY MEASUREMENTS

The viscosities were determined at 25°C. in Ostwald–Cannon type (3) viscometers with flow times for water of about 400 sec. The kinetic energy corrections were negligible.

The dependence of the reduced viscosities of sodium ligninsulphonate fractions on concentration in distilled water is shown in Figs. 4 and 5. The shape of these curves is typical for polyelectrolytes; at low concentrations the reduced viscosities are high, as the molecules are extended, and at high concentrations they are low, as the molecules are coiled. The dependence of the reduced viscosities of the sodium ligninsulphonates does not follow the empirical equation of Fuoss (9):

$$[1] \qquad z = \eta_{sp}/c = [A/(1+B\sqrt{c})]+D.$$

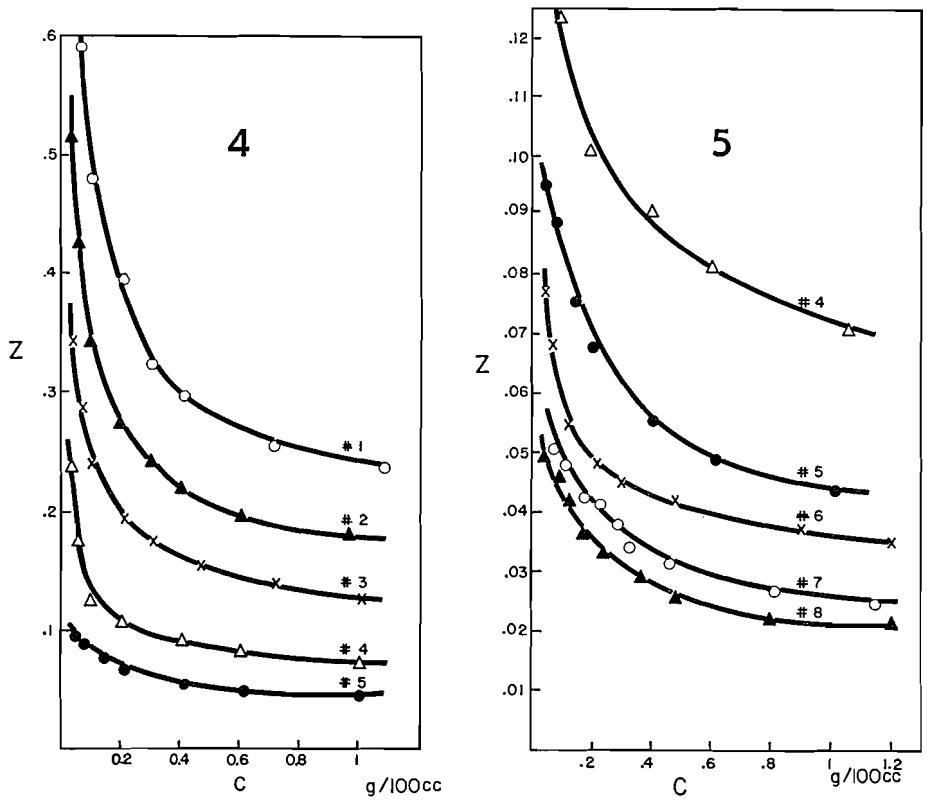

FIGS. 4 and 5. Reduced viscosities z at various concentrations of sodium ligninsulphonates in water. The molecular weights of the number fractions are given in Table I.

In the above equation, z is the reduced viscosity, c the concentration, B a constant depending on the dielectric properties of the solvent, $(A+D)$ is the intrinsic viscosity of the polyelectrolyte when the molecules are extended, and D is a measure of the intrinsic viscosity of the randomly coiled molecules. According to this equation, the $1/(z-D)$ vs. $\sqrt{c}$ plot should be linear, but a linear plot could not be obtained for ligninsulphonates. If, however, the term $c^{\frac{1}{2}}$ was replaced by c^x in equation [1],

$$[2] \qquad z = [A/(1+Bc^x)]+D,$$

linear plots of $1/(z-D)$ vs. c^x were obtained for the three highest molecular weight fractions (Fig. 6). D was taken to be the reduced viscosity of a 4% solution; the error in doing so was very small as the reduced viscosities of solutions with concentrations higher than 2% were practically constant. The constant x was established by trial and error. With an approximate value of A, $\log[1/(z-D)-1/A]$ was plotted against $\log c$. The value of A was so chosen that this plot yielded a straight line, the slope of which was x. When D and x were known, the curves of Fig. 6 could be plotted. The intercepts on the vertical axes obtained by an analytical extrapolation were equal to $1/A$.

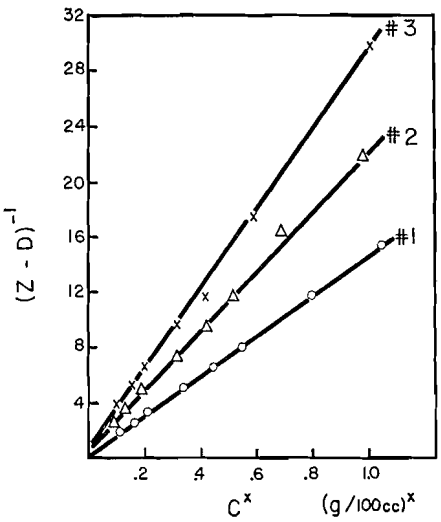

FIG. 6. $1/(z-D)$ vs. c^z plots for the three highest molecular weight fractions.

TABLE I

VISCOSITY DATA, DIFFUSION COEFFICIENTS, AND NUMBER-AVERAGE MOLECULAR WEIGHTS OF THE SODIUM LIGNINSULPHONATE FRACTIONS

		Fractions							
	Solvent	1	2	3	4	5	6	7	8
Molecular weight, gm.	0.5 *N* NaCl	58000	19200	15500	8500	5200	4600	3700	3650
Diffusion coefficient, cm./day	0.5 *N* NaCl	0.0314	0.0849	0.113	0.134	0.178	0.194	0.219	0.221
D, 100 cc./gm.	Water	0.172	0.134	0.0905	0.0563	0.0389	0.0328	0.0242	0.0211
$[\eta] = A+D$, 100 cc./gm.	Water	4–7	1.35–1.6	0.8–1.2	—	—	—	—	—
x	Water	0.71	0.73	0.78	—	—	—	—	—
$[\eta]$, 100 cc./gm.	2 *N* NaCl	0.0455	0.0425	0.0394	0.0262	0.0235	0.0220	0.0197	0.0190
k	2 N NaCl	4.9	5.0	5.42	6.00	4.75	4.15	4.6	4.6

Since this extrapolation was uncertain, the values of A thus obtained were not precise; values of $(A+D)$ are estimated to lie within the limits given in Table I. The values of x and D are also tabulated.

Equation [2] is empirical and does not have the theoretical significance of equation [1]. It is probable that the proportionality between $1/(z-D)$ and c^z is fortuitous and that the true equation describing the dependence of the reduced viscosity of the ligninsulphonates on their concentration is that of Schaefgen quoted by Katchalsky (20):

$$z = [A/(1+B\sqrt{c}+B'c)]+D.$$

The concentration dependence of the reduced viscosities of the other fractions cannot be expressed by equation [2]. Thus the intrinsic viscosities of the extended molecules could not be determined. The D values determined at a 4% concentration are given in Table I.

The reduced viscosities of the fractions in 2 N sodium chloride are shown in Fig. 7. The concentration dependence of the reduced viscosities can be

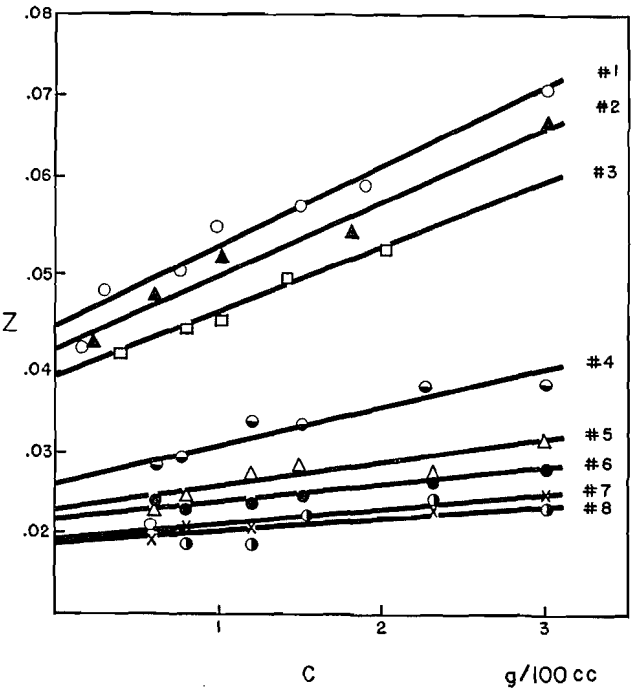

FIG. 7. Reduced viscosities at various concentrations of sodium ligninsulphonates in 2 N sodium chloride. The molecular weights of the various fractions are listed in Table I.

expressed by the equation of Simha (32) and Huggins (19) derived for non-charged interacting particles:

$$z = [\eta]+k[\eta]^2c+ \ldots \quad .$$

In this equation $[\eta]$ is the intrinsic viscosity and k is a constant characteristic for the homologous polymer series. Both $[\eta]$ and k are given for all fractions in Table I. As can be seen k changes between 4.2 and 6. Ligninsulphonates are approximately, but not truly, members of a homologous series and this may account for the variation of k.

RELATIONS BETWEEN INTRINSIC VISCOSITIES, DIFFUSION COEFFICIENTS, AND MOLECULAR WEIGHTS

According to the theories of Kuhn (23), Kirkwood and Riseman (21), and Debye and Bueche (5, 6), the constants a and b in the equations

$$[\eta] = K_2 M^a,$$
$$D_1 = K_1 M^{-b}$$

describing the dependence of the intrinsic viscosities $[\eta]$ and the diffusion coefficients D_1 on the molecular weights are both equal to unity, if the molecules are linear flexible chains, randomly coiled, and permeable to the solvent, and are equal to 0.5, if the randomly coiled flexible molecules are impermeable to the solvent. The constants K_1 and K_2 are characteristic of the homologous series. Kuhn and Kuhn (24) showed that these theories are also applicable to branched molecules if these chains are flexible and randomly coiled. The intrinsic viscosities of branched-chain molecular structures are lower than those of linear molecules of comparable size. Huggins (17, 18) has shown that $a = 2$ when the molecules behave as rigid rods.

It has been experimentally verified for a number of polyelectrolytes (20) that the values of a for the intrinsic viscosities $(A+D)$, corresponding to the extended molecules, approach 2 if the polyelectrolytes are linear, and are higher than unity but less than 2 if the polyelectrolytes are branched (31). As mentioned before, D is a measure of the intrinsic viscosity of a randomly coiled polyelectrolyte. Depending on the degree of ionization, D changes linearly with, or proportionally to the square root of, the molecular weight (20).

The diffusion coefficients, the D values, and the intrinsic viscosities in 2 N sodium chloride are plotted on a logarithmic scale against the number-average molecular weights of the ligninsulphonate fractions (Fig. 8). From the slopes

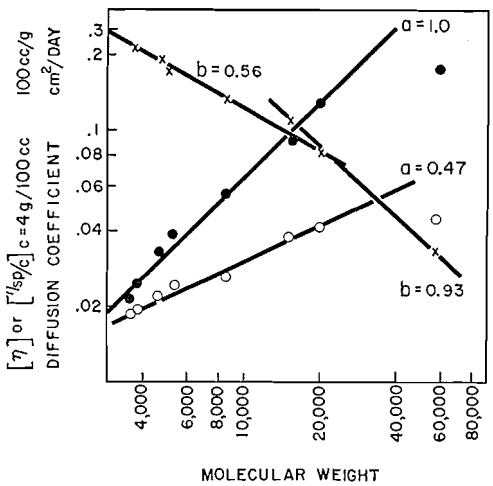

FIG. 8. Determination of constants a and b from reduced viscosities at 4% sodium ligninsulphonate in pure water (solid circles), intrinsic viscosities in 2 N sodium chloride (open circles), and diffusion coefficients in 0.5 N sodium chloride (crosses).

of these plots it can be concluded that $a = 1$ for the molecular weight dependence of D and 0.47 for the intrinsic viscosities in 2 N sodium chloride if the highest molecular weight fraction is disregarded. According to Debye (6)

the intrinsic viscosity is a measure of the true partial specific volume. As can be seen, the intrinsic viscosities in salt solution are smaller than the D values. Consequently in the sodium chloride solution, probably owing to the osmotic pressure of the sodium chloride, the coils are compressed, while in pure water the coils are expanded. The compressed coils are impermeable to water, the loose coils are permeable, and hence the values of a are in the range of 0.5 and 1 respectively.

Both the intrinsic viscosity in 2 N sodium chloride and the D value of fraction No. 1 are lower than predicted by the regularities described above. As shown in a previous communication (12), this fraction is more heterodisperse than the others and probably contains ligninsulphonates with molecular weights as high as 100,000. It is fair to assume that the higher the degree of polymerization, the greater the probability of branching during polymerization in the sulphite cook. If so, the reason for the relatively low D and low intrinsic viscosity of the highest molecular weight fractions is its higher degree of branching.

The diffusion coefficients were determined in 0.5 N sodium chloride (13). It seems that there are two b values describing the dependence of the diffusion coefficients on the molecular weight: $b = 0.56$ corresponds to all fractions but Nos. 1 and 3, while $b = 0.93$ corresponds to fractions Nos. 1, 2, and 3; this requires further investigation.

In connection with these experimental results, it is of interest to mention the work of Olleman, Pennington, and Ritter (28), who determined the diffusion coefficient, intrinsic viscosity, and partial specific volume of an ammonium ligninsulphonate in 1 N ammonium acetate solution. Using the Polson–Kuhn equation (29), they calculated the axial ratio to be 4.6. The weight-average molecular weight 21,000 calculated by them for a ligninsulphonate with 0.080 sq. cm./day diffusion coefficient compares favorably with the diffusion coefficient 0.0847 and number-average molecular weight 19,200 of fraction No. 2.

CONCLUSIONS

The results presented above lead to the conclusion that ligninsulphonates are flexible polyelectrolytes. At high concentrations of ligninsulphonates, and at low concentrations when sodium chloride is present, the molecules are coiled. At low ligninsulphonate concentrations and in the absence of sodium chloride the molecules become extended. There are indications that the low molecular weight fractions associate in solution and that the molecules of the highest molecular weight fraction are more branched than those of the other fractions. It is probable that the dispersive and adhesive properties of ligninsulphonates are due to their polyelectrolyte nature.

REFERENCES

1. ALEXANDER, A. E. and JOHNSON, P. Colloid science. Oxford University Press, London. 1949. pp. 667–696.
2. BRAUNS, F. E. The chemistry of lignin. Academic Press, Inc., New York. 1952. pp. 373–375, 621–669.
3. CANNON, M. R. and FENSKE, M. R. Ind. Eng. Chem. Anal. Ed. 10: 297. 1938.

4. CORRIN, M. L. and HARKINS, W. D. J. Am. Chem. Soc. 69: 679. 1947.
5. DEBYE, P. J. Chem. Phys. 14: 636. 1946.
6. DEBYE, P. and BUECHE, M. J. Chem. Phys. 16: 573. 1948.
7. EMSBERGER, F. M. and FRANCE, W. G. J. Phys. & Colloid Chem. 52: 267. 1948.
8. FLORY, P. J. Principles of polymer chemistry. Cornell Univ. Press, Ithaca, N.Y. 1953. pp. 629–637.
9. FUOSS, R. M. J. Polymer Sci. 3: 603. 1948.
10. FUOSS, R. M. Discussions Faraday Soc. No. 11: 125. 1951.
11. FUOSS, R. M. and STRAUSS, U. P. Die Physik der Hochpolymeren. Vol. II. *Edited by* H. A. Stuart. Verlag von Julius Springer, Berlin. 1953. pp. 680–700.
12. GARDON, J. L. and MASON, S. G. Can. J. Chem. 33: 1477. 1955.
13. GARDON, J. L. and MASON, S. G. Forthcoming publication.
14. HAGGLUND, E. Chemistry of wood. Academic Press, Inc., New York. 1951. pp. 230, 282–290.
15. HARTLEY, G. S. Trans. Faraday Soc. 30: 444. 1934.
16. HEARON, W. M. Tappi, 36(9): 14*A*. 1953.
17. HUGGINS, M. L. J. Phys. Chem. 42: 911. 1938.
18. HUGGINS, M. L. J. Phys. Chem. 43: 439. 1939.
19. HUGGINS, M. L. J. Am. Chem. Soc. 64: 2716. 1942.
20. KATCHALSKY, A. J. Polymer Sci. 12: 159. 1954.
21. KIRKWOOD, J. G. and RISEMAN, J. J. Chem. Phys. 16: 565. 1948.
22. KOENIG, F. Cellulosechemie, 2: 100. 1921.
23. KUHN, W. Kolloid-Z. 68: 2. 1934.
24. KUHN, W. and KUHN, H. Helv. Chim. Acta, 30: 159. 1947.
25. MCBAIN, J. W. Colloid science. D. C. Heath & Company, Boston. 1950. pp. 240–274.
26. MARSHALL, H. B. Pulp & Paper Mag. Can. 54: 113. 1953.
27. MELANDER, K. A. H. Cellulosechemie, 2: 41. 1921.
28. OLLEMAN, E. D., PENNINGTON, D. E., and RITTER, D. M. J. Colloid Sci. 3: 185. 1948.
29. POLSON, A. Kolloid-Z. 88: 51. 1939.
30. SAMEC, M. and RIBARIC, I. Kolloidchem. Beih. 24: 157–180. 1928.
31. SCHAEFGEN, J. R. and TRIVISONNO, C. F. J. Am. Chem. Soc. 74: 2715. 1952.
32. SIMHA, R. J. Research Natl. Bur. Standards, 42: 409. 1944.

STUDIES ON ALUMINA CATALYSTS

IV. THE PRODUCTION OF DIETHYLANILINE BY CONDENSATION OF ETHANOL AND ETHYLANILINE[1]

By L. A. Munro and R. A. Washington

ABSTRACT

The condensation of ethanol and ethylaniline was studied using alumina catalysts at 300°C. The gel water of the alumina affects its catalytic activity. Maxima and minima in activity occur at gel water values corresponding to those previously found for the dehydration of ethanol and formic acid. There is no concurrent change in crystal structure of the alumina gel. The results suggest the initial dehydration of alcohol to ether followed by condensation of the ether and ethylaniline to give diethylaniline. It is concluded that the best and poorest spatial arrangement of 'active points' or adsorption spaces is established by the amount of residual gel water.

In general, heterogeneous catalysis is pictured as involving adsorption of the reactants on the surface of the catalyst with activation of the substrate followed by reaction and removal of the products. The patent literature gives ample evidence of the specific and distinctive behavior of catalysts differing in chemical nature, e.g. metals such as nickel for hydrogenation and hydrous oxides and phosphates for dehydration. Many workers have found that even in the same type of catalysts there are not only differences in over-all activity but also in specificity. It is to be expected that one or both of these qualities may be affected by the size and valence of the metallic element present, by alteration of the crystal lattice, and by changes in porosity or total surface.

Activation of a hydrous oxide consists in the removal of the major portion of the gel water by heating. The temperature used in activation is cited repeatedly as a criterion of activity. In the case of alumina catalysts for the production of ether "optimum activation temperatures" from 310° to 600°C. have been reported by various authors. Of fundamental importance is the degree of removal of gel water and the crystal structure of the colloidal fibrils with concurrent alteration of the surface.

It has been found that alumina catalysts prepared by different workers in this laboratory at intervals of several years showed maxima (or minima) in activity at the same gel water irrespective of the temperature of activation (1, 9, 10). Furthermore, in the dehydration of formic acid and the production of ether and ethylene from ethanol, these maxima and minima were not due to changes in crystal lattice (9).

The present paper reports a similar study of the effect of gel water on the condensation of ethanol and ethylaniline to give diethylaniline.

This investigation was not concerned with the determination of conditions of temperature and space velocity which would give 100% conversion of ethylaniline to diethylaniline. Conditions were chosen such that the production of diethylaniline would be sufficiently high that variations in yields could be readily measured, while side reactions such as the dehydration of the ethanol

[1]*Manuscript received June 17, 1955.*
Contribution from the Department of Chemistry, Queen's University, Kingston, Ontario.

to ether and ethylene would be depressed as much as possible. A reaction temperature of 300°C. was chosen. At this temperature no appreciable change in the activation of the catalyst would occur.

The apparatus was essentially similar to that used in the previous work (9) except that the catalyst tube was half filled with pyrex wool. This acted as the vaporization chamber for the reaction mixture (1 mole ethylaniline to 1.05 moles ethanol). Reagents were analar grade. The ethylaniline was redistilled at 10 mm. The refractive index of the product was 1.5422 (n_D^{20}). The product was also analyzed for total and tertiary amines by the method of Siggia, Hanna, and Kervenski (12). The results showed the ethylaniline to be free of tertiary amines, and to have a total amine content of 8.27×10^{-3} M./gm. If the figure given in the literature is accepted (8.24×10^{-3} M./gm.) this would indicate a purity of 99.4%. The absolute alcohol tested 99.8%. The catalysts were prepared from a combined batch of alumina gel as described previously (9). The air-dried gel contained 36.7% water.

Reaction products were collected in a cold receiver and gaseous products in a gasometer over saturated brine at atmospheric pressure. The liquid products were allowed to separate into aqueous and amine layers and these analyzed. Diethylaniline was determined by an adaptation of the colorimetric method of English (5) using a Klett-Summerson photometer. The standardization curve was prepared by using a series of samples containing known mixtures (by weight) of carefully purified mono- and di-ethylaniline.

Analysis of the gaseous products indicated almost pure ethylene. Ether was detected in the liquid products but the amounts were so small that they have been neglected in calculating the materials balance, which with one exception is over 90, the average being 96.3%.

The apparatus was swept out with nitrogen before and at the conclusion of each run. A blank run with the catalyst tube packed with pyrex wool gave no ethylene, ether, or diethylaniline at 300°C.

TABLE I

Catalyst	G	M	K	L	P	N	J	I	O	R	Q
Gel water, %	9.4	7.0	6.6	6.2	5.2	4.5	3.8	3.5	1.8	0.5	0.0
% EtOH–$PhNEt_2$	13.7	15.0	17.3	15.0	25.0	16.6	22.8	22.1	17.2	22.1	22.9
% PhNHEt–$PhNEt_2$	14.9	15.7	18.1	15.7	26.1	17.3	23.8	23.0	18.0	23.1	23.9
% EtOH–C_2H_4	12.9	13.6	31.0	13.9	26.9	13.3	17.4	29.7	14.6	19.0	27.9
Total EtOH reacted	26.6	28.6	48.3	28.9	51.9	29.9	40.2	51.8	31.8	41.1	50.8

DISCUSSION OF RESULTS

The results of the experiments are summarized in Table I. In Fig. 1 is given a plot of the activity of the catalysts in the production of diethylaniline for gels differing in residual water. Included for comparison are curves from previous work on the decomposition of formic acid to carbon monoxide and water, using gels prepared from aluminum nitrate and chloride (9, Fig. 3). The points marked × on the second curve are per cent ethanol giving ether at

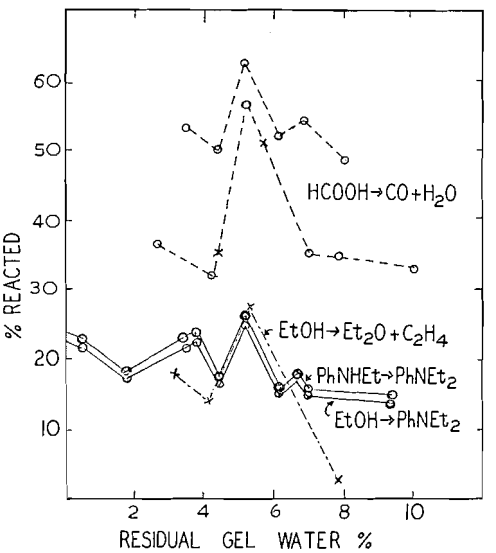

FIG. 1. The activity of catalysts differing in gel water.

250°C. (10). The bottom broken curve is for the production of both ether and ethylene at 318° (1).

It is apparent that alumina catalysts show a maximum in activity at 5.2% gel water. For the production of ethylene in the present work there is another maximum occurring between 2 and 4% gel water. This corresponds to the second maximum in the formic acid curve (9) and agrees with the position of the maximum in the ethylene to ether ratio (1, Fig. 1) although the latter differs from the point of maximum production of ethylene in the previous case.

That the activity of a catalyst may change with alteration in crystal lattice has been demonstrated by several workers (4, 8, 13). Taylor (14) and others (2, 6, 11) regard the catalytically active state of alumina as being due to the presence of gamma alumina having a cubic lattice A_0 7.90 (16), and consequently favor a method of preparation which is supposed to lead to the formation of this phase. Brown and Reid (3) however observed wide variations in the activity of their catalysts with slight variation in the method of preparation. Others have found no γ alumina in their most active catalyst (15).

The structural relations of the catalysts used in this work are shown in Figs. 2 and 3. In Fig. 2 X-ray patterns for catalysts M, N, I, and O, containing 7.0, 4.5, 3.5, and 1.8% residual water are obtained by plotting glancing angle as abscissa and intensity of the refracted beam as ordinate. No sharp peaks characteristic of crystalline samples were obtained. This indicates that the degree of crystallinity in all four samples was low, i.e. they were chiefly amorphous. Of these, catalysts M, N, and O exhibited low activity while catalyst I showed high activity. The patterns indicate no structural differences so that change in activity cannot be attributed to this factor.

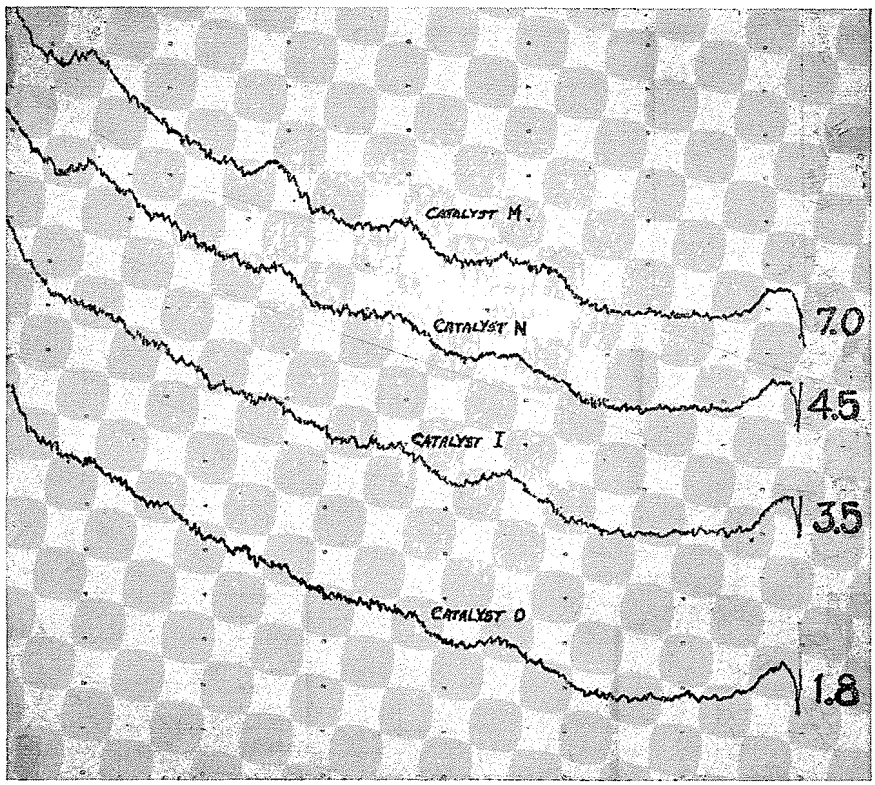

FIG. 2. X-ray diffraction patterns for catalysts containing 7.0, 4.5, 3.5, and 1.8% gel water. Catalyst I (3.5% water) had high activity, the others had low activity.

The X-ray photographs in Fig. 3 are for gels J, L, P, and Q, containing 3.8, 6.2, 5.2, and 0.0% gel water respectively. The first three obviously belong to the same type. The predominating structure appears to be that of Boehmite, with some gamma alumina. Catalysts J and P gave high activity, L much lower. These observations are similar to those made in the earlier work (9).

The catalyst containing zero water has a different structure. This catalyst also differs from that of zero water content used in the work cited above. The latter was prepared by blasting samples at 1200° resulting in conversion to alpha alumina or corundum. Such a catalyst showed a marked decrease in activity. In the present instance the anhydrous gel was obtained by activation in nitrogen at 550° which, according to Gregg and Sing (7), produces active gamma alumina. This is supported by its higher activity than the corundum sample and by the increase in activity over that of the gel containing 1.8% residual water.

Although an alumina catalyst containing 5.2% water had been found to be the best for the production of ether, both when ether alone is produced and when at higher temperatures ethylene and ether are formed, such a catalyst gave practically no ether in the present experiments. The very small amounts

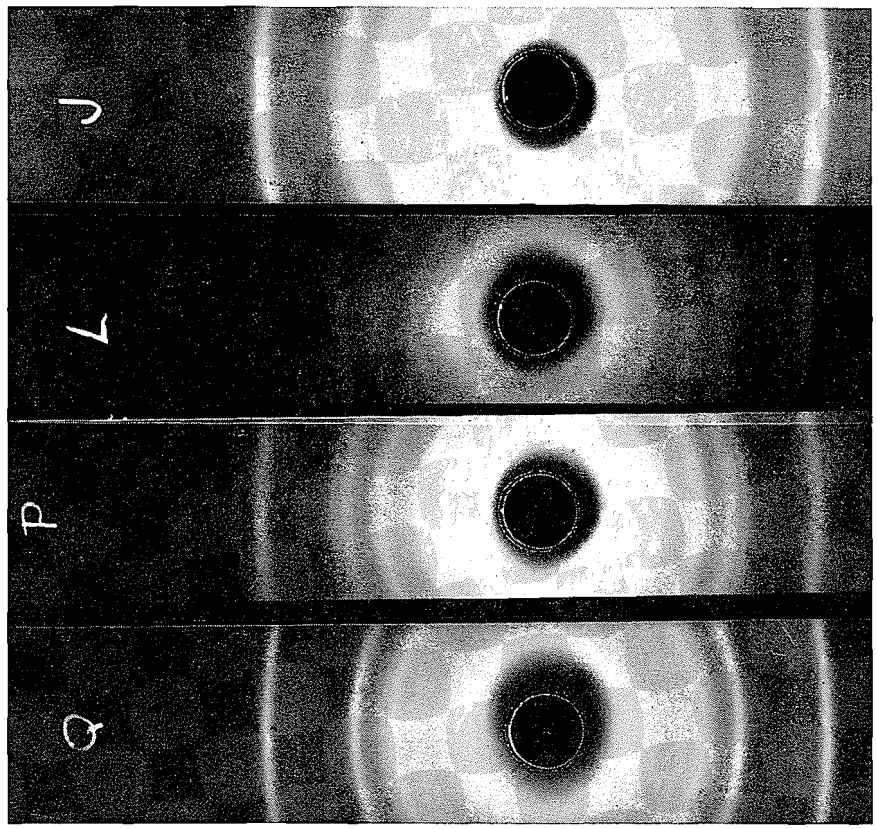

FIG. 3. X-ray photographs of catalysts containing 3.8, 6.2, 5.2, and 0% gel water.

of ether present in the reaction products can be explained if the reaction goes in two stages,

[1] $$2EtOH \rightarrow Et_2O + H_2O,$$

[2] $$Et_2O + PhNHEt \rightarrow PhNEt_2 + EtOH.$$

It was found that as the diethylaniline yield decreased the proportion of ethylene to diethylaniline decreased also. This would suggest that some of the ethylene was produced by decomposition of the reaction product, which might explain why maximum yields of ethylene were not obtained at the previously observed point on the activity – gel water curve.

SUMMARY AND CONCLUSION

From the above it may be concluded that while a change of surface geometry due to alteration of the crystal lattice can affect catalyst activity, the best and poorest surface condition of the catalyst may be established primarily by the extent to which constituent water is removed from the gel.

ACKNOWLEDGMENT

The authors wish to express their indebtedness to Dr. L. G. Berry, Department of Mineralogy, Queen's University, and to the management and staff of Aluminium Laboratories, Ltd., Arvida, for their assistance in obtaining X-ray diffraction patterns of the catalysts.

REFERENCES

1. ALEXANDER, W. H., HORN, W. R., and MUNRO, L. A. Can. J. Research, B, 15: 438. 1937.
2. BENTLEY, F. J. L. and FEACHAM, C. G. J. Soc. Chem. Ind. (London), 64: 148. 1945.
3. BROWN, A. B. and REID, E. E. J. Phys. Chem. 28: 1067. 1924.
4. EISENHAUT, O. and KAUPP, E. Z. Elektrochem. 36: 392. 1930.
5. ENGLISH, F. L. Anal. Chem. 19: 457. 1947.
6. FEACHAM, C. G. and SWALLOW, H. F. S. J. Chem. Soc. 267. 1948.
7. GREGG, S. J. and SING, K. S. W. J. Phys. Chem. 56: 388. 1952.
8. LONG, J. R., FRASER, J. W., and OTT, E. J. Am. Chem. Soc. 56: 1101. 1934.
9. MUNRO, L. A., DEWAR, D. J., GERTSMAN, S., and MONTEITH, G. Can. J. Research, B, 21: 21. 1943.
10. MUNRO, L. A. and HORN, W. R. Can. J. Research, 12: 707. 1935.
11. NAHIN, P. G. and HUFFMANN, H. C. Ind. Eng. Chem. 41: 2021. 1949.
12. SIGGIA, S., HANNA, J. G., and KERVENSKI, I. R. Anal. Chem. 22: 1296. 1950.
13. STORFER, E. Z. Elektrochem. 41: 540. 1935.
14. TAYLOR, R. J. J. Soc. Chem. Ind. (London), 68: 23. 1949.
15. THIBON, H., MAILLARD, H., and SAVON, L. Chimie & industrie, 57: 117. 1946.
16. WYCKOFF, R. W. G. The structure of crystals. Reinhold Publishing Corporation, New York. 1935.

CONDUCTANCES OF AQUEOUS LITHIUM NITRATE SOLUTIONS AT 25.0°C. AND 110.0°C.[1]

By A. N. Campbell, G. H. Debus[2], and E. M. Kartzmark

ABSTRACT

The conductances, densities, and viscosities of aqueous solutions of lithium nitrate have been determined, at temperatures of 25.0° and 110.0°C., at concentrations up to 14 molar. The results have been compared with the conductances calculated by means of the Robinson–Stokes equation and good agreement found up to about 7 molar. A short discussion of the theoretical implications is given.

In pursuance of our work on the conductances of concentrated solutions we have determined those of lithium nitrate solutions at 25° and 110°C. up to a concentration of 14 molar, which represents saturation at 110°C. We have also determined the viscosities and thus we have been able to compare our results with those calculated from the Robinson and Stokes equation (9). The agreement is surprisingly good.

After we had commenced this work, we came upon a paper by Klotschko and Grigorjew (7), in which the authors appeared to have anticipated our work completely, in that they have determined the specific conductances, viscosities, and densities of aqueous lithium nitrate solutions at concentrations varying from 0.22 to 71.64 weight per cent and at temperatures of 25°, 75°, and 100°. In this article and elsewhere (8), the authors prefer the specific to the equivalent conductance as a basis of theoretical interpretation. They also seek to use the equilibrium diagram for the system lithium nitrate – water to interpret their results. For instance, they state (with approximate truth) that the composition at which the maximum specific conductance occurs is that of the eutectic at which ice and lithium nitrate trihydrate coexist. However, on plotting the experimental values of specific conductance obtained by Klotschko and Grigorjew against concentration, and comparing them with our own, we feel that they are too inaccurate to be of great value. For example, the specific conductance of their weakest solution (at 25°) would give a value of the equivalent conductance in excess of the limiting value, calculated as the sum of the ionic conductances.

EXPERIMENTAL

The lithium nitrate used was a Fisher "Certified Reagent". The principal impurity was described as "other alkalis 0.35%". The lithium nitrate was recrystallized from water and small samples ignited in platinum, immediately before weighing. The more dilute solutions were made up by direct weighing, while solutions which were supersaturated at room temperature were analyzed by the conductance of a weighed aliquot. All the details of conductance measurements have been previously described (3). Viscosity measurements

[1]*Manuscript received June 22, 1955.*
Contribution from the Department of Chemistry, University of Manitoba, Winnipeg, Manitoba.
[2]*Holder of an N.R.C. Postdoctorate Fellowship.*

at 25° were made in a viscometer designed by Cannon and Fenske (2), while at 110° the simple apparatus of Fig. 1 was used. This apparatus was sealed after it had been filled, to prevent boiling and evaporation of the liquid; it was calibrated with water. Obviously, the total volume of liquid in the viscometer is not critical, so long as there is sufficient to fill the calibrated bulb. A number of different viscometers were used, having different capillary bores, in order to get a suitable flow time; this was never less than 30 sec. and, since time was measured with a stop-watch to one-fifth second, the accuracy of our viscosity determinations is better than one per cent, as far as this factor is concerned. As previously described (5) our high temperature density measure-

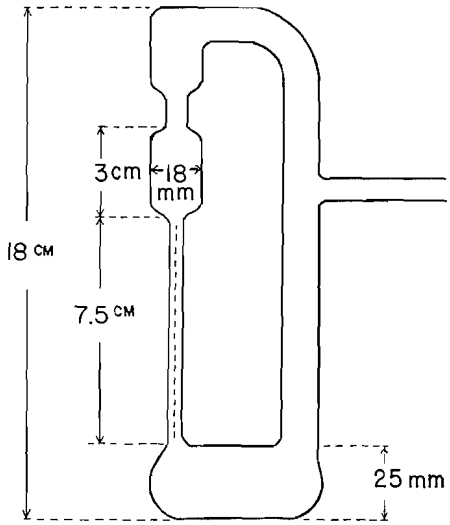

FIG. 1. Viscosity apparatus for high temperatures.

ments, carried out in a closed bomb, are probably not better than one in a thousand but this should not appreciably affect the viscosity. The apparatus (Fig. 1) could be rotated through 180°, while still in the thermostat, by means of a rack and pinion, and was automatically set in the same vertical position. The whole apparatus was placed in a tall thermostat filled with silicone. Temperature (at 110°) was maintained constant (using an Archimedean stirrer) within 0.1° which was sufficient for the purpose of our viscosity measurements. Temperature control for the conductance measurements was much better than this. For details of the high temperature conductance work, the paper by Campbell, Kartzmark, Bednas, and Herron (5) should be consulted.

EXPERIMENTAL RESULTS

The experimental results are contained in Table I, which is self-explanatory.

DISCUSSION OF RESULTS

As usual, the specific conductance is observed to pass through a maximum at about 5.337 molar at 25°, and 5.459 molar at 110°; the composition of the

TABLE I

CONDUCTANCES, DENSITIES, AND VISCOSITIES OF LITHIUM NITRATE SOLUTIONS

Wt. %	Conc., in moles per liter	Density, gm. per ml.	Relative viscosity, water = 1.0	Specific cond. κ, in mhos	Λ_{exp}	$\Lambda\eta$	Λ_{calc} $\mathring{a}$ = 4.5Å	Λ_{calc} $\mathring{a}$ = 5.0Å	Temperature coefficients: Conductance	Temperature coefficients: Viscosity
Temperature = 25°C.										
0.0635	0.00997	0.997	1.005	0.001025	102.79	103.31	102.3	102.5		
0.6878	0.0990	1.001	1.013	0.009083	91.74	92.93	90.88	91.46		
3.739	0.553	1.018	1.063	0.04244	76.86	81.70	75.18	76.82		
6.384	0.958	1.035	1.109	0.06730	70.26	77.89	68.75	70.15		
6.624	0.995	1.036	1.111	0.06942	69.78	77.50	68.33	69.86		
12.13	1.885	1.070	1.221	0.1112	58.95	71.98	58.22	59.44		
17.13	2.740	1.103	1.351	0.1387	50.60	68.35	50.41	52.01		
18.35	2.957	1.111	1.390	0.1448	48.98	68.06	—	—		
21.09	3.456	1.130	1.490	0.1545	44.72	66.65	44.44	45.96		
22.39	3.698	1.139	1.534	0.1583	42.81	65.70	42.78	44.26		
28.32	4.857	1.182	1.826	0.1685	34.68	63.31	34.89	35.86		
30.65	5.337	1.201	1.984	0.1694	31.66	62.81	31.43	32.58		
32.37	5.703	1.215	2.122	0.1685	29.54	62.67	—	—		
37.88	6.916	1.259	1.637	0.1626	23.52	62.06	22.69	23.50		
40.09	7.427	1.277	1.914	0.1578	21.24	61.89	20.31	20.99		
45.46	8.726	1.323	3.849	0.1441	16.51	63.54	14.86	15.40		
46.97	9.124	1.339	4.218	0.1388	15.21	64.15	13.34	13.93		
47.02	9.135	1.340	4.236	0.1387	15.18	64.30	—	—		
50.33	9.986	1.368	5.142	0.1277	12.79	65.76	10.81	11.18		
55.56	11.50	1.427	7.987	0.1067	9.28	74.03	6.67	7.15		
57.66	12.17	1.456	—	0.0972	7.99	—	—	—		
62.36	13.55	1.498	14.88	0.0817	6.03	89.72	3.45	3.56		
Temperature = 110°C.							Λ_0=360 $\mathring{a}$=3.0Å	Λ_0=356 $\mathring{a}$=3.5Å		
0.701	0.0972	0.956	1.010	0.02765	284.56	287.4	285.39	284.53	2.336	2.950
3.499	0.4936	0.973	1.053	0.1114	225.71	237.7	222.55	225.86	2.223	2.953
6.41	0.9177	0.988	1.094	0.1843	200.81	219.7	194.30	199.57	2.166	2.987
12.14	1.802	1.024	1.185	0.2955	164.03	194.4	165.97	166.22	2.045	3.020
17.25	2.634	1.053	1.276	0.3649	138.53	176.8	137.26	144.87	1.971	3.127
20.49	3.198	1.076	1.346	0.3989	124.75	167.9	125.73	133.22	1.960	3.218
26.25	4.252	1.117	1.516	0.4390	103.25	156.5	104.33	111.51	1.958	3.364
32.45	5.459	1.160	1.739	0.4476	82.00	142.6	85.78	92.01	1.961	3.710
40.13	7.109	1.222	2.197	0.4408	62.00	136.2	63.65	68.50	1.974	3.956
45.67	8.411	1.270	2.658	0.4254	50.57	134.4	50.20	54.20	2.187	4.427
49.00	9.237	1.300	3.097	0.4127	44.67	138.3	41.88	45.35	2.351	4.585
55.90	11.06	1.364	4.481	0.3705	33.50	150.1	27.29	29.24	2.687	
60.40	12.31	1.405	5.48	0.3658	29.72	162.8	17.82	23.37	3.31	
67.10	14.36	1.476	7.92	0.3317	23.10	182.9	13.76	15.24	4.22	

maximum changes but little with temperature. The very low value (6.03 mhos) to which the equivalent conductance falls, at 25°, is remarkable. It should be noted that the last four figures at 25° represent supersaturated solutions, which are easy to obtain. Although no particular interest now attaches to the calculation, the values of $\Lambda\eta$ have been worked out and a glance at column 7 of Table I shows that, as usual, the product drops rapidly from 103 at 0.01 molar to 68 at 2.74 molar, after which it drops very slowly to 61.9 at 7.4 molar, and then rises slowly to 89.7 at 13.6 molar (all at 25°). Similar behavior is observed at 110°. If the Robinson–Stokes equation were valid throughout the concentration range, it is easy to see from the form of the equation that the product should decrease continuously. The concentration

at which the product actually starts to increase (about 7 M) is the concentration beyond which the Robinson–Stokes equation is no longer valid.

In order to calculate Λ by means of the Robinson–Stokes equation it is necessary to know Λ_0 and to know (or assume) å, the distance of closest approach. In order to obtain the (theoretical) constants (B, B_1, and B_2) of the Robinson–Stokes equation, it is also necessary to know the dielectric constant and viscosity of water. The dielectric constant of water is now known up to the critical temperature of water (1), while good values for the viscosity of water are available up to 125° (6). Hence, at 25°, the only doubtful parameter is the distance of closest approach of the ions. We have made two sets of calculations, using å = 4.5 Å and å = 5.0 Å. It will be observed that both values give rather good agreement up to 7 M, but å = 4.5 Å is the better value, on the whole. Observed and calculated results are graphed in Figs. 2 and 3. At 110° we had the usual difficulty of not knowing Λ_0. We have assumed

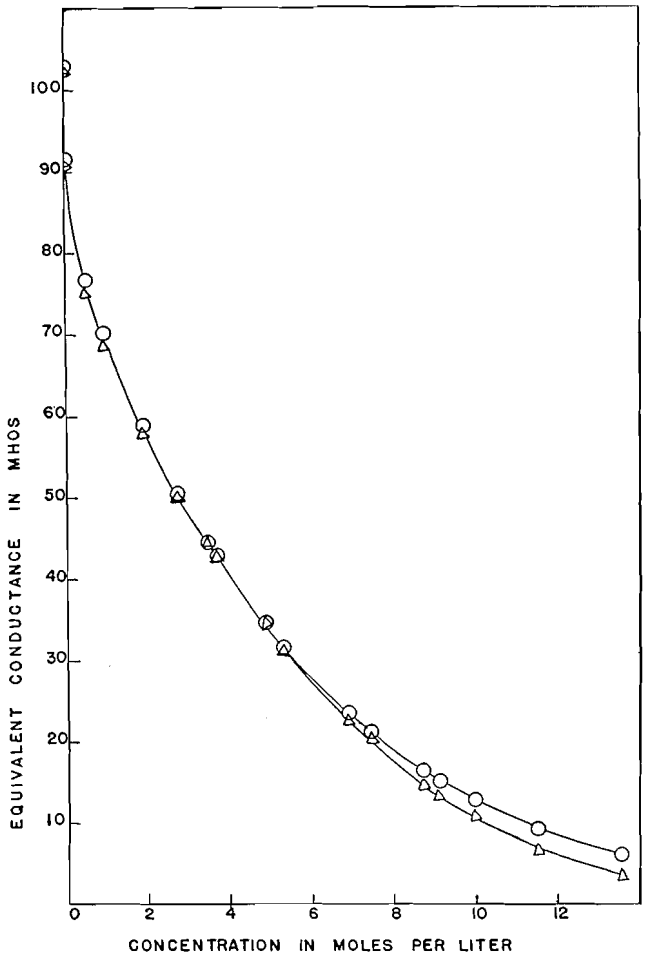

FIG. 2. ○ Experimental at 25°.
△ Calculated Λ_0 = 110.13, å = 4.5.

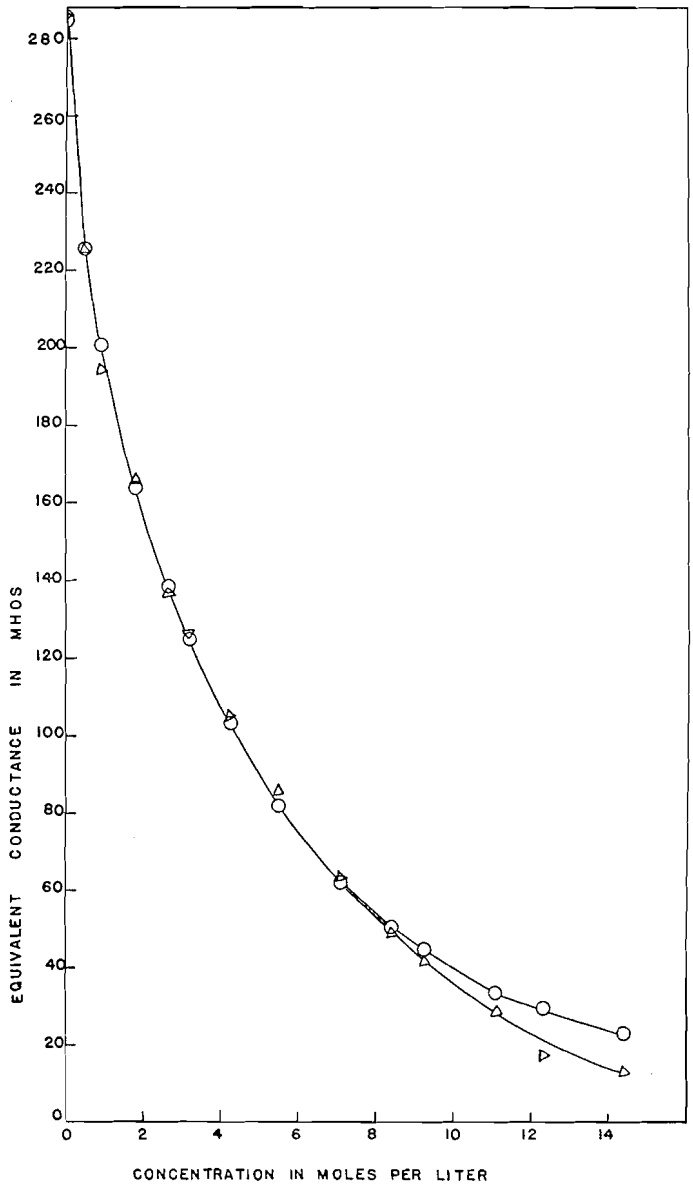

FIG. 3. ○ Experimental at 110°.
△ Calculated $\Lambda_0 = 360$, $\mathring{a} = 3.0$.

a value of $\Lambda_0 = 360$ mhos when using $\mathring{a} = 3.0$ Å, and of $\Lambda_0 = 356$ mhos when using $\mathring{a} = 3.5$ Å. Using the former set of values we obtain reasonably good agreement up to 4.2 *M*. Considering the uncertainty of Λ_0, better results can hardly be expected.

Despite the insistence of Stokes himself that $\mathring{a}$ must not be a temperature function, we have boldly used a much smaller value for $\mathring{a}$ at 110° than that

at 25° and for this we consider there may be justification. It is widely admitted that the lithium ion is highly and strongly hydrated. It seems reasonable to suppose, however, that the coordination number of hydration will decrease at higher temperatures and hence the distance of closest approach become smaller. Alternatively, if the coordination number does not change, or does not change very much, it may be that the attached water molecules may become more mobile at the higher temperature, and that they can then be pushed aside and thus allow the electrical centers of the ions to come closer together.

The agreement between calculated and observed equivalent conductances for lithium nitrate is so good, that it has not been necessary to resort to the hypothesis of ion-pair formation, though such an explanation has been offered to explain the fact that the calculated equivalent conductances are higher than the experimental values for silver nitrate and for ammonium nitrate. On the other hand, the agreement is good for ammonium chloride and potassium chloride (4). It seems reasonable to attribute ion-pair formation to the unsymmetrical form of the nitrate ion and therefore the Robinson–Stokes equation should be tested by further work on chlorides, etc.

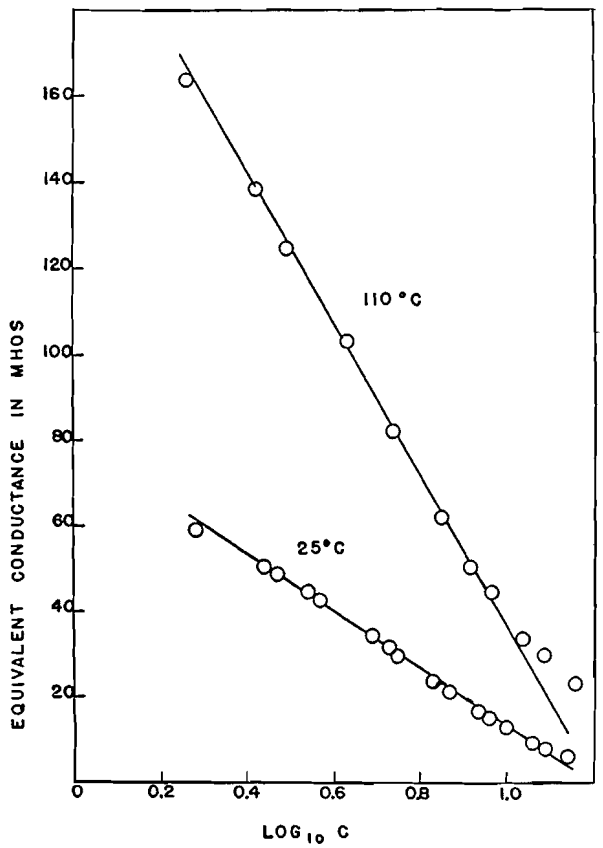

FIG. 4. Λ vs. log C.

We have elsewhere alluded to the fact that if equivalent conductance is plotted against the logarithm of the concentration, a straight line is obtained in the region of high concentration (5). The same effect is observed with lithium nitrate (Fig. 4), the straight line behavior beginning at about the concentration (say 5 to 7 molar) at which the Robinson–Stokes equation begins to break down. In the case of lithium nitrate, however, the straight line relation also breaks down at the very highest concentrations, where the lithium ion must be losing its water of hydration. If a coordination number of four is assigned to the lithium ion (Stokes believes it to be much higher than this) there must, at high concentrations, be insufficient water present to hydrate the ion. The lithium nitrate concentration corresponding to $Li^+.4H_2O$ is 49%; we have proceeded to a lithium nitrate concentration of 67% (by weight), which corresponds to less than $2H_2O$.

Finally, in the last two columns of the table of numerical results (Table I) the temperature coefficients of conductance and of viscosity have been obtained, assuming that both are straight line functions of temperature (they are not) between 25° and 110°. As usual, they are not equal and they behave in a somewhat erratic manner. The very high values of the temperature coefficient of viscosity in the region of high concentration (as high as 4.585 per degree) are, however, significant. These high values are in harmony with our belief that the lithium ion loses water of hydration at the higher temperature. This may also be true of the silver and ammonium ions but we see no reason to believe that these ions have any chemical or firmly bound water molecules. No doubt, all ions bind large numbers of water molecules in a more or less loose fashion, analogous to adsorption, but water of this kind will scarcely affect the distance of closest approach, or the viscosity, very much.

REFERENCES

1. Akerlof, G. C. and Oshry, H. I. J. Am. Chem. Soc. 72: 2844. 1950.
2. Cannon, M. J. and Fenske, M. R. Ind. Eng. Chem. Anal. Ed. 10: 299. 1938.
3. Campbell, A. N. and Kartzmark, E. M. Can. J. Research, B, 28: 43, 161. 1950; Can. J. Chem. 30: 128. 1952. Campbell, A. N., Kartzmark, E. M., Bissett, D., and Bednas, M. E. Can. J. Chem. 31: 303. 1953. Campbell, A. N., Gray, A. R., and Kartzmark, E. M. Can. J. Chem. 31: 617. 1953. Campbell, A. N., Kartzmark, E. M., Bednas, M. E., and Herron, J. T. Can. J. Chem. 32: 1051. 1954.
4. Campbell, A. N. and Kartzmark, E. M. Can. J. Chem. 33: 887. 1955.
5. Campbell, A. N., Kartzmark, E. M., Bednas, M. E., and Herron, J. T. Can. J. Chem. 32: 1051. 1954.
6. Hardy, R. C. and Cottington, E. M. Natl. Bureau Standards (U.S.), Research Paper RPL 1994. J. Research Natl. Bur. Standards, 42: 573. 1949.
7. Klotschko, M. A. and Grigorjew, I. G. Akad. Wiss. (U.S.S.R.), Nachr. Abt. physik.-chem. Analyse, 21: 303. 1950.
8. Klotschko, M. A. and Grigorjew, I. G. Akad. Wiss. (U.S.S.R.), Nachr. Abt. physik.-chem. Analyse, 21: 288. 1950. A German translation of these papers can be obtained from the Library of the National Research Council, Ottawa, Canada.
9. Robinson, R. A. and Stokes, R. H. J. Am. Chem. Soc. 76: 1991. 1954. Wishaw, B. F. and Stokes, R. H. J. Am. Chem. Soc. 76: 2065. 1954.

STEROIDS AND RELATED PRODUCTS. III. THE SYNTHESIS OF 17β-METHYL-17-ISODESOXYCORTICOSTERONE[1,2]

By Ch. R. Engel[3] and G. Just[4]

ABSTRACT

The synthesis of 17β-methyl-17-isodesoxycorticosterone, an epimer of the biologically active hormone homologue 17α-methyldesoxycorticosterone, is described.

In the first communication of this series (5) and in a second paper (7) syntheses of 17α-methyldesoxycorticosterone (IV), a biologically active homologue of the adrenal cortical hormone desoxycorticosterone (I), were reported. The present communication deals with the synthesis of 17β-methyl-17-isodesoxycorticosterone (XII), a new homologue of the "unnatural" 17-isodesoxycorticosterone (14).

The synthesis proceeded from methyl Δ^4-3-keto-17β-methyl-17-isoetienate (VI); this substance has previously been obtained (5) together with its 17 epimer V by a rearrangement of the Aston–Greenburg or Faworsky type (2, 6) of 21-chloroprogesterone (II*b*) or of a mixture of this compound with 21-tosyloxyprogesterone (II*a*), as well as by Oppenauer oxidation of methyl Δ^5-3β-hydroxy-17β-methyl-17-isoetienate (III), an intermediate in the synthesis of 17-β-methyl-17-isoprogesterone (8). The transformation of the not easily saponifiable keto ester VI to the keto acid VIII was carried out similarly to the experiments in the natural series (5). The alkaline sensitive α,β-unsaturated ketone was protected by the formation of the enol ethyl ether IX, the latter was heated at high temperatures in a sealed tube with methanolic potassium hydroxide, and, after acidification of the reaction product, the free acid VIII isolated in good yield.

We decided to transform the acid VIII to the diazoketone X through the acid chloride VII, to convert the diazoketone X to the chloroketone XI, and to substitute the highly inert chlorine atom of the latter by an acetoxy grouping (XII*a*), using the method described previously (5, 7). As reported earlier, the direct hydrolysis of the 17 epimer of the diazoketone X to the epimer of the ketol XII had been possible under well-defined conditions, but the ketol obtained was accompanied by appreciable amounts of the corresponding chloroketone (5).

In the series of experiments described in this paper the acid chloride VII was at first prepared from the sodium salt VIII*a* by the action of oxalyl chloride in the presence of pyridine, according to a method originated by Adams and Ulich (1) and developed in the field of steroid chemistry by Wilds and

[1]*Manuscript received May 9, 1955.*

Contribution from the Collip Medical Research Laboratory and the Department of Chemistry, the University of Western Ontario, London, Ontario, Canada. Abstracted from part of the Ph.D. thesis of G. Just, to be presented to the Faculty of Graduate Studies of the University of Western Ontario. The subject of this publication was part of a communication presented before the annual meeting of the Chemical Institute of Canada, Toronto, June, 1954.

[2]*For Paper II of this series see Reference 4.*

[3]*Holder of a Medical Fellowship of the Canadian Life Insurance Officers Association.*

[4]*Holder of an Ontario Research Council Special Fellowship 1953–54 and of a National Research Council Studentship 1954–55.*

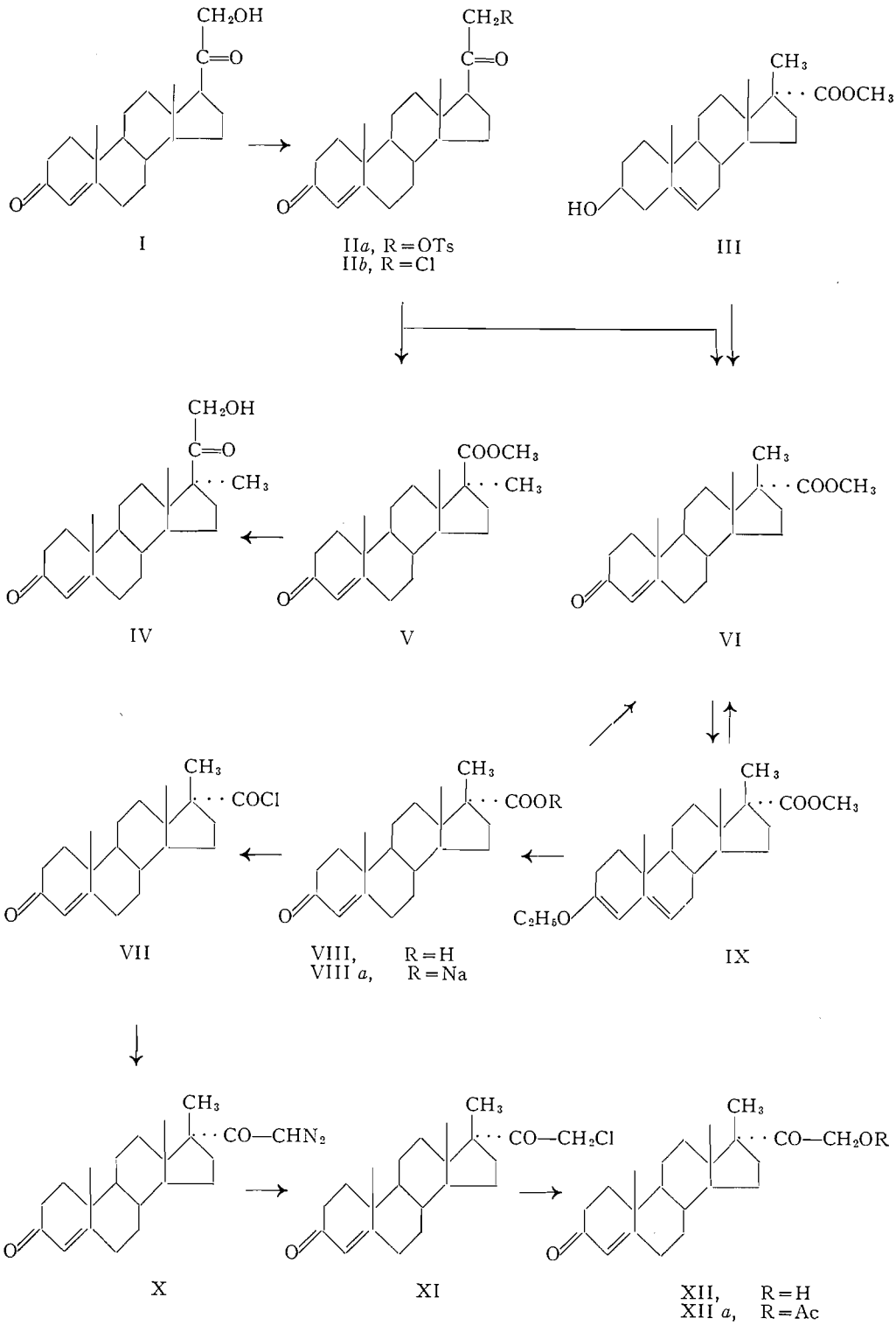

Shunk (16, 17). The crude acid chloride prepared by this procedure was subjected to the action of diazomethane, under the experimental conditions employed in the 17 α-methyl series (5), and the resulting crude diazoketone X was treated with an excess of hydrogen chloride in ether–benzene (compare 7, 12, 15). The desired chloroketone XI was thus obtained but the yields in this series of reactions were unsatisfactory. Reichstein and co-workers (13) have lately experienced similar difficulties in obtaining in good yield Δ^4-3-keto-21-diazopregnene from Δ^4-3-ketoetienic acid, using Wild's experimental conditions (16, 17) for the preparation of the intermediate acid chloride. However, the Swiss authors obtained satisfactory results when subjecting the free acid to the action of oxalyl chloride without addition of pyridine, a procedure which had also been developed as a general method by Adams and Ulich (1). In a second series of experiments we therefore applied Reichstein's experimental conditions (10, 13); the crude acid thus obtained was then transformed to the chloroketone XI, as mentioned above. The yields in this series of reactions showed a marked increase over those obtained when using the acid chloride prepared from the sodium salt VIII*a*. The very inert chlorine atom of the chloroketone XI was replaced by an acetoxy grouping by the action of silver acetate in acetic anhydride – pyridine (compare 5, 7). The resulting 17β-methyl-17-isodesoxycorticosterone acetate (XII*a*) was hydrolyzed to the free 17β-methyl-17-isodesoxycorticosterone (XII) by the prolonged action of potassium bicarbonate in methanol–water at room temperature and in a nitrogen atmosphere. Acetic anhydride in pyridine reacetylated the free ketol XII to the acetate XII*a*.

Similar to the findings in the 17β-methyl-17-isoprogesterone series (8) and in the 17-isoprogesterone (3) and 17-isodesoxycorticosterone series (14), all the here-described 17β-methyl-17-isosteroids are more levorotatory than their stereoisomers with the "natural" configuration in position 17.

Using a modification of the bioassay described by Marcus *et al.* (11), 17β-methyl-17-isodesoxycorticosterone acetate was found to produce no sodium retention in adrenalectomized fasting rats, at dose levels up to 300 μgm. Desoxycorticosterone acetate showed marked activity in the same test at 6.25 μgm.[5] This lack of biological activity affecting the electrolyte metabolism is in contrast to the life maintaining action of 17α-methyldesoxycorticosterone acetate (7), and shows close analogy to the inactivity of 17-isodesoxycorticosterone acetate in the life maintenace test (14) and to the lack of progestational activity of 17β-methyl-17-isoprogesterone (8) and of 17-isoprogesterone (3).

EXPERIMENTAL[6,7,8]

Methyl $\Delta^{3,5}$-3-Ethoxy-17β-methyl-17-isoetiadienate (IX)

Following the procedure previously described by Julian and co-workers (9)

[5]*The biological tests were kindly carried out by Professor J. A. F. Stevenson, Department of Physiology, University of Western Ontario. Details of these experiments will be published elsewhere.*

[6]*All melting points were taken in evacuated capillaries and the temperatures corrected.*

[7]*The microanalyses were carried out by Mr. J. F. Alicino, Metuchen, N.J., to whom we wish to express our high appreciation.*

[8]*The aluminum oxide used in the chromatographic absorption was treated as described under footnote 31 of Reference (5). We wish to thank Messrs. Merck and Co., Montreal, for kindly providing us with their aluminum oxide for chromatography.*

and by Engel and Just (5), 1.633 gm. of ester VI, m.p. 152–154°, was transformed to its enol ethyl ether. The crude product afforded upon recrystallization from acetone–methanol, in the presence of a few drops of pyridine, 1.48 gm. of IX, m.p. 105–106°, and a second crop of 155 mgm., m.p. 100–106° (92.6%). A sample was recrystallized three times for analysis; shiny plates, m.p. 109–110°, $[\alpha]_D^{21}$ −132.8° (*c*, 0.982 in $CHCl_3$–pyridine). Anal. Calc. for $C_{24}H_{36}O_3$: C, 77.37; H, 9.74. Found: C, 77.20; H, 9.72.

Hydrolysis.—Following the experimental conditions described previously (5), 53 mgm. of enol ether IX was hydrolyzed with hydrochloric acid in methanol–water. Crystallization of the amorphous reaction product from acetone–hexane afforded 35 mgm. of the ester VI, m.p. 151–152.5° (71%). Further crystallization raised the melting point to 153–154°. The melting point was not depressed upon admixture of authentic ester VI.

The mother liquors from the recrystallizations of ether IX were subjected to a similar hydrolysis. Purification of the crude reaction product by chromatography and crystallization gave 33 mgm. of ester VI, m.p. 147–152°. Thus the total yield of ether IX from keto ester VI was raised to 94.5%.

Δ^4-3-Keto-17β-methyl-17-isoetienic Acid (VIII) from Enol Ether IX

In a sealed tube 1.636 gm. of enol ether IX was heated with 80 cc. of a 7% methanolic potassium hydroxide solution for 48 hr. at 168–170°. After cooling, the reaction mixture was poured into water and acidified with sulphuric acid. The chloroform extraction of the precipitate gave 1.663 gm. of crude acid, m.p. 203–207°, which afforded upon recrystallization from acetone 982 mgm. of long blades, m.p. 217–222° (62.6%). A sample was recrystallized four times for analysis; m.p. 223–225°, $[\alpha]_D^{24}$ 83.3° (*c*, 1.286 in $CHCl_3$). Anal. Calc. for $C_{21}H_{30}O_3$: C, 76.33; H, 9.15. Found: C, 76.60; H, 9.26.

Methylation of acid VIII.—Acid VIII (110 mgm.) was dissolved in absolute ether and methylated with an ethereal solution of diazomethane at 0° for 15 hr. The solvent was removed *in vacuo*. Chromatography of the resulting amorphous product (150 mgm.) on 5 gm. of aluminum oxide and recrystallization of the petroleum ether – benzene fractions from acetone–hexane yielded 79 mgm. of colorless needles, m.p. 150–152°, which gave no depression of melting point upon admixture of authentic ester VI.

Similar methylation of the mother liquors from the recrystallizations of acid VIII (545 mgm.) afforded 262 mgm. of ester VI, m.p. 144–152°. Considering this recovery of starting material, the yield of the saponification was 74.5%.

21-Chloro-17β-methyl-17-isoprogesterone (XI)

(*a*) *From the sodium salt of Δ^4-3-keto-17β-methyl-17-isoetienic acid (VIIIa).*—According to the procedure described previously (5, 16, 17), 1 gm. of acid VIII was transformed to its sodium salt, which after being dried for 10 hr. at 105° in a high vacuum was suspended in 21 cc. of absolute benzene containing seven drops of pyridine and treated with 10 cc. of oxalyl chloride at −15°; after 25 min. the temperature was raised to 25°, and after a further 15 min. the mixture was worked up in the usual manner. A solution of the product in 25 cc. of absolute benzene was slowly added, with vigorous stirring, to 33 cc.

of a 3.3% ethereal diazomethane solution at −15°. The mixture was kept seven hours at −5° and 90 min. at room temperature, and the excess solvents were removed *in vacuo*. To a suspension of this crude diazoketone in 50 cc. of absolute ether was added, with swirling, a solution of 876 mgm. of hydrogen chloride in 20 cc. of absolute ether. After 45 min., the reaction mixture was poured into water; the ether extraction of the precipitate gave 1.5 gm. of an oil which was chromatographed on 30 gm. of aluminum oxide. Recrystallization of the petroleum ether – benzene (4:1; 1:1; 1:4) and benzene elutions from acetone–hexane afforded 341 mgm. of the chloroketone, m.p. 175–180° (31%). A sample was recrystallized from acetone–hexane five times for analysis; colorless plates, m.p. 182.5°, $[\alpha]_D^{24}$ 43.2° (*c*, 1.02 in $CHCl_3$), λ_{max}^{EtOH} 239 mμ (log ε 4.2). Anal. Calc. for $C_{22}H_{31}O_2Cl$: C, 72.80; H, 8.61, Cl, 9.77. Found: C, 72.97; H, 8.81; Cl, 9.73.

(*b*) *From acid VIII.*—According to Reichstein's modification (10, 13) of Wilds' method (16, 17), 3.3 cc. of oxalyl chloride in 8.2 cc. of absolute benzene was added to a suspension of 660 mgm. of Δ^4-3-keto-17β-methyl-17-isoetienic acid (VIII), m.p. 221–222°, in 25 cc. of benzene at 0°. The acid went into solution after five minutes. The mixture was shaken for 45 min. at frequent intervals at room temperature. The excess solvents were removed *in vacuo* at 15° and the reaction product was dried with absolute benzene at 20°. The solution of the crude acid chloride VII in 18 cc. of absolute benzene was added slowly, with stirring and exclusion of moisture, to 26 cc. of a 1.8% ethereal diazomethane solution at −15°. The mixture was allowed to stand at 0° for 18 hr., then 30 min. at room temperature. The solvents were removed *in vacuo* at 15°. The crude diazoketone X was treated with 402 mgm. of hydrogen chloride in ether–benzene, as described above. The amorphous reaction product (950 mgm.) gave upon chromatography and recrystallizations 16 mgm. of methyl ester VI, m.p. 146–151°; 235 mgm. of 21-chloro-17β-methyl-17-isoprogesterone (XI), m.p. 178–181°; 83 mgm. of XI melting at 173–177° (43.9%); and 60 mgm. crude acid VIII. Methylation of the latter gave after chromatographic purification 40 mgm. of ester VI, m.p. 147–153°. Taking into account this recovery of acid, the yield of the chloride was 47.5%.

17β-Methyl-17-isodesoxycorticosterone Acetate (XIIa) from Chloroketone XI

To a solution of 560 mgm. of the chloroketone XI, m.p. 173–177°, in 7.7 cc. of acetic anhydride was added 1.8 gm. of silver acetate in 6.4 cc. of hot pyridine. The mixture was refluxed for 100 min. at 135–140° bath temperature in a nitrogen atmosphere. The usual working up gave 600 mgm. of a dark brown oil which was dissolved in 8 cc. of benzene and chromatographed on 20 gm. of aluminum oxide. Petroleum ether – benzene (1:4), benzene, and benzene–ether (95:5; 4:1) eluted 115 mgm. of fine needles, m.p. 140–154° (19.2%). A sample was recrystallized three times for analysis; m.p. 154.5–155.5°, $[\alpha]_D^{26}$ 33.2° (*c*, 1.11 in $CHCl_3$), λ_{max}^{EtOH} 241 mμ (log ε 4.24). Anal. Calc. for $C_{24}H_{34}O_4$: C, 74.57; H, 8.87. Found: C, 74.62; H, 8.68.

17β-Methyl-17-isodesoxycorticosterone (XII)

To a solution of 83 mgm. of the acetate XII*a*, m.p. 150–153°, in 7.6 cc. of methanol was added 83 mgm. of potassium bicarbonate in 1.4 cc. of water.

The mixture was kept at room temperature in an atmosphere of nitrogen for four and one-half days. The usual working up afforded 72 mgm. (97.3%) of needles, m.p. 134–136°, giving a depression of the melting point upon admixture of the acetate XII*a*. The product was recrystallized three times for analysis; m.p. 137.5–138°, $[\alpha]_D^{22}$ 60.5° (*c*, 0.82 in $CHCl_3$), λ_{max}^{EtOH} 241 mμ (log ε 4.23). Anal. Calc. for $C_{22}H_{32}O_3$: C, 76.70; H, 9.36. Found: C, 76.65; H, 9.23.

Acetylation.—Isodesoxycorticosterone XII (66 mgm.) was acetylated with 1 cc. of acetic anhydride in 2 cc. of pyridine and worked up in the usual way. The resulting product (79 mgm.) crystallized upon trituration with ether–hexane, m.p. 131–145°. The product was chromatographed on 3 gm. of aluminum oxide. Recrystallization of the petroleum ether – benzene (1:4), benzene, and benzene–ether (4:1) elutions from ether–hexane afforded 25 mgm. of the acetate XII*a*, m.p. 151–153°, and 20 mgm. melting at 145–148°. Admixture of authentic acetate XII*a* gave no depression of the melting point.

ACKNOWLEDGMENTS

We wish to express sincere thanks to Professor James A. F. Stevenson for the biological tests reported in this paper. We are very grateful to Dean J. B. Collip for his interest and encouragement during this study. We should also like to thank Professor J. A. Gunton for extending the facilities of his Department to this work.

REFERENCES

1. Adams, R. and Ulich, L. H. J. Am. Chem. Soc. 42: 599. 1920.
2. Aston, J. G. and Greenburg, R. B. J. Am. Chem. Soc. 62: 2590. 1940.
3. Butenandt, A., Schmidt-Thomé, J., and Paul, H. Ber. deut. chem. Ges. 72: 1112. 1939.
4. Engel, Ch. R. J. Am. Chem. Soc. 77: 1064. 1955.
5. Engel, Ch. R. and Just, G. J. Am. Chem. Soc. 76: 4909. 1954.
6. Faworsky, A. J. prakt. Chem. [2] 88: 658. 1913.
7. Heusser, H., Beriger, E., and Engel, Ch. R. Helv. Chim. Acta, 37: 2166. 1954.
8. Heusser, H., Engel, Ch. R., and Plattner, Pl. A. Helv. Chim. Acta, 33: 2237. 1950.
9. Julian, P. L., Meyer, E. W., Karpel, W. J., and Cole, W. J. Am. Chem. Soc. 73: 1982. 1951.
10. Lardon, A. and Reichstein, T. Helv. Chim. Acta, 37: 388,443. 1954.
11. Marcus, F., Romanoff, L. P., and Pincus, G. Endocrinology, 50: 286. 1952.
12. Plattner, Pl. A., Heusser, H., and Herzig, P. T. Helv. Chim. Acta, 32: 270. 1949.
13. Reber, F., Lardon, A., and Reichstein, T. Helv. Chim. Acta, 37: 45. 1954.
14. Shoppee, C. W. Helv. Chim. Acta, 23: 925. 1940.
15. Steiger, M. and Reichstein, T. Helv. Chim. Acta, 20: 1164. 1937.
16. Wilds, A. L. U.S. Patent No. 2,538,611. 1951.
17. Wilds, A. L. and Shunk, C. H. J. Am. Chem. Soc. 70: 2427. 1948.

CARBOHYDRATES OF SUNFLOWER HEADS[1]

By C. T. Bishop

ABSTRACT

Extractive-free, ash-free sunflower seed heads contained lignin (12.3%), pectin (27.5%), alkali-soluble polysaccharides (8.2%), and α-cellulose (52.0%). Pectin and polysaccharides were separated by successive extraction of the seed heads with ammonium oxalate – oxalic acid solution and 5% aqueous sodium hydroxide. The pectin was 37% esterified with methyl groups and yielded only galacturonic acid when hydrolyzed. The polysaccharides yielded, on hydrolysis, a mixture of neutral sugars and an aldobiouronic acid. The neutral sugars consisted of D-xylose (59.3%), D-glucose (23.5%), D-galactose (16.2%), and traces of arabinose and rhamnose. Fractionation of the polysaccharide acetate indicated that the three main sugars were constituents of three different polysaccharides. The aldobiouronic acid (1.53% of the polysaccharides) was shown to be 3-*O*-α-(D-glucopyruronosyl)-D-xylopyranose.

INTRODUCTION

Sunflowers are grown commercially in Southern Manitoba for the edible oils obtained from the seeds. The sunflower heads are not recovered after harvesting the seeds but are plowed back into the the ground and represent an agricultural waste of considerable importance. In 1948 Stoikoff (12) reported that sunflower seed heads gave good yields of pectin and suggested that they might become a commercial source for this product. Shewfelt (11) evaluated this possibility by studying the effect of isolation procedures on gelling properties of sunflower pectin. Highest yields of good-gelling preparations were obtained by extracting the sunflower seed heads with a hot dilute solution of ammonium oxalate – oxalic acid.

Pectin and polysaccharides are closely associated in plants and it has not been shown whether this association is chemical or physical (9). It has been difficult to isolate either of the two materials without concurrent degradation of the other. Polysaccharides are usually extracted by alkaline solutions which decompose pectin, and pectin is extracted by acidic solution which may hydrolyze the more labile polysaccharides (8).

This report deals with the effectiveness of the ammonium oxalate – oxalic acid extraction, developed by Shewfelt (11), for separating pectin from polysaccharides, and with the chemical composition and properties of these two products from sunflower seed heads.

Extraction Procedure

Diagram 1 shows the fractionation procedure used to separate the carbohydrate components of sunflower seed heads. Chromatography of Fraction 1 (mother liquors from precipitation of pectin) before and after hydrolysis showed the fraction to be free of sugars and proved that no degradation of the polysaccharides occurred during removal of the pectin. In a similar way, a hydrolyzate of Fraction 2 (pectin) was found to contain no sugars other than

[1]*Manuscript received June 28, 1955.*
Contribution from the Division of Applied Biology, National Research Laboratories, Ottawa, Canada. Issued as N.R.C. No. 3712.

DIAGRAM 1

FRACTIONATION OF SUNFLOWER SEED HEADS*

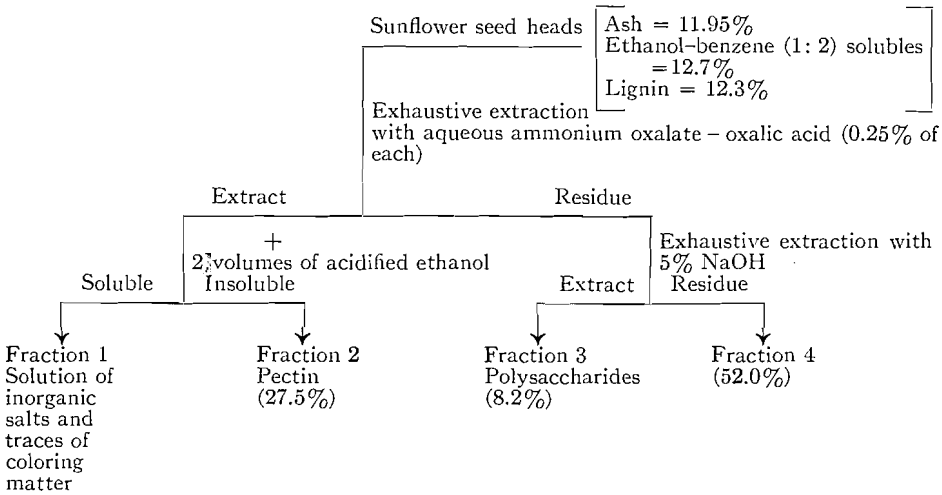

**Lignin analysis and yields of fractions are on an ash-free, extractive-free basis.*

galacturonic acid, and therefore no polysaccharides were coextracted with the pectin. Complete removal of pectin by extraction with the ammonium oxalate – oxalic acid solution was confirmed by the absence of galacturonic acid in hydrolyzates of Fractions 3 (polysaccharides) and 4 (largely cellulose). These results showed that the pectin and polysaccharides of sunflower seed heads could be completely separated by first removing the pectin with a dilute solution of ammonium oxalate – oxalic acid. This procedure may prove useful in investigating carbohydrates of other plant materials when pectin interferes with the purification of polysaccharides.

Pectin

Sunflower pectin yielded only galacturonic acid on hydrolysis and was therefore devoid of contaminating polysaccharides. Ninety-seven per cent of the product was soluble in water, forming a clear 0.5% solution and having a specific rotation (+249°) in good agreement with that reported (+250°) by Luckett and Smith (10) for a highly purified sample of citrus pectin. Sunflower pectin, as isolated, contained 6% of methyl ester groups and was therefore only 37% esterified, fully esterified pectin requiring 16% of methyl ester groups. The pectin was fully esterified by diazomethane and then saponified, the difference in methoxyl contents corresponding to a uronic acid content of 95.6%. Oxidation of the pectin with nitric acid gave a 60% yield of mucic acid. Sunflower pectin was resistant to all attempts at methylation with (*a*) dimethyl sulphate and alkali, (*b*) diazomethane, (*c*) methyl iodide and silver oxide, and (*d*) thallous hydroxide and methyl iodide; hence no detailed structure could be determined. However, the properties and reactions described above were the same as those reported (8) for pectin from many other sources

and there seems little doubt that sunflower pectin has the same basic structure, i.e. D-galacturonic acid units joined by α, $1 \rightarrow 4$ glycosidic bonds.

Polysaccharides

Acid hydrolysis of the polysaccharides yielded an aldobiouronic acid (1.53%) and five neutral sugars: D-xylose (59.3%), D-glucose (23.5%), D-galactose (16.2%), arabinose (trace), and rhamnose (trace). The neutral sugars crystallized and were identified by melting points and rotations except for arabinose and rhamnose which were present in such small amounts that they could only be identified chromatographically.

Attempts were made to fractionate the polysaccharides to obtain a chemically homogeneous portion for structural studies. The polysaccharides gave a soluble and insoluble fraction with Fehling's solution, both containing all five monosaccharides in the same proportions.

The polysaccharide preparation was acetylated and fractionated by precipitation from chloroform solution with petroleum ether. Table I represents a

TABLE I

FRACTIONATION OF THE ACETATES OF POLYSACCHARIDES FROM SUNFLOWER HEADS

Fraction	Volume (ml.) of pet. ether per 400 ml. chloroform	Yield (gm.)	Rotation $[\alpha]_D^{25}$ (c = 1% in $CHCl_3$)	Constituent sugars*			
				Xylose	Glucose	Galactose	Arabinose
1	160	1.65	−47.6	85	10	5	Trace
2	250	1.71	−32.6				
3	365	2.71	+37.3	70	20	10	Trace
4	440	0.70	+93.8				
5	640	2.84	+123.0	25	40	35	Nil

**No rhamnose could be found in any of the fractions. It may have been spread throughout all fractions in quantities too small for detection.*

fractionation of 10 gm. of this material. The differences in specific rotation indicated a mixture of chemically different polysaccharides and the change in a dextrorotatory direction corresponded with an increase in hexosan material and a decrease in pentosans. Naturally occurring xylans have high negative rotations, in the order of −90° to −110° after purification, and usually contain some arabinose units (13). It was probable, then, that the first two acetate fractions consisted of an arabo-xylan contaminated by some hexosan material. The results also showed that there was no constant ratio between any of the component monosaccharides, good evidence that the three main sugars were present in different polysaccharides: a levorotatory arabo-xylan, and a dextrorotatory glucosan and galactan. This is similar to results found by Gilles, Meredith, and Smith (7) who isolated three polysaccharides from barley gum: a levorotatory arabo-xylan and two polyglucosans, one dextrorotatory and the other levorotatory. However, the three polysaccharides of sunflower heads could not be completely separated either by repeating or by extending the fractionation, i.e. by further fractionation of each fraction. The difficulty in

separation was probably caused by similarities in molecular size of the components. Because of the dubiousness of interpreting results of methylation studies on a mixture of polysaccharides no further structural investigations were carried out.

Aldobiouronic Acid

The aldobiouronic acid (I), isolated from the hydrolyzate of the polysaccharides by ion exchange resins, had an acid equivalent of 318 (calculated 326) and yielded glucuronic acid and xylose when hydrolyzed. Its dextrorotatory specific rotation (+59.7°) indicated that the glycosidic linkage was in the α-configuration. This compound was methylated (II), reduced (III), and hydrolyzed to yield the partially methylated glucose (IV) and xylose (V) derivatives. The glucose fragment was identified as 2,3,4-tri-*O*-methyl-D-

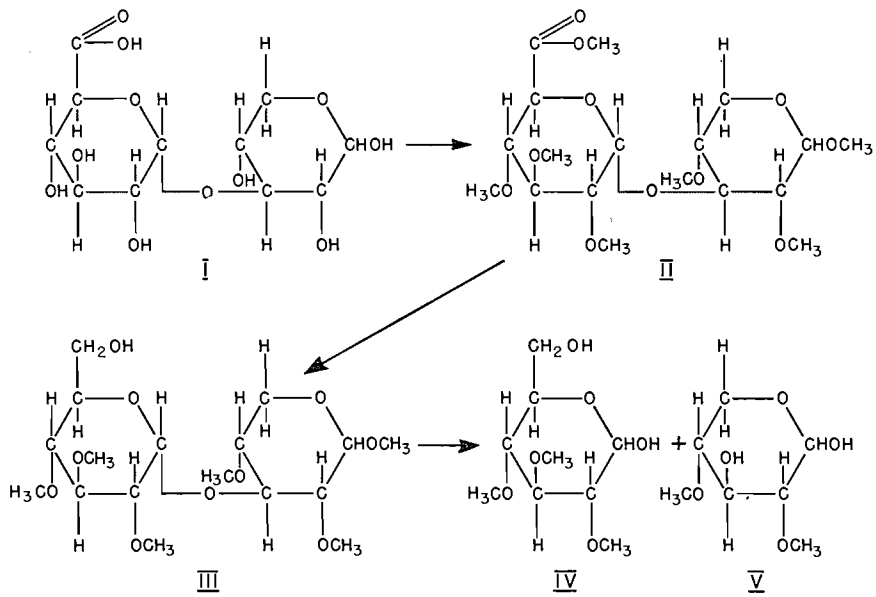

glucopyranose (IV) by oxidation and esterification to the crystalline methyl ester of 2,3,4-tri-*O*-methyl-D-glucosaccharolactone. The xylose portion of the molecule was shown to be 2,4-di-*O*-methyl-D-xylopyranose (V) by conversion to the crystalline amide of 2,4-di-*O*-methyl-D-xylonic acid. These results proved that the aldobiouronic acid was 3-*O*-α-(D-glucopyruronosyl)-D-xylopyranose. This compound has also been isolated from xylans of pear cell wall (5) and wheat straw (1, 2).

EXPERIMENTAL

Chromatograms were run by the descending method using: (*A*) ethyl acetate – pyridine – water, 2:1:2; (*B*) ethyl acetate – acetic acid – water, 9:2:2; (*C*) butanol – acetic acid – water, 4:1:5; and (*D*) butanol – ethanol – water, 5:1:4. Sugars were detected on chromatograms by aniline oxalate or silver nitrate sprays. Evaporations were carried out under reduced pressure

at 40°C. or less. All melting points are corrected and rotations are equilibrium values.

Isolation of Pectin and Polysaccharides from Sunflower Heads

Sunflower seed heads (ash, 11.95%) were extracted exhaustively in a Soxhlet with ethanol–benzene, 1:2 (v/v). This procedure removed 12.7% as waxes and pigments. All analyses and yields that follow were calculated on an ash-free, extractive-free basis. Extractive-free sunflower heads (Klason-lignin, 12.3%) were stirred in an aqueous solution of ammonium oxalate – oxalic acid (0.25% of each) at 75°C. for one and one-half hours. A solid: liquid ratio of 1:22 was used. The extracts were removed by filtration through a linen cloth, and addition of two volumes of ethanol, acidified with 5 ml. of concentrated hydrochloric acid per liter, caused the formation of a gelatinous precipitate of pectin. The extraction procedure was repeated until no more ethanol-insoluble material was obtained, three extractions being required. The pH of the extracts varied from 3.6 to 4.0. The precipitated pectin (Fraction 2, Diagram 1) was filtered, with suction, on Whatman No. 1 paper, washed several times with ethanol and then with ether, and dried at 0.1 mm. over paraffin and phosphoric anhydride (yield, 27.5%). The alcoholic mother liquors (4 liters, Fraction 1, Diagram 1) from the pectin precipitation were evaporated to 250 ml. and examined by paper chromatography (solvent *A*). No sugars were detected. The solution was then made 2 *N* with respect to hydrochloric acid and was heated on a boiling water bath for six hours. The hydrolyzate was neutralized with Dowex-2 (carbonate form) and examined by chromatography as before. No sugars were found.

The pectin-free residue was stirred at room temperature in 5% aqueous sodium hydroxide using a solid: liquid ratio of 1:20. After 24 hr. the extract was removed by suction filtration through linen cloth and the residue was extracted three more times in the same way. The combined extracts were neutralized with acetic acid and dialyzed in cellophane against distilled water for 36 hr. The solution of non-dialyzable material was evaporated to one-quarter its volume and diluted with three volumes of 95% ethanol to precipitate the polysaccharides. The precipitate was removed by centrifuging, washed several times with ether, and finally dried at 0.1 mm. over paraffin and phosphoric anhydride (yield 8.2%, Fraction 3, Diagram 1).

The residue from the alkali extraction of the polysaccharides was washed successively with 10% aqueous acetic acid, water, and acetone before drying *in vacuo* over phosphoric anhydride (yield 52.0%, Fraction 4, Diagram 1). This fraction was not examined further but probably consisted largely of cellulose.

Pectin

Ninety-seven per cent of sunflower pectin was soluble in water, forming a clear solution having $[\alpha]_D^{25} = +249°$ ($c = 0.49$). The pectin as isolated had a methoxyl content of 6.0% which was completely removed by saponification with alkali showing that the methoxyl groups were present as methyl esters. Since the calculated methoxyl content for fully esterified pectin ($C_6H_7O_5$.-

$OCH_3)_n$ is 16.3%, sunflower pectin was only 36.8% esterified. A sample (1 gm.) of pectin was allowed to stand at 5°C. for seven days in an ethereal solution of diazomethane. The diazomethane solution was replaced from time to time as the yellow color faded. Evaporation of the ether left fully esterified sunflower pectin as a white powder (1.07 gm., MeO = 19.5%). This fully esterified, partially etherified pectin was shaken with *N* alcoholic sodium hydroxide for 24 hr. to saponify the ester groups. The de-esterified pectin was recovered by centrifuging and after being washed with ethanol, ether, and petroleum ether, it was dried *in vacuo*. This product (0.98 gm.) was a white powder having a methoxyl content of 3.9%. The saponification therefore reduced the methoxyl content by 15.6% corresponding to a uronic acid content of 95.6%. Pectin (1 gm.) was heated on a steam bath with nitric acid (10 ml., sp. gr. 1.2) until the volume was reduced by about two-thirds, and the solution was kept at room temperature for 10 hr. Crystals of mucic acid (0.65 gm.) were filtered and recrystallized from alkaline solution by acidification with hydrochloric acid. The crystals had a melting point and mixed melting point with mucic acid of 212–213°C. A sample (50 mgm.) of sunflower pectin was heated in a sealed tube at 110°C. for 17 hr. with 2.5% sulphuric acid (10 ml.). The hydrolyzate was neutralized with barium carbonate and the neutral solution freed of barium by Amberlite IR-120. When this solution was examined by chromatography, using glucuronic acid, galacturonic acid, xylose, arabinose, and glucose as reference sugars, only galacturonic acid could be found with solvents *A*, *B*, and *C*.

Pectin (40 gm.) was methylated 10 times with dimethyl sulphate and potassium hydroxide to a constant methoxyl content of 11.9% (calculated for $C_8H_{11}O_6K$, MeO = 25.6%). This product (8.4 gm.) was then converted to the thallium complex, which was methylated with methyl iodide. This procedure gave a product (2.1 gm., MeO = 34.5%) which was methylated twice more with Purdie's reagents to a constant methoxyl content of 38.5% (calculated for $C_6H_5O_3{\cdot}3OCH_3$, MeO = 42.6%). Fractionation of this material from acetone by precipitation with petroleum ether did not yield any fractions with a higher methoxyl content. When sunflower pectin was allowed to stand under ethereal diazomethane at 5°C. for several weeks, the methoxyl content was raised to 29%. Further methylations of this product with Purdie's reagents, by the thallium – methyl iodide method, and with dimethyl sulphate and alkali gave low yields of products with methoxyl contents no higher than 37%.

Polysaccharides

The polysaccharides (Fraction 3, Diagram 1) of sunflower heads were isolated as a light, tan powder having $[\alpha]_D^{25} = +110°$ (c = 2% in 4% sodium hydroxide). Hydrolysis of a small sample (50 mgm.) by heating with 2% sulphuric acid (3 ml.) at 97° for 10 hr. released xylose, glucose, galactose, glucuronic acid, and traces of arabinose and rhamnose. These sugars were detected by paper chromatography in solvents *A*, *B*, *C*, and *D* using known sugars as reference compounds. The polysaccharides, treated with Fehling's

solution (4), gave an insoluble copper complex, which was separated by filtration. Polysaccharide material isolated from both the precipitate and filtrate, after removal of copper salts by acidification and dialysis, yielded the same sugars on hydrolysis as the original polysaccharide preparation. The polysaccharides (43.6 gm.) were acetylated twice by the formamide – pyridine – acetic anhydride method (3). The acetate (59.3 gm.) was fractionated from chloroform solution by successive precipitation with petroleum ether (60–100°C.). Table I represents the fractionation of 10 gm. of the acetate by this method. Constituent sugars were estimated, after deacetylation of small aliquots (*ca.* 10 mgm.) of each fraction by alcoholic potassium hydroxide, by hydrolysis and quantitative paper chromatography (6). This fractionation was carefully repeated five times on the total acetate mixture and was extended by further fractionation of the individual fractions. The procedure was also carried out in reverse by extracting the acetate mixture with petroleum ether containing increasing amounts of chloroform. No improvement of the separation shown in Table I could be obtained.

Identification of Component Sugars

Deacetylated polysaccharides of sunflower heads (30.27 gm.) were heated on a boiling water bath in 2% sulphuric acid (500 ml.). After 10 hr. an insoluble residue (2.11 gm.) was filtered and the filtrate was heated again to constant rotation, $[\alpha]_D^{25} = +27.6°$. The hydrolyzate was brought to pH 3.0 with saturated barium hydroxide solution to remove a large amount of the sulphuric acid and was clarified by centrifuging. To remove barium, the centrifugate was passed through a column of Amberlite IR-120, which was then washed with water until the eluates gave a negative anthrone test. The eluates were evaporated to 500 ml. and passed through a column of Amberlite IR-4B to remove uronic acids (see below) and last traces of sulphuric acid. Evaporation of this eluate left a mixture of neutral sugars (25.05 gm.) which was shown by quantitative paper chromatography (solvent *A*) to consist of xylose (59%), glucose (23%), and galactose (16%). Arabinose and rhamnose were also present in trace quantities. A portion (1 gm.) of this mixture of sugars was separated by preparative paper chromatography to yield: D-xylose, m.p. 146–147°C., $[\alpha]_D^{25} = +19.5$ ($c = 3.18$ in water); D-glucose, m.p. 143–144.5°C., $[\alpha]_D^{25} = +54.0$ ($c = 1.11$ in water); and D-galactose, m.p. 165–166°C., $[\alpha]_D^{25} = +78.0$ ($c = 0.41$ in water). Since the quantities of arabinose and rhamnose were insufficient for isolation, these two sugars could only be identified as being chromatographically indistinguishable from arabinose and rhamnose in solvents *A*, *B*, *C*, and *D*.

Aldobiouronic Acid

The uronic acids were removed from the column of Amberlite IR-4B by elution with *N* sulphuric acid until an anthrone test was negative. The eluate was neutralized (pH 7.0) with saturated, aqueous barium hydroxide and inorganic barium salts were removed by filtration. The filtrate, evaporated to 200 ml., was passed through a column of Amberlite IR-120 to remove barium from the uronic acids. Evaporation of the eluate and examination by

chromatography revealed some xylose still mixed with the uronic acids. This mixture (1.40 gm.) was separated on a cellulose column, the xylose being eluted first with water-saturated butanol. Butanol – formic acid, 50: 1, then removed traces of glucuronic acid, and this was followed by elution with water, which removed the aldobiouronic acid. Evaporation of the aqueous eluate left the aldobiouronic acid as a thick yellow sirup (429.2 mgm.) having $[\alpha]_D^{25} = +59.7$ ($c = 7.5$ in water) and an acid equivalent, by titration, of 318 (calculated for $C_{11}H_{18}O_{11}$, 326). The aldobiouronic acid (400 mgm.) in water (5 ml.) was added to dimethyl sulphate (5 ml.) and the mixture was stirred vigorously at 0°C. during the dropwise addition of 30% aqueous sodium hydroxide (7.5 ml.) over a period of eight hours. The mixture was then stirred for an additional 18 hr. during which it was allowed to warm to room temperature. The mixture was again cooled to 0°C. followed by the addition of solid sodium hydroxide (4.5 gm. all at once), and dimethyl sulphate (5 ml., drop by drop, during six hours). After another 18 hr. of stirring the mixture was cooled, acidified with 10% sulphuric acid, and extracted continuously with chloroform for three days. The chloroform extract was dried over anhydrous magnesium sulphate and evaporated leaving a thick sirup (130.2 mgm.). This product was methylated three times with Purdie's reagents after which no hydroxyl groups were detectable by infrared analysis. This fully methylated product (130 mgm.) in dry ether (10 ml.) was added, drop by drop, to a stirred suspension of lithium aluminum hydride (0.5 gm.) in anhydrous ether (25 ml.). After addition was complete the mixture was heated under gentle reflux for three hours. Excess lithium aluminum hydride was destroyed by cautious addition of ethyl acetate and, after acidification with 10% sulphuric acid, the mixture was filtered. The filtrate was freed of organic solvents by evaporation and the residual aqueous solution (25 ml.) was extracted continuously with ether for 24 hr. Evaporation of the dried (sodium sulphate) ether extract left a sirup (92.1 mgm.) of which an infrared spectrum showed the absence of a carbonyl group, which was present before reduction, and the presence of a hydroxyl group, which had not been found in the unreduced product. The reduced product was hydrolyzed by heating for six hours on a boiling water bath with 1% hydrochloric acid (2 ml.). The hydrolysis could not be followed polarimetrically because the solution was too highly colored. The hydrolyzate was neutralized with Dowex-2 (carbonate form) and examination by chromatography (solvent *D*) revealed the presence of 2,4-di-*O*-methyl xylose and 2,3,4-tri-*O*-methyl glucose. These two compounds were separated by preparative paper chromatography (solvent *D*) and extracted from the papers with acetone. The extracts were evaporated to sirups, which were taken up in water and filtered through charcoal. Evaporation of these clarified solutions left 2,4-di-*O*-methyl-D-xylose (15.2 mgm., $[\alpha]_D^{25} = +25.5$ ($c = 1.52$ in water)) reported (15) $[\alpha]_D^{25} = +24.7$; and 2,3,4-tri-*O*-methyl-D-glucose (14.0 mgm., $[\alpha]_D^{25} = +65.7$ ($c = 1.4$ in water)) reported (14) $[\alpha]_D^{20} = +65°$.

The 2,4-di-*O*-methyl-D-xylose was taken up in water (2 ml.) to which 0.5 ml. of bromine was added. The mixture was stored in the dark at room temperature for 48 hr., after which excess bromine was removed by aeration. The

clear solution was neutralized with Dowex-2 (carbonate form) and the neutral solution was evaporated to dryness. The residue was dissolved in methanol (5 ml.) and anhydrous ammonia was passed through the solution for one-half hour. After it was stored at 5°C. for 18 hr., the solution was evaporated to dryness leaving a semicrystalline residue which was recrystallized from ethyl acetate to yield the amide of 2,4-di-*O*-methyl-D-xylonic acid, m.p. 98–99°C., reported (15) m.p. 98–100°C.

The 2,3,4-tri-*O*-methyl-D-glucose was oxidized by heating at 90°C. for three hours with nitric acid (5 ml., sp. gr. 1.2). Nitric acid was removed by repeated distillation with water and methanol and the residue was esterified by ethereal diazomethane. Evaporation of the ethereal solution left a residue, which was extracted with ether. Removal of the ether gave a sirup which crystallized completely after four days at room temperature. The crystals, after trituration and washing with cold ether, had m.p. 105–106°C., reported (14) for the methyl ester of 2,3,4-tri-*O*-methyl-D-glucosaccharolactone, m.p. 106–107°C.

ACKNOWLEDGMENTS

The author is indebted to Dr. A. L. Shewfelt, Department of Agriculture, Experimental Station, Morden, Manitoba, who provided the sunflower seed heads used in this work. The careful technical assistance of Mr. W. R. Rowsome is gratefully acknowledged as is also the assistance of Mr. F. Rollin, who carried out the infrared spectra.

REFERENCES

1. ASPINALL, G. O. and MAHOMED, R. S. J. Chem. Soc. 1731. 1954.
2. BISHOP, C. T. Can. J. Chem. 31: 134. 1953.
3. CARSON, J. F. and MACLAY, W. D. J. Am. Chem. Soc. 70: 293. 1948.
4. CHANDA, S. K., HIRST, E. L., JONES, J. K. N., and PERCIVAL, E. G. V. J. Chem. Soc. 1289. 1950.
5. CHANDA, S. K., HIRST, E. L., and PERCIVAL, E. G. V. J. Chem. Soc. 1240. 1951.
6. FLOOD, A. E., HIRST, E. L., and JONES, J. K. N. J. Chem. Soc. 1679. 1948.
7. GILLES, K. A., MEREDITH, W. O. S., and SMITH, F. Cereal Chem. 29: 314. 1952.
8. HIRST, E. L. and JONES, J. K. N. Advances in Carbohydrate Chem. 2: 235. 1946.
9. KERTESZ, Z. I. and MCCOLLOCH, R. J. Advances in Carbohydrate Chem. 5: 82. 1950.
10. LUCKETT, S. and SMITH, F. J. Chem. Soc. 1106. 1940.
11. SHEWFELT, A. L. Ph.D. Thesis, Oregon State College, Corvallis, Oregon. June, 1952.
12. STOIKOFF, S. Mitt. Gebiete Lebensm. u. Hyg. 39: 292. 1948.
13. WHISTLER, R. L. Advances in Carbohydrate Chem. 5: 269. 1950.
14. WHITE, E. V. J. Am. Chem. Soc. 76: 4906. 1954.
15. WINTERSTEINER, O. and KLINGSBERG, A. J. Am. Chem. Soc. 71: 939. 1949.

THE VAPOR-PHASE PHOTOLYSIS OF ACETIC ACID[1]

By P. Ausloos[2] and E. W. R. Steacie

ABSTRACT

The photolysis of acetic acid (CH_3COOD) vapor has been investigated in the temperature range from room temperature to 285°C. Since CH_3D formation is independent of temperature, it is certain that the primary process

$$CH_3COOD + h\nu \rightarrow CH_3D + CO_2$$

occurs to the extent of about 10%. The results are complex and suggest that three other primary processes may occur, viz.

$$CH_3COOD + h\nu \rightarrow CH_3CO + OD$$
$$\rightarrow CH_3 + COOD$$
$$\rightarrow CH_3COO + D.$$

The abstraction reaction

$$CH_3 + CH_3COOD \rightarrow CH_4 + CH_2COOD$$

is of importance, and the results indicate that it has an activation energy of 10.2 kcal., and a steric factor of the order of 10^{-3}.

INTRODUCTION

The photolysis of acetic acid in the gas phase was first investigated by Farkas and Wansborough-Jones (5), who suggested the primary processes:

$$CH_3COOH + h\nu \rightarrow CH_4 + CO_2$$
$$(CH_3COOH)_2 + h\nu \rightarrow CH_4 + CO_2 + CH_3COOH$$
$$(CH_3COOH)_2 + h\nu \rightarrow C_2H_6 + CO_2 + CO + H_2O.$$

Burton (2) investigated the photolysis by mirror methods and suggested that radicals were formed by

$$CH_3COOH + h\nu \rightarrow CH_3 + COOH,$$

followed by

$$COOH \rightarrow CO_2 + H, \text{ etc.}$$

In later work (3) he rejected this mechanism and suggested that H-atoms but no CH_3 radicals were formed. He therefore proposed the primary step

$$CH_3COOH + h\nu \rightarrow CH_3COO + H.$$

Clusius and Schanzer (4) investigated the photolysis of CH_3COOD in the liquid phase, and concluded that two primary processes occur:

$$CH_3COOD + h\nu \rightarrow CH_3 + COOD$$
$$CH_3COOD + h\nu \rightarrow CH_3D + CO_2,$$

the first process being the more important. They suggested that CH_4, found in the methane fraction, could be accounted for by the abstraction reaction

$$CH_3 + CH_3COOD \rightarrow CH_4 + CH_2COOD.$$

In the present work the photolysis of CH_3COOD has been investigated in the vapor phase over a more extended temperature range.

EXPERIMENTAL

The apparatus has been described previously (1). A Hanovia S-500 medium pressure mercury arc was used as a light source. The full radiation was used

[1]*Manuscript received June 10, 1955.*
Contribution from the Division of Pure Chemistry, National Research Council, Ottawa, Canada. Issued as N.R.C. No. 3717.
[2]*National Research Council of Canada Postdoctorate Fellow, 1952–54.*

to obtain the maximum intensity. The intensity was varied by the use of calibrated screens. Two samples of CH_3COOD were used, containing respectively 20% and 15% CH_3COOH. The analysis of the products was done by taking off two fractions, one at −196°C., and one at −150°C. These were then analyzed by a mass spectrometer. No attempt was made to determine condensable reaction products.

One experiment was made with a Corning 7-54 filter, with a cutoff below 2400 Å. This gave a rate approximately one quarter the normal rate. Since the filter has a transmission of about 40% at 2537 Å and decreases sharply below this, it appears that the effective radiation was mainly in the range from 2400 Å to 2537 Å.

RESULTS AND DISCUSSION

The results are given in Table I. The main reaction products found were CO, CO_2, CH_4, CH_3D, and C_2H_6. At temperatures above 150°C. H_2 and HD were also present, and they constituted about 10% of the reaction products at temperatures above 250°C. Very small amounts of CH_2D_2 and C_2H_5D were also detected. The amounts of these products were always less than two per cent of the methane or ethane fraction, and their formation is probably due to the presence of small amounts of CH_2DCOOD in the starting material.

The Primary Process

The results in Table I indicate that for runs at constant intensity the rate of formation of CH_3D is constant within experimental error, and is independent of temperature in the range from 27 to 287°C. On the other hand, the rate of formation of CH_4 increases steadily with increasing temperature as might be expected if it is formed in a secondary reaction. This constitutes a definite proof of the occurrence of the primary process

$$CH_3COOD + h\nu \rightarrow CH_3D + CO_2. \qquad [I]$$

If runs 9, 12, and 15 are compared it can be seen that the rate of formation of CO decreases sharply below 100°C., while at higher temperatures (compare runs 2–7) it is nearly independent of temperature. This suggests that CH_3CO is formed in the primary process

$$CH_3COOD + h\nu \rightarrow CH_3CO + OD, \qquad [II]$$

and decomposes thermally.

A comparison of CH_3D with CO_2 shows that primary process [I] accounts only for about 10% of the CO_2 formed. Nevertheless the rate of CO_2 formation is nearly independent of temperature over the whole range. This excludes the formation of CO_2 by a secondary process unless it is one with a very low activation energy. There appear to be two possibilities:

(*a*) $$CH_3COOD + h\nu \rightarrow CH_3 + COOD \qquad [III]$$

followed by

$$COOD \rightarrow CO_2 + D. \qquad [1]$$

TABLE I

Run	Temp., °C.	Pressure, cm.	Time, min.	Relative intensity	Products, cc./min. × 10^4							$k_6/k_7^{\frac{1}{2}} \times 10^{13}$ cm.$^{3/2}$ molecules$^{-\frac{1}{2}}$ sec.$^{-\frac{1}{2}}$	$\frac{2CH_4+2C_2H_6}{CO+CO_2-CH_3D}$
					CO	CO_2	CH_3D	CH_4	C_2H_6	H_2	HD		
Sample 1													
1	97	1.29	140	1	2.80	3.50	0.326	0.154	2.30			0.73	0.79
2	132	1.20	120	1	3.30	3.30	0.325	0.220	2.28			1.66	0.79
3	156	1.23	120	1	3.25	3.22	0.320	0.320	2.30			3.00	0.83
4	187	1.22	120	1	3.38	3.32	0.300	0.510	2.05	0.051	0.100	6.10	0.81
5	212	1.24	120	1	3.67	3.54	0.330	0.805	1.85	0.100	0.145	11.10	0.77
6	237	1.35	100	1	3.75	3.70	0.340	1.300	1.70	0.220	0.370	18.40	0.83
7	269	1.20	100	1	3.90	3.70	0.350	1.780	1.44	0.335	0.390	34.00	0.90
8	285	1.20	100	1.2	4.65	3.90	0.430	2.260	1.36	0.306	0.320	45.40	0.89
Sample 2													
9	27	1.51	100	1.28	1.33	5.30	0.410	0.142	2.13			0.44	0.73
10	28	1.50	200	0.58	0.57	2.36	0.195	0.075	0.88			0.34	0.70
11	27	1.48	1190	0.08	0.104	0.40	0.016	0.029	0.151			0.7	0.75
12	107	1.45	90	1.28	5.10	5.65	0.35	0.205	3.72			0.96	0.77
13	106	1.50	160	0.58	2.11	2.30	0.158	0.106	1.54			0.80	0.77
14	105	1.48	1080	0.08	0.287	0.345	0.021	0.034	0.225			0.87	0.85
15	232	1.45	80	1.30	6.15	5.98	0.405	1.78	2.51			19.8	0.73
16	236	1.53	135	0.08	2.17	2.52	0.196	1.21	0.91			21.7	0.94
17	168	1.28	100	0.85	2.65	3.00	0.223	0.355	1.58			4.55	0.71
18	169	1.32	200	0.35	2.14	1.25	0.100	0.230	0.76			4.30	0.60
19	168	1.35	1420	0.055	0.554	0.21	0.011	0.070	0.100	0.002	0.006	3.80	0.97
20	187	1.40	95	0.85	2.925	2.83	0.207	0.552	1.65	0.027	0.067	6.95	0.79
21	187	1.40	1156	0.055	0.194	0.187	0.018	0.108	0.09	0.0022	0.0045	6.10	1.11

This will only account satisfactorily for CO_2 production if [1] is very fast, which appears to be the case (8). The analogous reaction

$$COOCH_3 \rightarrow CO_2+CH_3 \qquad [2]$$

is known to occur readily (7). Reaction [1] will be less exothermic than [2], but is probably feasible thermochemically.

(*b*) $$CH_3COOD+h\nu \rightarrow CH_3COO+D \qquad [IV]$$

followed by

$$CH_3CO_2 \rightarrow CH_3+CO_2. \qquad [3]$$

In solution the acetate radical appears to have considerable stability (6), which casts some doubt on the rapid formation of CO_2 by [3] at low temperatures.

Either mechanism involves the formation of D-atoms. Since no D_2 is formed, and H_2 and HD are only formed at higher temperatures, recombination is apparently negligible compared with the abstraction reaction

$$D+CH_3COOD \rightarrow HD+CH_2COOD. \qquad [4]$$

H_2 will be formed from the CH_3COOH present in the acetic acid. The quantity of H_2 is, however, rather large compared with that of HD, and the possibility of the loss of an H-atom from the methyl group in the primary process is not excluded.

In any case the very small amount of H_2 and HD relative to CO_2 shows that most H- or D-atoms disappear in some other way to form condensable products, such as HDO and D_2O. The independence of CH_3D formation with temperature rules out the reaction

$$CH_3+D \rightarrow CH_3D. \qquad [5]$$

It is also possible to explain the above results in a somewhat simpler way by postulating the occurrence of reactions such as

$$CH_3COOD^*+CH_3COOD \rightarrow CH_3CO_2+CH_3CO+D_2O$$

or

$$(CH_3COOD)_2+h\nu \rightarrow CH_3CO_2+CH_3CO+D_2O.$$

It should be noted that at 27°C. under the experimental conditions used about 90% of the acetic acid is in the form of double molecules. At 150°C., however, the number of double molecules is negligible for the pressures used in this work. It should be pointed out that processes [I], [II], and [III] are nearly independent of temperature. It may therefore be concluded that double molecules do not affect the primary processes.

The Abstraction Reaction

The fact that the formation of CH_3D is essentially independent of temperature, while that of CH_4 increases rapidly with increasing temperature, indicates that only H-atoms on the methyl group are involved in abstraction reactions to an appreciable extent, viz.

$$CH_3+CH_3COOD \rightarrow CH_4+CH_2COOD. \quad [6]$$

If this is the only way in which CH_4 is formed, and if all C_2H_6 results from recombination,

$$2CH_3 \rightarrow C_2H_6, \quad [7]$$

then $$R_{CH_4}/R^{\frac{1}{2}}_{C_2H_6}[A] = k_6/k_7^{\frac{1}{2}},$$

where R_{CH_4} and $R_{C_2H_6}$ are the rates of formation of the products indicated and A represents acetic acid. In applying this relationship it is necessary to correct the CH_4 for the small amount formed by a process analogous to [I] from the small amount of CH_3COOH present.

The results given in Table I show that $k_6/k_7^{\frac{1}{2}}$ is not appreciably affected by a variation of the intensity by a factor of 15. The corrected values of $k_6/k_7^{\frac{1}{2}}$ are given in Fig. 1 in the form of an Arrhenius plot. A good straight line is

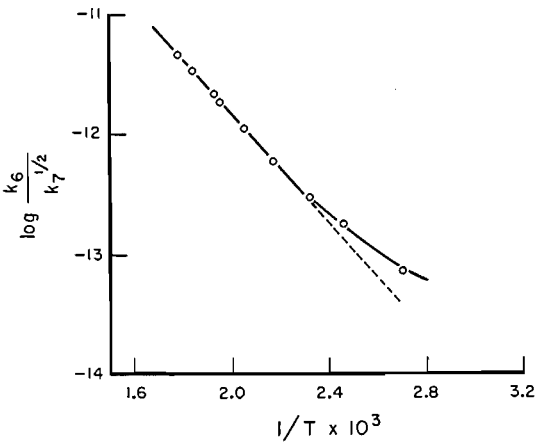

FIG. 1. Arrhenius plot of $k_6/k_7^{\frac{1}{2}}$.

obtained at higher temperatures with some curvature at low temperatures. The curvature may be connected with the presence of double molecules and wall reactions. The slope of the curve leads to a value of 10.2 kcal. for $E_6-\frac{1}{2}E_7 = E_7$. This is of the expected order of magnitude for such a reaction. The steric factor of reaction [7] is estimated to be $\sim 10^{-3}$.

Material Balance

On the basis of the above mechanism primary process [I] implies that

$$CH_3D = CO_2.$$

All other primary processes lead to $1CH_3$ for each CO_2 or CO formed. Hence it would be expected that

$$CO_2+CO-CH_3D = CH_4+2C_2H_6.$$

However, nothing has been said of the fate of the CH_2COOD radical formed

by abstraction. If it is assumed that this disappears only by recombination with methyl, then

$$(2CH_4+2C_2H_6)/(CO_2+CO-CH_3D) = 1. \qquad [A]$$

This ratio will be greater than unity if some CH_2COOD radicals disappear by dimerization, but will be low if CH_2COOD is formed by reaction [4] and is followed by the addition of methyl. A value of $[A]$ somewhat less than unity is therefore to be expected. Any other processes leading to condensable products with elimination of CO or CO_2 will also lower the ratio.

The last column of Table I gives values of the ratio $[A]$. There is considerable scatter, but it will be seen that from 80 to 90% of the methyls are accounted for, which seems quite satisfactory in the absence of a detailed knowledge of the condensable products.

REFERENCES

1. AUSLOOS, P. and STEACIE, E. W. R. Bull. soc. chim. Belges, 63: 87. 1954.
2. BURTON, M. J. Am. Chem. Soc. 58: 692. 1936.
3. BURTON, M. J. Am. Chem. Soc. 58: 1645. 1936.
4. CLUSIUS, K. and SCHANZER, W. Ber. 75, B: 1795. 1942.
5. FARKAS, L. and WANSBOROUGH-JONES, O. H. Z. physik. Chem. B, 18: 124. 1932.
6. FRY, A., TOLBERT, B. M., and CALVIN, M. Trans. Faraday Soc. 49: 1444. 1953.
7. KUTSCHKE, K. O. Unpublished work.
8. WEST, W. and ROLLEFSON, G. K. J. Am. Chem. Soc. 58: 2140. 1936.

REACTIONS OF ARYLSULPHONIC ESTERS

III. ON THE HYDROLYSIS OF METHYL *p*-METHYLBENZENESULPHONATE[1]

By R. E. Robertson

ABSTRACT

A study of the temperature dependence for the rate of hydrolysis of methyl *p*-methylbenzenesulphonate shows the specific heat of activation for this reaction in water to be 33.45±3 cal./mole degree. A comparison with the corresponding term for other methyl compounds reveals differences apparently characteristic of the anionic portion of the molecule. These differences are discussed in terms of specific solvation.

The possibility that the energy of activation for reactions in solution may be temperature dependent has been predicted and occasionally reported[2], but in general this property has been largely neglected. This is hardly surprising, since little interest was likely in such a derived quantity when the utility of the energy of activation was questionable (5, 6), especially since useful qualitative relationships, such as the S_N1–S_N2 classification, were more readily developed from a comparison of relative rates. Recently, Winstein, Grunwald, and Jones (16) and Swain and Scott (15) have suggested more quantitative classifications based on relative free energies. Such an approach, however, fails to take account of the many effects which result in compensating changes of energy and entropy. Nor will the substitution of the Arrhenius parameters or the equivalent energy and entropy of activation necessarily remove this objection unless it is known that the temperature dependence of the energy of activation is negligible.

Moelwyn-Hughes and co-workers (3, 10, 12) have shown that the specific heat of activation is by no means negligible for the hydrolysis of methyl halides and methyl nitrate. For these reactions ΔC_p[3] is not only large, but varies appreciably between the halides (10) and the nitrate, and may itself be temperature dependent. While it is probably too soon to assess the general significance of these results, and Moelwyn-Hughes has put forward two apparently unrelated hypotheses to account for the value he reports, it is clear that the magnitude of the ΔC_p term is such that it may not be neglected in any quantitative discussion relating structure and energy. In view of the prominent place given to ΔC_p values in discussion of the dissociation of weak acids, one may hope that the corresponding kinetic factor will prove a useful parameter in the quantitative study of reactions in solution.

Because of this possibility, a study was begun on the temperature dependence of the rate of hydrolysis for a series of benzenesulphonic esters. In this paper we report the results for methyl *p*-methylbenzenesulphonate.

[1]*Manuscript received June 10, 1955.*
Contribution from the Division of Pure Chemistry, National Research Council, Ottawa, Canada. Issued as N.R.C. No. 3713.
[2]*Theoretical and experimental results prior to 1935 are noted by LaMer, Ref. (7).*
[3]*The term ΔC_p indicates the specific heat of activation, as defined by the equation*

$$dE_A/dT = C_{act} - C_{int} = \Delta C_p$$

EXPERIMENTAL DETAIL

Water

Distilled water flowed through an 80 cm. × 35 mm. Acid–Base Ion Exchange column at the rate of 500 cc. per min. The first 600–800 cc. was rejected and the subsequent delivery used to make up solutions and rinse cells.

Methyl p-Methylbenzenesulphonate

Eastman Kodak white label methyl *p*-methylbenzenesulphonate was fractionally frozen to give material melting at 28.0–28.1°C.

Toluenesulphonic Acid

Eastman Kodak white label grade was used without further purification.

The Conductance Bridge

The conductance bridge was built about a Tinsley No. 4896 Electrolytic Conductivity Bridge. The 1000 cycle supply was from a Model 200 AB Hewlett-Packard Oscillator. This was passed through a phase shifter, opposite phases being supplied to the bridge through an isolating transformer, and to the X input of the detecting oscilloscope (Dumont-304H).

The output from the bridge passed through an isolating transformer (GR, 578A), a band pass filter (General Radio, 830-R), and a GR Amplifier (1231 B) and thence to the Y input of the oscilloscope. The Wagner ground of the Tinsley bridge was modified by the introduction of a Leeds and Northrup Decade Resistor (No. 4755) in series with the variable resistance, and balance was observed on a second oscilloscope between the high side of the output of the bridge and ground. This separate balancing was of particular advantage in following fast reaction rates and simultaneous reactions. All wiring was with RG-62U low-loss shielded cable and the leads to the bridge from the cells were carefully shielded, observing the usual precautions.

The Conductance Cells

In control experiments the first order rate was shown to be independent of the design of the cell, provided the resistance was of the proper order. One important restriction was that with more insoluble esters (8), certain precautions had to be taken to avoid the effects of adsorption of appreciable amounts of ester on the glass walls. The obvious precautions of avoiding cells with high surface to volume ratios and further of adopting the Guggenheim method (4) of determining the rate were usually sufficient. Shiny platinum or gold-plated platinum electrodes proved satisfactory. Platinum gray or black electrodes gave evidence of adsorption at low concentrations. While the presence of air did not alter the rate, it was standard practice to partially evacuate the cells to avoid separation of gas on the electrodes at higher temperatures.

Temperatures were determined by a Leeds and Northrup Mueller Bridge and a platinum resistance thermometer calibrated by the Heat Section of these laboratories. Temperatures were controlled within limits of ±0.003°C. Time was determined by either an electric clock driven by current from our

Standard Frequency Laboratory or for shorter runs by a split second-hand stop watch which was checked against the standard time.

EXPERIMENTAL PROCEDURE

After the cells were cleaned with hot chromic acid and repeatedly washed with distilled water, they were filled with a solution of toluenesulphonic acid of the same concentration used as supporting electrolyte in the solution to be studied. A solution containing ester (0.2 gm./l.) and toluenesulphonic acid (0.2 gm./l.) was then prepared. The cells were filled with this solution, evacuated, and sealed off. The presence of backing electrolyte reduced the relative change in electrolyte concentration during a run, and created a more reproducible environment. It was customary to preheat the cells in a subsidiary bath to the temperature under study, to avoid disturbing the main thermostat.

Resistances were measured at times t_1, t_2, t_3, etc., and $t_1+\sigma$, $t_2+\sigma$, $t_3+\sigma$, etc., where $\sigma = 1$ to 2 half-lives, and the slope of the plot of $\log[1/(R_{t_i}+\sigma)-1/R_{t_i}]$ versus t_i gave the rate.

The use of this direct method involves the following approximation. Bolam and Hope (1) have shown that the equivalent conductance of benzenesulphonic acid in water is given by the equation

$$\Lambda = 383-(0.227_4\ \Lambda_0+59.79)\ \sqrt{c} \qquad [1]$$

which may be rewritten for any particular experiment as

$$M/R_x = C-0.38349\ C^{3/2} \qquad [2]$$

where M is a constant, characteristic of the system, and R_x is the measured resistance. If the concentration of backing electrolyte and ester is 1×10^{-3} molar at t_0 and hence 2×10^{-3} molar with respect to benzenesulphonic acid at t_∞ this will introduce a systematic positive error of approximately 1% in all the equivalent values. But the rate is derived from a difference of concentrations or (in the approximation) from the equivalent reciprocal ohms, so that the magnitude of this approximation is reduced to the order of 0.2%. The assumption that this argument applies equally at all temperatures and for similar strong acids does not seem unreasonable since the equivalent conductance of the proton is common to all. The application of this direct method was shown to give the same results, within the reproducibility possible, as those obtained using a calibration curve relating concentration and conductivity, and also was in agreement with values determined by our intermittent titration technique (13).

Precision

The errors introduced by fluctuations in temperature, time, and resistance readings were small compared to the errors arising as a result of what appears to be the adsorption of the ester on the glass walls of the cell. In Fig. 1 is shown a plot of the data for three typical runs done simultaneously. The resulting rates (37.04×10^{-5}, 37.14×10^{-5}, 36.72×10^{-5}) derived from these plots vary from the mean by 0.35% while the scatter of the points in

any run is estimated to be of the order of 0.1%. If care was taken that the concentration of ester did not fall below $5 \times 10^{-5}M$ during the run, this lack of reproducibility was reduced but probably not entirely eliminated by calculating rates by the Guggenheim method (4). With methyl esters this was easily achieved. With less soluble esters, errors from this source became the limiting factor. A further error for slow runs arose from what is generally called "glass-error" and rendered the data at 0° and 10°C. less reliable than the remainder.

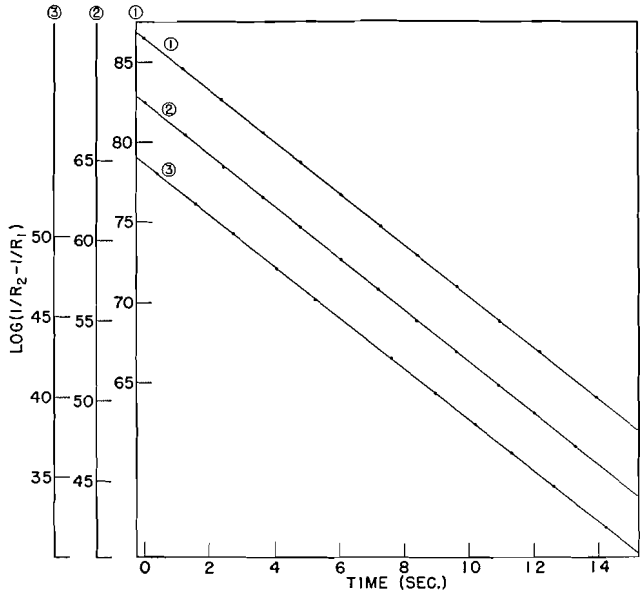

FIG. 1.

RESULTS

The initial concentrations of ester and the backing electrolyte were made up to 0.2 gm./l. in all experiments, and no attempt was made to explore salt effects (9), save for some preliminary experiments which indicated that a 10-fold increase in concentration of benzenesulphonic acid increased the rate by only a few per cent. Average rates corresponding to a series of temperatures are given in Table I, together with the average deviation from the mean, the number (n) of runs involved in the average, and the rate calculated from equation [4]. Prior to deriving such an equation by the direct application of the least mean squares to the data (average rates were used) it is advantageous to test the data for internal consistency by an adaptation of the graphical method of Everett and Wynne-Jones (2) based on equation [3],

$$[3] \qquad \Delta_{1,2}(T \log K)/\Delta_{1,2}(T) = (\Delta C_{p1,2}\, T \log T + B')/R\, \Delta_{1,2}(T),$$

by which these authors calculated the thermodynamic parameters from the ionization constants of weak acids, or more directly by the application of a plot of calculated E_A versus T such as was used by Moelwyn-Hughes (12). Our data

TABLE I

RATE DATA FOR THE HYDROLYSIS OF METHYL *p*-METHYLBENZENESULPHONATE IN WATER FOR A SERIES OF TEMPERATURES

Temperature, °C.	n	k_1 av.(sec.$^{-1}$) $\times 10^5$ (obs.)	k_1 (sec.$^{-1}$) $\times 10^5$ (calc.)
80.161	6	221 ±3.5	221.8
75.216	4	147.5 ±0.4	146.6
69.983	2	92.95 ±0.1	93.05
65.128	5	60.1 ±0.4	60.08
59.992	3	37.0 ±0.2	37.15
55.894	4	25.05 ±0.06	24.96
54.996	5	22.67 ±0.12	22.84
50.008	4	13.81 ±0.03	13.80
45.130	4	8.36 ±0.05	8.27
40.142	4	4.789 ±0.007	4.795
40.007	4	4.716 ±0.017	4.724
35.138	5	2.71 ±0.04	2.716
30.008	5	1.485 ±0.007	1.481
24.850	4	0.778 ±0.003	0.7839
20.009	4	0.421 ±0.001	0.4208
14.998	3	0.2150 ±0.007	0.2152
10.012	3	0.1082 ±0.0002	0.1073
0.0621	4	0.02541 ±0.00011	0.02438

plotted according to equation [3] are shown in Fig. 2. Where $\Delta_{1,2}T \backsim 10°C.$, this plot provides a test of consistency, and on the basis of this test the data for 0° and 10°C. were omitted from the least mean square calculation. While the possibility that the systematic deviation noted in the rates for these temperatures may reflect some structural change in the solvent was considered, we believe that these data deviate from the remainder because of a larger glass-error resulting from the slowness of the runs. The slope of the curve in Fig. 2

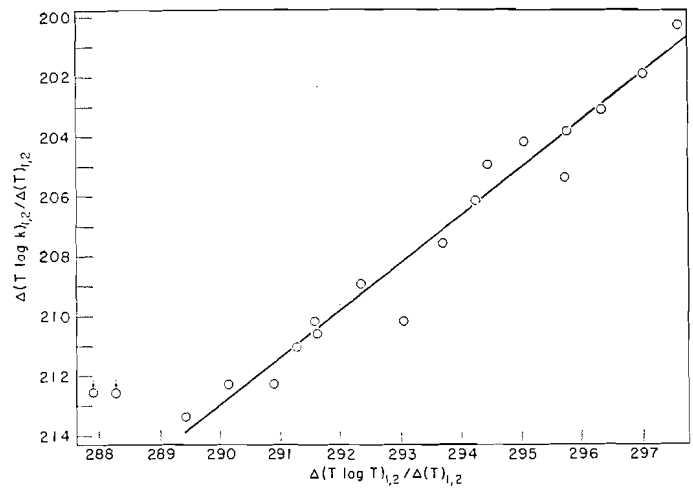

FIG. 2.

leads by the method of least mean squares to a value of ΔC_p of -33.9 ± 3 cal./deg. mole. The thermodynamic constants for equation [4] were then calculated by the method of least squares.[4]

[4]*See Hyne and Robertson. This issue.*

[4] $$\log_{10}k = (A/T)+B\log_{10}T+C$$

where $$A = -\Delta H_0/2.3026\,R = -7036.861,$$
$$B = \Delta C_p/R = -16.8385,$$
$$C = \Delta S_0 - C_p/2.3026\,R = 60.1695,$$
$$0°C. = 273.16°K. \text{ and } R = 1.9865,$$

[5] $$\Delta H_T = \Delta H_0+(-16.8385)RT.$$

Thermodynamic constants for the activation process at 298.16°C. are given in Table II.

TABLE II

THERMODYNAMIC CONSTANTS FOR THE ACTIVATION PROCESS AT 298.16°K.

ΔF = +6953.5 cal./mole
ΔH = −22220.4 cal./mole
ΔS = −51203 cal./mole deg.
ΔC_p = −33.45±3 cal./mole deg.

The error in ΔH is probably less than ±100 cal./mole. The random scatter of the points in Fig. 2 and the deviations between calculated and observed data in Table I show that the data are not sufficiently accurate to justify any claim for a change in ΔC_p with temperature in striking contrast to the results of Moelwyn-Hughes for the methyl halides (12).

DISCUSSION

In Table III, kinetic data are given for the hydrolysis of six methyl compounds. Large differences in the rates compared to that for methyl *p*-methylbenzenesulphonate are accompanied by corresponding changes in ΔH_T, but it is noted that the observed differences in this latter term would correspond to

TABLE III

A COMPARISON OF KINETIC DATA FOR HYDROLYSIS AT T = 303.19°K.

Compound	$k_1(\times 10^{-8}$ sec.$^{-1})$	$\Delta H_{303.19}$(kcal.)	ΔC_p	Notes
Me *p*-Me	1480	22.04	33.4₇±3	(*a*)
MeBr	84	26.36	(66)	(*b*)
MeI	17.3	28.31	(66)	(*b*)
MeCl	5.43	28.07	(66)	(*b*)
MeF	0.622	27.53	67	(*c*)
$MeNO_2$	0.201	29.300	42.6±14	(*d*)

Notes: (*a*) *This work.*
(*b*) *Ref. (11). The E_A values are recorded here. The ΔC_p values are merely approximate.*
(*c*) *Data calculated from equation [9], Ref. (3).*
(*d*) *Data calculated from equation [3], Ref. (9).*

rate differences from 2 to 700 times greater than actually found. It is interesting to note that the closest agreement on this basis (assuming constant entropy) is for the comparison with methyl fluoride, although the ratio of the rates is greater than 2000/1. The slope of the curve in Fig. 2 and the close agreement of the observed and calculated rates (Table I) leave no doubt that the activation energy for the hydrolysis of methyl *p*-methylbenzenesulphonate

changes with temperature in a systematic manner expressed by equation [5]. This change is of the same sign as, but of about one-half the magnitude of the values reported for the methyl halides in the lower temperature range, and there is no perceptible change in ΔC_p with temperature as was found for the halides.

Now it has long been recognized that the change in the bulk dielectric constant with temperature will lead to a corresponding change in the activation energy in the order of -13 cal./mole deg. for ionogenic reactions. It is clear that this factor will account neither for the magnitude of ΔC_p found for the above hydrolytic reactions, nor for the specific differences between compounds, nor would it be expected to lead to a difference in ΔC_p with temperature.

The fact that ΔC_p values for the hydrolysis of the methyl halides are roughly the same, in spite of widely differing bond strengths, led Moelwyn-Hughes to the conclusion that this coefficient is related to specific differences in the solvation of the reacting molecule. In view of the large difference between the sulphonate and the halides and to a lesser degree the nitrates, it seems probable that the specific solvation of the anionic part of the esters may play a major part in determining the value of this coefficient, and our explanation of the difference between the sulphonate ester and the corresponding halides is based on this postulate.

Reasoning on the basis of average specific heat values, Glew and Moelwyn-Hughes (3) calculate that the large and approximately equal ΔC_p values found for the hydrolysis of the methyl halides could be accounted for by the "freezing" of six water molecules (the freezing process for water involving a ΔC_p of -9 cal./mole deg.) about the transition state—the activation energy involving the breaking of water–water bonds. Such a model applied to the $\Delta C_p = -33$ cal./mole deg. found for the hydrolysis of methyl *p*-methylbenzenesulphonate would lead to a mechanism involving two water molecules reminiscent of the termolecular mechanism of Swain (14). If E_A is largely accounted for by the breaking of water–water bonds, as suggested in this hypothesis, the lower activation energy observed by us is not low enough to support such a hypothesis.

Qualitatively it is well known that the addition of a sulphonic group renders many organic molecules more soluble in water—an effect which points to strong interaction with the water of the initial state in hydrolysis of sulphonic esters. In attempting to account for the difference between the ΔC_p for the hydrolysis of the methyl halides and methyl *p*-methylbenzenesulphonate, in terms of solvation, it is reasonable to assume that the relative differences will be greater for the initial states where dipole–dipole interactions are weaker than for the transition states which involve partial charges. On this hypothesis, the lower value of ΔC_p reported for methyl *p*-methylbenzenesulphonate may be accounted for by assuming that the stronger solvation accompanying the initial state results in a smaller change in solvation on passing to the transition state as compared to the corresponding changes in solvation for the methyl halides. A similar explanation would also account for the lower value of ΔC_p

reported by McKinley-McKee and Moelwyn-Hughes (10) for the hydrolysis of methyl nitrate.

ACKNOWLEDGMENT

The author wishes to acknowledge the technical assistance of Mr. Allan Relf throughout this investigation. The advice of Dr. A. F. Dunn was very helpful in connection with modifying the bridge circuit.

REFERENCES

1. BOLAM, T. R. and HOPE, J. J. Chem. Soc. 843. 1941.
2. EVERETT, D. H. and WYNNE-JONES, W. P. K. Trans. Faraday Soc. 35: 1380. 1939.
3. GLEW, D. N. and MOELWYN-HUGHES, E. A. Proc. Roy. Soc. (London), A, 211: 254. 1952.
4. GUGGENHEIM, E. A. Phil. Mag. 2: 538. 1926.
5. HAMMETT, L. P. Physical organic chemistry. McGraw-Hill Book Company, Inc., New York. 1940. Chap. IV.
6. INGOLD, C. K. Structure and mechanism in organic chemistry. Cornell Univ. Press, Ithaca, N.Y. 1953. p. 255.
7. LAMER, V. K. and MILLER, M. L. J. Am. Chem. Soc. 57: 2674. 1935.
8. LAUGHTON, P. M. and ROBERTSON, R. E. Can. J. Chem. 33: 1207. 1955.
9. MCCLEARY, H. R. and HAMMETT, L. P. J. Am. Chem. Soc. 63: 2254. 1941.
10. MCKINLEY-MCKEE, J. S. and MOELWYN-HUGHES, E. A. Trans. Faraday Soc. 48: 247. 1952.
11. MOELWYN-HUGHES, E. A. Proc. Roy. Soc. (London), A, 164: 295. 1938.
12. MOELWYN-HUGHES, E. A. Proc. Roy. Soc. (London), A, 220: 386. 1953.
13. ROBERTSON, R. E. To be published.
14. SWAIN, C. G. J. Am. Chem. Soc. 70: 1119. 1948.
15. SWAIN, C. G. and SCOTT, C. B. J. Am. Chem. Soc. 75: 141. 1953.
16. WINSTEIN, S., GRUNWALD, E., and JONES, H. A. J. Am. Chem. Soc. 73: 2700. 1951.

ON THE TEMPERATURE DEPENDENCE OF THE REACTION VELOCITY[1]

By J. B. Hyne[2] and R. E. Robertson

ABSTRACT

The temperature dependence of the rates of three reactions in solution which the Arrhenius equation fails to express has been analyzed in terms of equations involving higher powers of the temperature and an improved fit of the experimental results obtained. The significance of the equations in terms of the thermodynamic parameters of the activation process is discussed.

There is a growing body of evidence to show that for important classes of reactions the Arrhenius equation fails to express fully the temperature dependence of reaction velocity. The Arrhenius equation assumes the activation energy to be temperature independent but this has not been fully tested in the majority of reactions in solution, since the temperature dependency has been derived from data over a limited temperature range with but an accuracy of a few per cent. With a few possible exceptions, such as in discussions of steric hindrance (3, 4), the activation energy has found little use save in converting rate data to a common temperature. Existing relationships between structure and the rate have been based on a comparison of rate data, the validity of such relations resting on the temperature independence of the Arrhenius parameters.

Both LaMer and Miller (15) and Moelwyn-Hughes and co-workers (8, 16, 17, 18), among others, have published results which indicate a marked temperature dependence of activation energy in particular systems. Neglect of such a measurable parameter at the present stage in the development of the kinetics of organic processes is not warranted and it is the object of this paper to present an analysis of kinetic data which considers the higher order temperature dependence of reaction velocity.

It must be recognized that the work of Harned *et al.* (11, 12), Everett and Wynne-Jones (7), and others (19, 23) on the analysis of acid and base dissociation constants as a function of temperature has already established a set of equations for the treatment of data for equilibrium systems. Accepting the assumption that the initial and transition states in a reaction are in equilibrium (5), such a system of equations may be applied to the analysis of rate–temperature data. The treatment of rate–temperature data in a manner analogous to the work on dissociation constants, however, presents problems peculiar to this field arising from difficulties attendant upon obtaining kinetic data of an accuracy comparable to e.m.f. data.

Refinement of the rate–temperature relationships for kinetic data would engender little interest were it not a necessary step in the long term problem of developing a more quantitative statement of the theory of the mechanism of reactions. A more immediate gain is the possibility that such refinement

[1]*Manuscript received June 16, 1955.*
Contribution from the Division of Pure Chemistry, National Research Council, Ottawa, Canada. Issued as N.R.C. No. 3721.
[2]*National Research Council Postdoctorate Fellow.*

will provide a parameter (14) which can be interpreted in a thermodynamic sense and will provide a means of obtaining quantitative measurement of the factors involved in solvation processes accompanying reactions in solution; heretofore, such problems in solvation have been dealt with on an empirical basis (10, 22) by the study of reactions in mixed solvents or as a function of the bulk dielectric constant of the system (1).

TYPES OF EQUATION

Skrabal (21) has set down the various types of equation which have been suggested as representing the temperature dependence of rate data. Harned and Robinson (12) in particular, however, have treated the problem of progressive refinement of equations relating the equilibrium constants of dissociation processes and temperature and it is upon this work that our analysis of kinetic data is based. The Arrhenius equation

$$\log k = (A/T)+B, \qquad [1]$$

where $A = -E_a/2.303R$, assumes that the activation energy, E_a, is temperature independent. If the activation energy, or heat content change of the activation process ΔH, is expressed as a power series in T,

$$\Delta H = a+bT+dT^2,$$

the expression for the temperature dependence of the rate becomes

$$\log k = (A/T)+B \log T+DT+C \qquad [2]$$

where the thermodynamic functions of the activation process are given by

$$\begin{aligned} \Delta H &= -2.303RA+BRT+2.303RDT^2, \\ \Delta C_p &= RB+2.303R(2DT), \\ \Delta S &= 2.303R(B \log T+2DT+C)+RB. \end{aligned}$$

Harned and Robinson (12) and Everett and Wynne-Jones (7) have simplified this four-constant equation and have obtained two three-constant equations which, within the limit of accuracy of the data available to them for analysis, were found to represent the temperature dependence of the log k function studied.

$$\log k = (A/T)+B \log T+C \text{ (Everett and Wynne-Jones)} \qquad [3]$$

where

$$\begin{aligned} \Delta H &= -R(2.303A-BT), \\ \Delta C_p &= BR, \\ \Delta S &= 2.303R(C+B \log T)+RB; \end{aligned}$$

$$\log k = (A/T)+DT+C \text{ (Harned and Robinson)} \qquad [4]$$

where

$$\begin{aligned} \Delta H &= -2.303R(A-DT^2), \\ \Delta C_p &= 2.303R(2DT), \\ \Delta S &= 2.303R(C+2DT). \end{aligned}$$

The progressive refinement implied in equations [1] to [4] is seen when the thermodynamic parameters are expressed in terms of the constants of the

equations. Equation [1] as stated previously assumes ΔH to be temperature independent; equation [3] assumes a linear dependence of ΔH on temperature leading to a specific heat of activation term ΔC_p, which is temperature independent; equation [4] expresses ΔC_p as directly proportional to the absolute temperature; equation [2], the general case of [3] and [4], requires ΔC_p to be a linear function of the temperature. It is on the basis of equations [1] to [4] that the results of Robertson for the hydrolysis of methyl *p*-methylbenzenesulphonate (20), of LaMer and Miller for the dealdolization of diacetone alcohol (15), and of Moelwyn-Hughes for the hydrolysis of methyl chloride (18) have been analyzed.

CALCULATION

In Fig. 1 are shown plots of the activation energy against temperature for the three systems analyzed in this work. The data were analyzed by means

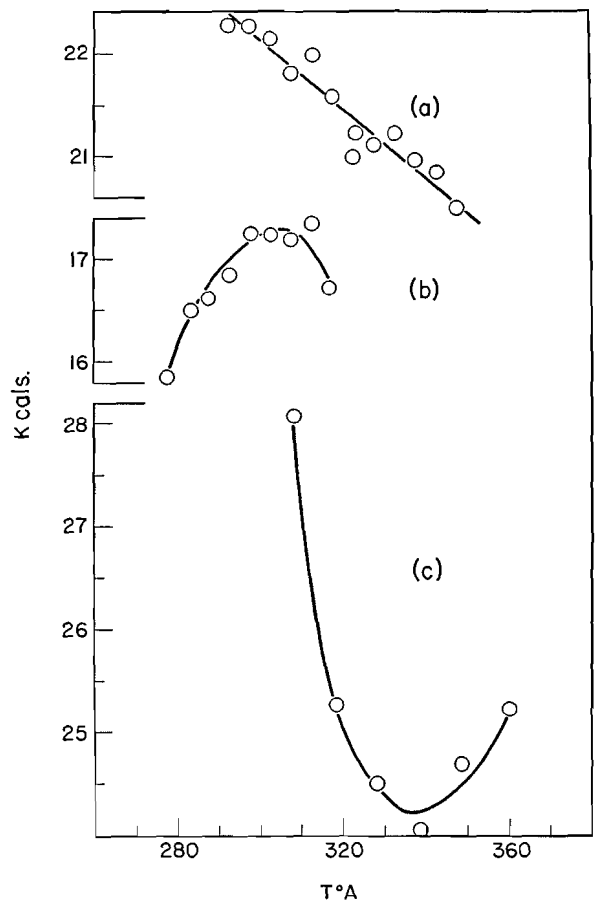

FIG. 1. Activation energy against temperature: (*a*) hydrolysis of methyl *p*-methylbenzenesulphonate; (*b*) dealdolization of diacetone alcohol; (*c*) hydrolysis of methyl chloride.

of the Arrhenius equation in the form [1′] using 10°C. temperature intervals, and the activation energies calculated for these intervals were associated with the mean temperature of the intervals:

$$[1'] \qquad \log(k_1/k_2) = E_a(T_1-T_2)/2.303R\ T_1T_2.$$

In the case of methyl *p*-methylbenzenesulphonate (Fig. 1(*a*)) the activation energy is a linear function of the temperature indicating a unique value of dE_a/dT over the temperature range studied, or in terms of thermodynamic parameters, a ΔC_p term which is temperature independent. In both the dealdolization of diacetone alcohol (Fig. 1(*b*)) and the hydrolysis of methyl chloride (Fig. 1(*c*)) the activation energy is a non-linear function of temperature indicating that the ΔC_p terms are temperature dependent. The curvature of the plot over the temperature range available is more marked in the case of methyl chloride than in that of diacetone alcohol hinting that the temperature dependence of the ΔC_p term is more complex in the former case. Such preliminary plots in the detailed analyses of rate–temperature data serve to indicate, in addition to the nature of the ΔC_p temperature dependence, any determinations which are not internally consistent with the other data since they will appear as deviating widely from the general trend of neighboring points. Calculation of the activation energy at intervals of less than 10°C. requires exceptionally accurate experimental data and is not necessary for preliminary plots such as in Fig. 1 when a temperature range of 40 to 50 degrees is available for study.

Figs. 2, 3, and 4 show, for the three systems studied, the deviations between observed and calculated log k values after the manner of Pitzer (19). The rate–temperature data for each system have been analyzed in terms of the various equations set down in the previous section until a minimum deviation between the observed log k value and that calculated from the equation fitted was obtained. The constants of the various equations were determined by a least mean square fit method applied directly to the data except in the case of the four-constant equation where an empirical graphical correction was applied to obtain the fourth constant C. The least mean square method used was that outlined by Goulden (9) using the method of Gauss Multipliers.

In work where rates of reaction of several systems are determined at a fixed series of temperatures the Gauss Multiplier method has much to recommend it since the Gauss Multipliers are dependent only on the temperature data and once calculated can be applied to any set of rate data determined for that particular set of temperatures.

In the design of experiments the extent of the temperature range studied is of considerable importance. In the application of the least mean square method to the results the inclusion of one determination at a temperature 10°C. outside the initially studied range (say 10° to 60°C.) is equivalent to increasing the number of determinations within the range by a factor of 1.7. The importance of determinations at the extremes of the temperature range has been pointed out previously (2) and great care is necessary in establishing the accuracy of these points.

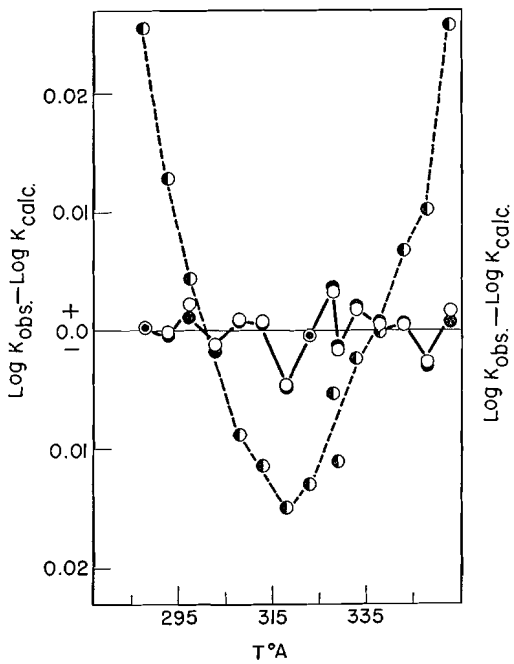

FIG. 2. Methyl *p*-methylbenzenesulphonate.

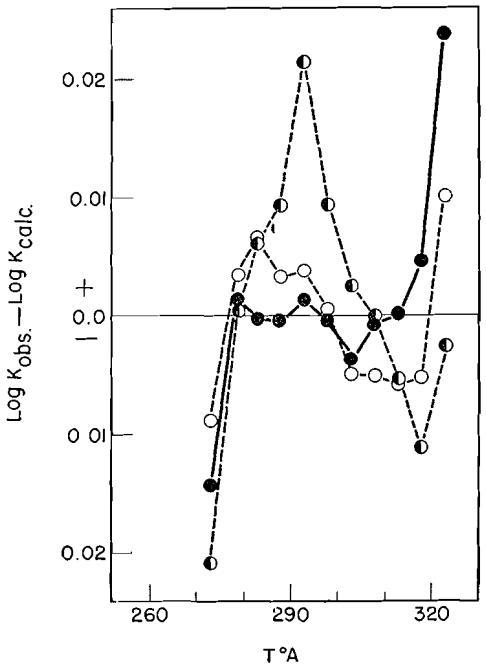

FIG. 3. Diacetone alcohol.

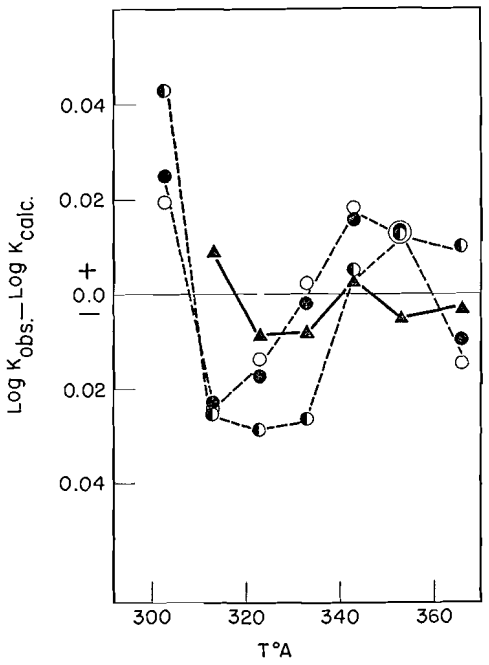

FIG. 4. Methyl chloride.

◐ $\log k = (A/T)+B$
○ $\log k = (A/T)+B \log T+C$
● $\log k = (A/T)+DT+C.$
▲ $\log k = (A/T)+B \log T+DT+C$

The equations derived for the three systems by the method of least mean squares were:

Methyl p-methylbenzenesulphonate (*Fig.* 2)

[1*a*] $\log k = (-4706.257/T)+10.6902$

[3*a*] $\log k = (-7036.861/T)-16.8385 \log T+60.1695$

[4*a*] $\log k = (-5885.250/T)-0.0115793\ T+18.0932$

Diacetone alcohol (*Fig.* 3)

[1*b*] $\log k = (-3681.667/T)+10.7035$

[3*b*] $\log k = (-1874.496/T)+14.0194 \log T-30.0565$

[4*b*] $\log k = (-2571.561/T)+0.0129521\ T+3.1090$

Methyl chloride (*Fig.* 4)

[1*c*] $\log k = (-5492.118/T)+10.8925$

[3*c*] $\log k = (-8708.034/T)-22.2727 \log T+76.7500$

[4*c*] $\log k = (-6739.194/T)-0.0112566\ T+18.4003$

[2*c*] $\log k = (-4474.950/T)+7.0453 \log T-0.001067\ T-9.5704$

DISCUSSION

Methyl p-Methylbenzenesulphonate

The failure of the Arrhenius equation [1*a*] to represent the data is clearly shown in Fig. 2, a systematic deviation between the observed and calculated log k values being observed. Analysis of the data in terms of equations [3*a*] and [4*a*] resulted in a random scatter of the deviation about the zero line in Fig. 2 showing that it is impossible to distinguish between the accuracy of fit of the two equations. Both equations take into consideration temperature dependence of the activation energy, i.e. they include a ΔC_p term, equation [3*a*] assuming ΔC_p to be temperature independent and [4*a*] requiring ΔC_p to be directly proportional to the absolute temperature. As Harned and Robinson (12) have pointed out, the fact that both equations fit the data equally well indicates that any temperature dependence of ΔC_p must be very small. The best fit of equations [3*a*] and [4*a*] also agrees with the linearity found in the E_a/T plot of Fig. 1(*a*).

Diacetone Alcohol

As in the methyl *p*-methylbenzenesulphonate system the failure of the Arrhenius equation [1*b*] is seen in Fig. 3. In this system, however, somewhat better agreement between observed and calculated log k values is found for equation [4*b*], where allowance is made for ΔC_p being directly proportional to the absolute temperature, compared with equation [3*b*], where the ΔC_p is assumed to be temperature independent. The preliminary plot of E_a against T established the non-linearity of the temperature dependence of E_a and hence the temperature dependence of the corresponding ΔC_p term. Inspection of the deviation curves in Fig. 3 shows that even the three-constant equation [4*b*], allowing temperature dependence of ΔC_p, does not give good agreement between the observed and calculated log k values especially at the limits of the temperature range employed. It does, however, provide evidence of the existence of data for a system exhibiting temperature dependence of ΔC_p.

Methyl Chloride

Fig. 4 again illustrates the failure of the Arrhenius equation [1*c*] to express the temperature dependence of the rate of hydrolysis of methyl chloride. In this system, however, although the two three-constant equations [3*c*] and [4*c*] give a better fit, the deviation between observed and calculated log k values is still systematic and not random. The four-constant equation [2*c*], which considers a linear dependence of ΔC_p on temperature (but not direct proportionality), gives a still better fit with all points except that at the lowest temperature. Furthermore, it should be noted that the coefficient of the log T term in [2*c*] has changed sign compared with that in the three-constant equation [3*c*] resulting in a change in sign of the ΔC_p term. The reason for this can be seen by considering the effect of neglecting the lowest temperature determination in Fig. 1(*c*) which will result in the slope of the best straight line through the points changing from negative to positive, and hence the change of sign of the ΔC_p. Investigation of the form of the systematic deviations between the observed and calculated values of log k for the methyl chloride system has shown that an improved over-all fit would require an equation involving at least a cubic term in T. Calculation of the constants of such an equation is an extremely laborious process and even with such an equation the physical significance of the coefficients of the higher powers of T could not be established on the basis of the present theory. The apparent complexity of the equation required to express the temperature dependence of rate in this case suggests the possibility that the hydrolysis of methyl chloride is not a simple reaction but is accompanied by a parallel reaction having a different activation energy (13). Moelwyn-Hughes does not consider this possibility in his presentation of the data although he offers several possible suggestions as explanations of the complex temperature dependence of the activation energy. Confirmation of the data, particularly at the extremes of the temperature range, is obviously desirable. The methyl chloride example is paralleled by the results for methyl bromide and methyl iodide also given by Moelwyn-Hughes (18) but not analyzed here.

The importance of choice of equation when the fit is not good is illustrated in Table I by a comparison of the ΔC_p terms calculated for the various systems

TABLE I

Equation	$\Delta C_p^{313.16}$ (cal./deg. mole)		
	Methyl *p*-methyl-benzenesulphonate	Diacetone alcohol	Methyl chloride
[3]	−33.5	−27.9	−44.2
[4]	−33.2	−37.1	−32.2
[2]			+10.4

from the corresponding coefficients of the equations used. For methyl *p*-methylbenzenesulphonate, where both equations [3*a*] and [4*a*] fit the data within the experimental error, the ΔC_p values are in excellent agreement. The diacetone alcohol system, where the fit is somewhat poorer, gives two

values of ΔC_p differing by 10 cal./deg.mole, while in the methyl chloride system, where the fit is poor even in the case of the four-constant equation [2*c*], the ΔC_p value calculated by the four-constant equation [2*c*] is of opposite sign to those evaluated from equations [3*c*] and [4*c*]. In no case, it should be noted, does the value of the ΔC_p determined by a least mean square method agree with the value quoted by Moelwyn-Hughes (17).

These systems suggest that kinetic data may well require more complex expressions to describe their temperature dependence than the corresponding dissociation constant temperature dependence relationships where Harned and Robinson (12) and Everett (6) found no evidence for discriminating between equations of the type [3] and [4]. Whether this apparent necessity for more complex equations to account for rate–temperature behavior is a reflection of a more complex activation process or is due to the fact that systems exhibiting complex temperature dependence of dissociation constants have not as yet been studied, is a question which only further work in both fields will answer.

ACKNOWLEDGMENTS

We gratefully acknowledge helpful advice of Mr. K. A. Brownlee and Mr. L. J. Savage, Committee on Statistics, University of Chicago, and of Mr. P. P. F. Clay, Section on Biometrics, of these laboratories.

REFERENCES

1. AMIS, E. S. The kinetics of chemical change in solution. The MacMillan Co., New York. 1949. Chap. 9.
2. BATES, T. G. and PINCHING, G. D. J. Research Natl. Bur. Standards, 42: 419. 1949.
3. BROWN, H. G. J. Am. Chem. Soc. 75: 14. 1953.
4. DOSTROVSKY, I., HUGHES, E. D., and INGOLD, C. K. J. Chem. Soc. 173. 1946.
5. EVANS, M. G. and POLANYI, M. Trans. Faraday Soc. 32: 1333. 1936.
6. EVERETT, D. H. Private communication.
7. EVERETT, D. H. and WYNNE-JONES, W. F. K. Trans. Faraday Soc. 35: 1380. 1939.
8. GLEW, D. N. and MOELWYN-HUGHES, E. A. Proc. Roy. Soc. (London), A, 211: 254. 1952.
9. GOULDEN, C. H. Methods of statistical analysis. 2nd ed. John Wiley & Sons, Inc., New York. 1952. Chap. 8.
10. GRUNWALD, E. and WINSTEIN, S. J. Am. Chem. Soc. 70: 486. 1948.
11. HARNED, H. S. and OWEN, B. B. The physical chemistry of electrolytic solutions. Reinhold Publishing Corporation, New York. 1950. Chap. 15.
12. HARNED, H. S. and ROBINSON, R. A. Trans. Faraday Soc. 36: 973. 1940.
13. HINSHELWOOD, C. N. The kinetics of chemical change. The Clarendon Press, Oxford. 1940. p. 15.
14. LAMER, V. K. J. Chem. Phys. 1: 289. 1933.
15. LAMER, V. K. and MILLER, M. L. J. Am. Chem. Soc. 57: 2674. 1935.
16. MCKINLEY-MCKEE, J. S. and MOELWYN-HUGHES, E. A. Trans. Faraday Soc. 48: 247. 1952.
17. MOELWYN-HUGHES, E. A. Proc. Roy. Soc. (London), A, 164: 295. 1938.
18. MOELWYN-HUGHES, E. A. Proc. Roy. Soc. (London), A, 220: 386. 1953.
19. PITZER, K. S. J. Am. Chem. Soc. 59: 2365. 1937.
20. ROBERTSON, R. E. Can. J. Chem. 33: 1536. 1955.
21. SKRABAL, A. Monatsh. 63: 23. 1933.
22. SWAIN, C. G. J. Am. Chem. Soc. 75: 4627. 1953.
23. WALDE, A. W. J. Phys. Chem. 39: 477. 1935.

SOME CORRELATIONS OF THE MOLECULAR STRUCTURE OF ORGANIC PHOSPHORUS COMPOUNDS WITH THEIR INFRARED SPECTRA[1]

By R. B. Harvey[2] and J. E. Mayhood[3]

ABSTRACT

The infrared spectra of fourteen organic esters of phosphorus containing dimethylamino groups, and two esters containing diethylamino groups have been examined over the region 5000 to 670 cm.$^{-1}$ (2 to 15 microns). Correlations have been obtained between absorption band frequencies and the presence of dialkylamino groups in the molecule as an aid to their identification in the spectra of phosphorus compounds. A number of compounds of the pyrophosphate type have been examined and absorption associated with the (P—O—P) linkage has been found in the 950 to 910 cm.$^{-1}$ (10.5 to 11.0 micron) region. Some criteria are proposed to distinguish absorption by the (P—O—P) linkage in this region.

INTRODUCTION

Some convenient method for the identification of compounds or of specific groupings present in compounds is desirable either from the standpoint of process or quality control in industrial application, or for the chemist in laboratory operations. Since the development of the theory of infrared spectra is not yet adequate to interpret the observations without accessory data except in the simplest cases, a system of correlations is required between known molecular configurations and absorption spectra. The present paper is concerned with such a series, characteristic of the dimethylamino (Me_2N) group in esters of phosphorus compounds. Some limited data are presented on absorption bands attributed to the (P—O—P) bond.

EXPERIMENTAL

A Perkin-Elmer Model 21 double beam recording spectrophotometer was used to obtain the spectra presented in Figs. 1 to 19. The particular instrument is set up to scan on a linear wavelength scale, but all references to absorption bands have been converted to wave numbers (cm.$^{-1}$). The absorption of energy was read in units of optical density or absorbance; the ordinate of the absorption curves in the figures is labelled "% transmission", the origin being 0% and the topmost index line being 100% transmission. Most of the samples were run as contact films; any exceptions to this are noted on the spectra concerned. Since many of the compounds are highly hygroscopic, care was taken to eliminate moisture both from the windows and from the cell surfaces coming into contact with the samples, and by preparing the samples in a dry box or under the beam of an infrared lamp. The presence of (OH) bands is usually a fairly good test of water that may have been present in the sample or that may have been picked up during sample preparation. Water bands in the majority of the spectra were of negligible importance. Spectra were obtained at room temperature.

[1]*Manuscript received June 13, 1955.*
Contribution from the Physics Section, Suffield Experimental Station, Ralston P.O., Alberta.
[2]*Present address: Suffield Experimental Station, Ralston P.O., Alberta.*
[3]*Present address: University of British Columbia, Vancouver, B.C.*

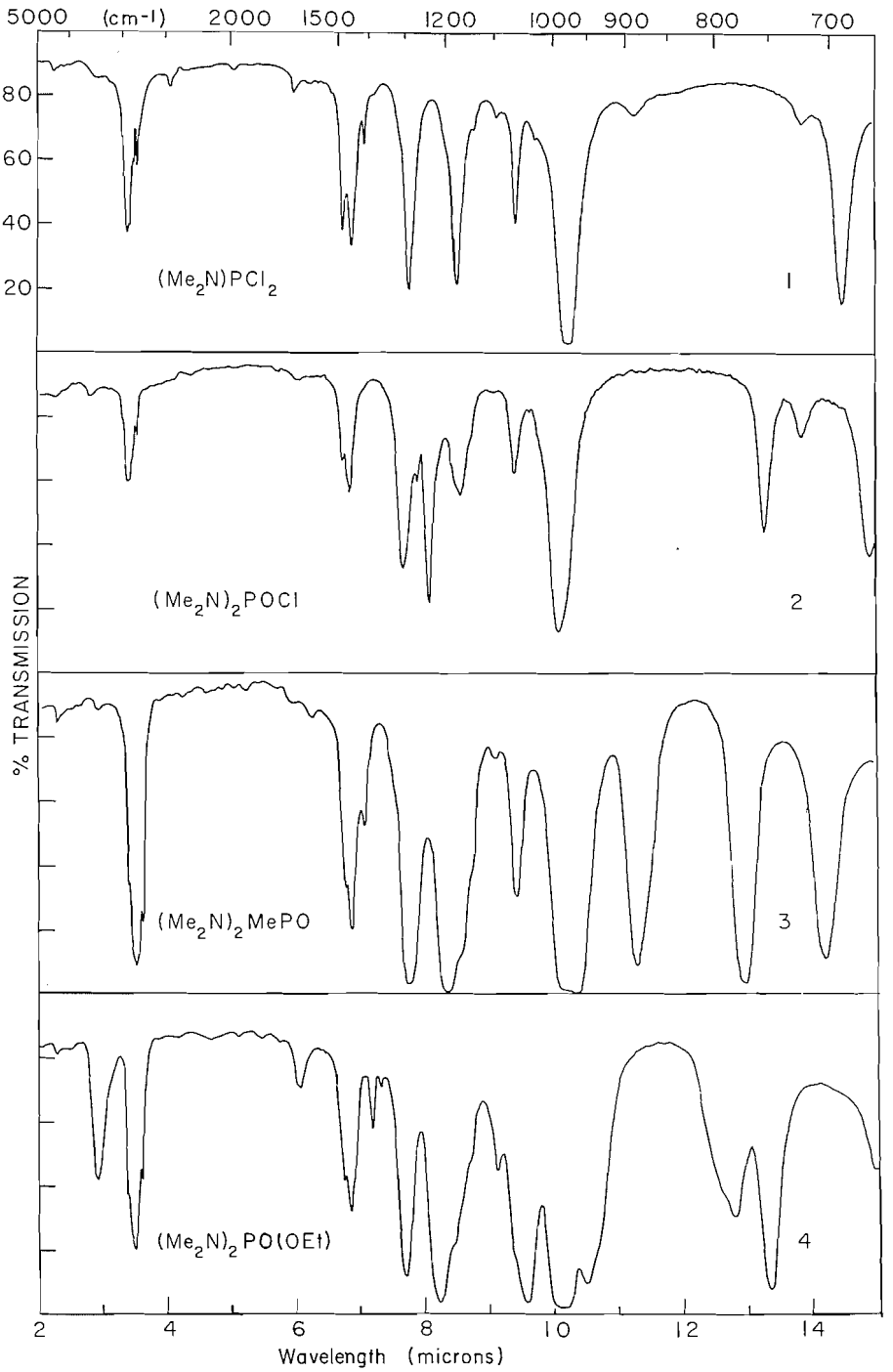

FIGS. 1 to 4.

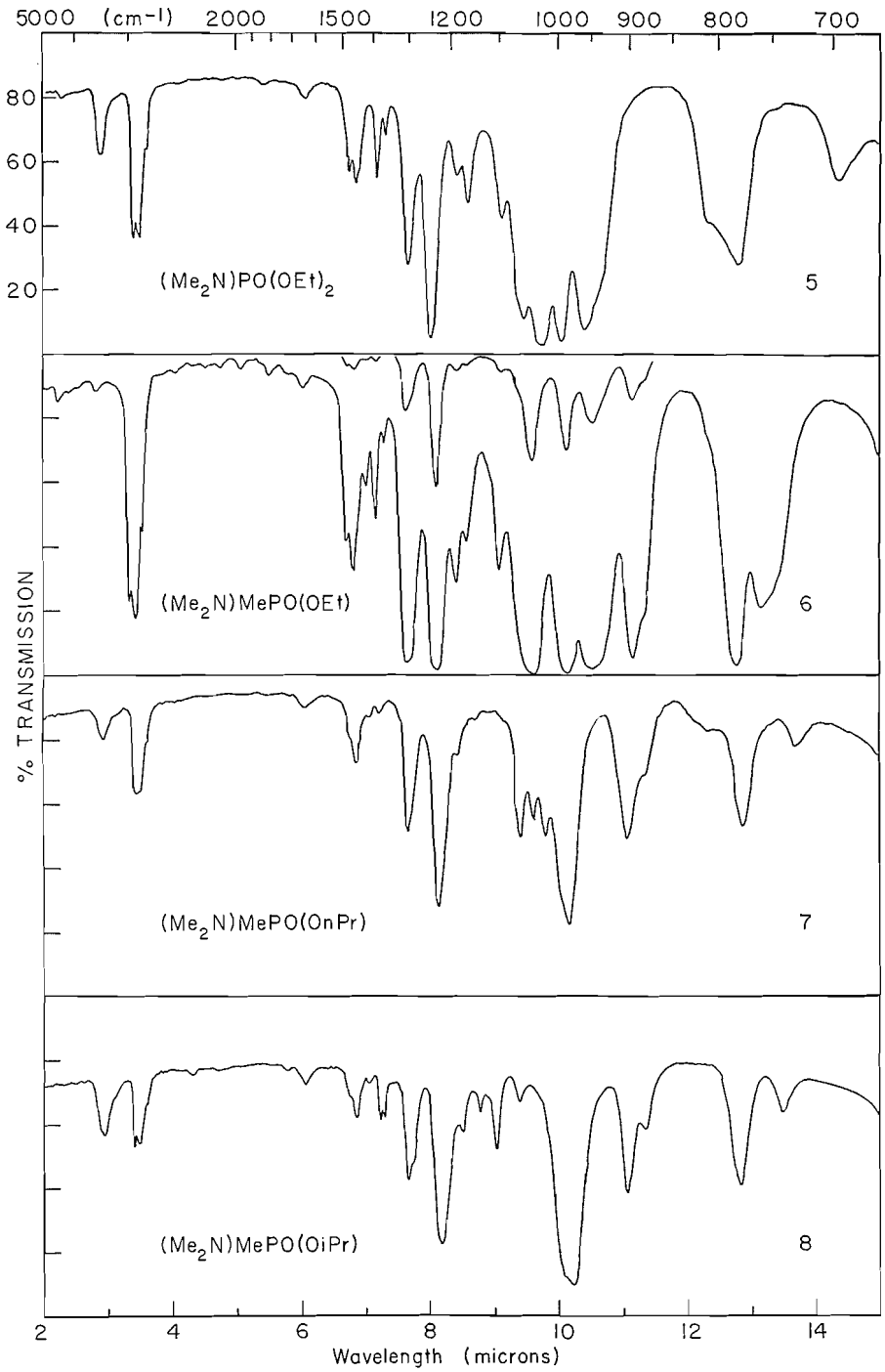

FIGS. 5 to 8.

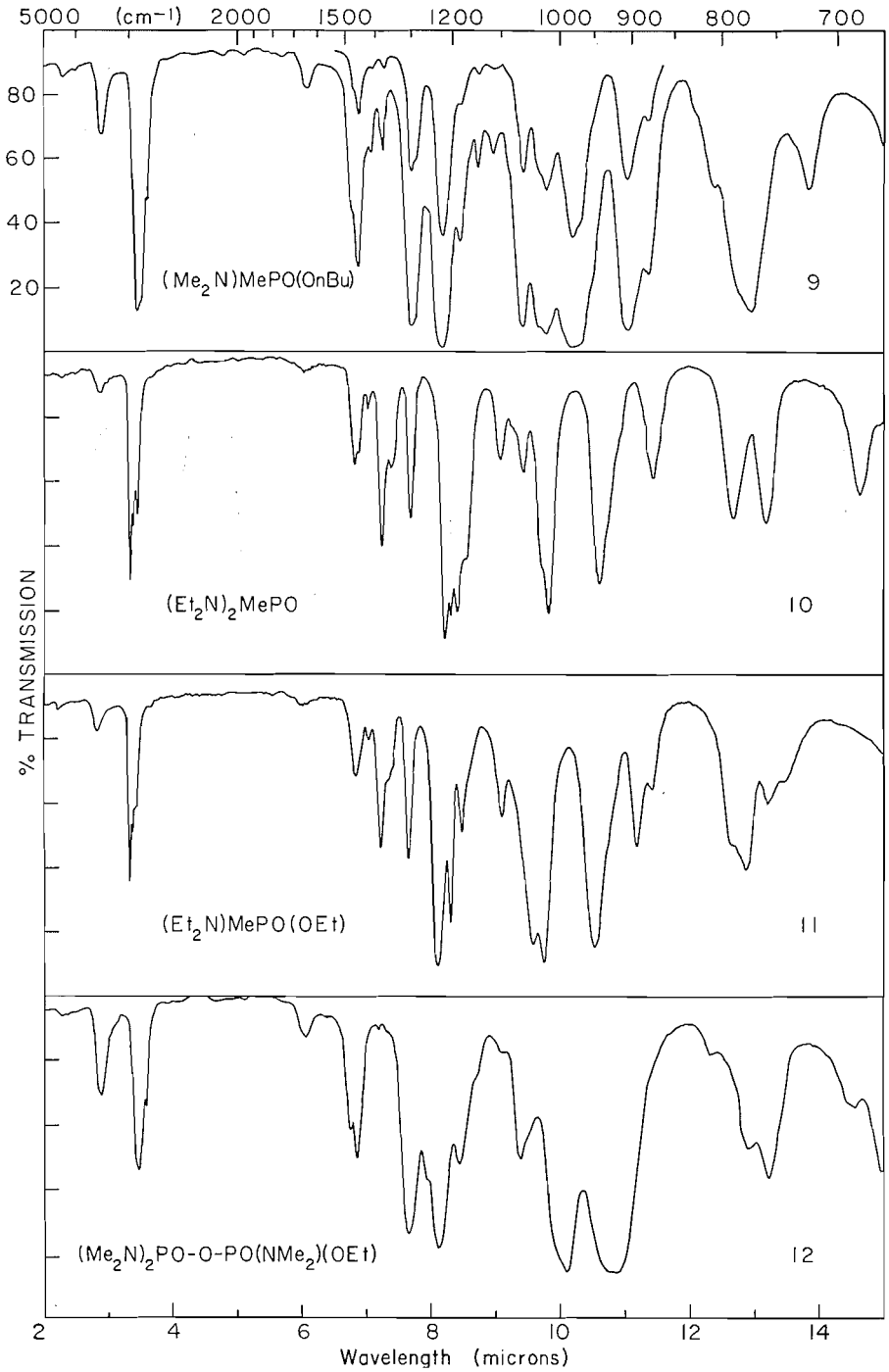

FIGS. 9 to 12.

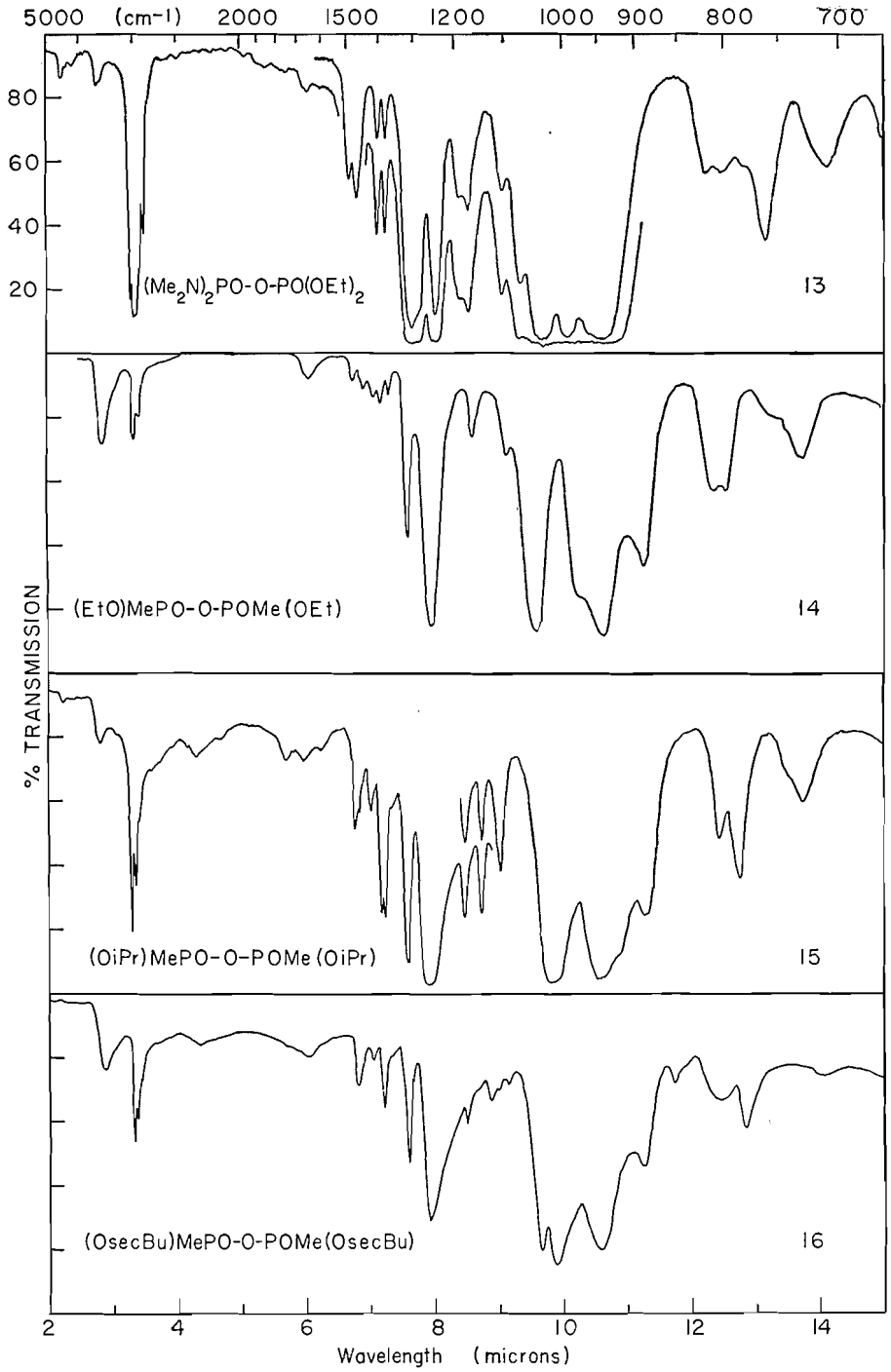

FIGS. 13 to 16.

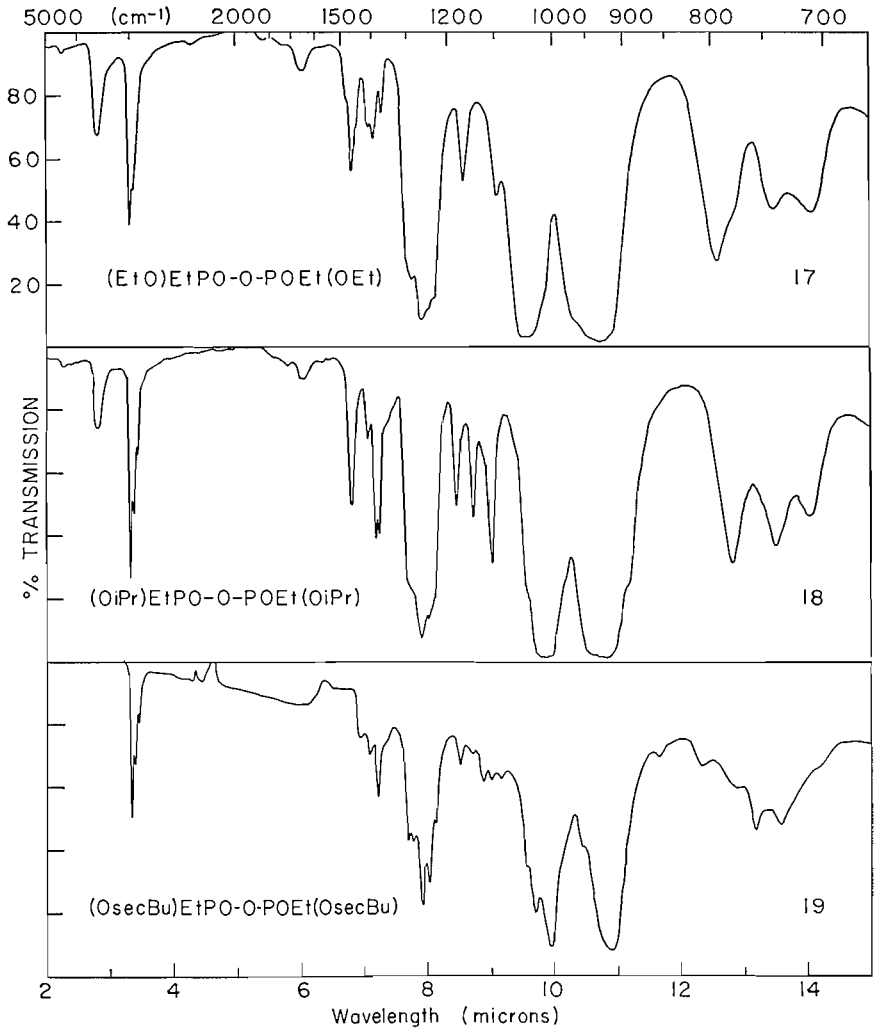

FIGS. 17 to 19.

Most of the compounds whose spectra are presented were prepared through the co-operation of the Chemistry Section of the Suffield Experimental Station. Redistilled materials were used, and where possible, separate preparations of the same compound were examined for deviations in the spectrum. The spectrum of any compound of doubtful purity is marked. In Table I are listed compounds that we are concerned with in this paper, together with their boiling points and refractive indexes. Formulas are given for compounds to avoid confusion in the nomenclature.

TABLE I*

COMPOUNDS EXAMINED BY INFRARED METHODS FOR STRUCTURAL CORRELATIONS

Compounds	Figure number	Boiling point, °C./mm.	Refractive index, °C./index	Remarks
$(Me_2N)PCl_2$	1	41/12.5	—	Chlorine: calc. 48.5%; found 48.42%
$(Me_2N)POCl_2$	—	88/25	22/1.4634	Chlorine: calc. 43.8%; found 44.0%
$(Me_2N)_2POCl$	2	76/2.5	28/1.4635	
$(Me_2N)_2MePO$	3	60.5/0.6	26.5/1.4560	
$(Me_2N)_2PO(OEt)$	4	59/1	24/1.4343	
$(Me_2N)PO(OEt)_2$	5	64/3	24/1.4175	
$(Me_2N)MePO(OEt)$	6	55/1	—	
$(Me_2N)MePO(OnPr)$	7	62.2/1	25.5/1.4320	
$(Me_2N)MePO(OiPr)$	8	42.5/0.04	22/1.4300	
$(Me_2N)MePO(OnBu)$	9	64/0.5	26/1.4341	
$(Et_2N)_2MePO$	10	91/1	21/1.4580	
$(Et_2N)MePO(OEt)$	11	54/1	21/1.4360	
$(Me_2N)_2PO—O—PO(NMe_2)_2$	—	82–83/10^{-3}	24/1.4620	
$(Me_2N)_2PO—O—PO(NMe_2)(OEt)$	12	—	20/1.4564	Purity not checked
$(Me_2N)(OEt)PO—O—PO(OEt)(NMe_2)$	—	—	18/1.4300	Purity not checked
$(Me_2N)_2PO—O—PO(OEt)_2$	13	101–103/5×10^{-4}	25/1.4380	
(EtO)MePO—O—POMe(OEt)	14	68–70/3.5×10^{-4}	20/1.4360	Analysis for carbon and hydrogen for all oxygen compounds checks well with theory
(OiPr)MePO—O—POMe(OiPr)	15	77–80/0.07	25/1.4270	
(O*sec*Bu)MePO—O—POMe(O*sec*Bu)	16	86/0.07	23/1.4329	
(EtO)EtPO—O—POEt(OEt)	17	70/7×10^{-4}	25/1.4342	
(OiPr)EtPO—O—POEt(OiPr)	18	65/6×10^{-4}	25/1.4304	
(O*sec*Bu)EtPO—O—POEt(O*sec*Bu)	19	85–87/0.07	20/1.4391	
(EtO)(EtO)PO—O—PO(OEt)(OEt)	—	110/0.05	25/1.4177	

**The compounds in this table were supplied by the Chemistry Section of the Suffield Experimental Station. Their data are quoted for boiling points, refractive indexes, and analytical results.*

RESULTS AND DISCUSSION

(*a*) *The Dimethylamino Grouping* (Me_2N)

Interest in the dimethylamino grouping, 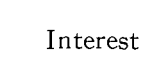 , has arisen from the compound Schradan, in which all the ethoxy groups (EtO) of tetraethyl pyrophosphate have been replaced by dimethylamino groups. Many phosphonic acid esters containing the dimethylamino group have been synthesized and spectra have appeared in some publications. Bellamy and Beecher (2) and Colthup (4) have ascribed an absorption band at about 7.8 μ (1280 cm.$^{-1}$) to secondary aromatic amines. Holmstedt and Larrson (11) suggest that bands at 9.94 to 10.11 μ (1006 to 989 cm.$^{-1}$) and 13.7 to 14.25 μ (730 to 702 cm.$^{-1}$) are characteristic of dimethylamino compounds. They suggest the latter absorption may be the result of stretching vibrations of the (P—N) bond in the combination 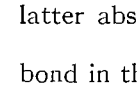 ; the former they suggest may be associated with vibration in the (C—N) bond. Corbridge and Lowe (5) have calculated the absorption wavelength to be expected from a (P—N) stretching vibration by Gordy's relation (9) to be about 13.5 μ (740 cm.$^{-1}$). This is in agreement with their observation of a strong absorption near 14.3 μ (700 cm.$^{-1}$) in each of their phosphoramidates. Absorption in the 6.18 and 6.8 μ (1620 and 1470 cm.$^{-1}$) regions may be ascribed to zwitterion formation in this type of compound.

The spectra of 13 of the 16 compounds considered are presented here, 11 of them containing the dimethylamino group, and 2 containing the diethylamino group (see Figs. 1 to 13). Some characteristic absorption bands of the compounds are assembled in Table II. Compounds containing alkyl hydrocarbon groups usually exhibit absorption from 3130 to 2860 cm.$^{-1}$, which is the region attributed to the (C—H) stretching vibrations. Absorption arising from dimethylamino groups appears in a narrow band from 2850 to 2780 cm.$^{-1}$. The absorption band in this region is usually rather weak and may consist of a subsidiary peak or shoulder. The dimethylamino group appears to absorb at 2910 and 2890 cm.$^{-1}$ respectively in the two compounds.

Absorption in the region of 1470 cm.$^{-1}$ appears to be enhanced when dimethylamino groups are attached to phosphorus. A comparison of the spectra of compounds containing the dimethylamino group with the spectra of similar compounds without the group indicates a predominant absorption peak at 1460 to 1450 cm.$^{-1}$. Absorption is almost continuous over the region 1480 to 1430 cm.$^{-1}$ for the compound $[(Me_2N)(EtO)PO]_2O$. The two compounds containing diethylamino groups exhibit absorption in the region 1390 to 1350 cm.$^{-1}$, rather than at 1470 to 1450 cm.$^{-1}$, considerably greater than is normally observed for ethyl esters of phosphonic acids—compare for instance, the spectrum of tetraethyl pyrophosphate.

Compounds containing the methyl phosphoryl group (Me—P=O) exhibit a single sharp absorption band at about 1308 cm.$^{-1}$ with a width at half

TABLE II

CORRELATION OF ABSORPTION BANDS WITH (NMe_2) GROUPS IN SOME PHOSPHORO-ESTERS

Compound	Figure number	2860–2780 cm.$^{-1}$ region	1470 cm.$^{-1}$ region	1320–1280 cm.$^{-1}$ region	1190 cm.$^{-1}$ region	1070 cm.$^{-1}$ region	1000–980 cm.$^{-1}$ region	710–670 cm.$^{-1}$ region
$(Me_2N)PCl_2$	1	2840 2790	1478 1450	1287 (25)*	1175	1063	978	690 s
$(Me_2N)POCl_2$	—	2820	1486 1468	1315 (33)	1175	1070	994	723 s
$(Me_2N)_2POCl$	2	2820	1485 1468	1307 (36)	1175	1068	995	755 m 672 m
$(Me_2N)_2POMe$	3	sh 2800 2760	1480 1460	1300 (36)	1184	1065	988 970	704 s
$(Me_2N)_2PO(OEt)$	4	2750	— 1460	1303 (34)	1184	sh 1070	989	665
$(Me_2N)PO(OEt)_2$	5	2760	1458 1450	1308 (22)	1190	1062	998	698
$(Me_2N)POMe(OEt)$	6	2810	1465 sh 1450	1303 (33)	1188	sh 1068	988	660
$(Me_2N)POMe(OnPr)$	7	2770	1460 sh 1440	1308 (34)	1188	1067	sh 999 985	660 w
$(Me_2N)POMe(OiPr)$	8	2760	1458 sh 1448	sh 1295 (41)	1178	1067	sh 994 980	662 w
$(Me_2N)POMe(OnBu)$	9	2770	— 1462	1305 (33)	1190	1067	986 sh 975	660 mw
$(Et_2N)_2POMe$	10	2890	1472 1459	1305 (16)	1192 1177	1065	—	684 m
$(Et_2N)POMe(OEt)$	11	2910	1467 sh 1453	1310 (16)	1184	sl sh 1065	—	662 mw
$(NMe_2)_2PO—O—PO(NMe_2)_2$	—	2810	— 1466	1310 (36)	1188	1070	992	668 s
$(NMe_2)_2PO—O—PO(NMe_2)(OEt)$	12	2790	— 1460	1310 (41)	1188	1068	993	668 mw
$(NMe_2)(OEt)PO—O—PO(NMe_2)(OEt)$	—	2790	1460 1448	Very broad	1188	Very broad	982 (absorption from 900 to 1100 cm.$^{-1}$)	Not clear
$(NMe_2)_2PO—O—PO(OEt)_2$	13	2850	— 1468	1305 Very broad Several peaks merged	1190	1070	994	710 m 667 w

The figures in brackets indicate the width of the absorption band at half the maximum height of the peak.

height ($\Delta\nu_{1/2}$,)* of about 16 cm.$^{-1}$. Absorption is shown in the region 1320 to 1280 cm.$^{-1}$ by compounds having a dimethylamino group, and if (Me—PO) and (Me_2N) groups both are present, the sharp absorption band of the former is obscured. Measurement of $\Delta\nu_{1/2}$ in such compounds gives values of 33 to 40 cm.$^{-1}$ (see Table II). In compounds that have no (Me—P) linkage, e.g. (Me_2N)PCl_2 and (Me_2N)$(OEt)_2PO$ the $\Delta\nu_{1/2}$ value is usually about 22 to 36 cm.$^{-1}$. In two pyrophosphate compounds, $[(Me_2N)(OEt)PO]_2O$ and $(Me_2N)_2PO—O—PO(OEt)_2$, the band is merged with other absorption bands in the region and does not appear as a discrete peak. The $\Delta\nu_{1/2}$ value for two compounds with diethylamino groups is 16 cm.$^{-1}$ and, since both compounds contain (Me—PO) groups, there appears to be no absorption contributed by the diethylamino group in the region 1320 to 1280 cm.$^{-1}$. From the results of the spectra examined it appears that absorption in the region 1320 to 1280 cm.$^{-1}$ is characteristic of dimethylamino groups in phosphonic acid esters, and it may be distinguished from absorption arising from (Me—PO) groups by the $\Delta\nu_{1/2}$ values: $\Delta\nu_{1/2}$ = 30 cm.$^{-1}$ for (Me_2N), 16 cm.$^{-1}$ for (Me—PO), and 35 cm.$^{-1}$ for both groups on the phosphorus atom. In some pyrophosphates the band may not be clearly separated from bands lying at slightly longer wavelengths (see the last two compounds of Table II).

The regions near 1190 cm.$^{-1}$ and 1064 cm.$^{-1}$ give rise to consistent absorption for all the compounds studied (see Table II). The maximum and minimum values of the 1190 cm.$^{-1}$ band are 1175 and 1192 cm.$^{-1}$, and of the 1064 cm.$^{-1}$ band, 1063 and 1070 cm.$^{-1}$ respectively. It may be noticed that all compounds give a discrete peak in the 1190 cm.$^{-1}$ region with the exception of $(Et_2N)_2MePO$ with two peaks, at 1192 and 1177 cm.$^{-1}$. There appears to be no certain method of determining the assignment here, but tentatively the 1192 cm.$^{-1}$ peak was chosen as being the more intense. In two pyrophosphates the 1064 cm.$^{-1}$ peak is merged with other absorption bands.

Absorption in the region 1050–950 cm.$^{-1}$ is frequently associated with the (P—O—C) linkage, suggested to arise more specifically from the P—O—(C) bond. Examination of the spectra of three compounds without this linkage, e.g., (Me_2N)PCl_2, (Me_2N)$POCl_2$, and (Me_2N)$_2POCl$, discloses a strong absorption band in the 1000 to 980 cm.$^{-1}$ region. A similar absorption band can be found in the remainder of the compounds, the minimum and maximum values of wavelength being 998 and 978 cm.$^{-1}$. The range of absorption is

*$\Delta\nu_{\frac{1}{2}}$ *is defined as the width of the absorption band in cm.*$^{-1}$ *at half the maximum optical density. D. A. Ramsay has derived an expression (J. Am. Chem. Soc. 74: 72. 1952)*

$$A = (K/cl)\log_e[(T_0)/(T)\nu_{max}] \times \Delta\nu_{\frac{1}{2}}^{a}$$

where $K \simeq \pi/2$ *for condition of slit width much smaller than band width at half intensity,*
c is the concentration of the solution in moles per liter,
l is the absorption path length,
$\log_e[(T_0)/(T)\nu_{max}]$ *is the apparent peak intensity of the band at the frequency* ν_{max},
$\Delta\nu_{\frac{1}{2}}^{a}$ *is the apparent half intensity width of the band.*
This formula permits comparisons of integrated band intensities at different parts of the spectrum. For the comparison of bands on a quantitative basis linear wavelength absorption curves are replotted on a linear wave number scale and the area under the curve determined. For comparison of absorption bands common to a series of a molecular species, values of $\Delta\lambda_{\frac{1}{2}}$ *(microns) may be substituted for* $\Delta\nu_{\frac{1}{2}}$ *(cm.*$^{-1}$*) without serious error for bands occurring over a narrow range of frequencies.*

rather narrow and the substitution of ethyl for methyl appears to shift the absorption band out of this region.

A calculation of the absorption frequency of the (P—N) stretching vibration from Gordy's rule gives a value of 735 cm.$^{-1}$ or 13.6 μ. Corbridge and Lowe (5) have observed strong absorption near 14.3 μ (700 cm.$^{-1}$). The position of this band may be expected to be variable depending on the characteristics of the other groups associated with the phosphorus atom. The assignment of specific bands to any linkage is uncertain since the region 770 to 670 cm.$^{-1}$ is usually associated with skeletal vibrations which may be strongly influenced by comparatively small structural changes. The last column of Table II suggests absorption bands which may arise out of (P—NMe_2) vibrations. In this column the absorption bands are designated as weak (w), medium (m), or strong (s).

An examination of the position of the absorption band arising from the (P=O) bond indicates a shift toward longer wavelengths when a dimethylamino or a diethylamino group is substituted into the molecule. The shift of the (P=O) band position is shown in Table III for several compounds.

TABLE III

EFFECT OF (Me_2N) GROUPS AND (Et_2N) GROUPS ON THE POSITION OF (P=O) ABSORPTION BAND POSITION (CM.$^{-1}$)

Compound	Number of (Me_2N) substituent groups		
	0	1	2
$POCl_3$	1305	1268	1241
$(EtO)_3PO$	1277	1250	1220
$(EtO)_2PO—O—PO(OEt)_2$	1298	1268	1242 1234
$(EtO)_2MePO$	1243	1234	1205
$(EtO)_2MePO$*	1243	1238	1221

**The substituent group was (Et_2N) in place of (Me_2N).*

In all cases but the first, the shift of band position is greater on substitution of a second dialkylamino group into the molecule.

The effect of a substituted dimethylamino group on the magnitude of the band shift is greater than that of a diethylamino group for one set of compounds. A correlation between the substituent groups and the position of the (P=O) band has been put forward by several authors and elaborated in (1). The relationship is

$$\lambda(\mu)(P{=}O) = (39.96 - \sum x)/3.995$$

where $\lambda(\mu)$(P=O) is the expected wavelength for the phosphoryl absorption band in microns.

$\sum x$ is the sum of the "phosphoryl absorption shift constants" of the substitu-

ents attached to the phosphorus atom. Values are quoted for x for a wide range of atoms and radicals and a value of 3.0 is assigned to the (NR_2) group. Using this relationship the "phosphoryl absorption shift constants" for the dimethylamino and diethylamino groups have been calculated for the compounds in Table II. The values are 2.46±0.1 average deviation for the dimethylamino group (14 compounds), and 2.75±0.1 average deviation for the diethylamino group (2 compounds).

Absorption of radiation in the region of 3.4 μ (2940 cm.$^{-1}$) has been associated with (C—H) stretching vibrations (10, p. 195). The absorption bands observed in the region 2860 to 2780 cm.$^{-1}$ are probably attributable to (C—H) stretching in the dimethylamino group. The failure of diethylamino substituents to show absorption in this region is not clear since such absorption is present in the spectrum of diethylamine itself. Absorption in the region of 6.8 μ (1470 cm.$^{-1}$) is attributed to bending vibrations in the methyl group (6; 8; 10, p. 195). Absorption at 7.56 μ and 7.65 μ (1325 and 1308 cm.$^{-1}$) is associated with methyl symmetrical bending in Me_3PO (6). Absorption bands are observed in these two regions for compounds containing dimethylamino groups but they appear to be shifted when the substituent is diethylamino. Energy absorptions at 1190 cm.$^{-1}$ and 1064 cm.$^{-1}$ occur over rather narrow bands for a wide variety of substituents on the phosphorus atom and the vibration mode may not include the phosphorus atom itself. A calculation by Gordy's rule (9) suggests a wavelength of 8.5 μ (1178 cm.$^{-1}$) for the (C—N) stretching vibration and the bands at 8.4 μ and 9.4 μ (1190 cm.$^{-1}$ and 1064 cm.$^{-1}$) may arise out of the dialkylamino skeleton $\left(C\begin{smallmatrix}\diagup N\\ \diagdown N\end{smallmatrix}\right)$. This is supported by the fact that the wavelength varies only slightly from compound to compound, the band falls roughly in the same region as the (P)—O—C bands, and the terminal group may be ethyl or methyl without shifting the band position very much. The absorption band observed in the 1000 to 980 cm.$^{-1}$ region may involve the terminal methyl group since change of substituent from dimethylamino to diethylamino causes the band to be shifted from the region. The (P—N) stretching vibration should give rise to absorption near 13.6 μ (735 cm.$^{-1}$) according to Gordy's rule (9), but the assignment of specific bands in the 13 to 15 μ (770 to 670 cm.$^{-1}$) region to any linkage is uncertain, as the region is usually associated with skeletal vibrations, which may be strongly influenced by comparatively small structural changes.

In summary, the bands which appear to be specific for the dimethylamino group in phosphonic acid esters are 1330 to 1300 cm.$^{-1}$, 1000 to 980 cm.$^{-1}$, and possibly 2860 to 2780 cm.$^{-1}$. Other bands associated with the dimethylamino and diethylamino groups are 1470 to 1450 cm.$^{-1}$, 1190 cm.$^{-1}$, 1064 cm.$^{-1}$, and perhaps 770 to 670 cm.$^{-1}$, but in the absence of bands giving confirmation to assignments in the latter region, the added evidence is not strong. An additional bit of information may be derived from the position of the absorption band for the (P=O) bond which may be displaced toward longer wavelengths as much as 64 cm.$^{-1}$ when two substituent dimethylamino groups are put into the molecule.

(b) The Pyrophosphate Grouping (PO—O—PO)

Interest in the group of compounds of the Schradan type and in the pyrophosphates generally has led to an investigation of the possibility of distinguishing the (PO—O—PO) linkage from the point of view of recognition in unknowns, or of testing reaction products for the formation of the linkage. Holmstedt and Larrson (11) have suggested that the (P—O—P) linkage may give rise to absorption at about 14.1 μ (710 cm.$^{-1}$) on a basis of two derivatives of pyrophosphoric acid. Bergmann, Littauer, and Pinchas (3) have observed a band at 10.3 to 10.6 μ (970 to 944 cm.$^{-1}$) which they attribute to the (P—O—P) linkage. The band is not so apparent in the *n*-propyl and isopropyl esters and it is suggested that the wavelength is shifted so that the band cannot be distinguished from the 9.8 μ (1020 cm.$^{-1}$) absorption of the (P—O—C) linkage. Corbridge and Lowe (5) compared the (P—O—P) stretching vibration with the (Si—O—Si) stretching at 9.5–9.7 μ (1052 to 1031 cm.$^{-1}$) and the (P—O—C aliphatic) at 9.3–9.9 μ (1077 to 1010 cm.$^{-1}$). They observe that (P—O—P) stretching bands near 11 μ (910 cm.$^{-1}$) appear to shift toward longer wavelengths with increasing length of the (P—O—P) chain in the inorganic pyrophosphates they studied. Absorption in pyrophosphates is usually limited to a single band near 14.2 μ (704 cm.$^{-1}$), but this may become double in triphosphates and metaphosphates. They suggest that some bands observed near 14.2 μ (704 cm.$^{-1}$) may be due to (P—O) bending in the (P—O—P) link.

Some compounds prepared in these laboratories were examined in the 950 to 910 cm.$^{-1}$ and the 715 cm.$^{-1}$ regions of the spectrum and the results are given in Table IV, together with the characteristic absorptions from compounds of a similar type prepared by other workers (7). Since these compounds are limited to substituted pyrophosphates, the column labelled "Compound"

TABLE IV

ABSORPTION BANDS CHARACTERISTIC OF THE PO—O—PO LINKAGE

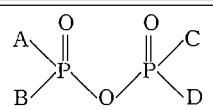

A	B	C	D		Absorption bands (cm.$^{-1}$) 950–900	$\Delta\nu_{\frac{1}{2}}$*	710–670‡
EtO	Me	Me	OEt	Fig. 14	943	62	<670
OiPr	Me	Me	OiPr	Fig. 15	945	60	<670
O*sec*Bu	Me	Me	O*sec*Bu	Fig. 16	947vb	64	714vw
OEt	Et	Et	OEt	Fig. 17	922†	—	712
OiPr	Et	Et	OiPr	Fig. 18	922	58	713
O*sec*Bu	Et	Et	O*sec*Bu	Fig. 19	928	51	704vw
EtO	EtO	EtO	EtO	—	940vb	—	697w
Me_2N	Me_2N	Me_2N	Me_2N	—	925	55	670s
Me_2N	Me_2N	OEt	Me_2N	Fig. 12	926	52	668, 690
Me_2N	OEt	Me_2N	OEt	—	938vb	—	—
Me_2N	Me_2N	OEt	OEt	Fig. 13	940	48	710
MeO	MeO	MeO	MeO	Ref. 7	980	—	704
$(P_2O_5)_2$				Ref. 7	1010	—	764
BuO	BuO	BuO	BuO	Ref. 7	953	—	700

*$\Delta\nu_{\frac{1}{2}}$ = *band width in cm.$^{-1}$ at half optical density.*
†*Spectrum was obtained from CS_2 solution.*
‡*Abbreviations in this column refer to band intensity: vw, very weak; w, weak; s, strong.*

gives the four substituents in the molecule. Strong absorption is observed in the 950 to 910 cm.$^{-1}$ regions in all compounds except two, viz. $(MeO)_2$-PO—O—PO $(OMe)_2$ and P_4O_{10}. With respect to the former compound, Bergmann, Littauer, and Pinchas (3) comment that the behavior of the first member of a homologous series may not be characteristic of the series. The absorption bands occur over a range of 947 cm.$^{-1}$ maximum to 922 cm.$^{-1}$ minimum. From an examination of the spectra of compounds without the (P—O—P) linkage, it appears unlikely that confusion would occur with other bands, with the exception of that from the ethyl ester group (EtO—P) which usually occurs at 962 to 944 cm.$^{-1}$ with a shoulder at 944 to 926 cm.$^{-1}$. Examination of the height and of the width at half height ($\Delta\nu_{1/2}$) indicates that the (EtO—P) band has a value of $\Delta\nu_{1/2}$ = 32 to 40 cm.$^{-1}$ in five phosphonic acid esters. The value of $\Delta\nu_{1/2}$ for the pyrophosphate derivatives varies from 48 to 64 cm.$^{-1}$ (average 56 cm.$^{-1}$) with two compounds exhibiting peaks broadened so that continuous absorption occurs over the 1000 to 910 cm.$^{-1}$ region.

Absorption in the region 715 to 670 cm.$^{-1}$ is strong and well defined in only a few cases—Fig. 13, and for the compounds $(NMe_2)_2PO—O—PO(NMe_2)_2$, $(MeO)_2PO—O—PO(OMe)_2$, P_2O_5, and $(BuO)_2PO—O—PO(OBu)_2$. The range of wavelength is considerable, and absorption bands occurring at the limit of the range of the instrument are labelled "<670". P_2O_5 exhibits a well-defined absorption at 763 cm.$^{-1}$ and this shortening may correlate with the band at 1010 cm.$^{-1}$ instead of 950 to 910 cm.$^{-1}$. In general it would not appear reliable to attribute absorption bands in the 715 to 670 cm.$^{-1}$ region to the (P—O—P) linkage but they may be confirmatory in the presence of strong broad absorption at 950 to 910 cm.$^{-1}$.

Briefly, organic esters of phosphorus-containing compounds with a linkage (P—O—P) may best be distinguished by the presence of a strong broad absorption band in the spectral region 950 to 910 cm.$^{-1}$. The ethyl ester grouping (EtO—P) is most likely to be confused, but the width of the band at half intensity ($\Delta\nu_{1/2}$) for five esters with this grouping is not greater than 40 cm.$^{-1}$, while the average value of $\Delta\nu_{1/2}$ for the pyrophosphates considered is 56 cm.$^{-1}$. An additional absorption band at 715 to 670 cm.$^{-1}$ may furnish additional evidence, but it is confirmatory only.

The authors wish to thank the Chemistry Section of the Suffield Experimental Station for preparation of the compounds and for the analytical work, and Mr. E. A. Jackman for obtaining many of the spectra and preparing the figures for this paper.

REFERENCES

1. Bell, J. V., Heisler, J., Tannenbaum, H., and Goldenson, J. J. Am. Chem. Soc. 76: 5185. 1954.
2. Bellamy, L. J. and Beecher, L. J. Chem. Soc. 475, 1701. 1952.
3. Bergmann, E. D., Littauer, U. Z., and Pinchas, S. J. Chem. Soc. 847. 1952.
4. Colthup, N. B. J. Opt. Soc. Amer. 40: 397. 1950.
5. Corbridge, D. E. C. and Lowe, E. J. J. Chem. Soc. 493. 1954.
6. Daasch, L. W. and Smith, D. C. J. Chem. Phys. 19: 22. 1951.
7. Daasch, L. W. and Smith, D. C. Anal. Chem. 23: 853. 1951.
8. Francis, S. A. J. Chem. Phys. 18: 861. 1950.
9. Gordy, W. J. Chem. Phys. 14: 305. 1946.
10. Herzberg, G. Molecular spectra and molecular structure. Vol. II. D. Van Nostrand Company, Inc., New York. 1945.
11. Holmstedt, B. and Larrson, L. Acta. Chem. Scand. 5: 1179. 1951.

THE ANALYSIS OF FLUOROCARBONS: USE OF INFRARED SPECTROPHOTOMETRY FOR THE ANALYSIS OF SMALL SAMPLES[1]

By P. B. Ayscough[2]

ABSTRACT

A method for the analysis of small quantities of mixtures of carbon tetrafluoride, hexafluoroethane, and fluoroform based on measurement of the intensity of infrared absorption bands is described. The relation between pressure and optical density for the main absorption bands of each gas was determined and used to calculate the composition of synthetic mixtures. These results were compared with those obtained by mass spectrometric analysis.

INTRODUCTION

Analytical procedures for handling small quantities of fluorocarbons are, as yet, largely undeveloped, though the physical and chemical properties of these compounds are well known. In order to make possible an examination of the reactions of trifluoromethyl radicals it was necessary to find an accurate and rapid method for the analysis of carbon tetrafluoride, hexafluoroethane, and fluoroform in quantities of 10 micromoles or less.

A summary of the various methods for analyzing fluorine compounds is to be found in Volume II of *Fluorine Chemistry* edited by J. H. Simons (Academic Press Inc., 1954). Procedures based on differences in vapor pressure or vapor density were shown to be of little value for analyzing these mixtures, and the chemical methods, such as pyrolysis over white-hot silica, combustion in moist hydrogen, and sodium fusion, give only values for the average carbon and fluorine content. Conventional oxidation methods cannot be used because of the high resistance to oxidation of fluorocarbons.

Mass-spectrometric analysis is one possible method since the mass spectra of most of the simple fluorine-containing compounds are known (2). However, a characteristic feature of the mass spectra of fluorocarbons is the almost complete absence of parent peaks and, for the straight-chain fluorocarbons, the preponderance of the mass 69 peak (CF_3^+). This means that the analysis depends on the magnitude of the relatively minor peaks which are frequently common to a large number of fluorocarbons. Carbon tetrafluoride is particularly difficult to estimate in this way because all of its peaks are shared by other fluorocarbons and it must be estimated from the residual 69 (CF_3^+) and 50 (CF_2^+) peaks.

Nevertheless, the method has been used successfully during the course of this work for the estimation of mixtures of carbon tetrafluoride, hexafluoroethane, and fluoroform in the presence of carbon monoxide and carbon dioxide. The results of a few analyses of test samples will be presented in a later section.

An examination of the infrared absorption spectra of carbon tetrafluoride,

[1]*Manuscript received July 11, 1955.*
Contribution from the Division of Pure Chemistry, National Research Council, Ottawa, Canada. Issued as N.R.C. No. 3716.
[2]*National Research Council Postdoctorate Fellow, 1953–1955.*

hexafluoroethane, and fluoroform showed the presence of a number of strong well-defined bands in the region 1000–1500 cm.$^{-1}$ which might be used for analysis. It was shown experimentally that with the exception of carbon tetrafluoride these compounds obey Beer's law in this region and that for samples of 5–10 micromoles an accuracy of $\pm 5\%$ can be obtained. The results of experiments designed to determine the relation between intensity and pressure for these compounds are presented in this paper, together with the analysis of some test samples.

Although the spectra of higher fluorocarbons are more complex it is reasonable to suppose that this method can be extended to estimate mixtures of other fluorocarbons in the same way as it is applied to the estimation of complex mixtures of hydrocarbons.

EXPERIMENTAL

Apparatus

Optical density measurements were made using a Perkin-Elmer Model 21 double beam recording spectrophotometer with a sodium chloride prism. The optical cell used in conjunction with this instrument was made of pyrex with polished sodium chloride windows fixed with Benolite cement. The cell had a volume of 155 ml. and was fitted with a stopcock and ground glass joint for admitting the samples of gas. Silicone grease was used on all joints to reduce absorption of the gas. No absorption of gas on the walls of the vessel was observed. The pressure of gas in the optical cell was calculated by measuring the pressure of the sample in a calibrated gas burette and then allowing the gas to expand into the cell. A pressure of 1 mm. in the cell is given by about 8 micromoles of gas.

Materials

Samples of carbon tetrafluoride, hexafluoroethane, and fluoroform of unspecified purity were supplied by E.I. du Pont de Nemours and Co. Inc. to whom we are greatly indebted. The gases were purified by bulb to bulb distillation in the vacuum system, a small middle fraction being taken in each case for calibration purposes. The mass spectra and infrared absorption spectra of these samples were identical with those published previously (1, 2, 5–8) and they were therefore assumed to be pure.

RESULTS AND DISCUSSION

For the purpose of analysis the important spectral region is from 1000 to 1500 cm.$^{-1}$. Since the spectra have already been published, they will not be reproduced here. The only strong line in the carbon tetrafluoride spectrum is that at 1284 cm.$^{-1}$, which is well separated from the strongest absorption bands of hexafluoroethane (1253 cm.$^{-1}$) and fluoroform (1152 cm.$^{-1}$), so that it is possible to use the intensity of these bands as a measure of the partial pressure of each gas in a mixture. Weaker bands in the hexafluoroethane spectrum (1117 and 1123 cm.$^{-1}$) and in the fluoroform spectrum (1380 cm.$^{-1}$) might be used under conditions in which the other bands are too intense.

Measurements of peak optical density were made for each band, using the pure gases, and although some deviation from Beer's law is observed in the

case of carbon tetrafluoride and fluoroform this is not serious enough to affect the validity of the method. All measurements were made with comparable slit widths with no matching cell in the control beam of the spectrophotometer. The base lines were obtained with the cell evacuated and all measurements of optical density were made from these reference lines. Tables I–III and Figs. 1–3 indicate the results of these experiments.

TABLE I

OPTICAL DENSITY OF CARBON TETRAFLUORIDE

Sample	Pressure (mm.)	Optical density, 1284 cm.$^{-1}$
A1	0.84	0.80
A2	0.646	0.75
A3	0.44	0.545
A4	0.24	0.344
A5	0.12	0.20
A6	0.95	0.92
A7	0.655	0.70
A8	0.46	0.52
A9	0.074	0.115

TABLE II

OPTICAL DENSITY OF HEXAFLUOROETHANE

Sample	Pressure (mm.)	Optical density		
		1253 cm.$^{-1}$	1123 cm.$^{-1}$	1117 cm.$^{-1}$
B1	0.470	0.690	0.130	0.200
B2	0.251	0.375	0.068	0.105
B3	0.157	0.215	0.042	0.054
B4	0.091	0.128	0.021	0.032
B5	0.652	1.032	0.215	0.302
B6	0.439	0.652	0.127	0.180
B7	0.273	0.402	0.077	0.109
B8	0.187	0.258	0.050	0.070
B9	0.129	0.173	0.033	0.047
B10	0.930		0.269	0.389

TABLE III

OPTICAL DENSITY OF FLUOROFORM

Sample	Pressure (mm.)	Optical density	
		1380 cm.$^{-1}$	1152 cm.$^{-1}$
C1	1.14	0.092	0.625
C2	0.695	0.064	0.400
C3	0.223	0.020	0.165
C4	0.152		0.105
C5	1.42	0.110	0.750
C6	0.970	0.073	0.520
C7	0.646	0.045	0.348
C8	0.385		0.236
C9	0.213		0.147
C10	0.643	0.051	0.363
C11	0.729	0.055	0.405
C12	1.73	0.123	0.80
C13	1.06	0.083	0.583

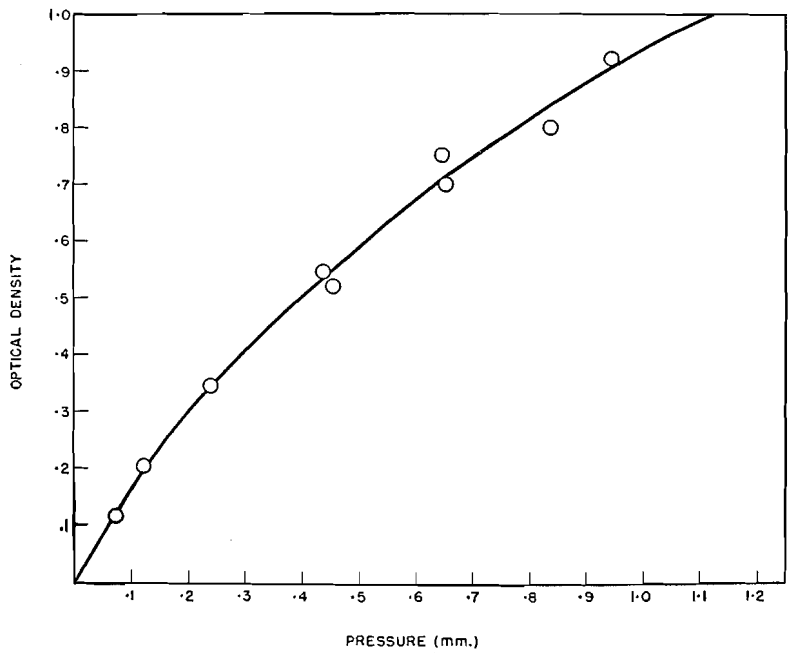

FIG. 1. Optical density of carbon tetrafluoride.

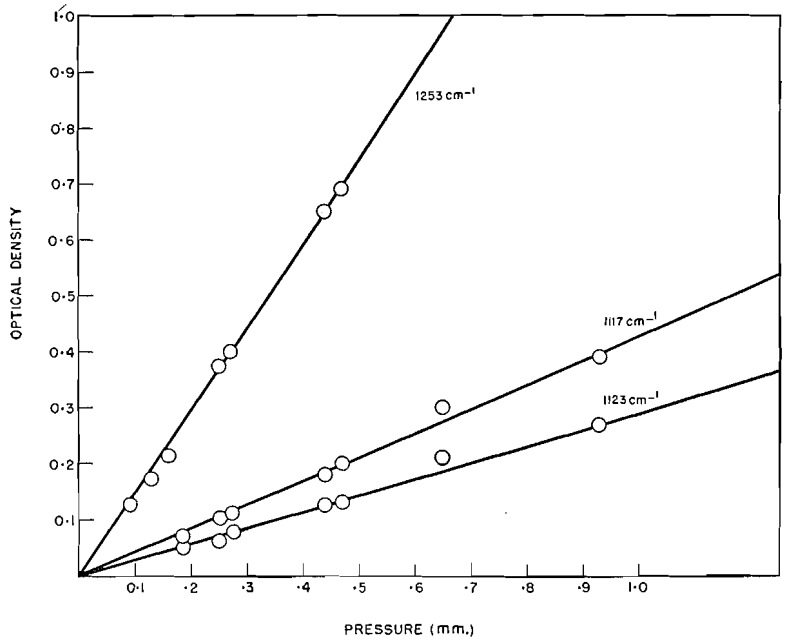

FIG. 2. Optical density of hexafluoroethane.

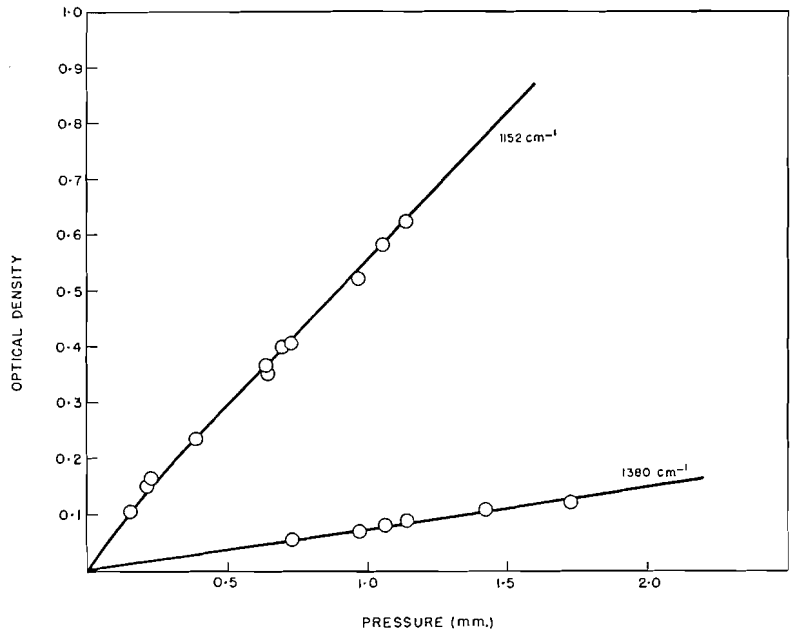

FIG. 3. Optical density of fluoroform.

Spectra of Mixtures

In order to check the accuracy of analyses using these absorption bands a number of mixtures were prepared. The absorption spectrum of each was observed under the same conditions as were used for the samples of pure materials, and from the peak heights the partial pressure of each was calculated and compared with the true values. There is very little overlap of absorption bands and it is necessary to apply a correction only in the case of the 1152 cm.$^{-1}$ band of fluoroform in the presence of hexafluoroethane. This correction becomes significant when C_2F_6/CF_3H is of the order of 5:1 or greater. The results of analyses of these test mixtures are shown in Table IV. It will be seen that there is good agreement between the values obtained in this way and those obtained by synthesis. In some cases the mixtures were also analyzed mass spectrometrically. The results of these analyses are added to the table for comparison.

Since the time this method of analysis was established, it has been used on numerous occasions in connection with a series of investigations of the reactions of trifluoromethyl radicals (3, 4). The mixtures have consisted, in general, of hexafluoroethane and fluoroform in the presence of small amounts of methane, ethane, and hexafluoroacetone. Small quantities of impurities such as these are of no importance since they do not absorb in the same region as the fluorocarbons. The only serious limitation so far observed is that resulting from pressure broadening of the fluoroform band in the presence of large amounts of hydrogen-containing material. Abnormally high results are obtained in this

TABLE IV

OPTICAL DENSITY OF MIXTURES

Sample	Volume (ml.) by synthesis			Volume (ml.) by infrared absn.			Volume (ml.) by mass spectrometer		
	CF_4	C_2F_6	CF_3H	CF_4	C_2F_6	CF_3H	CF_4	C_2F_6	CF_3H
M1	—	0.505	0.058	—	0.488	0.062	—	0.485	0.060
M2	—	0.335	0.323	—	0.344	0.320	—	0.331	0.316
M3	—	0.252	0.240	—	0.266	0.230	—	0.266	0.235
M4	—	0.146	0.249	—	0.160	0.251	—		
M5	—	0.114	0.528	—	0.120	0.510	—		
M6	—	0.040	0.657	—	0.042	0.667	—		
M7	0.030	0.183	—	0.034	0.165	—	0.034	0.170	—
M8	0.062	0.143	—	0.071	0.137	—	0.066	0.133	—
M9	0.156	0.033	—	0.152	0.035	—	0.147	0.037	—
M10	0.061	0.142	0.166	0.072	0.134	0.166	0.065	0.145	0.172
M11	0.160	0.088	0.098	0.162	0.087	0.099	0.153	0.085	0.096
M12	0.046	0.074	0.175	0.055	0.075	0.169	0.047	0.075	0.167
M13				—	0.102	0.025	—	0.104	0.026
M14				—	0.072	0.038	—	0.069	0.039
M15				—	0.096	0.044	—	0.093	0.045

way, and to overcome this difficulty new calibration curves have to be plotted for each total pressure. This is tedious, but under these conditions the mass-spectrometric method was equally unsatisfactory.

ACKNOWLEDGMENTS

The author is greatly indebted to Dr. R. N. Jones for the use of the infrared spectrophotometer and to Mr. R. Lauzon for its operation. Thanks are also due to Miss F. Gauthier for the mass-spectrometric analyses.

REFERENCES

1. American Petroleum Institute Research Project 44, Catalog of infrared spectral data.
2. American Petroleum Institute Research Project 44, Catalog of mass spectrometric data.
3. AYSCOUGH, P. B. J. Chem. Phys. In press. 1955.
4. AYSCOUGH, P. B., POLANYI, J. C., and STEACIE, E. W. R. Can. J. Chem. 33: 743. 1955.
5. BARCELO, J. J. Research Natl. Bur. Standards, 44: 521. 1950.
6. NIELSEN, J. R., RICHARDS, C. M., and MCMURRY, H. L. J. Chem. Phys. 16: 67. 1948.
7. PLYLER, E. K. and BENEDICT, W. S. J. Research Natl. Bur. Standards, 47: 202. 1951.
8. WOLTZ, P. J. H. and NIELSEN, A. H. J. Chem. Phys. 20: 307. 1952.

SOME MEASUREMENTS ON THE IRON (111) – THIOCYANATE SYSTEM IN AQUEOUS SOLUTION[1]

By M. W. Lister and D. E. Rivington

ABSTRACT

A spectrophotometric study of the ferric thiocyanate system is reported. The temperature and ionic strength of the solutions were carefully controlled, and suitable precautions were taken against fading. From the data, values of the equilibrium constant for the formation of $FeSCN^{++}$ from simple ions, and of the extinction coefficients of $FeSCN^{++}$ were obtained for different temperatures and ionic strengths, with results that differed somewhat from earlier values. The effect of varying acidity was also investigated. From more concentrated solutions, values for the equilibrium constants for the formation of $Fe(SCN)_2^+$ and $Fe(SCN)_3$ were obtained; it was not necessary to postulate higher complexes.

Many investigations have been made of aqueous solutions containing ferric and thiocyanate ions, starting with the original work of Gladstone (9) just over a hundred years ago. However it was only comparatively recently that Moeller (15) and, independently, Bent and French (3) showed that in dilute solution the color was due to the ion $FeSCN^{++}$. This put a new interpretation on the measurements made on this system, and as a result considerable further work was carried out (e.g. 6, 7, 10, 12, 18). This work mostly made use of the red color as a means of investigation, but some work was also done using solvent extraction (14), or electrochemical methods (15).

The present work was begun with the intention of using the red color of $FeSCN^{++}$ as a method of determining the concentration of free ferric ions in solution, and hence of evaluating the equilibrium constants of the dissociation of other complexes formed by ferric ions with other anions. This type of investigation was made by Lanford and Kiehl (13) for the ferric phosphate system. Although earlier work covered a fair range of conditions, it became apparent that in order to have an adequate picture of the system before adding other ions, it would be desirable to extend these measurements to cover systematically a range of temperature, hydrogen ion concentration, and ionic strength. These factors were therefore carefully controlled; temperature control, for instance, was provided by using absorption cells completely immersed in a thermostatted tank. The fading which occurs in these solutions had also to be taken into account, and it is believed conditions were found such that fading was negligible. It was also necessary to take into account the possible formation of the higher complexes, $Fe(SCN)_2^+$ and $Fe(SCN)_3$; and it was in fact possible to make a moderately accurate estimate of the extent to which these species were present, and so to determine their dissociation constants. In interpreting the experimental data, it is not necessary to assume that the extinction coefficients at various wave lengths were constant over a range of conditions; so that these experiments enable one to find the effect of temperature and ionic strength on the extinction coefficients. The effect of hydrogen ion concentration was

[1]*Manuscript received June 30, 1955.*
Contribution from the Department of Chemistry, University of Toronto, Toronto, Ontario.

also examined, especially as regards the possible formation of the ion $FeOH^{++}$ and of undissociated thiocyanic acid. It is hoped therefore that the present work provides a reasonably critical and detailed account of the ferric thiocyanate system, and one which can be used in measuring the dissociation constants of other ferric complexes.

APPARATUS AND MATERIALS

Spectrophotometer

All optical measurements were made with the Beckmann Model DU Spectrophotometer. For normal slit widths in the wave length region used in this work (4000–5000 Å) this instrument uses a band of wave lengths about 10 Å wide (8). As earlier workers do not entirely agree about the position of the maximum absorption of $FeSCN^{++}$, the wave length scale was calibrated using the hydrogen and mercury spectra, and was found to agree within 3 Å (i.e. within experimental error) at the wave lengths of the well-established lines of these elements. The absorption cuvettes used were made of silica, and were of conventional design. The light path was usually 1 cm. and was calibrated to $\pm 0.1\%$. For shorter light paths silica inserts, 0.9 cm. thick, were put in to reduce the light path to 1 mm.

The chief modification that was made on the spectrophotometer was the introduction of thermostatting for the absorption cells. The cells were placed directly in the thermostatting water in a bakelite box fitted with silica windows. The box was light-tight except for the windows. The light beam passed through the water, which was circulated by a pump from a larger reservoir. This reservoir, which contained the usual constant temperature devices, was made of stainless steel, as were the attached pipes and valves, and was filled with distilled water to minimize absorption by impurities in the water. The flow rate through the box was about 1 liter/min., and the temperature could be easily maintained to 0.1°C.

Ferric Perchlorate

The G. Frederick Smith product was used without further purification. A stock solution of about 0.5 *M* was prepared and then analyzed for iron by ammonia precipitation, ignition, and weighing as Fe_2O_3. No check for free acid was made since a high concentration of perchloric acid was added to the mixtures in all the runs.

Perchloric Acid

The 72% reagent grade product supplied by G. Frederick Smith was diluted to give a 1 *M* stock solution which was standardized volumetrically.

Sodium Perchlorate

A 5 *M* stock solution was prepared from the G. Frederick Smith reagent grade sodium perchlorate by dissolving it in water and filtering. This solution gave no test for chloride. The concentration was determined by evaporating a known volume of solution to dryness, heating to 160°C. to break up the mono-

hydrate, and weighing the residue. A check showed that this method gave the same result as prolonged heating at 300°C. This solution produced the same results as one prepared by neutralizing a known amount of perchloric acid with reagent sodium hydroxide, and diluting to the required volume.

Sodium Thiocyanate

A 1 *M* stock solution was prepared from Baker's Analyzed product, and standardized against silver nitrate with ferric alum as indicator. Solutions of thiocyanate slowly decompose on standing to produce a flaky white precipitate. It was found that this trouble could be largely avoided by keeping the solutions in black storage bulbs in an atmosphere of nitrogen. When the solution was needed, it was driven out by a stream of nitrogen.

Benzyl Alcohol

Merck reagent grade benzyl alcohol was used, and was stored in an atmosphere of nitrogen.

Standard Ferric Solutions

It was desirable to prepare a ferric solution with its concentration accurately known in order to have an independent check on the various batches of ferric perchlorate that were prepared. For this purpose the usual iron standards such as ferrous ammonium sulphate were of no value since the sulphate interferes strongly with the ferric thiocyanate color. Consequently a length of clean iron wire was weighed to 0.1%, and heated with the required amount of perchloric acid and a small amount of ammonium nitrate to oxidize ferrous to ferric ions. After cooling, the product was diluted to a known volume and used to produce a ferric thiocyanate solution in the same way as other ferric perchlorate solutions. The intensity of the color was compared with that from the latter solutions, whose concentration could thereby be checked. The results agreed within experimental error with those obtained by precipitating ferric hydroxide.

EXPERIMENTAL

Stock solutions of ferric perchlorate, sodium thiocyanate, perchloric acid, and sodium perchlorate were made up of known strength. Mixtures of known amounts of these were made, and diluted to a known volume, and the color was measured by the spectrophotometer. The color was always measured against a reagent blank which did not contain thiocyanate. In runs where the iron concentration was low this was also omitted in the reagent blank, but at higher concentrations it was included.

It was discovered early in this part of the investigation that solutions with the ferric concentration around 0.1 *M* and thiocyanate around 10^{-4} *M* were subject to serious fading. This was apparently not the same fading reaction that interfered with the colorimetric determination of iron as reported, for example, by Peters, MacMasters, and French (17), and that was later the subject of a kinetic investigation by Betts and Dainton (4), since this latter reaction occurred in solutions of very high thiocyanate concentration and very

low ferric concentration—just the reverse of the present case. The explanation of this fading reaction that was arrived at was that the thiocyanate is oxidized by dissolved oxygen, probably with ferric ion acting as a carrier. This is not an unfamiliar role to assign to ferric and other transition element ions (see, for example, Ref. 1). Jeu and Alyea (11) give a list of substances in order of their ability to inhibit the oxidation of sulphite. From this list benzyl alcohol was selected as a substance with good inhibitory properties, but still not likely to form complexes with ferric ions. In both respects this proved to be a happy choice. The ability of benzyl alcohol to inhibit fading was observed in many solutions, even at 45°C. Qualitatively, an inhibited solution stored in a glass-stoppered volumetric flask was still decidedly red after 18 months, whereas a companion solution with no inhibitor faded completely in about 10 days.

In order to check the possible interference of benzyl alcohol in the color formation, a series of solutions were set up in which the ferric and thiocyanate concentrations were maintained constant throughout and increasing amounts of benzyl alcohol were added; the optical densities of the solutions were read. As seen from the results given in Table I the benzyl alcohol does not interfere to any significant extent.

TABLE I

EFFECT OF BENZYL ALCOHOL

Iron and thiocyanate: 0.001 M; $(H^+) = 0.2$ M; 25°C.; volume: 25 ml.

Drops of benzyl alcohol	0	1	2	4	8
Optical density (460 mμ)	0.496	0.498	0.496	0.493	0.499

In measuring the optical density on the spectrophotometer, no reading was accepted if it showed more than 0.001 change in density after the 'dark current' and blank absorption were checked. At least two, and usually three, readings were taken for each wave length; the density reading was first taken for each wave length used, and then the whole series repeated. It was found that about six drops of benzyl alcohol in 50 ml. of solution were sufficient to reduce fading so that this degree of reproducibility could be obtained.

The results obtained are given in Tables II–VI, and the interpretation of these results will be discussed in the next section. However there is one general comment that should be made first. The ionic strength of 1.2 which was used in many runs may seem unduly high. It was originally chosen to allow, firstly, a sufficient concentration of acid to be present to suppress the formation of $FeOH^{++}$; and, secondly, to allow for a fairly high concentration of ferric perchlorate in some runs. As it turned out this ionic strength was higher than was needed in most runs, but it was thought to be advisable to keep it constant throughout the whole series. In Table III results are given which show the effect of altering the ionic strength.

In all of these tables the optical densities have been reduced to the density per centimeter by dividing by the calibrated cell width.

TABLE II

VALUES OF OPTICAL DENSITY FOR 1 CM. LIGHT PATH

All measurements in this table at 25°C., 1.2 ionic strength, and $(H^+) = 0.2\ M$

Series	(SCN^-), M	(Fe^{+3}), M	Wave length, mμ										
			400	420	430	440	450	460	470	480	490	500	520
1	.000125	.1667	.268	.411	.477	.523	.551	.560	.543	.511	.468	.416	.303
		.125	.266	.407	.469	.513	.543	.551	.539	.503	.461	.412	.300
		.100	.259	.399	.461	.508	.536	.540	.528	.498	.452	.401	.295
		.0833	.259	.395	.458	.500	.530	.537	.521	.491	.449	.396	.289
		.0667	.247	.385	.448	.489	.513	.522	.509	.479	.439	.387	.283
		.0500	.240	.370	.429	.471	.498	.502	.489	.461	.422	.373	.274
		.0333	.225	.347	.401	.441	.466	.471	.460	.436	.399	.352	.257
		.0200	.200	.309	.356	.391	.414	.420	.410	.385	.352	.313	.229
		.0100	.156	.239	.279	.305	.324	.325	.320	.301	.275	.243	.177
2	.000100	.1667	.207	.331	.385	.426	.448	.453	.440	.418	.379	.335	.244
		.125	.212	.329	.381	.420	.441	.449	.438	.412	.374	.331	.243
		.100	.209	.324	.376	.414	.437	.442	.430	.408	.370	.328	.240
		.0833	.205	.319	.370	.409	.430	.437	.423	.401	.363	.322	.237
		.0667	.200	.311	.360	.396	.419	.422	.412	.388	.355	.314	.229
		.0500	.192	.301	.350	.381	.404	.410	.400	.376	.344	.305	.225
3	.00025	.000985	—	.096	—	.121	.128	.130	.126	.119	.110	.097	—
	.00050		—	.189	—	.238	.250	.254	.247	.234	.214	.189	—
	.00075		—	.275	—	.350	.368	.373	.363	.343	.314	.279	—
	.00100		—	.358	—	.458	.479	.487	.470	.448	.411	.364	—
	.00125		—	.441	—	.559	.589	.598	.587	.555	.505	.449	—
	.00150		—	.510	—	.650	.683	.696	.681	.642	.590	.525	—
	.00175		—	.588	—	.752	.792	.810	.790	.743	.681	.604	—
	.00200		—	.661	—	.846	.889	.904	.879	.834	.762	.681	—
	.00225		—	.797	—	1.012	1.071	1.089	1.067	1.008	.929	.829	—
	.00250		—	.927	—	1.171	1.244	1.265	1.232	1.172	1.085	.966	—
4	.00040	.00197	—	.257	—	.333	.349	.356	.346	.327	—	.263	—
	.00060		—	.387	—	.495	.525	.534	.521	.489	—	.394	—
	.00080		—	.520	—	.663	.701	.709	.693	.653	—	.531	—
	.00100		—	.646	—	.830	.870	.886	.863	.814	—	.655	—
5	.00020	.00298	—	.187	—	.238	.250	.253	.246	.233	—	.188	—
	.00040		—	.364	—	.466	.487	.495	.484	.455	—	.367	—
	.00060		—	.545	—	.699	.733	.743	.725	.653	—	.582	—
	.00080		—	.722	—	.913	.967	.974	.950	.903	—	.727	—
6	.00015	.0167	.255	.394	.452	.498	.521	.527	.510	.480	.436	.384	.279
		.0150	.251	.385	.443	.487	.509	.514	.500	.469	.428	.375	.274
		.0125	.236	.365	.420	.460	.481	.489	.471	.443	.406	.357	.260
		.0100	.220	.338	.390	.428	.449	.451	.440	.411	.375	.331	.240
		.0075	.195	.300	.348	.381	.400	.405	.390	.367	.334	.296	.214
		.0050	.160	.249	.286	.315	.329	.331	.321	.304	.275	.245	.176
		.0025	.105	.163	.189	.205	.215	.217	.213	.199	.181	.159	.116

TABLE III

EFFECT OF IONIC STRENGTH

Optical densities at 1 cm. light path; 25°C.

Series	(SCN^-), M	(Fe^{+3}), M	Wave length, mμ					Ionic strength
			440	450	460	470	480	
1	.000250	.000985	.125	.130	.134	.128	.120	0.8
	.000500		.243	.255	.258	.251	.235	
	.000750		.355	.376	.380	.368	.349	
	.00100		.460	.486	.494	.479	.456	
	.001243		.566	.595	.604	.588	.554	
	.001492		.665	.703	.712	.694	.653	
	.001742		.766	.811	.823	.795	.752	
	.001989		.855	.905	.913	.891	.848	
	.002235		.950	.992	1.010	.986	.931	
	.002481		1.037	1.091	1.109	1.085	1.026	
2	.00025	.000995	.136	.141	.144	.140	.130	0.5
	.00050		.267	.278	.281	.274	.255	
	.00075		.390	.409	.412	.400	.379	
	.00100		.498	.528	.534	.517	.488	
	.001243		.620	.649	.657	.640	.607	
	.001492		.729	.764	.774	.752	.713	
	.001742		.842	.879	.889	.867	.816	
	.001989		.933	.976	.991	.966	.911	
	.002235		1.030	1.085	1.091	1.068	1.008	
	.002481		1.127	1.184	1.192	1.168	1.107	
3	.00025	.000990	.151	.157	.159	.155	.145	0.3
	.00050		.295	.310	.314	.304	.287	
	.00075		.433	.453	.458	.447	.420	
	.00100		.558	.587	.595	.579	.547	
	.001243		.685	.719	.725	.703	.663	
	.001492		.808	.848	.853	.832	.781	
	.001742		.915	.966	.972	.949	.895	
	.001989		1.032	1.085	1.093	1.068	1.008	
	.002250		1.133	1.190	1.204	1.182	1.113	
	.002500		1.230	1.289	1.309	1.283	1.210	
4	.00025	.000990	.169	.175	.179	.172	.164	0.2
	.00050		.329	.345	.350	.340	.319	
	.00075		.486	.508	.512	.499	.469	
	.00100		.616	.648	.656	.637	.604	
	.00125		.760	.798	.810	.784	.742	
	.00150		.893	.935	.948	.927	.875	
	.00175		1.014	1.069	1.083	1.053	.991	
	.00200		1.131	1.188	1.210	1.175	1.113	
	.00225		1.251	1.319	1.331	1.291	1.230	
	.00250		1.360	1.429	1.445	1.414	1.333	

TABLE IV

EFFECT OF TEMPERATURE

Optical densities at 1 cm. light path; ionic strength 1.2

Series	Temp., °C.	(SCN^-), M	(Fe^{+3}), M	Wave length, mμ						
				420	440	450	460	470	480	500
1	5.0	.000100	.100	.340	.431	.450	.452	.439	.410	.324
			.0833	.335	.427	.443	.448	.432	.407	.319
			.0667	.329	.419	.439	.440	.428	.399	.315
			.0500	.327	.414	.432	.437	.421	.393	.312
			.0333	.311	.390	.410	.411	.398	.371	.295
			.0200	.281	.352	.368	.370	.360	.333	.265
2	45.0	.000100	.1250	.304	.394	.420	.429	.421	.401	.334
			.0833	.296	.382	.408	.418	.410	.391	.325
			.0667	.289	.371	.396	.407	.400	.381	.318
			.0500	.279	.359	.381	.391	.385	.366	.306
			.0333	.259	.335	.356	.365	.359	.343	.285
3	5.3	.00040	.000985	.185	.233	.244	.248	.238	.224	.175
	5.6	.00060		.267	.335	.352	.354	.342	.318	.254
	5.4	.00080		.348	.438	.457	.459	.448	.419	.332
	5.4	.00100		.429	.541	.567	.569	.555	.517	.410
	5.2	.00020	.00197	.163	.205	.214	.215	.209	.195	.154
	5.2	.00040		.322	.407	.427	.428	.417	.387	.307
	5.2	.00060		.473	.598	.626	.631	.608	.565	.450
	5.2	.00080		.627	.782	.828	.831	.808	.745	.594
4	10.3	.00080	.000985	.329	.418	.437	.438	.428	.400	.319
		.00100		.409	.517	.544	.547	.528	.496	.397
		.00060	.00197	.445	.562	.592	.596	.580	.541	.430
		.00080		.592	.745	.784	.790	.768	.719	.572
5	14.9	.00040	.000985	.163	.205	.215	.218	.211	.199	.159
	14.8	.00060		.243	.304	.319	.323	.313	.293	.235
	15.0	.00080		.317	.401	.420	.427	.415	.387	.312
	15.1	.00100		.388	.490	.516	.522	.506	.476	.382
	14.9	.00040	.00197	.285	.366	.384	.387	.375	.350	.279
	14.9	.00060		.426	.543	.570	.575	.555	.525	.418
	14.9	.00080		.565	.713	.750	.756	.735	.694	.553
6	20.0	.00080	.000985	.302	.383	.404	.408	.397	.373	.302
	20.1	.00100		.372	.469	.496	.499	.487	.458	.372
	20.1	.00060	.00197	.406	.517	.543	.549	.537	.504	.406
	20.1	.00080		537	.683	.723	.732	.713	.671	.537
7	30.0	.00080	.000985	.279	.355	.376	.382	.373	.553	.288
		.00100		.343	.438	.463	.468	.458	.437	.356
		.00080	.00197	.495	.636	.674	.683	.671	.636	.517
8	35.0	.00040	.000985	.136	.175	.185	.189	.184	.174	.143
		.00060		.203	.260	.274	.279	.273	.259	.213
		.00080		.269	.343	.364	.370	.363	.343	.282
		.00100		.334	.427	.448	.457	.447	.427	.348
		.00060	.00197	.365	.467	.495	.504	.495	.467	.385
		.00080		.485	.624	.661	.670	.656	.626	.514
		.00100		.603	.772	.816	.834	.814	.774	.636
9	40.0	.00080	.000985	.263	.335	.355	.363	.357	.339	.280
		.00100		.323	.416	.438	.447	.439	.419	.347
		.00060	.00197	.349	.453	.479	.489	.483	.457	.378
		.00080		.465	.602	.636	.651	.641	.611	.504
10	45.2	.00040	.000985	.129	.168	.179	.184	.180	.171	.143
		.00060		.193	.248	.263	.269	.265	.253	.209
		.00080		.255	.327	.347	.354	.349	.332	.277
		.00100		.314	.407	.429	.438	.434	.415	.343

TABLE V

DATA FOR INVESTIGATION OF HIGHER COMPLEXES

Optical densities at 1 cm. light path; $(Fe^{+3}) = 0.001\ M$; $(H^+) = 0.2\ M$; ionic strength = 1.2, for all measurements; 25°C.

(SCN^-), M	Wave length, mμ							
	420	440	450	460	470	480	490	500
.00025	.096	.121	.128	.130	.126	.119	.110	.097
.00050	.189	.238	.250	.254	.247	.234	.214	.189
.00075	.275	.350	.368	.373	.363	.343	.314	.279
.0010	.358	.458	.479	.487	.470	.448	.411	.364
.00125	.441	.559	.589	.598	.587	.555	.505	.449
.0015	.510	.650	.683	.696	.681	.642	.590	.525
.00175	.588	.752	.792	.810	.790	.743	.681	.604
.0020	.661	.846	.889	.904	.879	.834	.762	.681
.00225	.735	.931	.988	1.006	.978	.927	.851	.760
.0025	.797	1.012	1.071	1.089	1.067	1.008	.929	.829
.0030	.927	1.171	1.244	1.265	1.232	1.172	1.085	.966
.0035	1.08	1.36	1.44	1.45	1.44	1.36	1.25	1.11
.0040	1.20	1.51	1.595	1.62	1.59	1.51	1.395	1.245
.0045	1.305	1.655	1.75	1.765	1.75	1.66	1.53	1.38
.0050	1.445	1.84	1.93	1.955	1.94	1.84	1.70	1.51
.0060	1.64	2.06	2.20	2.245	2.20	2.095	1.945	1.74
.0070	1.81	2.26	2.40	2.45	2.41	2.30	2.14	1.93
.0080	1.955	2.46	2.60	2.66	2.62	2.51	2.35	2.105
.0090	2.09	2.64	2.79	2.85	2.81	2.70	2.515	2.29
.0100	2.25	2.85	3.00	3.095	3.05	2.945	2.75	2.49
.0120	2.46	3.11	3.29	3.36	3.35	3.24	3.04	2.76
.0140	2.645	3.345	3.52	3.63	3.605	3.495	3.28	3.00
.0160	2.82	3.56	3.76	3.89	3.87	3.75	3.54	3.25
.0180	2.99	3.77	4.02	4.17	4.175	4.07	3.83	3.51
.0200	3.15	3.96	4.21	4.32	4.32	4.21	4.005	3.69
.0250	3.40	4.305	4.57	4.70	4.72	4.635	4.42	4.11
.0300	3.67	4.61	4.91	5.07	5.11	5.00	4.80	4.49
.0400	4.005	5.00	5.37	5.58	5.63	5.58	5.38	5.00
.0500	4.27	5.33	5.70	5.98	6.04	6.00	5.87	5.50
.0600	4.49	5.61	5.99	6.305	6.42	6.40	6.21	5.90
.0700	4.61	5.81	6.27	6.56	6.73	6.73	6.58	6.23
.0800	4.70	5.93	6.40	6.78	6.92	6.98	6.80	6.47
.0900	4.90	6.17	6.65	7.00	7.21	7.24	7.09	6.74
.1000	5.02	6.31	6.81	7.20	7.42	7.46	7.30	6.97
.1500	5.43	6.81	7.42	7.90	8.23	8.30	8.12	7.84
.2000	5.66	7.19	7.87	8.43	8.78	8.88	8.72	8.37
.2500	5.79	7.48	8.12	8.67	9.04	9.18	8.99	8.63

TABLE VI

EFFECT OF HYDROGEN ION CONCENTRATION

Optical densities at 1 cm. light path; $(Fe^{+3}) = 0.001\ M$; $(SCN^-) = 0.001\ M$; ionic strength = 1.2; 25°C.

(H^+), M	Wave length, mμ				
	440	450	460	470	480
0.500	.459	.482	.490	.479	.453
0.200	.459	.481	.489	.478	.451
0.150	.458	.480	.488	.474	.450
0.100	.448	.470	.477	.466	.442
0.075	.448	.469	.476	.466	.440
0.050	.443	.466	.472	.460	.435
0.025	.431	.452	.460	.450	.423
0.0175	.427	.448	.454	.442	.419
0.0100	.408	.428	.432	.422	.399
0.0075	.386	.408	.410	.400	.378
0.0050	.367	.384	.388	.376	.357
0.0025	.328	.344	.347	.337	.318
0.00175	.300	.315	.317	.308	.289
0.0010	.260	.271	.273	.265	.249

DISCUSSION OF RESULTS

In the treatment of data of this sort it is usual to assume that a reaction such as

$$Fe^{+3}+SCN^{-} \rightleftharpoons FeSCN^{++}$$

conforms to a Mass Law expression

$$a_{FeSCN^{++}}/a_{Fe^{+3}}.a_{SCN^{-}} = K_0$$

where $a_{Fe^{+3}}$, etc., are the activities of the various substances. Indeed this is little more than a matter of definition, the real assumptions being that the activity coefficients are dependent only on temperature and ionic strength, and that they approach unity as the ionic strength approaches zero. In practice it is usually simpler to evaluate an apparent constant, K, defined by the concentrations; and then to observe the variation of K with ionic strength. K is in fact the equilibrium constant at a certain ionic strength and temperature, and most of the constants derived below are of this sort.

In evaluating K from optical densities, it is always assumed that the densities obey Beer's Law: $D = \epsilon.c$; where D is the density, ϵ is the extinction coefficient, and c is the concentration of the colored substance. ϵ is, of course, dependent on the wave length, and to a lesser extent on the ionic strength and temperature; but we assume that it is independent of c, if c is fairly small. In the present work the concentration of the colored ion was 10^{-3} M or less, so that it can be reasonably assumed that the colored ions are sufficiently far apart not to affect each other's extinction coefficient. The results in Tables II–V enable the effect of temperature and ionic strength on the extinction coefficient to be determined.

To obtain values of K and ϵ from optical densities somewhat similar methods are available, devised by Rabinowitch and Stockmayer (19), and by Frank and Oswalt (7). The relation of these two methods can be seen from the following, which provides a simpler derivation of Frank and Oswalt's equation. If a is the total ferric concentration (present either as Fe^{+3} or $FeSCN^{++}$), b is the total thiocyanate concentration, and x that of the complex, $FeSCN^{++}$, then:

$$x/[(a-x)(b-x)] = K.$$

As $x = D/\epsilon$, we can substitute and rearrange to get

$$ab/D = (a+b)/\epsilon + 1/\epsilon K - D/\epsilon^2.$$

If we ignore D/ϵ^2 as small compared to the other terms, we get Frank and Oswalt's equation. By plotting ab/D against $a+b$, ϵ and K can be evaluated. Rabinowitch and Stockmayer, in effect, take Frank and Oswalt's equation and divide by b to get

$$a/D = a/b\epsilon + 1/b\epsilon K + 1/\epsilon.$$

They assume that $1/\epsilon$ is small and can be neglected; and by plotting a/D against a for runs at constant b, they can evaluate ϵ and K. It can readily be checked that this is precisely equivalent to assuming that x is negligible compared with a in $(a-x)$ in the original Mass Law equation. This method is

simple to apply, and is sufficiently accurate provided a is appreciably larger than b. It cannot be applied to all mixtures, but it is easy to check whether it is applicable or not. Of course, if b is larger than a, an analogous equation can be derived by ignoring x with respect to b. The Frank and Oswalt equation was valid for all the conditions that were used; but, as it is more difficult to apply, it was only used when its use was unavoidable.

These equations of course assume that no other reactions occur. There are three complicating reactions that must be considered. These are: (i) hydrolysis of Fe^{+3} to $FeOH^{++}$, (ii) formation of thiocyanic acid molecules, and (iii) formation of higher complexes, notably $Fe(SCN)_2^+$. An estimate can be made of the extent to which the first two reactions interfere, and conditions chosen so that this interference is not serious and can be allowed for. The third reaction presumably does not occur at great dilutions; the equilibrium giving the higher complex can be measured by observing the deviations from the simple equations at higher thiocyanate concentrations. The effect of the first two reactions can be estimated as follows.

If K_h is the equilibrium constant for the reaction:

$$Fe^{+3}+2H_2O \rightleftharpoons FeOH^{++}+H_3O^+$$

defined as

$$K_h = (FeOH^{++}) \cdot (H^+)/(Fe^{+3}),$$

then the total iron concentration is given by

$$a = (Fe^{+3})+(FeOH^{++})+(FeSCN^{++})$$

and $a = (Fe^{+3}) \cdot \{1+K_h/(H^+)\}+(FeSCN^{++})$.

The Rabinowitch–Stockmayer equation is modified to

$$\frac{a}{D} = \frac{a}{b\epsilon}+\frac{1+K_h/(H^+)}{Kb\epsilon}.$$

Reported values of K_h are given in Table VII. As the extrapolation from low ionic strengths to an ionic strength of 1.2 is somewhat uncertain, the results given above in Table VI were obtained, which show the effect of varying the hydrogen ion concentration in ferric thiocyanate mixtures. These results also provide some evidence on the possible existence of the ion $Fe(OH)(SCN)^+$.

TABLE VII

LITERATURE VALUES OF K_h

All measurements are at 25°C.

K_h	Ionic strength	Method	Reference
0.006	Small	Potentiometric	5
0.0035	Small	Conductivity	12*a*
0.0028	0.05	Spectrophotometric	15*a*
0.0065	Small	Spectrophotometric	20

The interpretation of these results must also take into consideration the possibility of thiocyanic acid formation. If thiocyanic acid is formed the Rabinowitch–Stockmayer equation should be modified much as above:

$$\frac{a}{D} = \frac{a}{b\epsilon} + \frac{1+(H^+)/K_a}{Kb\epsilon}$$

where K_a is the ionization constant of thiocyanic acid. Values of K_a are none too certain, though it is known (15*b*) that thiocyanic acid is a strong acid. Recently Gorman and Connell (9*a*) reported that sodium thiocyanate exerts no discernible buffering action on solutions of perchloric acid. This is confirmed by the results of Table VI in the following way. If the Rabinowitch–Stockmayer equation, allowing for both the above side reactions, is written down:

$$\frac{a}{D} = \frac{a}{b\epsilon} + \frac{(1+K_h/(H^+)) \cdot (1+(H^+)/K_a)}{Kb\epsilon}$$

and is differentiated to find the point where D is a maximum as (H^+) varies, with a and b constant, we get

$$\frac{\partial D}{\partial (H^+)} = \frac{D^2}{ab\epsilon K}(K_h/(H^+)^2 - 1/K_a).$$

Hence the maximum occurs when $(H^+) = \sqrt{(K_h K_a)}$. The results in Table VI give no definite maximum, but D scarcely increases as (H^+) goes from 0.2 to 0.5, so possibly a maximum occurs at about $(H^+) = 0.5\ M$. The value of K_h (obtained below) at this ionic strength is 1.55×10^{-3}, so K_a is 160 or more. This value of K_a has, of course, no precise quantitative significance, except to show that thiocyanic acid is a strong enough acid for its formation to be ignored. It may be added that the same conclusion about the position of the maximum is reached if the full Mass Law equation is used.

If we turn now to the evaluation of K_h, the Mass Law equation gives:

$$1+K_h/(H^+) = \frac{K}{x}(a-x)(b-x) \cong K\left(\frac{ab}{x} - a - b\right).$$

Calling D_0 the limiting density at high (H^+), this can be rearranged to:

$$K_h = (H^+) \cdot \left(\frac{D_0}{D} - 1\right)(1+Ka+Kb).$$

Hence to evaluate K_h we must know K. Anticipating later conclusions we can take K as 130. This is not arguing in a circle, since K, as evaluated later, is only slightly dependent on K_h. To obtain (H^+), it is necessary to note that while most of the hydrogen ions come from the added perchloric acid, a little comes from the hydrolysis of the ferric ions. The simplest way to deal with this is by successive approximation, an approximate value of K_h being used to correct (H^+). Table VIII gives the results of this calculation of K_h, based on the experimental results of Table VI. The average value of K_h is 1.55×10^{-3}. To compare this with the literature values which are reported at zero ionic strength some form of extrapolation must be used. Bray and Hershey (5) used an empirical equation, which, if applied to the present data, makes K_h^0 equal to 5.6×10^{-3}. Siddall and Vosburgh (20) used a form of the extended Debye-Hückel equation; with this, K_h^0 comes out at 6.4×10^{-3}. As these are in reasonable agreement with the literature values, our assumptions about the

TABLE VIII

EVALUATION OF K_h

$(H^+)_{uncorr.}$, M	$(H^+)_{corr.}$, M	K_h, $\times 10^{-3}$
0.0175	0.01757	1.61
0.0100	0.01012	1.58
0.0075	0.00765	1.57
0.0050	0.00521	1.77
0.0025	0.00282	1.42
0.00175	0.00214	1.43
0.0010	0.00148	1.44

ions present are presumably correct; in particular it is unlikely that any large concentration of $Fe(SCN)(OH)^+$ is present. This can be checked however by the same type of calculation that will be used later to demonstrate the existence of $Fe(SCN)Cl^+$. When (H^+) falls below 0.005 M, slight, but fairly consistent, deviations occur between the calculated and observed densities. If it is assumed that this is due to the presence of $Fe(SCN)(OH)^+$, the hydrolysis constant of $FeSCN^{++}$ can be calculated. The results do not permit any great accuracy, and the values of the constant vary by $\pm 20\%$, the average being

$$k = \frac{(FeSCNOH^+) \cdot (H^+)}{(FeSCN^{++})} = 6.5(\pm 1) \times 10^{-5}.$$

This means that $FeSCN^{++}$ would be half hydrolyzed at a pH of 4.2, as compared with Fe^{+++} which is half hydrolyzed at a pH of 2.8 at this ionic strength. As is to be expected the larger ion with the smaller charge is hydrolyzed less readily. The extinction coefficient of $Fe(SCN)(OH)^+$ can also be very roughly evaluated, the results being:

λ	4400	4500	4600	4700	4800 Å
ϵ	5400	4500	4600	4500	3900

EVALUATION OF THE DISSOCIATION CONSTANT AND EXTINCTION COEFFICIENTS OF $FeSCN^{++}$

A plot of a/D against a at constant b of the results in Table II gives curves which are very nearly straight lines. This in itself is some evidence of the correctness of this method of treatment. The values of ϵ obtained by the method of least squares from the first two series of runs in Table II are given in Table IX. The two runs agree, with an average deviation of about 1%. This difference

TABLE IX

EVALUATION OF ϵ

ϵ (series 1)	2240	3430	3980	4360	4600	4670	4530	4260	3890	3470	2530
ϵ (series 2)	2270	3450	4010	4460	4670	4730	4590	4370	3940	3480	2530
λ, mμ	400	420	430	440	450	460	470	480	490	500	520

cannot be attributed to the approximations made in deriving the Rabinowitch–Stockmayer equation; it is probably due partly to errors in measuring D, and partly to errors in the concentrations, particularly the very dilute thiocyanate.

Reference to earlier measurements of the same quantity (7, 14) shows appreciable deviation from the present results, though as this earlier work was done

at room temperature part of the difference may be due to different temperatures. Frank and Oswalt's results would agree well with ours, if all their wave lengths were shifted 100 Å to the red. Macdonald reports results that are consistently about 6% higher than ours, and the reason for this inconsistency is not obvious.

Evaluation of K from these data gives the results in Table X. As can be seen there is some range in the values of K, even ignoring the extreme points.

TABLE X

EVALUATION OF K

Wave length used, mμ	K from series 1	K from series 2
400	119	107
420	124	136
430	125	132
440	125	117
450	126	127
460	123	127
470	128	131
480	129	120
490	128	131
500	123	136

This is not due to algebraic approximations, as calculation of a second order correction only decreases K by 0.2%. However some improvement in the method of calculation can be made if ϵ is known, as it can now be taken to be from Table IX. K can be calculated directly from

$$K = \frac{D/\epsilon}{(a-D/\epsilon)(b-D/\epsilon)}.$$

Before calculating K directly, a small correction should be applied to the values of ϵ, because, in any given solution, the value of ϵ at various wave lengths must be proportional to D. The relative values of D at various wave lengths are known from a considerable number of measurements. Accordingly the values taken for ϵ have been smoothed out slightly to agree with the relative values of D; the final result is as follows:

λ	4000	4200	4300	4400	4500	4600	4700	4800	4900	5000	5200 Å
ϵ	2230	3440	3990	4380	4630	4680	4560	4310	3920	3475	2530

This is really applying another test of mutual consistency to our ϵ values, and adjusting them accordingly; the maximum adjustment is 0.7%. Using these ϵ values we can calculate K, with the results given in Table XI. In each run an average K was extracted from all the density readings; some of the readings at the highest thiocyanate concentrations have not been included in the over-all average, because it is evident that higher complexes are becoming important. The final result, corrected for hydrolysis of Fe^{+3}, is $130(\pm 1)$.

TABLE XI

MEAN VALUES OF K FROM EXTINCTION COEFFICIENTS AND OPTICAL DENSITIES

Series	(Fe^{+3}), M	(SCN^-), M	K
3	0.001	0.00025	131.1
		0.00050	131.7
		0.00075	132.2
		0.00100	132.4
		0.00125	134.0
		0.00150	132.6
4	0.002	0.0006	126.2
		0.0008	128.9
		0.0010	131.1
5	0.003	0.0002	128.3
		0.0004	126.6
		0.0006	129.1
		0.0008	129.0
			Mean 130.2±2

Variation of Ionic Strength

The runs reported in Table III were made in order to determine the effect of ionic strength on the dissociation constant and on the extinction coefficients. It seemed likely that the effect of varying ionic strength on the extinction coefficients might be small, but it could not be assumed to be negligible. The extinction coefficients were accordingly measured at the lowest ionic strength used, namely 0.2. In these runs the total thiocyanate ranged from about 1% to 7% of the total iron; as this seemed rather a high amount for the Rabinowitch–Stockmayer equation to hold accurately, the values of ϵ were first calculated by least squares in the usual way, and then a second least squares calculation was made in which the total iron was corrected for the amount present as $FeSCN^{++}$. Finally some of the values were slightly adjusted, as before, to bring them into agreement with the actual absorption spectrum. The results, for an ionic strength of 0.2, were:

λ	4000	4200	4300	4400	4500	4600	4700	4800	4900	5000	5200 Å
ϵ	2280	3490	4030	4415	4625	4670	4530	4250	3875	3420	2480

The results differ from those at an ionic strength of 1.2 by an amount that is little more than the experimental error, but there is a consistent shift of the absorption band to shorter wave lengths at the lower ionic strength: in fact the two bands would virtually coincide if the band at 1.2 ionic strength were shifted 20 Å to the violet.

Since these extinction coefficients were so nearly the same, they were interpolated for runs at intermediate ionic strengths. From these values and the data of Table III, K was calculated to have the values given in Table XII. As before, the values of K drifted at higher thiocyanate concentrations, presumably owing to the formation of $Fe(SCN)_2^+$.

Although it is a long extrapolation from these results to K at zero ionic strength, it is perhaps worth while seeing how well they agree with the extended Debye-Hückel equation:

$$\log K = \log K_0 + \frac{A.\Delta z^2.\sqrt{\mu}}{1+aB\sqrt{\mu}} + C\mu$$

where K_0 is the dissociation constant at zero ionic strength; Δz^2 is the change in the squares of the ionic charges in the reaction, here equal to -6; and A, B, C, and a are constants. If we give A and B their usual values for water of 0.509 and 0.330×10^8, and, following Rabinowitch and Stockmayer (19)

TABLE XII

VALUES OF K AT VARIOUS IONIC STRENGTHS

(SCN^-), M	Ionic strength 0.8	0.5	0.3	0.2
0.00025	133	145	165	189
0.00050	133	146	168	191
0.00075	134	147	169	195
0.00100	134	146	169	192
0.00125	135	149	171	196
Mean	134	146	169	192

and Betts and Dainton (4), if we take a as 4.5×10^{-8} and C as 0.30, we find that our results make K_0 equal to 1070. The degree of fit is best seen by calculating K at various ionic strengths and comparing with experiment:

Ionic strength (μ)	0.2	0.3	0.5	0.8	1.2
K (calculated)	193	165	140	133	140
K (observed)	192	169	146	134	130

While this is not a striking agreement, it is probably as good as could be expected over such a wide range of ionic strengths, and it shows general agreement with the form of the equation.

Temperature Variation

Experiment shows that the optical densities of ferric thiocyanate mixtures are markedly temperature dependent. In general it must be assumed that this is due to changes in both ϵ and K. It is simplest to determine first the dependence of the extinction coefficients on temperature, since it is unlikely that they will change by any large amount. The results given in Table IV for 5°C. and 45°C. enable a determination of ϵ for these temperatures to be made by the Rabinowitch–Stockmayer method; the values so obtained are given in Table XIII. The values at 25°C. are included for comparison. As might be expected the absorption band is slightly narrower at lower temperatures, but this effect is quite small. The chief change is that the maximum extinction coefficient decreases by about $4\frac{1}{2}\%$ in going from 5°C. to 45°C.; the maximum also shifts slightly to longer wave lengths (about 4570 Å at 5°C. to 4620 Å at 45°C.).

Using these values of ϵ it is possible to calculate K as before. Another series of runs at various intermediate temperatures was also made, the data being also given in Table IV. ϵ was interpolated from the results in Table XIII, and the average values of K for various temperatures were as follows:

Temp.	5	10	15	20	25	30	35	40	45 °C.
K	155	147	139	134	130	126	122	119	118

TABLE XIII

EXTINCTION TEMPERATURES AT VARIOUS TEMPERATURES

λ, mμ	5°C.	25°C.	45°C.
400	2460	2230	2060
420	3550	3440	3230
430	4110	3990	3760
440	4530	4380	4170
450	4710	4630	4440
460	4750	4680	4550
470	4600	4560	4470
480	4320	4310	4260
490	3870	3920	3940
500	3390	3480	3540
520	2400	2530	2670

A plot of log K against $1/T$ gives a somewhat curved line. This is straightened slightly by converting the concentrations used in obtaining K to molal quantities, which are more strictly applicable to calculations of the partial molar heat change in the reaction. In doing this it was assumed that the coefficient of expansion of water was the same as that of the solutions. It is evident that the heat change is small: an average over the range of temperatures gives 0.8 kcal./gm-mol.; and the results suggest that it changes appreciably over the temperature range, which is not inconceivable as it is such a small quantity. However the accuracy of the results did not seem to warrant a more detailed evaluation. If K is converted to K_0 by means of the extended Debye-Hückel equation, making allowance for the variation of the constants in this equation with temperature, we get:

Temp.	5	25	45 °C.
K_0	1090	1070	1100

Hence the heat change at zero ionic strength seems to be virtually zero.

Investigations on Higher Complexes

In almost every investigation dealing with $FeSCN^{++}$ deviations have been found at higher thiocyanate concentrations which have been ascribed to higher complexes (e.g. 3, 7, 18). This explanation is certainly plausible, but direct evidence for it can only be obtained if the dissociation constants of the higher complexes can be evaluated and are found to remain constant. Let us call K_2 the dissociation constant of the second complex, defined by

$$K_2 = \frac{(Fe(SCN)_2^+)}{(FeSCN^{++}) \cdot (SCN^-)}.$$

K_3 will be a similar expression for $Fe(SCN)_3$. Some previous attempts have been made to determine K_2 (with which we are chiefly concerned), but the results have admittedly been very approximate (e.g. 14). Betts and Dainton (4) arrived at a value of 20 by a trial and error method to fit their kinetic data.

We can probably assume that, just as there is a region where only $FeSCN^{++}$ is important, so at somewhat higher concentrations only $FeSCN^{++}$ and $Fe(SCN)_2^+$ are important. The second complex introduces two new constants (K_2 and the second extinction coefficient), and one additional equation (the Mass Law equation for K_2). Because of the complexity of the system, attempts

were made to measure (SCN^-) or (Fe^{+3}) directly by electrochemical means. These were not successful, so the attempts will be only very briefly described.

A silver – silver thiocyanate electrode was prepared essentially by the method of Pearce and Smith (16). Two such electrodes, prepared together, were placed in the two compartments of a cell; one compartment was filled with a sodium thiocyanate solution and the other with an identical solution except for the addition of a known concentration of ferric ions. The two compartments were separated by a sintered glass plug in a narrow tube, and side-arms allowed the cell to be kept filled with nitrogen during a run. The electrodes were moved up and down continuously during a run. The cell was immersed in a water thermostat, and its e.m.f. was measured on a Leeds and Northrup K2 potentiometer. In trial runs, using different thiocyanate concentrations in the two compartments, the cell quickly settled down to give steady readings which varied by less than 0.1 millivolt in an hour. Unfortunately when ferric perchlorate was introduced, the results were never sufficiently steady to be useful. It was calculated that only an e.m.f. steady to less than 0.1 mv. would be useful; and it was found after considerable trial that the e.m.f. did not stay constant and reproducible to this accuracy. A ferrous–ferric cell and polarographic methods were also tried, but did not prove accurate enough.

Another type of attack was made on the same problem by adding some other ion in small amount which forms a compound with either ferric or thiocyanate ions, and measuring the effect of this on the optical density. If the dissociation constant of the complex so formed is known, we have enough information to calculate all the concentrations in the solution. Chloride was tried, since the dissociation constant of $FeCl^{++}$ is known; unfortunately there are definite indications that $Fe(SCN)Cl^+$ is also formed, and this vitiates the calculation. The behavior of mixtures of this sort will be reported in a later paper. Ions which form complexes with thiocyanate were also tried. Monovalent thallium gives TlSCN, whose dissociation constant has been measured by Bell and George (2), but this gave no absorption spectrum within the range of the spectrophotometer. Cobalt (11), chromium (111), and molybdenum (111) produce complex ions, but it was found that their absorption spectrum overlaps too much with that of Fe^{+3} or $FeSCN^{++}$. Nickel (11) and manganese (11) were tried, but gave no absorption that could be attributed to a thiocyanate complex.

Finally spectrophotometric measurements were made, as for $FeSCN^{++}$, and the results interpreted in a way that, it is believed, gives a good, though slightly approximate, value for K_2 and ϵ_2, the second extinction coefficient. The data are given in Table V. The upper limit to the thiocyanate concentration is set by the fading of the sort investigated by Betts and Dainton (4); this is a different reaction from that encountered earlier, which was retarded by benzyl alcohol. At high concentrations fading is due to the reduction of ferric to ferrous ions by thiocyanate. Hydrogen peroxide prevents this (or reoxidizes the ferrous ions) up to a thiocyanate concentration of about 0.2 M.

The results show the previously observed shift of the maximum to longer

wave lengths; and the densities are greater than if only $FeSCN^{++}$ had been formed. To interpret the results, we note that there are eight quantities that we need to know: these are the four concentrations of Fe^{+3}, SCN^-, $FeSCN^{++}$, and $Fe(SCN)_2^+$, and the four constants, namely K, K_2, ϵ, and ϵ_2. K and ϵ have, of course, already been measured. We have five equations available: the Mass Law expressions for K and K_2, the two mass balances for total iron and thiocyanate, and Beer's law. We can eliminate the four concentrations from these five equations, and obtain a single equation in K, K_2, ϵ, and ϵ_2. By varying the concentrations, and hence D, we can get this equation with various known numerical coefficients; from any two such equations we can evaluate K_2 and ϵ_2. Thus it is possible in theory to disentangle the constants directly, but the algebra is so cumbersome that a method of successive approximations was used. It was assumed as a first approximation that

$$\epsilon_2 = 2.\epsilon,$$

i.e. that the absorption of an ion is proportional to the number of thiocyanate radicals attached. If this is so, then

$$[i] \qquad (SCN^-) = b - D/\epsilon$$

where b, as before, is the total thiocyanate present. The mass balance for iron can be put in the form:

$$a = (Fe^{+3}).\{1+K(SCN^-)+K.K_2(SCN^-)^2\},$$

from which we get:

$$D\{1+K(SCN^-)+K.K_2(SCN^-)^2\}/a = \epsilon K(SCN^-)+\epsilon_2 K.K_2(SCN^-)^2.$$

K_2 was adjusted in the left-hand side of this equation, with the use also of the value of (SCN^-) from equation [i] above, until the values of $\epsilon_2 K.K_2$ showed minimum deviation. The best value of K_2 was $15(\pm 1)$. The values of K_2 were effectively constant as (SCN^-) varied from 10^{-2} to 10^{-1} molar. As an example of the constancy obtained, the average deviation of the values obtained at a wave length of 4600 Å over this range was 0.2×10^6 for $\epsilon_2 K.K_2$, while the average value of $\epsilon_2 K.K_2$ was 17.3×10^6. This is an average deviation of about 1%.

This average value makes ϵ_2 equal to 8900 at 4600 Å, so $\epsilon_2 = 1.90\epsilon$. The first approximation that $\epsilon_2 = 2.\epsilon$ is altered only 5% for the next approximation. If we substitute this new value of ϵ_2, K_2 is raised by 3%. This method is equivalent to calculating (SCN^-) from K and the approximate value of K_2. As little thiocyanate is used up in forming the second complex, (SCN^-) is very little altered by any error in K_2. If we know (SCN^-), we can substitute it in the equations and find ϵ_2 and K_2 directly. Doing this gave a value of K_2 only $\frac{1}{3}$% different from the second approximation, and a value of ϵ_2 of 9130 at 4600Å. This is probably the best approximate method. The final value for K_2 was $15\frac{1}{2}(\pm 1)$.

Values of ϵ_2 at other wave lengths were obtained in a similar manner. The results were:

λ	4200	4400	4500	4600	4700	4800	4900	5000 Å
ϵ_2	6550	8030	8700	9130	9740	9980	10080	9740

It is interesting to note that the absorption maximum is shifted towards the red to 4870 Å.

At very high thiocyanate concentrations the calculated values of K_2 start to drift upwards; this is due, doubtless, to appreciable amounts of $Fe(SCN)_3$ being formed. If we include this possibility in our equations, and assume that the extinction coefficient of $Fe(SCN)_3$ is three times that of $FeSCN^{++}$ (this is analogous to our first approximation for $Fe(SCN)_2^+$), the value of K_3 comes out close to 1. K_3 is here defined as

$$K_3 = \frac{(Fe(SCN)_3)}{(Fe(SCN)_2^+) \cdot (SCN^-)}.$$

This is necessarily very rough, but it was impossible to continue measurements to higher thiocyanate concentrations.

REFERENCES

1. BAWN, C. E. H. Discussions Faraday Soc. No. 14: 181. 1953.
2. BELL, R. P. and GEORGE, J. H. B. Trans. Faraday Soc. 49: 619. 1953.
3. BENT, H. E. and FRENCH, C. L. J. Am. Chem. Soc. 63: 568. 1941.
4. BETTS, R. H. and DAINTON, F. S. J. Am. Chem. Soc. 75: 5721. 1953.
5. BRAY, W. C. and HERSHEY, A. V. J. Am. Chem. Soc. 56: 1889. 1934.
6. EDMONDS, S. M. and BIRNBAUM, N. J. Am. Chem. Soc. 63: 1471. 1941.
7. FRANK, H. S. and OSWALT, R. L. J. Am. Chem. Soc. 69: 1321. 1947.
8. GIBSON, K. S. Analytical absorption spectroscopy. *Edited by* M. G. Millon. John Wiley & Sons, Inc., New York. 1950. p. 235.
9. GLADSTONE, J. H. Trans. Roy. Soc. (London), 179. 1853.
   (*a*) GORMAN, M. and CONNELL, J. J. Am. Chem. Soc. 69: 2063. 1947.
10. GOULD, R. K. and VOSBURGH, W. C. J. Am. Chem. Soc. 64: 1630. 1942.
11. JEU, K. K. and ALYEA, H. N. J. Am. Chem. Soc. 55: 575. 1933.
12. VON KISS, A., ABRAHAM, J., and HEGEDÜS, I. Z. anorg. u. allgem. Chem. 244: 98. 1940.
    (*a*) LAMB, A. B. and JACQUES, A. G. J. Am. Chem. Soc. 60: 1215. 1938.
13. LANFORD, O. E. and KIEHL, S. J. J. Am. Chem. Soc. 64: 1630. 1942.
14. MACDONALD, J. Y., MITCHELL, K. M., and MITCHELL, A. T. S. J. Chem. Soc. 1574. 1951.
15. MOELLER, M. Kem. Maanedsblad, 18: 138. 1937. Chem. Abstr. 33: 9179. 1939.
    (*a*) OLSON, A. R. and SIMONSON, T. R. J. Chem. Phys. 17: 1322. 1949.
    (*b*) OSTWALD, W. J. prakt. Chem. 32: 305. 1885.
16. PEARCE, J. N. and SMITH, L. J. Am. Chem. Soc. 59: 2063. 1937.
17. PETERS, C. A., MACMASTERS, M. M., and FRENCH, C. L. Ind. Eng. Chem. Anal. Ed. 11: 502. 1939.
18. POLCHLOPEK, S. E. and SMITH, J. H. J. Am. Chem. Soc. 71: 3280. 1949.
19. RABINOWITCH, E. and STOCKMAYER, W. H. J. Am. Chem. Soc. 64: 335. 1942.
20. SIDDALL, T. H. and VOSBURGH, W. C. J. Am. Chem. Soc. 73: 4270. 1951.

FERRIC SULPHATE COMPLEXES, AND TERNARY COMPLEXES WITH THIOCYANATE IONS[1]

By M. W. Lister and D. E. Rivington

ABSTRACT

A spectrophotometric study of solutions containing ferric and sulphate ions, and also ferric, sulphate, and thiocyanate ions, is reported. The measurements were made at constant temperature and ionic strength; the effect of varying acidity was also investigated. The data were interpreted with the help of the results of the first paper of this series. It is believed that the data show that $FeSO_4^+$ and $FeHSO_4^{++}$ ions are formed. Values are obtained for the equilibrium constants for their formation from simple ions, and for their extinction coefficients. At higher sulphate concentrations there is evidence for the appearance of $Fe(SO_4)_2^-$ and $FeSO_4.HSO_4$, and estimates are made of their equilibrium constants. When thiocyanate is also present, the data can best be interpreted by assuming that the complex $FeSO_4.SCN$ is formed, and at higher sulphate probably also $Fe(SO_4)_2SCN^{--}$. Values are obtained for the equilibrium constants for the formation of these species, and the results would indicate that mixed complexes of this type are formed as readily as 'simple' ones such as $Fe(SO_4)_2^-$.

INTRODUCTION

One of the possible methods for investigating the complexes of ferric ions is to use thiocyanate as an indicator ion. It is generally observed that the red color of a ferric thiocyanate solution fades as another ion is added which also forms a complex with ferric ions; and by suitable colorimetric measurements it should be possible to determine the equilibrium constant of the formation of this other complex. This method has been employed in a few investigations, e.g. by Lanford and Kiehl (6) using phosphate ions; and it was also used in effect by Bent and French (1) for chloride ions in their early paper on ferric thiocyanate. In the latter case the equilibrium constant of the reaction $Fe^{+++} + Cl^- \rightleftharpoons FeCl^{++}$, as obtained with the help of thiocyanate, differs from the result obtained directly without thiocyanate. This matter has been investigated by the present authors, and will be reported in another paper. The present paper reports work on the application of this method to ferric sulphate complexes. Investigations of the sulphate complexes have been described in two papers appearing since the present work was started, though in neither case was the thiocyanate ion used as indicator. The first paper by Sykes (9) reported measurements on the effect of sulphate ions on the kinetics of the reaction between ferric and iodide ions: Sykes concluded that the equilibrium constant for $FeSO_4^+$,

$$k_1 = (FeSO_4^+)/(Fe^{+++}) \cdot (SO_4^{--}),$$

had a value of 15,000 at zero ionic strength. He did not investigate the ion $FeHSO_4^{++}$. Whiteker and Davidson (10) in the second paper decided that $FeHSO_4^{++}$ did not occur in significant amounts because of the rather small differences produced in the absorption spectra of ferric sulphate systems by alteration of the hydrogen ion concentration. On this basis they evaluated

[1]*Manuscript received June 30, 1955.*
Contribution from the Department of Chemistry, University of Toronto, Toronto, Ontario.

k_1 and found it to be 105 ± 15. The evidence against $FeHSO_4^{++}$ did not appear to be quite conclusive, and it was decided to investigate this particular matter in more detail. This was done directly on solutions of ferric and sulphate ions at different acidities. The alternative method of using thiocyanate as an indicator ion was also carefully examined, and it is believed that the results show that ternary complexes containing ferric, sulphate, and thiocyanate ions must be present. It is evident that similar work with other ions must also take into account the possible formation of ternary complexes.

APPARATUS AND MATERIALS

The extent of formation of the various complex ions was determined from the optical densities of the solutions as measured on a Beckmann DU spectrophotometer. The techniques used were generally the same as those used in the first paper of this series (7). The modification of the spectrophotometer and the methods of preparing the solutions were identical. The chemicals used were also the same, with the single addition of sulphuric acid, of which a stock solution was made by diluting the reagent grade acid.

EXPERIMENTAL RESULTS

As in the first paper of the series (7), runs were carried out at 25°C., and an ionic strength of 1.2, which was controlled by the addition of sodium perchlorate. Three series of runs were made. (i) Runs were made in which the ferric ion concentration was varied but the sulphate kept constant. The ferric ion was in considerable excess, so the results could be interpreted by the method devised by Rabinowitch and Stockmayer (8), though some extension of the method was necessary owing to the greater complexity of the sulphate systems.

TABLE I

OPTICAL DENSITIES OF FERRIC SULPHATE SOLUTIONS

Light path = 1 cm.; sulphate concentration = 0.001 M in all cases; ionic strength = 1.2

(Fe^{+3}), M	(H^+), M	Wave length, mμ					
		360	350	345	340	335	330
0.005	0.50	.019	.030	.037	.046	.055	.065
0.010		.035	.057	.071	.090	.106	.125
0.015		.045	.076	.099	.120	.145	.171
0.020		.060	.100	.124	.154	.183	.211
0.025		.069	.115	.144	.175	.209	.237
0.030		.080	.131	.165	.199	.226	.246
0.005	0.20	.034	.056	.071	.089	.106	.125
0.010		.060	.101	.126	.156	.190	.221
0.015		.084	.140	.175	.215	.255	.299
0.020		.100	.166	.207	.254	.301	.342
0.025		.115	.190	.236	.285	.330	.360
0.005	0.10	.049	.080	.102	.125	.151	.179
0.010		.086	.141	.179	.219	.261	.305
0.015		.112	.186	.233	.284	.335	.385
0.020		.127	.213	.262	.319	.369	.409
0.005	0.05	.060	.102	.128	.157	.190	.224
0.010		.099	.164	.205	.253	.300	.349
0.015		.120	.200	.247	.299	.346	.379

TABLE II

DEPENDENCE OF OPTICAL DENSITY ON (H^+) IN FERRIC SULPHATE SOLUTIONS
$(Fe^{+3}) = 0.001\ M$; $(SO_4^{--}) = 0.050\ M$; 25°C.; ionic strength = 1.2

	Wave length, mμ				
(H^+), M	350	345	340	335	330
0.20	.394	.491	.603	.722	.840
0.10	.458	.577	.709	.842	.974
0.05	.500	.631	.773	.920	1.058
0.02	.510	.642	.790	.939	1.073

TABLE III

OPTICAL DENSITIES OF SOLUTIONS CONTAINING FERRIC, THIOCYANATE, AND SULPHATE IONS
$(Fe^{+3}) = 0.001\ M$; $(SCN^-) = 0.001\ M$; $(H^+) = 0.2\ M$; 25°C.; ionic strength 1.2

	Wave length, mμ				
(SO_4^{--}), M	440	450	460	470	480
0	.450	.471	.480	.468	.443
0.0025	.430	.452	.460	.449	.423
0.005	.420	.441	.448	.437	.411
0.0075	.401	.421	.428	.417	.390
0.010	.387	.409	.412	.401	.377
0.0125	.372	.391	.396	.385	.363
0.015	.364	.381	.386	.376	.354
0.0175	.356	.375	.378	.367	.346
0.020	.342	.359	.361	.351	.330
0.025	.325	.339	.342	.331	.311
0.030	.309	.323	.325	.316	.295
0.035	.295	.307	.309	.299	.280
0.040	.280	.292	.294	.281	.265
0.050	.255	.265	.266	.256	.239

Various runs were made at different hydrogen ion concentrations, so that the possible formation of $FeHSO_4^{++}$ could be investigated. The results are given in Table I. (ii) A short series of runs were made at higher sulphate and lower ferric ion concentrations, with varying hydrogen ion concentrations. The results throw some light on the formation of higher complexes, and are given in Table II. (iii) A series were made with constant (and low) ferric and thiocyanate ion concentrations, and with sulphate also present in a fairly wide range of concentrations. The acidity was kept constant. This series gave a comparison of the equilibrium constants obtained with and without thiocyanate. The results are given in Table III.

DISCUSSION OF RESULTS

A discussion of the results in Table I should perhaps be prefaced by saying that the optical densities in the table are relative to solutions of identical composition except that no sulphate has been added. Qualitatively an examination of the solutions containing sulphate shows an absorption band with a maximum at 3050 Å, which is absent without sulphate. However ferric perchlorate solutions are themselves beginning to absorb at this wave length, so the measurements were made at wave lengths from 3300 to 3600 Å, where ferric perchlorate scarcely absorbs at all. Hence there is no doubt that the absorption is really due to ferric sulphate complexes.

It is apparent from Table I that a high hydrogen ion concentration reduces the optical density of ferric sulphate solutions, but that the relative densities at different wave lengths are scarcely altered. Hence the effect of hydrogen ion is either just to remove absorbing ions (presumably $FeSO_4^+$), or to introduce other ions of similar spectrum (presumably $FeHSO_4^{++}$), or both. To explain the results it is necessary to consider various possible equilibria. It seemed reasonable to suppose that, under the conditions of the first run (0.001 *M* sulphate, 0.005 to 0.03 *M* iron, and varying acidity), the following equilibria might be important:

$$Fe^{+++} + SO_4^{--} \rightleftharpoons FeSO_4^+,$$
$$Fe^{+++} + HSO_4^- \rightleftharpoons FeHSO_4^{++},$$
$$H^+ + SO_4^{--} \rightleftharpoons HSO_4^-.$$

The acidity was high enough to suppress the formation of $FeOH^{++}$ to more than a small extent. It was thought unlikely that ions containing two iron atoms would be formed (e.g. $Fe_2SO_4^{++}$), chiefly because in general it never seems necessary to postulate such ions in fairly dilute aqueous solutions; so this possibility was ignored.

The results in Table I can be treated by an extension of the Rabinowitch and Stockmayer (8) method. This method assumes that only a negligible fraction of the iron is complexed, the concentrations being such that this is a reasonably good approximation. If we represent the concentrations of the various ions by the following symbols:

$$p = (Fe^{+++}), \quad q = (SO_4^{--}), \quad r = (HSO_4^-),$$
$$x = (FeSO_4^+), \quad y = (FeHSO_4^{++}), \quad s = (H^+),$$

and a = total iron present,
b = total sulphate present,
c = total acid put in, measured in hydrogen ion concentration;

then: $x/pq = k_1$ (equilibrium constant for $FeSO_4^+$),
$y/pr = k_m$ (equilibrium constant for $FeHSO_4^{++}$),
$sq/r = k_a$ (ionization constant for HSO_4^-);

and for the mass balances:

$$a = p+x+y,$$
$$b = q+r+x+y,$$
$$c = s+r+y.$$

For the optical density, D, we have:

$$D = \epsilon_1 x + \epsilon_m y,$$

where ϵ_1 is the extinction coefficient of $FeSO_4^+$,
and ϵ_m is the extinction coefficient of $FeHSO_4^{++}$.

As a first approximation we can write $a = p$, i.e. little iron is complexed, and $c = s$, as only a little sulphate is present, so the formation of bisulphate ions

will not significantly alter the hydrogen ion concentration. The first assumption is equivalent to that made by Rabinowitch and Stockmayer. We can now rapidly eliminate p, r, s, x, and y from the above equations, when we get:

$$b = q(1+c/k_a+k_1a+k_mca/k_a),$$
$$D = aq(\epsilon_1 k_1+\epsilon_m k_m c/k_a).$$

Finally, eliminating q, and rearranging, we get:

[i] $$\frac{D}{a}\left(1+\frac{c}{k_a}\right) = k_1(b\epsilon_1-D)+k_m(b\epsilon_m-D)\frac{c}{k_a}.$$

This means that at any given wave length a plot of D/a against D should give a straight line. The slope of this line is given by:

[ii] $$\frac{\partial(D/a)}{\partial D} = -\frac{(k_1k_a+k_mc)}{k_a+c}.$$

Applying this to the data of Table I, moderately straight lines result; the straightness is best at fairly high acidity and not too high total iron. Averaging the data for all wave lengths, we get the results given below.

c	0.5	0.2	0.1	0.05
Average slope	16.5	28.5	46.3	71.0
Range of slope	14.9–18.5	26.9–30.9	42.8–49.1	63.5–79.2

By 'slope' is meant $-\partial(D/a)/\partial D$. There was a tendency for the slope to increase at higher values of a; where this was noticeable the slope was taken from the best line for the earlier points. 'Range of slope' gives the range over different wave lengths: there was no observable trend with wave length.

To evaluate k_1 and k_m, we must first know k_a. Various values of this constant have been reported (see for example Harned and Owen (5)), but the most reliable value is probably that from a critical survey of the data made by Davies, Jones, and Monk (3). They conclude that at zero ionic strength $k_a = 0.010$. This value is close to the more careful early estimates (4). The value of this constant at the ionic strength used here is open to some doubt, but fortunately the results in the present paper provide some check on the figure chosen. If we use the extended form of the Debye-Hückel equation, for instance in the form proposed by Davies (2), we get $k_a = 0.038$ at an ionic strength of 1.2. This extrapolation is too long for us to be able to conclude more than that a value near 0.04 would be plausible. Young and Blatz (11) from Raman spectra obtain values for the concentrations of sulphate and bisulphate ions in solutions of sulphuric acid. Taking solutions of the same ionic strength, their results would make k_a lie between 0.04 and 0.05 at an ionic strength of 1.2. It therefore seems probable that k_a should be taken as near 0.04.

Referring back to equation [ii], if we call the slope S, then

$$S(1+k_a/c) = k_1 k_a/c+k_m.$$

Hence a plot of $S(1+k_a/c)$ against k_a/c should give a straight line. If this plot is made, the result is reasonably straight for $k_a = 0.03$ and 0.04, but is definitely

curved for $k_a = 0.02$ or 0.05. The present results are not accurate enough to give more than a very rough value of k_a, but they are consistent with a value in the range 0.03 to 0.04. The values of k_1 and k_m that are obtained are:

k_a	0.03	0.04
k_1	178	153
k_m	6.8	5.6

We can therefore conclude that at this ionic strength, $k_1 = 165(\pm 10)$ and $k_m = 6(\pm 1)$. It seems definite that k_m is not zero, and that the species $FeHSO_4^{++}$ is present. It is also possible to calculate the ionization constant of $FeHSO_4^{++}$ considered as an acid: $FeHSO_4^{++} \rightleftharpoons FeSO_4^{+} + H^{+}$. The ionization constant equals $k_m/k_1 k_a$, which comes out close to unity. This is at least a reasonable figure, since $FeHSO_4^{++}$ would probably be a stronger acid than HSO_4^{-}.

If we take these values of k_1 and k_m, we can substitute in equation [i], and get a number of equations in ϵ_1 and ϵ_m at any wave length. From any pair of these, ϵ_1 and ϵ_m can be obtained separately with the following results:

λ	3600	3500	3450	3400	3350	3300 Å
ϵ_1	270	440	560	690	810	970
ϵ_m	160	265	340	390	470	560

It is interesting to note that ϵ_m is always about three fifths of ϵ_1. These extinctions might be expected to run parallel, but there seems to be no obvious reason for this ratio.

If we look now at the results in Table II, at relatively high sulphate, a rough calculation shows that the densities do not agree adequately with the densities calculated from the assumptions made in treating Table I. This presumably means that other species are present; the most probable one is $Fe(SO_4)_2^{-}$, and possibly $Fe(SO_4)(HSO_4)$. The rigorous treatment of a mixture of this sort is not easy, but we can make simplifying assumptions. As the mixtures in Table II all contained 0.001 M total iron, and 0.05 M total sulphate, a plausible approximation is that:

$$b = q + r,$$

i.e. the sulphate is almost all present as SO_4^{--} or HSO_4^{-}. The total acid added is also much more than the total iron, so approximately:

$$c = s + r,$$

i.e. the acid hydrogen is present either as H^{+} or as HSO_4^{-}. These approximations, and the ionization constant of HSO_4^{-} ($k_a = sq/r$), enable us to calculate s, q, and r. If we suppose that $Fe(SO_4)_2^{-}$ is the only new ion formed, and call its concentration z, its extinction coefficient ϵ_2, and its equilibrium constant k_2, where

$$k_2 = \frac{[Fe(SO_4)_2^{-}]}{[Fe^{+3}][SO_4^{--}]^2} = z/pq^2,$$

then we have from the mass balance for iron:

$$a = p + x + y + z$$

and for the optical density:

$$D = \epsilon_1 x + \epsilon_m y + \epsilon_2 z.$$

Eliminating p, x, y, and z, the result is:

$$a(\epsilon_1 k_1 q + \epsilon_m k_m r + \epsilon_2 k_2 q^2) = D(1 + k_1 q + k_m r + k_2 q^2).$$

Hence from the data in Table II, we get a series of equations in the two unknowns ϵ_2 and k_2. This equation is, in fact, of the form:

$$\epsilon_2 = \alpha/k_2 + D/a$$

where α is a function of known quantities. Values of α and D/a were calculated, and then by combining them in pairs with the result at $c = 0.1$, the following values for k_2 were obtained:

	Wave length, Å				
c	3500	3450	3400	3350	3300
0.2	3.24	2.78	2.79	3.14	3.13×10^4
0.05	1.67	1.58	1.67	1.65	1.68×10^4
0.02	1.72	1.69	1.67	1.69	1.62×10^4

The results at $c = 0.05$ and 0.02 are fairly constant and make $k_2 = 16{,}600$ as an average. The values at $c = 0.2$ give a discrepancy, although this discrepancy is not as big as it looks, since a change of only about 0.02 in the density readings would bring these points also into line. However we are faced with the choice that (i) our general picture of these mixtures is wrong, and the results in Tables I and II must be reconciled by postulating some other ionic species; or (ii) some other new species is beginning to make its appearance at $c = 0.2$ (high acidity). One is naturally loath to reject the idea that $Fe(SO_4)_2^-$ ions are responsible for the deviations in the optical densities at high sulphate concentrations, since this is the obvious explanation. Hence it seems most probable that the explanation is that at $c = 0.2$ the new species $Fe(SO_4)(HSO_4)$ is beginning to appear. A rough calculation can be made of the amount of this species present on the assumption that its extinction coefficient is equal to that of $Fe(SO_4)_2^-$ (see below), which is probably at least roughly true. The optical density at $c = 0.2$ was calculated assuming no $Fe(SO_4)(HSO_4)$. The results at different wave lengths were moderately consistent: the calculated concentrations ranged from 2.7 to 3.7×10^{-5} with a mean of 3.3×10^{-5}. This makes the equilibrium constant for the reaction

$$Fe(SO_4)(HSO_4) \rightleftharpoons Fe^{+3} + SO_4^{--} + HSO_4^-,$$

defined as

$$k_x = \frac{[FeSO_4.HSO_4]}{[Fe^{+3}][SO_4^{--}][HSO_4^-]},$$

about 380 (perhaps ± 50). Considered as an acid the ionization constant of $FeSO_4.HSO_4$ would be about 1.7, which is not far from that for $FeHSO_4^{++}$.

The extinction coefficients of $Fe(SO_4)_2^-$ are readily calculated once k_2 is known; the results are:

λ	3500	3450	3400	3350	3300 Å
ϵ_2	560	700	860	1030	1170

These extinction coefficients are parallel to ϵ_1 and are about 1.25 times as large.

Summarizing this part, it seems fair to say that the picture presented is simple and fairly consistent, and it is unlikely that an equally satisfactory alternative explanation could be found. The results show that $FeSO_4^+$ is first formed (equilibrium constant 165, or 170 to two significant figures), and it seems impossible to interpret the effect of acid unless we also suppose that $FeHSO_4^{++}$ is also formed. At higher concentrations of sulphate $Fe(SO_4)_2^-$ is formed, and perhaps $FeSO_4.HSO_4$. The extinction coefficients of the three species $FeSO_4^+$, $FeHSO_4^{++}$, and $Fe(SO_4)_2^-$ run nearly parallel.

Table III reports the densities of solutions containing ferric, sulphate, and thiocyanate ions. The first point to decide is whether such solutions could be used to obtain the equilibrium constant for $FeSO_4^+$. A rough examination of the results showed that in fact they did not give the same value for k_1, at least assuming that the only complex ions present are $FeSO_4^+$, $FeSCN^{++}$, and $FeHSO_4^{++}$. We are therefore driven to supposing that mixed complex ions are formed, such as $FeSO_4.SCN$. This situation is found to be repeated in systems containing ferric, thiocyanate, and chloride or bromide ions. Examination of the results of Table III also show the following: (i) the relative densities at different wave lengths for any given sulphate concentration stay very much the same throughout; (ii) at any one wave length the density falls off as sulphate is added, and at first the fall in density is proportional to the sulphate added; and (iii) at higher sulphate concentrations the fall in density is less rapid than at first.

We can discover the extent to which $FeSO_4.SCN$ is formed from the following considerations. Let us use the same symbols for the concentrations of various species with the following additions:

$$(SCN^-) = n, \quad (FeSCN^{++}) = m, \quad (FeSO_4SCN) = j,$$

and let us write for the equilibrium constants:

$$\frac{(FeSCN^{++})}{(Fe^{+3})(SCN^-)} = k_t, \quad \frac{(FeSO_4.SCN)}{(Fe^{+3})(SO_4^{--})(SCN^-)} = k_j.$$

As these measurements were made at wave lengths from 4400 to 4800 Å where the simple sulphate complexes scarcely absorb, the optical density is given by

$$D = \epsilon_j j + \epsilon_t m$$

where ϵ_j and ϵ_t are the extinction coefficients of $FeSCN^{++}$ and $FeSO_4.SCN$. As before, let a, b, and c represent the total concentrations of iron, sulphate, and acid hydrogen, and in addition let d be the total concentration of thiocyanate. As c is much larger than a, we shall assume as before that $c = s + r$. Also, when b is small, it seems reasonable to assume that no ions containing

two sulphates have yet been formed. Thus the following nine species may be present: Fe^{+3}, SO_4^{--}, HSO_4^-, $FeSO_4^+$, $FeHSO_4^{++}$, SCN^-, $FeSCN^{++}$, $FeSO_4.SCN$, and H^+. There are five Mass Law equations:

$$k_a = sq/r, \quad k_1 = x/pq, \quad k_m = y/pr, \quad k_t = m/pn, \quad k_j = j/pnq;$$

and four equations for the mass balances:

$$\begin{aligned} a &= p+x+y+m+j, \\ b &= q+r+x+y+j, \\ c &= s+r, \\ d &= n+m+j; \end{aligned}$$

and the equation, given above, for the optical density. Hence, in theory, the nine concentrations can be eliminated, and values of all the constants obtained by combining a sufficient number of measurements. It is not difficult to eliminate x, y, m, j, s, and r to get

$$\begin{aligned} a &= p\left[1+k_1q+\frac{k_mcq}{k_a+q}+n(k_t+k_jq)\right], \\ b &= q\left[1+\frac{c}{k_a+q}+k_1p+\frac{k_mcp}{k_a+q}+k_jpn\right], \\ n &= p\left(1+k_1q+\frac{k_mcq}{k_a+q}\right), \\ D &= pn(\epsilon_t k_t+\epsilon_j k_j q). \end{aligned}$$

These equations also use the fact that in Table III, $a = d$. When b is small, so is q, and we can at first ignore q compared with k_a. If we also call $k_1+k_m\, c/k_a=\alpha$, these equations reduce to:

$$\begin{aligned} a &= p[1+\alpha q+n(k_t+k_j\, q)], \\ b &= q(1+c/k_a+\alpha p+k_j\, pn), \\ n &= p(1+\alpha q), \\ D &= pn(\epsilon_t\, k_t+\epsilon_j\, k_j\, q). \end{aligned}$$

Let p_0, n_0, and D_0 be the values of these quantities when $b = 0$. Then since $q_0 = 0$

$$\begin{aligned} a &= p_0(1+k_t\, n_0), \\ n_0 &= p_0, \\ D_0 &= p_0\, n_0\, \epsilon_t\, k_t. \end{aligned}$$

If we differentiate the above equations with respect to b, and suppose that $b = 0$, we get equations giving the initial slopes of the quantities p, q, n, and D as sulphate is added. The resulting equations (with a little rearrangement) are:

$$\left(\frac{\partial q}{\partial b}\right)_0 = \frac{1}{1+c/k_a+\alpha p_0+k_j{p_0}^2},$$

$$\left(\frac{\partial p}{\partial b}\right)_0 = -\frac{(a\alpha+k_j{p_0}^2)}{(1+2k_t p_0)}\left(\frac{\partial q}{\partial b}\right)_0,$$

$$\frac{1}{D_0}\left(\frac{\partial D}{\partial b}\right)_0 = \frac{2}{p_0}\left(\frac{\partial p}{\partial b}\right)_0+\left(\alpha+\frac{\epsilon_j k_j}{\epsilon_t k_t}\right)\left(\frac{\partial q}{\partial b}\right)_0.$$

As $(\partial D/\partial b)_0$ is known from the data, and as $(\partial q/\partial b)_0$ and $(\partial p/\partial b)_0$ could be eliminated, we have in effect at each wave length an equation containing the unknowns ϵ_j and k_j. Since the shape of the absorption curve is virtually unaltered by adding sulphate, ϵ_j is presumably proportional to ϵ_i; and from the nature of the species concerned it seems reasonable to take $\epsilon_j = \epsilon_i$ as a first approximation. This last approximation can be checked to some extent from the results as more sulphate is added; but the effect of other ions, notably $Fe(SO_4)_2^-$, makes the whole system so complicated that this confirmation is not at all strong.

The observed values of $(1/D_0)(\partial D/\partial b)_0$, taken over the range $b = 0$ to 0.01, are:

λ	4400	4500	4600	4700	4800 Å
$(1/D_0)(\partial D/\partial b)_0$	−14.0	−14.1	−14.2	−14.3	−14.9

Probably the best average is −14.2. Substituting this in the equations above the value of k_j comes out at 11,500. The magnitude of this constant is not unexpected; since, combining it with other known constants, it means that the reaction

$$FeSO_4^+ + SCN^- \rightleftharpoons FeSO_4.SCN$$

has an equilibrium constant of 70; and the reaction

$$FeSCN^{++} + SO_4^{--} \rightleftharpoons FeSO_4.SCN$$

has an equilibrium constant of about 90. No very great accuracy can be claimed for k_j, but it probably lies between 10,000 and 13,000.

As the sulphate is increased, the optical density falls off linearly at first and then less rapidly. If we calculate the concentrations of the various species, assuming that no new ions are formed and that $\epsilon_i = \epsilon_j$, the results make a plot of D against b deviate only quite slowly from a straight line (the fact that a straight line is maintained for a moderate distance is some evidence that our assumptions about the solutions containing sulphate up to about 0.01 M were right). The deviation from this straight line must mean that some new colored ion is appearing that is competing successfully against the ions $Fe(SO_4)_2^-$ and $FeSO_4.HSO_4$ which will now be present. This was checked in another way. At higher sulphate concentrations (>0.02) the fraction of sulphate used up in complexes will be so small that we can write approximately:

$$b = q + r.$$

As $c = s + r$, and $k_a = sq/r$, this enables us to find q, r, and s. Allowing now for the presence of $Fe(SO_4)_2^-$ and $FeSO_4HSO_4$, it is possible to calculate D in terms of q and known constants. The observed densities were greater than the calculated ones. As mentioned above, the calculated curve only departs very slowly from a straight line. The only plausible new colored (at 4600 Å) ion is $Fe(SO_4)_2.SCN^{--}$, and a rough estimate of the extent to which it might be present was made in the following way.

If we assume that the species $Fe(SO_4)_2^-$ and $FeSO_4.HSO_4$ may now also be present, but not $Fe(SO_4)_2.SCN^{--}$, the equations for the various concentrations can be reduced to the following:

$$a = p[f(q)+n(k_t+k_j q)],$$
$$n = p.f(q),$$
$$D = pn(\epsilon_t k_t+\epsilon_j k_j q),$$

where

$$f(q) = 1+\left(k_1+\frac{k_m c}{k_a+q}\right) q+k_2\left(1+\frac{k_a c}{k_i(k_a+q)}\right) q^2.$$

k_t is the ionization constant of $FeSO_4.HSO_4$ as an acid. If we assume as above that $\epsilon_t = \epsilon_j$, and call $D/\epsilon_t = X$, we get

$$(a-X)^2 = Xf(q)/(k_t+k_j q).$$

As q is known, X can be calculated. The results of this calculation can be compared with experiment as in Table IV. There is evidently a very slight

TABLE IV

VALUES OF 10^5 X

	Wave length							
b	440	450	460	470	480	Mean X_{obs}	X_{calc}	Difference
0.025	7.42	7.32	7.31	7.26	7.22	7.31	7.03	0.28
0.03	7.05	6.98	6.94	6.93	6.84	6.95	6.49	0.46
0.035	6.74	6.63	6.60	6.56	6.50	6.61	6.00	0.61
0.04	6.39	6.31	6.28	6.16	6.15	6.26	5.56	0.70
0.05	5.82	5.72	5.68	5.61	5.55	5.68	4.80	0.88

shift of the absorption spectrum to the violet, the maximum being shifted about 30 Å. However as points on both sides of the maximum have been used, it is probably legitimate to compare a mean value of X as observed with the calculated X. The difference is given in the last column, and this may tentatively be taken as the concentration of $Fe(SO_4)_2.SCN^{--}$. This involves the assumptions (i) that the extinction coefficient of $Fe(SO_4)_2.SCN^{--}$ is the same as that of $FeSCN^{++}$ at these wave lengths, and (ii) that the amount of $Fe(SO_4)_2.SCN^{--}$ present is not enough to throw out the calculations of the concentrations of the other ions present by any great amount. The first assumption is fairly reasonable from the formulae of the ions, but its only other justification is that it gives a plausible and moderately constant value of the equilibrium constant of this ion. The second assumption is at least nearly true, since even at $b = 0.05$ the concentration of ferric ions is about 24 times, and that of thiocyanate ions is 110 times as great as that of $Fe(SO_4)_2.SCN^{--}$. The relevant concentrations are given in Table V. The last column gives the

TABLE V

b	$(Fe(SO_4)_2SCN^{--})$, M	(Fe^{+3}), M	(SO_4^{--}), M	(SCN^-), M	k_w
0.025	0.28×10^{-5}	4.19×10^{-4}	4.37×10^{-3}	9.30×10^{-4}	3.76×10^5
0.03	0.46	3.63	5.34	9.35	4.75
0.035	0.61	3.15	6.35	9.40	5.12
0.04	0.70	2.74	7.40	9.44	4.95
0.05	0.88	2.09	9.61	9.52	4.79

equilibrium constant:

$$k_w = \frac{(Fe(SO_4)_2.SCN^{--})}{(Fe^{+3})(SO_4^{--})^2(SCN^-)}.$$

The values obtained for it are fairly consistent, and the last four values average 490,000. This means that the equilibrium constant for the attachment of a second sulphate to $FeSO_4.SCN$ is 43, and for the attachment of a thiocyanate ion to $Fe(SO_4)_2^-$ is 29. These values are reasonably similar to the corresponding values for attachment of sulphate and thiocyanate ions to other complex ferric ions; however the constants obtained will be reviewed after results with chloride and bromide have been reported. In conclusion it may be said that while no great accuracy can be claimed for these constants, it seems very improbable that any other selection of complex ions would have explained the results, and that part of the support for the present picture indeed comes from the relative sizes of these constants.

REFERENCES

1. BENT, H. E. and FRENCH, C. L. J. Am. Chem. Soc. 63: 568. 1941.
2. DAVIES, C. W. J. Chem. Soc. 2093. 1938.
3. DAVIES, C. W., JONES, H. W., and MONK, C. B. Trans. Faraday Soc. 48: 921. 1952.
4. HAMER, W. J. J. Am. Chem. Soc. 56: 860. 1934.
5. HARNED, H. S. and OWEN, B. B. Physical chemistry of electrolytic solutions. 2nd ed. Reinhold Publishing Corporation, New York. 1950. p. 430.
6. LANFORD, O. E. and KIEHL, S. J. J. Am. Chem. Soc. 64: 291. 1942.
7. LISTER, M. W. and RIVINGTON, D. E. Can. J. Chem. 33: 1572. 1955.
8. RABINOWITCH, E. and STOCKMAYER, W. H. J. Am. Chem. Soc. 64: 335. 1942.
9. SYKES, K. W. J. Chem. Soc. 124. 1952.
10. WHITEKER, R. A. and DAVIDSON, N. J. Am. Chem. Soc. 75: 3081. 1953.
11. YOUNG, T. F. and BLATZ, L. A. Chem. Revs. 44: 93. 1949.

SOME FERRIC HALIDE COMPLEXES, AND TERNARY COMPLEXES WITH THIOCYANATE IONS[1]

By M. W. Lister and D. E. Rivington

ABSTRACT

A spectrophotometric study of solutions containing ferric and bromide ions; ferric, bromide, and thiocyanate ions; and ferric, chloride, and thiocyanate ions is reported. The measurements were made at constant temperature and ionic strength. The data were interpreted with the help of the results from the first paper of this series. The data show that $FeBr^{++}$ and $FeBr_2^+$ are formed, and values are obtained for the equilibrium constants for their formation from simple ions, and for the extinction coefficients of $FeBr^{++}$. When thiocyanate is also present, the data can best be interpreted by assuming that $FeSCNBr^+$ or $FeSCNCl^+$ is formed. At high chloride concentrations it seems necessary to postulate also $FeCl_2^+$ and $FeSCN.Cl_2$. Estimates are made for the equilibrium constants for the formation of all these species from simple ions. As with the corresponding sulphate complexes, there seems to be no particular reluctance to form mixed complexes such as $FeSCNCl^+$, as compared with the 'simple' complexes such as $FeCl_2^+$.

In the second paper of this series (3*b*), results were reported which showed that the color of ferric thiocyanate could only be used as a means of investigating complexes of ferric and sulphate ions, if allowance were made for the presence of species containing ferric, sulphate, and thiocyanate, such as $FeSO_4.SCN$. The present work deals with a similar investigation of solutions containing chloride or bromide ions, instead of sulphate. The intention was to make a critical examination of this method of investigating ferric complexes, and in particular to discover to what extent ternary complexes, such as $FeSCN.Cl^+$ or $FeSCN.Br^+$, were important. Rabinowitch and Stockmayer have already investigated solutions containing ferric and chloride or bromide ions, but not thiocyanate as well (6). They suggested that the discrepancy between their result for the equilibrium constant for the formation of $FeCl^{++}$, and the earlier results of Bent and French (1), who examined solutions made from ferric chloride and potassium thiocyanate, was due to the ion $FeSCN.Cl^+$. The present work attempts a more quantitative estimate of the formation of this ion, and of the analogous $FeSCN.Br^+$. It is believed that the results demonstrate the existence of these ions, and values for the equilibrium constants of their formation from simple ions have been obtained.

APPARATUS AND MATERIALS

All optical measurements were made with a Beckmann Model DU spectrophotometer, modified so that the temperature of the solutions could be controlled, as described in the first paper of this series (3*a*).

The reagents used were the same as described in this same paper, with the following additions.

Hydrochloric acid.—The concentrated reagent grade acid was diluted to give a stock solution of about 1 *M* concentration. This was standardized volumetrically against borax.

[1]*Manuscript received June 30, 1955.*
Contribution from the Department of Chemistry, University of Toronto, Toronto, Ontario.

Sodium chloride.—The reagent grade chemical was dissolved to give a stock solution of about 5 *M* concentration. This was standardized volumetrically against silver nitrate.

Sodium bromide.—A pure grade of sodium bromide was dissolved to give a 5 *M* stock solution, which was standardized by titration against silver nitrate.

The general technique used in making up and storing solutions, in preventing fading of the ferric thiocyanate color, and in measuring the optical densities was exactly the same as described in the first paper (3*a*). The mixtures in the present work contained ferric perchlorate, perchloric acid (to suppress hydrolysis), sodium perchlorate (to adjust the ionic strength), sodium thiocyanate, and sodium chloride or bromide.

EXPERIMENTAL RESULTS

It was first necessary to check that the ions $FeCl^{++}$ or $FeBr^{++}$ did not absorb light appreciably in the region of measurement which was 4400 to 4800 Å. Solutions containing 0.001 *M* ferric ions in 0.2 *M* perchloric acid and a large excess of sodium chloride (about 0.6 *M*) show a strong absorption band with a maximum at 3270 Å; however the absorption falls rapidly at longer wave lengths, and is negligible at 4400 Å. Similar measurements with bromide substituted for chloride show only a very slight absorption in the ultraviolet besides that due to ferric ions, but there is a long 'tail' extending into the visible with a very weak subsidiary maximum at about 4100 Å. Accordingly solutions containing ferric, bromide, and thiocyanate ions were measured against a 'reagent blank' which contained the same concentrations of the various ions except for thiocyanate. Some measurements were also made on ferric bromide solutions (without thiocyanate) in which case the reagent blank was simply a ferric perchlorate solution. These measurements with ferric, bromide, and thiocyanate solutions against this reagent blank require a slight correction which will be described later.

Effect of chloride ion.—In order to investigate the effect of chloride ion on the ferric thiocyanate equilibrium, a series of solutions having 0.001 *M* total iron, 0.00125 *M* total thiocyanate, 0.200 *M* hydrogen ions, an ionic strength of 1.2, and total chloride varying from zero to 1.2 *M* were prepared. The optical densities of these solutions at 25°C. were measured from 4400 to 4800 Å. The results are given in Table I.

Effect of bromide ion.—As the $FeBr^{++}$ complex has only been examined once before (6), it was thought worth while to check the value of its equilibrium constant. Accordingly measurements were made on solutions containing ferric perchlorate, perchloric acid, sodium perchlorate, and sodium bromide only, without thiocyanate. The results are given in Table II. The value of the dissociation constant of $FeBr^{++}$, and its extinction coefficients, will be deduced in the next section.

Solutions containing ferric, thiocyanate, and bromide ions were also examined. The results are given in Table III; as was mentioned above, these results are against a reagent blank of the same composition as the test solutions except that the thiocyanate is omitted.

TABLE I

OPTICAL DENSITIES OF SOLUTIONS CONTAINING FERRIC, CHLORIDE, AND THIOCYANATE IONS (Fe^{+3}) = 0.001 *M*; (SCN^-) = 0.00125 *M*; (H^+) = 0.2 *M*; ionic strength = 1.2; light path = 1 cm.; temperature 25°C.

(Cl^-), *M*	Wave length, mμ				
	440	450	460	470	480
0	.562	.592	.599	.587	.557
0.025	.539	.568	.572	.561	.530
0.050	.511	.541	.549	.535	.503
0.075	.492	.519	.528	.512	.483
0.100	.471	.498	.502	.492	.464
0.125	.459	.481	.489	.479	.452
0.150	.447	.469	.472	.462	.439
0.200	.419	.441	.448	.438	.411
0.250	.395	.417	.422	.411	.389
0.300	.370	.390	.396	.386	.365
0.350	.352	.371	.376	.368	.346
0.400	.336	.353	.359	.350	.330
0.450	.322	.339	.344	.336	.318
0.500	.309	.325	.329	.323	.304
0.600	.284	.299	.304	.297	.280
0.700	.266	.281	.286	.279	.265
0.800	.250	.265	.269	.262	.248
1.000	.225	.239	.241	.235	.222
1.200	.205	.216	.220	.215	.204

TABLE II

OPTICAL DENSITIES OF SOLUTIONS CONTAINING FERRIC AND BROMIDE IONS (Fe^{+3}) = 0.001 *M*; (H^+) = 0.2 *M*; ionic strength = 1.2; light path 1 cm.; 25°C.

(Br^-), *M*	Wave length, mμ					
	380	400	420	440	450	460
0.10	.025	.028	.025	.020	.016	.013
0.20	.047	.054	.050	.037	.030	.025
0.30	.065	.075	.068	.050	.041	.034
0.40	.084	.095	.088	.065	.054	.044
0.50	.099	.113	.105	.078	.064	.051
0.60	.115	.131	.120	.091	.075	.060
0.70	.130	.148	.136	.102	.085	.066
0.80	.143	.161	.149	.110	.092	.075
0.90	.154	.174	.160	.120	.099	.080
1.00	.161	.184	.167	.125	.105	.085

TABLE III

OPTICAL DENSITIES OF SOLUTIONS CONTAINING FERRIC, BROMIDE, AND THIOCYANATE IONS (Fe^{+3}) = 0.001 *M*; (SCN^-) = 0.001 *M*; (H^+) = 0.2 *M*; ionic strength 1.2; temp. 25°C.; light path 1 cm.

(Br^-), *M*	Wave length, mμ					
	400	420	440	450	460	470
0	.234	.360	.459	.481	.488	.478
0.10	.223	.345	.440	.466	.471	.461
0.20	.210	.328	.424	.449	.457	.447
0.30	.200	.318	.409	.431	.439	.429
0.40	.193	.305	.395	.420	.428	.420
0.50	.185	.294	.381	.406	.411	.406
0.60	.176	.285	.368	.391	.401	.394
0.70	.170	.273	.355	.380	.386	.381
0.80	.156	.254	.333	.356	.366	.361
0.90	.150	.246	.324	.345	.354	.350
1.00	.141	.232	.305	.327	.334	.330

DISCUSSION OF RESULTS

1. Solutions Containing Bromide

The results in Table II will be considered first as these are most simply dealt with. The method of Rabinowitch and Stockmayer (6) can be used to interpret these results. If we use the following symbols:

a = total ferric concentration,
b = total bromide concentration,
D = optical density,
ϵ = extinction coefficient of $FeBr^{++}$,
k = equilibrium constant of $FeBr^{++}$ = $(FeBr^{++})/(Fe^{+3})(Br^{-})$;

then Rabinowitch and Stockmayer show that

$$b/D = b/a\epsilon + 1/ka\epsilon$$

holds to a good approximation. In Table II, a is kept constant and b is varied; hence a plot of b/D against b should give a straight line from which k and ϵ can be evaluated. The results of Table II, when plotted in this way, do give reasonably straight lines; and by drawing lines by the method of least squares through the experimental points, we obtain the values of k and ϵ given in Table IV. The best average value of k is probably 0.61, as the result at 4500 Å

TABLE IV

VALUES OF k AND ϵ FOR $FeBr^{++}$

λ, mμ	ϵ	k
380	435	0.601
400	491	0.606
420	457	0.594
440	328	0.630
450	295	0.562
460	225	0.607

is somewhat divergent. This can be compared with the value of 0.5 obtained by Rabinowitch and Stockmayer. The values for the extinction coefficients make the absorption maximum close to 4050 Å, and the maximum extinction coefficient is about 495. This is lower than the value obtained by Rabinowitch and Stockmayer, but the reason for the discrepancy is not clear.

The equation given above assumes that $FeBr^{++}$ is the only complex formed. At high concentrations there is a slight but consistent deviation from the optical densities calculated on the above assumptions. This is presumably due to $FeBr_2^{+}$ being formed. If we call the equilibrium constant of this ion k_2, where $k_2 = (FeBr_2^{+})/(Fe^{+3})(Br^{-})^2$, and ϵ_2 is its extinction coefficient, and if we assume that at these high concentrations the concentration of free bromide is virtually equal to the total bromide, then

$$a(\epsilon\, k + \epsilon_2\, k_2\, b) = D(1/b + k + k_2 b).$$

This equation contains two unknowns, and so these can be evaluated from any two measurements at one wave length. Unfortunately a very small error

in the density can lead to a considerable error in the value of k_2. If we take the points at $b = 1.0$ and 0.7 as the two measurements to calculate k_2, we get the following values of k_2 from the measurements at various wave lengths:

λ	3800	4000	4200	4400	4500	4600 Å
k_2	0.17	0.18	0.24	0.43	0.07	0.19

An error of 0.001 in the density could give an error of 0.1 in k_2; so the most that can be said is that k_2 is probably close to 0.2. The values of ϵ_2 are not reliable enough to be worth reporting: they seemed to run parallel to ϵ, but to be unduly low.

Turning now to the results when both bromide and thiocyanate are present, we shall attempt to explain them on the assumption that the complex ions $FeBr^{++}$, $FeSCN^{++}$, and $FeSCN.Br^{+}$ are present, and at higher concentrations $FeBr_2^{+}$ also. A rough calculation showed that the observed densities did not agree with those calculated if only $FeBr^{++}$ and $FeSCN^{++}$ are formed, so that some other ion must be formed; we shall be justified in assuming that this is $FeSCN.Br^{+}$ if the results give a reasonably constant value for its equilibrium constant. It will readily be appreciated that this system leads to rather complicated expressions for the constants, so that some approximations have to be made. If the concentrations of the various species are indicated by the following letters: $(Fe^{+3}) = p$, $(SCN^{-}) = q$, $(FeSCN^{++}) = x$, $(Br^{-}) = r$, $(FeBr^{++}) = u$, $(FeSCN.Br^{+}) = z$, there are three equations for the equilibrium constants of the complex ions:

$$FeBr^{++} : k_a = u/pr,$$
$$FeSCN^{++} : k_1 = x/pq,$$
$$FeSCN.Br^{+} : k_m = z/pqr.$$

The total iron (a), total bromide (c), and total thiocyanate (b) in the solution lead to equations for the mass balances:

$$a = p+x+u+z,$$
$$b = q+x+z,$$
$$c = r+u+z.$$

Finally the observed density is given by

$$D' = \epsilon_1 x+\epsilon_m z+\text{correction},$$

where ϵ_1 and ϵ_m are the extinction coefficients of $FeSCN^{++}$ and $FeSCN.Br^{+}$. The correction is small owing to the fact that there is a slightly different amount of $FeBr^{++}$ in the reagent blank and in the test solution, as some of the ferric ions are used up forming $FeSCN^{++}$ in the test solution. This correction was evaluated from a rough value of k_m (and of course the other constants) in a way that will be described in a moment. There are thus seven equations and six concentrations, so that in theory the two unknown constants, ϵ_m and k_m, can be found from any two measurements.

The results in Table III are for solutions in which $a = b$, and the total bromide (c) is much larger than a or b. Therefore it seemed reasonable to put

$r = c$, as a good approximation. If D is the corrected optical density, given by

$$D = \epsilon_1 x + \epsilon_m z,$$

we can eliminate p, r, u, x, and z from the above equations to get:

[i] $$\frac{q^2(k_1+k_m c)}{1+k_a c} + q - a = 0,$$

[ii] $$q = \frac{D(1+k_a c)}{a(\epsilon_1 k_1 + \epsilon_m k_m c) - D(k_1 + k_m c)}.$$

These make use of the fact that, in these solutions, $a = b$.

Before dealing with these equations further, we must explain how D' was corrected to give D. The correction is evidently $\epsilon_a(u_0 - u)$, where ϵ_a is the extinction coefficient of $FeBr^{++}$ obtained above, and u_0 is the concentration of this ion when no thiocyanate is present. Putting $b = 0$, u_0 is readily obtained as

$$u_0 = k_a ca/(1+k_a c).$$

When thiocyanate is present, as $a = b$:

$$u = k_a cq/(1+k_a c);$$

and equation [i] can be converted into a quadratic in u:

$$u^2(k_1 + k_m c) + u.k_a c - [a(k_a c)^2/(1-k_a c)] = 0.$$

Very rough calculation showed that k_m was not far from 25, and this value was used to obtain u and hence $u_0 - u$. The values of $u_0 - u$ so obtained were

c	0.1	0.2	0.4	0.6	0.8	1.0
$u_0 - u$	0.62	1.05	1.82	2.40	2.73	3.03×10^{-5}

Hence as ϵ_a is known the correction can be calculated; it is always less than 0.015, usually much less, and not particularly sensitive to changes in k_m: hence the rough value of k_m was quite adequate here.

Before we turn to the main method used to determine k_m, a word should be said about applying the initial slope method, used for the mixed sulphate–thiocyanate complexes in the second paper of this series. This method assumed that the mixed complex (in that case $FeSO_4.SCN$) absorbed light to nearly the same extent as $FeSCN^{++}$, at least in the region of the main absorption band of the latter. However $FeBr^{++}$ also absorbs somewhat in the region where $FeSCN^{++}$ absorbs, (while $FeSO_4^+$ absorbs there scarcely at all), so it cannot be assumed that $FeSCN^{++}$ and $FeSCNBr^+$ have nearly the same extinction coefficient. Actually if this assumption is made, the equilibrium constant for $FeSCNBr^+$ comes out as 30, while (to anticipate) the most reliable value is probably 21. Accordingly a more laborious, but probably more accurate, method was used to evaluate k_m.

Equations [i] and [ii] above are the starting point of the method. q could be eliminated readily enough, but the resulting equation in ϵ_m and k_m is very cumbersome. A method of successive approximations was therefore used, as follows. First let us assume that $\epsilon_1 = \epsilon_m$; in spite of the considerations given

in the last paragraph, this is unlikely to be totally wrong, in view of the formulae of the ions concerned, and at the next approximation we can discard this assumption. If $\epsilon_1 = \epsilon_m$, equations [i] and [ii] can be readily combined, and reduced to

$$k_1+k_mc = \frac{(1+k_ac)D/\epsilon_1}{(a-D/\epsilon_1)^2}.$$

Hence a rough value of k_m can be obtained from each density reading, and with this value of k_m, q can be calculated from equation [i]; then everything in equation [ii] is known except ϵ_m, which can thus be evaluated to a first approximation. With these values of ϵ_m and k_m, improved values of q can be obtained from equation [ii], and then used in equation [i] to obtain improved values of k_m. In theory these approximations could be repeated; in effect we are adjusting k_m and ϵ_m until the two equations give the same values of q for each value of c, the total bromide concentration. However the first approximation $\epsilon_1 = \epsilon_m$ is actually a fairly good approximation so the process did not need to be carried very far.

Table V gives the results of the first approximation for k_m. Ignoring the rather deviant values at 4000 Å, k_m averages as 21.2. The first approximation for ϵ_m gives the values in Table VI. These values are not very constant, but it is easily seen that a relatively small change in D will give a considerable change in ϵ_m. The absorption band of $FeSCNBr^+$ is evidently similar to that of $FeSCN^{++}$ shifted somewhat to the red. If we use these mean values of ϵ_m from Table VI, we get as our next approximation for k_m the results in Table VII. The results in Table VII are more consistent but the average is little changed.

TABLE V

FIRST APPROXIMATE VALUES FOR k_m

c	Wave length, mμ					
	400	420	440	450	460	470
0.1	31.5	27.5	25.7	26.5	24.2	31.4
0.2	13.2	15.2	22.2	22.8	27.1	29.3
0.3	12.0	20.5	21.0	18.4	21.3	21.9
0.4	15.4	17.9	20.0	21.5	23.5	25.6
0.5	14.8	17.2	18.3	20.0	19.1	23.0
0.6	12.0	17.9	17.1	17.7	20.4	21.9
0.7	14.7	14.8	15.4	17.6	17.6	19.9

TABLE VI

FIRST APPROXIMATE VALUES OF ϵ_m

c	Wave length, mμ					
	400	420	440	450	460	470
0.1	(3100)	4290	4930	5570	5360	(6340)
0.2	1540	2650	4560	4920	5760	5990
0.3	1420	3350	4350	4110	4680	4680
0.4	1720	2990	4170	4680	5110	5350
0.5	1660	2900	3880	4410	4330	4880
0.6	1410	2990	3670	3980	4540	4680
Mean	1530	3190	4260	4610	4960	5120
ϵ_m/ϵ_1	0.69	0.93	0.97	0.995	1.06	1.12

TABLE VII

VALUES OF k_m; SECOND APPROXIMATION

	Wave length, mμ					
c	400	420	440	450	460	470
0.1	(46.9)	29.4	24.9	26.1	23.1	26.7
0.2	21.3	17.2	22.8	22.7	24.9	25.1
0.3	19.5	22.3	21.7	18.7	19.9	19.2
0.4	24.3	19.7	20.7	21.5	21.9	22.2
0.5	23.2	19.1	19.1	20.2	18.3	20.1
0.6	19.3	19.8	18.0	18.0	19.2	19.2
0.7	19.7	—	16.4	17.9	16.8	17.6
Mean	21.2	21.2	20.5	20.75	20.6	21.45

The best value for k_m is 21, probably 21±2. The constancy of the values in Table VII seems to be sufficient to justify the initial assumption that the ion $FeSCNBr^+$ is indeed present. It is scarcely worth correcting the ϵ_m values further; however it was found that if k_m is reduced to 21.0, ϵ_m is raised by about ¾%. Therefore the best values of ϵ_m, rounded off to the nearest 50, are:

λ	4000	4200	4400	4500	4600	4700 Å
ϵ_m	1550	3200	4300	4650	5000	5150

At high bromide concentrations some deviation occurs, probably owing to the appearance of $FeBr_2^+$. An estimate of its effect can be made as follows. With the constants already known the densities at high bromide concentrations can be calculated; no systematic deviations from experiment were found until $[Br^-]$ is 0.7, but after this the observed densities were consistently higher. If we attribute this to $FeBr_2^+$, which removes some of the iron from possible equilibrium with $FeSCN^{++}$, the concentration of $FeBr_2^+$ can be calculated, and hence its equilibrium constant, k_2, which was defined earlier. The mean value of k_2 at various wave lengths was:

k_2	0.29	0.18	0.19	0.20	0.17
λ	4200	4400	4500	4600	4700 Å

This makes the mean value of k_2 about 0.2. This is a very rough calculation; but as the result agrees with the same constant obtained from solutions without thiocyanate, it seems plausible that this really is the cause of the deviation.

2. Solutions Containing Chloride

The first constant for the association of ferric ions with chloride ions has been measured before, e.g. Rabinowitch and Stockmayer (6), Bray and Hershey (2), Moeller (4), Olerup (5). These authors all used solutions which did not contain thiocyanate, and hence interference by ions such as $FeSCNCl^+$ could not occur. The best value for this constant, $K_1 = (FeCl^{++})/(Fe^{+3}) \cdot (Cl^-)$, under the conditions of the present experiments is probably 4.1. Both Rabinowitch and Stockmayer, and Moeller get results very close to this. Bent and French (1), using mixtures containing ferric, chloride, and thiocyanate ions, arrived at a value of 1.3; this difference is presumably due to $FeSCNCl^+$ ions. Our own results in Table I do not agree with the calculated densities, assuming that K_1 is 4.1 and no $FeSCNCl^+$ is present; hence we shall assume that $FeSCNCl^+$ really is present and attempt to evaluate its equilibrium constant.

Examination of Table I shows that as the chloride concentration is increased the densities at all wave lengths are reduced by the same fractional amount, at least to within the experimental error. Hence $FeSCNCl^+$ must have very nearly the same absorption spectrum as $FeSCN^{++}$; all the extinction coefficients of $FeSCNCl^+$ could be larger than those of $FeSCN^{++}$, but they would all have to be larger in the same ratio. It can also be seen that at any one wave length the densities fall off at first by an amount proportional to the chloride added. When the total chloride exceeds about 0.1 M, the fall slowly becomes less steep. The interpretation of the results was attempted by two methods: (i) as for the bromide solutions above, and (ii) as for the sulphate solutions, described in the second paper of this series. As a result of applying the first method, the values for ϵ_M, the extinction coefficient of $FeSCNCl^+$, which were obtained were all within 1% of those for $FeSCN^{++}$, which is within the experimental error. This is not surprising since $FeCl^{++}$ scarcely absorbs at all in this region. Since this is so, we can apply the second method, that is, the initial slope of the plot of D against total chloride as a means of determining k_M. Here k_M, the equilibrium constant for $FeSCNCl^+$, is defined as

$$k_M = (FeSCNCl^+)/(Fe^{+3}) \cdot (SCN^-) \cdot (Cl^-).$$

The evaluation of k_M is very similar to the method used for sulphate; but as here the concentrations of iron and thiocyanate are not equal, and as there is no complication from ions such as $FeHSO_4^{++}$, it is perhaps worth outlining the calculation. If we write for the concentrations:

$$(Fe^{+3}) = p, \quad (SCN^-) = q, \quad (FeSCN^{++}) = x,$$
$$(Cl^-) = r, \quad (FeCl^{++}) = u, \quad (FeSCNCl^+) = z,$$

we have from the Mass Law:

$$k_1 = x/pq, \quad K_1 = u/pr, \quad k_M = z/pqr,$$

where k_1, K_1, and k_M are the equilibrium constants for $FeSCN^{++}$, $FeCl^{++}$, and $FeSCNCl^+$ respectively. If a, b, and c are respectively the total concentrations of iron, thiocyanate, and chloride present, mass balances give:

$$a = p+x+u+z,$$
$$b = q+x+z,$$
$$c = r+u+z.$$

If ϵ_1 and ϵ_M are the extinction coefficients of $FeSCN^{++}$ and $FeSCNCl^+$, then

$$D = \epsilon_1 x + \epsilon_M z.$$

We shall assume for the reasons given above that $\epsilon_1 = \epsilon_M$. Eliminating x, u, and z:

$$a = p(1+k_1 q+K_1 r+k_M qr),$$
$$b = q(1+k_1 p+k_M pr),$$
$$c = r(1+K_1 p+k_M pq),$$
$$D = pq\ \epsilon_1(k_1+k_M r).$$

Differentiating these with respect to c, and (as we are interested in the initial slope) putting $c = r = 0$ in the result, we get

$$0 = \frac{\partial p}{\partial c}(1+k_1 q)+p\left(k_1\frac{\partial q}{\partial c}+K_1\frac{\partial r}{\partial c}+k_M q\frac{\partial r}{\partial c}\right),$$

$$0 = \frac{\partial q}{\partial c}(1+k_1 p)+q\left(k_1\frac{\partial p}{\partial c}+k_M p\frac{\partial r}{\partial c}\right),$$

$$1 = \frac{\partial r}{\partial c}(1+K_1 p+k_M pq),$$

$$\frac{\partial D}{\partial c} = \epsilon_1 k_1\left(p\frac{\partial q}{\partial c}+q\frac{\partial p}{\partial c}\right)+pq\epsilon_1 k_M\frac{\partial r}{\partial c}.$$

The initial concentrations, p_0 and q_0, are easily found as

$$a = p_0(1+k_1 q_0),$$
$$b = q_0(1+k_1 p_0).$$

D_0, the initial density, equals $\epsilon_1 k_1 p_0 q_0$. The equation in the initial slope of D reduces to

$$\frac{1}{D_0}\frac{\partial D}{\partial c} = \frac{1}{p_0}\frac{\partial p}{\partial c}+\frac{1}{q_0}\frac{\partial q}{\partial c}+\frac{k_M}{k_1}\frac{\partial r}{\partial c}.$$

Substituting for $\partial p/\partial c$, $\partial q/\partial c$, and $\partial r/\partial c$ from the equations above and simplifying, the result is finally:

$$\frac{1}{D_0}\frac{\partial D}{\partial c} = \frac{k_M/k_1-K_1}{(1+K_1 p_0+k_M p_0 q_0)(1+k_1 p_0+k_1 q_0)}.$$

The values of $(1/D_0)\,\partial D/\partial c$ at various wave lengths are

λ	4400	4500	4600	4700	4800 Å
$-(1/D_0)\partial D/\partial c$	1.62	1.59	1.62	1.62	1.67

The mean value is -1.62. With this and the values of a and b (and hence p_0 and q_0) from Table I, we get $k_M = 260$, to two significant figures. An error of about 1% in the slope would lead to about 1% error in k_M.

As the density falls off more gradually at high chloride concentrations it is evident that some other colored species must then have appeared. We can feel sure that $FeCl_2^+$ must be formed to some extent, and the new colored species is presumably $FeSCN.Cl_2$. As the position and shape of the absorption maximum does not change at high chloride concentration, it is reasonable to assume to a first approximation that the extinction coefficients of $FeSCNCl_2$ are roughly the same as those of $FeSCN^{++}$. With this assumption it is possible to evaluate the equilibrium constants of $FeCl_2^+$ and $FeSCNCl_2$. Let these constants be

$$k_2 = (FeCl_2^+)/(Fe^{+3})\,.\,(Cl^-)^2,$$
$$k_n = (FeSCNCl_2)/(Fe^{+3})\,.\,(SCN^-)\,.\,(Cl^-)^2.$$

When the chloride concentration is high, it must be nearly true that $c = r$. The equations given above for the Mass Law, etc., can then be reduced to:

$$X(1+K_1 c+k_2 c^2) = (a-X)(b-X)(k_1+k_M c+k_n c^2)$$

where $X = D/\epsilon_1$. The results of Table I give virtually the same values of X at all wave lengths for a given value of c. The average values of X are as follows (using the values of ϵ_1 given in the first paper in this series):

X	1.015	0.956	0.902	0.846	0.804	0.766	0.735	0.705	0.649	0.610	0.574	0.515	0.470×10^{-4}
c	0.15	0.20	0.25	0.30	0.35	0.40	0.45	0.50	0.60	0.70	0.80	1.0	1.2

The equation above in X contains two unknowns, k_2 and k_n. It could be written in the form:

$$Ak_2 = B + k_n$$

where

$$A = X/(a-X)(b-X),$$

$$B = (1/c^2)\{k_1 + k_M c - A(1+K_1 c)\}.$$

The values of A and B obtained from the data are:

c	0.15	0.20	0.25	0.30	0.35	0.40	0.45	0.50	0.60	0.70	0.80	1.0	1.2
A	98.4	91.6	85.5	79.3	74.8	70.7	67.4	64.3	58.6	54.6	51.1	45.3	41.0
B	484	409	370	363	333	309	284	265	240	212	193	164	143

A plot of A against B gives a reasonably straight line from $c = 0.3$ to 0.8. At lower c values the points are rather erratic, and the last two points drift away a little from the line. The fact that the plot is linear over a considerable length is some evidence that this is the correct explanation. The line makes $k_2 = 6.1$ and $k_n = 120$.

Finally it seems worth while to summarize all the constants evaluated for the complex ions considered in this work. The constants are the equilibrium constants for the formation of the complex ions from simple ions, written with the concentration of the complex ion on top. They are at the same ionic strength.

$FeSCN^{++}$	130;	$FeCl^{++}$	4.1;	$FeBr^{++}$	0.61;	$FeSO_4^+$	170;			
$Fe(SCN)_2^+$	1950;	$FeCl_2^+$	6.1;	$FeBr_2^+$	0.2;	$Fe(SO_4)_2^-$	17000;			
$FeSCNCl^+$	265;	$FeSCNBr^+$	21;	$FeSCN.SO_4$	12000;	$FeHSO_4^{++}$	6;			
$FeSCNCl_2$	120;			$FeSCN(SO_4)_2^{--}$	490000;	$FeHSO_4.SO_4$	380			

By dividing these constants, the constants for the attachment of further simple ions to the various complex ions can be obtained. As is to be expected, further ions are held less firmly than the first one attached; and generally speaking the numbers so obtained seem fairly consistent, or, at least, provide no obvious contradictions. The chief point to note is that the mixed ions, such as $FeSCNCl^+$, are formed as readily (or very nearly so) as those derived from only two simple ions, such as $FeBr_2^+$. This is perhaps slightly unexpected, but it is difficult to think of any reason why this should not be so.

REFERENCES

1. BENT, H. E. and FRENCH, C. L. J. Am. Chem. Soc. 63: 568. 1941.
2. BRAY, W. C. and HERSHEY, A. V. J. Am. Chem. Soc. 56: 1889. 1934.
3*a*. LISTER, M. W. and RIVINGTON, D. E. Can. J. Chem. 33: 1572. 1955.
3*b*. LISTER, M. W. and RIVINGTON, D. E. Can. J. Chem. 33: 1591. 1955.
4. MOELLER, M. J. Phys. Chem. 41: 1123. 1937.
5. OLERUP, H. Svensk Kem. Tidskr. 55: 324. 1943. Chem. Abstr. 40: 2720_3. 1946.
6. RABINOWITCH, E. and STOCKMAYER, W. H. J. Am. Chem. Soc. 64: 335. 1942.

THEORY OF THE TRANSIENT PHASE IN KINETICS, WITH SPECIAL REFERENCE TO ENZYME SYSTEMS[1]

By Keith J. Laidler[2]

ABSTRACT

The steady-state hypothesis is discussed for enzyme systems, and the conditions under which the steady-state equations will be valid over the main course of the reaction are obtained. It is shown that this is so if the substrate is in great excess, and also under several other circumstances. Equations are derived for the kinetic behavior during the transient phase of the reaction. Two-substrate systems, and the special case of catalase, are considered.

In the theoretical formulation of the rates of complex reactions in terms of the concentrations of reactants and other substances (e.g. inhibitors) it is customary to make use of the steady-state hypothesis. This hypothesis, according to which the rates of change of the concentrations of reaction intermediates can be neglected, is easily justified for systems in which the intermediates are present in much lower concentrations than the reactants. In enzyme systems, however, this condition is not necessarily satisfied, since in many instances the concentration of intermediate—the enzyme–substrate complex—is close to the total concentration of the enzyme.

The object of this paper is to examine the steady-state hypothesis as applied to simple enzyme systems, and to see under what conditions it may be expected to be valid. Consideration is also devoted to the question of the kinetics during the transient phase of the reaction—the period during which the steady-state concentration is being established. A single-substrate system is treated first, after which a two-substrate system is briefly considered.

Some of the kinetic equations obtained in this paper have previously been derived, particularly by Chance (3, 4, 5) and by Beers (1, 2), but the methods here employed are more general and permit application to a wider variety of cases.

THE SINGLE-SUBSTRATE SYSTEM

The single-substrate system, uncomplicated by the effects of activators and inhibitors, may be represented by the Michaelis-Menten scheme:

$$\underset{e_0-y}{\mathrm{E}} + \underset{s_0-y-p}{\mathrm{S}} \underset{k_{-1}}{\overset{k_1}{\rightleftharpoons}} \underset{y}{\mathrm{ES}} \xrightarrow{k_2} \underset{e_0-y}{\mathrm{E}} + \underset{p}{\mathrm{P}}.$$

Here E represents enzyme, S the substrate, P the product or products of reaction, and ES the binary complex between enzyme and substrate. If e_0 is the *total* concentration of enzyme (including that bound to substrate), s_0 the *initial total* concentration of substrate, p the amount of product at time t, and y the amount of complex at time t, the various concentrations at time t are as represented above. The rate equations are therefore

[1]*Manuscript received June 6, 1955.*
Contribution from the Department of Chemistry, The Catholic University of America, Washington, D.C.
[2]*Present address: Department of Chemistry, The University of Ottawa, Ottawa, Canada.*

[1] $$dy/dt = k_1(e_0-y)(s_0-y-p)-\bar{k}y$$

and

[2] $$dp/dt = k_2y$$

where $\bar{k}$ is equal to $k_{-1}+k_2$.

Steady-state Treatment

The steady-state treatment involves setting dy/dt equal to zero in equation [1] and solving for y. The result is

[3] $$y=\left[\bar{k}+k_1(e_0+s_0-p)\pm[\bar{k}+k_1(e_0+s_0-p)]\left(1-\frac{4k_1^2e_0(s_0-p)}{[\bar{k}+k_1(e_0+s_0-p)]^2}\right)^{\frac{1}{2}}\right]\Big/ 2k_1.$$

In this solution the negative sign must be taken, as otherwise it becomes possible for y to be greater than e_0. In the event that

[4] $$[\bar{k}+k_1(e_0+s_0-p)]^2 \gg 4\,k_1^2e_0(s_0-p)$$

we can expand the square root and accept only the first term; the solution then reduces to

[5] $$y = \frac{k_1e_0(s_0-p)}{\bar{k}+k_1(e_0+s_0-p)}.$$

We may now enquire under what circumstances the condition [4] is satisfied. The inequality [4] transforms into

[6] $$\bar{k}^2+k_1^2[e_0^2+(s_0-p)^2]+2\bar{k}k_1(e_0+s_0-p) \gg 2k_1^2e_0(s_0-p)$$

or into

[7] $$\frac{\bar{k}^2}{2k_1^2e_0(s_0-p)}+\frac{e_0}{2(s_0-p)}+\frac{s_0-p}{2e_0}+\frac{\bar{k}(e_0+s_0-p)}{k_1e_0(s_0-p)} \gg 1.$$

This relationship can be true in various ways. Since p cannot be greater than s_0, it is evident that [7] is true if

[8] $$s_0 \gg e_0$$

or if

[9] $$e_0 \gg s_0.$$

It is also true if

[10] $$\bar{k} \gg k_1e_0$$

or if

[11] $$\bar{k} \gg k_1s_0.$$

The inequality [8] of course corresponds to a situation that usually exists in enzyme systems. However even if s_0 and e_0 are of comparable magnitudes equation [5] is valid provided that either [10] or [11] is true. If $s_0 \gg e_0$ equation [5] can be written as

[12] $$y = \frac{k_1e_0(s_0-p)}{\bar{k}+k_1(s_0-p)}$$

and the steady-state rate is then

$$[13] \qquad \frac{dp}{dt} = \frac{k_1 k_2 e_0 (s_0 - p)}{k + k_1 (s_0 - p)}.$$

The Maximum Concentration of Complex

It is unfortunately not possible to obtain an exact explicit solution of the differential equations [1] and [2]. It is possible, however, to arrive at some conclusions about the circumstances under which the steady-state assumption will be reasonably accurate.

For this purpose it is convenient to note that the relationships derived in the last section are satisfactory in giving the *maximum* concentration of complex, y_m, in terms of the concentration of product, p_m, present at the maximum. Thus if in equations [3], [5], [12], and [13] we replace y by y_m and p by p_m we obtain equations relating y_m and p_m which are independent of the steady-state assumption; the relationship

$$[14] \qquad y_m = \frac{k_1 e_0 (s_0 - p_m)}{k + k_1 (e_0 + s_0 - p_m)},$$

for example, is true provided that one of the four conditions [8], [9], [10], and [11] is satisfied. It is clear, therefore, that the steady-state equations are *exact* at the maximum. As the reaction proceeds the steady-state assumption predicts only a gradual diminution in y as p increases, and the exact theory predicts such a change during the later stages of the reaction. The steady-state assumption will, however, lead to error in the early stages of reaction, when the concentration of complex is building up, but if this occurs during the *very* early stages of the reaction the error will not be considerable over the main course of reaction.

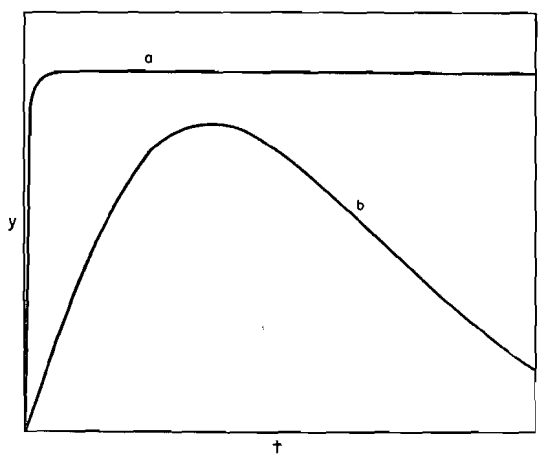

FIG. 1. Schematic curves showing concentration of enzyme–substrate complex vs. time. In curve *a* the steady state is established rapidly; in *b* the concentration of complex varies significantly throughout the course of reaction.

In view of this it is desirable to obtain an estimate of the time taken for the maximum concentration to be attained, in order to see whether it represents an appreciable fraction of the entire reaction. One may envisage two extreme cases, as represented in curves *a* and *b* of Fig. 1. In curve *a* the maximum is reached in the very early stages of the reaction, and in this case the steady-state treatment is satisfactory for the most part. In curve *b* on the other hand, the maximum is a fairly sharp one and the steady-state assumption is therefore unjustified.

The Transient Phase

A kinetic expression will now be obtained for the behavior during the transient phase. The equation will of necessity be an approximate one, but will be sufficiently correct to allow dependable conclusions to be drawn with regard to the circumstances under which the transient phase will constitute a small fraction of the half-life of the reaction.

In place of equation [1] we start with the approximate equation

$$dy/dt = k_1(e_0-y)(\bar{s}-y)-\bar{k}y. \qquad [15]$$

In this equation s_0-p has been replaced by $\bar{s}$, which is treated as constant; $\bar{s}$ may be regarded as the average concentration of the substrate during the transient phase. The circumstances under which this will be a close approximation are discussed later. Equation [15] integrates to

$$t = \frac{1}{\sqrt{Q}} \ln \frac{2ay+b-\sqrt{Q}}{2ay+b+\sqrt{Q}} + \text{constant} \qquad [16]$$

where

$$Q = b^2-4ac, \qquad [17]$$

$$a = k_1, \qquad [18]$$

$$b = -(k_1e_0+\bar{k}+k_1\bar{s}), \qquad [19]$$

$$c = k_1e_0\bar{s}. \qquad [20]$$

The boundary condition $t = 0$, $y = 0$ gives rise to

$$t = \frac{1}{\sqrt{Q}} \ln \frac{by+2c+y\sqrt{Q}}{by+2c-y\sqrt{Q}}. \qquad [21]$$

At the maximum

$$ay_m^2+by_m+c = 0, \qquad [22]$$

whence

$$y_m = (-b-\sqrt{Q})/2a. \qquad [23]$$

From equations [17] and [23] it can be shown that

$$\sqrt{Q} = -ay_m+(c/y_m), \qquad [24]$$

$$b = -ay_m-(c/y_m). \qquad [25]$$

The rate equation [21] therefore reduces as follows:

$$t = \frac{1}{\sqrt{Q}} \ln \frac{c - a y_m y}{c - c y / y_m} \quad [26]$$

$$= \frac{1}{\sqrt{Q}} \ln \frac{y_m - a y y_m^2 / c}{y_m - y} \quad [27]$$

$$= \frac{1}{[(k_1 e_0 + \bar{k} + k\bar{s})^2 - 4k_1^2 e_0 \bar{s}]^{\frac{1}{2}}} \ln \frac{y_m(1 + y y_m / e_0 \bar{s})}{y_m - y} \quad [28]$$

$$= \frac{y_m}{k_1 e_0 \bar{s} - k_1 y_m^2} \ln \frac{y_m(1 + y y_m / e_0 \bar{s})}{y_m - y}. \quad [29]$$

It is now possible to arrive at an estimate of the amount of product, p_m, that has been produced during the transient phase. The time that it takes for y to reach $0.99 y_m$ is given by (from equations [27] and [28])

$$\tau = \frac{1}{\sqrt{Q}} \ln 100 \left(1 + \frac{y y_m}{e_0 \bar{s}}\right). \quad [30]$$

Since y and y_m are necessarily less than the smaller of e_0 and $\bar{s}$ it follows that

$$\tau < (1/\sqrt{Q}) \ln 200 \quad [31]$$

$$< 5.3/\sqrt{Q}. \quad [32]$$

Since y is always less than y_m during the induction period, an *upper limit* to the rate of formation of product is therefore given by

$$dp/dt < k_2 y_m. \quad [33]$$

This integrates to

$$p < k_2 y_m t \quad [34]$$

since $p = 0$ when $t = 0$. An upper limit to the amount of product produced until $y = 0.99 y_m$ (and therefore essentially an upper limit to the amount of product produced in the transient phase) is therefore given by

$$p < 5.3\, k_2 y_m / \sqrt{Q}. \quad [35]$$

Using equations [17] and [23] this becomes

$$p < \frac{5.3 k_2}{2a} \left(-\frac{b}{\sqrt{Q}} - 1\right) \quad [36]$$

$$< \frac{5.3 k_2}{2k_1} \left(-\frac{b}{\sqrt{Q}} - 1\right), \quad [37]$$

$$\frac{p}{s_0} < \frac{5.3 k_2}{2k_1 s_0} \left[\frac{1}{\sqrt{(1 - 4ac/b^2)}} - 1\right]. \quad [38]$$

From this it follows that p/s_0 is small, i.e. that not much product has been produced during the transient phase, if

$$4ac \ll b^2. \quad [39]$$

The circumstances under which this is so were considered earlier, and are expressed by the inequalities [8]–[11] above. It may further be noted that b^2 is necessarily greater than $4ac$ (cf. [6] above), so that the term in the square brackets in [38] can never become very large; p/s_0 will therefore also be small if

$$k_1 s_0 \gg k_2. \qquad [40]$$

The conclusion that has been reached is therefore that the transient phase will be a relatively short one provided that one or more of the inequalities [8], [9], [10], [11], and [40] are satisfied. The situation is then as represented in curve *a* of Fig. 1. In any of these circumstances the kinetic equations derived in the present section for the transient phase will be obeyed with high accuracy since the approximation involved in equation [15] is justified *a posteriori*.

A Special Case: The Substrate Is Present in Great Excess

In view of the fact that in most enzyme systems the concentration of enzyme is very much less than that of the substrate it is now convenient to write down those relationships that are particularly applicable to this case. For this purpose the starred quantities, y^*, y_m^*, p^* will be used when the relationships between them only apply in the case that $s_0 \gg e_0$.

The value of y_m^* is given by (cf. equation [12])

$$y_m^* = \frac{k_1 e_0 s_0}{\bar{k}+k_1 s_0} \quad . \qquad [41]$$

During the induction period the rate equations are

$$dy^*/dt = k_1 s_0 (e_0 - y^*) - \bar{k} y^*, \qquad [42]$$

$$dp^*/dt = k_2 y^*. \qquad [43]$$

Since in equation [29] $k_1 y_m^{*2} \ll k_1 e_0 \bar{s}$ and $y y_m \ll e_0 \bar{s}$ (since y and y_m must be less than e_0, which is much less than $\bar{s}$), and $\bar{s}$ can be replaced by s_0, the kinetic law during the transient phase is

$$t = \frac{y_m^*}{k_1 e_0 s_0} \ln \frac{y_m^*}{y_m^* - y^*} \, . \qquad [44]$$

This may be written as

$$y^* = y_m^* [1 - \exp(-k_1 e_0 s_0 t / y_m^*)] \qquad [45]$$

and using equation [41] this becomes

$$y^* = \frac{k_1 e_0 s_0}{\bar{k}+k_1 s_0} [1 - \exp\{-(\bar{k}+k_1 s_0)t\}]. \qquad [46]$$

The variation of the concentration of product during the transient phase is obtained by using equation [43]:

$$\frac{dp^*}{dt} = \frac{k_1 k_2 e_0 s_0}{\bar{k}+k_1 s_0} [1 - \exp\{-(\bar{k}+k_1 s_0)t\}]. \qquad [47]$$

With the boundary condition $t = 0$, $p = 0$ this integrates to

$$[48] \qquad p^* = \frac{k_1k_2e_0s_0}{\bar{k}+k_1s_0}t+\frac{k_1k_2e_0s_0}{(\bar{k}+k_1s_0)^2}[\exp\{-(\bar{k}+k_1s_0)t\}-1].$$

When t is sufficiently large, i.e. at the maximum, the kinetics are seen to be first order. At lower times more complex behavior is observed. If t is sufficiently small that

$$[49] \qquad (\bar{k}+k_1s_0)t \ll 1$$

it is permissible to expand the exponential and accept only the first two terms; the result is

$$[50] \qquad p^* = \tfrac{1}{2}k_1k_2e_0s_0t^2.$$

This particular relationship has previously been given by Roughton (8).

Equations for the rate of disappearance of substrate during the transient phase can readily be obtained by making use of the fact that

$$[51] \qquad -ds/dt = (dp/dt)+(dy/dt).$$

Another result of interest is the time that it takes for the steady state to be established. Equation [32] gives the time that it takes for y to reach 0.99 y_m, and for the special case of $s_0 \gg e_0$ we obtain

$$[52] \qquad \tau \approx 5.3/(\bar{k}+k_1s_0).$$

It is of interest that this time is independent of the concentration of the enzyme. An experimental determination of the length of the induction period should therefore allow an estimate to be made of the magnitude of $\bar{k}+k_1s_0$, i.e. of $k_{-1}+k_2+k_1s_0$, and since k_2 and $k_1/(k_{-1}+k_2)$ can be determined by conventional kinetic methods the constants can be separated. Work along these lines has been carried out by Gutfreund (6). A more accurate, but experimentally more difficult, procedure for separating constants is to follow the rate of increase of y^* during the induction period; $\bar{k}+k_1s_0$ can then be determined using equation [46].

After y has attained the value of y_m the steady state is established, and the remaining course of the reaction is in accordance with equation [13]. This equation integrates to

$$[53] \qquad k_1k_2e_0 = \frac{1}{t}\ln\frac{s_0}{s_0-p}+\frac{k_1p}{\bar{k}t},$$

which is equivalent to the well-known Henri equation(7). The behavior is zero order as long as $k_1(s_0-p) \gg \bar{k}$ and first order when $\bar{k} \gg k_1(s_0-p)$.

The conclusion that has been reached in the present treatment is that as long as $s_0 \gg e_0$ the kinetic behavior can be closely represented by two sets of

equations, one referring to the transient phase and the other to the steady-state period. The situation is represented schematically in Fig. 2. Here the curve ABC corresponds to equation [46] for the transient phase, the value of y approaching $y_m{}^*$ asymptotically. The curve DBF, corresponding to equation [12], is that predicted by the steady-state theory. The treatment proposed in the present paper involves regarding ABF as representing the true course of the reaction. Strictly speaking it gives a discontinuity at B, but since y_m is very close to $y_m{}^*$ the error is evidently very slight.

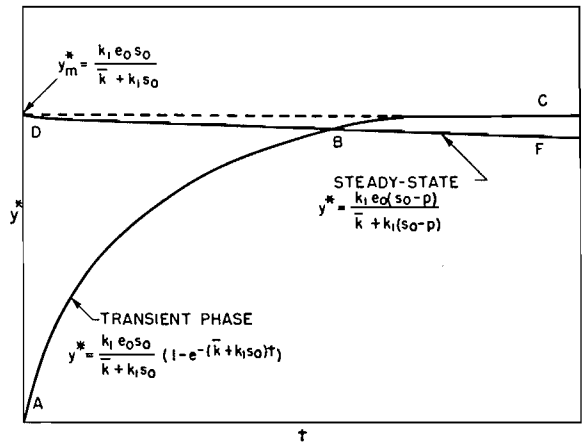

FIG. 2. Schematic curves showing complex concentration vs. time, for the case in which the substrate concentration is in great excess. The true course of the reaction is closely represented by ABF.

The above treatment at once leads to a useful graphical procedure for arriving at the variation of y with t in terms of known rate constants and initial conditions. The curve ABC can readily be plotted, and from equation [48] the amount of product at various times can be calculated. Curve DBF can then be constructed, and ABF will then represent the course of the reaction to a high approximation.

It may be noted that curves and equations of the same *form* as in Fig. 2 and the present section apply also if any of the conditions [9], [10], [11], and [40] apply. The constants appearing in the equations are, however, different for these cases, but may easily be written down by applying the methods of the present section.

The General Case

When none of the conditions [8], [9], [10], [11], and [40] applies it is no longer the case that only a small fraction of the substrate has been transformed into product by the time y has reached its maximum value. The situation is now more as represented in Fig. 3. The true curve, AGF, now deviates considerably from the transient-phase and steady-state curves in the region of

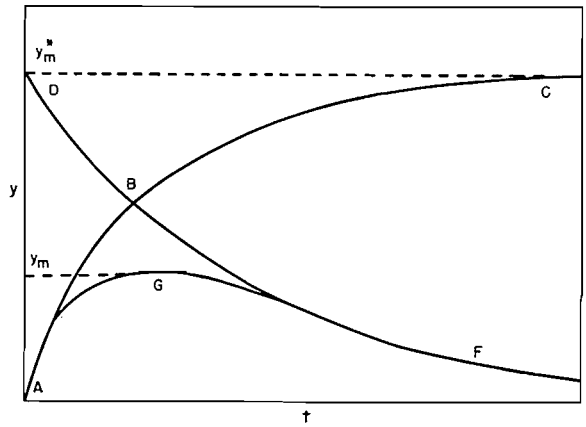

FIG. 3. Schematic curves showing complex concentration vs. time, for the case in which none of the inequalities [8], [9], [10], [11], and [40] is applicable.

the maximum, but corresponds at the beginning and end of the reaction. In the very early stages of the reaction equation [28] is valid and since y and p are small it may be written as

$$[54] \qquad t = \frac{1}{[(k_1e_0+\bar{k}+k_1s_0)^2-4k_1^2e_0s_0]^{\frac{1}{2}}} \ln \frac{y_m^*}{y_m^*-y}$$

or

$$[55] \qquad y = y_m^*(1-\exp\{-[(k_1e_0+\bar{k}+k_1s_0)^2-4k_1^2e_0s_0]t\})$$

where y_m^* is defined by equation [41]. This equation is of the same form as equation [46], and enables the function in the square brackets to be determined from the experimental results. A further separation of constants would, however, appear to be very difficult for this general case without the use of a differential analyzer.

TWO-SUBSTRATE SYSTEMS

A somewhat similar type of analysis can be applied to systems in which there are two substrates. The simplest kinetic scheme corresponding to this situation is the following:

$$\underset{e_0-y}{\mathrm{E}} + \mathrm{S} \underset{k_{-1}}{\overset{k_1}{\rightleftharpoons}} \underset{y}{\mathrm{ES}}, \qquad \begin{matrix} \\ s_0-y-p \end{matrix}$$

$$\underset{y}{\mathrm{ES}} + \underset{r_0-p}{\mathrm{R}} \xrightarrow{k_2} \underset{e_0-y}{\mathrm{E}} + \underset{p}{\mathrm{P}}.$$

Here R, the second substrate, does not form a ternary complex ESR but reacts with ES to give products in a single step; the case of the ternary complex is considerably more difficult to work out. Examples of the above scheme are to be found in the peroxidatic reactions of peroxidase and catalase; in these reactions S is hydrogen peroxide and R an acceptor molecule.

The rate equations for this system are

[56] $$dy/dt = k_1(e_0-y)(s_0-y-p)-k_2(r_0-p)y-k_{-1}y,$$

and

[57] $$dp/dt = k_2y(r_0-p).$$

Steady-state Treatment

The general steady-state equation for this system is equation [3] with $\bar{k}$ replaced by $k_2(r_0-p)+k_{-1}$. In the event that any one of the conditions [8], [9], [10], and [11] holds the steady-state equation reduces to

[58] $$y = \frac{k_1e_0(s_0-p)}{k_{-1}+k_1(e_0+s_0-p)+k_2(r_0-p)}.$$

According to the steady-state treatment the concentration of y therefore starts at an initial value of

[59] $$y_0 = \frac{k_1e_0s_0}{k_{-1}+k_1(e_0+s_0)+k_2r_0}$$

when $t = 0$ and gradually diminishes as product accumulates.

The situation is again that steady-state conditions may, under certain circumstances, be expected to exist during the main course of the reaction. When this is the case a simple rate equation will apply to the early stages of the reaction, as will now be considered.

The Transient Phase

The procedure will again be to employ an approximate rate equation for the first part of the reaction, and to justify it *a posteriori* under certain circumstances.

The equation that will be used is

[60] $$dy/dt = k_1(e_0-y)(\bar{s}-y)-(k_2\bar{r}+k_{-1})y$$

where $\bar{s}$ and $\bar{r}$ are the average amounts of S and R during the transient phase. This equation is seen to be of the same form as equation [15], and the remainder of the argument is therefore exactly as previously except that $\bar{k}$ is now given the significance of $k_2\bar{r}+k_{-1}$. The general kinetic equation for the transient phase is now (cf. equation [28])

[61] $$t = \frac{1}{[(k_1e_0+k_1\bar{s}+k_2\bar{r}+k_{-1})^2-4k_1^2e_0s_0]^{\frac{1}{2}}} \ln \frac{y_m(1+yy_m/e_0\bar{s})}{y_m-y}$$

where y_m is as given previously (except that $\bar{k}$ is now $k_2\bar{r}+k_{-1}$). The conclusion is again that during the induction period only a very small amount of product is produced provided that one or more of the conditions [8], [9], [10], [11], and [40] are satisfied.

In the event that the two substrates are greatly in excess of the enzyme the rate equation during the induction period is (cf. equation [46])

[62] $$y^* = \frac{k_1e_0s_0}{k_{-1}+k_1s_0+k_2r_0}[1-\exp\{-(k_{-1}+k_1s_0+k_2r_0)t\}].$$

The course of the formation of product can then be readily obtained by proceeding as previously (equations [47]–[50]). Chance (3) has previously treated this type of situation using numerical methods.

THE CATALATIC REACTION

A slight variant of the above treatment is provided by the catalatic reaction —the decomposition of hydrogen peroxide catalyzed by the enzyme catalase. The reaction scheme is now (4)

$$\underset{e_0-y}{\mathrm{E}} + \underset{s_0-y-p}{\mathrm{S}} \overset{k_1}{\underset{k_{-1}}{\rightleftharpoons}} \underset{y}{\mathrm{X}},$$

$$\underset{y}{\mathrm{X}} + \underset{s_0-y-p}{\mathrm{S}} \overset{k_2}{\rightarrow} \underset{e_0-y}{\mathrm{E}} + \underset{p}{\mathrm{P}}.$$

The rate equations for this system are

$$[63] \qquad dy/dt = k_1(e_0-y)(s_0-y-p)-k_2y(s_0-y-p)-k_{-1}y,$$

$$[64] \qquad dp/dt = k_2y(s_0-y-p).$$

In the event that one of the conditions equivalent to [8], [9], [10], or [11] holds the steady-state equation reduces to

$$[65] \qquad y = \frac{k_1e_0(s_0-p)}{k_{-1}+(k_{-1}+k_2)(s_0-p)}.$$

Chance (4, 5) has shown that k_{-1} is exceedingly small so that almost invariably it is true that

$$[66] \qquad y = k_1e_0/(k_1+k_2).$$

The Transient Phase

In order to obtain an approximate expression for the transient phase the procedure will be, as above, to write equation [63] as

$$[67] \qquad dy/dt = k_1(e_0-y)(\bar{s}-y)-k_2y(\bar{s}-y)$$

where $\bar{s}$ is the average amount of free substrate during the transient phase. The solution of this is equations [16] and [21] above, but a, b, and c now have a slightly different significance, namely

$$[68] \qquad a = k_1+k_2,$$

$$[69] \qquad b = -(k_1e_0+k_1\bar{s}+k_2\bar{s})+k_1e_0\bar{s},$$

$$[70] \qquad c = k_1e_0\bar{s}.$$

The remainder of the treatment is then as given previously. It again follows that the transient phase will be short compared with the over-all duration of the reaction if, among other possibilities, $s_0 \gg e_0$.

For this case the final result for the kinetic equation during the transient phases is again found to be equation [44]. Such a result has previously been obtained, using another procedure, by Chance *et al.* (5) and by Beers and Sizer (2).

REFERENCES

1. Beers, R. F. J. Phys. Chem. 58: 197. 1954.
2. Beers, R. F. and Sizer, I. W. J. Phys. Chem. 57: 290. 1953.
3. Chance, B. J. Biol. Chem. 151: 553. 1943.
4. Chance, B. Acta Chem. Scand. 1: 236. 1947.
5. Chance, B., Greenstein, D. S., and Roughton, F. J. W. Arch. Biochem. and Biophys. 37: 311. 1952.
6. Gutfreund, H. Discussions Faraday Soc. No. 17: 220. 1954.
7. Henri, V. Lois générales de l'action des diastases. 1903.
8. Roughton, F. J. W. Discussions Faraday Soc. No. 17: 116. 1954.

NOTES

A NEW TYPE OF ULTRAFILTER

By J. L. Gardon[1] and S. G. Mason

INTRODUCTION

Most ultrafilters (2, 3, 6) have perforated or porous plates as membrane supports, use membranes of small area, and to get appreciable rates of filtration are operated at relatively high pressures. The solution, being under pressure, cannot readily be stirred and, becoming increasingly concentrated on the membrane surface, has a tendency to block the membrane pores (1). Such ultrafilters are not suitable for handling large quantities of materials.

A simple and inexpensive method of supporting membranes which was developed by the authors for an osmometer cell and which inhibits ballooning in membranes as large as 200 sq. cm. in area is described elsewhere (4). In the present note we describe an ultrafiltration unit consisting of a number of slightly modified osmometer cells which has been used for the fractionation of ligninsulphonates (5).

Since the membrane area is large, the unit may be used at relatively low pressure differentials using water aspirators. It is fully automatic, simple to construct, leakproof, and allows thorough stirring of the liquid.

ULTRAFILTER CELLS

Each ultrafilter cell consists mainly of two lucite disks and two rubber rings (Fig. 1). The membrane is clamped between the rubber rings, reinforced with fine-mesh stainless steel screens, and supported on both sides by two layers of tightly packed glass beads. To avoid leakage at the edges of the screens, rings of dental dam rubber are placed between them and the membrane and between them and the rubber rings, forming the body of the cell. When the unit is compressed, the dental dam penetrates into the meshes of the screen reinforcers and seals the cell effectively. The necessary parts for a typical cell are described in Table I.

A simple leakproof connection between the glass parts and the lucite can be made without cement. For this purpose tygon tubing with 1.5 mm. wall thickness and 10 mm. O.D. is placed into 8 mm. bore holes in the lucite. To introduce the tubing into the hole the end of it is cut off conically along the length and pulled into the hole by the tongue thus formed, and the tongue is then cut away.

Each lucite disk is equipped with the connectors before assembling the cell. To prevent glass beads from dropping into the tygon tubing, a small piece of stainless steel screen is placed in the tubing.

[1]*Holder of the Anglo-Paper Research Fellowship and of a Studentship from the National Research Council of Canada. Present address: Industrial Cellulose Research Ltd., Hawkesbury, Ontario.*

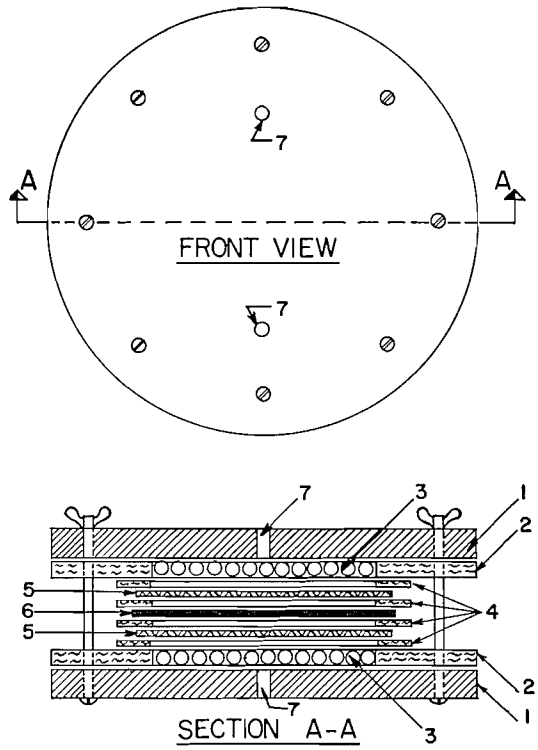

FIG. 1. Details of the ultrafilter cell: (1) lucite disks, (2) rubber rings, (3) glass beads, (4) dental dam gaskets, (5) stainless steel screens, (6) membrane, (7) inlet hole.

TABLE I

CELL COMPONENTS

1. 2 lucite disks
   - Diameter 25 cm.
   - Thickness 1 cm.
   - 8 holes with centers on a 23 cm. diameter circle concentric with the disks to accommodate the screws
   - 2 holes with centers on the same diameter 17.5 cm. apart—bore diameter 8 mm.
2. 8 rubber rings
   - Inside diameter 18 cm.
   - Outside diameter 25 cm.
   - Thickness 0.3 to 0.32 cm.
   - 8 holes drilled in identical positions as in the lucite for holding the screws
3. 4 dental dam gaskets
   - Inside diameter 18 cm.
   - Outside diameter 22 cm.
   - Thickness about 0.03 cm.
4. 2 stainless steel screens
   - Diameter 20 cm.
   - 125 mesh
5. 1 membrane
   - Diameter 21 cm.
6. Glass beads
   - Diameter 0.28 to 0.3 cm.
7. 8 screws, 8 wing nuts, 16 washers

THE CIRCULATING PUMP

Stirring in the cells is provided by circulating the solution from a reservoir. The pumping unit, shown in detail in Fig. 2, consists of a membrane pump (A) governed by an oscillating mercury pump (B).

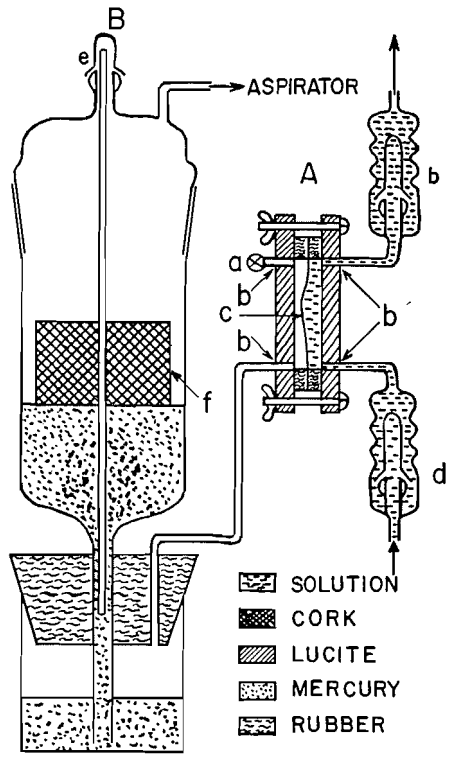

FIG. 2. Details of the circulating pump: (A) membrane pump, (a) stopcock, (b) inlet holes, (c) dental dam membrane, (d) valves, (B) oscillating mercury pump, (e) valve, (f) cork floater.

The construction of the membrane pump is similar to that of the ultrafilter cells. It is made up of two lucite disks of 12 cm. diameter, two rubber rings 5 mm. thick with 10 cm. outside diameter and 8 cm. inside diameter, and an elastic dental dam membrane disk (c) of 10 cm. diameter clamped between the rubber rings. To accommodate the screws, both lucite disks have four holes with centers on an 11 cm. diameter circle concentric with the disks and two 8 mm. bore holes (b), with centers 3.75 cm. from the center of the disk and on the same diameter, in which tygon tubing is placed in the same manner as described above. The membrane is made of two dental dam rubber sheets stuck together with silicone grease. This method of preparation gives the membrane a life of at least several months of continuous operation.

The two check valves (d) are made of spherical glass joints of 12 mm. diameter.

The oscillating mercury pump functions as follows. By applying vacuum in the upper chamber, mercury is sucked into it. The rising mercury raises the cork float (f) and thus opens valve (e). Consequently air enters into the upper chamber, the mercury level drops, valve (e) is closed, and a new pumping cycle starts. The lower chamber of this pump is connected with the membrane pump, and the membrane in the latter forcibly has to follow the movements of the mercury. In practice the oscillating mercury pump is put into

operation first, independently of the membrane pump, and stopcock (a) is closed afterwards. The difference in level between the mercury in the lower and upper chambers should alternate between 10 and 14 cm. The diameter in both the upper and lower chambers of the oscillating mercury pump is 7 cm. and the length of the pump is 25 cm. The valve (e) is made of a 12 mm. diameter spherical glass joint.

The capacity of this pumping unit is around 200 cc. per minute.

OPERATION

The assembled ultrafilter is shown in Fig. 3. The solution chambers of the different cells are connected in series and the solution is circulated from reservoir (C) to provide adequate stirring.

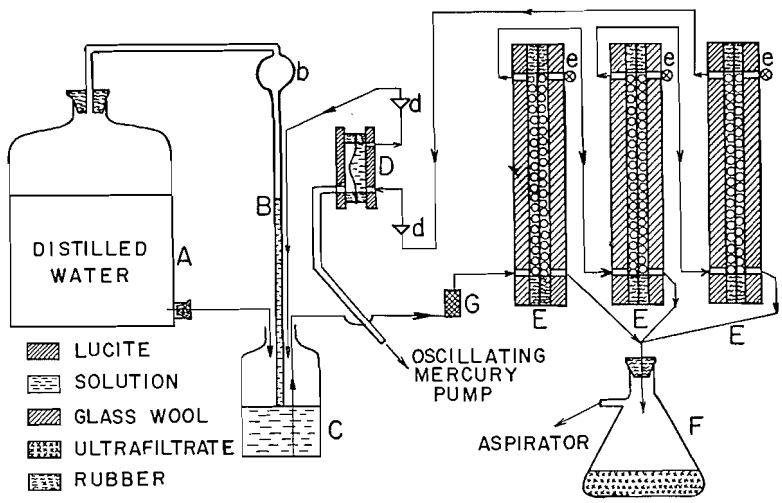

FIG. 3. The assembled ultrafiltration unit: (A) water reservoir, (B) constant head device, (b) solution trap, (C) solution reservoir, (D) membrane pump, (d) valves, (E) ultrafilter cells, (e) stopcocks, (F) suction flask, reservoir for ultrafiltrate, (G) glass wool filter.

The volume of the liquor is kept constant by the constant head device (B). If the level in reservoir (C) drops sufficiently to expose the end of the tube (B) to the air, air will enter into the distilled water container (A) and consequently water will flow into reservoir (C). The rising level in the reservoir closes tube (B) and thus stops the water flow. Trap (b) is needed to prevent the solution from entering the distilled water container.

The ultrafiltrate is fed into suction flask (F) by gravity.

Keeping the residual liquor at constant volume allows good control of the process. If V_0 is the volume of the residual liquor, K the volume of ultrafiltrate produced in unit time, $c(t)$ the concentration of the component to be removed, and $\gamma\, c(t)$ its concentration in the ultrafiltrate passing through the membrane at time t (γ is the partition coefficient between the solutions inside and outside

the membrane, $0 < \gamma < 1$), the following relation may be derived for the variation of $c(t)$ with time:

$$-V_0\,dc = \gamma\,K\,c(t)\,dt,$$

which on integration yields

$$c(t) = c(0).e^{-\gamma K t/V_0}.$$

By determining K, V_0, c_0, and several values of $c(t)$ at different time intervals, γ can be evaluated and the time necessary for the removal of any arbitrary portion of the component in question can be calculated.

The rate of ultrafiltration is readily varied by changing the number of cells in the unit.

1. BECHHOLD, H. Z. physik. Chem. 60: 257. 1907.
2. CUMMINGS, A. P. Technique of organic chemistry. Vol. III. Edited by A. Weissberger. Interscience Publishers, Inc., New York. 1950. pp. 558–563.
3. FERRY, J. D. Chem. Revs. 18: 374. 1936.
4. GARDON, J. L. and MASON, S. G. Can. J. Chem. 33: 1453. 1955.
5. GARDON, J. L. and MASON, S. G. Can. J. Chem. 33: 1477. 1955.
6. MCBAIN, J. W. Colloid science. D. C. Heath & Company, Boston. 1950. pp. 121–130.

RECEIVED JUNE 10, 1955.
PULP AND PAPER RESEARCH INSTITUTE OF CANADA,
AND
CHEMISTRY DEPARTMENT, MCGILL UNIVERSITY,
MONTREAL, QUEBEC.

THE REMOVAL OF FLUORIDE ION FROM AQUEOUS SOLUTION BY MAGNESIUM OXIDE

BY JOHN C. BARTLET AND ROSS A. CHAPMAN[1]

Venkateswarlu and Narayana Rao (1, 2, 3) reported that magnesium oxide takes up fluoride ion from hot solution, basic to phenolphthalein. Light magnesium oxide was reported to remove up to 20 μgm. of fluoride per mgm. of magnesium oxide. This procedure was used to reduce the fluoride content of water (1, 2) and as an aid in the determination of fluoride in tea (3).

In this laboratory, it was found that the removal of fluoride could be increased manyfold if the original solution was acidic. Table I shows the effect

TABLE I

THE EFFECT OF pH ON THE TAKING UP OF FLUORIDE FROM AQUEOUS SOLUTION BY MAGNESIUM OXIDE

pH		% Removal of fluoride
Before addition of MgO	After addition of MgO	
12.5	12.4	10
11.7	11.6	50
8.6	10.5	88
5.6	10.3	94
1.7	8.9	100

[1]*Present address: World Health Organization, Geneva, Switzerland.*

the membrane, $0 < \gamma < 1$), the following relation may be derived for the variation of $c(t)$ with time:

$$-V_0\,dc = \gamma\,K\,c(t)\,dt,$$

which on integration yields

$$c(t) = c(0).e^{-\gamma K t/V_0}.$$

By determining K, V_0, c_0, and several values of $c(t)$ at different time intervals, γ can be evaluated and the time necessary for the removal of any arbitrary portion of the component in question can be calculated.

The rate of ultrafiltration is readily varied by changing the number of cells in the unit.

1. BECHHOLD, H. Z. physik. Chem. 60: 257. 1907.
2. CUMMINGS, A. P. Technique of organic chemistry. Vol. III. Edited by A. Weissberger. Interscience Publishers, Inc., New York. 1950. pp. 558–563.
3. FERRY, J. D. Chem. Revs. 18: 374. 1936.
4. GARDON, J. L. and MASON, S. G. Can. J. Chem. 33: 1453. 1955.
5. GARDON, J. L. and MASON, S. G. Can. J. Chem. 33: 1477. 1955.
6. MCBAIN, J. W. Colloid science. D. C. Heath & Company, Boston. 1950. pp. 121–130.

RECEIVED JUNE 10, 1955.
PULP AND PAPER RESEARCH INSTITUTE OF CANADA,
AND
CHEMISTRY DEPARTMENT, MCGILL UNIVERSITY,
MONTREAL, QUEBEC.

THE REMOVAL OF FLUORIDE ION FROM AQUEOUS SOLUTION BY MAGNESIUM OXIDE

BY JOHN C. BARTLET AND ROSS A. CHAPMAN[1]

Venkateswarlu and Narayana Rao (1, 2, 3) reported that magnesium oxide takes up fluoride ion from hot solution, basic to phenolphthalein. Light magnesium oxide was reported to remove up to 20 μgm. of fluoride per mgm. of magnesium oxide. This procedure was used to reduce the fluoride content of water (1, 2) and as an aid in the determination of fluoride in tea (3).

In this laboratory, it was found that the removal of fluoride could be increased manyfold if the original solution was acidic. Table I shows the effect

TABLE I

THE EFFECT OF pH ON THE TAKING UP OF FLUORIDE FROM AQUEOUS SOLUTION BY MAGNESIUM OXIDE

pH		% Removal of fluoride
Before addition of MgO	After addition of MgO	
12.5	12.4	10
11.7	11.6	50
8.6	10.5	88
5.6	10.3	94
1.7	8.9	100

[1]*Present address: World Health Organization, Geneva, Switzerland.*

of pH on the taking up of 1 mgm. of fluoride ion in 100 ml. of hot solution by 100 mgm. of magnesium oxide. The pH of the solutions was adjusted with sodium hydroxide or perchloric acid. The solution of pH 1.7 contained sufficient perchloric acid to dissolve approximately 40 mgm. of the original 100 mgm. of magnesium oxide added. From a hot solution at pH 1.7 containing 20 mgm. of fluoride as sodium fluoride in 100 ml., 100 mgm. of magnesium oxide took up 18.8 mgm. or 94% of the fluoride. This represents a removal of 188 μgm. of fluoride per mgm. of original magnesium oxide or 312 μgm. of fluoride per mgm. of magnesium oxide remaining in the solid phase.

The solid residue prepared under several different conditions with an excess of fluoride present was found to be of variable composition ranging from approximately the composition $2Mg(OH)_2 \cdot MgF_2$ to $4Mg(OH)_2 \cdot 3MgF_2$. These products were slightly soluble in hot water. Examination by the X-ray diffraction powder method showed that the products consisted of a mixture of $Mg(OH)_2$ and MgF_2 with no lines attributable to a new compound.

We wish to thank Dr. W. H. Barnes of the National Research Council of Canada who carried out the X-ray diffraction studies.

1. VENKATESWARLU, P. and NARAYANA RAO, D. Indian J. Med. Research, 41: 135. 1953.
2. VENKATESWARLU, P. and NARAYANA RAO, D. Indian J. Med. Research, 41: 473. 1953.
3. VENKATESWARLU, P. and NARAYANA RAO, D. Anal. Chem. 26: 766. 1954.

RECEIVED JULY 11, 1955.
FOOD AND DRUG LABORATORIES,
DEPARTMENT OF NATIONAL HEALTH AND WELFARE,
OTTAWA, CANADA.

A SYNTHESIS OF L-ISOGLUTAMINE FROM γ-BENZYL GLUTAMATE

BY M. KRAML AND L. P. BOUTHILLIER

In the course of our studies on histidine metabolism (5) it became necessary to prepare some L-isoglutamine. Bergmann and Zervas (1) obtained the desired product by cleaving N-carbobenzyloxy-L-glutamic anhydride with anhydrous ammonia followed by catalytic hydrogenation to remove the carbobenzyloxy (CBZ) group. Recently, Chambers and Carpenter (3) achieved a similar synthesis by blocking the amino acid with the *p*-nitrobenzyloxycarbonyl group. Paper chromatography (3) has revealed that these methods, while favoring L-isoglutamine formation, invariably yield small amounts of L-glutamic acid and L-glutamine as contaminants. Swan and duVigneaud (6) have published the only unambiguous synthesis of L-isoglutamine. It consists in the preparation of N-*p*-toluenesulphonyl-L-glutamic acid, the conversion to N-tos-5-oxo-2-pyrrolidine-carboxyl chloride, the amidation to N-tos-5-oxo-2-pyrrolidine-carboxamide, the conversion to N-tos-L-isoglutamine, and the subsequent hydrogenation with sodium in liquid ammonia to give L-isoglutamine. We have found it more convenient to prepare L-isoglutamine by the amidation of N-CBZ-γ-benzyl-L-glutamate by the mixed anhydride procedure

of pH on the taking up of 1 mgm. of fluoride ion in 100 ml. of hot solution by 100 mgm. of magnesium oxide. The pH of the solutions was adjusted with sodium hydroxide or perchloric acid. The solution of pH 1.7 contained sufficient perchloric acid to dissolve approximately 40 mgm. of the original 100 mgm. of magnesium oxide added. From a hot solution at pH 1.7 containing 20 mgm. of fluoride as sodium fluoride in 100 ml., 100 mgm. of magnesium oxide took up 18.8 mgm. or 94% of the fluoride. This represents a removal of 188 μgm. of fluoride per mgm. of original magnesium oxide or 312 μgm. of fluoride per mgm. of magnesium oxide remaining in the solid phase.

The solid residue prepared under several different conditions with an excess of fluoride present was found to be of variable composition ranging from approximately the composition $2Mg(OH)_2 \cdot MgF_2$ to $4Mg(OH)_2 \cdot 3MgF_2$. These products were slightly soluble in hot water. Examination by the X-ray diffraction powder method showed that the products consisted of a mixture of $Mg(OH)_2$ and MgF_2 with no lines attributable to a new compound.

We wish to thank Dr. W. H. Barnes of the National Research Council of Canada who carried out the X-ray diffraction studies.

1. VENKATESWARLU, P. and NARAYANA RAO, D. Indian J. Med. Research, 41: 135. 1953.
2. VENKATESWARLU, P. and NARAYANA RAO, D. Indian J. Med. Research, 41: 473. 1953.
3. VENKATESWARLU, P. and NARAYANA RAO, D. Anal. Chem. 26: 766. 1954.

RECEIVED JULY 11, 1955.
FOOD AND DRUG LABORATORIES,
DEPARTMENT OF NATIONAL HEALTH AND WELFARE,
OTTAWA, CANADA.

A SYNTHESIS OF L-ISOGLUTAMINE FROM γ-BENZYL GLUTAMATE

BY M. KRAML AND L. P. BOUTHILLIER

In the course of our studies on histidine metabolism (5) it became necessary to prepare some L-isoglutamine. Bergmann and Zervas (1) obtained the desired product by cleaving N-carbobenzyloxy-L-glutamic anhydride with anhydrous ammonia followed by catalytic hydrogenation to remove the carbobenzyloxy (CBZ) group. Recently, Chambers and Carpenter (3) achieved a similar synthesis by blocking the amino acid with the *p*-nitrobenzyloxycarbonyl group. Paper chromatography (3) has revealed that these methods, while favoring L-isoglutamine formation, invariably yield small amounts of L-glutamic acid and L-glutamine as contaminants. Swan and duVigneaud (6) have published the only unambiguous synthesis of L-isoglutamine. It consists in the preparation of N-*p*-toluenesulphonyl-L-glutamic acid, the conversion to N-tos-5-oxo-2-pyrrolidine-carboxyl chloride, the amidation to N-tos-5-oxo-2-pyrrolidine-carboxamide, the conversion to N-tos-L-isoglutamine, and the subsequent hydrogenation with sodium in liquid ammonia to give L-isoglutamine. We have found it more convenient to prepare L-isoglutamine by the amidation of N-CBZ-γ-benzyl-L-glutamate by the mixed anhydride procedure

of Boissonnas (2), followed by catalytic hydrogenolysis of the resulting amide. The method is evidently unambiguous and L-isoglutamine is the only product formed. This was verified by paper chromatography in four solvent systems.

EXPERIMENTAL[1]

N-CBZ-γ-benzyl-L-glutamate

γ-Benzyl-L-glutamate, m.p. 168–169°, was condensed with carbobenzyloxy chloride in the presence of sodium bicarbonate as suggested by Hanby *et al.* (4). The N-CBZ-γ-benzyl-L-glutamate was crystallized from hot carbon tetrachloride, m.p. 77–78°. Calculated for $C_{20}H_{21}NO_6$, N: 3.77. Found N: 3.75.

N-CBZ-γ-benzyl-L-isoglutamine

N-CBZ-γ-benzyl-L-glutamate (32.8 mM.) was dissolved in 150 ml. of dioxane (redistilled from sodium) containing 7.80 ml. of tri-*n*-butylamine. The solution was cooled to 10° and 3.16 ml. of ethyl chlorocarbonate was added. The solution was shaken for 10 min. at 10° after which anhydrous ammonia was bubbled through for 15–30 min. The solution was evaporated to a white powder on a water bath at a temperature not exceeding 50°. The residue was suspended in 50 ml. of carbon tetrachloride and 50 ml. of water was added. The mixture was agitated vigorously and the N-CBZ-γ-benzyl-L-isoglutamine was filtered off and washed with cold water, carbon tetrachloride, and ether to remove any trace of starting material. The compound was recrystallized from hot ethanol, m.p. 126–127°, yield 80%. N-CBZ-γ-benzyl-L-isoglutamine has not been previously described in the chemical literature. Calculated for $C_{20}H_{22}N_2O_5$, C: 64.86; H: 5.96; N: 7.56. Found C: 65.16; H: 6.19; N: 7.52.

L-*Isoglutamine*

N-CBZ-γ-benzyl-L-isoglutamine (5 gm.) was dissolved in 100 ml. of 50% ethanol and hydrogenated for 12 hr. at room temperature and atmospheric pressure in the presence of palladium catalyst (5% Pd on calcium carbonate). The catalyst was filtered off and a trace of calcium ions was removed with oxalic acid. The solution was evaporated to dryness, the residue dissolved in a small amount of hot water, and the solution treated with charcoal. Alcohol was added to the cloud point and L-isoglutamine was recovered from the chilled solution as fine white crystals, m.p. 186–188°, yield 65%. Calculated for $C_5H_{10}N_2O_3$, N: 19.16. Found N: 18.94. Chambers and Carpenter (3) reported a melting point of 175–176°, whereas Swan and duVigneaud (6) found 186°. Chambers and Carpenter have reported $[\alpha]_D^{24}$ +19.4 to 20.5 (*c* 3, water) and Swan and duVigneaud, $[\alpha]_D^{21}$ +20.5° (*c* 6.1, water). We have measured $[\alpha]_D^{24}$ +20.0° (*c* 2.3, water). Paper chromatograms of our product revealed only one bluish-purple spot in each of the four solvent systems employed. The R_f in *n*-butanol – glacial acetic acid – water (15:3:7) was 0.28 and there was no

[1]*Analyses by the Geller Microanalytical Laboratories, Hackensack, New Jersey. All melting points were taken by the capillary method and are uncorrected.*

trace of L-glutamine (R_f 0.18); the R_f in phenol–water (4:1) was 0.56 and L-glutamic acid (R_f 0.30) was absent.

ACKNOWLEDGMENTS

The authors are indebted to the 'Fondation J. Rhéaume' for supporting this research.

1. BERGMANN, M. and ZERVAS, L. Ber. 65: 1192. 1932.
2. BOISSONNAS, R. A. Helv. Chim. Acta, 34: 874. 1951.
3. CHAMBERS, R. W. and CARPENTER, F. H. J. Am. Chem. Soc. 77: 1522. 1955.
4. HANBY, W. E., WALEY, S. G., and WATSON, J. J. Chem. Soc. 3239. 1950.
5. KRAML, M. and BOUTHILLIER, L. P. Can. J. Biochem. Physiol. 33: 590. 1955.
6. SWAN, J. M. and DUVIGNEAUD, V. J. Am. Chem. Soc. 76: 3110. 1954.

RECEIVED JUNE 27, 1955.
DEPARTMENT OF BIOCHEMISTRY,
FACULTY OF MEDICINE,
UNIVERSITY OF MONTREAL,
MONTREAL, P.Q.

Canadian Journal of Chemistry

Issued by THE NATIONAL RESEARCH COUNCIL OF CANADA

VOLUME 33 NOVEMBER 1955 NUMBER 11

SOME FLUORINE SUBSTITUTED TOLANES[1]

BY C. S. ROONEY[2] AND A. N. BOURNS

ABSTRACT

p-Trifluoromethyltolane and *p*-fluorotolane have been synthesized by the action of sodium or potassium amide in liquid ammonia on *para*-substituted 1,1-diphenyl-2-bromoethylenes. The geometrical isomers of 1-(*p*-trifluoromethylphenyl)-1-phenyl-2-bromoethylene have been separated and their configurations assigned on the basis of dipole moment measurements. *p*-Trifluoromethyltolane has been converted to a dibromide, which on oxidation gave benzoic and *p*-trifluoromethylbenzoic acids. Both tolanes have been reduced to the correspondingly substituted 1,2-diphenylethanes.

INTRODUCTION AND DISCUSSION

The syntheses and some reactions of (*p*-trifluoromethylphenyl)phenylacetylene (*p*-trifluoromethyltolane) (I) and (*p*-fluorophenyl)phenylacetylene (*p*-fluorotolane) (II) are described. These compounds were prepared in the course of some work which was to have been preliminary to a carbon-tracer investigation of the rearrangement of 1,1-diaryl-2-haloethylenes to tolanes in the presence of strong base (5, 6). A related investigation of this reaction, using a different system, was completed recently in another laboratory (4) and for this reason our mechanism studies were discontinued.

1-(*p*-Trifluoromethylphenyl)-1-phenylethylene (III) was prepared by the interaction of acetophenone and *p*-trifluoromethylphenylmagnesium bromide, as well as from *p*-trifluoromethylbenzophenone (IV) and methylmagnesium iodide. Compound IV was synthesized by the action of antimony trifluoride on *p*-trichloromethylbenzophenone at an elevated temperature. Bromination of III, followed by dehydrobromination, yielded 1-(*p*-trifluoromethylphenyl)-1-phenyl-2-bromoethylene (V), which, by a combination of elution chromatography on alumina and fractional crystallization at low temperatures, was separated into two geometrical isomers. On the basis of dipole moment measurements, the crystalline isomer (VA) was assigned the *cis* configuration, and the other (VB), a liquid at room temperature, the *trans* configuration. Isomer VB could not be obtained completely free of its higher-melting, less-soluble isomer.

[1]*Manuscript received July 18, 1955.*
Contribution from the Department of Chemistry, Hamilton College, McMaster University, Hamilton, Ontario.
[2]*National Research Council Postdoctorate Fellow, Department of Chemistry, Hamilton College, McMaster University, 1952–1954.*

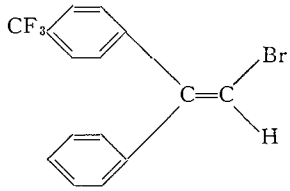

Compound VA

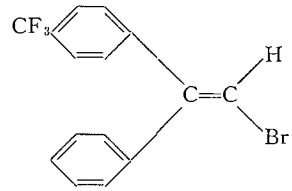

Compound VB

Compounds VA and VB on interaction with sodium or potassium amides in liquid ammonia solution both gave *p*-trifluoromethyltolane (I) in about 75% yield. Bromination of I yielded the dibromide VI, which on oxidation with chromic anhydride in acetic acid solution produced a mixture of benzoic and trifluoromethylbenzoic acids. Oxidation of I directly with potassium permanganate in acetone gave a low yield of these acids. Catalytic hydrogenation of compound I, using Raney nickel or Adam's catalyst at low pressure, produced 1-(*p*-trifluoromethylphenyl)-2-phenylethane (VII).

p-Fluorotolane (II) was prepared from 1-(*p*-fluorophenyl)-1-phenyl-2-bromoethylene (VIII) in a manner analogous to the synthesis of I. The bromo compound, VIII, prepared by the action of bromine on 1-(*p*-fluorophenyl)-1-phenylethylene, could not be crystallized, or separated into pure geometrical isomers by distillation or chromatography. Catalytic hydrogenation of II produced 1-(*p*-fluorophenyl)-2-phenylethane (IX).

EXPERIMENTAL*†

p-Trifluoromethylbenzophenone (IV)

p-Trichloromethylbenzophenone (10) (7.6 gm.) and 8.5 gm. of antimony trifluoride were mixed intimately and heated on a hot plate for 15 min. at a temperature sufficient to fuse the mixture. Water and benzene were added and 2.3 gm. of benzene-soluble material was isolated. Recrystallization from ethanol–water gave 1.53 gm., or 23% yield, melting at 116–118°C. Calc. for $C_{14}H_9OF_3$: C, 67.18; H, 3.63. Found: C, 67.24, 67.08; H, 3.75, 3.68.

1-(p-Trifluoromethylphenyl)-1-phenylethylene (III)

Method A

p-Bromobenzotrifluoride (9) (9.16 gm.) and 1.04 gm. of magnesium were allowed to react in 50 ml. of anhydrous diethyl ether. To the resulting red-colored Grignard reagent 4.88 gm. of acetophenone in 50 ml. of ether was added. The reaction mixture was worked up in the usual way. The resulting crude carbinol was dehydrated by heating at 150°C. in a nitrogen atmosphere for one and one-half hours. Distillation yielded 5.3 gm. of product (52.5% of theory), b.p. 78–79°C. at 0.1 mm., which crystallized. Recrystallization from methanol, or vacuum sublimation, gave the pure compound, m.p. 38–39°C.

**Melting points are corrected.*

†Carbon and hydrogen analyses were performed by Dr. F. G. Harcsar of McMaster University, and Miss G. Rotermann of the Dominion Rubber Company, Guelph, Ontario. Bromine analyses were carried out by the authors using the Carius combustion procedure.

Method B

p-Trifluoromethylbenzophenone (IV) (1.50 gm.) was added to an ether solution containing methylmagnesium iodide (0.22 gm. magnesium, 0.94 gm. methyl iodide) and the product was worked up as described under Method *A*. The yield of compound III, m.p. 38–39°C., was 1.12 gm. or 75% of theory. Calc. for $C_{15}H_{11}F_3$: C, 72.58; H, 4.47. Found: C, 71.82, 71.63; H, 4.98, 4.57.

Oxidation of compound III (0.068 gm.) with a solution containing 1.50 gm. of potassium permanganate, 10 ml. of acetone, and 7 ml. of water gave 0.043 gm. or a 76% yield of *p*-trifluoromethylbenzophenone.

1-(p-Trifluoromethylphenyl)-1-phenyl-2-bromoethylene (V)

Compound III (2.83 gm.) was brominated using bromine in acetic acid and the resulting dibromide dehydrobrominated by the procedure of Bergmann and Szmuszkowicz (2). On evaporation of the acetic acid solution, 3.78 gm., or 101% of theory, of a liquid product was isolated. After the product had been left overnight in the refrigerator, 1.54 gm. of crystalline solid (VA), m.p. 71–74°C., separated. This material was isolated by dissolving the surrounding liquid selectively in ethanol. The ethanol-soluble portion was chromatographed on an alumina* column using *n*-hexane as the developing solvent. A further 0.17 gm. of the solid isomer was obtained in this way, it being the last fraction removed from the column. Recrystallization of the combined solid product from ethanol gave pure VA, m.p. 74–75°C. The liquid fractions, which were eluted from the alumina column first, had n_D^{25} 1.5670–1.5690. When cooled to 0°C., or when cooled in ethanol solution to dry ice temperatures, these partially crystallized. Repeated chromatography, as well as fractional crystallization in ethanol solution, however, failed to give a sharply melting substance. What was probably the purest sample isolated had a melting point of 8–12°C., and n_D^{25} 1.5684. Anal. Calc. for $C_{15}H_{10}F_3Br$: C, 55.07; H, 3.08; Br, 24.4. Found: Solid isomer; C, 55.11, 55.11; H, 3.09; 3.07, Br, 25.9, 24.3. Liquid isomer; Br, 26.5, 24.8.

Dipole moment measurements determined using the resonance method (7) gave 3.46 D for the solid isomer (VA) and 2.26 D for the liquid product (VB). One therefore can assign with considerable certainty the *cis* (*p*-trifluoromethylphenyl and bromine *cis*) and *trans* configurations to the high- and low-melting isomers respectively. The moment of the liquid product was high for a pure compound of the *trans* configuration, indicating some contamination by the less soluble *cis* isomer.†

Oxidation of 0.072 gm. of compound VA in a solution containing 11 ml. of water, 15 ml. of acetone, 0.05 gm. of acetic acid, and 1.59 gm. of potassium permanganate yielded 0.045 gm. of *p*-trifluoromethylbenzophenone (81.5% yield).

**British Drug Houses chromatographic grade alumina, activated by heating for three hours with a Meeker burner, was used.*

†It is of interest that a larger-than-expected moment has also been observed (1) for the trans isomer of 1-(p-bromophenyl)-1-phenyl-2-bromoethylene, although in this case the compound appears to be free of its geometrical isomer (4). This would suggest that our liquid product was purer trans isomer than the dipole moment might imply.

p-Trifluoromethyltolane (I)

Compound VA, or VB, (0.61 gm.) in 15 ml. of diethyl ether was added to a liquid ammonia solution (70 ml.) containing 0.42 gm. of sodium amide. The mixture was evaporated to dryness after 15 min., 50 ml. of water added, and the insoluble product filtered. Recrystallization from ethanol–water, following vacuum sublimation, gave 0.135 gm., or 75% of theory, of the tolane melting at 104–105°C. Calc. for $C_{15}H_9F_3$: C, 73.17; H, 3.66. Found: C, 73.39, 73.38; H, 4.05, 4.02.

p-Trifluoromethyltolane Dibromide (VI)

To compound I (0.26 gm.), dissolved in 15 ml. of acetic acid, was added a slight excess of bromine in acetic acid and the solution heated at about 100°C. for 15 min. Following evaporation to 5 ml. and dilution with 20 ml. of water, 0.30 gm., or 72% of theory, of solid bromide was isolated, which after recrystallization from ethanol–water or isooctane melted at 159–161°C. Calc. for $C_{15}H_9F_3Br_2$: C, 44.30; H, 2.22; Br, 39.3. Found: C, 44.09, 43.86; H, 2.32, 2.22; Br, 37.0.

The dibromide VI (0.143 gm.) was added to a solution containing 0.40 gm. of chromic anhydride, 0.5 ml. of water, and 4 ml. of acetic acid. The mixture was heated at the boiling point for 15 min. and then 20 ml. of water was added. The precipitated solid (0.080 gm.) was filtered. A further 0.027 gm. was recovered from the filtrate by extraction with 60:40 benzene–ether. Extraction of the first product with 5% sodium hydroxide solution followed by acidification with dilute hydrochloric acid gave 0.046 gm. of acidic material. The combined solid products (0.073 gm.) were subjected to partition chromatography on a silicic acid column using methanol and isooctane as the stationary and mobile phases, respectively (8). The first compound removed from the column (0.038 gm.) melted at 218–220°C. and gave no depression when mixed with authentic *p*-trifluoromethylbenzoic acid. A later fraction gave 0.012 gm. of an acid whose melting point, 120–122°C., was unchanged in admixture with benzoic acid.

1-(p-Trifluoromethylphenyl)-2-phenylethane (VII)

Hydrogenation of compound I (1.33 gm.) in ethanol solution, using a Raney nickel catalyst at room temperature and 40 p.s.i., yielded 1.23 gm. of product (92% yield). Recrystallization from ethanol–water, or vacuum sublimation, gave the pure compound, m.p. 37.3–38.6°C. Calc. for $C_{15}H_{13}F_3$: C, 71.95; H, 5.23. Found: C, 71.77, 71.33; H, 5.15, 5.15.

1-(p-Fluorophenyl)-1-phenyl-2-bromoethylene (VIII)

This compound was prepared by bromination of 1-(*p*-fluorophenyl)-1-phenylethylene (X) (3) using the method of Bergmann and Szmuszkowicz (2). Compound X (21.2 gm.) gave 27.2 gm. (92% yield) of a product (VIII) boiling at 129–133°C. at 0.1 mm. Fractional distillation through a laboratory column *in vacuo* gave fractions with refractive indices varying from n_D^{25} 1.6131 to n_D^{25} 1.6162. Chromatography on an alumina column failed to give separation

into two distinct fractions. Calc. for $C_{14}H_{10}FBr$: C, 60.60; H, 3.61; Br, 28.8. Found: C, 59.97, 59.50; H, 3.59, 3.55; Br, 29.0, 28.4.

p-Fluorotolane (II)

Compound VIII (5.57 gm.) was added in ether solution to 100 ml. of liquid ammonia containing 2.5 gm. of potassium (as potassium amide) and the mixture was worked up as described for compound I. A crude solid (3.84 gm.) was isolated, which after recrystallization from ethanol–water weighed 3.01 gm. (75.5% yield) and melted at 109–110°C. Calc. for $C_{14}H_9F$: C, 85.71; H, 4.59. Found: C, 86.36, 86.29; H, 4.83, 4.68.

1-(p-Fluorophenyl)-2-phenylethane (IX)

Hydrogenation of compound II (0.128 gm.) with Raney nickel catalyst in ethanol solution at room temperature and 18 p.s.i. yielded 0.128 gm. of crude product, which after recrystallization from ethanol–water melted at 61–62.5°C. Calc. for $C_{14}H_{13}F$: C, 83.96; H, 6.50. Found: C, 83.16, 82.98; H, 6.49, 6.42.

ACKNOWLEDGMENT

One of us (C. S. Rooney) wishes to acknowledge the financial support of the National Research Council.

REFERENCES

1. BERGMANN, E., ENGEL, L., and MEYER, H. Ber. 65, B: 446. 1932.
2. BERGMANN, F. and SZMUSZKOWICZ, J. J. Am. Chem. Soc. 69: 1777. 1947.
3. BERGMANN, F. and SZMUSZKOWICZ, J. J. Am. Chem. Soc. 70: 2748. 1948.
4. BOTHNER-BY, A. A. J. Am. Chem. Soc. 77: 3293. 1955.
5. COLEMAN, G. H., HOLST, W. H., and MAXWELL, R. D. J. Am. Chem. Soc. 58: 2310. 1936.
6. COLEMAN, G. H. and MAXWELL, R. D. J. Am. Chem. Soc. 56: 132. 1934.
7. DANIELS, F., MATHEWS, J. H., WILLIAMS, J. W., BENDER, P., MURPHY, G. W., and ALBERTY, R. A. Experimental physical chemistry. 4th ed. McGraw-Hill Book Company, Inc., New York. 1949.
8. HUNT, C. F. M.Sc. Thesis, McMaster University, Hamilton, Ontario. 1953.
9. MARKARIAN, M. J. Am. Chem. Soc. 74: 1858. 1952.
10. THÖRNER, W. Ann. 189: 83. 1877.

THE ACTION OF SULPHURIC ACID ON GLIADIN: WITH SPECIAL REFERENCE TO THE N-PEPTIDYL→O-PEPTIDYL BOND REARRANGEMENT[1]

By L. K. Ramachandran[2] and W. B. McConnell

ABSTRACT

Treatment of gliadin with sulphuric acid transposes peptide bonds of serine from the amino to the hydroxyl group. Maximum transposition, 60–70% of the theoretical, occurs when the protein is treated with anhydrous sulphuric acid at 0°C. for 35 hr. No rearrangement was detected at threonine residues. Examination of the peptide material, obtained from the rearranged protein by Elliott's degradation method, indicates apparent "homogeneity". In an alternative scheme for the degradation, nitrous acid deamination of free amino groups was used. The resulting loss in serine content of the protein is direct evidence for the acyl migration of peptide bonds. Incorporation of sulphur and partial disappearance of several amino acids accompany the sulphuric acid treatment. The occurrence of these secondary reactions imposes limitations on the use of sulphuric acid as a reagent for the specific fission of peptide bonds.

INTRODUCTION

Attention has recently been directed towards methods which effect fragmentation of protein molecules in a predictable manner. Especially significant is Elliott's procedure for the cleavage of peptide bonds (7, 8, 9) at the amino groups of the β-hydroxyamino acids, serine and threonine. It is based on the strong acid-induced N-acyl→O-acyl transformations studied earlier by Bergmann, Brand, and Weinmann (2), Desnuelle and Casal (5), and Desnuelle and Bonjour (6), and is briefly outlined in the equations below:

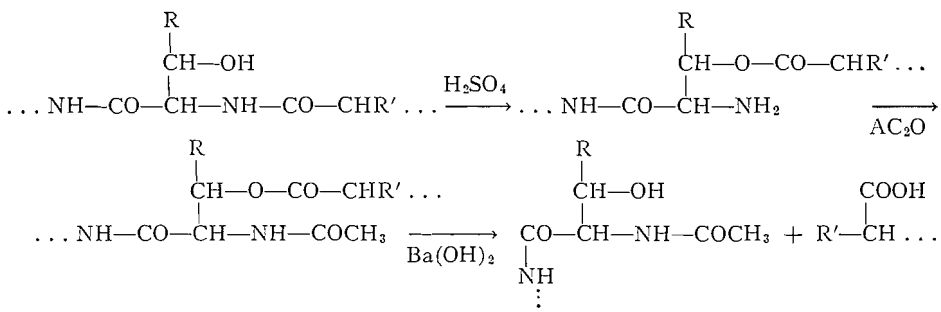

This N-acyl→O-acyl migration might also occur where the ε-amino groups of δ hydroxylysine (26) are linked in a peptide bond.

The treatment of silk fibroin with 97.5% sulphuric acid for three days at 20°C. (8) caused rearrangement in only 66% of the serine residues, the major N-terminal residue detected by the dinitrofluorobenzene method (24) being serine. The non-reactivity of the other serine residues was thought to result

[1]*Manuscript received May 26, 1955.*
Contribution from the National Research Council of Canada, Prairie Regional Laboratory, Saskatoon, Saskatchewan. Issued as Paper No. 201 on the Uses of Plant Products and as N.R.C. No. 3728. Presented in part at the Western Regional Conference of the Chemical Institute of Canada at Vancouver, British Columbia, September 1954.
[2]*National Research Council of Canada Postdoctorate Fellow 1953–1955.*

from factors like steric hindrance. With lysozyme (9) nearly all the serine groups and a third of the threonine residues participated in the reaction. The non-dialyzability of the lysozyme derivative and the absence of the Ehrlich test for tryptophan suggested that cross linking occurred through those residues. Wiseblatt and McConnell (37), who applied the method to wheat gluten, also observed the preferential release of serine amino groups and suggested that the product was highly cross linked.

In the present study the action of anhydrous sulphuric acid in effecting bond transposition in gliadin has been studied from the quantitative aspects of time of reaction and temperature, to determine suitable conditions for further degradation studies on wheat proteins. The gliadin fraction was chosen because of its discrete characteristics. The reactivity of the liberated amino groups towards nitrous acid was determined. This treatment would convert the N-terminal serine residues to glyceric acid. After saponification of the O-acyl bond, the reactivity of the terminal dihydric alcohol towards periodic acid was studied. The above alterations in Elliott's scheme avoid the necessity for protecting the free amino N with a substituent often difficult to remove without other alterations to the material.

An effort has also been made to detect changes in some of the amino acids, arising from sulphuric acid treatment of the protein. Uchino (33) reported that silk fibroin was stable towards sulphuric acid at 7–8°C. for 11 days, but that later there was slow liberation of amino groups. Reitz *et al.* (28) noted that although appreciable hydrolysis of γ-globulin occurred in one week at room temperature there was only 2–3% hydrolysis in 10 days at 4°C. Work on wool (11) indicated considerable non-ionic combination of sulphate ions with the amino groups to form sulphamates. With other proteins (28) it seemed possible to account for all bound sulphate on the basis of ester formation with aliphatic hydroxyl groups, formation of sulphonic acids, and formation of thiosulphates by reaction with the sulphydryl groups. Although some workers observe very little destruction of tryptophan, cystine, and serine (28) other reports (20) indicate appreciable alteration besides the sulphamate formation. When wool was treated with sulphuric acid at low temperatures 10% of the serine and 25% of the arginine was lost. Phenylalanine and tyrosine showed a decrease which, as with tryptophan, may be partly accounted for by sulphonation of the benzene ring.

EXPERIMENTAL

Analytical Methods

Total N was determined by the micro-Kjeldahl method with mercuric oxide catalyst. *Free amino groups* were estimated by the Van Slyke nitrous acid method and a ninhydrin colorimetric procedure (31).

The difference in free amino groups before and after treatment of the materials with pH 9.1 borate buffer for 12–16 hr. was taken as a measure of the *bond transposition* (8).

Standard methods were employed for determination of the following: *amide N* (24), *cystine* (16), *methionine* (13), *arginine* (21), *tryptophan* (10). *Tyrosine* was determined by the 1,2-nitrosonaphthol reaction (25, 34).

Total S was estimated by a combined micro-combustion and volumetric method (32) and *formaldehyde* by the chromotropic acid color reaction (23). The method of Rice, Keller, and Kirschner (30) was used for the identification of the aldehydes as the 2,4-dinitrophenylhydrazones.

Treatment of Gliadin with Sulphuric Acid

One gram of gliadin (N—17.64%, prepared by the method of Blish and Sandstedt (3)) and 10 ml. anhydrous sulphuric acid (prepared by addition of the calculated amount of oleum to 97.5% sulphuric acid) were shaken together for the required time at the temperature desired. The reaction mixture was then poured with stirring into 20 times its volume of cold ether and the precipitated material washed repeatedly with ether. The material was dissolved in the minimum volume of 60% (v/v) ethanol, transferred to a Visking cellophane bag, and dialyzed exhaustively against distilled water. The contents of the bag were lyophilized. The recovery of the products was close to 97% based on nitrogen analyses.

Degradation of the Sulphuric Acid Treated Gliadin

The material obtained above was *acetylated* at pH 5.0 using acetic anhydride (8) or *formylated* with a mixture of formic acid and acetic anhydride (35). *Deacylation* was effected by means of anhydrous MeOH – HCl (1.5 *M* in regard to HCl) under conditions used by Boissonnas and Preitner (4). *Saponification* of the O-acyl bond was achieved using 0.01 *N* NaOH or 0.02 *N* $Ba(OH)_2$ (8).

Deamination of Sulphuric Acid Treated Gliadin

Two methods were employed. In the first, the reaction mixture was treated at 0.5°C. with solid $NaNO_2$ (1 gm. for every gram of protein), added in small portions during 20 min. In the other method 0.5 gm. of the material in 30 ml. 50% acetic acid was treated at room temperature with 1 gm. $NaNO_2$ added in small portions during 20 min. with agitation. The reaction mixtures were exhaustively dialyzed against distilled water and lyophilized. The latter method gave products free of color.

Reaction of Terminal Amino Groups with 1-Fluoro-2,4-dinitrobenzene (DNFB)

Conditions for the reaction and hydrolysis of the products for the release of the dinitrophenyl amino acids were those recommended by Porter (24). Separation of the 2,4-dinitrophenol and 2,4-dinitroaniline from the amino acid derivatives was effected on a chloroform – silicic acid column (19). The dinitrophenyl amino acids were identified by paper chromatography (22) and determined quantitatively by spectrophotometry at 360 mμ (24).

RESULTS

To establish a basis for assessing the results the serine content of gliadin was determined (27) and found to be 4.9% by weight. Gliadin, of molecular weight 30,000, on cleavage of all peptide bonds attached to serine N should therefore yield material containing about 15 fragments with an average chain length of 15–16 residues and with 0.65% amino N (3.7% of total N)

due to exposed serine amino groups. The original gliadin contained 1.01% of the total N as free amino N.

Figs. 1, 2, and 3 contain results obtained for total amino N, amino N arising from bond transposition alone, and amino N other than that arising from bond transposition when samples of gliadin were treated with H_2SO_4 at

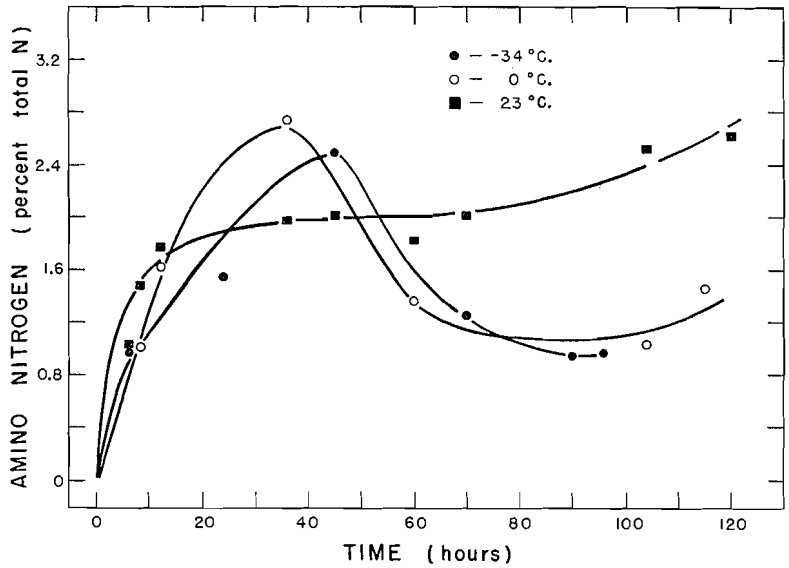

FIG. 1. Effect of time and temperature on free amino N released from gliadin by sulphuric acid.

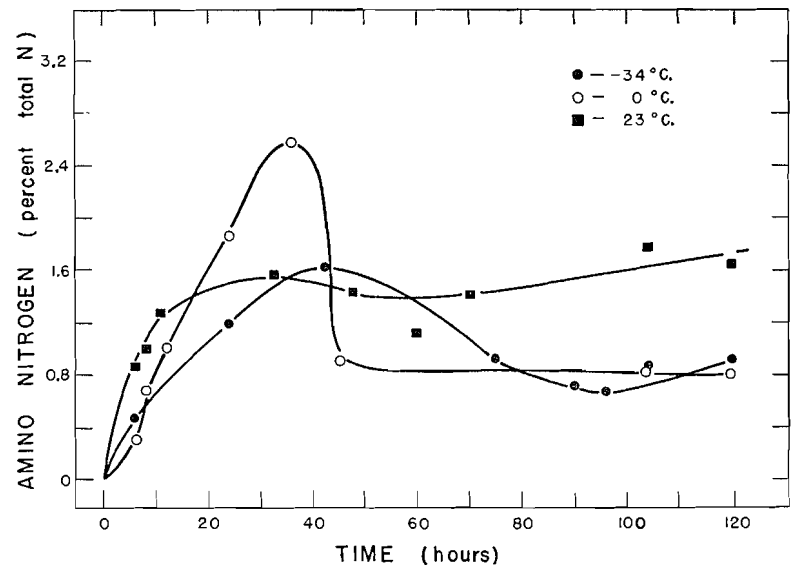

FIG. 2. Effect of time and temperature on the release of amino nitrogen by bond transposition alone during the sulphuric acid treatment of gliadin. Free amino nitrogen expected from a quantitative bond transposition at serine is 3.7% of total nitrogen.

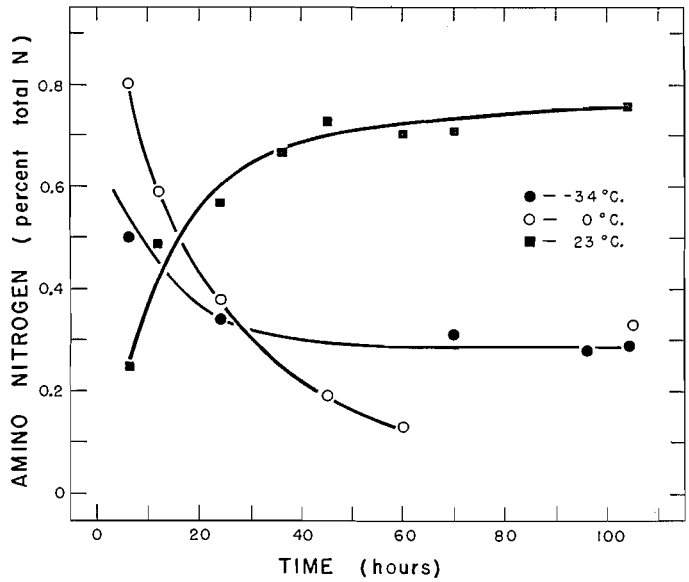

FIG. 3. Effect of time and temperature on amino nitrogen not arising from bond transposition during the sulphuric acid treatment of gliadin.

0°, 23°, and −34°C. for different lengths of time. The data were obtained on lyophilized products, isolated from the reaction mixtures, as described above.

The data indicate that in samples treated at 0°C. and −34°C. the total amino N increases during 35–45 hr. and thereafter falls to 50–65% of the maximum, remaining practically constant. At 23°C. amino groups increase rapidly for about 45 hr. after which there is a slow but continuous rise. Changes in amino N arising specifically from bond transposition follow the same pattern (Fig. 2). The pattern of changes in content of amino N other than those involved in the bond transposition is depicted in Fig. 3. In samples treated at −34° and 0°C. the values decrease gradually to a low value. Since the free amino N content of the original gliadin was measured to be 1.01% the initial decrease at 23°C. is relatively rapid but thereafter there is a progressive increase in free amino groups which may be the result of non-specific hydrolysis.

The difference between analytical values on duplicate preparations was of the order of 10%. The observed trends are therefore significant. The average deviation of the mean for determinations of amino N by the colorimetric method was ±1.5%.

Acylation and Saponification of the Treated Gliadin to Peptides

Two samples, one treated at 0°C. for 45 hr. and another treated at 23°C. for 60 hr. with sulphuric acid (0.312% and 0.221% of amino N, respectively, exposed by the bond shift), were subjected to acetylation, saponification, and deacetylation by methods referred to earlier. Material from saponification (after precipitation of barium either by passing in CO_2 at pH 6.5–7.0 or by

adding dilute sulphuric acid) had a high ash content which was retained even after the treatment with MeOH – HCl. To determine the serine end groups, the peptide samples obtained were oxidized with periodic acid. The amounts of formaldehyde obtained corresponded to 107.8 and 92.2% of the theoretical calculated from the amino N values for bond transposition.

The peptide samples were subjected to paper electrophoresis (Whatman 3 mm. 11×30 cm. sheet) using a pH 6.0 phthalate (0.05 *M*) buffer and 0.05 *N* acetic acid. The material was spotted along a line drawn across the middle of the sheet, which had been previously wetted with the electrolyte, and a potential of 220 v. was applied for a period of from two and one-half to three hours. No appreciable part of the material migrated toward either electrode so that although analyses indicated cleavage of the molecule at five to eight sites, no heterogeneity in the resulting material was demonstrable by paper electrophoresis. This observation is similar to results obtained in studies on gluten (37), where the suggestion was made that the material resulting from the treatments employed may consist of cross-linked polypeptide material of colloidal dimensions exhibiting marked homogeneity by physiochemical criteria. It was emphasized that the electrophoretic homogeneity may have resulted from polar groups introduced by the chemical treatments used. It thus appeared of some interest to avoid, at least, the steps of acylation and deacylation.

Deamination with Nitrous Acid and Saponification of the O-Peptide Bond

Some experiments were done therefore on deamination of the products from the sulphuric acid treatment. The reaction should convert the free amino groups to hydroxy groups and subsequent saponification should then yield a mixture of peptides with terminal glyceric acid. The reaction could be represented as follows:

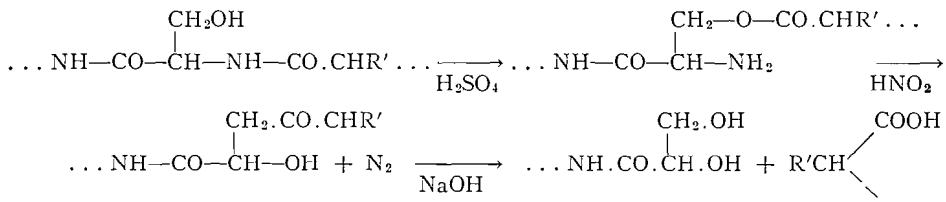

Gliadin treated with sulphuric acid at 0°C. for 45 hr. was deaminated and saponified according to the above scheme of reactions. The isolated product was then oxidized with periodate (37) to determine terminal dihydric alcohols. Formaldehyde* equivalent to 105.5% of that calculated from bond transposition was recovered. The second method of deamination was applied to gliadin treated with sulphuric acid at 23°C. for 60 hr. The sample had a serine amino N value of 0.221% and total amino N 0.298%. After deamination the product had only 0.013% amino N, indicating destruction of 95.6% of the free amino

**Although the amounts of formaldehyde estimated in several samples examined were nearly equivalent to the bond transposition effected, the periodate consumed during the oxidation of the products was found to be several times higher than that expected. The sites in the protein-derivatives responsible for this reduction of periodate have not yet been determined.*

groups. Saponification with NaOH resulted in a product which on periodate oxidation yielded only a trace of periodate ammonia, indicating complete destruction of the serine amino groups. The formaldehyde produced during this oxidation corresponded to 112.8% of the calculated amount. The absence of acetaldehyde in the reaction mixture by the *p*-hydroxydiphenyl test indicated that no threonine residues were involved in the arrangement. This was confirmed when the aldehydes present were reacted with 2,4-dinitrophenylhydrazine and the hydrazones extracted and identified on paper chromatograms. Only one spot corresponding to formaldehyde was present.

The nitrous acid treated samples were hydrolyzed with 6 *N* HCl for 20 hr. as was a control sample of gliadin. The hydrolyzates were chromatographed in two dimensions (36) and the combined intensity of the ninhydrin spots due to serine and glycine was determined spectrophotometrically after extraction with 10% isopropanol. The values indicated that 80–90% of the serine determined as involved in the rearrangement had been destroyed by nitrous acid. However, application of both the dye test (17) and the biuret test (14) to electrophorograms of the two samples (deaminated H_2SO_4-treated gliadin, one at 0°C. for 45 hr. and the other at 23°C. for 60 hr.), prepared as described above, showed a single major component, which moved slowly towards the anode, but did not separate into differing fragments. Both the materials moved a distance of 2.3 cm. in three hours in 0.05 *N* acetic acid.

C-Terminal Groups of Degradation Products

Reaction of the degradation products with carboxypeptidase in a qualitative study indicated the following amino acids occupying C-terminal positions—tyrosine, "leucine",* valine, alanine, glutamic acid, and glycine. No amino acids were released when undegraded gliadin was treated with the enzyme, although application of the modified Schlack and Kumpf procedure (1) for C-terminal groups had indicated the presence of glutamic acid and "leucine" in less than molar amounts (unpublished results of the authors). It is thus possible that bond fission occurred at sites where serine is linked to the above amino acids.

Reaction of Exposed Amino Groups with DNFB

Gliadin was treated with sulphuric acid at 23°C. for four days, precipitated, acetylated, saponified, and then deacetylated with MeOH – HCl and the material fractionated roughly into MeOH – HCl soluble and insoluble fractions (37). The methanol insoluble sample (the amount of material recovered thus accounted for 25% of the nitrogen in the starting material) had very low amino N (0.137%) whereas the soluble fraction had a value of 0.490%. The free serine amino N was 0.082 and 0.183% respectively. The latter sample had a very high ash content and the formaldehyde values on periodate oxidation were abnormally high. It was considered desirable to determine the amount of free serine amino groups by condensing with DNFB and measuring the DNP-serine formed. The dinitrophenyl derivative was hydrolyzed and the DNP-amino acids in the ether extract and aqueous phase examined for their

**No differentiation has been made between leucine and isoleucine.*

identity by paper chromatography (22) after initial purification on silicic acid (19). DNP-serine was found in the ether phase and the aqueous phase contained DNP-histidine. The presence of DNP-histidine is to be expected since histidine occupies the N-terminal position in gliadin (15, unpublished data of the authors). The DNP-serine amounted to 10.65 μM. while the amount theoretically expected from the other analyses was 12.59 μM. Although the recovery for serine amino groups thus appeared to be nearly quantitative, the condensation with the other free amino groups, known to be present from ninhydrin amino N analysis, could not be detected.

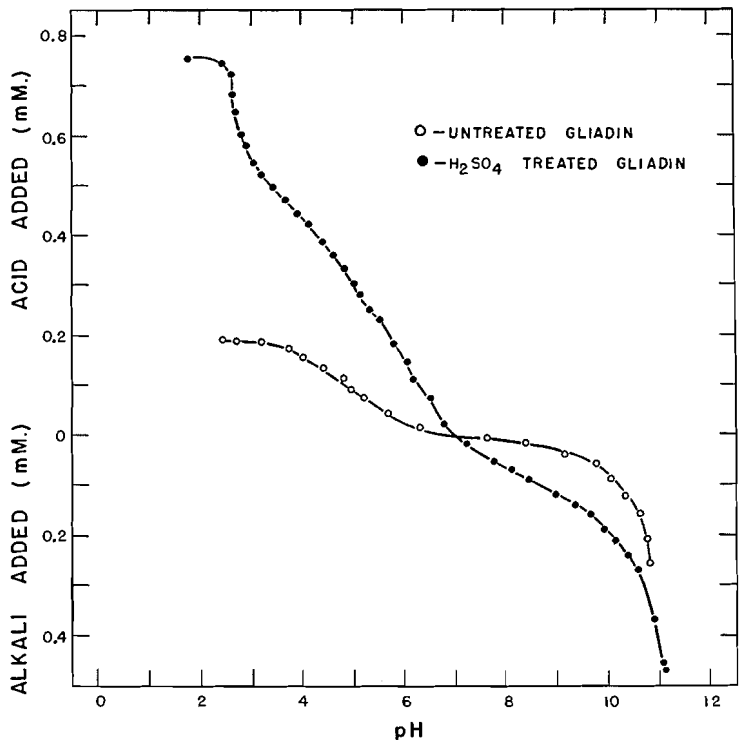

Fig. 4. Titration curve of gliadin before and after treatment with sulphuric acid.

The Effect of Sulphuric Acid Treatment on Some Amino Acid Residues

The titration curves of a sample of gliadin in 60% ethanol, before and after treatment with sulphuric acid at 23°C. for 70 hr., are indicated in Fig. 4. The shape of the curves suggests appreciable changes in the groups titrated in the pH region 2.5–8.5.

Table I contains the results of analyses for bound sulphate, amide N, arginine, methionine, and tyrosine. A single determination of tryptophan in the sample treated for 70 hr. at 23°C. indicated a decrease from 1.15 to 1.02%, of cystine from 2.35 to 1.85%, and of phenylalanine (12) from 5.45 to 4.72% on moisture and ash-free protein.

TABLE I

AMINO ACID CONTENT OF THE SULPHURIC ACID TREATED SAMPLES*

Reaction time, hr.	Reaction temp., °C.	Total S, %	Amide N, as % total N	Methionine	Arginine	Tyrosine
Untreated		0.943	25.6	1.53	4.52	3.5
6	23		23.3	1.11	3.83	2.49
24	23	2.32	23.91		3.67	1.97
70	23		19.75	0.971	3.84	0.71
120	23	3.24	18.69	0.71	3.40	0.65
6	0	1.62		0.75	3.57	2.27
60	0	2.17	25.63	0.67	3.62	0.95
104	0		22.92	0.55	3.41	
6	−34	1.05	20.74	1.22	3.66	2.94
90	−34	1.30	16.20	1.10	3.47	2.14
192	−34	2.40		0.98	2.79	2.29

**All values for amino acids as gm./100 gm. protein.*

DISCUSSION

The results presented show that time of treatment is a factor of importance in the sulphuric-acid-induced acyl migration of peptide bonds in gliadin. Although this study of transposition as a function of time indicates the best conditions (40 hr. at 0°C.), the complete migration of peptide bonds was not obtained under any of the conditions. The shape of the curves in Fig. 3 suggests partial disappearance of amino N during acid treatment at the two lower temperatures, whereas at 23°C. a non-specific hydrolytic cleavage appears to be superimposed. Amino groups might undergo reaction to form sulphamates (11, 29) or be involved in other reactions. If some of the newly formed amino groups participate in such reactions under the conditions of treatment used, it would be impossible to detect or make use of a complete shift of the peptide bonds. Apparent incompleteness in the shift cannot be explained solely on the basis of factors like reactivity of the residues in the protein molecule. Elliott (9) suggested the occurrence of polymerization reactions involving tryptophan residues in the case of lysozyme, but quantitative fission at serine groups and at a third of the threonine residues had occurred. In silk fibroin the cleavage at serine residues was of the order of 66% (8). In gliadin the maximum observed is of the same order (Fig. 2). Thus the effective cleavage of these bonds seems to vary with different proteins.

The present observations indicate that problems arising in the blocking of amino groups and removal of the blocking agent later could be avoided by deamination and that, with gliadin, the removal of the amino groups by nitrous acid is quantitative. This treatment would however convert terminal serine residues to glyceric acid. In theory, this simplification in procedure could distinguish between serine residues rearranged in the first step and those encountered later. Samples of treated protein deaminated in this way showed a decrease in content of serine in the hydrolyzate, of the same order as involved in the bond rearrangement. This in effect constitutes direct evidence of a shift of peptide bonds attached to the serine N in gliadin. Desnuelle (see Ref. 9, p. 140) however has encountered difficulty with some proteins in dimethylating or deaminating the amino groups exposed by sulphuric acid.

The results obtained indicate the incorporation of considerable amounts of undetermined forms of sulphur into the protein during the treatment with acid. Extensive chemical modification of the original protein is also shown by the changes in the content of amide bonds, methionine (cf. 18), arginine, tyrosine, cystine, and phenylalanine. The tryptophan reaction was still strong in some of the products examined. Side reactions involving free amino groups in the sulphuric acid medium are indicated by the gradual diminution of non-serine amino N with time. This perhaps involves, amongst other possibilities, sulphamate formation. The differences observed in the titration curves of gliadin, before and after treatment, possibly result from rather extensive alterations.

The incomplete nature of the rearrangement and the chemical modification of several of the constituent amino acids in the protein severely limit the scope and usefulness of sulphuric acid as a reagent for the selective fission of peptide bonds. The results presented herein do nevertheless provide direct evidence for strong acid-induced acyl migration in gliadin and indicate that a fairly specific cleavage of peptide bonds can thereby be obtained. More satisfactory schemes for selective protein hydrolysis will probably be developed in the future but, for the present, degradation based upon the sulphuric-acid-induced bond transposition remains a useful tool in the study of proteins. Improved understanding of the various effects of sulphuric acid on proteins will lead to rational applications of the procedure and facilitate interpretation of the results.

ACKNOWLEDGMENT

The authors are indebted to Mr. J. A. Baignee for determinations of sulphur.

REFERENCES

1. BAPTIST, V. H. and BULL, H. B. J. Am. Chem. Soc. 75: 1727. 1953.
2. BERGMANN, M., BRAND, E., and WEINMANN, F. Z. physiol. Chem. 131: 1. 1923.
3. BLISH, M. J. and SANDSTEDT, R. M. Cereal Chem. 3: 144. 1926.
4. BOISSONNAS, R. A. and PREITNER, G. Helv. Chim. Acta, 36: 875. 1953.
5. DESNUELLE, P. and CASAL, A. Biochim. et Biophys. Acta, 2: 64. 1948.
6. DESNUELLE, P. and BONJOUR, G. Biochim. et Biophys. Acta, 7: 451. 1951.
7. ELLIOTT, D. F. Chemistry & Industry, 86. 1952.
8. ELLIOTT, D. F. Biochem. J. 50: 542. 1952.
9. ELLIOTT, D. F. *In* Ciba symposium on "Chemical structure of proteins". *Edited by* G. E. W. Wolstenholme and M. P. Cameron. J. & A. Churchill Ltd., London. 1953. p. 129.
10. GOODWIN, T. W. and MORTON, R. A. Biochem. J. 40: 628. 1946.
11. HARRIS, M., MEASE, R., and RUTHERFORD, H. J. Research Natl. Bur. Standards, 18: 343. 1937.
12. HESS, W. C. and SULLIVAN, M. X. Arch. Biochem. 5: 165. 1944.
13. HORN, M. J., JONES, D. B., and BLUM, A. E. J. Biol. Chem. 166: 313. 1946.
14. KILLANDER, A. Upsala Läkareförens. Förhandl. 53, (5/6): 283. 1948.
15. KORÓS, Z. Magyar Kém. Folyóirat, 56: 131. 1950.
16. KRISHNASWAMY, T. K. Proc. Indian Acad. Sci. 15: 135. 1942.
17. KUNKEL, H. G. and TISELIUS, A. J. Gen. Physiol. 35: 89. 1951.
18. LAVINE, T. F. and FLOYD, N. F. J. Biol. Chem. 207: 97. 1954.
19. LI, C. H. and ASH, L. J. Biol. Chem. 203: 419. 1953.
20. LUSTIG, B. and KONDRITZER, A. A. Arch. Biochem. 8: 51. 1945.
21. MACPHERSON, H. T. Biochem. J. 40: 470. 1946.
22. MELLON, E. F., KORN, A. H., and HOOVER, S. R. J. Am. Chem. Soc. 75: 1675. 1953.
23. NEISH, A. C. Analytical methods for bacterial fermentations. Report 46-8-3. Natl. Research Council Can., Saskatoon. 1950. p. 32.

24. PORTER, R. R. Methods in medical research. Vol. 3. *Editor-in-Chief* R. W. Gerard. Year Bk. Pubs. Inc., Chicago. 1950. p. 256.
25. RAMACHANDRAN, L. K. and SARMA, P. S. J. Sci. Ind. Research, (India), 10, B: 246. 1951.
26. RAMACHANDRAN, L. K. and SARMA, P. S. J. Sci. Ind. Research, (India), 12, B: 4. 1953.
27. REES, M. W. Biochem. J. 40: 632. 1946.
28. REITZ, H. C., FERREL, R. E., FRAENKEL-CONRAT, H., and OLCOTT, H. S. J. Am. Chem. Soc. 68: 1024. 1946.
29. REITZ, H. C., FERREL, R. E., OLCOTT, H. S., and FRAENKEL-CONRAT, H. J. Am. Chem. Soc. 68: 1031. 1946.
30. RICE, R. G., KELLER, G. J., and KIRSCHNER, J. G. Anal. Chem. 23: 194. 1951.
31. ROSS, A. F. and STANLEY, W. M. J. Gen. Physiol. 22: 165. 1938.
32. SUNDBERG, O. E. and ROYER, G. L. Ind. Eng. Chem. Anal. Ed. 18: 719. 1946.
33. UCHINO, T. J. Biochem. (Japan), 20: 65. 1934.
34. UDENFRIEND, S. and COOPER, J. R. J. Biol. Chem. 196: 227. 1952.
35. WALEY, S. G. Chemistry & Industry, 107. 1953.
36. WELLINGTON, E. F. Can. J. Chem. 30: 581. 1952.
37. WISEBLATT, L., WILSON, L., and MCCONNELL, W. B. Can. J. Chem. 33: 1295. 1955.

THE REACTION OF ACTIVE NITROGEN WITH AZOMETHANE[1]

By D. A. Armstrong[2] and C. A. Winkler

ABSTRACT

The main products of the reaction between active nitrogen and azomethane were hydrogen cyanide and ethane. Traces of methane, ethylene, and acetylene were also formed, together with small amounts of an unstable product. Activation energies of about 0.5 ± 0.4 and 1.9 ± 0.3 kcal. per mole, with corresponding steric factors of 10^{-1} to 10^{-3} and 10^{-2} to 10^{-4}, were estimated for the reactions of active nitrogen with methyl radicals and azomethane respectively, on the assumption that atomic nitrogen is the reactive component of active nitrogen. Azomethane appeared to catalyze the deactivation of active nitrogen.

INTRODUCTION

Free alkyl radicals have been postulated as intermediates in many of the hydrocarbon – active nitrogen reactions studied in this laboratory, and it has been invariably assumed that they were very rapidly destroyed by reaction with active nitrogen. The present study represents an attempt to evaluate experimentally the kinetic characteristics of the methyl radical – active nitrogen reaction.

EXPERIMENTAL

The apparatus and analytical methods have been described in earlier papers (4). Two concentrations of active nitrogen, which differed by a factor of approximately ten, were used. For the higher concentration, molecular nitrogen at a flow rate of 9.75×10^{-5} mole/sec. was admitted to the condensed discharge. The lower concentration was obtained by reducing the flow of nitrogen to 3.53×10^{-6} mole/sec., while the pressure in the system was maintained at the previous value (*ca.* 1.0 mm.) by introducing argon into the discharge tube at a flow rate of 7.28×10^{-5} mole/sec. In two experiments on the hydrogen atom – azomethane reaction, a comparable hydrogen–argon mixture was passed through the discharge tube.

Three samples of azomethane were prepared from dimethylhydrazine by the method of Leitch* (11); these showed identical vapor pressure – temperature relations.

Reaction temperatures were measured with two copper–constantan thermocouples. One of these was situated directly below the hydrocarbon inlet tube in the center of the reaction vessel, while the other was located near the top of the vessel at the active nitrogen inlet.

[1]*Manuscript received July 22, 1955.*
Contribution from the Physical Chemistry Laboratory, McGill University, Montreal, Quebec, with financial assistance from the Consolidated Mining and Smelting Co., Trail, B.C., and the National Research Council of Canada.
[2]*Holder of a National Research Council Studentship, 1953–1954, and a Cominco Fellowship, 1954–1955.*
**The authors are grateful to Dr. L. C. Leitch of the National Research Council, Ottawa, for one sample of azomethane and for some of the dimethylhydrazine. Further supply of the latter was obtained from Brickman and Company of Montreal.*

RESULTS

A preliminary experiment with azomethane mixed with molecular nitrogen in approximately the proportions used in the subsequent studies of the active nitrogen reaction showed no significant thermal decomposition of azomethane under these flow conditions at 400°C. Also no decomposition was observed when argon alone was passed through the discharge tube and allowed to mix with azomethane in the reaction vessel.

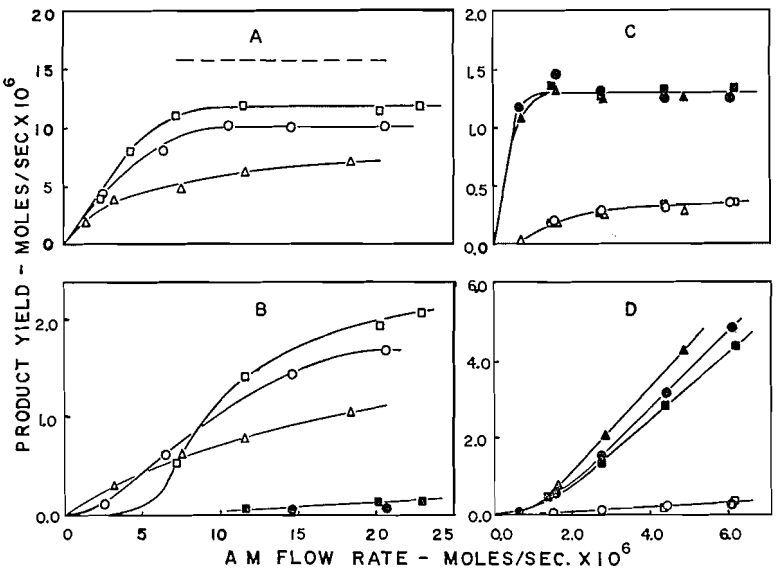

FIG. 1. Relations between flow rate of azomethane and yields of products in the reaction between azomethane and active nitrogen.

A: HCN production at high active nitrogen concentration:

HCN	Temp. (°C.)
□	390
○	160
△	85

B: Production of C_2 hydrocarbons at high active nitrogen concentration:

C_2H_6	C_2H_4	Temp. (°C.)
□	■	390
○	●	160
△		85

C: Production of HCN and C_2 hydrocarbons at low active nitrogen concentration:

HCN	C_2H_6	Temp. (°C.)
■	□	400
●	○	180
▲	△	50

D: Production of the unstable product and azomethane recovery at low active nitrogen concentration:

Recovered AM	Unstable product	Temp. (°C.)
■	□	400
●	○	180
▲		50

The condensable products of the active nitrogen – azomethane reaction consisted mainly of hydrogen cyanide and ethane. Unreacted azomethane was also recovered. A Le Roy still (10) was used to separate the ethane fraction, which was subsequently analyzed with a mass spectrometer.*

The HCN content of the remaining fraction was estimated by absorption in KOH solution and titration with standard $AgNO_3$ solution (9). Unreacted azomethane was obtained by difference. The yields of HCN and C_2 hydrocarbons for three different temperatures, at each of the active nitrogen flow rates used, are shown in Fig. 1A, B, and C.

Analysis of the uncondensed gases from two experiments at the higher active nitrogen flow rate indicated that methane was produced only in small amounts in the azomethane – active nitrogen reaction and that the hydrogen production approximated to the HCN yield.

In all of the active nitrogen – azomethane experiments small amounts of methane and nitrogen (in roughly equal proportions as determined by mass spectrometer analysis of several samples) were evolved when the condensable products were evaporated from one vessel to another, and also during distillation in the Le Roy still. The evolution of these gases in the same proportion was also observed from the products of the two experiments with the hydrogen atom – azomethane reaction. These observations indicate that the formation of an unstable product in the active nitrogen – azomethane reaction is a result of secondary hydrogen atom – azomethane reactions. From the total amounts of methane and nitrogen formed by complete decomposition of the unstable product, it was possible to estimate its yield on the assumption that one molecule of the unstable material decomposed to one molecule of methane and one molecule of nitrogen. The data obtained from such estimates, together with the recovery of azomethane, have been plotted in Fig. 1D as a function of the azomethane flow rate for a number of experiments at the lower active nitrogen flow rate.

No products other than residual azomethane and hydrogen cyanide were detected in significant amounts by mass spectrometric analysis of the final fraction from two experiments at 45° and 177°C. with the lower active nitrogen concentration. The hydrogen cyanide yields calculated from these analyses agreed with those obtained by the chemical method mentioned previously.

At the lower temperatures material balances were within a few per cent of the theoretical. However, at higher temperatures the material balances were between 88 and 100% and some polymer formation was observed.

Experiments with ethylene and propylene at high temperatures and high flow rates, such that consumption of the active nitrogen should be complete (4), indicated a value of about $1.60 \pm 0.10 \times 10^{-5}$ mole/sec. for the higher active nitrogen flow rate (dotted line, Fig. 1A). Similar experiments with ethane and ethylene gave a value of $1.31 \pm 0.06 \times 10^{-6}$ mole/sec. for the lower flow rate.

Apart from the unstable product, the hydrogen atom – azomethane experiments yielded large quantities of ethane and a higher boiling fraction. Material

The authors are indebted to Dr. H. I. Schiff of this department for the mass spectrometer analyses.

balances, calculated on the assumption that the latter fraction was residual azomethane or dimethylhydrazine, were well over 100%, a feature in which the hydrogen atom – azomethane experiments differed from those with active nitrogen.

DISCUSSION

Although evidence has recently been obtained (3) to indicate the presence of more than one reactive species in active nitrogen, the identities of the species have not been established. As in most of the previous studies, therefore, the present results will be discussed on the assumption that atomic nitrogen is the only reactive species involved.

At the lower active nitrogen concentration the hydrogen cyanide production increased rapidly with azomethane flow rate, and attained a constant maximum value which was virtually independent of temperature. The close agreement between this maximum hydrogen cyanide yield and the corresponding yields from ethane and ethylene suggests that the hydrogen cyanide production from azomethane represents the complete consumption of the relatively small amount of active nitrogen available in these experiments.

On the other hand, the hydrogen cyanide production from azomethane at the higher active nitrogen flow rate never approached the value obtained with ethylene and propylene, although the constant yield observed for higher azomethane flow rates would again imply complete consumption of the available active nitrogen at 160° and 400°C.

The apparent loss of active nitrogen in the presence of azomethane might be due to catalyzed recombination of nitrogen atoms with azomethane as a third body; thus:

$$N+N+CH_3{-}N{=}N{-}CH_3 \rightarrow N_2+CH_3{-}N{=}N{-}CH_3{}^*. \qquad [1a]$$

This would be in competition with the reaction:

$$N+CH_3{-}N{=}N{-}CH_3 \rightarrow HCN+N_2+H_2+CH_3 \qquad [1b]$$

which appears to be the most reasonable process for the initial nitrogen atom attack on azomethane.

Both of these reactions are first order in respect of azomethane. A competition between them would thus explain the constant hydrogen cyanide production observed at azomethane flow rates in excess of the critical flow rate. A difference in activation energy would explain the increase in hydrogen cyanide production with temperature. Also, since the recombination reaction is second order in respect of the nitrogen atom concentration, a significant reduction in the concentration of this reactant should favor conversion of the active nitrogen to hydrogen cyanide, and the apparent difference in behavior at high and low active nitrogen concentrations can be explained.

It might be noted parenthetically that if excited or metastable nitrogen molecules, rather than atoms, were the major component of active nitrogen it would be difficult to account for this behavior, which has also been observed with other compounds (1, 2).*

**It is hoped that a general discussion of the behavior may be published shortly.*

Methyl radicals formed in the initial process may react with nitrogen atoms as follows:

$$N+CH_3 \rightarrow HCN+2H \quad [2a]$$

$$\rightarrow HCN+H_2 \quad [2b]$$

$$\rightarrow CN+H_2+H. \quad [2c]$$

Reaction [2*c*] is probably slightly endothermic; moreover if it were extensive, cyanogen might have been expected as a significant product. Although reaction [2*a*] is thermodynamically less favorable than [2*b*], it permits conservation of spin (1), while [2*b*] does not.

Ethane formation presumably occurred by the reaction:

$$CH_3+CH_3+M \rightarrow C_2H_6 \quad [3]$$

which seems to have a negligible activation energy and a steric factor close to unity (12).

Methane, ethylene, and acetylene are all minor products and were probably produced in relatively unimportant processes (for example methane might have been formed in reactions involving hydrogen abstraction by methyl radicals).

From the results of the present investigation and from previous studies of the hydrogen atom – azomethane reaction (5) it would seem that secondary hydrogen atom – azomethane reactions must have been relatively insignificant in the reaction of active nitrogen with azomethane. However, formation of the unstable product implies that a small concentration of atomic hydrogen was present in the system. This may be taken as evidence for the occurrence of reaction [2*a*]. Indeed it is possible to infer from the relative proportions of HCN, C_2H_6, and the unstable product that this reaction largely predominated over reaction [2*b*].

The chain characteristics observed in previous studies of the hydrogen atom – azomethane (5) indicated that hydrogen atom – azomethane complexes might be relatively stable. Since such complexes might decompose to yield methane and nitrogen in roughly equal proportions (and possibly other products which are condensable in liquid nitrogen) they might well be identical with the unstable product recovered in the present investigation.

By making certain simplifying assumptions it is possible to obtain estimates for the activation energies of reactions [1*b*] and [2] from the results of the experiments at the lower active nitrogen concentration where the occurrence of reaction [1*a*] could be neglected.

On the basis of the mechanism already outlined the equations required for these calculations may be formulated as follows:

$$N+AM \xrightarrow{k_1} HCN+H_2+N_2+CH_3 \quad [1b]$$

$$N+CH_3 \xrightarrow{k_2} HCN+2H \text{ (or } H_2) \quad [2]$$

$$CH_3+CH_3 \xrightarrow{k_3} C_2H_6 \quad [3]$$

$$d(\mathrm{HCN})/dt = k_1(\mathrm{AM})(\mathrm{N}) + k_2(\mathrm{Me})(\mathrm{N}) = R_1$$

$$d(\mathrm{Me})/dt = k_1(\mathrm{AM})(\mathrm{N}) - k_2(\mathrm{Me})(\mathrm{N}) - k_3(\mathrm{Me})^2$$

$$d(\mathrm{C_2H_6})/dt = \tfrac{1}{2}k_3(\mathrm{Me})^2 = R_2.$$

The usual steady state approximation for the methyl radical concentration gives:

$$\frac{k_2}{k_3^{\frac{1}{2}}} = \frac{(Q_1 - 2Q_2)}{2^{3/2} \cdot F_n \cdot Q_2^{\frac{1}{2}}} \times \frac{RT}{pV^{\frac{1}{2}}} \times (\text{total molar flow rate}) \qquad [\text{i}]$$

$$\frac{k_1 \cdot k_3^{\frac{1}{2}}}{k_2} = \frac{2^{\frac{1}{2}} \cdot (Q_1 + 2Q_2)}{(Q_1 - 2Q_2)} \times \frac{Q_2^{\frac{1}{2}}}{F_a} \times \frac{RT}{pV^{\frac{1}{2}}} \times (\text{total molar flow rate}) \qquad [\text{ii}]$$

$$k_1 = \frac{(Q_1 + 2Q_2)}{2 \cdot F_n \cdot F_a} \times \left(\frac{RT}{pV^{\frac{1}{2}}}\right)^2 \times (\text{total molar flow rate})^2 \qquad [\text{iii}]$$

F_a and F_n are the flow rates of azomethane and nitrogen atoms in the reaction zone, and Q_1 and Q_2 are the observed rates of production of hydrogen cyanide and ethane respectively.

Calculations were made for the higher azomethane flow rates, where the reaction flame was confined to the upper part of the reaction vessel and the reading of the upper thermocouple could be assumed to indicate the reaction temperature. With the assumption of completely turbulent flow in the reaction zone, F_a and F_n may be assigned steady-state values. As a rough approximation the values of F_a and F_n in the reaction zone were assumed to be equal and independent of temperature. A value of 1.30×10^{-6} mole/sec. (equal to the average hydrogen cyanide production) was therefore taken to represent both F_n and F_a.

The reaction volume V was assumed to remain constant over the temperature range studied and was estimated from the dimensions of the reaction flame to be about 50 cm^3. It was also necessary to assume negligible ethane consumption by the reaction:

$$\mathrm{N} + \mathrm{C_2H_6} \rightarrow \mathrm{HCN} + \mathrm{CH_3} + \mathrm{H_2}.$$

Collision diameters of 3.0, 3.5, and 5.5 Å for nitrogen atoms (4), methyl radicals (6), and azomethane (8) respectively were used in the calculation of the collision numbers and estimation of the steric factors.

The ratios $k_2/k_3^{\frac{1}{2}}$ calculated for the three different temperatures gave a value of 0.5 ± 0.4 kcal. per mole for $E_2 - \frac{1}{2}E_3$ and the ratio $P_2/P_3^{\frac{1}{2}}$ was found to be between 10^{-1} and 10^{-2}. Allowing for the possible decreases in P_3 at low pressures (7) a lower limit of 10^{-3} may be set for P_2. If secondary hydrogen atom – azomethane reactions, which led to the formation of methyl radicals or ethane, were responsible for some of the decomposition of the azomethane, the fraction of hydrogen cyanide formed in the methyl radical – active nitrogen reaction would be greater than indicated and the ratios $k_2/k_3^{\frac{1}{2}}$ and $P_2/P_3^{\frac{1}{2}}$ would be correspondingly greater. The values of the ratios $k_2/k_3^{\frac{1}{2}}$ and $P_2/P_3^{\frac{1}{2}}$ calculated above can thus be regarded as lower limits.

A value of 2.0 ± 0.3 kcal. with a corresponding steric factor between 10^{-2} and 10^{-4} was estimated for E_1 from the values of k_1 calculated by equation [iii] for the three temperatures. Relation [ii], which is independent of F_n, gave a value of 1.4 ± 0.3 kcal. for $E_1-E_2+\frac{1}{2}E_3$. This is consistent with the values of 2.0 ± 0.3 and 0.5 ± 0.4 kcal. per mole calculated for E_1 and $E_2-\frac{1}{2}E_3$ with the other two relations. These calculations indicate that the reaction of nitrogen atoms with azomethane was far more rapid than their reaction with saturated hydrocarbons and comparable in rate with their attack on unsaturated hydrocarbons.

REFERENCES

1. Evans, H. G. V. Ph.D. Thesis, McGill University, Montreal, Quebec. 1955.
2. Forst, W. Ph.D. Thesis, McGill University, Montreal, Quebec. 1955.
3. Freeman, G. R. and Winkler, C. A. J. Phys. Chem. 59: 371. 1955.
4. Greenblatt, J. H. and Winkler, C. A. Can. J. Research, B, 27: 721, 732. 1949.
5. Henkin, H. and Taylor, H. A. J. Chem. Phys. 8: 1. 1940.
6. Hill, T. L. J. Chem. Phys. 17: 503. 1949.
7. Ingold, K. U., Henderson, I. H., and Lossing, F. P. J. Chem. Phys. 21: 2239. 1953.
8. Jones, M. H. and Steacie, E. W. R. J. Chem. Phys. 21: 1019. 1953.
9. Kolthoff, I. M. and Sandell, E. B. Textbook of quantitative inorganic analysis. The MacMillan Co., New York. 1948.
10. Le Roy, D. J. Can. J. Research, 3, 28: 492. 1950.
11. Renaud, R. and Leitch, L. C. Can. J. Chem. 32: 545. 1954.
12. Steacie, E. W. R. Atomic and free radical reactions. 2nd ed. Reinhold Publishing Corporation, New York. 1954.

DISINTEGRATION-RATE DETERMINATION BY 4π-COUNTING

PART III. ABSORPTION AND SCATTERING OF β RADIATION[1]

By B. D. Pate[2] and L. Yaffe

ABSTRACT

The "coincident discharges" in a 4π-counter have been examined and found to be due in the main to gas and wall back-scattering. This can be resolved into two components—scattering near to and far from the source. Curves have been obtained for the back-scattering of β radiation by the source-mounting film and for the absorption of the incident and back-scattered radiation. Back-scattering by the film is shown to be great enough to introduce a large error into the "sandwich" method which is currently in use for correcting for source-mount absorption.

INTRODUCTION

Previous publications in this series (37, 38, 39) have described experimental work aimed at improving the accuracy of absolute counting using a 4π-counter. In this paper additional experimental data are presented, which enable identification to be made of the agency giving rise to the discharges occurring coincidently in both half-counters, and examination to be effected of some of the scattering and absorption processes involved in using a 4π steradian geometrical arrangement.

The penetration of electronic radiation through matter is a complex phenomenon owing to the variety of processes by which interaction may occur (5). With an initially collimated beam of monoenergetic electrons, interaction with a layer of material up to a superficial density of a few hundred μgm./cm.^{2} occurs by means of a few scattering events per electron. This results in the beam spreading without too great an energy or intensity loss. With thicker layers, more scattering events per electron occur and a transition to "multiple scattering" takes place. With still thicker layers the electrons no longer have a preferred direction of motion and the process resembles diffusion. The number of electrons now emerging from the foil decreases with increasing foil thickness, i.e. absorption of the radiation occurs.

The single scattering of electrons has been treated theoretically (2, 33) and the multiple scattering has been treated in an approximate way (4). When the system is further complicated by an uncollimated β radiation with a continuous energy spectrum, a theoretical analysis is very difficult. Consequently the absorption and scattering of β radiation have only been described empirically, principally with counting geometries of less than 2π steradians.

The absorption process, of interest both as a source of error in disintegration-rate measurements and as an energy determination method, has been the subject of a voluminous literature (6, 17, 19, 20, 21, 27, 29, 41, 42). Our knowledge

[1]*Manuscript received July 11, 1955.*
Contribution from the Radiochemistry Laboratory, Department of Chemistry, McGill University, Montreal, Quebec, with financial assistance from the National Research Council of Canada and Atomic Energy of Canada Ltd.
[2]*Holder of a National Research Council Studentship.*

of the back-scattering of β radiation is largely due to experimental work performed in connection with disintegration-rate determinations using $\ll 2\pi$ geometry systems (12, 16, 22, 26, 50, 51).

Absorption measurements in a 4π-counting geometry are of interest for two reasons. First, the effects observed are due to absorption alone, and scattering effects which cause complications like maxima in absorption curves (15, 18, 34, 45) are virtually absent. Secondly, measurements in the absorber thickness range below a few hundred μgm./cm.^{2} (not hitherto reported), particularly with sources with minimal self-absorption, will provide absorption data regarding the lowest energy electrons in the β spectrum. The results given in an earlier paper in this series (39) and those of Suzor and Charpak (47, 48) indicate large absorption effects in this region.

Prior to the present investigation no detailed study of absorption effects in a 4π-counter has been reported. Measurements of the variation of total counter, half-counter, and coincidence counting rates have previously been made(25, 44, 47, 48). However these have all been done at a relatively high source-mount superficial density.

Previous observations of phenomena interpreted as due to back-scattering from a source mount in a 4π-counter have been reported (16, 25, 31). These were large compared with the corresponding effects in $\ll 2\pi$ geometries. The reason for this was attributed by Mann and Seliger (28) to a large contribution in the 4π geometry due to small-angle single-scattering.

"Coincidences in a 4π-counter" may be defined as events where both halves of the counter are discharged within the resolving time of the apparatus by a *single* disintegration. This is, of course, an entirely different phenomenon from that by which resolution losses occur at high counting rates, because the counter is unable to differentiate between *two successive* disintegrations. The "coincidences" obviously do not result in any error in the disintegration-rate determination.

This phenomenon was previously observed by Haxel and Houtermans (24), who ascribed it to conversion electrons emitted simultaneously with the β radiation of Rb^{87}. A fairly comprehensive study by Suzor and Charpak (13, 14, 46, 47, 48) pointed out three possible causes for these coincidences:

(i) Secondary electronic radiation resulting from interaction of the primary beta radiation with the source mount.

(ii) Electrons from the source, in addition to the β particle.

(iii) Very soft gamma radiation from the source.

Smith (44) interpreted his data for S^{35} on the basis of (ii) and (iii). However, Meyer-Schützmeister and Vincent (31) came to the conclusion that, in the case of S^{35} at least, the main cause was back-scattering of radiation by the counter gas and counter walls from one half-counter to the other. They considered that $<0.1\%$ of the effect observed could be attributed to inner bremsstrahlung electrons in the cases of S^{35} and P^{32}. This latter observation agrees with recent experimental work (8, 40) where inner bremsstrahlung electron emission was found to occur very much less frequently than reported by Bruner (11).

The first problem attempted in this paper is the identification of the phenomena leading to coincident discharges. Back-scattering and absorption curves, as observed in a 4π steradian counter geometry, are then obtained.

EXPERIMENTAL AND RESULTS

The counter and most of the associated equipment were the same as described earlier (38). The total counting rate N_T (with the two half-counter anodes connected in parallel) is related to the counting rates above (n_a) and below (n_b) the source mount and to the coincidence rate (n_c) by the relationship

$$N_T = n_a + n_b - n_c. \qquad [1]$$

n_c may be obtained by measuring N_T, and then n_a and n_b separately by disconnecting each anode in turn. n_c is then obtained by subtraction of two large quantities, which gives rise to a large statistical error. Alternatively, as in this work, one may use an electronic coincidence circuit which obtains the result directly.

The two counter anodes were connected to different high voltage supplies. The outputs were fed separately into Atomic Instrument Co. Ltd. 205-B Pre-Amplifiers, Atomic Energy of Canada AEP 1448 non-overloading amplifiers, and Marconi AEP 908 scalers. The output signals of the two amplifiers, taken after discrimination from the output of the multivibrator stage, were fed into an Atomic Energy of Canada AEP 1509 coincidence unit and thence to a third AEP 908 scaler. A block diagram of the equipment appears in Fig. 1.

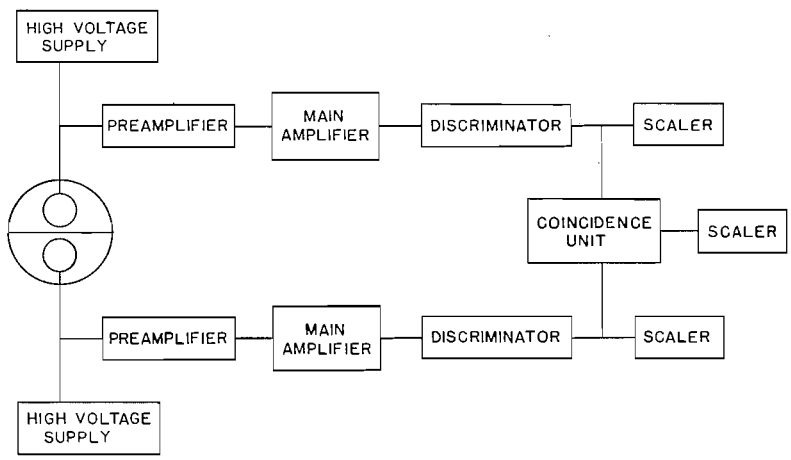

FIG. 1. Block diagram of electronic apparatus for coincidence experiments.

The two systems were shown to be matched using the threshold of the Ni^{63} plateau as a criterion.

The coincidence rates as measured were corrected for random coincidences. The rate at which random coincidences are recorded (N) when unrelated

sources of pulses occurring at rates of n_1 and n_2 are connected to the two inputs of the coincidence circuit is given by

$$N = n_1 n_2 t \quad [2]$$

where t is the effective resolution time of the circuit. The latter was determined to be 10.3 μsec. for a range of values for n_1 and n_2 (supplied by two independent proportional counters) and this value substituted into equation [2] was used to correct all subsequent data for random effects.

A disadvantage of measuring the coincidence rate directly, involving as it does an electrical separation of the two anode systems, is the appearance of positive pulses at the amplifier output, in addition to the usual negative pulses from the electron cascade. The amplitude of these positive pulses is observed to be a function of the diameter of aperture in the diaphragm separating the two half-counters, and of the polarization potential applied to the half-counter opposite to that in which they are produced. They are found to be in coincidence with negative pulses in the other half-counter, and to be nearly independent of the state of polarization of the hemisphere in which they are observed.

All the foregoing is consistent with this effect being due to induction of a positive pulse in one anode by the movement of the electron cascade away from it, towards the other. In normal counter operation, connection of the anodes in parallel eliminates the effect since the small positive pulse merely slightly reduces the amplitude of the negative pulse normally measured. In the coincidence experiments, the positive pulses are amplified but fail to trigger the discriminator circuit and so do not register. However, above 2.6 kv. polarization potential, the negative overshoot following the larger positive pulses begins to be effective in triggering the discriminator, and with the relatively long resolving time in use (10.3 μsec.), spurious coincidence counts are produced. In the experiments to be described below, conditions were always such that these spurious coincidences did not occur. The presence of these induced pulses of opposite sign, however, should always be considered in experiments where two halves of a 4π-counter are used separately.

The experimental results to be presented here fall into two main categories:

(*a*) The coincidence rate n_c was determined as a function of various diaphragm aperture sizes at a suitable polarization potential using β emitters with maximum energies covering the range 67 to 1700 kev. Methane, and argon +10% methane were the two counter filling gases used. In all cases but that of Ni^{63}, the sources were point sources prepared by evaporation of a carrier-free solution. For Ni^{63} the source was prepared as nickel dimethylglyoxime by a vacuum distillation method to be described in a forthcoming publication. Each source was prepared on a gold-coated VYNS film (5–10 μgm./cm.^{2}) which had been mounted over 5 cm. aperture. Measurements of n_a, n_b, n_c were made and N_T computed. A diaphragm with a smaller aperture was then placed over the film, and the measurements were repeated for a series of aperture sizes in this manner. The results of this series are plotted in Figs. 2 and 3. N_T was found to be independent of aperture size.

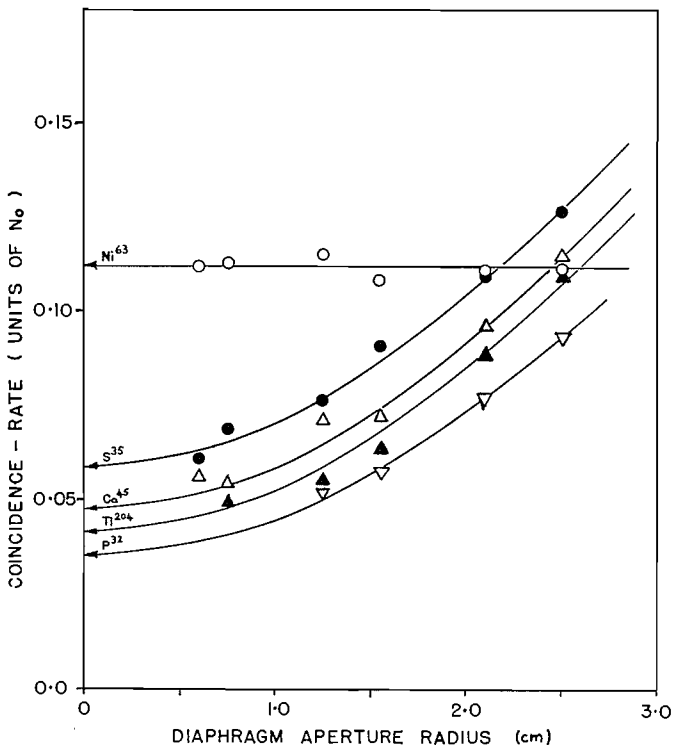

FIG. 2. Coincidence rate as a function of diaphragm aperture radius and beta end-point energy for methane counting gas.

(*b*) n_c, n_a, and n_b were measured for the same series of nuclides plus the α emitter Po^{210} as a function of source-mounting film-thickness with each of the counting gases mentioned. The aperture diameter remained constant at 2.5 cm. The sources were identical to those described previously. The results are shown in Fig. 4. In addition a thick source of Ni^{63} (2.6 mgm./cm.) was prepared. These curves show no features differing from those observed with the thin source, other than the expected additional absorption.

In all experiments at least 1000 coincidence events were recorded, giving a standard deviation of $\pm 3\%$.

In order to check on the operation of the counter with the greater mount thicknesses, the Ni^{63} characteristic was periodically checked. This at no time showed any unexpected features.

DISCUSSION

(*a*) *The Coincident Discharges*

The frequency of occurrence of the coincident discharges (as high as 20% of the disintegration-rate of pure β emitters even with very thin source mounts) allows one to eliminate many of the possible causes of this phenomenon. A low production probability, coupled in the relevant cases with a low counter response to photons, is sufficient to eliminate nuclear gamma radiation,

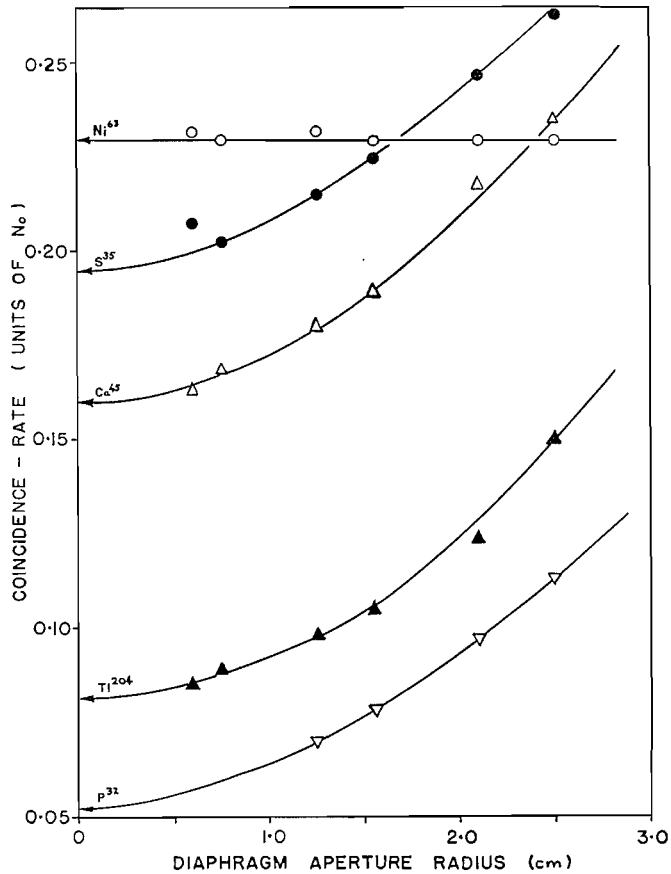

FIG. 3. Coincidence rate as a function of diaphragm aperture radius and beta end-point energy for argon + 10% methane counting gas.

conversion electrons, inner bremsstrahlung, and inner bremsstrahlung electrons (7, 9, 10, 35, 43, 49). Similarly bremsstrahlung production (3, 49) and secondary electron production (32, 33, 36) in the very thin film can be shown to be several orders of magnitude too low. Corresponding processes in the counter gas and walls may also be ruled out owing to absorption in the source-mount diaphragm and unfavorable geometrical conditions.

It appears that the only process of sufficient magnitude which could be responsible for a significant proportion of the coincidence events is back-scattering of radiation by the counter gas and counter walls into the other half-counter. (Back-scattering effects with $\ll 2\pi$ counters, e.g. end-window counters, have been shown to be of the necessary order of magnitude.) The rate of occurrence of coincidences due to scattering close to the source will be independent of the aperture diameter. That due to scattering further away from the source will increase with aperture diameter while that due to scattering at large distances will be proportional to the square of the aperture diameter.

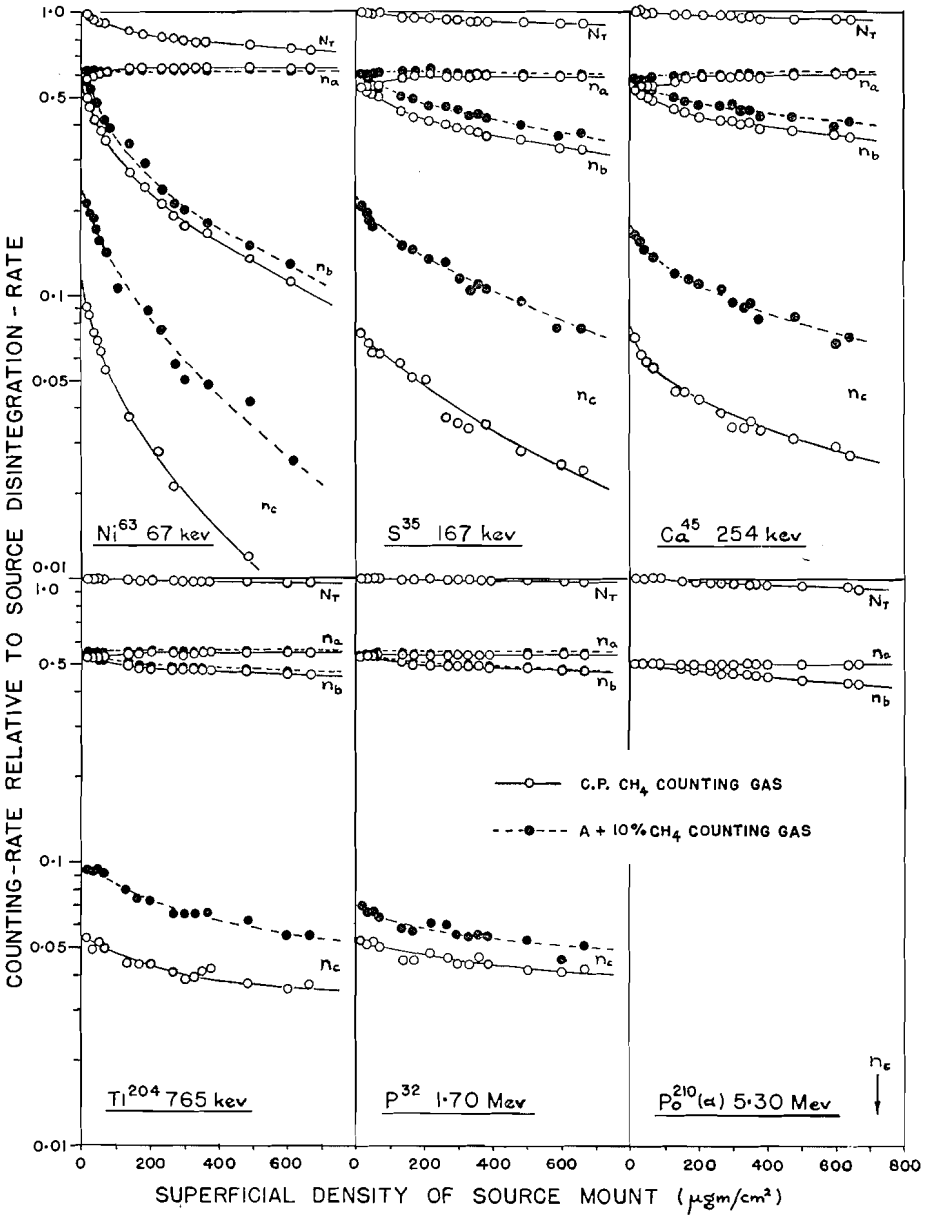

FIG. 4. Total counter, half-counter, and coincidence counting rates as a function of source-mount superficial density for beta emitters of increasing end-point energy and for Po^{210} alpha radiation for methane and argon+10% methane counting gases.

The contribution from either or both of these processes may be obtained from the data in Figs. 2 and 3. If the curves are extrapolated to $r = 0$, that part of the coincidence phenomenon which is independent of r can be separated. In Fig. 5 the values of n_c at $r = 0$ are plotted against the maximum energy of the β emitter. The values obtained for each counter gas lie on a smooth

curve and can be attributed to back-scattering from the gas in the neighborhood of the source. The relative positions of the curves for argon–methane ($\bar{Z} = 16$) and methane ($\bar{Z} = 2$) are consistent with the increased scattering expected (4) and observed by Yaffe and Justus (50) using material of higher atomic number. The form of the curves obtained here is similar to that observed by these authors for back-scattering from a constant thickness back-scatterer as a function of particle energy, if one neglects the fall-off they observed at very low energies. (This fall-off is undoubtedly due to preferential absorption of the back-scattered radiation in the counter window.)

The value of n_c for Ni^{63} is independent of aperture size as shown in Figs. 2 and 3. This is to be expected owing to the soft nature of this β radiation. An appreciable scattering will occur close to the source. Any other radiation will be absorbed by the counter gas.

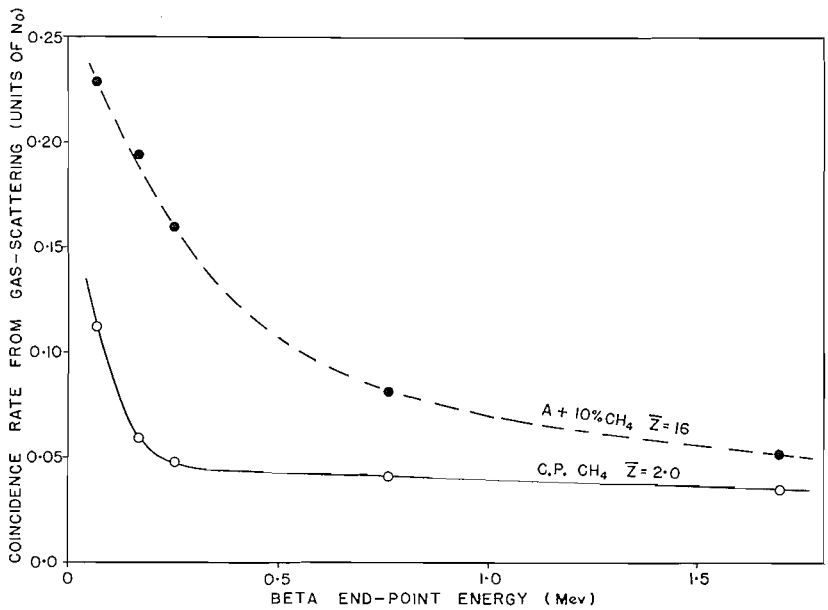

FIG. 5. Coincidence rate due to gas-scattering near the source, as a function of beta end-point energy for methane and argon+10% methane counting gases.

Measurements of Po^{210} α particles, as shown in Fig. 4, give values for n_c of less than 0.1% of the disintegration rate. This agrees with the foregoing interpretation since α radiation, for which the diffusion mechanism does not occur, can only back-scatter by large-angle single or plural scattering events, which are highly improbable. This value of 0.1% also serves as an upper limit enabling one to confirm that many of the processes suggested by other workers, e.g. secondary electron production by interaction with the source mount, are unimportant in this case.

Our conclusions regarding the origin of the coincidence phenomena agree with those of Hawkings (23), who studied the variation of coincidence rate with counting gas pressure using a S^{35} source.

(b) Absorption and Scattering of β Radiation by the Source-mounting Film

The curves shown in Fig. 4 can be resolved into the appropriate absorption and scattering components using methods somewhat similar to those used previously in calculations of this type (28, 44). Our treatment will however consider these components as functions of β particle energy and film thickness. One can assume a response probability of the counter of unity towards electrons and can neglect all processes involving the production of secondary electronic radiation as before. The relevant processes are absorption and elastic scattering in the source-mount film and back-scattering of electrons by the electron diffusion process near and far from the source.

During this part of the experiment the aperture diameter of the diaphragm between the two half-counters remained constant at 2.5 cm. If E is the maximum energy of the β radiation and d the film thickness, one can let

$p_1(E, d)$ = transmission of the film to the incident β radiation from the source,

$p_2(E, d)$ = the probability that β radiation originally emitted into the 2π steradian solid angle towards hemisphere A will be scattered by the film so as to enter the other hemisphere B,

$p_3(E)$ = the probability that the β radiation incident into either hemisphere is back-scattered by the counter gas at a distance small compared to the aperture diameter so as to enter the other hemisphere (one can neglect the small energy degradation by the film),

$p_4(E)$ = the probability that the β radiation incident into either hemisphere is back-scattered by the counter gas and/or counter walls at a distance comparable to or greater than the aperture diameter so as to enter the other hemisphere,

$p_5(E, d)$ = the transmission of the film to the back-scattered radiation arising from processes 3 and 4.

Other second-order effects may justifiably be neglected, e.g. wall scattering of back-scattered particles.

Using the above probabilities, the following expressions for the half-counter and coincidence counter rates are obtained where N_0 is the disintegration rate of the sample.

[3] $$n_a = \tfrac{1}{2}N_0[(1+p_2) + p_1 p_3 p_5 + p_1 p_4 p_5]$$

(incident + film scattering; near gas back-scattering from other hemisphere; far gas and wall back-scattering from other hemisphere)

[4] $$n_b = \tfrac{1}{2}N_0[(1-p_2)p_1+p_3 p_5+p_4 p_5]$$

[5] $$n_c = \tfrac{1}{2}N_0[p_3 p_5+p_1 p_3 p_5+p_1 p_4 p_5+p_4 p_5].$$

At $d = 0$, $p_5 = p_1 = 1$, and $p_2 = 0$,

$$n_{a_0} = n_{b_0} = \tfrac{1}{2}N_0[1+p_3+p_4],$$

and $$n_{c_0} = N_0[p_3+p_4].$$

Also $$N_T = n_a+n_b-n_c = \tfrac{1}{2}N_0[1+p_2+(1-p_2)p_1],$$

and at $d = 0$ $$N_T = N_0.$$

This agrees with the expectation that N_T will be independent of the factors governing the magnitude of the coincidence rate and differs from N_0 only owing to absorption in the film of that part of the radiation which escapes back-scattering. The values of n_a, n_b, and n_c can be obtained from Fig. 4. p_3 and p_4 are taken from Figs. 5 and 2 respectively. The unknown quantities p_1, p_2, and p_5 are obtained by substituting a series of values of E and d in equations [3], [4], and [5], and solving them simultaneously. The results are shown in Figs. 6 and 7.

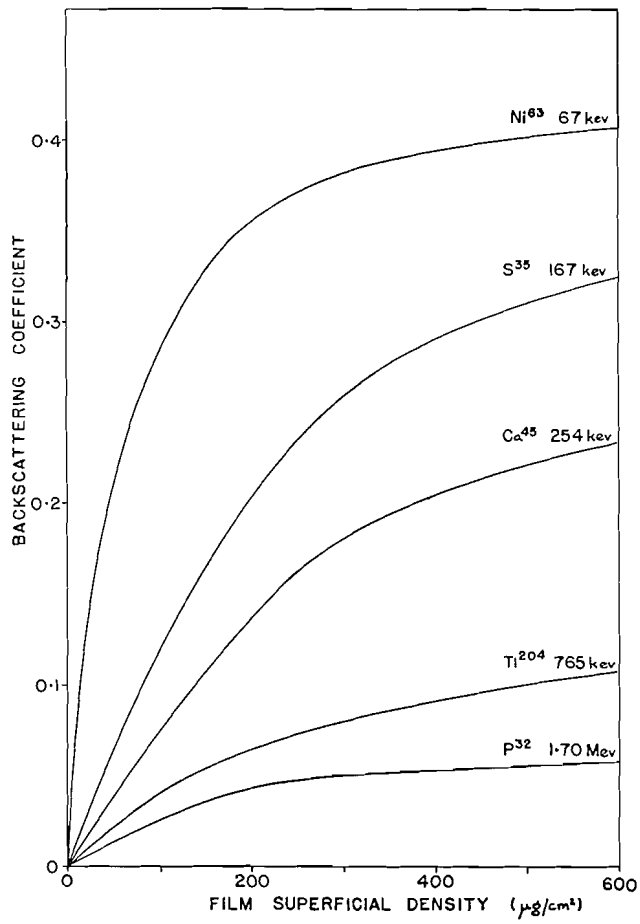

FIG. 6. Source-mount back-scattering coefficient (p_2) as a function of film superficial density for beta emitters of increasing end-point energy.

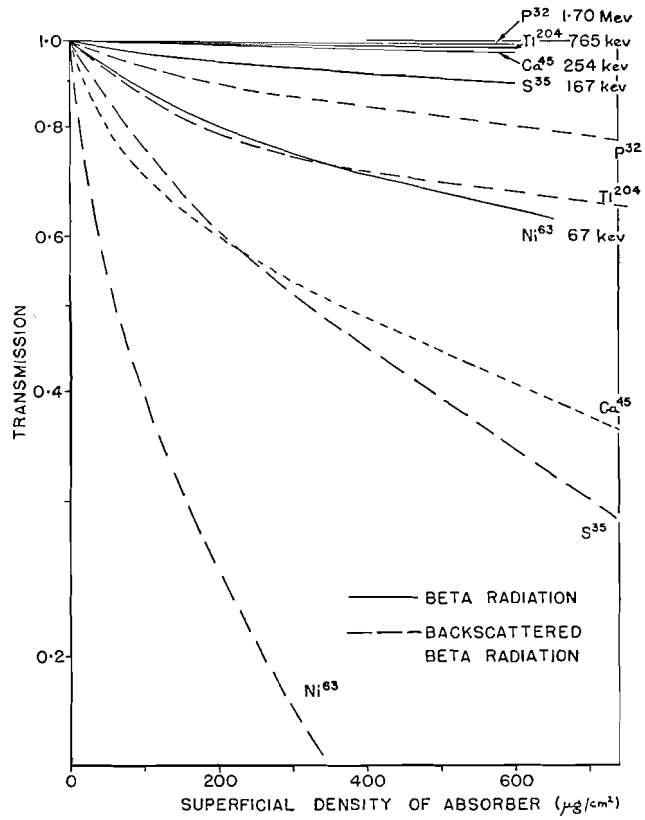

FIG. 7. Transmission of source mount to incident beta radiation (p_1) and to back-scattered beta radiation (p_5) as a function of film superficial density for beta emitters of increasing end-point energy.

Back-scattering of β Radiation from Thin Films

The curves of p_2, the film back-scattering coefficient, bear a superficial resemblance to the results of previous work using $\ll 2\pi$ counter systems. The magnitude of the effect observed here is much larger at low film thicknesses in agreement with the previous observations by other workers (14, 47, 48), who used much thicker films than we did. In contradistinction to the $<2\pi$ systems, back-scattering at a given mount thickness was found to be greatest for the lowest energy β emitter. This is consistent with the suggestion that the scattering effects observed here are due to single scattering events involving electrons incident at small angles to the film, rather than to the electron diffusion type of back-scattering. The Rutherford-type scattering of relativistic electrons by atoms, described for example by McKinley and Feshbach (30), will occur predominantly at very small angles, will fall off rapidly as the scattering angle increases, and will be greatest for small electron energies.

Absorption of Incident and Back-scattered Radiation

In Fig. 7 the absorption curves for the incident and the back-scattered β radiation are compared. The energy degradation of the back-scattered radi-

ation is found to be much greater than that observed in the $\ll 2\pi$ system. In the latter case a ratio of 0.4–0.8 for the ratio of half-thicknesses or ranges of the back-scattered to the incident radiation is found. In this work, for Ni^{63} for example, we find a half-thickness ratio of about 0.05. Our results, in agreement with those of Balfour (1), clearly indicate the existence of a large proportion of very low energy particles in the spectrum of the back-scattered radiation. This is observable because of the "windowless" nature of the counter.

(c) "Sandwich" Procedure for Correcting for Source-mount Absorption Losses

It was shown in an earlier publication (39) that the correction for source-mount absorption losses by the "sandwich" method leads to erroneous values being obtained for the source disintegration rate. Mann and Seliger (28) formulated the following expression for the fractional absorption τ in a film,

$$\frac{\tau}{2} = \frac{N_T - N_S}{2N_T - N_S},$$

where N_T and N_S are the counting rates observed for a source mounted on one film and in a "sandwich" respectively.

By inspection, using nomenclature as defined above, $N_S = N_0 . p_1$ and

$$\frac{\tau}{2} = \frac{(1-p_1)(1+p_2)}{2(1+p_2-p_1p_2)}.$$

If one assumes as Mann and Seliger have done that p_2, the back-scattering by the film, is negligible, then τ would equal $(1-p_1)$, the film absorption as expressed in our nomenclature. However one can see from Fig. 6 that p_2 cannot be neglected without introducing a fairly large error. Mann and Seliger assumed also that

$$N_T = N_0 - \tfrac{1}{2} N_0 . \tau,$$

i.e. that half the emitted radiation entered the film and a fraction of this would be absorbed. However this half is reduced by the back-scattered portion. This introduces an error in the opposite direction. Despite this fortuitous cancellation of errors, the "sandwich" process can only be considered as an approximation in disintegration-rate determinations.

ACKNOWLEDGMENTS

The authors wish to thank the National Research Council of Canada and Atomic Energy of Canada Ltd. for grants-in-aid. We would also like to express our appreciation to Dr. R. E. Bell for valuable discussions during the preparation of this manuscript. One of us (B. D. P.) wishes to thank N.R.C. for assistance in the form of a studentship.

REFERENCES

1. Balfour, J. G. J. Sci. Instr. 31: 395. 1954.
2. Bethe, H. Ann. Physik, 5: 325. 1930.
3. Bethe, H. and Heitler, W. Proc. Roy. Soc. (London), A, 146: 83. 1934.
4. Bethe, H. A., Rose, M. E., and Smith, L. P. Proc. Am. Phil. Soc. 78: 573. 1938.
5. Bethe, H. A. and Ashkin, J. *In* Experimental nuclear physics. *Edited by* E. Segrè. Vol. I. Section II. John Wiley & Sons, Inc., New York. 1953.

6. BLEULER, E. and ZÜNTI, W. Helv. Phys. Acta, 19: 375. 1946.
7. BLOCH, F. Phys. Rev. 50: 272. 1936.
8. BLUE, J. W. and BLEULER, E. Bull. Am. Phys. Soc. 30: 59. 1955.
9. BOLGIANO, P., MADANSKY, L., and RASETTI, F. Phys. Rev. 89: 679. 1953.
10. BRADT, H., GUGELOT, P. G., HUBER, O., MEDICUS, H., PREISWERK, P., and SCHERRER, P. Helv. Phys. Acta, 19: 77. 1946.
11. BRUNER, J. A. Phys. Rev. 84: 282. 1951.
12. BURTT, B. P. Nucleonics, 5 (No. 2): 28. 1949. Conference on absolute β counting. Preliminary Rept. No. 8. Nuclear Sci. Ser. N.R.C., Washington, D.C. 1950. p. 1.
13. CHARPAK, G. and SUZOR, F. Compt. rend. 231: 1471. 1950.
14. CHARPAK, G. and SUZOR, F. Compt. rend. 232: 322. 1951.
15. COLLIE, C. H., SHAW, P. F. D., and GALE, H. J. Proc. Phys. Soc. 63, A: 282. 1950.
16. Conference on Absolute β Counting. Preliminary Rept. No. 8. Nuclear Sci. Ser. N.R.C., Washington, D.C. 1950.
17. FEATHER, N. Proc. Cambridge Phil. Soc. 34: 599. 1938.
18. FEATHER, N. British Atomic Energy Rept. B.R. 504. 1944.
19. FLAMMERSFELD, A. Z. Naturforsch. 2, A: 370. 1947.
20. GLENDENIN, L. E. and CORYELL, C. D. U.S. Atomic Energy Commission Rept. M.D.D.C. 19. 1946.
21. GLENDENIN, L. E. Nucleonics, 2(No. 1): 12. 1948.
22. GLENDENIN, L. E. and SOLOMON, A. K. Science, 112: 623. 1950.
23. HAWKINGS, R. C. Private communication.
24. HAXEL, O. and HOUTERMANS, F. G. Z. Physik, 124: 705. 1948.
25. HOUTERMANS, F. G., MEYER-SCHÜTZMEISTER, L., and VINCENT, D. H. Z. Physik, 134: 1. 1952.
26. KOVARIK, A. F. Phil. Mag. 20: 849. 1910.
27. LIBBY, W. F. Anal. Chem. 19: 2. 1947.
28. MANN, W. B. and SELIGER, H. H. J. Research Natl. Bur. Standards, 50: 197. 1953.
29. MARSHALL, J. S. and WARD, A. G. Can. J. Research, A, 15: 39. 1937.
30. MCKINLEY, W. A., JR. and FESHBACH, H. Phys. Rev. 74: 1759. 1948.
31. MEYER-SCHÜTZMESITER, L. and VINCENT, D. H. Z. Physik, 134: 9. 1952.
32. MØLLER, C. Ann. Physik, 14: 531. 1932.
33. MOTT, N. F. Proc. Roy. Soc. (London), A, 126: 259. 1930.
34. NOVEY, T. B. and ELLIOTT, N. Natl. Nuclear Energy Ser. Div. IV. Vol. 9. Paper 3. McGraw-Hill Book Co. Inc., New York and London. 1949.
35. NOVEY, T. B. Phys. Rev. 89: 672. 1953.
36. PAGE, L. A. Phys. Rev. 81: 1062. 1951.
37. PATE, B. D. and YAFFE, L. Can. J. Chem. 33: 15. 1955.
38. PATE, B. D. and YAFFE, L. Can. J. Chem. 33: 610. 1955.
39. PATE, B. D. and YAFFE, L. Can. J. Chem. 33: 929. 1955.
40. RUBINSON, W. Private communication.
41. RUTHERFORD, E., CHADWICK, J., and ELLIS, C. D. *In* Radiations from radioactive substances. Cambridge University Press, London. 1930.
42. SARGENT, B. W. Can. J. Research, A, 17: 82. 1939.
43. SAUTER, F. Ann. Physik, 20: 404. 1934.
44. SMITH, D. B. British Atomic Energy Rept. A.E.R.E. I/R 1210. 1953.
45. SOLOMON, A. K., GOULD, R. G., and ANFINSEN, C. B. Phys. Rev. 72: 1097. 1947.
46. SUZOR, F. and CHARPAK, G. Compt. rend. 232: 720. 1951.
47. SUZOR, F. and CHARPAK, G. Compt. rend. 234: 720. 1952.
48. SUZOR, F. and CHARPAK, G. J. phys. radium, 13: 1. 1952.
49. WU, C. S. Phys. Rev. 59: 481. 1941.
50. YAFFE, L. and JUSTUS, K. M. J. Chem. Soc. Suppl. S. 341. 1949.
51. ZUMWALT, L. R. U.S. Atomic Energy Commission Rept. M.D.D.C. 1346. 1949.

A DIELECTRIC STUDY OF PLASTICIZED POLYVINYLIDENE CHLORIDE[1]

By B. L. Funt and T. H. Sutherland[2]

ABSTRACT

The electrical response of plasticized polyvinylidene chloride has been studied over a wide range of frequency, temperature, and plasticizer content. The dispersion region was shifted to lower temperatures at a given frequency on the addition of alpha chloronaphthalene as plasticizer, but remained practically unchanged with hexachlorobenzene as plasticizer. Comparison was made with mechanical measurements for plasticized vinylidene chloride copolymers and reasonable agreement between electrical and mechanical properties was found. Enthalpies and entropies for dielectric relaxation were calculated on the theory of absolute reaction rates and were compared with values for plasticized polyvinyl chloride. A calculation of plasticizer efficiency from electrical measurements was attempted on the basis of a method suggested by Dyson. An interesting empirical relationship between enthalpy and entropy of activation and plasticizer content in polyvinyl chloride and polyvinylidene chloride is presented.

Previous studies of the electrical response of plasticized polymers have contributed to the elucidation of the mechanism of interaction between a polar polymer and a plasticizer. In general the presence of a plasticizer serves to decrease the attractive forces between neighboring polymer chains and results in a softer and more pliable material. In a polar polymer, this increased freedom of molecular movement will be evident in a corresponding increase in the ability of polar groups to respond to an applied alternating electric field. The ease with which dipoles follow the impressed field can be measured by the characteristic Debye dispersion curves at a given temperature. Where a strong intermolecular attraction exists dielectric dispersion will occur at a relatively low frequency at which a sigmoidal change of dielectric constant with frequency and the appearance of a loss factor maximum will be exhibited. On the addition of plasticizer the dispersion region shifts to higher frequencies indicating a lower internal viscosity and a greater freedom of chain movement.

While the general features of plasticizer action and their investigation by dielectric methods were established by Fuoss (7, 8, 9, 10, 11, 12, 13, 14, 17) there has been considerable latitude in the quantitative interpretation of the data. Attempts have been made to relate plasticizer efficiency to size, shape, and polarity of the plasticizer molecule and to correlate electrical and mechanical properties (19). Although a relatively large number of investigations have been reported almost all of them have been confined to the study of plasticized polyvinyl chloride (2, 3, 4, 5, 6, 7, 8, 9, 10, 11, 12, 13, 14, 17). Consequently the validity and generality of many of the theoretical comparisons have rested on the experimental confirmation found with this polymer.

It therefore appeared advisable to initiate experimental work with other similar polar plasticized polymers in order to test some of the current views

[1]*Manuscript received June 23, 1955.*
Contribution from the Department of Chemistry, University of Manitoba, Winnipeg, Manitoba. Presented in part before the sixth Canadian High Polymer Forum, April, 1955.
[2]*Present address: Department of Chemistry, Royal Military College, Kingston, Ontario.*

of the dielectric interpretation of plasticizer action. Vinylidene chloride was selected for its chemical similarity to vinyl chloride.

APPARATUS

The electrical apparatus has been described previously (6, 18). In the current work a General Radio precision sample holder was used. The side plates were removed from the holder in order to permit its being thermostatted in an air thermostat maintained to ±0.05°C. A thermocouple was inserted in the housing of the sample holder to provide a further check of the sample temperature.

CHEMICALS

Polyvinylidene chloride (Saran A) of weight average molecular weight 10,000 and 100,000 was provided through the courtesy of the Dow Chemical Company.

Alpha chloronaphthalene, Eastman, reagent grade, was used as obtained. The lead stearate used was Wittco No. 10, and was not purified further.

The samples were prepared by treating the pulverized polymer in a 70:30 mixture of benzene and 2-butanone to which the plasticizer was added. After refluxing for four to five hours the samples were dried *in vacuo* for 24 hr. and then pressed into thin disks at a temperature of 135–165°C. and a pressure of 5000 lb./in^2.

After cooling, the samples were coated with aquadag and then placed into the sample holder.

RESULTS

The dielectric constant and loss factor of each sample was measured at frequencies of 50, 100, 300, 1000, 3000, 10,000, 30,000, and 100,000 cycles per second at temperature intervals of 5°C. throughout the dispersion range. The data are shown graphically in Figs. 1 to 6 for concentrations of 0 to 24.8% alpha chloronaphthalene plasticizer by weight.

The addition of a good plasticizer progressively decreases the temperature at which dispersion occurs at a given frequency. For instance, the maximum of the loss factor curve (f_{max}) changes by 35°C. from the unplasticized to the most plasticized sample at 3 kc. A plot of log f_{max} versus reciprocal temperature is expected to yield a straight line whose slope determines ΔH^*, the free enthalpy of activation. Such plots are shown in Fig. 7 for the data obtained at 3 kc. with alpha chloronaphthalene. Pronounced curvature is shown, particularly if the 100 kc. points are included. For the data in Table I the slopes were determined by the method of least squares, and weighting factors were used to compensate for the lower precision at the extremes of frequency. The relative weighting factors at each frequency were 50 c.p.s. (3), 100 c.p.s. (3), 300 c.p.s. (4), 1 kc. (4), 3 kc. (4), 10 kc. (4), 30 kc. (3), and 100 kc. (1). The curvature shown in the plots for activation energy is not new; a similar phenomenon is shown in Dyson's data for polyvinyl chloride (3).

The free energies, enthalpies, and entropies for dielectric relaxation were calculated by the method described by Kauzmann (16) and are also tabulated in Table I.

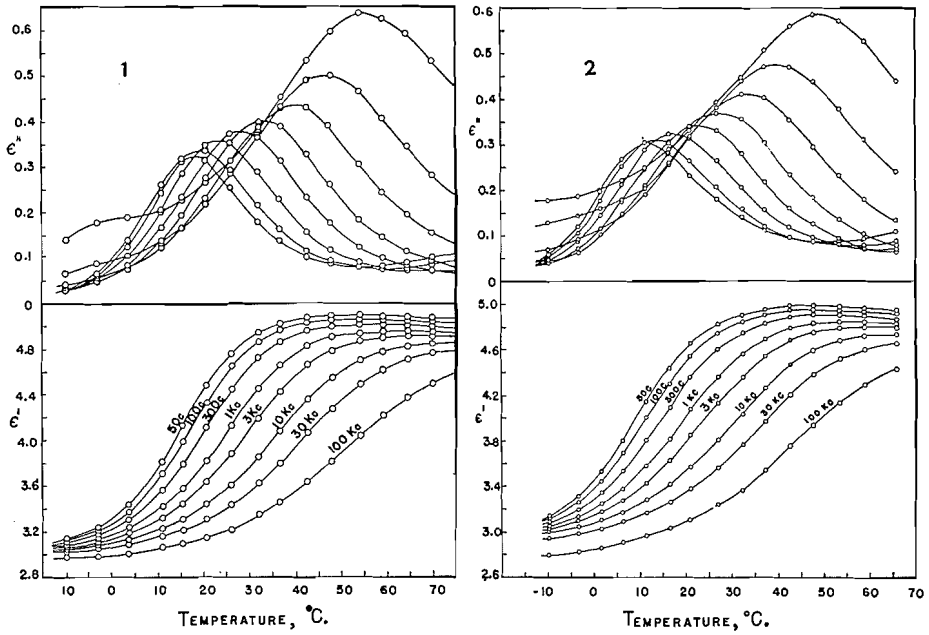

FIG. 1. Dielectric dispersion in polyvinylidene chloride of molecular weight 10,000 stabilized with 1% by weight of lead stearate.

FIG. 2. Dielectric dispersion in polyvinylidene chloride of molecular weight 10,000 containing 3.1% by weight alpha chloronaphthalene and 1% lead stearate.

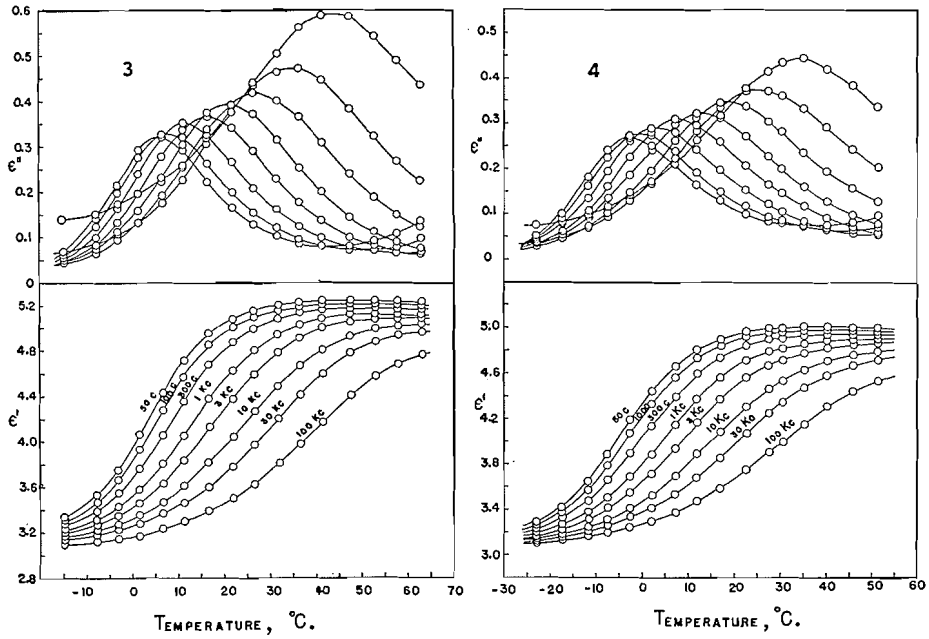

FIG. 3. Dielectric dispersion in polyvinylidene chloride of molecular weight 10,000 containing 6.0% by weight alpha chloronaphthalene and 1% lead stearate.

FIG. 4. Dielectric dispersion in polyvinylidene chloride of molecular weight 10,000 containing 10.1% by weight alpha chloronaphthalene and 1% lead stearate.

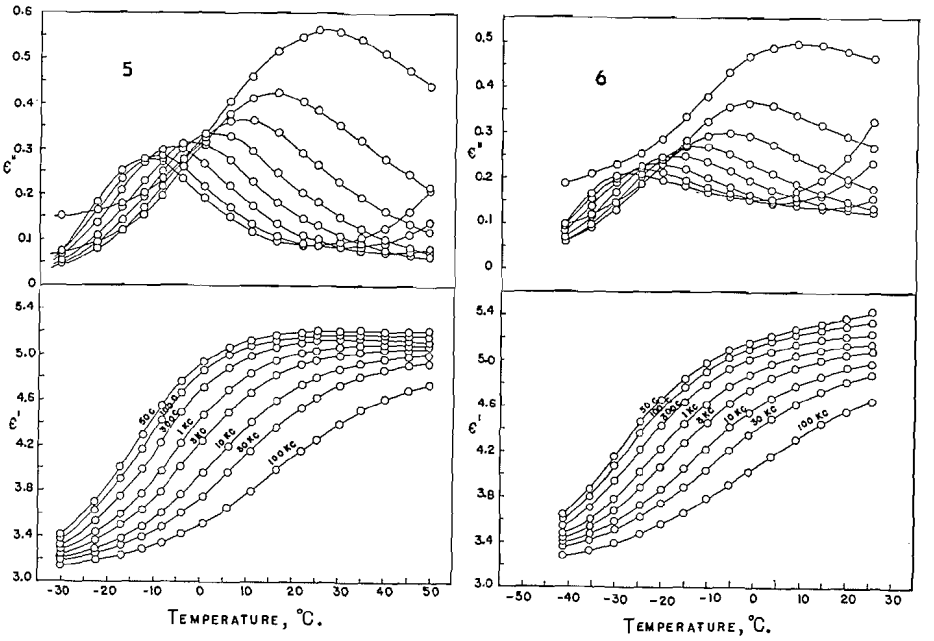

FIG. 5. Dielectric dispersion in polyvinylidene chloride of molecular weight 10,000 containing 15.1% by weight alpha chloronaphthalene and 1% lead stearate.

FIG. 6. Dielectric dispersion in polyvinylidene chloride of molecular weight 10,000 containing 24.8% by weight alpha chloronaphthalene and 1% lead stearate.

TABLE I

ENTHALPIES ΔH^*, ENTROPIES ΔS^*, AND CHARACTERISTIC TEMPERATURES (T_z) FOR SYSTEMS INVESTIGATED, AS FUNCTIONS OF POLYMER AND PLASTICIZER CONCENTRATION

Sample	ΔH^* (kcal.)	ΔS^* (e. u.)	Mole fraction polymer	Weight % polymer	Density (gm./cc.)	T_z (°C.)
Hexachlorobenzene						
B $\frac{1}{2}$	42.55	100.2	99.5	98.0	1.741	268.1
B1 $\frac{1}{2}$	39.53	91.8	98.2	94.6	1.736	263.0
B2 $\frac{1}{2}$	41.29	96.6	96.9	91.1	1.762	266.2
B3 $\frac{1}{2}$	40.56	94.1	95.2	86.7	1.781	265.8
B4 $\frac{1}{2}$	41.20	96.5	92.0	79.2	1.812	265.7
B5	40.46	93.8	89.6	74.3	1.804	265.5
B6	40.97	96.3	74.4	49.5	1.886	264.6
B7	41.41	96.7	46.2	24.8	1.933	266.7
Alpha chloronaphthalene						
C1	39.56	92.2	97.6	95.9	1.752	262.5
C2	37.76	88.7	95.8	93.0	1.702	256.5
C3	36.12	86.9	93.3	89.0	1.697	248.5
C4	34.21	84.5	89.9	84.0	1.678	239.5
C5	29.94	76.0	82.8	73.9	1.635	223.1
Unplasticized polymers						
P	40.08	91.2	99.5	99.0	1.751	267.6
S-1	40.75	90.0	100.0	100	1.736	272.6
S-2	41.93	93.7	100.0	100	1.732	275.3
T	38.45	83.9	100.0	100	1.290	269.8

The data of Table I can be compared with similar data obtained from dielectric investigations of other polymer systems, and for plasticized polyvinyl chloride. For a given comparison the relative magnitudes of the enthalpies and entropies of activation are significant, and reflect freedom of movement of segments of the polymer chains.

It can be seen from Table I that for alpha chloronaphthalene, which is a relatively good plasticizer for polyvinylidene chloride, the dispersion region is shifted to lower temperatures with increasing plasticizer content. The enthalpy and entropy values are also lowered corresponding to increased freedom of segmental motion in the polymer chains. With hexachlorobenzene, however, the effect of plasticizer is very slight, the temperature range of the dispersion region remains unchanged, and the enthalpy and entropy values remain relatively constant even at plasticizer concentrations of 75% by weight. One must conclude that true plasticization is not occurring in this instance, and that a macro dispersion of plasticizer in polymer is being obtained.

The results with different unplasticized polymers are also shown in Table I. Polymer S-1 was a Dow Chemical Co. sample of weight average molecular weight 10,000 and S-2 was a similar sample of molecular weight 100,000. Sample P was obtained from S-1 on the addition of 1% by weight of lead stearate as a thermal stabilizer. Sample T was obtained by emulsion polymerization of vinylidene chloride under nitrogen at 25°C. using a persulphate activator, and was not fractionated.

The results obtained with these materials confirm the slight dependence of the position of the dispersion region on molecular weight. This is doubtless due to the segmental nature of the electrical response (16).

The mechanical properties of a vinylidene chloride 85% – vinyl chloride 15% copolymer have been reported by Havens (15). These data can be compared with the electrical results obtained in the present work. For this purpose we define temperature T_x obtained by extrapolation of the electrical data to a relaxation time τ of one second, where the relaxation time is defined as 2π times frequency of maximum absorption. The relaxation time of one second is comparable to that of a mechanical test, and is usually chosen where a comparison of electrical and mechanical properties is desired.

In Fig. 7 the flex temperatures determined by Havens and T_x values obtained in this work are plotted against plasticizer content for comparison. It is evident that quite good agreement is obtained.

A most detailed interpretation of data on plasticized polymers has been attempted by Dyson (3). If a typical relaxation mechanism involves n monomer units, then the enthalpy of activation, ΔH^*, is nM calories per mole where M is the attractive energy between two chains per monomer length. For vinylidene chloride M has been reported as 1890 cal. per unit (1). If there are r alternative configurations available in the excited state the n monomer units will have r^n configurations available and the entropy of activation can be expressed as

$$S^* = R \ln r^n$$

where R is the gas law constant.

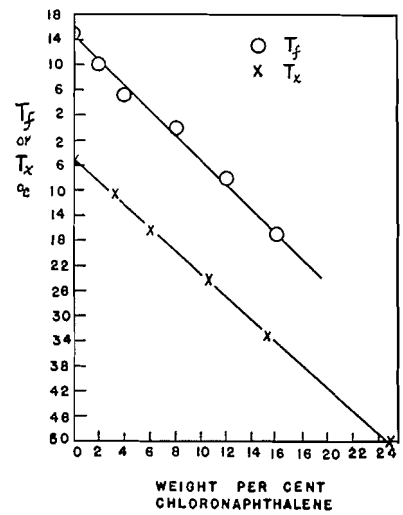

FIG. 7. Comparison of mechanical and electrical data.

Dyson has further elaborated his argument to include plasticized systems. He suggests that a plot of $1/\Delta H^*$ against volume fraction plasticizer should yield a straight line whose slope could be interpreted to indicate the tendency for plasticizer molecules to 'cluster'. The present data (and some of the data on polyvinyl chloride) do not yield a good linear relationship. Nevertheless the slope of the best line was taken and using the appropriate data a value for q of 6 was obtained for alpha chloronaphthalene, and a value approaching infinity for hexachlorobenzene. The significance of q on this picture is that it represents the number of plasticizer molecules in a cluster. One would interpret a large value of q as indicative of poor plasticizer action and a low value as giving high plasticizer efficiency. Corresponding values for polyvinyl chloride are 4.4 and 2.3 with tricresyl phosphate, 4.8 with diphenyl, and 1.7 with dioctyl phthalate, according to Dyson. These latter values would be reduced by the factor 1040/1520 if Bunn's recent values for cohesive energy (1) are used instead of those adopted by Dyson.

An interesting empirical relationship between plasticizer content and enthalpy and entropy of activation was discovered. It was found that on a logarithmic plot of enthalpy of activation against mole per cent polymer the data for all good plasticizers for a given polymer were found to fall on the same straight line. This is shown in Fig. 8 where the data of Fuoss for tetralin and diphenyl and of Daniels, Miller, and Busse for tricresyl phosphate as recalculated by Dyson (3), and of Fitzgerald and Miller (5) for dimethyl thianthrene plasticizers in polyvinyl chloride are shown. It should be noted that Dyson's treatment of enthalpy data yields different slopes for different plasticizers. The present empirical relationship shows agreement for all good plasticizers in a given polymer. Our data for polyvinylidene chloride plasticized with alpha chloronaphthalene are shown in Fig. 9. Again the agreement with a

linear relationship is reasonable, but the slope of the line is different for this polymer than for polyvinyl chloride.

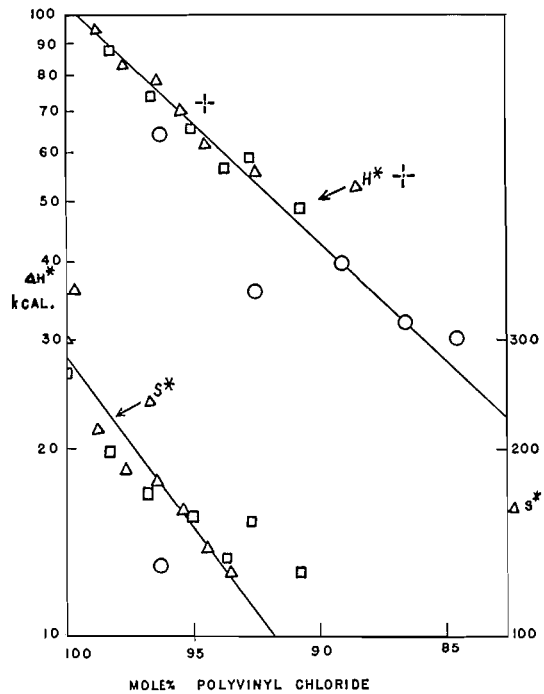

FIG. 8. Enthalpy and entropy of plasticized polyvinyl chloride as a function of polymer content. Plasticizer: tetralin (O), diphenyl (Δ), tricresyl phosphate (□), dimethyl thianthrene (+).

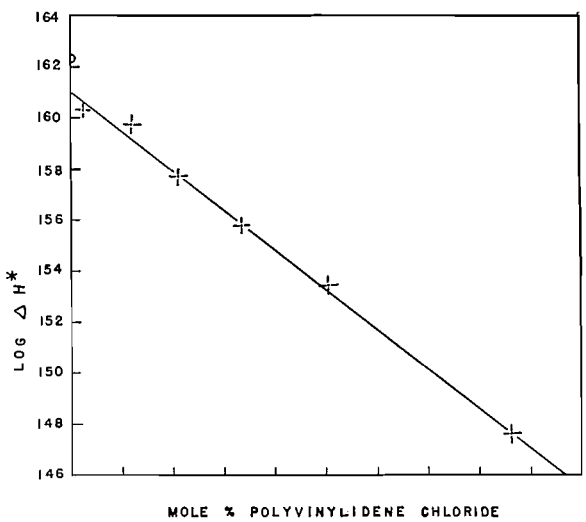

FIG. 9. Enthalpy of polyvinylidene chloride plasticized with alpha chloronaphthalene as a function of mole per cent polymer.

ACKNOWLEDGMENTS

The authors are indebted to the National Research Council of Canada for a grant in aid of this work and for scholarship aid to one of us (T. H. S.). The courtesy of the Dow Chemical Company in supplying samples is also gratefully acknowledged.

REFERENCES

1. BUNN, C. W. J. Polymer Sci. 16: 323. 1955.
2. DANNIS, M. L., NIELSEN, L. E., BUCHDAHL, R., and LEVREAULT, R. J. Appl. Phys. 21: 607. 1950.
3. DYSON, A. J. Polymer Sci. 7: 133. 1951.
4. FERRY, J. D. and FITZGERALD, E. R. J. Colloid Sci. 8: 224. 1953.
5. FITZGERALD, E. R. and MILLER, R. F. J. Colloid Sci. 8: 148. 1953.
6. FUNT, B. L. and SUTHERLAND, T. H. Can. J. Chem. 30: 940. 1952.
7. FUOSS, R. M. J. Am. Chem. Soc. 60: 451. 1938.
8. FUOSS, R. M. J. Am. Chem. Soc. 60: 456. 1938.
9. FUOSS, R. M. J. Am. Chem. Soc. 61: 2320. 1939.
10. FUOSS, R. M. J. Am. Chem. Soc. 61: 2334. 1939.
11. FUOSS, R. M. J. Am. Chem. Soc. 63: 385. 1941.
12. FUOSS, R. M. J. Am. Chem. Soc. 63: 2401. 1941.
13. FUOSS, R. M. J. Am. Chem. Soc. 63: 2410. 1941.
14. FUOSS, R. M. and KIRKWOOD, J. G. J. Am. Chem. Soc. 63: 378. 1941.
15. HAVENS, C. B. Ind. Eng. Chem. 42: 315. 1950.
16. KAUZMANN, W. Revs. Mod. Phys. 14: 12. 1942.
17. MEAD, D. J., TICHENOR, R. L., and FUOSS, R. M. J. Am. Chem. Soc. 64: 283. 1942.
18. SUTHERLAND, T. H. and FUNT, B. L. J. Polymer Sci. 11: 177. 1953.
19. TUCKETT, R. F. Trans. Faraday Soc. 40: 498. 1941.

SOME CALCULATIONS OF THE SURFACE ENERGY OF MAGNESIUM OXIDE[1]

By G. C. Benson and R. McIntosh[2]

ABSTRACT

Calculations of the surface energy of an undistorted {100} face of crystalline magnesium oxide have been made. An exponential form of the repulsive energy term was used, and the van der Waals attractive energy between dipoles was included, as in the Born–Mayer treatment of cohesive energy. Comparison with earlier work is made, and it is shown that results are markedly dependent upon the form of the repulsive potential term, the inclusion of the van der Waals term, and, indeed, the choice of coefficients of the van der Waals term. This is not the case so far as the calculated cohesive energies are concerned. The results indicate that a Born–Mayer model may be inadequate in the case of magnesium oxide, and that caution must be exercised before accepting surface energies arrived at by such calculations.

INTRODUCTION

In early theoretical calculations concerning the properties of ionic crystals the potential energy of interaction between ions was taken to be the sum of the coulombic and the repulsive terms. Originally the latter was represented through an inverse power law, but this was later replaced by an exponential form more in accord with a quantum mechanical consideration of the interaction between closed shells of electrons. A further refinement was the inclusion of terms for the van der Waals attraction between the ions. This model of an ionic crystal, usually referred to as the Born–Mayer model, has been quite successful in explaining the cohesive properties of the alkali halides and other ionic crystals. It has also been adopted in calculations of the surface energy of such crystals. In this case the theoretical problem is complicated by the asymmetrical field at the surface, which leads to polarization of the ions and distortion of the lattice near the surface. Consideration of these effects by Lennard-Jones and Dent (12) and Verwey (21) indicates that they will lead to a decrease of the surface energy below the value calculated for an undistorted crystal. Calculations due to Shuttleworth (18) show that although the van der Waals terms play a rather minor role in the cohesive energy of the alkali halides, they make a substantial contribution to the calculated surface energy of these crystals.

Unfortunately there are very few experimental data on which to base a judgment of the utility of the Born–Mayer theory in calculating surface energies. In the case of sodium chloride (3) the experimental evidence, though admittedly inconclusive, is that the surface energy is higher by a factor of two or three than the value obtained by the application of the Born–Mayer theory. The only other material for which data are available is magnesium oxide, for which Jura and Garland (10) have reported a surface energy of 1040 ergs per cm.^{2}, in good agreement with the only available theoretical value calculated

[1]*Manuscript received July 21, 1955.*
Contribution from the Division of Pure Chemistry, National Research Council, Ottawa, Canada. Issued as N.R.C. No. 3739.
[2]*Professor of Chemistry, University of Toronto, Toronto, Ontario.*

by Lennard-Jones and Taylor (13) some thirty years ago. Since in their calculation Lennard-Jones and Taylor employed the older form of repulsive potential (an inverse 10th power) and did not consider the van der Waals contribution, a reinvestigation of the problem is of some interest and is the purpose of the present communication.

METHOD OF COMPUTATION

According to the Born–Mayer (4) theory, the cohesive energy at 0°K. of a bivalent ionic crystal of sodium chloride type structure is given by

$$U = 1.7476 \times \frac{4\epsilon^2}{r_0} + \left[a_{+-}A_6' + \left(\frac{a_{++}+a_{--}}{2} \right) A_6'' \right] \frac{1}{r_0^6} - 6b[(e^{(r_+ + r_-)/\rho})\, e^{-r_0/\rho} + (1.5\, e^{2r_+/\rho} + 0.5\, e^{2r_-/\rho})\, e^{-\sqrt{2}\, r_0/\rho}].$$

In this equation zero point energy and van der Waals terms higher than those between dipoles have been omitted. The symbols employed are defined as follows:

r_0 is the nearest neighbor distance at 0°K.,

ϵ is the value of the electronic charge,

a_{++}, a_{--}, a_{+-} are van der Waals coefficients,

A_6', A_6'' are lattice sums tabulated by Jones and Ingham (9),

r_+, r_- are the Pauling radii of the ions,

b, ρ are the constants in the expression for the repulsive potential.

The corresponding expression for the surface energy of an undistorted {100} face of the crystal, that is, neglecting polarization of ions and changes of lattice spacing, is

$$\sigma = \frac{1}{2r_0^2}\left\{ 0.065246 \times \frac{4\epsilon^2}{r_0} + \left[a_{+-}B_6' + \left(\frac{a_{++}+a_{--}}{2} \right) B_6'' \right] \frac{1}{r_0^6} - b[(e^{(r_+ + r_-)/\rho})\, e^{-r_0/\rho} + 2(1.5\, e^{2r_+/\rho} + 0.5\, e^{2r_-/\rho})\, e^{-\sqrt{2}\, r_0/\rho}] \right\}$$

where B_6', B_6'' are lattice sums tabulated by Shuttleworth (18).

In applying these equations to magnesium oxide, difficulties arise in connection with the choice of the van der Waals coefficients and the constants in the term for the repulsion. Mayer and Maltbie (15) in their calculations of the cohesive energy employed $\rho = 0.345 \times 10^{-8}$ taken from previous work on the alkali halides. This choice was apparently dictated by the fact that the authors wished to deal with a series of alkaline earth oxides, and compressibility and other data necessary for a more direct adjustment of ρ were not available for the entire series. de Boer and Verwey (7) in repeating these calculations have also taken $\rho = 0.345 \times 10^{-8}$. Both groups of authors pointed out that this value of ρ is probably too small. In the present work, Bridgman's data for the compressibility and thermal expansion of magnesium oxide (5), together with a nearest neighbor spacing of 2.101_5 Å (22) at 30°C., have been used to calculate ρ and b in the manner outlined by Born and Mayer (4).

In treating the van der Waals term there is considerable uncertainty in the

choice of the "a" coefficients. Several possibilities have been considered, and thus this term is:

(a) Omitted.

(b) Evaluated from the London formula (14) using the ionization potential of Mg^{++} (1), the electron affinity of O^- in the crystal estimated from the edge of the ultraviolet absorption spectrum of the magnesium oxide crystal* (19), and the polarizabilities of the Mg^{++} (17) and O^{--} (20) ions.

TABLE I

COEFFICIENTS USED IN THE VAN DER WAALS INVERSE SIXTH POWER ATTRACTIVE POTENTIAL TERM

Source of coefficients	$a_{+-} \times 10^{60}$	$a_{++} \times 10^{60}$	$a_{--} \times 10^{60}$
(b) London formula and ultraviolet absorption	3.25	0.854	50.7
(c) Kirkwood–Müller formula	8.64	1.19	143
(d) Fowler	14.5	2.38	135

TABLE II

COHESIVE ENERGY OF MAGNESIUM OXIDE IN 10^{-12} ERG PER MOLECULE

Specification of model	$r_0 \times 10^8$, cm.	$\rho \times 10^8$, cm.	$b \times 10^{12}$, ergs	$\epsilon \times 10^{10}$, e.s.u.	Contributions from: Electrostatic term	Repulsive term	van der Waals term	Total omitting zero point energy
Our calculation (a) no van der Waals term	2.093	0.4427	1.871	4.8024	77.0	−14.5	—	62.5
Our calculation (b) van der Waals coefficients from London formula	2.093	0.4353	1.966	4.8024	77.0	−15.2	0.8	62.6
Our calculation (c) van der Waals coefficients from Kirkwood–Müller formula	2.093	0.4245	2.134	4.8024	77.0	−16.4	2.2	62.8
Our calculation (d) van der Waals coefficients from Fowler	2.093	0.4220	2.179	4.8024	77.0	−16.6	2.6	63.0
Lennard-Jones and Taylor r^{-11} force of repulsion	2.10	—	—	4.77	75.7	− 7.4	—	68.3
Mayer and Maltbie exponential repulsion with ρ from alkali halides and includes a van der Waals term	2.09	0.345	—	—	76.3	−11.5	0.1	64.9
de Boer and Verwey treated as in preceding entry	2.10	0.345	1.58	—	76.0	−11.2	0.1	64.9
Exponential repulsion with $\rho = 0.345 \times 10^{-8}$ and van der Waals coefficients as in (c)	2.10	0.345	1.85_2	4.77	75.7	−13.1	2.2	64.8

Suggested in a private communication from Professor Mayer.

TABLE III*

SURFACE ENERGY OF MAGNESIUM OXIDE IN ERGS PER CM.^{2}

Specification of model	Contributions from:			Total
	Electrostatic term	Repulsive term	van der Waals term	
Our calculation (*a*) no van der Waals term	3284	−3582	—	−298
Our calculation (*b*) van der Waals coefficients from London formula	3284	−3742	307	−151
Our calculation (*c*) van der Waals coefficients from Kirkwood–Müller formula	3284	−4024	853	113
Our calculation (*d*) van der Waals coefficients from Fowler	3284	−4100	927	111
Lennard-Jones and Taylor r^{-11} force of repulsion	3194	−1832	—	1362
de Boer and Verwey's values of b and ρ but no van der Waals terms	3206	−2687	—	519
Exponential repulsion with $\rho = 0.345\times10^{-8}$ and van der Waals coefficients as in (*c*)	3206	−3150	829	885

**Values of r_0, ρ, etc. are those given in Table II.*

(*c*) Evaluated from the Kirkwood–Müller formula (14), using, in addition to the polarizabilities referred to above, the diamagnetic susceptibilities of the ions calculated by Slater's method as has been recommended by Myers (16).

(*d*) Taken from the table compiled by Fowler (8).

See Table I for numerical values of these coefficients.

The particular choice made caused some variation of the constant ρ deduced from compressibility data. It should be noted that whatever method was utilized to obtain the van der Waals coefficients, the contribution to the cohesive energy obtained by us was greater than the values recorded by Mayer and Maltbie (15) and by de Boer and Verwey (7). We have not been able to ascertain the source of their values.

Results are recorded in Tables II and III. The choices made in dealing with the van der Waals term are indicated, as well as the parameters of the crystal which were employed. Both our computations and those of earlier workers have been summarized. Where individual terms are given which were not stated in the work of the original authors, these were evaluated by us from their publications.

DISCUSSION

Attention should be drawn to the range of values which may be obtained for the surface energy of magnesium oxide due both to the choice of the function employed for the energy of repulsion and to the values selected for the van der Waals attractive terms. These choices are of minor importance in the case of the cohesive energy, but are of extreme importance in the case of the surface energy.

The results raise the general question whether or not the use of the Born–Mayer model is justified to calculate the surface energy of ionic crystals, or whether the discrepant results are due to its inadequacy in the special case of magnesium oxide. Brill, Hermann, and Peters (6) have stated on the basis of X-ray measurements of electron density that magnesium oxide is not completely ionic in character in the solid state. They support their contention by reference to the work of de Boer and Verwey (7), in which the electron affinity of O is calculated for the series of alkaline earth oxides, by means of cohesive energies and the Born cycle. It is pointed out that the oxides of beryllium and magnesium have high values of the electron affinity when determined in this way. It should be noted, however, that these values are based upon the use of $\rho = 0.345 \times 10^{-8}$, which, as has been pointed out above, may lead to erroneous results. The experimental evidence must be recognized, however, and since de Boer and Verwey also point out that the bond in the gaseous magnesium oxide molecule is quite covalent in character, the treatment of the problem by a model assuming complete ionic character may not be justified. This does not, however, explain the wide variations in the computed values which are recorded in Table III. These arise from changes in the assumed values of the coefficients, changes which did not materially affect the cohesive energy. The results emphasize the sensitivity of calculated values of surface energy to the details of computation. They also suggest that the agreement between the Lennard-Jones and Taylor result and the experimental value of Jura and Garland may be fortuitous. The result obtained by Jura and Garland is of a preliminary nature as the authors have stressed (11) and the general procedure must be carefully assessed as Bauer (2) has emphasized. It would therefore seem that further experimental data are urgently required, and that some caution must be exercised in the use of calculated values until experimental results have been accumulated.

REFERENCES

1. BACHER, R. F. and GOUDSMIT, S. Atomic energy states. McGraw-Hill Book Company, Inc., New York. 1932.
2. BAUER, S. H. J. Am. Chem. Soc. 75: 1004. 1953.
3. BENSON, G. C. and BENSON, G. W. Can. J. Chem. 33: 232. 1955.
4. BORN, M. and MAYER, J. E. Z. Physik, 75: 1. 1932.
5. BRIDGMAN, P. W. Proc. Am. Acad. Arts Sci. 67: 345. 1931–1932.
6. BRILL, R., HERMANN, C., and PETERS, C. Z. anorg. Chem. 257: 151. 1948.
7. DE BOER, J. H. and VERWEY, E. J. W. Rec. trav. chim. 55: 443. 1936.
8. FOWLER, R. H. Statistical mechanics. 2nd ed. Cambridge University Press, London. 1936. p. 326.
9. JONES, J. E. and INGHAM, A. E. Proc. Roy. Soc. (London), A, 107: 636. 1925.
10. JURA, G. and GARLAND, C. W. J. Am. Chem. Soc. 74: 6033. 1952.
11. JURA, G. and GARLAND, C. W. J. Am. Chem. Soc. 75: 1006. 1953.
12. LENNARD-JONES, J. E. and DENT, B. M. Proc. Roy. Soc. (London), A, 121: 247. 1928.
13. LENNARD-JONES, J. E. and TAYLOR, P. A. Proc. Roy. Soc. (London), A, 109: 476. 1925.
14. MARGENAU, H. Revs. Mod. Phys. 11: 1. 1939.
15. MAYER, J. E. and MALTBIE, M. Z. Physik, 75: 748. 1932.
16. MYERS, W. R. Revs. Mod. Phys. 24: 15. 1952.
17. PAULING, L. Proc. Roy. Soc. (London), A, 114: 181. 1927.
18. SHUTTLEWORTH, R. Proc. Phys. Soc. (London), A, 62: 167. 1949.
19. STRONG, J. and BRICE, R. T. J. Opt. Soc. Amer. 25: 207. 1935.
20. TESSMAN, J. R., KAHN, A. H., and SHOCKLEY, W. Phys. Rev. 92: 890. 1953.
21. VERWEY, E. J. W. Rec. trav. chim. 65: 521. 1946.
22. WYCKOFF, R. W. G. The structure of crystals. 2nd ed. The Chemical Catalog Co., Inc., New York. 1931.

THE PREPARATION OF L-SORBOSE FROM 5-*KETO*-D-GLUCONIC ACID (L-SORBURONIC ACID)[1]

By J. K. N. Jones[2] and W. W. Reid[3]

ABSTRACT

L-Sorbose has been prepared from 5-*keto*-D-gluconic acid.

INTRODUCTION

The most convenient method of preparation of L-sorbose is undoubtedly from the biochemical oxidation of sorbitol (1). The purpose of this communication is to demonstrate how D-glucose can be converted to L-sorbose by purely chemical transformations. The starting product was the calcium salt of 5-*keto*-D-gluconic acid (L-sorburonic acid) which had been prepared by biochemical oxidation of D-glucose (4). Salts of this acid can be prepared by prolonged oxidation of D-glucose with bromine (3) or electrolytically (2). When the calcium salt was shaken with methanolic hydrogen chloride it dissolved with the formation of a mixture of products composed mainly of the methyl glycoside methyl ester of 5-*keto*-D-gluconic acid. The carbomethoxy group of this glycoside was reduced with sodium borohydride to the alcohol with the formation of methyl L-sorbofuranoside from which L-sorbose was prepared by hydrolysis.

Since the oxidation of sugars by bromine water to 5-*keto*hexonic acids is a general reaction (3) the interconversion of aldoses to ketoses with concomitant inversion of the chain of hydroxyl groups becomes possible.

EXPERIMENTAL

Solutions were evaporated under reduced pressure. Optical rotations were measured in water at 20°±2° (unless otherwise stated). Sugars were separated chromatographically in either (*a*) ethyl acetate – acetic acid – formic acid – water (18:3:1:4, v/v) or (*b*) *n*-butanol–water–pyridine (18:3:3, v/v), and detected with the *p*-anisidine–hydrochloride spray.

Methyl 5-keto-D-Glucofuronic Acid Methyl Ester

The calcium salt of 5-*keto*-D-gluconic acid hydrate ($2\frac{1}{2}$, H_2O) (22 gm.) was suspended in methanol (500 ml.) and hydrochloric acid (d. 1.12, 20 ml.) added. The mixture was stirred overnight when a clear solution resulted. The pale yellow reaction mixture was heated at 40°C. for 24 hr., cooled, and then passed down columns of Amberlite resin 1R120 and 1R4B, which had been washed previously with dry methanol. The effluent was concentrated to a sirup (17 gm.) which was dissolved in acetone and filtered from insoluble material. The resultant methyl ester methyl glycoside was obtained as a pale yellow

[1]*Manuscript received July 7, 1955.*
Contribution from the Department of Chemistry, Queen's University, Kingston, Ontario and Research Department, H. W. Carter and Company Limited, Coleford, Gloucester, England.
[2]*Department of Chemistry, Queen's University, Kingston, Ontario.*
[3]*Research Department, Catteras Limited, 221, Stanhope Street, London, N.W. 1, England.*

non-reducing sirup (14.2 gm.) $[\alpha]_D$ −24° (*c*, 3.6 in MeOH). Found: OMe, 28.1%. Calc. for $C_8H_{14}O_7$: OMe, 27.9%. The product contained three components, detected chromatographically, which moved, relative to rhamnose (R_{RH}), at the rates 1.25, 1.59, and 1.98 (solvent (*b*)). They gave yellow orange spots with the *p*-anisidine spray. The fastest moving material was present in traces only. 5-*keto*-D-Gluconic acid had R_{RH} 0.95 in solvent (*a*).

Methyl L-*Sorbofuranoside and* L-*Sorbose*

The methyl ester methyl glycoside (2 gm.) was dissolved in water (10 ml.) and sodium borohydride (0.5 gm.) added. The solution became warm and changed color from pale yellow to pale green. After 24 hr., excess of acetic acid was added and the solution was deionized on Amberlite resins 1R120 and 1R4B. On concentration a sirup (1.28 gm.) remained which contained five components. These materials moved on the chromatogram relative to rhamnose at the rates 0.38, 0.91, 1.07, 1.87, and 2.12 (solvent (*b*)). The slowest moving component which reduced Fehling's solution was identified as sorbose, and results probably from the hydrolytic action of the acidic resin on the methyl furanoside. The components with R_{RH} 0.91 and 1.07 behaved like methyl sorbofuranoside whilst the fastest two components which were present in trace amounts only were not identified. The mixture was heated with *N* sulphuric acid for three hours at 100°C., cooled, neutralized ($BaCO_3$), and filtered. The filtrate on concentration gave crystalline L-sorbose, which was recrystallized from methanol. The product (0.71 gm.) had m.p. 165°C. not depressed on admixture with an authentic specimen, moved on the chromatogram at the same rate as sorbose, and had $[\alpha]_D$ −41° (*c*, 1.1). Found: C, 40.1; H, 6.9%. Calc. for $C_6H_{12}O_6$: C, 40.0, H, 6.7%.

ACKNOWLEDGMENT

The authors are grateful to the National Research Council for financial assistance.

REFERENCES

1. BERTRAND, G. Compt. rend. 126: 762. 1898.
2. COOK, E. W. and MAJOR, R. T. J. Am. Chem. Soc. 57: 773. 1935.
3. HART, J. P. and EVERETT, M. R. J. Am. Chem. Soc. 61: 1822. 1939.
4. LOCKWOOD, L. B., TOBENKIN, B., and WOOD, G. E. J. Bacteriol. 42: 51. 1941.

MERCURY PHOTOSENSITIZED DECOMPOSITION OF ETHYLENE OXIDE[1]

By R. J. Cvetanović

ABSTRACT

Some aspects of the mercury photosensitized decomposition of ethylene oxide at room temperature have been reinvestigated. At least two, and probably more than two, distinct primary steps occur. The previously assumed major primary formation of hydrogen by a molecular process is shown to occur to a relatively small extent only. Hydrogen atoms play an important role in the process, as well as the following radicals: CH_3, CHO, CH_2CHO, and C_2H_5, and probably to a lesser extent also CH_2. The products formed are CO, H_2, C_2H_6, a little CH_2CO and C_2H_4, and large amounts of aldehydes. The presence of higher aldehydes has been demonstrated. While there is a general similarity to the other modes of decomposition of ethylene oxide, a unique and unambiguous solution of the complete reaction mechanism is at present not possible.

In a previous publication (5) an investigation of the reaction of oxygen atoms with ethylene has been reported. The primary step of the readily occurring reaction is believed to be a direct addition of the oxygen atom to the double bond in ethylene. Very little or no ethylene oxide is found, however, and a variety of products is formed instead, presumably as a result of further reactions of the initially produced energy rich molecule

$$C_2H_4+O \rightarrow C_2H_4O^* \qquad [1]$$
$$C_2H_4O^* \rightarrow \text{products.}$$

A support for this view is found in the similarity of the products formed in this process with those reported in the literature for the thermal, photolytic, and mercury photosensitized decomposition of ethylene oxide. All these processes appear to be quite complex and are difficult to treat in an unambiguous manner. While their courses cannot be expected to be identical, the over-all similarity suggests that a comparative study may yield useful information regarding the more important features of the respective mechanisms.

An investigation of the mercury photosensitized decomposition of ethylene oxide was reported in 1948 by Phibbs, Darwent, and Steacie (12). The observed products were CO, H_2, CH_3CHO, and a polymer, as well as smaller amounts of CH_4, HCHO, and of a fraction indicated as "C_2 hydrocarbons" but not further analyzed. It was postulated that initially an energy rich ethylene oxide molecule was formed and that it was capable of isomerizing to acetaldehyde or splitting in the following manner

$$C_2H_4O^* \rightarrow H_2+CO+CH_2. \qquad [2]$$

Only a small portion of the primary process was considered to proceed by the reaction

$$C_2H_4O+Hg^* \rightarrow C_2H_3O+H+Hg \qquad [3]$$

(Hg* refers to Hg $6(^3P_1)$ atoms). All the hydrogen is, therefore, supposed to

[1]*Manuscript received July 18, 1955.*
Contribution from the Division of Applied Chemistry, National Research Council, Ottawa, Canada. Issued as N.R.C. No. 3741.

be formed by a molecular process and a very minor role is ascribed to hydrogen atoms.

Direct photolysis of ethylene oxide in the far ultraviolet was reported in 1950 by Gomer and Noyes (8). The products formed were CO, H_2, CH_4, C_2H_6, smaller amounts of HCHO and CH_3CHO, and almost certainly some C_2H_5CHO. The authors were led to assume for the primary step the reaction

$$C_2H_4O+h\nu \rightarrow CH_3+HCO \qquad [4]$$

followed by (or simultaneous with)

$$HCO \rightarrow H+CO. \qquad [5]$$

A considerable amount of work has been done on thermal decomposition of ethylene oxide. A recent investigation was conducted by Lossing, Ingold, and Tickner (10) who were able to observe directly by a mass spectrometer the products of the pyrolysis at 800 to 1000°C. They found CO, H_2, CH_4, C_2H_6, CH_2CO, and an abundant formation of methyl but no methylene radicals. Propane, formaldehyde, and acetaldehyde, reported previously at lower temperatures, were not formed. Mueller and Walters (11) found that at 400°C. acetaldehyde, ketene, and some formaldehyde were formed but not propionaldehyde, at least not in amounts comparable to those of acetaldehyde.

Both Lossing and his co-workers and Mueller and Walters find it necessary to ascribe an important role in the thermal decomposition of ethylene oxide to the primary splitting into CH_3 and HCO, analogous to the reactions [4] and [5] proposed by Gomer and Noyes, and to abandon the classical view of a primary formation of methylene radicals and formaldehyde. The well-known use of ethylene oxide as an excellent source of methyl radicals is thus made more easily understandable. In the reaction of oxygen atoms with ethylene the products formed (CO, paraffinic aldehydes, H_2, CH_4, C_2H_6, C_3H_8, and probably some CH_2CO) suggest a somewhat similar mode of decomposition of the initially formed intermediate. The mechanism proposed for the mercury photosensitized decomposition, on the other hand, is very different. The present work has been carried out, therefore, in order (1) to obtain further information on products formed in the mercury photosensitized decomposition of ethylene oxide, (2) to test the postulated molecular production of hydrogen and other features of the previously proposed mechanism, (3) to attempt to correlate the main features of this process with the other modes of decomposition of ethylene oxide, and (4) to attempt, by analogy, to formulate the more important of the secondary reactions following the addition of oxygen atoms to ethylene.

EXPERIMENTAL

The reaction was studied at room temperature using a conventional type of apparatus, including a cylindrical quartz reaction vessel (5 cm. in diameter, 10 cm. long). The apparatus and the analysis of products have been described in detail previously (3, 5).

Ethylene oxide was obtained from Matheson Co., Inc., ethylene was supplied by Ohio Chemicals Canada, Ltd., and butene-1 was a Phillips reagent grade

product. All the three reagents were further purified by repeated bulb to bulb distillation *in vacuo*. Deuterated ethylene oxide was kindly supplied by Dr. D. J. Worsfold of these laboratories.

The quantum yields of reaction products were determined relative to the formation of hydrogen by mercury photosensitized decomposition of 200 mm. of *n*-butane, and taking 0.50 for the value of ϕH_2, as found by Bywater and Steacie (1).

RESULTS

The pressure dependence of the quantum yields of formation of some of the products in the mercury sensitized decomposition of ethylene oxide is shown in Fig. 1. The trends in the H_2, CO, and CH_4 formation are in agree-

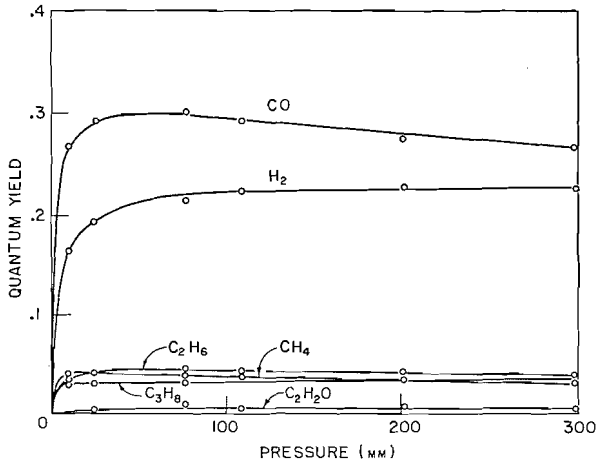

FIG. 1. Pressure dependence of the quantum yields of formation of some of the products in the mercury photosensitized decomposition of ethylene oxide (static experiments, exposure 90 min., mean $I_a = 3.27 \times 10^{15}$ quanta sec.$^{-1}$).

ment with those established by Phibbs, Darwent, and Steacie (12). The "C_2 fraction" reported by these authors is seen to consist mainly of C_2H_6 and C_3H_8. Small amounts of ketene (identified and estimated by mass spectrometer) are separated out with the propane. In addition very small amounts of C_4H_{10} are usually found with the propane and there is indication that traces of ethylene accompany ethane. In this series of experiments no determinations of aldehydes nor of ethylene oxide consumption were attempted. Determinations of these quantities were reported previously (12).

The effect of the addition of very small amounts of ethylene to ethylene oxide is shown in Table I for static (*A*) and circulating (*B*) experiments and for the latter also in Fig. 2. The inhibiting effect of ethylene is extremely pronounced; hydrogen production is strongly suppressed and to a somewhat smaller extent the production of carbon monoxide and methane. On the other hand, the amount of propane formed is much increased. The figures for ethane are uncertain since small amounts of this compound were determined

TABLE I

THE INHIBITING EFFECT OF ETHYLENE
(Exposure 90 min.)

Run	C_2H_4O, mm.	Mean C_2H_4/C_2H_4O	Quantum yields CO	H_2	CH_4	C_2H_6	C_3H_8	$H_2-C_2H_2$	$-\Delta C_2H_4$
A. Static experiments (mean $I_a = 2.95 \times 10^{15}$ quanta sec.$^{-1}$)									
49	200.0	—	.278	.217	.034	.043	.043	Not detd.	Not detd.
48	199.2	.00567	.149	.046	.012	.010	.083	Not detd.	Not detd.
45	201.1	.0160	.121	.028	.015	.022	.078	Not detd.	Not detd.
47	199.3	.0206	.109	.026	.013	.014	.083	Not detd.	Not detd.
43	200.0	.0285	.104	.025	.012	.021	Not detd.	Not detd.	Not detd.
44	201.2	.0336	.099	.022	.012	.014	.067	Not detd.	Not detd.
B. Circulating experiments (mean $I_a = 3.27 \times 10^{15}$ quanta sec.$^{-1}$)									
8	99.8	—	.284	.220	.043	.048	.037	.220	—
11	199.0	.00261	.170	.053	.021	.051	.075	.051	.307
10	198.5	.00584	.146	.036	.019	.051	Not detd.	Not detd.	.329
12	198.0	.0122	.131	.029	.017	.043	.075	.023	.342
9	100.9	.0432	.096	.042	.011	.032	.050	.027	Not detd.

in the presence of excess ethylene. Large amounts of ethylene are consumed in the process. Determination of eventual butane formed proved not to be feasible in the presence of a huge excess of ethylene oxide. For this reason a

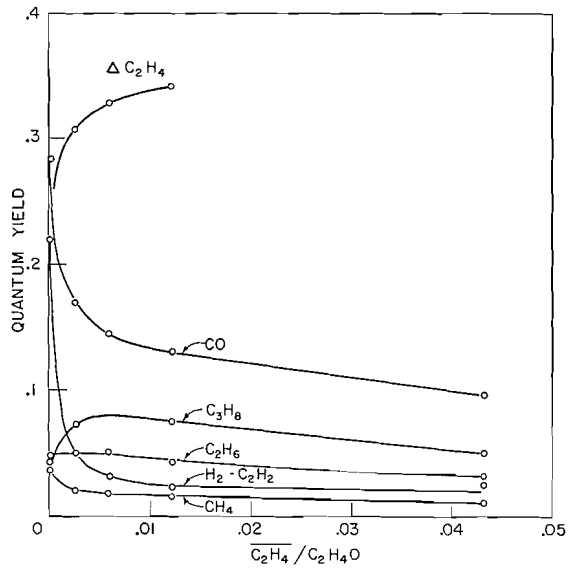

FIG. 2. The inhibiting effect of ethylene (circulating experiments, exposure 90 min., mean $I_a = 3.27 \times 10^{15}$ quanta sec.$^{-1}$).

series of experiments was performed using butene-1 instead of ethylene as the inhibitor. The results are presented in Table II and the effect shown is very

TABLE II

EFFECT OF ADDITION OF BUTENE-1 TO 100 MM. OF ETHYLENE OXIDE
(Mean $I_a = 3.67 \times 10^{15}$ quanta sec.$^{-1}$)

Run	C_4H_8-1, mm.	Irradn. time, min.	Quantum yields							
			CO	H_2	CH_4	C_2H_6	C_2H_4	C_3H_8	Total RCHO	Room temp. fraction
2	—	90	.291	.222	.037	.043	Trace	.039	Not detd.	Very small
74	2.8	100	.138	.033	.021	.020	.044	.001	.175	Not detd.
75	2.4	150	.155	.038	.023	.021	.034	Not detd.	.225	Not detd.
76	5.5	150	.100	.022	.017	.018	.030	Trace	.178	.14
78	5.2	150	.100	.021	.017	Not detd.	Not detd.	Not detd.	Not detd.	.13[a]

[a]*Composed mainly of higher saturated aldehydes (propanal to hexanal) and octane (probably 3,4-dimethylhexane).*

much the same as with ethylene. The following distinctions, however, are to be noted: propane is nearly completely suppressed, appreciable amounts of ethylene are produced, and appreciable quantities of less volatile substances ("room temperature fraction") are formed. By a combination of mass-spectrometer analysis and the removal of the aldehydes by polymerization on solid KOH, this fraction is found to be quite complex, being composed mainly

TABLE III

PRODUCTS OF MERCURY SENSITIZED DECOMPOSITION OF 100 MM. OF ETHYLENE OXIDE ALONE AND OF 100 MM. OF ETHYLENE OXIDE WITH 3.45 MM. ETHYLENE ADDED
(Mean $I_a = 4.93 \times 10^{15}$ quanta sec.$^{-1}$, 25±1°C.)

Run	Irradn. time, min.	Mean C_2H_4, mm.	Quantum yields							
			CO	H_2	CH_4	C_2H_6	C_3H_8	CH_2CO	H_2–C_2H_2	RCHO
A. Ethylene oxide alone										
55	30	—	.287	.217	.044	.048	.030	.010	.217	.169
59	60	—	.295	.223	.043	.044	.027	.016	.223	.166
53	90	—	.294	.226	.041	.042	.026	.008	.226	Not detd.
61	90	—	.297	.224	.041	.040	Not detd.	Not detd.	.224	.139
57	120	—	.295	.216	.042	.041	.026	.009	.216	.084
B. Ethylene oxide+ethylene										
56	30	3.18	.118	.039	.015	.043	.043	.024	.025	.248
60	60	3.02	.120	.045	.012	.046	.046	.026	.027	Not detd.
54	90	2.84	.129	.042	.014	.044	.045	.021	.027	.236
58	120	2.71	.132	.040	.015	.038	.045	.020	.027	.225

of higher paraffinic aldehydes (propanal to hexanal) and of higher paraffins (up to octane).

In order to establish in greater detail the effect of ethylene addition on the formation of various products, alternate experiments were performed with 100 mm. of ethylene oxide alone and 100 mm. of ethylene oxide with 3.45 mm. ethylene added. The time of exposure was varied and the results are given in Table III. In addition to the already indicated suppression of H_2, CO, and CH_4, and the increase of C_3H_8 production on addition of ethylene, it is also seen that ketene and especially aldehyde formation is much increased. Aldehyde was determined by infrared absorption measurement on the basis of calibrations with acetaldehyde (in the presence of analogous quantities of ethylene oxide). The quantities for aldehyde obtained in this manner are approximate because besides acetaldehyde its higher homologues appear to be present in quite appreciable quantities. This was evident from the details of the infrared absorption spectra and also from a partial separation, by the use of gas–liquid partition chromatography (2), of some higher aldehydes from the huge excess of ethylene oxide and their subsequent identification by mass spectrometer. A few determinations of HCHO were made in the manner described previously (5). Only very small amounts of this substance were found. There might have been, however, an appreciable loss of this compound by polymerization.

The inhibiting effects of C_2H_4 and C_4H_8-1 indicate that in the uninhibited reaction most of the hydrogen is formed through action of hydrogen atoms. In the inhibited reaction hydrogen production is not completely suppressed, suggesting that it may be formed by a molecular rather than an atomic process. In order to test this possibility several experiments were carried out with mixtures of C_2H_4O and C_2D_4O. The results are given in Table IV. In the uninhibited reaction (run 64) such mixtures form large amounts of HD, while in the inhibited reaction (runs 62 and 61) HD is suppressed to the level that appears when C_2D_4O is used in the absence of C_2H_4O (runs 63 and 65). In the inhibited reaction, therefore, hydrogen is formed by a molecular process. The interpretation of the ratios of the isotopic methanes formed is somewhat more difficult because the figures for CH_3D and CH_4 may be subject to large errors. The ratios CD_4 to CD_3H should, on the other hand, be accurate and the indications are that both in the inhibited and uninhibited reaction, methane is probably formed predominantly, but possibly not entirely, from free methyl radicals.

It is of interest also that there are pronounced isotopic effects in the rates of hydrogen formation, both the abstraction and the molecular formation of deuterium taking place less readily than those of hydrogen. This is in agreement with the observations of other workers in abstractions of the two isotopes of hydrogen and explains the fact that in the uninhibited decomposition of the 1:1 C_2D_4O–C_2H_4O mixture (run 64) the relative rate of HD formation is not as large as would be expected on probability grounds. An isotopic effect in a molecular reaction has recently been found in the mercury photosensitized decomposition of ethylene (6).

TABLE IV

EXPERIMENTS WITH C_2H_4O AND C_2D_4O
(Mean $I_a = 2.34 \times 10^{15}$ quanta sec.$^{-1}$)

Run	Initial pressures (mm.)				Irradn. time, min.	Quantum yields									
	C_2H_4O	C_2D_4O	C_2H_4	C_4H_8-1		CO	Total H_2	Total methane	H_2	HD	D_2	CD_4	CD_3H	CH_3D	CH_4
49	200	—	—	—	90	.278	.217	.034	.217	—	—	—	—	—	.034
64	100	100	—	—	120	.259	.168	.026	.075	.071	.022	.008	.007	.004	.007
43	200	—	6.3	—	90	.104	.025	.012	.025	—	—	—	—	—	.012
62	100	100	5.4	—	300	.116	.022	.012	.014	.003	.005	.004	.003	.0015	.005
57	100	—	—	—	120	.295	.216	.042	.216	—	—	—	—	—	.042
65	—	100	—	—	120	.229	.088	.037	—	.004	.084	.032	.005	—	—
63	—	100	—	5.6	240	.066	.012	.012	.001	.003	.008	.007	.004	.0004	.0005
61	50	50	—	5.4	150	.099	.021	.014	.012	.0031	.0055	.003	.003	.002	.006

DISCUSSION

The quenching efficiency of ethylene is 10 times greater than that of ethylene oxide (4) and even for the largest ratios of ethylene to ethylene oxide used in the present experiments the fraction of the exciting radiation quenched by ethylene is small and cannot be responsible for the large inhibiting effects observed. It appears safe to conclude that the inhibition is due to the addition of H-atoms to ethylene or butene-1. In the former case the increased ethyl radical concentration leads to an increased propane formation, by combination with methyl radicals, which also leads to some decrease in methane formation. With butene-1 propane is not formed at all, but higher paraffins instead. The experiments with butene-1 show that quite appreciable amounts of ethylene are formed in the decomposition of ethylene oxide but, in the absence of excess butene, H-atoms add on to it readily; the ethyl radicals thus formed explain the production of propane in the "uninhibited" reaction.

An inspection of the magnitude of the inhibiting effect produced by ethylene and of the large consumption of this compound shows that large quantities of H-atoms are formed in the sensitized decomposition of ethylene oxide. This finding rules out the previously suggested (12) formation of hydrogen by a molecular process as the major primary step. The amounts of CH_4, C_2H_6, and C_3H_8 produced indicate that substantial quantities of methyl radicals are also formed. Formation of methane at room temperature by abstraction of hydrogen indicates that a relatively loosely bound hydrogen atom is available. All these considerations point to a primary step of the type suggested by Gomer and Noyes (8) for the direct photolysis: primary production of CH_3 and HCO radicals, the latter readily decomposing into H and CO. In order to explain the formation of higher aldehydes it is then necessary to assume also the occurrence of the reactions

$$R+HCO\ (+M) \rightarrow RCHO\ (+M) \qquad [6]$$

in addition to

$$R+HCO \rightarrow RH+CO \qquad [7]$$

and

$$H+HCO \rightarrow H_2+CO. \qquad [8]$$

The major features of the process are then qualitatively readily explainable. When ethylene is added, reaction [8] is suppressed and at the same time large quantities of C_2H_5 are formed which, through an increase in aldehyde formation, lead to more rapid removal of HCO radicals and therefore their decreased decomposition to yield CO. Thus, a drastic suppression of H_2, partial suppression of CO, and a large increase in aldehydes is observed. A slight pressure dependence of reaction [6] could explain the pressure dependence of CO formation. Alternately, there may be a slight collisional deactivation of an initially produced excited ethylene oxide molecule. The very slight increase in the yield of hydrogen with increasing pressure may be due to pressure dependence of reaction [5], as suggested by Horner, Style, and Summers (9).

It would appear, on the basis of the foregoing conceptions, that H-atoms undergo preferentially reaction [8], CH_3 radicals both reactions [6] and [7], and C_2H_5 and any higher radicals predominantly reaction [6]. These differences

may be due to different availability of degrees of freedom for a distribution of the heat of the reaction. It should be pointed out at the same time that a combination of CH_3 and CHO radicals to give acetaldehyde is, on the basis of the existing experimental information, indistinguishable from a direct primary isomerization to this compound without decomposition. The formation of higher aldehydes, on the other hand, would seem to require the occurrence of reactions [6].

While a primary split into CH_3 and CHO may explain in a qualitative way the major features of the process, it is evident that at least one more primary process has to be considered. The experiments with mixtures of C_2H_4O and C_2D_4O show that a small fraction of hydrogen is formed by a primary molecular process possibly by reaction [2] or by the similar reaction

$$C_2H_4O^* \rightarrow H_2+CH_2CO. \qquad [9]$$

It appears, therefore, to be reasonably certain that there are at least two primary processes. A primary molecular formation of methane, if it occurs at all, does not seem to be very important. A primary split into H-atoms and C_2H_3O radicals, (reaction [3]), on the other hand, is very likely in view of the seemingly largely saturated character of the ethylene oxide molecule. The properties of the C_2H_3O radicals have been investigated by Gomer and Noyes (8) and it appears that there is about equal probability of decomposition of these radicals into CH_3 and CO and of their stabilization by isomerization, presumably to CH_2CHO radicals. The latter could then lead to aldehyde formation. It can be seen that the qualitative consequences of such a primary step, followed by a number of feasible secondary reactions, are similar to those of a primary split into CH_3 and HCO. Attempts to exclude the latter primary step, however, lead to quantitative difficulties. Complete and unambiguous stoichiometric and kinetic treatment is at present impossible because of the lack of detailed quantitative information on the aldehydes formed and a very limited knowledge of the relative values of rate constants of the different reactions involved. Some conclusions, on the other hand, can be drawn from a comparative analysis of the various modes of decomposition of ethylene oxide.

The stoichiometry of the reaction of oxygen atoms with ethylene (5) can be approximately represented by

$$\begin{aligned} O+1.38\ C_2H_4 \rightarrow\ & .50\ CO+.15\ CH_3CHO+.20\ C_2H_5CHO+.05\ C_3H_7CHO \\ & +.03\ C_2H_4O+.04\ CH_2CO+.09\ H_2+.11\ CH_4 \\ & +.17\ C_2H_6+.17\ C_3H_8+.03\ (C_2H_4O\text{-polymer}). \end{aligned}$$

A stoichiometric balance of the likely processes involved can be written as follows:

$$O+C_2H_4 \rightarrow C_2H_4O^* \rightarrow \begin{cases} .03\ \text{polymer} \\ .03\ C_2H_4O \\ .05\ H_2+CH_2+CO \\ .04\ H_2+CH_2CO \\ .10\ H+C_2H_3O \\ .75\ CH_3+HCO \end{cases}$$

$$.10\ C_2H_3O \rightarrow .05\ CH_2CHO + .05\ CH_3 + .05\ CO$$
$$.05\ CH_2 + .05\ CH_3 \rightarrow .05\ C_2H_4 + .05\ H$$
$$.32\ CH_3 \rightarrow .16\ C_2H_6$$
$$.11\ CH_3 + .11\ HCO \rightarrow .11\ CH_4 + .11\ CO$$
$$.17\ CH_3 + .17\ C_2H_5 \rightarrow .17\ C_3H_8$$
$$.15\ CH_3 + .15\ HCO \rightarrow .15\ CH_3CHO$$
$$.28\ HCO \rightarrow .28\ H + .28\ CO$$
$$.43\ H + .43\ C_2H_4 \rightarrow .43\ C_2H_5$$
$$.20\ C_2H_5 + .20\ HCO \rightarrow .20\ C_2H_5CHO$$
$$.01\ C_2H_5 + .01\ HCO \rightarrow .01\ C_2H_6 + .01\ CO$$
$$.05\ C_2H_5 + .05\ CH_2CHO \rightarrow .05\ C_3H_7CHO.$$

The proposed scheme involves some simplifications and for some of the steps alternative reactions may be written. The small primary split into H and C_2H_3O, in particular, is suggested only in order to explain the formation of C_3H_7CHO and may prove to be unnecessary if this compound is found to arise by some other type of radical combination. Regardless of these uncertainties, in its main outline, the scheme appears feasible on the basis of the present knowledge. Considering the reactions

$$CH_3 + CH_3 \rightarrow C_2H_6 \qquad [10]$$
$$CH_3 + CHO \rightarrow CH_4 + CO \qquad [11]$$
$$CH_3 + CHO \rightarrow CH_3CHO \qquad [11']$$

and

$$CHO \rightarrow H + CO \qquad [5]$$

it is likely that reactions [11] and [11′] have each a collision efficiency of about 0.5. Assuming that (1) the collision efficiency of reaction [10] is unity and of reaction [11] 0.5, (2) the collision diameters of CH_3 and HCO have the same value of 3.5 Å, (3) the effective reaction volume is 10 cc., and (4) $k_5 = 10^{13} \exp(-E_5/RT)$, a value of 14.4 kcal./mole can be calculated for E_5 from the observed rate of reaction [10] and the ratio of the rates of reactions [5] and [11] as given in the foregoing stoichiometric balance (.28/.11). Even with an ample allowance for uncertainties in the assumptions made, E_5 remains within the range of the values for the same quantity quoted in the literature (13).

Inasmuch as the primary decomposition of ethylene oxide in the mercury photosensitized reaction follows the same course, the relative amounts of the products formed when ethylene is present should be very much the same as in the reaction of O-atoms with ethylene. A comparison of the rates of formation of all but some of the minor products detected is given in Table V. The figures given should be regarded as approximate since there is an appreciable uncertainty in some of the analytical results, particularly those for the total aldehydes and ketene. Nevertheless, it is clear that there is a broad similarity, as evidenced by the values reduced to equal CO production. There are also some important differences. In the mercury sensitized decomposition of ethylene oxide in the presence of ethylene less fragmentation products (CO, CH_4, C_2H_6, C_3H_8) and more aldehydes are formed, and also, relative to equal CO formation, there is less methane while propane remains about the same. These differences are qualitatively explainable by a decreased initial split into CH_3 and HCO and a considerably increased primary split

TABLE V

COMPARISON OF THE RATES OF FORMATION OF THE MAIN PRODUCTS IN THE MERCURY SENSITIZED DECOMPOSITION OF ETHYLENE OXIDE AND IN THE REACTION OF OXYGEN ATOMS WITH ETHYLENE (For ethylene oxide decomposition the rates are relative to the total number of moles of products containing oxygen, i.e., to the sum of CO, total aldehyde, and CH_2CO; the bracketed figures are relative to CO taken as 0.50. For the reaction of oxygen atoms with ethylene, the rates are expressed per oxygen atom consumed)

	CO	H_2	CH_4	C_2H_6	C_3H_8	CH_2CO	RCHO	C_2H_4
Ethylene oxide alone	.60	.46	.10	.10	.07	.03	.37	Small
Ethylene oxide $+C_2H_4$	.35 (.50)	.07 (.10)	.04 (.16)	.10 (.14)	.12 (.17)	.06 (.08)	.59 (.85)	Not detd.
Ethylene oxide $+C_4H_8$	.34 (.50)	.07 (.10)	.05 (.08)	.06 (.09)	.002 (.002)	.01 (.02)	.65 (.89)	.10 (.15)
O atoms $+C_2H_4$	.50	.09	.11	.17	.17	.04	.40	Not detd.

into H and C_2H_3O radicals. The CH_2CHO radicals, formed from C_2H_3O, could be visualized as being responsible for increased aldehyde formation by combination with free radicals. While this view seems to fit better all the experimental observations, it is also possible that the increased aldehyde formation could be due to a direct primary isomerization to acetaldehyde. An analysis of the material balance of the process, which could remove much of the ambiguity, is impossible until detailed and accurate determinations of the aldehydes formed are available.

An observation arising from the butene-1 inhibited experiments is that some ethylene is formed in the mercury sensitized decomposition of ethylene oxide. Two ways of formation of this compound appear possible: a primary split into C_2H_4 and an O-atom, or some reaction involving CH_2 radicals. In connection with the latter possibility it is of interest that some preliminary work of Gesser (7) indicates that C_2H_4 is formed in the reaction of CH_2 radicals with ethylene oxide.

The results of the experiments reported in the literature and in the present work indicate that there is a significant similarity between the different modes of decomposition of ethylene oxide: the thermal, photolytic, mercury photosensitized, and the decomposition of the energy rich molecule formed in the reaction of oxygen atoms with ethylene. The differences observed appear to be largely of a quantitative rather than a qualitative character and may be ascribed to a variation in the relative importance of the different primary processes and, in the case of thermal decomposition, also to a variation with temperature of the stability and the reactivity of the intermediate free radicals and atoms formed.

ACKNOWLEDGMENT

The author is thankful to Dr. A. W. Tickner for mass-spectrometer analyses, to Mrs. P. M. Schreiber and Mr. D. S. Russell for infrared analyses, and to Mr. L. C. Doyle for valuable technical assistance. A number of helpful suggestions made by Dr. E. W. R. Steacie are gratefully acknowledged.

REFERENCES

1. BYWATER, S. and STEACIE, E. W. R. J. Chem. Phys. 19: 319. 1951.
2. CALLEAR, A. B. and CVETANOVIĆ, R. J. Can. J. Chem. 33: 1256. 1955.
3. CVETANOVIĆ, R. J. J. Chem. Phys. 23: 1203. 1955.
4. CVETANOVIĆ, R. J. J. Chem. Phys. 23: 1208. 1955.
5. CVETANOVIĆ, R. J. J. Chem. Phys. 23: 1375. 1955.
6. CVETANOVIĆ, R. J. and CALLEAR, A. B. J. Chem. Phys. 23: 1182. 1955.
7. GESSER, H. Private communication.
8. GOMER, R. and NOYES, W. A., JR. J. Am. Chem. Soc. 72: 101. 1950.
9. HORNER, E. C. A., STYLE, D. W. G., and SUMMERS, D. Trans. Faraday Soc. 50: 1201. 1954.
10. LOSSING, F. P., INGOLD, K. U., and TICKNER, A. W. Discussions Faraday Soc. No. 14: 34. 1953.
11. MUELLER, K. H. and WALTERS, W. D. J. Am. Chem. Soc. 76: 330. 1954.
12. PHIBBS, M. K., DARWENT, B. DEB., and STEACIE, E. W. R. J. Chem. Phys. 16: 39. 1948.
13. STEACIE, E. W. R. Atomic and free radical reactions. 2nd ed. Reinhold Publishing Corporation, New York. 1954. Chap. V.

SOLUBILITY CRITERIA FOR THE EXISTENCE OF HYDROXYAPATITE[1]

By J. S. Clark

ABSTRACT

The solubilities of synthetic basic calcium phosphate precipitates in carbon dioxide free aqueous systems were studied over a wide range of conditions. The pH of the suspensions and the calcium and phosphate concentrations in the solutions were determined both after precipitation and after dissolution of the solid phases. Solubility criteria applied to these measurements indicated that hydroxyapatite has a definite solubility product.

INTRODUCTION

Although hydroxyapatite is generally considered to be one of the stable basic calcium phosphates in nature, its existence as a compound with a fixed crystalline form and a unique solubility is controversial. Neumann and his co-workers (6, 7) considered the basic calcium phosphate system to be a solid phase of variable composition so that the principle of solubility product would not apply. In contrast to this opinion, the thermodynamic properties of crystalline hydroxyapatite have been reported by the Chemical Engineering Division of the TVA (8). Since in a previous paper solubility criteria were proposed as a means of establishing the existence of calcium phosphate compounds in soils (2), it was considered desirable to resolve the contrasting views on the solubility of hydroxyapatite in order to evaluate the validity of this approach. The object of the work reported here was to determine whether hydroxyapatite possesses a definite solubility product over a wide range of conditions.

EXPERIMENTAL

The solid phase calcium phosphates used for the solubility measurements were prepared by reacting dilute solutions of $Ca(OH)_2$ and H_3PO_4 at different temperatures for various periods of time while N_2 (CO_2 free) was passed through the systems. Following reaction at elevated temperatures, the flasks containing the suspensions were placed in a water bath at 25°C. for 96 hr. and the pH was measured with a glass electrode in the presence of N_2. The suspensions were filtered rapidly and phosphate and calcium determinations were made on the filtrates by the molybdenum blue (4) and the versene (1) methods, respectively. The activities of the ions were estimated by means of the Debye–Huckel equation (5).

In some cases, the precipitates were separated from the solutions and redispersed at 25°C. in CO_2-free water through which N_2 was passed. After 24 hr., the pH was measured and calcium and phosphate determinations were made on these suspensions in the manner described above.

[1]*Manuscript received July 28, 1955.*
Contribution No. 285, Chemistry Division, Science Service, Department of Agriculture, Ottawa, Canada.

RESULTS AND DISCUSSION

In preliminary experiments, it was found that reproducible solubilities could not be obtained in the presence of CO_2 even after reaction for long periods at relatively high temperatures. For this reason, a CO_2-free atmosphere was used in all experiments. In addition, it was found that, although satisfactory results were obtained by rapid mixing of the $Ca(OH)_2$ and H_3PO_4 solutions below a final pH of about 7.8, it was necessary to combine the reacting solutions slowly above this pH in order to obtain equilibrium.

The solubility measurements made on precipitates which had reacted at 90°C. for 120 hr. are reported in Table I, and those obtained by redispersing some of these precipitates in water are presented in Table II. The values for

TABLE I

SOLUBILITY OF HYDROXYAPATITE MEASURED AFTER PRECIPITATION

No.	pH	pCa	pH_2PO_4	pPO_4	$pH-\frac{1}{2}pCa$	$pH_2PO_4+\frac{1}{2}pCa$	$pK_{sp}=10pCa+6pPO_4+2pOH$
1	5.04	2.66	2.24	11.69	3.71	3.57	114.66
2	5.10	2.79	2.48	11.81	3.70	3.88	116.56
3	5.29	2.87	2.50	11.45	3.85	3.94	114.82
4	5.37	3.03	2.65	11.44	3.85	4.17	116.20
5	5.40	3.05	2.55	11.28	3.87	4.08	115.38
6	5.42	2.97	2.54	11.23	3.93	4.03	114.24
7	5.58	3.15	2.77	11.14	4.00	4.35	115.18
8	5.78	3.39	3.02	10.99	4.08	4.72	116.28
9	5.82	3.41	3.05	10.94	4.11	4.76	116.10
10	5.83	3.39	3.04	10.91	4.13	4.74	115.70
11	5.88	3.47	3.15	10.92	4.14	4.89	116.46
12	5.94	3.52	3.11	10.76	4.18	4.87	115.88
13	6.02	3.56	3.33	10.82	4.24	5.11	116.48
14	6.08	3.62	3.27	10.64	4.27	5.08	115.88
15	6.44	3.85	3.58	10.23	4.51	5.51	115.00
16	6.57	4.09	3.49	9.88	4.52	5.54	115.04
17	6.60	4.00	3.71	10.04	4.60	5.71	115.04
18	6.78	4.04	3.97	9.94	4.76	5.99	114.48
19	7.26	4.34	4.70	9.71	5.09	6.87	115.14
20	7.30	4.40	4.77	9.70	5.10	6.97	115.60
21	7.30	4.50	4.69	9.62	5.05	6.94	116.12
22	7.54	4.46	5.17	9.62	5.31	7.40	115.24
23	7.69	4.45	5.43	9.58	5.41	7.66	114.60
24	7.70	4.74	5.17	9.30	5.33	7.54	115.80
25	8.36	4.72	6.60	9.41	6.00	8.96	114.94
26	8.51	4.52	7.20	9.71	6.25	9.46	114.44
27	8.91	5.4*	6.68	8.39	6.21	9.38	114.52

**Approximate Ca^{++} activity.*

TABLE II

SOLUBILITY OF HYDROXYAPATITE MEASURED AFTER DISSOLUTION

No.	pH	pCa	pH_2PO_4	pPO_4	$pH-\frac{1}{2}pCa$	$pH_2PO_4+\frac{1}{2}pCa$	$pK_{sp}=10pCa+6pPO_4+2pOH$
D2	6.31	3.75	3.41	10.32	4.43	5.29	114.80
D6	5.62	3.22	2.85	11.14	4.01	4.46	115.80
D8	6.36	3.90	3.41	10.22	4.41	5.36	115.60
D15	7.13	4.28	4.43	9.70	4.99	6.57	114.74
D20	7.56	4.50	5.05	9.46	5.31	7.30	114.64
D24	6.94	4.28	4.22	9.87	4.80	6.36	116.14
D27	8.48	4.76	6.83	9.40	6.10	9.21	115.04

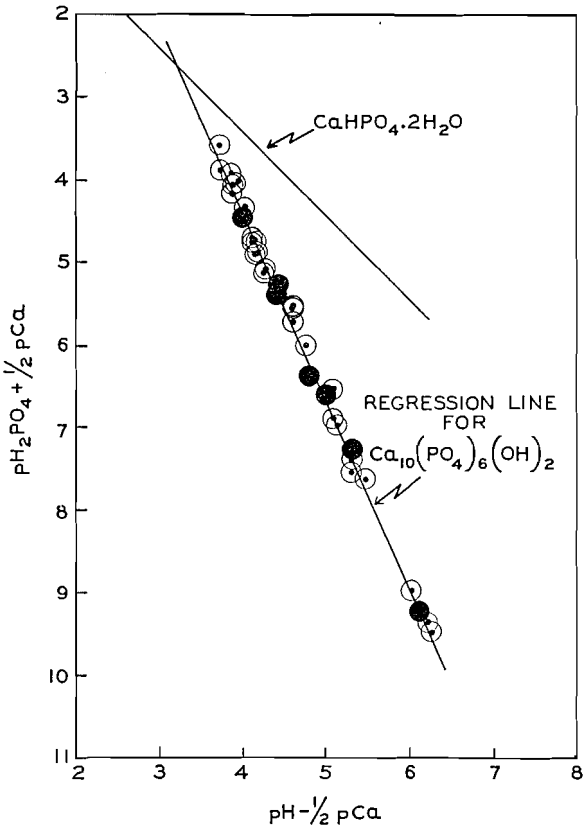

FIG. 1. Solubility diagram.
Legend: ⊙ Solubility measured after precipitation.
● Solubility measured after dissolution.

$pH-\frac{1}{2}pCa$ and $pH_2PO_4+\frac{1}{2}pCa$ in these tables are plotted on the solubility diagram in Fig. 1. Details with respect to the construction and interpretation of the diagram were presented in earlier publications (2, 3). The regression line relating $pH-\frac{1}{2}pCa$ and $pH_2PO_4+\frac{1}{2}pCa$ was calculated from the data and the corresponding value for the negative logarithm of the solubility product was 115.5. The slope of the regression line was similar to that for hydroxyapatite (actual slope 2.26 as compared with a theoretical value of 2.11) indicating that, although the calcium concentration varied from 10^{-3} to 10^{-6} M, the phosphate concentration from 10^{-3} to 10^{-6} M, and the pH from 5 to 9, hydroxyapatite possesses a definite solubility product.

To ascertain if heating to 90°C. for 120 hr. was sufficient to establish equilibrium, solubility measurements were made with precipitates that were prepared by reaction for 24 and 120 hr. at 40°C., 8 and 120 hr. at 60°C., and 4 and 120 hr. at 90°C. The solubilities, measured after equilibration at 25°C., are plotted on the enlarged section of the solubility diagram in Fig. 2. It is seen from Fig. 2 that increasing the reaction temperature decreased the solubilities

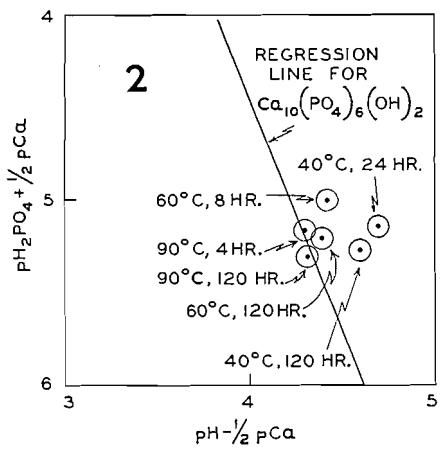

FIG. 2. The influence of reaction temperature and time of reaction at a given temperature on the solubility of hydroxyapatite.

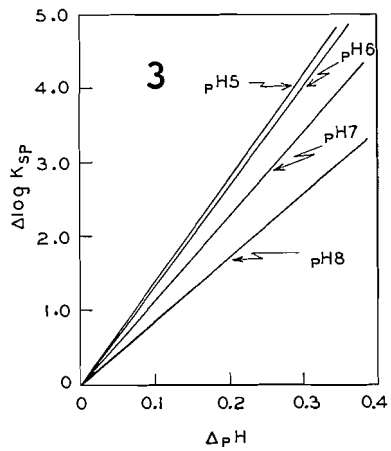

FIG. 3. The effect of errors in the measurement of pH on the calculated solubility product of hydroxyapatite.

of the precipitates. The solubilities were also decreased by increasing the length of the reaction period except at 90°C. The solubility after 4 hr. at 90°C. was as low as that after heating for 120 hr. at this temperature, and it is noted further that the solubility was only slightly higher after heating for 120 hr. at 60°C. Thus, heating for 120 hr. at 90°C. evidently was sufficient to produce stable conditions in these basic calcium phosphate systems.

As it was possible that the systems which had reacted at temperatures below 90°C. were in a state of supersaturation, the precipitates were separated from the solution and dispersed in water at 25°C. and the solubility measured 24 hr. later. The solubilities of precipitates formed at 90°C. were measured in this way and showed good agreement with the values obtained by precipitation (compare Tables I and II). On the other hand, after the solid phase of the system which had reacted for 24 hr. at 40°C. was redispersed in water the value obtained for $pH - \frac{1}{2}pCa$ was 5.14 and that for $pH_2PO_4 + \frac{1}{2}pCa$ was 6.10. Comparing these values with those for the corresponding precipitated system in Fig. 2, it is seen that the solubility did not decrease, indicating that the solution was not simply supersaturated. Similarly, when the other precipitates formed below 90°C. were redispersed in water, the solutions remained at the same degree of apparent supersaturation as in the original precipitated system. Increasing the reaction temperature and the length of the reaction period apparently served to age the precipitates producing better defined crystals with a lower solubility. Although the rate of precipitation and aging of hydroxyapatite is slow, its rate of dissolution is rapid since stable conditions were reached in 24 hr. when the precipitates were dispersed in water. These experiments on the dissolution of hydroxyapatite support the contention that a state of virtual equilibrium had been attained by heating to 90°C., and they indicate that the nature of the solid phase was not changed by heating.

In the light of these experiments on the effect of reaction time and temperature on the solubility of hydroxyapatite, it is improbable that the variability of the solubility products reported in the last columns of Tables I and II was caused by the failure to obtain stable conditions. The variability can be attributed to a great extent to the influence of analytical errors in the calculation of the solubility product where the ion activities are raised to such high exponents. As illustrated in Fig. 3, relatively small errors in pH may have a marked effect on the value of the calculated solubility product. Considering the effect of possible errors in the measurement of pH, the discrepancies observed in the pK_{sp} values do not appear serious.

In these unbuffered systems, errors in the measurement of pH coupled with errors in the determination of calcium and phosphate concentrations were probably sufficient to account for the observed differences in the values obtained for the solubility products. Further refinements in experimental technique would be necessary to obtain an accurate experimental value but these experiments were adequate to demonstrate that, within accountable errors, hydroxyapatite has a definite solubility product over a wide range of conditions.

REFERENCES

1. BERSWORTH CHEMICAL CO. The Versenes. Tech. Bull. No. 2. 6th ed. Bersworth Chemical Co., Framingham, Mass. 1953.
2. CLARK, J. S. and PEECH, M. Soil Sci. Soc. Amer. Proc. 19: 171. 1955.
3. CLARK, J. S. and TURNER, R. C. Can. J. Chem. 33: 665. 1955.
4. DICKMAN, S. R. and BRAY, R. H. Ind. Eng. Chem. Anal. Ed. 12: 665. 1940.
5. GLASSTONE, S. Introduction to electrochemistry. D. Van Nostrand Company, Inc., New York. 1942.
6. LEVINSKAS, G. J. and NEUMANN, W. F. J. Phys. Chem. 59: 164. 1955.
7. NEUMANN, W. F. and NEUMANN, M. W. Chem. Revs. 53: 1. 1953.
8. TENNESSEE VALLEY AUTHORITY. Phosphorus, properties of the element and some of its compounds. Chem. Eng. Rept. No. 8. 1950.

PERIODATE–PERMANGANATE OXIDATIONS

I. OXIDATION OF OLEFINS[1]

By R. U. Lemieux[2] and E. von Rudloff[3]

ABSTRACT

It was discovered that olefinic double bonds are readily oxidized in an aqueous solution of periodate which contains only catalytic amounts of permanganate. The data suggest that in the effective pH range of 7 to 10 the permanganate is not reduced at once beyond the manganate state and that it is regenerated from this state by periodate action. Evidence was obtained that the main course of the oxidation of an olefin of type —CH=CH— involves first permanganate oxidation to hydroxyketones which are then rapidly cleaved by periodate to products which may subsequently be oxidized by the permanganate.

INTRODUCTION

The use of a mildly alkaline solution of periodate containing permanganate as a reagent for the detection of carbohydrates on paper chromatograms was described by Lemieux and Bauer (6). This communication deals with the ability of the reagent to oxidize olefins smoothly.

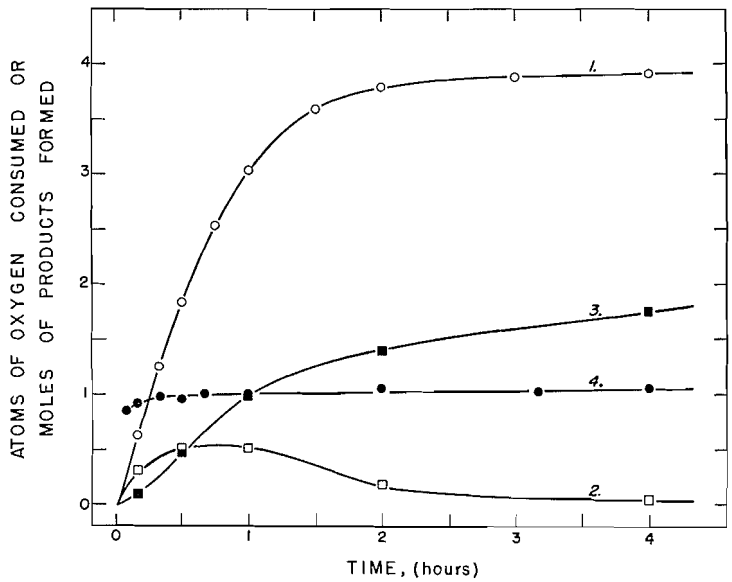

FIG. 1. Plot 1: Periodate (0.0197 *M*) – permanganate (0.00034 *M*) oxidation of oleic acid (0.0025 *M*) in the presence of potassium carbonate at pH 7.7 and 20°C. (atoms of oxygen consumed per oleate ion). Plot 2: Aldehyde formed during the oxidation of oleic acid (plot 1; moles per oleate ion). Plot 3: Acids formed during the oxidation of oleic acid (plot 1; moles per oleate ion). Plot 4: Oxidation of 9,10-dihydroxystearic acid and 9,10-keto hydroxystearic acids under the conditions of plot 1, but without the permanganate (atoms of oxygen consumed per stearate ion).

[1]*Manuscript received August 9, 1955.*
Contribution from the National Research Council of Canada, Prairie Regional Laboratory, Saskatoon, Saskatchewan. Issued as Paper No. 205 on the Uses of Plant Products and as N.R.C. No. 3742. Presented in part at the Second Western Regional Conference of the Chemical Institute of Canada, Vancouver, B.C., September 9–11, 1954.
[2]*Present address: Department of Chemistry, University of Ottawa, Ottawa, Ontario.*
[3]*National Research Council of Canada Postdoctorate Fellow, 1953–54.*

The data presented in Fig. 1 (plot 1) show that a reagent consisting of 0.0197 *M* periodate and 0.00034 *M* permanganate at pH 7.7 and 20°C. efficiently oxidized 0.0025 *M* oleate ion with the consumption of the amount of oxidant theoretically required to cleave the olefin to carboxylic acid.

$$\begin{matrix} -CH \\ \| \\ -CH \end{matrix} + 4[O] \longrightarrow 2\,-COOH$$

The fact that after 20 hours' reaction time these conditions gave a product from which azelaic and pelargonic acids were isolated in quantitative yields shows that the oxidation was specific for the olefinic linkage. Periodate alone did not oxidize the olefin. Therefore, the ability of the reagent to bring about complete cleavage of the olefin must depend on an ability of the periodate ions to regenerate permanganate from its reduced state. We have observed that the addition of sodium *meta*-periodate to an alkaline solution of manganate ion (11) resulted in the immediate formation of permanganate ion. This observation provided a satisfactory explanation for the regeneration of the permanganate in the above periodate–permanganate oxidation since Drummond and Waters (2) have recently produced evidence that olefins and other organic compounds do not reduce permanganate at once beyond the manganate stage. This conclusion was supported by the effect of pH on the ability of the reagent to oxidize substances stable toward periodate. The data presented in Fig. 2 show that, in acidic media, the oxidation of mesityl oxide did not go to completion and that the extent of oxidation was least when the pH was lowest. The cessa-

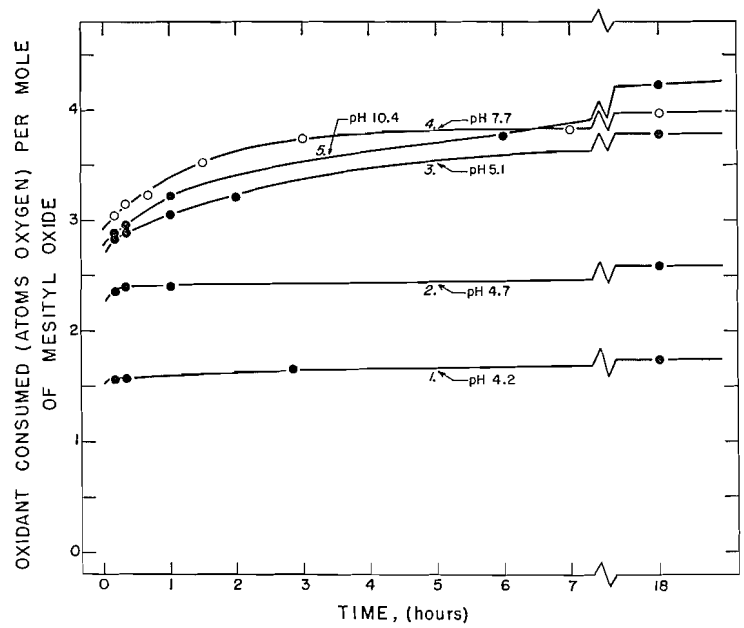

FIG. 2. Experimental rates for the oxidation of mesityl oxide (0.0025 *M*) at 20°C. Relative molar concentrations: mesityl oxide, 1; sodium *meta*-periodate, 7.9; potassium permanganate, 0.13; potassium carbonate, 0 (plot 1), 0.125 (plot 2), 0.25 (plot 3), 1 (plot 4), 10 (plot 5).

tion of oxidation was accompanied by precipitation of manganese dioxide. It is well known that manganate ions disproportionate into manganese dioxide and permanganate ions in acidic media. Since periodate does not oxidize manganese dioxide to permanganate in alkaline media, the oxidations which had ceased to operate in acidic media did not resume when the solution was rendered alkaline. The periodate oxidation of α-glycols usually becomes very slow in strongly alkaline media (1, 10). Since this is a step in the periodate–permanganate oxidation of olefins, high pH's are not favorable. Furthermore, strongly alkaline media lead to disappearance of the typical permanganate color. Therefore, it was concluded that the most favorable pH range for the periodate–permanganate reagent is from 7 to 10.

Permanganate has been widely used to hydroxylate olefins. Treatment of oleic acid with an alkaline solution of permanganate yields racemic *erythro*-9,10-dihydroxystearic acid (3, 5). The reaction results in a green solution containing manganate ion. However, when the oxidation is carried out near neutrality and an excess of permanganate is avoided, the main product is a mixture of 9-keto-10-hydroxy and 9-hydroxy-10-keto-stearic acids (3). 9,10-Dihydroxystearic acid is formed only in smaller amounts. Since King (3) was unable to prepare the ketohydroxy acids by a similar oxidation of the 9,10-dihydroxy acid, it was evident that the mechanism of the permanganate oxidation of olefins is strongly dependent on pH.

The periodate–permanganate oxidation of oleate ion described in Fig. 1 was carried out at pH 7.7, i.e. in the pH range where the main product of the permanganate oxidation of oleate ion is the mixture of ketohydroxy acids. If this product was also intermediate in the periodate–permanganate oxidation, then it could be concluded that the initial stages of the periodate–permanganate oxidation involve true permanganate oxidation. Direct evidence that the ketohydroxy acids were in fact intermediates was obtained by oxidizing oleate ion (0.0025 M) at pH 7.7 using a relatively high concentration of permanganate (0.000806 M) to speed up the initial stage of the reaction and only a relatively small amount of periodate (0.00106 M). The reaction was stopped by the addition of bisulphite at the first indication that the permanganate was not being regenerated as evidenced by the appearance of manganese dioxide. This procedure restricted the reaction to the conditions which prevail in periodate–permanganate oxidation. The product contained the mixture of ketohydroxystearic acids in near quantitative yield based on the amount of periodate added. Elaidic acid was also in part converted to the ketohydroxystearic acids and 10-undecenoic acid was oxidized in part to 10-keto-11-hydroxyundecanoic acid under similar reaction conditions. Since 9,10-epoxystearic acid was not oxidized under these conditions, the intermediate formation of epoxides was ruled out.

Furthermore, the periodate–permanganate oxidation of ethylene resulted in the formation of only about one mole of formaldehyde on the consumption of oxidant equivalent to four oxygen atoms. Had ethylene glycol alone been produced in the first stage of the reaction, a consumption of oxidant equivalent to only two oxygen atoms would have yielded two moles of formaldehyde. Therefore, it seems clear that the periodate–permanganate oxidation of an

olefin in the pH range 7 to 8 has a strong tendency to proceed by way of an acyloin. It is noteworthy in this respect that the permanganate oxidation under near neutral conditions may prove to be a useful means for converting certain olefins to acyloins.

The products isolated after different reaction times in the course of the oxidation of oleate ion under the conditions described in Fig. 1 were analyzed for their aldehyde and carboxylic acid contents. The results, plotted in Fig. 1 (plots 2 and 3), form a picture of the reaction sequences involved in terms of the isolable products. Since periodate alone rapidly oxidized the 9,10-dihydroxy and ketohydroxystearic acids (plot 4), the concentration of these substances must always have been relatively small. The fact that the amount of aldehyde passed through a maximum at 0.52 mole per gram ion of oleate ion oxidized supports the above conclusion that the ketohydroxystearic acids were intermediates in the over-all reaction.

Thus, in terms of the isolable organic products, the periodate–permanganate oxidation can be considered to take place in three stages. The first stage appears to be a complex sequence of reactions which involve permanganate ion in one-electron exchanges leading, near neutrality, mainly to hydroxyketone. The rapid periodate cleavage of the hydroxyketone (and any diol which may have been formed) can be considered as the second stage. This property of the periodate–permanganate reagent is undoubtedly that mainly responsible for the high specificity of the over-all reaction. The oxidation of the products formed in the periodate cleavage through permanganate action can be considered as the third stage. It is noteworthy that the fact that the reagent requires only mildy alkaline conditions is conducive to the oxidation of an aldehyde without degradation.

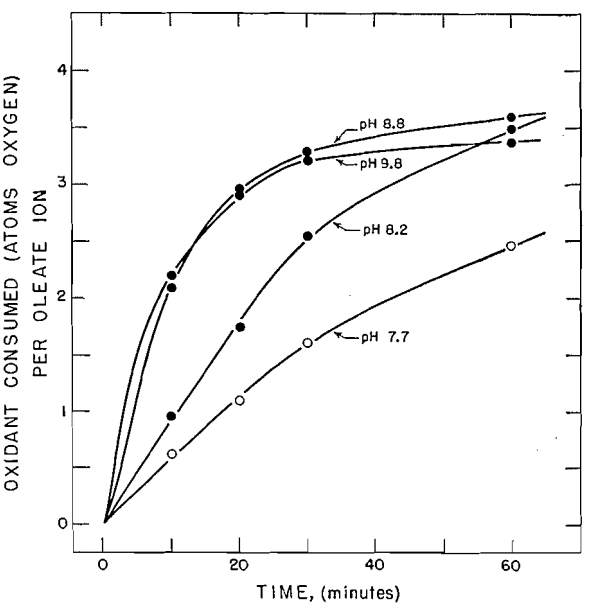

FIG. 3. Effect at 20°C. of pH on the rate of periodate (0.02 *M*) – permanganate (0.00034 *M*) oxidation of oleate (0.0025 *M*).

Although the periodate–permanganate reagent is limited in application to the oxidation of compounds which are soluble in slightly alkaline media, the high yields obtained and the convenience of operation render it likely that the reagent will find application for degradative and analytical purposes. Thus, for example, the oxidation of 10-undecenoic acid gave sebacic acid and formaldehyde in excellent yield. The fact that formaldehyde resisted oxidation suggests the use of the reagent for determining terminal methylene groups (7). The oxidation of mesityl oxide at pH 7.7 gave a quantitative yield of acetone. This result forms a convenient basis for the determination of terminal isopropylidene groups and will be described in a later communication (12).

In view of these possible uses for the reagent, a study was made of the effect of certain variables on the rate of reaction using oleate ion as substrate. The data plotted in Fig. 3 show that the rate of the over-all reaction increases with increase in pH. The effect of temperature on the rate of reaction is illustrated in Fig. 4. The plots of Fig. 5 show clearly that permanganate is involved in the rate controlling stages. The results presented in Fig. 6 show that an increase in the periodate ion concentration has a retarding effect on rate of reaction. This interesting effect was not to be expected. Nevertheless, these results serve as further evidence that in these oxidations the steps which involve periodate ion are fast as compared to those which involve permanganate ion. It should be noted in this respect that the periodate cleavage of glycols is strongly dependent on pH in basic media with the rate of reaction decreasing with increasing pH (1, 10). This fact may account for the slower rate of the second stage of periodate–permanganate oxidation of oleate ion on going from pH 8.8 to 9.8 (see Fig. 3).

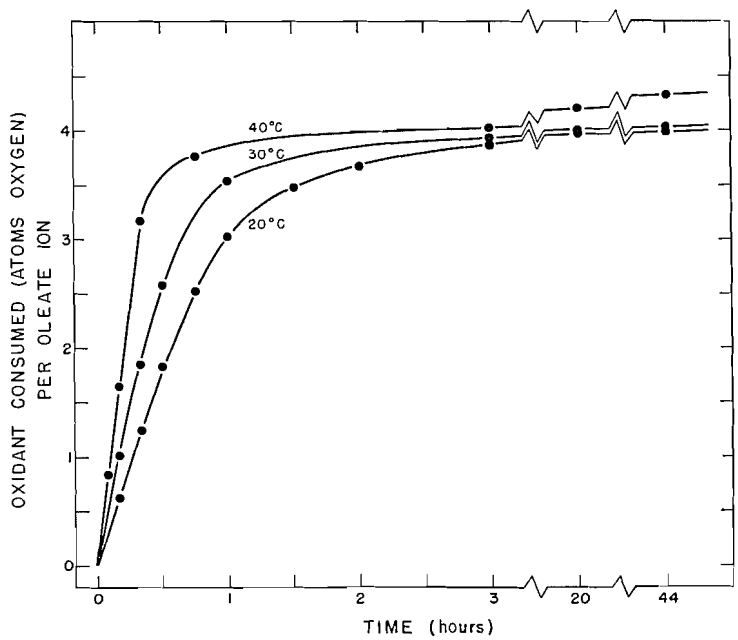

FIG. 4. Effect of temperature on the rate of periodate–permanganate oxidation of oleate using the conditions of Fig. 1, plot 1, except for temperature.

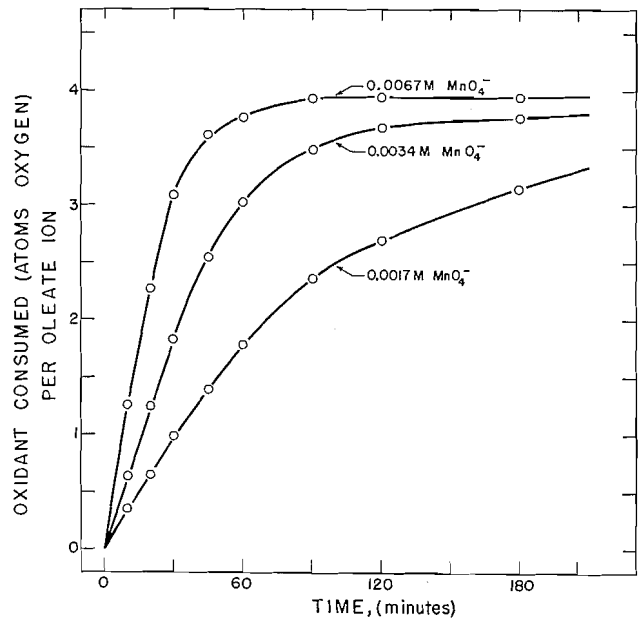

FIG. 5. Effect of the permanganate concentration on the rate of periodate–permanganate oxidation of oleate using the conditions of Fig. 1, plot 1, except for the permanganate concentration.

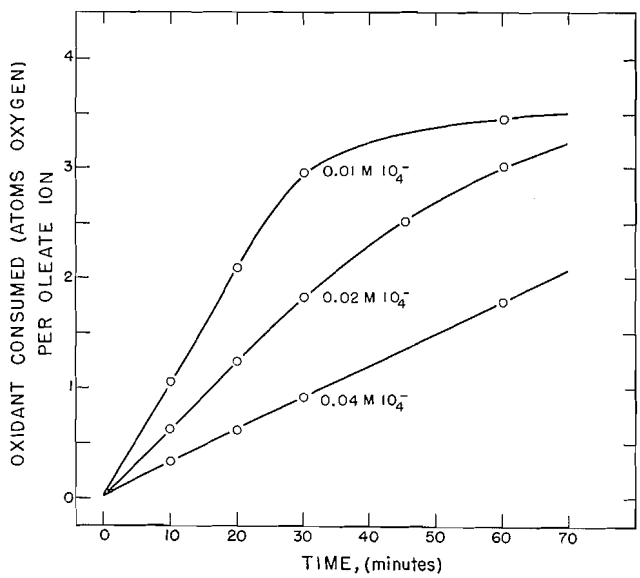

FIG. 6. Effect of the periodate concentration on the rate of periodate–permanganate oxidation of oleate using the conditions of Fig. 1, plot 1, except for the periodate concentration.

EXPERIMENTAL

Methods

The following procedure was used to follow the rates of oxidation. The required amounts of olefin and potassium carbonate were dissolved in water and the solution was made up to 100 ml. The periodate–permanganate reagent was made up freshly before use by mixing the required amounts of standard solutions of sodium *meta*-periodate and potassium permanganate and diluting to 100 ml. At zero time, 5-ml. volumes of the two solutions at the desired temperature were mixed in a glass-stoppered flask. The reaction was stopped by rapidly adding about 0.5 gm. sodium bicarbonate, a measured volume of standard arsenite solution, and a few crystals of potassium iodide. After this solution was left for at least 10 min., the excess arsenite was determined by slow titration of the stirred solution with standard iodine solution to the starch end point. The difference between the titers for a run and a reagent blank was taken as equivalent to the oxidant consumed. The pH values reported were measured soon after the reaction mixture was made up. In some experiments, potassium hydroxide was added to achieve the desired pH. The following procedure was used to determine the amounts of aldehyde and acid present in the reaction mixture (see Fig. 1). After a given reaction time, the oxidant was destroyed and the solution rendered strongly acid by the addition of an excess arsenite solution and 10% sulphuric acid. The resulting mixture was extracted continuously with ether. The extract was filtered and concentrated to a small volume. The acid content in the residue was determined by titration with standard methanolic sodium hydroxide to the phenolphthalein end point. The aldehyde content was determined by the hydroxylamine procedure of Siggia (13).

Runs with mixtures of heptanal, azelaic acid, and oleic acid showed the method reliable to within ±2% for the acid content and to within ±10% for the aldehyde content. Formaldehyde was determined colorimetrically using chromotropic acid (4, 7). The acetone liberated in the oxidation of mesityl oxide was removed from the oxidation mixture by distillation and determined by iodometric titration (9).

Oxidations of Oleic Acid

A reaction mixture, 400 ml., which contained initially 0.2824 gm. (1 mM.) of pure oleic acid, 3 mM. of potassium carbonate, 8 mM. sodium *meta*-periodate, and 0.134 mM. potassium permanganate was kept at 20°C. for 20 hr. The solution was rendered strongly acid by addition of 10% sulphuric acid and extracted with ether. The extraction yielded 0.354 gm. of material which on trituration with petroleum ether gave 161 mgm. of an oil with neutral equivalent 164. The oxidation would theoretically yield 0.158 gm. of pelargonic acid and 0.188 gm. of azelaic acid. The oil was distilled *in vacuo* and then gave a hydrazide of m.p. 93.5–94.5°C. (undepressed by pelargonic acid hydrazide m.p. 94–95°C. (8)). The residue from the trituration melted at 102–104.5°C. (undepressed by azelaic acid m.p. 106.5–107.5°C.) and was pure azelaic acid after recrystallization first from water and then from ethyl acetate.

A reaction mixture, 200 ml., was made up at 20°C. which contained 0.1412 gm. (0.5 mM.) oleic acid, 1.5 mM. potassium carbonate, 0.162 mM. potassium permanganate, and 0.2 mM. sodium *meta*-periodate. The initial pH was 7.7. Discoloration of the permanganate began in about three minutes and a large excess of sodium bisulphite was immediately added. The precipitate which formed on acidification was filtered off and triturated with cold petroleum ether to yield 35 mgm. of a substance, which was recrystallized from petroleum ether. The melting point, 60–62°C., of the material, 31 mgm., was not depressed by the mixture of ketohydroxystearic acids, m.p. 62–63.5°C., prepared by the method of King (3).

Almost exactly the same result was obtained when elaidic acid, m.p. 42.5–43.5°C., was oxidized under the above conditions except that the low solubility of the elaidate ion required that the reaction mixture be 2.5 times more dilute.

Oxidations of 10-Undecenoic Acid

10-Undecenoic acid was oxidized in the manner described above for oleic acid (Fig. 1, plot 1). Commercial undecenoic acid was distilled *in vacuo* to give a product of about 96% purity (iodine value 132); 0.190 gm. of the distilled acid yielded 0.192 gm. petroleum ether insoluble material, m.p. 126–131°C. Recrystallization from water and ethyl acetate yielded a product of m.p. 131–132.5°C. (undepressed by sebacic acid, m.p. 132–133°C.). The yield of formaldehyde was 73% (7).

The following procedure for preparing 10,11-dihydroxyundecanoic acid is similar to that described by Lapworth and Mottram (5) for the preparation of 9,10-*erythro*-dihydroxystearic acid. 10-Undecenoic acid, 0.68 gm., was dissolved with 1 gm. sodium hydroxide in 100 ml. of water and the solution was diluted to 800 ml. with ice-cold water. A 1% solution of potassium permanganate, 80 ml., was added with stirring. The mixture immediately changed in color to a dark green and was decolorized with sodium bisulphite after five minutes' reaction time. The solution was concentrated to 150 ml., made strongly acid with sulphuric acid, and extracted with ether. Evaporation of the dried ether extract to small volume led to the deposition of 0.50 gm. of a crystalline solid, m.p. 72–78°C. The material was recrystallized alternately from ethyl acetate and water to yield a substance, m.p. 67–69°C. Upon rapid recrystallization from acetone at −20 to −30°C. an acid was obtained, m.p. 83–84°C., which was undepressed in admixture with and possessed the same infrared spectrum as 10,11-dihydroxyundecanoic acid (m.p. 83–85°C.) prepared by the method of Swern *et al.* (14). The high and low melting forms could be readily interconverted by crystallization and both gave a *p*-bromophenacyl ester of m.p. 105–106°C. The material gave a negative 2,4-dinitrophenylhydrazine test, consumed oxidant equivalent to two atoms of oxygen on periodate–permanganate oxidation (as described above) with the formation of a mole of formaldehyde, and possessed the neutral equivalent (218) expected for 10,11-dihydroxyundecanoic acid (calc. 218.29).

10-Undecenoic acid (0.924 gm., 5 mM.) and potassium carbonate (5 mM.) were dissolved in 500 ml. of ice-cold water. An ice-cold solution of 5 mM.

potassium permanganate and 10 mM. sodium *meta*-periodate in 500 ml. water was added with stirring. After one minute, an excess of sodium bisulphite was added. The solution was concentrated to about 200 ml., cooled to about 2°C., and made strongly acid with cold 10% sulphuric acid. After the mixture had stood in the cold for 15 to 20 min., the precipitate was collected and dried, m.p. 83–89°C. Recrystallization from chloroform raised the melting point to 89–94°C. The following observations established the substance to be substantially pure 10-keto-11-hydroxyundecanoic acid. The infrared spectrum showed two bands in the carbonyl region and the material gave a positive 2,4-dinitrophenylhydrazine test. The material, neutral equivalent 220, liberated 1 mole of formaldehyde on periodate oxidation with the liberation, by titration, of 0.84 equivalent of acid per mole of periodate consumed. In a separate experiment, periodate oxidation gave a quantitative yield of crude sebacic acid, m.p. 119–129°C.; after two recrystallizations the compound had m.p. 130–132°C.

Oxidation of Ethylene

Ethylene, about 0.13 mM., was admitted to 200 ml. of solution containing 0.034 mM. potassium permanganate, 1.97 mM. sodium *meta*-periodate, and 0.25 mM. potassium carbonate kept in a nitrogen atmosphere. Highly erratic results were obtained when the reaction was performed in air. These results were probably due to the ability of permanganate to catalyze autoxidation (15). After it was shaken for 18 hr., the solution, pH 7.6, was analyzed as described above for oxidant content and for formaldehyde (7). Since the consumption of oxidant equivalent to 0.402 milliatoms of oxygen resulted in the formation of only 0.11 mM. formaldehyde, it is apparent that glycollic aldehyde is the first product of the reaction. It was established (7) that formaldehyde is oxidized only very slowly under these conditions.

ACKNOWLEDGMENTS

The authors wish to express their gratefulness to Dr. B. M. Craig who kindly supplied the oleic and 9,10-epoxystearic acids and to Miss Agnes Epp for the infrared-spectrographic measurements.

REFERENCES

1. BUIST, G. J. and BUNTON, C. A. J. Chem. Soc. 1406. 1954.
2. DRUMMOND, A. Y. and WATERS, W. A. J. Chem. Soc. 435. 1953.
3. KING, G. J. Chem. Soc. 1788. 1936.
4. LAMBERT, M. and NEISH, A. C. Can. J. Research, B, 28: 83. 1950.
5. LAPWORTH, A. and MOTTRAM, E. N. J. Chem. Soc. 1628. 1925.
6. LEMIEUX, R. U. and BAUER, H. F. Anal. Chem. 26: 920. 1954.
7. LEMIEUX, R. U. and RUDLOFF, E. VON. Can. J. Chem. 33: 1710. 1955.
8. PAJARI, K. Fette u. Seifen, 51: 347. 1944.
9. PREGL, F. and GRANT, J. Quantitative organic microanalysis. The Blakiston Co., Philadelphia. 1946. p. 170.
10. PRICE, C. C. and KROLL, H. J. Am. Chem. Soc. 60: 2726. 1938.
11. RUBY, C. E. J. Am. Chem. Soc. 43: 294. 1921.
12. RUDLOFF, E. VON. Can. J. Chem. 33: 1714. 1955.
13. SIGGIA, S. Quantitative organic analysis via functional groups. John Wiley & Sons, Inc., New York. 1949. p. 17.
14. SWERN, D., BILLEN, G. N., FINDLEY, T. W., and SCANLAN, J. T. J. Am. Chem. Soc. 67: 1786. 1945.
15. WATERS, W. A. Trans. Faraday Soc. 42: 184. 1946.

PERIODATE–PERMANGANATE OXIDATIONS

II. DETERMINATION OF TERMINAL METHYLENE GROUPS[1]

By R. U. Lemieux[2] and E. von Rudloff[3]

ABSTRACT

The periodate–permanganate oxidation of a terminal methylene ($CH_2{=}C<$) group can be made to produce formaldehyde in high although not quantitative yield. Since the yields compare favorably with those obtained by ozonolysis, the reagent can serve as the basis for a convenient micromethod for the estimation of terminal methylene groups. The less than theoretical yields of formaldehyde are believed mainly due to the conversion of the olefin in part to α-hydroxyaldehyde in the initial stage of the reaction.

INTRODUCTION

Results were reported in our first communication in this series (12) which indicated that the periodate–permanganate oxidation of a terminal methylene group (I) produces, simultaneously, in the first stage of the reaction, glycol (II), ketol (III), and hydroxyaldehyde (IV). Subsequent periodate oxidation of these substances produces formaldehyde from II and III but not from IV. Glycol formation did not appear extensive in weakly alkaline media since the oxidation of ethylene gave very nearly one mole of formaldehyde. However, oxidation of 10-undecenoic acid gave a 73% yield of formaldehyde (12). It was therefore evident that the ketol formation can be the preferred route and since the oxidant attacked formaldehyde only very slowly, it was apparent that the reagent deserved attention as a means for the semiquantitative estimation of terminal methylene groups.

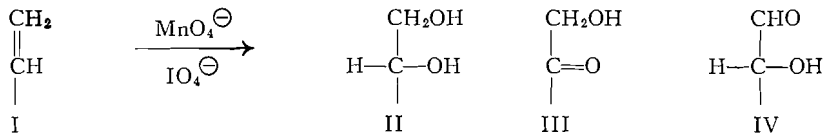

We now wish to report on evidence that any attempt to obtain a maximum yield of formaldehyde in the periodate–permanganate oxidation of a terminal methylene group should consider: (*a*) the effect of pH on the reaction route, (*b*) the effect of pH on the rate of the periodate oxidation of glycols and acyloins, (*c*) the effect of pH on the rate of the permanganate oxidation of formaldehyde, and (*d*) the solubility of the compound in aqueous media.

Evidence has been obtained (12) that hydroxylation of the olefin is favored at a pH of 9–10 with acyloin formation predominating at a slightly lower pH. On this basis, it would appear desirable to operate at a high pH. However, the periodate–permanganate reagent does not operate above about pH 10 (12). Also, even at pH 10, the periodate oxidation of glycols is relatively slow (3, 14).

[1]*Manuscript received August 9, 1955.*
Contribution from the National Research Council of Canada, Prairie Regional Laboratory, Saskatoon, Saskatchewan. Issued as Paper No. 203 on the Uses of Plant Products and as N.R.C. No. 3743.
[2]*Present address: Department of Chemistry, University of Ottawa, Ottawa, Ontario.*
[3]*National Research Council of Canada Postdoctorate Fellow, 1953–54.*

Furthermore, as seen in Fig. 1, formaldehyde is oxidized fairly rapidly at pH 10. Therefore, it is evident that should the pH of the media be maintained at a pH about 10, loss of formaldehyde would result from the oxidation of the formaldehyde and degradation of the glycol by the permanganate. Also, the use of alkaline media can be expected to give rise to formaldehyde from the enol

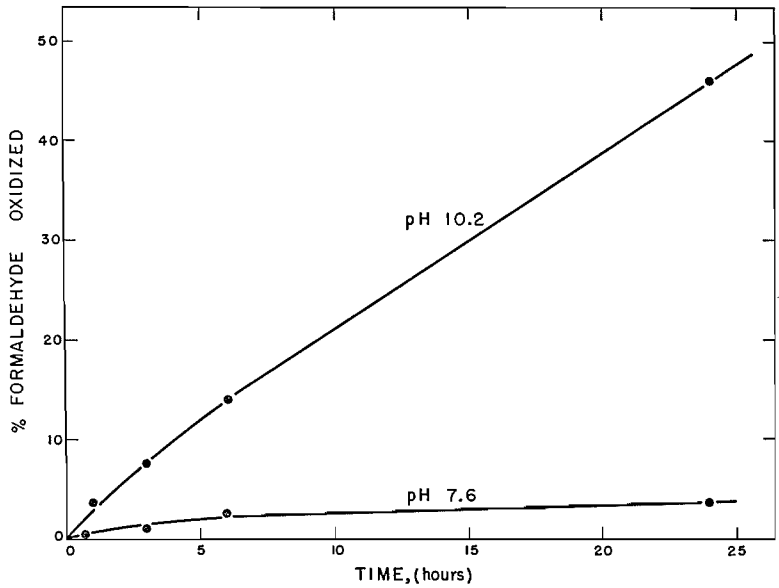

FIG. 1. Effect of pH on the rate of the oxidation of formaldehyde by the periodate–permanganate reagent.

form of methyl ketones thus complicating the results. On the other hand, the maintenance of the medium at near neutrality can be expected to result in the formation of appreciable amounts of hydroxyaldehyde. As a compromise to these conflicting effects, it was decided to carry out the oxidation for a short period of time at pH 10 and then to adjust the pH to near neutrality for completion of the reaction. The data listed in Table I show that this expedient gave in most cases a much improved yield of formaldehyde over that obtained when near neutral conditions were maintained throughout the reaction.

The yields of formaldehyde listed in Table I were determined colorimetrically using the chromotropic acid reagent according to the procedure of Lambert and Neish (10). The formaldehyde can also be determined by precipitation as the methone derivative (10, 13). In this case, larger samples are required and it is best to isolate the formaldehyde by distillation of the acidified reaction mixture before carrying out the precipitation. The present procedure should prove of value since it is easier to use than the standard methods of ozonolysis (4, 5), obviates the need of an expensive ozonizer, appears to provide higher yields of formaldehyde in many instances (see Table I), and may prove to be more reliable (6, 9, 15). The latter point is of importance since the detection of a terminal methylene group by infrared spectral analysis (2) must

TABLE I

TERMINAL METHYLENE GROUP ESTIMATIONS

(Maximum yields (per cent of theory) of formaldehyde obtained at pH∼7 and at pH∼10 with subsequent lowering to pH∼7)

Compound	Moles of CH_2O expected per mole of compound	pH∼7	pH∼10 → pH∼7	Reference
10-Undecenoic acid	1	73	97	
Itaconic acid	1	83	60	
Quinine	1	59	71	(9)[a]
Gelsemine	1	76	43	(8)
Isoatisine	1	76	50	(7)
Hydroxylactone	1	60	—	(1)[b]
Vinyl acetate	1	87	12(unstable)	(11)[c]
Allyl acetate	1	50	100(unstable)	
Allyl alcohol	2	57	—	
Allylamine	2	44	49	
Diallyl ether	2	55	89	
Allyl ethyl ether	1	56	81	
1-Allyl-2-thiourea	1	42	51	
Methacrylamide	1	45	69	(11)[c]
Acrylonitrile	1	14	50	
3-Butenenitrile	1	25	50	
3-Bromopropene	1	45	56	
Styrene	1	62	64	(4)[d]

[a]*Ozonolysis gave a 46% yield.*
[b]*Ozonolysis gave a 24% yield.*
[c]*Ozonolysis of a vinyl group and methyl methacrylate gave only 5% yields.*
[d]*Ozonolysis gave a 30% yield.*

be checked by chemical means. The method in its present form is restricted in scope by the fact that water is used as solvent. This limitation is not great, however, since only extremely low concentrations are required.

EXPERIMENTAL

The following procedures were used to determine the data listed in Table I and plotted in Fig. 1.

The compound, 0.005 mM., was dissolved in 5 ml. (or less) water contained in a 25 ml. volumetric flask. A quantity of 0.1 *N* potassium carbonate solution was then added to give the final solution a pH of 7 to 7.6. At zero time, 10 ml. of a solution of 0.02 *M* sodium *meta*-periodate and 1 ml. of 0.005 *M* potassium permanganate solution were added. The solution was made up to volume. Aliquots, 5 ml., were then transferred to 10 ml. volumetric flasks and after the desired time intervals, 15, 30, and 60 min., the reaction was stopped by the addition of 2 ml. of 1 *M* sodium arsenite solution and 2 ml. of 2 *N* sulphuric acid to a flask. The resulting solutions were then analyzed for their formaldehyde contents as described below, following the procedure of Lambert and Neish (10).

When it was desired to carry out the oxidation at higher pH's, 0.1 *N* potassium hydroxide was added to the solution before the addition of the oxidant. If it was desired to lower the pH back to near neutrality after a given period

of oxidation, an equivalent amount of hydrochloric acid was added before the solution was made up to volume. The data listed in Table I for pH about 10 with return to pH about 7 were obtained by adding 5 ml. of 0.1 *N* potassium hydroxide solution followed by 5 ml. of 0.1 *N* hydrochloric acid after about one minute's reaction time.

After the oxidation had been stopped, the solutions were allowed to stand for about 15 min., made up to volume (10 ml.), and 1-ml. aliquots were transferred to 25 × 200 mm. test tubes. Chromotropic acid reagent (1 gm. chromotropic acid in 100 ml. water, filtered and the filtrate made up to 500 ml. with 2:1 v/v concentrated sulphuric acid – water mixture), 10 ml., was added and the mixtures heated in a boiling water bath for 30 min. After the contents were cooled to room temperature, they were transferred to cuvettes for measurement of the per cent transmission at 570 mμ when compared to a reagent blank. Erythritol was used as standard for the production of known amounts of formaldehyde (2 moles of formaldehyde per mole of erythritol) in the setting up of a standard curve.

ACKNOWLEDGMENT

The authors are indebted to Dr. O. E. Edwards who supplied the alkaloids listed in Table I.

REFERENCES

1. ANET, F. A. L. and MARION, L. Can. J. Chem. 33: 849. 1955.
2. BERNARD, D., BATEMAN, L., HARDING, A. J., KOCH, H. P., SHEPPARD, N., and SUTHERLAND, G. B. B. M. J. Chem. Soc. 915. 1950.
3. BUIST, G. J. and BUNTON, C. A. J. Chem. Soc. 1406. 1954.
4. CLEMO, G. R. and MACDONALD, J. M. J. Chem. Soc. 1294. 1935.
5. DOEUVRE, J. Bull. soc. chim. 3: 612. 1936.
6. DURLAND, J. R. and ADKINS, H. J. Am. Chem. Soc. 61: 429. 1939.
7. EDWARDS, O. E. and SINGH, T. Can. J. Chem. 32: 465. 1954.
8. GOUTAREL, R., JANOT, M.-M., PRELOG, V., SNEEDON, R. P. A., and TAYLOR, W. I. Helv. Chim. Acta, 34: 1139. 1951.
9. KARRER, P. and KEBRLE, J. Helv. Chim. Acta, 35: 862. 1952.
10. LAMBERT, M. and NEISH, A. C. Can. J. Research, B, 28: 83. 1950.
11. LANGMAN, I., MCKAY, A. F., and WRIGHT, G. F. J. Org. Chem. 14: 550. 1949.
12. LEMIEUX, R. U. and RUDLOFF, E. VON. Can. J. Chem. 33: 1701. 1955.
13. MACFADYEN, D. A. J. Biol. Chem. 158: 107. 1945.
14. PRICE, C. C. and KROLL, H. J. Am. Chem. Soc. 60: 2726. 1938.
15. STOLL, M. and ROUVÉ, A. Helv. Chim. Acta, 27: 950. 1944.

PERIODATE–PERMANGANATE OXIDATIONS

III. DETERMINATION OF ISOPROPYLIDENE GROUPS[1]

By E. von Rudloff

ABSTRACT

The reaction of the periodate–permanganate reagent with olefinic double bonds was applied to the determination of isopropylidene groups. The oxidation of compounds containing such groups gave a quantitative yield of acetone which could be readily determined by known iodometric and colorimetric procedures. Use of aqueous solutions of pyridine or dioxane as solvent permitted analysis of water-insoluble compounds. The colorimetric determination of acetone was then preferred. This method also allowed a simultaneous estimation of terminal methylene groups. The content of isopropylidene groups of commercial samples of three terpenes of the geraniol type was determined.

INTRODUCTION

The oxidation of olefinic double bonds with the periodate–permanganate reagent was described in part I of this series (2). From the general characteristics of this reaction the oxidation of an isopropylidene group would be expected to proceed as follows at pH 7–8:

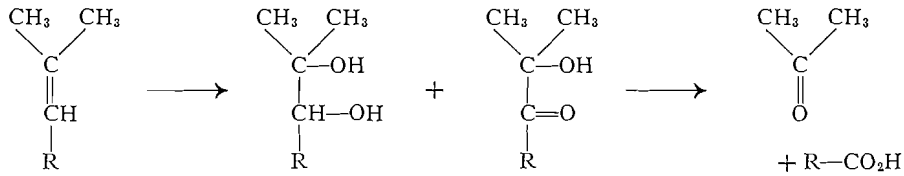

each isopropylidene group yielding one molecule of acetone. At neutrality the acetone formed by the oxidation of mesityl oxide did not appear to react further with the reagent (2). The yield of acetone could, therefore, be used as a convenient measure of isopropylidene groups in general. In conjunction with the semiquantitative estimation of terminal methylene groups, described in part II (3), such a procedure should also make it possible to distinguish readily between these two positions of unsaturation, which would be of special interest in the study of terpenes and resin acids.

RESULTS AND DISCUSSION

In preliminary experiments the effect of pH on the stability of acetone in the oxidation mixture was determined. Table I shows the amount of oxidant consumed when acetone was oxidized at varying pH values with five times the amount of oxidant used in the standard procedure (2).

Since the hydroxylation and cleavage steps are relatively fast reactions (2), it is safe to assume that the amount of acetone lost owing to oxidation will be insignificant at a pH below 8.0.

Acetone can be conveniently determined both iodometrically (5) and colori-

[1]*Manuscript received August 9, 1955.*
Contribution from the National Research Council of Canada, Prairie Regional Laboratory, Saskatoon, Saskatchewan. Issued as Paper No. 204 on the Uses of Plant Products and as N.R.C. No. 3744.

TABLE I

OXIDANT CONSUMED BY ACETONE
Atoms oxygen/mole of acetone

	pH					
	5.4	6.6	6.9	7.3	7.7	8.0
After 70 hr.	0	0.03	0.04	0.05	0.10	0.40
After 142 hr.	0	0.06	0.07	0.10	0.19	0.78

metrically (7). In the former method the acetone was distilled from an alkaline solution after the excess oxidant had been destroyed with sodium arsenite solution. This method could not, however, be used when volatile compounds were present which react with iodine or alkaline iodine solution, unless these were removed by prior oxidation. The colorimetric method proved to be less accurate (the error was $\pm 2\%$), but it had the advantage that aliquots could be used directly from the reduced reaction mixture. In addition, the color reaction is more specific and no interference was obtained when formaldehyde was present in concentrations more than twice that of acetone.

Water-soluble Compounds

From experiments using mesityl oxide as test substance the following conclusions were drawn:

(1) The amount of oxidant should be at least twice the theoretical amount required for complete oxidation as deduced from the above reaction scheme.

(2) Increasing the amount of permanganate in the periodate–permanganate reagent increases the rate of reaction (2), but too high a permanganate concentration results in a more rapid oxidation of the acetone formed.

(3) If other volatile compounds, such as aldehydes, are formed during the oxidation, these may be removed from the distillate by dichromate oxidation (4) in acidic medium at room temperature. Acetone itself is not oxidized under these conditions, but a second distillation step is then introduced into the procedure. As an alternative, the more convenient, though slightly less accurate, colorimetric determination of acetone may be used.

Under optimum conditions the yield of acetone was 95 to 96% of the theoretical. This represented a practically quantitative result, since the sample of mesityl oxide used gave after oxidation a yield of about 2% formaldehyde, indicating the presence of 2 to 3% of the isomer having the double bond in the 4,5-position. The presence of this isomer in mesityl oxide has been reported before (1).

Because of the possible interference with the iodometric determination by volatile reaction products or unreacted starting material from the oxidation of mesityl oxide, 3-methyl-2-butenoic acid appeared to be a more satisfactory test substance and was consequently prepared by hypochlorite oxidation of mesityl oxide (6). On oxidation this acid would be expected to yield acetone, oxalic acid, and carbonic acid, with glyoxylic acid and formic acid as intermediates. The only distillable product at any stage of the periodate–permanganate oxidation from an alkaline reaction mixture would therefore be acetone.

The rate of oxidation of 3-methyl-2-butenoic acid was similar to that of mesityl oxide, e.g. at pH 7 the amount of oxidant consumed was equivalent to 2.08, 3.09, 3.65, and 3.88 oxygen atoms after 0.05, 0.5, 3, and 70 hr. respectively. A formaldehyde determination indicated the presence of up to 2% of the Δ^3-isomer. The yield of acetone was determined iodometrically after different reaction times (from 5 to 360 min. at 5 to 10 min. intervals) with the reagent containing the normal and twice and four times the normal amount of potassium permanganate. A practically quantitative yield was obtained (98.8, 98.8, and 98.4 $\pm$0.4% respectively) within one hour of reaction time, and this yield did not appear to drop during a further period of two hours.

Water-insoluble Compounds

When the above procedure was applied to terpenes of the geraniol group, difficulty was encountered because of their insolubility. A study was therefore made of certain organic solvents which, when added to the aqueous reaction mixture, would increase the solubility sufficiently without interfering with the periodate–permanganate oxidation. Of the solvents tested only pyridine and dioxane proved suitable. Reagent blanks containing these solvents, especially dioxane, consumed appreciable amounts of iodine in excess of the aqueous reagent blank (Table II), but the oxidation of mesityl oxide appeared to be little altered in rate and degree by their presence (Table III). When pyridine

TABLE II

TITRATION OF REAGENT BLANKS CONTAINING 25% ORGANIC SOLVENTS TAKING COMPARATIVE AQUEOUS BLANKS AS 0
Ml. 0.025 *N* iodine solution

Medium	Time (hr.)				
	$\frac{1}{4}$	$\frac{1}{2}$	1	3	24
25% Pyridine solution	0.10	0.15	0.22	0.36	0.72
25% Dioxane solution	1.34	1.36	1.39	1.54	3.58

TABLE III

OXIDANT CONSUMED (ATOMS OXYGEN/MOLE) BY MESITYL OXIDE IN VARIOUS MEDIA UNDER STANDARD CONDITIONS

Medium	pH	Time (hr.)							
		$\frac{1}{12}$	$\frac{1}{6}$	$\frac{1}{2}$	1	3	22	46	72
Aqueous	7.2	3.0	3.05	3.20	3.50	3.75	3.97	4.00	4.04
Aqueous	7.7	3.05	—	3.28	3.56	3.82	3.98	4.02	4.06
25% Pyridine	8.4	3.12	—	3.24	—	3.48	3.90	4.05	4.11
25% Dioxane	7.3	2.94	3.22	3.44	—	3.84	—	—	—

was used the pH of the reaction mixture was 8.4 and the addition of potassium carbonate was therefore omitted. The reaction mixture containing 25% dioxane decolorized overnight and the reaction stopped. This may have been due to the regeneration of permanganate by periodate being slowed down to a critical value. When 30% or more solvent was used, this phenomenon was

noticed at an earlier stage. However, the early part of the reaction involving the formation of acetone is relatively fast and a quantitative yield of acetone could still be obtained.

Difficulties were experienced when the iodometric method for determining acetone was used since most of the solvent distilled over with the acetone. With dioxane the error introduced was not large, but when pyridine was used the procedure had to be modified by introducing a second distillation step. After the acetone and pyridine from the first distillation was collected, excess 10% sulphuric acid (20–25 ml.) was added and the acetone was redistilled. Although the results obtained by this modification were satisfactory, the procedure was cumbersome and the colorimetric method was preferred. The latter method gave results similar to those with aqueous solutions as long as the reagent blank and reference samples contained the same amount of solvent.

3-Methyl-2-butenoic acid was oxidized in the different solvent systems under the usual conditions, and aliquots were analyzed colorimetrically after various reaction times. The time required to reach a maximum yield of acetone was different for each medium, but the maximum values were maintained for 5 to 10 min. After this period the yield dropped somewhat faster than would be expected from the rate of oxidation of the acetone (in an aqueous medium) alone. The results obtained were:

(1) in aqueous solution = 99% of theoretical (maximum after 10 min.),
(2) solution containing 25% pyridine = 100% (maximum after 30 min.),
(3) solution containing 25% dioxane = 99% (maximum after 20 min.).

The foregoing results show that the procedures outlined should be of value in both structure determination and routine analysis, especially since as little as 0.01 mM. of a substance was sufficient for quantitative results. The use of the reagent for determining the position of double bonds in unsaturated fatty acids and related compounds will be the subject of a future communication.

Application to Terpenes

The method was applied to the analysis of three commercial samples of terpenes. Each compound gave the maximum yield of acetone (see Table IV)

TABLE IV

YIELDS OF ACETONE* FROM TERPENES
Per cent of the theoretical

Medium	Terpene		
	Geraniol	Citronellol	Citronellal
Solution containing 25% pyridine	88	79	77
Solution containing 30% dioxane	89	81	79

**Colorimetric procedure.*

already after 5 to 10 min. These results show that in each of the terpenes the isomer having the isopropylidene grouping is the major component. The same

reaction mixtures were also analyzed for their content of formaldehyde resulting from the presence of terminal methylene groups. The maximum yields for geraniol, citronellol, and citronellal were 43%, 4%, and 8.5% respectively.

EXPERIMENTAL

Apparatus

The condenser was constructed of capillary glass-tubing surrounded by an ordinary cooling jacket. The tubing extended into the receiver so that the distillate was collected under 10 to 15 ml. of water. The receiver was surrounded by ice water. The connection to the distillation flask was through a standard glass joint.

The colorimetric measurements were carried out with a Coleman electrophotometer (Junior 6A).

Reagents

Analytical grade reagents and solvents were used. Mesityl oxide (Eastman Kodak) was redistilled through a Podbielniak fractionating column. Pyridine and dioxane were further purified by treating with weak alkaline permanganate solution for 16 hr. at room temperature and redistilling over solid potassium hydroxide after the excess permanganate had been reduced.

3-Methyl-2-butenoic acid was synthesized by hypochlorite oxidation of mesityl oxide (6) and was purified by recrystallization from water and light petroleum, m.p. 67–68°C. (reported m.p. 66–67.5°C.); neutralization equivalent found 100.7, calc. 100.1. The terpenes were of technical or practical grade (Eastman Kodak) and were not purified further.

Periodate–Permanganate Oxidant

The stock solution of the oxidant contained 20.980 gm. (98.33 mM.) sodium *meta*-periodate and 167 ml. 0.01 *M* (1.67 mM.) potassium permanganate per liter. In experiments using two or four times the concentration of permanganate, the amount of periodate was reduced in order to maintain the total concentration of oxidant at 100 mM. per liter.

Standard Procedure of Oxidation

The substance to be oxidized, 0.5 mM., was dissolved in distilled water, or where necessary, in the required amount of organic solvent, and the solution was made up to 100 ml. with distilled water. To 50 ml. of this solution sufficient potassium carbonate was added (about 25 mgm. for a neutral substance) to give the final reaction mixture a pH of 7.2 to 7.5. To this solution 20 ml. stock oxidant solution was added with shaking, the time of addition being noted, and the solution was quickly made up to 100 ml. Aliquots of 10 ml. were analyzed at the desired time intervals by the method described in part I (2).

Periodate–Permanganate Oxidation and Iodometric Acetone Determination

Aliquots of 10 ml. of the oxidation mixture were placed in 100 ml. flasks having ground glass joints. At the required time interval the oxidation was stopped by adding to each aliquot 1 ml. 1 *M* sodium arsenite, 1 ml. 2 *N* NaOH, and 10 to 15 ml. water. About half the volume of this solution was distilled,

the distillate being collected in 10 to 15 ml. ice-cooled water. Five milliliters 2 *N* sodium hydroxide and 5.0 ml. 0.1 *N* iodine solution were added to the distillate and this solution was allowed to stand out of contact with direct sunlight for 10 to 15 min. Five milliliters 10% sulphuric acid was then added and the liberated iodine was titrated with 0.025 *N* sodium thiosulphate to the starch end point. When dioxane was present 10–15 ml. sulphuric acid had to be added. When pyridine was present the distillate was treated with excess 10% sulphuric acid (approx. 20 ml.) and redistilled. In this way the iodometric determination could be carried out without interference from the pyridine.

Periodate–Permanganate Oxidation and Colorimetric Acetone Determination

The solution of the compound to be oxidized, 2.0 ml., was pipetted into a 25 ml. volumetric flask and 2.0 ml. 0.1 *N* potassium carbonate, 10 ml. water, and 8.0 ml. stock oxidant solution were added. The solution was made up to 25 ml. after noting the time when the oxidant was added. Aliquots of 5.0 ml. of this reaction mixture were pipetted into 10 ml. volumetric flasks and after 5, 10, 20, or 30 min. reaction time 2.0 ml. 1 *M* sodium arsenite and 2.0 ml. 2 *N* sulphuric acid were added. The solutions were allowed to stand for 15 to 30 min., when 0.4 ml. 10 *N* sodium hydroxide (enough to neutralize the solution) was added to each sample, and these were then made up to 10 ml. These solutions could be kept for several hours before colorimetric analysis. Aliquots of 2.0 ml. of each sample were pipetted into a 25 × 200 mm. test tube and 3.0 ml. distilled water was added. When all samples, reagent blanks, and reference standards were thus prepared, 4.0 ml. 10 *N* sodium hydroxide was added with a syringe and finally, with mixing, 1.0 ml. of salicylic aldehyde solution. The salicylic aldehyde solution (1 volume of the aldehyde and 4 volumes ethanol) was used within five to six hours after preparation. The test tubes were immediately placed in a water-bath at 50°C., kept at 45–50°C. for 20 min. and then at room temperature for 30 min. The contents were transferred to 19 mm. cuvettes for immediate measurement of the percentage transmission at 530 mμ as compared to a reagent blank.

Formaldehyde Determinations

Aliquots of 1.0 ml. from the reaction mixture in the 10 ml. volumetric flasks could be used directly and these were analyzed as described in part II (3).

ACKNOWLEDGMENT

The author wishes to express his thanks to Drs. A. C. Neish and A. S. Perlin for helpful advice.

REFERENCES

1. DUPONT, G. and MENUT, M. Bull. soc. chim. France [V], 6: 1215. 1939.
2. LEMIEUX, R. U. and RUDLOFF, E. VON. Can. J. Chem. 33: 1701. 1955.
3. LEMIEUX, R. U. and RUDLOFF, E. VON. Can. J. Chem. 33: 1710. 1955.
4. NEISH, A. C. Nat. Research Council of Can. Rept. No. 46-8-3. 2nd revision, 1952.
5. PREGL, F. and GRANT, J. Quantitative organic microanalysis. The Blakiston Co., Philadelphia. 1946. p. 170.
6. SMITH, L. I., PRICHARD, W. W., and SPILLANE, L. J. Organic synthesis. Vol. 23. John Wiley & Sons, Inc., New York. 1946. p. 27.
7. SNELL, F. D. and SNELL, C. T. Colorimetric methods of analysis. Vol. III. D. Van Nostrand Company Inc., New York. 1953. p. 285.

OZONOLYSIS OF 1-SUBSTITUTED CYCLOOLEFINS[1]

By D. G. M. Diaper[2]

ABSTRACT

Extension of an aliphatic chain by five, six, or seven carbon atoms may be achieved by adding to it a 5-, 6-, or 7-membered olefinic alicycle and subsequently breaking the double bond. Addition of the ring is achieved by a Grignard reaction between an alkylmagnesium bromide and a cyclic ketone, and the resulting 1-alkylcycloolefin is opened by ozonolysis. The end product is a 5-, 6-, or 7-keto acid.

Methods for extension of the aliphatic chain fall into two main groups; those in which one or two carbon atoms are added, and those in which the starting material and added fragment are of comparable chain length. To the former class belong the familiar cyanide and malonic ester syntheses. These are regarded as inferior in long-chain work because end products and starting materials have similar chain-lengths (and thus similar physical properties) and are difficult to separate from each other. Methods of the latter class include the Robinson (5), Noller and Adams (4), and Blaise (1) syntheses, in which a large increment is added in one step and end product is easily separated from relatively short-chain starting materials. These methods suffer from the limited accessibility of such necessary chain-extending reagents as ω-bromo, -cyano, or -aldehydo esters or ω-carbalkoxy acid halides.

Extension using an alicyclic fragment which is subsequently opened to become part of the chain is a tempting approach. Fieser and Smuszkovicz (2) showed that 1-substituted cycloalkanols (from cycloalkanones and a Grignard reagent) may be oxidized to keto acids by chromic acid at 30° in the presence of large amounts of anhydrous acetic acid. Kelkar, Phalnikar, and Bhide (3) encountered difficulty in an attempt to make a keto acid from a 1-alkylcyclohexene by strong oxidation. Schneider and Spielman (7) concluded that chromic acid oxidation of a 1-alkylcyclohexene was inferior to the alkylzinc synthesis of a keto acid. In all investigations there was evidence of concurrent reactions. If linkages other than those intended are attacked, as may well happen when oxidizing agents of poor selectivity are employed, the same problem of separation of end product from lower homologues may be encountered.

In the present investigation, opening of the alicyclic system was achieved by ozonolysis and the resulting keto aldehydes were oxidized by performic acid to the corresponding keto acids. These are "clean" reagents of high specificity and the end products in all cases were nearly white and reasonably pure. A prerequisite for success of the synthesis is unambiguity of location of the olefinic linkage. Wallach (10) has shown that, in general, dehydration of a 1-alkylcyclohexanol gives the olefin with the cyclic rather than the semicyclic double bond. During ozonolysis of the olefins of this investigation, no evidence of alkylidenecycloalkanes was encountered.

[1]*Manuscript received July 13, 1955.*
Contribution from the Department of Chemistry, Royal Military College, Kingston, Ontario.
[2]*Department of Chemistry, Royal Military College.*

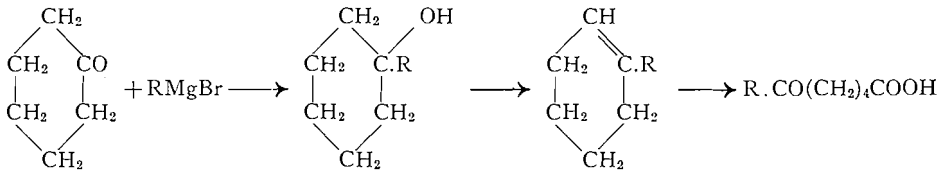

The use of cyclohexanone is illustrated above in the extension of a chain by six carbon atoms giving a 6-keto acid. It is also found that a 5-keto acid may be obtained from cyclopentanone and a 7-keto acid from cycloheptanone. Yields in the two-step synthesis are indicated in Tables I and II.

TABLE I

OLEFINS

Name	Yield, %*	B.p., °C./mm.	n_D^{20}	C and H, % Calc. C	Calc. H	Found C	Found H
1-*n*-Butylcyclopentene	56	51–53/18	1.4478				
1-*n*-Butylcyclohexene	40	71–73/18	1.4592				
1-*n*-Amylcyclopentene	52	176–177/760	1.4540				
1-*n*-Butylcycloheptene	40	87–92/19	1.4695†	86.8	13.2	86.7	13.2
dl-1-(2-Methylbutyl)cyclohexene	25	193–194/760	1.4600	86.8	13.2	86.6	12.9
1-Phenylcyclohexene	62	122–125/11	1.5669†				
1-*n*-Hexylcyclohexene	43	104–109/19	1.4560	86.7	13.3	86.6	13.0
1-*n*-Octylcyclohexene	36	121–127/12	1.4683				
1-(10-Undecenyl)cyclopentene	28	139–151/13	1.4908	87.3	12.7	87.1	13.0

**Based on cyclic ketone.*
†*25°*.

TABLE II

KETO ACIDS

Name	Yield, %	M.p., °C.	Acid equivalent Calc.	Acid equivalent Found	Semicarbazone M.p., °C.	N analysis, % Calc.	N analysis, % Found
5-Ketononanoic acid	43	44			132–133	18.3	18.2
6-Ketodecanoic acid	61–68	46–47			160	17.3	17.2
5-Ketodecanoic acid	67–73	57			111	17.3	17.1
7-Ketoundecanoic acid	63	51.5–52	200	202	133	16.3	16.3
6-Keto-8-methyldecanoic acid	76	33–34	200	204	120	16.3	15.9
5-Benzoylpentanoic acid	69	78			182–183		
6-Ketododecanoic acid	71	62.5–63	214	216	130–131	15.4	15.5
6-Ketotetradecanoic acid	60	66	242	246	120–121	14.0	14.0
4-Ketotridecane-1,13-dicarboxylic acid	27	108	286	286	130		

Losses in the synthesis of 1-alkylcycloolefins are attributable (cf. 6, 8) to two main causes, "coupling" of the Grignard reagent giving a paraffin hydrocarbon and reduction of the cyclic ketone giving an olefin and cycloalkanol. "Coupling" appears to be more serious when higher alkyl halides are employed, and reduction appears to be favored by branching of the Grignard reagent and by increase in the size of the alicycle. It was found to be least in the reaction involving phenylmagnesium bromide.

EXPERIMENTAL

Synthesis of 1-Substituted Cycloolefins

The procedure outlined below in the synthesis of 1-*n*-butylcyclohexene from cyclohexanone and *n*-butylmagnesium bromide is typical for all olefins listed in Table I (cf. Signaigo and Cramer (8)). Cyclohexanone (47 gm., 0.48 mole) was added during eight and one-half hours to the Grignard reagent from *n*-butyl bromide (71 gm., 0.52 mole) and magnesium (12 gm., 0.50 mole) in 200 cc. of dry ether, cooled with solid carbon dioxide to maintain an internal temperature of −40 to −20°C. Next day, the mixture was added to ice and hydrochloric acid in excess, and the ethereal solution was washed with water, three times with a saturated aqueous solution of sodium bisulphite (to remove cyclohexanone), and with potassium carbonate solution before it was dried over sodium sulphate. The product, a tertiary alcohol, was not purified, but used directly in the next stage.

Dehydration of 1-*n*-butylcyclohexanol was achieved by heating with iodine (0.2 gm., cf. 11) at reflux in an apparatus provided with a water separator. The theoretical quantity of water was collected in one and one-half hours, and the liquid remaining was fractionally distilled through a 15 cm. Widmer column. To avoid overheating during dehydration of higher tertiary alcohols it was found desirable to add xylene as a diluent. 1-*n*-Butylcyclohexene (26 gm., 40%) boiled at 71–73° at 17 mm. and had n_D^{20} 1.4592. On standing in air, the liquid darkened somewhat, became more viscous, and had a higher refractive index. This was taken to indicate polymerization, and the olefin was utilized as soon as possible in the next step.

Oxidation of 1-Substituted Cycloolefins to Keto Acids

The general procedure employed is described here for the case in which 1-*n*-butylcyclohexene was converted, by ozonolysis, to 6-ketodecanal, and this aldehyde was oxidized to the corresponding acid by performic acid, generated *in situ*. A slow stream of oxygen containing approximately 6% of ozone was passed into 1-*n*-butylcyclohexene (20 gm., 0.15 mole) in acetic acid (20 cc.) until a test sample failed to decolorize bromine and for 10 min. afterward. A technique similar to that of Noller and Adams (4) was used to decompose the ozonide as follows: The viscous solution was diluted with an equal volume of ether, cooled in ice, and treated cautiously with several cubic centimeters of water and 1 gm. (0.01 mole) of zinc dust. There ensued a violent reaction after an induction period, and next day the solution was filtered and separated. The ether solution was washed with water, and then 20 cc. of hydrogen peroxide (30%, 0.2 mole), 25 cc. of formic acid (90%), and 1 gm. of ammonium acetate were added. After 24 hr. at room temperature the mixture was diluted with ether and water and separated. The ethereal layer was shaken with several portions of aqueous ferrous sulphate until free from peroxides, and the acidic product was freed from neutral impurities using potassium carbonate solution in the usual manner. After removal of ether, 6-ketodecanoic acid was recrystallized from petroleum ether; the yield was 61–68% in several runs and the acid melted at 46–47°.

A simplification of the oxidation procedure was made possible by the obser-

vations that formic acid may replace acetic acid as an ozonization solvent and that performic acid oxidation appears to be unaffected by the presence of zinc salts. In the modified procedure, 21 gm. of 1-*n*-butylcyclohexene in an equal volume of formic acid was treated with ozonized oxygen as before except that care was necessary in using the bromine test as the formic acid gradually decolorized bromine. After treatment with zinc, water, and ether, the reaction mixture was filtered but not washed before treatment with a further 20-cc. portion of formic acid and 20 cc. of 30% hydrogen peroxide. The yield of keto acid was 16.5 gm. (58%).

A neutral fraction was obtained in varying quantity after performic acid oxidation of 6-ketodecanal. It was shown to contain unchanged aldehyde, as a second treatment with performic acid gave some 6-ketodecanoic acid. There remained, however, a residual neutral fraction, corresponding to 10–15% of the starting material, which was not an aldehyde and showed evidence of unsaturation. This material will be further studied.

Ozonolysis of 1-Phenylcyclohexene

A modified procedure was employed in the ozonolysis of the aromatic hydrocarbon 1-phenylcyclohexene. By a technique similar to that of Dawson (9) this substance was ozonized in ethyl acetate at −70° under conditions designed to avoid over-ozonization with attack of the benzene nucleus. Following catalytic hydrogenation of the ozonide, the ethyl acetate solution containing 5-benzoylpentanal was treated with performic acid as previously described. From 11.4 gm. of starting material, the yield of 5-benzoylpentanoic acid was 10.3 gm. (69%), melting at 75°.

Undecenyl Bromide

1-Bromoundec-10-ene (undecenyl bromide) made by the action of phosphorus tribromide upon the corresponding alcohol must be freed from unchanged alcohol before use in the Grignard reaction. This cannot be achieved by distillation, as the two compounds have similar boiling points. The crude bromide (80 gm.) was taken up in dry ether (150 cc.) and treated with 20 gm. of phosphorus pentoxide. Next day, a further 20-gm. portion of phosphorus pentoxide was added, and the mixture was frequently shaken during the next four hours and then decanted into 250 cc. of 50% aqueous methanol. Concentrated aqueous ammonia was quickly added until the mixture was alkaline to phenolphthalein, and after it was washed with a similar portion of aqueous-methanolic ammonia and with water, the ether solution was dried and distilled.

REFERENCES

1. Blaise, E. E. and Koehler, A. Compt. rend. 148: 489. 1909.
2. Fieser, L. F. and Smuszkovicz, J. J. Am. Chem. Soc. 70: 3352. 1948.
3. Kelkar, G. M., Phalnikar, N. L., and Bhide, B. V. J. Univ. Bombay, 15: 17. 1947.
4. Noller, C. R. and Adams, R. J. Am. Chem. Soc. 48: 1074. 1926.
5. Robinson, R. and Robinson, G. M. J. Chem. Soc. 127: 175. 1925.
6. Sabatier, P. and Mailhe, A. Ann. chim. et phys. (8), 10: 545. 1907.
7. Schneider, A. K. and Spielman, M. A. J. Biol. Chem. 142: 345. 1942.
8. Signaigo, F. K. and Cramer, P. L. J. Am. Chem. Soc. 55: 3326. 1933.
9. Symes, W. F. and Dawson, C. R. J. Am. Chem. Soc. 75: 4952. 1953.
10. Wallach, O. Ann. 396: 264. 1913.
11. Wibaut, J. P. *et al.* Rec. trav. chim. 58: 329. 1939.

NOUVELLES SYNTHÈSES DE L'ACIDE GLUTARIQUE, DE LA GLUTARIMIDE ET DE L'ACIDE GLUTAMIQUE

PRÉPARATION DE LA N-BROMOGLUTARIMIDE[1]

PAR GÉRARD PARIS, ROGER GAUDRY ET LOUIS BERLINGUET

RÉSUMÉ

La monoamide de l'acide glutarique a été obtenue par condensation du cyanure de potassium avec la γ-butyrolactone, suivie de neutralisation et d'hydrolyse partielle du sel de potassium du nitrile intermédiaire. Cette monoamide a été facilement hydrolysée pour donner quantitativement l'acide glutarique. La glutarimide a été obtenue avec un excellent rendement, en cyclisant par chauffage, la monoamide de l'acide glutarique. L'ester éthylique monobromé de l'acide glutarique, préparé à partir de l'acide glutarique, a été condensé avec la phtalimide de potassium par chauffage dans la diméthylformamide. L'hydrolyse de ce dérivé phtalimidé a donné l'acide glutamique avec un bon rendement. La N-bromoglutarimide a été préparée à partir de la glutarimide par bromuration en présence d'hydroxyde de potassium. Cette N-bromoglutarimide s'est comportée, dans les quelques essais effectués à date, comme un bon agent de bromuration, comparable à la N-bromosuccinimide.

Les synthèses de l'acide glutarique et de la glutarimide sont assez nombreuses. On s'est servi comme produits de départ de l'acide L-glutamique naturel (6), du dicyanure de triméthylène (16, 21), de la cyclopentanone (14), de la δ-hydroxyvaléraldéhyde (3) de l'acrylonitrile et des esters β-cétomaloniques (17), du dihydropyranne (8), et enfin de la pipéridine (27).

Les produits de départ des principales synthèses de l'acide glutamique sont aussi nombreux: acide lévulique (25), acide β-aldéhydopropionique (12), acide α-cétoglutarique (13, 15, 24), ester acylaminomalonique (7, 9, 22).

Toutefois peu de ces synthèses sont pratiques, soit à cause des faibles rendements, soit à cause de la rareté relative des produits de départ.

Récemment Pichat, Baret et Audinot (18) ont montré que la β-méthylbutyrolactone s'ouvrait facilement en présence de cyanure de potassium à une température de 280°C. pour donner le sel de potassium du mononitrile correspondant. Ce sel de potassium leur a permis d'obtenir avec d'excellents rendements l'acide β-méthylglutarique et la β-méthylglutarimide.

Dans le but d'élaborer une synthèse simple et facile de l'acide glutarique et de la glutarimide, nous avons repris cette synthèse et l'avons appliquée à la γ-butyrolactone, produit facilement accessible.

La γ-butyrolactone a été condensée avec le cyanure de potassium à 190°C. Le sel de potassium du mononitrile formé n'a pas été isolé mais immédiatement neutralisé par l'acide chlorhydrique concentré, soit à une température de 25°C. pour donner la monoamide de l'acide glutarique avec un rendement de 80%, soit à 0°C. pour donner le mononitrile de l'acide glutarique avec un rendement de 65%. Par hydrolyse de ces deux derniers produits, l'acide glutarique a été obtenu avec un rendement quantitatif dans le cas de la monoamide et un rendement de 80% dans le cas du mononitrile.

[1]*Manuscrit reçu le 25 juillet, 1955.*
Contribution du Département de Biochimie, Faculté de Médecine, Université Laval, Québec, Québec.

La glutarimide est formée avec un rendement de 84% par cyclisation de la monoamide de l'acide glutarique à une température de 210°C.

Cette synthèse permettait de préparer facilement et avec d'excellents rendements l'acide glutarique et la glutarimide. Ces deux produits intermédiaires ont été utilisés pour de nouvelles synthèses de l'acide glutamique et de la N-bromoglutarimide.

Dans une nouvelle synthèse de l'acide glutamique, nous avons d'abord préparé le diester éthylique monobromé de l'acide glutarique suivant la méthode décrite par Ingold (11). Ce diester fut condensé avec la phtalimide de potassium. Le produit de condensation fut hydrolysé pour donner l'acide glutamique avec un rendement total de 50%, calculé à partir de l'acide glutarique.

La N-bromoglutarimide a été préparée à partir de la glutarimide suivant une méthode de synthèse identique à celle de la N-bromosuccinimide. Le rendement brut en N-bromoglutarimide est de 62%.

La N-bromoglutarimide ainsi préparée semble se comporter dans les essais effectués à date comme un bon agent de bromuration. C'est ainsi que nous avons bromé l'acétanilide, la triéthylamine. Nous avons oxydé l'alanine et finalement, nous avons effectué la bromuration allylique du méthylcrotonate. Les rendements obtenus se comparent avantageusement avec ceux décrits pour la N-bromosuccinimide.

PARTIE EXPÉRIMENTALE

Monoamide de l'acide glutarique

On ajoute du cyanure de potassium (17 g., 0.26 mole) à de la γ-butyrolactone (20.9 g., 0.24 mole) et on agite mécaniquement. On élève rapidement la température du mélange et on la maintient à 190°C. pendant trois heures après quoi on refroidit la solution. Le solide formé est repris à l'eau (50 ml.) et neutralisé avec un équivalent d'acide chlorhydrique (ou d'acide sulfurique concentré) à une température de 25°C. On ajoute un léger excès d'acide chlorhydrique (19.5 ml. en tout) et on laisse reposer quelque temps. On extrait la monoamide à l'éther. L'éther est séché sur du sulfate de sodium anhydre, puis évaporé à sec sous pression réduite. L'huile résiduelle brunâtre pèse 25.5 g. Rendement brut: 80%.

Par distillation fractionnée de cette huile, on obtient la monoamide contaminée par un peu de la glutarimide formée par chauffage lors de la distillation, lequel mélange distille à 150–155°C. sous 4.5 mm. La monoamide pure est extraite à l'éther. Point de solidification 14–15°C., $n_{20} = 1.450$. Calculé pour $C_5H_9O_3N$: N, 10.69%. Trouvé: N, 10.60%.

Acide glutarique

(*a*) *À partir de la monoamide*

On dissout la monoamide brute (5 g., 0.038 mole) dans 50 ml. d'eau et on ajoute 50 ml. d'acide chlorhydrique concentré. Le mélange est chauffé à reflux pendant une heure. On évapore la solution à sec sous pression réduite. On dissout le résidu dans l'eau chaude et on le décolore au noir animal. L'eau

est évaporée sous pression réduite. Par recristallisation du chloroforme bouillant, on obtient l'acide glutarique, débarrassé du chlorure d'ammonium insoluble. Le rendement est quantitatif: 5.02 g. P. f. 98–99°C. Litt: 97.5°C. (16).

(*b*) *À partir du mononitrile*

Le mononitrile (5 g., 0.04 mole) est hydrolysé de la même façon sauf que la durée de l'hydrolyse est portée de une à trois heures. Rendement: 4.67 g., 80%. P. f. 98–99°C. Litt: 97.5°C. (16).

Mononitrile de l'acide glutarique

La neutralisation lente à 0°C. avec un équivalent d'acide chlorhydrique concentré (19 ml.) du produit de condensation obtenu en traitant la γ-butyrolactone (16.5 g., 0.19 mole) par le cyanure de potassium (13 g., 0.20 mole) donne le mononitrile correspondant. On extrait le nitrile à l'éther lequel est séché sur du sulfate de sodium anhydre, puis évaporé à sec sous pression réduite. Le nitrile ainsi obtenu est recristallisé d'un petit volume d'éther pour enlever les traces de monoamide présente laquelle est beaucoup plus soluble. Rendement: 14.1 g., 65% P. f. 41–42°C. Litt: 45°C. (5). Calculé pour $C_5H_7O_2N$: N, 12.39%. Trouvé: N, 12.42%.

Glutarimide

(*a*) *À partir de la monoamide*

Dans un ballon de 50 ml. à un col surmonté d'un réfrigérant à air, on place la monoamide brute (5 g., 0.04 mole). On élève rapidement la température et on la maintient à 210–215°C. pendant trois heures. La solution est refroidie, après quoi on dissout le résidu dans l'eau chaude et on le décolore au noir animal. L'eau est évaporée sous pression réduite. Le résidu est recristallisé de l'alcool éthylique. Rendement 3.6 g., 84%. P. f. 154°C. Litt: 154.5°C. (27). Calculé pour $C_5H_7O_2N$: N, 12.38%. Trouvé: N, 12.39%.

(*b*) *À partir de l'acide glutarique*

Le chauffage de l'acide glutarique en présence d'ammoniaque concentré suivant la méthode habituelle (1) donne la glutarimide avec un bon rendement quoique le rendement total, calculé à partir de la γ-butyrolactone, soit inférieur à celui obtenu en passant par la monoamide.

Diester éthylique de l'acide 2-bromoglutarique

Le diester éthylique de l'acide 2-bromoglutarique est préparé à partir de l'acide glutarique par traitement au chlorure de thionyle, bromuration et réaction avec l'alcool éthylique, suivant la méthode décrite par Ingold (11). Le rendement a toutefois été augmenté de 50% à 80–85% en effectuant la bromuration avec l'aide de rayons ultraviolets.

Acide glutamique

Dans un ballon à trois cols, muni d'un agitateur et d'un réfrigérant surmonté d'un tube de chlorure de calcium, on ajoute de la phtalimide de potassium (18 g., 0.097 mole) à un mélange du diester éthylique de l'acide 2-bromoglutarique (25 g., 0.094 mole) et de 100 ml. de diméthylformamide. On agite une heure à la température d'ébullition de la diméthylformamide (152–154°C.).

La solution est refroidie. On filtre le précipité de bromure de potassium (9.5 g., théorie 11.1 g.). On évapore la solution à sec sous pression réduite et on ajoute de l'acide chlorhydrique concentré. On chauffe à reflux pendant 15 h. puis on évapore à sec. On reprend à l'eau et, après refroidissement, on filtre l'acide phtalique (15.5 g., théorie 16.1 g.) La solution est concentrée à faible volume, amenée à un pH de 3.2 au moyen de NaOH 10%, et placée à la glacière pendant plusieurs heures. Une première fraction (8.5 g.) précipite. Au bout de plusieurs jours on obtient une seconde fraction (2 g.). Rendement brut en acide glutamique: 10.5 g., 76%. Après recristallisation de l'acide aminé de l'alcool et de l'eau le p. f. est de 180–185°C. Litt.: 198°C. (26). Calculé pour $C_5H_9O_4N$: N, 9.52%. Trouvé: N, 9.48%. L'acide glutamique fut identifié par chromatographie sur papier ascendante et circulaire avec la pyridine à 80% comme solvant: R_f 0.21. De plus l'acide glutamique, étant un acide aminé monoaminé dicarboxylique, a été analysé par électrophorèse sur papier (pH 8.6, 4 ma., 200 volts). La bande obtenue après révélation à la ninhydrine correspondait exactement avec celles d'échantillons commerciaux d'acide glutamique.

L'acide glutamique fut aussi préparé à partir du diester éthylique monobromé de l'acide glutarique en présence d'ammoniaque sous pression. La présence de sels d'ammonium interfère toutefois dans l'isolement de l'acide libre.

N-Bromoglutarimide

On ajoute avec agitation rapide de la glutarimide (5 g., 0.044 mole) à une solution d'hydroxyde de potassium (2.78 g. de KOH dans 10 cc. d'eau) maintenue à −5°C. Au bout d'une minute, on ajoute rapidement et en une seule addition 7.1 g. de brome. Le solide formé (5.3 g., 62%) est filtré, lavé à l'eau froide, et recristallisé immédiatement de l'eau chaude. Rendement de la N-bromoglutarimide: 4.4 g., 52%; p.f. 185–190°C. d. Calculé pour $C_5H_6O_2NBr$: C, 31.40%; H, 3.14%; N, 7.13%; Br, 41.62%. Trouvé: C, 28.60%; H, 3.02%; N, 6.30%; Br, 44.08%. On peut aussi recristalliser la N-bromoglutarimide de l'acide acétique glacial.

Lorsqu'on solubilise la glutarimide dans une solution d'hydroxyde de potassium au lieu d'une solution d'hydroxyde de sodium, la N-bromoglutarimide obtenue est plus pure et plus facile à recristalliser, quoique les rendements obtenus lors de la bromuration soient inférieurs.

Réactions effectuées à l'aide de la N-bromoglutarimide

(*a*) *p-Bromoacétanilide*

La méthode est identique à celle décrite par Buu-Hoi' (4) pour la N-bromosuccinimide. Le résidu obtenu est recristallisé d'un mélange d'alcool et d'eau. Le rendement en *p*-bromoacétanilide est quantitatif. P. f. 167°C. Litt: 167°C. (10). Calculé pour C_8H_8ONBr: N, 6.5%; Br, 37.4%. Trouvé: N, 6.5%; Br, 37.5%.

(*b*) *Bromhydrate de la triéthylamine*

La méthode est la même que celle décrite par Braude et Waight (2) pour la N-bromosuccinimide. On ajoute en faibles portions de la N-bromoglutarimide à une solution de triéthylamine dans du tétrachlorure de carbone

refroidie à 0°C. Le solvant est évaporé. La glutarimide est extraite à l'acétone. Le bromhydrate fond à 245°C. Litt: 245–246°C. (2).

(*c*) *Dérivé 2,4-dinitrophénylhydrazone de l'acétaldéhyde, obtenu à partir de l'alanine*

La méthode est la même que celle décrite par Schönberg et collaborateurs (23) pour la N-bromosuccinimide. On ajoute de la N-bromoglutarimide à une solution aqueuse d'alanine. Après 10 min., on refroidit la solution et on ajoute du chlorhydrate de la 2,4-dinitrophenylhydrazine. Après recristallisation de l'alcool le dérivé fond à 146°C. Litt: 147°C. (19).

(*d*) *γ-Bromométhylcrotonate*

La méthode est la même que celle décrite par Ziegler et collaborateurs (28) pour la N-bromosuccinimide. On ajoute de la N-bromoglutarimide à un grand excès de méthylcrotonate et on chauffe à reflux pendant une heure. La solution est ensuite refroidie et la glutarimide formée est filtrée. Le γ-bromométhylcrotonate distille à 65°–68°C. sous 4.5 mm. $n_{20} = 1.495$. Litt: $n_{19} = 1.498$ (20).

REMERCIEMENTS

Les auteurs sont heureux de remercier le Conseil National des Recherches du Canada pour l'octroi à l'un d'eux (G. P.) d'une bourse qui a permis la réalisation de ce travail.

BIBLIOGRAPHIE

1. Bernheimer, M. O. Gazz. chim. ital. 12: 281. 1882.
2. Braude, E. A. et Waight, E. S. J. Chem. Soc. 1122. 1952.
3. Bremner, J. G. M., Jones, D. G. et Taylor, A. W. C. (Imperial Chemical Industries Ltd.) U.S. Patent No. 2,389,950. 27 nov., 1945.
4. Buu-Hoi', Ng. Ph. Ann. 556: 8. 1944.
5. Dieckmann, W. Ber. 33: 588. 1900.
6. Dittmar, W. J. prakt. Chem. 5: 338. 1872.
7. Dunn, M. S., Smart, B. W., Redemann, C. E. et Brown, K. E. J. Biol. Chem. 94: 599. 1931.
8. English, J., Jr. et Dayan, J. E. Organic syntheses. Vol. 30. John Wiley & Sons, Inc., New York. 1950. pp. 48–50.
9. Galat, A. J. Am. Chem. Soc. 69: 965. 1947.
10. Hübner, H. Ann. 209: 355. 1881.
11. Ingold, C. K. J. Chem. Soc. 1: 316–317. 1921.
12. Keimatsu, S. et Sagasawa, S. J. Pharm. Soc. Japan, 531: 369. 1925.
13. Knoop, F. et Oesterlin, H. Z. physiol. Chem. 170: 186. 1927.
14. McAllister, S. H. (Shell Development Co.) U.S. Patent No. 2,286,559. 16 juin, 1942. Chem. Abstr. 36: 7031 p. 1942.
15. McIlwain, H. et Richardson, G. M. Biochem. J. 33: 44. 1939.
16. Markownikoff, W. Ann. 182: 341. 1876.
17. Mikeska, L. A. (Standard Oil Development Co.) U.S. Patent No. 2,461,336. 8 février, 1949. Chem. Abstr. 43: 4689 *g*. 1949.
18. Pichat, L., Baret, C. et Audinot, M. Bull. soc. chim. France, 88–92. 1954.
19. Purgotti, A. Gazz. chim. ital. 24, I: 565. 1894.
20. Rambaud, R. Bull. soc. chim. France, Mém. 1: 1317–1341. 1934.
21. Reboul, E. Compt. rend. 82: 1197, 1502. 1876.
22. Redemann, C. E. et Dunn, M. S. J. Biol. Chem. 130: 341. 1939.
23. Schönberg, A., Moubasher, R. et Barakat, M. Z. J. Chem. Soc. 2504. 1951.
24. Shemin, D. et Herbst, R. J. Am. Chem. Soc. 60: 1954. 1938.
25. Wolff, L. Ann. 260: 79. 1890.
26. Wolff, L. Ann. 260: 122. 1890.
27. Wolffenstein, R. Ber. 25: 2777. 1892.
28. Ziegler, K., Spath, A., Schaaf, E., Schumann, W. et Winkelmann, E. Ann. 551: 80–119. 1942.

NOTES

A QUARTZ SPIRAL-TORSION MICROBALANCE*

By W. Bushuk† and C. A. Winkler

During a study of the adsorption of vapors and gases on porous powders with a Gulbransen type (1) torsion balance it was found that the instrument (at least the particular one available) lacked stability over a range of pressures and temperatures. A McBain–Bakr (2) quartz spiral balance had the necessary stability but had inadequate load capacity for a spiral with sufficient sensitivity. This note describes a null-point microbalance in which a torsion wire supports the load and the increase in weight during adsorption is determined with a highly sensitive quartz spiral.

A practically self-explanatory schematic diagram of the complete balance assembly is shown in Fig. 1. It has been found an advantage to have suitable

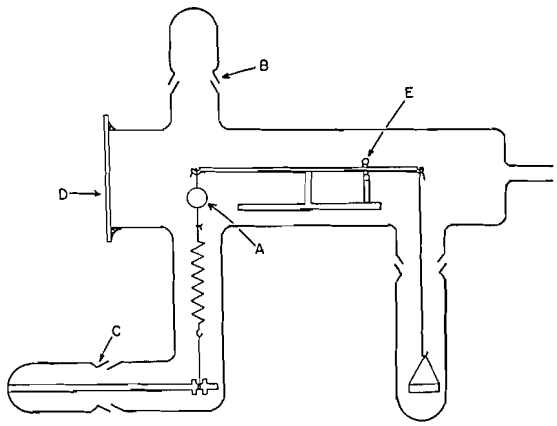

Fig. 1.

arrests (E) on the balance frame to limit the movement of the beam and thereby reduce the possibility of damage to the beam or the spiral. The quartz spiral is attached, as shown, from a hook on the counterpoise, A, at the opposite end of the beam from which the sample is suspended. Access to the balance may be had through B. The tension in the spiral is varied by winding or unwinding a very thin silk thread, which hangs from the lower end of the spiral, on a glass rod fitted through a ground glass joint C. Increase in weight during adsorption is determined from the extension of the spiral necessary to bring the beam to a null-point in the field of a microscope focused through the window D.

This type of balance has the calibration characteristics of the spiral‡

*Financial assistance was provided by the National Research Council of Canada.

†Graduate student, holder of National Research Council Studentship.

‡Quartz spirals are obtainable from: Houston Technical Laboratories, 2424 Branard Street, Houston 6, Texas, U.S.A.

employed. The balance used in this laboratory gave a linear weight–extension relation over at least 30 mm. extension of the spiral, in the temperature range −80°C. to 65°C. and the pressure range 10^{-4} mm. to atmospheric pressure, and the sensitivity was 0.163 ± 0.002 mgm./mm.

1. GULBRANSEN, E. A. Rev. Sci. Instr. 15: 201. 1944.
2. MCBAIN, J. W. and BAKR, A. M. J. Am. Chem. Soc. 48: 690. 1926.

RECEIVED AUGUST 10, 1955.
PHYSICAL CHEMISTRY LABORATORY,
MCGILL UNIVERSITY,
MONTREAL, QUEBEC.

THE VISCOSITIES OF AMMONIUM NITRATE SOLUTIONS AT 180°C.

BY A. N. CAMPBELL AND G. H. DEBUS*

Because of our interest in the Robinson–Stokes conductance equation (4), which requires a knowledge of the viscosity in order to calculate the equivalent conductance for any given concentration, we have determined the viscosities, at 180°C., of ammonium nitrate solutions ranging in concentration from 0.80% by weight up to 100% (molten salt). The conductances of these solutions had previously been determined in this laboratory (2). After obtaining the viscosities, however, we realized that not even a reasonable guess could be made at the value of Λ_0, the limiting conductance, at 180°. Elsewhere, we have made such guesses for temperatures of 35°, 95°, and even 110°C. (1) but the more the temperature is removed from 25°C., the only temperature at which Λ_0 is known experimentally, the greater the uncertainty. We therefore feel that our viscosity figures should be published at this time.

It is apparent that, if as much importance is attached to the Robinson–Stokes equation by others as by us, this must result in a stimulation of work in the dilute region at temperatures other than 25°C. The data might then be profitably treated by Stokes' simplified equation (3) to obtain Λ_0. A rigorous test of the Robinson–Stokes equation could then be made at temperatures other than 25°, since good data on conductances of concentrated solutions are beginning to accumulate.

EXPERIMENTAL

The method used has been described elsewhere (1). We express our results to the third decimal, the third decimal being uncertain. The viscosity is given as relative viscosity only, since the absolute viscosity of water is not known with great accuracy at 180.0°C.

RESULTS

The results are contained in Table I.

National Research Council Postdoctorate Fellow.

employed. The balance used in this laboratory gave a linear weight–extension relation over at least 30 mm. extension of the spiral, in the temperature range −80°C. to 65°C. and the pressure range 10^{-4} mm. to atmospheric pressure, and the sensitivity was 0.163 ± 0.002 mgm./mm.

1. GULBRANSEN, E. A. Rev. Sci. Instr. 15: 201. 1944.
2. MCBAIN, J. W. and BAKR, A. M. J. Am. Chem. Soc. 48: 690. 1926.

RECEIVED AUGUST 10, 1955.
PHYSICAL CHEMISTRY LABORATORY,
MCGILL UNIVERSITY,
MONTREAL, QUEBEC.

THE VISCOSITIES OF AMMONIUM NITRATE SOLUTIONS AT 180°C.

BY A. N. CAMPBELL AND G. H. DEBUS*

Because of our interest in the Robinson–Stokes conductance equation (4), which requires a knowledge of the viscosity in order to calculate the equivalent conductance for any given concentration, we have determined the viscosities, at 180°C., of ammonium nitrate solutions ranging in concentration from 0.80% by weight up to 100% (molten salt). The conductances of these solutions had previously been determined in this laboratory (2). After obtaining the viscosities, however, we realized that not even a reasonable guess could be made at the value of Λ_0, the limiting conductance, at 180°. Elsewhere, we have made such guesses for temperatures of 35°, 95°, and even 110°C. (1) but the more the temperature is removed from 25°C., the only temperature at which Λ_0 is known experimentally, the greater the uncertainty. We therefore feel that our viscosity figures should be published at this time.

It is apparent that, if as much importance is attached to the Robinson–Stokes equation by others as by us, this must result in a stimulation of work in the dilute region at temperatures other than 25°C. The data might then be profitably treated by Stokes' simplified equation (3) to obtain Λ_0. A rigorous test of the Robinson–Stokes equation could then be made at temperatures other than 25°, since good data on conductances of concentrated solutions are beginning to accumulate.

EXPERIMENTAL

The method used has been described elsewhere (1). We express our results to the third decimal, the third decimal being uncertain. The viscosity is given as relative viscosity only, since the absolute viscosity of water is not known with great accuracy at 180.0°C.

RESULTS

The results are contained in Table I.

National Research Council Postdoctorate Fellow.

TABLE I

VISCOSITIES OF AMMONIUM NITRATE SOLUTIONS AT 180.0°C.

No.	Wt. %	Density, gm./ml.*	Relative viscosity
1	0.80	0.892	1.011
2	8.51	0.928	1.093
3	16.06	0.957	1.168
4	23.97	0.993	1.268
5	32.06	1.030	1.395
6	38.68	1.061	1.524
7	45.24	1.099	1.715
8	50.19	1.121	1.862
9	54.89	1.145	2.055
10	58.59	1.166	2.237
11	61.96	1.184	2.397
12	69.70	1.225	2.819
13	76.50	1.272	3.34
14	84.07	1.322	3.98
15	88.63	1.356	4.65
16	100.00	1.44	10.1

**Calculated by interpolation of earlier results (2).*

1. CAMPBELL, A. N., DEBUS, G. H., and KARTZMARK, E. M. Can. J. Chem. 33: 1508. 1955.
2. CAMPBELL, A. N., KARTZMARK, E. M., BEDNAS, M. E., and HERRON, J. T. Can. J. Chem. 32: 1051. 1954.
3. ROBINSON, R. A. and STOKES, R. H. J. Am. Chem. Soc. 76: 1991. 1954.
4. WISHAW, B. F. and STOKES, R. H. J. Am. Chem. Soc. 76: 2065. 1954.

RECEIVED AUGUST 2, 1955.
DEPARTMENT OF CHEMISTRY,
UNIVERSITY OF MANITOBA,
WINNIPEG, MANITOBA.

THE DETERMINATION OF HYDROGEN CHLORIDE IN TITANIUM TETRACHLORIDE*

BY T. R. INGRAHAM†

INTRODUCTION

Titanium tetrachloride, as prepared by the chlorination of titanium oxide in the presence of carbon, generally contains appreciable quantities of dissolved hydrogen chloride. The hydrogen chloride may form during the chlorination owing to the presence of moisture or hydrocarbons. Unlike the other impurities present (Cl_2, $COCl_2$, $VOCl_3$, $SiCl_4$, etc.) it is not completely eliminated during subsequent purification procedures. Also, since titanium tetrachloride is strongly hydroscopic, additional amounts of hydrogen chloride form and contaminate the product during handling in moist air.

When titanium tetrachloride is reduced to metallic titanium, the presence of HCl causes embrittlement of the metal due to hydrogen absorption. Hence,

**Published by permission of the Acting Deputy Minister, Department of Mines and Technical Surveys, Ottawa, Canada.*
†Metallurgist, Extractive Metallurgy Section, Division of Mineral Dressing and Process Metallurgy, Mines Branch, Ottawa, Canada.

TABLE I

VISCOSITIES OF AMMONIUM NITRATE SOLUTIONS AT 180.0°C.

No.	Wt. %	Density, gm./ml.*	Relative viscosity
1	0.80	0.892	1.011
2	8.51	0.928	1.093
3	16.06	0.957	1.168
4	23.97	0.993	1.268
5	32.06	1.030	1.395
6	38.68	1.061	1.524
7	45.24	1.099	1.715
8	50.19	1.121	1.862
9	54.89	1.145	2.055
10	58.59	1.166	2.237
11	61.96	1.184	2.397
12	69.70	1.225	2.819
13	76.50	1.272	3.34
14	84.07	1.322	3.98
15	88.63	1.356	4.65
16	100.00	1.44	10.1

**Calculated by interpolation of earlier results (2).*

1. CAMPBELL, A. N., DEBUS, G. H., and KARTZMARK, E. M. Can. J. Chem. 33: 1508. 1955.
2. CAMPBELL, A. N., KARTZMARK, E. M., BEDNAS, M. E., and HERRON, J. T. Can. J. Chem. 32: 1051. 1954.
3. ROBINSON, R. A. and STOKES, R. H. J. Am. Chem. Soc. 76: 1991. 1954.
4. WISHAW, B. F. and STOKES, R. H. J. Am. Chem. Soc. 76: 2065. 1954.

RECEIVED AUGUST 2, 1955.
DEPARTMENT OF CHEMISTRY,
UNIVERSITY OF MANITOBA,
WINNIPEG, MANITOBA.

THE DETERMINATION OF HYDROGEN CHLORIDE IN TITANIUM TETRACHLORIDE*

BY T. R. INGRAHAM†

INTRODUCTION

Titanium tetrachloride, as prepared by the chlorination of titanium oxide in the presence of carbon, generally contains appreciable quantities of dissolved hydrogen chloride. The hydrogen chloride may form during the chlorination owing to the presence of moisture or hydrocarbons. Unlike the other impurities present (Cl_2, $COCl_2$, $VOCl_3$, $SiCl_4$, etc.) it is not completely eliminated during subsequent purification procedures. Also, since titanium tetrachloride is strongly hydroscopic, additional amounts of hydrogen chloride form and contaminate the product during handling in moist air.

When titanium tetrachloride is reduced to metallic titanium, the presence of HCl causes embrittlement of the metal due to hydrogen absorption. Hence,

**Published by permission of the Acting Deputy Minister, Department of Mines and Technical Surveys, Ottawa, Canada.*
†Metallurgist, Extractive Metallurgy Section, Division of Mineral Dressing and Process Metallurgy, Mines Branch, Ottawa, Canada.

to control the embrittlement due to hydrogen, it is necessary to have a convenient analytical method for determining the amount of HCl dissolved in $TiCl_4$ and for following its removal by vacuum distillation. With the exception of an infrared spectroscopic determination recently published by the U.S. Bureau of Standards (1), little attention appears to have been given to this determination.

EXPERIMENTAL

Apparatus

Since the freezing points of HCl and $TiCl_4$ differ widely (−112°C. and −30°C. respectively), and since it was found that HCl was readily liberated from cold $TiCl_4$ solutions under vacuum, a method was developed to measure the pressure developed by a known volume of HCl liberated from $TiCl_4$ solutions. The apparatus is shown diagrammatically in Fig. 1.

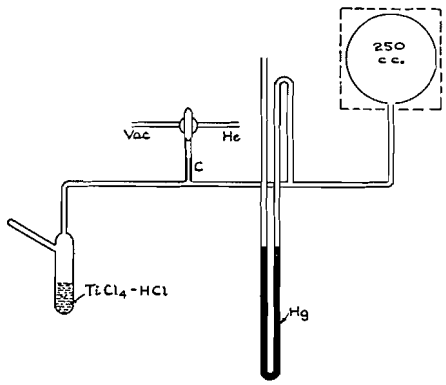

FIG. 1. Apparatus for determining HCl in $TiCl_4$.

The apparatus was constructed entirely of pyrex glass. Stopcocks were greased with Dow-Silicone stopcock grease. It was found that under the experimental conditions used in HCl determinations, no protection was required for the mercury in the manometer, or its alternative, a McLeod Gage. Volumes of all sections of the apparatus were determined before assembly by filling with water.

Procedure

The apparatus was thoroughly evacuated and flushed, using a mechanical pump and helium. With the apparatus at atmospheric pressure, an entry was blown into the $TiCl_4$ bulb and a specified (25.0 ml.) quantity of $TiCl_4$ admitted by pipette against a gentle countercurrent of helium. Helium was chosen because of its low condensation temperature. The apparatus was then resealed, the $TiCl_4$ sample frozen with liquid air, and the helium evacuated from the apparatus. As a precaution against attack of the stopcock grease by HCl, the capillary section C was then sealed, thus isolating the system.

When the liquid air was removed from the $TiCl_4$ container, the $TiCl_4$ melted slowly with a visible liberation of gas. When the $TiCl_4$ had melted completely, but had not been heated sufficiently to develop an appreciable

vapor pressure, it was refrozen with a slurry of CO_2 in a CCl_4–$CHCl_3$ mixture. This reduced the vapor pressure of $TiCl_4$ in the system to a very small value but did not alter the pressure developed by the HCl.

RESULTS

From the pressure of HCl developed in the system, and the known volume of the system, the quantity of HCl originally dissolved in the $TiCl_4$ was calculated assuming the Ideal Gas Law.

It was found that no change took place in the original pressure when the $TiCl_4$ was repeatedly refrozen and remelted. It was also shown that once a sample had been degassed by this procedure, the removal of HCl was virtually complete, as indicated by a zero HCl content when the determination was repeated on the same sample. Repeat determinations on previously degassed samples also showed that the helium used did not dissolve in or become mechanically trapped in the $TiCl_4$ during the determination.

Examination of the evolved gas with an infrared spectroscope has shown that HCl was the only constituent present.

The following results were obtained from triplicate samples of reagent grade $TiCl_4$:

Sample	% HCl
1	0.032%
2	0.034%
3	0.030%

When a sample of $TiCl_4$ at room temperature had been saturated with HCl at atmospheric pressure, it was found to contain 0.117% HCl.

CONCLUSIONS

The proposed method yields reproducible results for HCl within the range usually found in $TiCl_4$ (less than 0.1%).

1. JOHANNESEN, R. B., GORDON, C. L., STEWART, J. E., and GILCHRIST, R. J. Research Natl. Bur. Standards, 53: 4, 197. 1954.

RECEIVED MAY 26, 1955.
DEPARTMENT OF MINES AND TECHNICAL SURVEYS,
MINES BRANCH,
OTTAWA, CANADA.

Canadian Journal of Chemistry

Issued by THE NATIONAL RESEARCH COUNCIL OF CANADA

VOLUME 33 DECEMBER 1955 NUMBER 12

THE ACTION OF PYRIDINE ON D-MANNITOL HEXANITRATE[1]

BY J. R. BROWN AND L. D. HAYWARD

ABSTRACT

From a 0.368*M* solution of D-mannitol hexanitrate in pyridine at 30±5°C. a gas consisting of nitric oxide, nitrous oxide, and nitrogen was evolved and D-mannitol-1,2,4,5,6-pentanitrate and pyridinium nitrate were recovered after dilution with water. The amount and composition of the gas mixture were sensitive to traces of moisture in the pyridine. Establishment of a material balance for the reaction indicated that approximately two moles of pyridine suffered ring cleavage while 0.25 mole of hexanitrate was completely denitrated and 0.75 mole of pentanitrate was formed. Some features of the mechanism of the denitration reaction are discussed.

In earlier papers it was shown that pyridine caused selective partial denitration of dulcitol (22) and D-mannitol (18) hexanitrates; the corresponding pentanitrates were recovered in 67–73% yield and identified as the 3-hydroxy derivatives in each case. Elrick and collaborators have recently confirmed these results with D-mannitol hexanitrate and have also shown that treatment with an aqueous acetone solution of ammonium carbonate gave a similar yield of the same D-mannitol pentanitrate (11).

The pyridine denitration amounted to the replacement of nitronium ion by a proton at the oxygen atom of carbon 3 in the hexitol hexanitrates since no racemization or inversion of the asymmetric centers occurred. In the present research the nonhexitol products of the reaction of pyridine with D-mannitol hexanitrate were explored in an attempt to reveal further details of this unusual selective reaction (32).

Pure D-mannitol hexanitrate dissolved readily in pyridine in a molar ratio of 1:34 to give an initially colorless solution which rapidly turned yellow and then deep red while external cooling was required during the first hour to maintain the temperature below 35°C. When the reaction was carried out in an open vessel (Runs F and G), small bubbles of gas rapidly rose through the solution and a red-brown vapor collected in the upper part of the flask. After the solution was left for 24 hr. at room temperature a thin film of colorless crystals was observed on the inner walls of the flask above the solution. This material was collected and identified as pyridinium nitrate. In other runs (A to E), contact with the atmosphere was avoided during the reaction and the temperature maintained at 30±2°C. by combining the reactants in the

[1]*Manuscript received August 15, 1955.*
Contribution from the Department of Chemistry, University of British Columbia, Vancouver, B.C. This paper is based on a thesis submitted by J. R. Brown in partial fulfillment of the requirements for the degree of Master of Science in Chemistry, April, 1953, and was presented in part before the second Western Regional Conference, the Chemical Institute of Canada, Vancouver, September, 1954.

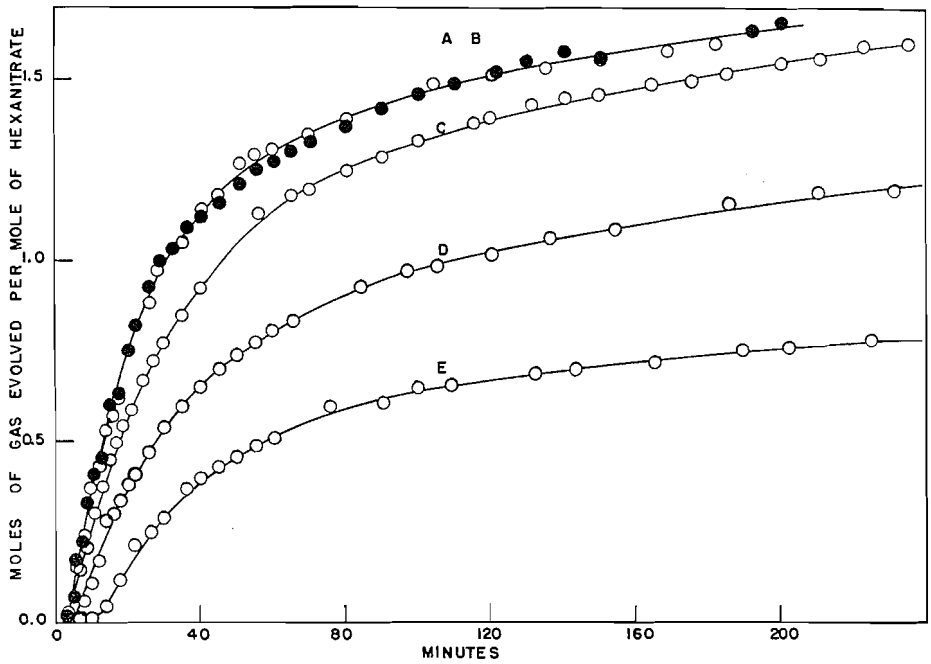

FIG. 1. Gas evolved in the denitration of D-mannitol hexanitrate with dried (A, B) and with moist (C, D, E) pyridine.

Toricellian vacuum of a water-cooled du Pont nitrometer, and in these cases the gas evolved was colorless and no crystals of pyridinium nitrate appeared.

The volume of the gas evolved in the nitrometer was measured at intervals, corrected for the vapor pressure of pyridine (34), and plotted against time (Fig. 1, Runs A and B). Extrapolation of the nearly linear, later portion of these rate plots to zero time indicated the production of about 1.33 moles of gas per mole of hexanitrate in the initial vigorous reaction. The addition of small amounts of water to the pyridine considerably reduced the amount of

TABLE I

COMPOSITION OF THE GAS EVOLVED FROM A 0.368 *M* SOLUTION OF D-MANNITOL HEXANITRATE IN PYRIDINE AT 30°C.

Run	Time of reaction (min.)	Composition of the gas evolved			
		% N_2O	% NO	% N_2	% Pyridine
A[a]	180	63.6	16.5	17.4	2.5
		63.3	16.3	17.9	2.5
B[a]	200	62.1	17.5	18.0	2.4
C[b]	240	61.1	18.1	18.2	2.5
D[c]	240	58.6	19.3	19.4	2.8
E[d]	240	56.5	18.5	22.2	2.8

[a]*Pyridine was freshly distilled over barium oxide.*
[b]*Dried pyridine was exposed to the laboratory atmosphere for three minutes before use.*
[c]*Water, 0.17% by weight, was added to the pyridine.*
[d]*Water, 0.34% by weight, was added to the pyridine.*

gas evolved (Fig. 1, Runs C, D, and E). The compositions of the gaseous products collected during four hours in each of Runs A to E are compared in Table I.

Chemical (20) and mass-spectrometric (17) methods for determining nitrous oxide, nitric oxide, and nitrogen in admixture have but recently been reported; the procedure developed in the present case appeared to be new and although probably less accurate, was considerably more straightforward than the above. Nitric oxide was determined in the evolved gas by mixing it with an excess of pure oxygen and exposing the mixture to a fine stream of mercury droplets until it became colorless and constant in volume. Previous reports of this reaction (10, 23, 24) were qualitative in nature; our experiments with samples of the pure gases showed the reaction to be quantitative and to be represented by the following equation at room temperature:

$$NO_{(g)}+O_{2(g)}+Hg_{(l)} \rightarrow HgNO_{3(s)}.$$

After removal of the nitric oxide the remaining gas was analyzed for nitrous oxide, carbon dioxide, and the known excess of oxygen in an Orsat apparatus (28) and for nitrogen by gas-density measurements on the nonabsorbable residual gas (19, 28). Appropriate corrections were made for the pyridine vapor and its coabsorption with the nitrous oxide. The over-all accuracy of the method was assessed at 1.5% with known samples of the individual gases.

Crystalline D-mannitol-1,2,4,5,6-pentanitrate was recovered from the pyridine solutions as previously described (18) when these were diluted with water; the yields obtained at different reaction times are shown in Table II.

TABLE II

YIELD OF D-MANNITOL-1,2,4,5,6-PENTANITRATE WITH DRIED AND WITH MOIST PYRIDINE

Run	Time of reaction (min.)	% Yield
A	180	70.8
B	200	71.6
C	240	73.0
D[a]	240	77.8
E[a]	240	76.5
F[b]	1080	73.0
G[b]	1440	69.0

[a] *Water was added to the pyridine before reaction, see Table I.*
[b] *The reaction mixture was exposed to air (18).*

An orange-brown, partially crystalline residue, 42% of the weight of the hexanitrate used, was obtained by careful evaporation of an aliquot of the yellow aqueous filtrate, and crystalline pyridinium nitrate (31% of the residue) was isolated from this solid by adsorption of the colored material on charcoal. Paper chromatography of the aqueous filtrate indicated about 14 components to be present, but no clear-cut separation of these substances could be achieved by fractional crystallization, solvent partition, dialysis, adsorption chromatography on silica gel, or by treatment with an anion exchange resin. Attempts

to separate pyridine quantitatively from the residue by precipitation from acetic acid solution as the perchlorate salt (4) or from aqueous solution as the copper thiocyanate complex (30) were unsuccessful and nitrogen analyses for nitrate were hampered by the presence of pyridine.

Potentiometric titration of aliquots of the aqueous pyridine filtrate first with alkali and then with acid revealed the concentration of *bound* and of *free* pyridine. The accuracy of this method was assessed as 1.1% with suitable aqueous solutions containing pyridine and pyridinium nitrate. *Bound* pyridine was recorded as equivalent to nitrate ion and the sum of *bound* and *free* pyridine as unreacted pyridine. These assumptions were supported by the actual isolation of 0.41 mole of pyridinium nitrate per mole of hexanitrate and by the agreement between the pH values measured potentiometrically at the beginning of the titration (7.57) and at the equivalence points (10.1, 4.2) and those calculated from the apparent ionization constant (pK_b 7.82) (26) measured in the known solution (initial pH, 7.55; calculated at equivalence points: 10.0, 3.3). A summary of the analyses of the four-hour runs C, D, and E is given in Table III.

TABLE III

COMPONENTS IN THE REACTION OF PYRIDINE WITH D-MANNITOL HEXANITRATE

	Run C	Run D	Run E
Reactants (moles)			
D-mannitol hexanitrate	1.00	1.00	1.00
Pyridine	40.5	40.5	40.5
Water	Trace	0.25	0.50
Elementary composition of reactants (gm-atoms)			
C	208.5	208.5	208.5
H	210.5	211.0	211.5
O	18.0	18.3	18.5
N	46.5	46.5	46.5
Products (moles)			
D-mannitol pentanitrate	0.73	0.77	0.76
Pyridine unreacted[a]	38.4	38.5	38.9
Nitrous oxide[b]	1.24	0.94	0.67
Nitric oxide	0.30	0.24	0.15
Nitrogen gas	0.30	0.24	0.18
Nitrate ion	1.63	1.66	1.73
Elementary composition of products identified (gm-atoms)			
C	196.4	197.1	199.1
H	198.6	199.4	201.3
O	18.1	18.4	18.3
N	47.1	46.6	46.3

[a]*Corrected for losses in manipulations.*
[b]*Including nitrous oxide dissolved in the pyridine (29).*

As shown in Table III the total nitrogen and oxygen content of the reactants was accounted for, within the experimental error, as mannitol pentanitrate, nitrogen, nitrogen oxides, nitrate ion, and unreacted pyridine. The mannitol hexanitrate not represented by the pentanitrate recovered, an average of 0.25 mole, was therefore completely denitrated in the aqueous solution. One mole

of hexanitrate yielded on the average 0.75 mole of pentanitrate while approximately 2.0 moles of pyridine disappeared. That some of this pyridine suffered ring cleavage in the initial vigorous reaction was certain since, in Runs A, B, and C, the total nitrogen content of the pentanitrate and gases isolated, excluding that of nitrate ion and pyridine, exceeded the nitrogen content of the original amount of hexanitrate by 0.88, 1.19, and 1.03 gm-atoms per mole respectively. In Runs D and E these figures were substantially lowered (0.45 and -0.35) by the presence of water in the pyridine. The material balance calculated for the three runs (Table III) indicated that the unidentified, water-soluble, and dialyzable products were probably nitrogen-free and approximated to the composition $C_xH_x(OH)_y$ of a mixture of unsaturated aldehydes and alcohols of low molecular weight. A possible major component was glutaconaldehyde (I and II), $C_5H_6O_2$, which has been shown by Zincke and others (5, 13, 14, 36, 37) to be formed by ring opening of pyridine under salt-forming and oxidizing conditions and to have indicator properties, existing in basic media as the dark red enolate ion (I) and in acid solution as

$\bar{O}$—CH=CH—CH=CH—CHO+H^+ OHC—CH_2—CH=CH—CHO

I or

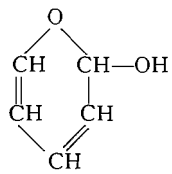

II

the yellow-brown dialdehyde (II). The aqueous pyridine denitration solutions showed a reversible change in color from pale yellow to orange with alteration of pH from 4 to 10, but attempts to isolate the dianilide of glutaconaldehyde (12) were unsuccessful and were hampered by the presence of pyridinium nitrate. Evaporation of the aqueous pyridine solution in the presence of excess potassium hydroxide left a dark, tarry, pyridine-free substance. Steam distillation of an alkaline solution of glutaconaldehyde was shown by Baumgarten and Glatzel (6) to cause decomposition of the dialdehyde to acetaldehyde, formic acid, crotonaldehyde, and other fragments.

Since several reaction products, amounting to 4 to 5% of the carbon and hydrogen content of the reactants, remained unidentified, the over-all mechanism for the denitration reaction was not obvious; some salient features of the reaction, however, were indicated:

(*a*) The source of the proton substituted for nitronium ion in the nitryloxy-fission (3) appeared to be traces of active hydrogen remaining in the pyridine after distillation from barium oxide. Nitronium ion substitution on carbon atoms of the pyridine nucleus was ruled out as the source of the proton since pyridine has been shown to stubbornly resist such substitution (16, 27). Tanberg (33) showed that samples of pyridine distilled from barium oxide

contained 0.013 to 0.028% by weight active hydrogen and Zerewitinoff (35) considered that this active hydrogen might have been present as dihydropyridine formed in the drying operation. The yield of pentranitrate obtained in Run C would require 0.028% active hydrogen to be retained in the pyridine; in Runs A and B the pyridine was exposed to the moist laboratory air for shorter periods of time and the yield of pentanitrate was lowered (Table II). Addition of small amounts of water (0.17 and 0.34% by weight) in Runs D and E considerably reduced the amounts of gas evolved but only slightly increased the yield of pentanitrate.

(*b*) Nitrogen cleaved from the pyridine ring in the anhydrous reaction appeared in part in the gaseous form, the proportion so evolved decreased with increasing moisture content although the amount of pyridine ring-opened was only slightly reduced by added water. Freytag (14, 15) showed that hygroscopically absorbed moisture reacted with pyridine to form pyridinium hydroxide which subsequently suffered ring opening, slowly in the dark, more rapidly in sunlight and in the presence of nitrate ion, to give the colored ammonium salt of the enolic glutaconaldehyde (I), "photopyridine". Lane (21) has reported colored polymeric material to be formed in addition to pyridinium nitrate and alkenes when pyridine was treated with some simple alkyl secondary and tertiary nitrate esters at reflux temperature.

(*c*) Nitrogen dioxide, if released from the hexanitrate, could be expected to form first an addition compound with the pyridine of the type described by Spencer (31) and others (1, 9) and this complex would then undergo oxidation–reduction reactions (9) to give the gaseous products observed.

(*d*) The 0.25 mole of hexanitrate not recovered in the form of pentanitrate was rendered soluble in water and, from the nitrogen balance (Table III), was probably denitrated to a tetranitrate stage in the first vigorous reaction with dried pyridine and then completely saponified during the titration of the aqueous pyridine solution with 0.2 *N* alkali.

It is of interest that in the partial denitration of other polynitrates (19, 28) the presence of free hydroxylamine in the pyridine inhibited the color formation, caused the evolution of gaseous nitrogen only, and increased the rate of reaction. The formation of the colorless dioxime of glutaconaldehyde (7) might account for the very slow development of color in those reactions.

EXPERIMENTAL

Materials and Methods

Pure D-mannitol-1,2,3,4,5,6-hexanitrate was prepared as described previously (18). The usual precautions (18, 19, 22) were observed in handling this high explosive and its derivatives.

Analytical reagent grade pyridine supplied by the British Drug Houses was dried by distilling over anhydrous barium oxide with care to avoid exposure to moist air.

Gas Evolved from D-*Mannitol Hexanitrate and Pyridine*

Pure, finely divided mannitol hexanitrate, 2.500 gm., was placed in the cup

of the reaction vessel of a du Pont nitrometer which was fitted with a thermometer well and water-cooling jacket and connected to two gas burettes by a three-way stopcock. The nitrate was quickly washed into the reaction chamber with pyridine, 15.0 ml., with care to prevent the entry of air, and the volume and temperature of the colorless gas evolved were noted at two to four minute intervals. The rate plots with the most carefully dried pyridine were closely grouped (Fig. 1, Runs A and B) and were corrected for the vapor pressure of pyridine (34). Similar experiments were carried out with pyridine to which water had been added from a graduated pipette (Fig. 1, Runs D and E) and with pyridine previously exposed to the moist air of the laboratory for three minutes before use (Fig. 1, Run C).

Admission of air or oxygen to a sample of the evolved gas caused the immediate appearance of red-brown nitrogen dioxide indicating nitric oxide to be present. The brown gas reacted slowly with the surface of the confining mercury forming a gray to white powder. When a continually renewed, fresh surface of mercury was exposed to the gas mixture by adjusting the mercury levelling bulbs so that a fine stream of mercury droplets flowed through it, the color of the gas disappeared and the residual volume became constant in about two hours at room temperature. To test the value of this reaction as a means of determining nitric oxide, 16.20 ml. of nitric oxide was generated by the nitrometer reaction from pure potassium nitrate and mixed with 16.40 ml. of dry oxygen (99.0% soluble in alkaline pyrogallol) at 757.0 mm. and 20.5°C. The mercury stream was passed through this mixture and the residual volume of colorless gas was 0.30 ml. after two hours indicating that the reaction was 99.4% complete. The grayish white powder trapped by the mercury against the walls of the gas burette partially dissolved in water to give an acid solution. It dissolved readily in dilute nitric acid and appeared to be mercurous nitrate (23, Vol. 4, p. 987).

After four hours' reaction time the pyridine denitration solution was removed from the nitrometer chamber which was flushed with pyridine (3.00 ml.) and then with water (10 ml.) and dried with acetone. Dry oxygen, approximately one half the volume of the evolved gas, was then admitted through the chamber to the burette and the mixed gases were treated with mercury as before. The volume of the colorless residual gas became constant in about two hours and the gas was then analyzed in an Orsat apparatus equipped with pipettes containing 95% ethanol, 40% potassium hydroxide, and alkaline pyrogallol solutions for absorption of nitrous oxide (28), ethanol vapor and carbon dioxide, and oxygen respectively. The percentage of nitrous oxide was given by $aV_2/V_1-p\ 100/P$, of nitrogen by bV_2/V_1, and of nitric oxide by $100-(a+b)V_2/V_1$, where a and b were respectively the percentage of the mercury-and-oxygen-treated gas absorbed by ethanol and 40% potassium hydroxide, and the percentage of the nonabsorbable gas. V_1 was the volume of the gas before admission of oxygen, V_2 the volume of the gas after treatment with oxygen and mercury, p the vapor pressure of pyridine (34), and P the atmospheric pressure. The nonabsorbable gas was found to have a molecular weight of 29.1 ± 0.5 (average of six experiments) by the method of Daniels,

Mathews, and Williams (8) and was assumed to be nitrogen (19, 28); any carbon monoxide present in the evolved gas would have been oxidized at room temperature to the dioxide by the nitrogen dioxide. In the analysis of the oxygen-and-mercury-treated gas a repass through the ethanol pipette established that the loss in volume of the gas ($<1.5\%$) on passage through the potassium hydroxide solution was probably due to absorption of ethanol vapor and not to acid gases. The results of these analyses are shown in Table I. A sample of commercial nitrous oxide was found to be 98.5% soluble in 95% ethanol, the absorption requiring 90 min.

Isolation of D-*Mannitol*-1,2,4,5,6-*pentanitrate*

The reaction mixture removed from the nitrometer was poured into water, 200 ml., contained in a ground-glass stoppered flask. The pyridine and water washings were added and after the solution had stood for two hours the precipitation of solid material was complete. The crystalline, nearly colorless product was recovered on a fritted glass crucible, washed thoroughly with water, and dried *in vacuo*. After two recrystallizations from aqueous ethanol the pure D-mannitol-1,2,4,5,6-pentanitrate melted correctly at 81–82°C. (11, 18). This melting point was not altered by further recrystallization from carbon tetrachloride. The specific rotation in alcohol was $+47.7°$ (c, 4.426).* The yields of crude pentanitrate obtained at several different reaction times with dried and moist pyridine are given in Table II.

The Aqueous Pyridine Solution from the Denitration Reaction

The combined filtrate and washings from the denitration of 5.00 gm. of hexanitrate (Run F) were evaporated to dryness *in vacuo*. The solid, odorless, orange-brown residue contained some crystals and weighed 2.61 gm. From Run G 2.1 gm. of the residue was similarly obtained. This material was readily soluble in water, methanol, ethanol, and acetic acid and to the extent of about 75% in boiling acetone. It was slightly soluble in ether, benzene, and petroleum ether.

A portion of the solid residue, 0.78 gm., dissolved in 50 ml. of water was heated to boiling with 1 gm. of activated charcoal and filtered through Kieselguhr. Evaporation of the slightly yellow filtrate and recrystallization of the residual product from acetone gave 0.24 gm. of colorless, odorless needles melting at 115.0–116.2°. The substance was pyridinium nitrate since it immediately produced a strong odor of pyridine on contact with caustic solution and did not depress the melting point (115.5–117.2°) of authentic pyridinium nitrate prepared from pyridine and yellow fuming nitric acid (2, 25). Crude pyridinium nitrate, 0.12 gm., was also recovered in Run G from the inner walls of the reaction flask which had been exposed to the laboratory atmosphere during the denitration. Further small amounts of pyridinium nitrate were obtained by fractional crystallization of an acetone extract of the residue.

Other attempts to fractionally crystallize or partition the residue with a variety of solvents gave only highly colored amorphous products. A sample of the residue (*ca.* 5 mgm.) was chromatographed on paper for 24 hr. by the

*An incorrect value of $+43.6°$ was reported earlier (18).

descending technique with butanol–water–ethanol–ammonia (40: 49: 10: 1) as irrigating solvent. The dried chromatogram was inspected under ultraviolet light, which revealed 14 distinct spots ranging in color from pink to blue with R_f values from 0.02 to 0.90. D-Mannitol pentanitrate and pyridinium nitrate did not fluoresce under the same conditions. Adsorption chromatography of the acetone extract of 0.8 gm. of residue on a column of unactivated silica gel (80–115) mesh, 1.3×52 cm.) with acetone followed by methanol as eluting solvents gave six separate fractions detected by diphenylamine reagent, each of which was amorphous and yellow to orange in color and was not investigated further.

To 0.62 gm. of pyridinium nitrate dissolved in 10 ml. of glacial acetic acid was added a 1 *N* solution of perchloric acid in acetic acid until precipitation of the colorless pyridinium perchlorate (14) was complete. The dried precipitate (0.75 gm.) represented 98% of the pyridinium nitrate. An attempt to precipitate pyridinium perchlorate from a glacial acetic acid solution of the residue (0.70 gm.) gave a dark colored solid product (0.73 gm.) which was not investigated further. Dialysis against water of a solution of 0.80 gm. of the residue in 100 ml. of water contained in a cellophane bag caused all but 0.01 mgm. of the residue to move into the dialyzing liquid in 24 hr. The brown product from the evaporated dialyzate could not be crystallized. Amberlite I-R-45 anion exchange resin, 20 gm., completely removed nitrate ion (diphenylamine test) from a solution of 1 gm. of pyridinium nitrate in 100 ml. of water. When 0.68 gm. of the residue was treated in a similar manner with the exchange resin, and the treated solution was evaporated to dryness, 0.11 gm. of a hard, amorphous, dark brown solid remained which gave a paper chromatogram similar to that of the untreated residue, but showing only nine separate spots under ultraviolet light.

A portion of the residue, 1.31 gm., was dissolved in anhydrous methanol, 50 ml., treated with sodium hydroxide pellets, 0.4 gm., and warmed with stirring on the steam bath for five minutes. When all the hydroxide had dissolved the solution became turbid and a fine brown precipitate separated while the solution gave off a distinct odor of pyridine. Concentrated hydrochloric acid (1.70 ml.; d., 1.18) was then added with stirring and the solution once more became clear and yellow in color. Aniline, 2.00 ml., was added and the solution gradually became deep cherry-red in color. Evaporation of the solution left a large amount of colorless crystalline product covered with a sticky, deep-red sirup which could not be induced to crystallize. N-(2,4-Dinitro-)-phenylpyridinium hydrochloride in ethanol solution gave an immediate precipitate of the dianilide hydrochloride of glutaconaldehyde (12) as cherry-red needles (44% of theory) when treated with hydrochloric acid and aniline under the same conditions.

Titrimetric Estimation of Pyridine and Nitrate in the Reaction Products

Twenty-five-milliliter aliquots of a 250 ml. aqueous solution containing 1.340 gm. of pyridinium nitrate and 18.2 gm. of pyridine were titrated first with 0.2 *N* potassium hydroxide solution for estimation of nitrate ion and then

with 0.6 *N* sulphuric acid for estimation of total pyridine (*free* pyridine added plus *bound* pyridine released from the pyridinium nitrate). The end points, detected with a Beckman model G pH-meter, occurred at pH 10.23 for the alkali titration and at pH 4.13 for the acid titration and had a sharpness of about 0.16 pH units per 0.20 ml. at the maxima. Found: pyridinium nitrate, 0.134, 0.135 gm. (100.3%); pyridine, 1.81, 1.81 gm. (99.5%).

Each filtrate from the isolation of D-mannitol pentanitrate in Runs C, D, and E was combined with the water washings and made up to 250 ml. and aliquots of these solutions were titrated by the above procedure. The value from the alkali titration was recorded as nitrate ion concentration and that from the acid titration as concentration of unreacted pyridine in Table III. Losses of pyridine in the manipulations were estimated at 1.1% by carrying out the procedure of denitration with a pyridine blank.

Evaporation of 25-ml. aliquots of the denitration solutions from Runs C, D, and E after addition of a measured excess of potassium hydroxide left 0.097, 0.046, and 0.102 gm. of dark amorphous residues respectively.

ACKNOWLEDGMENT

The authors wish to thank the National Research Council of Canada for Grant G 249 which helped to defray the cost of this research. They are indebted to Dr. Milton Kirsch for many helpful discussions.

REFERENCES

1. ADDISON, C. C., HODGE, N., and SHELDON, J. C. Chemistry & Industry, 1338. 1953.
2. ANDERSON, T. Ann. 105: 335. 1858.
3. ANSELL, E. G. and HONEYMAN, J. J. Chem. Soc. 2778. 1952.
4. ARNDT, F. and NACHTWEY, P. Ber. 59, B: 448. 1926.
5. BAUMGARTEN, P. Ber. 57, B: 1622. 1924.
6. BAUMGARTEN, P. and GLATZEL, G. Ber. 59, B: 2658. 1926.
7. BAUMGARTEN, P., MERLÄNDER, R., and OLSHAUSEN, J. Ber. 66, B: 1802. 1933.
8. DANIELS, F., MATHEWS, J. H., and WILLIAMS, J. W. Experimental physical chemistry. 3rd ed. McGraw-Hill Book Company, Inc., New York. 1941. p. 3.
9. DAVENPORT, D. A., BURKHARDT, H. J., and SISLER, H. H. J. Am. Chem. Soc. 75: 4175. 1953.
10. DIVERS, E. and SHIMIDZU, T. J. Chem. Soc. (Trans.), 47: 630. 1885.
11. ELRICK, D. E., MARANS, N. S., and PRECKEL, R. F. J. Am. Chem. Soc. 76: 1373. 1954.
12. FISHER, N. I. and HAMER, F. M. J. Chem. Soc. 189. 1933.
13. FIX, D. D. Org. Chem. Bull. 25 (No. 3). 1953.
14. FREYTAG, H. Ber. 67, B: 1995. 1934; 69, B: 32. 1936.
15. FREYTAG, H. Phot. Korr. 73: 17, 37, 57. 1937.
16. FRIEDEL, F. Chem.-Ztg. 36: 589. 1912; Chem. Abstr. 7: 1483. 1913.
17. FRIEDEL, R. A., SHARKEY, A. G., JR., SHULTZ, J. L., and HUMBERT, C. R. Anal. Chem. 25: 1314. 1953.
18. HAYWARD, L. D. J. Am. Chem. Soc. 73: 1974. 1951.
19. HAYWARD, L. D. and PURVES, C. B. Can. J. Chem. 32: 19. 1954.
20. JOHNSON, C. L. Anal. Chem. 24: 1572. 1952.
21. LANE, E. S. J. Chem. Soc. 1172. 1953.
22. MCKEOWN, G. G. and HAYWARD, L. D. Can. J. Chem. 33: 1392. 1955.
23. MELLOR, J. W. A comprehensive treatise on inorganic and theoretical chemistry. Vol. 8. Longmans, Green and Co. Ltd., London. 1928. p. 545.
24. NOYES, W. A., JR. J. Am. Soc. 53: 514. 1931.
25. PINCUSSOHN, L. Z. anorg. Chem. 14: 379. 1897.
26. PRIDEAUX, E. B. R. Trans. Faraday Soc. 15: 137. 1919.
27. SCHOFIELD, K. Quart. Revs. (London), 4: 382. 1950.
28. SEGALL, G. H. and PURVES, C. B. Can. J. Chem. 30: 860. 1952.

29. SEIDELL, A. Solubilities of inorganic and metal organic compounds. 3rd ed. Vol. I. D. Van Nostrand Company, Inc., New York. 1940. p. 1142.
30. SPACU, G. Bul. soc. stiinte Cluj, 1: 284. 1922; Chem. Abstr. 17: 1772. 1923.
31. SPENCER, J. F. Chem. News, 87: 176. 1903.
32. SUGIHARA, J. M. *In* Advances in carbohydrate chemistry. Vol. 8. *Edited by* C. S. Hudson and M. L. Wolfrom. Academic Press, Inc., New York. 1953. p. 1.
33. TANBERG, A. P. J. Am. Chem. Soc. 36: 335. 1914.
34. VAN DER MEULEN, P. A. and MANN, R. F. J. Am. Chem. Soc. 53: 451. 1931.
35. ZEREWITINOFF, T. Ber. 47: 2417. 1914.
36. ZINCKE, T. Ann. 330: 361. 1904.
37. ZINCKE, T., HEUSER, G., and MÖLLER, W. Ann. 333: 396. 1904.

INTENSITY IN THE RAMAN EFFECT

IV. RAMAN INTENSITY SUM RULES AND FREQUENCY ASSIGNMENTS FOR CH_3CN, CD_3CN, CH_3CCl_3, AND CD_3CCl_3 [1]

By J. C. Evans[2] and H. J. Bernstein

ABSTRACT

The standard intensities of the Raman bands of CH_3CN, CD_3CN, CH_3CCl_3, and CD_3CCl_3 have been obtained for the liquids with a photoelectric, grating spectrometer. The intensity sum rules for isotopic homologues are valid within the experimental error. The infrared spectra of CD_3CN and CD_3CCl_3 have been obtained in the liquid phase and in the vapor phase. A definitive assignment of $\nu_{11}(e)$ has been made for methyl chloroform.

In Paper III (1) of this series the theoretical rules relating the intensities of vibrational Raman bands in isotopic molecules were applied to benzene and its deuterium substituted homologues. Within the experimental uncertainty the rules were found to be valid. Further intensity data have been obtained and tests of the rules have been made for CH_3CN and CD_3CN and for CH_3CCl_3 and CD_3CCl_3.

The vibrational spectra of the two deuterium substituted molecules have not been reported previously, but methyl cyanide (10, 11) and methyl chloroform (8) have been studied extensively. However, there are available only qualitative values for the depolarization ratios of the Raman bands of CH_3CN (3) and only 10 of the 12 fundamental modes of CH_3CCl_3 are well-established. Of the two remaining modes one is inactive in both Raman and infrared, while the other has been assigned differently by various authors (8). The Raman spectrum of CD_3CCl_3 enabled this last difficulty to be resolved.

EXPERIMENTAL

The CH_3CN and CH_3CCl_3 were Eastman Kodak samples; they were fractionally distilled. The methods of preparing the deuterium substituted compounds will be described: CD_3CN (6), CD_3CCl_3 (7).

A White, grating Raman spectrometer with photoelectric recording (12) and a Perkin Elmer model 112 double pass spectrometer were used to record the spectra. Depolarization ratio measurements were made (5) and corrected for convergence error (9). Standard intensities of scattering per molecule referred to the 458 cm.$^{-1}$ band of CCl_4 were obtained (2).

The observed Raman spectra and the corrected depolarization ratios for CH_3CN and CD_3CN are summarized in Table I, and the infrared data for CD_3CN are given in Table II. Figs. 1 and 2 illustrate the spectra. The doubtful Raman band reported at 1124 cm.$^{-1}$ in previous investigations on CH_3CN was not observed here. In CD_3CN, ν_1, ν_2, $2\nu_3$, and $2\nu_6$ appear to be in Fermi reson-

[1]*Manuscript received August 15, 1955.*
Contribution from the Division of Pure Chemistry, National Research Council, Ottawa, Canada. Issued as N.R.C. No. 3758. Presented in part at the Symposium on Molecular Structure, Columbus, Ohio, June 1955.
[2]*N.R.C. Postdoctorate Research Fellow 1953–55.*

TABLE I

RAMAN SPECTRA OF CH_3CN AND CD_3CN IN THE LIQUID STATE

Assignment	CH_3CN			CD_3CN		
	cm.$^{-1}$	Corrected depol. ratio		cm.$^{-1}$	Corrected depol. ratio	
$\nu_5(e)$	3001	0.86		~2258	Overlapped by ν_2	
$\nu_1(a_1)$	2941	0.09	F.R.*	2112	0.12	F.R.
$2\nu_6(A_1+E)$	2882	P	F.R.*	2057	0.13	F.R.
$\nu_3+\nu_4(A_1)$	2289	0.26	F.R.	—		
$\nu_2(a_1)$	2248	0.20	F.R.	2258	0.29	F.R.
$2\nu_3(A_1)$	—			2209	0.44	F.R.
$\nu_6(e)$	1443	0.85		1041	0.86	
$\nu_3(a_1)$	1371	0.52		1103	0.70	
$\nu_4(a_1)$	919	0.17		834	0.23	
$2\nu_8(A_1+E)$	750	0.51		684	0.43	
$\nu_7-\nu_8(A_1+A_2+E)$	674	0.46		—		
$\nu_8(E)$	379	0.86		348	0.86	

In this and in the other tables, wave number values are corrected to vacuum.
**Fermi resonance.*

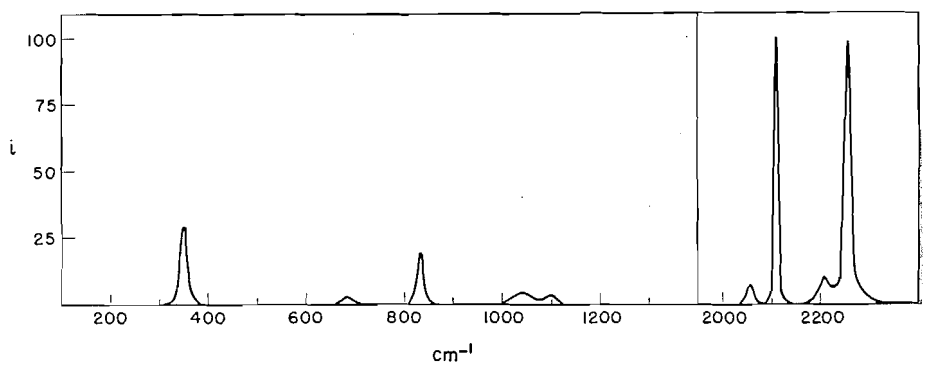

FIG. 1. The observed Raman spectrum of CD_3CN. The intensity of the band with greatest peak height is 100. Slits were 6.5 cm.$^{-1}$ in the 3000 cm.$^{-1}$ region and 7.5 cm.$^{-1}$ in the region 0–1600 cm^{-1}.

ance. Several minor features in the infrared spectrum of CD_3CN remain to be explained. The band at 1375 cm.$^{-1}$ in the vapor was not observed in the liquid spectrum while the band at 2692 cm.$^{-1}$ in the liquid has no simple explanation. The band at 1246 cm.$^{-1}$ in the vapor and one of the two bands at 1266 and 1282 cm.$^{-1}$ in the liquid seem to correspond to $4\nu_8$. (Some support for this assignment is that ν_8 also shifts to higher wave number from vapor to liquid.) The assignments of the fundamentals and of the other observed bands are straightforward.

TABLE II

INFRARED SPECTRUM OF CD_3CN BETWEEN 300 AND 3400 CM.$^{-1}$

Wave number (Liquid)		Wave number (Vapor)	Assignment*
3376	vw	3380	$\nu_2+\nu_3 = 3361\ (A_1)$
3286	vw	~3300	$\nu_2+\nu_6 = 3299\ (E)$
3200	vvw	—	$\nu_1+\nu_3 = 3215\ (A_1)$
3096	w	3115	$\nu_2+\nu_7 = 3108\ (E)$ or $\nu_2+\nu_4 = 3092\ (A_1)$
2965	vw	2985	$\nu_1+\nu_7 = 2962\ (E)$
2962	w	—	
2607	w	2600	$\nu_2+\nu_8 = 2606\ (E)$
2263	s	2289, 2279, 2270	$\nu_2(a_1)$
		~2270 (overlapped)	$\nu_5(e)$
2212	vvw	—	$2\nu_3 = 2206\ (A_1)$
2116	w	2137, 2126, 2117	$\nu_1(a_1)$
2059	w	2088, 2073, 2065	$2\nu_6 = 2082\ (A_1+E)$
1945	vw	1950	$\nu_3+\nu_7 = 1953\ (E)$
1931	vw	~1930	$\nu_3+\nu_4 = 1937\ (A_1)$
1884	vw	~1900	$\nu_7+\nu_6 = 1891\ (A_1+A_2+E)$
		1375 w	$\nu_6+\nu_8 = 1389\ (A_1+A_2+E)$
1282	w	~1246	$4\nu_8 \approx 1300\ (A_1+2E)$
1266	w		
1197	m	1181, 1166	$\nu_7+\nu_8 = 1198\ (A_1+A_2+E)$
1103	m	~1115 (overlapped by ν_6)	$\nu_3(a_1)$
1039	vs	Resolved: center 1052	$\nu_6(e)$
850	m	~850 (overlapped by ν_4)	$\nu_7(e)$
833	vs	~845, 833, 820	$\nu_4(a_1)$
687	w	670, ?, 645 (overlapped by CO_2)	$2\nu_8 = 696\ (A_1+E)$
348	m	335	$\nu_8(e)$

**Liquid phase data were used in computing the frequencies in the last column of this table and Table III.*

The Raman and infrared data for CD_3CCl_3 are collected in Table III and are illustrated in Figs. 3 and 4. Corresponding to the band at 343 cm.$^{-1}$ in the liquid phase spectrum of CH_3CCl_3, there are in CD_3CCl_3 two bands, 335 (a_1) and 315 (e). This latter band is the controversial e-type mode which in CH_3CCl_3 must be at 343 cm.$^{-1}$ in the liquid and at 350 cm.$^{-1}$ in the vapor. Pitzer and Hollenberg's suggestion (8) (which is based on the observed combination tones in the far infrared) that the 350 cm.$^{-1}$ band in CH_3CCl_3 vapor is composed of an a_1 type and an e-type band is therefore confirmed.

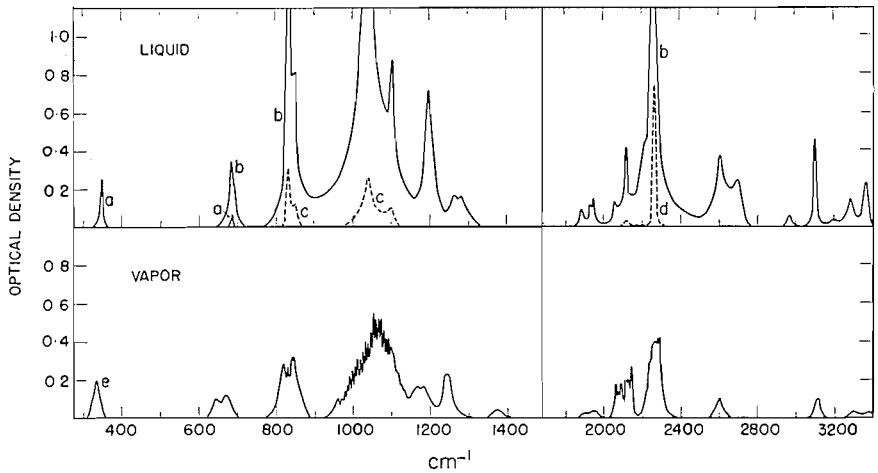

FIG. 2. The infrared spectrum of CD_3CN.
Liquid: *a*, capillary film; *b*, 0.1 mm. film; *c*, another capillary film; *d*, another capillary film.
Vapor: *e*, 6 cm. cell at 60°C.; vapor pressure ~370 mm. The remainder of the spectrum was obtained with a 1 meter cell at 20°C.; vapor pressure ~70 mm.

TABLE III

EXPERIMENTAL DATA FOR CD_3CCl_3

Raman data (liquid phase)		Infrared data		Assignment
cm.$^{-1}$	Corrected depol. ratio	Liquid	Vapor	
		3426 vvvw	3445	$3\nu_2 = 3420\ (A_1)$
		3301 vvw	3307	$2\nu_2+\nu_8 = 3323\ (E)$
				$\nu_7+\nu_8 = 3299\ (A_1+A_2+E)$
		3233 vvw	3242	$\nu_1+\nu_2 = 3269\ (A_1)$
				$\nu_3+\nu_7 = 3230\ (E)$
		3178 vvw	3190	$\nu_1+\nu_8 = 3175\ (E)$
				$\nu_7+\nu_9 = 3172\ (A_1+A_2+E)$
				$2\nu_2+\nu_9 = 3196\ (E)$
		3054 vvw	3064	$\nu_1+\nu_9 = 3048\ (E)$
				$2\nu_2+\nu_3 = 3062\ (A_1)$
		3008 vvw } Broad		$2\nu_8+\nu_9 = 3004\ (A_1+A_2+2E)$
		2974 vvw } ill-defined		$\nu_2+\nu_4+\nu_{12} = 2994\ (E)$
		2929 vvw } absorption		$2\nu_2+\nu_{10} = 2937\ (E)$
2277	0.19	2280 vw	—	$2\nu_2 = 2274\ (A_1)$
2256	0.86	2257 vw	2265	$\nu_7(e)$; ν (CD_3)
2150	0.24			$\nu_8+\nu_9+\nu_{12} = 2179\ (A_1+A_2+3E)$
2132	0.10	2136 vw	2152, 2143, 2135	$\nu_1(a_1)$; ν (CD_3)
2099	0.08	2103 vw	—	$\nu_2+\nu_3 = 2111\ (A_1)$
2068	0.13	2072 vvw	—	$2\nu_8 = 2088\ (A_1+E)$
		1312 vw	1325	$2\nu_{10} = 1314\ (A_1+E)$
		1280 vw	1285	$\nu_3+\nu_{11} = 1293\ (E)$
		1260 vw	—	$\nu_8+\nu_{12} = 1275\ (A_1+A_2+E)$
		1165 w sh	1170	$\nu_4+\nu_{10} = 1160\ (E)$
1137	0.68	1140 vs	1153, 1145, 1138	$\nu_2\ (a_1)$; δ (CD_3)
		1120 vw sh	—	$\nu_{10}+\nu_{12}+\nu_{12} = 1127\ (A_1+A_2+2E)$

TABLE III (*Concluded*)

Raman data (liquid phase)		Infrared data		Assignment
cm.$^{-1}$	Corrected depol. ratio	Liquid	Vapor	
		1105 vw	? 1110 1102	$\nu_6+\nu_9\sim 1116\ (E)$
1043	0.86	1044 m	1059 1050 1042	$\nu_8\ (e)$; $\delta\ (CD_3)$
		1013 vw	1020	$2\nu_4 = 1014\ (A_1)$
		992 vw sh	1000	$\nu_5+\nu_{10} = 992\ (E)$
974	0.50	976 m	977 967	$\nu_3\ (a_1)$; $\nu\ (c-c)$
		943 m sh	950	$\nu_4+\nu_{12}+\nu_6\sim 940\ (E)$
916	0.86	919 vs	932 925	$\nu_9\ (e)$; $\delta\ (CD_3)$
		893 vw	896	$\nu_{10}+\nu_{12} = 888\ (A_1+A_2+E)$
		866 m	876 869	$\nu_6+\nu_{10}\sim 857\ (E)$
		812 vw	818	$\nu_4+\nu_{11} = 823\ (E)$
		790 vvw	795	$2\nu_{12}+\nu_5 = 797\ (A_1+E)$
		727 w	728	$\nu_4+\nu_{12} = 736\ (E)$
			700 w	$2\nu_5 = 676\ (A_1)$
657	0.86		665 vvs	$\nu_{10}\ (e)$; $\nu\ (CCl_3)$
		605 vvw		$2\nu_{11} = 630\ (A_1+E)$
		580 vvw		$\nu_9-\nu_5 = 581\ (E)$
553 vvw	P	—	—	$\nu_{11}+\nu_{12} = 546\ (A_1, E)$
503	0.09	506 s	516 507 497	$\nu_4\ (a_1)$; $\nu\ (CCl_3)$
		466 vvw	—	$2\nu_{12} = 462\ (A_1+E)$
445 vvw	P?	—	—	$\nu_6+\nu_{12}\sim 440\ (E)$
		413 vvw	—	$2\nu_6\sim 420\ (A_1)$
364 vvw	P	—		$\nu_9-(\nu_{11}+\nu_{12}) = 366\ (A_1+A_2+3E)$
335	0.40	338 m	347 338 327	$\nu_5\ (a_1)$; $\delta\ (CCl_3)$
315	0.86	317 m	327 317	$\nu_{11}\ (e)$; $\delta\ (CCl_3)$
231	0.86			$\nu_{12}\ (e)$; $\delta\ (CCl_3)$

In CD_3CCl_3, $2\nu_8$, and $\nu_2+\nu_3$, which are presumably in Fermi resonance with ν_1, appear in the liquid spectra but are absent from the infrared vapor spectrum. This may be due to the removal or reduction of Fermi resonance by the separation of levels which are influenced differently by intermolecular interaction. The band at 2280 cm.$^{-1}$ in the liquid, assigned as $2\nu_2$, is also absent from the spectrum of the vapor.

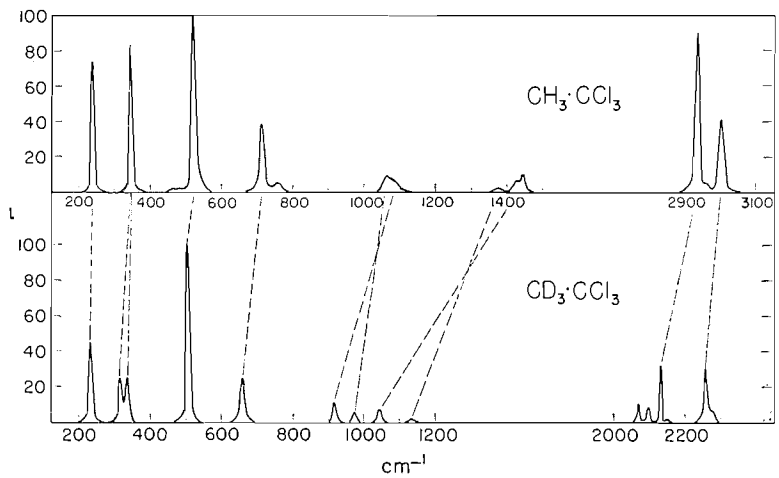

FIG. 3. The observed Raman spectra of CH_3CCl_3 and CD_3CCl_3. In each spectrum the band with greatest peak height is 100; the two scales are therefore not identical. Slits were 5 $cm.^{-1}$ in the 3000 $cm.^{-1}$ region and 6.5 $cm.^{-1}$ in the region 0–1600 cm^{-1}.

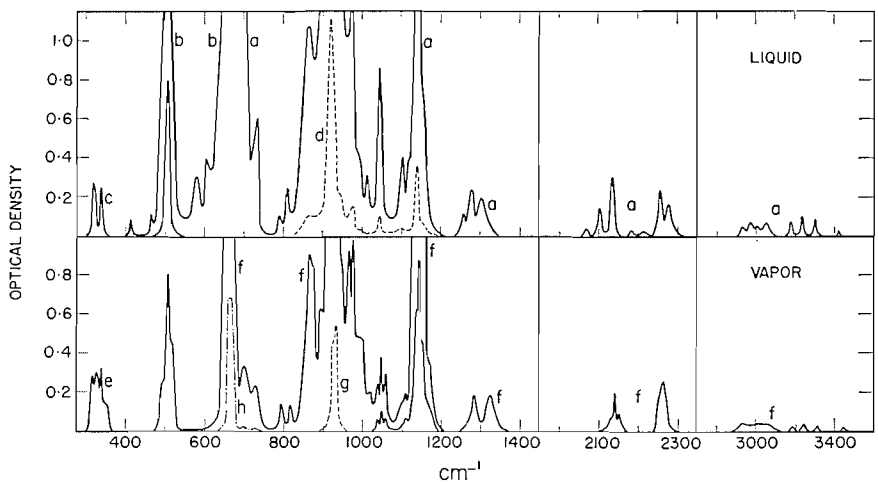

FIG. 4. The infrared spectrum of CD_3CCl_3.
Liquid: *a*, 0.1 mm. film; *b*, 0.24 mm. film; *c*, capillary film; *d*, another capillary film.
Vapor: *e*, 6 cm. cell at 60°C.; vapor pressure ~500 mm. *f*, 1 meter cell at 20°C.; vapor pressure ~90 mm. *g* and *h*, 1 meter cell at 20°C. with lower pressures of vapor. Slits were 8, 4, 5, 3, 2, 3, and 1.5 $cm.^{-1}$ in the regions 3000, 2000, 1400, 1100, 900, 700, and 400 $cm.^{-1}$ respectively.

The theoretical product rule ratios* for both pairs of molecules have been calculated and, in Table IV, these values are compared with the observed ratios. The agreement is satisfactory.

**Dimensions for calculating moments of inertia: CH_3CN and CD_3CN; C—H and C—D = 1.09 Å, C—C = 1.46 Å, C≡N = 1.16 Å, angles tetrahedral (Kessler et al. Phys. Rev. 79:54. 1950). CH_3CCl_3 and CD_3CCl_3: C—H and C—D = 1.09 Å, C—C = 1.53 Å, C—Cl = 1.76 Å, angles tetrahedral.*

TABLE IV

TELLER–REDLICH PRODUCT RULE APPLIED TO CH_3CN AND CD_3CN AND TO CH_3CCl_3 AND CD_3CCl_3

	Symmetry species	Observed ratio	Theoretical ratio
CH_3CN and CD_3CN	a_1	0.522	0.512
	e	0.412	0.396
CH_3CCl_3 and CD_3CCl_3	a_1	0.516	0.506
	e	0.375	0.371

RAMAN INTENSITIES

Crawford's (4) $\sum^F$ rule relating the intensities of the vibrational Raman bands of isotopic molecules may be written in the form

$$[1] \qquad \sum_a \frac{I_{1a}}{K_{1a}\Delta\nu_{1a}} = \sum_a \frac{I_{2a}}{K_{2a}\Delta\nu_{2a}}$$

if the conditions of irradiation and observation are the same for the isotopic molecules. Here, subscripts 1 and 2 refer to the two isotopic species; I_{1a} is the intensity of the "a"th fundamental of Raman shift $\Delta\nu_{1a}$ in isotopic molecule 1, and

$$K_{1a} = (\nu - \Delta\nu_{1a})^4(1-e^{-1.44\Delta\nu_{1a}/T})^{-1}$$

where ν is 22,938 cm.$^{-1}$, the frequency of the exciting line, and T is the absolute temperature. The assumptions made in deriving the rule are: (*a*) isotopic substitution does not change the force constants of the most general quadratic potential function, (*b*) nor does it change the polarizability and anisotropy derivatives with respect to the internal coordinates, and, (*c*) anharmonicity effects may be neglected. Assumption (*b*) is very nearly true if there is no rotation which changes the equilibrium polarizability of the molecule in the species of vibration considered. The a_1 species of CH_3CN and CH_3CCl_3 are of this type.

Written in terms of standard intensities S (1), the rule is

$$[2] \qquad \sum_a \frac{S_{1a}}{(\Delta\nu_{1a})^2} = \sum_a \frac{S_{2a}}{(\Delta\nu_{2a})^2}.$$

Although the rule was derived for the vapor phase it has been applied here to liquid phase intensities since it is expected that intermolecular interaction effects are the same for isotopic molecules.

The rule has been applied in both forms given by equations [1] and [2], and the results for the a_1 modes of CH_3CN and CD_3CN are given in Table V. There are several cases of Fermi resonance and in each case the total intensity of fundamental and overtone or combination tone was taken. Correction for overlapping of ν_2 by $\nu_5(e)$ was also necessary for CD_3CN. These bands are coincident so that the usual method of drawing symmetrical contours which is

TABLE V

	$\Delta\nu$	$\bar{S}$	$(\bar{S}/K\Delta\nu)\times10^{22}$	S	$S/(\Delta\nu)^2\times10^7$
			CH_3CN a_1 species		
ν_1	2941	0.79	16.8	4.74	5.48
	2882	0.03	0.7	0.20	0.37
ν_2	2289	0.05	1.2	0.18	0.35
	2248	0.43	10.5	1.62	3.21
ν_3	1371	0.14	4.5	0.20	1.06
ν_4	919	0.12	5.4	0.14	1.66
		Sum	39.1		12.1
			CD_3CN a_1 species		
ν_1	2112	0.52	13.1	1.86	4.18
	2057	0.05	1.2	0.17	0.40
ν_2	2258*	0.75	18.1	2.58	5.06
	2209	0.14	3.5	0.43	0.87
ν_3	1103	0.05	2.1	0.06	0.47
ν_4	834	0.14	6.8	0.14	2.00
		Sum	44.8		13.0

$\bar{S}$ is the integral intensity of the Raman band corrected for the spectral sensitivity of the phototube. The unit of the intensity scale is the intensity of the 458 cm.$^{-1}$ band of CCl_4.
S is the standard intensity.
**Correction for overlap by ν_5 was necessary.*

applicable to partially overlapping bands was inapplicable here. The assumption was made that the ratio $\bar{S}_{\nu_2}/\bar{S}_{\nu_1}$ (see Table V) was unchanged by isotopic substitution. The calculated contribution of ν_2 was subtracted from the band

TABLE VI

	$\Delta\nu$	$\bar{S}$	$(\bar{S}/K\Delta\nu)\times10^{22}$	S	$S/(\Delta\nu)^2\times10^7$
			CH_3CCl_3 a_1 species		
ν_1	2938	0.35	7.5	4.18	4.8
ν_2	1378	0.01	0.4	0.04	0.2
ν_3	1067	0.10	4.0	0.19	1.6
ν_4	521	0.61	42.4	0.74	27.3
ν_5	343*	0.25	22.4	0.13	11.5
		Sum	76.7		45.4
			CD_3CCl_3 a_1 species		
	2277	0.03	0.8	0.26	0.5
	2150	0.01	0.2	0.06	0.1
ν_1	2132	0.19	4.7	1.37	3.0
	2099	0.06	1.4	0.40	0.9
	2068	0.07	1.8	0.47	1.1
ν_2	1137	0.01	0.3	0.01	0.1
ν_3	974	0.06	2.4	0.11	1.2
ν_4	503	0.70	49.8	0.81	32.2
ν_5	335	0.25	22.4	0.13	11.5
		Sum	83.8		50.6

$\bar{S}$ and S are defined in Table V.
**Correction for overlap by ν_{11} was necessary.*

at 2258 cm.$^{-1}$ in CD_3CN to leave $\bar{S}_{\nu_2}$. Apart from being without basis, this assumption is complicated by the fact that ν_1 and ν_2 in CD_3CN may be in Fermi resonance. Unfortunately, ν_2 makes a large contribution to the total sum and introduces a large uncertainty, probably in excess of $\pm 5\%$, to this sum. For CH_3CN conditions are more favorable, and the estimated uncertainty in the total sum is $\pm 5\%$. Within $\pm 8\%$ the sums are the same.

The results for CH_3CCl_3 and CD_3CCl_3 are presented in Table VI. One case of Fermi resonance involving ν_1 in CD_3CCl_3 arises here, but a more serious uncertainty is introduced by the coincidence of ν_5 and ν_{11} in CH_3CCl_3. The ratio $\bar{S}_{\nu_5}/\bar{S}_{\nu_{11}}$ was assumed to be the same for the two molecules ($\bar{S}_{\nu_5}+\bar{S}_{\nu_{11}}$ was observed to be the same and a comparison of the depolarization ratios of the three observed bands suggests that the assumption is not unreasonable). It is again unfortunate that the overlapped band makes an important contribution to the sum, but a comparison of the total sums shows that within $\pm 6\%$ they are the same.

TABLE VII

e SPECIES

	CH_3CN			CD_3CN		
	$\Delta\nu$	$\bar{S}$	S	$\Delta\nu$	$\bar{S}$	S
ν_5	3001	0.27	0.96	2258*	0.18	0.42
ν_6	1443	0.13	0.18	1041	0.09	0.09
ν_7	1047	0	0	850	0	0
ν_8	379	0.23	0.06	348	0.32	0.07

$\bar{S}$ and S are defined in Table V.
ν_7 was not observed in the Raman spectra.
**Correction for overlap by ν_1 was necessary.*

TABLE VIII

e SPECIES

	CH_3CCl_3			CD_3CCl_3		
	$\Delta\nu$	$\bar{S}$	S	$\Delta\nu$	$\bar{S}$	S
ν_7	3005	0.45	3.39	2256	0.36	1.75
ν_8	1444 1428	0.17	0.44	1043	0.08	0.12
ν_9	1081	0.08	0.15	916	0.18	0.26
ν_{10}	712	0.53	0.58	657	0.44	0.43
ν_{11}	343*	0.30	0.11	315	0.30	0.11
ν_{12}	239	0.53	0.12	231	0.51	0.11

$\bar{S}$ and S are defined in Table V.
**Correction for overlap by ν_5 was necessary.*

The experimental data for the *e*-type modes of CH_3CN and CD_3CN are given in Table VII and the data for CH_3CCl_3 and CD_3CCl_3 are collected in Table VIII. Here the intensity sum rules are not expected to be valid since

molecular rotations which change the equilibrium polarizability occur. The quantities in equations [1] and [2] were however determined and are:

For CH_3CN and CD_3CN		
Equation [1]:	L.H.S. 30.2	R.H.S. 36.3
Equation [2]:	L.H.S. 5.76	R.H.S. 7.52
and for CH_3CCl_3 and CD_3CCl_3		
Equation [1]:	L.H.S. 132	R.H.S. 130
Equation [2]:	L.H.S. 49.2	R.H.S. 50.1

In each case, the deuterium substituted compound is on the right-hand side. The sum rule seems to be obeyed better for the *e*-type modes of the two methyl chloroform molecules than for the *e*-type modes of the two methyl cyanide molecules. This is proably due to the fact that the *e*-type rotational frequency changes less upon deuterium substitution in methyl chloroform than it does in methyl cyanide.

ACKNOWLEDGMENTS

The authors wish to express their thanks to Dr. L. C. Leitch and Mr. J. Francis for preparing the samples of CD_3CN and CD_3CCl_3, and to Mrs. C. A. Hunt for assistance in reducing the spectra.

REFERENCES

1. ALLEN, G. and BERNSTEIN, H. J. Can. J. Chem. 33: 1137. 1955.
2. BERNSTEIN, H. J. and ALLEN, G. J. Opt. Soc. Amer. 45: 237. 1955.
3. BISHUI, B. M. Indian J. Phys. 22: 167. 1948.
4. CRAWFORD, B. J. Chem. Phys. 20: 977. 1952.
5. EDSALL, J. T. and WILSON, E. B. J. Chem. Phys. 6: 124. 1938.
6. LEITCH, L. C. To be published.
7. LEITCH, L. C. and FRANCIS, J. To be published.
8. PITZER, K. S. and HOLLENBERG, J. L. J. Am. Chem. Soc. 75: 2219. 1953. References to earlier work are given.
9. RANK, D. H. and KAGARISE, R. E. J. Opt. Soc. Amer. 40: 89. 1950.
10. THOMPSON, H. W. and WILLIAMS, R. L. Trans. Faraday Soc. 48: 502. 1952.
11. VENKATESWARLU, P. J. Chem. Phys. 19: 293. 1951.
12. WHITE, J. U., ALPERT, N., and DEBELL, A. G. J. Opt. Soc. Amer. 45: 154. 1955.

THE EFFECT OF ADDITION AGENTS ON CATHODE POLARIZATION DURING ELECTRODEPOSITION OF COPPER AT SINGLE CRYSTAL COPPER CATHODES[1]

By K. Ekler[2] and C. A. Winkler

ABSTRACT

The polarization–time relations for the initial (P_i), maximum (P_{max}), and pseudo-steady-state (P_s) polarizations on copper single crystals in the absence and presence of gelatin and gelatin plus chloride ion were found to depend upon crystal orientation. The P_i and P_{max} in the absence of gelatin, the P_i in its presence, and the static potentials were all similarly related to the reticular density. The P_i increased, and the time to maximum polarization (t_{max}) decreased, with increase of current density; the relations between these quantities showed marked differences for the different crystals. The variation with reticular density of P_i and P_{max} in the absence of addition agents and of P_i in its presence probably represents differences in activation overpotential at the various crystal faces. The adsorption of gelatin on different crystal faces was also found to be markedly different. Polarization in the presence of gelatin was decreased by small amounts of chloride ion; a linear relation for all the crystals used was obtained by plotting the increase in polarization caused by gelatin against the decrease caused by 2 mgm./liter chloride ion in the presence of gelatin. In the absence of addition agent, change of acid concentration from 50 to 200 gm./liter had no effect on P_i and addition of chloride ion had no effect on P_s at single crystal cathodes.

INTRODUCTION

A number of papers from this laboratory have discussed the changes in cathode polarization at polycrystalline cathodes during electrodeposition of copper from acid copper sulphate electrolyte containing addition agents. Since the earliest of these studies (4), it has been of interest to examine the behavior with single crystal copper cathodes under similar conditions. Ample evidence exists that significantly different lattice energies are associated with different crystal faces of a single crystal, and such differences might be expected to influence not only the adsorption of an addition agent, hence the polarization in its presence, but perhaps also the polarization values in the absence of addition agent. The present paper represents a re-examination with single crystal cathodes of the more prominent features found previously to characterize the polarization behavior with polycrystalline cathodes.

EXPERIMENTAL AND RESULTS

Crystals $1\frac{1}{2}$ in. $\times$ $\frac{1}{2}$ in. $\times$ $\frac{1}{4}$ in. were purchased from Horizons Inc., Cleveland, Ohio. Their orientations were specified to be (111), (100), (110), (211), (410), and (322), referred to the longitudinal axis.

The interplanar spacings shown in Table I were calculated from the relation (3):

$$d = s/\sqrt{(h^2+k^2+l^2)}$$

where h, k, and l are the Miller indices and s is a term which for a face centered

[1]*Manuscript received July 28, 1955.*
Contribution from the Physical Chemistry Laboratory, McGill University, Montreal, Quebec, with financial assistance from the International Nickel Company of Canada, and the National Research Council.
[2]*Holder of an International Nickel Company Graduate Research Fellowship 1952–1955.*

cubic lattice, e.g. copper, is equal to 0.5 if one or two indices are odd; otherwise it is unity.

It should be noted that although two lattice planes of different Miller indices may have the same interplanar distances, e.g. (410) and (322), hence the same reticular densities (2), examination of a space lattice model readily revealed that the environment of a given atom in the two cases is quite different.

The polarization measurements were made in a modified Haring cell as described previously (4).

Prior to every experiment after the first one with a given crystal, deposited copper was carefully removed with a succession of files of decreasing roughness. A special guide was designed to ensure uniform removal of the deposit and thus preserve the original orientation of the crystal face. A rectangular groove was milled along a 10 in. brass bar to accommodate interchangeable files, while the crystal to be ground was placed in a slot milled into a brass block 2 in. long. When the block was inverted over the bar, and allowed to slide on it, the deposit of copper was removed while retaining parallelism of the crystal faces as indicated by micrometer measurements. The crystal was ground finally on metallographic papers 0 to 4/0 after which it was transferred to a suitable holder and all of the crystal surface coated with paraffin wax except the face under examination. The dimensions of the exposed area were determined with a table cathetometer so that the current could be adjusted to the desired apparent current density for the next operation of electropolishing. Chemical etching did not allow reproducible polarization values to be obtained.

The electropolishing bath consisted of 42.5% orthophosphoric acid (6). To minimize gassing, a copper cathode of area approximately 20 times that of the crystal was used. The potential between the electrodes was 4 volts and the spacing approximately three and one-half inches. The crystal was anodically polished for eight minutes at a starting current density of 12 amp./dm^2. An increase of polishing time to 20 min. gave identical results. Pitting of the surface was largely avoided by dislodging gas-bubbles as soon as their formation was detected.

After it had been electropolished, the crystal was rinsed with distilled water and immediately placed in a Haring cell containing electrolyte in presence of air at 25$\pm$0.1°C. Unless otherwise stated the electrolyte contained 125 gm./liter Merck's reagent grade copper sulphate pentahydrate and 100 gm./liter Baker's C.P. sulphuric acid in freshly distilled water. It was not stirred during polarization measurements.

Potentials were measured with a recording potentiometer (Brush Development Co., Cleveland, Ohio, Recorder BL 201, DC-Amplifier BL 932) and a potentiometer (Tinsley, Type 3184 D).

A reproducibility within $\pm$5 millivolts was required and generally obtained without difficulty.

For all experiments in the absence of addition agents the cathode was allowed to remain in contact with the electrolyte for 10 min. before starting

electrolysis. An increase of this immersion time to 30 min. gave identical polarization values. When addition agent was present in the electrolyte the immersion time was 15 min. An increase from 15 to 120 min. did not show any detectable polarization changes.

(*i*) *No Addition Agent Present*

The polarization–time relations for the various crystals at 2 amp./dm.^{2} are shown in Fig. 1. From the original tracings of these curves on the recording

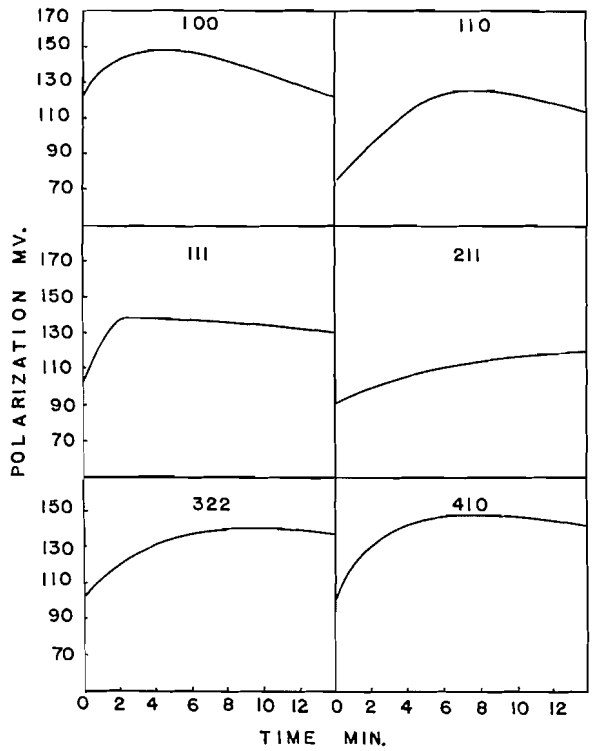

FIG. 1. Polarization–time relations at single crystal cathodes.

potentiometer, values of the initial (P_i) and maximum (P_{max}) polarization respectively were obtained and are recorded for the six crystals in Table I.*

The relative static potentials of the crystals are also shown in the table. To obtain these values, each crystal was immersed in the standard electrolyte in the presence of air and the electrode potential measured relative to a capillary probe filled with the same electrolyte in contact with a calomel half-cell through a closed, ungreased stopcock. Potential measurements were taken every five minutes until a steady state was obtained after 70 to 120 min.

The initial polarization and times required to attain the maximum polarization values for current densities from 0.2 to 4.0 amp./dm.^{2} are summarized

**While various quantities may be graphically represented in relation to the d-values, it should be noted that d is not a "running parameter", hence such plots are of doubtful significance.*

TABLE I

INITIAL (P_i) AND MAXIMUM (P_{max}) POLARIZATION VALUES, AND STATIC POTENTIALS, AT SINGLE CRYSTAL CATHODES IN THE ABSENCE OF ADDITION AGENT

Crystal (Miller indices)	Interplanar distance (d)* (Å)	P_i (mv.)	P_{max} (mv.)	Static potential (mv.)
(111)	0.5774	102	132	84
(100)	0.5000	120	148	90
(110)	0.3536	78	123	83
(211)	0.2041	90	118	69
(410)	0.1213	99	140	77
(322)	0.1213	101	147	80

**Referred to edge of unit cube.*

in Fig. 2. (For clarity the curves for only four crystals are shown; the other two are similar.) The latter quantity for a given crystal shifted systematically to lower values as the current density was increased.

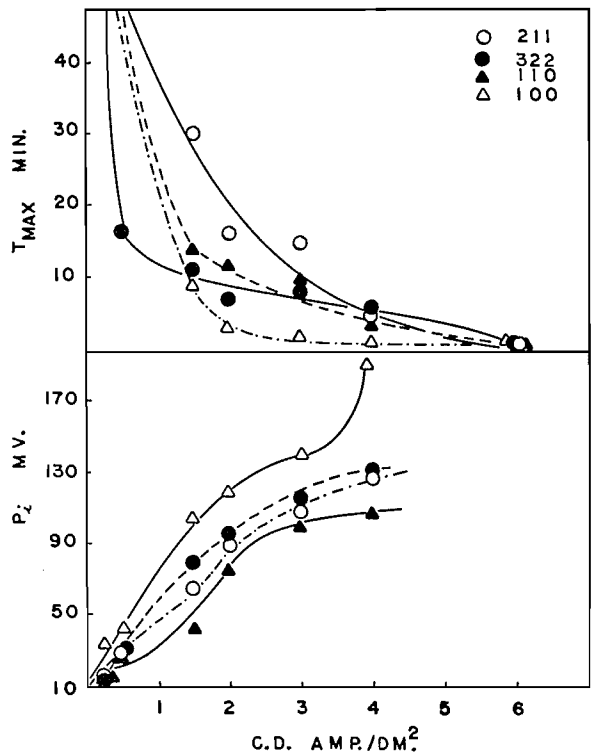

FIG. 2. Variation with current density of initial polarization (P_i) and time to maximum polarization (t_{max}).

The concentration polarization for the (100) face at 2 amp./dm.^{2} was determined with an oscilloscope (11) (Dumont 304H) and was found to be 17 ± 2 mv. This is comparable with the value (20 mv.) observed for polycrystalline copper under similar conditions.

An attempt was made to study perpetuation of the base structure at 0.5 and 0.2 amp./dm^2. The deposition was interrupted after 10 min. and the polarization allowed to dissipate. The current was then turned on again and the second recorded pattern compared with the original. It was noted that at 0.5 amp./dm.^{2} only the (111) face seemed to repeat the original pattern; all the other crystals gave somewhat higher initial polarization values in the second pattern. At 0.2 amp./dm.^{2} the values of the initial pattern appeared to be repeated in the second pattern only with the (111) and (410) crystal faces.

At 2 amp./dm.^{2} microscopic examination of the deposits showed islands of varying reflectivity, indicative of polycrystallinity after deposition times of three minutes or less.

Change of the sulphuric acid concentration of the electrolyte from 50 to 200 gm./liter resulted in no pronounced or systematic changes of polarization, as indicated by the following values:

Acid conc. (gm./l.)	Polarization values for crystal faces					
	(110)		(111)		(410)	
	P_i	P_{max}	P_i	P_{max}	P_i	P_{max}
50	75	111	105	116	102	140
100	78	118	102	130	101	146
200	67	105	99	120	91	124

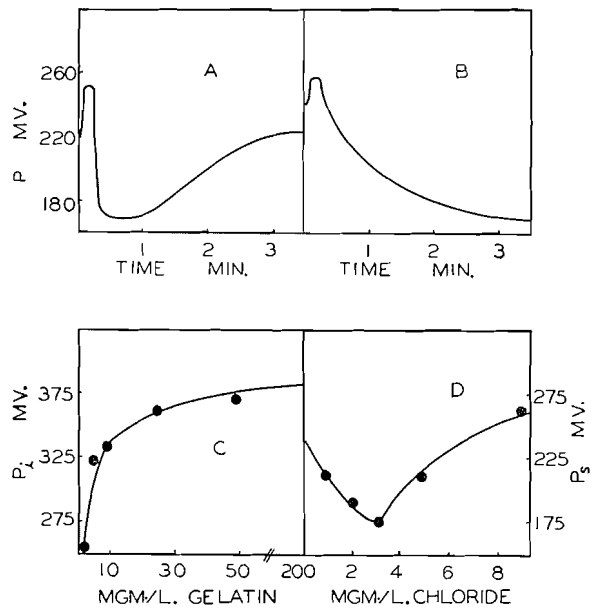

FIG. 3. A: Polarization–time relation at a single crystal cathode in the presence of gelatin.
B: Polarization–time relation at a single crystal cathode in the presence of gelatin and chloride.
C: Relation between initial polarization at a single crystal cathode and gelatin content of the electrolyte.
D: Relation between steady-state polarization at a single crystal cathode and chloride content of the electrolyte in the presence of gelatin.

(ii) Addition Agent Present

An experiment in the presence of addition agent was usually made following an experiment in the standard electrolyte, after removing the previous copper deposit and preparing the crystal anew by electropolishing.

In the presence of gelatin (25 mgm./liter), the single crystal cathodes gave polarization–time curves similar to those observed previously (9) with polycrystalline cathodes (Fig. 3A). The initial polarizations (P_i) for the six crystals varied from 265 to 365 mv., while the steady-state polarization (P_s)* showed a variation with orientation ranging from 200 to 270 mv. The curve relating initial polarization (P_i) to gelatin concentration was similar in shape for the six crystals (Brush oscillograph). Typical of the behavior is the plot shown in Fig. 3C, for the (100) crystal. However the polarization values for a given amount of gelatin differed for the different crystal faces, as shown in Table II.

TABLE II

RELATION BETWEEN INITIAL POLARIZATION AND GELATIN CONTENT OF THE ELECTROLYTE

Gelatin conc. (mgm./l.)	Initial polarization (mv.)					
	(111)	(100)	(110)	(211)	(322)	(410)
0	105	120	75	90	101	102
2	164	205	178	207	190	255
5	222	325	220	230	240	280
10	254	335	260	266	274	290
25	271	365	265	274	290	350
50	284	370	287	292	296	356
200	304	387	290	300	307	366
Adsorption (%) from electrolyte containing 1.5 mgm./l. gelatin	18	38	7	7	25	21
Interplanar spacing (d-value)	0.5774	0.5000	0.3536	0.2041	0.1213	0.1213

It is interesting to note that P_i changes with interplanar spacing in a similar manner for all the systems, including that which contained no gelatin.

The dependence of P_i on d-value in the presence of gelatin prompted an attempt to determine the relative extents of adsorption of gelatin on the six crystals. A calibration curve was first established, to relate P_s measured at a *polycrystalline* cathode (which had been given a steady-state surface) to the gelatin concentration in the electrolyte (up to 2 mgm./liter). Electrolyte containing 1.5 mgm./liter gelatin and a polycrystalline cathode with a steady-state surface were then placed in the Haring cell and the single crystal of copper, with known area exposed, was immersed during one hour with constant agitation but no passage of current, to permit adsorption of gelatin on the crystal. The crystal and stirrer were then removed from the cell and the value of P_s in the gelatin-depleted electrolyte determined. The corresponding gelatin

**This really corresponds only to a pseudo steady state for the short deposition times involved. Had deposition been continued for a sufficiently long time, it is probable that the true steady-state values would all have been similar at the eventual polycrystalline surfaces.*

concentration remaining in the electrolyte could then be obtained from the calibration curve, and the extent of adsorption of gelatin calculated. Adsorption of gelatin on the cell walls and polycrystalline cathode was eliminated as a factor by allowing the cell to stand with the appropriate electrolyte for 10 min. before each experiment, after which fresh electrolyte was introduced. All conditions used in establishing the calibration curve were reproduced as precisely as possible in the adsorption experiments; the only difference was immersion of the single crystal in the latter. The procedure gave values for adsorption on a given crystal that were reproducible within $\pm 4\%$. The relative extents of adsorption at the different crystal surfaces are shown in Table II. It will be noted that the variation of per cent adsorption with d-value parallels rather closely corresponding changes in P_i.

When chloride (2 mgm./liter) was added to the electrolyte in the absence of gelatin the polarization behavior was substantially the same as that in the standard electrolyte. This was true for immersion times of 1 to 30 min. With polycrystalline cathodes the addition of chloride to the electrolyte had little effect with the immersion time of one minute but caused about 15 mv. increase in polarization when the immersion time was increased to 30 min.

The results reported so far were obtained on the six crystals of known orientation. A second group of crystals available in this investigation consisted of 25 crystals, each 3 in. $\times \frac{1}{4}$ in. $\times \frac{1}{4}$ in., grown from melts of spectroscopically pure copper without benefit of seed crystal.* As a consequence the Miller indices of most of these crystals were quite complex and not suitable for estimation of interplanar distances.

With these single crystals, as with the ones previously used, the addition of chloride (2 mgm./liter) to electrolyte containing gelatin (25 mgm./liter) had a pronounced effect on P_s, though not on P_{max} (cf. Figs. 3A and 3B as typical). There appeared to be no significant effect of immersion time (up to 120 min.) on P_{max} or P_s in such systems. Experiments with two of the single crystals showed that the relation between P_s and chloride concentration (Fig. 3D) in the presence of gelatin (25 mgm./liter) was similar to that observed with polycrystalline cathodes.

When all the available data† for the various crystals were considered, it was found that the decrease in P_s caused by the chloride in the presence of gelatin ($-\Delta P_{Cl}$) was correlated with the increase in P_s caused by the gelatin alone (ΔP_{gel}) (Fig. 4A; line drawn by least squares).

In the above experiments, a given amount of chloride appeared capable of nullifying polarization increments which differed because of different cathode surfaces. This suggested that a similar study be made in which the polarization increments at a given cathode face were varied by addition of different amounts of gelatin. For this purpose, steady-state *polycrystalline* cathodes were used (5) and the behavior was examined not only with a constant amount of chloride (2 mgm./liter) (broken line, Fig. 4B) but with the amount of chloride deter-

*We are indebted to Mr. C. Cupp, Department of Metallurgy, University of Toronto, for preparing these crystals and determining their orientations.

†*With most of the crystals data were obtained for two orientations corresponding to two faces of the crystal at right angles.*

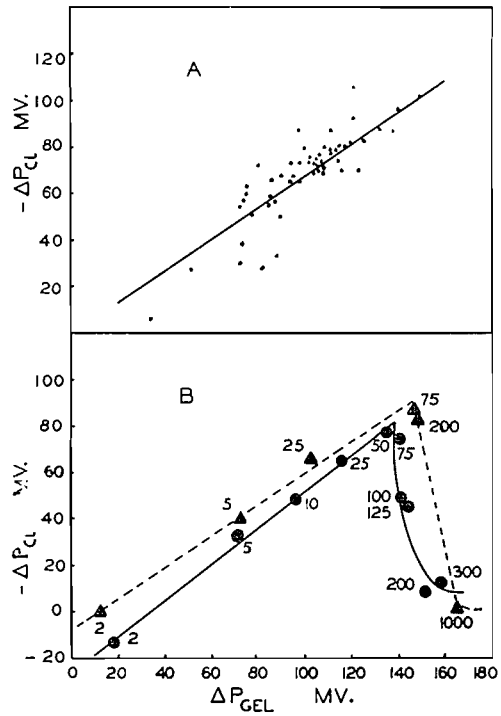

FIG. 4. Relation between decrease ($-\Delta P_{Cl}$) in steady-state polarization caused by chloride in the presence of gelatin and the increase (ΔP_{gel}) in steady-state polarization caused by gelatin alone.

Top: Single crystal cathodes, with 25 mgm./liter gelatin, 2 mgm./liter chloride.

Bottom: Polycrystalline cathodes with amounts of gelatin (mgm./liter) shown on figure.

mined experimentally (8) that gave the minimum polarization for each gelatin concentration (full line, Fig. 4B).

When the effect of chloride (2 mgm./liter) in the presence of gelatin (25 mgm./liter) was examined for the six crystals of known orientation, the values of $-\Delta P_{Cl}$ were found to relate in much the same way as P_i to the d-values for these crystals.

DISCUSSION

The results of the present study in the absence and presence of addition agents demonstrate rather marked differences in behavior of the cathode polarization with the changes in crystal orientations and changes from single- to poly-crystallinity. A polycrystalline metal surface consists of an array of crystal faces of diverse orientations, edges, corners, and boundaries. Each type of orientation has its characteristic arrangement of atoms which influences the surface free energy of the crystal face. The properties of the polycrystalline surface therefore depend upon the properties of these individual parts. In some cases, e.g. cold rolled metal, there may be a preponderance of certain

preferred orientations and the properties of the surface therefore may be weighted in one direction or the other.

(*i*) *No Addition Agent Present*

The initial polarization on electropolished *polycrystalline* copper, in the absence of addition agent, lies between the values for single crystals; this is reasonable because of the composite nature of the former. The value, 85 mv., is biased towards the lower values for the crystals investigated. This might be attributed to a preponderance of certain orientations on the rolled polycrystalline copper cathodes. The static potential for the polycrystalline cathode, 73.7 mv., is similarly related to the static potentials of the crystals, probably for a like reason.

The maxima observed in the polarization–time relations for the six crystals of specified orientations indicate that opposing processes are involved in the polarization changes. It seems reasonable that these processes might be:

(*a*) Increase of total polarization due to build-up of concentration and hydrogen-ion interference polarizations.

(*b*) Increase of polarization due to deposition of nuclei of orientations different from that of the base crystal, such that discharge of atoms requires a higher activation polarization than on the original base matrix.

(*c*) Decrease of total polarization due to increase of true surface area of the cathode, hence decrease of true current density.

The pseudo-steady-state value might be expected when the single crystal base eventually becomes overgrown with nuclei of diverse orientations to such an extent that the increase of true surface area, with the attendant decrease of true current density, hence of polarization, finally predominates.

As expected, t_{max} decreased systematically with an increase in current density, owing in all probability to increased rate of nucleation with consequent increase in rate of surface roughening.

The values of the initial polarization, i.e. in the absence of significant concentration polarization, must contain an activation overpotential and presumably also an ohmic component due to hydrogen ion interference. In the present study, no effect of increased acid concentration on this initial polarization at three different crystal cathodes was observed in the range of 50 to 200 [illegible]gm./liter acid. On the other hand, with polycrystalline cathodes, a linear increase of polarization with acid concentration was previously observed in this laboratory (10). The extent of the increase was the same in the absence and presence of addition agent (cystine), and the opinion was expressed that adsorption of hydrogen ion was probably not involved. However, there seems no alternative to assuming optimal adsorption of hydrogen ion on the single crystal cathodes over the range of acid concentrations studied, to account for the absence of an acid effect with these cathodes. The behavior with polycrystalline cathodes might then be ascribed to an adsorption which is less than optimal, if it is further assumed that the adsorption–concentration relations for hydrogen ion and cystine are comparable in the ranges of concentrations concerned.

If, as seems reasonable, the contribution to the polarization at single crystal cathodes due to hydrogen ion is comparable with or less than that at polycrystalline cathodes (30), the *differences* in the hydrogen ion effect at the different single crystals would be less, probably much less than 30 mv., and the observed differences in P_i may be taken to reflect mainly differences in activation overpotentials at different crystal faces.

The differences in P_{max} might also be due largely to differences in activation overvoltage for the different crystal orientations, but it must be remembered that by the time P_{max} occurs, the single crystal surface might have undergone considerable change due to the formation of nuclei with orientations other than that of the crystal base.

The variation of P_i and P_{max} with d-value for the crystal might reasonably be expected to reflect changes in the surface free energy, which in turn should presumably be associated with the different static potentials of the crystals. In general, the P_i and P_{max} values appear to be related to the reticular density in much the same way as the static potentials. However, there is not a linear relation between either P_i or P_{max} and the static potentials when all the data are considered. It would appear therefore that polarization is not determined solely by the surface lattice energy. It is interesting to note, however, that the plot of P_i-values against static potentials may be considered to yield a roughly linear relation for five of the six crystals used; the P_i value for the (110) face only seems to deviate to an unacceptable extent from the relation. For the dynamic conditions that prevail in polarization measurements, it seems likely that the spatial distribution and density of atoms in the lattice may play a part which is not reflected in the contribution of these factors to a thermodynamic quantity such as the static potential.

(*ii*) *Addition Agent Present*

A satisfactory explanation of the P_i–time pattern observed in the presence of gelatin seems to be possible along the lines suggested by Parsons and Winkler (9). The rise in polarization to the early maximum is readily explained by cataphoretic migration of cuprous–gelatin complexes to the cathode when the circuit is completed, thus increasing the amount of addition agent on the cathode with consequent increase of polarization. Simultaneously, slight depletion of the gelatin in the immediate neighborhood of the cathode must occur. When deposition is initiated, new copper surface is laid down (either with growth of the existing crystal or as new nuclei) in an environment of electrolyte partially depleted of gelatin, such that adsorption of gelatin on the newly formed surface is hindered and the true current density decreases with increase in extent of cathode area free from addition agent. The polarization therefore tends to decrease again, and a maximum is observed in the polarization–time curve. Eventually, of course, the supply of gelatin at the cathode face is replenished by convection and the polarization passes through a minimum to a steady-state value. The effect of immersion time on the polarization pattern with polycrystalline electrodes was attributed to corrosion which would serve to expose different crystal faces and change the true surface area until

a steady state was reached. The absence of any effect of immersion time when single crystals were used may reasonably be attributed to the absence of such change in true surface area due to corrosion.

The value of P_i in the presence of gelatin consists probably of an activation overpotential, an ohmic component due to adsorbed cuprous–gelatin complexes, and possibly some component due to hydrogen ion interference. The observation that the presence of gelatin makes no substantial change in the relation between d-value and P_i suggests that the activation overpotential in the presence and absence of gelatin is the same, and corresponds to the deposition of aquo-complexes in both cases, while the ohmic and hydrogen ion components of the polarization are practically constant for the different crystals. This latter condition, in turn, would probably prevail if all the crystals were almost completely covered by adsorbed cuprous–gelatin complexes.

The effect of chloride ion in reducing the polarization is readily explained by assuming that the chloride ion acts as an electron bridge as suggested by Heyrovsky (7). Consideration of Fig. 4B indicates that a limit is reached, perhaps when the cathode becomes so heavily overladen with adsorbed complexes that access of the chloride ion to effective positions is virtually precluded. This view would gain support from the polarization – gelatin concentration curve, from which it would appear that a plateau, presumably corresponding to essentially complete coverage of the cathode by gelatin or its copper complexes, occurs in the neighborhood of 75 mgm./liter gelatin.

In the presence of gelatin plus 2 mgm./liter chloride the polarization gradually decreased from P_i to P_s with no minimum in the polarization–time curve. This behavior seems reasonable enough since, after the maximum is passed and new surface is laid down in the presence of chloride ion, any tendency for polarization to increase again because of adsorption of complexes should be offset by the facilitated electron transfer effected by the chloride ion. Hence, as deposition continues and the polycrystalline character of the cathode surface is increased, the polarization should merely decrease to that corresponding to deposition on a polycrystalline surface in the presence of gelatin plus chloride.

With single crystals, 2 mgm./liter chloride ion (no gelatin present) had no effect on the pseudo-steady-state polarization, whereas with polycrystalline cathodes the steady-state polarization was increased about 15 mv. (8). Adamek has suggested that this increase be associated with migration of atoms into lattice positions following their deposition in out-of-lattice positions in the presence of chloride by the dismutation reaction (1)

$$2Cu^{+} = Cu + Cu^{++}.$$

Failure to observe the increase with single crystals might be expected on this basis, since deposition on the single crystals until the pseudo steady state was established presumably consisted largely of nucleus formation, with limited crystal growth, and dismutation could occur freely on the crystal face without subsequent migration of atoms into an established lattice.

REFERENCES

1. ADAMEK, S. and WINKLER, C. A. Can. J. Chem. 32: 931. 1954.
2. BARRETT, C. S. Structure of metals. McGraw-Hill Book Company, Inc., New York. 1952.
3. DAVEY, W. P. Study of crystal structure and its applications. McGraw-Hill Book Company, Inc., New York. 1934.
4. GAUVIN, W. and WINKLER, C. A. Can. J. Research, A, 21: 37. 1943.
5. GAUVIN, W. and WINKLER, C. A. Can. J. Research, B, 21: 81. 1943.
6. GWATHMEY, A. T. Pittsburgh Intern. Conf. on Surface Reactions. 1948.
7. HEYROVSKY, J. Discussions Faraday Soc. No. 1: 212. 1947.
8. MANDELCORN, L., MCCONNELL, W. B., GAUVIN, W., and WINKLER, C. A. J. Electrochem. Soc. 99: 84. 1952.
9. PARSONS, B. I. and WINKLER, C. A. Can. J. Chem. 32: 581. 1954.
10. SUKAVA, A. J. and WINKLER, C. A. Can. J. Chem. 33: 961. 1955.
11. TURNER, R. C. and WINKLER, C. A. J. Electrochem. Soc. 99: 78. 1952.

THE TERTIARYBUTYLBENZENES

III. THE SYNTHESIS OF 2,4,6-TRI-*t*-BUTYLBENZOIC ACID AND THE DISSOCIATION OF DI- AND TRI-*t*-BUTYLBENZOIC ACIDS[1]

By Eileen E. Betts[2] and L. Ross C. Barclay

ABSTRACT

2,4,6-Tri-*t*-butylbromobenzene, m.p. 177–177.5°, was prepared by the bromination of 1,3,5-tri-*t*-butylbenzene in the presence of silver nitrate. The reaction of 2,4,6-tri-*t*-butylbromobenzene and *n*-butyllithium gave 2,4,6-tri-*t*-butylphenyllithium, which on carbonation yielded 2,4,6-tri-*t*-butylbenzoic acid, m.p. 297°. A solution of this acid in fuming sulphuric acid yielded a methyl ester, m.p. 96–98°, when it was poured into absolute methanol. Similar treatment of 1,4-di-*t*-butylbenzene with bromine gave 2,5-di-*t*-butylbromobenzene, which on reaction with *n*-butyllithium and subsequent carbonation gave 2,5-di-*t*-butylbenzoic acid. The reaction of 1,3,5-tri-*t*-butylbenzene with acetyl chloride in the presence of aluminum chloride gave a liquid ketone, and hypohalide oxidation of this ketone yielded 3,5-tri-*t*-butylbenzoic acid. The ultraviolet absorption spectra of the two bromo compounds and the three acids were measured and are discussed. The considerable acid-weakening effect in 2,4,6-tri-*t*-butylbenzoic acid is attributed to steric hindrance to the formation of the carboxylate anion.

We have been interested in the synthesis of derivatives of 1,3,5-tri-*t*-butylbenzene required in a study of the influence of two bulky ortho *t*-butyl groups on aromatic functional groups. The present communication describes the synthesis of 2,4,6-tri-*t*-butylbenzoic acid. As a preliminary study of steric hindrance in such a structure, the ultraviolet spectrum and apparent dissociation constant of this acid are measured and compared with those of 3,5-di-*t*-butyl- and 2,5-di-*t*-butyl-benzoic acids.

1,3,5-Tri-*t*-butylbenzene, prepared by the alkylation of 1,4-di-*t*-butylbenzene with *t*-butyl chloride (1), was brominated with bromine in the presence of silver nitrate by a procedure similar to the one used by Derbyshire and Waters (7) for the bromination of chloro- and bromo-benzenes. The 2,4,6-tri-*t*-butylbromobenzene prepared by this method was identical with 2,4,6-tri-*t*-butylbromobenzene prepared by the Sandmeyer reaction on 2,4,6-tri-*t*-butylaniline. Attempts to react 2,4,6-tri-*t*-butylbromobenzene with magnesium were unsuccessful.

2,5-Di-*t*-butylbromobenzene was prepared by the addition of bromine to 1,4-di-*t*-butylbenzene in the presence of silver nitrate. The procedure of Thiec (15) was used to prepare 2,5-di-*t*-butylbenzoic acid from 2,5-di-*t*-butylbromobenzene by refluxing with *n*-butyllithium and carbonation of the resulting 2,5-di-*t*-butylphenyllithium. Similar treatment of 2,4,6-tri-*t*-butylbromobenzene with *n*-butyllithium gave 2,4,6-tri-*t*-butylphenyllithium, which on hydrolysis gave 1,3,5-tri-*t*-butylbenzene or on carbonation gave 2,4,6-tri-*t*-butylbenzoic acid, m.p. 297°. The methyl ester, m.p. 96–98°, of 2,4,6-tri-*t*-butylbenzoic acid was prepared from the acid by the procedure of Newman (11).

[1]*Manuscript received August 18, 1955.*
Contribution from the Department of Chemistry, Mount Allison University, Sackville, New Brunswick.
[2]*Recipient of a National Research Council of Canada Bursary.*

The reaction of 1,3,5-tri-*t*-butylbenzene with acetyl chloride in the presence of aluminum chloride for two hours at room temperature gave a brown liquid ketone, 3,5-di-*t*-butylacetophenone, whose 2,4-dinitrophenylhydrazone melted at 212–214°. Hypohalide oxidation of this ketone gave an acid, 3,5-di-*t*-butylbenzoic acid, m.p. 173–174°. Carpenter and Easter (6) report 3,5-di-*t*-butylbenzoic acid, m.p. 169.5–170.5°, by oxidation of a hydrocarbon described as 3,4-di-*t*-butyltoluene by Capeller (5), but given the 1,3,5 configuration by Schlatter (14). No conclusive evidence has been given for the structure of this acid. Brown (4) has shown that inherent strain in an *o*-di-*t*-butyl configuration makes the existence of such a structure highly improbable. On this basis, and from comparison of the absorption spectrum and ionization constant with those of 2,5-di-*t*-butylbenzoic acid, we have assigned the structure 3,5-di-*t*-butylbenzoic acid. This product requires a replacement of a *t*-butyl group by an acetyl group during the Friedel-Crafts acetylation of 1,3,5-tri-*t*-butylbenzene. This result is analogous to the anomalous acetylations obtained by Nightingale and Hucker (12) where *p*-di-*t*-butylbenzene yielded *p*-*t*-butylacetophenone.

The ultraviolet absorption spectra of 2,4,6-tri-*t*-butylbromobenzene and 2,5-di-*t*-butylbromobenzene (Fig. 1), and of 2,4,6-tri-*t*-butylbenzoic, 2,5-di-*t*-butylbenzoic, and 3,5-di-*t*-butylbenzoic acids (Fig. 2) were measured in cyclohexane with a Beckman DU spectrophotometer. In Fig. 1, 2,5-di-*t*-butyl-

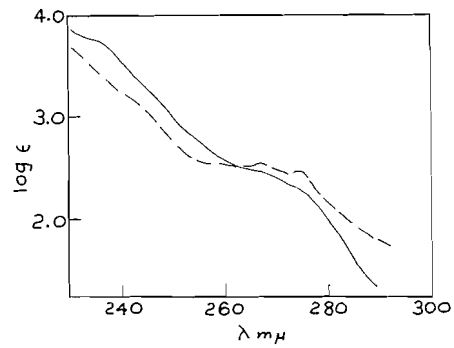

FIG. 1. Ultraviolet spectra in cyclohexane:
— — 2,5-di-*t*-butylbromobenzene (b.p. 150° (12–13 mm.));
—— 2,4,6-tri-*t*-butylbromobenzene (m.p. 177–177.5°).

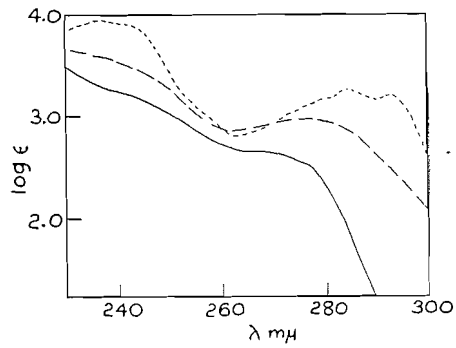

FIG. 2. Ultraviolet spectra in cyclohexane:
—— 2,4,6-tri-*t*-butylbenzoic acid (m.p. 297°);
— — 2,5-di-*t*-butylbenzoic acid (m.p. 128°);
- - - - 3,5-di-*t*-butylbenzoic acid (m.p. 173–174°).

bromobenzene shows slight absorption at 2750 and 2670 Å, while 2,4,6-tri-*t*-butylbromobenzene has no bands. The presence of the second *t*-butyl group ortho to the bromine in 2,4,6-tri-*t*-butylbromobenzene evidently blots out resonance interaction between the bromine and the benzene ring. A similar effect of the bulky *t*-butyl groups is more noticeable in the spectra of the *t*-butylbenzoic acids (Fig. 2). In the case of the di-*t*-butylbenzoic acids a shift of

a *t*-butyl group from a meta position, as in 3,5-di-*t*-butylbenzoic acid, to a position ortho to the carboxyl group removes the K-band near 2360 Å. In addition, the benzenoid "fine structure" absorption of 3,5-di-*t*-butylbenzoic acid (2800–2950 Å) is replaced by weaker general absorption at 2700 Å. When two *o*-*t*-butyl groups are present this effect is very pronounced—so much so that 2,4,6-tri-*t*-butylbenzoic acid has no characteristic absorption maxima, only rising absorption towards shorter wave lengths.

The relative dissociation constants of benzoic, 2,5-di-*t*-butylbenzoic, 3,5-di-*t*-butylbenzoic, and 2,4,6-tri-*t*-butylbenzoic acids (Table I) were measured by potentiometric titration in 50% methanol–water using a Beckman pH meter, with a glass electrode and a calomel reference electrode. The results for benzoic acid agree well with that of pK_a 5.15 obtained by Bright and Briscoe (3) but not with the value of 5.62 recently obtained by Hammond and Hogle (9). Other workers (8) have used aqueous dioxane media. Although our procedure yielded reliable comparative pK_a values the necessity for some standard technique is apparent.

TABLE I

Acid	pK_a ($\frac{1}{4}$ point)	pK_a ($\frac{1}{2}$ point)	pK_a ($\frac{3}{4}$ point)
Benzoic	5.19	5.21	5.20
2,5-Di-*t*-butylbenzoic	5.03	5.05	5.05
3,5-Di-*t*-butylbenzoic	5.78	5.80	5.84
2,4,6-Tri-*t*-butylbenzoic		6.25	

A number of effects can be brought into play in the steric effect of ortho-substituted benzene derivatives. These effects have been discussed by Ingold (10) and recently summarized by Hammond and Hogle (9). Ingold explains that aromatic conjugation weakens a benzoic acid and that the often-observed acid-strengthening effect in *o*-substituted benzoic acids is due to a twisting of the carboxyl group from the plane of the benzene ring. In the case of 2,5-di-*t*-butylbenzoic acid this acid-strengthening effect is greater than the hindering effect of one *t*-butyl group to the formation of the anion and the acid-weakening effect of electron-repelling *t*-butyl groups. The latter effect is important in 3,5-di-*t*-butylbenzoic acid where there is a considerable rise in the pK_a value. 2,4,6-Tri-*t*-butylbenzoic acid is a much weaker acid than benzoic. We attribute this to the controlling hindering effect of two *o*-*t*-butyl groups which decrease the stability of the carboxylate ion.

EXPERIMENTAL[3]

2,4,6-Tri-t-butylbromobenzene

(*a*) *By Direct Bromination*

1,3,5-Tri-*t*-butylbenzene, m.p. 74° (2.46 gm., 0.01 mole), was dissolved in

[3]*Melting points are uncorrected.*

30 ml. of glacial acetic acid in a 100 ml. round-bottom flask. To this solution was added 0.60 ml. (a slight excess of 0.01 mole) of bromine, solutions of 5 ml. of concentrated nitric acid in 10 ml. of water and of 1.7 gm. of silver nitrate in 5 ml. of water, the addition of the last solution taking one half-hour. Another 20 ml. of glacial acetic acid was added and the reaction mixture heated on the steam cone for an hour with occasional shaking, a loose cork being placed in the mouth of the flask to prevent excess escape of bromine. At the end of the hour most of the bromine color had disappeared and the oil which had appeared on the solution when it was first heated had solidified. The hot reaction mixture was poured into 200 ml. of water, a little sodium sulphite added to destroy excess bromine, and then 5% sodium hydroxide until the solution was approximately neutral. The cooled solution was extracted three times with ether, the ether extracts washed with water, and most of the ether removed by distillation. The yellow solid, which separated from the residue on cooling, was collected on a filter paper, water was added to the filtrate and more product was collected (total yield 1.7 gm., 50%). After four recrystallizations from ethanol, the shining white plates melted at 177–177.5°. In a subsequent bromination the yield was 67%. Anal. Found: C, 66.52, 66.57; H, 9.09, 8.86; Br, 24.51, 24.40. Calc. for $C_{18}H_{29}Br$: C, 66.46; H, 8.98; Br, 24.57.

(*b*) *By the Sandmeyer Reaction*

1,3,5-Tri-*t*-butylbenzene was nitrated by the addition of 6.1 gm. of fuming nitric acid (sp. gr. 1.5) to 22 gm. of the hydrocarbon dissolved in a solution of 30.5 ml. of acetic acid and 23.6 ml. of acetic anhydride. The yellow precipitate, 2,4,6-tri-*t*-butylnitrobenzene, which was isolated 45 min. later by filtration, melted at 204–206° after recrystallization from petroleum ether (yield 80%).

2,4,6-Tri-*t*-butylaniline, m.p. 146–148°, was prepared by the reduction of 2,4,6-tri-*t*-butylnitrobenzene using the procedure of Bartlett and co-workers (2).

Three grams of 2,4,6-tri-*t*-butylaniline was added to 30 ml. of glacial acetic acid, 15 gm. of 48% hydrobromic acid was then added, the suspension warmed until solution was complete and then cooled with stirring to 0°. The slow addition of a solution of 1.5 gm. of sodium nitrite in 7.5 ml. of water caused the formation of a yellow precipitate. This was added to a solution of 5 gm. of cuprous bromide in 30 gm. of 48% hydrobromic acid. After it was left for two hours at room temperature, the purple reaction mixture was heated on the steam cone for 30 min., cooled, water added until the reaction mixture was yellow, then concentrated hydrochloric acid until it was clear. The organic layer, which was a semisolid mass on the bottom of the flask, was removed, washed with water, and placed on a filter paper. A yellow oil was drawn off with suction, leaving colorless needles, m.p. 100–176° (wt. 0.370 gm.). After two recrystallizations from ethanol the reaction product, in the form of shining plates, melted at 177.5–178° and did not depress the melting point of the 2,4,6-tri-*t*-butylbromobenzene prepared by direct bromination. The ultraviolet absorption spectra of the two samples were identical.

Attempts to react 2,4,6-tri-*t*-butylbromobenzene with magnesium or sodium in absolute ether failed.

2,5-Di-t-butylbromobenzene

2,5-Di-*t*-butylbromobenzene was prepared by the addition of bromine to 5.7 gm. (0.03 moles) of 1,4-di-*t*-butylbenzene using the same procedure as for the direct bromination of 1,3,5-tri-*t*-butylbenzene. The reaction mixture was heated for eight hours on the steam cone and the product was distilled *in vacuo* to give 1.7 gm. (21% yield) of 2,5-di-*t*-butylbromobenzene, a yellow liquid (b.p. 150° at 12–13 mm.).

2,5-Di-t-butylbenzoic Acid

An approximately 0.1 molar *n*-butyllithium solution was prepared by the procedure given in *Organic Reactions* (13).

2,5-Di-*t*-butylbromobenzene (1 gm.), 5 ml. of the *n*-butyllithium solution, and 10 ml. of absolute ether were refluxed in an atmosphere of dry nitrogen for 40 min. Dry carbon dioxide was passed over the surface of the reaction mixture for four hours at room temperature. Dilute sodium hydroxide was added to the reaction mixture, the resulting solution warmed, and the aqueous layer filtered. Acidification of the filtrate with hydrochloric acid gave a precipitate which, after standing overnight, was collected on a filter paper (0.25 gm., about 35% yield). The 2,5-di-*t*-butylbenzoic acid after repeated recrystallizations from ethanol–water melted at 128° (lit. (15), 128°). Anal. Neutralization equivalent found: 237. Calc. for 2,5-di-*t*-butylbenzoic acid: 234.

The Synthesis of 2,4,6-Tri-t-butylbenzoic Acid

2,4,6-Tri-*t*-butylbromobenzene (1.4 gm.), 12 ml. of 0.1 molar *n*-butyllithium solution, and 25 ml. of absolute ether were refluxed together for one hour. Hydrolysis of a small amount of the reaction mixture with 10% hydrochloric acid gave a white crystalline product, which did not depress the melting point of authentic 1,3,5-tri-*t*-butylbenzene.

Dry carbon dioxide was passed over the reaction mixture for three hours. Sodium hydroxide (10%) was then added, the resulting solution warmed, filtered, and the filtrate acidified with hydrochloric acid. The mixture was allowed to stand overnight, then filtered (0.5 gm., 40% yield). The 2,4,6-tri-*t*-butylbenzoic acid, which crystallized from petroleum ether in thick white needles, melted at 297°. In a subsequent preparation a 60% yield was obtained. Anal. Found: C, 78.83, 78.75; H, 10.40, 10.53; N.E., 296, 292. Calc. for tributylbenzoic acid: C, 78.57; H, 10.41; N.E., 290.

2,4,6-Tri-*t*-butylbenzoic acid (0.1 gm.) was dissolved in 2.5 ml. of fuming sulphuric acid and after several minutes this solution was added slowly to 25 ml. of absolute methanol. Most of the methanol was removed under reduced pressure, 6 ml. of water added, and the remaining methanol removed, leaving a white precipitate. Water (100 ml.) was added to the residue and the solid methyl ester of 2,4,6-tri-*t*-butylbenzoic acid was isolated by filtration, washed with water, dried, and recrystallized from ethanol, m.p. 96–98° (yield 0.08 gm., about 80%).

When 0.01 gm. of the methyl ester of 2,4,6-tri-*t*-butylbenzoic acid was dissolved in fuming sulphuric acid and the resulting solution added to ice, the starting acid was regenerated.

3,5-Di-t-butylbenzoic Acid

A 500 ml. three-neck flask was fitted with a dropping funnel, stirrer, and gas trap. Aluminum chloride (7.3 gm.) and 10 ml. of carbon disulphide were placed in the flask and cooled with ice–salt to −10°. A solution of 15.6 gm. of 1,3,5-tri-*t*-butylbenzene in 8.5 gm. of acetyl chloride was added with stirring over a 45 min. period. The reaction mixture was then allowed to warm to room temperature and after two hours it was decomposed by adding it to water. The organic layer was separated and the solvent removed by evaporation, leaving a semisolid reaction product. This was cooled to −10° and filtered immediately. The white solid (0.4 gm.) thus isolated after recrystallization from ethanol melted at 69–72°. A mixed melting point with authentic 1,3,5-tri-*t*-butylbenzene showed this to be the starting material.

The filtrate from the filtration of the reaction product was a brown liquid, 3,5-di-*t*-butylacetophenone (wt. 4.2 gm.). The 2,4-dinitrophenylhydrazone of the ketone was prepared and after recrystallization from ethanol the derivative melted at 212–214°.

One gram of 3,5-di-*t*-butylacetophenone was dissolved in 20 ml. of dioxane, 10 ml. of 10% sodium hydroxide added, then iodine – potassium iodide solution until the dark color of iodine remained for over five minutes at 60°. The dark color was removed by the addition of a little 10% sodium hydroxide, water was then added until no more cloudiness appeared, and after 15 min. the solution was filtered and the filtrate acidified. The precipitate, which formed in the filtrate on standing overnight, was isolated by filtration. After two recrystallizations from ethanol–water the 3,5-di-*t*-butylbenzoic acid melted at 173–174°. Carpenter and Easter (6) report 169.5–170.5° as the melting point of their 3,5-di-*t*-butylbenzoic acid prepared by the oxidation of 3,5-di-*t*-butyltoluene. Anal. Found: N.E., 234. Calc. for dibutylbenzoic acid: N.E., 234.

Measurement of the Ionization Constants

The ionization constants (Table I) were measured by the method of Hammond and Hogle (9) in 50 volume % methanol–water solution at 21° using a Beckman pH meter with calomel and glass electrodes, standardized against buffer solutions of pH 4 and 10. About 0.01 meq. of the acid was dissolved in 10 ml. of 50% methanol and titrated with 0.0095 *N* methanolic NaOH. In the case of 2,4,6-tri-*t*-butylbenzoic acid, a saturated solution of the acid in 50% methanol was used.

ACKNOWLEDGMENTS

The authors thank Dr. L. Marion for having ultimate analyses done for them at the National Research Council Laboratories.

One of us (E. E. B.) gratefully acknowledges financial assistance provided by a National Research Council Bursary.

REFERENCES

1. BARCLAY, L. R. C. and BETTS, E. E. Can. J. Chem. 33: 672. 1955.
2. BARTLETT, P. D., ROHA, M., and STILES, R. M. J. Am. Chem. Soc. 76: 2349. 1954.
3. BRIGHT, W. L. and BRISCOE, H. T. J. Phys. Chem. 37: 787. 1933.
4. BROWN, H. C. J. Am. Chem. Soc. 75: 24. 1953.
5. DE CAPELLER, R. Helv. Chim. Acta, 11: 166. 1928.
6. CARPENTER, M. S. and EASTER, W. M. J. Org. Chem. 19: 87. 1954.
7. DERBYSHIRE, D. H. and WATERS, W. A. J. Chem. Soc. 573. 1950.
8. GOERING, H. L., RUBIN, T., and NEWMAN, M. S. J. Am. Chem. Soc. 76: 787. 1954.
9. HAMMOND, G. S. and HOGLE, D. H. J. Am. Chem. Soc. 77: 338. 1955.
10. INGOLD, C. K. Structure and mechanism in organic chemistry. Cornell Univ. Press, Ithaca, N.Y. 1953. pp. 743–750.
11. NEWMAN, M. S. J. Am. Chem. Soc. 63: 2431. 1941.
12. NIGHTINGALE, D. V. and HUCKER, H. B. J. Org. Chem. 18: 1529. 1953.
13. Organic reactions. Vol. VIII. *Edited by* R. Adams. John Wiley & Sons, Inc., New York. 1954. p. 285.
14. SCHLATTER, M. J. U.S. Patent No. 2,635,114. Apr. 14, 1953.
15. THIEC, J. Ann. chim. (Paris), 9: 51. 1954.

HEAT OF HYDROLYSIS OF URANIUM (IV) IN PERCHLORIC ACID SOLUTIONS[1]

By R. H. Betts

ABSTRACT

The heat of hydrolysis of uranium (IV) in perchloric acid solution has been measured by a spectrophotometric technique. A value of 10.7±1 kcal. per mole was obtained, in good agreement with a previous value determined by a calorimetric method. The entropy of association of uranium (IV) with hydroxyl ion is +52 e.u.

INTRODUCTION

In a kinetic study of the oxidation of uranium (IV) by iron (III) (1), a value was required for the heat of hydrolysis of uranium (IV). This quantity, ΔH, is related to the temperature variation of the hydrolysis constant K for reaction [1] according to $d(\ln K)/dT = \Delta H/RT^2$.

$$U^{4+} + H_2O \rightleftharpoons UOH^{3+} + H^+ \qquad [1]$$

The hydrolysis constant K is defined by:

$$(UOH^{3+})(H^+)/(U^{4+}) = K, \qquad [2]$$

where the brackets indicate concentrations in gram-ions per liter.

A value of 11 kcal./mole has been reported for ΔH (2). This result is based on the difference between the measured heats of solution of solid uranium tetrachloride in 0.5 M perchloric acid and in water. The accuracy of the value obtained by this method depends on the assumptions that:

(i) UOH^{3+} is the only species of uranium (IV) in very dilute acid solutions,
(ii) U^{4+} is the only uranium species in 0.5 M perchloric acid solution, and
(iii) chloride ion does not form complex ions with uranium (IV).

However, Kraus and Nelson (3) have shown in a careful study of equilibrium [1] at 25°C. that none of these assumptions is strictly correct. Further, the precision of the value of 11 kcal./mole depends on a single measurement of the heat evolved when uranium tetrachloride is dissolved in water (2).

In the present work, the value of ΔH has been calculated more directly from measurement of the hydrolysis constant K as a function of temperature. The method used depends on measurement of the changes in optical density of partially hydrolyzed uranium (IV) solutions with temperature, and is based on the technique described in Reference (3). The principle of the method may be summarized.

The optical density D for a 1-cm. thickness of solution containing U^{4+} and UOH^{3+} as the only light-absorbing species is

$$D = (U^{4+})E_4 + (UOH^{3+})E_3, \qquad [3]$$

where E_3 and E_4 are the extinction coefficients of UOH^{3+} and U^{4+}, respectively,

[1]*Manuscript received August 4, 1955.*
Contribution from the Chemistry and Metallurgy Division, Atomic Energy of Canada Limited, Chalk River, Ontario. Issued as A.E.C.L. No. 235.

for the wave length used. If the total concentration of uranium (IV) is a molar, then the hydrolysis constant K is given by:

$$K = (H^+)(E_4 - E_{obs})/(E_{obs} - E_3), \quad [4]$$

where E_{obs} = observed extinction coefficient
$= D/a$.

It follows from equation [4] that if E_4 and E_3 are known, measurements of E_{obs} and (H^+) permit the calculation of K. Kraus and Nelson (3) have shown that their data at 648 mμ (the wave length at the maximum of a characteristic U^{4+} absorption peak) are best described by $E_4 = 60.0$ and $E_3 = 6.1$, independent of ionic strength.

The principal assumption made in the application of this method to the present work is that the activity coefficient terms, which are implicit in the definition of the hydrolysis constant by equation [2], are unaffected by changes in temperature between 15.2°C. and 24.7°C. The assumption, although not strictly correct, is frequently made in other studies of similar equilibria (see, for example, Reference (4)). A second assumption is that the extinction coefficients E_3 and E_4 are temperature-independent. Further discussion bearing on this latter assumption is given below.

EXPERIMENTAL

Solutions of U^{IV} of the desired concentration and acidity were prepared by dilution of weighed portions of a stock solution 0.0787 M in U^{IV}, 1.010 M in perchloric acid. Other details of the preparation and analysis of the solutions are given elsewhere (1).

Two series of experiments have been made. (i) The first set were carried out with 2.44 M perchloric acid. At this concentration of acid, the hydrolysis of U^{4+} is very largely suppressed ($K \sim 0.01$ at 25°C. (3)). Such measurements served therefore to fix the value of E_4, the extinction coefficient of U^{4+}. (ii) The second set of experiments, made with 0.104 M perchloric acid, provided the values of E_{obs} required for the calculation of K as a function of temperature.

The optical measurements were made with a Beckman DU spectrophotometer. The instrument was adapted to permit control of the temperature of solutions in the cell compartment to ±0.05°C. in the temperature range used here. The optical density at 648 mμ was read vs. a blank cell containing either 0.10 M or 2.44 M perchloric acid. The two 1-cm. cells used were matched to ±0.1% transmission at this wave length.

The optical density for solutions 2.44 M in perchloric acid showed no tendency to drift with time. However a slight decrease with time was noted for the solutions 0.104 M in perchloric acid, presumably as a result of slow air oxidation of U^{IV} which is known to occur more readily in solutions of low acidity. For these samples, the readings of optical density vs. time were extrapolated back to the time of preparation of the samples. These extrapolated values never differed by more than 0.5% from the optical density first recorded.

RESULTS AND DISCUSSION

Tables I and II give the relevant data for solutions 2.44 M and 0.104 M in

perchloric acid. The excellent agreement of our value of 59.9±0.05 for E_4 at 25°C. with the value of 60.0 (3) is to be noted (Table I). However, the apparent dependence of E_4 on temperature (−0.2% per degree) shown in Table I is unexpected. To account for this relatively large change in the optical density on the basis of hydrolysis alone, it would be necessary to assume that the true value of E_4 is 63 or 64, and that $K = 0.14$ at 25°C. Such a value of K is 10 to 15 times higher than one would expect from the careful work of Kraus and Nelson. A more reasonable explanation is that K is indeed of the order of 0.01 at 25°C., and that the extinction coefficient of U^{4+} is temperature dependent. This uncertainty in interpretation fortunately does not appreciably alter the value of ΔH calculated from the experimental results. (See below.)

TABLE I

EXTINCTION COEFFICIENTS* OF URANIUM (IV) IN 2.44 *M* PERCHLORIC ACID

Temp., °C.	*M* U^{IV} (×10³)	E_4	E_4 (average)
24.7	8.56	59.9	59.9_5
24.7	8.57	60.0	
20.4	8.47	60.4	60.5
20.4	8.52	60.6	
15.2	8.51	61.1†	61.2
15.2	8.49	61.3	

Ionic strength = 2.53.
**For λ = 648 mμ.*
†This sample was heated to 24.7°C., and gave E_4 = 59.9. On cooling again to 15.2°C., E_4 = 61.3, indicating a reversible change.

TABLE II

EXTINCTION COEFFICIENTS* OF URANIUM (IV) IN 0.104 *M* PERCHLORIC ACID

Temp., °C.	*M* U^{IV} (×10³)	E_{obs}	E_{obs} (average)
24.7	8.47	38.6_1	38.6_4
24.7	8.50	38.6_8	
20.4	8.49	42.2_3	42.3_9
20.4	8.52	42.5_5	
15.2	8.50	46.5_6	46.5_1
15.2	8.52	46.4_6	

Ionic strength = 0.19 (including contribution from $U(ClO_4)_4$).
**For λ = 648 mμ.*

Table III gives the values of the hydrolysis constants calculated from the experimental results by means of equation [4]. Since $E_{obs} \gg E_3$, an error of ±20% in E_3 has only a small effect on ΔH, and the Kraus and Nelson value of 6.1 (3) has therefore been accepted for this constant. Because of the uncertainty regarding possible variations of E_4 with temperature, K has been calculated using three sets of values for E_4. The second and third columns of Table III give the values of K based on $E_4 = 64$ and 63 respectively. In the last column are shown values of K deduced on the basis that E_4 is temperature-dependent. In this case, the appropriate value of E_4 for each temperature is given in Table I. The values of ΔH listed in Table III were calculated from a plot of

TABLE III

VALUES FOR THE EQUILIBRIUM CONSTANT AND ΔH FOR HYDROLYSIS OF URANIUM (IV)

Temp., °C.	K*	K†	K‡
24.7	0.0810	0.0778	0.0680
20.4	0.0619	0.0591	0.0519
15.2	0.0450	0.0424	0.0378
ΔH, kcal./mole =	10.5	10.9	10.6

Ionic strength = 0.19.
**Assuming* $E_4 = 64$.
†*Assuming* $E_4 = 63$.
‡*Assuming* E_4 *is temperature-dependent.*

log K vs. $1/T$°K. (Fig. 1). The values of ΔH obtained from these three sets of values of K are identical within experimental error, i.e., 10.7 ± 1.0 kcal./mole.

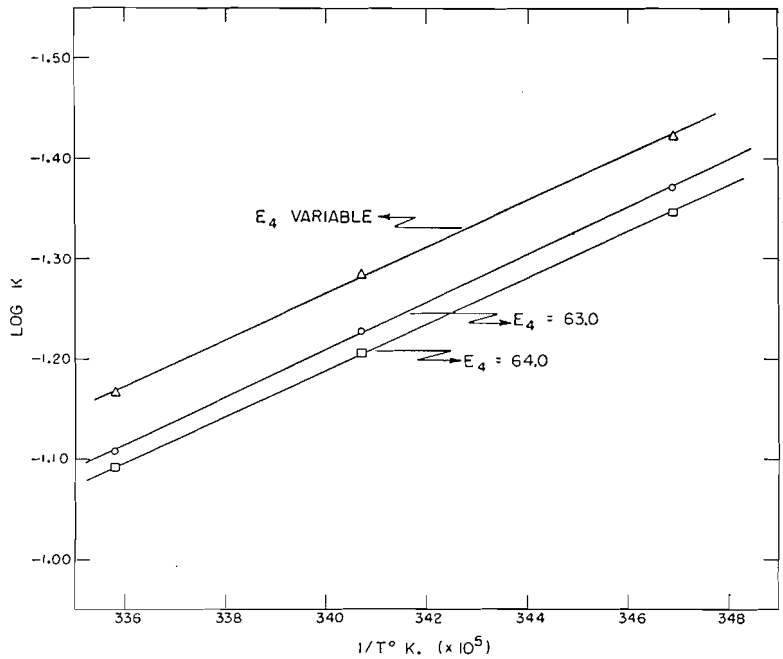

FIG. 1. Dependence of the hydrolysis constant on temperature (Table III).

The agreement of this result with that found earlier (2) is striking, in view of the completely different experimental methods employed; however the almost exact coincidence of the two values must be regarded as fortuitous.*

Table III shows that K is about 0.075 at 24.7°C., the exact value depending on the value of E_4 assumed. For comparison, the Kraus and Nelson result (3) is 0.05 at 25°C., for ionic strength 0.19. This agreement is as good as can be

*NOTE ADDED IN PROOF: *In a paper published after completion of present manuscript, Kraus and Nelson (J. Am. Chem. Soc. 77:3721. 1955) report* $\Delta H = 11.7$ *kcal./mole for heat of hydrolysis of uranium (IV) in perchlorate media, in agreement with value obtained in present work.*

expected, since in the present study, uranium (IV) perchlorate contributes almost 50% of the total ionic strength at $\mu = 0.19$, whereas the value of 0.05 applied to solutions in which sodium perchlorate and perchloric acid were the principal electrolytic components.

The entropy of association of U^{4+} with a hydroxyl ion can now be estimated. For this purpose the hydrolysis constant at zero ionic strength, K_a, must be used— 0.21 ± 0.02 at 25°C. (3). Using the relation $\Delta F^\circ = -RT \ln K_a$, and $\Delta F^\circ = \Delta H^\circ - T\Delta S^\circ$, ΔS° and ΔF° at 25°C. are found to be +33 e.u. and +0.92 kcal./mole, respectively. These values refer to reaction [1] above. This result may be combined with the dissociation equilibrium of water (4) to derive the thermodynamic constants for the association reaction proper:

	ΔF°, kcal.	ΔH°, kcal.	ΔS°, e.u.
$U^{4+}_{aq} + H_2O \rightarrow UOH^{3+}_{aq} + H^+_{aq}$	+0.9	+11.0	+33
$H^+_{aq} + OH^-_{aq} \rightarrow H_2O$	−19.1	−13.5	+19
$U^{4+}_{aq} + OH^-_{aq} \rightarrow UOH^{3+}_{aq}$	−18.2	−2.5	+52

The large positive value of ΔS° for the association reaction is in qualitative agreement with the suggestion of Rabinowitch and Stockmayer (4), viz., the partial neutralization of charge which occurs releases water molecules from the hydration shells around the separated ions, and thereby increases the disorder (and hence the entropy) of the system as a whole.

REFERENCES

1. BETTS, R. H. Can. J. Chem. 33: 1780. 1955.
2. FONTANA, B. J. Declassified Report MDDC 1452. U.S. Atomic Energy Comm., Oak Ridge, Tennessee.
3. KRAUS, K. A. and NELSON, F. J. Am. Chem. Soc. 72: 3901. 1950.
4. RABINOWITCH, E. and STOCKMAYER, W. H. J. Am. Chem. Soc. 64: 335. 1942.

KINETICS OF THE OXIDATION OF URANIUM (IV) BY IRON (III) IN AQUEOUS SOLUTIONS OF PERCHLORIC ACID[1]

By R. H. Betts

ABSTRACT

The kinetics of oxidation of uranium (IV) by iron (III) in aqueous solutions of perchloric acid have been investigated at four temperatures between 3.1°C. and 24.8°C. The reaction was followed by measurement of the amount of ferrous ion formed. For the conditions $(H^+) = 0.1$–$1.0\ M$, ionic strength = 1.02, $(Fe^{III}) = 10^{-4}$–$10^{-5}\ M$, and $(U^{IV}) = 10^{-4}$–$10^{-5}\ M$, the observed rate law is $d(Fe^{2+})/dt = -2d(U^{IV})/dt$

$$= 2(U^{IV})(Fe^{III})\left[\frac{K'(H^+)+K''}{(H^+)^2+(K_1+K_2)(H^+)+K_1K_2}\right] \text{ mole/liter/sec.}$$

K_1 and K_2 are the first hydrolysis constants for Fe^{3+} and U^{4+}, respectively, and K' and K'' are pseudo rate constants. At 24.8°C., $K' = 2.98$ sec.$^{-1}$, and $K'' = 10.6$ mole liter^{-1} sec^{-1}. The corresponding temperature coefficients are $\Delta H' = 22.5$ kcal./mole and $\Delta H'' = 24.2$ kcal./mole. The kinetics of the process are consistent with a mechanism which involves, as a rate-controlling step, electron transfer between hydrolyzed ions.

INTRODUCTION

Oxidation–reduction reactions between cations in aqueous solution have been thought until recently to proceed very rapidly, and the term "instantaneous" has frequently been used to characterize their rates. However recent studies with radioactive tracers have shown that even such elementary reactions as electron transfer between iron (II) and iron (III), or between Ce (III) and Ce (IV), do not proceed instantaneously (18, 8). Such results have reawakened interest in the whole subject of both isotopic and nonisotopic electron transfer reactions between cations in solution. Some kinetic information is now available relating to the reactions between the nonisotopic pairs Sn (II) – Fe (III) (5), Tl (III) – Fe (II) (2), and Np (IV) – Fe (III) (10). Several review articles have recently appeared in which the current status of theory and experiment have been summarized for both isotopic and nonisotopic electron transfer reactions (1, 14, 19). The proceedings of a symposium held in 1954 on this subject have also been published (12).

As a further example of this type of reaction, the present paper describes experiments relating to the kinetics of the oxidation of uranium (IV) by iron (III) in aqueous acidic media. Perchloric acid and sodium perchlorate were chosen as the principal electrolytes, since amongst the common inorganic anions, perchlorate has the least tendency to form ion-pairs with cations. To bring the rate of reaction into a range suitable for study, it has been necessary to work with solutions 10^{-4} to $10^{-5}\ M$ in uranium (IV) and iron (III).

The course of the reaction has been followed by measurement of the rate of formation of iron (II). Such measurements, in conjunction with a knowledge of the stoichiometry of the reaction, were sufficient to enable a kinetic analysis of the results to be made. It would have been useful, as confirmatory evidence,

[1]*Manuscript received August 4, 1955.*
Contribution from the Chemistry and Metallurgy Division of Atomic Energy of Canada, Limited, Chalk River, Ontario. Issued as A.E.C.L. No. 236.

to measure also the rate of disappearance of uranium (IV). However no method could be devised which was specific for uranium (IV) at the low concentrations involved.

EXPERIMENTAL

A. Reagents

Doubly distilled water was used in the preparation of all reagents and in all experiments in the present investigation.

Uranyl perchlorate was prepared by dissolving reagent grade uranium trioxide in an excess of standard perchloric acid. An aqueous solution of uranium (IV) perchlorate was prepared from this solution by electrolytic reduction of the uranium at a mercury cathode in a two compartment cell. The uranium (IV) content was determined by titration with standard potassium permanganate.

Sodium perchlorate, which was used to adjust the ionic strength of solutions as required, was prepared from reagent grade stock by two recrystallizations from water.

A stock solution of iron (III) perchlorate was prepared by methods described previously (4). Solutions of iron (II) perchlorate, which were required for standardization of the analytical procedures used in the kinetic experiments, were made by dissolving iron (II) ammonium sulphate in 1.0 *M* perchloric acid, and were standardized against potassium permanganate.

All other chemicals used were reagent grade, and were not further purified.

B. Procedure

Unless indicated otherwise, all experiments were made with solutions of ionic strength 1.02.

The kinetic experiments were carried out in glass-stoppered flasks which were suspended in a water bath at the desired temperature. All of the reagents except uranium (IV) were added to the flask, after which the required amount of this reactant was added carefully by micropipette. The reaction was started by inverting the flask, and mixing thoroughly the added uranium (IV) with the rest of the solution.

The course of the reaction was followed by measurement of the amount of iron (II) formed as a function of time. For this purpose, 4 to 5 ml. samples were withdrawn at measured times, and run rapidly into a mixture which stopped the reaction, and which also served as a means for analysis of ferrous ion formed (see below). Generally eight samples were taken during each experiment, together with two more when the reaction had gone to completion. The purpose of the last two samples was to give an independent measure of the initial concentration of either uranium (IV) or iron (III), depending on which of these two was in excess initially. In most of the experiments, iron (III) was in large excess over uranium (IV), and hence the final measurement of ferrous ion formed was used as a measure of the initial concentration of uranium (IV) ion. Confirmatory evidence regarding the validity of this procedure is given later.

The quenching mixture referred to above consisted of 5 ml. of an aqueous

solution of *o*-phenanthroline; it contained also an equimolar mixture of ammonium fluoride and ammonium acetate in sufficient quantity to raise the pH of the final reaction mixture to 4.0. At this pH, *o*-phenanthroline reacts immediately with ferrous ion to form the highly colored complex $Fe(o\text{-phen})_3^{++}$. The concentration of this complex was determined by measurement of the optical density at 511 mμ of portions of the quenched mixture with a Beckman DU spectrophotometer. The exact dilution of the reacting mixture by the quenching solution was calculated from the weight of the latter before and after addition of the sample for analysis.

The analytical scheme was calibrated by addition of known amounts of iron (II) perchlorate to solutions similar to those used in the kinetic studies. A small blank was observed which depended on the total amount of iron (III) present. This was taken into account as required. The presence of either uranium (IV) or uranium (VI) had no measurable effect on the analysis. Separate experiments showed that the quenching agent did not induce the oxidation of uranium (IV) by iron (III); it was also shown that ferrous ion has no tendency to form in quenched solutions containing both uranium (IV) and iron (III).

The detailed mechanism of the quenching action of this mixture is not completely understood. However, the omission of ammonium fluoride from the mixture completely destroys the quenching action; it is probable therefore that the reaction is stopped by fluoride ion complexing of the reactants at pH 4.0.

C. Experimental Results

(*i*) *Stoichiometry of the Reaction*

Table I presents the data for seven experiments relating to the stoichiometry of the reaction. The initial concentrations of reactants in each experiment were calculated from the amounts of standardized stock solutions used. In column four is given the final concentrations of iron (II) found when the reaction had gone to completion. Each value in this column is based on at least two concordant analyses which were made on samples taken several hours apart. Values of iron (II) concentrations given in column five are those calculated according to

TABLE I

STOICHIOMETRY OF THE REACTION

Run No.	$(U^{IV})_0$, $M \times 10^5$	$(Fe^{III})_0$, $M \times 10^5$	Fe^{2+}, $M \times 10^5$	
			Found	Calc.
1	3.75	52.4	7.30	7.50
3	3.72	21.1	7.26	7.44
4	3.63	10.60	7.04	7.26
5	9.10	10.65	10.57	10.65
6	9.10	5.41	5.41	5.41
7	18.20	2.26	2.27	2.26
8	36.20	1.21	1.22	1.21

$$2Fe^{III} + U^{IV} = 2Fe^{II} + U^{VI}. \quad [1]$$

The slight differences between the corresponding values in columns four and

five of Table I are not greater than the combined probable errors involved; it is concluded therefore that Equation [1] represents the stoichiometry of the reaction.

(*ii*) *Kinetic Order of the Reaction*

Experiments which were made to deduce the kinetic order of the reaction are summarized in Table II. These experiments were carried out at a perchloric acid concentration of 1.021 *M*, at 24.8°C. The second order rate constant k_0 shown in the last column of Table II is defined by Equation [2]:

$$\frac{+d(\mathrm{Fe^{II}})}{dt} = \frac{-d(\mathrm{Fe^{III}})}{dt} = \frac{-2d(\mathrm{U^{IV}})}{dt} = 2\,k_0\,(\mathrm{U^{IV}})(\mathrm{Fe^{III}}). \qquad [2]$$

The constant k_0 was calculated from the results in the following way. If $(\mathrm{U^{IV}})_0$ and $(\mathrm{Fe^{III}})_0$ represent the total concentrations of these species at time zero,

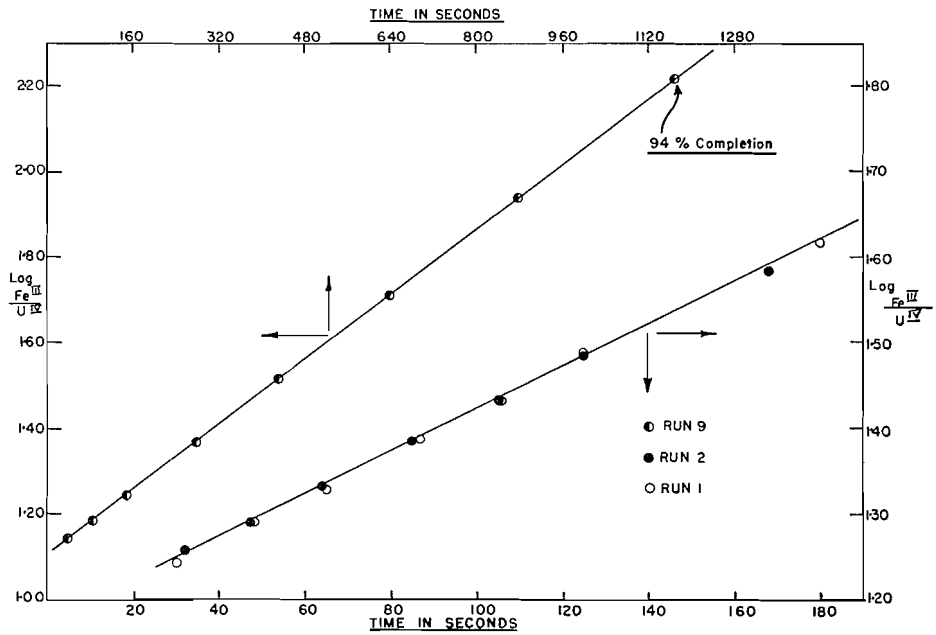

FIG. 1. Plot illustrating second order behavior of the reaction.

and if $(\mathrm{Fe^{II}})_t$ is the concentration of iron (II) measured at time t, then the corresponding concentrations of reactants are given by:

$$(\mathrm{U^{IV}}) = (\mathrm{U^{IV}})_0 - 0.5(\mathrm{Fe^{II}})_t, \qquad [3]$$

$$(\mathrm{Fe^{III}}) = (\mathrm{Fe^{III}})_0 - (\mathrm{Fe^{II}})_t. \qquad [4]$$

Substitution of Equations [3] and [4] into [2] and integration in terms of $(\mathrm{Fe^{II}})$ leads to

$$k_0 t = \frac{2.303}{(\mathrm{Fe^{III}})_0 - 2(\mathrm{U^{IV}})_0} \log \frac{(\mathrm{Fe^{III}})}{(\mathrm{U^{IV}})} + B, \qquad [5]$$

where B is an integration constant related to the (arbitrary) initial concen-

trations of uranium (IV) and iron (III). Equation [5] implies that a plot of log $(Fe^{III})/(U^{IV})$ vs. t should give a straight line if the reaction is of first order in both iron (III) and uranium (IV). Fig. 1 shows such plots for the data of Runs 1, 2, and 9 of Table II. In these cases, and for all experiments in this study, such plots gave good straight lines up to at least 80% completion of the reaction. Table II shows also that the value of k_0 deduced from the slope of these plots is unaffected by a 30-fold variation in $(U^{IV})_0$, and a 40-fold variation in $(Fe^{III})_0$. We conclude therefore that at constant hydrogen-ion concentration, the reaction is first order with respect to both uranium (IV) and iron (III).

TABLE II

VALUES OF SECOND ORDER RATE CONSTANT AT 24.8°C. $(HClO_4) = 1.021\ M$; $\mu = 1.02$

Run No.	$(Fe^{III})_0$, $M \times 10^5$	$(U^{IV})_0$, $M \times 10^5$	k_0 (mole^{-1} liter^1 sec.$^{-1}$)
1	52.4	3.75	12.9
2	52.4	3.72	12.9
3	21.1	3.72	12.7
4	10.6	3.63	12.2
5	10.6	9.10	11.9
6	5.41	9.10	10.8
7	2.26	18.2	11.5
8	1.21	36.2	13.2
9	21.1	1.69	12.4
10	21.1	3.13	12.6

Fig. 1 also gives some idea of the reproducibility of the kinetic experiments. Evidently the slope of the log $(Fe^{III})/(U^{IV})$ vs. t plot can be reproduced to $\pm 2\%$. However the derived rate constant is not known with this precision, since it also depends on the difference $(Fe^{III})_0 - 2(U^{IV})_0$. Judging from the spread of results in Table II, an over-all uncertainty of ± 4–5% is associated with the rate constants obtained in this work.

(iii) Dependence of the Rate on Hydrogen-ion Concentration

Table III summarizes the results for experiments at varying concentrations of hydrogen ion, for each of four temperatures. The ionic strength of each solution was maintained at 1.02 by addition of sodium perchlorate as required. For each run a good straight line was observed when log $(Fe^{III})/(U^{IV})$ was plotted vs. t. From the slope of such plots, the corresponding second order rate constants shown in Table III were calculated.

TABLE III

VALUES OF SECOND ORDER RATE CONSTANT k_0 AS A FUNCTION OF ACIDITY AND TEMPERATURE

Temp., °C.	$HClO_4$, M					
	1.021	0.821	0.6167	0.4125	0.2083	0.1045
24.8	12.3*	19.2	30.7	64.7	233	—
16.8	4.16	6.57	10.4	21.8	74	304
7.8	1.17	1.81	2.92	6.15	22.4	80
3.1	0.54	0.82	1.36	3.01	10.3	33.6

**Average of 10 values listed in Table II.*
The units of k_0 are mole^{-1}. liter^{+1}. sec^{-1}.

The apparent order of the reaction with respect to hydrogen ion at each temperature has been calculated from these results by using the following empirical rate expression:

$$\text{Rate} = 2k'[H^+]^n\,[U^{IV}][Fe^{III}]. \qquad [6]$$

In Equation [6], $k'[H^+]^n$ is to be identified with k_0 for each experiment. The value of n can therefore be deduced from a plot of log $[H^+]$ vs. log k_0 for each temperature. These plots are shown in Fig. 2, from which it was found that n

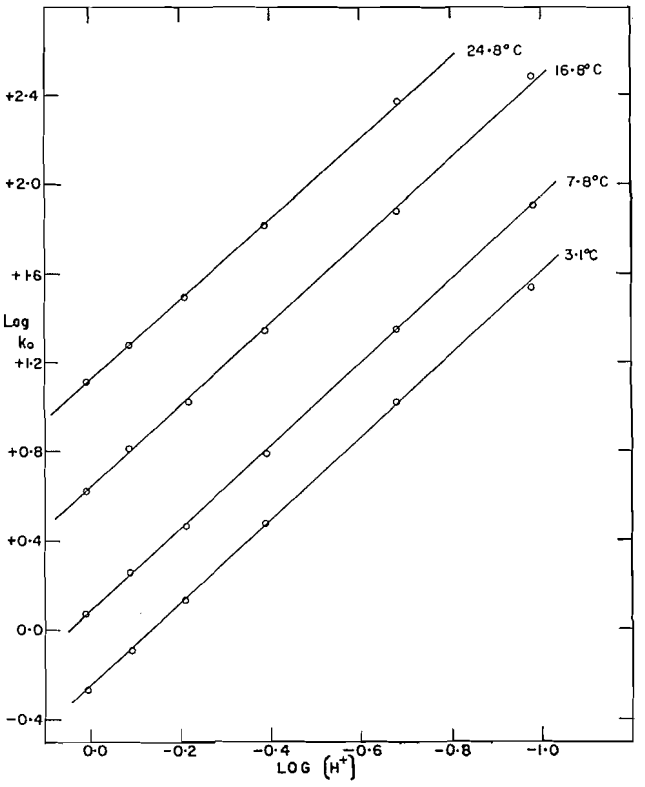

FIG. 2. Variation of the observed rate constant k_0 with temperature and acidity.

has a value of -1.81 ± 0.02, independent of temperature. This result implies that the rate of oxidation of uranium (IV) by iron (III) is dependent on very nearly the inverse second power of the hydrogen-ion concentration.

(*iv*) *Effect of Ionic Strength on the Reaction*

A few experiments were made to determine the effect of an inert electrolyte (sodium perchlorate) on the rate of the reaction. The results of these experiments are summarized in Table IV. Evidently, the rate of the reaction increases slowly with ionic strength in the region $\mu = 0.4$ to $\mu = 1.02$.

TABLE IV

EFFECT OF IONIC STRENGTH ON RATE OF REACTION AT 5°C.
$HClO_4 = 0.413\ M$; $(Fe^{III})_0 = 2.11 \times 10^{-4}\ M$; $(U^{IV})_0 = 2.3 \times 10^{-5}\ M$

$NaClO_4$, M	μ	k_0 (mole^{-1} liter^{+1} sec.$^{-1}$)
0.0	0.414	3.57
0.195	0.609	3.96
0.405	0.819	4.06
0.609	1.023	4.35

DISCUSSION

Stoichiometry and Kinetic Order of the Reaction

The kinetic order of the reaction at constant acidity and the stoichiometry of the process are most simply accounted for by the following scheme:

$$U^{IV} + Fe^{III} \xrightarrow{k_0} U^{V} + Fe^{II}, \text{ slow and rate-controlling,} \quad [7]$$

$$U^{V} + Fe^{III} \rightarrow U^{VI} + Fe^{II}, \text{ fast.} \quad [8]$$

U^V represents an undetermined form of pentavalent uranium (11). These equations have not been balanced with respect to hydrogen ion, nor are the ionic configurations of the reactants specified. These aspects are discussed further below. Assuming that $d(U^V)/dt = 0$, this scheme leads directly to the observed rate expression (Equation [2] above). The factor 2 in Equation [2] arises from the fact that for every Fe(II) formed in Reaction [7], a second Fe(II) is formed by Reaction [8].*

The absence of terms like $(U^{IV})^2$ or $(Fe^{III})^2$ in the empirical rate expression rules out any significant contribution from dimeric ions, e.g., $(FeOHFe)^{+5}$; this ion is known to be present at very low concentration in aqueous solutions of ferric salts (9, 15).

Effect of Hydrogen-ion Concentration

The appearance of the nonintegral order $[H^+]^{-1.81}$ in the rate expression suggests that at least two paths involving hydrolyzed ions contribute to the slow stage of the reaction. The slight departure of this exponent from -2.00 points to the principal path as one involving two hydroxyl groups, with some minor participation from reactions involving only one hydroxyl group.

The principal hydrolyzed species present in solution are $FeOH^{2+}$ and UOH^{3+} (15, 17, 13), which exist in equilibrium with the parent fully hydrated ions according to:

$$Fe^{3+} + H_2O \rightleftharpoons FeOH^{2+} + H^+; \qquad K_1 = (FeOH^{2+})(H^+)/(Fe^{3+}), \quad [9]$$

$$U^{4+} + H_2O \rightleftharpoons UOH^{3+} + H^+; \qquad K_2 = (UOH^{3+})(H^+)/(U^{4+}). \quad [10]$$

The doubly hydrolyzed ion $Fe(OH)_2^+$ is also present at very low concentration (8, 9, 16, 17):

$$Fe^{3+} + 2H_2O \overset{K_3}{\rightleftharpoons} Fe(OH)_2^+ + 2H^+. \quad [11]$$

**A rapid disappearance of U^V by disproportionation according to: $2U^V \rightarrow U^{VI} + U^{IV}$ would also satisfy the observed stoichiometry and kinetic order. This reaction is known to be rapid in solutions of high acidity (11). However the low concentration of U^V makes it unlikely that this mechanism would compete favorably with Reaction [8] above.*

Although there is no quantitative information available, it is reasonable to assume, by analogy with the chemistry of iron (III), that the ion $U(OH)_2^{++}$ also is present at very low concentration:

$$U^{4+}+2H_2O \overset{K_4}{\rightleftharpoons} U(OH)_2^{++}+2H^+. \qquad [12]$$

The rate-controlling step (Equation [7] above) may therefore consist of the following competitive reactions:

$$Fe^{3+}+UOH^{3+} \xrightarrow{k_1} Fe^{2+}+U^{V}, \qquad [13]$$

$$U^{4+}+FeOH^{2+} \xrightarrow{k_2} Fe^{2+}+U^{V}, \qquad [14]$$

$$UOH^{3+}+FeOH^{2+} \xrightarrow{k_3} Fe^{2+}+U^{V}, \qquad [15]$$

$$Fe(OH)_2^{+}+U^{4+} \xrightarrow{k_4} Fe^{2+}+U^{V}, \qquad [16]$$

$$U(OH)_2^{++}+Fe^{3+} \xrightarrow{k_5} Fe^{2+}+U^{V}. \qquad [17]$$

Reactions [13] and [14] involve one hydroxyl group and are of course kinetically indistinguishable. The remaining reactions, which involve two hydroxyl groups, are also kinetically equivalent. These two groups of processes are referred to below as the 1-OH and the 2-OH processes, respectively.*

The following rate expression is derived on the basis of these postulated reactions:

$$\frac{d(Fe^{2+})}{dt} = 2\,(U^{IV})(Fe^{III})\,\frac{K'(H^+)+K''}{(H^+)^2+(K_1+K_2)(H^+)+K_1K_2}. \qquad [18]$$

Equation [18] is based on the assumption that the concentrations of the species $U(OH)_2^{++}$ and $Fe(OH)_2^{+}$ are negligible in comparison to the total concentration of uranium (IV) and iron (III). In this equation:

$$K' = k_1K_2+k_2K_1, \qquad [19]$$

$$K'' = k_3K_1K_2+k_4K_3+k_5K_4. \qquad [20]$$

Equation [18] describes the variation of the observed rate constant k_0 with acidity (Table III) provided:

$$k_0 = \frac{K'(H^+)+K''}{(H^+)^2+(K_1+K_2)(H^+)+K_1K_2}. \qquad [21]$$

If the denominator on the right-hand side of Equation [21] is represented by D, then

$$k_0D = K'[H^+]+K''. \qquad [22]$$

The left-hand side of Equation [22] can be calculated from the results in Table III together with a knowledge of the hydrolysis constants K_1 and K_2. The appropriate values of K_1 and K_2 for each temperature were calculated from

**In reactions [13] to [17] the products have been written as Fe^{2+} and U^{V}; if, as is probable, uranium (V) exists in solution as UO_2^{+}, one or more rapid hydrolyses may take place following electron transfer between the reactant ions indicated in the L.H.S. of these equations. It is not possible to specify the exact sequence of these hydrolytic reactions, nor for the present purpose, is it necessary.*

data in the literature (17, 15, 3, 6, 13), and are given in Table V. A test of Equation [22] can therefore be made, since a plot of k_0D vs. $[H^+]$ should give a straight line, with a finite intercept. Fig. 3 shows the data from the present

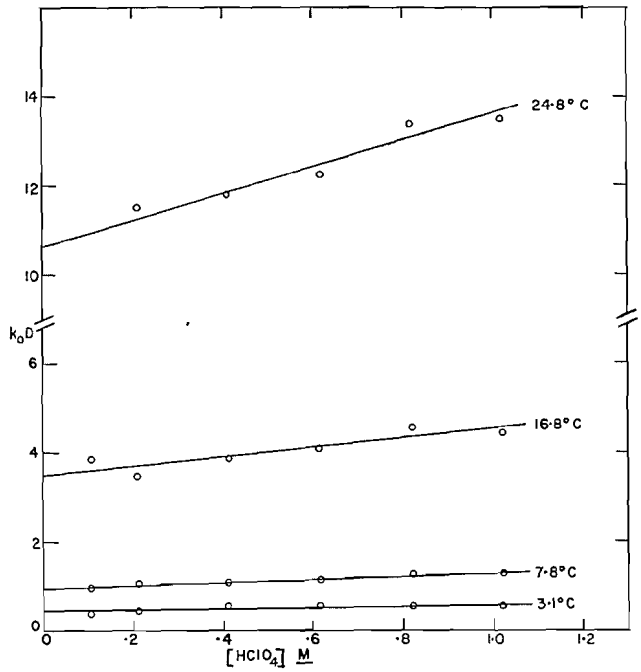

FIG. 3. Application of Equation [22] to the experimental results.

work treated in this manner. Within experimental error, Equation [22] describes the results at each temperature, and lends support to the suggestion that a duality of mechanism is involved in the rate-controlling step of the process.

TABLE V

VALUES OF THE HYDROLYSIS CONSTANTS K_1 AND K_2

Temp., °C.	K_1, mole liter^{-1} ($\times 10^3$)	K_2, mole liter^{-1} ($\times 10^3$)
3.1	0.311	6.8
7.8	0.452	9.4
16.8	0.85	17.0
24.8	1.59	27.8
25.0	1.61*	28.2†

*Value at 25.0°C. from Ref. (15), for μ = 1.02.
†Value at 25.°0C. from Ref. (13), for μ = 1.02.
Values at other temperatures calculated from
ΔH_1 = 12.3 kcal./mole (17)
and ΔH_2 = 10.6 kcal./mole (3)
according to $d \ln K/dt = \Delta H/RT^2$.
K_1 and K_2 are defined by Equations [9] and [10] in the text.

Values of the constants K' and K'' at each temperature can be obtained from the slopes and intercepts, respectively, of the lines in Fig. 3. These values

are given in Table VI. The variation of these pseudo rate constants with temperature is shown in Fig. 4, in which are plotted log K' or log K'' vs. $1/T$°K.

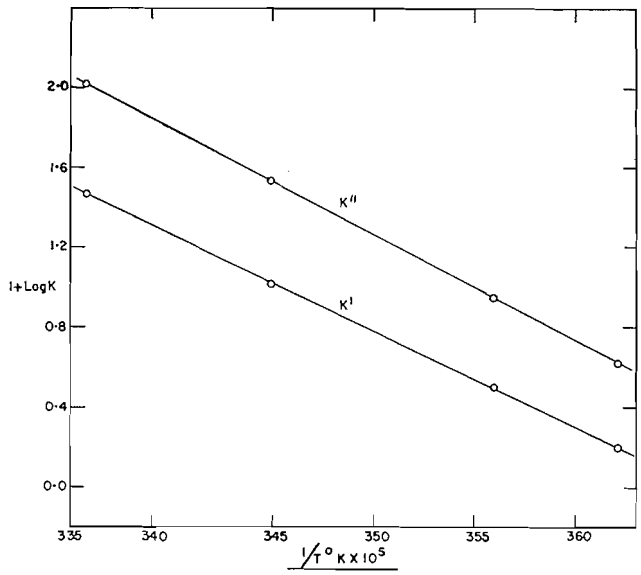

FIG. 4. Variation of the pseudo rate constants K' and K'' with temperature.

From the slopes of these lines, values of the corresponding temperature coefficients $\Delta H'$ and $\Delta H''$ were found to be 22.5 and 24.5 kcal./mole, respectively. These ΔH terms may be thought of as the apparent energies of activation for the 1-OH and 2-OH processes.

TABLE VI

VALUES OF THE PSEUDO RATE CONSTANTS K' AND K''

Temp., °C.	K' (sec.$^{-1}$)	K'' (mole liter^{-1} sec.$^{-1}$)
3.1	0.158	0.420
7.8	0.320	0.936
16.8	1.05	3.48
24.8	2.98	10.6

K' and K'' are defined by Equations [19] and [20] in the text.

The relative contributions of the 1-OH and 2-OH processes can be assessed from the values of K' and K''. For example, at 24.8°C., in 1.021 M perchloric acid, the mechanisms involving two hydroxyl groups make up 78% of the total reaction.

The positive identification of the constants K' and K'' with the rate constants for the individual processes shown in Equations [13] to [17] cannot of course be made with any certainty. This is evident from Equations [19] and [20] which define K' and K''. However, two points emerge from a more detailed examination of the results.

(i) A possible assumption would be that since $Fe(OH)_2^+$ and $U(OH)_2^{++}$ are present in very low concentration, they contribute nothing to the reaction, i.e., k_4 and $k_5 = 0$. The apparent energy of activation $\Delta H''$ for the 2-OH process would then be:

$$\Delta H'' = 24.2 \text{ kcal.} = E_3 + \Delta H_1 + \Delta H_2, \qquad [23]$$

where ΔH_1 = heat of hydrolysis of iron (III),
ΔH_2 = heat of hydrolysis of uranium (IV),
and E_3 = true energy of activation for the electron transfer reaction between UOH^{3+} and $FeOH^{2+}$ (Reaction [15] above).
Since $\Delta H_1 = +12.3$ kcal./mole (17) and $\Delta H_2 = +10.6$ kcal./mole (3, 6), then E_3 could not be more than 1 or 2 kcal./mole. This is an extraordinarily low value for the activation energy of an electron transfer reaction between cations in solution (19). It is suggested therefore that the main contribution to the 2-OH process is *not* that indicated by Reaction [15], and that Reactions [16] and [17], involving $Fe(OH)_2^+$ and $U(OH)_2^{++}$, are the principal contributors to the 2-OH process.

This admittedly qualitative method of distinguishing between kinetically equivalent paths cannot be extended to the other 2-OH processes, since we have insufficient knowledge of the thermodynamics of formation of either $U(OH)_2^{++}$ or $Fe(OH)_2^+$.

(ii) We finally consider the relation between K' and the individual rate constants k_1 and k_2 for the 1-OH processes. The *maximum* values of these rate constants can be calculated from the experimental results in the following way:

(*a*) If $k_2 = 0$, the whole of the 1-OH contribution is carried by Reaction [13]:

$$UOH^{3+} + Fe^{3+} \xrightarrow{k_1}, \text{ and } k_{1(\max)} = K'/K_2.$$

(*b*) Similarly, if $k_1 = 0$, then $k_{2(\max)} = K'/K_1$.

Table VII gives the maximum values for k_1 and k_2 derived in this way, together with the corresponding energy and entropy of activation terms (E_{act} and $\Delta S^{\ddagger}$, respectively). The E_{act} terms in Table VII were calculated from the value of $\Delta H'$ and either ΔH_1 or ΔH_2, in a manner similar to that shown in Equation [23]. Values of $\Delta S^{\ddagger}$ were calculated from the data in columns two and three of Table VII by reaction rate theory (7).

TABLE VII

MAXIMUM VALUES OF RATE CONSTANTS k_1 AND k_2 AT 25°C.

Condition assumed	Rate constant, mole^{+1} liter^{-1} sec.$^{-1}$	E_{act}, kcal./mole	$\Delta S^{\ddagger}$, e.u./mole
$k_2 = 0$ $k_1 = K'/K_2$	107	11.9	−11.2
$k_1 = 0$ $k_2 = K'/K_1$	1860	10.2	−11.3

Perhaps the most significant feature of the results in Table VII is that E_{act} for either process is ~10 to 12 kcal./mole. Most of the simple cationic electron transfer reactions which have been examined in any detail yield values between 8 and 11 kcal./mole for this factor (19).

CONCLUSION

The principal conclusion of the present work is that the rate of reaction between iron (III) and uranium (IV) is controlled by the concentration of hydrolyzed forms of the reactants. Two independent paths appear to be present, the predominant one involving two hydroxyl groups. The experimental evidence suggests, but does not prove, that the reactions $Fe(OH)_2^+ + U^{4+} \rightarrow$ and $Fe^{3+} + U(OH)_2^{2+} \rightarrow$ predominate over the kinetically equivalent 2-OH path involving $FeOH^{2+}$ and UOH^{3+}. The energy of activation for the 1-OH path is in qualitative agreement with other data for similar systems, and in this respect the result is unexceptionable.

The marked reactivity of hydrolyzed species in this system has also been observed in the other studies already cited. For example, the oxidation of neptunium (IV) by iron (III) requires the participation by three hydroxyl groups (10). Also, the conclusions we have reached regarding the presence of two concurrent paths for reaction find a counterpart in several other systems. Thus, the isotopic electron transfer reaction between iron (II) and iron (III) proceeds in perchlorate media via the pairs Fe^{2+}–Fe^{3+} and Fe^{2+}–$FeOH^{2+}$; the rate constant for the reaction involving $FeOH^{2+}$ is about 1000-fold greater than that for the reaction between the fully hydrated ions (18).

REFERENCES

1. AMPHLETT, C. B. Quart. Revs. (London), 8: 219. 1954.
2. ASHURST, K. G. and HIGGINSON, W. C. E. J. Chem. Soc. 3044. 1953.
3. BETTS, R. H. Can. J. Chem. 33: 1775. 1955.
4. BETTS, R. H. and DAINTON, F. S. J. Am. Chem. Soc. 75: 5721. 1953.
5. DUKE, F. R. and PINKERTON, R. C. J. Am. Chem. Soc. 73: 3045. 1951.
6. FONTANA, B. J. Report MDDC 1452. U.S. Atomic Energy Comm. Oak Ridge, Tennessee. 1947.
7. GLASSTONE, S., LAIDLER, K. J., and EYRING, H. The theory of rate processes. McGraw-Hill Book Company, Inc., New York. 1941. p. 417.
8. GRYDER, J. W. and DODSON, R. W. J. Am. Chem. Soc. 73: 2890. 1951.
9. HEDSTRÖM, B. O. A. Arkiv. Kemi, 6: 1. 1953.
10. HUIZENGA, J. R. and MAGNUSSON, L. B. J. Am. Chem. Soc. 73: 3202. 1951.
11. KERN, D. M. H. and ORLEMANN, E. F. J. Am. Chem. Soc. 71: 2102. 1949.
12. Kinetics and Mechanism of Inorganic Reactions in Solution. Report of a Symposium held at the Chem. Soc., London, Feb. 4, 1954. The Chemical Society, London. 1954.
13. KRAUS, K. A. and NELSON, F. J. Am. Chem. Soc. 72: 3901. 1950.
14. MARCUS, R. J., ZWOLINSKI, B. J., and EYRING, H. J. Phys. Chem. 58: 432. 1954.
15. MILBURN, R. M. and VOSBURGH, W. C. J. Am. Chem. Soc. 77: 1352. 1955.
16. MULAY, L. N. and SELWOOD, P. W. J. Am. Chem. Soc. 76: 6207. 1954.
17. RABINOWITCH, E. and STOCKMAYER, W. H. J. Am. Chem. Soc. 64: 335. 1942.
18. SILVERMAN, J. and DODSON, R. W. J. Phys. Chem. 56: 846. 1952.
19. ZWOLINSKI, B. J., MARCUS, R. J., and EYRING, H. Chem. Revs. 55: 157. 1955.

THE VIBRATIONAL SPECTRA OF CH_2=CHCl AND CH_2=CDCl[1]

By J. C. Evans[2] and H. J. Bernstein

ABSTRACT

The infrared and Raman spectra of CH_2=CDCl and the Raman spectrum of CH_2=CHCl have been obtained and depolarization ratios of the Raman bands have been measured. The spectra of the two molecules have been correlated.

While the vibrational assignment of vinyl chloride has been satisfactorily made with the aid of the observed envelopes of the infrared absorption bands (8), the vibrational spectrum of CH_2=CDCl has not previously been examined. Since a sample of the latter compound was available in this laboratory, its vibrational spectrum was examined and correlated with that of vinyl chloride. Furthermore, since previous Raman studies (6) did not include depolarization measurements, the Raman spectrum of vinyl chloride was obtained and depolarization ratios measured.

EXPERIMENTAL

Samples of both compounds were provided by Mr. J. Francis and Dr. L. C. Leitch. A commercial sample (Matheson Co.) of vinyl chloride was distilled. The preparation of the deuterium substituted compound will be described (3). This sample contained a small amount of vinyl chloride which was detected spectroscopically.

The spectra were obtained with a Perkin-Elmer Model 112 double pass infrared spectrometer and a White, grating Raman spectrometer with photoelectric recording (9), using 4358 Hg as exciting line. The infrared spectrum of CH_2=CDCl in the vapor phase was measured using LiF, CaF_2, NaCl, and CsBr optics and the Raman spectra of both compounds in the liquid phase were obtained at $-100°C. \pm 5°C.$ A low temperature cell, in which the sample tube was cooled by a controlled stream of air passed through liquid nitrogen, was used. The cooled central part of the cell was surrounded by an evacuated jacket which in turn was surrounded by an outer jacket containing saturated aqueous sodium nitrite solution. The filter and the low temperature inhibited polymerization of the samples. Depolarization measurements were made by wrapping polaroid film around the entire cell, first with its axis parallel to the length of the sample tube and then at right angles (2). The observed ratios were corrected for convergence (7).

The Raman and infrared data for the two molecules are collected in Tables I and II. The Raman spectra are reproduced in Fig. 1, and Fig. 2 illustrates the infrared spectrum of CH_2=CDCl.

[1]*Manuscript received September 6, 1955.*
Contribution from the Division of Pure Chemistry, National Research Council, Ottawa, Canada. Issued as N.R.C. No. 3761.
[2]*National Research Council Postdoctorate Research Fellow 1953–1955.*

TABLE I

RAMAN SPECTRUM OF CH_2=CHCl (LIQUID)

Assignment	Approximate description	cm.$^{-1}$	$\rho_{corr.}$
$2\nu_4$ (A')		3203	0.33
ν_1	ν_{as} (CH_2); a'	3112	0.75
ν_2	ν (CH); a'	3079	0.46
ν_3	ν_s (CH_2); a'	3027 *	0.25
$\nu_5+\nu_6+\nu_9$ = 3033 (A')		3014 sh. *	0.22
$\nu_4+\nu_5$ = 2966 (A')		2950	0.2
ν_4	ν (C=C); a'	1603	0.39
$\nu_{11}+\nu_{12}$ = 1523 (A')		1515	?
ν_5	CH_2 def.; a'	1363	0.63
ν_6	CH rock.; a'	1274	0.60
$2\nu_{12}$ = 1246 (A')		~1242	P
ν_7	CH_2 rock.; a'	1026	~0.76
ν_{11}	Out-of-plane; a''	901	~0.85
ν_8	ν (C—Cl); a'	706	0.42
ν_{12}	Torsion; a''	623	Dp
ν_9	δ (C=C—Cl); a'	396	0.52

ν_{10}, at 942.5 cm.$^{-1}$ in the infrared, was not observed.

Fermi resonance.

TABLE II

THE INFRARED AND RAMAN SPECTRA OF CH_2=CDCl

Infrared spectrum (vapor phase)			Raman spectrum (liquid phase)	
cm.$^{-1}$	Type	Assignment	cm.$^{-1}$	Corrected depolarization ratio
3535	?	3186+385 = 3571 (A')		
3430 — 3410	a'	3034+385 = 3419 (A')		
3175 sh.	?	2 × 1593 = 3186 (A')	3168	0.24
3133 — 3111	a'	ν_1: ν_{as} (CH_2)	3110	0.77
3080 sh.		ν_2 of CH_2=CHCl impurity	3079	~0.55
3045 — 3024	a'	ν_3: ν_s (CH_2)	3020	0.33 *
2980	?	2308+714 = 3022 (A')	2985	P *
2464 2453 2445	a'	1117+1358 = 2476 (A')		
2319 2308 2299	a'	ν_2: ν (C—D)	2300	0.47
2230 2220 2210	a'	2 × 1117 = 2234 (A')		
1812 1798 1791	a'	2 × 900 = 1800 (A')		
~1730	?	1358+385 = 1743 (A')		
		or 2×866 = 1732 (A')		
		2×803 = 1606 (A')	1603	~0.7
		or CH_2=CHCl impurity		

TABLE II (*Concluded*)

Infrared spectrum (vapor phase)			Raman spectrum (liquid phase)	
cm.$^{-1}$	Type	Assignment	cm.$^{-1}$	Corrected depolarization ratio
1604 1593 1584	a'	ν_4: ν (C=C)	1586	0.32 *
		861+697 = 1558 (A')	1530	P *
1498 1487 1478	a'	385+1117 = 1502 (A')	1493	P
1427 sh.		587+861 = 1448 (A'')	1437	Dp?
1406		2 × 714 = 1428 (A')	1395	P *
1367 1358 1347	a'	ν_5: CH_2 def.	1349	0.50 *
1292 — 1270	a'	CH_2=CHCl impurity		
1192 — 1165	a'	2 × 587 = 1174 (A')		
1125 1117 1104	a'	ν_7: CH_2=CD rocking	1100	0.35
950		385+587 = 972 (A'')		
943		CH_2=CHCl impurity		
900	a''	ν_{10} out-of-plane	905	~0.83
		ν_6: CH_2=CD rocking	861	0.63
804	a''	ν_{11} out-of-plane	803	~Dp
722 714 702	a'	ν_8: ν (C—Cl)	697	0.36
587	a''	ν_{12}: torsional	590	Dp
— 385 —	a'	ν_9 δ (C=C—Cl)	393	0.57

**Fermi resonance; sh. shoulder.*

TABLE III

TELLER–REDLICH PRODUCT RULE RATIOS FOR CH_2=CHCl AND CH_2=CDCl

Species	a'	a''
Observed ratio	0.518	0.812
Theoretical ratio	0.516	0.807

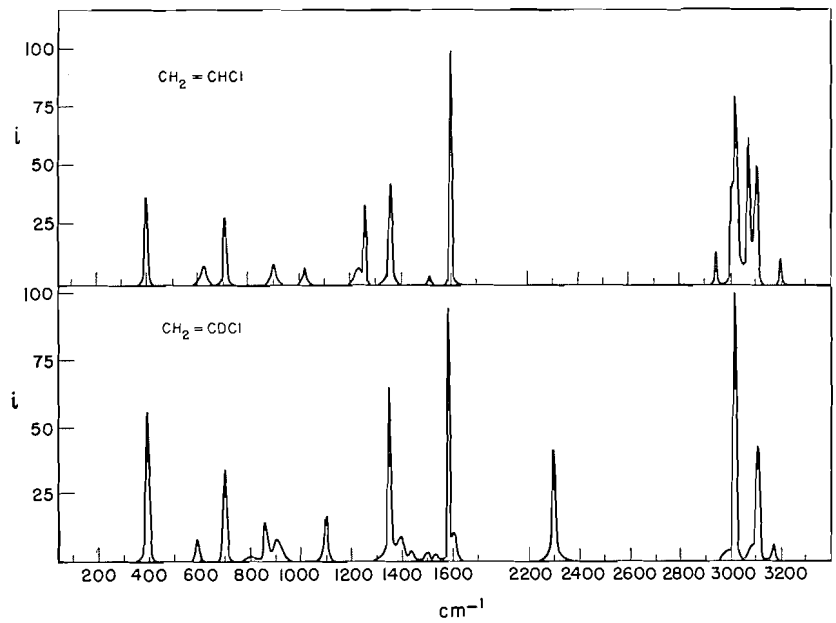

FIG. 1. Raman spectra of CH_2=CHCl and CH_2=CDCl in the liquid state. Temp. −100°C. ±5°C. Volume of sample 6 ml. Slit widths: ~7.5 cm.$^{-1}$ between 300 and 1600 cm.$^{-1}$; ~6.5 cm.$^{-1}$ in 3000 cm.$^{-1}$ region. The scales are different in the two spectra. In each case the band with highest peak is 100.

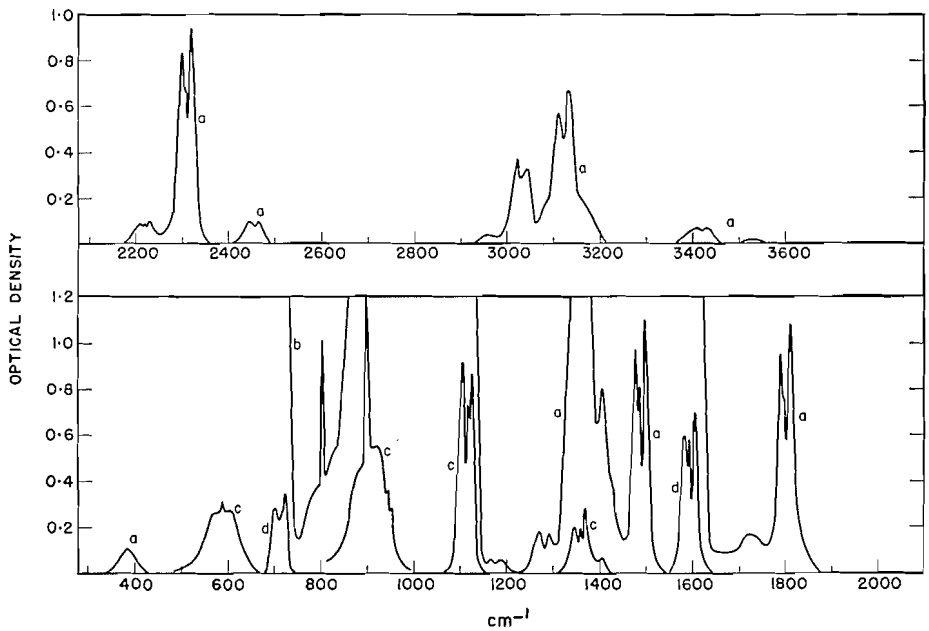

FIG. 2. Infrared spectrum of CH_2=CDCl in the vapor state. 10 cm. cell at 20°C. Vapor pressures: *a*, 760 mm.; *b*, 370 mm.; *c*, 75 mm.; *d*, 19 mm. Slit widths: 8, 3, 3, 4, 3, 3, and 2 cm.$^{-1}$ in the regions 3000, 2000, 1600, 1300, 1000, 700, and 400 cm.$^{-1}$ respectively.

DISCUSSION

Both molecules have the same symmetry, Cs, (5) and all twelve modes of each should be infrared and Raman active. The nine planar modes, species a', and the three out-of-plane modes, species a'', should give rise to polarized and depolarized Raman bands respectively.

Little need be said about the Raman spectrum of CH_2=CHCl. The depolarization ratios confirmed the assignment, based on the observed envelopes of the infrared bands of the vapor, which was made by Thompson and Torkington (8). The a'' mode at 942.5 cm.$^{-1}$ in the infrared was not observed in the Raman spectrum.

For CH_2=CDCl the bands were readily separated into the a' and a'' species by means of the depolarization ratios in the Raman spectrum and the vapor band contours in the infrared. The molecule approximates to a symmetric rotator* with moments of inertia C = 18.7; and $A = B = 149 \times 10^{-40}$ gm. cm.^{2}. The a'' modes are essentially perpendicular modes and should give rise to infrared bands with strong central peaks. The three bands with such a structure correspond to three depolarized Raman bands. The PR separation calculated using Gerhard and Dennison's formula (4) for parallel bands of a symmetric rotator with moments of inertia of 18.7 and 149.5 is approximately 20 cm^{-1}. Most of the infrared bands have a triplet structure with two strong outer peaks separated by ~20 cm.$^{-1}$, and a very weak central peak. The fundamental modes were readily identified. One mode, the a' mode at 861 cm.$^{-1}$ in the Raman, was not observed in the infrared spectrum probably because it was obscured by the strong a'' band at 900 cm^{-1}.

The agreement between the theoretical and observed product rule ratios was satisfactory. The results are collected in Table III.

When a correlation of the fundamentals of CH_2=CHCl and CH_2=CDCl is attempted using the approximate descriptions of the modes given in Table I, it is apparent that an unexpected change has occurred. Two bands, that arising from the in-plane rocking mode of the CH group (1274 cm.$^{-1}$) and that arising from the in-plane rocking mode of the CH_2 group (1026 cm.$^{-1}$), have shown major changes upon deuterium substitution. The explanation for the large change ($>\sqrt{2}$) in the former band's position and the anomalous increase in frequency of the latter must presumably be looked for in the coupling, in CH_2=CDCl, of vibrational modes which, in CH_2=CHCl, are well separated, thus allowing only a small interaction. A closely similar situation occurs in the corresponding bromo compounds where the following tentative assignment was made (1):

	CH_2=CHBr	CH_2=CDBr
CH_2 rocking	1006	1091
CH, CD rocking	1256	841

More data are available for the bromo compounds where all the possible hydrogen–deuterium homologues of vinyl bromide have been examined (1).

Using the dimensions (5): C—Cl = 1.73 Å, C=C = 1.33 Å, C—H = 1.08 Å, C—C—Cl = 122°, C—C—H = 120°, the moments of inertia were calculated to be:

$$I_A = 18.7,\ I_B = 140.2,\ I_C = 158.9 \times 10^{-40}\ gm.\ cm^2.$$

Comparison of the spectra of CD_2=$CHBr$ and CD_2=$CDBr$ shows that the CD rocking mode lies just below 1000 cm^{-1}. Deuterium substitution at the CH_2 group has only a relatively small effect upon the CH rocking mode as is shown by the band positions in CH_2=$CHBr$ (1256 $cm.^{-1}$) and in CD_2=$CHBr$ (1239 $cm.^{-1}$). So it is not unreasonable to assume that the CH_2 rocking mode will also be relatively unaffected by deuterium substitution at the other carbon atom. On this basis, both the CH_2 rocking and the CD rocking modes in CH_2=$CDBr$ would be expected near 1000 cm^{-1}. It is probable that strong coupling of the modes occurs, giving rise to two new vibrational levels at 841 $cm.^{-1}$ and 1091 cm^{-1}. These modes cannot therefore be described simply as CH_2 rocking and CD rocking.

For the two vinyl chlorides the argument is the same; only the band positions differ. The remaining a' modes in the two molecules may readily be correlated in accordance with the approximate descriptions in Table I.

One of the a'' modes, the torsional mode, is easily identified in both molecules but the correlation of the other two out-of-plane modes is uncertain. In CH_2=$CHCl$ they are about 40 $cm.^{-1}$ apart while in CH_2=$CDCl$ the separation is increased to about 100 cm^{-1}.

REFERENCES

1. Charrette, J. and De Hemptinne, M. Bull. classe sci., Acad. roy. Belg. 38: 934. 1952.
2. Edsall, J. T. and Wilson, E. B., Jr. J. Chem. Phys. 6: 124. 1938.
3. Francis, J. and Leitch, L. C. To be published.
4. Gerhard, S. L. and Dennison, D. M. Phys. Rev. 43: 197. 1933.
5. Goldstein, J. H. and Bragg, J. K. Phys. Rev. 75: 1453. 1949.
6. Kohlrausch, K. W. F. Ramanspektren. J. W. Edwards, Ann Arbor, Mich. 1943. p. 127.
7. Rank, D. H. and Kagarise, R. E. J. Opt. Soc. Amer. 40: 89. 1950.
8. Thompson, H. W. and Torkington, P. Proc. Roy. Soc. (London), A, 184: 21. 1945.
9. White, J. U., Alpert, N., and DeBell, A. G. J. Opt. Soc. Amer. 45: 154. 1955.

THE MESOMORPHIC BEHAVIOR OF ANHYDROUS SOAPS

PART II. DENSITIES OF ALKALI METAL STEARATES[1]

By D. P. Benton,[2] P. G. Howe,[2] R. Farnand, and I. E. Puddington

ABSTRACT

The densities of the series of alkali metal stearates and of a number of sodium stearates having substituents in the hydrocarbon chain have been measured over a temperature range of 25–380°C. Discontinuities in the density–temperature relationships indicate the transitions between the various mesomorphic forms in which these soaps exist and the results are compared with transition data obtained by an optical method, described in Part I of this series. Mesomorphism is found to be much less pronounced in the substituted stearates examined than in the normal soaps.

INTRODUCTION

In the extensive and varied studies that have been made of the mesomorphic behavior of salts of the long chain fatty acids, dilatometric measurements have been found particularly useful, since many of the thermal transformations between successive phases are accompanied by conspicuous changes in specific volume (2, 4, 5, 7, 8).

This paper presents the results of a study of the density–temperature relationships of the series of alkali metal stearates and of a number of sodium stearates having substituents in the hydrocarbon chain. The work parallels the previously reported transition data, obtained by an optical method, for the same soaps (1). To facilitate comparison of the data for the different soaps and for use in connection with electrical conductivity and viscosity data, to be presented in subsequent papers in this series, the density measurements have been made on an absolute basis.

EXPERIMENTAL

The sources of materials and methods of preparation of the soaps used in this work were as described previously (1). J-shaped, weight dilatometers were used. A weighed quantity of soap, previously fused under vacuum to remove last traces of water and alcohol (1), was introduced to the dilatometer before sealing to the capillary. The apparatus was then evacuated to a pressure not exceeding 10^{-5} mm. Hg, at a temperature above the final melting point of the soap and, after cooling, mercury was admitted to fill the dilatometer. A 2 meter length of 0.5 mm. diam. capillary was sealed to the capillary outlet and the dilatometer was set in an air thermostat so that the long capillary protruded vertically. The thermostat consisted of heavily lagged, hollow dural block which was heated electrically and controlled by a well-distributed mercury regulator. Calibrated complete immersion thermometers were used within the air bath and temperature control was better than ±0.5°C. over the range 25–355°C.

The upper ends of the capillaries were bent over and dipped below the

[1]*Manuscript received July 25, 1955.*
Contribution from the Division of Applied Chemistry, National Research Council, Ottawa, Canada. Issued as N.R.C. No. 3770.
[2]*National Research Council Postdoctorate Fellow, 1953–55.*

surface of mercury in small weighing bottles. The weights of mercury expelled from the dilatometers as the temperature was raised were determined at 5–10° intervals. Not more than two determinations were made per day, thus allowing a time found to ensure attainment of equilibrium values. The use of the 2 meter length of capillary gave a total pressure of about four atmospheres on a soap sample and appeared to prevent vacuole formation within the sample on cooling (6). Using this device, reproducible values of the weight of mercury expelled at a given temperature were obtained in every case on passing through the cycle of melting to isotropic liquid and cooling to room temperature.

After completion of the above measurements, the capillary was broken at the point of exit from the thermostat and the dilatometer, containing soap and mercury, was weighed. The dilatometer was then emptied, cleaned, and weighed and finally weighed when completely filled with mercury. The density of a soap at temperature T was calculated using the equation

$$\text{density of soap at temp. } T = W_s/[W_0/\rho_t - (W_M - W_T)/\rho_T]$$

where W_s = weight of soap, W_0 = weight of mercury required to fill dilatometer at temperature t, W_M = weight of mercury in dilatometer with soap at temperature t, W_T = weight of mercury expelled at temperature T ($W_T = 0$ when $t = T$), ρ_t and ρ_T = densities of mercury at t and T. The assumptions thus made are that the expansion of the glass dilatometer and the expansion of the small quantity of mercury in the capillary outside the thermostat are negligible.

In order to check the accuracy of the absolute density values, some subsidiary measurements were made in the higher temperature regions, by means of a different experimental method. A small glass bulb, of approximately 0.25 ml. capacity, was formed at the end of a uniform, calibrated 2 mm. capillary and the bulb calibrated. This container was baked out at 380°C. under vacuum, let down under dry nitrogen, and the required amount of soap weighed in. The apparatus was evacuated, the soap melted, and dry nitrogen introduced into the tube above the soap. An amount of soap was used so that, at about the melting point, the meniscus lay somewhere near the center of the capillary. The apparatus was mounted in a dural block furnace, fitted with a glass covered viewing slot. The slot was illuminated at one side and readings of the height of the meniscus made with a telescopic cathetometer through the other, after equilibration at various temperatures. An etched ring on the capillary tube, used for the volume calibration, was used as a reference point for readings. Measurements below the final melting points of the soaps could only be made in some cases where the soap–glass adhesion was sufficiently low. However, this method provided a check on the values obtained at the highest temperatures with the mercury dilatometers and allowed observations to be extended to about 380°C.

RESULTS AND DISCUSSION

Results for the series of alkali metal stearates are shown graphically in Fig.1. The curve for lithium stearate shows only three transitions, at 229°, 176°, and

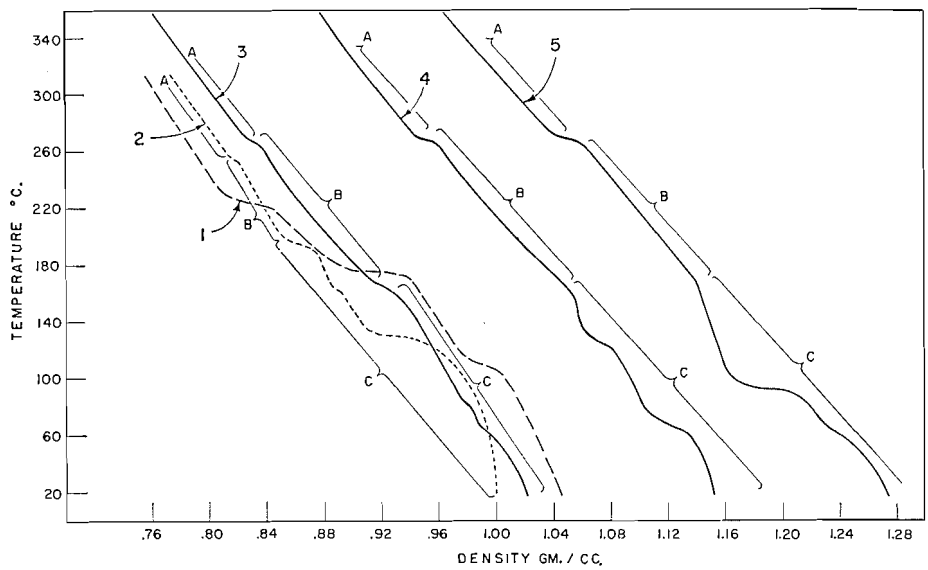

FIG. 1. Densities of alkali metal stearates. 1. Lithium stearate. 2. Sodium stearate. 3. Potassium stearate. 4. Rubidium stearate. 5. Cesium stearate.

115°C. This is similar to the behavior of lithium palmitate (8), which exhibits transitions at 223°, 190°, and 103°C. Supercooling occurred at the final melting point, cf. Part I (1).

The density–temperature curves for the four other alkali metal stearates may each be divided into three major portions, viz., the linear region A, the second linear region B, and the remaining region C.

(1) The linear region A. These regions contain the neat phase and isotropic liquid in each case. The temperatures at the terminations of regions A agree closely with the subneat–neat transition temperatures for the four soaps, determined by the optical method (1). The final melting points of these four soaps are not manifested by sufficiently substantial discontinuities in the density–temperature relationships to produce noticeable deviations from linearity in the graphs.

(2) The linear region B. The next break in the curve for sodium stearate occurs at 190–200°C. This is doubtless a manifestation of the transition which caused a major discontinuity in the light transmission – temperature curve for this soap at 188°C. (1) and ascribed to the change from the subneat to the superwaxy phase. The corresponding terminations of the linear regions in potassium, rubidium, and cesium stearates occur at 160–165°C., 160°C., and about 170°C. respectively. It is noteworthy that these are close to the temperatures at which these soaps were found to become opaque (1). It is suggested that these changes indicate transitions in potassium, rubidium, and cesium stearates corresponding to the subneat–superwaxy transition in sodium stearate.

The regions B would thus represent the subneat phases of this series of soaps. We may note that the optical studies (1) indicated minor transitions within

the subneat phases at 220°, 242°, and 222°C. for sodium, potassium, and rubidium stearates respectively. However, it would appear from dilatometric measurements that no radical changes in molecular packing occur within this region.

(3) The region C. The curve, in region C, for sodium stearate is seen to show an irregularity at about 165°C., corresponding to the discontinuity found by light transmission (1) at this temperature. At 132°C., the temperature ascribed to the transition waxy–subwaxy soap (7), a large density change commences and proceeds in an apparently continuous manner to that of the room temperature crystalline soap. The continuous nature of the density–temperature relationship for sodium stearate in this range, 25–132°C., has been observed previously (2, 6) in spite of very considerable precautions to ensure attainment of equilibrium values, although it has been shown by differential thermal analysis (7) that at least two thermal transitions, at approximately 90° and 117°C., do in fact occur.

The curves in region C for potassium, rubidium, and cesium stearates are seen to be basically of similar form to that for sodium stearate. However, by consideration of the property of density alone, a choice of possible interpretation into corresponding phases is afforded. The lowest temperature regions at 25–70°C., 25–75°C., and 25–70°C., in the curves for potassium, rubidium, and cesium stearates respectively, may correspond to the 25–132°C. region for sodium stearate. In this case the discontinuities at 90°, 130°, and 100°C. presumably would correspond to that at 165°C. in sodium stearate. On the other hand, the regions 25–90°, 25–130°, and 25–100°C. in potassium, rubidium, and cesium stearates may correspond, as a whole, to the 25–132°C. region in sodium stearate. If this is the case, then discontinuities within these regions might correspond to the transitions in sodium stearate that become apparent by reason of their heats of transition.

Consideration of the behavior of the soaps in dispersion in oil is of interest in this connection. The transition at 117°C. in sodium stearate is close to the temperature at which an unsheared dispersion in oil, of this soap, precipitates soap on cooling from a higher temperature or, conversely, close to the swelling temperature of the soap in oil (3). Loosening of the interactions in the hydrocarbon tail–tail planes of the soap lattice is believed to be involved at this temperature. Although observation of the like phenomenon with potassium, rubidium, and cesium stearates is rendered more difficult, by virtue of the greater difficulty of their initial dispersion by application of heat alone, comparable precipitation of these soaps appears to occur at about 70°C. This observation would appear to favor the second of the alternative interpretations postulated above. However, X-ray studies in the temperature ranges in question may be desirable before a choice is made between the two interpretations.

To supplement the graphical presentation of the density data, the numerical values within some of the phase ranges are given in Table I. This table also shows the density values for the isotropic liquids determined by the supplementary experimental method. Agreement between results obtained by the two methods is within 0–2%.

TABLE I

	Lithium stearate		Sodium stearate		Potassium stearate		Rubidium stearate		Cesium stearate	
Phase	Temp.	Density	Temp.	Density	Temp.	Density	Temp.	Density	Temp.	Density
Curd	25–100°	1.04–1.00	25–130°	1.00–0.93	25–165°	1.02–0.92	25–165°	1.15–1.05	25–90°	1.27–1.21
and waxy	110–170°	1.00–0.94	135–190°	0.91–0.87					100–170°	1.17–1.14
Subneat	180–220°	0.90–0.84	195–258°	0.86–0.82	165–265°	0.92–0.84	165–265°	1.05–0.96	170–270°	1.14–1.05
Neat			260–283°	0.81–0.795	270–*353*°	0.83–0.77	270–*357*°	0.94–0.88	275–*351*°	1.04–0.97
			*260–280°	0.82–0.805						
Isotropic	229–*310*°	0.81–0.76	283–*310*°	0.795–0.78						
liq.	*235–350°	0.82–0.75	*285–330°	0.80–0.77	*360–380°	0.78–0.77	*360–380°	0.885–0.87	*360–380°	0.99–0.97

Numbers in italics are the limit of measurements with Hg dilatometers.
**Values obtained by supplementary experimental method.*

The molecular volumes of the series of alkali metal stearates, as functions of temperature, are shown graphically in Fig. 2. It is seen that the magnitudes of

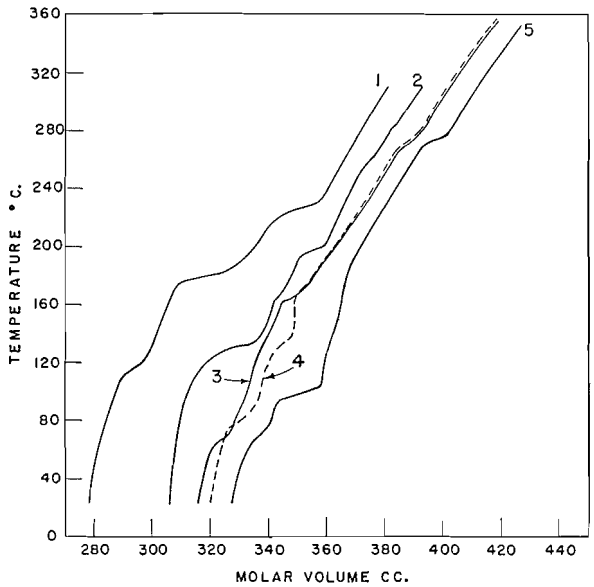

FIG. 2. Molecular volumes of alkali metal stearates. 1. Lithium stearate. 2. Sodium stearate. 3. Potassium stearate. 4. Rubidium stearate. 5. Cesium stearate.

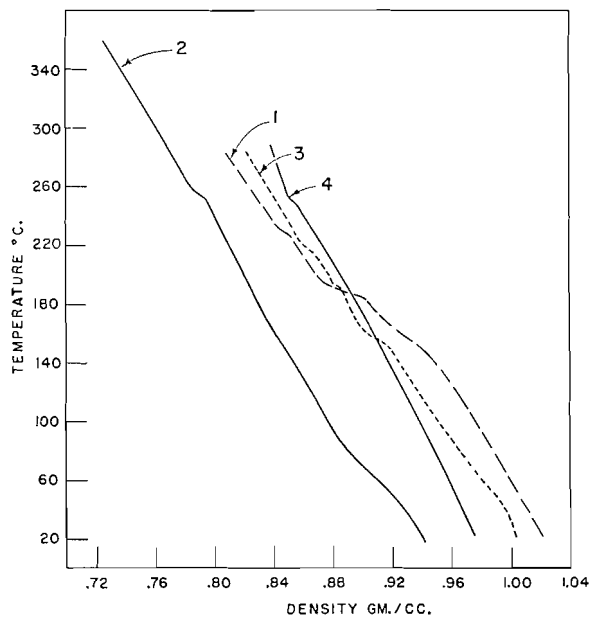

FIG. 3. Densities of substituted sodium stearates. 1. Sodium 12-hydroxy stearate. 2. Sodium 10-methyl stearate. 3. Sodium 9-keto 10-methyl stearate. 4. Sodium 9(10)-phenyl stearate.

this property increase from lithium stearate to cesium stearate, although the values for potassium and rubidium stearates in the subneat and neat phases and in the isotropic liquid are virtually identical.

Results of density determinations for the substituted sodium stearates are shown graphically in Fig. 3. It is apparent that the introduction of these substituent groups into the hydrocarbon chain of sodium stearate has greatly reduced the gross discontinuities in the density–temperature relationship. In the case of the phenyl stearate this relationship is virtually linear. A definite specific volume change is indicated at the final melting point, 250°C., of this soap.

The curves for sodium 9-CO-10-Me stearate and sodium 10-Me stearate also show only small departures from linearity. In the former case small discontinuities provide support for the minor transitions at 195° and 160°C. and the final melting point at 216°C. (1). The 10-Me stearate shows several slight deviations from a linear relationship at the lower temperature regions but the most conspicuous discontinuous specific volume change occurs at 255–260°C., in good agreement with the temperature at which this soap exhibited the major change in translucency (1).

The density–temperature curve for sodium 12-OH stearate is less linear than those for the other substituted soaps. Definite discontinuities occur at 185–195°C., and 225–230°C., again conforming with the results obtained by the light transmission technique (1).

Table II gives some numerical density data for the substituted stearates.

TABLE II

Soap	Temp.	Density
Sodium 10-Me stearate	25–255°	0.94–0.79
	265–355°	0.78–0.73
Sodium 9(10)-Ph stearate	25–245°	0.975–0.86
	255–280°	0.85–0.84
Sodium 9-CO-10-Me stearate	25–155°	1.005–0.915
	160–190°	0.90–0.885
	195–215°	0.88–0.87
	220–280°	0.86–0.825
Sodium 12-OH stearate	25–180°	1.20–0.905
	195–225°	0.875–0.855
	235–280°	0.84–0.81

Fig. 4 shows the molecular volumes of the substituted stearates plotted as a function of temperature. Progressive increase in molecular volume is exhibited as the size of the substituent group is increased. It is to be noted that the size of the substituent hydrocarbon group is indicated to be of primary importance in the effect on the nature of the crystal packing. Perhaps surprisingly, the further introduction of the polar keto grouping into the 10-methyl stearate does not substantially affect the molecular volume. Also, on comparing the

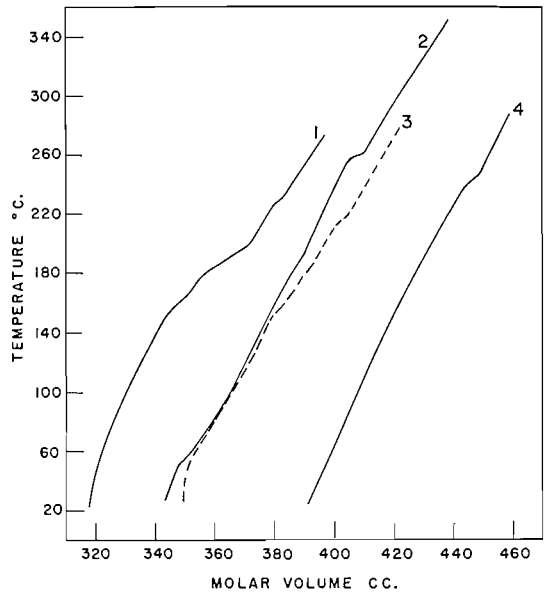

FIG. 4. Molecular volumes of substituted sodium stearates. 1. Sodium 12-hydroxy stearate. 2. Sodium 10-methyl stearate. 3. Sodium 9-keto 10-methyl stearate. 4. Sodium 9(10)-phenyl stearate.

molecular volume curves for sodium stearate and sodium 12-OH stearate, it is found that the effect of the polar hydroxyl group is less pronounced than that of the hydrocarbon substituents.

The density–temperature relationships of these substituted stearates indicate that the relative balance of polar and van der Waals interactions has been modified to a great degree and the stepwise structural changes of the normal soap, on heating, reduced in number or virtually eliminated. These substituted soaps appear to be very useful in grease preparation and likely to give lubricating materials with much more uniform behavior, over a range of operating temperatures, than those prepared with normal soaps.

REFERENCES

1. BENTON, D. P., HOWE, P. G., AND PUDDINGTON, I. E. Can. J. Chem. 33: 1384. 1955.
2. GALLAY, W. and PUDDINGTON, I. E. Can. J. Research, B, 21: 202. 1943.
3. GALLAY, W. and PUDDINGTON, I. E. Can. J. Research, B, 22: 90. 1944.
4. LAWRENCE, A. S. C. Trans. Faraday Soc. 34: 660. 1938.
5. SOUTHAM, F. W. and PUDDINGTON, I. E. Can. J. Research, B, 25: 121. 1947.
6. STAINSBY, G., FARNAND, R., and PUDDINGTON, I. E. Can. J. Chem. 29: 838. 1951.
7. VOLD, M. J., MACOMBER, M., and VOLD, R. D. J. Am. Chem. Soc. 63: 168. 1941.
8. VOLD, R. D. and VOLD, M. J. J. Phys. Chem. 49: 32. 1945.

THE POLAROGRAPHY OF MALEIC HYDRAZIDE[1]

By D. M. Miller

ABSTRACT

Maleic hydrazide was found to be similar to maleic acid in its polarographic behavior. Two pairs of double waves are produced, one in the region around pH 5.9 and the other around 8.2. The theory that the double waves are a result of the reduction of the undissociated acid followed by that of its anion at a higher negative potential appears to explain the first of these double waves but fails to explain the second.

INTRODUCTION

The polarographic behavior of maleic hydrazide (MH) was studied with the intention of using the polarographic method to follow some of the reactions of MH. It was also hoped that some information concerning the tautomeric

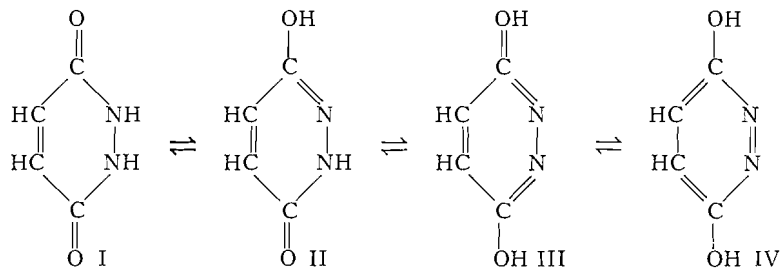

forms of MH might be obtained. The pyridazine ring in structures III and IV should make these forms highly aromatic with a possible similarity to hydroquinone. No anodic wave was found in the voltage range available to the dropping mercury electrode however, but a well-defined cathodic wave was produced. This cathodic wave is probably the result of the reduction of the carbon–carbon double bond of structure I. MH might then be expected to be polarographically analogous to maleic acid (MA), and since no information on the polarography of MH appears to have been published, reference will be made to the work on MA.

Elving and Teitelbaum (4) obtained waves for MA over the pH range of 0.7 to 12, and found a complicated relationship between $E_{\frac{1}{2}}$ and pH. A double wave occurred in the region of pH 5.9 but with increase in buffer concentration to one molar the two waves merged. The double wave was considered to be the result of insufficient buffering and all subsequent work was done at a buffer concentration of one molar. Elving and Rosenthal (3) reinvestigated MA using buffer concentrations ranging from 0.1 to 1.0 M and confirmed the existence of the double wave. These waves did not appear to be normal however, showing characteristics attributed to adsorption and kinetic control. A value of 4 was found for the polarographic constant $I_d = i_d/Cm^{2/3}t^{1/6}$ for the first wave

[1]*Manuscript received July 22, 1955.*
Contribution 57, Science Service Laboratory, Canada Department of Agriculture, University Sub Post Office, London, Ontario.

in the pH range 0 to 4. As the pH increased beyond this range however I_d decreased reaching 0 at pH 6.5. I_d for the second wave increased as the first decreased, becoming equal to it at pH 6, and then passing through a maximum at pH 7 became 0 at pH 10. Similar results were found with fumaric acid.

Double waves having equal heights at pH 5.8 were reported for pyruvic acid by Müller and Baumberger (6), while Brdicka (1) showed that phenolglyoxylic acid produced a double wave but its ethyl ester and ethyl pyruvate produced only single waves. This would indicate that the two waves are a result of the reduction of the free acid followed by the reduction of its anion at a more negative potential, a theory which received quantitative treatment by Brdicka and Wiesner (2) for monobasic acids and by Hanus and Brdicka (5) for dibasic acids. It was shown (2) that the pH at which the double waves are of equal height could occur several pH units higher than the pK_a for the acid, provided the formation of the free acid from its anion is fast enough.

EXPERIMENTAL

Polarograms were obtained with a Sargent Model XXI Recording Polarograph. Applied e.m.f. and pH measurements were made with a Beckman Model "G" pH meter. A saturated calomel electrode was used as reference in an H-cell maintained at 25±0.05°C. The resistance of all solutions was measured by an a-c. bridge and correction for *IR* drop applied where necessary. Reagent grade chemicals were used as supplied except for the MH which was recrystallized from water. All polarograms were obtained on solutions of 5.0×10^{-4} *M* with respect to MH except where otherwise noted.

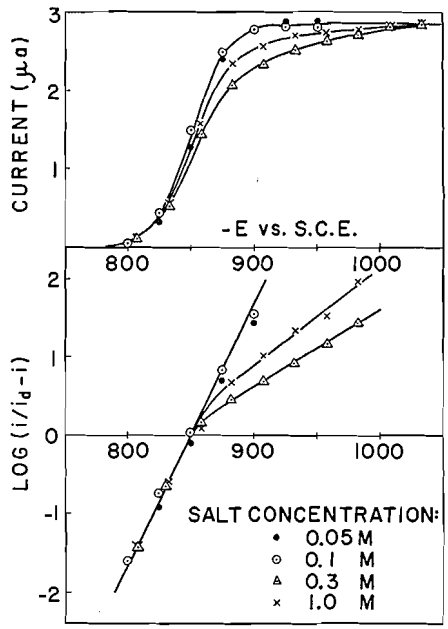

FIG. 1. Top: Polarographic curves of MH in 0.01 *M* HCl with KCl added to give indicated salt concentration ($-E$ in mv.).
Bottom: Log $i/(i_d-i)$ vs. $-E$ for above.

RESULTS

The effect of salt concentration on the polarographic waves was first investigated. Fig. 1 shows the results of increasing the salt concentration of a solution of MH in 0.01 *M* HCl (pH 2.19) from 0.05 *M* to 1.0 *M* using KCl. The top of Fig. 1 shows the polarograms and the bottom the log $i/(i_d-i)$ vs. $-E$ plot. Both plainly show distortion at salt concentrations in excess of 0.1 *M*. Similar results were obtained with other buffer solutions whether KCl or the buffer itself was used to increase the salt concentration. In some cases $E_{\frac{1}{2}}$ was also found to be altered. As a result of these findings all subsequent polarograms were made on solutions of approximately 0.1 *M* with respect to the salt component. A list of the buffer systems used is given in Table I. Elving and

TABLE I

COMPONENTS AND APPROXIMATE CONCENTRATIONS OF BUFFERS

pH	Buffer system
1.21	0.1 *M* HCl
2.19	0.1 *M* KCl and 0.01 *M* HCl
3.50	0.1 *M* sodium formate and 0.1 *M* formic acid
4.89	0.05 *M* pyridine and 0.1 *M* pyridine hydrochloride
5.21	0.1 *M* pyridine and 0.1 *M* pyridine hydrochloride
5.51	0.1 *M* KH_2PO_4 and 0.005 *M* K_2HPO_4
5.80	0.1 *M* KH_2PO_4 and 0.01 *M* K_2HPO_4
6.15	0.1 *M* KH_2PO_4 and 0.02 *M* K_2HPO_4
6.85	0.1 *M* KH_2PO_4 and 0.1 *M* K_2HPO_4
7.40	0.1 *M* Triethanolamine (TEA) and 0.1 *M* TEA·HCl
7.87–8.88	0.1 *M* NH_4Cl titrated with NH_4OH
9.18	0.1 *M* NH_4Cl and 0.1 *M* NH_4OH
10.80	0.1 *M* K_2HPO_4 titrated with KOH
11.70	0.1 *M* KCl and 0.01 *M* KOH

Rosenthal (3) reported anomalous results from the use of acetate buffer and since similar difficulties were encountered in this work it was decided to avoid the use of acetate using pyridine in its place. The polarograms obtained for MH over the pH range 1.2 to 11.7 are shown in the top of Fig. 2. Three distinct waves are apparent. The first wave (I), existing at the lowest pH, exhibits a constant height up to about pH 5, beyond which it gradually decreases being replaced by a second wave (II) which is in turn replaced at higher pH by a third wave (III).

A plot of log $i/(i_d-i)$ vs. $-E$ for each of these waves is shown in the lower section of Fig. 2. Where double waves occur, a separate plot is made for each wave. In all cases the straight line plots obtained indicate that the waves are of normal shape. One anomaly is apparent, however, in that the theoretical number of electrons ($n = 2$) involved in the electrode reaction, as obtained from the slope of these plots, is only realized in the lowest pH range. The slope of the remaining lines indicates a change to one electron (see column six, Table II) which must be fictitious since no reduction in I_d occurs simultaneously.

The half wave potentials ($-E_{\frac{1}{2}}$) and polarographic constants (I_d) of the three waves are given in Table II and plotted against pH in Fig. 3. The curves for I_d vs. pH (top of Fig. 3) show a striking similarity to those of Elving and Rosenthal for MA, the addition of the third wave (III) being the only essential

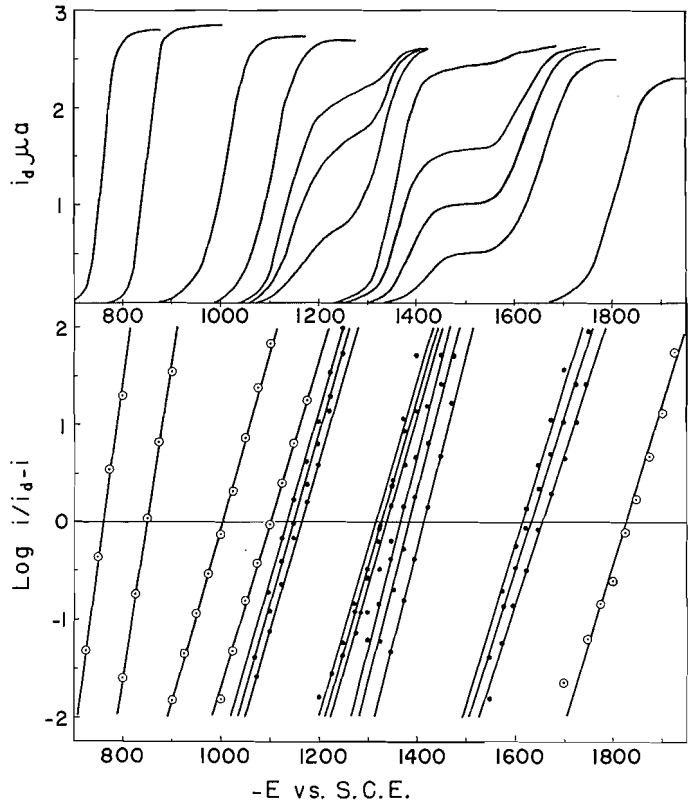

FIG. 2. Top: Polarographic curves of 5×10^{-4} *M* MH at pH of 1.21, 2.19, 3.50, 4.89, 5.51, 5.80, 6.15, 6.85, 7.87, 8.38, 9.18, and 11.70 respectively ($-E$ in mv.).
Bottom: Log $i/(i_d-i)$ vs. $-E$ for above.

TABLE II

pH	Wave	$-E_{\frac{1}{2}}$ vs. S.C.E., mv.	i_d, μa.	I_d	n
1.21	I	759	2.80	3.94	2.18
2.19	I	850	2.86	4.02	1.90
3.50	I	1002	2.75	3.85	1.07
4.89	I	1100	2.68	3.80	0.98
5.21	I	1125	2.60	3.68	1.09
5.51	I	1140	2.08	2.91	1.03
	II	1310	0.58	0.84	0.98
5.80	I	1152	1.60	2.28	1.05
	II	1325	1.00	1.44	1.09
6.21	I	1163	0.72	1.03	1.02
	II	1320	1.90	2.74	1.09
6.85	II	1356	2.42	3.48	1.05
7.40	II	1345	2.20	3.17	1.03
7.87	II	1368	1.57	2.28	1.18
	III	1615	1.06	1.57	1.02
8.38	II	1389	1.02	1.48	1.13
	III	1633	1.62	2.42	0.92
8.88	II	1410	0.66	0.96	1.20
	III	1648	1.94	2.90	0.92
9.18	II	1417	0.51	0.74	1.13
	III	1658	2.00	3.00	0.94
10.80	III	1780	2.40	3.58	0.83
11.70	III	1805	2.50	3.71	0.94

difference. It should be noted that in both cases curves start at I_d equal to 4 at pH 0 and that the crossover point of curves I and II occurs at pH 5.9. The $-E_{\frac{1}{2}}$ vs. pH plots for waves I and II (bottom of Fig. 3) are generally similar to those for MA. Both show a straight line portion for wave I at low pH but tend to become parallel to the pH axis as the crossover point is approached, while wave II appears more or less sigmoid.

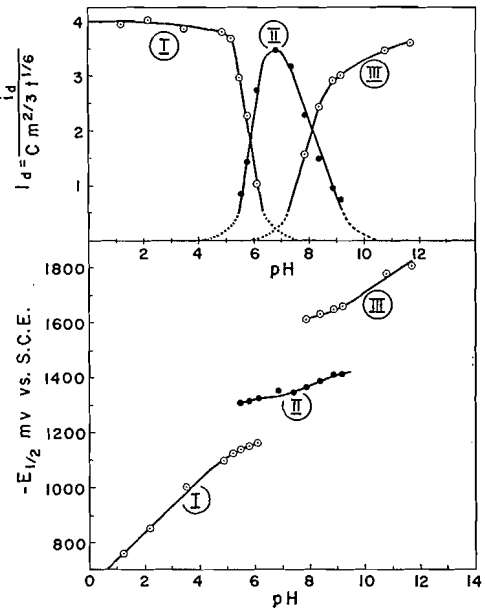

FIG. 3. Top: Polarographic constant I_d of MH vs. pH.
Bottom: Half wave potential of MH vs. pH.

The three curves for MH could be the result of the existence of three species. According to the theory of Brdicka *et al.* these species should be the free acid, its singly charged anion, and its doubly charged anion. There must therefore be two pK_a values for MH, the first being less than 5.9 (the first crossover point) and the second less than 8.2 (the second crossover point). An attempt to determine these by titration with NaOH gave a value of pK_{a1} equal to 5.67 but no value for pK_{a2} was found although the titration was carried to pH 12. The ultraviolet spectra of MH were then recorded at various pH values between 0.92 and 12.10. Two changes occurred with increasing pH as shown in Fig. 4. The height of the peak at 217 mμ (A in Fig. 4) increased and the position of the peak at 300 mμ shifted to 330 mμ (B in Fig. 4). These changes were plotted against pH in the usual way giving for pK_{a1} a value of 5.61 from A and 5.65 from B. No change in the spectra was noticeable from pH 7 to 12. Thus the second ionization constant, if it existed, must be greater than 12.

A test for the constancy of I_d with change in MH concentration was made and the values of I_d resulting are shown in Table III. For any given pH there appears to be little change in I_d for either waves I or II over the concentration range 0.5 to 2.0 mM.

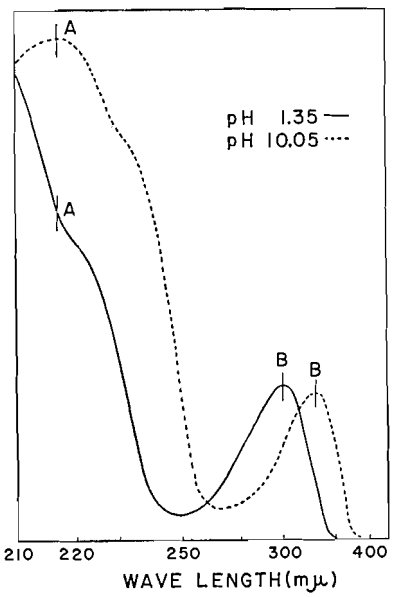

FIG. 4. Ultraviolet absorption curve for MH.

TABLE III

pH	Wave	MH, mM	i_d, μa.	I_d
1.21	I	0.50	2.82	3.94
		1.00	5.58	3.94
		1.50	8.40	3.95
		2.00	11.7	4.12
5.80	I	0.50	1.60	2.28
		1.00	3.44	2.42
		1.50	5.40	2.54
		2.00	7.00	2.47
5.80	II	0.50	1.00	1.44
		1.00	1.90	1.34
		1.50	2.95	1.38
		2.00	3.85	1.36

DISCUSSION

The polarography of MH presents two main anomalies:

1. The apparent number of electrons (n) involved in the electrode process changes from two at low pH to one as the pH increases (Table II). This may be the result of a two step reduction, one step of which becomes irreversible as the pH increases.

2. Two sets of double waves are produced. The first of these may be explained using the concept of Brdicka *et al.* Treating MH as a monobasic acid HA, we may write:

$$HA \rightleftharpoons H^+ + A^- \text{ and } K_a = [H^+][A^-]/[HA].$$

The total concentration of MH is given by

$$C = [HA]_B + [A^-]_B$$

where $[HA]_B$ and $[A^-]_B$ represent concentrations in the bulk of the solution. From these expressions it follows that

[1] $$[HA]_B = C[H^+]/([H^+]+K_a),$$

[2] $$[A^-]_B = C K_a/([H^+]+K_a).$$

At potentials such that the diffusion current of the first wave alone has been reached, all HA molecules, but no A^- ions, arriving at the electrode are reduced immediately and the following processes occur:

$$\begin{array}{lll} (HA)_B \xrightarrow{R} & (HA)_0 \longrightarrow & (HR) \\ & \uparrow k & \\ (A^-)_B \xrightarrow{R} & (A^-)_0 & \end{array}$$

where $(MA)_B$ and $(A^-)_B$ represent the species in the bulk of the solution and $(HA)_0$ and $(A^-)_0$ those at the electrode interface, R is the diffusion rate constant which is assumed to be approximately the same for HA and A^-, k is the rate constant for the association, and HR the reduced form of HA. In a well-buffered solution the hydrogen ion concentration can be assumed to be the same in the bulk and at the interface; thus if i_d is the diffusion current and Q a factor converting it to the proper units, the following steady state equations may be written:

[3] $$d[HA]/dt = R[HA]_B + k[A^-]_0[H^+] - Qi_d = 0,$$

[4] $$d[A^-]/dt = R([A^-]_B - [A^-]_0) - k[A^-]_0[H^+] = 0.$$

If i_d^0 is the diffusion current measured at large $[H^+]$ (i.e. pH = 0) so that $[A^-]_B$ is essentially 0, then

[5] $$Qi_d^0 = RC.$$

From expressions [1] to [5] it can be shown that the ratio of the rate constants for association to that for diffusion is:

[6] $$\frac{k}{R} = \frac{K_a[i_d/(i_d^0 - i_d)] - [H^+]}{[H^+]^2 + K_a[H^+]}.$$

Expression [6] may be checked by substituting $K_a = 2.24 \times 10^{-5}$ moles liters^{-1}, $i_d^0 = 2.83$ μa., and the appropriate values of i_d and $[H^+]$ into [6] to obtain k/R which should be constant over a wide range of hydrogen ion concentrations. The results obtained in this way follow:

$[H^+]$	k/R
1.29×10^{-5} M	1.3×10^5 liters moles^{-1}
6.17×10^{-6}	2.6×10^5
3.09×10^{-6}	1.9×10^5
1.59×10^{-6}	2.2×10^5
6.17×10^{-7}	0.8×10^5

Although the ratio shows some variation, probably due to errors in pH measurements to which expression [6] is sensitive, there is no definite trend with change in pH; thus a value of 2×10^5 liters moles^{-1} can be taken for k/R.

By substituting $i_d = \frac{1}{2}i_d^0$ into equation [6] the dependence of the hydrogen ion concentration at the crossover point ($[H^+]_{\frac{1}{2}}$) on the other factors is given by the expression

$$[7] \qquad k/R = K_a - [H^+]_{\frac{1}{2}}/([H^+]_{\frac{1}{2}}^2 + K_a[H^+]_{\frac{1}{2}}).$$

This equation is similar to the one obtained by Brdicka and Wiesner for similar conditions ($i_+ = i_-$ in their paper). It must be emphasized that since R is a complex function of diffusion and reaction rates, no absolute values of k can be obtained from the above form of the equation. It does give a fairly adequate qualitative picture, however, showing that the crossover point is not only a function of K_a but is dependent also on the relative rates of the diffusion and recombination processes.

On the basis of the above theory the second crossover point would occur when the reduction rate of the singly and doubly charged anions is equal. The second ionization constant, however, was found to be less than 10^{-12}, which is so much lower than $[H^+]_{\frac{1}{2}}$ that substitution in [7] would result in a negative value for k/R. This is of course meaningless, and the above theory must be discarded as an explanation of the second set of double waves. Elving and Teitelbaum (4) reported a double wave in the case of the diethyl esters of maleic and fumaric acids at a higher pH than for the acids themselves. This would indicate that the second set of waves cannot be attributed to normally ionized species but to some other pH dependent feature of the reduction. An explanation of these waves would most likely be found in a study of the mechanism of the electrode reaction. It would also seem advisable to reinvestigate the polarography of all acids giving a double wave, as well as their esters, under conditions similar to those used in this work, with the view to determining which compounds give a second set of double waves at higher pH. The methyl esters of MH are being investigated to this end.

REFERENCES

1. BRDICKA, R. Collection Czechoslov. Chem. Communs. 12: 212. 1947.
2. BRDICKA, R. and WIESNER, K. Collection Czechoslov. Chem. Communs. 12: 138. 1947.
3. ELVING, P. J. and ROSENTHAL, I. Anal. Chem. 26: 1454. 1954.
4. ELVING, P. J. and TEITELBAUM, C. J. Am. Chem. Soc. 71: 3916. 1949.
5. HANUS, V. and BRDICKA, R. Chem. Listy, 44: 291. 1950.
6. MÜLLER, O. H. and BAUMBERGER, J. P. J. Am. Chem. Soc. 61: 590. 1939.

THE REACTION OF HYDROGEN ATOMS WITH METHYL CYANIDE[1]

By W. Forst[2] and C. A. Winkler

ABSTRACT

Hydrogen atoms produced in a discharge tube were found to react with methyl cyanide to produce hydrogen cyanide as the main product, together with smaller amounts of methane and ethane. The proposed mechanism involves the formation of hydrogen cyanide and a methyl radical in the initial step; methane and ethane are attributed to secondary reactions of the methyl radicals.

INTRODUCTION

The reaction of hydrogen atoms with methyl cyanide seems never to have been studied. A limited investigation of it has been made, partly for its intrinsic interest, and partly to provide information about the possible significance of hydrogen atom reactions during the reaction of active nitrogen with methyl cyanide, which will be reported in a later communication.

EXPERIMENTAL

The apparatus was essentially identical with that used for active nitrogen studies in this laboratory (1, 5) except for the methyl cyanide feed system. Methyl cyanide was stored as a liquid in a wide flat-bottomed bulb immersed in a thermostat regulated at 20.25 ± 0.05°C., and the vapor drawn directly from the liquid surface. The methyl cyanide flow rate was varied by placing jets of different sizes in a flowmeter.

The molecular hydrogen flow rate was 7.95×10^{-5} mole/sec., corresponding to an operating pressure of 0.95 mm. Hg in the system.

Methyl cyanide, "chemically pure", was purchased from Brickman and Company and thoroughly dehydrated by one distillation over calcium chloride, followed by six distillations over P_2O_5 (13), and a final distillation over freshly fused potassium carbonate (9).

The condensable products of the reaction were distilled into a low temperature still of the type described by LeRoy (8). The C_2 fraction was distilled off at −140°C. and by mass-spectrometric analysis* was found to contain only ethane. The remainder of the products were distilled into an absorber containing $N/2$ KOH immersed in liquid air. After the solution had melted, the cyanide was determined by titration with silver nitrate (6). Three experiments were made in which the products were analyzed for cyanogen by the method due to Rhodes (11); the result in each case was negative. Samples of non-condensable products were withdrawn from the hydrogen stream by a Toepler pump and analyzed on the mass spectrometer. They contained only methane,

[1]*Manuscript received July 25, 1955.*
Contribution from the Physical Chemistry Laboratory, McGill University, Montreal, Quebec, with financial assistance from the National Research Council, Ottawa, Canada.
[2]*Holder of the Alexander McFee Fellowship, and two National Research Council Studentships.*
**The authors are indebted to Dr. H. I. Schiff of this department for permission to use the mass spectrometer, and to Mr. G. Verbeke for the analyses.*

in addition to excess hydrogen. There were traces of a white solid on the walls of the tube leading from the reaction vessel into the first trap.

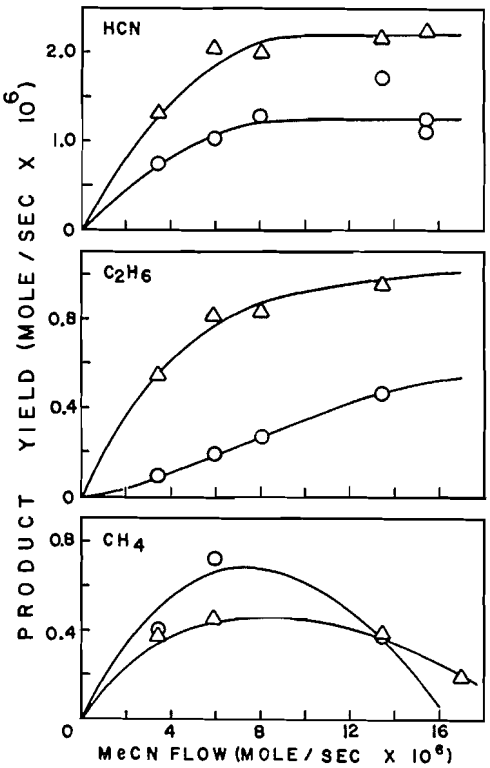

FIG. 1. Yields of hydrogen cyanide, ethane, and methane as functions of methyl cyanide flow rate.
Circles: 107°C. Triangles: 237°C.

The yields of hydrogen cyanide, ethane, and methane at 107° and 237°C. are plotted in Fig. 1 as functions of the methyl cyanide flow rate.

DISCUSSION

The initial attack of a hydrogen atom on the methyl cyanide molecule can be represented in three ways:

$$H+CH_3CN \rightarrow CH_4+CN-2 \text{ kcal.} \quad [1]$$

$$H+CH_3CN \rightarrow H_2+CH_2CN+3 \text{ kcal.} \quad [2]$$

$$H+CH_3CN \rightarrow HCN+CH_3+10 \text{ kcal.} \quad [3]$$

The heats of reaction in each case were calculated from heats of formation given in Reference (10). The heat of formation of the CH_2CN radical was estimated at about -70 kcal., and the heat of formation of the CN radical was taken as -93 kcal. (2, 10).

If reaction [1] occurs to an appreciable extent, some of the cyanide radicals formed in [1] should, at least at low MeCN flow rates, recombine to cyanogen. Since HCN but no cyanogen was found, every cyanide radical formed in [1] would have to be removed quantitatively by reactions leading ultimately to hydrogen cyanide. Moreover, with reaction [1] as initial step, there should be one molecule of methane produced for every cyanide radical disappearing. Fig. 1 shows that no such relation exists between the formation of HCN and CH_4. It would also be difficult to account for the presence of ethane in the products on this basis. Hence reaction [1] must be ruled out as a possible primary step.

If reaction [2] is the initial step, it is difficult to visualize how methane, ethane, and hydrogen cyanide could arise by further reactions of the cyanomethyl radicals produced. While it is true that recombination of the CH_2CN radicals to succinonitrile would account for the white deposit observed on the walls of the reaction vessel, this cannot be taken as proof that reaction [2] occurs, since CH_2CN radicals may also be formed in the reaction

$$CH_3+CH_3CN \rightarrow CH_4+CH_2CN$$

which is known to occur (12). While reaction [2] does not appear to be attractive for the primary step, the present experiments do not permit its importance to be assessed directly.

If reactions [1] and [2] are considered unimportant, and the primary step is assumed to be reaction [3], methane and ethane would have to arise by subsequent reactions of methyl radicals, and at any flow rate of methyl cyanide the following relation between the products of the reaction should exist:

$$2(\text{moles of ethane})+(\text{moles of methane}) = (\text{moles of HCN}).$$

Inspection of Fig. 1 shows that this is approximately true, within the relatively large experimental error. This agreement may, perhaps, be taken as evidence that, compared with reaction [3], reaction [2] does not occur to an appreciable extent.

The two curves in Fig. 1 representing the production of hydrogen cyanide as a function of methyl cyanide flow rate show that above a flow rate of about 8×10^{-6} mole/sec. MeCN, further increase in MeCN flow rate does not increase the production of hydrogen cyanide. A reasonable explanation of this behavior seems to be that the available supply of hydrogen atoms becomes exhausted.

If the flat portion of each curve represents complete consumption of all the available hydrogen atoms, there is reason to expect that the plateau should be higher at the lower temperature, since presumably more hydrogen atoms should be available at the lower temperature owing to a decreased number of collisions (in the gas phase and at the wall) leading to their recombination. From the relative positions of the two plateaus in Fig. 1, the experimental results seem to imply that the opposite is true. On the basis of a detailed mathematical treatment, it will be shown in a later communication that the change of plateau values with temperature could be accounted for on the assumption that

methyl cyanide acts as an efficient third body in the recombination of hydrogen atoms.

There are four obvious possibilities for secondary reactions of methyl radicals:

$$CH_3+H \rightarrow CH_4 \quad [4]$$

$$CH_3+CH_3 \rightarrow C_2H_6 \quad [5]$$

$$CH_3+H_2 \rightarrow CH_4+H \quad [6]$$

$$CH_3CN+CH_3 \rightarrow CH_4+CH_2CN. \quad [7]$$

Reactions [4] and [5] have low activation energies, and both probably require a third body. Reactions [6] and [7] are both known to have activation energies of the order of 10 kcal. (14, 15). On the basis of this information, reactions [4] and [5] should be equally likely at 107°C. and 237°C., with reactions [6] and [7] becoming important only at the higher temperature. This conclusion appears to be borne out by the pattern of methane production shown in Fig. 1. At 107°C. the amount of methane formed rises with increasing methyl cyanide flow rate up to a maximum which corresponds roughly to the point where complete consumption of hydrogen atoms occurs, and then drops off sharply as the methyl cyanide flow rate is increased further. This suggests a strong dependence of methane production on hydrogen atom supply, and consequently reaction [4] must be responsible for a major part of the methane produced at this temperature. At 237°C. the decrease of methane production at MeCN flow rates corresponding to complete consumption of hydrogen atoms is less pronounced than at 107°C., and this may be taken as evidence that at this temperature reactions [6] and [7]—in addition to reaction [4]—contribute significantly to the formation of methane, as expected.

It is difficult to assess the relative importance of reactions [6] and [7]. It will be noted however that in reaction [6] a hydrogen atom is formed for each molecule of methane produced. If reaction [6] were the only important methane-producing step at high MeCN flow rates, a chain reaction could conceivably be set up in conjunction with reaction [3], resulting in continued increase of hydrogen cyanide yield at high MeCN flow rates. Since the hydrogen cyanide production curve (Fig. 1) reaches a flat plateau (within experimental error), it is very improbable that at high flow rates appreciable amounts of methane are produced in reaction [6].

There can be little doubt that ethane is due to recombination of methyl radicals, and by reference to the discussion of methane production the only other important reaction competing at both temperatures for methyl radicals at low MeCN flow rates should be reaction [4]. The fact that production of ethane increases markedly with a rise in temperature would then seem to be a matter of methyl radical concentration. The increased amount of reaction at 237°C. increases $[CH_3]$ relative to its value at 107°C., and this should profoundly affect the rate of formation of ethane, which depends on the second power of $[CH_3]$. The rate of formation of methane (reaction [4]) should also increase, though to a lesser extent.

Actually, a decline in the yield of methane is observed at 237°C., and this appears to be attributable to a decrease in hydrogen atom concentration. At low MeCN flow rates, only relatively few hydrogen atoms are removed in reactions [3] and [4], and in third order recombination with methyl cyanide as the third body. As a result, under these conditions, an appreciable part of the hydrogen atoms will recombine by $H–H_2$ collisions and at the wall, and, as mentioned, such recombination can be expected to exhibit a positive temperature coefficient. It appears that at 237°C. this hydrogen atom recombination is much more pronounced than at 107°C., to the extent that it may offset the effect of the temperature increase on $[CH_3]$, hence on the rate of formation of methane, and lead to a reduced yield of methane at the higher temperature.

The reaction of hydrogen atoms with methyl cyanide appears to be essentially similar to the reactions of methyl halides with hydrogen atoms (3, 4, 7). This is perhaps not surprising since in many inorganic reactions the cyanide group exhibits a strong resemblance to the halogens.

REFERENCES

1. BLADES, H. and WINKLER, C. A. Can. J. Chem. 29: 1022. 1951.
2. BREWER, L., TEMPLETON, L. K., and JENKINS, F. A. J. Am. Chem. Soc. 73: 1462. 1951.
3. CHADWELL, H. M. and TITANI, T. J. Am. Chem. Soc. 55: 1363. 1933.
4. CREMER, E., CURRY, J., and POLANYI, M. Z. physik. Chem. B, 23: 445. 1933.
5. GREENBLATT, J. H. and WINKLER, C. A. Can. J. Research, B, 27: 721. 1949.
6. KOLTHOFF, I. M. and STENGER, V. A. Volumetric analysis. 2nd ed. Vol. II. Interscience Publishers, Inc., New York. 1947. p. 282.
7. LEE, G. L. and LEROY, D. J. Can. J. Research, B, 28: 500. 1950.
8. LEROY, D. J. Can. J. Research, B, 28: 492. 1951.
9. LEWIS, G. L. and SMYTH, C. P. J. Chem. Phys. 7: 1085. 1939.
10. MCDOWELL, C. A. and WARREN, S. W. Trans. Faraday Soc. 48: 1084. 1952.
11. RHODES, F. H. J. Ind. Eng. Chem. 4: 652. 1912.
12. Selected Values of Chemical Thermodynamic Properties. National Bureau of Standards, Washington, D.C. 1952.
13. WALDEN, P. and BIRR, E. J. Z. physik. Chem. 144: 269. 1929.
14. WIJNEN, M. H. J. J. Chem. Phys. 22: 1074. 1954.
15. WIJNEN, M. H. J. and STEACIE, E. W. R. Discussions Faraday Soc. No. 14: 118. 1953.

THE PREPARATION OF *o*- AND *p*-ACETAMINOBENZALDEHYDES[1]

By J. J. Brown[2] and R. K. Brown

ABSTRACT

Treatment of N,N-diacetyl-*o*-toluidine with N-bromosuccinimide followed by hydrolysis of the intermediate dibromo compound gave *o*-acetaminobenzaldehyde. The reaction was applied successfully to N,N-diacetyl-*p*-toluidine, N,N-diacetyl-4-chloro-*o*-toluidine, 2,4-bis(diacetamino)toluene, and 4-acetoxy-N,N-diacetyl-*o*-toluidine.

Both *o*- and *p*-acetaminobenzaldehyde were required for synthetic work in this laboratory. These compounds have been prepared in the usual way by the acetylation (6, 7) of *o*- and *p*-aminobenzaldehyde. However, the methods described in the literature for the preparation of *o*-aminobenzaldehyde by the reduction of *o*-nitrobenzaldehyde with ferrous sulphate and ammonia (15) and for *p*-aminobenzaldehyde by the action of sodium polysulphide upon *p*-nitrotoluene (3) are tedious, and the products must be used immediately in order to avoid self-condensation.

A direct preparation of *o*- and *p*-acetaminobenzaldehyde was suggested by the hydrolysis of N,N-diacetyl-*p*-toluidine (16) using aqueous sodium carbonate which gave a quantitative yield of *p*-acetotoluidide, and also by the work of Brown and Newbold (2) who used N-bromosuccinimide to oxidize 4-chloromethylmeconin(I) to 3-formylopianic acid (II).

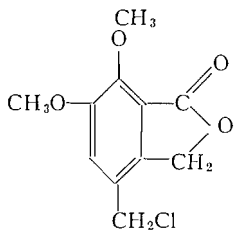

I

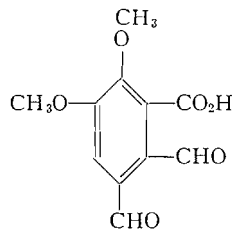

II

We found that treatment of N,N-diacetyl-*p*-toluidine with two moles of N-bromosuccinimide in carbon tetrachloride, followed by aqueous sodium carbonate hydrolysis without isolation of the intermediate bromo compound, gave *p*-acetaminobenzaldehyde in 70% yield. Similarly, N,N-diacetyl-*o*-toluidine (16) gave *o*-acetaminobenzaldehyde in 66% yield.

The reaction was investigated further with respect to certain 4-substituted N,N-diacetyl-*o*-toluidines prepared by prolonged refluxing of the toluidine or its acetyl derivative in acetic anhydride. N,N-Diacetyl-4-chloro-*o*-toluidine, 2,4-bis(diacetamino)toluene, and 4-acetoxy-N,N-diacetyl-*o*-toluidine when

[1]*Manuscript received August 29, 1955.*
Contribution from the Department of Chemistry, University of Alberta, Edmonton, Alberta.
[2]*National Research Council of Canada Postdoctoral Fellow, 1954–1955. Present address: The Converse Memorial Laboratory, Harvard University, Cambridge 38, Mass., U.S.A.*

treated with N-bromosuccinimide as above gave 2-acetamino-4-chlorobenzaldehyde (69%), 2,4-bis(acetamino)benzaldehyde (79%), and 2-acetamino-4-hydroxybenzaldehyde (70%) respectively.

The reaction was also applied to N,N-diacetyl-4-nitro-*o*-toluidine but the acetaminobenzaldehyde could not be isolated from the reaction mixture.

EXPERIMENTAL

Brominations using N-bromosuccinimide were carried out with irradiation from a Westinghouse Sunlamp (type R.S.-275 Watt) placed close to the flask.

p-Acetotoluidide

N,N-Diacetyl-*p*-toluidine (5 gm.) was treated with anhydrous sodium carbonate (10 gm.) and water (100 ml.) on the steam bath for one hour. Partial solution took place, and the solid which separated on cooling was crystallized from benzene to give *p*-acetotoluidide as blades, m.p. and mixed m.p. 149–150°.

p-Acetaminobenzaldehyde

A solution of N,N-diacetyl-*p*-toluidine (5 gm.) in carbon tetrachloride (100 ml.) containing 10.3 gm. of N-bromosuccinimide was heated under reflux on the steam bath for one hour. The filtered solution was evaporated under reduced pressure, and the residual red oil was heated with anhydrous sodium carbonate (10 gm.) in water (100 ml.) for one hour on the steam bath. The solution was decanted from a small amount of tar, extracted with ether (3×100 ml.), and the combined extracts were dried with sodium sulphate. Removal of solvent under reduced pressure gave a yellow solid which was crystallized from benzene – light petroleum (b.p. 30–60°) to give *p*-acetaminobenzaldehyde as needles (3 gm., 70%), m.p. 152–153° (lit.(7) 154.5–155°). Oxime, m.p. 206–207° (lit.(7) 205–206°). Calc. for $C_9H_9O_2N$: C, 66.2; H, 5.6. Found: C, 66.4; 5.5%.

o-Acetaminobenzaldehyde

N,N-Diacetyl-*o*-toluidine (5 gm.) was brominated as above, with the reflux time extended to eight hours. After hydrolysis of the product, the dried (Na_2SO_4) ethereal extract was evaporated to a dark red oil which was extracted thoroughly with boiling light petroleum (b.p. 30–60°). The extract was reduced to a small volume and placed in the refrigerator for one hour when *o*-acetaminobenzaldehyde separated as needles (2.8 gm., 66%), m.p. 68–70°. A specimen recrystallized from light petroleum (b.p. 30–60°) melted at 70–71° (lit. (6) 70–71°). Found: C, 66.6; H, 5.6%. Oxime, m.p. 193–194° (lit.(1) 194°).

N,N-Diacetyl-4-chloro-o-toluidine

4-Chloro-*o*-toluidine was prepared in good yield by the method of Hodgson and Moore (8). Twenty grams of 4-chloro-*o*-toluidine in acetic anhydride (50 ml.) was heated under reflux for 17 hr. The cooled solution was diluted with water (200 ml.) and the brown oil which separated was extracted with ether (3×50 ml.). The combined ethereal extracts were washed with water (2×50 ml.), 10% sodium bicarbonate solution (3×50 ml.), and water (50 ml.) and then dried (Na_2SO_4). The red oil obtained on removal of the solvent under reduced pressure was distilled to give N,N-diacetyl-4-chloro-*o*-toluidine as a

colorless oil which rapidly crystallized as needles (24 gm.), m.p. 40–42°, b.p. 154° at 8.5 mm. Calc. for $C_{11}H_{12}O_2NCl$: C, 58.5; H, 5.4. Found: C, 58.6; H, 5.6%.

2-Acetamino-4-chlorobenzaldehyde

N,N-Diacetyl-4-chloro-*o*-toluidine (5 gm.), N-bromosuccinimide (9 gm.), and carbon tetrachloride (100 ml.) were heated under reflux on the steam bath for three hours. The filtered solution when evaporated gave a yellow solid which was heated under reflux for 30 min. with a solution of anhydrous sodium carbonate (10 gm.) in water (50 ml.). The cooled reaction mixture was extracted with chloroform (3×50 ml.) and the combined chloroform extracts were dried (Na_2SO_4). Evaporation of solvent under reduced pressure, followed by crystallization of the yellow solid from aqueous ethanol, gave 2-acetamino-4-chlorobenzaldehyde as yellow blades (3 gm., 69%), m.p. 124–125°. Calc. for $C_9H_8O_2NCl$: C, 54.7; H, 4.1. Found: C, 54.7; H, 4.1%. The oxime crystallized from aqueous ethanol as needles, m.p. 215–216°. Calc. for $C_9H_9O_2N_2Cl$: C, 50.9; H, 4.3. Found: C, 50.8; H, 4.4%.

2-Acetamino-4-chlorobenzaldehyde was hydrolyzed to 2-amino-4-chlorobenzaldehyde by heating the former compound (1 gm.) with sodium hydroxide solution (40 ml., 2 *N*) and methanol (20 ml.) on the steam bath for 15 min. with occasional shaking. The solution was decanted from a small amount of tar, cooled, and extracted with ether (3×30 ml.). The combined ethereal extracts were washed with water (30 ml.), dried (Na_2SO_4), and evaporated to a yellow oil which soon solidified. Crystallization from aqueous ethanol gave 2-amino-4-chlorobenzaldehyde as needles (550 mgm.), m.p. 86–87°. Calc. for C_7H_6ONCl: C, 54.0; H, 3.9. Found: C, 53.8; H, 3.8%. Sachs and Sichel (14) give a melting point of 86° for the same compound obtained by reduction of 4-chloro-2-nitrobenzaldehyde using titanous chloride.

2,4-Bis(diacetamino)toluene

2,4-Bis(acetamino)toluene was prepared from 2,4-diaminotoluene (11) by the method of Lumière and Barbier (10). The compound melted at 219–223° (lit.(9) 223°). 2,4-Bis(acetamino)toluene (40 gm.) and acetic anhydride (200 ml.) were heated under reflux for 17 hr. The acetic anhydride was removed under reduced pressure and water (50 ml.) was added to the residue which was then extracted with chloroform (3×50 ml.). The combined chloroform extracts were washed with water (50 ml.), 10% sodium bicarbonate solution (50 ml.), and water (50 ml.) and then dried (Na_2SO_4). Removal of the solvent under reduced pressure gave a dark brown oil which solidified on standing. The solid, which was filtered with the aid of some ether and then washed with a small amount of ether, crystallized from benzene – light petroleum (b.p. 30–60°) to give 2,4-bis(diacetamino)toluene as prisms (20 gm.), m.p. 109–110°. Calc. for $C_{15}H_{18}O_4N_2$: C, 62.0; H, 6.25. Found: C, 62.2; H, 6.4%.

2,4-Bis(acetamino)benzaldehyde

2,4-Bis(diacetamino)toluene (5 gm.), N-bromosuccinimide (6.75 gm.), and carbon tetrachloride (100 ml.) were heated under reflux on the steam bath for

three hours. Evaporation of the solvent after filtration gave a yellow oil which was heated on the steam bath for 15 min. with a solution of anhydrous sodium carbonate (10 gm.) in water (50 ml.). The solid which separated on cooling was collected and crystallized from ethanol to give 2,4-bis(acetamino)benzaldehyde as plates (3 gm., 79%), m.p. 233–235°. Calc. for $C_{11}H_{12}O_3N_2$: C, 60.0; H, 5.5. Found: C, 59.8; H, 5.5%. Sachs and Kempf (13) give m.p. 235.5° for the compound obtained by treating the product of the ammonium sulphide reduction of 2,4-dinitrobenzaldehyde with acetic anhydride. The phenylhydrazone melted at 252–254° (lit.(13) 246–252°).

2-Amino-p-cresol (Me = 1)

2-Nitro-*p*-toluidine, prepared in excellent yield by the method of Cohen and Dakin (4) for 4-nitro-*o*-toluidine, was converted into 2-nitro-*p*-cresol (17). Sodium dithionite (50 gm.) was added in small portions, with stirring, to 2-nitro-*p*-cresol (5 gm.) in a solution of potassium hydroxide (12 gm.) in water (100 ml.). After 15 min. at room temperature, the solution was acidified to Congo red with hydrochloric acid (d., 1.16) and heated on the steam bath to remove sulphur dioxide. The filtered solution was neutralized with 10% sodium bicarbonate, extracted with ether (4×100 ml.), and the combined ethereal extracts were washed with water (100 ml.) and dried (Na_2SO_4). Evaporation of solvent under reduced pressure yielded 2-amino-*p*-cresol as a brown solid (3 gm.), m.p. 147–150°. Copisarow (5) reports a melting point of 157–159° for the compound obtained by sodium sulphide reduction of 2-nitro-*p*-cresol.

4-Acetoxy-N,N-diacetyl-o-toluidine

2-Amino-*p*-cresol (5 gm.) and acetic anhydride (20 ml.) were heated under reflux for 17 hr. The cooled solution was diluted with water (100 ml.) and the product was isolated with ether as before. Removal of solvent gave a red oil which was extracted with boiling light petroleum (b.p. 30–60°). The solvent was reduced in volume and the remaining solution cooled in a refrigerator for one hour. The 4-acetoxy-N,N-diacetyl-*o*-toluidine separated as needles (4 gm.), m.p. 72–73°. Calc. for $C_{13}H_{15}O_4N$: C, 62.6; H, 6.1. Found: C, 62.4; H, 6.2%.

2-Acetamino-4-hydroxybenzaldehyde

4-Acetoxy-N,N-diacetyl-*o*-toluidine (2 gm.) and N-bromosuccinimide (3.15 gm.) in carbon tetrachloride (30 ml.) were heated under reflux for two and one-half hours on the steam bath. The yellow oil, obtained by evaporation of the filtered solvent, was heated on the steam bath for 30 min. with a solution of anhydrous sodium carbonate (4 gm.) in water (25 ml.). The solution was acidified with acetic acid and extracted with ether (5×50 ml.). The dried solution (Na_2SO_4), freed of solvent under reduced pressure, gave 2-acetamino-4-hydroxybenzaldehyde as a light brown solid. Crystallization from aqueous ethanol gave needles (1 gm., 70%) melting at 238–239°. Calc. for $C_9H_9O_3N$: C, 60.3; H, 5.1. Found: C, 60.2; H, 5.4%. The oxime crystallized from water as needles, m.p. 215° (decomp.). Calc. for $C_9H_{10}O_3N_2$: C, 55.7; H, 5.2. Found: C, 55.5; H, 5.5%.

N,N-Diacetyl-4-nitro-o-toluidine

4-Nitro-*o*-toluidine (20 gm.) (prepared according to Cohen and Dakin (4)) in acetic anhydride (50 ml.) was heated under reflux for 17 hr. The cooled solution was diluted with water (200 ml.) and the product, a dark red oil, was isolated with chloroform. The oil was dissolved in a few milliliters of benzene and the 4-nitro-*o*-acetotoluidide (5 gm.) which separated was filtered off, m.p. 151–153° (lit.(12) 150–151°). Evaporation of the filtrate gave a dark oil which soon solidified. Crystallization from benzene – light petroleum (b.p. 30–60°) gave N,N-diacetyl-4-nitro-*o*-toluidine as prisms (16 gm.), m.p. 81–83°. Calc. for $C_{11}H_{12}O_4N_2$: C, 55.9; H, 5.1. Found: C, 56.1; H, 5.2%.

ACKNOWLEDGMENT

The authors wish to thank the National Research Council of Canada for generous financial support.

REFERENCES

1. BISCHLER, A. Ber. 26: 1891. 1893.
2. BROWN, J. J. and NEWBOLD, G. T. J. Chem. Soc. 4878. 1952.
3. CAMPAIGNE, E., BUDDE, W. M., and SCHAEFER, G. F. Organic synthesis. Vol. 31. John Wiley & Sons, Inc., New York. 1951. p. 6.
4. COHEN, J. B. and DAKIN, H. D. J. Chem. Soc. 81: 1324. 1902.
5. COPISAROW, M. J. Chem. Soc. 251. 1929.
6. FRIEDLÄNDER, P. Ber. 15: 2572. 1882.
7. GABRIEL, S. and HERZBERG, M. Ber. 16: 2000. 1883.
8. HODGSON, H. H. and MOORE, F. H. J. Chem. Soc. 2036. 1926.
9. KELBE, W. Ber. 16: 1199. 1883.
10. LUMIÈRE, A. L. and BARBIER, H. Bull. soc. chim. 33: 783. 1905.
11. MAHOOD, S. A. and SCHAFFNER, P. V. L. Organic synthesis, Collective Vol. 2. John Wiley & Sons, Inc., New York. 1943. p. 160.
12. NÖLTING, E. and COLLIN, A. Ber. 17: 268. 1884.
13. SACHS, F. and KEMPF, R. Ber. 35: 2704. 1902.
14. SACHS, F. and SICHEL, E. Ber. 37: 1861. 1904.
15. SMITH, L. I. and OPIE, J. W. Organic synthesis, Collective Vol. 3. John Wiley & Sons, Inc., New York. 1955. p. 56.
16. SUDBOROUGH, J. J. J. Chem. Soc. 79: 533. 1901.
17. ULLMANN, F. and DOOTSON, P. Ber. 51: 9. 1918.

DEGRADATION OF D-GLUCOSE-1-C^{14} TO TRIOSE-REDUCTONE-C^{14} [1]

By H. F. Bauer and Carol Teed

ABSTRACT

Triose-reductone-C^{14} was obtained by treating D-glucose-1-C^{14} with sodium hydroxide in the presence of lead acetate at elevated temperatures. Carbon atoms four, five, and six, as well as carbon atoms one, two, and three, of the D-glucose molecule are shown to contribute to the triose-reductone yield. The formation of triose-reductone was found not to be accompanied by glycerol formation. Mechanisms for fragmentation of reducing sugars are discussed in the light of these findings.

INTRODUCTION

Triose-reductone, often called "glucoreductone" or "reductone", was discovered and isolated in a crystalline state by Euler and Martius (6) when they treated D-glucose with strong solutions of sodium hydroxide. It was subsequently shown that many reducing sugars yield triose-reductone under the same conditions but the methods for its isolation have been modified only slightly and D-glucose still remains the only practical source. By analogy with the ascorbic acids triose-reductone was assigned an α-carbonyl-α-enediol structure (I). This structure, though still widely accepted, cannot account for all of the observed properties of reductone and a resonance hybrid (II) has been suggested recently (12) as a more adequate alternative.

It was the object of this work to gain information about the mechanisms of decomposition of a hexose molecule to three-carbon fragments, especially triose-reductone, under the influence of alkali.

Two main mechanisms have been suggested for this disintegration. The older of these, postulated by Nef (10), involves an alkali-induced 1,2-enediol formation followed by a migration of the double bond via the 2- and 3-ketose to yield a 3,4-enediol. Fragmentation at the double bond was then assumed to result in the formation of two molecules of glyceraldehyde, which in turn could undergo a Lobry de Bruyn – Alberda van Ekenstein rearrangement to dihydroxyacetone or be enolized and oxidized to give triose-reductone. However, the step involving cleavage at the double bond has made this mechanism no longer acceptable since it was shown that the bond energy of a carbon–carbon double bond is much higher than of a single bond and that cleavage of a carbon chain occurs preferentially in α,β-position to a double bond (11, 14).

The other theory, first suggested by Evans and co-workers (1, 2), avoids the shortcomings of Nef's mechanism. Again a 1,2-enediolate ion (III) initiates the degradation reaction. The formation of triose-reductone and elucidation of its structure as an enediol have actually served as evidence for the existence of a 1,2-enediol (2) and other evidence can also be cited (7, 13), although the enediolic forms of the common reducing sugars themselves have never been

[1]*Manuscript received August 29, 1955.*
Contribution from the National Research Council of Canada, Prairie Regional Laboratory, Saskatoon, Saskatchewan, Canada. Issued as Paper No. 208 on the Uses of Plant Products and as N.R.C. No. 3765.

isolated. The 2-ketose formed via the 1,2-enediolate can still undergo 2,3-enolization (IV) (16). The fragmentation to three-carbon fragments is then thought to occur by a reverse aldolization of the 1,2- or 2,3-enediolate between C-3 and C-4. The possibility of formation of a 3,4- and 4,5-enediolate to explain epimerizations observed on C-4 and C-5 is today regarded as very unlikely and the epimerizations are explained by a recombination of three-carbon fragments (18). A fragmentation as indicated in III and IV would lead to two molecules of triose, one being in an enolized form. Oxidation of the triose could then give rise to triose-reductone, a possibility that is suggested by the formation of triose-reductone by the action of alkali on dihydroxyacetone (17). According to Euler (3) a fragmentation as indicated by V would lead, however, directly from D-glucose to one molecule of triose-reductone and one molecule of glycerol.

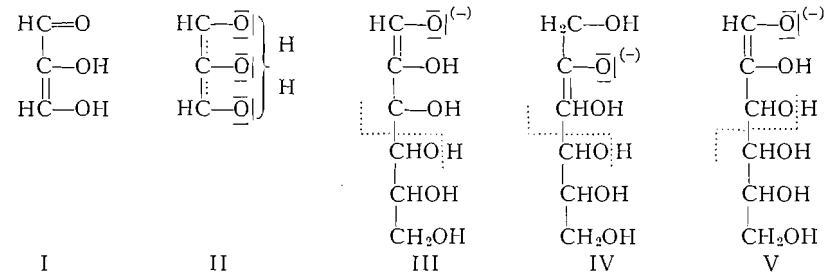

I II III IV V

The use of carbon-14 tracer techniques in recent studies of the action of alkali on carbohydrates (9, 15) has provided a deeper understanding of some aspects of the degradation reactions. It appeared, therefore, that preparation of triose-reductone from carbon-14 labelled sugars might likewise yield information suitable for evaluating the mechanisms discussed above. D-Glucose-1-C^{14} was dissolved in water and heated in a stream of nitrogen in the presence of lead acetate and small amounts of potassium cyanide (4, 6) and cupric acetate (5). Sodium hydroxide was then added and after the desired reaction time the mixture was neutralized with acetic acid. The triose-reductone lead salt was analyzed for its lead content and decomposed with the calculated amount of phosphoric acid. The purification was simplified and the yield of pure material increased by the finding that the triose-reductone obtained from the decomposition sublimes easily *in vacuo*. To determine the C^{14} content of the triose-reductone the compound was combusted to carbon dioxide, which was either analyzed as such in a gas phase counter, or counted as barium carbonate at infinite thickness in a gas flow counter (Table I).

TABLE I

CONTRIBUTION OF THE CARBON ATOMS OF D-GLUCOSE TO THE YIELD OF TRIOSE-REDUCTONE

Activity in mμc./mM. CO_2		Contribution by	
D-Glucose-1-C^{14}	Triose-reductone-C^{14}	C-1+C-2+C-3	C-4+C-5+C-6
38.9	42.8	55.1%	44.9%
70.5	74.2	52.6%	47.4%

From the results of these analyses and by examining the mother liquors it could be shown that:

(*a*) Carbons 4, 5, and 6 of the D-glucose molecule as well as carbons 1, 2, and 3 contribute to the triose-reductone formation.

(*b*) The contribution of the bottom half of D-glucose to the yield of triose-reductone nearly equals that of the top half.

(*c*) No glycerol is formed from D-glucose in the degradation by alkali.

These findings strongly suggest that a fragmentation according to Euler (4) is not possible and that triose-reductone is a secondary reaction product derived from a three-carbon compound possibly by a fragmentation according to III and IV with triose-enediol as an intermediate. The small deficiency of triose-reductone formed from the bottom half of D-glucose might best be explained by the fact that the glyceraldehyde formed on the reverse aldolization has first to be converted to its enediolate before being oxidized to triose-reductone. Since enolization is not an instantaneous reaction (13), the top half of the molecule, already present as enediolate before fragmentation, is therefore converted to triose-reductone at a slightly faster rate. It was noted above that formation of triose-reductone has been taken as evidence for the existence of a 1,2-enediolate (III) in an alkaline solution of a hexose (2). However, since the compound is also derived from the bottom half of the molecule, its formation may not necessarily serve as a direct proof of this postulate.

EXPERIMENTAL

Triose-reductone-C^{14} from D-*Glucose-1-C^{14}*

D-Glucose-1-C^{14}, 25 gm., was dissolved in 375 ml. of water. Lead acetate, 13.5 gm., potassium cyanide, 3 mgm., and copper acetate (5), 50 mgm., were added and the solution was heated in a stream of nitrogen to 92°C. Sodium hydroxide, 8.5 gm. in 25 ml. of water, was added and the mixture was shaken for two to three minutes. It was then acidified with glacial acetic acid, 4 ml., and quickly cooled. The lead salt of triose-reductone-C^{14}, 12.5 gm., was isolated by centrifuging, washed in succession with water, acetone, and ether, and dried *in vacuo*. The lead content of the salt was 58.8%. The lead salt was suspended in dry acetone, 50 ml., and phosphoric acid, 4.5 ml. of 85% acid, was added and the mixture was shaken for 30 min. at room temperature. The lead phosphate was filtered off and the acetone solution was concentrated *in vacuo* and cooled to −15°C. The crude crystals obtained on filtration were sublimed at 5μ pressure and a bath temperature of 60–80°C. to yield 0.85 gm. of pure triose-reductone-C^{14}, m.p. 153°C.

For determination of their radioactivity the samples of D-glucose-1-C^{14} and triose-reductone-C^{14} were combusted in an apparatus used for carbon–hydrogen microdeterminations. The carbon dioxide was converted to barium carbonate, which was plated by filtration on paper disks and counted at infinite thickness. A parallel determination was always carried out by combusting a sample with Van Slyke solution and measuring the activity of the carbon dioxide in a gas phase counter. The results obtained are listed in Table I.

In calculating the contribution of the different carbon atoms of D-glucose to the formation of triose-reductone, the following considerations were made: the maximum activity possible for triose-reductone is twice the activity of the hexose, and this value is attained through direct conversion of only carbons 1, 2, and 3 to reductone. In experiment 1, for example, the maximum theoretical value is 38.9×2, or 77.8 mμc./mM. CO_2. The activity of the derived reductone was 42.8 mμc./mM. CO_2. Hence carbons 1, 2, and 3 of D-glucose contributed $(42.5/77.8) \times 100$, or 55.1% of the yield of the reductone. Dilution of the activity of the reductone from the maximum to the observed value was due, therefore, to the contribution of carbons 4, 5, and 6 (44.9%).

Large Scale Preparation of Triose-reductone

In general the preparation was carried out as described for the triose-reductone-C^{14}. For the fragmentation of kilogram quantities of D-glucose it was advantageous to heat the solution by blowing in steam and to add the sodium hydroxide when the D-glucose solution had reached 87–88°C. Addition at higher temperatures was dangerous since the reaction mixture tended to boil vigorously. After neutralization the solution was cooled with crushed ice, 2–3 kgm., and the triose-reductone lead salt isolated by allowing it to settle and decanting the supernatant. The salt was washed in succession with water, acetone, and ether, always allowing the salt to settle and decanting the supernatant. This procedure required several hours but resulted in a purer lead salt since a cake obtained on filtration could not be washed efficiently. The crude triose-reductone isolated from the lead salt was sublimed in 20–30 gm. batches. One thousand grams of D-glucose yielded 32–35 gm. of pure triose-reductone.

Determination of Glycerol in the Reaction Mixture of D-Glucose with Alkali

D-Glucose, 25 gm., treated as described for D-glucose-1-C^{14}, yielded a dark brown solution after the lead salt of triose-reductone was filtered off. This solution was concentrated *in vacuo* to a thin sirup and extracted continuously with ethyl acetate. The ethyl acetate extract and the original sirup were examined for the presence of glycerol (8). None could be detected. Addition of known amounts of glycerol to the sirup showed that the limit of identification (5γ) and the limit of concentration (1:10,000) of glycerol was the same in the presence of sugars as in pure glycerol solutions.

ACKNOWLEDGMENT

The technical assistance of J. A. Baignee and J. Dyck is gratefully acknowledged.

REFERENCES

1. BERNIER, C. L. Ph.D. Thesis, The Ohio State University, Columbus, Ohio. 1935.
2. BUSCH, K. G. A., CLARK, J. W., GENUNG, L. B., SCHROEDER, E. F., and EVANS, W. L. J. Org. Chem. 1: 1. 1936.
3. EULER, H. v. and HASSELQUIST, H. Arkiv Kemi, Mineral. Geol. 26, A: No. 25. 1949.
4. EULER, H. v. and HASSELQUIST, H. *In* Reductone, Sammlung chemischer und chemisch-technischer Vorträge. *Edited by* R. Pummerer-Erlangen. Verlag Ferd. Enke, Stuttgart. 1950. p. 10.

5. EULER, H. v., HASSELQUIST, H., and HANSHOFF, G. Arkiv Kemi, 6: 471. 1953.
6. EULER, H. v. and MARTIUS, C. Svensk Kem. Tidskr. 45: 73. 1933.
7. EVANS, W. L. Chem. Revs. 31: 537. 1942.
8. FEIGL, F. *In* Qualitative analysis by spot tests. 3rd ed. *Translated by* R. E. Oesper. Elsevier Publishing Company, Inc., New York. 1946. p. 408.
9. GIBBS, M. J. Am. Chem. Soc. 72: 3964. 1950.
10. NEF, J. U. Ann. 357: 214. 1907; 376: 1. 1910.
11. NEUBERG, C. Chem. Ber. 68, B: 505. 1935.
12. PETUELY, F. and BAUER, H. F. Monatsh. Chem. 83: 758. 1952.
13. PETUELY, F. and MEIXNER, N. Chem. Ber. 86: 1255. 1953.
14. SCHMIDT, O. Chem. Revs. 17: 137. 1935.
15. SOWDEN, J. C. and KUENNE, D. J. J. Am. Chem. Soc. 75: 2788. 1953.
16. SOWDEN, J. C. and SCHAFFER, R. J. Am. Chem. Soc. 74: 505. 1952.
17. WEYGAND, F. Arkiv Kemi, 3: 11. 1950.
18. WOLFROM, M. L. and SCHUMACHER, J. N. J. Am. Chem. Soc. 77: 3318. 1955.

LIGHT ABSORPTION STUDIES

PART II. ULTRAVIOLET ABSORPTION SPECTRA OF SUBSTITUTED BENZOIC ACIDS AND PHENYL BENZOATES[1]

By W. F. Forbes and M. B. Sheratte

ABSTRACT

The spectra of a number of substituted benzoic acids, acetanilides, and phenyl benzoates are discussed in terms of the electronic and steric effects of substituents.

INTRODUCTION

The absorption band observed in the 230 mμ region of the absorption spectrum, and designated by Moser and Kohlenberg (12) as the B-band, is of interest in the *ortho*-substituted benzoic acids, since the usual explanation of the steric effect due to an *ortho*-substituent must be modified in order to account for the observed spectra.

The formula of benzoic acid may be written in two forms, one possessing an intact carboxyl group (type IA), the other a hydrogen-bridged structure (type IB). On steric considerations alone, neither form accounts satisfactorily

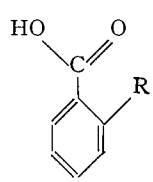

IA

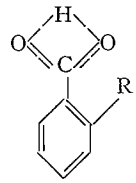

IB

for all of the *ortho*-substituted benzoic acid spectra (see Table I). For example, supposing *o*-toluic acid exists as structure IA (R = Me), no unusual loss of intensity should be apparent since a similar conformation may be shown to be relatively insensitive to steric effects involving excited states only in *o*-methylacetophenone (8), where the OH group of IA is replaced by a methyl group. In *o*-toluic acid, however, there is observed a pronounced hypsochromic shift accompanied by almost complete loss of intensity of absorption as compared to *p*-toluic acid. Similarly, if IB (R = Me) alone were the correct configuration, and one *ortho*-methyl substituent was to produce a twist in the carbon–carbon linkage sufficient to accommodate the substituent, a second methyl substituent in the other *ortho*-position would not be expected to bring about much further change in the observed spectrum. However, in 2,6-dimethylbenzoic acid the band in this region has disappeared completely (12).

Hence it may be concluded that the observed changes in the B-band of the spectra of substituted benzoic acids are primarily due to the *electrical* effects of substituents, which is not unexpected since an isolated C=O group is known

[1]*Manuscript received August 9, 1955.*
Contribution from the Department of Chemistry, Memorial University of Newfoundland, St. John's, Newfoundland.

to be relatively small. Thus only very bulky substituents in the *ortho*-position would be expected to make steric overlap the primary factor in the observed changes of the spectra.

Electrical effects may be divided into *inductive* effects, and *mesomeric* (or resonance) effects. Bearing in mind the geometrically small hydroxyl group in benzoic acids, the *inductive* effect would be of greater importance in the *ortho*-position. Mesomeric effects are generally considered to be of equal importance in *ortho*- and *para*-positions. Of the substituents discussed here, methyl groups have a positive inductive effect (i.e. they repel electrons) while nitro, hydroxyl, and methoxyl groups, and halogens exert a negative inductive effect, the halogens being in the order F > Cl > Br > I. Only the nitro group exerts a negative mesomeric effect, while all the other groups referred to exert a positive mesomeric effect; the positive mesomeric effect of the halogens is in the order I > Br > Cl > F.

ULTRAVIOLET ABSORPTION SPECTRA

Para-substituted Benzoic Acids

Table I shows that all *para*-substituted benzoic acids, with the exception of *p*-nitrobenzoic acid, exhibit pronounced bathochromic shifts accompanied by enhanced intensity of absorption which are both approximately parallel to the *mesomeric* effect of the substituent, for example I > Br > Cl > F. The *inductive* effect in *para*-halogen compounds appears to be of secondary importance, since both the bathochromic shifts and the observed intensities of absorption may be correlated with the *mesomeric* effect, but not with the *inductive* effect of the substituent. In the above-mentioned example, the latter would suggest, in both bathochromic shifts and intensities, an order F > Cl > Br > I. In this connection the reported value of the absorption maximum for *p*-bromobenzoic acid (12), i.e. λ_{max} 240 mμ, ϵ = 12,500, appeared to us to be slightly inaccurate with respect to the intensity at maximal absorption and a careful redetermination gave a value of ϵ = 16,000 at 238.5 mμ, the wave-length of

TABLE I

ABSORPTION SPECTRA OF SUBSTITUTED BENZOIC ACIDS IN ABSOLUTE ETHANOL
Wave-lengths and intensities of the B-band maxima (values in italics represent inflections)

Acid	Position of substituent					
	Ortho		Meta		Para	
	λ_{max}, mμ	ϵ_{max}	λ_{max}, mμ	ϵ_{max}	λ_{max}, mμ	ϵ_{max}
Benzoic			(227	11000)		
Toluic* (12)	228	5000	232	9000	236	14,000
Fluorobenzoic	223	9500	225	10000	228	11,000
Chlorobenzoic* (12)	*229*	*5000*	230	8500	234	15,000
Bromobenzoic* (12)	*224*	*6500*	*225*	*8500*	238.5	16,000†
Iodobenzoic	*233*	*7000*	284	9500	252	17,000
Hydroxybenzoic* (12)	236	7500	236	6000	251	12,500
Anisic* (12)	230	6000	230	7000	249	14,000
Nitrobenzoic	~*255*	*3500*	255	7500	258	11,000

* *Values in 95% ethanol.*
†*See experimental.*

maximal absorption. This value of $\epsilon = 16{,}000$, as expected, lies between the values for the intensities at wave-length of maximal absorption of *p*-chlorobenzoic acid ($\epsilon = 15{,}000$) and *p*-iodobenzoic acid ($\epsilon = 17{,}000$) (see Table I).

p-Nitrobenzoic acid, because of the negative *mesomeric* effect of the nitro group, does not exhibit any enhanced intensity of absorption, and the spectrum resembles that of nitrobenzene itself (see below).

Meta-substituted Benzoic Acids

For *meta*-substituted benzoic acids, according to the above hypothesis, the *inductive* effect increases in importance, owing to the greater proximity of the heteroatoms and the more effective transmission of the electron release (or *mesomeric* effect) to the *ortho*- and *para*-positions. This will normally prevent the *mesomeric* effect of the substituent from making its contribution, and the molecular spectrum resembles that of the unsubstituted benzoic acid, but with a slightly decreased absorption intensity owing to the adverse *inductive* effect. Appreciable changes in the location of maximal absorption are observed only for *m*-iodo- and *m*-nitro-benzoic acid, and this may be ascribed to the characteristic behavior of iodo atoms and nitro groups. In the iodobenzoic acids the interaction of the carboxyl group and the iodo atom is readily apparent. The *meta*-compound, compared to the *para*-compound, exhibits appreciable loss of intensity of absorption together with a pronounced change in the location of maximal absorption. This is of interest since in that region 2-iododiphenyl also exhibits a similar unusual absorption band—for a compound containing an iodophenyl group—which becomes apparent under conditions of slight steric strain (7). In the nitrobenzoic acids, the carboxyl groups, from an electrical point of view, appear to be of relatively little consequence. The spectrum of *p*-nitrobenzoic acid is altered as might have been expected from steric considerations, namely the *meta*-compound exhibits an hypsochromic shift accompanied by loss of intensity of absorption, and neither spectrum is radically different from that of nitrobenzene which was found to absorb maximally at 258 mμ, $\epsilon = 8500$. A fuller discussion of these effects, together with a semiquantitative examination of various theoretical formulas to account for these effects, will be the subject of a separate communication.

A similar explanation, that is in terms of steric factors, holds for the spectra of toluic acids, in which the *inductive* effect of the substituent is small. This steric effect becomes readily apparent in *increasing* magnitude *ortho* > *meta* > *para*. The increased sensitivity of benzoic acids to steric effects, compared with acetophenones, is ascribed to the more appreciable concentration of electrons *in the excited state* of the benzoic acid in the carboxyl group as compared with the acetyl group, and/or less double bond character in the carbon–carbon linkage. Thus the hindrance occurs chiefly in the excited state, which, as has previously been pointed out (8), explains the observation that the steric effect consists chiefly of decreased absorption intensity rather than of a pronounced hypsochromic shift of the band. The intermediate steric effect of the methyl group in the *meta*-position may be accounted for by the known but-

tressing effect of a methyl group in that position (3), that is the methyl group exerting a buttressing effect on the *ortho*-hydrogen atom which in turn sterically interacts with the carboxyl group.

The spectrum of benzoic acid may now also be correlated with other spectra in accordance with the above hypothesis. Benzoic acid absorbs maximally with smaller intensity of absorption than acetophenone and this may again be ascribed to steric inhibition of resonance *in the excited state* due to the *ortho*-hydrogen atoms. Both acetophenone and benzoic acid from dipole moment and X-ray crystallographic data (both of which measure ground state contributions only) appear to be planar, or nearly planar, in the ground state (4, 5, 14), which corroborates the postulated hindrance in the excited state. The steric hindrance in benzoic acid would therefore be expected to give rise to reduced absorption intensity and a slight hypsochromic shift. However, the ground state of benzoic acid is more stabilized by resonance forms than that of acetophenone, because the replacement of the methyl group in acetophenone, or the hydrogen atom in benzaldehyde, by the hydroxyl group of benzoic acid aids the setting up of polar excited states because of the negative *inductive* effect of the hydroxyl group; thus the energy level of the ground state of benzoic acid is reduced relative to that of acetophenone, and this together with the relative *increase* in the energy level of the excited state of benzoic acid with respect to acetophenone gives rise to a considerably greater energy difference in benzoic acid between the ground state and the excited state. Thus benzoic acid absorbs maximally at much shorter wave-length and lower intensity (227 mμ, ϵ = 11,000) than either acetophenone (240 mμ, ϵ = 12,500) or benzaldehyde (244 mμ, ϵ = 13,000).

Ortho-substituted Benzoic Acids

Although as Moser and Kohlenberg (12) point out—from evidence involving comparisons with van der Waals radii—shifts in the wave-lengths of the B-band should not be assigned only to steric interference with coplanarity, the conclusion that the recorded values of maximal absorption of the *ortho*-substituted benzoic acids can best be rationalized by consideration of the steric factors involved appears to us irrefutable. Also van der Waals radii are rather unsatisfactory as a measure of *intra*molecular interference properties of atoms, particularly for groups containing heteroatoms whose electronegativity largely differs from that of the carbon atom. Heteroatoms may give rise to appreciable *mesomeric* and *inductive* effects, the latter especially affecting any semiquantitative interpretation of the values.

Toluic acids have already been discussed. It is supposed that both benzoic and *o*-toluic acid and possibly also 2,6-dimethylbenzoic acid are near-planar in the ground state, but the permitted planar or near-planar excited states are sharply reduced in the order benzoic acid > *ortho*-toluic acid > 2,6-dimethylbenzoic acid.

All the other above-mentioned *ortho*-substituted benzoic acids also show the expected hypsochromic shift of the absorption maxima accompanied by loss of intensity of absorption compared with the corresponding *para*-substituted compound.

Acetanilides

Applying this hypothesis to the recently investigated ultraviolet absorption spectra of acetanilides (15; see Table II) it is seen that the data correspond with the generalizations made. Thus acetanilide itself, to which the steric

TABLE II

ABSORPTION SPECTRA OF SUBSTITUTED ACETANILIDES IN ABSOLUTE ETHANOL ACCORDING TO UNGNADE (15)
Wave-lengths and intensities of the main maxima

Acetanilide	Position of substituent					
	Ortho		Meta		Para	
	λ_{max}, mμ	ϵ_{max}	λ_{max}, mμ	ϵ_{max}	λ_{max}, mμ	ϵ_{max}
Acetanilide			(242	14,500)		
Methyl-	230	6500	245	14,000	245	15,000
Fluoro-	239	12500	242	15,100	240	13,000
Chloro-	240	10500	245	14,900	249	18,000
Bromo-	234	7500	246	14,000	252	18,500
Iodo-	Shoulder		246	13,500	254	23,000
Methoxy-	244	10500	245	11,500	249	15,000
Nitro-	233	17000	242	22,500	222	13,000

considerations referred to under benzoic acid do not apply, absorbs maximally in a similar manner to acetophenone, because of transitions involving polar excited states of type II (13). In *para*-substituted acetanilides, the shifts in the locations of maximal absorption and intensity changes again generally

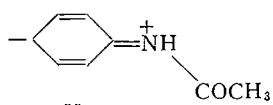

II

correspond to the *mesomeric* effect of the substituents, for example I > Br > Cl > F. The *para*-nitro group gives rise to a pronounced hypsochromic shift because of the negative *mesomeric* effect of the nitro group and interaction with the $NHCOCH_3$ group (compare Table I for the spectrum of *p*-nitrobenzoic acid, where there appears to be no interaction).

For *meta*-substituted acetanilides, because of the *ortho–para* directive properties of the $NHCOCH_3$ group, that is its powerful electron-releasing properties, the spectra will even more resemble that of the unsubstituted acetanilide than was the case for *meta*-substituted benzoic acids. An exception is provided by the *m*-nitroacetanilide where the combination of a negative *inductive* effect together with the negative *mesomeric* effect of the nitro group appears to stabilize excited states of type II, thus giving rise to considerably increased intensity of absorption. Steric effects also become noticeable in some of the compounds, particularly where the substituent is large, such as in *m*-bromo- or *m*-iodo-acetanilide (see Table II). The nitroacetanilides as described above are of special interest. The negative *mesomeric* effect of the nitro group lessens the electron density of all ring carbon atoms, but the

ortho- and *para*-positions are deactivated almost exclusively, leaving the *meta*-position with the greatest concentration of electrons. Thus the *meta*-nitro compound exhibits the largest absorption intensity. It is tentatively proposed that in *o*-nitroacetanilide the steric hindrance of the *ortho*-substituents inhibits the deactivation mechanism and thus the spectrum of the *ortho*-compound reverts to a spectrum where the opposing *mesomeric* effect of the nitro group is less noticeable (see Table II).

In the other *ortho*-substituted acetanilides, steric effects play their expected part. This steric *ortho*-effect is generally strikingly similar to that observed in substituted benzoic acids and thus lends additional support to the proposed polar excited states of type II; comparison of Tables I and II indicates this, as for instance the halogen-substituted compounds, where the combination of *mesomeric*, *inductive* and steric effects gives rise to similar spectra. Discussing *ortho*-substituted acetanilides, Ungnade (15) states that there are no steric effects in *o*-methoxyacetanilide, but we believe that a steric effect hypothesis accounts more satisfactorily for the observed spectrum. Ungnade argues that although the primary band of *o*-methoxyacetanilide is somewhat less intense than that of the *meta*-isomer, the order of intensities is reversed for the secondary bands and the wave-lengths of corresponding bands in the *ortho-* and *meta*-isomers are virtually identical. In our view, the *ortho*-compound exhibits a typical steric effect of a type which has been discussed fully elsewhere (3, 4, 8), in which the location of maximal absorption remains approximately the same, while the intensity of absorption is reduced. This effect becomes readily apparent if the *ortho*-compound is compared with the corresponding *para*-compound rather than with the *meta*-compound. This seems justified, since it has been shown in the study of acetophenones (4, 8) that the former comparison has greater validity. We would propose a similar steric effect for the anisidine spectra referred to by Ungnade (15). Further, since it has been shown in a number of other examples (12, 8) that the secondary band is not apparently affected by steric interference of resonance, we would not expect the secondary band to exhibit a corresponding steric effect.

Aromatic Esters

In the light of these hypotheses an examination of the spectra reported by Cilento (6) and the extension of this work to a number of other esters appeared to be of interest. The spectrum of phenyl benzoate we explain as follows: The spectrum of benzoic acid compared to acetophenone has been correlated by the *inductive* effect of the hydroxyl group and by consideration of steric factors operative largely in the excited state of benzoic acid. This steric effect in benzoic acid, postulated to be due to a concentration of electrons in the carboxyl group, is reduced somewhat in phenyl benzoate since the phenyl group attached to the oxygen atom (henceforth referred to as ring B in accordance with Cilento's nomenclature) is an electron-attracting group. It therefore removes some of the electrons responsible for the steric effect, and hence transitions to excited states of type III are aided, accounting for the increased intensity of absorption and the slight bathochromic shift. The value for the observed absorption intensity, however, also includes some absorption

TABLE III

ABSORPTION SPECTRA OF AROMATIC ESTERS AND REFERENCE COMPOUNDS IN ABSOLUTE ETHANOL
Wave-lengths and intensities of the main maxima (values in italics represent inflections)

Compound	Substituent in:		Ring A band		Ring B band	
	Ring A	Ring B	λ_{max}, mμ	ϵ_{max}	λ_{max}, mμ	ϵ_{max}
(Benzoic acid)			(227	11,000)		
Phenyl benzoate	—	—	230	15,000	*~274*	*2000*
Phenyl *p*-chlorobenzoate	*p*-Chloro	—	242	20,000	—	—
Phenyl *p*-iodobenzoate	*p*-Iodo	—	259	21,000	—	—
Phenyl *p*-anisate (6)	*p*-Methoxy	—	261	22,000	—	—
Phenyl *p*-nitrobenzoate (6)	*p*-Nitro	—	259	15,500	*~305*	*2500*
p-Nitrophenyl *p*-anisate (6)	*p*-Methoxy	*p*-Nitro	276	27,400	—	—
p-Nitrophenyl *p*-nitrobenzoate (6)	*p*-Nitro	*p*-Nitro	266	20,600	—	—
p-Anisyl benzoate (6)	—	*p*-Methoxy	228	19,400	275	5000
p-Anisyl *p*-anisate (6)	*p*-Methoxy	*p*-Methoxy	261	23,500	—	—
p-Anisyl *p*-nitrobenzoate (6)	*p*-Nitro	*p*-Methoxy	258	15,500	*~300*	*4000*
p-Chlorophenyl *p*-chlorobenzoate	*p*-Chloro	*p*-Chloro	249	22,000	*274*	*3000*
p-Iodophenyl *p*-iodobenzoate	*p*-Iodo	*p*-Iodo	260	22,000	—	—
m-Anisyl benzoate	—	*m*-Methoxy	225	17,000	271	3500
m-Anisyl *p*-anisate	*p*-Methoxy	*m*-Methoxy	259	21,000	—	—
m-Anisyl *p*-nitrobenzoate	*p*-Nitro	*m*-Methoxy	256.5	20,000	*~295*	*3000*
p-Chlorophenyl benzoate	—	*p*-Chloro	232	17,500	*~273*	*2500*
p-Iodophenyl benzoate	—	*p*-Iodo	233	23,800	*~270*	*4000*
p-Nitrophenyl benzoate (6)	—	*p*-Nitro	235	14,100	270	14300
	Cyclohexane ring					
Phenyl cyclohexane-carboxylate	—	—	—	—	258	2500
p-Nitrophenyl cyclohexanecarboxylate	—	*p*-Nitro	—	—	268	10000
p-Anisyl cyclohexanecarboxylate	—	*p*-Methoxy	—	—	275	2000
m-Anisyl cyclohexanecarboxylate	—	*m*-Methoxy	—	—	273	3000

due to ring B, that is, due to transitions involving excited states of type IV. In agreement with Cilento we ascribe bands to transitions involving either ring A or ring B, although both bands will be influenced by the neighboring ring.

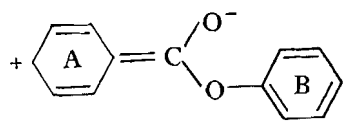

III

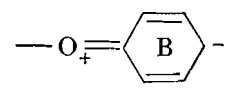

IV

From Tables I and III it is seen that substituents in ring A produce changes as might be expected from a consideration of the corresponding benzoic acid spectra. Since the *para*-substituent on account of its *mesomeric* effect will also influence the electron density in the carboxyl group, the change due

to the introduction of the B-ring phenyl group will also be affected. However, in most cases, these additional changes from the benzoic acids to the corresponding phenyl esters are similar and roughly the same as between benzoic acid and phenyl benzoate, that is, a wave-length shift $\Delta\lambda$ of about 3 mμ and intensity increase $\Delta\epsilon$ of approximately 4000. The greatest change is observed in the *para*-methoxy compound ($\Delta\lambda_{max}$ 12 mμ, $\Delta\epsilon$ = 8000) which may be ascribed to a combination of favorable *mesomeric* and *inductive* effects stabilizing resonance forms of type III. The smallest change occurs in the *para*-nitro compound ($\Delta\lambda_{max}$ 1 mμ), presumably because of the negative *mesomeric* effect of the nitro group.

With a view to investigating the conjugation of the non-bonding *p*-electrons of the oxygen atom and the π-electrons of the B-ring, which Cilento considers to be rather weak, we may consider a number of compounds in which this conjugation might manifest itself. Taking phenyl *p*-anisate as an example where conditions favoring this conjugation already exist, we should expect the introduction of a *para*-nitro group in the B-ring to enhance this effect; the nitro group by withdrawing electrons from the B-ring should stabilize polar excited states of type III. This in fact occurs, and a further bathochromic shift relative to phenyl *p*-anisate accompanied by increased intensity of absorption is observed. Cilento (6) classifies this band separately, but this seems to us to be unnecessary, since we believe it to be due to what is essentially the same type of transition. Introduction of a *para*-nitro group in the B-ring generally would be expected to give rise to a similar effect, and a second example is in fact provided by *p*-nitrophenyl *p*-nitrobenzoate where this change is again observed on comparison with the parent compound, that is phenyl *p*-nitrobenzoate. In these compounds the B-band is not apparent since its maximal absorption closely approximates that of the A-band (see Table III). This was confirmed by determining the maximal absorption of *p*-nitrophenyl cyclohexanecarboxylate, which as expected absorbs maximally in the same region (λ_{max} 268 mμ, ϵ = 10,000). Occasionally the ester spectra exhibit the absorption due to the B-ring as maximal absorption, but often this occurs as an inflection. It seems to us unfortunate that Cilento does not record these inflections, that is the submerged maxima, in his table (6), even though the absorption in that region includes some absorption due to the secondary band of ring A.

Reversing the substituents in the above examples has the expected effect. A *para*-methoxy group in the B-ring, because of its *mesomeric* effect, causes a slight hypsochromic shift relative to phenyl benzoate. This is ascribed to the increased electron-availability in the carboxyl group, which enhances the steric effect in that area. The intensity of absorption does not exhibit the expected decrease, since the increased intensity of absorption due to ring B outweighs the supposed decrease accompanying the hypsochromic shift. An analogous effect is observed in *p*-anisyl *p*-anisate relative to phenyl *p*-anisate and in *p*-anisyl *p*-nitrobenzoate relative to phenyl *p*-nitrobenzoate (see Table III). In B-ring *para*-halogen substituted compounds an intermediate effect is observed; the *para*-substituent does bring about a bathochromic shift, which, however, is smaller than that observed for a *para*-nitro substituent in ring B

(see Table III for the spectra of *p*-chlorophenyl *p*-chlorobenzoate and *p*-iodophenyl *p*-iodobenzoate compared to those of phenyl *p*-chlorobenzoate and phenyl *p*-iodobenzoate respectively). This is readily explained by the intermediate *mesomeric* effects in these compounds.

Meta-methoxy substituents in the B-ring produce a low-intensity band in the 270–280 mμ region. This band is not appreciably influenced by an unsubstituted A-ring as may be seen from the similar B-ring absorption bands in the spectra of *m*-anisyl benzoate and *m*-anisyl cyclohexanecarboxylate. Substituents in the A-ring, however, again give rise to the preferential absorption of the A-ring band (see Table III for the spectra of *m*-anisyl *p*-anisate and *m*-anisyl *p*-nitrobenzoate) which masks the low-intensity absorption due to the B-band.

Finally a number of other B-ring substituted esters are listed in Table III. Sometimes the absorption due to the B-ring is negligible, and the absorption due to the A-ring almost completely predominates as in *p*-chlorophenyl or *p*-iodophenyl benzoates; compounds like *p*-nitrophenyl benzoate, on the other hand, serve as examples where the two bands are of almost the same intensity.

EXPERIMENTAL

The ultraviolet absorption spectra were determined in duplicate by standard methods using a Unicam SP 500 spectrophotometer as described in Part I (8).

Melting points are uncorrected; analyses were carried out in the microanalytical laboratory (Mr. F. H. Oliver) of the Department of Organic Chemistry, Imperial College, London, England, and in the microanalytical laboratory (Mr. A. Bernhardt) of the Max-Planck Institut für Kohlenforschung, Mülheim, Ruhr, Germany.

Benzoic Acids

The commercially available compounds were crystallized to constant melting point and intensity of absorption. *o*-Fluoro-, *m*-fluoro-, *p*-bromo-, and *m*-nitro-benzoic acids were obtained by the oxidation with permanganate of the appropriate toluene according to the method described by Vogel (16). *p*-Bromobenzoic acid had melting point 251–253° (Heilbron and Bunbury (10) give melting point 251–253°). Anal.: Calc. for $C_7H_5O_2Br$: Br, 39.75%. Found: Br, 40.1%. Light absorptions in ethanol: see Table I.

Phenyl Benzoates

The esters were prepared by standard methods. Solid esters were crystallized from methanol or aqueous methanol to constant melting point and intensity of absorption; liquid esters were distilled to constant refractive index and intensity of absorption.

Phenyl benzoate crystallized as prisms, melting point 70° (Heilbron and Bunbury (10) give melting point 71°); phenyl *p*-chlorobenzoate crystallized as plates, melting point 100° (Birkenbach and Meisenheimer (2) give melting point 100°); *phenyl p-iodobenzoate* crystallized as plates, melting point 133°.

Anal.: Calc. for $C_{13}H_9O_2I$: C, 48.2; H, 2.8; I, 39.15%. Found: C, 47.9; H, 2.6; I, 39.0%. *p*-Chlorophenyl *p*-chlorobenzoate crystallized as plates, melting point 71° (Birkenbach and Meisenheimer (2) give melting point 71°); *p-iodophenyl p-iodobenzoate* crystallized as plates, melting point 148°. Anal.: Calc. for $C_{13}H_8O_2I_2$: C, 34.7; H, 1.8; I, 56.4%. Found: C, 34.7; H, 2.1; I, 56.1%. *m-Anisyl benzoate* distilled at 163°, 3 mm., n_D^{27} 1.5751. Anal.: Calc. for $C_{14}H_{12}O_3$: C, 73.7; H, 5.3%. Found: C, 73.9; H, 5.5%. *m-Anisyl p-anisate* crystallized as prisms, melting point 102°. Anal.: Calc. for $C_{15}H_{14}O_4$: C, 69.75; H, 5.5%. Found: C, 69.95; H, 5.7%. *m-Anisyl p-nitrobenzoate* crystallized as needles, melting point 126°. Anal.: Calc. for $C_{14}H_{11}O_5N$: C, 61.5; H, 4.1; N, 5.1%. Found: C, 61.4; H, 4.3; N, 4.9%. *p*-Chlorophenyl benzoate crystallized as needles, melting point 87° (Autenrieth and Müllinghaus (1) give melting point 86°); *p*-iodophenyl benzoate crystallized as needles, melting point 119° (Willgerodt and Wiegand (17) give melting point 118.5–119.5°).

The light absorption properties of the above-described compounds are recorded in Table III.

Phenyl Cyclohexanecarboxylates

Cyclohexanecarboxylic acid was prepared from cyclohexyl chloride according to the method of Gilman and Zoellner (9) and distilled at 179°, 17 mm.; n_D^{30} 1.4620 as a colorless liquid, which solidified on standing to a solid, melting point 28° (Hiers and Adams (11) give boiling point 105°, 4 mm.; n_D^{38} 1.4520; melting point 29–30°). The esters were prepared in the above-described manner.

Phenyl cyclohexanecarboxylate distilled at 129°, 3 mm.; n_D^{27} 1.5107. Anal.: Calc. for $C_{13}H_{16}O_2$: C, 76.4; H, 7.9%. Found: C, 76.5; H, 8.0%. *p-Nitrophenyl cyclohexanecarboxylate* crystallized as needles, melting point 53.5°. Anal.: Calc. for $C_{13}H_{15}O_4N$: C, 62.6; H, 6.1; N, 5.6%. Found: C, 62.3; H, 5.9; N, 5.7%. *p-Anisyl cyclohexanecarboxylate* crystallized as needles, melting point 64°. Anal.: Calc. for $C_{14}H_{18}O_3$: C, 71.8; H, 7.7%. Found: C, 71.5; H, 7.8%. *m-Anisyl cyclohexanecarboxylate* distilled at 80°, 3 mm.; n_D^{28} 1.5460. Anal.: Calc. for $C_{14}H_{18}O_3$: C, 71.8; H, 7.7%. Found: C, 72.0; H, 7.9%.

The light absorption properties in ethanol of the above-described compounds are recorded in Table III.

ACKNOWLEDGMENTS

The authors gratefully acknowledge a research grant from the National Research Council of Canada. They are also much indebted to Professor E. A. Braude and Dr. H. J. Anderson for discussions concerning this and the preceding part of these studies.

REFERENCES

1. Autenrieth, W. and Müllinghaus, P. Ber. 39: 4102. 1906.
2. Birkenbach, L. and Meisenheimer, K. Ber. 69: 723. 1936.
3. Braude, E. A. and Forbes, W. F. J. Chem. Soc. In press. 1955.
4. Braude, E. A., Sondheimer, F., and Forbes, W. F. Nature, 173: 117. 1954.
5. Brooks, C. S. and Hobbs, M. E. J. Am. Chem. Soc. 62: 2851. 1940.

6. CILENTO, G. J. Am. Chem. Soc. 75:3748. 1953.
7. DUNN, T. M. and IREDALE, T. J. Chem. Soc. 1592. 1952.
8. FORBES, W. F. and MUELLER, W. A. Can. J. Chem. 33:1145. 1955.
9. GILMAN, H. and ZOELLNER, E. A. J. Am. Chem. Soc. 53:1945. 1931.
10. HEILBRON, Sir I. and BUNBURY, H. M. Dictionary of organic compounds. Eyre & Spottiswoode Ltd., London. 1946.
11. HIERS, G. S. and ADAMS, R. J. Am. Chem. Soc. 48:2385. 1926.
12. MOSER, C. and KOHLENBERG, A. I. J. Chem. Soc. 804. 1951.
13. PICARD, J. P. and MCKAY, A. F. Can. J. Chem. 31:896. 1953.
14. SIM, G. A., MONTEATH ROBERTSON, J., and GOODWIN, T. H. Acta Cryst. 8:157. 1955.
15. UNGNADE, H. E. J. Am. Chem. Soc. 76:5133. 1954.
16. VOGEL, A. I. A textbook of practical organic chemistry. Longmans, Green & Co., Ltd., London. 1951. p. 720.
17. WILLGERODT, C. and WIEGAND, G. Ber. 42:3768. 1909.

PHOTOLYSIS OF DIETHYL KETONE AT LOW PRESSURES: THE PRESSURE DEPENDENCY OF THE COMBINATION OF ETHYL RADICALS[1]

By R. K. Brinton[2] and E. W. R. Steacie

ABSTRACT

The photolysis of diethyl ketone has been investigated in the pressure range 0.01–30 mm. at 100°, 150°, 200°, and 250° with a variation in absorbed intensity of 1000-fold. Over this wide variation in experimental conditions the kinetics of the reaction show excellent agreement with the mechanism of Kutschke, Wijnen, and Steacie. Under conditions where the production of ethylene by decomposition of the pentanonyl radical was negligible (high light intensity and low ketone pressure), the ratio of the rate of ethylene formed to the rate of butane produced was determined to be 0.12 independent of the temperature. These data indicate that both the disproportionation and combination of ethyl radicals are homogeneous and pressure independent to as low as 0.01 mm. pressure. In addition it is probable that the two reactions are the result of different reaction intermediates as was postulated by Wijnen and Steacie. The abstraction reaction

$$C_2H_5+C_2H_5COC_2H_5 \rightarrow C_2H_6+C_2H_4COC_2H_5$$

showed definite heterogeneous character at low pressures similar to the analogous reaction of methyl radicals with acetone studied by Ausloos and Steacie.

INTRODUCTION

The absolute values of the rate constant for the combination of methyl radicals as determined in several independent investigations (2, 5, 10, 11) have differed significantly. Recent papers by Dodd and Steacie (3) and Kistiakowsky and Roberts (7) treat this reaction by a pressure dependent mechanism,

$$2CH_3 \leftrightharpoons C_2H_6^*$$

$$C_2H_6^*+M \rightarrow C_2H_6+M,$$

in an attempt to reconcile these apparent discrepancies. Both studies were made on the photolysis of acetone at low pressures whereby it is possible to compare the rate of ethane formation by combination to the rate of methane formed by the abstraction mechanism,

$$CH_3+CH_3COCH_3 \rightarrow CH_4+CH_2COCH_3.$$

The magnitude of the pressure effects on the relative rates of methane and ethane production can be explained for the most part by such a mechanism, but the lower pressure experiments of Dodd and Steacie indicate other anomalies which are strongly surface dependent. These latter effects have been verified by similar low pressure experiments of Ausloos and Steacie (1).

This paper reports on a similar investigation of the pressure dependency of the combination of ethyl radicals formed in the photolysis of diethyl ketone. It was expected that the experimental difficulties would be somewhat greater than in the acetone photolysis since, presumably, the more complex ethyl

[1]*Manuscript received August 26, 1955.*
Contribution from the Division of Pure Chemistry, National Research Council, Ottawa, Canada. Issued as N.R.C. No. 3777.
[2]*On leave from Department of Chemistry, University of California, Davis, California, U.S.A.*

radicals would not show the effect of third body deactivation for the combination reaction at such high pressures as observed for methyl radicals. On the other hand the disproportionation reaction of ethyl radicals into ethylene and ethane seemed to offer a more reliable comparison reaction than the abstraction reaction which most certainly is partly heterogeneous at low pressures in the case of the acetone photolysis.

EXPERIMENTAL

The photolysis apparatus was similar to that of Dodd and Steacie (3). A majority of the experiments were conducted in a cylindrical silica cell of 3.9 cm. diameter and 100 cm. length (volume = 1210 cm.^{3}, surface = 1260 cm.^{2}). Another cell of similar dimensions but having two concentrically mounted inner silica tubes (volume = 1040 cm.^{3}, surface = 3580 cm.^{2}) was used in a series of photolyses at 200° in order to evaluate the effect of increased surface and shorter diffusion distance. The method of temperature control of the cells was identical to that used by the above workers. It was possible to maintain the temperature along the cell's length to ±1°. No correction was made for that part of the reaction taking place at the cooler end windows since these cold zones represent a rather small fraction of the total reaction volume.

The light which completely filled the reaction cell in all experiments was a well-collimated beam from a B.T.H. ME/D 250 watt high pressure mercury arc operated on a regulated d-c. supply. A Corning 9-53 filter and the long wave length absorption limit of diethyl ketone limited the absorption region to λλ2800–3200 Å. A plane aluminized mirror was used at the back cell window to increase the light intensity in some of the photolyses and neutral density filters of chromel deposited on silica plates were used to decrease the intensity in other cases.

The per cent decomposition of diethyl ketone was limited in most of the experiments to 0.5 to 4%. However it was necessary to exceed this amount in those photolyses at pressures less than 0.1 mm. pressure and some decompositions were as much as 20%. In all cases the concentration of diethyl ketone used in the various calculations was the average over the run. A supplementary volume of 15 liters was used in conjunction with the photolysis cell in the photolyses under 1 mm. pressure. This additional gas supply was circulated through the reaction cell at frequent intervals during the photolysis by a mercury diffusion pump. Circulation was not carried out during irradiation since the pumping caused considerable pressure differentials within the cell system. Measurement of diethyl ketone pressure was made by a McLeod gauge.

The analytical vacuum system and the diethyl ketone circulation system employed mercury cutoffs throughout, thus eliminating possible errors due to the absorption of diethyl ketone and reaction products in stopcock grease. Photolysis products were separated by use of a Ward–LeRoy still (9) into three fractions: (*a*) CO fraction (volatile at −210°), (*b*) C_2 fraction (volatile at −175°), (*c*) C_4 fraction (volatile at −115°). These three fractions were analyzed mass spectrometrically. Fraction (*a*) was essentially pure CO. Analysis showed <0.2% CH_4 to be present. Fraction (*b*) contained C_2H_6, C_2H_4, and

traces of C_3H_8, C_3H_6, and CO_2. Fraction (*c*) was predominantly C_4H_{10} with small amounts of butene and propene in experiments carried out at high temperature and low intensity.

Eastman Kodak Company diethyl ketone was dried with anhydrous $CaSO_4$ and fractionated in a 15 plate column. Small portions of the fraction boiling from 100.8° to 101.0° (uncorrected) used as a main supply were thoroughly outgassed before each trial in the vacuum system. The perfluorodimethyl cyclohexane obtained from Halogen Chemicals Inc., Columbia, S.C., was distilled and degassed *in vacuo*.

EXPERIMENTAL RESULTS

In all about 90 runs were made at four different temperatures. The pertinent data for the experiments conducted on diethyl ketone alone are shown in Table I; those shown in Table III refer to the photolyses made in the presence of added perfluorodimethyl cyclohexane, C_8F_{16}.

TABLE I

THE RATES OF PRODUCT FORMATION IN THE PHOTOLYSIS OF DIETHYL KETONE

[D], mole cm.$^{-3}\times10^{7}$	R_{CO}	$R^{total}_{C_2H_4}$	$R^{total}_{C_2H_6}$	$R_{C_4H_{10}}$
	mole cm.$^{-3}$ sec.$^{-1}\times10^{13}$			
		100°		
0.0320	0.840	0.0875	0.0960	0.715
0.0373	1.26[6]	0.134	0.140[0]	1.09[3]
0.0961	2.47	0.268	0.292	2.12
0.0975	3.92	0.391	0.428	3.38
0.409	2.64	0.272	0.405	2.21
0.468	3.00	0.282	0.475	2.53
0.901	2.92	0.292	0.668	2.26
2.31	4.54	0.428	1.248	3.41
3.69	0.744	0.0519	0.511	0.345
4.29	0.169[0]	0.0123	0.178[8]	0.0415
4.29	0.214	0.0122	0.201	0.0520
4.29	0.772	0.0605	0.545	0.328
4.46	0.861	0.0638	0.630	0.368
4.67	1.62[5]	0.161[6]	0.986	0.835
4.29	3.48	0.307	1.56[0]	2.18
4.33	16.2[5]	1.53[4]	4.49	11.9[6]
4.29	63.2	6.25	11.9[7]	51.5
8.63	4.15	0.202	2.32	1.67[3]
		150°		
0.00345	0.475	0.0468	0.0633	0.385
0.00412	0.587	0.0490	0.0770	0.432
0.00810	1.10[0]	0.102[8]	0.129	0.908
0.194	2.85	0.249	0.298	2.40
0.0348	3.64	0.356	0.442	3.13
0.0619	6.08	0.564	0.720	5.27
0.196	7.25	0.684	1.09	6.10
0.353	7.18	0.665	1.41	5.78
0.763	1.06[5]	0.0876	0.546	0.653
3.78	0.354	0.0130	0.495	0.0352
3.76	1.63[0]	0.0930	1.67[5]	0.373
3.76	7.10	0.486	5.05	2.99
3.76	12.0[5]	0.910	7.21	5.87
3.71	66.1	5.56	22.7	45.1
3.68	199.[0]	17.6	48.9	152.[6]
8.27	6.08	0.292	6.65	1.37[5]

TABLE I (*Concluded*)

THE RATES OF PRODUCT FORMATION IN THE PHOTOLYSIS OF DIETHYL KETONE

[D], mole cm.$^{-3}\times10^{7}$	R_{CO}	$R^{total}_{C_2H_4}$	$R^{total}_{C_2H_6}$	$R_{C_4H_{10}}$
	mole cm.$^{-3}$ sec.$^{-1}\times10^{13}$			
		200°		
0.00408	0.703	0.0655	0.0934	0.567
0.00430	0.651	0.0607	0.0955	0.556
0.00425	0.575	0.0645	0.0853	0.478
0.00644	0.813	0.0795	0.116^{4}	0.704
0.00752	0.914	0.0914	0.131^{5}	0.755
0.00792	1.00^{0}	0.103^{0}	0.149^{5}	0.769
0.0170^{4}	1.94^{2}	0.186^{0}	0.268	1.69^{5}
0.0192^{1}	2.12^{0}	0.203	0.306	1.72^{1}
0.0351	4.28	0.418	0.631	3.49
0.165^{8}	8.12	0.766	1.63^{8}	6.53
0.341	6.14	0.553	2.03	4.25
1.56^{0}	2.95	0.189^{0}	2.98	0.707
1.57^{9}	148.^{8}	45.5	12.3^{6}	0.107^{0}
1.62^{9}	0.492	0.683	0.0252	0.571
3.24	6.13	6.92	0.336	0.300
5.40	308	157.8	26.2	0.153^{0}
5.52	2.86	4.25	0.139^{5}	0.623
6.84	4.03	6.11	0.143	0.382
8.81	0.513	0.904	0.0244	0.960
9.72	0.942	1.62^{2}	0.0412	1.29^{8}
10.1^{4}	43.0	49.4	2.75	0.366
10.4^{8}	4.71	7.33	0.220	1.04
11.0^{5}	454	311	36.1	0.184
		250°		
0.00273	0.638	0.0770	0.133^{0}	0.473
0.00444	1.07^{4}	0.118^{5}	0.212	0.738
0.00720	1.09^{0}	0.123	0.213	0.836
0.00806	1.66^{3}	0.181^{6}	0.307	1.32^{1}
0.169^{3}	2.96	0.316	0.531	2.41
0.0345	5.43	0.615	1.025	4.37
0.0839	9.65	1.03^{2}	2.09	7.19
0.278	27.1	2.70	8.67	18.6^{5}
0.337	6.94	0.828	3.86	3.47
0.708	2.92	0.479	2.82	0.605
1.56^{3}	147.^{3}	12.4^{0}	74.5	66.7
1.61^{5}	8.12	0.902	9.33	1.16^{6}
2.85	203	18.4^{7}	144.^{2}	86.0
6.43	4.87	0.598	7.70	0.0975
8.68	1.81^{5}	0.377	2.89	0.0240
10.0^{5}	399	32.4	422	87.2
		200° "packed cell"		
0.0114^{5}	0.456	0.0499	0.101^{6}	0.402
0.0352	1.60^{4}	0.1675	0.332	1.29^{4}
0.0933	4.17	0.419	0.898	3.43
0.0348	15.6^{5}	1.51^{6}	4.17	12.3^{0}
0.0933	40.1	3.74	14.4^{1}	28.8
2.35	87.2	7.53	40.6	52.5
4.72	154.^{0}	11.3^{0}	85.8	82.5

DISCUSSION

The Photolysis Mechanism

Recently a detailed study of the photolysis of diethyl ketone has been made

by Kutschke, Wijnen, and Steacie (8). They explained their results on the basis of the following mechanism—

[1] $$C_2H_5COC_2H_5+h\nu \xrightarrow{\phi I_a} 2C_2H_5+CO$$

[2] $$2C_2H_5 \xrightarrow{k_2} C_4H_{10}$$

[3] $$2C_2H_5 \xrightarrow{k_3} C_2H_4+C_2H_6$$

[4] $$C_2H_5+C_2H_5COC_2H_5 \xrightarrow{k_4} C_2H_6+C_2H_4COC_2H_5$$

[5] $$C_2H_5+C_2H_4COC_2H_5 \xrightarrow{k_5} C_4H_9COC_2H_5$$

[6] $$2C_2H_4COC_2H_5 \xrightarrow{k_6} [C_2H_4COC_2H_5]_2$$

[7] $$C_2H_4COC_2H_5 \xrightarrow{k_7} C_2H_4+C_2H_5+CO$$

If the rate of formation of a product, P, is expressed by R_P and the concentration of diethyl ketone by [D] the following expression may be derived.[3]

$$\log(R^{ab}_{C_2H_6}/R_{C_4H_{10}}) = \log(k_4/k_2^{\frac{1}{2}})+\log([D]/R^{\frac{1}{2}}_{C_4H_{10}})$$

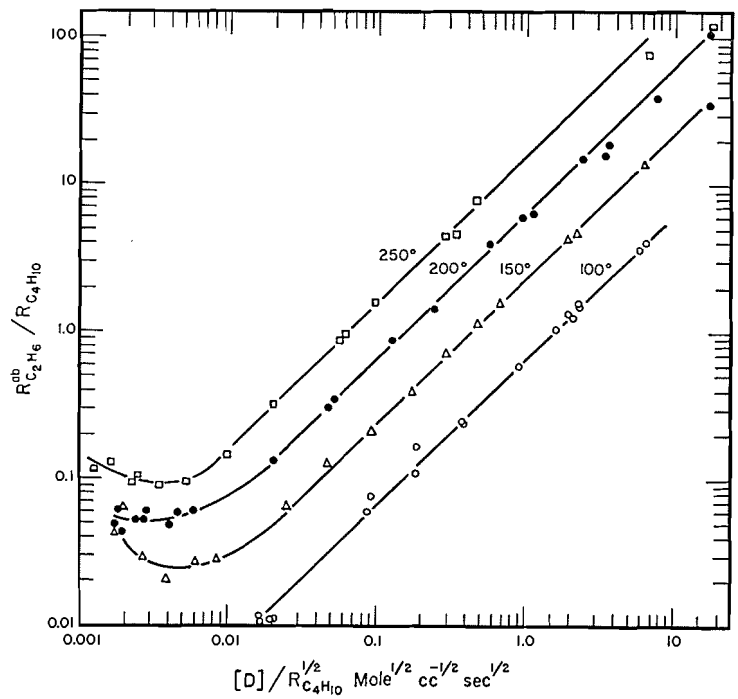

FIG. 1. Plot of $\log R^{ab}_{C_2H_6}/R_{C_4H_{10}}$ vs. $\log [D]/R^{\frac{1}{2}}_{C_4H_{10}}$.

[3] *$R^{ab}_{C_2H_6}$ represents the rate of ethane formation by the abstraction reaction [4] to differentiate it from $R^{dp}_{C_2H_6}$, the rate of ethane formed by the disproportionation reaction [3]. This quantity was calculated from the expression $R^{ab}_{C_2H_6} = R^{total}_{C_2H_6} - 0.12\ R_{C_4H_{10}}$ assuming tacitly that the ratio $k_3/k_2 = 0.12$, independent of experimental conditions. Justification for this procedure is given in the subsequent discussion. $R^{ab}_{C_2H_6}$ is greater than $\Delta R_{C_2} = R^{total}_{C_2H_6} - R^{total}_{C_2H_4}$, the rate calculated by Kutschke, Wijnen, and Steacie, by the amount of the additional ethylene produced by the decomposition of the pentanonyl radical, $C_2H_4COC_2H_5$, in reaction [7]. In most cases, however, the difference between $R^{ab}_{C_2H_6}$ and ΔR_{C_2} is small.*

The results of the present investigation are shown in Fig. 1 as a plot of $\log R^{ab}_{C_2H_6}/R_{C_4H_{10}}$ vs. $\log [D]/R^{\frac{1}{2}}_{C_4H_{10}}$. Data at the four temperatures cover the pressure range 0.01–30 mm. and represent a variation in absorbed intensity of more than 1000-fold. The series of straight lines of unit slope fit the experimental points well except at the low and high extremes of the variables. Deviations in the low region which occur at pressures under *ca.* 0.4 mm. are treated in detail in a later section; those in the high region are most pronounced at high [D] and low absorbed intensity and are apparent at the two higher temperatures only. A reasonable explanation of these latter anomalies has not been formulated but it is possible that some mode of butane formation in addition to reaction [2] is becoming significant under these conditions. This reaction seemingly must be of the type

$$R + C_2H_5COC_2H_5 \rightarrow C_4H_{10} + \text{other products}$$

where R represents some radical present in the system. Production of detectable amounts of 2-butene and a pentene (2-pentene probably) accompanying the extra amounts of butane could well be the result of the same or a closely related mechanism.

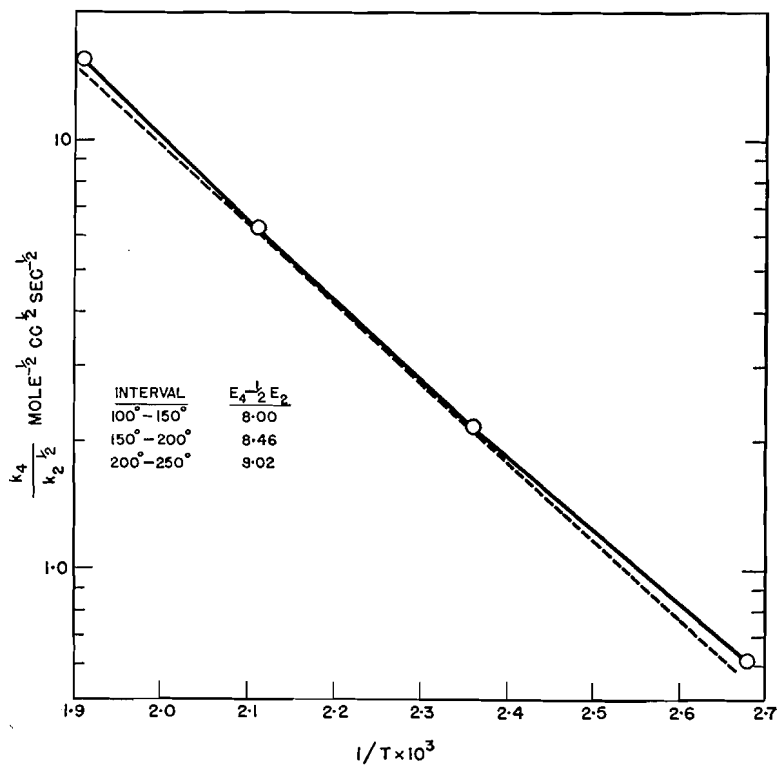

FIG. 2. Arrhenius plot of $k_4/k_2^{\frac{1}{2}}$.

Fig. 2 shows values of $\log k_4/k_2^{\frac{1}{2}}$ calculated from the straight line portions of the curves of Fig. 1 plotted vs. $1/T$. The line connecting the four points shows a

curvature so the values of $E_4-\frac{1}{2}E_2$ were calculated for each of the three intervals. These activation energies are all higher than the $E_4-\frac{1}{2}E_2 = 7.4$ kcal./mole reported by Kutschke, Wijnen, and Steacie. Reasons for these differences are not altogether clear but it may be pointed out that almost all of their experiments were conducted at ketone pressures greater than 10 mm. In this region it has been indicated that the values of $k_4/k_2^{\frac{1}{2}}$ tend to be too small at higher temperatures, and hence a calculated activation energy would be low in value. The curvature, although not large, seems to be real and is perhaps the consequence of the diethyl ketone molecules having both a primary and secondary hydrogen atom available for the abstraction process. Activation energies of these two processes would be expected to differ by several kcal./mole (13) and lead to a curvature of the type observed.

No attempt was made in the course of the study to analyze for the products of reactions [5] and [6], ethyl butyl ketone and bipentanonyl respectively. However, it is possible to calculate the rate of production of these two substances by a consideration of the balance of the radicals involved,

$$R_{CO}-R^{p}_{C_2H_4} = R_{C_4H_{10}}+R^{dp}_{C_2H_4}+R_{C_2H_5COC_4H_9}+R_{(C_2H_4COC_2H_5)_2}$$

(total radical balance)

$$R^{ab}_{C_2H_6} = R_{C_2H_5COC_4H_9}+2R_{(C_2H_4COC_2H_5)_2}+R^{p}_{C_2H_4}$$

(pentanonyl radical balance).

Then

$$\frac{R_{C_2H_5COC_4H_9}[D]}{R^{\frac{1}{2}}_{(C_2H_4COC_2H_5)_2}R^{ab}_{C_2H_6}} = \frac{k_5}{k_6^{\frac{1}{2}}k_4} \text{ and } \frac{R_{C_2H_5COC_4H_9}}{R^{\frac{1}{2}}_{(C_2H_4COC_2H_5)_2}R^{\frac{1}{2}}_{C_4H_{10}}} = \frac{k_5}{k_6^{\frac{1}{2}}k_2^{\frac{1}{2}}}.$$

Ratios of rates shown in the latter two equations have been calculated for those experiments at the three higher temperatures in which the amount of ethylene formed by reaction [7] was large enough to justify such a procedure. These ratios shown in the second and third columns of Table II have a good

TABLE II

MECHANISM VALIDITY OF THE DIETHYL KETONE PHOTOLYSIS

	$k_5/k_6^{\frac{1}{2}}k_4$, mole$^{\frac{1}{2}}$ cm.$^{-3/2}$ sec$^{\frac{1}{2}}$.	$k_5/k_6^{\frac{1}{2}}k_2^{\frac{1}{2}}$
150° (6 runs)	0.666±0.136	1.50±0.30
200° (10 runs)	0.311±0.061	1.61±0.35
250° (4 runs)	0.135±0.029	1.92±0.35
	$E_4-E_5+\frac{1}{2}E_6 = 7.1$ kcal./mole	
	$E_5-\frac{1}{2}E_6-\frac{1}{2}E_2 \sim 1$ kcal./mole	

precision at each temperature considering the indirect nature of the calculations involved. In addition $E_4-E_5+\frac{1}{2}E_6 = 7.1$ kcal./mole estimated from the second column ratios compares well with $E_4-\frac{1}{2}E_2 \backsim 8.0$ kcal./mole determined directly while $E_5-\frac{1}{2}E_6-\frac{1}{2}E_2$ from the third column data is about zero.

Since E_2, E_5, and E_6 are activation energies of radical–radical combination reactions and are probably near zero, the agreement of the calculated values with those predicted by analogy to other similar mechanisms is excellent. The above treatment gives strong evidence that only the seven reactions enumerated by Kutschke, Wijnen, and Steacie are required to describe the photolysis of diethyl ketone adequately in the temperature range 150°–250°. The actual magnitude of the derived quantities must be accepted with some reservation because of the type of operations necessary in making the calculations.

The Formation of Ethylene

The ratio $R^{\text{total}}_{C_2H_4}/R_{C_4H_{10}}$ at temperatures under 150° was shown by Kutschke, Wijnen, and Steacie to be about constant at ∽0.1. However, at higher temperatures, and especially at high diethyl ketone concentrations and low absorbed intensities, this ratio increased. It was this latter evidence that led them to add reaction [7] to the mechanism of Dorfman and Sheldon (4). In the present study the absorbed intensity and ketone concentration have been varied over a much wider range and the essentials of this study are shown in Fig. 3 where $R^{\text{total}}_{C_2H_4}/R_{C_4H_{10}}$ is plotted vs. R_{CO}.[4] It is evident that $R^{\text{total}}_{C_2H_4}/R_{C_4H_{10}}$ tends toward a constant value of about 0.11–0.12 as the absorbed intensity is

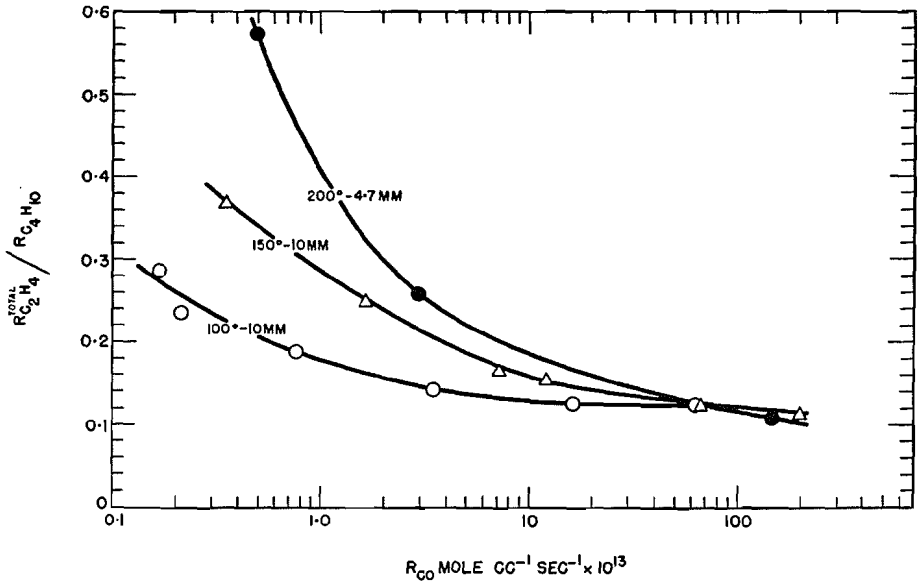

FIG. 3. Plot of $R^{\text{total}}_{C_2H_4}/R_{C_4H_{10}}$ vs. R_{CO}.

[4]*The quantum yield of diethyl ketone was carefully determined by Dorfman and Sheldon (4) at 60° and 120°. They found* $\Phi_{CO} = 1.0$ *within experimental error and consequently wrote reaction [1] as given previously. Thus it would seem that even at 60° any propionyl radical formed by* $C_2H_5COC_2H_5 \xrightarrow{h\nu} C_2H_5 + C_2H_5CO$ *would decompose before appreciable participation in other reactions causing its disappearance. At higher temperatures reactions [4] and [7] constitute a chain mechanism for CO production. However, a calculation from the data of Table I shows that no more than ca. 13% of the total CO is formed by reaction [7] in even the most unfavorable case at 250°. For this reason* R_{CO} *may be taken as a good approximation of the absorbed intensity.*

increased. For a given intensity the deviation from this value is greater at higher temperatures, and, although not indicated in Fig. 3, for fixed temperature and intensity a higher pressure is accompanied by greater deviations. The values of relatively few of the ratios are shown in Fig. 3 but those of all the photolyses follow the generalizations just given in a very regular manner as may be verified by simple calculations from Table I. At 250° the ratio was never lower than about 0.13 even in the very low pressure region. In fact at constant maximum *incident* intensity the minimum of 0.131 was at $[D] = 0.0345 \times 10^{-7}$ mole cm.$^{-3}$; both higher and lower concentrations produced a larger ratio. It is probable that the lower absorbed intensities due to the smaller percentage absorption at the concentrations below $[D] = 0.0345 \times 10^{-7}$ more than offset the effects of the lower concentrations of diethyl ketone tending to decrease the value of $R^{\text{total}}_{C_2H_4}/R_{C_4H_{10}}$. Limits on the intensity imposed by the B.T.H. lamp prevented a real test of this latter explanation.

The evidence given in the preceding sections indicates rather clearly that the disproportionation of ethyl radicals in the photolysis of diethyl ketone in the 3000 Å region is essentially independent of experimental conditions of temperature, intensity, and pressure over a very wide range. The variation in $R^{\text{total}}_{C_2H_4}/R_{C_4H_{10}}$ seems well explained by the production of extra ethylene formed by pentanonyl radical decomposition, reaction [7]. Calculation of $R^{\text{dp}}_{C_2H_4} = 0.12\ R_{C_4H_{10}}$ made earlier in the paper is justified on the basis of such a mechanism. The apparent value of the disproportionation to combination for other systems, especially in the photolysis of diethyl mercury, differs markedly from this value. Discussions of these other determinations are given by Ivin, Wijnen, and Steacie (6) and LeRoy and co-workers (12), and it appears that all recent evidence is in agreement with $k_3/k_2 = 0.12$–0.15.

The Combination of Ethyl Radicals. Third Body Effects

The influence of a third body effect on the combination of ethyl radicals in the photolysis process is conveniently demonstrated by comparing the rate of the combination reaction to the rate of some other reaction occurring simultaneously. This comparison reaction must not be dependent on such a third body deactivation. Both Dodd and Steacie (3) and Kistiakowsky and Roberts (7) used the methyl radical abstraction of a hydrogen atom from acetone for this purpose. An analogous treatment in the case of the diethyl ketone photolysis leads to the equations,

$$2C_2H_5 \xrightarrow{k_a} C_4H_{10}^*$$

$$C_4H_{10}^* \xrightarrow{k_b} 2C_2H_5$$

$$M + C_4H_{10}^* \xrightarrow{k_c} C_4H_{10} + M$$

$$R_{C_4H_{10}} = \frac{k_a[M]}{k_b/k_c + [M]}[C_2H_5]^2$$

$$[M] \gg k_b/k_c, \quad R_{C_4H_{10}} = k_a[C_2H_5]^2;$$

$$[M] \ll k_b/k_c, \quad R_{C_4H_{10}} = \frac{k_a k_c}{k_b}[M][C_2H_5]^2.$$

Thus if [M] is limited to diethyl ketone as a third body, the formation of butane should be independent of [D] above some low pressure. By using the

rate of ethane formation by the abstraction reaction [4], $R^{ab}_{C_2H_6} = k_4[C_2H_5][D]$, as a measure of the ethyl radical concentration, equations [I] and [II],

$$\frac{R^{ab}_{C_2H_6}}{R^{\frac{1}{2}}_{C_4H_{10}}[D]} = \frac{k_4}{k_a^{\frac{1}{2}}}\left[1+\frac{k_b}{k_c[D]}\right]^{\frac{1}{2}}, \qquad [I]$$

$$\frac{R^{ab}_{C_2H_6}}{R^{\frac{1}{2}}_{C_4H_{10}}[D]^{\frac{1}{2}}} = \frac{k_4}{k_a^{\frac{1}{2}}}\left[\frac{k_b}{k_c}+[D]\right]^{\frac{1}{2}}, \qquad [II]$$

may be derived. At a single temperature the first of these expressions should approach a constant value with increasing [D] while the latter should tend toward constancy at low [D] values. These two functions are plotted vs. [D] in Figs. 4 and 5. The curves of Fig. 4 follow in a general way the predicted

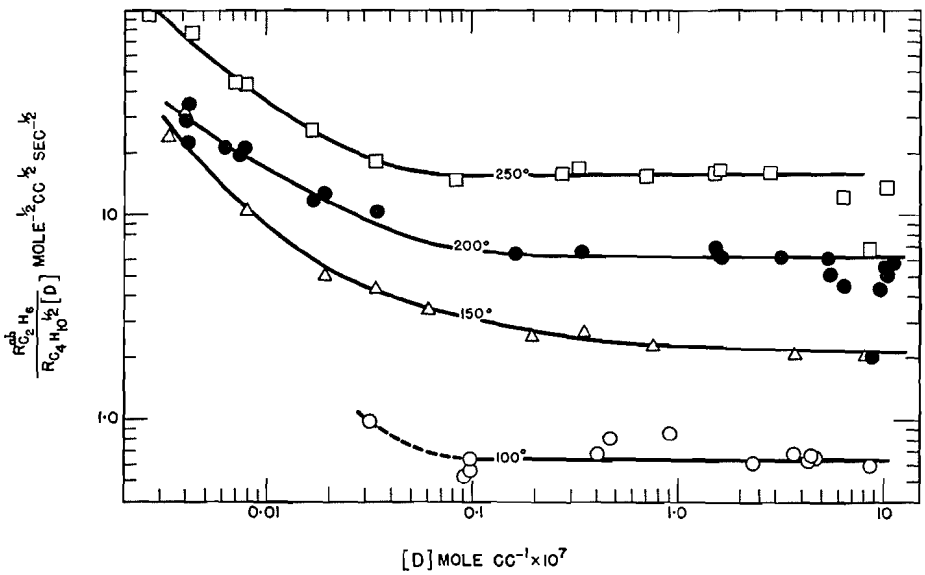

FIG. 4. Plot of $R^{ab}_{C_2H_6}/R^{\frac{1}{2}}_{C_4H_{10}}[D]$ vs. [D].

trend except for the experiments at the highest pressures in which the absorbed intensity was low. A possible explanation of this deviation has been given previously. The curves of Fig. 5 all show a decided increase in the low pressure region where they should be essentially constant if they were to behave as predicted by equation [II]. The dotted curve of Fig. 5 indicates that the data obtained at 200° in the cell with the increased surface area deviate to a still greater extent. It is evident that some heterogeneous reaction is affecting the variables of equations [I] and [II] in the low pressure region. How much of the total defect in the low pressure values of equation [I] from the high pressure value of $R^{ab}_{C_2H_6}/R^{\frac{1}{2}}_{C_4H_{10}}[D]$ is due to surface effects and how much is due to a third body deactivation anomaly is difficult to assess by this treatment. It seems significant that the minima in the curves of Fig. 5 occur at lower pressures (*ca.* 0.1 mm.) than do the corresponding ones (0.5–2 mm.) for the photo-

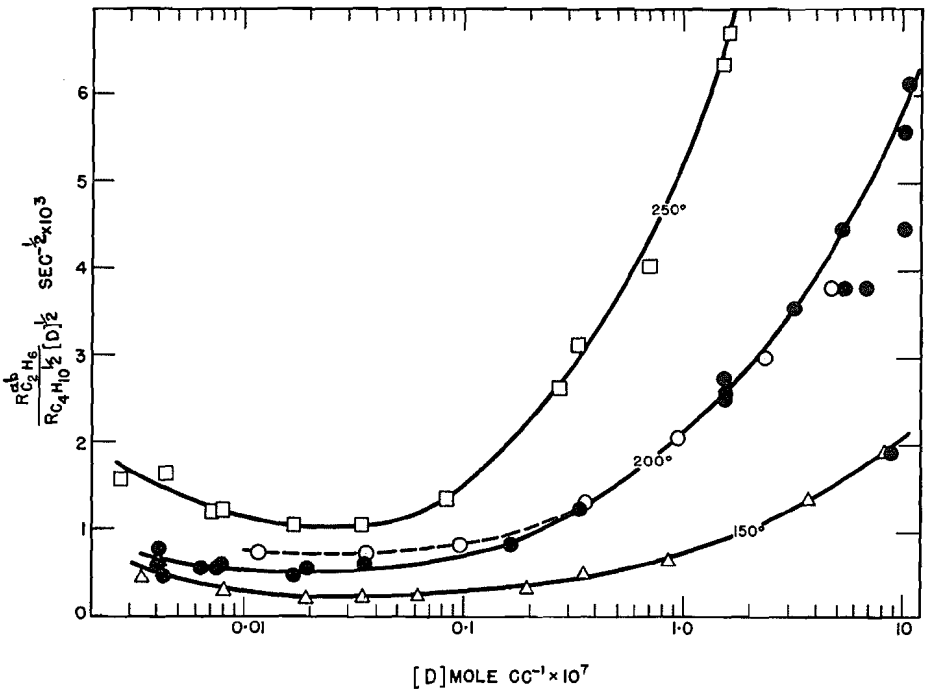

FIG. 5. Plot of $R^{ab}_{C_2H_6}/R^{\frac{1}{2}}_{C_4H_{10}}[D]^{\frac{1}{2}}$ vs. [D].

lysis of acetone given by Ausloos and Steacie (1). Since the influence of a heterogeneous reaction should not be appreciably different for the two ketones, the minima at lower pressures in the case of diethyl ketone could well indicate a much smaller third body effect.

A less complex and seemingly more meaningful treatment of the third body effect in the case of diethyl ketone is to compare the rate of disproportionation to the rate of combination. Although the reactants are identical in the two reactions it will be assumed that the two reaction intermediates differ and that the complex for the disproportionation reaction is not influenced by a third body effect. The disproportionation scheme will be

$$2C_2H_5 \xrightarrow{k_\alpha} C_4H_{10}^{**}$$

$$C_4H_{10}^{**} \xrightarrow{k_\beta} 2C_2H_5 \qquad R^{dp}_{C_2H_4} = [k_\alpha k_\gamma/(k_\beta+k_\gamma)]\,[C_2H_5]^2$$

$$C_4H_{10}^{**} \xrightarrow{k_\gamma} C_2H_4+C_2H_6$$

If this latter rate is combined with the expression already derived for the third body mechanism for butane formation, the rate of disproportionation to combination becomes

$$\frac{R^{dp}_{C_2H_4}}{R_{C_4H_{10}}} = \frac{k_\alpha k_\gamma/(k_\beta+k_\gamma)}{k_a k_c[D]/(k_b+k_c[D])}.$$

Since it has been found that this ratio is 0.12 independent of experimental conditions, it must be true that $[M]k_c \gg k_b$ or that the combination reaction is not showing a dependency on a third body deactivation down to pressures as low as 0.01 mm.

It is necessary to substantiate the two postulates made in the previous discussion: (*a*) the reaction intermediates of the disproportionation and combination reactions differ, and (*b*) the disproportionation complex will not be third body dependent. The two complexes may be represented as

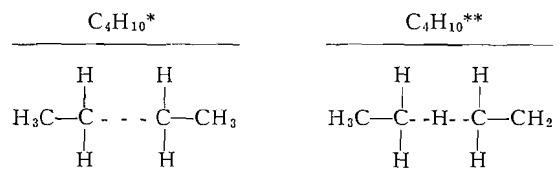

These same complexes were postulated by Wijnen and Steacie (14) to explain the composition of the various deuterated ethylenes formed in the photolysis of 2,2′4,4′ tetradeuterodiethyl ketone. Their evidence strongly supports a "head to head" intermediate for the combination and a "head to toe" intermediate for the disproportionation.

A consideration of the possible fates of the two complexes and the energetics involved leads to the conclusion that they should have very different response to a collisional deactivation. The combination of two ethyl radicals to form C_4H_{10}* produces a molecule essentially of the butane configuration which is "hot" by about 80 kcal./mole compared to the final butane product. If the possibilities of H atom rearrangements are ruled out as seems to be the case from Wijnen and Steacie's results (14), the only possible reactions available for C_4H_{10}* are deactivation by collision and dissociation into the original ethyl radicals. The C_4H_{10}** complex, on the other hand, cannot be deactivated to a stable molecule without an H atom shift. In addition the complex is not as "hot" as is C_4H_{10}* when it is compared to its end products, C_2H_4 and C_2H_6 ($2C_2H_5 \rightarrow C_2H_4+C_2H_6$, $\Delta H = -59$ kcal./mole). Most important, however, is the ability of the two product fragments of almost equal mass to distribute this excess energy between them so that the 30 kcal./mole carried by each product is far below that necessary to decompose either the ethylene or ethane.

A further test of the role of a third body was attempted by adding perfluorodimethyl cyclohexane to the reaction system. This gas was chosen because (*a*) its physical characteristics allowed an easy separation from the products of the photolysis, (*b*) it was transparent to the radiation used in the photolysis, (*c*) it was inert to the various radicals formed in the photolysis, and (*d*) the data of Dodd and Steacie indicated that its efficiency as a third body was quite high. Runs were made at 200° and 250° using essentially constant intensity and ketone concentration but with varying amounts of C_8F_{16} added. Experimental data and various calculated parameters for these runs are given in Table III. The most significant and unexpected result of the experiments was the increase in $R^{\text{total}}_{C_2H_4}/R_{C_4H_{10}}$ with an increase in C_8F_{16} concentration. Inas-

TABLE III

THE EFFECT OF ADDED PERFLUORODIMETHYL CYCLOHEXANE, C_8F_{16}

[D] (mm.)	C_8F_{16} (mm.)	R_{CO}	$R^{total}_{C_2H_4}$	$R_{C_4H_{10}}$	$R^{ab}_{C_2H_6}$	$R^{total}_{C_2H_4}/R_{C_4H_{10}}$	$R^{ab}_{C_2H_6}/R^{\frac{1}{2}}_{C_4H_{10}}[D]$
		mole cm.$^{-3}$ sec.$^{-1}\times10^{13}$					
			200°				
0.0234	0	1.00	0.103[0]	0.769	.0535	0.134	24.4
0.0234	0.552	0.958	0.106[6]	0.783	.0404	0.136	18.2
0.0215	1.60	0.933	0.107[8]	0.746	.0367	0.144	17.9
0.0235	4.95	0.971	0.127[5]	0.710	.0389	0.180	20.8
			250°				
0.0236	0	1.09[0]	0.123	0.836	.108	0.147	53.3
0.0246	0.177[2]	1.18[8]	0.127	0.874	.107	0.145	48.1
0.0248	1.16[2]	1.19[5]	0.162	0.794	.149	0.204	72.0
0.0238	4.99	1.19[6]	0.169	0.767	.120	0.220	59.4

much as the formation of butane would not be expected to be made less favorable by an added gas, the increase in the ratio must be attributed to an enhanced C_2H_4 formation. It seems likely that the unimolecular pentanonyl radical decomposition, reaction [7], is in its pressure dependent region at 0.02 mm. of diethyl ketone. Addition of C_8F_{16} must aid in the deactivation of the pentanonyl reaction complex thus increasing the C_2H_4 formation.

Values of $R^{ab}_{C_2H_6}/R^{\frac{1}{2}}_{C_4H_{10}}[D]$ in the last column of Table III, although not constant to a high degree of precision, show no trend with increasing C_8F_{16} concentration. The poorer agreement between the values is compatible with the difficulty of analyzing for the photolysis products contained in the very large amounts of added C_8F_{16}. The lack of any appreciable effect of even high C_8F_{16} concentrations on $R^{ab}_{C_2H_6}/R^{\frac{1}{2}}_{C_4H_{10}}[D]$ may substantiate the independence of the ethyl radical combination to pressure. Unfortunately this latter evidence is complicated by the unevaluated effect of the added gas on the heterogeneous formation of ethane. It might be expected that the greater gas concentration would reduce the rate of radical diffusion to the wall and in addition perhaps reduce the concentration of adsorbed substrate. Since both these effects would tend to decrease the heterogeneous ethane formation it is surprising that the values in the last column of Table III do not decrease at the high C_8F_{16} concentrations.

REFERENCES

1. AUSLOOS, P. and STEACIE, E. W. R. Can. J. Chem. 33: 47. 1955.
2. DODD, R. E. Trans. Faraday Soc. 47: 56. 1951.
3. DODD, R. E. and STEACIE, E. W. R. Proc. Roy. Soc. (London), A, 223: 283. 1954.
4. DORFMAN, L. M. and SHELDON, Z. D. J. Chem. Phys. 17: 51. 1949.
5. GOMER, R. and KISTIAKOWSKY, G. B. J. Chem. Phys. 19: 85. 1951.
6. IVIN, K. J., WIJNEN, M. H. J., and STEACIE, E. W. R. J. Phys. Chem. 56: 967. 1952.
7. KISTIAKOWSKY, G. B. and ROBERTS, E. K. J. Chem. Phys. 21: 1637. 1953.
8. KUTSCHKE, K. O., WIJNEN, M. H. J., and STEACIE, E. W. R. J. Am. Chem. Soc. 74: 714. 1952.
9. LEROY, D. J. Can. J. Research, B, 28: 492. 1950.
10. LUCAS, V. E. and RICE, O. K. J. Chem. Phys. 18: 993. 1950.
11. MILLER, D. M. and STEACIE, E. W. R. J. Chem. Phys. 19: 73. 1951.
12. SMITH, M. J., BEATTY, P. M., PINDER, J. A., and LEROY, D. J. Can. J. Chem. 33: 821. 1955.
13. TROTMAN-DICKENSON, A. F. and STEACIE, E. W. R. J. Chem. Phys. 19: 329. 1951.
14. WIJNEN, M. H. J. and STEACIE, E. W. R. Can. J. Chem. 29: 1092. 1951.

NOTE

A FURTHER OBSERVATION ON THE BIOGENESIS OF HYOSCYAMINE[1]

By Léo Marion and Alan F. Thomas[2]

It has been shown previously that in mature *Datura stramonium* plants putrescine is not involved in the formation of either hyoscine or hyoscyamine (3), and that ornithine is a precursor of hyoscyamine but not of hyoscine (7, 8). This fact has been interpreted as implying a different mode of formation for the two alkaloids (8), although the conclusion that hyoscine is no longer synthesized in the mature plant, while hyoscyamine is, is equally plausible (cf. 12).

In all cases of nitrogen methylation in plants studied so far methionine has always been found to act as a precursor of the methyl groups (1, 2, 4, 9) although formate and choline did not always perform that role (4, 9). Therefore, it appeared legitimate to assume that in *D. stramonium* methionine would perform the same function. On feeding C^{14}-methyl-labelled methionine to mature *D. stramonium*, both hyoscyamine and hyoscine should be radioactive because of the presence of an $N—C^{14}H_3$ group in each, if both alkaloids were still being synthesized, albeit by different pathways. On the other hand, were hyoscine no longer synthesized at the time of the experiment, then only the hyoscyamine should be radioactive.

It has now been found that when C^{14}-methyl-labelled methionine was fed to the mature plant and the alkaloids isolated, only the hyoscyamine but not the hyoscine was radioactive. There seems to be little doubt, therefore, that as stated by Trautner (12) hyoscine is formed at a comparatively early stage in the development of the plant, after which hyoscyamine is formed exclusively. Although it is possible that hyoscine could be synthesized from a different precursor, the fact that this base is no longer produced in the mature plant accounts for the failure of ornithine-2-C^{14} to give rise at this stage to radioactive hyoscine (7, 8).

Very recently, in a study of the metabolism of glycine-2-C^{14} in vigorously growing *D. ferox*, Evans and Partridge (6) found that both hyoscine and meteloidine were radioactive, but also they observed that the labelling of the alkaloids varied significantly with the state of maturity of the plant.

In reporting the results of previous experiments on feeding ornithine-2-C^{14} to *D. stramonium*, the radioactivity of the amino acid fraction obtained from the plant extract was assumed to be due to the presence of excess labelled ornithine (8). Examination of this fraction has now revealed that it contained practically no ornithine, and hence the radioactivity of this fraction must be attributed to other amino acids arising from the metabolism of ornithine.

EXPERIMENTAL

dl-C^{14}-Methionine prepared from *dl*-homocysteine according to the method of Melville, Rachele, and Keller (10) had an activity of 1.07×10^7 counts per

[1]*Constitutes Part XV of the series on the Biogenesis of Alkaloids. Issued as N.R.C. No. 3756.*
[2]*National Research Council of Canada Postdoctorate Fellow, 1954–1955.*

min. per mgm. (1.59×10^9 counts per min. per millimole); and 74 mgm. was fed to a mature *D. stramonium* plant as described previously (3). The methionine was rapidly taken up by the plant, over 90% having been absorbed in four days at which time it was harvested. The radioactivity then was distributed as follows in counts per min. per mgm. (before drying): roots, 1000; leaves, 9; seeds, 4. The whole plant was dried at 100° in an oven for 48 hr., and the crude alkaloids isolated as described already (8). To the crude mixture of alkaloids 250 mgm. each of hyoscine and hyoscyamine was added and the mixture was dissolved in ether. The total activity of the crude solution at this stage was 6.34×10^6 counts per min. (i.e. *ca.* 1% of the total activity administered). Separation of the alkaloids was effected by chromatography on a kieselguhr column as described by Evans and Partridge (5) since the method previously used (8, 11) was found to be unreliable. The alkaloids were purified finally by recrystallization of the aurichlorides to constant activity. Hyoscyamine was found to have an activity of 5.8×10^4 counts per min. per millimole, while that of hyoscine, although faintly positive at first, had dropped to zero after three recrystallizations from water.

The N-methyl group was eliminated from the hyoscyamine in a Herzig-Meyer determination, the reaction being carried out as described by Dubeck and Kirkwood (4) up to the precipitation of the tetramethylammonium reineckate. The precipitate was dissolved in acetone and chromatographed on alumina which retained the impurities while the tetramethylammonium reineckate passed through the column. The solution was concentrated under reduced pressure at room temperature and diluted with water. The salt crystallized as pale pink leaflets, m.p. 288–289° (decomp.). Its activity was 5.4×10^4 counts per min. per millimole.

As reported previously (8), *D. stramonium* fed with C^{14}-labelled ornithine yielded when extracted, besides labelled hyoscyamine, a radioactive amino acid fraction. This fraction has now been examined further by two-dimensional paper chromatography. It was found to contain mainly the following free amino acids: asparagine, glycine, alanine, proline (trace), methionine, and aspartic acid. Neither ornithine nor glutamic acid was present in appreciable concentration.

1. Byerrum, R. U., Flokstra, J. H., Dewey, L. J., and Ball, C. D. J. Biol. Chem. 210: 633. 1954.
2. Dewey, L. J., Byerrum, R. U., and Ball, C. D. J. Am. Chem. Soc. 76: 3997. 1954.
3. Diaper, D. G. M., Kirkwood, S., and Marion, L. Can. J. Chem. 29: 964. 1951.
4. Dubeck, M. and Kirkwood, S. J. Biol. Chem. 199: 307. 1952.
5. Evans, W. C. and Partridge, M. W. J. Pharm. and Pharmacol. 4: 769. 1952.
6. Evans, W. C. and Partridge, M. W. J. Pharm. and Pharmacol. 6: 702. 1954.
7. Leete, E., Marion, L., and Spenser, I. D. Nature, 174: 650. 1954.
8. Leete, E., Marion, L., and Spenser, I. D. Can. J. Chem. 32: 1116. 1954.
9. Matchett, T. J., Marion, L., and Kirkwood, S. Can. J. Chem. 31: 488. 1953.
10. Melville, D. B., Rachele, J. R., and Keller, E. B. J. Biol. Chem. 169: 419. 1947.
11. Schill, G. and Agren, A. Svensk Farm. Tidskr. 56: 55. 1952. Chem. Abstr. 46: 6324. 1952.
12. Trautner, E. M. Australian Chem. Inst. J. & Proc. 14: 411. 1947.

Received August 12, 1955.
Division of Pure Chemistry,
National Research Council,
Ottawa, Canada.